ISCI 2011

Copyright and Reprint Permission: Abstracting is permitted with credit to the source. Libraries are permitted to photocopy beyond the limit of U.S. copyright law for private use of patrons those articles in this volume that carry a code at the bottom of the first page, provided the per-copy fee indicated in the code is paid through Copyright Clearance Center, 222 Rosewood Drive, Danvers, MA 01923. For other copying, reprint or republication permission, write to IEEE Copyrights Manager, IEEE Operations Center, 445 Hoes Lane, Piscataway, NJ 08854. All rights reserved. Copyright ©2011 by IEEE.

2011 IEEE Symposium on Computers & Informatics

IEEE Catalog Number: CFP1163N-CDR

ISBN: 978-1-61284-690-3

Menu

Welcome Message

Table of Contents

International Advisory / Liason

Organizing Committee

Reviewers

Technical Program Overview

Technical Program / Abstract

Author Index

Manuscripts

CD-ROM Support: ISCI 2011 Secretariat *Phone*: (+603) 5543 5052 *Fax*: (+603) 5544 276 *Email*: ieeeisci@gmail.com

Sponsor

IEEE Advancing Technology for Humanity

IEEE computer society

IEEE Malaysia Computer Chapter

pels ies IAS IEEE INDUSTRY APPLICATIONS SOCIETY

IEEE Malaysia PEL/IE/IA Joint Chapter

Organizer

Universiti Teknologi MARA Malaysia

RMI

Research Management Institute
Universiti Teknologi MARA

WELCOME MESSAGE

On behalf of the Organizing Committee of the three events of IEEE Symposium on Computers and Informatics (ISCI 2011) it gives me great pleasure in welcoming all delegates to Kuala Lumpur, Malaysia. The event is held from 20 to 22 March 2011 at the Renaissance Kuala Lumpur Hotel, Kuala Lumpur, Malaysia. The event is sponsored by the IEEE Malaysia, the IEEE Malaysia Power Electronics (PEL)/Industrial Electronics (IE)/ Industrial Applications (IA) Joint Chapter, the IEEE Malaysia Computer Chapter and co-organised with the Research Management Institute and Centre of Computer Engineering Studies, Faculty of Electrical Engineering, Universiti Teknologi MARA, Malaysia.

The symposium is to create a forum for scientists, engineers and practitioners on the varied disciplines and its associated applications. In line with IEEE's vision of Advancing Technology for Humanities beyond traditional boundaries, tracks on Humanities, Finance and Business applications has been introduced.

We are very glad to mention that the Proceedings of ISCI2011 will be included in the IEEE Xplore database.

We have received approximately 394 full paper submissions. Over 600 reviewers worldwide volunteered to evaluate papers of which finally more than 147 papers are to be presented at the event through 4 parallel sessions and 3 parallel tutorials. The event is scheduled with 16 half-day oral sessions. There is a welcome reception on Sunday evening (20 March 2011) and a Gala Dinner on Monday evening (21 March 2011). Throughout these events, we hope to create an opportunity for old friends and colleagues to get together, and more importantly, to welcome new peers in diverse areas of expertise.

On behalf of the organizing committee we would like to take this opportunity to express our gratitude to all reviewers who have been working hard to finish reviews on time and hence ensured the success of this event. Members of the International Advisory Committee deserve special appreciation as they played key supportive role in the symposium organization. We would like to thank all authors, session chairpersons, reviewers and delegates for your great support and contribution to the event. Last but not least are the Organizing Committee, colleagues and friends who have been working behind-the-scenes; who deserve special mention. Without their unfailing cooperation, hard work and dedication, this event would simply not be possible.

I understand that many delegates are here in Malaysia for the first time. I would like to encourage you to explore the beautiful sights of Malaysia during your stay and do enjoy the conference.

MUSTAFAR KAMAL HAMZAH
Chair, IEEE Malaysia PEL/IE/IA Joint Chapter
General Chair, ISCI 2011

TABLE OF CONTENTS

WELCOME MESSAGE ..... **i**
TABLE OF CONTENTS ..... **ii**
INTERNATIONAL ADVISORY / LIAISON ..... **iii**
ORGANIZING COMMITTEE ..... **iii**
REVIEWERS ..... **iv**
TECHNICAL PROGRAM OVERVIEW ..... **viii**
TECHNICAL PROGRAM / ABSTRACT ..... **ix**

Tutorial 1 (Sanjeev Sofat & Divya): Security Issues in Wireless Mesh Networks
Tutorial 2 (Anitawati Mohd Lokman): Human Factors in Interface Design
Tutorial 3 (Mohd Khairul Mohd Salleh): Side-Coupled Ring Resonators for Pseudo-Elliptic Microwave Bandpass Filters
A11: Artificial Intelligence I
D11: Network & Communications Technology I
B11: Applications I
C11: Signal & Image Processing I
A12: Artificial Intelligence I (cont)
D12: Network & Communication Technology I (cont)
B12: Applications I (cont)
C12: Signal & Image Processing I (cont)
A13: Artificial Intelligence & Computer Engineering
D13: Network & Communication Technology II
B13: Applications II
C13: Signal & Image Processing II
A14: Artificial Intelligence & Computer Engineering (cont)
D14: Network & Communication Technology II (cont)
B14: Applications II (cont)
C14: Signal & Image Processing II (cont)
D21: Network & Communication Technology III
B21: Applications III
C21: Signal Processing & Communications Technology
A21: Software Engineering & Applications
C22: Signal Processing & Communications Technology (cont)
D22: Network & Communications Technology III (cont)
B22: Applications III (cont)
A22: Software Engineering & Applications (cont)
A23: Autonomic and Trusted Computing
C23: Bioinformatics & Computational Biology
B23: Human Factors & Applications
D23: Network & Communication Technology IV
B24: Human Factors & Applications (cont)
D24: Network & Communication Technology IV (cont)

AUTHOR INDEX **0**
MANUSCRIPTS **1**

INTERNATIONAL ADVISORY / LIAISON

Okyay Kaynak, Bogazici Univ, *Turkey*

Abdul Halim Mohd Yatim, *Universiti Teknologi Malaysia*

Norman Mariun, *Universiti Putra Malaysia*

Abu Bakar Majeed, *Universiti Teknologi MARA*

Marzuki Khalid, *Universiti Teknologi Malaysia*

Mohd Nasir Taib, *Universiti Teknologi MARA, Malaysia*

Mohamed Rawidean Mohd Kassim, *MIMOS, Malaysia*

ORGANIZING COMMITTEE

General Chair:
Mustafar Kamal Hamzah (General Chair)
Mohamed Rawidean Mohd Kassim

Secretary:
Roslina Mohammad

Finance Chair:
Yuslinda Wati Mohamad Yusof

Publication Chair:
Mohammad Nawawi Seroji
Mohd Zafran Abd Aziz

Local Arrangement Chair:
Ruhani Abdul Rahman

Publicity & Website Chair:
Ihsan Mohd Yassin

Program Chair:
Nooritawati Md Tahir
Habibah Hashim
Mohd Khairul Mohd Salleh

REVIEWERS

A Rahim, Mohamad Kamal
A., Jasmin
Aazam, Mohammad
Ab Kadir, Rosmalini
Ab Wahab, Norfishah
Abbas, Nidaa
Abd Aziz, T. J. Iskandar
Abd Khalid, Noor Elaiza
Abd Latiff, Muhammad Shafie
Abd Malek, Mohd Fareq
Abd Wahab, Mohd Helmy
Abdallah, Omari
Abdul Aziz, Mohd Zafran
Abdul Aziz, Noor Hafizah
Abdul Ghani, Nor Maniha
Abdul Kadir, Herdawatie
Abdul Mutalib, Ariffin
Abdulal, Wael
Abdulla, Mouhamed
Abdullah, Azian Azamimi
Abdullah, Azizol
Abdullah, Azween
Abdullah, Junaidi
Abdullah, Lazim
Abdullah, Noor Ezan
Abg Jawawi, Dayang Norhayati
Abu Bakar, Nordin
Abu Bakar, Raudah
Abu Bakar, Zahari
Abu Hassan, Hasliza
Aburas, Akram
Achmad, Balza
Adeyeye, Michael
Adhicandra, Iwan
Agrawal, Himanshu
Ahamed, Imthias
Ahmad, Idawaty
Ahmad, Mohd Ashraf
Ahmad, Noraziah
Ahmad Fauzi, Mohammad Faizal
Ahmed, Louazani
Ahmed, Nisar
Ahmed, Shaftab
Ahmed, Syed
Ahmed, Syed Khaleel
Ahrary, Alireza
AÃsa, JesÃºs
Akmeliawati, Rini
Al Harbi, Fatima
Al Jadaan, Omar
Al Junid, Syed Abdul Mutalib
Al Soufy, Khaled Abdullah
Al-Ani, Muzhir
Al-Azzawi, Nemir
Al-Humoud, Sarah
Al-Nasser, Faisal
Al-Saif, Abdulwahid
Al-waely, Waail
Alam, Mahtab
Alam, Muhammad Raisul
Aldawibi, Omar
Alhaffa, Alaa
AlHaj, Dr. Salahideen
Alharbi, Fahd
Alhmiedat, Tareq
Ali, Abdul Halim
Ali, Md.
Ali, Syed Faisal
Ali Munir, Handy
Almisreb, Ali
Alnoukari, Mouhib
Alomari, Abdallah
Alqudah, Yazan
AlSabbagh, Haider
Alzoabi, Zaidoun
Amanatiadis, Angelos
Aminudin, Norziana
Amirtharajan, Rengarajan
Ammar, Ammar
Amutha Prabha.N,
Anagnostopoulos, Ioannis
Anani, Nader
Andrews, Samraj
Ang, Li Minn
Annamalai, Muthukkaruppan
Anwar, Muhammad
Anwari, Makbul
Arbain @ Sulaiman, Norakmar
Arnia, Fitri
Asirvadam, Vijanth
Askari, Mohsen
Aslam, Saira
Asmat, Arnis
Atan, Rodziah
Atani, Reza
Awad, Mohammed
Awang, Robi'atun Adayiah
Awang, Robiatun
Awang Rambli, Dayang
Ayadi, Ahmed
Aye, Win
Ayu, Media
Ayyadurai, Velmurugan
Aziz, Khurram
Azman, Afizan
Azzouzi, Messaouda
B, Chandra Mohan
B, Chitti Babu
B, Janet
Baba, Noor Hasimah
Bahari Jambek, Asral
Bahrami, Mehdi
Balakrishnan, Arunkumar
Baloch, Javed
Baluapuri, Apoorva
Banerjee, Usha
Banimelhem, Omar
Bany Mohammed, Ashraf
Bao, Paul
Barukang, L.
Bashar, Abul
Battula, Krishna
Beeran Kutty, Suhaili
Belkhamza, Zakariya
Bhakthavatchalu, Ramesh
Bhatia, Komal
Bodini, Giovanni
Bouzari, Hamed
Bushehrian, Omid
Calvo-Gallego, Jaime
Castiglione, Aniello
Castro, Gerson
Celebi, M. Emre
Chai, Douglas
Chaki, Ayan
Chandra, Aniruddha
Chatterjee, Bijoy
Chattopadhyay, Tanushyam
Chaudhary, Ankit
Chaurasia, Parul
Che Abdullah, Syahrul Afzal
Cheah, Cheng Lai
Chen, Tsung Teng
Chen, Uei_Ren
Cheong, Marc
Chetouani, Aladine
Chetty, Girija
Chiang, Ming-Chin
Chilamkurti, Naveen
Chin, Siew Wen
Choudhary, Deepak
Chowdhury, Iqbal
Chrysoulas, Christos
Chu, Chung-Hua
Chuah, Teong Chee
Chuprat, Suriayati
Connie, Tee
Cullen, Jeff
Da Costa, Daniel Benevides
Dadhich, Reena
Dalal, Upena
Dalvi, Ashwini
Dani Baba, Mohd
Danyaro, Kamaluddeen
David, Sumam
De Silva Lokuge, Kulari
Debita, Grzegorz
Dehghantanha, Ali
Derakhshan-Barjoei, Pouya
Desai, Anirudhha
Deshmukh, Sudarshan
Dettori, Paolo
Djemaiel, Yacine
Do, Van Thanh
Doomun, Razvi
Dorn, Marcio
Duarte, Carlos
Dubey, Ashutosh
Dundas, Jitesh
Duraisamy, Lenine. D
Edalati, Homa
El-Saleh, Ayman
ElÃ§i, Atilla
Esro, Mazran

Farquad, Mohammed
FernÃ¡ndez Del Carpio, Gonzalo
Fessi, Boutheina
FiaschÃ©, Maurizio
Fiorini, Michele
Fonseca, David
Forouzanfar, Mohamad
Fu, Chong
Furuie, Sergio
G p, Sajeev
Ganapathy, Gopinath
Garg, Hitendra
Gawanmeh, Amjad
George, Abraham
Georgiev, Georgi
Ghaffar, Rosniwati
Ghafoor, Kayhan
Ghahari, Alireza
Ghani, Imran
Giri, Debasis
Goel, Anisha
Goh, Jung Hean
GonzÃ¡lez, Norton
Gopalakrishnan Nair, Nithya
Govindaswamy, Visvasuresh Victor
Gui, Guan
Gulati, Ruchir
Gull, Sonia
Guo, Ya
Gupta, Brij
Habbal, Adib
Habib, Sami
Habibi Lashkari, Arash
Hafeez, Moaaz
Halim, Abdul Karimi
Hamid, Fazrena
Hamouid, Khaled
Hamzah, Mustafar Kamal
Han, Byeong-jun
Handigund, Shivanand
Hari, Om
Hariharan, Shanmugasundaram
Haron, Muhammad Adib
Hashim, Habibah
Hashizume, Ayako
Hassab Elgawi, Osman
Hassan, Hasmarina
Hassan, Sa'adah
Hassan, Taysir
Herawan, Tutut
Herman, Sukreen Hana
Hidayat, Mas Irfan
Ho, Chee-Kit
Hoque, Rezaul
Hossain, Shahadat
Hosseini, Mostafa
Hussin, Hanim
Ibrahim, Ahmad Fauzi
Ibrahim, Hamidah
Ibrahim, Idnin Pasya
Ibrahim, Zaidah
Idoudi, Hanen
Imtiaz, Hafiz
Imtiaz Bin Hamid, Nafiz
Indera Putera, Siti Hazurah
Islam, Md.
Islam, Md. Rajibul
Ismail, Marina
Ismail, Roslan
Ismail, Yusof
Israr, Nauman
Issac, Biju
Jaiswal, Manish
Jamaluddin, Jehana Ermy
Jamaludin, Md Zaini
Jamil, Nursuriati
Jat, Dharm
Jayabalan, Sudharsan
Jayakumar, Geetha
Jeoti, Varun
Jha, Rakesh
Jia Yew, Teh
JimÃ©nez MacÃas, Emilio
Johari, Ayob
Joseph, Annie
Joseph, Gnana
Joshi, Madhuri
Jotsov, Vladimir
Jusoh, Shaidah
JÃ¸nvik, Tore
Kalwar, Santosh
Kamalrudin, Massila
Kamaluddin, Mohd Uzir
Kamarudin, Latifah Munirah
Kamaruzaman, Fairus
Kameas, Achilles
Kannan, S
Kannan, Subarmaniam
Kar, Rajib
Karim, Aymen
Karimi, Abbas
Karmakar, Subrata
Karmakar, Sushanta
Kassim, Murizah
Katuk, Norliza
Kenzi, Adil
Kerdvibulvech, Chutisant
Khairnar, Vaishali
Khalid, Fatimah
Khan, M Ayoub
Khan, Muhammad Fahim
Khan, Muhammad Imran
Khani, Naser
Khanjary, Mohammad
Kheyrihassankandi, Jahangir
Khin Wee, Lai
Khokhar, Rashid
Khong, Chee Weng
Kim, Geun-Hyung
Kim On, Chin
Kisku, Dakshina Ranjan
KÃ¶bel, Christian
Korchiyne, Redouan
Korhonen, Vesa
Kotchasarn, Chirawat
Kotwal, Mohammed
Kourgli, Assia
KR, Chetan
Kraidi, Aaras
Kranthi Rekha, Chennaboina
Krishna Kumar, M
Kuang, Yu
Kuehnhausen, Martin
Kumar, Alok
Kumar, Mohit
Kumar, Pramod
Kumar, Pravin
Kumar, Rajesh
Kumar, Rajinder
Kumar, Rangaraju Naveen
Kumar, S
Kumar, Samaksh
Kumar, Vijay
Kumar, Vikash
Kumbhakar, Pathik
Kumngern, Montree
Kurundkar, Sangeeta
Labadin, Jane
Lagha, Mohand
Lahtela, Antti
Lakhtaria, Kamaljit
Lalbakhsh, Pooia
Lauwens, Ben
Lazar, Cosmin
Le, Tan
Le Ngo, Anh Cat
Lee, DongJin
Lee, Gordon
Lee, Wookwon
Lee, Yih-Jiun
Lendak, Imre
Li, Kin Fun
Li, Xiaohang
Li, Xu
Liao, Iman
Lim, King Hann
Logeswaran, Rajasvaran
Lopes, Rafael
Lotfi, Ehsan
Lu, Chao
M Thampi, Sabu
M. Thamrin, Norashikin
Mahmud, Jamaluddin
Mahmud, Mufti
Mahmuddin, Massudi
Maity, Tanmoy
Man, Mustafa
Manangi, Suhas
Mandal, Durbadal
Manickam, Karthikeyan
Maniktala, Saurabh
Mantoro, Teddy
Manzoor Qasim, Syed
Marchetti, Eda
Marimuthu, Paulvanna Nayaki
Martinez Castillo, Juan Jose
Martinez Perez, Gregorio
Mashinchi, M. Reza
Mason, Alex
Masoumi, Behrooz
Masrie, Marianah
Masud, Abdullah

Mat Isa, Mohd Anuar
Mat Jubadi, Warsuzarina
Mat Jusoh, Rizal
Mat Yamin, Fadhilah
Mayron, Liam
Mazalan, Lucyantie
McLauchlan, Lifford
Md Enzai, Nur Idawati
Md Noor, Rafidah
Md Norwawi, Norita
Md Tahir, Nooritawati
Mehdi, Hamid
Meher, Sukadev
Mehrotra, Rishabh
Memon, Qurban
Miaji, Yaser
Millham, Richard
Mirmotahhary, Navid
Mishra, Prabhakar
Mittal, Varun
Mohamad, Roslina
Mohamad Anas, Nuzli
Mohamad Mohsin, Mohamad Farhan
Mohamad Yusof, Yuslinda Wati
Mohamad Zaini, Norliza
Mohamed @ Omar, Hasiah
Mohamed Said, Mohamed Faidz
Mohamed Suffian, Muhammad Dhiauddin
Mohammad, Suraya
Mohammed, Jafar
Mohd, Masnizah
Mohd Ali, Darmawaty
Mohd Ali, Mohd Alauddin
Mohd Aripin, Norazizah
Mohd Fauzi, Shukor Sanim
Mohd Hussin, Naimah
Mohd Kassim, Mohamed Rawidean
Mohd Lokman, Anitawati
Mohd Noor, Uzer
Mohd Salleh, Mohd Idzwan
Mohd Yussoff, Yusnani
Mohd. Daud, Salwani
Mohd. Sani, Nor Fazlida Mohd. Sani
Mokhsin, Mudiana
Moorthi, Sridharan
Mostafavi Isfahani, Sayed Mohammad
Moumen, Hamouma
Mourad, Amad
Mozi, Aiza Mahyuni
Mridha, Muhammad
MS, Sricharan
Muddenahalli Nagendrappa, Thippeswamy
Mueller, Juergen
Muhammad, Ghulam
Mukahar, Nordiana
Murugappan, M
Musfiqur Rahman, Sharif Mohammad
Mustaf, Omar
Muthusamy, Hariharan
N, Prabaagarane
Nabil, Waleed
Nabiollahi, Akbar
Nadian, Ali
Nani Fadzlina, Naim
Narote, Sandipan
Nassar, Mahmoud
Nasseri, Mona
Nauman, Mohammad
Nazir, Muhammad
Nejadmorad, Fatemeh
Ng, Hu
Ng, Jia Tsing
Ngan, Henry Yuk-tung
Niazi, Muaz
Nisar, Humaira
Noor, Norliza
Noor Batcha, Mohamed Farid
Noruzi Nashalji, Mostafa
Nusrath Ali, K A
Nyamasvisva, Elisha
Olatunji, Sunday
Olivares Bueno, JoaquÃn
Omar, Dr. Khairuddin
Omar, Hasmila Akmar
Omara, Fatma
Osman, Rasha
Othman, Mohamed
Othman, Mohd Shahizan
Oztekin, Halit
Ozyurt, Ozcan
P v, Arun
Padmapriya, Arumugam
Panakala, Rajesh Kumar
Pandey, Punit
Pandit, Amit
Pang, Grantham
Pang, Ying Han
Park, Sang Kyu
Patel, Ahmed
Patel, Bhavesh
Patil, Rajendrakumar
Patil, Varsha
Payakpate, Janjira
Pemmaraju, Ananda Mohan
Peng, Chin-Hung
Permpoontanalarp, Yongyuth
Persis Urbana Ivy, Persis Urbana Ivy
Pileggi, Salvatore
Pinheiro, Eduardo
PirahanSiah, Farshid
Po, Lai Man
Poppe, Chris
Potuganuma, Jaswini Reddy
Prabhu, Cmr
Prakash Raj, E. George
Prasad, Lalji
Puteh, Mazidah
R Porle, Rosalyn
Radha Charan, Chandragiri
Rahim, Aneel
Rahman, Kazi Atiqur
Rahman, Tarif
Rajendran, Sabapathy
Rajput, Anshul
Ramadan, Rabie
Ramesh, Maneesha
Ramli, Arnidza
Ramli, Dzati Athiar
Ramli, Suzaimah
Ranathunga, Lochandaka
Rangel-Magdaleno, Jose
Rao, Suryakari
Rashidi-Bajgan, Hannaneh
Rawoof, Fathima
Reddy, Ganta
Reel, Parminder Singh
Rekhis, Slim
Rezvanian, Alireza
Rind, Abdul
Riyadi, Munawar
Rizvi, Syed
Rohani, Vala Ali
Romano, Paolo
Romoozi, Mojtaba.
Romsaiyud, Walisa
Rosman, Rafidah
Ruthramurthy, Balachandran
Ryu, Eun
S, Issac Niwas
Saad, Hasnida
Saaidin, Shuria
Sadeghzadeh, Ramezan Ali
Sadistap, Shashikant
Sadkhan, Sattar
Sadrolhosseini, Amir
Sah, Nagendra
Saha, Amit Kumar
Saha, Arun
Sahari @ Ashaari, Noraidah
Sahula, Vineet
Saini, Sandeep
Salatian, Apkar
Saleem, Kashif
Saleh, Moutaz
Salehinejad, Hojjat
Salgia, Ankit
Samad, Mustaffa
Sanaatiyan, Mohammad Mehdi
Sanap, Pratap
Sandoval Orozco, Ana Lucila
Saparon, Azilah
Sarkar, Nurul
Sarkar, Sajal
Sarnin, Suzi
Sathyamoorthy, Dinesh
Satyanarayana Murthy sarma, Nimushakavi
Sauli, Zaliman
Sayeed, Md. Shohel
Schaffa, Frank
Seifi Majdar, Reza
Selamat, Ali
Seman, Kamaruzzaman
Sen, Jaydip
Sh Ahmad, Sabarinah
Sha Sadeghi, Mokhtar
Shah, Kriyang
Shah, Nimit
Shah, Peer
Shah, Satish
Shah, Sumiran
Shahbudin,
Shahid Manzoor, Rana

Shaik Mohamed, Shahrizat
Shaikh, Fatema
Shaker, Sherif
Shanmugalingam, Sivasothy
Sharifi, Mohammad
Sharma, Ankit
Sharma, Hemant
Sharma, Madhu
Sharma, Manoj
Sharma, Nitinipun
Sheeja, M. K.
Sheikholeslami, Arman
Shinghal, Kshitij
Siddique, Uzma
Sim, K. Y.
Simeonov, Stanislav
Sin Ban, Ho
Singh, Buddha
Singh, Jagbeer
Singh, Neeta
Singh, Satish
Singhal, Priyank
Sinha, Adwitiya
Skliarova, Iouliia
Sklyarov, Valery
Souza, Andre
Soyturk, Mujdat
Sreelal, Sreedharan Pillai
Sridevi, Balu
Srikrishnan, Rangamani
Srinivasan, Madhan Kumar
Srivastava, Rajeev
Srivastava, Viranjay
Staniec, Kamil
Suandi, Shahrel
Subahir, Suhaila
Sudarsan, Rajesh
Sugiyama, Kazunari
Sulaiman, Ahmad Asari
Sulaiman, Ir. Riza
Suliman, Saiful
Sumari, Putra
Sundaraj, Kenneth
Suresh, Sankaranarayanan
Syed Adnan, Syed Farid
Tahat, Ashraf
Taib, Mohd Nasir
Talbar, Sanjay
Talluri, Kalyan chakravarthy
Tan, Alan
Tan, Chong Eng
Tan, Su Wei
Tan, Wooi Haw
Tang, Adelina
Tanveer, Tamleek
Tavassoli, Sude
Tay, Kai Meng
Tay, Tee Tiong
Taylor, Ken
Tee, Sim-Hui
Teixeira, Otavio
Thekkeyil Kunnath, Abishek
Thomas, Bindu
Thompson, John
Thuneibat, Saed
Tian, Tian
Tiwari, Navneet Tiwari
Tohidi, Shahab-o-din
Tong, Hau Lee
Toorani, Mohsen
Trivedi, Harsh
Tyagi, Priti
Tyagi, Sapna
Udgata, Siba
Ukil, Arijit
Upadhyay, Amit
Usman, Mohammed
Usman, Muhammad
Varshneya, Gopalji
Varzakas, Panagiotis
Vasumathi, Balasubramaniam
Vattakuzhy, Renju
Verma, Seema
Veselovsky, Gennady
Vidhate, Amarsinh
Viswacheda, Duduku V
Vu, Thao
W.Muhamad, Wan Norsyafizan W Muhamad
Wan Ishak, Wan Hussain
Wan Mohd Isa, Wan Abdul Rahim
Wan Zainal Abidin, Wan Azlan
Wang, Jie
Wang, Kun-Ching
Werner, Martin
Winandy, Marcel
Wong, Chi-Ming
Wong, Chui Yin
Xiao, Xiaoqiang
Ya'acob, Norsuzila
Yahya Dawod, Ahmad
Yang, Jui-Pin
Yassin, Ihsan
Yin, Shuangye
You, Kok Yeow
Yu, Fan
Yussof, Salman
Zaim, A. Halim
Zaini, Norliza
Zainol Abidin, Husna
Zakaria, Zulkarnay
Zaman, Noor
Zaman, Rafi
Zamli, Kamal Zuhairi
Zarafshan, Faraneh
Zargari, Farzad
Zawawi, Mohd Anwar
Zhang, Chaohai
Zhang, Haipeng
Zhao, Gang
Zolkapli, Maizatul

TECHNICAL PROGRAM OVERVIEW

Time	Function Room 5	Function Room 6	Function Room 7	Function Room 9
Sunday, March 20				
02:10 PM	R1: *Registration (Foyer)*			
02:40 PM	Tutorial 1 (Sanjeev Sofat & Divya): *Security Issues in Wireless Mesh Networks*	Tutorial 2 (Anitawati Mohd Lokman): *Human Factors in Interface Design*		Tutorial 3 (Mohd Khairul Mohd Salleh): *Side-Coupled Ring Resonators for Pseudo-Elliptic Microwave Bandpass Filters*
03:40 PM	AB1: *Afternoon Break (Foyer)*			
04:00 PM	Tutorial 1 (Sanjeev Sofat & Divya): *Security Issues in Wireless Mesh Networks (Cont)*	Tutorial 2 (Anitawati Mohd Lokman): *Human Factors in Interface Design (cont)*		Tutorial 3 (Mohd Khairul Mohd Salleh): *Side-Coupled Ring Resonators for Pseudo-Elliptic Microwave Bandpass Filters*
06:00 PM	CT1: *Welcoming Cocktail (Poolside)*			
Monday, March 21				
08:00 AM	R2: *Registration (Foyer)*			
08:20 AM	W1: *Welcome Coffee (Foyer)*			
09:00 AM	A11: *Artificial Intelligence I*	B11: *Applications I*	C11: *Signal & Image Processing I*	D11: *Network & Communications Technology I*
10:40 AM	MB2: *Morning Break (Foyer)*			
11:00 AM	A12: *Artificial Intelligence I (cont)*	B12: *Applications I (cont)*	C12: *Signal & Image Processing I (cont)*	D12: *Network & Communication Technology I (cont)*
01:00 PM	LUNCH2: *Lunch Break (TEMPTationS)*			
02:00 PM	A13: *Artificial Intelligence & Computer Engineering*	B13: *Applications II*	C13: *Signal & Image Processing II*	D13: *Network & Communication Technology II*
03:40 PM	AB2: *Afternoon Break (Foyer)*			
04:00 PM	A14: *Artificial Intelligence & Computer Engineering (cont)*	B14: *Applications II (cont)*	C14: *Signal & Image Processing II (cont)*	D14: *Network & Communication Technology II (cont)*
08:00 PM	GALA (Ballroom): *GALA DINNER*			
Tuesday, March 22				
08:20 AM	W2: *Welcome Coffee (Foyer)*			
09:00 AM	A21: *Software Engineering & Applications*	B21: *Applications III*	C21: *Signal Processing & Communications Technology*	D21: *Network & Communication Technology III*
10:40 AM	MB3: *Morning Break (Foyer)*			
11:00 AM	A22: *Software Engineering & Applications (cont)*	B22: *Applications III (cont)*	C22: *Signal Processing & Communications Technology (cont)*	D22: *Network & Communications Technology III (cont)*
01:00 PM	LUNCH3: *Lunch Break (TEMPTationS)*			
02:00 PM	A23: *Autonomic and Trusted Computing*	B23: *Human Factors & Applications*	C23: *Bioinformatics & Computational Biology*	D23: *Network & Communication Technology IV*
03:40 PM	AB3: *Afternoon Break (Foyer)*			
04:00 PM		B24: *Human Factors & Applications (cont)*		D24: *Network & Communication Technology IV (cont)*

TECHNICAL PROGRAM / ABSTRACT

Tutorial 1

Tutorial 1

Security Issues in Wireless Mesh Networks

Time: 2:40 PM - 5:00 PM **Presenter: Sanjeev Sofat & Divya**
Room: Function Room 5 **Chair: Habibah Hashim (Universiti Teknologi MARA, Malaysia)**

Abstract
The rapid proliferation of wireless networks and mobile computing applications has changed the landscape of network security. The traditional ways of protecting networks using firewalls and encryption software are not enough. A lot of institutions, business homes etc. are providing this latest facility to be used by the people. With the increasing popularity of wireless networks, the need to be adequately protected against the threats becomes paramount. However limited awareness about the risks of using unsecured or poorly secured wireless network devices, coupled with the wide spread availability of affordable wireless network equipment has exposed users to potential misuse of these unsecured wireless network. The challenges faced by WMNs need to be solved in order to effectively use WMNs as reliable and effective networking solution for tactical, semi-tactical, or civilian communications. One of the core components which can make WMNs successful and an enabler into different markets is security. A core challenge in securing the WMN is the large number of communication links over the air; as each mesh device may be static or mobile and deployed outdoors, each mesh link presents an exposure and vulnerability into the mesh network. Security solutions in the form of network architecture, protocol, and algorithmic design are essential for solving the network performance impediments that tactical networks face. The tutorial presents a comprehensive analysis of the types of attacks that are being leveled upon wireless mesh networks and results in designing a secure framework for WMNs. This tutorial will also discuss the security challenges faced by WMNs, attempts at solving them, and lessons learned, besides the approaches to be considered while solving some of the experimental, and deployment challenges.

Tutorial 2

Tutorial 2

Human Factors in Interface Design

Time: 2:40 PM - 5:00 PM **Presenter: Anitawati Mohd Lokman**
Room: Function Room 6 **Chair: Nooritawati Md Tahir (Universiti Teknologi MARA, Malaysia)**

Abstract
Design principles are generally applied to any piece of work one may create. However, the principles often include human as evaluation source and not requirements generator. This session will address the nature of human experience in product interface design. It will introduce scientific way in which appropriate design principle could be formulated geared to human experience, so that product interface can be designed embedding the requirements generated by human experience. Using this design principle, product interface is designed in such a way that it predicts what human would feel when interacting with the product, thus facilitate success strategies. Subsequently, this session will introduce the general problem of human interaction in online systems. Various efforts were done by online stores to capture visitor's attention and much knowledge was gained through cognitive functionality and usability research. Yet, the knowledge fails to notice that visitors will not stay long on the website if it does not capture their interest, especially when competitors are just a click away. Captivating visitors' interest in a website will enhance persuasion to stay even longer on the website, which is the first step before one can be influenced to go to further actions and judgements such as purchasing decision. In order to capture visitors' attention, a website needs to embed the element of positive experience in its interface design. Adopting Kansei Engineering methodology, this session will introduce how website interface can be designed embedding positive experience so that it can predict what consumers would experience when interacting with the website and capture consumers attention to the website.



Tutorial 3

Side-Coupled Ring Resonators for Pseudo-Elliptic Microwave Bandpass Filters

Time: 2:40 PM - 5:00 PM **Presenter: Mohd Khairul Mohd Salleh**
Room: Function Room 9 **Chair: Ihsan M. Yassin (Universiti Teknologi Mara, Malaysia)**

Abstract
The rapid and inevitable increase in demand of telecommunication market necessitates optimal exploitation of frequency spectrum. This is explained by the fact that the number of users, applications and services have been multiplied many times recently leading to the needs of imposing very rigorous specifications on the end elements of the emission/reception chain, especially on the high frequency filters. Thus, these filters are expected to possess, not only very good selectivity while remaining compact and low-cost, but also the agility in terms of centre frequency and bandwidth. Ring resonators have found special attention since several years for their capability in supporting dual resonance and pseudo-elliptic behaviour in their frequency response that make them very good resonators for compact and selective filters. The study on such interesting structure continues nowadays in more positive ways since the introduction of side-coupling concept of the ring that led to the development of its global synthesis while opening to other paths of improvement. This tutorial introduces the basic concept of microwave bandpass filters that involve the use of side-coupled ring resonators and discusses in details about their pseudo-elliptic response and its control parameters, their global synthesis and their design concepts. Other aspects of the ring resonators that are also covered include the higher-order cascading possibility, frequency tunability, and their dual-band features.

A11

Artificial Intelligence I

Time: 9:40AM - 10:40AM **Chair: Oi Mean Foong (Universiti Teknologi PETRONAS, Malaysia),**
Room: Function Room 5 **David Yap (Universiti Teknikal Malaysia Melaka, Malaysia)**

9:00 ***Genetic Algorithm for Null Synthesizing of Circular Array Antennas by Amplitude Control***
Naren. Tapaswi Yallaparagada *(National Institute of Technology, Durgapur, West Bengal, India); Gopi Ram Hardel (National Institute of Technology, Durgapur, India); Durbadal Mandal (National Institute of Technology, Durgapur, India); Anup Bhattacharjee. (National Insttitute of Technology, India)*

In this paper, the method of imposing of nulls in the radiation pattern of an antenna array is hashed out using Real coded Genetic Algorithm (RGA). Circular array antennas lying on x-y plane is assumed. The array is assumed to have the maximum radiation along positive z- axis. Single and multiple nulls are imposed by optimizing the current amplitude excitations of each element through RGA. Various simulated results are presented and hence nulling performance is analyzed.

9:20 ***Rank Based Genetic Algorithm for Solving the Banking ATM's Location Problem Using Convolution***
Alaa Hekmat Alhaffa *(Osmania University, India); Omar Al Jadaan (, India); Wael Ahmed Abdulal (Osmania University, India); Ahmad Jabas (Osmania University, India)*

In order t o satisfy the client needs, his Utility should be increased by covering his Demand. The service Utility should be maximized through effective deployment of ATMs. Genetic Algorithm is one of widely used techniques to solve complex optimization problems, such as Banking ATM's Location Problem. This paper proposes a novel Rank Based Genetic Algorithm using convolution for solving the Banking ATM's Location Problem (RGAC). This paper proposes a novel Rank Based Genetic Algorithm using convolution for solving the Banking ATM's Location Problem (RGAC). The proposed RGAC maximizes Demand Coverage Percentage with less number of ATM machines. The novel RGAC speeds up the convergence using Rank Concept, with limited number of iterations to obtain a high quality feasible scheduling solution in reasonable time. The proposed algorithm RGAC performs more effectively in the large scale deployments, thus it can be used in the marketing study of Banks which have highly complex operations. The simulation results show that RGAC improves the Percentage Coverage up to 16.2 over the previous algorithm [1] using the same number of ATMs. Also they exhibit that RGAC reduces the number of ATM machines up to ten (10).

9:40 ***Artificial Immune System Based on Hybrid and External Memory for Mathematical Function Optimization***
David Yap *(Universiti Teknikal Malaysia Melaka, Malaysia); Johnny Koh (Universiti Tenaga Nasional, Malaysia); Sieh Kiong Tiong (UNITEN, Malaysia)*

Artificial immune system (AIS) is one of the nature-inspired algorithm for optimization problem. In AIS, clonal selection algorithm (CSA) is able to improve global searching ability. However, the CSA convergence and accuracy can be further improved because the hypermutation in CSA itself cannot always guarantee a better solution. Alternatively, Genetic Algorithms (GAs) and Particle Swarm Optimization (PSO) have been used efficiently in solving complex optimization problems, but they have a tendency to converge prematurely. Thus, a hybrid PSO-AIS and a new external memory CSA based scheme called EMCSA are proposed. In hybrid PSO-AIS, the good features of PSO and AIS are combined in order to reduce any limitation. Alternatively, EMCSA captures all the best antibodies into the memory in order to enhance global searching capability. In this preliminary study, the results show that the performance of hybrid PSO-AIS compares favourably with other algorithms while EMCSA produced moderate results in most of the simulations.

10:00 ***Robust Combining Methods in Committee Neural Networks***
Seyed Ali Jafari Kenari *(University Putra Malaysia, Faculty of Engineering, Malaysia); Syamsiah Mashohor (Universiti Putra Malaysia, Malaysia)*

Combining a set of suitable experts can improve the generalization performance of the group when compared to single experts alone. The classical problem in this area is to answer the question about how to combine the ensemble members or the individuals. Different methods for combining the outputs of the experts in a committee machine (ensemble) are reported in the literature. The popular method to determine the error in every prediction is Mean Square Error (MSE), which is heavily influenced by outliers that can be found in many real data such as geosciences data. In this paper we introduce Robust Committee Neural Networks (RCNNs). Our proposed approach is the Huber and Bisquare function to determine the error between measured and predicted value which is less influenced by outliers. Therefore, we have used a Genetic Algorithm (GA) method to combine the individuals with the Huber and Bisquare as the fitness functions. The results show that the Root Mean Square Error (RMSE) and R-square values for these two functions are improved compared to the MSE as the fitness function.

10:20 ***Comparison Between Adaptive and Fuzzy Logic Controllers for Advance Microwave Biodiesel Reactor***
Wasan Wali (Liverpool John Moores University, United Kingdom); Jeff Cullen (Liverpool John Moores University, United Kingdom); Kadhim H Hassan (Liverpool John Moores University, United Kingdom); Ahmed I Al-Shamma'a (Liverpool John Moores University, United Kingdom); Alex Mason (Liverpool John Moores University, United Kingdom)

Biodiesel reactor is the heart of biodiesel system. These reactors involve a highly complex set of chemical reactions and heat transfers. The high nonlinearity requires an efficient control algorithm to handle the variation of operational process parameters and the effect of process disturbances efficiently. In this paper, Fuzzy logic and Adaptive controllers are compared for advance microwave biodiesel reactor. The process control is complex and nonlinear, the Adaptive control have longer time and unreliability in dealing with the system parameters including temperature, microwave power, liquid flow rate as well as the prediction of chemical reaction. The proposed fuzzy logic control will provide precise temperature control and faster warm-up phase with quicker response to disturbances with minimal overshoot and undershoot where Adaptive control techniques can not meet these extra challenges. A closed loop fuzzy and adaptive controllers are used to automatically and continuously adjust the applied power of microwave reactor under different perturbations. Labview based software tool will be presented and used for measurement and control of the full system, with real time monitoring.

D11

Network & Communications Technology I

Time: 9:40AM - 10:40AM
Room: Function Room 9

Chair: Faisal Al-Nasser (King Fahd University of Petroleum & Minerals, Saudi Arabia), Nurul I Sarkar (Auckland University of Technology, New Zealand)

9:00 ***Performance Studies of 802.11G for Various AP Configuration and Placement***
Nurul I Sarkar (Auckland University of Technology, New Zealand); Eric Lo (AUT University, New Zealand)

Using indoor radio propagation measurements, the impact of access point (AP) configuration as well as placement on throughput of IEEE 802.11g ("802.11g") wireless local area networks (WLANs) is investigated. By using a pair of wireless laptops and APs we conducted several experiments involving 802.11g computer links, which were carried out in a controlled environment at AUT University within the School of Computing and Mathematical Sciences office building. The AP configuration and placement is found to have the significant effect on the link throughput of 802.11g. Results obtained show that a different throughput performance be achieved with a different AP configuration and placement and the resulting throughput variation is found to be significant. By using an appropriate AP configuration and placement, an optimum system performance can be achieved.

9:20 ***Implementation of VoIP Over Malaysian Research and Education Network (MYREN) Emulator Testbed***
Husna Zainol Abidin (Universiti Teknologi MARA, Malaysia); Muhammad Ramlan (Universiti Teknologi MARA, Malaysia); Ihsan M. Yassin (Universiti Teknologi Mara, Malaysia)

Quality of Service (QoS) of a network has become the core research area in a computer communication field. Normally researchers will be using simulation software to carry out their research works. However, it is found that simulation software has its own limitations as it does not really reflect the actual network environment. Thus, most research and development works now are exploiting emulation technology to replicate the real network environment by injecting real traffic into the network model. This paper describes the implementation of an emulator testbed for Voice over Internet Protocol (VoIP) transmitted over the Malaysian Research and Education Network (MYREN). The emulator software used in this paper is known as WAN Emulator (WANem) and it is found that the QoS obtained from the emulator are considered acceptable.

9:40 ***Simulation of Dynamic Traffic Control System Based on Wireless Sensor Network***
Faisal Al-Nasser (King Fahd University of Petroleum & Minerals, Saudi Arabia); Hosam Rowaihy (King Fahd University of Petroleum and Minerals, Saudi Arabia)

The use of wireless sensor network in the smart traffic control systems is very beneficial and starting to be very promising in the design and implementation for such systems. It will help in saving people time and adapt the intersections traffic lights to the traffic loads from each direction. In this paper we present an intelligent traffic signals control system based on a wireless sensor network (WSN). It uses the vehicle queue length during red cycle to perform better control in the next green cycle. The main objective is to minimize the average waiting time that will reduce the queues length and do better traffic management based on the arrivals in each direction. The system also includes an approach to alert the people about the red light crossing to minimize the possibility of accidents due to red light crossing violations. The system was simulated and results are shown in the end of this paper.

10:00 ***Evaluation of 6To4 and ISATAP on a Test LAN***
Mohammad Aazam (Mohammad Ali Jinnah University Islamabad, Pakistan)

Coexistence of IPv4 and IPv6 bears problem of incompatibility, as IPv6 and IPv4 headers are different from each other. To counter this problem, three solutions are possible: a) making every device dual stack, b) translation, c) tunneling. Tunneling stands out as the best possible solution. Among the IPv6 tunneling techniques, this paper evaluates the performance of two recent IPv6 tunneling techniques: 6to4, and ISATAP. These protocols were implemented on real test bed setup, on Microsoft Windows (MS Windows XP and MS Windows Server 2003) and Linux operating systems. Five to six devices were used to setup the whole test bed. Each protocol was then implemented on the setup using specific configuration commands. UDP audio streaming, video streaming and ICMP-ping traffic was run. Four different runs of traffic were routed over the setup for each protocol. The average of the data was taken to generate graphs and final results. The performance of these tunneling techniques has been evaluated through certain parameters, namely: throughput, end to end delay (E2ED), round trip time (RTT), and jitter.

10:20 ***Optimization of Energy Usage in Wireless Sensor Network Using Position Responsive Routing Protocol (PRRP)***
Noor Zaman (King Faisal University KSA, Saudi Arabia); Azween Bin Abdullah (Universiti Teknologi Petronas, Malaysia); Tang Jung Low (Universiti Teknologi PETRONAS, Malaysia)

Wireless Sensor Networks (WSNs) are consist of very tiny nodes structure, with very small batteries without having facility to recharge it. It works under any hard circumstances, hence this type of network is gaining high importance day by day. Maximum focus of researchers is to enhance or optimized its energy efficiency level. Routing protocol is the main energy expensive operation of sensor networks which utilize maximum energy resources of sensor network. Already a good number of routing protocols has been designed for energy efficiency or optimization with different approaches under controlled conditions. With this research we try to propose energy optimization of wireless sensor network through our proposed position response routing protocol (PRRP), under certain controlled parametric consideration. Research results shows a significant energy optimization in the life cycle of WSN.



Applications I

Time: 9:40AM - 10:40AM **Chair: Tanmoy Maity (Indian School of Mines, Dhanbad, India),**
Room: Function Room 6 **Aparna P (National Institute of Technology Karnataka, India)**

9:00 ***A Strategic Evaluation Model for Knowledge Relationship Among Members in Enterprise Communities***
Fariba Haghbin (Universiti Teknologi Malaysia, Malaysia); Othman Bin Ibrahim (Universiti Teknologi Malaysia, Malaysia); Seyed Mohammad Attarzadeh (Universiti Teknologi Malaysia, Malaysia)

With the development of online communities, there has been a dramatic increase in the number of members using Enterprise Communities (ECs) over the past few years. Many join ECs with the objective of sharing their knowledge on the specific issue and seeking relative knowledge from others. Despite the eagerness of sharing knowledge and receiving knowledge through ECs, there is no standard of assessing ones knowledge sharing capabilities and prospects of knowledge sharing in order to get great level of efficiency of knowledge sharing collaboration. This paper developed evaluation model to assess knowledge relationship behavior among ECs members with the aim of Vector Space Model.

9:20 ***Multilevel Coset Coding of Video with Golay Codes***
Aparna P (National Institute of Technology Karnataka, India); Sumam David (National Institute of Technology Karnataka, India)

This paper presents a video coding method based on the principle of distributed source coding. This work aims in shifting the encoder complexity to the decoder to support uplink friendly video applications, simultaneously achieving the rate-distortion performance of the conventional predictive coding system. In this work concept of syndrome coding with Golay codes is adopted for compression. The simulation results presented in this paper reveals the superior performance of this distributed video coder over the Intraframe coders and predictive coders for video data with less correlation between frames.

9:40 ***Model for Courseware Development of Teaching and Learning Traditional Craft (CDTC Model): Initial Validation***
Salyani Osman (Universiti Selangor, Malaysia); Nor Azan Haji Mat Zin (Universiti Kebangsaan Malaysia, Malaysia); Noraidah Sahari @ Ashaari (Universiti Kebangsaan Malaysia, Malaysia); Yuhanis Omar (Universiti Kebangsaan Malaysia, Malaysia)

Alternative method to reduce dependency on instructors in teaching and learning traditional crafts will be greatly benefited from electronic learning practices. In order to make sure the courseware for teaching and learning traditional craft is applicable, effective and support teaching and learning pedagogy, a model for courseware development of teaching and learning traditional craft was developed and derived from methodologies synthesized from related research areas. Through an extensive review of literature, the model was specifically designs to meet the needs of adult learners in a web-based environment with concentrating on designing strategic learning using cognitive apprenticeship approaches. The aim of this study is to verify the components of the proposed model namely CDTC model through initial validation for each component by Evaluator Committee composed of selected craft instructors. The verification is purposely to examine, evaluate, and score the efficacy of each proposed components according to its relevance to the model and was realized through quantitative investigation using questionnaire among instructors from National Craft Institute, Rawang, Malaysia (Institut Kraf Negara (IKN)). The committee, evaluated the model and made recommendations for improving the model. Components validated by committee were used in designing a preliminary version of the model. A significant contribution in this research is providing relevant preliminary CDTC model for courseware development of teaching and learning traditional craft that will support and preserve our traditional heritage for future generation. With the development of the CDTC model, hopefully it will encourage courseware designers to develop more multimedia applications for teaching and learning traditional craft as well as a good reference for educators, instructional designers, and product developers for developing interactive multimedia applications.

10:00 ***Evaluation and Routing of Power Transmission Lines by Using AHP Method and Genetic Algorithm***
Mostafa Hosseini (Science And Research branch of Azad University, Iran); Homa Famil Bahmani (Tehran Power Distribution Company, Iran)

Today optimization is one of the most important issues in all engineering fields. According to importance of this issue in planning power transmission lines, appropriate areas have been accreted for numerous researches. Widespread usages of GIS application and its combination with GA base methods offer practical solution for power transmission lines design. In this paper, we first study about efficient criteria for selecting appropriate points for installing towers, and then we can evaluate available points for installing power towers by one of the multi-criteria decision-making analysis, named AHP. As we know, all of these nodes are not suitable for being one of the transmission line Points. So by using this procedure (AHP) we calculate cost function of transmission line between towers. Finally, with GA algorithm, the best and the most optimum route between source and destination will be selected.

10:20 ***A Novel Three Phase Energy Meter Model with Wireless Data Reading and Online Billing Solution***
Tanmoy Maity (Indian School of Mines, Dhanbad, India); Partha S. Das (Durgapur Institute of Advanced Technology and Management, WB, India)

Measurement of data electronically leads a combination of benefits that go well beyond the traditional rotor-plate energy meter design. In this paper with the help of an energy chip, an improved novel three phase energy metering solution is developed. Automating the progression of measurement through digital wireless communication technique is done to get high accuracy, smooth control and better reliability. The developed energy meter calculates the total average active power mainly for industrial and commercial applications. The hardware circuit accepts three phase voltages and currents as its inputs and provides the output in the form of serial interfaced data equivalent to the average real power. This serial data is fed to a remote personal computer through the wireless ZigBee network that represents the concept of distant wireless metering, practically involving no manpower. The paper also presents a software solution developed for total electrical energy billing and data management system.

C11 Signal & Image Processing I

Time: 9:40AM - 10:40AM **Chair: Abid Yahya (University Malaysia Perlis, Malaysia), Kwang Hooi Yew (Universiti Teknologi PETRONAS, Malaysia)**
Room: Function Room 7

9:00 ***Carving JPEG Images and Thumbnails Using Image Pattern Matching***
Kamaruddin Malik Mohamad (Universiti Tun Hussein Onn Malaysia, Malaysia); Ahmed Patel (Universiti Kebangsaan Malaysia, Malaysia); Mustafa Mat Deris (University Tun Hussein Onn Malaysia, Malaysia)

Digital forensics is a branch of forensic science to monitor, analyze and examine digital media or devices. File carving is the art of recovering files from digital data storage with corrupted or unavailable file system metadata and it is very useful in a digital forensics investigation. However, earlier generation file carver like Scalpel and Foremost only deals with non-fragmented files. We proposed an automatic image and thumbnail carving tool called myKarve which is useful in digital forensics investigation and presentation of evidential information that is able to carve contiguous and linearly fragmented images caused by garbage. myKarve is designed on a new architecture by extending Scalpel features to deal with thumbnail and fragmentation issues. The tool is tested with images obtained from the Internet. myKarve is found to be a more efficient automated image and thumbnail carver compared to the original Scalpel with the following advantages: detects more headers using validated headers; carves more images and thumbnails by using the newly introduced image patterns; and is able to discard garbage from linearly fragmented images. The results from myKarve are invaluable in the field work of digital forensic analysis that can produce technical evidence against cybercrime activities to prosecution cases.

9:20 ***Design and Implementation of Smart Driving System Using Context Recognition System***
Taehyun Kim (Sejong University, Korea); Soohan Kim (Samsung Electronics Co., LTD, Korea); Dongkyoo Shin (Sejong University, Korea); Dongil Shin (Sejong University, Korea)

In this paper, we develop a context recognition system that is based on multimodal biometric signals and applicable to smart driving system. The context recognition system includes a biometric analysis module that analyzes and recognizes human biometric signal patterns. The context recognition system can recognize a user's emotion and level of concentration by analyzing ECG (electrocardiogram) and EEG (electroencephalogram) patterns. To predict the concentration and stress status of the user, the electroencephalogram rendering system utilizes 5 signal values: MID_BETA, THETA, ALPHA, DELTA, and GAMMA. Also, electrocardiogram analysis system utilizes 5 basic signal values: P, Q, R, S, T wave. To recognize the user's electrocardiogram signal patterns, a deformation K-means-based EM algorithm was applied.

9:40 ***Detecting Emotion From Voice Using Selective Bayesian Pairwise Classifiers***
Jangsik Cho (Nagoya Institute of Technology, Japan); Shohei Kato (Nagoya Institute of Technology, Japan)

This paper describes a method for detecting a dialogist's emotion from his or her voice. The method is based on pairwise classification by probability from the selective pairwise classifiers. In this research, we focus on the elements of emotion included in a dialogist's voice. Thus, as training datasets for learning the pairwise classifiers, we extract acoustic features from emotionally expressive voice samples spoken by unspecified actors and actresses in films, and TV dramas. The acoustic features adopt duration per mora, fundamental frequency, energy, and formant. All features except duration per mora have statistics extracted standard deviation, mean, maximum, minimum, median, timezone of maximum, and timezone of minimum. Pairwise classification classifies a multi-class problem by using a series of binary classifiers. Pairwise classifiers used tree augmented naive bayes, which constructs tree structure among the attributes in naive bayes, by selected subset features. The subset features are selected on every pair of emotions by using naive bayes. This paper reports the accuracy rates of emotion detection by using our method. In experimental results from our voice samples, the emotion classification rates improved.

10:00 ***Facial Emotion Detection Considering Partial Occlusion of Face Using Bayesian Network***
Yoshihiro Miyakoshi (Nagoya Institute of Technology, Japan); Shohei Kato (Nagoya Institute of Technology, Japan)

Recently, robots that communicate with human have attracted much attention in the research field of robotics. In communication between human, almost all human recognize the subtleties of emotion in each other's facial expressions, voices, and motions. Robots can communicate more smoothly with human as they detect human emotions and respond with appropriate behaviors. Usually, almost all human express their own emotions with their facial expressions. In this paper, we propose an emotion detection system with facial features using a Bayesian network. In actual communication, it is possible that some parts of the face will be occluded by adornments such as glasses or a hat. In previous studies on facial recognition, these studies have been had the process to fill in the gaps of occluded features after capturing facial features from each image. However, not all occluded features can always be filled in the gaps accurately. Therefore, it is difficult for robots to detect emotions accurately in real-time communication. For this reason, we propose an emotion detection system taking into consideration partial occlusion of the face using causal relations between facial features. Bayesian network classifiers infer from the dependencies among the target attribute and explanatory variables. This characteristic of Bayesian network makes our proposed system can detect emotions without filing in the gaps of occluded features. In the experiments, the proposed system succeeded in detecting emotions with high recognition rates even though some facial features were occluded.

10:20 ***Technique to Correct Displacement of Vector Drawings on Scaled Underlying Raster Image***
Kwang Hooi Yew (Universiti Teknologi PETRONAS, Malaysia); Siew Yoong Leong (Universiti Tunku Abdul Rahman, Malaysia)

The problems of vector graphics displacement over raster drawing due to magnification in Java Graphics2D are described. Demarcation of engineering drawing is a process of highlighting sections of interest by drawing clouds. The clouds were stored as an array of points that are combined with background image at runtime. Magnification of background causes unexpected displacement of newly drawn clouds. This may be a common but unreported problem for interactive drawing in Java Graphics2D. The paper proposed a technique that successfully corrects the issue.

A12

Artificial Intelligence I (cont)

Time: 11:40AM - 1:00PM **Chair: Oi Mean Foong (Universiti Teknologi PETRONAS, Malaysia),**
Room: Function Room 5 **David Yap (Universiti Teknikal Malaysia Melaka, Malaysia)**

11:00 ***Focusing on Rule Quality and Pheromone Evaporation to Improve ACO Rule Mining***
Pooia Lalbakhsh (Islamic Azad University-Borujerd Branch, Iran); Mohammad Sajjad Khaksar Fasaei (Islamic Azad University - Arak Branch, Iran); Mehdi Fesharaki (Islamic Azad University, Iran)

In this paper an improved version of Ant-Miner algorithm is introduced and compared to the previously proposed ant-based rule mining algorithms. Our algorithm modifies the rule pruning process and introduces a dynamic pheromone evaporation strategy. The algorithm was run on five standard datasets and the average accuracy rate and numbers of discovered rules were analyzed as two important performance metrics of rule mining. As simulation results show, not only the accuracy rate and rule comprehensiveness is improved by our algorithm, the algorithm runtime is also reduced.

11:20 ***Harmonic Estimation Using Modified ADALINE Algorithm with Time-Variant Widrow - Hoff (TVWH) Learning Rule***
Balasubramaniam Vasumathi (National Institute of Technology, India); Sridharan Moorthi (National Institute of Technology, India)

Algorithms are well developed for adaptive estimation of selected harmonic components in Digital Signal Processing. In power electronic applications, objectives like fast response of a system is of primary importance. An effective active power filtering for estimation of instantaneous harmonic components is presented in this paper. A signal processing technique using Modified Adaptive Neural Network (Modified ANN) algorithm has been proposed for harmonic estimation. Its primary function is to estimate harmonic components from selected signal (Current or Voltage) and it requires only the knowledge of the frequency of the component to be estimated. This method can be applied to a wide range of equipments. The validity of the proposed method to estimate voltage harmonics is proved with a dc/ac inverter as an example and the simulation results are compared with ADALINE algorithm for illustrating its effectiveness.

11:40 ***A Near Linear Shortest Path Algorithm for Weighted Undirected Graphs***
Muhammad Aasim Qureshi (Universiti Teknologi PETRONAS, Malaysia); Mohd Fadzil Hassan (Universiti Teknologi PETRONAS, Malaysia); Sohail Safdar (Universiti Teknologi PETRONAS, Malaysia); Rehan Akbar (Universiti Teknologi PETRONAS, Malaysia)

This paper presents an algorithm for Shortest Path Tree (SPT) problem. The presented algorithm is an improvement over a previously published work of the authors. The effort is put in to improve the running/execution time of the SPT problem. Introduced improvement is simple and easy to incorporate in to the existing algorithm. This algorithm uses DFS like graph traversal during a BFS like traversal i.e. combines and take advantage of the inherent properties of the two heuristic graph search techniques so that vertex weights can be kept balanced. The need of improvement is discussed in detail and the expected improvement in overall processing time is shown with the example

12:00 ***An Unsupervised Center Sentence-based Clustering Approach for Rule-based Question Answering***
Shen Song (MIMOS Berhad, Malaysia); Yu-N Cheah (Universiti Sains Malaysia, Malaysia)

Question answering (QA) systems have widely employed clustering methods to improve efficiency. However, QA systems with unsupervised automatic statistical processing do not seem to achieve higher accuracies than other approaches. Therefore, with the motivation of obtaining optimal accuracy of retrieved answers under unsupervised automatic processing of sentences, we introduce a syntactic sequence clustering method for answer matching in rule-based QA. Our clustering method called CEnter SEntence-baseD (CESED) Clustering is able to achieve accuracies as high as 84.62% for WHERE-type questions.

12:20 ***A Hybrid PSO Model in Extractive Text Summarizer***
Oi Mean Foong (Universiti Teknologi PETRONAS, Malaysia); Alan Oxley (Universiti Teknologi PETRONAS, Malaysia)

The World Wide Web has caused rapid growth of information explosion. Readers are often drown in information while starve for knowledge. This paper presents a hybrid Particle Swarm Optimization (PSO) framework in extractive text Summarizer to tackle the information overload problem. Readers are bombarded with too many lengthy documents in which a shorter summarized text with its main contents of its original documents is desirable. The PSO is a suitable technique for solving complex problems due to its simplicity and fast computational convergence. However, it could be trapped in a local minimal search space in the midst of searching for optimal solutions. The objective of this research is to

investigate whether the proposed hybrid harmony PSO model is capable of condensing the main gist of its original electronic documents into shorter summarized text more efficiently and accurately. Empirical results show that the proposed Hybrid PSO model improves the search accuracy of extractive text summarizer.

D12

Network & Communication Technology I (cont)

Time: 11:40AM - 1:00PM
Room: Function Room 9

Chair: Faisal Al-Nasser (King Fahd University of Petroleum & Minerals, Saudi Arabia), Nurul I Sarkar (Auckland University of Technology, New Zealand)

11:00 ***Fast Analysis of On-Chip Power Distribution Networks***
Hedi Harizi (Leibniz University of Hannover, Germany)

The verification of the power distribution network is of critical importance to ensure reliable performance. However, with the increasing number of transistors on a chip, the complexity of the power network has also grown. The available computational power and memory resources impose limitations on the size of the networks that can be analyzed using currently known techniques. In this paper, we present a fast and efficient method to analyze power distribution networks in the time-domain. The new contributions of this work are the use of PWL data point reduction and correction factors (CF) to reduce the number of current source models and to speed up the characterization time. The proposed techniques provide good analysis results compared to the reference with a reduction of the run-time by a factor of 400, although the cell pre-characterization is based on SPICE simulations. Our model is independent of power network parasitic, which implies that different power network scenarios may be analyzed based on the same model and the same cell characterizations. The run-time and accuracy of the proposed approach are demonstrated on some industrial designs.

11:20 ***Performance Analysis of Full Adder (FA) Cells***
Azrul Ghazali (Universiti Tenaga Nasional, Malaysia)

Since full adders play a vital role in electronics design, new ideas, investigations and study cases for constructing full-adders are required. This paper presents a comprehensive study in total of 24 different single-bit full adder (FA) topologies. The aim of this paper is to conduct performance analysis in term of power and delay of those designs using 0.18μm Silterra transistor models in order to find the best full adder cells. Simulations and results of FA performance are demonstrated and analyzed using Hspice. The results of this paper are expected to assist designers to select the appropriate FA cell that meet their specific applications.

11:40 ***Dynamic Candidate Keypad for Stroke-based Chinese Input Method on Touchscreen Devices***
Lai Man Po (City University of Hong Kong, Hong Kong); Chi Kwan Wong (City University of Hong Kong, Hong Kong); Chi Wang Ting (City University of Hong Kong, Hong Kong); Ka-Ho Ng (City University of Hong Kong, Hong Kong); Ka-Man Wong (City University of Hong Kong, Hong Kong); Chun Ho Cheung (City University of Hong Kong, Hong Kong); Kwok-Wai Cheung (City University of Hong Kong, Hong Kong)

With the popularity of touchscreen devices, physical button-based keyboards are being replaced by finger-operated virtual keyboards. Entering text on these touchscreen devices is no longer limited by finger tapping activities on the keys. Text input can be performed by finger sliding over the virtual keyboard, which is well realized by the Swype technology on a typical QWERTY keyboard. Such shorthand gesturing for text input, however, may be inefficient when directly applied to Chinese input, especially in Chinese stroke-based input method. In this paper, a novel dynamic candidate keypad with use of unidirectional finger gesture on the stroke key for character selection is proposed for enhancing stroke-based Chinese input method. The new design can enhance frequently used Chinese characters searching and input using stroke-based input. The new method is implemented on the Android 2.2 platform for performance evaluation using Traditional Chinese characters set. Experimental results show that the proposed method enables users to input popular Chinese characters easier than conventional stroke-based input methods.

12:00 ***A MAC Approach for Dynamic Power Control in Wireless Sensor Network***
Buddha Singh (JNU new Delhi, India); Daya Krishan Lobiyal (Jawaharlal Nehru University, New Delhi, India)

To design energy efficient Medium Access Control (MAC) protocol for maximizing the network lifetime in Wireless Sensor Network (WSN), is evolving as a challenging portal in research area. The overall radio energy inherently depends on network workload as well as the radio characteristics. Therefore, we have proposed a Dynamic Power Control MAC (DPCMAC) protocol which supports variable power level transmission of packets according to data rate of sources. Our novel approach minimizes the aggregate energy consumption in all power states according to the network traffic.

Moreover in our protocol, we calculate the desired power level for the transmission of packets for two types of scenarios: low and high network workload. The protocol is simulated for the variable size of networks and its performance is analyzed on the basis of success rate and energy consumption. The simulation results show that our protocol outperforms the existing Sensor MAC (SMAC) protocol.

12:20 ***Evaluation of RASTA Approach with Modified Parameters for Speech Enhancement in Communication Systems***
Satish K Shah (The M. S. University of Baroda, India); Jigar H. Shah (Faculty of Technology and Engineering, M. S. University of Baroda, Vadodara, India); Nishant N. Parmar (G. H. Patel College of Enginerring & Technology, Vallabh Vidyanagar, India)

The purpose of speech enhancement techniques is to improve quality and intelligibility of speech without producing any artifact. The speech enhancement algorithms are designed to suppress additive background noise and convolutive distortion or reverberation. The need for enhancement of noisy speech in communication systems increases with the spread of mobile and cellular telephony. Calls may originate from noisy environments such as moving vehicles or crowded public gathering places. The corrupting noise is not always white rather it is colored and contains reverberation. The currently employed noise suppressors in communication systems use spectral subtraction based on short time spectral attenuation (STSA) algorithms as a preprocessor in speech coder. They can perform well in white noise condition but failed in real colored noise environments with different SNRs. This leads to the use of RelAtive SpecTrAl (RASTA) algorithm for speech enhancement which was originally designed to alleviate effects of convolutional and additive noise in automatic speech recognition (ASR). RASTA does this by band-pass filtering time trajectories of parametric representations of speech in the domain in which the disturbing noisy components are additive. This paper evaluates the performance of RASTA algorithm for white and colored noise reduction as well as suggests modifications in parameters and filtering approach to perform quite well than original RASTA approach. The NOIZEUS database is used for objective evaluation in different noise conditions with 0 to 10dB SNRs. The results shown here give improvements compared to spectral subtraction methods.

B12

Applications I (cont)

Time: 11:40AM - 1:00PM **Chair: Tanmoy Maity (Indian School of Mines, Dhanbad, India), Aparna P (National Institute of Technology Karnataka, India)**
Room: Function Room 6

11:00 ***A Modified Planar Monopole Antenna for UWB Applications***
Ramezan Ali Sadeghzadeh (Khaje nasir toosi university of Technology, Iran); Yashar Zehforoosh (Islamic Azad University of Urmia Branch, Iran); Navid Mirmotahhary (Islamic Azad University Science and research Branch, Iran)

In this paper, we present a novel design of printed monopole antenna for UWB applications. The radiating element of the proposed antenna is composed of an octagonal patch fed by a 50 ohm microstrip. It has a very compact size of 20mm×12mm, which can be integrated easily with other RF front-end circuits. The antenna parameters and performances have been investigated through a large amount of EM simulations. It has been demonstrated that the proposed antenna provides an ultra wide bandwidth from 2.95 GHz to 13.35 GHz, completely covering the range set by the Federal Communication Commission (FCC) for UWB operations (3.1GHz to 10.6GHz). It also enjoys advantages such as low profile, low cost, high gain and satisfactory radiation characteristics.

11:20 ***Variable Forgetting Factor RLS Adaptive Equalizer for DS-CDMA System***
Adisaya Charoenphol (King Mongkut's Institute of Technology Ladkrabang, Thailand); Chawalit Benjangkaprasert (King Mongkut's Institute of Technology Ladkrabang, Thailand)

In this paper, a variable forgetting factor RLS adaptive equalizer is proposed for direct sequence code division multiple access (DS-CDMA) communication system. We consider an adaptive Laguerre lattice equalizer which applies an optimal method based on the variable step-size least mean square (VSLMS) algorithm for adaptable forgetting factor RLS algorithm for improve performance of the receiver.

11:40 ***Eliciting Essential Requirements for Social Networks in Academic Environments***
Vala Ali Rohani (University of Malaya, Malaysia); Siew Hock Ow (Universiti Malaya, Malaysia)

Recent years have witnessed the generation of online social networking web sites, in which millions of members publicly articulate mutual friendship relations and share user-created contents. But it is just a few years that we have seen some efforts to create special social networks to be used in academic environments. Considering the increasing needs for this

kind of web sites, we did a comprehensive survey on more than 20 academic social networks for gathering and categorizing the essential requirements for this kind of web sites. Hence, having some good experiences by creating the Iranian Experts Social Network with more than 120,000 official members, in this paper we try to clarify the features of Social Networks in academic environments and propose a category for their requirements.

12:00 ***New Metric for Measuring Programmer Productivity***
Marwa Solla (The National University of Malaysia UKM, Malaysia); Ahmed Patel (Universiti Kebangsaan Malaysia, Malaysia)

Measuring programmer productivity is a challenging exercise because it is not well understood since it is without bounded rules and ill-defined meanings of complicated set of parameters. This is made worse by new software development paradigms such as agile and mashup methods and the ensuing advances in software engineering practices and ways of designing and developing software. The existing metrics for measuring performance of solo and pairs of programmers does not appear to be suitable to meet these new forms of software development. This paper presents a new metrics which can be used to measure performance productivity of programming effort by solo and pair programmers in a much more comprehensive manner. All of the key parameters are looked at objectively and defined for and from software engineering life cycle points of view to make productivity performance calculations for solo and pair programmers. The methodology used for formulating and composing the formula and defining the parameters as coefficients is explained. These parameters are based on a weighting system to derive the effective performance results. It is a more objective and quick way for the performance analysts to define a table of weights for the parameters based on several criteria within the different aspects of the software development life cycle. The composition of the formula and the metric for measuring programmer productivity performance is presented and examples are used to illustrate the method and the outcomes.

12:20 ***Computer System for Navigating a Mobile Robot***
Stanislav Simeonov (Burgas Free University, Bulgaria); Penka Georgieva (BFU, Bulgaria); Vladimir Germanov (Burgas Free University, Bulgaria); Atanas Dimitrov (Burgas Free University, Bulgaria); Dimitar Karastoyanov (BAS, Bulgaria)

In this paper a fuzzy and communication system for managing and controlling the basic movements of a mobile robot is proposed. Several ultrasound and infrared sensors are installed on the robot and the collected data is operated with the means of fuzzy logic and thus decisions for the robot route are made. This intelligent system is created to navigate the mobile robot indoors in an unknown environment.The paper is funded by Bulgarian National Science Fund - NSF Grand No RNF_09_0037 "Improved Infrastructure for Embedded and Mobile Device Research".

C12

Signal & Image Processing I (cont)

Time: 11:40AM - 1:00PM **Chair: Abid Yahya (University Malaysia Perlis, Malaysia), Kwang Hooi Yew (Universiti Teknologi PETRONAS, Malaysia)**
Room: Function Room 7

11:00 ***Current-Controlled Current-Mode Multiphase Oscillator Using CCCDTAs***
Montree Kumngern (King Mongkut's Institute of Technology Ladkrabang, Thailand)

This paper presents a new current-controlled current-mode multiphase sinusoidal oscillator using current controlled current differencing transconductance amplifiers (CCCDTAs). The proposed oscillator circuit, which employs one CCCDTA, one grounded capacitor and one MOS resistor for each phase, can generate arbitrary n output current equal-amplitude signals that are equally spaced in phase (n being even or odd), all at high output impedance terminals. The frequency of oscillation and the condition of oscillation can be controlled electronically and independently through adjusting the bias currents of the CCCDTAs. The proposed multiphase oscillator is highly suitable for integrated circuit implementation. The theoretical results were verified by PSPICE simulation.

11:20 ***An Analysis of Multiple Size Region of Interest in Disparity Mapping for Stereo Vision Application***
Rostam Affendi Hamzah (Universiti Teknikal Malaysia Melaka, Malaysia)

This paper presents an analysis of multiple size region of interest in selected area or segment of disparity mapping in application of stereo vision. The mapping is about to deal with the intensities of pixels which allocate the depths of an image and can be extracted to get the distance values. This region is a reference view of the stereo camera and stereo vision baseline is based on horizontal configuration. The block matching technique is briefly described with the performance of its output. The disparity mapping is generated by the algorithm with the reference to the left image coordinate. The algorithm uses Sum of Absolute Differences (SAD) which is developed using Matlab software. The rectification and block matching processes are also briefly described in this paper.

11:40 ***Error Concealment Using Multiple Description Coding and Lloyd-max Quantization***
Ali Farzamnia (Universiti Teknologi Malaysia, Malaysia); Sharifah K. Syed-Yusof (Universiti Teknologi Malaysia, Malaysia); Norsheila Fisal (Universiti Teknologi Malaysia, Malaysia)

There has been increasing usage of Multiple Description Coding (MDC) for error concealment in non ideal channels. This paper attempts to conceal the error and reconstruct the lost descriptions by combining MDC and Lloyd-max quantizer. At first original image downsampled to four subimages then by using wavelet transform each subimage is mapped to transform domain then descriptions are quantized by Lloyd-max and coded. Since in proposed method wavelet transform is been used, there could be no blocking effect as compared to DCT transform. The results show that average MSE (mean square error) for our proposed method in comparison with DCT method (in other paper) has decreased from 240 to 152 in 0.625 bpp (bit per pixel), from 161 to 107 in 1 bpp and from 96 to 73 in 2 bpp in rate- distortion performance. Therefore, this method is suitable for low capacity channels. By losing descriptions, the obtained image is still in good quality (subjective evaluation and PSNR values) as compared to method which is DCT and MDSQ (multiple description scalar quantization).

12:00 ***Current-Controlled Voltage-Mode Multifunction Filter Using CCDDCCs***
Montree Kumngern (King Mongkut's Institute of Technology Ladkrabang, Thailand)

This paper presents a new voltage-mode multifunction filter with four inputs and three outputs employing three current controlled differential difference current conveyors (CCDDCCs) and two grounded capacitors. By appropriately selecting the input and output terminals, the proposed circuit can provide low-pass, band-pass, high-pass, band-stop and all-pass voltage responses at a high impedance input terminal, which enable easy cascadability. The circuit parameters Wo and Q can be set orthogonally by adjusting the circuit components. PSPICE simulation results are also performed to confirm the theoretical analysis.

12:20 ***New QC-LDPC Codes Implementation on FPGA Platform in Rayleigh Fading Environment***
Abid Yahya (University Malaysia Perlis, Malaysia); Abdul Kader (University Malaysia Perlis, Malaysia)

This paper presents performance of Quasi-Cyclic low-density parity-check (QC-LDPC) codes on a flat Rayleigh fading channels by employing DPSK modulation scheme. The BER curves show that large girth and diversity level robust the system performance. Moreover, Prototype architecture of the LDPC codes has been implemented by writing Hardware Description Language (VHDL) code and targeted to a Xilinx Spartan-3E XC3S500E FPGA chip. Simulation results show that the proposed QC-LDPC codes achieve a 0.1dB coding gain over randomly constructed codes and perform 1.3 dB from the Shannon-limit at a BER of 10^-6 with a code rate of 0.89 for block length of 1332.

A13

Artificial Intelligence & Computer Engineering

Time: 2:00PM - 3:40PM
Room: Function Room 5

Chair: Alex Mason (Liverpool John Moores University, United Kingdom), Saeed Sabamoniri (Islamic Azad University- Soufian Branch, Iran)

2:00 ***Development of User Interfaced for 3D Reconstruction Algorithm Using Modified Grangeat Method***
Nimit Shah (FTE, M. S. University of Baroda, India); Satish K Shah (The M. S. University of Baroda, India)

Image transformation is one of the important digital image processing techniques widely used in medical science. Typical applications of image transformation include creation of 3D volumetric models from 2D images. 2D images may be obtained energy source used for hard tissue imaging are x-rays. 3D model of hard tissue are created by traditional tomography using CT scans. Since scanners are very expensive they are not easily available at most of health care centers. The algorithm presented in the paper is based on 2D image data of hard tissues obtained from basic x-rays equipments. It is unique in context of data gathering collected via arbitrary path to impart maximum flexibility for 3D models compared to some other approaches. A series of experiments performed with various data sets validates claim MATLAB® platform is used for implementation.

2:20 ***Image Denoising Using Gabor Filter Banks***
Ashek Ahmmed (Politecnico di Milano, Italy)

We introduce a method for denoising a digital image corrupted with additive noise. A dyadic Gabor filter bank is used to obtain localized frequency information. It decomposes the noisy image into Gabor coefficients of different scales and orientations. Denoising is performed in the transform domain by thresholding the Gabor coefficients with phase preserving threshold and non-phase preserving threshold where both approaches have been formulated as adaptive and data-driven.

For the non-phase preserving approach the BayesShrink thresholding methods have been used. Finally using the thresholded Gabor coefficients of each channel the denoised image has been formed. It has been found that for smoothly varying images the modified BayesShrink method outperforms both the BayesShrink and the phase preserving approaches whereas for images with high variations the phase preserving approach performs better.

2:40 *PESYMO: a Pervasive System for Mobile Life Long Learners*
Wiem Taktak (ISG-University of Tunis, Tunisia); Hilali jaghdam (University of Tunisn, Institut Supérieur de Gestion Tunis, Tunisia); Jalel Akaichi (SOIE-ISG, Tunisia)

In this paper, we present PESYMO (PErvasive SYstem for MObile lifelong learning) a solution for Mobile Professionals (MP) that motivates workers to improve their skills through lifelong learning. In fact, they have to move from one place to another to accomplish their duties. This makes very complex the mapping of their timetable to Lifelong Learning Centers (LLCs) learning schedules. Consequently, they logically fail to get their diploma enhance mobile professional success. PESYMO is performed in 4 steps: LLCs localization, LLCs courses matching with MP curriculum and level, LLCs courses schedules matching with MP free time, and MP subscription according to LLCs vacancy. Moreover a database is designed to support MP and LLCs activities in order to generate decisions guiding to the enhancement of this mobile learning system.

3:00 *Improving CBRLA Algorithm to Variable Size Problems*
Saeed Sabamoniri (Islamic Azad University- Soufian Branch, Iran); Behrooz Masoumi (Islamic Azad University, Qazvin Branch, Iran); Mohammad Reza Meybodi (Amirkabir University of Technology, Iran)

In this paper an improved approach based on CBR-LA model is proposed for static task assignment in heterogeneous computing systems. The proposed model is composed of case based reasoning (CBR) and learning automata (LA) techniques. The LA is used as an adaptation mechanism that adapts previously experienced cases to the problem which must be solved (new case). The goal of this paper is to expressing some weak points of the CBR-LA and proposing new algorithm called ICBR-LA which has improved performance in terms of Makespan performance metric. The results of experiments have shown that the proposed model performs better than the previous one.

3:20 *Autonomic Computing Approach in Service Oriented Architecture*
Muhammad Agni Catur Bhakti (Universiti Teknologi Petronas, Malaysia); Azween Bin Abdullah (Universiti Teknologi Petronas, Malaysia)

Service oriented computing is a computing paradigm that utilizes existing services as the basic construct to compose new service / application, with service oriented architecture (SOA) as its architectural concept. A service architecture that is capable of changing its structure and functionality autonomously with little human intervention is required to address the issue of complexity and dynamism in the current network systems, due to unpredictable events which could cause services unavailability in the event of crashes or other network problems. In this paper, we elaborate and discuss the idea of incorporating the autonomic computing paradigm into SOA and utilizing case-based reasoning approach to achieve a more autonomous SOA, and our current work shows the feasibility of its implementation.

D13

Network & Communication Technology II

Time: 2:00PM - 3:40PM
Room: Function Room 9

Chair: Tamleek Ali Tanveer (Institute of Management Sciences, Pakistan), Valapadasu Vijaya (Vaagdevi college of engg, India)

2:00 *FPGA Implementation of RS232 to Universal Serial Bus Converter*
Valapadasu Vijaya (Vaagdevi college of engg, India); Rama Valupadasu (National Institute of Technology, India); B Rama Rao Chunduri (National Institute Of Technology, Warangal, India); Chennaboina Kranthi Rekha (Linton Universiti College, India); Bobbala Sreedevi (Vaagdevi college of engg, India)

Universal Serial Bus (USB) is a new personal computer interconnection protocol, developed to make the connection of peripheral devices to a computer easier and more efficient. It reduces the cost for the end user, improves communication speed and supports simultaneous attachment of multiple devices (up to127)RS232, in another hand, was designed to single device connection, but is one of the most used communication protocols. An embedded converter from RS232 to USB is very interesting, since it would allow serial-based devices to experience USB advantages without major changes. This work describes the specification and development of such converter and it is also a useful guide for implementing other USB devices. The main blocks in the implementation are USB device, UART (RS232 protocol engine) and interface FIFO logic. The USB device block has to know how to detect and respond to events at a USB port and it has to provide a

way for the device to store data to be sent and retrieve data that have been received UART consists of different blocks which handle the serial communication through RS232 protocol. There are a set of control registers to control the data transfer. The interface FIFO logic has FIFOs to bridge the data rate differences between USB and RS232 protocols

2:20 *Routing Mechanisms and Cross-Layer Design for Vehicular Ad Hoc Networks: a Survey*
Harsh Trivedi (La Trobe University, Australia); Prakash Veeraraghavan (La Trobe University, Australia); Seng W Loke (La Trobe University, Australia); Anirudhha Desai (La Trobe University, Australia); Jugdutt Singh (La Trobe University, Australia)

Vehicular Ad-Hoc Network (VANET) will pave the way to advance automotive safety and occupant convenience. The potential VANET applications present diverse requirements. VANET shows unique characteristics and presents a set of challenges. The proposed VANET applications demand reliable and proficient message dissemination techniques. Routing techniques proposed for Mobile Ad-Hoc Network (MANET) do not cater for the characteristics of VANET. The need for novel routing techniques, exclusively designed for VANET has been recognized. This paper analyses different routing techniques proposed specifically for VANET. Unique characteristics of VANET pose challenges to traditional layered architecture where different layers make independent decisions. Mobility, absence of global view of network, random changes in topology, poor link quality and varied channel conditions have encouraged the paradigm shift to cross-layer approach. In order to optimise the performance of VANET, architectures based on cross-layer approach have been proposed by the researchers. The paper also surveys such cross-layer paradigm based solutions for VANET and concludes with an analytical summary.

2:40 *Introducing Deeper Nulls for Time Modulated Linear Symmetric Antenna Array Using Real Coded Genetic Algorithm*
Gopi Ram Hardel (National Institute of Technology, Durgapur, India); Naren. Tapaswi Yallaparagada (National Institute of Technology, Durgapur, West Bengal, India); Durbadal Mandal (National Institute of Technology, Durgapur, India); Anup Bhattacharjee. (National Insttitute of Technology, India)

A novel approach based on the real coded genetic algorithm (RGA) is proposed to improve nulling performance of time modulated linear antenna arrays. The RGA adjusts the excitation amplitude of each radiating element to place deeper nulls in the desired direction. Various results are presented to show the advantages of this approach considering one and multiple desired nulls.

3:00 *FPGA Implementation of DSSS-CDMA Transmitter and Receiver*
Bobbala Sreedevi (Vaagdevi college of engg, India); Valapadasu Vijaya (Vaagdevi college of engg, India); Chennaboina Kranthi Rekha (Linton Universiti College, India); Rama Valupadasu (National Institute of Technology, India); B Rama Rao Chunduri (National Institute Of Technology, Warangal, India)

The DS - CDMA is expected to be the major medium access technology in the future mobile systems owing to its potential capacity enhancement and the robustness against noise. The CDMA is uniquely featured by its spectrumspreading randomization process employing a pseudo-noise (PN) sequence, thus is often called the spread spectrum multiple access (SSMA). As different CDMA users take different PN sequences, each CDMA receiver can discriminate and detect its own signal, by regarding the signals transmitted by other users as noise-like interferences. In this project Direct sequence principle based CDMA transmitter and receiver is implemented in VHDL for FPGA. The digital frequency synthesizer principle is used in generating the carrier signals both at transmitter and receiver modules. The transmitter module mainly consists of symbol generator, programmable PN sequence generator, digital local oscillator, spreader and BPSK modulator blocks. The receiver module consists of BPSK demodulator, matched filter, programmable PN sequence generator and threshold detector blocks. The CDMA receiver gets this input and recovers the data using matched filter.Modlesim Xilinx Edition 5.8 (MXE) tool will be used for functional simulation and logic verification at each block level and system level. The Xilinx Synthesis Technology (XST) of Xilinx ISE tool will be used for synthesis of transmitter and receiver on FPGAs. Applications of the developed CDMA system for ADHOC networks and defense communication links will be studied. The possible extensions of work in view of advancements in software defined radio principles will be discussed.

3:20 *SIP Over Peer-to-Peer - Implications and Existing Approaches*
Md. Safiqul Islam (Royal Institute of Technology (KTH), Bangladesh); Rezaul Hoque (The Royal Institute of Tehcnology, Denmark)

In contemporary communication system, Peer-to-Peer Session Initiation Protocol (P2PSIP) is the forthcoming migration from the traditional client-server based SIP system. Traditional centralized server based SIP system is vulnerable to several problems like performance bottleneck, single point of failure. So, integration of Peer-to-Peer system (P2P) with Session Initiation Protocol (SIP) will improve the performance of a conventional SIP system because a P2P system is highly scalable, robust, and fault tolerant because of its decentralized manner and self-organization of the network. However, P2PSIP architecture faces several challenges including trustworthiness of peers, resource lookup delay, Network Address Translation (NAT) traversal, etc. This paper focuses on understanding the needs of integration of P2P and SIP. It reviews the existing approaches to identify how they have integrated P2P and SIP and solved the challenges introduced by P2PSIP.

B13

Network & Communication Technology II

Time: 2:00PM - 3:40PM
Room: Function Room 6

Chair: S Balasubramaniam (Bharathiyar University, India), Mas Irfan Purbawanto Hidayat (Institute of Technology Sepuluh Nopember, Indonesia)

2:00 ***Traffic Sign Recognition Model on Mobile Device***
Hwee Ling Wong (Multimedia University, Malaysia); Woo Chaw Seng (University of Malaya, Malaysia)

Incorporation of a good machine vision into mobile device can create a powerful application. With such advancement, mobile users can use their existing Smartphone as their third-eye to perceive the world. This paper introduces a framework using the Smartphone to increase ambient intelligence and road safety of moving vehicles through traffic sign alert application. The driver is alerted of the incoming traffic signs in different modes depending on the user's preference. However, the competency of the application is still bounded with the capability of a normal human vision. Unlike conventional research work, this paper emphasizes on portability and expandability. Portability means there is no additional installation or placement of electronic hardware required in the vehicle in order to make the system work. Expandability focuses on the transparency of the traffic sign recognition output to other applications within same hardware device or external devices. This provides an option to other developers to use or expand their own applications by using the result of the proposed application. An interaction model of the traffic sign recognition system on mobile device is introduced.

2:20 ***Neural Networks with NARX Structure for Material Lifetime Assessment Application***
Mas Irfan Purbawanto Hidayat (Institute of Technology Sepuluh Nopember, Indonesia); Puteri Sri Melor (Universiti Teknologi Petronas, Malaysia); Wajan Berata (Institute of Technology Sepuluh Nopember, Indonesia)

In the present paper, neural networks (NN) with non-linear auto-regressive exogenous inputs (NARX) structure is developed and further applied for material lifetime assessment application. Rational of the use of the NARX structure in the application is emphasized and linked to the concept of constant life diagram (CLD), the well known concept in fatigue of material analysis and design. Fatigue life assessment is then performed and realized as one-step ahead prediction with respect to each stress level corresponding to stress ratio values arranged in such a way that transition took place from a fatigue region to another one in the CLD. As a result, material lifetime assessment can be fashioned for a wide spectrum of loading in an efficient manner. The simulation results for different materials and loading situations are presented and discussed.

2:40 ***The Parallel AGE Variances Method for Temperature Prediction on Laser Glass Interaction***
Lizawati Mi Yusuf (Universiti Teknologi Malaysia, Malaysia); Norma Alias (Universiti Teknologi Malaysia, Malaysia); Mohammed Shariff Bashir Ghouse (Universiti Teknologi Malaysia, Malaysia); Siti Mariyam Shamsuddin (Universiti Teknologi Malaysia, Malaysia); Mohd Shahizan Othman (Universiti Teknologi Malaysia, Malaysia)

This paper describes the formula of three-dimensional parabolic equations for cylindrical coordinate glass that is used for the mathematical simulation in simulating the temperature behavior of laser glass cutting. There are three methods been use for simulation purposes which is the Alternating Group Explicit (AGE) which compromising two variances that is Brian and Douglas variant, and Gauss Seidel Red Black method. The simulation for these three methods is done in a parallel computing environment to speed up the calculation process and to achieve an accurate and convergence result. From the simulation, the results will be compared by conducting parallel performance measurement, which are execution time, speedup, efficiency, effectiveness and temporal performance.

3:00 ***Design and Implementation of MPPT Controlled Grid Connected Photovoltaic System***
Md. Ismail Hossain (International Islamic University Chittagong, Bangladesh); Shakil Ahamed Khan (Dhaka International University, Bangladesh); Md. Shafiullah (BUET, Bangladesh); Mohammad Jakir Hossain (Dhaka University of Engineering and Technology, Bangladesh)

This paper proposes an intelligent method for maximum power point tracking (MPPT) of a photovoltaic system under variable temperature and insolation conditions and conversion of this solar energy into stabilized sine wave having low distortion factor (DF), so that the solar energy can be supplied to grid and can operate electrical and electronic devices efficiently. For the reduction of tracking time of maximum power from photovoltaic array and to obtain stabilized sine wave with very fast rise time for voltage stability, fuzzy logic control algorithm is implemented with the embedded microcontroller for improved performance as compared to conventional techniques. The system includes a photovoltaic array; a PWM controlled DC-DC, DC-AC converters, sensor circuits and zero crossing detector (ZCD). The designed MPPT controller regulates the converter output voltage by varying modulation index of the PWM pattern using MPPT algorithm and it maximizes the output power extracted from photovoltaic array. This paper discusses the low cost implementation of MPP

algorithm in a 8-bit microcontroller using the tools and techniques to generate optimized real time code in C for ATMega8 microcontroller which will demonstrate how maximum power point tracker might provide elegant and efficient solution for increasing the efficiency of a solar system and connection of the extracted energy to grid which is based on experimental results rather than on mathematical models.

3:20 ***Water Pipe Leak Detection Using Electromagnetic Wave Sensor for the Water Industry***
Jung Hean Goh (Liverpool John Moores University, United Kingdom); Andrew Shaw (Liverpool John Moores University, United Kingdom); Jeff Cullen (Liverpool John Moores University, United Kingdom); Ahmed I Al-Shamma'a (Liverpool John Moores University, United Kingdom)

This project concerns the use of an electromagnetic sensor for the detection of leaks/cracks in water pipes. As old metal pipes corrode, they start to become brittle, resulting in the potential for cracks to appear in the pipes. In addition corrosion can build up resulting in a restricted flow of water in the pipe. Using an electromagnetic (EM) sensor to monitor the signal reflected from the pipes in real time, provides the necessary information to determine where a leak in the pipe has occurred. Analysis of the reflected signal can provide the operator with information about the condition of the leak within the pipe. This work describes how the system was designed, and also its construction at a scale suitable for insertion into a 100mm diameter water pipe.

C13

Signal & Image Processing II

Time: 2:00PM - 3:40PM
Room: Function Room 7

Chair: Mansour Alsulaiman (King Saud University, Saudi Arabia), Paul Bao (University of South Florida, USA)

2:00 ***Design of Tunable Folded Cascode Differential Amplifier Using PDM***
Ashis Kumar Mal (NIT Durgapur, India); Rishi Todani (NIT Durgapur, India); Om Prakash Hari (NIT Durgapur, India)
Operational Amplifiers (op-amps) are one of the most commonly used blocks in analog and mixed signal VLSI design.

Designers often spend considerable time in designing op-amps analytically, and then realize that the simulated circuits do not match with analytical expectations. This is primarily due to the modeling of short channel MOS devices using long channel equations. Finally an adhoc mechanism is adopted to realize the op-amp with the help of a simulator. Proposed Potential Distribution Method (PDM) is a method where the design methodology is based on actual behaviour of the devices and it is free from any analytical expression. This paper demonstrates the design approach for realizing a fully differential folded cascode op-amp using PDM, which is based on simulator results obtained with predefined bias conditions. The dependency of various performance parameters, like slew rate (SR), unity gain bandwidth (UGB), phase margin (PM), etc. on potentials and current distribution at different nodes is presented. It is found that using these dependencies, the target specifications for an op-amp can be achieved with shorter design time. Also, fine tuning the performance metric can be achieved using PDM. Finally, a fully differential folded cascode op-amp is thus designed and the simulation results are presented.

2:20 ***Automatic Enlargement of Speech Corpus for Speaker Recognition***
Mansour Alsulaiman (King Saud University, Saudi Arabia)

Development of an automatic speaker recognition system using different clustering and stochastic approaches to achieve higher recognition rate has been continuing for last three decades. This research deals with the problem of recognition when only a few samples are available for training of the system. To avoid the low recognition rate caused by such type of speech corpus, automatic techniques for the enlargement of speech corpus are proposed in this paper. Different combinations of samples, generated by proposed techniques, are used to obtain the high recognition rate. These techniques have shown promising result of 89.90%.

2:40 ***Regional Skin Detection Based on Eliminating Skin-Like Lambertian Surfaces***
Ali Nadian (Shahid Beheshti University, Iran); Alireza Talebpour (Shahid Beheshti university, Iran); Mohammad Basseri (Shahid Beheshti university, Iran)

Skin color is an often used feature in machine vision application related to humans, regarded as pixel-based skin color detection. This method has an inherent problem when color overlaps between skin and none skin regions In this paper a skin detection system based on a regional property of objects, called; Lambertian reflection is proposed. Skin is a none-Lambertian surface. In order to use this feature, first, a Single Gaussian Model (SGM) is used to detect skin like pixels in an image. From detected skin regions, ones having none-Lambertian surface property are detected as final skin regions. To detect none-lambertian skin regions, an exponential is fit the the histogram of potential skin regions and based on the

fit, it is decided if the region is skin or not. By incorporating this feature the False Positive detect rate (FPR) is greatly decreased.

3:00 ***A Face Recognition Scheme Using Wavelet-based Local Features***
Hafiz Imtiaz (Bangladesh University of Engineering and Technology, Bangladesh); Shaikh Anowarul Fattah (Concordia University, Canada)

In this paper, a multi-resolution feature extraction algorithm for face recognition is proposed based on two-dimensional discrete wavelet transform (2D-DWT), which efficiently exploits the local spatial variations in a face image. For the purpose of feature extraction, instead of considering the entire face image, an entropy-based local band selection criterion is developed, which selects high-informative horizontal segments from the face image. In order to capture the local spatial variations within these high-informative horizontal bands precisely, dominant wavelet coefficients corresponding to each local region residing inside those horizontal bands are selected as features. In the selection of the dominant coefficients, a threshold criterion is proposed, which not only drastically reduces the feature dimension but also provides high within-class compactness and high between-class separability. A principal component analysis is performed to further reduce the dimensionality of the feature space. Extensive experimentation is carried out upon standard face databases and a very high degree of recognition accuracy is achieved by the proposed method in comparison to those obtained by some of the existing methods.

3:20 ***Pixel-Based Skin Detection Using Sinc Function***
Ali Nadian (Shahid Beheshti University, Iran); Alireza Talebpour (Shahid Beheshti university, Iran)

Skin detection is a major key in most human-related recognition systems. Parametric models have been proposed to effectively model the distribution of skin pixels. Some limitations of these methods have been reviewed and a new model based on the sinc function is proposed to overcome these limitations. Three different color spaces are chosen for experiment. The results are compared with the results of Gaussian, GMM and Elliptic boundary models. The method significantly outperforms Gaussian and Elliptic method and in also the results show that the model slightly outperforms GMM with 2 Gaussians used. Steepest decent method was used for data fitting and COMPAQ database has been used for training purposes.

A14

Artificial Intelligence & Computer Engineering (cont)

Time: 4:00PM - 5:40PM
Room: Function Room 5

Chair: Alex Mason (Liverpool John Moores University, United Kingdom), Saeed Sabamoniri (Islamic Azad University- Soufian Branch, Iran)

4:00 ***Processing Tree-like Data Structures for Sorting and Managing Priorities***
Valery Sklyarov (University of Aveiro, Portugal); Iouliia Skliarova (University of Aveiro, Portugal); Dmitri Mihhailov (Tallinn University of Technology, Estonia); Alexander Sudnitson (Tallinn University of Technology, Estonia)

The paper describes the hardware implementation and optimization of parallel algorithms that sort data using tree-like structures combined with sorting networks. The emphasis is done on applications that require fast resorting for any new portion of incoming data items. Parallel processing is achieved by constructing N binary trees (N>1) and applying concurrent sorting to the N trees at the same time with the aid of N communicating processing modules. Experiments and comparisons demonstrate that the performance is increased significantly compared to other known implementations

4:20 ***Data Driven Approach for Low-Power Pre-Computation-Based Content Addressable Memory***
Tsung-Sheng Lai (National Taiwan University, Taiwan); Chin-Hung Peng (National Taiwan University, Taiwan); Lai Feipei (National Taiwan University, Taiwan)

Content addressable memory (CAM) plays an important role in the performance of many applications such as DCT transforms, processor caches, database accelerators, and network routers because it enables high-speed search operations with hardware acceleration. However, the power consumption of CAM is rather high because within CAM, searching is conducted in parallel for all registered words. Hence, pre-computation-based CAM, i.e., PB-CAM, was proposed in [1] in order to reduce the number of parallel-operated words by first filtering using a precomputation circuit called the parameter extractor. We observed that the efficiency of the parameter extractor was limited by the locality of precomputed data and the circuit structure itself. In this work, we propose a data driven algorithm—local grouping (LG)—to synthesize a parameter extractor for PB-CAM such that the registered data can be uniformly mapped to construct

parameters; the cost of implementing the parameter extractor is also decreased. Moreover, we also adopt a discard and interlace (DAI) method that can further reduce the impact on non-uniform cases, which happens when most data are identical in some data blocks before LG processing. In experiments, average power consumption reduction of 60.4% was achieved and the number of CMOSs used was also reduced by 0.52%, when compared with the conventional gate-block selection algorithm [2].

4:40 ***A New NoC Architecture Based on Partial Interconnection of Mesh Networks***
Sudhanshu Choudhary (Indian Institute of Technology, Kanpur, India); Shafi Qureshi (IITK, India)

A new network on chip (NoC) topology called partially interconnected mesh network is proposed and a routing algorithm supporting the proposed architecture is also developed. The proposed architecture is based on standard mesh networks, here four extra bidirectional channels are added which remove the congestion and hotspots compare to standard mesh networks with fewer channels. The proposed architecture and routing algorithm are compared to measure performance benefits over standard mesh network in terms of delay and throughput. Significant improvement in delay (60% reduction) and throughput (60% increased) were observed when using the proposed network. Although an increase in number of channels makes the switches expensive and could increase the area and power consumption. However, the proposed network can be useful in high speed applications where speed is more important and a tradeoff between speed, area and power is acceptable.

5:00 ***Principles and Dynamics of Block-based Programming Approach***
Siti Nor Hafizah Mohamad (University Kebangsaan Malaysia, Malaysia); Ahmed Patel (Universiti Kebangsaan Malaysia, Malaysia); Yiqi Tew (University Kebangsaan Malaysia, Malaysia); Rodziah Latih (Universiti Kebangsaan Malaysia, Malaysia); Qais Janabi (UKM, Malaysia)

Block-based programming approach is based on the principles and dynamics of combining component-based programming approach with end-user programming paradigm which is purported to be more advanced and easier to use in practice. We perform a state of the art review of block-based programming by accessing the different forms of programming approaches and paradigms pertaining to it and establish the core fundamental principles, mechanics and dynamics with examples to illustrate the essence of this approach as well as any metrics to measure its performance. The important characteristics of block-based programming are gathered together and tabulated with clear definition of meaning and purpose. Correspondingly, we establish the criterion and metric by which to measure the effectiveness and efficiency of programming effort in developing software systems based on the block-based approach. In addition, we illustrate more on the block specification and identification to give brief understanding. Finally, we identify aspects of block-based programming which need further investigation, research and development.

5:20 ***Comparison Between PID and Fuzzy Logic Controllers for Advance Microwave Biodiesel Reactor***
Wasan Wali (Liverpool John Moores University, United Kingdom); Jeff Cullen (Liverpool John Moores University, United Kingdom); Kadhim H Hassan (Liverpool John Moores University, United Kingdom); Ahmed I Al-Shamma'a (Liverpool John Moores University, United Kingdom); Alex Mason (Liverpool John Moores University, United Kingdom)

The proportional integral derivative (PID) controllers are widely applied in industrial process owing to their simplicity and effectiveness for both linear and nonlinear systems, and the tuning methods still a hot research area to give the optimum result for control behavior. Fuzzy logic and proportional integral derivative (PID) controllers are designed and compared for use in control on-line an advanced biodiesel microwave reactor system which converts waste cooking oil into biodiesel by transesterification chemical process. A closed loop fuzzy and PID controllers are used to automatically and continuously adjust the applied power of microwave reactor under different perturbations. Labview based software tool will be presented and used for measurement and control of the full system, that will make charts real time display as well as state real time monitoring.

5:40 ***Samsung ARM9 S3C2440A Hardware Core Circuit Design***
Azlan Sulaiman (Research Department, Malaysia)

Samsung S3C2440A is advance microprocessor available now, offered very competitive in term of performance and price. The microprocessor, 32-bit CMOS is developed with ARM920T core, with 0.13 um CMOS standard cells and memory complier. The attractive features by this microprocessor are consumed less power and fully static design for the cost and power sensitive application. This paper will demonstrated the hardware design of core circuitry for this microprocessor that can be implemented for various applications, including mobile and desktop model devices. The core design consists of basic microprocessor design platform which utilize the features offered by S3C2440 microprocessor.

D14

Network & Communication Technology II (cont)

Time: 4:00PM - 5:40PM
Room: Function Room 9

Chair: Tamleek Ali Tanveer (Institute of Management Sciences, Pakistan), Valapadasu Vijaya (Vaagdevi college of engg, India)

4:00 ***Medium Access Control for Collaborative Transmit Beamforming in Wireless Networks***
Suhanya Jayaprakasam (Multimedia University, Malaysia); Teong Chee Chuah (Multimedia University, Malaysia); Su Wei Tan (Multimedia University, Malaysia)

A new medium access control (MAC) scheme to enable collaborative transmit beamforming in IEEE 802.11 based wireless networks is proposed. The proposed scheme allows information sharing and simultaneous transmission in collaborative transmit beamforming, and is compatible with the existing distributed coordination function protocol. Performance comparisons with multi-hop and direct communications of the IEEE 802.11g wireless standard employing carrier sense multiple access with collision avoidance MAC are made. Results show that the proposed approach provides better throughput when greater distances or more hops are needed to complete communications, especially in a noisy environment.

4:20 ***A Probabilistic Measure of Extended Reservation Aloha MAC Protocol Against Some MAC Problems in MANET***
Kazi Atiqur Rahman (University of Windsor, Canada); Khaja Shazzad (University of Windsor, Canada); Kemal Tepe (University of Windsor, Canada)

Mobile hidden station and neighborhood capture problems severely affect the communication in the MAC layer of a mobile ad hoc network. IEEE 802.11 cannot prevent blocking due to neighborhood capture problem and collisions due to mobile hidden station problem. Extended reservation Aloha (ERA) solves these two problems in a probabilistic manner along with solving widely known hidden station and exposed station problems. This paper provides a probabilistic view of ERA to neighborhood capture and mobile hidden station problems. The analysis shows that the channel accessing probability of a station facing neighborhood capture problem is more than 90 percent with 60 percent traffic.

4:40 ***Usage Control Framework for Mobile Ad-hoc Applications***
Tamleek Ali Tanveer (Institute of Management Sciences, Pakistan); Mohammad Nauman (Computer Science Research and Development Unit (CSRDU), Pakistan)

Mobile ad-hoc applications create a link with other applications in an ad-hoc manner. Resources may be released to the peer applications. Access and usage control is an important requirement while sharing resources with peer application. Currently there is no controlling framework for the usage of shared resources in mobile ad-hoc applications. In this paper we introduce the notion of a usage control administrative system (UCAS) that manages the usage of individual objects registered with it. Whenever a node joins the ad-hoc network, it may share and use one or more objects while being part of the ad-hoc application domain. While releasing resources to UCAS it attaches the policy along with the resource. This policy may describe the number of total usages, the number of individual usages, location and timings etc. We have proposed a framework with the XML based policy for usage control of the shared resources. We show that our design effectively enforces usage control in the highly dynamic mobile ad hoc applications network.

5:00 ***A Novel Method for Achieving Load Balancing in Web Clusters Based on Congestion Control and Cost Reduction***
Ahmad Yousofi (Islamic Azad University Naein Branch, Iran)

The World Wide Web is fundamental infrastructure for different services. The number of accessing to web sites is significantly increasing. Cluster-based web systems (web-cluster) are a new solution to implement a web server system with high efficiency and availability. In practice, a web cluster consists of several web servers, and a web switch which distributes user's requests among server nodes. Achieving high efficiency from web cluster requires load balancing between web servers. In this paper, we propose a novel dispatching policy, namely Multi-Class Round Robin with Congestion Control and Cost Reduction (MC-RR-CC-CR), for web switches operating at layer 7 of the OSI protocol stack. The results of a real scenario showed that the proposed method can significantly balance the load of web cluster and substantially improve the system efficiency. Particularly when web cluster is heterogeneous and web site content is dynamic.

5:20 ***A Mobile Service Architecture for Improving Availability and Continuity***
Nor Shahniza Kamal Bashah (Norwegian University of Science and Technology, Norway); Ivar Jørstad (Ubisafe AS, Norway); van Thuan Do (Linus AS, Norway); Tore Jønvik (Oslo University College, Norway); Van Thanh Do (Telenor/ Norwegian University of Science and Technology, Norway)

In modern mobile multi-network multi-domain environments services can be anything and can have any name. This poses problems for the service availability and consequently service continuity since services may not be discovered in time for being used. Services offering equivalent functions and capabilities such as GSM voice, IP telephony, etc. are usually considered as different by the network system and are not interchangeable. This paper proposes a mobile service architecture which enables the discovery and consumption of equivalent services. The solution provides also seamless service continuity by incorporating dynamic discovery of equivalent services with dynamic switching of available services. The solution offers personalisation while preserving both flexibility and control of the user. Although most of the storage and processing of data are located in the network the service continuity process is initiated, controlled and decided by the mobile device's side. A proof-of-concept including a client implementation on Android is presented.

B14

Applications II (cont)

Time: 4:00PM - 5:40PM
Room: Function Room 6

Chair: S Balasubramaniam (Bharathiyar University, India), Mas Irfan Purbawanto Hidayat (Institute of Technology Sepuluh Nopember, Indonesia)

4:00 ***BZK.SAU.FPGA10.0: Microprocessor Architecture Design on Reconfigurable Hardware as an Educational Tool***
Halit Oztekin (University of Bozok, Turkey)

The Computer Architecture and Organization course in Computer and Electrical Engineering departments faces with a big problem: the migration from theory to practice. In order to solve this problem, a Computer Architecture simulator named BZK.SAU[1] is designed using an emulator program for educational purpose. This approach has important limitations. While students can complete and simulate their designs using software, they do not have the chance to implement and to run their designs in actual hardware. This work presents our solution to this problem: the FPGA implementation of BZK.SAU so that it would look and behave like the computer architecture simulator published in [1]. So we have implemented BZK.SAU Computer Architecture Simulator by using Altera® FPGA board that is a reconfigurable hardware prototyping development platform.

4:20 ***Cascade Multi-level Converter Based DVR and D-STATCOM for Voltage Sag and Swell Reduction***
Bahr Eldin Suliman Osmsn (University Technology PETRONAS, Malaysia); K S Rama Rao (Universiti Teknologi Petronas, Malaysia); Perumal Nallagownden (Universiti Teknologi Petronas, Malaysia)

This paper presents the modeling and simulation of three and seven-level cascade multilevel converter (CMC) based dynamic voltage restorer (DVR) and distribution static compensator (D-STATCOM), aimed at correcting the supply voltage sag/swell and interruption in low voltage distribution networks. The proposed design models of CMC based DVR and D-STATCOM are expected to be most powerful solutions to minimize supply voltage disturbances of the sensitive loads. The proposed models of DVR and D-STATCOM together with the controllers are simulated by using electromagnetic transient simulation program (PSCAD/ EMTDC) and the results are presented to assess the performance of each device.

4:40 ***G-Flash: an Authoring Tool for Guided Digital Storytelling***
Jumail Wastam (Universiti Teknologi PETRONAS, Malaysia); Dayang Rohaya Awang Rambli (Universiti Teknologi PETRONAS, Malaysia); Suziah Sulaiman (Universiti Teknologi Petronas, Malaysia)

This paper describes the conceptual design of G-Flash, an authoring tool for supporting guided digital storytelling among young children. The basic idea of G-Flash revolves around guidance concept with the aim of assisting young children quickly generate a story according to the intended learning objectives. Tutored condi-tion, a mid-level form of guidance giving was selected as the guided learning approach to allow the student getting only the right amount of assistance without compromising on the learner's creativity and motivation as well as to learn on their own within the assistance withholding condition. An important feature of G-Flash is the use of flashcards, a familiar and widely used tool to teach children, as the main media element to create the digital story was highlighted. A review of existing tools was provided and benefits of guidance concept, not present in existing digital storytelling tool, were discussed.

5:00 ***GIS Integrated DNA Computing for Solving Travelling Salesman Problem***
Sridhar R (Bharathiyar University, India); S Balasubramaniam (Bharathiyar University, India)

DNA computing is a new method of simulating biomolecular structure of DNA and computing by means of molecular biology technological computation. It introduces a fire-new data structure and calculating method, providing a new way of solving NP-complete problem of traveling salesman. It is a new computational method by harnessing the enormous parallel computing ability and high memory density of bio-molecules, which brings potential challenges and opportunities to cryptography, steganography, Signature and Authentication. In this paper, DNA computing is integrated with GIS to find shortest path of traveling salesman problem with geocomputational method and DNA Computing method without using laboratory. Both methods show the same result proving that problems of GIS could be solved using DNA computing.

5:20 ***Illuminance Distributions, Visual Response and Limits for Conservation of Exhibits in Admiral Cheng Ho Gallery, Malaysia***
Noraini Ahmad (University of Technology MARA, Malaysia); Sabarinah Sh Ahmad (Universiti Teknologi MARA, Malaysia); Anuar Talib (Universiti Teknologi MARA, Malaysia)

This paper presents i) literature review of illuminance limits for conservation of exhibits; ii) pilot study on illuminance levels and distributions, air temperatures and relative humidity, RH and iii) survey results on visitors' visual feedbacks on the exhibits' conditions conducted at the Admiral Cheng Ho Gallery (Museum of History and Ethnography), Stadthuys, Melaka, Malaysia. Indicators for visual discomfort are observed from objectives ii and iii. The fieldwork was a pilot survey in the west facing gallery during high period of daylight distributions (14.00 -16.00hr) for a full week in March 2010. Results showed illuminance levels exceeded allowable exposure limits for some showcases. Measured air temperatures were much higher than accepted comfort range especially with opened windows in the afternoon and the RH levels were within the prescribed range. The survey identified the combination of natural daylight and artificial lighting deteriorated the exhibits' conditions through fading, distortion, dirt and dust. The showcases were placed against and opposite the fully opened windows. Thus, the presence of sunlight, daylight and provision for external views in the gallery produced glare and veiling reflections problems on the glass showcases. These situations may demonstrate the need for proper maintenance and appropriate controlled shading system. The evaluation of daylight distributions may serve as future conservation measure for the exhibits.

C14

Signal & Image Processing II (cont)

Time: 4:00PM - 5:40PM
Room: Function Room 7

Chair: Mansour Alsulaiman (King Saud University, Saudi Arabia), Paul Bao (University of South Florida, USA)

4:00 ***Finite Difference Error Analysis of Geometry Properties of Implicit Surfaces***
Pan Zheng (Universiti Sains Malaysia, Malaysia); Bahari Belaton (Universiti Sains Malaysia, Malaysia); Iman Yi Liao (Universiti Sains Malaysia, Malaysia); Zainul Ahmed Rajion (Universiti Sains Malaysia, Malaysia)

In this paper we investigate the impact of different finite difference method (FDM) on estimation of the curvatures and other geometry properties of an implicit surface extracted from volumetric data. The FDM estimations are conducted on the surface in different resolutions: refined surface, medium surface and coarse surface. A ground truth is established on each resolution to be compared with the experiment results. Then we apply relative error analysis on the results to find the suitable FDM that can be utilized in the estimation.

4:20 ***Image Mosaics with Wavelet Domain Seam-lines***
Paul Bao (University of South Florida, USA)

Scene mosaics are a technique for building a panoramic view of a scene from a set of small views. When overlapped scene images are pasted, the mixed radiometry of the overlap areas may cause artifacts and blurred areas. The seam-line scene mosaics can avoid such artifacts and blurred areas. We propose a seamless scene mosaic scheme in the wavelet domain of the edge images, where the correspondence search and the seam-line search are performed. The homographic transformation obtained through wavelet domain correspondence research is applied for the original scene images for the geometric correction and the seam-line in the wavelet domain is reverse wavelet transformed to form a seam-line in the original spatial domain for the image pasting. This scheme can significantly improve the performance of the scene mosaics while achieving seamless scene mosaics of the scene. The experiment shows that the scheme outperforms the spatial domain seam-line scene mosaics scheme three times as much.

4:40 ***Contour Layer Extraction From Colour Topographic Map by Feature Selection Approach***
Banda Sandhya (University of Hyderabad, India); Arun Agarwal (University of Hyderabad, India); Raghavendra Rao Chillarige (University of Hyderabad, India); Rajeev Wankar (University of Hyderabad, India)

Contour layer of topographic maps can provide useful information for many vector based GIS applications. A topographic map consists of various semantic layers of overlapping information, differentiated primarily based on colour. Hence, to extract the contour layer from a topomap, colour segmentation algorithms are employed. However due to scanning and inherent properties of topomap, colour space selection which provides efficient segmentation results becomes essential. The method proposed uses PCA as feature selection approach to select the colour features of topomap. The clusters are further processed to map to the layers of topomap using spatial properties.

5:00 ***An Efficient Multimodal Face Recognition Method Robust to Pose Variation***
Ali Cheraghian (Amir Kabir University of Technology (Tehran Polytechnic), Iran); Karim Faez (Amirkabir University of Technology, Iran); Hamid reza Dastmalchi (Tehran Polytechnic (AUT), Iran); Farhad Bagher Oskuie (Amir Kabir University of Technology (Tehran Polytechnic), Iran)

In recent years, face recognition has obtained much attention. Using combined 2D and 3D face recognition is an alternative method to deal with face recognition. .A multimodal face recognition algorithm based on Gabor wavelet information is presented in this paper. The Principal Component Analysis (PCA) and the Linear Discriminant analysis (LDA) have been used for size reduction. The system has combined 2D and 3D systems in the decision level that presented higher performance in contrast with methods which only 2D and 3D systems, separately. The proposed algorithm examined in FRAV3D database that has faces with pose variation and performance of 95% achieved in rank one for fusion experiment.

5:20 ***Towards MPEG4 Compatible Face Representation Via Hierarchical Clustering-Based Facial Feature Extraction***
Alireza Ghahari (University of Connecticut, USA); Mohsen Mosleh (Sharif University of Tech, Iran)

Multi view imaging and display systems has taken a divide and conquer approach to 3D sensing and visualization. We aim to make more reliable and robust automatic feature extraction and natural 3D feature construction from 2D features detected on a pair of frontal and profile view face images. We propose several heuristic algorithms to minimize possible errors introduced by prevalent non-perfect orthogonal condition and non-coherent luminance. In our approach, we first extract the 2D features that are visible to both cameras in both views. Then, we estimate the coordinates of the features in the hidden profile view based on the visible features extracted in the two orthogonal views. After that, based on the coordinates of the extracted features, we deform a 3D generic model to perform the desired deformation based modeling. Finally, the face model is texture-mapped by projecting the input 2D images onto the vertices of the face model. As the reconstructed 3D face model is MPEG4 compliant, it can be readily animated by standard MPEG4 facial animation parameters (FAPs). Present study proves the scope of resulted facial models for practical applications like face recognition and performance driven facial animation.

D21

Network & Communication Technology III

Time: 9:00AM - 10:40PM
Room: Function Room 9
Chair: Yoong Choon Chang (Multimedia University, Malaysia), Hanen Idoudi (ENSI-Manouba University, Tunisia)

9:00 ***Performance of Real Time Cooperative MIMO Using an SDR Platform***
Hassaan Ajaz (National University of Sciences and Technology, National Radio Telecommunication Corporation, Pakistan); Omer Ihsan (National University of Sciences and Technology, Pakistan); Usman Javed (National University of Sciences and Technology, National Radio Telecommunication Corporation, Pakistan); Moaaz Hafeez (National University of Sciences and Technology, Pakistan); Safwat Irteza Butt (Ilmenau University of Technology, Germany)

Fading remains the prime problem in wireless communications, and line of sight communication is not possible everywhere. Multiple Input Multiple Output (MIMO) is a technique used to fight off multi path fading effects by physically placing multiple antennas to create independent channel realizations. The paper identifies performance gains of cooperative communication networks over conventional SISO and multiple collocated antenna array systems. An experimental testbed is developed on a Software Defined Radio (SDR) platform comprising of three distributed network nodes operating in the 2.4GHz unlicensed ISM band. A Selective Decode and Forward (DF) cooperative protocol is developed and established between the nodes. The results have been evaluated in terms of diversity gains as measured from the experimental curves of frame error rate versus average signal to noise ratio. A comparative analysis is drawn between different communication techniques.

9:20 ***Video Transmission Over WiMedia-UWB Using Subpacket Hybrid ARQ***
Gek Hong Sim (Multimedia University, Malaysia); Yoong Choon Chang (Multimedia University, Malaysia); Teong Chee Chuah (Multimedia University, Malaysia)

Ultra-wideband (UWB) serves the high bandwidth demand for high definition video transmission over short-range wireless networks. Nevertheless, bursty errors due to harsh channel conditions during video transmission greatly deteriorate video quality. In order to improve the quality of video transmission over UWB, we propose the use of a subpacket based hybrid automatic repeat request (HARQ) scheme instead of the conventional packet based HARQ scheme. The proposed subpacket based HARQ scheme only retransmits erroneous subpackets and avoids retransmission of other correctly decoded subpackets. Simulation results show that in comparison with the conventional packet based HARQ scheme, the proposed subpacket based HARQ scheme achieves significant performance improvement in terms of delay, percentage of overhead, throughput and reconstructed video quality.

9:40 ***Improving Connectivity and Coverage of Wireless Sensor Networks Using Mobile Robots***
Chiraz Houaidia (ENSI, University of Manouba, Tunisia); Hanen Idoudi (ENSI-Manouba University, Tunisia); Leila Saidane (ENSI, University of Manouba, Tunisia)

Wireless sensor networks are often deployed in hardly accessible or hazardous fields. Their main goal is to monitor the target field and transmit surveillance data to a sink. Therefore, connectivity of the sensor network and the coverage ratio of the monitored area are the most relevant concerns to reach these goals. In this paper, we propose to use several mobile robots to assist sensor networks redeployment in order to enhance the network connectivity and the coverage ratio of the monitored area. We model the sensor network as an islets-based topology and we propose to use robots to detect and heal connectivity and coverage holes availing the sensors redundancy. Preliminary simulations showed that our new scheme can significantly enhance the connectivity ratio of the initial network and improve the coverage ratio by using few numbers of robots.

10:00 ***Mobility Models for Vehicular Ad-hoc Network Simulation***
Vaishali Khairnar (University of Mumbai, India); Shrikant Pradhan (Nirma University, India)

One of the emerging applications that belongs to ambient systems is to transparently and directly interconnect vehicles on roads, making an ad-hoc network that enables a variety of applications through distributed software's without the need of any fixed and dedicated infrastructure. The network as well as the embedded computers and sensors in the vehicle will be invisible to the driver, who will get the required services during his journey. New type of ad-hoc network is the Vehicular Ad-hoc Network (VANET), in which vehicles constitute the mobile nodes in the network. Due to the prohibitive cost of deploying and implementing such as system in a real world, most research work in VANET relies on simulations for evaluation purpose. The key concept for VANET simulations is a real world vehicular mobility model which will ensures conclusions drawn from simulation experiments will carry through to real world deployments. In this paper we present a tool SUMO, MOVE that allows users to easily generate real world mobility models for VANET simulations. MOVE tool is built on top of SUMO which is open source micro-traffic simulator. Output of MOVE is a real world mobility model and can used by NS-2 and qualnet simulator. In this paper we evaluate and compare ad-hoc routing performance for vehicular nodes using MOVE, which is using random waypoint model. The simulation results are obtained when nodes are moving according to a real world mobility model which is significantly different from that of the generally used random waypoint model.

10:20 ***BER Performance Evaluation for Multicarrier Code Division Multiple Access Over Generalized κ-M Fading Channels***
James Osuru Mark (Universiti Teknologi Petronas, Malaysia); Brahim Belhaouri Samir (Universiti Technologi PETRONAS, Malaysia)

Multicarrier code division multiple access (MC-CDMA)system has received a considerable attention from researchers owing to its great potential in achieving high data rates transmission in wireless communications. Due to the detrimental effects of multipath fading the performance of the system degrades. Similarly, the impact of non-orthogonality of spreading codes can exist and cause interference. This paper addresses the performance of multicarrier code division multiple access system under the influence of frequency selective generalized κ-μ fading channel and multiple access interference caused by other active users to the desired one. The average bit error rate is derived and expressed in Gauss hypergeometric functions. Maximal ratio combining diversity technique is utilized to alleviate the deleterious effect of multipath fading.

B21

Applications III

Time: 9:00AM - 10:40PM **Chair: Omid Bushehrian (Shiraz University of Technology, Iran), Debnath Mukherjee (Tata Consultancy Services, India)**
Room: Function Room 6

9:00 ***The Application of FSP Models in Software Performance Engineering: a Multi-Threaded Case-Study***
Omid Bushehrian (Shiraz University of Technology, Iran); Hassan Ghaedi (Shiraz University of Technology, Iran)

Detecting and fixing the performance obstacles of software during the early stages of software development process is the main objective of Software Performance Engineering(SPE) activities. SPE is mostly depended on the formal modeling languages due to the fact that these languages enable us to simulate the software and analyze the performance parameters. Various modeling languages such as queuing networks(QN), layered queues (LQ), Petri Nets and Stochastic Process Algebras are suggested for modeling distributed systems. There are several issues that are needed to be addressed when translating software architectural models to a target formal model, which are synchronous and asynchronous invocations, active and reactive objects, multi-threading, object deployment over computational nodes and process (thread) scheduling for resource utilization. In this paper, first we present a one-to-one translation rule set that is used to translate software Sequence and Deployment Diagrams into their corresponding FSP(Finite State Process) model considering the above mentioned issues. The resulting model then is analyzed through discrete event simulation tools such as LTSA from the performance perspective. Second, we have applied our translation rule set on a real world multi-threaded web application to obtain its FSP model. The simulation results are also presented.

9:20 ***Research and Implementation of ARINC653 Configuration Tool Based on AADL***
Yang Meng (University Electronic Science and Technology of China, P.R. China)

Applications must be integrated into a system confi-guration which satisfies all the requirements of applications in the ARINC653 system. The goal of this paper is to assist system integrator to generate correct configuration tables. Architecture Analysis and Design Language (AADL) is widely used in avionics systems modeling and analysis. In order to model and analyze avionics systems that meet the ARINC653 standard, we need to extend AADL existing standard to satisfy the requirements of ARINC653. This paper presents an approach to augment the modeling ability of AADL to describe ARINC653 configuration instance, details a modeling approach exploiting the new property sets of AADL for the design of ARINC653 architectures, and implement an automatic ARINC653 configuration tool based on AADL which generates the static configuration files that meet the qualification of ARINC653 schema for the instance model. The correct configurations generated by this tool verify the validity and feasibility of this method.

9:40 ***An Insight Into Real Software Industry Paradigms and Software Engineering Research***
Rehan Akbar (Universiti Teknologi PETRONAS, Malaysia); Mohd Fadzil Hassan (Universiti Teknologi PETRONAS, Malaysia); Azrai Abdullah (UTP, Malaysia); Sohail Safdar (Universiti Teknologi PETRONAS, Malaysia); Muhammad Aasim Qureshi (Universiti Teknologi PETRONAS, Malaysia)

Since years software development industry is trying hard to show a remarkable performance in its project development work. Inspite of standardized processes and practices, the expected increase in project's success is not seen yet. Issues related to the software processes improvement, risk management, people's factors and effective project management still exist. Though academic researchers have produced good quality work on software industry issues, but unluckily, software industry could not get benefit of it as it was being expected. Software engineering research also seems unable to identify and understand the real industry problems and providing hands on solutions. The gap between researchers and actual industry practitioners is the sole reason behind it. Actual software development practices and processes are slightly different from those models and frameworks presented in software engineering research. It is the foremost need to bridge this gap by learning from the academic research work and experiences of real software development industry practitioners. In this paper reasons behind this academic-industry gap are critically discussed. Such factors are identified that need to be considered both by the researchers and industry practitioners to uplift the industry. The aim of this study is the realization of importance of industry focused research by highlighting flaws in the entire process. An analysis of real industry projects, academic projects, research publications, and industry people is made to complete this research work. This research would help to produce such software engineering research which is more close to industry work and will provide realistic solutions to the real software industry problems.

10:00 ***A Collective Intelligence Based Business-Matching and Recommending System for Next Generation E-Marketplaces***
Youssef Iguider (The University of Electro-Communications, Japan); Hiroyoshi Morita (University of Electro-Communications, Japan)

The present work proposes and describes a novel approach to business-matching and recommending systems, for next-generation e-marketplaces. The introduced matching system makes use of Collective Intelligence (IC) means to identify and recommend the most relevant business opportunities to the user. At first, the content of business proposals and companies' profiles are parsed and indexed. The search engine starts by expanding the keyword of interest, to enable an intuitive-like search. The look-up results are then filtered based on a compatibility scoring mechanism. The personalized business matching results and recommendations are later served to the user via a novel visual interactive graphical interface. We believe that this approach can take the business-matching process and the capabilities of e-marketplaces to a new level. While focusing on the needs and realities of small businesses, a prototype system applying the proposed and described approach is currently being developed and experimentally tested, to fully demonstrate the capabilities of the proposed system on real-world data. Although the prototype is at an early stage, the initial experiments show promising results.

10:20 ***Three-phase Four-Leg Shunt Active Power Filter to Compensate Harmonics and Reactive Power***
Izzeldin Idris Abdalla (Universiti Technologi PETRONAS, Malaysia); K S Rama Rao (Universiti Teknologi Petronas, Malaysia); Perumal Nallagownden (Universiti Teknologi Petronas, Malaysia)

This paper presents a compensating system for the harmonics and the reactive power using four-leg shunt active power filter (SAPF) in a three-phase four-wire distribution network and aims to minimize the harmonics and neutral current. Two control approaches p-q theory based hysteresis current control and load current detection based hysteresis current control are proposed. To validate the compensation performance of SAPF a distribution network with nonlinear loads is simulated using MATLAB/Simulink software. Simulation results are presented to assess the performance of SAPF to minimize the total harmonics distortion (THD) and neutral current, as well as to compensate the reactive power.

C21

Signal Processing & Communications Technology

Time: 9:00AM - 10:40PM
Room: Function Room 7

Chair: Divya Bansal (PEC University of Technology & PEC University of Technology, India), Noureddine A. Boudriga (University of Carthage, Tunisia)

9:00 ***3D Object Tracking Using Three Kalman Filters***
Yasir Salih (Universiti Teknologi PETRONAS, Malaysia); Aamir S Malik (Universiti Teknologi Petronas, Malaysia)

In the recent years, 3D tracking has gained attention due to the perforation of powerful computers and the increasing interest in tracking applications. One of the most common tracking algorithms used is the Kalman filter. Kalman filter is a linear estimator that is based on approximating system's dynamics using Gaussian probability distribution. In this paper, we provide a detailed evaluation of the most common Kalman filters, their use in the literature and their implementation for 3D visual tracking. The main types of Kalman filters discussed are linear Kalman filter, extended Kalman filer and unscented Kalman filter.

9:20 ***Unbiased Plain Gradient Adaptive IIR Notch Filter for Echo Cancellation***
Sasita Dhanawan (King Mongkut's Institute of Technology Ladkrabang, Thailand); Adisaya Charoenphol (King Mongkut's Institute of Technology Ladkrabang, Thailand); Chawalit Benjangkaprasert (King Mongkut's Institute of Technology Ladkrabang, Thailand)

In this paper, an adaptive echo canceller based on adaptive IIR notch filter with unbiased plain gradient algorithm for the echo cancellation in telephone network is presented. The unbiased plain gradient algorithm employs the bias removal techniques to remove the bias existing in the estimated parameter, resulting in obtaining good estimate of parameter for the echo canceller. The computer simulation results in terms of echo return loss enhancement (ERLE) are provided to confirm the performances of the presented adaptive echo canceller.

9:40 ***Efficient Design of Local Binary Pattern for Image Retrieval***
Rafi Md Najmus Sadat (Monash University, Australia); Abdur Rakib (Rajshahi University, Bangladesh); Md. Musfequs Salehin (Rajshahi University of Engineering and Technology, Bangladesh); Naurin Afrin (Rajshahi University of Engineering and Technology, Bangladesh)

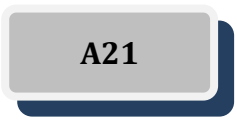
A novel image description method named Half-LBP has been proposed in this paper for image retrieval applications. Half-LBP transforms the relationship between two intensity levels of image pixels into binary pattern in such a way which reduces the descriptor dimension significantly while keeping the retrieval accuracy comparable with the state of art methods. The basic operation is quite similar to texture operator Local Binary Pattern (LBP). However, the dimension of the LBP method and its variants are too high and take substantial amount of time to retrieve the images. To address this issue, Half-LBP image descriptor has been proposed which takes comparatively less time to find out the matched images from the database.

10:00 ***Mobility Tolerant TDMA Based MAC Protocol for WSN***
Sandhya Thaskani (IIIT-Hyderabad, India); K. Vinod Kumar (National Institute of Technology, Warangal, India); Rama Garimella (IIIT Hyderabad, India)

Recent advancements in wireless communications and electronics have enabled the development of low cost sensor networks. Among the protocols of wireless Sensor Networks (WSN), Medium Access Control (MAC) protocols are given more priority as traditional MAC protocols are not suitable for Wireless communication. As many of the MAC protocols consider the sensor nodes to be stationary, and when these protocols are used in mobile environment the network performance decreases. In this paper, we introduce a new TDMA based MAC protocol which can be used in mobile wireless sensor network. This protocol uses TDMA based MAC scheme where the time will be divided into frames and then time slots. These slots are further divided into sections as channel request (CR), channel allocation (CA) and data section. We will also design an algorithm considering the energy efficiency of a wireless sensor network. Therefore the life time of the sensor nodes deployed in a wireless sensor network will be increased.

10:20 ***A New Hierarchal and Scalable Architecture for Performance Enhancement of Large Scale Underwater Sensor Networks***
Majid Hamidzadeh (Sharif University - Iran, Iran)

The different characteristics of UWSN and trade off between UWSN and WSN have been discussed in many researches. Here we aim to propose a new architecture for very large scale underwater sensor network. In deployment part of sensors topology plays a crucial role in issues such as communication performance, power consumption, network reliability and fault tolerance capabilities. Hence, it is so critical and should be analyzed how we deploy sensors in targets environment. For instance it is so important to avoid deploying underwater sensors with single point of failure and bottleneck to improve reliability of our networks in harsh conditions. For this purpose we present enhanced clustering algorithm to build a topological architecture and we try to set some topological features for our proposed model. Given scalability is regarded as the main advantage of clustering algorithms. In this paper we comprise the pyramidal architecture with our proposed architecture for building scalable UWSN with capability of fault tolerance and end to end delay estimation. We tried to calculate optimized number of nodes for using maximum number of deployed sensors into the water. Tree of Wheels (ToWs) improved our work for finding enhanced results. To the best of our knowledge, there is no study addressing the organized architecture due to enhance communication in underwater sensor networks. For the simulation purpose we have developed some MATLAB code. Performance results are obtained taking into consideration different number of level and number of sensors and the future works are mentioned. We believe such a scalable architecture presents information that help network designers to choose proper protocol and clustering algorithms depending on network situation and deployment environments.



Software Engineering & Applications

Time: 9:00AM - 10:40PM **Chair: Imthias Ahamed (King Saud University, Riyadh, Saudi Arabia),**
Room: Function Room 5 **Douglas Chai (Edith Cowan University, Australia)**

9:00 ***Cache Balancing with Proportionate Cutting Strategy***
Mohd Rohaizat Abdul Wahab (Universiti Putra Malaysia, Malaysia); Muhamad Taufik Abdullah (University Putra Malaysia, Malaysia); Mat Rofa Ismail (Universiti Putra Malaysia, Malaysia)

Caching mechanism had been widely used in many applications particularly in CPU optimization, internet application, data structure etc. Our research in text processing reveals that caching mechanism is also applicable to solve performance problem of text analyzers. In this paper we describe the strategy called 'proportionate cutting' for balancing (maintaining) limited size cache. Our experiment shows that by proportionate cutting at 0.5 threshold's value gives good performance to the cache. This actually allows of using limited cache in text processing with high frequency words.

9:20 ***Verification of Embedded System by a Method for Detecting Defects in Source Codes Using Model Checking***
Yoshitaka Aoki (Graduate School of Engineering, Shibaura Institute Technology, Japan); Saeko Matsuura (Graduate School of Engineering, Shibaura Institute Technology, Japan)

We have proposed a method based on model checking for detecting hard-to-discover defects in enterprise systems. We apply our method to embedded system development to easily discover some defects caused by input/output data of the hardware which are influenced by the external environment before the software is integrated into the hardware. This paper discuss the effectiveness of our method using a case study to develop a line tracing robot.

9:40 ***Model-Based Methodology for Implementing MARTE in Embedded Real-Time Software***
Mohd Zulkifli Mohd Zaki (Universiti Teknologi Malaysia, Malaysia); Dayang Norhayati Abg Jawawi (Universiti Teknologi Malaysia, Malaysia)

This paper presents an integration of a model-based methodology for embedded real-time software with MARTE. However, although has being introduced as a new profile to overcome problem in previous profile, a sound and systematic methodology is necessary to tackle complexity problem that arise. The objective of this paper is to propose an integration of profile and method for satisfying embedded real-time software requirements and helping engineers to model their system, enhancing the structure and behavior modeling. For that, this paper describes a proposed methodology for the integration process, involving two elements: a profile and a method. The integration result will support to solve complexity whereby the profile is used to solve the lack of specific modeling language notation for embedded real-time system and the method can provide a systematical software process. The proposed integration component model is applied on a case study to show its enhancements.

10:00 ***Software Engineering Education: the Gap Between Industry's Requirements and Graduates' Readiness***
Nurul Ezza Asyikin Mohamed Almi (Universiti Sains Malaysia, Malaysia); Najwa Abdul Rahman (Universiti Sains Malaysia, Malaysia); Durkadavi Purusothaman (Universiti Sains Malaysia, Malaysia); Shahida Sulaiman (Universiti Sains Malaysia, Malaysia)

Software engineering is one of the most demanding jobs in software industry nowadays and its demand keeps on increasing. However, there are several issues arise with regard to readiness of Information Technology (IT) or Computer Science (CS) graduates from the point of views of software industry such as lack of technical skills. This perspective causes the supply of graduates mainly in software engineering field seems to be insufficient. The industry claims that the software engineering graduates are not able to meet their requirements in software industry. This is really surprising to the academia that offers software engineering specialisation or related programmes in IT or CS field. This phenomenon creates the gap between industry's requirements and graduates' readiness which indirectly reflects the gap between software engineering education and industry. A number of studies and frameworks are available to ponder the issues on software engineering education and industry. However, in this paper we report the gap between industry's requirements and graduates' readiness in software engineering perspectives. The study focuses the expectations of the industry or employers towards graduates and the readiness of graduates to face the real world. From the findings, we conclude that there is a gap due to high demands from the industry in highly skilled fresh graduates. In contrast, future graduates are still lack of confidence and readiness though they specialise in software engineering field that has more job opportunities in IT field.

10:20 ***The Process of Quality Assurance Under Open Source Software Development***
Atieh Khanjani (UKM (University Kebangsaan Malaysia), Malaysia); Ir. Riza Sulaiman (UKM, Malaysia)

Open Source Software (OSS) is software products available to the public, with its source code to study, change, and improves its design. Open Source Software Development (OSSD) is the process by which open source software is developed within the confines of software engineering life-cycle methods. However when open source used for commercial purpose, then an open source license is required. Open source software is very often developed in a public and collaborative manner. The quality assurance principle under open source software development is an approach to improve software product quality against traditional methods and techniques. Despite the fact that the open source developments have seen remarkable successful in recent years, there are a number of product quality issues and challenges facing the open source development model. Many industries and business sectors are following or using OSSD, since they realize the benefits, but they do have some reservations concerning quality assurance in the form of program code quality, maintenance of the code and its quality, over the life-cycle of the product and third party usage. This paper reviews the literature of the process of the latest quality assurance, under open source software development methods and techniques. The result from this review is to show the process of quality assurance of open source software and that how it can affect the overall quality assurance principal.

C22

Signal Processing & Communications Technology (cont)

Time: 11:00AM - 1:00PM
Room: Function Room 7

Chair: Divya Bansal (PEC University of Technology & PEC University of Technology, India), Noureddine A. Boudriga (University of Carthage, Tunisia)

11:00 ***A Hybrid TCP Congestion Mechanism to Improve Mobile WiMAX Network***
Jhonny Tay (University of Malaya, Malaysia)

The traditional TCP was designed for a wired net- work; implementing TCP protocol in wireless network may lead inaccuracy prediction and will results degradation performance in a network. The experiment results have shown that the conventional TCP is not performed well and offered high delay issues. A proposed hybrid TCP congestion mechanism is presented in this article to address the issues by improving the TCP performance in wireless environments such as a mobile WiMAX. The model adapted the existing TCP congestion control which is based on a TCP Vegas and adopting a Scalable TCP aggressive rule to increase a window size. A Hybrid TCP implements in two way modes which are a loss-based and delay-based congestion control mechanism.

11:20 ***Cooperative Architecture for QoS Management in Wireless 4G Networks***
Nejd Ben Hamza (Communication Networks and Security research lab., Tunisia); Slim Rekhis (University of the 7th of November at Carthage, Tunisia); Noureddine A. Boudriga (University of Carthage, Tunisia)

The dynamics of the wireless links represent serious problems in guaranteeing quality of services (QoS). Combined with mobility, additional problems, arise like handoff delays and resource management, arise. In this work, we consider an interworking architecture composed of IEEE 802.11 and IEEE 802.16 access networks. We define a new set of Hybrid Units in charge of QoS management and handoff decisions, allowing to map quality of service classes, reduce the handoff blocking probability, and guarantee a fair distribution of users among the different access networks if they cover the same network area. The simulation results validate the efficiency of our approach.

11:40 ***SL2R-HT and SL2R- LH: Securing Layer-2 Routing Protocol for WMN***
Divya Bansal (PEC University of Technology, India); Sanjeev Kumar (PEC University of Technology, India); Prafulla Kumar (Department of IT, India)

Earlier research efforts mainly focused on securing adhoc routing mechanisms. However, recently there has also been growing research interest in studying the security of the medium access control (MAC) and its impact on network performance. The impact will be even more severe in case of multi hop wireless networks. IEEE 802.11s being a multihop technology also derives similar security concerns. It also hence needs to ensure correct route establishment mechanisms, protection of routing information, and security of packet forwarding. In this paper two new schemes have been proposed to protect the IEEE 802.11s (draft) routing protocol: HWMP which is currently defined as the default protocol. The proposed schemes have been implemented in a simulation environment and the results have been compared with the existing protocol.

12:00 ***Energy Efficient Cross-Layer Design Protocol by Using Token Passing Mechanism for WSN***
K. Vinod Kumar (National Institute of Technology, Warangal, India); Sandhya Thaskani (IIIT-Hyderabad, India); Rama Garimella (IIIT Hyderabad, India)

Recent advancements in processor, memory and radio technologies have enabled cheap and small sensors which are capable of sensing, communication and computation. Most of the Wireless Sensor Networks have limitation of battery power and in most of the applications it is not possible to replace the battery of a node. Considering this scarce energy and processing resources of WSN, we try to establish a joint optimization and design of networking layers i.e., cross layer design which could be a promising alternative to the inefficient traditional layered protocol design. In this paper we propose energy efficient cross layer design of the MAC and Routing protocol namely Energy Efficient cross-layer design protocol by using token passing mechanism for WSN. This proposed protocol proves to be better than some of the existing protocols and it is shown with the help of simulations.

12:20 ***A Review on Modulation Techniques in Multiband-Orthogonal Frequency Division Multiplexing in Ultra-Wideband Channel***
Roslina Mohamad (University Teknologi Mara, Malaysia); Wahidah Mansor (Universiti Teknologi MARA, Malaysia); Chempaka Mohd Din (Universiti Teknologi MARA, Malaysia)

This paper describes a review on mapping or modulation techniques used in multiband orthogonal frequency division multiplexing (MB-OFDM) in ultra-wideband (UWB) channel. QAM, BPSK and QPSK modulation techniques are commonly

used in this system due to their smooth power spectrum, low bit error rate (BER) and low receiver complexity. The new constant envelop modulation technique is proposed since it has the capability to improve the power spectrum density and BER performance. Continuous phase modulation (CPM) scheme could be used to reduce the complexity at the receiver. The constant envelop characteristics of CPM has to be analyzed in order to adapt this scheme in (MB-OFDM) UWB system.

D22

Network & Communications Technology III (cont)

Time: 11:00AM - 1:00PM
Room: Function Room 9

Chair: Yoong Choon Chang (Multimedia University, Malaysia), Hanen Idoudi (ENSI-Manouba University, Tunisia)

11:00 ***Defense Triangular of Routers (DTR) Against Traffic of Packets in Internet Data Centers (IDC)***
Hamid Mehdi (Islamic Azad university, Andimeshk Branch, Iran)

These days many of the data centers are looking for new ways in order to increase the amount of responding to requests and also offering effectual and optimal services. Hence, in many of the data centers procedures like cache management of physical resources same as routers, load balancing, controlling over load, QOS mechanisms are utilized. One of the reasons that decrease the effectiveness of a router after a period of time is the reduction of the buffer level and the elimination of the packets by the router. It makes many unanswered requests or at least prolonged answering time. This article tries to offer an approach in order to increase the amount of the routers to improve the efficiency of an Internet Data Center (IDC). The article has shown an appropriate correspondence between the results and the hypothesis.

11:20 ***An Integrated Fusion Protocol for Congregating Sensor Data in Wireless Sensor Network***
Buddha Singh (JNU new Delhi, India); Adwitiya Sinha (Jawaharlal Nehru University, India); Priti Narwal (Manav Rachna International University, India)

Effective fusion of data, accumulated from the sensors, can be regarded as a direct proportional factor to the successful deployment of a wireless sensor network. Two important fusion properties in support of the concerned area are: Correlation and Aggregation. This paper proposes an energy efficient data fusion protocol, which apart from employing power saving aggregation schemes, also implements network throughput enhancing routines via correlation of sensor signals. The protocol operates in dual mode to provide a perfect balance between the workload distributions among the sensor nodes during several parameter calculations. The notion of Connected Correlation Dominating Set is used to find out the clusters of active alive sensors, which actually involves in the transmission of data. On the basis of an Energy Model, the cluster heads are determined. To keep track of the error parameters, Least Squares (LS) estimation method along with the Linear Predictive Model is taken into consideration. Moreover, we simulate our algorithm using the Network Simulator (NS-2.34).

11:40 ***Studies on the Planarity, Reliability and Energetic Efficiency in Wireless Sensor Networks***
Kamil Staniec (Wroclaw University of Technology, Poland); Grzegorz Debita (Wroclaw University of Technology, Poland)

In the paper three most popular methods for spanning the wireless sensor networks (WSN) have been studied with respect to their offered reliability and intra-network radio interference. The authors proposed an algorithm for creating fully planar and reliable WSN structures that, unlike the other algorithms, considerably increase the Signal-To-Noise and Interference (SNIR) ratio in mesh networks, which advantage is particularly emphasized when directional antennas are used. Next, the influence of the number of sink nodes has been studied which ended with conclusion that a properly chosen sink nodes configuration may remarkably extend the network lifetime by bringing the number of necessary hops minimum.

12:00 ***A QoS-Aware Routing Protocol for Mitigating End-to-End Delay in IEEE 802.11-Based Mobile Ad Hoc Networks***
Khaled Abdullah Mohammed Al Soufy (Aligarh Muslim University, India); Ash Mohammad Abbas (Aligarh Muslim University, India)

Providing quality of service (QoS) in a mobile ad hoc network is a challenging task due to its peculiar characteristics. This paper aims at presenting a routing protocol which identifies multiple node-disjoint paths between a given source and a destination. These multiple node-disjoint paths are examined for satisfying QoS in terms of end-to-end delay. In this paper, we analyze the end-to-end delay along the paths taking into account the IEEE 802.11 contention delays. To study the performance of our protocol, we have carried out simulation. The results show that the proposed protocol performs better in terms of QoS satisfaction ratio and the throughput as compared to an existing protocol proposed in the literature.

12:20 ***Fair and Reliable Multicast Routing for Wireless Mesh***
Nasrin Razavi (Islamic Azad University, qazvin Branch, Iran); Mohammad Reza Meybodi (Amirkabir University of Technology, Iran)

Multicast is a fundamental routing service in wireless mesh networks (WMNs) due to its many potential applications such as video conferencing, online games, and webcast. Recently, researchers proposed using link-quality-based routing metrics for finding highthroughput paths for multicast routing. However, the performance of such link-quality-based multicast routing is still limited by severe unfairness. Two major artifacts that exist in WMNs are fading which leads to low quality links, and interference which leads to unfair channel allocation in the 802.11 MAC protocol. These artifacts cause the multicast application to behave unfairly with respect to the performance achieved by the multicast receivers. In some applications such as electronic test, competitions and etc. in addition to need for establishing the fairness among the members of the multicast group, it is need to reliable routing with 100% packet delivery ratio (PDR). one of proposed method for increasing PDR is Automatic Repeat Request(ARQ). Previously, numerous multicast protocols based on ARQ have been proposed to improve the packet delivery ratio. Therefore, these ARQ-based protocols can lead to excessive control overhead and drastically reduced throughput. Another technique for increasing PDR is Forward Error Correction (FEC) this method unlike the ARQ prevents of forward control packets and decreases overhead network partly.

B22

Applications III (cont)

Time: 11:00AM - 1:00PM Chair: Omid Bushehrian (Shiraz University of Technology, Iran)
Room: Function Room 6

11:00 ***An Architecture for Real Time Television Audience Measurement***
Debnath Mukherjee (Tata Consultancy Services, India); Tanushyam Chattopadhyay (Tata Consultancy Services, Kolkata, India); Siddharth Bhattacharya (Tata Consultancy Services, India); Avik Ghose (Tata Consultancy Services, India); Prateep Misra (Tata Consultancy Services, India)

Currently, audience measurement reports of television programs are only available after a significant period of time, for example as a daily report. This paper proposes an architecture for real time measurement of television audience. Real time measurement can give channel owners and advertisers important information that can positively impact their business. We show that television viewership can be captured by set top box devices which detect the channel logo and transmit the viewership data to a server over internet. The server processes the viewership data and displays it in real time on a web-based dashboard. In addition, it has facility to display charts of hourly and location-wise viewership trends and online TRP (Television Rating Points) reports. The server infrastructure consists of in-memory database, reporting and charting libraries and J2EE based application server.

11:20 ***Recognizing User Activity Based on Accelerometer Data From a Mobile Phone***
Media A Ayu (International Islamic University Malaysia, Malaysia); Teddy Mantoro (International Islamic University Malaysia, Malaysia)

Activity recognition refers to the ability of a machine/device to recognize the activity of users. This area of research has attracted many works especially related to the context aware and ubiquitous computing area. Wearable accelerometers have been explored for this activity recognition purpose; however the impracticality of attaching accelerometers to the user presents significant issues. Accelerometers today are embedded in many mobile devices. This paper explores the potential of using these accelerometer data to determine user activity recognition. The initial experiments show encouraging results with a very good accuracy rate of 92%.

11:40 ***InteractiveDisplay: a Computer-Vision-Based Solution to Retrofit Existing Flat Displays Into Interactive Surfaces***
Lahiru L Priyadarshana (Informatics Institute of Technology, Sri Lanka); Kulari De Silva Lokuge (Informatics Institute of Technology, Sri Lanka)

This paper outlines InteractiveDisplay, a novel and cost effective solution to create vision-based interactive surface systems by retrofitting existing regular displays. The proposed solution uses a regular off-the-shelf web camera as the main input device, and the raw image data captured by the web camera are processed using several image processing algorithms such as, background subtraction and skin color detection, to identify foreground objects. InteractiveDisplay's configuration addresses complexity and cost related issues with currently available computer-vision-based interactive surfaces. The proposed system provides an opening for more people to experience a new level of interactions with computing systems using the existing and commonly available technologies. The presented system is capable of

responding in real-time for user interactions and provides a cost-effective configuration that requires minimum engineering efforts to set-up.

12:00 ***An Electronic Policy Integrated Approach for Software Development (EPISoDe): a Case Study***
Shahida Sulaiman (Universiti Sains Malaysia, Malaysia); Umi Kalsom Yusof (Universiti Sains Malaysia, Malaysia); Wan Mohd Nazmee Wan Zainon (Universiti Sains Malaysia, Malaysia); Wan Muhammad Zulhafizsyam Wan Ahmad (Universiti Sains Malaysia, Malaysia); Sarina Sulaiman (Universiti Teknologi Malaysia, Malaysia)

Official websites of an organisation is a gateway to inform the public about its profiles, products or services, and other related information for the interested parties. Nevertheless such websites are sometimes not updated, do not provide required information or the worst case they are abandoned despite the fact that software developers have fulfilled the requirements of the users, and the systems have been deployed successfully. Hence, such websites require a dynamic web design that can delegate responsibility to each staff in ensuring the contents are always updated either to be shared among the staff or the public. This paper proposes an approach called EPISoDe that directly integrates organisations' policies as part of functional requirements in software development in this case we focus on website design and its implementation of higher learning institutions. We have deployed the proposed EPISoDe approach in a prototype called DyWeMS that provides an engine of a dynamic web design. We evaluated the approach on an official website of a school in a higher learning institution using DyWeMS dynamic engine. It implies that an organisational official website has the potential to be a one-stop information and knowledge centre that reflects organisations' history and legacy using the proposed EPISoDe approach that promotes delegation of responsibilities among the staff with the support of dynamic web design.

12:20 ***Review of Pricing Models for Grid & Cloud Computing***
Parnia Samimi (University Kebangsan Malaysia (UKM), Malaysia); Ahmed Patel (Universiti Kebangsaan Malaysia, Malaysia)

Distributed system resources have become prevalent in ICT departments to lessen the burden of huge expenses incurred by very expensive storage computer systems. Add to this the continuous introduction and ever-growing evolution of simple to complex applications, the demand to access huge quantities of data, intensive computations, powerful simulations, maintaining and offering system resources and middleware infrastructure services the need to do all of this at an affordable and reasonable price is crucial. Distributed grid and cloud computing resources are currently considered to be one of the best technology options to provide this. They have many similar features and functions, and both of them are classed as distributed systems. They are capable of offering unaffordable resources and services at a reasonable price in a mass marketplace. The big question is: what is a reasonable price? How is pricing modeled and on what kind of economic principles is it based? Much of the issues surrounding these questions are very complex in themselves. This paper provides a comparative review of grid and cloud computing economic and pricing models from which appropriate tariffs and charging models can be chosen to meet particular business objectives. The actual choice depends on many other factors like enterprise regulations, tax laws, service level agreements and return on investments, are very important but outside the scope of this paper. In this paper we give the basic core principles and a comparative review of the latest and most appropriate economic and pricing models applicable to grid and cloud computing in order to propose better models for the future.



Software Engineering & Applications (cont)

Time: 11:00AM - 1:00PM **Chair: Imthias Ahamed (King Saud University, Riyadh, Saudi Arabia),**
Room: Function Room 5 **Douglas Chai (Edith Cowan University, Australia)**

11:00 ***Requirement Engineering Techniques in Developing Expert Systems***
Ang Jac Ky (University Sains Malaysia, Malaysia); Leong Sook Bing (University Sains Malaysia Malaysia, Malaysia); Lee Chin fei (University Sains Malaysia, Malaysia); Umi Kalsom Yusof (Universiti Sains Malaysia, Malaysia)

Expert system has the least focus on requirement engineering. Nevertheless, requirement engineering is important to get all the requirements needed for an expert system. The expert system is considered fail although it works perfectly, if the requirements do not meet the clients' needs.Currently, there are a lot of studies proposing and describing the development of expert systems. However, they are focusing in a specific and narrow domain of problems. Also, the major concern of most researchers is the design issues of the expert system. Therefore, we emphasize on the very first step of success expert system development - requirement engineering. Hence, we are focusing in the requirement engineering techniques in order to present the most practical way to facilitate requirement engineering processes. In this study, we analyze expert system attributes, requirement engineering processes in expert system developments and the possible techniques that can be applied to expert system developments. We propose the appropriate techniques for the expert system

developments based on the analysis of requirement engineering. We also provide a set of techniques for expert system development will be provided.

11:20 ***The Aspects of Choosing Open Source Versus Closed Source***
Atieh Khanjani (UKM (University Kebangsaan Malaysia), Malaysia); Ir. Riza Sulaiman (UKM, Malaysia)

Closed source software, is a type of software that is licensed under the exclusive legal right of its owner. It is also purchasable by users by paying amount of money. Open Source Software (OSS) is software available with its source code under an open source license to study and modify the code. Open Source Software Development (OSSD) is the process to develop OSS. Many industries try using OSSD as they see the advantages of open source compared to closed source software development. This research presents the reasons of recently using OSSD model rather than traditional closed source approach. The result is to show the differences between closed source and open source process and how open source can effect on quality through its particular features. It also identifies and addresses the challenges and benefits faced by the users against traditional closed source model.

11:40 ***Reinforcement Learning in Power System Scheduling and Control: a Unified Perspective***
Imthias Ahamed (King Saud University, Riyadh, Saudi Arabia); Jasmin E. A. (Govt.Engg.College, Thrissur, India); Essam A. Al-Ammar (King Saud University, Saudi Arabia)

Reinforcement Learning (RL) has been applied to various scheduling and control problems in power systems in the last decade. However, the area is still in its infancy. In this paper, we present various research work in this area in a unified perspective. In most of the applications, power system problems - control of FACTS devices, reactive power control, Automatic Generation Control, Economic Dispatch, etc - are modeled as a multistage decision making problem and RL is used to solve the MDP. One important point about RL is it takes considerable amount of time to learn. However, RL can learn off line using a simulation model. Once the control strategy is learned decision making can be done almost instantaneously. A major draw back of RL is most of the application does not scale up and much work need to be done. We hope this paper will generate more interest in the area and RL will be utilized to its full potential.

12:00 ***A Robust Mobile Business Card Reader Using MMCC Barcode***
Siong Ong (Edith Cowan University, Australia); Douglas Chai (Edith Cowan University, Australia); Alexander Rassau (Edith Cowan University, Australia)

Business cards have existed since the 19th century and exchanging of business cards is common during introduction. The digital version, an electronic business card, helps to share information quickly and accurately. Also, it allows information to be stored and easily located. However, the current state of the art in business card readers using OCR technology usually fail in correctly reading all elements of the business card. Hence, in this paper, we proposed the use of an Mobile Multi-Colour Composite (MMCC) barcode printed on the business card. Containing the electronic version of the business card, the MMCC barcode allows cheap and accurate reading of the business card with a mobile phone camera. To highlight the effectiveness of the proposed method, we compared the results against commercially available business card readers, both in desktop and mobile versions.

12:20 ***On Sequence Based Interaction Testing***
Mohd Hazli Mohamed Zabil (Universiti Tenaga Nasional, Malaysia); Kamal Zuhairi Zamli (Universiti Sains Malaysia, Malaysia); Rozmie Razif Othman (Universiti Sains Malaysia, Malaysia)

T-way strategies aim to generate effective test data for detecting fault due to interaction. Different levels of interaction possibilities have been considered as part of existing t-way strategies including that of uniform strength interaction, variable strength interaction as well as input-output based relations. Many t-way strategies have been developed as a result (e.g. GTWay, TConfig, AETG, Jenny and GA for uniform strength interaction; PICT, IPOG and ACS for variable strength interaction; and TVG, Density and ParaOrder for input-output based relations). Although useful, all aforementioned t-way strategies have assumed "sequence-less" interactions amongst input parameters. In the case of reactive system, such an assumption is invalid as some parameter operations (or events) occur in sequence and hence, creating a possibility of bugs or faults triggered by the order (or sequence) of input parameters. If t-way strategies are to be adopted in such a system, there is also a need to support test data generation based on sequence of interactions. In line with such a need, this paper discusses the sequence based t-way testing (termed sequence covering array) as an extension of existing t-way strategies. Additionally, this paper also highlights the current progress and achievements.

A23

Autonomic and Trusted Computing

Time: 2:00PM - 3:40PM **Chair: Habibah Hashim (Universiti Teknologi MARA, Malaysia)**
Room: Function Room 5

2:00 ***IPSec Authentication Using Certificateless Signature in Heterogeneous IPv4/IPv6 Network***
Nazrul Muhaimin Ahmad (Multimedia University, Malaysia); Asrul Hadi Yaacob (Multimedia University, Malaysia); Ridza Fauzi (Multimedia University, Malaysia); Alireza Khorram (Multimedia University, Malaysia)

This paper studies the incompatibilities issues on deploying IPSec ESP in providing end to end security between heterogeneous IPv4 and IPv6 networks. The presence of IPv4/IPv6 translation gateway violates the TCP/UDP intrinsic functionalities due to the translation of the IP addresses in IP packets. We address these interoperability issues by modifying IKE negotiation with NAT-Traversal capability and some improvements on IPSec software. However, the implementation of the conventional IKE authentication mechanisms such as pre-shared key and Public Key Infrastructure (PKI) certificate-based requires both nodes either to be manually configured, or to exchange the certificates and the necessity to enroll to certain Certificate Authority (CA). This paper proposes a new IKE authentication based on certificateless public key infrastructure in order to alleviate the limitation of the conventional IKE authentication. We also propose an efficient public and shared parameters distribution mechanism whereby the translation gateway acts as Key Generator Centre (KGC).

2:20 ***Improved Extreme Programming Methodology with Inbuilt Security***
Bala Musa S. (Universiti Sains Islam Malaysia, Malaysia); Norita Md Norwawi (Universiti Sains Islam Malaysia, Malaysia); Mohd. Hasan Selamat (Universiti Putra Malaysia, Malaysia); Khaironi Yatim Sharif (Universiti Putra Malaysia, Malaysia)

Security in e-commerce is becoming an important issue to deal with as people are increasingly making businesses online and several cases of attacks to users' data are also increasing exponentially. Therefore, there is absolute need for using the appropriate framework in developing e-commerce web application with proper checks and balances for mitigation of lapses. This paper thus, improved the Extreme Programming Methodology by tightening security controls across the development stages without necessarily extending the process.

2:40 ***Data Hibernation Framework in Workflows Under Intrusion Threat***
Sohail Safdar (Universiti Teknologi PETRONAS, Malaysia); Mohd Fadzil Hassan (Universiti Teknologi PETRONAS, Malaysia); Muhammad Aasim Qureshi (Universiti Teknologi PETRONAS, Malaysia); Rehan Akbar (Universiti Teknologi PETRONAS, Malaysia)

The main objective of the research is to define and propose a framework for data hibernation in the workflows under intrusion threat. When the intrusion is detected, the data services need to be discontinued immediately to retain the security and the integrity of the valuable data, till the system is recovered from the threat. By discontinuing data services, the end users may face inconveniences in using the system because of its temporary unavailability. Data hibernation addresses a mechanism of secure transferring of data and providing an access of the data alternatively keeping the data integrity intact. Data hibernation involves three steps i.e. designing an alternate schema for storing data, transferring data to that alternate storage and providing an access to that data. Hence the system can continue to provide data services securely to the end user even in the threat situations.

3:00 ***Intrusion Tolerant Serializability for Transaction-based SAN Environments***
Yacine Djemaiel (Sup'Com. CN&S Research Lab., Tunisia); Noureddine A. Boudriga (University of Carthage, Tunisia)

The serializability of transactions is among the properties that should be implemented in order to ensure the correct processing in transaction-based environments. When the system is compromised, the serializability in addition to the relevant properties of transaction-based environments may be affected. Ensuring the serializability of transactions in compromised systems is among the needs in order to enable the processing of interrelated transactions and avoiding blocking situations with the inability of committing transactions or some available sub-transactions. In this context, this paper proposes an approach to ensure an intrusion tolerant serializability in a compromised transaction-based environment. This approach is built on a new concept that is based on the definition and the use of virtual nodes instead of the detected malicious nodes. These virtual entities ensures the processing of transactions and sub transactions in a secure manner even if the running environment is compromised. They ensure the continuous running of transactions without experimenting the blocking of interleaved transactions and therefore to ensure the serializability even if the monitored system is compromised. A serial schedule graph is also generated and used by the Central Security Node in order to make decisions concerning the nodes and the set of data and transactions that are threatened by a malicious activity by attaching to each component a set of security parameters. The behavior of the proposed intrusion tolerant serializability scheme in addition to its efficiency is illustrated through a case study describing a SAN system that ensures

the monitoring of cars activity and determines infractions and generates warning messages on road in order to prevent the occurrence of car accidents.

3:20 ***Distributed Cross Layer Approach for Detecting Multilayer Attacks in Wireless Multi- Hop Networks***
Divya Bansal (PEC University of Technology, India); Sanjeev Kumar (PEC University of Technology, India); Prafulla Kumar (Department of IT, India)

To deter internal attacks, Intrusion Detection Systems are the most favorable solutions for detecting intrusions and raising alerts for desired action since using encryption software for secure communication is not enough. A number of intrusion detection systems have been proposed for ad-hoc networks. Such intrusion detection systems cannot perform well for wireless mesh networks due to its multihop decentralized architecture. The selection of optimal and secure routing path and detection of multilayer security attacks cannot be achieved using traditional single layer IDS. Most of the MAC layer attacks occur due to non compliance of protocols by the nodes. Such a malicious behavior cannot be detected using conventional IDS. In this paper, a Cross Layer based Intrusion detection system has been proposed which takes advantage of the information available across different layers of protocol by activating multiple layer monitoring and detection. The proposed Cross layer based IDS is novel in its architecture and is able to detect multi layer attacks of compound nature. It can also detect low intensity attacks and attack switching behaviors which have been the major shortcoming of most of the existing IDS for Wireless Networks.

C23

Bioinformatics & Computational Biology

Time: 2:00PM - 3:40PM
Room: Function Room 7

Chair: Mansour Alsulaiman (King Saud University, Saudi Arabia), Sim-Hui Tee (Multimedia University, Malaysia)

2:00 ***Automatic Arabic Digit Speech Recognition and Formant Analysis for Voicing Disordered People***
Ghulam Muhammad (King Saud University, Saudi Arabia); Khalid Almalki (King Saud University, Saudi Arabia); Tamer Mesallam (King Saud University, Saudi Arabia); Mohamed Farahat (King Saud University, Saudi Arabia); Mansour Alsulaiman (King Saud University, Saudi Arabia)

In this paper, analysis of speech from voice disordered people is performed from automatic speech recognition (ASR) point of view. Six different types of voicing disorder (pathological voice) are analyzed to show the difficulty of automatically recognizing their corresponding speech. As a case study, Arabic spoken digits are taken as input. The distribution of first four formants of vowel /a/ is extracted to show a significant deviation of formants from the normal speech to disordered speech. Experiment result reveals that current ASR technique is far from reliable performance in case of pathological speech, and thereby we need attention to this.

2:20 ***Measuring Pairwise Distances Among Sequences of the miR-15/107 Group of miRNA Gene***
Sim-Hui Tee (Multimedia University, Malaysia)

The miR-15/107 group of miRNA gene has been recognized as an important regulatory mechanism for main biochemical pathways in human. It has significant role to play in regulating gene expression that relevant to cardiovascular diseases, cancers and neurodegenerative diseases. Notwithstanding the fact of strong implication on human health, an exhaustive taxonomic classification for the miR-15/107 group is impossible as the phylogeny of this group is incomplete. This paper aims at measuring pairwise distances among sequences of the miR-15/107 group of miRNA gene. The distance function allows bioinformaticians to compare the sequence of miR-15/107 group of miRNA gene and predict its target site.

2:40 ***Using Emergency Re-admission Time Window to Design the Re-admission Prediction Feature in Electronic Medical Record (EMR) Systems***
Sim-Hui Tee (Multimedia University, Malaysia)

Electronic Medical Record (EMR) systems are the most innovative information technology infrastructure in the recent decades that facilitate the improvement of healthcare quality, efficiency and safety. EMRs are used by medical practitioners in storing, handling, and consulting the patients' data. Decision support is one of the most useful and promising features of EMRs, which is yet to be fully adopted in healthcare sector. The reason of the uncommon use of the decision support feature is partly due to the complexity of medical processes and protocols, and partly due to the technological constraint. In this research, the re-admission prediction feature was investigated as a part of decision support in EMRs. The emergency readmission time window was used to design the proposed readmission prediction feature. This research also examined how the appropriateness of the width of a time window contributes to the design factor of the proposed re-admission prediction feature. This research demonstrated that the use of emergency

readmission time window is appropriate in the design of readmission prediction feature. The research outcome allows the users of EMRs to manage the re-admission case in hospital.

3:00 ***Medical Simulation Platform***
Jairo Melo (University of Brasília (UnB), Brazil); Lourdes Brasil (University of Brasília (UnB), Brazil); Remis Balaniuk (Catholic University of Brasília (UCB), Brazil); Edilson Ferneda (Catholic University of Brasília (UCB), Brazil)

The Medical Simulation Platform (MSP), developed and validated by teachers and students of the medical area, tried to present the architecture of a virtual platform that integrates formal content in the form of texts, ontologies, 3D images and simulation. A case study was accomplished in the area of the skull bone anatomy for graduation courses in the area of Health.

3:20 ***Emerging Computational Strategy for Eradication of Malaria***
Monday Eze (Universiti Malaysia Sarawak, Malaysia); Jane Labadin (Universiti Malaysia Sarawak, Malaysia); Terrin Lim (Universiti Malaysia Sarawak, Malaysia)

Even with a lot of efforts by researchers, malaria eradication is yet to become a reality. The link between malaria infected and non-infected human beings, which led to transmission of the disease, is bridged by infected malaria vectors, through blood sucking bites. Such bites take place either in residential homes or public places. Suppose the residential homes are placed under reliable vector control, malaria transmission will still persist unless the public places are taken into consideration. The emerging computational strategy is about leveraging on the interactions between human beings and mosquitoes in public places to build realistic network models with the ultimate aim of applying relevant search techniques to such models, so as to determine the public places which act as reservoir of infected malaria vectors. The overall result will form a key resource for realistic vector control. Hence the idea is to be more proactive and offensive against malaria vectors, by locating the vectors in their hiding places, rather than human beings being located and bitten by the infected vectors. The emerging computational strategy discussed here is part of an ongoing research project in application of computational techniques towards eradication of malaria. This paper documents the result of an initial survey on malaria vector existence in public places.



Human Factors & Applications

Time: 2:00PM - 3:40PM **Chair: Shaftab Ahmed (Bahria University Islamabad, Pakistan), Jaume**
Room: Function Room 6 **Duran (Universitat de Barcelona, Spain)**

2:00 ***Relationships Between Emotional Evaluation of Music and Acoustic Fluctuation Properties***
Ryosuke Yamanishi (Nagoya Institute of Technology, Japan); Yuya Ito (Nagoya Institute of Technology, Japan); Shohei Kato (Nagoya Institute of Technology, Japan)

We studied the relationships between the acoustic fluctuation properties of music and the emotional evaluations of music as a component technology for an automated song selecting system based on instinct and human emotion. When people listen to music, they select songs reflect their own feelings at the time, and then they emotionally evaluate the song. We believe that our emotional evaluation of songs are influenced by the fluctuation properties of both the volume and pitch of songs. Thus, we focused on the fluctuation properties containing dynamic ideas concerning music, and extracted thirty six fluctuation properties concerning both the volume and pitch from each song using the Fast Fourier Transform. We also prepared a subjective evaluation experiment for plural songs using the Semantic Differential method, and obtained an emotional evaluation of the songs. Then, we studied the relationships between the extracted properties and the emotional evaluations of the songs by conducting a multiple discriminant analysis. As a result, a high percentage of the questions were answered correctly and low discriminant errors were shown, and therefore, we suggested that the fluctuation properties of the songs influenced the emotional evaluations of them. Furthermore, we confirmed the especial properties related with the emotional evaluation of the music by taking into consideration the coefficients of the liner discriminants of the canonical variates that describe the discriminant spaces.

2:20 ***A-Class: a Classroom Software with the Support for Diversity in Aptitudes of Autistic Children***
Md. Ridwanur Rahman (Bangladesh University of Engineering and Technology, Bangladesh); Shujon Naha (Bangladesh University of Engineering and Technology, Bangladesh); Proteek Chandan Roy (Bangladesh University of Engineering and Technology, Bangladesh); Ishrat Ahmed (Bangladesh University of Engineering and Technology, Bangladesh); Samiha Samrose (Bangladesh University of Engineering and Technology, Bangladesh); Md. Mizanur Rahman (Bangladesh University of Engineering and Technology, Bangladesh); Syed Ishtiaque Ahmed (Bangladesh University of Engineering and Technology, Bangladesh)

The burgeoning growth of the e-Learning technologies implies the fact that the future education system will largely depend upon the electronic devices and computer aided technologies. It has already been proved that the computer aided teaching techniques are much more effective for the children than the traditional teaching system in most of the cases. A large number of software has been designed to assist the teachers in the classroom to teach and evaluate the students. Although those software systems are good enough for a class with normal (neurotypical) children, those very often fail to address the special needs of the autistic children. Hence, the autistic children face various challenges in participating with neurotypicals in the same classroom. We have addressed this problem by designing and implementing an intelligent classroom software, named "A-Class", which takes care of the diversity of tastes among the autistic children of a classroom and helps the teacher to teach in a class participated by both autistic and neurotypical children. In this paper we discuss the idea, design and implementation of A-Class based upon our five months of intervention with the autistic children at Autism Welfare Foundation (AWF) in Dhaka.

2:40 ***Architectural Digital Images. Quality and Emotional Evaluation Based on the Visualization Environment***
David Fonseca (Enginyeria Arquitectura La Salle (Universitat Ramon Llull), Spain); Jaume Duran (Universitat de Barcelona, Spain)

The visualization of architectural images has always been associated with physical models, panels and displays on large format computer screens. However, technological developments in the past decades have produced new devices such as Smartphones or immersive displays as HMD (Head Mounted Display), that have increasingly larger screens and more sophisticated technical characteristics. The emergence of these devices has made both the non expert and advanced user a consumer of such devices. This evolution has created a new workflow that enables on-site management, virtual visualization and decision making through the viewing of information on those devices. In this paper, we will study the emotional differences on visualization architectural images in different environments (computer screen, HMD and mobile phone) and the relationship with the quality perceived by the users.

3:00 ***Measuring User Reaction to Reduce Internet Anxiety***
Santosh Kalwar (Lappeenranta University of Technology, Finland); Kari Heikkinen (Lappeenranta, University of Technology, Finland); Jari Porras (Lappeenranta University of Technology, Finland)

The Internet has recently emerged with new kind of services, applications and countless contents. User reaction plays essential role in interacting with the Internet. The theoretical concepts on feelings are extracted from psychology, phenomenology and computer science. It is understood that feelings are subjective experience of users aroused from different emotions. As feelings changes based on time, circumstance, people and environment, it is extremely difficult to assess feelings objectively. User's interaction on the Internet is based on contents (text, audio and video materials) and context (past experience, surroundings, circumstances, environment, background, or settings). Thus, the potential of understanding feelings and its measure is very important. In this paper, a systematic measure of feelcalc module is introduced to measure user's reaction in order to reduce human anxiety on the Internet.

3:20 ***Study on Service Diffusion in Mobile Social Network***
Feng Chen (University of Science and Techology of China, P.R. China); Rui Ni (University of Science and Technology of China, P.R. China); Leixin Mai (University of Science and Techology of China, P.R. China); Xiaowei Qin (University of Science and Technology of China, P.R. China); Guo Wei (University of Sci. & Tech. of China, P.R. China)

How to popularize the own Mobile Value-added Services (MVSs) in the mobile networks is interesting and important to many SP/CPs. In this paper, we investigate the service diffusion from a new perspective of epidemic spread. Firstly, we argue about the characteristics of Mobile Social Network (MSN), which is composed of mobile users, and analyze various factors that impact the subscribers to customize the MVSs. Then epidemic dynamics is used to depict the service diffusion and some conclusions including marketing strategy have been carried out in this paper. Finally, through a series of experiments, we find that: 1) by using Acquaintance-First marketing strategy, the MVSs will quickly pop up at a low cost; 2) SP/CPs should do efforts to the effective spreading rate, which can result in a higher popularity of the service.

D23

Network & Communication Technology IV

Time: 2:00PM - 3:40PM
Room: Function Room 9

Chair: Batool Abadi Khasragi (Islamic Azad University OSKU Branch, Iran), Vishal A Wankhede (SVNIT, India)

2:00 ***Capacity and Resource Reservation in Broadband Internet***
Raenu Kolandaisamy (University of Malaya, Malaysia); Rafidah Md Noor (University of Malaya, Malaysia)

The aim of this paper is to introduce a model to providing Internet service charging according to a capacity and usage based charging. A charging model is introduced according to the user interests and preferences. The model provides resource optimization to the mobile network through a capacity and resource parameters where it generates a cost-effective method to optimize the resources. Experiments are conducted using a network simulator to evaluate the model and analyze the results. The results will be useful for Telecommunication Networks and accounting policy planning for the Broadband Internet Charging Quality of Service.

2:20 ***Resource Allocation Algorithm for WiMAX Systems***
Vishal A Wankhede (SVNIT, India); Rakesh Kumar Jha (SVNIT, India); Upena D. Dalal (Sardar Vallabhbhai National Institue of Technology, Surat, India)

Interest in broadband wireless access has been growing due to increased user mobility and the need for data access at all times. IEEE 802.16e based WiMAX networks promises the best availability quality of experience for mobile data service users. WiMAX presents a very challenging multiuser communication problem: Different users in same geographic area requiring high on-demand data rates in a finite bandwidth with low latency. To make resource allocation more practical, in mobile WiMAX instead of individual subcarriers a group of them is allocated to different users in both frequency and time. There are several ways to allocate subchannels in mobile WiMAX, three for downlink:FUSC (Fully Utilised Sub channelization), PUSC (Partially Utilized Sub channelization) and AMC (Adaptive Modulation and Coding). This paper aims to study the performance of low complexity adaptive resource allocation in downlink of OFDMA for WiMAX systems with variable rate requirements. Objective of the proposed algorithm is to maximize total throughput while maintaining rate proportionality among the users. The proposed algorithm prioritizes the user with the high sensitivity to the subcarrier allocation. Simulation results shows that proposed method performs better than previous method in terms of significantly decreasing the computational complexity and achieve higher capacities, while being applicable to a more general class of systems.

2:40 ***Study of Mobility Effect on Energy Efficiency in Medium Access Control Protocols***
Mahdi Zareei (Universiti Sains Malaysia, Malaysia)

Wireless sensor networks (WSN) became popular in recent years, with big variety of applications from environmental monitoring to disaster recovery. Energy efficiency is a key characteristic of todays wireless sensors. In energy constraint sensor network, mobility handling can cause some additional challenges in sensor protocol design. Recently there are many MAC protocols have been proposed and adopted specially for sensor networks. Most of the proposed MAC protocols in wireless sensor network assumed nodes to be static. However some application like medical care and disaster response make use of mobile sensors essential. In this paper, we take closer look at S-MAC, T-MAC (which are well-known energy efficient MAC protocols) and IEEE 802.15.4 (which is the ZigBee standard) MAC protocols and studies their performance in terms of energy efficiency in different situation of mobility.

3:00 ***Performance of Alamouti Coded MIMO Systems with Switch and Examine Combining***
Gourab Maiti (NIT Durgapur, India); Aniruddha Chandra (National Institute of Technology, Durgapur, India)

In this paper, we have considered a 2 x L multiple input multiple output (MIMO) system employing Alamouti coding at transmitter and switch and examine combining (SEC) at receiver. At first, analytical expressions for capacity and outage probability, in Rayleigh fading channel, are found. Next, the symbol error rate (SER) for M-ary phase shift keying (MPSK) modulation is calculated. The derived expressions are in closed-form and conform to the simulation results. For more than two (L > 2) receiver antennas, SEC performs significantly better than the traditional switch and stay combining (SSC).

3:20 ***Energy Balanced Clustering Method with Use of Learning Automata***
Batool Abadi Khasragi (Islamic Azad University OSKU Branch, Iran)

Increasing miniaturization and sensor communication abilities make them invisible and expand the availability everywhere and in any time. Sensor network applications, increase the challenging issues related to design network protocols have emerged. One of them is increasing energy efficiency and lifetime in the network. Sensor nodes with limited energy

reserves are deployed, so the network must operate with minimal energy overhead. This article focuses on improving the network lifetime by using energy efficient arrangement of nodes in a state primary goal to reduce energy waste with using energy balance. Therefore, learning automata capabilities - to solve issues in sensor networks is appropriate - this tool is used. For the purpose mentioned above, energy balanced clustering technique based on learning automata is proposed that learning automata residing in the cluster head, for balance, the best node according to the amount of energy remaining as the new cluster head is selected. Proposed technique with the NS2 simulator to simulate the behavior is evaluated. Results show that the calculated energy balance improves the life time of sensor network substantially.

B24

Human Factors & Applications (cont)

Time: 4:00PM - 5:40PM
Room: Function Room 6

Chair: Shaftab Ahmed (Bahria University Islamabad, Pakistan), Jaume Duran (Universitat de Barcelona, Spain)

4:00 ***Telemedicine in a Cloud - a Review***
Shaftab Ahmed (Bahria University Islamabad, Pakistan); Azween Bin Abdullah (Universiti Teknologi Petronas, Malaysia)

The Information communication Technologies (ICT) has assumed an important role in all domains of life today. The computation requirements are often larger than resources available at hand in an enterprise and it would like to outsource it for high speed computation or data management requirements. In other cases a small enterprise would like to lease computation or data archiving resources as per demand. Cloud computing is a new paradigm which may be used to handle such situations. It offers a virtual environment at a small initial investment by entrepreneurs planning to develop large applications scalable as the scope and workload increases. The computer hardware and software are available in virtualized environments of cloud computing offering Software as a Service (SaaS), Infrastructure as a Service (IaaS), and Platform as a Service (PaaS) through Datacenters and Cloud Service Providers (CSP). The paradigm shift provides elastic infrastructure, efficiency of resource utilization, reduction in upfront capital investment and focus on core activities. A model for cloud computing for telemedic services is being developed to cater for large data archive of Clinical Data Records (CDR), Decision Support Systems (DSS) and event based notification and monitoring system in a typical hospital. In this paper we have reviewed the rapid growth in cloud computing activities, available opportunities and services with the early birds in this technology. Beside this the hospital information and medical data services architecture using cloud services has been discussed in the context of the model being developed. Data storage service, Security service, scalability and performance issues have been discussed.

4:20 ***A Parametric Study to Investigate Skin Prestretch***
Jamaluddin Mahmud (Universiti Teknologi MARA, Malaysia); Cathy Holt (Cardiff University, United Kingdom); Sam Evans (Cardiff University, United Kingdom)

This paper for the first time assesses the significance of skin pre-stretch using numerical analysis. The derivations of mathematical models based on Ogden's constitutive equation which both ignore and include the pre-stretch term are presented. A programme was written to conduct the parametric study. This is novel as no similar approach has been reported before. The results show that pre-stretch is a significant parameter in describing skin behaviour. It is found that a 0.1 unit difference in prestretch, λp ($\Delta\lambda p = 0.1$) produced a larger effect than a 10 unit difference in Ogden's coefficient, μ ($\Delta\mu = 10$ Pa) and 4 unit difference in Ogdens's exponent, α ($\Delta\alpha = 4$).The current stress-stretch graph is also compared and seems in good agreement with results found by the other researchers. The result of this study could contribute to the development of the constitutive models for skin in the future. Therefore, further analysis should be carried out to investigate this. Nevertheless, this study has contributed to the knowledge about skin behaviour.

4:40 ***Name Extraction for Unstructured Malay Text***
Mohd Yunus Sharum (Universiti Putra Malaysia, Malaysia); Muhamad Taufik Abdullah (University Putra Malaysia, Malaysia); Md Nasir Sulaiman (Universiti Putra Malaysia, Malaysia); Masrah Azrifah Azmi Murad (Universiti Putra Malaysia, Malaysia); Zaitul Azma Zainon Hamzah (Universiti Putra Malaysia, Malaysia)

Names are categorized as proper nouns. Identifying nouns in unstructured text is very challenging since the number is almost unlimited. Name recognition can be used for POS tagging or automatic term acquisition in Natural Language Processing (NLP). In this paper we proposed a general approach to recognize names in Malay text. Using the proposed approach, we implement an application of free indexing for indexing names from a collection of Malay texts. Our evaluation shows that the application reach 92% Precision, 54% Recall, and F-score 68% in indexing names from news' articles.

D24

Network & Communication Technology IV (cont)

Time: 4:00PM - 5:40PM
Room: Function Room 9

Chair: Batool Abadi Khasragi (Islamic Azad University OSKU Branch, Iran), Vishal A Wankhede (SVNIT, India)

4:00 ***Electromagnetic (EM) Cavity Resonance Residual Life Indicator***
Alex Mason (Liverpool John Moores University, United Kingdom)

This paper presents part of a joint venture between Dstl and LJMU. The purpose of this work is to investigate the interaction of electromagnetic (EM) waves within a resonant microwave cavity to sense and characterise filter materials for residual life indication. This paper looks at a single filter material, ASZM-TEDA activated carbon, which is commonly used for military applications where personnel are likely to come under attack from chemical agents. The paper briefly introduces activated carbon, discusses theory relevant to the work, the methodology used for investigation, and finally a selection of pertinent measurements taken using a bespoke microwave cavity resonator.

4:20 ***Development of a Non-Deterministic Input-Output Based Relationship Test Data Set Minimization Strategy***
Hui Yeh Ong (Universiti Sains Malaysia, Malaysia); Kamal Zuhairi Zamli (Universiti Sains Malaysia, Malaysia)

Numerous efficient interaction testing strategies have been proposed in the past literatures to generate optimized test cases for software system under test (SUT). Meanwhile, most of the reported tools enumerate their test cases by covering all t-interactions of parameters involved, which are also known as uniform strength interaction testing. Later on, variable strength interaction testing has been proposed to allow certain subsets to cover higher t-interactions. Nevertheless, this consideration is still insufficient to generate test cases based on actual interactions. In fact, recent researches claimed that neither uniform nor variable strength interaction testing is capable to exactly cover actual factors interaction. Recently, interaction testing based on input-output relationship is reported to accommodate the actual interactions for SUT. This approach claimed that the interaction testing should focus on those input combinations that affect a program output, rather than considering all possible input combinations. The problem of generating minimal test cases is considered NP-complete as no single strategy in input-output interaction testing can generate the most efficient test cases. Therefore, a non-deterministic input-output based relationship test data sets minimization strategy, TIOR, has been proposed in this paper. The benchmarking inputs that have been reported in the literatures [12] are compared with that of TIOR in order to demonstrate its effectiveness. In most cases, TIOR gives competitive results against other strategies.

4:40 ***Multi-Sensor Spot Welding Monitor Using Wireless Sensor Network Technology***
Jeff Cullen (Liverpool John Moores University, United Kingdom); Andrew Shaw (Liverpool John Moores University, United Kingdom); Ahmed I Al-Shamma'a (Liverpool John Moores University, United Kingdom); Alex Mason (Liverpool John Moores University, United Kingdom)

Resistance welding is used extensively in manufacturing industries, the most popular being spot welding in the automotive industry. Despite spot welding being in use for over a century, there has been relatively little development of sensors for monitoring the process in real-time. Most existing systems use current, voltage and electrode force to give an indication of welding quality, however these systems do not provide warning of changes in the welding environment. These changes could include material variability or electrode condition, which could result in weak weld nuggets. Presented in this paper is an investigation of a system that utilises an array of sensors, including current, voltage, infrared and ultrasonic that is capable of monitoring the spot welding process as it is performed. This system utilises wireless sensor technology to transmit data from the welding arms to a sensor connected to a base computer where the data can be analysed. The wireless link is particularly useful when retrofitting the sensor cluster to existing installations.

AUTHOR INDEX

NAME	SESSION CODE
A	
A., Jasmin	A22
Aazam, Mohammad	D11
Abadi Khasragi, Batool	D23
Abbas, Ash Mohammad	D22
Abdalla, Izzeldin Idris	B21
Abdul Rahman, Najwa	A21
Abdul Wahab, Mohd Rohaizat	A21
Abdulal, Wael	A11
Abdullah, Azrai	B21
Abdullah, Azween	A13
Abdullah, Azween	B24
Abdullah, Azween	D11
Abdullah, Muhamad Taufik	B24
Abdullah, Muhamad Taufik	A21
Abg Jawawi, Dayang Norhayati	A21
Afrin, Naurin	C21
Agarwal, Arun	C14
Ahamed, Imthias	A22
Ahmad, Nazrul Muhaimin	A23
Ahmad, Noraini	B14
Ahmed, Ishrat	B23
Ahmed, Shaftab	B24
Ahmed, Syed	B23
Ahmmed, Ashek	A13
Ajaz, Hassaan	D21
Akaichi, Jalel	A13
Akbar, Rehan	B21
Akbar, Rehan	A12
Akbar, Rehan	A23
Al Jadaan, Omar	A11
Al Soufy, Khaled Abdullah	D22
Al-Ammar, Essam	A22
Alhaffa, Alaa	A11
Alias, Norma	B13
Almalki, Khalid	C23
Al-Nasser, Faisal	D11
Al-Shamma'a, Ahmed	A11
Al-Shamma'a, Ahmed	A14
Al-Shamma'a, Ahmed	B13
Alsulaiman, Mansour	C13
Alsulaiman, Mansour	C23
Aoki, Yoshitaka	A21
Attarzadeh, Seyed Mohammad	B11
Awang Rambli, Dayang	B14
Ayu, Media	B22
Azmi Murad, Masrah Azrifah	B24
B	
Bagher Oskuie, Farhad	C14
Balaniuk, Remis	C23
Balasubramaniam, S	B14
Bansal, Divya	A23
Bansal, Divya	C22
Bao, Paul	C14
Bashir Ghouse, Mohammed Shariff	B13
Basseri, Mohammad	C13
Belaton, Bahari	C14
Ben Hamza, Nejd	C22
Benjangkaprasert, Chawalit	B12
Benjangkaprasert, Chawalit	C21
Berata, Wajan	B13
Bhakti, Muhammad Agni Catur	A13
Bhattacharjee., Anup	A11
Bhattacharjee., Anup	D13
Bhattacharya, Siddharth	B22
Bin Ibrahim, Othman	B11
Boudriga, Noureddine	A23
Boudriga, Noureddine	C22
Brasil, Lourdes	C23
Bushehrian, Omid	B21
C	
Chai, Douglas	A22
Chandra, Aniruddha	D23
Chang, Yoong Choon	D21
Charoenphol, Adisaya	B12
Charoenphol, Adisaya	C21
Chattopadhyay, Tanushyam	B22
Chaw Seng, Woo	B13
Cheah, Yu-N	A12
Chen, Feng	B23
Cheraghian, Ali	C14
Cheung, Chun Ho	D12
Cheung, Kwok-Wai	D12
Chillarige, Raghavendra Rao	C14
Chin fei, Lee	A22
Cho, Jangsik	C11
Choudhary, Sudhanshu	A14
Chuah, Teong Chee	D14

NAME	SESSION CODE
Chuah, Teong Chee	D21
Chunduri, B Rama Rao	D13
Chunduri, B Rama Rao	D13
Cullen, Jeff	A11
Cullen, Jeff	A14
Cullen, Jeff	B13
D	
Dalal, Upena	D23
Das, Partha S.	B11
Dastmalchi, Hamid reza	C14
David, Sumam	B11
De Silva Lokuge, Kulari	B22
Debita, Grzegorz	D22
Desai, Anirudhha	D13
Dhanawan, Sasita	C21
Dimitrov, Atanas	B12
Djemaiel, Yacine	A23
Do, Van Thanh	D14
Do, van Thuan	D14
Duran, Jaume	B23
E	
Evans, Sam	B24
Eze, Monday	C23
F	
Faez, Karim	C14
Famil Bahmani, Homa	B11
Farahat, Mohamed	C23
Farzamnia, Ali	C12
Fattah, Shaikh Anowarul	C13
Fauzi, Ridza	A23
Feipei, Lai	A14
Ferneda, Edilson	C23
Fesharaki, Mehdi	A12
Fisal, Norsheila	C12
Fonseca, David	B23
Foong, Oi Mean	A12
G	
Garimella, Rama	C21
Garimella, Rama	C22
Georgieva, Penka	B12
Germanov, Vladimir	B12
Ghaedi, Hassan	B21
Ghahari, Alireza	C14
Ghazali, Azrul	D12
Ghose, Avik	B22
Goh, Jung Hean	B13
H	
Hafeez, Moaaz	D21
Haghbin, Fariba	B11
Haji Mat Zin, Nor Azan	B11
Hamidzadeh, Majid	C21
Hamzah, Rostam Affendi	C12
Hardel, Gopi	D13
Hardel, Gopi	A11
Hari, Om	C13
Harizi, Hedi	D12
Hassan, Kadhim	A11
Hassan, Kadhim	A14
Hassan, Mohd Fadzil	A12
Hassan, Mohd Fadzil	A23
Hassan, Mohd Fadzil	B21
Heikkinen, Kari	B23
Hidayat, Mas Irfan	B13
Hilali jaghdam,	A13
Holt, Cathy	B24
Hoque, Rezaul	D13
Hossain, Md.	B13
Hossain, Mohammad	B13
Hosseini, Mostafa	B11
Houaidia, Chiraz	D21
I	
Idoudi, Hanen	D21
Iguider, Youssef	B21
Ihsan, Omer	D21
Imtiaz, Hafiz	C13
Irteza Butt, Safwat	D21
Islam, Md.	D13
Ismail, Mat Rofa	A21
Ito, Yuya	B23
J	
JÃ¸nvik, Tore	D14
JÃ¸rstad, Ivar	D14
Jabas, Ahmad	A11
Jac Ky, Ang	A22
Janabi, Qais	A14
Javed, Usman	D21
Jayaprakasam, Suhanya	D14
Jha, Rakesh	D23
K	
Kader, Abdul	C12
Kalwar, Santosh	B23
Kamal Bashah, Nor Shahniza	D14
Karastoyanov, Dimitar	B12
Kato, Shohei	C11
Kato, Shohei	C11
Kato, Shohei	B23
Kenari, Seyed Ali	A11
Khairnar, Vaishali	D21
Khaksar Fasaei, Mohammad Sajjad	A12
Khan, Shakil	B13
Khanjani, Atieh	A21
Khanjani, Atieh	A22
Khorram, Alireza	A23
Kim, Soohan	C11
Kim, Taehyun	C11
Koh, Johnny	A11
Kolandaisamy, Raenu	D23
Kranthi Rekha, Chennaboina	D13
Kranthi Rekha, Chennaboina	D13
Kumar, K. Vinod	C22
Kumar, K. Vinod	C21
Kumar, Prafulla	A23
Kumar, Prafulla	C22

NAME	SESSION CODE
Kumar, Sanjeev	A23
Kumar, Sanjeev	C22
Kumngern, Montree	C12
Kumngern, Montree	C12
L	
Labadin, Jane	C23
Lai, Tsung-Sheng	A14
Lalbakhsh, Pooia	A12
Latih, Rodziah	A14
Leong, Siew Yoong	C11
Liao, Iman	C14
Lim, Terrin	C23
Lo, Eric	D11
Lobiyal, Daya	D12
Loke, Seng	D13
Low, Tang	D11
M	
Mahmud, Jamaluddin	B24
Mai, Leixin	B23
Maiti, Gourab	D23
Maity, Tanmoy	B11
Mal, Ashis	C13
Malik, Aamir	C21
Mandal, Durbadal	A11
Mandal, Durbadal	D13
Mansor, Wahidah	C22
Mantoro, Teddy	B22
Mark, James	D21
Mashohor, Syamsiah	A11
Mason, Alex	D24
Mason, Alex	A11
Mason, Alex	A14
Masoumi, Behrooz	A13
Mat Deris, Mustafa	C11
Matsuura, Saeko	A21
Md Noor, Rafidah	D23
Md Norwawi, Norita	A23
Mehdi, Hamid	D22
Melo, Jairo	C23
Melor, Puteri	B13
Meng, Yang	B21
Mesallam, Tamer	C23
Meybodi, Mohammad Reza	D22
Meybodi, Mohammad Reza	A13
Mi Yusuf, Lizawati	B13
Mihhailov, Dmitri	A14
Mirmotahhary, Navid	B12
Misra, Prateep	B22
Miyakoshi, Yoshihiro	C11
Mohamad, Kamaruddin	
Malik	C11
Mohamad, Roslina	C22
Mohamad, Siti Nor Hafizah	A14
Mohamed Almi, Nurul Ezza Asyikin	A21
Mohamed Zabil, Mohd Hazli	A22
Mohd Din, Chempaka	C22
Mohd Zaki, Mohd Zulkifli	A21
Moorthi, Sridharan	A12
Morita, Hiroyoshi	B21
Mosleh, Mohsen	C14
Muhammad, Ghulam	C23
Mukherjee, Debnath	B22
Musa S., Bala	A23
N	
Nadian, Ali	C13
Nadian, Ali	C13
Naha, Shujon	B23
Nallagownden, Perumal	B14
Nallagownden, Perumal	B21
Narwal, Priti	D22
Nauman, Mohammad	D14
Ng, Ka-Ho	D12
Ni, Rui	B23
O	
Omar, Yuhanis	B11
Ong, Hui Yeh	D24
Ong, Siong	A22
Osman, Salyani	B11
Osmsn, Bahr Eldin	B14
Othman, Mohd Shahizan	B13
Othman, Rozmie Razif	A22
Ow, Siew Hock	B12
Oxley, Alan	A12
Oztekin, Halit	B14
P	
P, Aparna	B11
Parmar, Nishant	D12
Patel, Ahmed	A14
Patel, Ahmed	B12
Patel, Ahmed	B22
Patel, Ahmed	C11
Peng, Chin-Hung	A14
Po, Lai Man	D12
Porras, Jari	B23
Pradhan, Shrikant	D21
Priyadarshana, Lahiru	B22
Purusothaman, Durkadavi	A21
Q	
Qin, Xiaowei	B23
Qureshi, Muhammad Aasim	A12
Qureshi, Muhammad Aasim	A23
Qureshi, Muhammad Aasim	B21
Qureshi, Shafi	A14
R	

NAME	SESSION CODE
R, Sridhar	B14
Rahman, Kazi Atiqur	D14
Rahman, Md. Mizanur	B23
Rahman, Md. Ridwanur	B23
Rajion, Zainul	C14
Rakib, Abdur	C21
Ramlan, Muhammad	D11
Rao, K S	B14
Rao, K S	B21
Rassau, Alexander	A22
Razavi, Nasrin	D22
Rekhis, Slim	C22
Rohani, Vala Ali	B12
Rowaihy, Hosam	D11
Roy, Proteek Chandan	B23
S	
Sabamoniri, Saeed	A13
Sadat, Rafi Md Najmus	C21
Sadeghzadeh, Ramezan Ali	B12
Safdar, Sohail	A23
Safdar, Sohail	A12
Safdar, Sohail	B21
Sahari @ Ashaari, Noraidah	B11
Saidane, Leila	D21
Salehin, Md. Musfequs	C21
Salih, Yasir	C21
Samimi, Parnia	B22
Samir, Brahim Belhaouri	D21
Samrose, Samiha	B23
Sandhya, Banda	C14
Sarkar, Nurul	D11
Selamat, Mohd. Hasan	A23
Sh Ahmad, Sabarinah	B14
Shafiullah, Md.	B13
Shah, Jigar	D12
Shah, Nimit	A13
Shah, Satish	D12
Shah, Satish	A13
Shamsuddin, Siti Mariyam	B13
Sharif, Khaironi Yatim	A23
Sharum, Mohd Yunus	B24
Sharum, Mohd Yunus	A21
Shaw, Andrew	B13
Shazzad, Khaja	D14
Shin, Dongil	C11
Shin, Dongkyoo	C11
Sim, Gek Hong	D21
Simeonov, Stanislav	B12
Singh, Buddha	D12
Singh, Buddha	D22
Singh, Jugdutt	D13
Sinha, Adwitiya	D22
Skliarova, Iouliia	A14
Sklyarov, Valery	A14
Solla, Marwa	B12
Song, Shen	A12
Sook Bing, Leong	A22
Sreedevi, Bobbala	D13
Sreedevi, Bobbala	D13
Staniec, Kamil	D22
Sudnitson, Alexander	A14
Sulaiman, Azlan	A14
Sulaiman, Ir. Riza	A21
Sulaiman, Ir. Riza	A22
Sulaiman, Md Nasir	B24
Sulaiman, Sarina	B22
Sulaiman, Shahida	B22
Sulaiman, Shahida	A21
Sulaiman, Suziah	B14
Syed-Yusof, Sharifah	C12
T	
Taktak, Wiem	A13
Talebpour, Alireza	C13
Talebpour, Alireza	C13
Talib, Anuar	B14
Tan, Su Wei	D14
Tanveer, Tamleek	D14
Tay, Jhonny	C22
Tee, Sim-Hui	C23
Tee, Sim-Hui	C23
Tepe, Kemal	D14
Tew, Yiqi	A14
Thaskani, Sandhya	C21
Thaskani, Sandhya	C22
Ting, Chi Wang	D12
Tiong, Sieh Kiong	A11
Todani, Rishi	C13
Trivedi, Harsh	D13
V	
Valupadasu, Rama	D13
Valupadasu, Rama	D13
Vasumathi, Balasubramaniam	A12
Veeraraghavan, Prakash	D13
Vijaya, Valapadasu	D13
Vijaya, Valapadasu	D13
W	
Wali, Wasan	A11
Wali, Wasan	A14
Wan Ahmad, Wan Muhammad Zulhafizsyam	B22
Wan Zainon, Wan Mohd Nazmee	B22
Wankar, Rajeev	C14
Wankhede, Vishal	D23
Wastam, Jumail	B14
Wei, Guo	B23
Wong, Chi Kwan	D12
Wong, Hwee Ling	B13

NAME	SESSION CODE
Wong, Ka-Man	D12
Y	
Yaacob, Asrul Hadi	A23
Yahya, Abid	C12
Yallaparagada, Naren	A11
Yallaparagada, Naren.	D13
Yamanishi, Ryosuke	B23
Yap, David	A11
Yassin, Ihsan	D11
Yew, Kwang Hooi	C11
Yousofi, Ahmad	D14
Yusof, Umi Kalsom	B22
Yusof, Umi Kalsom	A22
Z	
Zainol Abidin, Husna	D11
Zainon Hamzah, Zaitul Azma	B24
Zaman, Noor	D11
Zamli, Kamal Zuhairi	A22
Zamli, Kamal Zuhairi	D24
Zareei, Mahdi	D23
Zehforoosh, Yashar	B12
Zheng, Pan	C14

Genetic Algorithm for Null Synthesizing Of Circular Array Antennas by Amplitude Control

N. Tapaswi Yallaparagada, Gopi Ram Hardel, Durbadal Mandal, Anup Kr. Bhattacharjee.
National Institute of Technology Durgapur, West Bengal, India- 713209
Department of Electronics and Communication Engineering,
renswi@gmail.com, gopi203hardel@gmail.com, durbadal.bittu@gmail.com, akbece12@yahoo.com

***Abstract*—In this paper, the method of imposing of nulls in the radiation pattern of an antenna array is hashed out using Real coded Genetic Algorithm (RGA). Circular array antennas lying on *x-y* plane is assumed. The array is assumed to have the maximum radiation along positive *z*- axis. Single and multiple nulls are imposed by optimizing the current amplitude excitations of each element through RGA. Various simulated results are presented and hence nulling performance is analyzed.**

***Keywords*— Circular array antennas; First Null Beamwidth; Side lobe Level; Nulls; Real Coded Genetic Algorithm.**

I. INTRODUCTION

A lot of research works have been carried out in the past few decades on different antenna arrays in order to get improved nulls. Antenna Array is formed by assembly of radiating elements in an electrical or geometrical configuration. Total field of the Antenna Array is found by vector addition of the fields radiated by each individual element. There are several parameters by varying which the radiation pattern can be modified. These parameters are, geometrical configurations (e.g. linear, circular, planar, spherical etc.), inter element spacing, individual excitations (amplitude and phase) and relative pattern of individual elements. A circular array has all its elements placed along a perimeter of a circle. Circular array is an array that has a configuration of very practical interest. Its application span radio detection finding, air and space navigation, underground propagation, radar sonar and many other systems. The goal in antenna array geometry synthesis is to determine the current excitation amplitude values of each element of the array that produces the radiation pattern that is closest to the desired pattern. In this paper the design goal is to improve a null or to insert a null at desired direction for an asymmetric circular antenna array. In the present case, the current excitation amplitude values of elements are taken as the parameter for modifying the radiation pattern. A radiation pattern with deeper nulls or improved nulls is preferred in the present case. RGA is used in this paper to get the desired pattern. The rest of the paper is arranged as follows: in section II, the general design equations for the non-uniformly placed asymmetric circular antenna array are stated. Then, in section III, RGA is introduced in brief. Numerical simulation results are presented in section IV. Finally the paper concludes with a summary of the work in section V.

II. DESIGN EQUATION

Fig. 1 assumes the geometry of a circular array of N isotropic sources is laid on x-y plane having a radius 'a' and scanning at point P in the far field.

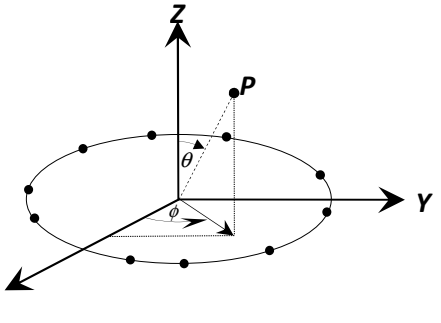


Fig 1. A Symmetric non-uniform circular array lay in the *x-y* plane with N isotropic elements scanning at a point P in the far field.

Array factor (AF (θ,ϕ)) of such an array can be given by (1).

$$AF(\theta,\phi)=\sum_{n=1}^{N} I_n e^{[jka\sin\theta\cos(\phi-\phi_n)+\alpha_n]} \quad (1)$$

Where,

I_n = individual excitation amplitude,

$k = 2\pi / \lambda$, λ being the wavelength of operation,

θ is the azimuth angle,

ϕ is the elevation angle,

ϕ_n is the angular location of nth element along the x-y plane.

$\alpha_n = -ka \sin\theta_0 \cos(\phi_0 - \phi_n)$

$(\theta_0 - \phi_0)$ is the desired direction of scanning.

Therefore there should be maxima of $AF(\theta,\phi)$ at that point. In the present case, the maximum scanning is required along the z- axis. Therefore θ_0=0for this case. Moreover, in the paper, the pattern in the x-z plane is taken for experiment. So, $\phi = 0$ in the present case. Thus, (1) changes to,

$$AF(\theta,\phi_n) = \sum_{n=1}^{N} I_n e^{jka\sin\theta\cos\phi_n} \qquad (2)$$

In this case, ϕ_n was set to 2πn/N i.e. all the elements were uniformly spaced. The design goal in the paper is to find the optimum set of values of I_n in order to get the improved nulls in the radiation pattern in the desired direction θ. Element positions are varied asymmetrically in order to get the desired pattern. A radiation pattern that gives better null is preferred for this paper. In this paper, radius of the array, i.e. 'a' is taken such that 'a' =1.414. Any value of 'a' can be taken and here the 'a' value was taken in order to have good array factor figure. All the antenna elements are assumed isotropic. Only Amplitude excitations of each element are used to change the antenna pattern.

The Cost Function (CF) for imposing null is given below

$$CF = \frac{\left| \prod_{i=1}^{m} AF\ (null_i) \right|}{|AF|} \qquad (3)$$

'm' is the possible number of positions where nulls can be imposed. In this paper, one has been considered as the value of 'm'. *AF (null $_i$)* is the Array factor value at the particular null. AF is the maximum of the array factor. In cost function, both the numerator and denominator are absolute values. Smaller value of the cost function means that array factor values at predefined positions are less. Consequently, GA controls the amplitude excitations in order to minimize the cost function.

III. REAL CODED GENETIC ALGORITHM

GA is mainly a probabilistic search technique, based on the principles of natural selection and evolution. At each generation it maintains a population of individuals where each individual is a coded form of a possible solution of the problem at hand and called chromosome. Chromosomes are constructed over some particular alphabet, e.g., the binary alphabet {0, 1}, so that chromosomes' values are uniquely mapped onto the decision variable domain. Each chromosome is evaluated by a function known as fitness function, which is usually the fitness function or the objective function of the corresponding optimization problem.

Steps of RGA as implemented for optimization of spacing between the elements and current excitations are:

- Initialization of real chromosome strings of np population, each consisting of a set of excitations. Size of the set depends on the number of excitation elements in a particular array design.
- Decoding of strings and evaluation of *CF* of each string.
- Selection of elite strings in order of increasing *CF* values from the minimum value.
- Copying of the elite strings over the non-selected strings.
- Crossover and mutation to generate off-springs.
- Genetic cycle updating.
- The iteration stops when the maximum number of cycles is reached. The grand minimum *CF* and its corresponding chromosome string or the desired solution are finally obtained.

IV. NUMERICAL SIMULATION RESULTS

This section gives simulated results of the performance of the imposed nulls at various positions of the radiation pattern. Three circular antenna array structures having 10, 12, 14 elements are assumed, each maintaining a fixed spacing between the elements. For predefined nulls of the radiation pattern, the nulling performances are improved. Similarly at predefined peak positions, the nulls are imposed. Every time GA executed with 100 iterations. The population size was fixed at 120.For

the real coded GA, the mutation probability was set to 0.15 and uniform crossover was taken. GA algorithm is initialized using random values.

Figures 2-4 show the imposing of deeper nulls over 2nd null. For 10, 12, 14-element, the null has improved up to -72.72 dB, -72.2 dB, and -75.9 dB with initial values of -58.64 dB, -56.93 dB, -60.43 dB respectively. The Initial values of Beam width between first nulls (BWFN) has been given for all the array structures in the TABLE I, whereas TABLE II shows the resulting amplitude excitation distribution. In this case the weighting for the array elements $I_1, I_2 \ldots\ldots\ldots I_N$ are normalized using max (I_N) =1.

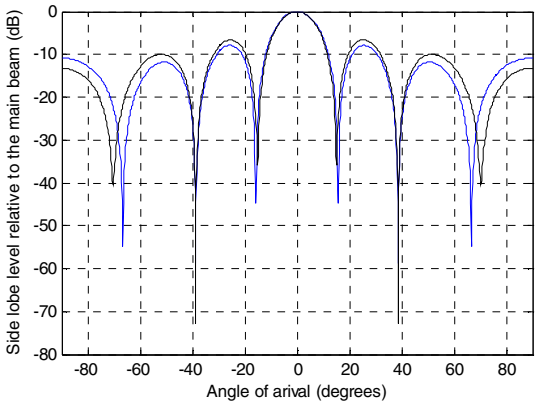


Fig. 2. Best array pattern found by GA for the 10-element array case with an improved null at 2nd null i.e. $\theta = \pm 38.7$.

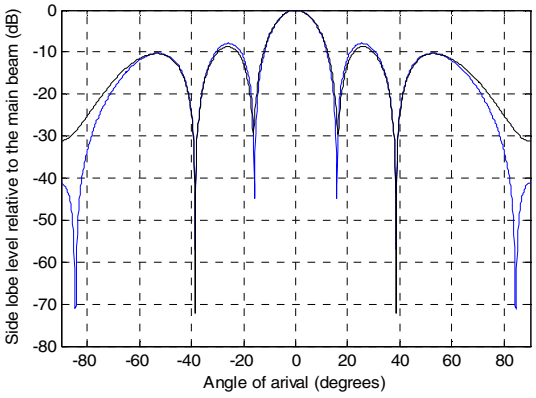


Fig. 3. Best array pattern found by GA for the 12-element array case with an improved null at 2nd null i.e. $\theta = \pm 38.52$.

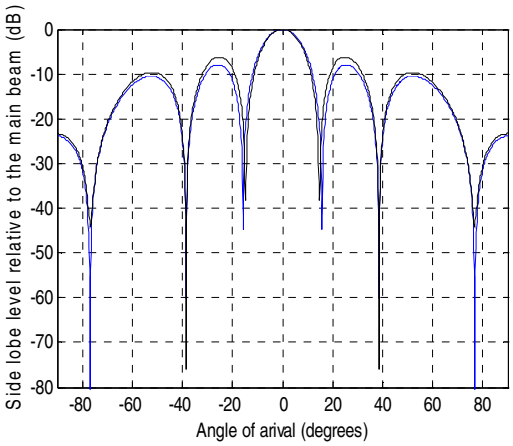


Fig. 4. Best array pattern found by GA for the 14-element array case with an improved null at 2nd null i.e. $\theta = \pm 38.52$.

Figures 8-10 show the imposing of nulls over 2nd peak. For 10, 12, 14-element, the null has improved up to -70.86 dB, -69.28 dB, and -70.65 dB with initial values of -11.83 dB, -10.3 dB, and -10.47 dB respectively. The improved values are shown in TABLE IV.

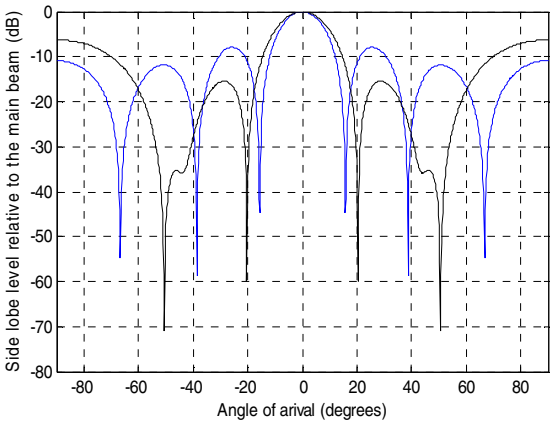


Fig. 5. Best array pattern found by GA for the 10-element array case with a null imposed at 2nd peak i.e. $\theta = \pm 50.58$.

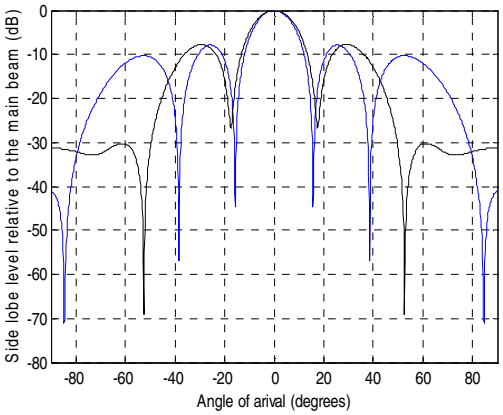


Fig. 6. Best array pattern found by GA for the 12-element array case with a null imposed at 2nd peak i.e. $\theta = \pm 52.56$.

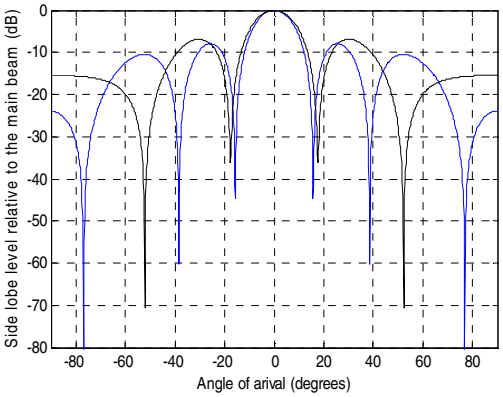


Fig. 7. Best array pattern found by GA for the 14-element array case with a null imposed at 2nd peak i.e. $\theta = \pm 52.2$.

V. CONVERGENCE PROFILE OF RGA

The minimum *CF* values against number of iteration cycles are recorded to get the convergence profile of each set. Figures 8-9 portray the convergence profiles of minimum of circular array set having 20 elements with improved null and null imposed at a peak respectively. The programming has been written in MATLAB language using MATLAB 7.5 on dual core(TM) processor, 2.88 GHz with 1 GB RAM.

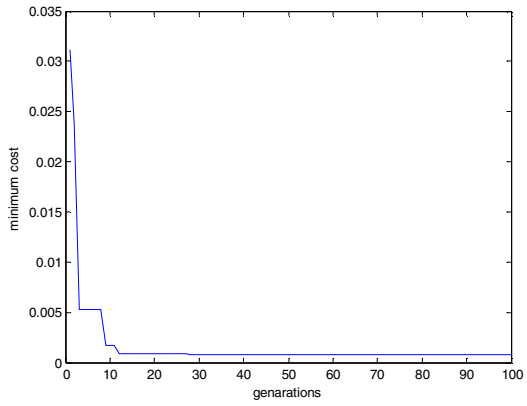


Fig 8. Convergence profile for RGA in case of non-uniformly excited 20-element linear array with improved nulls.

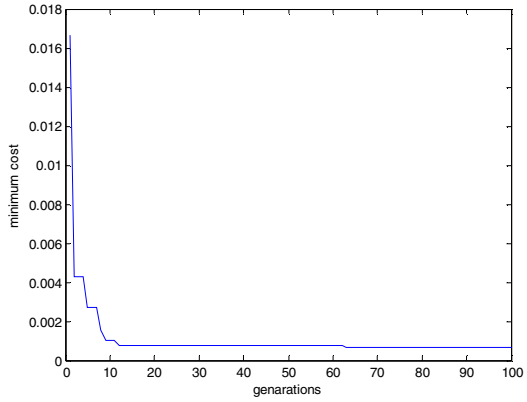


Fig 9. Convergence profile for RGA in case of non-uniformly excited 20-element linear array with nulls imposed at peaks.

TABLE I. INITIAL VALUES OF BWFN FOR UNIFORMLY EXCITED ($I_N = 1$) ARRAYS

Number of Elements (El.)	Initial BWFN (θ degrees)
10	31.32
12	31.32
14	31.32

TABLE II. ONE NULL IMPOSED IN THE 2ND NULL POSITION

El.	$(I_1, I_2 ..... I_N)$				Initial Value (dB)	Final value (dB)
10	0.4229	0.6578	0.7257	0.6381	-58.64	-72.72
	0.5739	0.5802	0.2383	0.3625		
	0.8563	0.5679				
12	0.7156	0.6705	0.7188	0.5920	-56.93	-72.2
	0.5519	0.3244	0.7377	0.6695		
	0.5653	0.4058	0.2587	0.6786		
14	0.5430	0.6731	0.2895	0.1160	-60.43	-75.9
	0.4230	0.5152	0.4354	0.4429		
	0.4871	0.5607	0.4103	0.2440		
	0.2417	0.7085				

TABLE III. ONE NULL IMPOSED IN THE 2ND PEAK POSITION

El.	$(I_1, I_2 ..... I_N)$				Initial Value (dB)	Final value (dB)
10	0.1476	0.9430	0.8351	0.3733	-11.83	-70.86
	0.3490	0.2895	0.5614	0.4865		
	0.4859	0.2590				
12	0.5768	0.8195	0.1133	0.7207	-10.3	-69.28
	0.1982	0.1926	0.6387	0.8785		
	0.7778	0.8999	0.4443	0.3091		
14	0.0912	0.6711	0.4353	0.4468	-10.47	-70.65
	0.5914	0.1150	0.5649	0.2076		
	0.9430	0.1704	0.5983	0.9861		
	0.1353	0.1127				

Table IV. FINAL VALUES OF BWFN FOR DIFFERENT CASES OF NON UNIFORMLY EXCITED

El.	BWFN when deeper null imposed on 2nd Null	BWFN when null imposed on 2nd peak
10	30.24	40.68
12	32.4	34.92
14	29.52	35.28

VI. CONCLUSION

In this paper, the design of a non-uniformly excited symmetric circular antenna array with uniform spacing between the elements has been described using the optimizing techniques of RGA. Simulated results reveal that optimizing the excitation values of the elements of the array antenna can impose nulls at a desired direction for a given number of the array elements. For example for a 10 element circular array antenna after optimizing, a null with the value -70.86 dB was imposed at a peak having initial value -11.83 dB. The BWFN of the initial and final radiation pattern remains approximately same.

REFERENCES

[1]. C. A. Ballanis, "Antenna theory analysis and design," 2ndedition, John Willey and Son's Inc., New York, 1997.

[2]. R. L. Haupt, and D. H. Werner, Genetic Algorithms in Electromagnetics, IEEE Press Wiley-Interscience, 2007.

[3]. Diogenes Marcano and Filinto Duran, "Synthesis of Antenna Arrays Using Genetic Algorithms", IEEE Antennas Propagat.Magazine, Vol. 42, No. 3, June 2000.

[4]. N. Pathak, G. K. Mahanti, S. K. Singh, J. K. Mishra and A. Chakraborty, "Synthesis of Thinned Planar Circular Array Antennas Using Modified Particle Swarm Optimization", Progress In Electromagnetics Research Letters, Vol. 12, pp. 87-97, 2009.

[5]. K. Murthy and A. Kumar, "Synthesis of Linear Antenna Arrays," IEEE Trans. Antennas Propagat. Vol. AP-24, pp. 865-870, November 1976.

[6]. M. A.Panduro ,A. L. Mendez, R. Dominguez and Romero,' Design of non-uniform circular antenna arrays for side lobe reduction using the method of genetic algorithms," *Int. J.Electron.Commun. (AEÜ)* vol. 60 pp. 713-717, 2006.

[7]. L. L. Wang and D. G. Fang, "Synthesis of nonuniformly spaced arrays using genetic algorithm," Asia-Pacific Conference on Environmental Electromagnetics, pp. 302- 305, Nov. 2003.

[8]. D. Mandal, S. P. Ghoshal, and A. K. Bhattacharjee, " Novel Particle Swarm Optimization Based Optimal Design of Three-Ring Concentric Circular Antenna Array," IEEE International Conference on Advances in Computing Control, and Telecommunication Technologies. 2009, ACT'09, pp. 385-389, 2009

[9]. D. Mandal, S. P. Ghoshal, and A. K.Bhattacharjee,"Determination of the Optimal Design of Three-Ring Concentric Circular Antenna Array Using Evolutionary Optimization Techniques," International Journal of Recent Trends in Engineering. vol. 2(5), pp. 110- 115, 2009.

Rank Based Genetic Algorithm for Solving the Banking ATM's Location Problem Using Convolution

Alaa Alhaffa
Osmania University, Economics Dept.,
Hyderabad 500-007, India
Alaa.haffa@yahoo.com

Omar Al Jadaan
Medical and Health Sciences
University, Ras Al-Khaimah
United Arab Emirates
o_jadaan@yahoo.com

Wael Abdulal, Ahmad Jabas
Osmania University, CSE Dept., EC
Hyderabad 500-007, India
wael.abdulal@ymail.com
jabas@ieee.org

***Abstract*— In order t o satisfy the client needs, his Utility should be increased by covering his Demand. The service Utility should be maximized through effective deployment of ATMs. Genetic Algorithm is one of widely used techniques to solve complex optimization problems, such as Banking ATM's Location Problem. This paper proposes a novel Rank Based Genetic Algorithm using convolution for solving the Banking ATM's Location Problem (RGAC). The proposed RGAC maximizes demand Coverage Percentage with less number of ATM machines. The novel RGAC speeds up the convergence using Rank Concept, with limited number of iterations to obtain a high quality feasible solution in resonable time.**

The proposed algorithm RGAC performs more effectively in the large scale deployments, thus it can be used in the marketing study of Banks which have highly complex operations. The simulation results show that RGAC improves the Percentage Coverage up to 16.2 over the previous algorithm [1] using the same number of ATMs. Also they exhibit that RGAC reduces the number of ATM machines up to ten (10).

Key–Words: Genetic Algorithms (GAs), Rank, Automated Teller Machines (ATM), Percentage coverage (PC),Client Utility matrix (CU), Service Utility Matrix (SU)

.

I. Introduction

After years of growth in E-Banking sector, the expansion of ATM supply exceeds the demand on this service and has put profit margins under pressure, thus many ATM deployers struggle to stay in business. The installed base of ATMs worldwide has grown from 640 thousand machines in 1996, to about 1.56 million machines in 2006, and is estimated to reach 2.4 million machines by 2017, averaging an annual growth rate about 9 percent [1]. On the contrary, the growth rate of ATM demand has slowed down, and is expected to remain at 2 percent per year. Consequently, the challenges have emerged between Banks and ATM deploying companies (Third Party) in capturing the higher number of customers by targeting the high demand areas and optimal exploitation of the existing number of ATMs.

A bank's decision to deploy ATMs should be a rational Economic decision using the best ATM deployment strategy, that takes into account the high computation complexities [2]. This paper introduces a new Rank Based Genetic Algorithm for solving the banking ATM location problem using Convolution (RGAC). Experimental studies show that RGAC finds an escape route from a local minimum and goes directly to the global minimum through applying the best allocation of ATMs and computing Percentage Coverage (PC) for each deployment process in order to realize the highest PC.

The experimental studies show that RGAC outperforms the Heuristic Algorithm based on Convolution (HAC) used in [3].

In order to increases search efficiency, RGAC uses random generation of initial population and improving the evolutionary process while meeting a feasible result. Moreover, RGAC is a robust approach for the ATMs deployment problem and is able to provide high quality solutions in a reasonable time. The rest of the paper is structured as follows: Section II indicates some important related work, as well as the improvements that have been introduced by this sudy. A detailed description of the problem encoding and specific operators are explained in Section III. Section IV gives explanation of RGAC, while section V describes the computer simulation results. Concluding remarks are contained in Section VI.

II. Related Work

The case study which was undertaken in Saudi Arabia [3] proposes a simple heuristic approach using convolution operation which can be performed very efficiently by simply centering the elements of degradation of service quality matrix(A) at the location of each machine. According to the authors in [3] the elements of Demand matrix (D) are real values taken from the market, and the elements of Supply matrix (S) are percentages of A, Difference matrix (E) is the resultant of substructing D from S as in equation (10).

In order to make the model more realistic, this study modifies D to be Client Utility Matrix (CU), and S as the Service Utility Matrix (SU). Consequently, all elements of SU and CU matrices become percentages which denote Utility of Service and Utility of Client. In addition, HAC binds ATMs sequentially, thus, it selects the location of first machine then

moves to the next one, and so on. In this way HAC has solved the ATM location problem with less flexibility.

The main advantage of the proposed scheme is to provide high flexibility for location specialists to choose arbitrary SU and CU Matrices. The previous work [4] uses all costs accompanied with the provision of ATM service as a parameter to choose the ATM's type and location. This study sheds light on the demand side in order to cover all potential clients in the market. Therefore, RGAC can be considered as a complementary study to [4]. Michael Wagner developed a framework to derive the optimal cash deployment strategy for a network of ATMs [1]. The same author applies the Wagner-Whitin algorithm for optimal inventory and Dantzing Fulkerson and joneson integer program for identifying routes of least total distance. Another study [5] describes the application of a Hybrid Grouping Genetic Algorithm (HGGA) for deploying metropolitan wireless networks.

III. Problem formulation

The ATM placement problem is modeled and defined mathematically. The variables used in modelling of the intended problem are shown in the table I. The optimization problem is organized in such a way as to realize market clearing. In other words, the difference between CU and SU should be minimized. This difference can be expressed mathematically in equation 1:

$$E = SU - CU \geqslant \theta \tag{1}$$

where E is the difference matrix of size (I×J) after assigning total number of machines, SU is the service utility matrix of all ATMs, CU is the client utility matrix, Θ is the zeros matrix. The generation of previous matrices SU, and CU are explained as follows:

A- Client Utility Matrix CU:

Clients are a source of returns to banks, therefore, their main objective is to satisfy client's needs. Thus, Banks try to capture higher potential clients through expanding the ATM network in the market. This study assumes that the bank will invest in the unserviced area as such no competition exists in that area. The generating of CU is made by using two methods:

I- First method:

1) Randomly generate the binary matrix Q(i×j).
2) Divide Q(i×j) into smaller submatrices qq .
3) Calculate number of ones in each qq and equate it to g(x×y), when g(x×y) is highest it means that the area has the highest demand intensity, in contrast, when g(x×y) is smallest it means lowest demand intensity.
4) Jump to the step 2 for the second method.

II- Second method:

1) Randomly generate G(x×y) matrix, the elements of G(x×y) range from 0 to 10.
2) Generate sub-matrices (cu_r), the matrix of cu_r is presented in equation 2.

$$cu_r = G(x \times y) \times U(m \times n) \tag{2}$$

where $r = 1, 2, \cdots, \frac{I \times J}{m \times n}$.

U(m×n) is the degradation of Client Utility, by assuming m =3,n=3, U(m×n) is given in figure 1.

$$U(m \times n) = \begin{bmatrix} 1/m & 2/m & 1/m \\ 2/m & 1 & 2/m \\ 1/m & 2/m & 1/m \end{bmatrix}$$

Fig. 1. Degradation of Client Utility matrix

3) CU matrix can be obtained by replacing each element in G(x×y) by its corresponding matrix cu_r. The reason behind calculating CU is that the Client Utility will be strongest at the center of the area, and it will degrade as one moves away from it.

B- Service Utility Matrix SU:

Once the deployment of ATMs is a one off project, hence it is done once. It is essential to distribute the limited number of ATMs in such a way as to maximize the utility of services. In order to find SU, this study assumes that ATMs are homogeneous, in line with this there exists only one matrix A. Matrix A (represents the degradation of ATM's utility as one moves away from its location) is predetermined and held constant for all ATM machines. The rectilinear distance model is adopted as shown in figure 2:

The matrix L_n indicates the location of the nth machine. If this location is denoted by the coordinates (u_n, v_n) then all elements of Ln are equal to zero except for coordinates (u_n, v_n) where they are equal to one as in the equation 3:

$$L_n = \begin{cases} 1 & \text{at } (u_n, v_n); \\ 0 & \text{elsewhere.} \end{cases} \tag{3}$$

The matrix SU can be obtained from the convolving of two matrices A and L as in equation 4:

$$SU = A * L \tag{4}$$

where the symbol $*$ indicates the convolution.

C- Percentage Coverage (PC):

In order to satisfy the client, his Utility should be satisfied by covering his demand, and service Utility should be maximized through effective deployment of ATMs, this will save the cost of providing additional ATM (i.e., deploying more ATMs than it needs). PC is computed as the percentage of ψ (ψ is equal to one in all points in E that have SU greater than CU) divided by the number of elements in E . PC is given as in equation (5)

$$PC = \frac{\sum_{i=1}^{I} \sum_{j=1}^{J} (\psi \times 100)}{I * J} \tag{5}$$

where ψ is given in equation(6).

$$\psi = \begin{cases} 1 & \text{if } E(i,j) \geqslant 0 \\ 0 & \text{otherwise} \end{cases} \tag{6}$$

In addition to PC, another important measure (the total Client Utility satisfied γ) is calculated. The formula of γ is given in equation(7).

Variable	Variable Description
N	Total number of machines
SU	Service Utility matrix which represents the service supply side
CU	Client Utility matrix which represents the demand side
E	Difference or market clearing matrix
A	Matrix that represents degradation of service utility as a client moves away from each machine
L_n	Location Matrix indicats the location of the nth machine
(u_n, v_n)	Coordinates of the nth machine
θ	Zero matrix

TABLE I
PROBLEM FORMULATION

$$A = \begin{bmatrix} 0 & 10 & 40 & 10 & 0 \\ 10 & 40 & 70 & 40 & 10 \\ 40 & 70 & 100 & 70 & 40 \\ 10 & 40 & 70 & 40 & 10 \\ 0 & 10 & 40 & 10 & 0 \end{bmatrix}$$

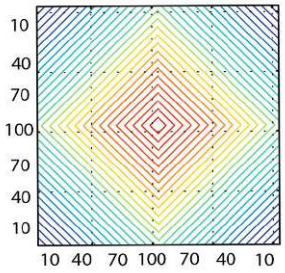


Fig. 2. Service matrix A (The rectilinear distance model)

$$\gamma = \frac{\sum_{i=1}^{I}\sum_{j=1}^{J}|B(i,j)|}{\sum_{i=1}^{I}\sum_{j=1}^{J}|CU(i,j)|} \tag{7}$$

Where:

$$B(i,j) = \begin{cases} CU(i,j) & \text{if } E(i,j) > 0; \\ Q(i,j) & \text{otherwise.} \end{cases} \tag{8}$$

The algorithm returns both γ and PC values with the solution as will be shown in the simulations section. PC and γ values are essential in measuring the goodness of deployment of ATMs. The value of γ ranges between [0,1] and it approaches one only when all elements in E are zeros or positive values, denoting the saturation level of Client Utility. In order to deploy less number of ATMs without affecting negatively on PC and γ, this study uses trial method such that, the trial starts with number of ATMs which can be determined from the HAC output and then run (RGAC) to compute the best PC and γ. If the value of PC is equal to hundred (100), then next step the number of ATMs is reduced by one, the trial continues reducing N as long as PC is within the acceptable limit (i.e. more than the lower limit 99). otherwise when the value of PC is less than the acceptable limit, then trial increases number of ATMs till PC reaches the acceptable limit. The previous conditions are presented in Mathematical equation 9.

$$Deploy \;\; (M) \;\; ATMs \;\; if \begin{cases} PC_{(M=N-K)} = 100 \\ Or \\ |PC_{(M=N+K)} < 99 \end{cases} \tag{9}$$

where K=1,2,. . . ,.

IV. Rank Based Genetic Algorithm for solving the Banking ATM's Location Problem

GA is used to solve optimization problems by imitating the genetic process of biological organisms [6]. A potential solution to a specific problem may be represented as a chromosome containing a series of genes. A set of chromosomes makes up the population. By using Selection, Crossover and Mutation Operators, GA is able to evolve the population to generate an optimal solution.

$$E_N = (\sum_{n=1}^{N} A * L_n) - CU \geqslant \theta \tag{10}$$

A. Chromosome Representation

The efficiency of GA depends largely on the representation of a chromosome which is composed of a series of genes. In this paper, each gene represents an ATM location which is equal to one or zero based on binding of the ATM to its location as in equation 3. As a result, L represents the chromosome. Population Initialization is generated randomly.

B. Fitness Equation

A fitness equation must be devised to determine the quality of a given chromosome and always returns a single numerical value. In determining the fitness equation, it is necessary to maximize the Percentage Coverage PC of CU. RGAC takes the PC value as a fitness equation for a given chromosome, which presented in equation 5.

C. Evolutionary Process

Evolutionary process is accomplished by applying Rank-based Roulette Wheel Selection (RRWS) [7], [8], Crossover and Mutation Operators from one generation to the next. Selection Operator determines how many and which individuals will be kept in the next generation. Crossover Operator controls how to exchange genes between individuals, while the Mutation Operator allows for random gene alteration of an individual. Besides the standard genetic operators discussed above,the Elitism Phase is used to preserve the best candidates. These stages are discussed in details as below.

Firstly, in order to carry out the RRWS, the Relative Probability (shown in equation 11) and cumulative proportion of each chromosome are calculated.

$$P_i = Rank_{(fitness)}; \tag{11}$$

Algorithm 1 One point Crossover

```
for i=1 to popSize/2 do
    Select two chromosomes p1, p2 randomly
    Select Crossover point Point randomly
    Save coordinates of ATM locations of two chromosomes p1, p2 in row1, col1, row2, col2.
    if random[0,1] < probCrossover then
        for k=Point+1:ChromosomeLength do
            Swap the coordinates of ATM locations of two chromosomes p1, p2
        end for
        Keep the newly produced chromosomes as candidates
    end if
end for
```

Algorithm 2 Mutation

```
for i=1 to popSize do
    Select chromosome p randomly
    Save coordinates of ATM locations of chromosome p in row, col
    if random[0,1] < probMutation then
        Select one ATM location of chromosome p randomly and make it equals to zero
        Generate one ATM location of chromosome p randomly and make it equals to one
        add the newly produced chromosomes as candidates
    end if
end for
```

After that, one-Point Crossover and mutation Operators, the algorithms(1, 2), are applied to the chromosomes from the selection phase.

Mutation operator runs through the genes in each of the chromosomes and mutates each gene according to a Mutation Rate P_m.

Finally, Elitism combines the parent population with the modified population (the candidates generated by Crossover and Mutation Operators), and takes the best chromosomes to the next generation. The purpose of this phase is to preserve the best chromosomes from being lost. After this phase, the algorithm continues to the next iteration. RGAC is presented in the algorithm 3.

D. Performance Analysis

RGAC needs to execute some hundreds of iterations to come up with an optimal solution. However, the shortcoming of HAC is convergence to a local optimum. According to the simulation results, it is proved that RGAC is effective in speeding up convergence while meeting a feasiable result. Also RGAC outperforms HAC, in the PC and γ values to obtain the final schedule.

TABLE II
PARAMETERS USED IN THIS STUDY

Parameters of RGAC algorithm	Value
Crossover Rate	1
Mutation Rate	1
Maximum Generations	700
Population Size	$(I \times J \times 2)$
Stopping Criterion	If 100 iterations of RGAC are not showed improvement in *PC* value Or *PC* value equals to hundred (100)

V. SIMULATION RESULTS

Tests were run on a machine with Intel P4 2.2GHz CPU, 2GB memory and Linux operating system. The simulation results of RGAC are compared with those of HAC. The parameters of RGAC are listed in table II. HAC and RGAC are simulated using MATLAB.

In this work, figures (5, 4) represent RGAC solution for ATMs deployment problem expressed in figure 3. The simulation results are shown in table III for four different groups of CU matrices;(12×12), (18×18), (24×24), and (30×30), respectively. Each experiment uses five samples for each group of CU matrix seeking more reliabilty to the results. The reason of testing grouping is to explore the performance of RGAC in the dynamic banking environment.

In the table III, the values of PC, γ and N, for both RGAC and HAC are compiled together for purposes of comparison.

The table III shows that:

1) Using the same N for both algorithms, RGAC shows a significant improvement in both *PC* and γ over those of HAC. For example, in table III, CU(12×12), sample 1, exhibits 15.3 improvement in *PC* value.
2) In the case of satisfying the second condition, of deploying less N, in equation 9, RGAC contributes effectively in reducing the cost of providing extra ATMs without affecting negatively on the value of *PC*. For instance, in table III, CU(24×24), sample 3 shows a reduction in the number of ATMs by ten (10) keeping the *PC* better than that of HAC.
3) RGAC overcomes one limitation of HAC, that is, when a certain number of ATMs are deployed, the value of *PC* reaches a ceiling and remains constant. For example, in table III, CU(12×12),sample 3, shows that HAC after deploying nineteen (19) ATMs the value of *PC* approches 86.8 and gets stuck at that value. However, in RGAC each increase in ATMs will lead to an increase in the value of *PC*.
4) The fitness equation 5 gives very good results and high quality solutions, even though the complexity of the problem increases.

5) As it has been discussed before, RGAC is scalable and effective in Banking environment. The simulation results are consistent with the performance analysis in section IV-D, which clarifies that the improvement to the evolutionary process is reasonable and effective.

Algorithm 3 RGAC

Generate Initial Population P of size $N1$ randomly.
    Evaluate each chromosome using equations (1, 5, and 7) }
for $g = 1$ to *MaximumGenerations* **do**
    Generate offspring Population from P
        {Rank based Roulette Wheel Selection
        Crossover and Mutation (algorithms 1, and 2)
            Evaluate each chromosome resulting from Crossover and Mutation stages using equations (1, 5, and 7) }
    (Elitist) Select the members of the combined population based on minimum fitness, to make the population P of the next generation.
        Evaluate each chromosome using equations (1, 5, and 7) }
    if Stopping criterion has reached **then**
        return PC, γ values and best ATM Location Matrix L found;
        break;
    end if
end for

VI. Conclusions and Future Work

This paper presents the RGAC technique, for deploying ATMs in the Banking world, which increases search efficiency by improving the evolutionary process while meeting a feasible result. Moreover, RGAC has proved to be a robust approach for solving the ATMs deployment problem and is able to provide high quality solutions in a reasonable time. The simulation results show that, RGAC solves the optimization problem of ATMs deployment by maximizing PC and minimizing N,thus RGAC matches the two objectives of banks, namely, attaining the highest client utility as well as improving the cost effeciency of the banks. In the future, it is appropriate to extend the goodness of results by including other measures like variance or standard deviation in order to obtain less dispersion in matrix E. So far as studies move towards the real banking world, they should consider the dynamic features and the interrelated factors of this world in order to have the most feasible solution.

TABLE III
Simulation Results

Parameters	N	PC	γ	N	PC	γ	ΔPC	ΔN
Algorithm	HAC			RGAC				
Sample No.	$CU(12 \times 12)$							
1	13	84.7	95	13	100	100	15.3	0
2	11	93	97.6	11	98.61	99.45	5.61	0
	12	93	97.6	12	100	100	7	0
3	19	86.8	93.6	14	100	100	13.2	5
4	15	100	100	13	100	100	0	2
5	14	87.5	92.6	13	100	100	12.5	1
Sample No.	$CU(18 \times 18)$							
1	33	97.5	99	28	100	100	2.5	5
2	26	95.4	99	26	99	100	3.6	0
3	25	92	87	25	99	100	7	0
4	26	97.2	98.1	26	99.3	100	2.1	0
5	25	88.6	96	24	98.77	99.28	10.17	0
	27	88.6	96	27	99.69	99.96	11.09	0
Sample No.	$CU(24 \times 24)$							
1	45	82.6	92.2	45	98.8	99.4	16.2	0
	47	82.6	92.2	47	99.13	99.49	16.53	0
2	48	96.2	98.7	45	99	99.5	2.8	3
	48	96.2	98.7	46	99.65	99.91	3.45	2
3	57	95.1	97.5	47	99.3	99.5	4.2	10
4	42	91.3	95.3	42	97.39	98.14	6.09	0
	45	91.3	95.3	45	99.48	99.86	8.18	0
5	41	85.93	94.3	41	94.44	97	8.51	0
	48	85.93	94.3	48	99.3	98.87	13.37	0
Sample No.	$CU(30 \times 30)$							
1	66	87.8	94	66	97	97	9.2	0
	74	87.8	94	74	99.11	99.55	12.3	0
2	77	89.5	95	76	99.1	99.5	9.6	1
3	80	92.1	97	76	98.5	99	6.4	4
	80	92.1	97	78	99.44	99.52	7.34	2
4	65	91.7	96.7	65	95.67	97.05	3.97	0
	75	91.7	96.7	75	99.56	99.53	7.83	0
5	60	87.7	93.4	60	96	96.5	8.3	0
	71	87.7	93.4	71	99.56	99.81	11.86	0

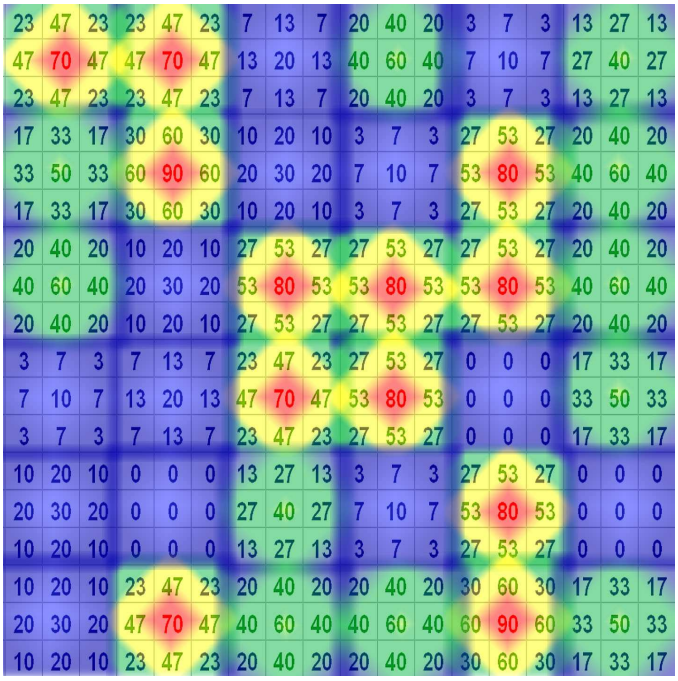


Fig. 3. CU(18 × 18) Sample No.1

References

[1] M. Wagner, "The optimal cash deployment strategy modeling a network of automated teller machines," *thesis in Master of Science in Accounting, Hanken- Swedish School of Economics and Business Administration*, 2007.

$$A = \begin{bmatrix}
0 & 1 & 0 & 0 & 0 & 0 & 0 & 0 & 0 & 0 & 0 & 0 & 0 & 0 & 1 & 0 & 0 \\
0 & 0 & 0 & 0 & 1 & 0 & 0 & 0 & 0 & 0 & 1 & 0 & 0 & 0 & 0 & 0 & 0 & 0 \\
0 & 0 & 0 & 0 & 0 & 0 & 0 & 0 & 0 & 0 & 0 & 0 & 0 & 0 & 0 & 0 & 1 & 0 \\
0 & 1 & 0 & 0 & 0 & 0 & 0 & 1 & 0 & 0 & 0 & 0 & 0 & 0 & 0 & 0 & 0 & 0 \\
0 & 0 & 0 & 0 & 1 & 0 & 0 & 0 & 0 & 0 & 0 & 0 & 0 & 1 & 0 & 0 & 0 & 0 \\
0 & 0 & 0 & 0 & 0 & 0 & 0 & 0 & 0 & 0 & 0 & 0 & 0 & 0 & 0 & 0 & 0 & 0 \\
0 & 0 & 0 & 0 & 0 & 0 & 0 & 0 & 0 & 0 & 1 & 0 & 0 & 0 & 0 & 0 & 0 & 1 \\
0 & 0 & 1 & 0 & 0 & 0 & 0 & 1 & 0 & 0 & 0 & 0 & 1 & 0 & 1 & 0 & 0 & 0 \\
0 & 1 & 0 & 0 & 0 & 0 & 0 & 0 & 0 & 0 & 0 & 0 & 0 & 0 & 0 & 0 & 0 & 0 \\
0 & 0 & 0 & 0 & 0 & 0 & 0 & 0 & 0 & 0 & 0 & 0 & 0 & 0 & 0 & 0 & 0 & 0 \\
0 & 0 & 0 & 0 & 0 & 1 & 0 & 0 & 0 & 0 & 1 & 0 & 0 & 0 & 0 & 0 & 1 & 0 \\
0 & 0 & 0 & 0 & 0 & 0 & 0 & 0 & 0 & 0 & 0 & 0 & 0 & 0 & 0 & 0 & 0 & 0 \\
0 & 0 & 0 & 0 & 0 & 0 & 0 & 1 & 0 & 0 & 0 & 0 & 0 & 0 & 0 & 0 & 0 & 0 \\
0 & 1 & 0 & 0 & 0 & 0 & 0 & 0 & 0 & 0 & 0 & 0 & 1 & 0 & 0 & 0 & 0 & 0 \\
0 & 0 & 0 & 0 & 0 & 0 & 0 & 0 & 0 & 0 & 0 & 0 & 0 & 0 & 0 & 0 & 0 & 0 \\
0 & 0 & 0 & 0 & 0 & 0 & 0 & 0 & 0 & 0 & 1 & 0 & 0 & 0 & 0 & 0 & 0 & 0 \\
0 & 0 & 1 & 0 & 0 & 1 & 0 & 1 & 0 & 0 & 0 & 0 & 0 & 1 & 0 & 0 & 1 & 0 \\
0 & 0 & 0 & 0 & 0 & 0 & 0 & 0 & 0 & 0 & 0 & 0 & 0 & 0 & 0 & 0 & 0 & 0
\end{bmatrix}$$

Fig. 4. Location Matrix for CU(18 × 18) Sample No.1

[2] E. Agustín-Blas, S. Salcedo-Sanz, P. Vidales, G. Urueta, A. Portilla-Figueras, and M. Solarski, "A hybrid grouping genetic algorithm for citywide ubiquitous wifi access deployment," in *CEC'09: Proceedings of the Eleventh conference on Congress on Evolutionary Computation*. Piscataway, NJ, USA: IEEE Press, 2009, pp. 2172–2179.

[3] M. A. Aldajani and H. K. Alfares, "Location of banking automatic teller machines based on convolution," *Comput. Ind. Eng.*, vol. 57, no. 4, pp. 1194–1201, 2009.

[4] A. Qadrei and S. Habib, "Allocation of heterogeneous banks' automated teller machines," in *INTENSIVE '09: Proceedings of the 2009 First International Conference on Intensive Applications and Services*. Washington, DC, USA: IEEE Computer Society, 2009, pp. 16–21.

[5] L. B. J. F. P. D. Rimvydas Simutis, Darius Dilijonas, "Optimization of cash management for atm network," in *Information Technology and Control*, 2007.

[6] D. E. Goldberg, *Genetic Algorithms in Search, Optimization, and Machine Learning*. New York, NY: Addison-Wesley, 1989.

[7] W. Abdulal, O. A. Jadaan, A. Jabas, and S. Ramachandram, "Genetic algorithm for grid scheduling using best rank power," in *Nature & Biologically Inspired Computing, NaBIC 2009*. IEEE, 2009, pp. 181–186.

[8] A. J. S. R. Wael Abdulal, Omar Al Jadaan, "Rank based genetic scheduler for grid computing systems," in *The International Conference on Computational Intelligence and Communication Networks (CICN 2010)*. IEEE, 2010.

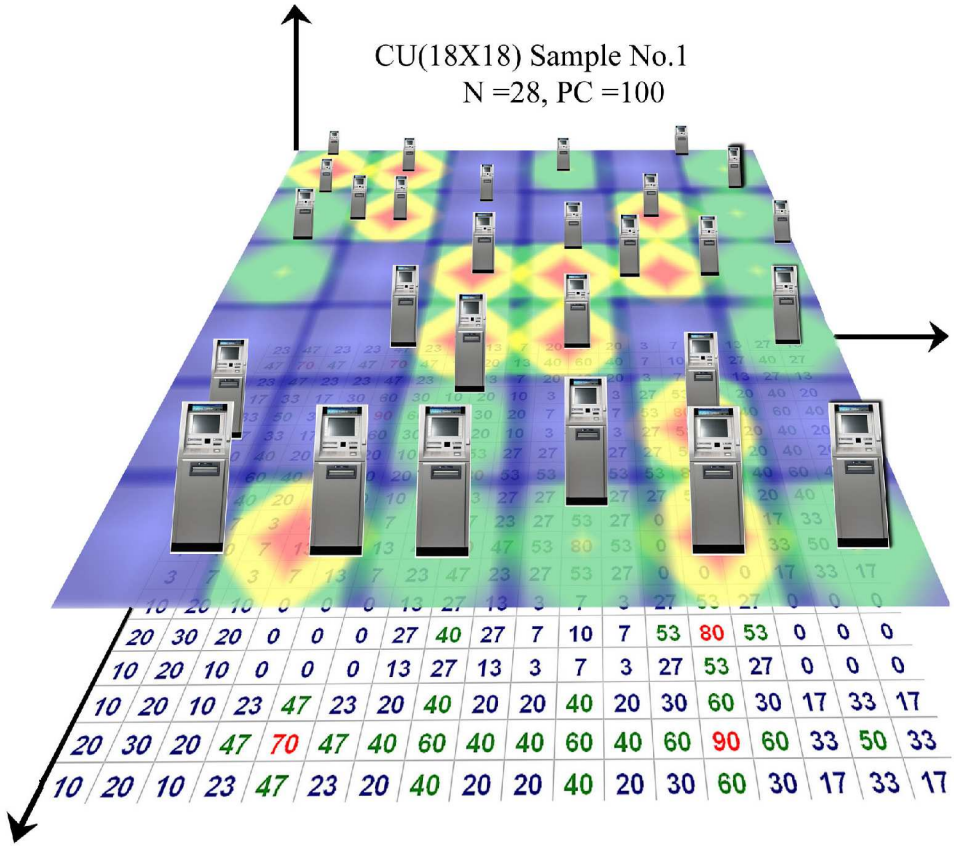


Fig. 5. RGAC solution for CU(18 × 18) Sample No.1

Artificial Immune System based on Hybrid and External Memory for Mathematical Function Optimization

David F. W. Yap*
Faculty of Electronic and Computer Engineering,
Universiti Teknikal Malaysia Melaka (UTeM),
Hang Tuah Jaya,76100 Durian Tunggal, Melaka, Malaysia.
*david.yap@utem.edu.my

S. P. Koh, S.K.Tiong
College of Engineering,
Universiti Tenaga Nasional (UNITEN),
Km 7, Kajang-Puchong Road, 43009 Kajang, Selangor
Darul Ehsan, Malaysia.

Abstract—**Artificial immune system (AIS) is one of the nature-inspired algorithm for optimization problem. In AIS, clonal selection algorithm (CSA) is able to improve global searching ability. However, the CSA convergence and accuracy can be further improved because the hypermutation in CSA itself cannot always guarantee a better solution. Alternatively, Genetic Algorithms (GAs) and Particle Swarm Optimization (PSO) have been used efficiently in solving complex optimization problems, but they have a tendency to converge prematurely. Thus, a hybrid PSO-AIS and a new external memory CSA based scheme called EMCSA are proposed. In hybrid PSO-AIS, the good features of PSO and AIS are combined in order to reduce any limitation. Alternatively, EMCSA captures all the best antibodies into the memory in order to enhance global searching capability. In this preliminary study, the results show that the performance of hybrid PSO-AIS compares favourably with other algorithms while EMCSA produced moderate results in most of the simulations.**

Keywords-component: clonal selection, antibody, antigen, affinity maturation, mutation.

I. INTRODUCTION

Optimization problem has been a challenge to many researchers in order to find the best local searching method. This problem also leads to a branch of knowledge which is the evolutionary computing. The methods were greatly influenced by nature. Few decades ago, many methods have been developed, for instance, GA, PSO or Artificial Immune System (AIS). In this study, the hybrid CSA and modified CSA are evaluated in comparison to conventional CSA and other evolutionary algorithms such as PSO and GA. These algorithms are described in the following paragraphs.

PSO was originally proposed by Kennedy and Eberhart [1]. The PSO is inspired from social behavior of individual organisms living together in groups [2]. Each individual in a group imitates other groups that are better, in order to improve its own group.

GA was inspired from a set of chromosome where each chromosome represents an individual solution (genes). The GA uses a search technique where genes in the population are improved across generation through a set of operation. During each generation, the genes go through the process of selection, cross-over and mutation [3].

AIS is one of the nature-inspired approach in solving the optimization problem. The AIS is greatly reinforced by the immune system of a living organism such as human and animal. In humans, the immune system is responsible in maintaining stability of the physiological system such as protection from pathogens. In AIS, CSA is able to improve global searching ability as it uses the principle of clonal expansion and affinity maturation as the main forces of the evolutionary process [4]

In this research, the hybrid PSO-AIS and EMCSA are studied to improve the performance of diversity and convergence that are responsible in finding the global solution of single objective function. The ease of implementation is sustained in both of the proposed algorithms.

II. PSO, GA AND AIS ALGORITHMS

Particle Swarm Optimization

The PSO algorithm starts with a group of random particles that searches for optimum value for each updated generation. The i_{th} particle is denoted as $X_i = (x_{i1}, x_{i2}, x_{i3}, ..., x_{in})$. During generation updating, each particle is updated by ensuing two best values. These values are the best solution (*mbest*) and the global best value (*gbest*) that has been obtained by particles in the population at particular generation. With the inclusion and inertia factor ω, the velocity equations are shown in Eqs. (1) and (2).

$$v_{i+1} = v_i\omega + \alpha_1 \cdot rnd() \cdot (mbest_i - x_i) + \alpha_2 \cdot rnd() \cdot (gbest_i - x_i) \quad (1)$$

$$x_{i+1} = x_i + v_i \quad (2)$$

Where *rnd()* is a random number between 0 and 1, α_1 and α_2 are learning factors to control the knowledge and the neighbourhood of each individual respectively. The PSO algorithm is described in the following steps.

Step	Process
1	Generate initial random particle swarms assigned with its random position and velocity
2	Compute the fittest value of N particles according to fitness function
3	Update values of the best position of each particle and the swarm
4	Update the position and velocity for each particle according to equation 1 and 2
5	Repeat steps 3 and 4 until pre-defined stopping condition is achieved

Genetic Algorithm

As described earlier, GA uses three main processes i.e. selection, crossover and mutation to improve genes through each generation. The selection process uses the objective function to assess the quality of the solution. Then, the fittest solutions from each generation are kept. The function of crossover generates new solutions given a set of selected members of the current population. In the crossover process, genetic material between two single chromosome parents is exchanged. After that, mutation triggers sudden change in the chromosomes unexpectedly. However, the mutation process is expected to avoid genes from trapping in local minima by adding random variables. The GA algorithm is described in the following steps.

Step	Process
1	Generate initial random population of individuals
2	Compute the fittest value of each individual in the current population
3	Select individuals for reproduction
4	Apply crossover and mutation operators
5	Compute the fittest value of each individual
6	Select the best individuals to generate new population
7	Repeat steps 3 to 6 until pre-defined stopping condition is achieved

Artificial Immune System

The biological immune system has been modeled into AIS for engineering application. In AIS, CSA was inspired from the fact that only antibodies (Abs) that are able to recognize antigens (Ags) are selected to proliferate. The selected Abs then enters the affinity maturation process. The algorithm was verified to be capable to solve complex problem such as multi-modal and combinatorial optimization [5].

The clonal selection theory describes how Abs detects the Ags and proliferates by cloning. As shown in Fig. 1, the immune cells will reproduce against the Ags. The new cloned cells are then differentiated into plasma cells and memory cells. The plasma cells produce Abs and go through mutation process to promote genetic variation. The memory cells are responsible for future Ags invasion. Finally, the selection mechanism keeps the Abs with the best affinity to the Ags in the next population [4]. The CSA pseudocode is described in the following steps.

Step	Process
1	Generate an initial random population of antibodies, Abs
2	Compute the fittest value of each Ab according to fitness function
3	Generate clones by clonning all cells in the Ab population
4	Mutate the clone population to produce a mature clone population
5	Evaluate the affinitiy value for each clone population
6	Select the best Ab to compose the new Ab population
7	Repeat steps 2 to 6 until a pre-defined stopping condition is achieved

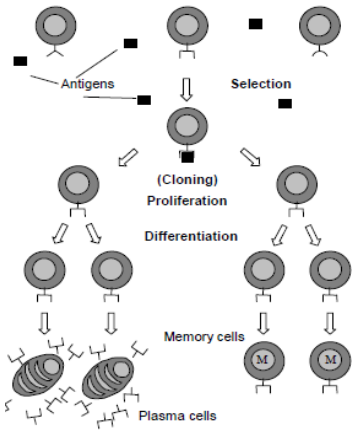


Figure 1. Clonal Selection Principle [4]

Hybrid PSO-AIS

AIS have the advantage to prevent the population from being trapped into local optimum. Besides, PSO has the ability to improve itself but tend to converge prematurely [6]. Therefore, the combination between PSO and AIS (PSO-AIS) is expected to improve the global search ability and avoid being trapped in local minima even though the population size is relatively small. Hence, the hybrid PSO-AIS pseudocode is described in the following steps.

Step	Process
1	Select the best particles from PSO to be half of AIS initial population, N_1
2	Generate randomly other half of initial population of Abs, N_2
3	Combine N_1 and N_2 and compute fittest values of each Ab
4	Generate clones by cloning all cells in Ab population
5	Mutate the clone population to produce a mature clone population
6	Evaluate the affinity value for each clone in the population
7	Select the best Ab to compose the new Ab population
8	Repeat steps 4 to 7 until pre-defined stopping condition is achieved

EMCSA

In AIS, clonal selection adapts B-cells (and T-cells) to kill the invader through affinity maturation by hypermutation. However, the adaptation requires B-cells to be cloned many

times [7, 8], and the hypermutation process cannot always guarantee that the next generation will provide better solution. The stochastic factor (randomization) at times can even produce worse result from previous solution. Therefore, *N* number of the best Abs from the previous generation are kept in the external memory database and then combined with the initial random Abs of the next generation to compose a new population for that next generation. Thus, the good Abs of every generation that are stored in the database will keep on growing until the last generation. Finally, on the last generation, all the good Abs that are kept in the database from the previous generations are combined with the Abs of the last generation. Moving forward, when new Ags are required to be detected, the external memory database would be very useful to speed up the performance. The pseudocode of EMCSA is shown as below.

Step	Process
1	Generate an initial random population of antibodies, Abs
2	Combine Abs with Ab_{ext} (if any)
3	Compute the fittest value of each Ab according to fitness function
4	Generate clones by clonning all cells in the Ab population
5	Mutate the clone population to produce a mature clone population
6	Evaluate the affinitiy value for each clone population
7	Select the best Ab, *N*, to compose the new Ab population
8	Save a range of good Abs N_{ext} into external memory, Ab_{ext}
9	Repeat steps 1 to 8 until a pre-defined stopping condition is achieved

All methods described above are evaluated using nine mathematical test functions. The termination criteria for all methods will be met if minimum error value is achieved or maximum number of evaluation allowed is exceeded.

III. EXPERIMENTS ON TEST FUNCTION

The computing platform used for the experiment is AMD Phenom 9600B Quad-Core CPU running at 2.30 GHz, 2GB of RAM and Windows Vista Enterprise operating system. Each algorithm is evaluated based on 500 iterations. The minimum error is set as 1e-25. The population size P_0 is set to 20.

In the EMCSA, a total of five antibodies, Ab_{ext}, from every iteration would be stored into the external memory. However, the maximum number of antibodies that can be kept in the memory is fixed to only 50 antibodies. Thus, whenever the memory size have reached 50 antibodies, the worst five would be removed from the memory and replaced with the current Ab_{ext}. This is repeated until a pre-defined stopping condition is achieved.

The CSA, EMCSA, PSO, PSO-AIS and GA algorithms are evaluated using nine benchmark functions (objective functions) which are described as follows.

1. Rastrigin's Function (TF1) :

Rastrigin's function is mathematically defined as follows.

$$f_1(x) = \sum_{i=1}^{n} \left(x_i^2 - 10\cos\left(2\pi x_i\right) + 10 \right) \quad (3)$$

where $-5.12 \le x_i \le 5.12$, $i = 1\ldots,n$

and global minimum is located at the origin and its function value is zero.

2. De Jong's Function (TF2):

De Jong's function is mathematically defined as follows.

$$f_2(x) = \sum_{i=1}^{n} x_i^2 \quad (4)$$

where $-5.12 \le x_i \le 5.12$, $i = 1\ldots,n$

and global minimum is located at the origin and its function value is zero.

3. Axis Parallel Hyper-ellipsoid Function (TF3):

Axis parallel hyper-ellipsoid function is mathematically defined as follows.

$$f_3(x) = \sum_{i=1}^{n} i \bullet x_i^2 \quad (5)$$

where $-5.12 \le x_i \le 5.12$, $i = 1\ldots,n$

and global minimum is located at the origin and its function value is zero.

4. Rosenbrock's Function (TF4):

Rosenbrock's function is mathematically defined as follows.

$$f_4(x) = \sum_{i=1}^{n-1} 100 \bullet \left(x_{i+1} - x_i^2 \right)^2 + \left(1 - x_i\right)^2 \quad (6)$$

where $-2.048 \le x_i \le 2.048$, $i = 1\ldots,n$

and global minimum is located at the origin and its function value is zero.

5. Sum of Different Power Function (TF5):

Sum of different power function is mathematically defined as follows.

$$f_5(x) = \sum_{i=1}^{n} \left| x_i \right|^{(i+1)} \quad (7)$$

where $-1 \le x_i \le 1$, $i = 1\ldots,n$

and global minimum is located at the origin and its function value is zero.

6. Rotated Hyper-ellipsoid Function (TF6):

Rotated hyper-ellipsoid function is mathematically defined as follows.

$$f_6(x) = \sum_{i=1}^{n} \left(\sum_{j=1}^{i} x_j \right)^2 \quad (8)$$

where $-65.536 \le x_i \le 65.536$, $i = 1. . . ,n$

and global minimum is located at the origin and its function value is zero.

7. Moved Axis Parallel Hyper-ellipsoid Function (TF7):

Moved axis parallel hyper-ellipsoid function is mathematically defined as follows.

$$f_7(x) = \sum_{i=1}^{n} 5i \bullet x_i^2 \quad (9)$$

where $-5.12 \le x_i \le 5.12$, $i = 1. . . ,n$

and global minimum is located at the origin and its function value is zero.

8. Griewangk Function (TF8):

Griewangk's function is mathematically defined as follows.

$$f_8(x) = \sum_{i=1}^{n} \frac{x_i^2}{4000} - \prod_{i=1}^{n} \cos\left(\frac{x_i}{\sqrt{i}} \right) + 1 \quad (10)$$

where $-600 \le x_i \le 600$, $i = 1. . . ,n$

and global minimum is located at the origin and its function value is zero.

9. Ackley Function (TF9):

Ackley's function is mathematically defined as follows.

$$f_9(x) = 20 + e - 20e^{-0.2\sqrt{\frac{1}{n}\sum_{i=1}^{n} x_i^2}} - e^{\frac{1}{n}\sum_{i=1}^{n} \cos(2\pi x_i)} \quad (11)$$

where $-32.768 \le x_i \le 32.768$, $i = 1. . . ,n$

and global minimum is located at the origin and its function value is zero.

IV. Result and Discussion

The results for the test functions are shown in Fig. 2 to 10 and Table I. For Rastrigin's function, Fig. 2 shows that PSO suffers from premature convergence while GA and CSA are comparable in giving the fitness value. On the other hand, PSO-AIS and EMCSA performed moderately.

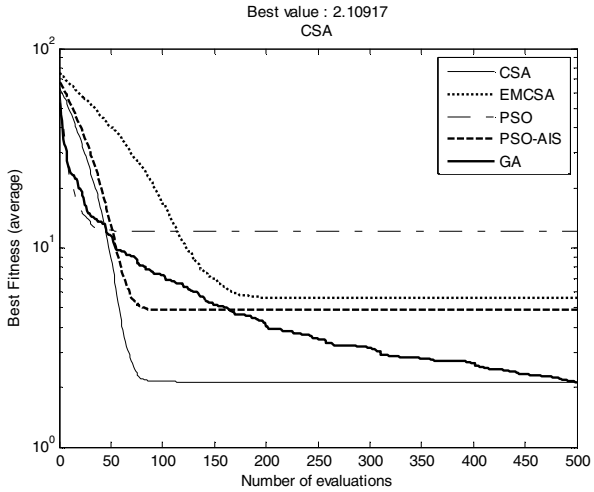


Figure 2. Algorithms evaluation on Rastrigin's function

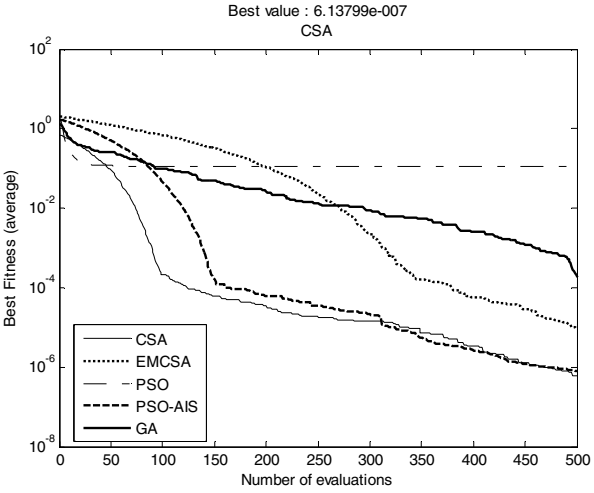


Figure 3. Algorithms evaluation on Dejong's function

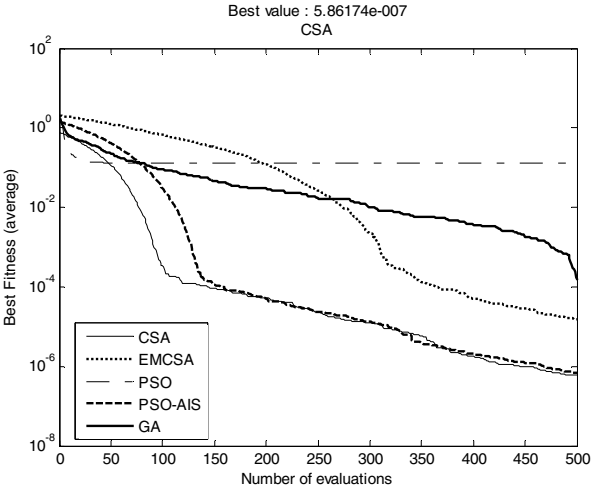


Figure 4. Algorithms evaluation on Axis Parallel Hyper-ellipsoid function

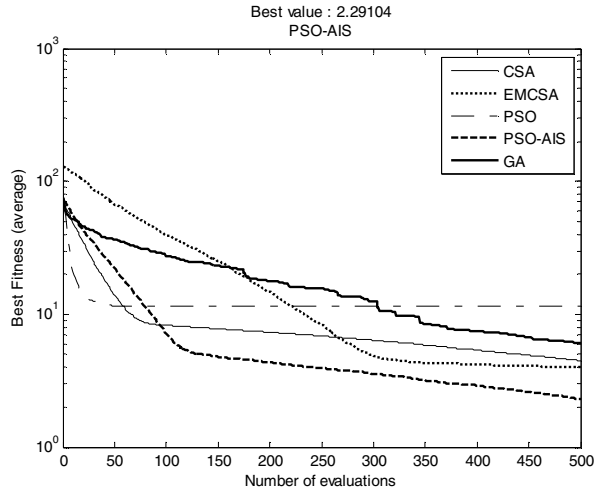


Figure 5. Algorithms evaluation on Rosenbrock function

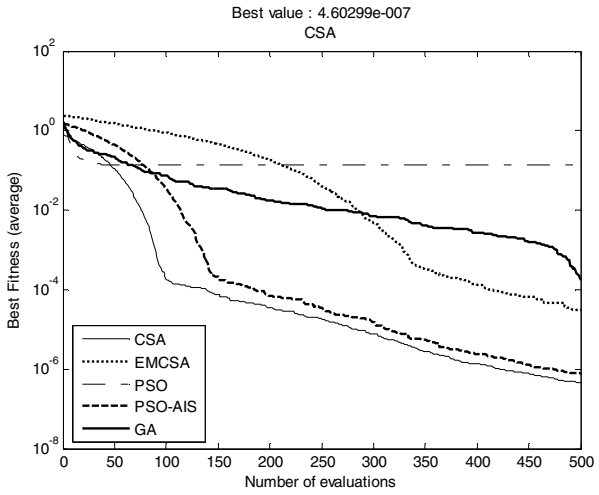


Figure 6. Algorithms evaluation on Sum Differential Power function

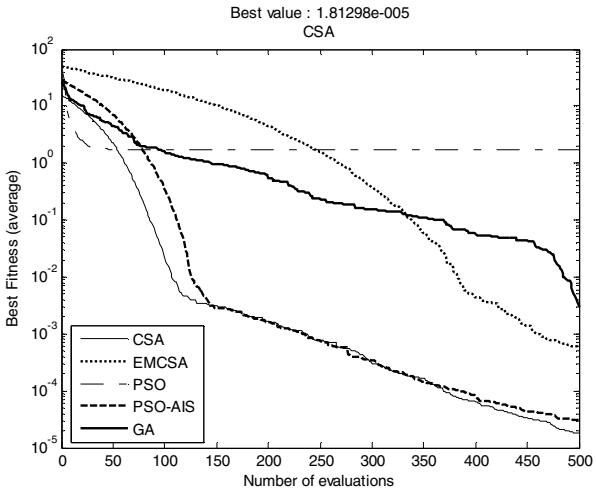


Figure 7. Algorithms evaluation on Rotated Hyper-ellipsoid function

For fitness function of Figures 3, 4, 6, 7, 8 and 9, PSO again suffers from premature convergence while PSO-AIS and CSA are comparable in performance. The EMCSA only achieved moderate performance among all the algorithms.

Figure 5 shows that PSO-AIS outperformed other algorithms. The EMCSA is second best, followed by CSA. GA and PSO performed poorly where these algorithms converge very slowly.

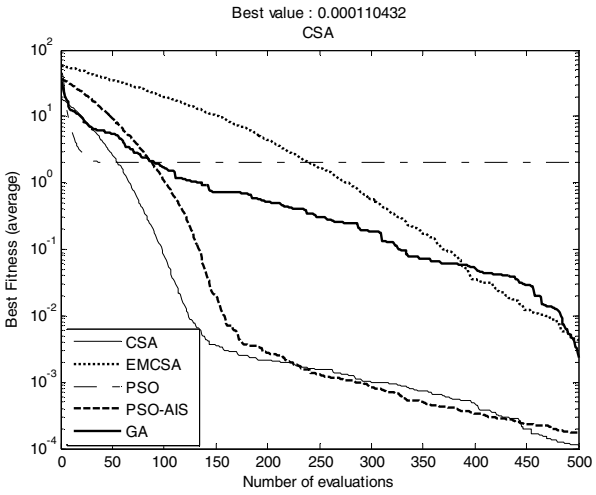


Figure 8. Algorithms evaluation on Moved Axis Parallel Hyper-ellipsoid function

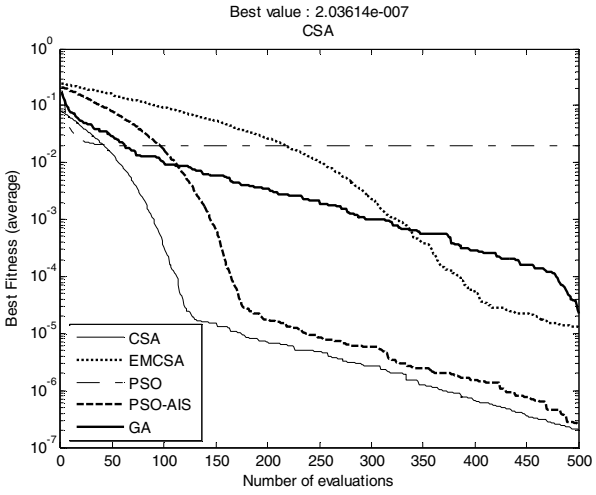


Figure 9. Algorithms evaluation on Griewangk function

The Ackley function in Fig. 10 shows that GA outperformed all other algorithms, followed by CSA. The rest of the algorithms, PSO, PSO-AIS and EMCSA performed poorly.

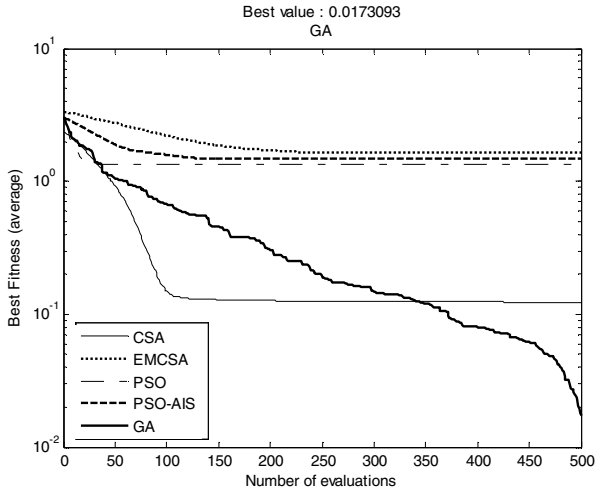


Figure 10. Algorithms evaluation on Ackley function

Table I shows the mean and standard deviation value for nine test functions used, to evaluate the algorithms performance. The CSA outperformed all other algorithms in almost all of the test functions except TF4 and TF9. The algorithms that performed the best in TF4 and TF9 are PSO-AIS and GA respectively.

V. CONCLUSION

A hybrid PSO-AIS algorithm and an external memory-based clonal selection AIS algorithm were proposed. From initial simulation work done on both of the algorithms, the performance of PSO-AIS is comparable to CSA while EMCSA only achieved moderate performance among all the algorithms compared. More work would be done in tweaking certain parameters in EMCSA such as the memory allocation factor, best memory selection criteria or the number of best memory to be taken into consideration, in order to improve the performance of the algorithm.

Table I. Mean and Standard Deviation for each of the algorithm based on the given transfer function

Function	CSA		EMCSA		PSO		PSO-AIS		GA	
	Mean	Std Dev	Mean	Std Dev	Mean	Std Dev	Mean	Std Dev	Mean	Std Dev
TF1	**2.10917**	**1.51617**	5.58652	1.56830	12.1057	5.61802	4.8883	1.09404	2.1186	1.18767
TF2	**6.1E-07**	**4.8E-07**	9.5E-06	7.4E-06	0.11565	0.07709	8.2E-07	6.3E-07	0.00019	0.00014
TF3	**5.9E-07**	**3.9E-07**	1.56E-05	2.03E-05	0.12653	0.0811	6.9E-07	4.6E-07	0.00015	7.1E-05
TF4	4.48752	1.38984	4.00733	2.18162	11.414	3.75693	**2.29104**	**1.304**	6.05602	2.18913
TF5	**4.6E-07**	**1.5E-07**	2.9E-05	2.8E-05	0.13601	0.08611	7.4E-07	5.4E-07	0.00017	6.6E-05
TF6	**1.8E-05**	**1.3E-05**	0.0029	0.0016	1.7223	2.46831	3E-05	3.3E-05	0.00293	0.00165
TF7	**0.00011**	**0.00011**	0.0023	0.00075	1.9966	1.08895	0.00017	0.00033	0.00239	0.00075
TF8	**2E-07**	**1.3E-07**	1.24E-05	1.17E-05	0.0194	0.02263	2.6E-07	2.1E-07	2.2E-05	1.6E-05
TF9	0.12283	0.36299	1.6293	0.70439	1.33007	0.8346	1.47366	0.85525	**0.01731**	**0.00304**

ACKNOWLEDGMENT

The authors would like to thank Universiti Teknikal Malaysia Melaka and The Ministry of Higher Education Malaysia for the financial support under PJP/2009/FKEKK (20D) S614 and Fundamental Research Grant Scheme No. FRGS/2010/FKEKK/TK03/1 – F0085 respectively.

REFERENCES

[1] J. Kennedy and R. Eberhart, 1995. Particle Swarm Optimization. Proc. IEEE Int. Conf. Neural Networks, 4:1942-1948.

[2] J. Kennedy and R. Eberhart, 1995. Swarm Intelligence. 1st Edition. , Academin Press., San diego. CA.

[3] C. Emmeche, 1994. Garden in the Machine: The Emerging Science of Artificial Life. Princeton University Press, New Jersey, USA.

[4] L. N. De Castro and J. Timmis, 2002. Artificial Immune System: A New Computational Approach. Springer-Verlag, NewYork.

[5] A. Acan and A. Unveren, "A Memory-Based Colonization Scheme for Particle Swarm Optimization," IEEE Congress on Evolutionary Computation, pp. 1965-1972, 2005.

[6] J. Vesterstrom and R. Thomsen, "A Comparative Study of Differential Evolution, Particle Swarm Optimization, and Evolutionary Algorithms on Numerical Benchmark Problems," pp. 1980-1987.

[7] S. M. Garret, "How Do We Evaluate Artificial Immune System", Evoluationary Computation, vol. 13, pp. 145-178.

[8] F. M. Burnet, 1969. The Clonal Selection Theory of Acquired Immunity. Cambridge University Press.

Robust Combining Methods in Committee Neural Networks

S.A.Jafari, S.Mashohor

Department of Computer and Communication Systems Engineering, Faculty of Engineering, University Putra Malaysia

***Abstract*- Combining a set of suitable experts can improve the generalization performance of the group when compared to single experts alone. The classical problem in this area is to answer the question about how to combine the ensemble members or the individuals. Different methods for combining the outputs of the experts in a committee machine (ensemble) are reported in the literature. The popular method to determine the error in every prediction is Mean Square Error (MSE), which is heavily influenced by outliers that can be found in many real data such as geosciences data. In this paper we introduce Robust Committee Neural Networks (RCNNs). Our proposed approach is the Huber and Bisquare function to determine the error between measured and predicted value which is less influenced by outliers. Therefore, we have used a Genetic Algorithm (GA) method to combine the individuals with the Huber and Bisquare as the fitness functions. The results show that the Root Mean Square Error (RMSE) and R-square values for these two functions are improved compared to the MSE as the fitness function and the proposed combiner outperformed other five existing training algorithms.**

***Keywords*—Committee Machine; Neural Network; genetic Algorithms; Bisquare and Huber Function**

I. INTRODUCTION

An ensemble is a set of learning machines that their outputs are combined to improve the performance of the whole system. The ensemble has a successful performance when its members are in disagreement. In such an intelligent system, each member estimates a target variable. These estimated outputs then combined with different methods which will be discussed later in the next section. Both theoretical [1] and empirical studies [2, 3] have shown that the ensemble output can be enhanced when individuals are accurate enough and the error of each member is occurred on a different part of the input space. In the past two decades a number of researchers have shown that a simply combining the output of many individuals can improve their prediction than single network alone [4, 5]. In particular, combining separately trained neural networks has been demonstrated to be successful [6, 7]. Therefore the main reason to use ensembles is due to improvement in the generalization ability. Different committee members can be created by different types of input training data, initialization, topology or different training algorithms and so on. There are many methods to create individuals for an ensemble in literature such as, Bootstrap aggregation or Bagging [4], Cross-validation [1], Stacking [5], Boosting by filtering [8], AdaBoost [9], and etc. After selecting individuals and training them, their generated results will be combined by some methods. Many investigations have been done to find accurate and useful combining methods to combine the network outputs and produce the final outputs such as Simple averaging [10], Majority voting [11], Naive Bayesian fusion [12], Ranking [13], Weighted averaging [14], Fuzzy integral [15], Decision templates [16], Dumpster Shafer combination [17], weighted majority voting [18], and etc. Some of them are suitable for classification and some of them are more applicable for regression. In this paper, we provide a review on robustness issues in ensemble neural network. A general ensemble structure can be viewed in Figure 1.

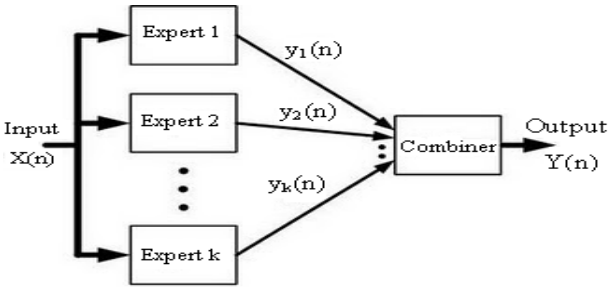


Figure 1: A graphical illustration of ensemble k experts.

II. COMBINATION METHODS

As mentioned in introduction part, an ensemble approach can implemented using two methods: generating individuals or committee members and combining the individual predictions. In this section we explain a brief description on second parts and introduce some of the traditional methods.

A. Simple Averaging

This combining method is most commonly used in ensemble. The final output in this method is obtained by averaging the whole individual outputs. It is easy to illustrate by Cauchy's inequality which the MSE for Committee Neural Network (CNN) with the simple averaging method is less than or equal to the average of MSE for whole networks. The disadvantage of this method is due to giving equal weights to all the individuals so the important individuals cannot be emphasized.

B. Weighted Averaging

In this method every committee member has a suitable weight related to their ability to generalization. In [14] the researcher introduced a gating method to determine the weight of every experts. The authors in [19] have used GA to determine the weight of each member. To obtain the optimal weights for combining with GA algorithm, the fitness function is defined as below:

$$MSE_{GA} = \sum_{i=1}^{n} \frac{1}{n} (w_1 y_{1i} + w_2 y_{2i} + ... + w_k y_{ki} - T_i)^2 \; ; \qquad \sum_{i=1}^{k} w_i = 1 \qquad (1)$$

where, y_{1i} is the output of first network on the *ith* input or *ith* training pattern, T_i is the target value of *ith* input, and n is the number of training data. The major disadvantage of this method is that it depends on the distribution of environmental variables; highly roughly distributions can scramble the order of weighted averaging of different species[20].

C. Ranking

This method uses experimental results obtained from applying the experts on a set of datasets to generate rankings for those experts. All experts are ranked by an input dataset in each experiment. This act is repeated for all datasets of a set. The rankings obtained are then used in suitable methods such as average rank, success rate ration, significant wins, etc to evaluate the experts and to generate their final rankings [21]. The number of classes that has the same ranks depends on the number of classifiers used. Therefore, this method is useful only if the number of classifiers is small relative to the number of classes. Therefore the drawback in this method is that the combined ranking may have many ties. Otherwise, most of the classes are involved in ties and the final ranking is not interesting[22].

D. Majority Voting

This combination method is most popular for classification problems. If more than half of the individuals vote a prediction, majority voting selects this prediction to be the final output. Majority voting also has some disadvantages, for example, a winning expert that obtains only a minority of correct results is often neglected by the majority voting decision rules and this downgrades the diversity of the ensembles which is the basic reason for using ensembles.

However, there is no unique criterion for selecting a combination method and it is mainly dependent on the specific application under the focus. The nature of application in addition to the size and quality of datasets and the generated errors on the region of the input space are the most significant parameters involved in such selection [23].

III. A REVIEW ON ROBUST STATISTICS

The focus of classical statistics is mainly on optimal procedures where the assumptions about the models are true. For example, the mean value is the most efficient estimator for the expected value only when a sample comes from a normal distribution. Also the accuracy of the Least Squares (LS) method for linear regression is totally dependent on such assumptions in a same fashion. As long as the model assumption (in Equation 2), where the e_is are independent and identically distributed (i.i.d), [24].

$$y_i = b_0 + b_1 x_{i1} + ... + b_m x_{im} + e_i = X_i^{'} b + e_i \qquad (2)$$

However, it is obvious that even single outliers are capable of changing the mean value or the predicted coefficient of the regression function. Also the classical statistics presumes that the data is made up of independent samples from an optimal distribution, where in contrast the robust statistics considers the data to be mixed with an unknown noise distribution [24]. The extended discussions about these subjects and the related methods are provided in [25].

IV. M-ESTIMATORS FOR GA METHODS

Let us consider the case of GA method to obtain the weight of individuals in neural network ensemble. The most common, fitness function in GA method is based on the MSE which is optimal for the normal error distribution. In the MSE, the square of the residuals is minimized to achieve the best fitting between ensemble output and the targets. However, when the errors are generated even from different Gaussian distributions with different means and variances, the MSE method may lose its efficiency. The robust method is decreasing the influence of this data by using another error function which is less influence by them. Given training data $D = \{(X,T)\}$ where $X = (X_1,...,X_n)$ is input data and $T = (T_1,...,T_n)$ is the target data. The fitness function is minimized as follows:

$$\sum_{i=1}^{n} \rho(e_i) = \sum_{i=1}^{n} \rho(Y_i - T_i); \quad Y_i = \sum_{j=1}^{k} w_j y_{ij} \quad and \quad \sum_{j=1}^{k} w_j = 1 \qquad (3)$$

Where ρ is a suitable error measure, w_j is the weight of each member, and y_{ij} is the output of the jth individual from ith input and e_i is the ith error. A suitable error function must satisfy the conditions in (4).

$$\rho(e_i) \geq 0, \quad \rho(e) = \rho(-e), \quad \rho(e_i) \geq \rho(e_j) \ if \ i \geq j \qquad (4)$$

A parameter estimation based on an objective (fitness) function of equation (3) and (4) is called an M-estimator. Figure 2 shows a graph of the error function and the weighting function for the Least Square (LS) method. LS means that the overall solution minimizes the sum of the squares of the errors made in solving every single equation but MSE means the average of this errors. Figure 3 and 4 provides the error function ρ and the weight function w for the Huber and Bisquare methods respectively.

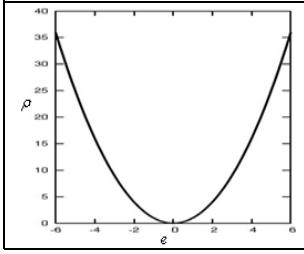
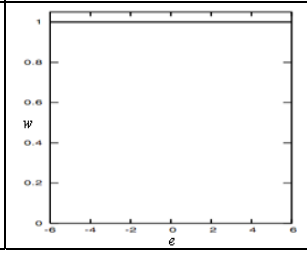
$\rho(e)$	$w(e)$
e^2	1
	

Figure 2: The error function ρ and the weight function w for the LS method.

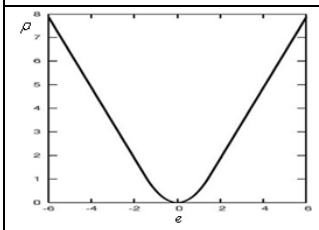
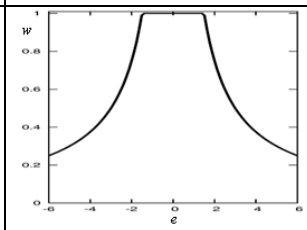
$\rho(e)$	$w(e)$
$\begin{cases} \frac{e^2}{2} & if \lvert e\rvert \leq k \\ k\lvert e\rvert - \frac{k^2}{2} & if \lvert e\rvert > k \end{cases}$	$\begin{cases} 1 & if \lvert e\rvert \leq k \\ k/\lvert e\rvert & if \lvert e\rvert > k \end{cases}$
	

Figure 3: The error function ρ and the weight function w for Huber.

In LS method, the function ρ increases in the quadratic manner with increasing distance, but the weights are always constant. In the Huber and Bisquare methods, the error function ρ is divided in two parts. In first part (small errors; means the absolute of errors are less than the constant k), the ρ is quadratic, and for second part (large errors; means the absolute of errors are greater than the constant k), the ρ is linearly increasing. Furthermore as shown in figure 2, 3 and 4, the Bisquare and Huber methods are stronger than MSE function, because for larger errors the weight w not only is not constant, but also decreases for extreme outliers.

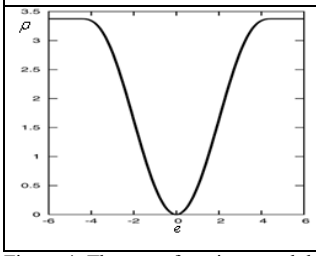
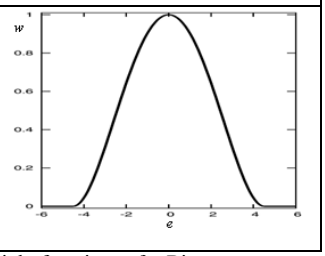
$\rho(e)$	$w(e)$
$\begin{cases} \frac{k^2}{6}\left(1-\left(1-\left(\frac{e}{k}\right)^2\right)^3\right); & if \lvert e\rvert \le k \\ \frac{k^2}{6}; & if \lvert e\rvert > k \end{cases}$	$\begin{cases} \left(1-\left(\frac{e}{k}\right)^2\right)^2; & if \lvert e\rvert \le k \\ 0; & if \lvert e\rvert > k \end{cases}$
	

Figure 4: The error function ρ and the weight function w for Bisquare.

V. SIMULATION RESULTS

The simulation is performed on Matlab on a personal computer with Intel core 2 duo 2.2 GHZ processor and 2 GB of memory. In this section, the performances of five neural networks with different training algorithms are evaluated. These five training algorithms were:

1) Levenberg–Marquardt (LM), [26] and [27],

2) Scaled Conjugate Gradient (SCG), [28],

3) Bayesian regularization (BR), [29],

4) Resilient Back-Propagation (RP), [30],

5) Gradient Descent with momentum and adaptive learning rate backpropagation (GDX), [31].

GA Parameters	Configuration
Population	Population type: double vector, Population size: 50, Initial range: [0; 1]
Scaling function	Rank
Selection function	Stochastic uniform
Reproduction	Elite count: 2, crossover fraction: 0.8
Mutation function	Use constraint dependent default
Crossover function	Scattered
Migration	Direction: forward, Fraction: 0.2, Interval: 20
Stopping criteria	Generations: 1000, Time limit: Inf, Fitness limit: Inf, Stall generations: 1000, stall time: Inf

Table 1: The configurations of GA Parameters for calculate the weight of individuals.

After that three methods for combining the outputs of individuals are implemented. All of these three methods are based on GA, with different fitness functions; MSE, Huber, and Bisquare. GA Parameters of the Matlab which used in this work are listed in Table 1. The data points used for this experiment consists of two independent variables and one dependent variable such as data sets that have been described in [32]. The input data are generated in the range of [-2, 2], and the equation (5) is used to calculate the dependent variable. After that the data points are corrupted in both x and y-coordinates with Gaussian noise with dB=20 using Matlab software. Pictures of the corrupted X1, X2 and Y are illustrated in figure 5 with the corresponding histograms.

$$y = x_1 e^{-m}, \quad m = x_1^2 + x_2^2; \quad x_1, x_2 \in [-2,2] \tag{5}$$

To assess the performance for each estimator and compare them, the RMSE and R-square has been used.

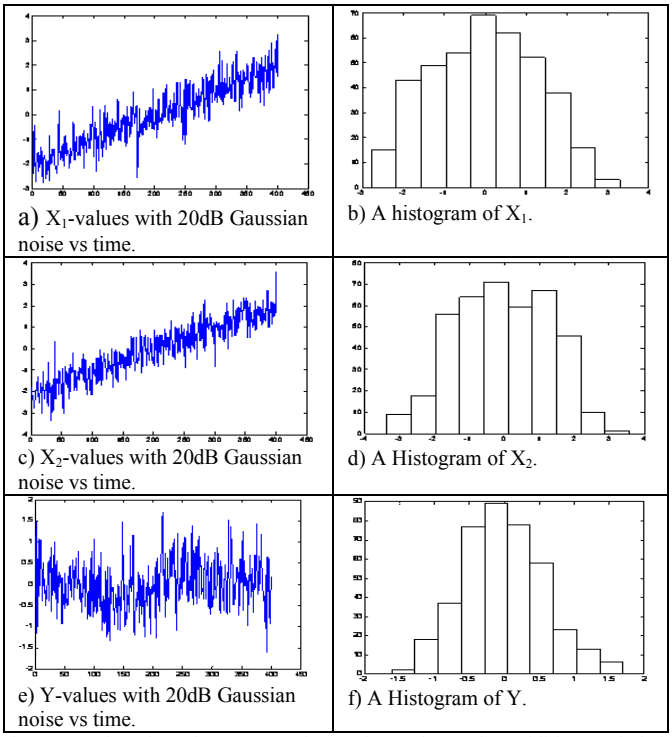


Figure 5: The plot of X_1, X_2 and Y values after noise addition and their corresponding histograms.

VI. RESULTS AND DISCUSSIONS

In this paper we presented two robust fitness (objective) functions for neural network ensemble with GA as combining method. It is based on the robust estimator and introduces two robust approaches to the error criterion to reduce the influence of the outliers. The performance of the weighted averaging with GA constructed from combining five different training algorithms are shown in figure 6. According to result, the GA with MSE as fitness function using LM, SCG, BR, RP, and GDX methods has produced the minimum error whereas, combination of these algorithms with Huber and Bisquare are associated with the minimum error. The GA-MSE derived values for w_1, w_2, w_3, w_4 and w_5 corresponding to LM, SCG, BR , RP, and GDX estimations are 0.091, 0.161, 0.01, 0.717 and 0.022 respectively, also are 0.025, 0.746, 0.098, 0.083, 0.047 for Huber and 0.083, 0.13, 0.144, 0.643, 0.001 for Bisquare fitness functions. Over all estimation of outputs by RCNN was calculated as below:

$$Output_{RCNN} = w_1 y_1 + w_2 y_2 + w_3 y_3 + w_4 y_4 + w_5 y_5 \tag{6}$$

Figure 6 shows the comparison of RMSE and R-square testing data points from different algorithms including LM, SCG, BR, RP, GDX and figure 7 shows the comparison of RMSE and R-

square data points from GA as combination method with different fitness function including GA-MSE, GA-Huber, and GA-Bisquare (all learning algorithms).

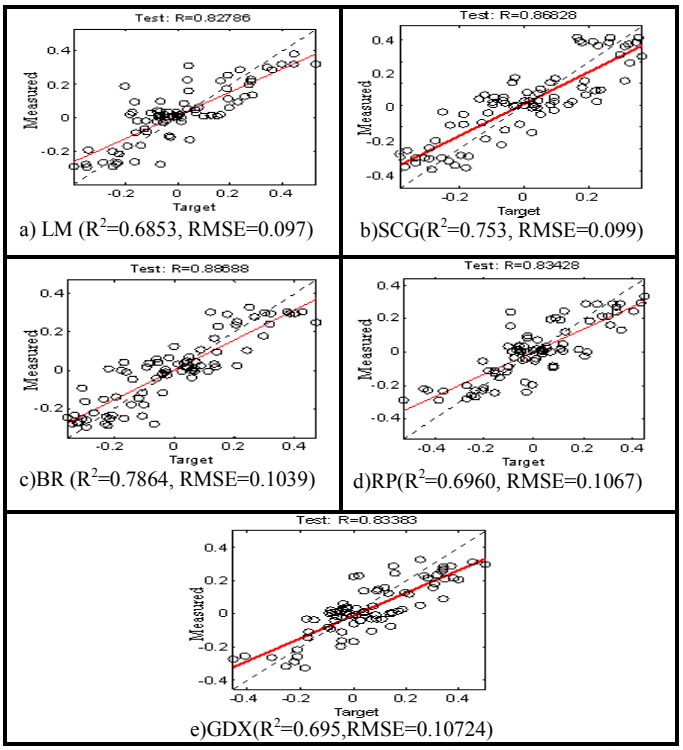
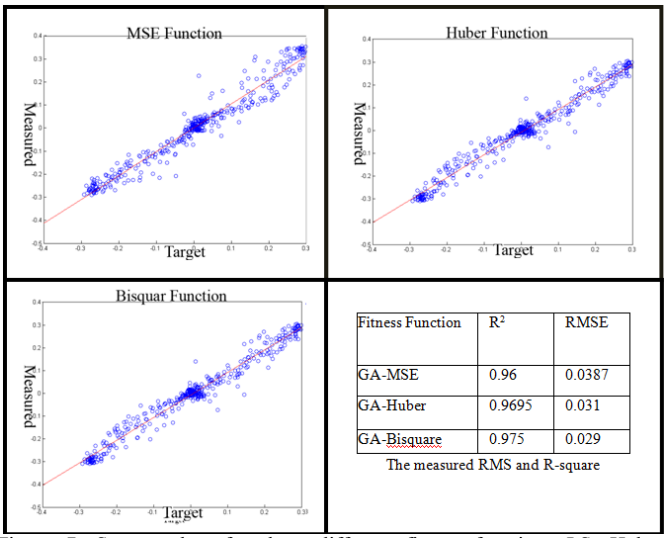


Figure 6: Scatter plots, RMSE and R-square for five training algorithms (a) LM, (b) SCG, (c) BR, (d) RP, (e) GDX.

Considering cross plots of Fig 6 (a–e), among the five neural networks with different training algorithms used, the smallest error and highest R-square are 0.097 and 0.7864 respectively. Based on Figure 6 and 7, the weighted averaging with applying GA for construction committee neural network using LM, SCG, BR, RP and GDX methods has produced the minimum error and maximum R-square algorithms than each training algorithm individually.



Fitness Function	R^2	RMSE
GA-MSE	0.96	0.0387
GA-Huber	0.9695	0.031
GA-Bisquare	0.975	0.029

The measured RMS and R-square

Figure 7: Scatter plots for three different fitness functions LS, Huber, Bisquare, and the measured RMS and R-square using genetic algorithm.

Also according to Figure 7, the genetic algorithm with Bisquare function has provided the smallest error (RMSE=0.0295) and R-square value of 0.97 then genetic algorithm with Huber and MSE function. This indicates that Bisquare function had a significant improvement as objective function for GA. Namely; Bisquare function performs better than any of the individual training algorithms acting alone for prediction. Also it has provided better results than constructed CNN with GA as combining method by Huber and MSE function. It might be noticed that in our case study the GA with Bisquare as objective function performed better than Huber or MSE function; in some cases it may not be so.

VII. CONCLUSION

The results for GA based combiner have shown an improved R-square and RMSE values in Huber and Bisquare function compared with MSE function. Robustness issues have been ignored in ensemble methods and have not been investigated in this type of machine learning approach, especially application with real data which generally are not clear-cut and most of times are associated with uncertainties such as geosciences data. These robust methods can be easily adapted to many types of ensemble neural networks and committee machine with different type of members and applications. This indicates that robust fitness functions have a significant improvement than any of the individual training algorithms acting alone and also GA with conventional fitness function (MSE function).

REFERENCES:

[1] A. Krogh and J. Vedelsby, "Neural network ensembles, cross validation, and active learning " *Advances in Neural Information Processing Systems,* vol. 7, pp. 231-238, 1995.

[2] S. Hashem, *et al.*, "Optimal linear combinations of neural networks: an overview," in *IEEE World Congress on Computational Intelligence., 1507-1512 vol.3*, 1994.

[3] D. Opitz and R. Maclin, "Popular Ensemble Methods: An Empirical Study," *Journal of Artificial Intelligence Research,* vol. 11, pp. 169 - 198, 1999.

[4] L. Breiman, "Bagging predictors," *Machine Learning,* vol. 24, pp. 123-140, 1996.

[5] D. H. Wolpert, "Stacked Generalization," *Neural Networks,* vol. 5, pp. 241-259, 1992.

[6] H. Drucker, *et al.*, "Boosting and Other Ensemble Methods," *Neural Computation,* vol. 6, pp. 1289-1301, 1994.

[7] Maclin and Opitz, "An empirical Evaluation of bagging and Boosting," in *Proceedings of the Fourteenth National Conference on Articial Intelligence, 456-551*, 1997, pp. 456-551.

[8] R. E. Schapire, "The Strength of Weak Learnability," *Mach. Learn.,* vol. 5, pp. 197-227, 1990.

[9] Y. Freund and R. Schapire, "A decision-theoretic generalization of on-line learning and an application to boosting," in *European Conference on Computational Learning Theory*, 1995, pp. 23-37.

[10] W. Lincoln and J. Skrzypek, "Synergy of clustering multiple back propagation networks," *Advances in Neural Information Processing systems-2,* pp. 650-657, 1990.

[11] L. K. Hansen and P. Salamon, "Neural Network Ensembles," *IEEE Trans. Pattern Anal. Mach. Intell.,* vol. 12, pp. 993-1001, 1990.

[12] L. Xu, *et al.*, "Methods of combining multiple classifiers and their applications to handwriting recognition," *Systems, Man and Cybernetics, IEEE Transactions on,* vol. 22, pp. 418-435, 1992.

[13] H. Tin Kam, *et al.*, "Decision combination in multiple classifier systems," *Pattern Analysis and Machine Intelligence, IEEE Transactions on,* vol. 16, pp. 66-75, 1994.

[14] R. A. Jacobs, "Methods For Combining Experts' Probability Assessments," *Neural Computation,* vol. 7, pp. 867-888, 1995.

[15] S.-B. Cho and J. H. Kim, "An HMM/MLP architecture for sequence recognition," *Neural Comput.,* vol. 7, pp. 358-369, 1995.

[16] L. I. Kuncheva, *et al.*, "Decision templates for multiple classifier fusion: an experimental comparison," *Pattern Recognition,* vol. 34, pp. 299-314, 2001.

[17] M. R. Ahmadzadeh and M. Petrou, "Use of Dempster-Shafer theory to combine classifiers which use different class boundaries," *Pattern Analysis & Applications,* vol. 6, pp. 41-46, 2003.

[18] L. I. Kuncheva, "Classifier Ensembles for Changing Environments," ed, 2004, pp. 1-15.

[19] D. W. Opitz and J. W. Shavlik, "Actively Searching for an Effective Neural Network Ensemble," *Connection Science,* vol. 8, pp. 337 - 354, 1996.

[20] J. C. J. R. H. G. Jongman, C. W. N. Looman, C. J. F. ter Braak, O. F. R. van Tongeren, P. A. Burrough, j. a. f. oudhof, a. barendregt, t. j. van de Nes, "Data Analysis in Community and Landscape Ecology," p. 324, 1997.

[21] P. Brazdil and C. Soares, "A Comparison of Ranking Methods for Classification Algorithm Selection," ed, 2000, pp. 63-75.

[22] T. K. Ho, *et al.*, "Decision Combination in Multiple Classifier Systems," *IEEE Trans. Pattern Anal. Mach. Intell.,* vol. 16, pp. 66-75, 1994.

[23] S. Yang and A. Browne, "Neural network ensembles: combining multiple models for enhanced performance using a multistage approach," *Expert Systems,* vol. 21, pp. 279-288, 2004.

[24] F. Klawonn and F. Höppner, "Fuzzy Cluster Analysis from the Viewpoint of Robust Statistics," in *Views on Fuzzy Sets and Systems from Different Perspectives*, ed, 2009, pp. 439-455.

[25] P. J. Huber, *Robust Statistics* Wiley Series in Probability and Statistics, 2004.

[26] K. Levenberg, "A method for the solution of certain non-linear problems in least squares," *Quart. Appl. Math., 2 (1944), pp. 164-168.,* 1994.

[27] D. Marquardt, "An Algorithm for Least-Squares Estimation of Nonlinear Parameters," *SIAM Journal on Applied Mathematics* vol. 11, pp. 431–441, 1963.

[28] M. F. Møller, "A scaled conjugate gradient algorithm for fast supervised learning," *Neural Networks,* vol. 6, pp. 525-533, 1993.

[29] D. J. C. MacKay, "Bayesian interpolation," *Neural Comput.,* vol. 4, pp. 415-447, 1992.

[30] M. Riedmiller and H. Braun, "A direct adaptive method for faster backpropagation learning: the RPROP algorithm," in *IEEE International Conference on Neural Networks*, 1993, p. 586-591, pp. 586-591 vol.1.

[31] L. Baird and A. Moore, "Gradient descent for general reinforcement learning," presented at the Proceedings of the 1998 conference on Advances in neural information processing systems II, 1999.

[32] M. El-Melegy, *et al.*, "Robust Training of Artificial Feedforward Neural Networks," in *Foundations of Computational Intelligence (1)*, ed, 2009, pp. 217-242.

Comparison between Adaptive and Fuzzy Logic Controllers for Advance Microwave Biodiesel Reactor

W.A.Wali, J.D.Cullen, K.H.Hassan, A.Mason, A.I.Al-Shamma'a
Environment, Sustainable and Renewable Technologies Center (BEST)
School of the Built Environment, Liverpool John Moores University, Byrom Street, Liverpool L3 3AF,U.K
E-mail: W.Wali@2009.ljmu.ac.uk

***Abstract*- Biodiesel reactor is the heart of biodiesel system. These reactors involve a highly complex set of chemical reactions and heat transfers. The high nonlinearity requires an efficient control algorithm to handle the variation of operational process parameters and the effect of process disturbances efficiently. In this paper, Fuzzy logic and Adaptive controllers are compared for advance microwave biodiesel reactor. The process control is complex and nonlinear, the Adaptive control have longer time and unreliability in dealing with the system parameters including temperature, microwave power, liquid flow rate as well as the prediction of chemical reaction. The proposed fuzzy logic control will provide precise temperature control and faster warm-up phase with quicker response to disturbances with minimal overshoot and undershoot where Adaptive control techniques can not meet these extra challenges.**

A closed loop fuzzy and adaptive controllers are used to automatically and continuously adjust the applied power of microwave reactor under different perturbations. Labview based software tool will be presented and used for measurement and control of the full system, with real time monitoring.

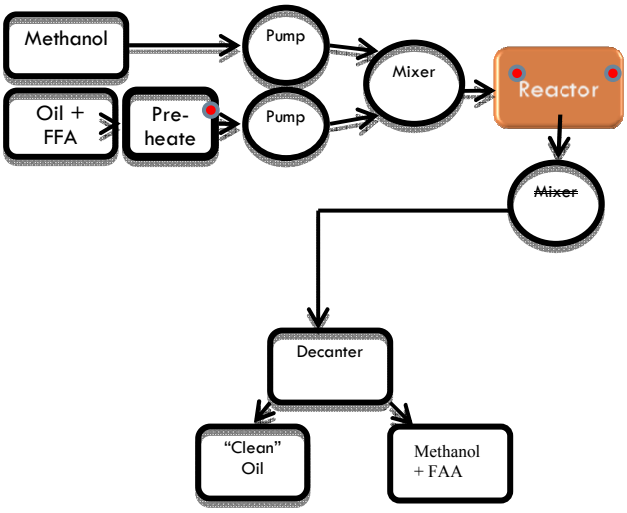


Fig.1 The general waste cooking oil conversion process.



Fig.2. biodiesel from waste oil.

I. INTRODUCTION

The increasing production of waste frying oils (WFO) from household and industrial sources is growing problem worldwide [1]. Oils are generally poured down the drain, resulting in problems for waste water treatment plants and energy loss. Fig.1 shows the general biodiesel production process and Fig.2 shows the production of biodiesel from waste oil.

*Biodiesel Rea*ctor

Diesel fuel that is derived from plant or animal oils [2]. It is synthesized by the reaction of triglyceride molecule (the main constituent of oils) with an acid or base catalyst [3]. The breadth of biodiesel production technologies has exploded along with the expansive growth of the industry in the past several years [4]. Novel process design provides a new way of thinking about the heating process. Conventional thermal heating relies on conduction current within the sample to provide an overall rise in temperature [4]. Energy consumption studies show that the continuous-flow preparation of biodiesel using microwave heating proves to be more energy efficient than the conventional synthesis of biodiesel in large tank reactor[4].

Microwave

The major advantage of using microwave for industrial processing are rapid heat transfer, volumetric and selective

heating, compactness of equipment, speed of switching on and off and pollution-free environment as there are no products of combustion [5]. Microwave chemistry has become increasingly more prominent in laboratories over the last decade, and has become a standard technique in the synthesis of organic compounds [6].

Microwave As Reactor

Most organic reactions requiring heat have been heated using traditional heat transfer equipment such as oil baths, sand baths or heating mantles. These techniques are rather slow and create a temperature gradient within the sample. Moreover, the hot surface of the reaction vessel may result in localized overheating leading to product, substrate and reagent decomposition when heated for prolonged periods. Microwaves, representing a non- ionizing radiation, influence molecular motions such as ion migration or dipole rotations, but not altering the molecular structure [7]. Polar solvent of low molecular weight and high dielectric constant irradiated by microwaves increase their temperature very rapidly, reaching boiling point in a short time. In biodiesel production using microwave irradiation, rapid heating is observed and very efficient heating can be obtained for shorter times, much greater than the overall recorded temperature of the bulk reaction mixture [7]. In these conditions with use catalysts enables organic reaction to occur expeditiously at ambient pressure, leads to a substantial reduction in the catalyst and solvent required for the transesterification reaction.

Control of the biodiesel system.

Because of many industrial processes are of a complex nature, it is difficult to develop a closed loop control model for this high level process. Also the human operator is often required to provide an on line adjustment which make the process performance greatly dependent on the experience of the individual operator. One of these systems is the control of biodiesel reactor, including the complex set of chemical reaction and heat transfer, and the system is subject to many unexpected disturbance during operation such as noise, parameter variation, model uncertainties, etc. The reactor has high nonlinearity, frequent overshoot of temperature and oscillation of its internal pressure. In this work a Fuzzy logic and Adaptive controllers are implemented and compared in advance microwave biodiesel reactor to maintain the temperature of reaction mixture at set points under disturbances.

Adaptive Control

Adaptive control has been the subject of active research for over three decades now, and the last ten years have seen an impressive growth in the availability of commercial adaptive control [8]. In the 1950s, it was motivated by problem of designing autopilots for aircraft operating at a wide range of speed and altitudes. The Adaptive Controller is a form of control in which the control parameters are automatically adjusted as condition change so as to optimize performance for systems to be controlled have parameter uncertainty and system dynamics experience unpredictable parameter variation as the control operation goes on.

There is a model reference Adaptive control(direct Adaptive control) and self tuning regulators Adaptive control (indirect Adaptive control) which the last one is in this work.

Fuzzy logic controller

Fuzzy system is one of the succeed controller used in the process control in case of model uncertainties [9]. It is initiated by the pioneering work of Mamdani and Assilian (1975) and emerged as one of the most active fruitful areas for research in the application of Fuzzy set theory, Fuzzy logic and Fuzzy reasoning [10]. Fuzzy logic control has been considered as an alternative to traditional control schemes implementation without relying on the detailed mathematical model of the plant to deal with complicated, ill defined and poorly mathematically understood processes by incorporating human control knowledge directly into the controlled system [10]. The work presented in this paper covers full design of Fuzzy logic controller.

Labview

Labview is a graphical programming language that has been widely adopted throughout industry academic and research labs as a standard of data acquisition and instrument control software. It is a powerful and flexible instrumentation and analysis software system [11]. Labview is short for **Lab**oratory **V**irtual **I**nstrument **E**ngineering **W**orkbench. Fig.3 shows the front panel for the biodiesel system in Labview. The control system, implemented in Labview, is required to control the flow reactor in such a way that it can be operated in a failsafe manner suitable for industry.

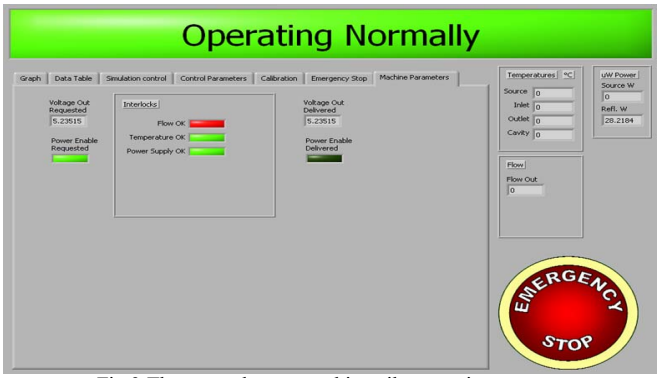


Fig.3 The general waste cooking oil conversion process.

In this work the two controllers are designed and implemented to online control the designed advance biodiesel microwave reactor system which convert waste cooking oil into biodiesel

II. *Experimental system setup*

Automated microwave system

The low energy automated microwave system will be used as a heating source for the reactor to produce biodiesel from waste cooking oil and animal fats. Microwave operation at frequency 2.45GHz is used to reduce chemical reaction time,

from hours under conventional heating, to minutes for the same volume of waste input. This novel microwave reactor is capable of operating at commercial production rates (kg/hr) instead of laboratory scale (g/day) as shown in Fig.4.

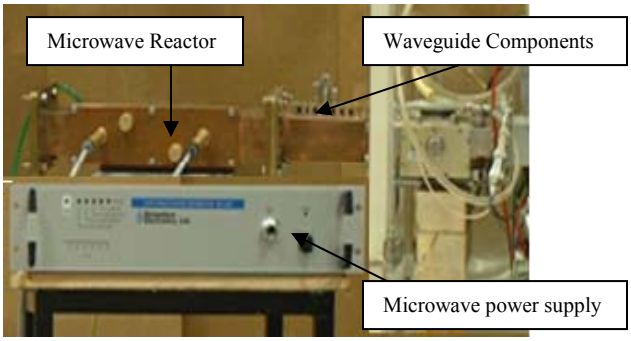


Fig.4 Novel microwave laboratory reactor heating system.

Laboratory biodiesel system *setup*

The biodiesel system as shown in Fig.5 was connected with computer through a compact DAQ, and data displayed using Labview. The Labview system has two main parts, the front panel and block diagram. The front panel provides the user interface for data inputs and outputs. The block diagram is responsible for the actual data flow between the inputs and outputs. The sensors have their reading captured using compact data aquistion and recorded in computer. A labview-based microwave biodiesel reactor control system was built in order to run Fuzzy and adaptive algorithms. All the changes in control system can be observed in real time and also user commands can be accepted during the process.

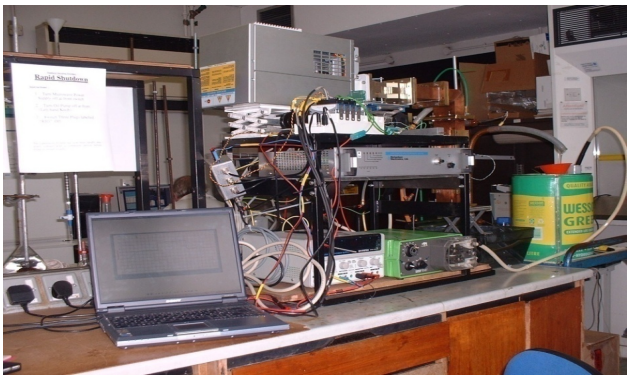


Fig.5 The biodiesel system.

III. Controllers

Fig.6 shows the close loop block diagram of biodiesel system with controller and Fig.7 shows the systems parameters under control. In this paper it was aimed that set point temperature tracking and online control under sudden changes in input flow rate of the oil in biodiesel system.

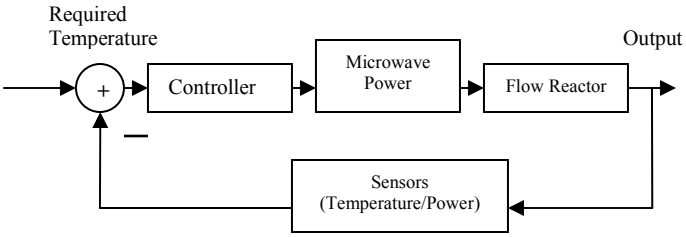


Fig.6 The close loop block diagram of biodiesel system with controller.

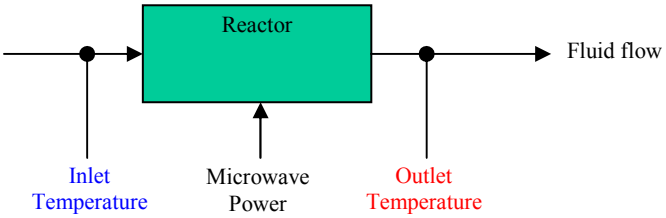


Fig.7 The systems parameters under control.

Adaptive controller design

Adapt means change a behavior to conform to new circumstance. So an Adaptive controller is a controller that can modify its behavior in response to changes in the dynamics of the process and character of the disturbances. Adaptive controller tunes its own parameters or otherwise modifies its control law so as to accommodate fundamental changes in the behavior of the process [12] . Fig. 8 shows the indirect self-tuning regulator controller block diagram.

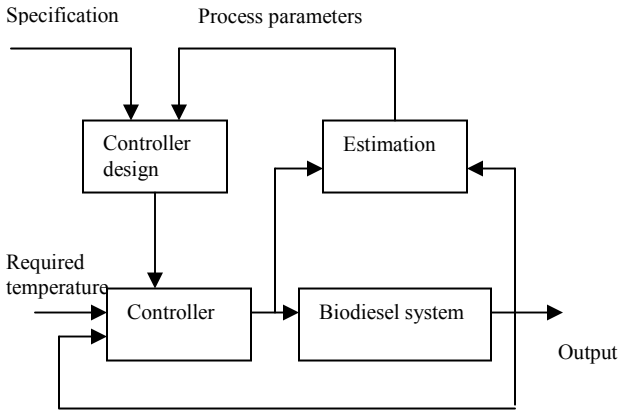


Fig.8 The indirect self-tuning regulator controller block diagram.

In labview programming, the adaptive controller has several of parameters to be taken into consideration:

1) Output power : parameter to be controlled
2) Output target : set point that is required
3) Temp Window : 'dead band' around the target point where the controller gain is not adjusted
4) Output Temperature : parameter that is required to be controlled
5) Source Temperature : temperature of the input oil

6) *Gain* : provides the output power from the temperature difference, i.e. gain* (output target – source temperature)
7) Pass response : how much the gain is adjusted on each pass through the controller (either increase or decrease)
8) Proportional response: proportional increase based upon the difference between actual and desired output temperatures (either increase or decrease)
9) Loop delay : the delay after the parameters are executed, before the loop restarts
The Adaptive controller algorithm process as flows:
On each pass through the loop the following commands are executed:
- If output temperature is within Output Target ± Temp Window then do not change gain otherwise adapt according to following rules
- If Output Temperature > Output target then
gain = gain - pass response
gain = gain - (proportional response * |output temperature – output target |)
- If Output Temperature < Output target then gain = gain + pass response
gain = gain + (proportional response * |output temperature – output target |)
Output power = gain * (output target – source temperature)
Wait for loop delay
Restart loop.

Fuzzy Logic controller design
In this research, Mamdani Fuzzy logic operations are applied. Mamdani fuzzy system is the main type examples of fuzzy inference systems. Fig.9 illustrates how a two-rule Mamdani fuzzy inference system derives their overall output Z when subjected to two numeric inputs x and y [13].

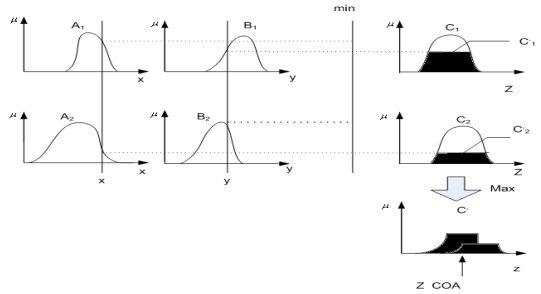


Fig.9 Mamdani Fuzzy Inference System
If x is A_1 and y is B_1 Then Z is C_1
If x is A_2 and y is B_2 Then Z is C_2

A Fuzzy controller is composed of three calculation steps [14].:
1) Fuzzification: the function of accepting input values and determining the degree of membership to some pre-select lingusitic terms.

2) Fuzzy Inference: consists of determing relationships based upon If-Then rules used to obtain more weighted outputs. These outputs are also linguistic variables in nature and have a nonlinear relationship.

3) Defuzzification: involves converting the output term into a crisp value such that it is compatible with all systems.

Fuzzy logic control design try accounting the human's knowledge about how to control a system without requiring a mathematical model. The basic block diagram for fuzzy controller is shown in Fig.10.

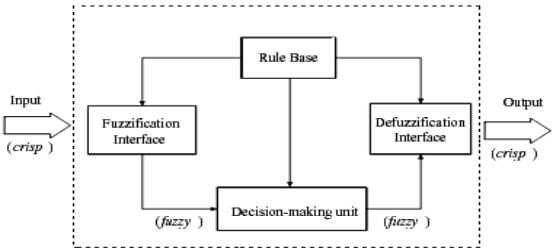
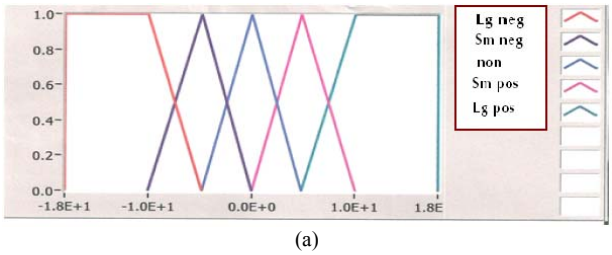
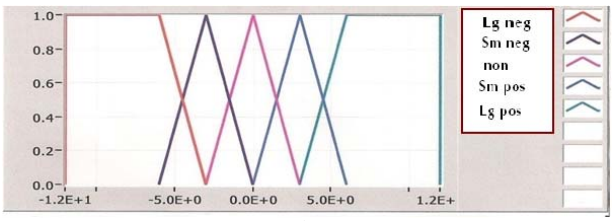


Fig.10 The basic block diagram for fuzzy controller

Fuzzy control based on Labview Fuzzy Toolkit. First Fuzzy input represents the error between measured temperature and set point. The second Fuzzy input represent the change in error. Fig.11 shows the membership function for error and change of error over the range of input variable values and linguistically describes the variables universe of discourse. Five membership functions are selected with triangle shape as follows : large positive, small positive, zero, small negative, large negative. The universe of discourse for the error and change of error from -18 to 18 and -12 to 12 respectively. The left and right half of the triangle membership functions for each linguistic label was chosen to provide membership overlap with adjacent membership functions.



(a)



(b)

Fig.11 Fuzzy inputs membership functions (a) error, (b) change of error.

Fuzzy logic controller output is delivered power which is applied to microwave reactor. Fig.12 shows the membership functions of the output linguistic variables of Fuzzy output.

Output variable is chosen to interval from -100 to 100 with seven triangle membership functions; large positive, medium positive, small positive, zero, small negative, medium negative, large negative.

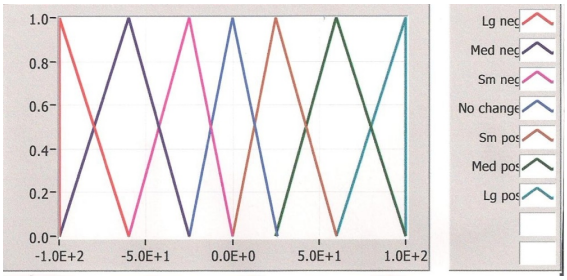


Fig.12 Membership functions of the output linguistic variables .

The rule base of the fuzzy controller gives the decision that in which of the five memberships function have to fire. Rule evaluation part has 25 fuzzy rule. Table 1 presents shows the Fuzzy logic control rules developed to the proposed system. Selection of the number of membership functions and control rules are based on process knowledge and intuition. The main idea is to define partitions over the plant operating region that will adequately represent the process variables.

TABLE I
Fuzzy Rules Table For Biodiesel System

Δe \ e	Lg neg	Sm neg	Zero	Sm pos	Lg pos
Lg neg	Lg neg	Med neg	Med pos	Med neg	Sm pos
Sm neg	Med neg	Sm neg	Sm pos	Zero	Sm pos
Zero	Sm neg	Sm neg	Zero	Sm pos	Sm pos
Sm pos	Sm neg	Zero	Zero	Sm pos	Med pos
Lg pos	Sm neg	Sm pos	Zero	Med pos	Lg pos

IV. Experimental results

The Fuzzy logic and Adaptive controllers were online implemented for our advanced biodiesel microwave reactor. All the experimental results are in (5000ms control sample interval) and (300 ml/min flow rate). The controllers subjected to a multiple set point tracking beginning from the nominal temperature value of 30°C and changing rise to 35°C then down to 30°C as shown in Fig.13. The Fuzzy logic controller successfully fast tracks the demands of reactor temperature setpoint accurately with minimum overshoot and undershoots. Fig.14 shows the controllers set point tracking beginning from the inlet temperature, no oscillations and no steady state error if it compared with the adaptive controller .
The controllers were then tested under an introduced disturbance in the feed to the flow rate of the reactor. After the start up of the processes, the reactor temperature was left regulated by the controllers at 30°C. The disturbance was then introduced. When the nominal feed in flow rate was reduced by 20%, it was observed that the Fuzzy controller was able to bring back the process to its initial set point of 30C, the adaptive controller was bring the system to the set point but with long time and steady state error as shown in Fig.15. For further test under disturbance, the input flow rate was reduced 10% then sudden rising by 30%, the Fuzzy controller shows a good ability to reject these disturbances.

VI. Conclusions

An advance control approach using Fuzzy logic and adaptive controllers were introduced for real time temperature control in biodiesel microwave reactor. Experimental results reported in this paper indicate that the Fuzzy control is able to regulate and tracking the reactor desired temperature precisely in minimal overshoot with fast worm –up phase. The disturbance in the form of varying flow rate in the process input poses good rejection by this controller.
Because of the system to be controlled is not identified; this leads to undesirable behavior for the indirect adaptive control underlying control criterion.

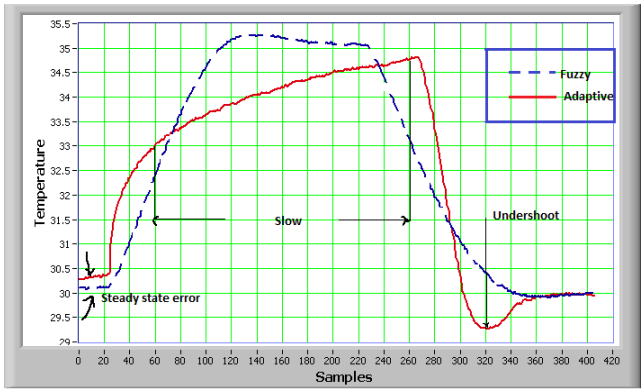


Fig.13 Online implementation of Fuzzy and adaptive (setpoint tracking).

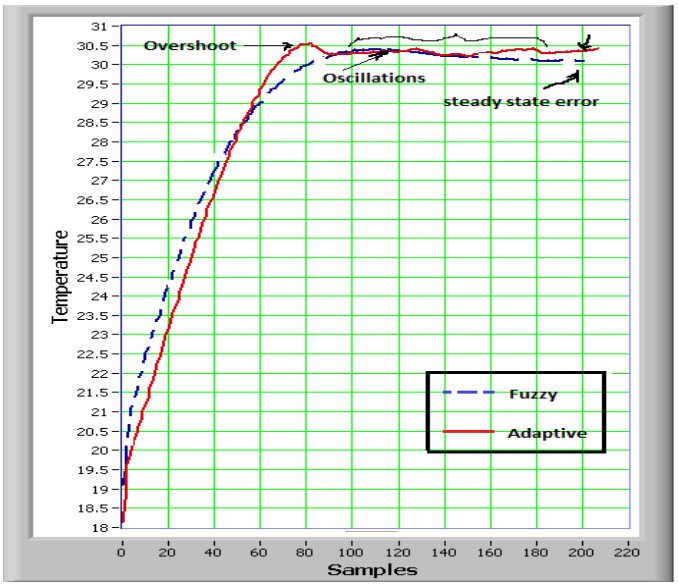
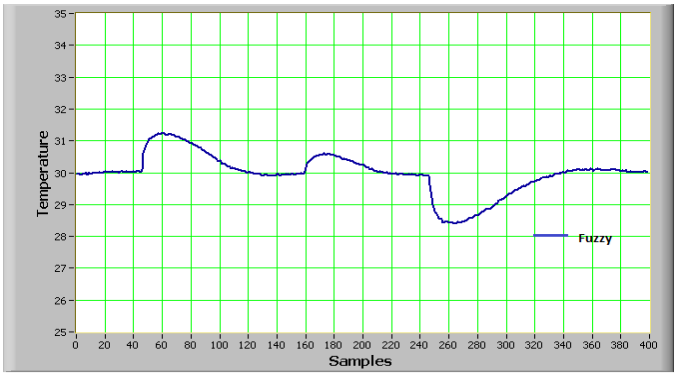
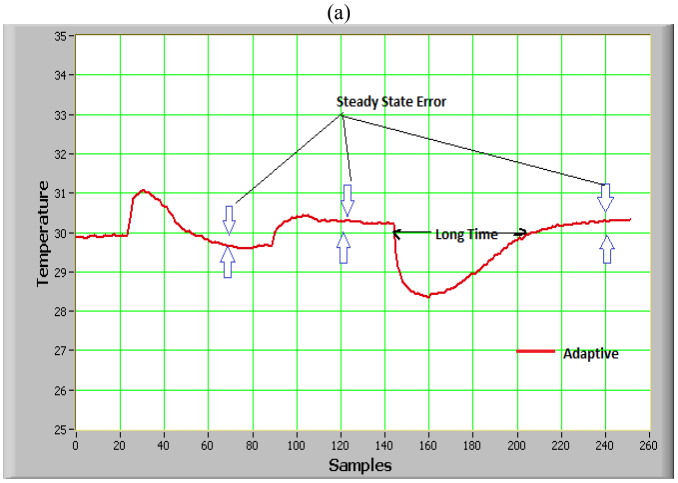


Fig.14 Fuzzy and adaptive controllers (setpoint tracking from inlet temperature).



(a)



(b)

Fig.15 Disturbance rejection of (a) Fuzzy and(b) Adaptive Controllers with change in the input flow rate (-20%, -10%, +30%).

REFERENCES

[1] T. Sabudak, M.Yildiz,“ Biodiesel Production from Waste Frying Oils and its Quality Control”, *Waste Management*, 2010, doi:10.1016/j.2010.01.007.

[2] V. Rudolph , Y.He “ Research and Development Trends in Biodiesel” *Dev. Chem. Eng. Mineral Process*, Vol.12, PP.461-474, 2004.

[3] Christopher J. Chuck, Chris D. Bannister, J. Gary Hawley, Matthew G. Davidsn, ” Spectroscopic Sensor Techniques Applicable to Real-Time Biodiesel Determination “,*Fuel*, Vol.89, PP.457- 461 , 2009.

[4] T. Mchael Barnard , Nicholas E. Leadbeater , “ Microwave Technology and Continuous –Flow Production”, *Biodiesel Magazine*, october 2007 Issue.

[5] A.C. Metaxas, Roger J. Meredith,” Industrial Microwave Heating*”, Peter Beregrinus Ltd.*, London, U.K. 1993, ISBN:0906048 89 3.

[6] G.P.Lewis, S.R. Wylie , A. Shaw, A.I. Al-Shamma’a, D Phipps, R. Alkhaddar, G . Bond, “Monitoring and Control System for Tuneable High Frequency Microwave Assisted Chemistry*”, Journal of Physics: Conference Series* 76 , 2007, doi:10.1088/1742-6596/76/1/0120 6596/76/1/012058.

[7] A. A.Refaat, S.T Elsheltawy, k.U. Sadek, “Optimum reaction time, performance and exhaust emissions of biodiesel produced by microwave irradiation”,*Int.J.Environ.Sci.Tech,* Vol.5, PP.315-322,2008.

[8] S.Sastry, M. Bodson, “Adaptive Control Stability, Convergence, and Robustness”,*Prentice-Hall,Inc.,* 1989.

[9] Saravanan S, Shubhalaxmi Kher, “Fuzzy Control of Multivariable Process by Modified Error Decoupling”, *ISA Transactions*, Vol.41, PP.437-444, 2002.

[10] K. Gowrishankar, Vasanth Elancheralath , “ Adaptive Fuzzy Controller to Control Turbine Speed”, *Ubicc Journals*, Vol.3, No.5, 2008.

[11] J.Travis , J.kring,”Labview for Every one Graphica Programming Mode Easy And Fan”, *Prentice Hall*, Third Edition 2007.

[12] J. H. Taylor, K. M. Akida,” Indirect Adaptive Model Predictive Control Of A Mechanical Pulp Bleaching Process”, *Nith IASTED International Conference on Control and applications*,2007.

[13] T. Takagi and M Sugeno "Fuzzy Identification of Systems and its Application to Modeling and Control", IEEE Transaction on Systems, Man, and Cybernetics,Vol. 15, PP. 116-132, 1985.

[14] D. Ruan,” Intelligent Systems: Fuzzy Logic Neural Networks and Genetic Algorithms”, *Kluwer Academic Publishers*,USA,1997.

Performance Studies of 802.11g for Various AP Configuration and Placement

Nurul I Sarkar and Eric Lo
School of Computing and Mathematical Sciences
Auckland University of Technology
Auckland, New Zealand
nurul.sarkar@aut.ac.nz

Abstract- **Using indoor radio propagation measurements, the impact of access point (AP) configuration as well as placement on throughput of IEEE 802.11g ("802.11g") wireless local area networks (WLANs) is investigated. By using a pair of wireless laptops and APs we conducted several experiments involving 802.11g computer links, which were carried out in a controlled environment at AUT University within the School of Computing and Mathematical Sciences office building. The AP configuration and placement is found to have the significant effect on the link throughput of 802.11g. Results obtained show that a different throughput performance be achieved with a different AP configuration and placement, the resulting throughput variation is found to be significant. By using an appropriate AP configuration and placement, an optimum system performance can be achieved.**

I. INTRODUCTION

There has been a significant growth in the deployment of 802.11-based WLANs worldwide in recent years. This growth is due to low-cost, simplicity in operation, and user mobility offered by the technology. A typical WLAN can be setup either as an ad-hoc or an infrastructure network [1]. An ad-hoc network is a peer-to-peer network that can be setup easily by linking two or more wireless stations ("clients") without any infrastructure and APs. In contrast, one or more APs are required to set up an infrastructure network. An AP coordinates transmission among the active clients in the network. Infrastructure-based networks are widely deployed in the organizations worldwide [2]. In this paper we consider an 802.11g infrastructure network to study its performance under various AP configurations and placements using radio propagation measurements.

To gain a better understanding of 802.11g AP configuration and to obtain unbiased results in an indoor environment, we first conducted radio propagation measurements (using real hardware/software) in a controlled room at the AUT University within the School of Computing and Mathematical Sciences office building. We then study the impact of AP placements on 802.11g throughput. An optimum network performance can be achieved by carefully configuring and placing APs. A study on the effect of AP configuration and placement on an 802.11g throughput is required to assist an efficient planning and deployment of such systems.

A detailed discussion of wireless networks, and of radio propagation, in general, can be found in numerous wireless networking literature [3-5]. The network throughput with 2.4 GHz products as well as monitoring of actual exchange of frames has been investigated in [6]. Pelletta and Velayos [7] presented a method of measuring the maximum saturation throughput of 802.11 WLANs. They also analyzed the performance of five 802.11b APs. The AP selection strategy for the (re)association procedure in large-scale WLANs is investigated in [8]. Many previous studies in indoor WLAN deployments have adopted the engineering approach of carefully characterizing the radio propagation channel by modeling the physical environment and measuring the properties of the received signal [9-13].

In this paper we obtain some insights into 802.11g link throughput under various AP configurations and placements in a typical indoor environment (at the AUT University) without using any complex mathematical modeling or radio channel characterization. Our approach is straightforward. Using a pair of wireless laptops and APs, we study the effect of AP configurations as well as placements on the file transmission time as well as the link throughput of 802.11g.

The remainder of this paper is organized as follows. Section II provides an overview of 802.11. The AP configuration scenarios are described in Section III. The experimental details and summary of findings are presented in Section IV. Section V highlights measurement accuracy and validation. Section VI concludes the paper.

II. IEEE 802.11 TECHNOLOGY DEFINED

The IEEE released the 802.11 standard for WLANs in 1997. This standard supports data rates of 1 and 2 Mbps. It defines protocols for medium access control (MAC) layer and physical layer (PHY) transmissions in the unlicensed 2.4 GHz (2.4-2.4835 GHz in North America). The standard employs frequency-hopping spread spectrum (FHSS) and direct-sequence spread spectrum (DSSS) techniques for radio transmission [14].

After a successful implementation by various companies, including Lucent Technologies, an amendment was made for higher data rates and the resulting standard was 802.11b with data rates of 5.5 and 11 Mbps. 802.11b differs from the 802.11 in the MAC layer only (keeping the physical layer unchanged), and retains compatibility with 802.11. The 802.11b was approved in 1999 and during that year the term wireless fidelity (Wi-Fi) was introduced. 802.11b has proven to be very successful in the commercial domain. In parallel with the 802.11b, another variant of the original 802.11 called 802.11a was introduced in 1999. The 802.11a differs from both 802.11 and 802.11b by using 5 GHz band rather than 2.4 GHz. The 5 GHz is unlicensed in the USA but not in many other countries especially in Europe.

The 802.11b adopts high rate direct sequence spread spectrum (HR/DSSS) and complementary code keying (CCK) modulation schemes in providing high data rates (5.5 and 11 Mbps). Since 802.11b operates in the 2.4 GHz band, it also adopts DSSS to support low data rates (1 and 2 Mbps).

The 802.11a [15] supports up to 54 Mbps by using orthogonal frequency division multiplexing (OFDM). The use of high-frequency band (5 GHz) in 802.11a has an advantage of having less signal interference than the 802.11b. However, this high carrier frequency in 802.11a results in limited transmission range than the 802.11b [16].

To support the growing applications of wireless and mobile communications, high performance networks are required. The 802.11g was introduced in June 2003 operating at 2.4 GHz. 802.11g is one of the most popular WLANs worldwide. It offers the combined advantages of 802.11a and 802.11b [17]. For example, high data rate (up to 54 Mbps), longer transmission range, low-cost, and backward compatible with the 802.11b. The 802.11g has three compulsory components: Extended Rate Physical (ERP)-DSSS, ERP-CCK and ERP-OFDM, and two optional components: ERP-PBCC and DSSS-OFDM [18]. The ERP-DSSS and ERP-CCK module are backward compatible with the 802.11b. The ERP-OFDM is a core component of the 802.11g. As 802.11a, the 802.11g uses OFDM as spread spectrum technology to provide high data rates. In DSSS-OFDM, DSSS is used for header to encode packet and OFDM for encoding payload. DSSS-OFDM provides backward compatibility with the 802.11b. More details about 802.11g can be found in [19]. The AP configuration scenarios are described next.

III. AP Configuration Scenarios

The following four AP configuration scenarios are considered in this study: (1) AP mode; (2) WDS mode; (3) WDS with AP mode; and (4) AP mode with Ethernet connection.

Most of the commercially available APs have an Ethernet port for linking them to another AP or an Ethernet switch [20]. We conducted experiments using the 802.11g wireless APs (D-Link DWL-2100AP). The AP configuration is generally straightforward. The AP can be configured using the vendor supplied software that comes with the device. Figure 1 shows the main D-Link AP configuration interface.

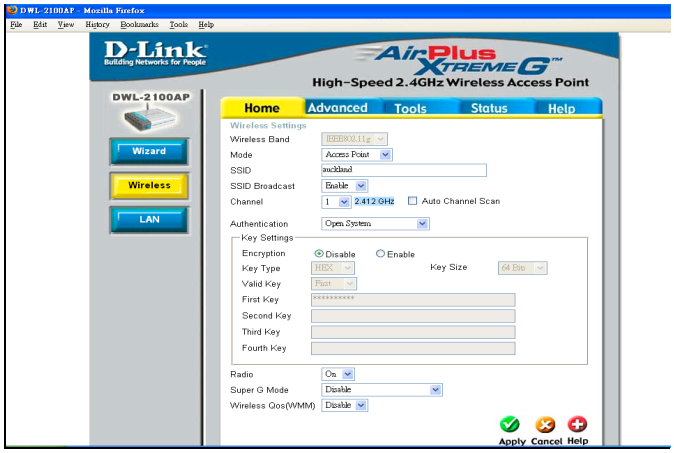


Figure 1. Screenshoot of AP configuration interface.

By using the above interface (Fig. 1), one can easily set up SSID (service set identifier), channel, user authentication, encryption, SSID broadcast, and quality of service (QoS). In the experiments (Section IV) both encryption and wireless QoS were disabled. The AP mode was configured using default settings for 802.11g AP. For WDS and WDS with AP modes, the remote AP MAC address was used in the remote AP selection menu. The four AP configurations are briefly described below.

AP mode: The throughput measurement scenario for 'AP mode' configuration is shown in Fig. 2(a). This configuration is a popular one for use in office and home environments. In this configuration, the AP acts as a coordinator in which wireless stations ('clients') are link to the AP for communications. The AP receives data from a wireless client and forwards it to another client.

WDS mode: The network scenario for 'WDS mode' configuration is shown in Fig. 2(b). In this configuration, an AP acts as a wireless bridge only and hence the wireless clients cannot associate with the AP. In the experimentation, two Ethernet Cat 5e cables were used for linking two wireless clients to the AP. This configuration can be used for connecting two or more wireless networks located on multiple buildings, which is a common scenario for a campus network.

WDS with AP mode: The AP configuration using 'WDS with AP mode' is shown in Fig. 2(c). In this configuration the AP acts as both the coordinator and wireless bridge. Therefore, this configuration has the combined advantages of AP mode and WDS mode. The radio signal coverage extension is also an advantage of using WDS with AP mode configuration.

AP mode with Ethernet connection: The network scenario for AP mode with Ethernet connection is shown in Fig. 2(d). In this configuration, the APs are configured as AP mode and a Cat 5e UTP cable is used for linking two APs.

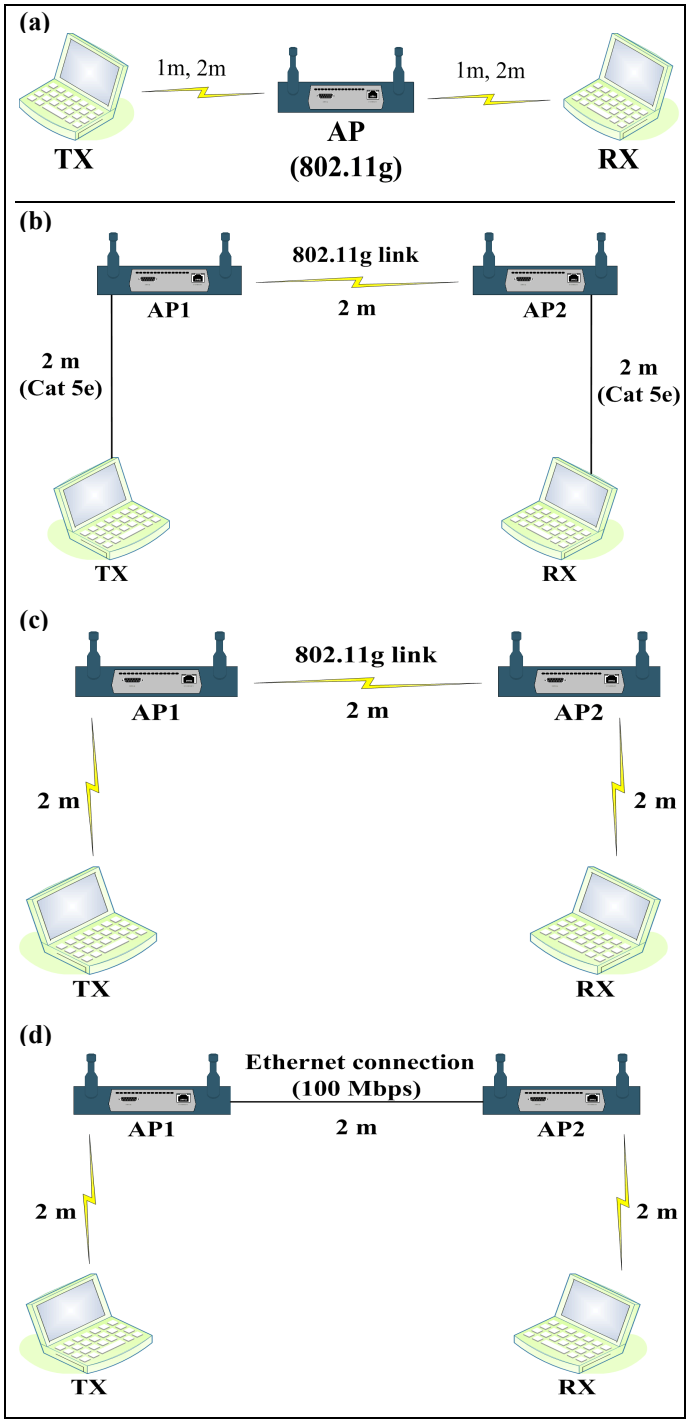


Figure 2. AP configuration scenarios. (a) AP mode; (b) WDS mode; (c) WDS with AP; and (d) AP with Ethernet connection.

IV. Experiment Details and Results

The 802.11g AP throughput measurements were conducted in the staff meeting room (control environment) located on the first floor of WY building at AUT University (Fig. 3). The staff meeting room is made of plasterboards with a glass door, and its dimension is 4m×3m.

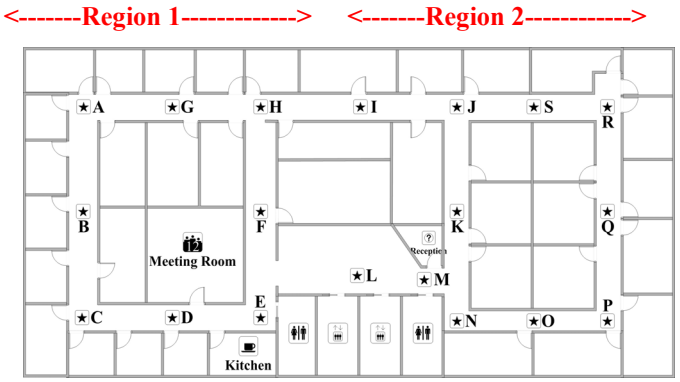


Figure 3. Layout of floor 1 of WY Building and measurement locations.

Two wireless laptops with identical configuration (Intel Celeron 2.4 GHz; 512 MB RAM; MS Windows XP Professional) were used in the experiment. The IEEE 802.11g wireless adapters were D-Link DWL-G132 (54 Mbps) USB cards (omnidirectional) with a power output of 15 dBm [21]. The wireless APs were D-Link DWL-2100AP [20].

One of the laptops was set as the transmitting-antenna (TX) and the other as the receiving-antenna (RX). The transmitting and receiving laptops and APs were positioned on trolleys (1 m height) during the experimentation. The distance between TX and AP, AP and RX, and two APs was set to 2 m each, to obtain strong received signal strengths (RSSs). Having conducted experiments under strong RSSs avoided retransmission and packet losses due to bit error-rate (BER).

By conducting measurements in a controlled environment minimizes the effect of external noise and interference on system performance. Network throughput is the main performance metric considered in this study.

Several data files were sent from the TX to the RX (through APs) using the 'Send Files' feature of the Colligo TM Workgroup Edition 3.2 (www.colligo.com), which allows us to obtain the file transmission time. For each observation, we record the file transmission time and throughput (in Mbps) was computed by dividing the file size (Mbits) with the total transmission time (seconds).

The empirical results for the AP mode configuration are summarized in Table I. The four different data files are transmitted serially from the TX to the RX is indicated in column 1. The file transmission time and the corresponding link throughput for the TX-AP separation of 1 m and 2 m are shown in column 2, 3, 4, and 5, respectively.

As shown in Table I, the effect of file size on the 802.11g link throughput is not very significant. We observe that the mean throughput for the TX-AP separation of 1m is about 21% lower than the throughput obtained for TX-AP separation of 2 m. This decrease in throughput is due to the fact that when two wireless stations (TX and AP) are closely located (up to 1 m)

resulted in weak RSS and consequently low throughput is achieved.

The propagation measurement results for WDS mode, WDS with AP, and the AP mode with Ethernet connection are summarized in Tables II, III, and IV, respectively.

TABLE I
MEASUREMENT RESULTS FOR AP MODE

File Size (MB)	TX-AP separation: 1 m		TX-AP separation: 2 m	
	Time (seconds)	*Throughput (Mbps)*	*Time (seconds)*	*Throughput (Mbps)*
109	107.7	8.149	83.9	10.461
256	248.7	8.252	200.5	10.236
263	258.9	8.150	202.4	10.425
274	271.6	8.079	212.9	10.306
Mean Throughput (Mbps)	8.157		10.357	

TABLE II
MEMEASUREMENT RESULTS FOR WDS MODE

File Size (MB)	TX-AP separation: 2m	
	Time (seconds)	*Throughput (Mbps)*
109	46.7	18.794
256	104.7	19.603
263	108.4	19.465
274	113.9	19.264
Mean Throughput (Mbps)		19.281

TABLE III
MEMEASUREMENT RESULTS FOR WDS WITH AP MODE

File Size (MB)	TX-AP separation: 2m	
	Time (seconds)	*Throughput (Mbps)*
109	151.5	5.793
256	355.2	5.778
263	369.1	5.717
274	382.7	5.733
Mean Throughput (Mbps)		5.755

For ease of comparison and interpretation, the empirical results for four AP configurations as shown in Tables I to IV are compared in Table V. The effect of data file size on the 802.11g throughput performance is not very significant for all four AP configurations studied (Table V). Of the four AP configurations, the highest (19.281 Mbps) and the lowest (5.755 Mbps) throughputs are obtained for WDS mode and WDS with AP mode, respectively.

TABLE IV
MEMEASUREMENT RESULTS OF AP MODE WITH ETHERNET CONNECTION

File Size (MB)	TX-AP separation: 2m	
	Time (seconds)	*Throughput (Mbps)*
109	78.7	11.152
256	174.6	11.755
263	168.7	12.507
274	182.3	12.036
Mean Throughput (Mbps)		11.863

TABLE V
COMPARISON OF THROUGHPUTS OBTAINED FOR FOUR AP CONFIGURATIONS

File Size (MB)	Throughput (Mbps) of four AP configurations			
	AP mode	WDS with AP	AP with Ethernet	WDS mode
109	10.461	5.793	11.152	18.794
256	10.236	5.778	11.755	19.603
263	10.425	5.717	12.507	19.465
274	10.306	5.733	12.036	19.264
Mean Throughput (Mbps)	10.357	5.755	11.863	19.281

By comparing the AP mode with Ethernet connection and WDS with AP mode, we observe that the mean throughput obtained for AP with Ethernet connection is much higher than the throughput obtained for WDS with AP mode. This increase in throughput is as a result of an Ethernet (100 Mbps) link between two APs which handles more traffic loads.

By comparing the AP mode and the WDS with AP mode, we observe that the mean throughput for the AP mode (10.357 Mbps) is significantly higher than the throughput obtained for WDS with AP mode (5.755 Mbps). This increase in throughput is mainly due to the single-hop communication between the TX and the RX.

TABLE VI
MEAN THROUGHPUT OF 802.11G FOR DIFFERENT AP POSITIONS

AP position	Region 1 Mean TP (Mbps).	Region 2 Mean TP (Mbps).	Mean TP (Mbps).
A	8.838	3.857	6.384
G	8.554	5.006	6.780
H	6.935	4.845	5.890
F	6.964	4.273	5.619
**E-3m	8.949	5.617	7.283
I	7.043	6.631	6.837
L	6.972	6.823	6.898
J	5.767	8.972	7.369
K	4.072	7.239	5.655
**N-3m	4.776	10.085	7.430
R	5.305	8.820	7.062

** E-3m: 3 meters away from the measured point E
** N-3m: 3 meters away from the measured point N
TP: Throughput

The effect of AP placements on 802.11g throughput is demonstrated in Table VI. The mean throughputs of Region 1 (i.e. left-hand side of the office block in Fig.3) are slightly better for AP positions at A, G and E-3m (3 m away from the measured point E). For Region 2 (right-hand side of the office block), the higher throughputs are achieved when the AP was placed at J, R and N-3m. The throughputs at I and L are 6.837Mbps and 6.898 Mbps, respectively which are not adequate to cover both regions of the office block. It was observed that multiple APs could provide better throughputs and coverage than a single AP in the office block.

TABLE VII
COMBINED EFFECT OF AP CONFIGURATION AND PLACEMENT ON THROUGHPUT

AP position in Fig.3	AP configuration	AP separation (m)	Throughput (Mbps)
A-R	APs configured as WDS with AP mode	32	3.235
A-J		21	3.663
G-R		26	5.281
G-J		17	4.271
E-3m-N-3m		12	5.610
E-3m-N-3m	AP mode (Cat5 cable linking two APs)	12	14.834

The combined effect of AP configuration and placement on 802.11g throughput is shown in Table VII. When APs are configured as "WDS with AP" mode, higher throughputs are achieved for APs at E-3m and N-3m than any other positions. This is because of the shorter AP separation at E-3m-N-3m and also it had favorable (i.e. less harsh) radio propagation environment at these locations. This clearly shows that the AP position/placement has a significant impact on throughput.

By comparing the last two rows of Table VII, one can observe that AP configuration has a significant effect on 802.11g throughput. For example, when two APs are configured as "AP mode" and a Cat 5 Ethernet cable is linked them, a significantly higher throughput is achieved (compared to the throughput obtained under WDS with AP mode).

V. MEASUREMENT ACCURACY AND VAIDATION

The following factors are considered to improve the accuracy of the propagation measurement results.

- **People movement:** The measurements were conducted after hours and weekends to avoid the impact of the movement of people on system performance.
- **Co-channel interference:** To reduce the impact of co-channel interference on system performance, all external radio sources were detected and the experimental APs were adjusted accordingly prior to measured data collection.
- **Validation:** The propagation measurements were repeated several times to ensure the correctness of the measured data. The throughputs presented in Section IV closely agree with the results obtained from data sheet for D-link cards and APs [20, 21]. In addition, the measurement results obtained from this study were compared with the work of other network researchers for correctness [9, 22-24].

VI. CONCLUSIONS

This paper investigated the impact of AP configuration as well as placement on 802.11g throughput in an obstructed office block. Empirical results have shown that of the four AP configurations studied, WDS offered the highest and the WDS with AP mode has the lowest throughput and the throughput difference between these two configurations is about 70%. AP with an Ethernet connection offered slightly better mean throughput than the throughput obtained for AP mode. The combined effect of AP configuration and placement on 802.11g throughput is found to have significant. The throughput of an 802.11g can be optimized by carefully configuring and placing APs during WLAN deployments.

An investigation of the impact of WDS configuration using an omnidirectional antenna in the outdoor environment is planned as an extension of the present study.

ACKNOWLEDGMENT

The financial support provided by AUT University and UTM (Malaysia) for the presentation of this work is greatly acknowledged.

REFERENCES

[1] J. Khan and A. Khwaja, *Building Secure Wireless Networks with 802.11*. Indianapolis: Wiley Publishing, Inc., 2003.

[2] A. R. Prasad, N. R. Prasad, K. A., H. Moelard, and A. Eikelenboom, "Indoor wireless LANs deployment," presented at the 51st IEEE Vehicular Technology Conference (VTC'00), May 15-18, 2000, pp. 1562-1566.

[3] T. S. Rappaport, *Wireless communications: principles and practice*, 2nd ed. Englewood Cliffs, NJ: Prentice-Hall, 2002.

[4] W. Stallings, *Data and computer communications*, 8th ed. New Jersey: Prentice Hall, 2007.

[5] J. F. Kurose and K. W. Ross, *Computer networking: a top-down approach*, 4th ed. New York: Addison Wesley, 2008.

[6] A. Kamerman and G. Aben, "Throughput performance of wireless LANs operating at 2.4 and 5 GHz," presented at 11th IEEE International Symposium on Personal, Indoor and Mobile Radio Communications (PIMRC), September 18-21, 2000, pp. 190-195.

[7] E. Pelletta and H. Velayos, "Performance measurements of the saturation throughput in IEEE 802.11 access points," presented at Third International Symposium on Modeling and Optimization in Mobile, Ad Hoc, and Wireless Networks, 2005, pp. 129-138.

[8] D. Lei, B. Yong, and C. Lan, "Access point selection strategy for large-scale wireless local area networks," presented at the IEEE Wireless Communications and Networking Conference (WCNC'07), March 11-15, 2007, pp. 2161-2166.

[9] T. M. Schafer, J. Maurer, and W. Wiesbeck, "Measurement and simulation of radio wave propagation in hospitals," presented at IEEE 56th Vehicular Technology Conference (VTC '02-Fall), September 24-28, 2002, pp. 792-796.

[10] S. S. Ghassemzadeh, R. Jana, C. W. Rice, W. Turin, and V. Tarokh, "Measurement and modeling of an ultra-wide bandwidth indoor channel," *IEEE Transactions on Communications*, vol. 52, no. 10, pp. 1786-1796, 2004.

[11] D. Pena, R. Feick, H. Hristov, and W. Grote, "Measurement and modeling of propagation losses in brick and concrete walls for the 900-MHz band," *IEEE Transactions on Antennas and Propagation*, vol. 51, no. 1, pp. 31-39, 2003.

[12] D. C. K. Lee, M. J. Neve, and K. W. Sowerby, "The impact of structural shielding on the performance of wireless systems in a single-floor office building," *IEEE Transactions on Wireless Communications*, vol. 6, no. 5, pp. 1787-1695, 2007.

[13] D. Xu, J. Zhang, X. Gao, P. A. Zhang, and Y. A. Wu, "Indoor office propagation measurements and path loss models at 5.25 GHz," presented at the IEEE 66th Vehicular Technology Conference (VTC-2007 Fall), September 30 - October 3, 2007, pp. 844-848.

[14] "IEEE 802.11b WG, Part II: wireless LAN medium access control (MAC) and physical layer (PHY) specifications: high-speed physical layer extension in the 2.4 GHz band, IEEE 802.11b Standard," New York, April 1999.

[15] "IEEE 802.11a WG/D5.0, Part II: wireless LAN medium access control (MAC) and physical layer (PHY) specifications: high-speed physical layer in the 5 GHz band, IEEE 802.11a Standard," New York, April 1999.

[16] M. J. Ho, M. S. Rawles, M. Vrijkorte, and L. Fei, "RF challenges for 2.4 and 5 GHz WLAN deployment and design," presented at IEEE Wireless Communications and Networking Conference, 2002, pp. 783-788.
[17] C. Sunghyun and J. del Prado Pavon, "802.11g CP: a solution for IEEE 802.11g and 802.11b inter-working," presented at the 57th IEEE Semiannual Vehicular Technology Conference (VTC'03-Spring), April 22-25, 2003, pp. 690-694.
[18] IEEEStd802.11g-2003, "IEEE Std 802.11g-2003 (Amendment to IEEE Std 802.11, 1999 Edn. (Reaff 2003) as amended by IEEE Stds 802.11a-1999, 802.11b-1999, 802.11b-1999/Cor 1-2001, and 802.11d-2001)," 2003. Retrieved 18 February, 2007, from
[19] "IEEE 802.11g WG. Amendment to IEEE Std 802.11, 1999 Edn. (Reaff 2003) as amended by IEEE Stds 802.11a-1999, 802.11b-1999, 802.11b-1999/Cor 1-2001, and 802.11d-2001. IEEE 802.11g Standard," New York, 2003.
[20] *D-Link Wireless Access Point (802.11 b/g) DWL-2100AP*. Retrieved March 15, 2010, from http://www.dlink.com/products/
[21] *D-Link Wireless USB Adapter (802.11g) DWL-G132*. Retrieved March 15, 2010, from http://www.dlink.com/products/
[22] P. C. Ng and S. C. Liew, "Throughput analysis of IEEE 802.11 multi-hop ad hoc networks," *IEEE/ACM Transactions on Networking*, vol. 15, no. 2, pp. 309-322, 2007.
[23] M. K. Awad, K. T. Wong, and Z.-B. Li, "An integrated overview of the open literature's empirical data on the indoor radiowave channel's delay properties " *IEEE Transactions on Antenna and Propagation*, vol. 56, no. 5, pp. 1451-1468, 2008.
[24] N. I. Sarkar and K. W. Sowerby, "Wi-Fi performance measurements in the crowded office environment: a case study," presented at the 10th IEEE International Conference on Communication Technology (ICCT ' 06), Guilin, China, November 27-30, 2006, pp. 37-40.

Implementation of VoIP over Malaysian Research and Education Network (MYREN) Emulator Testbed

Husna Zainol Abidin, Muhammad Imran Ramlan, Ahmad Ihsan M. Yasin
Faculty of Electrical Engineering
Universiti Teknologi MARA,
40450 Shah Alam, Selangor, Malaysia
E-mail:husnaza@salam.uitm.edu.my

Abstract—**Quality of Service (QoS) of a network has become the core research area in a computer communication field. Normally researchers will be using simulation software to carry out their research works. However, it is found that simulation software has its own limitations as it does not really reflect the actual network environment. Thus, most research and development works now are exploiting emulation technology to replicate the real network environment by injecting real traffic into the network model. This paper describes the implementation of an emulator testbed for Voice over Internet Protocol (VoIP) transmitted over the Malaysian Research and Education Network (MYREN). The emulator software used in this paper is known as WAN Emulator (WANem) and it is found that the QoS obtained from the emulator are considered acceptable.**

Keywords- **VoIP, MYREN, Emulator, WANem, testbed, performance, QoS**

I. INTRODUCTION

Voice over Internet Protocol (VoIP) has become one of the popular applications nowadays as the Internet usage has increased for various purposes. VoIP delivers voice communication over an IP network such as the Internet or other packet-switched networks. In VoIP, the voice signal is digitized, compressed and sliced into packets which will be sent with other packets across the packet switched network. Packets will be re-assembled and converted back to analog signal as a normal sound voice call at the receiver. There are two protocols that are normally used to transmit this voice signal which are known as Session Initiation Protocol (SIP) and Real-time Transport Protocol (RTP) [1]. SIP is an application-layer control protocol that can establish, modify and terminate multimedia sessions or calls [2] while RTP provides end-to-end network transport functions which is suitable for transmitting real time data over multicast or unicast network services [3].

Codec is used to convert an analog voice signal to digitally encoded version. There are different types of codec with different sound quality, bandwidth required, delay, the computational requirements and others. Thus, codec will be chosen based on the network that will be used to transmit the voice signal.

The National Research and Education Network (NREN) is a network that is dedicated for research and education purposes within a country. It is supported by a high-speed backbone network where consequently, researchers and educators will be provisioned with a higher bandwidth network with no interruption from background traffic. If NRENs are properly implemented, it could be used in future as a testbed for new technologies, applications and governing policies that will lead to a larger national network [4]. MYREN is the Malaysian Research and Education Network used by researchers for collaborative research [5]. It offers a high bandwidth network where researchers would be able to carry out their research projects involving data-intensive applications as well as sharing resources across the network. The network can also be used as a platform for the researchers to run a pilot test and to validate the findings prior to the deployment into the market without jeopardizing the main network in their respective institutions. As depicted in Figure 1, MYREN currently connects eighteen members that consists of universities and research institutes.

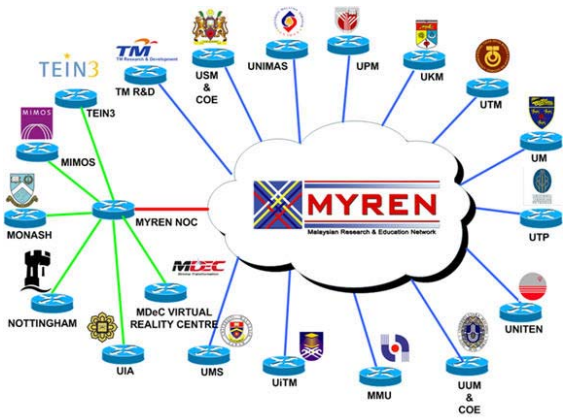


Figure 1. MYREN Topology [2]

This paper describes the implementation of an emulator testbed that replicates the VoIP communications between Universiti Teknologi MARA (UiTM) and Universiti Tenaga Nasional (UNITEN) via the MYREN link. It is envisaged that, with this emulator testbed, the real MYREN network will not

be interrupted if researches wish to test their findings on VoIP research. The rest of the paper is organized as follows. Section II will discuss some related works on emulator testbed that have been done by other researchers while Section III focuses on the development process. Results are presented in Section IV while Section V will finally conclude the whole paper.

II. RELATED WORKS

Researches carried out in the area of computer networking are widely focusing on the traffic performance or normally known as Quality of Service (QoS). Simulation is well known for its specialty in assisting researchers to perform their research and development works compared to analyzing complex mathematical modeling. However, simulation has its own limitations as it does not really reflect the actual network environment. Thus, most researchers are now deploying the emulator technology. Emulator replicates real network where real traffics will be injected into the emulated network to represent the actual network environment.

Shuai et al. in [6] study the QoS parameters and video quality scores using a network emulator called NIST Net while Shin et al. compare results obtained from simulator and emulator of Network Simulator (NS2) [7][8]. United States Army Research Laboratory (ARL) and Naval Research Lab (NRL) have come out with a mobile ad hoc network emulator software called MANE or Mobile Ad Hoc Network Emulator as presented in [9] and [10]. On top of that, an emulator software known as Wireless IP Scalable EmulatR (WISER) has been deployed by Kaplan et al. in reference [11] to replicate a mobile ad hoc network. Kumar et al. in their paper [12] stated that, network emulation studies are preferred during the design phase of a product design. Thus they have developed a WiMAX emulation testbed to benchmark the streaming multimedia QoS.

III. METHODOLOGY

The topology of this project is based on the real network as shown in Figure 2. As depicted in Figure 3, the testbed consists of a switch, an Internet Protocol Private Branch Exchange (IP PBX) server, two hosts that represent UiTM and UNITEN with softphone application installed and finally an emulator software called Wide Area Network Emulator (WANem) that controls the properties of the network. A router is needed to let the traffic pass trough VoIP server before reaching the end user. The testbed components will be briefly described in the following subsections.

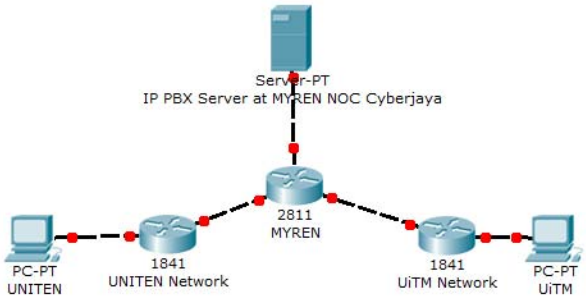


Figure 2. Real Network Topology

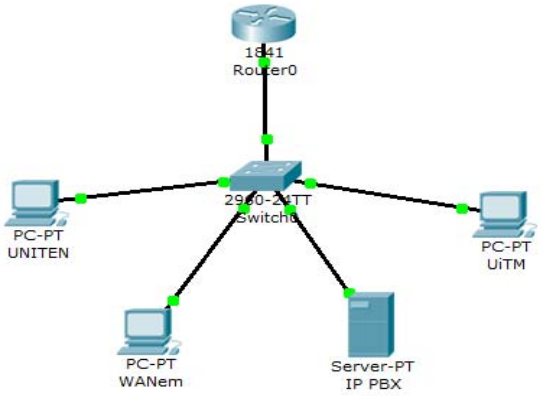


Figure 3. Emulator Testbed Topology

A. *Trixbox (IP PBX)*

Trixbox is a line of Asterisk-based IP-PBX server [13]. It is an open source software. Rebooting the Compact Disc (CD) will prompt the installer to automatically format the hard disk and copy all required packages for it to work as an IP PBX server. Initially, user needs to create a root password before copying the installation package file. Next, the static IP address of Trixbox need to be set. Maintanance password is also needed to enable the remote access to Trixbox. Figure 4 illustrates the remote access Graphical User Interface (GUI) of Trixbox and as shown in Figure 5, all softphones will be assigned with a unique extension .



Figure 4. Trixbox GUI from Remote Access

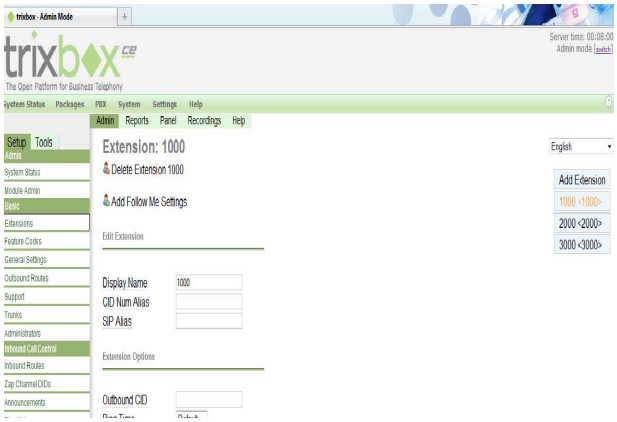


Figure 5. Trixbox Extension Setup

B. *X-Lite (Softphone)*

There are many types of softphone available. An open source software called X-Lite has been chosen for the softphone because it is easy to use, have all codecs needed and easy to setup. Moreover, X-Lite also support video calls. Figure 6 and Figure 7 show the interface and extension setting of X-Lite softphone.



Figure 6. X-Lite Softphone

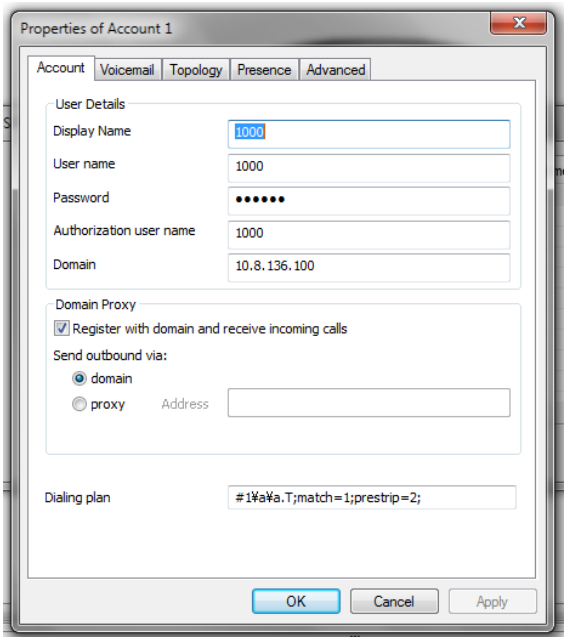


Figure 7. Extension Setting

C. *Wide Area Network Emulator (WANem)*

WANem is a Wide Area Network Emulator [14] that provide a real experience of a Wide Area Network (WAN) or Internet, environment which is normally used for teaching and research purposes. WANem allows the application development team to setup a transparent application gateway which can be used to simulate WAN characteristics such as delay, packet loss, jitter and many more. WANem need to be used on a workstation to emulate the network where it only needs to be boot from the CD. After the emulator has been boot, user will need to set its IP address. Then, the emulator can be remote access from other computer by entering its IP address on internet browser as shown in Figure 8.

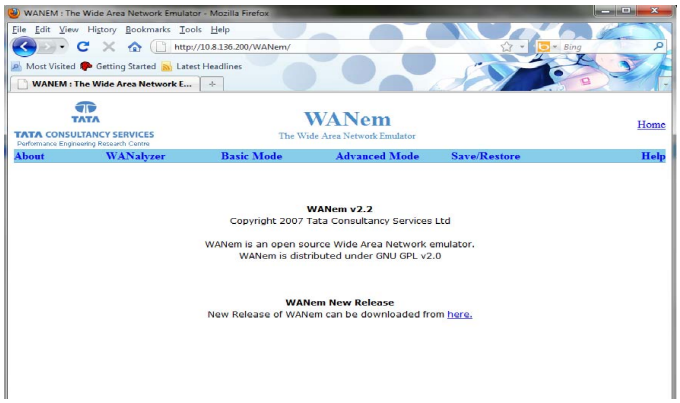


Figure 8. WANem GUI

This emulator contains two modes of emulation known as Basic and Advance. It also contains one analyzing mode known as WANalyzer mode. Basic mode only allows user to enter the bandwidth and delay of traffic but the Advance mode will give more freedom where user can modify more properties. WANem also provide its own analyzer which can measure latency, packet loss, jitter and available bandwidth. Figure 9 and Figure 10 illustrate the Basic and Advance Modes respectively.

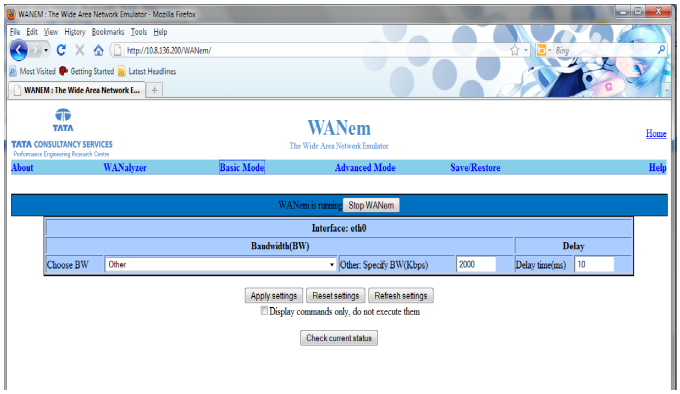


Figure 9. WANem Basic Mode

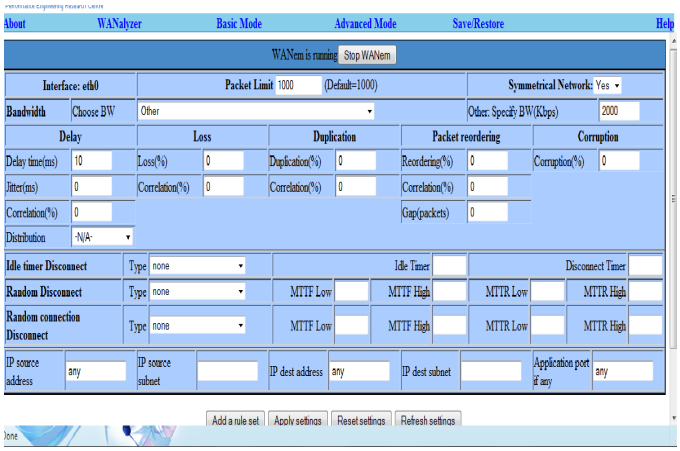


Figure 10. WANem Advance Mode

D. *SIPp (VoIP generator)*

SIPp is a performance testing tool for the SIP protocol [15]. It establishes and releases multiple calls using the INVITE and BYE method. By using SIPp traffic generator tool, thousands of user agents calling in SIP protocol can be emulated to the IP PBX server.

IV. RESULT AND DISCUSSION

As mentioned earlier, this project is emulating the VoIP over MYREN network between UiTM and UNITEN. Thus, the parameters that are need to be configured in WANem are based on the MYREN link between the two institutions. The bandwidth was set to 2Mbps while the delay was set to 0ms. X-Lite softphone is configured with G.711 codec as used by the IP PBX server located in MYREN Network Operation Centre (NOC). The data which comprises of delay, packet loss and jitter were captured by using WireShark.

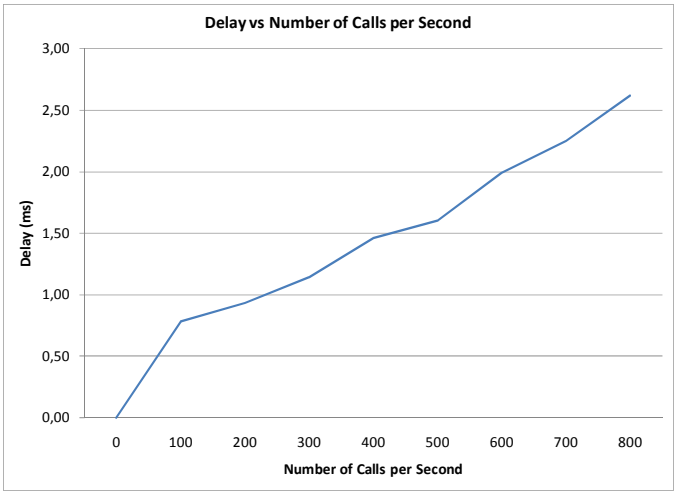


Figure 11. Delay

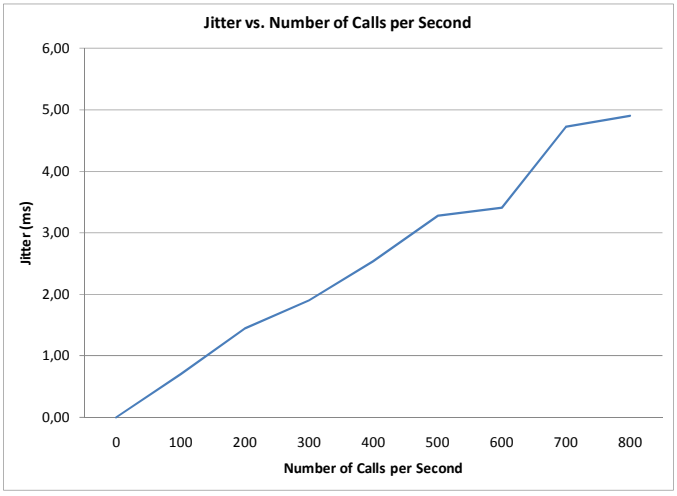


Figure 12. Jitter

Figure 12 and Figure 13 demonstrate the delay and jitter for the VoIP traffic. As expected, both delay and jitter are directly proportional to the load. This is due to the fact that the network will become congested as the load increases. Consequently, the transmission rate will become slower which will affect the end-to-end delay and jitter of the traffic.

TABLE I. PACKET LOSS

Number of calls per second	Packet Loss
0	0
100	0
200	0
300	0
400	0
500	0
600	0
700	0
800	0

Table I shows measurement of packet loss. Based on the table, it can be seen that there is no packet drop while transmitting the voice traffic over the testbed as there is no background traffic has been injected into the testbed. However, it is envisaged that the packet drop will occur if some background traffics are injected into the network.

V. CONCLUSION AND FUTURE WORKS

Testbed can be use for learning and research without disturbing a real network. This paper has detailed out the development of a emulator testbed that imitate the VoIP communications between UiTM and UNITEN via the MYREN link. The developed testbed is considered functioning well as the performances of the VoIP traffic obtained are acceptable. In future, background traffics such as video and File Transfer Protocol (FTP) may be added to reflect the real network situation.

REFERENCES

[1] CISCO's website, http://www.cisco.com/univercd/cc/td/doc/product/voice/sipsols/biggulp/bgsipov.htm Accessed on 3 October 2009 10:32PM (GMT +8)

[2] CISCO Support Forum's website, https://supportforums.cisco.com/docs/DOC-1422 : Accessed on 3 October 2009 11:00PM (GMT +8)

[3] Penn State University's website, http://citeseer.ist.psu.edu/183712.html : Accessed on 30 October 2009 4:32 PM (GMT +8)

[4] M. Kapor, "Building the Open Road: The NREN as Test-Bed for the National Public Network," RFC1259, September 1991.

[5] Official Myren Website, www.myren.net.my, Accessed on 25 March 2010 8:25PM

[6] H. Shuai, H. Xiaohong and M. Yan, "Application QoS for Video: Benchmarking, Control Strategies abn Business Systems," 5th International Conference on Wireless Communications, Networking and Mobile Computing (WiCom '09), 2009, pp.1-4.

[7] J-Y. Shin, J-W. Jang and J-M. Kim, "Result based on NS2, Simulation and Emulation Verification," International Conference on New Trends in Information and Service Science (NISS '09), 2009, pp. 807-811.

[8] J-Y. Shin and J-W. Jang, "Verification and Method Act Comparison of the Simulator and Emulator Result based on NS-2," Fourth International Conference on Digital Telecommunications (ICDT '09), 2009, pp. 34-38.

[9] N. Ivanic, B. Rivera and B. Adamson, "Mobile Ad Hoc Network Emulation Environment," IEEE Military Communications Conference, 2009 (MILCOM 2009), 2009, pp.1-6.

[10] N. Ivanic, B. Rivera, R. Gopaul, B. Luu, D. Gwyn, R. Hardy, K. Marcus, L. Scott, G. Tran and B. Nguyen, "A Scalable Testbed for Emulating Wireless Mobile Ad-Hoc Networks," IEEE Military Communications Conference, 2008 (MILCOM 2008), 2008, pp.1-5.

[11] M. A. Kaplan, T. Chen, M. A. Fecko, P. Gurung, I. Hokelek, S. Samtani, L. Wong, M. Patel, A. Staikos and B. Greear, "Realistic Wireless Emulation for Performance Evaluation of Tactical MANET Protocols," IEEE Military Communications Conference, 2009 (MILCOM 2009), 2009, IEEE pp 1-7.

[12] R.K.K, M. Raj, K. Balakrishnan and D. Das, "WEBS: WiMAX Emulation Testbed to Benchmark Streaming Multimedia QoS," IEEE International Conference on Internet Multimedia Services Architecture and Applications (IMSAA), 2009, pp. 1-6.

[13] Trixbox Website, http://www.trixbox.org/, Accessed on 10 January 2010 10:55PM

[14] WANem Website, http://wanem.sourceforge.net/ , Accessed on 9 November 2009 3:10PM

[15] SIPp Website, http://sipp.sourceforge.net/, Accessed on 20 February 2010 11:03 PM

Simulation of Dynamic Traffic Control System Based on Wireless Sensor Network

Faisal A. Al-Nasser *, Hosam Rowaihy

College of Computer Sciences and Engineering
King Fahd University of Petroleum and Minerals
Dhahran 31261, Saudi Arabia

*faisal_1997_n@yahoo.com; rowaihy@kfupm.edu.sa

***Abstract*— the use of wireless sensor network in the smart traffic control systems is very beneficial and starting to be very promising in the design and implementation for such systems. It will help in saving people time and adapt the intersections traffic lights to the traffic loads from each direction. In this paper we present an intelligent traffic signals control system based on a wireless sensor network (WSN). It uses the vehicle queue length during red cycle to perform better control in the next green cycle. The main objective is to minimize the average waiting time that will reduce the queues length and do better traffic management based on the arrivals in each direction. The system also includes an approach to alert the people about the red light crossing to minimize the possibility of accidents due to red light crossing violations. The system was simulated and results are shown in the end of this paper.**

I. INTRODUCTION

The sensors applications nowadays are involved in many fields. For example, in home automation, weather and environmental monitoring, military, health, agricultural, traffic monitoring and other commercial applications like smart vehicles. One important application is the Traffic Signal Control System that is based on a Wireless Sensor Network. It gathers the traffic information and control the traffic flow according to the incoming traffic data. Many traffic light systems operate on a timing mechanism, preset cycle time that changes the lights after a given interval. An intelligent traffic light system senses the presence or absence of vehicles then it controls the traffic lights accordingly. The idea behind intelligent traffic systems is that drivers will not spend unnecessary time waiting for the traffic lights to change which may lead them to some traffic violations and accidents when some drivers start to lose their patience. An intelligent traffic system detects traffic in many different ways. The older system uses weight as a trigger mechanism. Current traffic systems react to motion to trigger the light changes based on the infrared object detector that picks up the presence of a car or some proximity switches. Then, a switch causes the lights to change. In order to accomplish this, algorithms are used to govern the actions of the traffic system. We need to understand the function of traffic signals so that we can improve driving habits by controlling the speed and the red light crossing in order to reduce the number of associated traffic accidents. The more the drivers know about the operation of traffic signals, the less frustrated they are going to be while waiting for the lights to change. Usually, in the intelligent traffic signal systems, the main aim is to reduce the cars waiting time at each signal and also to maximize the total number of cars that can cross an intersection safely with the green signal time.

In this paper, the main goal is to gather the information of incoming vehicles via WSN for the deployed smart traffic light signals that can do the following while maintaining fairness among the other traffic lights:

1. Intelligent traffic management system based on the queue length of cars in each signal side.
2. Optimize the following (trade-off):
    a. Average waiting time (minimize).
    b. Average service time (maximize).
    c. Average number of cars of the same queue not passing from the first time (minimize).
3. Handling of the red light crossing violation to minimize the number of accidents by giving and alarm to the car which is about to start moving from the green light side.
4. The system can also give indication to the police traffic control room in case the road is blocked due heavy traffic to take an immediate action.

The paper is organized as follows: Related Work, Problem Statement, System Model, Control Algorithms Design, Crossing Red Light Handling, Simulation Setup, Results & Discussions, Future Work and Conclusion.

II. RELATED WORK

The roads intersection is a bottleneck point in the urban traffic network and it is very critical node. Traffic may

978-1-61284-690-3/11/$26.00 ©2011 IEEE

accumulate quickly and traffic jam can occur quickly in case the traffic control system is not efficient to properly manage the vehicles queues in fast and smart manner. One of the hot topics these days is how to gather the traffic information and control the traffic flow around. There are two main methods in signal control: periodical signal control, time based, and sensor-based signal control [4]. Usually, the nature of traffic flow is random and predicting the traffic behavior is not easy. So, to use the periodical signal control method is not suitable and it will not be able to adapt the signal control to the dynamic traffic flow. However, it may work for the less busy intersections. Developing a smart dynamic traffic light control system is complicated task and involves many logics. For example, the work in [1] proposed a decentralized traffic light control using wireless sensor network. They used layered system architecture where sensors will detect vehicles' number, speed, etc. and send these data to the nearest Intersection Control Agent (ICA) which determines the flow model of the intersection. The work in [2] presented a traffic light control simulator that depends on the sensors to sense the presence or absence of vehicles within certain range by setting the appropriate calculated duration for the traffic signals to react accordingly where the initial time before the start was set to 1 sec.

According to the number of detecting points, traffic forecasting algorithms can be classified as single-point, double-point and multi-point where the first one is the mostly used in the traditional traffic control [3]. Also, there are several choices to construct a traffic monitoring based on WSN, such as the ad hoc self-organized network, the mixed mode of short-range and long-range wireless communication and the hybrid mode of wired/wireless communication [3]. One disadvantage [4] of most conventional vehicle detection methods in a traffic control system is that they can only detect the vehicle in a fixed position. The hybrid mode WSN was used to detect and monitor the vehicles dynamically. It consists of three layers: City layer (top layer) that consisting of traffic monitoring. Region layer, it presents traffic information cabinets installed at intersections, roads and residential paths. Finally, the bottom layer which is the field layer consisting of the WSN nodes on roads. One possible way to control the traffic is to optimize the flow over a junction using information from the optical information systems (OIS) sensors which cannot be measured using normal sensors [5]. An Agent based traffic lights logic algorithm which uses the length of a jam in front of a traffic light as input. The length of each jam lane is measured and if at one of these lanes the jam gets longer, this lane gets green for a longer time. The open source traffic Simulation "SUMO" (Simulation of Urban Mobility) was used to simulate the system. The work in [6] is meant to simulate a busy traffic light by recognizing patterns related to time in the intersection and use the information (e.g. traffic density , No. of lanes) to make the light as efficient as possible.

An intelligent traffic lights controller based on fuzzy logic technology was shown in [7] and [8] to simulate the design and implementation of traffic control system. Another real-time traffic signal control strategy was introduced in [9] using genetic algorithms to provide near optimal traffic performance for intersections and effective real-time traffic signal control for a large complex traffic network. The work in [10] they used multi agents approach while in [11, 12] they used a video/image processing techniques for calculating the system parameters to control the traffic.

In this paper, we simulate a dynamic traffic control system to improve the traffic management in many signals that works based on weight trigger method which is sometimes not fair. Also, we can apply it to many cities where they used timing based traffic signals. Moreover, a new idea proposed in our work is to implement an alerting system for red light crossing scenarios to alert the drivers in other sides to save their lives. The Industrial Jubail City has excellent roads and highways which encourage some people to drive so fast. Unfortunately, many accidents are due to red light violations which are increasing in scary manner.

III. PROBLEM STATEMENT

Controlling the traffic light intersection requires a prior knowledge of that intersection and the traffic load to be able set the proper parameters for the control algorithm, especially if the system used is not an intelligent system like time based traffic control. Basically most of the traffic signals intersections have four directions, North (N), South (S), East (E) and West (W) as shown in Fig.1. The other possibilities are North West (NW), South East (SE), East South (ES) and West North (WN) as shown in the Fig.2.
The model in Fig.1 simply shows that two directions can be open at the same time, for example, N and S direction will move then W and E at the same time because there is no turning in other directions like NW or SE. The other scenario is when we have the other directions NW, SE, ES and WN, then the control algorithm will be more complicated and more sensing elements are required. So, the main goal is to provide a controlling mechanism to minimize the waiting time for vehicles waiting in the red signal and maximize the service time for cars passing the green signal to avoid if possible the number of cars not able to pass from the first time or at least minimize this number.

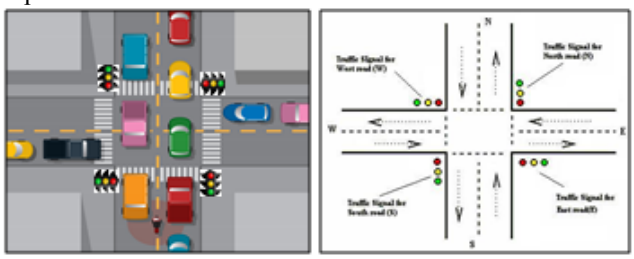


Fig. 1: Basic Traffic Intersection



Fig. 2: More Complicated Traffic Intersection

IV. SYSTEM MODEL

The simplest approach to model vehicle arrivals is to assume a uniform arrival. This will results in a deterministic, uniform arrival pattern which means constant time headway between all vehicles. However, this assumption is usually unrealistic, as vehicle arrivals typically follow a random process. Thus, a model that represents a random arrival process is needed and the most suitable one is the Poisson distribution with arrival rate of λ . In general, the car arrival is part of the queuing model (e.g. M/M/1 or M/G/1) which simulates the traffic signal operations. Basically the queue model is any service station with the following:

- One or multiple servers
- A waiting area or buffer

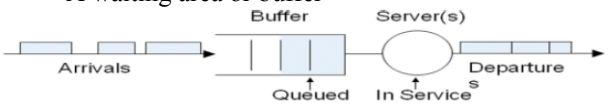


Fig. 3. Basic Queue System

The time τ_n is interarrival time between cars n and $n+1$ and it is a random variable. The traffic light system is following the stochastic process behavior.

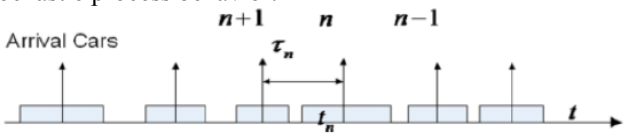


Fig. 4. Arrivals Cars in time

V. CONTROL ALGORITHMS

The basic traffic model can be controlled in timing mechanism since there is no much of complications and also can be controlled by smart system in case the traffic load is high in such intersection. Assume that T_G is the time period when the signal is green, T_R is when it is red, Q_L is the queue length, T_w is the average waiting time, T_{max} is maximum allowed time for one lane having the green signal even if it's queue not finished yet, τ_s is the service time required to pass one raw of cars at the same time, T_s is the total service time required to pass a queue of cars waiting for green signal and it depends on τ_s and number of lanes in that direction as shown in equation (3). T_{max} is used to avoid other lanes drivers to get lose their patience in case the signal of longer queue will take long time with green signal and F is a flag for programming purpose to make sure that each signal will get the required service. The choice of T_G is based on the total service time required for the present queue length plus some threshold time Δ. In other words:

$$T_G = T_s + \Delta \quad (1)$$

When the service time required is greater than the T_{max} then we will take the minimum of them which means:

$$T_G = min\ (T_s + \Delta\ ,\ T_{max}) \quad (2)$$

Where $$T_s = (\tau_s * Q_L) / NoOfLanes \quad (3)$$

The queue length can be detected by Ultrasonic Vehicle Detector placed before the signal by certain distance in each lane of the road to detect the cars arrival and the count will be saved in the controller unit. Another way by using cameras that can be placed at height and based on video or image processing results, the queue length is calculated.

In this paper, we considered four types of control strategies:

1- Model 1: in this model we control only the main directions as in Fig.1 where North and South signals are green at the same time, then, East and West are green at the same time. In some countries, it is allowed to turn but there is no signal controlling it, the driver has to look for the chance to pass which is in our opinion could be not safe.

2- Model 2: only one signal direction at a time. For example, as in Fig.2, North and North West will start together. Then, South with South East, East with East South and finally West with West North.

3- Model 3: allowing the parallel directions to move together, like North with South, East with West, East South with West North and North West with South East.

4- Model 4: is a Static model that works on timer for each direction regardless of the queue length in each direction.

In all algorithms we initialize the system by a timer which is giving certain time for some directions as a start. Then, start analysing the sensors data for that signal direction and find which direction has the lengthiest queue of vehicles. Based on the queue length (Q_L), the T_G is given to pass the traffic for that side as per equation (1) and (2). If $T_G = T_{max}$ then stop this side and open for the other side. Also, in case of the opened lane has no more cars and the other lanes has some new arrivals then $F = 0$ for the open lane and $F = 1$ for the other one. For the 1st control algorithm the directions will be N/S then W/E directions. So, if it is green for N/S the next will be the other side which is E/W. In the 2nd control we consider each direction with its sub directions like North and North West directions at the same time. In contrast, in the 3rd model the sequence will be North with South, West with East, North West with South East, East South with West North, all parallel directions at the same time. Finally, the static model works by giving a fixed window time for each side similar to model 2 but not in smart way. It will start, for example with North and NW, and then wait for a window time to stop. Then shift to next side one by one according to predetermined order. The static

model could be useful in highly traffic signals where the probability of cars will not pass from the first time near to 1 especially at the peak time. So, in this case it could be not feasible to spend money to have a smart traffic control system using WSN.

VI. CROSSING RED LIGHTS HANDLING

There are many factors that encourage some drivers to cross the red light signals like: Careless attitude, driving at high speeds, the prior knowledge of signals behaviour and the Time between T_G and T_R for the other sides, high traffic or very low traffic and the long waiting time in case if it is timing mechanism. So, by using an intelligent traffic control system, it can also give an alarm in case of someone cross the red light. In case the vehicles are moving from N to W or from S to E, then crossing for red lights could be from other sides and that will lead to accident.

The following scenarios can happen:

- Cars waiting in one lane and it is about to have Green signal for them, a sensors will detect if other lanes have full occupancy then no chance to have a high speed car trying to cross.
- In case some of the lanes are empty which most common at non peak hours, there is a chance to have one car at a high speed to cross and hit the other cars where they have Green signal.

This can be handled by the following:

- When T_G for the moving lane is becoming equal to T_{max} , then sensors will detect if there are vehicles coming at high speed while F becomes 0 and the F about to be 1 for the other lane, then red alarm will flash for people before they moved to look one more time before moving to avoid accidents.
- In case traffic is low in all directions, the same can be applied when somebody is coming toward a red signal with high speed.

VII. SIMULATION SETUP

MATLAB R2008b was used to implement the control algorithms on DELL Latitude 6400, 2.4 GHz personal laptop with 2 GB of memory with operating system Windows Vista Business. Vehicles arrivals are modeled using Poisson arrival λ which is calculated from historical data collected from one Main Signal Intersection near Jubail Industrial Colleague in Industrial Jubail City as shown in the Fig.5. This signal is always busy and in peak hours it has a lot of traffic. The average rate of cars arrival in peak hours found to be greater than 30 cars per minute. The North and South Direction have two lanes and the third one for turning direction in each. The East and West have three lanes and one more for the turn. In the simulation we considered this and also we have done a simulation in case all directions have same number of lanes which is 3. Also, there is something called safe time (T_{safe}) which is the time margin between the Red signal ON until the next direction green signal is ON and usually is around 5 sec. The time for which the green signal is ON in one direction was found to be 45 seconds as an average and we used this value in our simulation as T_{max}. The service time (τ_s) is around 1 second means that in 1 sec the cars in all lanes ,e.g. 3 lanes have 3 cars so the 3 cars will move in 1 sec time, and also we simulate it for $\tau_s = 2$.

VIII. RESULTS & DISCUSSIONS

The first simulation we assumes that all directions has same number of lanes which is 3 plus the sub directions for turning and the arrival rate fixed for each direction but changed along with simulations runs then we averaged the results. Also, we set $\tau_s = 1$ and $T_{safe} = 5$ sec. The results in Table 1 and Fig.6 shows that model 1 is providing much lower waiting time compared to model 2 and 4 because we don't count the waiting time for the sub directions. Model 1 and 3 give almost the same service time which guarantees no remaining cars as shown in the Table 1 but model 4 shows that on average 5 cars were not able to pass from the first time when $\lambda = 50$.

The second simulation is same as the first but with different λ for each direction and as shown in each experiments in Table 2 and we set the $T_{safe} = 0$, $\tau_s = 2$ sec. It shows that at rate 70 cars/min some cars were not able to pass from the first time which is logical due to the very long queue. Also, we shows the information for the sub directions which we have considered in the Model 3 as shown in Table 3. In the third simulation we assign λ for each direction based on realistic scenarios and also we shows the results for the sub direction in separate graph as shown in Table 5. Also, the number of lanes for North and South is 2 plus one for the sub direction as it is in the Fig.5 while the East and West has 3 lanes plus the sub direction.



Fig. 5. Simulated Intersection in Industrial Jubail City

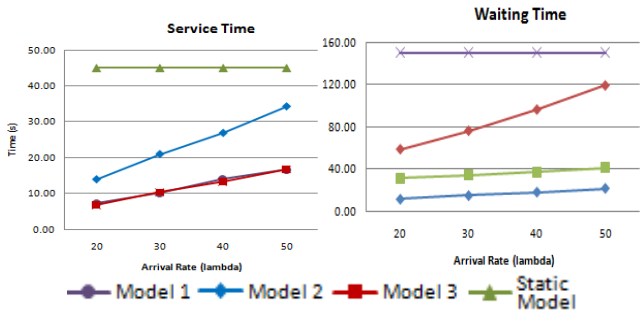


Fig. 6. Service & Waiting Time for First Simulation, λ is same for all directions

The static model will deal with all directions in same manner while the weight triggered system will give the priority to whom is coming first weather this side has long queue or not and this will allow one or two cars to pass before longer queue of cars in other side just because they have arrived by one or two seconds in advance. Model 3 provides better control by considering the queue length in all directions and sub directions and giving it a priority. However, Model 1 shows lower waiting time in the main signals because we don't consider the waiting time for the sub directions and that is why it shows better results. If we tried to calculate the waiting time for cars trying to cross in the sub direction it will be more than the mean T_s for the two parallel directions and we will have some cars not able to pass in case of high arrival rates in sub directions.

Table 1: First Simulation Results

		Ts = 1, Tsafe = 5	Cars Arrival				Service Time				Waiting Time				Car Not Pass			
	Signal	Model	1	2	3	4	1	2	3	4	1	2	3	4	1	2	3	4
Experiment 1	North	λ = 20	21	21	21	21	7.02	13.81	6.89	45.00	11.93	58.52	31.30	150	0.00	0.00	0.00	0.00
	South	λ = 20	22	21	21	21	7.22	13.86	6.76	45.00	11.93	58.01	31.30	150	0.00	0.00	0.00	0.00
	East	λ = 20	20	21	21	21	6.83	14.10	6.59	45.00	12.12	58.23	31.22	150	0.00	0.00	0.00	0.00
	West	λ = 20	21	21	21	21	7.04	14.28	6.53	45.00	12.12	57.83	31.22	150	0.00	0.00	0.00	0.00
Experiment 2	North	λ = 30	31	31	31	31	10.38	20.64	10.45	45.00	15.30	76.16	34.32	150	0.00	0.00	0.00	0.00
	South	λ = 30	30	31	31	31	10.07	20.93	10.33	45.00	15.30	75.87	34.32	150	0.00	0.00	0.00	0.00
	East	λ = 30	31	31	30	31	10.22	20.52	10.06	45.00	15.23	76.28	34.21	150	0.00	0.00	0.00	0.00
	West	λ = 30	31	30	30	30	10.38	19.70	9.88	45.00	15.23	77.10	34.21	150	0.00	0.00	0.00	0.00
Experiment 3	North	λ = 40	41	42	41	41	13.53	27.96	13.52	45.00	18.53	96.30	37.40	150	0.00	0.00	0.00	0.00
	South	λ = 40	42	40	40	41	14.02	26.83	13.31	45.00	18.53	97.42	37.40	150	0.00	0.00	0.00	0.00
	East	λ = 40	40	42	39	40	13.30	27.73	12.93	45.00	18.78	96.52	37.60	150	0.00	0.00	0.00	0.00
	West	λ = 40	41	40	40	40	13.76	26.73	13.30	45.00	18.7	97.52	37.60	150	0.00	0.00	0.00	0.00
Experiment 4	North	λ = 50	51	52	51	51	16.91	34.99	16.96	45.00	22.02	119.19	41.14	150	0.00	0.53	0.53	5.00
	South	λ = 50	50	51	50	50	16.59	34.24	16.72	45.00	22.02	119.85	41.14	150	0.00	0.03	0.03	5.00
	East	λ = 50	50	51	51	51	16.68	34.07	17.06	45.00	21.75	120.06	40.91	150	0.00	0.23	0.00	5.00
	West	λ = 50	52	54	51	52	17.36	35.92	16.98	45.00	21.75	118.17	40.91	150	0.00	0.00	0.00	5.00

Table 2: Simulation Results for Second Simulation (varying λ)

		Ts = 2, Tsafe = 0	Cars Arrival				Service Time				Waiting Time				Car Not Pass			
	Signal	Model	1	2	3	4	1	2	3	4	1	2	3	4	1	2	3	4
Experiment 1	North	λ = 60	60	64	59	61	40.19	42.54	39.10	40.61	32.03	86.84	52.03	135	0.35	6.73	0.00	0.00
	South	λ = 55	56	55	57	56	37.08	36.88	37.74	37.23	32.03	91.41	52.03	135	0.35	0.00	0.00	0.00
	East	λ = 75	74	73	75	74	49.36	48.61	49.70	49.22	38.58	84.02	58.72	135	0.00	26.20	0.00	5.00
	West	λ = 20	22	22	21	22	14.71	14.58	13.76	14.35	38.58	122.53	58.72	135	0.00	0.00	0.00	0.00
Experiment 2	North	λ = 70	72	71	70	71	48.07	47.37	46.40	47.28	23.04	79.92	39.07	135	15.58	21.60	10.00	2.00
	South	λ = 65	67	65	66	66	44.77	43.17	44.09	44.01	23.04	81.70	39.07	135	15.58	7.10	10.10	0.00
	East	λ = 30	32	32	31	31	21.08	21.10	20.51	20.98	43.86	107.83	60.06	135	0.00	0.00	0.00	0.00
	West	λ = 35	38	36	37	37	25.00	23.93	24.70	24.54	43.86	101.61	60.06	135	0.00	0.00	0.00	0.00
Experiment 3	North	λ = 20	20	21	20	21	13.66	13.88	13.45	13.67	32.33	76.67	52.13	135	0.00	0.00	0.00	0.00
	South	λ = 15	17	16	15	16	11.20	10.36	10.00	10.56	32.33	80.13	52.13	135	0.00	0.00	0.00	0.00
	East	λ = 55	54	57	52	54	36.03	37.78	34.90	36.25	12.43	52.92	32.13	135	0.00	3.07	0.00	0.00
	West	λ = 45	43	44	43	43	28.63	29.34	28.60	28.89	12.43	60.84	32.13	135	0.00	0.00	0.00	0.00
Experiment 4	North	λ = 25	26	26	24	25	17.26	17.64	16.31	16.97	27.08	86.58	44.74	135	0.00	0.00	0.00	0.00
	South	λ = 50	49	50	50	50	32.98	33.33	33.56	33.29	27.08	70.91	44.74	135	0.00	0.10	0.00	0.00
	East	λ = 25	26	26	26	26	17.38	17.00	17.38	17.25	25.12	87.51	42.93	135	0.00	0.00	0.00	0.00
	West	λ = 55	55	55	54	55	36.78	36.80	36.11	36.54	25.12	67.68	42.93	135	0.00	1.27	0.00	0.00

Table 3: Simulation Results for Second Simulation for Sub Directions (Average)

Ts = 2, Tsafe = 0		Cars Arrival	Service Time	Waiting Time	Car Not Pass
	Model 3				
NW	λ = 5	6.0	12.0	68.6	0.0
SE	λ = 5	5.8	11.6	68.6	0.0
ES	λ = 5	5.6	11.3	66.0	0.0
WN	λ = 5	5.7	11.4	66.0	0.0

In third simulation we can see the power of model 3 in terms of waiting time and number of car not pass from the first time as shown in Fig. 7 and 9. For the sub directions Table 5 shows the data for Model 3 as we only include it in this model. Comparing with first simulation where service time was 1 sec still the model 3 provides minimum waiting time. However, model 1 shows lower waiting time for the main directions because we don't consider the sub directions but crossing the running signal from the sub directions requires driving experience from the drivers to decide when it is the proper time to move otherwise an accident will occur. It is clearly in third simulation the effects of number of lanes on the remaining car and even on the service and waiting time. In general, the static model will deal with all directions in same manner while the weight triggered system will give the priority to whom is coming first weather this side has long queue or not and this will allow one or two cars to pass before longer queue of cars in other side just because they have arrived by one or two seconds in advance. Model 3 provides better control by considering the queue length in all directions and sub directions and giving it a priority.

Table 4: Simulation Results for third Simulation (Two Lanes)

		Ts = 2, Tsafe = 0	Cars Arrival			Service Time			Waiting Time			Car Not Pass		
	Signal	Model	2	3	4	2	3	4	2	3	4	2	3	4
Experiment 1	North	λ = 10	11	10	10	11.12	10.03	45.00	48.99	27.42	135.00	0.00	0.00	0.00
	South	λ = 10	11	10	10	10.02	9.60	45.00	50.09	27.42	135.00	0.00	0.00	0.00
	East	λ = 30	28	28	28	19.17	18.98	45.00	40.94	18.65	135.00	0.00	0.00	0.00
	West	λ = 30	29	27	28	19.81	18.20	45.00	40.30	18.65	135.00	0.00	0.00	0.00
Experiment 2	North	λ = 20	22	20	21	21.52	20.43	45.00	73.58	39.59	135.00	0.00	0.00	0.00
	South	λ = 20	21	21	21	21.17	19.90	45.00	74.75	39.59	135.00	0.00	0.00	0.00
	East	λ = 40	40	40	40	26.29	25.80	45.00	67.40	33.74	135.00	0.00	0.00	0.00
	West	λ = 40	39	39	39	26.87	25.50	45.00	67.27	33.74	135.00	0.00	0.00	0.00
Experiment 3	North	λ = 30	31	30	31	31.02	30.45	45.00	98.26	48.00	135.00	0.00	0.00	0.00
	South	λ = 30	30	30	30	30.38	29.83	45.00	98.89	48.00	135.00	0.00	0.00	0.00
	East	λ = 50	50	49	50	33.61	32.54	45.00	95.66	45.78	135.00	0.00	0.00	5.00
	West	λ = 50	51	48	50	34.30	32.19	45.00	95.01	45.78	135.00	0.00	0.00	5.00
Experiment 4	North	λ = 40	42	41	41	41.50	40.62	45.00	117.20	58.67	135.00	5.87	0.83	1.00
	South	λ = 40	41	39	40	40.70	39.45	45.00	117.40	58.67	135.00	2.66	0.83	1.00
	East	λ = 60	61	59	60	40.40	39.10	45.00	115.36	59.29	135.00	3.83	0.69	10.00
	West	λ = 60	62	59	60	41.00	39.53	45.00	114.74	59.29	135.00	1.43	0.68	10.00

Table 5: Simulation Results for third Simulation for sub Directions

		Ts = 2, Tsafe = 0	Cars Arrival	Service Time	Waiting Time	Car Not Pass
		Model 3				
Experiment 1	NW	λ = 2	2.90	5.80	33.44	0.00
	SE	λ = 2	2.50	5.00	33.44	0.00
	ES	λ = 2	2.58	5.17	32.21	0.00
	WN	λ = 2	2.45	4.90	32.21	0.00
Experiment 2	NW	λ = 3	3.78	7.57	54.93	0.00
	SE	λ = 3	3.55	7.10	54.93	0.00
	ES	λ = 3	4.05	8.10	52.33	0.00
	WN	λ = 3	3.82	7.63	52.33	0.00
Experiment 3	NW	λ = 4	5.03	10.07	72.08	0.00
	SE	λ = 4	4.57	9.13	72.08	0.00
	ES	λ = 4	4.75	9.50	68.58	0.00
	WN	λ = 4	4.82	9.63	68.58	0.00
Experiment 4	NW	λ = 5	5.90	11.80	90.66	0.00
	SE	λ = 5	6.18	12.37	90.66	0.00
	ES	λ = 5	6.23	12.47	86.86	0.00
	WN	λ = 5	6.10	12.20	86.86	0.00

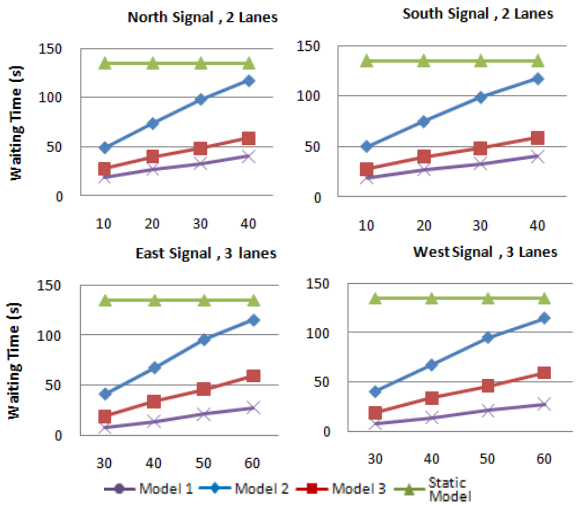


Fig. 7. Waiting Time for third Simulation for Each Signal

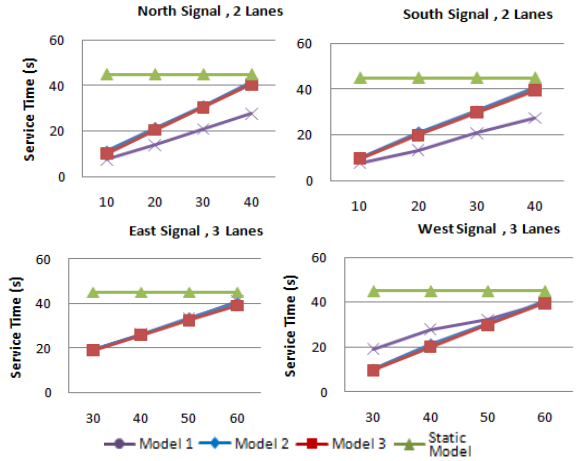


Fig. 8. Service Time for third Simulation for Each Signal

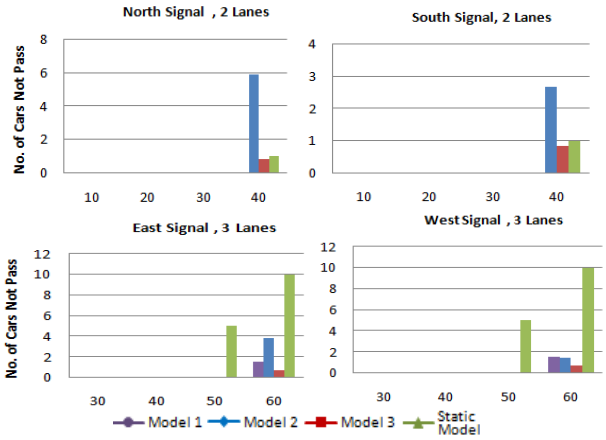


Fig. 9. Number of cars not pass for third Simulation for Each Signal

I. Future Work

It will be good if we could design a specific simulator using Java or .Net to show the animations of cars arrivals and movements and allow the changing different parameters online to see the effects.

II. Conclusion

In this paper, we have shown one application of WSN in designing and simulating a smart traffic signal control system by measuring the queue length in each side. The simulation was done using four models were all models are used in one place or another around the world. Model 3 and Model 1 shows competing results in terms of waiting time and number of cars not served from the first time.

References

[1] Tubaishat, Malik; Shang, Yi; Shi, Hongchi; "Adaptive Traffic Light Control with Wireless Sensor Networks" , Consumer Communications and Networking Conference, 4th CCNC 2007.

[2] A. Albagul, M. Hrairi, Wahyudi and M.F. Hidayathullah; "Design and Development of Sensor Based Traffic Light System ", American Journal of Applied Sciences 3 : 1745-1749, 2006.

[3] WEN Y, PAN J. L. and LE J. F; "Survey On Application Of Wireless Sensor Networks For Traffic Monitoring", International Conference on Transportation Engineering 2007 (ICTE 2007).

[4] L. K. Chien, "A Real-time Dynamic Traffic. Control System Based on Wireless Sensor Network ". International Conference on Parallel Processing Workshops (ICPPW'05).

[5] Daniel Krajzewicz, Elmar Brockfeld, Jürgen Mikat, " Simulation of modern Traffic Lights Control Systems using the open source Traffic Simulation SUMO ",

[6] Lynn Jepsen, "Learning Traffic Light Simulation" , Computer Systems Lab, 2006-2007.

[7] Kok Khiang Tan, 1Marzuki Khalid and Rubiyah Yusof, "Intelligent Traffic Lights Control By Fuzzy Logic" . Malaysian Journal of Computer Science, Vol. 9 No. 2, December 1996, pp. 29-35.

[8] Wu WEI, YI Zhang and Jean Bosco, "Traffic Signal Control Using Fuzzy Logic and Moga", IEEE-SMC, 2001.

[9] Leena Singh, Sudhanshu Tripathi, Himakshi Arora. "Time Optimization for Traffic Signal Control Using Genetic Algorithm". International Journal of Recent Trends in Engineering, Vol 2, No. 2, November 2009.

[10] Visit Hirankitti, Jaturapith Krohkaew, and Chris Hogger, "A Multi-Agent Approach for Intelligent Traffic-Light Control" Proceedings of the World Congress on Engineering 2007 Vol I, WCE 2007, July 2 - 4, 2007, London, U.K.

[11] M.Y. Siyal1, M. Fathi1 and M. Atiquzzaman "A Parallel Pipeline Based Multiprocessor System For Real-Time Measurement of Road Traffic Parameters" Real-Time Imaging 6, 241-249 (2000).

[12] Hajime sakakibara, masanori aoki and hiroshi matsumoto, "Advanced Traffic Signal Control System Installed in phuket city, Kingdom Of Thailand" Information & Communication Systems, SEI Technical Review , number 60 · June 2005.

Evaluation of 6to4 and ISATAP on a Test LAN

Mohammad Aazam[1, 2], Adeel M. Syed[3], Syed Atif Hussain Shah[4]
[1]Mohi-ud-Din Islamic University
[3]Bahria University
[4]Shaheed Zulfikar Ali Bhutto Institute of Science and Technology (SZABIST)
[1, 2, 3, 4, 6]Islamabad, Pakistan
[1]aazam@ieee.org, [3]adeelmuzaffar@gmail.com,
[4]a.shahgee@gmail.com

Imran Khan[5, 2], Muhammad Alam[6]
[5]Telecom Paris Tech
Department Informatique et Resseaux (INFRES)
46 Rue de Barrault
Paris, France
[6]Bahria University
[2]Center of Research in Networks and Telecom
[2]Mohammad Ali Jinnah University
[5]imran@ieee.org, [6]muhammad.alam@ieee.org

***Abstract*— Coexistence of IPv4 and IPv6 bears problem of incompatibility, as IPv6 and IPv4 headers are different from each other. To counter this problem, three solutions are possible: a) making every device dual stack, b) translation, c) tunneling. Tunneling stands out as the best possible solution. Among the IPv6 tunneling techniques, this paper evaluates the performance of two recent IPv6 tunneling techniques: 6to4 and ISATAP. These protocols were implemented on real test bed setup, on Microsoft Windows (MS Windows XP and MS Windows Server 2003) and Linux operating systems. Five to six devices were used to setup the whole test bed. Each protocol was then implemented on the setup using specific configuration commands, available online at various sources. UDP based audio streaming, video streaming, and TCP based ICMP-ping traffic was run. Four different runs of IPv6 traffic were routed over the setup for both IPv6 tunneling protocols. The average of the data was taken to generate graphs and final results. The performance of these tunneling techniques has been evaluated through certain parameters, namely: throughput, end to end delay (E2ED), round trip time (RTT), and jitter.**

Keywords: IPv6 tunneling, 6to4, ISATAP

I. INTRODUCTION

Transitioning towards IPv6 is inevitable and very soon IPv6 will be running on every IP device. Transitioning towards IPv6 won't be an overnight project. It would be incremental and step by step. IPv4 and IPv6 will coexist even after about a decade of IPv6 deployment [1]. Keeping in view the importance of IPv6, the transition from IPv4 to IPv6 has started [6]. To make this transition manageable and easy, a lot of research has been done. It is not practical to change the Internet, or any large network altogether into an IPv6 network at once. All the routers cannot be upgraded simultaneously [7]. Hence transition is only feasible in a gradual manner, due to complexity of the Internet and huge number of devices accessing it. Migration towards IPv6 should be in such a manner that for certain time, both IPv4 and IPv6 capable devices will co-exist [2]. Also, there will be islands of both IPv4 and IPv6 networks. For example, two IPv6 devices want to communicate with each other but there is an IPv4 network between them, IPv6 packets has to be routed from that IPv4 network. As IPv4 and IPv6 headers are different from each other (fields, the address format and address size are different), so IPv6 packet has to be tunneled to route through the incompatible IPv4 network. Tunneling is a technique in which one protocol is encapsulated in another protocol, according to the network where the packet is to be routed [9]. In case of IPv6 tunneling, if an IPv6 source communicating with an IPv6 destination and an IPv4 network is between them, then IPv6 packets must be tunneled into the IPv4 header so that the IPv6 packet gets routed through the IPv4 network and reaches its IPv6 destination.

A. IPv6 Tunneling Techniques

1) 6to4: 6to4 is an automatic way to connect isolated IPv6 sites (domains/hosts) attached to an IPv4 network that has no native IPv6 support. 6to4 Relay is provided for such IPv6 sites to visit IPv6 native network before they can obtain native IPv6 connectivity [4]. With 6to4, the current IPv4 network is treated as the link layer, and the existing IPv4 routing infrastructure is utilized to forward IPv6-in-IPv4 encapsulated packet. The host in 6to4 site uses a 6to4 IPv6 address (2002:IPv4Address::/80) as the communication identifier [13]. When the IPv6 packet goes through the 6to4 router, the IPv4 address of tunnel end point can be found within the 6to4 address, then a tunnel is formed without explicit configuration. 6to4 is designed only as a temporary mechanism, and it will be replaced in future by other mechanisms using permanent IPv6 addresses [6].

2) Intra-Site Automatic Tunnel Addressing Protocol (ISATAP): ISATAP is designed for the intra-site scope. ISATAP connects isolated nodes within IPv4 sites via automatic IPv6-in-IPv4 tunnels. That is why it is called intra-site [5]. With ISATAP, the intra-site IPv4 network is viewed as a link layer for IPv6, and other nodes in the intra-site network are viewed as potential IPv6 hosts/routers. An automatic tunneling abstraction is supported, which is similar to the Non-Broadcast Multiple Access (NBMA) model. An ISATAP host gets a 64-bit prefix from the ISATAP Server. Then an ISATAP address is formed with its own interface identifier (::0:5EFE:IPv4Address). After that, the ISATAP hosts can connect with each other via the IPv6-in-IPv4 tunnel

with ISATAP addresses. Furthermore, ISATAP can be used to provide connectivity to the outside IPv6 network together with other transition mechanisms. For example, if the site gateway is supported with 6to4 and holds the 6to4 prefix as an ISATAP Server and the IPv6 hosts among this site can use ISATAP to get intra/inter-site IPv6 connectivity.

II. Performance Evaluation Using Test bed Setup

The most widely followed way to evaluate performance of protocols is to simulate them using the most widely used simulation tools, like: NS2/NS3, OMNeT++, and OPNET. But, there were no simulation patches available for these techniques. For this research activity, the other option was to deploy these techniques practically on a test lab and then run the traffic using each technique. The biggest challenge that has been faced is that which tunneling technique is to be deployed in what circumstances and in which scenario [16]. This comparison shows the tunneling overhead and traffic comparison of the most widely deployed IPv6 tunneling techniques.

A. Test-bed Setup Description

IPv6 test-bed setup was needed to evaluate the performance of these protocols. Using minimum possible nodes required to set-up the test bed, IPv6 was configured and tested. It required 5 nodes to setup the test-bed, which was first configured for IPv6 and later on each protocol was deployed on it. These five nodes are: two hosts, one DNS server, two routers. Cables and hubs/switches were used to connect them. The following figure depicts the setup more comprehensively.

ISATAP works where one node (dual stack ISATAP node) is residing inside an IPv4 network and it has to communicate to an IPv6-only node, sitting inside an IPv6 network [5]. When ISATAP node wants to communicate to the other end IPv6-only node, then an ISATAP setup was in such a way that Host 1 (H1), as shown in the fig. 1, is a dual stack node, residing in an IPv4 network. This node has to communicate to another dual stack node, residing in an IPv6 network. Now, the traffic of and from both, H1 and H2, has to go through IPv4 network. Those IPv6 packets have to be tunneled through IPv4 network. By default, the IPv6 protocol for Windows XP Professional with SP2 and Windows Server 2003 with SP1, Standard Edition, configures a link-local ISATAP address on the Automatic Tunneling Pseudo-Interface for each IPv4 address assigned to a computer. To configure global ISATAP addresses, or to communicate beyond the logical subnet defined by the IPv4 intranet, an ISATAP router is needed [8]. ISATAP router performs two functions: a). advertises its presence and address prefixes, enabling global ISATAP addresses to be configured. b). optionally forwards IPv6 packets between ISATAP hosts on the IPv4 intranet and IPv6 hosts beyond it [10].

"An ISATAP router is typically configured to perform both functions, but can perform either individually. Most often, an ISATAP router acts as the forwarder between ISATAP hosts on an IPv4 intranet and IPv6 hosts on an IPv6-enabled portion of an intranet" [17]. To demonstrate the use of an ISATAP router between IPv6 and IPv4 intranets, first the test lab was separated into a portion that has IPv4 and IPv6 connectivity and another that has IPv4 connectivity only [11]. Then, router1 is configured as an ISATAP router so that hosts on the IPv4-only portion of the intranet can communicate with hosts on the IPv6-enabled portion of the intranet. To do this, IPv6 forwarding and advertising was disabled on the Subnet 2 Connection interface of router1 and both interfaces of router2. This emulates an intranet in which a portion is IPv6-enabled (Subnet 1) and a portion is not (Subnet 2 and Subnet 3) [17].

Just like ISATAP, 6to4 requires two routers, configured as 6to4 routers and capable of providing 6to4 tunnel address prefix to the client asking for that. The dual host was configured as 6to4 host, so that it could ask for 6to4 prefix from the nearest 6to4 router. For this setup, no standalone 6to4 server was required because the setup was small and there was only one client asking for the prefix. When deployed over the Internet or on a large network, there would be standalone 6to4 server required.

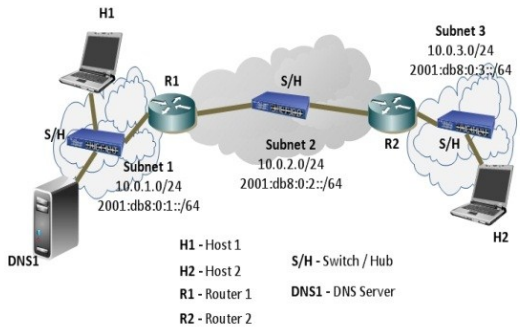


Fig. 1 Test bed setup

B. Performance Evaluation

The performance was evaluated based on certain parameters. The parameters were selected keeping in view the attributes related to tunneling and network layer or routing, like: throughput, round trip time, jitter, and end to end delay, were used to evaluate the performance.

- *Throughput*

It describes the overall throughput of the protocols. i.e. number of packets received per second.

Formula to calculate throughput is:

$$Throughput_{pps} = No_of_pkts_rcvd / timestamp_{sec} \text{ pps} \quad (1)$$

Where pps is packets per second.

UDP audio streaming traffic was run end to end to calculate the throughput. There were basically four runs of traffic, whose average was calculated and the final graph, shown below, was generated. Figure 2 shows that ISATAP has got relatively better throughput as compared to 6to4.

The packet size remained 1500 bytes. Traffic was run for about five minutes over the test bed setup, which was sniffed using the most widely used packet sniffing tool, called Wireshark. The graph shows that ISATAP performs better in respect of throughput. Its throughput remained 40-45 packets per second. 6to4's throughput remained 35-38 packets per second.

The ultimate, average throughput in Kbps comes out as:

Throughput = ((No_of_pkts_rcvd / $timestamp_{sec}$) X 1500 X 8) / 1000 Kbps (2)

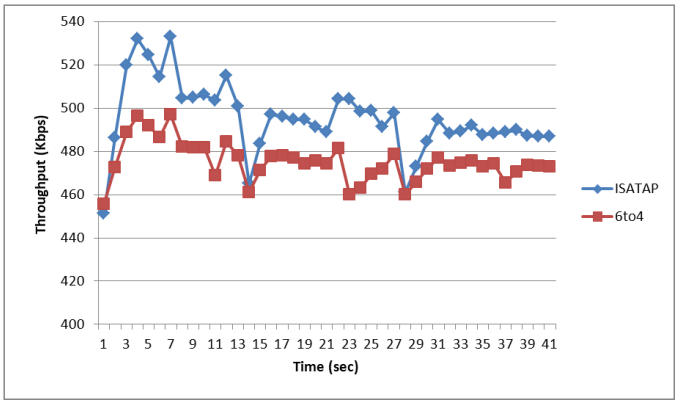


Figure 2. 6to4-ISATAP throughput (in Kbps)

Average throughput is shown in the following table:

Table 1. Average throughput in Kbps

Protocol	6to4	ISATAP
Average Throughput (Kbps)	468.83	495.11

As the network conditions were more or less stable, because it was a test bed setup, so there is apparently not a huge difference among the protocols. But when deployed over the Internet, this difference will surely increase. The average throughput was calculated to make things more comprehensive. As shown in the table 1, in relatively stable conditions, ISATAP has the edge of around 25 Kbps on 6to4.

- *End to End Delay (E2ED)*

It describes delay in milliseconds the traffic incurs.

The formula for end to end delay is:

E2ED = $timestamp_{msg_rcvd}$ - $timestamp_{msg_sent}$ milliseconds (3)

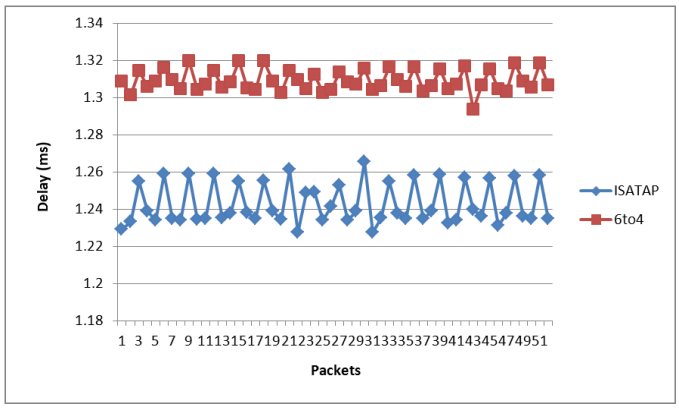


Figure 3. 6to4-ISATAP end to end delay

Delay was also calculated on UDP audio streams. It was calculated by subtracting the timestamp of packet received at the receive end with the timestamp of packet sent by the sender. Again, in terms of delay, ISATAP has got the edge. Its performance is better than 6to4. 6to4 traffic incurs more delay. This is because 6to4 has to deal with larger communication identifier. As discussed before, the host in 6to4 site uses a 6to4 IPv6 address (2002:IPv4Address::/80) as the communication identifier.

Average delay is shown in the following table:

Table 2. Average end to end delay in milliseconds

Protocol	6to4	ISATAP
Average Delay (ms)	1.3103	1.2427

Table 2 shows that ISATAP incurs least amount of delay in comparison with 6to4. When these techniques are deployed over the Internet, there would be lot more devices each packet has to travel through. This difference would be lot more then. The scenario used for this research activity, in which conditions remained stable, shows basic difference between performances of these two protocols. This difference suggests that in wide area network, the performance difference of ISATAP and 6to4 would of this much ratio, most probably.

- *Jitter*

Jitter, variation in delay, was calculated on the basis of the end to end delay. The formula is given below;

Jitter = Absolute ($delay_{current_pkt}$ – $delay_{prev_pkt}$) milliseconds (4)

The first packet won't be having any previous packet, so its jitter is 0.

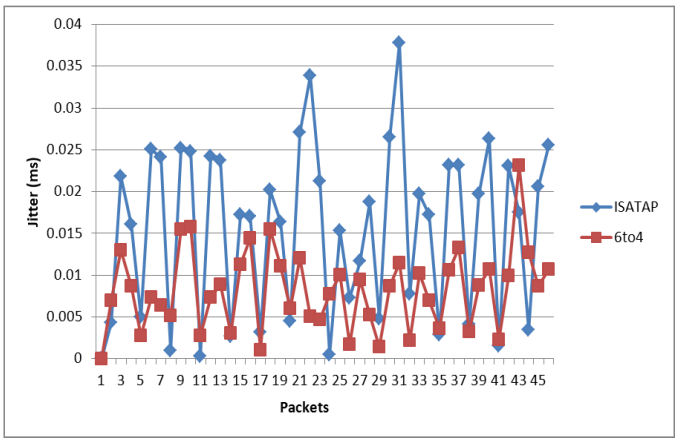


Figure 4. 6to4-ISATAP jitter

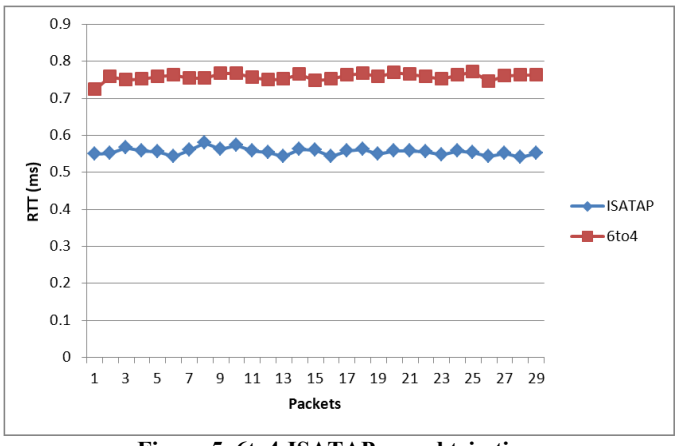


Figure 5. 6to4-ISATAP round trip time

Jitter is the only parameter in which ISATAP's performance is inferior from 6to4. This is because in ISATAP, tunnel refresh packets; which are meant to refresh the tunnels; are send more frequently. They are sent after every 13 data packets. When the tunnel is being refreshed and maintained, the data traffic is halted for that while. In 6to4, tunnel refresh packets are sent randomly, but less frequently; after around 18-19 data packets. This is the reason for 6to4 being less jittery. When real time streaming traffic has to be tunneled through IPv4 network, then 6to4 is the better option.
Average jitter is shown in the following table:

Table 3. Average jitter in milliseconds

Protocol	6to4	ISATAP
Average Jitter (ms)	0.0078	0.0152

The difference revealed from the above mentioned table 3 shows that when these techniques would be deployed over the Internet, ISATAP tunneled traffic would be containing even more jitter, because when there would be lot more devices involved and the network conditions would also be unpredictable, then those refresh packets would take more time to travel through the network between the client and the ISATAP server. Thence, incurring more jitter and also, affecting the bandwidth as well.

- *Round Trip Time (RTT)*

Round trip time is also regarded as one of the key parameter when talking about networks and network layer protocols. RTT is the time taken in total starting from the moment packet left the sending machine till the reply packet received by the sender. To get this, TCP based ICMP-ping traffic was used.

Formula is given below:

$$RTT = timestamp_{pkt_rcvd} - timestamp_{pkt_sent} \text{ milliseconds} \quad (5)$$

The difference between E2ED and RTT is that different traffics were used to calculate each. For E2ED, UDP audio/video streams were used, while for RTT, TCP based ICMP-ping traffic was used.

Average RTT is shown in the following table:

Table 4. Average round trip time in milliseconds

Protocol	6to4	ISATAP
Average RTT (ms)	0.7193	0.5516

In terms of RTT, ISATAP is again the better choice, because of the very reason of lesser encapsulation overhead.

CONCLUSION

For the tunneling overhead and tunneled traffic comparison of these IPv6 tunneling techniques: ISATAP and 6to4; UDP audio streams, video streams, and ICMP-ping traffic were used. Traffic was run end to end and sniffed at every node for better analysis. Four separate runs of traffic were routed over the most common and recommended setup for each protocol. At the end, the average of those four runs of traffic was calculated to generate final results.

After all this research activity, it is concluded that based on the parameters used: end to end delay, round trip time, throughput, and jitter; ISATAP has got the edge. ISATAP would be the most efficient and economical solution to tunnel IPv6 packet over IPv4 networks. Although, 6to4 has got its own significance, as it would be the best solution real-time traffic, as it is relatively less jittery. This is because 6to4 nodes send tunnel refresh packets less frequently, as compared to ISATAP. But in otherwise cases, ISATAP remains the most suitable choice.

REFERENCES

[1] R. Gilligan, E. Nordmark, Transition Mechanisms for IPv6 Hosts and Routers, RFC 1933, April 1996

[2] C. Huitema, et al, Evaluation of IPv6 Transition Mechanisms for Unmanaged Networks, RFC 3904, September 2004

[3] B. Carpenter, K. Moore, Connection of IPv6 Domains via IPv4 Clouds, RFC 3056, February 2001

[4] Savola, P., Observation of IPv6 Traffic on a 6to4 Relay, Proceedings of the ACM SIGCOMM, Philadelphia, USA, January 2005

[5] F. Templin, et al, Intra-Site Automatic Tunnel Addressing Protocol (ISATAP), RFC 5214, March 2008

[6] Jun Bi, Jianping Wu, and Xiaoxiang Leng, IPv4/IPv6 Transition Technologies and Univer6 Architecture, International Journal of Computer Science and Network Security (IJCSNS), VOL.7 No.1, Beijing, China, January 2007

[7] Ra'ed AlJa'afreh, John Mellor, and Irfan Awan, A Comparison between the Tunneling process and Mapping schemes for IPv4/IPv6 Transition, in the proceedings of 2009 International Conference on Advanced Information Networking and Applications Workshops, Bradford, UK, 2009

[8] Sang-Do Lee, Myung-Ki Shin, and Hyoung-Jun Kim, Implementation of ISATAP Router, In the proceedings of The 8th International Conference of Advanced Communication Technology (ICACT 2006), Phoenix Park, Korea, February, 2006

[9] Jivika Govil, Jivesh Govil, Navkeerat Kaur, and Harkeerat Kaur, "An Examination of IPv4 and IPv6 Networks: Constraints and Various Transition Mechanisms", IEEE Region 3 Huntsville Section (IEEE SoutheastCon 2008), April 3-6, 2008, Huntsville, Alabama, USA

[10] Shubhangi Kharche and B D Biranale, IPv4 to IPv6 Transition Using Windows OS, Proceedings of the SPIT-IEEE Colloquium and International Conference, Mumbai, India, February 2008

[11] Vasaka Visoottiviseth and Niwat Bureenok, Performance Comparison of ISATAP Implementations on FreeBSD, RedHat, and Windows 2003, Proceedings of the IEEE 22nd International Conference on Advanced Information Networking and Applications, Okinawa, Japan, 2008

[12] Manageable Transition to IPv6 using ISATAP, IPv6 Integration Paper Series, Cisco Systems, May 2006

[13] Malone, D., Counting 6to4 Relay Routers, Proceedings of the ACM SIGCOMM, Pisa, Italy, January 2006

[14] Marc Blanchet, Migrating to IPv6 – A practical guide to impelenting IPv6 in mobile and fixed networks, John Wiley and Sons Ltd., 2006

[15] Pete Loshin, IPv6 Theory Protocol & Practice 2nd edition, Elsevier, Morgan Kaufmann Publishers, 2004

[16] IPv6 Transition Test Challenges, Agilent Technologies, April 2004

[17] Mohammad Aazam et. al., Comparison of IPv6 Tunneled Traffic of Teredo and ISATAP over Real Test-bed Setup, in the poceedings of 2nd IEEE International Conference on Information and Emerging Technologies (ICIET) 2010, Karachi, Pakistan

Optimization of Energy Usage In Wireless Sensor Network Using Position Responsive Routing Protocol (PRRP)

Noor Zaman
Department of Computer & Information Science, Universiti Tecknologi PETRONAS, Malaysia.
noorzaman650@hotmail.com
Azween B Abdullah, Low Tan Jung
Department of Computer & Information Science, Universiti Tecknologi PETRONAS, Malaysia.
azweenabdullah@petronas.com.my, lowtanjung@petronas.com.my

***Abstract*- Wireless Sensor Networks (WSNs) consist of numerous tiny nodes powered by very small batteries that are normally non-rechargeable. Many researchers have thus focused on the issue of optimizing energy efficiency in WSNs. Their research have shown that routing operation is in fact the main energy expensive operation in the WSN because it tends to utilize maximum energy resources in the network. A good number of routing protocols have been designed in the past in the context of energy efficiency/optimization using different approaches under certain predefined control conditions. We propose in this paper an energy optimization protocol called Position Response Routing Protocol (PRRP) that incorporated the global positioning system (GPS). Our simulation results show a significant improvement in the life cycle of the WSN with respect to the proposed protocol.**

I. INTRODUCTION

WSN is a wireless network consisting of small nodes with sensing, computation, and wireless communications capabilities [1]. Each sensor collects data from its monitored area (such as temperature, sound, vibration, pressure, motion or pollutants). Then it routes the data back to the base station (BS) [2]. Data transmission is usually in multi-hop manner from a source toward the BS. Sensor nodes are often equipped with small irreplaceable batteries that have a certain life span limit. The nodes always come with wireless modem to jointly accomplish a monitoring or control task.

An important concern in WSN is its working lifetime. As nodes run out of power, the connectivity decreases and the network is finally partitioned and shall become dysfunctional [3,4,10]. Routing in WSNs is always a challenging problem due to the inherent characteristics which differentiate it from other types of wireless network such as ad hoc networks and cellular networks [3,14,18]. Many algorithms have been proposed for the routing issue in WSNs. The minimum energy routing problem has been addressed in various published papers [7,8,12,13,15,9,16]. The minimum total energy routing approaches in those papers were mainly focusing on minimizing the total energy consumed. However, if all traffic is routed through the minimum energy path to the destination, the nodes along that path will soon run out of battery energy quickly rending other nodes useless due to the network partition even if they do have available energy. Instead of trying to minimize the total energy consumed on the path, the main objective would be to maintain the connected network for as long as possible. If sensor nodes consume energy more equitably, they would be able to provide connectivity for a longer period thus increasing the network lifetime [4,5,6,13, 11,17,18]. As sensor networks have specific requirements on energy saving, data-oriented communication, and inter-connection between non-IP and IP, therefore sensor-network-dedicated routing protocols may be required for energy optimization and routing efficient.

The rest of the paper is organized as follow. Section II described the problem statement and the network model. Section III briefly touches on the topology used in the simulation works. Section IV describes the simulation and the results obtained. Section V concludes the paper.

II. PROBLEM STATEMENT AND NETWORK MODEL

Routing in WSNs has a primary task to transfer data from a source node to the sink node in the case of any physical triggered event or a time driven query run. Initially the routes are defined by the nodes and after which the nodes shall use those routing paths to send or receive the data.

A. Problem Statement

Ample number of different routing protocols had been designed by various researchers. Topology-based routing protocols include, Flat Routing Protocols, Hierarchal Routing Protocols, and Location Based Routing Protocols. Among these protocols, hierarchal routing protocol technique is preferred regarding the power saving in sensor nodes. This protocol works on the basis of forming several clusters (a sub network) within a network. The cluster is responsible for transferring data from a node to the sink. However direct data sending approach from each node is not supported with this method. Cluster communications is via a cluster leader known as cluster head. Communication with the sink is accomplished

with the help of clusters' head. A cluster head collects data from neighboring nodes and send them to another cluster head, which is responsible for any other cluster, this mechanism continuous until the data reaches the sink. The current energy efficient routing protocols including LEACH and HEED are designed on the basis of clustering.

The main issue with these method is that the cluster heads normally remain active for more time than other nodes in the cluster resulting in energy depletion quicker than other nodes. So if the cluster head used up its energy earlier than other nodes in the cluster then it is highly possible that one segment of the network is considered lost. Even though those routing protocols work fine up to a limited size of a sensor network, they are not suitable for large amount (size) of networks. This is due to the fact that they need to broadcast messages to find out their neighbors. Then to form new clusters by finding new cluster heads will directly cause an ample amount of energy to be consumed.

Hence there is highly a need to design an energy efficient routing protocol with assumptions closer to the real practical implementation constraints. We are proposing a Position Responsive Routing Protocol (PRRP) with the help of global positioning system (GPS) which is to be more energy optimized and efficient than the existing protocols. In this approach nodes and cluster heads will be informed about their position through the GPS.

B. Network Model

Our model assumes that the sensor network nodes are randomly distributed over an area of 90 x 90 meters with the following network properties.

1) Network is static and nodes are distributed in random format and the area is divided into equal square grid format.
2) There exists only one BS, which is deployed at a fixed place outside.
3) The energy of sensor nodes cannot be recharged.
4) Sensor nodes are position responsive through GPS.
5) The radio power can be controlled i.e. a node can vary its transmission power.

The fifth assumption is the main cause of energy saving. Moreover since all nodes are aware of their locations respectively via the GPS hence the amount of energy, which are normally used by the nodes in the network to find out their initial location, can be saved.

Routing capabilities would be tested in two ways. Initially it was tested with a normal approach and then in second phase it was tested through our PRRP. The second routing approach gave excellent results in terms of energy optimization or power saving. The results obtained are discussed in the following sections.

III. TOPOLOGY

The entire simulation of the proposed protocol was conducted on the ns2 simulator. Various topologies were applied. Two mesh topology samples are shown in Fig 1.

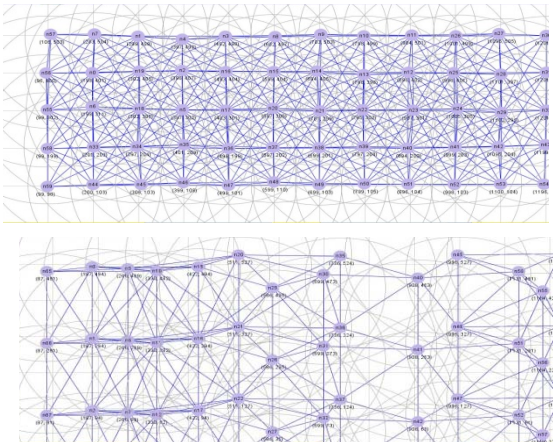


Fig. 1. Mesh topology samples

IV. SIMULATION

Simulation was conducted using the ns2 simulator. The ns2 is an object-oriented, discrete event driven network simulator written in C++ that allows OTcl simulation scripts (Tcl script language with Object-oriented extensions). It implements network protocols such as TCP and UPD; traffic source behavior such as FTP, Telnet, Web, CBR and VBR; router queue management mechanism such as Drop Tail, RED and CBQ; routing algorithms such as Dijkstra. ns2 also implements multicasting and some of the MAC layer protocols for LAN simulation.

The ns-2 includes a tool, called NAM, which is a Tcl/TK based animation tool for viewing network simulation traces and real-time packet data trace. Through its user interface, NAM provides control over many aspects of animations.

A Simulation Parameters

Standard Simulation parameters are shown in Fig. 2.

Channel type	Channel/WirelessChannel
Propagation model	Propagation/TwoRayGround
Phy type	Phy/WirelessPhy
Mac protocol type	Mac/802_11
Queue type	Queue/DropTail/PriQueue
Link layer type	LL
Antenna type	Antenna/OmniAntenna
Max packet in queue	50
Routing protocol	DSDV
Agent trace	ON
Router trace	ON
Mac trace	ON
Movement trace	ON

Gt_	1
Gr_	1
L_	1.0
freq_	2.472e9
bandwidth_	11Mb
Pt_	0.031622777
CPThresh_	10.0
CSThresh_	5.011872e-12
RXThresh_	5.82587e-09
dataRate_	11Mb
basicRate_	1Mb

Fig. 2. Simulation parameters.

B. *Results and Discussions*

Sample screenshot of the initial simulation output with NAM is shown in Fig. 3 where 50 nodes are scattered randomly over a 90 x 90 meters space.

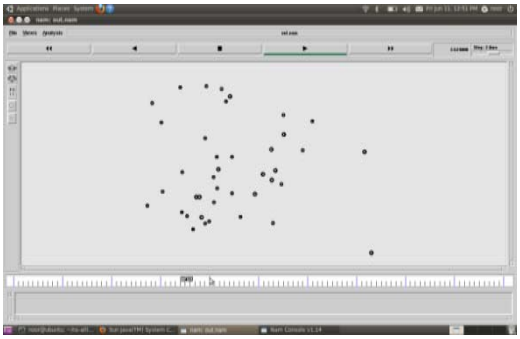


Fig. 3. Screenshot of simulation

WSN Nodes Without PRRP approach:

Simulation results without applying PRRP approach, is shown in graphs ranging from Fig. 4 to Fig. 6 for multiple hops. These graphs are plotted with respect to two parameters where the x-axis is for time in seconds while y-axis is for cumulative energy level for sensor nodes. These graphs are plotted with the assumption that the nodes are not position responsive and are scattered in random fashion over an area of 90 x 90 meters. Fig. 4. shows the energy drained from the nodes as over a routing time frame of 25 seconds. Fig. 5 shows the nodes life measured in terms of energy level over the same time fame and Fig. 6 represents the energy consumed by the nodes for multi-hop over the specific routing time. These graphs represent the relationship between routing data and sensor nodes energy. Fig. 4 shows that all 50 nodes (or 100%) are alive when the process starts and all nodes drained off their energy after about 22 seconds of active routing.

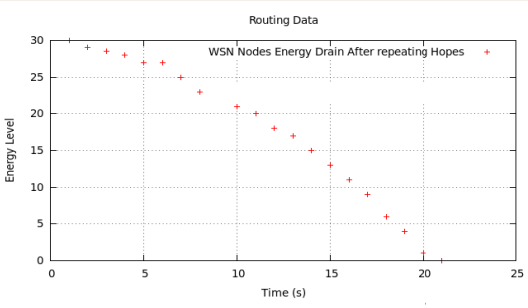


Fig. 4. WSN energy drain after multiple hops

The nodes life in Fig. 5 shows the similar pattern as that of Fig. 4 whereby the nodes die off gradually (so does the network) when their energy is drained off over time.

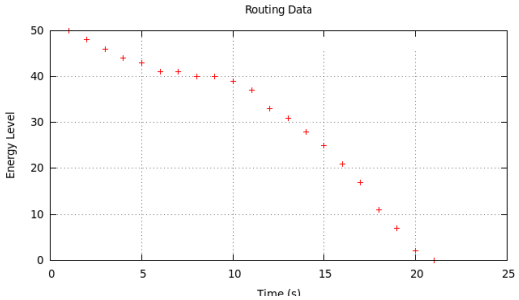


Fig.5. WSN nodes life against time after multiple hops

It can be seen in Fig. 6 that in multiple hop routing the energy consumption is almost a linear function against time which indicates that the number of hops increases as time went by and therefore more energy is consumed.

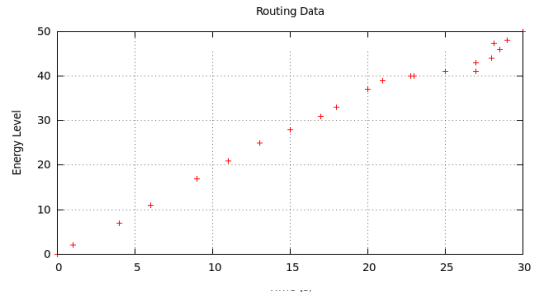


Fig. 6. Energy consumption in multiple hop routing

Fig.7 shows the result for entire energy usage for hoping simultaneously in different shades (colors). It shows that during the initial hops the energy level of the nodes were sufficient enough (shown in dark/blue color). However when the number of hops increases the energy level drastically went up as shown with different shading/colors ranging from light blue to yellow and finally towards red, which is the maximum level of energy. At this level almost all energy of the nodes has drained off completely.

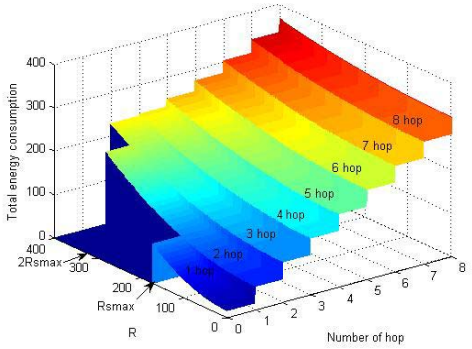


Fig. 7. Number of hops vs energy consumption

WSN Nodes With PRRP approach:

Graphs ranging from Fig. 8 to Fig. 10 are plotted with the same parameters but with the proposed PRRP applied. Again three different plots were taken into consideration. However the nodes are now position responsive, and are again assumed to be scattered in random fashion over an area of 90 x 90 meters. The results shown in the graphs of Fig.8 to Fig.10 are noticeably different from those shown in Fig. 4 to Fig. 6.

With PRRP all nodes are position responsive, that is, they are all aware of their neighboring nodes' positions through the GPS positioning function. By applying this protocol each node can save a certain amount of its initial energy due to the fact that there is no need for them to broadcast or send request-to-send (RTC) signaling data packets to its neighbors to find out the position of the sink node. In this way, nodes life can be enhanced approximately from 22 seconds to almost 35 seconds. This life enhancement time shall allows the network to have a longer remaining life and consequently more data can be transferred thus optimization of sensor network energy becomes higher. In a nutshell, PRRP routing approach increases the time span of sensor network which in turn may enhance network energy optimization and efficiency.

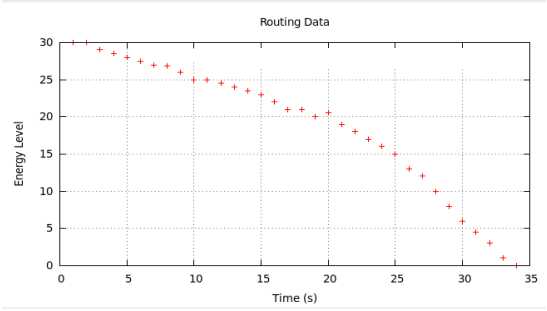


Fig.8 PRRP WSN nodes energy drain after multiple hops

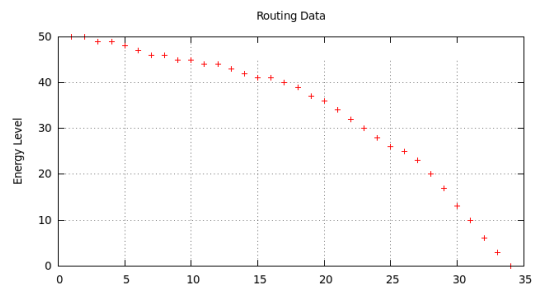


Fig. 9. PRRP WSN nodes life against time after multiple hops

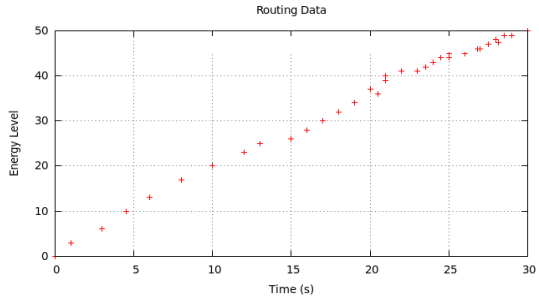


Fig. 10. PRRP energy consumption in multiple-hop routing

V. CONCLUSION

Energy optimization and thus efficiency is one of the major issues in WSN. In this paper we have address this issue by proposing a Global Positioning System (GPS) based routing protocol called Position Responsive Routing Protocol (PRRP) to provide energy optimization and thus creating a more energy efficient network. Our simulated results show that this protocol is able to provide significant enhancement to the network life span and making the network more energy efficient. Benchmarking PRRP against other routing protocols would be our next step in the course of this research.

REFERENCES

[1] Jamal N. Al-Karaki, Ahmed E Kamal, " Routing Techniques in Wireless Sensor Network: A Survey", IEEE Wireless Communication December 2004.

[2] I.F. Akyildiz, W. Su, Y. Sankarasubramaniam, and E. Cayirci, "A Survey on Sensor Network", IEEE Communication Magazine, vol. 40, no.8, pp. 102-116, August 2002.

[3] Akyildiz, I. F., W. Su, Y. Sankarsubramaniam and E. Cayirci, A survey on sensor networks, IEEE, Communications Magazines, vol.40, no.8, pp.102-114, 2002.

[4] Bhardwaj, M. and A. Chandrakasan, Bounding the lifetime of sensor networks via optimal role, assignments, Proc. of the INFOCOM'02, pp.1587-1596, 2002.

[5] Chang, J. H. and L. Tassiulas, Routing for maximum system lifetime in wireless Ad Hoc networks, Proc. of the ACCCC'99, 1999.

[6] Chang, J. H. and L. Tassiulas, Maximum lifetime routing in wireless sensor networks, IEEE/ACM Trans. on Networking, vol.12, no.4, pp.609-619, 2004.

[7] Ettus, M., System Capacity, Latency, and power consumption in multihop-routed SS-CDMA wireless networks, Proc. of RAWCON'98, pp.55-58, 1998.

[8] Rodoplu, V. and T. H. Meng, Minimum energy eobile wireless networks, IEEE JSAC, vol.17, no.8, pp.1333-1344, 1999.

[9] Singh, S., M. Woo and C. S. Raghavendra, Power-aware routing in mobile Ad Hoc networks, Proc. of the MobiCom'98, pp.181-190, 1998.

[10] Zussman, G. and A. Segall, Energy efficient routing in Ad Hoc disaster recovery networks, Proc. Of the INFOCOM'03, pp.682-691, 2003.

[11] Rentala, P.; Musunnuri, R.;Gandham, S. and Saxena U., "Survey on Sensor Networks ," Available online at: http://www.mdpi.net/sensors.

[12] Estrin, D.; Govindan, R.; Heidemann, J. and Kumar, S., "Next Century Challenges: Scalable Coordination in Sensor Networks ," Proceedings of 5th annual IEEE/ACM international conference on Mobile Computing and Networking, pp. 263-270, 1999.

[13] Anna Hac,Wiley. Wireless Sensor Network Design, 2003.

[14] Q. Cao, T. Abdelzaher, T. He, and R. Kravets, "Cluster-Based Forwarding for Reliable End-to-End Delivery in Wireless Sensor Networks", IEEE Infocom'07, May 2007.

[15] Wood, A. D., and Stankovic, J. A., Security of Distributed, Ubiquitous, and Embedded Computing Platforms, to appear in Wiley Handbook of Science and Technology for Homeland Security, Voeller, J. G. (Ed.), John Wiley & Sons, Hoboken, NJ, 2008.

[16] A. K. Sadek, W. Su, and K. J. R. Liu "Multinode cooperative communications in wireless networks," IEEE Trans. Signal Processing, vol. 55, no. 1, pp. 341-355, 2007.

[17] A. K. Sadek, Z. Han, and K. J. Ray Liu, "A distributed relay-assignment algorithm for cooperative communications in wireless networks," in Proc. IEEE International Conference on Communications (ICC), vol. 4, pp. 1592-1597, June 2006.

[18] Charles Pandana and K. J. Ray Liu "Robust Connectivity-Aware Energy-Efficient Routing for Wireless Sensor Networks " , IEEE transactions on wireless communications, vol. 7, no. 10, october 2008.

A Strategic Evaluation Model for Knowledge Relationship Among Members in Enterprise Communities

Fariba Haghbin
Department of Computer Science and Information System
Universiti Teknologi Malaysia
Johor Bahru,Malaysia
Email: haghbin@live.utm.my

Othman Bin Ibrahim
Department of Computer Science and Information System
Universiti Teknologi Malaysia
Johor Bahru,Malaysia
Email: othmanibrahim@utm.my

Mohammad Reza Attarzadeh Niaki
Department of Mechanical Engineering
Universiti Teknologi Malaysia
Johor Bahru,Malaysia
Email: smran@live.utm.my

***Abstract*—With the development of online communities, there has been a dramatic increase in the number of members using Enterprise Communities (ECs) over the past few years. Many join ECs with the objective of sharing their knowledge on the specific issue and seeking relative knowledge from others. Despite the eagerness of sharing knowledge and receiving knowledge through ECs, there is no standard of assessing ones knowledge sharing capabilities and prospects of knowledge sharing in order to get great level of efficiency of knowledge sharing collaboration. This paper developed evaluation model to assess knowledge relationship behavior among ECs members with the aim of Vector Space Model.**

***Index Terms*—Knowledge Sharing Relationship;Enterprise Community; Vector Space Model**

I. Introduction

The impressive development of electronic communication techniques has totally changed the overall picture of social communication methods. Collective writing, e-mail handling, shared database accessing, electronic conferencing and newsgroup, discussion lists, co-ordination by means of Web pages and other computer-mediated communication methods have greatly accelerated the speed, size and ease of human communication. Internet is no doubt a major phenomenon of our time. These new electronic techniques have given rise to new groupware which names enterprise community. Using enterprise community allows companies to extend their enterprise resource planning implementation to the Internet. Enterprise community can support and energize a Web site, which enables companies to communicate online with their customers and partners. Moreover, companies can implement enterprise community through their Intranet to help networked teams collaborate effectively [1]-[2].

A major contribution of enterprise community is its capability of knowledge sharing from all over the world [2].It makes environment for people to contribute their knowledge and acquire valuable knowledge to fulfill their needs from enterprise communities. Knowledge sharing seems to be the most important reason for participating in ECs [2].

Members are the most important resource for actual knowledge of enterprise community. They must interact with each other in order to obtain and share knowledge. In general the significance of social context to knowledge sharing has been accepted by researchers [3]-[4]-[5]-[6].

According to cognitive theories, an individual can only contribute knowledge he/she knows, which is currently a part of his/her cognitive structure. He/she can acquire knowledge if it is comprehensible, given his current cognitive structure [8]-[11]. Thus there is more possibility that members with similar knowledge structure are eager and capable to share knowledge with each other in ECs. Thus knowledge relationship among members should be considered in investigating knowledge sharing in ECs, but this part was often neglected in previous studies on knowledge sharing in ECs.

In this paper, we focused on the online network, forming in EC members knowledge sharing interactions, named knowledge sharing enterprise network and we purposed a model to investigate members knowledge sharing behavior in ECs in order to reduce the redundancy of knowledge which is usually happens at each community and raise the power of collaboration among members aimed by effective knowledge.

II. Enterprise Community And Knowledge Sharing Network

The important reason for participating in ECs is knowledge sharing. Knowledge sharing requires interaction between contributor and consumer of knowledge [14]-[16]. Each member can be a contributor or requester as they have own knowledge in knowledge sharing interactions. Thus knowledge relationship could be a metric used to measure the degree of contributors knowledge being similar with requesters knowledge structure .Based on the above explanation, our model will explain as follow: (A) The individual knowledge structure for each member is based on the tags added by him/her self and rating from others to his/her posting in past knowledge sharing interactions.(B): Knowledge relationship between each

member is evaluated by calculating the similarity of their knowledge structure.

The next step is how to calculate knowledge relationship based on Vector Space Model.

III. Calculating The Knowledge Relationship of Knowledge Sharing Network in Enterprise Community

When we talk about knowledge we should consider both sides, tacit and explicit knowledge. Tacit knowledge is more difficult to code, eloquent, and transfers from the owners mind. In contrast, explicit knowledge can be expressed into signs, text and words, so it can be more easily codified and documented[12]-[13]-[17].By the mean time, measuring knowledge would be more problematical by its intangible nature, especially measuring tacit knowledge. However, when tacit knowledge is transformed into explicit knowledge through socialization or interaction [12]-[15]-[18] and shared by members of an organization, measuring the knowledge can be made.

In ECs, members interact with each other to share their knowledge mainly through posting and replying. Although these posts and replies themselves by definition do not contain tacit knowledge, they point to those who own knowledge related to the content and reflects their knowledge status [19]-[20]. The individual knowledge structure construction starts from a collection of posting and replying documents related to a user. The most common way to represent text document in an automated text mining system is Vector Space Model [21]-[22].

In this model, each text document is transformed into a vector with the entire vocabulary of the document body as dimensions. The document vector contains a weight for each of these dimensions. If a weight is 0 indicates that word from the vocabulary is not present. However, this simple word-count based method is not accurate to represent the actual knowledge express in the document. Thus many semantic analysis methods are developed for this reason. In our research, we used to figure out the users knowledge structure by rating information of these posting and replying related to a user. Tagged post or reply, counted and rated during members interaction can be used to figure out each members knowledge status more precisely, tags added by the author indicate the knowledge domains the member is proficient at and ratings from other members represent his/her proficiency level in these knowledge domains. After identification of the posted documents relevant to an EC member, they are used to profile users knowledge structure. For a document Di, the knowledge shown in it can be expressed using a knowledge vector KDi as in (1) which Lij is proficiency level in each domain (j) of the knowledge in document Di and N is the number of domains:

$$KDi = [Li1, Li2, Li3, ..., Lin]^T \quad (1)$$

Then next step is show the knowledge structure of EC member (k) that can be expressed by using a knowledge vector as follow (2):

$$Xk = [Lk1, Lk2, Lk3, ..., Lkn]^T \quad (2)$$

The result of this is a new knowledge vector in the same vector space as the document knowledge vectors. If the member is newcomer, there is no reviewing and replying record so to overcome cold-start problem, his/her proficiency level in each knowledge domain is set to a medium value. Then the knowledge relationship between member i and j can be calculated by the similarity between their knowledge structure represented using knowledge vectors X i and X j as in (3):

$$R(i,j) = \cos\theta = \frac{Xi.Xj}{||Xi||.||Xj||} \quad (3)$$

Knowledge transferring will be easier if the knowledge requester and knowledge contributor share more common knowledge, i.e., they have more similar knowledge structures.

On the other hand, if the knowledge structure of knowledge contributor is very similar to that of the knowledge requester, then what can be transferred is limited.

IV. Conclusion

To acquire and share knowledge, EC members must interact with each other. As the members interact, they become more and more familiar with each other, their knowledge structures co-evolve over time, and a multiple-relationship network, named knowledge sharing enterprise network, is formed among members. At the heart of each community lies a social network which affects members knowledge sharing behavior. In this paper, knowledge relationship of the network was modeled by Vector Space Model. In prior studies on knowledge sharing in ECs, the knowledge relationship was often neglected.

In this paper, our work was focused on the modeling of a component of knowledge sharing enterprise network .What we proposed in this paper is just a model of the knowledge relationship in knowledge sharing enterprise network in ECs. The application of the model to extracting the network from practical enterprise community web sites need to be considered carefully.

References

[1] G. David and C. Yen , *A synergic analysis for Web-based enterprise resources planning systems*, 2002.

[2] Lee,F.S.,Vogel, D., Limayem,M, *Virtual community informatics: a review and research agenda*, Journal of Information Technology Theory and Application. 5(1),pp 47-61. 2003.

[3] Koh J, Kim Y G, *Knowledge Sharing in Virtual Communities: an Ebusiness Perspective* ,Expert Systems with Applications, 2004, 26(2), pp. 155-166.

[4] Chao-Min Chiu, Meng-Hsiang Hsu, Eric T G Wang, *Understanding knowledge sharing in virtual communities: An integration of social capital and social cognitive theories*, Decision Support Systems, 2006(42), pp 1872-1888.

[5] Hall, Hazel, Dianne Graham, *Creation and recreation: motivating collaboration to generate knowledge capital in online communities*, International Journal of Information Management, 2004, pp 235-246.
[6] Meng-Hsiang Hsu, Teresa L JU, Chia-Hui Yen, Chun-Ming Chang, *Knowledge sharing in virtual communities:The relationship between trust, self-efficacy and outcome expectations*,International Journal of human-computer studies, 2007, pp 153-169.
[7] Andrew C. Inkpen et.al, *Social capital, network and knowledge transfer* ,Academy of Management Review, 2005, Vol. 30(1), pp 146-165.
[8] Stephen J.H. Yang and Irene Y.L. Chen, *A social network-based system for supporting interactive collaboration in knowledge sharing over peer-to-peer network*,Int. J. Human-Computer Studies, 66(2008), pp 36-50.
[9] Hall, Hazel, Dianne Graham, *Creation and recreation: motivating collaboration to generate knowledge capital in online communities*,International Journal of Information Management, 2004(24), pp 235- 246.
[10] Robin Cowan, Nicolas Jonard, *Network structure and the diffusion of knowledge*, Journal of Economic Dynamics and Control, 2004, pp 1557-1575.
[11] Ray Reagans, Bill McEvily, *Network Structure and Knowledge Transfer: The Effects of Cohesion and Range* , Administrative Science Quarterly, 48 (2003), pp240267.
[12] Davis F. *Perceived usefulness, perceived ease of use, and user acceptance of information technology* MIS Quarterly, 1989,13(3), pp 319-340.
[13] Luria, A. R, *Cognitive Development*,Cambridge, MA. Harvard University Press. 1978.
[14] Wang Jyun-Cheng and Chiu Chiu-Chen, *Recommending trusted online sellers using social network analysis* ,Expert Systems with Applications, 2008 (34), pp 1666-1679.
[15] Peter Moka., *Flink: Semantic web technology for the extraction and analysis of social networks*,Web Semantics: Sciences, Services and Agents on the World Wide Web 3(2005), pp 211-223.
[16] Hansen M, *The Search - Transfer Problem: The Role of Weak Ties in Sharing Knowledge Across Organizational Subunits*, Administrative Science Quarterly, 1999, pp 82-111.
[17] R Burt, *Structural Holes* MA Cambridge, Harvard UniversityPress,1992.
[18] Granovetter,*The Strength of Weak Ties*, American Journal of Sociology, 1973 (78).
[19] Nonaka., *A dynamic theory of organizational knowledge creation*, Organization Science, 1994,5 (1), pp 14-37.
[20] Wasko, M.M., Faraj, S. *Why should I share? Examining social capital and knowledge contribution in electronic networks of practice* , MIS Quarterly, 2005,29 (1), pp 3557.
[21] Joon Koh, young-Gul kim, Brain Butter and Gee-Woo Bock, *Encouraging participation in virtual communities*,Communication of ACM, 2007,50(2), pp 69-73.
[22] Sangman Han and Beom Jun Kim., *Network analysis of an online community* Physica A 387(2008), pp 5946-5951.
[23] R. Baeza-Yates, R. Ribeiro-Neto, *Modern Information Retrieval*, Addison-Wesley,1999.

Multilevel Coset coding of video with Golay codes

Aparna.P , Dr Sumam David
Department of Electronics and Communication Engineering
National Institute of Technology Karnataka, Surathkal
Email: p.aparnadinesh@gmail.com, sumam@ieee.org

Abstract -**This paper presents a video coding method based on the principle of distributed source coding. This work aims in shifting the encoder complexity to the decoder to support uplink friendly video applications, simultaneously achieving the rate-distortion performance of the conventional predictive coding system. In this work concept of syndrome coding with Golay codes is adopted for compression. The simulation results presented in this paper reveals the superior performance of this distributed video coder over the Intraframe coders and predictive coders for video data with less correlation between frames.**

Keywords: predictive coding, coset, uplink, distributed video coding (DVC)

I. INTRODUCTION

Extensive developments in VLSI technology and computing capabilities have made a number of advanced video applications like video conferencing, video telephony, DVD, video-on demand etc possible. With increased technology power more complex video applications like HDTV, 3-D movies, 3-D games have come in to existence demanding higher compression performance. Current popular video standards like ISO MPEG and ITU-H.26x have been successful in delivering the required compression and quality standards. These standards have an interframe coding model that exploits source statistics at the encoder resulting in a very high compression performance at an acceptable quality level. The interframe coding model uses motion estimation and compensation algorithm at the encoder that removes the temporal redundancy between frames. The motion estimation and compensation process amounts to 80% of the encoder complexity and computational resources resulting in a bulky encoder with higher power consumption. This feature makes it inappropriate for uplink friendly applications like mobile video cameras, wireless video sensor networks, wireless surveillance etc. These wireless video applications demand a simple encoder since power, size and the computational resources are of primary concern in the wireless scenario. Distributed Video Coding is a new coding paradigm that attempts to fulfill the requirement of wireless- video applications. In this scheme the complex motion search algorithm at the encoder is eliminated, but can be incorporated at the decoder. Distributed video coder thus exploits the source statistics at the decoder alone, interchanging the traditional balance of complex encoder and simple decoder. A video codec working on this principle is thus very promising for uplink friendly video applications. In such a coding system the encoder encodes each video frame separately with respect to the correlation statistics between itself and the side information. The decoder decodes the frames jointly using the side information available only at the decoder. This video paradigm is as opposed to the conventional coding system where the side information is available both at the encoder and decoder. Alternatively, we have the intraframe coding scheme (Motion- Jpeg) with a low complexity encoder but a poor rate-distortion performance as the temporal redundancy across the frames are not taken care. However it provides robustness against channel errors [1] as every frame is coded independent of others. All these factors lead to the development of a new coding paradigm called the Distributed video coding that needs to incorporate within itself the merits of interframe coding scheme and intraframe coding scheme. Such an architecture promises higher compression efficiency, robustness to wireless channel errors and at the same time distribution of complexity between encoder and decoder. In this paper, we present an approach used for video coding based on the principle of multilevel coset coding using Golay codes and compare it with H.263+ Intra coding [6], H.264 Intra coding [7], H.263+ Inter coding [6]. We also compare the complexity and performance of this work with [8] which presents a syndrome coding approach based on LDPC codes.

II. PRINCIPLE

Distributed Video coding concept is based on the information theoretic bounds established in 1970s by Slepian-Wolf [2] for distributed lossless coding and by Wyner-Ziv [3] for lossy coding with decoder side information. Practical distributed video coders specifically work on the principle of Wyner-Ziv coding considering a distortion measure. In conventional coding system, the source is coded with respect to the side information that is available both at the encoder and decoder. In distributed video coding system side information is not available at the encoder, but the encoder encodes each frame separately with respect to the correlation statistics between itself and the side information. The decoder has access to the side information and hence decodes the frames jointly using the side information. In distributed video coding environment side information Y is treated as the noisy version of the source X i.e $X = Y + N$. Statistically dependent side information Y, is available only at the decoder and if X is the source that is to be transmitted using least average number of bits. The encoder must therefore encode X in the absence of Y, whereas the decoder jointly decodes X using Y. In this context

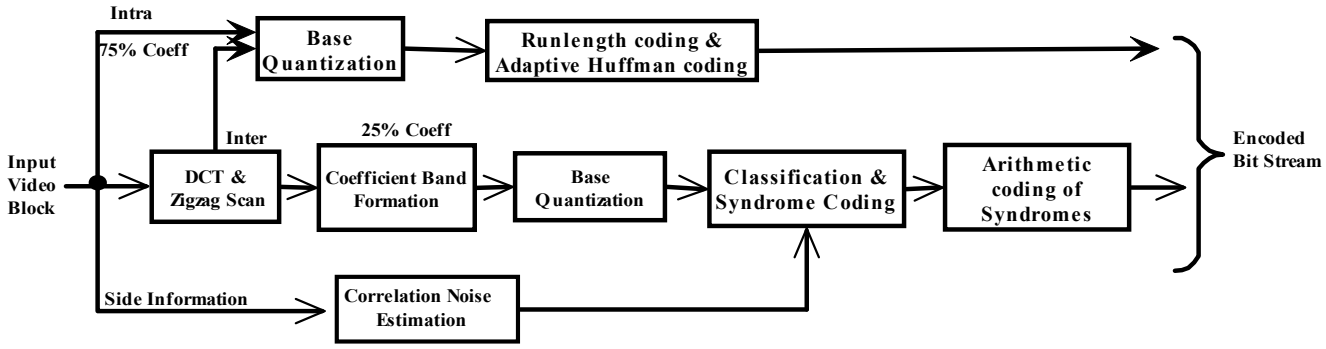


Fig.1 Video Encoder Block Diagram of the Proposed Method

X is compressed to syndrome S of a channel code [5]. These syndromes identify the coset to which X belongs to. The receiver on receiving the syndrome S identifies the code word from the corresponding coset that is close to the side information Y. This corresponds to coset channel coding. This is done by using a parity check matrix H of a (n, k) linear channel code. Compression is achieved by generating syndrome bits of length $(n - k)$ for each n bits of data.

III. PROPOSED SCHEME

Encoder: The encoder block diagram of the current implementation is as shown in the Fig.1. The first frame is coded as the intra frame. Each of the consecutive frames are intercoded. An intra frame is introduced after an interval of p frames. Each 8 × 8 block of the frame is transformed using Discrete Cosine Transform. The transformed coefficients are zig zag scanned so that they are arranged in the order of their importance. For the frames to be coded as intra, these coefficients are scalar quantized and entropy coded using Huffman and run length coding. For the frames to be intercoded, these transformed coefficients are formed into coefficient bands such that each coefficient at the same spatial location within a block is combined together in one coefficient band. The first coefficient band corresponds to all DC coefficients and hence is very significant. Around 1/4 of the coefficients in a block are chosen for intercoding and hence number of bands is limited to 16 in a block of size 8 × 8. The remaining 3/4th of the coefficients are less important and hence can be quantized and entropy coded like intra blocks. These coefficients are insignificant and hence contribute less to the compression performance. Each of the coefficient bands is assigned different number of bits for quantization. More number of bits are assigned to higher bands and less number of bits to lower bands. Proper decoding of the syndrome coded bits requires that the band step size is greater than the correlation noise. Hence a different set of bit allocation is pre-defined. One of these data sets is chosen based on the input data. The bit allocation data set is chosen based on the average of the correlation noise between each band and the corresponding coefficient band of the side information, such that the above criterion is fulfilled. Each of these coefficients bands are uniformly quantized with reference to the bits allocated for each band. Syndrome generation for these bits is based on the principle of multilevel coset code proposed in [5]. Syndrome for each quantized coefficient is generated based on the correlation noise between the source and the side information. In this case syndrome corresponds to the bits that cannot be inferred from the best side information. The Fig.2 shows the quantization bin, where X_i represents the source, X_{qi} quantized value of the source, Y_i represents side information, $\triangle$ represents the stepsize of the corresponding band. The N_i represents the correlation noise, given by $N_i = X_{qi} - Y_i$. In the presence of side information Y_i the number of least significant bits that needs to be communicated to the encoder is given by

$$l_i = 2 + \left\lfloor \log_2\left(\frac{|(N_i)|}{\Delta}\right) \right\rfloor ; N_i > \Delta \qquad (1)$$

$$l_i = 0; \text{else} \qquad (2)$$

The syndrome bits to be communicated to the decoder can be obtained by:

$$S_i = X_{qi} \,\&\, (2^{li} - 1) \qquad (3)$$

where & represents bitwise AND operation. The number of least significant bits l_i , for each coefficient should also be sent along with these bits. Hence for each coefficient, the value of l_i and l_i number of least significant bits are mapped to a unique symbol :

$$S_{ti} = 2^{li} + S_i \qquad (4)$$

where + denotes bitwise OR operation. Transmitting syndrome bits is equivalent to dividing the quantization lattice into sub lattices as shown in the Fig.2 up to the level specified by l_i . Thus the number of least significant bits that needs to be communicated to decoder is dependent on the correlation noise between the source X and the side information Y. Bit planes marked in gray in Fig.3 are transmitted to the decoder and the bit planes in white can be inferred from the side information. More the correlation noise, more number of bits are to be transmitted to the decoder. This corresponds to Wyner-Ziv coding where in the least significant bits that cannot be obtained from the side information is transmitted to

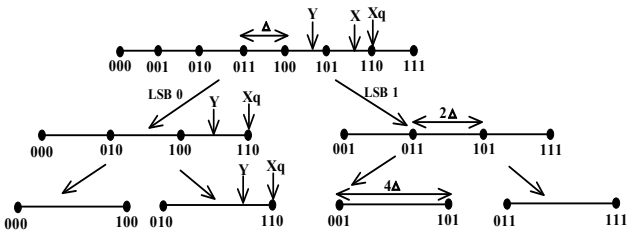


Figure 2. The quantization bin [5]

the decoder. The unique symbol S_{ti} obtained from l_i and S_i is then arithmetic coded and transmitted to the decoder.

Coset Channel Coding using Golay code : In order to reduce the bitrates further, some of the bitplanes can be coset channel coded. These bits as shown in Fig.3 cannot be generated by side information and hence are transmitted to the decoder. However this may incur higher bitrate. In order to further reduce the bitrate, some of the least significant bitplanes are further compressed based on the principle of distributed source coding [5]. Distributed video coding in [8] uses LDPC codes for coset channel coding. This gives only a marginal gain in the bitrate with reasonable quality, but at the cost of very high complexity at the decoder. It also needs a very long block length n to give a good performance. In this method (23,12,7) Golay code is used where the block length n is 23 and the message bit length k is 12 and the hamming distance d_{min} between the code words is 7. In this method the parity check matrix H of a (23,12,7) Golay code is used to generate the syndrome bits S_i from the input bits X_i . One or two least significant bitplanes of the syndrome bitplanes can be considered for coset channel coding which are formed into a block of n bits each as shown in Fig.3. Each of the n bits of X_i say b_{xi} block is transformed into $(n - k)$ syndrome bits Z_i by using the parity check matrix H according to

$$Z_i = Hb_{xi} \qquad (5)$$

Thus n data bits are compressed to $(n - k)$ syndrome bits giving a compression rate of $(n /n - k)$. Two methods can be adopted for side information generation. If a less complex decoder is desirable we consider the co- located block of the reference frame as side information. The other method of generating the side information is by performing the motion search for the candidate predictor Y. This is done by transmitting some cyclic Redundancy check (CRC) bits generated on the quantized codewords which helps the decoder to find the best side information.

2) Decoder: The block diagram of the decoder is shown in the Fig.4. The frames that are intracoded are passed through an entropy decoder, then dequantized and inverse transformed to get back the intra coded frame. The coefficients that are syndrome coded are first passed through the arithmetic decoder to decode the unique symbol S_{ti} . From this symbol S_{ti} the number of least significant bits l_i and the syndrome bits Z_i are obtained. At the decoder only the syndrome bits Z_i and the side information bits Y_i are available. As long as the hamming

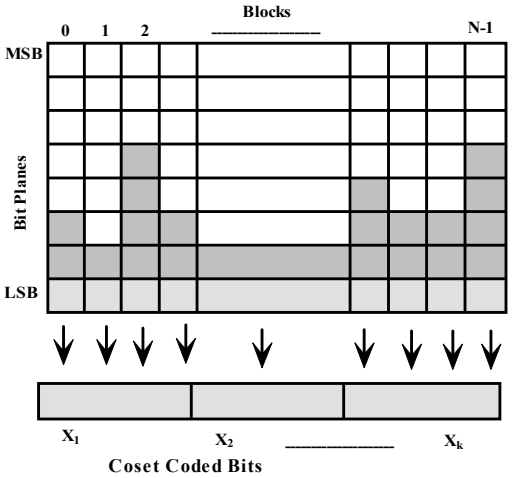


Figure 3. Bitplanes of a single coefficient Band

distance between X_i and Y_i is less than d_{min} of the Golay code, the data b_{xi} can be recovered. The syndrome bits Z_i indicates the coset to which b_{xi} belongs to. The coset leader of that coset is chosen as say A_i . We then find Y_i' such that $Y_i^{'} = Y_i \oplus A_i$, where $\oplus$ is bitwise EXOR operation. We then find b_{xi}' a codeword corresponding to the Golay code closest to Y_i'. The required data bits X_i is then obtained from b_{xi}' as $b_{xi} = b_{xi} \oplus A_i$. These decoded bits b_{xi} are combined with rest of the multilevel coset coded bits to reconstruct back the current frame. Side information generation unit provide the best side information Y_i for the current frame. Based on the side information Y_i the rest of the MSBs are retrieved and combined together with the LSBs to form the current frame coefficient band for X. The coefficient bands are uniform dequantized based on the bit allocation set chosen. Rest of the coefficient that are intracoded are further combined with syndrome decoded coefficients and then block inverse DCT is applied to get back the original frame. In case of complex decoder side information is generated by performing the motion search and quantizing the candidate block and computing the CRC. If the CRC matches, that block is considered as side information. By using a (n, k) linear channel code, the encoding rate achieved is $(n - k)/n$. In the work [8] the syndrome coding of the inter coefficients was done using 3/4 and 1/2 rate LDPC code. It is observed that for a 1/2 rate LDPC code, the correlation of the sources with the side information should be very high, which other wise would result in high distortion. On the other hand the use of 3/4 rate LDPC encoder results in less distortion, but the compression achieved is quite low. The other issue with the LDPC code is the parity check matrix H which needs to be generated in real-time or stored at the encoder. This would increase the complexity of the encoder as storing increases the resource requirement and power consumption. Also LDPC codes require long block lengths and high decoding complexity. As the block length of the data to be coset channel coded is small, LDPC code seems to be unsuitable for the current implementation. Hence in this work Golay codes have been considered for coset channel coding. The encoder of this

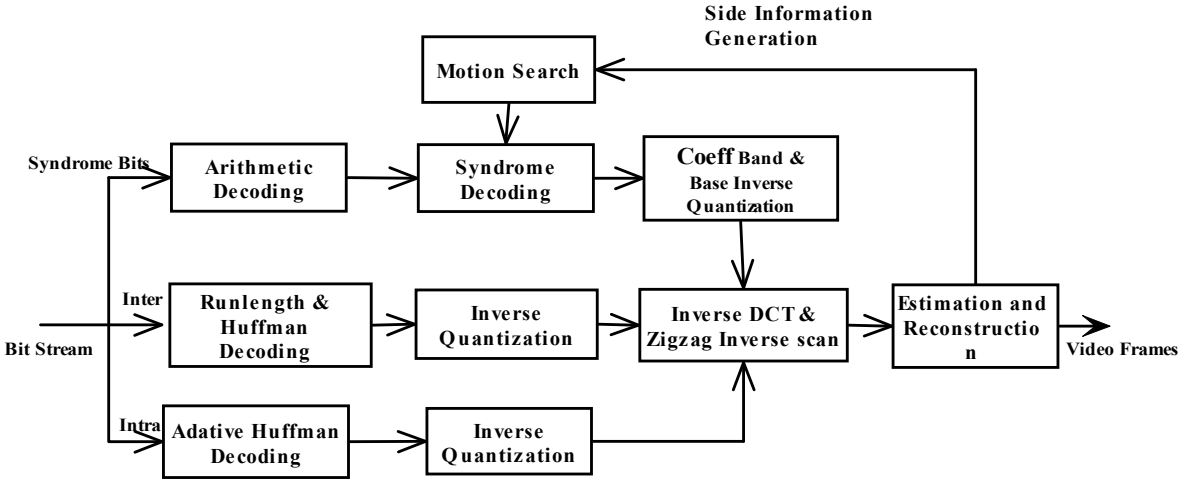


Figure 4. Video Decoder of the proposed scheme

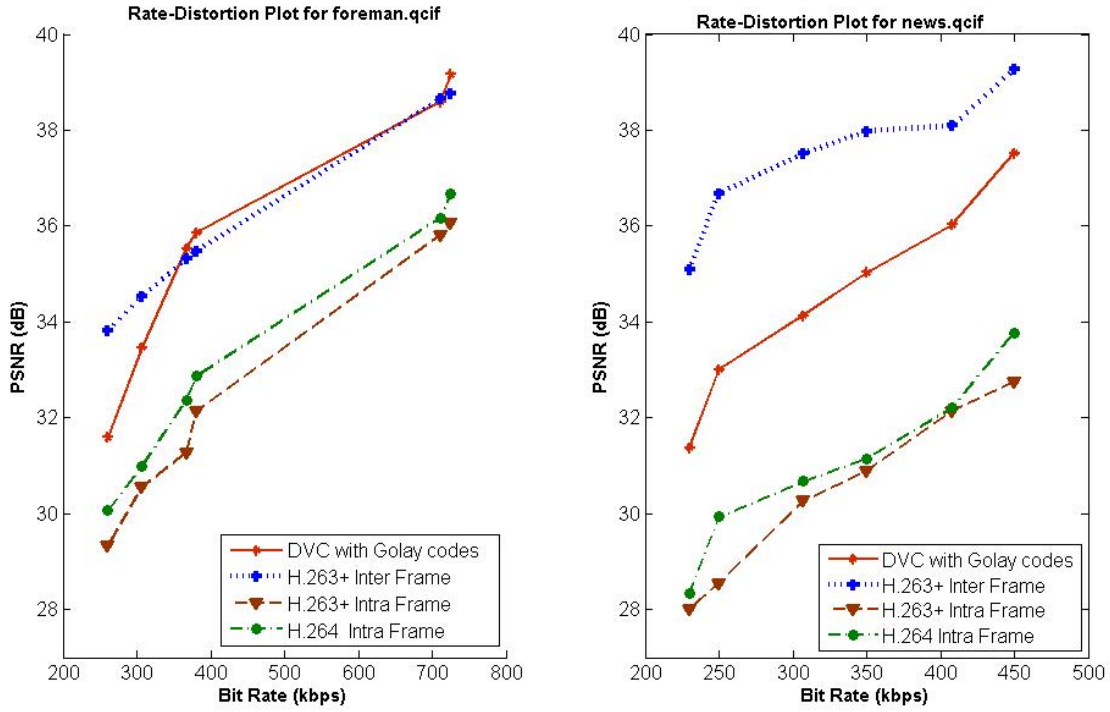


Fig. 5. Comparison of rate-distortion performance of various methods for a frame rate of 30 fps

method is simple satisfying the main objective of this work. Also quality of the reconstructed sequence is good with Golay codes for a 1/2 rate encoder.

IV. SIMULATION RESULTS

Video Codec is designed to support an application to wireless network of video camera equipped with cell phones. Encoder allows the storage of one previous frame. Objective performance evaluation of the system is done by comparing the bit rate and the Peak Signal to Noise Ratio (PSNR) between the original and the reconstructed video sequence. The method discussed above has been simulated and the results are presented in this paper. Two test video QCIF sequences with a resolution of 176 × 144 are considered for evaluating the rate distortion. These video files are considered based on their motion content. The frames of foreman.qcif have less correlation when compared to news.qcif file. As seen in the Fig.5, the Luma PSNR is plotted against different bitrates for different methods. The performance of distributed

video codec discussed in this paper is compared with H.263+ Intra Frame coder [6], H.264 Intra Frame coder [7], H.263+ In- ter Frame coder [6] for foreman.qcif and news.qcif at a frame rate of 30 fps. From the simulation results we can see that the DVC implementation performs considerably well for video sequences with higher motion content i.e foreman.qcif. For video sequences with less motion content (i.e more correlation between adjacent frames) H.263+ Inter coder performs better than DVC implementation. Also an improvement of at least 3dB is seen in the current implementations when compared to the syndrome coding with LDPC codes [8]. However the results of DVC implementations are consistently better than H.263+ Intracoder and H.264 Intra coder.

V. CONCLUSION

Coset channel coding using Golay Code has been introduced in this method. Use of simple block codes will improve the rate-distortion performance further without increasing the encoder complexity. Use of LDPC codes for coset channel coding is eliminated as it increases decoder complexity and the requirement of resources at the encoder without contributing much to the rate distortion performance. Also a proper statistical model for classification will drastically improve the performance of the coder. The main aim of this work is to reduce encoder complexity making it pertinent to uplink friendly architecture which seems to be satisfied. It is also observed that the current implementation operates well in high quality (PSNR of order of 30dB) regime. The extension to lower bit rates without any compromise in the quality so that it is comparable with the conventional codecs can be further considered without increasing the complexity.

REFERENCES

[1] Bernd Girod, Anne Margot Aaron, Shantanu Rane and David Rebollo- Monedero, "Distributed Video Coding ", Proceedings of the IEEE, Volume 93, Issue 1, pp 71 - 83 , Jan 2005

[2] J. D. Slepian and J. K. Wolf, "Noiseless coding of correlated information sources", IEEE Transactions on Information Theory, vol. IT-19, pp. 471- 480, July 1973.

[3] A. D. Wyner and J. Ziv, "The rate-distortion function for source coding with side information at the decoder ", IEEE Transactions on Information Theory, vol. IT-22, no. 1, pp. 1-10, Jan. 1976.

[4] A. D. Wyner, "Recent Results in the Shannon Theory ", IEEE Transactions on Information Theory, vol. 20, No. 1, pp. 2-10, Jan. 1974.

[5] S. S. Pradhan and K. Ramchandran, "Distributed source coding using syndromes (DISCUS): Design and construction", Proc. IEEE Data Compression Conference, Snowbird, UT, pp. 158 -167, Mar. 1999.

[6] G.Cote, B.Erol, M.Gallant, and F.Kosssentini, "H.263+:Video coding at low bitrates ", IEEE Transactions. Circuits Sys. Video Technology, Vol 8, No 7, pp 849-866, November 1998.

[7] T. Wiegand, G.J.Sullivan, G.Bjontegaard and A.Luthra, "Overview of the H. 264/AVC video coding standard ", IEEE Transactions on circuits and systems for video technology, Vol 13, No 7, pp 560-576, 2003.

[8] Aparna P, Sivaprakash Reddy, Sumam David, "Distributed video coding using LDPC codes for wireless video ", Journal on Wireless Sensor Networks, Scientific Research Publishing, Inc. USA, pp 334-339, Nov 2009,

[9] Rohit Puri, Abhik Majumdar and Kannan Ramachandran, "PRISM: A video Coding Paradigm with Motion Estimation at the Decoder", IEEE Transactions On Image Processing, Vol 16, No 10, October 2007.

[10] R. Puri and K. Ramchandran, "PRISM: A new robust video coding architecture based on distributed compression principles", Proc. Allerton Conference on Communication, Control and Computing, Allerton, IL,Oct. 2002.

Model for Courseware Development of Teaching and Learning Traditional Craft (CDTC Model): Initial Validation

Salyani Osman, Nor Azan Haji Mat Zin, Noraidah Sahari@Ashaari and Yuhanis Omar
Faculty of Information Science and Technology
Universiti Kebangsaan Malaysia
Selangor, Malaysia
salyani@unisel.edu.my, azan@ftsm.ukm.my, nsa@ftsm.ukm.my, yuhanis3207@gmail.com

Abstract— **Alternative method to reduce dependency on instructors in teaching and learning traditional crafts will be greatly benefited from electronic learning practices. In order to make sure the courseware for teaching and learning traditional craft is applicable, effective and support teaching and learning pedagogy, a model for courseware development of teaching and learning traditional craft was developed and derived from methodologies synthesized from related research areas. Through an extensive review of literature, the model was specifically designs to meet the needs of adult learners in a web-based environment with concentrating on designing strategic learning using cognitive apprenticeship approaches. The aim of this study is to verify each component of the proposed model (namely CDTC Model) through initial validation by an Evaluator Committee that was appointed among selected craft instructors from National Craft Institute, Rawang, Malaysia (Institut Kraf Negara (IKN)). The validation is purposely to examine, evaluate, and score the efficacy of each proposed components according to its relevance to the model and was realized through quantitative investigation using questionnaire among Evaluator Committee. The committee, evaluated the model and made recommendations for improving the model. Components validated by committee were used in designing a preliminary version of the model. A significant contribution in this research is to provide relevant preliminary CDTC model for courseware development of teaching and learning traditional craft that will support and preserve our traditional heritage for future generation. With the development of the CDTC model, hopefully it will encourage courseware designers to develop more multimedia applications for teaching and learning traditional craft as well as a good reference for educators, instructional designers, and product developers for developing interactive multimedia applications.**

Keywords — **Electronic Learning; Traditional Craft; Traditional Apprenticeship; Teaching and Learning**

I. INTRODUCTION

Preservation of traditional crafts should be seriously done to make sure this cultural heritage can be everlasting presented and inherited to future generations. Although the crafts were very popular among the local community in the past, but now they are less enthused by the young generation to learn these crafts. The use of mechanical equipments in the production of traditional crafts is also a threat and led to neglecting traditional teaching and learning of hand crafts. A better approach is needed to attract young people to learn these traditional crafts in order to avoid boredom and boring learning, and most important can be easily learned at any desired paced and time. Basically, the conventional way of learning a traditional craft is through direct observation of the instructor called traditional apprenticeship [4]. This is the most common means of educating students in the fields of practices to obtain practical skills, guidance and assistance from instructors. As the learning is mostly done through observation, student has put high level of dependency to instructor [2]. There is an obvious problem in conventional approach when instructor needs to teach a group of students. It is potentially limiting the support from instructor to monitor, focus and assess student individually. The most major problem found in this type of learning also reducing students' ability to solve their own problems especially at the beginning of learning as they much like referring and asking to the instructors. This also reduces the students' cognitive and construction of knowledge. To reduce dependency on instructors and to conserve teaching and learning of traditional crafts, it is appropriate to provide digital learning of traditional craft as in the past decades there have been many efforts to integrate technology into teaching and learning practices. In order to make sure the courseware for teaching and learning traditional craft is applicable and support teaching and learning pedagogy, a model (CDTC model) for courseware development of teaching and learning traditional craft was developed as a guide to courseware developers and other researchers. Through an extensive review of literature, CDTC model was specifically designs to meet the needs of adult learners with concentrating on designing strategic learning using cognitive apprenticeship approaches. Cognitive apprenticeship (CA) has been developed essentially to place learner in an authentic work environment as a partial participant. The focus of this learning-through-guided experience is on cognitive and meta-cognitive skills, rather than on the physical skills and processes of traditional apprenticeships [5].With the

development of the model, it will encourage courseware designers to develop more multimedia applications for teaching and learning traditional craft. Thus, this effort will preserve our traditional heritage for future generation. Therefore, the aim of this study is to verify the components of the proposed CDTC model developed by previous study [7] through initial validation for each component by selected craft instructors.

In this paper, a review of proposed CDTC model for courseware development of teaching and learning traditional craft were discussed in Section 2. Section 3 presents the methodology and results from initial validation of the proposed CDTC model that has been done. Section 4 is the conclusions.

II. Review of Proposed CDTC Model

A. Establishing Components of Model

In order to produce well-developed model, some main aspects have been considered including analysis of relevant teaching and learning theories; and analysis of existing learning models and multimedia applications for teaching and learning crafts. As a result of the analysis, important components were absorbed into the development of proposed CDTC model which comprised of two main components (i) teaching and learning components and (ii) digital traditional craft components. The model is embedded in virtual learning environment (VLE) which consists of four flexible utility frameworks 1) Presentation Framework (PF) 2) Control Framework (CF) 3) Data Storage Access Framework (DSAF) and 4) - eLearning Framework (eLF') [6].

The teaching and learning components consist of six (6) primary elements as follows: 1. *Teaching and learning goal setting* which emphasize on the teaching and learning objectives. It is very important to clearly define teaching and learning goal setting in order to accomplish teaching and learning goals for selected traditional craft. 2. *Teaching and learning theories adaption* enable to provide the appropriate learning environment and improve learning effectiveness. Such theories are Social Learning Theory, Cognitive Theory, Constructivism Theory, Behaviorism Theory, Mastery Theory and Adult Learning Theory (Andragogy) 3. *Course Materials Design* - Designing course material involves selecting contents and elements used for appropriate craft learning. It is tailored to selected teaching and learning theories. This component divides the contents into sequence of delivery 4. *Teaching and Learning Strategy* which determine the approach for achieving the learning objectives. The strategies are usually tied to the needs and interests of students to enhance learning and are based on many types of learning styles [3]. Cognitive apprenticeship method is identified to be used and can be highlighted through simulations, discussion, tutorials and exercises 5. *Course Structure Design* involves designing layout of the elements in the presentation. The elements such as visual, verbal, animation and chunking of information will be drawn on as the way of information is placed on the screen and 6. *Delivery design* will be divided into several parts such as introduction, body, conclusion and assessment for the whole presentation.

Meanwhile for digital traditional crafts components are based on the following primary elements: 1. *Multimedia Technology and Elements* - Selective multimedia technology will stretch the multimedia experience to envelop the user. This technology and their elements allow learners to visualize craft learning and thereby improving their learning (retention) and their performance when transferring from the virtual world to the real world 2. *Immersive* - Courseware should make learners absorbed with the environment and the student can experience a sense of presence and interact with the other characters within that place (virtual world) 3. *Interactive Design* allows users to control what elements are to be delivered and when they are to be delivered. Interactivity is important as intermediary between learners and contents 4. *Adaptive Crafts Modules* are designed based on learning goals and it is structured using course materials design 5. *Self-assessment* - Through self-assessment, learners can track their personal development and deepen their learning experience. They take more responsibility for their own learning and become more aware of their own knowledge gaps too. Learners can evaluate their performance based on level of difficulties and 6. *Rewards* - Each exercise determines the level of learner's performance. Reward is given after completing each exercise.

III. Initial Validation

The aim of this study is to verify the components of the proposed CDTC model through initial verification for each component by selected craft instructors. The validated components will be used for designing a preliminary version of the model.

A. Method

Research instrument was established to verify the components of the proposed model. This initial verification study is conducted through a survey based on a Likert Scale among Evaluator Committee comprised of sixteen (16) experts in the areas of traditional crafts from National Craft Institute, Rawang, Malaysia. This committee was established to assist in determining the appropriate components and also assist in providing feedback to improve and enhance the proposed model.

The questions were designed based on the proposed CDTC model components. A total of 16 copies of the questionnaire were distributed on 18 May 2010 among instructors of the Fakulti Seni Kraf Tenunan, Fakulti Seni Kraf Kayu and Fakulti Seni Kraf Rotan. All of them had completed their diplomas and degree in the respective craft field. Instructors that have been chosen as Evaluator Committee must have at least one year experience in teaching traditional craft. Evaluator Committee will examine and evaluated the importance and efficacy of each component listed according to its relevance to the design of the model. The proposed components was rated on a Likert Scale using the following five categories listed in Table 1, as refer to previous study [1]. It was agreed by all evaluators that components receiving an average rating

less than 2.0 would be removed from the list. Evaluator Committee also allowed to suggest any appropriate components that relevant to proposed CDTC model. The proposed component that was suggested by more than five (5) members from Evaluator Committee will be considered and then will be verified through second validation session with five (5) selected evaluators that were randomly chosen from Evaluator Committee members. The second validation method was basically same as Initial Validation using five categories of Likert Scale listed in Table 1.

B. Results

The results are based on all completed questionnaire by 16 Evaluator Committee comprised from 56.2% (n=9) males and 43.8% (n=7) females and came from 37.5% (n=6) from Fakulti Seni Tenunan, 31.25% (n=5) from Fakulti Seni Kraf Kayu and 31.25% (n=5) from Fakulti Seni Kraf Rotan. Table II shows mean score for each component of the proposed model. From the table it shows all listed components in the proposed CDTC model received average rating higher than 2.0 except component 8 which was ranked at an average mean score of 1.94. Because the score of this component was below the 2.0 scoring margin, it was agreed to remove it from the list.

TABLE I.
COMPONENT RATING SCALES

Rating	Category
1	Very Low: The component is not relevant to the model. *(Not a consideration at all)*
2	Low: Will have minimal impact on the model. *(Unimportant/minimum consideration)*
3	Moderate: The component should be included in the model. *(Neutral consideration)*
4	High: The component will add value to the model. *(Important consideration)*
5	Very High: The component is central to the efficacy of the model. *(Very important consideration)*

TABLE II.
MEAN SCORE FOR EACH COMPONENT OF THE PROPOSED CDTC MODEL

Proposed Model Components	Mean Score
A. Teaching and Learning Components	
1. Teaching and learning goal setting	3.94
2. Teaching and learning theories adaption	3.63
3. Course Materials Design	4.00
4. Teaching and Learning Strategy	4.00
5. Course Structure Design	3.63
6. Delivery design	3.88
B. Digital Craft Components	
7. Multimedia Technology and Elements	3.94
8. Immersive	1.94
9. Interactive Design	3.63
10. Adaptive Crafts Modules	3.75
11.Self-assessment	4.19
12. Outcomes / Rewards	4.13

From the reviewed questionnaire, it was found that one (1) new proposed component (multimedia database) was recommended by seven (7) members from Evaluator Committee as suggestions for improving the model and to make sure the model is meeting user needs.

Result from second validation for the proposed component shows the component should be listed as one of the primary component in the CDTC model because it received average rating of 4.4.

C. Summary

Through discussion with Evaluator Committee, many committee members argued that component 8 (immersive) did not belong on the list. The general consent was it was unnecessarily to include virtual reality elements in digital teaching and learning traditional craft as the term of immersive is synonym with virtual reality environment. Meanwhile from their point of view, they agreed that multimedia database component is appropriate to the model to allow accessibility of data and enable more flexible learning and provides more options in hosting one or more primary media file types.

After the primary components of the model were determined (from initial validation and second validation for the proposed component), a preliminary CDTC model was developed as shown in Figure 1.

IV. CONCLUSION

This paper presented the preliminary CDTC model that will be used to assist and guide educators or developers in developing multimedia courseware for teaching and learning traditional craft. In order to provide a relevant model to users, the proposed CDTC model was examined in this study through initial validation by selected committee to improve and enhance the proposed components. Further research will be done to investigate the effectiveness of preliminary CDTC model applied in web-based courseware for teaching and learning traditional craft.

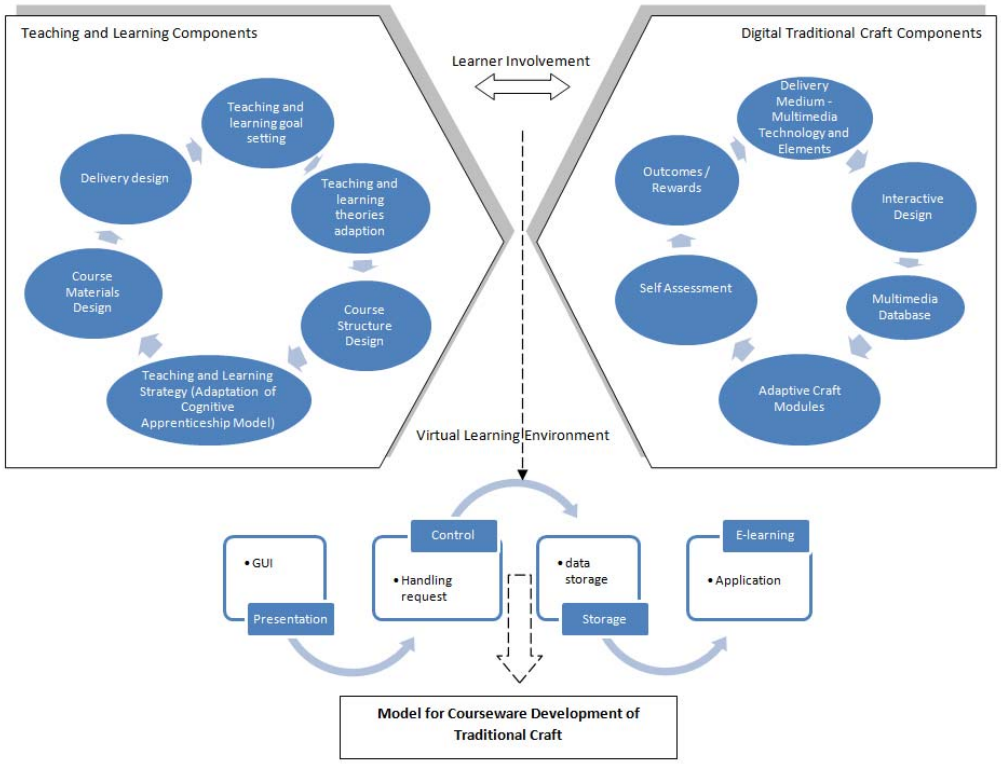


Figure 1. Preliminary CDTC model for courseware development of teaching and learning traditional craft

REFERENCES

[1] Biello, A. D., "A Model for Developing Interactive Instructional Multimedia Applications for Electronic Music Instructors," *Proquest Dissertations And Theses 2006*. Florida: Nova Southeastern University; 2006. Publication Number: AAT 3206011.

[2] Collins, A., Brown, J.S., Newman, S., "Cognitive Apprenticeship: Teaching the Crafts of Reading, Writing and Mathematics," In: Resnick, L.B. (Ed.), Knowing, Learning and Instruction: *Essays in Honor of Robert Glaser*. Lawrence Erlbaum Associates, New Jersey,1989, pp. 453–494.

[3] Ekwensi, F., Moranski, J., & Townsend-Sweet, M., "E-Learning Concepts and Technique," Bloomsburg University of Pennsylvania's Department of Instructional Technology. *Instructional Strategies for Online Learning*, 2005.

[4] Gamble, J. "Modelling the Invisible: the pedagogy of craft apprenticeship". *Studies in Continuing Education*, 23, 2 , 2001, pp.185-200.

[5] Judith Conway, "Educational Technology's Effect on Models of Instruction," unpublished.

[6] Marius Dragomiroiu', Marian Ventuneac, Ioan Salomie and Tom Coffey, "Application Framework Development for Virtual Learning Environments", *25th Int. Conf. lnformation Technology lnterfaces IT/ 2003*, June 16-1 9, 2003, Cavtat, Croatia

[7] Osman, S. and N. A. H. M. Zin, "Proposed Model for Courseware Development of Virtual Teaching and Learning Traditional Craft," in *IEEE Proc. on The 4th International Symposium on Information Technology (ITSim) 2010*, June 2010, pp.293-298.

Evaluation and Routing of Power Transmission Lines by Using AHP Method and Genetic Algorithm

Mostafa Hosseini

Department of Artificial Intelligence

Science and Research branch of Azad University

Mostafah@systemgroup.net

Homa Famil Bahmani

Tehran Power Distribution

Company, IRAN

Bahmani.Homa@gmail.com

Abstract- Today optimization is one of the most important issues in all engineering fields. According to importance of this issue in planning power transmission lines, appropriate areas have been accreted for numerous researches. Widespread usages of GIS application and its combination with GA base methods offer practical solution for power transmission lines design. In this paper, we first study about efficient criteria for selecting appropriate points for installing towers, and then we can evaluate available points for installing power towers by one of the multi-criteria decision-making analysis, named Analytic Hierarchy Process. As we know, all of these nodes are not suitable for being one of the transmission line Points. So by using this procedure (AHP) we calculate cost function of transmission line between towers. Finally, with GA algorithm, the best and the most optimum route between source and destination will be selected.

Keywords: Power Distribution Line, Geographical Information System, Genetic Algorithm, AHP Method

I. INTRODUCTION

The first step in installation of power lines is to find adequate criteria for assessment and selection of nodes. In this context, GIS techniques have been used as efficient methods for finding an appropriate assessment model. In order to select the best route for constructing a network of power transmission lines.At first it is needed to find appropriate nodes for installing power tower furthermore,a function for calculating costs between nodes have to be found. In this paper both of mentioned processes are implemented by one of the multi-criteria decision analysis named AHP.

Intelligent algorithms are always helpful in complicated cases. Due to high flexibility and its quality variations, genetic algorithm is an appropriate strategy for calculating the best route for power transmission from a determined source to any destination.The value of genetic algorithm is defined when numerous nodes with their distances are available. Because in these situations old methods with fixed order such as Dijkstra's algorithm usually become frustrating and have high computational load.

In the beginning of this paper we will explain intended criteria for selecting appropriate nodes and also MCDA methods and their implementation necessity will be explain, and AHP method will represent as an optimum solution.

Then AHP algorithm will be implemented on specified criteria and we will find functions for calculating efficiency rate of power tower installation nodes and cost between the edges.

After that we will implement genetic algorithm on obtained routes to find the most optimized route in the minimum time. Finally we will demonstrate the resulting and will compare it with a similar method.

II. EVALUATION CRITERIA FOR INSTALLING POWER TOWER POINTS

To find an appropriate fitness function for selecting power tower points we need a series of criteria to make decision based on them and select the most optimal and the least costly nodes. Because of using AHP we can classify and prioritize our criteria. According to the research, the most important effective factors on selecting power tower nodes are divided into three categories: technical factors, natural environment factors and social environment factors [1]. Since engineering of lines construction has high importance, technical factors have more priorities. Of course each of three mentioned criteria divides to sub-criteria that we name them factor. Each factor has criteria for itself which are in lowest structure level and related expert is bound to give them weight. We say to these criteria index. Table 1 represents available criteria set in each layer.

Available criteria are selected among the several criteria and they are more important than the other ones in author's opinion so they can be ignored.

TABLE 1
Evaluatio Criteria for Appropriate Points

Criteria	Factors	Indicators
Technical	Executive	The observance of Authorized and legal-privacy Absence of noise interferencing Points with lower angle
	Maintenance	Accessibility Resistance in difficult weather condition Security
	Economic	Establishing Time Minimum Cost
Natural environment	Absence of enviromental-danger	Earthquake Flood Hurricane No damaging to the natural environment
Social-environment	Observing the general-rules	Avoid crossing the residential-areas and public facilities Avoid crossing agricultural-land and antiquities Coordination with regional Construction plans

III. EVALUATION CRITERIA OF ROUTE

After finding recommended nodes for installing power towers, we need to calculate route cost function between nodes to select the most optimal route. For calculating of this function, we need to have a series of evaluation criteria. Certainly score achieved by each node in previous level is an appropriate criterion for this level. But we shouldn't neglect from economic cost of route between two nodes because it is more important than the other criteria. Environmental noises and avoidance of passing forbidden areas are the other factors.

IV.EVALUATION BASED ON MULTI-CRITERIA

MC Harg (1968) presented Systematic method for planning on using appropriate locations by using the Compatibility concept of several appropriate points [2],[3]. He mentioned that there are effective factors in the selection of nodes that have different values. Therefore, optimizing them for a unique application is hard. He defined a simple matrix to determine the degree of compatibility. The main idea of MCDA is based on this concept. Over time the idea of multiple criteria decision by GIS system were advanced and converted to the multi criteria methodology concepts.

A. Integration of GIS and multi-criteria methods

Jankowski has proposed two methods for integrating GIS and Multi-criteria techniques: the loose coupling strategy and the tight coupling strategy. The main idea of the loose coupling strategy is to facilitate the integration by using a file exchange mechanism. The assumption behind this strategy is that multi-criteria techniques already exist in the form of stand-alone computer programs. The results of the decision analysis may be sent to GIS for display and spatial visualization. The loose coupling architecture is based on linking three modules (GIS module, Multi-criteria technique module and file exchange module), as seen in figure 1[4].

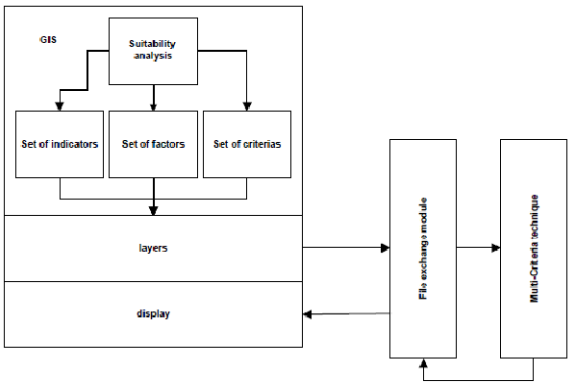


Fig. 1. Architecture of Loose Coupling

B. Analytic Hierarchy Process

It is a MCDA method and uses hierarchical architecture for showing the problem and spread of criteria and their priority based on user's judgment. This method was developed by Saaty (1980). Saaty showed that weighing process in multi-criteria decision is carried out effectively by using hieratical structures and two by two comparisons. Two by two comparisons based on judgment between two specific elements are done instead of comparison between all of the elements together.

C. Calculating the rules of criteria

At first we find importance of each criterion rather than the other. Their importance level is depending on the judgment of experts. In AHP standard, following table is used to calculate the level of importance.

If our criteria to be n, we place all the criteria in an n × n square matrix and we enter the degree of importance of corresponding elements. Suppose aij is the importance of element i (criterion) to element j, in this case aij is equal to the reverse of them. For example technical criteria are much more important than natural environment criteria. Therefore, its corresponding value is equal to 5 and the amount of its corresponding element in row and column reversed is equal to 1/5. Table 2 represents values assigned to each element.

TABLE 2
Fundamental Scale

Importance level	Concept	*aij*	*aji*
1	Equal	1	1
2	Between	2	$\frac{1}{2}$
3	More important	3	$\frac{1}{3}$
4	Between	4	$\frac{1}{4}$
5	Essential	5	$\frac{1}{5}$
6	Between	6	$\frac{1}{6}$
7	Very strong	7	$\frac{1}{7}$
8	Between	8	$\frac{1}{8}$
9	Absolute	9	$\frac{1}{9}$

D. Calculating fitness function for selection of nodes
Since we have 3 main criteria, coefficient matrix will be a 3×3 matrix.

TABLE 3
Criteria Importance Coefficient

	Technical	Natural invironment	Social invironment
Technical	1	5	3
Natural invironment	$\frac{1}{5}$	1	$\frac{1}{3}$
Social invironment	$\frac{1}{3}$	3	1

After calculating the importance of criteria, it is needed to normalize elements.At last, the percentage of the overall importance of each of the 3 criteria is determined with taking the average of its related row. Table 4 shows the stages of this process. As you see in this table technical criteria with 63% has the most importance.

TABLE 4
Normalized Value and Final Weight of Criteria

	Technical	Natural invironment	Social invironment	Final weight
Technical	0.65	0.55	0.69	$\sum \frac{1.89}{3} = 0.63$
Natural invironment	0.13	0.11	0.08	$\sum \frac{0.32}{3} = 0.11$
Social invironment	0.21	0.33	0.23	$\sum \frac{0.77}{3} = 0.26$

E. Evaluation of Factors and Indicators
Each of calculated criteria at previous level includes some factors that sub factors of each criterion are standardized separately. Each factor is also included a few indicators and it is necessary to standardize them. For calculation, we will do the same operation for each of the factors.

F. Calculating cost function of nodes
After calculating the value of different criteria, we have a hierarchical structure with specified coefficient like following figure. Now we can find appropriate evaluation function according to formula *1*.

$$F(a_1 \dots \mu) = (.138)\alpha_1 + (.027)\alpha_2 + (.012)\alpha_3 + (.028)\beta_1 + (.012)\beta_2 + (.005)\beta_3 + (.068)\delta_1 + (0.336)\delta_2 + (.059)\phi_1 + (.017)\phi_2 + (.008)\phi_3 + (.028)\gamma + (.192)\partial_1 + (.038)\partial_2 + (.032)\mu \quad (1)$$

G. Evaluating the cost of route selection
As we said, for calculation of this function we have to consider 5 criteria. According to selected criteria for the level of selection nodes, the criteria of this level just have one stage and are not layering.

H. Calculation of route cost function
Figure 2 represents criteria structure and their coefficient.

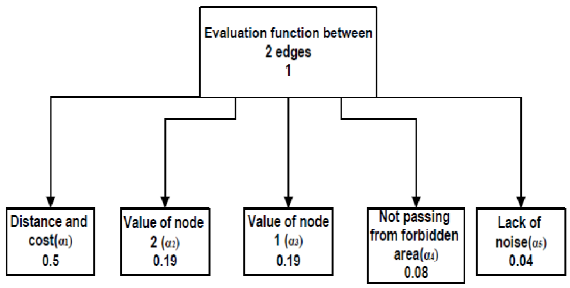


Fig. 2. Structure of criteria for selecting appropriate cost

According to above coefficients, cost function is like this:

$$F(\alpha_1 \dots \alpha_5) = 0.5\alpha_1 + 0.19\alpha_2 + 0.19\alpha_3 + 0.08\alpha_4 \; 0.04\alpha_5 \quad (2)$$

V. DISCUSSION ON CONSISTENCY IN AHP ALGORITHM

An important issue in distribution of coefficients and weighing to criteria is consistency discussion that represents rate of dependencies. In one consistent matrix, dominant eigenvalue is equal to rank of matrix. So for rate of inconsistency, we can calculate eigenvalue deviation from rank of matrix with formula 3 [6],[7] :

$$IC = \frac{\lambda_{max} - n}{n-1} \quad (3)$$

Now for more accurate calculation of inconsistency coefficient it's better to compare it with inconsistency coefficient of a random matrix that has high inconsistency. The coefficients of random matrices are written in table 5 with rank from 3 to 9.

TABLE 5
Inconsistencies Index for Random Matrix

n	3	4	5	6	7	8	9
C.R	0.58	0.9	1.12	1.24	1.32	1.41	1.45

Thus formula 4 is obtained:

$$CR = \frac{IC}{CR_{rand}} = \frac{\lambda_{max} - n}{(n-1).CR_{rand}} \quad (4)$$

Until this coefficient is less than 0.1, we have a consistent matrix. For instant in table 5 the value of λ_{max} is equal to 2.976 that with use of above formula the value of CR is equal to 0.02 that represents the consistency of matrix. But when this rate goes higher than 0.1 we need to review for finding evaluation error. This error can be caused by typing mistake in entering a coefficient or be outcome of a bad interpretation. In this case, it is better to review the coefficients and if it is necessary, we should revise the amount of coefficients. Finally, this task can be delegated to someone who will be able to create stable matrix.

VI. IMPLEMENTATION OF GENETIC ALGORITHM FOR FINDING OPTIMUM ROUTE

Use of genetic algorithm due to operating randomized for complicated and high cost issues is customary. When we are facing the vast volume of data and we don't have appropriate and stable solution, artificial intelligence techniques, especially genetic algorithms will help us. We want to find the best route among the available routes between determined source and destination. An appropriate solution with clear computational order for routing is Dijkstra's algorithm. However, the computational order at best state is equal to $O(|E| + |V| \log|V|)$, Which E is edges and V is vertices. With little pause we realized that for large number of nodes and routes, this algorithm requires high computational time. So we use genetic algorithm to reduce the computational load with the following algorithm techniques that we mention to them .Of other reasons for choosing the genetic algorithm are high diversity and high flexibility which prevent significant changes in computational load despite of change in network size [8]. A genetic algorithm includes several parts. First, we have to define the desired issue in a way that any solution can be placed in a chromosome. Genes form Parameters of this chromosome guide us to the solutions. Then we create a sample population of chromosomes (parents), (which it is called initialization stage) and we perform mutation and crossover operation on them until new chromosomes (offspring) are created. By using a suitable criterion, we can select chromosomes among the offspring for next generation. Also we can perform this selection among the parents. Now we repeat previous cases on the new generation produced as much as we reach an optimal answer. We need an appropriate Fitness Function so as to reach optimal answer. We run this function in each repetition of loop and if we achieve optimum answer or after several repetitions the best answer does not change, we end this algorithm.

A. Creation of chromosome

Since selecting the best route between the source and destination is our issue so, we form the chromosomes that its genes are route nodes. The first gene is source point and the last gene is destination point and the genes which are between them are nodes of a choice route. Since different routes have different number of nodes, chromosomes are not fixed-length. However there are methods provided with fixed-length that in regard to their computational complexity, their performance are less effective than this method [10].

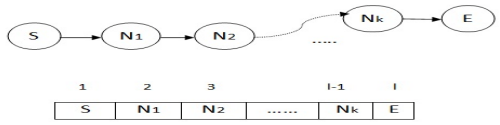


Fig. 3. Structure of intended chromosome

B. Initialization stage

At this stage we want to create initial population proportional to intended population size. There are several ways to perform this method. We can randomly place nodes on the chromosomes. Since this method may be producing small number of chromosomes that have a route from beginning to end, it does not seem as a suitable solution. At first It is better to randomly choose a node among the nodes which are linked to the initially node by an edge. Then we should do the same for the nodes connected to the selected following node and continuing this loop to reach destination node. Another way is using heuristic methods to perform initialization. Although this method probably causes to have better routes in the beginning, it would reduce the diversity of chromosomes. It is worth noting that the more population size cause the more probability of reaching optimum answer but it also cause higher computational load.

C. Crossover operation

We randomly choose two chromosomes for crossover and then we identify Nodes which are common in both chromosomes (except the initial and final node) and we choose a node among them. Now from the following point, we perform crossover operation and then we attach second part of each chromosome to the next chromosome like the following figure. The

important point is the possibility of loop existence in the new created chromosome that we must have a correction function for such conditions to identify the loop and remove it by omitting edges and repetitive nodes. The coefficient considered for probability of crossover operation (PC) is equal to 0.7. This means that crossover operation act on 70 percent of each generation of chromosomes. The high of this coefficient is due to crossover operation that causes to reach better solutions. There are also other methods for crossover operation which are not mentioned in this paper. [9], [10].

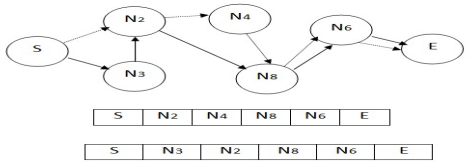


Fig. 4. Two separate routes before crossover operation

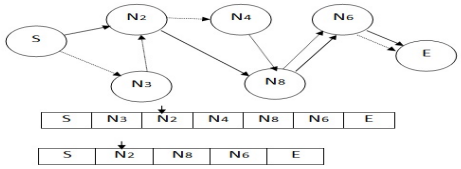


Fig. 5. The new routes resulting from crossover operation

D. Mutation operation

For mutation, we randomly select a chromosome. Then we choose one of the genes (except the first and last genes). If we randomly replace this gene with another gene, the chromosome may no longer represent one answer; we do not perform any operation on the genes between source and selected case. For the point after that, we consider the intended gene as the source node and again we perform the operation like initialization operation to reach the destination node. This method may increase computational cost little more but, this little impact is not felt, because the mutation operation is done on the chromosomes with very low percent probability. The coefficient considered for probability of mutation operation (Pm) is equal to 0.1 in this paper. Mutation operation is used when the issue is trapped in the local minimum points and it needs a mutation to be lead to the global minimum.

E. Fitness Function

Since we want to find the best route based on cost, fitness functions is equal to reverse of total cost of available edges in the route. The larger outcome of this function means lower cost of the route.

$$F(i) = \frac{1}{\sum_{i=1}^{l} Cost(Node(i),Node(i+1))} \quad (5)$$

F. Selection criterion

In each generation after performing crossover operation, if chromosomes produced by the operation have more fitness than their parent, they are added to the population. After adding of chromosomes from mutation and crossover, a pool of chromosomes is caused by parents and offspring. By using tournament method with k=2 (size of tournament), the next generation of chromosomes are selected. However, the most valuable and the least valuable chromosome is transferred to the next generation to improve each generation.

VII. IMPLEMENTATION RESULTS

We evaluate our genetic algorithm in different topologies with 10 up to 50 nodes. We assume there is a path between every two nodes. Cost of routes is determined by evaluation functions that have calculated in last steps. In these examples, costs are generated randomly for any iteration. Table 6 shows final results of every topology with 100 iterations. For certainty we compare our results with Dijkstra's algorithm.

TABLE 6
Accuracy and Speed of Proposed Algorithm (Population Size=100)

Avarege of elapsed time(second)	Optimum results (%)	Number of nodes
0.13	100	10
0.67	100	20
4.06	98	30
6.2	95	40
9.23	95	50

Figure 6 is the chart that illustrates percentage of correct answeres. As you see, percentage of correct answers didn't have any obviouse diffrence by changing number of nodes. For example in state of 50 nodes, there are 1225 paths that the optimum answer was found in 9 secends with 95% confidence.

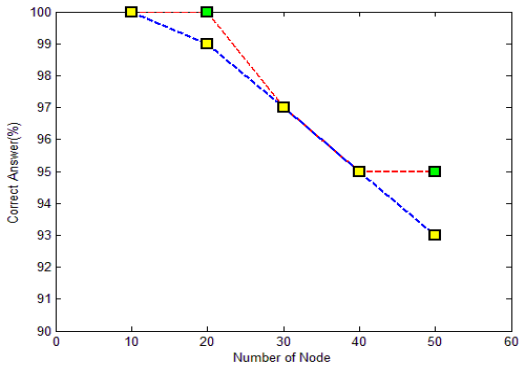


Fig. 6. Percentage of correct answers(Red :Popzie 100, Blue:Popsize 50)

It is obviouse that by enhancement of iteration, the percentage of correct answers are increased, but complexity and computational time increase too. Also this is right about size of population.

TABLE 7
Accuracy and Speed of Proposed Algorithm (Population Size=50)

Avarege of elapsed time(second)	Optimum results (%)	Number of nodes
0.15	100	10
0.46	99	20
1.04	97	30
3.8	95	40
7.75	93	50

For more understanding we compared obtained results with another research by 100 nodes and with population size equal to 50 [11]. It is observable from following table that both accuracy and complexity improved by our algorithm.

TABLE 8
Comparision Between Proposed Algorithm and Another Research

Algorithm	Number of nodes	Accuracy	Elapsed time(second)
Proposed algorithm	100	72	17.64
Compared algorithm	100	64	634.42

IIX. CONCLUSION

In this paper we proposed a method based on MCDA for selecting appropriate points for installing power towers. Because of wide usage of MCDA methods (especially AHP) in problems with high complexity, we calculated cost of intended points with AHP method. These points create several routes with variant costs. Since genetic algorithm has high diversity and consistency in front of changing size of route nodes, using this algorithm is very suitable for finding best route. For more realization we implement this method on several topologies and at the end we compare our proposed method with another implementation. Obtained results show that our proposed algorithm has higher accuracy than the compared algorithm. It is also true about elapsed time. Of course we can reduce computational time by using paralleling method and multi population method that will be a good idea for future researchs.

REFRENCES

[1] General Standard for Designing and Engineering Power Transmission Lines in Iran, By Tavanir

[2] Omkarprasad S. Vaidya, Sushil Kumar Analytic hierarchy process: An overview of applications, European Journal of Operational Research 169 (2006) 1–29, ScienceDirect

[3] Kirti Peniwati, Criteria for evaluating group decision-making methods, Mathematical and Computer Modelling 46 (2007) 935–947, ScienceDirect

[4] Elianne GonÇalves Gomes and Marcos Pereira Estellita lins, Integrating Geographical Information Systems and Multi-Criteria Methods: A Case Study, Annals of Operations Research 116, 2002, 243–269

[5] J. Aran Carrion, A.Espın Estrella, F.Aznar Dolsa,M. Zamorano Torob,Environmental decision-support systems for evaluating the carrying capacity of land areas,Renewable and Sustainable Energy Reviews 12 (2008) 2358–2380,ScienceDirect

[6] A. Ishizaka and M. Lusti, An expert module to improve the consistency of AHP matrices, Intl. Trans. in Op. Res. 11(2004) 97–105

[7] Germano Lambert-Torres, Cláudio Inácio de Almeida Costa, Manoel Clementino Barros Neto, Decision-Making using a Paraconsistent Analytic Hierarchy Process, 2008 IEEE

[8] Chang Wook Ahn,and R. S. Ramakrishna, A Genetic Algorithm for Shortest Path Routing Problem and the Sizing of Populations,IEEE Transactions on Evolutionary Computation, VOL. 6, NO. 6, December 2002

[9] Masaharu Munetomo, Yoshiaki Takai,A Migration Scheme for the Genetic Adaptive Routing Algorithm, 1998 IEEE

[10] Jan Inajaki, Miki Haseyarna, and HideoKitajima, A Genetic Algorithm For Determining Multiple Routes And Its Applications, 1999, IEEE

[11] Salman Yussof, Rina Azlin Razali,A Parallel Genetic Algorithm for Shortest Path Routing Problem, 2009 International Conference on Future Computer and Communication,IEEE

[12] Keiron Bailey, Principles of the EP-AMIS GIS/Multicriteria methodology for Participatory Electric Power Transmission Line Routing, 2006 IEEE

[13] Chen, Y, J. Yu, K. Shahbaz, and E. Xevi, A Weights, 18th World IMACS / MODSIM Congress, Cairns, Australia 13-17 July 2009

[14] Optimal reserve site selection with distance requirements, Justin C.Williams, Computers & Operations Research 35 (2008) 488 – 498, Scence Direct

[15] Salman Yussof, Azimah Abdul Ghapar, Marina Md Din, A Coarse-grained Parallel Genetic Algorithm with Migration for Shortest Path Routing Problem, 2009 11th IEEE International Conference on High Performance Computing and Communications

[16] Basela S. Hasan, Mohammad A. Khamees, Ashraf S. Hasan Mahmoud,A Heuristic Genetic Algorithm for the Single Source Shortest Path Problem, 2007 IEEE

[17] Yinzhen Li Ruichun He Yaohuang Guo, Faster Genetic Algorithm for Network Paths, The Sixth International Symposium on Operations Research and Its Applications (ISORA'06) Xinjiang, China, August 8–12, 2006 ORSC & APORC,pp. 380–389

A Novel Three phase Energy Meter Model with Wireless data reading and online Billing solution

Tanmoy Maity
Department of Electrical Engineering
Indian School of Mines
Dhanbad, INDIA
tanmoy_maity@yahoo.com

Partha Sarathi Das
Department of Electrical Engineering
Durgapur Institute of Advanced Technology and Management, Durgapur, INDIA
partha_san79@rediffmail.com

Abstract— **Measurement of data electronically leads a combination of benefits that go well beyond the traditional rotor-plate energy meter design. In this paper with the help of an energy chip, an improved novel three phase energy metering solution is developed. Automating the progression of measurement through digital wireless communication technique is done to get high accuracy, smooth control and better reliability. The developed energy meter calculates the total average active power mainly for industrial and commercial applications. The hardware circuit accepts three phase voltages and currents as its inputs and provides the output in the form of serial interfaced data equivalent to the average real power. This serial data is fed to a remote personal computer through the wireless ZigBee network that represents the concept of distant wireless metering, practically involving no manpower. The paper also presents a software solution developed for total electrical energy billing and data management system.**

Keywords- Energymeter, wireless, automatic meter reading, online billing. Introduction

I. INTRODUCTION

This paper describes a complete three phase wireless Energy Meter Reading system (WEMR)- an integrated and programmable meter reading and management system which can give us perfect measurement of parameters wirelessly. WEMR is a specific application of automatic Meter Reading (AMR) where the remote collection of consumption data are done from customers' utility meters over telecommunication, radio, power-line and other links [1]. The Electronic energymeters used for this system, are able to handle higher currents, have low power consumption and stable over time and temperature. They don't have gears that wear out or magnets that saturate with dc current. Electronic meters more easily enable new functionalities such as multi-tariff billing, tamper proofing, load shedding, power outage detection and power factor detection [2]. These offer flexibility of design, and can easily be reconfigured and updated. They have easy and stable calibration without hardware adjustment and are simpler to manufacture, transport, and install. This system can also reduce the total number of meters in a particular area if necessary. AMR is where the communication link is complete from the meter to the utility headquarters [3]. The automatic meter-reading systems may employ distributed structure, which consists of meters, sensors, intelligent terminals, management centre and wireless communication network [4]. The meter reading and management processes are free from human errors. Accuracy, speed, efficiency, reliability and cost-effectiveness are the usual benefits achieved using this system. This system also gives special advantages over the traditional metering system such as the eradication of manual meter reading costs, improvement of customer services by reducing the maltreatment of data, replacement of difficulties like involvement of distance and accessibility of measurement points. With the advancement of new modern computer technologies, chances for more well-organized management of electric power distribution are there. The increasing importance of more accurate energy measurement data and real-time access to that data is accelerating acceptance of the digital metering technology [5]. The data communication is an important part of the AMR system. To evaluate the type of communications network needed to carry metering data it is necessary to review the type of customer infrastructures that could be interfaced to such a network [6]. The primary role of the WEMR systems is to provide daily usage, total usage and real time usage data to the consumers. As for the automation of the power distribution system, its development and practical application have become an urgent task to achieve efficient and reliable operation of equipment.

For the successfully wireless data transmission, in this paper the ZigBee specification is utilised. There has been increased interest in the ZigBee standard, in particular for building automation and industrial controls since its release in 2004 [7]. Though the specification was available publicly in 2005, people prefer using this standard among different wireless protocol for diversified applications. In [8], an agent-based wireless local positioning system with ZigBee technology is proposed, mainly for factory level applications. A cost effective ZigBee-based wireless mine supervising system with early-warning intelligence on methane, temperature, humidity in mining area is proposed in [9]. Again, another article [10] presents the development of a system integrated to a ZigBee network to measure the whole human body vibration, for the persons exposed to vibratory environment. ZigBee specification is incorporated by many manufacturers in their devices because of its low power consumption and decreasing development cost. In the work presented here, Chipcon make CC2430 product is used for transmitting and receiving data wirelessly from a three-phase energymeter.

II. DESCRIPTION OF THE SCHEME

The developed system can be divided into three sections. First is a hardware based chipset solution of Energymeter that measures real-time active power from any three phase based system. Second part is the data transmission, where a number of meter reading data can be transferred through a wireless ZigBee based network to a remote server. The third part is the user friendly improved data management system based on software with two separate access support – one for consumer and another for the electric supply company. The first two sections are shown in a block diagram in Fig. 1. The separate sections are described briefly below.

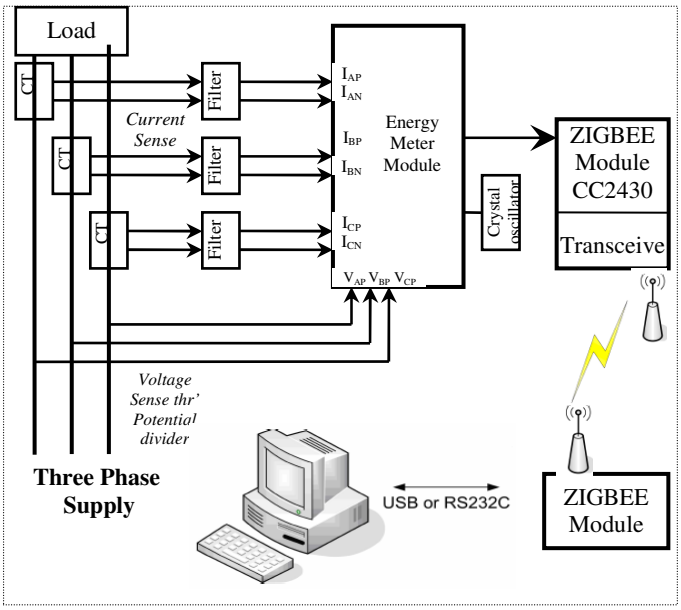


Figure 1. General Block Diagram of the Scheme

A. Energymeter

The analog IC chip ADE 7754 is the heart of this hardware system. It is a high accuracy polyphase electrical energy measurement chip with a serial interface, suitable for active power measurement from 3-phase/4-wire, 3-phase/3-wire or 4-wire delta system. The three phase supply voltages are fed directly to the chip and three line currents are fed through current transformers (CT). CTs are used here to get high current, low power performance. Burden resistors are used across the CTs which are calculated from the maximum current value and the number of turns in the CT. Antialiasing filters (RC LPF) are required at the input terminals to prevent possible distortion due to the sampling in the ADC. The analog ground plane and digital ground plane are physically separated from each other and are connected only at one point. ADE7754 calibration is done using the registers through the SPI interface.[11].

All data transfer operations are synchronized to a serial clock input SCLK provided through a crystal oscillator of 10 MHz frequency. Data is shifted out of the chip at the DOUT logic output on a rising edge of SCLK. The CS input should be driven low for the entire data transfer operation. The functional block diagram of AD7754 is shown from the data sheet [11] in Fig. 2.

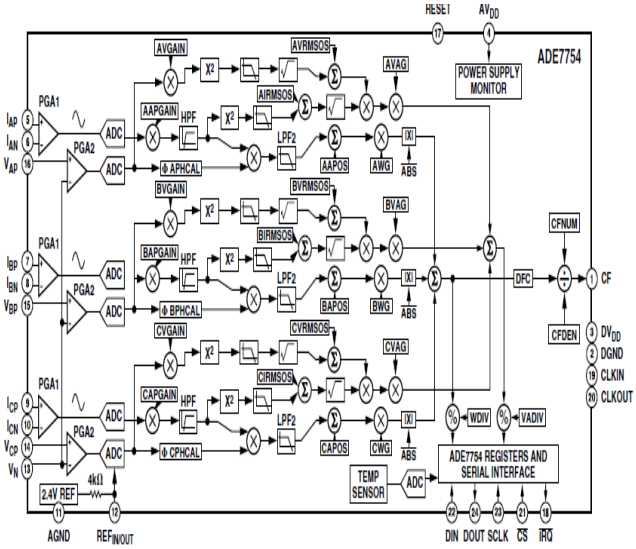


Figure 2. Functional internal Diagram of the IC ADE7751

B. Data transmission through ZigBee network

The main characteristics of ZigBee network are simple implementation, low power consumption, low cost interface, redundancy of devices, high node density per physical layer (PHY) and medium access control layer (MAC). Besides, they allow the network to work with a great number of active devices. ZigBee is based on IEEE 802.15.4 standard in terms of the PHY and MAC layers [12]. IEEE 802.15.4 defines two kinds of devices: the Full Function Device (FFD) and the Reduced Function Device (RFD). The FFD has the function to coordinate the network and consequently has access to all other devices. The RFD is limited to a star topology configuration, not being able to work as a network coordinator, so it does not have all the protocol services. The FFD and RFD devices can operate in three different ways at the ZigBee standard as the ZigBee coordinator (ZC), ZigBee Router (ZR), or ZigBee End Device (ZED) [12]. The network layer supports three topologies: star, cluster tree and mesh as shown in Fig. 3. A star topology consists of a coordinating node and of one or more FFD or RFD which communicates with the ZC. At the cluster tree, the final devices can be associated to the network by the ZC and the ZR helping the increasing of number of nodes and the network scope. At the mesh topology, the FFD can distribute messages directly to other FFD. To enter the network, each device receives an address given by ZC or a ZR.

The meter reading system adopts a distributed structure according to its characters. The system consists of data collector, wireless communication networks and the server system. Digital meter data is transmitted through two separate boards i.e. ZigBee transmission module to the data collector module. The ZigBee true System-on-Chip CC2430 is suitable for the purpose. It combines the excellent performance of the leading CC2420 RF transceiver with an industry-standard enhanced 8051 MCU, 32/64/128 KB flash memory, 8 KB RAM and many other powerful features. [13] It has low noise, low power consumption.

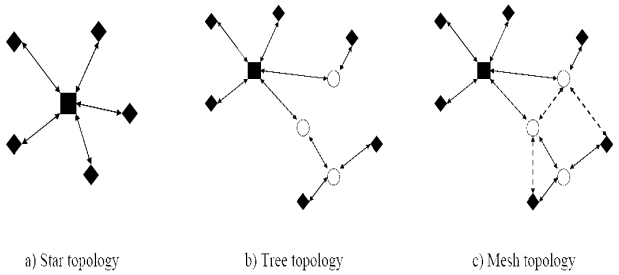


Figure 3. Different topologies of ZigBee network

The data collection rate (may be every an hour) can be adjusted according to the system requirement. The data collector is also a ZigBee gateway which is also a protocol conversion used to transform data package. The data package is transformed from ZigBee protocol to TCP/IP protocol before transmitting. So, the data collector sends the meter data to the receiver server through internet TCP/IP protocol. The socket client /server programming plays major role in case of long distance transmission. In the Fig. 4 a ZigBee wireless sensor communication network scheme is shown where a multiple data from energymeters installed at different location are transferred to the data base server. In case of short distance (within the range of ZigBee network i.e. 100 meter [14]) the data collector is interfaced with a PC through RS-232 or USB (shown in the diagram Fig.1).

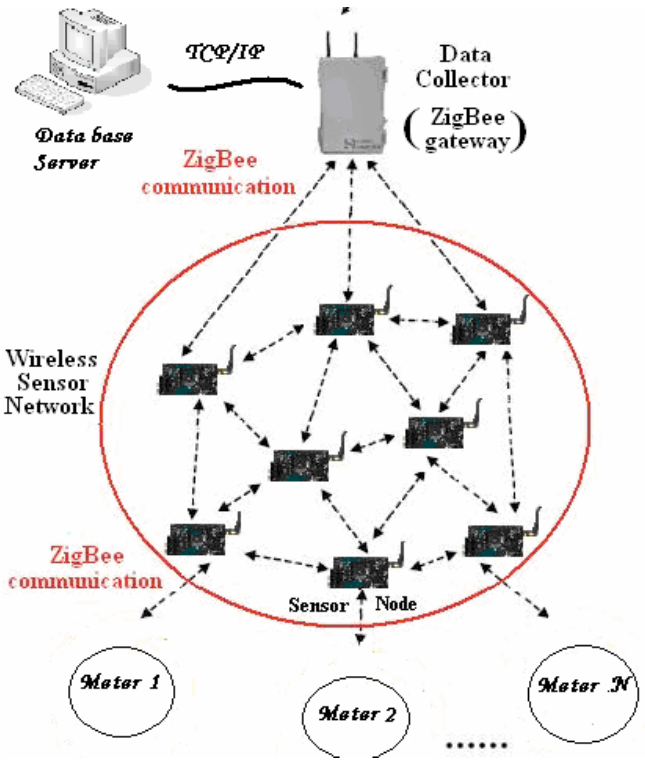


Figure 4. Long distance EM reading through ZigBee network

III. DATA MANAGEMENT SOFTWARE

The software developed here is to make an interactive, reliable and transparent relationship between the consumer and the electric supply agency. The system software is made using Visual Basic[15] which helps to form graphical user interface.

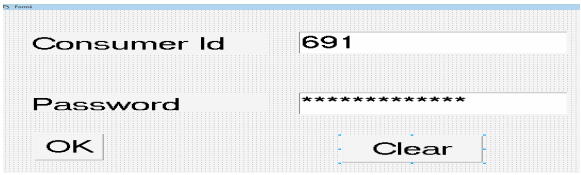


Figure 5. Consumer access starting window.

The program developed reads the data through the ZigBee receiver and gives the corresponding energy reading continuously, similar to a connected conventional electromechanical meter. The software also gives user the opportunity of automatic billing i.e. the software makes the bill based on the current energy reading and the standard rates of energy consumption given by the Energy Board. At any time, the consumers can verify the meter reading, current billing information, next due date, the other facilities as provided by the electric supply agency from their internet connected computer by simply typing its unique consumer ID and password as shown in the window (Fig. 5). The electric supply agency can also see the status of it's any consumer without physically sending its employees there. This is the main benefit of this software. The electric supply agency also can access the individual consumer's information by its own password and user name. A sample of the information window is shown in Fig. 6.

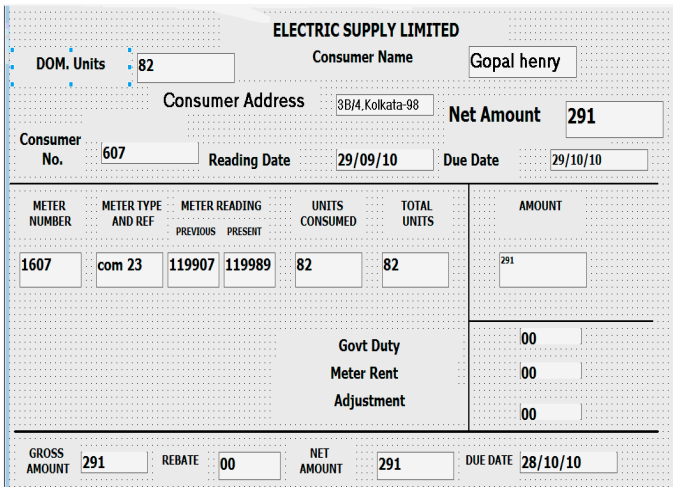


Figure 6. Consumer information window.

One database management is here which gives us the facility to store and access data, and also helps us to process those data. This data base shows the current billing information of different consumers. This database helps in the monthly

billing preparation. In this single database window the consumers details like name, address, consumer number, meter number, meter type are stored. This database window shown in the Fig.7 opts for administrator only and no change is possible by the consumer.

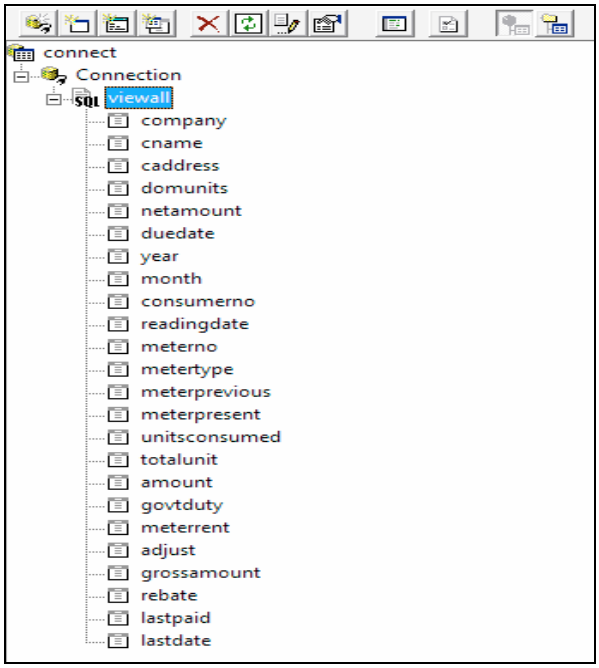


Fig.7. Consumer database.

There is also a Billing Information window in general, corresponds to the unit rates of energy under different levels of monthly consumption. As the unit rate varies normally with type of consumer, this is developed for five category of consumers viz. domestic, commercial, institute, public utility service and private hospitals/ educational institute. Though the access to this window is available for both consumer and administrator, only the administrator has the option to change the rates of the unit consumption. Again, the administrator can add new consumer to the database based on their valid consumer number through the user-friendly data entry window.

IV. CONCLUSION

Developing this wireless energymeter-reading system is not only to have high accuracy over a wide power range, better reliability and robustness but also to face the weakening competence in meter reading in increasingly over crowded localities and remote places. In order to accommodate the advanced requirements, not available in electromechanical meters, this all-electronic solution will be well accepted by the Electric distribution companies. The data like reactive power, apparent power and power factor with sign also can be sensed through this network by simply tracking the internal register of the chip. With the system described, customer service is improved through remote and automated meter reading, more credible utility bills and efficient data management. New features such as multi-tariff billing, power quality monitoring and reactive energy management are also possible in this system to improve generation, distribution, customer service and billing. Tampering in energy measurement as well as line to earth fault do not affect the accuracy in measurement and also can be diagnosed easily.

This will not only help the service providers of power to offload the manpower, trouble to collect energymeter readings and organising bill preparation, but also provide consumers an online tracking system to regulate the energy consumption intelligently.

REFERENCES

[1] Sridharan, K., and Schulz, N.: 'Outage Management Through AMR Systems Using an Intelligent Data Filter', IEEE Trans. Power Delivery, 2001, 16(4), pp. 669-675.

[2] http://www.analog.com,accessed Sep2010

[3] Holmes, J., and Campbell, D.: 'Communicating with domestic electricity meters', Schlumberger Industries UK, pp. 129-133.

[4] Cao, L., Tian, J., and Zhang, D.: ' Networked Remote Meter-Reading System Based on Wireless Communication Technology', Proc. IEEE Int. Conf. Information Acquisition, China, 2006, pp. 172-176.

[5] Maity,T., Das, S., and Datta, B.: 'A PC based Intelligent Wireless Energy Metering and Online Billing Solution for Domestic Consumers', Institution of Engineers (India) Journal (ET), 2009, 89, pp. 8-12.

[6] [6] Newbury, J., and Miller,W.: 'Multiprotocol Routing for Automatic Remote Meter Reading Using Power Line Carrier Systems', IEEE Power Delivery, 2001, 16(14), pp. 1-4.

[7] [7] Egan. D.: 'The Emergence of ZigBee in building automation and industrial controls', IEE Computing & Control Engineering, 2005, 16(2), pp. 14-19.

[8] [8] Chan, H. K.: 'Agent-Based Factory Level Wireless Local Positioning System with ZigBee Technology', IEEE Systems Journal, 2010, 4(2), pp. 179-85.

[9] [9] Qiang, C., Ping, S. J., Zhe, Z., and Fan, Z.: 'ZigBee Based Intelligent Helmet for Coal Miners', IEEE World Congress on Computer Science and Information Engineering, 2009, pp. 433-35.

[10] [10] Koenig, D.,Chiaramonte, M.S., and Balbinot, A.: ' Wireless Network for Measurement of Whole-Body Vibration', Sensors, 2008, 8, pp. 3067-81.

[11] [11] http://www.analog.com,accessed Sept 2010.

[12] [12]http://www.citeseerx.ist.psu.edu/viewdoc/download, accessed August 2010.

[13] [13] http://www.focus.ti.com/docs/prod.html,accessed Sept 2010.

[14] [14] Lee, J., Su, Y., and Shen, C.: 'A Comparative Study of Wireless Protocols. Bluetooth, UWB, ZigBee, and Wi-Fi', Proc. 33rd Annual Conf. IEEE Industrial Electronics Society, Taiwan, 2007, pp. 46-51.

[15] [15] Gottfried, B.S.: 'Schaum's outline of theory and Problems of Programming with Visual Basic', (Tata Mcgraw Hill, 1st edn, 2002), pp. 01-50.

Carving JPEG Images and Thumbnails Using Image Pattern Matching

Kamaruddin Malik Mohamad[1], Ahmed Patel [2] and Mustafa Mat Deris[3]

[1,3]Faculty of Computer Science and Information Technology
Universiti Tun Hussein Onn Malaysia
86400 Parit Raja, Batu Pahat, Johor, Malaysia

[2]Department of Computer Science, Faculty of Information Science and Technology
Universiti Kebangsaan Malaysia 43600 Bangi, Selangor Darul Ehsan, Malaysia

[2]Faculty of Computing Information Systems and Mathematics
Kingston University,
Penrhyn Road, Kingston upon Thames KT1 2EE, United Kingdom

[1]kamaruddin.malik *at* gmail.com, [2]apatel *at* ftsm.ukm.my, [3]mustafamatderis *at* yahoo.com

***Abstract- Digital* forensics is a branch of forensic science to monitor, analyze and examine digital media or devices. File carving is the art of recovering files from digital data storage with corrupted or unavailable file system metadata and it is very useful in a digital forensics investigation. However, earlier generation file carver like Scalpel and Foremost only deals with non-fragmented files. We proposed an automatic image and thumbnail carving tool called *myKarve* which is useful in digital forensics investigation and presentation of evidential information that is able to carve contiguous and linearly fragmented images caused by *garbage*. myKarve is designed on a new architecture to deal with thumbnail and fragmentation issues. The tool is tested with images obtained from the Internet. myKarve is found to be a more efficient automated image and thumbnail carver compared to the original Scalpel with the following advantages: detects more headers using validated headers; carves more images and thumbnails by using the newly introduced image patterns; and is able to discard garbage from linearly fragmented images. The results from myKarve are invaluable in the field work of digital forensic analysis that can produce technical evidence against cybercrime activities to prosecution cases.**

Keywords: file carving, digital forensics, myKarve, hidden information, side channels

I. INTRODUCTION

Digital forensics focuses on developing evidence pertaining to digital files that relate to a computer document, email, text, digital photograph, software program, or other digital record which may be at issue in a legal case. It is a branch of forensic science to monitor, analyze and examine digital media or devices [1]. There are many ways to examine data in cybercrimes such as recovering lost or purposely deleted files [2]

File carving is one of the techniques used to gather digital evidence from cyber-crime related digital storage. It is the art of recovering files from data storage with corrupted or unavailable file system metadata and it is very useful in a digital forensics investigation.

In this paper, we propose myKarve architecture that extends the capability of Scalpel to carve linear fragmented files caused by garbage. This paper is based on our full paper [3].

The paper is organized as follows. Section II describes related works. Section III describes about JPEG and thumbnail. Section IV describes myKarve's architecture, image patterns, image carving and garbage elimination. Experimentation, result and discussion; and conclusion will be discussed in Section V, VI and VII respectively.

II. RELATED WORKS

Currently, there are various tools and techniques available for file carving. Foremost [4] and Scalpel [5] are among the popular open-source carving tools. Scalpel is built on Foremost engine with improvement on its performance and memory usage. It is able to run on machines with modest resources and performs carving operations very rapidly.

To perform file carving, Scalpel makes only two sequential passes over each disk image. The first pass reads the entire disk image in large chunks (of user-definable size, with a default size of 10MB). Once the first pass over the disk image is complete, Scalpel has a complete index of header and footer locations, which is used to populate a set of work queues that control file carving operations during the second pass over the disk image. For each file header in the index, an attempt is made to match the header with an appropriate footer, subject to rules in the configuration file. The carving operation is carried out in the second pass using work queues.

However, Scalpel simply extract data between a known header and footer or ending point determined by size, with the assumption that the file is not fragmented and there is no missing information between the header and the footer. It is

also unable to detect thumbnail with non-standard header and unable to eliminate garbage that is located between the header and footer. In this paper, garbage is referred to a complete non-JPEG file or specifically PDF, Word documents and Excel spreadsheet that caused fragmentation to a JPEG image.

III. JPEG FILES AND IMAGES

JPEG files are segmented by special two-byte hexadecimal codes called markers. All these markers are assigned with two-byte codes, 0xFF byte followed by a byte which is not equal to 0x00 or 0xFF. The list of markers used in this paper is shown in Table 1.

According to [6], all JPEG images begin with the hexadecimal sequence of 0xFFD8FF followed by 0xE0 or 0xE1 which is a standard header pattern; and end with 0xFFD9. The probability of these patterns occurring randomly in an arbitrary object is 2 in 248. Nevertheless, few more hex patterns should be included following the 0xFFD8FF pattern; namely 0xE2, 0xC4 and 0xDB. The inclusion of these hex patterns is crucial for carving thumbnails. File carvers that use standard header pattern matching will definitely miss out some thumbnails, including Scalpel. The images carved from Digital Forensics Research Workshop (DFRWS) 2007 test set images have been analyzed to contain thumbnails that have 0xE0, 0xE1, 0xE2, 0xC4 and 0xDB following the 0xFFD8FF sequence.

Application markers APP0, APP1 and APP2 that appear directly after SOI will be referred to as APPx. Validated headers are illustrated in Fig. 1 as SOI that is followed by APPx, DHT or DQT.

Thumbnails are as important as JPEG images because corrupted images can still be known based on their thumbnails. Thumbnail is a smaller image embedded in a bigger image with its own start-of-image and end-of-image (SOI-EOI) pair. An image can have one or two thumbnails or none at all. Thumbnails are usually carved successfully due to their smaller sizes. One advantage of carving a thumbnail is that, we can roughly guess how a corrupted image should look like as shown in Fig. 1.

TABLE I
LIST OF JPEG MARKERS

Markers	Hexadecimal Values
Application marker APP0	0xFFE0
Application marker APP1	0xFFE1
Application marker APP2	0xFFE2
Define Huffman Table (DHT)	0xFFC4
Define Quantization Table (DQT)	0xFFDB
End-of-image (EOI)	0xFFD9
Start-of-image (SOI)	0xFFD8
Start-of-frame (SOF)	0xFFC0
Start-of-scan (SOS)	0xFFDA

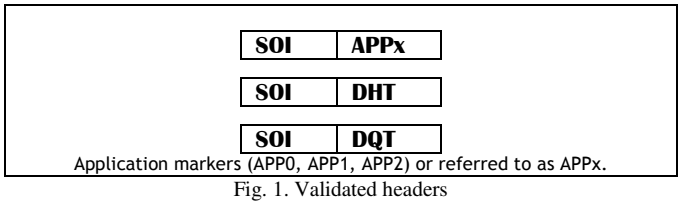


Fig. 1. Validated headers

IV. MYKARVE FILE CARVING SYSTEM

The proposed automated image carving tool called myKarve is discussed in this section. For this new carver to be feasible as a tool, issues in three areas need to be addressed. Firstly, it must able to carve automatically using work instructions in *Automated Work Queue* (AWQ), in order to eliminate human intervention and manual configuration. This is aligned with the objective of the DFRWS 2007 carving challenge, aimed to improve research in fully or semi-automated carving techniques [7]. Secondly, it should be able to carve more thumbnails. Thumbnails are much smaller in size and have better chances for full recovery without corruption. Thus, corrupted images can still be known based on their thumbnails. Finally, it should have the ability to detect and clean garbage that caused the linear fragmentation into two or more parts. Fig. 2 illustrates an image that is fragmented into three fragments due to PDF, Word document and Excel garbage.

Three components are required by myKarve automatic carving operation: *Validated JPEG Header* (VJH) list, *Address DataBase* (ADB) and AWQ. VJH list stores the addresses of all validated headers, ADB maintains addresses of validated headers and selected markers and AWQ is used to initiate automated carving. *Selected markers* are referred to a group of markers specifically APPx, DHT, DQT, SOF, SOS and EOI. These markers are the standard markers used in different JPEG image formats. myKarve, the automated carving tool requires no configuration skill.

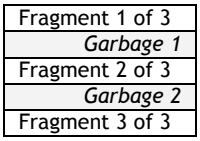


Fig. 2. Non-contiguous JPEG image with garbage

Besides performing automated carving, this tool is also capable of discarding garbage from linearly fragmented images to yield a clean image. *Shift-Key-Matching* (SKM) technique is employed in myKarve for detecting garbage in carved images or thumbnails.

myKarve is designed to carve not only images, but also thumbnails embedded in these images. Three image patterns are introduced to detect images with one or two thumbnails; or none at all. Therefore, corrupted images can still be known based on their thumbnails.

Architecture of myKarve

myKarve only makes two complete sequential passes over a disk image. The first pass reads the entire disk image, searching for validated headers and selected markers. The addresses of these items are stored in ADB. Validated headers that are stored in ADB are also maintained in the VJH list. Both the VJH list and ADB are now used to generate a set of work instructions for AWQ. AWQ is then used to automate file carving operations in the second pass. After the second pass, all carved images are scanned for garbage and there after cleaned. This architecture is illustrated in Fig. 3.

A. *Address DataBase (ADB)*

ADB is one of the components in myKarve. It contains selected markers for determining the patterns of an image or thumbnail. An image or thumbnail is carved between a validated header obtained from VJH list and EOI from ADB or in other words between a SOI-EOI pair. Based on Fig. 3, the first pass reads the entire disk image searching for headers and selected markers. There are two significant advantages of using validated headers. Firstly, false positive carving results are reduced since only SOI of validated headers are stored in ADB and VJH list, therefore eliminating false headers. Secondly, more JPEG thumbnail headers or base fragments are detected because some thumbnails are using non-standard header patterns of 0xFFD8FFC4 and 0xFFD8FFDB. Indirectly, this would increase the number of carved thumbnails.

B. *Validated JPEG header (VJH) list*

VJH list is the second component in myKarve. It contains validated headers or base-fragments of images and thumbnails. During the first pass, only validated headers that are found in the disk image will be stored into the ADB and VJH list. The difference between an ADB and VJH list is that VJH list contains only validated header addresses, whereas ADB also includes selected markers. Both, VJH list and ADB will be used for generating work instructions for AWQ where VJH list will be used to initiate the process.

C. *Automated Work Queue (AWQ)*

AWQ is the third component of myKarve. The automatic carving capability of myKarve depends entirely on the efficiency of work instructions in an AWQ. Each work instruction represents one carving job to be queued inside an automated work queue, AWQ.

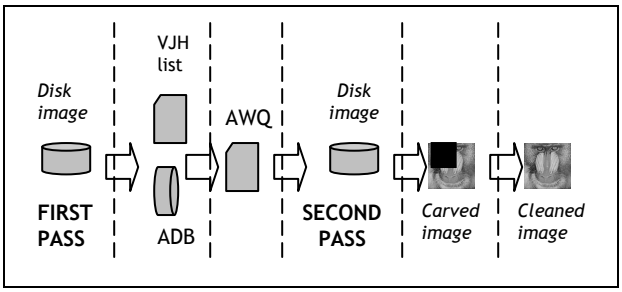


Fig. 3. Architecture of myKarve Tool

Work instructions in AWQ are generated using data from two sources, namely the VJH list and ADB. Initially, a validated header address is read from the VJH list. The markers related to this validated header are accumulated from ADB. Then, a work instruction for AWQ will be generated. A work instruction for AWQ will be generated only for validated headers with at least one of each of these markers: SOI, DHT, DQT, SOF, SOS and EOI, while APPx is optional for some thumbnails. This observation is supported by DFRWS test sets and image samples taken from websites on the Internet [8-11]. It is found that some of these thumbnails do not have APPx; instead, SOI is followed by either DHT or DQT. AWQ will be used to automate carving.

AWQ contains a set of work instructions. START_STOP_CARVE_JPEG is the only command used in a work instruction. The syntax for a work instruction is:

<INDEX> <COMMAND> <1st. ADDR.> <2nd. ADDR.>

and can be written as:

1 START_STOP_CARVE_JPEG 100 1200

'*Index*' is the position of the work instruction in AWQ, '*Command*' is the directive for carving, '*1st. ADDR.*' is the offset address of SOI and '*2nd. ADDR.*' is the offset address of EOI. The work instruction shown above can be translated as the first carving job in AWQ for carving a JPEG image which is located between the offset addresses of 100 and 1200.

The advantage of using AWQ is that there will be no incomplete carving operations due to missing footers. Only those blocks of data in the disk image that are located between a pair of SOI-EOI in the work instructions are carved.

Image patterns

Another feature of myKarve is its image pattern detections. myKarve generates work instructions for only three JPEG image patterns; 1) image only; 2) image with one thumbnail; and 3) image with two thumbnails. These patterns are illustrated in Table II. These introduced image patterns plays an important role in pairing the right SOI and EOI. *Pattern 1* is used for matching an image without thumbnail, *pattern 2* for matching an image with a single thumbnail and finally *pattern 3* is used for matching an image and two thumbnails. The introduced set of image patterns is one of the novelties of the myKarve. Work instruction will not be generated for any validated header with non-matching image pattern, in which case the validated header is simply discarded.

Carving Images

The carving operation starts after the AWQ generation process is completed. Initially, work instruction is read from AWQ to initiate the carving of image or thumbnail. It uses the seek operation to jump directly to the first address taken from the work instruction. Thereafter, it starts carving from there to the second address. Carved image/thumbnail is then saved as a file with running numbers (1.jpg, 2.jpg etc.). The whole process will be repeated for every work instructions in AWQ.

After executing all work instructions from AWQ in the carving operation sequentially, then all carved images and thumbnails will be scanned for garbage. In simple terms, an image without garbage is a contiguous or non-fragmented image while an image with garbage is a non-contiguous or linearly fragmented JPEG image. The non-contiguity of the image can be caused by garbage that is located within the image. This garbage can be of many file types. For this research, only a few garbage types or specifically PDF, Word document and Microsoft Excel are tested. Further garbage types will be dealt with in future undertakings.

TABLE II
THREE JPEG IMAGE PATTERNS USED FOR GENERATING WORK INSTRUCTION IN AWQ

PATTERN 1: Simple type	
Option 1	Option 2
SOI_1	SOI_1
$APPx_1$	**DQT_1 /DHT_1**
DQT_1	SOF_1
SOF_1	DHT_1 /DQT_1
DHT_1	SOS_1
SOS_1	EOI_1
EOI_1	

PATTERN 2: Single thumbnail	
Option 1	Option 2
SOI_1	SOI_1
$APPx_1$	$APPx_1$
SOI_2	SOI_2
***$APPx_2$**	**DQT_2 /DHT_2**
DQT_2	SOF_2
SOF_2	DHT_2/DQT_2
DHT_2	SOS_2
SOS_2	EOI_2
EOI_2	DQT_1
DQT_1	SOF_1
SOF_1	DHT_1
DHT_1	SOS_1
SOS_1	EOI_1
EOI_1	

PATTERN 3: Two thumbnails	
Option 1	Option 2
SOI_1	SOI_1
$APPx_1$	$APPx_1$
SOI_2	SOI_2
***$APPx_2$**	**DQT_2/DHT_2**
DQT_2	SOF_2
SOF_2	DHT_2/DQT_2
DHT_2	SOS_2
SOS_2	EOI_2
EOI_2	SOI_3
SOI_3	**DQT_3/DHT_3**
***$APPx_3$**	SOF_3
DQT_3	DHT_3/DQT_3
SOF_3	SOS_3
DHT_3	EOI_3
SOS_3	DQT_1
EOI_3	SOF_1
DQT_1	DHT_1
SOF_1	SOS_1
DHT_1	EOI_1
SOS_1	
EOI_1	

Eliminating Garbage

SKM technique is introduced to detect header and footer of garbage. This technique is illustrated in Fig. 4 where a *4-byte header* and *5-byte footer* structure or simply called as *header* and *footer keys* are used. Single-byte-marker [12] and dual-byte-marker [13] techniques are more suitable for detecting fixed sized headers or footers, but SKM is more suitable for detecting header/footer of variable size such as PDF with header *%PDF* and footer *%%EOF*.

Given the values for the header key is *%%EO*, current values for the footer key is *Z%%EO* and the currently read byte are F or 0x46. The initial values are:

Current header key [%][%][E][O]
Current footer key [Z][%][%][E] [O]
Current byte read from carved image is *F*

These initial values are then used in the algorithm for SKM technique as illustrated in Fig. 4.

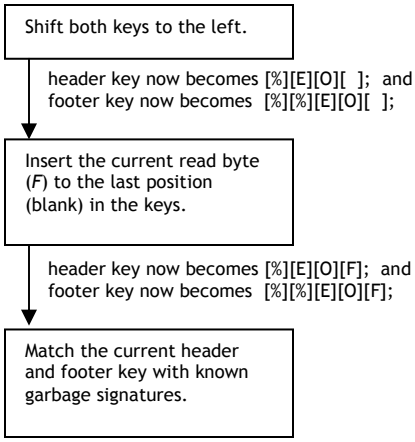


Fig. 4. Algorithmic function for SKM technique

V. EXPERIMENT

Test on Images with Thumbnails

A new 8MB hard disk partition is created. Five images with thumbnails and three images without thumbnails from [8-11] are copied over. Thumbnails for the first four images are with non-standard headers while the thumbnails for the fifth image are with standard headers. The other three images without thumbnail are used in this test just for comparison. Disk image of the partition is taken using Helix Live CD [14] and named as *hdd.dd.* Disk image hdd.dd is then tested with myKarve and Scalpel 1.6. This experiment test is performed to determine the efficiency of myKarve against Scalpel on carving images with thumbnails.

Garbage Elimination Test

Ten images without thumbnail are used in this experiment. Each image is inserted with garbage according to scenarios. These images are then copied over to an 8MB hard disk partition. Disk image of the partition is taken using Helix Live CD and named as *garbage.hdd*. Disk image garbage.dd is then tested with myKarve and Scalpel 1.6. This experiment is performed in order to test garbage elimination from JPEG images that caused linear fragmentation.

V1. RESULT AND DISCUSSIONS

Result for Test on Images with Thumbnails

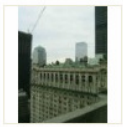
The main focus of myKarve implementation is on its carving efficiency, not on its processing time. The results of this test are shown in Table III. Only the successful carved images and thumbnails that are without corruptions are tabulated.

From the result, it is clearly shown that myKarve is able to successfully carve all images with or without thumbnails. Scalpel has successfully carved three images that are without thumbnails, two thumbnails with standard header while the other four corrupted images are not recorded in the result. These carved images are corrupted due to Scalpel non-efficient header-footer pairing mechanism. For example,

Scalpel incorrectly paired SOI_1 of image1.jpg to EOI_2 that belongs to SOI_2 as illustrated in Table IV.

TABLE III

CARVE RESULTS FOR SCALPEL AND MYKARVE ON HDD.DD DISK IMAGE

Test Images	Scalpel 1.6		myKarve	
	Image	Thumbnail	Image	Thumbnail
image1.jpg with a thumbnail [8] 	0	0	1	1
image2.jpg with two thumbnails [8] 	0	0	1	2
image3.jpg with two thumbnails [9] 	0	0	1	2
image4.jpg with two thumbnails [9] 	0	0	1	2
image5.jpg with two thumbnails [11] 	0	2	1	2
image6.jpg (no thumbnail) [8] 	1	no thumbnail in image	1	no thumbnail in image
image7.jpg (no thumbnail) [8] 	1	no thumbnail in image	1	no thumbnail in image
image8.jpg (no thumbnail) [10] 	1	no thumbnail in image	1	no thumbnail in image
TOTAL	3	2	8	9

Another observation that can be made from Table III is that, Scalpel only able to carve thumbnails that are using the standard header pattern (image5.jpg). Even though thumbnails with standard header for image5.jpg are carved, but the image for image5.jpg is failed to be carved due to mismatch of SOI-EOI pair. This is shown as in Table V. Finally, the results from Table III are graphically shown in Fig. 5(a) and Fig 5(b).

From these results, we can conclude that the validated headers helps to detect non-standard headers that normally will be missed out by other tools; and the introduced set of patterns used by myKarve are able to pair SOI-EOI more efficiently. Thus, *images with thumbnails* are able to be carved more efficiently.

Result for Garbage Elimination Test

The results for garbage elimination test are shown in Table VI. From the results, it is shown that myKarve has successfully eliminated garbage for all the test scenarios while Scalpel is unable to delete any garbage because it only works for non-fragmented files and does not have any feature for garbage detection and deletion.

TABLE IV

COMPARISON OF CARVED FILE PATTERN BETWEEN SCALPEL AND MYKARVE ON HDD.DD DISK IMAGE

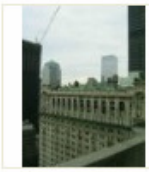
Test Image	Scalpel 1.6		myKarve	
	Image Pattern	Thumbnail Pattern	Image Pattern	Thumbnail Pattern
image1.jpg with a thumbnail [8] 	SOI_1 SOI_2 EOI_2 CORRUPT: mis-match SOI_1 to EOI_2	NOT DETECTED	[PATTERN 2] SOI_1 $APPx_1$ SOI_2 DQT_2 SOF_2 DHT_2 SOS_2 EOI_2 DQT_1 SOF_1 DHT_1 SOS_1 EOI_1	[PATTERN 1] SOI_2 DQT_2 SOF_2 DHT_2 SOS_2 EOI_2

TABLE V

SCALPEL UNABLE TO CARVE IMAGE FOR IMAGE5.JPG

	Scalpel 1.6			myKarve
Test Image	Image Pattern	1st Thumbnail	2nd Thumbnail	Pattern 3
image5.jpg with two thumbnails [11] 	SOI_1 SOI_2 EOI_2 CORRUPT: mis-match SOI_1 to EOI_2	SOI_2 EOI_2 Thumbnail with standard header	SOI_3 EOI_3 Thumbnail with standard header	SOI_1 APPx APPx SOI_2 APPx DQT SOF DHT SOS EOI_2 SOI_3 APPx DQT SOF DHT SOS EOI_3 APPx DQT SOF DHT SOS EOI_1

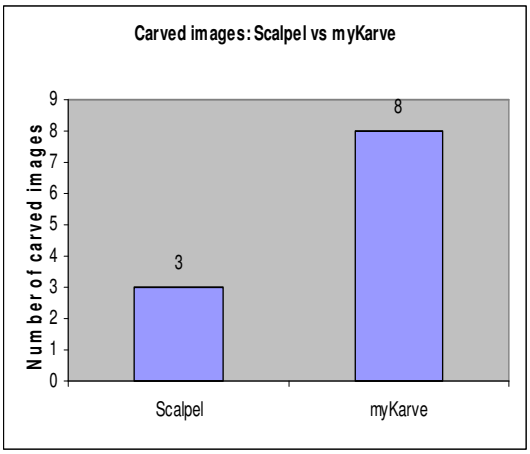


Fig. 5(a). Summary of carving results

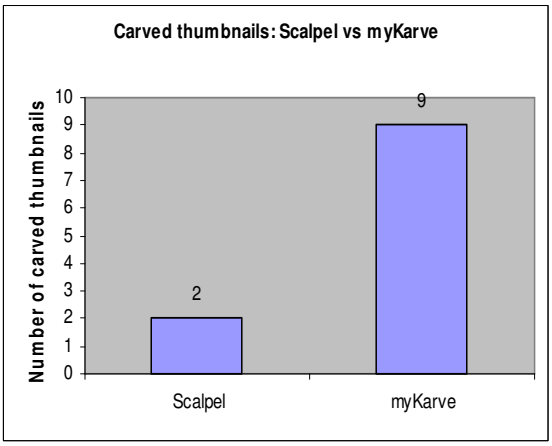


Fig. 5(b). Summary of carving results

TABLE VI
GARBAGE ELIMINATION TEST RESULT

Scenario	Garbage successfully eliminated	
	Scalpel 1.6	myKarve
Image with a single piece of garbage (PDF)	NO	YES
Image with two pieces of garbage (PDF)	NO	YES
Image with three pieces of garbage (PDF)	NO	YES
Image with single piece of garbage (Word)	NO	YES
Image with two pieces of garbage (Word)	NO	YES
Image with three pieces of garbage (Word)	NO	YES
Image with single piece of garbage (Excel)	NO	YES
Image with two pieces of garbage (Excel)	NO	YES
Image with three pieces of garbage (Excel)	NO	YES
Image with few garbage pieces of various types (PDF and Word in a single image)	NO	YES

IV. CONCLUSIONS

An automatic JPEG image carver called *myKarve* has been introduced. This tool is able to carve non-fragmented and linearly-fragmented images and thumbnails caused by *garbage*. The newly introduced validated headers and image patterns enable myKarve to carve more images and thumbnails. myKarve is also able to discard garbage from linearly fragmented images.

Our contributions were four-fold. Firstly, a novel automated carving technique has been introduced by using myKarve architecture. Secondly, the newly introduced *validated headers* are able to detect more base-fragments. Thirdly, the introduced set of *image patterns* is able to pair SOI-EOI more efficiently, which results in carving images and thumbnails more efficiently. Fourthly, the *Shift-Key-Matching* (SKM) technique is introduced for detecting garbage, thus enabling the tool to clean and carve images and thumbnails that are fragmented into two or more parts. The results from this research work is invaluable in the field work of digital forensic analysis concerned with image files to produce hard core technical evidence against cybercrime criminals and their activities.

ACKNOWLEDGMENT

We wish to sincerely thank the publisher Taylor & Francis Group LLC for allowing us to base this paper on the full published paper given as reference [3]. We also wish to note that this work was partially supported by Universiti Tun Hussein Onn, Malaysia.

REFERENCES

[1] A. Patel, and S. Ó Ciardhuáin. The Impact of Forensic Computing on Telecommunications. IEEE Communications Magazine, 38 (11), pp. 64–67, November 2000.

[2] K. Kalajdzic and A. Patel. A fast practical method for recovery of lost files in digital forensics, Journal of Internet Technology, 10(5), pp. 539-546, October 2009.

[3] K. M. Mohamad, A. Patel, T. Herawan and M. Mat Deris. "myKarve: JPEG Image and Thumbnail Carver". Journal of Digital Forensic Practice, vol. 3, pp. 74-97, 2011.

[4] SourceForge.net: Download and Develop Open Source Software for Free, Foremost 1.5.7, http://foremost.sourceforge.net, accessed, Oct 2010.

[5] G. G. Richard III and V. Roussev, "Scalpel: A Frugal, High-Performance File Carver." *Proceedings of the 2005 Digital Forensics Research Workshop*, *Louisiana, US,* 2005, pp. 1-10, 17-19.

[6] S. Garfinkel, "Carving Contiguous and Fragmented Files with Fast Object Validation." *Proceedings of Digital Forensics Research Workshop (DFRWS)*, *Pittsburg, PA,* 2007, pp. 2–12.

[7] DFRWS 2007 Forensics Challenge Data and Submission Details, http://www.dfrws.org/2007/challenge/submission.shtml, accessed, Oct 2010.

[8] Flickr: Jordan Davis' Photostream, http://www.flickr.com/photos/jordandavis, accessed on Oct 2010.

[9] Flickr: Leef Smith's Photostream, http://www.flickr.com/photos/leef_smith, accessed on Oct 2010.

[10] Flickr: Pirana Snaps' Photostream, http://www.flickr.com/photos/Phaebique, accessed on Oct 2010.

[11] DFRWS 2006 Forensics Challenge File Image Details. Retrieved Jan. 09, 2011 from Digital Forensics Research Conference (DFRWS): http://www.dfrws.org/2006/challenge/submission.shtml

[12] K.M. Mohamad and M. Mat Deris, "Single-byte-marker for Detecting JPEG JFIF Header using FORIMAGE-JPEG." *Proceedings of Fifth International Joint Conference on INC, IMS and IDC (NCM),* 2009, pp. 1693-1698.

[13] K.M. Mohamad, T. Herawan and M. Mat Deris, "Dual-byte-marker for Detecting JFIF Header." *Proceedings of 4th International Conference on Information Security and Assurance (ISA),* 2010, pp. 27-36.

[14] e-fense: E-Discovery Forensics Security Training, Helix Live CD, http://www.e-fense.com, accessed, Oct 2010.

Design and Implementation of Smart Driving System using Context Recognition System

Taehyun Kim[1], Soohan Kim[2], Dongkyoo Shin[1], Dongil Shin[1]*
[1] Department of Computer Engineering, Sejong University, Korea
[2] Div. Internet Infra Planning Team, Samsung Electronics CO.,LTD NW
[1] 98 Kunja-Dong Kwanjin-Gu 143-747, Seoul, Korea
[2] 416 Metan-3dong, Yeongtong-gu, Suwon-city, Korea
crowlid82@gce.sejong.ac.kr, {ksoohan, myungsu.lee}@samsung.com, {dshin, shindk}@sejong.ac.kr

***Abstract*- In this paper, we develop a context recognition system that is based on multimodal biometric signals and applicable to smart driving system. The context recognition system includes a biometric analysis module that analyzes and recognizes human biometric signal patterns. The context recognition system can recognize a user's emotion and level of concentration by analyzing ECG (electrocardiogram) and EEG (electroencephalogram) patterns. To predict the concentration and stress status of the user, the electroencephalogram rendering system utilizes 5 signal values: MID_BETA, THETA, ALPHA, DELTA, and GAMMA. Also, electrocardiogram analysis system utilizes 5 basic signal values: P, Q, R, S, T wave. To recognize the user's electrocardiogram signal patterns, a deformation K-means-based EM algorithm was applied.**

I. INTRODUCTION

The human body is a large complex system composed of a hundred trillion cells. Even though science and technology in the 21st century are developing very rapidly, humans still know themselves only to a very limited extent. The digital human project aims to build all of the human body datasets, from nano to macro, including cells, DNA, tissue, organs and the complex system that contains them all. The information may be anatomical, physical and functional, depending on the stage of the database's development. Until intelligence inundates "to create intelligence how" the problem which is than "to deliver how" to be important, this becomes conclusion with problem of interface. Currently, it is entering the stage where the progress of technique surpasses user requirements, and the interface will become an efficient means for reducing the gap between the product and the user. Renovation of the interface will become an efficient means of making a priority of the effect over performance upgrade. In the future, the importance of the interface will be augmented largely by the product's competitive power. Also, must develop it applies the interface technique of the sense which is diverse widely and renovation and the human being the interface which is affinity. The present paper surveys the body of the target customer and recognition and sensitivity property enough and the interface which raises a user's experience it develops. Especially, the antenna and the olfactory sense, sensitivity etc. a fact feeling and a use usability the positive it applies a base one up-to-date interface technique in the sense which is diverse and it raises, the competitive product and will discriminate. It stares the development trend of the sensors and the interface part by advanced enterprises, it strengthens strategic alliance with these enterprise by which it will be able to secure an element technique. IBM, with Emotive System Corporation, established a collaborative relationship for the application of a brain interface. Also, Microsoft (Xbox) and many IT companies have applied EMERGEN company's HAPTIC techniques.

The industry of commercial games that use primarily human body intelligence is in its elementary phase. The government researched sonar enterprises are coming out to make existing games feel more realistic, but they are still in development. In addition, their current status is not as a commercial business product, and only there will only be experimental use when they do come to market. It is difficult to make a character where the user uses biometric signals. Also, the game console is not developed enough, so these commercial business products develop slowly.
Making the biofeedback interface technique more natural and effective is the focus of the field of virtual reality, which is developed with technique in the visual/auditory sense centers.

Smart driving system applied context recognition uses various sensor links in the body; and the electroencephalogram/electrocardiogram/electromyograms signals of the user whom it measures are reflected with in real time.

II. PREVIOUS WORK

A. Brain Computer Interface (BCI) & Recognition Research

The multimodal of human body signals to interactively recognize emotions rely on the detection of a physiological change caused by an affective stimulus and then the adequate classification of such change. Hitherto, the majority of methods employed to classify emotions using biometric signals have been based on off-line analysis of statistical features extracted from large quantities of data

*Dongil Shin is corresponding author.

[1]. Systems to dynamically detect, classify, and utilized emotions, based on instantaneous responses from the autonomic system are still lacking. Using a combination of Auto associative Neural Networks (AANNs) and sequential analysis, a novel mechanism to detect changes in biometric signals associated with emotional states was developed [2]. Brain Computer Interface (BCI) technology represents a rapidly rising field of research with application systems ranging from prosthetics and control systems through to medical diagnostics. In this research, the experiment only considers BCI technologies that use sensors that measure and interpret brain activity (commonly termed neural bio-recorders [5]) as a source of input. The longest established method of neural bio-recording, developed in 1927 by Berger [4], is the application of electrodes that survey the changes in field potential over time arising from synaptic currents. "In 2003, taxonomy by Mason and Birch identified MEG, PET and fMRI as unsuitable for BCI applications, due to the equipment required to perform and analyze the scan in real-time, but more recent attempts to use fMRI as a BCI input device have demonstrated significant future potential in this area."[3].

In our research, we control car speed by concentration value of brain signals at driving simulation content. Also, when the stress value is excessively high, the car flies for overcome obstacles

B. Smart Driving System

In our experiment, the topography modeling such as car embodies, racing track and obstacle such as object modeling, offer correct attribute in each propensity used this technology. Also, advanced moving information applied the Bayesian algorithm to measure information about interior game environment from a database. First, the transferred automobile's position had to be known, including the velocity of vehicles and input angle values. Second, it was necessary to measure the elapsed time for each course and analyze incidental values. That information was measured with a driving analysis system, which is shown in figure 1. This module has analyzed data that were collected through functions that referred to and organized necessary information. Figure 2 expresses a plan that was needed when composing the necessary data and the actuality tracks for the composed module. In the next step, select a turning angle among those that are offered in an upper part of experiment that is recognized in the safest state when a stumbling block and turning angle become horizontal. That is to say, calculate the amount of damage from the collision impact [6].

One of the important things that made an important contribution was the database for the analyzed data that used a Bayesian network to embody the Artificial Intelligent Drive System. Figure 3 shows a table that was created to store data values that were generated selectively through intelligence physics engine implementation module. Also, as previously described, we embody smart driving system that applied context recognition system [6].

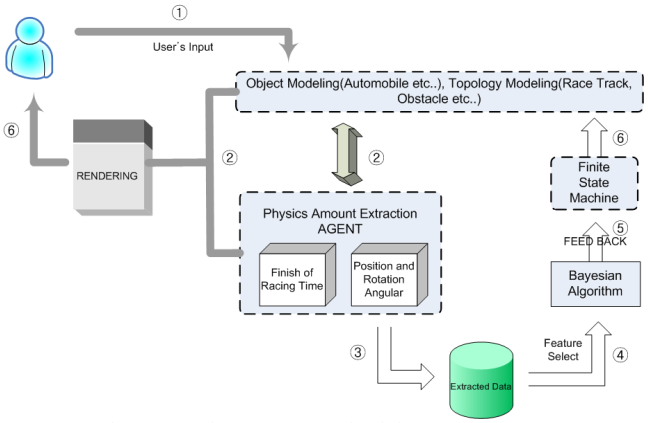


Fig. 1. Experiment Process of Driving Agent System

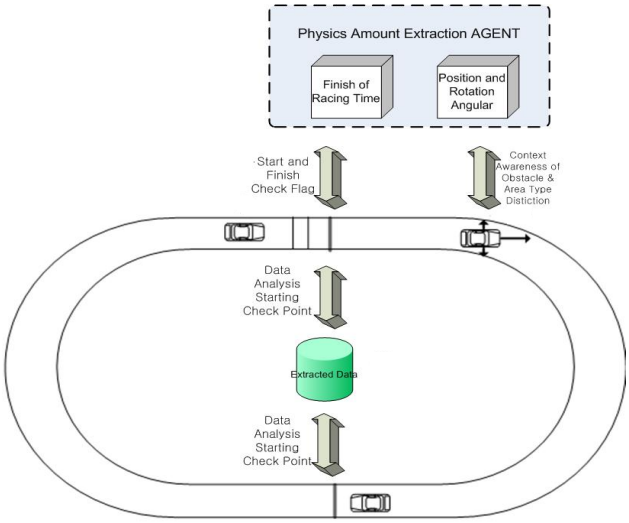


Fig. 2. Module Design of Intelligent Physics Engine

LineNum	POS X	POS Y	Rot	Front	Left	Right	Time	Course Select	WeghitVAR	Bayesresult	Warning	ProposeROT	Velocity
1	50	90	0.99	50	15	32	00:00:00	GoStraight	0	0.91	0	0	0
2	52	88	0.95	48	16	31	00:00:02	GoStraight	0	0.89	0	0	55
3	56	87	0.89	44	13	34	00:00:04	TurnLeft	0	0.90	0	15	89
4	65	84	0.55	35	16	31	00:00:06	TurnLeft	0	0.88	0	25	102
5	75	79	0.23	15	12	46	00:00:08	TurnLeft	0	0.91	0	10	115
6	86	65	0.13	165	13	32	00:00:10	GoStraight	0	0.90	0	0	132
7	87	45	0.17	146	16	30	00:00:12	GoStraight	0	0.87	0	0	166
8	88	15	0.13	114	18	29	00:00:14	GoStraight	0	0.88	0	0	189
9	87	-22	0.11	78	21	26	00:00:16	GoStraight	0	0.89	0	0	211
10	84	-58	0.19	42	17	30	00:00:18	GoStraight	0	0.86	0	0	223
11	73	-81	-0.75	127	15	32	00:00:20	GoStraight	0	0.88	0	0	231
12	60	-77	-0.45	112	17	30	00:00:22	GoStraight	0	0.92	0	0	240
13	42	-82	-0.85	142	16	34	00:00:24	TurnLeft	0	0.93	0	16	211
14	12	-83	-0.87	112	13	43	00:00:26	TurnLeft	0	0.80	0	21	205
15	-20	-85	-0.99	80	14	41	00:00:28	TurnLeft	0	0.94	0	11	200
16	-59	-75	-0.64	41	11	32	00:00:30	GoStraight	0	0.85	0	0	201
17	-73	-43	-0.04	75	15	35	00:00:32	GoStraight	0	0.89	0	0	213
18	-88	-9	-0.10	109	13	36	00:00:34	GoStraight	0	0.83	0	0	223
19	-86	25	-0.12	75	17	33	00:00:36	GoStraight	0	0.87	0	0	231
20	-87	42	0.05	61	18	30	00:00:38	GoStraight	0	0.80	0	0	239
21	-80	60	0.21	40	21	28	00:00:40	GoStraight	0	0.93	0	0	245
22	-77	82	0.75	22	12	32	00:00:42	GoStraight	0	0.94	0	0	249

Fig. 3. Feature Database for drawing in Game Environment

III. DESIGN AND DEVICE FOR BIOFEEDBACK RECOGNITION SYSTEM

A. Design for Acquirement Devices of Biometric Signals

We developed two different devices to measure EEG and ECG signals. Figure 4 shows the EEG sensor device. The four sensors should be attached to the forehead positions of the human brain.

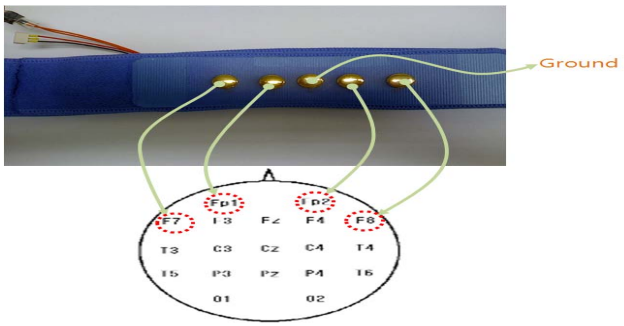


Fig. 4. EEG sensor device: 4 channels with electrode disposition

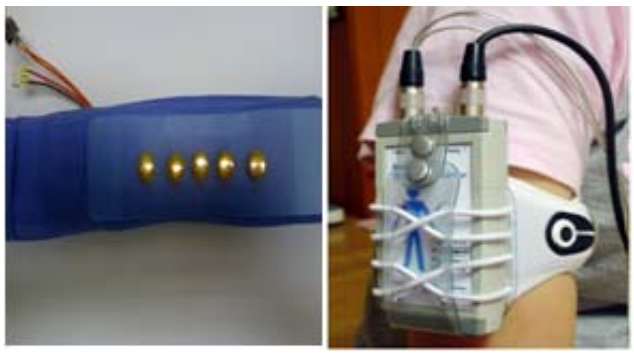


Fig. 5. EEG sensor device (right) and ECG sensor device (left)

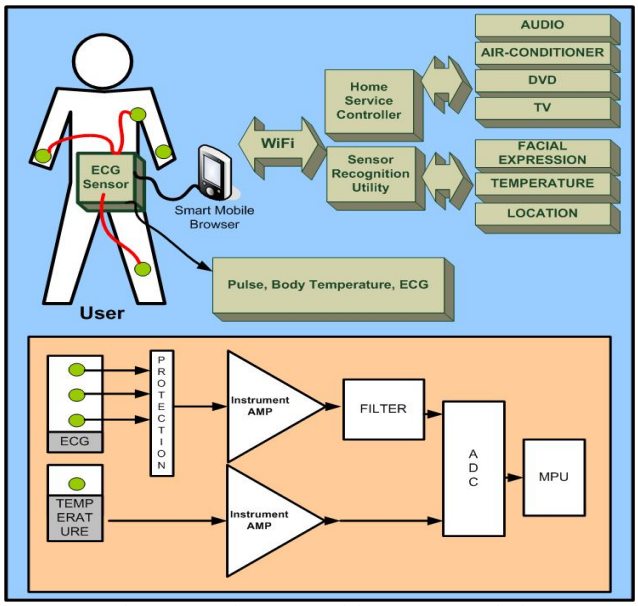


Fig. 6. Internal Structure of the ECG sensor device

The left device in Figure 5 acquires brainwave signals from the frontal lobe of the brain. EEG device have 4 channels with electrode disposition. Right device of figure 5 is to measures ECG signals from the user body. Figure 6, the ECG sensor device uses four tags to acquire the user's pulse, body temperature, and electrocardiogram.

B. Software Molules for Bio Signal I/O Device

Software modules are divided two parts. First part is network software module with I/O device. And second part is context manager software module for biometric data. First part has two base modules about client and server.

One, EEG/ECG network client module has three modules. The modules are initialize module, and connect module, and data manager module. Data manager module takes charge of the radio communication data reception department, a data processing department and the data transmission department.

Two, contents network server module are network server modules which will interpolate in game contents. Likewise, contents network server module has three parts. Initializer module is initialize server. Client manager module manages EEG/ECG client module part.

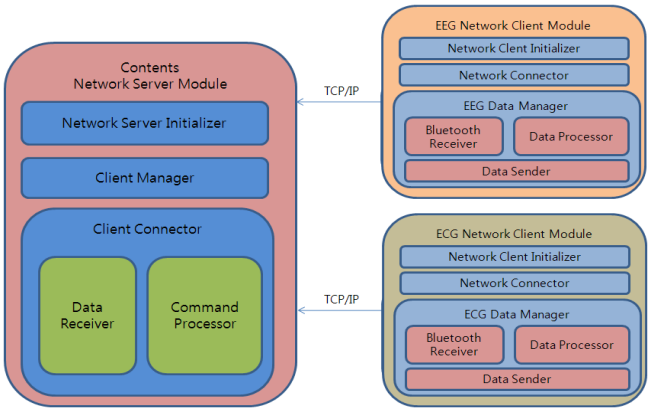


Fig. 7. Network software module for I/O device

Command	To Server	From Client		Comment
		ACK	Value	
SPEED_UP	0x02	0x02	0~100	Concentration Value
SPEED_DOWN	0x03	0x03	0~100	
LEFT	0x04	0x04		Eye's Wikling One time
RIGHT	0x05	0x05		Eye's Wikling two times
FLY ON	0x06	0x06	0~100	Stress and Non Stress State
FLY DOWN	0x07	0x07	0~100	
HAPPY	0x09	0x09	0~100	Analyze Emotion as 2 Part(Happy, Sad)
SAD	0x10	0x10	0~100	

Fig. 8. Interlock protocol definition for contents

Figure 7 is view of network software module. Figure 8 is interlock protocol definition for biometric I/O device between software modules and contents. Figure 9 shows structure of context manager for acquiring and analyzing biometric signals.

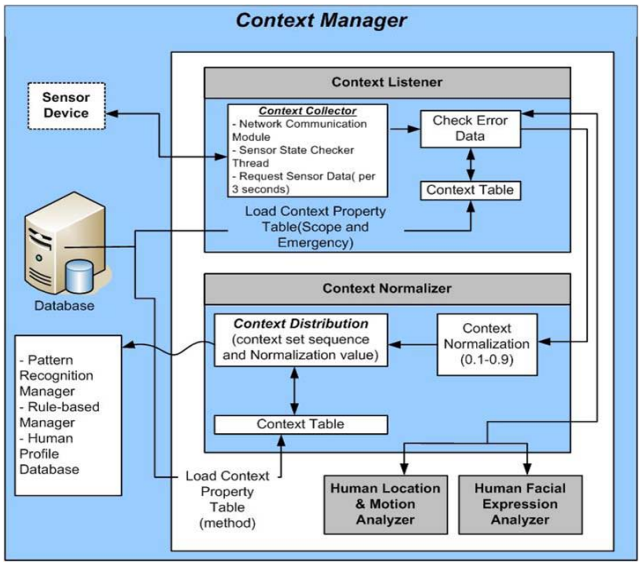


Fig. 9. Structure of context manager

A design of biometric (EEG, ECG) analyzing algorithm have three part as next.

1) Normalization Module: In about biometric signal from person deviation by normal function
2) Post Processing Module: Analysis function of wavelet by signals/nonlinear dynamics/high dimensional statistical/laplacian mapping
3) Analytical Study Module: Analytical function of user's intention about biometric signals

The contents composed of car and two tracks and obstacles in this experiment. Each object needs physics engine and rendering engine. Also, the contents program has network thread for network processing. And contents embody car's position and course data acquirement system for sending and receiving data to another pc.

IV. IMPLEMENTATION AND EXPERIMENTAL RESULTS

A. Implementation of Biofeedback Interface

We are still developing a program to analyze a user's concentration status from brainwave signals. Thus, this paper only presents the evaluation results from analyzing ECG signals. Figure 10 shows the program that classifies EEG signals. It measures the dimension of the power of concentration with EEG signals, and it finds the direction where the power of concentration is displayed by the winkling of the eye. Figures 11 show emotion recognition module. This program assesses and displays the user's current state of emotion or stress. The experimental game decides the direction of the automobile by using the eye winkling of the user. And it moves according to intensive state of EEG. Further, the user feels plentiful stress; the automobile slows down, embodied with the artificial intelligence model. Figure 12 is the implementation screen of the smart driving system applied multimodal context recognition interface.

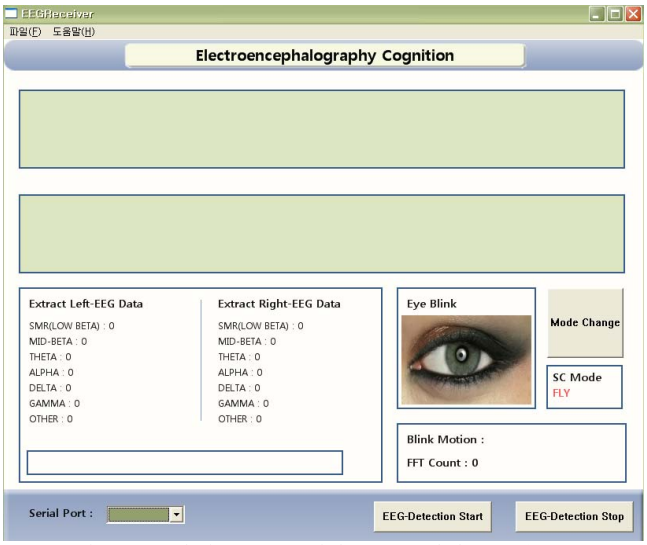


Fig. 10. Analysis program of electroencephalogram (EEG)

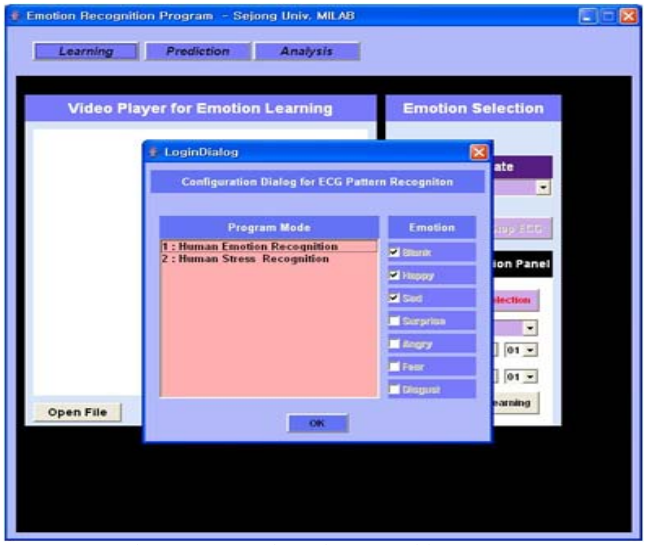


Fig. 11. Screen of emotion recognition program

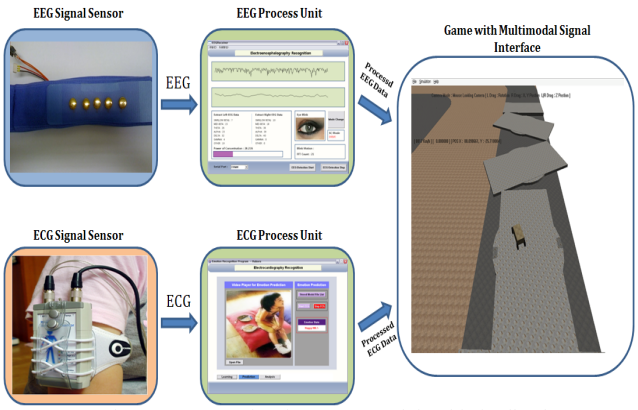


Fig. 12. Screen of racing game applying biofeedback

B. Experimental Results

EM bases K-means which are applied in the research which it sees deformation used unsupervised learning with supervised learning algorithms. To verify the performance of the Human Emotion Recognition module, we applied a protein data set as the input value of the human emotion recognition module program. Protein data sets have a rich structure that includes its primary structure, a sequence of amino acids, and its secondary structure, a sequence of folding patterns The Protein Data Set is offered in the UCI Machine Learning Repository. Figure 13 shows the ECG wave that was analyzed by the human emotion analyzer. The electrocardiogram wave includes P, Q, R, S, T waves. The human emotion analyzer applied peak values of all waves and intervals between the R waves as input values.

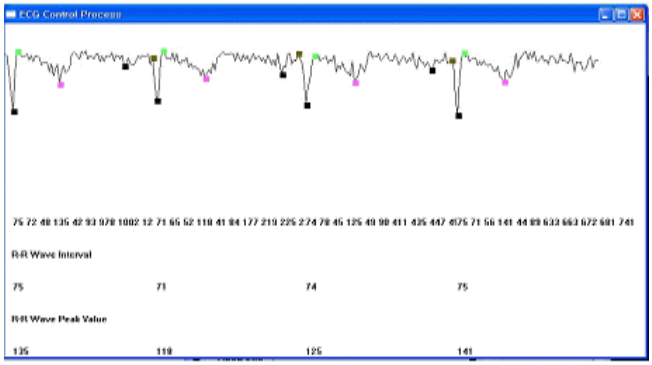


Fig. 13. ECG wave analyzed by the human emotion analyzer

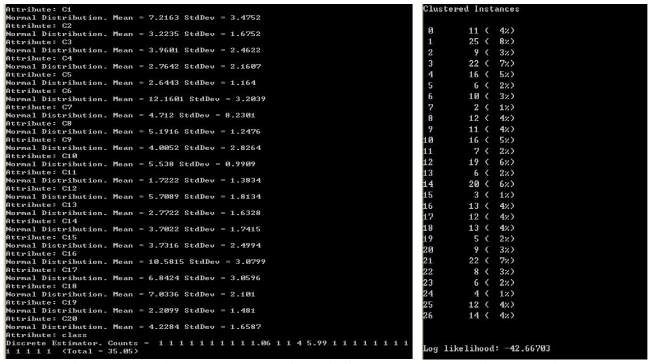


Fig. 14. Performance Results of the Human Emotion Analyzer

Figure 14 shows the accuracy performance results for the Human Emotion Analyzer. When unsupervised algorithm deformation applying with supervised algorithm, the accuracy error confirmed a nil. (The deformation algorithm is 100% accuracy of analysis in all protein instances.)

The Human Emotion Recognition module acquires electrocardiogram data (p, q, r, s, t waves) from the electrocardiogram sensor device and applies the peak of all waves and the RRV(r-r interval) as input values. As shown in Figures 17, all distributions were normal. In our experiment, only the R-R Interval and R peak showed small differences in emotion and stress changes. Table 1 shows the performance results of human emotion recognition. The neural emotion showed the highest accuracy, with the range of the three emotions at 55.8 to 75.1%. Stress recognition showed a high performance result of 83.2%. Figure 15, 16 shows experimental data of concentration and non-concentration state from brain waves.

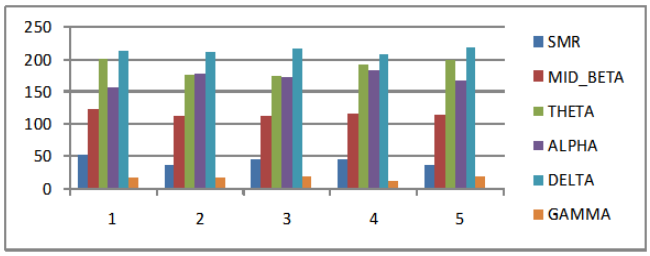


Fig. 15. Brain wave data of normal (non-concentration) state

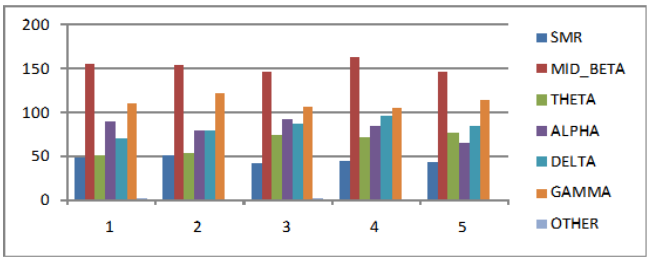


Fig. 16. Distribution of RRV and R Peak of Stress (yes, no)

TABLE I
PERFORMANCE RESULTS OF THE HUMAN EMOTION ANALYZER

Emotion	Correctly Classified Instances	Incorrectly Classified Instances	Accuracy (%)
Fear	662	524	55.8
Neural	891	295	75.1
Joy	801	385	67.5
Stress(yes)	1348	272	83.2
Stress(No)	1348	272	83.2

* 10-fold cross validation was used

** The stress data were extracted from 10 different users. Each user was tested for 5 minutes for each emotion.

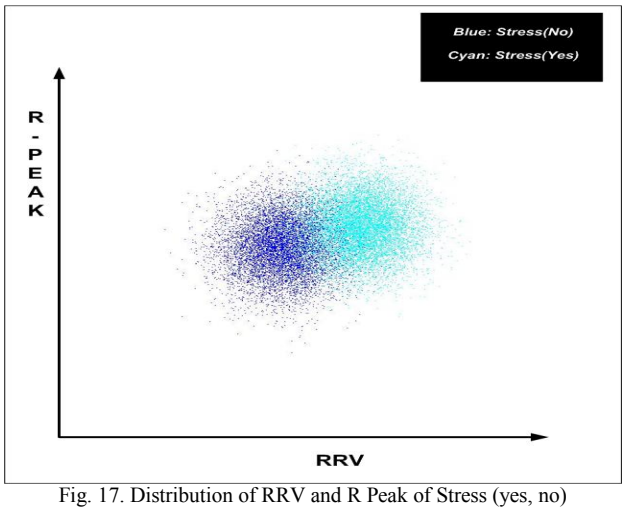


Fig. 17. Distribution of RRV and R Peak of Stress (yes, no)

V. CONCLUSION AND FUTURE WORK

In this paper, we produced architecture for building smart system effects that had more efficiency than the requirement of a user's status recognition and expediency environment. The Human Emotion Recognition module evaluates differences in emotion or stress levels. To recognize an occupant's emotional pattern, we applied deformation K-means-based EM as the HEA's pattern recognition. In emotion recognition, the neural emotion showed the highest accuracy, and three emotions were in a range of 55.8 to 75.1% accuracy. Stress recognition showed a high performance result of 83.2% accuracy.

We also show the sensor device acquires continuous brainwave signals from frontal lobe. This result of recognition was applied to smart driving system. In this experiment, we develop the analysis system of multimodal biometric signal. The technology which analyzes a brain wave is very important in foundation research. The analysis method was embodied in this research. It will use diversity field in future work.

ACKNOWLEDGMENT

This research is supported by Ministry of Culture, Sports and Tourism(MCST) and Korea Creative Content Agency(KOCCA) in the Culture Technology(CT) Research & Development Program 2009

REFERENCES

[1] R. Picard, E. Vyzaz and J, Healey, "Toward Machine Emotional Intelligence: Analysis of Affective Physiological State," *IEEE Transl. Pattern Analysis and Machine Intelligence*, vol. 23, no. 10, 2001, 1175-1191.

[2] M. A. Kramer, "Autoassociative Neural Networks, Computers and Chemical Engineering," vol. 16, no. 4, 1992, pp. 313-328.

[3] Vaughan, T., et al., "Brain-computer interface technology: a review of the second international meeting," *IEEE Transactions on Neural Systems and Rehabilitation Engineering*, 11 vol. 2, 2003, 94–109.

[4] Haynes, J.D., Rees, G., "Decoding mental states from brain activity in humans," *Nature Neuroscience*, vol.7(7), 2006.

[5] Poli, R., Cinel, C., Citi, L., Sepulveda, F., "Evolutionary brain computer interfaces," *in Giacobini, M, eds. EvoWorkshops LNCS, vol.4448*, Springer, Heidelberg, 2007, 301–310.

[6] Taehyun Kim, Dongkyoo Shin, Dongil Shin, "Design and Implementation of Intelligent Physics System," *Proc. Computer Games, Multimedia and Allied Technology 09*, 2009, 291-298.

Detecting Emotion from Voice using Selective Bayesian Pairwise Classifiers

Jangsik Cho, and Shohei Kato
Dept. of Computer Science and Engineering
Nagoya Institute of Technology
Gokiso-Cho, Showa-ku, Nagoya 466-8555, Japan
Email: {cho, shohey} @juno.ics.nitech.ac.jp

***Abstract*—This paper describes a method for detecting a dialogist's emotion from his or her voice. The method is based on pairwise classification by probability from the selective pairwise classifiers. In this research, we focus on the elements of emotion included in a dialogist's voice. Thus, as training datasets for learning the pairwise classifiers, we extract acoustic features from emotionally expressive voice samples spoken by unspecified actors and actresses in films, and TV dramas. The acoustic features adopt duration per single mora, fundamental frequency, energy, and formant. All features except duration per single mora have statistics extracted standard deviation, mean, maximum, minimum, median, timezone of maximum, and timezone of minimum. Pairwise classification classifies a multi-class problem by using a series of binary classifiers. Pairwise classifiers used tree augmented naive bayes, which constructs tree structure among the attributes in naive bayes, by selected subset features. The subset features are selected on every pair of emotions by using naive bayes. This paper reports the accuracy rates of emotion detection by using our method. In experimental results from our voice samples, the emotion classification rates improved.**

***Keywords*—Detecting Emotion from Voice; Tree Augmented Naive Bayes; Pairwise Classification; Feature Selection**

I. Introduction

Human service robots and anthropomorphic software agents have been developed thanks to advances in information technology and robotics. In particular, man-machine interface and human-computer interaction (HCI) technologies, for expressive communication with humans, have been developed (e.g., [1], [2], [3]). Communication involves not only conveying messages or instructions but also psychological interactions, such as comprehending mutual sentiments, sympathizing with the other person, and enjoying the conversation itself. Humans communicate expressively by recognizing their dialogist's emotions, having emotions, and expressing emotions. To communicate expressively, HCI technology requires several mechanisms to make up for its lack of human intelligence.

The target of our research is to develop fundamental technology to recognize, control, and express the emotional content within human computer interactions[4], [5], [6]. This study focused on recognition of the dialogist's emotion. Humans can understand the dialogist's emotion by acquiring knowledge from the dialogist's expressive features, such as, level, speed and volume of his voice, gesture and face of him. For emoiton detection, this study uses the acoustic features of voice that can be precisely recognized as the emotions expressed in voice data. Emotional vocal expression is different in each language. In our previous work[7], we compared the sensibilities of emotion detection from speech between Japanese and Korean. This study focuses on Japanese speech.

Several researchers have reported methods for detecting emotions from the human voice. Ververidis and Kotropoulos [8] proposed a method to classify voice samples into five emotions (anger, happiness, neutral, sadness, and surprise) by using a bayes classifier. This method detects emotion from specified four participants. Lee and Narayanan [9] proposed a method to classify voice samples into two emotions (negative, non-negative) by using a linear discriminant classifier and k-nearest neighborhood classifier as combining acoustic, lexical, and discourse. This method had the accuracy rates over 80% from free sentences of unspecified participants in the two emotions. In our previous works[4], [10], we detected emotion using single bayesian network as a multi-class classifier. This study adopts pairwise classifiers that detect emotion using a series of selective tree augmented naive bayes classifiers in two emotions.

Pairwise classification [11], [12], [13] converts a multi-class problem into the series of binary class problems. C classes is classified by $C(C-2)/2$ binary classifiers. Furthermore, tree augmented naive bayes [14], [15], [16] is a bayesian network classifier that constructs a tree structure among the attributes in naive bayes. It has high classification performance ability, and reduces independency on the attributes from naive bayes.

In this paper, we propose a method for human-computer interaction that detects emotion. The method is pairwise classification: using selective tree augmented naive bayes in which the emotional content of the voice are modeled by their selected acoustic features on every pair of emotions.

II. Pairwise Classification

Generally, a binary class has higher classification ability than a multi-class. Thus, a multi-class sometimes resolves a series of binary class classifiers. Pairwise classification [12] converts a C class problem into $C(C-1)/2$ binary problems for a pair of classes. Otherwise, one against all classifies the C class problem into $C-1$ binary problems for one class and other class. Pairwise classification is more common

between multi binary classifiers, because pairwise classification has relatively high ability. In pairwise classification, each binary classifier C_{ij}(classifiers for class i, j) is learned on the subset of training examples that belong to the classes C_i and C_j, all other examples are ignored for the training of C_{ij}. Classification from each binary classifier adopts voting system that classifies the most selected class by using each binary classifiers. However, the voting system can not classify if two classes have an equal amount of wins. Therefore, pairwise classification as a voting system adopt classifiers probability[11], [13]. This study adopts weighted probability pairwise classification using pairwise classifiers probability to detect emotion from a voice.

III. Bayesian Classifier

A. Naive Bayes

Naive bayes (NB) is a simple bayesian classifier with strong independence assumption of attributes. Class C classifies from attributes $x = a_1 \cdots a_n$ as follows:

$$\begin{aligned} C &= \underset{c_i \in C}{\operatorname{argmax}} P(c_i|x) \\ &= \underset{c_i \in C}{\operatorname{argmax}} P(c_i)P(a_1 a_2 \cdots a_n|c_i) \\ &= \underset{c_i \in C}{\operatorname{argmax}} P(c_i)P(a_1|c_i)P(a_2|c_i)\cdots P(a_n|c_i) \\ &= \underset{c_i \in C}{\operatorname{argmax}} P(c_i)\prod_{j=1}^{n} P(a_j|c_i) \end{aligned} \quad (1)$$

It sometimes has high classification performance ability, although it is unrealistic for strong independence assumption of the attributes. This study adopts naive bayes as a classifier for feature selection.

B. Tree Augmented Naive Bayes

Tree augmented naive bayes (TAN) [14], [15], [16] is a bayesian network classifier that constructs a tree structure among the attributes in naive bayes. The tree structure is constructed by conditional mutual information between the attributes. Conditional mutual information is defined as [14]

$$I_P(\mathbf{X};\mathbf{Y}|\mathbf{Z}) = \sum_{\mathbf{x},\mathbf{y},\mathbf{z}} P(\mathbf{x},\mathbf{y},\mathbf{z}) \log \frac{P(\mathbf{x},\mathbf{y}|\mathbf{z})}{P(\mathbf{x}|\mathbf{z})P(\mathbf{y}|\mathbf{z})} \quad (2)$$

The tree structure is constructed as follows:

1) Compute $I_{\hat{P}_D}(a_i; a_j|c)$ beween each pair of attributes, $i \neq j$.
2) Build a complete undirected graph in which nodes are attributes $a_1, \cdots, a_n$. Annotate the weight of an edge connecting a_i to a_j by $I_{\hat{P}_D}(a_i; a_j|c)$.
3) Build a maximum weighted spanning tree.
4) Transform the resulting undirected tree into a directed one by choosing a root variable and setting the direction of all edges to be outward from it.
5) Construct a TAN model by adding a vertex labeled by c and adding an arc from c to each a_i.

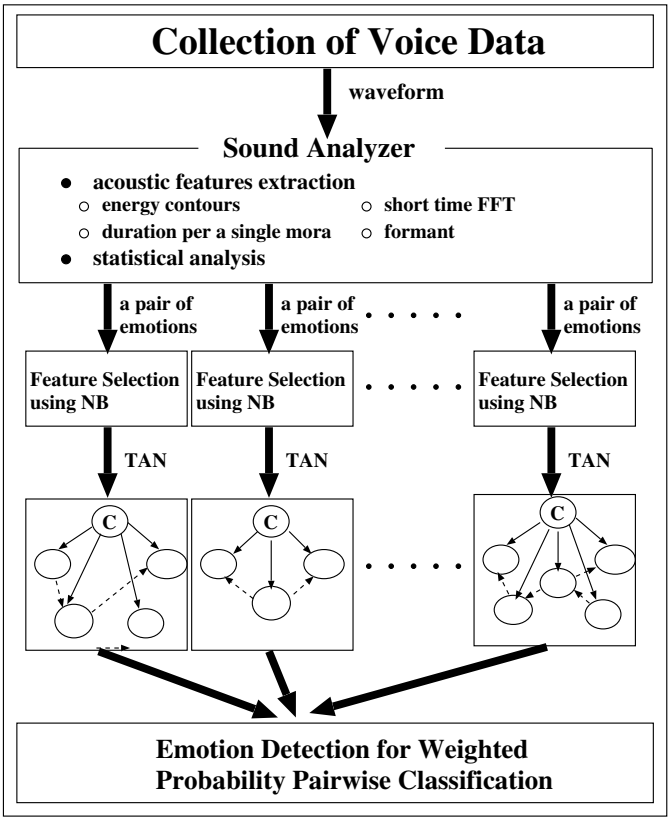


Fig. 1. Overview of pairwise classification for emotion detection

All attribute nodes except the root node of the tree can have only one parent from another attribute node. Class C is classified from the attributes as follows:

$$C = \underset{c_i \in c}{\operatorname{argmax}} P(c_i)\prod_{j=1}^{n} P(a_j|c_i, Pa(a_j)) \quad (3)$$

$Pa(a_j)$ is a parent node of a_j but not of class node. TAN reduces independence of the attributes for constructing the tree structure, and it keeps on classification efficiency. This study adopts TAN as the pairwise classifiers for detecting emotion.

IV. Emotion Detection Engine

In this paper, we focus on the acoustic features of the speaker's voice as a clue to what emotion he or she expresses. This section describes a pairwise classifiers learned for emotion detection as shown Fig. 1.

A. Voice Data

To construct the emotion detection engine, the voice data that have expressive of emotions are necessary as a learning data. A researcher collected segments of Japanese voice samples that were spoken by unspecified actors and actresses from free utterances in films, TV dramas, and so on. The segments we collected do not have loud noises. In this paper, we supposed that the segments have single emotion. All segments are labeled with one label from the five emotions (anger,

TABLE I
ACOUSTIC FEATURES

Acoustic features	Statistics						
	Standard deviation	Mean	Maximum	Minimum	Median	Timezone of maximum	Timezone of mininum
Fundamental frequency	$F0_1$	$F0_2$	$F0_3$	$F0_4$	$F0_5$	$F0_6$	$F0_7$
Energy	PW_1	PW_2	PW_3	PW_4	PW_5	PW_6	PW_7
First formant frequency	$F1_1$	$F1_2$	$F1_3$	$F1_4$	$F1_5$	$F1_6$	$F1_7$
Second formant frequency	$F2_1$	$F2_2$	$F2_3$	$F2_4$	$F2_5$	$F2_6$	$F2_7$
Third formant frequency	$F3_1$	$F3_2$	$F3_3$	$F3_4$	$F3_5$	$F3_6$	$F3_7$
Fourth formant frequency	$F4_1$	$F4_2$	$F4_3$	$F4_4$	$F4_5$	$F4_6$	$F4_7$
First formant bandwidth	$BW1_1$	$BW1_2$	$BW1_3$	$BW1_4$	$BW1_5$	$BW1_6$	$BW1_7$
Second formant bandwidth	$BW2_1$	$BW2_2$	$BW2_3$	$BW2_4$	$BW2_5$	$BW2_6$	$BW2_7$
Third formant bandwidth	$BW3_1$	$BW3_2$	$BW3_3$	$BW3_4$	$BW3_5$	$BW3_6$	$BW3_7$
Fourth formant bandwidth	$BW4_1$	$BW4_2$	$BW4_3$	$BW4_4$	$BW4_5$	$BW4_6$	$BW4_7$
Duration per single mora	T_m						

sadness, disgust, surprise, or happiness) by a researcher. The appropriateness of the emotional labels are confirmed through subjective evaluation experiments.

B. Features Extraction

Acoustic features used for emotion detection is fundamental frequency, energy, duration, formant, mel-frequency cepstral coefficients, duration, speech rate [17], [18]. In this paper, as attributes of voice data, we chose acoustic components as: duration, fundamental frequency ($F0$), energy (PW), from first to fourth formant frequency ($F1$, $F2$, $F3$, $F4$), and from first to fourth formant bandwidth ($BW1$, $BW2$, $BW3$, $BW4$). Acoustic analysis was done on 11 ms frames passed through a Hamming window extracted from voice waveforms sampled at 22.05 kHz. Then, we extract statistics of fundamental frequency, energy, and formant: standard deviation, mean, maximum, minimum, median, timezone of maximum, and timezone of minimum. We measured the average duration per a single single mora (T_m). Table I shows extracted seventy one features for emotion detection.

C. Feature Selection

Feature selection (FS) [19], [20] is a data preprocessing step for classification. Generally, feature selection is done by selecting efficient features that determine the class label. This can also reduce the dimensionality, which can otherwise worsen the performance of the pattern classifiers. In this paper, we used the forward-backward stepwise selection method. In this approach, variables once entered may be dropped if they are no longer significant as other variables are added. Feature selection conducts on every pair of emotions for pairwise classification. They obtain the important subset features for classification on every pair of emotions. Thus, we expect that feature selection done on each pair of emotions improves emotion detecting ability for pairwise classification and reduces computational effort of emotion detection. In this paper, subset features criterion use the accuracy rate of classification by naive bayes, and the accuracy rate is estimated by the leave one out method.

D. Learning Emotion Detection Engine

In this paper, we learned the pairwise classifiers using TAN on every pair of emotions. For detecting the five emotions, we learned ten pairwise classifiers. Each classifier used different features that selected every pair of emotions from all features, and classifies them into only included two emotions by posterior probability.

E. Emotion Detection Algorithm

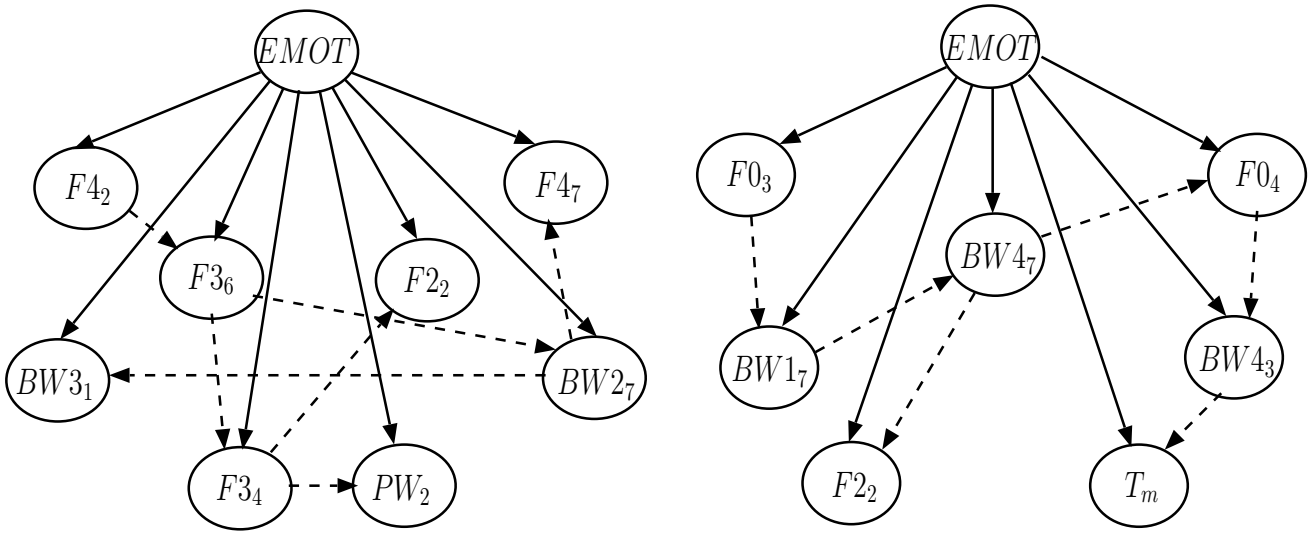
The voting system is a common pairwise classification. However, if the win scores are tied over two classes, classification randomly occurs among classes with the most wins. In this paper, we detected emotion as weighted voting for posterior probability by TAN classifiers. Emotions are detected as follows:

for $i = 1$ to k-1 **do**
  for $j = i + 1$ to k **do**
    Compute probability P_i, P_j using classifier $C_{i,j}$
    if $P_i > P_j$ **then**
      $w = P_i$
      $sum_i = sum_i + w$ //weighted probability
    else if $P_i < P_j$ **then**
      $w = P_j$
      $sum_j = sum_j + w$ //weighted probability
    else if $P_i = P_j$ **then**
      Continue
    end if
  end for
end for
Detect emotion as $\underset{c=1\cdots k}{\operatorname{argmax}} sum_c$

In algorithms, C_{ij} is classifier of i, j class, P_i is posterior probability of i as classifier C_{ij}, and k is class number.

V. EXPERIMENTAL EVALUATION

The section describes an experimentation of emotion detection. First, we collected 200 segments of male and female voice waveforms (400 segments in total) and labeled them with the five emotions, as described in Section IV-A. Voice samples are same number segments for each emotion (40 segment per emotion). Then, we extracted 71 acoustic features in each of the segments and assigned them to the attributes, as described in Section IV-B. The acoustic analysis used the Snack sound toolkit [21]. Then, we conducted feature selection on every pair of emotions, as described in Section IV-C. Then



(a) An example of male TAN

(b) An example of female TAN

Fig. 2. Examples of TAN classifiers between anger and disgust

TABLE II
ACCURACY RATES OF EMOTION DETECTION

Emotion	Accuracy rates(%)		
	Male	Female	Total
Anger	**60**	**85**	**72.5**
Sadness	35	37.5	36.25
Disgust	57.5	42.5	50
Surprise	47.5	52.5	50
Happiness	57.5	37.5	47.5
Total	51.5	51	51.25

we learned pairwise classifiers, as described in Section IV-D, with Bayes Net Toolbox [22]. Then, we detected emotion from voice samples, as described in Section IV-E. To evaluate emotion detection performance, we adopted ten fold cross-validation. For ten fold cross-validation, we partitioned voice samples into ten subsamples in which each subsample had the same number of emotion segments. One subsample assigns the test data, and the remaining nine subsamples are used as training data. Then we repeated this ten times as changing test data.

Fig. 2 shows the examples of the TAN model that classifies male and female segments into anger and disgust. The male model for anger and disgust uses eight selected subset features ($F4_2$, $F3_6$, $BW3_1$, $F3_4$, PW_2, $F2_2$, $F4_7$, $BW2_7$) (Table VI). It constructs tree among eight attributes as $F4_2$ is root node. Also the female model use seven selected subset features ($F0_3$, $BW1_7$, T_m, $F2_2$, $BW4_3$, $BW4_7$, $F0_4$) (Table VI). It also constructs tree among seven attributes as $F0_3$ is root node.

A. Results of Emotion Detection

We examined the emotion detection performance of pairwise classification. Table II shows the accuracy rates for emotion detection. The total accuracy rates of male and female emotion detection are higher than 50%. The accuracy rates for male and female anger was higher than the other emotions, whereas those for male and female sadness, and female disgust and happiness were lower than the other emotions.

Table III shows the number of classified samples from each emotion. Many male sadness voice samples are mis-detected as anger or disgust. This result indicates that the accuracy rate for male sadness is low because of mis-detecting many sadness voice as anger and disgust. Many female sadness and disgust voice samples are mis-detected for each other. This result indicates that mis-detecting a lot of female sadness and disgust voice for each other cause low accuracy rates of female sadness and disgust. Furthermore, many female happiness voice samples are classified as anger. This result also indicates that the accuracy rate for female happiness is low because of mis-detecting many happiness voice as anger.

B. Comparing Results for Emotion Detections

To confirm the influence of feature selection and pairwise classification on emotion detection, we examined emotion detection by pairwise classification and multi-class classification for weak FS and without FS. Weak FS detects emotion with feature selection on all emotions, and selects subset features($F0_5$, PW_4, $F0_3$, $F1_4$ for male, and $BW1_4$, $F4_7$, $F0_6$, $BW2_4$, $F0_3$, $BW2_4$, $F3_5$, $F1_4$, $F2_4$ for female). And without FS occurs emotion detection by all features. Table IV shows the accuracy rates. The accuracy rates of weak FS are higher than those of without FS on both pairwise classification and multi-class classification. This result indicates that feature selection improves emotion detection ability from voice. Furthermore, although the accuracy rates between pairwise classification and multi-class classification as to weak FS almost are unchanged, total accuracy rate of strong FS is higher than that of weak FS. This result indicates that our method improves emotion detection ability from voice.

For comparison of pairwise classification methods for emotion detection, we detected emotion by simple voting system.

TABLE III
THE NUMBER OF CLASSIFIED SAMPLES

Gender	Emotion of voice	The number of classified samples					
		Anger	Sadness	Disgust	Surprise	Happiness	Total
Male	Anger	**24**	3	8	1	4	40
	Sadness	**11**	**14**	**9**	3	3	40
	Disgust	11	3	**23**	3	0	40
	Surprise	5	2	7	**19**	7	40
	Happiness	6	2	3	6	**23**	40
Female	Anger	**34**	1	1	2	2	40
	Sadness	7	**15**	**11**	4	3	40
	Disgust	6	**10**	**17**	4	3	40
	Surprise	6	4	5	**21**	4	40
	Happiness	**11**	5	3	6	**15**	40

TABLE IV
ACCURACY RATES OF EMOTION DETECTION METHODS

Emotion	Accuracy rates(%)				
	Pairwise classification			Multi-class classification	
	Strong FS(Our method)	Weak FS	without FS	Weak FS	without FS
Anger	**72.5**	71.5	53.75	68.75	58.75
Sadness	36.25	40	28.75	43.75	32.5
Disgust	**50**	36.25	22.5	37.5	20
Surprise	**50**	28.74	31.5	31.25	32.5
Happiness	**47.5**	27.5	28.75	26.25	25
Total	**51.25**	40.75	33	41.5	33.75

TABLE V
ACCURACY RATES OF PAIRWISE CLASSIFICATIONS

Emotion	Accuracy rates(%)		
	Our method	Simple voting	Sum of probability
Anger	**72.5**	60	68.5
Sadness	36.25	32.5	41.25
Disgust	**50**	35	47.5
Surprise	**50**	36.25	50
Happiness	**47.5**	37.5	42.5
Total	**51.25**	40.25	49.95

The algorithm is as follows:

for $i = 1$ to k-1 **do**
  for $j = i + 1$ to k **do**
    Compute probability P_i, P_j using classifier C_{ij}
    if $P_i > P_j$ **then**
      $sum_i = sum_i + 1$ //simple voting system
    else if $P_i < P_j$ **then**
      $sum_j = sum_j + 1$ //simple voting system
    else if $P_i = P_j$ **then**
      Continue
    end if
  end for
end for
if One emotion is max win **then**
  Detect emotion as $\underset{c=1\cdots k}{\operatorname{argmax}}\, sum_c$
else
  Emotion detection is failure
end if

This method mis-detects emotion to equal amount of wins on more than two emotions. Table V (middle) shows the accuracy rates. The accuracy rates of our method (Table V (left)) are quite higher than those of simple voting system. This result indicates that our method improves emotion detection ability.

We also detected emotion by sum of probability. The algorithm is as follows:

for $i = 1$ to k-1 **do**
  for $j = i + 1$ to k **do**
    Compute probability P_i, P_j using classifier C_{ij}
    $w_i = P_i$
    $sum_i = sum_i + w_i$ //sum of probability
    $w_j = P_j$
    $sum_j = sum_j + w_j$ //sum of probability
  end for
end for
Detect emotion as $\underset{c=1\cdots k}{\operatorname{argmax}}\, sum_c$

This method adds all posterior probability from TAN classifiers. Table V (right) shows the accuracy rates. Total accuracy rate of our method is higher than sum of probability. The result indicates that our method has more acceptable accuracy rates.

C. Results of Feature Selection

Table VI shows the results of feature selection on pairs of emotions for male and female. The selected features are important for detecting emotion, and are different for gender, and pairs of emotions. T_m(duration per single mora) is selected on many pairs of emotions. T_m is mainly selected on pairs of emotions containing anger for female. This result indicates that T_m is important for detecting female anger. Also $BW2_7$ (timezone of minimum for second formant bandwidth) is selected on pairs of emotions containly disgust for male. This result indicates that $BW2_7$ is important for detection of male disgust.

TABLE VI
RESULTS OF FEATURE SELECTION

Gender	Pair of emotions	Selected subset features
Male	Anger, Sadness	$BW3_1, F4_7, PW_3, F0_4, F3_7$
	Anger, Disgust	$F4_2, F3_6, BW3_1, F3_4, PW_2, F2_2, F4_7, \mathbf{BW2_7}$
	Anger, Surprise	$\mathbf{T_m}, BW1_4, BW4_1, F4_2, F1_7, F3_2, F0_7, F1_4$
	Anger, Happiness	$F1_2, BW4_1, \mathbf{T_m}, F3_4, PW_3, PW_7$
	Sadness, Disgust	$PW_2, \mathbf{BW2_7}, F0_5, BW2_2, F4_6, PW_1, \mathbf{T_m}$
	Sadness, Surprise	$\mathbf{T_m}, BW4_1, F3_4, PW_2, F3_7$
	Sadness, Happiness	$F1_5, F2_7$
	Disgust, Surprise	$\mathbf{T_m}, BW4_4, \mathbf{BW2_7}, F2_6, PW_2, F4_6, F4_1, BW2_4$
	Disgust, Happiness	$F0_2, F1_2, F0_1, BW4_4, PW_3, \mathbf{BW2_7}, BW4_5, BW4_6, BW1_6, BW3_6, F3_6, F3_4, F0_7$
	Surprise, Happiness	$BW4_3, F2_2, \mathbf{BW2_7}, BW2_2, F2_1, F1_2, PW_6, BW1_5, BW4_1, BW4_4, PW_3, PW_5, BW1_7$
Female	Anger, Sadness	$BW1_2, F2_2, F0_3, \mathbf{T_m}, BW2_4, PW_3$
	Anger, Disgust	$F0_3, BW1_7, \mathbf{T_m}, F2_2, BW4_3, BW4_7, F0_4$
	Anger, Surprise	$\mathbf{T_m}, PW_5, BW4_7, PW_6$
	Anger, Happiness	$\mathbf{T_m}, BW3_2, F0_7, PW_1, F2_1, PW_3$
	Sadness, Disgust	$F0_1, BW1_2, F1_4$
	Sadness, Surprise	$F0_3, F1_4, F3_6, PW_1, F2_2, PW_7, F0_5, BW4_6, F1_6, F3_4$
	Sadness, Happiness	$F0_3, F3_5, F2_7, BW2_7, BW1_2$
	Disgust, Surprise	$F0_1, \mathbf{T_m}, BW1_6$
	Disgust, Happiness	$F0_3, BW1_7, F1_3$
	Surprise, Happiness	$PW_5, F4_4, BW2_4, BW4_6, PW_1, F3_5, BW3_3, F3_4, F1_1$

VI. CONCLUSION

This paper proposed a method for human computer intraction that detects emotions. The method provides pairwise classification using selective tree augmented naive bayes of acoustic features from human voice for emotion detection. Considering the practical constraints of human computer interaction, voice analysis can not be fully guaranteed. However, selective pairwise classifiers proposed in this paper improve emotion detection ability for freely uttered voice samples from many and unspecified actors and actresses.

In the future, we will aim to improve emotion detection ability and reduce computational effort of pairwise classification. We consider that emotional content is conveyed not only by voice but also by verbal and facial expression and gesture. In the future, we will attempt to combine verbal information and facial expression for emotion detection.

ACKNOWLEDGMENT

This work was supported in part by the Ministry of Education, Science, Sports and Culture, Grant–in–Aid for Scientific Research under grant, and the Hori Information Science Promotion Foundation.

REFERENCES

[1] R. A. Brooks, C. Breazeal, M. Marjanović, B. Scassellati, and M. M. Williamson, "The cog project: building a humanoid robot," *Lecture Notes in Artificial Intelligence*, vol. 1562, pp. 52–87, 1999.

[2] W. Burgard, A. B. Cremers, D. Fox, D. Hähnel, G. Lakemeyery, and et al., "The interactive museum tour-guide robot," *Proc. of the Fifteenth National Conference on Artificial Intelligence (AAAI-98)*, 1998.

[3] S. Kato, S. Ohsiro, H. Itoh, and K. Kimura, "Development of a communication robot ifbot," *In IEEE International Conference on Robotics and Automation*, pp. 697–702, 2004.

[4] J. Cho, S. Kato, and H. Itoh, "Bayesian-based inference of dialogist's emotion for sensitivity robots," *IEEE International Conference on Robot & Human Interactive Communication*, pp. 792–797, 2007.

[5] H. Shibata, M. Kanoh, S. Kato, and H. Itoh, "A system for converting robot 'emotion' into facial expressions," *IEEE International Conference on Robotics and Automation*, pp. 3660–3665, 2006.

[6] C. Itoh, S. Kato, and H. Itoh, "Mood-transition-based emotion generation model for the robot's personality," *IEEE International Conference on Systems, Man, and Cybernetics*, pp. 2957–2962, 2009.

[7] J. Cho, S. Kato, and H. Itoh, "Comparison of sensibilities of japanese and korean in recognizing emotions from speech by using bayesian networks," *IEEE International Conference on Systems, Man, and Cybernetics*, pp. 2866–2871, 2009.

[8] D. Ververidis, C. Kotropoulos, and I. Pitas, "Automatic emotional speech classification," *IEEE International Conference on Acoustic, Speech, and Signal Processing*, vol. 1, pp. I–593–596, 2004.

[9] C. M. Lee and S. S. Narayanan, "Toward detecting emotions in spoken dialogs," *IEEE Trans. on Speech and Audio Processing*, vol. 13, pp. 293–303, 2005.

[10] S. Kato, Y. Sugino, and H. Itoh, "A bayesian approach to emotion detection in dialogist's voice for human robot interaction," *Lecture Notes in Computer Science*, vol. 4252, pp. 961–968, 2006.

[11] S. H. Pack and J. Fürnkranz, "Efficient pairwise classification," *Machine Learning:ECML 2007*, vol. 4701, pp. 658–665, 2007.

[12] E. Hüllermeier and S. Vanderlooy, "Combining predictions in pairwise classification: An optimal adaptive voting strategy and its relation to weighted voting," *Pattern Recognition*, vol. 43, pp. 128–142, 2010.

[13] D. Price, S. Knerr, L. Personnaz, and G. Dreyfus, "Pairwise neural network classifiers with probabilistic outputs," *in Advances in Neural Information Processing Systems*, vol. 7, pp. 1109–1116, 1995.

[14] N. Friedman, D. Geiger, and M. Goldszmind, "Bayesian network classifiers," *Machine Learning*, vol. 29, pp. 131–163, 1997.

[15] L. Jiang, H. Zhang, Z. Cai, and J. Su, "Learning tree augmented naive bayes for ranking," *Lecture Notes in Computer Science*, vol. 3453, pp. 688–698, 2005.

[16] J. Cheng and R. Greiner, "Comparing bayesian network classifiers," *In Proceeedings of the 15th Conference on Uncertainty in Artificial Intelligence(UAI'99)*, pp. 101–107, 1999.

[17] R. Cowie, E. Douglas-Cowie, N. Tsapatsoulis, G. Votsis, S. Kollias, and et al., "Emotion recognition in human-computer interaction," *IEEE Trans. on IEEE Signal Processing Magazine*, vol. 18, pp. 32–80, 2001.

[18] D. Ververidis and C. Kotropoulos, "Emotion speech recognition:resourcesfeaturesand methods," *Speech Communication*, vol. 48, pp. 1162–1181, 2006.

[19] H. Liu and H. Motoda, *Feature Extraction Construction and Selection: A Data Mining Perspective*. Kluwer Academic Publishers, 1998.

[20] R. Kohavi and G. H. Jone, "Wrappers for feature subset selection," *Artificial Intelligence*, vol. 97, pp. 273–324, 1997.

[21] K. Sjölander, the Snack Sound Toolkit, http://www.speech.kth.se/snack.

[22] K. Murphy, bayes Net Toolbox, http://www.cs.ubc.ca/˜murphyk/Software/BNT/ bnt.html.

Facial Emotion Detection Considering Partial Occlusion of Face Using Bayesian Network

Yoshihiro Miyakoshi, and Shohei Kato
Dept. of Computer Science and Engineering
Nagoya Institute of Technology
Gokiso-cho, Showa-ku, Nagoya 466–8555, Japan
Email: {miyakosi, shohey}@juno.ics.nitech.ac.jp

***Abstract*—Recently, robots that communicate with human have attracted much attention in the research field of robotics. In communication between human, almost all human recognize the subtleties of emotion in each other's facial expressions, voices, and motions. Robots can communicate more smoothly with human as they detect human emotions and respond with appropriate behaviors. Usually, almost all human express their own emotions with their facial expressions. In this paper, we propose an emotion detection system with facial features using a Bayesian network. In actual communication, it is possible that some parts of the face will be occluded by adornments such as glasses or a hat. In previous studies on facial recognition, these studies have been had the process to fill in the gaps of occluded features after capturing facial features from each image. However, not all occluded features can always be filled in the gaps accurately. Therefore, it is difficult for robots to detect emotions accurately in real-time communication. For this reason, we propose an emotion detection system taking into consideration partial occlusion of the face using causal relations between facial features. Bayesian network classifiers infer from the dependencies among the target attribute and explanatory variables. This characteristic of Bayesian network makes our proposed system can detect emotions without filling in the gaps of occluded features. In the experiments, the proposed system succeeded in detecting emotions with high recognition rates even though some facial features were occluded.**

***Keywords*—Facial Emotion Detection; Bayesian Network; Feature Selection; K2 Algorithm; Partial Occlusion of Face**

I. Introduction

Recently, diverse type of robots designed not only for industrial activities but also for communicating with human have been researched and developed. Therefore, opportunities for human who rarely use computers to have contact with robots are increasing. In addition, communication robots are aimed at accomplishing smooth communication with human. For these reasons, communication robots need more intuitive interaction systems.

It is reasonable to suppose that robots that give human a sense of familiarity can communicate more smoothly with human. According to reports in the field of human communication, human feel familiarity with one's counterpart as they synchronize with their nonverbal information, e.g., facial expressions and voices [1], [2]. Robots can communicate more smoothly with human as they detect human emotions and respond with appropriate behaviors. Usually, almost all human express their own emotions with their facial expressions. In this paper, we propose an emotion detection system with facial features using a Bayesian network.

In actual communication, it is possible that some parts of the face will be occluded by adornments such as glasses or a hat. In previous studies on facial recognition, these studies have been had the process to fill in the gaps of occluded features after capturing facial features from each image [3], [4]. However, not all occluded features can always be filled in the gaps accurately. Therefore, it is difficult for robots to detect emotions accurately in real-time communication. For this reason, we propose an emotion detection system considering partial occlusion of the face using causal relations between facial features. Bayesian network classifiers infer from the dependencies among the target attribute and explanatory variables. This characteristic of Bayesian networks makes our proposed system can detect emotions without filling in the gaps of occluded features.

II. Emotions in communication

According to reports in the field of evolutionary psychology, emotions have been selected in the evolution [5], [6]. These reports indicate that emotions are important for human life. Especially, in communication between human, almost all human recognize the subtleties of emotion each other. Moreover, in previous studies on human communication, the meaning of emotions have been debated for make smooth communication [7]. So, we consider that emotions are also important for make smooth communication between robots and human. For these reasons, communication robots need the emotion detection system to make emotional communication with human.

A. Relationships between emotions and facial expressions

Human express emotions in diverse ways, e.g., facial expressions, voices and body languages. However, voices contain verbal information, and the voice pitch is associated with a gender gap. Likewise, the meaning that is expressed through body language differs among cultures. Nevertheless, Paul Ekman and his colleagues found evidence to support universality in facial expressions [8]. Moreover, according to reports in the field of human emotions, when human mimic an emotional face, they then generate the same emotion [9]. These evidences indicate strong relationships between emotions and facial expressions. For these reasons, we focus on facial expressions to

detect human emotions. In this paper, we use six different human emotions: happiness, anger, sadness, surprise, disgust, and fear as target attributes of the detection system. These emotions are represented as "universal facial expressions" by Ekman, et al. They studied facial expressions in different cultures, including preliterate cultures, and found much commonality in the expression and recognition of emotions on the face. For this reason, we believe that a system that detects these emotions is effective for people of different races and cultures.

III. Facial features for emotion detection

In this paper, we use magnitudes of some predefined motion of various facial features as explanatory variables of the detection system. Magnitudes of these motions are calculated by movements of facial features from a neutral face for each facial expression. Our proposed system is designed to detect human emotions for communication robots. We believe that it is the appropriate assumption that communication robots can get a neutral face of the interlocutor. The facial features are shown in Fig. 1, and are described in TABLE I. Each facial feature corresponds to a simple deformation on the face referring to Motion-Units [10].

IV. Bayesian network classifier for facial expression detection

Bayesian networks are powerful tools for knowledge representation and inference under conditions of uncertainty.

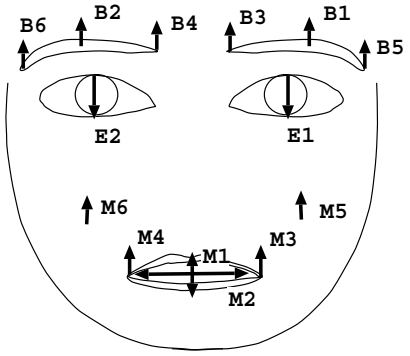


Fig. 1. Facial features.

TABLE I
Description of Facial Features

Index	Description
E1	Blinking of right eye
E2	Blinking of left eye
B1	Vertical movement of right brow
B2	Vertical movement of left brow
B3	Vertical movement of right brow left corner
B4	Vertical movement of left brow right corner
B5	Vertical movement of right brow right corner
B6	Vertical movement of left brow left corner
M1	Horizontal stretch of mouth height
M2	Vertical stretch of mouth width
M3	Horizontal movement of right mouth corner
M4	Horizontal movement of left mouth corner
M5	Lifting of right cheek
M6	Lifting of left cheek

According to reports on classification, Bayesian networks are also effective as classifiers [11].

A Bayesian network classifier represents the dependencies among the target attribute and explanatory variables in a directed acyclic graph. This graph is the structure of the Bayesian network. Many Bayesian network classifiers have been proposed in previous works, for example [11], [12], [13]. However, these Bayesian network classifiers almost no consider causal relations among explanatory variables. Therefore, we propose a Bayesian network classifier considering causal relations among explanatory variables. We construct the Bayesian network composed of the emotions and the facial features. The proposed system learns the structure of the Bayesian network in two phases: an internal phase and an external phase. Because of these phases, proposed system constructs a more robust Bayesian network classifier. Fig. 2 shows the process flow of learning the structure in the proposed system.

A. Gaussian distribution

Bayesian network classifiers calculate the maximum likelihood to classify the target attribute based on Bayes' theorem. The optimal classification rule under the maximum likelihood is expressed by the following equation.

$$\hat{c} = \underset{c \in \{1,\ldots,|C|\}}{\arg\max}\ P(X_1, \ldots, X_n | c; \Theta), \tag{1}$$

where, c, $X_1, \ldots, X_n$, and Θ each shows one of class label of the target attribute, explanatory variables, and the parameter set.

There is the problem that how to model $P(X_1, \ldots, X_n | c; \Theta)$ that is the probability of explanatory variables given the class label c. In general Bayesian networks, the explanatory variables are treated as discrete, in which case the distributions are probability mass functions. The

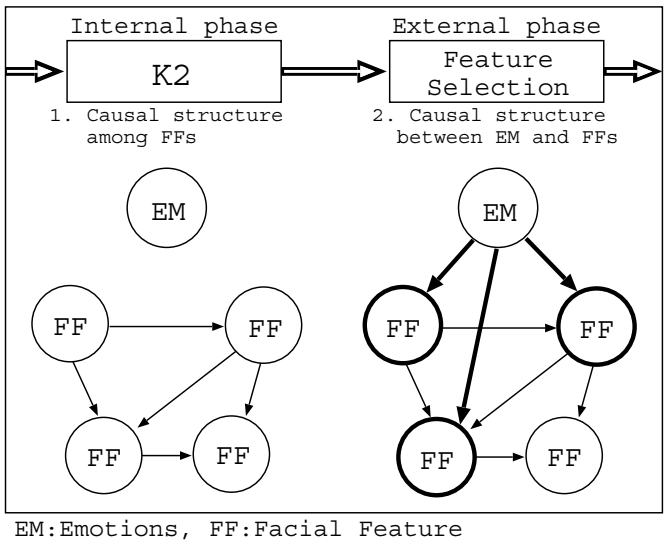


Fig. 2. Process flow of learning the structure of the Bayesian network.

explanatory variables can also be continuous as use the Gaussian distribution. The maximum likelihood can be used to obtain the estimate of the parameters (mean and variance). In this paper, we treat the facial features as continuous by using the Gaussian distribution.

B. Internal phase

In the internal phase, the system learns the structure among facial features using the K2 algorithm [14]. K2 is a greedy algorithm that learns the structure of the Bayesian network from given data. Therefore, the structure learned by using the K2 approximates real causal relations among facial features.

1) K2 algorithm: K2 algorithm is a Bayesian method for inducting a structure from given data. K2 attempts to select the network that maximizes the posterior probability of the network given the database of cases. K2 is a scoring-based learning algorithm. We use the Bayesian Information Criterion to determine the scores. When M, $\hat{\theta_M}$, and d each shows an explanatory variable, explanatory variables that have dependencies with M, and the number of $\hat{\theta_M}$; the $BIC(\hat{\theta_M}, d)$, which is the score of M, is expressed by the following equation.

$$BIC(\hat{\theta_M}, d) = \sum_{i=1}^{N} \log P(D_i) - \frac{d \log N}{2}, \tag{2}$$

where N, D_i, and $P(D_i)$ each shows the size of the database, a data, and a occurrence probability of D_i. K2 needs to be given a total order of the explanatory variables for learning the structure. In this paper, we arrange explanatory variables in descending order by the degree of separation of emotions. The ordering on the explanatory variables is shown by the following equation. The index in the following equation shows each facial feature (refer to TABLE I).

$$\begin{aligned} &B4 \prec M4 \prec M3 \prec E1 \prec B3 \prec B6 \prec M1 \\ &\prec B5 \prec M6 \prec M5 \prec M2 \prec B2 \prec B1 \prec E2. \end{aligned} \tag{3}$$

C. External phase

In the external phase, the system learns the structure between emotions and facial features with causal relations using feature selection. In previous studies on Bayesian network classifiers, the importance of selection to find a good subset of explanatory variables has been reported [15], [16], [17]. However, these studies selected features without considering causal relations among explanatory variables. We believe that proposed system can select the more appropriate subset of facial features for emotion detection because of using causal relations among facial features. In this paper, we use stepwise selection to find a good subset of facial features for emotion detection, and use the average recognition rate for all emotions as evaluation values.

V. Related study

Cohen, et al. studied an emotion detection system with facial features using a Bayesian network [18]. Their system learns the structure of the Bayesian network using Tree-Augmented-Naive Bayes (TAN) [12]. TAN forms strong relationships between emotions and facial features. On the other hand, relationships among facial features become a tree structure. So, a facial feature has at most one parent. When some parts of the face are occluded, it is difficult for TAN to correctly detect emotions because it does not have sufficiently relationship to make up for the occluded features. In contrast, the structure of our proposed system forms strong relationships among facial features. We believe that the proposed system can handle the occlusion of facial features robustly by using causal relations between facial features. We discuss here the effectiveness of the proposed system by comparing the recognition rates between the proposed Bayesian network classifier (Proposed method) and the TAN classifier (Conventional method).

A. Tree-Augmented-Naive Bayes

The algorithm for learning TAN first learns a tree structure over explanatory variables, using mutual information tests conditioned on the target attribute. It then adds a link from the target attribute to each explanatory variable. When X_i and X_j, which $i \neq j$, and C each shows an explanatory variable, and the target attribute, then $I_P(X_i; X_j|C)$ that the average mutual information conditioned on a target attribute is shown by the following equation.

$$I_P(X_i; X_j|C) = \sum_{X_i, X_j, C} P(x_i, x_j, c) \log \frac{P(x_i, x_j|c)}{P(x_i|c)P(x_j|c)}. \tag{4}$$

When using the Gaussian distribution for explanatory variables, Equation (4) is replaced by the following equation.

$$I_P(X_i; X_j|C) = -\frac{1}{2} \sum_{c=1}^{|C|} P(C = c) \log\left(\frac{1}{1 - \rho^2_{(ij)|c}}\right), \tag{5}$$

where $\rho_{(ij)|c}$ is the correlation coefficient between X_i and X_j given the class label c.

VI. Experiments

To verify the effectiveness of the proposed method, we use the Japanese Female Facial Expression (JAFFE) database collected by Lyons, et al., [19]. JAFFE is composed from facial images that are acted by ten Japanese female subjects, and posed giving three or four examples of each emotion as well as a neutral face, for a total of two hundred thirteen images (one hundred eighty three images are emotional faces and thirty images are neutral faces). We calculate magnitudes of the motion of facial features from the neutral face for each facial expression. We use one hundred eighty three data for the experiments, with at least three data for each emotion for each subject. In order to normalize each image, we set the distance between the inner corners of one's eyes to 30 pixels.

In the experiment, we conduct ten-fold cross validation: nine subjects are used for training data, and another one subject is used for test data in each validation. In a validation, we learn the structures of the Bayesian network using proposed method,

and conventional method, respectively. With the learned structures, we then conduct following two experiments, Ex.1 for detecting facial emotions with all of the facial features, and Ex.2 for detecting facial emotions with facial features that are occluded in some way. Moreover, in Ex.2, we also detect the occluded facial features.

A. Learning the structure of the Bayesian network

Fig. 3 and 4 each shows an example of the structure of the Bayesian network using the proposed method and the conventional method respectively. In the figures, the bold arrowed lines show the causal relations between the emotions and facial features, and the thin arrowed lines show the causal relations among facial features. TABLE II lists the selected rates of facial features by stepwise selection over cross validation. Facial features getting high selected rates are E1, E2, B1, B2, B4, M1, M2, and M4. These facial features indicated a strong relationship with emotions in Ekman's report. Therefore, we consider that the proposed method is able to find a good subset of facial features for emotion detection. In terms of relations among facial features, we can see that the proposed method is able to form strong relationships among facial features compared with the conventional method. Moreover, as a result of using K2, facial features are linked by the strength of the relationship between them. We suggest that the proposed method is able to approximate real causal relations among facial features.

B. Ex.1: Experiment on emotion detection

We conduct an experiment on emotion detection with the learned structure of the Bayesian network using the proposed method , and the conventional method, respectively.

TABLE III lists the results of emotion detection using the proposed method. The columns show the induced emotions and the rows show the detected emotions. TABLE IV shows the comparison of recognition rates between the proposed and conventional methods. The total is the average recognition rate for all emotions.

In TABLE IV, the total recognition rate of the proposed method outperforms that of the conventional method. The recognition rate for disgust using the conventional method is below 50%. On the other hand, all of the recognition rates with the proposed method are above 55%. This result is due to the difference in the structure between emotions and facial features. The conventional method overfits the training data because it forms a relationship between emotions and all facial features. In comparison, the proposed method selects a good subset of facial features for emotion detection. The proposed method obtain high recognition rates for total recognition, and especially happiness and surprise are relatively high. In terms of emotions with low recognition rates, angry, sadness, and disgust are mistaken for each other. These mistakes occur caused by the similarity of the facial expressions among these emotions, e.g., brows and corners of one's mouth are lowered. In addition, according to Ekman's report, it is even difficult for human to distinguish between angry and disgust. For these reasons, we suggest that the proposed method achieves a human-like emotion detection system.

Fig. 5 shows occurrence probabilities of each emotion for each facial feature selected by the proposed method over all cross validations. It seems that detecting emotions with only one facial feature is difficult, however almost all emotions can be detected by inferring from all selected features. We can confirm that the proposed method is able to select facial features that have effect to detect emotions from Fig. 5.

C. Ex.2: Experiment on emotion detection considering facial occlusion

In actual communication, not all facial features can always be captured accurately. We conduct an experiment when some facial features are occluded in order to verify the effectiveness for the robustness about facial occlusion of the proposed method. Emotion detection systems using Bayesian networks can detect emotions without filling in the gaps of occluded features. In addition, these systems can also detect occluded features by using relationships among facial features. So, we first detect emotions considering facial occlusion, and then detect occluded features. Parts of occluded facial features are eyes (E1, E2), brows (B1, B2, B3, B4, B5, B6), and mouth (M1, M2, M3, M4, M5, M6). These parts can easily be occluded by adornments such as glasses, a hat, or a surgical mask. In this study, we assumed that two or more occlusions of facial parts would not occur at the same time. We conduct ten-fold cross validation the same way as in VI-B.

TABLES IV, V, and VI list the recognition rates of emotion detection for the partial occlusion. TABLE VIII(a), (b), and (c) give the average absolute errors for actual measurement values based on estimated values inferred from relationships among

TABLE II
SELECTED RATES OF FACIAL FEATURES

Facial Feature	E1	E2	B1	B2	B3	B4	B5
Rates (%)	**100**	**90**	**100**	**80**	70	**100**	20

Facial Feature	B6	M1	M2	M3	M4	M5	M6
Rates (%)	60	**80**	**80**	40	**90**	60	40

TABLE III
CONFUSION MATRIX BY PROPOSED METHOD

Emotion	Happiness	Anger	Sadness	Surprise	Disgust	Fear
Happiness	**25**	1	0	4	0	2
Anger	2	**19**	0	0	7	2
Sadness	0	3	**19**	0	2	6
Surprise	3	0	0	**27**	0	0
Disgust	0	6	5	1	**16**	1
Fear	1	0	4	3	1	**23**

TABLE IV
RECOGNITION RATES

	Happiness	Anger	Sadness	Surprise	Disgust	Fear	Total
Proposed (%)	78.1	63.3	**63.3**	**90.0**	**55.2**	**71.9**	**70.3**
Conventional (%)	**84.4**	**73.3**	53.3	86.7	48.3	59.4	67.6

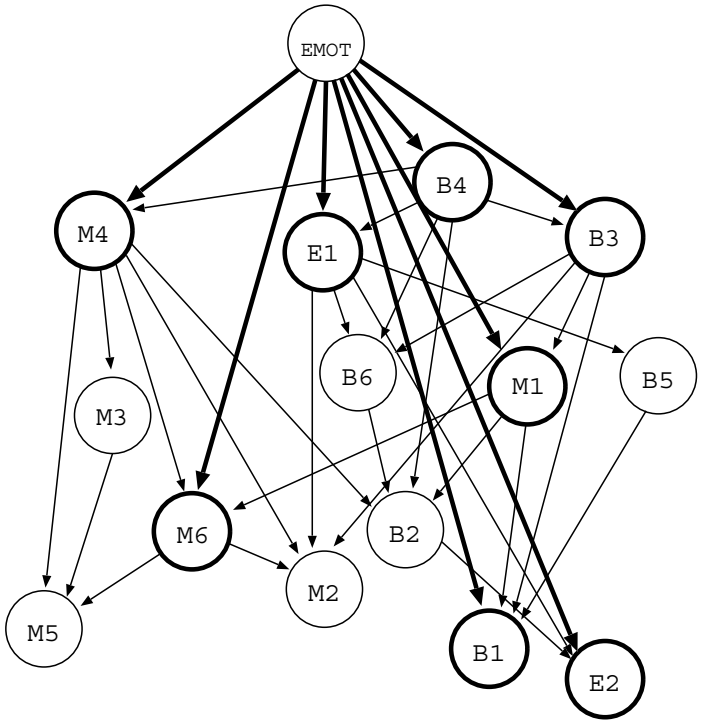


Fig. 3. Learned structure using conventional method.

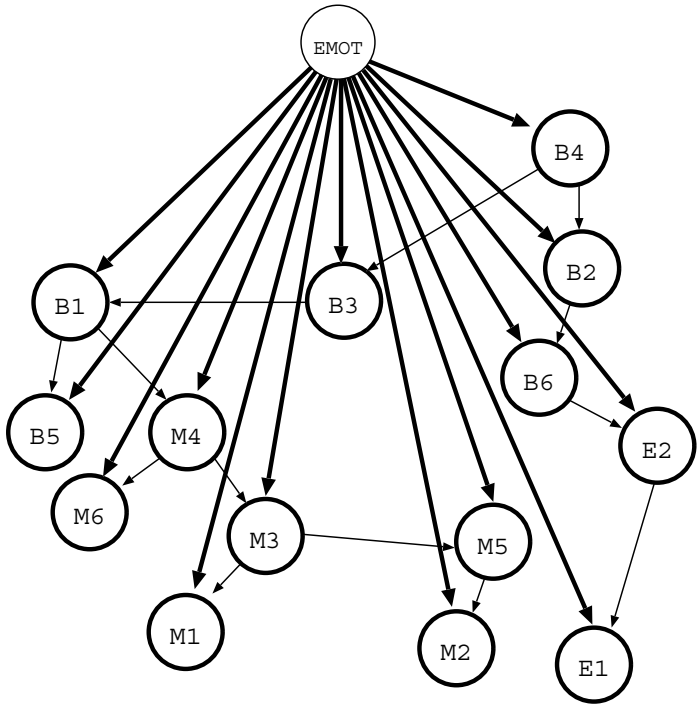
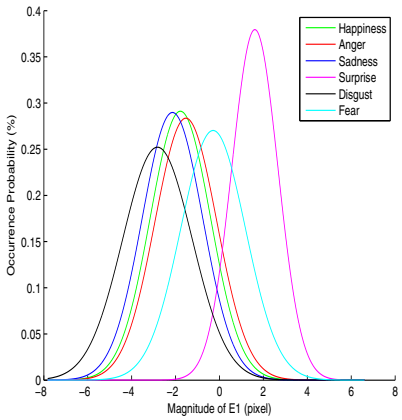
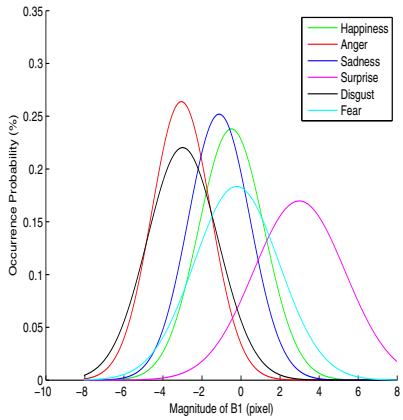


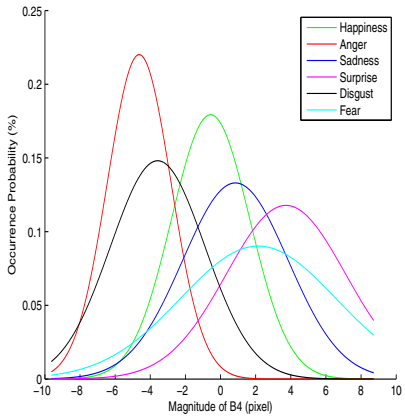
Fig. 4. Learned structure using proposed method.



(a) Facial feature: E1



(b) Facial feature: B1



(c) Facial feature: B4

Fig. 5. Occurrence probabilities of each emotion for each facial feature.

facial features. The index in the tables indicates each facial feature (refer to TABLE I).

The total recognition rate of the proposed method outperform that of the conventional method for each occlusion. Recognition rates for some emotions using the conventional method show a sharp downturn. On the other hand, almost all recognition rates using the proposed method remain above 50%. In terms of errors, the proposed method outperform the conventional method for all facial features. The error for M1 with the conventional method is abnormally large. In contrast, the facial feature is in the same range as other facial features with the proposed method. Because of the abnormally large error, we consider that the recognition rates of the conventional method for occluded mouth are not obtained from the correct inference. Moreover, we can see from Fig. 4 and TABLE VIII that the errors of facial features that have only one relation between facial features, e.g., B5, M2, and M6 tend to be large compared with the proposed method. The errors of the proposed method are sufficiently small considering the fact that the distance between the inner corners of one's eyes is 30 pixels. We can suggest that the proposed method is more effective in recognizing emotions despite facial occlusion compared with the conventional method because of strong relationships among facial features.

TABLE V
RECOGNITION RATES FOR OCCLUDED EYES

	Happiness	Anger	Sadness	Surprise	Disgust	Fear	Total
Proposed (%)	78.1	70.0	66.7	83.3	48.3	56.3	**67.1**
Conventional (%)	68.8	73.3	53.3	83.3	41.4	56.3	62.7

TABLE VI
RECOGNITION RATES FOR OCCLUDED BROWS

	Happiness	Anger	Sadness	Surprise	Disgust	Fear	Total
Proposed (%)	71.9	56.7	50.0	70.0	34.5	53.1	**56.0**
Conventional (%)	71.9	26.7	53.3	70.0	13.8	65.6	50.2

TABLE VII
RECOGNITION RATES FOR OCCLUDED MOUTH

	Happiness	Anger	Sadness	Surprise	Disgust	Fear	Total
Proposed (%)	56.3	46.7	40.0	70.0	31.0	53.1	**49.5**
Conventional (%)	46.9	66.7	23.3	80.0	24.1	43.8	47.5

TABLE VIII
AVERAGE OF ABSOLUTE ERRORS

(a) Occluded Eyes

	E1	E2
Proposed ($pixels$)	1.3	1.4
Conventional ($pixels$)	5.6	3.6

(b) Occluded Brows

	B1	B2	B3	B4	B5	B6
Proposed ($pixels$)	1.6	1.8	2.5	2.7	1.4	1.7
Conventional ($pixels$)	1.8	2.0	2.8	3.1	3.1	2.3

(c) Occluded Mouth

	M1	M2	M3	M4	M5	M6
Proposed ($pixels$)	3.9	3.6	3.5	3.5	4.2	4.3
Conventional ($pixels$)	**314.2**	4.3	3.9	4.0	4.7	5.0

VII. CONCLUSION

We proposed an emotion detection system considering partial occlusion of the face using a Bayesian network. The proposed Bayesian network forms strong relationships among explanatory variables. In experiments, we confirmed high recognition rates for total recognition, and especially for happiness and surprise. Moreover, in the experiment on emotion detection considering facial occlusion, we confirmed that almost all recognition rates with the proposed method remained above 50%, and the errors were small compared with the conventional method. These results indicate that the propose method was more effective in recognizing emotions than the conventional method even if facial features were partially occluded.

The future direction of this study will be follows.

- Increasing the recognition rate:
  In this paper, we learned the structure among facial features using the K2. In terms of relationships among facial features, they have been researched in the field of anatomy [20]. We will reform relationships learned by K2 based on researches on anatomy and form real causal relations. And also, we will confirm whether proposed structure can comply with a larger database.
- Communication between robots using our proposed system and human:
  Our proposed system is designed to detect human emotions for communication robots, and is aimed at accomplishing smooth communication with human. We will compose robots using our proposed system, and then confirm the usability of the robots for communication with human.

ACKNOWLEDGMENT

This work was supported in part by the Ministry of Education, Science, Sports and Culture, Grant–in–Aid for Scientific Research under grant #20700199.

REFERENCES

[1] J. L. Lakin and T. L. Chartrand, "Using nonconscious behavioral mimicry to create affiliation and rapport," *Psychological Science*, vol. 14, pp. 334–339, 2003.
[2] T. Hayashi, S. Kato, and H. Itoh, "A synchronous model of mental rhythm using paralanguage for communication robots," *Lecture Notes In Artificial Intelligence*, vol. 5925, pp. 376–388, 2009.
[3] A. M. Martinez and Y. Zhang, "Subset modelling of face localization error, occlusion, and expression," *Face Processing: Advance Modeling and Methods*, 2005.
[4] I. Kotsia, I. Buciu, and I. Pitas, "An analysis of facial expression recognition under partial facial image occlusion," *Journal of Image and Visual Computing*, vol. 26, pp. 1052–1067, 2008.
[5] M. Ridley, *The Origins of Virtue: Human Instincts and the Evolution of Cooperation*. Penguin Books, 1998.
[6] V. Johnston, *Why We Feel: The Science of Human Emotions*. Basic Books, 2000.
[7] P. A. Andersen and L. K. Guerrero, *Handbook of Communication and Emotion: Research, Theory, Applications, and Contexts*. Elsevier Science and Technology Books, 1997.
[8] P. Ekman, "Strong evidence for universals in facial expressions: a reply to russell's mistaken critique,," *Psychol Bull*, vol. 115, pp. 268–287, 1994.
[9] L. K. Bush, C. L. Barr, G. J. McHugo, and J. T. Lanzetta, "The effects of facial control and facial mimicry on subjective reactions to comedy routines," *Motivation and Emotion*, vol. 13, pp. 31–52, 1989.
[10] H. Tao and T. S. Huang, "Bõzier volume deformation model for facial animation and video tracking," *Lecture Notes In Computer Science*, vol. 1537, pp. 242–253, 1998.
[11] P. Langley, W. Iba, and K. Thompson, "An analysis of bayesian classifiers," *Proceedings of the tenth national conference on artificial intelligence*, pp. 223–228, 1992.
[12] N. Friedman, D. Gieger, and M. Goldszmidt, "Bayesian network classifiers," *Machine Learning*, vol. 29, pp. 131–163, 1997.
[13] J. Cheng and R. Greiner, "Comparing bayesian network classifiers," *Proceedings of the Uncertainty in Artificial Intelligence*, pp. 101–108, 1999.
[14] G. F. Cooper and E. Herskovits, "A bayesian method for the induction of probabilistic networks from data," *Machine Learning*, vol. 9, pp. 309–347, 1992.
[15] P. Langley and S. Sage, "Induction of selective bayesian classifiers," *Proceedings of the Uncertainty in Artificial Intelligence*, pp. 399–406, 1994.
[16] M. Singh and G. M. Provan, "Efficient learning of selective bayesian network classifiers," *Proceedings of the International Conference on Machine Learning*, 1996.
[17] R. Kohavi and G. H. John, "Wrappers for feature subset selection," *Artificial Intelligence*, vol. 97, pp. 273–324, 1997.
[18] I. Cohen, N. Sebe, A. Garg, L. S. Chen, and T. S. Huanga, "Facial expression recognition from video sequences: temporal and static modeling," *Computer Vision and Image Understanding*, vol. 91, pp. 160–187, 2003.
[19] M. J. Lyons, S. Akamatsu, M. Kamachi, and J. Gyoba, "Coding facial expressions with gabor wavelets," *Proc. the 3rd IEEE International Conference on Automatic Face and Gesture Recognition*, pp. 200–205, 1998.
[20] R. C. Jacobs, *Royal's Guide to Muscular Anatomy*. Royal Jacobs Publishing Company, 2010.

Technique to Correct Displacement of Vector Drawings on Scaled Underlying Raster Image

Yew Kwang Hooi[#1], Leong Siew Yoong[*2]
[#]*Universiti Teknologi PETRONAS, Bandar Seri Iskandar, 31750 Tronoh, Perak, Malaysia.*
[1]yewkwanghooi@petronas.com.my
[*]*Universiti Tunku Abdul Rahman, 31900 Kampar, Malaysia.*
[2]leongsy@utar.edu.my

***ABSTRACT* – The problems of vector graphics displacement over raster drawing due to magnification in Java Graphics2D are described. Demarcation of engineering drawing is a process of highlighting sections of interest by drawing clouds. The clouds were stored as an array of points that are combined with background image at runtime. Magnification of background causes unexpected displacement of newly drawn clouds. This may be a common but unreported problem for interactive drawing in Java Graphics2D. The paper proposed a technique that successfully corrects the issue.**

I. INTRODUCTION

Demarcation is the use of geometrical lines or transparent shapes to highlight areas of interest of an engineering drawing. Demarcated areas are called clouds. In this study, we have developed an application to view engineering drawing with tools to create and edit clouds on top of the drawing. Engineering drawing, though done initially in vector format through Computer Aided Design (CAD), is often converted into postscript or appropriate raster image formats for ease of viewing and better portability [1]. Hence, demarcation is done by placing clouds, which are vector graphics, over a rasterized engineering drawing in the background.

The intended users are an engineering safety audit team who has the need to focus on design safety by inspecting electrical single-line diagrams (SLDs). SLD is a simplified notation of a power system often used for power flows studies. Audit team would eyeball the SLD systematically to identify possible safety hazards and to make necessary recommendations.

If any of the design components in an SLD are thought to compromise safety, then a cloud is drawn to mark the identified component(s) for a discussion of the areas of concern and to recommend changes. Clouding is done by drawing transparent geometrical shapes over an area of interest, see Fig. 1. The clouds should be editable to accommodate further changes if any.

The shape and position of cloud perimeters are stored in vector form on the computer. The background SLD is stored in raster form. Both are combined only during loading and refreshed repeatedly at viewing time.

In a program for displaying an SLD and drawing cloud perimeters, a magnification feature is necessary in order to enlarge or shrink certain sections of the drawing. Other necessary features to draw or edit various clouds are displayed in Fig. 2.

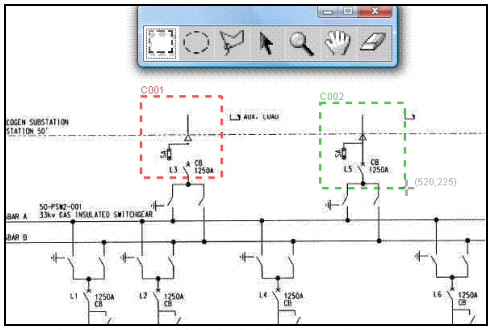


Fig. 1. Clouds (marked by dashed geometries) are demarcated on engineering drawing such as Single Line Diagram.

978-1-61284-690-3/11/$26.00 ©2011 IEEE

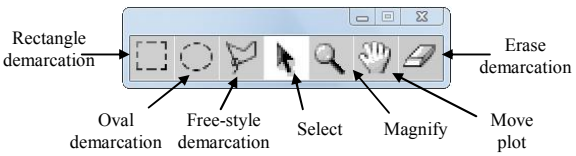


Fig. 2 Clouding tools.

The displacement problem occurs if any cloud is drawn after the background is rescaled. Cloud appears elsewhere except at its intended location, see Fig. 3. The size of the cloud relative to its background also appears disproportionately magnified.

This paper shows how the Java drawing mechanism can be exploited to mix vector and raster graphics and to magnify both types of graphics. The paper pointed out the deficiency of standard Java's graphics library in addressing maintaining relative positions of vector and raster graphics due to scaled coordinate systems. Graphics, is an object used to draw to a surface in Java, .Net and some graphics systems. An algorithm to address the problem is proposed. The final section discusses the result prospect and some limitations of the technique.

2. RELATED WORKS

Despite rescaling graphics is a common feature in almost all graphics system, there are not much literature on how rescaling mechanism works for systems with both vector and raster graphics mixed at run-time. To the best of the author's knowledge, there seems to be no mention of similar displacement problem in Java graphics system, much less of the solution. The following review literature is aimed at showing that the drawing mechanism assumed by the author is common in most graphics system regardless of its implementation.

Reference [1] stated that a large amount of engineering drawings stored in database are available in raster form instead of vector. Boeing, for example stores hundreds of thousands of illustrated parts. The paper explored techniques to identify lines through Optical Character Recognition (OCR) and domain-specific knowledge about the set of drawings in order to enhance the quality.

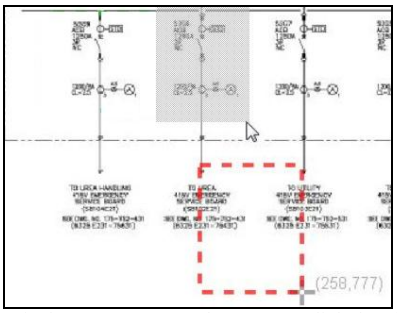


Fig. 3. Displacement occurs when mouse-click drawing (at position hinted by gray rectangle) produces the cloud elsewhere (as indicated by dashed rectangle).

References [2,3] pointed out that graphics systems for engineering drawing should store vector-valued parameters and provide scaling ability because the features allow easier manipulation of shapes and if necessary, to undo some drawings.

Several research [4,5] studied new scaling technique to enhance display of image or document content, such as a new metaphor and scaling ratio automated by rate of scrolling a document or image. In all the literature mentioned, the design seemed to be working with rasterized images only. The authors' work focuses on rescaling a medium which is an aggregation of both raster and vector graphics.

3. DRAWING MECHANISM

The application was developed using Java Swing and Java Graphics2D. Java offers better portability and improving performance due to availability of faster hardware.

The standard Java library provides rich object-oriented facilities to develop Graphical User Interface windows, components and graphics output through AWT and Swing packages. Extending standard Java package is Java3D which renders 3D objects or scenes. The scope of this work is a 2D graphics, hence 2D drawing mechanism using Java's Graphics2D object is described, as summarized in Fig. 4 block diagram.

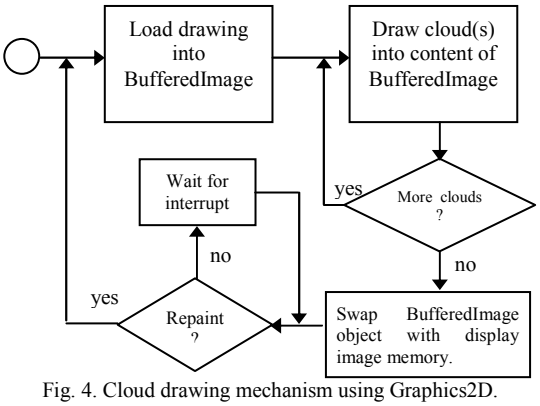


Fig. 4. Cloud drawing mechanism using Graphics2D.

Every time a cloud is drawn, mouse-click and mouse-dragged events are generated. The events invoke Graphics2D object's repaint() method to update drawings on the image:

Step 1: Retrieve Image's Graphics2D object.
Step 2: Use Graphics2D object to draw.
Step 3: Repeat at next repaint() method.

Graphics2D object draws image into a BufferedImage object instead of displaying directly. Double-buffering image helps reducing flickers in interactive drawing [6].

Next, Graphics2D object checks for any cloud object in the array. Each cloud object contains a pair of array for the x and y coordinates. Graphics2D uses the coordinate points, to draw the cloud(s) on the buffered image.

Finally, the completed drawing is copied to canvas for display. The BufferedImage object is then cleared for the next refresh cycle.

4. MAGNIFICATION MECHANISM

Magnifying requires simultaneous proportionate enlargement of both cloud(s) and underlying raster image using zoom factor described in Table 1:

TABLE 1
VALUES OF ZOOM_FACTOR VARIABLE

ZOOM_FACTOR	Image size and cloud size
1.0	Default sizes
< 1.0	Shrunken sizes
> 1.0	Magnified sizes.

The default sizes of graphics are in the code represented as a double value 1.0, see Fig. 5.

```
double ZOOM_FACTOR = 1.0;
```
Fig. 5. Zoom factor declaration.

Resizing the size is an iterative multiplication of zoom factor with itself triggered by mouse-click event. To magnify, the zoom factor must be greater than 1.0. For example, to magnify by 10%, the following code in Fig. 6 would be executed.

```
ZOOM_FACTOR  *=1.1;
```
Fig. 6. Code to increase graphics sizes.

To shrink the current sizes, the zoom factor is multiplied with a value less than 1.0. For example, to shrink by 10%, the code in Fig. 7 would be executed.

```
ZOOM_FACTOR  *=0.9;
```
Fig. 7. Code to decrease graphics sizes.

The ZOOM_FACTOR is passed as an argument to the Graphics2D object, see Fig. 8. To resize, the current width and height of the display (composed of both engineering drawing and overlaying clouds) are multiplied with the value stored in ZOOM_FACTOR.

```
Graphics2D drawGraphics
= (Graphics2D)copyImage.getGraphics();
drawGraphcs.scale(ZOOM_FACTOR,ZOOM_FACTOR);
```
Fig. 8. Scaling method of Graphics2D in code

5. CAUSES OF DISPLACEMENT AND SOLUTIONS.

Two coordinate systems are involved in drawing clouds:- JFrame container (container) and BufferedImage (image), as implied by references [7,8]. Using two coordinate systems pose a significant problem because both do not share the same origin. The mouse coordinate is based on coordinate system of JFrame whilst Graphics2D object (which draws graphics) is based on coordinate system of image canvas, see Fig. 9.

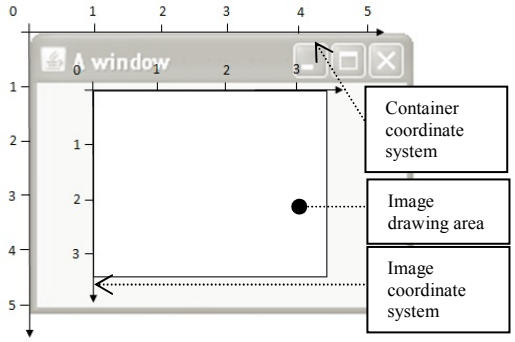


Fig. 9. Coordinate systems of container and image.

Characteristics of displacement are given in Table 2.

TABLE 2
TASK OBSERVATION

Task	Observation
Clouding at default size.	Cloud is drawn correctly within perimeter coordinates pointed by the mouse pointer.
Zoom 1.5x, then redraw similar cloud.	Instead of appearing within perimeter clicked using mouse pointer, cloud is displaced with disproportionate enlargement. The displacement distance from actual point is consistent for all new clouds drawn after a single magnification.
Zoom 3x, then redraw similar cloud.	Displacement distance increases. The displacement distance that occurs after 3x zoom is twice longer than displacement that occurs after 1.5x zoom.
Repeat with different zoom factors.	Subsequent tests reveal a pattern that displacement lengthens coherently with magnification ratio.

To address differences of both coordinate systems, one way is to determine the container coordinates registered by mouse pointer are mapped to the image coordinates. This can be done by calculating the offsets, i.e. the distance between both origins using equations (1) and (2).

$$x_{offset} = (Width_{container} - Width_{image}) \div 2 \quad (1)$$
$$y_{offset} = (Height_{container} - Height_{image}) \div 2 \quad (2)$$

However, adjusting the offsets is not sufficient to prevent displacement of cloud drawn after magnification. Prior to magnification, the problem is hidden because the lengths of unit scales in both coordinate systems are by default the same, see Fig. 10. However, magnification increases the scale of the image coordinate system but not the container's, thus resulting in the displacement.

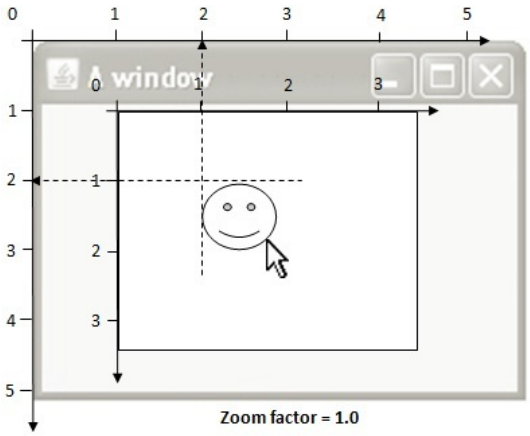


Fig. 10. Consistent scale size of both coordinate systems prior to magnification.

As an example of erroneous output, see Fig. 11. The cloud represented by a smiley should be drawn at coordinate (0.9, 0.9) but actually appears at position (2,2). Mistakenly, the mouse clicking and dragging register the coordinate location and size of the drawing to the coordinate system of the container. They should be with respect to the coordinate system of image.

On the other hand, drawing is done by Graphics2D object using enlarged coordinates and scale of the magnified image. Dashed smiley face is the actual draw location but it appears at where the solid line smiley is. Finding the offset of the origins is not enough because the unit scales of both coordinate systems become different after magnifying.

Any coordinate registered by mouse click event should be transformed to an image's coordinate. The calibration is necessary because we want to store the coordinates of the points of the shape drawn relative to the coordinate of the image, not that of the container. Calibration is done on the arrays of x and y coordinates registered by mouse-clicks. The x and y coordinates make up the shape of the cloud. The formulae to calibrate the coordinate points are given as follows:

$$x_{image} = (x_{container} - x_{offset}) \div zf \quad (3)$$
$$y_{image} = (y_{container} - y_{offset}) \div zf \quad (4)$$

where zf is zoom factor

(3) subtracts x-coordinate offset value from x coordinate returned by mouse event. The result is

divided by zoom factor in order to factor out the scaling of the image coordinate. Similar steps are repeated for the y-coordinate in (4).

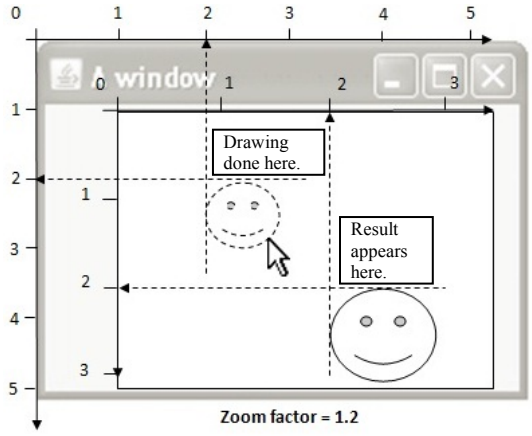


Fig. 11. Displacement error due to different scale sizes of different coordinate systems referred.

Algorithm in Fig.12 outlines the calibration step. The converted coordinates are stored into memory of each cloud. These coordinate values are used by Graphics2D object to draw on buffered image, see Fig. 4. Calibration is done for every new cloud drawn.

```
Input: container x-coordinate CX,
container y-coordinate CY, zoom factor
ZF, container width CW, container height
CH, image width IW and image height IH.

Output: an array A containing image x-
coordinate and image y-coordinate.

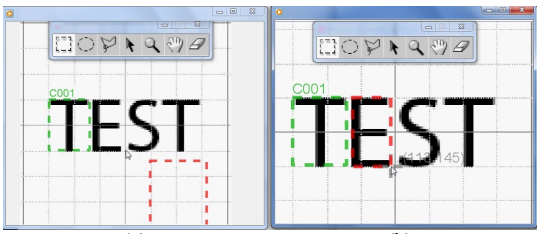
RESOLVE-DISPLACEMENT(CX,CY)
1. Let A be an new 2-dimensional array.
2. Offset coordinate CX and CY
2.1   OFFSETX=CW/2 - IW/2
2.2   OFFSETY=CH/2 - IH/2
2.3   CX  CX - OFFSETX
2.4   CY  CY - OFFSETY
3. Calibrate unit scales of coordinates
3.1   A[0]  CX/ZF
3.2   A[1]  CY/ZF
4. Return A
```

Fig. 12: Calibration algorithm to translate container coordinates to image coordinates.

6. RESULT AND DISCUSSION

Unit testing was conducted to evaluate correctness of the algorithm. An image with gridded background was loaded. A control experiment was carried out by leaving the image at its default size. Demarcation was done by enclosing letter "T" without the corrective algorithm implemented, see cloud labeled C001 in Fig. 13a. Then, demarcation was repeated on another application but this time with the corrective algorithm implemented, see cloud labeled C001 in Fig. 13b. As expected, the demarcation appeared correctly and exactly at where it was intended in both due to similar scale sizes despite different coordinates referred, as illustrated by the earlier example in Fig. 10.

The second demarcation was done after scaling with letter "E". Fig. 13a, i.e. the one without corrective algorithm, shows unwanted displacement - the bounding rectangle does not contain letter "E". Similar test was repeated with the corrective algorithm implemented and the result is positive, see Fig. 13b. Test was repeated with various images of various zooming degrees using all demarcation shapes available.



(a) (b)

Fig. 13: Images without (a) and with (b) corrective algorithm.

The algorithm resolves the problem of displacement for all demarcation shapes in all possible magnification ratios without loss of sensitivity or appreciable delay during interactive execution. Existing clouds are not affected and the number of clouds drawn does not slow down the refresh. This is because the coordinates of the clouds are calibrated only once, that is only when drawing a new cloud. Then, the Graphics2D object automatically retrieves the already calibrated coordinates of each cloud to refresh the display, as illustrated earlier in Fig. 4.

User acceptance testing was carried out with actual users. Users were requested to demarcate and magnify images repeatedly on sample engineering drawings. The algorithm has proven its practical purpose: - ease of use, precision and

sensitivity. It had also been used in at least 9 actual risk assessment activities.

This technique is designed and tested in Java environment. Hence the technique may work only for graphics applications developed using similar library or architecture. It is applicable to solve a generic problem with necessity to mix both vector graphics and raster graphics but affected by displacement due to unsynchronized magnification.

The algorithm used in this technique is implemented as a class method. Java applications with misalignment problem can import the class and use the method to rectify displacement problem.

7. CONCLUSION

This work provides a simple yet useful insight to calibrate two or more coordinate systems used for positioning vector shapes accurately on raster background in spite of different scale sizes caused by image scaling.

The problem can be resolved by first resolving origin offset and then converting container coordinate to image coordinate. Finally, image coordinates are stored for repeated use by Graphics2D to generate vector drawings correctly on scaled image of any zoom factor.

Future work investigates how other graphics systems with similar specifications and requirements can benefit from the technique.

8. ACKNOWLEDGEMENT

We thank A. P. Dr. Azmi Shaarif(Chemical Eng.), Mr. Fakhizan Romlie(E&E Eng.), Ir. Salmey Hassan(Petronas), Dr. Jubair Al-Mujawar, Dr. Etienne Schneider, Prof. Dr. Alan Oxley and Dr. Suziah Sulaiman for constructive comments. Our gratitude also goes to reviewers, Dr. M. Fadzil (program head of CISD) and A.P. Dr. Hilmi Mukhtar (director of Undergraduate Studies) of Universiti Teknologi PETRONAS for their supports and guidance.

9. REFERENCES

[1] Boose et. al., "A scalable solution for integrating illustrated parts drawings into a Class IV Interactive Electronic Technical Manual",Document Analysis and Recognition, 2003. Proceedings. Seventh International Conference, 2003.

[2] Sonmez, A.I. ,"Interactive computer aided drawing, manipulating, storing, retrieving and analyses of overall facility layout", Factory 2001- Integrating Information and Material Flow, Second International Conference, Cambridge, 1990.

[3] Y. C. Kuo, "An Interactive Design System for Engineering Drawings", IEEE Computer Software and Applications Conference, Proceedings. COMPSAC 79. The IEEE Computer Society's Third International, p.738-743, 1979.

[4] R. St. Amant, T. E. Horton, "A tool-based interactive drawing environment" , ACM International Conference Proceeding Series; Vol. 24 Proceedings of the 2nd International Symposium on Smart Graphics, p. 86 - 93, Hawthorne, New York, 2002.

[5] A. Cockburn., J. Savage and A. Wallace, "Tuning and Testing Scrolling Interfaces that Automatically Zoom", ACM CHI 2005, Portland, Oregon, USA, 2005.

[6] A. Denault, J. Kienzle, "Avoid Common Pitfalls when Programming 2D Graphics in Java – Lessons Learnt from Implementing the Minueto Toolkit. ",ACM Crossroads 13.3: Computer Graphics (2007): p.100

[7] Oracle, "Mouse Event", Java TM 2 Platform SE v.1.4.2 2010, 12 April 2010, http:// download.oracle.com/javase/1.4.2/docs/api/java/awt/event/MouseEvent.html.

[8] Oracle, "Class BufferedImage", Java TM 2 Platform SE v.1.4.2 2010, 12 April 2010, http:// www.jdk5.ru/api/java/awt/image/BufferedImage.html.

Focusing on Rule Quality and Pheromone Evaporation to Improve ACO Rule Mining

[1]Pooia Lalbakhsh, *Member, IEEE,* [2]M. Sajjad Khaksar Fasaei, and [3]Mehdi N. Fesharaki
[1]Islamic Azad University- Borujerd Branch, Young Researchers Club, Borujerd, Lorestan, Iran
[2]Islamic Azad University- Arak Branch, Arak, Iran
[3]Islamic Azad University- Science & Research Branch, Tehran, Iran
[1]Lalbakhsh@ieee.org, [2]sajjadkhaksar@yahoo.com, [3]mehfesharaki@yahoo.com

***Abstract*- In this paper an improved version of Ant-Miner algorithm is introduced and compared to the previously proposed ant-based rule mining algorithms. Our algorithm modifies the rule pruning process and introduces a dynamic pheromone evaporation strategy. The algorithm was run on five standard datasets and the average accuracy rate and numbers of discovered rules were analyzed as two important performance metrics of rule mining. As simulation results show, not only the accuracy rate and rule comprehensiveness is improved by our algorithm, the algorithm runtime is also reduced.**

I. INTRODUCTION

The domination of the concept of information in the new age, and transforming the concept of power from technology to information, introduced new data and information challenges in the fields of classification, mining and management. The most important challenge lies in the time dependent characteristic of information and the problem of unmanaged raw data which worsens the related complexities. Although most of the industrial age systems deal with raw data, the new age systems prefer to work with upper levels of the awareness pyramid contain the extracted knowledge and finally the awareness [1]. Semantic web services, the doctrine of NCW, and the other ontology-based systems can be mentioned as such systems that keep track of high level information products [2].

Rule mining is an important process which is responsible for extracting knowledge from data. This knowledge is created as some comprehensive rules with permissible level of accuracy and simplicity which can be applied by human entities or machine-to-machine interacting systems [3, 4]. It should be noted that rule mining is a step within the knowledge discovery process in which models and patterns are extracted from large data bases [5].

Our paper focuses on ant colony optimization strategy applied in rule mining. The first ACO rule mining algorithm was proposed in [5] termed Ant-Miner, which is responsible for discovering classification rules. This algorithm takes advantage of a kind of supervised learning strategy making use of predetermined training sets to learn classification rules and apply them on the real datasets. Ant-Miner not only considers ACO characteristics such as stigmergy, evaporation, and heuristic operations, it also makes use of some of the data mining characteristics such as rule quality and rule pruning.

II. THE ANTMINER FAMILY

The successful results of ACO in different applications are the consequences of its underlying robust theoretical concepts. ACO lies in the field of swarm intelligence, in which simple interactions among a group of dispersed agents, lead to complex results. ACO takes advantage of groups of artificial ants exploring the problem search space. Each ant conveys the gathered experiences to the others through an indirect communication strategy called stigmergy. This cooperative process converges to better action selections in the sense of learning automata and consequently the optimum or near optimum condition is achieved. Because of the evolutionary and iterative nature of this strategy, it is used to solve various combinatorial problems from traveling salesman problem to data mining [6].

The general pseudo code for Ant-Miner algorithm is presented in pseudo code 1 [7]. As shown in the code, Ant-Miner is based on four main parts namely: Pheromone Initialization, Rule Construction, Rule Pruning, and Pheromone Update.

Pseudo Code 1

```
Training set = All training cases;
WHILE (number of uncovered cases in the training set > msx_uncovered_cases)
i = 0;
Initialize all trails with the same amount of pheromone;
REPEAT
i = i + 1;
Ant_i incrementally construct a classification rule;
Prune the just constructed rule;
Update the pheromone of the trail followed by Ant_i;
UNTIL (i ≥ number of ants ) OR (Ant_i constructed the same rule as the previous No_Rules_Coverg – 1 Ants)
Select the best rule among all constructed rules;
Remove the cases correctly covered by the selected rule from training set;
END WHILE
```

In the initialization phase, the pheromone tables are initialized according to a predetermined value. In all ACO algorithms, each artificial ant incrementally constructs or modifies a solution for the problem. Considering rule mining, the goal is to discover classification rule from data sets. Each classification rule can considered as:

IF < term1 AND term2 AND …> THEN <class>

As mentioned above, each rule contains a condition part as the antecedent and a predicted class. Each term is a triple <*attribute*, *operator*, *value*> where *value* is a value belonging to the domain of *attribute,* and o*perator* corresponds to a relational operator. We consider the operator "=" in all of our experiments. In all experiments attributes are assumed to be categorical. Let us assume a rule condition such as $term_{ij} \approx A_i = V_{ij}$, where $A_i$is the i^{th} attribute and V_{ij} is the j^{th} value in the domain of A_i. Finally $term_{ij}$ is added to the current partial rule according to the amount of deposited pheromone and a heuristic factor.

The rule pruning is a commonplace technique in data mining. The main goal of rule pruning is to remove irrelevant terms that might have been unduly include in the rule [5]. The rule pruning procedure iteratively removes the term whose removal will cause a maximum increase in the quality of the rule which is measured by:

$$Q = \frac{TP}{TP+FN} \times \frac{TN}{FP+TN} \quad (1)$$

Where *TP* is the acronym for True Positive, which is the number of cases covered by the rule that have the class predicted by the rule. *FP* stands for False Positive, which reflects the number of cases covered by the rule that have a class different from the class predicted by the rule. *FN* refers to the False Negatives, indicating the number of cases that are not covered by the rule but that have the class predicted by the rule. *TN* stands for True Negatives, which implies the number of cases that are not covered by the rule and that do not have the class predicted by the rule. The value of *Q* is within the range [0, 1] and larger values of *Q*, results in higher rule quality.

After each ant completes the construction of its rule, pheromone updating is carried out. The pheromone update step is supported by two basic ideas [5] namely:

1. The amount of pheromone associated with each $term_{ij}$occurring in the rule found by the ant is increased proportional to the quality of that rule.
2. The amount of pheromone associated with each $term_{ij}$ that does not occur in the rule is decreased, simulating the pheromone evaporation in real ant colonies.

The following sub-sections reviews three main proposals on ant-based rule mining called ANT-MINER 1.0, ANT-MINER 2.0, and ANT-MINER 3.0.

A. Ant-Miner 1.0

This part is going to review the first ACO rule mining algorithm called ANT_MINER 1.0 presented in [5]. In ANT_MINER 1.0 the mentioned four parts are organized as follows:

In the pheromone initialization phase, the pheromone tables are equally initialized by the following value:

$$\tau_{ij}(t=0) = \frac{1}{\sum_{i=1}^{a} b_i} \quad (2)$$

Where *a* corresponds to number of attributes, and b_i is the number of values in the domain of attribute *i*. In the construction phase of ANT-MINER 1.0 the probability of adding this condition to the current partial rule is given by:

$$P_{ij}(t) = \frac{\tau_{ij}(t).\eta_{ij}}{\sum_i^a \sum_j^{b_i} \tau_{ij}(t).\eta_{ij}, \forall\, i \in I} \quad (3)$$

Where $\eta_{ij}$is a problem-dependent heuristic value for $term_{ij}$, and $\tau_{ij}(t)$ is the amount of pheromone currently available at time *t* on the connection between attribute *i* and value j. *I* is the set of attributes that are not yet used by the ants. ANT-MINER 1.0 generates the heuristic value according to the following:

$$\eta_{ij} = \frac{\log_2 k - H(W|A_i=V_{ij})}{\sum_{i=1}^{a} x_i . \sum_{j=1}^{b_i} (\log_2 k - H(W|A_i=V_{ij}))} \quad (4)$$

In the above relation, *W* is the class attribute, *k* is the number of classes, and $x_i$corresponds to 1 if attribute A_i was not yet used by the current ant, or 0, otherwise. *H* is entropy for $term_{ij}$ calculated as:

$$H(W|A_i = V_{ij}) = -\sum_{w=1}^{k} (P(w|A_i = V_{ij}).\log_2 P(w|A_i = V_{ij}) \quad (5)$$

Where $P(w|A_i = V_{ij})$ is the empirical probability of observing class *W* conditional on having observed $A_i = V_{ij}$.

The pruning strategy in ANT-MINER 1.0 follows the method suggested in [8] but the rule quality is determined according to (1).

ANT-MINER 1.0 updates the pheromone trails according to the rule quality defined by (1). Pheromone updating for $term_{ij}$is performed by:

$$\tau_{ij}(t+1) = \tau_{ij}(t) + \tau_{ij}(t).Q,\ \forall\, i,j \in R \quad (6)$$

Where *R* is the set of terms occurring in the rule constructed by the ant at iteration *t*.

In ANT-MINER 1.0 pheromone evaporation is achieved by normalizing the value of each pheromone τ_{ij}. This normalization is performed by dividing the value of each τ_{ij} by the summation of all τ_{ij}, $\forall i,j$.

B. Ant-Miner 2.0

ANT-MINER 2.0 [9] uses identical value as ANT-MINER 1.0 for pheromone initialization, but it uses a different relation for heuristic value. This algorithm proposes the following simpler equation for density estimation, which does not need accurate information as in (4):

$$\eta_{ij} = \frac{majority_class\, T_{ij}}{|T_{ij}|} \quad (7)$$

Where majority_class T_{ij} is the majority class in partition T_{ij}, which contains the cases where attribute A_i has value V_{ij}. $|T_{ij}|$ is the total number of cases in partition T_{ij}. Although using this strategy reduces the computational overhead for calculating heuristic value, the accuracy rate and number of rules are not changed in simulation runs.

C. Ant-Miner 3.0

Although the pheromone initialization of ANT-MINER 3.0 is identical to previous algorithms, it modifies the rule construction and pheromone update methods to increase the accuracy of classification by ACO [7]. The authors have focused on two vital characteristics of ACO called exploration and stagnation, and tried to balance these two features to improve the term selection for each rule. In the previous ANT-MINER algorithms, the pheromone of each term is changed after an ant constructs a rule, while η is always the same, so the next ant tends to choose terms used in the previous rule whose pheromone is increased and is unlikely choose unused terms, whose pheromone is decreased which leads to stagnation and prevents to produce alternative potential rules.

In order to enhance the role of exploration, the authors apply transition rule as illustrated in pseudo code 2. In this code $q_1$and q_2 are random numbers and φ is a parameter in [0, 1]. J_i is the number of i^{th} attribute values, and P_{ij} is possibly calculated using (3).

Pseudo Code 2

IF $q_1 \leq \varphi$
LOOP
IF $q_2 \leq \sum_{j \in J_i} P_{ij}$ **THEN** Choose $term_{ij}$
ENDLOOP
ELSE
Choose $term_{ij}$ with max P_{ij}

According to Pseudo code 2, $q_1 > \varphi$ corresponds to an exploitation of knowledge available about the problem, whereas $q_1 \leq \varphi$ results in more exploration.

After an ant constructs a rule, the amount of pheromone associated with each term that occurs in the constructed rule is updated by the following equation:

$$\tau_{ij}(t+1) = (1-\rho).\tau_{ij}(t) + \left(1 - \frac{1}{1+Q}\right).\tau_{ij}(t) \qquad (8)$$

Where ρ is the pheromone evaporation rate, which controls the influence of the history on the current pheromone trail which is fixed as 0.1.

III. OUR PROPOSAL: IMPROVED ANT-MINER

The proposed algorithm focuses on two main points namely: rule pruning process and evaporation ratio. Other aspects of the algorithm follow the strategies used in ANT-MINER 3.0.The other modification accomplished on determining the evaporation factor. Unlike ANTMINER 3.0 which considers a constant value for evaporation rate, our algorithm takes a dynamic regime to evaporate pheromone trails. These modifications are studied in the following subsections.

A. Modification in the Rule Pruning Process

In the rule pruning process, another step is added to the algorithm in which some of the low-quality terms are removed from the constructed rule. Pseudo code 3 shows this situation. In this code, parameters q_1, q_2 are constant values determined according to our experiments and valued as 2, 3 respectively. φ is set according to the number of attributes and valued as 12. According to pseudo code 3 The extra overhead of this strategy can be calculated as *O(Number_of _Attributes)*.

Pseudo Code 3

i = 0;
REPEAT
Calculate Quality of the constructed rule considering $term_i$ only
i = i+ 1;
UNTIL (i ≤ number of attributes)
IF (number of attributes ≤ φ) **THEN** $\theta = q_1$;
ELSE $\theta = q_2$;
Remove the θ lowest quality of terms
Prune the rule according to strategy used in ANT-MINER

Pruning strategy used in ANT-MINER 3.0 does not analyze the overall term combinations in the constructed rules. So a limited part of the problem search space is covered. Applying the proposed pruning algorithm, more extensive part of the search space is considered. On the other hand, eliminating low quality terms will lead to much optimal rules.

A. Modification in the Evaporation Ratio

Unlike ANT-MINER 3.0 which fixes the pheromone as a constant value, we propose a dynamic approach in which the amount of evaporation is proportional to the amount of current pheromone value τ_{ij}. Pheromone evaporation factor is calculated as (9) while the pheromone update process is still identical to (8) which is introduced by ANT-MINER 3.0.

$$\rho = \frac{1}{1+\frac{(\tau_{ij}-\alpha)^4}{\sqrt{(2\times\alpha)}}} \qquad (9)$$

Fig. 1 shows the functionality of the proposed evaporation strategy (9). The figure diagrams $(1-\rho)$ which is used in (8). As shown in the figure, a large pheromone value earns less evaporation factor which enhances the effects of the much-optimal terms in the current rule. This strategy can speed up the overall convergence towards constructing much permissible classification rules. In our simulation we fix α as 0.3.

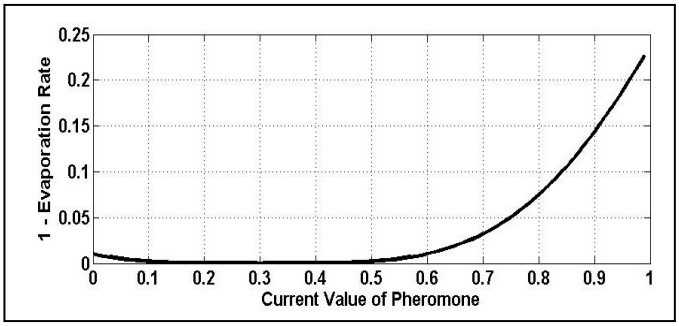


Fig. 1 diagram of (1- ρ) according to (9)

IV. EXPERIMENTAL RESULTS

In our experiments we use five standard databases from the UCI Irvine Machine Learning Data Set Repository available at: http://archive.ics.uci.edu/ml. The characteristics of these data sets are tabulated in Table 1.

TABLE 1. DATA SETS USED IN THE EXPERIMENTS (Tic. Stands for Tic-Tac-Toe; L.B.C. Stands for Ljubljana Breast Cancer; W.B.C. stands for Wisconsin Breast Cancer, D.T.Y. stands for Dermatology, H.P. stands for Hepatitis)

Data Set	No. of Cases	Categ. Attributes	Cont. Attributes	Classes
Tic.	282	9	-	2
L.B.C	683	-	9	2
W.B.C	985	9	-	2
D.T.Y	366	33	1	6
H.P	155	13	6	2

The first column of Table 1 is the data set name, while the other columns refers to the number of cases, the number of categorical attributes, the number of continuous attributes, and the number of classes of each data set respectively. The experiments are accomplished through GUIANTMINER developed by Fernando Meyer under the orientation of Rafael Stubs Parpinelli [5] which is freely available at: http://sourceforge.net.

The results are the average of 10 independent experiment runs. We analyzed three important metrics namely: accuracy rate, number of rules and the total elapsed time. We use the rule list produced by a training set to predict the class of each case in the test set. The accuracy rate is calculated as [7]:

$$Accuracy\ Rate = \frac{TP+TN}{TP+FN+FP+TN} \quad (10)$$

Table 2 contains accuracy rate for the rule sets produced by ANT-MINER 3.0 and our improved version. As the values imply, our algorithm works well in the sense of accuracy rate. Table 3 tabulates the number of rules for both algorithms. Finally Table 4 tabulates the total elapsed time for both algorithms. As Table 4 infers, eliminating low quality terms caused by the novel pruning process and the efficiency of dynamic evaporation, compensate the overhead imposed by the added loop in the pruning process.

TABLE 2. COMPARISON OF ACCURACY RATES FOR IMPROVED *ANT-MINER* AND *ANT-MINER 3.0* (The acronyms are used as Table 1)

Algorithm	Tic.	L.BC.	W.B.C	D.T.Y	H.P
Improved-Ant-miner	74.19	78.39	93.13	97.12	84.07
Ant-Miner 3.0	70.53	75.02	90.66	97.28	81.13

TABLE 3. COMPARISON OF DISCOVERED RULES FOR IMPROVED *ANT-MINER* AND *ANT-MINER 3.0*

Algorithm	Tic.	L.B.C	W.B.C	D.T.Y	H.P
Improved-Ant-miner	8.4	6.1	12.6	7.5	5.6
Ant-Miner 3.0	8.5	6.4	12.4	7.4	5.9

TABLE 4. COMPARISON OF TOTAL ELAPSED TIME FOR IMPROVED ANT-MINER AND ANT-MINER 3.0

Algorithm	Tic.	L.B.C	W.B.C	D.T.Y	H.P
Improved-Ant-miner	9 s	3 s	28 s	58 s	5 s
Ant-Miner 3.0	9 s	3 s	30 s	94 s	5 s

V. CONCLUSIONS

Knowledge engineering and cognitive systems are the foundations of the future cyber world which are based on the extracted concepts from raw data. Processing time, accurate data analysis, and the comprehensiveness of the emerged knowledge can be considered as the vital characteristics in this era. ACO data mining showed up as an efficient method in rule mining because of its multi-agent nature, swarm behavior and learning strategy which forms an adaptive roadmap for the future huge data repositories. Our proposed algorithm is an improved version of previously proposed ant-based rule mining algorithms in which two steps of evaporation and pruning are modified. In the sense of evaporation, a novel dynamic approach is proposed in which evaporation factor is determined according to the amount of the current value of the pheromone. This strategy weakens the terms with lower amounts of pheromone; therefore the algorithm converges toward much permissible terms. In the proposed pruning method the low quality terms are removed which enhances the rule construction process.

REFERENCES

[1] D. Alberts, and R. Hayes, *Power to the Edge: Command and Control in the Information Age,* CCRP Publications, 2003.

[2] P. Lalbakhsh, and M. N. Fesharaki, *Highly Reliable Interconnection Network for C4ISR Framework,* M.S.c Thesis, School of Computing, Islamic Azad University – Science & Research Campus, Tehran, Iran, 2006.

[3] K. P. Soman, S. Diwakar, and V. Ajay, *Insight into Data Mining – Theory and Practice,* Prentice-Hall of India, 2006.

[4] P. Lalbakhsh, A. Goodarzi, and M. N. Fesharaki, "Towards Virtual Audio/Video Environments using Semantic Service Composition on a Service Oriented Infrastructure," *Proc. Int. Conf. Advanced Computer Control,* Singapore, pp. 485-492, 2008.

[5] R. S. Parpinelli, H. S. Lopes, and A. A. Freitas, "Data Mining with an Ant Colony Optimization Algorithm," *IEEE Trans. Evolutionary Computing,* vol. 6(4), 2002.
[6] M. Dorigo, and T. Stutzle, *Ant Colony Optimization,* MIT Press, USA, 2004.
[7] B. Liu, H. A. Abbass, and B. Mckay, "Classification Rule Discovery with Ant Colony Optimization," *Proc. IEEE/WIC Int. Conf. Intelligent Agent Technology,* China, pp. 83-88, 2003.
[8] L. A. Brewlow, and D. W. Aha, "Simplifying Decision Tree: A Survey," *Knowledge Engineering Rev.,* vol. 12(1), pp. 1-40, 1997.
[9] B. Liu, and H. A. Abbass, and B. Mckay, "Density-based Heuristic for Rule Discovery with AntMiner," *Proc. 6th Australia-Japan Joint Workshop on Intelligent and Evolutionary Systems,* Canberra, Australia, pp. 180-184, 2002.

Harmonic Estimation Using Modified ADALINE Algorithm with Time-Variant Widrow – Hoff (TVWH) Learning Rule

B.Vasumathi S.Moorthi
Department of Electrical and Electronics Engineering
National Institute of Techonology
Trichy 15, India.

Abstract– **Algorithms are well developed for adaptive estimation of selected harmonic components in Digital Signal Processing. In power electronic applications, objectives like fast response of a system is of primary importance. An effective active power filtering for estimation of instantaneous harmonic components is presented in this paper. A signal processing technique using Modified Adaptive Neural Network (Modified ANN) algorithm has been proposed for harmonic estimation. Its primary function is to estimate harmonic components from selected signal (Current or Voltage) and it requires only the knowledge of the frequency of the component to be estimated. This method can be applied to a wide range of equipments. The validity of the proposed method to estimate voltage harmonics is proved with a dc/ac inverter as an example and the simulation results are compared with ADALINE algorithm for illustrating its effectiveness.**

Keywords: Harmonics; ADALINE; Artifical Neural Networks (ANN)

I. INTRODUCTION

Harmonics generated by non-linear loads are causing great concern and have attracted special interests. The harmonics interfere with sensitive electronic equipment and cause undesired power losses in electrical equipment. Array of problems are caused by harmonics such as overheating, frequent tripping of circuit breakers, frequent fuse blowing, capacitor failures, excessive neutral currents and power-metering inaccuracy. It is prerequisite to compensate harmonics to avoid unwanted losses and maintain electrical equipments with IEEE: 519 standards [1]. Active power filtering has been an effective way for harmonic compensation. It works basically in two steps: Harmonic estimation and elimination.

Harmonic detection in active filters can be done by a variety of methods: FFT (Fast Fourier Transformation) technique [2], p-q theory, Synchronous d-q reference frame theory or by using suitable analog or digital filters. Recent works on harmonic elimination in inverters can be seen in [3] - [8]. The harmonic voltage determination in FFT is delayed by more than two cycles, one cycle to acquire data and another cycle for analysis of data. In case of digital filters, the notch filters makes implementation difficult.

The Adaptive Linear Element (ADALINE) as seen in [9] - [12], when considered for harmonic detection can determine harmonics in just half cycle of the fundamental period. This algorithm serves good for harmonic tracking in a real time environment due to its faster convergence rate. In this paper, a Modified ADALINE algorithm with a Time-Variant Widrow – Hoff rule has been proposed for harmonic detection. This algorithm incorporates all the merits of ADALINE together with a reduced error, to attain maximum convergence. Thus detection reaches its maximum value of exactness. A dc/ac inverter is used for simulation to verify the effectiveness of the developed algorithm. The effectiveness is investigated by simulation to estimate harmonics by both ADALINE and Modified ADALINE algorithms and the results are compared.

II. MODIFIED ADALINE ALGORITHM WITH TIME-VARIANT WIDROW – HOFF (TVWH) LEARNING RULE

A. ADALINE Algorithm

This ANN approach adaptively estimates harmonics using Fourier linear combiner. The linear combiner is realized using a linear adaptive neural network called ADALINE. ADALINE has an input sequence, an output sequence and a desired response-signal. It also has a set of adjustable parameters called weight vector which are random generated initially [7], [9]. Weight vector of ADALINE [7], [9], generates the Fourier co-efficients of the signal using a non-linear weight adjustment algorithm and a stable difference equation given by (1). The weight updation rule given by (2) does not incorporate the time factor, which means the instant of iteration, is not considered.

$$e(k) = y(k) - y\hat{}(k) \tag{1}$$

Where,

$e(k)$	is error at time k
$y(k)$	is actual signal amplitude at time k
$y\hat{}(k)$	is estimated signal amplitude at time k
α	is learning parameter (Reduction factor)
$X(k)$	is input vector at time k

The weight vector of ADALINE is updated using Widrow – Hoff delta rule as,

$$W(k+1) = W(k) + (\alpha e(k) X(k) / X^T(k).X(k)) \quad (2)$$

Where,

$w(k) = [w_1(k) \ldots w_{2N}(k) w_{2N+1}(k) w_{2N+2}(k)]^T$ is weight vector at time k

The amplitude of harmonics is calculated further after error convergence, using the final updated weight vector.

B. Modified ADALINE Algorithm

Among various optimization algorithms, Particle Swarm Optimization (PSO) is one of the most widely used algorithms. When the literature of such algorithms were reviewed, [13]-[16] it was found that, in PSO algorithm, initially developed by Shi and Eberhart, each particle keeps track of its own position and velocity in problem space. The position and velocity of a particle are initially random generated. Then at each iteration, the new positions and velocities of the particles are updated [17]. The updation rule of PSO used linearly varying inertia weight over iteration and is given by (3) which incorporate the instant of iteration as a time factor for updation. This is referred to as Time-Varying Inertia Weight factor PSO (PSO-TVIW).

$$w(k) = w_{\min} + \frac{iter_{\max} - iter}{iter_{\max}} .(w_{\max} - w_{\min}) \quad (3)$$

Where,

$iter_{\max}$ is maximum number of iterations

$iter$ is current iteration number

$w_{\min}$ is minimum value of the inertia weight vector

$w_{\max}$ is maximum value of the inertia weight vector

Also on surveying further literatures of PSO [18] - [21], it was found that all updation rules of PSO incorporated the Time-Varying inertia factor $\frac{iter_{\max} - iter}{iter_{\max}}$.

In Time-Varying Acceleration Co-efficient PSO (PSO-TVAC) [17], the cognitive parameter and social parameter change according to,

$$c_1(k) = c_{1\min} + \frac{iter_{\max} - iter}{iter_{\max}} (c_{1\max} - c_{1\min}) \quad (4)$$

$$c_2(k) = c_{2\max} + \frac{iter_{\max} - iter}{iter_{\max}} (c_{2\min} - c_{2\max}) \quad (5)$$

In the Time-Varying Non-linear function modulated inertia weight updation [17],

$$w(k) = w_{\min} + ((iter_{\max} - iter) / iter_{\max})^{\alpha} .(w_{\max} - w_{\min}) \quad (6)$$

In Non-linear Time-Varying Evolution PSO (PSO-NTVE) [17], the cognitive parameter and social parameter are given as,

$$c_1(k) = c_{1\min} + ((iter_{\max} - iter) / iter_{\max})^{\beta} .(c_{1\max} - c_{1\min}) \quad (7)$$

$$c_2(k) = c_{2\max} + ((iter_{\max} - iter) / iter_{\max})^{\gamma} .(c_{2\max} - c_{2\min}) \quad (8)$$

Where,

$c_{1\max}$ and $c_{1\min}$ are maximum and minimum values of cognitive parameter

$c_{2\max}$ and $c_{2\min}$ are maximum and minimum values of social parameter

α, β, γ are constant co-efficients

The idea of incorporating this Time-Varying inertia factor into the updation rule of ADALINE was thus inferred from PSO. The Modified ADALINE algorithm was then devised with time factor $\frac{iter_{\max} - iter}{iter_{\max}}$ in the updation rule proposed by Widrow and Hoff. Thus the weight updation rule of Modified ADALINE algorithm with ***Time-variant Widrow – Hoff learning rule*** is given as,

$$W(K+1) = W(k) + ((iter_{\max} - iter) / iter_{\max}).(\alpha e(k) X(k) / X^T(k).X(k)) \quad (9)$$

Where,

$w(k) = [w_1(k) \ldots w_{2N}(k) w_{2N+1}(k) w_{2N+2}(k)]^T$ is weight vector at time k

$e(k)$ is error at time k

$y(k)$ is actual signal amplitude at time k

$y\hat{}(k)$ is estimated signal amplitude at time k

α is learning parameter (Reduction factor)

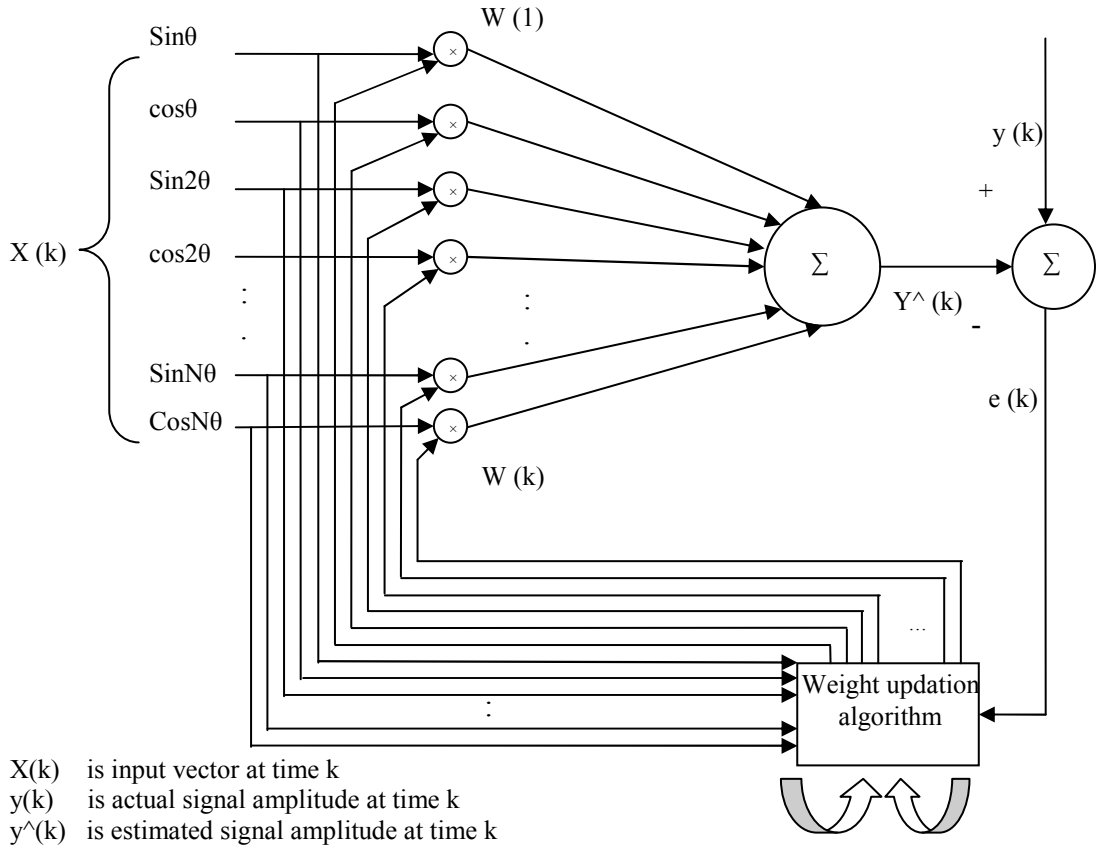
$X(k)$ is input vector at time k

$iter_{\max}$ is maximum number of iterations

$iter$ is current iteration number

III. Harmonic Estimation Using Modified Adaline Algorithm

The task of estimating the undesirable harmonic components from a signal can be done by Modified ADALINE algorithm with TVWH rule, in the following way. The Modified ADALINE algorithm with the newly developed updation rule (9) is trained using Neural Network. Fig. 1 shows the block diagram of proposed Modified ADALINE algorithm with TVWH rule for harmonic estimation. The flow chart of the proposed algorithm is shown in Fig. 2.



X(k) is input vector at time k
y(k) is actual signal amplitude at time k
y^(k) is estimated signal amplitude at time k
e(k) is error vector at time k
w(k) is weight vector at time k
N_s is Sampling rate

Fig. 1 Block representation of Modified ADALINE algorithm with TVWH learning rule

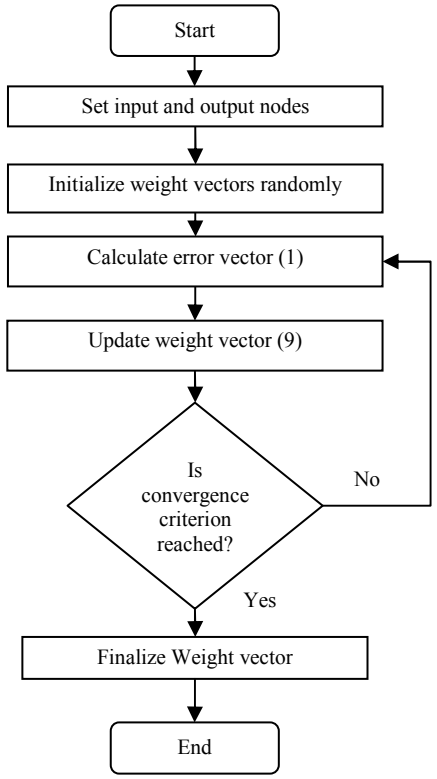


Fig. 2 Flow chart for Modified ADALINE algorithm with TVWH learning rule

The general form of a waveform for voltage or current from a non-linear load with an angular frequency ω, is the sum of harmonics of unknown magnitudes and phases [9]. It is represented as,

$$y(t)=\sum_{l=1}^{N}A_l\sin(l\omega t+\Phi_l)+\varepsilon(t) \tag{10}$$

Where,

A_l is amplitude of harmonics

Φ_l is phase of harmonics

$\varepsilon(t)$ is noise

t is the time instant of measurement]

The discrete-time version of the signal can be given as,

$$y(k)=\sum_{l=1}^{N}A_l\sin((2\pi lk/N_s)+\Phi_l)+\varepsilon(k) \tag{11}$$

$$=\sum_{l=1}^{N}A_l\cos\Phi_l.\sin\frac{2\pi lk}{N_s}+\sum_{l=1}^{N}A_l\sin\Phi_l.\cos\frac{2\pi lk}{N_s}+\varepsilon(k) \tag{12}$$

Where,

$N_s=\frac{f_s}{f_o}$ is sampling rate

f_s is sampling frequency

f_o is nominal system frequency

Input to Modified ADALINE algorithm is given as

$$X(k)=\left[\sin\frac{2\pi k}{N_s}\cos\frac{2\pi k}{N_s}\sin\frac{4\pi k}{N_s}\cos\frac{4\pi k}{N_s}\ldots\sin\frac{2N\pi k}{N_s}\cos\frac{2N\pi k}{N_s}\right]^T \quad (13)$$

Where,

T refers the transpose of a quantity

The error vector is calculated as given by (1) and is,

$$e(k)=y(k)-y\hat{}(k)$$

The weight vector is updated using the ***Time-Variant Widrow – Hoff (TVWH) learning rule*** (9).

$$W(K+1)=W(k)+((iter_{\max}-iter)/iter_{\max}).(\alpha e(k)X(k)/X^T(k).X(k))$$

After the convergence of tracking error, the amplitude of harmonics can be calculated from the final set of updated weight vectors

The amplitude and phase of N^{th} harmonics is given by

$$A_N=\sqrt{W_0^2(2N-1)+W_0^2(2N)} \quad (14)$$

and

$$\phi_N=\tan^{-1}\{W_0(2N-1)/W_0(2N)\} \quad (15)$$

Where,

W_0 is the weight vector obtained after convergence

IV. Application Example on a DC/AC Inverter

The main problem being faced by a dc/ac inverter in producing a sinusoidal ac voltage is due to harmonics. Harmonic isolation is hence needed for the better performance. The proposed algorithm (Modified ADALINE algorithm) is thus incorporated to enhance the performance of the inverter. Dedicated software in MATLAB is developed for the implementation of the proposed algorithm.

In Modified ADALINE algorithm, training vectors of 50 x 50 samples are formed. The number of rows of the training vector is chosen to be 50, so as to compute up to 25^{th} harmonic order. The number of columns in training vector is chosen to be 50 to accommodate 50 samples taken over one cycle of 50Hz. The learning parameter α is taken to be 0.02 by trial and error to yield the best solution.

The weight vectors of the proposed algorithm are random generated initially. A dc/ac inverter with a resistive load is considered for the application. The load voltage is discretized into 50 samples at an interval of 400μs with a total cycle span of 20ms.

The discretized non-linear load voltage serves as the input for adaptation for which harmonics are to be estimated. To compare the effectiveness of the proposed algorithm, harmonic estimation is done in both ADALINE and Modified ADALINE algorithms.

The input along with the training vector is trained to minimize the error difference of the differential error equation (1) and update the weight vector (9). Training process continues until convergence of error to its least approximation towards zero. Training up to 1000 epochs was performed to verify convergence. The convergence graph up to 60 epochs of error vector and weight vector for α = 0.02 are represented in Fig. 3 and 4 for Modified ADALINE algorithm for clarity.

For α = 0.02, ADALINE algorithm starts converging at 20^{th} epoch and converges to a minimum error of -0.0282 at 1000^{th} epoch. Modified ADALINE algorithm starts converging at almost 30^{th} epoch and converges to a minimum error of -0.0214 at 1000^{th} epoch. This improves the error approximately by 24.11%. To show the improvement of Modified ADALINE algorithm over ADALINE, plot of the error vector value of both algorithms for learning parameter α = 0.02 is shown in Fig. 5. With the final weight vector obtained after convergence, the harmonic components are obtained using (14) and (15)

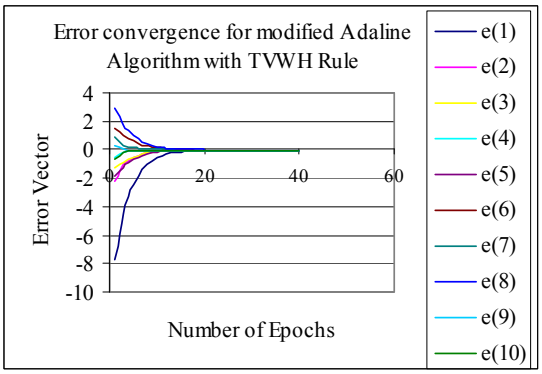


Fig. 3 Error convergence graph of Modified ADALINE algorithm learning parameter α = 0.02

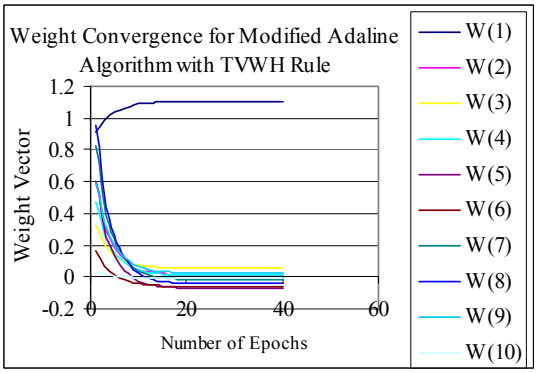
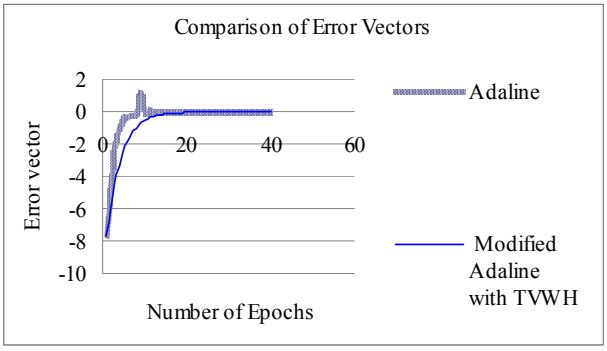
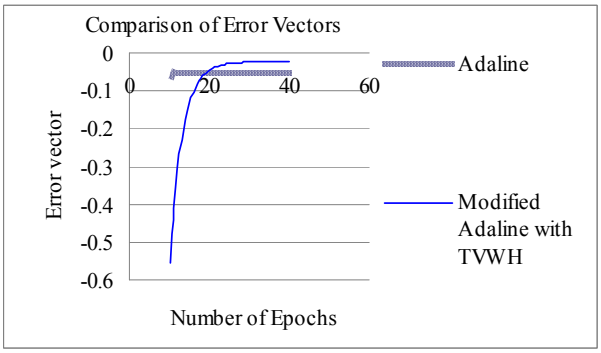


Fig. 4 Weight convergence graph of Modified ADALINE algorithm for learning parameter α = 0.02



Graph showing complete convergence



Expanded Graph

Fig. 5 Comparison of error convergence of Modified ADALINE algorithm and ADALINE algorithm for $\alpha = 0.02$

V. Results and Discussion

To illustrate the effectiveness of the proposed algorithm, the operation of a single phase dc/ac inverter is simulated for both ADALINE algorithm and Modified ADALINE algorithm. Thus the harmonics of the output voltage of the inverter is computed with the two approaches, for learning parameter $\alpha = 0.02$ and are shown in Table. I. As the error convergence is closer to zero in Modified ADALINE the computed harmonics are more exact than ADALINE algorithm. When real time implementation is considered further, certain performance parameters may be lesser due to practical considerations but this applies also to other algorithms and hence the proposed algorithm will stay good even under such circumstances.

From the computational output of the two methods, it is evident that, both the approaches are iterative based approaches in which the final convergence does not depend on initial random selection of weight vectors. The processing steps are too simple and both the methods converge at almost same rate. The convergence towards a minimum error is obtained with a uniform convergence in Modified ADALINE algorithm. Thus the ADALINE algorithm is tuned to a finer error value when the Time-Variant Widrow – Hoff rule is incorporated. These advantages are proven for different initial values and to brief it they are not included. One of the disadvantages of Modified ADALINE algorithm is that it slows down its convergence when the error reaches to a near minimum

TABLE. I
COMPARISON OF ESTIMATED HARMONICS

Comparison of estimated harmonics of Modified ADALINE and ADALINE algorithm		
S.No	Modified ADALINE algorithm	ADALINE algorithm
1	79.5876	79.8962
2	4.1197	4.2683
3	6.6944	6.6295
4	3.4346	3.4249
5	1.8727	1.9356
6	10.1475	10.0993
7	6.8683	6.8394
8	6.0772	6.0974
9	10.4092	10.4202
10	0.2047	0.1776
11	12.5016	12.479
12	9.1076	9.0831
13	6.3326	6.3564
14	11.204	11.2278
15	5.9164	5.8929
16	7.7553	7.7709
17	7.8141	7.8362
18	8.7381	8.7168
19	19.6317	19.6413
20	2.8298	2.8457
21	17.9185	17.9038
22	2.1313	2.1511
23	1.4642	1.4453
24	4.6517	4.644
Total Harmonic Distortion (THD %)	THD % = 52.51 %	THD % = 52.39 %

value. But this convergence rate does not stay much apart from ADALINE algorithm. Though the two methods differ significantly in their convergence towards a minimal error, the two methods exhibit very good convergence properties.

VI. Conclusion

The concept of Modified ADALINE algorithm with Time-Variant Widrow – Hoff rule is developed for an optimization problem with selective harmonic elimination in PWM inverter. A clear description of various stages of the algorithm is provided in this paper. The proposed algorithm stays computationally simple with a random initial guess and converges faster towards its optimal solution. The task of minimizing the error which has already been narrowed down, is achieved through the proposed algorithm. The results are presented to demonstrate the validity of the proposed algorithm. It is shown that Modified ADALINE algorithm is on its excellence when compared with normal ADALINE algorithm.

References

[1] C.K. Duffey and R.P.Stratford, "Update of harmonic standard IEEE – 519 : IEEE recommended practices and requirements for harmonic control in electric power systems," *IEEE Trans. Ind. Appl*., vol. 25, no. 6, pp. 1025 – 1034, Nov/Dec. 1989.

[2] James W. Cooley and John W. Turkey, "An algorithm for the machine calculation of complex fourier series," *Mathematics of Computation*, vol. 19, no.6, pp. 297 – 301. 1965.

[3] Cristian Lascu, Lucian Asiminoaei, Ion Boldea and Frede Blaabjerg, "Frequency response analysis of current controllers for selective harmonic compensation in active power filters," *IEEE Trans. Ind. Electron*., vol. 56, no.2, pp.337 – 347, Feb. 2009.

[4] Kinattingal Sundareswaran, Krishna Jayant and T.N. Shanavas, "Inverter harmonic elimination through a colony of continuously exploring ants," *IEEE Trans. Ind. Electron*., vol. 54, no. 5, pp. 2558 – 2565, Oct. 2007.

[5] Kinattingal Sundareswaran , and V.T.Sreedevi, "Boost converter controller design using queen – bee assisted GA," *IEEE Trans. Ind. Electron*., vol. 56, no. 3, pp. 778 – 783, Mar. 2009

[6] Shouling He and Xuping Xu, "Hardware/softwarre co-design approach for an adaline based adaptive control system*," Journal of Computers*, vol. 3, no.2, pp.29 – 36, Feb. 2008.

[7] K.R.Valluvan and A.M. Natarajan, "Implementation of adaline algorithm on a FPGA for computation of total harmonic distortion of load current," *ICGST-ACSE Journal*, vol. 8, no. 2. pp. 35 – 41, Dec. 2008.

[8] Vladimir Blasko, "A novel method for selective harmonic elimination in power electronic equipment," *IEEE Trans. Power Electron*., vol. 22, no.1, pp. 223 – 228, Jan. 2002.

[9] P.K. Dash, D.P. Swain A.C. Liew and Saifur Rahman, "An adaptive linear combiner for on-line tracking of power system harmonics," *In Proc. of IEEE/PES Winter Meetin*g, vol.11, no.4, pp. 1730 – 1735. Nov. 1996.

[10] R.K.Hartana, G.G. Richards, "Harmonic source monitoring and identification using neural networks," *IEEE Trans. on Power Syst*., vol. 5, no. 4, pp. 1098 – 1104, Nov. 1990.

[11] Mohd Amran Mohd Radzi and Nasrudin Abd. Rahim, " Neural network and bandless hysteresis approach to control switched capacitor active power filter for reduction of harmonics," *IEEE Trans. on Ind. Electron*., vol. 56, no.5, pp. 1477 – 1483, May. 2009.

[12] J.R. Vazquez, P. Salmeron, "Active power filter control using neural network technologies. *In Proc. IEE Electric Power Appl*., vol. 150, no. 2, pp.139 – 145, Mar. 2003.

[13] Russell Eberhart and James Kennedy, "A new optimizer using article swarm theory," *In proc. of IEEE Sixth International Symposium on Micro Machine and Human Science*, pp. 39 – 43, 1995.

[14] James Kennedy, "The particle swarm: social adaptation of knowledge," *In proc. of IEEE International Conference on Evolutionary Computation*. pp. 303 -308, 1997.

[15] Yuhui Shi and Russell Eberhart, "Parameter selection in particle swarm optimization.," *In Proc. of IEEE 7th Annual conference on Evolutionary Programming*, pp. 69 – 73, 1998.

[16] Yuhui Shi and Russell C. Eberhart, "Empirical study of particle swarm optimization," *In the Proc. of IEEE 12th International Conference on Artificial Intelligence (IJCA),* pp. 1945 – 1950, 1999.

[17] Chia-Nan Ko, Ying-Pin Chang and Chia-Ju Wu, "A PSO method with nonlinear time-varying evolution for optimal design of harmonic filters," *IEEE Trans. on Power Syst*., vol. 24, no. 1, pp.437 – 444, Feb. 2009

[18] Emad Elbeltagi and Tarek Hegazy, "Comparison among five evolutionary-based optimization algorithms," *Advance Engineering Informatics*, vol.19, no.1, pp. 43 – 53, Jan. 2005.

[19] C. Thanga Raj, S.P. Srivastava and Pramod Agarwal, "Induction motor design with limited harmonic currents using Particle Swarm Optimization," *International Journal of Science and Engineering*, vol.1, no.3, pp.201 –207, summer 2008.

[20] Ioan Cristian Trelea, "The particle swarm optimization algorithm: convergence analysis and parameter selection," *Information Processing Letters*, 85, pp. 317 – 325, 2002

[21]. Yuhui Shi, "Particle swarm optimization," Feature article: Electronic Data Systems, Inc., *IEEE Neural Network Society*. pp. 8 – 13, Feb. 2004

A Near Linear Shortest Path Algorithm for Weighted Undirected Graphs

Muhammad Aasim Qureshi, Mohd Fadzil Hassan, Sohail Safdar, Rehan Akbar

Computer and Information Science Department
Universiti Technologi PETRONAS
Perak, Malaysia
maasimq@hotmail.com, mfadzil_hassan@petronas.com.my, sagi_636@yahoo.com, rehankb@yahoo.com

***Abstract*: This paper presents an algorithm for Shortest Path Tree (SPT) problem. The presented algorithm is an improvement over a previously published work of the authors. The effort is put in to improve the running/execution time of the SPT problem. Introduced improvement is simple and easy to incorporate in to the existing algorithm. This algorithm uses Depth First Search (DFS) like graph traversal during a BFS like traversal i.e. combines and take advantage of the inherent properties of the two heuristic graph search techniques so that vertex weights can be kept balanced. The need of improvement is discussed in detail and the expected improvement in overall processing time is shown with the example.**

Keywords: *Theoretical Computer Science(TCS), Graph Theory, Algorithm, Shortest Path Problem.*

I. Introduction

Shortest Path Problem is one of the classic problems in algorithmic graph theory. Shortest Path Problem plays a vital role in solving many optimization problems and achieving the efficient solutions. It is used in many domains of computer sciences such as networks, communication, computer systems, and transportation networks [1].

Formally Shortest Path Problem is defined as follows: Let G be a graph such that G = (V, E), where V = { v_1, v_2, v_3, . . . , v_n} and E = { e_1, e_2, e_3, . . . , e_m} such that |V| = n and |E| = m. G is an undirected weighted connected graph with no negative weight edges and pre-specified source vertex 's' and destination vertex 'd' such that s ∈ V and d ∈ V. The problem is to find the simple path from source to destination with the minimum most total edge weight known as single source shortest path problem (SSSP).

SSSP is considered as a challenging area in the domain of theoretical computer science [19] [20]. It has been extensively used in many practical problems such as routing and communication problems in networks. Since 1959, most of the theoretical developments in SSSP for general directed and undirected graphs are based on Dijkstra's algorithm.

Dijkstra's algorithm emphasized on finding the path with lowest cost such that it starts from the source and visits the vertices with the increasing distance. To solve the shortest path problem with Disjisktra's algorithm, minimum weight is calculated using linear search [2] and the complexity of Dijkstra's algorithm [10] is determined as $O(n^2 + m)$.

Later on Williams and Hershberger presented a new heap data structure to calculate the minimum weight [4] [5]. The work presented by [4] and [5] improved the complexity of the algorithm to O(m log n). Fibonacci Heap, developed by Fredman and Tarjan [9] improved the efficiency as well as time complexityof many algorithms including SSSP. The work presented by Fredman and Tarjan [9] was an optimal implementation of Dijkstra's algorithm in contrast to the common implementation of Dijkstra's algorithm which visits the vertices in sorted order.

Fredman and Willard proposed the use of fusion trees to solve the shortest path problem [8]. The use of fusion trees provides the complexity as O(m (log n) ½) with randomized bound. Later atomic heaps gave an O(m + n log n/log log n) bound as presented in [7]. Afterwards, in [11] [12] [16] priority queues were introduced which gave an O(m log log n) bound and an O(m + n(log n1+ε)½) bound. These bounds are randomized assuming that the linear space is used. Afterwards [14] reduced the complexity to O(m + n(log n log log n) ½) and it was further improved with randomized bound to O(m + n(log $n^{1+\varepsilon}$) $^{1/3}$) by [15].

Much work is also done by using the weights of the edges. Priority queue presented in [6] improved the shortest path cost giving a running time of O(m + n(log C) ^{½}) where C was the cost of the heaviest edge. The work by [13] reduced the complexity to O(m + n (3 log C log log C)$^{1/3}$) and [15] presented a further improvement to O(m + n(log C) $^{1/4+\varepsilon}$). The work reported in [3] presented an algorithm and claimed that it will out class Dijkstra's algorithm.

II. Basic Idea of the Algorithm

This research is continuation of the works presented in [24][22][23]. Basic idea of the algorithm is the classification and identification of the vertices that have high probability of causing problem/error during a Breadth First Search (BFS) like traversal. To reduce that error, DFS like traversal is being incorporated, in such a way that vertices' weights are kept balanced. Previously, processing through such vertices was delayed until all possible updates were done on them but now this delay is tackled and covered through increase in branch length using DFS.

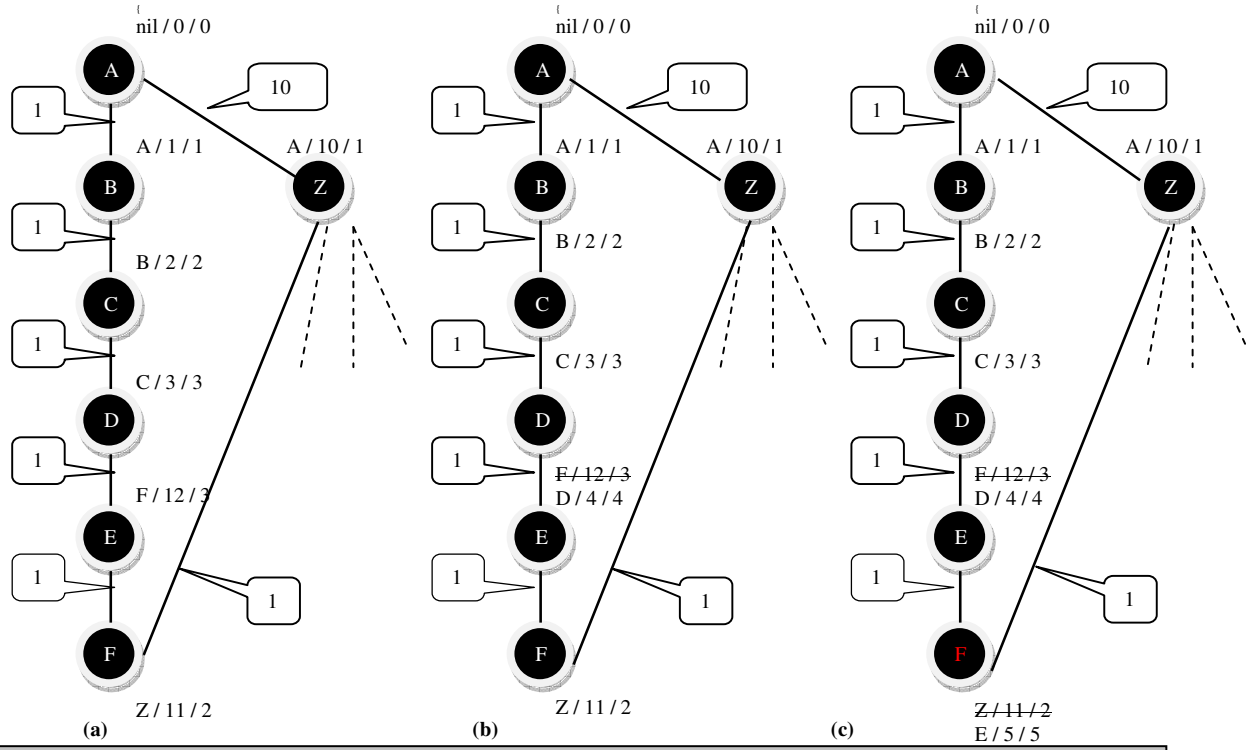


Fig 1: (a) F explored E, and C explored D (b) E tried to explore D but could not update, D explored and updated E but it is not marked CULPRIT as difference of levels is < 2 (c) E explored F and as difference of level is >= 2 so F is marked as CULPRIT vertex; NOTE: *(Parent / Distance / Level) is the legend being used to express the information used at each vertex*

III. Summary of Previous Work

A. Two Phase SPT Algorithm and its Improvements

To start with let's briefly discuss the algorithm discussed in [24]. The algorithm comprises of two almost similar phases but the purpose of the two is somewhat different. First phase provides initialization of data structure for second phase that include calculation of vertex weights, identification of the levels of the vertices as well as marking of initial level CULPRIT vertices.

Second phase accepts the initializations of previous phase and continues with vertices level by level skipping and identifying CULPRIT vertices. Fig 1 provides a brief example of the working of this algorithm.

In [25] two improvements and their effectiveness are presented. A new data structure – avgQ was introduced to give priority to the light weight vertices. The improvements discussed in this paper are very effective leading to the worst case complexity close to that of Dijkstra's using Fibonacci heap.

To start with, all vertices except source vertex are colored WHITE, designated with no parent, assigned ∞ as distance value, marked with Normal type and level '-1'. While source is colored Gray, designated with no parent, given distance value as 0, marked with Normal type and level 0 and source is enqueued in a normal queue. This algorithm proceeds in BFS fashion. One vertex is dequeued and its adjacent vertices are explored, one by one, and enqueued in the same queue. When a vertex explores one of its adjacent vertices, adjacent vertex's color is updated to GRAY, it is marked with level (level of exploring vertex + 1), and min(Distance of exploring vertex+edge weight, old distance) is marked and if distance changes then exploring vertex will become parent of the vertex that was being explored. If this vertex updates some vertex that is at least two levels up then it is marked CULPRIT and it is put in avgQ. The same processing is repeated for all adjacent vertices. As soon as all adjacent vertices are explored, the color of the vertex (vertex that was exploring) is marked BLACK. This process continues level by level until all vertices are marked black except destination vertex.

Phase II uses the results of Phase I as its initialization except all vertices are repainted WHITE and all CULPRIT vertices are painted GRAY. After initialization, lowest Phase II level Culprit vertex is dequeued from avgQue. All its adjacent vertices are explored and then it is colored BLACK and enqueued in avgQ (rules of insertion can be seen in fig. 2). Processing continues level by level meanwhile if some BLACK vertex's distance is updated and the difference between old level and new level is of 2 or more then the vertex is marked as CULPRIT and is colored GRAY again. And in this way the algorithm proceed until all vertices are colored BLACK (except destination). (for further details please refer to [24][25])

IV. Scope for Improvements

The complexity discussed in [24][25] is based upon the frequency of the CULPRIT vertices. So if somehow we can control the generation of the CULPRIT vertices we can improve the execution time of the algorithm.

A. *Why a vertex is marked CULPRIT*

In order to reduce CULPRIT vertices, it is necessary to understand the causes that lead to a CULPRIT vertex.

Formally a vertex will be called CULPRIT vertex if it has following properties:

Len(Pi(s,w)) >= Len(Pj(s,w) + 2

$$\sum_{i=0}^{k-1} w(x_i, x_{i+1}) \angle \sum_{i=0}^{l-1} w(y_i, y_{i+1})$$

for Pi *for Pj*

where **k ≠ l, l ≠ l,**
and **x0 = y0 = s**
and **xk = yk = w**

and **Pi** and **Pj** are paths from **s** to **w** such that **Pi ≠ Pj**
and **Pi = { x0 ,x1 ,x2 , . . . ,xk }**
and **Pj = { y0 ,y1 ,y2 , . . . ,yl }**

It is very important to understand why a vertex is marked CULPRIT. Suppose a vertex, '**w**' has multiple paths of varying lengths from source, '**s'**, it will be a candidate of being CULPRIT vertex. Let's take two paths, **Pi** and **Pj**, such that **Pi** has at least two more edges than **Pj.** It shows that **Pi**, generally, will be having light weight edges than **Pj**. Given the scenario, '**w**' will definitely be marked as CULPRIT vertex. As the difference of number of edges is greater than 1 so '**w**' will be explored first through **Pj** and then after few levels it will again be updated through **Pi** resulting in its new distance to be derived and causing the prior processing through '**w**' to be marked as incorrect.

B. *Scope*

As in Phase II the processing restarts as soon as a new CULPRIT vertex is found and previously processed vertices of the sub-tree rooted at CULPRIT vertex needs to be reprocessed. This paper is an attempt to reduce, further, the number of CULPRIT vertices that appear during the execution of the algorithm. In [24], in order to give priority to the light weight vertices avgQ data structure was introduced that very effectively reduced the number of CULPRIT vertices. Along with the introduction of avgQ the cascading effect of the CULPRIT vertices were also rectified. This can be seen in fig 1 as **F** is marked as CULPRIT vertex, due to cascading effect of **Z**.

Thorough analysis of the reasons of how and why CULPRIT vertices generate, it was found that the main cause of it is unbalanced weights of the vertices in the avgQ. Though it gives priority to smallest weight vertex but still there is need to give priority to almost all the light weight vertices.

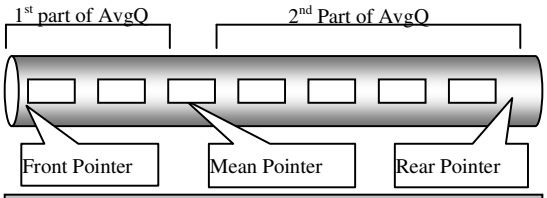


Fig 2: AvgQ Insertion in queue

```
if (d[v_y] < d[vertex at front])
    then insert v_y infront of first vertex
else if (d [v_y] < μ)
    then insert v_y in front of the point being pointed by μ
else if (d [v_y] > d[vertex at rear])
    then insert v_y at the end of the queue
else insert after the average pointer of the AvgQ
```

V. Improvements

In the light of above findings the following improvements has been proposed:

A. *Improvement 1: Merging the Two Phases*

The Main reason of the first phase was the initializations. Along with it served the cause of marking of the levels of vertices as the whole algorithm was based on BFS and traversal needed level by level growth. But in this update the levels are not being considered. Though algorithm will be moving level by level but at points it will traverse in the branches to balance the weights of the vertices (i.e. keeping the weight of all branching as balanced as possible) as well as giving priority to the light weight vertices.

B. *Improvement 2: Depth covering in BFS*

This improvement suggests that we must give priority to lightweight vertices (i.e vertices having less distance shows lightweight path/branch) over heavyweight vertices such that no paths ever face starvation (stuck at one point and seldom gets its turn). The mean of all the GRAY vertices should be kept track of using the formula

$$\mu = \frac{\sum_{i=1}^{k} \Delta[\ v_i\ ]}{k} \quad \text{.....(i)}$$

Where **v_i:** any GRAY vertex at any point
$\Delta[v_i]$: distance of v_i
k: total number of GRAY vertices at the current moment

The vertices that have weight less than the average weight of the vertices should be given chance to explore further and if newly explored vertex has weight less than the new average then exploration should continue from that vertex in a DFS fashion. So this algorithm is making use of the power of the two heuristic searches i.e. DFS and BFS. Starts with BFS and mixes it with DFS to balance the weight of the vertices/branches/paths in hand

VI. Algorithmic Details

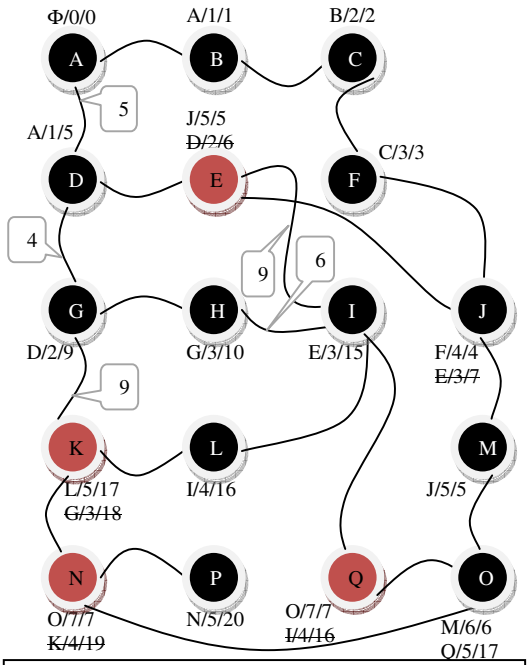


Fig 3: Execution of Original Two Phase Algorithm's Phase I only. 4 CULPRIT vertices are found that will lead to more CULPRIT vertices in the next phase (edges that have no weights are weighted 1)
NOTE: (Parent / Distance / Level) is the legend being used to express the information used at each vertex

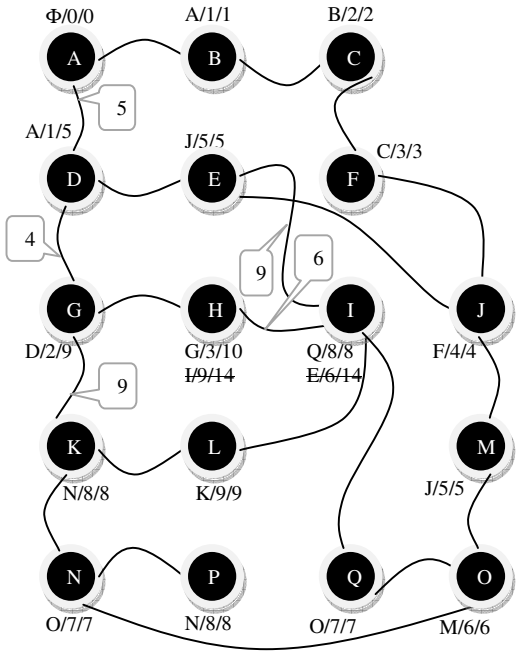


Fig 4: Execution of the Improved algorithm presented in this paper using avgQ. It can easily be seen that no CULPRIT vertex is found. (edges that have no weights are weighted 1)
NOTE: (Parent / Distance / Level) is the legend being used to express the information used at each vertex

Starting from the source vertex all its adjacent vertices are explored (all these vertices are now GRAY and are have new distance values) and enqueued in avgQ. A vertex (say $\mathbf{x_i}$) is then extracted and all its adjacent vertices (say $\mathbf{y_1}$, $\mathbf{y_2}$, $\mathbf{y_3}$ … $\mathbf{y_k}$) are explored one by one. But before inserting a GRAY vertex $\mathbf{y_i}$ into avgQ its distance (i.e. Δ) is compared to μ. If $\Delta[\mathbf{y_i}] < \mu$ then DFS starts from this vertex. $\mathbf{y_i}$ then explores its adjacent vertices and again if some vertex's weight is found less than μ, control switches to that vertex to continue DFS. Process continues until a $\Delta[\mathbf{r}] > \mu$ where r is current vertex, and r is enqueued. When all the vertices are explored control returns to the parent vertex and completes its remaining explorations and returns until it reaches to the point from where DFS was initially started. Then a new vertex is dequeued and algorithm continues until there is any element in the avgQ. When a vertex is explored μ is updates using formula

$$\mu = \frac{\mu \times k - \Delta[x_i] + \Delta[y_j]}{k} \quad \text{.....(ii)}$$

when $\mathbf{y_j}$ is the first vertex that is extracted as adjacent vertex of $\mathbf{x_i}$

or $$\mu = \frac{\mu \times k + \Delta[y_j]}{k+1} \quad \text{.....(iii)}$$

when $\mathbf{y_j}$ is not the first vertex that is extracted as adjacent vertex of $\mathbf{x_i}$

If at some point during the explorations, value of μ changes in such a way that it becomes less than the Δ of that vertex, even then this vertex will cover all its adjacent vertices.

VII. Working Example

In order to show and strengthen the arguments provided in above discussion two versions of the algorithm, original and the one discussed in this paper are executed on same graph having 17 vertices and 21 edges. The edge weights are specially taken in such a way that it could cause worst scenario as there are few edges that have high weights and few have very low weights. The dry runs are shown in table 1 and table 2 respectively.

When a vertex is picked its μ is calculated. If it is less than the Δ of the vertex then its parent is marked and

Legend that is being used in the Table 1 and Table 2
***:** No update is made, previous state holds
+: **v** is removed from the queue and enqueued again at the tail
-: A CULPRIT vertex is found as a black vertex's weight was updated
↓: Go deep; explore the adjacent vertices of **v**
↑: Go back; return back to the parent vertex
u: vertex that is exploring its adjacent vertices, clored BLACK afterwards
v: Vertex being explored (one of the adjacent vertices of u.
Π_v: Parent of v
D_v: Distance of v
L_v: Level of v
Q: Queue to keep track of explored vertex

Table 1: Step by step execution of the Two-Phase Shortest Path Algorithm (without improvement) on the graph whose final outcome is fig.3. Total 4 CULPRIT vertices are found

u	v	π_v	Δ_v	L_v	C_v	C_u	Remarks	Q
A	B	A	1	1	G	G		B
	D	A	5	1	G	B		DB
B	A						*	D
	C	A	2	2	G	B		CD
D	A						*	
	E	D	6	2	G	G		EC
	G	D	9	2	G	B		GEC
C	B	A					*	
	F	C	3	3	G	B		FGE
E	D	A					*	
	J	E	7	3	G	G		JFG
	I	E	15	3	G	B		IJFG
G	D	A					*	
	H	G	10	3	G	G		HIJF
	K	G	18	3	G	B		KHIJF
F	C	B						
	J	F	4	4	G	B	+	JKHI
I	L	I	16	4	G	G		LJKH
	H	G					*	LJKH
	D	J					*	LJKH
	Q	I	16	4	G	B		QLJKH
H	G	D					*	QLJK
	I	E					*	QLJK
K	G	D					*	QLJ
	L	I					*	
	N	K	19	4	G	B		NQLJ
J	F	C					*	NQL
	E	J	5	5	G	G	-	NQL
	M	J	5	5	G	B		MNQL
L	I	E					*	MNQ
	K	L	17	5	5	B	-	MNQ
Q	I	E					*	MN
	O	Q	17	5	G	B		OMN
N	K	L					*	QM
	O	Q					*	QM
	P	N	20	5	G	B		POM
M	J	F					*	
	O	M	6	6	G	B	+	OP
P	N	O					*	O
O	M	J					*	Empty
	N	O	7	7	G	G	-	Empty
	Q	O	7	7	G	G	-	Empty

one of its adjacent vertices are explored. When B was picked μ calculated is 3 and Δ is 1 which is smaller than μ. B has 2 neighbors A and C. A cannot be updated, so exploring C, its Δ is updated and B is marked as its parent and it is painted gray. Now it can be seen that $\Delta[C] < \mu$ so control switches to C. Now new μ is calculated. C has two adjacent vertices. No update is possible on B but C updates F. As $\Delta[F] > \mu$ so F is inserted into avgQ. Control is not transferred to F and returned back to C

Table 2: Step by step execution of the Algorithm discussed in this paper on the graph whose final outcome is fig.4. No CULPRIT vertex is found.

u	μ	v	π_v	Δ_v	Rem	avgQ
A		B	A	1		B
		D	A	5		DB
B	(1+5)/3=3	C	B	2	↓	D
C	(1+2+5)/3=2.7	F	C	3	↑	DF
B	All adjacent vertices are covered. Paint it black and return					
F	(3+5)/2=4	J	F	4	↑	DJ
	All adjacent vertices are covered. Paint it black and return					
J	(4+5)/3=4.5	M	J	5	↑	DM
		E	J	5	↑	DME
	All adjacent vertices are covered. Paint it black and return					
E	(5+5+5)/3=5	D	A		*	
		I	E	14	↑	IDM
	All adjacent vertices are covered. Paint it black and return					
M	(14+5+5)/3=8	J	F		*	ID
		O	M	6	↓	ID
O	(14+5+5+6)/4=7.5	Q	O	7	↓	ID
Q	(14+5+5+6+7)/5=7.4	I	Q	8	↑	ID
O	(8+5+5+6)/4=6	N	O	7	↑	IND
	All adjacent vertices are covered. Paint it black and return					
M	All adjacent vertices are covered. Paint it black and return					
D	(8+7+5)/3=6.7	E	J		*	IN
		G	D	9		GIN
	All adjacent vertices are covered. Paint it black and return					
N	(9+8+7)/3=8	O	M		*	GI
		P	N	8	↑	GIP
		K	N		↑	GIPK
	All adjacent vertices are covered. Paint it black and return					
K	(9+8+8)/3=8.3	L	K	9	↑	LGIP
	All adjacent vertices are covered. Paint it black and return					
P	(9+9+8+8)/4=8.5					LGI
	All adjacent vertices are covered. Paint it black and return					
I	(9+9+8)/3=8.7	E			*	LG
		H	I	14	↑	HLG
		L			*	HLG
		Q			*	HLG
G	(9+9+14)/3=10.7	H	G	10	↓	HL
H	(10+9+9+10)/4=9.5	I	Q		*	HL
	All adjacent vertices are covered. Paint it black and return					
G	10.7	D			*	L
		K			*	L
	All adjacent vertices are covered. Paint it black and return					
L	9	I	Q		*	Empty
		K	N		*	Empty

where it checks for the other adjacent vertices of C to explore and as there is no other adjacent vertex so it returns to B. Now new element, F, is dequeued from avgQ and process continues until avgQ is empty.

VIII. CONCLUSION

The results are very promising and show immense improvement in processing time (almost near to that of

BFS or DFS). The improved algorithm is using AvgQ which is very much similar to normal queue having constant time complexity of all operations and is very easy to implement.

Unlike Dijkstra, vertices are being picked in a pseudo random way. Priority is given to the light weight vertices (i.e. low cost paths) in order to keep the Δ's of working vertices balanced. In the example Phase I of Two Phase SPT algorithm is executed and 4 CULPRIT vertices are found. On the other hand this new algorithm resulted in zero CULPRIT vertices. Hence completed the execution in O(|V|+|E|) (only this example)

The process can be more refined and complexity can be more improved deciles logic (nine pointers) in place of mean or using buckets of same length and so on.

The results of the algorithm are very promising with θ(|V|+|E|) time best case complexity (when no CULPRIT vertex is found) but still some work needs to be done to calculate, and prove mathematically, worst case time complexity of the algorithm. The execution of the algorithm on different graphs has shown that complexity is quite close to that of Dijkstra's implementation using Fibonacci heap. It is also seen that if the graph is of hierarchical form then there appear hardly any CULPRIT vertices or very few resulting in O(V + E) overall time complexity.

IX. References

[1] Binwu Zhang, Jianzhong Zhang, Liqun Qi :The shortest path improvement problems under Hamming distance. In Springer Science+Business Media, LLC 2006, (Published online: 20 September 2006)

[2] Mikkel Thorup :Undirected Single-Source Shortest Paths with Positive Integer Weights in Linear Time. In AT&T Labs Research, Florham Park, New Jersey, Journal of the ACM, vol. 46, No. 3, pp. 362–394 (May 1999)

[3] Seth Pettie, Vijaya Ramachandran, and Srinath Sridhar :Experimental Evaluation of a New Shortest Path Algorithm_ (Extended Abstract). In D. Mount and C. Stein (Eds.): ALENEX 2002, LNCS 2409, pp. 126–142, 2002. Springer-Verlag Berlin Heidelberg (2002)

[4] Williams, J. W. J. :Heapsort. Commun. In ACM 7, 6 (June), 347–348. (1998)

[5] John Hershberger, Subhash, and Amit Bhosle :On the Difficulty of Some Shortest Path Problems. In ACM Transactions on Algorithms, Vol. 3, No. 1, Article 5 (2007)

[6] Ahuja, R. K., Melhorn, K., Orlin, J. B., and Tarjan, R. E. :Faster algorithms for the shortest path problem. J.ACM 37, 213-223 (1990)

[7] Fredman, M. L., and Willard, D. E. :Trans-dichotomous algorithms for minimum spanning trees and shortest paths. In J. Comput. Syst. Sci. 48, 533–551. (1994)

[8] Fredman, M. L., and Willard, D. E. : Surpassing the information theoretic bound with fusion trees. J. Comput. Syst. Sci. 47, (1993)

[9] Fredman, M. L., and Willard, D. E. : Fibonacci heaps and their uses in improved network optimization algorithms. J. ACM 34, 3 (July), 596 – 615. (1987)

[10] Dijekstra, E. W. 1959. A note on two problems in connection with graphs. Numer. Math. 1, 269 –271.

[11] Therup, M. :On RAM priority queues. In Proceedings of the 7th Annual ACM-SIAM Symposium on Discrete Algorithms. ACM, New York, pp. 59 – 67 (1996)

[12] Thorup, M. :Floats, integers, and single source shortest paths. In Proceedings of the 15th Symposium on Theoretical Aspects of Computer Science. Lecture Notes on Computer Science, vol. 1373. Springer-Verlag, New York, pp. 14 –24.(1998)

[13] Cherkassky, B. V., Goldberg, A. V., and Silverstein, C. :Buckets, heaps, lists, and monotone priority queues. In Proceedings of the 8th Annual ACM-SIAM Symposium on Discrete Algorithms. ACM, New York, pp. 83–92.(1997)

[14] Raman, R.: Priority queues: small monotone, and trans-dichotomous. In Proceedings of the4th Annual European Symposium on Algorithms. Lecture Notes on Computer Science, vol. 1136, Springer-Verlag, New York, pp. 121–137. (1996)

[15] Raman, R.: Recent results on the single-source shortest paths problem. SICACT News 28, 81– 87.(1997)

[16] Andersson, A. Miltersen, P. B. and Thorup, M. :Fusion trees can be implemented with AC0 instructions only. Theoret. Comput. Sci., 215, 337–344. (1999)

[17] Rehan Akbar, Mohd Fadzil Hassan, Sohail Safdar and Muhammad Aasim Qureshi, Client's Perspective: Realization as a New Generation Process for Software Project Development and Management, Proceedings of 2nd International Conference on Communication Software and Networks (ICCSN'10). February 26-28, 2010. IEEE. Singapore.pp.191-195.

[18] Rehan Akbar, Mohd Fadzil Hassan, A Collaborative-Interaction Model of Software Project Development: An Extension to Agile Based Methodologies, International Symposium on Information Technology 2010. IEEE, K.L., Malaysia.

[19] Muhammad Aasim Qureshi, Onaiza Maqbool, 2007, *Complexity of Teaching: Computability and Complexity* In '*International Conference on Teaching and Learning 2007*' organized by INTI International University College at Putrajaya, Malaysia.

[20] Muhammad Aasim Qureshi, Onaiza Maqbool, 2007, Complexity of Teaching: Computability and Complexity, *INTI Journal Special Issue on Teaching and Learnning 2007*

[21] Rehan Akbar, Mohd Fadzil Hassan, Limitations and Measures in Outsourcing Projects to Geographically Distributed Offshore Teams, International Symposium on Information Technology 2010. IEEE, K.L., Malaysia.

[22] Muhammad Aasim Qureshi, Mohd Fadzil Hassan, Sohail Safdar, Rehan Akbar, Rabia Sammi; 2009, An Edge-wise Linear Shortest Path Algorithm for Non-Negative Weighted Undirected Graphs, *Frontiers of Information Technology* (FIT 09) Pakistan, December 2009.

[23] Muhammad Aasim Qureshi, Mohd Fadzil Hassan, Sohail Safdar, Rehan Akbar; 2009, A O(|E|) time Shortest Path Algorithm for Non-Negative Weighted Undirected Graphs, *International Journal on Computer Science and Information Security Volume 6* (No 1) October 2009.

[24] Muhammad Aasim Qureshi, Mohd Fadzil Hassan, Sohail Safdar, Rehan Akbar; 2010, Two Phase Shortest Path Algorithm for non Negative Weighted Undirected Graphs, International Conference on Communication Software and Networks (ICCSN 2010) Feb 2010,pp 223-227, accepted

[25] Sohail Safdar, Mohd Fadzil Hassan, "Moving Towards Two Dimensional Passwords", International Symposium on Information Technology 2010, ITSIM 2010, June 2010, Malaysia (In press).

[26] Sohail Safdar, Mohd Fadzil Hassan, Muhammad Aasim Qureshi, Rehan Akbar, "Framework for Alternate Execution of workflows under threat", 2nd International Conference on Communication Software and Networks, ICCSN 2010, Feb 2010, Singapore.

[27] Sohail Safdar, Mohd Fadzil Hassan, Muhammad Aasim Qureshi, Rehan Akbar, "Biologically Inspired Execution Framework for Vulnerable Workflow Systems", International Journal of Computer Science and Information Security, Vol.6 No.1, IJCSIS 2009.

An Unsupervised Center Sentence-based Clustering Approach for Rule-based Question Answering

Shen Song
MIMOS Berhad,
Technology Park Malaysia,
57000 Kuala Lumpur,
Malaysia.
shen.song@mimos.my

Yu-N Cheah
School of Computer Sciences,
Universiti Sains Malaysia,
11800 USM Penang,
Penang, Malaysia.
yncheah@cs.usm.my

***Abstract*- Question answering (QA) systems have widely employed clustering methods to improve efficiency. However, QA systems with unsupervised automatic statistical processing do not seem to achieve higher accuracies than other approaches. Therefore, with the motivation of obtaining optimal accuracy of retrieved answers under unsupervised automatic processing of sentences, we introduce a syntactic sequence clustering method for answer matching in rule-based QA. Our clustering method called CEnter SEntence-baseD (CESED) Clustering is able to achieve accuracies as high as 84.62% for WHERE-type questions.**

Keyword- question answering; clustering; structural rule generation

I. INTRODUCTION

To reduce the dependence of time-consuming manual work, machine learning (ML) approaches are commonly used in natural language processing (NLP) [1], in which unsupervised clustering is regarded as a popular method due to its automatic processing of knowledge [2]. Generally, unsupervised clustering techniques are divided into two major families: 1) *hierarchical clustering* (e.g. agglomerative hierarchical approach [3]) and 2) *partitioning (or non-hierarchical) clustering* (e.g. K-means clustering approach [4]). As one of the important research fields in NLP, question answering (QA) has widely employed clustering methods to improve system efficiency as well.

Generally, a typical QA system consists of a question analysis phase, an answer analysis phase, and an answer matching phase. In question analysis, clustering approaches are mainly used for query extension [5][6]. For the answer analysis phase, summarization of documents is mostly the main purpose for using clustering approaches [7][8]. In the answer matching phase, clustering approaches are for generating sets of rules for searching possible answer candidates. Traditionally, rule-based QA systems mostly utilize pattern overlapping for answer matching. However, QA systems with unsupervised automatic statistical processing do not seem to achieve higher accuracies than other ML approaches. Therefore, with the motivation of obtaining optimal accuracy of retrieved answers under unsupervised automatic processing of sentences, we introduce a syntactic sequence clustering method for answer matching in rule-based QA. The clustering method is called CEnter SEntence-baseD (CESED) Clustering.

II. LITERATURE REVIEW

Many ML-based QA work have been done. In C5 [9][10], question-sentence pairs are defined as feature vectors to provide useful information to the learning algorithm. Sentences' feature vectors with the highest confidence are regarded as answers. The maximal accuracy of this system is 39.3% when all features are considered.

A single Maximum Entropy multiclass classifier for question processing and a Support Vector Machine (SVM) classifier for answer extraction have also been utilized for QA [11]. The best accuracy of this ML technique is less than 45% by using the Mean Reciprocal Rank (MRR) score.

For the QA system in [12], a SVM method is used for both the question classifier and answer matching components. The features of the classification module are basically the output of the shallow question parsing module. The features for question classifier are assisted by statistical information of the corpus. To answer finder module, SVM is utilized by means of considering question features and word corpus features. The highest accuracy for the best answer is 31.5% while for the top five answers is 58.5%.

Based on the survey, we found out that most ML approaches for QA assign a similarity value to each individual training unit. Meanwhile, the features for similarity measurement are extracted within one training unit. However, ML approaches are implemented in a different way in the biological research field. The similarity value is assigned to a pair of training units, e.g. in Quality Threshold (QT) Clustering, which is an alternative method of partitioning data invented originally for gene clustering [13]. In the QT clustering algorithm, a central object is randomly selected from the set of data. The algorithm determines which gene has the greatest similarity to this

central object by setting a threshold value. With inspiration from QT clustering, we propose a clustering method by considering the relationship of the sequence of the sentences for answer matching in rule-based QA.

TABLE I
COMPREHENSION ARTICLES' WHAT-TYPE QUESTION SENTENCES AND ANSWER SENTENCES

NO.	Q-Sentence	Original A-sentence	Reworded A-Sentence
1	What was the president of Yugoslavia indicted for?	Judge Arbour's last major act as chief prosecutor was to indict Slobodan Milosevic for crimes against humanity.	The president of Yugoslavia was indicted for crimes against humanity.
2	What is the estimated size of the seal herd?	Mr. Efford says the seal herd, which is estimated at six million, needs to be cut in half.	The estimated size of the seal herd is six million.
3	What is the name of the Portuguese anti-landmine film?	In Brasilia, the capital city of Brazil, anti-landmine pamphlets were distributed and there were screenings of "Spotlight on a Massacre".	The name of the Portuguese anti-landmine film is Spotlight on a Massacre.
4	What kind of animal do the inmates hunt in the summertime?	In the summer they go after seals.	The inmates hunt seals in the summertime.

TABLE II
POS-TAGGED WHAT-TYPE QUESTION-ANSWER PAIRS

Sentence No.	Training Q-Sentence	Training A-Sentence
1	WP VBD DT NN IN NP VVD IN	DT NN IN NP VBD VVN IN NNS IN NN
2	WP VBZ DT JJ NN IN DT NN NN	DT JJ NN IN DT NN NN VBZ CD CD
3	WP VBZ DT NN IN DT JJ NN NP	DT NN IN DT JJ NP NP VBZ NN IN DT NP
4	WP NN IN NN VVP DT NNS VVP IN DT NN	DT NNS VVP NNS IN DT NN

III. CESED CLUSTERING METHOD

We now present our CESED clustering method to generate structural rules from training data (i.e. question-answer pairs). The methodology consists of two phases: (1) preprocessing of training question-answer pairs, and (2) automatic rule generation.

A. Phase One: Preprocessing of Training Question-Answer Pairs

In this phase, the training data (question-answer pairs) is prepared based on a reading comprehension corpus. Following the compilation of the training data, part-of-speech (POS) tagging is carried out.

1. Compilation of Question-Answer Pairs

The question-answer pairs are compiled from the CBC Reading Comprehension Corpus and made available by MITRE Corporation [14]. However, the answer-tagged version of the CBC Reading Comprehension Corpus tags whole sentences that contain the answer to a particular question and also other irrelevant information. As a result, these tagged sentences may only answer the question implicitly. Therefore, for our purposes, these answer sentences are reworded accordingly. Table I shows examples of WHAT questions with original and reworded answer sentences.

400 question-answer pairs are selected for our research and categorized into 4 WH-question types (WHAT, WHERE, WHEN and WHO) respectively. Due to the complexity of HOW and WHY questions, these two types of questions are excluded. Half of the question-answer pairs were utilized to assist in generating structural rules, while the remainder will be used for testing.

2. Analysis of Question-Answer Pairs

Following the compilation of question-answer pairs, we utilize the Tree Tagger [15] parser to produce a part-of-speech (POS) representation of the question-answer pairs. Table II shows examples of the POS-tagged question-answer pairs (with reworded answers) based on those in Table I.

B. Phase Two: Automatic Rule Generation

In this phase, we aim to generate rules concealed in the structures of the question-answer pairs. The rule generation algorithm consists of two sub-phases: similarity measurement and rule generation via clustering.

1. Similarity Measurement

We utilize the BLEU mechanism to measure the similarity distance between two sentences, which were originally proposed for automatic machine translation evaluation [16]. The following modified BLEU formula is utilized:

$$\textbf{BLEU} = \exp \sum_{n=1}^{N} w_n \log p_n \qquad (1)$$

In (1), $w = 1 - \frac{1}{e^{s.f.}}$ ($w = 1$, when $s.f. = 0$) and $p = \frac{matches}{length}$. w refers to the weight for the sequence difference (*s.f.*) of any two sentences, which indicates the number of differences in the token sequence of these two sentences (i.e. if any two

TABLE III

COMPARISONS OF WHAT TYPE QUESTION PAIRS FOR RULE CLUSTERING

Pair No.	Question No.	Main-Sentence	Question No.	Co-Sentence
1	1	WP VBD DT NN IN NP VVD IN	2	WP VBZ DT JJ NN IN DT NN NN
2	1	WP VBD DT NN IN NP VVD IN	3	WP VBZ DT NN IN DT JJ NN NP
3	1	WP VBD DT NN IN NP VVD IN	4	WP NN IN NN VVP DT NNS VVP IN DT NN
4	2	WP VBZ DT JJ NN IN DT NN NN	3	WP VBZ DT NN IN DT JJ NN NP
5	2	WP VBZ DT JJ NN IN DT NN NN	4	WP NN IN NN VVP DT NNS VVP IN DT NN
6	3	WP VBZ DT NN IN DT JJ NN NP	4	WP NN IN NN VVP DT NNS VVP IN DT NN

sentences have the same tokens and sequence, then sequence differences = 0). The value of matches indicates the number of the same tokens in any two sentences, while *length* indicates the average number of tokens in any two sentences. The BLEU similarity measurement technique is based on N-grams.

To further illustrate the calculation of the BLEU values, we name one question as Main-sentence (i.e. the one compared from) and the other one as Co-sentence (i.e. the one compared to). The idea here is to determine which Co-sentence and the Main-sentence are more similar to each other as compared to the other pairs of question sentences. The POS tokens of the Main-sentence are used to locate matching POS tokens in the Co-sentence. Each cycle starts by comparing the first unmatched POS token of the Main-sentence with the first unmatched POS tokens of the Co-sentence, and the Co-sentence is examined token-by-token until a match is found or the tokens have all been examined. When a match is found in the Co-sentence, the searching pauses at that Co-sentence token. If the search continues until the end of the Co-sentence, this means that a match was not found in the Co-sentence. The search then continues by comparing the second POS token of Main-sentence with the remaining unmatched POS token of the Co-sentence. The matching ends when all the POS tokens of the Main-sentence have been searched through in the Co-sentence.

Table III presents an example of the various comparisons between Main-sentence and Co-sentence pairs based on POS-tagged question sentences from Table II.

To determine the BLEU parameters, the similarity of the Main-sentence-Co-sentence pair is determined in terms of the number of matched POS tokens (i.e. matches). In the case of the sequence of matched POS tokens (i.e. sequence difference), we set the Main-sentence as the base, and determine how dissimilar the Co-sentence and Main-sentence are. This is evaluated by two factors:

(a) The *relative position* of Main-sentence and Co-sentence, which indicates the distance between the matched POS token in Co-sentence and the first unmatched POS token in Co-sentence.

(b) The *relative sequence* of Main-sentence and Co-sentence, which indicates the distance between the matched POS token of Co-sentence and the one of Main-sentence.

Relative Position

Let us represent the matched POS token number in the Co-sentence and Main-sentence as *m* and *n* respectively. The total relative position of the Main-sentence-Co-sentence is $\sum_{i=1}^{k} |n-m|$, where *k* is the total number of matched tokens between Main-sentence and Co-sentence. For each matched POS token of Co-sentence,

- If $n = m$, the relative position value of the matched POS tokens is zero.
- If $n \neq m$, the relative position value of the matched POS token of Co-sentence is $|n - m|$.

Relative Sequence

We assign each matched POS token number of Co-sentence to D_i ($1 \leq i \leq$ number of matched POS tokens between Main-sentence-Co-sentence pair, where *i* represents the *i*-th matched POS token). The total relative sequence of Main-sentence-Co-sentence pair is $\sum_{i=1}^{i-1} |D_{i+1} - D_i|$. For each two neighboring POS tokens that matches (i.e. D_i and D_{i+1}) between Main-sentence-Co-sentence,

- If $D_{i+1} > D_i$, then the relative sequence is zero.
- If $D_{i+1} < D_i$, then the relative sequence value is $|D_{i+1} - D_i|$.

In view that N-gram is utilized in CESED, we have set the maximum N-gram as 3. Hence, for our purposes, 3 sets of BLEU values are produced, i.e. with N-gram = 1, 2, and 3. As an example, Table IV presents BLEU values for the WHAT-type questions from Table II using N-gram = 3. Therefore, Table IV presents an example of the output of this similarity measurement sub-phase, and the BLEU values that have been obtained are used as the dataset for the next sub-phase of rule generation.

TABLE IV
BLEU VALUES FOR WHAT-TYPE QUESTION SENTENCE PAIRS FROM TABLE 2 (N-GRAM = 3)

Pair No.	Main–sentence	Co-sentence	BLEU value
	Question No.	Question No.	
1	1	2	0.753
2	1	3	0.721
3	1	4	0.757
4	2	3	0.950
5	2	4	0.803
6	3	4	0.816

2. Rule Generation via Clustering

The learning strategy of CESED is to learn a rule that covers part of the given training instances. The clustering begins by examining the question sentences of the training data. A Main-sentence would be examined as a potential center of a cluster. In other words, the objective of the clustering process is to judge whether a Co-sentence is more similar (or closer) to the Main-sentence than all the other Co-sentences. For this purpose, a threshold value is set.

If the BLEU value of a particular Main-sentence-Co-sentence pair is greater than the threshold value, then the other Main-sentence-Co-sentence pairs involving that particular Co-sentence will be selected and their respective BLEU values compared against this BLEU value. If and only if this particular BLEU value is greater than the other selected BLEU values, that particular Co-sentence will be clustered into the Main-sentence group. Consequently, all the Main-sentence-Co-sentence pairs related to the particular Co-sentence are removed from future clustering. However, if the BLEU value of this particular pair of Main-sentence-Co-sentence is not the greatest, then the Co-sentence will not be clustered to that particular Main-sentence. The comparison terminates when all BLEU values of all the pairs involving that particular Main-sentence (as the center) has been examined. If all these Main-sentence-Co-sentence pairs cannot satisfy the conditions, then that Main-sentence would be the sole member of the cluster. Clustering the question sentences would form the main clusters.

Following the clustering of the question sentences, the corresponding answer sentences are also clustered in the same way. In view that a particular sentence is closest to their respective "centers" of a particular cluster or sub-cluster, the center sentences are selected to represent their clusters or sub-clusters to form rules (see Table V).

The CESED clustering method employed here is an unsupervised clustering method. This is desired due to the uncertainty of rule numbers, and also in view that there should be no overlaps between different clusters. This avoids confusion while extracting answer candidates. Therefore, in contrast to other clustering techniques in NLP, feature weights are not assigned to the sentences. Instead, a similarity distance is assigned to each sentence pair.

IV. IMPLEMENTATION

To evaluate the syntactic clustered rules, we implemented a QA system called QASARG (Question Answering System via Automatic Rule Generation) for this purpose. To optimize the results, we employed both the clustered structural rule matching and keyword matching.

In QASARG, the input natural language question will be analyzed to capture its structural information and keywords. Then, the question's structural information will be used for matching purposes against the structural rules. This is to locate a suitable rule that has the IF part (or question-side) that matches the structure of the input question. The structure of the candidate answers would then be known based on the THEN part (or answer-side) of the rule. Based on this, and also the relevant keywords, the answer matching phase involves extracting the answer from the repository of documents (or question-answer pairs).

V. EVALUATION

Three parameters were considered when evaluating the rules, i.e. N-gram value, question threshold, and answer threshold. Here, we consider parameters that produce fewer rules with higher accuracy as being superior. Based on the evaluation, Table VI shows the average number of rules produced and the amount of reduction.

TABLE VI
AVERAGE NUMBER OF RULES PRODUCED AND AMOUNT OF REDUCTION

Question Type	Total Number of Training Q-A pairs	Average Number of Rules	Reduction	N-Gram
WHAT	78	52.6	32.6%	1
WHERE	39	22.1	43.3%	2
WHEN	33	21.1	36.1%	1
WHO	43	20.1	53.3%	2

TABLE V
SUMMARY OF RULES GENERATED VIA CLUSTERING

Rule No.	Question Side	Answer Side
	IF	THEN
1	WP VBD DT NN IN NP VVD IN	DT NN IN NP VBD VVN IN NNS IN NN
2	WP VBZ DT JJ NN IN DT NN NN	DT JJ NN IN DT NN NN VBZ CD CD
3	WP NN IN NN VVP DT NNS VVP IN DT NN	DT NNS VVP NNS IN DT NN

We compared the answer accuracy produced by QASARG with the results obtained by Quarc [17]. The corpus to extract and evaluate rules for QASARG and Quarc was the same. However, in QASARG, the testing data was QA pairs (reworded and original) rather than the comprehension passages. The average accuracy comparison between QASARG and Quarc is shown in Fig. 1.

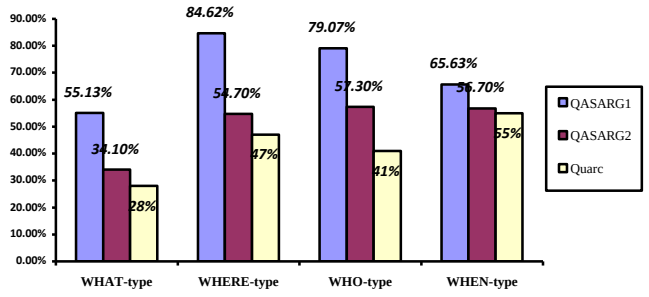


Fig.1. Differences in the accuracies of retrieved answers between QASARG 1 (reworded), QASARG 2 (original) and Quarc

In general, both results from QASARG are higher than that of Quarc. With the reworded testing data, the WHERE-type test achieves the highest accuracy in QASARG with 84.62%. With the original testing data (not reworded), the WHO-type test is the highest with 57.30%. However, the highest accuracy in Quarc is from the WHEN-type test with 55.00%. WHAT-type questions achieves the lowest average accuracy in both QA systems, which implies that WHAT-type questions is more difficult to cope with, not only from a semantic perspective but also from a syntactic perspective in view that it covers a variety of answers, i.e. actions, time, objects, etc. The test data used in Quarc was based on entire reading comprehension passages. Therefore, all these candidate sentences in passages would potentially not share more similar words or phrases. Keyword matching might not narrow down the search space effectively, which might cause the accuracy of Quarc to suffer.

VI. Conclusion

The ability to answer questions automatically in natural language has far reaching implications especially now that machines are expected to be more and more human-like. In the future we hope to suggest techniques to automate the rewording of the answer sentences for the training and testing data until a more suitable QA corpus could be identified. Possible ways of doing this is to use rules or heuristics on acceptable ways of answering natural language questions.

The work on QASARG has contributed to improve the understanding of human language and expression, and would be useful for technological advancement as well. Nevertheless, there is still much to do in view that the sources and modalities for question answering, in line with the freedom of expression and creativity of humans, are practically boundless.

References

[1] R. Andrew, "Machine Learning in Natural Language Processing", www.comp.leeds.ac.uk, Oct, 2003.

[2] K.W. Church and P. Hanks, "Word association norms, mutual information and lexicography", *In Proceedings of the 27th Annual Conference of the Association of Computational Linguistics*, pp. 76-83, Vancouver Canada, 1989.

[3] H.H. Bock, "Classification and Clustering: Problems for The Future" *In Proceedings of New Approaches in Classification and Data Analysis*, Springer-Verlag, Berlin, pp. 3-24, 1994.

[4] C.D. Manning and H. Schütze, "Foundations of Statistical Natural Language Processing" *MIT Press, Cambridge. MA:* 1999.

[5] E. Agichtein, S. Lawrence, and L. Gravano, "Learning to find answers to questions on the Web", *In ACM Transactions on Internet Technology (TOIT)*, Vol. 4, No. 2, pp. 129-162. New York, 2004.

[6] Y.-C. Wang, J.-C. Wu, T. Liang and J.S. Chang, "Web-Based Unsupervised Learning for Query Formulation in Question Answering", *In Proceedings of 2nd International Joint Conference on Natural Language Processing (IJCNLP)*, LNAI 3651, pp. 519-529, Berlin, 2005.

[7] Y. Guo and G. Stylios, "A New Multi-document Summarization System", *In Proceedings of the Document Understanding Conference*, NIST. Edmonton, Canada,2003.

[8] Y. Chali, S.R. Joty and S.A. Hasan, "Complex Question Answering: Unsupervised Learning Approaches and Experiments", *Journal of Artificial Intelligence Research*, Vol. 35, No. 1, pp.1-47, May 2009.

[9] J.R. Quinlan, "C4.5: Programs for Machine Learning", *Morgan Kaufmann Publishers*, 1993.

[10] H.T. Ng, L.H. Teo, J. Lai and P. Kwan, "A Machine Learning Approach to Answering Questions for :Reading Comprehension Tests", *In Proceedings of EMNLP/VLC-2000 at ACL-2000*, Hong Kong, 2000.

[11] D. Dominguez-Sal and M. Surdeanu, "A Machine Learning Approach for Factoid Question Answering", *In Proceedings of the 22nd Congreso de la Sociedad Espanola para el Procesamiento del Lenguaje Natural (SEPLN 2006)*, Andalucia Spain,September 2006.

[12] A. Purwarianti, M. Tsuchiya and S. Nakagawa, "A machine learning approach for an Indonesian-English cross language question answering system", *In Proceedings of IEICE TRANSACTIONS on Information and Systems*, Vol. E90-D, No.11, pp.1841-1852, Oxford, November 2007.

[13] M. Basu and K.H. Tin, "Data Complexity in Pattern Recognition". XVI, 300 p. 95 illus. *Springer*, London, 2006.

[14] M. Light, G. Mann, L. Hirschmann, E. Rilo, and E. Breck, "Analyses for Elucidating Current Question Answering Technology". *Journal of Natural Language Engineering, Special Issue on Question Answering*, Vol. 7, No. 4, pp. 325-342, 2001.

[15] S. Helmut, "Probabilistic Part-of-Speech Tagging Using Decision Trees", *In Proceedings of the International Conference on New Methods in Language Processing*, pp. 44-49, Manchester, UK ,1994.

[16] K. Papineni, S. Roukos, T. Ward and W.J. Zhu, "BLEU: A Method or Automatic Evaluation of Machine Translation", *In Proceedings of the 40th Annual Meeting of the Association for Computational Linguistics (ACL)*, pp.311-318, Philadelphia, July 2002.

[17] E. Riloff and M. Thelen, "A Rule-Based Question Answering System for Reading Comprehension Tests", *In Proceedings of the ANLP/NAACL 2000 Workshop on Reading Comprehension Tests as Evaluation for Computer-Based Language Understanding Systems*, Stroudsburg,PA,USA.

2000.

A Hybrid PSO Model in Extractive Text Summarizer

Oi-Mean Foong, Alan Oxley
Universiti Teknologi PETRONAS
Computer and Information Sciences Department, Seri Iskandar, Tronoh 31750, Perak, Malaysia

Abstract- **The World Wide Web has caused an information explosion. Readers are often drowned in information while starved of knowledge. Readers are bombarded with too many lengthy documents where shorter summarized texts would be preferable. This paper presents a hybrid Harmony Particle Swarm Optimization (PSO) framework in an Extractive Text Summarizer to tackle the information overload problem. Particle Swarm Optimization is a suitable technique for solving complex problems due to its simplicity and fast computational convergence. However, it could be trapped in a local minimal search space in the midst of searching for the optimal solutions. The objective of this research is to investigate whether the proposed hybrid harmony PSO model is capable of condensing original electronic documents into shorter summarized texts more efficiently and accurately than the alternative models. Empirical results show that the proposed hybrid PSO model improves the efficiency and accuracy of composing summarized text.**

I. INTRODUCTION

Automatic text summarization has drawn substantial interest from researchers and software developers since it provides a solution to the information overload problem for users in this digital era of the World Wide Web. Readers are overloaded with too many lengthy text documents when they are more interested in shorter versions. Two fundamental techniques are identified to automatically summarize texts, i.e. extractive and abstractive summarization. The former technique creates summaries using terms, phrases and sentences extracted from the source texts at surface level. The frequency of words are counted and analyzed based on their occurrences, where they appear in the source documents. This is sometimes known as knowledge-poor processing [1].

On the other hand, more complex summarization technique is adopted through abstraction. The latter technique uses computer generated analyses and synthesis of the source documents into a completely new documents. Not only is the summarized document shorter but also cohesive, readable and intelligible. Multi disciplinary approaches in information retrieval, linguistics, machine learning and artificial intelligence have been applied to achieve the abstractive summarization [2]. The objective of this research is to investigate whether the proposed hybrid harmony PSO model is capable of condensing original electronic documents into shorter summarized texts more accurately than the alternative models.

Research on single document summarization based on word frequency was pioneered by Luhn [3]. Baxendale applied sentence position as a useful feature to extract the salient parts of documents [4]. Edmundson used cue words and title as important features to produce the summarized text [5]. Isfahani et al. applied fuzzy logic for the improvement of text summarization [6]. Wang et al used neural networks to train and learn the relevant features of sentences that should be included in the summary of text documents [7]. Fattah and Ren applied a model based on a genetic algorithm (GA) and mathematical regression (MR) in order to obtain a suitable combination of feature weights to summarize one hundred English articles [8]. Binwahlan et al. have adopted Particle Swarm based features selection to produce summary text [9]. Binwahlan and Salim used Fuzzy Swarm Diversity Hybrid Model for Text Summarization [10]. The latter Fuzzy Swarm Hybrid outperforms the Particle Swarm model when leverages on the summaries generated manually by human.

This paper is organized as follows: Section I introduces the background of text summarization. Section II states the main research motivation and contribution. Section III describes Particle Swarm Optimization. Section IV explains the Harmony Search algorithm. Section V highlights Hybrid PSO. Section VI discusses the experimental results. Section VII states the conclusion and future work.

II. RESEARCH MOTIVATION AND CONTRIBUTION

The information retrieved from the World Wide Web is growing exponentially. The number of relevant hits based on user's query is huge inclusive of the false positive hits or irrelevant hits. Each electronic document could be very lengthy. Readers find that it is too time consuming to condense the main gist of a document. Although there is a number of software tools (MS AutoSum, Summarist, etc.) available to automatically facilitate the text summarization process, but the summarized text output is still imprecise. Thus, there is still room for improvement.

The main research contributions in this paper are: (1) Hybrid Harmony PSO model is proposed. (2) A new Hybrid Harmony PSO algorithm is explored and implemented. The hybrid model condenses the original electronic documents into shorter summarized texts more accurately without intervention from human.

978-1-61284-690-3/11/$26.00 ©2011 IEEE

III. PARTICLE SWARM OPTIMIZATION

Particle swarm optimization (PSO) is a population based stochastic optimization technique developed by R.C. Eberhart [11]. PSO mimics the social behavior of a swarm of insects, a flock of birds or a school of fish. PSO shares many similarities with evolutionary computation techniques like Genetic Algorithms, Artificial Neural Networks and Artificial Immune Systems. It is initialized with a population of random solutions and searches for optima by updating generations. If one of the particles discovers a good path to food, the rest of the swarm will be able to follow instantly, e.g. swarm of ants or even school of fish. The swarm behavior is modeled by particles in multidimensional search space with position and velocity as characteristics. These particles forage through the hyperspace by adjusting their own position and velocity.

IV. HARMONY SEARCH

The proposed hybrid consists of the harmony search and PSO algorithms. The harmony search (HS) algorithm is based on natural musical performance processes that occur when a musician seeks to find musically pleasing harmony as determined by aesthetics [12]. During music improvisation, each instrument player sounds any pitch within a possible range; together this makes one harmony vector. If the pitches make a good harmony solution, that solution will be stored in each variable's memory. In this HS algorithm, three optimization operators, namely harmony memory (HM), harmony memory considering rate (HMCR), and the pitch adjusting rate (PAR) were explored to investigate the performance of the text summarizer.

The followings steps are considered in the attempt to find a suitable harmony state.

Step 1: Initialize the problem and algorithm parameters.
Step 2: Initialize the harmony memory (HM).
Step 3: Improvise a new harmony from the HM.
Step 4: Update the HM.
Step 5: Repeat steps 3 and 4 until the termination criterion is satisfied.

V. PROPOSED HYBRID PSO MODEL

Extensive optimization techniques such as neural networks, evolutionary algorithms, genetic algorithms and swarm intelligence algorithms have been successfully deployed to solving complex problems. To improve the PSO performance, several methods have been developed. Recently, hybrid techniques which include NM-PSO (Nelder-Mead PSO) and CPSO (Chaotic PSO) and Fuzzy PSO have been implemented to solve real world complex problems [13][14][15].

A. Hybrid Harmony PSO Algorithm

The steps below elaborate on how to incorporate HS with PSO for automatic text summarization:

Step 1: Initialize the parameters of PSO and HS.
Step 2: Initialize the particles.
Step 3: Evaluate particles according to their fitness functions then sort them in descending order.
Step 4: Perform HS and generate a new solution.
Step 5: If the new solution is better than the worst particle then replace it with the new one.
Step 6: Update the particles according to the PSO formula.
Step 7: The algorithm is finished only if the terminating condition is met otherwise go to step 3.

The hybrid theory is implemented by using HS at steps 4 and 5. Using HS parameters, the PSO weight assigned to every sentence by PSO is further optimized by the pitch adjustment algorithm of HS. The adjustment is done based on the parameters of HS, which are Harmony Memory Considering Rate (HMCR) and Pitch Adjusting Rate (PAR).

B. Hybrid Harmony PSO Flowchart

Features are crucial in determining the accuracy of the summarized text. In this paper, the following features were examined which affect the sentence weight:

- Title Feature
- Keywords
- Similarity to first and last sentence
- Sentence Cohesion

These features determine the rank of the sentences from the raw text. Using the PSO encoding, every sentence in the document will have a 4-bit binary value, each representing the score of every feature [9]. Sentence features determine what attribute of the text that should be considered in the swarm-based text summarization model. These features are extracted after pre-processing is done to the text itself. Each sentence will have its own score. Sentence with the highest value will be ranked first. All subsequent sentences will be ranked in descending order in the summarized text. The final output will be determined based on the compression rate from the user.

The extracted features from electronic document are further elaborated as follows:

- *Title Feature*

A sentence's resemblance to the title is measured by comparing the keywords in sentence *s* with those in the document title. This can be achieved by using Eq.1 [8]:

$$tf(s) = \frac{Keywords\ in\ s \cap Keywords\ in\ Title}{Keywords\ in\ s \cup Keywords\ in\ Title} \quad \textbf{(1)}$$

- *Keywords*

Words that are being repetitively used in the document are considered as important. The words with the top ten scores, according to Eq. 2, are considered as the keywords of a particular document [7][16]. In order to calculate the keyword score, we use Eq. 2:

$$Score\ (w) = f(w) \times \frac{\log N}{S(w)} \quad \textbf{(2)}$$

where *f(w)* is the frequency of the word in a sentence. *N* indicates the number of words in that particular sentence while *S(w)* is the number of sentences in which the word occurs.

- *Similarity to First and Last Sentence*

This feature $S_f(s)$ is used to compute the sentence score based on its similarity to the first and last sentence of the document. The average score of both similarities can be achieved by using Eq. (3) (4) (5):

$$S_f(s) = \frac{s_1 + s_2}{2} \quad \textbf{(3)}$$

where

$$s_1 = \frac{Keywords\ in\ s\ \cap\ Keywords\ \ in\ First\ Sentence}{Keywords\ in\ s\ \cup\ Keywords\ \ in\ First\ Sentence} \quad \textbf{(4)}$$

$$s_2 = \frac{Keywords\ in\ s\ \cap\ Keywords\ \ in\ \ Last\ Sentence}{Keywords\ in\ s\ \cup\ Keywords\ \ in\ \ Last\ Sentence} \quad \textbf{(5)}$$

- *Sentence Cohesion*

Sentences that have continuity are extracted to ensure a continuous summarized text flow and to reduce redundancy. The sentence cohesion feature's score can be achieved by using Eq. 6 [8]:

$$Sc(s) = \frac{Keywords\ \ in\ \ s \cap Keywords\ \ in\ another\ \ Sentence}{Keywords\ \ in\ \ s \cup Keywords\ \ in\ another\ \ Sentence} \quad \textbf{(6)}$$

To determine the scores, all of the output summary were set to 50% compression rate, to match the compression rate provided by the benchmark summary in order to obtain the most accurate comparison between output summaries and benchmark summaries.

Let us consider Fig. 1. The 'Update' box uses the following Eq. 7 and Eq. 8 [11]:

$$V_i(t+1) = w * v_i(t) + c_1 * \phi_1(p_l - x_i(t)) + c_2 * \phi_2(p_g - x_i(t)) \quad \textbf{(7)}$$

$$X(t+1) = X_i(t) + V_i(t+1) \quad \textbf{(8)}$$

where c_1 and c_2 are positive constants; w is an inertia weight; φ_1 and φ_2 are random numbers between 0 and 1; p_l is the previous best location of the particle; p_g is the previous best location of all of the particles.

The values chosen for the HS parameters are PAR = 0.2 and HMCR = 0.9. At step 4, a Harmony Memory (HM) is created based on the particle position of the PSO. We apply Eq. 9 to modify HM [12]:

$$x_i'(t) \leftarrow \begin{cases} x_i' \in \{x_i^1, x_i^2, ..., x_i^{HMS}\}\ with\ probability\ \ HMCR \\ x_i' \in X_i\ with\ \ probability\ \ 1 - HMCR \end{cases} \quad \textbf{(9)}$$

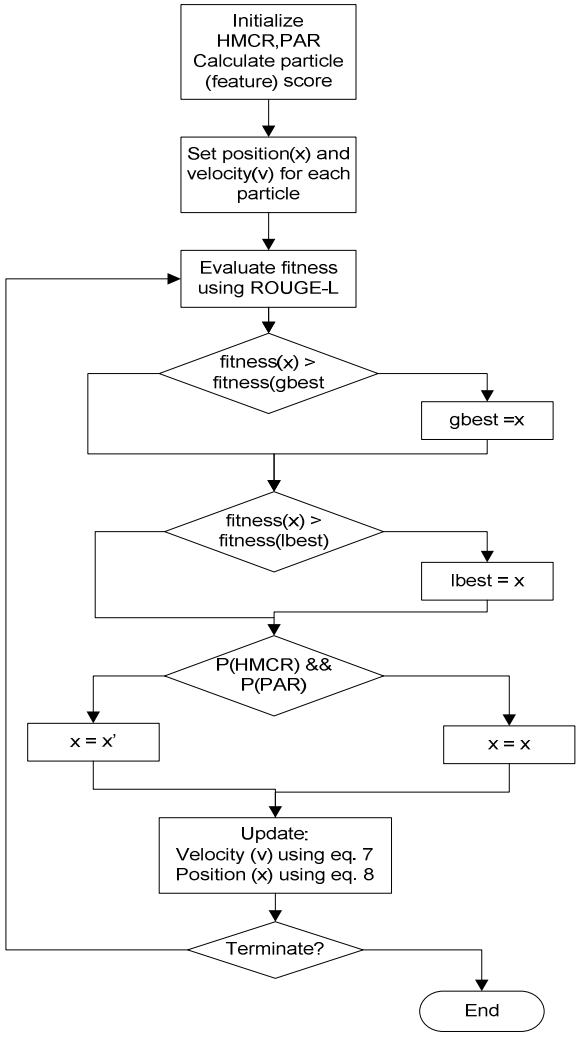


Fig.1. Proposed Hybrid Harmony PSO Flowchart

HMCR is the probability of choosing one value from the historic values stored in the HM, and (1-HMCR) is the probability of randomly choosing one feasible value not limited to those stored in the HM. Every component of the new harmonic vector x_i' is examined to determine whether it should be pitch-adjusted. The pitch adjusting decision is shown in Eq.10 [12]:

$$x_i'(t) \leftarrow \begin{cases} Yes\ with\ probability\ \ PAR \\ No\ \ with\ probability\ 1 - PAR \end{cases} \quad \textbf{(10)}$$

The new position determined by HMCR is examined to determine whether or not to undertake pitch-adjustment. If it is adjusted, the new position will be based on the HM.

VI. RESULTS AND DISCUSSION

A. Experimental Setup

The method used in evaluating the output summary is an intrinsic method which aims to evaluate the quality of the summaries as compared to other summaries or extracts. For

a start, a total of 8 electronic documents are downloaded from the internet for testing and validating the hybrid model. A document repository that is often used by automatic text summarization researchers is DUC [17]. There are different versions of this repository, such as DUC 2007. A typical DUC 2007 document has 20,000 or more words. This large file size has made it infeasible to undertake preliminary testing of our Hybrid Swarm Text Summarizer. Similarly, DUC 2002 documents are prohibitively large.

Our reluctance to benchmark our text summarizer against DUC has meant that we have tried to find an alternative way of assessing the summaries produced. We took documents from the internet and automatically summarized them. Each document summary was evaluated, by English linguists from the Management and Humanities Department, based on readability and cohesion. In addition, we also decided to compare our system's summaries with those produced by an existing market text summarizer - the Microsoft Word Auto Summarizer. The output produced by these two summarizers is compared with a benchmark summary using the measures of Recall, Precision and F-score. These measures are calculated using ROUGE-L.

An important metric relates to the extent to which sentences of the automatically generated summary overlap with those of the benchmark summary.

B. Performance Evaluation Metrics

The performance measures used for the evaluation of the summary generated by the system are Recall, Precision, and F-score [18]. 'Recall' is a measure of how effective the system is at including relevant sentences in the summary. 'Precision' is a measure on how effective the system is at excluding irrelevant sentences from appearing in the summary. Meanwhile, the F-score is a composite score that combines the precision and recall measures.

ROUGE-L is a widely used evaluation package for text summarization that has been developed by Lin [19]. It has been used by many researchers to evaluate the scores of automatically generated summaries. ROUGE-L compares two generated summaries produced by different text summarizers. It gives the Precision, Recall and F-score values for both summarizers.

C. Discussion and Analyses

Initially, using some sample articles and summaries, the author managed to obtain an average F-score in the range 0.42 to 0.64 for PSO model, as shown in Table III. This score was due solely to the choice of PSO features, as the Harmony Search algorithm had not yet been implemented.

After the strong positive indication given by this initial result, the author added the Harmony Search algorithm. The new system was then compared with Microsoft Word Auto Summarizer, using benchmark documents and their summaries. Table I and Table II show the benchmarking results of average Recall and average Precision respectively among PSO, Hybrid PSO and MSWord summarized text output.

TABLE I
Recall Comparison among PSO, Hybrid PSO & MS Word

Document	PSO	Hybrid PSO	MSWord
1	0.72	0.72	0.47
2	0.74	0.63	0.38
3	0.65	0.64	0.50
4	0.56	0.49	0.46
5	0.58	0.58	0.59
6	0.67	0.66	0.57
7	0.72	0.73	0.49
8	0.75	0.76	0.42
Avg Recall	**0.68**	**0.65**	**0.49**

TABLE II
Precision Comparison among PSO, Hybrid PSO & MS Word

Document	PSO	Hybrid PSO	MSWord
1	0.54	0.56	0.58
2	0.52	0.65	0.57
3	0.57	0.61	0.55
4	0.46	0.58	0.56
5	0.41	0.61	0.52
6	0.61	0.62	0.61
7	0.54	0.58	0.57
8	0.61	0.69	0.54
Avg Precison	**0.53**	**0.61**	**0.56**

TABLE III
F-Score Comparison among PSO, Hybrid PSO and MS Word

Document	PSO	Hybrid PSO	MSWord
1	0.55	0.58	0.56
2	0.54	0.65	0.58
3	0.61	0.61	0.55
4	0.47	0.57	0.55
5	0.42	0.60	0.53
6	0.62	0.63	0.60
7	0.56	0.60	0.57
8	0.64	0.71	0.53
Avg F-Score	**0.55**	**0.62**	**0.56**

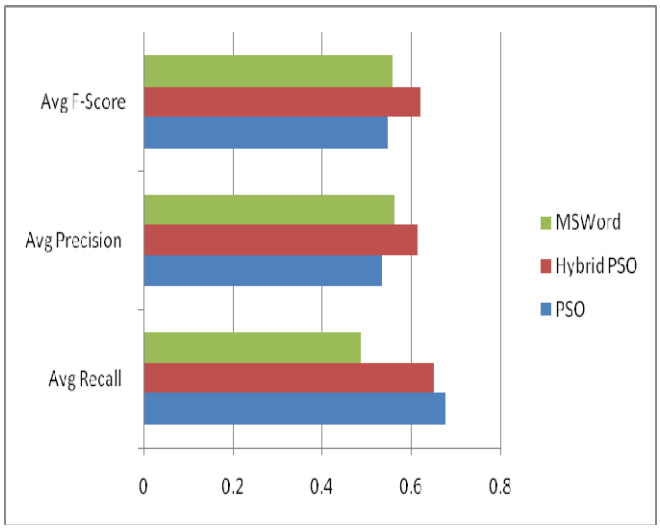


Fig. 2 Overall average performance comparison among PSO, Hybrid PSO and MS Word

Fig. 2 produces the overall performance of average Recall, average Precision, and average F-score among PSO, Hybrid PSO and MS Word Summarizers. From the experimental results, PSO, Hybrid PSO and MS Word Summarizers yield an average F-score of 0.55, 0.62 and 0.56 respectively. In spite of the high average Recall of 0.68 obtained by PSO in Table I, the proposed hybrid PSO produces the best F-score of 0.62 among the three models.

VII. CONCLUSION AND FUTURE WORK

The proposed Hybrid PSO Text Summarizer performs better than PSO and MS Word Auto Summarizer. Our new hybrid algorithm produces an average F-Score of 0.62. We conclude that the proposed hybrid harmony PSO model is capable of condensing original electronic documents into shorter summarized texts more accurately than the alternative models. For future work, the prototype will benchmark against DUC 2007 documents. Typically each document has over 20,000 words, which is equivalent to over 100,000 characters. In order to undertake this work a high performance computing machine will be used. Other techniques will be explored to investigate the performance of hybrid PSO in solving complex optimization problems [20] [21] [22].

ACKNOWLEDGMENT

Special thanks to Research Innovative Office (RIO) for funding this research. I would like to thank the reviewers who have given invaluable comments and feedback for this paper.

REFERENCES

[1] I. Mani, M. T. Maybury, *Advances in Automatic Text Summarization.* U.S.A.: MIT Press, 2001.
[2] C. Prakash, A. Shukla, "Automatic Summary Generation from Single Document using Information Gain", *Communications in Computer and Information Science*, vol. 94 CCIS, issue PART 1, pp. 152-159, 2010.
[3] P.H.Luhn, "The Automatic Creation of Literature Abstracts", IBM *Journal of Research Development*, vol.2, no.2, pp.159-165, 1958.
[4] P. Baxendale, "Machine-made Index for Technical Literature –An Experiment", *IBM Journal of Research Development*, vol.2, no.4, pp. 354-361, 1958.
[5] H.P. Edmundson. "New Methods in Automatic Extracting", *Journal of ACM*, vol.16, no.2, pp. 264-185, 1969.
[6] F.R. Isfahani, F.Kyoomarsi, H. Khosravi, E. Eslami, A. Tajodin, P.K. Dehkordy, "Application of Fuzzy Logic in the Improvement of Text Summarization", IADIS International Conference Informatics, pp. 3-10, 2008.
[7] J.B. Wang, P. Hong, J.S. Hu, "Automatic Keyphrases Extraction from Document using Neural Network", *Springer-Verlag LNAI 3930*, pp.633-641, 2006.
[8] Mohamed Abdel Fattah, Fuji Ren, "Automatic Text Summarization", *International Journal of Computer Science*, Vol., No.1, pp.25-28, 2008.
[9] M.S. Binwahlan, N. Salim, L. Suanmali, "Swarm Based Features Selection for Text Summarization", *International Journal of Computer Science and Network Security (IJCSNS)*, vol.9, no.1, pp. 175-179, 2009.
[10] M.S. Binwahlan, N. Salim, "Fuzzy Swarm Diversity Hybrid Model for Text Summarization", *Journal of Information Processing and Management*, vol. 46, no. 5, pp. 571-588, 2010.
[11] R.C. Eberhart, J. Kennedy, "A New Optimizer using Particle Swarm Theory", Sixth International Symposium on Micro Machine and Human Science, pp. 39-43, 1995.
[12] Z.W. Geem, "Music-Inspired Harmony Search Algorithm: Theory and Applications", *Studies in Computational Intelligence* 191, Springer, 2009. ISBN 978-3-642-00184-0.
[13] S.K.S. Fan, Y.C. Liang, E. Zahara, "A Genetic Algorithm and a Particle Swarm Optimizer Hybridized with Nelder-Mead Simplex Search", *Journal of Computers and Industrial Engineering*, vol. 50, no. 4, pp. 401-425, 2006.
[14] B. Liu, L.Wang, Y.H.Jin, F.Tang, D.X.Huang, "Improved Particles Swarm Optimization Combined with Chaos", *Chaos Solitons & Fractals*, pp. 1261-1271, 2005.
[15] K.E. Permana, S.Z.M. Hashim, "Fuzzy Membership Function Generation using Particle Swarm Optimization", *International Journal Open Problems Compt. Math.*, vol. 3, no. 1, pp.27-41, 2010.
[16] G. Ercan, Y. Cicekli, "Using Lexical Chains for Keyword Extraction", *Information Processing & Management*, vol.43, no.6, pp: 1705-1714, 2007.
[17] http://duc.nist.gov
[18] C. Goutte C, E. Gaussier, "A Probabilistic Interpretation of Precision, Recall and F-score with Implication for Evaluation", *Advances in Information Retrieval, LNCS 3408*, pp. 345-359, 2005.
[19] C. Lin, "Rouge: A Package for Automatic Evaluation of Summaries", Workshop on Text Summarization, 42nd Annual Meeting of the Association for Computational Linguistics, pp.74-81, 2004.
[20] Kiran Yadav, Ranjit Bisbas, "An Intelligent Search Path", *International Journal of Intelligent Systems*, vol. 25, no.9, pp.970-980, 2010.
[21] M.C. Schut, "On Model Design for Simulation of Collective Intelligence", *Information Sciences, Elsevier*, vol. 180, no.1, pp. 132-155, 2010.
[22] C.L. Huang, J.F. Dun, "A Distributed PSO-SVM Hybrid System with Feature Selection and Parameter Optimization", *Applied Soft Computing*, vol.8, no. 8, pp.1381-1391, 2008.

Fast Analysis of On-Chip Power Distribution Networks

Hedi Harizi
Institute of Microelectronic Systems
Leibniz University of Hannover
Hannover, Germany
Email: Hedi.Harizi@hotmail.com

***Abstract*—The verification of the power distribution network is of critical importance to ensure reliable performance. However, with the increasing number of transistors on a chip, the complexity of the power network has also grown. The available computational power and memory resources impose limitations on the size of the networks that can be analyzed using currently known techniques. In this paper, we present a fast and efficient method to analyze power distribution networks in the time-domain. The new contributions of this work are the use of PWL data point reduction and correction factors (CF) to reduce the number of current source models and to speed up the characterization time. The proposed techniques provide good analysis results compared to the reference with a reduction of the run-time by a factor of 400, although the cell pre-characterization is based on SPICE simulations. Our model is independent of power network parasitics, which implies that different power network scenarios may be analyzed based on the same model and the same cell characterizations. The run-time and accuracy of the proposed approach are demonstrated on some industrial designs.**

***Keywords*-Voltage drop modeling; circuit simulation; hierarchical analysis; correction factors; PWL data point reduction;**

I. Introduction

IR drop analysis is an important step in the design flow since it affects signal and power integrity, which may result in timing and silicon failures. Due to the nature of localized switching events, static IR drop analysis no longer provides sufficient accuracy. Designers are currently looking for accurate dynamic IR drop analysis to ensure the power integrity of their designs in the sub-nanometer era.

One of the critical issues in the analysis of power distribution networks is the extremely large size of the network due to the rapid increase of the number of transistors on a chip. At the current technological level, it is obvious that the available computing resources and the usage of a flat model are insufficient to simulate very large power grids of today's microprocessors. Therefore, the analysis should be performed at the gate level. It should be fast enough in order to enable an interactive what-if analysis. Although gate level approaches are less accurate, as pointed out in [1], dynamic gate-level power analysis will be the most promising method for full chip analysis [2], [3], [4].

In this paper, we propose a new approach to transient analysis of large P/G grids. In a first step, we apply a coarse analysis based on a selection approach (SA) to determine the voltage drop-critical cells in the netlist. Typical examples of voltage drop-critical cells are clock buffers, I/O buffers and bus drivers. These cells are then replaced by accurately abstracted models and precharacterized with respect to the corresponding modeling requirements. With the abstracted models, the original network can be significantly reduced and sufficient transient analysis of large P/G networks at minimal computational effort becomes possible.

The remainder of the paper is organized as follows. We briefly describe the power distribution network (PDN) analysis at gate level in Section II. Section III describes the PDN analysis at block level, the model optimization using corrections factors (CF) and the approach for the PWL data point reduction. Section V gives an overview of the proposed voltage drop analysis flow. Experimental results on some industrial designs are described in Section VI. Section VII concludes the paper.

II. PDN Analysis at Gate Level

The analysis at gate level is based on the voltage drop model presented in Figure 1. This current source-based model (CSM) enables dynamic gate-level PG analysis, which provides the actual currents drawn from the power network at any given time for individual cells. The model represents the time-domain behaviour of the current drawn by a CMOS cell corresponding to each input event. The CSM internally consists of two models: A non-switching cell model (NSCM) and a switching cell model (SCM). NSCM represents a library cell, if it does not switch. The SCM represents a switching library cell.

Each cell in the netlist is replaced by a corresponding current source-based model (CSM) consisting of a capacitance C_{CSM}, a current source $i_0(t)$ and a non-linear resistor r_{CSM}. The current $i_0(t)$ is the switching current at the nominal supply voltage V_0, and $r_{CSM}(v)$ is a voltage controlled resistor (VCR), which depends on the actual supply voltage $v(t)$. The switching cell model is time and voltage dependent. The time dependency is in the current source, and the voltage dependency is in the VCR. The VCR makes the CSM more accurate and independent of the PG parasitics. The library cells are then characterized, using SPICE simulation, for each voltage in a given voltage range (in our approach from 0 to 300 mV voltage drop peak).

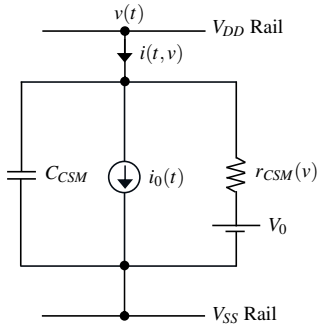


Figure 1. Corresponding abstracted current source model for a library cell

III. PDN Analysis at Block Level

Once the cells are characterized, cell models can be used for the analysis of different power grid alternatives. Each cell in the netlist is replaced by a corresponding (characterized) CSM. A power grid with the reduced netlist is now simulated using SPICE. A SPICE reference simulation using the original netlist is performed to evaluate the accuracy of the current source model. Within this simulation voltage drop is measured at each node in the power grid. Voltage drop waveforms as well as voltage drop peak (VDP) characteristics (value, location, and time) are then compared to the reference values.

Using the corresponding CSM model for each instance in the netlist, the new model provides a voltage drop analysis error less of $+10$ % in VDP value and about $+4$ % in VDP time at block level [5]. The overestimation is due to the fact, that the input/output transition times used in CSM are estimated using a standard STA approach (based on PrimeTime), which implicitly assumes that within the circuit the power supply voltage is uniformly constant at each cell. In a real scenario due to variations in the supply voltage, the cell-input transition times are larger than those used in the CSM model, which has an impact on the VDP values.

The output ramp duration τ_{OUT} of a CMOS structure depends on its supply voltage v. As proposed in [6] τ_{OUT} can be obtained from $\tau_{OUT} = \alpha \cdot v$, with $\alpha = \frac{C_L}{I_{MAX}}$. C_L is the output loading capacitance and I_{MAX} represents the maximal switching current. This implies that a k variation in the supply voltage results in a $\alpha \cdot k$ variation in transition time.

Figure 2 shows the voltage drop impact on the signal output transition time for a switching library cell at the nominal supply voltage V_0 and at a supply voltage $v_1(t)$. The transition output time (40 %-60 %) is 1.5875 ps at V_0 and 2.017 ps at $v_1(t)$. This means, a 10 % deviation in the VDP value causes a deviation of 27 % in transition time.

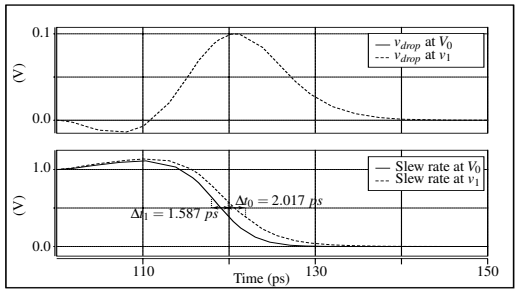


Figure 2. Signal transition time at V_0 and at $v_1(t)$

The impact in turn of transition time deviation on the supply voltage can be given by $V = \frac{\tau_{OUT}}{\alpha}$. The result of the SPICE simulation for a switching library cell at $v_1(t)$ with a nominal input transition time and with a modified transition time caused by the voltage drop at the driving cell shows that 30 % deviation in transition time results in less than 1 % deviation in VDP value and less than 4 % deviation in VDP time.

In order to take into account the impact of the transition time deviations on VDP value and VDP time, correction factors (CF) are introduced and used in the following.

A. Model Optimization Using Correction Factors

Figure 3 presents the result of SPICE simulations for all inverter cells in an industrial circuit. These cells are put in a switching situation ($0 \rightarrow 1$). For each voltage drop peak value, the output transition time is measured for each cell. Figure 3 shows that transition time deviation (TTD) and voltage drop peak (VDP) value are linearly dependent. For example, a 5 % larger voltage drop results in 8 % to 25 % larger transition time, depending on the cell. This means, it is up to 25 % larger than the estimated transition time with PrimeTime.

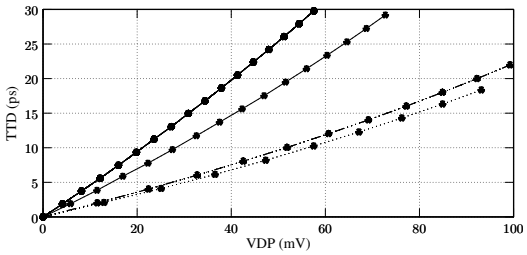


Figure 3. Transition time deviation (TTD) as a function of voltage drop peak (VDP) value

TTD for each cell c_i is approximately given by

$$\text{TTD } (\%) \approx k_{transition_{c_i}} \cdot \text{VDP}, \; k_{transition_{c_i}} > 0, \quad (1)$$

and the cell transition time CTT can be given by

$$\text{CTT} \approx \textit{nominal CTT} \cdot (1 + \text{TTD}). \quad (2)$$

Equations 1 and 2 yield

$$\text{CTT} \approx \textit{nominal CTT} \cdot (1 + k_{transition_{c_i}} \cdot \text{VDP}).$$

$k_{transition_{c_i}}$ is estimated without any additional computational effort by just adding a transition measure statement in current simulations.

In order to estimate the impact of TTD on the current source model, which depends on the inputs' transition times, the inverter cells are simulated with different transition times. VDP value and VDP time are then compared to the reference. The reference values are measured at nominal supply voltage. Figure 4 shows the impact of TTD on VDP value and VDP time.

The value and the time of the voltage drop peak (VDP) are both linearly dependent of TTD. The larger the transition time, the less the VDP value, the later, however, the VDP time. As a result, the peak value deviation (PVD) and the peak time deviation (PTD) can approximately be given for each cell c_j by

$$\text{PVD} \approx \alpha_{c_j} \cdot \text{TTD}, \; \alpha_{c_j} < 0, \quad (3)$$

$$\text{PTD} \approx \beta_{c_j} \cdot \text{TTD}, \; \beta_{c_j} > 0. \quad (4)$$

Equations 1, 3 and 4 yield

$$\text{PVD} \approx \alpha_{c_j} \cdot k_{transition_{c_i}} \cdot \text{VDP}, \quad (5)$$

$$\text{PTD} \approx \beta_{c_j} \cdot k_{transition_{c_i}} \cdot \text{VDP}. \quad (6)$$

Equations 5 and 6 finally give

$$\text{VDPvalue} \approx \textit{nom VDPvalue} \cdot (1 + \alpha_{c_j} \cdot k_{transition_{c_i}} \cdot VDP),$$

$$\text{VDPtime} \approx \textit{nom VDPtime} \cdot (1 + \beta_{c_j} \cdot k_{transition_{c_i}} \cdot VDP).$$

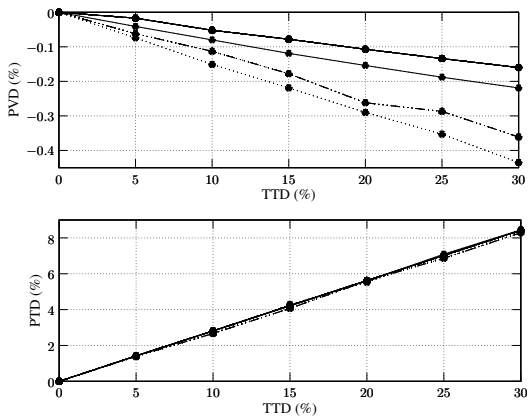


Figure 4. Peak value deviation (PVD) and peak time deviation (PTD) as a function of transition time deviation (TTD)

The nominal VDP value (time) corresponds to the VDP value (time) with the nominal transition time. $k_{transition_{c_i}}$ is the transition coefficient of the cell c_i, the output of which is connected to the input of the cell c_j.

The modified current source model CSM_{mod} now contains a modified current source $i_{0mod}(t)$. The modified current is saved as PWL source, where a current value $i_{j_{mod}} = i_{0mod}(t_{j_{mod}})$ corresponds to each $t_{j_{mod}}$. With

$$\begin{cases} t_{j_{mod}} = t_{j_{org}} \cdot (1 + \beta_{c_j} \cdot k_{transition_{c_i}} \cdot VDP), \\ i_{j_{mod}} = i_{j_{org}} \cdot (1 + \alpha_{c_j} \cdot k_{transition_{c_i}} \cdot VDP). \end{cases}$$

The current $i_{j_{org}}$ is the corresponding current at time $t_{j_{org}}$ in the original current source model CSM_{org} with the nominal transition time.

As a result, the corresponding current source for each cell c_j with a supply voltage v_j is given by

$$\begin{cases} t_{j_{mod}} = t_{j_{org}} \cdot (1 + \beta_{c_j} \cdot k_{transition_{c_i}} \cdot (V_0 - v_j)), \\ i_{j_{mod}} = i_{j_{org}} \cdot (1 + \alpha_{c_j} \cdot k_{transition_{c_i}} \cdot (V_0 - v_j)), \end{cases}$$

where α_{c_j}, β_{c_j} are correction factors that compensate the overestimations from the original CSM presented in Section III

Using correction factors (CF) the CSM becomes more accurate than without CF. Although the cell characterizations are based on SPICE simulations, the new model provides a two order of magnitude speedup compared to the reference SPICE for small circuits. However, to maintain this speedup advantage for much larger designs, a reduction approach for PWL data points proved to be more effective in enhancing the current source model.

IV. Reduction of PWL Current Sources

From the initial polyline, which is already given by a finite set of points as a result of a SPICE simulation, a smaller subset of points is constructed with respect to some predefined error tolerances. Eventually, only the most significant points are used in the PWL curve approximation.

A. Problem Statement

a. Let p_i, where $i = 0, \cdots, n$, be vertices of the source polyline P. Let decomposition vertices p_{q_j} divide P into the set

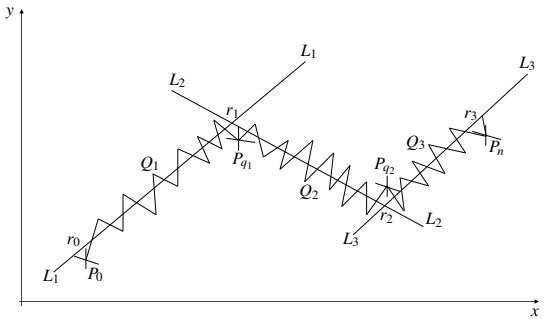


Figure 5. Decomposition of the source polyline P into polygonal sectors

of non-overlapping polygonal sectors, where q_j $(j = 0, \cdots, m)$, are the indices of source polyline vertices (see Figure 5). The number of decompositions of P into m sectors is C_{n-1}^{m-1}. The number of all possible decompositions of P is 2^{n-1}.

b. Each polygonal sector Q_j is approximated with a straight line L_j minimizing integral square error $\epsilon_{q_j,q_{j-1}}$. The minimum integral square error can approximately be given by [7]

$$\epsilon_{j_1,j_2} = \frac{1}{2}\left(V_{xx} + V_{yy} - \sqrt{(V_{xx} - V_{yy})^2} + 4V_{xy}^2\right),$$

where the parametric description of the source line is $(x(t), y(t))$, $t \in [0, T]$, $(x(t), y(t))$ are the coordinates, t is the distance between the beginning and the current point measured along the polyline, T is the polyline length, l_j is the distance between the beginning of the polyline and j-th vertex measured along the polyline,
$V_x = \int_{l_{j_1}}^{l_{j_2}} x(t)dt,\ V_y = \int_{l_{j_1}}^{l_{j_2}} y(t)dt,$
$V_{xx} = M_{xx} - V_x^2,\ V_{xy} = M_{xy} - V_x.V_y,\ V_{yy} = M_{yy} - V_y^2,$
$M_{xx} = \int_{l_{j_1}}^{l_{j_2}} x^2(t)dt,\ M_{xy} = \int_{l_{j_1}}^{l_{j_2}} x(t)y(t)dt,\ and\ M_{yy} = \int_{l_{j_1}}^{l_{j_2}} y^2(t)dt.$

c. Let the measure of the error of the polyline approximation be a functional

$$F(m, \{q\}, \Delta) = \sum_{j=1}^{m} \epsilon_{q_{j-1},q_j} + m \cdot \Delta, \tag{7}$$

where Δ $(\Delta \geq 0)$ is a penalty for each straight segment of the result polyline.

d. For a given Δ, let the optimal decomposition be the decomposition for which functional F is minimal. Approximation accuracy depends on the penalty Δ. The smaller the Δ, the higher the number of the found decomposition points. If Δ = 0, all vertices of the source polyline are decomposition points and $F = 0$. As $\Delta \to \infty$, the source polyline becomes one polygonal sector.

As the CSM model is characterized and optimized at the current peak value, Δ = 0 for each decomposition point q_j, if it fulfills the condition

$$y_{q_j} \geq \alpha \cdot I_{max},\ \alpha \geq \frac{3}{4}$$

and $\Delta \to \infty$ if $y_{q_j} = \beta \cdot I_{max},\ \frac{-1}{10} \leq \beta \leq \frac{1}{10}$.

Using β, the selection of decomposition points with small current peak values is avoided.

e. After finding the optimal decomposition or critical points, polygonal sectors have to be approximated by optimal straight lines. Then, the intersections of the lines approximating the adjusted polygonal sectors should be found. The new polyline goes through these intersections $r_j, (j = 0, \cdots, m)$. The beginning and the end of the new polyline are built as projections of the beginning and the end points of the source polyline to the first and the last straight segments of the new polyline.

B. Iterative Algorithm for an Optimal Solution

Let $P_i, i \leq n$ be polylines defined by the first i straight segments of the source polyline P.

Given that optimal decompositions of $P_k, P_{k-1}, \cdots, P_1$ are known, the optimal (minimal) values of functional (7), the number of decomposition sectors $m_i, (i = 1, \cdots, k)$, and the decomposition points $q_s^i, (i = 1, \cdots, k; s = 1, \cdots, m_i)$ for each of these polylines can be determined.

To find the optimal decomposition of P_{k+1}, an exhaustive search, as presented in [7], may be applied.

Let M_{k+1}^j be the minimum value of the functional, when the last decomposition point of polyline P_{k+1} is p_j. Obviously, $M_{k+1}^j = M_j + \epsilon_{j,k+1} + \Delta$ and $M_0 = 0$.

Let M_{k+1}^j be minimal when the value of $j, (j = k, k-1, \cdots, 0)$ is equal to j^*, or $M_{k+1} = M_{k+1}^{j^*}$.

The optimal decomposition of the source polyline will be built when $k = n - 1$.

The PWL current source reduction procedure requires a total run time of only a few seconds and provides a data point reduction of at least 70 % without the loss of accuracy in the characterization of cells with SIS as well as MIS events, as shown in Chapter VI. This is due to the fact that the cell models are characterized and optimized at the maximum cell current, where the lowest error tolerance is set.

V. Dynamic Voltage Drop Analysis Flow

The flowchart depicted in Figure 6 describes the proposed dynamic voltage drop analysis flow. Using a selective approach the voltage drop critical cells are chosen depending on the placement of the cells in the layout, logic states, consumed energy, input pattern, input transition times, and output loads. Only the selected cells are replaced by abstracted current source-based models.

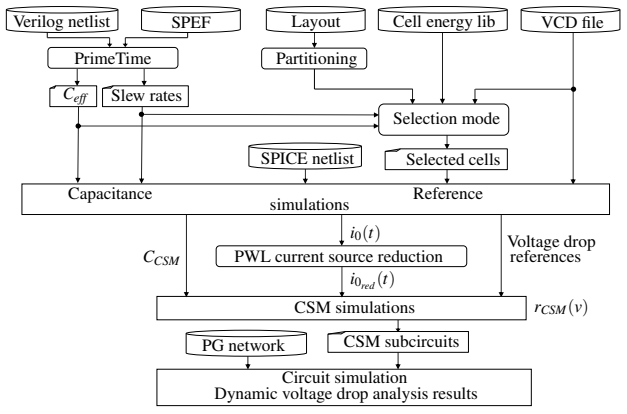


Figure 6. Dynamic voltage drop analysis flow

The characterization of the selected cells consists of two SPICE simulations. In the first step two different simulations are carried out in parallel, as they are independent of each other. The capacitance simulation estimates the capacitance C_{CSM} for each cell in the netlist. For each single input switching (SIS) and multiple input switching (MIS) event the corresponding current waveform $I_0(t)$ at nominal supply voltage V_0 is determined from the reference simulation using the original RC-netlist of the library cell. $I_0(t)$ is converted to a reduced current source $I_{0_{red}}(t)$. The reference voltage drop waveforms as well as the voltage drop peak values are estimated for each switching cell in the netlist.

In the second simulation (CSM simulation), with the reduced $I_{0_{red}}(t)$ and C_{CSM} drawn from the first simulation, a SPICE simulation is carried out for each switching cell. For each voltage drop peak (0-300 mV) the corresponding voltage controlled resistor r_{CSM} is determined. The parameters of the current source model (C_{CSM}, $I_{0_{red}}(t)$, $r_{CSM}(V)$) are then saved in a CSM subcircuit for each selected cell.

The third simulation is the SPICE simulation of the RC extracted power supply network with the cell coordinates, where the abstracted CSM subcircuits are connected. During this simulation the voltage drop is measured on each node in the PDN. Location, time, and value of the critical (worst) voltage drop are determined.

The cell characterization consisting of the first and second simulation is independent of the PDN parasitics. This means that these simulations are carried out only one time (for the first PDN). For each further PDN scenario, only the third simulation (circuit simulation) is needed.

VI. Experimental Results

This section shows the results obtained using SA and CF. The dynamic voltage drop flow is applied to standard cell-based circuits designed in 90 nm process technology. The voltage drop characteristics (peak value, location, time), total run-time and memory demand are compared to reference SPICE simulations at different abstraction levels.

A. Results at Block Level

For the voltage drop simulation at block level each switching cell is replaced by an abstracted CSM that guarantees a VDP analysis error of less than 1 % at the gate level. Each non-switching cell is considered inactive and is, therefore, replaced by a capacitance C_{CSM}. The parasitic capacitances and resistances of the power supply network are extracted from the layout.

Figure 7 shows the voltage drop simulation result for the industrial circuit based on a 16 bit multiplier designed in 90 nm technology. The VDP characteristics (worst peak, time, location) provided by the CSM are compared to SPICE.

Our approach shows +6 % VDP deviation compared to the reference. This overestimation is due to the fact, that on the one hand, the input transition times used in our model are estimated using a standard STA approach, which implicitly assumes that within the circuit block the power supply voltage is uniformly constant at each cell. In a real case scenario and due to fluctuations in the supply voltage, the cell-input transition times are larger than those used in CSM model, which has an impact on the VDP values. On the other hand, the toggle times are based on the VCD pattern. This pattern is the result of a gate-level Verilog simulation, which

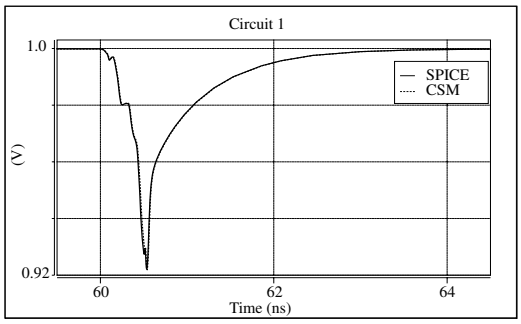


Figure 7. Voltage drop result at block level, Circuit 1

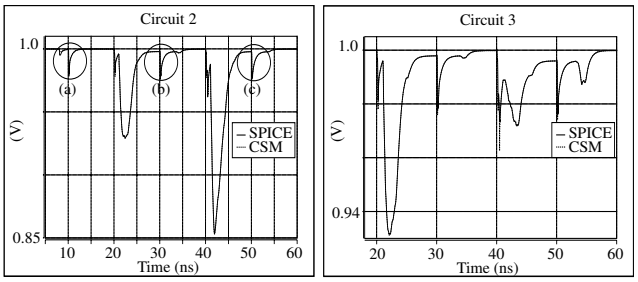


Figure 8. Voltage drop result at block level, Circuit 2 and Circuit 3

is less accurate than an analog simulation. Our investigations have shown that inaccuracy in transition times can produce errors up to +10 % in the VDP value and +8 % errors in the VDP time. We have introduced a correction factor in our approach to take these inaccuracies into account which reduces the VDP errors to +6 % in value and under +2 % in time. On the one hand these deviations are not very big. On the other hand, if relevant at all, they slightly overestimate the true effects. So the method indeed is capable to provide the designer with estimates of the voltage drop effects usually sufficiently accurate, but which are still reliable even in the case of deviations since they slightly overestimate the true effects, which is acceptable from the designers point of view.

Table I shows the analysis result of different power network alternatives. Since the CSM approach is independent of power

Power Network (PN)	CSM run-time(s)		Voltage Drop Peak error (%)	
	Cell characterization	Block simulation	Block level	Cell level
PN-1	3000	632.5	6	< 1
PN-2	-	600.43	5.8	
PN-1	-	620.25	5.7	
PN-2	-	629.19	6	

Table I
ANALYSIS OF DIFFERENT POWER NETWORKS

network context, the cell characterization is needed only for the analysis of the first power network (PN-1). As shown in column 2 and 3, the total runtime for the analysis of PN-1 consists of cell characterization time and block simulation time. For each further power network we need only a block simulation to analyze the power network. This means, the block simulation time is the total run-time. Column 4 and 5 show the accuracy of the proposed approach. One finds a voltage drop peak analysis-error of less than 1 % at cell level and less than 6 % at block level.

Figure 8 presents the voltage drop analysis results for two other different circuits. The voltage waveform of the library cell, which has the worst voltage drop in circuit 2, is presented in Figure 8. This cell switches at 21 ns and 41 ns and is, therefore, replaced by a SCM at these times. For all other times, the cell is replaced by an NSCM consisting of only the capacitance C_{CSM}.

The VDP deviations provided by the NSCM are due to the errors in the estimation of the effective capacitance C_{eff}. These errors are considered to be negligible due to the fact that the critical voltage drops are caused more by the switching than by the non-switching states. Using the effective capacitance model and the NSCM approach, the netlist can be extremely reduced, which speeds up the circuit simulation.

The new voltage drop model provides the same VDP location in the layout as the SPICE simulation. Using the correction factors (CF) the new model shows $+5$ % error in the VDP value and $+2$ % error in VDP time. A comparison between CSM with CF and CSM without CF is presented in Figure 9 for different industrial circuits. Using CF for the Circuit 3, CSM provides a 5 % VDP value error (7 % without CF) and a 3 % VDP time error (7 % without CF). The CF improve the CSM up to 3 % in VDP value and 4 % in VDP time.

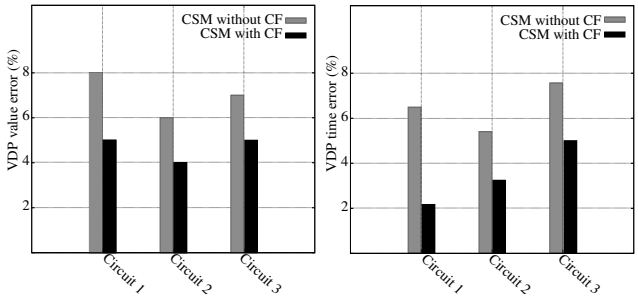


Figure 9. Voltage drop results using correction factors

	Run-time (sec)				Memory (MB)	
	CSM			SPICE	CSM	SPICE
	Characterization	Simulation	Total			
C1	3000	630	3630	64875	29	600
C2	4025	850	4875	104950	57	1020
C3	2563	705	3268	84152	40	875
C4	10495	4032	14527	270919	100	1600

Table II
RUN-TIME AND MEMORY COMPARISON

Table II compares the performance of the new voltage drop model with that of SPICE simulations for different industrial circuits. Two metrics are compared, the peak memory demand and the total run-time. Column 4 shows the total run-time required by the CSM. This time consists of the cell characterization time in Column 2, and the circuit simulation time in Column 3. For example, for

Circuit 1 the CSM approach provides a reduction of the total run-time by a factor of 18, where 82 % are characterization time. Columns 5 and 6 show the peak memory demand, in Megabyte, during the PG analysis with CSM and SPICE. The effect of size reduction is clearly reflected here. A 20x to 30x reduction in memory requirement is possible with the proposed approach.

The library cells are characterized for different voltage drop peak values, which makes the CSM independent of the PG parasitics. As a result, the cell characterization is needed only for the first analysis, where the total run-time consists of cell characterization time and circuit simulation time. For each further PG analysis (different power network alternatives) only the circuit simulation is needed. The circuit simulation time represents in this case the total run-time. The reduction factor of the total run-time is 102, as shown in Table II.

B. Results at Chip Level

The voltage drop analysis at chip level consists of two steps. The analysis of the individual blocks and the PG simulation of a chip. Although all blocks in the chip are analyzed in parallel, the PG simulation can be carried out only after all blocks have been analyzed. Hence, the smaller the individual blocks, the earlier the PG simulation is performed.

The reduced netlist for each block is now connected to the global power grid using the coordinates of the cells. The voltage drop analysis at chip level is then performed using SPICE simulation. During this simulation the voltage drop is measured on each node in the PG. The worst voltage drop value as well as VDP time and VDP location are determined.

Table III presents the voltage drop analysis results of two testchips with different number of blocks. Different blocks are analyzed. The reduced netlists are connected to the RC extracted PG and are simulated using SPICE. The CSM provides a reduction of the total run-time by a factor of 17 for Testchip1 and a factor of 30 for Testchip2. Compared to the reference, the new model provides the same location of the worst voltage drop in the PG, with a VDP value error of less than 8 %.

	#Cells	#Blocks	CSM run-time		SPICE	VDP error (%)
			Blocks analysis	PG simulation		
Chip1	100k	4	4h	6h	7 days	7.45
Chip2	160k	10	3h	5h	10 days	7.85

Table III
VOLTAGE DROP RESULTS USING CORRECTION FACTORS

VII. CONCLUSION

In this paper, new voltage drop modeling techniques have been analyzed and their performance and accuracy on some industrial circuits designed in 90 nm technology have been discussed.

Based on the standard cell properties, a current source-based model (CSM) has been developed. This abstracted model represents the dynamic voltage drop behaviour of the cell and can efficiently handle single input switching as well as multiple input switching events. The library cells are precharacterized for each voltage in a given voltage range using the voltage controlled resistor in CSM with a predefined error tolerance of less than 1 %.

Using the abstracted CSM obtained at the cell level, voltage drop analysis at block level is performed. Each cell in the block, depending on its switching activity, is replaced by a CSM. Correction factors are used at the block level to improve the model in term of VDP value and VDP time.

In order to reduce the complexity of the analysis at chip level, the analyzed circuits have been partitioned into small blocks. These blocks are analyzed in parallel. Using the selective approach, only the voltage drop-critical cells are replaced with CSM. This method extremely reduces the netlist of the individual blocks and, thus, the whole netlist of the circuit.

The proposed voltage drop analysis techniques are compared to reference SPICE simulations at different abstraction levels. The new CSM techniques provide a VDP analysis-error of less than 1 %, 5 %, and 8 % at cell-, block-, and chip-level, respectively. A reduction of the total run-time by a factor of 18 compared to the reference is possible. However, the CSM total run-time consists of 60-80 % cell characterization time and 20-40 % PG simulation time. The library cells' characterization is needed only for the first PG analysis, as it is independent of the PG parasitics. For each further PG scenario, only the PG simulation is needed. The result is a reduction of the total run-time required by the CSM techniques by a factor of up to 200.

The advantage of the CSM model lies in its independency of the voltage variations in the supply networks, which makes an interactive 'what-if' analyses possible. The ability of the CSM model to handle the increasing size of the power networks gives it an excellent perspective as a viable alternative to traditional approaches. The model should be of a great help for the designers in analyzing different power network alternatives. Its effectiveness in finding out if resizing is needed or if decoupling capacitances should be placed is another important advantage.

REFERENCES

[1] F. Rouatbi, B. Haroun, and A. Al-Khalili, "Power estimation tool for sub-micron cmos vlsi circuit," *European Design Automation Conference*, pp. 204–209, 1992.

[2] D. Bountas, G. Stamoulis, and N. Evmorfopoulos, "A macro-model technique for vlsi dynamic simulation by mapping pre-characterized transitions," *International Conference on Computer Design*, pp. 450–456, 2008.

[3] N. Evmorfopoulos, D. Karampatzakis, and G. Stamoulis, "Precise identification of the worst-case voltage drop conditions in power grid verification," *International Conference on Computer-aided Design*, pp. 112–118, 2006.

[4] A. B. Kahng, B. Liu, and X. Xu, "Constructing current-based gate models based on existing timing library," *International Symposium on Quality Electronic Design*, pp. 37–42, 2006.

[5] H. Harizi, R. Haeußler, M. Olbrich, and E. Barke, "Efficient modeling techniques for dynamic voltage drop analysis," *Design Automation Conference*, pp. 706–711, June 2007.

[6] J. M. Daga and D. Auvergne, "A comprehensive delay macromodelling for submicron cmos logics," *IEEE Journal of Solid State Circuits*, vol. 34, no. 1, pp. 42–55, 1999.

[7] T. Pavlidis and S. L. Horwitz, "Segmentation of plane curves," *IEEE Trans. on Computers*, vol. 23, no. 8, pp. 860–870, 1974.

PERFORMANCE ANALYSIS OF FULL ADDER (FA) CELLS

Phuong Thi Yen, Noor Faizah Zainul Abidin, Azrul Bin Ghazali,
Center for Communication Service Convergence Technologies (CCSCT)
Department of Electronics and Communication, University Tenaga Nasional
Kajang, Selangor, Malaysia

***Abstract*- Since full adders play a vital role in electronics design, new ideas, investigations and study cases for constructing full-adders are required. This paper presents a comprehensive study of 24 different single-bit full adder (FA) topologies. All FA cells are designed using 0.18µm Silterra transistor models. Each FA cell is analyzed in terms of power and delay. The design and simulation of each FA cell are performed using Hspice simulator. The results of this paper are expected to assist designers to select the appropriate FA cell that meets their specific applications.**

I. INTRODUCTION

With the extremely fast development of Very Large Scale Integrated (VLSI) technology, demand for widespread use of high performance portable integrated circuit (IC) devices such as MP3, PDA, mobile phones is increasing rapidly. Most of the VLSI applications, such as digital signal processing, image and video processing and microprocessors, extensively use arithmetic operations. Therefore, the integrated circuit performances highly depend on how the arithmetic modules are implemented. Since addition between two binaries is the most fundamental operation in arithmetic logic unit, a full adder (FA) is the core element of complex arithmetic circuits like subtraction, multiplication, division, exponentiation, etc [1]. Consequently, enhancing performance of full adder is crucial to improve the performance of overall modules.

There are numerous research efforts of designing the best VLSI system with high speed, low power dissipation and compact implementation since they are the main factors which directly affect performance of an entire system. Therefore, various full adder cell topologies were designed and developed by electronics designers in order to achieve the best performances. However, currently, VLSI designers faces two conflicting design challenges: first is to discover high performance design and implementation techniques that can meet the stringent speed constraints; second is to consider low-power design approaches to prolong the operating time of devices [2]. Since power and speed are usually trade-off, it is necessary for the designer to consider and choose the best design which meets a specific requirement and application.

The full adder cell can be implemented in two types of logic structures, namely static style and dynamic style. Static full adders are commonly more reliable, simpler and lower power than dynamic ones. However, dynamic full adders are faster and sometimes more compact than static full adders. However, dynamic full adders suffer from charge sharing, high power due to high switching activity, clock load and complexity [4]. In this paper, only static style of full adder is presented due to its regularity of design.

Since the objective of the paper is to search for a high performance full adder, the most efficient method is to design from structural level. This approach requires the FA cell to be decomposed into smaller modules for further analysis and improvement. Then, an optimized full adder cell can be constructed by connecting these improved smaller modules [3]. The paper presents a comprehensive study that compares and examines the performance of currently used cells. Simulations and results of full adder performances are demonstrated and analyzed using Hspice.

The structure of the paper is organized as follows: Section II explores the full adder designs in different logic styles; Section III discusses the performance analysis and the results; Lastly, Section IV concludes the paper.

II. A SINGLE-BIT FULL ADDER AND ITS MODULES

A full adder has three inputs and two outputs. The single-bit full adder's functionality can be described directly as followings.

$$Sum = (A \oplus B) \oplus Cin = H \oplus Cin \quad (1)$$

$$Cout = A.B + Cin(A \oplus B) = A.\overline{H} \oplus Cin.H \quad (2)$$

where $H = A \oplus B$

A full adder cell can be implemented in many different logic structures due to different derivations from (1) and (2). However, in general, it is constituted by three main modules which are shown Fig. 1.

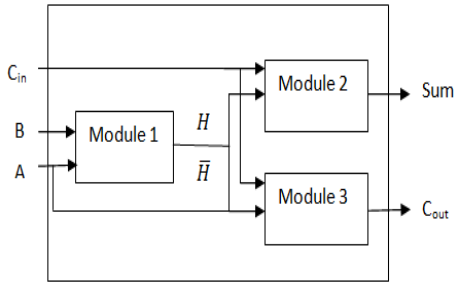


Fig. 1. 1-bit full adder building block

The first module is required to generate XOR or XNOR function, or both of them. The second module is to generate Sum and the last module is to produce C_{out}. The main requirement of the last two modules is to provide enough driving power to the following stage. In other words, the driving cell must provide almost full swing outputs to the driven cell. Otherwise, the performance of the circuit will be degraded dramatically or become non-operative at low supply voltage. Since the paper employs structural approach to design a high performance adder cell, it is necessary to study each module of a full adder thoroughly. Three main modules of a full adder are discussed in the next subsections.

A. Module 1: XOR/XNOR circuit

The XOR/XNOR module is an important function in an FA cell. Therefore, designing a good XOR/XNOR circuit plays a major role in creating an effective and efficient FA cell. Fig. 2 shows several designs of XOR and XNOR circuits.

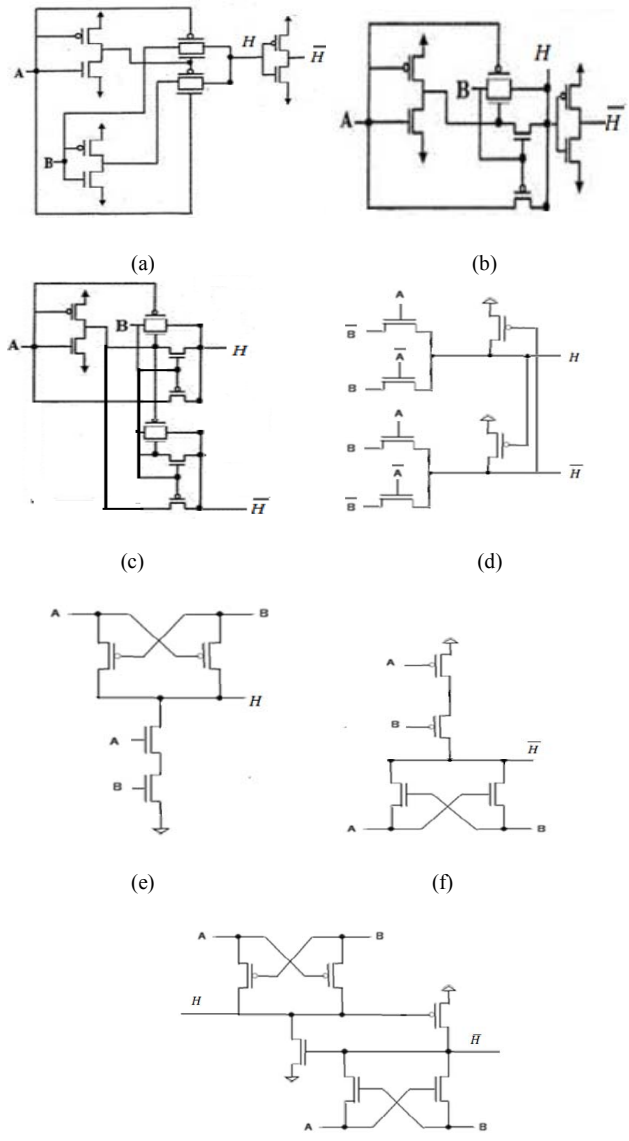


Fig. 2. Different XOR/XNOR circuits

Fig. 2(a), 2(b), 2(c) use transmission gates and inverters to generate XOR and XNOR circuits. The advantage of this type of circuits is the ability to produce full swing outputs. However, a large amount of power is consumed due to short circuit current between the power supply and ground from inverters. Fig. 2(d) employs Complementary Pass Transistor (CPL) to realize the first module. The XOR circuit shown contains a pMOS pull-up arrangement configured like a latch. It reduces the power consumption of the circuit but introduces the threshold voltage drop like any other pass transistor implementations. Fig. 2(e), 2(f) and 2(g) show another topology of XOR/XNOR circuit which is currently used in a full adder. This topology of pass transistor logic (PTL) not only improves the voltage drop problem but also consumes less power than previous designs.

B. Module 2: Sum circuit

From (1), Sum circuit can be realized by an XOR function or a multiplexer function. Fig. 3(a) shows an XOR function designed using PTL structure as introduced in previous subsection. Since pass transistor logic suffers from threshold voltage drop, it produces weak logic '0' and '1' for certain input combinations. Therefore, Sum circuits in Fig. 3(b), 3(c) and 3(d) combine transmission gate and pass transistor logic to take their advantages. Fig. 3(b) shows a 4-transistor Sum circuit which uses one transmission gate and two pass transistors to produce a XOR circuit. Its structure is based on multiplexer function derived from (1). By interchanging H and $\bar{H}$ in XOR circuit, the complement, XNOR circuit is created. Thus, the Sum circuit is also implemented by building a XNOR circuit with an inverter as in Fig. 3(c). Although it produces perfect output, the circuit consumes more static power due to the inverter and bigger transistor count.

By employing almost the same structure as 4-T Sum circuit, 5-T Sum circuit in Fig. 3(d) uses one extra nMOS to create two feedback nMOS transistors instead of one feedback nMOS in Sum circuit. The advantage of this structure is reduction in power dissipation since the two feedback nMOS transistors turn ON only when $H = C_{in} = 0$.

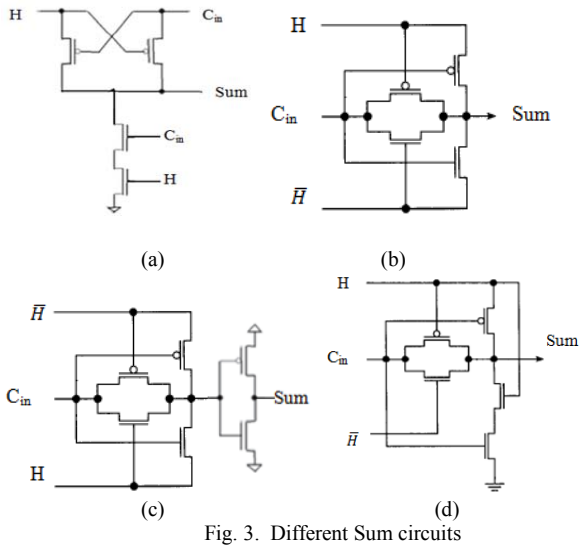


Fig. 3. Different Sum circuits

C. Module 3: C_{out} circuit

Four different designs of a C_{out} circuit are introduced in this paper. Fig. 4(a) uses transmission gate logic with four transistors. This structure produces perfect output C_{out} but consumes quite a large power due to its big transistor count.

The other three designs utilize the advantage of PTL by having lower power dissipation due to small transistor counts. Fig. 4(b) shows that only two transistors are needed to form a multiplexer C_{out} circuit. However, this structure suffers from threshold problem. Therefore, to achieve desirable output, a buffer is added. This results in higher power dissipation. Also, double-nMOS or double pMOS transistors can be employed to produce C_{out} circuit as in Fig. 4(c) and 4(d). Similarly, this structure may require buffer at the output, to achieve desirable outputs. However, double nMOS structure is preferred since it dissipates lower power and has a better speed compared to double-pMOS structure.

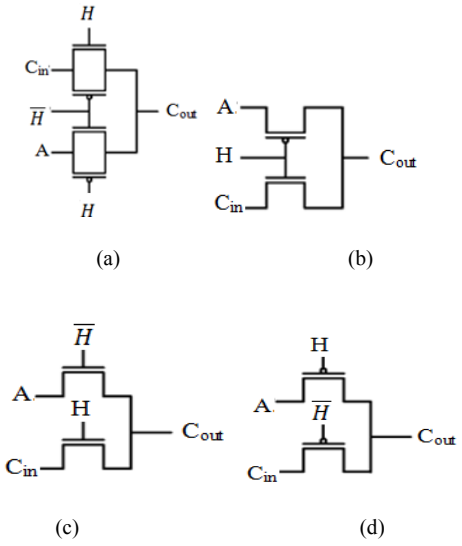


Fig. 4. Different C_{out} circuits

As shown in the previous subsections, each of the three modules in an FA cell can be designed using various topologies. Hence, a full adder can be built by assembling these three modules together. This paper introduces twenty four designs out of all structures that can be made from those modules for purpose of analysis and comparison.

III. PERFORMANCE ANALYSIS AND THE RESULTS

A. Simulation Environment

Twenty four different FA designs are simulated using Hspice simulator. All the cells are implemented using 0.18µm Silterra CMOS transistor models with power supply set to 1.8V. Three sets of frequencies were selected; 100 MHz, 250 MHz and 500 Mhz with 50% duty cycle. Propagation delay was measured from 50% of voltage level of input to 50% of voltage level of output.

Performances of full adder cells are evaluated in term of power and delay, where power is the total average power consumption of the circuit, which is calculated from the following equation:

$$P_{avg} = \frac{E}{T} = \frac{V_{DD}}{T}\int_0^T i_{DD}(t)dt \qquad (3)$$

where $i_{DD}(t)$ is the instant current drawn from power supply and T is period.

Also, it is assumed that the 'high' state is above 70% of the maximum value of voltage supply and the 'low' state is below 30%. The delay of a digital circuit is defined as the time it takes for a change in the input to produce a change in the output [1]. Three different delays are mentioned in a digital circuit: maximum, typical and minimum delay. In this paper, only maximum delay is mainly discussed. The maximum delay is associated with the longest path in the circuit. The maximum delay of a single-bit FA is measured by finding the longest delay of all the different combinations of inputs.

Another important parameter which should be considered when analyzing a FA performance is power-delay product (PDP) as in (4).

$$\text{PDP} = \text{Power (ave)} \times \text{Delay} \qquad (4)$$

Sizes of all transistors are set at L =0.18um and W_n = 1.4um while W_p of pMOS in MUX circuits are properly tuned to produce the lowest power and better output waveforms.

B. Results and Discussion

The simulation results for different full adders are tabulated in Table I. As can be seen, the power consumption of all FA cells increases as frequency increases. Table I shows that CCMOS, Cell 1- 4 and Cell 9-12 have larger dynamic power consumption than the rest of analyzed cells. The reason is that they employ transmission gates and inverters in XOR/XNOR module while the rest of the cells employ pass transistors which reduce large amount of power dissipation and transistor counts. As shown in Table I, Cell 21-23 dissipate a large amount of static power. It is due to the first module structure which is combination of 4-T XOR circuit and an inverter. The results from power consumption graph in Fig. 6 shows that the best cells which consume the least power are Cell 14 and Cell 16.

Since the delays at three different frequencies are almost equal, Table I shows the delay results at 250 MHz only. The delay graph in Fig. 7 shows that Cell 5 and Cell 6 have the least amount of delay among all of the cells whereas Cell 17 and Cell 19 have the largest delay value due to the buffer circuit at the C_{out} output.

As mentioned, power and delay are usually trades-off, which implies the fastest circuit is not always the most efficient power consumer. Therefore, PDP is introduced to evaluate the overall performance of a FA circuit. Fig. 8 indicates that Cell 5, Cell 14 and Cell 16 are the best cells with the lowest PDP values. As a result, it shows that the best FA cell utilizes the advantage of pass transistor logic and transmission gates.

TABLE 1
SIMULATION RESULTS OF 24 SINGLE-BIT FULL ADDERS

Cell name	Static Power(pW)	Dynamic Power (uW)			Delay(pS)	PDP (10^{-18} J)
		At 100 MHz	At 250 MHz	At 500 MHz	At 250 MHz	At 250 MHz
CCMOS	361.363	5.813	14.515	29.057	86.971	1262.384
CELL 1	249.733	8.360	20.889	41.641	83.555	1745.380
CELL 2	299.877	8.656	21.637	43.295	80.374	1739.052
CELL 3	372.973	11.556	28.888	57.872	74.672	2157.125
CELL 4	353.528	9.014	22.505	45.252	70.543	1587.570
CELL 5	238.390	2.746	6.854	13.730	8.452	57.932
CELL 6	311.486	5.594	13.984	28.121	8.674	121.301
CELL 7	379.453	4.000	10.004	20.004	78.531	785.624
CELL 8	360.008	2.201	7.076	14.147	75.300	532.845
CELL 9	299.871	7.022	17.550	35.114	85.843	1506.545
CELL 10	250.002	7.030	17.560	35.114	84.996	1492.530
CELL 11	545.498	17.466	27.539	39.510	123.570	3402.979
CELL 12	246.684	16.424	25.026	34.724	70.978	1776.269
CELL 13	188.513	1.485	3.710	7.423	100.100	371.328
CELL 14	187.354	0.201	0.522	1.075	60.839	31.752
CELL 15	138.636	1.291	3.227	6.455	98.222	316.969
CELL 16	137.476	0.101	0.273	0.573	60.913	16.625
CELL 17	250.003	5.292	10.832	19.115	272.070	2947.140
CELL 18	175.553	1.614	4.038	8.071	101.640	410.453
CELL 19	200.125	5.126	10.414	18.300	271.080	2823.092
CELL 20	125.675	1.430	3.575	7.234	96.810	346.120
CELL 21	22101.000	1.117	2.790	5.573	82.054	230.726
CELL 22	22051.000	0.799	1.990	3.975	83.685	168.417
CELL 23	22038.000	0.804	2.005	3.993	103.450	209.718

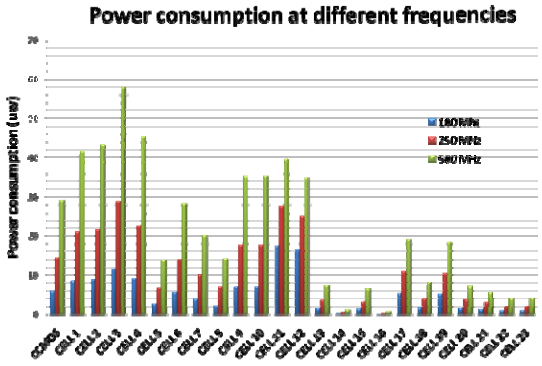


Fig. 6. Power consumption for twenty four different cells

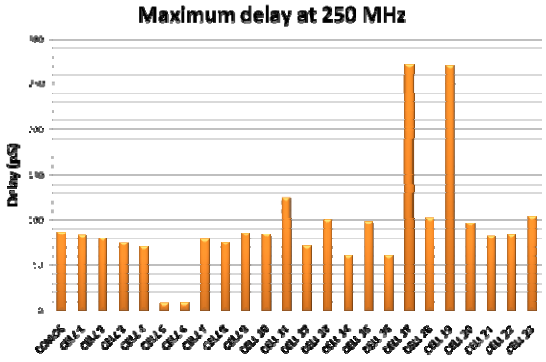


Fig. 7. Maximum delay for twenty four different cells

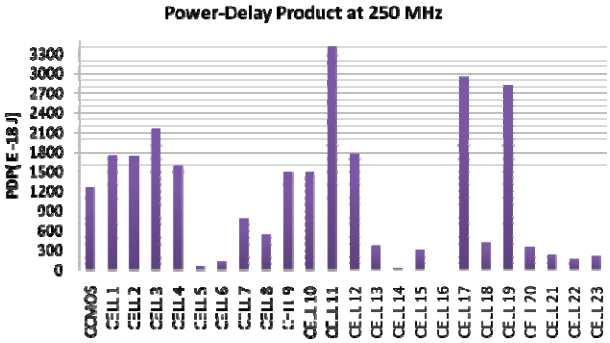


Fig. 8. PDP for twenty four different cells

IV. CONCLUSION

This paper presents a comprehensive study on single bit full adders. Twenty four different topologies of FA cells are implemented in 0.18µm Silterra technology and analyzed using Hspice simulator. From simulation results and analysis, a designer should utilize the advantage of different topologies in order to design the best FA cell, to meet a specific performance target. Also, beside factors directly affecting the performance of a FA such as power consumption, delay and PDP, load capacitance and driving capability should be taken into consideration when designing a FA.

V. ACKNOWLEDGEMENT

We would like to express our gratitude to Silterra Malaysia Sdn. Bhd. for allowing us to use their device models for our FA cell designs.

REFERENCES

[1] Chip Hong Chang, Jiangmin Gu, Mingyan Zhang, "A Review of 0.18um Full Adder Performances for Tree Structured Arithmetic Circuits", *IEEE Trans, VLSI systems*, Vol.13, No. 6, pp. 686-694, June, 2005.

[2] Arash Shoarinejad, Sue Ann Ung, Wael Badawy, "Low power single-bit full adder cells," *IEEE Xplore*, *Computer engineering,* Vol.28, No.1, January, 2003.

[3] Dan Wang, Wu Cheng, Xuguang Guan, Zhangming Zhu, Yintang Yang, "New low power full adder cells in 180nm CMOS technology", *IEEE Xplore, circuit and system*, pp. 430-433, 2009.

[4] M. Hosseinghadiry, H. Mohammadi, M. Nadisenejani, "Two new low power high performance full adders with minimum gates," *IEEE Trans, circuit and system*, pp. 124-130, 2009.

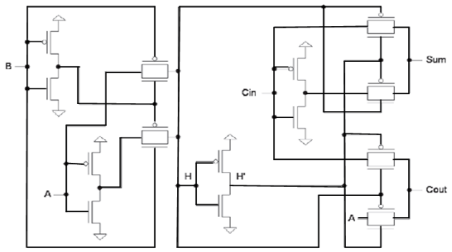
[5] Neil H.E Weste, David Harris, *CMOS VLSI design: A circuit and systems perspective*, third edition, Addison Wesley Longman, 2005.

[6] John P. Uyemura, *Introduction to VLSI circuits and systems*, Wiley, 2002.

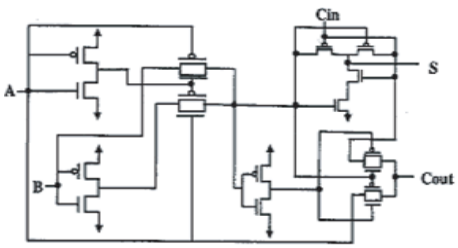
[7] Keivan Navi, Neda Khandel "The Design of a High-Performance Full Adder Cell by Combining Common Digital Gates and Majority Function," *European Journal of Scientific Research*, ISSN 1450-216X Vol.23 No.4, p626-638, 2008.

[8] Omid Kavehei, Mostafa Rahimi Azghadi, Keivan Navi, Amir-Pasha Mirbaha, "Design of Robust and High-Performance 1-Bit CMOS Full Adder for Nanometer Design," ISVLSI, *IEEE Computer Society Annual Symposium on VLSI*, pp.10-15, 2008.

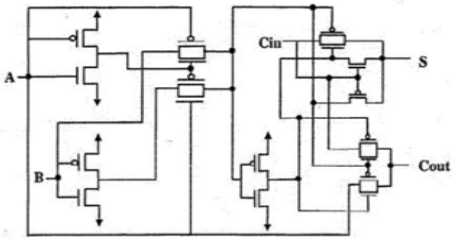
[9] Ahmed M. Shams, Tarek K. Darwish, Magdy A. Bayoumi, "Performance analysis of low -power 1-bit CMOS full adder cells", *IEEE Trans, VLSI systems*, Vol.10, No 1, pp. 20-27, February, 2002.



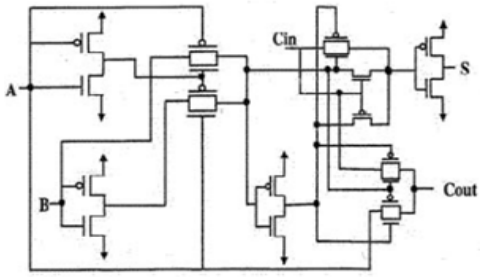
Conventional cell CCMOS



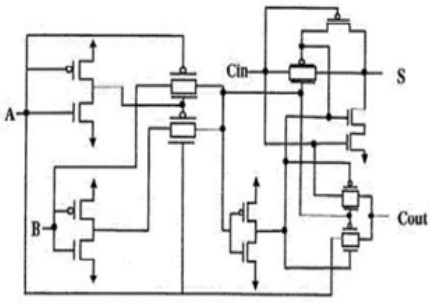
Cell 1



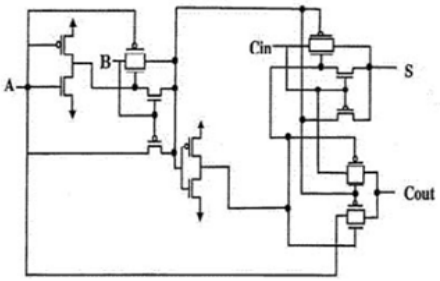
Cell 2



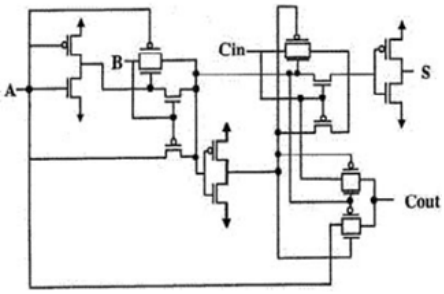
Cell 3



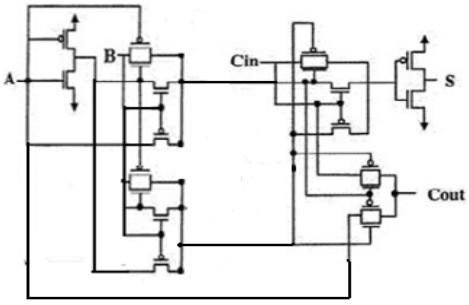
Cell 4



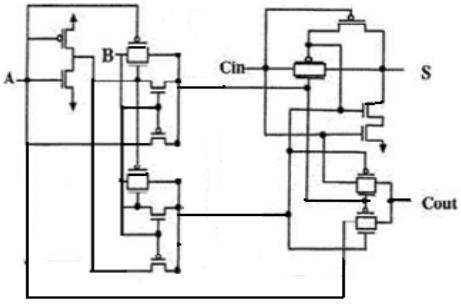
Cell 5



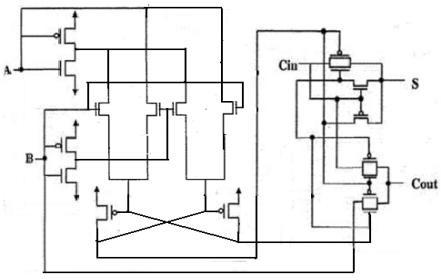
Cell 6



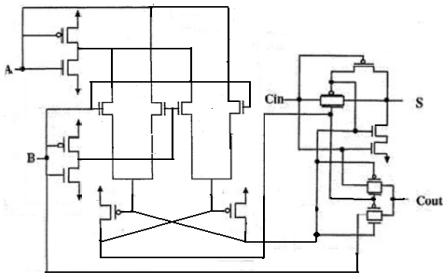
Cell 7



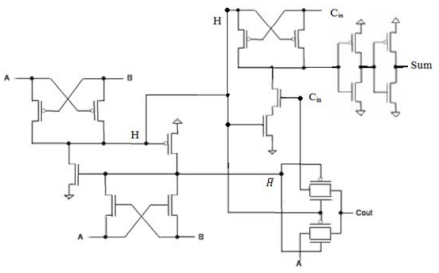
Cell 8



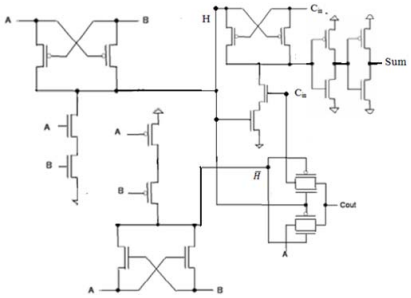
Cell 9



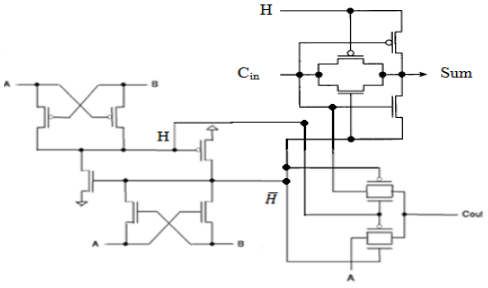
Cell 10



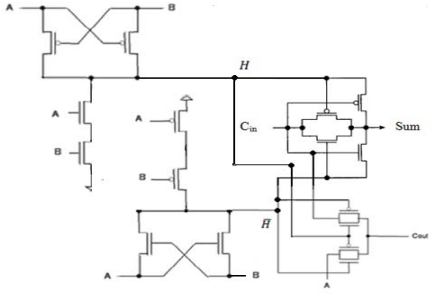
Cell 11



Cell 12



Cell 13



Cell 14

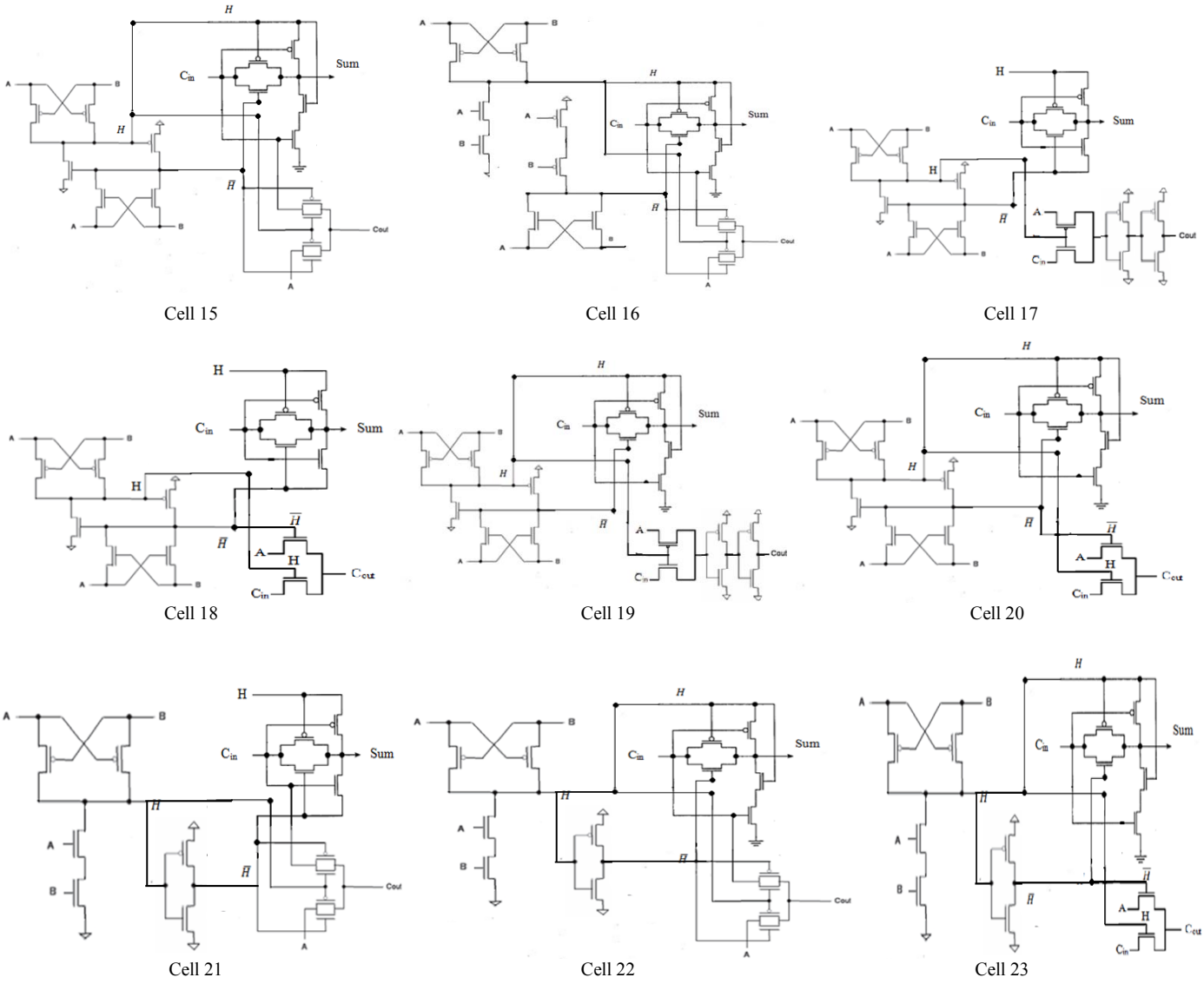


Fig. 5. Twenty four FA cells

Dynamic Candidate Keypad for Stroke-based Chinese Input Method on Touchscreen Devices

L.M. Po[1], C.K. Wong[1], C.W. Ting[1], K.H. Ng[1], K.M. Wong[1], C.H. Cheung[2], K.W. Cheung[1,3]

[1]Department of Electronic Engineering, City University of Hong Kong, Tat Chee Avenue, Kowloon, Hong Kong SAR, China
[2]Department of Information Systems, City University of Hong Kong, Tat Chee Avenue, Kowloon, Hong Kong SAR, China
[3]Department of Computer Science, Chu Hai College of Higher Education, N.T., Hong Kong SAR, China

***Abstract* - With the popularity of touchscreen devices, physical button-based keyboards are being replaced by finger-operated virtual keyboards. Entering text on these touchscreen devices is no longer limited by finger tapping activities on the keys. Text input can be performed by finger sliding over the virtual keyboard, which is well realized by the Swype technology on a typical QWERTY keyboard. Such shorthand gesturing for text input, however, may be inefficient when directly applied to Chinese input, especially in Chinese stroke-based input method. In this paper, a novel dynamic candidate keypad with use of unidirectional finger gesture on the stroke key for character selection is proposed for enhancing stroke-based Chinese input method. The new design can enhance frequently used Chinese characters searching and input using stroke-based input. The new method is implemented on the Android 2.2 platform for performance evaluation using Traditional Chinese characters set. Experimental results show that the proposed method enables users to input popular Chinese characters easier than conventional stroke-based input methods.**

Keywords: virtual keyboard, touchscreen, dynamic keypad, Chinese input method, stroke-based, gesture, handheld devices.

I. INTRODUCTION

One trend in smartphone is to replace physical keyboard with touchscreen finger-operated virtual keyboard [1-6], which is controlled by finger's gestures or tapping instead of key pressing. Recently, touchscreen-based smartphone users are rapidly increasing and on-screen virtual keyboard can also be found in tablet PCs, game consoles, kiosks, television, and remote controls. The revolutionary touchscreen device available in early 2010 is the Apple iPad with a 9.7-inch display. Companies such as Samsung, Dell, Motorola and HTC have also released various kinds of touchscreen devices, e.g. Samsung Galaxy Tab with 7-inch touchscreen; Dell Streak with 5-inch screen; Motorola and HTC continue to manufacture smartphones or tablet devices with screen sizes varied from 3.7 to 7 inches. Most of these companies see the finger-operated virtual keyboard as future text input interface for mobile devices.

Fig. 1 and 2 show typical touchscreen virtual QWERTY and Cangjie (倉頡) keyboards of smartphone, respectively. Due to the limited screen size of smartphones, however, key sizes of these virtual keyboards are relatively small as compared with our fingertips especially for the portrait (vertical) display mode. Users find it difficult to tap the correct key due to these small keys are placed very close together. This drawback significantly reduces the accuracy of the text input and results in many typos as well as requiring undo or corrective activities.



Fig. 1. A virtual QWERTY keyboard of an Android Smartphone.



Fig. 2. A virtual Cangjie (倉頡) keyboard for Traditional Chinese character input.



Fig. 3. An example of entering "chinese" by Swype.

Solutions that try to improve the input accuracy do exist. Localized zooming is an alterative method to tackle this problem, in which the keyboard's software increases the size of keys near the pointer to give a better visibility [7]. Shift technique [8] has also been proposed for selecting small targets with a finger. Another way to address the problem of key's size is to reduce the number of keys that are displayed [9, 10]. This leads to a multiple-page keyboard or to ambiguity due to more than one character assigned to each key. In short, these methods have not yet provided a complete solution.

Recently, Swype technology [11] was employed in some smartphones to improve the typing speed and accuracy of virtual keyboards. Besides tapping on an individual key, Swype allows users to input a word by sliding a finger from alphabet to alphabet and lifting only between words. There is a visual blue trail that marks the finger movement. Fig. 3 shows how the word "chinese' is entered by using Swype. It uses error correction

algorithms and a language model to predict the possible word intended to be input by the users. Thus, it does not matter if other keys are touched when sliding the inputting word, as the Swype dictionary will recognize the intended word. If more than one words are estimated, a popup box containing some suggested words will appear. The estimated maximum speed for entering English characters using Swype is up to 55 words per minute.

Similar to Swype, shorthand gesturing technique [12] can be applied to Chinese input methods such as Pinyin (拼音), Zhuyin (注音), Cangjie (倉頡), Wubi (五筆), and Stroke-based method (筆劃) [15]. The improvement, however, to the above conventional Chinese input methods may not be as effective as English input, particularly in stroke-based method. It is because the stroke-based Chinese input method has only five keys such that the virtual key size can be much larger than the alphabet keys of QWERTY keyboard. In addition, the character collision rate of stroke-based method is very high and it always needs to use the candidate window to select the intended character.

In this paper, a new dynamic candidate keypad (DCK) with the use of unidirectional finger gesture on the stroke key for character selection is proposed for enhancing stroke-based Chinese input method. The most likely Chinese characters are dynamically updated on every input of stroke key and eight unidirectional finger gestures are designed to directly select the intended character on the stroke key. The proposed method is implemented and evaluated on a HTC Desire smartphone running Android version 2.2.

This paper is organized as below. Section II gives a brief review of conventional Chinese input methods for touchscreen devices and particularly more details on stroke-based method. The proposed DCK for stroke-based Chinese input method is described in section III and performance evaluation of the proposed method is given in section IV. Finally, a conclusion is drawn in section V.

II. Touchscreen Chinese Input Methods

Chinese input on touchscreen devices is usually realized by handwriting recognition or virtual keyboard for Pinyin, Cangjie and stroke-based method. In handwriting recognition, the Chinese character is drawn on the touchscreen and the software tries to recognize the pattern and come up with a candidate list for selection. The input speed is slow as users are required to draw the Chinese characters stroke-by-stroke and some of the characters are very complex with many strokes. Pinyin is the pronunciation of a Chinese character in the form of Roman characters such that it can be implemented by virtual QWERTY keyboard on touchscreen devices as shown in Fig. 1. Cangjie is a radical-based input method while it also uses the Roman letter keys to map the pre-defined Chinese character's radicals and strokes. The virtual Cangjie keyboard is shown in Fig. 2 and it can achieve very high input speed for well-trained users using physical keyboard. However, the typing speed and accuracy of Pinyin and Cangjie are significantly reduced when using virtual keyboards on small touchscreen devices. This is because tapping small targets on these virtual keys is a difficult task.



Fig. 4. A virtual keypad for stroke-based Chinese input method.

On the other hand, stroke-based Chinese input method [15], that uses only 5 basic strokes to code Chinese characters, is very popular on mobile phones. It is because the stroke-based method conforms to the conventional writing practice (from top to bottom, and from left to right) providing easy and intuitive Chinese input. Those who know how to write Chinese should understand the 5 basic types of strokes and their writing order. Moreover, stroke-based input method also meets the stroke order specification that standardized and established by China's State Language Commission. The five basic stroke types are:

(1) Horizontal strokes [横]: 一
(2) Vertical strokes [豎] : 丨
(3) Left-falling strokes [撇]: 丿
(4) Right-falling strokes or Dot strokes [點, 捺]: 丶
(5) Turning strokes [折]: フ

Users simply type in the basic strokes of a character according to the writing order. For example, the strokes for typing the Chinese characters of "不" and "的" are as follows:

不 : 一丿丨丶
的 : 丿丨フ一一丿フ丶

A typical stroke-based Chinese input virtual keypad for touchscreen based mobile phones is shown in Fig. 4. Because of 5 strokes only, the virtual keypad can allow much larger keys than the alphabet-symbol keys in QWERTY keyboard. Thus, stroke-based Chinese input method can achieve relatively higher key tapping accuracy. Moreover, an important feature of stroke-based method implementation is the fast built-in intelligence. For each stroke input, the software will update the candidate window with the most likely Chinese characters for selection. In Fig. 4, for example, only the first two strokes of "一丿" are tapped, the most likely characters like "不,在,有,大,而,成,面,感,原,研" are listed for selection in the candidate window. These are frequently used Chinese characters and they can be predicted based on the first two strokes. By using a linguistic database, the software can ensure the most likely characters are always presented first (in leftmost position). Thus, the user can instantly select the desired character with a few strokes input for most frequently used characters. In this paper, a new stroke-based keypad with most likely characters dynamically updated around the stroke keys is proposed to further improve the searching and input speed of the

most frequently used Chinese characters. Moreover, the character selection is replaced by unidirectional finger gesture on the stroke keys instead of tapping on the character.

III. Dynamic Keypad for Stroke-based Chinese Character Input Method

National Language Committee of China for Chinese character frequency research indicates that the top 1000 Chinese characters can cover about 92% cases [12, 13]. The top 600 Chinese characters are normally sufficient for written communication. Recent results on mobile short message context indicate that top 600 can cover about 93% of all the used Chinese characters. That means if we can improve the stroke-based Chinese input method for searching and entering these Top 600 characters will significantly enhance the efficiency of stroke-based input method even for inexperience users.

3.1 Dynamic Stroke Keys with Candidate Characters

As mentioned in section II, the keys of the stroke-based Chinese input method can be quite large even on a 3-inch touchscreen. It is, therefore, possible to display the most likely characters in the padding space of the stroke keys, surrounding the stroke symbol as shown in Fig. 5. These eight candidate characters are the most likely characters based on the usage frequency and these characters start with the stroke of that key.

In order to make the candidate's priority listing to be consistent and understandable, the candidate characters are displayed from left-to-right and top-to-bottom manner, as shown in Fig. 6. The most likely character is displayed at upper-left corner of the key as indicated in position (1), and then second most likely character is displayed in position (2), etc. With this dynamic candidate stroke keys design, 40 frequently used characters can be displayed on the keypad without any code input. In Traditional Chinese character set, these 40 characters are all within the top 600 and top 1000 frequently used characters as shown in Table 1. That means these 40 characters are possible to input with one single touch of the virtual keypad.

If the users cannot find their intended character on the initial dynamic keypad, they can input the first stroke of the intended character. Then the dynamic keypad will be updated with new candidate characters on each stroke key as shown in Fig. 7, in which candidate characters of each stroke key are updated after entering the first stroke of "—". Theoretically, it can display another 200 frequently used characters on this dynamic keypad after one stroke input as there are five types of stroke and each stroke with 40 candidates (5x40=200). Due to some of the characters being repeated in the first 40 characters in the initial keypad, the total number of distinct characters can be displayed, is a little bit lower than 200. Based on the Traditional Chinese character set, 193 distinct characters including the first 40 characters can be displayed on the dynamic keypad with one or no stroke key input as shown in Table 1. Within these 193 characters, there are 171 and 181 characters belonging to top 600 and top 1000 frequently used Chinese characters, respectively. They also represent 28.5% and 18.1% of top 600, and top 1000 characters, respectively. Users can continue to enter strokes for



Fig. 5: The proposed dynamic keypad with eight most likely characters displaying around the stroke keys.

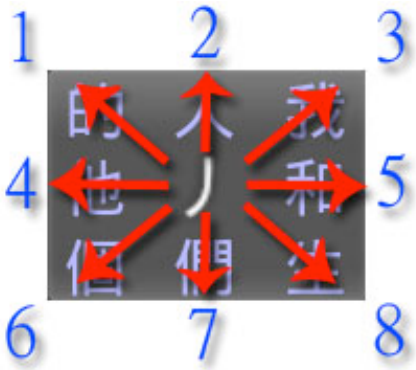


Fig. 6: The candidate characters displaying positions and the eight unidirectional gestures for the "丿" stroke key.

Traditional Chinese Character Set			
Number of Stroke keys input	Distinct Characters	Characters in Top 600 (covered %)	Characters in Top 1000 (covered %)
Initial keypad	40	40 (6.7%)	40 (4%)
After 1 key Input	193	171 (28.5%)	181 (18.1%)
After 2 keys Input	740	372 (62%)	474 (47.4%)
After 3 keys Input	2593	547 (91.2%)	832 (83.2%)

Table 1: The number of distinct Chinese characters can be displayed on the dynamic candidate keypad against number of keys input.

searching the intended character. Fig. 8 shows the dynamic keypad after entering two strokes of "—丿". Table 1 also shows the number of distinct characters that can be displayed after inputting 2 and 3 strokes. From these results, we can find that 2,593 distinct characters will be displayed using this dynamic keypad design with input no more than 3 keys. Moreover, 547 and 832 frequently used characters of top 600 and top 1000 are covered. That represents 91.2% and 83.2% of the top 600 and top 1000 characters can be searched with no more than 3 keys input using the proposed dynamic stroke keys design. This feature can significantly enhance the efficiency of stroke-based input method, especially for inexperience users.

3.2 Character Selection by Unidirectional Finger Gesture

To improve the input speed of these frequently used characters on the new dynamic candidate keypad and make use of the touchscreen feature, unidirectional finger gesture is proposed to directly select the intended character on the stroke key. That means the candidate characters can be directly entered from one of the eight unidirectional gestures on the stroke key as shown in Fig. 6. For example, to enter the most popular Chinese character "的", we can just slide toward the upper-left corner of the "丿" stroke key. This unidirectional finger gesture on the relatively large stroke keys is indeed much faster than tapping on the intended character from the candidates listed. In addition, these sliding gestures on the stroke keys are especially handy for entering text with thumb fingers. It is because people are most likely to use the thumbs to input Chinese characters due to their way on holding the smartphones.

As shown in Fig. 5, for example, sliding our finger vertically upward on the "一" key can directly enter the "不" character. For entering the "雲" character, we just need one tap on the "一" key and then a horizontal right gesture on the "丶" key as shown in Fig. 7. With experience, the user does not have to look at the dynamic keys, because the candidates are presented in a consistent location of the stroke keys and the selection of choice depends on direction only. An experienced user can soon get used to the candidate's direction as a part of the shorthand for that character. In addition, this design does not affect the normal stroke-based input style. User can still use the conventional stroke-based input method for entering some of non-frequently used characters.

IV. Performance Evaluation

To measure the impact of Dynamic Candidate Keypad (DCK) on improving stroke-based Chinese input method, user performance data with and without DCK was collected using G6 stroke-based Chinese input method [14]. The details of the evaluation are described in the following subsections.

4.1. Participants

Ten participants of ages from 22 to 30 were recruited. Nine are male and one is female. All participants were native speakers of Chinese (Cantonese). Nine are right-handed and one is left-handed. All participants were experienced users of touchscreen smartphones. Four participants, called Group1, are inexperienced users of conventional stroke-based Chinese input methods. Four participants, called Group2, were experienced users of T9, which are the stroke-based Chinese input method widely implemented in 12-key mobile phones in Hong Kong. In order to measure the trends in performance, two participants, called Group3, were experienced users of T9 and were given the proposed DCK before the experiment, which allows them to have a couple hours of experience on it.

4.2. Apparatus

As mentioned before, the proposed DCK was evaluated using G6 stroke-based Chinese input method [14]. G6 encodes a Chinese character with at most six strokes using the conventional 5 basic stroke types of horizontal (一), vertical (丨), left-falling (丿), right-falling or dot (丶) and turning (乛). The G6 coding rule is

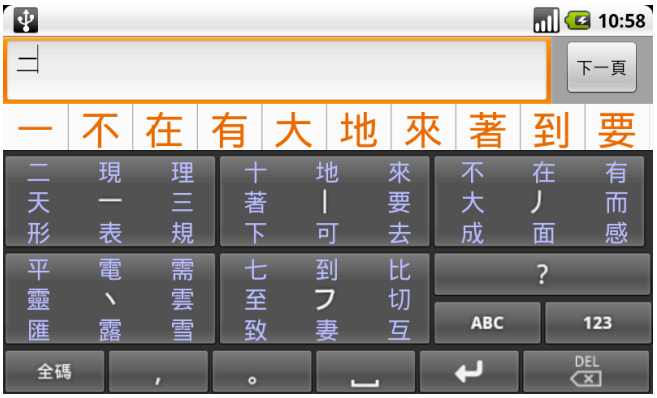


Fig. 7: The character candidates list of each stroke key is updated after tapping one stroke of "一".

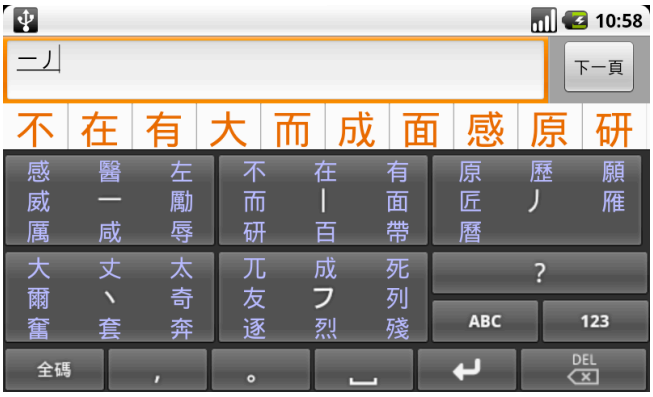


Fig. 8: The character candidates list of each stroke key is updated after tapping two strokes of "一丿".

very simple that it is based on the (3+3) rule by using the first 3 strokes and the last 3 strokes. Two G6 stroke-based Chinese input methods using conventional keypad depicted in Fig. 4 and DCK depicted in Fig. 5 were implemented on HTC Desire smartphone with 3.7-inch touchscreen and running Android 2.2 OS for user testing. These two input methods were developed with Eclipse IDE for Java EE (JEE) Developers, Java SDK 6 and Android SDK 2.2 on Windows XP.

4.3. Procedures

The participants were given instructions for entering two paragraphs of text, which were randomly selected in the newspaper. One of the paragraphs contains 41 Chinese characters and the other one contains 45 Chinese characters. Half of the participants use G6 with and without DCK to enter first paragraph, respectively, and then enter the second paragraph using G6 with and without DCK, respectively. Another half of the participants would be on the contrary order.

Participants were instructed to input the text, excluding punctuations, as quickly and accurately as possible. Correction was allowed only using the backspace, no other navigation on the typed text was allowed. Associated character function was not allowed to be used during the test. The participants can hold the mobile phone and input texts with their own comfortable positions. During experiment, participants were seated in a quiet

room to minimize distractions. Three kinds of the data would be analyzed. They are Key Strokes Per Character (KSPC) [15], including delete key and extra strokes due to errors, Error Rate, including wrong stroke identification, wrong character selection and other errors, and the Character Per Minute (CPM). These parameters are computed as follows:

$$KSPC = \frac{C+IC+F}{N} \quad (1)$$

$$Error\ Rate = \frac{E}{N} \quad (2)$$

$$CPM = \frac{N}{T} \quad (3)$$

where ***C*** is the correct keystrokes, ***IC*** represents the incorrect keystrokes, ***F*** is the keystrokes to fix errors, ***N*** is the total number of characters, ***E*** is the total number of errors and ***T*** is the total time.

4.4. Results

The KSPC, Error Rate and CPM for analyzing the impact of the proposed DCK are shown in Fig. 9, Fig. 10 and Fig. 11, respectively. These results indicated that Group3, the experienced DCK users, had improvement on all of the tests, which are 14.7% on KSPC, 61.3% on Error Rate and 19.3% on CPM. DCK method also reduced the 15% of Error rate for the Group1, which are the inexperienced users of stroke-based Chinese input methods. However, the experienced T9 users cannot be benefited with the DCK method, because they have already been used to the traditional stroke-based Chinese input methods and the custom cannot be changed at once.

4.5. Future Work

The above experimental result is encouraging. The DCK approach will be implemented to other developing input methods and which will be tested by more participants in order to reveal the full benefit of adopting proposed DCK.

V. Conclusion

A novel dynamic candidate keypad (DCK) with use of unidirectional finger gesture on the stroke key for character selection is proposed for enhancing stroke-based Chinese input method. The proposed DCK can display 547 frequently used Chinese characters of top 600 characters with no more than 3 keys tapped. This feature can significantly enhance the efficiency of stroke-based input method, especially for inexperience users. User performance data also shows that experienced DCK users can achieve 14.7% on KSPC, 61.3% on Error Rate and 19.3% on CPM. The new input methods can be applied across a variety of devices such as phones, tablets, game consoles, kiosks, televisions, virtual screens and more.

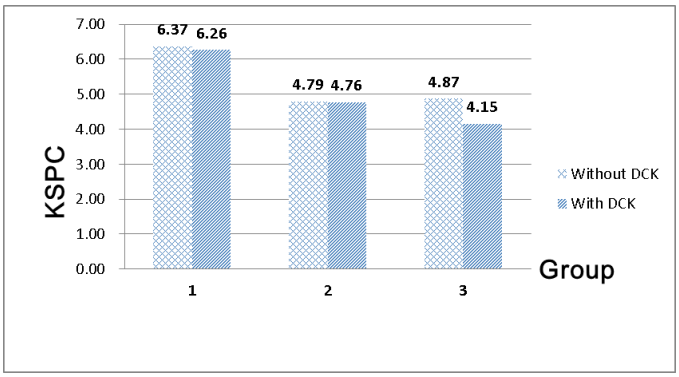


Fig. 9: KSPC of the 3 groups.

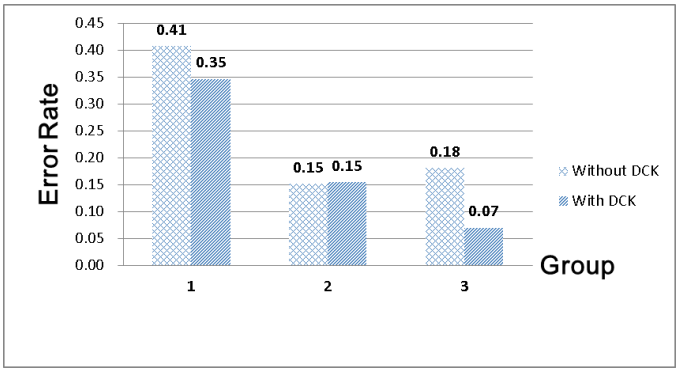


Fig. 10: Error Rate of the 3 groups.

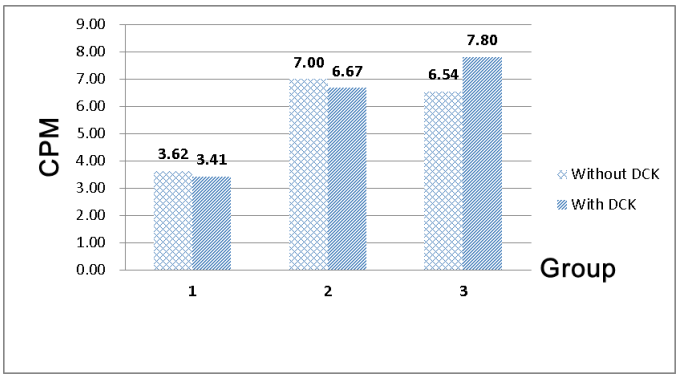


Fig. 11: CPM of the 3 groups.

References

[1] B. Martin, P. Isokoski, F. Jayet, T. Schang, "Performance of finger-operated soft keyboard with and without offset zoom on the pressed key," Proceedings of the 6th International Conference on Mobile Technology, Application & Systems, Nice, France, 2009.

[2] J. Goodman, G. Venolia, K. Steury, C. Parker, "Language modeling for soft keyboards," Proceedings of the 7th international conference on Intelligent user interfaces, January 13-16, 2002, San Francisco, California, USA.

[3] P. Isokoski, "Performance of menu-augmented soft keyboards," Proceedings of the SIGCHI conference on Human factors in computing systems, p.423-430, April 24-29, 2004, Vienna, Austria.

[4] I. S. MacKenzie, S. X. Zhang, and R. W. Soukoreff, "Text entry using soft keyboards," Behaviour & Information Technology, 18, 235--244, 1999.

[5] Edgar Matias , I. Scott MacKenzie , William Buxton, "One-handed touch typing on a QWERTY keyboard," Human-Computer Interaction, v.11 n.1, p.1-27, March 1996.

[6] Pekka Parhi , Amy K. Karlson , Benjamin B. Bederson, "Target size study for one-handed thumb use on small touchscreen devices," Proceedings of the 8th conference on Human-

computer interaction with mobile devices and services, September 12-15, 2006, Helsinki, Finland.
[7] Resco Keyboard Pro for Windows Mobile, Accessed 5 Jan 2011, http://www.resco.net/pocketpc/keyboard/
[8] Vogel, D., and Baudisch, P., "Shift: a technique for operating pen-based interfaces using touch," In Proc. of. CHI 07, 657-666, 2007.
[9] Matias, E., MacKenzie, I., S., and Buxton, W., "One-Handed Touch-Typing on a QWERTY Keyboard," In Human- Computer Interaction, Vol. 11, No. 1, 1-27, 1996.
[10] MacKenzie, I. S., and Soukoreff, R. W., "Text entry for mobile computing: Models and methods, theory and practice," In Human-Computer Interaction, Vol. 17, 147-198, 2002.
[11] Katie Boehret, WaltMossberg'sArchive, "Virtual Keyboard Makes Smudges a Must," Accessed 5 Jan 2011, http://solution.allthingsd.com/20100810/swype-virtual-keyboard-review/
[12] S. Zhai and P.-O. Kristenssion, "Shorthand Writing on Stylus Keyboard," *CHI 2003,* April 5–10, 2003, Ft. Lauderdale, Florida, USA
[13] Q Yan, "The Birth of Mobile Chinese Keypad & Hybrid Input Methods," CHK 2009, Design Community Vignettes, April 4-9, 2009. Boston, MA, USA.
[14] L. M. Po, C. K. Wong, Y. K. Au, K. H. Ng and K. M. Wong, "Six-digit Stroke-based Chinese Input Method," 2009 International Conference on Systems, Man, and Cybernetics, San Antonio, Texas, USA, October, 2009.
[15] I. Scott MacKenzie, "KSPC (Keystrokes per Character) as a Characteristic of Text Entry Techniques", Proceedings of the Fourth International Symposium on Human Computer Interaction with Mobile Devices, 2002, pp. 195-210, Springer-Verlag.

A MAC Approach for Dynamic Power Control in Wireless Sensor Network

Buddha Singh
Sch. of Comp. & System Sciences
Jawaharlal Nehru University
New Delhi, India
e-mail: b.singh.jnu@gmail.com

D. K. Lobiyal
Sch. of Comp. & System Sciences
Jawaharlal Nehru University
New Delhi, India
e-mail: lobiyal@gmail.com

Abstract- **To design energy efficient Medium Access Control (MAC) protocol for maximizing the network lifetime in Wireless Sensor Network (WSN), is evolving as a challenging portal in research area. The overall radio energy inherently depends on network workload as well as the radio characteristics. Therefore, we have proposed a Dynamic Power Control MAC (DPCMAC) protocol which supports variable power level transmission of packets according to data rate of sources. Our novel approach minimizes the aggregate energy consumption in all power states according to the network traffic. Moreover in our protocol, we calculate the desired power level for the transmission of packets for two types of scenarios: low and high network workload. The protocol is simulated for the variable size of networks and its performance is analyzed on the basis of success rate and energy consumption. The simulation results show that our protocol outperforms the existing Sensor MAC (SMAC) protocol.**

Keywords- Power controlled multiple access; Basic power control protocol; Sensor MAC (SMAC) protocol; Dynamic power control MAC (DPCMAC) protocol.

I. INTRODUCTION

The Wireless Sensor Network (WSN) consists of three components: the sensing component, which senses the environment; the processing component, which performs local computations on the gathered (sensed) data; and the communication component which is responsible for message exchange with neighboring sensor nodes (nodes) through the wireless channel. The networking is fault-tolerant as many nodes sense the same events. There are various specialized Medium Access Control (MAC) protocols that are developed or modified to suit sensors networks for the major operations of data dissemination and gathering. WSNs have scarce resources, such as - restricted processing power, lack of memory and limited energy, because the sensor nodes are battery operated devices. Therefore, it gives rise to many challenges of designing protocols at different layers of OSI model for communication among the nodes in the sensor networks. The WSNs are regarded as special kinds of Ad Hoc networks. However it differs in several ways. In the sensor network, energy efficiency is one of the most important attribute. In WSN, sensor nodes are deployed in harsh environment conditions without human intervention. Therefore, it is very difficult to replace or recharge batteries for these nodes.

To model an energy efficient MAC layer, is thus evolving as a major issue in sensor network for prolonging the network lifetime. Moreover, the radio activities consume more energy and are directly controlled by the MAC layer. Therefore, at the MAC layer, power control becomes one of the major issues to be addressed. The transmission power of nodes needs to be regulated as it should be high enough to reach the intended receiver, however causing minimal interference to other nodes.

The MAC layer directly controls radio activities, and its energy savings significantly affect the overall node lifetime. Gomez and Campbell [1-2] analyzed the benefits of transmission power control in the wireless multi-hop networks. The authors showed that per-link range adjustments outperform global range transmission adjustments by 50%. Thus, instead of globally defining a uniform transmission range that keeps the network connected, wireless networks should adjust transmission ranges on each link. The power control problem in sensor networks is that of choosing the transmit power for each packet in a distributed fashion at each node [3]. The problem is complex since the choice of the power level fundamentally affects many aspects of the operation of the network. Transmission power control is the key attribute and plays vital role in wireless sensor networks. Several MAC protocols employing this technique have been proposed. PCMA (Power Controlled Multiple Access) [4]. Therefore, it is clarified that a WSN should reduce the energy consumed in each of the power states (i.e., transmission, reception, and idle) of radio in order to minimize its energy consumption. This requires a sensor network to effectively apply all of the afore-mentioned approaches. As we will show in this article, however, the correlations between the different approaches are dependent on the network load and hence cannot be combined in a straightforward fashion. For example, when network workload is low, the energy consumption of a WSN is dominated by the idle state. In such a case, scheduling nodes to sleep saves the most energy. It is therefore more energy efficient for active nodes to use long communication

ranges, since this will require fewer nodes to remain awake in order to relay packets. Conversely, short radio ranges may be preferable when the network workload is high, as the radio tends to spend more time in the transmission and reception states. is one such protocol, which provides communication at minimum propagation ranges, allowing spatial reuse. The transmission power control techniques developed for adhoc networks do not apply to sensor networks. Since the calculation performed is complex & imprecise in transceivers employed in the network, currently few MAC protocols implement the transmission power control [7-9].

Some existing MAC protocols, like- Sensor MAC (SMAC) and Power controlled Sensor MAC (PSMAC) protocol has been designed for static environment as well as not minimizing radio energy according to network workload. Therefore, in this article, we propose Dynamic Power Control MAC (DPCMAC) protocol for mobile environment. We show through analysis that the network configuration that minimizes the total radio energy depends on network workload as well as radio characteristics of nodes. To evaluating its performance in mobile environment with consideration data rate of sources with that in static environment only. We propose to make certain changes in the existing MAC protocols. Nodes with a high mobility, or sensor nodes around a highly mobile sensor, look for additional schedules much more frequently and adopt schedules with a lower latency. A second improvement is in static duty cycle of SMAC and PSMAC protocol. Sensor nodes may not change their duty cycle based on network workload or density conditions, and thus can consume more energy than required. This results in the limitation of performance of the protocol.

In sensor networks must create a network infrastructure to establish communication links among the thousands of randomly scattered sensors. It must also ensure fair and efficient sharing of communication resources among the nodes, so that the overall lifetime of the network can be maximized.

II. Related Work

A. Basic Power Control Protocol

In basic power control scheme, to save battery power the *Request-To-Send* and *Clear-To-Send* (RTS-CTS) packets uses normal (maximal) power level, while DATA-ACK uses the minimal needed power level. When the receiver node B receives an RTS packet, it responds with a CTS packet at the usual maximum power level P_{max}. When source node receives this CTS packet, it calculates $P_{desired}$ based on the received power level P_r and transmitted power level P_t^{max} as following:

$$P_{desired} = \frac{P_t^{max}}{P_r} R_r^{th} C \qquad (1)$$

where R_r^{th} is the minimum necessary received signal strength and C is constant. The source node uses power level $P_{desired}$ mentioned in (1) to transmit the DATA packet. Similarly, the receiver uses the signal power of received RTS packet for the reception of packets, as shown in Fig. 1. The receiver makes use of the $P_{desired}$ power level for sending the ACK packet.

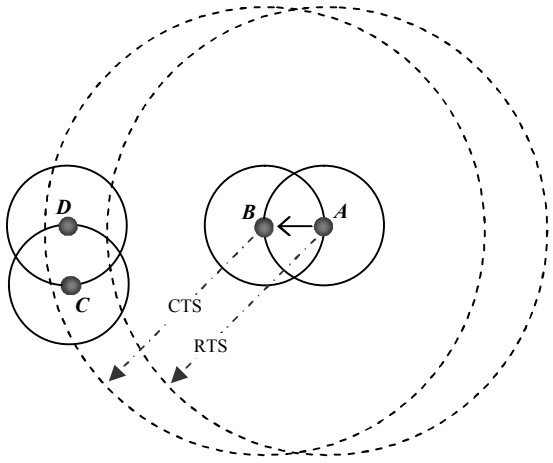


Fig. 1. Packet transmissions in the basic power control scheme

B. Sensor MAC Protocol (SMAC)

SMAC [5] protocol is a MAC protocol designed for sensor networks. WSNs use battery-operated computing and sensing devices, so reducing energy consumption is the primary goal in SMAC protocol. SMAC uses a few novel techniques to reduce energy consumption and support self-configuration. It enables low-duty-cycle operation in a multi-hop network. Nodes form virtual clusters based on common sleep schedules to reduce control overhead and enable traffic-adaptive wakeup. SMAC makes use of in-channel signaling to avoid overhearing unnecessary traffic. Moreover, SMAC applies message passing to reduce the contention latency for applications that require network data processing. The primary mechanisms for SMAC protocol adopts as follows [6]:

1) Periodic Listen and Sleep: In many sensor network applications, nodes are idle for long time if no sensing event happens. Given the fact that the data rate is very low during this period, it is not necessary to keep nodes listening all the time. SMAC reduces the listen time by putting nodes into periodic sleep state. The basic scheme is that each node sleeps for some time, and then wakes up and listens to see if any other node wants to talk to it. During sleeping, the node turns off its radio, and sets a timer to awake it later. All nodes are free to choose their own listen/sleep schedules. However, to reduce control overhead, it prefers neighboring nodes to synchronize together. Nodes exchange their schedules by periodically broadcasting a SYNC packet to their immediate neighbors.

2) Collision Avoidance: If multiple neighbors want to talk to a node at the same time, they will try to send when the node starts listening. In this case, they need to contend for the medium. SMAC adopts virtual and physical carrier sense, and the RTS/CTS exchange for the hidden terminal problem. All senders perform carrier sense before initiating

a transmission. If a node fails to get the medium, it goes to sleep and wakes up when the receiver is free and listening again. Broadcast packets are sent without using RTS/CTS. Unicast packets follow the sequence of RTS/CTS/ DATA/ACK between the sender and the receiver. After the successful exchange of RTS and CTS, the two nodes will use their normal sleep time for data packet transmission. They do not follow their sleep schedules until they finish the transmission.

3) Adaptive Listening: The scheme of periodic listen and sleep is able to significantly reduce the time spent on idle listening when traffic load is light. However, when a sensing event indeed happens, it is desirable that the sensing data can be passed through the network without too much delay. SMAC proposes an important technique, called adaptive listen, to improve the latency caused by the periodic sleep of each node in a multi-hop network. The basic idea is to let the node who overhears its neighbor's transmissions (ideally only RTS or CTS) wake up for a short period of time at the end of the transmission. In this way, if the node is the next-hop node, its neighbor is able to immediately pass the data to it instead of waiting for its scheduled listen time. If the node does not receive anything during the adaptive listening, it will go back to sleep until its next scheduled listen time.

4) Overhearing Avoidance: SMAC tries to avoid overhearing by letting interfering nodes go to sleep after they hear an RTS or CTS packet. Since DATA packets are normally much longer than control packets, the approach prevents neighboring nodes from overhearing long DATA packets and following ACKs.

5) Message Passing: A message is the collection of meaningful, interrelated units of data. The receiver usually needs to obtain all the data units before it can perform in-network data processing or aggregation. The disadvantages of transmission a long message as a single packet is the high cost of re-transmitting the long packet if only a few bits have been corrupted in the first transmission. However, if we fragment the long message into many independent small packets, we have to pay the penalty of large control overhead and longer delay. The reason is that the RTS and CTS packets are used in contention for each independent packet. SMAC fragments the long message into many small fragments, and transmit them in a burst. Only one RTS and one CTS are used. They reserve the medium for transmitting all the fragments. Every time a data fragment is transmitted, the sender waits for an ACK from the receiver. If it fails to receive the ACK, it will extend the reserved transmission time for one more fragment, and retransmit the current fragment immediately.

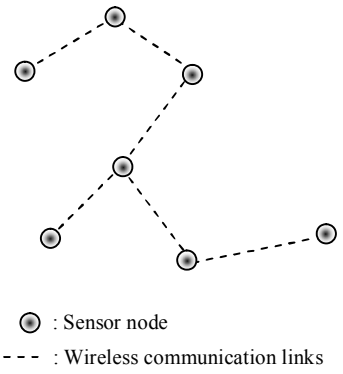


Fig. 2. Random deployment of sensor nodes leading to the formation of wireless sensor network

III. Dynamic Power Control Algorithm for MAC (DPCMAC) Protocol

In static sensor networks, we assume that the transmission power used during communication is almost equal for all the sensor nodes. The main idea of the proposed algorithm is to send RTS, CTS, DATA, and ACK frames with appropriate transmission power levels, instead of the fixed power level. The illustration of our proposed DPCMAC protocol is given in the following section.

First, we show through analysis that the minimum power configuration of a network is inherently dependent on the data rates of sources in the network. Second, we provide a new problem formulation that models the energy conservation problem. Our formulation further considers the overall energy consumption from all power states of the radio according to the network workload. The sensor network is formed by the random deployment of sensor nodes over the sensing region (Fig. 2).

We assess the ideal transmission power for the communication between sender and receiver nodes in the synchronization period for both high and low network workload scenarios. Moreover, the overhead of assessing ideal transmission power in synchronization period is very small. The average power consumption is further computed for both the type network workloads. A weightage factor (or channel utilization ratio) β , is used in the formulation of average power consumption. It is defined as:

$$\beta = \left(\frac{R}{B} \right) \tag{2}$$

where, R denotes the data rate and B refers to the bandwidth of the sensor network. In the low network workload (Fig. 3), most of the sensors remain in idle state as data transmission becomes a rare event. Therefore, major energy is consumed by the idle sensors. Our strategy during low traffic increases the transmission power level to use direct links rather than a number of smaller hops. The average power consumption in such situation is given by $P_{direct\text{-}hop}$ and is computed in (3):

$$P_{direct-hop} = \left(\beta \times P_{t(|AB|)}\right) + \left(\beta \times P_r\right) + \left[2 \times (1-\beta) \times P_{id}\right] + P_s \tag{3}$$

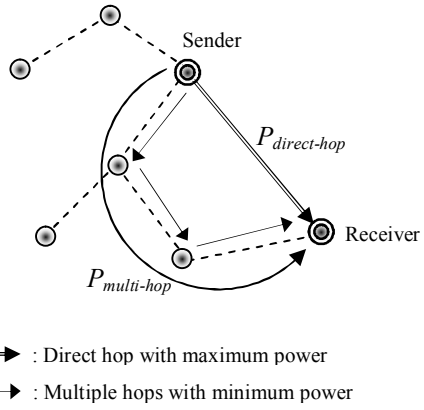


Fig. 3. Using maximum power for direct hop (low network workload) and using minimum power for multiple hops (high network workload)

where, $P_{t(|.|)}$, P_r , P_{id} , P_s denotes the power required in the transmission (along a path), reception, idle and sleep states respectively.

However, the network workload increases (Fig. 3) when the data rate of the sensor network is very high, i.e. the packet transmission among the sensor nodes is quite frequent and most of the nodes remain in the active state. In such case, energy exhaustion occurs mainly because of sensor communication. Therefore, to balance the power usage, we propose to use multiple hops which in turn will require less transmission power. The average power consumption for high network workload is represented by $P_{multi\text{-}hop}$ and is calculated as following in (4):

$$P_{multi-hop} = \beta \times \left[\left(P_{t(|AC|)} + P_{t(|CD|)} + P_{t(|DB|)}\right)\right] + \left(3\beta \times P_r\right) + \left[3 \times (1-\beta) + (1-3\beta)\right] \cdot P_{id} + P_s$$

$$P_{multi-hop} = \beta \times \left[\left(P_{t(|AC|)} + P_{t(|CD|)} + P_{t(|DB|)}\right)\right] + \left(3\beta \times P_r\right) + \left[2 \times (2-3\beta) \times P_{id}\right] + P_s \quad (4)$$

A. Transmission Power in DPCMAC for Low Network Workload

In low network workload, the energy consumption of a WSN is dominated by the idle state. In such a case, scheduling nodes to sleep saves the most energy. It is therefore more energy efficient for active nodes to use long communication ranges (with maximum transmission power), since this will require fewer nodes to remain awake in order to relay packets.

The power received by a destination node which is separated from a sender node by a distance d is given by:

$$P_r = P_t \frac{G_t G_r \lambda^2}{L (4\pi)^2 d^n} \quad (5)$$

where λ is the carrier wavelength, n is the path loss coefficient, G_t and G_r is the transmitter antenna gain and is the receiver antenna gain. The value of n is usually chosen between 2 and 6 (we have chosen n = 2) depending upon the physical environment. L is the loss in transmission lines, antennas and other.

B. Transmission Power in DPCMAC for High Network Workload

When network workload is high, short radio ranges may be preferable. This is because of the reason that the radio tends to spend more time in the transmission and reception states. There are three steps to calculate the transmission power in DPCMAC:

1) Determining Transmission Power level of P_t^{min}

We explain how the proposed algorithm determines the transmission power level for a packet. Our scheme is based on the following assumptions:

a) The physical layer can transmit a frame with one of the discrete power levels notified by the MAC layer.

b) The physical layer can measure (Received Signal Strength Indicator) RSSI of a received frame.

c) The communication links are bidirectional and symmetric.

The minimum transmission power level P_t^{min} at the sender is calculated as:

$$P_t^{min} = P_r^{min} \frac{L (4\pi)^2 d^n}{G_t G_r \lambda^2} \quad (6)$$

Combining (5) and (6), we obtain:

$$P_t^{min} = P_r^{min} \left(\frac{P_t}{P_r}\right) \quad (7)$$

where P_r^{min} is the receiver's sensitivity. P_t is the maximum transmission power level of the sender of RTS frame. After the receiver node receives the RTS frame, it received maximum power level (P_r) of the RTS frame.

The receiver calculates the required transmission power level P_t^{min} by using (7). The receiver sends the CTS frame, with the P_t^{min} in it, back to the sender node. After the RTS/CTS handshake, the sender node has the information of the required minimum transmission power level.

Therefore the DATA packet can be transmitted at the required transmission power level. Each sensor node stores the values of the P_t^{min} for its neighbors, and uses the corresponding P_t^{min} to transmit DATA packet in the next communication cycle with its neighbors.

2) Build Transmission Power Control Table

We divide the transmission power of the nodes into eight levels, i.e. $P_t^1, P_t^2, P_t^3, P_t^4, P_t^5, P_t^6, P_t^7$ *and* P_t^{max} . It represents the transmission power for variable range of transmissions (say d meters).

In the synchronization period, each of the nodes transmits the SYNC packets with the maximal transmission power. When a node N_a receives a SYNC packet from its neighbor N_b , the node N_a calculates the power intensity of the receiving SYNC packet according to the RSSI readings, which is represented by P_r. The minimum desired power intensity to ensure that the nodes can normally receive packets, is called the *threshold power* and is represented by P_r^{th}. So the minimum transmission power P_t^{min} that can be received by node N_a must satisfy (5) and (6):

$$\frac{P_t^{max}}{P_r} = \frac{P_t^{min}}{P_r^{th}} \tag{8}$$

$$P_t^{min} = \left(\frac{P_t^{max}}{P_r} \right) P_r^{th} \tag{9}$$

In order to store the minimum transmission power, a table, named power control table, is built in each sensor node, as shown in Table 1. The power control table consists of two fields, its neighbors' node ID and the corresponding transmission power level.

TABLE I
POWER CONTROL TABLE

S.No.	Attribute Details		
	Attribute Name	Type	Unit
1.	Neighbor_Node_Id	Integer	-
2.	Power_Level	Double	watts

a. The Neighbor_Node_Id is stored in array structure.

3) Assessing the Ideal Power

The node A access desired power level for transmission of packets as follows:

while $\left(P_r^{\,i} \le P_r^{\,min} \right)$ && $\left(P_t^{\,i} \le P_t^{\,i+1} \right)$

{

$P_t^{\,i} = P_t^{\,i+1}$;

$P_t^{\,ideal} = P_t^{\,i+1}$;

}

The ideal transmission power between node N_a and node N_b is represented by P_t^{ideal}, it satisfies (10). The method of assessing the ideal transmission that we adopt avoids the frequent fluctuations in the estimates as small changes happen in the surrounding environment.

$$P_t^{\,ideal} = P_t^{\,i+1} \tag{10}$$

C. The Process of Dynamic Transmission Power Control In DPCMAC

Due to variation in WSNs, the power control table need to be update in each transmission cycle At first, we add a new field P_t^{ideal} in the neighbor list of each node, which denotes the ideal transmission power used when transmit data to the neighbor. Base on the SMAC protocol, we add the content as follows:

a) At the beginning, a node, say node A, broadcast the SYNC packet with the maximal transmission power during synchronization period, The neighbors in active mode receive the SYNC. They calculate the corresponding transmission power level separately each receiver node sends the power level back ton the node A.

b) If a node A receives a SYNC packet from node B, node A calculates the ideal transmission power when communication with node B according to the algorithm of assessing the ideal transmission power. If node B is a new neighbor of node A, node A inserts the neighbor B in the neighbor list and records the ideal transmission power. If node B is a known neighbor of node A, node A updates the ideal transmission power to node B.

c) If the RTS/CTS handshake fails, we go to step (d) Otherwise the node A uses the latest power level to update the power control table. DATA frames are transmitted with the corresponding P_t^{min} in the table.

d) Handshake failure may occur due to two situations given below:

- When the RTS arrives, the receiver node is in sleep mode. To solve the problem, the sender sends RTS for a pre-defined number of times. Based on the SMAC protocol, there is always a time window that the receiver is in active mode while sender transmits RTS.
- After the pre-defined number of times, if the sender has not received the CTS from the destination, the sender will assume the transmission channel and/or receiver state have changed. The sender will gradually increase its power level and repeat above process until it receives CTS from the destination. If the sender transmits the RTS with its maximum power level and still can't receive the CTS, it will delete the node from its power control table because the destination node is no longer within its transmission range or runs out of the battery.

e) The sensor nodes used variable power level for transmission of unicast packets. They use the power table for transmission where the different power level is recorded in the sensor nodes for communicate with different neighbors.

f) When sensor nodes want to broadcast packets, they transmit packets with the maximal transmission power.

V. SIMULATION RESULTS

The emergence of wireless sensor networks has created many open issues in network design. In the proposed work, we have used a new sensor network simulator, called SENSE [11] for simulating our proposed work. We have evaluated the performance of our proposed algorithms under the

different node densities and length of data frame. In our simulation, nodes are spread in a terrain of 2000×2000. We have considered network of size 110, 220, 330, 440, 550, 660, 770, 880, 990, and 1000. Nodes are placed randomly within the simulation area and each node has same transmission range. Moreover, Ad-hoc On-demand Distance Vector [10] (AODV) protocol is used for routing. Results of experiments are obtained by taking the average of 10 simulation runs for randomly deployed sensor nodes.

The results of the simulation are expressed using following metrics: success rate and energy consumed. *Success rate* is defined as the ratio of total packet received to the total number of packets sent. In our simulation, it is a ratio of total number of received and sent by a MAC layer. *Energy consumption* is expressed in terms of the total energy consumed (in joules) by all the nodes in transmission as well as receiving the packets.

The Fig. 4 shows the success rate of our proposed protocol. Success rate of DPCMAC is found to increase with increase of network size between nodes 110 to 210. Success rate becomes constant between 220 to 440 nodes. Further, there is marginal decrease up to 750 nodes. Finally, it starts decreasing for network size of 1000 nodes. In Fig. 5 DPCMAC reduces the energy consumption in comparison to SMAC protocol with the increase of network size, varying the nodes 330 to 1000. The results obtained from simulation, reveals that the overall performance of DPCMAC is superior in terms of energy consumption than SMAC, for both the network scenarios (low/high network workload). This modification of controlled power level transmission of packets results in improving the performance of the existing SMAC protocol.

VI. CONCLUSION

Our proposed MAC protocol (DPCMAC) supports variable power level transmissions according to data rate of source that minimize the aggregate energy consumption in all radio states. This modification is suggested to improve the performance of existing SMAC protocol in terms of energy consumption with network workload. Therefore, the current work contributed to the knowledge in a modest way by simulating and realizing that SMAC indeed will perform better with controlled power usage, achieved by saving energy and increasing success rate.

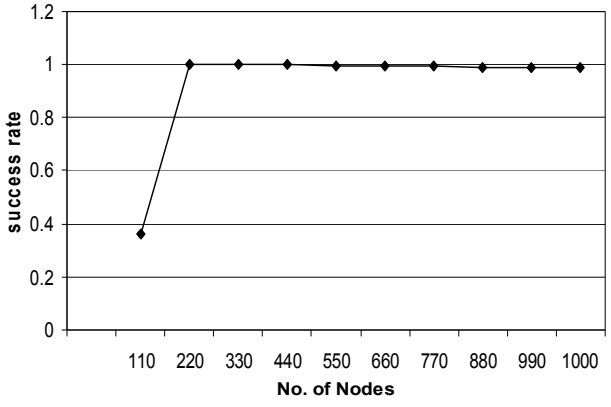


Fig. 4. Success rate of packet transmissions in the DPCMAC protocol

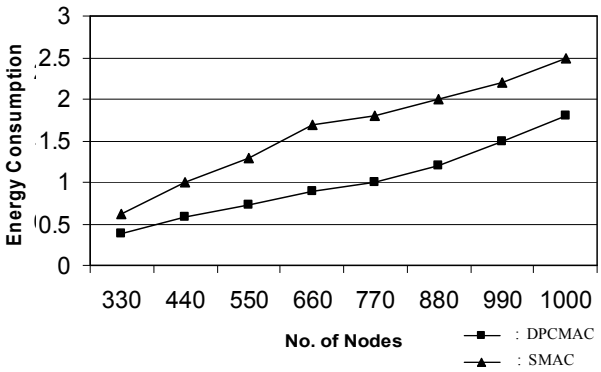


Fig. 5. Comparison of energy consumption between DPCMAC and SMAC

REFERENCES

[1] J. Gomez, A. T. Campbell, "Variable-range transmission power control in wireless ad hoc networks," *IEEE Transactions on Mobile Computing*, vol. 6 , issue. 1, 2007, pp. 87-89.

[2] J. Gomez, A. T. Campbell, "A case for variable range transmission power control in wireless multihop networks," *INFOCOM'04 Twenty-third Annual Joint Conference of the IEEE Computer and Communications Societies*, vol. 2, 2004, pp. 1425-1436.

[3] S. Kostin, L. B. de Pinho, C. L. de Amorim, "Transmission power levels prediction for distributed topology control protocols within parameterized scenarios," *ICT'08 International Conference on Telecommunications*, 2008, pp. 1-7.

[4] Jeffrey P. Monks, "Transmission power control for enhancing the performance of wireless data packet networks," Doctor of Philosophy, Univ. of Illionis at Urbana-Champaign, 2001, pp. 30-81.

[5] Zhiwei Zhao, Xinming Zhang, Peng Sun, Pengxi Liu, "A transmission power control MAC protocol for wireless sensor networks," *ICN'07 Sixth International Conference on Networking*, 2007, pp. 1-5.

[6] Jian Xiao, Fengqi Yu, "An efficient transmission power control algorithm for wireless sensor networks," *WiCom'07 International Conference on Wireless Communications, Networking and Mobile Computing*, 2007, pp. 2767-2770.

[7] Luiz H. A. Correia, J. M. S. Nogueira, "Transmission power control techniques for MAC protocols in wireless sensor networks," *NOMS'08 Network Operations and Management Symposium, IEEE*, 2008, pp 1049-1054.

[8] Luiz H. A. Correia, Daniel F. Macedo, Daniel A. C. Silva, Aldri L. dos Santos, Antonio A. F. Loureiro, Jose Marcos S. Nogueira, "Transmission power control in MAC protocols for wireless sensor networks", *Proceedings of the 8th ACM international symposium on Modeling, Analysis and Simulation of Wireless and Mobile Systems*, ACM Press, 2005, pp. 282-289.

[9] M. Kubisch, H. Karl, A. Wolisz, L. C. Zhong, J. Rabaey, "Distributed algorithms for transmission power control in wireless sensor networks," *WCNC'03 Wireless Communications and Networking, IEEE*, vol. 1, 2003, pp. 558-563.

[10] C. Perkins, E. Royer, "Adhoc On-Demand Distance Vector Protocol," *In C. Perkins, editor, Ad hoc Networking*, 2000, pp. 173-219.

[11] The SENSE Simulator, *www.ita.cs.rpi.edu/sense/index.html*

Evaluation of RASTA Approach with Modified Parameters for Speech Enhancement in Communication Systems

S.K.Shah[1], J.H.Shah[2], N.N.Parmar[3]

[1] Electrical Engg. Dept., Faculty of Tech. and Engg, The M.S. Uni. of Baroda, Rajmahel Road, Vadodara, India

[2,3] Electronics and Telecom. Engg. Dept,. S.V.M. Institute of Tech., Old NH 8, College Campus, Bharuch, India

[1]satishkshah_2005@yahoo.com

[2]jhs707in@yahoo.com

[3]parmar_nishant@rediffmail.com

***Abstract*- The purpose of speech enhancement techniques is to improve quality and intelligibility of speech without producing any artifact. The speech enhancement algorithms are designed to suppress additive background noise and convolutive distortion or reverberation. The need for enhancement of noisy speech in communication systems increases with the spread of mobile and cellular telephony. Calls may originate from noisy environments such as moving vehicles or crowded public gathering places. The corrupting noise is not always white rather it is colored and contains reverberation. The currently employed noise suppressors in communication systems use spectral subtraction based on short time spectral attenuation (STSA) algorithms as a preprocessor in speech coder. They can perform well in white noise condition but failed in real colored noise environments with different SNRs. This leads to the use of RelAtive SpecTrAl (RASTA) algorithm for speech enhancement which was originally designed to alleviate effects of convolutional and additive noise in automatic speech recognition (ASR). RASTA does this by band-pass filtering time trajectories of parametric representations of speech in the domain in which the disturbing noisy components are additive. This paper evaluates the performance of RASTA algorithm for white and colored noise reduction as well as suggests modifications in parameters and filtering approach to perform quite well than original RASTA approach. The NOIZEUS database is used for objective evaluation in different noise conditions with 0 to 10dB SNRs. The results shown here give improvements compared to spectral subtraction methods.**

***Keywords*—short time spectral attenuation, temporal processing, time trajectories, modulation frequency, objective measures.**

I. INTRODUCTION

The need for noise reduction and suppression technology is more important than ever. Mobile phones, portable communication devices and other phones are widely used in noisy environments. As a result, phone calls contain, in addition to the speaker's voice, unwanted signals like other people talking around, vehicle engine noise and horns, wind noise, keyboard-strokes etc. A background noise suppression system developed by Motorola is included as a feature in IS-127, the TIA/EIA standard for the Enhanced Variable Rate Codec (EVRC) to be used in CDMA based telephone systems [1]. EVRC was modified to EVRC-B and later on replaced by Selectable Mode Vocoder (SMV) which retained the speech quality at the same time improved network capacity. Recently, however, SMV itself has been replaced by the new CDMA2000 4GV codecs. 4GV is the next generation 3GPP2 standards-based EVRC-B codec [2]. The EVRC based codec uses combination of STSA based approaches: multiband spectral subtraction (MBSS) and minimum mean square error (MMSE) gain function estimator for background noise suppression as a preprocessor. The voice activity detector (VAD) used to decide speech/silence frame is embedded within the algorithm. Its quality has been proven good through commercial products. Nevertheless, the quality may not be sufficiently good for a wide range of SNRs, which were not given much attention when it was standardized. Another algorithm suggested by A.Sugiyama, M.Kato and M. Serizawa [3] uses modified MMSE-STSA approach based on weighted noise estimation. The subjective tests on this algorithm claim to give maximum difference in mean opinion score (MOS) of 0.35 to 0.40 compared to EVRC and hence its later version is equipped within 3G handsets [3].

However, the STSA based approaches have their common problems of musical noise and speech distortion. Hence it is needed to shift the enhancement domain itself. This leads to investigate the use of RASTA processing of speech originally proposed by Hermansky and Morgan [4-6] and designed to alleviate effects of convolutional and additive noise in automatic speech recognition (ASR). Recently, RASTA was also applied to direct enhancement of noisy speech in communication systems [4-6]. This paper evaluates the performance of RASTA algorithm with original and modified parameters in the context of additive noise removal in white and colored noise environments with SNRs 0 to 10dB and compares it with the STSA based approaches by using perceptual estimation of speech quaility (PESQ) objective measure.

II. RASTA IN ADDITIVE NOISE REDUCTION

Speech signal reflects the geometry of the vocal organs, and

the linguistically dominant component is in the shape of the vocal tract. At any given point in time, the shape of the vocal tract is reflected in the short-time spectral envelope of the speech signal. The rate of change of the vocal tract shape appears to be important for the identification of linguistic components. This rate of change or the rate of change of the short-time spectral envelope can be described by the modulation spectrum, i.e. the spectrum of the time trajectories described by the short-time spectral envelope [7]. For a wide range of frequency bands, the modulation spectrum of speech exhibits a maximum at about 4 Hz, the average syllabic rate. Disturbances such as additive noise may have different modulation spectrum properties than speech and often have modulation frequency components outside the speech range, and could in principle be attenuated without significantly affecting the range with relevant linguistic information. The RASTA processing suppresses the spectral components outside the typical modulation spectrum of speech. The maximum modulation frequency of the modulation spectrum is half of the sampling frequency of RASTA filter. The sampling frequency of RASTA filter is decided by frame rate. The frame rate is obtained by taking ratio of sampling frequency of speech signal to the number of shift points in a frame.

RASTA based speech enhancement for additive noise suppression suggested in [6] involves linear filtering of the trajectory of the short-term power spectrum of noisy speech signal as shown in fig. 1. The spectral values of input speech signal are compressed by a nonlinear compression rule (a=2/3) before performing the filtering operation and expanded after filtering (b=3/2). The filter suggested for each temporal trajectory is fixed IIR band pass filter [4] or non causal Wiener like FIR filter [8].

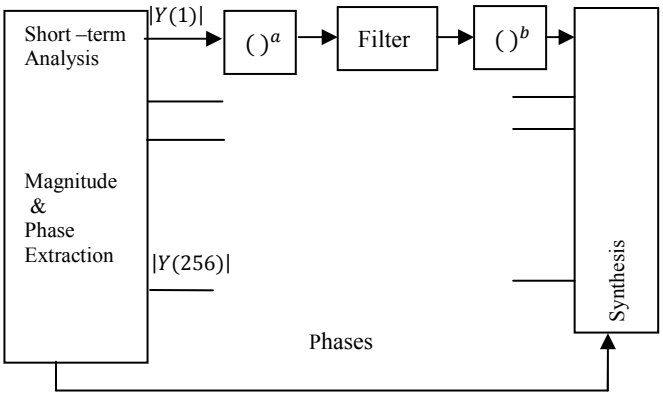


Fig. 1. Block diagram of RASTA algorithm for additive noise suppression.

III. Simulation Of RASTA Algorithm And Modifications

In simulation of original RASTA filter; the filter for each time trajectory is implemented by fixed IIR band pass filter [4] with transfer function given by

$$H(z) = 0.1z^4\left(\frac{2+z^{-1}-z^{-3}-2z^{-4}}{1-0.94z^{-1}}\right). \qquad (1)$$

To perform the RASTA filtering a Hamming window of 256 samples length with an overlap of 128 samples is used. With 8 kHz sampling frequency this gives 32 ms window duration and 16 ms overlap. The frame rate and hence the sampling frequency of RASTA filter is 100Hz. The maximum modulation frequency is 50Hz. The filter is designed with lower cut-off frequency of 0.26Hz. The filter slope decline 6dB/octave from 12.8Hz with sharp zeros at 28.9Hz and at 50Hz. The frequency response of the filter is shown in fig. 2. The algorithm used for obtaining FFT generates 256 points complex FFT, which gives magnitude and phase for first 129 points. Each spectral value is filtered using the filter described in (1). These filtered spectral values are combined with the phase of noisy spectrum, 256 point IFFT is applied and overlap-add operation is performed to reconstruct the enhanced speech.

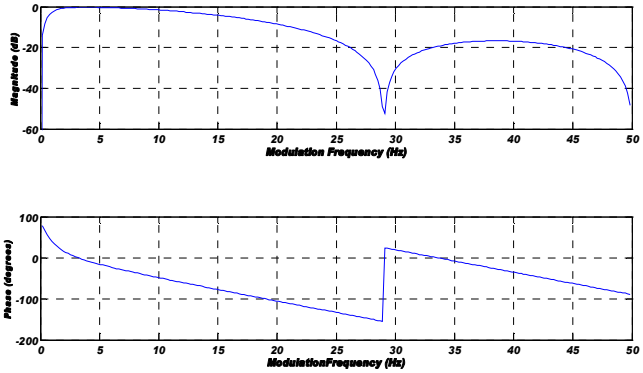


Fig. 2. Frequency response of fixed RASTA filter.

As per auditory principles; the nonlinear compression and expansion is critical in RASTA approach. In simulation experiment the parameters a and b are tested for different values. The simulation is carried out with originally fixed values of parameters a and b as well as with the modified values. From the listening experience the parameter values a=3/4 and b=4/3 are found more satisfactory. The objective evaluation done using PESQ also backs the results. Also the original fixed RASTA filter is modified and it is replaced by multiband filters. For very low frequency band 0-100 Hz no filtering is performed. The filters for the band 300-2300 Hz are approximated by band-pass filter with lower cut-off frequency of 0.07 Hz and higher cutoff frequency of 20 Hz. The filters for the bands 100-300 Hz and 2300-4000Hz are approximated by low pass filters with cut-off frequency of 15 Hz. The filter coefficients for four different frequency bands are shown in table I. The frequency responses of these filters are shown in fig. 3 and 4.

IV. Evaluation And Results

To test and evaluate performance of speech enhancement algorithms; the objective measure called perceptual estimation of speech quality (PESQ) score is used [9]. It gives score out of 5. The test files obtained from NOIZEUS database [10] are used in the experiment. A noisy speech corpus (NOIZEUS) was developed to facilitate comparison of speech enhancement

algorithms among research groups. The noisy database contains 30 IEEE sentences (produced by three male and three female speakers and recorded in a sound-proof booth using Tucker Davis Technologies (TDT) recording equipment) corrupted by eight different real-world noises at 0,5 and 10dB SNRs. The noise includes train, babble, car, exhibition hall, restaurant, street, train-station and airport noise. Speech enhancement for white noise, car noise, restaurant noise and airport noise at different SNR level is carried out using two spectral subtraction algorithms: MBSS and MMSE-LSA and using the RASTA filtering algorithm with two different cases of parameters *a* and *b*. The performances of these methods are evaluated using the perceptual estimation of speech quaility (PESQ) objective measure.

TABLE I
COEFFICIENTS OF MODIFIED RASTA FILTER

Filter coefficients	Frequency band	
	300-2300Hz	100-300Hz 2300-4000Hz
b_0	0.2466	0.0229
b_1	0	0.0915
b_2	-0.4932	0.1372
b_3	0	0.0915
b_4	0.2466	0.0229
a_0	1.0	1.0
a_1	-1.9933	-1.4120
a_2	1.3253	1.2228
a_3	-0.4983	-0.408
a_4	0.1781	0.0632

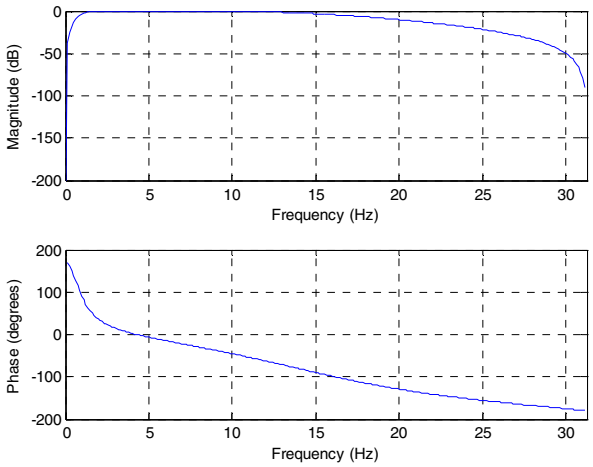


Fig. 3. Frequency response of Modified RASTA filter in 300-2300Hz band.

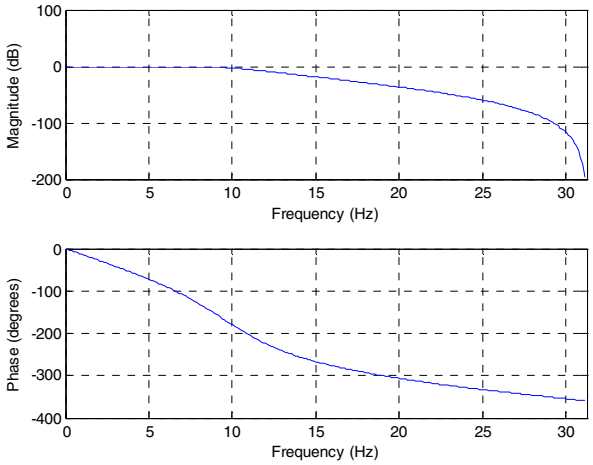


Fig. 4. Frequency response of Modified RASTA filter in 100-300Hz and 2300-4000Hz band.

Fig. 5,6,7 and 8 illustrate mean PESQ score bar chart comparison of all five algorithms with white noise, car noise, restaurant noise and airport noise respectively at 0, 5 and 10dB SNRs. The noisy speech PESQ score is also included for reference. The theoretical limit bar is obtained by taking magnitude of clean speech and phase of noisy speech. This defines the maximum limit for particular method at particular SNR level. It can be observed that at relatively high SNR two STSA algorithms are performing well compared to RASTA algorithms. But at the lower SNRs the STSA algorithms are inferiored compared to RASTA algorithms. Also the perfromance of RASTA algorithms are consistent in white and colored noise environments. The modified RASTA algorithm performs well in most noise conditions compared to its orignial version.

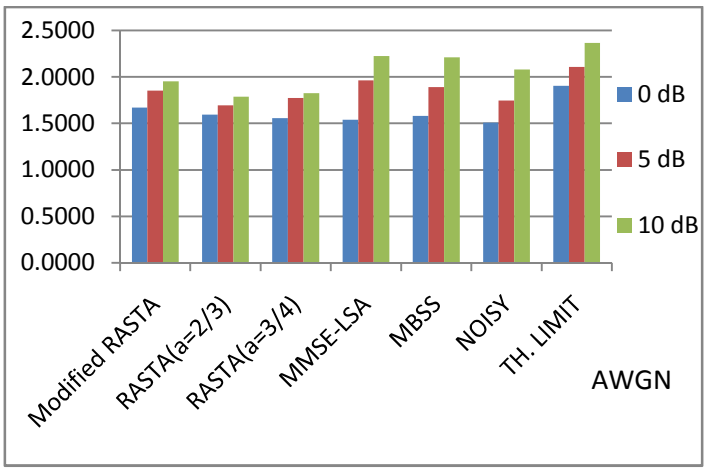


Fig. 5. PESQ score comparison in white noise.

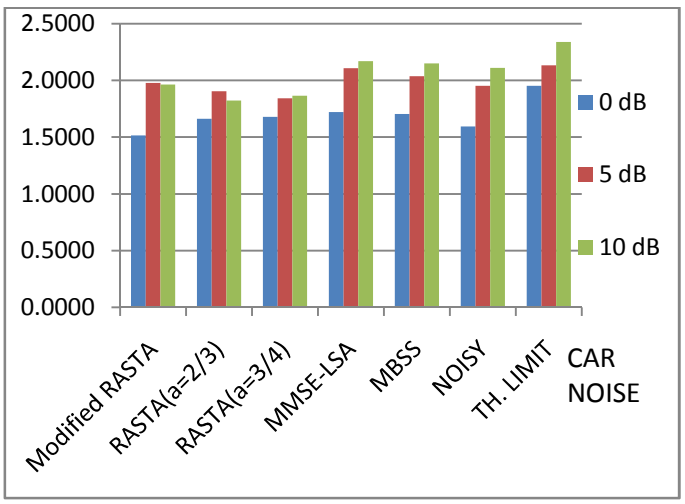


Fig. 6. PESQ score comparison in car noise

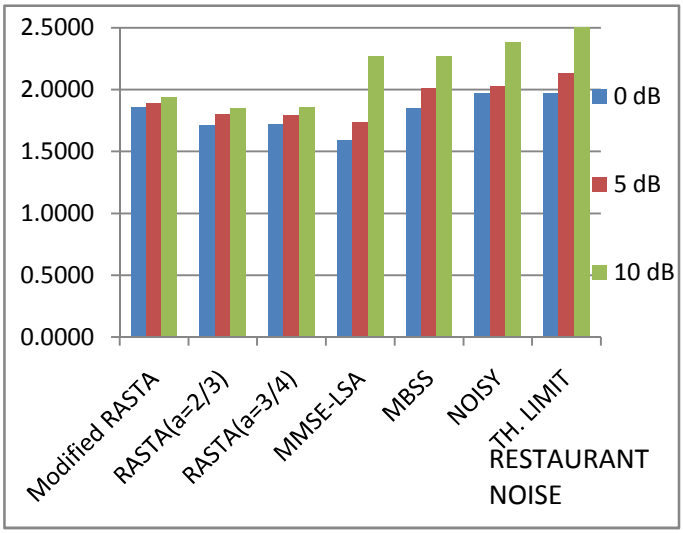


Fig. 7. PESQ score comparison in restaurant noise.

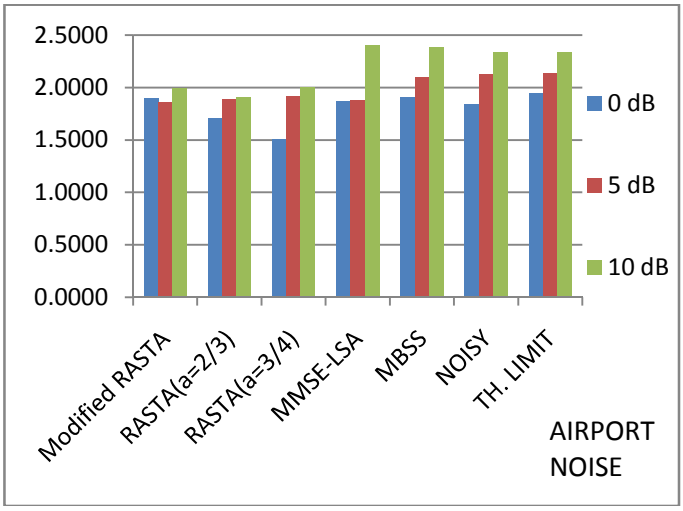


Fig. 8. PESQ score comparison in airport noise

V. Conclusion And Future Scopes

The RASTA algorithm is evaluated here and compared with spectral subtraction methods. The objective measure using PESQ is obtained. The RASTA algorithm has unique advantage that it does not require voice activity detector (VAD). The RASTA algorithm with modified parameters outperforms all the five algorithms in low SNR conditions. Further hardware complexity can be evaluated by implementing the algorithms on hardware platforms like DSP or FPGA. Further optimization can be obtained by implementing the algorithms using artificial neural network and fuzzy logic. Also the RASTA approach can be combined in some way with the STSA approaches to have better results.

References

[1] T.V.Ramabadran,J.P.Ashley,M.J.McLauglin, "Background noise suppression for speech enhancement and coding", *IEEE Workshop on Speech Coding for Telecommunications Proceedings*, 1997.

[2] 3GPP2 Specifications (2007). Available: http://www.3gpp2.org/Public_html/specs/index.cfm

[3] J. Benesty, S.Makino, J.Cheng, *Speech Enhancement*, Springer series of signals and communication technology, 2005.

[4] Hynek Hermansky, Nelson Morgan "RASTA processing of speech," *IEEE Trans. on acoustics, speech and signal processing*, Vol.2, pp. 578-589, Oct.1994.

[5] H. Hermanskey, E.A. Wan, C.Avendano, "Noise suppression in cellular communications," *2nd IEEE workshop on Interactive Voice Technology for Telecommunications Applications IVTT 94*, Kyoto, Japan, Sept. 1994.

[6] Hynek Hermansky, Nelson Morgan, Hans-Gunter Hirsch, "Recognition of speech in additive and convolutive noise based on RASTA spectral processing", *IEEE International Conference on Acoustics, Speech, and Signal Processing, ICASSP-93,* 1993.

[7] Hynek Hermansky, Eric A. Wan, and Carlos Avendano, "Speech enhancement based on temporal processing", *International Conference on Acoustics, Speech, and Signal Processing,5. ICASSP-95,* 1995.

[8] Carlos Avendano and Hynek Hermansky, "On the Properties of Temporal Processing for Speech in Adverse Environments", in *Proc. WASPA'97*, Mohonk, New York, 1997.

[9] A. Hu, P. Loizou, "Subjective comparisons of speech enhancement algorithms," in *Proc. IEEE International conference on Acoustics, Speech and Signal Processing,* May 2006.

[10] The NOIZEUS database (2009). Available: http://www.utdallas.edu/~loizou/speech/noize

A Modified Planar Monopole Antenna for UWB Applications

Yashar Zehforoosh
Department of electrical engineering
Islamic Azad University, Urmia Branch
Urmia, Iran
y.zehforoosh@iaurmia.ac.ir

Ramazanali Sadegzadeh
Department of electrical engineering
Khajenasir Tosi University
Tehran, Iran
sadeghzadeh@kntu.ac.ir

Navid Mirmotahhary
Department of electrical engineering
Islamic Azad university, science &research branch
Tehran, Iran
n.mirmotahhary@srbiau.ac.ir

Abstract— **In this paper, we present a novel design of printed monopole antenna for UWB applications. The radiating element of the proposed antenna is composed of an octagonal patch fed by a 50 ohm microstrip. It has a very compact size of**
20mm×12mm, which can be integrated easily with other RF front-end circuits. The antenna parameters and performances
have been investigated through a large amount of EM simulations. It has been demonstrated that the proposed antenna provides an ultra wide bandwidth from 2.95 GHz to 13.35 GHz, completely covering the range set by the Federal Communication Commission (FCC) for UWB operations (3.1GHz to 10.6GHz). It also enjoys advantages such as low profile, low cost, high gain and satisfactory radiation characteristics.

***Keywords*—planar antenna,monopole,UWB**

I. INTRODUCTION

As a candidate for the so called "short fat pipe" Ultra wideband (UWB) radio has recently been researched for the
possibilities of providing a short range (10m or less) high bandwidth (> 1 Gbps) communications link. The average emission limits as defined by the FCC for the regulation of indoor UWB systems [1] shows that UWB is essentially now a low power technology. This has presented many opportunities and challenges for antenna designers. Several kinds of antennas, such as bow-tie, conical, TEM horn, vivaldi, IRA, porcupine, spiral, fractal and log-periodic antennas have been introduced and they have good impedance stability over a very large frequency band [2-8]. In short-range UWB communications, the trade off between
bandwidth, size, radiation efficiency, and low cost should be optimized to obtain an acceptable design. Some trade offs such as size-bandwidth and size-gain are more challenging [9]. Patch antennas are extensively used in wireless communications because of their light weight, low cost, and ease of fabrication. These features are desirable for both indoor and outdoor handheld UWB antenna applications. Ideally, UWB antennas should be non-dispersive or dispersive in a controlled fashion that is amenable to compensation. Planar dipoles perform well in commercial applications [10]. Among the UWB antenna designs in the recent literatures, planar monopole antennas have become one of the considerable candidates for UWB applications owing to the features of nearly omni-directional radiation pattern. Several designs of planar monopole UWB antennas have been proposed [11-15]. However, some of these monopole UWB antennas only cover partial parts of the UWB band and some designs are difficult to integrate with other RF fronts because of their large size.

In this paper, we present a novel planar microstrip-fed modified rectangular monopole antenna that exhibits broadband performance. The design of the proposed structure is based on the simple rectangular monopole antenna, but has a significantly large operational bandwidth.

The antenna's ground-plane is also truncated symmetrically.

This antenna designed operates across 2.95 to 13.35 GHz with VSWR < 2. Unlike other antennas reported in the literature to date, the proposed antenna displays a good omni-directional radiation pattern even at higher frequencies. The monopole antenna is analyzed using Ansoft's High Frequency Simulator (HFSS™) [16]. Simulated results are presented to validate the usefulness of the proposed antenna structure for UWB applications.

II. ANTENNA DESIGN

Fig. 1 shows the configuration of the proposed ultra wideband monopole antenna which consists of rectangular structure which three sides of the rectangular patch filled with same size stubs and positioned above a triangular. The ground-plane is truncated, as shown in

Fig. 1 and envelops the feedline to the radiating triangular patch including two stairs at its both sides. The proposed antenna is constructed from FR4 substrate with thickness of 1.6 mm and relative dielectric constant of 4.4. The proposed antenna is investigated by changing one parameter at a time, while fixing the others. Optimum physical parameters of the antenna presented in table I. To fully understand the behavior of the antenna's structure and to determine the optimum parameters the antenna was analyzed using Ansoft's high-frequency structure simulator (HFSS™). The proposed shape of the truncated groundplane acts as an effective impedance matching network to realize an antenna with a very wide impedance bandwidth. This is because the truncation creates capacitive loading that neutralizes the inductive nature of the patch to produce nearly pure resistive impedance present at the antenna's input [12].

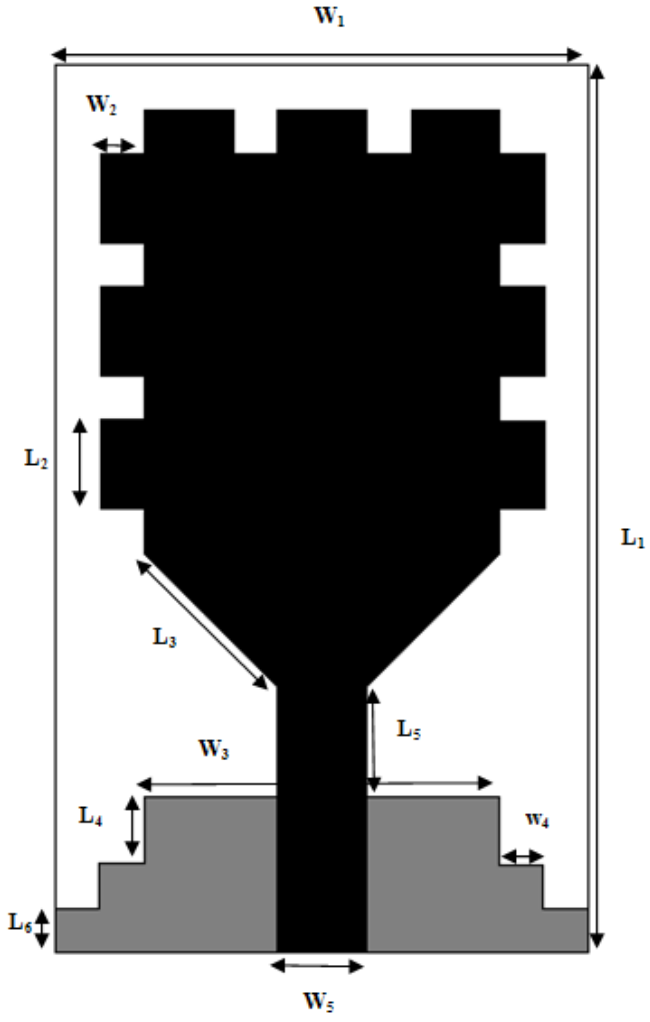


Figure1. Configuration of proposed monopole antenna

Table I.
Physical parameters of the proposed antenna

L_1	L_2	L_3	L_4	L_5	L_6
20(mm)	2(mm)	4.24(mm)	1.5(mm)	2.5(mm)	1(mm)
W_1	W_2	W_3	W_4	W_5	
12(mm)	1(mm)	8(mm)	1(mm)	2(mm)	

III. RESULTS

Fig. 2 shows a comparison of the return-loss characteristics of the proposed antenna with simple rectangular monopole antenna. As shown the simple rectangular monopole antenna has a relatively narrow bandwidth. As observed in Fig. 2 the successive modifications improve the bandwidth of the rectangular monopole antenna. With the inclusion of stubs on the radiation patch and modifying the groundplane, as in Fig. 1, has a significant effect on increasing its bandwidth. Figure 3 shows the antenna gain from 3 to 10 GHz for the proposed antenna. The maximum gain variation is less than 2 dB with the peak antenna gain of about 4.3 dB.

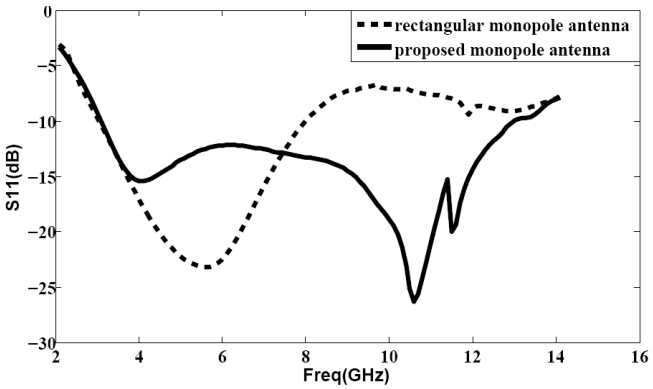


Figure2. S_{11} plot of a rectangular monopole and proposed monopole Antenna

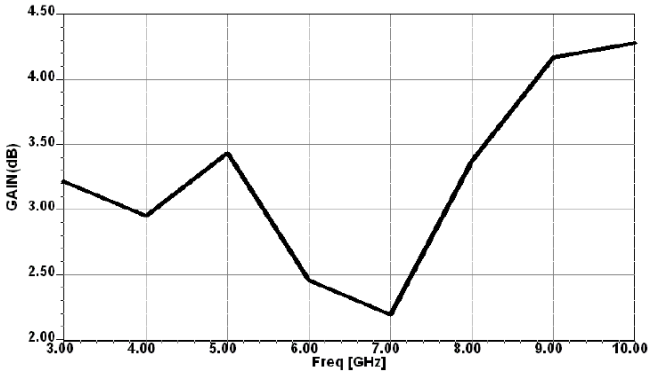


Figure3. Gain plot of the proposed monopole antenna

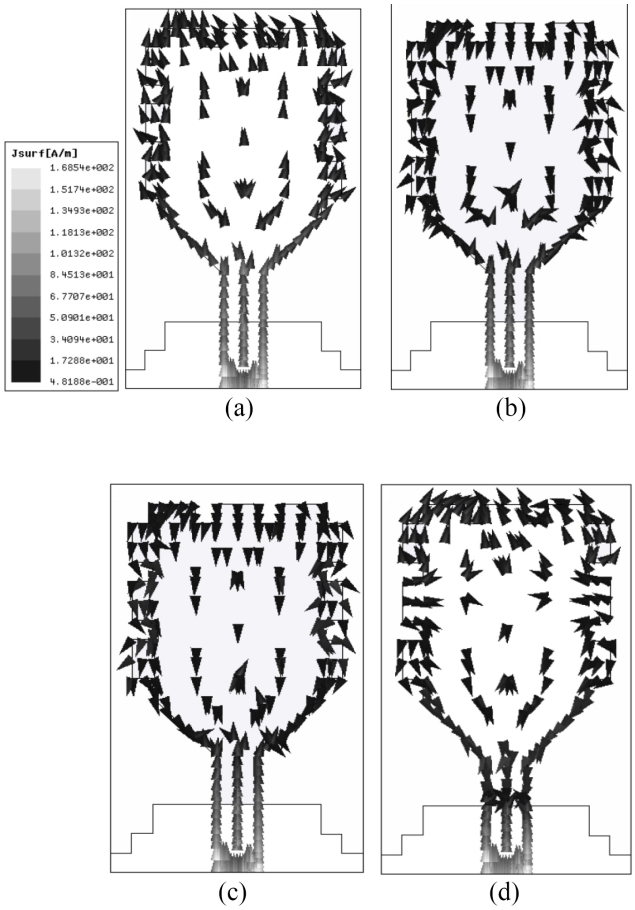


Figure4. Current distribution of the proposed monopole antenna at (a) 4, (b)
6, (c) 8 and (10) GHz.

The spectrum of the antenna in Fig. 2 shows several resonances. These resonances correspond to the different modes of field distribution. Fig. 4 shows the simulated current distribution at frequency of 4 GHz, 6GHz, 8 GHz, and 10 GHz. Fig. 4(c) and (d) show a strong current distribution located around the radiating patch on the stubs, as well as the current flow directed towards the side stubs. This indicates that the modifications in the radiating patch excite resonance modes at a higher frequency which effectively extend the antenna's bandwidth. The proposed antenna's far-field radiation patterns are presented in the two principle planes, *y-z* plane for the *E* plane and *x-z* plane for the *H*-plane. Figs. 5 show the radiation patterns plots at several different frequencies are stable. It is noticed that the *H*-plane pattern is omnidirectional at lower frequency and is near omni-directional at higher frequencies.

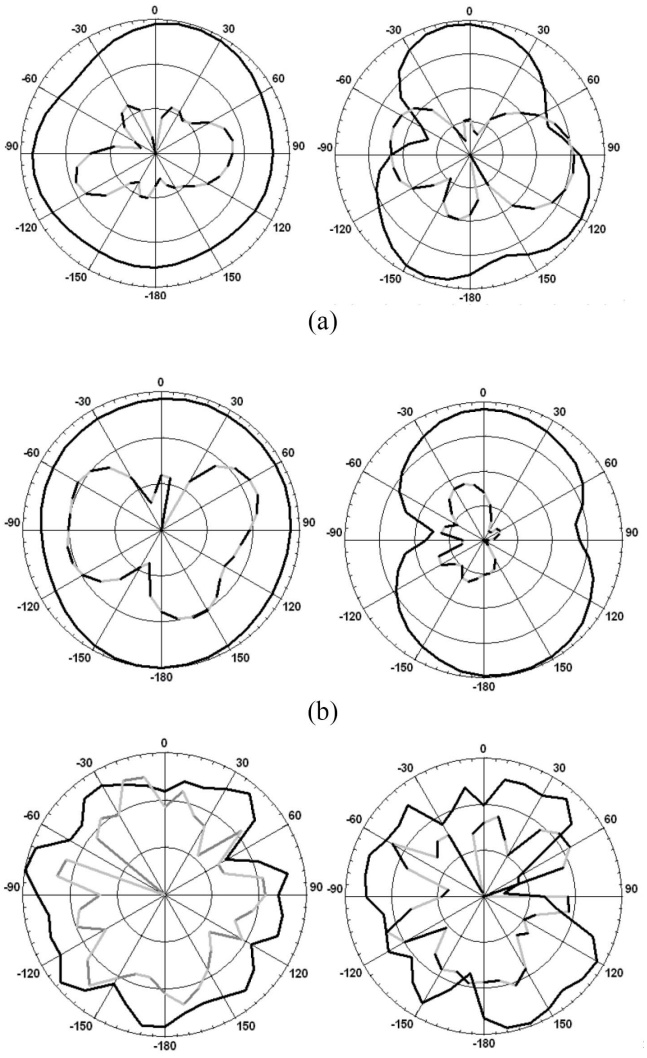


Figure5. Measured radiation patterns of the proposed antenna in x-z and yz
plane at: (a) 4 GHz, (b) 7 GHz, and (c) 11 GHz.

IV. CONCLUSION

In this paper a compact planar monopole antenna is proposed that exhibits ultra wide bandwidth performance and easily satisfies the requirements for UWB applications. The results show that the impedance bandwidth of the proposed antenna is significantly improved with the inclusion of square stubs on the radiating patch, a triangular shape piece on the connection section of feedline and radiating patch, and using a truncated ground-plane. The proposed antenna exhibits an impedance bandwidth of 127.6% over a very wide frequency range from 2.95 to 13.35 GHz with return-loss better than -10 dB also results show good radiation patterns within the UWB frequency range.

REFERENCES

[1] J Gary Breed; "A Summary of FCC Rules for Ultra Wideband communications", *High Frequency Electronics,*January 2005

[2] K. Y. Yazdandoost and R. Kohno, “Bow-tie antenna for UWB communication frequency,” IEEE Antennas and Propagation Society International Symposium, Vol. 3, pp. 2520-2523, 2004.
[3] S. Licul, J. A. N. Noronha, W. A. Davis, D. G. Sweeney, C. R. Anderson and T. M. Bielawa, “A parametric study of time-domain characteristics of possible UWB antenna architectures,” Proc of IEEE Vehicular Tech. Conference., Vol. 5, pp. 3110- 3114, 2003.
[4] C. E. Baum and E. G. Farr, “Impulse Radiating Antennas,” in Ultra Wideband/Short-Pulse Electromagnetics, edited by H. L. Bertoni et al, Plenum Press, New York, pp.139-147, 1993.
[5] H. Aliakbarian, M.M. Danai, M. Azarbadegan and J. Rashed-Mohassel, “A new miniaturized ultra-wideband high gain antenna,” IEEE Antennas and Propagation Symposium, pp. 4823-4826, 2006.
[6] T. W. Hertel, and G. S. Smith, “Analysis and design of conical spiral antennas using the FDTD method,” IEEE Antennas and Propagation Society International Symposium, Vol. 3, pp. 1540-1543, 2000.
[7] D. H. Werner and S. Ganguly, “An overview of fractal antenna engineering research,” IEEE Antennas and Propagation Magazine, Vol. 45, Issue 1, pp. 38-57, Feb. 2003.
[8] K. M. P. Aghdam, R. Faraji-Dana and J. Rashed-Mohassel, “Compact dualpolarisation planar log-periodic antennas with integrated feed circuit,” IEE Proc.Microwaves, Antennas & Propagation Journal, Vol. 152, No. 5, pp. 359-366, 2005.
[9] H. G Schantz, “Introduction to ultra-wideband antennas,” IEEE Conference on Ultra Wideband Systems and Technologies, pp.1-9, 2003.
[10] Jianxin Liang, Choo C., Xiaodong Chen, Chiau Clive G. Parini, “Study of a Printed Circular Disc Monopole Antenna for UWB Systems”, IEEE TRANSACTIONS ON ANTENNAS AND PROPAGATION, VOL 53, NO 11, NOVEMBER 2005.
[11] E. Antonino-Daviu, M. Cabedo-Fabre’s, M. Ferrando-Bataller, A. Valero-Nogueira, : ‘Wideband double-fed planar monopole antennas,’ Electron. Lett., Nov. 2003, vol. 39, no. 23, pp. 1635–1636.
[12] A.A. Eldek, :’Numerical analysis of a small ultra wideband microstrip-fed tap monopole antenna,’ Progress In Electromagnetics Research, 2006, PIER 65,pp. 59-69.
[13] W.-C. Liu, P.-C. Kao, :’CPW-fed triangular monopole antenna for ultra-wideband operation,’ Microwave Opt. Technol. Lett., Dec. 2005, vol. 46, no. 6, pp.580–582.
[14] C.-C. Lin, Y.-C. Kan, L.-C. Kuo, H.-R. Chuang, :’A planar triangular monopole antenna for UWB communication,’ IEEE Microw. Wireless Compon. Lett., Oct. 2005, vol. 15, no. 10, pp.624–626.
[15] C.-C. Lin, H.-R. Chuang, Y.-C. Kan, :’A 3–12 GHz UWB planar triangular monopole antenna with ridged ground-plane’ Progress in Electromagnetics Research, 2008, PIER 83, 307–321.
[16] Ansoft High Frequency Structure Simulation (HFSS). ver. 10, Ansoft
Corp., 2005.

Variable Forgetting Factor RLS Adaptive Equalizer for DS-CDMA System

A. Charoenphol, C. Benjangkaprasert
Faculty of Engineering, King Mongkut's Institute of Technology Ladkrabang,
Bangkok 10520, Thailand.

Abstract – **In this paper, a variable forgetting factor RLS adaptive equalizer is proposed for direct sequence code division multiple access (DS-CDMA) communication system. We consider an adaptive Laguerre lattice equalizer which applies an optimal method based on the variable step-size least mean square (VSLMS) algorithm for adaptable forgetting factor RLS algorithm for improve performance of the receiver.**

I. INTRODUCTION

The recursive least squares (RLS) algorithm is the one of the most popular adaptive filter [1]. The main feature of RLS algorithm is its fast convergence rate, especially for highly correlated input signal. The performance of RLS algorithm is influenced by forgetting factor, which is mainly used to increase the weight of new data and to enhance the adaptability of non-stationary signals, so the adaptive filter has a rapid response capability to the characteristics of changes in the process of input signal.

Let us consider a direct sequence-code division multiple access (DS-CDMA) system, that widely used for multiplexing users in wireless communications [2]. However, its performance is limited by multiple access interference (MAI) due to a typical of DS-CDMA system involves multiple users sharing spectrum by use different spreading codes and intersymbol interference (ISI) with a long impulse response environment due to multipath channels. There have been extensive research effort to introduce a reliable multi-user detector, apt to alleviate the effect of both MAI and ISI [1]-[12]. While the maximum likelihood (ML) estimation based detector offers the best possible performance, its unrealistic complexity renders it unsuitable for downlink applications owing to handset constraints. Alternatively, sub-optimal schemes such as the MMSE multi-user equalizer offer moderate complexity and generally good performance.

The adaptive filter with long impulse response has found various application in adaptive signal processing. Because of the stability of Laguerre filter is compromise between the finite impulse response (FIR) filter and infinite impulse response (IIR) filter. This structure forms the apparent that a hybrid approach of combining the advantage of FIR and IIR filters, that be properly to solve problem of designing an adaptive filter with a long impulse response[3]-[7].

Lattice filter have an advantage of lower sensitivity to round-off error in comparison with FIR filter. This round-off error effects the performance of filter, and especially, this error is serious in fixed-point processing. On the other hand, system design using fixed-point processing is strongly desired as a means of reducing the production cost. The low sensitively of lattice filter is an attractive characteristic for such system design. The Laguerre filter has been extended to lattice adaptive filter, as for the same order, its computational complexity is high compared to that of the transversal. The Laguerre lattice adaptive filter [8]-[9] not only provides a performance that is either same or better as that of a normal lattice algorithm [10].

The performance of RLS algorithm is heavily dependent on the choice forgetting factor, the question of how to choose these value has not been studies in detail. The main contribution of this paper is to derive RLS algorithm which adaptively varies the forgetting factor to minimize the mean output error and thus achieve joint MAI and ISI suppression. A method of adaptable forgetting factor[11]-[12] is variable step-size least mean squares (VSLMS) algorithm and considered to improve the performance of the RLS algorithm for DS-CDMA system.

The paper organized as follows. In Section II describes the DS-CDMA system model. Section III presents the adaptive equalizer based on adaptive Laguerre lattice filter and followed by adaptive forgetting factor RLS algorithm. Computer simulation to demonstrate the performance of the system and conclusion are given in sections IV and V, respectively.

II. SYSTEM MODEL

We consider a single cell DS-CDMA system of K users. All the K users are active. A BPSK modulation is employed. User K transmits a baseband signal given by

$$x_k(n) = \sum_i A_k d_k(i) s_k(n - iT) \qquad (1)$$

where $\boldsymbol{d_k(i)}$ is the symbol transmitted by user $\boldsymbol{K}$ at time $\boldsymbol{i}$, $\boldsymbol{s_k(n)}$ is the associated spreading code, an $\boldsymbol{A_k}$ is the real amplitude. We assume binary signals, and that the symbols $\boldsymbol{d_k(i) \epsilon \{-1, +1\}}$ are independent and identically distributed. The spreading sequence of user $\boldsymbol{K}$ can be written as

$$\boldsymbol{s_k(n) = \sum_{i=0}^{N-1} c_{k,i} P_{T_c}(n - iT_c)} \qquad (2)$$

with

$$\boldsymbol{P_{T_c}(n) = \begin{cases} 1, & 0 < n < T_c \\ 0, & otherwish \end{cases}}$$

where $\boldsymbol{c_{k,i} \epsilon \{\pm 1/\sqrt{N}\}}$, the processing gain is given by $\boldsymbol{N = T/T_c}$, where $\boldsymbol{T_c}$ is the chip period and $\boldsymbol{T}$ is the symbol period. We assume DS-CDMA, so that the chip sequence $\boldsymbol{P_{T_c}(t)}$ is a constant.

The equivalent impulse response of the channel of $\boldsymbol{M}$ paths between the base station and $\boldsymbol{K^{th}}$ user can be represented by

$$\boldsymbol{h_k(n) = \sum_{m=0}^{M-1} a_{k,m} \delta(n - \tau_{k,m})} \qquad (3)$$

where $\boldsymbol{\tau_{k,m}}$ is the propagation delay for path $\boldsymbol{m}$ of the $\boldsymbol{K^{th}}$ user. $\boldsymbol{\tau_{k,m}}$ is assumed to be a multipath of $\boldsymbol{T_c}$. The path attenuation $\boldsymbol{a_{k,m}}$ is complex Guassian random process with zero mean, where $\boldsymbol{a_{k,m}}$ can be written by [1]

$$\boldsymbol{a_{k,m}} = \begin{cases} \boldsymbol{0.5\left\{1 + cos\left(\frac{2\pi}{B}(m-2)\right)\right\}}, & \boldsymbol{m = 1,2,3,\ldots} \\ \boldsymbol{0} \qquad\qquad\qquad\quad , & \boldsymbol{otherwish} \end{cases} \tag{4}$$

where the parameter $\boldsymbol{B}$ is introduced to allow scaling to customize the simulated ISI that varied from 2.9 to 3.5 in step 0.2.

The baseband received signal sampled at the chip rate $\boldsymbol{1/T_C}$ can be written as

$$\boldsymbol{r(n) = \sum_{k=1}^{K}\sum_{j} g_k(n - jN)d_k(j) + b(n)} \tag{5}$$

where $b(n)$ is a complex AWGN with power spectral density $N_0/2$, zero mean and variance of σ^2. The $g_k(n) = s_k(n)h_k(n)$, is the convolution of the K^{th} user's spreading code with the channel impulse response, and represents the K^{th} user's signature waveform.

III. ADAPTIVE EQUALIZER

A. Laguerre Lattice Structure

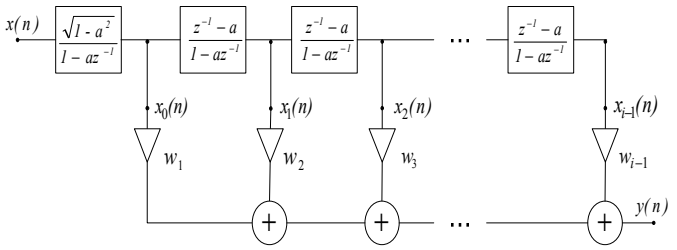


Fig. 1. Laguerre filter.

The basic Laguerre filter is shown in Fig. 1. A transversal filter is converted to a Laguerre filter by inserting a single pole low-pass filter, $L(z)$ at the input and by replacing the delay unit at each stage by a first order all-pass filter $A(z)$. $L(z)$ and $A(z)$ are given by

$$\boldsymbol{L(z,a) = \frac{\sqrt{1-a^2}}{1-az^{-1}}}, \tag{6}$$

and

$$\boldsymbol{A(z,a) = \left(\frac{z^{-1}-a}{1-az^{-1}}\right)}, \qquad \boldsymbol{|a| < 1} \tag{7}$$

here, $\boldsymbol{a}$ is the Laguerre parameter, which denotes a pre-determined pole location for the low-pass filter $\boldsymbol{L(z,a)}$ and all-pass filter $\boldsymbol{A(z,a)}$. Note that for $\boldsymbol{a = 0}$ becomes exactly the transfer function of FIR filter. It is very interesting to verify that in the stationary case the correlation matrix of the internal signals of Laguerre filter, which are given by

$$\boldsymbol{x_i(n) = L(z,a)A^i(z,a)x(n)} \tag{8}$$

is a Toeplitz matrix. This observation suggests immediately that these filters have also a lattice version, which is indeed case [8]. It is interesting to note that this so-called Laguerre lattice filter is very similar to generalized lattice filter, in which the delays of the standard lattice filter are replace by copies of an arbitrary all-pass filter. In the Laguerre lattice filter this all-pass filter is of first order, and these is a first order low-pass preprocessing stage. These are also differences between the transversal filters and Laguerre filters.

The lattice structure of the Laguerre filter is shown in Fig. 2. The update parameters are given as follows :

$$\begin{bmatrix} \boldsymbol{x_i^f(n)} \\ \boldsymbol{x_i^b(n)} \end{bmatrix} = \begin{bmatrix} \boldsymbol{1} & \boldsymbol{k_i^f} \\ \boldsymbol{k_i^b} & \boldsymbol{1} \end{bmatrix} \begin{bmatrix} \boldsymbol{x_{i-1}^f(n)} \\ \boldsymbol{\tilde{x}_{i-1}^b(n)} \end{bmatrix} \tag{9}$$

with

$$\boldsymbol{x_0^f(n) = x_0^b(n) = L(z,a)x(n)} \tag{10}$$

where

$$\boldsymbol{k_i^f = \frac{E\left\{x_{i-1}^f(n)\tilde{x}_{i-1}^{*b}(n)\right\}}{E\left|\tilde{x}_{i-1}^b(n)\right|^2}} \tag{11a}$$

$$\boldsymbol{k_i^b = \frac{E\left\{\tilde{x}_{i-1}^b(n)x_{i-1}^{*f}(n)\right\}}{E\left|x_{i-1}^f(n)\right|^2}} \tag{11b}$$

and where $\boldsymbol{\tilde{x}_{i-1}^b(n) = A^i(z,a)x_i^b(n)}$, and $\boldsymbol{k_i}$ is the reflection coefficients.

B. RLS algorithm with an adaptive forgetting factor

The RLS algorithm is one of the most efficient techniques for estimating the channel response. In this paper, RLS algorithm is used to update the coefficient of the filters. Denoting by $\boldsymbol{w_n}$ the matrix of coefficient at time $\boldsymbol{n}$. The most important key factor affected the performance of the algorithm is the forgetting factor, $\boldsymbol{\beta}$, that we have to select the appropriate value for the conditions of the filter.

The RLS algorithm for update $\boldsymbol{w_n}$ is summarized as follows:

$$\boldsymbol{k(n) = \frac{P(n-1)x(n)}{\beta(n) + x^H(n)P(n-1)x(n)}} \tag{12}$$

$$\boldsymbol{e(n) = d(n) - w^H(n-1)x(n)} \tag{13}$$

$$\boldsymbol{P(n) = \frac{1}{\beta(n)}[P(n-1) - k(n)x^H(n)P(n-1)]} \tag{14}$$

$$\boldsymbol{w(n) = w(n-1) + k(n)e^*(n)} \tag{15}$$

where $\boldsymbol{P(0) = \delta^{-1}I}$, $\boldsymbol{I}$ is identity matrix$(\boldsymbol{M \times M})$and $\boldsymbol{\delta}$ is small positive constant, $\boldsymbol{k(n)}$ is the Kalman gain vector, $\boldsymbol{w(n)}$ is coefficient of the filters, where $\boldsymbol{w(0) = 0}$, and the forgetting factor, $\boldsymbol{\beta}$, is adaptable in order to match with the instantaneous channel conditions. Note that we have added the time $\boldsymbol{n}$ to $\boldsymbol{\beta(n)}$ to emphasize that it may vary with time. The

objective is to find the particular value of $\boldsymbol{\beta}$ that derived by the variable step size least mean square (VSLMS) algorithm[4].

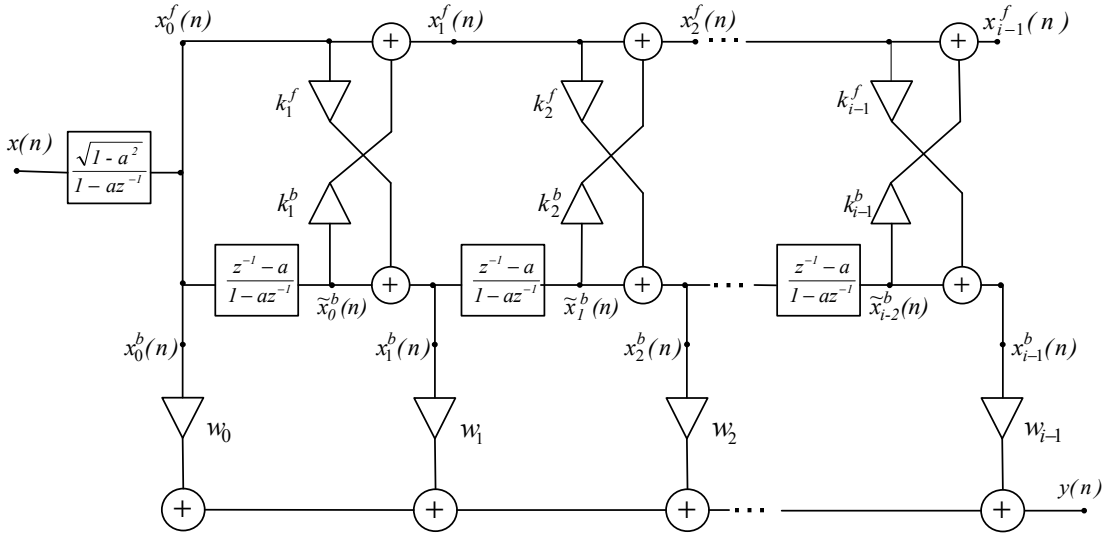


Fig. 2. Laguerre lattice filter.

We may summarized the RLS algorithm with adaptive forgetting factor as follows:

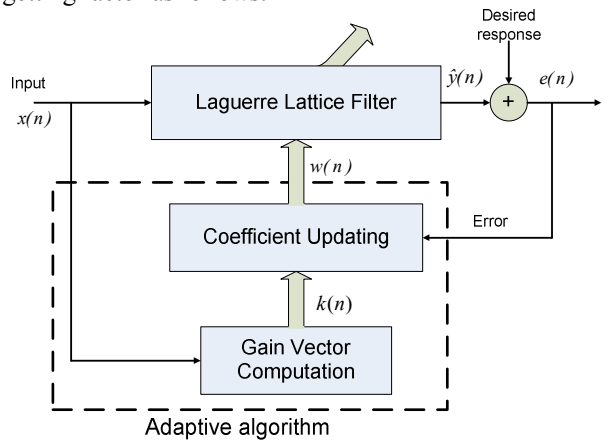


Fig. 3. Adaptive Laguerre lattice equalizer with the variable forgetting factor RLS algorithm.

$$\alpha(n-1) = 1 - \beta(n-1) \tag{16}$$

$$\alpha(n) = \{1 + \rho sign[z(n)]\}\,\alpha(n-1) \tag{17}$$

$$sign[z(n)] = sign[e(n)e(n-1)] \times sign[x^H(n)k(n-1)] \tag{18}$$

$$\beta(n) = 1 - \alpha(n) \tag{19}$$

where starting with value $\beta(n-1)$ close to unity and ρ is constant positive large.

Block diagram of the adaptive equalizers with the variable forgetting factor RLS algorithm is shown in Fig. 3.

IV. Simulation Results

We consider a synchronous DS-CDMA system, where over both MAI and ISI channels. The adaptive equalizer processes begin with decision of the optimal pole and initial value of tap-weight of the Laguerre filter and Laguerre lattice filter. The main system parameters are defined as follows: support 4 users that each user transmits 10,000 bits, processing gain = 4 for spread spectrum and with long impulse response 25 paths. Adaptive forgetting factor RLS algorithm's parameter define as positive constant $\boldsymbol{\delta = 0.3}$. The VSLMS was run initialized at $\boldsymbol{\beta = 0.996}$ and the value of step size is set to $\boldsymbol{\rho = 9 \times 10^{-6}}$.

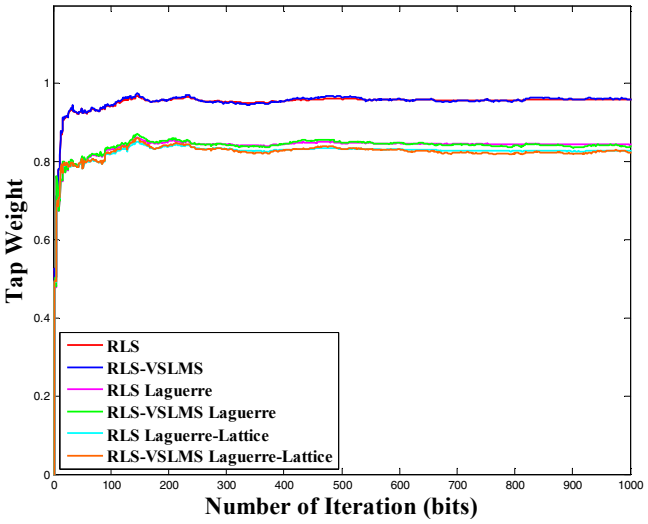


Fig. 4. Convergence process of adaptive equalizers.

Fig. 4 compares the convergence performance of the RLS algorithm and the variable forgetting factor RLS algorithm for the conventional adaptive Laguerre equalizer and adaptive Laguerre lattice equalizer. From Fig. 4, it is evident that the variable forgetting factor RLS adaptive equalizer by using VSLMS algorithm with Laguerre lattice structure is potentially more suited to DS-CDMA system because that fast convergence.

Fig. 5 shows the average BER for each SNR. From the simulation results can be observed that the variable forgetting factor RLS adaptive Laguerre lattice structure equalizer by

using VSLMS algorithm has lowest BER when compared to the conventional adaptive equalizer for every SNR.

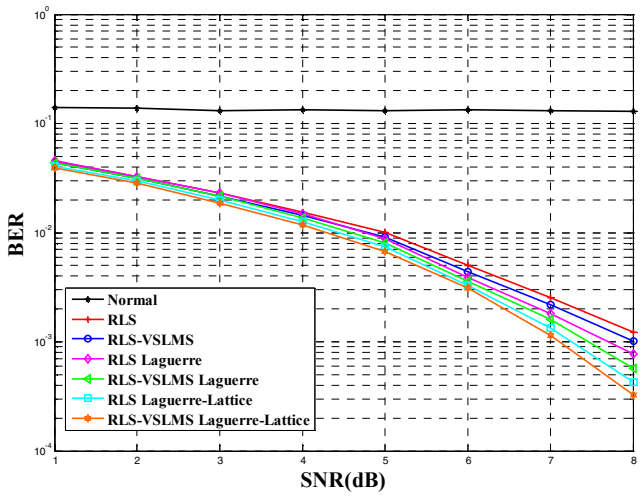


Fig. 5 Average BER performance of adaptive equalizers.

V. Conclusions

We have presented a variable forgetting factor RLS adaptive equalizer for DS-CDMA multi-user communication system based on adaptive Laguerre lattice filter that can eliminates the effect of AWGN, ISI and MAI. The proposed scheme achieves much better equalization performance than the conventional adaptive equalizer.

References

[1] Dimitris G. Manolakis, Vinay K. Ingle, Stephen M. Kogon, *Statistical and Adaptive Signal Processing*, Artech House, Inc., London, 2005.

[2] R. Michael Buehre, *Code Division Multiple Access (CDMA)*, Morgan & Claypool, 2006.

[3] A. Charoenphol, M. Lertwateechakul and C. Benjangkaprasert, "Adaptive equalization for DS-CDMA multi-user communication system based on adaptive Laguerre lattice filter," *International Conf. on Control, Automation and Systems*, pp.1970-1973, Oct. 2010.

[4] S. Haykin, *Adaptive Filter Theory*, 4th edition, Prentice-Hall, 2002.

[5] B. Farthang-Boroujeny, *Adaptive Filters Theory and Applications*, John Wiley & Sons, 1998.

[6] H.J.W. Belt, A.C. den Brinker, "Laguerre filters with adaptive pole optimization," *International Symposium on Circuits and Systems*, Vol. 2, pp. 37-40, May. 1996.

[7] S. He and X. Shan, "Adaptive equalization for multipath fading channels using laguerre filters," *IEEE Pacific Rim Conf. on Communications, Computers and Signal Processing*, vol. 1, pp. 450-453, Aug. 2003.

[8] T. Oliveira e Silva, "Optimality conditions for Laguerre lattice filters," *IEEE Signal Processing Letters*, Vol. 2, no. 5, pp. 97-98, 1995.

[9] Z. Fejzo, H. Lev-Ari, "Adaptive Laguerre-lattice filters," *IEEE Trans. Signal Processing*, Vol. 45, no. 12, pp. 3006-3016, 1997.

[10] S. Veena, S.V. Narasimhan, "Improve active noise control performance based on Laguerre lattice," *IEEE Trans. Signal Processing*, Vol. 84, pp. 695-707, Apr. 2004.

[11] V. Krishnamurthy and S. Singh, "Adaptive forgetting factor recursive least squares for blind interference suppression in DS/CDMA systems," *International Conf. on Acoustics, Speech, and Signal Processing*, vol. 5, pp. 2469–2472, Jun. 2000.

[12] S. Md Salleh, M.O. Tokhi and M. Mohamand, "Modelling of a flexible plate using RLS with variable and directional forgetting factor," *International Conf. on Mechatronics*, pp. 1-6, Apr. 2009.

Eliciting Essential Requirements for Social Networks in Academic Environments

Vala Ali Rohani
Department of Software Engineering
Faculty of Computer Science
University of Malaya
Kuala Lumpur, Malaysia

Siew Hock Ow
Department of Software Engineering
Faculty of Computer Science
University of Malaya
Kuala Lumpur, Malaysia

Abstract: Recent years have witnessed the generation of online social networking web sites, in which millions of members publicly articulate mutual friendship relations and share user-created contents. But it is just a few years that we have seen some efforts to create special social networks to be used in academic environments. Considering the increasing needs for this kind of web sites, we did a comprehensive survey on more than 20 academic social networks for gathering and categorizing the essential requirements for this kind of web sites.

Hence, having some good experiences by creating the Iranian Experts Social Network with more than 120,000 official members, in this paper we try to clarify the features of Social Networks in academic environments and propose a category for their requirements.

Keywords: Social Networks, Academic Social Networks, Requirement Elicitation

INTRODUCTION

The majority of Internet users have visited thousands of social networking sites. They have taken advantage of the free services of such sites in order to stay connected online with their offline friends and new online acquaintances, or to share user-created contents, such as photos, videos, bookmarks, blogs, etc.

Most of these social networks are developed for public purposes which allow a wide range of internet users in different ages, interests, social and academic levels to join them and make their own friendship network.

As two most popular ones, MySpace claims over 250 million registered users while Just recently, Facebook has announced that it has passed the 500 million member mark [14,15]. Twitter, the social networking site that features 140-character messages, called microblogs, are so popular in the US that it has spawned such words as twitter, tweed, and twitterati [16]. Half the Internet users in Brazil are registered in orkut while 87% of the Internet users in the Philippines are members of Friendster. These two social networks originated in the US, but have been overshadowed by other sites and instead enjoy popularity elsewhere. [17].

Universities, Colleges and higher education institutions are constantly being refreshed with new members while being connected with graduates seems to be vital too. In most cases, Students use the systems only out of necessity rather than choice, preferring to self create study groups on Facebook.

But is obvious that the academic society and definitely their members, need some special facilities to leverage the regarding communication between students, graduates, instructors and all other members of academic environments.

The Social Friend in MySpace sometimes equates to ‘‘an old and valued friend’’ but also equates to a ‘‘celebrity fan’’. The Social Friend in an academic network has status, trust, funding, tenure and potential associated with it [18].

In 2007 the University of Cambridge experimented with exposing secure content from its Virtual Learning Environment to sites like FaceBook and iGoogle, as well as desktop ‘Widgets’ such as Mac Desktop Widgets, Windows Vista Sidebar Widgets and Google Desktop Gadgets. During the same period the University carried out a ‘Learning Landscape’ study that investigated, among other things, student use of technology. Our conclusion was that use of, and dependence on, external sites for mainstream learning support has significant drawbacks - such as lack of access to content for marking and record keeping, lack of even student control over content, privacy concerns, etc.

However, it was equally clear that students found their interactions with social networking sites far more rewarding and intuitive than their interaction with institutional software [19].

LITERATURE REVIEW

There are thousands of social Web sites and several ones in academic environments which differ in details and layouts of the features they provide. Further, they continue to add new features and make changes to existing features. In this section we tried to do a literature review on social networks in academic environments with the aim of eliciting features which cover the essential needs of academic social networks.

During our research in this field, we faced to 10 popular social networks which specially were used in academic environments such as Academia.edu, ResearchGate.com, mendeley.com, UniversityNetwork.org, classmates.com, teachstreet.com, gradeguru.com, campusbuddy.com, Digication.com and Sakai.

As the result of our survey, we introduce the features of the four most popular academic social networks.

A. Academia.edu

This section is about Academia.edu, a social networking website for academics which leverages powerful techniques from the social networking web in a way that is easy and accessible for academics. But it overlooks some the most fundamental social networking techniques as well.

When you sign up, you create a user profile as you would on most social networks, but with one big difference: you tag yourself with topics that are related to your research. The site can be used to keep in touch with your peers, but one of its biggest selling points is its News Feed, which includes a stream of research items that the site believes you'll be interested in based on those tags. This is similar in some ways to Facebook's News Feed, with one key difference: Facebook tends to suggest items your friends are interested in. Academia.edu does this too, but it has more of a discovery focus, and tries to surface articles you'll be interested in even if they haven't been shared by one of your coworkers.

As the positive points, we can mention to its functionality, database and interface. Academia.edu is a free and easy way for academics to publish their bios, publications, contact information, and Twitter-like status updates for the entire world to see. Further to that, users can use specialized search terms like research interests and departmental affiliations to find like-minded individuals and forge potential connections. I briefly mentioned that users can post publications, but I want to emphasize what an easy way this is for academics to highlight the work they feel best represents what they're currently interested in. Furthermore, the Academia.edu site allows users to easily write blog posts that become part of their online profile.

The information about thousands of post-secondary institutions has been populated into the Academia.edu database. So when a new academic user first registers, the site intuitively auto-populates the information about their academic institution and department. A simple example of this is the fact a PhD candidate from, say, the University of Waterloo's English department, can choose the appropriate departmental title, the "Department of English Language and Literature," instead of simply a generic title like the "Department of English." Academia.edu achieves this by allowing users to populate the database as they register. So the first registrant of a given department paves the way for subsequent registrants to easily select their department from a list of options.

In terms of user interface, Academia.edu has done everything right. The layout is clean and clear with solid web architecture. And one of the most noticeable aspects of the site is the visual layout of academic departments. Once a user has chosen their institution and department, they can see the other faculty members, graduate students, and staffs who are also Academia.edu users.

Of course, it has some problems too. Users can't filter the site's feeds. The feeds are scrolling updates about users posting papers, status updates, profile changes, etc. You'll be most familiar with this user interface from Facebook. Academia.edu claims that the site uses your reported research interests to populate your feed with information you'll find relevant. Well this is just not true.

In most cases, the users are interdisciplinary researcher with interests in different areas. Perhaps this diversity is the reason his/ her feed is constantly clogged with information about academics who he/she not interested in and papers.

Although the site allows you to "Follow" the work of some academics, this doesn't occlude the work of academics you've never heard of from appearing in your newsfeed.

B. ResearchGate.com

ResearchGATE is a free social networking site and collaboration tool aimed at scientific researchers from all

disciplines of science (Fig. 1). It provides web applications including semantic searching (whole abstract searching), file-sharing, publication database sharing (e.g. endnote libraries), forums, methodology discussions, groups etc. Members can create their personal blog within the network. Since May 2008, ResearchGATE has gathered a user base of more than 250,000 researchers from 196 countries [3].

The custom designed semantic search engine built by ResearchGATE represents a new way to search for information. Instead of simply relying on matching keywords, semantic search returns hits that are meaningfully related to what you're looking for. Using semantic search allows you to be more efficient and effective than ever before.

The semantic search engine also uses your profile information to recommend fellow researchers, groups, literature, and other ResearchGATE resources that may be of interest to you.

Using ResearchGATE's internal search engine allows you to simultaneously search seven major databases consisting of over 35,000,000 articles and conference abstracts. All databases are updated daily.

The databases are: Pubmed , Arxiv , Pubmed Central , IEEE , RePEc , Citeseer , NASA Library and Directory of Open Access Journals.

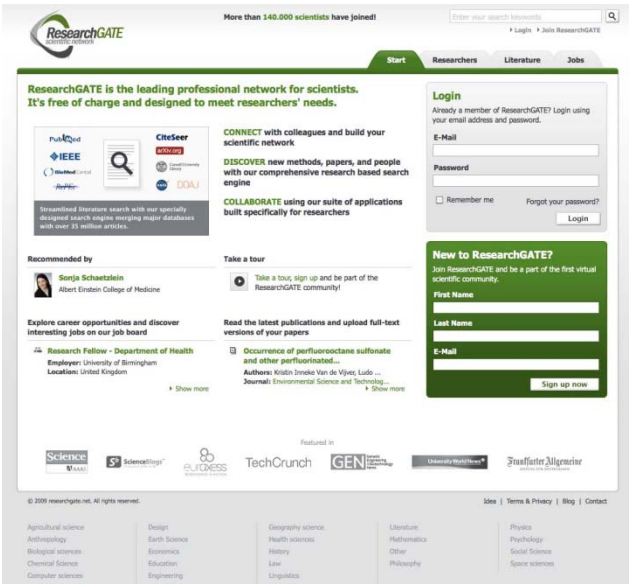


Figure1. ResearchGATE web site

When you view an article you can see other members that have added it to their personal library which you can then view.

Every scientific paper accessible via our search engines can be rated and commented on by ResearchGATE members. This unique tool creates a new way of discussing and sharing research results within the scientific community. Since our publication database of more than 35 million articles is updated daily, you can rate even the most recent publications. You can select between five different rank levels from „not interesting“ to „remarkable“. The number of rankings and the average ranking level will be displayed.

C. Mandely.com

Mendeley is a research management tool for desktop & web. You can also explore research trends and connect to other academics in your discipline. Mendeley is used at, and endorsed by, some of the world's leading research institutions (Fig. 2). Based in London, it is funded by some of the people behind Skype, Last.fm, and Warner Music [5].

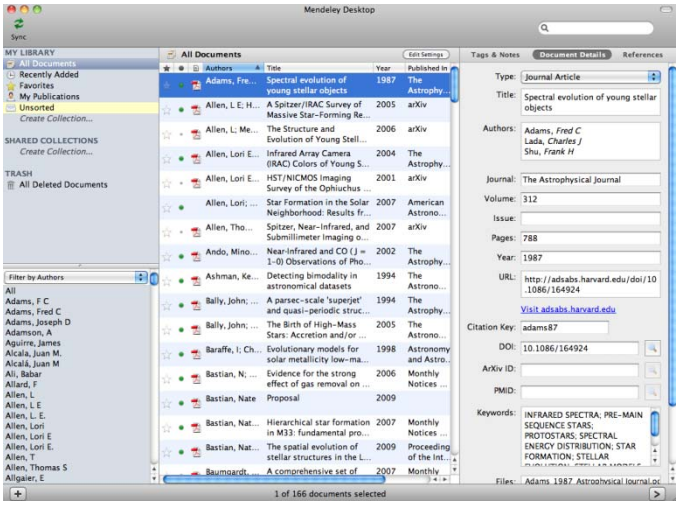


Figure2. Mendeley web site User Interface

Mendeley Desktop organizes your research paper collection and citations. It automatically extracts references from documents, generates bibliographies, and is freely available on Windows, Mac OS X and Linux. It automatically extracts bibliographic data, keywords, and cited references from your PDFs and turns them into a searchable full-text database. Also it imports and exports different file formats like BibTeX, RIS or EndNoteTM XML. It also syncs continuously with other reference managers like Zotero or CiteULike.

Mendeley Web lets you access your research paper library from anywhere, share documents in closed groups, and collaborate on research projects online. It connects you to like-minded academics and puts the latest research trend statistics at your fingertips.

D. TeachStreet.com

TeachStreet is a dynamic online community that brings motivated learners and talented teachers together. On one hand, this is a place where people who love to learn can find classes that are just right for them. On the other, we offer a public forum that helps teachers, coaches, and other experts share what they know. In the process, TeachStreet helps these experts grow their businesses with simple online tools they can use to promote their classes, workshops and special events.

In short, the TeachStreet team is a bunch of dreamers and tech geeks who want to encourage people to get away from their computers, get out into the real world, and learn something new. So we support that goal by helping people find experts in their own neighborhoods who can teach them face-to-face.

TeachStreet is privately-funded and located in downtown Seattle, WA. It has formally launched in major cities all over the U.S. and are growing bigger all the time. In fact, customers have listed classes in more than 500 cities across the country.

E. Sakai

Leading educational institutions throughout the world choose Sakai to enable powerful teaching and learning and research collaboration. Depending on where you are in the world, Sakai might be called a Course Management System (CMS), a Virtual Learning Environment (VLE) or Learning Management System (LMS). While Sakai is typically used for teaching and learning (similar to products like Blackboard and Moodle) we call it a Collaboration and Learning Environment (CLE) because it embraces uses beyond the classroom.

Sakai's open approach allows institutions to deploy, host and modify the software in whatever manner best supports institutions skills, needs and goals. Sakai's open development process allows local enhancements to be incorporated into future versions of the software.

This social network embraces both open source and open standards. We use open source software within our technology whenever possible and base as much work as we can on open standards. Sakai enables an open approach to support models allowing choices between institutional support, community support and commercial support, each with unique benefits and costs [12].

Sakai provides users with a suite of capabilities that best meet the needs of today's teachers and learners. The functionality can be assembled to create spaces for a variety of purposes. The list of Sakai current core tools is provided below. In addition, there are a large number of add-on tools (called "contrib") available that are in use by many Sakai institutions.

The Sakai CLE is a flexible, enterprise application that supports teaching, learning and scholarly collaboration in either fully or partially online environments. Sakai also has a robust and full-featured online portfolio system built-in. The Sakai CLE is distributed as free, open-source software, which offers the ultimate in flexibility and avoids the risks of vendor lock-in and escalating license costs.

ESSENTIAL FEATURES OF ACADEMIC SOCIAL NETWORKS

In this section, we will provide taxonomy of essential features of academic social web sites and then, compare them to current social networks features in academic environments.

They are separated in 4 categories:

a) Administrative Features
b) Collaborative Features
c) Reporting Features
d) Integrating Features

As mentioned in TABLE 1, the administrative features of academic social networks are categorized to 6 groups. The first 6 capabilities are common between all types of users are considered as General. The assignment uploading is considered for students who use this model and join this academic social network. Lecturers also need some special feature for handling their tasks in this model. Four features are considered for lecturers. There are other types of users which we can them as Researchers. They are not necessarily the lecturers. So we consider Research Field Following Management and My Publications Management for this kind of users. There are two level of administration in this model which will be handled by university and social network administrators. The last two groups of features is dedicated to this type of users.

TABLE 1. Administrative Features of Academic Social Networks

A) Administrative Features					
General	1.Create and Editing profile 2.Editing Privacy Settings 3.Uploading Publications 4.Billboard management 5.File Repository Management 6.Freinds Network Management 7.Membership 8. Forum activities	**For Students**	1. Assignment Uploading	**For Lecturers**	1.Uploading assignments 2.Building Courses 3.Managing Course Student Forums 4.Course Membership Management
For Researchers	1.Research Field Following management 2.My Publications management	**For University Administrators**	1.Editing University Information 2.Managing Faculties Information 3.Abuse Report Management 4.News Letter Management	**For Social Network Admin**	1.Confirming a University 2.Abuse Report Management

For persuading the social network users to check their profiles continuously, we should pay special attention to the collaborative features. TABLE 2 shows the list of suggested collaborative features in academic social networks. Personal billboards are amazing capability for announcing the personal feelings while the general billboard can be helpful in informing the last news of an organization (e.g. a university). All of the social network users need peer-to- peer message passing system and friendship network to be connected to their friends. Discussion forums and online groups can play a significant role in mechanizing the organizations in academic environments. We cannot forget the online chat as one of the most favorite features of social networks.

TABLE 2. Collaborative Features of Academic Social Networks

B) Collaborative Features	
1. Personal and General Billboard	5.Discussion Forums
2.Peer-to-Peer Message passing	6.Online Groups
3.General Announcement	7.Online Chat
4.Friendship Network	

Reporting services in social network can update the user information about his/her current position among the other users. TABLE 3 shows the list of necessary reporting features for our model in academic social networks.

Pointing and ranking mechanism can create an enthusiasm for users to increase their rank and enhance their position in the social network of their university or colleges. We can consider different parameters for using in pointing mechanisms. Usually the number of invites, the count of scientific posts and also rate of user activities in answering to other members' questions are considered as basic parameters for this purpose.

Sending daily scientific news to members email is one of the most effective alternatives for encouraging users to login to their profile periodically.

TABLE 3. Reporting Features of Academic Social Networks

C) Reporting Features
1.Points & Ranks Management and Reporting
2.Daily Scientific News Letter Sending
3.Different Transaction Notifications

The most important feature group of this model is Integrating Features (TABLE 4).

TABLE 4. Integrating Features of Academic Social Networks

A) Integrating Features					
General	1.Common Billboard 2.Single Signup Mechanism 3.Common Calendar	**For Students**	1.Group Building 2.Common Assignments	**For Lecturers**	1.Common Course Management 2.Common Q&A Service 3.Common Paper Reviewing Service
For Researchers	1.Common Research Following UP 2.Common Paper Reviewing Service	**For University Administrator**	1.Common News Letter 2.Common Discussion Forum Topics 3.Common Survey		

According to survey in academic environment, we face to the need of integration between academic organizations social networks. Hence, we categorize these types of features in five groups according to its user domains.

Some features like Common Billboard and Calendar are common among all social network members. Also, this model should prepare a special service to enable the its users to have several profiles regarding different social networks while having just a single Username and password. We named this service the Single Signup Mechanism.

Regarding the students view point, this model provides some features for building scientific groups and also some services for doing teamwork in group assignments.

This kind of features helps lecturers managing the shared course contents as well as handling the common Question and Answers services. Usually, the lecturers and researchers needs to cooperate with each others in some scholarly tasks such as paper reviewing. They can use the prepared service in this manner to interact with each other as well as possible.

Maybe it would be too amazing for autonomous universities to share some services of their separated social networks with each other. In these cases, the integrating features which considered for University Administrators level can enable them to have inter-organization newsletters and discussion forums.

CONCLUSION

This paper did a survey on current academic social networks for eliciting the social networks necessary requirements in academic environments. According to our investigations, each of them had their own positive and negative points.

After investigating their most popular ones, we categorized the most important and necessary features of a model for developing academic social networks in four categories includes Administrative, Collaborative, Reporting and Integrating features.

This set of requirements can be used to design an architecture for autonomous and integrated social networks to enhance the interaction and teamwork between the students, graduates, lecturers, official staffs and researchers. By using this architecture, Universities and higher education colleges will be able to have their own social network for managing the academic e-content in their domains.

ACKNOWLEDGMENT

The authors wish to acknowledge the collaborative funding support from the Fundamental Research Grant Scheme (FRGS). Under grant no. FRGS/1/10/TK/UM/02/14.

We also wish to acknowledge the valuable contributions of the numerous companies and individuals who participated in the surveys.

REFERENCES

[1] http://allanmcdougall.wordpress.com/2010/03/16/academic-pr-2/, Accessed 10 Feb. 2010.

[2] http://techcrunch.com/2010/04/28/academia-edu-raises-1-6-million-to-help-researchers-connect-with-each-other, Accessed 5 Feb. 2010.

[3] http://en.wikipedia.org/wiki/ResearchGate#cite_note-2, Accessed 10 Feb. 2010.

[4] http://help.researchgate.net/Literature, Accessed 4 Aug. 2010.

[5] http://www.mendeley.com/organize-research-collaboration/, Accessed 12 June. 2010.

[6] http://www.universitynetwork.org, Accessed 10 Feb. 2010.

[7] http://www.teachstreet.com/about-teachstreet, Accessed 12 Feb. 2010.

[8] http://proquest.umi.com/pqdweb?index=2&did=1818538211&SrchMode=2&sid=5&Fmt=3&VInst=PROD&VType=PQD&RQT=309&VName=PQD&TS=1276160065&clientId=18803, Accessed 25 July. 2010.

[9] http://proquest.umi.com/pqdweb?index=6&did=1594495261&SrchMode=2&sid=5&Fmt=3&VInst=PROD&VType=PQD&RQT=309&VName=PQD&TS=1276160065&clientId=18803, Accessed 3 Feb. 2010.

[10] http://proquest.umi.com/pqdweb?index=10&did=1125986851&SrchMode=1&sid=5&Fmt=3&VInst=PROD&VType=PQD&RQT=309&VName=PQD&TS=1276160275&clientId=18803, Accessed 13 July. 2010.

[11] PR Newswire. New York: Sep 12, 2006.

[12] http://sakaiproject.org/product-overview, Accessed 8 June. 2010.

[13] http://sakaiproject.org/features, Accessed 12 May. 2010.

[14] Adam Ostrow, It's Official: Facebook Passes 500 Million Users, Mashable/Social Media, 24 July 2010, http://mashable.com/2010/07/21/facebook-500-million-2/

[15] B. Stone, Is Facebook growing up too fast, The New York Times, March 29, 2009.

[16] D. Pogue, Twitter? It's what you make it, The New York Times, February 12, 2009.

[17] The future of social networking sites like Orkut, Ryze, Friendster, /http://www.webtalkguys.com/020704.shtmlS.

[18] Ian Boston, "Racing towards academic social networks", ON THE HORIZON, VOL. 17 NO. 3 2009, pp. 218-225, Q Emerald Group Publishing Limited, ISSN 1074-8121.

[19] Laura James, "JISC Academic Social Networking Final Report", 22 April 2010

New Metric for Measuring Programmer Productivity

Marwa Solla[1], Ahmed Patel[2], Christopher Wills[3], Raed Alsaqour[4]

[1, 2,4]Department of Computer Science, Faculty of Information Science and Technology
Universiti Kebangsaan Malaysia 43600 Bangi, Selangor Darul Ehsan, Malaysia

[1]Department of Computer Science, Faculty of Sciences
AlFateh University, Tripoli, Libya

[2,3]Faculty of Computing Information Systems and Mathematics
Kingston University,
Penrhyn Road, Kingston upon Thames KT1 2EE, United Kingdom

[1]marwa.solla *at* gmail.com, [2]whinchat2010 *at* gmail.com, [3]ccwills *at* kingston.ac.uk, [4]raed.saqour *at* ftsm.ukm.my

***Abstract*- Measuring programmer productivity is a challenging exercise because it is not well understood since it is without bounded rules and ill-defined meanings of complicated set of parameters. This is made worse by new software development paradigms such as agile and mashup methods and the ensuing advances in software engineering practices and ways of designing and developing software. The existing metrics for measuring performance of solo and pairs of programmers does not appear to be suitable to meet these new forms of software development. This paper presents a new metrics which can be used to measure performance productivity of programming effort by solo and pair programmers in a much more comprehensive manner. All of the key parameters are looked at objectively and defined for and from software engineering lifecycle points of view to make productivity performance calculations for solo and pair programmers. The methodology used for formulating and composing the formulae and defining the parameters as coefficients is explained. These parameters are based on a weighting system to derive the effective performance results. It is a more objective and quick way for the performance analysts to define a table of weights for the parameters based on several criteria within the different aspects of the software development lifecycle. The composition of the formulae and the metric for measuring programmer productivity performance is presented and examples are used to illustrate the method and the outcomes.**

Keywords: solo and pair programming, software metric, parameters, weights, calculation, measurement, lifecycle software development methods, agile, mashups

I. INTRODUCTION

Software engineering has become a scientific discipline that is concerned with methods, principles, approaches, measurements and tools for the development of all kinds of software systems, from initial life-cycle stages of problem definition, requirements capture, system specification, through to testing and maintaining the system throughout the life of its use [1]. Currently, various methods such as *agile development methods*, *component-based software engineering*, *aspect-oriented software development*, and *mashup application development* are in vogue [2]. They have gained popularity within the industry and have become areas for academic research. On the one hand, much attention has been given to these methods as the software industry strives for better production quality because they are designed to produce useful working software quickly. On the other hand, increasing productivity with higher levels of quality assurance and measurements programmer performance has been lagging behind. Hitherto the measurement of productivity, the determination of the costs of production which itself may inform the determination of the selling price of software, has not been an exact science. A more appealing way to do this would be to have advanced metrics. This is best achieved by including software metrics in the software development life cycle itself so as automatically to facilitate measuring the productivity performance of the development and quality of software. Software metrics are an important part of software development and as such should be used from the early stages of every phase of the software development life- cycle so as to ensure that maximum benefit is derived. Although at first glance, the solutions proposed by the metric seem generic, it requires customization for each individual software project. Moreover, productivity benchmarks and quality measures, the allocation of weights to parameters by each software house or company are likely to be different depending on variances in production and cost factors. Even in the same company, different software projects will have different requirements and cost structures, depending on the type and scope of the individual project. While the complexity of software projects is not underestimated, one has to strive to provide realistic and simplified reasoned metrics to measure, forecast and determine the duration and cost of such projects. We attempt to do this within the context of solo and pair programming.

Our metric offers the generic structure within which project managers, analysts, project leaders and developers can plug-in the parameters and adjust the weights to meet their specific circumstances. These software measurement metrics should also be used to improve the productivity and quality of software through measuring programmer performance.

The paper is organized as follows: In Section II, the definitions of solo and pair programming are given. In Section III, solo and pair programming methods are compared which includes their benefits and weaknesses. Section IV outlines

software measurement techniques. Section V reviews related works of using metrics to measure programming effort. Section VI reports the problems experienced in the use of existing metrics. Section VII presents our new metric for measuring programmer productivity performance. Finally Section VIII offers a brief discussion and conclusion.

II. Solo And Pair Programming

Definitions:

Solo Programming (SP): refers to a programmer working as a developer and coder alone on software development tasks, without necessarily sharing programming thinking or workspace with other programmers. The single programmer reads the program specification as to what software to develop, designs the program, codes the program and often reviews the code while testing and debugging until the program works as required by the specification.

Pair Programming (PP): is a method in which two programmers work at a single computer, sitting side-by-side to develop the software. They work jointly on the same design, algorithm and code and they debug and test the program as they develop the complete piece of software. One programmer is called a *driver* who writes down the design and focuses on entering the code. The second programmer is called the *navigator*, whose work is to observe the driver as necessitates, discuss, look for flaws or strategic defects, and to forecast in order to point out problems, offer suggestions or alternative methods while planning the next set of steps in the task functions of the software development job [3].

III. Comparing Pair versus Solo Programming

The studies of PP technique have increased in recent years, with quite a number performed on the effectiveness of PP over SP [4]. There are many opposing views on the effectiveness of pair programming. Some argue that PP is not as productive as SP, whereas others agree that PP has brought many benefits to software industry [3]. An experiment run by professional programmers showed that pair programmers outperformed the solo programmers [5] in agile developments[1]. PP improves and produces better design quality [6,7]. Some accepted that PP is useful for learning complex tasks [8]. Pair programmers complete their tasks faster than solo programmers [7]. However, this is not always the case. In some tasks, pair programmers spent the same amount of time as solo programmers but the SP teams were much more successful in finding and fixing defects than the PP teams [9]. Another controlled experiment showed that pair programming is less efficient than SP [10,11]. The variation of results between the experiments proves that there is no constructive evidence to suggest that PP is far more productive than SP or vice versa. Table I summarizes the pros and cons of both SP and PP.

TABLE I
Comparsion Between Pair And Solo Programming

Technique / Task	Pair programming	Solo programming
Methodology	Agile software development method	Traditional software development method
Advantages	• Higher design quality with fewer defects. • Knowledge transfer. • Higher satisfaction and confidence in work. • Students were more likely to complete their course. • Shorter time to complete a programming task.	• Within SP method used, person's time management is easier; no partner to wait for. • Many developers feel they cannot achieve the same level of concentration & creativity when working with a partner.
Disadvantages	• Scheduling time • Disagreement between PP. • Some developers may receive undeserved credit for completion of a program. • PP increases the cost of software development.	• More time consuming to deliver the new system. • No sharing of ideas with other programmers • Programming alone could cause misconstruing of the requirements task more than a team programming.

IV. Metrics And Measurement

Several metrics have been used to measure programmer productivity and quality of software, the most common ones includes lines of code, function points, McCabe method, C&K method and COCOMOII [1].

Lines of code are the oldest software size metric. They are used to measure the amount of code in a software program to estimate productivity and measure the production ratio of programmers [12]. This metric has a drawback. It fails to measure programmer productivity since a professional programmer may produce fewer lines of code to implement a task than another less experienced programmer. Despite its weaknesses, it is still used because of its simplicity [13].

Function points are one of the most common techniques for measuring the size and complexity of a development task. They are useful in estimating projects and measuring functional requirements [14]. Function points measure can be used as an input to estimate effort and cost of software [15], and are widely used in software development. However, function points are not easy to do properly [13].

McCabe's cyclomatic metric is popular with the researchers because it is simple to calculate by static analysis. It is a measure of module control flow complexity based on graph theory. It also provides a quantitative measure of the logical complexity of the program. This method is calculated by using the control flow graph of the program, which then transfers the control flow chart into the flow graph [16].

C&K method is object oriented and is a well known design metric for measuring design quality. It includes six object oriented parameters in the metric [16] based on measurement theory and reflects the viewpoint of experienced OO software programmers [17].

COCOMO II model: Constructive Cost Model II has been developed as a major revision of the original COCOMO model. It has three stages; in the first stage COCOMO II estimates size using object points. In stage 2 COCOMO II applies function points as size measure. In the final stage,

[1] The development of large systems with many lines of code is organized and managed quite differently, particularly in relation to the development of safety-critical software.

development has begun and more information would be made available [18]. This model is used for both the early design and post- architecture cost model.

V. Related Work

PP has gained popularity within both industry as well as academic research [19], and the research on its effectiveness against SP has been reported by several experiments [4]. Most of these experiments have studied the effect of PP in terms of time, effort and quality. Various metrics have been used to measure the performance of both techniques. A single measurement Relative Effort Afforded by Pairs (REAP) and Elapsed time (t) are used as metric to measure the time and the effort spent to complete a task [6, 5, 10]. The productivity effort of paired team increased by 42% as compared to solo teams [5], while a 15% increase in given in [6], and a 100% increase in [10], and more recently experiment [11] shows an increase of about 84%. Quality is evaluated by the number of test cases passed in several experiments [6, 18], and the score on programming assignment and of the final exam was quality metric [4, 20]. Quality was measured also by evaluating the readability and functionality of the problem solution [5]. These experiments suggested that PP improves quality of software. Productivity is measured by counting lines of code [9, 10]. Additionally, number of solutions that satisfy test cases, and the McCabe`s cyclomatic complexity were used [8]. Different results between PP and SP was reported which depend on the metric used [9]. Other research studies used defects count to estimate the quality of the developed software [6, 17, 4], as well as Chidamber & Kemerer's metric [21] was used to measure program complexity. However, these metrics are restrictive in that they only take a subset of measuring parameters into account, and also they are inappropriate for measuring programmer performance within the new paradigms and aspects of designing and developing software. Advanced software engineering practices and comprehensive measurements of not only productivity, but also other factors like cost and pricing have to be taken into account for the metrics to be meaningful.

VI. Problems With Existing Metrics

Software measurement should be used during every phase of the software development life cycle. When the metrics are used from the early stages of software development life cycle, its effect can be the greatest, assuming that the functionality of the software has been correctly specified [12]. However, if some of the current metrics are used for a particular stage in software development process such as LOC, they concentrate only on the coding phase. This makes it difficult to estimate early in the lifecycle, and cannot be applied until the typing code is completed. On the other hand, more lines of code do not necessarily mean better productivity, nor do they imply quality. Although Function points can be applied in the early stage of the lifecycle but is difficult to do properly [13]. The McCabe method is used just with procedure-oriented programming development [15].

VII. A New Metric Defined For Measuringing Programmer Performance

Measuring programmer productivity can be performed in many different ways as exemplified [22]. While these metric methods are acceptable for what they do in the specific context of the performance measurement and analysis, they are constraining to the point that they fail to take all aspects of the software engineering cycle and working conditions into account through a single composite metric. To overcome this deficiency, a metric to measure performance of a programmer by measuring each phase of software development, working conditions and other environmental factors into account separately and then combining them into a single composite formula to derive the final results. Typically, each component sub-part is a parameter which may have many sub-parts represented by their own parameters to be a key parameter in the top-level formula which gives the overall programmer productivity performance.

The new metric presented here has not been done before. It is a unique way of measuring overall programmer productivity performance. *Solo* and *Pair* programming methods are used to demonstrate the effective use of the metric and benefits supported by the parameters shown in Table II.

TABLE II.
The Main Parameters Of The Metric

The Parameter	***Definition***	***Measure***
Understanding the problem **UP**	Means understand what user requirements are and get feeling of what the developer should do to provide the customer need, what are the methods and techniques he should use to get correct requirements.	How much time does the developer spend on understanding the problem? Could be in minutes/hours/days
Experience of developer **E**	Practical knowledge, skill, or practices has gained by developer. The experience can be in programming, designing, or testing	How many years of experience does the developer have? I.e. a developer has 5 years experience in programming.
Number of the requirements **R**	User requirements that meet costumer's need, and requirements of what the system should provide to users	Does the software meet the requirements of customer's need?
Design Quality **DQ**	How good the design of the software, a good design is elegant and simple; we look at it in term of interface design.	Normally measured by ordinal scale (excellent, very good, good, etc.)
Communication **CO**	Cost of Communication among programmers team has impact on the cost of software development. There are few types of communication patterns between developers such as F2F, online chat, emails, phone calls, and SMS	How is the cost of using communication specially, between the programmers who need to communicate with each other?
Collaborative Work **CW**	Two or more developers work together developing the system. Software developers interact with each other to solve a problem.	Normally measured in terms of the cost of collaborate developers working together in a given time period.
Checking and Reviewing code **CRC**	Check and review code is systematic examination of source code to find and fix defects. Software developers review each other's code.	Normally measured by how much time spent in reviewing code and how many defects can be found, and then how much all of these cost. Measured as cost of time spent to review, check, and fix defects.
Quality of code	Good code is easy to understand	Normally measured by

QC	and readable, it meets all requirements and works right without defects. As well as it should be testable, supportable and maintainable	nominal scale so we consider as agreement (Yes or no)
Defects **D**	Defects or errors found when developer validates requirements, errors found in code	Normally measured by number of errors that we find during running and testing the system
Time (in hours or days) **T**	How much time spent to complete the exercise?	Normally measured by recording time from start to finish of completing the exercise
Satisfaction **S**	It is one of the core outcome measures, how satisfied is the developer and the user?	Normally measured by using Ordinal scales (dissatisfied, satisfied, etc)

These parameters are applied to the software development life cycle. Some of these parameters have sub parameters such as e*xperience, communication, collaborative work,* and *satisfaction*, which can be applied in appropriate phases of software development. The years of experience of programmer are one of the most important parameters that affect the productivity of programmer. Experience can be in programming in General *(EPG)*, in Particular Programming Language *(EPL)*, Experience as Architecture Designer *(EAD)*, or in Experience in Testing *(ET)*. Experience and productivity are inextricably linked. Communication between developers is measured by computing the cost of each sub parameter used in the different phases of the software development life cycle. Collaborative working can be measured by calculating the effort and cost of developers spending time together on a given job and accumulated over the life of the project. Checking and reviewing code is measured in terms of the time effort spent on checking and fixing defects translates into tangible cost. Put all these effort and cost elements together and add other costs such as office space, lighting, insurance etc, give a composite cost value, which translates into money.

Weights distribution is used as well to make our metric more flexible and can be applied by many organizations. These weights are defined in a generic manner so that different analysts can use them according to their perception and judgment of the importance of the metric in question. The weight distribution scale from runs from 1, which means a less important stage of software development, to 10, which in turn means the most important stage in that particular exercise. This gives the flexible ability of using the metric. For instance, suppose that for a particular programming task the analyst perceives that coding is more important than design, and then he can change the weights accordingly within the weighting range to obtain a more balanced result or outcome by taking the maximum value of 10on the scale. Table III shows the full set of the weights distribution.

TABLE III
TABLE OF WEIGHTS FOR THE METRIC

Parameter	***Weights***									
Understanding the problem	1	2	3	4	***5***	6	7	8	9	10
Experience of developer	1	2	3	4	5	6	***7***	8	9	10
Number of requirements	1	2	3	4	5	6	7	8	***9***	10
Design quality	1	2	3	4	***5***	6	7	8	9	10
Communication	1	2	3	***4***	5	6	7	8	9	10
Collaborative work	1	2	***3***	4	5	6	7	8	9	10
Checking and reviewing code	1	2	3	***4***	5	6	7	8	9	10
Quality of code	1	2	3	4	5	***6***	7	8	9	10
Defects	1	2	3	4	***5***	6	7	8	9	10
Time	1	2	3	4	5	6	7	***8***	9	10
Satisfaction	1	2	3	4	***5***	6	7	8	9	10

The weights colored in *red* which are the selecting weights of a particular calculation are set by us and can be changed by the analyst of the exercise at anytime. To calculate the efficiency of each phase that is required to be applied in the top-level formula to obtain the final result, six equations are used. Each equation is for one phase and it has its own parameters. However, we use a general equation for each phase of the software development life cycle, which is:

$$\text{Efficiency of each phase} = \frac{\sum_i Wi*Pi}{\sum_i Wi} \qquad (1)$$

where *i* is the parameter, *W* is the weight distribution, *P* is the percentage parameter value.

A. *Requirement phase:*

The requirements reflect the function which the customers need in the system. This phase contains five parameters as shown in Table IV.

TABLE IV
PERCENTAGE PARAMETER VALUE FOR REQUIREMENT PHASE

% parameter Value	***R%***	***CO***	***CW***	***UP***	***T***
100	100%	0-19	0-16	1	14
90	90%	20-39	17-33	2	16
80	80%	40-59	34-50	3	18
70	70%	60-79	51-67	4	20
60	60%	80-99	68-84	5	22
50	50%	100-119	84-101	6	24
40	40%	120-139	102-119	7	26
30	30%	140-159	120-135	8	28
20	20%	160-179	136-152	9	30
10	10%	180-199	153-169	10	32
0	0	> 200	> 170	> 10	> 32

From this table we can compute the percentage of requirement phase using the following equation:

$$\text{Efficiency of requirement phase} = \frac{(WR*PR)+(WUP*PUP)+(WT*PT)+(WCO*PCO)+(WCW*PCW)}{(WR+WUP+WT+WCO+WCW)} \qquad (2)$$

where *WR* = weight of requirement, *PR* = percentage parameter value of requirement, *WUP* = weight of understanding the problem, *PUP* = *perce*ntage parameter value of understanding the problem, WT = weight of Time, *PT* = percentage parameter value of Time, *WCO* = weight of cost of communication, *PCO* = percentage parameter value of communication, *WCW* = weight of collaborative work, and *PCW* = percentage parameter value of Collaborative work.

B. *Design phase:*

This stage has five parameters as well as shown in Table V.

TABLE V
PERCENTAGE PARAMETER VALUE FOR DESIGN PHASE

% Parameter Value	***DQ***	***CO***	***CW***	***EAD***	***T***
100	Excellent	0-19	0-16	> 11	14

80	Very good	20-39	17-33	10	16
70	Good	40-59	34-50	8	18
60	Adequate	60-79	51-67	6	20
40	Inadequate	100-119	85-101	4	24
30	Poor	120-139	102-119	2	26
20	Very poor	> 140	> 120	1	> 28

To calculate the percentage parameter value of design phase we use the following equation:

$$\text{Efficiency of design phase} = \frac{(WDQ*PDQ)+(WEAD*PEAD)+(WT*PT)+(WCO*PCO)+(WCW*PCW)}{(WDQ+WEAD+WT+WCO+WCW)} \quad (3)$$

where *WDQ* = weight of design quality, *PDQ* = percentage parameter value of design quality, *WEAD* = weight of years of experience as architecture designer, *PEAD* = percentage parameter value of experience as architecture designer, WT = weight of Time, *PT* = percentage parameter value of Time, *WCO* = weight of cost of communication, *PCO* = percentage parameter value of communication, *WCW* = weight of collaborative work, and *PCW* = percentage parameter value of Collaborative work. To obtain years of experience for pair programming, the average of years of experience for both developers is taken into account because we want to derive a single number (years of experience) to apply it equation.

C. Validation of the requirement phase:

Requirements validation is the process of checking if the requirements are defined as the customer really wants, assuming that the customer's needs and wants are not dynamic and change often unrealistically. This phase has four parameters as shown in Table VI.

TABLE VI
PERCENTAGE PARAMETER VALUE FOR VALIDATION OF REQUIREMENT PHASE

% Parameter Value	*D*	*CW*	*S*	*T*
100	0-1	0-16	Completely satisfied	14
90	2-3	17-33	Mostly satisfied	16
80	4-5	34-50	satisfied	18
70	5-6	51-67	Slightly satisfied	20
60	7-8	85-101	Average	22
50	9-10	102-119	Slightly dissatisfied	24
40	11-12	120-130	Dissatisfied	26
30	12-13	131-140	Mostly dissatisfied	28
20	> 13	> 140	Completely dissatisfied	30

To calculate the percentage parameter value of validation of the requirement phase we use the following equation:

$$\text{Efficiency of Validation of requirements phase} = \frac{(WD*PD)+(WCW*PCW)\ (WS*PS)+(WT*PT)}{(WD+WCW+WS+WT)} \quad (4)$$

where *WD* = weight of defects, *PD* = percentage parameter value of defects, *WCW* = weight of collaborative work, *PCW* = percentage parameter value of Collaborative work, *WS* = weight of satisfaction, *PS* = percentage parameter value of satisfaction, *WT* = weight of Time, and *PT* = percentage parameter value of Time.

D. Implementation phase

This is one of the most important phases, which has six parameters as shown in Table VII.

The experience of programmers is one of the most important parameters that can affect implementation phase; the average experience is computed for PP. To calculate the percentage parameter value of implementation phase we use the following equation:

$$\text{Efficiency of implementation phase} = \frac{(WEPG*PEPG)+(WEPL*PEPL)+(WCO*PCO)+(WCW*PCW)+(WCRC*PCRC)+(WT*PT)}{(WEPG+WEPL+WCO+WCW+WCRC+WT)} \quad (5)$$

where *WEPG* = weight of years of experience in programming in general, *PEPG* = percentage parameter value of experience in programming in general, *WEPL* = weight of years of experience in particular language, *PEPL* = percentage parameter value of experience in particular language, here as pair programming to get the years of experience for general programming and particular language, we find the average experience of both developers. *WCO* = weight of cost of communication, *PCO* = percentage parameter value of communication, *WCW* = weight of collaborative work, and *PCW* = percentage parameter value of Collaborative work. *WCRC* = weight of checking and reviewing code. PCRC = percentage parameter value of checking and reviewing code. *WT* = weight of Time and *PT* = percentage parameter value of Time.

TABLE VII
PERCENTAGE PARAMETER VALUE FOR IMPLEMENTATION PHASE

% Parameter Value	*EPG*	*EPL*	*CO*	*CW*	*CRC*	*T*
100	> 10	> 10	0-19	0-16	0-15	12
90	9	9	20-39	17-33	16-25	13
80	8	8	40-59	34-50	26-35	15
70	7	7	60-79	51-67	36-45	17
60	6	6	80-99	68-84	46-55	20
50	5	5	100-119	85-101	56-65	24
40	4	4	120-139	102-118	66-75	30
30	3	3	140-159	119-135	76-85	40
20	2	2	160-179	136-152	86-95	60
10	1	1	180-199	153-169	96-105	120
0	0	0	> 200	> 170	> 105	> 32

E. Testing phase

One of the most essential phases is the testing phase, which has five parameters as shown in Table VIII.

TABLE VIII
PERCENTAGE PARAMETER VALUE FOR TESTING PHASE

% Parameter Value	*QC*	*ET*	*D*	*S*	*T*
100	100 %	> 10	0-1	Completely satisfied	12
90	90%	9	2-3	Mostly satisfied	13
80	80%	8	4-5	satisfied	15
70	70%	7	6-7	Slightly satisfied	17
60	60%	6	8-9	Average	20
50	50%	5	10-11	Slightly dissatisfied	24
40	40%	4	12-13	Dissatisfied	30
30	30%	3	14-15	Mostly dissatisfied	40
20	20%	2	16-17	Completely dissatisfied	60
10	10%	1	18-19	-	120
0	0%	0	> 20	-	> 32

Given Table VIII, we can calculate the percentage of testing phase by using the following equation:

$$\text{Efficiency of testing phase} = \frac{(WQC*PQC)+(WET*PET)\,(WD*PD)+(WS*PS)+(WT*PT)}{(WQC+WET+WD+WS+WT)} \quad (6)$$

where *WQC* = weight of quality of code, *PQC* = percentage parameter value of quality of code, *WET* = weight of experience as tester, *PET* = percentage parameter value of experience as tester, *WD* = weight of defects, *PD* = percentage parameter value of defects, *WS* = weight of satisfaction, *PS* = percentage parameter value of satisfaction, *WT* = weight of Time, *PT* = percentage parameter value of Time.

F. Verification and validation phase

Verification and validation is the process of checking that a product meets user's need, and to determine whether it satisfies specified requirements. This phase has three parameters as shown in Table IX.

TABLE IX
PERCENTAGE PARAMETER VALUE FOR VERIFCATION AND VALIDATION PHASE

% Parameter Value	*D*	*S*	*T*
100	0-1	Completely satisfied	8
90	2-3	Mostly satisfied	10
80	4-5	satisfied	12
70	6-7	Slightly satisfied	14
60	8-9	Average	16
50	10-11	Slightly dissatisfied	18
40	12-13	Dissatisfied	20
30	14-15	Mostly dissatisfied	22
20	16-17	Completely dissatisfied	24
10	18-19	-	26
0	> 20	-	> 26

To compute the percentage parameter value of verification and validation phase we use the following equation:

$$\text{Efficiency of verification and validation phase} = \frac{(WD*PD)+(WS*PS)+(WT*PT)}{(WD+WS+WT)} \quad (7)$$

where WT = weight of Time, PT = percentage parameter value of Time. WD = weight of defects, PD = percentage parameter value of defects, WS = weight of satisfaction, and PS = percentage parameter value of satisfaction. After we define and calculate the efficiency of each phase, we apply these equations to our top level formula to obtain overall programmer productivity performance as:

$$\text{Efficiency} = \frac{\sum_i PHi}{n} \quad (8)$$

where *i* is the phase, *PH* is the efficiency of the phase, *n* is the number of phases of software life cycle.

After all, the appropriate measures have to be taken to ensure that the user knows how to use the metric. It is a bit like mathematics. Understanding of the use of the metric and the formula would be experience gained through practice, which is the mother of all teachers. Otherwise, the formula will be deemed obviously complex and undoable without practice.

VIII. DISCUSSION AND CONCLUSION

Programmer productivity is a valuable essential in software development attracting a great deal of attention in developing software. In order to successfully measure programmer's performance, software metrics must be used and considered. This enhances our decisions. Software metrics are used to obtain data to support the software goals for the project. Their primary goal is to measure software quality and productivity. From our research, the basic motivation for proposing such a metric is to be able to measure performance productivity of pair and solo programming in exhaustive behavior. It can be used to evaluate efficiency of any phase of software life cycle, therefore, can be applied to early phases of software development.

REFERENCES

[1] I. Sommerville, "SOFTWARE ENGINEERING 9," *Inc.,publishing as Addison-Wesley*, 2009.

[2] A. Patel, *et al.*, "Ahmed Patel, Liu Na, Rodziah Latih, Christopher Wills, Zarina Shukur and Rabia Mulla," *Journal of Computer Science,*, vol. 6 No. 11, pp. 1406-1415, 2010. doi: 10.3844/jcssp.2010.1406.1415

[3] L. Williams and R. Kessler, "Pair Programming Illuminated," *Addison Wesley, July* 2002. 288 pages, ISBN: 0-201-74576-3

[4] J. E. Hannay, *et al.*, "The effectiveness of pair programming: A meta-analysis," *ScienceDirect, July* 2009. vol. 51, pp. 1110-1122 DOI: 10.1016/j.infsof.2009.02.001

[5] J. T. Nosek, "The Case for Collaborative Programming," *ACM, March* 1998. vol. 41 issue No. 3, pp.105-108, doi:10.1145/272287.272333

[6] L. Williams, *et al.*, "Strengthening the Case for Pair Programming," *IEEE Software, July* 2000. Vol. 17 NO. 4, doi:10.1109/52.854064

[7] A. Cockburn and L. Williams, "The Costs and Benefits of Pair Programming," *presented at extreme Programming and Flexible Processes in Software Engineering -- XP2000. Cagliari, Sardinia, Italy, 2000*. doi: 10.1.1.26.9064

[8] H. Hulkko and P. Abrahamsson, "A Multiple Case Study on the Impact of Pair Programming on Product Quality," *IEEE International Conference on Software engineering*, pp. 495-504, 2005. doi: 10.1145/1062455.1062545

[9] J. Vanhanen and C. Lassenius, "Effects of Pair Programming at the Development Team Level: An Experiment," *IEEE*, 2005. pp. 336-345. doi: 10.1109/ISESE.2005.1541842

[10] J. Nawrocki and A. Wojciechowski, "Experimental Evaluation of Pair Programming," *proc. European Software Control and Metrics(Escom)*, 2001. doi: 10.1.1.19.1689

[11] E. Arisholm, *et al.*, "Evaluating Pair Programming with Respect to System Complexity and Programmer Expertise," *IEEE Computer Society*, 2007. VOL. 33, NO. 2. doi:10.1109/TSE.2007.17

[12] R. Gunnalan, *et al.*, "Pseudo Dynamic Metrics," *IEEE Computer Society*, 2005. ISBN:0-7803-8735-X

[13] N. E. Fenton and M. Neil, "Software metrics: successes, failures and new directions," *The Journal of Systems and Software 47 (1999) 149-157*, 1999.

[14] G. Sikka, *et al.*, "Estimating Function points: Using Machine Learning and Regression Models," *2nd International Conference on Education Technology and Computer (ICETC)*, 2010. doi:10.1109/ICETC.2010.5529600

[15] D. J. Ram and S. V. G. K. Raju, "Object Oriented Design Function Points," *Quality Software, 2000. Proceedings. First Asia-Pacific Conference ,IEEE*, pp. 121-126, 2000 DOI: 10.1109/APAQ.2000.883785

[16] T. Honglei, *et al.*, "The Research on Software Metrics and Software Complexity Metrics," *IEEE International Conference on Cognitive Informatics*, 2009. pp. 131-136. doi: 10.1109/IFCSTA.2009.39

[17] S. R. Chidamber and C. F. Kemerer, "A Metrics Suite for Object Oriented Design," *IEEE TRANSACTIONS ON SOFTWARE ENGINEERING, VOL. 22, issue No. 6*, 1994. doi:10.1109/32.295895

[18] R. Dillibabu and K. Krishnaiah, "Cost estimation of a software product using COCOMO II.2000 model – a case study," *ScienceDirect*, 2005. Vol 23, Issue 4, May 2005, pp 297-307, doi:10.1016/j.ijproman.2004.11.003

[19] K. M. Lui and K. C. C. Chan, "Pair programming productivity: Novice–novice vs. expert–expert," *ScienceDirect*, 2006, Vol. 64 Issue 9, September 2006. doi:10.1016/j.ijhcs.2006.04.010

[20] C. McDowell, *et al.*, "The impact of pair programming on student performance, perception and persistence," *International Conference on Software Engineering, IEEE Computer Society*, 2003. http://doi.ieeecomputersociety.org/10.1109/ICSE.2003.1201243

[21] T. Bipp, *et al.*, "Pair programming in software development teams – An empirical study of its benefits," *ScienceDirect*, 2008. Vol. 50, Issue 3. doi:10.1016/j.infsof.2007.05.006

[22] L. F. Johnson, "On Measuring Programmer Team Productivity " *Electrical and Computer Engineering, IEEE Canadian Conference.*, vol. vol. 2, pp. 701-705, 1998. DOI: 10.1109/CCECE.1998.685594

Computer System for Navigating a Mobile Robot

Stanislav Simeonov
Department of Informatics and Computer Science
Burgas Free University
Burgas, Bulgaria
stan@bfu.bg

Penka Georgieva
Department of Informatics and Computer Science
Burgas Free University
Burgas, Bulgaria
pgeorg@bfu.bg

Vladimir Germanov
Department of Informatics and Computer Science
Burgas Free University
Burgas, Bulgaria
germanov@bfu.bg

Atanas Dimitrov
Department of Informatics and Computer Science
Burgas Free University
Burgas, Bulgaria
atanas@bfu.bg

Dimitar Karastoyanov
Institute of Information and Communication Technologies
Bulgarian Academy of Sciences
Sofia, Bulgaria
dkarast@iinf.bas.bg

***Abstract*—In this paper a fuzzy and communication system for managing and controlling the basic movements of a mobile robot is proposed. Several ultrasound and infrared sensors are installed on the robot and the collected data is operated with the means of fuzzy logic and thus decisions for the robot route are made. This intelligent system is created to navigate the mobile robot indoors in an unknown environment. The application areas of the robot are for embedded and mobile device, guiding of visual impaired people, mobile vehicle in technological lines, etc.**[*]

***Keywords*—Mobile Robot; Fuzzy Logic; Embedded**

I. INTRODUCTION

Mobile robots are widely applied in a range of applications in transportation, surveillance, health care etc. The ability to analyze and control the performance of the mobile robot is of primary importance in all applications. This article introduces methods and procedures from system identification that can be applied to address these important problems. The core objective is to try to explain the interaction between the robot, the task and the environment in a transparent manner such that system characteristics can be analyzed, controllers can be designed, and behaviors can be replicated in a systematic and structured manner. This aim of constructing a formalized approach for task-achieving mobile robots represents a refreshingly new approach to this complex set of problems.

The modeling and realization of a mobile robot is a long term project of team. The main goals of the project are:

- contribution to real problems understanding and solving;
- supporting people with disabilities;
- providing the opportunity to the university students to extend their knowledge and skills.
- The specific tasks that the team had faced in the process of developing the device have been defined as follows:
- developing an autonomous mobile explorer which can be navigated in close space, public building and local areas;
- building up a construction that is easy to manage using fuzzy logic, neural networks and other tools of Soft computing;
- the complete concept is based on the module principle – each module has a defined interface and thus the construction shows the interaction between the separate details in the context of laws of Physics, Mechanics, Electronics and Computer Science.

II. PROTOTYPE OF THE MOBILE ROBOT

A. Construction

The principle of development of the robot is modular – the robot is build up of mechanical, electronic and program modules each of them being easily substituted or modified according to the specific research problem.

B. Navigation

Managing the navigation and controlling the basic movements of the mobile robot are realized by software applications and drivers, embedded in an operation system specifically designed for Ebox 2300 [9]. Using Ebox 2300 as a base system gives an opportunity for defining additional interfaces. The microcontrollers that are running the stepper and the dc motors communicate with Ebox2300 throw USB, Ethernet or RS232 interface [8].

The main regime of the mobile agent constitutes of orientation and moving indoors. There are different ways for navigating such a mobile agent: GPS maps, navigation algorithms, laser navigation and etc. [1], [2], [4].

The authors propose different approach in this paper: using the tools of fuzzy logic for managing and controlling the basic movements indoors of the robot [1], [5].

[*] The paper is partially sponsored by NSF Grand № RNF_09_0037, D002-13, DID 02-14

The size of the mechanical construction of the mobile robot defines the preconditions for designing the fuzzy system. The basic movements of the robot are defined as follows: moving forward, moving backwards, turning left, turning right and stopping. The turning to the left and right is carried out as a rotation around the central point of the robot and thus the whole robot stays in a circle with radius R which depends on the size of the robot.

III. FUZZY SYSTEM FOR NAVIGATION

The input data for the fuzzy system are received from ultrasound sensors for measuring distances to different obstacles in the environment from 3 cm up to 10 m and infrared sensors for detecting the height of eventual obstacles not less than 10 cm [7].

The implementation of the fuzzy system uses the universal fuzzy logic library created by a team of Burgas Free University, working on a research projects supported by Bulgarian National Science Fund NSF Grand №: RNF_09_0037, D002-13, DID 02-14.

Fig. 1 shows the scheme of decision making fuzzy system for navigating the robot indoors. The input variables of the system are the fuzzy variables: *DF=Distance Forward, DL=Distance Left, DR=Distance Right* and *H=Height.* The decision for action *A* is made under the "if-then" aggregation rules.

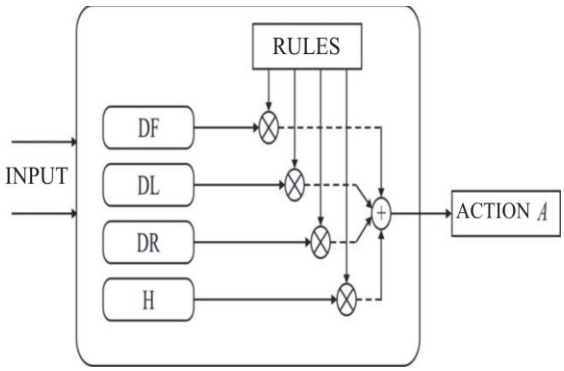


Figure 1. A scheme of fuzzy system for managing and control of basic movements

The input data as mentioned above are received from the sensors and are:

- the distance from the robot to the first object in front of it (*x1 – distance forward*);
- the distance from the robot to the first object in the left (*x2 – distance left*);
- the distance from the robot to the first object in the right (*x3 – distance right*);
- the height of the obstacle (*h – height of obstacle*).

In the next step the input data is fuzzified. The distance to the nearest object in front of the robot is a fuzzy variable *DF* with three terms defined as trapezoid fuzzy numbers - *DF1={too close}*, *DF2={close}*, *DF3={far}*, e.g.. *DF= {DF1, DF2, DF3} (Fig. 2).*

Because the robot should not go too close to the object forward in the definition of *DF* a parameter ε is used as a lower limit of the permissible distance forward. The distance *x1* detected by the sensors belongs to the three terms with the corresponding membership degrees. On fig. 2 an input parameter *x1* simultaneously belonging to

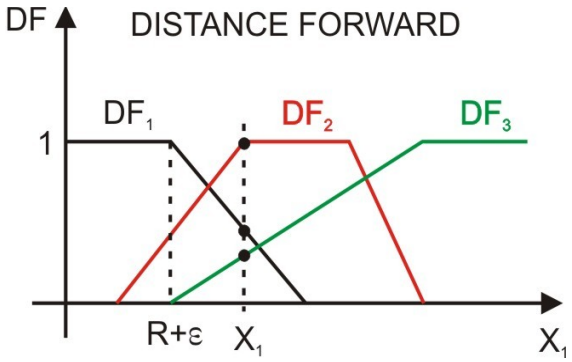


Figure 2. Fuzzy variable DF= {DF1, DF2, DF3}

the three terms with a membership degree to *DF2* equal to 1 is shown.

The fuzzy variable *DL* describes the distance from the robot to the nearest object to the left. This variable has to terms: *DL1= {too close}* and *DL2= {enough},* defined as

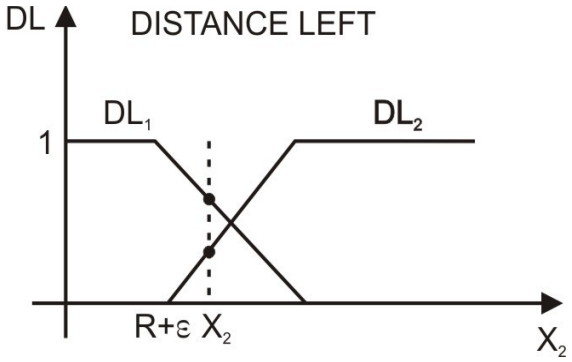


Figure 3. Fuzzy variable DL= {DL1, DL2}

trapezoid fuzzy numbers again and thus *DL= {DL1, DL2}* (fig. 3).

By analogy the fuzzy variable *DR= {DR1, DR2}* is defined for the distance to the right. It has two terms: *DR1= {too close}* and *DR2= {enough} that* are trapezoid fuzzy numbers as well (fig. 4).

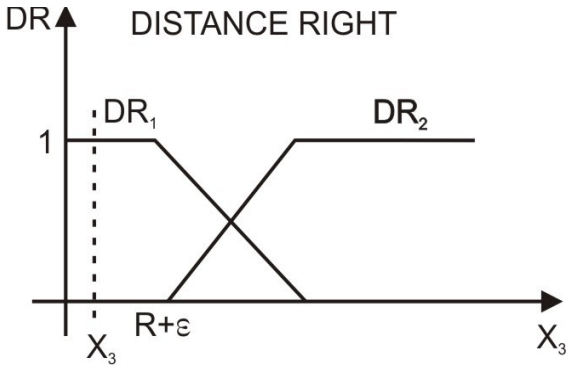


Figure 4. Fuzzy variable DR= {DR1, DR2}

The fuzzy variable *H= {H0, H1, H2}* describes the height of an eventual obstacle and has three terms: *H0= {ignorable}, H1= {surmountable}* and *H2= {insurmountable}* (fig. 5).

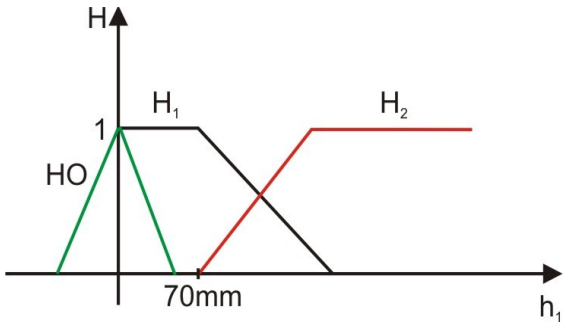


Figure 5. Fuzzy variable H= {H0, H1, H2}

The output *A* integrates three output variables Forward, Turn Left and Turn Right. They give the speed at which the mobile robot will move to the corresponding direction. The fuzzy variable Forward has three terms F1, F2 and F3 as shown on fig. 6. Each of the fuzzy variables Turn Left and Turn Right have two terms – L1, L2 and R1,R2 respectively (fig. 7 and fig. 8).

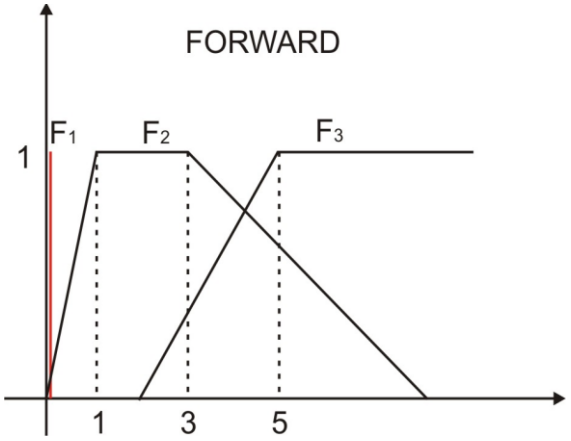


Figure 6. Fuzzy variable FORWARD={F1, F2, F3}

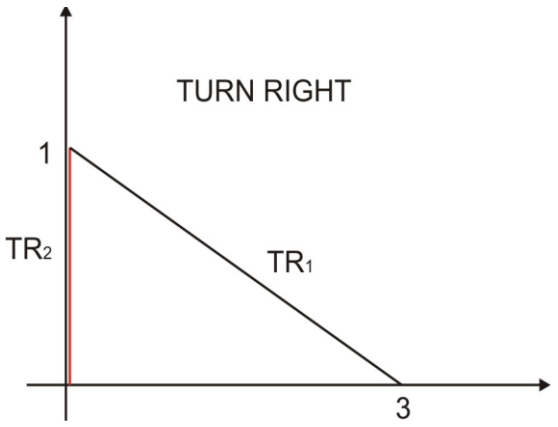


Figure 7. Fuzzy variable TURN RIGHT= {TR1, TR2}

The decision at which direction and at what speed the mobile robot should move is taken under several fuzzy aggregation rules "if-then" some of which are listed below:

1. If (Distance Forward is far and Height is ignorable) then (Forward is F3, Turn Right is TR2, Turn Left is TR2).
2. If (Distance Forward is close and Height is ignorable) then (Forward is F2, Turn Right is TR2, Turn Left is TR2).
3. If (Distance Forward is far and Height is surmountable) then (Forward is F2, Turn Right is TR2, Turn Left is TR2).
4. If (Distance Forward is close and Height is surmountable) then (Forward is F2, Turn Right is TR2, Turn Left is TR2).
5. If (Distance Forward is very close and Distance Right is enough) then (Forward is F1, Turn Right is TR1, Turn Left is TR2).
6. If (Distance Right is enough and Height is insurmountable) then (Forward is F1, Turn Right is TR1, Turn Left is TR2).
7. If (Distance Forward is very close and Distance Left is enough) and (Distance Right is very close) then (Forward is F1, Turn Right is TR2, Turn Left is TL1).
8. If (Distance Left is enough and Distance Right is very close) and (Height is insurmountable) then (Forward is F1, Turn Right is TR2, Turn Left is TL1).
9. If (Distance Forward is very close or Distance Left is very close or Distance Right is very close) or Height is ignorable) then (Forward is F1, Turn Right is TR2, Turn Left is TR2).

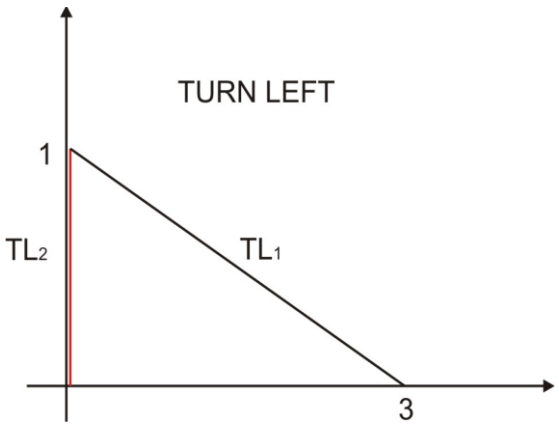


Figure 8. Fuzzy variable TURN LEFT= {TL1, TL2}

IV. Realization of Simple Series Communication Protocol

As we mentioned, Ebox 2300 use series protocol to communicate with speed & direction MCU. The choice of this type of communication is dictated by the simplicity and the fact that there is no need of extra components for hardware realization. To navigate the robot, the collected and translated information from the sensors passes only through one wire to the driver plate in four bytes. A simple block diagram shown in fig. 9 demonstrates the protocol and hardware realization.

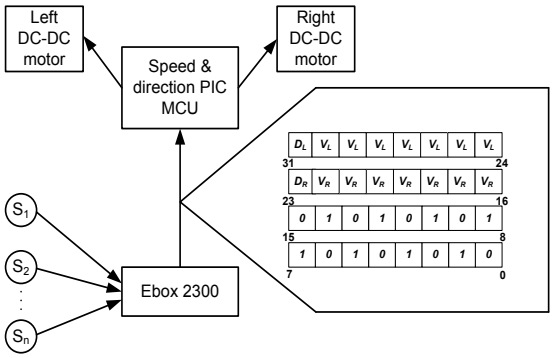


Figure 9. Protocol and hardware realization

First two bytes are control bytes. If driver MCU did not receive them in exact order, as shown in the figure, it ignores next two bytes. The third byte sets direction and velocity of the right dc-dc motor, and the fourth byte sets direction and velocity of the left dc-dc motor respectively. Direction bits are 23 for right engine and 31 for left engine. If these bits are equal to zero, the move direction is forward and if they are equal to one, the direction is reversed. The rest LSB 7 bits in third and fourth byte sets the for the velocity of motors. The actual speed of the motors depends on what movement we need. A simple picbasic pro code illustrate realized communication between Ebox 2300 and driver MCU:

```
recv_x VAR BYTE                ' variable for 3rd byte
recv_y VAR BYTE                ' variable for 4th byte
pwm_x VAR BYTE                 ' variable for speed of right dc-dc motor
pwm_y VAR BYTE                 ' variable for speed of left dc –dc motor
Main:
SERIN PORTC.4, N2400, 5, do_nothing, [$AA, $55], recv_x, recv_y
        IF recv_x >= 128 THEN
                pwm_x = recv_x - 128
                PORTB.0 = 0
        ELSE
                pwm_x = 127 - recv_x
                PORTB.0 = 1
        ENDIF
        IF recv_y >= 128 THEN
                pwm_y = recv_y - 128
                PORTB.1 = 0
        ELSE
                pwm_y = 127 - recv_y
                PORTB.1 = 1
        ENDIF
        HPWM 1, pwm_x*2, 20000
        HPWM 2, pwm_y*2, 20000
GOTO Main
do_nothing:
pwm_x = 0 : pwm_y = pwm_x
        HPWM 1, pwm_x, 20000
        HPWM 2, pwm_y, 20000
GOTO Main
END
```

Because the communication is one-way, i.e. Ebox use simplex operation to transmit data to driver MCU, in situation when no data is transmitted in 5 ms, the robot stops moving and waits until new data is received. In the main program, this is realized with do_nothing code.

V. EXPERIMENTS

A key step in building the navigation system is to conduct a number of simulations before the implementation. These simulations aim to check the validity of the fuzzy decision process and the correctness and functionality of the system.

The simulations have been held in MatLab environment and three of the possible outputs are shown in the figures below.

On the fig. 10 a decision for moving forward at the full speed of 5 km/h and no turning either to the right or to the left is shown. This speed is admissible because there is enough distance to the first obstacle in front of the robot – 145cm. Fig. 11 is for a decision for moving forward at the speed of 2.7 km/h, turning right with speed of 1 km/h which is a slow turn to the right because the first obstacle in front of the robot is becoming closer and the system is designed to give priority to the right turn. Fig. 12 is for a full left turn at the speed of 1 km/h.

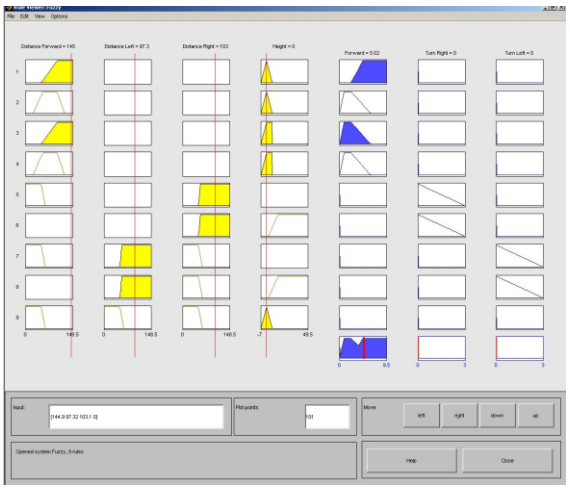


Figure 10. Moving forward at the full speed of 5 km/h

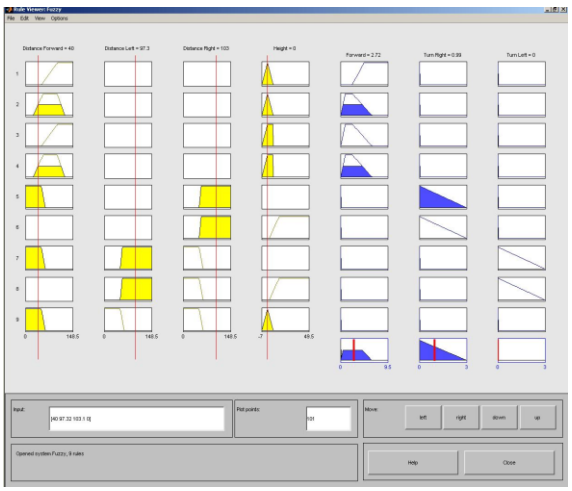


Figure 11. Moving forward at the speed of 2.7 km/h, turning right with speed of 1 km/h

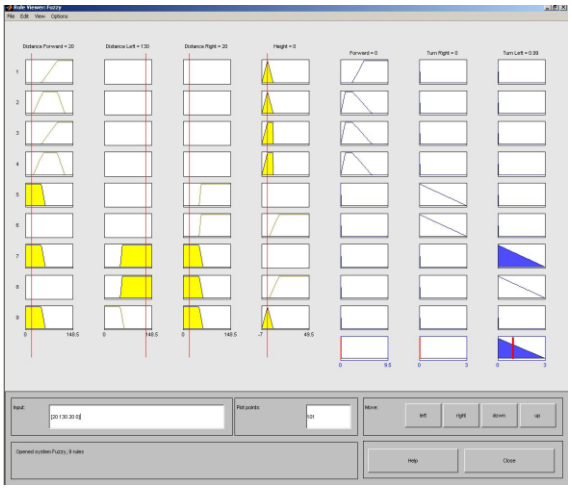


Figure 12. Full left turn at the speed of 1 km/h

VI. Conclusion and Future Research

The designing, realization and implementation of the mobile robot is an ongoing process.

In the near future the team intends to test several hybrid models based on integrated systems with fuzzy logic, artificial neural networks and genetic algorithm for navigating the robot.

The process of developing the mobile robot brings along different benefits:

- the mobile robot is used as universal model in the education of students in computer science and technologies, informatics in Burgas Free University;
- the mobile robot is used for realization and exploring many scheme and program solution;
- the mobile robot is a universal system for supporting scientific research in Burgas Free University for conducting different test.

From the other hand the mobile robot can be used as a base for development of:

- autonomous systems for detecting and dismantling of explosives device;
- autonomous system for detecting toxic materials in the environment;
- specialized cars with artificial intelligence for disabled and others.

References

[1] Driankov D. and Saffiotti A., Fuzzy Logic Techniques for Autonomous Vehicle Navigation, Springer-Verlag (Berlin, Germany) 2001

[2] Holland, J., Designing Autonomous Mobile Robots, Newnes-Elsevier, 2004

[3] Kasabov Nikola K., Foundations of Neural Networks, Fuzzy Systems, and Knowledge Engineering, Massachusetts Institute of Technology, England, 1996

[4] Saffiotti A., Fuzzy Logic in Autonomous Robotics: behaviour coordination, Proc. of the 6th IEEE Intl. Conf. on Fuzzy Systems, pp. 573-578. Barcelona, Spain, 1997

[5] Saffiotti A., The Uses of Fuzzy Logic in Autonomous Robot Navigation, Soft Computing 1(4):180-197, 1997

[6] Germanov Vl., Simeonov St., Georgieva P., Base Mechanical Construction for for Mobile Robot, AMTECH'07, 23 – 24 November 2007, GABROVO

[7] 6PAK Team, Final report, ImagineCup Competition, Microsoft, 2007

[8] http://imaginecup.com/

[9] http://www.embeddedpc.net/Default.aspx?tabid=110

Current-Controlled Current-Mode Multiphase Oscillator Using CCCDTAs

Montree Kumngern
Department of Telecommunications Engineering, Faculty of Engineering,
King Mongkut's Institute of Technology Ladkrabang,
Bangkok 10520, Thailand
E-mail: kkmontre@kmitl.ac.th

***Abstract*–This paper presents a new current-controlled current-mode multiphase sinusoidal oscillator using current controlled current differencing transconductance amplifiers (CCCDTAs). The proposed oscillator circuit, which employs one CCCDTA, one grounded capacitor and one MOS resistor for each phase, can generate arbitrary n output current equal-amplitude signals that are equally spaced in phase (n being even or odd), all at high output impedance terminals. The frequency of oscillation and the condition of oscillation can be controlled electronically and independently through adjusting the bias currents of the CCCDTAs. The proposed multiphase oscillator is highly suitable for integrated circuit implementation. The theoretical results were verified by PSPICE simulation.**

Keywords—Multiphase oscillator; Current-mode circuit, current controlled current differencing transconductance amplifier (CCCDTA)

I. INTRODUCTION

Multiphase sinusoidal oscillators (MSOs) have a wide range of application in communication, signal processing, power controlled systems, instrument control, and measurement system. As a result, a number of MSO circuits based on different design techniques have been developed in the literature [1]–[13]. In [1]–[4], the early systems exhibit good performance, but these circuits suffer complex circuitry from using a large of both active and passive components. Simpler circuits are available in the MSO based on the active-R technique [5]–[6], but it lacks the electronic tunability. Although the OTA-C realization [7] enjoys electronic tunability, it suffers from limited output voltage swing and temperature sensitivity. Additionally, the voltage-mode OTA-based MSO generally needs buffer to reduce the high output impedance associated with transconductance amplifiers. In [8]–[9], two MSO circuits, using a second-generation current conveyor (CCII) as an active component, have been proposed. However, a junction field-effect transistor (JFET) and three current conveyors are required for each phase in order to achieve electronically tenability. The current feedback operational amplifier (CFOA)-based MSO circuit is described by Wu et al. [10] exploits the internal pole of the device to operate at relatively high frequencies, but this approach requires access to the amplifier compensation terminal. This requirement is very restrictive since only one such device (AD844) is current available. The techniques to realize a MSO using operational amplifiers (op-amps) have been proposed [11]–[12]. However, the drawback of these circuits is the well-known limitations of the op-amps. Moreover, they utilize too many external passive components and a number of them float. A new technique for realizing MSO by using second-generation current controlled current conveyors (CCCIIs) has been presented in [13]–[14]. However, the implementation scheme is only suitable for bipolar technology.

Recently, a new current-mode active building block called the current differencing transconductance amplifier (CDTA) has been proposed [14]. This device is a synthesis of the well-know advantages of the current differencing buffered amplifier (CDBA) [16]. It is really current-mode element whom the input and the output are a current form.

The purpose of this paper is to developing a current-mode current-controlled multiphase sinusoidal oscillator employing the modified CDTAs, called a 'current controlled current differencing transconductance amplifiers (CCCDTAs)' [17]. Its properties of this device are similar to the conventional CDTA, but the CCCDTA has finite input resistances R_p and R_n at the p and n terminals, respectively, which is controllable by the bias current. The proposed CCCDTA-based current-mode MSO has the following features:

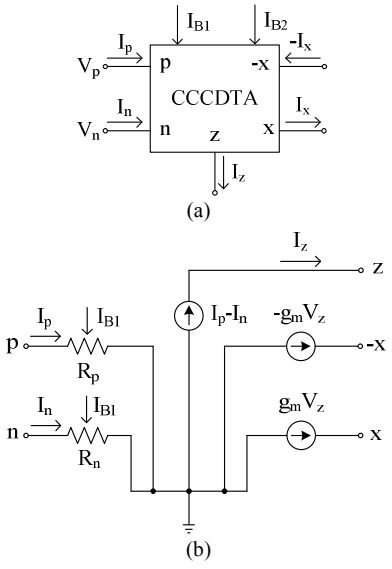


Figure 1. CDTA: (a) circuit symbol, (b) equivalent circuit.

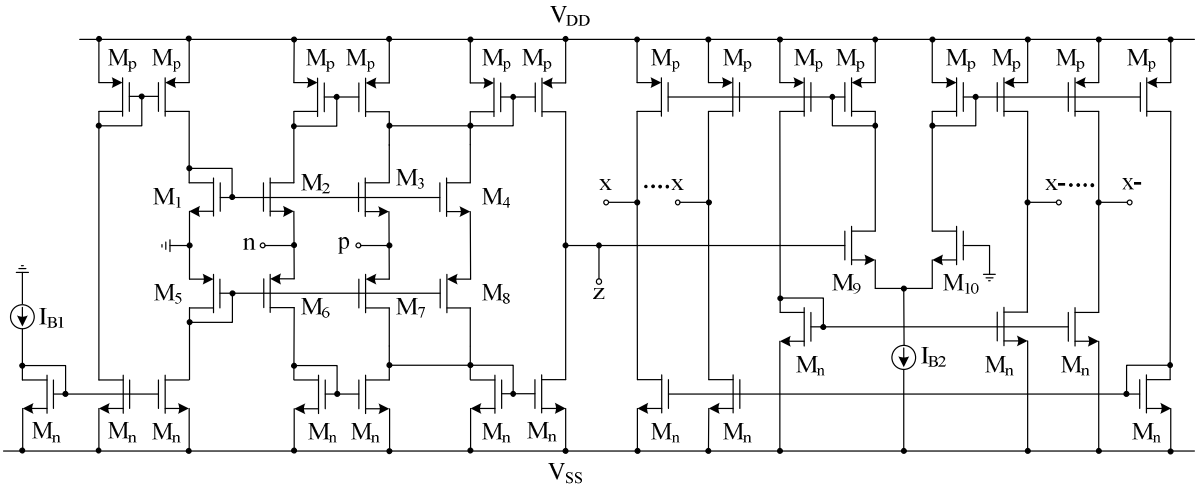


Figure 2. CMOS implementation for CCCDTA.

- It utilizes one CCCDTA, one grounded capacitor and one MOS resistor for each stage.
- It can realize either odd- or some even-phase output currents using the minimum number of passive components per section.
- The frequency of oscillation can be tuned by adjusting the bias current of CCCDTA.
- The condition of oscillation can be controlled by adjusting the transconductance gain of CCCDTA without disturbing the frequency of oscillation.
- It uses only grounded capacitor which is suitable for IC fabrication.

II. Circuit Descriptions

The electrical symbol of the CCCDTA is shown in Fig. 1. Its characteristic can be expressed by [17]

$$\begin{pmatrix} V_p \\ V_n \\ I_z \\ I_x \end{pmatrix} = \begin{pmatrix} R_p & 0 & 0 & 0 \\ 0 & R_n & 0 & 0 \\ 1 & -1 & 0 & 0 \\ 0 & 0 & 0 & \pm g_m \end{pmatrix} \begin{pmatrix} I_p \\ I_n \\ V_x \\ V_z \end{pmatrix}. \quad (1)$$

where R_p and R_n are the inner resistances at terminal p and n, respectively, and g_m is the transconductance gain. The x and z terminals have a high impedance level. Fig. 2 shows the CMOS implementation for CCCDTA. Assume that transistors, M_1 to M_8, are operated in saturation regions, the p and n resistances can be obtained, respectively, by

$$R_p = \frac{1}{g_{m3} + g_{m7}} \quad (2)$$

$$R_n = \frac{1}{g_{m2} + g_{m6}} \quad (3)$$

where g_{mi} denotes the transconductance parameter of transistor M_i. If transistors, M_1 to M_8, are identical, the p and n resistances can be approximately obtained as

$$R_p \cong R_n \cong \frac{1}{\sqrt{8\mu C_{ox}(W/L) I_{B1}}} \quad (4)$$

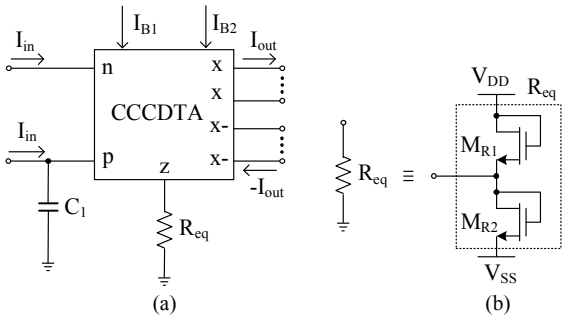


Figure 3. Basic building block for proposed MSO and (b) MOS resistor.

where μ is the carrier mobility, C_{ox} is the gate oxide capacitance per unit area, W and L are the effective channel width and length, respectively. From equation (4), the parasitic resistances R_p and R_n can be varied by adjusting the bias current I_{B1}. This property makes it different from conventional CDTA.

In addition, assume transistors, M_9 and M_{10}, are operated in saturation region, the transconductance gain (g_m) can be expressed by

$$g_m = \sqrt{\mu C_{ox}(W/L) I_{B2}}. \quad (5)$$

It can see that the transconductance gain can be electronically controlled by adjusting the bias current I_{B2}.

Fig. 3 shows the basic building block for the proposed multiphase oscillator. It consists of one CCCDTA, one grounded capacitor and one MOS resistor. The current transfer function of Fig. 3 can be given by

$$\frac{I_{out}}{I_{in}} = \pm R_{eq} g_m \frac{sCR_p}{1 + sCR_p}. \quad (6)$$

Fig. 4 shows the proposed odd-order MSO. It consists of N cascaded of Fig. 3. Each block uses the three minus-type output terminals and one plus-type output terminal of CCCCTA provides an additional 180° phase shift. Note that the proposed circuit employs only one CCCCTA, one grounded capacitor and one grounded resistor per stage. Using equation (6), the loop-gain of the structure in Fig. 4 can be expressed for N section by

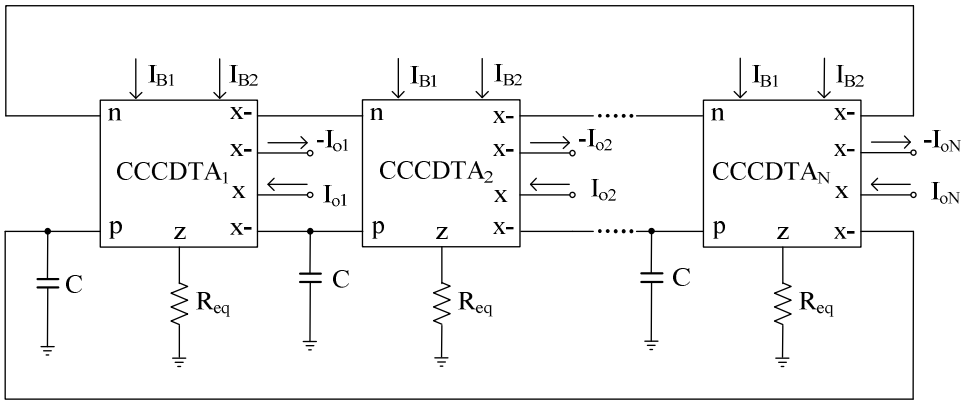


Figure 4. The proposed CCCDTA-based current-mode MSO.

$$L(s)=\left(-R_{eq}g_m\frac{sCR_p}{1+sCR_p}\right)^N. \quad (7)$$

The system can be set to provide a sinusoidal oscillation, if the loop gain is unity:

$$\left(-R_{eq}g_m\frac{sCR_p}{1+sCR_p}\right)^N_{S=j\omega_o}=1 \quad (8)$$

or

$$\left(1+j\omega_o CR_p\right)^N+\left(j\omega_o R_{eq}g_m\right)^N=0. \quad (9)$$

Equation (9) is the characteristic equation for an Nth-order sinusoidal oscillator of Fig. 4. By expanding equation (9), it can be shown that the scheme in Fig. 4 will only for odd number of N. By equating the imaginary and real parts of equation (9) to zero, the frequency of oscillation and the condition of oscillation for various odd values of N (N=3, 5, 7,····) can be obtained. The outputs at each of the sections of the scheme are symmetrical, i.e. equal in amplitude and equally spaced in phase at the oscillating frequency [5]. Returning to equation (9), for example in case of N=3, the frequency of oscillation and the condition of oscillation of a three-phase sinusoidal oscillator can be obtained, respectively, as

$$\omega_o=\frac{\sqrt{3}}{CR_p} \quad (10)$$

$$R_{eq}g_m\geq 2. \quad (11)$$

From equations (10) and (11), it can see that the frequency of oscillation and condition of oscillation can be orthogonally controlled. The condition of oscillation can be controlled by g_m through adjusting the bias current I_{B2} and the oscillation frequency can be controlled by resistor R_p through adjusting the bias current I_{B1}. The use of multiple-output CCCCTA provides an inverted version of the output current, hence there are 2n=6, 10, 14,····, even-phase available output currents. This shows that the scheme in Fig. 5 can generate odd-phase and some even-phase MSO into a single structure.

The resistor R_{eq} can be shown in Fig. 3(b) [18]. It consists two MOS transistors. Assume that the M_{R1} and M_{R2} have the same characteristics remaining in the saturation region, the resistance value can be expressed as [18]

$$R_{eq}=\frac{1}{2K(V_{DD}-V_{TH})} \quad (12)$$

where $K=\mu C_{ox}(W/L)$ is the transconductance parameter, V_{TH} is the threshold voltage, V_{DD} is the supply voltage (i.e. $V_{DD}=|V_{SS}|$).

It is to be further note that the proposed MSO can be realized even/odd order multiphase oscillator in a single system as same the one recent work [13]. It is formed of an odd-order of basic building blocks. While the first $CCCCTA_2$ blocks are identical, with each block using two minus-type x-outputs and one plus-type z-output, the transfer function of the Nth block, which uses two plus-type x-output and one minus-type x-output, provides an addition 180° phase shift.

III. Simulation Results

To the theoretical analysis of the proposed MSO, a three-phase sinusoidal oscillator design example has been simulated through PSPICE simulation program. The PSPICE model parameters for NMOS and PMOS transistors are simulated taken from TSMC 0.25μm process [19]. The aspect ratios of MOS transistors for CCCCTA in Fig. 2 are W/L=2μm/0.5μm for M_1–M_4, W/L=6μm/0.5μm for M_5–M_8, W/L=5μm/0.5μm for M_9–M_{10}, W/L=5μm/0.5μm for M_n and W/L=15μm/0.5μm for M_p [19]. The power supply is ±1V. The aspect ratios of MOS resistors (M_{R1} and M_{R2}) are W/L=2μm/2μm. Fig. 5 presents the simulation results of a three-phase sinusoidal oscillator (N=3) with C=500pF, I_{B1}=50μA, I_{B2}=100μA for n=3 (n=phase).

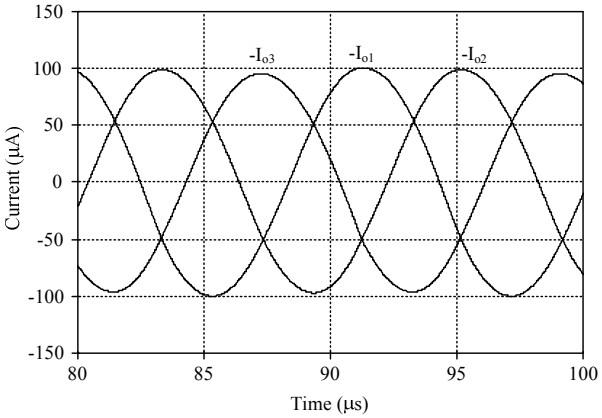


Figure 5. The simulated output waveform of three phase oscillator.

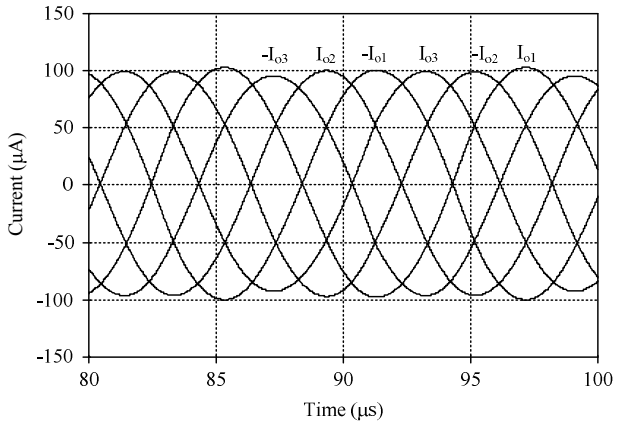


Figure. 6. Simulated output waveform of six phase oscillator.

In this case, g_m should be designed to be lesser than 2 times of R_{eq} to ensure the oscillation will start. The oscillation frequency is simulated to be 80kHz. Fig. 6 shows sinusoidal waveform for n=6. From Figs. 5 and 6, they can be expressed that the proposed oscillator can provide odd and some even phases into a single system.

IV. CONCLUSIONS

In this paper, a new electronically tunable current-mode MSO circuit has been presented. The proposed MSO is used CCCDTA-based current-mode high-pass section as building blocks. The circuit can provide an odd-number of equal-amplitude equally special in-phase output current, and all of them have high output impedance, which can be directly cascaded in current-mode operations. An orthogonal control between the condition of oscillation and the frequency of oscillation by electronic mean is achieved. Simulation results, which confirm the theoretical analysis, are also obtained.

ACKNOWLEDGMENTS

The author acknowledges with thank the support of Faculty of Engineering, King Mongkut's Institute of Technology Ladkrabang. The author also would like to express sincere thanks to the Telecommunications Research and Industrial Development Institute (TRIDI) of the office of National Telecommunications Commission of Thailand (NTC) for kindly supporting the equipments of the research laboratory.

REFERENCES

[1] B. Z. Kaplan and S. T. Bachar, "A versatile voltage controlled three phase oscillator," *IEEE Transactions on Industrial Electronics and Control Instrumentation*, vol. 26, pp. 192–195, 1979.

[2] A. Rahman and S. E. Haque, "A simple three-phase variable-frequency oscillation," *International Journal of Electronics*, vol. 53, pp. 83–89, 1982.

[3] V. P. Ramamurti and B. Ramaswami, "A novel three-phase reference sinewave generator for PWM inverter," *IEEE Transactions on Industrial Electronics*, vol. 29, pp. 235–240, 1982.

[4] W. B. Mikhael and S. Tu, "Continuous and switched-capacitor multiphase oscillators," *IEEE Transactions on Circuits and Systems*, vol. 31, pp. 280–293, 1984.

[5] M. T. Abuelma'atti and W. A. Almansoury, "Active-R multiphase oscillator," *IEE Proceeding, Part G, Circuit and Systems*, vol. 134 pp. 292–293, 1987.

[6] D. Stiurca, "On the multiphase symmetrical active-R oscillators," *IEEE Transactions on Circuits and Systems II: Analog and Digital Signal Processing*, vol. 41, pp. 156–158, 1994.

[7] I. A. Khan, M. T. Ahmed, N. Minhaj, "Tunable OTA-based multiphase sinusoidal oscillators," *International Journal of Electronics*, vol. 72, pp. 443–450, 1992.

[8] C. Hou and B. Shen, "Second-generation current conveyor-based multiphase sinusoidal oscillators," *International Journal of Electronics*, vol. 78, pp. 317-325, 1995.

[9] D.–S. Wu, S.–I. Liu, Y.–S. Hwang, and Y.–P. Wu, "Multiphase sinusoidal oscillator using second-generation current conveyors," *International Journal of Electronics*, vol. 78, pp. 645–651, 1995.

[10] D.–S. Wu, S.–I. Liu, Y.–S. Hwang, and Y.–P. Wu, "Multiphase sinusoidal oscillator using the CFOA pole," *IEE Proceedings of Circuits, Devices and Systems*, vol. 142, pp. 37–40, 1995.

[11] S. J. G. Gift, "Multiphase sinusoidal oscillator system using operational amplifiers," *International Journal of Electronics*, vol. 83, pp. 61–67, 1997.

[12] S. J. G. Gift, "Multiphase sinusoidal oscillator using inverting-mode operational amplifiers", *IEEE Transactions on Instrumentation and Measurement*, vol. 47, pp. 986–991, 1998.

[13] M. T. Abuelma'atti and M. A. Al-Qahani, "A new current-controlled multiphase sinusoidal oscillator using translinear current conveyor," *IEEE Transactions on Circuits and Systems-II: Analog and Digital Signal Processing*, vol. 45, pp. 881–885, 1998.

[14] M. Kumngern, S. Junnapiya, and K. Dejhan, "Current-mode multiphase sinusoidal oscillator using translinear conveyors," in *Proceeding of 6th International Conference on Electrical Engineering/Electronics, Computer, Telecommunications and Information Technology*, pp. 538–541, 2009.

[15] D. Biolek, "CDTA-building block for current-mode analog signal processing," in *Proceeding of the ECCTD'03*, III, pp. 397–400, 2003.

[16] C. Acar and S. Ozoguz, "A new versatile building block: current differencing buffered amplifier suitable for analog signal-processing filters," *Microelectronics Journal*, vol. 30, pp. 157–160, 1999.

[17] M. Siripruchyanun and W. Jaikla, "CMOS current-controlled current differencing transconductance amplifier and applications to analog signal processing," *International Journal of Electronics and Communications*, vol. 62, pp. 277–287, 2008.

[18] Z. Wang, "2-MOSFET transistor with extremely low distortion for output reaching supply voltage," *Electronics Letters*, vol. 26, pp. 951–952, 1990.

[19] M. Kumngern, "Current-mode multiphase sinusoidal oscillator using current-controlled current differencing transconductance amplifiers," in *Proceeding of 2010 IEEE Asia Pacific Conference on Circuits and Systems* (*APCCAS 2010*), Kuala Lumpur, Malaysia, December 6–9, 2010.

An Analysis of Multiple Size Region of Interest in Disparity Mapping for Stereo Vision Application

R A Hamzah, M. S. Hamid, H. N. Rosly, N. M. Z. Hashim
FKEKK, UTeM, Melaka, Malaysia.
rostamaffendi@utem.edu.my, saad@utem.edu.my, hasrul@utem.edu.my, nikzarifie@utem.edu.my

***Abstract* - This paper presents an analysis of multiple size region of interest in selected area or segment of disparity mapping in application of stereo vision. The mapping is about to deal with the intensities of pixels which allocate the depths of an image and can be extracted to get the distance values. This region is a reference view of the stereo camera and stereo vision baseline is based on horizontal configuration. The block matching technique is briefly described with the performance of its output. The disparity mapping is generated by the algorithm with the reference to the left image coordinate. The algorithm uses Sum of Absolute Differences (SAD) which is developed using Matlab software. The rectification and block matching processes are also briefly described in this paper.**

Keywords **– Stereo camera; disparity mapping; region of interest; rectification; block matching algorithm**

I. INTRODUCTION

The origin of the word "stereo" is the Greek word "stereos" which means firm or solid, with stereo vision, the objects are seen solid in three dimensions with range [1]. In stereo vision, the same seen is captured using two sensors from two different angles. The captured two images have a lot of similarities and smaller number of differences. In human sensitivity, the brain combines the captured to images together by matching the similarities and integrating the differences to get a three dimension model for the seen objects. In machine vision, the three dimension model for the captured objects is obtained finding the similarities between the stereo images and using projective geometry to process these matches. The difficulties of reconstruction using stereo is finding matching correspondences between the stereo pair.

A. Stereo Vision Application

A stereo vision application such as a stereo vision mobile robot navigation requires a number of various capabilities, including the ability to execute uncomplicated goal-achieving actions, like reaching a given location; to react in real time to unexpected events, like the sudden appearance of an obstacle; to build, use and maintain a map of the environment; to determine the robot's position with respect to this map; to form plans that pursue specific goals or avoid undesired situations; and to adapt to changes in the environment [2]. In a navigation of a stereo vision mobile robot research, the goal is to build up a vehicle that can navigate at a certain speeds using stereo camera whether in outdoor or indoor environments such as fields or building. These vehicles require massive computational power and suitable algorithm in order to adapt their sensitivity and control capabilities to the certain speed of motion and in avoidance of obstacles.

Basically, the stereo camera in Figure 1 takes pictures of a same object but with different view. The two dimension images on the plane of projection represent the object from camera view. These two images contain some encrypted information, the image-depth of each other. This information is the third dimension of two dimension images. Therefore, the object distance and its depth can be determined by using the stereo cameras [3]. With referring to Figure 2 the distance between two points of view is called the baseline [4]. The baseline's distance end to end affects on the range resolution, which establish the range of depth that can be calculated. A difference between scenes of the same object on the two images is called disparity [5]. The stereo system uses horizontal baseline. The cameras are placed at the same elevation. The process of stereo vision is then typically defined as finding a match between features in left and right images [6]. The stereo baseline b is the distance between the centres of the projection O_l and O_r. The x_l and x_r are the coordinates of p_l and p_r with respect to the principal points cl and cr. Where f is a focal length of the camera. The depth of P is uniquely determined by the following equation [4]:

$$\frac{b+x_l-x_r}{Z-f} = \frac{b}{Z} \quad (1)$$

And let the disparity $d = x_r - x_l$, then the depth of point P is:

$$Z = f\frac{b}{d} \quad (2)$$

The corresponding two images representing the same point of the scene is called disparity matching. The set of displacements between matched pixels is usually indicated as disparity map [6].



Figure 1. Stereo camera placement

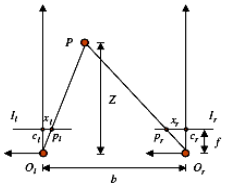


Figure 2. Basic principle of stereo vision

B. *Camera Calibration*

The calibration process is using Tsai's method. This method produces the values of extrinsic parameters such as the rotation and translation of images. Another result from Tsai's method is intrinsic parameters that generate focal length, principal point, skew, distortion coefficient and pixel size [7][8].

II. SOFTWARE ARCHITECTURE

The Matlab software is used to implement the software part. From Figure 3 images are captured by using the calibrated stereo camera. Then it will be changed to grey level scale to enhance the images using histogram equalization method [9]. The equation is:

$$q = T(w) = Imax \sum_{r=0}^{w} Pw(r) \quad (3)$$

The data from camera calibration using Tsai's method will be used to rectify the stereo images to obtain corresponding epipolar lines that parallel to the horizontal scan-lines for both images. The rectification process using equation (4) is to align the epipolar line for each image (left and right). With I_{old} and I_{new} are the original images and rectified image respectively with the combination of coefficient a_i for each camera.

$$I_{new}(x_0, y_0)=a_1 I_{old}(x_1, y_1) + a_2 I_{old}(x_2, y_2) + a_3 I_{old}(x_3, y_3) + a_4 I_{old}(x_4, y_4) \quad (4)$$

For example with referring to the dotted line left hand upper thumb of the model in Figure 4(a) shows stereo image before rectification process and Figure 4(b) is the image with rectification process. The output rectification process is look like a distortion image. But in fact that the image has been improved to be aligned each other with reference to epipolar line. The Sum of Absolute Differences (SAD) is applied to solve the stereo correspondence problem between two images. The SAD algorithm from the equation (5) shows an area-based correspondence algorithm [10][11][12]. It computes the intensity differences for each center pixel of (i, j) as follows:

$$SAD_v(x, y) = \sum_j \sum_i ||g_t(x+i, y+j) - g_{t-1}(x+v+i, y+ j)|| \quad (5)$$

The reference point of the left image g_t is minus with the right image g_{t-1} at the same epipolar plane. It sums up the intensities of all surrounding pixels in the neighbourhoods for each pixel in the left image. To calculate stereo correspondence of stereo images, this paper is using block matching technique. Each block from the left image is matched into a block in the right image by shifting the left block over the searching area of pixels in right image as shown in Figure 5. In order to find corresponding pairs of stereo points, they first have to be compared for different disparities, after which the best matching pairs can be determined. The maximum range at which the stereo vision can be used for detecting obstacles depends on the image and depth resolution. Absolute differences of pixel intensities are used in the algorithm to compute stereo similarities between points. By computing the sum of the absolute differences SAD for pixels in a window surrounding the points, the difference between similarity values for stereo points can be calculated. The disparity associated with the smallest SAD value is selected as best match [13].

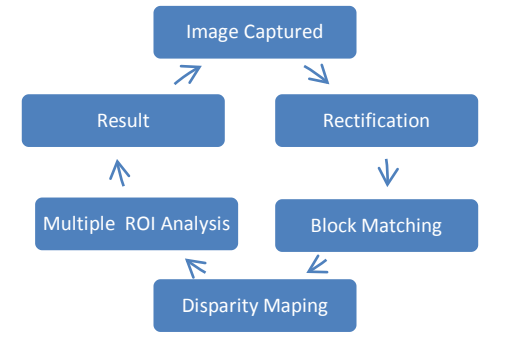


Figure 3. Software implementation for continuous process



Original Left Image Original Right Image

(a)



Rectified Left Image Rectified Right Image

(b)

Figure 4. Rectification process of stereo image

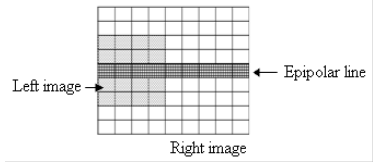


Figure 5. SAD block matching algorithm

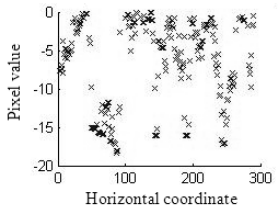


Figure 6. Pixel locations in region of interest

III. RANGE ESTIMATION AND OBSTACLE AVOIDANCE FILTER

Together with the stereo camera parameters from software calibration and the disparity between corresponding stereo points, real-world distances can be retrieved. In order to find corresponding pairs of stereo points, they first have to be compared for different disparities, after which the best matching pairs can be determined. The maximum range at which the stereo vision can be used for detecting obstacles depends on the image and depth resolution [13]. The equation below shows the distance or depth of obstacles that has been used in this paper.

$$Distance = ae^{bx} + ce^{bx} \quad (6)$$

The value of a, b, c and d is a constant value from curve fitting tool in Matlab. The value of *x* represents a pixel value in disparity mapping. The calculated distance has an effective range of detection for the stereo vision application. In the obstacle detection step, the points belonging to obstacles must be found. For data combination in image processing software, it is important to cluster or group the obstacle points Figure 6 in such a way that individual obstacles can be identified. If there are obstacles at closest range, the stereo program will filter using Gaussian lowpass filter [9](7) to determine the object and cluster the pixels location.

$$H(u,v) = e^{-\mathbf{D}^2(u,v)/2\sigma^2} \quad (7)$$

IV. RESULT OF SELECTED REGION OF INTEREST IN DISPARITY MAPPING AND PIXELS INTENSITIES

The disparity values from the SAD algorithm are mapped to disparity mapping with the reference to the left image coordinate. The region of interest is the area within the green line box that search for objects or obstacles Figure 7.



Figure 7. Region of interest for mobile robot

This area is a reference box for stereo camera to navigate if the application is applied on the stereo vision application such as a mobile robot. So, this paper is presenting the pixel intensities for every selected region of interest in graph. The idea is the pixels can be manipulated to certain applications such as the distance of the object detected and the shape of the object. The size of the region of interest is 320X20. From Figure 8 shows the pixels spread in the region of interest in pixel value with the horizontal coordinate.

A. Multiple Selected Region

With some illustrations of basic stereo theory shown by Figure 8, the obstacles detection for close object and far object can be concluded by Figure 9. Which is the baseline range are permanently setup and the left plane works as a reference plane. The result is the disparity values at a close object bigger than the disparity of a distant object. In disparity mapping the brighter pixels in the disparity map, the more close the corresponding pixel in the reference image. As a result Figure 10 (a), an obstacle could be identified as a group of pixels, which are generally brighter than their neighbourhood. The original images are gray level scale but not aligned each other (left and right). The rectification process produces aligned images with same image size about 320x240. At the border of both images the rectification process unable to allocate the pixel values because of the original images has been reconstructed. So, the SAD algorithm cannot identify the disparity values at the border of rectified images. Figure 10 (b) is a collection of multiple selected region. The range of disparity values about 1 until 40 and the size of selected region of interest from 320x20 until 320x50. The graphs show the total point of pixels with the coordinate systems detected each of selected green boxes on grey level scale image. the maximum or minimum value of pixel intensities can be manipulated according to the stereo vision application.

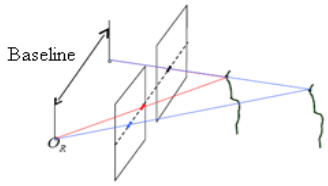


Figure 8. Stereo vision of obstacles detection

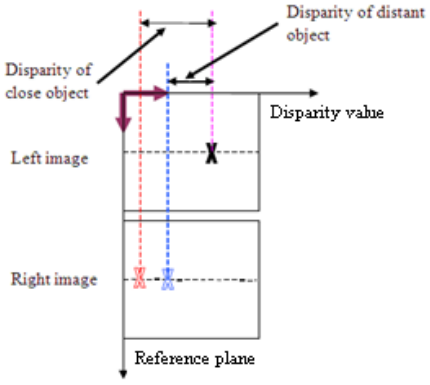
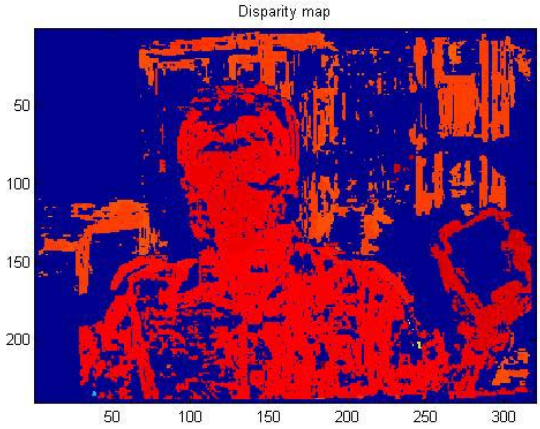
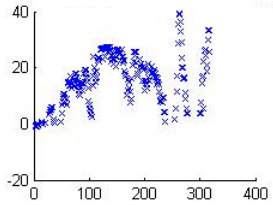
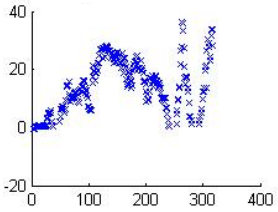
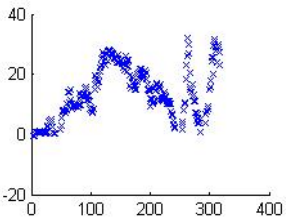
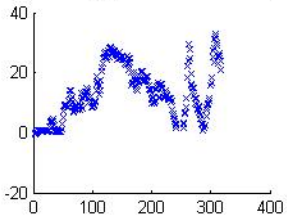


Figure 9. Relation of disparity and distance



(a) Disparity Mapping

	 Size: 320 x 20		Disparity Value Max: 40 Min: 1
	 Size: 320 x 30		Disparity Value Max: 40 Min: 1
	 Size: 320 x 40		Disparity Value Max: 40 Min: 1
	 Size: 320 x 50		Disparity Value Max: 40 Min: 1

(b) Multiple size of ROI

Figure 10. Multiple selected region of interest for a single image with the maximum disparity value 40 and minimum value 1

V. CONCLUSION

By changing the size region of interest, the pixel intensities could be manipulated depends on the application. A disparity map image is an efficient method for storing the depth or distance of each pixel in an image. Each pixel in the map corresponds to the same pixel in an image, but the grey level corresponds to the depth at that point rather than the gray-shade or color. From the colour mapping itself, the lighter are closer and darker are farther away. Viewing a gray level histogram equalized disparity map image, the objects also lighter are closer, and darker object are farther away. Stereo vision is also a type of passive sensor, meaning that it uses the radiation available from its environment. It is non-intrusive as it does not need to transmit anything for its readings.

ACKNOWLEDGEMENT

The authors would like to acknowledge the funding from Short Term Grant of Universiti Teknikal Malaysia Melaka.

REFERENCES

[1] Rovira-Más, F., Q. Zhang, and J. F. Reid., 2004. Automated agricultural equipment navigation using stereo disparity images. Trans. ASAE 47(4).

[2] Jones, E., J. Radford, D. Kumar, B. Fulkerson, R. Walters, and R. Mason, 2006. Autonomous off-road driving in the DARPA Grand Challenge. In Proc. PLANS Conference. IEEE

[3] Teerapat Chinapirom, U.W., and Ulrich Rückert, 2001. Steroscopic Camera for Autonomous Mini-Robots Applied in KheperaSot League. System and Circuit Technology, Heinz Nixdorf Institute, University of Paderborn.

[4] Konolige, K., 1999. Stereo Geometry. SRI International.

[5] B. Klaus, P.H., 1986. Robot Vision (MIT Electrical Engineering and Computer Science Series). MIT Press, McGraw-Hill Book Company, Cambridge, MA.

[6] Digney, S.S.a.B., 1999. Autonomous Cross-Country Navigation Using Stereo Vision. CMU-RI-TR-99-03, Carnegie Mellon University Technical report.

[7] Tsai, R.Y., 1986. An Efficient and Accurate Camera Calibration Technique for 3D Machine Vision. Proceedings of IEEE Conference on Computer Vision and Pattern Recognition, Miami Beach FL, 1986, pp. 364–374.

[8] J.Y. Bouguet, 2003, “Camera Calibration Toolbox for Matlab”, *MRL-Intel Corporation*, USA.

[9] Gonzalez, R.C., 2002. Digital Image Processing using Matlab. Pearson, Prentice Hall, pp 65-104

[10] Fusiello, E.T., and A. Verri, 2000. A compact algorithm for rectification of stereo pairs”, Machine Vision and Applications. 12(1) pp.16-22.

[11] Mattoccia, L.D.S.a.S., 2000. Fast stereo matching for the videt system using a general purpose processor with multimedia extensions. Fifth IEEE International Workshop on Computer Architecture for Machine Perception, Padova, Italy.

[12] Kuhl, A., 2005. Comparison of Stereo Matching Algorithms for Mobile Robots. The University of Western Australia Faculty of Engineering, Computing and Mathematics.

[13] Johan C. van den Heuvel, J.C.M.K., 2003. Obstacle Detectection For People Movers Using Vision And Radar. TNO Physics and Electronics Laboratory Oude Waalsdorperweg 63, The Netherlands.

Error Concealment Using Multiple Description Coding and LIoyd-max Quantization

Ali Farzamnia
Faculty of Electrical Engineering
Universiti Teknologi Malaysia
Johor Bahru, Malaysia
alifarzamnia@gmail.com

Sharifah K. Syed-Yusof
Faculty of Electrical Engineering
Universiti Teknologi Malaysia
Johor Bahru, Malaysia
kamilah@fke.utm.my

Norsheila Fisal
Faculty of Electrical Engineering
Universiti Teknologi Malaysia
Johor Bahru, Malaysia
sheila@fke.utm.my

***Abstract*- There has been increasing usage of Multiple Description Coding (MDC) for error concealment in non ideal channels. This paper attempts to conceal the error and reconstruct the lost descriptions by combining MDC and LIoyd-max quantizer. At first original image downsampled to four subimages then by using wavelet transform each subimage is mapped to transform domain then descriptions are quantized by LIoyd-max and coded. Since in proposed method wavelet transform is been used, there could be no blocking effect as compared to DCT transform. The results show that average MSE (mean square error) for our proposed method in comparison with DCT method (in other paper) has decreased from 240 to 152 in 0.625 bpp (bit per pixel), from 161 to 107 in 1 bpp and from 96 to 73 in 2 bpp in *rate- distortion* performance. Therefore, this method is suitable for low capacity channels. By losing descriptions, the obtained image is still in good quality (subjective evaluation and PSNR values) as compared to a method which is DCT and MDSQ (multiple description scalar quantization).**

I. INTRODUCTION

Multiple Description Coding (MDC) refers to source coding in which the encoder generates multiple descriptions of the source. The different descriptions are transmitted over various paths in an unreliable network. The decoder can rely on any subset of the descriptions to reconstruct the transmitted message. MDC is an interesting tool for robust communication over lossy networks such as the Internet, peer-to-peer, diversity wireless networks, and sensor networks [17].

MDC offers a potentially attractive framework for data transmission in scenarios where packet loss is inevitable. For instance, in real-time multimedia communications, packet retransmission is impossible due to severe latency constraints. In this situation, the receiver must rely on the packets available at the decoder to recover the transmitted signal. The quality of the recovered signal will depend on the level of packet loss on the network. MDC provides a mechanism to recover signals with reduced but acceptable quality even when some of the descriptions have been corrupted. This approach is fundamentally different from the use of scalable coding, where a specific enhancement layer can be used to improve the quality of the decoded signal provided that the base layer and all lower-level enhancement layers have been recovered by the receiver [17]. This feature has made MDC very attractive for multimedia communication over multi-path network which exploits network diversity to improve the transmitted signal quality. Several correlated representations of the signal are created and transmitted on different channels. Practical approaches to MDC include scalar quantization [2], polyphase decompositions [3–6]. In our method multiple description with LIoyd – max quantization is been applied so by using this kind of quantization and wavelet transform error concealed well.

The LIoyd-Max scalar quantization [7], [8] is to find a set of quanta $\{q_1,\ldots,q_{n-1}\}$ and a set of partition endpoints $\{x_1,\ldots,x_{n-1}\}$ that minimizes the mean square error (MSE) distortion, given a probability density function *p(x)*. The necessary condition of the LIoyd-Max process shows that each quantum is the centroid of the area of *p(x)* between two adjacent endpoints, whereas each obtained boundary is at the midpoint of two adjacent quanta. Because the centroid and midpoint equations are not in the closed form, a trial-and-error iterative process was proposed to successively adjust q_1 value until a stationary solution is obtained where q_n obtained from the midpoint condition is identical to that q_n^* from the centroid condition, i.e. $dq_n = q_n - q_n^* = 0$. Several heuristic methods to find a good initial q_1 have been proposed [9]-[11]. A multigrid method to speed up the LIoyd-Max iterative process was recently introduced [12].

The LIoyd-Max scalar quantization is to find a quantizer with *n* quanta $\{q_1,\ldots,q_{n-1}\}$ and $n-1$ endpoints $\{x_1,\ldots,x_{n-1}\}$ that minimizes the MSE distortion:

$$D = \sum_{i=1}^{n} \int_{x_{i-1}}^{x_i} (x - q_i)^2 \, p(x) \, dx \tag{1}$$

A quantization scheme is defined by *2 n – 1* numbers:

$$-\infty = x_0 \langle q_1 \langle x_1 \langle q_2 \langle \ldots \langle q_{n-1} \langle x_{n-1} \langle q_n \langle x_n = \infty. \tag{2}$$

The necessary conditions to minimize *D* for fixed n are

$$\frac{\partial D}{\partial x_i} = 0, \quad i = 1, \ldots, n-1 \tag{3}$$

and

$$\frac{\partial D}{\partial q_i} = 0, \quad i = 1, \ldots, n-1. \tag{4}$$

Equation (3) implies the midpoint condition:

$$x_i = \frac{1}{2}(q_i + q_{i+1}), \quad i = 1, \ldots, n-1. \tag{5}$$

Equation (4) implies the centroid condition:

$$\int_{x_{i-1}}^{x_i} (x - q_i) \, p(x) \, dx, \quad i = 1, \ldots, n. \tag{6}$$

The LIoyd-Max solution from the necessary conditions (5) and (6) yields a stationary solution which may be a saddle point or one of several local minimum. The sufficient conditions under which there exists only one locally optimal quantizer were investigated by Fleischer [13], Trushkin [14]-[16]. They showed that the concavity of $\ln p(x)$ on the interval of $p(x) > 0$ is the sufficient condition for the uniqueness of a locally optimal solution. This condition covers the cases of the Gaussian, Laplace, and Rayleigh distributions. In this case, the LIoyd-Max local method produces the globally optimal solution. Equations (5) and (6) form a set of simultaneous equations that are not in the closed form. The method, without using any other condition than (5) and (6), is to pick q_1, and then alternatively calculate the succeeding *xi*'s from the centroid condition (6) and the succeeding q_i 's from the midpoint condition (5). If q_n obtained from the midpoint condition:

$$q_n = 2x_{n-1} - q_{n-1} \tag{7}$$

where

$$q_n^* = \frac{\int_{x_{n-1}}^{\infty} x p(x) \, dx}{\int_{x_{n-1}}^{\infty} p(x) \, dx}, \tag{8}$$

then q_1 must be chosen again. The method consists of running through such chains using various q_1 values until the discrepancy $dq_n = q_n - q_n^*$ is zero. (2)

II. Simulations

The block diagram of proposed method is shown in Fig. 1. In this method Lena 512*512 grayscale image is downsampled to 4 subimages. Downsampling process is shown in Fig. 2. Downsampling block is applied for every 2 samples in rows and columns. So, four subimages (4 geometry shapes in 4 colors) are extracted. By using second order of wavelet type *Coiflet,* subimages mapped to transform domain and LIoyd – max quantization applied then coded and transferred along channels. At the receiver side, vice versa process is used and if one or some of the descriptions are lost along the channels by taking average of received data, lost data can be reconstructed.

Table 1 shows the result of proposed method in different *bpp* (bit per pixel) and number of description lost for Lena's image. Table 2 is average PSNR for [1]. In [1], MDSQ with spread 3 is used.

PSNR formula for 8 bit image is:

$$PSNR = 20 \log_{10}\left(\frac{255}{\sqrt{MSE}}\right). \tag{9}$$

Mean Square Error (MSE) for two *m*×*n* monochrome images *I* and *K* that one of the images is considered a noisy approximation of the other is defined as:

$$MSE = \frac{1}{mn} \sum_{i=0}^{m-1} \sum_{j=0}^{n-1} [\, I(i,j) - K(i,j)]^2 \tag{10}$$

As you compare our proposed worst situation (losing 3 descriptions) with [1]'s the worst situation (losing 7 descriptions), it is obvious that Table 1 has higher PSNR values. For example, if one description is received from proposed method in 0.5 bpp the PSNR is 26.21 dB but if one description is received from [1]'s method in 0.625 bpp the PSNR is 22.88 dB.

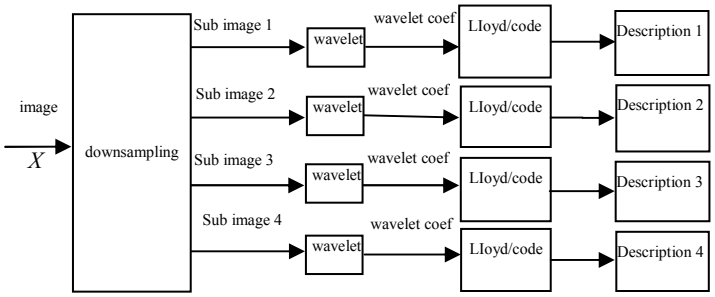


Fig. 1. Block diagram of error concealment using wavelet and LIoyd max quantization.

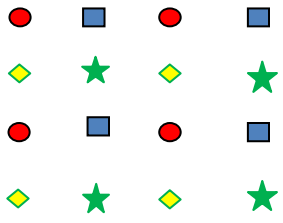


Fig. 2. Downsampling method.

Table 1. Average PSNR (dB) for Lena image from proposed method.

bit rate / Number of lost description	2 bpp	1 bpp	0.5 bpp
0	29.91	28.05	26.39
1	29.77	27.99	26.36
2	29.19	27.66	26.23
3	29.10	27.64	26.21

Table 2. Average PSNR (dB) values for Lena image in [1].

bitrate / number of lost description	2 bpp	1 bpp	0.625 bpp
0	29.80	27.67	26.44
1	29.01	26.85	25.21
2	28.99	26.36	24.57
3	28.25	26.00	23.93
4	27.96	25.71	23.78
5	27.71	25.48	23.38
6	27.50	25.40	23.24
7	27.14	25.07	22.88

In Fig. 3, reconstructed image is shown in 0.5 bpp and with three lost descriptions. In Fig. 4 Lena reconstructed image is plotted with one received description (7 lost descriptions) in 0.625 bpp from [1]. Since wavelet transform is used in proposed method, there is no blocking effect. In [1] as long as DCT is been used the blocking effect is inevitable. For better understanding, rate distortion plot is illustrated for Table 1 and Table 2 as shown in Fig. 5. As you see in every bit per pixel our MSE (mean square error) is lower than [1]. Furthermore slope of the blue lines (proposed method) are lower than the red lines ([1] method). It can be concluded that, by losing data (descriptions) in proposed method the quality or PSNR value is sustainable.



Fig. 3. Reconstructed image in 0.5 bpp with one received descriptions (3 lost).



Fig. 4. Reconstructed image with one received description (7 lost) in 0.625 bpp [1].

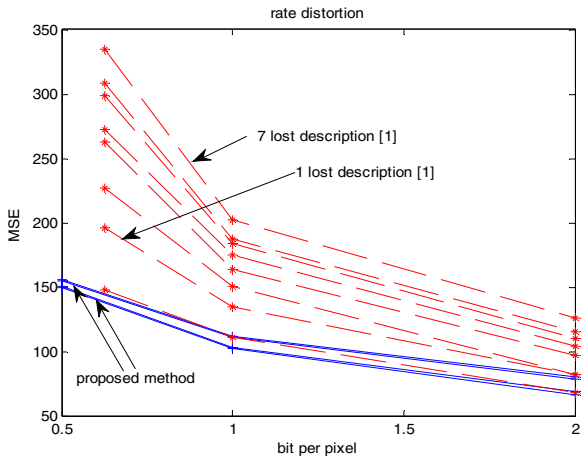


Fig. 5. Rate – distortion plot of proposed LIoyd method and method of [1].



Fig. 6. Original image of *dark-hair woman*.

Table 3. Average PSNR for dark-hair woman image from MDC, wavelet and Lloyd max.

bit rate / Number of lost description	2 bpp	1 bpp	0.5 bpp
0	35.13	33.02	31.55
1	34.95	32.92	31.50
2	34.04	32.44	31.24
3	33.82	32.28	31.12

Proposed method is also applied for grayscale 512*512 *dark-hair woman* image. The original image is shown in Fig. 6. Table 3 shows average PSNR (dB) values for this image in different bit rates and different number of lost descriptions.
Fig. 7 shows rate-distortion plot of Table 3. The top line is for the situation that 3 descriptions have been lost and the bottom line is for the no loss in description. In Fig. 8 image is reconstructed with one received description (3 lost) in 0.5 bpp and this is the worst situation as it is obvious, image is in good subjective evaluation quality. Fig. 9 shows the reconstructed image in 2 bpp with one lost description. So again in the low bpp there could be good quality (subjective evaluation and PSNR values) of reconstructed image.

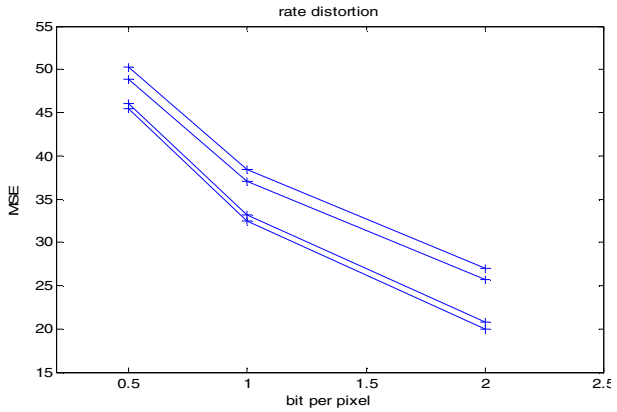


Fig. 7. Rate-distortion plot for *dark-hair woman*.

III. CONCLUSION:

Error concealment using wavelet and LIoyd quantization is used in this paper. Due to the usage of wavelet transform, there are no blocking effects. The quality of the reconstructed images is high even if three descriptions are lost in the channels. Moreover by losing data along channels PSNR values are sustainable. This method has good response in low capacity channels.



Fig. 8. Reconstructed image in 0.5 bpp with 3 lost descriptions.



Fig. 9. Reconstructed image in 2 bpp with 1 lost descriptions.

ACKNOWLEDGMENT

The authors would like to thank all those who contributed toward making this research successful. Also, we would like to thank to all the reviewers for their insightful comment. This work was sponsored by the Research Management Unit, Universiti Teknologi Malaysia.

REFERENCES

[1] X. Zhiming, L. Zhiping, and M. Anamitra, "Multiple Description Image Coding with Hybrid Redundancy," IEEE Asia Pacific conference on Circuits and Systems, APCCAS 2006, 4-7, pp: 382 – 385, Dec. 2006.

[2] V. A. Vaishampayan, "Design of multiple description scalar quantizers," IEEE Trans. on Inform. Theory, vol. 39, no. 3, pp. 821–834, 1993.

[3] P. L. Dragotti, S. D. Servetto, and M. Vetterli, "Analysis of optimal filter banks for multiple description coding," in Proceedings of the Data Compression Conference (DDC '00), pp. 323–332, Snowbird, Utah, USA, March 2000.

[4] P. L. Dragotti, S. D. Servetto, and M. Vetterli, "Optimal filter banks for multiple description coding: analysis and synthesis," IEEE Trans. on Inform. Theory, vol. 48, no. 7, pp. 2036–2052, 2002.

[5] X. Yang and K. Ramchandran, "Optimal multiple description subband coding," in Proceedings of IEEE International Conference on Image Processing (ICIP '98), Ill, USA, vol. 1, pp. 654–658, Chicago, Oct. 1998.

[6] X. Yang and K. Ramchandran, "Optimal subband filter banks for multiple description coding," IEEE Trans. on Inform. Theory, vol. 46, no. 7, pp. 2477–2490, 2000.

[7] S. P. LIoyd, "Least squares quantization in PCM," IEEE Trans. on Inform. Theory, vol. IT-28, pp. 129-137, Mar. 1982

[8] J. Max, "Quantizing for minimum distortion," IRE Trans. on Inform. Theory, vol. IT-6, pp. 7-12, Mar. 1960.

[9] G. M. Roe, "Quantizing for minimum distortion," IEEE Trans. on Inform. Theory, vol. IT-10, pp. 384–385, Oct. 1964.

[10] Y. Linde, A. Buzo, and R. M. Gray,"An algorithm for vector quantizer design," IEEE Trans. on Commun., vol. COM-28, pp. 84–95, Jan. 1980.

[11] X. Wu, "On initialization of Max's algorithm for optimum quantization," IEEE Trans. on Commun., vol. COM-38, pp. 1653–1656, Oct. 1990.

[12] Y. Koren, I. Yavneh, and A. Spira, "A multigrid approach to the scalar quantization problem," IEEE Trans. on Inform. Theory, vol. IT-51, pp. 2993-2998, Aug. 2005.

[13] P. E. Fleischer, "Sufficient conditions for achieving minimum distortion in a quantizer," in IEEE Int. Conv. Rec., vol. 12, pp. 104-111, 1964.

[14] A. V. Trushkin, "Sufficient conditions for uniqueness of a locally optimal quantizer for a class of convex error weighting functions," IEEE Trans. on Inform. Theory, vol. IT-28, pp. 187-198, Mar. 1982.

[15] A. V. Trushkin, "Monotony of LIoyd's Method II for log-concave density and convex error weighting function," IEEE Trans. on Inform. Theory, vol. IT-30, pp. 380-383, Mar. 1984.

[16] A. V. Trushkin, "On the design of an optimal quantizer," IEEE Trans. on Inform. Theory, vol. IT-39, pp. 1180-1194, Jul. 1993.

[17] V. K. Goyal, "Multiple description coding: compression meets the network", IEEE Signal Processing Magazine, vol. 18, pp. 74 - 93, 2001.

Current-Controlled Voltage-Mode Multifunction Filter Using CCDDCCs

Montree Kumngern
Department of Telecommunications Engineering, Faculty of Engineering,
King Mongkut's Institute of Technology Ladkrabang,
Bangkok 10520, Thailand
E-mail: kkmontre@kmitl.ac.th

***Abstract*–This paper presents a new voltage-mode multifunction filter with four inputs and three outputs employing three current controlled differential difference current conveyors (CCDDCCs) and two grounded capacitors. The proposed circuit can provide low-pass, band-pass, high-pass, band-stop and all-pass voltage responses by appropriately connecting the input and output terminals, at a high impedance input terminal which enable easy cascadability. The circuit parameters ω_0 and Q can be set orthogonally by adjusting the circuit components. PSPICE simulation results are also performed to confirm the theoretical analysis.**

***Keywords*—Multifunction filter, Voltage-mode circuit; Current controlled differential difference current conveyors (CCDDCCs)**

I. INTRODUCTION

Voltage-mode second-order active filters with high-input impedance are of great interest because several cells of this kind can be directly connected in cascade to implement higher order filters [1]. On the other hand, it is attractive for monolithic integrated circuit implementation, if the filters employ grounded capacitors [2]–[3]. Current conveyors are receiving growing attention as applications and advantages for realizing of various active filter transfer functions [4]. Recently, many voltage-mode universal biquadratic filters with multiple inputs using current conveyors have been proposed in the literature [5]–[12]. However, the reported filters suffer from one or more of the following disadvantages:

- They cannot provide high-input impedance for realizing five standard filter responses [5], [6], [10], [12],
- For realizing five standard filter responses, they require the component-matching condition [5], [6], [10].
- They use an excessive number of active or passive components [5], [8], [10].
- They use floating capacitors or require the capacitor injection of excitation signals in the circuit design [5]–[7], [9], [11].
- They use two kinds of active components [7], [8].
- They require additional voltage inverter for realizing all-pass filter responses [7], [9], [11].

Recently, Chiu et al. [13] proposed a new current conveyor circuit called the differential difference current conveyor (DDCC). The DDCC has the advantages of both the CCII and the differential difference amplifier (DDA) (such as high input impedance or arithmetic operation capability) [13]. Some DDCC-based voltage-mode universal biquadratic filters with multiple inputs have been proposed [14]–[18]. However, the multiple inputs universal filters in [14]–[15] still use two kinds of active components (DDCC and OTA) and the circuit in [16] uses the resistor injection of excitation signals in the circuit design.

The purpose of this paper is to developing a new high-input impedance voltage-mode universal biquadratic filter with four inputs and three outputs employing the modified DDCCs, called a "current controlled differential difference current conveyor (CCDDCC)" [17]. It properties are similar to the conventional DDCC, but the CCDDCC has finite input resistance R_x at the X-terminal, which is controllable by the bias current I_B. The proposed circuit uses two grounded capacitors and two grounded resistors, which is suitable for integrated circuit implementation. By appropriately connecting the input terminals, the circuit can realized five standard biquadratic filter functions. For the realization of all the filter responses, no critical component matching conditions are required. Also, the circuit has low active and passive sensitivities. The new universal filter configuration has not been found in the literature, although the proposed schemes employ the same number of active and passive components as the previous universal filters presented in [18]–[19] but the proposed circuit is the new topology.

II. CIRCUIT DESCRIPTIONS

Fig. 1 shows the electrical symbol of CCDDCC. The input and output of CCDDCC is defined by the following matrix equation:

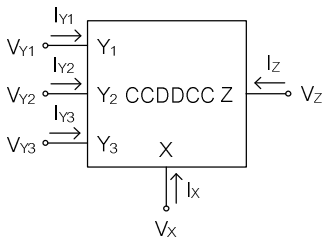


Figure 1. Electrical symbol of CCDDCC.

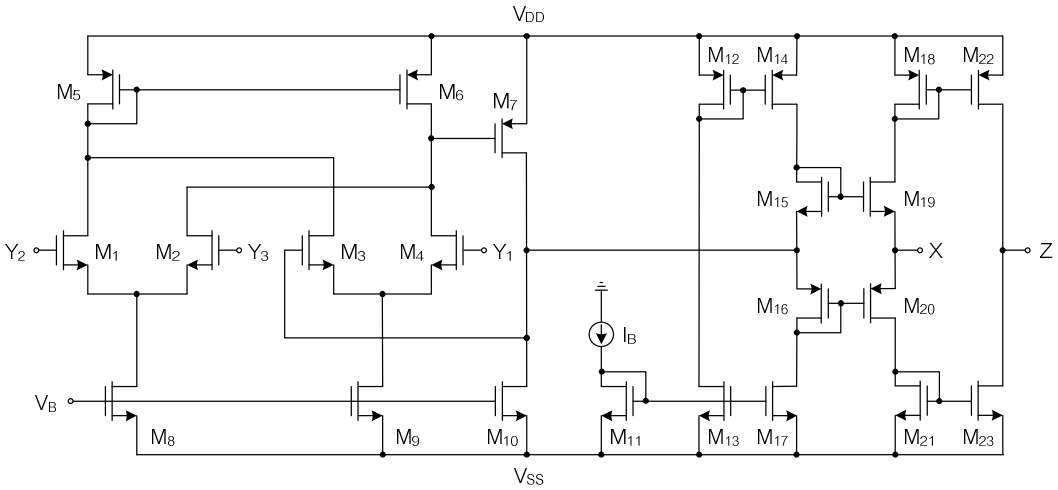


Figure 2. CMOS implementation for CCDDCC.

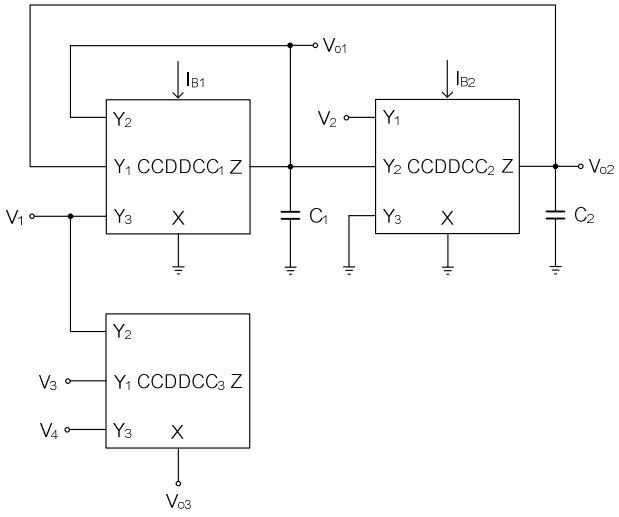


Figure 3. Proposed four-input three-output voltage-mode multifunction filter using CCDDCCs.

$$\begin{pmatrix} V_X \\ I_{Y1} \\ I_{Y2} \\ I_{Y3} \\ I_Z \end{pmatrix} = \begin{pmatrix} 1 & -1 & 1 & R_x \\ 0 & 0 & 0 & 0 \\ 0 & 0 & 0 & 0 \\ 0 & 0 & 0 & 0 \\ 0 & 0 & 0 & 1 \end{pmatrix} \begin{pmatrix} V_{Y1} \\ V_{Y2} \\ V_{Y3} \\ I_X \end{pmatrix}. \quad (1)$$

The CMOS implementation for CCDDCC is shown in Fig. 2 [17]. If matched transistors M_{19} and M_{20} are assumed, the X-terminal resistance can be approximated as

$$R_x \approx \frac{1}{\sqrt{8\mu C_{ox}(W/L)I_B}} \quad (2)$$

where μ, C_{ox}, W and L are, respectively, surface mobility, oxide capacitance, channel width and length of MOS transistors.

The proposed multifunction filter is shown in Fig. 3. It is composed of three CCDDCCs and two grounded capacitors. Using equation (1), the voltage output of the circuit in Fig. 3 can be expressed as

$$V_{o1} = \frac{sR_{x1}C_1V_1 + V_2}{D(s)} \quad (3)$$

$$V_{o2} = \frac{(sR_{x1}C_1 + 1)V_2 - V_1}{D(s)} \quad (4)$$

$$V_{o3} = \frac{-D(s)V_1 + V_3 + V_4}{D(s)} \quad (5)$$

where $D(s) = s^2R_{x1}R_{x2}C_1C_2 + sR_{x1}C_1 + 1$.

It is clearly seen from equations (3) to (5) that:

- The non-inverting LP response can be obtained when V_1=V_3=V_4=0 (grounded), V_2=V_{in} and V_{o1}=V_{out}.
- The inverting LP response can be obtained when V_2=V_3=V_4=0 (grounded), V_1=V_{in} and V_{o2}=V_{out}.
- The non-inverting BP response can be obtained when V_2=V_3=V_4=0 (grounded), V_1=V_{in} and V_{o1}=V_{out}.
- The inverting HP response can be obtained when V_4=0 (grounded), V_1=V_2=V_{in}, V_3=V_{o1} (connected) and V_{o3}=V_{out}.

- The inverting BS response can be obtained when V_2=V_4=0 (grounded), V_1=V_{in}, V_3=V_{o1} (connected) and V_{o3}=V_{out}.
- The inverting AP response can be obtained when V_2=0 (grounded), V_1=V_{in}, V_3=V_4=V_{o1} (connected) and V_{o3}=V_{out}.

Thus, the proposed filter can realize all the standard types of the biquadratic filtering function by appropriately connecting the input and output terminals without component-matching condition requirements as well as requiring no an inverting-type voltage input signal, hence the name "multifunction filter". Moreover, the four input signals V_1, V_2, V_3 and V_4, are connected to the high-input impedance input nodes of the CCDDCCs. Also, some output signals are connected to the low-output impedance output node of the CCDDCC. Then, the circuit enjoys the advantage of having high-input and some low-output impedance and therefore permitting easy cascadability. The parameters ω_o and Q of this filter are expressed by

$$\omega_o = \frac{1}{\sqrt{R_{x1}R_{x2}C_1C_2}} \tag{6}$$

$$Q = \sqrt{\frac{R_{x1}C_1}{R_{x2}C_2}}\,. \tag{7}$$

Under the condition of R_{x1}=R_{x2}=R, the circuit parameters are simplified to

$$\omega_o = \frac{1}{R\sqrt{C_1C_2}} \tag{8}$$

$$Q = \sqrt{\frac{C_1}{C_2}}\,. \tag{9}$$

From equations (8) and (9), the parameter Q can be setup by C_1 and C_2 and parameter ω_o can be set by resistance R without disturbing Q. Thus, the biquadratic filter has orthogonal tuning capability for the circuit parameters Q and ω_o. From equations (6) and (7), the incremental sensitivities of the parameters ω_o and Q are calculated as shown in Table 1. It shows that the active and passive sensitivities are low. Note from the proposed filter that it requires no component-matching condition for realization all filter responses. In fact, for the case of R_{x1}=R_{x2}, the component-matching condition is imposed. This problem can be solved by using multiple current sources using a single reference.

TABLE I.
SENSITIVITIES OF CIRCUIT COMPONENTS

X	$S_x^{\omega_0}$	S_x^Q
R_{x1}	-0.5	0.5
R_{x2}	-0.5	-0.5
C_1	-0.5	0.5
C_2	-0.5	-0.5

III. SIMULATION RESULTS

To verify the theoretical prediction of the proposed circuit, the multifunction filter in Fig. 3 has been simulated using PSPICE simulation program. The CCDDCC in Fig. 2 was simulated using the 0.25μm TSMC CMOS technology [17]. The transistor aspect ratios of CCDDCC are equaled to those reported in [17]. The supply voltages were ±1.25V. The bias voltage V_B and the bias current I_{B3} of $CCDDCC_3$ were taken as -0.9V and 120μA, respectively. For example design, the capacitors used are C_1=C_2=10pF. This setting has been designed to obtain the LP, BP, HP, BS and AP filter responses with f_o=3.18 MHz and Q=1. The simulated results for the LP, BS, HP and BP filter characteristics are shown in Fig. 4. In this figure, the pole frequency of 3.12MHz is obtained. This error would be caused by tracking errors of CCDDCCs. Fig. 5 shows the simulated frequency responses of the gain and phase characteristics of the AP filter. Then, it can be observed from Figs. 4 and 5 that the proposed filter in Fig. 3 performs five standard biquadratic filtering functions well. Fig. 6 shows the simulated a BP filter response of the proposed filter using parameters as C_1=C_2=10pF and I_B=1μA, 2.5μA, 5μA, and 20μA (i.e. I_{B1}=I_{B2}=I_B). This result is confirmed by equation (8). It can confirm that the proposed filter can be controlled electronically by adjusting the bias currents of the CCDDCCs.

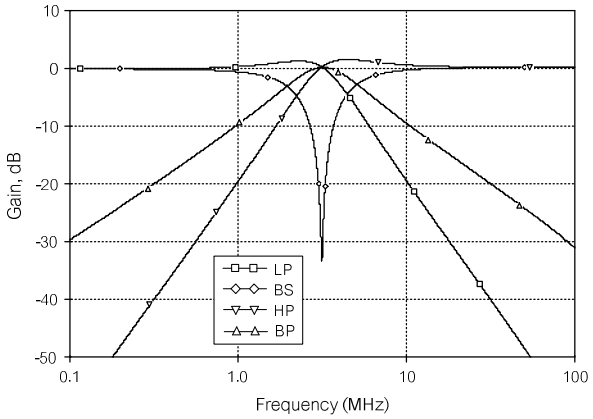


Figure 4. Simulated LP, BS, HP and BP voltage responses.

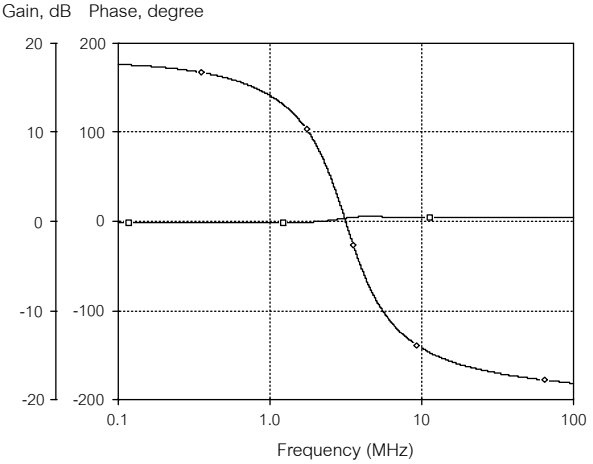


Figure 5. Simulated AP response of the proposed filter.

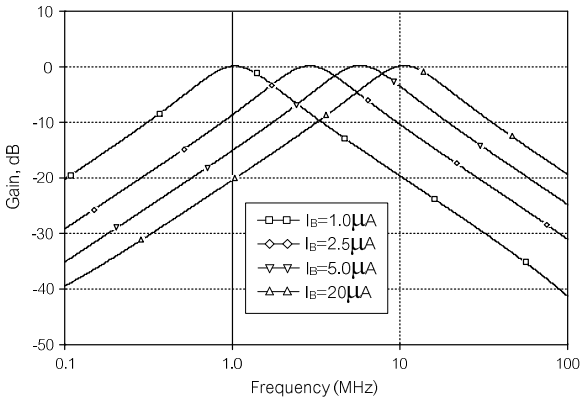


Figure 6. Simulated frequency responses of the BP filter when I_B is varied.

IV. CONCLUSIONS

In this paper, a new four-input three-output voltage-mode multifunction biquadratic filter is presented. The proposed circuit uses three CCDDCCs and two grounded capacitors and has high impedance input providing cascadibility feature to the circuit. The use only grounded capacitor makes the circuit suitable for integrated circuit implementation. The proposed filter provides five standard filter responses without component matching conditions, and offers low active and passive sensitivities. An orthogonal control between the natural frequency (ω_o) and the parameter ω_o/Q by electronic means is achieved. The simulation results verifying theoretical analyses are also included.

ACKNOWLEDGMENTS

The author acknowledges with thank the support of Faculty of Engineering, King Mongkut's Institute of Technology Ladkrabang. The author also would like to express sincere thanks to the Telecommunications Research and Industrial Development Institute (TRIDI) of the office of National Telecommunications Commission of Thailand (NTC) for kindly supporting the equipments of the research laboratory.

REFERENCES

[1] A. Fabre, F. Dayoub, L. Duruisseau, and M. Kamoun, "High-input impedance insensitive second-order filters implemented from current conveyors," *IEEE Transactions on Circuits and System-I*, vol. 41, pp. 918–921, 1994.

[2] M. Bhusan and R. W. Newcomb, "Grounding of capacitors in integrated circuits," *Electronics Letters*, vol. 3, pp. 148–149, 1967.

[3] K. Pal and R. Singh, "Inductorless current conveyor all-pass filter using ground capacitors," *Electronics Letters*, vol. 18, pp. 47–47, 1982.

[4] B. Wilson, "Recent developments in current conveyor and current-mode circuits," *IEEE Transactions on Circuits, Devices and Systems*, vol. 137, pp. 63–77, 1990.

[5] S. Ozoguz and E. O. Gunes, "Universal filter with three inputs using CCII+s," *Electronics Letters*, vol. 32, pp. 134–2135, 1996.

[6] S.–I. Liu and J.–L. Lee, "Voltage-mode universal filters using two current conveyors," *International Journal of Electronics*, vol. 82, pp. 145–149, 1997.

[7] J.–W. Horng, "High input impedance voltage-mode universal biquadratic filter using two OTAs and one CCII," *International Journal of Electronics*, vol. 90, pp. 183–191, 2003.

[8] T. Tsukutani, Y. Sumi, Y. Kinugasa, M. Higashimura, and Y. Fukui, "Versatile voltage-mode active-only biquad circuits with loss-less and lossy integrators," *International Journal of Electronics*, vol. 91, pp. 525–536, 2004.

[9] J.–W. Horng, "High-input impedance voltage-mode universal biquadratic filter using three plus-type CCIIs," *IEEE Transactions on Circuits and System-I*, vol. 48, pp. 996–997, 2001.

[10] C.–M. Chang, "Universal voltage-mode filter with four inputs and one output using two CCII+s," *International Journal of Electronics*, vol. 86, pp. 305–309, 1999.

[11] J.–W. Horng, "New configuration for realizing universal voltage-mode filter using two current feedback amplifier," *IEEE Transactions on Instrument and Measurement*, vol. 49, pp. 1043–1045, 2000.

[12] J.–W. Horng, C.–C. Tsai, and M.–H. Lee, "Novel universal voltage-mode biquad filter with three inputs and one output using only two current conveyors," *International Journal of Electronics*, vol. 80, pp. 543–546, 1996.

[13] W. Chiu, S.–I. Liu, H.–W. Tsao, and J.–J. Chen, "CMOS differential difference current conveyors and their applications," *IEE Proceeding of Circuits, Devices and System*, vol. 143, pp. 91–96, 1996.

[14] H.–P. Chen, S.–S. Shen, and J.–P. Wang, "Electronically tunable versatile voltage-mode universal filter," *International Journal Electronics and Communications*, vol. 62, pp. 316–319, 2008.

[15] H.–P. Chen, "Versatile multifunction universal voltage-mode biquadratic filter," *International Journal Electronics and Communications*, vol. 64, pp. 983–987, 2010.

[16] C.–M. Chang and H.–P. Chen, "Universal capacitor-grounded voltage-mode filter with three inputs and a single output," *International Journal of Electronics*, vol. 90, pp. 401–406, 2003.

[17] P. Prommee and M. Somdunyakanok, "CMOS-based current-controlled DDCC and its applications to capacitance multiplier and universal filter," *International Journal Electronics and Communications*, vol. 65, pp. 1–8, 2011.

[18] W.–Y. Chiu and J.–W. Horng, "High-input and low-output impedance voltage-mode universal biquadratic filter using DDCCs," *IEEE Transactions on Circuits and Systems-II*, vol. 54, pp. 649–652, 2007.

[19] J.–W. Horng, "High input impedance voltage-mode universal biquadratic filter with three inputs using DDCCs," *Circuits System and Signal Processing*, vol. 27, pp. 553–562, 2008.

New QC-LDPC Codes Implementation on FPGA Platform in Rayleigh Fading Environment

Farid Ghani, Abid Yahya and Abdul Kader

School of Computer and Communication Engineering
University Malaysia Perlis (UniMAP)
02000 Kuala Perlis, Perlis, MALAYSIA
faridghani@rediffmail.com, abidusm@gmail.com and kdr2k4@yahoo.com

***Abstract*—This paper presents performance of Quasi-Cyclic low-density parity-check (QC-LDPC) codes on a flat Rayleigh fading channels by employing BPSK modulation scheme. The BER curves show that large girth and diversity level robust the system performance. Moreover, Prototype architecture of the LDPC codes has been implemented by writing Hardware Description Language (VHDL) code and targeted to a Xilinx Spartan-3E XC3S500E FPGA chip. Simulation results show that the proposed QC-LDPC codes achieve a 0.1dB coding gain over randomly constructed codes and perform 1.3 dB from the Shannon-limit at a BER of 10^{-6} with a code rate of 0.89 for block length of 1332.**

***Keywords*— Bit error rate; Communication channels; Encoding; FPGA; QC-LDPC, Rayleigh Fading**

I. INTRODUCTION

Channel coding plays key role in providing a reliable communication method that can overcome signal degradation in practical channels. The breakthrough of convolutional codes [1] led off a new field of study into non-algebraic codes based on linear transformations using generator and parity-check matrices. Convolutional codes are encoded using a finite-state process, which generates them a linear order encoding scheme. Subsequently, convolutional codes led to the discovery of a class of codes called Turbo codes [2], which are the class of concatenated convolutional codes and randomize the order of some of the bits by using an interleaver.

Turbo codes are the first known capacity approaching error correction codes, which provide a powerful error correction capability when decoded by an iterative decoding algorithm [2]. The rediscovery of low density parity check (LDPC) code, which was originally proposed by Gallager [3] and was later generalized as MacKay-Neal code [4] puts back Turbo coding as the forward error correction (FEC) technique. LDPC codes were neglected for a long time as their computational complexity for the hardware technology was very high. LDPC codes have acquired considerable attention due to its near-capacity error execution and powerful channel coding technique with an adequately long codeword length [5]. LDPC codes have several advantages over Turbo codes. In the decoding part, Turbo code faces difficulty to apply parallelism due to the sequential nature of the decoding algorithm. In case of LDPC, decoding can be accomplished with a high degree of parallelism to attain a very high decoding throughput. LDPC codes do not need a long interleaver, which usually causes a large delay in Turbo codes. LDPC codes can be constructed directly for a desired code rate while Turbo codes, which are based on convolutional codes, require other methods such as puncturing to acquire the desired rate.

The codes are classified into two major categories, explicitly, block codes and convolutional codes. Hamming codes, Bose- Chaudhuri-Hocquenghem (BCH) codes; Reed-Solomon codes (RS) [6-7] and newly rediscovered LDPC codes are the example of block codes. Block codes like Hamming, BCH and RS codes have structures but with limited code length. A bounded-distance decoding algorithm is usually employed in decoding block codes except LDPC codes. In general, it is hard to use soft decision decoding for block codes.

Advances in error correcting codes have revealed that, using the message passing decoding algorithm, irregular LDPC codes can accomplish consistent communication at SNR very close to the Shannon limit as Compared to Turbo codes [8]. The numerical analysis method for calculating the threshold of the LDPC codes is examined by Hou *et al,*[9] over AWGN channel with uncorrelated flat Rayleigh fading channel. Additionally, using the nonlinear optimization technique of differential evolution, the degree distribution pairs are optimized for the uncorrelated Rayleigh fading channel and it has been observed that their threshold values are very close to the capacity of this channel for moderate block size with excellent performance. The two adaptive coded modulation schemes employing LDPC codes for Rayleigh fading channels are proposed by Zhang *et al.,* [10]. It is shown from their work that the proposed schemes have made good use of the time-varying nature of Rayleigh fading channel. It is also observed that the proposed schemes perform better by employing LDPC with large code length.

The performance of irregular LDPC codes is investigated in [11] with three BP based decoding algorithms, specifically the Uniformly Most Powerful (UMP) BP-based algorithm, the Normalized BP-based algorithm, and the Offset BP-based algorithm on a fast Rayleigh fading channel by employing density evolution (DE). It is observed from the study that the performance and decoding complexity of irregular LDPC codes with the offset BP-based algorithm can be very close to that with the BP algorithm on the fast Rayleigh fading channel. After successful evolution of irregular LDPC codes, Ohhashi and Ohtsuki [11] **then** analyze the performance of regular LDPC codes with the normalized BP-based algorithms on the fast Rayleigh fading channel. Formulas for short and long regular LDPC codes are derived based on the probability density function (PDF) of the initial likelihood information and DE for the normalized BP-based algorithm on the fast Rayleigh fading channel. Performance of the long regular LDPC codes with the Normalized BP-based algorithm in the proposed method outperforms the BP and the UMP BP-based algorithms on fast Rayleigh fading channel. In this paper new QC-LDPC codes [12] have been developed and then implement the newly designed codes on FPGA platform.

Simulation results demonstrate that the proposed QC-LDPC codes achieve a 0.1dB coding gain over randomly constructed codes and perform 1.3 dB from the Shannon-limit at a BER of 10^{-6} with a code rate of 0.89 for block length of 1332.

II. Representations For LDPC Codes

Basically there are two different underlying theories to represent LDPC codes. Like all linear block codes, LDPC codes can be described using matrices. Alternatively, it can be described using a graphical representation.

(a) Matrix Representation

LDPC codes are in the category of linear codes. They cater near capacity performance on a large data transmission and storage channels. LDPC codes are rendered with probabilistic encoding and decoding algorithms. LDPC codes are designated by a parity check H matrix comprising largely 0's and has a low density of 1's. More precisely, LDPC codes have very few 1's in each row and column with large minimum distance. In specific, a (n, j, k) low-density code is a code of block length n and source block length k. The number of parity checks is delimitated as $m = n - k$. The parity check matrix weight (number of ones in each column or row) for LDPC codes can be either regular or irregular. LDPC can be regular if the number of 1's is constant in each column or row and gets irregular with a variable number of 1's in each column or row. A regular LDPC code is a linear block code whose parity-check matrix constitutes exactly j 1's in each column and exactly $k = j(n/m)$ 1's in each row, with the code rate $R = 1 - j/k$.

(b) Graphical Representation

Tanner considered LDPC codes and showed how they represented effectively by a bipartite graph, now called a Tanner graph [13]. Tanner graphs provide a complete representation of the code and also help to explain the decoding algorithm.

In Tanner graphs the nodes of the graph are separated into two typical sets and edges are only connecting nodes of two different types. The two types of nodes in a Tanner graph are called variable nodes (v -nodes) and check nodes (c -nodes). The Tanner graph of a code is drawn according to the following rule: It consists of m check nodes (the number of parity bits) and n variable nodes (the number of bits in a codeword).Check node y_i is connected to variable node y_j if the element h_{ij} of H is a 1.

III. Quasi-Cyclic LDPC Codes

Quasi-Cyclic LDPC codes form a large class of codes with nice encoding and decoding, which have been comprehensively premeditated in the sense that their hardware is both cheap and easy to implement. Since both encoding and decoding require less memory, which have many gains for hardware and software implementations. This memory advantage is catered by being able to illustrate the matrices employing a series of short polynomials.

A code is pronounced to be quasi-cyclic (QC) if a cyclic shift of any codeword by p positions is still a codeword. Thus a cyclic code is a QC code with $p = 1$. The block length n of a QC code is a multiple of p, As a result

$$n = m \times p \tag{1}$$

Circulants, or cyclic matrices, are indispensable components in the generator matrix for a QC code.

A circulant matrix is defined as a square matrix, such that each row is incurred by a cyclic shift of the preceding. The parity-check matrix of a QC code is decomposed into $m \times m$ blocks of circulant matrices, with submatrix dimensions $vm \times \mu m$, where ν and μ are the circulants number in row and column, respectively.

Let C be a $m \times m$ matrix. We say that C is circulant if its rows are incurred by successive shifts. This means that a QC code can be distinguished by a generator matrix of the form [14-15]:

$$C = [C_0, C_1, C_2, C_3, \dots, C_{m-1}] \tag{2}$$

Where C_i, $i = 0,1,2, \dots, m-1$, are circulants of order $m \times m$ of the form:

$$C = \begin{bmatrix} C_0 & C_1 & C_2 & \cdots & C_{m-1} \\ C_{m-1} & C_0 & C_1 & \cdots & C_{m-2} \\ C_{m-2} & C_{m-1} & C_0 & \cdots & C_{m-3} \\ \vdots & \vdots & \vdots & & \vdots \\ C_1 & C_2 & C_3 & \cdots & C_0 \end{bmatrix} \tag{3}$$

We consider weight-1 and weight-2 circulants, in polynomial form, by referring the positions of the 1's in the first row of the circulant. Circulant with weight-2 is denoting in the polynomial form:

$$P(x) = x^{\alpha} + x^{\beta} \tag{4}$$

Great care has to be taken while dealing with the values of α and β, since efficient decoding and removal of short cycles depend on these values.

IV. New Algorithm for Quasi-Cyclic LDPC Codes

The proposed algorithm for the construction of the new QC-LDPC (N, j, k) code is as described in the following steps:

1. The codeword can be encoded as follows;

$$mod2(\mathbf{H} \times C^T) = 0 \tag{5}$$

where $\mathbf{H}$ represents parity check matrix and C denotes codeword.

2. For an efficient encoding the codeword's rows are split into sub rows with respect to group size.

$$C = (b, |p_1, p_2, \dots, p_k) \tag{6}$$

where b and p represent the information and parity check bits respectively.

3. The constraint of group's number on row weight size persists the row-column (RC) connections to generate variety of codes.

$$\mathbf{\Psi} = \sum_{i=1}^{\kappa} \boldsymbol{\chi} \tag{7}$$

where $\mathbf{\Psi}$ represents group size and $\boldsymbol{\chi}$ stands for number of row.

4. In each sub row the number of 1-component is selected in order to maintain the concentrated degree of distribution which results in random selection. Otherwise non-concentrated degree of distribution will appear.

$$\mathbf{H}_{QC} = \begin{bmatrix} H_{cir} & Z & H_{cir} & Z & H_{cir} & H_{cir} & Z \\ H_{cir} & H_{cir} & Z & H_{cir} & H_{cir} & Z & Z \\ Z & H_{cir} & Z & H_{cir} & H_{cir} & Z & H_{cir} \\ \dots\dots & & & & & & \end{bmatrix} \tag{8}$$

$$H_{cir} = \begin{bmatrix} I_1 & \cdots & I_{m^{k-1}} \\ I_n & \cdots & \vdots \\ \vdots & \ddots & \vdots \\ I_{n^{j-1}} & \cdots & I_{m^{k-1} n^{j-1}} \end{bmatrix} \tag{9}$$

A $p \times p$ $\mathbf{H}_{QC}$ array is obtained from the aforesaid equations, where $H_{cir}$is the permutation matrix with the location vector of the field elements, cyclically shifting codeword by one position. Therefore, each row of $H_{cir}$is obtained from shifting the rows of the identity matrix to the left. Hence $H_{cir}$is $p \times p$ circulant permutation matrix and $\mathbf{H}_{QC}$ is $p \times p$ array of $p \times p$ circulant permutation matrix.

Let $I_1, \ldots, I_{m^{k-1}}$ denote the rows of the parity check matrix **H**. First we consider splitting each row of **H** into the same number of sub rows. All the new sub rows have the same length as the original row. The weight (or "1s") of the original row is distributed among the sub rows. A regular row weight distribution can be done as follows. Let q be a positive integer, split each row $I_i$of **H** into q sub rows $I_{i,1}, I_{i,2}, \ldots, I_{i,q^{k-1}}$. The distribution of k "ones" of I_i into $I_{i,1}, I_{i,2}, \ldots, I_{i,q^{k-1}}$ is carried out in a rotating manner. In the first rotation, the first "1" of I_i is put in $I_{i,1}$, the second "1" of I_i is put in $I_{i,2}$ and so on. In the second rotation, the $(q+1)^{\text{th}}$ "one" of I_i is put in $I_{i,1}$, the $(q+2)^{\text{th}}$ "one" of I_i is put in I_{i+2} and so on. This rotating distribution of the "ones" of I_i continues until all the "ones" of I_i have been distributed into the q sub rows.

The above row's splitting results in a new parity check matrix **H** withqm^{k-1}rows which has the following structural properties: (1) each row has weight k (2) every column has weight j (3) any two rows (or columns) have at most one 1-component in common. Such a sparse parity-check matrix is said to be (j,k) regular and the code generated by it is called (j,k) a regular code. The constraint on the rows and columns of **H** given by property (3) is called the row-column (RC) constraint. Therefore, the above row's splitting results in a new parity check matrix with smaller density. Moreover, when the parity check matrix is systematic, one can easily use it to extract the density of the code.

5. Select the rows (a) find the row with the least distance (b) Store shift values of the submatrices (c) UNION ('rows')

The shift values of the submatrices are stored in order to reduce the memory requirement by a factor $1/p$, when $p \times p$ circulant permutation matrices are employed. This lead us to a point that a location of 1 is fixed in the first row and we determine the location of other 1 uniquely therefore the required memory for storing the parity check matrix of the QC-LDPC code can be reduced by a factor $1/p$.

V. Rayleigh Fading Channel

In this section, a statistical model for flat Rayleigh fading channels is presented. This channel model is used here to assess the dependability and performance of the system.

An impulse response is a broadband channel characterization which is used in designing a communication system. An impulse response comprises all entropy, essential to simulate and examine the radio transmission system through a communication channel.

The impulse response is a useful characterization of the channel, since it may be used to forecast and evaluate the performance of different mobile communication systems as well as the transmission bandwidths for a specific mobile channel condition [16].

The channel impulse response can be evinced as $h(d,t)$. Let the transmitted signal be set out by $x(t)$ and the received signal $y(d,t)$ at a position d is to be articulated as a convolution between (x) and $h(d,t)$ [16].

$$y(d,t) = x(t) \otimes h(d,t)$$
$$= \int_{-\infty}^{\infty} x(\tau) h(d, t-\tau) d\tau \qquad (10)$$

In case of a causal system the equation (10) turns into;

$$y(d,t) = \int_{-\infty}^{t} x(\tau) h(d, t-\tau) d\tau \qquad (11)$$

where d represents the position of the receiver at constant velocity v is denotative as;

$$d = vt \qquad (12)$$

Substituting the value of d in equation (11)

$$y(vt,t) = \int_{-\infty}^{t} x(\tau) h(vt, t-\tau) d\tau \qquad (13)$$

Given that v may be assumed as constant over a short time interval, therefore equation (13) can be stated as;

$$y(t) = \int_{-\infty}^{\infty} x(\tau) h(t,\tau) d\tau \qquad (14)$$

The impulse response $h(d,\tau)$ is a function of both t andτwhich entirely characterizes the channel. The time variation and time delay of multipath channel is represented by t and τ respectively.

Fading channel usually follows the Rayleigh fading characteristics. This also happen when simulating the wireless channel for mobile and macro cellular communications. If we put on a mobile station with carrier frequency f_c moving at a velocity v, then the Doppler shift brought in the n^{th} incident wave is set by;

$$f_{D,n}(t) = f_d \cos\theta_n(t) \qquad (15)$$

where $f_d = v/\lambda_c$

VI. Implementation And Design Flow

There are many aspects which are associated with the performance of LDPC codes such as the code rate, the choice of the ***H*** matrix, and even the selection of the design. One of the noticeable trade-off in the LDPC encoder-decoder design deals with code length and the area accessible in a design platform. In general, codes with larger block lengths have better performance. Now the FPGA platform gives the opportunity that one can fit more basic building block elements, thus letting for larger design.

Prototype architecture of the LDPC codes has been implemented by writing Hardware Description Language (VHDL) code and targeted to a Xilinx Spartan-3E XC3S500E FPGA chip. The block diagram of the overall design flow is shown in Figure 1. The Spartan-3E family reduces system cost by providing the lowest cost-per-logic of any FPGA family, supporting the lowest-cost configuration solutions including commodity serial and parallel flash memories, and competently integrating the functions of many chips into a single FPGA.

An USB interface is employed between the Spartan-3E Board and the PC for testing and verification of the architecture by transferring generated data between the PC and the FPGA architecture. The FPGA is programmed and configured with VHDL and the Xilinx integrated software environment (ISE). If the design needs changes, the device does not require being detached from the board just simply re-programmed in-system.

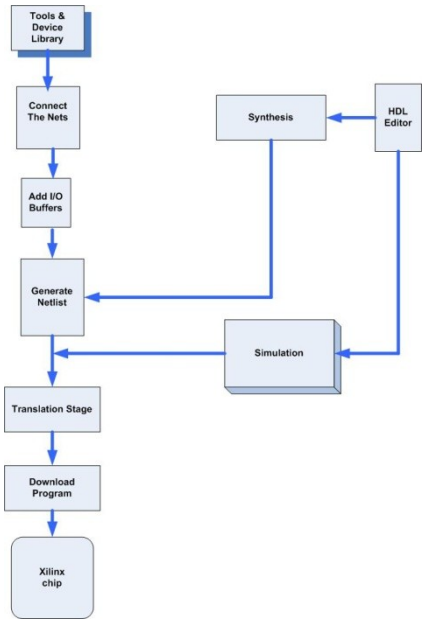


Fig.1 Overall LDPC codes design flow

VII. RESULTS AND DISCUSSION

In this section, we simulated the performance of two girth-twelve QC-LDPC codes. The allowable maximum number of iterations for decoder is set to 40,50 and 60 respectively, for diversity levels L=2, L=3 and L=4 with 5 microseconds symbol period and 1.1 milliseconds coherence time on a flat Rayleigh fading channels by employing BPSK modulation scheme. In this part of simulation, the noise variance is assumed to be known at the receiver. It can be observed in Figure 2 as the number of QC-LDPC decoding iterations and diversity levels increases; the decoder caters more reliable log likely ratio (LLR) values that are associated with the estimated demodulation vector. A large value of LLR points that the estimated bit of the demodulated vector has high reliability, due to this reason the probability of error goes down. The BER curves show that large girth and diversity level robust the system performance.

Figure 3 shows the performance of QC-LDPC codes, compares with that of randomly constructed LDPC code in term of their BER and block error rate (BLER) at fractional bandwidth $\rho = 0.1$. In each case, decoder runs for a 60 iterations to get the best possible performance. The performance of QC-LDPC codes is almost the same as that of random codes at low signal noise ratio (SNR), but the former is better than the later at high SNR.

Performance enhancement and comparison of the newly obtained codes is shown in Figure 4 employing different code rates. One way to accomplish the best and high rate LDPC code is the puncturing of low rate LDPC code and also some time puncturing columns. The drawback is that it reduces the block length and also effects in the performance. The proposed QC-LDPC codes take union of the rows in order to support the multiple coding rates as mentioned in point (5) of the proposed algorithm. It provides a simple overall architecture with a smaller chip area required to support all the needed rates.

Throughout the simulation BPSK modulation scheme has been employed with 50 maximum number iterations. Simulation results in Figure 4 portray that the proposed QC-LDPC codes achieve a 0.1dB coding gain over randomly constructed codes and perform 1.3 dB from the Shannon-limit at a BER of 10^{-6} with a code rate of 0.89 for block length of 1332. Simulation results show that the code optimization and girth conditioning not only improves the performance but also lowers the error floor for QC-LDPC codes. On the other hand random codes correspond to a smaller sub matrix. The rigid weight constraints of the optimization process do not allow many variations in the random codes construction. The structure of random codes confines the construction of codes with both good cycle and girth properties and directs to error floor.

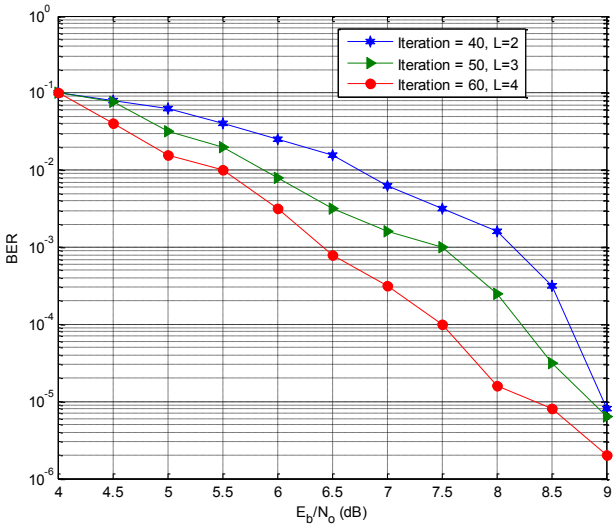


Fig.2 BER of two girth-twelve QC-LDPC codes for given value of E_b / N_o on Rayleigh fading channels with code rate 0.87

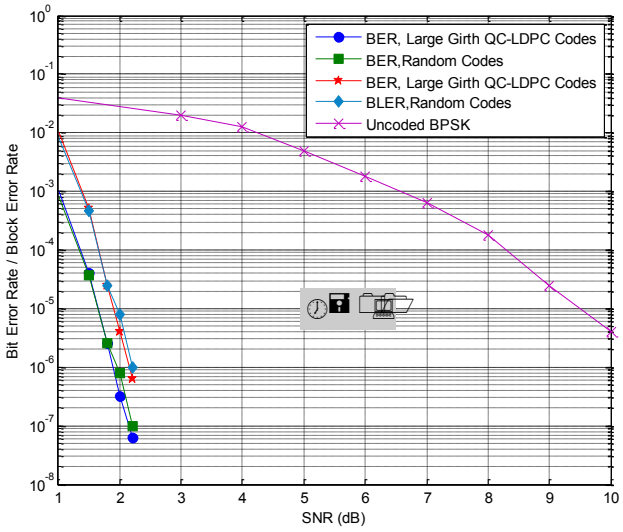


Fig.3 BER and BLER of the proposed codes and randomly constructed codes in partial band jamming environment

The method to calculate the Shannon's limit is as follows;

$$R \leq B \log2\left(1 + {}^{S}/_{N}\right) \quad (16)$$

where, R represents the code rate and replace the signal power S by RE_b and the noise power N by BN_0.

$$ {}^{R}/_{B} \leq \log2\left(1 + \left({}^{RE_b}/_{BN_0}\right)\right) \quad (17)$$

${}^{R}/_{B}$ is called the bandwidth efficiency in units of bit/second/Hz. Substituting ${}^{E_b}/_{N_0}$ with $\left({}^{E_b}/_{N_0}\right)min$ and rearranging;

$$\left({}^{E_b}/_{N_0}\right)min \geq {}^{\left(2^{\left({}^{R}/_{B}\right)} - 1\right)}/_{\left({}^{R}/_{B}\right)} \quad (18)$$

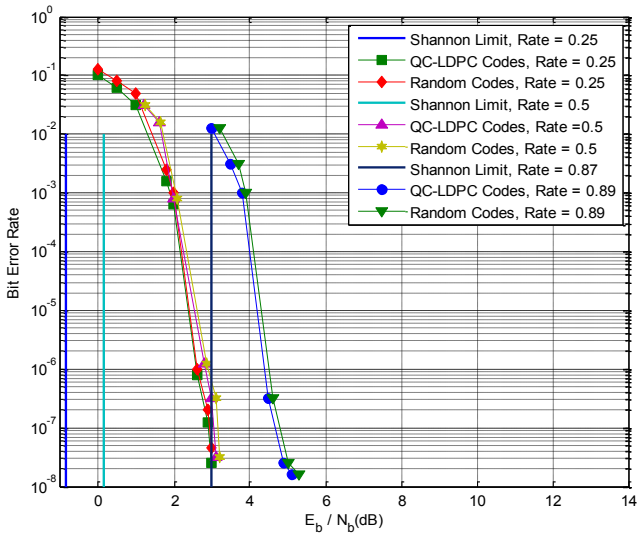


Fig.4 Shannon's limit of proposed QC-LDPC codes and randomly constructed codes, for block length 1332

VIII. CONCLUSION

Channel coding plays key role in providing a reliable communication method that can overcome signal degradation in practical channels. In this paper new QC-LDPC codes have been developed and then implement the newly designed codes on FPGA platform. Prototype architecture of the LDPC codes has been implemented by writing Hardware Description Language (VHDL) code and targeted to a Xilinx Spartan-3E XC3S500E FPGA chip. Simulation results demonstrate that the proposed QC-LDPC codes achieve a 0.1dB coding gain over randomly constructed codes and perform 1.3 dB from the Shannon-limit at a BER of 10^{-6} with a code rate of 0.89 for block length of 1332.

REFERENCES

[1] H. L. Charles, *Error-Control Convolutional* Coding,1st edition, Artech House, Inc. Norwood, MA, USA, 1997.

[2] C. Berrou, A.Glavieux and P. Thitimajshima, "Near Shannon limit error correcting coding and decoding: turbo-codes," IEEE ICC'93, Geneva, Switzerland, pp. 1064-1070, 1993.

[3] R. G. Gallager, Low-Density Parity-Check Code. Cambridge, MA: MIT Press, 1963.

[4] D. Mackay and R. Neal, "Near Shannon Limit Performance of Low Density Parity Check Codes," Electronic Letters, vol. 32, no.18, pp. 1645-1646, 1996.

[5] D. J. Mackay, "Good error-correcting codes based on very sparse matrices. IEEE Trans. Inform. Theory, vol. 45, pp. 399-431, 1999.

[6] S. Lin and D. Costello, *Error-Control Coding: Fundamentals and Applications*, Prentice-Hall, 2nd edition, 2004.

[7] S.B. Wicker and S. Kim, *Fundamentals of Codes, Graphs and Iterative Decoding*. Kluver International Series in Engineering and Computer Science, 2003.

[8] T. J. Richardson and R. L. Urbanke, "The capacity of low density parity-check codes under message-passing decoding," IEEE Transactions on Information Theory, vol. 47(2), pp. 599-618,2001.

[9] G. Huo and S. Alouini, "Another Look at the BER Performance of FFH/BFSK with Product Combining Over Partial-Band Jammed Rayleigh-Fading Channels," IEEE Transaction on Vehicular Technology, vol. 50(5),p p.1203-1215, 2001.

[10] H. Zhang and J. M. Moura, "The design of structured regular lpdc codes with large girth," GLOBECOM, pp. 4022–4027, 2003.

[11] A. Ohhashi and T. Ohtsuki, **Performance analysis of BP-based algorithms for irregular low-density parity-check codes on fast Rayleigh fading channel**," IEEE 60th Vehicular Technology Conference, 2004. VTC2004-Fall. vol. 4,pp.2530-2534, 2004.

[12] Y. Abid**,** S. Othman, M. F. M. Salleh, F. Ghani , "A New Quasi-Cyclic Low Density Parity Check Codes,"IEEE Symposium on Industrial Electronics and Applications (ISIEA 2009*)*, October 4-6, 2009, Kuala Lumpur, Malaysia, 2009.

[13] R. M. Tanner, "A recursive approach to low complexity codes," *IEEE Transactions on Information Theory*, vol. IT-27, pp. 533–547, 1981.

[14] Z. Chen, *"*Six New Binary Quasi Cyclic Codes*,"* IEEE Trans. I*nform.Theory, vol. 40; 1666-1667, 1994.*

[15] M. Rossi and M. Sala, *On a class of quasi-cyclic codes,* Technical Report 50, University College Cork, Cork, Ireland, 2005.

[16] T. S. Rappaport, *Wireless Communications - Principles and Practice*. 2nd edition, by Prentice Hall,2002.

Development of User Interface for 3D Reconstruction Algorithm using Modified Grangeat Method

Satish Shah
Department of Electrical Engineering, M. S. University, Baroda, India
Email: satishkshah_2005@yahoo.com
Nimit Shah
Department of Biomedical Engineering, C. U. Shah College of Engg & Tech, Wadhwan City, India
Email: shahnimit.82@gmail.com

***Abstract*-Image transformation is one of the important digital image processing techniques widely used in medical science. Typical applications of image transformation include creation of three dimensional volumetric models from two dimensional images. The two dimension images may be obtained energy source used for hard tissue imaging are x-rays. The three dimension models of hard tissue are created by traditional tomography using CT scans. Since scanners are very expensive they are not easily available at most of health care centers. The algorithm presented in the paper is based on two dimensional image data of hard tissues obtained from basic x-rays equipments. It is unique in context of data gathering collected via arbitrary path to impart maximum flexibility for three dimensional models compared to some other approaches. A series of experiments performed with various data sets validates claim MATLAB® platform is used for implementation.**

Keywords: Image transformation, computed tomography, volumetric reconstruction.

.

I. INTRODUCTION

3D model reconstruction of human hard tissue is one of the most powerful imaging processes widely used in case of critical injuries. The scope of usage is not only limited to the diagnosis part of treatment but can be extended to post operative recovery and subsequent rehabilitation. Tomography is the conventional, robust technique used for model reconstruction. Tomography is classified into two major categories based on the shape of beam it uses to illuminate the tissue parallel beam and fan beam. Over the years many new approaches are developed in tomography [1]. Limiting factor is that data needs to be gathered at fix and predefined trajectories. New Equipments, such as C-arm fluoroscope machine with capabilities similar to conventional CT scanners [2] are designed by Simens® for 3D reconstruction. But it lacks the flexibility for data gathering.

Algorithm presented provides flexibility of data collection via arbitrary path from any exiting C-arm fluoroscopy machine instead of fixed or predefined trajectory. The algorithm is based on modification of Grangeat's work for cone-beam tomography in order to include arbitrary data collection [3] due to its merit of straight implementation and exact formula relating the cone-beam x-ray transform to the first derivative of the 3D transform. Grangeat established an exact formula relating the cone-beam x-ray transform to the first derivative of the 3D radon transform [3, 6, 7, 9]. 2D radon transforms of the pre-weighted input images were used as samples of the 3D radon transform for interpolation, to the standard spherical coordinate system of the 3D radon transform. The 3D volumetric data is then recovered by inverting the3D radon transform.

Paper describes the implementation of the algorithm on the MATLAB® platform, which was followed by the testing of the algorithm by two different synthetic data sets and the result obtained were analyzed and to validate subjective evaluation and the geometric accuracy by using synthetic volume data set.

The paper contains five section where section II address the synthetic volume generation followed by projection of volume in section III for various trajectories, section IV describes the reconstruction algorithm followed by its implementation and user interface in section V.

II. VOLUME GENERATION

The first step includes the generations of the synthetic volume data sets which were used to test the reconstruction algorithm before using on human subjects. Two different synthetic volume data sets were generated used to match real world situation.

A .Constant Density Volume

Volume with four cylinders was generated which represents constant density volume. Inputs for data set generation are the size of the volume, radius of each cylinder and its distance from the center of the volume. Fig .1, shows the image of the rendered constant density volume

B .Multi Density Volume

A multi ellipsoid volume which contains a set of arbitrarily placed ellipsoids of different sizes and shapes was generated which represents multi density volume. The ellipsoids are parameterized (x, y. z) by the positions of their centroids and the length of their axis along each dimension. The possible inputs for generation of this data set are size of the volume and ellipsoidal parameters which includes parameterized along the three axes and the intensity value for each ellipsoid. Fig. 2 shows the image of the rendered multi density volume.



Fig. 1 Image of synthetic four column volume representing constant density volume

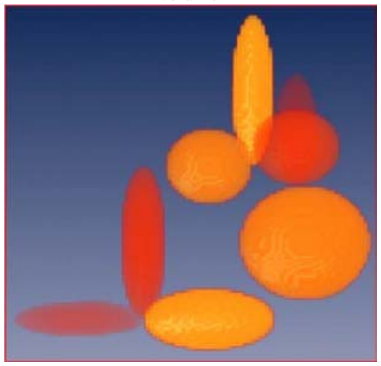


Fig. 2 Image of synthetic multi ellipsoid volume representing multi density volume

III. Volume Projection

Since arbitrary path may be represented as a combination of circle path, full circle path and full circle with arc, cone beam projection from the volume was generated for all types of trajectories. The trajectories were generated by varying values of the azimuth angle ψ_h and elevation angle ψ_v as defined in the Fig. 3 with respect to various coordinate systems used to obtain optimum origin.

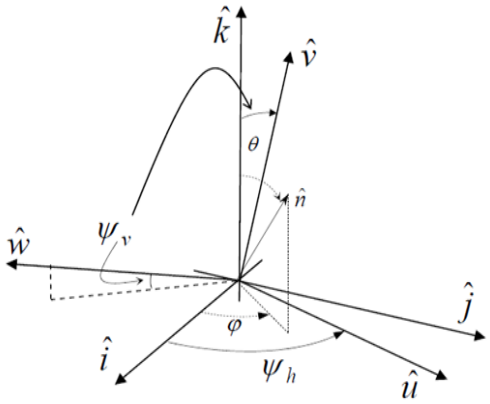


Fig 3: Illustration demonstrating definition of azimuth and elevation angel and relationship of unit vector.

IV. Reconstruction Algorithm

The volume reconstruction was done by implementing following three steps as follow:

1. Computation of 1st derivative of radon data from projections:

This step involves taking derivative radon transform of projected volume by using (1) [4, 8, 10]. This involves pre-weighing image as described in [5] followed by taking radon transform all the images resulting into three dimensional radon data for volume and lastly to differentiate in the two dimensional radon space along A, radial component by filtering the data with derivative filter, α is the angular component and inum is index of image.

$$R'f(A,\alpha,inum) = W_{post}\frac{\partial}{\partial A}\int_{-\infty}^{\infty} W_{pre}Xf(t,inum)dt \quad (1)$$

2. Resample to Spherical Coordinates

The reconstruction of volume is governed by equation described by (2). As the result obtained from the first step the data obtained is in (A,α inum) coordinate system and hence the data need to be resample to (ρ, θ, φ) coordinate system this can be archived by forward mapping or backward mapping.

$$f(x,y,z) = -\frac{1}{4\pi^2}\int_0^{\pi}\int_{-\frac{\pi}{2}}^{\frac{\pi}{2}}\frac{\partial}{\partial\rho}R'f(\rho,\theta,\varphi)sin\theta d\theta d\varphi \quad (2)$$

3Radon Inversion: Consecutive Back Projection

Once the data is resample to require coordinate system the last step to reconstruct model is performing inverse radon transformation that can be done by using consecutive back projection in vertical as well and in horizontal direction.

V. MATLAB® Implementation And GUI

Reconstruction algorithm was implemented on MATLAB® platform and for better usage the friendly user interface was developed. The user interface allows user to choose the type of volume, projection trajectory and there after reconstructs the volume. Fig. 3, Fig.4, Fig.5, Fig.6 shows the screen images of the user interface.

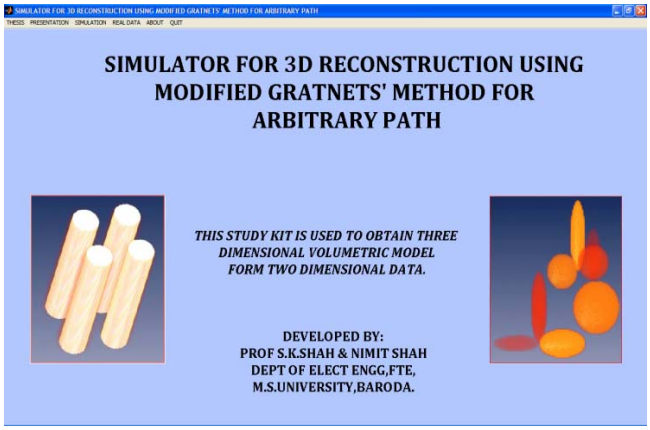


Fig 4: Screen Image of main window of User Interface

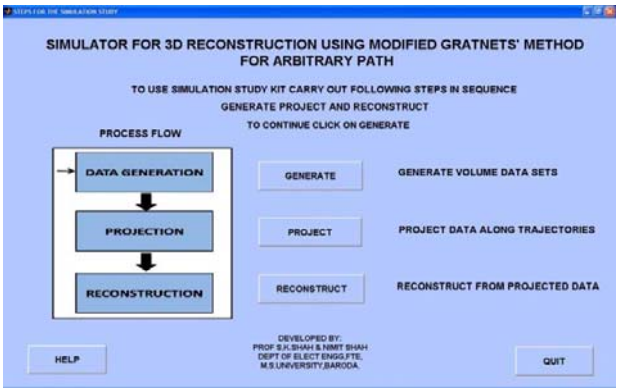


Fig 5: Screen Image of Simulation study of User Interface

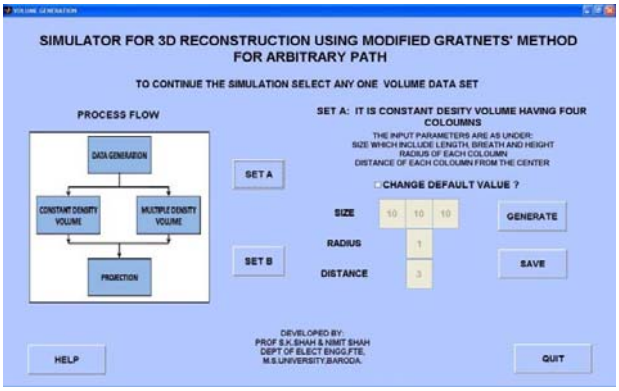


Fig 6: Screen Image of User Interface for generating Four Column Volume

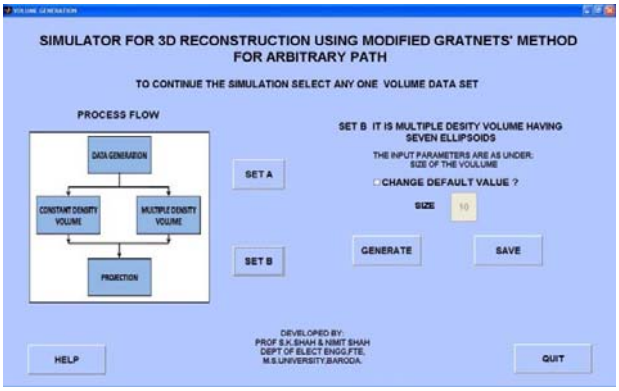


Fig 7: Screen Image of User Interface for generating Multi Ellipsoid Volume

VI. Results

The following are the results obtained after reconstructing synthetic volume by using algorithm described above. Results obtained were used for subjective evaluation and geometric accuracy.

A. Subjective Evaluation

Generated volumes were projected by different trajectories and then the data obtained was used for reconstruction. Fig 9 shows the slice of the original constant density volume and the volume reconstructed by different trajectories. By looking at the results obtained it can be seen that best contrasting results is obtained in full circle plus arc trajectories. Similarly Fig 10 shows the slice of original multi density volume and the volume reconstructed by different trajectories and similar conclusion can be drawn.

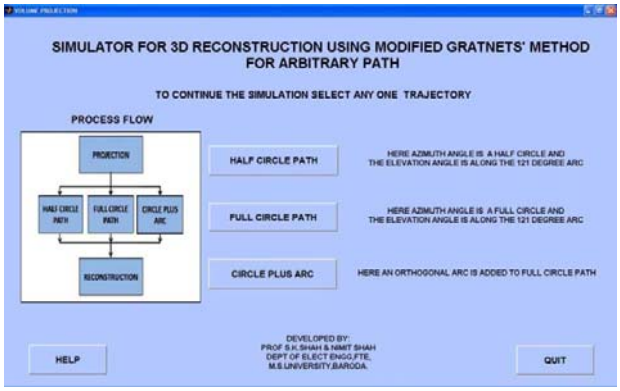


Fig 8: Screen Image for Projection of Volume.

B. Geometric Accuracy

In order to check the geometric accuracy of the algorithm the input parameters of the reconstructed multi ellipsoid volume were compared with the original multi ellipsoid volume the results obtained are listed in the table 1.

TABLE I:
Comparison of Parameters of Original Volume And Reconstructed Volume

	X-Cen	Y-Cen	Z-Cen	X-Axis	Y-Axis	Z-Axis
Mean	0.20	0.18	0.02	1.59	1.70	0.60
STD	0.50	0.47	0.13	1.29	0.82	0.52

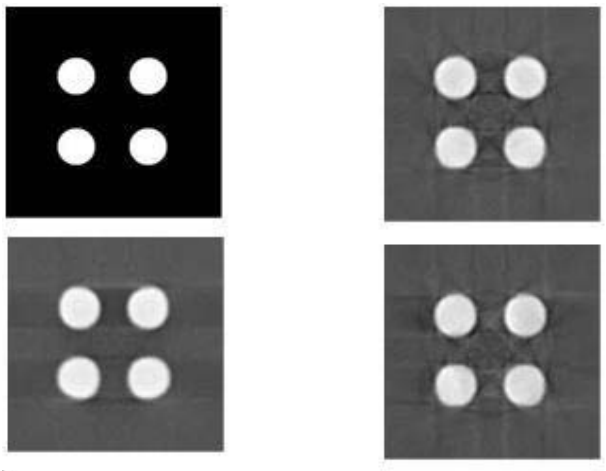


Fig 9: Result of four column volume reconstructed via different trajectories

VII. Conclusion And Future Scope

The modified algorithm has been implemented on MATLAB® platform and results for synthetic data sets are obtained which validates the algorithm. The algorithm can be

used for constructing three dimensional models of human tissue but in order to ensure more safety the algorithm must be used to test phantom data before using human subjects. As the data of human subjects need to obtained from the fluoroscopy machine some pre processing of data is needed before using our algorithm. Moreover corresponding volume rendering technique can also be developed.



Fig 10: Result of multi ellipsoid volume reconstructed via different trajectories

VIII. REFERENCES

[1] J. L. Semmlow, Bio signal and Biomedical Image Processing ,2nd ed.2004, New York: Marcel Dekker

[2] Siemens, Siremobil Iso-C 3D. 2002.

[3] Grangeat, P., Mathematical Framework of Cone Beam 3D Reconstructionvia the First Derivative of the Radon Transform in Mathematical Methods Tomography. 1992: Springer Verlag. p. 66.

[4] Banks, S.A. and W.A. Haodge, Accurate measurement of three-dimensional knee replacement kinematics using single-plane fluoroscopy. IEEE Transactions on Biomedical Engineering, 1996. 43(6): p. 638-649.

[5] Jacobson, C., Fourier Methods in 3D-Reconstruction from Cone-Beam Data. Linkoping Studies in Science and Technology Dissertations, 1996. 427.

[6] Gonzalez Woods & Eddins.,2nd ed.2009 Digital Image Processing Using Matlab

[7] Grimson, W.E.L., Object recognition by Computer.1990,Cambridge, Massachusetts: MIT Press.

[8] Jacobson, C., Fourier Methods in 3D-Reconstructionfrom Cone-Beam Data. Linkoping Studies in Science and Technology Dissertations, 1996. 427.

[9] Pratt, W.K., Digital Image Processing. 4th ed. 2007, New York: Wiley & Sons.

[10] Noo, F., M. Defrise, and R. Clack, Direct reconstruction of cone-beam dat acquired with a vertex path containing a circle. IEEE Trans. on Image Processing, 1998. 7(6): p. 854-867.

Image Denoising using Gabor Filter Banks

Ashek Ahmmed
Politecnico di Milano
Piazza L. Da Vinci 32, Milano 20133, Italy.
ashek02@yahoo.com

***Abstract*—We introduce a method for denoising a digital image corrupted with additive noise. A dyadic Gabor filter bank is used to obtain localized frequency information. It decomposes the noisy image into Gabor coefficients of different scales and orientations. Denoising is performed in the transform domain by thresholding the Gabor coefficients with phase preserving threshold and non-phase preserving threshold where both approaches have been formulated as adaptive and data-driven. For the non-phase preserving approach the *BayesShrink* thresholding methods have been used. Finally using the thresholded Gabor coefficients of each channel the denoised image has been formed. It has been found that for smoothly varying images the modified *BayesShrink* method outperforms both the *BayesShrink* and the phase preserving approaches whereas for images with high variations the phase preserving approach performs better.**

I. Introduction

In image denoising the problem in hand is that given a noisy version, $h(x,y)$, of an image $f(x,y)$ corrupted by an additive noise $\eta(x,y)$ such that:

$$h(x,y) = f(x,y) + \eta(x,y) \tag{1}$$

where $\eta(x,y)$ are *i.i.d.* as $N(0,\sigma^2)$ and $f(x,y) \perp \eta(x,y)$, having these we want to find an estimation $\hat{f}(x,y)$, of my original image $f(x,y)$, that minimizes the mean squared error(MSE) given by:

$$MSE(\hat{f}) = \frac{1}{M^2}\sum_{x,y=1}^{M}(f(x,y) - \hat{f}(x,y))^2 \tag{2}$$

That means two fold objectives associated with the problem: removal of the noise and retainment of important image features as much as possible.

Denoising of images is typically done in the following process:

A. The image is transformed into some domain from the original domain where the noise energy is well separated from the signal energy: $f_G = F_G(f)$
B. A thresholding operation is then applied to threshold the transform coefficients: $f_T = T(f_G, \tau)$
C. Finally applying the backward transformation onto the thresholded coefficients an approximation of the original noise free image is formed: $\hat{f} = B_G(f_T)$

For us F_G and B_G stand for forward Gabor transform and backward Gabor transform respectively. On the other hand $T(\cdot)$ corresponds to either phase preserving or non-phase preserving thresholding approach.

This paper is organized as follows: firstly we explain the Gabor filter bank. *BayesShrink* and modified *BayesShrink* are presented in the following section. Then the phase preserving thresholding approach is discussed in section four. In section five the performance of the different thresholding techniques are compared and the paper is concluded in section six.

II. Gabor Filter Bank

The theory behind Gabor filters has been developed by mimicking the properties of cells of visual cortex of human receptive fields. These cells are restricted to small regions of space and are highly structured. They respond differently to the stimuli with different spatial frequencies, orientations, and directions. Therefore, these cells can be thought of localized spatial filters that respond only to certain spatial frequency bands, orientations, and directions where altogether they form a tuned band pass filter bank structure. These filters are found to have Gaussian transfer functions in the spatial frequency domain. Thus, taking the inverse Fourier transform of this transfer function yields the filter characteristics in the spatial domain that closely resembles the Gabor filters. The Gabor filter is basically a Gaussian Band pass filter having spreads of σ_x and σ_y along the X and Y axes respectively [2].

A Gabor filter is obtained by modulating a sinusoid with a Gaussian. If a signal is modulated by a Gaussian window of a certain width and central time, the Fourier transform of the resulting signal can give us a measure of the local spectrum [2]. Since the width of the Gaussian is arbitrary so definitely such a spectrum is not unique. Now this also tells us that by varying the window positions we can generate a set of local spectra which can provide both temporal and frequency information.

In Gabor transform one tries to express a function $f(t)$ into a series of elementary functions which are the result of translation and modulation of a generic Gaussian function.

$$f(t) = \sum_{m,n\epsilon Z} c_{m,n} \cdot g_{m,n}(t)$$

where $g_{m,n}(t)$ is a typical Gabor function and $c_{m,n}(t)$ tells us "how much" the original function $f(t)$ does look like that particular Gabor function. The 1D Gabor function $g_{m,n}(t)$ is obtained by translating the mother Gabor and then modulating

by a complex sinusoid. We now discuss about the 2D Gabor function. But before that we would like to mention a great fact about Gabor filter bank. The Gabor representation has been shown to be optimal in the sense of minimizing the joint 2D uncertainty in space and frequency (cf.[1]).

A 2D Gabor function is defined as below:

$$g(x,y) = \frac{1}{2\pi\sigma_r\sigma_\theta} e^{-\frac{1}{2}(\frac{x^2}{\sigma_r^2}+\frac{y^2}{\sigma_\theta^2})} e^{j2\pi Ux} \tag{3}$$

where U is the center frequency of the filter, σ_r and σ_θ express the filter width i.e. the filter mask size as a "standard deviation" in terms of pixels. The Fourier transform of (3) is:

$$G(u,v) = e^{-2\pi^2[\sigma_r^2(u-U)^2+\sigma_\theta^2 v^2]} \tag{4}$$

This refers to an elliptical shape whose center is offset on the u axis by the center frequency U i.e. at (U,0) which can be seen from Figure 1.

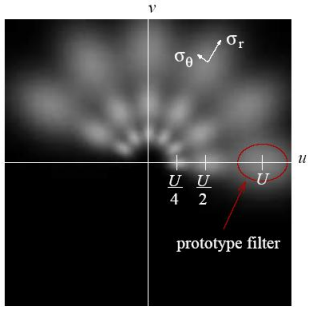


Fig. 1. A typical Gabor filter bank in the frequency domain [5]

.

The frequency coordinate system can then be rotated and scaled to create an array of filters of N different orientations and M different scales, using the substitution:

$$\begin{pmatrix} u \\ v \end{pmatrix} = s^m \begin{pmatrix} \cos(\frac{n\pi}{N}) & \sin(\frac{n\pi}{N}) \\ -\sin(\frac{n\pi}{N}) & \cos(\frac{n\pi}{N}) \end{pmatrix} \begin{pmatrix} \grave{u} \\ \grave{v} \end{pmatrix}$$

with m=0,1,...,M-1 ; n=0,1,...,N-1 ; $s > 1$. s is the scale ratio parameter. It defines both the ratio of the center frequencies of the filter of adjacent scales and their widths.

Since the Gabor functions are not orthogonal so the more filters we have, the more detailed as well as redundant representation of the image we get. On the other hand, fewer filters can not give us enough detailed representation. So one has to go for neither too big nor too small number of filters. To decompose the input image into spatial frequency subbands a dyadic Gabor filter bank is designed. Six levels of decomposition is considered in such a way that the radial frequency bandwidth is one octave i.e. the difference between successive center frequencies f_1 and f_2 are:

$$\log_2 \frac{f_2}{f_1} = 1$$

On the otherhand, if the the angular bandwidth = 45° is selected, this will yield the four orientations 0°, 45°, 90° and 135°. So $6 \times 4 = 24$ different subbands are obtained. In Table I each column corresponds to a specific orientation i.e. it contains subband detail coefficients for $M = 6$ different decomposition levels but of the same orientation.

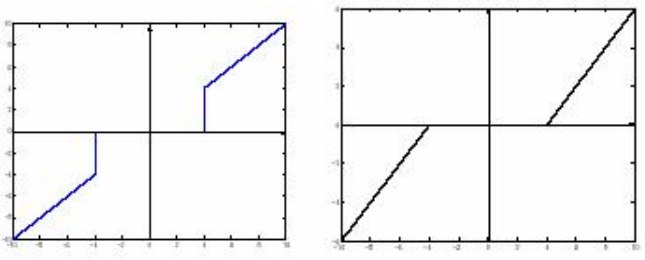
TABLE I
GABOR SUBBANDS.

m=1,θ = 0°	m=1,θ = 45°	m=1,θ = 90°	m=1,θ = 135°
m=2,θ = 0°	m=2,θ = 45°	m=2,θ = 90°	m=2,θ = 135°
m=3,θ = 0°	m=3,θ = 45°	m=3,θ = 90°	m=3,θ = 135°
m=4,θ = 0°	m=4,θ = 45°	m=4,θ = 90°	m=4,θ = 135°
m=5,θ = 0°	m=5,θ = 45°	m=5,θ = 90°	m=5,θ = 135°
m=6,θ = 0°	m=6,θ = 45°	m=6,θ = 90°	m=6,θ = 135°

III. BAYES SHRINK THRESHOLDING

Thresholding is a non-linear technique, yet it is very simple because it operates on one transform coefficient at a time. The theoretical formulation of filtering additive *i.i.d.* Gaussian noise of (zero mean and variance σ^2) via thresholding wavelet coefficients was pioneered by Donho and Johnstone. Two basic types of thresholding are:

A. *Hard thresholding*: it sets a transform coefficient to 0 if its magnitude is less than the threshold;otherwise it is kept i.e. $D(c,T) = c \quad \forall |c| > T$.
B. *Soft thresholding*: it sets a transform coefficient to 0 if its magnitude is less than the threshold;otherwise it is shrinked in magnitude.
i.e. $D(c,T) = sgn(c)\max(0, |c| - T)$



(a) hard thresholding (b) soft thresholding

Fig. 2. Basic thresholding types.

Most well known thresholding methods include *VisuShrink*, *SureShrink*, and *BayesShrink*. For image denoising *VisuShrink* is known to yield overly smoothed images. This is because its threshold choice: $\sigma\sqrt{2logM}$, known as the universal threshold, can be very large due to its dependence on the number of samples, M. *SureShrink* uses a hybrid of the universal threshold and the SURE method, derived by minimizing Stein's unbaised risk estimator and has been shown to perform well. The SURE threshold is data-driven, does not depend on M explicitly, and *SureShrink* estimates

it in a subband-adaptive manner. Moreover, *SureShrink* has yielded good image denoising performance and comes close to the true minimum MSE of the optimal soft-threshold estimator (cf. [4]). Then again it has been shown in [4] that the *BayesShrink* is typically within 5% of the MSE of the best soft-thresholding benchmark with the image assumed known, and it outperforms the *SureShrink* up to 8% most of the time or is within 1% if it is worse. Therefore, for our work we have used the *BayesShrink* thresholding approach.

The *BayesShrink* threshold is derived in a Bayesian framework, and the prior used on the transform coefficients is the generalized Gaussian distribution (GGD) widely used in image processing applications. A GGD with the shape parameter $\beta \in [0.5, 1]$ can adequately describe the transform coefficients of a large set of natural images [4]. And the threshold is given by the following equation:

$$\hat{T}_B(\hat{\sigma}_X) = \frac{\hat{\sigma}^2}{\hat{\sigma}_X} \tag{5}$$

where $\hat{\sigma}_X$ and $\hat{\sigma}^2$ stand for the estimated signal standard deviation and the estimated noise variance respectively.

To make the threshold adaptive and data-driven we estimate the noise standard deviation for each subband using the robust median estimator on the Gabor coefficients corresponding to that subband [4].

$$\hat{\sigma} = \frac{Median(|g_{m,n}(x,y)|)}{0.6745} \tag{6}$$

And from (1) with $f(x,y) \perp \eta(x,y)$ yields:

$$\hat{\sigma}_h^2 = \hat{\sigma}^2 + \hat{\sigma}_x^2$$

we can find $\hat{\sigma}_h^2$ empirically for each subband using once again the Gabor coefficients:

$$\hat{\sigma}_h^2 = \frac{1}{N^2} \sum_{i,j=1}^{N} |g_{m,n}(x,y)|^2 \tag{7}$$

this is because in (1) $h(x,y)$ is modeled as zero mean. Now having $\hat{\sigma}$ and $\hat{\sigma}_h$ we can estimate the signal standard deviation as below:

$$\hat{\sigma}_x = \sqrt{\max(\hat{\sigma}_h^2 - \hat{\sigma}^2, 0)} \tag{8}$$

That means for each subband we have a $(\hat{\sigma}_x, \hat{\sigma})$ pair. And using these pairs we can calculate the thresholds for each subband from (5) and then threshold the Gabor coefficients of the respective subbands. Just a note that if $\hat{\sigma}^2 \geq \hat{\sigma}_h^2$ then we get $\hat{\sigma}_x = 0$. This in turn produces the threshold,

$$\hat{T}_B(\hat{\sigma}_X) = \infty$$

In this case we have to take $\hat{T}_B(\hat{\sigma}_X) = \max(|g_{m,n}(x,y)|)$.

There is the problem of noise not being sufficiently removed in an image processed using *BayesShrink* method. But modified *BayesShrink* remove noise better than *BayesShrink* [6]. In modified *BayesShrink* the threshold is given by the following equation:

$$\hat{T}_B(\hat{\sigma}_X) = \frac{\beta\hat{\sigma}^2}{\hat{\sigma}_X} \tag{9}$$

where $\beta = \sqrt{\frac{\log M}{2j}}$ with M is the total number of Gabor coefficients and j is the decomposition level present in the subband coefficients under scrutiny.

IV. Phase preserving thresholding

Phase is very important for the human perception of images. To be able to preserve the phase data in an image we have to first extract the local phase and amplitude information at each point in the image. If we look at the expected response of the filters to a purely Gaussian white noise then the distribution of the magnitude of the response vectors will be a Rayleigh distribution [7], which is:

$$R(x) = \frac{x}{\sigma_g^2} e^{\frac{-x^2}{2\sigma_g^2}} \tag{10}$$

where σ_g^2 is the variance of the 2D Gaussian distribution that describes the position of the filter response vectors. From [7] the mean and variance of (10) is:

$$\mu_r = \sigma_g \sqrt{\frac{\pi}{2}} \tag{11}$$

$$\sigma_r^2 = \frac{4-\pi}{2}\sigma_g^2 \tag{12}$$

So if μ_r is known then σ_g and σ_r can be found and viceversa. Knowing these parameters one can set the noise threshold at each filter scale to be some multiple k of σ_r beyond the mean of the distribution μ_r [7].

$$T = \mu_r + k\sigma_r \tag{13}$$

We can obtain a robust estimate of μ_r for the smallest scale filter via the median of the Rayleigh distribution. The median of a Rayleigh distribution is the value x such that $\int_0^x R(x) = \frac{1}{2}$. This leads to:

$$median = \sigma_g \sqrt{-2\ln(\frac{1}{2})}$$

$$\hat{\mu}_r = \frac{\sqrt{\frac{\pi}{2}}}{\sqrt{-2\ln(\frac{1}{2})}} \cdot median = \frac{1}{2}\sqrt{-\frac{\pi}{\ln(\frac{1}{2})}} \cdot median$$

Having obtained an estimate of the noise amplitude distribution for the smallest scale filter pair we can simply scale this appropriately to form estimates of the noise amplitude distributions at all the other scales [7].



(a) (b) (c) (d)

Fig. 3. Test images from left to right: *lena*, *barbara*, *goldhill*, *mandrill*.

V. Experimental study

We have used the Gabor filter bank to decompose the test images into different subbands. Each image is of the size 256×256. Three different thresholding techniques namely the *BayesShrink* (BS), modified *BayesShrink* (mBS), and phase preserving thresholding (PhsP) are implemented to recover the noisy test images which are corrupted with additive white noise of different noise powers. The performance metric used is the peak signal-to-noise ratio (PSNR). For each case of different noise powers, σ_n^2 we repeat the denoising experiment of each test image using different thresholding approaches 20 times since we are introducing random noise in the test images. Each time we compute the PSNRs for the denoised images. And finally we take the mean values of these PSNRs and enlist them in the following tables.

TABLE II
PSNR(σ_n^2 = 0.01)

	BS	mBS	PhsP
lena	21.97	21.98	20.49
barbara	21.23	21.46	21.40
goldhill	24.20	23.82	19.56
mandrill	18.66	18.82	20.03

TABLE III
PSNR(σ_n^2 = 0.05)

	BS	mBS	PhsP
lena	21.23	21.36	20.01
barbara	20.69	20.96	20.83
goldhill	22.99	22.94	19.53
mandrill	19.00	19.13	19.65

TABLE IV
PSNR(σ_n^2 = 0.1)

	BS	mBS	PhsP
lena	20.48	20.69	19.64
barbara	19.92	20.25	20.35
goldhill	21.56	21.75	19.74
mandrill	18.67	18.84	19.29

From the results it is trivial that for the test image *mandrill* the phase preserving threshold is always clearly outperforming the *BayesShrink* based thresholding approaches. And this result is consistent with the increase of noise power. In this case between the *BayesShrink* based thresholding approaches the modified *BayesShrink* gives better performance than the *BayesShrink* thresholding approach. On the other hand, for smoothly varying images the pick of the techniques are the *BayesShrink* based approaches. And in these cases, the modified *BayesShrink* threshold performs better than the *BayesShrink* threshold in almost 80% of the cases.

VI. Conclusion

We analyzed the performance of phase preserving and non-phase preserving thresholds for image denoising. The decomposition was carried out by a dyadic Gabor filter bank. Modified *BayesShrink* overwhelmingly performed better than the *BayesShrink* based thresholding approach. But for the image with high variations the phase preserving threshold gave the best denoising performance. We plan to investigate this fact by using more test images with sufficient variations. One big limitations of the Gabor filter based approach is that the maximum bandwidth cannot be greater than 1 octave. This can be overcome with log-Gabor filters. Therefore examining the comparative performance of these discussed thresholds incorporated with log-Gabor filter bank demands attention.

References

[1] B. S. Manjunath, P. Wu, S. Newsam, H. D. Shin. A texture descriptor for browsing and similarity retrieval. *J. Signal Processing: Image Comm.*, 16:33–42, 2000.

[2] Vibha S. Vyas and Priti Regei. Automated Texture Analysis with Gabor filter. *GVIP J.*, 6(1):35–41, 2006.

[3] Nezamoddin Nezamoddini-KachouieS, Paul Fieguth. A Gabor Based Technique for Image Denoising. In *IEEE CCECE/CCGEI, Saskatoon*, May 2005.

[4] S. Grace Chang, Bin Yu, Martin Vetterli. Adaptive wavelet thresholding for image denoising and compression. November 16, 2007.

[5] Bill Christmas. Designing complex Gabor filters. In *IEEE Transactions on Image Processing*, 9(9): 1532–1546, 2000.

[6] Iman Elyasi, and Sadegh Zarmehi Elimination Noise by Adaptive Wavelet Threshold. In *World Academy of Science, Engineering and Technology*, 56: 462–466, 2009.

[7] Peter Kovesi. Phase Preserving Denoising of Images. In *The Australian Pattern Recognition Society Conference: DICTA*: 212–217, December 1999.

PESYMO: A Pervasive System for Mobile Life Long Learners

Wiem Taktak
wiem.taktak@isg.rnu.tn
ISG-University of Tunis
41, Rue de la Liberté, Cité Bouchoucha
2000 Le Bardo, Tunis-Tunisia

Jalel Akaichi
jalel.akaichi@isg.rnu.tn,
ISG-University of Tunis
41, Rue de la Liberté, Cité Bouchoucha
2000 Le Bardo, Tunis-Tunisia

Abstract: **In this paper, we present PESYMO (PErvasive SYstem for MObile lifelong learning) a solution for Mobile Professionals (MP) that motivates workers to improve their skills through lifelong learning. In fact, they have to move from one place to another to accomplish their sduties. This makes very complex the mapping of their timetable to Lifelong Learning Centers (LLCs) learning schedules. Consequently, they logically fail to get their diploma. PESYMO is performed in 4 steps: LLCs localization, LLCs courses matching with MP curriculum, LLCs courses schedules matching with MP free time, and MP subscription according to LLCs vacancy. Moreover a database is designed to support MP and LLCs activities in order to generate decisions guiding to the enhancement of this mobile learning system.**
Keywords**- lifelong learning, decision system, pervasive system, data warehouse, LLC, MP**

I. INTRODUCTION

Nowadays, lifelong learning programs offer new opportunities permitting persons to improve their skills and/or to get a new diploma. Nevertheless, they are penalized by their mobility and the inflexibility of LLCs. This inflexibility is seen from two perspectives: LLCs are physically static since they are located in unmovable address, and they provide a fixed schedule for delivering courses. Nevertheless, schedules may change, for various reasons such as instructor's availability, and become not adapted even if MP activities are planned in advance.

The advent of pervasive systems, positioning technologies, distributed databases, and internet technologies, may solve MP obstacles. Obviously, nothing can be done without enhancing LLCs flexibility. This flexibility is related to the fact of allowing MPs to assist to their classes at any LLCs offering their assigned courses. The LLCs accept MPs visitors and it is permanent in other LLCs. Consequently, this flexibility is guarantee in the system that runs the mobility of MPs.

The objective is to give the solution for MPs in order to achieve LLCs localization, LLCs courses matching with MP planned courses, LLCs courses schedules matching with MP available time, and MP subscription according to LLCs places availability. Also it serves to analyze different information concerning the relation of different elements of the environment of learning.

The rest of the paper is organized as follows: Section 2 presents the state of the art. Section 3 and section 4 present the design and the implementation of our system. Finally, we conclude the paper and give perspectives.

II. STATE OF THE ART

We present our approach PESYMO composed by four steps which are the LLCs localization, LLCs courses matching with MPs curriculum and level, LLCs courses schedules matching with MP free time, and MP subscription according to LLCs vacancies.

A. Learning system

The learning is populated by new concepts and technologies which might be used to enhance lifelong learning. Indeed, x-learning such as e-learning [20], m-learning [25] and p-learning [21], represent various approaches that were adopted for distance learning purposes. However the utility of x-learning don't reside only in being far from educational institution but also it lets the learning opened to any person, any age, at any educational level and social class or job [16].

E-learning involves the use of a computer in some way to provide training, educational or learning

material [20]. It is a principal solution for distance learning which has emerged considerably with the development of the internet. It is based on providing practical tools via the internet and provides the potential for cooperation and interaction [3]. In the e-learning system, the learner supports new forms of access to knowledge by surfing the net and seeking information and new patterns of reasoning and knowledge [11]. It allows the access to resources that are not available in traditional educational systems and it makes possible learning, checking knowledge, formulating and testing assumptions. However, e-learning is not adaptable to all situations [10] because it was initially designed for desktop computers connected with cables which stuck learners at defined locations and time. Mobile learning comes to liberate learners from time and space [14].

M-learning is defined as learning with mobile technologies when the learner is not in predetermined location. This system is related to cellular phones that are available and used by all people, such as Personnel Digital Assistant (PDA), pocket personal computers or smart phones. Thus, it is more oriented to academic and professional [24] [2] and ensures the effectiveness in the professional domain. It provides a way to learn wherever and whenever [13] [17]. So, the student can choose to learn in the appropriate days, places and circumstances [15]. Furthermore, the use of mobile devices for learning entails the creation of an environment for self-motivated learning [4] [9].

P-learning comes to enhance m-learning characteristics with intelligent environments and context awareness. It is considered as an immersive experience which mediates between the learner's mental (e.g. needs, preferences), physical (e.g. objects, other learners) and virtual contexts (e.g. content accessible with mobile devices, artifacts). Pervasive learning environment is a collection of mobile users, mobile services, mobile devices, contexts and policies [22]. It represents any setting in which students can become totally or partially immersed in the learning process. In that perspective, we aim to offer to MLs a p-learning environment able to answer efficiently their needs through a combination of the above tools with Location Based Services (LBS) concepts and tools.

X-learning approaches offer from endows opportunities. However, we think that interactions and discussions with teachers are necessary. They explain advice, support and motivate. The aim of our work is not to reject technological and methodological advances, but to allow mobile learners to get the opportunities to take profit of teachers by x-learning and experiences capabilities as much as they can. The x-learning may serve as a complement but not alternative way to get knowledge without teachers.

B. Pervasive system

Pervasive computing has great significance for many applications such as those related to domains of healthcare, mobile commerce, intelligent education, etc. It offers anytime, anywhere, human-centered features considered as an interesting know-how for lifelong learning applications. It was originally discussed as a new manner of thinking about computers [27] by considering the human world and giving the occasion to computers to be hidden in the background while being an integral but invisible part of people's life [19]. As, in the medical domain, locating the nearest medical organization is very important because it provides medical services to someone who needs medical assistance. There are many projects working in this field as *GSM-Schutzengel*, *Mobile Medical Emergency* used by SAMU, *Diabetics Medical Assistance* for the patients of Alzheimer [23]. They determine the user's current position, which ensures the fastest possible help. To achieve a more precise localization, Global Positioning System (GPS) is suited to assist. Technical solutions for systems localization by satellite are like GPS, GLONASS and terrestrial communications networks such as GSM and UMTS. Localization techniques exploit methods based on timing measurements such as Time Difference Of Arrival (TDOA), methods based on the direction of wave Angle Of Arrival (AOA) of signal strength [6].

Thanks to mobile computing and handheld devices and wireless communication, Location Based Service (LBS) has got an important place in the field of communication [26] [5]. LBS is no longer restricted to mobile computers, but can also be implemented with mobile phones. It can use information provided by the mobile network and the location of mobile device [26] that can be located using the GPS. It allows mobile users to use services based on their position and it allows learners to receive services [1]. An important class of problems in LBS is the research of Nearest Neighbors (NN) and continuous k-Nearest Neighbor (k-NN) taking account of the changes.

C. PESYMO design

The proposed system ensures a lifelong learning of the MP. It helps answering questions: What are the nearest LLCs to my current position? Are there some classes corresponding to my planned courses? Do those classes' schedules match with my free time? Is there a place in these classes?

With the assumption that LLC are distributed in various regions, students can follow one of the courses in the centers. This system doesn't just offer the LBS, but also gives to students the opportunity to research information such as coordinates and timetables LLCs and the scientific courses. Using his mobile device, a mobile learner interacts with a server based on one of main four agents. An agent is a program, a mobile software entity which works in an autonomous, flexible and intelligent way [7] [18]. Mobile agents collaborate between them and are adaptable to environment changes. They submit a query aiming to localize a LLC able to provide a suitable course. The query includes data describing MP position determined by a global positioning system to indicate his availability, and MP desired courses and levels. All these mobile objects are combined with LLCs data to deliver adequate answers.

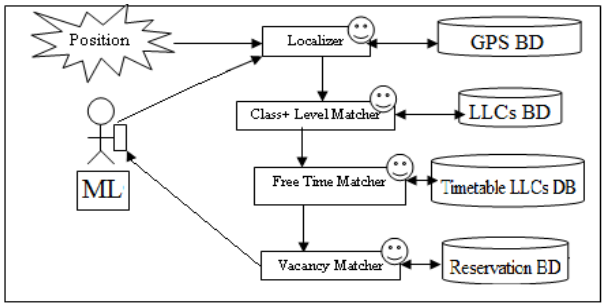


Fig. 1. System architecture

Our approach is performed to answer above questions through an application interface that communicates with following agents: localizer agent, Classes and Level Matcher, Free Time Matcher, and Vacancy Matcher. The output of one agent is the input of the other.

Localizer agent(LA): Following an MP query, the Localizer agent researches the k-NN LLCs close to the current MP position (k-LLCs) thanks to Delaunay Triangulation based on road (DTr) [8]. DTr provides a valid answer to continuous research of the k-Nearest Neighbors.

Classes and Level Matcher agent (CLM): The previous result is the input of CLM agent with LLCs DB. In fact, the MP allows distinguishing if these points enclose some classes corresponding to his planned courses and to his level. This is achieved through the CLM agent which is able to match the planned courses stored in the database of MP PDA with the located in the LLCs database.

Free Time Matcher agent (FTM): After the matching is realized, it is interesting to verify if the courses schedules corresponding to the MP given *free* time. This is achieved through a matching performed on the free time preferences stored in the database of MP PDA with the k-LLCs courses timetable.

Vacancy Matcher agent (VM): consists in determining if there is an available place for the MP. Availability Matcher agent looks for such availability. If it is the case, it subscribes into a class. This is achieved through a matching on the preferred free times stored in MP mobile device database with the k-LLCs schedules table.

To answer MP and localize for him the nearest neighbors LLC, basing on agents. The first step is performed thanks to LA that determines the continuous k nearest neighbors to MP current position. It uses DTr to filter a first list (L1) of LLCs. The second step consists on the matching of the planned courses stored in the database of MP PDA with the located LLCs databases by taking account the MP level and the course level provided by the LLCs. The result of second is filtering in a list L2 of LLCs. The list L2 is an input for the third step performed by FTMA which has to verify if the courses schedule corresponds to the MP proposed free time. This is achieved through a matching performed according to free time preferences stored in the database of MP PDA with the LLCs courses schedules table, and giving as a result the list of LLCs (L3). This latter serves as an input to VMA to determine if there is an available place for the MP in L3. VMA looks for such availability into the LLC database and informs the MP.

To explain our idea, we present a mathematical model. LLCs are basic elements to find the subset of LLCs who answers in need of MPs who can be of cardinality 0, 1 ..., or equal to the cardinality of the original set. This subset is generated by the basic functions determined by providing the values of their parameters. PESYMO has to localize the nearest k-LLCs depending on his position, his classes, his level, his free time and availability of place. So, it has to follow the flowing steps.

The localizer localizes a set of nearest LLC and it generates among X-LLCs the set L where L1= {LLC1…LLCk} and k>=0: L1=localizer (MyPosition, BD Geographic).

If it exists at least one LLC, the Classes and Level Matcher selects n-LLCs among the k- LLCs and it engenders a set L2 of nearest LLC takes into account the MP level and classes where L2 = {LLC1… LLCn} and 0<=n<=k: L2= Classes_Level_Matcher (L1, MyClasses, MyLevel, BD LLCs).

If (n=0) then it does not exist near LLC that contains MP classes and level, the Free Time Matcher selects m-LLCs among the n-LLCs and it engenders a set L3 of nearest LLC taking account MP classes and LLCs courses schedules matching

with MP free time where L3 = {LLC1…LLCm} and 0=<m<= n: L3=Free_Time_Matcher (L2, MyFreeTime, BD TimeTable).

If (m>0) then the Vacancy Matcher selects p- LLCs among the m-LLCs and it engenders a set L4 of nearest LLC taking account the MP classes and level and LLCs courses schedules matching with MP free time and it verifies the availability of places in specific classes where L4 = {LLC1… LLCp} and 0=<P<=M: L4=Vacancy_Matcher (L3, BD Reservation). Finally, MP can choose the LLC that verify all these characteristics by p-LLCs.

D. Implementation

The PESYMO architecture is characterized by distributed LLC and mobile MP. It is composed by the SGDB server that comports the DB of our system, server APPLICATION that comports the applications and we may add a WEB server. And the last level, the devices mobile is PDA or Pocket PC.The MP can record his program and especially the possible hours of study for some courses, then it receives alerts on his PDA in function of its position to indicate the possibilities and availability of LLCs and educational resources, in fact, PDA offers a list of centers near to him. It is easier to present this idea in a small algorithm that presents the idea with a more structured way.

```
Algorithm
Var
MyPosition: Data // MP position
N: Data // Time from position of MP to LLC
TimeBegin: Data // time of courses begin
TimeEnd: Data // end time of courses end
ListCourses: Data // the courses priority to MP
Begin
K=LLCs (MyPosition, N) // locate K LLCs close to MyPosition - N minutes
For i=1 to K do //For each LLCs
  Load (LLC, Courses) // each courses
    For j=1 to length (ListCourses) do
// Compatibility in time
     If (availabilityTime (LLC, cours, TimeBegin,TimeEnd)) then // Disponibility of place
          If (availabilityPlace (LLC, cours, TimeBegin,TimeEnd)) then
               Add (List, LLC) // add LLC in listing of LLC select
          End if
       End if
    End for
End for
End
```

Fig. 2. Algorithm

The database comports all information that support the MPs and answer their questions. The MP interrogates the databases to have courses information or localized LLCs. The database presents the interne organization of the LLCs, the classroom, block, sessions, professors, groups etc. The MP has two marks: the Mark of Continuous Control (MCC) and the Mark of Exams (ME). The ME are only marks of exams passed in his LLC, but the MCC is the average of some MCC given by different professors from different LLCs, so each professor gives his note depending on MP assiduity and work during his session. The justification of MP presence is stored in table *Reservation*. This table contains information related to MP for reserving a place at session. Information about session are in the table *Session*. So, we can know the professor by *id_Prof* saved in the table *Session* then takes his coordinated from table *Professor* .

PESYMO offers to the user a Mobile Graphical User Interfaces (MGUI) [12], this GUI aims to help MP to perform other tasks related to the use of some virtual learning resources that are designed. MPs have to provide minimal and sufficient information, to acquire responses to their requests. MGUI contains a set of sub-interfaces.

1. The connection interface allows filling cases by the login and password, when the user clicks on the button "Connection" a message contains this information would be received by the system that interrogates the database to subscribe. In case of error of seizure, user will be informed. Else, the MP is recognized by the system and shows him 4 choices of services under shape of radio flea: Location, Research, Diary and Disconnection.

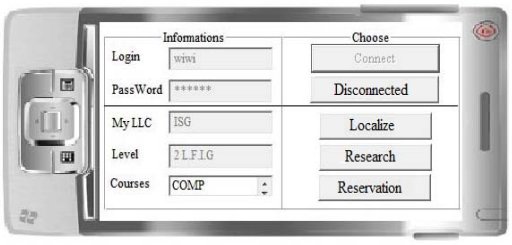


Fig. 3. Connection interface

2. The location interface allows the localizing of the more nearest LLCS according to criteria chosen by the MP. It gives a list of choice to the MP: Classes and Level Matching, Free Time Matcher and Vacancy Matcher. If the MP doesn't mark any of these choices and clicks on the button labeled "Localize" then the system will localize just k more nearest LLCs by showing their coordinates and their address. Otherwise if the MP marks one or

more choices then PESYMO takes in consideration MP's choices. The system will call the concerned agents and takes data information sources. The system asks DB for the statics data and the MP message for dynamic data. And the result will be shown diagrammatically.

To localize the LLCs, it is necessary to take account of marketing research of the MP which is going to be localized by the mobile device and to be integrated into the sent message. The "Localizer" agent interrogates the database to select the nearest LLCs in the ML by using the location algorithms. For matching between MP classes and the level supplied by the LLCS, the "CLM" agent takes the set selected by the agent "Localizer" and it interrogates the database to check correspondence between classes in the timetable of the LLCS by using matching algorithms. For matching between free time of the MP and the schedule of classes supplied by the LLCS, the "FTM" agent take into account the set selected by the "CLM" agent and it interrogates the database to verify correspondence. To verify the availability of place, the "VM" agent taking account the set selected by the "FTM" agent, it interrogates the database to verify the availability of places in the timetable by using the matching algorithms.



Fig. 4. Localization interface

3. The Research interface allows the MP to search classes, educational information, information on the LLCS, timetable of the corresponding LLC. The MP sends a message that will be received by the system and this last will interrogate the database and answer to the MP's question.



Fig. 5. Research interface

4. The diary interface allows administering diary of MP by booking a new place or cancelling a reserved one. This interface is almost a table of 3 columns: LLC, class and period. The MP clicks on the button "cancel" to cancel. After that, a small message will be sent to the system to update the table "reservation" in the database. But for the booking, the MP will choose the LLC, class and the schedule then he clicks on the button "reservation".

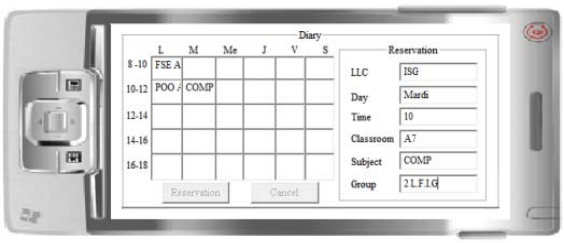


Fig. 6. Diary interface

V- CONCLUSION AND PERSPECTIVES

In this paper, we present a solution for the system of transmission through long distance. PESYMO permits to access to information by a mobile device anywhere and at anytime, it collaborates and allows interactivity between the actors of the system, in fact it facilities the communication, and it is sensible to context since it is intelligent and adaptable. Our approach can be put in exploitation with the use of a PDA or a smart telephone by MP. It is necessary to note that a server will be installed to manage all transmissions realized by PDAs and the LLCs. Despite its advantages, data warehouse can induce to the performance because of its traditional operators. But with new specific OLAP operators, it can better perform. So, we aim in our future research enriching traditional OLAP operators and adjusting them to trajectory analysis for better exploit the mobile data. So, it is necessary to think of TOLAP.

REFERENCES

[1] Aloizio P.S. Location Based Service. School of Information Technology and Engineering (SITE) University of Ottawa. April, 2003.
[2] Anderson P. and Blackwood. A Mobile and PDA technologies and their future use in education. JISC Technology & Standards Watch . JISC: Bristol,UK. 2004.
[3] Bourne J. R., McMaster E., Rieger J. and Campbell J.O. Paradigms for online learning: A case study in the design and implementation of an asynchronous learning networks (ALAN) course. In the 27th Annual Conference. Teaching and Learning in an Era of Change.1997.
[4] Chang, C., Y., and Sheu J., P. Design and implementation of ad hoc classroom and eSchoolbag systems for ubiquitous learning, Wireless and Mobile Technologies in Education, 2002. Proceedings of IEEE International Workshop on 29-30 Aug. 2002.
[5] Dao D., Rizos C. and Wang J. Location-Based Services: Technical and Business Issues. GPS Solutions, 6(3), pp 169-178. 2002
[6] Evennou F. Techniques et technologies de localisation avancées pour terminaux mobiles dans les environnements indoor. Thèse de doctorat 2007
[7] Gilbert N., Lucas L., Klein C., Menager M., Bonnet N. and Ploton D. Three-dimensional co-location of RNA polymerase I and DNA during interphase and mitosis by confocal microscopy Journal of cell science 1995;108 (Pt 1) 115-25.
[8] Khayati M. and Akaichi J. Incremental Approach for Continuous k-Nearest Neighbors Queries on Road. International journal of intelligent information and database systems, Volume 2/2008 Inder science Publishers.
[9] Lin, N.H., Shih, T.K., Hui-huang Hsu, Hsuan-Pu Chang, Han-Bin Chang, Wen Chieh Ko and Lin, L.J. "Pocket SCORM," icdcsw, vol. 1, pp.274-279, 24th International Conference on Distributed Computing Systems Workshops - W1: MNSA (ICDCSW'04), 2004.
[10] Marchand L, Conception de l'apprentissage chez les apprenants adultes qui suivent des cours à distance. Thèse de Doctorat, Université de Paris VIII. 1994
[11] Marchand L. L'apprentissage à vie. La pratique de l'éducation des adultes et de l'andragogie. Les éditions de la Chenelière, Montréal. 1997
[12] Follin, Jean-Michel. and Bouju, Alain, 2007. In: Meng L., Zipf A. and S. Winter (eds.), Map-Based Mobile Services – Design, Interaction and Usability, Chapter 4, pp. 57-79 (in press). Springer Verlag. Heidelberg.
[13] Jason G. Caudill. The Growth of m-Learning and the Growth of Mobile Computing: Parallel developments. The International Review of Research in Open and Distance Learning, Vol 8, No 2 (2007), ISSN: 1492-3831.
[14] Pavlekovic J. and Forkes A. Smartphone training content for disability learners; Catering staff with hearing impairments and learning difficulties such as dyslexia and literacy issues. November 2007.
[15] Poole D.M. Student participation in a discussion-oriented online course: A case study. Journal of Research on Computing in Education. 33(2), pp 162-177. 2000
[16] Reding V. Education in the 21 St Centuries: Education for the Knowledge Economy. Conference of the Asia-Europe Foundation. 2 May 2000.
[17] Schrum L. Oh, what wonders you will see: Distance education past, present, and future? Learning and Leading with Technology. Nov 2002
[18] Shoham Y. Agent Oriented Programming: a survey. In Software Agents, J.M. Bradshaw (ed.), MIT Press 1997.
[19] Stathis Th. Konstantinidis, and Panagiotis D. Bamidis. E-Learning environments in medical education: How pervasive computing can influence the educational process. Balkan Conference in Informatics (BCI 2007), Bulgarie (2007)
[20] Stockley D. E-learning Definition. Retrieved from: http://derekstockley.com.au/ elearningdefinition.html.2003
[21] Syvänen A., Beale R., Sharples M., Ahonen M., and Lonsdale P. Supporting Pervasive Learning Environments: Adaptability and Context Awareness in Mobile Learning. Poster. WMTE 2005 IEEE International Workshop on Wireless and Mobile Technologies in Education. Tokushima, Japan.
[22] Syukur E. and Loke S.W. Policy based control of context aware pervasive services. Journal of Ubiquitous Computing and Intelligence. No. 2. pp 110-131. 2006.
[23] Tao, Y., Kollios, G., Considine, J., Li, F., and Papadias, D. Spatio-temporal Aggregation Using Sketches, In proceedings of the International Conference on Data Engineering, ICDE, pp 214-226, Boston, MA.2004
[24] Traxler J. Current State of Mobile Learning. University of Wolverhampton United Kingdom. International Review on Research in Open and Distance Learning (IRRODL) 8, no. 2. 2007
[25] O'Malley C., Vavoula G., J.P. Glew, J. Taylor, M. Sharples and P. Lefrere. Guidelines for learning/teaching/tutoring in a mobile environment". MOBIlearn/UoN,UoB,OU/D4.1/1.0
[26] Virrantaus, K., Markkula, J., Garmash, A., and Terziyan, Y.V. Developing GIS-Supported Location-Based Services. Proc. of WGIS'2001 - First International Workshop on Web Geographical Information Systems, Japan, 2001, pp. 423-432.
[27] Weiser, M. The Computer for the twenty first Century. Scientific American 265, Nr. 3, S. 94-101, 1991.

Improving CBR-LA algorithm to variable size problems

S. Sabamoniri
Islamic Azad University, Soufian Branch, Iran
Saba_Moniry@Hotmail.com

B. Masoumi
Islamic Azad University, Qazvin Branch, Iran
bmasoumi@Qazviniau.ir

M. R. Meybodi
Amirkabir University of Technology, Department of Computer Engineering and IT, Tehran, Iran
mmeybodi@aut.ac.ir

***Abstract*- In this paper an improved approach based on CBR-LA model is proposed for static task assignment in heterogeneous computing systems. The proposed model is composed of case based reasoning (CBR) and learning automata (LA) techniques. The LA is used as an adaptation mechanism that adapts previously experienced cases to the problem which must be solved (new case). The goal of this paper is to expressing some weak points of the CBR-LA and proposing new algorithm called ICBR-LA which has improved performance in terms of Makespan performance metric. The results of experiments have shown that the proposed model performs better than the previous one.**

I. INTRODUCTION

Mixed-machine heterogeneous computing (HC) systems are used by a sequence of distributed high performance machines in order to being able to execute application programs that have different computing requirements. Assigning a set of tasks (Metatask) to the machines included in HC and scheduling them for executing on those machines is called *mapping*. The general problem of optimized mapping of tasks to machines in a HC sequence is known as a NP-complete problem [1]. The Metatask is defined as a set of independent tasks and there isn't any dependency among them [2]. The mapping can be done in a static or dynamic way. In the static mapping it is assumed that every machine executes one task at a time in the order which they had assigned to the machine. The goal of this mapping is to minimize the total execution time of the metatask, which is referred to as ***Makespan***. The size of Metatask and number of machines in HC are static and previously known. Some approaches for solving this problem include: graph theory based algorithms, simulated-annealing [3], MET, MCT, Min-Min, Max-Min, A* [4], GA [5,6], and LA [7] which all of them solve the problem without using the previous experiences. Also, a hybrid model so-called CBR-LA (consisting of LA and CBR techniques)_ proposed in [8] that its main goal was to reduce iteration number of LA approach and provide rapid access to the solution was based on using previous experiences. This model is used for recommending a quick mapping of tasks to a set of processors that exist in an HC environment. The goal of this paper is to evaluate the CBR-LA recommendations in terms of Makespan performance metric. So, this study intends to show that the CBR-LA solutions are not as optimal as other approaches such as Max-Min and Min-Min. To achieve this goal, some experiments were done and some modifications to the LA model of CBR-LA were proposed. The new proposed model (called ICBR-LA) is able to generate optimized mappings in contrast with the original CBR-LA.

In section II, the CBR-LA algorithm together with its CBR and LA models are introduced and in section III evaluation results about the CBR-LA are presented. Section IV presents experiments and their results about CBR-LA functionality against dynamic size problems. The proposed LA model which improves the CBR-LA will be described in section V. Section VI, proposes a modification about changing environment response model and its effect on ICBR-LA algorithm. Sections VII and VIII are respectively about the proposed algorithm's performance in comparison with other algorithms and the conclusions of this study.

II. CBR-LA ALGORITHM

Case-based reasoning (CBR) is a knowledge-based problem-solving technique, which is based on reusing of previous experiences. The CBR-LA algorithm is a model for static task assignment in heterogeneous computing systems and proposed in [8]. The proposed model is a combination of the CBR and LA models. The LA model is used as an adaptation mechanism that adapts previous experiences to the new problem. The aim of proposing of the model was to reduce the number of required iterations for finding a semi-optimum solution.

In this section the CBR-LA is briefly introduced and in the next sections it is shown that the solutions presented by the algorithm are quite different from those presented earlier. Then, a new model for improving the results is proposed.

A. The LA Model of CBR-LA

Learning Automata (LA) are adaptive decision-making devices operating on unknown random environments. The LA has a finite set of actions and each action has a certain probability (unknown for the automaton) rewarded by the environment of the automaton. Learning Automata can be classified into two main families: fixed structure and variable structure learning automata (VSLA). A VSLA is a quintuple $<\alpha, \beta, p, T(\alpha,\beta,p)>$, where α, β, p are an action set with s actions, an environment response set and the probability set p containing s probabilities, each being the probability of performing every action in the current internal automaton state, respectively. The function of T is the reinforcement algorithm, which modifies the action probability vector p with respect to the performed action and received β set responses. A general linear schema for updating action probabilities uses reward (a) and penalty (b)

parameters which the amount of their values classify automata. That is, when a=b, the automaton is called L_{RP}. If 0<a<<b<1 the automaton is called $L_{P\varepsilon R}$, and if 0<b<<a<1, the automaton is called $L_{R\varepsilon P}$ [8]. For more Information about LA the reader may refer to [9,10].

As mentioned earlier, LA is used as the case adaptation mechanism in the CBR-LA. Fig. 1 shows the schematic of the LA model. The model is constructed by associating every task s_i, which $1 \le i \le \tau$, in the metatask with a VSLA as $(\alpha(i), \beta(i), A(i))$. Since the tasks can be assigned to any of the μ machines, the action set of all LA are identical. So, there is $\alpha(i)=m_1,m_2,\ldots,m_\mu$ for each task s_i, $1 \le i \le \tau$. It is assumed that the environment is a P-model so the input set for each learning automaton A(i) is {0,1}.When $\beta(i)$ equals to 0 it indicates a favorable response, and when equals to 1 it indicates an unfavorable response. The general procedure for LA model is shown in fig. 2.

B. The Case Based Reasoning Model

CBR technique is a knowledge-based approach for solving problems which operates on reusing previous experiences and is emerged from cognitive science research [11, 12]. This approach assumes that similar problems could have similar solutions. Thus, the new problem might be solvable using the experienced solutions in previous similar problems. CBR collects its experiences into a case base (CB). Each experience of the CB is called *case*. A case consists of three parts: problem situation including the initial conditions and the goal, the solution and the performance [8]. The three parts of a case in CBR-LA model are ETC, Mapping and Makespan.

Main activities of problem solving by this approach that are described in CBR cycle have the following four steps: retrieve, reuse, revise, and retain. To solve the new problem, firstly, it must be formally described as a '*new case*'. Secondly, a case that is similar to this new case is retrieved from the CB. Thirdly, the solution in the retrieved case is reused (adapted) to solve the new problem. Finally, a new solution is obtained and presented to the user, who can verify and possibly revise the solution. During the last phase, a new solution is obtained which could be stored as a new experience in CB (this step realizes the learning phase of a CBR application). It should be noted that CBR does not offer a definite solution but proposes hypotheses and ideas for crossing the solution space [8]. Similarity criterion in retrieve phase is defined as similarity between two matrixes: ETC of the new case and ETCs of the stored cases, and is evaluated as the Euclidian distance of the two matrixes [8]. See [11, 13] for more information.

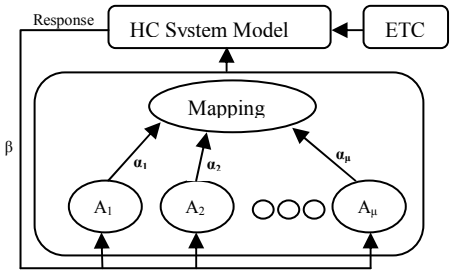


Fig. 1. Learning automata model [8].

while(true)
Begin
  LA_i *selects action* **for all** $1 \le i \le \tau$
  Evaluate the makespan
  If T_μ (n)<T_μ (n-1) **then** LA_i.Signal(0) **for all** $1 \le i \le \tau$
  Else LA_i.Signal(1) **for** $1 \le i \le \tau$
If no change in makespan occurs for 150 consecutive iterations **or** 10000 iterations is over **then exit**
End

Fig. 2. General procedure for learning automata model [8]

C. Describing Adaptation Phase of CBR-LA

After retrieving a set of similar cases, adaptation phase starts. Adaptation is the process of transforming the mappings of retrieved cases for finding a mapping for the new case. This process is done by means of the LA model. Let Φ be the set of selected cases. To build up the adaptation model for each case φ_k, $1 \le k \le |\Phi|$, every task s_i is associated with a VSLA $A^{\varphi}{}_k(i)$ and biased to the mapped machine m_j. To do this the automaton action probability has been initialized about *one* for corresponding to *mj* action. For a biased automaton, the rate of penalizing is set to a value much greater than the rate of rewarding. It helps a wrongly biased automaton to correct itself rapidly. LA model for each case φ_k starts iterating as explained in II-A. Mappings derived from Φ are compared with each other and the one with the minimum Makespan is selected as the final solution [8].

D. Conditions of Simulation

For the simulation studies, characteristics of the ETC matrices were varied in an attempt to represent a range of possible HC environments. The ETC matrices used were generated using the method introduced in [8, 14]. To generate different mapping scenarios, the characteristics of the ETC matrix were varied based on several different methods from [2]. The amount of variance among the execution times of tasks in the metatask for a given machine is defined as task heterogeneity. Machine heterogeneity represents the variation that is possible among the execution times for a given task across all the machines. To further vary the characteristics of the ETC matrices different ETC matrix consistencies were used. An ETC matrix is said to be consistent if a machine m_j executes any task s_i faster than machine m_k, then machine m_j executes all tasks faster than machine m_k [8, 14]. In contrast, inconsistent matrices characterize the situation where machine m_j may be faster than machine m_k for some tasks and slower for others. Eight different classes of ETC matrix characteristics are used in this paper: high (*Hi*) or low (*Lo*) task heterogeneity, high or low machine heterogeneity, and one type of consistencies; consistent (*cons.*) or inconsistent (*incons.*). Abbreviations are used for these kinds of heterogeneities such as HiHi-incons standing for high task heterogeneity, high machine heterogeneity and inconsistent environment. The experiments which were done in [8] were considered as a fixed size ETC matrices for all new cases but in this study, dynamic size of them are used to extend the algorithms power in solving different types of problems.

III. EVALUATING CBR-LA IN COMPARISION WITH MAX-MIN

In this section, the CBR-LA's performance from various aspects is evaluated. To achieve this, some equal experimental conditions as input to the CBR-LA algorithm along with Min-Min and Max-Min algorithms are used. In these experiments 160 new cases from 8 classes of heterogeneity were produced. In this section, the results are average of 10 executions. As it was made clear in [14] and our experiments in section VII, Min-Min algorithm acted better than Max-Min, so the results of it were not included in this part.

A. Comparison with Max-Min

Just like [8] 512 tasks and 16 machines for ETCs were used and the CB with 100 random cases were produced. And, the numbers of selected similar cases (Φ) were 3. As a result of equality of the ETC dimensions, all of automata will be biased. Due to time restriction, only the results of the HiHi-incons class were compared with max-min approach (shown in table1). As illustrated in table 1 CBR-LA results are about 17 times greater than Max-Min's results in terms of Makespan.

B. Evaluating CBR-LA with nonrandom CB

In this experiment we'll evaluate the capability of CBR-LA in using its CB experiences. In order to do this we had changed the CB of CBR-LA, it means that we used 100 nonrandom cases as experiences for the algorithm. To produce the CB we used Min-Min algorithm. As illustrated in table 2, in spite of better experiences, the CBR-LA still have a great difference with results of Max-Min.

C. Evaluating CBR-LA by changing the number of iterations in LA model

In this experiment the amount of iteration numbers for LA model were increased from 10000 to 50000, to let the automata search more in response spaces. According to table 3 and fig. 3, the results are the same as the previous experiments.

D. Evaluating the CBR-LA by changing the size of CB

In this experiment, the numbers of cases in CB were increased from 100 to 200. But as illustrated in table 4, the results are not so near to optimal.

As mentioned in section II, the main advantage of CBR-LA is its reduced number of iterations. But according to the result aspect of the CBR-LA (in terms of Makespan), this algorithm's recommendations are not so near to optimal in comparison with previously proposed algorithms such as Max-Min. Thus, in subsequent sections the LA model of this algorithm is modified to achieve improved results.

TABLE 1
COMPARISON BETWEEN RESULTS OF CBR-LA AND MAX-MIN ALGORITHMS IN HIHI-INCONS CLASS OF PROBLEMS

CBR-LA (with 3 selected Similar Case & random CB)		**Max-Min**
Makespan mean	31691687	1862188
amount of difference	17 times greater	-

TABLE 2
COMPARISON BETWEEN RESULTS OF CBR-LA (NONRANDOM CB) AND MAX-MIN ALGORITHMS IN HIHI-INCONS CLASS OF PROBLEMS

CBR-LA (random CB)	**CBR-LA (nonrandom CB)**	**Max-Min**
Makespan mean	31691687	32843660	1862188
amount of difference	17 times greater	17.64 times greater	-

TABLE 3
RESULTS OF COMPARISON OF DIFFERENT NUMBERS OF AUTOMATA ITERATION

CBR-LA (Nonrandom CB)			**Max-Min**
Mean results by 10000 iteration		Mean results by 50000 iteration	Mean results
26132244		25604685	1862188
Amount of difference	14.03 times greater	13.75 times greater	-

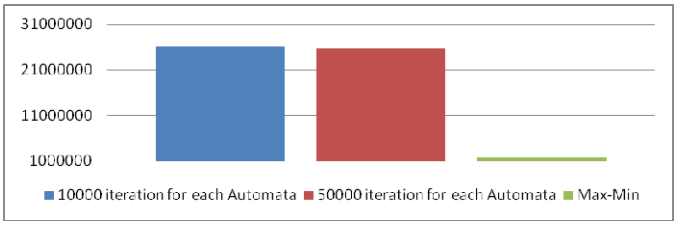


Fig. 3. Comparison of the results of different iteration numbers and max-min heuristic

TABLE 4
RESULTS OF INCREASING THE CB CASES IN CBR-LA

CBR-LA (Nonrandom CB)			**Max-Min**
Mean results by 100 experienced cases		Mean results by 200 experienced cases	Mean results
23483015		25492513	1862188
Amount of difference	12.61 times greater	13.69 times greater	-

IV. CBR-LA AGAINST DYNAMIC SIZE NEW CASES

As we described CBR model of CBR-LA in section II, in all experiments of [8] the ETC matrices had a fixed number of tasks and machines which it caused to biasing all of the automata. But depending on the number of tasks and machines there are in HC, the size of ETC matrix may vary in each new case. So, the algorithm was evaluated against new cases which had *dynamic size ETCs*. For creating the new cases it is assumed that task numbers are vary from 100 to 150 and the machine numbers are vary from 4 to 8 machines for ETC matrices. In the experiments of this section we'll use different reward and penalty values for biased and not biased automata. Also, the results presented in this section are average of 20 executions. Also, in subsection IV-B the improvement process of results by increasing the number of selected similar cases in CBR-LA evaluated.

A. Reward and penalty values for biased and unbiased automata to support dynamic size new cases

First of all it is better to examine the CBR-LA with the dynamic size problems. According to the LA model presented in II-A, L_{PeR} automata have a great penalty values in contrast with the reward. In order to found a meaningful amount for the penalty and rewards, two experiments were done and the parameters of tables 5 and 6 were selected to do the experiments (the original amounts in [8] were used as reward and penalty for the unbiased automata). Table 5 was used 10 times greater and table 6 was used 30 times greater penalties in contrast with

rewards. According to the table7, the results show better Makespan values when the amounts of table 5 were used. From here on, the table 5 values are used.

B. Evaluating the CBR-LA by selecting different numbers of similar cases

In this experiment, improvement process of results was examined by increasing the numbers of selected similar cases in CBR-LA. This feature was claimed in [8] but we will show that this improvement process is not so great and the algorithm still have a great difference by results that other algorithms produces.

In this experiment we performed the CBR-LA by 3, 5, 7 and 10 selected similar cases. The improvement process in results was shown in table 8 and fig. 4

As fig. 4, when the algorithm uses 10 experiences from CB, the results have about 8% improvements rather than when it uses 3 experiences. Then as expressed in [8] the CBR-LA produces better results if the number of experiences increases. But in case of using 10 experiences, the CBR-LA has 73% difference with Max-Min from results aspect.

V. The Proposed LA Model In Oreder To Improve CBR-LA

By evaluating the LA model we found out that in spite of better experiences in CB and biasing automata to these experiences, the CBR-LA can't benefit the experiences. In order to have improvements in results, it is decided to do some changes in the LA model.

TABLE 5
Penalty Is 10 Times Greater Than Rewards For Biased Automata

	Reward	Penalty
Biased Automata	0.01	0.1
Unbiased Automata	0.5	0.1

TABLE 6
Penalty Is 30 Times Greater Than Rewards For Biased Automata

	Reward	Penalty
Biased Automata	0.01	0.3
Unbiased Automata	0.5	0.1

TABLE 7
Results Achived By Different Reward And Penalties Used In Biased Automata

CBR-LA (CB with 100 Random cases)			**Max-Min's Makespan**
Penalty is 10 times greater than rewards for biased automata		Penalty is 30 times greater than rewards for biased automata	
Mean Makespan	18863346	21155754.1	4659276
Percentage of difference with Max-Min	75.29	77.98	-

TABLE 8
Results Achived By Increasing The Number Of Selected Similar cases

CBR-LA (Random CB with 100 cases)			**Max-Min**
Number of selected similar cases	Mean Makespans	percentage of difference with Max-Min	
3 cases	18863346	75.30	4659276
5 cases	18066344	74.21	
7 cases	17840050	73.88	
10 cases	17385551	73.20	

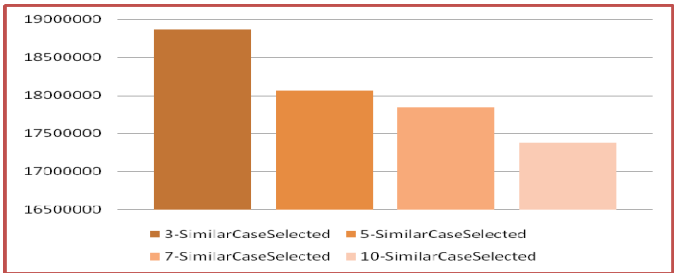


Fig.4. Comparing the CBR-LA results when it uses different number of experiences.

As introduced in section II-A, the LA model in CBR-LA assumed that the environment was a P-model so the input set for each LA was {0, 1}. As mentioned in fig. 2, if the Makespan value at iteration *n* was less than the value at iteration *n-1*, then the input for each automaton was favorable; otherwise it was unfavorable. It was found that this procedure has a major weak point. And as a result, the weak point prevents the CBR-LA to find a near to optimum results. Using the procedure automata always considers two recent results and rewards or penalties to LA actions were given according the results. By so doing, it causes to inefficiency of CBR-LA. In order to have a clear understanding about the weak point, assume that the results achieved in 3 recent iterations are as $T(n-1) << T(n) > T(n+1)$ which shows that in iteration *n-1* the automata has found a good result rather than in iterations *n* and *n+1*. But the procedure first evaluates the results of iterations *n-1* and *n*, then penalize automata and then compares the iterations *n* and *n+1* and in spite of an unfavorable result (in contrast with the *n-1* iteration's result) it rewards. E.g. assume that the Makespan value in iteration *n-1* is 1000 and this value in iterations *n* and *n+1* is 40000 and 15000 respectively. As you see, the value achieved in iteration *n+1* is better than 40000 but it is not favorable in contrast with 1000. This example illustrates that if the procedure of the LA model has a good memory, then it will lead to a better responses.

In this section the LA model was changed in a way that each automaton would compare its result with the best result achieved until yet. This new procedure is illustrated in fig. 5 as ICBR-LA that was abbreviated for Improved CBR-LA. By this algorithm, the automata can maintain its best result during its searches in response space of the problem.

A. Evaluating the functionality of ICBR-LA algorithm in contrast with the CBR-LA

In this part, the CBR-LA and ICBR-LA algorithms were evaluated to show improvements achieved by the new LA model in the results. Both of the algorithms were selected 3 and 5 similar cases to solve each problem in the experiments (results are shown in table11 and are mean values of 20 executions). According to the table 11, in both CBR-LA and ICBR-LA algorithms the mean Makespan were reduced by increasing the numbers of selected similar cases, but the ICBR-LA gives more optimized results (24 percent in the case that the algorithm uses 5 selected similar cases).

```
While (true)
Begin
  LA_i selects its action  for all 1≤ i ≤τ ;
  Evaluate the Makespan ;
  If  Current-Makespan < The-Best-Makespan Then
      Set Reward for all LA_i  that  1≤ i ≤τ ;
  Else
      Set Penalty for all LA_i  that 1≤ i ≤τ ;
  EndIf
  If (no change occurs  in Makespan for 150 consecutive iteration)   OR
(10000 iteration  is over)Then
      Exit ();
  EndIf;
End
```

Fig.5. The general procedure for ICBR-LA.

VI. Changing The Type Of Environment Responses

As described in II-A, the VSLA modifies its actions probability values as a result of analyzing the environment's responses. Also, the CBR-LA algorithm assumes the environment as a P-model. In order to the results that achieved in previous sections, it's likely that the environment model couldn't describe how the actions were favorable, so the responses were not useful for the automata. Then it is decided to use S-model environment. The ICBR-LA algorithm was examined by this new environment model and the results showed improvements in terms of Makespan.

In spite of P-model that uses only two values 0 and 1 as a response, an S-model environment generate responses in a continuous range (the responses lie in the interval [0, 1], that the smaller responses illustrate the more favorable ones). This feature will cause to describe the effect of automata actions better, and consequently it will be beneficial in making decisions about giving reward or penalty for automata actions depending on how well the action was. Parts of this section are dedicated to describe details of generating the S-model environment responses and the results achieved from experiments.

A. The algorithm for generating S-Model responses

The procedure of S-Model response generator is shown in pseudo code at fig.6. According to the procedure the difference of new actions Makespan and the best Makespan until yet is calculated first. In order to do this, after performing actions by LA, the Makespan related to current actions is calculated and the difference of new Makespan with the best one is calculated next. The result of recent calculation will be a value between 0 and 100. This value is a measure which presents the desirability of the actions was done by the automata.

Because of the effect that penalizing has on the probability set of the LA, for the situations which the Makespan is less than or equal to the best Makespan, the response of environment is considered as zero (the most favorable). Otherwise, depending on the amount of difference with the best Makespan, a number between 0 and 1 is generated as an S-model response. To do this, the amount of difference percentage with the best Makespan must be calculated (the result will be in range [0,100]), then the result is divided by 100. By so doing, the response of environment will always be in the continuous range of [0, 1].

B. The results achieved by using S-Model environment

In this section the effect of changing environment responses from P-Model to S-Model is presented. In order to have a full investigation on the results of ICBR-LA, the algorithm was examined over all classes of problems (section II-D). The results are shown in table 10 that each value is average of 20 executions of the algorithm. Also, the number of selected similar cases by the algorithm was 3 cases. According to the table 10, S-Model responses of the environment were improved the solutions of the ICBR-LA algorithm especially in case of the consistent classes of the problems.

VII. Comparing Proposed ICBR-LA With CBR-LA And Two Other Algorithms

In this section, the results achieved by the proposed ICBR-LA and its original form (CBR-LA) beside Max-Min and Min-Min algorithms were compared. Therefore, like the section VI-B we examined the algorithms over all classes of problems. The average results of running these algorithms for 20 problems of each class of heterogeneity are shown in tables 11, 12 and 13. Table 11 represents the amount of optimization that gained according to the proposed modifications in the CBR-LA. It is illustrated that at the worst case the proposed algorithm optimized the results of CBR-LA up to 25.20% and at the best case this optimization reaches to 39.95%, which is a great reduction. But as illustrated in tables 12 and 13, in spite of significant improvements that the proposed algorithm gained, there is still a great difference with other algorithms from results aspect, that is, at the best case ICBR-LA has 23.42% difference with Max-Min and 46.97% difference with Min-Min algorithm. Therefore we'll try to find other solutions to much more improving the proposed algorithm during our next researches.

VIII. Conclusion

In this paper, functionality of the hybrid CBR-LA model, which has proposed in [8] for task assignment in HC systems, evaluated and improved significantly. The main idea in this improvement was modifying the LA model (by changing the conditions which inspect the effect of automata actions on HC environment) and the type of responses which the environment generates, from P-model to S-model. Using computer simulations it was shown that by applying the both changes in the algorithm, the results improves significantly in terms of Makespan performance metric to generating near to optimal solutions (at the best case, 39.95% reduction). Finally we had presented some experiment results in order to representing comparison between the proposed ICBR-LA algorithm in contrast with Min-Min and Max-Min algorithms. The results showed that in spite of great improvements still the proposed algorithm has a great difference to reach other algorithms performance.

```
Calculate current-Makespan's difference percentage with best- Makespan;
If difference <=0 Then
   β=0;
Else
  Set β=difference percentage/100;
EndIf
```

Fig. 6. The general procedure for generating S-Model responses.

TABLE 9
RESULTS ACHIVED BY COMPARING THE ICBR-LA AND CBR-LA ALGORITHMS FOR 20 PROBLEMS

CBR-LA (with 100 Random Cases in its CB)			**ICBR-LA**(with 100 Random Cases in its CB)	
Number of selected similar cases	3 Cases	5 Cases	3 Cases	5 Cases
mean Makespan	18863346	18066344	13951096	13714116
Percentage of difference with CBR-LA	-	-	26.04124	24.09025

TABLE 10
THE RESULTS ACHIEVED BY EXECUTING ICBR-LA ALGORITHM IN P-MODEL AND S-MODEL ENVIRONMENTS

Consistency	**Task Heterogeneity**	**Machine Heterogeneity**	**ICBR-LA (P-Model)**	**ICBR-LA (S-Model)**	**Reduction in Makespan values**
Incons.	High	High	13951096	13747204.5	1.46
	High	Low	157053.3	154768.9	1.45
	Low	High	481184.3	473516.9	1.59
	Low	Low	5861.6	5777.35	1.44
Cons.	High	High	16967742	16147229	4.83
	High	Low	166106.2	159174.4	4.17
	Low	High	515709.2	510468.3	1.01
	Low	Low	5725.35	5492.9	4.06

TABLE 11
COMPARISION BETWEEN CBR-LA AND PROPOSED ALGORITHM (ICBR-LA)

Consistency	**Task Heterogeneity**	**Machine Heterogeneity**	CBR-LA	**ICBR-LA (S-Model)**	Reduction in Makespan values
Incons.	High	High	19316288	13747204.5	28.83
	High	Low	211800.6	154768.9	26.92
	Low	High	662140.3	473516.9	28.49
	Low	Low	7723.55	5777.35	**25.20**
Cons.	High	High	26888098	16147229	**39.95**
	High	Low	249500.8	159174.4	36.20
	Low	High	753277.2	510468.3	32.23
	Low	Low	8452.1	5492.9	35.01

TABLE 12
COMPARISION BETWEEN RESULTS ACHIEVED BY ICBR-LA AND MAXMIN ALGORITHMS.

Consistency	**Task Heterogeneity**	**Machine Heterogeneity**	Max-Min	ICBR-LA	Percentage of difference
Incons.	High	High	9135809	13951096	34.51
	High	Low	109420.9	157053.3	30.33
	Low	High	299151	481184.3	37.83
	Low	Low	4335.154	5861.6	26.04
Cons.	High	High	9078309	16967742	46.50
	High	Low	127206.1	166106.2	23.42
	Low	High	295614.4	515709.2	42.68
	Low	Low	4576.571	5725.35	20.06

TABLE 13
COMPARISION BETWEEN RESULTS ACHIEVED BY ICBR-LA AND MIN-MIN ALGORITHMS.

Consistency	**Task Heterogeneity**	**Machine Heterogeneity**	Min-Min	ICBR-LA	Percentage of difference
Incons.	High	High	5460156	13951096	60.86
	High	Low	63562.51	157053.3	59.53
	Low	High	169390.7	481184.3	64.80
	Low	Low	2494.503	5861.6	57.44
Cons.	High	High	5967740	16967742	64.83
	High	Low	88076.4	166106.2	46.97
	Low	High	191751.7	515709.2	62.82
	Low	Low	3035.603	5725.35	46.98

REFERENCES

[1] D. Fernandez-Baca, "Allocating Modules to Processors in a Distributed System," *IEEE Transaction on Software Engineering*, Vol.15, pp.1427-1436, 1989.

[2] T. D. Braun, H. J. Siegel, and N. Beck, "A Comparison of Eleven Static Heuristics for Mapping a Class of Independent Tasks onto Heterogeneous Distributed Computing Systems," *Journal of Parallel and Distributed Computing*, Vol.61, pp. 810-837, 2001.

[3] M. Coli, and P. Palazzari, "Real Time Pipelined System Design through Simulated Annealing," *Journal of Systems Architecture*, Vol.42, pp.465-475, 1996.

[4] K. Chow, and B. Liu, "On Mapping Signal Processing Algorithms to a Heterogeneous Multiprocessor System," *International Conference on Acoustics, Speech, and SignalProcessing*, Vol.3, pp.1585-1588, 1991.

[5] H. Singh, and A. Youssef, "Mapping and Scheduling Heterogeneous Task Graphs Using Genetic Algorithms," *5th IEEE Heterogeneous Computing Workshop*, pp. 86-97, 1996.

[6] L. Wang, H. J. Siegel, V. P. Roychowdhury, and A. A. Maciejewski, "Task Matching and Scheduling in Heterogeneous Computing Environments Using a Genetic-Algorithm-based Approach," *Journal of Parallel Distributed Computing,* Vol. 47, pp.1-15, 1997.

[7] R. D. Venkataramana, and N. Ranganathan, "Multiple Cost Optimization for Task Assignment in Heterogeneous Computing Systems Using Learning Automata," *IEEE 8th Heterogeneous Computing Workshop*, pp.137, 1999.

[8] S. Ghanbari, M. R. Meybodi, and K. Badie, "A Case-Based Recommender for Task Assignment in Heterogeneous Computing Systems", *Proceedings of the Fourth IEEE International Conference on Hybrid Intelligent Systems,* pp. 110-115, 2004.

[9] K. Narendra, and M. A. L. Thathachar, *Learning Automata: An Introduction*, Prentice Hall, Englewood Cliffs, New Jersey, 1989.

[10] K. Najim, and A. S. Poznyak, *Learning Automata: Theory and Application*, Tarrytown, NY: Elsevier Science Ltd., Pergamon Press, Cambridge, England, 1994.

[11] S. K. Pal, and S. C. K. Shiu, *Fundations of Soft Case-Based Reasoning*, Wiley Series on Intelligent Systems, A John Wiley & Sons INC. Publication, 2004.

[12] R. Bergman, "Engineering Applications of Case-Based Reasoning," *Journal of Engineering Applications of Artificial Intelligence*, Vol. 12, pp.805, 1999.

[13] A. Aamodt, and E. Plaza, "Case-Based Reasoning: Foundational Issues, " *Methodological Variations and System Approaches AI Communications*, IOS Press, Vol. 7: 1, pp. 39-59, 1994.

[14] M. Maheswaran, S. Ali, H. J. Siegel, D. Hensgen, and R. F. Freund, "Dynamic mapping of a class of independent tasks onto heterogeneous computing systems," *Journal of Parallel Distributed Computing*, Vol.59, pp.107-121, 1999.

Autonomic Computing Approach in Service Oriented Architecture

M. Agni Catur Bhakti, Azween B. Abdullah
Department of Computer and Information Sciences, Universiti Teknologi PETRONAS
Bandar Seri Iskandar 37150 Tronoh, Perak, Malaysia

Abstract

Service oriented computing is a computing paradigm that utilizes existing services as the basic construct to compose new service / application, with service oriented architecture (SOA) as its architectural concept. A service architecture that is capable of changing its structure and functionality autonomously with little human intervention is required to address the issue of complexity and dynamism in the current network systems, due to unpredictable events which could cause services unavailability in the event of crashes or other network problems. In this paper, we elaborate and discuss the idea of incorporating the autonomic computing paradigm into SOA and utilizing case-based reasoning approach to achieve a more autonomous SOA, and our current work shows the feasibility of its implementation.

I. Introduction

Service oriented architecture (SOA) is the main architectural concept in the field of service oriented computing, which is an emerging computing paradigm that utilizes services as the basic constructs to support the development of rapid and easy composition of distributed applications, even in heterogeneous environments. Using SOA, large distributed computational units can be built on the base of existing services, by composing complex composite services out of simple atomic ones [1]. The Organization for the Advancement of Structured Information Standards (OASIS) defines SOA as the following: "A paradigm for organizing and utilizing distributed capabilities that may be under the control of different ownership domains" [2]. The World Wide Web Consortium (W3C) defines SOA as the following: "A set of components which can be invoked, and whose interface descriptions can be published and discovered" [3]. In SOA, all functions, or services, are defined using a description language and have invoke-able, platform independent interfaces that can be called to perform business processes.

The current SOA frameworks offer service reusability, consistency, efficiency, and integration. However they are still lacking adaptability and robustness. Conventional service composition will be complete and correct with the assumption that there are no exceptions or errors occur from the initiating user to the terminating user. That is not the case with the current complex and dynamic systems. It is reported in [4] that the scale and complexity of current distributed systems are increasing and showing high dynamism as the global network systems grow. They also need to be able to cope with unpredictable events that could cause services unavailability, such as crashes or network problems. Therefore, a more robust, more adaptive and autonomous service architecture that can keep up with the dynamic changes in environments (including errors) and requirements is required. We proposed the adaptation of autonomic computing paradigm presented by IBM Research Center [5], [6] into SOA domain in order to meet those challenges.

The rest of this paper is structured as the following: section II presents brief literature reviews on autonomic computing paradigm and case-based reasoning as we are adapting those technologies; section III elaborates the proposed autonomic SOA; section IV describes the prototype development and initial results; lastly section V presents summary of this paper and direction for future work.

II. Literature Review

A. Autonomic Computing Paradigm

The autonomic computing paradigm, inspired by the human autonomous nervous system, was proposed by IBM as an approach to the development of computer and software systems that are able to manage themselves in accordance with only high-level guidance from administrators [6]. This paradigm has been used in many researches in various domains such as those in [7], [8].

Figure 1 shows the structure of autonomic element as given in [6]. The autonomic systems consist of autonomic elements, whose behavior is controlled by autonomic manager, which will relieve the human responsibility of directly managing the managed elements by monitoring these elements and its external environment to construct and execute plans based on the analysis of the gathered

information. Thus, the autonomic managers will carry out the autonomic computing cycle, i.e. monitor, analyze, plan, and execute, utilizing its knowledge base. Eventually, a system needs to exhibit four aspects of self-management, i.e. self-configuration, self-optimization, self-healing, and self-protection [6] in order to fully achieve the essence of autonomic computing, i.e. to self-managing.

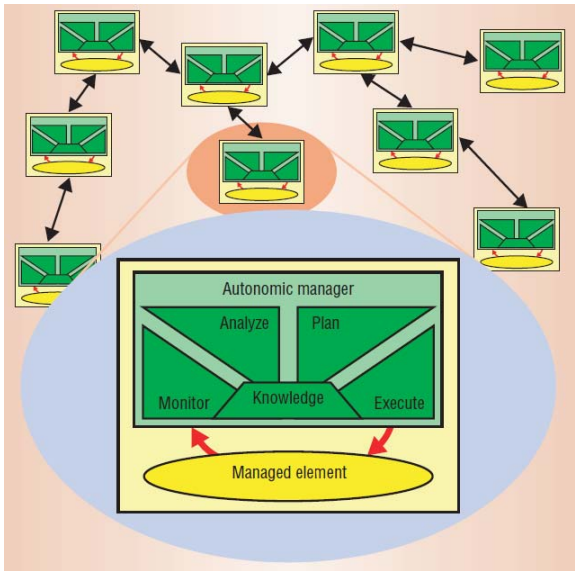


Fig. 1. Structure of an autonomic element [6]

B. Case-Based Reasoning

Case-based reasoning (CBR) [9] is the process of solving a new problem by remembering a previous similar situation and by reusing information and knowledge of that situation. CBR is able to utilize the specific knowledge of previously experienced, concrete problem situations, called 'cases'. In CBR, a new problem is solved by finding a similar past case, and reusing it in the new problem situation. CBR also is an approach to incremental, sustained learning, since a new experience is retained each time a problem has been solved, making it immediately available for future problems.

Some benefits of using CBR approach include the following: reasoning by re-using past cases is a powerful and frequently applied way to solve problems (inspired from human's problem solving); CBR favors learning from experience, since it is usually easier to learn by retaining a concrete problem solving experience than to generalize from it; and CBR is also known to be well suited for domain where formalized and recognized background knowledge may not be available.

Figure 2 shows the CBR cycle as given in [9]. A new problem is solved by retrieving one or more previously experienced cases, reusing the case in one way or another, revising the solution based on reusing a previous case, and retaining the new experience by incorporating it into the existing knowledge-base (case-base).

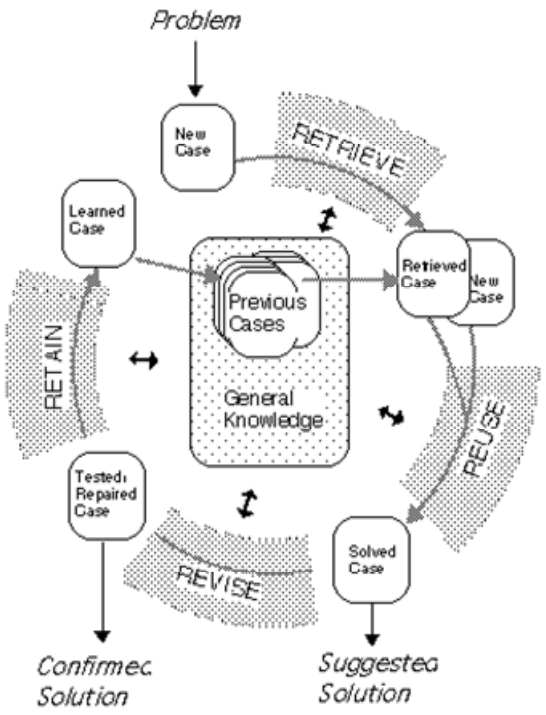


Fig. 2. Case-based reasoning cycle [9]

III. AUTONOMIC SOA

Based on the aforementioned background, our idea is to adapt autonomic computing paradigm into SOA to achieve a more adaptive and robust SOA. In pursuing the idea further, we have initiated our research with goals to provide new concepts of adapting autonomic computing paradigm into SOA, and to develop a SOA prototype based on these concepts. This paper extends and elaborates the framework in more details than the previous works in [10], [11]. Compared to conventional SOA, the proposed autonomic SOA has additional features which include the addition of autonomic agent / manager and the ability to learn and adapt in appropriate ways to solve problems based on the knowledge gained from previous cases (which are stored in the knowledge base). It will also be able to suggest other services related to the service currently being requested by the user.

Figure 3 shows the overall architecture of the proposed autonomic SOA that extends a typical SOA by incorporating the autonomic computing paradigm. The architecture is separated into three layers:

- On the top is a presentation layer that provides interfaces to various users.
- At the middle is a processing layer that performs and coordinates several jobs.

- At the bottom is a resource layer that enables utilization of the distributed resources via web services.

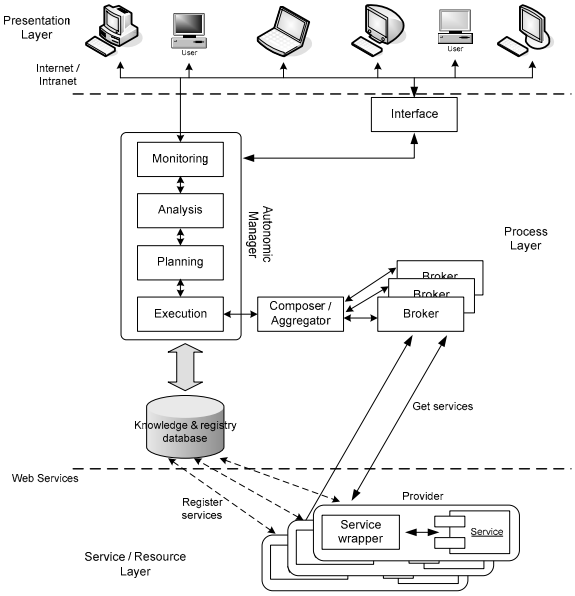


Fig. 3. Architecture of the autonomic SOA

The resource/service layer is a typical SOA framework which consists of service providers, service registry, and the broker agents act as service requestors in processing layer. We extend the functionality of the service registry by adding a knowledge base as required by the autonomic computing paradigm. Knowledge base provides the capability to store the previous services profiles (cases) whose features include:

- Name and description of the service.
- The type of service (atomic, composite).
- If the service is a composite service, then the profile will also include the list of atomic services needed to compose the composite service (the "ingredients").
- Where, when, how to access (and compose) the service (the "recipe").

The autonomic computing paradigm is incorporated in the intermediate processing layer which has the autonomic manager in it. In the context of autonomic computing paradigm, the autonomic manager will perform the autonomic cycle as the following:

A. Monitoring

Monitor the overall system which shall include the monitoring of the requests from users, sensing the availability of the services, addition of new services, removal of services, etc. A sentinel or monitoring agent will provide the monitoring service.

B. Analysis

The autonomic manager will analyze incoming service requests. It will retrieve related information (service profiles) from knowledge base and will use and/or revise the information as necessary to provide the requested service. It starts by first searching for information of the requested service in the knowledge base. If that particular service profile is available in the knowledge base, then this information is used to plan appropriate actions. However if it is not found in the knowledge base, the agent will look for similar ones and will reuse and/or revise if necessary to plan/create action plans.

We adapted the CBR cycle, i.e. retrieve, reuse, revise, and retain, for adaptive and learning functionality which include both the analysis and planning processes using the knowledge base as the case base. CBR is chosen based on its features and successful implementation in the autonomic system found in [8]. Figure 4 illustrates the adaptation of CBR and autonomic computing cycle. The CBR process is described below:

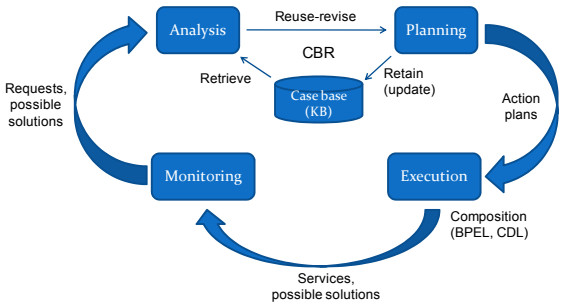


Fig. 4. Adaptation of autonomic cycle and CBR in the autonomic SOA

When the system receives request of service, it starts by first searching for that particular service profile (as represented by a case) in knowledge base/case base. If that particular service profile is available, then it is retrieved for action planning.

If there is no service profile of that particular service in the knowledge base, then cases that are having similar properties / features would be retrieved. Various metrics can be used to calculate the similarity distance. For example, the work in [8] used heterogeneous Euclidian-overlap metric [12]. The similar cases found shall then be used for action planning.

If there are no similar previous cases, the monitoring agent will search for the composite service in service registry (or search for atomic services that could be composed into the requested service). For scalability, the system should also be able to search in other service registries (e.g. online

service registry on the internet or other service ecosystems) if the local service registry does not have the needed services. The new service profile will then be used for action planning and added (retained) to the knowledge base.

The autonomic manager will also suggest other services to the users which are related to the requested services (e.g. other services that are also typically used) based on the previous cases in the knowledge base.

C. Planning

Autonomic manager plans the suitable actions for the requested service. If the requested service is a composite service then the action plan will include the list of available atomic services needed to compose the required composite service, where and how to access them, and the sequence of accessing them. The manager will also update the knowledge base if new action plan is created (or revised from old ones) so that these plans can be readily available when the same composite service is requested again in the future.

D. Execution

Autonomic manager executes the composed plan to provide the requested service. Broker or negotiator agent will assist in interacting and negotiating with the applications to obtain the required atomic services. The composer/aggregator will compose the atomic services to provide the service.

Figure 5 shows the sequence diagram that summarizes the overall process in the proposed autonomic SOA. Note that the monitoring process is running continuously and this is not shown. In the situations where the new profile is a composite service, the sequence might return to the analysis process if the new composite service does not match with the user's criteria/description/requirement.

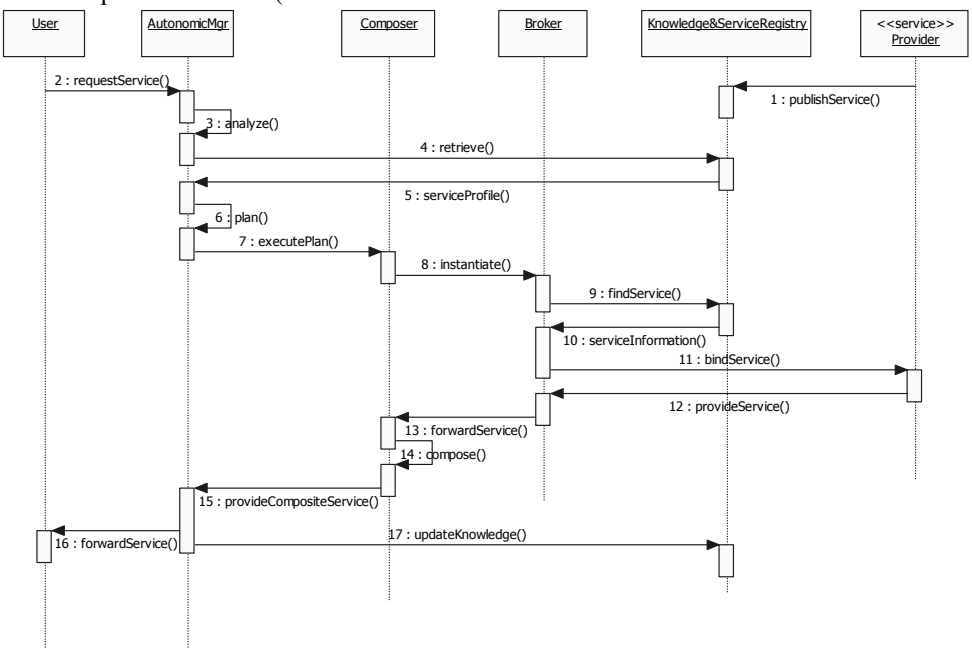


Fig. 5. Sequence diagram of the autonomic SOA

IV. Development and Implementation

Figure 6 illustrates an on-going project that has been initiated aiming to provide an integrated services framework for various distributed software used in computational engineering research, either in-house software or commercial software, including modeling software, simulation software, and visualization software. We have developed a prototype of the proposed autonomic SOA and we are currently implementing it in the project using Java-based platform Apache Axis2 [13] as the web services / SOAP engine and MySQL [14] for the database.

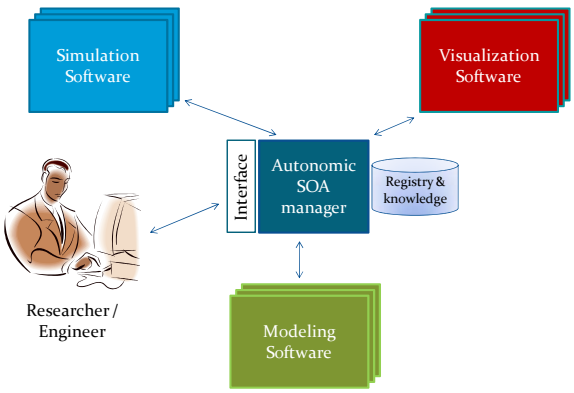


Fig. 6. Implementation model

Figure 7 shows a snapshot of some of the tables in the database. It is shown that we have integrated some applications via web services (i.e. survey visualizer and SunFlow [15] image rendering system). For the suggestion feature, we have the number of usage of each application (*service_count*). We have *app_uptime* and *app_downtime* to be used in measuring service availability as one of the performance metrics.

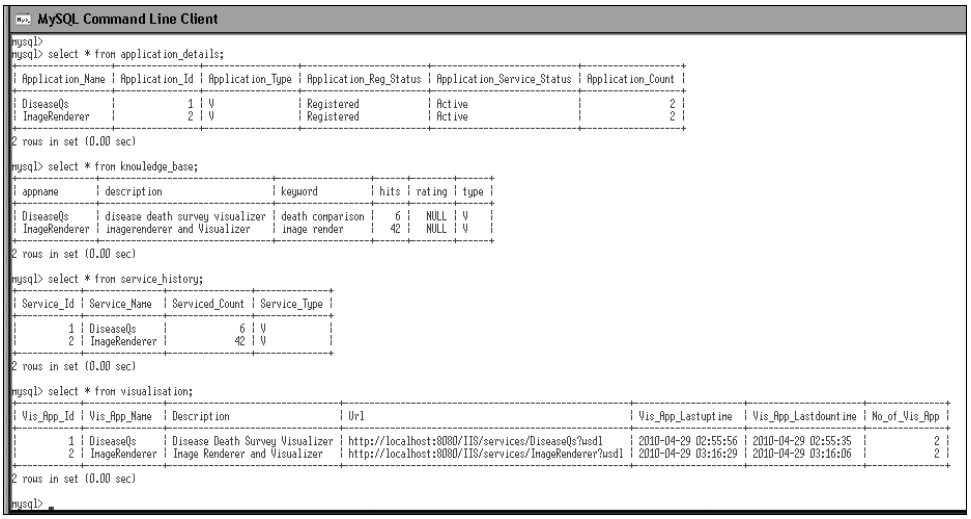


Fig. 7. A snapshot of the database

Figure 8 shows an example of the process choreography. First the user chose to use the ray-tracing modeling software. After the user finished with the modeling, based on the previous usage, the system suggests (and then executes) the finite-difference time-domain (FDTD) simulation and virtual reality visualization.

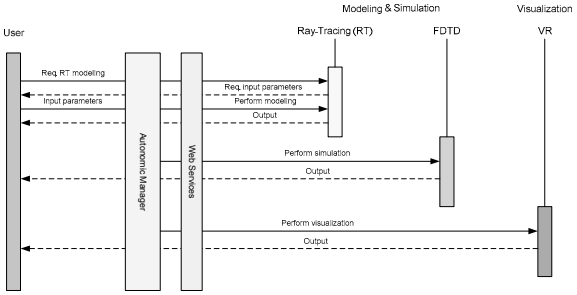


Fig. 8. Example of interaction model

It is shown above that some actions are initiated by the user and other actions are initiated by the autonomic manager automatically. The autonomic manager will learn and adapt appropriately the sequences of tasks to solve problems based on the previous cases stored in knowledge base.

V. Summary and Future Work

This paper presented and discussed an approach to achieve an autonomic SOA by applying autonomic computing paradigm and case-based reasoning. We have presented the design and elaborated the proposed architecture with comprehensive descriptions and models.

We are implementing the architecture in the mentioned project using SOA and web services framework, autonomic computing paradigm, and case-based reasoning technologies. The initial implementation that supports atomic services has successfully completed and we are moving towards composite services implementation. After which we will conduct thorough benchmarking between the autonomic SOA and conventional SOA framework.

We shall also work on formal analysis, for verification and simulation of formal properties of the proposed architecture using CPN Tools [16] to provide further insight on the behavior of the autonomic SOA, especially in situations where actual system testing is not applicable.

References

[1] A. Lazovik and F. Arbab, "Using Reo for Service Coordination," Proc. ICSOS 2007, LNCS 4749, Springer-Verlag, Berlin, Heidelberg, 2007, pp. 398-403.

[2] OASIS Reference Model for Service Oriented Architecture, OASIS Standard, 12 Oct. 2006

[3] H. Haas and A. Brown (Editors), "Web Services Glossary", W3C Working Group Note 11 Feb. 2004.

[4] A. Montresor, H. Meling, and O. Babaoglu, "Toward Self-Organizing, Self-Repairing, and Resilient Large-scale Distributed Systems", Technical Report UBLCS-2002-10, Department of Computer Science, University of Bologna, Italy, September 2002.

[5] IBM, "Autonomic Computing: IBM's Perspective on The State of Information Technology", http://www.research.ibm.com/autonomic/manifesto/
[6] J.O. Kephart and D.M. Chess, "The Vision of Autonomic Computing", *Computer*, IEEE Computer Society, vol. 36, no. 1, January 2003, pp. 41-50.
[7] H. Arora, T.S. Raghu, A. Vinze, and P. Brittenham, "Collaborative Self-Configuration and Learning in Autonomic Computing Systems: Applications to Supply Chain", Proc. IEEE International Conference on Autonomic Computing, June 2006.
[8] S. Montani and C. Anglano, "Achieving Self-Healing in Service Delivery Software Systems by Means of Case-Based Reasoning", *Applied Intelligence*, vol. 28, no. 2, Springer Netherland, April 2008, pp. 139-152.
[9] A. Aamodt and E. Plaza, "Case-Based Reasoning: Foundational Issues, Methodological Variations, and System Approaches," *AI Communications*, 7, 1994, pp. 39-59.
[10] M.A.C. Bhakti and A.B. Abdullah, "Nature-Inspired Self-Organizing Service Oriented Architecture: A Proposal", Proc. of the 6th International Conference on Information Technology in Asia (CITA 2009), Sarawak, Malaysia, July 2009.
[11] M.A.C. Bhakti and A.B. Abdullah, "Towards Self-Organizing Service Oriented Architecture", Proc. IEEE Conference on Innovative Technologies in Intelligent Systems & Industrial Application (CITISIA'09), Kuala Lumpur, Malaysia, July 2009.
[12] D.R. Wilson and T.R. Martinez, "Improved Heterogeneous Distance Functions", *Journal of Artificial Intelligence Research*, 6, 1997, pp. 1-34.
[13] Apache Web Services – Axis, http://ws.apache.org/axis/
[14] MySQL Open Source Database, http://www.mysql.com/
[15] SunFlow – Global Illumination Rendering System, http://sunflow.sourceforge.net/
[16] CPN Tools – Computer Tool for Coloured Petri Nets, http://wiki.daimi.au.dk/cpntools/cpntools.wiki

FPGA Implementation of RS232 to Universal serial bus converter

[1] V.Vijaya, (PhD) M.Tech
Assoc. Professor. VCEW
vsrtej@yahoo.co.in

[2] Rama Valupadasu (Ph D), M.Tech,
Asst.Professor, NIT, Warangal
agnivesh91@yahoo.co.in

[3].B.RamaRao Chunduri, PhD, M.Tech
Professor, NIT, Warangal
cbrr@nitw.ac.in

[4.] Ch.Kranthi Rekha, M.Tech,
Asst.Professor
LUC, Mantin, Malaysia
madakranthirekha@yahoo.co.in

[5.] B.Sreedevi, M.Tech,
Assoc. Professor. VCEW
vaagvijs_15@yahoo.co.in

Abstract— Universal Serial Bus (USB) is a new personal computer interconnection protocol, developed to make the connection of peripheral devices to a computer easier and more efficient. It reduces the cost for the end user, improves communication speed and supports simultaneous attachment of multiple devices (up to127)RS232, in another hand, was designed to single device connection, but is one of the most used communication protocols. An embedded converter from RS232 to USB is very interesting, since it would allow serial-based devices to experience USB advantages without major changes. This work describes the specification and development of such converter and it is also a useful guide for implementing other USB devices. The main blocks in the implementation are USB device, UART (RS232 protocol engine) and interface FIFO logic. The USB device block has to know how to detect and respond to events at a USB port and it has to provide a way for the device to store data to be sent and retrieve data that have been received UART consists of different blocks which handle the serial communication through RS232 protocol. There are a set of control registers to control the data transfer. The interface FIFO logic has FIFO to bridge the data rate differences between USB and RS232 protocols.

***Index Terms*— First-In-First-Out, RS-232, Universal Asynchronous Receive Transmit, Universal Serial Bus.**

I. INTRODUCTION

This paper describes the specification and implementation of a converter from RS232 to USB (Universal Serial Bus). This converter is responsible for receiving data from a peripheral device's serial interface and sending it to a computer's USB interface. In the same way, it must be able to send data from the PC's USB interface to the device. The problems faced with the old standards stimulated the development of a new communication protocol, which should be easier to use, faster, and more efficient. RS232 is a definition for serial communication on a 1:1 base. RS232 defines the interface layer, but not the application layer. To use RS232 in a specific situation, application specific software must be written on devices on both ends of the connecting RS232 cable. RS232 ports can be either accessed directly by an application, or via a device driver in the operating system.

USB is a new personal computer interconnection standard developed by industry and telecommunication leaders, which implements the Plug and Play technology. It allows multiple devices connection (up to 127) ranges. The use of a the devices attachment to PCs. USB is a low cost**,** easing solution and supports transfer rates up to 12Mbs, comprehending the low-speed and mid-speed data converter from a serial interface to USB would free a serial communication port to other applications, allowing a device that uses a serial interface to communicate using an USB interface. USB on the other hand is a bus system which allows more than one peripheral to be connected to a host computer via one USB port. Hubs can be used in the USB chain to extend the cable length and allow for even more devices to connect to the same USB port. The standard not only describes the physical properties of the interface, but also the protocols to be used. Because of the complex USB protocol requirements, communication with USB ports on a computer is always performed via a device driver. This way, we are not limited to the availability of a serial port and we can experience the USB advantages. Using a converter allows us to have the device unchanged, making the converter responsible for treating the differences between the protocols. This work was based on protocol engine which can be managed by exchanging data with a PC across a serial interface. Most of the times, this communication is not done constantly, since it is necessary to have a serial port available just for it. This paper presents the converter implementation, focusing on the development process, which comprehends the device itself and the PC-side software that will communicate with it. This methodology can be extended to other devices. We first present some important USB standard concepts. Then, we define the system specification, divided on host and device requirements. After, we describe the hardware (UART) features and software design and implementation. Finally, we discuss about achieved results and future work

II. PROBLEM DESCRIPTION

The USB specification describes bus attributes, protocol definition, programming interface and other features required to design and build systems and peripherals compliant with the USB standard. We briefly explain features used in our project.

The USB interface does not give this flexibility. When however an RS232 port is used via an USB to RS232 converter, this flexibility should be present in some way. Therefore to use an RS232 port via an USB port, a second device driver is necessary which emulates a RS232 UART, but communicates via USB. USB works as a Master/Slave bus, where the USB Host is the Master and the devices are the Slaves. The only system resources required by a USB system are the memory locations used by USB system software and the memory and/or I/O address space and IRQ line used by the USB host controller. USB devices can be functional (displays, mice, etc) or hubs, used to connect other devices in the bus. They can be implemented as low or high-speed devices. Low-speed devices are limited to a maximum 1.5 Mb/s rate. Each device has a number of individual registers - known as Endpoints which are indirectly accessed by the device drivers for data exchange. Each endpoint supports particular transfer characteristic has a unique address and direction. A special case is Endpoint 0, which is used for control operations and can do bi-directional transfers. It must be present in all devices. According to the device's characteristics, other types of endpoints can be defined. USB Host verifies the attachment and detachment of new devices, initiating the enumeration process and managing all the following transactions. It is responsible to install device driver (based on information provided by device descriptors), to automatically reconfigure the system (hot attachment) and to collect statistics and status of each device. USB on the other hand is a bus system which allows more than one peripheral to be connected to a host computer via one USB port. Hubs can be used in the USB chain to extend the cable length and allow for even more devices to connect to the same USB port. The standard not only describes the physical properties of the interface, but also the protocols to be used. Because of the complex USB protocol requirements, communication with USB ports on a computer is always performed via a device driver. Device's descriptors specify USB devices attributes and characteristics and describe device communication requirements (Endpoint Descriptors). The USB host uses this information to configure the device, to find its driver, and to access it. Devices with similar functions are grouped into classes [1, 2] in order to share common features and even use the same device drivers. Each class can define their own descriptors (class-specific descriptors), as for example, HID (Human Interface Device) Class Descriptors and Report Descriptors. The HID class consists of devices used by people to control computer systems. It defines a structure that describes a HID device, with specific communication requirements. According to the converter characteristics, it can be implemented as a HID device, using already developed HID drivers. A HID device's descriptors must support an Interrupt IN endpoint and the firmware must also contain a report descriptor that defines the format for transmitted and received device data.

A. Requests

The USB protocol is based on requests sent by the host and processed by the USB devices. These requests can be directed to a device or a specific endpoint in it. Standard requests must be implemented by all devices and are used for configuring a device and controlling the state of its USB interface, among other features. Two HID-specific requests must be supported by the converter: Set Report and Get Report. These requests enable the device to receive and send generic device information to the host. Set Report request is the only way the host can send data to a HID device, once it does not have an Interrupt OUT endpoint

B. Communication Flow

USB is a shared bus and many devices might use it at the same time. The devices share the bandwidth using a protocol based on tokens and commanded by the host. USB communication is based on transferring data at regular intervals called frames. A frame is composed by one or more transactions that must be executed in a 1 ms time. USB data transfers are typically originated by a USB Device Driver when it needs to communicate with its device. It supplies a memory buffer used to store the data in transfers to or from the USB device. The USB Driver provides the interface between USB Device Driver and USB Host Controller, translating transfer requests into USB transactions, consistent with the bandwidth requirements and protocol structure. Some of these transfers consist of a large block of data, which need to be splitted into several transactions. The Host Controller generates the transaction based on the Transfer Descriptor, which describes the frame sharing among the several devices requests. When a transaction is sent to the bus, all devices see it. Each transaction begins with a packet that determines its type and the endpoint address. The USB driver controls this addressing scheme. Inside the device, the USB Device Layer comprehends the actual USB communication mechanism and transfer characteristics. USB Logical Device implements a collection of endpoints that comprise a given functional interface, which can be manipulated by its respective USB client.

C. Transfer Types

The USB specification defines four transfer types: Control, Interrupt, Isochronous and Bulk. Control transfers send requests and data relating to the device's abilities and configuration. They can also be used to transfer blocks of information for any other purpose. Control transfers consist of a Setup stage, followed by a Data stage, which is composed of one or more Data transactions, and a Status stage. All data transactions in a Data Stage must be in the same direction (In or out). Interrupt transfers are typically used for devices that need to transfer data at regular period of time, and consequently must be polled periodically. The polling interval is defined in the Endpoint Descriptor. The data payload

for this kind of transfer for low-speed devices is 8 bytes. Error correction is done in this kind of transfer. Two other transfer types are Isochronous and Bulk**,** which are used for devices that need a guaranteed transfer rate or for large blocks of data transfers. They are not used in this work.

III. PROCEDURE/ALGORITHM

A. System Specification

To develop a USB peripheral we need all the following: A host that supports USB. Driver software on the host to communicate with the peripheral. An application executing in the host that communicates with the peripheral device. A UART with a USB interface. Code implementation on the USB controller to carry Out the USB communication. Code implementation on the USB controller to carry out the peripheral functions. Hardware specific problem arises from handshaking to prevent buffer overflows at the receiver's side. RS232 applications can use two types of handshaking, either with control commands in the data stream, called software flow control, or with physical lines, called hardware flow control. Not all USB to RS232 converters provide these hardware flow control lines. It is not always easily identified if an application needs them. Some applications do not use hardware flow control at all, and those cheap USB to RS232 converters will work without problems. Other applications use hardware flow control, but infrequently. Only with large data bursts, or in situations where the CPU is busy performing other tasks, hardware flow control might kick in to prevent data loss. In those situations, communications may seem error free, but with sometimes bytes lost, or unspecified errors in the communications. In a UART& FIFO used to store sent and received data in the USB communication process. Two endpoints were defined for the converter, where the first one is Endpoint 0, used for control operations and the second one is an Interrupt IN Endpoint, defined for sending data to the host. This way, a converter from a serial interface to USB can be implemented as a HID device with the features mentioned above.

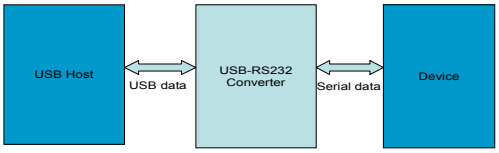


Fig 2.RS232 to USB Converter

B. HOST REQUIREMENTS

The choice of the Operating System used by the host was done in 1999, based on the USB support it provides. It should provide the entire drivers infrastructure and support the protocol characteristics, as for example, Plug and Play. The host must be able to receive USB data using its device drivers and make them available to the applications that have done the request. It is essential that we have a driver in the host to process USB transfers, recognizing the device, receiving and sending data to a USB device.

A. Device requirements

Some communication requirements, such as transmission speed, frequency and amount of data to be transferred, were essential in communication the process of defining the UART be used. Considering the speeds available for USB devices, it was clear that the converter could be implemented as a low speed device, where the communication speed varies from 10 to 100Kb/s. Considering the amount of data transferred and the transmission frequency, the converter was defined to use Interrupt transfers, a transfer type where considerable amounts of data must be transferred in pre defined amounts of time. The host is responsible for verifying if the device needs to transmit data from time to time. Interrupt transfers can be done in both directions, but needs to transmit data from time to time. Interrupt transfers can be done in both directions, but not at the same time. For the converter, they could be used to send and receive data from the PC. The Operating System provides HID drivers that allow us to use this transfer type. The maximum packet size for one transaction is 8 bytes for low speed devices. If we are sending larger amounts of data, they need to be splitted into many transactions, once USB is a shared bus. Another feature defined for the converter was the number of endpoints needed. As explained before, endpoints are buffers

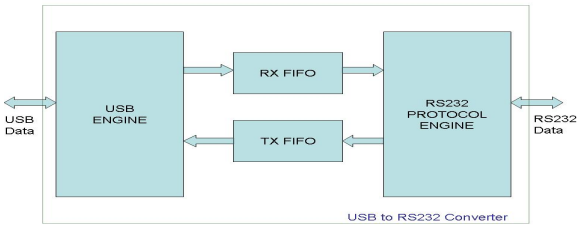


Fig 1.RS232 to USB Interface Diagram

III HARDWARE DESCRIPTION

It is a low-cost solution for low-speed applications with high I/O requirements. RS232 ports which are physically mounted in a computer are often powered by three power sources: +5 Volts for the UART logic, and -12 Volts and +12 Volts for the output drivers. USB however only provides a +5 Volt power source. Some USB to RS232 converters use integrated DC/DC converters to create the appropriate voltage levels for the RS232 signals, implementations, the +5 Volt voltages is directly used to drive the output The UART has serial interface to the RS232 driver. The operation of UART is controlled by an external host processor. There is an 8-bit data interface to host along with read and write control signals. Clock is fed from external crystal. The

family is USB specification [1] compliant and supports one address and three data endpoints *[5]*. The choice of a UART with three endpoint was done in order to allow us to have, beyond the Interrupt IN, an Interrupt OUT endpoint for receiving data from the host (OUT). Its definition requires we have an odd endpoint number besides Endpoint 0. This configuration could not be implemented at the time the project was being developed once the Operating System did not offer support for Interrupt OUT endpoints, which were defined in a later version of the specification. The instruction set has been optimized specifically for USB operations, USB controller provides one USB device address with three endpoints. The USB device address is assigned to the device and saved in the USB Device Address Register (7 bits) during the USB enumeration process. The USB controller communicates with the host using dedicated FIFO, one per endpoint. Each endpoint FIFO is implemented as 8 bytes of dedicated SRAM and the status and control of each of them can be done using its Mode Register and Count Register.

IV. SOFTWARE DESIGN AND IMPLEMENTATION

The development of the converter was divided in phases: Descriptors definition. Device detection and enumeration module (request treatment), Serial data exchange module, USB/serial modules interface be overlapped. USB data exchange module (request treatment). The phases definition does not imply that they cannot be overlapped.

A .Descriptors definition

The main structure to be data implemented consists of device descriptors, as defined by the USB specification [1] These descriptors store information about the device and the USB communication process, used by the host to identify the device and its characteristics. The Device Descriptor is the first descriptor the host reads on device attachment. It includes the basic information the host needs in order to retrieve further characteristics from the device. Its fields' values were defined according to the converter characteristics [7]. To implement a new device, some of these values must be re evaluated and changed if necessary. The converter was defined to use just one interface and two endpoints (Control and Interrupt IN). Interrupt OUT endpoints were defined just in a later version of HID specification. To solve this problem, data packets are sent to the UPS across Endpoint 0, using the SET REPORT request, and received through Endpoint 1**,** using Interrupt transfers. The data reception is done through Output Reports, which were defined as 16 8-bit fields, according to the largest command sent to the UPS. Sending data to the host is done through Input Reports, which were defined as 8, 8- bit fields. Report Descriptors define the size and uses for the data that implements the device's functionality.

B. Device Detection and Enumeration

The second phase consists of the implementation of the code that enables the host to detect and enumerate the device. The implementation of these routines was based on some example codes [8, 9, 10]. Inside the we must have the code to access the descriptors, to recognize and to respond to the request codes that the host sends when it enumerates the device.

C. The process of sending and receiving data

The process of sending data to the UPS is done through Control Transfers using SET REPORT on Endpoint 0. The host sends a request to the USB device, indicating it wants to send data. An interrupt informs the device when new data have arrived on Endpoint 0 and the corresponding Interrupt Service Routine copies it into a data buffer, which is used in the serial communication process.. The maximum packet size that is received from the host was defined according to the largest command that must be sent to the function must be changed to allow receiving an arbitrary number of bytes. These routines are called after the Host or the controller sends a packet to the bus. Endpoint 0 ISR receives. Using hardware flow control implies that more lines must be present between the sender and the receiver, leading to a thicker and more expensive cable. Therefore, software flow control is a good alternative if it is not needed to gain maximum performance in communications. Software flow control makes use of the data channel between the two devices which reduces the bandwidth. The reduce of bandwidth is in most cases however not so astonishing that it is a reason to not use it. First, the computer sets its RTS line to signal the device that some information is present. The device checks if there is room to receive the information and if so, it sets the CTS line to start the transfer. When using a null modem connection, this is somewhat different. There are two ways to handle this type of handshaking in that situation. One is, where the RTS of each side is connected with the CTS side of the other. In that way, the communication protocol differs somewhat from the original one. The RTS output of computer A signals computer B that A is capable of receiving information, rather than a request for sending information as in the original configuration. This type of communication can be performed with a null modem cable for full handshaking. Although using this cable is not completely compatible with the original way hardware flow control was designed, if software is properly designed for it it can achieve the highest possible speed because no overhead is present for requesting on the RTS line and answering on the CTS line. In the second situation of null modem communication with hardware flow control, the software side looks quite similar to the original use of the handshaking lines. The CTS and RTS lines of one device are connected directly to each other. This means, that the request to send query answers itself. As soon as the RTS output is set, the CTS input will detect a high logical value indicating that sending of information is allowed. This implies that information will always be sent as soon as sending is requested by a device if no further checking is present. To prevent this from happening, two other pins on the connector are used, the data set ready DSR and the data terminal ready DTR. These two lines indicate if the device attached is working properly and willing to accept data. When these lines are cross-connected (as in most null modem cables) flow control can be performed using these lines. A DTR output is set, if that computer accepts incoming characters.

V.RESULT ANALYSIS:

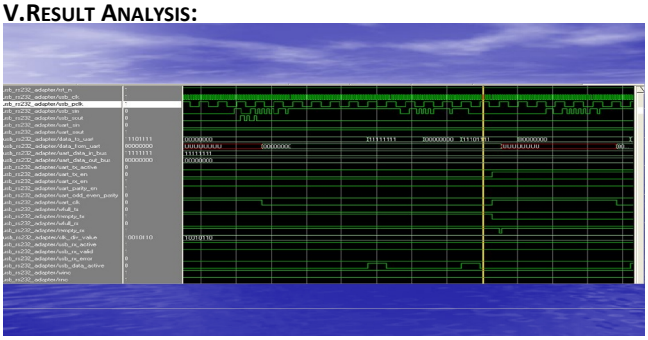


Fig.4.Shows the Waveforms of RS232USBconverter



FIG. 5. RTLSCHEMATICS

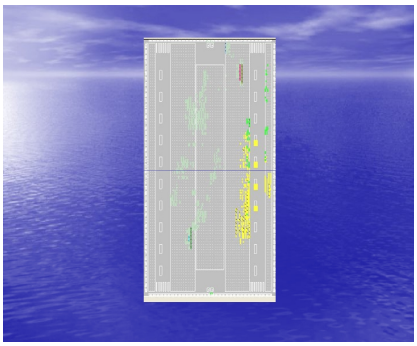


FIG. 6.The Routed design

VI. CONCLUSIONS

An embedded converter from RS232 to USB is designed in this project. VHDL will be used for implementing all these blocks. ModelSim Simulator tool will be used for functional simulation of the design. Reduces the cost for the end user, improves communication speed and supports simultaneous attachment of multiple devices (up to 127). USB protocol operates at 480 Mbps FPGA implementation of the design is done on Spartan 3E FPGA (XC3S500E). The design used 6% of the FPGA area and a maximum frequency of 130MHz is obtained.

ACKNOWLEDGMENT

We are grateful to management Vaagdevi college of Engineering, Warangal, NIT Warangal, Linton University College, and Mantin for the facilities to provide to complete the project in time.

REFERENCES

1. Ana Luiza de Almeida Pereira Zuquim, Claudionor **JosC** Nunes Coelho Jr, Antanio Ot6vio Fernández, Marcos **PCgo** de Oliveira, AndrCa Iabrudi Tavares, "An Embedded Converter from RS232 to Universal Serial Bus", IEEE
2. Jan axelson, "USB Complete, Everything you need to develop custom USB peripherals", Penram Intl. Publishing(India), 1999
3. Universal Serial Bus Specification Revision 2.0
4. http://www.usb.org
5. Charles H.Roth, Jr, "Digital Systems Design using VHDL", PWS publishing company, 1996.
6. ZainalabediNavabi,"VHDL Analysis and Modelling of Digital Systems", McGraw – Hill, Second Edition.
7. http://www.lvr.com
8. http://www.usbstuff.com
9. Douglas L. Perry ,"VHDL", Second Edition, McGraw-Hill, Inc, 1993
10. http://www.mrgadget.com.au/catalog/targus-usb-to-parallel-adapter-p-1160.html
11. USB Complete: The Developer's Guide, 4th Edition
12. USB Mass Storage: Designing and Programming Devices and Embedded Hosts14. FPGA Prototyping by VHDL Examples: Xilinx Spartan-3 Version. Pong P.Chu

Bibliographical notes

V.Vijaya obtained her B.Tech Degree in Electronics & Communication Engg., from (JNTU) Jawaharlal Nehru Technological University College of Engg., Ananthapur, and M.Tech. Degree in Instrumentation and Control Systems, from JNTUK college of Engg Kakinada and Pursuing PhD from JNTUH, Hyderabad. V.Vijaya worked at APEL Radio Communication Systems, Hyderabad and presently, she is working as Associate Professor in the ECE Dept of Vaagdevi College of Engineering at Warangal. She has 10 years of Teaching Experience and 2 years of Industrial Experience. Attended 15 workshops/refresher courses/short term courses at various places. Member of Project Review Committee (UG/PG); CRC for (UG/PG).She is the project coordinator for UG/PG. Her area of interest are Image processing, Signal processing, VLSI, Mobile Communications, Wireless Communications. She is life member of ISTE, IETE.She is the member of IEEE. She has published no. of papers in national conferences and international conferences.

V.Rama obtained her B.Tech in Electronics & Communication Engg., from JNTU, Kakinada, and M.Tech. from NIT, Warangal. Pursuing PhD from NIT, Warangal She is working as Asst Professor in the ECE Dept., at NIT, Warangal. Staff adviser of ECE Dept., Incharge for basic Electronics Lab. She involved in

extracurricular activites at institute. She has 12 years of Teaching Experience. She organized no. of UGC workshops in NITW. Her area of research is Bio Medical Signal Processing. Her areas of interest are Image processing, Signal processing, Tele medicine. She is the member of IEEE. She has published no. of papers in national and international conferences.

CH.Kranthi Rekha had received her B.E in Electronics and Communication Engineering from Madurai Kamaraj University in 2000 and Completed M.Tech from JNTUH, Hyderabad. Presently she is working as Lecturer in Linton university college, Mantin, Malaysia, She has more than 10 years of teaching experience. She is the Author of two Books (Digital communications and Digital Image processing). Organized student level technical symposium technocraft-'09. Attended 10 workshops/refresher courses/short term courses at various places. As a resource person to talk on Image processing. Member of Project Review Committee (UG/PG); CRC for (UG/PG). Her area of interest are Neural networks, Image processing, Signal processing, VLSI, Communications. She is life member of ISTE, IETE. She has published no. of papers in national conferences and international conferences.

B.Sreedevi obtained her AMIE Degree in Electronics & Communication Engg., from Institution of Engineers, Calcutta, and M.Tech. Degree in Digital System Computer Electronics, from JNTUA college of Engg Ananthapur. She is working as Associate Professor in the ECE Dept of Vaagdevi College of Engineering at Warangal. She has 10 years of Teaching Experience. Attended 12 workshops/refresher courses/short term courses at various places. Member of Project Review Committee (UG/PG); CRC for (UG/PG). Her area of interest are Image processing, Signal processing, VLSI, Communications. She is life member of ISTE, IETE. She has published no. of papers in national conferences and international conferences.

C.B.RamaRao obtained his B.Tech in Electronics & Communication Engg., from JNTU Kakinada, and M.Tech. from JNTU Kakinada, Ph.D from IIT, kharagpur. He is working as Professor in the ECE Dept., at NIT, Warangal. At present he is the Head of ECE Dept.,. He involved in various activities at institute. He acted as associate dean of academic affairs at NITW. He has 28 years of Teaching Experience. He organized no. of workshops at NITW. His area of research is in advanced digital signal processing. His areas of interest are Bio Medical Signal Processing, Image processing, Signal processing. He is the member of IEEE. He has published no. of papers in national and international conferences.

Routing Mechanisms and Cross-Layer Design for Vehicular Ad Hoc Networks: A Survey

Harsh Trivedi, Prakash Veeraraghavan, Seng Loke, Aniruddha Desai, Jack Singh
La Trobe University, Victoria, Australia – 3086
hrtrivedi@students.latrobe.edu.au, {p.veera, s.loke, a.desai, jack.singh}@latrobe.edu.au

Abstract— **Vehicular Ad-Hoc Network (VANET) will pave the way to advance automotive safety and occupant convenience. The potential VANET applications present diverse requirements. VANET shows unique characteristics and presents a set of challenges. The proposed VANET applications demand reliable and proficient message dissemination techniques. Routing techniques proposed for Mobile Ad-Hoc Network (MANET) do not cater for the characteristics of VANET. The need for novel routing techniques, exclusively designed for VANET has been recognised. This paper analyses different routing techniques proposed specifically for VANET. Unique characteristics of VANET pose challenges to traditional layered architecture where different layers make independent decisions. Mobility, absence of global view of network, random changes in topology, poor link quality and varied channel conditions have encouraged the paradigm shift to cross-layer approach. In order to optimise the performance of VANET, architectures based on cross-layer approach have been proposed by the researchers. The paper also surveys such cross-layer paradigm based solutions for VANET and concludes with an analytical summary.**

Index Terms— **Dedicated Short Range Communication, Routing, Survey, Vehicular Ad Hoc Network**

I. INTRODUCTION

Road accident related fatalities have become a major concern in today's society. Road traffic accidents have been recognised as a killer worldwide. Additionally, increased traffic delays and fuel wastage due to traffic jams also have global economic and environmental impacts. As a solution, to diminish road trauma and excessive financial burdens, governments and automotive manufacturers are working towards intelligent automobiles and smart transportation systems. Vehicular communications using 5.9 GHz Dedicated Short Range Communication (DSRC) technology is very active research field. Use of DSRC technology for Intelligent Transport System (ITS) is one such approach towards pervasive vehicular communications.

Vehicular Ad Hoc Network (VANET) applications are mainly categorised into safety, transport efficiency and information/entertainment applications [1]. Safety applications play a key role and broadcast useful information to the vehicles in the vicinity. Traffic management applications require data dissemination in a multi-hop fashion in different geographic locations to alert other vehicles regarding traffic situations. On the other hand, commercial applications require unicast routing. From this, it can be seen that routing protocols should be capable of serving a vast number of applications.

VANET has been considered as a practical endeavor of Mobile Ad Hoc Network (MANET). However, due to unique characteristics of VANET like mobility, distributed nature of operation, random changes in topology, poor link quality and varied channel conditions, routing protocols developed for MANET show degraded performance in vehicular scenarios. Development of VANET routing protocols has been a very dynamic field of research with a large number of routing protocols proposed in the literature. However, because of space limitation, this paper only outlines high-level classification of VANET routing protocols and presents recent developments.

VANET characteristics pose serious challenges to layered architecture of communication. In layered architecture, different layers interact with each other using standard interfaces and make independent decisions. This could lead to a poor network performance in VANET. For example packet loss due to harsh channel environments and interference can get interpreted by different layers in different ways. Medium access control (MAC) layer may misinterpret it as a result of excessive collisions, network layer may think that the node is out of reach and restart the process of node discovery and transport layer may interpret this as a result of excessive congestion. To cope with the challenges of VANET a paradigm shift to cross-layer approach has been recognised by the research community. Cross-layer design enables interaction among the layers and encourages joint decision making process. This paper also surveys such cross-layer design architectures. Due to space limitation, this paper limits the discussion to integration of lower layers. This paper includes architectures with network layer, MAC layer and physical layer. This paper also briefly discusses the concept of layer-triggering.

The reminder of the paper is organised as follows: Section II presents a brief discussion of VANET characteristics and performance evaluation of MANET protocols in VANET scenarios. Section III provides a survey of different routing protocols proposed for VANET. Section IV discusses the cross-layer design paradigm and proposals based on it, to achieve reliable message dissemination in VANETs, and Section V concludes this paper with an analytical summary.

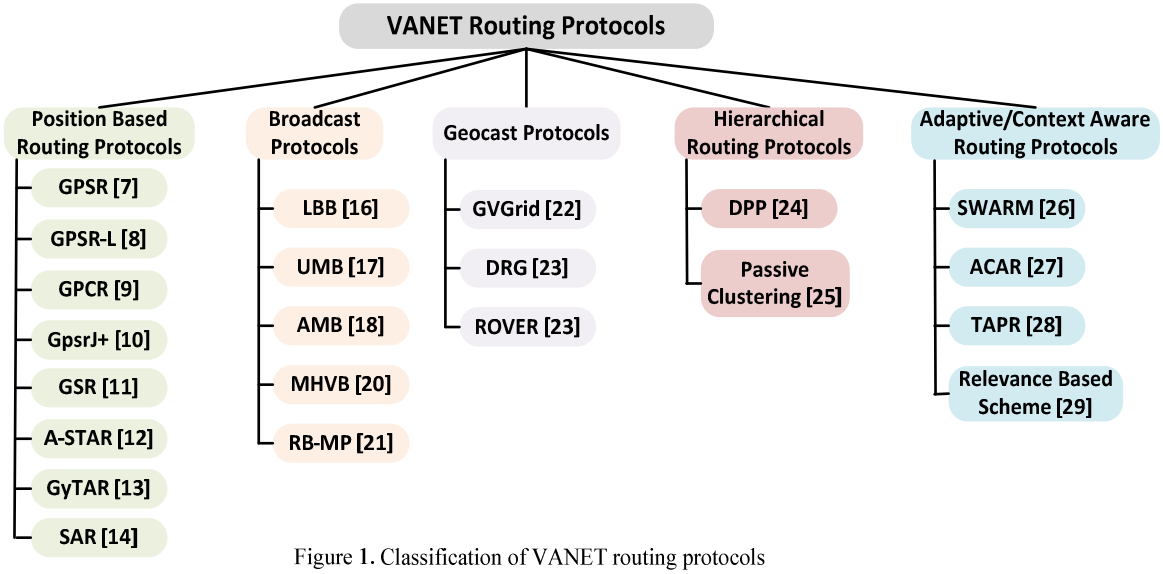


Figure 1. Classification of VANET routing protocols

II. MANET ROUTING PROTOCOLS

MANET has emerged as a platform for pervasive computing. Routing has been a very crucial research topic in MANET. VANET is being considered as a practical application of MANET. However, VANET involves vehicles travelling at high speeds yielding rapid network topology changes and so presents challenges to efficient and reliable message dissemination. Non-uniform node distribution, lack of a centralised administrative entity, frequent network fragmentation, dynamic changes in node density, large scale and stringent real time delay requirements, ample power availability, and the impact of driver's behavior on network topology are unique features of VANET [2]. Such features of VANET make adoption of MANET routing protocols in VANET nearly impossible. MANET routing protocols are known as topology based routing protocols and can be classified into three categories: proactive routing protocols, reactive routing protocols and hybrid routing protocols.

Extensive research has been carried out to evaluate the performance of MANET routing protocols in vehicular scenarios. Mobility of vehicles and the resulting highly dynamic network topology have been recognised as the main reason behind degraded performance of MANET routing protocols. Rapid topology changes make route discovery, optimal route selection and route maintenance very challenging in VANET. Proactive routing protocols tend to update routing information periodically. According to [3], proactive routing protocol performs satisfactorily in city environments (with low mobility) but shows degraded performance in highly mobile and dense scenarios when compared with reactive routing protocols. Work in [3, 4] show that the reactive Ad Hoc On Demand Distance Vector (AODV) protocol has promising performance when evaluated in both city and highway scenarios. VANET specific AODV extensions have been also proposed. The S-AOMDV [5] protocol combines speed with hop-count as a routing metric and shows improved performance in VANET. Prior AODV (PAODV) [6] routing protocol restricts the number of discovered routes to nodes between threshold distance and transmission range in order to reduce routing overhead.

These studies show that routing protocols must take VANET characteristics into account in order to facilitate reliable message dissemination in VANET.

III. VANET ROUTING PROTOCOLS: LAYERED PARADIGM

A vast number of protocols have been developed to cater for VANET specific reliability requirements. These protocols are classified in different categories as shown in Fig. 1. This section briefly analyses such protocols.

A. Position Based Routing Protocols

Position based routing protocols make use of position information obtained using the Global Positioning System (GPS) regarding destination and next hop neighbour. Position based routing protocols use location services like DREAM Location Service (DLS), Reactive Location Service (RLS) and Simple Location Service (SLS), which provides mapping of node ID to its geographic location. This geographic location information is flooded in the network using beacons. An important feature of position based routing is a forwarding mechanism. A wide range of forwarding mechanisms have been proposed in the literature, namely greedy forwarding, trajectory based forwarding, opportunistic forwarding, contention based forwarding and hybrid forwarding. Researchers around the globe have proved, by means of simulation, that position based routing protocols outperforms topology based routing protocols.

Greedy Perimeter Stateless Routing (GPSR) [7] uses a greedy forwarding technique that selects next hop which is closest to the destination. GPSR uses a perimeter mode when packets reach a local maximum (the forwarder fails in forwarding the packet to the destination). When the

closest node to the destination is found, again greedy forwarding is used by the GPSR. GPSR with Life time (GPSR-L) [8] improves the performance of GPSR by selecting the next hop neighbour with good link quality and a nonzero life-time. Greedy Perimeter Coordinator Routing (GPCR) [9] further improves the repair strategy of GPSR. GPCR uses nodes situated at junctions to decide which street the information should traverse in order to reach next junction and finally destination. Subsequently, the furthest node is selected as the next hop to forward the information. This way GPCR outperforms GPSR in city environments where interference is higher. Authors in [10] proposed prediction based GpsrJ+ to improve the recovery strategy of GPCR. GpsrJ+ outperforms GPCR and GPSR in terms of packet delivery ratio and hop count. To address issues allied with GPSR in mobile environments, Geographic Source Routing (GSR) protocol [11] was proposed. GSR combines position based routing with topological knowledge. GSR uses RLS to get correct message destination positions and a city map for a complete knowledge of city topology. To deal with the broadcast storm problem caused by RLS flooding packets, A-STAR [12] routing protocol computes a sequence of junctions (anchors) with traffic awareness which includes information about cars, buses and other roadway vehicles. The street map in use by the vehicle is assumed to be loaded with bus route information and a street with higher bus routes is given less weight. The authors proposed the use of dynamically rated maps to get the latest traffic information for a better weight-assignment scheme. Greedy Traffic Aware Routing (GyTAR) protocol [13] selects anchors on the fly based on real time traffic information. Furthermore, the next hop is selected on the basis of the vehicle's travel direction, speed and last known position. GyTAR also implements a store-and-forward method until the best next hop is found.

In trajectory based forwarding, messages are directed towards a destination using predefined trajectories. Spatial Aware Routing (SAR) [14] uses a spatial model to compute weights based on characteristics of interconnections, such as physical length, average vehicle density, average speed etc and computes the shortest path using Dijkstra's shortest path algorithm. Opportunistic routing dynamically selects the best relay node to forward the information. Authors in [15] have subdivided opportunistic routing protocols into timer-based protocols and MAC-based protocols. Contention Based Forwarding is an example of timer based protocols where single hop neighbors set random timers to contend for packet forwarding.

B. Broadcast Routing Protocols

Broadcasting is a preferred way of safety information dissemination to warn drivers about potential hazardous situations. Multihop broadcasting is also essential in VANET scenarios where there is a need to send the related information in longer region. Flooding is a very prominent technique of broadcasting. However, blind flooding would flood the network and generate broadcast storm problems like congestion, contention, excessive collisions and redundant rebroadcast. In Location Based Broadcast (LBB) [16], receivers decide regarding message relevance and proper responses. LBB uses relative position information, type of the warning message and highway traffic environment information for decisions. The protocol only broadcasts the information within a specified useful life time. The protocol uses the concept of flipping an unfair coin to determine if a node should transmit a packet or not. UMB [17] and AMB [18] are designed especially for multihop broadcast in urban scenarios addressing broadcast storm problems, hidden node and reliability issues in urban scenarios. UMB and AMB protocols divide roads (within vehicle's transmission range)_ into segments in a way that there is only one vehicle in each segment and selects vehicle from the furthest non-empty segment without a priori network topology information. Both protocols are composed of two sections (1) directional broadcast and (2) intersection broadcast. Both use the same directional broadcast mechanism but different intersection broadcast mechanisms. The directional broadcast employs Request to Broadcast (RTB) and Clear to Broadcast (CTB) handshaking packets to address the hidden node problem. Multihop Vehicular Broadcast (MHVB) [19] implements congestion suppression algorithm to suppress unnecessary messages in congestion conditions. It uses backfire algorithm to select the forwarding node (farthest node) to relay the message efficiently using knowledge about its distance from the receiver. In Enhanced MHVB [20], angle is added as an extra parameter to the backfire algorithm. In [21], Peiyuan et. al proposed the RB-MP-reliable broadcast routing protocol based on mobility prediction. In RB-MP, only a few selected nodes are allowed to rebroadcast information. Rebroadcast nodes are selected on the basis of Prediction Holding Time (PHT) of the connection between two nodes. The PHT indicates connection time such that one node may stay in transmission range of the other without going ahead of it. Simulation results from [21] have proved that RB-MP outperformed Flooding, V-TRADE and UMB in terms of packet delay under highly mobile scenarios.

C. Geocast Routing Protocols

A huge number of traffic management applications require information dissemination to the nodes located in specific geographic locations with end-to-end Quality of Service (QoS) requirement. These applications demand geocast routing.

GVGrid protocol [22] achieves geocasting in dense scenarios with vehicles travelling at normal speeds. GVGrid protocol partitions maps into equal-sized squares where a node selects the next hop node from its neighbouring grids and forwards packets for the desired destination region. Similarly in [23], authors have proposed Distributed Robust Geocast (DRG) protocol and

Robust Vehicular Routing (ROVER) protocol. DRG uses distance-based backoff mechanism for directed and restricted flooding and overcomes network fragmentation problem by scheduled retransmission. ROVER employs route discovery mechanism to generate a multicast tree from source vehicle to all vehicles in a Zone of Relevance (ZoR). Vehicle accepts the message, if at a time, it is within the rectangular ZoR specified by its corner coordinates.

D. Cluster Based/Hierarchical Routing Protocols

Clustering of nodes to achieve reliable networking is very attractive approach to address broadcast storm problems. Cluster based routing techniques reduce packet overhead and improve packet delivery ratio because only cluster heads and gateways are responsible for routing, control and update messages. However, highly mobile situations make election of cluster heads and cluster management very challenging as vehicles join and leave clusters randomly based on traffic situations and road topology.

To address these challenges, Little and Agrawal [24] proposed clustering schemes where clusters of vehicles are formed by taking their mobility into account. In their scheme, each cluster consists of a header and a trailer for communication with other clusters. To achieve end-to-end communication, Directional Propagation Protocol (DPP) exploits delay tolerant networking concepts, i.e. the custody transfer protocol. Other work [25] proposed the use of passive clustering techniques for V2V communication in order to reduce control overhead produced in cluster formation, based on the speed of the vehicles.

E. Adaptive and Context Aware Routing Protocols

Adaptive and context aware routing protocols adjust their routing parameters adaptively based on the contextual information regarding network conditions. Ant Colony Optimisation (ACO) has been recognized as a solution of NP-Hard problems. Performance comparison between the SWARM Intelligence routing protocol (that uses food searching behaviour of real ants and adaptively selects a path to the destination), with MANET routing protocols under VANET scenarios is provided in [26]. The results reveal that routing protocols using SWARM intelligence outperforms traditional MANET routing protocols. The performance gain is observed in terms of throughput, latency, packet delivery ratio and delivery cost.

Adaptive Connectivity Aware Routing (ACAR) protocol [27] models the transmission quality of each road segment and adaptively selects the next hop based on the ability to minimize packet error rates of the whole route. To accomplish this, an on-the-fly vehicle traffic density collection scheme is employed. The work in [28] proposed the Traffic Adaptive Packet Relaying (TAPR) protocol. The TAPR protocol extends the work presented in [24] by introducing an adaptive mechanism which decides whether to route through co-directional or oncoming clusters. VANET is intended to support a wide range of applications. Dissemination techniques required for one application may not be useful in another. To address this problem, an event-independent data dissemination scheme is presented in [29]. The proposed scheme calculates encounter probability (EP) to find out whether or not a vehicle is expected to encounter an event. Based on the EP, the information dissemination area, direction, distance and useful time-periods are calculated adaptively. Simulation results show that their scheme supersedes flooding techniques in VANET.

IV. ARCHITECTURES BASED ON CROSS-LAYER PARADIGM

To surmount the issues related to network performance, the concept of cross-layering has been widely recognised by ad hoc research community. A performance improvement over prevalent single layered communication architectures has made the cross-layer design paradigm attractive. In cross-layer design, protocols exchange the state information across the layers and make joint decisions. This section surveys the proposals based on cross-layer design paradigm.

A. Physical Layer – MAC Layer

In vehicular scenarios, the nature of wireless channel is observed as time-varying for large packets [30]. That means channel is changing its characteristics over a course of a packet transmission. This causes a high error rates as equalisation technique employed at the start of the packet cannot counterbalance changes during the packet time. Work in [31] presented comprehensive overview of DSRC technology, discussed issues allied with contention based non-deterministic IEEE 802.11 MAC protocol and reviewed a wide range of MAC layer protocols for VANET based on schedule based deterministic channel access mechanism.

To alleviate effects of time-variant channel, provide QoS and enhance throughput in high load network scenarios, authors in [32] proposed cross-layer scheme of fragmentation and priority scheduling (AFAE). The scheme estimates network load by monitoring the number of recent transmission bytes during the specified time period. Upon estimating network condition (NC), the Contention Window (CW) size is changed and the highest priority class is given the smallest CW size. Furthermore, authors proposed adaptive fragmentation algorithm to provide robust performance in higher bit error rates contributed by poor channel scenarios. The adaptive fragmentation algorithm estimates channel characteristics and selects the optimal packet size to reduce frame error rate. Authors observed that their cross-layer scheme outperformed IEEE 802.11e in all channel loads and provided higher throughput. In another work [33], authors proposed dynamic adaptation of transmission power and CW size of Enhanced Distributed Channel Access (EDCA). According to which each vehicle estimates local

vehicle density and sets transmission power dynamically. Authors used collision rate and the number of back off times as metrics to dynamically adapt the CW size. The main objective was to provide highest priority messages quickest channel access with higher transmission power so that safety messages can be broadcasted in larger region in single hop fashion. The simulation results proved that for high priority messages, proposed cross-layer scheme improved throughput with lower delays for a local node density.

B. MAC Layer – Network Layer

This sub-section provides a review of proposals based on integration between MAC layer and network layer. In one such cross-layer integration approach [34] vehicles are classified in different groups based on their location and the road they move in, to limit the propagation effects for vehicles on the same road. To achieve reliable forwarding of broadcast messages at intersection scenarios, authors combined MAC and routing protocols to improve the speed of sending packets by sending them directly from the routing layer to physical layer. In another approach [35], authors proposed a cross-layer Ad hoc On-Demand Multipath Distance Vector with retransmission counts metric (R-AOMDV) routing protocol. The key feature of the protocol is cross-layer routing metric to combat the poor link quality in urban VANET. R-AOMDV combines hop counts and MAC retransmission counts at MAC layer to make routing decisions. The protocol uses Maximum Retransmission Count (MRC) along the path in order to reflect link quality of the particular path. Furthermore, to reduce the end-to-end delay, the protocol uses hop-count information while selecting the best forwarding path. Thus cross-layer routing metric can provide smallest path (based on hop count) considering link quality of the path (based on retransmission attempts made at MAC layer) for successful and faster delivery of messages. The simulation results show improved Packet Delivery Fraction (PDF) and end-to-end delay performance in sparse as well as dense network scenarios.

Cross Layer Broadcast Protocol (CLBP) [36] focuses on selection of most appropriate relaying node. CLBP incorporates moving vehicle velocity along with channel conditions and geographical locations in order to establish a novel composite relaying metric. CLBP includes IEEE 802.11e MAC protocol for channel access with novel frames termed as Broadcast Request to Send (BRTS) and Broadcast Clear to Send (BCTS). According to the protocol, BRTS is transmitted by a node willing to broadcast the safety information. Upon reception of BRTS, the neighbour nodes decide whether to send BCTS based on the direction information or position information in the received BRTS. The eligible relaying node is selected using distance from sender, received Signal to Noise Ratio, Packet Error Rate and the relative velocity.

Cluster based cross-layer design is a very promising approach. This approach offers clustering of vehicles and an administrative entity in the form of cluster-head. Cluster-head vehicle gathers the information regarding its members and creates the schedule for medium access. All cluster member vehicles follow this medium access schedule and transmit only during their time slot on a specific channel. Cross-layer design combining MAC layer and cluster based routing technique was proposed in [37]. The proposed cross-layered cluster based packet forwarding (CCBF) scheme forms clusters at the MAC layer and shares cluster member information with network layer. Other proposals [38, 39] also includes cluster based cross-layer design with hybrid MAC techniques based on IEEE 802.11 for inter-cluster communication and Time Division Multiple Access (TDMA) for intra-cluster communication. Proposals described in [37-39] achieve low delay high priority information propagation over several hops. Their results prove that such cluster based cross-layer design can improve the network performance.

C. Layer Triggering

In layer triggering, one layer detects an issue and notifies the other layer about it using predefined signal. To alleviate network congestion problem in DSRC networks, authors in [40] proposed adaptive congestion control scheme. To control the rate at which application traffic is generated, authors proposed to exchange the information between MAC layer and application layer. According to their scheme, if MAC blocking is detected at node due to excessively long channel occupancy time, the channel is considered as congested for event driven safety messages. Consequently a congestion signal is sent to application layer to control the message generation rate.

V. ANALYTICAL SUMMARY AND CONCLUSION

VANET is an emerging research field. A large number of routing protocols have been proposed for VANET. This paper analyses such routing protocols. The routing protocols are classified under position based routing techniques, broadcast routing techniques, hierarchical/cluster based routing techniques, geocast routing techniques and adaptive and context aware routing techniques. Literature shows that MANET routing protocols do not cater for characteristics of VANET and thus routing techniques that take VANET characteristics in account are required. Different routing protocols can serve different VANET applications. Routing technique proposed for one type of application or one environment (urban or freeway) may underperform for the other considering different network conditions. A majority of work in literature focuses on development of routing techniques based on layered architecture without considering the impact of channel conditions and performance limitations of lower layers. Layered architecture may show restricted performance in VANET scenarios due to the nature of making independent decisions at different layers. This paper provides the discussion on the cross-layer design based architectures for VANET. The architectures that support cross-layer

integration and adaptive features will play a key role in bringing VANET to the reality.

ACKNOWLEDGMENT

This original research was proudly supported by the Commonwealth of Australia, through the Cooperative Research Centre for Advanced Automotive Technology.

REFERENCES

[1] H. Hartenstein and K. P. Laberteaux, "A tutorial survey on vehicular ad hoc networks," in *IEEE Commun. Mag.,* vol. 46, pp. 164-171, 2008.

[2] Y. Saleh, *et al.*, "Vehicular ad hoc networks (VANETs): Challenges and perspectives," in *Proc. 6th Int. Conf. on ITS Telecommun.* 2006, pp. 761-766.

[3] S. Jaap, *et al.*, "Evaluation of routing protocols for vehicular ad hoc networks in city traffic scenarios," in *Proc. 5th Int. Conf. on Intell. Transportation Systems Telecommun. (ITST), Brest, France, June*, 2005.

[4] J. A. Ferreiro-Lage, *et al.*, "Analysis of unicast routing protocols for VANETs," in *Proc. 5th Intl. Conf. on Networking and Services,* 2009, pp. 518-521.

[5] C. Yufeng, *et al.*, "An improved AOMDV routing protocol for V2V communication," in *Proc. IEEE Intell. Vehicles Symposium, 2009*, pp. 1115-1120.

[6] O. Abedi, *et al.*, "Improving route stability and overhead on AODV routing protocol and make it usable for VANET," in *Proc. 29th IEEE Int. Conf. on Distributed Computing Systems Workshops, 2009*, pp. 464-467.

[7] B. Karp and H. T. Kung, "GPSR: greedy perimeter stateless routing for wireless networks," in *Proc. 6th Annu. Int. Conf. on Mobile Computing and Networking*, Boston, Massachusetts, United States, 2000.

[8] S. A. Rao, *et al.*, "GPSR-L: Greedy perimeter stateless routing with lifetime for VANETS," in *Proc. 8th Int. Conf. on ITS Telecommun.*, 2008, pp. 299-304.

[9] C. Lochert, *et al.*, "Geographic routing in city scenarios," in *ACM SIGMOBILE Mobile Computing and Communications Review,* vol. 9, pp. 69-72, 2005.

[10] K. C. Lee, *et al.*, "Enhanced Perimeter Routing for geographic forwarding protocols in urban vehicular scenarios," in *Proc. IEEE Globecom Workshops,*2007, pp. 1-10.

[11] C. Lochert, *et al.*, "A routing strategy for vehicular ad hoc networks in city environments," in *Proc. IEEE Intell. Vehicles Symposium*, 2003, pp. 156-161.

[12] B.-C. Seet, *et al.*, "A-STAR: A mobile ad hoc routing strategy for metropolis vehicular communications," in *NETWORKING 2004*, pp. 989-999.

[13] M. Jerbi, *et al.*, "An improved vehicular ad Hoc routing protocol for city environments," in *Proc. IEEE Int. Conf. on Commun.,* 2007, pp. 3972-3979.

[14] T. Jing, *et al.*, "Spatially aware packet routing for mobile ad hoc inter-vehicle radio networks," in *Proc. IEEE Intell. Transportation Systems,* 2003, vol.2, pp. 1546-1551.

[15] B. Blaszczyszyn, *et al.*, "Opportunistic broadcast in VANETs (OB-VAN) using active signaling for relays selection," in *Proc. 8th Int. Conf. on ITS Telecommun.,* 2008, pp. 384-389.

[16] X. Qing, *et al.*, "Design and analysis of highway safety communication protocol in 5.9 GHz dedicated short range communication spectrum," in *Proc. 57th IEEE Semiannu. Veh. Technology Conf.,* 2003, pp. 2451-2455 vol.4.

[17] G. Korkmaz, *et al.*, "Urban multi-hop broadcast protocol for inter-vehicle communication systems," in *Proc. 1st ACM Int. Workshop on Veh. Ad Hoc Networks*, Philadelphia, PA, USA, 2004.

[18] G. Korkmaz, *et al.*, "An efficient fully ad-hoc multi-hop broadcast protocol for inter-vehicular communication systems," in Proc. *IEEE Int. Conf. Commun.,* 2006, pp. 423-428.

[19] O. Tatsuaki, *et al.*, "Multi-Hop Vehicular Broadcast (MHVB)," in *Proc. 6th Int. Conf. on ITS Telecommun.*, 2006, pp. 757-760.

[20] M. N. Mariyasagayam, *et al.*, "Enhanced Multi-Hop Vehicular Broadcast (MHVB) for active safety applications," in Proc. *7th Int. Conf. on ITS Telecommun.*, 2007, pp. 1-6.

[21] L. Peiyuan, *et al.*, "A reliable broadcast routing scheme based on mobility prediction for VANET," in *Proc. IEEE Intell. Vehicles Symposium,* 2009, pp. 1083-1087.

[22] W. Sun, *et al.*, "GVGrid: A QoS routing protocol for vehicular ad hoc networks," in *Proc. 14th IEEE Int. Workshop on Quality of Service,* 2006, pp. 130-139.

[23] M. Kihl, *et al.*, "Design and Evaluation of two Geocast protocols for vehicular ad-hoc networks," in *Journal of Internet Engineering,* vol. 2, 2008.

[24] T. D. C. Little and A. Agarwal, "An information propagation scheme for VANETs," in *Proc. IEEE Intell. Transportation Systems,* 2005, pp. 155-160.

[25] O. Kayis and T. Acarman, "Clustering formation for inter-vehicle communication," in *Proc. IEEE Intell. Transportation Systems Conf.,* 2007, pp. 636-641.

[26] S. S. Manvi, *et al.*, "Performance analysis of AODV, DSR, and Swarm Intelligence routing protocols in vehicular ad hoc network environment," in *Proc. Int. Conf. on Future Computer and Commun.,* 2009, pp. 21-25.

[27] Y. Qing, *et al.*, "ACAR: Adaptive connectivity aware routing protocol for vehicular ad hoc networks," in *Proc. 17th Int. Conf. on Computer Commun. and Networks,* 2008, pp. 1-6.

[28] M. Abuelela and S. Olariu, "Traffic-adaptive packet relaying in VANET," in *Proc. 4th ACM Int. Workshop on Veh. Ad Hoc Networks*, Montreal, Quebec, Canada, 2007.

[29] N. Cenerario, *et al.*, "Dissemination of information in inter-vehicle ad hoc networks," in *Proc. IEEE Intell. Vehicles Symposium,* 2008, pp. 763-768.

[30] I. Tan, *et al.*, "Measurement and analysis of wireless channel impairments in DSRC vehicular communications," in *Proc. IEEE Int. Conf. on Commun.,* 2008, pp. 4882-4888.

[31] H. Trivedi, *et al.*, "A survey of lower layer technologies for Vehicle-to-Vehicle communication," in *Proc. 9th IEEE Malaysia Int. Conf. on Commun.,* 2009, pp. 441-446.

[32] L. Hongfei, *et al.*, "A cross layer design of fragmentation and priority scheduling in vehicular ad hoc networks," in *Proc. 7th World Congress on Intell. Control and Automation,* 2008, pp. 6157-6160.

[33] D. B. Rawat, *et al.*, "Dynamic adaptation of joint transmission power and contention window in VANET," in *Proc.70th IEEE Veh. Technology Conf.,* 2009, pp. 1-5.

[34] A. Nasri, *et al.*, "A cross layered scheme for broadcasting at intersections in vehicular ad hoc networks," in *Proc. Int. Conf. on Future Networks,* 2009, pp. 13-17.

[35] C. Yufeng, *et al.*, "A cross-layer AOMDV routing protocol for V2V communication in urban VANET," in *Proc. 5th Int. Conf. on Mobile Ad-hoc and Sensor Networks,* 2009, pp. 353-359.

[36] B. Yuanguo, *et al.*, "Efficient and reliable broadcast in intervehicle communication networks: a cross-layer approach," in *IEEE Trans. on Veh. Technology,* vol. 59, pp. 2404-2417, 2010.

[37] B. Wiegel, *et al.*, "Cross-layer design for packet routing in vehicular ad hoc networks," in *Proc. 66th IEEE Veh. Technology Conf.,* 2007, pp. 2169-2173.

[38] S. Hang, *et al.*, "Cluster-based DSRC architecture for QoS provisioning over vehicle ad hoc networks," in *Proc. IEEE Global Telecommun. Conf.,* 2006, pp. 1-5.

[39] Z. Y. Rawashdeh and S. M. Mahmud, "Media access technique for cluster-based vehicular ad Hoc networks," in *Proc. 68th IEEE Veh. Technology Conf.,* 2008, pp. 1-5.

[40] H. Jianhua, *et al.*, "Adaptive congestion control for DSRC vehicle networks," in *IEEE Commun. Letters, ,* vol. 14, pp. 127-129, 2010.

Introducing Deeper Nulls for Time Modulated Linear Symmetric Antenna Array Using Real Coded Genetic Algorithm

Gopi Ram Hardel, N. Tapaswi Yallaparagada, Durbadal Mandal, Anup Kr. Bhattacharjee.
National Institute of Technology Durgapur, West Bengal, India- 713209
Department of Electronics and Communication Engineering,
gopi203hardel@gmail.com, renswi@gmail.com, durbadal.bittu@gmail.com, akbece12@yahoo.com

ABSTRACT--: **A novel approach based on the real coded genetic algorithm (RGA) is proposed to improve nulling performance of time modulated linear antenna arrays. The RGA adjusts the excitation amplitude of each radiating element to place deep nulls in the desired direction. Various results are presented to show the advantages of this approach considering one and multiple desired nulls.**

Index Terms— Linear **Antenna arrays, real coded genetic algorithm; deeper nulls; time modulation.**

I. INTRODUCTION

Time modulated linear arrays attracted the antenna designers for their advantages over conventional array antennas from a few years. Previous research works has shown Time modulated antenna arrays are attractive for the synthesis of low/ultralow side lobes [1-12]. In this paper, a novel approach was proposed in order to show that Time modulated linear arrays are good for getting deeper nulls. As compared to conventional antenna arrays, the time modulated antenna arrays introduce a fourth dimension—time—into the design. Consequently, it has more flexibility. An approach based on the real coded genetic algorithm (RGA) was proposed for imposing deeper nulls at predefined directions. In this paper, a novel approach to realize non uniform amplitude time modulated linear arrays with both single nulling and double nulling is proposed. The time modulation period is divided into numerous minimal time steps with the same length, where the ON-OFF status for each time step is followed by a scheme given in the paper.

In this paper, broadside uniform linear arrays with uniform spacing but non uniform amplitude distribution is considered. In this paper, a symmetric linear antenna array structure with equal spacing between any two consecutive elements has been considered. The phase difference between any two elements is kept zero. The excitations of each element are varied using genetic algorithm. A cost function is defined which keeps the nulls at lower levels.

II. DESIGN EQUATIONS

Consider a broadside linear array of 2M equally spaced isotropic elements as in Figure 1, in which each element is controlled by a high speed RF switch and excited with complex amplitude. The array is symmetric in both geometry and excitation with respect to the array center.

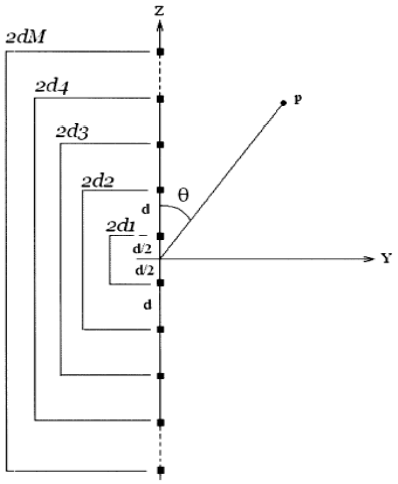


Fig. 1. Geometry of a 2M-element linear array along the z-axis.

The array is used to transmit a rectangular pulse of width T, with a pulse repetition frequency of $prf = 1/T_p$, and T_p is the pulse repetition period. For broadside beams, the array factor is given by

$$AF(\theta,t) = 2\sum_{n=1}^{M} U_n(t) I_n \cos[(\frac{2n-1}{2})kd\cos(\theta)] \quad (1)$$

where

θ = angle of radiation of electromagnetic plane wave

d = spacing between elements

k = propagation constant

2M = total number of elements in the array

I_n = Excitation amplitude of n th element

U_n = corresponding periodic switch on time sequence function in which each element is switch on for $\tau_n (0 \le \tau_n \le T)$.

The function of high speed RF switch is given by the following equation:

$$U_n(\tau_n) = 1 \qquad \text{if } \tau_n \le n * \frac{T}{M}$$

$$= 0 \qquad \text{Else} \qquad (2)$$

Where τ_n is the time for which n^{th} element will be ON and T is the pulse repetition time. All the antenna elements are assumed isotropic. Only Amplitude excitations of each element are used to change the antenna pattern.

The cost function (CF) for imposing null is given below

$$CF = \frac{\left|\prod_{i=1}^{m} AF(null_i)\right|}{|AF|} \qquad (3)$$

'm' is the possible number of positions where nulls can be imposed. In this paper, one and two has been considered as the value of 'm'. $AF(null_i)$ is the Array factor value at the particular null. AF is the maximum of the array factor. In cost function, both the numerator and denominator are absolute values. Smaller value of the cost function means that array factor values at predefined positions are less. Consequently, GA controls the amplitude excitations in order to minimize the cost function.

III. REAL CODED GENETIC ALGORITHM

GA is mainly a probabilistic search technique, based on the principles of natural selection and evolution. At each generation it maintains a population of individuals where each individual is a coded form of a possible solution of the problem at hand and called chromosome. Chromosomes are constructed over some particular alphabet, e.g., the binary alphabet {0, 1}, so that chromosomes' values are uniquely mapped onto the decision variable domain. Each chromosome is evaluated by a function known as fitness function, which is usually the fitness function or the objective function of the corresponding optimization problem.

Steps of RGA as implemented for optimization of spacing between the elements and current excitations are [13, 14]:

- Initialization of real chromosome strings of np population, each consisting of a set of excitations. Size of the set depends on the number of excitation elements in a particular array design.
- Decoding of strings and evaluation of CF of each string.
- Selection of elite strings in order of increasing CF values from the minimum value.
- Copying of the elite strings over the non-selected strings.
- Crossover and mutation to generate off-springs.
- Genetic cycle updating.
- The iteration stops when the maximum number of cycles is reached. The grand minimum CF and its corresponding chromosome string or the desired solution are finally obtained.

IV. NUMERICAL RESULTS

A 12-16-20 elements linear array of isotropic radiating elements, with λ/2 spacing, is considered for time modulated linear antenna array with T_p=16 μs .The required "switch-on" time intervals for each element can be calculated using (2). RGA is applied to get deeper nulls. Every time GA executed with 400 iterations. The population size was fixed at 120.For the real coded GA, the mutation probability was set to 0.15 and uniform crossover was taken. GA algorithm is initialized using random values.

Figures 2-4 show the imposing of deeper nulls over 3rd null. For 12, 16, 20-element, the null has improved up to -155.5 dB, -119.7 dB, and -134.3 dB with initial values of -57.94 dB, -56.44 dB, -40.97 dB respectively. The Initial values of Beam width between first nulls (BWFN) has been given for all the

array structures in the TABLE I, whereas TABLE II shows the resulting amplitude excitation distribution. In this case the weighting for the array elements $I_1, I_2 \ldots\ldots\ldots I_M$ are normalized using max (I_M) =1.

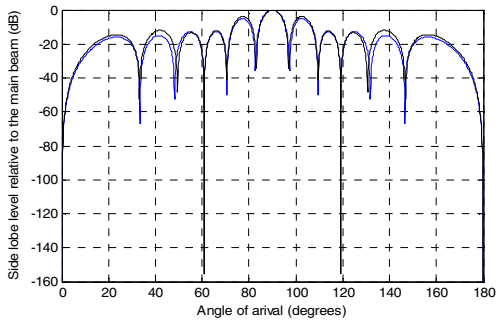


Fig. 2. Best array pattern found by GA for the 12-element array case with an improved null at 3rd nulls i.e. θ= 60.84 degrees.

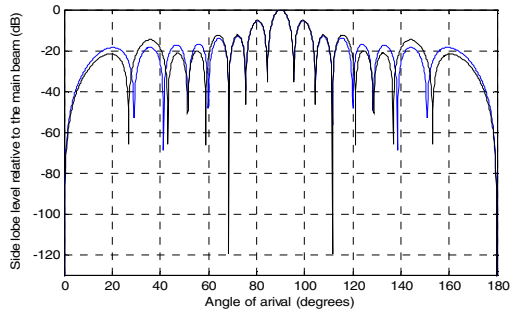


Fig. 3. Best array pattern found by GA for the 16-element array case with an improved null at 3rd null i.e. θ =68.4 degrees.

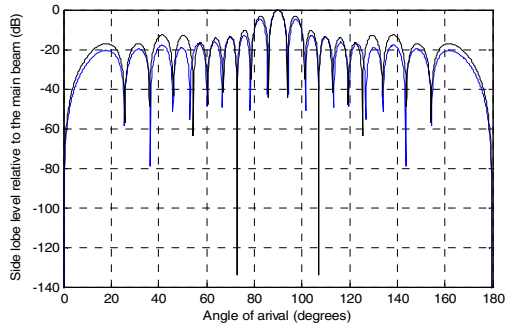


Fig. 4. Best array pattern found by GA for the 20-element array case with an improved nulls at 3rd null i.e. θ =72.9 degrees.

Figure 5-7 shows the imposing of nulls at the 3rd peak for 12, 16 and 20 element structures respectively. For 12, 16, 20-element, the pair of nulls has improved up to -179.1 dB, -124.2 dB, -124.2 dB with initial values of -12.81 dB, -13.79 dB, -13.79 dB respectively. The improved values are shown in TABLE III.

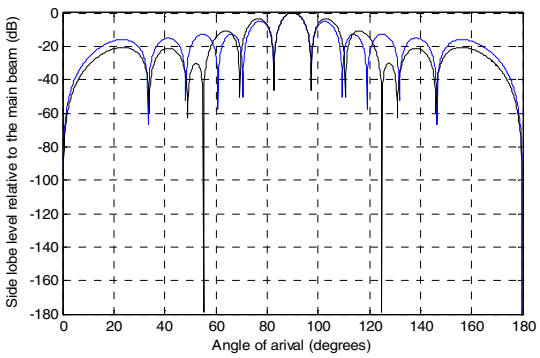


Fig. 5. Best array pattern found by GA for the 12-element array case with a null introduced at 3rd peak i.e. θ =55.08 degrees.

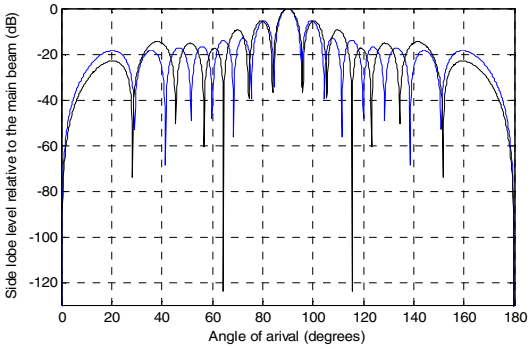


Fig. 6. Best array pattern found by GA for the 16-element array case with a null introduced at 3rd peak i.e. θ =64.44 degrees.

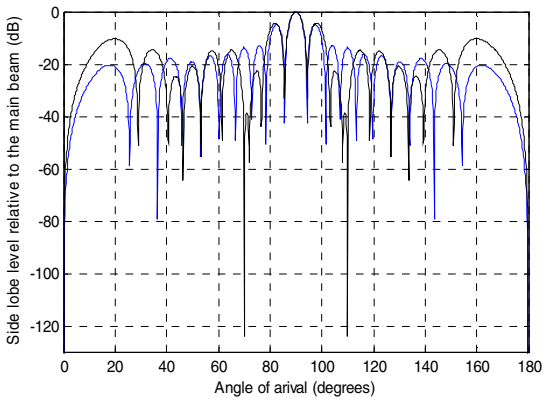


Fig. 7. Best array pattern found by GA for the 20-element array case with a null introduced at 3rd peak i.e. θ =70.02 degrees .

Figure 8-10 shows the imposing of nulls at the 2nd and 3rd peaks for 12, 16 and 20 element structures respectively. For 12, 16, 20-element, the pair of nulls has improved up to (-100.3 dB, -138.9 dB), (-99.54 dB, -78.21 dB), (-69.6 dB,-84.22 dB) with initial values of (-12.7 dB,-12.81 dB), (-12.84 dB,-13.9 dB), (-12.88 dB, -13.79 dB) respectively. The improved values are shown in TABLE IV.

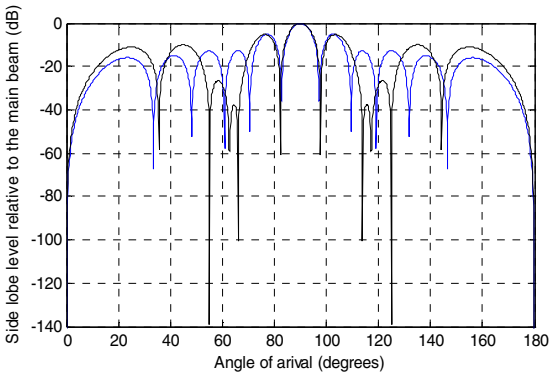


Fig.8. Best array pattern found by GA for the 12-element array case with nulls introduced at 2nd and 3rd peaks i.e. θ =66.06 and 55.08 degrees respectively.

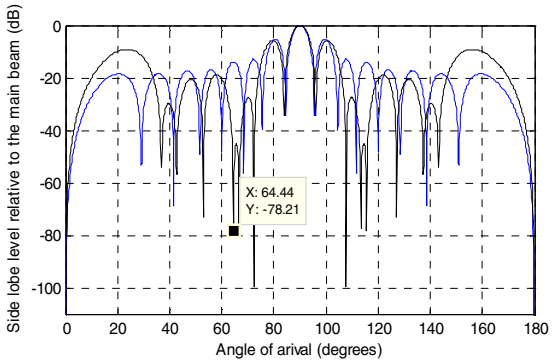


Fig. 9. Best array pattern found by GA for the 16-element array case with nulls introduced at 2nd and 3rd peak i.e. θ =72.36 and 64.44 degrees respectively.

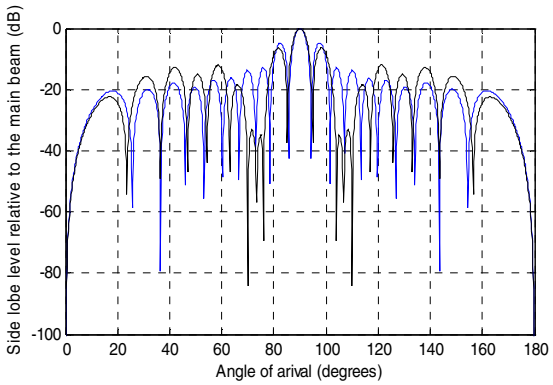


Fig. 10. Best array pattern found by GA for the 20-element array case with nulls introduced at 2nd and 3rd peak i.e. θ =75.96 and 70.02 degrees respectively.

Figure 11-13 shows the imposing of nulls at the 2nd and 3rd nulls for 12, 16 and 20 element structures respectively. For 12, 16, 20-element, the pair of nulls has improved up to (-130.1 dB, -91.43 dB), (-90.78 dB, -99.59 dB), (-86.83 dB,-83.69 dB) with initial values of (-50.3 dB,-57.94 dB), (-39.8 dB,-56.44 dB),(-50.83 dB, -40.97 dB) respectively. The improved values are shown in TABLE V.

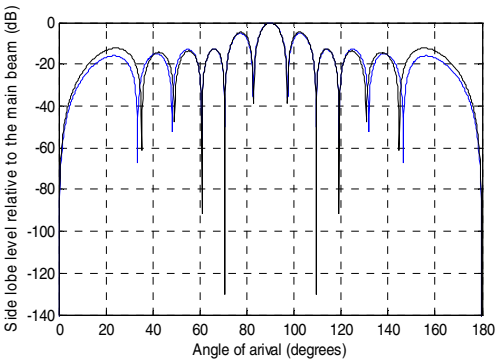


Fig. 11. Best array pattern found by GA for the 12-element array case with improved nulls at 2nd and 3rd nulls i.e. θ =70.56 and 60.84 degrees respectively.

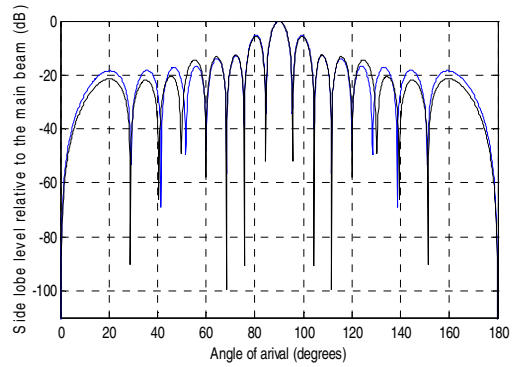


Fig. 12. Best array pattern found by GA for the 16-element array case with improved nulls at 2nd and 3rd nulls i.e. θ =75.6 and 68.4 degrees respectively.

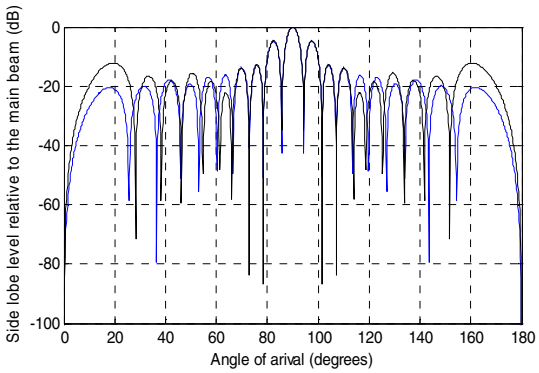


Fig. 13. Best array pattern found by GA for the 20-element array case with improved nulls at 2nd and 3rd nulls i.e. θ =78.48 and 72.9 degrees respectively.

V. CONCLUSION

In this paper, the design of a non-uniformly excited symmetric time modulated linear antenna array with uniform spacing between the elements has been described using the techniques of RGA. Simulated results reveal that optimizing the excitation values of the elements of the array antenna can impose nulls at a desired direction for a given number of the array elements. For example for a 12 element time modulated linear array antenna after

optimizing, a null with the value -179.1 dB was imposed at a peak having initial value -12.81 dB. The BWFN of the initial and final radiation pattern remains approximately same.

TABLE I. INITIAL VALUES OF BWFN FOR UNIFORMLY EXCITED (I_n =1) ARRAYS

Number of Elements (El.)	Initial BWFN (θ degrees)
12	14.4
16	10.8
20	8.64

TABLE II. ONE NULL IMPOSED IN THE 3rd NULL POSITION

El.	($I_1, I_2 ..... I_M$)	Initial value (dB)	Final value (dB)	BWFN (θ degrees)
12	0.3380 0.3573 0.7696 0.7844 0.7215 0.8130	-57.94	-155.5	13.68
16	0.5207 0.4127 0.8042 0.3923 0.5189 0.5964 0.5706 0.5316	-56.44	-119.7	10.8
20	0.4857 0.1632 0.1485 0.6547 0.5210 0.5668 0.8341 0.6848 0.6712 0.8833	-40.97	-134.3	7.92

TABLE III. NULLS IMPOSED IN THE 3rd PEAK POSITION

El.	($I_1, I_2 ..... I_M$)	Initial Value (dB)	Final value (dB)	BWFN (θ degrees)
12	0.6581 0.1580 0.5256 0.9435 0.7528 0.4425	-12.81	-179.1	14.4
16	0.7852 0.3439 0.1237 0.3921 0.3558 0.4048 0.4238 0.0446	-13.9	-124.2	11.88
20	0.2490 0.1216 0.2673 0.3990 0.5100 0.8590 0.3492 0.4640 0.1716 0.3945	-13.79	-124.2	9.00

TABLE IV. NULLS IMPOSED IN THE 2nd AND 3rd PEAK POSITIONS

El.	($I_1, I_2 ..... I_M$)	Initial Value (dB)	Final value (dB)	BWFN (θ degrees)
12	0.4860 0.2125 0.7099 0.7977 0.2199 0.4006	-12.7, -12.81	-100.3, -138.9	15.68
16	0.2344 0.5978 0.1940 0.8615 0.4404 0.5577 0.1637 0.2916	-12.84, -13.9	-99.54, -78.21	11.88
20	0.2786 0.8539 0.7236 0.5256 0.7271 0.7160 0.7666 0.2658 0.1654 0.4616	-12.88, -13.79	-69.69, -84.22	9.72

TABLE V. NULLS IMPOSED IN THE 2nd and 3rd NULL POSITIONS

El.	($I_1, I_2 ..... I_M$)	Initial Value (dB)	Final value (dB)	BWFN (θ degrees)
12	0.3543 0.4053 0.3958 0.5259 0.4023 0.4878	-50.3, -57.94	-130.1, -91.43	14.4
16	0.7405 0.3899 0.4722 0.5178 0.3940 0.4136 0.5051 0.4132	-39.8, -56.44	-90.78, -99.59	11.16
20	0.4476 0.4577 0.6987 0.7297 0.3471 0.6758 0.5798 0.7534 0.4266 0.6617	-50.83, -40.97	-86.83, -83.69	8.64

REFERENCE

[1] H. E. Schrank, "Low sidelobe phased array antennas," IEEE Antennas Propagat. Soc. Newslett., vol. 25, no. 2, pp. 4–9, Apr. 1983.

[2] Yang, S., Y. B. Gan, and P. K. Tan, "Linear antenna arrays with bidirectional phase center motion," IEEE Trans. Antennas Propagat., Vol. 53, No. 5, 1829–1835, 2005.

[3] S. Yang, Y. B. Gan, and A. Qing, "Sideband suppression in time-modulated linear arrays by the differential evolution algorithm," IEEE AntennasWireless Propag. Lett., vol. 1, pp. 173–175, 2002.

[4] S. Yang, Y. B. Gan, and P. K. Tan, "A new technique for power-pattern synthesis in time-modulated linear arrays," IEEE Antennas Wireless Propag. Lett., vol. 2, pp. 285–287, 2003.

[5] J. Fondevila, J. C. Brégains, F. Ares, and E. Moreno, "Optimizing uniformly excited linear arrays through time modulation," IEEE Antennas Wireless Propag. Lett., vol. 3, pp. 298–301, 2004.

[6] S.Yang, Y. B. Gan, A. Qing, and P. K. Tan, "Design of a uniform amplitude time modulated linear array with optimized time sequences," IEEE Trans. Antennas Propag., vol. 53, no. 7, pp. 2337–2339, Jul. 2005.

[7] "Comparative study of low sidelobe time modulated linear arrays with different time schemes," J. Electromagn. Waves Appl., vol. 18, no.11, pp. 1443–1458, Nov. 2004.

[8] R. L. Haupt, "Phase-only adaptive nulling with a genetic algorithm," IEEE Trans. Antennas Propagat., vol. 45, no. 6, pp. 1009-1015, Jun. 1997.

[9] H. Steyskal, R. A. Shore, and R. L. Haupt, "Methods for null control and their effects on the radiation pattern," IEEE Trans. AntennasPropagat., vol. 34, no. 3, pp. 404-409, Mar. 1986.

[10] R. L. Haupt, "Adaptive nulling in monopulse antennas," IEEE Trans. Antennas Propagat., vol. 36, no. 2, pp. 202-208, Feb. 1988.

[11] Y. C. Chung and R. L. Haupt, "Adaptive nulling with spherical arrays using a genetic algorithm," in Proc. IEEE AP-S Int. Symp. Dig., 1999, vol. 3, pp. 2000-2003.

[12] Yang, S., Y. B. Gan, and A. Qing, "Moving phase center antenna arrays with optimized static excitations," Microw. Opt. Tech.Lett., Vol. 38, 83–85, July 2003.

[13] D. Mandal, S. P. Ghoshal, and A. K. Bhattacharjee, "A Novel Particle Swarm Optimization Based Optimal

Design of Three-Ring Concentric Circular Antenna Array," IEEE International Conference on Advances in Computing, Control, and Telecommunication Technologies, 2009, ACT'09, pp. 385-389, 2009.

[14] D. Mandal, S. P. Ghoshal, and A. K. Bhattacharjee, "Determination of the Optimal Design of Three-Ring Concentric Circular Antenna Array Using Evolutionary Optimization Techniques," International Journal of Recent Trends in Engineering. vol. 2(5), pp. 110-115, 2009.

FPGA IMPLEMENTATION OF DSSS-CDMA TRANSMITTER AND RECEIVER FOR ADHOC NETWORKS

[1] B.Sreedevi, M.Tech
Assoc. Professor. VCEW
vaagvijs_15@yahoo.co.in

[2] V.Vijaya, (PhD) M.Tech
Assoc. Professor. VCEW,
vsrtej@yahoo.co.in

[3] Ch.Kranthi Rekh,
Asst.Professor LUC, Mantin, Malaysia
madakranthirekha@yahoo.co.in

[4] Rama Valupadasu (Ph D), M.Tech
Asst.Professor NIT, Warangal
agnivesh91@yahoo.co.in

[5] B.RamaRao Chunduri, PhD., M.Tech
Professor NIT, Warangal
cbrr@nitw.ac.in

Abstract— The DS - CDMA is expected to be the major medium access technology in the future mobile systems owing to its potential capacity enhancement and the robustness against noise. The CDMA is uniquely featured by its spectrum-spreading randomization process employing a pseudo-noise (PN) sequence, thus is often called the spread spectrum multiple access (SSMA). As different CDMA users take different PN sequences, each CDMA receiver can discriminate and detect its own signal, by regarding the signals transmitted by other users as noise- like interferences. In this project Direct sequence principle based CDMA transmitter and receiver is implemented in VHDL for FPGA. The digital frequency synthesizer principle is used in generating the carrier signals both at transmitter and receiver modules. The transmitter module mainly consists of symbol generator, programmable PN sequence generator, digital local oscillator, spreader and BPSK modulator blocks. The receiver module consists of BPSK demodulator, matched filter, programmable PN sequence generator and threshold detector blocks. The CDMA receiver gets this input and recovers the data using matched filter.Modlesim Xilinx Edition 5.8 (MXE) tool will be used for functional simulation and logic verification at each block level and system level. The Xilinx Synthesis Technology (XST) of Xilinx ISE tool will be used for synthesis of transmitter and receiver on FPGAs. Applications of the developed CDMA system for ADHOC networks and defense communication links will be studied. The possible extensions of work in view of advancements in software defined radio principles will be discussed.

Keywords—DDFS, DS-CDMA, LFSR, PN code, spread spectrum.

INTRODUCTION

Cellular technology has grown tremendously both in terms of traffic and the services it offers [1-2]. The mobile telecommunication industry facing the problem providing technology that be able to support a variety of services ranging from voice communication with a bit rate of few Kbps to wireless multimedia in which bit rate up to 2 Mbps. This tremendous growth has also been fueled by the recent improvements in the capacity of wireless links due to the use of multiple access techniques. The idea is to transmit signals simultaneously through a linear band limited channel without inter channel or inter symbol interference [5].

To design multi channel transmission must concentrate on reducing cross talk between adjacent channels. One of the most promising cellular standards is IS-95A code division multiple access (CDMA) system[2]. The advantages of IS-95A CDMA standard over other standards are optimum subscriber station power management, bandwidth recycling, efficient power control, multilayer diversity and compatability. The forward link frequency is in the range of (869-894) MHz and reverse link frequency is in the range of (824- 849) MHz. In the mobile communication transmission from the base station to mobile receiver are on the forward link and the transmission from the mobile user to the base station are on the reverse link[4].

VHDL implementation of DS-CDMA transmitter and receiver has been proposed in this thesis. In this project pseudo noise code is generated by using two six bit LFSRs.Code signal is called as chip signal. The chips modulated by the carrier using a digital modulation technique BPSK. The carrier is generated by using the technique discrete digital frequency synthesizer. CDMA base stations must be able to discriminate this different code sequences in order to distinguish one transmission from other .This discrimination is accomplished by means of a matched code filter .A matched code filter is a filter whose frequency spectrum is exactly designed to match the frequency spectrum of the input signal. Here matched code filter generating the pseudo noise code, generated noise code is correlated with the received code and detecting original data.

In the recent years the CDMA on FPGA platform has attracted attention of academic research and industry. The Spartan TM-3E family of Field-Programmable Gate Arrays (FPGAs) is specifically broadband designed to meet the needs of high volume, cost-sensitive consumer electronic applications. The five-member family offers densities ranging from 100,000 to 1.6 million system gates. Because of their exceptionally low cost, Spartan -3E FPGAs are ideally suited to a wide range of consumer electronics applications, including access, home networking, display/projection, and digital television equipment.

I. Code Division Multiple Access

Code Division Multiple Access (CDMA) is a spread spectrum technique that uses neither frequency channels nor time slots [3-5]. With CDMA, the narrow band message (typically digitized voice data) is multiplied by a large bandwidth signal that is a pseudo random noise code (PN code). All users in a CDMA system use the same frequency band and transmit simultaneously. The transmitted signal is recovered by correlating the received signal with the PN code

used by the transmitter. Figure 1 shows the general use of the spectrum using CDMA.

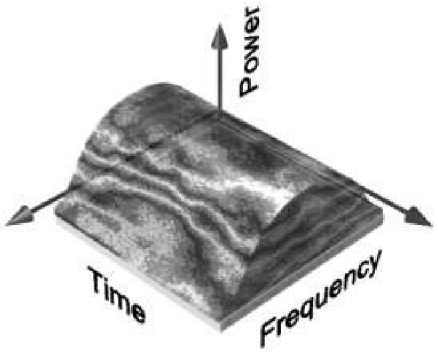


Figure 1 Code division multiple access (CDMA)

CDMA technology was originally developed by the military during World War II. Researchers were spurred into looking at ways of communicating that would be secure and work in the presence of jamming. Some of the properties that have made CDMA useful are [3]:

- Signal hiding and non-interference with existing systems.
- Anti-jam and interference rejection
- Information security
- Accurate Ranging
- Multiple User Access
- Multipath tolerance

A. CDMA Process Gain

One of the most important concepts required in order to understand spread spectrum techniques is the idea of process gain. The process gain of a system indicates the gain or signal to noise improvement exhibited by a spread spectrum system by the nature of the spreading and despreading process.

$$Gp = \frac{BW_{RF}}{BW_{info}}$$

Where transmitted bandwidth after the data is spread, and BW_{info} is the bandwidth of the information data being sent.

The data to be transmitted (a) is spread before transmission by modulating the data using a PN code. This broadens the spectrum as shown in (b). In this example the process gain is 125 as the spread spectrum bandwidth is 125 times greater the data bandwidth. Part (c) shows the received signal.

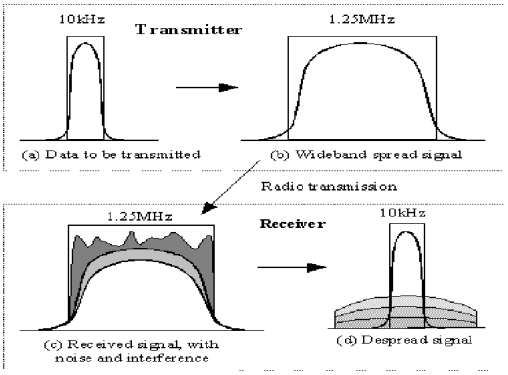


Figure 2 Basic CDMA transmissions.

B. CDMA Generation

CDMA is achieved by modulating the data signal by a pseudo random noise sequence (PN code), which has a chip rate higher then the bit rate of the data.. Figure 3 shows a basic CDMA transmitter [2-4].

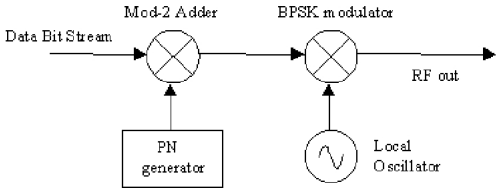


Figure 3 Simple direct sequence modulator

The PN code used to spread the data can be of two main types. A short PN code (typically 10-128 chips in length) can be used to modulate each data bit. Figure 4 shows the generation of a CDMA signal using a 10-chip length short code. Alternatively a long PN code can be used

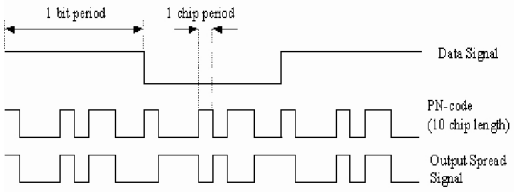


Figure 4 Direct sequence signals

C. CDMA Forward Link Encoding

The forward link, from the base station to the mobile, of a CDMA system can use special orthogonal PN codes, called Walsh codes, for separating the multiple users on the same channel. These are based on a Walsh matrix, which is a square matrix with binary elements and dimensions that are a power of two. It is generated from the basis that Walsh (1) = $W_1 = 0$ and that:

$$W_{2n} = \begin{bmatrix} W_n & W_n \\ W_n & \overline{W_n} \end{bmatrix}$$

Where W_n is the Walsh matrix of dimension n. For example:

$$W_2 = \begin{bmatrix} 0 & 0 \\ 0 & 1 \end{bmatrix}$$

$$W_4 = \begin{bmatrix} 0 & 0 & 0 & 0 \\ 0 & 1 & 0 & 1 \\ 0 & 0 & 1 & 1 \\ 0 & 1 & 1 & 0 \end{bmatrix}$$

Walsh codes are orthogonal, which means that the dot product of any two rows is zero. This is due to the fact that for any two rows exactly half the number of bits match and half do not. Each row of a Walsh matrix can be used as the PN code of a user in a CDMA system.

D.CDMA Reverse Link Encoding

The reverse link is different to the forward link because the signals from each user do not originate from a same source as in the forward link. The transmission from each user will arrive at a different time, due to propagation delay, and synchronization errors. Due to the unavoidable timing errors between the users, there is little point in using Walsh codes as they will no longer be orthogonal. For this reason, simple pseudo random sequences are typically used. These sequences are chosen to have a low cross correlation to minimize interference between users. The capacity is different for the forward and the reverse links because of the differences in modulation. The reverse link is not orthogonal, resulting in significant inter-user interference. For this reason the reverse channel sets the capacity of the system [1-2].

II.Types of CDMA techniques

Based on the modulation method the CDMA technique can be classified into three categories. CDMA: direct sequence (DS) CDMA: frequency hopping (FH) CDMA: time hopping (TH)

A . CDMA Properties

- Multiple access capability
- Protection against multipath interference
- Privacy, interference rejection
- Anti-jamming capability
- Low probability of interception

B. DIRECT Sequence

The spreading of the signal is done by using the pseudonoise sequence. Let's say that a binary information sequence with an information rate of R bits per second is to be spread. The bit interval of the signal is Tb = 1/R seconds and the available channel bandwidth is Bc Hz, where Bc >> R[4-5]

At the modulator the bandwidth of the information signal is expanded to W = Bc Hz by shifting the phase of the transmitted signal pseudorandomly at a rate of W times per second according to the pattern of the PN generator. The effective bit rate will therefore depend on the available bandwidth Bc, and the length of the PN-sequence N as

$$R_b = B_c * \left(\frac{1}{(1+N)} \right)$$

The results for various B_c and N are shown in the table 1.

CDMA-Table		
B_C (kHz)	N	R_b (kHz)
2	8	0.22
	16	0.12
	32	0.06
5	8	0.56
	16	0.29
	32	0.15
10	8	1.11
	16	0.59
	32	0.30

TABLE-1

In DS-CDMA the modulated information-bearing signal (the data signal) is directly modulated by a digital, discrete time, discrete valued code signal. It is from this direct multiplication that the direct sequence CDMA gets its name.

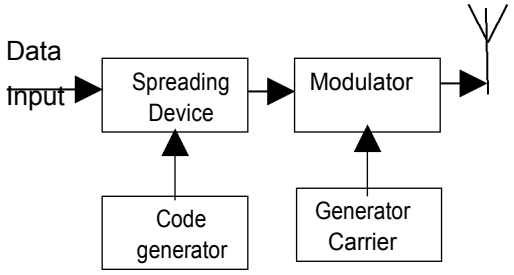


Figure 5 Block diagram of a DS-SS transmitter

The block diagram of a DS-CDMA transmitter as shown in Figure 5. The binary data signal is modulated by the code signal. This code signal consists of a number of code bits called “chips” that can be either +1 or –1. The spreaded signal is modulated by a RF carrier. For the modulation, various modulation techniques can be used, but usually some form of phase shift keying (PSK) like binary phase shift keying (BPSK), differential binary phase shift keying (D-BPSK), quadrature phase shift keying (QPSK), or minimum shift keying (MSK) is employed.The Figure 6 shows the block diagram of DSSS receiver.

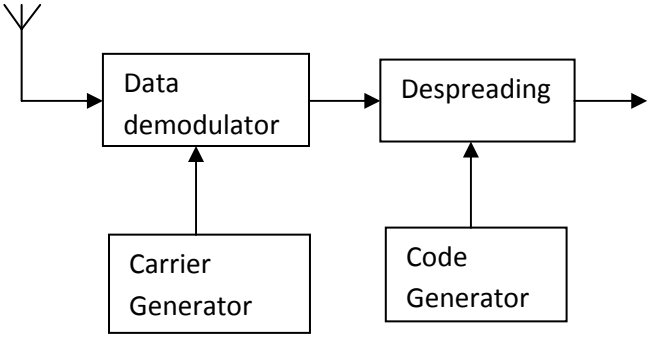


Figure 6 Receiver of a DS-SS signal

After transmission of the signal, the receiver shown in Figure 6 dispreads the SS signal using a locally generated code sequence.

A PN code is a sequence of chips valued -1 and 1 (polar) or 0 and 1 (non-polar) and has noise-like properties. This results in low cross- correlation values among the codes and the difficulty to jam or detect a data message. A usual way to create a PN code is by means of at least one shift-register. When the length of such a shift-register is n, the following can be said about the period N_{DS} of the above mentioned code-families:

$$N_{DS} = 2^n - 1.$$

Indirect- sequence systems the length of the code is the same as the spreading-factor with the consequence that:

$$Gp(DS) = N_{DS}.$$

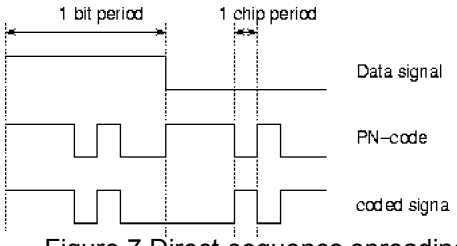


Figure 7 Direct-sequence spreading

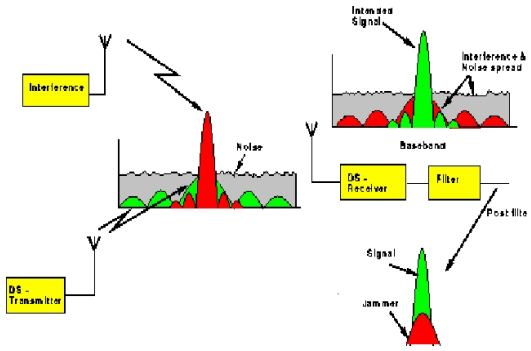


Figure 8 DS-concept, before and after despreading

In the receiver, the received signal is multiplied again by the same (synchronized) PN code. Since the code existed of +1s and -1s, this operation completely removes the code from the signal and the original data-signal is left. Another observation is that the despread operation is the same as the spread operation. The consequence is that a possible jamming-signal in the radio channel will be spread before data-detection is performed. So jamming effects are reduced

C. DSSS disadvantage

The main problem with applying Direct Sequence spreading is the so-called Near -Far effect which is illustrated in Figure 14 This effect is present when an interfering transmitter is much closer to the receiver than the intended

and B is low, the correlation between the received signal from the interfering transmitter and code A can be higher than the correlation between the received signal from the intended transmitter and code A. The result is that proper data detection is not possible [5].

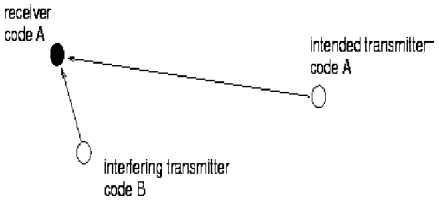


Figure 9: near-far effect illustrated

III. HARDWARE AND SOFTWARE DESIGN AND IMPLEMENTATION

A . DESIGN OF CDMA TRANSMITTER AND RECEIVER

The following specifications are considered for design and implementation of the CDMA transmitter and receiver.

TABLE.2

Type of Pn sequence	Gold code
LFSR Size	Two 6-bit LFSRs
PN sequence length	127
Number of communication links	127
Type of modulation	BPSK
Type of demodulation	Coherent BPSK
Type of correlator	Matched filter
Type of signal synthesis	ROM based DDFS
Phase resolution Choosen	5.625^0
Threshold type	Constant
Front end design	VHDL
Backend synthesis	Xilinx Spartan 3E FPGA

transmitter. Although the cross-correlation between codes A

DS- CDMA TRNSMITTER

The top level block diagram of CDMA transmitter which is implemented in this project is given in the below figure.

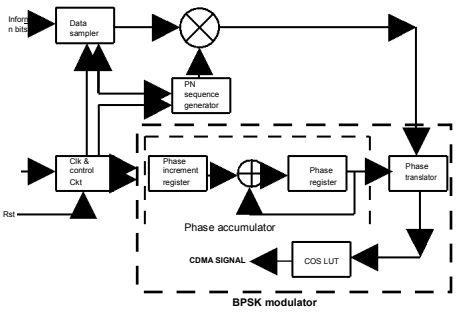


Figure 10 Block diagram of CDMA transmitter.

B . DS-CDMA RECEIVER

The DS-CDMA receiver implemented in this project with the specification mentioned in the above sections consists of following blocks.

The high level block diagram of CDMA receiver is shown in the Figure 11.

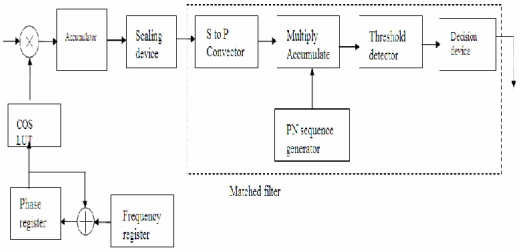


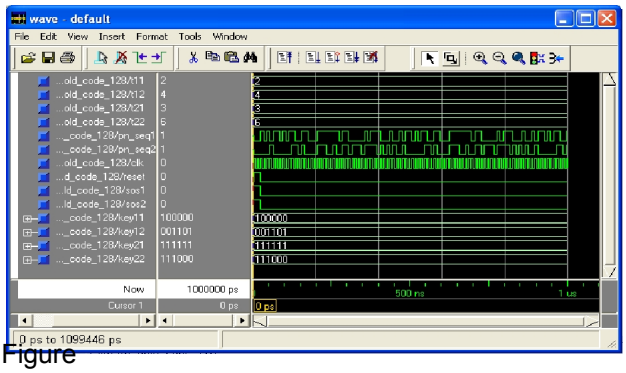
Figure 11: Block diagram of CDMA Rx

C . VHDL IMPLEMENTATION OF CDMA TRANSMITTER AND RECEIVER

A VHDL specification can be executed in order to achieve high level of confidence in its correctness before commencing design and may simulate one to two orders of magnitude faster than a gate level description

IV. Result Analysis:

PN Sequence generator:



Figure

The gold code generator is tested with input t11, t12, t21; t22, key and output observed are pn_seq1, pn_seq2.

Direct Digital Frequency Synthesizer

Direct Digital Frequency Synthesizer is a technique to produce desired out put with full digital control.

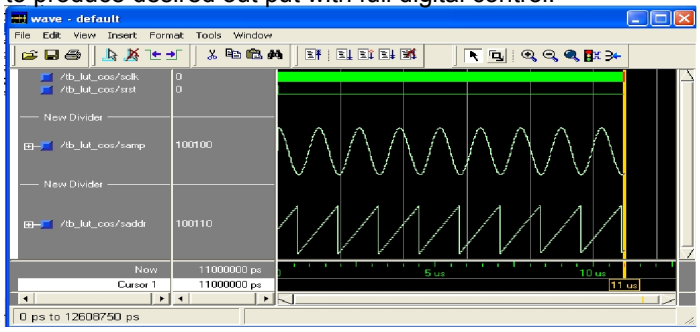


Figure 13 Simulation results for DDFS

Frequency of the carrier generated is $f_c = f_{clk}/64 = f_{ck}/2^6$

BPSK Modulator

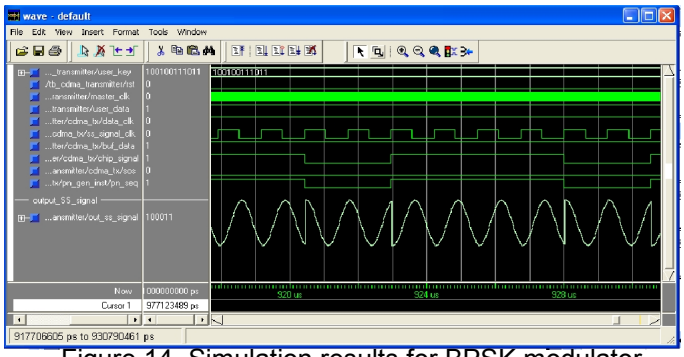


Figure 14 Simulation results for BPSK modulator

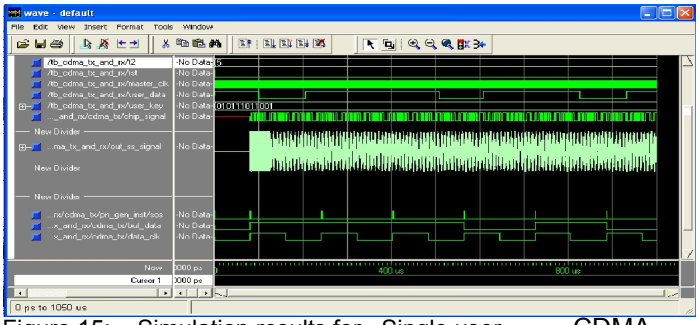


Figure 15: Simulation results for Single user CDMA Tx & Rx

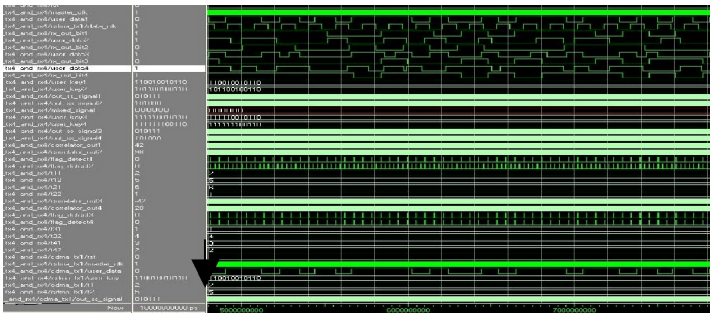


Figure 16: Simulation results for four user Tx & Rx

V. CONCLUSIONS

CDMA is one of the most impartant multiple access technique .In this project the transmitter and receiver were implemented on FPGA. After synthesis simulations are agreed before synthesis simmulations. The transmitter was connected to the receiver before synthesis was done to verify functionality of the transmitter and receiver. This has been tested using an arbitrary chosen data stream, where these data have been transmitted through implemented transmitter and then received by our implemented receiver. A comparison has been done betweenn the transmitted and received data and satisfactory results have been achieved. Increasing the number of bits using the same topology, it is possible to reach the standard rates specified for CDMA.

This work has the following applications.

- Custom CDMA communication setup with specified PN sequence length and number of users
- Standard CDMA systems designs such as used for mobiles and GPS

Implementation of a CDMA communication system with DSSS technique in VHDL has the following advantages

- The design is fully reconfigurable
- The number of bits and PN sequence can be changed very easily
- Useful for both FPGA and ASIC implementations. Disadvantages
- Complex hardware is involved in receiver design which increases the cost of the system.

FUTURE SCOPE

- The concept can be extended to design the GPS system which is CDMA system with 1023 chip length technique.

ACKNOWLEDGMENT

We are grateful to management Vaagdevi college of Engineering, Warangal for the facilities to provide to complete the project in time.

REFERENCES

[1] William C.Y.Lee, Mobile Cellular Telecommunications Systems, McGraw-Hill International Edditions , 1997.

[2] John G. Proakis and Masoud Salehi. "Communications Systems Engineering" Prentice Hall, Inc. Englewood Cliffs, New Jersey 1994.

[3] Rodger E. Ziemer and Roger L. Peterson. "Digital Communications and SpreadSpectrum Systems" Macmillian Publishing Company, New York 1985.

[4] S. Allevad, T. Andersen m,m. "Acoustic Communication System With Two Branch Diversity", Communication Project, Stockholm 2000.

[5] M.K. Simon, D.Divsalar and D.Raphaehi "improved parallel intereferencecancellation for CDMA" IEEE Trans. Commun..vol. 46 Feb 1998.

[6] "IS-95A CDMA," Technical report from Yonsei University, 2002

Bibliographical notes:

B.Sreedevi obtained her AMIE Degree in Electronics & Communication Engg., from Institution of Engineers, Calcutta, and M.Tech. Degree in Digital System Computer Electronics, from JNTUA college of Engg Ananthapur. She is working as Associate Professor in the ECE Dept of Vaagdevi College of Engineering at Warangal. She has 10 years of Teaching Experience. Attended 12 workshops/refresher courses/short term courses at various places. Member of Project Review Committee (UG/PG); CRC for (UG/PG). Her area of interest are Image processing, Signal processing, VLSI, Communications. She is the project coordinator for UG/PG.She is the course coordinator for PG course.She is life member of ISTE, IETE. She has published no. of papers in national conferences and international conferences.

V.Vijaya obtained her B.Tech Degree in Electronics & Communication Engg., from (JNTU) Jawaharlal Nehru Technological University College of Engg., Ananthapur, and M.Tech. Degree in Instrumentation and Control Systems, from JNTUK college of Engg Kakinada and Pursuing PhD from JNTUH, Hyderabad. V.Vijaya worked at APEL Radio Communication Systems, Hyderabad and presently, she is working as Associate Professor in the ECE Dept of Vaagdevi College of Engineering at Warangal. She has 10 years of Teaching Experience and 2 years of Industrial Experience. Attended 15 workshops/refresher courses/short term courses at various places. Member of Project Review Committee (UG/PG); CRC for (UG/PG).She is the project coordinator for UG/PG. Her area of interest are Image processing, Signal processing, VLSI, Mobile Communications, Wireless Communications. She is life member of ISTE, IETE.She is the member of IEEE. She has published no.of papers in national conferences and international conferences.

V.Rama obtained her B.Tech in Electronics & Communication Engg., from JNTU, Kakinada, and M.Tech. from NIT, Warangal. Pursuing PhD from NIT, Warangal She is working as Asst Professor in the ECE Dept., at NIT, Warangal. Staff adviser of ECE Dept., Incharge for basic Electronics Lab. She involved in extracurricular activites at institute. She has 12 years of Teaching Experience. She organized no. of UGC workshops in NITW. Her area of research is Bio Medical Signal Processing. Her areas of interest are Image processing, Signal processing, Tele medicine. She has published no. of papers in national and international conferences.

CH.Kranthi Rekha had received her B.E in Electronics and Communication Engineering from Madurai Kamaraj University in 2000 and Completed M.Tech from JNTUH, Hyderabad. Presently she is working as Lecturer in Linton university college, Mantin, Malaysia, She has more than 10 years of teaching experience. She is the Author of two Books (Digital communications and Digital Image processing). Organized student level technical symposium technocraft-'09. Attended 10 workshops/refresher courses/short term courses at various places. As a resource person to talk on Image processing. Member of Project Review Committee (UG/PG); CRC for (UG/PG). Her area of interest are Neural networks, Image processing, Signal processing, VLSI, Communications. She is life member of ISTE, IETE. She has published no. of papers in national conferences and international conferences.

C.B.RamaRao obtained his B.Tech in Electronics & Communication Engg., from JNTU, Kakinada, and M.Tech. from jNTU, Kagpur PhD from IIT, karagpur.He is working as Professor in the ECE Dept., at NIT, Warangal. Head of the ECE Dept.,. He involved in extracurricular activites at institute. He has 25 years of Teaching Experience. He organized no. of UGC workshops in NITW. His area of research is Bio Medicalsignalprocessing.

SIP Over Peer-to-Peer - Implications and Existing Approaches

Md. Safiqul Islam
School of Information and Communication Technology
Royal Institute of Technology
Stockholm, Sweden
islam3@kth.se

Rezaul Hoque
School of Information and Communication Technology
Royal Institute of Technology
Stockholm, Sweden
smrhoque@kth.se

Abstract- In contemporary communication system, Peer-to-Peer Session Initiation Protocol (P2PSIP) is the forthcoming migration from the traditional client-server based SIP system. Traditional centralized server based SIP system is vulnerable to several problems like performance bottleneck, single point of failure. So, integration of Peer-to-Peer system (P2P) with Session Initiation Protocol (SIP) will improve the performance of a conventional SIP system because a P2P system is highly scalable, robust, and fault tolerant because of its decentralized manner and self-organization of the network. However, P2PSIP architecture faces several challenges including trustworthiness of peers, resource lookup delay, Network Address Translation (NAT) traversal, etc. This paper focuses on understanding the needs of integration of P2P and SIP. It reviews the existing approaches to identify how they have integrated P2P and SIP and solved the challenges introduced by P2PSIP.

I. INTRODUCTION

The session initiation protocol (SIP) is a signaling protocol [1] standardized by IETF. It is also the default standard protocol for VoIP. The majority of the VoIP development is currently based on SIP. SIP is used to establish, modify, or tear down a multimedia session. Most VoIP systems rely on fixed set of SIP servers for which they suffer from performance bottlenecks, single point of failure, and Denial of Service (DoS) attacks. On the other hand, a Peer-to-Peer (P2P) system [2] is a popular technology which does not rely on central control and is very popular for resource sharing. As in a P2P system there is no centralized server, such a system has greater robustness, scalability and fault tolerance. If SIP can be made to work over P2P systems, it will improve the performance of traditional SIP systems and eliminate the problems of using centralized SIP servers. Integration of P2P technologies and SIP introduces several challenges such as resource lookup delays, node heterogeneity, NAT traversal, peers trustworthiness which has to be addressed before enjoying its advantages.

This paper describes the need to integrate P2P and SIP technologies and examines cost benefit of P2PSIP over the traditional fixed set of SIP servers. Further it discusses how P2P can be integrated with a traditional SIP system. We also examine some existing approaches to identify in achieving P2PSIP. The remainder of the paper is organized as follows. Section II gives an overview of traditional SIP systems and terminologies involved. P2P technology is demonstrated in section III. P2PSIP is introduced in section IV. In Section V, details out the current approaches for P2PSIP. Finally, Section VI takes an account of the conclusion.

II. SESSION INITIATION PROTOCOL (SIP)

SIP is an application-layer control protocol for initiating, terminating and modifying multimedia sessions (for example video, voice, instant messaging, online games and multimedia conferences). To establish a session, a traditional PSTN requires SS7 [3] signaling. In IP based telephony, the signaling protocol is SIP. However, Session Description Protocol (SDP) [4] and Real-Time Transport Protocol (RTP) [5] should be used together with SIP to provide complete IP telephony system.

Traditional SIP architecture uses client-server architecture. SIP servers are classified into proxy, registrar, and redirect servers [1]. A proxy server is an intermediate entity that can act as a server to accept a SIP request or act as a client to forward a SIP request. Redirect servers performs redirection of SIP request. A registrar server accepts Register request from clients and maintains location information in order to support mobility. SIP user agents are classified into user agent client (UAC) and user agent server (UAS). A user agent client [1] is a SIP entity that creates a new request. It uses client state machinery to send that request. A user agent server is also a SIP entity that receives SIP requests on behalf of users and responds to these requests.

Each user agent is identified by SIP uniform resource identifier (URI) for instance sip:username@somedomain.com. In order to initiate a session with another user, the caller first needs to know the SIP URI of that user. A caller can either send an INVITE request to a locally configured SIP server or directly send an INVITE to the IP address and port of the user's address. A user agent registers its location with the registrar server before initiating a session.

III. PEER-TO-PEER (P2P)

Peer-to-peer(P2P) technology, by definition, is a mesh network as opposed to a star network in a client/server model. In a peer-to-peer network, all nodes act simultaneously as client and server. Some of the advantages of P2P systems are:

- Scalability

- Robustness
- No single point of failure

There are two types of P2P systems [7], structured and unstructured. The structured networks impose techniques to tightly control the data placement and topology within the network, and currently only support search by identifier. On the other hand unstructured networks rely on flooding techniques. In many scenarios, the increased search efficiency makes structured networks preferable to the widely deployed unstructured networks. Most widely used structured P2P system is Distributed Hash Table (DHT). There are several flavors of DHT each with some advantages over another. It is very important to choose a proper DHT algorithm to have good performance of SIP running on P2P. Below is a table comparing the various features of different flavors of DHT algorithms:

Comparison among different DHT algorithms, adapted from [12] is show in Table 1.

TABLE I. Comparison of different DHT algorithm, adapted from [12]

	Chord	CAN	Pastry	Bamboo	Tapestry	Kademlia
Lookup Methods	Recursive Semi-Recursive Iterative	Recursive Semi-Recursive Iterative	Recursive Semi-Recursive Iterative	Recursive Semi-Recursive Iterative	Recursive Semi-Recursive Iterative	Iterative
Parallel Lookups	Not Suitable	No	Not suitable	Yes (on Iterative)	No	Yes
Complexity	Simple	Simple	Quite complex	Quite complex	Not complex	Simple
Bandwidth Consumption	Moderate	Moderate	High	Moderate	Quite high	Moderate
Node Join and Departure	Quite simple	Very simple	Complex join	Quite simple	Complex join	Simple

IV. PEER-TO-PEER SESSION INITIATION PROTOCOL (P2PSIP)

P2PSIP is the combination of a P2P network and SIP, where traditional fixed set of servers are replaced by a distributed mechanism. DHT can be used which is one of the possible distributed mechanisms available. All the address of record to contact URI mappings is distributed among the peers in the P2P overlay. Currently, the P2PSIP working group of the Internet Engineering Task Force (IETF) has defined the terminologies, concepts in [13] and use cases in [14]. Moreover, this working group is trying to standardize the P2PSIP peer protocol. P2PSIP can be implemented into two ways: one is SIP on top of P2P and the other implements P2P over SIP. SIP on top of P2P uses P2P protocol to implement SIP location service; while the other approach uses SIP messages to transport P2P traffic. Traditional a P2P node searching mechanism uses flooding mechanism to locate the node. However, to find a target node using P2PSIP for multimedia session, flooding mechanism should be avoided.

V. PINPOINTING CHALLENGES FOR P2PSIP

In the following section, we will discuss some common requirements to implement P2PSIP. In an IETF draft, Bryan, et al. defines a set of requirements for P2PSIP [15]. We have taken some important point from this paper.

First, P2PSIP peers should be capable of performing operations such as joining, leaving, storing information on behalf of the overlay, or transporting messages. Secondly, the peers must provide the functions offered by traditional SIP network. For example, P2PSIP should support the modification, establishment, and termination of multimedia sessions. Thirdly, the implementation should not prevent the use of existing protocols like SSL or TLS as used in the P2P or SIP network. NAT and firewall traversal should also be supported for P2PSIP. Finally, the functionality of the fixed set of centralized SIP servers should be distributed over the peers. Some of the other challenges are described in the following sections.

A. Resource Lookup Delay

Locating a peer or resources in P2PSIP networks takes much more time than the traditional SIP based network. Trying

to reduce this delay is significant challenge for P2PSIP.

B. Network Address Table (NAT) Traversal

Most of the P2P nodes may be behind a NAT or Firewall. There must be some relay in between them with a public IP address in order to establish communication with other peer. This is one of the most important challenges for P2PSIP network.

C. Node Heterogeneity

In order to maintain the scalability and service availability of P2PSIP, node heterogeneity should be handled appropriately. Node heterogeneity can be difference in bandwidth, CPU, storage, and uptime of the peer.

D. Security Issues and Trustworthiness of peers

Security of a distributed P2P communication system is another of the major challenges. Security issues concern user identification, authentication and trustworthiness.

VI. EXISTING APPROACHES

So far we have presented several challenges that must be faced while integrating P2P networks with SIP. As P2P has several advantages that will improve the performance of conventional SIP system, but there are several requirements that should be met also. We described those requirements in section V. In this chapter, we are going to analyze some existing approaches for P2PSIP.

A. *Hybrid Architecture of P2PSIP based InternetTelephony*

Singh and Schulzrinne proposes a hybrid architecture for the integration of P2P and SIP that introduces two additional advantages: interoperability with existing SIP servers and no maintenance cost besides P2P scalability and reliability [16]. Chord was used as an underlying DHT algorithm. Figure 1 shows the architecture proposed, based upon the user of super nodes and ordinary nodes. Figure 2 is the block diagram of a P2P node. Super nodes are powerful nodes having high bandwidth, lots of CPU power, and plenty of memory, long uptimes and public IP address. Super nodes will implement a DHT and ordinary nodes will be attached to one of its nearest super nodes. These authors have implemented a P2PSIP adaptor [17] which allows existing or new user agents to connect to the P2PSIP network without modifying the UA. They made their architecture open so that any new modules can be added or the underlying DHT algorithm can be replaced without affecting the existing architecture.

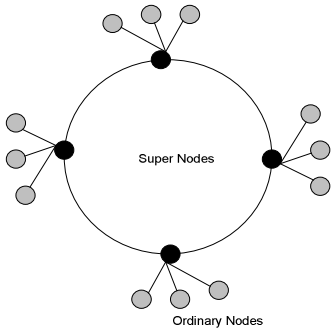


Fig. 1. P2PSIP architecture. Adapted from [16]

On startup, nodes sign in with the identifier and discover module detects whether the node is under NAT or firewall and also deals with SIP registration and peer discovery. User interfaces module keeps the buddy list and using user location module it detects the user's location. User location can be retrieved by SIP module or by the DHT module (Chord finger table). The most promising feature of this architecture is, if a super node fails or shut down, then all the registrations will be transferred to the another super node. Multicast registration is used to discover a multicast peer group. In order to find a super node in this architecture, ordinary nodes will use multicast addresses or use preconfigured super node addresses from their cache. SIP message routing is based on the Chord algorithm.

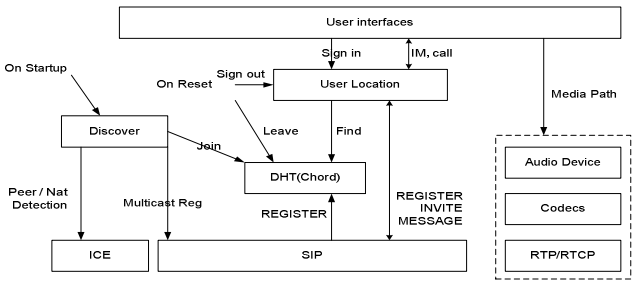


Fig. 2. A P2PSIP node block diagram. Adapted from [16]

This architecture introduces several advantages which are as follows:

- Use of a hybrid architecture that allows interconnection of tradition SIP networks with P2PSIP networks.
- Implementation of P2PSIP adaptor.
- NAT/Firewall detection based on the ICE [18] algorithm, then using a super node as a relay to help ordinary nodes to establish calls and participate in calls.
- Node heterogeneity is identified by the super nodes and ordinary nodes.
- Offline messaging services by combining the storage of sender and intermediate DHT nodes [19].
- Additional services like conference call,directory services and many more.

While analyzing the paper we have found the following limitation of their architecture:

- Their architecture fails to reduce call setup delay; which is higher than the traditional SIP networks.
- Peer trustworthiness and security issues are not described in their report.
- The paper does not propose any super node selection mechanism. Node heterogeneity is introduced, but they do not describe what will happen if a more powerful node than the current super node joins the existing network.
- Ordinary nodes always have to pay a high maintenance cost to maintain their Chord finger table and periodically send refresh messages to update their predecessors and successors.

B. *SOSIMPLE*

SOSIMPLE is a P2PSIP architecture where nodes are organized using the Chord DHT algorithm. SIP messages with a newly defined header are used to maintain the DHT, register users, locate resources and establish sessions. Based on the registration process, the SOSIMPLE architecture has two levels of REGISTER operations. One is user registration which is the traditional use of registration and another is node registration which is for DHT operation.

A joining node in the overlay will first locate the bootstrap node responsible for its region. If the bootstrap node is not responsible for that region, then it will respond with the necessary information for the joining node to find a suitable bootstrap node. To find a target node, a node hashes the username to produce a Resource-ID. Next, the node will check its finger table to locate the Node-ID nearest to this Resource-ID. Using the Chord algorithm, a search for the user will eventually find the target node.

The SOSIMPLE paper mentions several security and user authentication mechanisms such as user certificate, email verification, etc. that can be implemented on their architecture. However, this paper fails to describe the following:

- Node heterogeneity
- Bootstrap node selection
- Node maintenance cost for DHT operation.
- Resources look up delay.

C. Hierarchical and Breathing Overlay based P2PSIP

In order to alleviate the problems in [16] and [20], such as call setup delay, node heterogeneity, and high maintenance cost paid by the ordinary nodes, Le and Kuo [21] propose a hierarchical and breathing overlay based network. In a hierarchical overlay nodes forms different sub-overlays based on node heterogeneity. In a breathing overlay, the three states of a node are based on the up time or idle time which eliminates ordinary node maintenance costs. Besides this, they also introduced a node virtualization model which allows lower hierarchy nodes to share their capabilities with upper hierarchy nodes. The paper introduces several good features which are as follows:

- Session setup delay is reduced by introducing two types of lookups based on knowledge of the destination sub overlay: oriented lookup and un-oriented lookup. In oriented lookup, a node relays its request to its father node to establish the session. In the case of un-oriented lookup, a father node will receive the request from a son node and this (and if necessary other) upper level father node will do a DHT lookup in their sub over-lays.
- Node heterogeneity is introduced due to forming a hierarchical overlay.
- Lower DHT maintenance cost.
- Efficient offline message storage system using node virtualization.

The paper failed to address peer trustworthiness and other security issues. The following subsections will describe their three techniques briefly.

i. Hierarchical Overlay

Based on node heterogeneity, nodes form a hierarchical overlay. The top sub overlay consists of most powerful nodes. If any new node arrives it will first join the lower sub overlay and then it will share its capabilities with its upper sub overlay. Having greater capabilities will shift the node to the upper sub overlay. Le and Kuo introduce the concept of father node and son node. Figure 3 shows a three layer hierarchical overlay where N5 is the father node for N3 and a two step father node for N1 and N2.

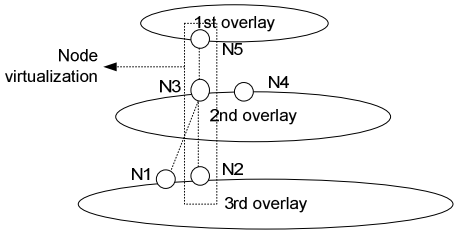


Fig. 3. Hierarchical overlay concept. Adapted from [21]

ii. Node Virtualization Model

By node virtualization model, a node will share their physical capabilities with its father nodes. Figure 4 shows how N2 forms a node virtualization model with N3 and N5. Two processes of Node virtualization were introduced in this system: one is collaborative processing and the other is storage sharing. By using the first method, a node can locate other node by sending a request to its upper father node. With the help of storage sharing a son node can share its resources with its upper nodes.

iii. Breathing Overlay

The breathing overlay proposed by Le and Kuo eliminates the high cost of maintaining the DHT when a node is idle. Three states of a node are defined in this paper: active, tired, and sleep. When the node is idle for some time it goes into the tired state. Before going from the tired state to sleeping state, the node will send a sleep indication to its upper node and send an address key-value pair to its successor.

D. Layered Architecture for P2PSIP

Dhara, et al. [22] propose a layered architecture that separates the P2P related issues from the underlying voice or transport layer. The advantage of this system is that it allows dynamic changes of overlays based on the requirements and properties of users and devices. There are three layers in this architecture: Feature Overlays, User Overlays, and Device Overlays.

Device overlays deal with the properties such as NAT and firewall traversal, connectivity, bandwidth, and based on the properties of the device organizes the nodes into P2P structures. The Feature overlays deals with advanced user communication features, such as voice conferencing, group features, etc. At last, a user overlay deals with the user identities and authentication information. Their paper describes a very good mechanism for the user trust overlay and user identity overlay.

The user trust overlay deals with trust management between the peers. A login server (LS) is introduced here which will issue a certificate to the joining node. When a peer wants to join a P2P network, it will send a SIP REGISTER message along with its public key, and then the login server will authenticate the node and provide it with a signed certificate. It will help the node to provide this certificate to the bootstrap node to join and build trust.

On the other hand the user identity overlay deals with distributing of user identity information in the network. While the peer sends its certificate to the bootstrap node to register itself in the network, the bootstrap node will verify the signature and identify whether the node will be its neighbor or not. If the node will be its neighbor, then it will update its finger table; otherwise it will send the necessary contact information.

Their paper focuses on a layered architecture that allows the choice of P2P overlay based on specific parameters. The architecture is a Public Key Infrastructure PKI [23] based trust management system where SIP is the transport protocol and chord is DHT algorithm for a P2P structure.

However, their paper fails to discuss to following issues:

- They have mentioned that the device overlay will focus on NAT and firewall traversal, but no such implementation or methods were introduced.
- DHT maintenance cost on an ordinary node.
- Bootstrap node selection.

E. Scalable Application-Layer Mobility Protocol

Besides the above approach, Scalable Application-Layer Mobility Protocol (SAMP) [24] deals with the session setup latency by introducing two optimization techniques: Hierarchical Registration (HR) and Two-Tier Caching (TTC). In this architecture, all SIP servers form a P2P overlay which increases the scalability, robustness, and load balancing capability in communications system. Each mobile node performs a local registration and location is tracked via SIP messages. In HR, when the mobile node (MN) is in a foreign domain it will register it's Care of Address with an anchor sip server instead of home SIP server, this is to reduce session setup delay. On the other hand, TTC introduces two phase cache lookup where the first cache lookup is based on the MN's cache and the second phase lookup is based on anchor SIP server's cache. If the target is not found in either cache then a traditional P2P lookup occurs.

F. Hierarchical P2PSIP

Hierarchical P2PSIP [25] is introduced to address the connectivity problem of heterogeneous P2P overlays and the overhead problem of extra SIP messages overhead when SIP is used to maintain the overlays. Shi, et al. introduce the concepts of a Higher Layer Overlay (HiLO) and a Lower Layer Overlay (LoLO). The HiLO interconnects the various LoLOs and HiLO peers are elected based upon the LoLO peer's capability. In previous sections, all the P2PSIP integrations were based on P2P-over-SIP which has extra SIP message overhead. Shi, et al. introduce SIP-using-P2P within each LoLO and P2P over SIP in inter-HILO peers. Peers within a LoLO speak the P2P protocol for DHT operation. While HiLO and LoLO peers speak using the SIP protocol. The architecture uses Bamboo as the underlying DHT algorithm for inter domain overlays; while LoLO can utilize any algorithm. Figure 4 illustrates the concept of H-P2PSIP network where HiLO peers establish communication between different P2P overlays running different DHT algorithm, thus solving connectivity problems.

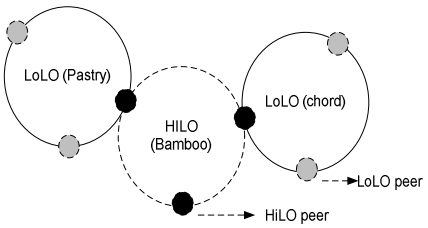


Fig. 4. H-P2PSIP architecture. Adapted from [25]

G. Other Existing Approaches

The main approaches for the integrating P2P and SIP have been described above. However, another approach to P2PSIP is described in [26]. This approach deals with the manageability of a P2P system. In this approach, the system architecture is divided into three layers: the signal control layer, the management layer, and the media transportation layer. In this architecture signaling is used to initiate the system, maintain the system topology, and for resource searching. The management layer deals with grouping, playing, and media uploading management. Inter-domain registers, resource locating and DHT creation and maintenance are the functions of the SIP signal control layer. Media transport layer deals with the storage management and media uploading. In Cooperative SIP (CoSIP) [27], both the server based and P2PSIP networking work together.

VII. CONCLUSION

This paper gave an overview of SIP and P2P and examines the integration of a P2P system with SIP. Moreover, it describes some advantages of their integration as well as challenges and implications were also discussed. Several current approaches to P2PSIP were discussed along with their approaches to mitigating the challenges of P2PSIP.

REFERENCES

[1] J. Rosenberg, H. Schulzrinne, G. Camarillo, A. Johnston, J. Peterson, R. Sparks, M. Handley, and E. Schooler. SIP: Session Initiation Protocol, RFC 3261, Internet Engineering Task Force, 2002.

[2] D.S. Milojicic, V. Kalogeraki, R. Lukose, K. Nagaraja, J. Pruyne, B. Richard, S. Rollins, and Z. Xu. Peer-to-Peer Computing. HP Laboratories Palo Alto, 2002.

[3] Performance Technologies, Inc. SS7 Tutorial, 2006. Available at: http://www.pt.com/tutorials/ss7/, Last Visited April 2008.

[4] M. Handley, V. Jacobson. SDP: Session Description Protocol RFC 2327, Internet Engineering Task Force,April 1998. Available at: http://www.ietf.org/rfc/rfc2327.txt

[5] H. Schulzrinne, S. Casner, R. Frederick, V. Jacobson. RTP: A Transport Protocol for Real-Time Applications RFC 1889, Internet Engineering Task Force, January 1996. Available at: http://www.ietf.org/rfc/rfc1889.txt

[6] H. Schulzrinne,A. Rao, R. Lanphier. RSTP: Real time streaming protocol RFC 2326, Internet Engineering Task Force, April 1998. Available at: http://www.ietf.org/rfc/rfc2326.txt

[7] D. Bryan, B. Lowekamp. Decentralizing SIP. ACM Portal, Vol.5, Issue 2, pages: 34-41, March 2007

[8] I. Stoica, R. Morris, D. Liben-Nowell, D.R. Karger, M.F. Kaashoek, F. Dabek, and H. Balakrishnan. Chord: A Scalable Peer-to-Peer Lookup Protocol for Internet Applications. IEEE/ACM Transactions on Networking, page 17, 2003.

[9] S. Rhea, D. Geels, T. Roscoe, and J. Kubiatowicz Kubiatowicz. Handling Churn in a DHT. In Proc. of USENIX Annual Technical Conference, 2004.

[10] A. Rowstron and P. Druschel. Pastry: Scalable, Distributed Object Location and Routing for Large-Scale Peer-to-Peer Systems. In IFIP/ACM International Conference on Distributed Systems Platforms, 2001.

[11] B.Y. Zhao, L. Huang, J. Stribling, S.C. Rhea, A.D. Joseph, and J.D. Kubiatowicz. Tapestry: A Resilient Global-scale Overlay for Service Deployment. Selected Areas in Communications, IEEE Journal on, 2004.

[12] J. Hautakorpi, G. Camarillo. Evaluation of DHTs from the viewpoint of interpersonal communications. ACM International Conference Proceeding Series; Vol. 284, Proceedings of the 6th international conference on Mobile and ubiquitous multimedia, pages 74-83, 2007

[13] D. Bryan, P. Matthews, E. Shim, and D. Willis. Concepts and Terminology for Peer to Peer SIP. draft-ietf-p2psip-concepts-01 (work in progress), Nov. 2007. Expires: May 18, 2008.

[14] D. Bryan, E. Shim, and B. Lowekamp. Use Cases for Peer-to-Peer Session Initiation Protocol (P2P SIP), draft-bryan-p2psip-usecases-00.txt , July 2007. Expires: January 3, 2008

[15] D. Bryan, S. Baset, M. Matuszewski, and H. Sinnreich. P2PSIP Protocol Framework and Requirements. draft-bryan-p2psip-requirements-00.txt , June 2007. Expires: Jan 2008.

[16] K. Singh and H. Schulzrinne. Peer-to-peer Internet Telephony Using SIP. In NOSSDAV '05: Proceedings of the international workshop on

Network and operating systems support for digital audio and video, pages 63-68. ACM Press, June 2005.
[17] K. Singh and H. Schulzrinne. SIPpeer: a session initiation protocol (SIP)-based peer-to-peer Internet telephony client adaptor. White paper, Computer Science Department, Columbia University, New York, NY, Jan 2005. http://www.cs.columbia.edu/ ~kns10/publication/sip-p2pdesign. pdf.
[18] J. Rosenberg. Interactive Connectivity Establishment (ICE): A Methodology for Network Address Translator (NAT) Traversal for Offer/Answer Protocols, draft-ietf-mmusic-ice-08. 2006.
[19] K. Singh and H. Schulzrinne. Peer-to-peer Internet telephony using SIP. Technical Report CUCS-044-04, Department of Computer Science, Columbia University, New York, NY, Oct. 2004.
[20] D. A. Bryan, B. B. Lowekamp, and C. Jennings. SOSIMPLE: A Serverless, Standards-based, P2P SIP Communication System. In Proceedings of the 2005 International Workshop on Advanced Architectures and Algorithms for Internet Delivery and Applications (AAA-IDEA 2005), June 2005.
[21] L. Le, G. Kuo. Hierarchical and Breathing Peer-to-Peer SIP System. Communications, 2007. ICC '07. IEEE International Conference. Pages:1887 – 1892, June 2007.
[22] K.K.Dhara, V. Krishnaswamy, S. Baset. Dynamic peer-to-peer overlays for voice systems. Pervasive Computing and Communications Workshops, 2006. PerCom Workshops 2006. Fourth Annual IEEE International Conference, March 2006.
[23] Public Key Infrastructure(PKI) tutorial. available at: http://www.cs.gmu.edu/~hfoxwell/EC511/pki.pdf. Last Visited- April 2008.
[24] S. Pack, K. Park, T. Kwon, Y. Choi. SAMP: scalable application-layer mobility protocol. IEEE Communications Magazine, Vol. 44, Issue 6,Page(s):86 – 92. JUNE 2006.
[25] J. Shi; Y. Wang; L. Gu; L. Li; W. Lin; Y. Li; Y. Ji; P. Zhang. A Hierarchical Peer-to-Peer SIP System for Heterogeneous Overlays Interworking. IEEE Global Telecommunications Conference. Page(s):93 –97, November 2007.
[26] H. Jie, H. Yongfeng, L. Xing. MSPnet: Manageable SIP P2P media distribution system. Journal of electronics(China). Volume 24, November, 2007
[27] A. Fessi, H. Niedermayer, H. Kinkelin, G. Carle. A Cooperative SIP Infrastructure for Highly Reliable Telecommunication Services. IPTCOMM, Proceedings of the 1st international conference on Principles, systems and applications of IP telecommunications, July 2007.

Traffic Sign Recognition Model on Mobile Device

Wong Hwee Ling[1, 2], Woo Chaw Seng[2]
[1]Faculty of Engineering, Multimedia University,
Persiaran Multimedia, 63100 Cyberjaya, Malaysia.
Phone: 603-831205419, Email: hlwong@mmu.edu.my
[2]Faculty of Computer Science and Information Technology, University of Malaya,
50603 Kuala Lumpur, Malaysia.
Phone: 603-79676400, Email: cswoo@um.edu.my

***Abstract*- Incorporation of a good machine vision into mobile device can create a powerful application. With such advancement, mobile users can use their existing smartphone as their *third-eye* to perceive the world. This paper introduces a framework using the smartphone to increase ambient intelligence and road safety of moving vehicles through traffic sign alert application. The driver is alerted of the incoming traffic signs in different modes depending on the user's preference. However, the competency of the application is still bounded with the capability of a normal human vision. Unlike conventional research work, this paper emphasizes on portability and expandability. Portability means there is no additional installation or placement of electronic hardware required in the vehicle in order to make the system work. Expandability focuses on the transparency of the traffic sign recognition output to other applications within same hardware device or external devices. This provides an option to other developers to use or expand their own applications by using the result of the proposed application. An interaction model of the traffic sign recognition system on mobile device is introduced.**

***Keywords*- traffic sign recognition, mobile platform, interaction model**

I. INTRODUCTION

Road safety is important for drivers and the passengers inside the vehicle. The driver usually relies on his/her vision to comprehend the visual inputs while driving. The visual inputs can be the weather condition, road condition, road signs, billboards, landmarks, presence of other automobiles and pedestrians. It is difficult for the driver to pay attention in a monotonous journey. The driver's attention span can also be affected by poor health physically or emotionally. Hence, there is a motivation to use machine to increase road safety via driver alert system. Machines can utilize information from proximity sensors, global positioning system (GPS) or/and camera to interpret the condition outside the vehicle. The problem of the current in-vehicle driver assistant unit is the requirement to purchase an additional electronic unit or software license. This usually comes with certain cost for the purchase and maintenance.

The objective is to propose a vision system based traffic signs warning application that can be downloaded and used in a smartphone without installation of any additional electronics hardware. Subsequently, this offers a lower cost to use the application as the users can use an existing but compatible smartphone. The application needs to be downloaded into that smartphone and then be installed. In order to utilize the application, the phone needs to be placed on the windscreen where the camera faces the road. Eventually, the maintenance cost tends to be lower, as a user only needs to maintain one smartphone instead of extra electronic devices. The cost friendly solution facilitates the second motivation, which is to enable the technology to benefit more users. The third objective is to make the result of the traffic sign recognition transparent to other applications or devices. An example of a third party application is an autonomous vehicle that is required to navigate on the road. The third party applicant can use the result to enhance their own application or system, without having to develop their own traffic sign recognition algorithm. Fig. 1 portrays few main functions performed on the smartphone for traffic sign recognition and the access to the recognition result by one or more users.

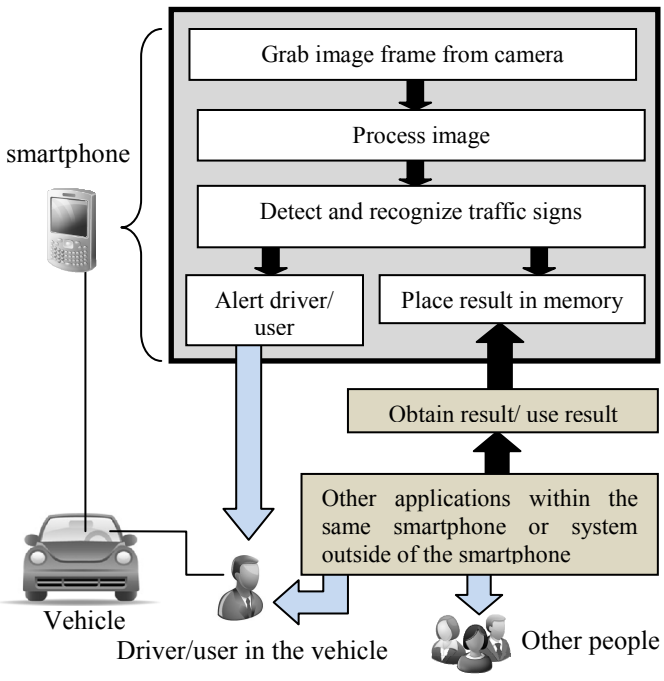


Fig. 1. Traffic sign recognition on smartphone

The difficulty faced in vision-based mobile application lies within both hardware and software. Smartphone application developers process image either fully on the phone itself or partially on the server side, where the phone is the client. For the later, a wireless connection is required. Most smartphones are equipped with camera with at least two mega-pixels. The processing power of smartphones is advancing. Memory capacity can be extended and the internal memory size is growing too. Hence, smartphone is a suitable candidate to be explored for the vision-based traffic signs warning application without requiring additional electronics hardware. The challenge is machine vision interpretation tends to consume high processing power and large memory space. Those features usually lack in smartphones, even today. Improvement in vision algorithm will be used to overcome the problem.

In this paper, background study is presented in section II to recapitulate the topics involved and to emphasize the importance of vision based traffic sign recognition framework. Later, framework of the application is described in section III together with a preliminary result of traffic sign recognition based on image processing. Last but not least, conclusion for the paper and the future work is shared in section IV.

II. BACKGROUND STUDY

The background study comprises of four main areas, which are traffic sign recognition, overview of mobile computing, vision application on mobile device and a quick review on in-vehicle infotainment trend. Traffic signs can be recognized through vision or through wireless identification. Traffic sign is erected by human and subjected to changes. Thus, it is difficult to keep track the exact location in order to enable its visibility on a GPS later. Traffic sign cannot be recognized by a very good resolution satellite image because the traffic signs are erected facing the horizon but not towards the sky. A wireless identification of traffic was proposed by sensing a transmitter placed on the traffic signs [1]. The disadvantage of the method is the need to have an access point facing the incoming vehicle for each traffic sign. The authors reported it is difficult to identify traffic signs which are relevant to the driver. Additional hardware required for that method may not be practical in near future. Vision based recognition is more practical than wireless identification method.

A. Traffic signs Recognition

Traffic sign recognition usually starts with detection, rectification and then recognition. Tracking method can also be employed to speed up recognition as a smaller area of detected object can be targeted for recognition. Research on traffic sign recognition has started since 1984 in Japan [2]. It is an important and widely researched topic in machine vision for road safety and autonomous ground vehicle. Several challenges of vision based traffic signs recognition are listed below:

1. Different road signs (e.g. shape, color, standardization)
2. Lighting variation (e.g. day, night)
3. Weather (e.g. rain, snow, dust, mist, reflection)
4. Location to deploy application (e.g. urban, rural area)
5. Background (e.g. presence of building, static/moving vehicle, road, signboard, trees)
6. Affine transformation of the road sign (e.g. scaling, rotation, shearing)
7. Occlusion of the road sign
8. Deformation of the road sign due to vandalism or weather
9. Difference in the hardware devices
10. Different placement or positioning of the camera
11. Different speed of the moving vehicle

Nguwi *et al.* [3] performed a study on road sign recognition methods. In other to perform road sign recognition, the road sign needs to be detected first. Color-based and shape-based methods are used due to distinction of the road signs based on colors and shapes. Examples of color based methods are static threshold, dynamic threshold and color indexing in various color spaces. Tsai *et al.* [4] proposed a novel Eigen color model for road sign detection based on the reflectance property that exist on the signage compared to the natural background. Comparison of separation ability between proposed method and various color spaces such as RGB, YIQ, LUV and L*a*b were performed. Fisher criterion was used to measure the separation ability and the result indicates that their proposed color model has higher separation ability. In contrast, shape based approach does not require color information. Thus, grayscale images are often used in this approach. Shape based method can be more robust during illumination invariance compared to color based method. However, shape based method tends to be difficult in situation where there is occlusion or affine transformation of the road signs viewed. Examples of shape based approaches are Hough transform, template matching and etc. Combination of both color and shape features are often utilized in detection process. Other more sophisticated methods that were used along with color and shape information for more robustness are support vector machines (SVM) [5], neural network and genetic algorithm.

Once the road sign is detected, the road sign needs to be recognized. Feature extraction needs to be performed to differentiate various road signs. Then, the feature will be compared with a standard representation of the specific road sign. The comparative value will determine whether the road sign is classified into the correct category. Examples of methods used for classification are template matching [6], Gaussian-kernel SVMs, character recognition for speed limit sign [7] and other hybrid classification techniques [8]. Saturnino *et al.* performed road sign detection and recognition based on SVM. The mean processing speed is 1.77s per frame and the best recognition success probability reported was 93.24%. Soigkas and Dermatas [6] reported an improvement of detection and recognition rate from below 45% to 81.2%, by employing tracking method. Fatmehsan *et al.* [8] obtained 93.1% accuracy using a hybrid one-vs.-rest SVM and naïve bayes classifier for detection and recognition of red color based road signs. The algorithms reported were mostly tested on generic computer and written in C/C++. It is also difficult to compare the actual performance as there is neither a standardized dataset nor a standardize procedure for evaluating the performance in terms of speed and accuracy.

B. Overview of Mobile Computing

A computer or controller that is portable is termed as a mobile hardware platform. Notebook, netbook, mobile phones or any other portable embedded systems are considered as a mobile platform. Hence, there could be millions of existing mobile platforms today. A mobile hardware platform has the capability to acquire data, process data and provide outputs. It has its own processor, memory, input-output devices and power supply to support portability.

Mobility of such platforms supports ubiquitous computing. Ubiquitous computing emerged as a post-desktop revolution with the advancement and miniaturization of technology. Mobile hardware interconnects with the sub-devices within the platform and connects with other devices using wired or wireless connectivity. The inter-connections and outer-connections are invisible to at the eyes of end user. Thus, mobile hardware platform has the ability to satisfy "*at anywhere, anytime*" utilization and "*disappearing computer*" concept of ubiquitous computing. The ambient intelligence paradigm builds upon ubiquitous computing. Ambient intelligence is accomplished through an electronic device that has reactive behavior to give the appropriate response to the human user in a specific environment. Mobile hardware platform is able assist in delivering ambient intelligence into dynamic environment, such as moving vehicles.

C. Vision Applications on Mobile Devices

Several vision-based mobile phone applications have been developed. The applications are a part of Augmented Reality (AR), where the real-world images or video are interpolated with computer generated graphics. Examples of vision based applications are landmark detection via Content Based Image Retrieval (CBIR) [9, 10], pose tracking of natural feature [11], face and eye detection [12]. In contrast with computer based vision approach, many of the AR approaches today rely mostly on the global positioning system (GPS) and sensors such as the accelerometer. According to Gammeter *et al.* [9], AR relaying on visual recognition tends to have more advantage on both stationary and non-stationary objects. Image processing on smartphone application can be conducted on the client and/or the server. The client is the phone, while the server is a super computer connected to the phone wirelessly. Most applications perform more complex image processing on the server, as the processing can be faster and huge database can be stored at the server side. Those applications require a persistent wireless connectivity, which may pose as a problem in some rural areas. On a single device processing, the challenge lies when the image processing algorithm gets complex that it takes up larger memory space and reduces the speed of recognition. The hardware limitation issue can be tackled either through software and/or hardware [13].

D. In-Vehicle Infotainment System

Few car manufacturers have turned to mobile application developers to built in-vehicle infotainment system. Ford introduces MyFord Touch which comprises of features such as media hub, phone, voice recognition, navigation, climate control, audio system, driver's personalization and other services [14]. MyFord Touch is a dedicated piece of electronics hardware embedded in certain models of Ford vehicles but with no capability for traffic sign recognition. Daimler has introduced Smart Drive Kit that works together with an iPhone to provide several in-vehicle infotainment functions for Smart car. In future, the designer intends to connect a camera to the Smart Drive Kit via wireless local area network (WLAN) to enable future applications such as traffic speed limit recognition [15]. Their proposed method requires three electronics devices which are the camera, a Smart Drive Kit and an iPhone. BMW was also spotted to seek Daimler for the vehicle infotainment solution as well. Other in-vehicle infotainment systems are Nokia's Terminal Mode [16] and Intel Atom chipset based in-vehicle infotainment system [17].

Several cars manufacturers have adopted Advance Driver Assisting System (ADAS), which includes traffic signs recognition. For instance in year 2008, Mobileye partnered with Continental AG launched three features in BMW 7 series, namely the lane departure warning, speed limit information based on traffic sign detection and intelligent headlight control [18]. Image processing is performed on a dedicated multi-core processor, namely the Mobileye EyeQ [19]. Mobileye uses both image and GPS mapping information to detect speed limit signs [20]. In contrast, Opel Eye on several models of Opel cars relies solely on image processing for traffic sign recognition. Opel Eye comprises of a set of dedicated hardware integrate into the car. The recognition capability is limited by speed and poor weather conditions [21].

From the commercialized or ongoing activities surrounding in-vehicle infotainment system, the companies emphasize on both software and hardware approach to enable their system. Most solutions are dedicated towards certain car models. We viewed a mobile application development problem at a different angle, as a software solution will be emphasized while the existing hardware resource is used. In addition, traffic sign recognition solely based on image processing method processed on the phone itself is unavailable.

III. FRAMEWORK

The traffic sign alert application is proposed to operate under different kinds of behavior in order to adapt to the needs of the user. The system is dependent upon machine vision as the sole engine for recognition. The behaviors are generalized below:

1. Warning mode: The driver is alerted for warning signs. Warning signs at a further distance can be recognized.
2. Long distance driving mode in rural area: The driver is alerted for incoming traffic signs.
3. Tracking mode: The traffic sign is continuously tracked.

The Maddix Human-Computer Interaction (HCI) model is used to initiate the framework for the mobile traffic sign alert system. Maddix HCI model consists of physical, syntactic and semantic level [22]. A HCI modeling intends to describe the interaction between human and computer which includes the software and hardware levels of the computer itself. In Maddix HCI model, the physical level involves the physical contact between the human and the computer to exchange information.

The human commands the computer of a task at the semantic level. The structural information is translated into meaningful information by the computer at the syntactic level. Maddix HCI model has been employed in Human-Robot Interaction (HRI) as well [23]. A model is proposed in this paper to elucidate the components involved and to exhibit the affiliation between the user and the smartphone. Fig. 2 summarizes the model for traffic sign alert system. The following subsections provide explanation in more details of each component within the model and their interaction.

A. Physical Level

The physical level consists of the physical component that resides in the mobile device itself such as the input, output and memory. The application requires at least a touch screen or a keypad input, in order for the user to initiate or change command. The screen acts as the main output interface. It is capable of displaying a graphical user interface (GUI) for behavior selection. Besides that, the result of the traffic sign recognition can be displayed as AR on the screen. The user should also have an option to run the application in background mode. This means that the application can run using sound alert instead of graphical AR. The memory is where the database of a standardize traffic sign are stored and can be updated from time to time. The database does not consist of images but rather a feature set that have reduced dimensionality to represent each traffic sign. Other important components are the processor and the camera. Most smartphones today should have sufficient physical components to perform simple image processing.

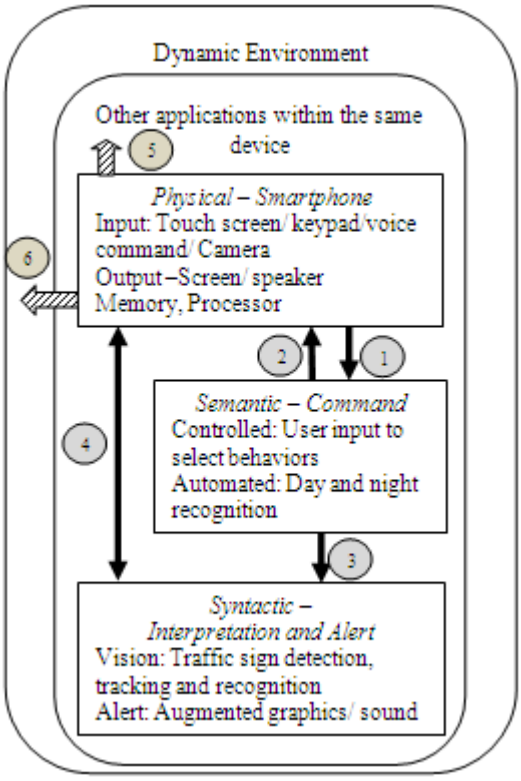


Fig. 2. A model for the traffic sign alert framework

B. Semantic Level

Semantic level consists of the input commands by the user. Upon starting the application, a simple GUI appears to prompt user on some information and options available. It is important to take note not to burden the user with too much information or options. Complexity of a GUI tends to make a user bored or impatient. Upon a mode selection, the application immediately detects day and night via the clock of the mobile device. Additional information such as the geographical location of the mobile device might be helpful to estimating the brightness of the environment. Identification of day and night is helpful for the image processing algorithm to adjust the recognition in dark and bright environment. Image processing methods can also be used to verify the brightness of the environment.

C. Syntactic Level

The syntactic level encompasses translation of the visual information into recognition of traffic signs for alert. The camera views the environment as video form. Hence, frame by frame of image must be grabbed to perform image processing. The image is processed to detect then recognize signs. Color and shape based features will be incorporated for the detection. Once detected, the region of interest will be segmented for recognition. The prominent feature of the region of interest will be computed. Then, a comparison will be made with the database of a standard feature set residing in the memory. Tracking method may be employed to increase the speed of detection and recognition at later stage. Upon recognition of the traffic sign, the user will be alerted through display or sound.

Fig. 3 portrays a preliminary methodology of a "no turning left" traffic sign recognition based on various low level image processing steps using color thresholding, shape indexing, edge detection and binary image template matching. Color and shape information are used to discard irrelevant information. Template matching is based on binary edge information. Similarity value between test image and template image is computed based on the equations (1) and (2):

$$Recognition = \begin{cases} True, & \text{if } Matching\ index > 0.3 \\ False, & \text{if } Matching\ index \leq 0.3 \end{cases} \quad (1)$$

where,

$$Matching\ index = \frac{No.\ of\ overlapping\ pixels}{No.\ of\ white\ pixels\ in\ edge\ object} \quad (2)$$

The size of edge object must be normalized to match the size of template object before matching proceeds. The *Matching index* value for test image in Fig. 3 compared with a standard template for "no turning left" sign is 0.37. In contrast, the *Matching index* value for the same test image compared with a standard template for "no turning right" sign is 0.16. Via the *Matching Index* value, the recognition of the actual "no turning left" sign from the test image can be discriminated. However, the image processing algorithm needs to be refined further before implementation on the smartphone to improve its robustness against changes in a dynamic environment.

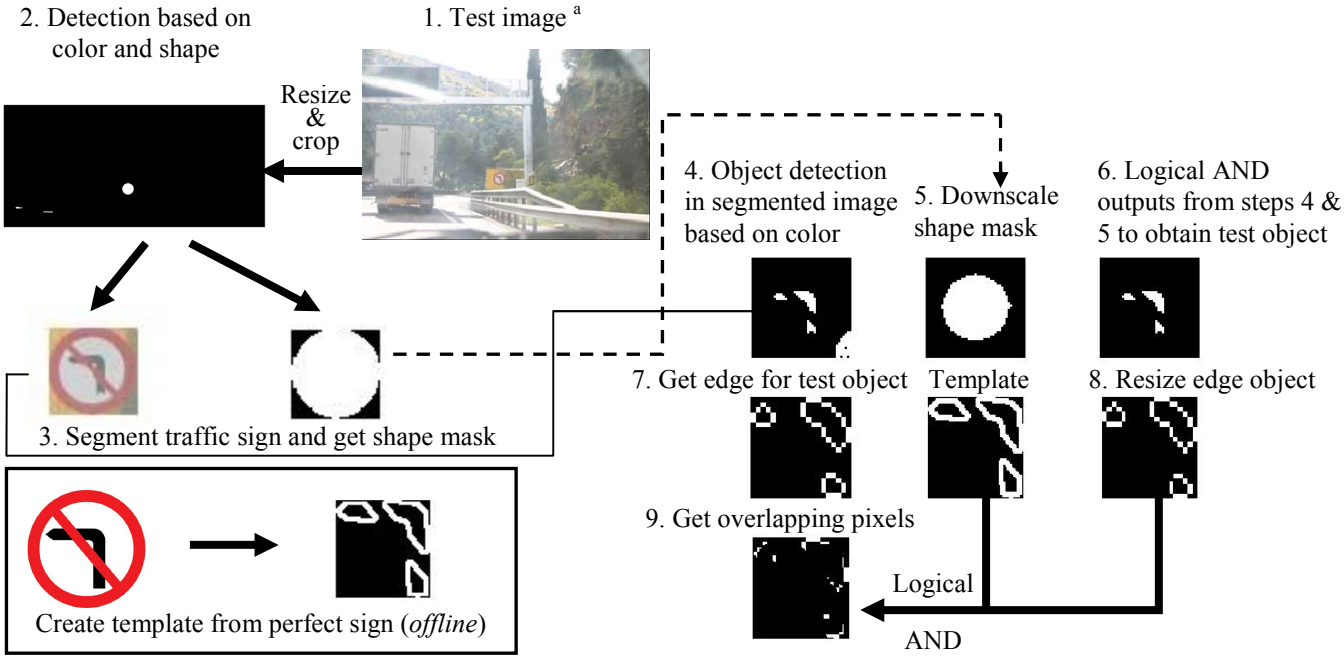


Fig. 3. Low level image processing for traffic sign detection and recognition

D. *Interaction*

Inter-connectivity of each component of the traffic sign alert model is illustrated in Fig. 2. Outer-connectivity of the application to the other applications on the mobile device and the environment are shown as well. The inter-connectivity is shown as arrows 1 to 4. Arrow 1 indicates that the input from the physical level is translated into commands. Arrow 2 indicates that a change in command can be displayed in the output device of the physical level.

Behavior selected by user and early information of day/night in semantic level is passed to the syntactic level via Arrow 3 in Fig. 2. Thus, the vision system could produce the suitable output for the corresponding behavior. The syntactic level also interacts with physical level directly and continuously for image processing. The processor and memory are used extensively during processing of the images. As recognition is performed, the user is alerted via the output devices in the physical level. The bidirectional data highway is represented as Arrow 4. Accuracy and speed of the application must meet the system's real-time and reliability constraints.

The traffic sign recognition result is continuously place in a location of the memory where it is made public to other applications. Other applications need to have their own means of method to retrieve the public data. The outer-connectivity is represented by arrows 5 and 6. Other applications refer to any other applications that reside within the mobile device. For instance, the traffic sign recognition result can be used along with a driver's attention detection application via Arrow 5. If the driver is detected to be sleepy, the volume of the speaker can be tuned up to inform the driver of a recognized traffic sign by the third-party application.

[a] Test image was obtained from http://agamenon.tsc.uah.es/Investigacion/gram/

Dynamic environment represents any element outside the mobile device. The environment is termed as dynamic as the vehicle is moving. Hence, the scene viewed by the mobile device is always changing. Optical flow of the scene may be inconsistent as a human can drive a vehicle at various speeds. The environment may also contain other electronic devices inside or outside the vehicle. Other electronic devices inside the vehicle can communicate with the smartphone wirelessly or through wired connection. Electronic devices outside the vehicle need to communicate with the smartphone wirelessly. These are represented by Arrow 6.

IV. Conclusions & Future Work

A conceptual framework of a traffic sign recognition system on mobile device is presented. The traffic sign alert framework proposed in this paper is an infant step to developing a fully functional application on a mobile device. The interaction model is designed to produce clarity on the complexity involved in realizing a machine vision on a mobile device that operates in dynamic environment. The model is divided into physical, semantic and syntactic levels to depict human and smartphone interaction during the mobile application utilization. Result of the application is proposed to be made available for applications that reside within the same mobile device or other electronic devices to assist in further expansion of other applications' capability.

The future work emphasizes on realizing the traffic sign recognition through vision techniques on a targeted smartphone. The aim is to enable the smartphone to recognize traffic signs as how a driver would perceive a sign. Through research on software based solution to overcome inadequacy of hardware computation power for image processing, traffic sign

recognition algorithm is intended to run on the smartphone alone. The phone's hardware resources will be used to capture image, process image and interact with user. Hence, the purchase and maintenance cost by an end user aimed to be lower than having to plug in additional piece of electronic hardware to run the image processing algorithms or other processes for interaction. A preliminary traffic sign recognition result based on low level image processing technique was presented. The authors hope to develop a novel image processing algorithm in the area of traffic sign recognition that can help to compensate the hardware limitation of the smartphone, operates in real-time and adaptable to some variations in the environment.

REFERENCES

[1] A. Katajasalo and J. Ikonen, "Wireless identification of traffic signs using a mobile device", in *Proc IEEE 3rd International Conference on Mobile Ubiquitous Computing, Systems, Services and Technologies*, Sliema, Malta, pp.130 - 134, Oct. 2009.

[2] P. Paclik, "Road Sign Recognition Survey", [Online: 08 Sep 2010]. Available: http://euler.fd.cvut.cz/research/ rs2/files/skoda-rs-survey.html

[3] Y.Y. Nguwi and A. Z. Kouzani, "A study on automatic recognition of road signs", in *Proc IEEE Conference of Cybernetics and Intelligent Systems*, Bangkok, Thailand, pp.1 – 6, Jun. 2006.

[4] L. W. Tsai, *et al.*, "Road sign detection using eigen color", *Journal of IET Computer Vision*, Vol. 2, No. 3, pp.164–177, 2008.

[5] M. B. Saturnino, L. A. Sergio, G. J. Pedro, G. M. Hilario and L. F. Francisco, "Road-sign detection and recognition based on support vector machines," *IEEE Transactions on Intelligent Transportation Systems*, Vol. 8, No. 2, pp.264 - 278, Jun. 2007.

[6] G. K. Siogkas and E. S. Dermatas, "Detection, tracking and classification of road signs in adverse conditions," in *Proc. IEEE Mediterranean Electrotechnical Conference*, Benalmádena (Málaga), Spain, pp.537 - 540, May 2006.

[7] Y. P. Wong, M. P. Shi and T. Wu, "A method of fast and robust for traffic sign recognition," in *Proc. IEEE Fifth International Conference on Image and Graphics*, Shanxi, China, pp.891 - 895, Sep. 2009.

[8] Y. R. Fatmehsan, A. Ghahari, R. A. Zoroofi, R.A, "Gabor wavelet for road sign detection and recognition using a hybrid classifier", in *Proc. IEEE International Conference on Multimedia Computing and Information Technology*, Sharjah, United Arab Emirates, pp.25 - 28, Apr. 2010.

[9] S. Gammeter, A. Gassmann, L. Bossard, T. Quack and L. V. Gool, "Server-side object recognition and client-side object tracking for mobile augmented reality", in *Proc. IEEE Computer Vision and Pattern Recognition Workshops*, California, U.S.A, pp.1 - 8, Jun. 2010.

[10] Y. Zhou, X. Fan, X. Xie, Y. Gong and W. Y. Ma, "Inquiring of sights from the web via camera mobiles", in *Proc. IEEE International Conference on Multimedia and Expo*, Ontario, Canada, pp.661 - 664, Jul. 2006.

[11] D. Wagner, G. Reitmayr, A. Mulloni, T. Drummond and D. Schmalstieg, "Pose tracking from natural features on mobile phones," in *Proc. IEEE International Symposium on Mixed and Augmented Reality*, Cambridge, U. K., pp.125 - 134, Sep. 2008.

[12] A. Hadid, J. Y Heikkild, O. Silven and M. Pietikdinen, "Face and eye detection for person authentication in mobile phones," in *Proc. ACM/IEEE 1st International Conference on Distributed Smart Cameras*, Vienna, Austria, pp.101 - 108, Sep. 2007.

[13] S. E. Lee, Y. Zhang, Z. Fang, S. Srinivasan, R. Iyer and D. Newell, "Accelerating mobile augmented reality on a handheld platform", in *Proc. IEEE International Conference on Computer Design*, California, U.S.A, pp.419 - 426, Oct. 2009.

[14] "MyFord™ Defines a New Driver Experience," [Online: 29 Sep. 2010]. Available: http://www. thefordstory.com/smart-technology/myford%E2% 84%A2-defines-a-new-driver-experience/

[15] "Smart Drive Kit for The iPhone," [Online: 29 Sep. 2010]. Available: http://500sec.com/smart-drive-kit-for-the-iphone/

[16] "Integration of Mobile Apps into the Vehicle HMI: Terminal Mode", [Online: 29 Sep 2010]. Available: http://www.nokia.com/NOKIA_ COM_1/Microsites/terminalmode/pdf/terminal_mode.pdf

[17] "In-Vehicle Infotainment," [Online: 29 Sep. 2010]. Available: http://www.intel.com/design/embedded/ infotainment/ products.htm

[18] "BMW", [Online: 28 Jan 2011]. Available: http://www.mobileye.com/manufacturer-products/product-launches/BMW

[19] P. S. Gideon, R. Elchanan, H. Gaby and S. Amnon, "A computer vision system on a chip: a case study from the automotive domain" in *Proc IEEE Computer Society Conference on Computer Vision and Pattern Recognition*, San Diego, CA, USA , pp. 130 - 134, Jun. 2005.

[20] "Test: traffic sign recognition systems", [Online: 28 Jan 2011]. Available: http://www.inautonews.com/test-traffic-sign-recognition-systems

[21] "Reward 2010 – Opel Eye", [Online: 28 Jan 2011]. Available: http://www.euroncap.com/rewards/opel_eye.aspx

[22] F. Maddix, Human-Computer Interaction: Theory and Practice, Ellis Horwood Limited, England, 1990.

[23] H. L. Wong and S. H. M. Amin, "Skin color detection based on various chrominance pairs from multiple color spaces for face detection in human-robot interaction", Jurnal Elektrika, Vol. 7, No. 1, pp.35-44, Jun. 2005.

Neural Networks with NARX Structure for Material Lifetime Assessment Application

Mas Irfan P. Hidayat
Materials Engineering Dept.
Sepuluh Nopember
Institute of Technology (ITS)
Surabaya 60111, East Java
Indonesia
Email: irfan@mat-eng.its.ac.id

Puteri Sri Melor M. Yusoff
Mechanical Engineering Dept.
Universiti Teknologi PETRONAS
Tronoh
31750 Perak Darul Ridzuan
Malaysia
Email: puteris@petronas.com.my

Wajan Berata
Mechanical Engineering Dept.
Sepuluh Nopember
Institute of Technology (ITS)
Surabaya 60111, East Java
Indonesia
Email: wayanb@me.its.ac.id

***Abstract*—In the present paper, neural networks (NN) with non-linear auto-regressive exogenous inputs (NARX) structure is developed and further applied for material lifetime assessment application. Rational of the use of the NARX structure in the application was emphasized and linked to the concept of constant life diagram (CLD), the well known concept in fatigue of material analysis and design. Fatigue life assessment was then performed and realized as one-step ahead prediction with respect to each stress level corresponding to stress ratio values arranged in such a way that transition took place from a fatigue region to another one in the CLD. As a result, material lifetime assessment can be fashioned for a wide spectrum of loading in an efficient manner. The simulation results for different materials and loading situations are presented and discussed.**

***Keywords* — Neural Networks; NARX; CLD; Lifetime Assessment**

I. INTRODUCTION

As one of soft-computing frameworks, neural networks (NN) found its application in fatigue life assessment of materials in recent years. The capabilities of NN lying in learning from examples, pattern or feature extraction in a collection of data and generalization to a new loading environment are the main reasons why NN found its path in the material lifetime assessment application and soon becomes the alternative route in the fatigue lifetime analysis [1, 2].

Recent authors have introduced and conducted the fatigue lifetime assessment analysis using NN with various configurations. The main objective of such analysis is to extract *S*-*N* relation from some fatigue loading conditions in a non-parametric fashion and to further utilize the pattern extraction for predicting the material lifetime under different loading conditions. Here, *S* represents stress magnitude, *N* represents material lifetime in cycles and loading condition or fatigue nature is represented by stress ratio, *R*. Following Lee and Almond [3], Al-Assaf and El-Kadi [4], and El-Kadi and Al-Assaf [5] performed fatigue life assessment of unidirectional glass fiber/epoxy laminate using several NN paradigms, namely feed-forward (FF), modular (MN), radial basis function (RBF) and principal component analysis (PCA) networks. The works have presented comprehensive analysis and discussion about the utilization of different NN models in predicting fatigue life of unidirectional composite laminate. Freire Junior et al. [6, 7] also noticed the potential of NN models of feed-forward and modular on building constant life diagrams (CLD) using only three *S*-*N* curves for predicting fatigue lives of multidirectional composite. Furthermore, Vassilopoulos et al. [8] also showed that using only randomly selected 40-50% of the experimental data were sufficient to produce reliable CLD using NN, emphasizing the NN convenience in performing fatigue life prediction of composite materials.

In the previous papers, studies were only focused on the application of various NN models in the task of material lifetime assessment. As a matter of fact, however, no further attempt has been made to link and ground the use of NN models to the one important concept of fatigue life analysis and design, namely CLD. It will be shown that the utilization of CLD concept could lead to the use of non-linear auto-regressive exogenous inputs (NARX) structure as a natural of choice of NN configuration for the task of material lifetime assessment. The concept of CLD will be briefly introduced and explained later in section II.

In the present paper, NN with NARX structure is developed and further applied for material lifetime assessment application. Rational of the use of the NARX structure in the application was emphasized and linked to the concept of CLD. Fatigue life assessment was then performed and realized as one-step ahead prediction with respect to each stress level corresponding to stress ratio values arranged in such a way that transition took place from a fatigue region to another one in the CLD. As a result, material lifetime assessment can be fashioned for a wide spectrum of loading in an efficient manner. Such an analysis constitutes to a variable amplitude or spectrum fatigue loading [9].

In addition, number of stress levels employed for a value of stress ratio is commonly limited, considering the fact that fatigue testing is very time consuming and costly. The use of three stress levels is not uncommon. Here, the use of five stress levels for each stress ratio, as the corresponding fatigue database utilized, is considered. Furthermore, two stress ratio values will serve as a basis for training data employed for dynamically predicting

fatigue lives of other stress ratios of CLD. Thus, the feasibility of using two *S-N* curves in material lifetime assessment is also investigated in the current study.

The remainder of the paper is organized as follows: section II presents briefly the concept of CLD for fatigue life analysis together with the NN with NARX structure employed. Section III presents the materials examined and methods chosen for the NN model. Fatigue life assessment results using the NN configuration and related discussion are presented in section IV, followed by conclusion casted through the simulation study along with future research direction in section V.

II. Constant Life Diagram (CLD) And NN with NARX Structure

A. CLD

CLD serves as a convenient way in fatigue life assessment analysis under spectrum loading. CLD is also another way to represent the *S–N* curve, with which design engineers are very familiar. Stress ratio *R*, which is a ratio between minimum and maximum alternating stresses, now in CLD also indicates what fatigue region the stress ratio value belongs to. Fig. 1 represents the CLD schematic.

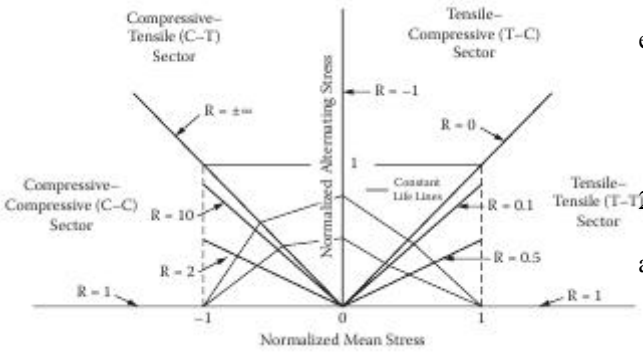


Figure 1. The schematic of CLD for fatigue life assessment analysis

The points along each radial line are the points of *S–N* curve for a specific stress ratio. Moreover, as one can see in Fig. 1, fatigue region moves from tensile-tensile to compressive-compressive sector in CCW direction forming a spectrum of loading conditions and all points with the same fatigue life *N* are connected with lines in a plane of amplitude stress (S_a) − mean stress (S_m) axes. The transition regions are marked by stress ratio values of $R = 1$ (ultimate static strength), $R = 0$ (minimum alternating stress equals zero), $R = -1$ (maximum alternating stress equals the absolute value of minimum alternating stress) and $R = \pm \sim$ (the absolute value of minimum alternating stress is much higher than the value of maximum alternating stress, which can be either positive or negative value).

B. NN with NARX Structure

NN with NARX structure has the signal vector applied to the NN input layer consisting of a data window made up by present and past values of *exogenous* (independent) inputs and by delayed values of the outputs. The NN model belongs to a class of recurrent neural networks (RNN) with one feed-back loop from the NN output layer to the input layer. Moreover, the presence of the feed-back loop has enabled such a configuration to acquire state representations. It also provides a unified representation for a wide class of discrete-time nonlinear systems [10, 11].

Mathematically, a NARX model can be represented as:

$$y(n+1) = f[\mathbf{y}(n); \mathbf{u}(n)]$$
$$y(n+1) = f[y(n),\ldots,y(n-d_y+1); u(n),u(n-1),\ldots,u(n-d_u+1)] \quad (1)$$

where *u(n)* and *y(n)*, respectively, state the input and output of the model at discrete time *n; u(n), y(n)* $\in \Re$. Moreover, d_y and d_u are the output-memory and input-memory orders. d_y represents the number of lagged output values, which is often referred to as the order of the model, d_u represents the number of lagged input values (d_u, $d_y \geq 1$ and $d_u \leq d_y$). The vectors $\mathbf{y}(n)$ and $\mathbf{u}(n)$, therefore, form the output and input regressors, respectively.

The NARX model is commonly trained using two basic modes, namely:

1. Parallel (P) Mode

Using this mode, the output regressor utilized the estimated outputs which are fed back to the regressor.

$$\hat{y}(n+1) = \hat{f}[\hat{y}(n),\ldots,\hat{y}(n-d_y+1); u(n),u(n-1),\ldots,u(n-d_u+1)] \quad (2)$$

2. Series-Parallel (SP) Mode

Using this mode, the output regressor utilized the actual output values.

$$\hat{y}(n+1) = \hat{f}[y(n),\ldots,y(n-d_y+1); u(n),u(n-1),\ldots,u(n-d_u+1)] \quad (3)$$

It is worth to note that, although NARX with SP mode acts as one-step ahead predictor, standard feed-forward architecture trained with back-propagation (BP) technique can be used directly in the mode. In addition, various learning algorithms are also widely applicable. A form of regularization may also be employed because the additive measurement errors, ε_n, which are zero-mean Gaussian variables with $\mathrm{Var}[\varepsilon_n] = \sigma^2$, can be also present in the model. Fig. 2 illustrates the NARX with input and output tapped delay lines, in parallel and series-parallel architectures [12].

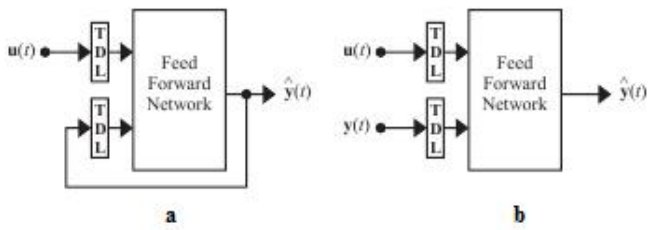


Figure 2. The NARX architecture with tapped delay lines: (a) parallel architecture, and (b) series-parallel architecture

III. Material and Methods

A. Materials

The investigated materials were two multidirectional laminates of E-glass/polyester, typical materials used in wind turbine blade applications. The first material had the corresponding lay-up of $[90/0/\pm45/0]_S$ and is called as DD16. It represented the earlier material used in the applications [13, 14]. The corresponding database containing fatigue data of various R values (R = 0.1, 0.5, 0.7, 0.8, 0.9, -0.5, -1, -2 and 10) makes it suitable for the study purpose. From the fatigue data, stress ratio R, maximum stress (S_{max}) and minimum stress (S_{min}) values were used as input set and the output was the corresponding fatigue cycles (log N) for the input set. For each particular R value, mean fatigue life values were used.

The second material had the corresponding lay-up of $[0/(\pm45)_2/0]_T$ and were cut by diamond saw wheel at on-axis (0°) and off-axis (15°, 30°, 45°, 60°, 75° and 90°) orientations [15] . For the material, fatigue data of on-axis and 45° orientations were examined with the corresponding R values of 0.1, 0.5, -1, and 10, for both the orientations. Also, all the data were normalized in range of -1 to 1.

Table 1 summarizes the materials examined together with the orientation and the training and testing sets employed. Note that stress ratio values R were arranged in CCW direction according to the CLD, moving across from tensile-tensile sector to compressive-compressive sector. In addition, fatigue data of R = 0.1 and 10 were chosen as training set because the best relative positions of the R values in the CLD. See again Fig. 1. Moreover, the fatigue testing on the R values are also commonly conducted. Note also that number of stress levels in each R value employed was 5.

TABLE I
Materials Examined Together with The Orientations and The Training and Testing Sets Employed

Material	Angle Orientation	Fatigue Data as Training Set	Fatigue Data as Testing Set
E-glass/polyester $[90/0/\pm45/0]_S$	On-axis	R = 0.1 and 10	R = 0.9, 0.8, 0.7, 0.5, -0.5, -1 and -2
E-glass/polyester $[0/(\pm45)_2/0]_T$	On-axis	R = 0.1 and 10	R = 0.5 and -1
	45°	R = 0.1 and 10	R = 0.5 and -1

B. Methods

In the present study, the training algorithm of Levenberg-Marquardt was chosen and utilized to result in fast and efficient NN model [16]. Moreover, to accommodate the noise may be present in the target data in the model and also to deal with limited training data employed, that may lead to ill-posed problem, Bayesian regularization technique was incorporated [17, 18]. Utilizing the regularization, the objective function of NN, $E(\mathbf{w})$, was modified into:

$$E(\mathbf{w}) = \beta \sum_{q=1}^{Q} \left[t_q - \hat{f}(\mathbf{p}_q; \mathbf{w}) \right]^2 + \alpha \sum_{i=1}^{W} {w_i}^2 \qquad (4)$$

where: α is a weight decay parameter, β is an inverse noise variance parameter, t_q is the target data, the estimate $\hat{f}$ realized by the NN, $\mathbf{p}$ is the vector of input sets, $\mathbf{w}$ is the vector of weights (and biases), Q is the number of training examples and W is the total number of weights.

Furthermore, fatigue life assessment of the materials was performed and realized as one-step ahead prediction with respect to each stress level S corresponding to stress ratio values R arranged in such a way that transition took place from a fatigue region to another one in the CLD. It is clear that the NARX-SP architecture is being currently employed and sliding over one-step to one-step of stress level, the prediction will be dynamically covering all the spectrum loadings of the testing sets according to the CLD. As a result, material lifetime assessment can be fashioned for a wide spectrum of loading in an efficient manner based upon solely the training data as the basis of the NARX regressor, thus developed variable amplitude or spectrum fatigue analysis. Fig. 3 describes the lifetime assessment process using NN with NARX model in the study.

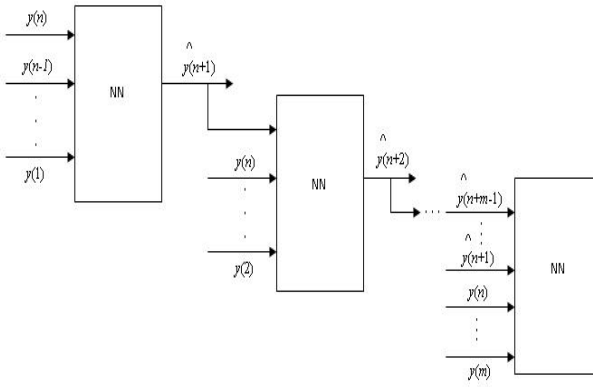


Figure 3. Spectrum fatigue life prediction made up by one-step ahead prediction using NN with NARX-SP structure

IV. Simulation Results and Discussion

Using the methods described previously, all simulation results of fatigue life assessment of the materials considered are presented in this section. E-glass/polyester of $[90/0/\pm45/0]_S$ will be denoted as Material I, E-glass/polyester of $[0/(\pm45)_2/0]_T$ whose on-axis orientation will be denoted as Material II-on-axis and E-glass/polyester of $[0/(\pm45)_2/0]_T$ whose 45° orientation will be denoted as Material II-45D. It is important to note also that the number of hidden nodes employed for the NN-NARX model was 10.

Fig. 4 presents fatigue life prediction of Material I at stress ratios R of the testing set.

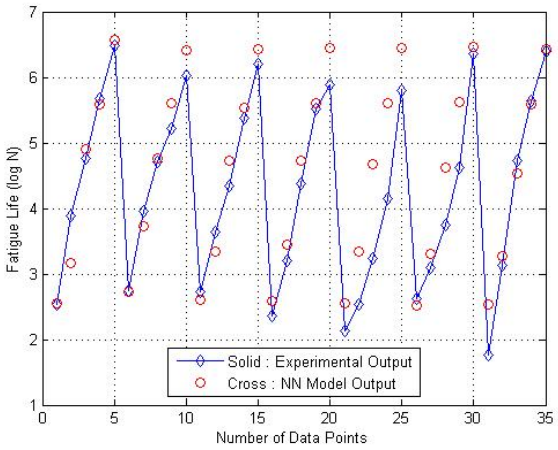


Figure 4. Fatigue lives predicted by the NN-NARX model for tested sets: R = 0.9, 0.8, 0.7, 0.5, -0.5, -1 and -2 of Material I (from left to right)

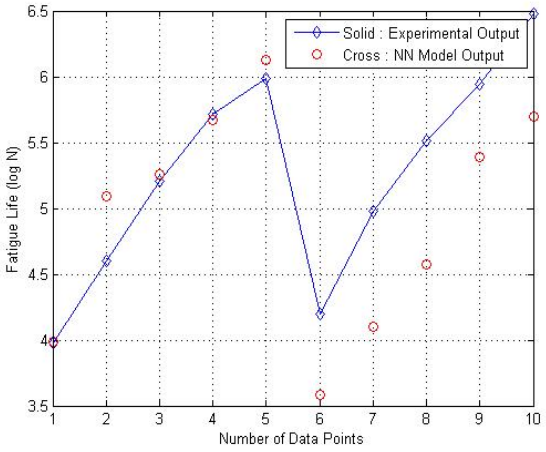


Figure 5. Fatigue lives predicted by the NN-NARX model for tested sets: R = 0.5 and -1 of Material II-on-axis (from left to right)

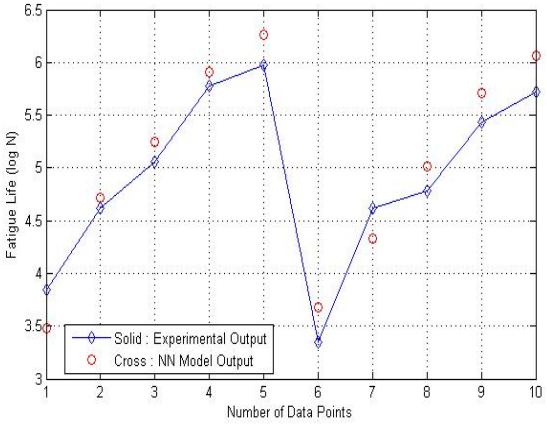


Figure 6. Fatigue lives predicted by the NN-NARX model for tested sets: R = 0.5 and -1 of Material II-45D (from left to right)

It can be seen that the NN-NARX model prediction results were consistent with the experimental data showing the applicability of the NN model to the problem considered. The NN model also shows its ability to dynamically predict the fatigue lives sliding over each stress level in a fashion of spectrum loading made up by several R values. It should be pointed out, however, that large enough discrepancies were also observed, in particular those belong to R = -0.5. Nevertheless, it can be said that in general the experimental data trend can still be followed well by that of the NN prediction results.

The accuracy of the NN-NARX model prediction compared to the experimental data was measured in mean squared error (MSE). The MSE prediction value for the Material I was 0.27.

Looking at the fatigue life prediction results for Material I produced by the NN architecture, it may be worth to also note that the results obtained were comparable with those obtained by the previous researchers investigating also the same material using NN. See, for instance, in [6,7] in particular for the NN fatigue life prediction results of R = -0.5 and 0.7, which were further casted in the corresponding S-N curves.

The application of the NN-NARX model was further applied for different laminate of E-glass/polyester whose different angle orientations, namely Material II-on-axis and Material II-45D. Figs. 5 and 6 depict, respectively, fatigue life prediction of Material II-on-axis and Material II-45D at stress ratios R of the testing sets examined.

It can be also seen that in general the NN-NARX model prediction results can fairly follow the experimental data trend. Moreover, for Material II-on-axis, the NN fatigue life prediction results of R = 0.5 were even quite good at some stress levels, while those of R = -1 were all underestimated compared to those of the experimental data. For the later, it can be said that although the corresponding NN fatigue life prediction results were far enough with those of the experimental data, the conservative prediction results, however, were still preserved.

Furthermore, for Material II-45D, the NN fatigue life prediction results of R = 0.5 and -1 were good for all stress levels involved. As can be seen clearly, the NN fatigue life prediction results can closely follow the experimental data trend. The MSE prediction values for the Material II-on-axis and Material II-45D were 0.32 and 0.07, respectively.

To further measure the closeness between both the experimental data trend and the prediction trend, the NN fatigue life prediction results were also presented in the corresponding S-N curves, with the corresponding coefficient of determination (R^2) between the NN fatigue life prediction results and the experimental data.

Figs. 7-8 show the S-N curves obtained by the NN-NARX model and the experimental data for stress ratios R = -0.5 and 0.7 of Material I, respectively. Note that the NN fatigue life prediction results of R = -0.5 represented "the worst prediction", while those of R = 0.7 represented the best one. In addition, those of R = 0.5 and -1 of Material II-on axis and of Material II-45D were also depicted by Figs. 9-10, respectively.

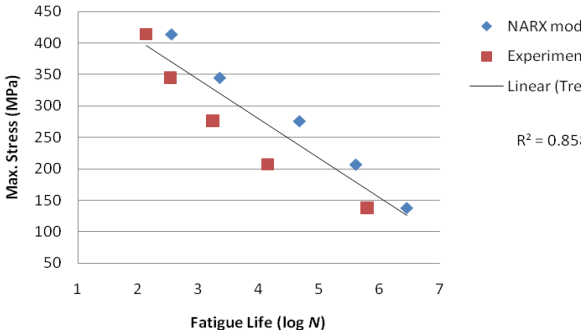


Figure 7. *S-N* curves obtained by the NN-NARX model and the experimental data for R = -0.5 of Material I

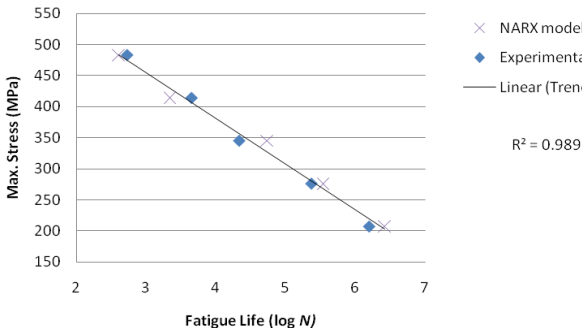


Figure 8. *S-N* curves obtained by the NN-NARX model and the experimental data for R = 0.7 of Material I

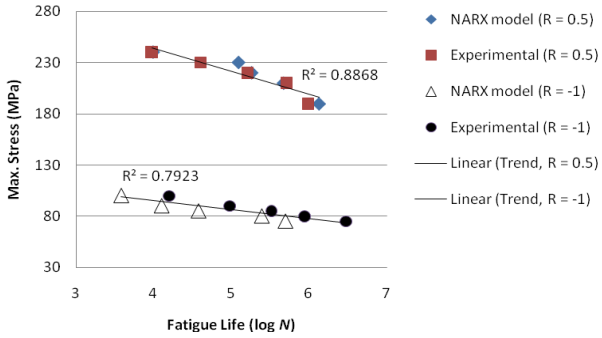


Figure 9. *S-N* curves obtained by the NN-NARX model and the experimental data for, respectively, R = 0.5 and -1of Material II-on-axis

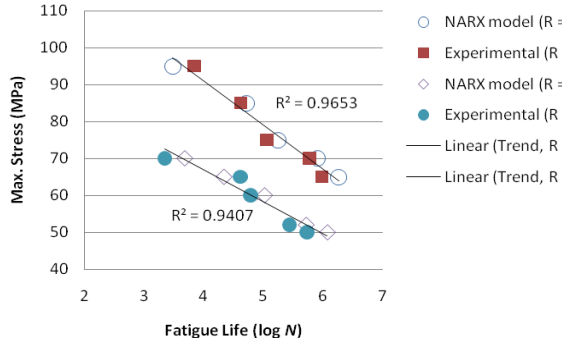


Figure 10. *S-N* curves obtained by the NARX model and the experimental data for, respectively, R = 0.5 and -1 of Material II-45D

From the results obtained, in general it can be seen again that for the discrepancies observed, fatigue lives predicted by the NN-NARX model were not excessively far from those of experimental data. The coefficient of determination (R^2) of fatigue life prediction produced thus can be considered high for all the laminates examined with the NN-NARX model. In addition, for Material I, the best prediction can even achieve the coefficient of determination of 0.989, while that of 0.9653 can be achieved in the fatigue life prediction of Material II-45D. For all the materials examined, the values of R^2 range from 0.7923 to 0.989.

Finally, it is important to note again here that the NN with NARX structure is first applied for the problem considered in the present study. The application has linked the concept of CLD to the selection of the NN with NARX structure, which has been shown here its applicability and feasibility. NARX model has been known previously in many fields of applications, among others, [19, 20]. Now, its application has been extended to spectrum fatigue life assessment and analysis.

Here, the improvement of the MSE prediction value that may be produced with respect to the variation of the hidden nodes number in a sensitivity analysis is still not further considered and left as further research and study.

V. Conclusions

Material lifetime assessment using NN with NARX structure has been presented in the present paper. Dynamic nature of both the CLD and the NARX model was emphasized and linked, resulting in the first application of the NARX model in spectrum fatigue analysis.

Fatigue life assessment was realized as one-step ahead prediction with respect to each stress level corresponding to stress ratio values arranged in such a way that transition took place from a fatigue region to another one in the CLD.

As a result, material lifetime assessment can be fashioned for a wide spectrum of loading in an efficient manner. The simulation results showed the applicability and the efficiency of the NN-NARX model when applied for different materials and loading situations in the study. For Material I, the MSE prediction value produced was 0.27, while those of Material II-on-axis and Material II-45D were 0.32 and 0.07, respectively. In addition, the results were obtained utilizing the available fatigue data composed of two stress ratio values. Meanwhile, in term of the coefficient of determination value (R^2) plotted in the corresponding *S-N* curves, for all the materials considered, the values of R^2 ranging from 0.7923 to 0.989 were produced, which are considered as high.

Further sensitivity analysis with respect to the variation of the hidden nodes number as well as further applications to other materials widely are recommended as further research and study.

Acknowledgement

The present authors would like to thank the Montana State University and A.P. Vassilopoulos and T.P. Philippidis (doi:10.1016/S0142-1123(02)00003-8) for the fatigue database published through the internet.

REFERENCES

[1] B. Harris, (ed.), *Fatigue in Composites*, Woodhead Publishing Ltd, Cambridge, England, 2003.

[2] S. Haykin, *Neural Networks and Learning Machines*, 3rd ed., Pearson Prentice Hall, USA, 2009.

[3] J.A. Lee, D.P. Almond, "A Neural-network approach to fatigue life prediction," *Fatigue in Composites*, edited by B. Harris, Woodhead Publishing Ltd, Cambridge, England, 2003, pp. 569-589.

[4] Y. Al-Assaf, H. El-Kadi, "Fatigue life prediction of unidirectional glass fiber/epoxy composite laminae using neural networks," *Composites Structures*, Vol. 53, No. 6, pp. 65-71, 2001.

[5] H. El-Kadi, Y. Al-Assaf, "Prediction of the fatigue life of unidirectional glass fiber/epoxy composite laminae using different neural network paradigms," *Composites Structures*, Vol. 55, No. 1, pp. 239-246, 2002.

[6] R.C.S. Freire Junior, A.D.D. Neto, and E.M.F. de Aquino, "Building of constant life diagrams of fatigue using artificial neural networks," *International Journal of Fatigue*, Vol. 27, No. 7, pp. 746-751, 2005.

[7] R.C.S. Freire Junior, A.D.D. Neto, and E.M.F. de Aquino, "Use of modular networks in the building of constant life diagrams," *International Journal of Fatigue*, Vol. 29, No. 3, pp. 389-396, 2007.

[8] A.P. Vassilopoulos, E.F. Georgopoulos, and V. Dionysopoulos, "Artificial neural networks in spectrum fatigue life prediction of composite materials," *International Journal of Fatigue*, Vol. 29, No. 3, pp. 20-29, 2007.

[9] A.P. Vassilopoulos, B.D. Manshadi, and T. Keller, "Influence of the constant life diagram formulation on the fatigue life prediction of composite materials," *International Journal of Fatigue*, Vol. 32, No. 4, pp. 659-669, 2010.

[10] S. Chen, S. A. Billings and P. M. Grant, "Non-linear system identification using neural networks," *International Journal of Control*, Vol. 51, No. 6, pp. 1191-1214, 1990.

[11] K. Narendra and K. Parthasarathy, "Identification and control of dynamic systems using neural networks," *IEEE Transactions on Neural Networks*, Vol.1, No. 1, pp. 4–27, 1990.

[12] Neural Network Toolbox™ User's Guide © COPYRIGHT 1992–2010 by The MathWorks, Inc.

[13] DOE/MSU Composite Material Fatigue Database, Montana State University, 2010.

[14] J.F. Mandell, D.D. Samborsky , *DOE/MSU Composite Material Fatigue Database: Test, Methods, Material and Analysis*, SAND97-3002, Sandia National Laboratories, 1997.

[15] A.P. Vassilopoulos and T.P. Philippidis, "Complex stress state effect on fatigue life of GRP laminates. Part I, experimental," *International Journal of Fatigue*, Vol. 24, No. 8, 2002, pp. 813-823.

[16] J. Nocedal and S.J. Wright, *Numerical Optimization*, 2nd ed., Springer, New York, 2006, Chap. 10.

[17] F.D. Foresee, M.T. Hagan, "Gauss-Newton approximation to bayesian learning," *IEEE International Conference on Neural Networks*, Vol. 3, No. 8, pp. 1930-1935, 1997.

[18] D.J.C. MacKay, *Information Theory, Inference and Learning Algorithms*, Cambridge University Press, England, 2004.

[19] M. Basso, L. Giarre, S. Groppi and G. Zappa, "NARX models of an industrial power plant gas turbine," *IEEE Transactions on Control System Technology*, 2004.

[20] Kao, C.Y., C.C. Tsang, C.C. Loh, and T.H. Wu, "Neural networks for nonlinear identification and diagnosis of structures," *Proc. of the First International Conference on Structural Health Monitoring and Intelligent Infrastructure (SHMII-1'2003)*, November 13-15, 2003, Tokyo, Japan.

The Parallel AGE Variances Method for Temperature Prediction on Laser Glass Interaction

Lizawati Mi Yusuf, Norma Alias, Mohammed Shariff Bashir Ghouse,
Siti Mariyam Shamsuddin and Mohd Shahizan Othman
Faculty of Computer Science and Information Systems,
Universiti Teknologi Malaysia, 81310 Skudai, Johor, Malaysia.
lizawati@utm.my, norma@ibnusina.utm.my, mshariff5@live.utm.my,
{mariyam, shahizan}@utm.my

***Abstract* - This paper describes the formula of three-dimensional parabolic equations for cylindrical coordinate glass that is used for mathematical simulation in simulating the temperature behavior of the laser glass cutting. There are three methods have been used for the simulation purposes which is the Alternating Group Explicit (AGE) which compromises two variances that is Brian and Douglas variant, and Gauss Seidel Red Black method. The simulation for these three methods is conducted in a parallel computing environment in order to speed up the calculation process and to achieve an accurate and convergence results. From the simulation, the results will be compared by conducting parallel performance measurement, which include execution time, speedup, efficiency, effectiveness and temporal performance.**

***Keywords* - Alternating Group Explicit Method (AGE); Gauss Seidel Red Black; Partial Differential Equation (PDE); Parallel Computing**

I. INTRODUCTION

The traditional method used on laser glass cutting use mechanical scribe and break processes. The diamond tip tool is used to create a mark or a scratching zone that will eventually break the glass [1]. This technique will produce fragmentation, micro cracks on the surface of the glass resulting an uneven glass structure. Then, came the laser technology to solve the problem arises in the traditional method. The laser technique serves a higher quality cutting and high precision compared to the mechanical scribe method [1, 2]. However, the laser technique is expensive and requires security aspects and expertise [1, 2, 3]. Hence, the mathematical simulation is needed to conduct the simulation of the laser glass technique.

To conduct mathematical simulation, a mathematical model is needed to represent the actual problem of the laser technique. In this research, the mathematical model that is used will be the partial difference equation (PDE). PDE is chosen because it can support high complexity, infinite dimensional and process that is difficult to estimate [4]. The PDE will need to undergo discretization to simplify the equation for numerical simulation. However, the discretization technique requires too many numerical analysis and iterations that will consume a lot of time particular in sequential computing platform [5]. Computer science field has advanced into a greater stage to help engineers and scientist to solve the problem by introducing a new platform using high-speed computing machine [6]. Thus, the parallel computing which is a high-speed computing machine is able to conduct mathematical simulation to simulate nanoscale temperature behavior on laser glass interaction.

The main objective of this paper is to compare the parallel performance of Alternating Group Explicit (AGE) method by using Brian and Douglass variances with Gauss Seidel Red Black (GSRB) in solving laser glass cutting problems in parallel environment.

II. PROBLEM FORMULATION

In solving large sparse problems, numerical methods are ideally used to solve partial difference equation (PDE), which is based on domain decomposition. Numerical methods can solve multidimensional problems such as the laser glass interaction problem which requires accurate results and highly convergent. Here is the three-dimensional parabolic equation for cylindrical coordinate glass that is used to formulate the laser glass interaction problem:

$$\frac{1}{a}\frac{\partial U}{\partial t} = \frac{\partial^2 U}{\partial r^2} + \frac{1}{r}\frac{\partial U}{\partial r} + \frac{1}{r^2}\frac{\partial^2 U}{\partial \theta^2} + \frac{\partial^2 U}{\partial z^2} + \frac{q}{k} \quad (1)$$

with the initial condition:

$$T(r,\theta,z,t)|_{r=0} = T_0 \quad (2)$$

with T_0 is the initial temperature, where the temperature of the glass cylinder before laser process and boundary conditions:

$$T(r,\theta,z,t)|_{s_1=0} = T_1 \text{ and } T(r,\theta,z,t)|_{s_2=0} = T_2 \quad (3)$$

where,

T_1, T_2 : Temperature (K) of inner and outer surface of glass cylinder
s_1, s_2 : Area of inner (m^2) and outer surface (m^2) of glass cylinder
r, θ, z : Radius (m), angle (^{o}) and length (m) of

glass cylinder

q : Rate of heat flow (W/m^2)
a : Density (Kg/m^3) and heat capacity (J)
K : Thermal conductivity (W)
t : Time (s)

The discretization of (1) is done by using Finite Difference Method (FDM). From the equation obtained after discretization, the AGE BRIAN method, AGE Douglas method and GSRB is used for simulation purposes.

A. AGE Brian Method

The method is based on linear interpolation that uses Brian variant and acceleration parameter, *r* with fractional concepts. The formula for BRIAN method for the three-dimensional cylindrical problems is as follows [7],

$$(G_1 + rI)u_{[xy]}^{\left(p+\frac{1}{7}\right)} = (rI - G_2 - G_3 - G_4 - G_5 - G_6)u_{[xy]}^{(k)} + f, \quad (4)$$

$$(G_2 + rI)u_{[xy]}^{\left(p+\frac{2}{7}\right)} = ru_{[xy]}^{\left(p+\frac{1}{7}\right)} + G_2u_{[xy]}^{p}$$

$$(G_3 + rI)u_{[xy]}^{\left(p+\frac{3}{7}\right)} = ru_{[xy]}^{\left(p+\frac{2}{7}\right)} + G_3u_{[xy]}^{p}$$

$$(G_4 + rI)u_{[xy]}^{\left(p+\frac{4}{7}\right)} = ru_{[xy]}^{\left(p+\frac{3}{7}\right)} + G_4u_{[xy]}^{p}$$

$$(G_5 + rI)u_{[xy]}^{\left(p+\frac{5}{7}\right)} = ru_{[xy]}^{\left(p+\frac{4}{7}\right)} + G_5u_{[xy]}^{p}$$

$$(G_6 + rI)u_{[xy]}^{\left(p+\frac{6}{7}\right)} = ru_{[xy]}^{\left(p+\frac{5}{7}\right)} + G_6u_{[xy]}^{p}.$$

$$u_{[xy]}^{(k+1)} = u_{[xy]}^{(p)} + 2(u_{[xy]}^{\left(p+\frac{6}{7}\right)} - u_{[xy]}^{(p)})$$

Based from the equations obtained from (4), it has been simplify further into 2×2 matrix block form and the matrix calculation using AGE Brian method for cylindrical coordinate system is as follows,

$$u_{1[xy]}^{\left(p+\frac{1}{7}\right)} = \bar{C}_{1,i}^{-1}(D_{1,i}u_{1[xy]}^{(p)} + E_{1,i}u_{2[xy]}^{(p)} + F_{1,i}u_{1[xy]}^{[N]} + H_{1,i}u_{2[xy]}^{[N]} + g_{1[xy]}) \quad (5)$$

$$u_{k[xy]}^{\left(p+\frac{1}{7}\right)} = \bar{C}_{2,i}^{-1}\left(\bar{E}_{1,i}u_{k-1[xy]}^{(p)} + E_{1,i}u_{k+1[xy]}^{(p)}\right) + D_{2,i}u_{k[xy]}^{(p)} + \bar{H}_{1,i}\left(u_{k-1[xy]}^{[N]} + H_{1,i}u_{k+1[xy]}^{[N]}\right) + F_{1,i}u_{k[xy]}^{[N]} + g_{k[xy]} \quad (6)$$

$$u_{k[xy]}^{\left(p+\frac{1}{7}\right)} = \bar{C}_{1,i}^{-1}(\bar{E}_{1,i}u_{k-1[xy]}^{(p)} + E_{1,i}u_{k+1[xy]}^{(p)} + D_{1,i}u_{k[xy]}^{(p)} + \bar{H}_{1,i}\left(u_{k-1[xy]}^{[N]} + H_{1,i}u_{k+1[xy]}^{[N]}\right) + F_{1,i}u_{k[xy]}^{[N]} + g_{k[xy]} \quad (7)$$

$$u_{m[xy]}^{\left(p+\frac{1}{7}\right)} = \bar{C}_{1,i}^{-1}(\bar{E}_{1,i}u_{m-1[xy]}^{(p)} + D_{1,i}u_{m[xy]}^{(p)} + \bar{H}_{1,i}u_{m-1[xy]}^{[N]} + F_{1,i}u_{m[xy]}^{[N]} + g_{m[xy]} \quad (8)$$

Equations (5) to (8) describe the point calculation for its fraction of the grid from $\frac{1}{7}$, $\frac{2}{7}$, $\frac{3}{7}$ until $\frac{7}{7}$. Thus, on calculation for every$(p+1)$,

$$u_{[x,y]}^{(p+1)} = u_{[xy]}^{(p)} + 2(u_{[xy]}^{\left(p+\frac{6}{7}\right)} - u_{[xy]}^{(p)}) \quad (9)$$

B. AGE Douglas Method

This method is based on the Douglas-Rachford formula which uses fractional scheme involves splitting a matrix system of linear equations [8]. Matrix A is been split into consistent symmetric and positive definite matrices $G_1, G_2, G_3, G_4, G_5, G_6$ and the calculation of these matrices will be simplified into four equations as follows,

$$u_{1[xy]}^{\left(p+\frac{1}{6}\right)} = \bar{C}_1^{-1}(D_1u_{1[xy]}^{(p)} + E_1u_{2[xy]}^{(p)} + F_1u_{1[xy]}^{[N]} + F_2u_{2[xy]}^{[N]} + 2g_{1[xy]}) \quad (10)$$

$$u_{k[xy]}^{\left(p+\frac{1}{6}\right)} = \bar{C}_2^{-1}(E_1(u_{k-1[xy]}^{(p)} + u_{k+1[xy]}^{(p)} + D_2u_{k[xy]}^{(p)} + F_2\left(u_{k-1[xy]}^{[N]} + u_{k+1[xy]}^{[N]}\right) + F_1u_{k[xy]}^{[N]} + 2g_{k[xy]} \quad (11)$$

$$u_{k[xy]}^{\left(p+\frac{1}{6}\right)} = \bar{C}_1^{-1}\left(E_1\left(u_{k-1[xy]}^{(p)} + u_{k+1[xy]}^{(p)}\right) + D_1u_{k[xy]}^{(p)} + F_2\left(u_{k-1[xy]}^{[N]} + u_{k+1[xy]}^{[N]}\right) + F_1u_{k[xy]}^{[N]} + 2g_{k[xy]}\right) \quad (12)$$

$$u_{m[xy]}^{\left(p+\frac{1}{6}\right)} = \bar{C}_1^{-1}\left(E_1\left(u_{m-1[xy]}^{(p)} + D_1u_{m[xy]}^{(p)}\right) + F_1u_{m[xy]}^{[N]} + F_2u_{m-1[xy]}^{[N]} + 2g_{m[xy]}\right) \quad (13)$$

Thus, based from (10) to (13), we can derive the calculation using AGE Douglas as (14).

$$u_{[x,z]}^{(p+1)} = (G_1 + rI)^{-1}[G_1u_{[xz]}^{(p)} + ru_{[xz]}^{(p+\frac{5}{6})} \quad (14)$$

C. Gauss-Seidel Red Black (GSRB) Method

The GSRB method is been used as the control scheme to solve three dimensional cylindrical glass interactions. GSRB method is based on domain decomposition for each odd sub domain, Ω^{R} and even sub domain, Ω^{H}[9]. GSRB calculation is as follows,

$$u_{i,j,k}^{(p+1)} = \frac{\begin{bmatrix} -a_iu_{i-1,j,k}^{(p)} - h_iu_{i,j-1,k}^{(p)} - du_{i,j,k-1}^{(p)} - \\ b_iu_{i+1,j,k}^{(p)} - gu_{i,j,k+1}^{(p)} + \bar{b}u_{i-1,j,k}^{[N]} + \\ \bar{d}_i\,u_{i,j,k}^{[N]} + \bar{h}\,u_{i,j-1,k}^{[N]} + \bar{d}u_{i,j,k-1}^{[N]} + \\ \bar{e}u_{i+1,j,k}^{[N]} + \bar{f}u_{i,j+1,k}^{[N]} + \bar{g}u_{i,j,k+1}^{[N]} + \frac{p}{k} \end{bmatrix}}{c_i} \quad (15)$$

where i, j and k are odd or even number depending on the type of subdomain.

III. Methodology

The flowchart in Fig. 1 is used to solve the laser glass interaction problem by using AGE method with Brian and Douglas variances in a parallel environment. This flowchart contains two levels of computers where the top level of the hierarchy is the master and the lower level contains numbers of worker. The master conducts the first task, t_1 that will initiate workers t_i where $i = 1,2,3,\ldots,N$. It is also responsible to process the domain decomposition, data distribution and output from workers. Whilst the workers will conduct data processing, establish communication between

neighboring processors and sending outputs back to the masters. This model is more practical and suitable to be implemented in the parallel program.

The initial boundary, domain size and task load are set to the master. The master will receive these information and it will initiate workers to activate them. As the main responsible for the master is domain decomposition, hence the master will start by decomposing data into data blocks. The data decomposition technique used is static data decomposition. Static data decomposition is a technique that sends data following the size of the domain and the task load. To ensure that all task loads are equally distributed to each processor, all processors must receive and process these data simultaneously. To allow this, iteration method is used by every processor will execute the same amount of arithmetic operation with the same quantity of data block distribution. This paper focuses on this decomposition technique to ensure that there are no processors idle during the simulation.

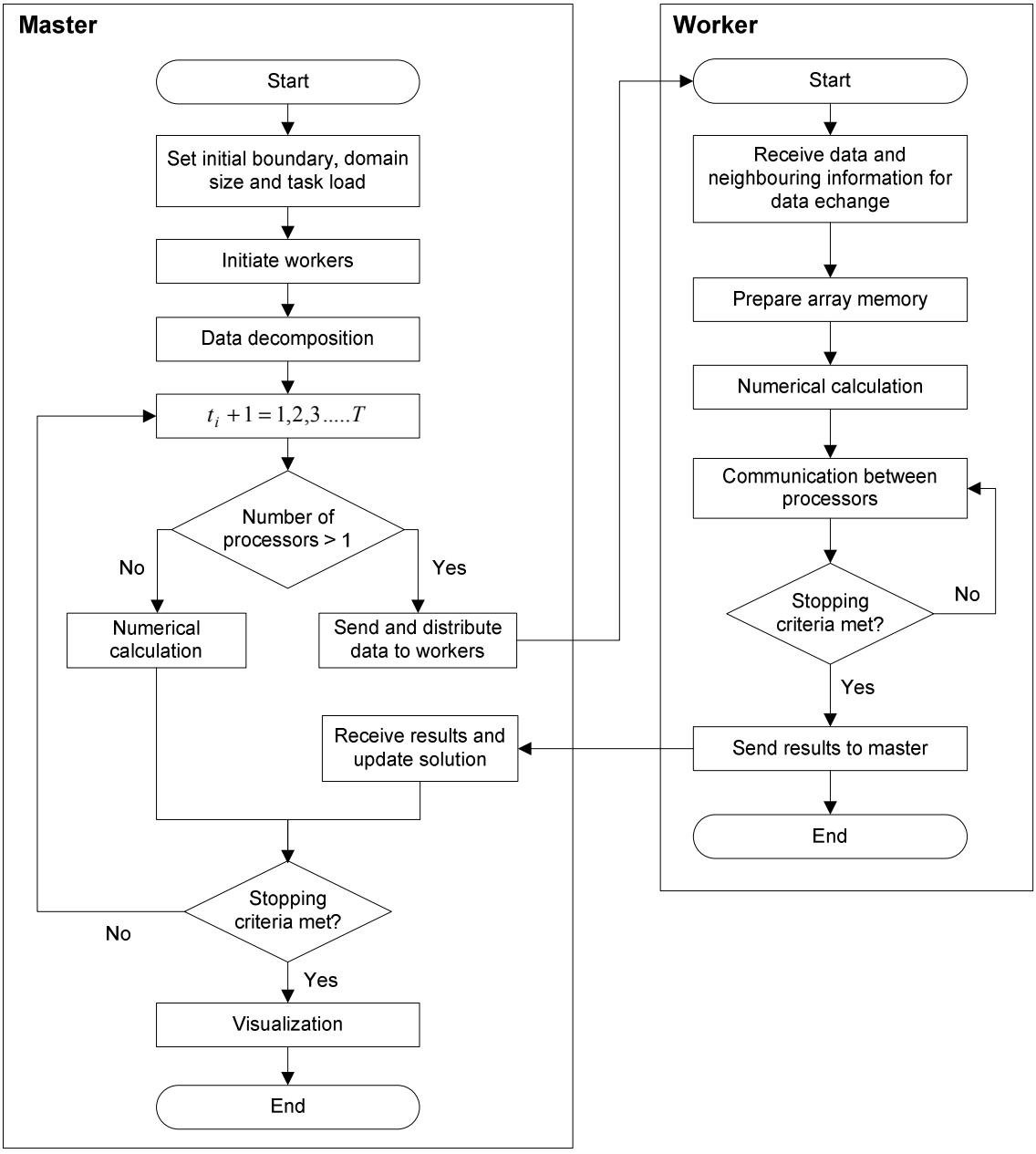


Figure 1. Parallelization flowchart

Then, the master will establish a global type of communication that is distributed to workers and received the data processed by the workers back to the master. Global communication occurs during the sending and receiving an absolute error, Ω for each iteration until the convergence needed is met then the communication will be terminated. At the workers level, each processor establishes a communication between them. The communication that is established is unstructured type of communication where it uses network of communication for any complex graph that requires domain decomposition. Moreover, this communication needs mapping s and algometric process. These processes will ensure the data that are passed do not depend on a

particular task to complete and prevent processors to be idle. Again, the global communication is used to determine the convergence criteria. If the criteria is met, then the data that been processed will be send back to the master for data collection to update the solution. The updated solution then will be visualized in a graph as shown in the next section.

IV. Experiment And Results

To measure the parallel performance on the simulation of the laser glass interaction, the following definitions are used,

Speed up: $S_p = T_1/T_p$ (16)

Efficiency: $C_p = S_p/p$ (17)

Effectiveness: $F_p = S_p/T_p$ (18)

Temporal Performance: $L_p = {T_p}^{-1}$ (19)

where, T_1 and T_p are execution time on one and p processors.

In determining the parallel performance, the parallelization is based on the a number of homogenous PC cluster systems which contains 20 units Intel Pentium processors that are supported by PVM software and C programming. The following graphs visualize the parallel performance in simulating the calculations on laser glass interaction.

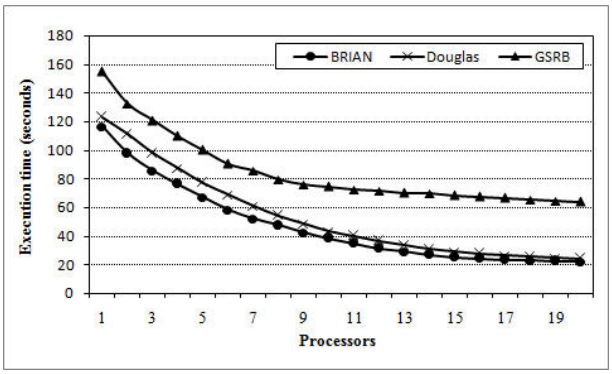


Figure 2. Execution time

Fig. 2 shows the results of parallel performance based on the execution time obtained from Brian, Douglas and GSRB methods. The results clearly show that as the number of processors p increases, the execution time decreases. It proves that when more processors are working together, the execution time will decrease gradually. However, by using Brian method the execution time has the lowest value compared with Douglas and GSRB methods.

Fig. 3 illustrates the performance of speed up using Brian, Douglas and GSRB methods. Based from the visualization obtained, BRIAN method records the highest value of speed up followed by Douglas and GSRB method. Speed up is a measurement on the speed of the processors to simulate the simulation in producing the results that intended. Thus, by using AGE Brian method, a large sparse point system is been used to decrease the execution time by increasing the speed during the calculation.

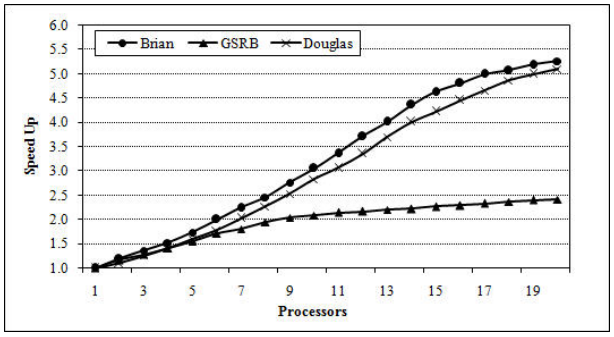


Figure 3. Speed up

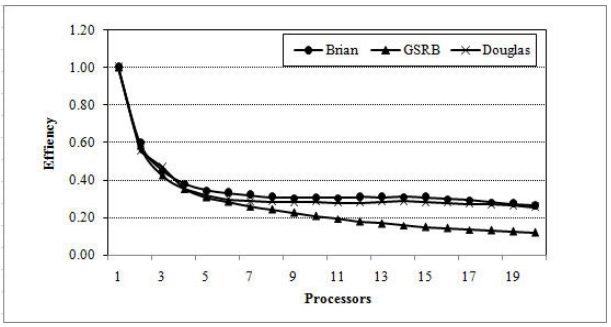


Figure 4. Efficiency

Based from Fig. 4, the efficiency slowly decreases as the number of processors p increases. However, by using Brian method, it produces a higher value of efficiency compared to Douglas and GSRB method. Hence, Brian method is much more efficient followed by Douglas and GSRB.

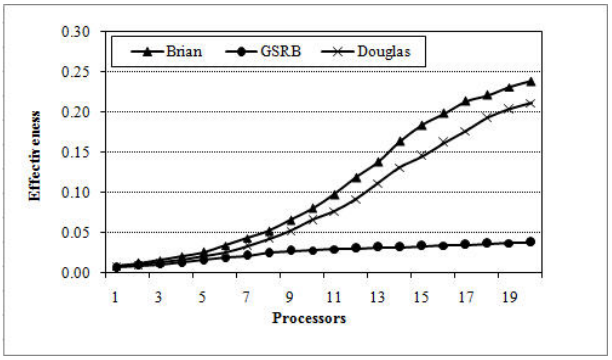


Figure 5. Effectiveness

Fig. 5 shows the effectiveness of the three methods used for the simulation on laser glass interaction. Effectiveness is the question on how the impact of these methods by cost and the accuracy provided by each method. AGE Brian method provide the highest effectiveness value compare to Douglas and GSRB methods. Therefore, AGE Brian method provides more accuracy and reduces the cost of calculation in the simulation process.

Fig. 6 shows the results of the temporal performance. Again, Brian method proves to be the better method. Brian method produces higher temporal performance followed by Douglas and GSRB methods.

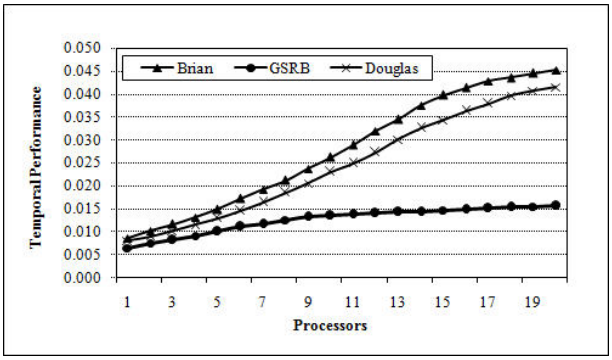


Figure 6. Temporal performance

V. CONCLUSION

To conclude, Brian method proves to be the better method to be used to simulate the laser glass interaction. From the visualization obtained, it supports Brian method to have better parallel performance compared to Douglas and GSRB methods. Douglas method shows that it is better than GSRB method. Thus to conclude, the Brian method is the best method that is more stable and more effective to simulate the temperature behavior on laser glass cutting followed by Douglas and GSRB method.

ACKNOWLEDGMENT

This material is based upon work supported by Fundamental Research Grant Scheme (FRGS), Malaysian Ministry of Higher Education under Vote No. 78598, 77264 and 78372. Any opinions, findings, and conclusions or recommendations expressed in this material are those from the authors and do not necessarily reflect the views of the Malaysian Ministry of Higher Education.

REFERENCES

[1] C. Hermans , "Laser Cutting of Glass", *Proceedings of SPIE - The International Society for Optical Engineering*, vol. 4102, pp. 219-226, 2000.

[2] I. Kono, A. Nakanishi, S. Warisawa and M. Mitsuishi " Non-Crack Laser Machining of Glass by using Absorbent Powder", *American Society for Precision Engineering (ASPE) Proceedings*, vol. 7, pp. 1793-1797, 2005.

[3] M. J. Weber, "Science and Technology of Laser Glass", *Journal of Non Crystalline Solids*, vol. 123, pp. 208-222, 2003.

[4] A. Tawai and C. Panjapornpon, "Nonlinear Model-Based Control for Parabolic Partial Differential Equation Systems", *Chia Mai Journal of Science*, vol. 35, pp.221-228, 2007.

[5] P. Solana, P. Kapadia, J. M. Dowden and P.J. Marsden, "An Analytical Model for the Laser Drilling of Metals with Absorption within Vapour", *London Journal of Physics*, vol. 32, pp. 942-952, 1999.

[6] W. Rheinboldt, "MANPAK: A Set of Algorithms for Computations on Implicity Defined Manifolds", *Computer Science and Applied Mathematics*, vol. 5, pp. 51-55, 1992.

[7] M. S. Sahimi, N. Alias, and E. Sundararajan, "The AGEB Algorithm for Solving the Heat Equation in Three Space Dimensional and its Parallelization using PVM", *Computational Science ICCS 2001*, vol. 2073, pp. 918-927, 2001.

[8] F. Fairag and M. S. Sahimi, "The Alternating Group Explicit (AGE) Iterative Method for Solving Ladyzhenskaya Model for Stationary Incompressible Vicous Flow". *International Journal of Computer Mathematics*, vol. 85(2): pp. 287-305, 2008.

[9] M. S. Sahimi, N. A. Mansor, N. M. Nor, N. M. Nusi and N. Alias, "A High Accurary Variant of the Iterative Alternating Decomposition Explicit Method for Solving the Heat Equation", *International Journal of Simulation and Process Modelling,* vol. 2(1/2): pp. 45-49, 2006.

Design and Implementation of MPPT Controlled Grid Connected Photovoltaic System

Md. Ismail Hossain
EEE Department
International Islamic University Chittagong (IIUC)
Dhaka, Bangladesh
Email: jewel04eee@yahoo.com

Shakil Ahamed Khan
EETE Department
Dhaka International University (DIU)
Dhaka, Bangladesh
Email: shakil_pilabs@yahoo.com

Md. Shafiullah
EEE Department
Bangladesh University of Engineering and Technology (BUET)
Dhaka, Bangladesh
Email: msu@fpvlbd.com

Mohammad Jakir Hossain
EEE Department
Dhaka University of Engineering and Technology (DUET)
Gazipur, Bangladesh
Email: jakir@duet.ac.bd

***Abstract*- This paper proposes an intelligent method for maximum power point tracking (MPPT) of a photovoltaic system under variable temperature and insolation conditions and conversion of this solar energy *into* stabilized sine wave having low distortion factor (DF), so that the solar energy can be supplied to grid and can operate electrical and electronic devices efficiently. For the reduction of tracking time of maximum power from photovoltaic array and to obtain stabilized sine wave with very fast rise time for voltage stability, fuzzy logic control algorithm is implemented with the embedded microcontroller for improved performance as compared to conventional techniques. The system includes a photovoltaic array; a PWM controlled DC-DC, DC-AC converters, sensor circuits and zero crossing detector (ZCD). The designed MPPT controller regulates the converter output voltage by varying modulation index of the PWM pattern using MPPT algorithm and it maximizes the output power extracted from photovoltaic array. This paper discusses the low cost implementation of MPP algorithm in a 8-bit microcontroller using the tools and techniques to generate optimized real time code in C for ATMega8 microcontroller which will demonstrate how maximum power point tracker might provide elegant and efficient solution for increasing the efficiency of a solar system and connection of the extracted energy to grid which is based on experimental results rather than on mathematical models.**

***Keywords*—PV module, MPP tracking, Voltage/current sensor, DC-DC converter, Fuzzy logic control, Grid connection.**

I. INTRODUCTION

Energy is the most basic and essential of all resources .All the energy we use on Earth comes from fission or fusion of atomic nuclei or from energy store in the Earth. The problem with both fission and fusion is that, they have dangerous radioactivity and side effect. Therefore, most of the generation of energy in our modern industrialized society is strongly depending on very limited non-renewable resources such as petroleum. As the world's energy demands rise and resources become scarce, the petroleum is getting more and more expensive. The search for alternative energy resources has become an important issue for our time. The people seek for new green and unlimited energy sources, e.g. wind energy, water energy, solar energy, etc. The most effective, reliable and harmless energy source is probably solar energy. Solar energy can be harvested by the use of photovoltaic (PV) array. But, there are still some drawbacks as follow: the install cost of solar panels is high, and the conversion efficiency is still lower. PV array has an optimum operating point to extract the maximum power called the maximum power point (MPP), which varies depending on cell temperature and insolation level, as shown in Fig. 1 and Fig. 2 respectively.

Variation in lighting intensity causes this trackers to deviate from the maximum power point when lighting conditions change, the tracker needs to response with in a short time to the change to avoid energy loss. Therefore, it is not easy to track the maximum power point of the PV cell quickly and effectively in the real application. To overcome this drawback, many MPPT algorithms were suggested for tracking the MPP of solar module [1], [8]. We have proposed a scheme as shown in Fig. 3, based on the use of conventional DC-DC converter, where combination of voltage and power feedback control system is implemented with the use of artificial intelligence algorithm which results in a two-dimensional tracking strategy that makes tracking response faster and maximizes the power extracted from the solar module and the power delivered to the load. Maximum power point tracking is assured by varying duty cycle of the PWM signal to control MOSFET switch applied to a boost converter [2]. The control logic is implemented to a microcontroller (ATMega8) with the use of fuzzy logic algorithm.

Designing a conventional controller presents problems since modelling the system is very difficult due to its non-linearity. For controlling such a complicated system, fuzzy logic control can be the best solution [3]. However, fuzzy technique, which has gained popularity in recent years, looks very promising for this application. The use of fuzzy logic in gate signals control in MPPT is tackled, analyzed, and implemented in this paper where MATLAB/SIMULINK simulation and experimental results are described. The

results show how well this controller eliminates the complexity and maximizes the power extracted from the solar module and the power delivered to the battery. For grid connected inverter design, which includes DC-DC converter, followed by a PWM inverter where feedback and fuzzy logic control is implemented to obtain output voltage stability so that the available energy can be supplied to the grid effectively. The output voltage is synchronized with the grid voltage by using Phase-Locked Loop (PLL) which is implemented software program and ZCD. Standalone operation is performed by detecting the abnormal grid condition.

II. MPP TRACKING

The characteristics of a PV system vary with temperature and insolation as shown in Fig. 1 and Fig. 2. So, the MPPT controller is also required to track the new modified maximum power point in its corresponding curve whenever temperature and/or insolation variation occurs.

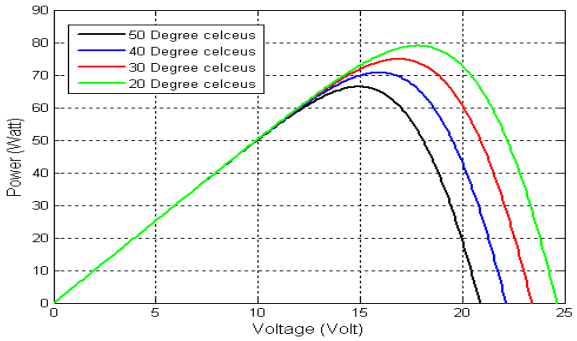


Figure1. Maximum power varies with different cell temperature at the same insolation

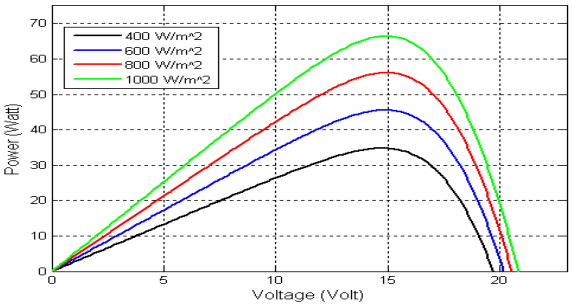


Figure2. Maximum power varies with different insolation at the same temperature

The MPPT algorithm employed based on voltage and power feedback control approach, with the step size being dependant on the slope of the power vs. voltage (P-V) curve as shown in Fig. 4. Conventionally with this methods,

$$\frac{dP}{dV_{PV}} = \frac{P(n) - P(n-1)}{V_{PV}(n) - V_{PV}(n-1)} \qquad (1)$$

MPP is defined by $\frac{dP}{dV_{PV}}(n) = 0$. When $\frac{dP}{dV_{PV}}(n) > 0$ (or $\frac{dP}{dV_{PV}}(n) < 0$), then the operation point is on the left (or right) of the MPP, and should be tuned toward opposite direction.

III. DESIGN CONSIDERATION

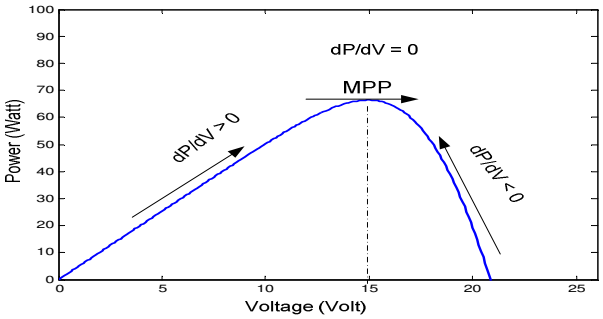


Figure4. P-V characteristic of a PV module

When a direct connection is carried out between the source and load, the output of the PV module is seldom maximum and the operating point is not optimal. So, a MPPT controller with a DC-DC converter is connected between the source and the load as shown in Fig. 3.

A. Hardware implementation

The feedback circuit consists of a voltage sensor and a current sensor. The sensors provide analog data as an output. For further processing of these data, A/D conversion is needed.

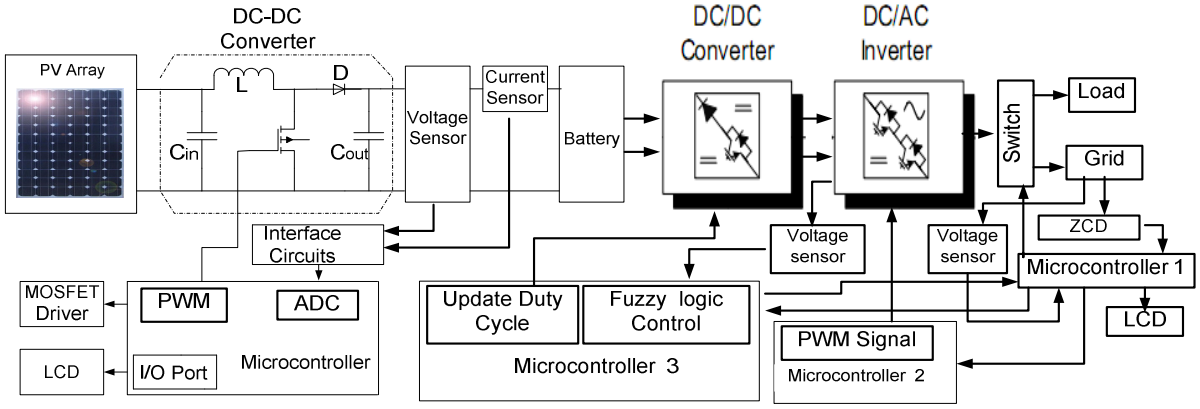


Figure3. Detailed system block diagram

Since ADC module contained in ATMega8 microcontroller and can work on voltage up to 5V, so it is an added advantage which reduces the cost of two A/D converters IC. The analog output of two sensors is connected to ADCO and ADC1 pin of ATMega8 microcontroller and the A/D conversion is completed by using software program. With a 10-bit ADC over the full range of mains voltage (0~30V) scaled to 0 to 5V. The resolution is 30/1024 or 0.03V. This is too high a resolution called for.

B. Voltage sensor for MPPT section

Voltage divider network is used as voltage sensor for the controller. The resistance values chosen are 22KΩ and 8.2KΩ. This gives the resistance ratio of 8.2KΩ/ (32KΩ+8.2KΩ) = 0.20 and therefore gives the maximum input voltage to the A/D conversion channel is 0.20×25=5.

C. Current Sensor for MPPT section

Differential amplifier circuit is used as current sensor for the controller. By connecting a current resistor at the inputs of the differential amplifier, the current from the PV array passing through the resistor and gives rise to a voltage drop across it. The voltage is then amplified by the differential amplifier. If the solar panel is assumed it operating its maximum capacity, the maximum output current is 4.85 amp, and if 0.5W dissipation is allowed for the current sensing resistor, the resistance value can be determined by $(0.5=4.85^2\times R)$ or $(R=0.5/4.85^2=0.0213\ \Omega)$. A 0.022 Ω surface-mount resistor is chosen for this design.

D. DC-DC Converter for MPPT section

The non-isolated boost DC-DC converter is widely used in stand alone PV system because it is simple, low cost and high efficiency. In general, the conversion efficiency is reading 90%. So, the boost is suitable for simple stand alone system. Here we adopted this converter as our regulator [4]. Fig. 3 depicts the circuits of the boost converter connected from the output of the solar cell. The power flow is controlled by varying the on/off duty cycle of the switching. The converter is operated at the switching frequency of 20 KHz. The average output voltage is determined by the Eq. (2) [5], [6].

$$\frac{V_{OUT}}{V_{IN}} = \frac{1}{1-D} \qquad (2)$$

Where, V_{OUT} is the output voltage V_{IN} is the input voltage and D is the duty cycle of controllable switch.

E. Hardware Implementation of grid connected inverter

The full bridge inverter stage is designed with MOSFET power transistors [6]. The drive signal for MOSFET power transistors is generated by the PWM (pulse width modulation) module contained in the microcontroller. The proper value of duty cycle is selected with the use of fuzzy logic control algorithm depending on the condition of inverter output voltage. With fuzzy logic, output voltage is stabilized while variation of the input range is 150V to 250V. For sensing the inverter output voltage, potential transformer is used to step down the output voltage and rectified by using full wave rectifier circuit. The output is then feed back to ADC0 pin of ATMega8 microcontroller. The ADC module contained in ATMega8 microcontroller is used to convert the voltage levels to digital value and can work on voltage up to 5V. A/D conversion is completed by using software program. With a 10-bit ADC over the full range of mains voltage (0~300V) scaled to 0 to 5V. The resolution is 300/1024 or 0.3V. This is too high a resolution called for. The rms value of the voltage is calculated by using the formula as given in (3).

$$V_{rms} = \sqrt{\frac{\sum_{n=1}^{4} V_n^{\,2}}{n}} \qquad (3)$$

If the output voltage decreases the *Vrms* voltage also decreases. The output voltage of inverter is rule-based. The rules logic is built into the software developed where fuzzy logic control system is applied so that whenever *Vrms* voltage decreases or increases; duty cycle of PWM varies to regulate the output voltage.

IV. FUZZY LOGIC IMPLEMENTATION ON EMBEDDED MICROCONTROLLER

Fuzzy logic controllers have the advantages of working with imprecise inputs, not needed an accurate mathematical model, and handling nonlinearity [7]. The inputs to a MPPT fuzzy logic controller are usually an error *E* and a change of error Δ*E* as given in (4) and (5) respectively [8].

$$E(n) = \frac{P(n)-P(n-1)}{V(n)-V(n-1)} \qquad (4)$$

$$\Delta E(n) = E(n)-E(n-1) \qquad (5)$$

The inputs to an AVR using fuzzy logic controller are usually an error voltage E and a change of error ΔE as given in (6) and (7) respectively.

$$E(n) = V(n)-V(n-1) \qquad (6)$$

$$\Delta E(n) = E(n)-E(n-1) \qquad (7)$$

E and ΔE are calculated and converted to the linguistic variables during fuzzification. Linguistic variables are non-precise variables that often convey a surprising amount of information. To simplify the control calculation, the values of error E and change of error ΔE can be normalized with (8) before fuzzification process:

$$Y_S = \begin{cases} -1, Y < -Y^* \\ Y/Y^*, |Y| < Y^* \\ 1, Y > Y^* \end{cases} \qquad (8)$$

Where, $Y^* = Y_{\max}$, so the scopes of error E and change of error ΔE will be [-1, 1]. Fig. 5 shows the relations between measured error and the linquistive term, such as positive small, positive medium and positive big. At some point the error is positive small and at some point the error is positive big the space between positive big and positive small indicates an error that is, to some degree, a bit of both. The horizontal axis in the following graph shows the measured or crisp value of error. The vertical axis describes the degree to which a linguistic variable fits with the crisp measured data.

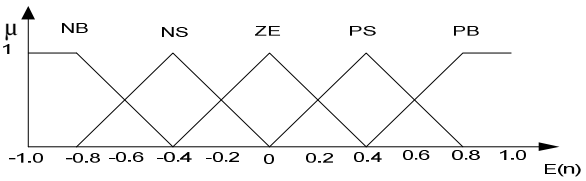


Figure5. The relationship between linguistics variable and error

To add the linguistics variable positive big to a computer program running in an embedded controller, translation the graphical representation into meaningful code is needed. The following C code fragment gives one example of how to do this. The function error- Positive Big ( ) returns a degree of membership, scaled between 0 and 1, indicating the degree to which a given error can be positive big. This type of simple calculation is the first tool required for calculations of fuzzy logic operations.

```
char Error_ Positive Big (int  CRISP)
   {
     if (CRISP < 0.4)
         return(0);
     else
        {
          if (CRISP >= 0.4)
             return(CRISP * 2.5);
          else
              {
                return(1);
   }}         }
```

Rule evaluation is done by using an algorithm where loops compare the antecedent value depending on the rule being evaluated in a repeated fashion until all rules are evaluated.

The fuzzy logic controller output is typically a change in duty ratio ΔD. The linguistic variables assigned to ΔD for the different combinations of E and ΔE as shown in Table I for MPPT and Table II for grid connected AVR system. If, for example, the operating point is far to the left of the MPP as shown in Fig. 4, that is E is PB, and ΔE is ZE, then we want to largely increase the duty ratio, that is ΔD should be PB to reach the MPP. The comparison of Matlab simulation for AVR using fuzzy logic and without fuzzy logic is shown in fig. 9.

TABLE I

FUZZY RULE BASE TABLE FOR MPPT

ΔE / E	NB	NS	ZE	PS	PB
NB	ZE	ZE	NB	NB	NB
NS	ZE	ZE	NS	NS	NS
ZE	NS	ZE	ZE	ZE	PS
PS	PS	PS	PS	ZE	ZE
PB	PB	PB	PB	ZE	ZE

The final step in the fuzzy logic controller is to combine the fuzzy output into a crisp systems output. The result of the defuzzification has to be a numeric value which determines the change of duty cycle of the PWM signal used to drive the MOSFET.

TABLE II

FUZZY RULE BASE TABLE FOR AVR

E / ΔE	NB	NS	ZE	PS	PB
NB	NB	NB	NS	ZE	ZE
NS	NB	NS	ZE	ZE	PS
ZE	NB	ZE	ZE	PS	PS
PS	ZE	ZE	PS	PS	PB
PB	ZE	PS	PS	PB	PB

There are various methods to calculate the crisp output of the system. Centre of Gravity (COG) method is used in our application due to better results it gives. The COG for our application is expressed mathematically as given in" (9),"

$$\Delta D = \frac{\sum_{n=1}^{4} Y[i] \times F[i]}{\sum_{n=1}^{4} Y[i]} \qquad (9)$$

Where Y[i] is the i^{th} members of the output vector and F[i] are the multiplying coefficients of the output membership function as shown in Table 1, and ΔD is the change of duty cycle, and this number represents a signed number which is added or subtracted from the present duty cycle to generate the next system response for reaching the MPP and inverter voltage stability.

V. FIRMWARE DESCRIPTION

A. MPPT section

The overview of fuzzy logic control MPPT is shown in Fig. 6. The Liquid Crystal Display is used to display output voltage, current, power and duty cycle. This information is used to tune fuzzy rules. The main loop is responsible for updating ADC value and calculating output voltage, current, power. Using these variables, duty cycle is calculated which is performed by using fuzzy logic control algorithm based on a single-chip unit ATMega8 microcontroller. With the output of controller, pulse generated from PWM can switch IRF540 MOSFET to change the duty cycle of the boost DC-DC

converter. Then the PV array output voltage can be adjusted to track the maximum power.

B. Grid connection Scheme

Fig. 3 shows the detail block diagram of the proposed scheme. The output of the grid voltage is stepped down by using potential transformer and rectified voltage is connected to ADC0 pin of microcontroller 1 for measuring grid voltage. Zero crossing detector circuit as shown in Fig. 6 is connected to INT0 pin of microcontroller 1 for measuring frequency of the grid voltage. The grid voltage is used as reference voltage for fuzzy logic input which is implemented in microcontroller 2 so that the duty cycle of the DC-DC converter will be updated to reduce the error voltage between inverter and grid.

The information of frequency from microcontroller 1 is supplied to microcontroller 2 for updating the number of pwm pulse to adjust the inverter frequency with the grid voltage.

When the difference voltage between grid and inverter is zero, then an interrupt pulse will be provided to microcontroller 1 from microcontroller 3. After receiving the interrupt signal, at zero crossing point of the grid voltage microcontroller 1 will provide a signal to microcontroller 2 for generating pwm signal from the beginning and will switch to grid supply simultaneously.
So the synchronization with grid is automatic in our system.

VI. TEST AND RESULT

The experimental layout for the real time test of fuzzy MPPT is shown in Fig. 10. From the experiment we observed that the implementation of the fuzzy logic algorithm in a low-cost microcontroller is capable of rapidly locking into the MPP for a photovoltaic panel under variable temperature and insolation conditions. Fig. 8 shows the control output surface of fuzzy logic using MATLAB/SIMULINK simulation. To adjust the grid voltage, the variation of duty cycle in DC-DC converter section is shown in Fig. 11. To obtain sine wave, the generation of PWM signal applied to DC-AC inverter is shown in Fig. 12 and the resultant sine wave is shown in Fig. 13.

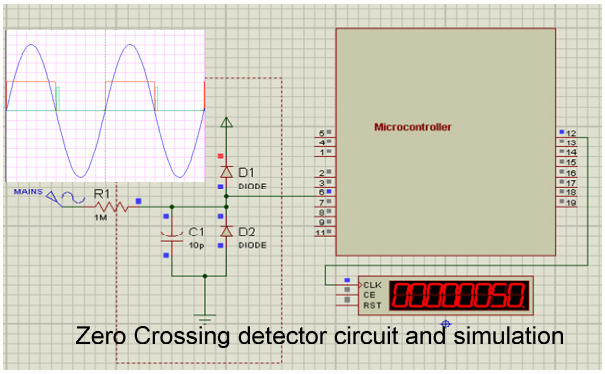


Figure6. Zero crossing detector

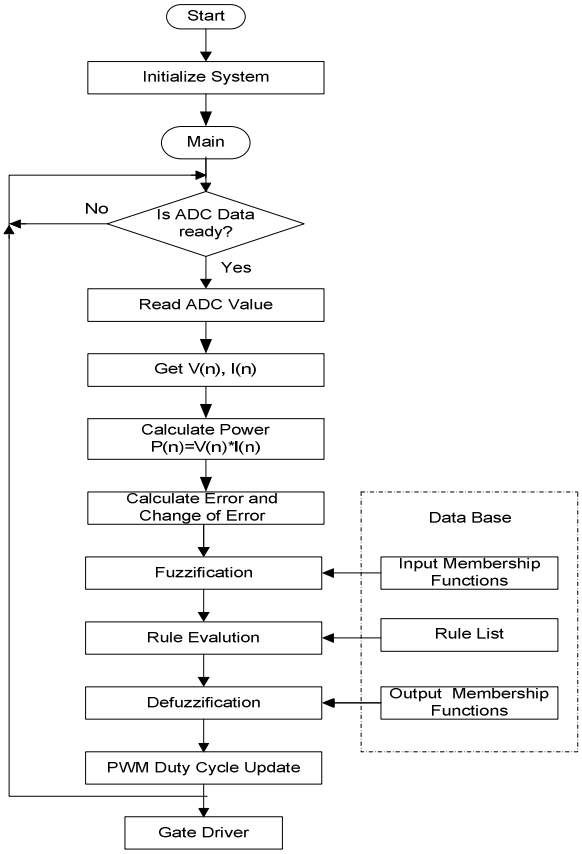


Figure7. Fuzzy MPPT algorithm

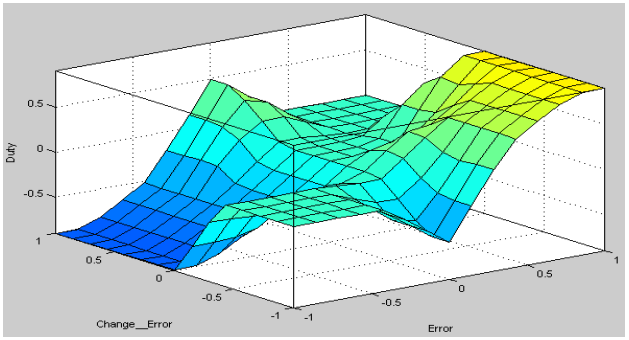


Figure8. Fuzzy control output surface

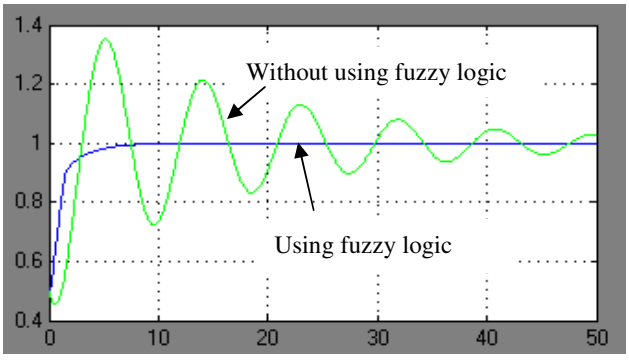


Figure9. MATLAB/SIMULINK result of fuzzy logic

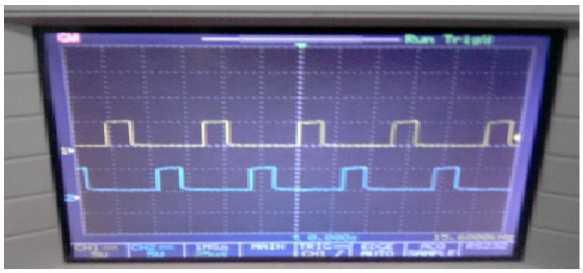


(a)

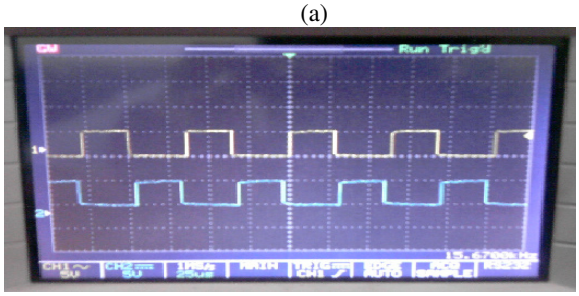


(b)

Figure10. Photos of MPPT controlled output, (a) Output results of MPPT controller (b) Tuned fuzzy MPPT controlled outputs for changing inputs



(a)



(b)

Figure11. (a) MOSFET gate pulse with 40% duty cycle in DC-DC converter section (b) 50% duty cycle

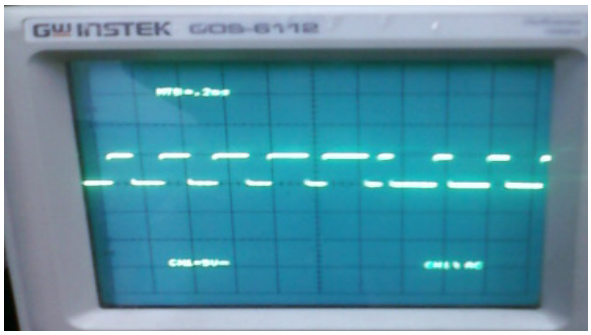


Figure12. PWM signal for sine wave inverter

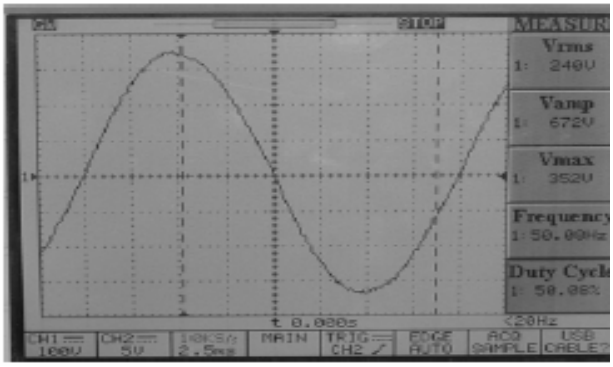


Figure13. Output sine wave of the inverter

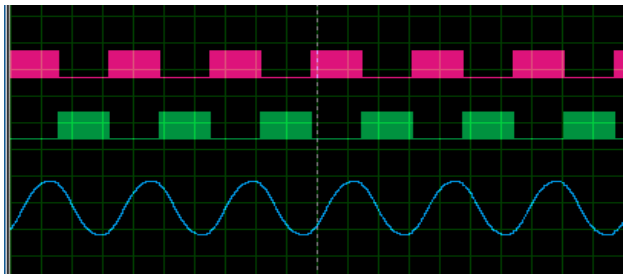


Figure14. Simulation of PWM and output sine wave in proteus software

VII. CONCLUSION

This paper has demonstrated the implementation of FLC to a microcontroller for MPPT of a PV module and AVR for an inverter which will be connected to grid in synchronizing condition. The FLC is easy to implement and require a small amount of inexpensive components in compact size. The designed controller is capable of rapidly locking into the MPP for a photovoltaic panel and very first rise time for voltage and frequency stability of the inverter.

REFERENCES

[1] H. P. Desai & H. K. Patel, "Maximum power point algorithm in PV generation: an overview." International conference on Power Electronics and Drive Systems, (PEDS07), Nov 27-30th, Thailand, 2007. pp. 637-641.

[2] H. Matsuo and F. Kurokawa., "New solar cell power supply system using a boost type bidirectional DC-DC converter", *IEEE Electron*, vol. 31, pp. 51- 55, Feb. 1984.

[3] Bor-SenChen, Chung-Shi Tseng and Huey-Jian Uang, "Robustness Design of Nonlinear Dynamic Systems via Fuzzy Linear Control," *IEEE Fuzzy Systems*, vol. 7, no. 5, pp. 571-585, Oct. 1999.

[4] N. Ozog, W. Xiao, and W. G. Dunford, "Topology study of Photovoltaic interface for maximum power point tracking," *IEEE Electron*., vol. 54, no. 3, pp. 1696–1704, Jun. 2007.

[5] Simoes, M. G., Franceschetti, N. N. and Friedhofer, M., "A Fuzzy Logic Based Photovoltaic Peak Power Tracking Controller," Proceedings of the IEEE Inter-National Symposium on Industrial Electronics, pp. 300-325 (1998).

[6] Mohammed H. Rashid. "*Power Electronics*" Prentice-Hall of India Private Limited, 2nd ed., 1994.

[7] M.Veerachary, T.Senjyu, and K.Uezato,"Neural-network-based maximum-power-point tracking of coupled-inductor interleaved-boost-converter-supplied PVsystem using fuzzy controller," *IEEE Electron*, vol.50, no.4,pp.749–758,Aug.2003.

[8] Trishan Esram and PatrickL. Chapman, "Comparison of Photovoltaic Array Maximum Power Point Tracking Techniques," *IEEE Energy Conversion*, Vol.22, No. 2, pp439-449, June 2007

Water Pipe Leak Detection Using Electromagnetic Wave Sensor for the Water Industry

J. H. Goh, A. Shaw, J.D. Cullen, A. I. Al-Shamma'a
Liverpool John Moores University, Built Environment and Sustainable Technologies (BEST) Research Institute,
RF and Microwave Research Group, Henry Cotton Building, 15-21 Webster Street, Liverpool, L3 2ET, UK

M. Oliver, M. Vines, M. Brockhurst
Balfour Beatty Utility Solutions, West Service Road, Raynesway, Derby, DE21 7BG, UK

***Abstract*- This project concerns the use of an electromagnetic sensor for the detection of leaks/cracks in water pipes. As old metal pipes corrode, they start to become brittle, resulting in the potential for cracks to appear in the pipes. In addition corrosion can build up resulting in a restricted flow of water in the pipe. Using an electromagnetic (EM) sensor to monitor the signal reflected from the pipes in real time, provides the necessary information to determine where a leak in the pipe has occurred. Analysis of the reflected signal can provide the operator with information about the condition of the leak within the pipe. This work describes how the system was designed, and also its construction at a scale suitable for insertion into a 100mm diameter water pipe.**

I. INTRODUCTION

The purpose of this project is to reduce the water loss from public water supply distribution networks by identifying leaks in cast iron pipes. This research has investigated whether EM waves can be used to pinpoint the exact location of leaks in water pipes by using an internal EM wave sensor. This sensor is launched into the live drinking water mains through any existing hydrant and deployed using a mechanical drive on the launch chamber developed by Balfour Beatty [1]. The aim is to design a new sensor that can obtain a level of accuracy well above industrial demands.

The present technology used in the detection of leaks is acoustic and ground penetrating radar (GPR). Both of these techniques have their advantages and limitations. The acoustic [2,3] techniques are the most widely used in leak detection. They are based on the continuous analysis of the pipeline pressure, flow, temperature and density. The acoustic failed to perform optimally within the criteria of response time, robustness, reliability, sensitivity, accuracy and cost.

The GPR [4,5,6] uses low frequency EM waves to create an image of the subsurface by detecting the reflected signals from subsurface structures. It transmits the EM wave into the ground, and when the wave hits a buried object, the receiving antenna records a reflected signal. The GPR technique cannot differentiate between water, gas or oil pipelines and DSP [7] analysis required takes hours to complete. The water companies therefore still require a quick, cost justified, large scale method of identifying areas of actual leakage.

As a result, a new method was introduced which uses electromagnetic wave propagation.

II. ELECTROMAGNETIC THEORY FOR LEAK DETECTION

Maxwell's equations [8] describe the relation of the electric and magnetic field to each other and to the position and motion of charged particles. Maxwell's equations relate the electric and magnetic fields to their sources, charge density and current density. The equations can be combined to show that light is an electromagnetic waves. The four fundamental electromagnetic equations are given in (1) to (4),

$$\nabla \cdot D = \rho \tag{1}$$

$$\nabla \cdot \mathrm{B} = 0 \tag{2}$$

$$\nabla \cdot \mathrm{E} = -\frac{\partial \mathrm{B}}{\partial t} \tag{3}$$

$$\nabla \cdot \mathrm{H} = J + \frac{\partial D}{\partial t} \tag{4}$$

In the above equations, E represents the electric field in volts per metre (Vm^{-1}) and H represents the magnetic field in amperes per metre (Am^{-1}). D is electric displacement field in coulombs per square metre (Cm^{-2}) and B is the magnetic flux density in tesla (T). J is the electric current density in amperes per square metre (Am^{-2}) and ρ is the electric charge density in coulombs per cubic metre (Cm^{-3}).

Water is transported in circular cross section metal pipes, which can be treated as a circular waveguide. Waveguide is a particular form of electrical transmission line that is generally used at microwave frequencies. When the pipe is filled with water, rather than air, it can operate at much lower frequencies, this is due to the speed of the EM wave in the two different mediums (water and air).

The speed of an EM wave in vacuum is approximately 3×10^{8}m/s, which is speed of light (c). The speed of an EM wave is reduced by a factor $\sqrt{\varepsilon_r \mu_r}$ when it travels through a material, where ε_r is the relative permittivity, and μ_r is the relative permeability of the material. ε_r for the water at the frequencies considered is approximately 81, at room temperature, and μ_r is 1, therefore, the speed of the EM wave

in fresh water at these frequencies is found approximately using equation 5,

$$c_{water} = \frac{c_{vacuum}}{\sqrt{\varepsilon_r \mu_r}} = \frac{3\times10^8}{\sqrt{81\times1}} = 3.33\times10^7\, m/s \qquad (5)$$

The electrical power is transported through a metal pipe by means of electromagnetic waves, which can take several different forms (modes), depending on the frequency the pipe dimensions and the material properties inside. This determines how the electric and magnetic fields appear in the pipeline.

The two most important modes in the circular waveguide are known as TE_{11} and the TM_{01} modes which are shown in Fig. 1. The solid line in Fig. 1 represents electric field and the dotted line represents the magnetic field. These modes differ from electromagnetic waves in free space because they have to be higher than a certain minimum frequency in order to be able to propagate through the pipe at all. For a typical 4 inch metal pipe, the so called cut off frequencies [9], below which there is no propagation is 192MHz for the TE_{11} mode and 251MHz for the TM_{01} mode. Consequently, between 192MHz and 251MHz, only the TE_{11} mode can propagate.

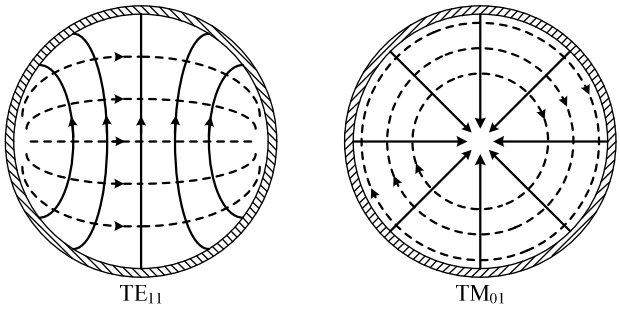


Fig. 1. Electromagnetic mode patterns in a circular waveguide [10]

III. Loop Antenna

The loop antenna is a directional type antenna which consists of one or more complete turns of a conductor [11]. The loop antenna has a very low radiation resistance because it acts as an inductive component [12,13]. The advantages of the loop antenna is that it strongly responds to the magnetic field (H) of the EM waves, and is less affected by the man-made interference. The loop antenna also picks up less noise, providing a better signal to noise ratio (SNR).

IV. HFSS Simulation

High Frequency Structure Simulator (HFSS) [14,15] is a full wave electromagnetic wave simulator software which can be used to designed RF structures. The advantage of HFSS is that it allows complex geometries to be created compared to other packages. To determine the most suitable frequency range for the loop antenna, a simulation was run in HFSS. Fig. 2 shows the HFSS model of a 4 inch diameter cast iron cylinder filled with fresh water an antenna at each port.

To validate the HFSS simulations for the antenna, Fig. 3 shows the experimental setup for the water pipe. The water pipe was filled with water and two antennas were used. The length of the cast iron pipe was 510mm. A vector network analyzer (VNA) was used to sweep the frequency from 200MHz to 600MHz. The $|S_{11}|$ and $|S_{21}|$ results for the HFSS simulation and the experimental results are shown in Fig. 4 and Fig. 5.

In Fig. 4 both set of $|S_{11}|$ results have a similar underlying shape. The minimum of the both results is approximately at the same frequency region around 480MHz although the amplitude is different. Therefore, the reflection spectrum $|S_{11}|$ shows a level of agreement between the HFSS simulation and the experimental results, which shows that the operational frequency range determined by simulation is correct.

In Fig. 5 the shape of the both results is also comparable. The peak of the both results is clearly shown, but there is a slightly different in the resonant frequency with that of the experimental results being around 310MHz while the peak of the HFSS simulation is around 350MHz. This is likely to be due to the concrete liner on the inner surface of the cast iron pipe supplied by Balfour Beatty.

There is no clear resonance shape for the $|S_{21}|$, so it will be difficult to use to determine a leak. A resonant peak is clearly shown at around 480MHz for $|S_{11}|$, so this can be used to determine if there is a leak in the water pipe using the EM wave sensor system.

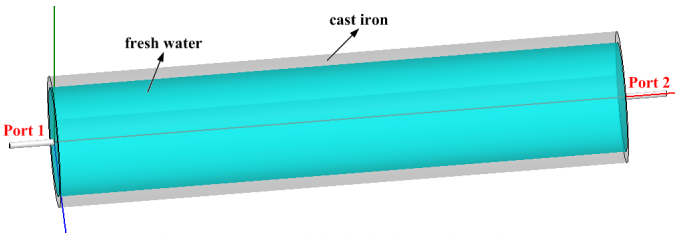


Fig. 2. HFSS model of 4 inch cast iron pipe

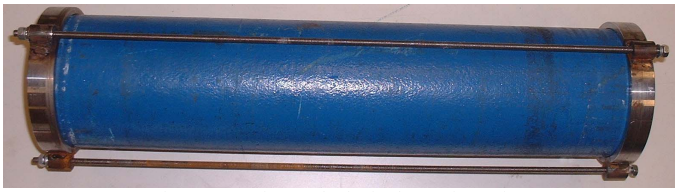


Fig. 3. Experimental of 4 inch cast iron pipe

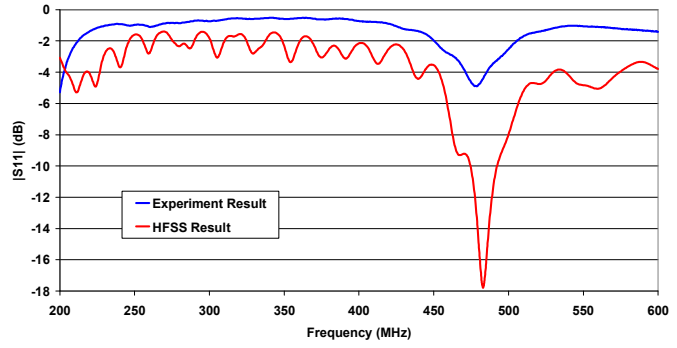


Fig. 4. Reflection signal $|S_{11}|$ of experiment and HFSS for loop antenna

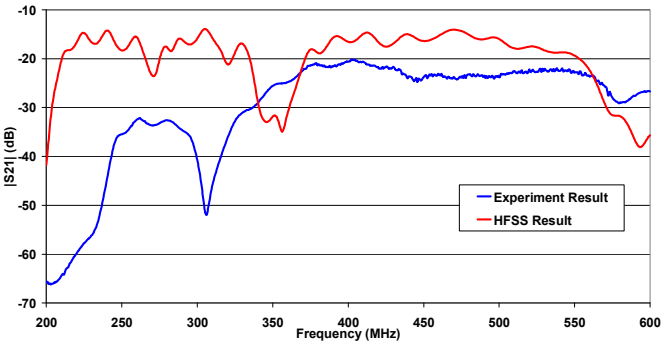


Fig. 5. Transmission signal $|S_{21}|$ of experiment and HFSS for loop antenna

It was then necessary to repeat the tests with a cracked pipe. A crack was made in the pipe and it was simulated using HFSS as shown in Fig. 6. The 4 inch cast iron cylinder is filled with fresh water and antennas at each port. A crack was made at the centre position on the cast iron cylinder. The simulation results for $|S_{21}|$ are shown in Fig. 7, and the attenuation caused for all crack widths, led to the signal dropping by 20dB. It can see the amplitude also falls as the width of the crack increases from 1mm to 10mm at 320MHz and 340MHz.

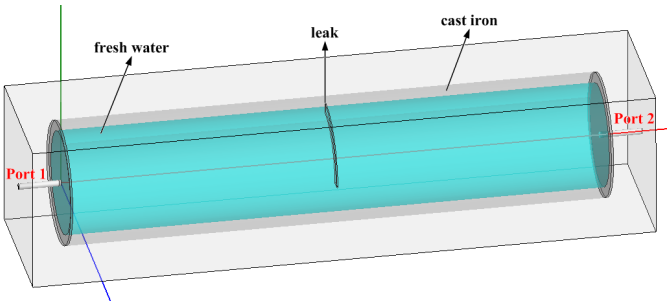


Fig. 6. HFSS simulation for water pipe leak

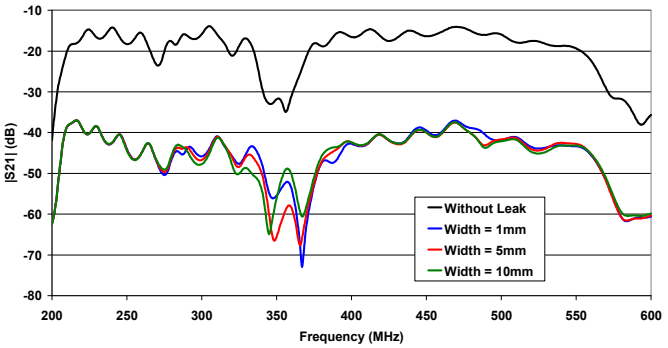


Fig. 7. Transmission signal $|S_{21}|$ of HFSS simulation result for water pipe leak

To validate the HFSS simulations for the water pipe leak, the experiment was setup as shown in Fig. 8. The pipe was totally filled with water and the two mild steel end caps were used to house an antenna at both ends. Then a 0.5mm crack was sawn in the central pipeline. The comparison results for this experiment with and without the crack are presented in Fig. 9. The attenuation at the lower frequencies the crack occurs on the signal for leakage pipe which same situation from the HFSS software simulation in previous simulation. The amplitude of the signals and the frequency of the resonance changes when the crack of the pipeline is made. The signal is down for 30dB at frequency region around 230MHz.

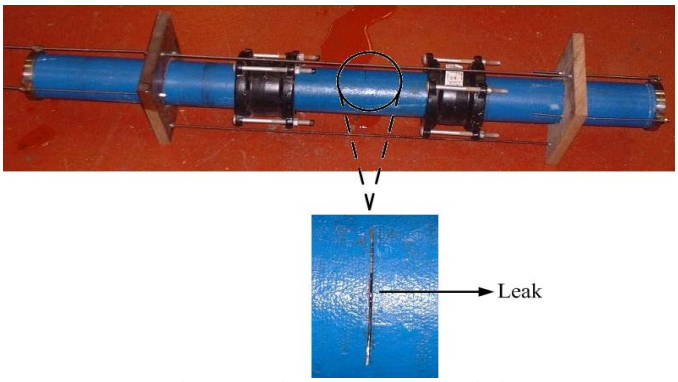


Fig. 8. Experimental for water pipe leak

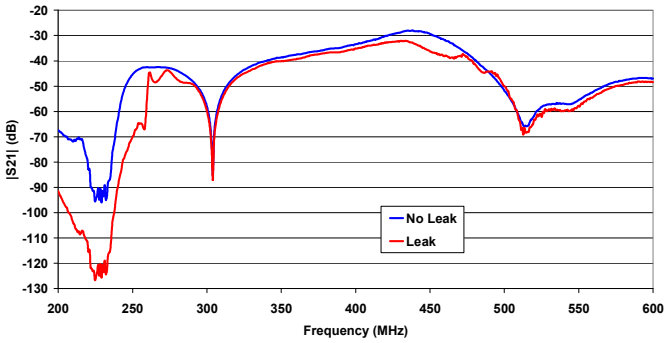


Fig. 9. Transmission signal $|S_{21}|$ versus frequency for water pipe leak

V. Prototype Sensor And PCB Design

The next stage was to construct a sensor that could be moved inside the pipe. This consisted of a stainless steel body to house the electronics with a nylon spacer and a loop antenna at the front. The electronic housing allows the electromagnetic radiation to radiate efficiently from the antenna. The antenna is connected to the VNA via a coaxial feed cable.

The next step was to design a surface mount version of the electronics that could fit within the stainless steel housing. Fig. 10 shows the complete PCB circuit board fully populated with the components for the sensor. The components include the voltage controlled oscillator (VCO) ROS-535+, voltage regulator LM317, voltage amplifier CA3140E, directional coupler ADC-10-1R+ and power detector MAX2015.

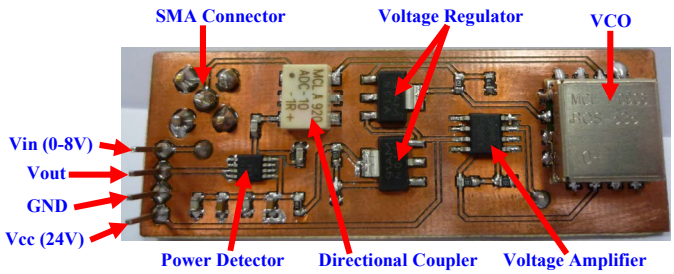


Fig. 10. Complete PCB circuit board with full components for the sensor

The PCB board was made using a computer numerical control (CNC) routing machine. The overall length of these circuit boards was 65mm and width was 22mm.

The block diagram for the electronics of a standalone EM wave sensor is shown in Fig. 11. For this circuit, a 24V power supply supplied the two voltage regulators (LM317) and the amplifier (CA3140E). The voltage regulators produced a 5V and 12V output voltages for the RF power detector MAX2015 and the voltage controlled oscillators (VCO) ROS-535+. LabVIEW programming software was used to control the NI Compaq DAQ with analogue output module NI9264 to produce an output voltage range from 0 to 8V, which was then amplified from 0 to 16V which will gives the full range of frequency output. The VCO produces a frequency sweep from 240MHz to 560MHz. The RF output from the VCO passes through a directional coupler ADC-10-1R+ and was then connecting to the antenna via an SMA connector. This allowed the reflected power to be measured via an RF power detector. The reflected signal power level is the $|S_{11}|$ parameter which is required for the RF signatures. The output from the RF power detectors is a DC voltage in the range of 0 to 2V which is then connected to the analogue input module NI9205 from which LabVIEW plots out the spectrum.

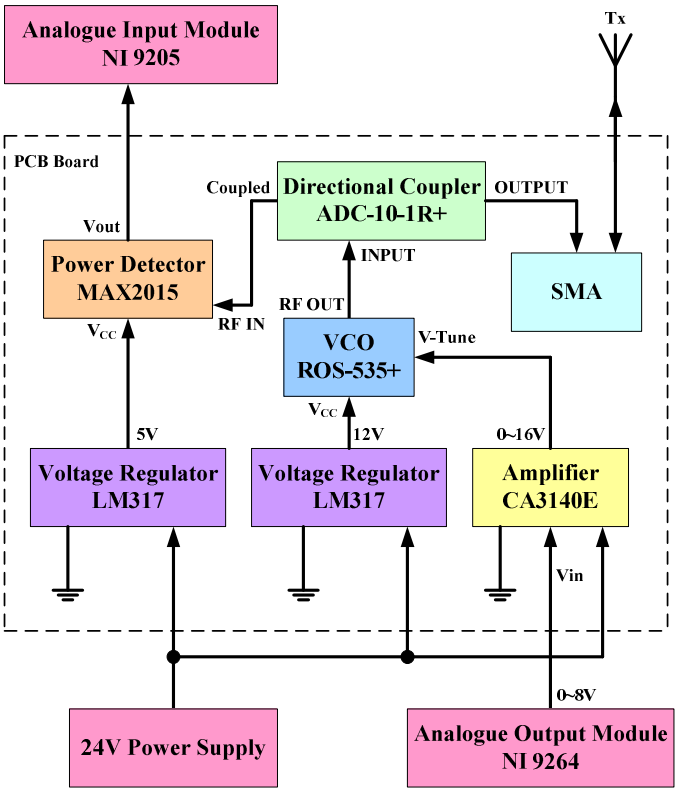


Fig. 11. Block diagram for PCB circuit board sensor

VI. Leak Detection

The final stage is to prove that the EM wave sensor can detect a leak in the pipeline. The first step is to obtain the reference signal spectrum for the 4 inch metal pipeline, then the sensor is put into the pipeline and the signal spectrum is compared with the reference signal. The signal comparison was done by the LabVIEW programme and the programme made a conclusion whether or not the pipeline needs further inspection.

Fig. 12 shows the experimental setup for leak detection. This experiment is setup with three 4 inch diameter pipelines sections connected together. These pipelines were mounted vertically and filled with water. The total length of the pipelines sections was 1480mm. The EM wave sensor with the electronics circuit which is shown in Fig. 10 was put into pipeline from the top of the pipe and the EM wave sensor passed through the centre of the pipeline.

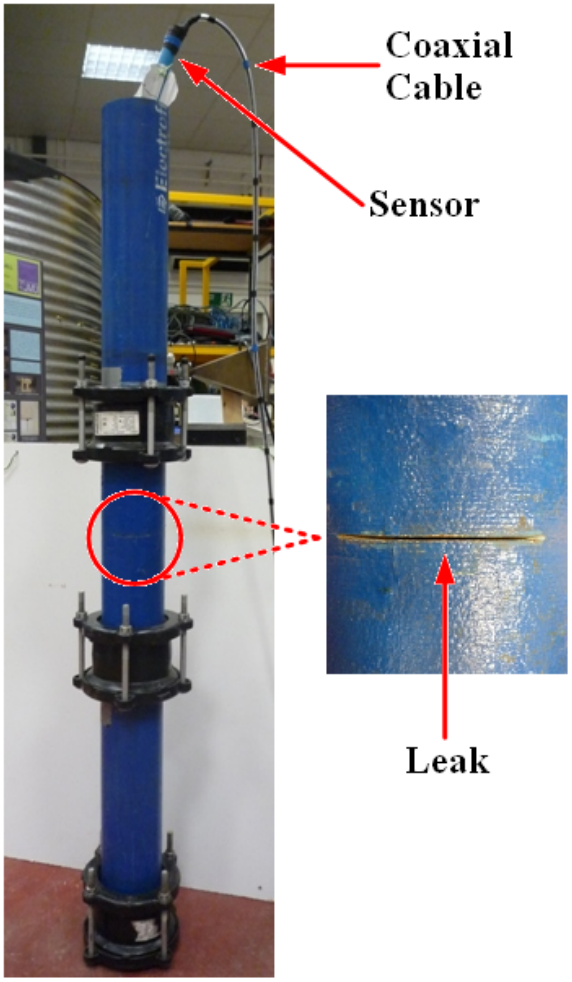


Fig. 12. Experimental setup for water pipe leak detection

The reference signal was taken at regular interval down the pipe and saved in a database. After that, a crack was made in the central pipeline to demonstrate that the EM wave sensor was able to detect leakage in the water pipeline. The crack was in the centre position of the second pipeline section away from any of the joints and at 74cm from top of the pipeline.

The measurements for the reflection signal $|S_{11}|$ were taken using the LabVIEW programme, and the reflection signal $|S_{11}|$ was compared with the reference signals that were obtained in the previous measurement. The LabVIEW programme then

made a conclusion on whether the pipeline needed further inspection. Fig. 13 shows the waveform comparison for the signal at 70cm depth in the pipeline. The waveforms were then compared using the Pearson correlation statistic method via the LabVIEW programme. The resonance peak has a huge change and attenuation occurs for the signal spectrum at 70cm depth compared to the reference signals. The LabVIEW programme shows the 'Pipe Needs Visual Inspection' in Fig. 13, which mean that a leak has been detected at this region of the pipeline and needs further inspection.

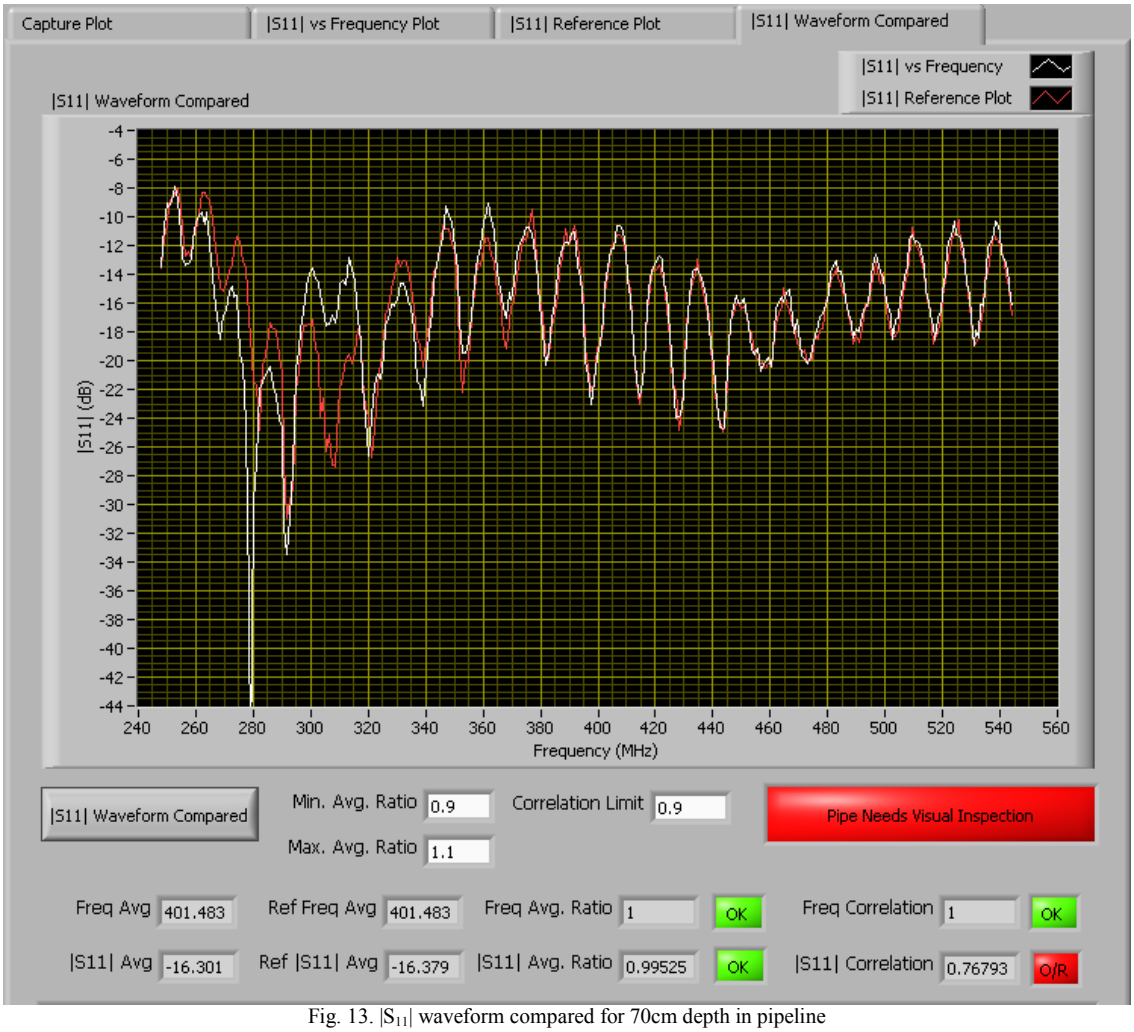


Fig. 13. $|S_{11}|$ waveform compared for 70cm depth in pipeline

VII. Conclusion

This research has proved that EM waves at high frequency in water are possible. Propagation of EM waves in water is affected by parameters including permittivity (ε) and conductivity (σ). The HFSS and experimental results showed good agreement throughout the project, and this helped in understanding the interaction between the water pipeline and the EM wave from the antenna. The attenuation was observed to be a good indication of water pipe leaks. The LabVIEW programme created for this project evaluates the output of the EM wave sensors and gives a recommendation about whether the water pipeline needs further investigation. For further work and development, leaks at different positions and the pipes with more than one leak should be investigated. Further work should also be done to improve the matching of the antenna to 50Ω which should improve signal strength.

References

[1] Balfour Beatty Utility Solutions, West Service Road, Raynesway, Derby, DE21 7BG, UK.

[2] D. B. Sharp and D. M. Campbell, "Leak Detection in Pipes Using Acoustic Pulse Reflectometry", Department of Physics and Astronomy, University of Edinburgh.

[3] M. J. Brennan, P. F. Joseph, J. M. Muggleton and Y. Gao, "Some Recent Research on the use of Acoustic Methods to Detect Water Leaks in Buried Plastic water Pipes", Institute of Sound and Vibration Research, University of Southampton.

[4] Mansor Nakhkash and Mohammad R. Mahmood-Zadeh, “Water Leak Detection Using Ground Penetrating Radar”, IEEE Tenth International Conference on Ground Penetrating Radar, 21-24 June, 2004, pp. 525-528.
[5] Seung-Yeup Hyun, Yu-Sun Jo, Heon-Cheol Oh and Se-Yun Kim, “An Experimental Study on a Ground Penetrating Radar for Detecting Water-Leaks in Buried Water Transfer Pipes”, IEEE Antennas, Propagation and EM Theory, 2003, pp. 597-599.
[6] S.R. Pennock, M.A. Redfern, and Q. Shan, “Subsurface Illumination And Propagation In Ground Penetrating Radar”, Department of Electronic & Electric Engineering, University of Bath, IEEE Antennas and Propagation, 2006, pp. 1-5.
[7] Yumei Wen, Ping Li, Jin Yang and Zhangmin Zhou, “Information Processing in Buried Pipeline Leak Detection System”, College of Opto-electronic Engineering, University of Chongqing , IEEE Information Acquisition, 2004, pp. 489-493.
[8] Joseph F. White, “High Frequency Techniques: An Introduction to RF and Microwave Engineering”, A John Wiley & Sons, Inc, 2004
[9] David M. Pozar, “Microwave Engineering, 2nd Edition”, John Wiley & Sons, Inc, 1998.
[10] John D. Kraus, “Electromagnetics, 4th Edition”, McGraw-Hill International Editions, 1992.
[11] K.F. Lee, “Principles of Antenna Theory”, Wiley, 1984.
[12] Joseph Carr, “Antenna Toolkit, 2nd Edition”, Newnes, 2001.
[13] John D. Kraus and Ronald J. Marhefka, “Antennas For All Applications, 3rd Edition”, McGraw-Hill International Editions, 2002.
[14] Ansoft Corporation, “Parametrics and Optimization using Ansoft HFSS”, Product Feature, Horizon House Publications, 1999.
[15] D. M. Park and J. J. Choi, “Three-Dimensional Simulation of X-Band Coupled Cavity Traveling Wave Tube Amplifier”, Journal of the Korean Physical Society, Vol.43, No. 6, Dec 2003, pp.1150-1111.

Design of Tunable Folded Cascode Differential Amplifier Using PDM

Ashis Kumar Mal*, Rishi Todani† and Om Prakash Hari‡
ECE Department, NIT Durgapur, INDIA - 713209
*akmal@ece.nitdgp.ac.in
†todani.rishi@gmail.com
‡om.nitd@gmail.com

***Abstract*—Operational Amplifiers (op-amps) are one of the most commonly used blocks in analog and mixed signal VLSI design. Designers often spend considerable time in designing op-amps analytically, and then realize that the simulated circuits do not match with analytical expectations. This is primarily due to modeling of short channel MOS devices using long channel equations. Finally an adhoc mechanism is adopted to realize the op-amp with the help of a simulator. Proposed Potential Distribution Method (PDM) is a method where the design methodology is based on actual behavior of the devices and it is free from any analytical expression. This paper demonstrates the design approach for realizing a fully differential folded cascode op-amp using PDM, which is based on simulator results obtained with predefined bias conditions. The dependency of various performance parameters, like slew rate (SR), unity gain bandwidth (UGB), phase margin (PM), etc. on potentials and current distribution at different nodes is presented. It is found that using these dependencies, the target specifications for an op-amp can be achieved with shorter design time. Also, fine tuning the performance metric can be achieved using PDM. Finally, a fully differential folded cascode op-amp is thus designed and the simulation results are presented.**

I. Introduction

This paper introduces a novel approach to analog design. Traditionally, analog designs are carried out by analytical methods [1]–[5], and then verified and fine tuned using a SPICE like simulator. Often, it is observed that final design variables (values) are far away from the estimated values obtained from analytical expressions. The difference in predicted design values can be reduced if complex models like BSIM etc. are used [6]–[8]. But then designer has to seek the help of another simulator, optimizer or programming method to handle those complex equations [9]–[12]. Whatever may be the approach, net time to design any analog block increases, specially for designs using short channel devices.

Potential Distribution Method (PDM) is an approach which is free from any mathematical expression and can be applied to both, long and short channel devices. Being free from analytical models, novice designers can design op-amps with reasonably good performance and within a shot period of time. This design methodology is independent of power supply (V_{DD}) and technology. It directly utilizes a simulator (SPICE) for designing any block satisfying the design specifications. PDM also enables us to fine tune the blocks AC response as per desired specifications. For example, to design an op-amp, a designer often finds it difficult to keep all the transistors in saturation. It is to be mentioned that PDM eliminates this problem and it forces all the transistors to be in saturation.

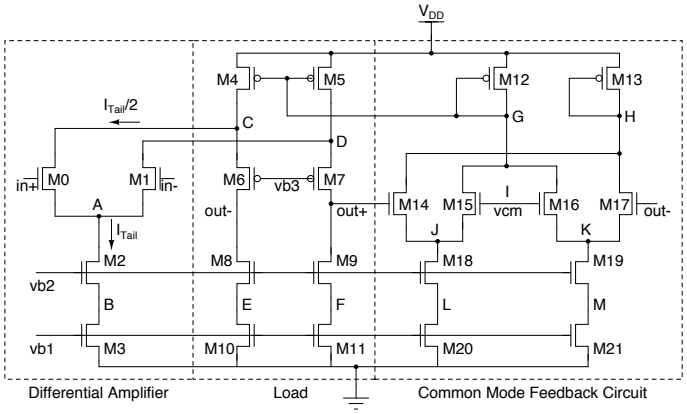


Fig. 1. Schematic of folded cascode differential amplifier

In the following sections, we illustrate how PDM can be employed to design a folded cascode differential amplifier.

II. Design of Folded Cascode Differential Amplifier

A differential amplifier with various subsections is shown in Fig. 1. A, B, C, etc. are the names of the various nodes in the design.

A. Threshold voltage estimation

It is known that stacking of transistors lead to body bias, which in turn increases the threshold voltage of the devices. For a typical 180 nm CMOS process, the effect of body bias on threshold voltage is shown in Fig. 2.

Let V_{Tuv} be the threshold voltage of all MOS devices of type v (NMOS or PMOS), with u numbers of v type MOS devices between itself and supply rail. Referring Fig. 1, since u takes value 0, 1 and 2, transistors M0 through M21 are diftributed into three categories, and their approximate threshold voltage is estimated using Fig. 2.

1) Transistors with $u = 0$: NMOS transistors M3, M10, M11, M20 and M21, do not experience any body bias. Referring Fig. 2, the threshold voltage of these transistors are equal to their zero bias threshold voltage given by $V_{T0n} \approx 0.45$

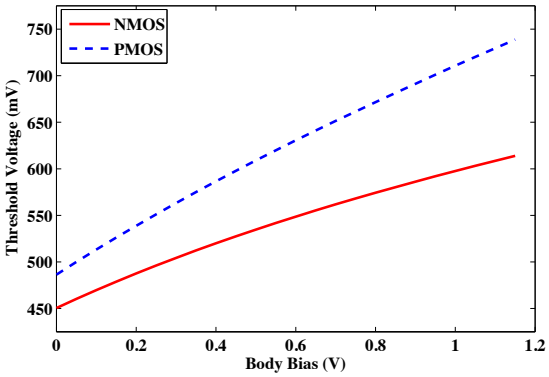


Fig. 2. Effect of body bias on threshold voltage in UMC 180 nm technology

V. Similarly, let the threshold voltage of PMOS transistors, M4, M5, M12 and M13, which also do not see any body bias be denoted by $|V_{T0p}| \approx 0.49$ V.

2) Transistors with $u = 1$: NMOS transistors M2, M8, M9, M18 and M19 are stacked by one transistor, thus $u = 1$. Assume a body bias for these transistors of around 10% of V_{DD}, which increases their threshold voltage by around 10% to $V_{T1n} \approx 0.475$ V. PMOS devices, M6 and M7, are stacked by current sources M4 and M5 respectively. The source to gate voltage of M4 and M5 are definitely more than V_{T0p} since it is derived from diode connected M12. Keeping M4 and M5 is deep saturation, we initially allow 33% of V_{DD} as their source to drain potential. Due to this body bias, for M6 and M7, we approximate $|V_{T1p}| \approx 0.625$ V.

3) Transistors with $u = 2$: The differential pair (M0 and M1) have a gate bias equal to V_{CM}, which is considered to be at $V_{DD}/2$ for this example. Just like 10% of V_{DD} was allowed across M3, additional 10% is allowed across M2. Thus, the differential pair sees a body bias of around 20% of V_{DD} leading to a threshold voltage $V_{T2n} \approx 0.5$ V. Care should be taken that the potential at node A is at least V_{T2n} less than V_{CM}, failing which, the differential pair transistors may enter cut-off region. Transistors M14 through M17 are also stacked in a similar manner and have a threshold voltage of V_{T2n}.

B. Voltage Constraints

To keep the transistors in saturation, the potential at nodes, labelled in Fig. 1, can be expressed with an upper and lower limit in terms of the threshold voltage and gate bias of other transistors. These constraints may be derived from the fact that the transistor is in saturation if $V_{DS} \geq V_{GS} - V_T$ with $V_{GS} \geq V_T$. In the following subsections, the upper and lower limits of the node and bias voltages are given. It should be noted that, although these conditions were proposed for long channel devices, the same can be used for even short channel devices in this design methodology while defining node potentials.

1) Node Voltages: The constraints on node voltages are,

$$vb1 - V_{T0n} \leq V_B \leq vb2 - V_{T1n} \tag{1}$$

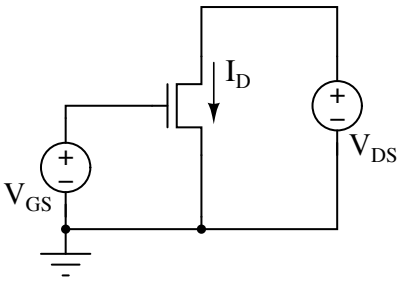


Fig. 3. Circuit used to determine device dimension at predefined bias point

$$vb2 - V_{T1n} \leq V_A \leq V_{CM} - V_{T2n} \tag{2}$$

$$V_{CM} - V_{T2n} \leq V_C \leq V_G - V_{T0p} \tag{3}$$

$$vb1 - V_{T0n} \leq V_E \leq vb2 - V_{T1n} \tag{4}$$

$$V_{CM} - V_{T2n} \leq V_G \leq V_{DD} - V_{T0p} \tag{5}$$

$$vb2 - V_{T1n} \leq V_J \leq V_{CM} - V_{T2n} \tag{6}$$

$$vb1 - V_{T0n} \leq V_L \leq vb2 - V_{T1n} \tag{7}$$

For initial simplicity of design, we consider

$$V_B = V_E = V_F = V_L = V_M \tag{8}$$

$$V_C = V_D; V_J = V_K; V_G = V_H \tag{9}$$

2) Bias voltages: The constraints on bias voltages are

$$V_{T0n} \leq vb1 \leq V_B + V_{T0n} \tag{10}$$

$$V_B + V_{T1n} \leq vb2 \leq V_A + V_{T1n} \tag{11}$$

$$V_{CM} - V_{T1p} \leq vb3 \leq V_C + V_{T1p} \tag{12}$$

To ensure operation of transistor in saturation region, the above equations should be satisfied when selecting the predefined bias conditions.

III. Transistor Sizing using PDM

In PDM, the designer designs the first version of the op-amp without caring much about its response. Once we have a working schematic, the bias conditions are tuned to achieve the target specifications. The strength of PDM is that, transistor sizing is done directly by the simulator. Transistor dimensions establishing the chosen current at the predefined bias conditions are determined. A simple circuit which may be used to determine the device dimension which sets a desired current at predefined bias point is shown in Fig. 3. The simulator is used to plot the drain current at different transistor widths, keeping the length fixed. In this example, supply voltage is assumed to be $V_{DD} = 1.8$ V.

A. Identify Node Voltages

To begin with, we identify those nodes which are to be kept at common mode level, $(V_{DD}/2)$ or approximately 0.9 V. It is identified that the input nodes (*in*+ and *in*-), output nodes (*out*+ and *out*-) and the common mode reference input in common mode feedback (CMFB) circuit, node *I*, must be kept at $V_{DD}/2$.

B. Tail Current I_{Tail}

From the slew rate requirement, we estimate the tail current (I_{Tail}) of the differential pair as given in [3]. Half of this tail current $(I_{Tail}/2)$ flows through each of the differential pair as shown in Fig. 1.

C. Differential Pair M0 and M1

The design starts from estimating the drop across the differential pair. As already seen, the gates of M0 and M1 are at $V_{CM} = V_{DD}/2 = 0.9$ V. The source terminal (node A) of these transistors will be at some positive potential, lower than V_{CM} by V_{T2n}, which will bias the tail transistors. As discussed in earlier sections, it is assumed that node A is at approximately 20% of V_{DD} or at 0.35 V. Thus the differential pair will have a gate-to-source voltage of 0.55 V and the remaining 0.35 V will be used to keep the tail transistors, M2 and M3, biased and in saturation region. It should be noted that the threshold voltage, V_{T2n}, of M0 and M1 should be less than 0.55 V with body bias 0.35 V. If not, then the potential of node A should be chosen lower than 0.35 V so as to lower the body bias and hence its threshold voltage. To keep the differential pair in deep saturation, node C and D is kept at 1.2 V. Thus for M0 and M1, $V_{GS} = 0.55$ V and $V_{DS} = 0.85$ V. Using the simulator, we get the dimensions of M0 and M1 so as to have a drain current of $I_{Tail}/2$ with the predefined bias conditions.

D. Tail Transistors M2 and M3

Transistor M3 does not experience any body bias and carries I_{Tail}. Thus, referring to Fig. 2, its threshold voltage $V_{T0n} =$ 0.45 V. Allowing an overdrive of 0.1 V, we assume $vb1 = 0.55$ V. With 0.1 V overdrive, a drain source of 0.175 V would be enough to keep the transistor in saturation. Thus, node B is kept at 0.175 V.

Transistor M2, experiencing a body bias of 0.175 V due to node B, its threshold voltage $V_{T1n} \approx 0.5$ V. Again, allowing 0.1 V overdrive, we choose $vb2 = 0.775$ V. As decided earlier, node A is at 0.35 V. Thus, for transistor M3, $V_{GS} = 0.55$ V and $V_{DS} = 0.175$ V, and for transistor M2, $V_{GS} = 0.6$ V and $V_{DS} = 0.175$ V. Just like for M0 and M1, we find the sizes of M2 and M3 to set the required current with the chosen DC bias.

E. Current Mirror M4 and M5

As a starting point, suggested in [3], let M4 and M5 carry around $1.5I_{Tail}$. As already discussed, for M4 and M5, $V_{SG} =$ 0.6 V and $V_{SD} = 0.6$ V. This sets potential at node G at 1.2 V.

TABLE I
NODE POTENTIALS AT INITIAL DESIGN

Node	Potential (V)	Node	Potential (V)
A	0.35	B	0.175
C	1.2	D	1.2
E	0.175	F	0.175
G	1.2	H	1.2
I	0.9	J	0.35
K	0.35	L	0.175
M	0.175	vb1	0.55
vb2	0.775	vb3	0.4
in+	0.9	in-	0.9
out+	0.9	out-	0.9

F. Transistors M12 and M13

The PMOS transistors M12 and M13 in the CMFB circuit do not see any body bias. Their source to drain potential now becomes 0.6 V. Both these transistors are in diode connected mode. Hence, $V_{SG} = V_{SD} = 0.6$ V. Initially, their dimensions are found assuming a drain current of I_{Tail}.

G. Transistors M6 and M7

The source and drain terminals of M6 and M7 are at 1.2 V and $V_{CM} = 0.9$ V respectively. They experience a body bias of 0.9 V and thus their threshold voltage $V_{T1p} \approx 35\%$ of $V_{DD} \approx 0.65$ V. We choose $vb3$ =0.4 V. Thus for M6 and M7, $V_{SD} = 0.3$ V and $V_{SG} = 0.8$ V and $I_D = I_{Tail}$. The device dimensions which set these conditions are found.

H. Transistors M14 through M21

Transistors M14 through M17 carry the same current as M0 and M1 and let them have the same potential drops. Since their gate potentials are also identical, transistors M14 through M17 may have the same dimensions as M0 and M1. Giving similar arguments, we may say that dimensions of M18 and M19 is same as M2 and that of M20 and M21 is same as that of M3.

I. Transistors M10 and M11

M10 and M11 do not see any body bias and carry I_{Tail} with their gate tied to $vb1$. Thus, M10 and M11 are sized same as M3.

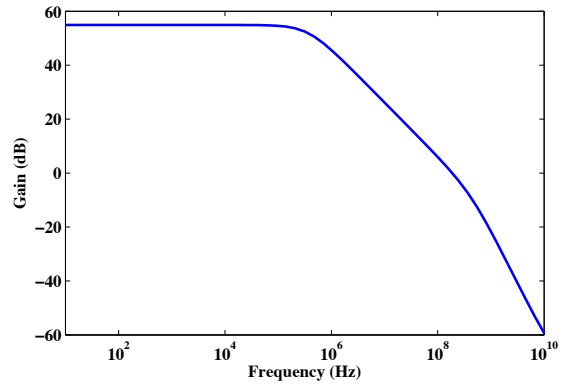
J. Transistors M8 and M9

Transistors M8 and M9 are under body bias of 0.175 V with their gates tied to $vb2$. The drains of M8 and M9 are the output nodes and hence are at $V_{CM} = 0.9$ V. They too carry a current of I_{Tail}. With these conditions, $V_{GS} = 0.6$ V and $V_{DS} = 0.725$ V, the widths of M8 and M9 are found.

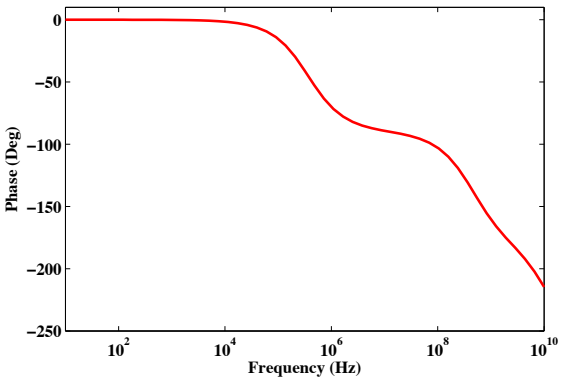
When all the device dimensions are found out, the complete op-amp schematic is drawn and simulated. In the proceeding sections, the simulation results are presented and it is shown how the performance metric of the op-amp can be tuned to match the specifications.

TABLE II
TRANSISTOR WIDTH AT INITIAL DESIGN ($L = 500\ nm$ / $L = 400\ nm$)

Transistor	Width (μm)	Transistor	Width (μm)
M0	4.72/4.69	M1	4.72/4.69
M2	3.79/3.73	M3	4.69/4.8
M4	30.76/24.22	M5	30.76/24.22
M6	13.37/10.59	M7	13.37/10.59
M8	3.22/3.08	M9	3.22/3.08
M10	4.69/4.8	M11	4.69/4.8
M12	20.55/16.27	M13	20.55/16.27
M14	4.72/4.69	M15	4.72/4.69
M16	4.72/4.69	M17	4.72/4.69
M18	3.79/3.73	M19	3.79/3.73
M20	4.691/4.798	M21	4.691/4.798



(a) Gain Plot



(b) Phase Plot

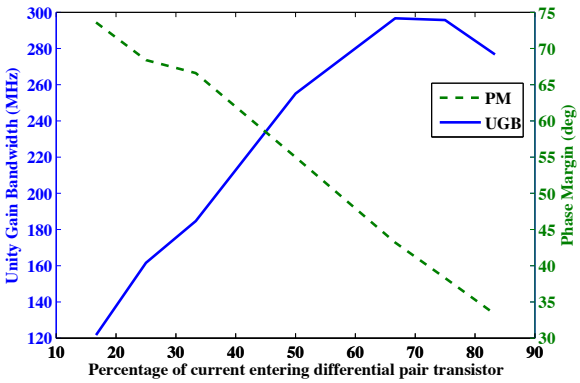
Fig. 4. Bode Plot of the designed op-amp with $L = 500\ nm$

IV. SIMULATION RESULTS

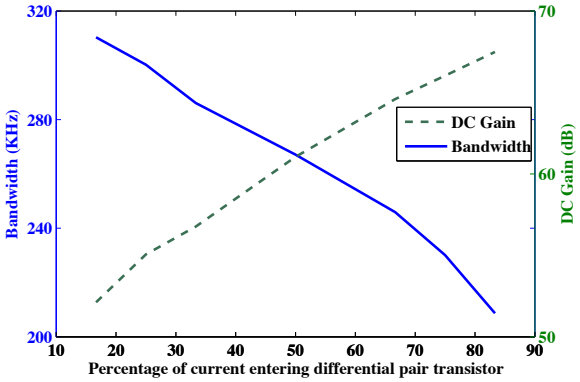
Using the design steps illustrated in earlier sections, a folded cascode differential amplifier was designed using proprietary 180 nm CMOS Process employing Cadence simulator. Current of 20 μA was chosen as the tail current of differential pair to achieve a defined slew rate. To begin with, M4 and M5 were assigned to carry a current of 30 μA, out of which 10 μA would flow into the differential pair and remaining 20 μA into the load. The node potentials as set up in the design is shown in Table I. Two op-amps are realized with lengths $L = 500$ nm and $L = 400$ nm (considering 2 to 3 times of minimum length). Their widths, as found from the simulator, are shown in Table II.

TABLE III
INITIAL DIFFERENTIAL AMPLIFIER RESPONSE

Performance Parameter	Response for $L = 500\ nm$	Response for $L = 400\ nm$
DC Gain	54.91 dB	53.09 dB
Bandwidth	358.1 KHz	491.3 KHz
UGB	186.8 MHz	210.8 MHz
Phase Margin	64.3°	70.2°



(a) UGB and PM dependency



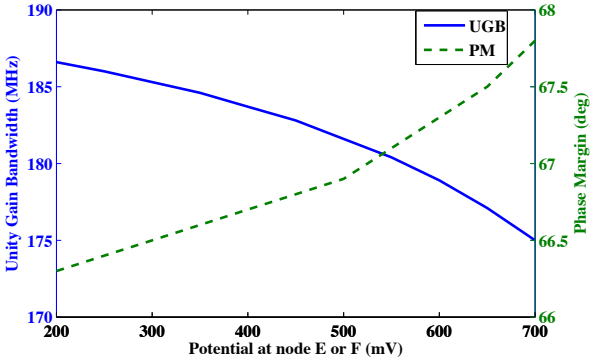
(b) Bandwidth and DC Gain dependency

Fig. 5. Effect of percentage current entering differential pair

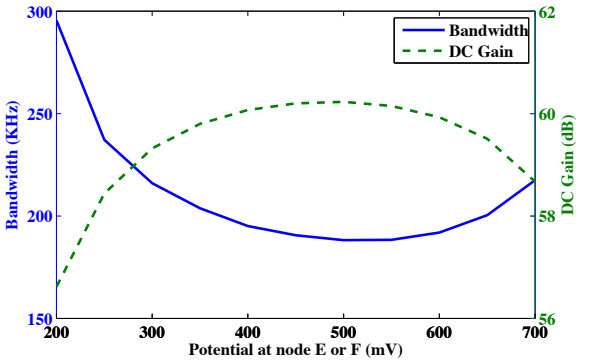
The op-amp realized with the estimated transistor width and $L = 500$ nm is now tested for AC response. The simulated results are shown in Fig. 4 and Table III.

V. TUNING CAPABILITIES

If appropriate choices of node voltages are made, PDM guarantees that all transistors will in operate saturation region. However, initially it may or may not perform as per the designers expectations. PDM possesses the capabilities of tuning the designed op-amp to achieve the target specifications.



(a) UGB and PM dependency



(b) Bandwidth and DC Gain dependency

Fig. 6. Varying Potential at node E or F

It is found that the AC response of the op-amp is a function of percentage of current flowing into the differential pair transistor, M0 or M1, from PMOS current source, M4 or M5 respectively. It is also found that the potential at node E or F (refer Fig. 1), keeping output common mode fixed, affects the AC response of the op-amp. These two dependencies may be exploited for tuning and fine tuning the op-amp performance.

A. Current Distribution

Fig. 5(a) depicts the dependency of unity gain bandwidth (UGB) and phase margin (PM) on the percentage of current diverted to the differential pair transistors. It is seen that as more and more current is branched into the differential pair, the UGB improves at the cost of the PM. The load current can thus be increased (decreased) to increase (decrease) the UGB, or decrease (increase) the PM, respectively. Fig. 5(b) shows the variation of DC gain and 3 dB bandwidth with current distribution. It may be noted that, if total power dissipation is more critical than slew rate requirement, then a simple distribution of drain currents of M4 and M5 can tune the AC response forgoing the value of I_{Tail}. If slew rate is critical and DC gain must be increased, then keeping I_{Tail} constant, the load current may be increased.

TABLE IV
TUNED DIFFERENTIAL AMPLIFIER RESPONSE WITH $L = 500\ nm$

Parameter	Response
DC Gain	59.32 dB
Bandwidth	216 KHz
UGB	185.3 MHz
Phase Margin	66.5°

B. Separate Bias for M8 and M9

Referring to Fig. 1, it may be seen that all the NMOS tail transistors share the same bias voltage. This topology makes the biasing circuit simple. However, if we use separate bias voltage for transistors M8 and M9, we can perform some additional fine tuning in the AC response of the op-amp. Let transistors M10 and M11 be biased by $vb1$ as before and output node fixed at 0.9 V. We can distribute this 0.9 V among the two stacked transistors, M8-M10 and M9-M11, in different proportions. Fig. 6 shows that fine tuning in the AC response of the op-amp can be achieved if potential at node E or F is modulated.

Let us consider that with no change in power dissipation or slew rate, the DC gain of the realized differential amplifier must be increased to around 59 dB. Referring to Fig. 6(b) it is seen that if the node potential is increased to around 0.3 V, the DC gain would be increased to a desired level. Reiterating for dimensions of M8 through M11, potential at node E and F is fixed at 0.3 V and gate bias of only M8 and M9 is increased to 0.9 V to compensate for the increased threshold voltage due to increase in body bias. The widths of M8 and M9 is found to be 4.196 μm and that of M10 and M11 as 4.42 μm. the tuned AC response if shown in Table IV. It should be noted, that other parameters like UGB, PM and bandwidth may also be tuned in a similar manner.

VI. CONCLUSION

Potential Distribution Method (PDM) is a hassle free and extremely simple design methodology, which can be applied to analog circuit design. Being free from any head scratching mathematical expression, even young analog designers can design op-amps in a few minutes. This methodology is not only quick in designing complex op-amp structures, but also independent of the supply voltage, process technology and MOSFET model used by the VLSI tool. Being directly based on the simulator, which uses state-of-the-the-art MOSFET models like BSIM, the accuracy of the results obtained from this method is is almost 100%.

The Potential distribution methodology proposed earlier is briefly explained in this paper and a fully differential folded cascode op-amp is designed using this method. The design approach for target specifications, like slew rate, UGB, PM, bandwidth and DC gain, is presented. The trade-off associated with percentage of current entering differential pair is also presented, which is actively used in the design procedure. It is also shown that modulating the distribution of output common mode level among the NMOS transistors in the load

branch fine tunes the performance metric of the op-amp. The op-amp is realized using proprietary 180 nm CMOS process and the simulation results are presented. PDM assures that all transistors will always be in saturation, even at the first run of the simulation.

ACKNOWLEDGMENT

The authors gracefully acknowledge Dr. Debashis Datta, Ministry of Communication and Information Technology, Govt. of India, for extending the SMDP project at NIT Durgapur. Prof. Anindya Sundar Dhar (E & ECE), IIT Kharagpur is thanked for all kind of support, whenever approached over phone/email. The present SMDP chair and Head of ECE department at NIT Durgapur is also thanked. Prof. Swapna Banerjee, SMDP chair of IIT Kharagpur, and Prof. Qureshi (EE), IIT Kanpur, are also acknowledged for extending to us the chip design opportunity. Dr. Pradip Mandal (E & ECE), IIT Kharagpur is also thanked for entertaining us at night in technical discussions. Finally, authors express their sincere gratitude to all above for giving us encouragement and time.

This paper would not have been possible without the support of our parents, who allowed us to work overnight. Prof. Swapan Bhattacharya, Director, NIT Durgapur, is thanked for his encouraging words. Dr. Mal also acknowledges his teachers Late Sri. Kanai Lal Samui, Prof. R. Saran (IIT Kanpur) and Prof. S. K. Lahiri (IIT Kharagpur). The authors also acknowledge Kanchan Maji, Project Engineer SMDP II, for his assistance.

REFERENCES

[1] K. Bult and G. Geelen, "A Fast-Settling CMOS Operational Amplifier for SC circuits with 90-dB DC Gain," *IEEE J. of Solid-State Circuits*, vol. 25, pp. 1379–1384, Dec. 1990.

[2] B. J. Hosticka, "Improvement of the Gain of CMOS Amplifiers," *IEEE J. of Solid-State Circuits*, vol. 14, pp. 1111–1114, Dec 1979.

[3] P. E. Allen and D. R. Holberg, *CMOS Analog Circuit Design*, Oxford University Press, 2007.

[4] Roubik Gregorian, Gabor C. Temes, *Analog MOS Integrated Circuits for signal processing*, John Wiley & Sons, 1986.

[5] B. Razavi, *Design of Analog CMOS Integrated Circuits, Analysis and Design*, Tata McGraw-Hill Publishing Company Limited, 2002.

[6] R. J. Baker, *CMOS Circuit Design, Layout, and Simulation*, Wiley-Interscience, 2005.

[7] S. Franco, *Design with Operational Amplifiers and Analog Integrated Circuits*, McGraw-Hill Companies, 1997.

[8] S. M. Kang, Y. Leblebici, *CMOS Digital Integrated Circuits, Analysis and Design*, McGraw-Hill Publishing Company Limited, 2003.

[9] P. Mandal and V. Visvanathan, "CMOS Op-Amp Sizing Using a Geometric Programming Formulation," *IEEE Trans. on Computer Aided Design of Integrated Circuits and Systems*, Vol. 20, No. 1, pp. 22-38, Jan. 2001.

[10] M. Hershenson, S. Boyd and T. Lee, "Optimal Design of a CMOS Op-amp via Geometric Programming", *IEEE Transactions on Computer-Aided Design*, Vol. 20, No. 1, pp. 1-21, Jan. 2001.

[11] DasGupta, S. and Mandal, P., "An automated design approach for CMOS LDO regulators," *Design Automation Conference, 2009. ASP-DAC 2009. Asia and South Pacific*, pp. 510-515, Jan. 2009.

[12] DasGupta, S. and Mandal, P., "An Improvised MOS Transistor Model Suitable for Geometric Program Based Analog Circuit Sizing in Submicron Technology," *23rd International Conference on VLSI Design, 2010. VLSID '10*, pp. 294-299, Jan 2010.

Automatic Enlargement of Speech Corpus for Speaker Recognition

Mansour M. Alsulaiman
Speech Processing Group, College of Computer and Information Sciences, King Saud University,
Riyadh, Saudi Arabia
E-mail: msuliman@ksu.edu.sa

Abstract- This research deals with the problem of recognition when only a few samples are available for training of the system. To avoid the low recognition rate caused by such type of speech corpus, automatic techniques for the enlargement of speech corpus are proposed in this paper. These techniques are: lengthening of sample by automatic segmentation, automatic noise addition at different sound-to-noise ratios (SNRs), and lengthening of reversed sample. Different combinations of samples, generated by the proposed techniques, are used to obtain the high recognition rate. These techniques have shown promising result.

Keywords- Database enlargement, Samples generation, Automatic segmentation, Speaker Recognition, MFCC, HMM.

I. INTRODUCTION

Speaker recognition with a speech corpus containing limited number of samples of each speaker for training the system is a difficult task. Solving such kind of problem is still a topic of research [1]. Speaker recognition with Hidden Morkov Model (HMM) and Gaussian Mixture Model (GMM) technique always required a large number of samples for the training of the system. In real life such data is sometimes not available or hard to collect. Modeling the system with small size data set will produce a system with poor performance. Therefore, automatic techniques to increase the number of samples in speech database are proposed in this paper.

Different manual techniques to increase the number of samples are discussed in [2]. These techniques are evaluated by performing different experiment on two types of speaker recognition systems. The first system is using Mel-frequency Cepstral Coefficients (MFCC) with HMM, while the other is using MFCC with GMM. The obtained results are encouraging. Another available solution to overcome the problem of small size of speech database is named as Bagging which was introduced by Breiman in [3], [4]. Bagging goal as introduced by Breiman was to reduce the classification error, but it is also used to deal with small size data in many fields [5], [6]. Different enhancements to bagging were introduced by Breiman [7], [8]. Some authors proposed other ways to enlarge the data set that were specific to the data type or application field [9], [10].

Different automatic techniques for generation of new samples from the single training sample are presented in this paper. These techniques are lengthening of sample by automatic segmentation, automatic noise addition at different SNRs, and lengthening of reversed sample. The number of training samples in the database is increased by 16 times than its original size after using the proposed techniques. The proposed technique, lengthening of sample, automatically detects the phoneme of the word and extracts 25 or 50 milliseconds around the center of the phoneme. Then, this segment is pasted at the end of place from where it was copied. Other methods of generating new samples are by adding noise and reversing the original sample. Different combinations of newly generated samples are used to make various groups to perform many experiments. Each group contains a combination of samples generated by the proposed techniques.

All of the changes are done in the time domain, without changing the original characteristics of the speaker. Several techniques for speech lengthening are proposed in literature, e.g. synchronized overlap-and-add (SOLA) procedure [11], waveform similarity overlap-and-add (WSOLA) [12], time domain pitch-synchronized OLA (TD-PSOLA) [13], segmental lengthening at prosodic boundaries and in accented syllables [14], etc. However these methods are computationally complex in the sense that they require either estimation of pitch, finding similarity, prosodic boundaries, etc.

A speech corpus of 50 speakers is used to evaluate the performance of the proposed techniques in which each speaker recorded five speech samples. One sample is treated as training sample and the remaining four samples for testing. The paper is organized as follows: section 2 describes the Speech corpus, and selection of data; section 3 defines speaker recognition system and its component; section 4 illustrates the proposed techniques to generate new samples; section 5 & 6 describes the experiments and their results respectively; section 7 provides the conclusion and gives suggestions for future work.

II. SPEECH CORPUS

This research is conducted with a local database recorded at King Saud University, College of Computer and

Information Sciences (CCIS), during the year 2007 [15]. The database consists of 91 native Arabic speakers, pronouncing the Arabic word "نعم" (/n/, /a/, /ʕ/, /a/, /m/), which stands for the word "yes" in English, in 5 different occurrences (samples).

The main characteristics, of this word, are of two aspects. The first aspect is that approximately all the Arab speakers frequently say "yes" (in Arabic) in any discussion. The second aspect is the richness of this word in the phonetic structure. It contains at the beginning the nasal phoneme [ن] (/n/), at the middle a very pertinent phoneme [ع] (/ʕ/), and the last phoneme is the bilabial phoneme [م]/m/. It also contains two occurrences of the vowel (فتحة /a/). This richness, plus the fact that it is a commonly pronounced word makes it a good choice for our investigation.

The HMM based system uses the phonemes of the word "نعم", for recognizing the speaker. The GMM based system models the speaker regardless of the text.

The five original samples are denoted as:

- First original sample: w_{1A}. From this sample we will generate the new samples, as will be explained later.
- Four other original samples are used for testing: w_{1B}, w_{1C}, w_{1D}, and w_{1E}.

In this work, a subset of the database is used. This subset consists of 50 different speakers (41 adult Male, 5 children and 4 Female). The speakers recorded their speech samples in one or two sessions.

The samples were recorded with 16 KHz sampling rate and 16 bits per sample resolution

III. Speaker Recognition System

Major components of speaker recognition system are feature extraction and modeling techniques. MFCC Feature vectors are used to extract the characteristics of speakers and, HMM and GMM are used as modeling techniques to construct speaker's templates in the developed recognition system to evaluate the proposed techniques.

A. Mel-Frequency Cepstral Coefficients

Speaker dependent features are extracted by using MFCC. MFCC simulates the behavior of human ear and use the Mel-Frequency scale [16]. The MFCC are the mostly used feature in speaker recognition due to their robustness against noise [17]. Major components for MFCC extraction are [18]: frame blocking, windowing, fast Fourier transformation, Mel-frequency filtering, and discrete Cosine Transformation. The system uses a 25 milliseconds hamming window duration with a step size of 10 milliseconds. In the HMM experiments we used 12 MFCC while in the GMM experiments we used 12 and 36 MFCC. The 36 coefficients consist of 12 MFCC and their first and second order derivatives.

B. Hidden Morkov Model

In text dependent applications, where there is a strong prior knowledge of the spoken text, additional temporal knowledge can be incorporated by using HMM, which is a stochastic modeling approach used for speech/speaker recognition.

The HMM system is built using the HTK (Hidden Markov Toolkit) software, which was developed by Steve Young at Cambridge University in 1989.

In our work each phoneme of the word is modeled by one HMM model with every speaker having his own phoneme model. Each phoneme model has three left to right active states; each state has one Gaussian. For a given speaker, each phoneme has its own model. These models can be used to find the speaker identity. The silence model is also included in the model set. This system is similar to our original work as presented in [2].

C. Gaussian Mixture Model

The second modeling technique used is GMM. GMM is a state of the art modeling technique that copes more with the space of the features, rather than the time sequence of their appearance. Each speaker is modeled by a GMM that represents, in a weighted manner, the occurrence of the feature vectors. The well known method to model the speaker GMM is the Expectation-Maximization algorithm, where model parameters (Mean, variance and mixture coefficients) are adapted and tuned to converge to a model giving a maximum log-likelihood value.

The GMM model is given by the weighted sum of individual Gaussians

$$p(X|\lambda) = \sum_{i=1}^{M} w_i g(X|\mu_i, \Sigma_i) \quad (1)$$

where X is a D-dimensional continuous-valued data vector (i.e. measurement or features), $w_i, i = 1..M$, are the mixture weights, and $g(X|\mu_i, \Sigma_i)$, $i = 1..M$, are the component Gaussian densities. Each component density is a D-dimensional Gaussian function of the form,

$$g(X|\mu_i, \Sigma_i) = \frac{1}{(2\pi)^{D/2}|\Sigma_i|^{1/2}} \exp\left\{-\frac{1}{2}(X-\mu_i)'\Sigma_i^{-1}(X-\mu_i)\right\} \quad (2)$$

with mean vector μ_i and covariance matrix Σ_i. The mixture weights satisfy the constraint that $\sum_{i=1}^{M} w_i = 1$. The model of the GMM is denoted as $\lambda = (\omega_i, \mu_i, \Sigma_i), i = 1..M$.

IV. Proposed Techniques

The proposed techniques for enlargement of the database are: lengthening of sample by automatic segmentation, automatic noise addition at different sound-to-noise ratios (SNRs), and lengthening of reversed sample. New samples for training of the recognition systems are developed by using these automatic techniques.

The lengthening of sample is performed automatically in two different ways with the help of HTK; first by using a 25 ms segment, say AS_1, and other by using a 50 ms segment, say AS_2. In AS_1, after the detection of phoneme, a segment of 25 milliseconds (12.5 milliseconds part taken from center to left side, say g_1, and 12.5 milliseconds part taken from

center to right, say g_2) is taken as shown in Fig. 1. Before pasting the segment, whole speech signal at the right side of g_2 is shifted, for the same amount of time (i.e. 25 milliseconds) to make the room for the extracted segment. While in AS_2, a segment of 50 milliseconds is extracted in the same way and pasted after g_2. In other words, a speech of 50 milliseconds is added after the right side part (g_2) of the extracted segment to generate new samples.

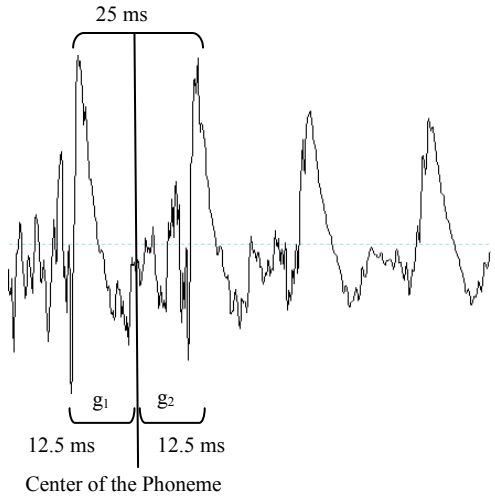


Fig.1. Extraction of Segment from Speech Signal.

The noise addition is done by adding one of two types of noises, Babble Noise and Train Noises, at SNR levels of 5db, 10db and 15db. For lengthening of reversed sample, AS_1 is applied on the reverse of the original sample.

V. EXPERIMENTS

All experiments are performed on two types of recognition system. Both systems have MFCC as a feature extraction technique but differ in modeling techniques. The first system is using HMM and the other uses GMM. Different combinations of samples, generated by the proposed techniques, are used to train the systems. The new samples for the experiments are generated as follow:

As discussed in section 2, Original speech signal w_{1A} contains three phonemes [ن], [ع] and [م]. Three new samples, say w_2, w_3 and w_4, are generated by applying AS_1 on the original sample, where w_2 is generated by detecting [ن], and samples w_3 and w_4 by detecting [ع] and [م] respectively. Similarly, three more samples, say w_5, w_6 and w_7, are generated by applying AS_2 on sample w_{1A}. Some more samples are generated by adding Babble Noise (BN) at SNR levels of 5db, 10db and 20db in the sample w_{1A} which produce samples w_8, w_9 and w_{10} respectively. Moreover, Train Noise (TN) of SNRs 5db, 10db and 20db create samples w_{11}, w_{12} and w_{13} respectively. One more sample is generated by reversing the original speech sample w_{1A}, and is named as w_{14}. To increase the size of database, further, three more samples, say w_{15}, w_{16} and w_{17}, are generated by applying AS_1 on the reversed sample w_{14}. Summary of generated samples is presented in the Table 1.

Now each speaker has 17 training samples to train the system. The recognition rate of the developed system is evaluated by using the four remaining original samples, i.e. w_{1B}, w_{1C}, w_{1D}, w_{1E}. Eight groups are constructed by making selected combination of the generated samples, as shown in Table 2, to perform the different experiment and to check the accuracy of the proposed techniques.

TABLE 1
Summary of Generated Samples and Methods of Generation

Name of Samples	Generated by
w_2, w_3, w_4	Lengthening of Sample by using 25 ms segment (AS_1)
w_5, w_6, w_7	Lengthening of Sample by using 50 ms segment (AS_2)
w_8, w_9, w_{10}	Adding Babble Noise (BN)
w_{11}, w_{12}, w_{13}	Adding Train Noise (TN)
w_{14}	Reversing Original Sample w_{1A} (RO)
w_{15}, w_{16}, w_{17}	Reversing & Lengthening of Sample by using 25 ms segment (RAS_1)

Groups are divided into three classes to according to method of generation. First class contains groups G_1, G_2 and G_3. Combinations of samples in the groups of the first class are generated by applying AS_1 and AS_2 on the original training sample. Second class includes the groups G_4 and G_5. Samples of groups of class 2 are generated by using combination of AS_1 and addition of noise. In the last class, groups G_6, G_7 and G_8 are obtained by combination of the following techniques: lengthening of sample by automatic segmentation, word reversal and, lengthening of reversed sample.

TABLE 2
List of the Groups

Class	Group	Training samples	Testing samples
First	G_1	Original Sample (OS), AS_1	w_{1B}, w_{1C}, w_{1D}, w_{1E}
	G_2	OS AS_2	
	G_3	OS, AS_1 & AS_2	
Second	G_4	OS, AS_1& BN	
	G_5	OS, AS_1, BN & TN	
Third	G_6	OS, AS_1, RAS_1	
	G_7	OS, AS_1,AS_2 & RAS_1	
	G_8	OS, RO, AS_1 & AS_2	

VI. RESULTS

The proposed techniques are tested with both modeling techniques. Results of each group are presented in this section and conclusion will be provided in the next section. In all these experiments training samples are taken from one of the groups, and testing samples are the four original samples as depicted in Table 2.

A. HMM Results

Recognition rates for HMM modeling technique by using different combination of generated samples for training of the system are provided in Table 3.

TABLE 3
Recognition Rates for HMM

Class	Group	Recognition Rates
First	G_1	85%
	G_2	79.40%
	G_3	88%
Second	G_4	68.90%
	G_5	77.78%
Third	G_6	71.72%
	G_7	67.17%
	G_8	69.70%

A comparison of the result of the groups is provided in Fig. 2. Groups are aligned in descending order of their recognition rates. It is obvious from Fig. 2 that recognition rates of all groups of class 1, speech lengthening, are much better than all other groups included in other classes. Group G_3 has very good recognition rate of 88% and other groups of the same class have also recognition rate close to 80% or above. Table 3 shows that recognition rate of G_5, also close to 80%. But groups of class 3, speech reversal, did not show promising results.

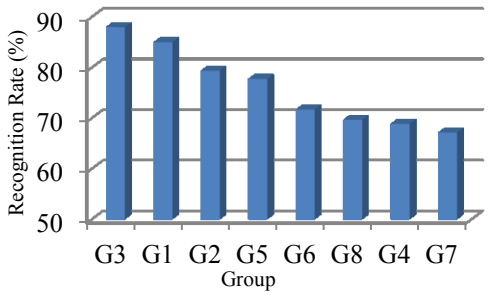


Fig. 2. Comparison of Groups for HMM.

B. GMM Results

To evaluate the accuracy of the proposed technique, different experiments are also performed by using GMM, while speaker dependent properties are captured by using MFCC. The experiments show that variation in number of MFCCs and number of GMMs affects the recognition rate, as presented in Table 4 and Table 5. Results in these tables are provided by considering 12 and 36 MFCCs with 4, 8, 16 and 32 GMMs.

Comparisons of all groups with different number of GMMs are depicted in Fig. 3 and Fig. 4. Recognition rates with 12 MFCCs are presented in Fig. 3 and that of with 36 MFCCs are provided in Fig. 4. Recognition rates for 4 and 8 GMMs with 12 MFCCs are almost same. But recognition rate with 4 GMMs clearly outperform the 8, 16 and 32 GMMs in the case of 32 MFCCs. For higher number of GMMs, recognition rates decrease as compared to 4 and 8 GMMs, for all MFCCs.

TABLE 4
Recognition rate (%) for GMM with 12 MFCCs

Class	Group	12MFCC			
		4 GMM	8 GMM	16 GMM	32 GMM
First	G_1	78.00	74.00	64.00	46.00
	G_2	77.50	80.50	79.00	64.00
	G_3	79.00	74.00	73.00	55.00
Second	G_4	77.78	80.30	73.23	63.13
	G_5	87.88	89.90	84.34	65.66
Third	G_6	85.35	77.78	77.78	63.13
	G_7	87.88	83.33	82.32	74.75
	G_8	80.81	81.82	76.26	53.03

TABLE 5
Recognition rate (%) for GMM with 36 MFCCs

Class	Group	36MFCC			
		4 GMM	8 GMM	16 GMM	32 GMM
First	G_1	79.00	60.00	47.00	28.00
	G_2	77.50	63.50	46.50	35.50
	G_3	83.00	75.00	60.00	37.00
Second	G_4	71.21	56.06	43.94	20.20
	G_5	88.38	84.85	71.72	50.00
Third	G_6	77.78	66.16	62.63	42.42
	G_7	89.39	78.28	70.71	46.97
	G_8	76.77	69.19	59.60	38.89

Overall and for all number of GMMs, the highest recognition rates of groups G_1, G_2 and G_3 of class1 are 79%, 80.50% and 83%, respectively, which is near or more than 80%. But comparison of Table 4 and Table 5 indicate that the highest recognition rate of group G_5 of class 2 is 89.90% with 12 MFCCs and 88.38% with 32 MFCCs, and in case of G_7, it is 87.88% and 89.39%, respectively. This can be due to the fact that samples contained in G_5 and G_7 are generated by more than one technique. So it can be concluded that combinations of the proposed techniques provide better recognition rate than one individual technique.

VII. Conclusion And Future Work

In this paper, we proposed different techniques to increase the size of a database automatically. The number of training samples, of 50 speakers, after implementation of proposed techniques was increased by 16 times than original training samples. Now each speaker has 17 training samples and 4 original testing samples in the database. The recognition systems were trained by using different combination of the generated samples and then tested by using four original samples. The results are very encouraging. The highest recognition rate with 12 MFCC is 89.80% and that of 88.38% with 36 MFCC. The maximum recognition rate achieved in all experiments is 89.80% for G_5, using 12 MFCC and 8 GMM.

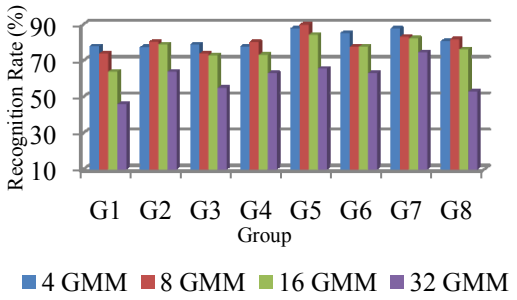


Fig. 3. GMM Recognition rate with 12 MFCC.

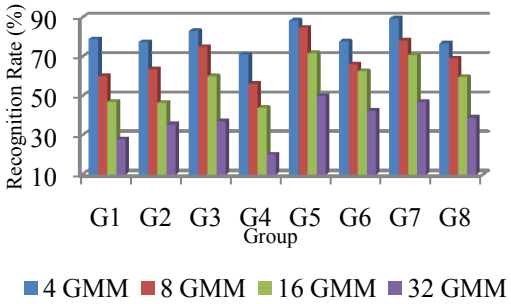


Fig. 4. GMM Recognition rate with 36 MFCC.

It can be concluded from the recognition rates of the developed system that proposed techniques presented in this paper can handle the severe situation in which only one sample of the person is available to train the system. Moreover, the complete process of segmentation and, training and testing of the system is automatic. Therefore, it can be deployed for the surveillance and security measures when little amount of information is available to recognize the person.

We are working on improving the system by improving the way we cut and append the segments and by finding better combinations. Moreover we are going to apply the techniques on a sentence instead of a word in a text independent system.

REFERENCES

[1] J. P. Campbell, et al., "Forensic speaker recognition: a need for caution", *IEEE Signal Processing Magazine*, pp. 95-103, March 2009.

[2] M. Alsulaiman, A. Mahmood, M. Ghulam, M. A. Bencherif, and Y. Alotaibi, "A Technique to Overcome the Problem of Small Size Database for Automatic Speaker Recognition", *Fifth International Conference on Digital Information Management*, *Thunder Bay, Canada* 2010, pp. 303-308.

[3] L. Breiman, "Bagging Predictors", *Technical Report No. 421, Dept. of Statistics, University of California (Berkley),* Sep 1994.

[4] L. Breiman, "Bagging Predictors", *Machine Learning, Springer Netherlands,* vol. 24, pp. 123-140, 1996.

[5] L. Yu, S. Wang, K. K. Lai, "Credit risk assessment with a multistage neural network ensemble learning approach", *Expert Systems with Applications,* vol. 34, Issue 2, pp. 1434-1444, Feb 2008,

[6] B. Drapper, K. Baek, "Bagging in Computer vision", *CVPR*, pp. 144-149, 1998.

[7] L. Breiman, "Random Forests", *Machine Learning*, vol. 45, no.1, pp. 5-32, Oct 2001.

[8] L. Breiman, "Using Iterated Bagging to Debias Regressions", *Machine Learning*, vol.45, no.3, pp. 261-277, Dec 2001.

[9] M. Mori, A. Susuki, A.Shio and S. Othsuka, "Generating new samples from handwritten numerals based on point correspondence", *Proceedings of the 7thIWFHR, Amsterdam, Netherlands*, 2000, pp. 281-290.

[10] L. Fei-Fei, R. Fergus, P. Perona, "Learning Generative Visual Methods from few training Examples: An incremental Bayesian Approach tested on 101 Object categories", *Computer vision and Image understanding*, vol. 106, issue 1, pp. 59-70, 2007.

[11] S. Roucos and A.M. Wilgus, "High Quality Time-Scale Modification for Speech", *IEEE Int. Conf. Acoust. Speech, Signal Process., ICASSP*, 1985, pp. 493-496.

[12] O. Erogul and I. Karagoz, "Time-scale modification of speech signals for language-learning impaired children", *Proc. The 2nd International Biomedical Engineering Days*, 1998, pp. 33-35.

[13] E. Moulines and F. Chanpentier, "Pitch-Synchronous Waveform Processing Techniques for text-to-Speech Synthesis Using Diphones", *Speech Communication*, vol. 9, pp. 453-467, 1990.

[14] C. Jianfen, "Restudy of segmental lengthening in Mandarin Chinese," *Proc. Of Speech Prosody 2004, Nara, Japan*, pp. 231-234.

[15] S.S. Al-Dahri, Y.H. Al-Jassar,Y.A. Alotaibi, M. M. Alsulaiman, K.A.B Abdullah-Al-Mamun, "A Word-Dependent Automatic Arabic Speaker Identification System", *Signal Processing and Information Technology, ISSPIT 2008,* IEEE, pp. 198-202.

[16] O. D. Richard, E. H. Peter, G. S. David, *Pattern Classification*, 2nd ed., John Willey Co., Nov 2000.

[17] Z. Ali, M. Aslam, M. E. Ana María, "A Speaker Identification System using MFCC Features with VQ Technique", *Proceedings of 3rd International Symposium on Intelligent Information Technology Application 2009, IEEE,* pp. 115-119.

[18] Z. Razak, N. J. Ibrahim, M. Y. Idna Idris, et al., "Quranic Verse Recitation Recognition Module for Support in J-QAF Learning: A Review", *International Journal of Computer Science and Network Security (IJCSNS),* vol. 8, no.8, pp. 207-216, Aug 2008.

Regional Skin Detection Based on Eliminating Skin-Like Lambertian Surfaces

A. Nadian Ghomsheh, A. Talebpour , and M. Basseri
Department of Electrical and Computer Engineering, Shahid Beheshti University, Tehran, Iran. e-mail: a_nadian@sbu.ac.ir, talebpour@sbu.ac.ir, Mohammad.basseri@gmail.com

Abstract **-Skin color is an often used feature in machine vision application related to humans, regarded as pixel-based skin color detection. This method has an inherent problem when color overlaps between skin and none skin regions In this paper a skin detection system based on a regional property of objects, called; Lambertian reflection is proposed. Skin is a none-Lambertian surface. In order to use this feature, first, a Single Gaussian Model (SGM) is used to detect skin like pixels in an image. From detected skin regions, ones having none-Lambertian surface property are detected as final skin regions. To detect none-lambertian skin regions, an exponential is fit the histogram of potential skin regions and based on the fit, it is decided if the region is skin or not. By incorporating this feature the False Positive detect rate (FPR) is greatly decreased.**

Keywords: **Skin detection, Lambertian reflection, Lambertian surface.**

I. INTRODUCTION

Skin detection is a major key in applications related to humans. Face detection [1], face tracking [1, 2], and human motion detection [3], all use skin detection as a preliminary step to find regions in an image that are of more interest for next step processing. The aim of skin detection is to find human skin pixels in an image and at the same try to avoid detecting none skin pixels that have color properties of skin; thus getting highest True Positive detection Rate (TPR) while at the same time keeping FPR as low as possible.

Many methods have been proposed to detect skin pixels based on color information. These methods are referred as pixel-based skin detection methods [4]. Pixel-based methods, despite their high detection speed, have a big disadvantage. When the color of skin pixels overlaps with none skin color pixels, classification based on color information does not have a good answer and no definite rule can be extracted to distinguish two classes. Due to this draw back high FPR is unavoidable.

Regional skin detection methods try to overcome this problem by incorporating information of regions that have high probability of being skin. Many methods have been proposed to incorporate regional features to refine skin detection, such as: texture information [5], entropy [6], histogram matching [7], and other features significant in a specific applications. A good examples of the latter are, skin shape and number of skin regions in the application of objectionable image filtering [8].

In this paper the effect of Lambertian reflection is investigated in order to decide if a region of interest which has skin color properties, is a Lambertian object or not. First skin-like pixels are determined using a Single Gaussian model (SG). The threshold is chosen so that most skin pixels, regardless of FPR, pass the first stage.

Since skin is a none-Lambertian surface; from the skin like regions, Lambertian objects are discarded and final skin regions are extracted. To compare the results of the proposed method, the detection rates are compared with the same results of the same trained Gaussian at its cutoff point. Gaussian Mixture Model (GMM) has also shown to have very good results when used for pixel based skin detection. GMM with 6 Gaussians has also been implemented in order to compare the result of pixel-based skin detection method with the proposed regional method.

The rest of the paper is organized as follows: in chapter 2, Lambertian reflection is described. In chapter 3 Lambertian reflection for skin regions is explained. The proposed algorithm is presented in chapter 4. Chapter 5 shows the results and the paper is concluded in chapter 6.

II. LAMBERTIAN REFLECTION

A surface exhibits Lambertian reflectance if light falling on it, is scattered such that the apparent brightness of the surface to an observer is the same regardless of the observer's angle of view; thus the surface luminance is isotropic. Wood finished with a glossy coat of polyurethane is a perfect Lambertian object, since specular highlights may appear at different locations on the surface and the surface has equal reflected intensity. When a surface is not Lambertian, the intensity of the reflected light varies from point to point on the surface of

an object. When angle, θ of incident light L with skin normal vector N at point X changes, the brightness of reflected light, changes also. This change can be formulated by:

$$I_S(X) = L.NC(X)I_L \qquad (1)$$

Where I_S is the intensity of the diffusely reflected light (surface brightness), C is color, I_L is the intensity of the incident light, and

$$L.N = |L||N|\cos\theta = \cos\theta \qquad (2)$$

Intensity will be the highest if the normal vector points in the same direction as the light vector $(\cos(0) = 1)$, and the lowest if the normal vector is perpendicular to the light vector $\cos(\pi/2) = 0$. [9]. In the next chapter it will be explained how this effect can be used to detect skin region in an arbitrary image.

III. LAMBERTIAN REFLECTION FOR SKIN REGIONS

Skin has a none-Lambertian surface [10, 11], therefore light reflected from its surface has different intensities at different points on the skin region. When the incident light and skin normal vector are parallel, intensity of the reflected light will be near white point, having specular reflectance.

By looking at Dichromatic Reflection Model [12], the apparent color of an object is the sum of the light reflected from the surface of an object L_s and the light that has once penetrated into the object and then reflected back into space, through the entering surface, called body reflectance L_b, and can be formulated by:

$$L(\lambda,\theta) = L_s(\lambda,\theta) + L_b(\lambda,\theta) \qquad (3)$$

When $\cos\theta \approx 0$ the intensity of the reflected light is minimized, and the color observed is the first term in the right hand of (3), which is true color of the object. Fig. 1.a shows two different points, A and B on the skin region of the Image. Point A is where the light is parallel to the surface of skin, and color is greatly saturated. At point B this angle should be near 90°, and the real color of the skin is observed. This effect can be better visualized when transferred to XYZ color space (fig. 1.b).

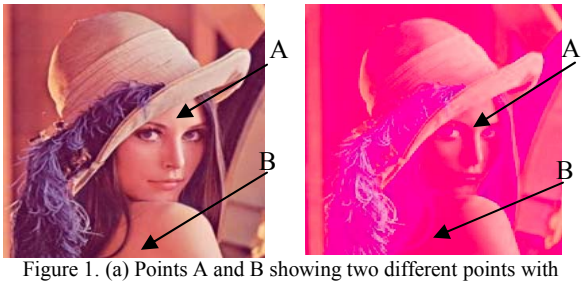


Figure 1. (a) Points A and B showing two different points with different reflection modes. (b) Same points on the image transferred to XYZ color space.

Through observing histograms of different skin images in XY plane (XYZ color space) it was found that dense part of the histogram follows an exponential which can be formulated by:

$$Y = 1 - e^{-(aX-b)} \qquad (4)$$

The reason for using XY plane can be found by looking at fig.2. Skin color changes mainly between colors yellow to red. These colors fall between 580 to 680 nm. So channel Z is not excited at these wavelengths and thus can be neglected in later processing.

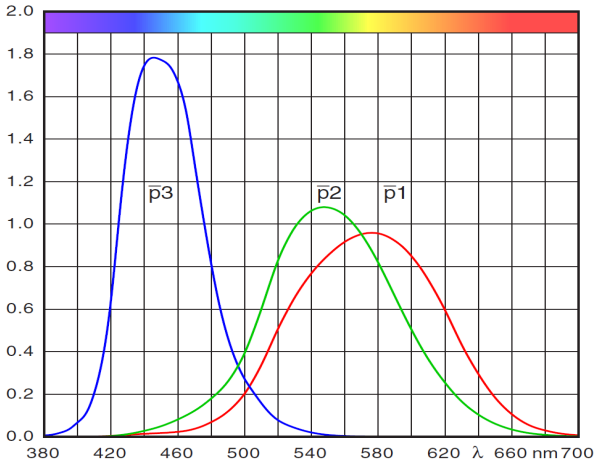
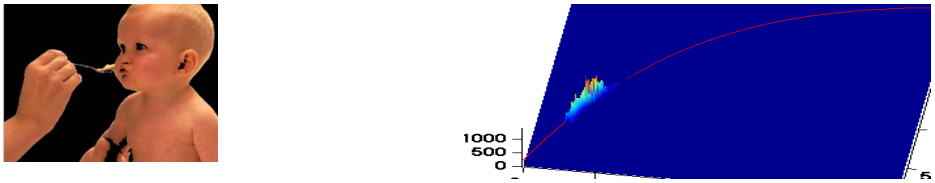
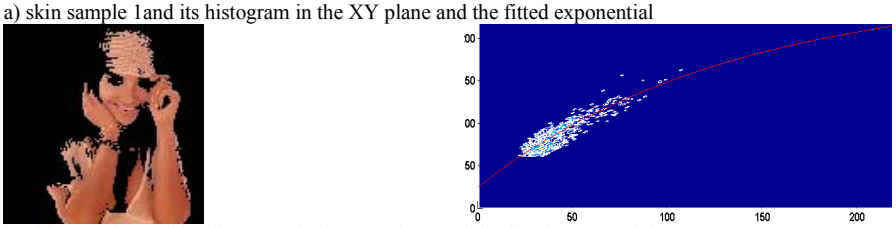


Figure 2. Skin color based on wavelength falls between 580-670 nm so Z channel does not hold information related to skin and can be neglected.

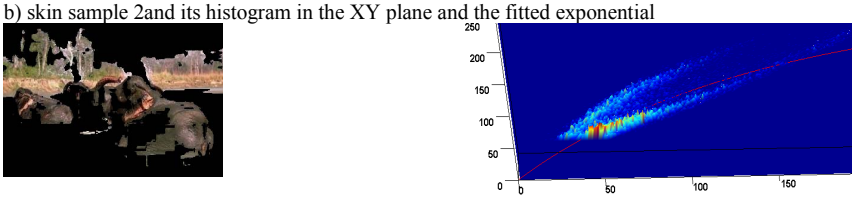
Fig. 3 shows some results of fitting the exponential,(eq. 4) to parts of image detected as skin. Fig 3.a and b show the histogram of regions correctly selected as skin region in the pre-filtering step, which will be explained in the next chapter. Fig 3.c shows the histogram of a wrongly detected skin region and the exponential fitted to it. It can be seen that true skin regions closely follow the exponential line while none skin regions do not show such property.



a) skin sample 1and its histogram in the XY plane and the fitted exponential



b) skin sample 2and its histogram in the XY plane and the fitted exponential



c) none skin sample and its histogram in the XY plane and the fitted exponential

Figure 3. Some samples detected as skin and their relative histogram in the XY plain with fitted Gaussian

IV. PROPOSED ALGORITHM

In previous section it was explained that skin is a none-Lambertian surface and observations showed that the histogram of a none-Lambertian surface with skin color characteristics follows equation (eq. 4).

The proposed algorithm first finds skin like regions in the image. None-Lambertian regions of the image are then selected and merged together. Finally another skin filter is applied to the image and final skin regions are detected. Overall structure of the proposed algorithm is described in fig. 4. Each part of the algorithm is next explained in detail.

A. Pixel-Based Skin Detection

To detect skin regions based on color information, chrominance information of YCbCr color space (Cb and Cr channels, respectively) is used. A single Gaussian is used to model the skin color distribution of skin pixels in this space. After finding the Gaussian distribution parameters, a threshold is selected to classify pixels as skin or none skin [13]. Threshold, T_1 set in this stage is high so that most skin color pixel pass through the initial filter.

B. Partitioning image and finding none Lambertian blocks in the image

In the next step the image is divided into 20×20 blocks. Calculation is then conducted on each

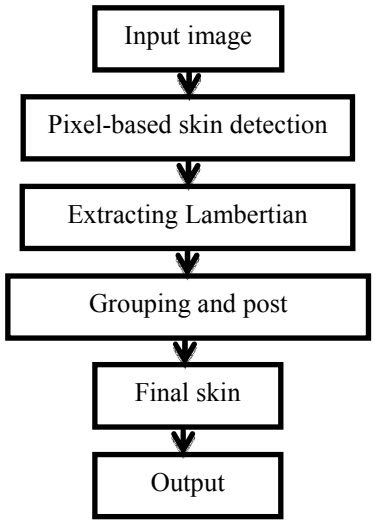


Figure 4. proposed skin detection method

block to decide if that block is Lambertian or not. Based on (4) the following can be calculated:

$$Ln(Y-1) = -(aX+b) \qquad (5)$$

By maximum likelihood estimation the best line that fits to the left hand term of (eq. 5) is calculated and parameters a and b are found. For skin regions, a is found to be in an interval [5 5.5] and b is between [-1 -2]. For blocks that a and b fall in these ranges, that block is considered as a pure skin block. Block size, parameters a and b are found through a training process. For 100 hundred images collected from the World Wide Web, skin regions were hand-labeled. Three different block size,

where checked for performance evaluation: 8×8, 20×20, and 32×32. A best block will be the one that is only consisted of skin pixels.

Choosing small size blocks takes too much processing time, and enlarging the block size, will discard many skin regions for later evaluation. 20×20 provided sufficient number of skin blocks for analysis. After choosing block size, parameters *a* and *b* were calculated for each skin block which the required information for choosing their relative intervals were extracted.

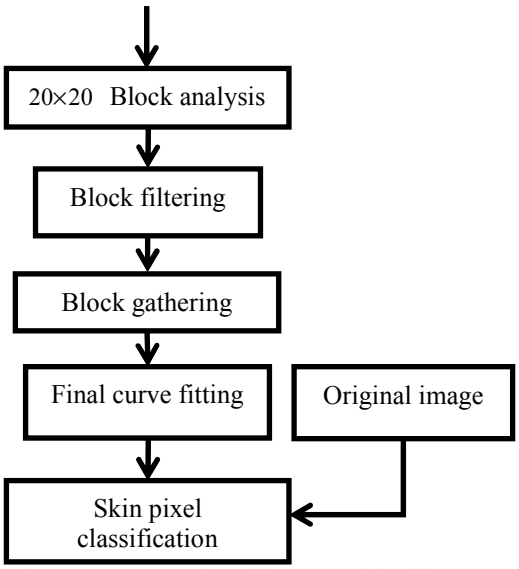


Figure 5- Stages B and C of the proposed algorithm

C. Grouping and post processing

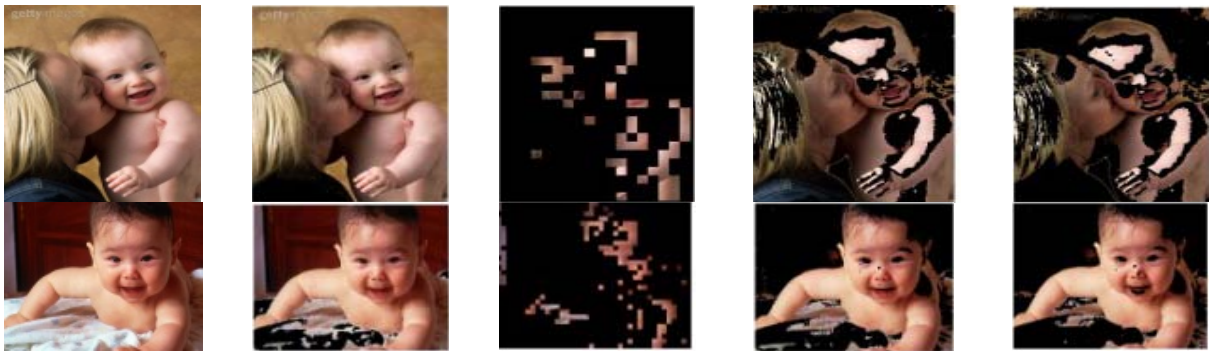
After finding none-Lambertian blocks, the other blocks are discarded. Many skin pixels in the previous section might not be selected because they were in blocks that either were not selected or discarded as Lambertian surface (because of their neighbors in the pixels corresponding block). In this step another exponential is fitted to the image resulted from grouping pure skin blocks. Since the remaining pixels are pure skin pixels the new fitted line is representative of skin pixels in the image. After curve fitting the distance of all pixels in the original image with the fitted exponential is calculated. Pixels closer that a predefined threshold are considered as skin pixel and added to the previously skin selected regions. Fig. 5 shows the blocks implementing stage B and C of the skin detection system.

D. Applying final filter

In the previous step some pixels that don't have skin color but are close to the final estimated exponential will be classified as skin pixels. Therefore another Gaussian filter is applied to the picture to eliminate such pixels. The only difference between this step and the original skin filter is that the threshold T_2 chosen is $T_2>T_1$. This is done in order to decrease FPR as much as possible. Fig. 6 shows 3 example images, with the resulting image after each step. Fig 6b shows the results of skin detection after applying the first skin filter. In fig. 6c the blocks that are chosen as pure skin blocks are shown, and in fig. 6d, the post processing step is shown. The last image in each row shows the final results after applying the final skin filter.

V. RESULTS

To investigate the performance of the proposed algorithm a dataset of pictures consisting of 200 skin and 200 none skin images were collected. The single Gaussian model was trained using the COMPAQ database using 1500 skin images [13]. Result of pixel based skin classification using different methods is shown in table 1.





a b c d e

Figure 6- Step by step results of the proposed algorithm. a) original image, b) first SGM, c) Lambertian blocks selected and merged, d) post processing, and e) final SGM.

Table 1- different results using YCbCr color space for skin detection

Authers	Detection mehotd	TP %	FP%
Jones and Rehg [13]	GMM (16)	90	15.5
Lee and You [14]	SGM	90	33
Phung et al [15].	Thresholding	85	10
	SGM	88	10

The selected results have all used YCbCr, chrominance information for skin detection. Comparisons have shown that when only chrominance data is used YCbCr is the best space for skin detection [16].

Although many results are available from previous work, but form table 1 it can be seen, even when the color space and the detection method used for skin detection are similar, very different results are achieved. To be able to properly see the improvement of the proposed method, SGM was tested on the same dataset used to test the proposed algorithm. GMM with 6 Gaussians was also tested on the same dataset for more comparisons. Table 2 shows the result of skin detection using the proposed method, SGM, and GMM. Two results showing FPR and TPR at cutoff point, shows the work point of the ROC curve. The proposed method yield 91% TPR and 5% FPR, therefore the corresponding detection rate in both SGM and GMM is also shown in the table. The Fig 7 shows the ROC curves for both models.

Results show that when regional information is used skin detection rate is improved significantly. Comparing the results of this work with other regional based method does not seem like a fair since the nature of such already proposed methods is different. But other regional methods such as texture, histogram matching can be used to gather for improving overall skin detection results.

Table 2- Results of SGM for skin detection

Model	TPR	FPR
Proposed regional method	91.2%	5.03%
SGM Cutoff point	85.9%	20%
SGM at 90% TPR	90%	29.5%
GMM cutoff point	88.1%	22%
GMM at 90% TPR	90%	25.7%

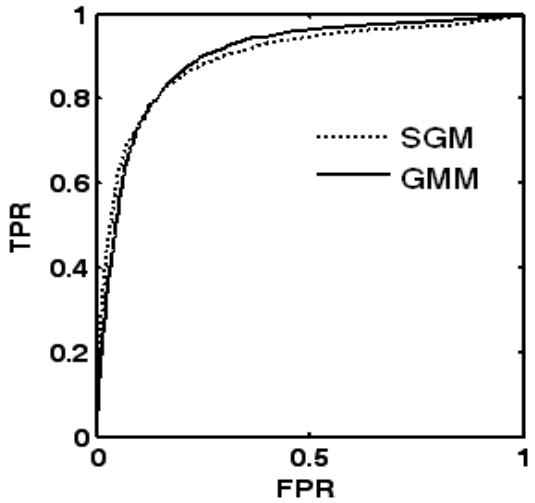


Figure 7. ROC curves of SGM and GMM

VI. CONCLUSIONS

In this paper, a new method based on Lambertian reflection was proposed. Through a pre-filtering stage, skin-like pixels were selected. None-Lambertian skin-like blocks were selected as pure skin blocks. From groping pure skin blocks, final skin mask was extracted. The results showed that using regional information skin detection rate can be improved significantly. The proposed method can be combined with other regional feature to further improve skin detection results.

REFERENCES

[1] A. Nasrabadi and J. Haddadnia, "Face detection base on fuzzy skin region segmentation," in international conference on education technology and computer, V5, 2010.

[2] F. Dadgostar, A. Sarrafzadeh, and C. Messom, "Multi-layered hand and face tracking for real-time gesture recognition," *Advances in Neuro-Information* vol. 5506 LNCS pp. 587-594, 2009.

[3] S. H. I. Jia-dong and W. Jian-zhong, "Detection of Human Motion Using a Fusion Method Based on Optical Flow and Skin Color," *Beijing Ligong Daxue Xuebao/Transaction of Beijing Institute of Technology,* vol. 29, pp. 347-350, 2009.

[4] V. Vezhnevets, V. Sazonov, and A. Andreeva, "A survey on pixel-based skin color detection techniques," in *GRAPHICON3*. vol. 85, 2003.

[5] M. Fotouhi, M. H. Rohban, and S. Kasaei, "Skin Detection using Contourlet-Based Texture Analysis," in *4th International Conference on Digital Telecommunications,*, pp. 59-64, 2009

[6] B. Jedynak, H. Zheng, and M. Daoudi, "Skin detection using pairwise models," *Image and Vision Computing,* vol. 23, pp. 1122-1130, 2005.

[7] Y. Yang, Z. Wang, M. Zhang, Y. Yang, and N. Cheng, "Skin Region Tracking Using Hybrid Color Model and Gradient Vector Flow," in *International Conference on Machine Vision and Human-machine Interface*, pp. 243-246, 2010.

[8] Z. Jiang, M. Yao, and W. Yi, "Filtering objectionable image based on image content " *Lecture Notes in Computer Science* vol. 4099 LNAI, pp. 1027-1031 2006.

[9] A. Edward,"*Interactive Computer Graphics: A Top-Down Approach Using OpenGL"* Adison-wiley, 2003.

[10] D. A. Forsyth, "Automatic detection of human nudes," *International Journal of Computer Vision* vol. 32, pp. 63-77, 1999.

[11] J. F. Lichtenauer, Reinders M. J. T., and H. E. A., "A Self-Calibrating Chrominance Model Applied To Skin Color Detection," in *Proceedings of the 2nd International Conference on Computer Vision Theory and Applications* 2007.

[12] J. M. Álvarez, T. Gevers, and A. M. López, "Learning photometric invariance for object detection " *International Journal of Computer Vision,* vol. 90, pp. 45-61, 2010.

[13] M. J. Jones and J. M. Rehg, "Statistical color models with application to skin detection " *International Journal of Computer Vision* vol. 46, pp. 81-96 2002.

[14] J. Y. Lee and S. I. Yoo, "An elliptical boundary model for skin color detection," in *the International Conference on Imaging Science, Systems and Technology*, 2002.

[15] S. L. Phung, A. Bouzerdoum, and D. Chai, "Skin segmentation using color pixel classification: analysis and comparison," *IEEE Transactions on Pattern Analysis and Machine Intelligence* vol. 27, pp. 148-154, 2005.

[16] P. Kakumanu, S. Makrogiannis, and N. Bourbakis, "A survey of skin-color modeling and detection methods," *Pattern Recognition,* vol. 40, pp. 1106-1122, 2007.

A Face Recognition Scheme Using Wavelet-based Local Features

Hafiz Imtiaz and Shaikh Anowarul Fattah
Department of Electrical and Electronic Engineering
Bangladesh University of Engineering and Technology
Dhaka-1000, Bangladesh
Email: hafiz.imtiaz@live.com, sfattah@princeton.edu

***Abstract*—In this paper, a multi-resolution feature extraction algorithm for face recognition is proposed based on two-dimensional discrete wavelet transform (2D-DWT), which efficiently exploits the local spatial variations in a face image. For the purpose of feature extraction, instead of considering the entire face image, an entropy-based local band selection criterion is developed, which selects high-informative horizontal segments from the face image. In order to capture the local spatial variations within these high-informative horizontal bands precisely, dominant wavelet coefficients corresponding to each local region residing inside those horizontal bands are selected as features. In the selection of the dominant coefficients, a threshold criterion is proposed, which not only drastically reduces the feature dimension but also provides high within-class compactness and high between-class separability. Extensive experimentation is carried out upon standard face databases and a very high degree of recognition accuracy is achieved by the proposed method in comparison to those obtained by some of the existing methods.**

***Index Terms*—Feature extraction, two-dimensional discrete wavelet transform, local intensity variation, face recognition, entropy.**

I. Introduction

Face recognition is very popular in biometric systems in operation primarily because of its non-intrusiveness and high degree of security and reliability. Automatic face recognition has widespread applications in biometric security, surveillance and criminal identification. Nevertheless, it is a complicated visual task even for humans. The primary difficulty in face recognition arises from the fact that different images of a particular person may vary largely, while images of different persons may not necessarily vary significantly. Moreover, some aspects of the image, such as variations in illumination, pose, position, scale, environment, accessories, and age differences, make the recognition task more complicated. Despite many relatively successful attempts to implement face recognition systems, a single approach, which combines speed, accuracy, and robustness to variations in poses, expressions, and aging, is yet to be developed.

Research on face recognition can be classified into two main categories: holistic and feature-based [1], [2]. Holistic or global approaches to face recognition involve encoding the entire facial image in a high-dimensional space [1]. It is assumed that all faces are constrained to particular positions, orientations, and scales. However, feature-based approaches rely on the detection and characterization of individual facial features and their geometric relationships prior to performing face recognition, which makes these approaches robust to variations in position and illumination [2]. Apart from those two approaches, face recognition can also be performed by modularizing the face images [3], [4]. It is well-known that, although face images are affected due to variations, such as non-uniform illumination, expressions and partial occlusions, facial variations are confined mostly to local regions. One way to localize these variations is to employ modularization. In this regard, wavelet analysis is also employed that possesses good characteristics of spatial-frequency localization to detect facial geometric structure [5]. Because of the property of shift-invariance, it is well known that wavelet based approach is one of the most robust feature extraction schemes, even under variable illumination [6]. Hence, it is motivating to utilize local variations of face geometry using wavelet transform for feature extraction and thereby develop a face recognition scheme incorporating the advantageous properties of both holistic- and feature-based approaches.

The objective of this paper is to develop a wavelet-based face recognition scheme, which, instead of the entire face image, considers only some high-informative local zones of the image for dominant feature extraction. An entropy based horizontal band selection criterion is developed to exploit the high-informative areas of a face image. In order to precisely capture the local spatial variation within a high-informative horizontal band, we propose to extract dominant wavelet coefficients corresponding to some smaller segments residing within the band based on a threshold criterion. Finally, the face recognition task is carried out using a distance based classifier.

II. Proposed Method

A. High-informative Zone Selection

It is to be noted that the concentration of information in certain regions of the human face image is greater than that of the other regions [7]. However, identification of these regions is not a trivial task. It can be shown that, if an image of a face is divided into certain windows, not all the windows would contain the same amount of information. It is expected that a close neighborhood of eyes, nose and lips contains more information than that possessed by the other regions of a human face image. Hence, estimating the amount of information from a given image can be used to identify those significant zones. In this paper, in order to determine the information content in a given area of a face image, an entropy based measure of intensity variation is defined as [8]

$$H = -\sum_{k=1}^{m} p_k \; log_2 p_k, \tag{1}$$

where the probabilities $\{p_k\}_1^m$ are obtained based on the intensity distribution of the pixels of a segment of an image. It is to be mentioned that the information in a face image

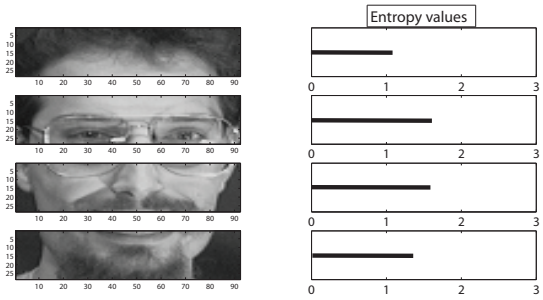


Fig. 1. Entropy values in different horizontal bands of a face image

exhibits variations more prominently in the vertical direction than that in the horizontal direction [9]. Thus, the face image is proposed to be divided into several horizontal bands and the entropy of each band is to be computed. It has been observed from our experiments that variation in entropy is closely related to variation in the face geometry. Fig. 1 shows the entropy values obtained in different bands of a sample face image. In this case, it is found that 63.10% of the total entropy is concentrated in two of the horizontal bands. Hence, such an entropy based facial band selection method is used in the proposed method prior to the feature extraction stage.

B. Wavelet Domain Dominant Feature Extraction

Feature extraction is a crucial step for a face recognition scheme, which directly dictates the recognition accuracy. Holistic face recognition methods, generally use some sort of transforms, such as the discrete cosine transform, Fourier transform, and wavelet transform, upon the entire image for the purpose of feature extraction [10]. Since it is shown in the previous section that certain zones of a face image consist considerably higher information in comparison to other zones, unlike conventional approaches, our objective is to extract features from the spatial data residing only in the high-informative facial bands. Obviously, such a method of feature extraction reduces the feature dimension, which results in significant computational savings. For feature extraction, we have employed two-dimensional discrete wavelet transform (2D-DWT), which, in comparison to the Fourier transform, possesses a better space-frequency localization. This property of the DWT is helpful for analyzing images, where the information is localized in space. The wavelet transform is analogous to the Fourier transform with the exception that it uses scaled and shifted versions of wavelets and the decomposition of a signal involves sum of these wavelets. The DWT kernels exhibit properties of horizontal, vertical and diagonal directionality.

The continuous wavelet transform (CWT) of a signal $s(t)$ using a wavelet $\psi(t)$ is mathematically defined as

$$C(a,b) = \frac{1}{\sqrt{a}} \int s(t)\psi(\frac{t-b}{a})dt, \tag{2}$$

where a is the scale and b is the shift. The DWT coefficients are obtained by restricting the scale (a) to powers of 2 and the position (b) to integer multiples of the scales, and are given by

$$c_{j,k} = 2^{j/2} \int_{-\infty}^{\infty} s(t)\psi(2^j t - k)dt, \tag{3}$$

where j and k are integers and $\psi_{j,k}$ are orthogonal baby wavelets defined as

$$\psi_{j,k} = 2^{j/2}\psi(2^j t - k) \tag{4}$$

The approximate wavelet coefficients are the high-scale low-frequency components of the signal, whereas the detail wavelet coefficients are the low-scale high-frequency components. The 2D-DWT of a two-dimensional data is obtained by computing the one-dimensional DWT, first along the rows and then along the columns of the data. Thus, for a 2D data, the detail wavelet coefficients can be classified as vertical, horizontal and diagonal detail.

In the process of feature extraction from a specific horizontal band of a face image using the 2D-DWT, if all the wavelet coefficients obtained were used as features, it would definitely result in a feature space with a very large dimension. In view of reducing the feature dimension, we propose to utilize the dominant wavelet coefficients as desired features. Wavelet coefficients, which are greater than a certain threshold value, are treated as the dominant coefficients.

For the purpose of feature extraction, we utilize only bands of face images with high entropy values as described in Section II-A and within a high-informative horizontal band of a face image, the image intensity distribution may drastically change at different localities. In order to select the dominant wavelet coefficients, if the thresholding operation were to be performed over the wavelet coefficients of the entire band, it would be difficult to obtain a global threshold value that is suitable for every local zone.

Use of a global threshold in a particular horizontal band of a face image may offer features with very low between-class separation. In order to obtain high within-class compactness as well as high between-class separability, we have considered wavelet coefficients corresponding to some smaller vertical segments residing in a horizontal band, which are capable of extracting variation in image geometry locally within a band. In this case, for each vertical segment, a different threshold value may have to be chosen depending on the coefficient values of that segment.

The wavelet coefficients (both approximate and horizontal detail) of a segment of the high-informative horizontal band are sorted in descending order and the top $\theta\%$ of the coefficients are considered as dominant wavelet coefficients and selected as features for the particular segment of the horizontal band. This operation is repeated for all the segments of a high-informative horizontal band.

Next, in order to demonstrate the advantage of extracting dominant wavelet coefficients corresponding to some smaller vertical segments residing in a horizontal band, we conduct an experiment considering two different cases: (i) when the entire horizontal band is used at a time and (ii) when all the vertical segments of that horizontal band are used separately for feature extraction. For these two cases, centroids of the dominant approximate wavelet coefficients obtained from several poses of two different persons are computed and shown in Figs. 2 and 3, respectively. It is observed from Fig. 2 that the feature-centroids of the two persons at different poses are not well-separated and even for some poses they overlap with each other, which clearly indicates poor between-class separability. In Fig. 3, it is observed that, irrespective of the poses, the feature-centroids of the two persons maintain a significant

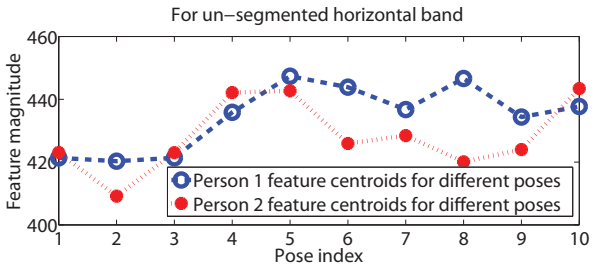


Fig. 2. Feature centroids of different poses for un-segmented horizontal band

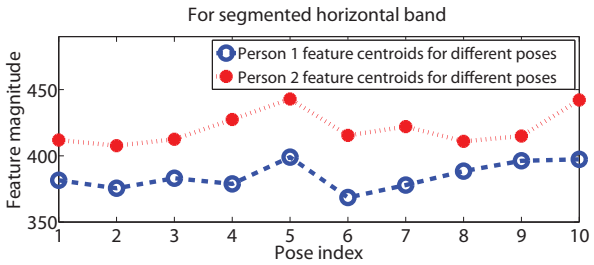


Fig. 3. Feature centroids of different poses for segmented horizontal band

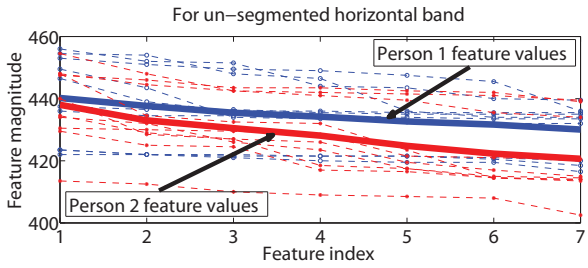


Fig. 4. Feature values for un-segmented horizontal band

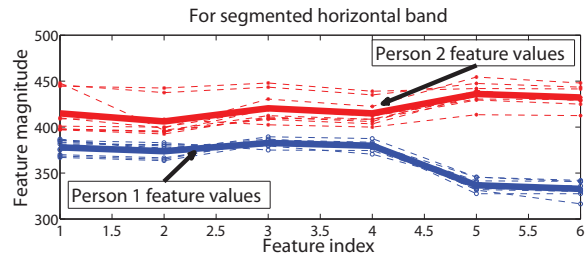


Fig. 5. Feature values for segmented horizontal band

separation indicating a high between-class separability, which strongly supports the proposed local feature selection algorithm.

We have also considered dominant feature values obtained for various poses of those two persons in order to demonstrate the within class compactness of the features. The feature values, along with their centroids, obtained for the two different cases, i.e., extracting the features from the horizontal band without segmentation and with segmentation, are shown in Figs. 4 and 5, respectively. It is observed from Fig. 4 that the feature values of several poses of the two different persons are significantly scattered around the respective centroids resulting in a poor within-class compactness. On the other hand, it is evident from Fig. 5 that the centroids of the dominant features of the two different persons are well-separated with a low degree of scattering among the features around their corresponding centroids. Thus, the proposed dominant features extracted locally within a band offer not only a high degree of between-class separability but also a satisfactory within-class compactness.

C. Distance Based Face Recognition

In the proposed method, for the purpose of face recognition using the extracted dominant features, a distance-based similarity measure is utilized. The recognition task is carried out based on the distances of the feature vectors of the training face images from the feature vector of the test face image. Given the m-dimensional feature vector for the k-th pose of the j-th person be $\{\gamma_{jk}(1), \gamma_{jk}(2), ..., \gamma_{jk}(m)\}$ and the f-th test pose with a feature vector $\{v_f(1), v_f(2), ..., v_f(m)\}$, a similarity measure between the test pose f of the unknown person and the sample poses of the j-th person is defined as

$$D_j^f = \sum_{k=1}^{q} \sum_{i=1}^{m} |\gamma_{jk}(i) - v_f(i)|^2, \tag{5}$$

where a particular class represents a person with q number of poses. Therefore, according to (5), given the f-th test sample face image, the unknown person is classified as the person j among the p number of classes when

$$D_j^f \leq D_g^f, \ \forall j \neq g \text{ and } \forall g \epsilon \{1, 2, ..., p\} \tag{6}$$

III. Experimental Results

Extensive simulations are carried out in order to demonstrate the effectiveness of the proposed method for face recognition using proposed feature vectors. The recognition performance is investigated for different standard face databases consisting a range of different face images varying in facial expressions, lighting effects, and presence/absense of accessories. The performance of the proposed method in terms of recognition accuracy is obtained and compared with that of some recent methods [10], [11]. Moreover, the effect of variation of feature dimension upon the recognition accuracy is also investigated.

A. Face Databases Used in Simulation

Performance of the proposed face recognition scheme has been tested upon two standard face databases, namely, the ORL database [12] and the Yale database [13]. Fig. 6 shows sample face images of different poses of two different persons taken from the ORL and the Yale databases. The ORL database contains a total of 400 images of 40 persons, each person having 10 different poses. Little variation of illumination, slightly different facial expressions and details are present in the face images. The Yale database, on the other hand, consists a total of 165 images of 15 persons, each person having 11 different poses. The poses exhibit large variations in illumination (such as central lighting, left lighting and right lighting, dark condition), facial expressions (such as wink, sad, happy, surprised, sleepy and normal) and other accessories (such as with glasses and without glass).

B. Performance Comparison

In the proposed feature extraction scheme, N number of high-informative horizontal bands are selected based on the entropy measure described in Section II-A. 2D-DWT coefficients (approximate and horizontal detail for one level decomposition) are extracted from the horizontal bands. The dominant wavelet coefficients corresponding to all the local

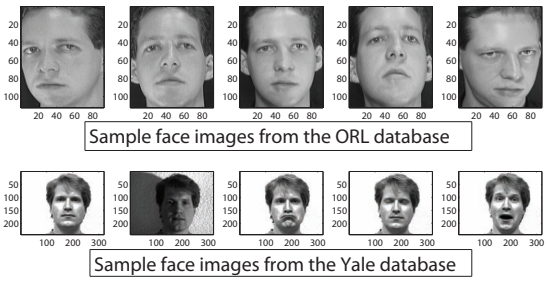


Fig. 6. Sample face images of two persons from the ORL and the Yale databases

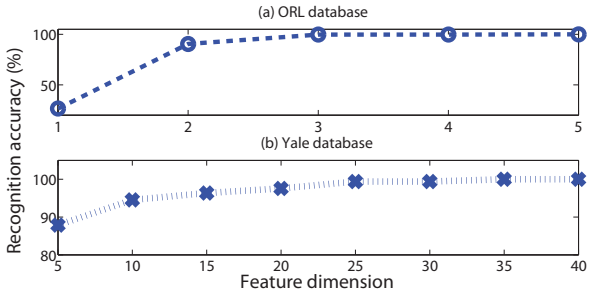


Fig. 7. Variation of recognition accuracy with feature dimension for (a) the ORL and (b) the Yale databases

TABLE I
COMPARISON OF RECOGNITION ACCURACIES

Method	Yale database	ORL database
Proposed method	98.71%	99.75%
Method [10]	98.18%	99.00%
Method [11]	97.70%	N/A

segments residing in the horizontal bands are then obtained, using $\theta = 20$ in our experiments, from a particular pose to form the feature vector of that pose. The recognition task is carried out on the reduced feature space as described in Section II-C. In our simulations, $N = 1$ and $N = 2$ are chosen for the ORL and the Yale databases, respectively.

The experiments were performed following the leave-one-out cross validation rule. For the purpose of comparison, recognition accuracies obtained using the proposed method along with those reported in [10] and [11] are listed in Table I. In case of the ORL database, the recognition accuracy for the method in [11], as not reported, is denoted as not available (N/A). It is evident from the table that the recognition accuracy of the proposed method is comparatively higher than those obtained by the other methods for both the databases. It indicates the robustness of the proposed method against partial occlusions, expressions and nonlinear lighting variations.

In Fig. 7(a), the variation in face recognition accuracy with the feature dimension obtained by the proposed method is shown for the ORL database. Here, the feature dimension is varied depending on the number of principal components utilized in the feature selection procedure maintaining a fixed segment size. It is observed from the figure that even for an extremely low feature dimension, the recognition accuracy remains very high. Similar performance is achieved for the case of the Yale database as shown in Fig. 7(b). It is to be mentioned that the size of the images in the Yale database is approximately nine times of those of the ORL database. The proposed feature extraction algorithm offers a reduction in feature dimension by an approximate order of 10^4 for both the databases.

IV. CONCLUSIONS

The proposed wavelet-based dominant feature extraction algorithm provides an excellent space-frequency localization, which is clearly reflected in the high within-class compactness and high between-class separability of the extracted features. Instead of using the whole face image for feature extraction at a time, first, certain high-informative horizontal bands within the image are selected using the proposed entropy based measure. The dominant wavelet coefficient features are then extracted from within the local zones of those horizontal bands. It has been found that the proposed feature extraction scheme offers an advantage of precise capturing of local variations in the face images, which plays an important role in discriminating different faces. Moreover, it utilizes a very low dimensional feature space, which ensures lower computational burden. From our extensive simulations on different standard face databases, it has been found that the proposed method provides high recognition accuracy even for images affected due to partial occlusions, expressions and nonlinear lighting variations.

ACKNOWLEDGMENT

The authors would like to express their sincere gratitude towards the authorities of the Department of Electrical and Electronic Engineering and Bangladesh University of Engineering and Technology (BUET) for providing constant support throughout this research work.

REFERENCES

[1] C. Villegas-Quezada and J. Climent, "Holistic face recognition using multivariate approximation, genetic algorithms and adaboost classifier: Preliminary results," *World Academy of Science, Engineering and Technology*, vol. 44, pp. 802–806, 2008.

[2] L. L. Shen and L. Bai, "Gabor feature based face recognition using kernal methods," in *Proc. IEEE Int. Conf. Automatic Face and Gesture Recognition*, 2004, pp. 386–389.

[3] C. BenAbdelkader and P. Griffin, "A local region-based approach to gender classification from face images," in *Proc. IEEE Comp. Society Conf. Computer Vision and Pattern Recognition*, 2005, pp. 52–57.

[4] R. Gottumukkal and V. K. Asari, "An improved face recognition technique based on modular PCA approach," *Pattern Recognition Lett.*, vol. 25, pp. 429–436, 2004.

[5] C.-C. Liu and D.-Q. Dai, "Face recognition using dual-tree complex wavelet features," *IEEE Trans. Image Processing*, vol. 18, pp. 2593–2599, 2009.

[6] Y. Utsumi, Y. Iwai, and M. Yachida, "Performance evaluation of face recognition in the wavelet domain," in *Proc. Int. Conf. Intelligent Robots and Systems*, 2006, pp. 3344–3351.

[7] S. Alirezaee, H. Aghaeinia, K. Faez, and F. Askari, "An efficient algorithm for face localization," *Int. Journal of Information Technology*, vol. 12, pp. 30–36, 2006.

[8] E. Loutas, I. Pitas, and C. Nikou, "Probabilistic multiple face detection and tracking using entropy measures," *IEEE Trans. Circuits and Systems for Video Technology*, vol. 14, pp. 128–135, 2004.

[9] S. C. Dakin and R. J. Watt, "Biological 'bar codes' in human faces," *World Academy of Science, Engineering and Technology*, vol. 9, pp. 1–10, 2009.

[10] F. M. de S. Matos, L. V. Batista, and J. v. d. Poel, "Face recognition using DCT coefficients selection," in *Proc. ACM symp. Applied computing*, 2008, pp. 1753–1757.

[11] X. Y. Jing and D. Zhang, "A face and palm print recognition approach based on discriminant DCT feature extraction," *IEEE Trans. Systems, Man, and Cybernetics*, vol. 34, pp. 2405–2415, 2004.

[12] "The ORL Database of Faces." [Online]. Available: http://www.cl.cam.ac.uk/Research/DTG/attarchive/pub/data/

[13] "The Yale Face Database." [Online]. Available: http://cvc.yale.edu/projects/yalefaces/yalefaces.html

Pixel-Based Skin Detection Using Sinc Function

A. Nadian and A. Talebpour
Department of Electrical and Computer Engineering, Shahid Beheshti University, Tehran, Iran.
e-mail: a_nadian@sbu.ac.ir, talebpour@sbu.ac.ir

Abstract- Skin detection is a major key in most human-related recognition systems. Parametric models have been proposed to effectively model the distribution of skin pixels. In this paper some limitations of these methods are reviewed and a new model based on the sinc function is proposed to overcome these limitations. Three different color spaces are chosen for experiments. The results are compared with the results of Gaussian, GMM and Elliptic boundary models. The method significantly outperforms Gaussian and Elliptic method and the results also show that the model slightly outperforms GMM with 2 Gaussians used. Steepest decent method was used for data fitting and COMPAQ database is used for training purposes.
Key Words- Sinc Function, Single and Mixture Gaussian Model, Skin Detection.

I. INTRODUCTION

Detecting human skin pixels has many applications in the field of machine vision such as face detection [1], hand gesture analysis [2], and objectionable image filtering [3]. Many approaches have been proposed to effectively detect skin pixels. Choices of color space and skin distribution model are two key problems of the matter at hand. Skin color modeling can be categorized to parametric and non-parametric methods. The disadvantages of using none parametric methods are the large memory space required and inability to interpolate or generalize the training data [4]. Parametric models on the other hand are not very dependent on the size of the data base, but they require a training phase where the model parameters are extracted. Gaussian distribution [5] and the Gaussian Mixture Model (GMM) [6] are widely used for detecting skin pixels. Elliptic model is proposed to overcome the problem of asymmetry of skin pixels around the mean of the Gaussian distribution [7].

In parametric modeling of the skin color distribution, a threshold is used as a decision rule to determine skin pixels, thus pixels with higher probability values than a predefined threshold are determined as skin pixels. Obviously, when moving towards the mean of the distribution probabilities of the respective pixels are high and therefore these pixels are determined as skin pixels. The detection error happens when a pixel value is far from the calculated mean of the distribution model and the occurrence probability of that pixel is low, therefore it will be selected as a non-skin pixel even though it actually is a skin pixel. A good approximation of pixels with lower occurrence frequency will result in a higher detection rate.

Sinc function behaves differently compared to Gaussian model and can better characterize the distribution of skin color pixels. This function can be fitted to the distribution of skin pixels with a small error which can consequently improve the skin detection rate.

The presented paper is organized as follows: in section 2, color spaces chosen for skin detection are reviewed. In section 3, parametric models are briefly looked at. In section 4, the Sinc model is proposed. Results are shown in section 5, and the paper is concluded in section 6.

II. COLOR MODELS FOR SKIN DETECTION

Skin pixels based on their color information strongly depends on the color space which is used to model the skin color distribution. There are many color spaces used for this purpose. In this paper three different color spaces are chosen for detecting skin pixels.

YCbCr color space is an orthogonal space, and is an encoded nonlinear RGB signal. The transformation simplicity and explicit separation of luminance and chrominance components makes this color space suitable for skin color modeling [8]. YCbCr color space has shown to perform better than other color spaces when only chrominance information is used for detecting skin pixels [4].

Normalized RGB (nRGB) space is simply normalization of the RGB color space and can be obtained by:

$$r=\frac{R}{R+G+B}, g=\frac{G}{R+G+B}, b=\frac{B}{R+G+B} \quad (1)$$

The sum of the three normalized components is known (r+g+b=1); hence the third component does not hold any significant information and can be omitted in order to reduce space dimensionality. The remaining components are often called "pure colors". This property, and simplicity of transformation makes this color space attractive for skin detection [9].

Perceptual uniformity represents how two colors differ in appearance to a human observer and hence uniform color spaces were defined such that all the colors are arranged by the perceptual difference of the colors. However, the perceptual uniformity in these color spaces such as CIE-Luv is obtained at the expense of heavy computational transformations. In these color spaces, the computation of the luminance (L) and chroma (uv) is obtained through a non-linear mapping of the XYZ coordinates [5]. Skin color is a perceptual phenomenon and therefore, color representation similar to the color sensitivity of human vision such as CIE-Luv system should help to obtain higher performance [10].

Figure 1 shows three different views of skin color distribution in two different color spaces; YCbCr and nRGB. Fig 1.a shows a 3D view of skin color distribution in YCbCr color space. It can be observed that in YCbCr the distribution

of skin color clusters in a small area of the space and follows the normal distribution, while in the nRGB space there is asymmetry around the mean of skin color distribution.

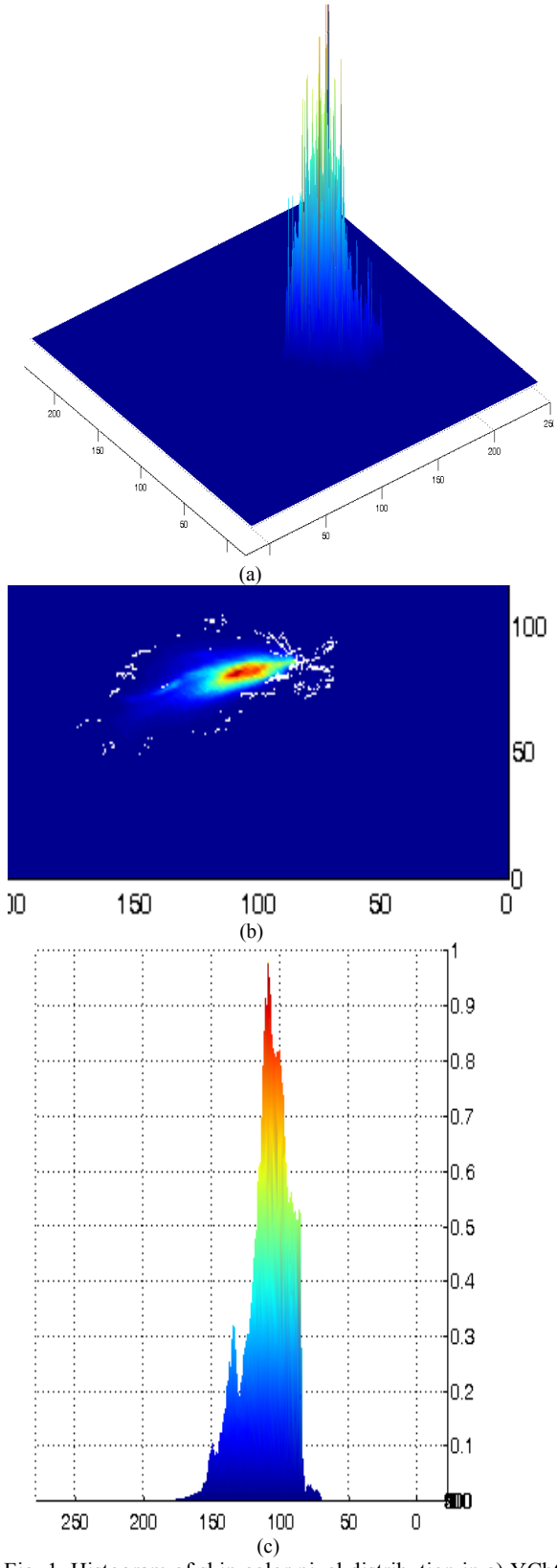


Fig. 1. Histogram of skin color pixel distribution in a) YCbCr b,c) nRGB color spaces with two different views.

For training, and testing purposes the Compaq data base has been used [8]. The data base contains over 4672 skin and 8966 non-skin images which are gathered from the World Wide Web. For the skin bank, a special tool was developed that allows the user to interactively segment regions of skin by controlling a connected-components algorithm. The tool was used to extract the relative skin mask for each image containing skin regions. In the training phase, 1500 images from the skin data base were used to build the required histograms which are used to train the models. In the training phase all model parameters are extracted.

A number of 1500 images from the skin bank and 4000 images from the non-skin data base have been used for test purposes. To achieve a suitable model for skin color distribution the chrominance information of skin pixels is considered. The chrominance 2D space is derived for the original 3D by eliminating intensity from that space [11].

For each color space the corresponding histogram showing the skin color distribution is constructed via histograms with 256×256 bin resolution.

III. PARAMETRIC SKIN COLOR MODELLING

A. Single Gaussian

Single Gaussian model is commonly used for detecting skin pixels [6-9]. Based on the training samples the parameters of the Gaussian function are derived. The skin likelihood of the input vector is calculated by;

$$P_{Gaussian}(X) = \frac{1}{2\pi|\Sigma|^{.5}} e^{-.5(X-\mu)^T|\Sigma|^{-1}(x-\mu)} \quad (2)$$

Where X is the input chrominance vector, μ and Σ are the mean and covariance values (model parameters) of the distribution given by;

$$\mu = \frac{1}{n}\sum_{j=1}^{n} X_j \quad (3)$$

$$\Sigma = 1/(n-1)\sum_{j=1}^{n}(x-\mu)(x-\mu)^T \quad (4)$$

n is the total number of skin pixel samples. After calculating model parameters, skin likelihood of each input data is calculated and if the likelihood $P_{Gaussian}$ is higher than a predefined threshold P_s that pixel is counted as a skin pixel.

B. Gaussian Mixture model (GMM)

Although skin pixels cluster in a small area of the color space, one Gaussian can't model all different types of skin color effectively [12]. GMM uses a determined number of Gaussians to model the skin color distribution. GMM is formulated by;

$$P(X \mid j) = \sum_{j=1}^{K} w_i . P_{gaussian,j}(X) \quad (5)$$

K is the number of Gaussians used; w is the mixing parameter which is trained by the EM algorithm. The number of Gaussians should be determined so that the model is well

representative of the skin color distribution and also the over-fitting problem is avoided [6].

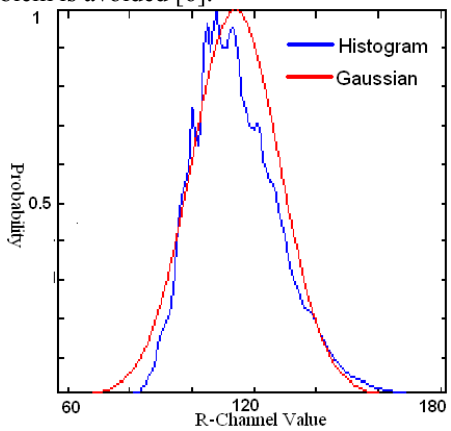


Fig. 2. Fitted Gaussian to the histogram of color band r in the nRGB color space

C. Elliptic model

Elliptic boundary model is proposed to overcome the problem of asymmetry of skin color distribution around the mean of single Gaussian model [7]. An ellipse is fitted to the skin distribution in the chrominance plane using the following formula:

$$\phi(X) = [X - \psi]^T \Lambda^{-1} [X - \psi] \tag{6}$$

X, (X_1, X_2, ..., X_n) are all the distinctive color vectors, ψ and Λ are the model parameters given by:

$$\psi = \frac{1}{n} \sum_{i=1}^{n} X_i \tag{7}$$

$$\Lambda = \frac{1}{N} \sum_{i=1}^{n} f_i (X_i - \mu)(X_i - \mu)^T \tag{8}$$

N is the total number of skin samples, μ is mean of chrominance vectors and f_i is the frequency of each chrominance vector X_j.

IV. SINC MODEL

It has been shown that skin pixels cluster in a small area in the chosen color space [5]. Fig. 2 shows skin color distribution in the nRGB color space. For better visualization only r – channel information is shown. A single Gaussian fitted to skin distribution is also shown in fig 2. Pixels near the mean value of the Gaussian distribution will score a high probability value, and will be determined as skin pixels.

If the input pixels were to be classified by this information, based on the fitted Gaussian, Pixels that have a value between [110 130] would score a probability of over .5 and will be selected as skin pixels (θ is normally chose much smaller than .5). These pixels have a value near the mean of the distribution. On the other hand the pixels far from the mean value of the model –near the tails of the distribution- will not score a high probability of being skin.

For these pixels to be detected as skin, a low threshold must be set. If the fitted model doesn't fit to skin color distribution where occurrence frequency of the skin pixels is low, a high false detection rate is inevitable. A model that can be better fit to skin data at low occurrence frequencies will lead to a better classification. Due to a better fit, for a low threshold more pixels will be counted as skin pixels, will keeping false detection rate at an acceptable level.

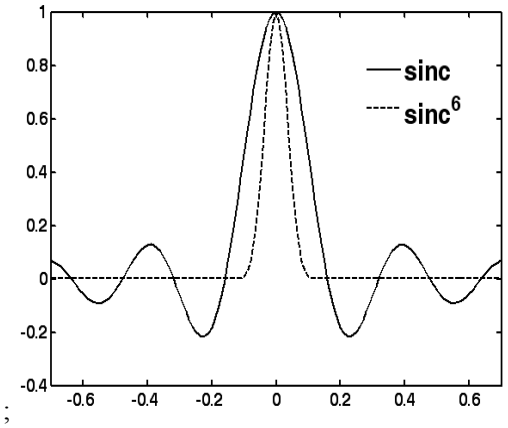


Fig. 3. Sinc function, and Sinc function to power of 6

Sinc function to power of a positive integer number, $n>0$, shows such property. By increasing the power of the function, oscillation start to disappear, and major envelop starts to get narrower (Fig. 3). This function can be formulated by:

$$\sin c(x) = \left(\frac{\sin \pi x}{\pi x} \right)^n \tag{9}$$

The gradient of the sinc function grows more rapidly near its tails compared to the Gaussian function Thus $sinc(mx-t)'-p_{Gaussian}(x)'>0$ for x close to the tails of both functions. Prime sign represents the derivative of the function with respect to x. Fig. 4.c shows the absolute value of derivatives of both sinc and Gaussian functions near their tails. The advantage of such difference between the two derivatives is that sinc function does not have to be as wide as the Gaussian function in order to be properly fitted to the skin color distribution and thus for small thresholds the detection rate still remains acceptable. The two-dimensional sinc function can be reformulated as:

$$f(x,y) = \sin c(\sqrt{m_1(x_1 - t_1)^2 + m_2(x_2 - t_2)^2})^n \tag{10}$$

t_1 and t_2 determine the center points of the function, m_1 and m_2 control skewness, n ensures that only the main envelope of the function remains significant and also controls the narrowness of the function. In order to fit the model to the skin color pixel histogram, the cost function

$$CF = \sum_{x=1}^{256} \sum_{y=1}^{256} (f(x,y) - h(x,y))^2 = error \ \ for\, x,y \mid h(x,y) \neq 0 \tag{11}$$

must be minimized. $h(x,y)$ is the respective normalized histogram. The next paragraphs will provide means for implementing the fitting process.

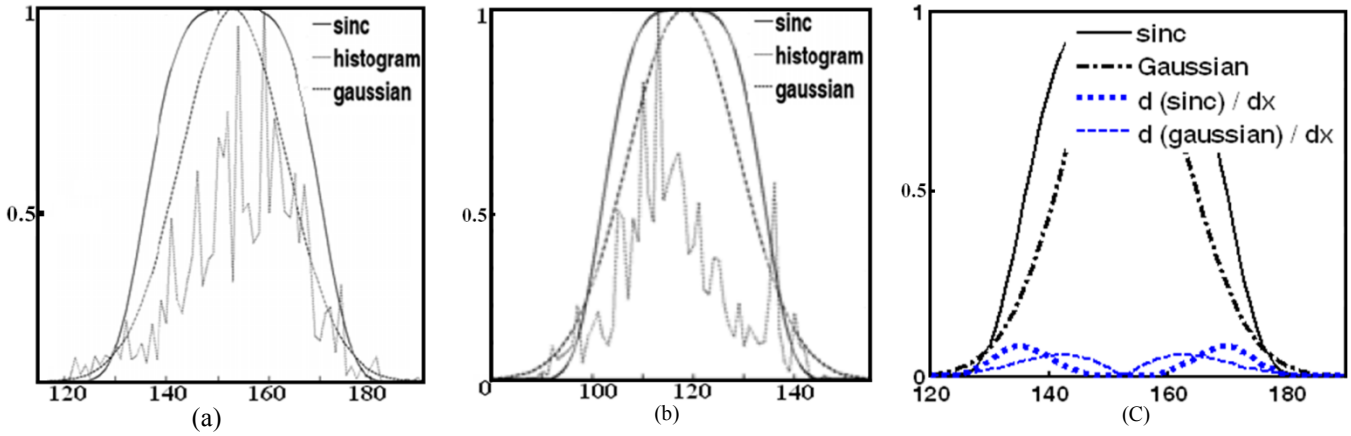


Fig. 4. a,b) fitted Sinc model to the Cb and Cr channels of the YCbCr color space respectively, c) derivatives of sinc and Gaussian functions. The blue solid, and dashed lines, show the derivatives of the since and Gaussian function respectively

To minimize the cost function, steepest descent method has been used where minimization is performed by an iterative algorithm [13]. The method provides numerical means to find local extremums of a multi variable function. Starting at an arbitrary point *x*, each time the gradient of the function at the current position x^{k} is calculated and the next point x^{k+1} is chosen in the opposite direction of the gradient vector, (trying to reach the point where gradient is zero) thus the updating formula is:

$$X^{K+1} = X^{K} + \alpha S^{K} \tag{12}$$

X is the updating vector with variables m_1, m_2, t_1, t_2, n , α is the pace chosen small enough to ensure convergence, and $s = -\nabla f$ given by:

$$\nabla f = \left[\frac{\partial f}{\partial m} \frac{\partial f}{\partial n} \frac{\partial f}{\partial t_1} \frac{\partial f}{\partial t_2} \frac{\partial f}{\partial n} \right]^{-1} \tag{13}$$

Gradient vector has 5 variables which have to be optimized (13). To speed up the search process of the optimization problem we guide the search by choosing start points $n=6$ and, t_1 and t_2 are chosen equal to the mean value of the chrominance vectors. Error at each iteration is calculated by:

$$error = (f(x, y)K - H_{skin})^2 \tag{14}$$

$f(x, y)$ is the fitted function. H_{skin} is the skin color distribution histogram. K is a 256×256 matrix which equals to 1 where $H_{skin} \neq 0$ and otherwise $K=0$. The error determines when to stop the iterative process. If the error is smaller than a predefined threshold the algorithm stops and vector X containing variables concerned with the 2D sinc function are obtained.

The fitted Sinc model and the respective histogram are shown in Fig. 4. The fitted Gaussian is also shown for comparison. For detection purposes, a predefined threshold P_θ is determined and if $P_{sinc} > P_\theta$, that pixel is classified as a skin pixel.

Fig. 4.a shows a plot of Sinc function fitted to the Cb channel in the YCbCr color space, and Fig. 4.b shows Sinc function fitted to color values in YCbCr color space in the Cr channel (for better visualization the fitted functions are shown separately for each channel). For comparison the fitted Gaussian is also shown in the figure.

V. EXPERIMENTAL RESULTS

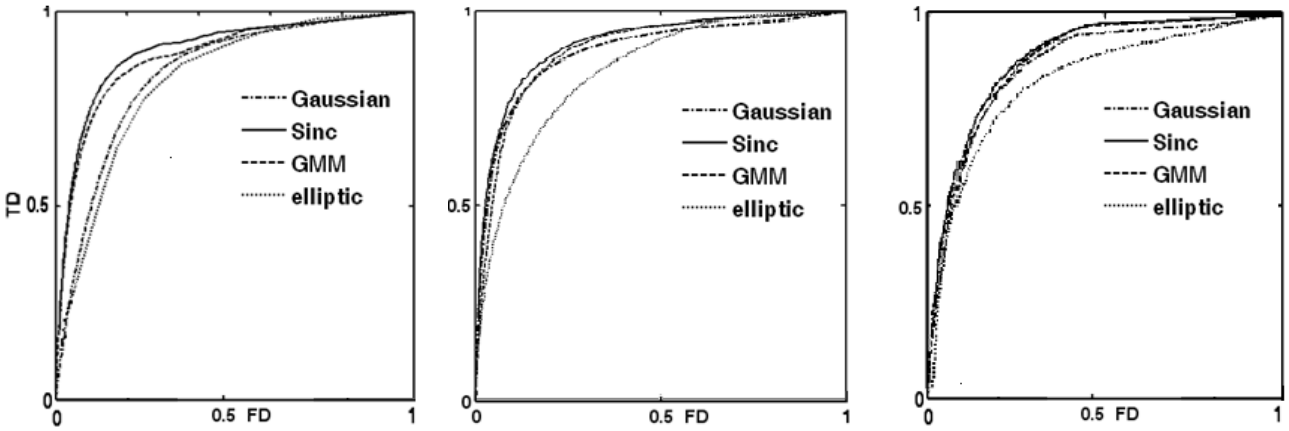
In this section, performance of the Sinc model is compared to SG, GMM, and the Elliptic boundary model. The Sinc model was optimized using steepest gradient method. Since the cost function has a negative gradient vector towards its minimum point, convergence is guaranteed. Table 1 shows the result of detecting skin pixels using 4 different methods in 3 different color spaces. As it was expected, YCbCr color space yields better results when compared to other color spaces.

The proposed method outperforms the other methods by a significant margin. In the YCbCr space, GMM was outperformed by 2.7 percent. But the improvement compared with SG is much more noticeable at 8.1%. Taking into account that GMM is harder to train and much computation time is needed, Sinc function is a much better choice for skin color detection when considering time and computation complexity.

It's worth mentioning that, as the number of Gaussians increase much better results is obtained at the price of much more complexity and computation time. The choice of 16 Gaussians was experimented by [8], were high detection rate is achieved, but calculations for 16 Gaussian is very time consuming.

CIE-Luv color space had the second best results in all cases, this is due to the face that again, chrominance information is provided in the u and v channel and L channel represents luminance.

Elliptic boundary model did not yield good results, since no chrominance vector was discarded in the process, which has a great effect on equation (6). Eliminating chrominance vectors from the skin color histogram reduces n and makes allot of difference in the resulting ψ.



(a) (b) (c)

Fig. 5. ROC curve analysis for all models in three different color spaces: a) nRGB, b) YCbCr, and c) Luv. Vertical axes is the True detection rate (TD), and the horizontal axes show the false detection rate (FD).

Table 1
Results of skin detection using 4 different skin modeling methods in 6 different color spaces

Color space	SG		GMM		Elliptic		Sinc	
	CD%	FD%	CD%	FD%	CD%	FD%	CD%	FD%
Ycbcr	90	31.1	90	25.7	90	44.3	90	23.05
	95	51.1	95	41.1	95	58.3	95	40.1
nRGB	90	39.32	90	38.98	90	43.2	90	26.28
	95	56.1	95	49.15	95	58.3	95	46.12
Luv	90	34.9	90	31.1	90	50.4	90	29.19
	95	42.6	95	39.67	95	69.1	95	39.7

VI. CONCLUSIONS

In this paper a new method based on Sinc function for detection skin pixels was proposed. The function is fitted to the skin color distribution histogram using steepest gradient method. The model was tested and the results were compared to SG, GMM, and Elliptic boundary model in three different color spaces. The results showed that the proposed method was superior to other methods tested for skin color detection.

REFRENCES

[1] M. Shamsi, R. A. Zoroofi, C. Lucas, M. S. Hasanabadi, and M. R. Alsharif, "Automatic facial skin segmentation based on EM algorithm under varying illumination" IEICE Transactions on Information and Systems, vol. E91-D, pp. 1543-1551 2008.

[2] S. Liang, W. Guijin, Y. Anbang, L. Xingang, and C. Xiujuan, "Hand posture recognition in video using multiple cues," in IEEE International Conference on Multimedia and Expo, ICME 2009, pp. 886-889.

[3] J. L. Shih, C. H. Lee, and C. S. Yang, "An adult image identification system employing image retrieval technique," Pattern Recognition Letters, vol. 28, pp. 2367-2374, 2007.

[4] V. Vezhnevets, V. Sazonov, and A. Andreeva, "A survey on pixel-based skin color detection techniques," pattern Recognition, vol. 85, 2003.

[5] P. Kakumanu, S. Makrogiannis, and N. Bourbakis, "A survey of skin-color modeling and detection methods," pattern Recognition, vol. 40, pp. 1106-1122, 2007.

[6] S. Muramatsu and H. Watanabe, "Fast algorithm for GMM-based pattern classifier" in IEEE International Conference on Acoustics, Speech and Signal Processing, pp. 633-636, 2009

[7] J. Y. Lee and S. I. Yoo, "An elliptical boundary model for skin color detection,," in Proceedings of the International Conference on Imaging Science, Systems and Technology, 2002.

[8] M. J. Jones and J. M. Rehg, "Statistical color models with application to skin detection," International Journal of Computer Vision, vol. 46, pp. 81-96, 2002.

[9] N. Sebe, T. Cohen, T. S. Huang, and T. Gevers, "skin detection: A Bayesian Network Approach," in International Conference on Pattern Recognition 2, pp. 903-906.

[10] F. Marqués and V. Vilaplana, "A morphological approach for segmentation and tracking of human face," in International Conference on Pattern Recognition 15 (1), pp. 1064-1067, 2000.

[11] W. L. J. Yang and A. Waibel, "Skin-Color Modeling and Adaptation," in Lecture Notes in Computer Science, Vol. 1352/1997, pp. 687-694, 1998

[12] M.H. Yang and N. Ahuja, "Gaussian Mixture model for human skin color and its application in image and video databases," in Proceedings of SPIE: Conference on Storage and Retrieval for Image and Video Databases, pp. 458–466, 1999

[13] P. Whittle, "Optimization under constraints: theory and application of nonlinear programming", John Wiley & Sons, 1971.

Processing Tree-like Data Structures for Sorting and Managing Priorities

Valery Sklyarov
DETI/IEETA,
University of Aveiro,
Aveiro, Portugal
skl@ua.pt

Iouliia Skliarova
DETI/IEETA,
University of Aveiro,
Aveiro, Portugal
iouliia@ua.pt

Dmitri Mihhailov
Computer Dept.,
TUT,
Tallinn, Estonia
d.mihhailov@ttu.ee

Alexander Sudnitson
Computer Dept.,
TUT,
Tallinn, Estonia
alsu@cc.ttu.ee

***Abstract*- The paper describes the hardware implementation and optimization of algorithms that sort data using tree-like structures combined with sorting networks. The emphasis is done on applications that require dynamic resorting for new incoming data items. Experiments and comparisons demonstrate that the performance is increased compared to other known implementations.**

I. INTRODUCTION

Using and taking advantage of application-specific circuits in general and FPGA-based accelerators in particular have a long tradition in data processing [1]. A number of research works are targeted to databases that use the potential of advanced hardware architectures. For example, the system [2] solves a sorting problem over multiple hardware shading units achieving parallelization through using SIMD operations on GPU processors. The algorithms [3,4,5] are very similar in nature, but target SIMD instruction sets of PowerPC 970MP, Cell, and Intel Core 2 Quad processors.

The application of FPGAs was studied within projects [6,7] implementing traditional CPU tasks on programmable hardware. In [8] FPGAs are used as co-processors in Altix supercomputer to accelerate XML filtering. The advantages of customized hardware as a database co-processor are investigated in different publications (*e.g.* [1]).

Data processing has many practical applications [9,10] and one of them is in the scope of distributed embedded systems and networks, targeted to the design of priority buffers (queues). Such buffer is a device that stores an incoming (sequential) flow of instructions (or other data) and allows outputs to be selectively extracted from the buffer for processing. The following list exemplifies some typical selection rules:

- Each instruction (data item) is provided with an extra field indicating its priority. The selection mechanism has to be able to extract the instruction with the highest priority;
- The system has to be able to remove from the buffer all the instructions that are not longer required;
- The system has to be able to check if a particular instruction is in the buffer.

The technique proposed in this paper can be used to design hardware circuits for sorting and managing priorities with fast resorting for new incoming data items. Let us consider two examples. Suppose, it is necessary to sort arriving data items during run-time. The data items are received by portions and we need to resort them as soon as a new portion has arrived. The known methods, such as [1,10,11] cannot be used efficiently because all existing data have to be resorted from the beginning after any new portion has been received and the resorting takes relatively long time. In the second example, we would like to design a priority buffer with characteristics described above. Many known methods targeted to the design of such buffers are based on sort and shift algorithms [12]. Once again, the existing hardware accelerators for sorting are not efficient, because they require frequent resorting, starting from the beginning that is not appropriate for time critical systems.

This paper suggests a technique for sorting and managing priorities that takes into account potential frequent changes in input data. The technique is based on the use of tree-like data structures and it has the following distinctive features: a) fast correction of output sorted sequence after any change in the input; b) optimization of sorting algorithms through parallelization and balancing the initial tree; c) acceleration through combining tree-like data structures with sorting networks.

The remainder of this paper is organized in four sections. Section II suggests methods for processing tree-like data structures. Section III is dedicated to the relevant hardware architectures. Section IV describes implementations and experiments. The conclusion is given in Section V.

II. PROCECCING OF TREE-LIKE DATA STRUCTURES

Tree-like data structures are frequently explored for data processing [10,12,13]. Let us consider an example of using a binary tree for sorting data [13]. Suppose that the nodes of the tree contain four fields: a pointer to the left child node (an address of the left child node) *LA*, a pointer to the right child node (an address of the right child node) *RA*, a counter *count* and a value *val* (*e.g.* an integer or a pointer to a string). Such fields can be described by the following C++ structure template tree_node:

```
template <class T> struct tree_node
{       T val;                  // Value of an item of type T
        int count;              // Number of items with value val
```

```
    tree_node <T>* lnode;  // Pointer to left child node
    tree_node<T>* rnode;   // Pointer to right child node
};
```

The nodes are maintained so that at any node, the left sub-tree only contains values that are less than the value at the node, and the right sub-tree contains only values that are greater. Such a tree can easily be built and traversed either iteratively or recursively. Taking into account the experiments in [14] we can conclude that hardware implementations of recursive and iterative algorithms over trees give very comparable results in terms of resource consumption and execution time. We will base our technique on recursive algorithms because they provide more clear and compact specification. The results of the paper are equally applied to both recursive and iterative implementations. A method that allows various sequences of operations over a tree to be executed in parallel will also be explored.

A. *General Functionality*

Let us consider a device (called a sorter - S) that receives input data from outside and generates a sorted sequence that is sent to other external devices (see Fig. 1a).

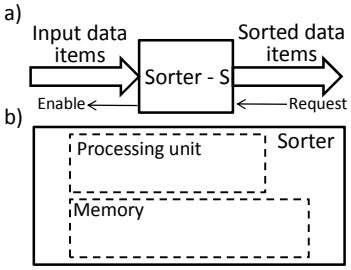


Fig. 1. Interaction with external devices (a), basic internal structure (b)

The number of receiving data items is generally unknown. A processing unit (see Fig. 1b) is responsible for four basic operations: a) receiving data while *Enable* signal is active; b) storing the received data in internal memory; c) sorting the data currently available in the memory; and d) outputting the sorted data on external requests. Thus, sorting has to be provided beginning with the first incoming data item. When any new data item has arrived, all available data in S have to be resorted as fast as possible. When any item is sent to the output it has to be removed from memory in Fig. 1b. In general the input transfer rate is not the same as the processing speed in S. Thus, buffering in internal memory is essential. If the memory is full the signal *Enable* becomes not asserted.

Such kind of processing differs from traditional data sorting when initial data are kept in memory and have to be sorted. In many cases the sorted sequence of data can be saved in the same memory. Thus, the number and values of data are fixed and cannot be changed after the relevant processing has started. We can call such sorting static as distinct from the considered sorting that is dynamic. In other words, we have to be able:

- To accommodate any incoming item in a proper position of the sorted sequence;
- To remove from the sorted sequence an item that is sent from sorter' output to external device;

At any time the memory of size R has to accommodate up to R data items. The total number P of inputs can be significantly bigger than R (because items are periodically removed from the head of the sorted sequence).

Thus, the number and values of data are not fixed and they are changed during processing time. As a result the majority of known methods developed for data sort either cannot be used or are very time consuming.

We suggest to process data through their addresses in internal memory. Potential techniques can involve linked lists and binary trees. We base our approach on trees because they permit to execute the required operations faster through applying both sequential and parallel processing.

B. *Sequential Sort*

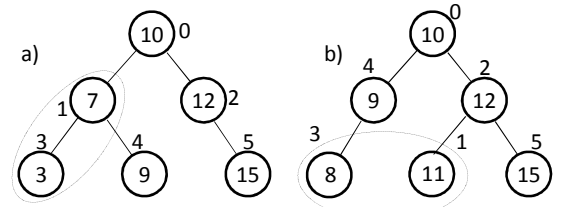
Two (following each other) sequential algorithms SA_1 and SA_2 have to be executed for data sort in [13]. The first one SA_1 constructs the tree. The second algorithm SA_2 outputs the sorted data from the tree. SA_1 executes the following steps: 1) compare the new data item with the value of the root node to determine whether the item should be placed in the sub-tree headed by the left node or the right node; 2) check for the presence of the node selected by 1) and if it is absent, create and insert a new node for the data item and end the process; 3) otherwise, repeat 1) and 2) with the selected node as the root. The following two C++ functions give additional details for sorting integers (*i.e.* in the structure above parameter *T* is *int*):

```
// SA1: Constructing the tree with the structure considered above
tree_node* build_tree(tree_node* node, int v)
{  if (node == 0)
   {  node = new tree_node;
      node->val = v;
      node->count = 1; // setting counter to 1
     node->rnode = node->lnode = 0;
   }
   else if (v == node->val)
      node->count++; // incrementing counter
   else if (v < node->val)
      node->lnode = build_tree(node->lnode,v);
      // traversing the left sub-tree
   else node->rnode=build_tree(node->rnode,v);
      // traversing the right sub-tree
   return node;
}
// SA2: traversing the tree
void tree_sort(tree_node* node)
{  if (node!=0)
   {   // if the node exists
       tree_sort(node->lnode); // sort left sub-tree
       // display value after any hierarchical return
       tree_sort(node->rnode); // now sort right sub-tree
   }
}
```

Fig. 2 demonstrates an example assuming that the following

sequence of input data has been received before the request for sorting: 10, 7, 9, 12, 3, 15 (see Fig. 2a). Since there is no repeated data, *count*=1 for all nodes.

Let us consider ascending sort: 3, 7, 9, 10, 12, 15 and suppose the sorted sequence has to be sent to output from left to right. Each word of memory has three fields: the value v, an address of the left sub-tree LA, and an address of the right sub-tree RA. For example, Fig. 2c demonstrates the representation in memory of the tree shown in Fig. 2a. Suppose the first two data items (*i.e.* 3 and 7) have been sent to the output of the sorter and two new data items (*e.g.* 8 and 11) have arrived. As a result, two nodes of the tree (3 and 7) have to be removed (see Fig. 2d) and two new nodes with the value 8 and 11 have to be inserted (see Fig. 2b and 2e). Finally, P=8 arrived data can be temporarily saved in the memory containing R=6 words.



A is memory address

c)

A	D	LA	RA
0	10	1	2
1	7	3	4
2	12	0	5
3	3	0	0
4	9	0	0
5	15	0	0

d)

A	D	LA	RA
0	10	~~1~~4	2
~~1~~	~~7~~	~~0~~	~~4~~
2	12	0	5
~~3~~	~~3~~	~~0~~	~~0~~
4	9	0	0
5	15	0	0

e)

A	D	LA	RA
0	10	4	2
1	11	0	0
2	12	1	5
3	8	0	0
4	9	3	0
5	15	0	0

Fig. 2. Pointer based dynamic data sort using binary trees

The considered above additional operations can be implemented using the following C++ functions:

```
// sending the smallest value to the output
void extract_value(tree_node* node)
{  if (node != 0)
   {   while (node->lnode != 0)
             node = node->lnode;
       // send node->val to the output
   }
}
// extracting the node (whose value was sent to the output)
// from the tree
void extract_from_tree(tree_node*& node, int v)
{  tree_node* temp_node;
   if (node != 0) // verifying if node exists
     if (v > node->val)
        // traversing the right sub-tree
        extract_from_tree(node->rnode,v);
     else if (v < node->val)
        // traversing the left sub-tree
        extract_from_tree(node->lnode,v);
     else
     {
       if ( (node->lnode == 0) && (node->rnode == 0) )
        // in this case the node has to be deleted
       {   delete node;          node = 0; }
       else if (node->rnode != 0)
       {   // changing pointers for the right node
           temp_node = node->rnode;
           if ((node->lnode) != 0)
             build_subtree(temp_node, node->lnode,
                           node->lnode->val);
           node->rnode = temp_node->rnode;
           node->lnode = temp_node->lnode;
           node->val = temp_node->val;
           node->count = temp_node->count;
           delete temp_node;
       }
       else
       {   // changing pointers for the left node
           temp_node = node->lnode;
           node->rnode = temp_node->rnode;
           node->lnode = temp_node->lnode;
           node->val = temp_node->val;
           node->count = temp_node->count;
           delete temp_node;
       }
     }
}
```

The build_subtree function is a simplified build_tree function with the following code:

```
tree_node* build_subtree
                (tree_node* node, tree_node* subnode, int v)
{  if (node == 0)
       node = subnode;
   else if(v < node->val)
       node->lnode = build_subtree(node->lnode, subnode, v);
   else
       node->rnode = build_subtree(node->rnode, subnode, v);
   return node;
}
```

The methods [15] enable us to convert the considered above C++ functions to hierarchical graph-schemes (HGSs), which can be seen as constrained flow charts [16]. The set of HGSs is a synthesizable specification making it possible to design the sorter hardware based on the model of hierarchical finite state machine (HFSM) [16]. At the beginning the HGSs are optimized in such a way that permits to take into account particularities of the target hardware platform such as rational use of dual-port memories applying methods [17].

Fig. 3 demonstrates a potential improvement for the function tree_sort. An address of the current sub-tree root is kept in a register. At the beginning left sub-trees of the current root are examined. If a left sub-tree (node) exists then it is checked again, i.e. to determine whether the left sub-tree also has either left or right sub-trees (nodes). Two addresses can be verified in parallel in dual-port memories [17]. If there is no sub-tree from the left node, then the value of the left node is

the leftmost data value and can be output as the smallest. In the last case the node addressed by the register holds the second smallest value and the relevant data value is sent to the output. Then similar operations are executed for right nodes.

Analogous optimization technique can also be applied to the other C++ functions when they are converted to HGSs.

The considered tree-like data structures possess the following important feature: it is not necessary to rebuild the existing tree when a new portion of input data items arrives. Thus, resorting for newly arriving items can be done very fast.

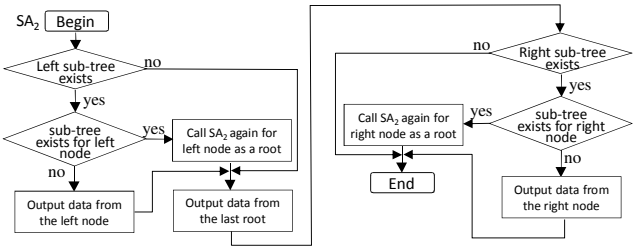


Fig. 3. Taking into account capabilities of dual-port memories for optimization of HGSs

C. Parallel Sort

In the considered parallel algorithm (let us call it PA), N trees (N>1) are built and then processed in parallel [18]. Let us consider an example for N=2. In this case the 1st, the 3d (N+1), the 5th (2N+1), etc. incoming data items are included into the 1st tree. Consequently, the 2nd, the 4th (N+1)+1, the 6th (2N+1)+1, etc. incoming data items are included into the 2nd tree. Fig. 4 shows N=2 trees that are built for our example (see the sequence of input data items given above and Fig. 2a).

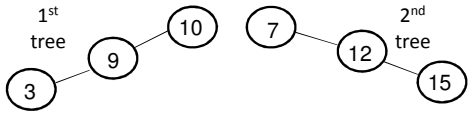


Fig. 4. Sorting data based on N=2 trees that are built and processed in parallel

It is known [18] that a set of such trees can be processed in parallel and the resulting performance of sorting is better.

Suppose a set of trees (like shown in Fig. 4) is built and each tree is stored in the relevant memory. Since N=2, there are totally N=2 blocks of processing memory. To output the sorted data the method [18] is used:

1) The trees in N=2 processing memories are traversed in parallel and there are also N=2 dual-port output memories. Data items from the tree *n* (1≤*n*≤N) are saved in the output memory *n* applying sequential sort for a single tree and using the first port. In other words, the output memory *n* is used to store the sorted data from the tree *n*.
2) This second point is executed in parallel with point 1) above but the second port of the output memories is used. At the beginning, all the addresses point to the first cell of the corresponding output memories. When all N addresses contain data items the smallest one is extracted and the address of the appropriate memory (from which the data item was extracted) is incremented.
3) Points 1) and 2) above are repeated until all data items are sorted.

D. Balancing

The tree that is built by the algorithm SA_1 can be balanced differently. For example, Fig. 5a shows a completely unbalanced tree that has just one linear branch. In the worst case, in order to add a new node we have to perform d steps where d is the depth of the tree. To reduce d the tree can be balanced at run-time. Fig. 5b demonstrates the result of balancing for the tree in Fig. 5a allowing d to be decreased from 14 to 3. Balancing allows inserting new nodes faster.

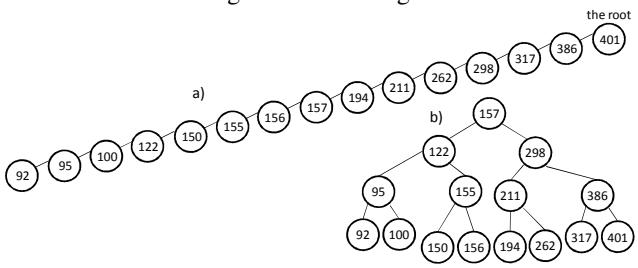


Fig. 5. Differently balanced trees

E. Using Sorting Networks

Some of the most efficient traditional approaches to sorting are also appropriate for hardware circuits [1]. One of such approaches is based on sorting networks [3,10] not requiring control flow of instructions or branches. Besides, sorting networks are parallel in nature. However, they are only suitable for relatively short sequences of data whose length is known a priori [1].

We suggest combining tree-like structures with sorting networks for data processing. The basic idea is the following. Suppose we need to sort m-bit data items. Let us apply the considered above algorithms for (m-k) most significant bits and sort the remaining k bits using sorting networks. In this case, the algorithms will sort up to 2^{m-k} groups of data items and up to 2^k data items within each group will be sorted by the networks. Such technique is additionally explained on an example shown in Fig. 6 for m=5, k=2 and the following sequence of inputs (that is the same as in Fig. 2a): 10(*010*10), 7(*001*11), 9(*010*01), 12(*011*00), 3(*000*11), 15(*011*11), where the binary code of the relevant decimal value is shown in parenthesis.

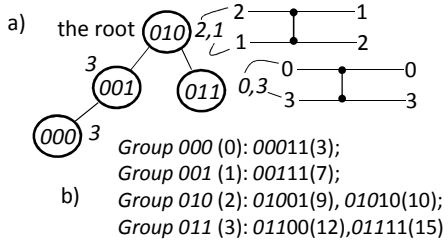


Fig. 6. Combining tree-like structure and sorting networks

For this example, m=3 most significant bits arrive in the following sequence: *010*, *001*, *011*, *000*. The relevant bits are shown in *Italic* in Fig. 6 and in the text. The tree for this sequence is shown in Fig. 6a. There is one less significant (k=2)-bit value associated with the group *000* namely 11 (3). Thus, an additional sort is not required. However, there are two values associated with the group *010*: 2 (10) and 1 (01). The values 2 and 1 are written near the node *010* in Fig. 6a. By analogy (k=2)-bit values associated with each group are shown

near the other nodes. All associated values are ordered in ascending sequence using sorting networks (see Fig. 6a where a trivial network is chosen). Thus, the groups are sorted using tree-like structures and the values associated with the groups are sorted using networks. Comparators needed for the networks are represented in Fig. 6a through the known Knuth notation [9]. The results of sorting are shown in Fig. 6b.

III. HARDWARE

A. Hardware Implementation of Sequential Sort

Sorting is provided by a processing module (PM) interacting with memory that keeps incoming data items that are received and stored sequentially by incrementing the memory address for any new item. An example is shown in Fig. 7a. The absence of a node is indicated by 0 because zero address is used just for the root and can easily be recognized.

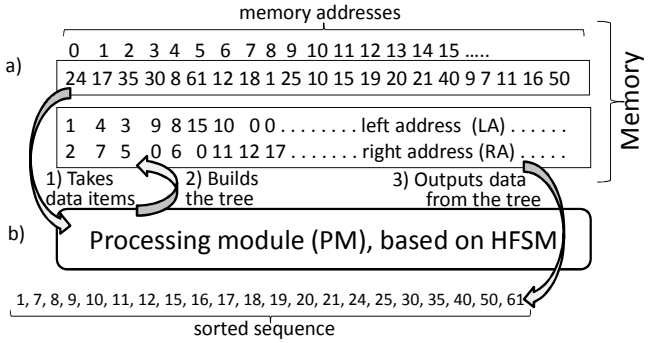


Fig. 7. Top-level hardware architecture

PM (Fig. 7b) builds the tree (point 2 in Fig. 7) from incoming data (point 1 in Fig. 7) through creating pointers between the data items shown in Fig. 7a, and outputs the sorted sequence from the tree. PM is based on a hierarchical finite state machine (HFSM) [16].

B. Hardware Implementation of Parallel Algorithms

Parallel sorting algorithm PA was implemented using the following technique:

- Parallel processing is done in concurrent communicating HFSMs;
- Each individual HFSM executes the sequential sort.

The top-level manager - TLM (top-level HFSM) receives input data items and distributes them between N concurrent HFSMs in such a way that the first data item is supplied to the first HFSM; the second data item is supplied to the second HFSM, etc. Data item N+1 can be supplied once again to the first HFSM as soon as the first HFSM completes the previous job (*i.e.* as soon as the first data item is allocated in the first tree). Suppose N=2 (see Fig. 4). In this case trees will be constructed in the processing memories (by $HFSM_1$ and $HFSM_2$). As soon as the trees are constructed, the TLM instructs the output circuit to generate the sequence of sorted data. The output circuit is built from multiplexers and comparators. Other details can be found in [18].

C. Implementation of Sorting Networks

Values, associated with each group, are coded using positional technique in memory that has 2^k 1-bit words. For example, the values 2,1 associated with the root in Fig. 6 are coded as: <address 0> 0; <address 1> 1; <address 2> 1; <address 3> 0. The memory has two ports with different sizes for addresses and data. The first port is used to store individual bits in accordance with the considered above example. The second port permits to read the recorded 1-bit values as a single binary vector V (V=0110 for our example). The V is used to assign k-bit values associated with a node to inputs of a predefined sorting network. It is done through the following expression:

for all i within the range $0,\ldots,2^k-1$ *do if* V(i) = 0 *then* 2^k-1 *else* i

Thus, if V(i) is 0, the relevant input of the sorting network is assigned the maximum value, else the actual value. The number of values that have to be taken from the network is determined with the aid of a counter that indicates the number of associated values for each group.

D. Dynamic Memory Allocation and De-allocation

The considered technique permits dynamic memory allocation/de-allocation to be provided. Indeed, data are saved in memory (see Fig. 1b) through the addresses of the nodes (see Fig. 2c, 2d, 2e). An availability of any memory cell is indicated by a one-bit flag. When a new node is saved in the memory the relevant flag is set to 1. When a data item is sent to the outputs on a request the relevant flag is set to 0. Thus the memory is filled in and freed dynamically, which is somehow similar to a circular buffer. However, the buffer permits to allocate cells sequentially from one side and free cells sequentially from the other side. In the considered memory cells can be taken and freed on any arbitrary address and permission for such address is determined just by the value of the flag. As soon as the memory is completely filled, the processing module sets disable signal (i.e. *Enable*=0 in Fig. 1a), which indicates that the sorter cannot accept input items. Thus, the sorter can be seen as a device that takes input data items, provides their buffering, and outputs the sorted sequence.

IV. IMPLEMENTATION AND EXPERIMENTS

Firstly, we simulated the sequential and parallel sort in software (in C++) running on HP EliteBook 2730p (Intel Core 2 Duo CPU, 1.87 GHz) tablet PC. The performance was evaluated through counting the number of clock cycles.

Secondly, the synthesis and implementation of the circuits from the specification in VHDL were done in Xilinx ISE 11 for FPGA Spartan3E-1200E-FG320 of Xilinx available on NEXYS-2 prototyping board of Digilent Inc.

For both types of experiments a random-number generator produces up to 2^{12} data items with a length of 14 bits that are supplied in portions to the actual and simulated circuits that have to sort the previously received portions of data and to resort them for a new portion as soon as possible. Besides, both types were evaluated without and with sorting networks for different values of k.

Fig. 8a, 8b permit to compare acceleration of resorting for a new portion (that includes from 10 to 120 data items) comparing with resorting all 2^{12} data items in

simulated/physical circuits respectively. Fig. 8a and 8b clearly demonstrate that the results of simulation are very similar to the results for physical circuits.

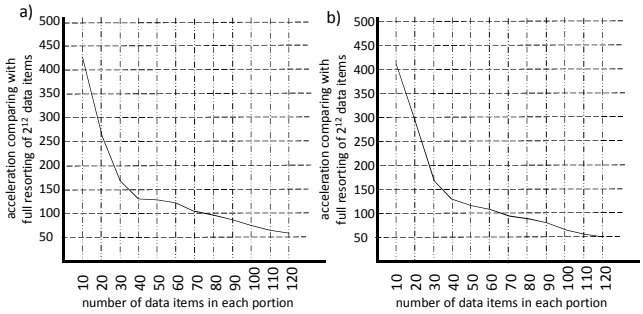


Fig. 8. The results of experiments

TABLE I permits to evaluate the parallel sort compared to sequential sort assuming that there is just one portion of data with 2^{12} items of 14 bits. It demonstrates that the number of clock cycles is decreased. The maximum clock frequency for the experiments is 75 MHz.

TABLE I.
The results of experiments

Number of data items	Number of clock cycles required for sorting		
	Sequential sort	Parallel sort (N=2)	Parallel sort (N=4)
4019	16075	5622	4047
3985	15939	5553	4013
3945	15779	5541	3969
3969	15875	5531	4001
3979	15915	5587	4013
3963	15851	5540	3989
4010	16039	5622	4037
3977	15907	5553	4013
4048	16191	5706	4072
3988	15951	5555	4014

When we combined tree-like structures and sorting networks for sequential and parallel algorithms we were able to provide additional acceleration on an average 1.6/3.1/4.7 times for different values of k: k=2/k=3/k=4 respectively. Regardless of parallelization of 2^k operations, acceleration cannot be equal to 2^k because the use of sorting networks gives significant delay in getting the results due to long paths in the relevant combinational circuits.

The considered technique is useful for different practical applications, such as priority buffers described in [19].

V. CONCLUSION

The paper suggests methods for the design and implementation in hardware of a device that receives input data items and executes sorting of these items dynamically in such a way that permits the accumulated data to be resorted properly when new items arrive. To satisfy the considered requirements data are stored in internal processing memory and relationships between data items are set through their addresses (pointers). The applicability and advantages of the proposed technique are demonstrated through simulation in software, prototyping in FPGA, and experiments.

ACKNOWLEDGMENT

This research was supported by the European Union through the European Regional Development Fund and the Estonian Doctoral School in Information and Communication Technology.

REFERENCES

[1] R. Mueller, J. Teubner, G. Alonso, "Data processing on FPGAs", Proc. VLDB Endowment 2(1), 2009.

[2] N.K. Govindaraju, J. Gray, R. Kumar, D. Manocha, "GPUTeraSort: High performance graphics co-processor sorting for large database management", Proc. 2006 ACM SIGMOD Int'l Conference on Management of Data, Chicago, IL, USA, 2006, pp. 325-336.

[3] H. Inoue, T. Moriyama, H. Komatsu, T. Nakatani, "AA-Sort: A new parallel sorting algorithm for multi-core SIMD processors", Proc. Int'l Conference on Parallel Architecture and Compilation Techniques (PACT), Brasov, Romania, 2007, pp. 189-198.

[4] B. Gedik, R.R. Bordawekar, P.S. Yu, "CellSort: High performance sorting on the Cell processor", Proc. 33rd Int'l Conference on Very Large Data Bases (VLDB), Vienna, Austria, 2007, pp. 1286-1297.

[5] J. Chhugani, A.D. Nguyen, V.W. Lee, W. Macy, M. Hagog, Y.K. Chen, A. Baransi, S. Kumar, P. Dubey, "Efficient implementation of sorting on multi-core SIMD CPU architecture", Proc VLDB Endowment 1(2), 2008, pp. 1313-1324.

[6] D.J. Greaves, S. Singh, "Kiwi: Synthesis of FPGA circuits from parallel programs", Proc. IEEE Symposium on Field-Programmable Custom Computing Machines (FCCM), 2008.

[7] S.S. Huang, A. Hormati, D.F. Bacon, R. Rabbah, "Liquid Metal: Object-oriented programming across the hardware/software boundary", European Conference on Object-Oriented Programming, Paphos, Cyprus, 2008.

[8] A. Mitra, M.R. Vieira, P. Bakalov, V.J. Tsotras, W. Najjar, "Boosting XML Filtering through a scalable FPGA-based architecture", Proc. Conference on Innovative Data Systems Research (CIDR), Asilomar, CA, USA, 2009.

[9] D.E. Knuth, The Art of Computer Programming, Volume 3: Sorting and Searching, 2nd edn., Addison-Wesley, 1998.

[10] T.H. Cormen, C.E. Leiserson, R.L. Rivest, C. Stain, Introduction to Algorithms, 2nd edition, MIT Press, 2002.

[11] R.D. Chamberlain, N. Ganesan, "Sorting on Architecturally Diverse Computer Systems", Proc. 3rd Int'l Workshop on High-Performance Reconfigurable Computing Technology and Applications, November 2009.

[12] P.A. Pietrzyk, A. Shaoutnew, "Message Based Priority Buffer Insertion Ring Protocol", Electronics Letters, vol. 27, no. 23, 1991, pp. 2106-2108.

[13] B.W. Kernighan, D.M. Ritchie, The C Programming Language, Prentice Hall, 1988.

[14] V. Sklyarov, I. Skliarova, and B. Pimentel, "FPGA-based Implementation and Comparison of Recursive and Iterative Algorithms", *Proc. FPL'05,* Finland, August, 2005, pp. 235-240.

[15] V. Sklyarov, "FPGA-based implementation of recursive algorithms", Microprocessors and Microsystems. Special Issue on FPGAs: Applications and Designs, vol. 28/5-6, pp. 197-211, 2004.

[16] V. Sklyarov, "Hierarchical Finite-State Machines and Their Use for Digital Control", *IEEE Trans. on VLSI Syst.,* vol. 7, no. 2, 1999, pp. 222-228.

[17] D. Mihhailov, V. Sklyarov, I. Skliarova, A. Sudnitson, "Hardware Implementation of Recursive Algorithms". In Proc. MWSCAS'2010, Seattle, August, 2010, pp. 225-228.

[18] D. Mihhailov, V. Sklyarov, I. Skliarova, A. Sudnitson, "Parallel FPGA-based Implementation of Recursive Sorting Algorithms", Proc. of ReConFig, Cancun, Mexico, December 2010, pp. 121-126.

[19] V. Sklyarov, I. Skliarova, "Modeling, Design, and Implementation of a Priority Buffer for Embedded Systems", *Proc. 7th Asian Control Conference* – ASCC'2009, Hong Kong, 2009, pp. 9-14.

Data Driven Approach for Low-Power Pre-Computation-Based Content Addressable Memory

Tsung-Sheng Lai
Department of Computer Science and Information Engineering
National Taiwan University
Taipei, Taiwan
r96922071@ntu.edu.tw

Chin-Hung Peng
Department of Computer Science and Information Engineering
National Taiwan University
Taipei, Taiwan
d94922023@ntu.edu.tw

Feipei Lai
Graduate Institute of Biomedical Electronics and Bioinformatics
National Taiwan University
Taipei, Taiwan
flai@ntu.edu.tw

***Abstract* - Content addressable memory (CAM) plays an important role in the performance of many applications such as DCT transforms, processor caches, database accelerators, and network routers because it enables high-speed search operations with hardware acceleration. However, the power consumption of CAM is rather high because within CAM, searching is conducted in parallel for all registered words. Hence, pre-computation-based CAM, i.e., PB-CAM, was proposed in [1] in order to reduce the number of parallel-operated words by first filtering using a precomputation circuit called the parameter extractor. In this work, we propose a data driven algorithm—local grouping (LG)—to synthesize a parameter extractor for PB-CAM such that the registered data can be uniformly mapped to construct parameters; the cost of implementing the parameter extractor is also decreased. Moreover, we also adopt a discard and interlace (DAI) method that can further reduce the impact on non-uniform cases, which happens when most data are identical in some data blocks before LG processing. In experiments, average power consumption reduction of 60.4% was achieved and the number of CMOSs used was also reduced by 0.52%, when compared with the conventional gate-block selection algorithm [2].**

***Index Terms* - local grouping, discard and interlace, content addressable memory, parameter extractor, PB-CAM, power consumption**

I. Introduction

In recent time, the speed of modern devices has increased considerably, and they can also be operated at high frequencies. However, simultaneously, power consumption and thermal issues have also increased, which are not suitable for portable devices and embedded systems. Therefore, achieving reductions in the power consumption of modern devices, while maintaining high-speed searching performance, is important. Devices with built-in content addressable memory (CAM) search content with all registered words using parallel operations. Hence, many devices such as network routers and DCT transforms, which are widely used in internet applications and image processing, respectively, use CAM to improve their performances.

Most researches on CAM have been well discussed and compared in [3]. Their methods used to reduce power consumption primarily focus on the match and search lines because many operations occur during search operations. An architectural technique for reducing the power consumption is pre-computation-based CAM (PB-CAM) [1]. The PB-CAM requires additional memory to store precomputed parameters; data are first compared with the incoming parameters produced by a precomputation circuit in order to reduce needless pre-charged operations on the match lines of the main data memory. In this manner, this method can significantly reduce power consumption.

We observed that the efficiency of the parameter extractor was limited by the locality of precomputed data and the circuit structure itself. In this study, we propose an adaptive local grouping (LG) algorithm to synthesize a proper parameter extractor with lower costs for specific applications. By using this adaptively selected parameter extractor, the registered data can be mapped to the synthesized parameters more uniformly; as a result, less registered banks will be selected, thereby reducing power consumption considerably. However, the PB-CAM suffers from a major disadvantage, partition conflict. Hence, we have also employed a discard and interlace (DAI) method that can further reduce the impact on non-uniform cases that occur when most data are identical in some data blocks.

Our LG-DAI approach can considerably reduce power consumption after a system trace is obtained while simultaneously preserving the synthesis algorithm efficiency. This implies that our approach can be implemented in electronic design automation (EDA) software to reconfigure PB-CAM and make parameter extractor hot swaps possible.

II. Related Works

A. One's Count PB-CAM

One's count PB-CAM [1] uses a 7T PB-CAM cell to reduce the area in the data memory and the power consumption on the search line. However, this PB-CAM cell cannot be applied to any parameter extractor; in [1], for example, the one's count parameter extractor was used to count the number of "binary ones" in the data. Moreover, the area and delay of extractor increase with the data word length, and random data cannot be distributed uniformly.

B. Block-XOR PB-CAM and Gate-Block Selection Algorithm

To improve the efficiency of the parameter extractor while generating more uniform data distribution, the Block-XOR scheme has been proposed in [4]. Here, two fan-in XOR logic gates are employed to construct the parameter extractor. An additional circuit is also combined with the parameter extractor to implement the valid bits in the CAM. The data can be distributed to parameters more uniformly using this scheme than with the one's count scheme when the input data is random. The parameter extractor performance can further be improved by obtaining the system trace. Therefore, the gate-block selection algorithm was proposed in [2] to synthesize such a parameter extractor for specific applications. However, the execution time of this algorithm increases when many types of logic gates are used in the algorithm. The data distribution is also restricted by the number of types of logic gates used in the algorithm.

III. Proposed Approach

In order to distribute the data to parameters more uniformly, we partition each data into several data blocks and uniformly map each block to one-bit parameters. The average match time in the parameter memory will then be close to the minimal value. Our LG algorithm for performing partition is based on this idea.

A. Top Level of Local Grouping (LG) Algorithm

The variables used in the algorithm are defined below.

- d_i: One bit of the data at bit position *i*.
- p_i: One bit of the parameter at bit position *i*.
- n: Word length of data. Thus, the data are $d_{n-1}d_{n-2}\ldots d_1d_0$.
- m: The number of unique data in the system trace. Unique data implies that only one datum is chosen from the original data and the other duplicate data are discarded.
- S: Set of unique data. Thus, |S| = m.
- B_i: Each data is partitioned into several blocks logically. See Fig. 2.
- bs: Size of each block. In the LG algorithm, *bs* = two bits.
- C_i: A set $C_i = \{(0, c_0), (1, c_1), \ldots, (2^{bs}-1, c_{2^{bs}-1})\}$ contains several pairs for each bs-bit data block B_i. The first elements of the pairs are the decimal representation of the bs-bit data in the block B_i. The second elements of the pairs are the number of times the data appears in data block B_i of a set S; this is relative to the first elements of the pairs.
- g_{i_j}: Synthesized gate type of the parameter extractor at the i-th level and position j.

The LG algorithm is shown in Fig. 1. The number of times each 2-bit data block appears is analyzed, and the statistics is collected in lines 11 to 16. A one-level parameter extractor can then be synthesized by the ***Find Gate*** function in lines 18 to 21. This function uses these statistics to find an appropriate gate type that enables each data block to be mapped to one-bit parameters uniformly.

```
1   Local Grouping (LG) Algorithm
2   Input:
3   S: Set of unique data.
4   n: Word length of data. Thus, data is d_{n-1}d_{n-2} … d_1d_0.
5   level: The number of levels of the parameter extractor for our
    synthesis.
6   Output: Parameter extractor.
7   Local variable:
8   C_i: Set of counting pairs {(0, c_0), (1, c_1), (2, c_2), (3, c_3)} for 2-
    bit block B_i. Initial values of c_0, c_1, c_2, and c_3 are zero.
9   li: Index of the level in the parameter extractor. Initial value is
    one.
10  {
11    for all data ∈ S {
12      for all 2-bit data block d_{2i+1}d_{2i}, i = 0 to ⌊n/2⌋−1 {
13        j = decimal presentation of d_{2i+1}d_{2i}.
14        c_j = c_j + 1 in the (j, c_j) of C_i.
15      }
16    }
17
18    for i = 0 to ⌊n/2⌋−1 {
19      Sort the elements (0, c_0), (1, c_1), (2, c_2), and (3, c_3) of C_i
        in descending order by c_j, where j ∈ {0,1,2,3} .
20      Find Gate (sorted C_i) and record the gate type at the
        li-th level and i-th position of the parameter extractor.
21    }
22
23    if ( li < level ) {
24      Use S and the generating gates in the li-th
        level of the parameter extractor to compute the new data
        set. Then replace S with the new dataset.
25      n = word length of new data.
26      Initialize C_i for new data. // i = 0 to ⌊n/2⌋−1
27      li = li + 1.
28      Goto line 11.
29    }
30  }
```

Fig. 1 Top level of synthesis algorithm.

After synthesizing the one-level parameter extractor, if the number of levels reaches our requirements, the algorithm is completed. Otherwise, new data are computed using the old data, and the one-level parameter extractor is again generated. The next-level parameter extractor can then be synthesized by analyzing the new data, as shown in lines 23 to 29. Fig. 2 presents a 2-level parameter extractor for every two 2-bit data blocks.

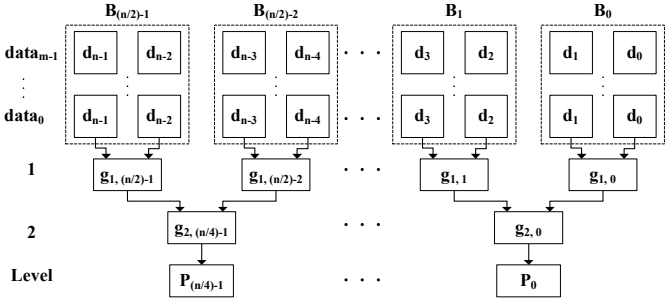


Fig. 2 An example of synthesized 2-level parameter extractors.

B. Grouping Function

The ***Grouping*** function is the kernel of the LG algorithm and is responsible for grouping the data into two groups; subsequently, these two groups can be mapped to 0 or 1. The gate type can thus be determined from these two groups. The general ***Grouping*** function for two groups is shown in Fig. 3. The sorted C_i is input into this function. Next, each pair of the sorted C_i is assigned to one group by the second element of each pair in the sorted C_i and a greedy method. This greedy method ensures that the sum of the second element of each pair in one group is close to that in the other. Each data block can then be mapped to one-bit parameters uniformly.

Now, we must find the appropriate gate type. The total combinations of the groups and relative gate type are derived from the grouping function for a 2-bit data block; see Table 1. Table 1 can then be translated into the ***Distinguish All Gate Type*** function shown in Fig. 4 using the ***Grouping*** function. The ***Grouping*** and ***Distinguish All Gate Type*** functions can then be employed to implement the ***Find Gate*** function.

```
1   Grouping Function // General version for two groups
2   Input:
3   Sorted C_i = {(j_0, c_j0), (j_1, c_j1), ..., (j_k, c_jk)} and
    c_j0 ≥ c_j1 ≥ ... ≥ c_jk ; here k = 2^bs − 1 and bs is block size.
    j_0, j_1, ..., j_k ∈ {0,1,...,2^bs − 1} and j_0 ≠ j_1 ≠ ... ≠ j_k .
4   Output: Two groups G0 and G1. Initial is empty.
5   Local variable: gc0 = gc1 = 0, p = 1, q=0.
6   {
7     Place j0 into G0 and j1 into G1.
8     gc0 = gc0 + c_j0 ,  gc1 = gc1 + c_j1 .
9     for i = 2 to 2^bs - 1
10    {
11      place ji into Gp.
12      gc_p = gc_p + c_ji .
13      if (gcp ≧ gcq) swap (p, q)
14    }
15  }
```

Fig. 3 General grouping function.

TABLE I

TOTAL COMBINATIONS OF GROUPS FOR 2-BIT BLOCK

Mapping / Grouping	G_p map to 0 G_q map to 1	G_p map to 1 G_q map to 0	Identity of Gate Type
G_p = {0} G_q = {1, 2, 3}	a[1] or b[2] = not (a nor b)	a nor b	gt1
G_p = {1} G_q = {0, 2, 3}	a or (not b) = (not a) nand b	(not a) and b = a nor (not b)	gt2
G_p = {2} G_q = {0, 1, 3}	(not a) or b = a nand (not b)	a and (not b) = (not a) nor b	gt3
G_p = {3} G_q = {0, 1, 2}	a nand b	a and b = not (a nand b)	gt4
G_p = {0, 1} G_q = {2, 3}	a	not a	gt5
G_p = {0, 2} G_q = {1, 3}	b	not b	gt6
G_p = {0, 3} G_q = {1, 2}	a xor b	a xnor b	gt7

[1] msb of 2-bit block [2] lsb of 2-bit block

```
1   Distinguish All Gate Type Function
2   Input: Groups G0 and G1.
3   Output: Gate type.
4   {
5     if ( |G0| = 1 ){
6       if ( j0 = 0 ) return gt1.
7       else if ( j0 = 1 ) return gt2.
8       else if ( j0 = 2 ) return gt3.
9       else return gt4.
10    }
11    else if( |G0| = 2 ) {
12      Bitwise xor two elements of G0 and store the decimal
        presentation of the result in the variable i.
13      if ( i = 1) return gt5.
14      else if ( i = 2 ) return gt6.
15      else if ( i = 3 ) return gt7.
16    }
17  }
```

Fig. 4 Function for distinguishing all gate types.

C. Find Gate Function

The ***Find Gate*** function must find the proper gate type with lower costs. Moreover, this gate type must uniformly map each data block to one-bit parameters. Hence, we analyzed the relation between the groups and the order of the count for a 2-bit data block, as shown in Table 2. For example, when the order of the relative count is $c_{j_0} = c_{j_1} > c_{j_2} > c_{j_3}$ (3rd row), the cardinality of each group must be two because the sums of the count in each group must be close. Since the relative counts of j_0 and j_1 are also equal, j_0 and j_1 can be exchanged. Therefore, there are two available combinations of groups that are related to this order.

In Table 2, the available combinations of methods 1 and 3 cover gt5, gt6, and gt7, and hence, we can choose one of these three gate types. Methods 5 and 6 can also use the concept of the ***Grouping*** and ***Distinguish All Gate Type*** functions to choose a gate type. However, methods 2 and 4 require one additional function to choose a lower-cost gate type. Accordingly, we analyzed the total combinations of the elements in each group for these two methods, as shown in Table 3. The relationship between these methods and the relative gate types can now be found. The characteristic value *cv* in the first column of Table 3 can be used to choose a gate type. The value of *i* is zero here, but it can also be two. From Tables 2 and 3, the ***Distinguish Gate Type567*** and ***Find Gate*** functions are constructed in Fig. 5 and Fig. 6, respectively.

TABLE II

RELATION BETWEEN GROUPS AND ORDER OF COUNT

Order of Relative Counts $(j_0, j_1, j_2, j_3 \in \{0,1,2,3\}$ $j_0 \neq j_1 \neq j_2 \neq j_3)$	Available Combinations of Groups $(p, q \in \{0,1\}, \quad p \neq q)$	Method of Finding Gates Related to The Comment of The Find Gate Function
$c_{j_0} = c_{j_1} = c_{j_2} = c_{j_3}$ $c_{j_0} = c_{j_1} = c_{j_2} > c_{j_3}$	$G_p = \{j_0, j_1\}$ $G_q = \{j_2, j_3\}$	Method 1
	$G_p = \{j_0, j_2\}$ $G_q = \{j_1, j_3\}$	
	$G_p = \{j_0, j_3\}$ $G_q = \{j_1, j_2\}$	

$c_{j_0} = c_{j_1} > c_{j_2} > c_{j_3}$ $c_{j_0} = c_{j_1} > c_{j_2} = c_{j_3}$	$G_p = \{j_0, j_2\}$ $G_q = \{j_1, j_3\}$	Method 2
	$G_p = \{j_0, j_3\}$ $G_q = \{j_1, j_2\}$	
$c_{j_0} > c_{j_1} = c_{j_2} = c_{j_3}$	$G_p = \{j_0, j_1\}$ $G_q = \{j_2, j_3\}$	Method 3
	$G_p = \{j_0, j_2\}$ $G_q = \{j_1, j_3\}$	
	$G_p = \{j_0, j_3\}$ $G_q = \{j_1, j_2\}$	
	$G_p = \{j_0\}$ $G_q = \{j_1, j_2, j_3\}$	Method 5
$c_{j_0} > c_{j_1} > c_{j_2} = c_{j_3}$	$G_p = \{j_0, j_2\}$ $G_q = \{j_1, j_3\}$	Method 4
	$G_p = \{j_0, j_3\}$ $G_q = \{j_1, j_2\}$	
	$G_p = \{j_0\}$ $G_q = \{j_1, j_2, j_3\}$	Method 5
$c_{j_0} > c_{j_1} > c_{j_2} > c_{j_3}$ $c_{j_0} > c_{j_1} = c_{j_2} > c_{j_3}$	$G_p = \{j_0, j_3\}$ $G_q = \{j_1, j_2\}$	Method 6
	$G_p = \{j_0\}$ $G_q = \{j_1, j_2, j_3\}$	

TABLE III

CHARACERISTIC VALUES OF METHODS 2 AND 4

cv = $j_i + j_{i+1}$ (i = 0)	Gate type	Method 2				Method 4			
		j_0	j_1	j_2	j_3	j_0	j_1	j_2	j_3
1	gt 6 gt 7	0	1	2	3	0	1	2	3
				3	2	1	0		
		1	0	2	3	0	1	3	2
				3	2	1	0		
2	gt 5 gt 7	0	2	1	3	0	2	1	3
				3	1	2	0		
		2	0	1	3	0	2	3	1
				3	1	2	0		
3	gt 6 gt 5	0	3	1	2	0	3	1	2
				2	1	3	0		
		3	0	1	2	0	3	2	1
				2	1	3	0		
3	gt 6 gt 5	1	2	0	3	1	2	0	3
				3	0	2	1		
		2	1	0	3	1	2	3	0
				3	0	2	1		
4	gt 5 gt 7	1	3	0	2	1	3	0	2
				2	0	3	1		
		3	1	0	2	1	3	2	0
				2	0	3	1		
5	gt 6 gt 7	2	3	0	1	2	3	0	1
				1	0	3	2		
		3	2	0	1	2	3	1	0
				1	0	3	2		

```
1   Distinguish Gate Type567 Function.
2   Input: cv is the characteristic value of groups.
3   Output: Gate type.
4   {
5       if (cv is odd) return gt6 according to Table 5(b).
6       if (cv is even) return gt5 according to Table 5(b).
7   }
```

Fig. 5 Function for distinguishing gate types 5, 6, and 7.

```
1   Find Gate function.
2   Input:  Sorted C_i = {(j0, c_j0), (j1, c_j1), (j2, c_j2), (j3, c_j3)}
                and c_j0 ≥ c_j1 ≥ c_j2 ≥ c_j3
3   Output: One gate type. Local variable: G0 and G1
4   {
5       Boolean j3toG0 = false.
6       if (cj1 + cj2 >= cj0)  j3toG0 = true.
7       if (cj0 = cj1) {
8           if (cj1 = cj2)  return either gt5, gt6, or gt7.  // Method 1
9           else {  // Method 2
10              temp = j0 + j1.
11              return Distinguish Gate Type567 ( temp ).
12          }
13      } // end if (cj0 = cj1)
14      else if (cj2 = cj3) {
15          if ( j3toG0 = true ) {
16              if (cj1 = cj2)  return either gt5, gt6, or gt7. // Method 3
17              else {  // Method 4
18                  temp = j0 + j1.
19                  return Distinguish Gate Type567 ( temp ).
20              }
21          }
22          else  // Method 5, Grouping function for 2-bit block
23              Place j0 into G0.  Place j1, j2 and j3 into G1.
24      } // end else if (cj2 = cj3)
25      else { // Method 6
26          // Grouping function for 2-bit block
27          Place j0 into G0.  Place j1 and j2 into G1.
28          if ( j3toG0 = true ) Place j3 into G0.
29          else Place j3 into G1.
30      } // end else
31      return Distinguish All Gate Type (G0, G1).
32  }
```

Fig. 6 Functions for distinguishing and finding gate type.

D. *Demonstration of Local Grouping Algorithm*

For example, five 4-bit data are shown in Table 4(a). All five data are logically divided into two 2-bit data blocks in Table 4(b). The appearance times are then counted for each data block in Table 4(c) and sorted by the counts in Table 4(d). The sorted C_0 in Table 4(d) matches that of method 2 in Table 2 because c0 = c1 > c3 > c2. Hence, we get the characteristic value that is 0 + 1 = 1. We can then choose either gt6 or gt7; here, we choose gt6. In the same manner, the sorted C_1 in Table 4(d) matches that of method 3 in Table 2 because c3 > c0 = c1 = c2 and c0 +c1 >= c3. Therefore, we can choose either gt5, gt6, or gt7; here, we choose gt6 according to the configurations specified in Table 5(b). If we implement gt6 using a buffer, then the first level of the parameter extractor comprises two buffers. Subsequently, the new data are computed using the original data and the first level of the parameter extractor, as given in Table 4(e). The new data block is also counted and sorted (Table 4(f)). The gate is found in an identical manner, and gt6 is chosen as the second level of the parameter extractor. Therefore, the synthesized parameter extractor requires two buffers to implement it in the hardware but the gate-block selection algorithm requires one each of NAND, NOR, and XOR logic gates in this example. Furthermore, the data are also mapped to parameters uniformly.

TABLE IV

AN EXAMPLE TO DEMONSTRATE LOCAL GROUPING ALGORITHM

Data
0011
1101
0100
1100
1001

(a)

Block B_1	Block B_0
00	11
11	01
01	00
11	00
10	01

(b)

Binary	C_1	C_0
	(Decimal, Count of B_1)	*(Decimal, Count of B_0)*
00	(0, 1)	(0, 2)
01	(1, 1)	(1, 2)
10	(2, 1)	(2, 0)
11	(3, 2)	(3, 1)

(c)

Sorted C_1	Sorted C_0
(Decimal, Count of B_1)	*(Decimal, Count of B_0)*
(3, 2)	(0, 2)
(0, 1)	(1, 2)
(1, 1)	(3, 1)
(2, 1)	(2, 0)

(d)

Block B_0 of new data
01
11
10
10
01

(e)

C_0	Sorted C_0
(Decimal, Count of B_0)	*(Decimal, Count of B_0)*
(0, 0)	(1, 2)
(1, 2)	(2, 2)
(2, 2)	(3, 1)
(3, 1)	(0, 0)

(f)

E. Time Complexity of LG Algorithm

The time complexities of the LG algorithms and gate-block selection algorithms are O(mn). Hence, the LG algorithm is also a polynomial-time algorithm. However, the execution time of LG algorithm is faster than that of gate-block selection algorithms when the number of unique data is considerably larger than the word length of the data. This is because the ***Find Gate*** function is used for each data block in gate-block selection algorithms. Moreover, the new data for the next level of the parameter extractor is calculated once in each level. However, in the gate-block selection algorithm, the new data are calculated for each gate type and counted for all blocks of each unique data. Therefore, the LG algorithm is suitable for large amounts of unique data.

F. Discard and Interlace (DAI) Method

If most data in one block are identical, then the data will be centralized in some parameters. This causes match time in the parameter memory, which implies that the power consumption in the match line is still high. Therefore, we propose a method, shown in Fig. 7, to reduce the impact on mapping data. If most data are identical in one block, then the standard deviation of the appearance times of the data in this block is large. Hence, the standard deviation is used to find such data blocks. Subsequently, such data blocks are discarded, and the remaining data blocks are then used to construct new data for the synthesized algorithm. For example, if the data format is $d_7d_6\ldots d_1d_0$, and moreover, if most data are identical in $d_7d_6d_5d_4$ and different in d_1d_0, we divide the data into four 2-bit data blocks—$B_3 = \{d_7, d_6\}$, $B_2 = \{d_5, d_4\}$, $B_1 = \{d_3, d_2\}$, and $B_0 = \{d_1, d_0\}$. Subsequently, the standard deviation of each block is calculated. Because the standard deviations of B_3 and B_2 are larger than those of the others, B_3 is discarded and B_2 is interlaced with the copied B_0. We then construct the new data $d_5d_0d_4d_1d_3d_2d_1d_0$ and remove the duplicate data. The synthesizing algorithm can then use these data as input data to synthesize the parameter extractor.

IV. EXPERIMENTAL RESULTS

In order to evaluate our algorithm and method, we compared them experimentally with the Block-XOR and Gate-block selection schemes. We used MiBench [5] as the benchmark in our experiment and modified sim-cahce.c in SimpleScalar [6] to dump the data address that are used to access data TLB as test data. Moreover, the configurations used in this experiment are shown in Table 5(a), (b), and (c). In the configuration of the DAI method, we divide the data into four 8-bit data blocks and calculate the standard deviation of these data blocks of the benchmark; we found that the standard deviations are high in the case of blocks 3 and 2 but low in the case of block 0. Hence, we discarded block 3, interlaced block 2, and copied block 0 as the new input data when the DAI method is applied.

1 ***Discard and Interlace Method.***

2 Divide unique data into *t* blocks.
3 Compute the standard deviation of each block.
4 Discard Block BS_0 with the highest standard deviation.
5 Find Block BS_1 with the second highest standard deviation.
6 Choose and copy Block BS_2 with the smallest standard deviation.
7 Interlace the blocks BS_1 and BS_2 as new big Block BS_{new0}. Use Block BS_{new0} and remaining part of original data as new input data of the parameter extractor.

Fig. 7 Discard and interlace method.

TABLE V

EXPERIMENTAL CONFIGURATIONS

Spice Simulation Tool	Synopsys NanoSim
High-Level Simulation Tool	HLSRC[a]
Technology	CIC [7] 0.18 um SPICE Model
Supply Voltage	1.8 V
CAM Cell	Conventional 9T XOR type
Parameter Comparison Circuit	As in [1]
Match Line Structure of Data Memory	NOR type match line
Word Structure	Static [1]
Capacity of Parameter Memory	4 bits × 128 words

Capacity of Data Memory	32 bits × 128 words
Replacement Policy	Counter-based LRU
Pre-fetch Data	Yes
Size of Data Block for Each Level of Parameter Extractor	2 bits
Number of Levels of Parameter Extractor	3 levels

(a) For all schemes.

Schemes	Configurations
Block-XOR	Without valid bit design
Gate-block selection algorithm	The priority of selecting gates is NAND > NOR > XOR when C_{avg} is equal.
LG algorithm	gt1 = a nor b, gt2 = a nor (not b), gt3 = (not a) nor b, gt4 = a nand b, gt5 = a, gt6 = b, gt7 = a xor b gt5 and gt6 are implemented by two inverters
	The priority of selecting gate types is gt6 > gt5 > gt7 when we need to choose a gate type to return.

(b) For each scheme.

Blocks	Original	DAI method
Block 3	$d_{31}d_{30}\ldots d_{25}d_{24}$	$d_{23}d_0d_{22}d_1\ d_{21}d_2d_{20}d_3$
Block 2	$d_{23}d_{22}\ldots d_{17}d_{16}$	$d_{19}d_4d_{18}d_5\ d_{17}d_6d_{16}d_7$
Block 1	$d_{15}d_{14}\ldots d_9d_8$	$d_{15}d_{14}\ldots d_9d_8$
Block 0	$d_7d_6\ldots d_1d_0$	$d_7d_6\ldots d_1d_0$

(c) For DAI method.

In order to evaluate the power consumption, we use Synopsys NanoSim to simulate the circuits. The average reduction rate is also shown in Table 6.

TABLE VI

AVERAGE REDUCTION RATE OF POWER CONSUMPTION AND NUMBER OF CMOS ELEMENTS IN ALL CIRCUITS

LG-DAI (Power)		***LG-DAI (Area)***	
VS. gsel	***VS. xor***	***VS. gsel***	***VS. xor***
60.4%	60.7%	0.52%	0.59%

When our schemes are used, the average reduction rate is 60% better than that of the original gate-block selection and block-XOR schemes; further, the average reduction rate of the number of CMOS elements is also better by 0.5%. The simulation result was conducted by mixing multiple search/write operations of PB-CAM while we write a row of memory and perform the comparisons with other rows of memory in parallel. In practice, the network router is configured once during the cool down period and later carries out search operations for a long time. In order to imitate this scenario, we have altered the simulation configuration to search 128 different data consecutively, the average reduction rate of our approach is also about 40% better than the gate-block selection scheme and is about 50% better than the block-XOR scheme too.

CONCLUSIONS

In this paper, we propose an LG algorithm to synthesize a parameter extractor for PB-CAM whenever the trace of the system is obtained. A DAI method is also proposed to reduce the impact on mapping when most data in some computed data blocks are identical. The experiment results show that the power consumption and number of CMOS elements can be reduced when our schemes are used for PB-CAM. Moreover, our LG-DAI approach can probably be extended to reconfigurable environments when the system trace is known and a new hot-swap precomputation circuit is required to leverage known data locality. In this manner, low power operations can be sustained for longer time. Our approach may be useful to EDA researchers and others involved in developing framework for Hardware-Software Co-Design of embedded systems.

REFERENCES

[1] C.-S. Lin, J.-C. Chang, and B.-D. Liu, A low-power precomputation-based fully parallel content-addressable memory, *IEEE J. Solid-State Circuits*, vol. 38, no. 4, pp. 654-662, Apr. 2003.

[2] J.-Y. Hsieh and S.-J. Ruan, Synthesis and design of parameter extractors for low-power pre-computation-based content-addressable memory using gate-block selection algorithm, in *Asia and South Pacific Design Automation Conference (ASPDAC)*, Mar. 2008, pp. 316-321.

[3] K. Pagiamtzis and A. Sheikholeslami, Content-addressable memory (CAM) circuits and architectures: a tutorial and survey, *IEEE J. Solid-State Circuits*, vol. 41, no. 3, pp. 712-727, Mar. 2006.

[4] S.-J. Ruan, C.-Y. Wu, and J.-Y. Hsieh, Low Power Design of Precomputation-Based Content-Addressable Memory, *IEEE Trans. Very Large Scale Integr. (VLSI) Syst.,* vol. 16, no. 3, pp. 331-335, Mar. 2008.

[5] M. R. Guthaus, J. S. Ringenberg, D. Ernst, T. M. Austin, T. Mudge, and R. B. Brown, MiBench: A free, commercially representative embedded benchmark suite, in *IEEE International Workshop on Workload Characterization (WWC-4)*, Dec. 2001, pp. 3-14.

[6] *SimpleScalar LLC*. Available: http://www.simplescalar.com/

[7] *National Chip Implementation Center*. Available: http://www.cic.org.tw/cic_v13/

A New NoC Architecture Based on Partial Interconnection of Mesh Networks

S. Choudhary and S. Qureshi
Department of Electrical Engineering, Indian Institute of Technology, Kanpur, India-208016.
E-mail: suds@iitk.ac.in and qureshi@iitk.ac.in

***Abstract*- A new network on chip (NoC) topology called partially interconnected mesh network is proposed and a routing algorithm supporting the proposed architecture is also developed. The proposed architecture is based on standard mesh networks, here four extra bidirectional channels are added which remove the congestion and hotspots compare to standard mesh networks with fewer channels. The proposed architecture and routing algorithm are compared to measure performance benefits over standard mesh network in terms of delay and throughput. Significant improvement in delay (60% reduction) and throughput (60% increased) were observed when using the proposed network. An increase in number of channels makes the switches expensive and could increase the area and power consumption. However, the proposed network can be useful in high speed applications with some compromise in area and power.**

I. INTRODUCTION

As reported by the researchers in [1–5], it will not be possible for the dedicated wires and shared busses to fulfill the communication requirements of future ICs. On chip interconnection architecture is commonly based on dedicated wires or shared busses. As the system complexity increases the number of dedicated wires grows which means they are effective only for small core systems. Also there are issues of poor reusability and flexibility with dedicated wires. A shared bus can be more scalable and reusable compared to dedicated wires but they cannot support the communication parallelism and bandwidth requirements of multi core systems [6–7].

NoCs have emerged as a solution to the existing interconnection architecture constraints [8–10] due to the following characteristics: (i) energy efficiency and reliability [3], (ii) scalability of bandwidth when compared to traditional bus architectures, (iii) reusability and (iv) distributed routing decisions [4–5]. NoC is an on-chip interconnection network [4] composed by cores (IP blocks) connected to switches (routers) which are in turn connected among themselves by communication channels. Two main resources that compose NoCs are buffers and channels. To increase the resources allocation for each packet, a physical channel is multiplexed into a number of virtual channels [4, 5]. Each virtual channel has one or more buffers which provide multiple buffers for each physical channel. The performance of NoC with virtual channels can be evaluated and the important parameters can be fixed by the designers for specific applications [10].

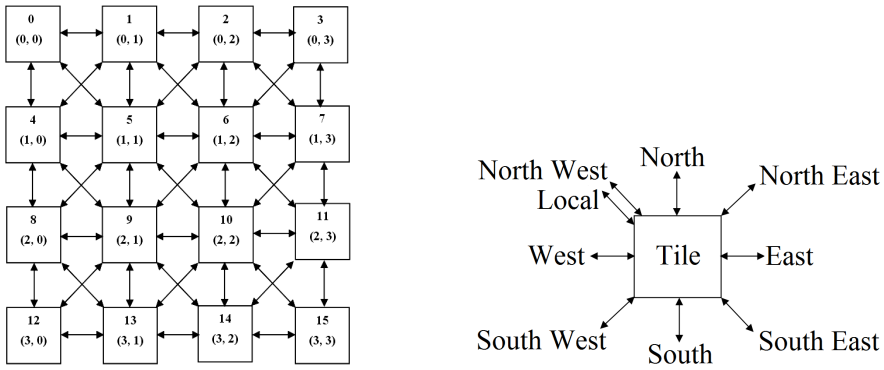
The main steps of a NoC design are architecture specification, traffic modeling, and performance evaluation. Fully adaptive routing is considered the best for mesh networks [11-18], we verified the same using Noxim simulator [19] (details not shown in this paper). The key contribution of this paper is a new NoC architecture (partially interconnected mesh topology) and a suitable routing algorithm for the new design. In section 2, partially interconnected mesh network topology and a routing scheme [20] for this topology is proposed. This proposed architecture and routing algorithm is compared with the best configured ideal mesh network architecture proposed by previous research works [11-18] [20]. We used Nirgam simulator [21] to build the proposed architecture and routing scheme, the simulator was modified to support the new topology and routing scheme. Conclusion is presented in section 3.

II. PROPOSED ARCHITECTURE AND ROUTING

Full mesh topology is a network topology in which all nodes are directly connected to each other. In a fully connected network with n nodes, there are n(n-1)/2 direct links. Full mesh networks are very costly to setup, but provide a highly reliable data transfer because of the availability of multiple paths to a node. This topology is used when there are only a small number of nodes to be interconnected. These networks are usually seen in military applications.

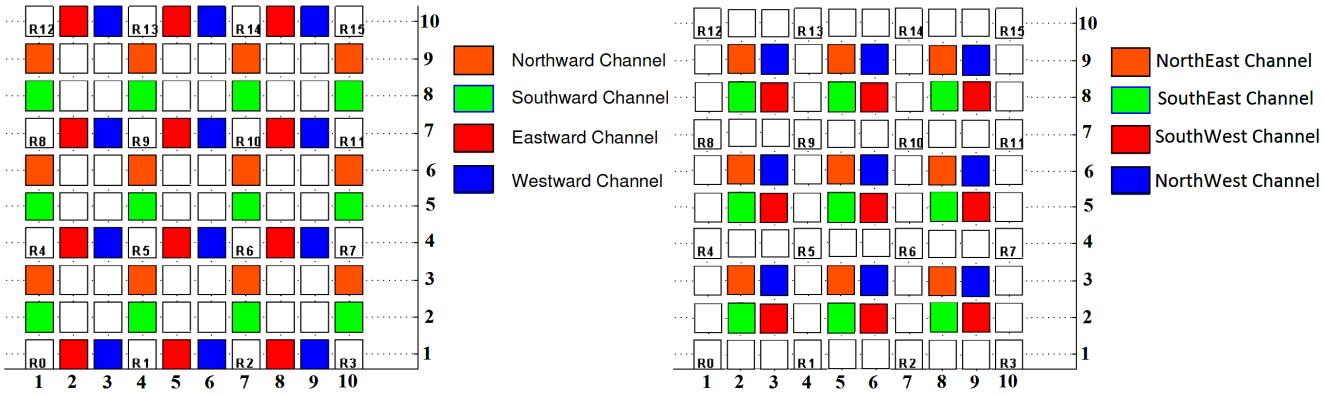
Partially connected mesh is a network topology in which some of the nodes of the network are connected to more than one other node in the network with a point-to-point link. This makes it possible to take advantage of some of the redundancy that is provided by a physical fully connected mesh topology without the expense and complexity required for a connection between every node in the network [22]. In this section, a new architecture based on partially connected mesh topology and a routing algorithm for this new topology is proposed. We use Nirgam [21] simulator for evaluation.

This simulator supports both mesh and torus networks. The simulator was modified to support the proposed new architecture, a routing algorithm was also written for the simulator to send packets on the proposed network. In this



(a) (b)

Fig. 1. (a) Proposed partially connected mesh topology where tiles are connected through bidirectional channels (b) Representation of a tile with its bi-directional channels.



(a) (b)

Fig. 2. Representation of Performance metrics on per channel basis (a) North, South, East and West channels (b) North-East, South-East, North-West and South-West channels. R0-R15 represents the routers.

new architecture we add four extra bidirectional channels to each router of the mesh network, so that there are nine bidirectional communication channels in each router namely East, West, North, South, Local, North-East, South-East, North-West and South-West (see Fig. 1).

The performance of NoC is evaluated on per-channel basis. Fig. 2(a) shows representation of performance metrics in matlab generated graphs. R0 - R15 shows the placement of tiles/routers. Red bar between R0 and R1 represents metric for east channel from R0 to R1. Blue bar between R0 and R1 represents metric for west channel from R1 to R0. Green bar between R0 and R4 represents metric for south channel from R0 to R4. Orange bar between R0 and R4 represents metric for north channel from R4 to R0. Similarly in Fig. 2(b), Red bar between R1 and R4 represents metric for South-West channel from R1 to R4. Blue bar between R5 and R0 represents metric for North-West channel from R5 to R0. Green bar between R0 and R5 represents metric for South-East channel from R0 to R5. Orange bar between R4 and R1 represents metric for North-East channel from R4 to R1.

In a standard mesh network each router/tile has four bidirectional ports/channels for communicating other routers in the network and has one bidirectional channel for communicating with the local IP attached to tile. Routing algorithms for such network are mainly based on communication in x-direction and y-direction, using turn models that routes the packet by turning in x-direction (using East or West channel) or y-direction (using North or South channel). Dead-locks in some unique cases in turn models are avoided by prohibiting few turns while routing a packet from source node to destination node. In the new architecture, packets can also be routed in z-direction (NE, SE, NW and SW) along with the usual x and y-directions. This saves the number of routers traversed which in turn applies the use of free router channels by other communications. For example, if a packet has to move from source tile number 12 to destination tile number 7 using standard mesh network, the path could be through tiles 12-13-14-15-11-7. However, the path is through tiles 12-9-6-7 when network of Fig. 1(a) is used, that saves time by routing through fewer tiles and also allows the free channels/paths for other communications. Higher throughput

```
if(dest_yco > yco)                  else if(dest_yco < yco)          else if(dest_yco == yco)
   {                                   {                                {
      if(dest_xco < xco)                  if(dest_xco < xco)               if(dest_xco < xco)
           return NE;                          return NW;                       return N;
        else if(dest_xco > xco)             else if(dest_xco > xco)          else if(dest_xco > xco)
           return SE;                          return SW;                       return S;
        else if(dest_xco == xco)            else if(dest_xco == xco)         else if(dest_xco == xco)
           return E;                           return W;                        return C;
     }                                                                 }
                                        }
```

Fig. 3. Cross-routing algorithm; 'xco' and 'yco' are x and y-coordinates of source tile; 'dest_xco' and 'dest_yco' are coordinates of destination tile.

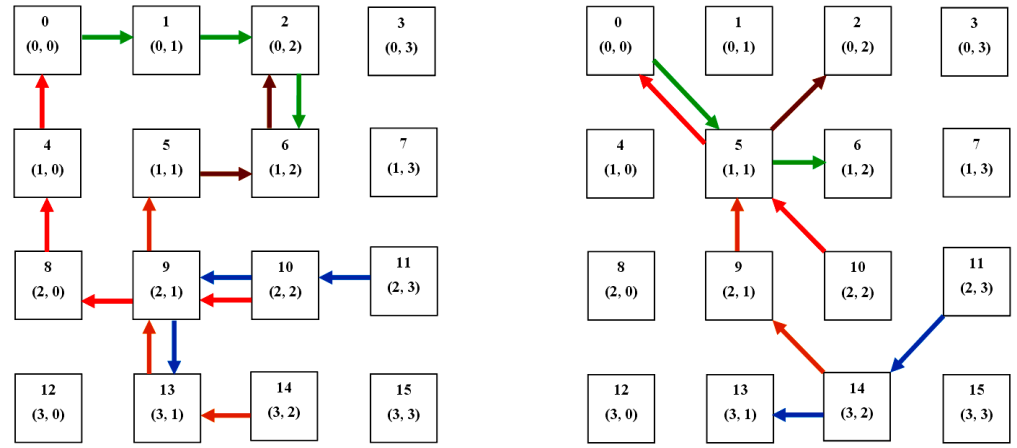
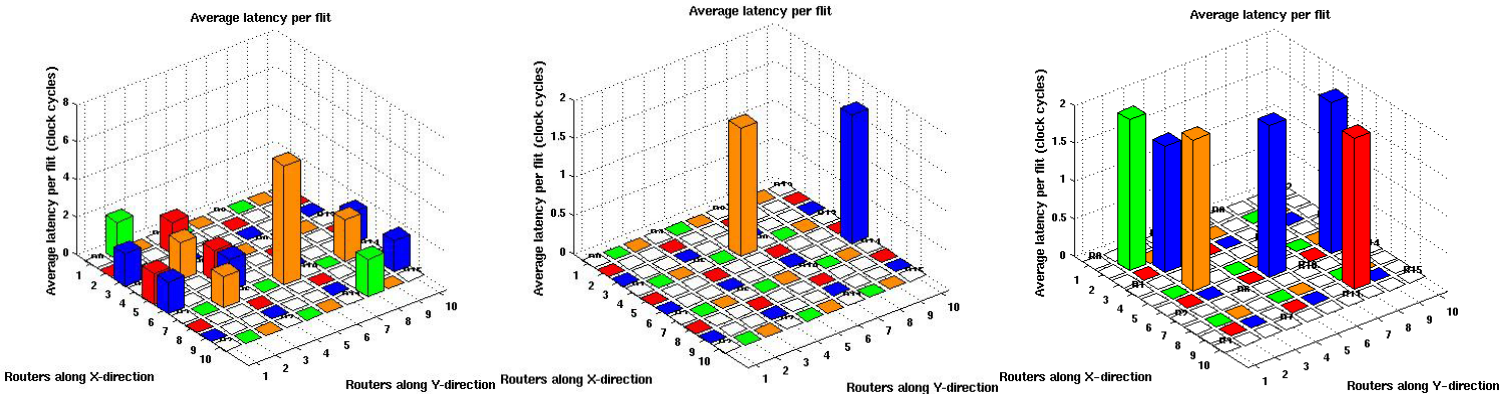
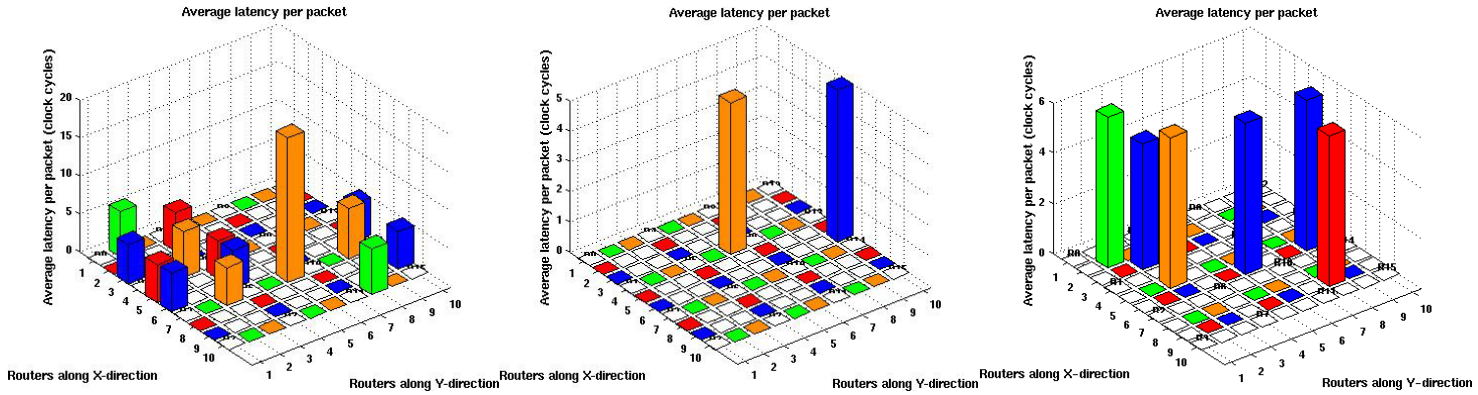


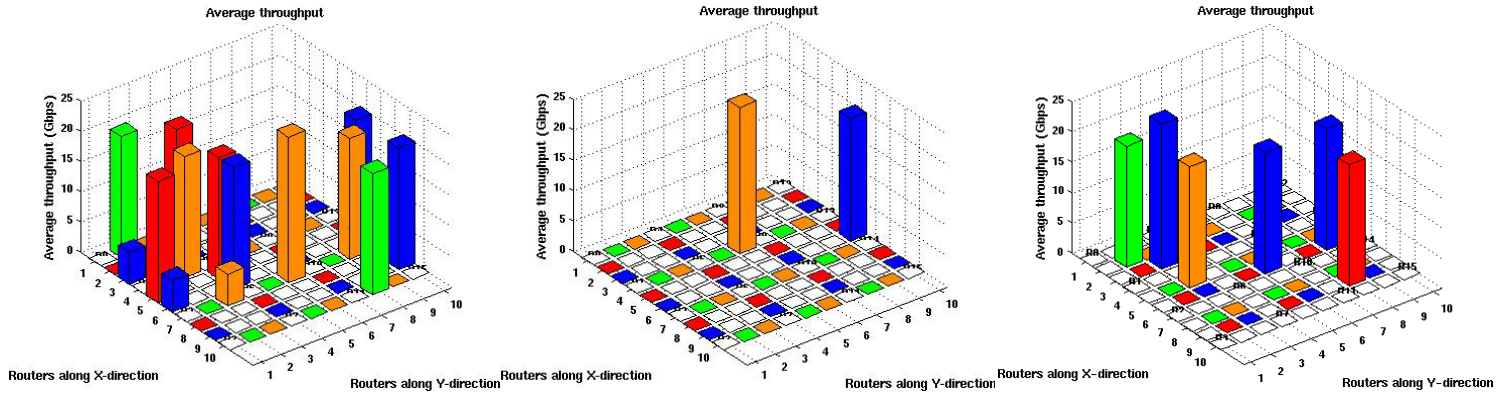
Fig. 4. CBR with fixed destination on (a) standard mesh with fully adaptive routing (b) partially connected mesh with cross-routing



(a) Latency per flit on per channel basis

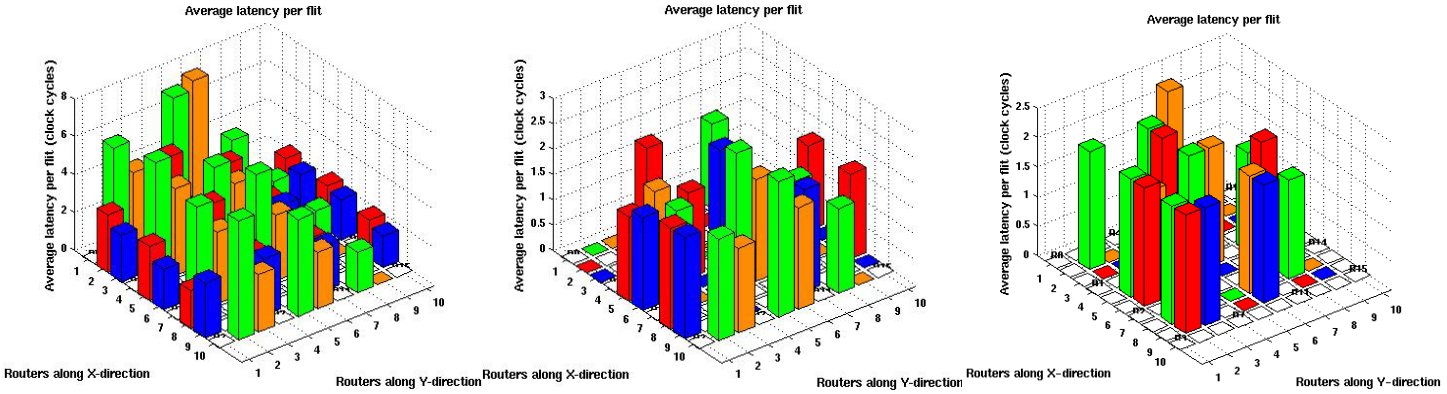


(b) Latency per packet on per channel basis

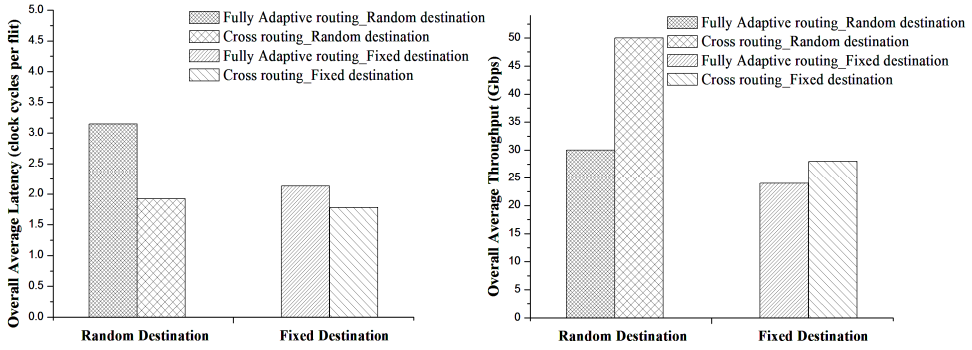


(c) Throughput per channel

Fig. 5. Simulation results for fixed destination corresponding to Fig. 4; (a) latency per flit, (b) latency per packet and (c) Throughput. Three results are shown in each case where first result is obtained for mesh network using fully adaptive routing, second and third results are for the proposed network topology on cross- routing. Also in each case, second result shows measurements on East, West, North and South channel and third result shows measurements on North East, South East, North West and South West channels.



(a) Latency per flit for random destination, other details remain same as in Fig. 5 above.



(b) (c)

Fig. 6. (a) Latency per flit for random destination, (b) Overall Average latency for fixed and random destination and (c) Overall Average Throughput for fixed and random destination.

and smaller latency is confirmed through simulations on this architecture.

Routing algorithm for this architecture is called cross-routing and is given in Fig. 3. While moving a packet, the x-coordinate and y-coordinate of source and destination tiles are compared. If both x and y-coordinates of source and destination tiles are not equal, packet is moved in z-direction (using NE, SE, NW or SW channels), else packet moves in either x or y-direction depending on whether the x-coordinate or y-coordinate of source tile is equal to that of destination tile. Cross-routing is free of dead-locks since it does not form loops, third turn is prohibited so that a packet reaches the

destination by taking maximum two turns, one in z-direction and other in x or y-direction. Simulation results using cross-routing on the proposed architecture show significant improvement in latency and throughput when compared to fully adaptive routing on ideal mesh networks.

A. Experimental Results and Discussion

The performance evaluation is based on standard 4x4 mesh network with five bi-directional ports and partially connected mesh network with nine bidirectional channels (see Fig. 1(a)). It was found earlier that fully adaptive routing is superior to all other routing schemes [11-18]. Hence we evaluate and compare the performance of these networks on fully adaptive and cross-routing algorithm. Also, we consider tiles of both the networks transmitting packets at constant bit-rate (CBR) with random destinations and at constant bit-rate with fixed destinations. In CBR with random destinations, each tile behaves as a source as well as sink, implying that it is capable of generating as well as receiving flits. Each tile generates CBR traffic to randomly chosen destination. For CBR with fixed destinations, we consider an example shown in Fig. 4, where, tile 0 sends CBR traffic to tile 6, tile 5 sends CBR traffic to tile 2, tile 10 sends CBR traffic to tile 0, tile 11 sends CBR traffic to tile 13 and tile 14 sends CBR traffic to tile 5. Fig. 4(a) shows the possible path taken by the packets to move from sources to fixed destinations on standard mesh network using fully adaptive routing, while Fig. 4(b) uses partially connected mesh network of Fig. 1(a) with cross-routing.

Performance of both the NoCs are measured on per channel basis. Traffic generation begins after 5 clock cycles, and continues until 300 clock cycles. Simulation stops after 1000 clock cycles. Latency and throughput per-channel for CBR with fixed destination are measured and plotted in Fig. 5. Overall average latency is shown in Fig. 5(a), which is smaller in case of cross-routing (1.78, in clock-cycles per flit) compare to fully adaptive routing on standard mesh NoC (2.13, in clock cycles per flit). Overall average throughput (see Fig. 5(b)) is also higher for cross-routing scheme (28 Gbps) compare to fully adaptive routing on standard mesh NoC (24 Gbps). Similar results are obtained for CBR with random destinations and are shown in Fig. 6. The results in Fig. 6(b) and (c) show that for cross-routing the overall average latency reduces by 60% and the overall average throughput increases by 60% in comparison to fully adaptive routing on standard mesh NoC. This improvement in performance is possible because lesser nodes are traversed during packet transmission thus offering greater number of available free channels which could be utilized by other communications.

III. CONCLUSION

In this paper we have evaluated the performance of standard mesh-based NoC architecture and compared it with the proposed partially interconnected network architecture. We started by evaluating different routing algorithms and switching schemes on a standard mesh topology and then proposed a partially interconnected mesh topology with cross-routing algorithm. From the performance comparison, it was found that the proposed network and routing algorithm can be efficiently used for future NoCs. The experiments were also performed on larger networks and performance measurements gave significant improvements. While the proposed topology provides some improvements (e.g. increased bandwidth, decreased latency) over standard mesh, it effectively duplicates the number of links making switches expensive. It is also expected that this topology could increase the die area and power consumption but still it can be useful for high speed applications with some compromise in power and area.

ACKNOWLEDGMENT

The authors would like to thank Ministry of Communication and Information Technology, Govt. of India for their support.

REFERENCES

[1] [1] S. Kumar, A. Jantsch, J. P. Soininen, M. Forsell, M. Millberg, J. Oberg, K. Tiensyrja and A. Hemani, "A network on chip architecture and design methodology," *IEEE Computer Society Annual Symposium on VLSI (ISVLSI'02)*, April 2002, pp. 105–112.

[2] M. Millberg, E. Nilsson, R. Thid, S. Kumar and A. Jantsch, "The Nostrum backbone—a communication protocol stack for networks on chip," *Proceedings of the VLSI Design Conference*, January 2004.

[3] L. Benini and G. De Micheli, "Powering networks on chips: energy-efficient and reliable interconnect design for SoCs," *14th International Symposium on Systems Synthesis (ISSS'01)*, October 2001, pp. 33–38.

[4] L. Benini and G. De Micheli, "Networks on chips: a new SoC paradigm," *IEEE Compute*r, vol. 35, no. 1, pp. 70–78, 2002.

[5] P. Guerrier and A. Greiner, "Ageneric architecture for on-chip packet-switched interconections," *Design Automation and Test in Europe (DATE'00)*, March 2000, pp. 250–256.

[6] E. Bolotin, I. Cidon, R. Ginosar and A. Kolodny, "Cost Considerations in Network on Chip," *Integration: The VLSI Journal*, no. 38, pp. 19-42, 2004.

[7] C.A. Zeferino, M.E. Kreutz, L. Carro and A.A. Susin, "A Study on Communication Issues for Systems-on-Chip," *Symposium on Integrated Circuits and Systems Design,* 2002, pp. 121-126.

[8] E. Rijpkema, K. Goossens, A. Radulescu, J. Dielissen, J. van Meerbergen, P. Wielage and E. Waterlander, "Tradeoffs in the design of a router with both guaranteed and best-effort services for networks on chip," *Design, Automation and Test in Europe (DATE'03)*, March 2003, pp. 350–355.

[9] E. Rijpkema, K. Goossens and P. Wielage, "A router architecture for networks on silicon," *2nd Workshop on Embedded Systems (PROGRESS'2001)*, November 2001, pp. 181–188.

[10] B. S. Feero and P. P. Pande, "Networks-on-Chip in a Three-Dimensional Environment: A Performance Evaluation," *IEEE Trans. on Computers*, vol. 58, no. 1, pp. 32-45, 2009.

[11] M. Palesi, G. Longo, S. Signorino, S. Kumar, R. Holsmark and V. Catania, "Design of Bandwidth Aware and Congestion Avoiding Efficient Routing Algorithms for Networks-on-Chip Platforms," *IEEE International Symposium on Networks-on-Chip*, 7th-11th April 2008, Newcastle University, UK, pp. 97-106.

[12] G. Longo, S. Signorino, M. Palesi, S. Kumar, R. Holsmark and V. Catania, "Bandwidth Aware Routing Algorithms for Networks-on-Chip," *2nd Workshop on Interconnection Network Architectures: On-Chip, Multi-Chip*, Goteborg, Sweden, January 27, 2008.

[13] R. Tornero, J. M. Orduna, M. Palesi and J. Duato, "A Communication-Aware Task Mapping Technique for NoCs," *2nd Workshop on*

Interconnection Network Architectures: On-Chip, Multi-Chip, Goteborg, Sweden, January 27, 2008.

[14] M. Palesi, S. Kumar, R. Holsmark and V. Catania, "Exploiting Communication Concurrency for Efficient Deadlock Free Routing in Reconfigurable NoC Platforms," *IEEE International Parallel and Distributed Processing Symposium*, Long Beach, CA, March 2007, pp. 1-8.

[15] G. Ascia, V. Catania, M. Palesi and D. Patti, "Neighbors-on-Path: A New Selection Strategy for On-Chip Networks," *Fourth IEEE Workshop on Embedded Systems for Real Time Multimedia*, Seoul, Korea, October 26-27, 2006, pp. 79-8.

[16] M. Palesi, R. Holsmark, S. Kumar and V. Catania, "A Methodology for Design of Application Specific Deadlock-free Routing Algorithms for NoC Systems," *International Conference on Hardware-Software Codesign and System Synthesis,* Seoul, Korea, October 22-25, 2006, pp. 142-147..

[17] M. Palesi, S. Kumar and R. Holsmark, "A Method for Router Table Compression for Application Specific Routing in Mesh Topology NoC Architectures," *SAMOS VI Workshop: Embedded Computer Systems: Architectures, Modeling, and Simulation,* Samos, Greece, July 17-20, 2006, pp. 373-384.

[18] G. Ascia, V. Catania, M. Palesi and D. Patti, "A New Selection Policy for Adaptive Routing in Network on Chip," *International Conference on Electronics, Hardware, Wireless and Optical Communications*, Madrid, Spain, February 15-17, 2006.

[19] Noxim-the NoC Simulator, http://sourceforge.net/projects/noxim/

[20] S. Choudhary and S. Qureshi, "Performance Evaluation for Mesh-based NoCs: Implementation of a New Architecture and Routing Algorithm," springer, IJAC, submitted.

[21] NIRGAM: A Simulator for NoC Interconnect Routing and Application Modeling, http://www.nirgam. ecs.soton.ac.uk, 2008.

[22] http://en.wikipedia.org/wiki/Tree_and_hypertree_networks#Tree

Principles and Dynamics of Block-based Programming Approach

Siti Nor Hafizah Mohamad[1], Ahmed Patel[2], Yiqi Tew[3], Rodziah Latih[4], Qais Qassim[5]

[1, 2, 3, 4,5]School of Computer Science, Faculty of Information Science and Technology
Universiti Kebangsaan Malaysia
43600 Bangi, Selangor Darul Ehsan, Malaysia

[2]Visiting Professor
Faculty of Computing Information Systems and Mathematics
Kingston University
Kingston upon Thames KT1 2EE, United Kingdom.

[1]fiza410 *at* gmail.com, [2]whinchat2010 *at* gmail.com, [3]yiqi01 *at* gmail.com [4]ggiemel *at* gmail.com, [5]qaisjanabi *at* gmail.com

***Abstract*- Block-based programming approach is based on the principles and dynamics of combining component-based programming approach with end-user programming paradigm which is purported to be more advanced and easier to use in practice. We perform a state of the art review of block-based programming by accessing the different forms of programming approaches and paradigms pertaining to it and establish the core fundamental principles, mechanics and dynamics with examples to illustrate the essence of this approach as well as any metrics to measure its performance. The important characteristics of block-based programming are gathered together and tabulated with clear definition of meaning and purpose. Correspondingly, we establish the criterion and metric by which to measure the effectiveness and efficiency of programming effort in developing software systems based on the block-based approach. In addition, we illustrate more on the block specification and identification to give brief understanding. Finally, we identify aspects of block-based programming which need further investigation, research and development.**

Keywords: programming skills, software development, component-based model, component development, end-user development, mashups.

I. INTRODUCTION

Block-based programming approach is defined in the principles and dynamics based on combined approaches between component-based programming and end-user programming that are said to be more comprehensive and easy to be used in practice. In a world of computer programming, a block is declared as a section of a code combined together to consist of one or more declarations and statements [1]. Basically, a block is a program component being developed to be combined with other blocks to generate specific applications without the need of any programming skills. The block-based programming is an approach that integrates programming blocks for developing some applications in a short period of time and within estimated cost [2]. The main aim of this approach is to allow the application to be developed directly by the end-users.

The paper is comprised as follows: In Section 2, the background study on component-based programming and end-user programming is described in a simple manner with a review on their advantages and disadvantages to clearly judge their strengths and weaknesses. In Section 3, we present a state of the art literature review of block-based programming by comparing similar mashups composition tools such as Google App Inventor and IBM WebSphere sMash [3] which are using the same approaches as being studied in this paper. Section 4, shows the important characteristics of block-based programming which allow further understanding of the approach and is being explained by a clear definition of the meaning and purpose. We also identify the block by giving a real-example. Furthermore, we clarified the criterion and metric which was used to measure the effectiveness and efficiency of block-based programming of the software systems. Finally Section 5 offers a brief discussion and our conclusion for future work.

II. BACKGROUND

A. What is component-based programming?

Component-based programming approach is a rational addition of good code organizing principles where a component or software object is developed, encapsulated certain functionality or a set of functionalities [4]. This component will then be integrated into a larger piece of software. Essentially, this process is the concept that software components are written in such a manner that they provide functions common to many different systems. By using ideas from different hardware components, component-based software systems have to be flexible to accept new replacement of software component and functionality equivalent components where possible. Another significant characteristic of software component is reusability where they are to be designed, implemented and reused in many different programs.

Component-Based Development (CBD) is how to produce new software by merging *prefabricated components* with *new programs* that provide bonding between the components and their new functionality [5]. As shown in Table I, there are several key technical concepts of Component Based Software Engineering (CBSE) such as component, interfaces, contract, component model and component framework [5].

TABLE I
KEY TECHNICAL CONCEPT OF CBSE

Key Concepts	Description
Component	A component is an obscure implementation of a contract of its provided interface, subject to the third party composition and conformant with component model. To implement such contract, the component may use services provided by other components which was called required services and are specified as a contract of an interface that is called the required interface. Component combines two perspective component as an implementation and component as an architectural abstraction.
Interfaces	Interfaces describe all of the properties of a component that probably guide to inter-component dependencies. Without providing any semantic information of the interface's designs and implementations, the interface proclaims a set of fields and a set of operation signatures.
Contract	A contract of an interface of component provides semantic information that identifies on how the interface can be used and allows them to define the dynamic behavior of the component on the interface. There are two senses of contract which are component contract and interaction contract. A component contract identifies a pattern of interaction rooted on that component. An interaction contract specifies a pattern of interaction among different roles and the reciprocal obligation of component that fill those roles.
Component Model	Specifies the design rules that must be obeyed by the component which improves the ability of the composition by encapsulating a variety of sources of interface mismatches through a common API.
Component Framework	Component framework provides services to sustain and impose a component model. The framework manages resources shared by components and provides the underlying mechanisms that allow interaction among components.

A Critical aspect of CBSE is the need for a system that will predictably demonstrate the quality attributes compulsory to them. The end user of commercial component technologies must rely upon off-the-shelf component models and framework to provide basis for achieving system quality attributes. Although component technology vendors make claims concerning on how their products yield these attributes, the technical basis for these claim is being doubtful [5]. The main advantages and disadvantages of the component-based programming also can be referred to Table II [6].

TABLE II
THE ADVANTAGES AND DISADVANTAGES OF COMPONENT-BASED APPROACH

Advantages	Disadvantages
• Eases work distribution • Eases maintainability • Parallel development • Extensibility	• Communication overhead • Development timing • Difficult integration due to the independency of the component

B. What is End-user Programming?

Most people in a society will encounter experiences in a computer's world as "end-users" of package programs. Unfortunately the writers of these programs do not know the particulars of the work that the developers are trying to implement. Struggling to meet the needs of these diverse users, they expand their programs with hundreds of features most people never use. Life would be much simpler if each user could add the functions he or she wanted.

The programs must be designed to accept user-written components in appropriate places. There must be a method to store and manage them. Importantly, since most users do not have the time or awareness to study the tools and skills of a professional programmer, rational compromises are necessary. The clarity and overview of developed programming languages are trades for usability by a variety of metaphors and tricks. Metaphor helps to do the programming in much easier manner.

Since the appropriate metaphors have some of their capabilities and limitations which diverge commonly depending on the users and theirs purposes, there is no specific method of end-user programming. As a substitute, there is a variety of techniques, such as Programming by Demonstration, visual programming, and many domain-specific languages and formalisms. Ideally there is a smooth progression from simple but limited metaphors, to more complex and powerful techniques as the user-programmer advances.

TABLE III
THE ADVANTAGES AND DISADVANTAGES OF END-USER DEVELOPMENT

Advantages	Disadvantages
• Frees IS resources for higher priority projects • May help reduce the hidden backlog • Faster design/implementation cycle • More acceptable to users • Reduces communications problems between users and IS • Encourages innovation and creative solutions.	• Duplication of effort and waste of resources • Greatly increased costs • Loss of control over data • Loss of control of quality in both programs and data • Incompatibles prevent sharing • Can be used to circumvent control processes such as the steering committee • Generally produces narrow, inflexible systems with short lives.

End-User Development (EUD) is a study within the field of computer science and human-computer interaction which explains the activities or techniques that allow amateur developers to produce or modify a software artifact. Early attempts in End-user development were concentrated in adding simple scripting programming languages to expand and familiarize oneself to an existing application, such as an office suite.

There are two basic reasons why EUD has being accepted:- one is that organizations are encountering delays on projects and by using EUD they can effectively reduce the time of completion of a project. The second is that software tools are more powerful and easier to use. Table III shows the main advantages and disadvantages of end-user development [7].

According to Nardi [9], three criteria are essential for end user programming to achieve a success level. The following three criteria are considered to be essential:

- A visual environment.
- A tack specific language.
- Support for collaborative practices.

III. State Of Art Literature Review

This review is to show the two new free mashup software tools which were released by Google called Google App Inventor for Android [10] and WebSphere sMash [11] which was released by IBM. These software tools were reviewed to show the similarity on using block-based approach in their application.

A. *Google App Inventor for Android*

Google App Inventor tool is intended to make it easy for people to build applications for its Android operating system. The tool enables people to drag and drop blocks of code which shown as graphic images and representing different Smartphone's capabilities and put them together, similar to snapping together Lego blocks. The result is an application on that person's Smartphone [10].

For example, one student made a program to inform a selected list of friends, with a short text message, where the user was every 15 minutes. The program was created by assembling three graphic code blocks together: one block displayed the phone's location sensor; another displayed a clock which he set for 15-minute intervals, and third linked to a simple database on a website, listing the selected friends.

In Figure 1, the screenshot which was taken from the website [10] shows the interview or the looks of the Google App Inventor which consist of several blocks. The 'Viewer' block which was in the center allows any element from the 'Palette' block to be *dragged and dropped* into it. The tool, specifically works only for phones which running Android operating systems. A sign-up with a Google Gmail is required. The tool is Web-based except for a small software download that automatically syncs the programs created on a personal computer, connected to the application inventor website, with an Android Smartphone. When making programs, the phone must be connected to a computer with USB link.

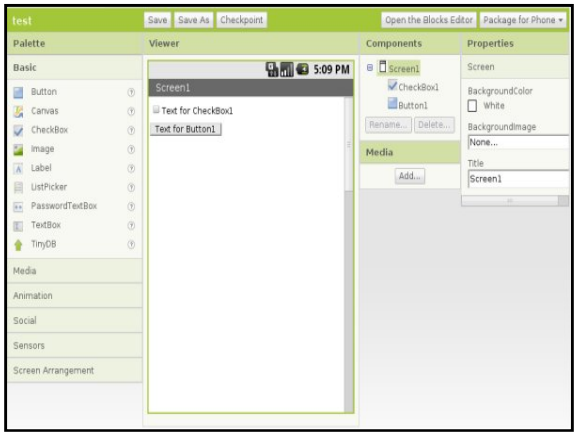


Fig. 1. The screenshot of the Google App Inventor

To use the App Inventor, a user does not need to be a developer. This is because instead of writing a code, the user visually designs the way the application looks and uses blocks to specify the application's behavior. The App Inventor team has created blocks for just about everything the user can do with an Android phone, as well as blocks for doing "programming-like" stuff such as blocks to store information, blocks for repeating actions, and blocks to perform actions under certain conditions. A block to talk to services such Twitter also had been made available for user.

B. *IBM WebSphere sMash*

IBM WebSphere sMash is an agile Web application platform that contributes in developing and running modern Web applications which introduces a simple environment for creating, assembling and running applications based on popular Web technologies.

IBM WebSphere sMash enables the following Web technologies [11]:

- A dynamic scripting runtime for Groovy and PHP.
- Java as a system programming language.
- Application programming interfaces optimized for producing Representational state Transfer (REST) services
- Rich Ajax Web user interfaces.
- Integration mashups and feeds.

TABLE IV
The Main Advantages Of WebSphere sMash

Advantages	Details
Speed	• Dynamic scripting languages. • Fewer lines of code. • Browser-based tooling.
Simplicity	• Leverage pre-existing content. • Use the web as your SOA platform. • Visual Assembly-style development.
Agility	• Small footprint. • Easily modify your applications. • Restart the server in seconds.

IBM WebSphere sMash software provides development and execution platform which based on the public incubator Project Zero [11]. Project Zero is an online development community that entitled the people who build and use this software. WebSphere sMash advances Smart Service Oriented Architecture's (SOA) properties and increase the alignment between Business and IT by allowing developers to rapidly deliver dynamic Web 2.0 based applications. Table IV shows the main advantages of IBM WebSphere sMash. The software's design is intended to increase the developer's productivity and efficiency through the support of dynamic scripting language [11].

Users can get several benefits from IBM WebSphere sMash software such:

- Improved developer productivity and efficiency by providing a runtime environment for Groovy and PHP scripts which allows developers to write applications and services leverage the assets of both Java and PHP community.
- Simplified deployment of applications which assembly the application to acts as the server and enable applications to connect to other resources through a Hypertext Transfer Protocol (HTTP) or Hypertext Transfer Protocol Secure (HTTPS), Java Message Service (JMS) and Simple Mail Transfer Protocol (SMTP).
- Increased customer satisfaction and business productivity line by streamlining the end-users interaction with Web-based application which provides a visual editor for designing user interface where dragging and dropping of blocks is possible.
- Access to a growing online development community of consumers and the WebSphere sMash development team which allows the developers to interact directly with the development team, download the latest builds, submit bugs, access source code, read documentation and access to the latest browser-based tools for WebSphere sMash.

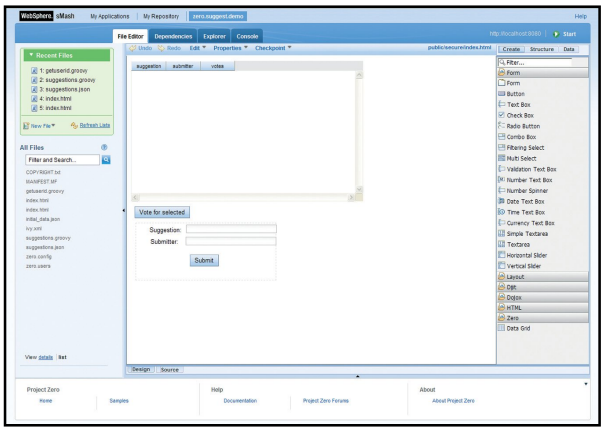


Fig. 2. The screenshot of the IBM WebSphere sMash

Figure 2 shows the screenshot of the web-based visual page editing tool in WebSphere sMash which applies the features of drag and drop design, automatic Hypertext Markup Language (HTML) source generation, widgets and Cascading Style Sheet (CSS) property editing and data binding. The screenshot was taken from the paper published by the IBM [11].

IV. Block-Based Programming (BBP) Approach

A. *Historical Background of BBP*

Block-based programming approach is a combined idea of component-based programming approach with end-user programming paradigm. The component-based programming attempts to generate tighter and better documented contracts so that the user can have some idea of what to expect from the component. Once the protocols between components are defined, this then allows the development of a component from different vendors to work together. Thus, one can buy off-the-shelf components from different vendors and plug it together into applications. In end-user programming, the user is allowed to develop web applications without knowing or writing the code. The concept of end-user programming is to provide and facilitate the users with controls such as pages, buttons, links, input fields, rules, and database records that the user needed to compose their applications.

The idea of combining these two programming is to reveal each of their advantages and eliminate each other's disadvantages. The component-based programming will effectively complete the job in a faster development mode. They also deployed in the real world. The programming is fairly safe, reliable, less code is needed to be written and also the plug-and-play systems are easy to modify. By combining the component-based programming and the end-user programming, the block-based programming will be able to satisfy the users with no programming skill to allow them to create their own application without even knowing any programming code. It's also allowed the block-based programming to be able to provide a powerful component from other vendor to plug it together as one application which later will satisfy the end-user.

Fundamentally, the term BBP is defined as an approach which integrating the programming blocks in a form to develop applications [11]. The main aim of BBP is to enable end-users to develop application directly. Several features for Block-Based Programming Approach have been identified as follows:

- Most of the blocks will be made available for a problem domain.
- Each block supports certain tasks.
- Users are allowed to customize blocks and to build applications adapting to their needs.
- Application software development can be performed by integrating those blocks.

The efficiency of any process approach is determined by the satisfaction of the consumer of its results. So, in terms of software development, the success is defined whether the software product can be produced on time, within budget, and the most important one, the continuous customer satisfaction. Even though, the continuity cannot be guaranteed, the high level of extensibility endorses it. In the Table V, shows the

advantages in terms of such attributes. Based on the initial characteristics of the component which was identified by Ian Sommerville [12], the desired characteristics of block-based programming as shown in Table VI.

TABLE V
THE ADVANTAGES OF BLOCK-BASED PROGRAMMING APPROACH

Advantages
• Existing applications are made possible to be reused. • High decrease of the associated application development costs. • Professional IT skills are not necessarily required. • Rapid application development is made possible. • There is no need to go for anyone's approval once a user wants to add an API to the internet. • Users' needs can be perfectly met by applications since the users are now able to incorporate content that they could not develop by themselves due to resource or time constraints.

TABLE VI
DESIRED CHARACTERISTICS OF BLOCK-BASED PROGRAMMING

Characteristics	Description
Standardized	Each block needs to conform to some standardized model which may include some attributes, variables, functions and classes.
Independent	Each block should be able to execute successfully without the need to depend on other blocks.
Composable	The block should provide external interactions and access to information about itself, such as attributes and method.
Deployable	The block has to be self contained and must be able to operate as a standalone entity.
Documented	The class or function library in the block has to be fully documented because a page of documentation is far more intelligent than a page of source code.
Testable	The block should conform to specific standards and to ensure the created block meets the user's needs.

In block-based approach, there are some criterion and metric to measure the effectiveness and efficiency of the programming effort in developing software system. Such criterions and metrics are:

- **Project management**: This explains how difficult or easy it is for the developer to manage the project in order to develop the system. In this case, it should be easy due to less work in programming because the block's service was made available by the third party.
- **Design quality**: The quality been measured in terms of effectiveness toward user's perspective. This shows how the design could help the user to understand the system easily.
- **Development speed**: These clarify that whether the system is able to execute within or over the timeline.
- **Testing**: This is to ensure the reliability of the system and to certify that all defined requirements are met. Such tests includes testing the performance of the application, testing each block, testing the integration of each blocks or finally testing the application in various environments.
- **Development cost**: This cost is basically considered on the complexity of the software system, the development environment and characteristic of the software system that is planned to be developed.
- **Maintainability**: This is based on how certain software systems manufactured were able to sustain correcting faults, to cope with new requirements, to make future maintenance easier or cope with a changing environment.
- **Reusability**: This indicates whether the modules and classes in the programming code could be used again to add new functionalities with slight or no modification which will helps in reducing implementation time, increase the likelihood that prior testing and use has eliminated bugs.
- **Satisfaction**: This includes the satisfaction from both of the developers such as the programmers and the end-users. The satisfaction was measured based on how the software system meets these users' requirement.

B. Block Identification

In a software application, especially while using the block-based programming approach, each of the blocks needs to be identified to show the individuality of each of them. Therefore, a block consists of one or more declarations and statements in terms of block's name, attributes, behaviors, variables, methods, classes, functions and interface which differentiate one block to another as shown in Figure 3.

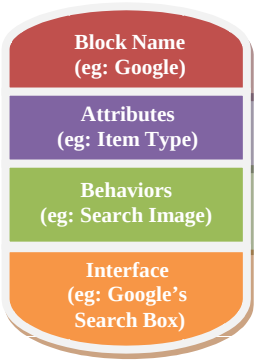


Fig. 3. Block Specification

In Figure 4, it shows the examples of block identification in an application by using declarations and statement. The example indicates the block services from Google Map and Youtube application services.

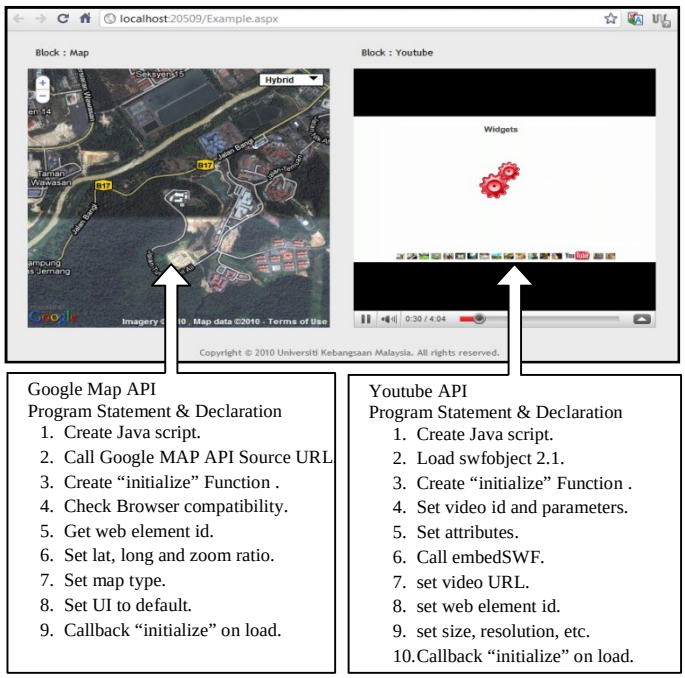


Fig. 4. Block Identification using statement and declaration

C. *The Proposed Model for Block-based Programming*

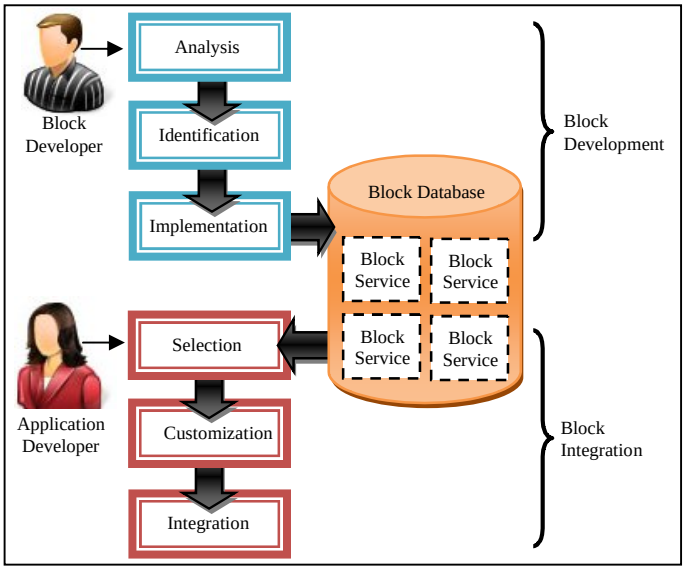


Fig. 5.The Proposed Model of Block-based Programming Approach

The proposed model for block-based programming form of two types of system developers, as illustrated in Figure 5, those will contribute to the block-based programming development approach. The first developer is the *Block Developer* (BD) or *Programmers*, who are responsible in identifying and implementing the blocks. The *Application Developers* (AD) or *end-users*, are responsible for selecting the suitable blocks from the list that was already developed by the BD. From the selection, the end-user will customize the block interface based on their needs and these selected block services will then be integrated as one application. The block database acts as storage for all blocks that have been developed by the BD and which will be used by the AD in order to create an application.

V. Conclusion And Discussion

In this paper, a CBP and EUP was been studied to understand fully the principles and dynamic of block-based programming approach. The block-based programming approach is a combined tool of the component-based programming approach with end-user programming paradigm. Also elaborated in the paper were the advantages and disadvantages of both component-based and end-user programming. The characteristics of block-based programming approach have been classified together with the metric involvement in the block-base to measure its the performance. Finally, the proposed model for block-based programming was introduced in order to develop the application. In future work, we will do further investigation, research and development on the framework architecture, and the programming involved in the block-based programming approach.

References

[1] Block (programming), Creative Commons Attribution-ShareAlike License. Wikipedia. http://en.wikipedia.org/wiki/Block_(programming), 2010. (Accessed 21-9-2010)

[2] A. Ismail, M. Djasmir, N. Omar, A. M. Zin. *Designing and Implementing Blocks for Developing Educational Software for Children with Learning Disabilities.* Universiti Kebangsaan Malaysia. 2009.

[3] Ahmed Patel, Liu Na, Rodziah Latih, Christopher Wills, Zarina Shukur and Rabia Mulla, 2010. A Study of Mashup as a Software Application Development Technique with Examples from an End-user Programming Perspective. Journal of Computer Science, Vol. 6, No. 11, pp. 1406-1415.

[4] A. Seyfi, A. Patel. *Briefly Introduced and Comparative Analysed: Agile SD, Component-Based SE, Aspect-Oriented SD and Mashups.* Data. International Symposium on International Technology (ITSim 2010). Volume 2, 2010, pp. 977-982.

[5] F. Bachman, L. Bass, C. Buhman, S. Comella-Dorda, F. Long, J. Robert, R. Seacord, K. Wallnau. *Technical Concepts of Component-Based Software Engineering.* CMU/SEI, Volume 2, 2000.

[6] M. Perez. *Component-based Development in Geographically Dispersed Teams*. MSE 17-652, 6 May 2002.

[7] H. Prahofer, D. Hurnaus, H. Mossenbock. *Building End-User Programming Systems Based on a Domain-SpecificLanguage*. Keba AG. Austria.

[8] Raymond S. Kulzick. *End-User Development: Advantages and Disadvantages.* Publication last modified: September 13, 2008, http://www.kulzick.com/endusrad.htm. (Accessed 26-9-2010)

[9] E. Kandogan, E. Haber, R. Barrett, A. Cypher, P. Maglio. *End-User Programming for Web-based System Administration.* UIST'05, October 23-27 2005, Seattle Washington.

[10] S. Lohr. *Google's Do-It-Yourself App Creation Software*. (2010), http://www.nytimes.com/2010/07/12/technology/12google.html?_r=1 (Accessed 18-10-2010)

[11] IBM Software Group. *IBM WebSphere sMash Version 1.1.* IBM Corporation. United State of America. 2008. http://www-01.ibm.com/software/webservers/smash/reqs/. (Accessed 30-10-2010)

[12] Ian Sommerville. 2006. *Software Engineering* Eighth Edition. Addison-Wesley, pp.443. ISBN: 7-111-19770-4.

Comparison between PID and Fuzzy Logic Controllers for Advance Microwave Biodiesel Reactor

W.A.Wali, J.D.Cullen, K.H.Hassan, A.Mason, A.I.Al-Shamma'a
Environment, Sustainable and Renewable Technologies Center(BEST)
School of the Built Environment, Liverpool John Moores University, Byrom Street, Liverpool L3 3AF,U.K
E-Mail: W.Wali@2009.ljmu.ac.uk

Abstract- **The proportional integral derivative (PID) controllers are widely applied in industrial process owing to their simplicity and effectiveness for both linear and nonlinear systems, and the tuning methods still a hot research area to give the optimum result for control behavior. Fuzzy logic and proportional integral derivative (PID) controllers are designed and compared for use in control on-line an advanced biodiesel microwave reactor system which converts waste cooking oil into biodiesel by transesterification chemical process. A closed loop fuzzy and PID controllers are used to automatically and continuously adjust the applied power of microwave reactor under different perturbations. Labview based software tool will be presented and used for measurement and control of the full system, that will make charts real time display as well as state real time monitoring**.

I. INTRODUCTION

In 1930s and 1940s vegetable oils were used as diesel fuels but only in emergency situations [1]. Alternative fuels are becoming increasing important due to energy is an essential requirement for economic and social development of any country, biodiesel yields a 78% carbon dioxide (CO_2) reduction compared to petroleum diesel under life-cycle analysis, increasing production of waste frying oil from household and industrial sources is growing problem worldwide, resulting in problems for waste water treatment plant and energy loss and biodiesel can be used in any diesel motor in any percent from 0-100% with little or no modifications to the engine.

The term biodiesel refers to the Fatty Acid Alkyl Esters (FAAE) derived from vegetable, animal or waste oil feedstock. Biodiesel is synthesized by the reaction of triglyceride molecule(the main constituent of oils) with an acid or base catalyst[2]. Because of high cost of biodiesel from virgin oil the use of waste cooking oil instead of virgin oil to produce biodiesel is an effective way to reduce the raw material cost because it is estimated to be about half the price of virgin oil[3]. Fig.1 shows the general biodiesel production process.

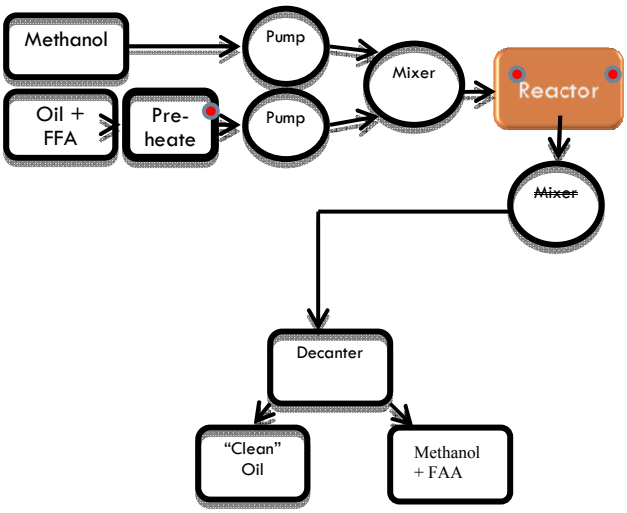


Fig.1 The general waste cooking oil conversion process.

Transesterification

The most common way to produce biodiesel is by transesterification,, which refer to a catalyzed chemical reaction involving vegetable oil and an alcohol to yield fatty acid alkyl esters(biodiesel) and glycerol [3]. Fig.2 shows the biodiesel with glycerin.

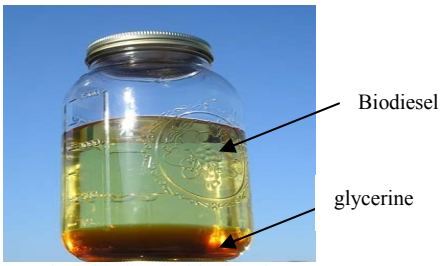


Fig.2. biodiesel with glycerin

The effective variable on biodiesel from transesterification : reaction temperature , molar ration of alcohol and oil, catalyst, reaction time, presence of moisture and free fatty acids (FFA), and mixing intensity [4].

Microwave reactor

Microwave heating is now widely used because it is small scale, with the advantages of fast reaction times, improved impurity profiles and convenient access to super heated solvents [5]. Microwave energy has become an essential part in many technical applications in chemical and related industries since the 1950s [6]. Microwave can be used for the production of the alternative energy source, biodiesel [7]. Most organic reactions requiring heat have been heated using traditional heat transfer equipment such as oil baths, sand baths or heating mantles. These techniques are rather slow and create a temperature gradient within the sample. Moreover, the hot surface of the reaction vessel may result in localized overheating leading to product, substrate and reagent decomposition when heated for prolonged periods. In biodiesel production using microwave as reactor, rapid heating is observed and very efficient heating can be obtained and the heat generated can be, for short times, much greater than the overall recorded temperature of the bulk reaction mixture [7]. In these conditions with use catalysts enables organic reaction to occur expeditiously at ambient pressure, give a special offer to decrease to amount of catalyst required reaction time due to the increased chemical activity.

Control of the biodiesel process with labview

The biodiesel systems are complex nature, so it requires a good controller to meet the challenges such as noise, parameter variation, model uncertainties, frequent overshoot of reactor temperature and oscillation of its pressure. In this work a Fuzzy logic and PID controllers are implemented and compared in advance microwave biodiesel reactor to maintain the temperature of reaction mixture at set points under disturbances by using a labview. A labview as the man machine interface to compute the controller output and communication between the computer and biodiesel systems, it is widely used in instrument control, data acquisition, data analysis and data displays. Labview is short for **Lab**oratory **V**irtual **I**nstrument **E**ngineering **W**orkbench. Fig.3 shows the front panel for the biodiesel system in labview [8].

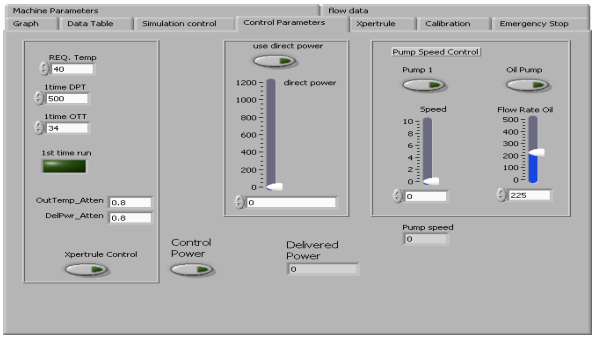


Fig.3 Front panel for the biodiesel system in labview.

Fuzzy Logic and PID controllers.

PID stands for **P**roportional, **I**ntegral and Derivative [9]. Conventional PID controller has been successfully used in the process industries since 1940s [10]. However it is difficult to achieve the desire control performance in the presence of unknown nonlinearities, time delays and disturbances [11]. There is some internal relationship between fuzzy controllers and PID controllers. In fact, for single–input single-output systems, most of fuzzy logic controllers are essentially of PD type, PI type or PID type with nonlinear gains [12], or multi-inputs and single- output are PID controller with nonlinear element [13]. Because of this nonlinearity on the control, fuzzy PID controllers achieve better performance over conventional PID controller [12]. If PID controller is properly tuned, it will produce an acceptable control for most industrial processes. In this work we will show how the PID controller give a good result if it has good tuning parameters which compare with Fuzzy controllers but improve on (overshoot and undershoot, steady state error) for the temperature which is a very important factor in biodiesel production. The classical PID control is widely used with its gains manually tuned based on the thermal mass and the temperature set point [14].

Fuzzy system is one of the succeed controller used in the process control in case of model uncertainties [15]. It is initiated by the pioneering work of Mamdani and Assilian (1975) has emerged as one of the most active fruitful areas for research in the application of Fuzzy set theory, Fuzzy logic and Fuzzy reasoning [16]. Fuzzy logic control has been considered as an alternative to traditional control schemes implementation without relying on the detailed mathematical model of the plant to deal with complicated, ill defined and poorly mathematically understood processes by incorporating human control knowledge directly into the controlled system [16]. The work presented in this paper covers full design of Fuzzy logic controller.

II. *Experimental system setup*

The low energy automated microwave system will be used as reactor to produce biodiesel. Microwave operation at low power (100W to 200W) and frequency 2.45GHz is used to reduce chemical reaction time, from hours under conventional heating, to minutes using the same volume of input material. This novel microwave reactor is capable of operating at commercial production rates (kg/hr) instead of laboratory scale (g/day). Figure 4 shows part of the microwave system.

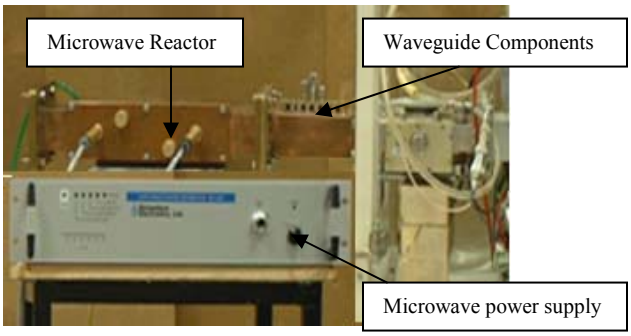


Fig. 4 Novel microwave labratory system as new biodiesel reactor

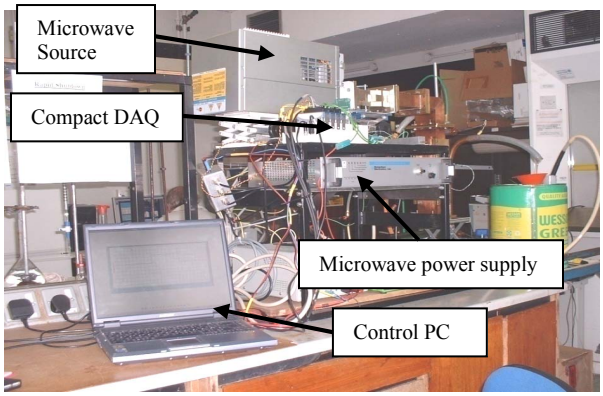


Fig. 5 The biodiesel system

The biodiesel system shown in Fig.5 is connected with a computer through a compact DAQ, shown in Fig.6. The sensors have their reading captured using the data aquistion modules and recorded to the computer. A labview-based microwave biodiesel reactor control system was built in order to run Fuzzy and PID controlers and analyze their works. All the changes in control system can be observed in real time and also user commands can be accepted during the process.

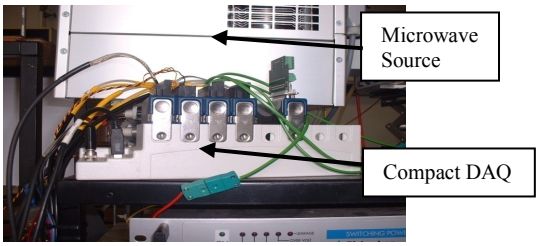


Fig.6 compact DAQ for the biodiesel system

III. Controllers

Fig.7 shows the closed loop block diagram of the biodiesel system with controller and Fig.8 shows the system parameters under control. In this paper the aim is to show set point temperature tracking and online control under sudden changes in input flow rate of the oil in biodiesel system.

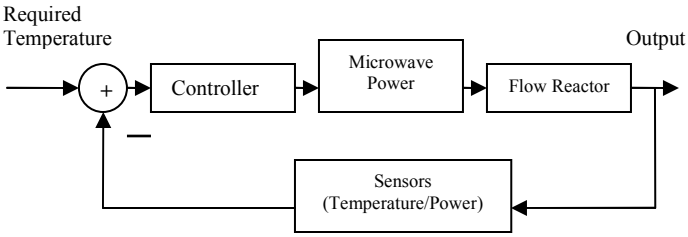


Fig.7 The close loop block diagram of biodiesel system with controller.

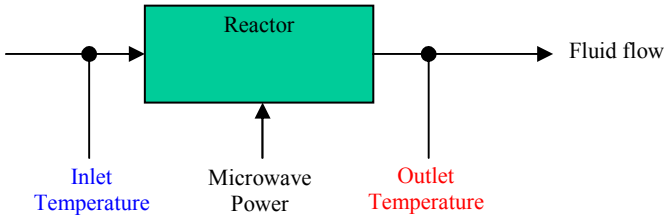


Fig.8 The systems parameters under control

PID controller design

It is a generic control loop feedback mechanism (controller) widely used in industrial control systems even though many advance control strategies have been proposed [17]. Fig. 9 shows the PID controller block diagram.

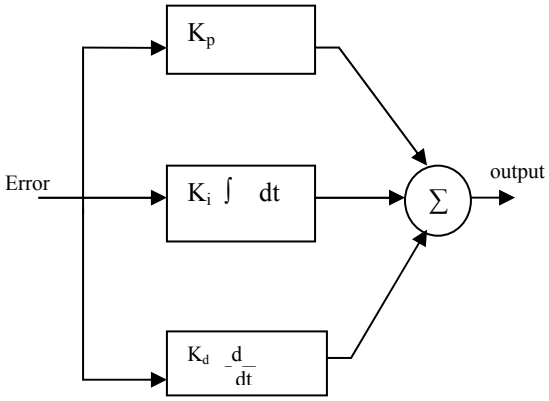


Fig. 9 The PID controller block diagram.

The mathematic ideal PID controller algorithm is described in the following equations.

$$y(t)=K_p[e(t)+T_d\ (d(e)/dt) +(1/T_i) \int_0^t e(t)\ d(t)\ ] \qquad (1)$$

$$y(t)= [\ K_p\ e(t)+Kd\ (d(e)/dt) + K_i \int_0^t e(t)\ d(t)] \qquad (2)$$

where

y(t)= Controller's output

e(t)=Error signal

K_p=Proportional gain

$K_i = K_p/T_i$=Integral gain

$K_d=K_p.T_d$=Derivative gain

T_d=Derivative time constant

T_i= Integral time constant

Proportional part: action repeats the change of deviation.

Derivative part: action an increment of manipulated variable so that the proportional plus derivative action is shifted ahead in time.

Integral part: action adds further increment of manipulated variable proportional to the area under the deviation line.

The PID control based on Labview PID Toolkit. The input of the controller represents the error between measured temperature and setpoint. The output of PID is the control signal applied to the biodiesel plant.
The manual tuning proposed by Ziegler and Nichols of the PID controller is off line practical method of PID constants determination, and there is a chance of the system becoming unstable [18]. In this work, experimental online tuning was used to find out a set of PID Parameters. As we know that when a system is operating too close to its stability limit, it tends to oscillate, so reduce the integral gain to reduce phase shifts and increase the derivative gain to improve damping. But if the system response is too heavily damped, increase the integral gain to respond more quickly and decrease the derivative gain to reduce excess damping. So after more than one on line try of balancing, successively the values are determined.

Fuzzy Logic controller design
In this research, Mamdani Fuzzy logic operations are applied. Mamdani fuzzy system is the main type examples of fuzzy inference systems. Fig.10 illustrates how a two-rule Mamdani fuzzy inference system derives their overall output Z when subjected to two numeric inputs x and y [19].

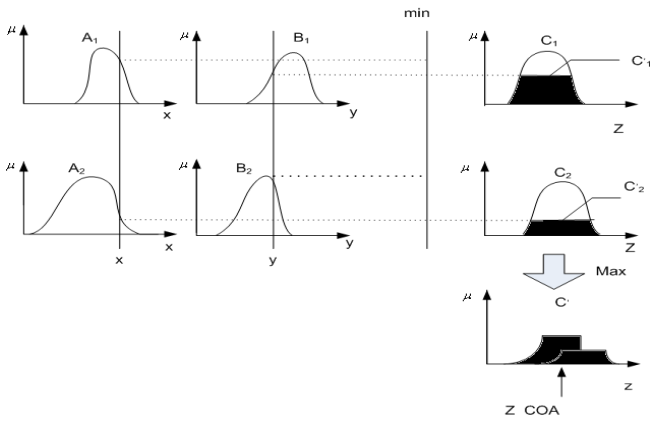


Fig.10 Mamdani Fuzzy Inference System
If x is A_1 and y is B_1 Then Z is C_1
If x is A_2 and y is B_2 Then Z is C_2

A Fuzzy controller is composed of three calculation steps[20]:
1) Fuzzification: the function of accepting input values and determining the degree of membership to some pre-select lingusitic terms.

2) Fuzzy Inference: consists of determing relationships based upon If-Then rules used to obtain more weighted outputs. These outputs are also linguistic variables in nature and have a nonlinear relationship.

3) *Defuzzification:* involves converting the output term into a crisp value such that it is compatible with all systems.

Fuzzy logic control design try accounting the human's knowledge about how to control a system without requiring a mathematical model. The basic block diagram for fuzzy controller is shown in Fig.11.

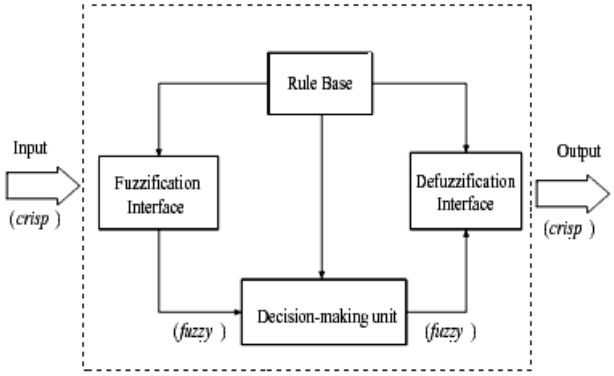
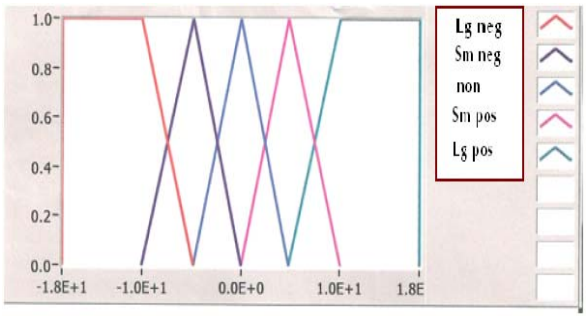
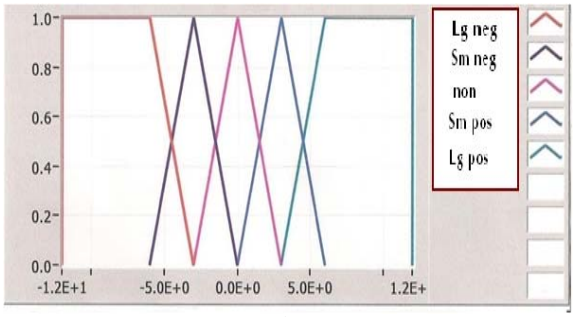


Fig.11 The basic block diagram for fuzzy controller.

Fuzzy control based on Labview Fuzzy Toolkit. First Fuzzy input represents the error between measured temperature and set point. The second Fuzzy input represent the change in error. "Fig.12" shows the membership function for error and change of error over the range of input variable values and linguistically describes the variables universe of discourse. The triangular membership functions are chosen with a five linguistic labels large positive, small positive, zero, small negative, large negative. The universe of discourse for the error and change of error from -18 to 18 and -12 to 12 respectively. The left and right half of the triangle membership functions for each linguistic label was chosen to provide membership overlap with adjacent membership functions.



(a)
Fig.12 Fuzzy inputs membership functions (a) error.



(b)

Fig.12 Fuzzy inputs membership functions (b) change of error.

Fuzzy logic controller output is delivered power which is applied to the microwave reactor system. Fig.13 shows the membership functions of the output linguistic variables of Fuzzy output. Design of Fuzzy output variable is scaled to interval from -100 to 100 with seven triangle membership functions; large positive, medium positive, small positive, zero, small negative, medium negative, large negative.

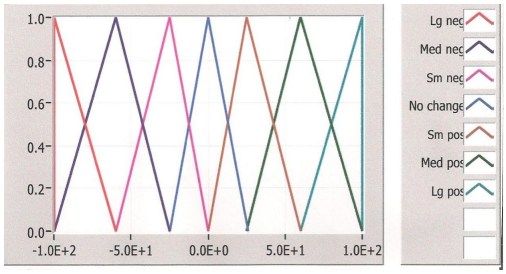


Fig. 13 Membership functions of the output linguistic variables

The rule base of the fuzzy controller gives the decision that in which of the five memberships function have to fire. Rule evaluation part has 25 fuzzy rules. The Table 1 shows the Fuzzy logic control rules developed to the proposed system. Selection of the number of membership functions and control rules are based on process knowledge and intuition. The main idea is to define partitions over the plant operating region that will adequately represent the process variables.

TABLE I
Fuzzy Rules Table For Biodiesel System

Δe \ e	Lg neg	Sm neg	Zero	Sm pos	Lg pos
Lg neg	Lg neg	Med neg	Med pos	Med neg	Sm pos
Sm neg	Med neg	Sm neg	Sm pos	Zero	Sm pos
Zero	Sm neg	Sm neg	Zero	Sm pos	Sm pos
Sm pos	Sm neg	Zero	Zero	Sm pos	Med pos
Lg pos	Sm neg	Sm pos	Zero	Med pos	Lg pos

IV. Experimental results

The Fuzzy logic and PID controllers were online implemented for the LJMU advance biodiesel microwave reactor. All the experimenting results in (5000ms control sample interval) and (300 ml/min flow rate) The controllers subjected to a multiple set point tracking beginning from the nominal temperature value of 30°C and changing rise to 35°C then down to 30°C as shown in "Fig.14" . The results show that Fuzzy logic controller successfully tracking the demands of reactor temperature setpoint accurately with minimum overshoot and undershoot.

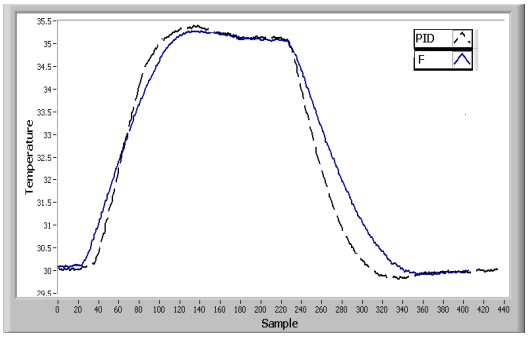


Fig.14 Time response for Fuzzy Logic and PID controllers.

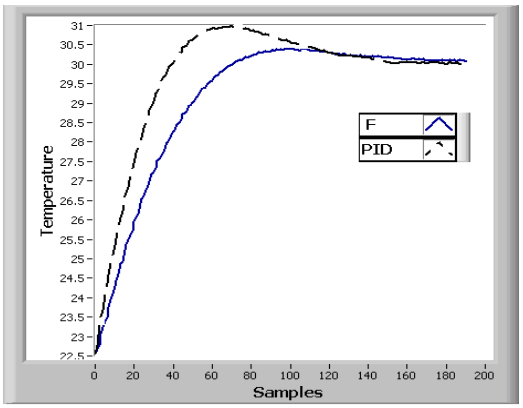


Fig.15 Fuzzy Logic and PID controllers (setpoint tracking from inlet temperature)

Fig.15 shows the controllers set point tracking beginning from the inlet temperature, it appears that the overshoot and steady state error in PID controller. The controllers were then tested under an introduced disturbance in the feed to the flow rate of the reactor. After the start up of the processes, the reactor temperature was left regulated by the controllers at 30°C . The disturbance was then introduced. When the nominal feed in flow rate was reduced by 20%, it was observed that the Fuzzy and PID controllers were able to bring back the process to its initial set point of 30°C, as shown in Fig.16, but in fuzzy controller the overshoot and the undershoot less than PID controller as shown in Fig.17. For further test under disturbance, the input flow rate was reduced 10% then sudden rising by 30% as shown in Fig.16.

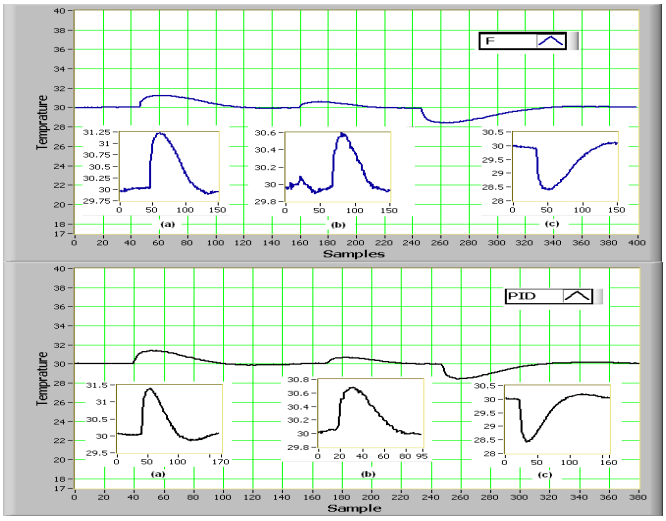


Fig.16 Disturbance rejection of Fuzzy and Adaptive Controllers with change in the input flow rate (-20%, -10%, +30%).

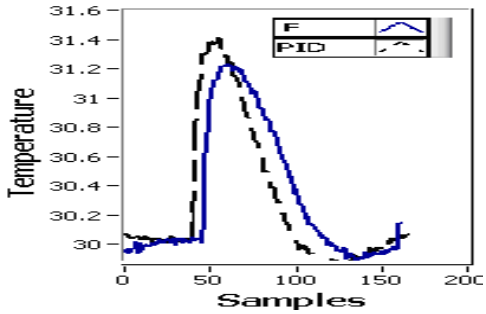


Fig.17 Fuzzy and PID controllers in disturbance rejection with change in the input flow rate -20%.

A performance response of Fuzzy and PID controller were tested under different flow rates of input oil. Fig. 18 illustrates the Fuzzy and PID response under a chosen three flow rates (250,300,350) ml/min. The figure shows the Fuzzy controller minimizes the overshoot as compared to PID controller.

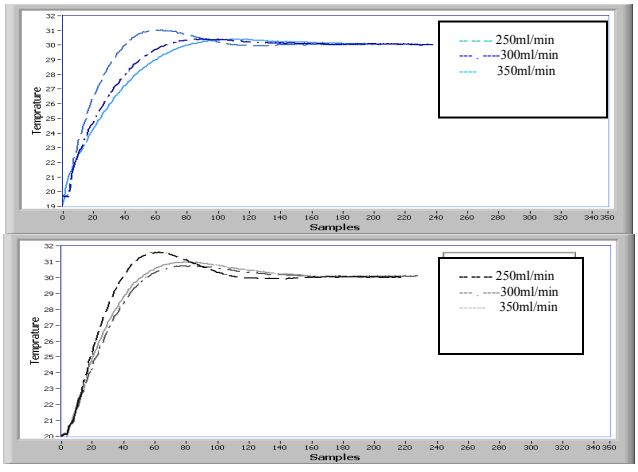


Fig.18 Performance of the Fuzzy and PID controllers under different flow rate

VI. Conclusions

Experimental results reported in this paper indicate that the PID controller with a good tuning give a good performance if its compared with Fuzzy controller, so the controllers are able to regulate and tracking the reactor desired temperature . The disturbance in the form of varying flow rate in the process input poses good rejection by this controllers, Fuzzy controller has minimum overshoot and undershoot and steady state error in temperature control which its important parameter in biodiesel production.

References

[1] G.Najafi, B.chobadian, T.Yusaf,H.Ralin ,"Combustion Analysis of a CI Engine Performance Using Waste Cooking Biodiesel Fuel with an Neural Network Aid", *American Journal of Applied Sciences,* Vol:4 PP:756-764, 2007.

[2] V. Rudolph , Y.He " Research and Development Trends in Biodiesel" *Dev. Chem. Eng. Mineral Process*, Vol.12, PP.461-474, 2004.

[3] Y. Zhang, M. Dube, D. Mclean, M. Kates, "Biodiesel Production From Waste Cooking Oil: 1 Process Design and Technologicaln Assessment", *Bioresource Technology,* Vol:89,PP:1-16, 2003.

[4] N. Nazir, N.Ralmil, D. Mangunwidja, E. Hambali, D.Setyaningsih, S.Yuliani, M. Ambar, J.Salimon, "Extraction, transesterification and Process Control in Biodiesel Production from Jatropha Curcas", *Eur.J. Lipid Ssci..Technol*, Vo:111,PP:1185-1200, 2009.

[5] J. Mosely, E. Woodman, "Energy Efficiency of Microwave-and Conventionally Heated Reactors Compared at Meso Scale for Organic Reactions" *Energy Fuels,* Vol:23,PP:5438-5447, 2009.

[6] T. Glasnov, C.Kappe," Micro-Assisted Synthesis Under Continuous-Flow Conditions", *Macromol, Rapid Commun,* Vo:28,PP:395-410,2007.

[7] A. A.Refaat, S.T Elsheltawy, k.U. Sadek, "Optimum reaction time, performance and exhaust emissions ofbiodiesel produced by microwave irradiation",*Int.J.Environ.Sci.Tech,* Vol.5, PP.315-322,2008.

[8] J.Travis , J.kring, " Labview for Every one Graphica Programming Mode Easy And Fan", *Prentice Hall*, Third Edition 2007.

[9] Y.Chee Wei, " Servo Motor System Control Usin Labview", *Bachelor of Engineering (Hons) Thesis, The Queensland University , Department ,Australia*, May 2003.

[10] E,Natsheh, K.Buragga,"Comparision Between Conventional and Fuzzy Logiic PID Controllers for Controlling DC Motors",*IJCSI International Journal of Computer Science* , Vol:7, PP;128-134 , 2010.

[11] A.Khan, N.Rapal , "Fuzzy PID Controller: Design, Tuning and Comparison with Conventional PID Controller" ,*Engineering of Intelligent systems,IEEE, International Conference,* PP:1-6, 2006.

[12] C.Liu, J.Xihxu, C.Hang," Comparison between a Fuzzy PID Controller and a Kind of Nonlinear PID ", *Proceedings of the 36th Conference on Decision &Control San Digo, California USA,* December,1997.

[13] H.Li, C.Philipchen,"Relationship between Fuzzy Controllers and PID Controllers", *Proceedings of the international Conference on Intelligent Robots and Systems,IEEE,*1999.

[14] Farouq S. Mjalli and M. Hussain, " Approximate Predictive versus Self-Tuning Adaptive Control Strategies of Biodiesel Reactors", *Ind. Eng. Chem. Res*., Vol.48, PP.11034-11047, 2009.

[15] G.P.Lewis, S.R. Wylie , A. Shaw, A.I. Al-Shamma'a, D Phipps, R.Alkhaddar, G . Bond, "Monitoring , Control System for Tuneable High Frequency Microwave Assisted Chemistry", *Journal of Physics: Conference Series* 76 , 2007, doi:10.1088/1742-6596/76/1/012058.

[16] K. Gowrishankar, Vasanth Elancheralath , " Adaptive Fuzzy Controller to Control Turbine Speed", *Ubicc Journals*, Vol.3, No.5, 2008.

[17] D.Koo, J. Lee,D.Lee,C.Han,L.Cyu,J.Jung, M.Lee,"A Tuning of the Nonlinear PI Controller and its Experimental Application", *Korean J.Chem. Eng..,*Vol:18,PP:451-455,2001.

[18] S.Gade, S.Shendage,M.Uplane, "Performance Comparison of Online Auto Tune PID Controller" , *International Journal of Computer Science & Communication*, Vol: 1,PP:1273-277,2010.

[19] T. Takagi and M Sugeno "Fuzzy Identification of Systems and its Application to Modeling and Control", IEEE Transaction on Systems, Man, and Cybernetics,Vol. 15, PP. 116-132, 1985.

[20] D. Ruan," Intelligent Systems: Fuzzy Logic Neural Networks and Genetic Algorithms", *Kluwer Academic Publishers*,USA,1997.

Samsung ARM9 S3C2440A Hardware Core Circuit Design

Azlan Bin Sulaiman, Mohd Sharifuddin Bin Mohd Nordin, Namazi Bin Azhari , Dr. Jalil Md. Desa
Department IP Core
Telekom Research & Development Sdn Bhd
TMR&D Innovation Center
Lingkaran Teknokrat Timur
63000 Cyberjaya
azlan@tmrnd.com.my

***Abstract* – The Samsung S3C2440A is an advance microprocessor available with good performance for cost. The 32-bit CMOS microprocessor contained ARM920T core, with 0.13 um CMOS standard cells and memory complier. The interesting features are consumed less power and fully static design for the cost and power sensitive applications. This paper described the hardware design of core circuitry and PCB layout for the microprocessor that can be implemented for various applications, including mobile and desktop model devices. The core design consisted of basic development platform which utilized the features offered by the S3C2440 microprocessor.**

***Index Terms* - Samsung S3C2440A, microprocessor, hardware design, core circuitry, ARM920T.**

I. INTRODUCTION

No doubt the applications of the microprocessor are drastically increased day by day especially ARM core, which is famous due for its efficiency and very low power consumption. One of the most famous and the biggest manufacture for ARM microprocessor is Samsung Electronics Co. Ltd., where the S3C2440A is one of its famous products line. The S3C2440A consists of a 16/32-bit ARM920T RISC core which implements the AMBA BUS and Harvard cache architecture with separate 16KB instruction and data caches, each with 8-word line length. One of the interesting features of S3C2440A it required less power supplies voltages compared to ARM microprocessor made by Marvel, Atmel and ST.

The minimum power supply requirements are 1.3V for its core and 3.3V for the rest etc. memory interface and external I/O. In this case, the power management circuit can be made simple as well as the cost can be minimized. The operating speed for the core of S3C2440A is linear to its core voltage rating. The S3C2440A's core frequency can go up to 400 MHz as the core voltage supply is 1.3V. 300MHz if the core voltage is 1.2V and 133MHz if the core voltage is 1.0V

II. POWER MANAGEMENT

The S3C2440A required a minimum of at least two voltages in order to start functioning as in the table 1; 1.3V for the core and 3.3V for the rest. For mobile device application the memory selection supposes to low power version where the minimum voltages available is 1.8V.

Parameters	Symbol	Typical
DC Supply for alive block	$V_{DDalive}$	1.3V
DC Supply voltage for internal	V_{DDi} V_{DDiarm} V_{DDMPL} V_{DDUPLL}	3.3V
DC supply voltage for IO block	V_{DDOP}	3.3V
DC supply voltage for memory interface	V_{DDMOP}	1.8V/2.5V/3.3V
DC supply for analogue core	V_{DD}	3.3V
DC supply for RTC	V_{DDRTC}	1.8V/2.5V/3.3V
DC input voltage	V_{IN}	3.3V
DC output voltage	V_{OUT}	3.3V
Operating temperature	T_{OPR}	-40 TO 85 °C

Table 1: Recommended operating voltages for S3C2440A

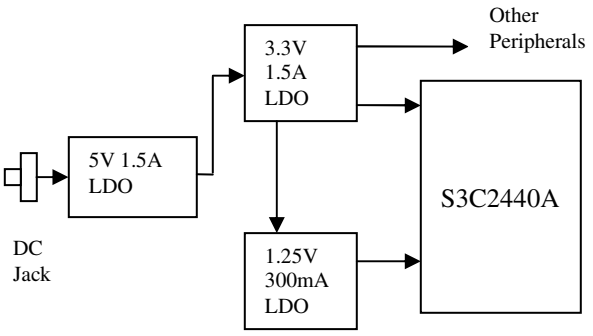


Figure 1A: Basic power management block topology for S3C2440A

The topology purposed in per figure 1A is a cost effective approach, where 5V regulated voltage supply source from external DC jack supplying to LDO (Low Dropout) chipset in providing regulate 3.3V for internal SC3440A, consist of IO block, memory interface and 1.3V for SC3440A's core. For the mobile application which the power supply consumption is critical, the power management topology as per figure 1B is

suggested to make used of DVS (dynamic voltage scaling) which is to reduce power consumption in idle or in sleep mode.

The basic concept of DVS is to drop the core and internal voltage and reduce the power consumption when those blocks in rest state. There are two methods to reduce power consumption; one is drop the voltage while the internal blocks does not work or the system operates slowly. The other is lengthening the system clock speed to reduce power consumption. DVS uses the two methods, voltage scaling and change clocking. In the figure 1B, the DVS controller collecting the input from S3C2440A which is the microprocessor current states (etc. active, turbo, idle, sleep) and assigned an appropriate voltages for the core. The core voltages generator must be able to generate 0.1V step voltages, where the initial value is 0.9V (operating frequency 66MHz) and maximum 1.35V (operating frequency 400MHz) as well as enough current to support at maximum frequency.

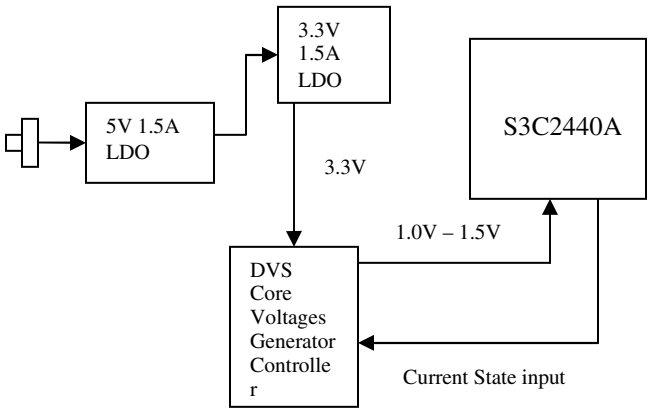


Figure 1B: Power management block topology via DVS implementation as the core voltage can varies from 1.0V up to 1.5V.

Linear regulator, Maxim MAX 1793 LDO is used to convert voltage from 5V to 3.3V and it is guaranteed to deliver 1A current with 210 mV dropouts where it is suitable to supply adequate power to external peripherals.[2]. Maxim MAX8860 LDO is used to convert 3.3V to 1.25V for power supply requirement of the S3C2440A's core. It is capable of delivering 300mA with typical dropout of 105mV [3].

III. Memory Interface

The S3C2440A included external buses for SDRAM and NOR Flash. It even provided a dedicated port for NAND flash memory interface since, the memory is targeted low cost application. The boot code can be executed on an external NAND flash memory through the usage of internal SRAM buffer called "Steppingstone'.

The NAND flash memory used is the Samsung K9F1208U0C, 64M x 8-bit NAND Flash memory. The R/B output signal from K9F1208U0C indicate the status of the device operation which is an open drain output type, therefore pull-up resistor is needed so that the pin does not float to high-Z condition when the chip is deselected or when the outputs are disabled. The S3C2440A consists of 8 memory banks (1GB/8 per banks), of which are six, are dedicated for ROM and SRAM and remaining 2 banks are for dedicated SDRAM. The bas is programmable in width size for all banks except bank 0 which support only 16/32.

SDRAM from Micron MT48LC16M16A2 is used, which are 4 Mb x 16 x 4 banks, is used. It is operated by a single supply 3.3V and supports self-refresh mode. With two pieces of MT48LC16M16A2, the total requires a 64 MB address bus which A[25] and A[24] are used for the selection of active bank for READ, WRITE and PRECHARGE process [4].

IV. Reset Circuit

The reset circuit is vital role in microprocessor system which the threshold voltages need to be carefully selected according to application. The main task of this device is to assert a reset signal whenever the supply voltage to microprocessor Vcc falls below a preset threshold in order to prevent the system into an unknown state. The part used for reset component is Maxim MAX811.The MAX811 has an active low reset, guaranteed to assert active low reset pulse for S3C2440A [5]. Since the supply voltage for S3C2440A's internal is 3.3V, the reset threshold value for this part is 3.08V.

V. Flash Programming

To program the boot loader to NAND flash memory for S3C2440A system, JFlash software is one of the cheapest option available. JFlash is an open source programmer originally designed for Samsung SMDK 2440 platform. It is capable of programming many types of flash memory including Samsung K9S1208, Intel E28F128 and AMD29LV800BB through the JTAG port and performed rear/write data from or to a specified address as shown in figure 2 below.

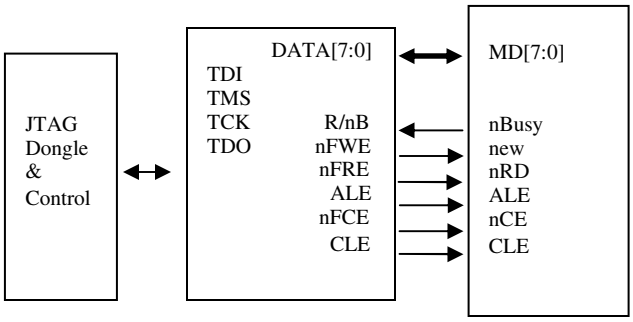


Figure 2: Hardware Interface for K91208 NAND flash programming.

VIII. PCB DESIGN AND ROUTING CONSIDERATION

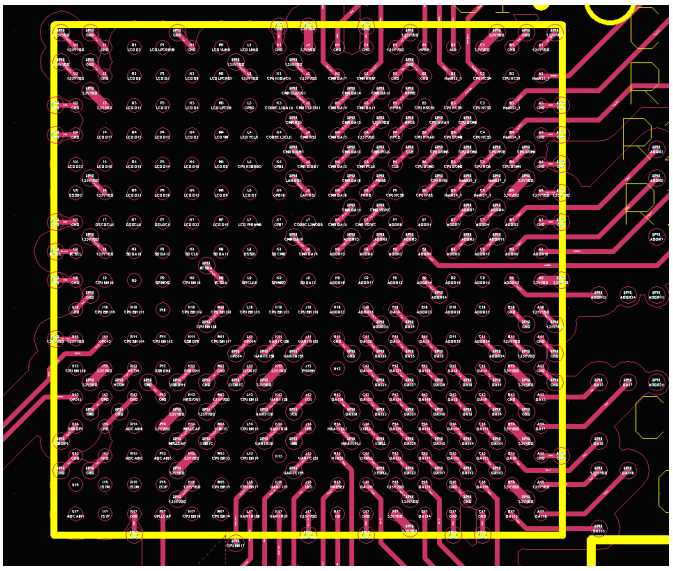


Figure 3: Top Layer of the S3C2440A PCB footprint.

Figure 3 show the surface of the top layer of the S3C2440 designed PCB (printed circuit board). The optimum size of FBGA (fine ball grid array) pads is 0.36mm and the size of the traces between 2 pads or via is 0.56mm.

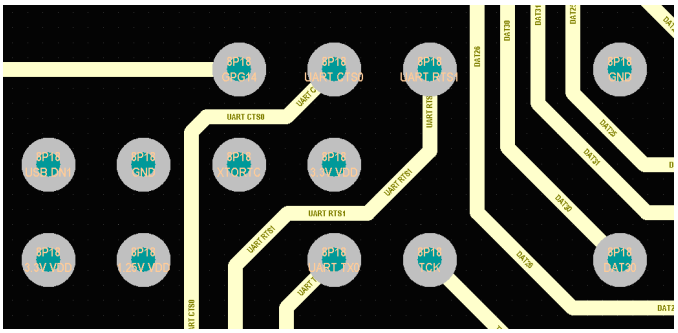


Figure 4: Vias, pads and traces.

In figure 4 showed the close-up view of the micro via where the hole size is 0.2 mm and the diameter is 0.45 mm. It is required to extract many signal traces from narrow space and it is not easy for each trace to maintain desired characteristic impedance. Using too narrow trace might cause a problem in PCB manufacture or increase the costs of PCB manufacture. In normal case, recommended trace's widths are between 0.1 ~ 0.15 mm.

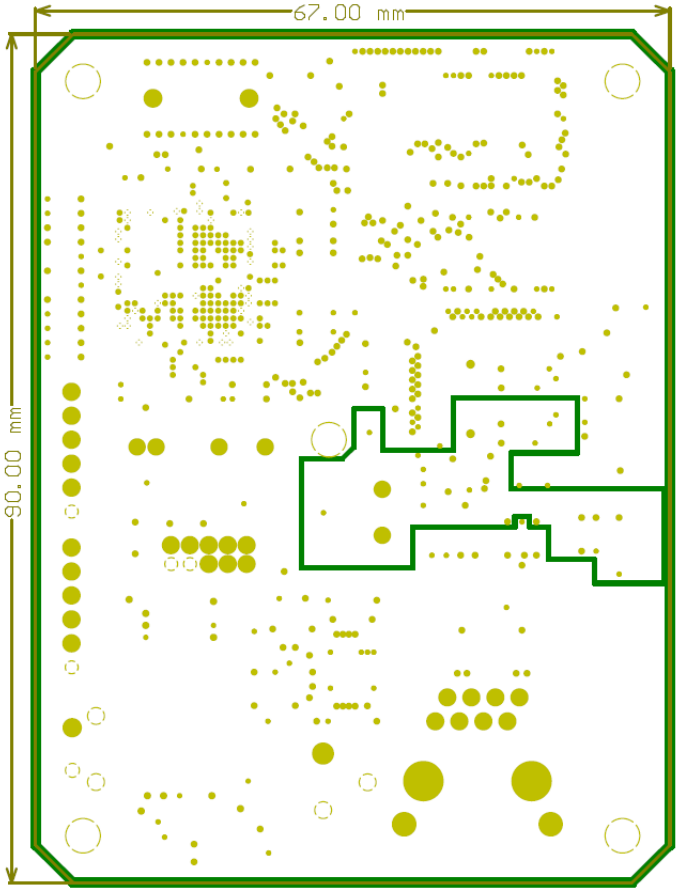


Figure 5: Ground plane of the S3C2440A PCB.

Good ground-plane design is another trick in order to improve signal integrity in high speed PCB design as well as EMC. The ground-plane provides ubiquitous return path for signal traces in a PCB. The transmission-line impedance of a signal traces, 50 ohm remained constant with respect to the ground-plane. Another good reason is to provide some shielding for high speed signals.

Because the ground plane needs a large area (compared to traces) it forms a good antenna at relatively low frequencies eventually lead to problems EMC and immunity. Resonance occurs at frequencies where an integer multiple of half wavelength is equal to one of the physical dimensions of the ground plane. One solution involves isolating sensitive circuits in their own small areas off the ground-plane [8].

The S3C2440 PCB incorporated split planes where the signal plane and large solid ground plane for the rest to isolate digital and analogue ground which less sensitive. Both of the planes are connected to each other via bridge as shown in figure 5.

VIII. 20-H RULE

As the operating frequency of electronic circuits continues to increase, today's package and printed circuit board designers face more radiation problem than ever before. To make the package comply with radiation constraint radiated emission should be in control which is the most important factors of the EMC study [6].

20-H rule is used in the design of the S3C2440 PCB board in order to contain fringing field induced by on boards power and ground plane. The ground planes are extended beyond the power planes about 20 the distance between the planes. The 20-H rule structure is shown in 6 below.

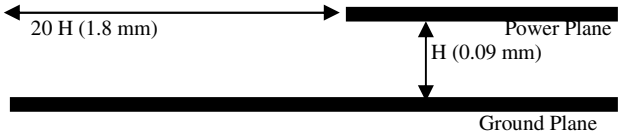


Figure 6: 20-H rule.

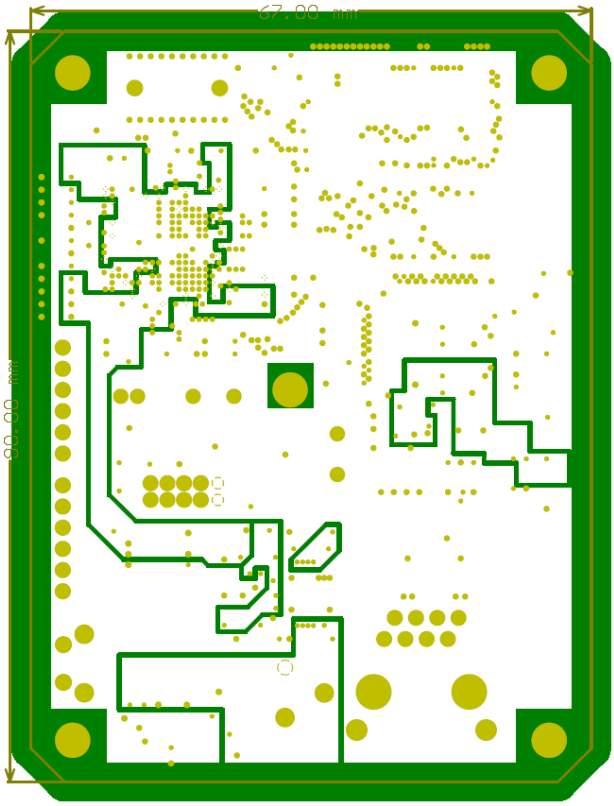


Figure 7: The copper area of power-plane of S3C2440 which limited up to 1.8 mm before reaching the edge of the PCB compare to ground-plane shown in figure 5, complied the 20-H rule.

VIII. PCB BOARD LAYERS

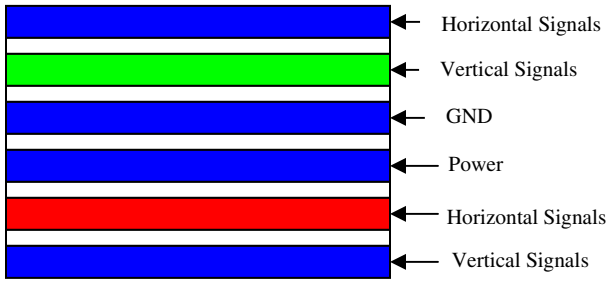


Figure 8: The S3C2440 PCB board stack-up layers.

The S3C2440 PCB board consists of six stack-up layers in figure 8, optimum for the EMC consideration and gave good signal integrity. Some of the distributed capacitance between the power and the ground signals is lost, but it can be compensated by adding additional decoupling with discrete devices [7].

The combination of a power plane and ground plane sandwich (plane-pair) within the PCB provides free power supply decoupling capacitance and current spreading within these planes which improved the noise isolation between power pins [8].

VII. CONCLUSION

This paper covered the essential steps of the core design circuitry for S3C2440, as a reference platform for high performance of embedded system. Various applications will benefit from the usage of S3C2440A ARM processor such as camera vision, surveillance system, and mobiles devices due to it high performance in term of processing capability as well as lower cost.

The challenges for the future works is to shrink the PCB board areas 50% less than the current designed PCB of S3C2440 (90mm x 67mm board size) or the upgrade version of the microprocessor which the core speed not less than 1Ghz. Is not the matter of the external parts is chosen to be smaller but utilising the high speed PCB design techniques and increasing in layers are crucial in order to avoid unwanted issues such signal integrity or EMC.

The DVS module for power management topology is crucial in order to save power consumption for mobile application platform. The challenges are to design the low dropout voltage regulator where the default minimum core voltage can be increased 0.1V step up to the maximum of

S3C2440A's core voltage while maintaining high current support for the S3C2440A's core usage.

VIII. ACKNOWLEDGMENT

We would like to thank Telekom Malaysia for sponsoring the work through research project RDTC080707, where everything began and not to forget the involved team members who make it a reality.

REFERENCES

[1] S3C2440A 32- Bit CMOS Micro controller User's Manual Revision 1.3
[2] MAXIM MAX1793 Low-Dropout, Low I_Q 1A Linear regulator Revision 1; 11/00
[3] MAXIM MAX 8860 Low-Dropout 300mA Linear Regulator Revision 2; 1/01
[4] MT48LC64M4A2 Synchronous DRAM 256MSDRAM_1.fm - Rev. M 12/08 EN
[5] MAXIM MAX811 4-upin Voltage Monitors 19-0411; Rev 4; 12/05
[6] Effect of 20-H Rule and Shielding Vias on Electromagnetic Radiation From Printed Circuits Boards. Huabo Chen, Student Member, IEEE, and Jiayuan Fang, Senior Member, IEEE Dept. of Electrical Engineering, University of California at Santa Cruz, Santa Cruz, CA 95064
[7] NXP AN10897 A guide to designing for ESD and EMC Rev02-19 January 2010
[8] Practical Power Planes for EMC; T.P.Jarvis, RadioCAD Ltd, t.jarvis@radiocad.com

Medium Access Control for Collaborative Transmit Beamforming in Wireless Networks

Suhanya Jayaprakasam, Teong Chee Chuah, Su Wei Tan
Faculty of Engineering
Multimedia University
Jalan Multimedia, 63100 Cyberjaya, Selangor D.E., Malaysia
suhanya@mmu.edu.my

***Abstract*- A new medium access control (MAC) scheme to enable collaborative transmit beamforming in IEEE 802.11 based wireless networks is proposed. The proposed scheme allows information sharing and simultaneous transmission in collaborative transmit beamforming, and is compatible with the existing distributed coordination function protocol. Performance comparisons with multi-hop and direct communications of the IEEE 802.11g wireless standard employing carrier sense multiple access with collision avoidance MAC are made. Results show that the proposed approach provides better throughput when greater distances or more hops are needed to complete communications, especially in a noisy environment.**

I. INTRODUCTION

Collaborative transmit beamforming is a technique where distributed nodes in a wireless network cooperate together to form a virtual directed antenna to transmit a common signal to a common destination [1]. Assuming a fixed transmit power at each node, an ideal transmit beamforming with N nodes will result in N^2–fold gain in the receive power at the receiver node [1, 2]. As a result, collaborative transmit beamforming provides the advantage of increased transmission range compared to single node communications.

The process of forming a beam collaboratively consists of two stages. The first stage is the information sharing stage, where a source node that intends to transmit its data to a destination will broadcast the data to all nodes within its transmission range. The nodes that receive the data become the collaborating nodes and will act as a distributed antenna system along with the source node to forward the data to the intended destination during the second stage. One of the nodes will be appointed as the cluster head (CH) as a reference point to all the collaborating nodes.

During the second stage, each collaborating node will multiply the received signal with a complex weight, which is computed independently by each node, before simultaneously transmitting the common data towards the intended destination. The complex weight multiplied to the signal by each node is relative to the position of the CH, hence eliminating phase offsets, allowing signals from all the collaborating nodes to add coherently at the destination node.

While the process of forming a good beampattern towards the destination is a physical (PHY) issue, the process of information sharing among the nodes is a medium access control (MAC) problem. Considerable research has been carried out on the PHY issues of collaborative beamforming [1, 3, 4]. However, the subject of MAC modelling for collaborative beamforming received little attention.

Existing wireless MAC schemes cannot be used directly for collaboratively beam-formed communications because they do not provide sufficient information for collaborating nodes to perform phase alignments during the first stage of collaboration, nor do they provide details regarding the collaborative transmission time. Furthermore, with the current MAC schemes, a destination that receives copies of the same data from different nodes deciphers them as separate interference, thus defeating the purpose of collaborative transmit beamforming.

In this paper, a new MAC scheme called Collaborative MAC (Coll-MAC), which is an extended version of the existing carrier sense multiple access/collision avoidance (CSMA/CA) scheme, is proposed to perform medium access for collaborative beamforming. Though the CSMA/CA scheme allows relaying of information along nodes, it cannot be used for collaborative communications as it has not been modelled to specify phase alignment of signals or coordinate simultaneous transmissions of data by a group of nodes. The proposed MAC scheme handles information sharing and passing to the PHY layer for phase alignment and the subsequent collaborative data transmission.

This paper is organized as follows. Section II provides the basic theory of collaborative beamforming. The proposed applications of collaborative beamforming concept and the Coll-MAC scheme are presented in Section III and IV respectively. Section V describes the simulation setup, while Section VI presents and discusses the results obtained. Finally, conclusions are drawn in Section VII.

II. INTRODUCTION TO THE CONCEPT OF COLLABORATIVE TRANSMIT BEAMFORMING

A brief introduction to the fundamentals of collaborative beamforming is provided in this section. Consider nodes with a geometrical composition as depicted in Fig. 1. Each node is equipped with a single isotropic antenna. It is assumed that the

system is operating under perfect channel conditions and all nodes transmit identical power of σ^2.

One of the nodes involved in forming the collaborative beam is chosen as the CH, which will become the geometrical reference point for all the other nodes in the system. The polar coordinates of all nodes in Fig. 1 are derived relative to the CH. The notation in Fig. 1 and recurring variables used in this paper are tabulated in Table I.

During the first stage of the communications, the source node broadcasts the data meant for the destination to the nodes within its transmission range.

Each node then aligns its phase by multiplying the received data symbol with a complex weight relative to the position of the CH, such that signals from all the nodes are received in phase at the destination.

Assuming that the source node is appointed as the CH, the corresponding weight for each node, c_k is represented by

$$c_k(\phi) = e^{-j\frac{2\pi}{\lambda}d_{k,a}} \quad (1)$$

In the second stage, the source node and the collaborating nodes will collaboratively transmit the data towards the destination. Since phase corrections were made by each node during the first stage, the data will be added constructively at the destination node.

Neglecting the time and phase asynchronism and path loss effects, the resultant received signal, y becomes

$$y = \sum_{k=1}^{N} \sigma_k . e^{-j\psi_k} . e^{-j\frac{2\pi}{\lambda}d_{k,a}} \quad (2)$$

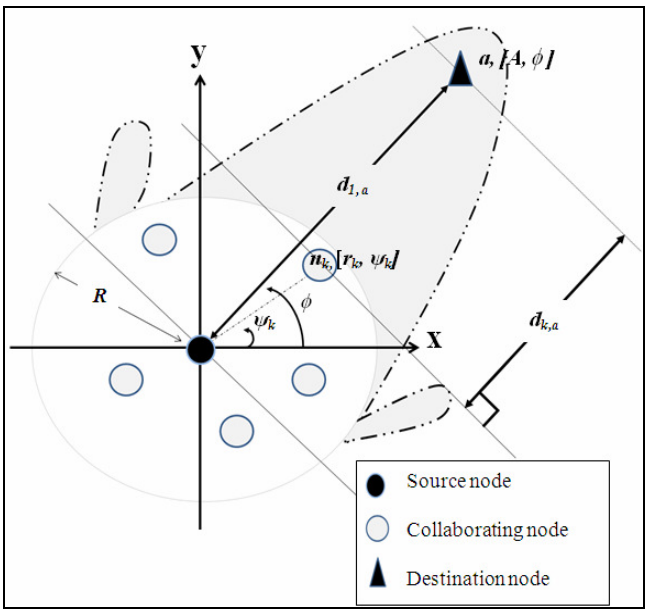


Fig. 1. Geometrical configuration of collaborative beamforming

TABLE I.
NOTATIONS AND VARIABLES USED THROUGHOUT THE PAPER

Notations	Description
N	Total number of collaborating nodes (inclusive of the source node)
k	1, 2,…, N, k=1 refers to the source
n_k	The k-th collaborating node, polar coordinate
a	Destination node
$d_{k,a}$	Distance between n_k and a
R	The transmit range of the cluster head
σ_k	Energy of the transmitted signal at the k-th node
A	Distance of a relative to the CH
ϕ	Elevation angle of the a relative to the CH
r_k	Distance of n_k relative to the CH
Ψ_k	Elevation angle of the n_k relative to the CH
λ	Wavelength of the signal

All nodes are assumed to be transmitting identical power; hence Equation (2) can be rewritten as

$$y = N\sigma \sum_{k=1}^{N} e^{-j\psi_k} . e^{-j\frac{2\pi}{\lambda}d_{k,a}} \quad (3)$$

Equation (3) proves that the receive power when N nodes are collaborating is $|N\ \sigma|^2$, while a single node transmission could only yield a receive power of σ^2 under ideal system assumptions.

III. POTENTIAL APPLICATIONS OF COLLABORATIVE BEAM-FORMED COMMUNICATIONS

Although collaborative beamforming has been originally proposed for wireless sensor network applications, recent findings [3, 5] have shown that this method is feasible to be applied to conventional wireless network applications.

Collaborative beamforming approach can be used as an alternative to CSMA/CA based multi-hop and direct communications in areas with low node density or limited gateway to the Internet, for example, in rural areas.

Most rural wireless projects adopt the IEEE 802.11 wireless standard to provide low cost wireless connections, since the IEEE 802.11 equipment are affordable and easily available off the shelf compared to other wireless standards' equipment. Services and applications targeted for the rural communities using this standard are basic Internet surfing, video conferencing, and Voice over Internet Protocol (VoIP) services.

The IEEE 802.11 standard switches to lower modulation/data rate when the distance between a source and a destination node becomes greater and the expected bit error performance is not achievable. Hence, the greater the range of the transmission, the lower the data rates and therefore causing

underutilization of spectrum. Since collaborative beamforming is able to increase the transmission power, longer transmission range can be covered with higher data rates, provided that the source node has a few neighbouring nodes which are ready to collaborate.

Collaborative transmission can also be used as an alternative to multi-hop communications. Though multi-hop can be used to cover long distance transmission by relaying packets through multiple hops, this type of network is prone to problems such as bandwidth degradation, radio interference and network latency as the number of hops increases. Use of collaborative beam-formed communications instead could reduce the number of hops and thus the problem caused by multi-hop communications.

IV. COLLABORATIVE MEDIUM ACCESS PROTOCOL

A. *Assumptions*

The following are the assumptions made in modelling the proposed MAC protocol:

1. The source node is the cluster head of a collaboratively beam-formed transmission.
2. There exists a line-of-sight for all nodes.
3. The channel is modeled as Rician fading with additive white Gaussian noise.
4. The fading gain of a given path stays the same during the duration of a single packet transmission.
5. All nodes are static.
6. Each node knows its location's coordinate.
7. Each node has information about its neighbours.
8. The location of the destination is known *a priori*.
9. All nodes have perfect time and phase synchronization.

B. *The Proposed MAC Scheme*

The frame format of the proposed Coll-MAC is summarized in Table II. The proposed MAC scheme adopts the distributed coordination function (DCF), which is the standard coordination function of the IEEE 802.11 standard. Hence, according to the DCF scheme, a node in the network will set its network allocation vector (NAV) to defer from accessing the medium when it senses a busy medium, and employs the back-off algorithm scheme in instances of collisions.

Suppose a station wishes to transmit data to a destination via collaborative beamforming, the station will first appoint itself as a cluster head (CH).

The flow of the proposed Coll-MAC can be divided into 3 stages; handshake, information sharing and collaborative transmission.

1) *The CH- collaborating nodes handshake*

Each node will maintain a collaborating nodes vector which stores the IDs of all the potential collaborative nodes.

TABLE II.
FRAME FORMATS AND DESCRIPTIONS

Frame	Mnemonic	Size (Bytes)	Description
Request to Collaborate	RTC	50	Multicast packet to neighbours, with unique time slot for each neighbour to respond
Consent to Collaborate	CTC	39	
Collaborative data	COLL-DATA	50+data	Contains tentative collaborative transmit time information and unique time slot for each collaborating node to respond
Collaborative Acknowledgement	ACK-COLL	47	Acknowledgement from a collaborating node to the CH during the first stage
Data	DATA	39+data	
Acknowledgement	ACK	39	From the destination

Initially, the collaborating nodes vector of a node will list all of its neighbours as its potential collaborating nodes.

The CH sends a Request to Collaborate (RTC) to its neighbours. The RTC frame is similar to the Request to Send (RTS) frame of CSMA/CA, but it contains additional information on the location coordinate of the CH and the time slot allocation for each potential collaborating node.

Neighbour nodes which are free to collaborate will respond with Consent to Collaborate (CTC) packet, which is sent according to the time slot allocated by the CH in its RTC packet. The format of the CTC frame is similar to the format of Clear to Send (CTS) frame in the CSMA/CA scheme. Apart from acting as the response to the CH, this frame also ensures that hidden nodes which are out of the CH's range are notified about the imminent collaborative transmission, so that these hidden nodes do not attempt to access the medium during this duration and cause collisions.

Once the CTCs from the neighbouring nodes are received by the CH, a successful handshake is established, and the CH will proceed with the information sharing process.

2) *Information sharing*

The CH will update its collaborating nodes vector according to the CTCs received from the neighbouring nodes. The data intended to be transmitted to the destination is packaged as a COLL-DATA frame and sent to all the collaborating nodes via multicast. This frame is similar to the data frame of the CSMA/CA scheme, but it contains extra fields to include timing information to collaboratively send the packet to the destination.

Each collaborating node responds by sending an acknowledgement (ACK) frame back to the CH according to

the pre allocated time slot. This frame is the same as the existing ACK frame in the CSMA/CA scheme.

3) Collaborative transmission

The received data's signal phase will be aligned by each collaborating node with respect to its location from the CH. The collaborating nodes will repackage the data received in the DATA-COLL packet as the DATA packet, which is similar to the data packet of the CSMA/CA scheme. However, instead of using its own address, each node will fill in the sender address field of the DATA frame with the address of the CH node.

All the collaborating nodes and CH will transmit the DATA frame towards the intended destination at the time mentioned by the CH in the DATA-COLL packet. The phase alignment will ensure that signals from separate nodes add constructively at the destination while the masking of the address field allows the receiver to perceive the added signals to have originated from one node, i.e. the CH.

If the data is successfully received by the receiver, the receiver will send out an ACK frame (with the same format as the existing ACK frame) to the source node (CH), completing a transmission cycle of collaborative transmit beam-formed communications.

V. Simulation System Model

An IEEE 802.11g standard wireless network in rural area is assumed as the network model. Each node in the network is equipped with an omni directional antenna and an IEEE 802.11g radio.

An empirical path loss (PL) model of the IEEE 802.11 rural links as suggested in [8] is adopted in this work. The channel is characterised as a mostly flat terrain with a few scattered trees, coupled with atmospheric dust, moisture and effect of earth curvature. The path loss model is as given by

$$35.45+20\log(f)+20\log(d)+0.15d \quad (4)$$

where f and d denote the operating frequency and transmission distance in km, respectively. Other physical parameters used in the simulation model are listed in Table III.

The performance of the proposed COLL-MAC based collaborative beamforming is compared with the existing IEEE 802.11 CSMA/CA based direct communications and CSMA/CA based multi-hop communications.

A. Collaborative Beamforming as an Alternative to Direct Communications

Direct communications are communications where a source node transmits data to the destination node without the help of relay nodes.

Assume that there are two neighbouring nodes within 100m of the source node as shown in Fig 2. The destination is separated from the source node with a distance of d km. The throughput of the CSMA/CA based direct communications is

TABLE III.
MULTI-HOP VS. COLLABORATIVE COMMUNICATIONS

Parameters		Notes
802.11 standard	802.11g	
Operating frequency	2.4GHz	Unlicensed band
Transmit power, Ptx	17dBm	Transmit power of the radio
Transmit antenna Gain, Gtx	16dBi	Omnidirectional antenna
Receive antenna gain, Grx	16dBi	
Forwarding scheme	AAF	Amplify and forward scheme
Path loss model	DGPPL	
Fading	Ricean	K factor=3

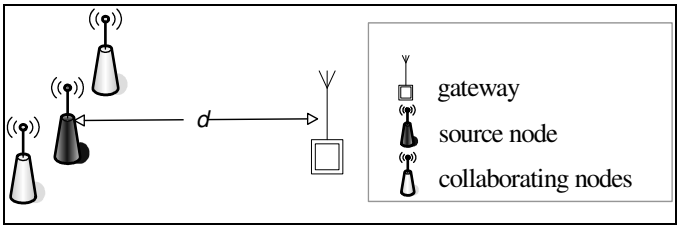


Fig. 2.Direct / collaborative beamforming communications setup

compared to that of COLL-MAC based collaborative communications when the distance between the source and destination, d and the noise figure (Nf) are varied.

B. Collaborative Beamforming as an Alternative to Multi-hop Communications

Consider a random topology as shown in Fig. 3. In multi-hop communications, data is passed to the destination by retransmissions over a chain of relay nodes. Assuming that each node employs 24Mbps/QPSK for transmission, three scenarios are analysed; 1 hop, 2 hops and 3 hops communications. The throughput performance of collaborative communications using Coll-MAC for the same scenarios is studied. The source node for each scenario, corresponding number of hops and route for multi-hop communications and corresponding collaborative nodes for collaborative communications are summarized in Table IV.

VI. Simulation Results and Discussions

A. MAC Overhead Comparison

The MAC layer overhead of Coll-MAC is compared to the CSMA/CA based direct communications and multi-hop communications. The overhead of the proposed Coll-MAC relies on the number of collaborating nodes. The more collaborative nodes used, the higher the MAC overhead of collaborative communications. Though the overhead is larger compared to that of direct communications, collaborative communications provide a good trade off by enabling the use of higher data rates when the transmission range is long. The results also show that the MAC overhead of collaborative beam formed communications is essentially lower than that of multi-hop communications.

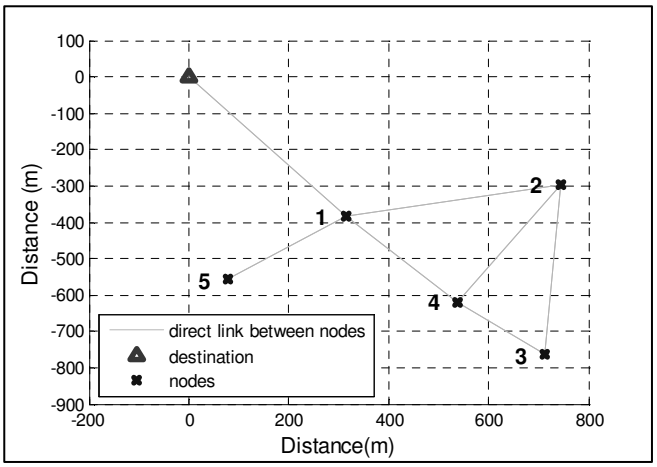


Fig. 3.Random topology to compare performance of collaborative beamforming communications with multi-hop communications

TABLE IV.
MULTI-HOP VS. COLLABORATIVE COMMUNICATIONS SCENARIOS

Source node	Multi-Hop Communication	Collaborative Beam formed Communication
1	1hop (1→destination)	2 collaborating nodes (nodes 5 &2)
4	1hop (4→1→destination)	2 collaborating nodes (nodes 1 &2)
3	1hop (3→4→1→destination)	2 collaborating nodes (nodes 4 & 2)

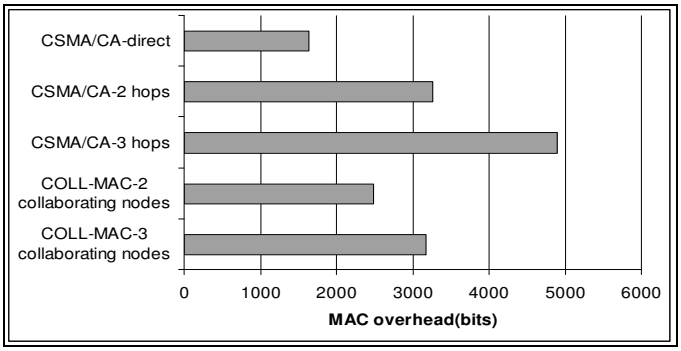


Fig. 3. MAC overhead comparison of COLL-MAC to CSMA/CA

B. *Throughput of Direct vs. Collaborative Communications*

The throughput of CSMA/CA based direct communications are compared to that of Coll-MAC based collaborative communications when the distance between source and destination, *d* and the noise figure are varied, are depicted in Fig 4.

It is evident that collaborative communications perform better when distance between source and destination is greater and when the overall noise figure is high.

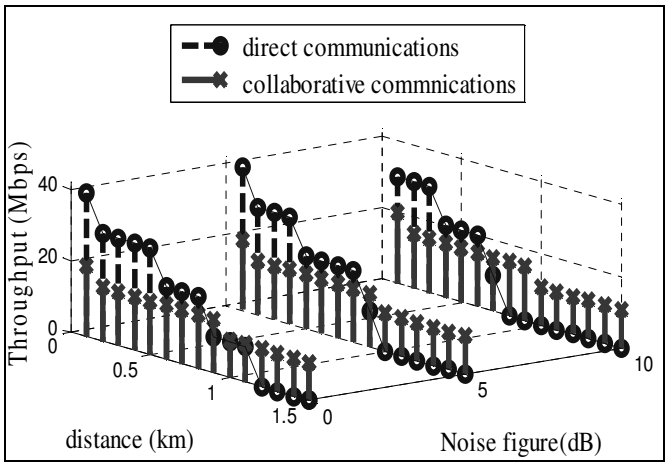


Fig. 4. Throughput comparison of direct and collaborative communications under different distances and noise figures

C. *Throughput of Multi-hop vs. Collaborative Communications*

Throughput comparison for the scenarios tabulated in Table III for noise figures ranging from 0dB to 5dB are summarised in the bar chart in Fig 5.

Although collaborative communications are not the ideal solution when single hop communications are possible between the source and the destination; however, when the number of hops is more than two and the noise figure is high, collaborative communications are a better alternative as they provide stable throughput and are less susceptible to noise.

VII. CONCLUSIONS

A new MAC scheme based on the DCF scheme is introduced to enable collaborative transmit beamforming in wireless networks. Results show that collaborative based communications can achieve better throughput for long transmission distances and noisy scenarios.

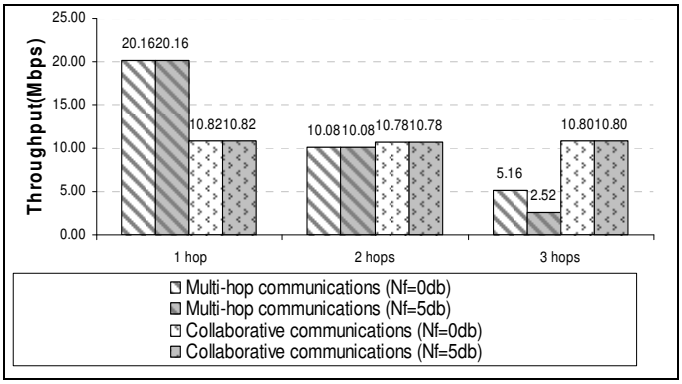


Fig. 5. Throughput comparison of multi- hop and collaborative communications under different noise figures

REFERENCES

[1] H. Ochiai, P. Mitran, H. V. Poor, and V. Tarokh, "Collaborative beamforming for distributed wireless ad hoc sensor networks," *Signal Processing, IEEE Transactions on*, vol. 53, pp. 4110-4124, 2005.

[2] P. Mitran, H. Ochiai, and V. Tarokh, "Space-time diversity enhancements using collaborative communications," *Information Theory, IEEE Transactions on*, vol. 51, pp. 2041-2057, 2005.

[3] R. Mudumbai, G. Barriac, and U. Madhow, "On the Feasibility of Distributed Beamforming in Wireless Networks," *Wireless Communications, IEEE Transactions on*, vol. 6, pp. 1754-1763, 2007.

[4] R. Mudumbai, D. R. Brown, U. Madhow, and H. V. Poor, "Distributed transmit beamforming: challenges and recent progress," *Communications Magazine, IEEE*, vol. 47, pp. 102-110, 2009.

[5] D. Lun, A. P. Petropulu, and H. V. Poor, "A Cross-Layer Approach to Collaborative Beamforming for Wireless Ad Hoc Networks," *Signal Processing, IEEE Transactions on*, vol. 56, pp. 2981-2993, 2008.

[6] "Solving the Wireless Mesh Multi- Hop Dilemma," Strix Systems. Inc 2005.

[7] Cisco, "Cisco Aironet 1240AG Series 802.11A/B/G Access Point," Cisco Systems, Inc., 2008.

[8] B. Raman, "Digital Gangetic Plains: 802.11based LowCost Networking for Rural Areas, 2001-2004: A Report," B. Raman, Ed. Kanpur, India: Department of CSE, IIT Kanpur, 2004.

A Probabilistic Measure of Extended Reservation Aloha MAC Protocol Against Some MAC Problems in MANET

Kazi Atiqur Rahman
ECE, University of Windsor
Ontario, Canada
rahman1h@uwindsor.ca

Khaja Shazzad
ECE, University of Windsor
Ontario, Canada
shazzad@uwindsor.ca

Kemal E. Tepe
ECE, University of Windsor
Ontario, Canada
ktepe@uwindsor.ca

***Abstract*—Mobile hidden station and neighborhood capture problems severely affect the communication in the MAC layer of a mobile ad hoc network. IEEE 802.11 cannot prevent blocking due to neighborhood capture problem and collisions due to mobile hidden station problem. Extended reservation-Aloha (ERA) solves these two problems in a probabilistic manner along with solving widely known hidden station and exposed station problems. This paper provides a probabilistic view of ERA to neighborhood capture and mobile hidden station problems. The analysis shows that the channel accessing probability of a station facing neighborhood capture problem is more than 90 percent with 60 percent traffic.**

***Index Terms*—Neighborhood capture problem, Mobile hidden station problem, hidden station problem, ALOHA, medium access control (MAC), IEEE 802.11.**

I. INTRODUCTION

The mobility of stations in wireless networks increases MAC layer challenges [1]. Hidden station (HS), exposed station (ES), mobile hidden station (MHS) and neighborhood capture (NC) problems are common and inevitable in a mobile ad hoc network (MANET) due to its multi-hopping mobile nature.

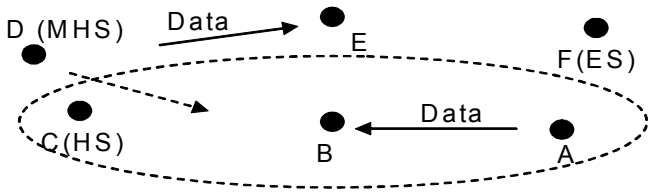
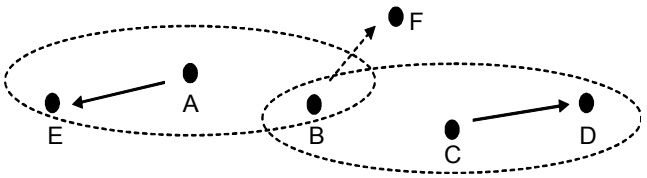
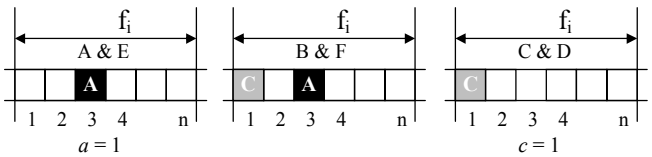


Fig. 1. HS, ES and MHS in a simple scenario.

If any mobile station enters any receiver's interference range, and disturbs their communication, that mobile station is called a mobile hidden station. Suppose, Station A is transmitting to Station B in Fig. 1, and all stations are using IEEE 802.11 MAC [2] protocol. Let us consider that Station D is transmitting to any other station, and at the same time moving into the transmission range of B without any knowledge of a clear to send (CTS) from B. Here, Station D may disturb Station A's transmission to B. So, Station D is a mobile hidden station to A. Thus, IEEE 802.11 MAC cannot prevent packet losses due to the MHS problem in MANET. IEEE 802.11 MAC protocol solves HS and ES problems forcing them to remain idle. If two stations (i.e. A and C in Fig. 2(a)) are out of their interference ranges from each other, they may acquire the channel simultaneously for their transmissions to other stations. If Stations A and C have a common neighbor (i.e. B in Fig. 2(a)), this neighbor will not sense the channel idle as long as its neighbors will not release that channel simultaneously. So, Stations like B may not sense the channel idle for a long period of time. This problem is called neighborhood capture problem [3, 4]. As IEEE 802.11 is a distributed MAC protocol, stations using IEEE 802.11 MAC do not release the channel simultaneously. That is why it does not solve the NC problem.



(a) A simple MANET scenario to show the neighborhood capture problem.



(b) A's reservation. (c) B's observation. (d) C's reservation.

Fig. 2. Neighborhood capture problem with example reservations of stations in a frame.

IEEE 802.11p is an amendment standard of IEEE 802.11 and will be used by vehicular communications [5, 6]. Since it is similar to IEEE 802.11, it does not address NC and MHS problems. Global channel release (GCR) MAC protocol forces all stations to release the channel at synchronized pre-specified times. This ensures that all competing stations would have an equal chance to seize the channel [4]. As all contending stations using GCR release the channel simultaneously, the NC problem is solved. However, GCR uses carrier sense multiple access with collision avoidance (CSMA/CA), it does not solve

the MHS problem. Dual busy tone multiple access (DBTMA) MAC protocol [7, 8] uses two busy tones to remove HS and ES problems. Like any other distributed protocol, DBTMA prevents collisions due to HS and ES forcing them to remain idle. An MHS in transmitting mode cannot hear the receiver initiated busy tone. That is why, an MHS disturbs that communication. As the DBTMA is distributed in nature, it does not solve the NC problem [3]. An interleaved MAC protocol [9] uses two frequency channels for any successful communication e.g. one for RTS and DATA, another for CTS and acknowledgement (ACK). The interleaved MAC protocol uses the RTS/CTS handshaking as in IEEE 802.11, and does not address MHS or NC problems. Reservation Aloha (R-Aloha) is a packet access scheme based on time division multiplexing (TDM) [10]. R-Aloha also does not address access related problems (i.e. HS, ES, NC and MHS problems) in MANETs. Extended reservation Aloha (ERA) is an enhanced version of R-Aloha to address HS, ES, NC and MHS problems in MANETs. ERA completely solves HS and ES problems, and decreases collision losses due MHSs. This paper provides detailed calculations of the quantitative analysis to show that ERA provides significant chances to stations under a neighborhood capture situation. The discussions throughout the paper compare ERA with IEEE 802.11 analytically. Section II contains a view of the ERA MAC protocol. Its effectiveness to HS, ES, NC and MHS problems is analyzed in Section III. The paper is concluded in Section IV.

II. EXTENDED R-ALOHA MAC PROTOCOL

The extended R-Aloha MAC protocol uses the principle of the R-Aloha protocol with the following modifications:

(1) Two stations under a communication use the same slot in consecutive frames one after another. They establish a bi-directional connection by sharing the same slot in consecutive frames.

(2) Any of the two stations uses one slot in the current frame, and reserves the same slot in next two subsequent frames.

(3) While accessing a slot for the first time, the sender (who wants to start a communication) follows the following rules:

I. The sender senses the idle slot for a small random amount of time. This is done by starting a back-off timer.

II. The contending station with a lower back-off timer value has a priority to access and reserve a slot first.

III. If there is a collision, the contending station resets the back-off timer again, and tries to access to the channel in the next idle slot.

(4) Depending on the intensity of the traffic, any station may reserve more than one slot.

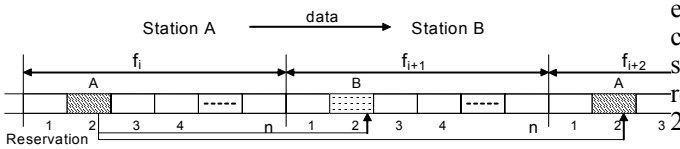


Fig. 3. ERA reservation scenario.

Fig. 3 shows a reservation scenario using the ERA MAC protocol. If Station A wants to start a communication with Station B in frame f_i, it acquires a slot (i.e. slot 2) in frame f_i, and reserves the same slot in frames f_{i+1} and f_{i+2}. Consequently, Station B sends an acknowledgement to A using slot 2 of frame f_{i+1}, and reserves slot 2 of frames f_{i+2} and f_{i+3}. Thus reservations continue until end of the communication. A detailed analysis of the ERA MAC protocol is presented in the next section.

III. ANALYSIS

The ERA MAC protocol has been analyzed for HS, ES, NC, and MHS problems in this section.

A. Extended R-Aloha as a Solution to Hidden and Exposed Station Problems

Station A is transmitting data to Station B as shown in Fig. 1. In this scenario, Station C is a HS, and Station F is an ES to Station A. After A's transmission using slot 2 of frame f_i as shown in Fig. 3, Station F knows about A's reservation of slot 2 in frames f_{i+1} and f_{i+2}. When Station B sends an acknowledgement to A using slot 2 of frame f_{i+1}, F knows that this slot is already reserved by A. After B's transmission of the acknowledgement to A using slot 2 of frame f_{i+1}, C knows about B's reservation of slot 2 in frames f_{i+2} and f_{i+3}. When A sends data to B using slot 2 of frame f_{i+2}, exposed Station F and hidden Station C are aware of this reservation. So, the ERA MAC protocol ensures that there are no collisions from both HSs and ESs. Stations A and B are using only slot 2 for their communication. Stations C and F are able reserve any other slot of the frame if they want to communicate with other stations. So, the ERA does not force HSs and ESs to remain idle during the whole frame.

B. Extended R-Aloha as a Solution to the Neighborhood Capture Problem

A simple MANET scenario as shown in Fig. 2(a) is used to illustrate the neighborhood capture problem. Let us consider that all stations in Fig. 2(a) are using the IEEE 802.11 MAC protocol. Station B is one hop neighbor of both Stations A and C. Stations A and C are out of the interference ranges of each other this is why they cannot hear each other, and use the channel independently. If B wants to transmit packets, it must have to wait until both Stations A and C release the channel simultaneously. Consequently, Station B may not get access to the channel for long time, which is the NC problem. The NC problem will be severe if A and C both have many packets in their queues. Now, we will see what happens if the ERA is applied in this scenario as a MAC protocol. According to the ERA, Station B knows about A's and C's reservation of slots as shown in Fig. 2(c). So, B may continue its communication with any other stations (i.e. Station F in Fig. 2(a)) by reserving a slot free from both A and C. So, Station B is out of the effect of the NC problem. For example, A is communicating with E reserving one slot in frame f_i as shown in Fig. 2(b), and C is communicating with D reserving one slot in the same frame as shown in Fig. 2(d). B observes both A's and C's reservations, and selects any slot from the rest of $(n-2)$ slots of the frame f_i as shown in Fig. 2(c). But, high traffic load

reduces B's chance to access to the channel. Let us consider that Station B wants to reserve one slot per frame, and there are n number of slots per frame, and number of slots reserved by Station A is a, and number of slots reserved by Station C is c. If summation of all slots reserved by A and C is less than the total number of slots in a frame, B can always access the channel, which is the best case scenario for B. Therefore, the probability of B's chance to access the channel, P_B, based upon the condition $a + c < n$ is 1, this is

$$P_B = 1. \tag{1}$$

B has a probability to access the channel for the boundary conditions $a + c \geq n$ and $a + c \leq 2n$. Let us consider that A has the possibility to use the frame in U_1 ways, and C has the possibility to use the frame in U_2 ways. Therefore, the number of events in which station A is reserving a number of slots out of n slots in a frame in all possible ways is

$$U_1 = {}^{n}C_a. \tag{2}$$

The number of events in which C is reserving c number of slots out of n slots in a frame in all possible ways is

$$U_2 = {}^{n}C_c. \tag{3}$$

Since A and C choose the slots independently, the total number of events (i.e. U) in which A and C both use the frame is

$$U = U_1 \times U_2 = {}^{n}C_a \times {}^{n}C_c. \tag{4}$$

Let us consider only one case first, where A is reserving the first a number of slots of the frame, and C can reserve its c number of slots out of n slots in that frame in all possible ways. In this case, the number of slots remaining in the frame or not reserved by A is $(n-a)$. We need to find the number of events V in which C must use the rest of $(n-a)$ number of slots of the frame in its reservation. B will not get a chance to access to the channel in V number of events. Because, stations A and C are covering all the slots of the frame in these V events. As $c \geq (n-a)$, V can be found by taking a combination of $(c-(n-a))$ out of a slots. Therefore, the number of events in which B will not get chance to access to the channel is

$$V = {}^{a}C_{(c-n+a)}. \tag{5}$$

Now, total number of events for all cases of A in which B will not get chance to access to the channel is

$$W = V \times {}^{n}C_a = {}^{a}C_{(c-n+a)} \times {}^{n}C_a. \tag{6}$$

Therefore, the probability of B's chance to access to the channel based upon the condition $n \leq a + c \leq 2n$ is given by

$$P_B = \frac{U - W}{U}. \tag{7}$$

Using (4), (6), and (7), we obtain

$$P_B = \frac{n! \times (c+a-n)! - a! \times c!}{n! \times (c+a-n)!}. \tag{8}$$

According to the IEEE 802.11, Station B in Fig. 2(a) is exposed to both Stations A and C, and forced to remain idle. As there is no guarantee that A and C will release the channel simultaneously, B's chance to access the channel is completely uncertain. So, IEEE 802.11 blocks stations like B for an indefinite time. ERA provides a good channel accessing probability to these stations (i.e. B) as revealed in (1) and (8).

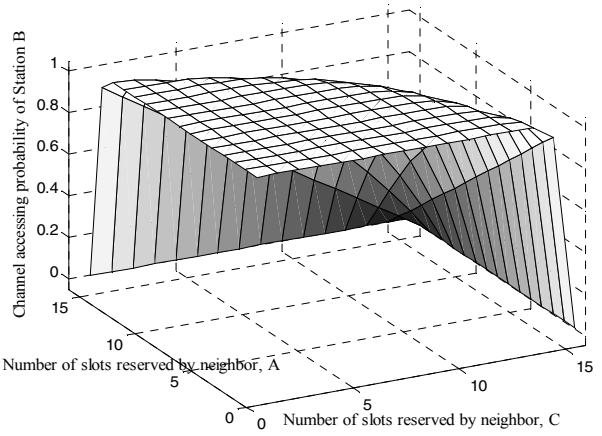


Fig. 4. Channel accessing probability of B with the variation of the number of slots reserved by Station A and Station C.

ERA has the provision to reserve more than one slot if necessary. Fig. 4 shows a mesh diagram where Stations A and C are reserving variable numbers of slots in a 16-slot frame. The channel accessing probability of B is plotted against different combinations of slots reserved by A and C. Fig. 4 shows that the channel accessing probability of B is always 1 for any combination of slot reservations of A and C where the summation of the number reserved slots by them is less than 16. The probability decreases if this summation is greater than 16. For example, if the number of slots reserved by A is 14, and the number of slots reserved by C is 15, the channel accessing probability of B is 0.25. The worst case occurs if either of A or C reserves the whole frame. But, that is a rare case.

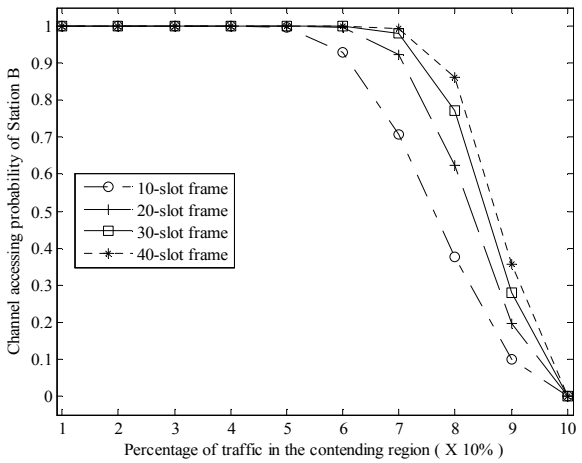


Fig. 5. Channel accessing probability of B with the variation of traffic in the contending area.

Fig. 5 shows the effect of percentage of traffic on the channel accessing probability of B. The percentage of traffic is defined as the ratio of the total number of reserved slots in a frame and total number of slots in a frame. In this case, we have considered that all stations in the contending region of B are allowed to reserve only one slot per frame. The channel accessing probability of B starts decreasing when the traffic is more than fifty percent. Fig. 5 also shows that channel accessing probability increases for larger frame size. The ERA promises 100 percent channel accessing probability for the traffic less than or equal to 50 percent in the contending region. Alike the analysis in Fig. 5, if all stations in the contending region of B are allowed to reserve only one slot per frame, the channel accessing probability of Station B decreases with increasing the number of contending neighbours while using ERA as a MAC protocol. So, unlike IEEE 802.11 MAC, ERA solves the NC problem with neighbours more than two.

The discussion in this sub-section highlights that the severity of the NC problem increases with the IEEE 802.11 MAC, where as the ERA MAC protocol solves the NC problem in a probabilistic manner. The stations using the ERA MAC protocol are not severely affected by the NC problem compared to the IEEE 802.11 or similar distributed-type protocols. The next sub-section contains an analysis how ERA solves the MHS problem.

C. Extended R-Aloha as a Solution to the Mobile Hidden Station Problem

The mobile hidden station scenario in Fig. 1 is used for our analysis in this sub-section. Let us consider that Station A is transmitting data to B, and C is HS to A. Station D is moving towards the transmission range of Station B, and transmitting data to Station E at the same time. When Station D enters into the transmission range of B, D's transmission collide with A's transmission at B. So, Station D is an MHS to A. According to the principle of ERA, each transmitting station can reserve a slot per frame. Let us consider that Station A reserved a slot, and is communicating with B using that slot. Similarly, Station D reserved a slot, and is communicating with E. If A's reservation and D's reservation are same, there will be a collision at B, and A's data will be lost. Otherwise, there is no problem with the MHS, D. So, the ERA provides a good probability that an MHS does not affect any ongoing communication. Let us consider that Station A and Station D reserve a and d number of slots per frame respectively. Total number of slots per frame is n. If summation of all the slots reserved by Station A and Station D is greater than the total number of slots in a frame, a successful transmission by Station A is not possible. Therefore, the probability of collision, P_c, at Station B based on the condition $a+d>n$ is given by

$$P_c = 1. \quad (9)$$

There is always a chance of successful transmission by Station A for the following condition, $a+d \le n$. So, the probability of collision for this condition is calculated by

$$P_c = \frac{(n-a-d)!\times n! \; - \; (n-a)!\times(n-d)!}{(n-a-d)!\times n!}. \quad (10)$$

According to the IEEE 802.11, Station D does not know about A's transmission to B. Whenever D will enter the interference range of B, D's transmission will collide with A's transmission. So, the severity of probability of collision due to MHSs is high. ERA promises to reduce the probability of collisions due to MHSs as revealed in (10). According to the principle of ERA, any station has a provision to reserve more than one slot if necessary.

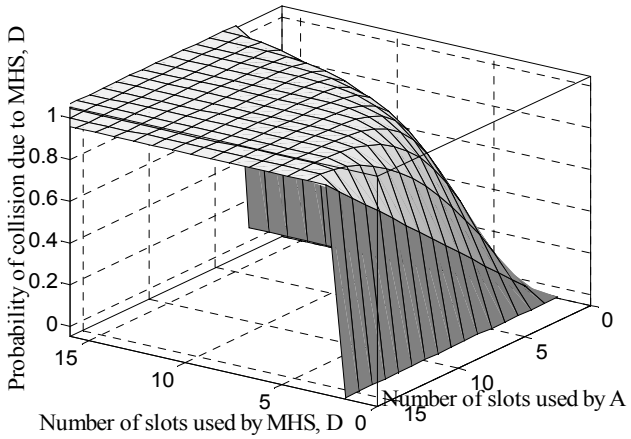


Fig. 6. Probability of collision due to MHS, D with the variation of the number of slots reserved by A and D.

The mesh diagram in Fig. 6 illustrates that Stations A and D are reserving variable numbers of slots in a 16-slot frame. The probability of collision at B due to MHS, D is plotted against different combinations of slots reserved by A and D. Fig. 6 shows that the probability of collision at B is always less than one for any combination of slot reservations of A and D, where summation of the number of their reserved slots is less than or equal to 16. For example, if the number of slots reserved by A is one, and the number of slots reserved by MHS, D is one, the probability of collision at B is 0.07. So, A has 95 percent probability to make a successful transmission in this situation. The probability of collision increases if the summation of reservations by A and D increases. The worst case arises if the summation of reservations of slots by A and D exceeds the number slots in a frame (i.e. 16 in this case). In these cases, the probability of collision is 100 percent (see top flat portion of Fig. 6). But, these are not usual cases.

Equation (10) reveals that stations in the contending region are also affected by the amount of traffic in the contending region. If summation of a and d is equal to n, the traffic in the contending region is 50 percent. Equation (9) shows that it is not possible to have a successful transmission when traffic is more than 50 percent. If the traffic is less than or equal 50 percent, there is a chance of successful transmission. Thus the analysis in this sub-section shows that ERA outperforms the IEEE 802.11 and other similar distributed-type MAC protocols in solving the MHS problem.

VI. CONCLUSION

In this paper, MAC problems of MANETs, namely hidden station, exposed station, neighborhood capture, and mobile hidden station problems, are discussed. IEEE 802.11 solves HS and ES problems, but does not solve neighborhood capture and mobile hidden station problems. The extended R-Aloha solves HS and ES problems, and deals NC and MHS problems in a probabilistic manner. If all the stations use the IEEE 802.11 as a MAC protocol, at least two stations hidden to each other may block their common neighbor for an indefinite span of time. This blocking gets more severe when number of stations gets larger. The ERA MAC protocol provides a good channel accessing probability to the blocked station even if the number of the neighbors of the blocked station is more than two. The ERA reduces collisions due to MHSs, and thereby provides good chances of successful transmissions.

REFERENCES

[1] N. Enneya, K. Oudidi, and M. Elkoutbi, "Network Mobility in Ad hoc Networks", Proc. of Int. Conference on Computer and Communication Engineering, Kuala Lumpur, Malaysia, May 2008.

[2] LAN/MAN Standard Committee of the IEEE Computer Society, "IEEE Standard for Wireless LAN Medium Access Control (MAC) and Physical Layer (PHY) specifications", IEEE Standard, Jun. 1997.

[3] K.A. Rahman, K. Am. Rahman, M. Lott, and K.E. Tepe, "Characterization of the Adverse Effect of Neighborhood Capture in MANET and on the Way to a Remedy", Proc. of IEEE EIT 2009, Windsor, ON, Canada, Jun 2009.

[4] M. Benveniste, "Wireless LANs and Nieghborhood Capture", Proc. of 13th IEEE PIMRC, vol. 5, pages 2148-2154, Lisboa, Portugal, Sep. 2002.

[5] W. Alasmary, and W. Zhuang, "Mobility Impact in IEEE 802.11p Infrastructureless Vehicular Networks", Elsevier Journal of Ad Hoc Networks, In press, 2010.

[6] D. Jiang, and L. Delgrossi, "IEEE 802.11p: Towards an International Standard for Wireless Access in Vehicular Environments", Proc. Of IEEE VTC, Pages 2036-2040, Singapore, May 2008.

[7] Z.J. Haas, and J. Deng, "Dual busy tone multiple access (DBTMA)-a multiple access control scheme for ad hoc networks," *IEEE Trans. Comm.*, vol. 50, pp. 975-985, June 2002.

[8] P. Wang, H. Jiang, and W. Zhuang, "A dual busy-tone MAC scheme supporting voice/data traffic in wireless ad hoc networks," *Proc. of IEEE Globecom*, Nov. 2006.

[9] S. Jagadeesan, B.S.Manoj, and C. Siva Ram Murthy, "Interleaved Carrier Sense Multiple Access: An Efficient MAC Protocol for Ad hoc Wireless Networks", Proc. Of ICC, Vol. 2, Pages 1124-1128, Alaska, USA, May 2003.

[10] S.S. Lam, 1980. "Packet Broadcast Networks – A performance analysis of the R-ALOHA protocol.", IEEE Trans. Of Computers, vol. C-29, no.7 July 1980.

Usage Control Framework for Mobile Ad-hoc Applications

Tamleek Ali, Asad Khan, Mohammad Nauman
Institute of Management Sciences, Peshawar Pakistan.
tamleek,asad,nauman@imsciences.edu.pk

***Abstract*—Mobile ad-hoc applications create a link with other applications in an ad-hoc manner. Resources may be released to the peer applications. Access and usage control is an important requirement while sharing resources with peer application. Currently there is no controlling framework for the usage of shared resources in mobile ad-hoc applications. In this paper we introduce the notion of a usage control in mobile ad hoc application scenarios that manages the usage of individual objects registered with it. Whenever a node joins the ad-hoc network, it may share and use one or more objects while being part of the ad-hoc application domain. While releasing resources to UCAS it attaches the policy along with the resource. This policy may describe the number of total usages, the number of individual usages, location and timings etc. We have proposed a framework with the XML based policy for usage control of the shared resources. We show that our design effectively enforces usage control in the highly dynamic mobile ad hoc applications network.**

I. Introduction

Increasing popularity of mobility and location based services has introduced the concept of mobile ad-hoc applications which is getting popularity in the scientific literature. With the increase in mobile services deployment, the issues of security are getting to surface. These includes issues is protecting resources after they have been released to devices outside the control of the original owner. One way to protect resources in such scenarios is through the use of access control models to protect access to these resources. However, in such models, the decision to allow or deny access is made only before the object is released and control is lost over the object after it leaves the boundary of the owner's control. Therefore, there is a need of a reference monitor that can enforce policies attached to these protected resources even after they are outside this direct control. This is the concept termed as 'usage control' [1]. The concept of distributed usage control has also been studied in detail in the past [2], [3]. To the best of our knowledge, the implications and semantics of usage control in the context of mobile ad-hoc networks have never been studied before. In the following section, we describe how the marriage of usage control models with mobile ad-hoc networks can truly open new vistas for secure ad-hoc applications on devices such as smart phones.

In this paper, we define a comprehensive framework that incorporates the UCON model in the context of mobile ad hoc applications. The primary strength of this framework is that it works without relying on a centralized infrastructure – a primary limitation of any ad hoc network-based scenario. Most of the access control models fail in the scenarios of ad hoc applications because of the lack of infrastructure in the underlying networks. We, on the other hand, rely on a decentralized reference monitor deployed on each node in the network to achieve optimal control over the objects released to other nodes. We describe the policy semantics and the enforcement model at a high level of abstraction. The implementation aspects of our framework are described in detail.

Outline: The rest of the paper is organized as follows: Section II provides some background information on the related technologies. A use case is provided in Section II-C to motivate the idea. Section III describes in detail, our proposed architecture along with policy specification semantics and other important concerns. Implementation is covered in Section IV and the paper is concluded in Section V.

II. Background

A. Mobile Ad-hoc Applications

A large amount of scientific literature covering Mobile Ad-hoc NETworks (MANETs) has been generated in the recent past. Mobile ad-hoc networks are characterized by a decentralized networking infrastructure that is centered around mobile entities coming together to form dynamic collaborations. One of the most important characteristics of these networks is the absence of a centralized authority or controlling infrastructure. Peer-to-peer collaborative ad-hoc networks are also discussed in the literature [4], [5], [6], [7]. Rising above the low-level network layer details of MANETs, Garbinato and Rupp [8] have proposed the concept of "Mobile Ad-hoc Applications". A mobile ad-hoc application is a "self-organizing application composed of mobile and autonomous devices, interacting as peers and [in] which relationships are made possible because of relative physical distance". They describe *mobility*, *peer-to-peer communication* and *collocation* – physical closeness – as the three tenets of mobile ad-hoc applications. In this way, the application layer is decoupled from the network layer thus rendering the problem a lot simpler to implement i.e. any type of network - GSM, WLAN or ad hoc - can be used. This decoupling is fundamental in understanding the key issues underlying ad hoc applications and in providing reusable solutions to solve these issues (in order to ease the development of ad hoc applications). Figure 1 describes a use case of mobile ad hoc applications which gives motivation (cf. II-C) to this paper.

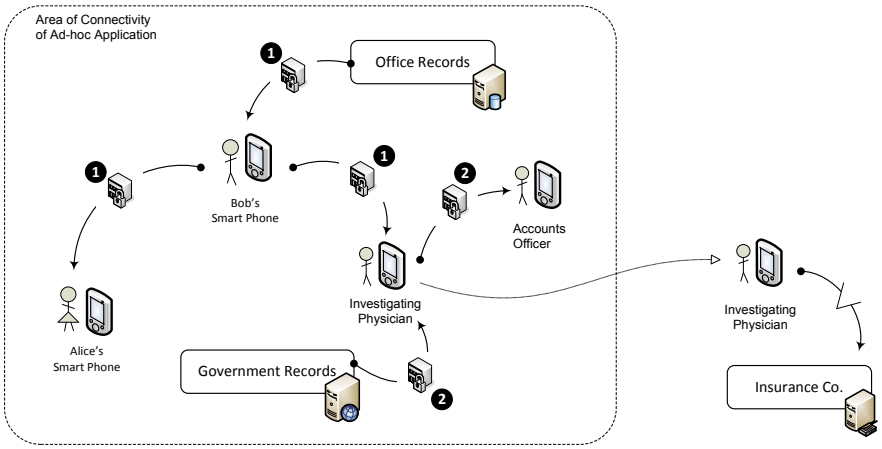


Fig. 1. An Example Ad-hoc Application

B. Usage Control

Usage control is a relatively new area in scientific research through which the usage of protected resources can be controlled. Contrary to traditional access control models, which specify the conditions under which an object can be accessed, usage control models allow the object owner to specify policies that dictate how an object is to be used. This broad definition encompasses such policy requirements as those specifying the purpose of the usage (privacy requirements), the extent to which the object can be used (DRM requirements) and even those that are the concern of traditional access control models. Thus, usage control is a superset of access control. Park and Sandhu [1] have introduced the concept of usage control and proposed a highly expressive and very powerful usage control model called UCON. This model formalizes the abstract idea of usage control through the concept of a usage session that is divided in *states*. Figure 2 shows these states. A subject can request an object from state *requesting* and can transition to *accessing* (if access is granted) or *denied* (if it is not). While in accessing state, the conditions are continuously checked to ensure that they are still being satisfied. If they are not satisfied at any time, access is *revoked*. This feature is called *continuity of access decisions*. If the subject ends access itself, the usage session moves to state *end*. Moreover, values of attribute associated with objects can be updated before access is granted (*preupdate*), while in accessing state (*onupdate*) or after access has been revoked or ended by the subject (*postupdate*). This is termed as *mutability of attributes*. Semantics of UCON have been studied at length in [9], [10].

The concept of distributed usage control has also been studied in detail in the past [2], [3].

C. Motivating Usecase

We motivate the need for creating a usage control architecture for mobile ad-hoc applications through a real-world use case describing the handling of an insurance claim. Consider a scenario in which a meeting room is arranged for the handling of an insurance claim filed by Bob. In figure 1 the dotted line shows the boundaries of the application network domain. The meeting is attended by Bob, his secretary, an accounts officer from Bob's firm and an investigating physician from the insurance company. It is the responsibility of the investigating physician to establish that Bob's claim is in fact genuine. Bob shares his health records with all of the participants of the meeting but requires that they only have access to the records during the meeting. After the meeting finishes (signified by the departure of all participants) or if a participant leaves the meeting room, the data released to his or her device must be purged and no longer accessible to the device owner. This way, Bob's medical records are keep secure while still enabling their use during a meeting session enabled by an ad-hoc application. shows the Below, we describe how a usage control engine running on the mobile devices operated by the participants can cater to these and other fine-grained requirements.

III. Usage Control for Mobile Ad-hoc Applications

We base our architecture on the work of Cai [11]. Our meeting room is a 'capable zone'. a circular region centered on its current position with a user-defined radius. Any mobile node having mobile application can run in promiscus mode where it can get to know about the neighboring applications and share resources along side. Each application interacts with the context manager for any object usage. The context manager can get envoironment attributes such as location and time etc. In this section first we define the requirements of the system

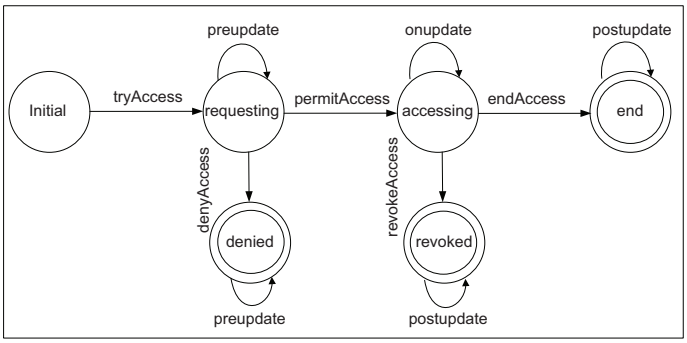


Fig. 2. The UCON Model States

and then specify the policy while in the third section discuss the revocation issue.

A. Requirements

We propose the following requirements for the design of our usage control system:

1) *Expressive power:* Usage control is one of the most expressive policy models thus requires to cover various types of policies. Further it should covers many real-world scenarios. Implementation of usage control engine in MA-APP must be able to specify various usage control features like *attribute mutability* and *decision continuity*.
2) *Efficiency:* As the continuous observation of the object during its use needs alot of computational resources, therefore our usage control engine should introduce little overhead. The applicability of the usage control in this scenario depends on efficiency of this system.
3) *Easy to use:* End user should be able to specify usage policies in an easy way. Although the policy language for usage control will not be that simple for novice users still it should be easy to understand for them.
4) *Battery Life:* Battery life has been a major problem in the mobile devices. Our target architecture should be optimized to use less battery i.e. should be less computationally intensive to consume less battery. The primary objective of the decentralized usage control architecture is to generate less traffic and take decisions locally.
5) *Standardization:* There are certain policy specification standards available for complex policy specifications. So our policy language should also be based on some standardized syntax. An esoteric or proprietary policy syntax is not desirable in normal scenarios.
6) *Portable:* A successful implementation of a UCON engine can be portable to different platforms without major code changes. As the engine needs to be deployed on different type of systems including mobile and hand held devices.

Now we mention how do we meet these requirements in a platform independent deployment of mobile ad hoc application. Our architecture is based upon the widely accepted usage control model – UCON [1] – that divides a *usage session* in different states as shown in figure 2. These modules are discussed in detail below (cf. Figure 3):

1) **Authentication Module:** UCON while being an authorization model still needs to have an authentication module as its integral portion to provide identity of the peer applications and nodes. The implementation of the authentication mechanism is still remains outside our scope. However authentication module provides the abstraction of the authentication details from the rest of the UCON engine.
2) **Context Manager:** Context of the usage is one of important aspect of the design. The main responsibility of the context menager is to take all the requests to the objects and forwarding them to the corresponding modules within the UCON engine. This module is also responsible for managing the continuity requirements of the system and recording information related to various subjects and objects. It has the capability of communication with the access manager to allow state transitions and to receive notifications of decisions regarding different requests from the access manager.
3) **Access Manager:** Because of the expressive nature of the usage policies it allows the specification of various types of policies. These policies are parsed and evaluated by the 'policy evaluation module' through the access manager. The PEP requests the policy evaluation module through access manager to evaluate the different policies associated with their respective objects. This module is also responsible for providing updates to the attribute update manager and attribute reader to change and retrieve the attributes associated with subjects and objects.
4) **Policy Evaluation Module:** In UCON there are different policies associated with different states of access e.g. requesting, accessing etc. When the access manager requests for the evaluation of an individual policy of the corresponding state of the system, this module parse the policies, evaluate the predicates and calculate update values. After retrieval of the attributes through attribute reader and updated using update managers this information is passed through the access manager.
5) **Schemas:** In accordance with the requirement of standardization, the policies and attributes for subjects and objects are defined through the widely adopted standard of inter-operability – XML. The policies and metadata must adhere to the schemas defined for their respective types. Note that subjects are a subset of objects in UCON and therefore, their schema are derived from that of the objects.
6) **Resource Manager:** This entity is responsible for the protection of the resource from any unauthorized access. A hardware based security chip can ascertain the proper enforcement of the policy. This particular chip being introduced by the Trusted Computing Group is known as TPM. This cryptographic chip comes built-in to most of todays commodity systems that is capable of providing trusted execution and is based on strong security. The binding security feature of this chip allows an object to be associated with a specific system state. In our case only a trusted machine would be to decrypt the object. By binding the data using the public portion of a specific TPM's key, it can be ensured that only an application which has the private portion of the key can access the object. For further capabilities of the TPM we refer the reader to [12].

B. Policy Specification

Usage control policy like other access control policies has a set of subjects, objects and rights. Subjects are the users at mobile nodes while objects are the shared entities that can be used by the subjects. In addition to that certain conditions are also stated to specify the constraints on the usage of the

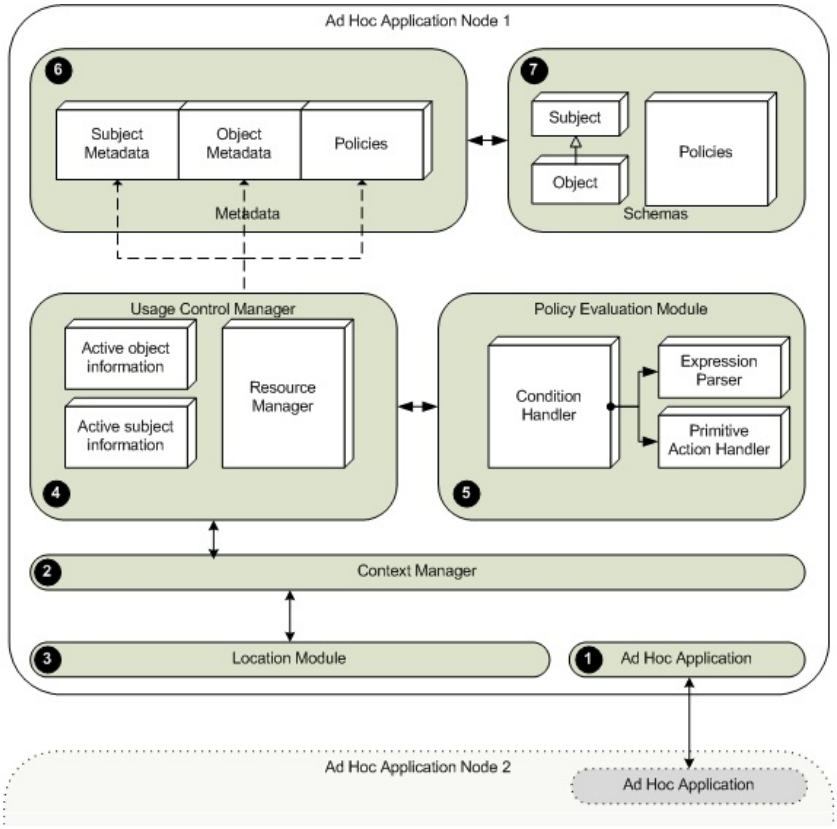


Fig. 3. Usage Control Framework for Ad Hoc Applications

object by a specified subject. In the example policy depicted in figure 4, show list of subject as *Physician* and *Alice*, object as *HealthRec*. Conditions are specified as an expression which can further have sub-expression that as whole needs to give a positive result for enabling subjects to execute the specified permission on objects. The conditions specified in the example policy states mentioned subjects can read the document if the location is MeetingRoom, and time is between 1:00PM to 5:00PM. Further at a time only two subjects can access this document. Usage control policy specification has been studied in detail [13], [3], [14] but we need to keep a minimal set of policies that can suffice the use of ad hoc application requirements.

C. Revocation Concerns

One of the most important issue that needs to be addressed while enforcing usage control is that of revocation of the resource when it is already given to a peer node for usage. As resources are released to the peers with the policy, according to which the resource needs to be used. The context awareness of the ad hoc applications makes the usage control engine aware of the location of the node that

IV. Implementation

For the realization of the usage control in mobile ad hoc applications we use the already existing framework Pervaho [15]. The Pervaho platform is founded on a location-based service, which allows mobile peers to interact in a flexible and anonymous manner, based on their collocation at the time of the interaction. We have changed the libraries of Pervaho middleware to enable the applications to enforce usage policies based on the location of the peers.

One contribution in this paper is that we enable ad hoc applications to enforce usage control while they release documents to the peers. Further through usage control engine, we ensure that the network traffic is kept to a minimum thus increasing battery life i.e. instead of transmitting and receiving all data, we keep copies on the device. The policies specified by the owner of the resources are enforced at the peer node.

V. Conclusion

Mobile adhoc applications are fast gaining popularity due to their added advantages of being mobile and more personal for the end users. Releasing sensitive information in such applications to parties outside the owner's control is an important security concern. Existing access control models fail to address the needs of such scenarios. In this paper, we have described the use of UCON – a comprehensive usage control model – for controlling access to resources even after they have been released outside the owner's boundary of control. We have provided a comprehensive XML-based policy language – that allows owners to specify their policies – as well as the implementation details of our architecture. Our architecture enables specification of fine-grained policies based on subject and object attributes including environment attributes such as location and time of day etc.

```
<?xml version="1.0" ?>
<p:PolicySet xmlns:p="http://our-domain-omitted/mbar/UCONPolicy"
  xmlns:xsi="http://www.w3.org/2001/XMLSchema-instance"
  xsi:schemaLocation="http://our-domain-omitted/mbar/UCONPolicy ../schemas/UCONPolicy.xsd ">

  <p:Policy PolicyType="PermitAccess">
    <p:Target>
      <p:Subjects>
        <p:Subject>Alice</p:Subject>
        <p:Subject>Physician</p:Subject>
      </p:Subjects>
      <p:Objects>
        <p:Object>HealthRec</p:Object>
      </p:Objects>
      <p:Rights>
        <p:Right>Read</p:Right>
      </p:Rights>
    </p:Target>
    <p:Condition CombiningAlgorithm="edu.serg.mbar.algorithms.combiningalgorithms.All">
      <p:Expression FunctionID="edu.serg.mbar.algorithms.functions.LogicalAnd">
        <p:Expression
          FunctionID="edu.serg.mbar.algorithms.functions.StringEqual">
          <p:ObjAttribute>
            <p:RequestingSubject ></p:RequestingSubject>
            <p:AttrName>Location</p:AttrName>
          </p:ObjAttribute>
          <p:Constant DataType="String">MeetingRoom</p:Constant>
        </p:Expression>
        <p:Expression
          FunctionID="edu.serg.mbar.algorithms.functions.LessThan">
          <p:ObjAttribute>
            <p:RequestedObject/>
            <p:AttrName>
              SimultaneousReads
            </p:AttrName>
          </p:ObjAttribute>
          <p:Constant DataType="Integer">3</p:Constant>
        </p:Expression>
        <p:Expression FunctionID="edu.serg.mbar.algorithms.functions.LogicalAnd">
          <p:Expression FunctionID="edu.serg.mbar.algorithms.functions.TimeGreaterThan">
            <p:Expression FunctionID="edu.serg.mbar.algorithms.functions.EnvironmentVariable">
              <p:Constant DataType="String">CurrentTime</p:Constant>
            </p:Expression>
            <p:Constant DataType="Time">1300</p:Constant>
          </p:Expression>

          <p:Expression FunctionID="edu.serg.mbar.algorithms.functions.TimeLessThan">
            <p:Expression FunctionID="edu.serg.mbar.algorithms.functions.EnvironmentVariable" >
              <p:Constant DataType="String">CurrentTime</p:Constant>
            </p:Expression>
            <p:Constant DataType="Time">1700</p:Constant>
          </p:Expression>
        </p:Expression>
      </p:Expression>
    </p:Condition>
  </p:Policy>
```

Fig. 4. A Sample Usage Control Policy for the Budget Document

One of the important future directions along this line of research is the deployment of our architecture on an existing real-world mobile adhoc application. This will allow us to measure the adaptability of our architecture to third party applications. By making our architecture modular, we have the problem half solved. However, taking the final steps in making this architecture adaptable to any existing application would be an important new step in the mobile adhoc application research.

REFERENCES

[1] Park, J., Sandhu, R.: Towards Usage Control Models: Beyond Traditional Access Control. In: SACMAT '02: Proceedings of the seventh ACM Symposium on Access Control Models and Technologies, New York, NY, USA, ACM Press (2002) 57–64

[2] Pretschner, A., Hilty, M., Basin, D.: Distributed usage control. Communications of the ACM **49**(9) (2006) 39–44

[3] Hilty, M., Pretschner, A., Basin, D., Schaefer, C., Walter, T.: A policy language for distributed usage control. Computer Security–ESORICS 2007 (2008) 531–546

[4] Kortuem, G., Schneider, J., Preuitt, D., Thompson, T., Fickas, S., Segall, Z.: When peer-to-peer comes face-to-face: Collaborative peer-to-peer computing in mobile ad hoc networks. p2p (2001) 0075

[5] Ding, G., Bhargava, B.: Peer-to-peer file-sharing over mobile ad hoc networks. In: Pervasive Computing and Communications Workshops, 2004. Proceedings of the Second IEEE Annual Conference on, IEEE (2004) 104–108

[6] Klemm, A., Lindemann, C., Waldhorst, O.: A special-purpose peer-to-peer file sharing system for mobile ad hoc networks. In: Vehicular Technology Conference, 2003. VTC 2003-Fall. 2003 IEEE 58th. Volume 4., IEEE (2004) 2758–2763

[7] Joa-Ng, M., Lu, I.: A peer-to-peer zone-based two-level link state routing for mobile ad hoc networks. Selected Areas in Communications, IEEE Journal on **17**(8) (2002) 1415–1425

[8] Garbinato, B., Rupp, P.: From ad hoc networks to ad hoc applications. In: Proceedings of the 7th International Conference on Telecommunications, Citeseer (2003) 145–149

[9] Zhang, X., Parisi-Presicce, F., Sandhu, R., Park, J.: Formal Model and

Policy Specification of Usage Control. ACM Trans. Inf. Syst. Secur. **8**(4) (2005) 351–387
[10] Katt, B., Zhang, X., Breu, R., Hafner, M., Seifert, J.: A General Obligation Model and Continuity: Enhanced Policy Enforcement Engine for Usage Control. In: Proceedings of the 13th ACM symposium on Access control models and technologies, ACM New York, NY, USA (2008) 123–132
[11] Cai, Y., Xu, T.: Design, analysis, and implementation of a large-scale real-time location-based information sharing system. In: MobiSys '08: Proceeding of the 6th international conference on Mobile systems, applications, and services, New York, NY, USA, ACM (2008) 106–117
[12] TCG: Trusted Computing Group (2010) http://www.trustedcomputinggroup.org/.
[13] Zhang, X., Parisi-Presicce, F., Sandhu, R., Park, J.: Formal model and policy specification of usage control. ACM Transactions on Information and System Security **8**(4) (2005) 351–387
[14] Katt, B., Zhang, X., Breu, R., Hafner, M., Seifert, J.: A general obligation model and continuity: enhanced policy enforcement engine for usage control. In: Proceedings of the 13th ACM symposium on Access control models and technologies, ACM (2008) 123–132
[15] Eugster, P., Garbinato, B., Holzer, A.: Pervaho: A development & test platform for mobile ad hoc applications. In: Mobile and Ubiquitous Systems-Workshops, 2006. 3rd Annual International Conference on, IEEE (2007) 1–5

A Novel Method for Achieving Load Balancing in Web Clusters Based on Congestion Control and Cost Reduction

Ahmad Yousofi
Computer Department, Islamic Azad University Naein Branch, Iran
a.yousofi@yahoo.com

Mostafa Banitaba
Computer Department, Islamic Azad University Naein Branch, Iran
ma_banitaba@yahoo.com

Saeed Yazdanpanah
Computer Department, Islamic Azad University Khorramabad Branch, Iran
yazdanpanah_saeed@yahoo.com

***Abstract* - The World Wide Web is fundamental infrastructure for different services. The number of accessing to web sites is significantly increasing. Cluster-based web systems (web-cluster) are a new solution to implement a web server system with high efficiency and availability. In practice, a web cluster consists of several web servers, and a web switch which distributes user's requests among server nodes. Achieving high efficiency from web cluster requires load balancing between web servers. In this paper, we propose a novel dispatching policy, namely Multi-Class Round Robin with Congestion Control and Cost Reduction (MC-RR-CC-CR), for web switches operating at layer 7 of the OSI protocol stack. The results of a real scenario showed that the proposed method can significantly balance the load of web cluster and substantially improve the system efficiency. Particularly when web cluster is heterogeneous and web site content is dynamic.**

1. INTRODUCTION

Most public web sites are suffering from severe congestion, when thousand requests arrive at them every second. Moreover, heterogeneity and complexity of services and application provided by web service systems is continuously increasing.

To deal with this problem three solutions are considered as follows.

1- Replacing existing machine with a faster model
2- Geographically distributed web servers [3].
3- Cluster systems.

In [1,2] it is shown that the third solution is best and most effective solution.

A cluster refers to a group of independent computers that working together (run program) to provide an integrated image of system for users and costumers. The cluster increases scalability, accessibility and reliability.

A new solution for increasing operational power of web sites, is the application of a cluster which increase scalability, accessibility and reliability of web sites [1,2,4]

One of main operational aspects of a cluster-based web system is the availability mechanism that shares the load among over the server nodes.

Unlike the traditional distributed systems, a web cluster is subject to quite different workload, especially when the web cluster provides heterogeneous services. Thus, the load characteristics reaching a web cluster have motivated proposals of global scheduling strategies based on dynamic server state information. So far different methods have been presented in aim of increasing load balance using dynamic information. Unfortunately none of them has considered congestion control of web cluster and its cost reduction.

In this paper, we propose a novel dispatching policy, namely Multi-Class Round Robin with Congestion Control and Cost Reduction (MC-RR-CC-CR), which distributes the load based of client and server state information. It avoids congestion in servers and it uses fewer server when the input load of web is low therefore it reduces the web cost. The next sections of the present study are organized as follow:

In section 2, briefly present the web cluster architecture, with real examples, web switches and the goals of load distribution algorithms in web switches. In section 3, describe the suggested algorithms. In section 4, a model is presented to evaluate the suggested method with previous methods. In section 5 evaluation and results are presented.

Finally in section 6 conclusions are presented.

2. Web Cluster

2.1. Architecture

A cluster-based web system (briefly, Web cluster) refers to a set of server machines that are situated in a single location and are interconnected through a high speed network and present a single system image to the outside world.

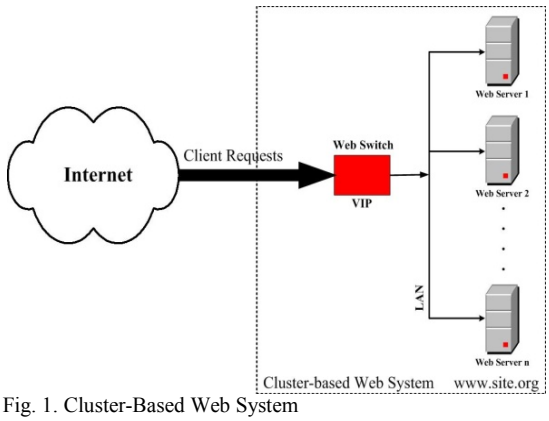


Fig. 1. Cluster-Based Web System

As it is shown in "Fig.1," a web cluster may consist of tens of nodes. But this set is identified with a name (www.site.org) and a virtual IP address. It should be noted that VIP address is corresponds to web switch address.

Today scientific and business products emphasize on the usefulness of this kind of web architecture. for example we can refer to IBM TCP[5], Mgicrouter[6], Distributed packet Rewriting [7], Cisco Local Director[8], IBM network dispatcher[9].

2.2. Web Switches

A key element of any web cluster is web switch. Because a web switch dispatches client requests among server nodes. Generally they can be divided into two groups according to the OSI protocol stack layer at which they operate: layer-4 and layer-7 web switches [4].

Layer-4 web switches work at TCP/IP level. Layer-4 web switch algorithms are content information blind, because they choose the target server when the client asks for establishing a TCP/IP connection, on the arrival of the first TCP SYN packet at the web switch. As the client packets do not reach the application level, the routing mechanism is efficient but the dispatching policies are unaware of the content of the client request.

Layer-7 web switches can execute content-aware routing. The switch first establishes a complete TCP connection with the client examines the HTTP request at application level and then relays it to the target server. This routing mechanism is much less efficient, but it can support more sophisticated dispatching policies. Therefore layer-7 web switches can achieve a better load balance in comparison with layer 4 web switches

In [21] it is shown that content-aware algorithms can improve the efficiency of cache in comparison with content-blind algorithms.

2.3. Web Switch Algorithms

The web switch cannot use the sophisticated dispatching algorithms, because it has to make fast decisions for thousand requests per second. Generally, web switch's algorithms can divide in two static and dynamic groups. Due to higher efficiency of dynamic algorithms, we will describe this group in more details. Dynamic algorithm's classes are as follow:

Server state aware policies: in this method, web switch chooses the target serve based on some server state information, such as current and past load condition, latency time, network throughput, and availability.

Work-load aware policy distributes the requests based on workload of servers.

For example, can see WARD strategy [15].

Client state aware policies: in this method, web switch chooses the target server based on some client information. For example, can see SITA-E policy [14], and MC-RR policy [13].

Server and client state aware policies: in this method, web switch chooses the target server by combining client and server state information. For example, for layer-4 web switch, can see WRR policy [16] and for layer-7 web switch, can see LARD policy [12].

3. Suggested policies

Generally for obtain good performance of web cluster requires load balancing and minimize disk accesses [22].

In this paper, we focused on load balancing. To this end, we propose a novel dispatching policy, namely Multi-Class Round Robin with Congestion Control and Cost Reduction (MC-RR-CC-CR). Since the main idea of this policy results from Multi-Class Round Robin policy and Token Bucket, we first introduce Multi Class Round Robin policy and then Token Bucket in sections 3-1, 3-2 respectively. Then in section 3-3 the suggested policy with some real examples are completely described.

3.1. Multi-Class Round Robin policy [13]

Multi-Class Round Robin policy estimates the requested service time in order to improve load sharing in web cluster. In fact, most load balancing problems occur when the web site hosts heterogeneous services that make an intensive use of different web server's components.

For this reason, MC-RR policy divides services, based on using of main resources into four main classes:

1. Static and lightly dynamic services (SLD).
2. CPU bound services (CB).
3. Disk bound services (DB).
4. CPU and disk bound services (CDB).

Although a web switch cannot estimate precisely the service time of a client request, from the URL it can distinguish the class of the request and its impact on main web server recourses.

3.2. Token Bucket Algorithm

A token bucket is a common algorithm used to control the amount of data that is injected into a network, allowing for bursts of data to be sent.

The bucket contains tokens, each of which can represent a unit of bytes or a single packet of predetermined size. Tokens in the bucket are removed for the ability to send a packet. The network traffic engineer specifies how many tokens are needed to transmit how many bytes. When tokens are present, a flow is allowed to transmit traffic. If there are no tokens in the bucket, a flow cannot transmit its packets.

In "Fig. 2," you observe a computer whose bucket has 3

tokens. Five packets are waiting for sending .whenever a packet is going to sent it first has to get a token and then destroy it. In "Fig. 3," you can see 3 packets out of 5 packets are sent by computer. Due to lack of token the other 2 packets are waiting for sending.

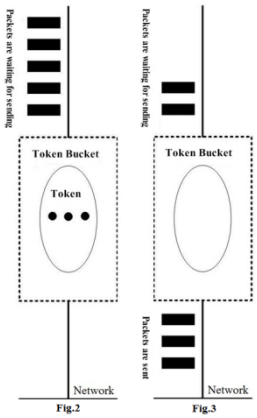


Fig. 2. Computer before Sending Packets
Fig. 3. Computer after Sending Packets

Based on the above mentioned subject, a bucket is considered in web switch. Considering the operational power of web cluster, there are number of tokens in bucket. A client request is accepted only when there is a token in the bucket, otherwise request is not accepted. So congestion is avoided in web cluster.

3.3. Multi Class Round Robin Policy with Congestion Control and Cost Reduction

Multi class Round Robin policy with congestion control and cost reduction (MC-RR-CC-CR) is implemented on layer-7 web switch. This policy is a content aware and dynamic policy. On the other hands this policy uses client and server state information. Also this policy by congestion control algorithm named token bucket carry out congestion control in web cluster. And it attempts to reduce the cost of web cluster to the minimum level.

Better to describe this policy the following questions must be answered:

1. how does this policy become aware of customer state?
2. how does this policy become aware of server state?
3. how does this policy carry out control congestion in web cluster?
4. how does this policy reduce the web cluster's cost?
5. how does this policy carry out load balancing among web servers?

Answer to the question 1:
A web switch can obtain the kind of requested services from URL; hereto web switch becomes aware of client state.

Answer to the question 2:
Each Web server has to inform its load to Web switch when its load is 0% or 25% or 75% or 100%, hereto web switch becomes aware of servers state.

Answer to the question 3:
This policy has a manager named token manager that generates number of tokens for each web server. In practice the number of tokens for each server can be estimated based on server's processing power.

Achieving a goal, token manager are numerated server nodes from 1 to n and considers C_1 to C_n to their processing power.
Now considering the above mentioned hypothesis, the number of tokens for each server is estimated from formula 1:

$$N_{Max,i} = \alpha_i \times N_{Max} \quad (1)$$

$N_{Max,i}$: Maximum number of tokens for i^{th} server

$\alpha_i = C_i / C_{Max} \qquad 0 \le \alpha_i \le 1$

C_{Max} : Maximum (C_1,C_2,…C_n)
N_{Max} : The number of token for C_{Max}

Whenever a web server reports its load to web switch, token manager using of formulae 2 correction number of tokens i^{th} server and thus to avoid the congestion in web cluster.

$$N_i = (100\% - L_i) \times N_{Max,i} \quad (2)$$

N_i : the number of tokens of i^{th} server
L_i : the current load of i^{th} server.

Answer to question 4:
This policy has a manager named cost manager, that whenever a web server reports its load to web switch, cost manager using of formulae 3 and 4 activate or inactivate the number of servers and thus reduces the web cluster's cost .

$$L_S = \sum_{i=1}^{n} L_i \quad (3)$$

n: is the number of active servers
L_i : the current load of servers i

$$1 \le m < n \quad \square \quad L_s \le 75 \times m \quad (4)$$

If m was founded
Inactivate (n-m-1) server
Else
Activate one of the inactive servers.

It should be noted that it is possible to combine cost and token managers. Because they need same information. For more clarity they are considered separately.

Answer to question 5:
To obtain load balance, this policy divides the services of web cluster in to four groups. Then for each service considers the number of different tokens (see table1).

Table 1
TOKEN ASSIGN AT SERVICE

Type Service	Number of tokens
static and dynamic light	1
CPU bound	4
disk bound	6
CPU and disk bound	8

The policy has a scheduler that operates as follow:

When a client request was accepted and was selected target server, scheduler is correct the number of tokens target server according to formula 5 (if the number of tokens less than number of tokens request, client request will not be accepted).

$$N_i = N_i - n_j \qquad \text{j=SDL, CB, DB, DCB} \qquad (5)$$

Scheduler for each type provided service in web cluster, should consider a circular queue.

Although a web switch cannot estimate precisely the service time of a client request, from the URL it can distinguish the class of the request and its impact on main web server recourses.

According to these points, whenever a scheduler receive a request, given URL of that request, it identify the type of services. Then using circular queue, it finds the target servers. Scheduler acts in accordance with the following pseudo code:

```
While (true)
        {
          Accept (client);
          Receive (request);
          j=Analyze_Request (request);
          i=Select_Server (Request_type );
          K=1;
          While ( nj > Ni  and  K<= number of server )
             {
                i =Next_server(Request_type);
                 K=K+1;
             }
          If (K > number of server )
                Reject(client) ;
          else
             {
                Send request to ith  server;
                Ni = Ni - nj
             }
        }
```

Analyze_Request function: return type of service

Select_Server function: return number 's server according to type of service and circular queue considered for type of service

Next_server function: return next number's server according to type of service and circular queue considered for type of service

According to the above mentioned point a web switch which is going to use MC-RR-CC-CR should have main modules as it is shown in "Fig. 4," : token manager, cost manager and scheduler.

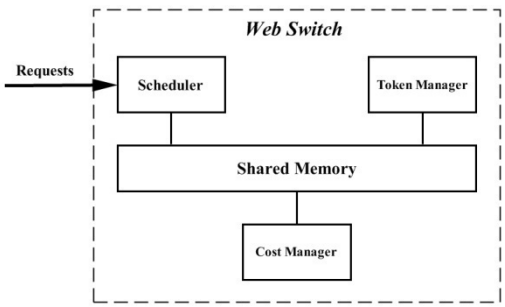


Fig. 4. Block Diagram of Web Switch Which is Going to Use MC-RR-CC-CR

4. A Model for Testing:

In order to compare the suggested policy (MC-RR-CC-CR) to the previous policy we applied an empirical study.

By connecting five computers using, local Ethernet with bandwidth 100Mbps, we produced a web cluster at laboratory level. Of these five nodes, four are considered as a server and one is considered as web switch (see "Fig. 5").

For simulation of client we used two separate computer with webstone[18] software.

The general procedure is that two separated machines send the request to web switch using web stone software. Then our parameters are stored in several files. Then through these parameters we compare the related policies.

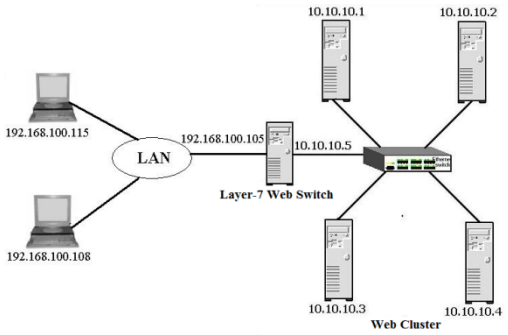


Fig. 5. A Model for Testing

5. Evaluation

5.1. Comparison of CD-CC-MC-RR policy with MC-RR:

Since CD-CC-MC-RR policy is derived from MC-RR policy, evaluation of these two policies considering load balance doesn't seem appropriate. Since load distribution method is the same in both policies with the exception that CD-CC-MC-RR policy avoids congestion in the cluster, and attempts to reduce the cost of cluster, we examine these two policies according to their congestion control and the number of active servers when increases the number of requests.

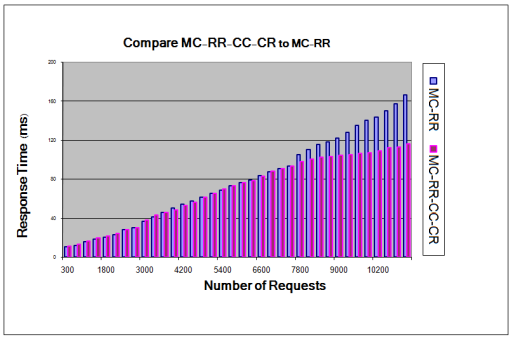


Fig. 5. Comparison of CD-CC-MC-RR Policy with MC-RR (Congestion Control)

Based on "Fig. 5," it is observed that the average response time in MC-RR is higher in comparison with CD-CC-MC-RR policy when congestion occurs in web cluster. Because in MC-RR policy congestion is not controlled.

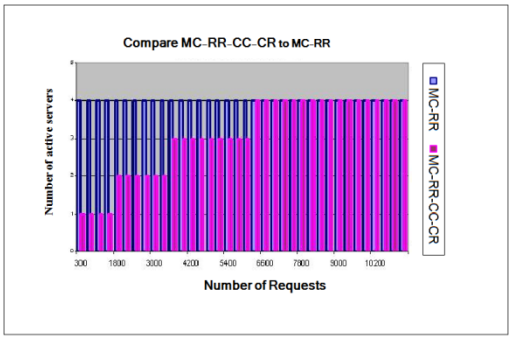


Fig. 6. Comparison of CD-CC-MC-RR Policy with MC-RR (Number of Active Servers)

According to "Fig. 6," it is shown that when the number of requests are low, in MC-RR-CC-CR policy the fewer servers are used. Because in MC-RR cost control is not performed.

5.2. The Comparison of MC-RR-CC-CR Policy with Random and Round Robin Policies:

Since the MC-RR-CC-CR policy is quite different from Round Robin (RR) and random policies in nature, to compare these policies, the measurement is the amount of unbalance factor of load in server processors.

The amount of unbalance factor (UF) is derived from load balance measurement (LBM) [23]. but LBM is presented for a system with n servers and m sampling is expressed as Formula 6.

$$LBM = \frac{\sum_{j=1}^{m} peak_load_j}{\sum_{j=1}^{m}\sum_{i=1}^{n} load_{i,j} / n} \quad (6)$$

$Load_{i,j}$: load of server i (of n server) at the j^{th} sampling point (of m such points).

$Paek_load_j$: highest load on any server at the j^{th} sampling point.

In fact, LBM represents the ability of dispatcher policy; share the load among services of cluster.

Given the above mentioned points, UF equals the difference between LBM from the best value of LBM when the load is quite balanced among servers.

Then through formulate we estimate the degree of UF. The more it approaches to zero, the more balanced is the load in web.

$$UF = \frac{LBM - 1}{n - 1} \quad (7)$$

It should be noted that we have to register the amount of processor load of each server every ten second. Then using formulate 7, we calculate the amount of unbalance factor. To improve the comparison of these policies the following scenarios are considered.

1. 80% of requests are static and 20% is dynamic.
2. 60% of requests are static and 40% are dynamic. The results of these scenarios are presented in "Fig. 7 and Fig. 8," respectively.

As it stated "Fig. 7 and Fig. 8," shows the amount of unbalance factor among server node. It is clear that the amount unbalance factor in MC-RR-CC-CR policy compared to Round Robin and Random policies is low. This shows that MC-RR-CC-CR significantly balance load of the web cluster system.

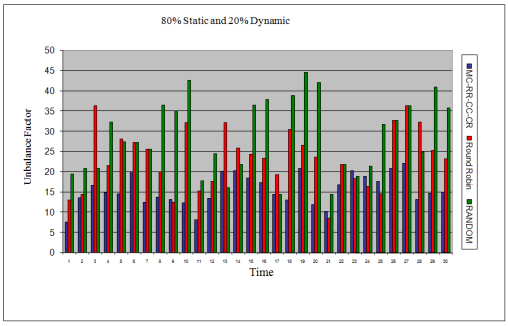


Fig. 7. Comparison of MC-RR-CC-CR Policy with Random and Round Robin Policies (80% Static and 20% Dynamic)

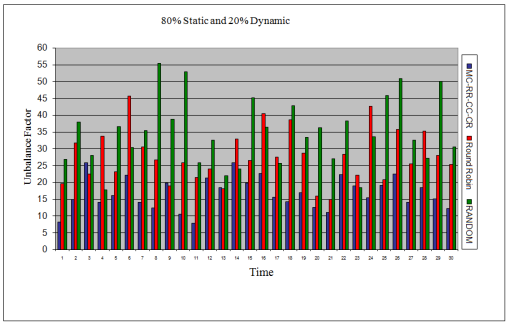


Fig. 8. Comparison of MC-RR-CC-CR Policy with Random and Round Robin Policies (60% Static and 40% Dynamic)

6. CONCLUSION

web cluster is a fundamental solution to support web sites whose access to which increases exponentially. They have heterogeneous services: in this paper, we proposed a new algorithm named Multi Class Round Robin policy with Congestion Control and Cost Reduction. (MC-RR-CC-CR) for a web switch which operates in layer 7 of stack protocol OSI.

Then we showed that MC-RR-CC-CR can improve the efficiency business sites and transactional sites whose services are a combination of dynamic and security services. Moreover, we showed that MC-RR-CC-CR is an appropriate policy for those web clusters that provide heterogeneous services or whose server nodes don't possess the same operational power or those clusters that are the combination of these two states. Then showed that, it policy improves performance of web cluster significantly, and reduces the cost of web cluster.

REFRENCE

[1] A. Yousofi, M.K. Akbari, "Content aware dispatcher algorithm for heterogeneous web clusters", Proc. Of 12th international CSI Computer

Conference (CSICC2007), Electrical and Computer Engineering Faculty, Shahid Beheshty University, 20–22 February 2007.
[2] A. Yousofi, M.K. Akbari, " New dynamic algorithm for load balancing of homogeneous and heterogeneous web clusters base on congestion control", Proc. Of 15th Int. Iranian Conference Electrical Engineering (ICEE2007), Iran Telecom Research Center(ITRC), 15-17 may 2007.
[3] V. Cardellini, M. Colajanni and p.s. Yu, "Geographic load balancing for scalable distribution web system.", proc. Of MASCOTS' 2000, IEEE computer society, San Francisco, CA, Aug. 2000.
[4] T. Schroeder, S. Goddard, B. Ramamurthy, "scalable web server clustering technologies" IEEE Network, May-jun 2000, pp. 38-45.
[5] D.M. Dias, W. kish, R.Mukherjee, R.Tewari, "A scalable and highly available web server", Proc. Of 41st IEEE Computer Society Intl. Conf. Feb. 1996, pp. 58-92.
[6] E.anderson, D. Patterson and E. Brewer, "The Magicrouter, an application of fast packet interposing", unpublished Tech. Rep., Computer Science Department, University of Berkeley, May 1996.
[7] A. Bestavros, M. E. Crovella, J.Liu, D. Martin, "distributed Packet Rewriting and its application to scalable server architectures", Tech. Rep. BUCS-TR-98-003, Computer science Department, Boston University, Dec. 1997.
[8] Cisco's LocalDirector. Available online at http://www.cisco.com/warp/public/cc/pd/cxsr/400/
[9] G.D.H. Hunt, G.S. Goldszmidt, R.P. King and R.Mukherjee, "Network Web switch: A connection router for scalable Internet services", Proc. Of 7th Int. World Wide Web Conf., Brisbane, Australia, April 1998.
[10] M.Harchol-Balter, M.Crovella, C.Murta, "On choosing a task assignment policy for a distributed server system", J. of parallel and Distributed Computing, Vol.59, pp. 204-228, 1999.
[11] C.-S. Yang and M.-Y. Luo, "A content placement and management system for distributed Web-server systems", Proc. Of IEEE 20th Int. Conf. on Distributed Computing System, Taipei, Taiwan, Apr. 2000.
[12] Vivek S.pui, M.Aron, G.Banga, M.Svendsen, P.Druschel, W. Zwaenepcel and E.Nhum, "locality-aware request distribution in cluster-based network servers", In Proc. Of 8th ACM Conf. on Architectural Support for Programming languages and operating system, Sun Jose, CA, Oct.1998.
[13] E. Casalicchio and M. Colajanni, "Content-aware Dispatching Algorithms for Web clusters providing multiple service, in: Proc. Of 10th Int'l Word Wide Web Conf., Hong Kong (May 2001).
[14] M. Harchol-Balter, M. E. Crovella, and C.D. Murta, On choosing a task assignment policy for a distribution server system, J. of Parallel and Distribution Computing, 59(2) (1999) 204-228.
[15] L.Cherkasova, M.Karlsson. "Scalable Web Server Cluster Design with Workload-Aware Request Distribution Strategy WARD," wecwis, pp. 212-221, Third International Workshop on Advanced Issues of E-Commerce and Web-Based Information Systems (WECWIS '01), 2001.
[16] E. Casalicchio and M. Colajanni, "Scalable Web Clusters with Static and Dynamic Contents"", Proc. Of IEEE 20th Int. Conf. on Distributed Computing System, Taipei, Taiwan, Apr. 2000.
[17] Computer Networks (FOURTH EDITION).
Tanenbaum, Andrews. 2003.
[18]Mindcraft Software, http://www.mindcraft.com/webstone.
[19] M. Andreolini, M. colajanni, and M. Nuccio, "Scalability of content-aware server switch for cluster-based Web information system," WWW2003, May 20-24, 2003, Budapest, Hungary.
[20] P.D.Michailids and K.G.Margaritis, Performance valuation of load balancing strategies for approximate string matching application on an MPI cluster of heterogeneous workstations, Future Generation Computer System (FGCS), pp. 1705-1104, 11 March 2003.
[21] X.Tang and S.T.Chanson, On caching effectiveness of web clusters under persistent connections, Distributed Computing, pp. 981-995, 14 May 2003.
[22]W.H.Ahn, W.J.Kim and D.Park, Content-aware cooperative caching for cluster-based web servers, The Journal of System and Software 69 (2004), pp. 75-86.
[23] R.B. Bunt, D. L. Eager, G. M. Oster, and C.L. Williamson. Achieving load balance and effective caching in clustered Web server. In proc. Of 4th Int'l Web Caching Workshop, page 150-169, San Diego, CA, Apr. 1999

A Mobile Service Architecture for improving Availability and Continuity

Nor Shahniza Kamal Bashah[1], Ivar Jørstad, [2] Do van Thuan[3], Tore Jønvik[4] & Do van Thanh[5]

[1]Department of Telematics, NTNU, O.S. Bragstads Plass 2E, NO-7491 Trondheim, Norway- nor@item.ntnu.no
[2]Ubisafe, Gamleveien 252, 2624 Lillehammer, Norway- ivar@ubisafe.no
[3]Linus AS, Norway- t.do@linus.no
[4]Oslo University College, Norway- tore.jonvik@iu.hio.no
[5]Telenor & NTNU, Snaroyveien 30, 1331 Fornebu, Norway

***Abstract*- In mobile multi-network multi-domain environments services can be anything and can have any name. This poses problems for the service availability and consequently service continuity since services may not be discovered in time for being used. Services offering equivalent functions and capabilities such as GSM voice, IP telephony, etc. are usually considered as different by the network system and are not interchangeable. This paper proposes a mobile service architecture which enables the discovery and consumption of equivalent services. The solution provides also seamless service continuity by incorporating dynamic discovery of equivalent services with dynamic switching of available services. The solution offers personalisation while preserving both flexibility and control of the user. Although most of the storage and processing of data are located in the network the service continuity process is initiated, controlled and decided by the mobile device's side. A proof-of-concept including a client implementation on Android is presented.**

Keywords: Service continuity, service availability, voice call continuity, service transfer, handover, service personalisation

I. INTRODUCTION

A modern mobile environment consists of multiple network systems own and managed by different players such as home, enterprise, airport, shopping center, etc. The services offered by these network systems are usually not standardised. Consequently, the same services may have different names and different services may have same name. This creates problems for service availability and continuity simply because services are not discovered in order to be used. For example, a user talking using GSM voice service will have problem to find an IP telephony called chIPhone offered by a shopping center in order to transfer his call over. In fact, even though the user perceives the GSM voice service and chIPhone as equivalent these two services are completely different in terms of implementation, user interface and ownership and there is no relationship between them. In order to improve the service availability and to provide service continuity across network systems this paper proposes a new mobile service architecture that enables the unification of equivalent services and hence enhances the service availability and continuity for the user. The paper starts with an explanation of the motivations of the proposed architecture. Next, the related works are briefly reviewed. The concept of service is then clarified before the main part of the paper, which is the elaboration of the service continuity architecture. The proof-of-concept implementation is described thoroughly. Further works are given in the conclusion.

II. MOTIVATION

A. *Handling of equivalent services*

In a multi-network environment a service can be implemented using different architecture and technologies for different network systems resulting to different user interfaces. For example, the telephony or voice service can be implemented as GSM voice or chIPhone using IP technologies. Seen from the user these two services are equivalent since they both offer human-to-human voice communication. However, they are currently considered as completely unrelated. When the mobile device is moving connections to the network systems are also changing, a service currently in use e.g. GSM voice may no longer be available and another one e.g. chIPhone may appear. Unfortunately, the mobile device is not aware of the availability of this equivalent service in order to use it. Of course, the detection and swapping to the pop up service is not only motivated by the availability but also other factors like ease of use, performance, security, price, etc. Furthermore, when a service e.g. voice service is ongoing it is desirable that it is not interrupt. Service continuity is another required characteristic. Seen from the user it is valuable to be able to manage this sort of equivalent services in a uniform and simple way to improve service availability and preserve service continuity.

B. *Providing location-based services*

When travelling the mobile user will want to have access to the same services such as taxi, hotel, restaurant, flight booking, etc. which enable the necessary booking, modification, cancellation, etc. when needed. At first glance, the mentioned services look the same everywhere but a closer

look reveals the opposite. Indeed, when being in Trondheim the user will need to communicate with the Trondheim Taxi service and not the one in London. It is also desirable that the generic Taxi service switches to the right service according to the location automatically without the intervention of the user. In fact, it may be sometime difficult for the user to find the Taxi service in a country, e.g. China, Cambodia, etc. where a different language is used. Seen from the user it is valuable to seamlessly access the right service based on the location.

C. Offering personalised service

As human being each user will have some preferences related to the services and it will be very convenient if these preferences are remembered and dynamically re-applied to every equivalent service in use. In addition, the personal data such as personal details, address, phone numbers, contact list, etc. should also be shared between all the services. Seen from the user it is valuable to be able to use the service in a personalised way and personal data can be handled at one place.

III. Related Works

A. Service continuity works at NTNU

There have been works on service continuity related to the future mobile research activities carried out by Do and Jørstad [1][2]. The following definitions have been proposed in [3]:

"Seamless service continuity is the ability to pick up a service at a new Location, where service abruptness is bounded by the time it takes the user to move between the two Locations."

"Non-seamless service continuity is the ability to pick up a service at a new Location, where service usage can proceed from the 'point'/state where it was left at the previous Location, but where additional disruption is introduced due to a required reorganization of the service composition."

Several interesting concepts and theoretic models have been developed but no real implementation or usage has been achieved.

B. TISPAN (Telecoms & Internet converged Services & Protocols for Advanced Networks)

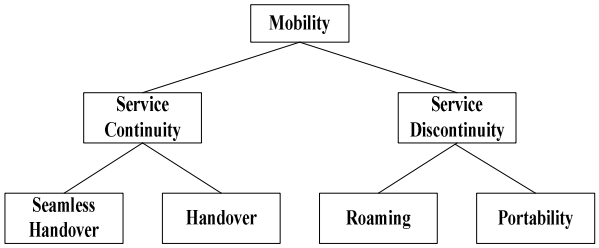


Fig. 1. TISPAN's mobility components

In their works of defining the European view of the Next Generation Networking (NGN), TISPAN has studied all the potential service capabilities and requirements [4] and defined the concept of service continuity as a component of mobility [5] as shown in Fig. 1.

More specifically, service continuity is defined as "*the ability for a user to maintain an ongoing service during mobility*"

Unfortunately, although the definition may imply continuity across different devices, it is not clearly stated.

C. 3GPP Voice Call Continuity (VCC) and GSMA VoLTE

The 3GPP has conducted studies described in TR 23.806 [6] and has elaborated in TS 23.2006 [7] the specifications of the Voice Call Continuity (VCC) which ensure the persistence of a voice call when the mobile phone moves between circuit switched and packet switched radio domains.

With the emergence of LTE (Long Term Evolution) paving the way for VoIP over all-IP mobile networks, it is necessary to ensure the continuity of voice calls when a user moves from an LTE coverage area to another without LTE. The GSM Association VoLTE (Voice over LTE) initiative endorses the IMS solution specified by 3GPP. VoLGA (over LTE Via Generic Access) is ensuring continuity by tunneling GSM voice over IP.

The focus of all these activities is the seamless switching between circuit switched voice and IMS voice, which are two well-defined services provided by mobile operators. Our work extends service continuity over non-standardised services.

D. IEEE Media Independent Handover (MIH)

The IEEE Working Group has introduced the 802.21 Media Independent Handover (MIH) Services [8] which allows the mobile terminal to detect the communication channels and services that are available in the vicinity. It facilitates the handover between heterogeneous networks and ensures seamless connectivity via the Media Independent Handover Function (MIHF) which is a logical entity in the mobility-management protocol stack of both the mobile node and the network elements.

With the 802.21, the Mobile Node can communicate with the visited MIH Information Server to acquire network information necessary for carrying out handover and preserving connectivity.

However, it can only support the service continuity if the same service implementation is used across all heterogeneous access networks. We extend the service continuity for future mobile service architecture where the services offered by different types of networks could be different in service implementation and using different components.

IV. Enhancing Availability And Providing Continuity

A. Clarification of the service concept

Service is a concept which is broadly used by numerous communities and hence quite confusing. To avoid confusion, the definition used in this paper is adopted from [9] as follows

"A service is a mechanism enabling the end-user's access to one or more capabilities"

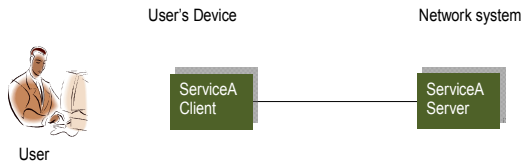


Fig. 2. A common service architecture

In a mobile environment, a service can be conceptually realised by two components:

- A **server** on the network, which can be both hardware and software and distributed over multiple network elements.
- A **client** on the user's device, which can be:
  - **Generic client** such as the Web browser that is capable to collaborate with any service server.
  - **Specific or dedicated client** that could collaborate only with some specific service servers.

In this paper, the focus is only on specific clients and how to provide service continuity on these clients.

B. A Service Continuity architecture

When the user is moving the service A as shown in Fig. 3 currently in use may cease to be available. However, a service B which is perceived as equivalent to service A by the user is emerging. The user will probably want to use service B instead of service A and the replacement should preferably be carried out in smooth and seamless way. Until now this is not possible since the two services are considered as completely different and there is no mechanism enabling the service switching.

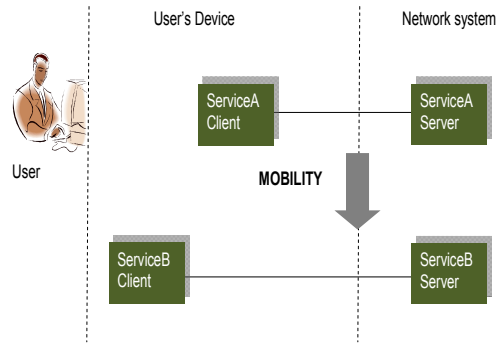


Fig. 3. Services in a mobile environment

To enhance the service availability and continuity we propose to introduce a new entity called **Generic Service** on the user's device. The Generic Service is equipped with a user interface that enables to receive commands from the user and to generate output. Depending on their availability the Generic Service will either invoke service A or service B.

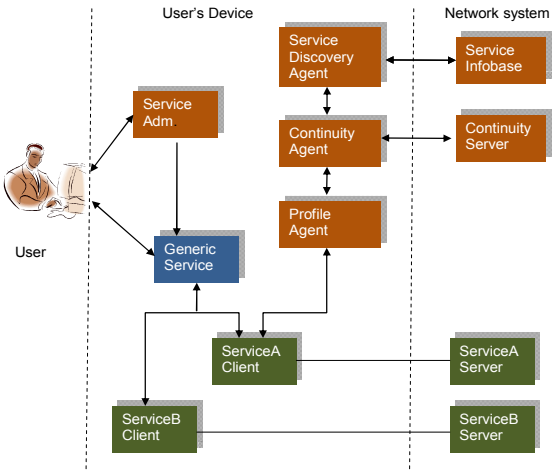


Fig. 4. A Service Continuity architecture

Now, the challenge is to know when and how to switch the Generic Service to either service A or service B. Another entity called **Continuity Agent** is proposed to assist the Generic Service in the switching process between services. It will perform the necessary initialisation and configuration such that the replacing service can continue from the point the former service stops. In the case where a new service client is required the Continuity Agent should also be capable of downloading, installing and initiating this new client. The Continuity Agent gets assistance from the **Continuity Server** on the network system to carry out seamless transfer of synchronous services like telephony.

The Continuity Manager needs assistance to find dynamically the available services at every place. An entity called **Service Discovery Agent** is introduced to perform the discovery of available services in collaboration with an entity called **Service Infobase** in the network system. The Service Infobase is a service registry that contains information about all the services available at a location. It has also capabilities to provide a complete list of available services to carry out matchmaking to find the specific services requested by the Service Discovery Agent. The service information stored in the Service Infobase should include details about service equivalence as specified in [10] which allows the discovery of equivalent services. The Service Infobase is also equipped with an open interface enabling all the service providers, including the end-users to register the services they are providing. The Service Infobase provides also an *Event service* that the Service Discovery Agent can subscribe to receive notification when networks and services emerge due to the user's mobility.

At service switching, to avoid cumbersome repetition it is convenient for the user if the preference settings and personal data can be shared among the equivalent services. For that the **Profile Agent** is introduced to store and administer the user profile. It has interface allowing the Continuity Agent to fetch the necessary data to configure the service and to save all the changes done by the user when using the services.

The whole service continuity process is illustrated in Fig. 5.

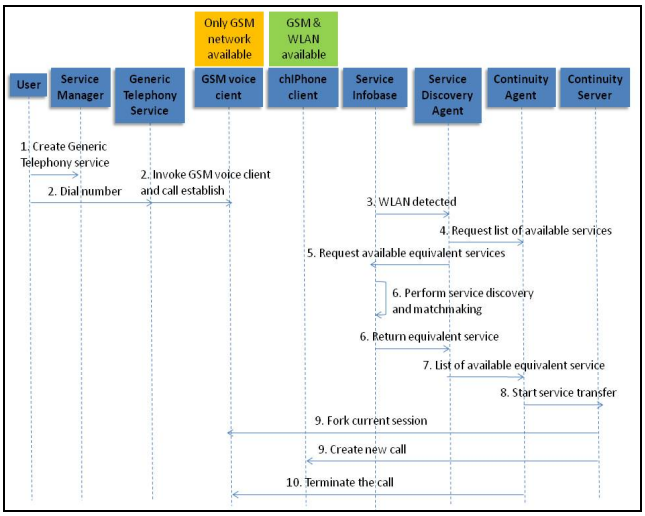


Fig. 5. Sequence diagram for the service continuity process

1. The user communicates with the *Service Manager* to create a *Generic Telephony service*, which includes either *GSM voice* service or *chIPhone*, a SIP-based IP telephony service. The GSM voice client is factory installed at while *chIPhone* is downloaded and installed by the user.
2. The user dials a number on the Generic Telephony service at a place where only GSM voice is available. The *Generic Telephony service* invokes the *GSM voice client* and the call is established.
3. The user is moving to a place where there is WLAN network offering an IP telephony service. The *Service Infobase* sends notification to the *Service Discovery Agent.*
4. The *Service Discovery Agent* requests the list of services demanding availability and continuity from the *Continuity Agent*, which contains *GSM voice* and *chIPhone.*
5. The *Service Discovery Agent* requests the *Service Infobase* to find all the available services that are equivalent to *GSM voice* and *chIPhone.*
6. The *Service Infobase* carries out the service discovery and matchmaking, and returns to the *Service Discovery Agent* a list containing a service *sIPhone*, which is SIP-based telephony and equivalent to *chIPhone*.
7. The *Service Discovery Agent* hands the list of available services over to the *Continuity Agent* for the initiation of the service transfer
8. Since the chIPhone client is already a SIP client, the *Continuity Agent* does not have to download and install any SIP client but only initialize the *chIPhone client*. The *Continuity Agent* requests the *Continuity Server* to start the service transfer.
9. The *Continuity Server* forks the current session between a B-party and the *GSM voice* client and creates a new call leg towards the *chIPhone client*.
10. When the *chIPhone client* is ready and running the Continuity Agent terminates the call leg with the *GSM voice client*. This is a typical soft handover since there is a short overlapping period where both clients are operating.

V. IMPLEMENTATION

A proof-of-concept prototype demonstrating the proposed service continuity architecture is under development.

The **Continuity Server** is realised by the Voice server inherited from the EUREKA Mobicome[1] project [11], which is focusing on providing service continuity across multiple devices. For example, the user is talking to the mobile phone while walking to his office. When arriving to his office, he transfers the call to his multimedia PC and continues the conversation while taking notes since he does not have to hold the phone anymore. However, it is worth noting that changing devices is conceptually similar to changing voice clients in the same device. The only difference is that in the first case the user is fully aware and actively participating to the switching of devices while in the latter case service continuity should preferably be seamless.

A simplified version of the **Service Infobase** supporting the discovery of equivalent services in different languages has been successfully implemented [12]. In addition, the discovery of partially matched services; i.e. services satisfying only a subset of the functionality has been realised.

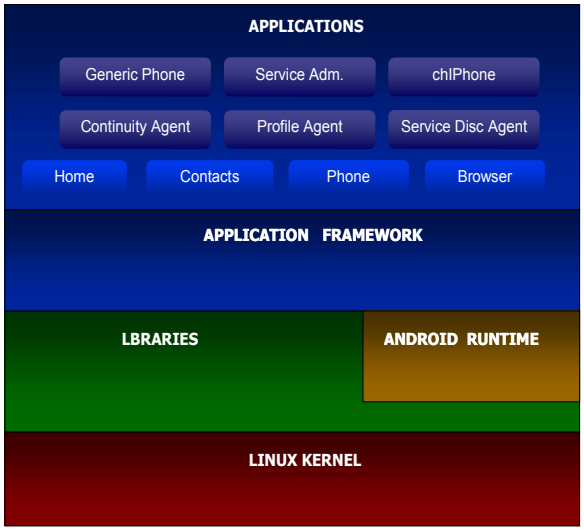


Fig. 6. A Service Continuity implementation on Android

The development of entities on the mobile device is carried out on Android [13], which is a software stack for mobile devices that includes an operating system, middleware and key applications. As shown in Fig. 6 the service continuity entities are introduced as applications. The *Generic Phone* will switch between the native *Phone* application and *chIPhone*, a SIP client. The *Profile Agent* will communicate with the native *Contacts* application to provide proper configuration and contacts for *Phone* and *chIPhone*.

[1] The EUREKA Mobicome project (2007-2010) is aiming at providing fixed-mobile convergent IMS environment with the participation of Telenor, Telefonica, Ericsson, Huawei, Linus, Ubisafe, HiQ, Oslo University College, Polytechnical University of Madrid and Blekinge Institute of Technology

VI. CONCLUSION

This paper demonstrates the needs for improving service availability and continuity in a heterogeneous networks environment where there are equivalent services with different names. To enable the use of these equivalent services it is proposed a service architecture, which incorporates dynamic discovery of equivalent services and dynamic switching of available services. The solution also ensures the re-use of the user's preference settings and personal data including personal details, contact, pictures, etc. Although most of the storage and processing of data are located in the network the service continuity process is initiated, controlled and decided by the mobile device's side. Currently, the only criterion for the transfer of service is the service availability. As further work it is quite relevant to introduce additional handover criteria such as QoS, security, price, etc.

REFERENCES

[1] Ivar Jørstad, Schahram Dustdar and Do van Thanh, "Service Continuity and Personalisation in Future Mobile Services", Proceedings of the 10th Eunice Summer School, ISBN 952-15-1187-7 (pp. 128-134), Tampere, Finland, June 14-16, 2004.

[2] Ivar Jørstad, Do van Thanh and Schahram Dustdar, "An analysis of service continuity in mobile services", Proceedings of the 2nd International Workshop on Distributed and Mobile Collaboration (DMC 2004), IEEE Computer Society Press, ISBN 0-7695-2183-5 (pp. 121-126), University of Modena and Reggio Emilia, Italy, June 14-16, 2004.

[3] Ivar Jørstad, Do van Thanh and Schahram Dustdar, "A Service Continuity Layer for Mobile Services", Proceedings of the IEEE WCNC Wireless Communications and Networking Conference 2005, ISBN 0-7803-8967-0, New Orleans, USA, Mar 13-17, 2005.

[4] Telecommunications and Internet converged Services and Protocols for Advanced Networking (TISPAN): Services Capabilities, Requirements and strategic direction for NGN services – Technical Report – ETSI TR 181 003 V1.1.1 (2006 05).

[5] Telecommunications and Internet converged Services and Protocols for Advanced Networking (TISPAN): NGN Terminology - Technical Report – ETSI TR 180 000 V1.1.1 (2006 02).

[6] 3rd Generation Partnership Project: 3GPP Technical Specification Group Services and System Aspects; Voice Call Continuity between CS and IMS (Release 7) – Technical Report TR 23.806 V7.0.0 (2005-12).

[7] 3rd Generation Partnership Project: 3GPP Technical Specification Group Services and System Aspects; Voice Call Continuity (VCC) between Circuit Switched (CS) and IP Multimedia Subsystem (IMS); Stage 2 3GPP TS 23.206 V7.5.0 (2007-12).

[8] IEEE Computer Society, "IEEE Standard for Local and Metropolitan Area Networks. Part 21: Media Independent Handover Service", IEEE Std. 802.21™ – 2008, 21 January 2009.

[9] Nor Shahniza Kamal Bashah, Natalia Kryvinska & Do van Thanh, "Service Discovery in Ubiquitous Mobile Computing Environment", Proceedings of the 8th International Conference on Advances in Mobile Computing & Multimedia (MoMM2010), ISBN 978-1-4503-0440-5, Paris, Nov 8-10, 2010.

[10] Nor Shahniza Kamal Bashah, Ivar Jørstad & Do van Thanh, "Service Discovery in Future Open Mobile Environments", Proceedings of the 4th International Conference on Digital Society (ICDS 2010), IARIA, ISBN: 9780769539539, St. Maarten, Netherlands Antilles, February 10 – 16, 2010.

[11] Do van Thuan, Ivar Jørstad, Boning Feng, Tore Jønvik & Do van Thanh, "Service Continuity for IMS converged services", Proceedings of the 10th International Conference on Intelligence in Next Generation Networks (ICIN 2008), ISBN 978-1-60702-868-0.

[12] Nor Shahniza Kamal Bashah, Atif Bhatti, Imran Aslam Choudhary, Ivar Jørstad & Do van Thanh, "Service Discovery for mobile multi-domain multi-language environments", Proceedings of the 6th IEEE International Conference on Wireless and Mobile Computing, Networking and Communication (WiMOB 2010), ISBN 978-4244-7741-8, Niagara Falls, Canada, October 11-13, 2010.

[13] Android developers – http://developer.android.com/index.html

BZK.SAU.FPGA10.0: Microprocessor Architecture Design on Reconfigurable Hardware as an Educational Tool

Halit Oztekin[1,2]
[1]Electrical and Electronics Eng.
Bozok University
Yozgat, Turkey
oztekinhalit@gmail.com

Feyzullah Temurtas[1]
[1]Electrical and Electronics Eng.
Bozok University
Yozgat, Turkey
temurtas@gmail.com

Ali Gulbag[2]
[2]Institute of Science Technology
Sakarya University
Sakarya, Turkey
agulbag@sakarya.edu.tr

***Abstract*— The Computer Architecture and Organization course in Computer and Electrical Engineering departments faces with a big problem: the migration from theory to practice. In order to solve this problem, a Computer Architecture simulator named BZK.SAU[1] is designed using an emulator program for educational purpose. This approach has important limitations. While students can complete and simulate their designs using software, they do not have the chance to implement and to run their designs in actual hardware. This work presents our solution to this problem: the FPGA implementation of BZK.SAU so that it would look and behave like the computer architecture simulator published in [1]. So we have implemented BZK.SAU Computer Architecture Simulator by using Altera® FPGA board that is a reconfigurable hardware prototyping development platform.**

***Keywords* — Computer Architecture and Organization; FPGA; Educational Tool; Microprocessor; Digital Logic Design; Microcomputer Design**

I. INTRODUCTION

Traditionally, teaching concepts in the computer architecture and organization course to computer and electrical science students can be inefficient if the teaching method is only on textbook materials. One common solution to this state is to provide an active learning environment for teaching computer architecture and organization course by taking advantage of software technology [2]. In other words, students can obtain a better understanding of the internal operation of a unit like processor by simulating. There are many computer architecture simulators [3-14] in the literature. These simulators are developed by using software programming languages or emulator programs. The open literature offers a variety of simulators for teaching courses in computer architecture and organization. The basic characteristics of selected simulators are shown in Table I. Their detailed descriptions are not given in the paper for reasons of length. In order to provide readers with the detailed features of these simulators, more data are given in [1].

Computers are digital systems, formed either by a composition of several subsystems or even centered on a single very large scale integration (VLSI) chip. Thus, an excellent way to teach and to understand their capabilities and limitations is by effectively designing them [15]. There are two recent technological advances: field-programmable gate arrays (FPGAs) and complex programmable logic devices (CPLDs). Previous research has revealed that the students enjoyed using programmable logic to augment their education [15]. More educational applications in reconfigurable design were found at literature in recent years as follows:

1) Reference [16] proposed a 16-instruction RISC processor was designed and downloaded in a FPGA board with 70.000 gate-count Altera chip. To utilize each logical module in the design of a sequence of simulation and implementation projects for teaching computer organization and architecture was her emphasis.

2) Reference [17] proposed a 10-instruction 16-bit RISC processor. An effective and practical education

TABLE I.
THE BASIC PROPERTIES OF SELECTED COMPUTER ARCHITECTURE SIMULATORS

Simulator Name	HW/SW	#Instruction	#Addressing Modes	Interrupt/ Stack
BZK.SAU	Fully HW	59	6	Interrupt and Stack
Marie Computer by Null and Lobur	SW	13	2	-
Marie Computer by Timothy D.Stanley	Limited HW	13	2	-
p88110	SW	NA	NA	NA
Easy CPU	SW	NA	2	Stack
LittleMan	SW	11	NA	NA
RTLSim	SW	NA	NA	NA
Z80	SW	NA	NA	NA
68000	SW	NA	NA	NA
Simple CPU	SW	8	3	-
Relatively Simple CPU	SW	16	NA	-
Very Simple CPU	SW	4	NA	-
SIMPLE	SW	28	1	-

NA: Not Available HW:Hardware SW: Software

approach for understanding and developing pipelined RISC processor was his emphasis.

3) Reference [18] proposed a 47-instruction 8-bit microprocessor. It was designed and implemented on Xilinx FPGA chip. He emphasizes that the modular, hierarchical design method adopted makes it is to modify.

4) Reference [19] proposed a 32-bit simplified MPIS-liked [21] CPU design.

5) Reference [20] proposed a 16-bit processor named TINYCPU. It is designed using Verilog HDL. He emphasizes that the students were able to learn digital circuit design using processor architectures.

6) Reference [22] proposed a 40 instructions 16-bit and 32-bit microcomputer named Edulent.

7) Reference [23] proposed an 8-bit microprocessor named Micro-FIMEE-08. it has the advantage to be an open core which benefits the students with the hands-on experience on microprocessor design.

Table II summarizes the basic properties of selected Fpga-Based Microprocessor Architecture Designs. The main concerns of the above educational FPGA applications were to introduce the concepts handled in Computer Architecture and Organization course, especially CPU design concept. Almost every application was designed using any hardware description language and very few are educationally oriented. The advantage of the approach is that BZK.SAU.FPGA.10.0 is fully designed at logic gate level using Altera's QuartusII CAD software tool. Additionally, it is free and can be downloaded from our website [24]. Since all modules are designed at logic gate level, the students can easily examine the internal structure of all modules in the design and use the required modules in the courses like Introduction to Logic Circuits, Digital Electronics etc.

This paper consists of the FPGA implementation of BZK.SAU. All units of BZK.SAU.FPGA.10.0 are fully designed at logic gate level. It was implemented and tested on Altera's FPGA development board which is connected to personal computer.

In the remaining of this paper, we show the architecture of BZK.SAU.FPGA.10.0 and its instruction set. Then we implement on FPGA board and run the sample application on BZK.SAU.FPGA.10.0. Finally, we present our conclusions.

II. THE ARCITECTURE OF BZK.SAU.FPGA.10.0

The 16-bit microcomputer architecture was designed on Altera FPGA board accordingly to the Computer Architecture Simulator named BZK.SAU[1] used by Computer Engineering Department in Sakarya University in Turkey since 2009 year. Basic features are listed as the following:

- The instruction set consists of 51 instructions: 21 instructions for memory and accumulator, 8 instructions for index and stack registers, 22 instructions for control

- Support six addressing modes: immediate, direct, indirect, index, relative and inherent mode.

- It has eight registers: Address Register (AR), Data Register (DR), Accumulator (AC), Program Counter (PC), Stack Pointer (SP), Index Register (IX) and Temporary Register (TR) are 16-bit; Instruction Register (IR) is 8-bit.

TABLE II.
THE BASIC PROPERTIES OF SELECTED COMPUTER ARCHITECTURE SIMULATORS

System Name	HW or SW	#Instruction	#Addr. Modes	Av.
BZK.SAU.FPGA.10.0	Fully HW	51	6	Free
SIMPLE RISC COMPUTER, Ref. [17]	HW	16	3	NA
ASAP-0/f0,f1,f2	SW	10	NA	NA
No-Name, Ref. [19]	SW	47	7	NA
No-Name, Ref. [20]	SW	NA	NA	NA
TINYCPU	SW	28	NA	NA
Edulent	HW and SW	40	4	NA
Micro-FIMEE-08	SW	100	4	NA

Av:Availability NA: Not Available HW:Hardware SW: Software

- 16-bit data bus and address bus.

- The unit for calculating of the effective address in the control instructions.

Instructions that use direct, immediate, indirect addressing modes take 3 bytes to execute in the memory. Instructions that use index and relative addressing modes take 2 bytes to execute while inherent addressing mode instructions take 1 byte to execute. In order to provide readers with the detailed features of instructions and instruction structures, more data are given [1]. Table III shows the list of all instructions of BZK.SAU.FPGA.10.0. Fig. 1 illustrates the block diagram of BZK.SAU.FPGA10.0 Microprocessor Architecture Design.

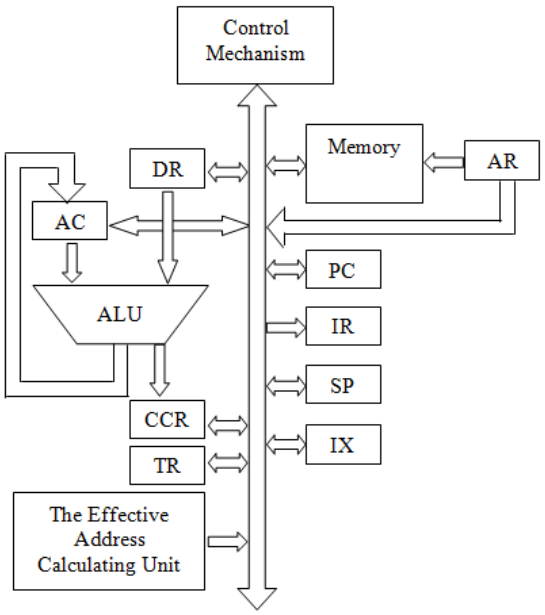


Figure 1. BZK.SAU.FPGA.10.0 Microcomputer Architecture

TABLE III.
THE INSTRUCTION SET OF BZK.SAU.FPGA.10.0

	Machine Code (HEX)-First Byte					
Mnemonic	Mod1	Mod2	Mod3	Mod4	Mod5	Mod6
ADD	10	20	30		40	
ADDC	11	21	31		41	
AND	12	22	32		42	
CLR						01
CMP	13	23	33		43	
DECR						02
DIV	15	25	35		45	
XOR	16	26	36		46	
INCR						03
COM						04
NEG						05
LDA	1A	2A	3A			
OR	1B	2B	3B		4B	
PSH						06
PUL						07
SAR						08
SAL						09
SUB	1E	2E	3E		4E	
SUBC	1F	2F	3F		4F	
STA		A0	B0		C0	
MUL	95	A5	B5		C5	
LDAX	91	A1	B1		C1	
LDAS	92	A2	B2		C2	
STAX		A3	B3			
STAS		A4	B4			
DECX						0A
INCX						0B
DECS						0C
INCS						0D
BRA				50		
BCC				51		
BCS				52		
BZR				53		
BGE				54		
BGR				55		
BHI				56		
BLE				57		
BLS				58		
BLT				59		
BMI				5A		
BNE				5B		
BVC				5C		
BVS				5D		
BPL				5E		
BSR				5F		
RTS						8A
JMP		A7			4C	
JSR		A8			4D	
RTI						81
NOP						89
HLT						0E

Mod1: Immediate addressing mode-- Mod2: Direct addressing mode

Mod3: Indirect addressing mode-- Mod4: Relative addressing mode

Mod5: Index addressing mode-- Mod6: Inherent addressing mode

III. IMPLEMENTATION OF BZK.SAU.FPGA.10.0

BZK.SAU.FPGA.10.0 was fully designed using web edition of Altera's Quartus II software with schematic design entry. Modular design is an important factor for the educational training of CPU design. Only Bo Hatfield [16] mentioned the approach of modularization. So we took the approach of modularization in order to avoid having students be overwhelmed by the complexity of a complete computer system design. Fig. 2. only shows the ALU module of BZK.SAU.FPGA.10.0 using Altera's Quartus II CAD tool. Other modules can be examined and used by downloading from our web-site [24] since it is free.

Fig. 3 shows Altera's Cyclone II development board with EP2C35F672C6N Chip. There are 17-slide switch from SW0 to SW17 on the board. We used the slide switch named SW1 to store the machine codes that are entered from the keyboard. If SW1 is logic 1(forward position) then the machine codes are stored on memory. The slide switch named SW0 is required to run the machine codes in the memory. If SW0 is logic 1 (forward position) then the machine codes are run. Also, there are 8-green led from LEDG0 to LEDG7 and 18-red led from LEDR0 to LEDR17 on the board. We used 8-green led and 8-red led from LEDR0 to LEDR7 to show the value of 16-bit Accumulator in the binary format. Additionally, the development board has 8-7 segment display from HEX0 to HEX7. 7-segment displays named HEX7 and HEX6 are used to show the machine code pressed from the keyboard in the hex format. 7-segment displays named HEX5 and HEX4 are used to show the value of last instruction in the Instruction Register (IR). 7-segment displays named HEX3, HEX2, HEX1 and HEX0 are used to show the value of Accumulator (AC), Data Register (DR), Address Register (AR) and Program Counter (PC) depending on the position of slide-switches named SW17 and SW16 and the positions of slide-switches are shown in Table IV.

IV. TEST APPLICATION FOR BZK.SAU.FPGA.10.0

Let us take a simple program in the high-level programming languages. The program is:

```
a:=5;
for i=1 to 10
{
a=a+i;
}
```

The assembler program developed for BZK.SAU can be downloaded from our web-site [26] and for information how to use the assembler program was published in [27]. Assembler code of the sample program is as follows using the instruction set of BZK.SAU design:

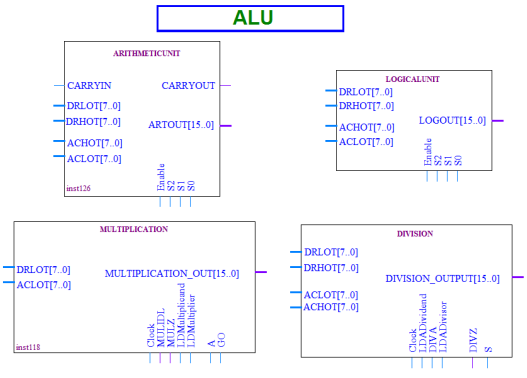


Figure 2. The ALU Module of BZK.SAU.FPGA.10.0

TABLE IV.
THE POSITION TABLE OF SW17 AND SW16

SW17	SW16	The values in HEX3, HEX2, HEX1, HEX0
0	0	Accumulator (AC)
0	1	Data Register (DR)
1	0	Address Register (AR)
1	1	Program Counter (PC)

LDA #0005h \\ the Accumulator is loaded with hex 0005h. (a variable)

STA $005Ah \\ the data in the Accumulator is stored the address 005Ah.

BZR *09h \\ If the Accumulator is zero, then branch "End_Process" label.

LDA $005Ch \\ the Accumulator is loaded the data in address 005Ch. (AC←i)

INCR \\ the Accumulator is incrementing. (AC←AC+1)

STA $005Ch \\ the data in the Accumulator is stored the address 005Ch.

BRA *E6h \\ branching "Add_Process" label

End_Process:HLT \\ the program is finished.

This program is written using the assembler program [26-27] and the machine code generated from the program is stored the memory on the FPGA by using the keyboard. The result is seen in Fig. 3.

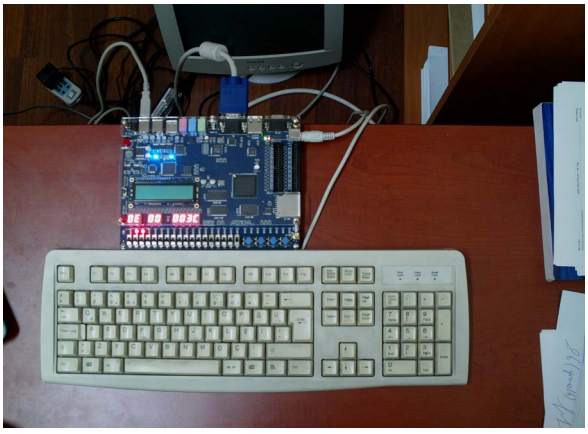


Figure 3. The result of test application in Altera Cyclone II Development Card

V. CONCLUSIONS

It is indicated that FPGA boards helps computer and electrical science students learn digital logic design [25]. In this paper, microprocessor design and its FPGA implementation were described. It is an improvement of design previously done [1] by means of an emulator program. The proposed microprocessor design makes it possible to utilize each module in the design for teaching computer organization and architecture, Introduction to Logic Circuits, Digital Electronics etc. since each module is designed at logic gate level. It is believed that the presented microprocessor design will be received since it is available [24] at no cost. Also, it is expected that the students will better prepare for advanced computer architecture designs since BZK.SAU.FPGA10.0 has modular nature.

An additional advantage is that the design will provide a consistent teaching platform across a range of courses. This design will be used at Computer Architecture and Organization course and similar courses at Sakarya University and Bozok University in Turkey in 2011 academic year. We expect that this design considerably will enhance the students learning experience.

ACKNOWLEDGMENT

This work was fully supported under TUBITAK (The Scientific and Technological Research Council of Turkey) project no. 110E069.

REFERENCES

[1] H. Oztekin, F. Temurtas, and A. Gulbag, "BZK.SAU: Implementing a hardware and software-based computer architecture simulator for educational purpose," *Proceedings of 2010 International Conference on Computer Science and Applications (ICCDA 2010)*, vol. 4, pp. 90-97, June 2010.

[2] W. Yurcik, G. S. Wolffe, M.A. Holliday, "A Survey of simulators used in computer organization/architecture courses", *Proceedings of the 2001 Summer Computer Simulation Conference (SCSC)*, July 2001.

[3] C. Yehezkel, W. Yurcik, M. Pearson, and D. Armstrong, "Three simulator tools for teaching computer architecture: EasyCPU, little man computer, and RTLSim," *Journal on Educational Resources in Computing (JERIC)*, vol. 1, no. 4, pp. 60-80, 2001.

[4] D. Colton, G. Embrey, L. Fife, S. Mikolyski, D. Prigmore, and T. D. Stanley, "Pedagogic value in understanding computer architecture of implementing the marie computer from null and lobur in the logic emulation software, multimedia logic", *Workshop On Computer Architectur Education. Procedings of the 2007 workshop on Computer Architecture education*, pp. 66-71, 2007.

[5] J. Lobur, and L. Null, The essentials of computer organization and architecture, Sudbury: Jones and Barlett Publishers, 1997.

[6] D. Colton, G. Embrey, L. Fife, S. Mikolyski, D. Prigmore, and T. D. Stanley, "From archi torture to architecture: undergraduate students design and implement computers using the multimedia logic emulator," *Computer Science Education*, vol. 17, no. 2, pp. 141-152, June 2007.

[7] T. Kawamura, Y. Kawaguchi, S. Nakanishi, and K. Sugahara, "Machine cycle CPU simulator for educational use based on Squeok environment," *First Conference on Creating Connecting and Collaborating through Computing*, p. 120, 2003.

[8] D. Dechow, G. Korienek, and T. Wrensch, SQUEAK- A Quick trip to object land, Boston: Addision Wesley, p. 320, 2002.

[9] J.D. Carpinelli, "The very simple CPU simulator," *32nd Annual Frontiers in Education(FIE'02)*,vol.1, pp.T2F11-14, 2002.

[10] J. R. Arias, and D. F. Garcia, "Introducing computer architecture education in the first course of computer science career," *IEEE Computer Society*, pp. 37-40, July 1999. [Online]. Available: http://tab.computer.org/tcca/NEWS/feb99/index.html. [Accessed: Oct 15, 2009]

[11] J. Carpinelli, and T. Zaman, "Instructional tools for designing and analysing a very simple CPU," *International Journal of Electrical Engineering Education*, vol. 43, no. 3, pp. 261-270, July 2006.

[12] M. I. Garcia, S. Rodriguez, A. Perez, and A. Garcia, "p88110: A graphical simulator for computer architecture and organization courses," *IEEE Transactions on Education*, vol. 52, no. 2, May 2009.

[13] H. B. Diab, and I. Demashkieh, "A computer-aided teaching package for microprocessor systems education," *IEEE Transactions on Education*, vol. 34, no. 2, pp. 179-183, May 1991.

[14] W.D. Henderson, "Animated models for teaching aspects of computer system organization," *IEEE Transactions on Education*, vol. 37, no.3, pp. 247-256, August 1994.

[15] N.L.V. Calazans, and F.G. Moraes, "Integrating the teaching of computer organization and architecture with digital hardware design early in undergraduate courses" *IEEE Transaction on Education*, vol. 44, no. 2, pp. 109-119, May 2001.

[16] B. Hatfield, M. Rieker, and L. Jin, "Incorporating simulation and implementation into teaching computer organization and architecture", *35th. ASEE/IEEE Frontiers in Education Conference*, October 2005.

[17] H. Ochi, "ASAver.1: An FPGA-based education board for computer architecture/system design", *Design Automation Conference 1997. Proceedings the ASP-DAC '97*, pp. 157-165, January 1997.

[18] X. Tiejun, and L. Fang, "16-bit teaching microprocessor design and application," *Proceedings of 2008 IEEE International Symposium on IT in Medicine and Education*, pp. 160-163, 2008.

[19] M. Pearson, D. Armstrong, and T. McGregor, "Design of a processor to support the teaching of computer systems," *Proceedings The first IEEE International Workshop on Electronic Design, Test and Applications*, vol. 29-31, pp. 240-244, January 2002.

[20] K. Nakano, and Y. Ito, "Processor, assembler and compiler design education using an FPGA," *14th IEEE International Conference on Parallel and Distributed Systems*, pp. 723-728, 2008.

[21] D. A. Patterson, and J. L. Hennessy, *Computer organization and* design, 3rd ed., San Francisco: Morgan Kaufmann, 2005.

[22] I. Mazei, and V. Malbasa, "Using VHDL to improve an FPGA based educational microcomputer," *EUROCON 2005*, pp.799-802, 2005.

[23] R. de J. Romero-Troncoso, A. Ordaz-Moreno, J. A. Vite-Frias, and A. Garcia-Perez, "8-bit CISC microprocessor core for teaching applications in the digital systems laboratory,"*IEEE International Conference on Reconfigurable Computing FPGA's*, pp. 1-5, 2006.

[24] "BZK.SAU.FPGA.10.0," Aug 19, 2010[Online]. Available: http://eem.bozok.edu.tr/database/1/BZK_SAU_FPGA10_0.rar. [Accessed: Aug. 25, 2010]

[25] Y. Zhu, T. Weng, and C. Keng, "Enhancing learning effectiveness in digital design courses through the use of programmable logic boards," *IEEE Transactions on Education*, vol. 52, no. 1, pp. 151-156, February 2009.

[26] "Assembler Program," Dec. 15, 2009. [Online]. Available: http://eem.bozok.edu.tr/database/1/Assembly_Program_For_BZK_SAU.rar. [Accessed: Dec. 16, 2009]

[27] H. Oztekin, F.Temurtas, and A. Gulbag, "An assembler and compiler program design for an educational purpose computer architecture simulator being used computer and electrical engineering education," *Elec Lett Sci Eng*, vol. 5(1), pp. 9-16, 2009.

Cascade Multi-level Converter Based DVR and D-STATCOM for Voltage Sag and Swell Reduction

B. S. Mohammed, K. S. Rama Rao, N. Perumal
Department of Electrical and Electronic Engineering
Universiti Teknologi PETRONAS
Bandar Seri Iskandar, 31750 Tronoh, Perak, Malaysia

***Abstract*- This paper presents the modeling and simulation of three and seven-level cascade multilevel converter (CMC) based dynamic voltage restorer (DVR) and distribution static compensator (D-STATCOM), aimed at correcting the supply voltage sag/swell and interruption in low voltage distribution networks. The proposed design models of CMC based DVR and D-STATCOM are expected to be most powerful solutions to minimize supply voltage disturbances of the sensitive loads. The proposed models of DVR and D-STATCOM together with the controllers are simulated by using electromagnetic transient simulation program (PSCAD/ EMTDC) and the results are presented to assess the performance of each device.**

Keywords **— Cascade Multilevel Converter; Dynamic Voltage Restorer; Distribution Static Compensator**

I. INTRODUCTION

With the increased use of high efficiency variable speed drives and power electronic controllers, both electric utilities and end users of electrical power are becoming increasingly concerned about the quality of electric power. Voltage sag is the most common type of power quality disturbance in the distribution system. The effect of voltage sag can be very expensive for the customer because it may lead to production downtime and damage. Voltage sag can be mitigated by voltage and power injections into the distribution system using power electronics based devices, which are also known as custom power devices [1]. DVR and D-STATCOM are the most effective custom power devices preferred to address the voltage sag and swell problems. Most of the research work published on DVR and D-STATCOM has been based on two-level voltage source converter (VSC) as in [2]-[8]. Very few publications dedicated to multilevel VSC based DVR and D-STATOM are presented in [9]-[11]. CMC is one of the most popular converter topologies used in high-power medium-voltage applications. The CMC synthesizes a desired voltage from several independent sources of dc voltages, which may be obtained from batteries, fuel cells or solar cells. The adoption of CMC for DVR and D-STATCOM applications leads to reduced injection of harmonics and decrease the cost and the voltage of power switching devices. This paper is aimed at the design and simulation of CMC based three-level DVR and D-STATCOM for power quality enhancement and a PI controller is used to provide better voltage stabilization, sag suppression and power factor correction. The simulation results are then compared with the results of seven-level CMC based DVR and D-STATCOM. The results reveal that the seven-level CMC offers higher efficiency and reduced voltage THD levels than a three-level CMC.

II. PHASE-SHIFT MULTI-CARRIER MODULATION (PSHM)

Cascade multilevel converter with m voltage levels requires (m – 1) triangular carriers. In the phase-shifted multi-carrier modulation, all the triangular carriers have the same frequency and the same peak-to-peak amplitude, but there is a phase shift between any two adjacent carrier waves, given by $\Phi = 360/(m-1)$. The gate signals are generated by comparing the modulating wave with the carrier wave. Fig.1 shows the principle of PSHM for a seven-level CMC, where six triangular wave carriers are required with a 60° phase displacement between any two adjacent carriers. The advantage of PSHM is that the switching frequency and conduction period are same for all devices, and rotation of switching patterns is not required.

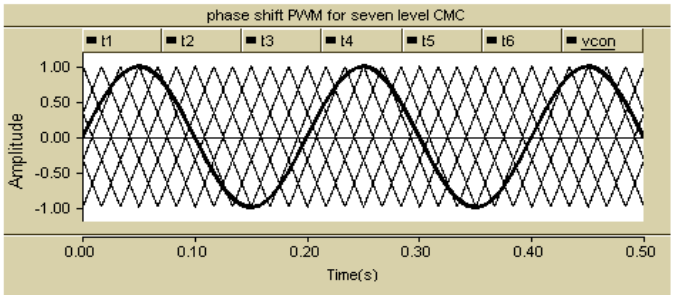


Fig. 1. PSHM for seven-level CMC

III. DYNAMIC VOLTAGE RESTORER (DVR)

A power electronic converter based series compensator that can protect critical loads from all supply side disturbances other than outages is called a DVR. The DVR is capable of generating or absorbing independently controllable real and reactive power at its ac output terminal. The DVR injects a set of three-phase ac output voltages in series and in synchronism with the distribution feeder voltages. The amplitude and phase angle of injected voltages are variable there by allowing control of the real and reactive power exchange between the DVR and the distribution system. The reactive power exchange is internally generated by the DVR without ac passive reactive

components. The real power exchanged at the DVR output ac terminals is provided by the DVR input dc terminal or by an external energy source or energy storage system [1]. Fig. 2 shows a typical DVR connected in series with a 11 kV distribution feeder that supplies a sensitive load. The DVR can protect the sensitive load by injecting voltage of controllable amplitude, phase and frequency into the distribution feeder via a series injection transformer. Thus DVR can only supply partial power to the load during very large variations (sag or swells) in source voltage [1].

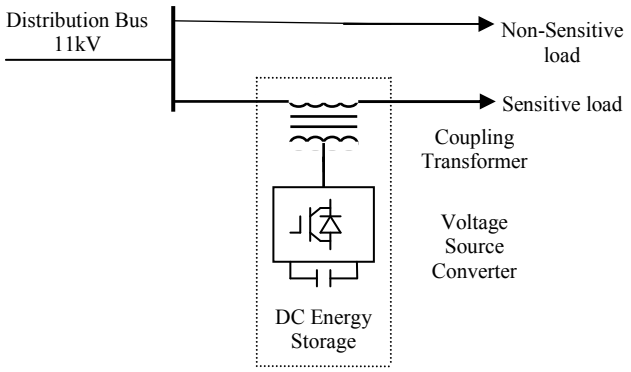


Fig. 2. Schematic representation of the DVR

IV. Distribution Static Compensator (D-STATCOM)

A D-STATCOM connected in shunt with the ac system, consists of a VSC, switching control scheme, a DC energy stored device and a three-winding coupling transformer. Fig. 3 shows a D-STATCOM connected to a 230 kV power system having three loads and two circuit breakers. The controller of the D-STATCOM continuously monitors the load voltages and currents and determines the amount of compensation required by ac system for a variety of disturbances.

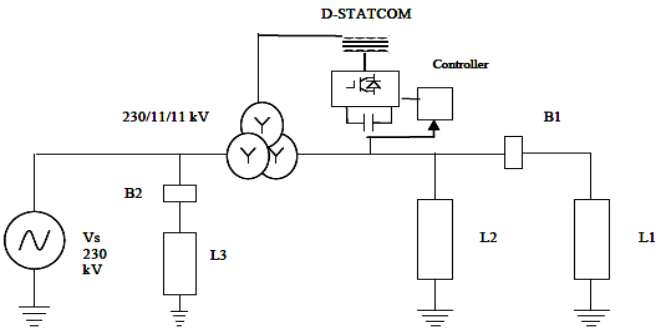


Fig. 3. Schematic diagram of test system including D-STATCOM

V. Uni-Polar and PSHM Based PWM Controller

The aim of the control scheme is to maintain constant voltage magnitude at the point where a sensitive load is connected, under system disturbances without incurring significant switching losses. The three-level CMC switching strategy based on uni-polar modulation and the seven-level CMC based on PSHM which are sinusoidal PWM (SPWM) technique, offers simplicity and good response. Since custom power is a relatively low-power application, SPWM methods offer a more flexible option than the fundamental frequency switching (FFS) methods favored in FACTS applications. Besides, high switching frequency can be used to improve on the efficiency of the converter, without incurring significant switching losses. The main parameters of the uni-polar and PSHM used in the simulation are the amplitude modulation index m_a of sinusoidal signal and the frequency modulation index m_f of the triangular signal. The amplitude modulation index m_a is kept fixed at 1 p.u, in order to obtain the highest fundamental voltage component at the controller output [2], [3], [4]. The switching frequency is set at 600 Hz and m_f is selected as 12 for simulation. The control system only measures the V_{rms} at the load point. The controller operates for an error signal obtained by comparing the reference voltage, V_{ref} with the measured load voltage, V_{rms}. The PI controller processes the error signal and generates the required angle delta to drive the error to zero, the load V_{rms} is brought back to the reference voltage. The modulated signal is compared against two triangle signals $V_{carrier1}$ and $V_{carrier2}$ in three-level CMC using uni-polar modulation scheme and with six triangles in seven-level CMC using PSHM, in order to generate the switching signals for the CMC. The speed of response and robustness of the control scheme are clearly shown in the simulation results. Modulating angle delta is applied to the uni-polar and PSHM generators in phase A and the angles for phases B and C are shifted by 240 and 120, respectively.

VI. Case Study and Simulation Results

Simulation case studies are performed on three-phase power system using PSCAD/ETMDC for (i) normal three and seven-level CMC (ii) three and seven-level CMC based DVR and (iii) three and seven-level CMC based D-STATCOM.

A. Simulation of three-phase three and seven-level CMC

Figs.4 to 9 shows the simulated results of three and seven-level CMC using uni-polar and PSHM modulation techniques. The phase and line-to-line output voltages of the CMC and output phase voltage harmonic spectrum demonstrates the capability of uni-polar and PSHM schemes for improving frequency spectrum and hence the reduction of output THD.

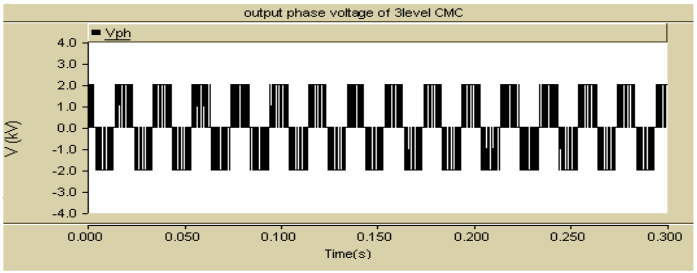


Fig. 4. Output phase voltage of three-level CMC

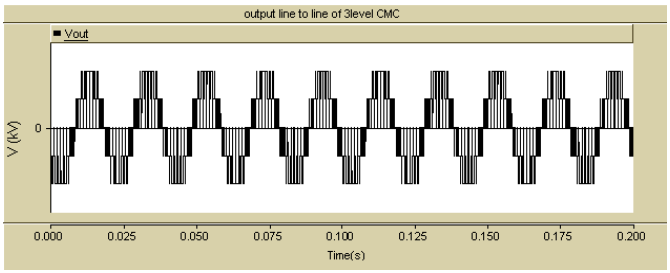


Fig. 5. Output line-to-line voltage of three-level CMC

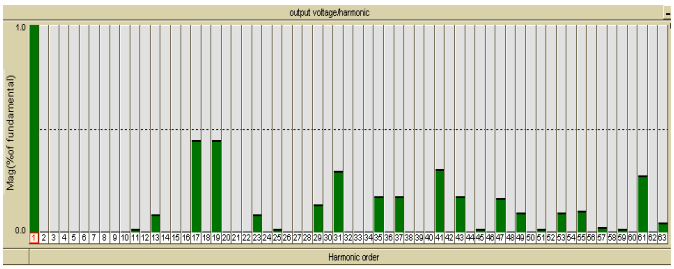


Fig. 6. Three level CMC output phase voltage /harmonics (THD = 38.86 %)

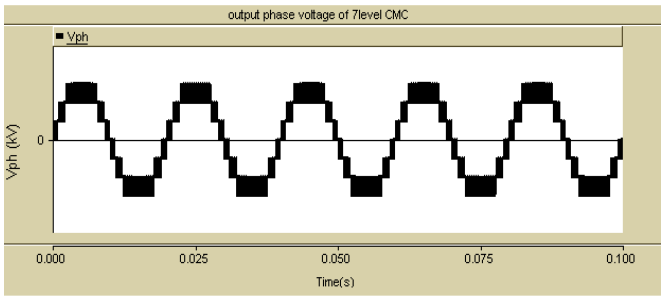


Fig. 7. Output phase voltage of seven-level CMC

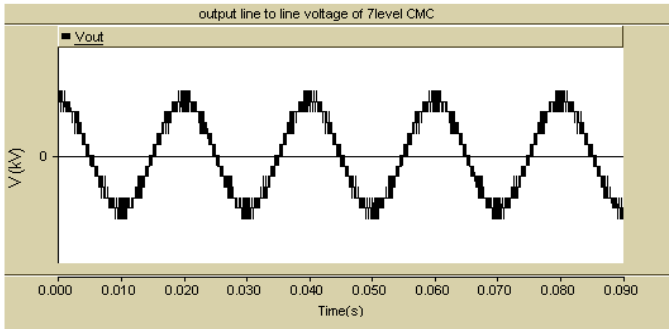


Fig. 8. Output line-to-line voltage of seven-level CMC

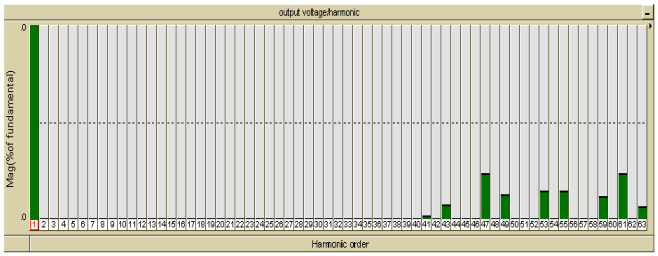


Fig. 9. Seven-level CMC output phase voltage /harmonics (THD=10.554 %)

B. Simulation of three and seven-level CMC based DVR

A test system comprising a 230 kV, 100 MVA, 3-phase transmission line, represented by Thevenin equivalent, feeding into the primary side of a three-winding transformer is selected as shown in Figs. 10 and 11. Two loads are connected to the tertiary windings via two two-winding transformers. The DVR is connected in series with a sensitive load 2 through a coupling transformer, with a leakage reactance of 10 %. A unity transformer turn ratio used for the DVR coupling transformer with no booster capabilities. The capacity of storage device of each CMC cell is 2 kV for three-level and 1 kV for seven- level. CMC based DVR is connected to the 11 kV tertiary winding to provide instantaneous voltage support at the load point. Two different simulations are carried out using PSCAD/EMTDC as follows.

In the first case the system is tested without the DVR for different types of faults via a fault resistance of 0.36 Ω. Various faults such as line-to-ground fault, line-to-line fault, line-to-line-to-ground fault, three-phase-to-ground fault and three-phase fault are simulated from 0.3s – 0.6s and the voltage sag is observed as shown in Figs. 12(a) to 16(a).

The second simulation is carried out using the same scenario as above but now with the three and seven-level CMC based DVR in operation and the simulation results are as shown in Figs. 12(b) -12(c) to 16(a) - 16(c).

The three and seven-level CMC based DVR is simulated to be in operation only for the duration of the fault of 0.3 s and the total simulation period is observed to be 0.9 s. The simulation results for both cases are presented as shown in Figs.12 to 16. It can be seen that when the DVR is in operation, the voltage sag is mitigated almost completely and the rms voltage at the sensitive R-L load 2 is maintained as shown in Table 1. It is also observed that the DVR maintained 100 % voltage at the sensitive load with seven-level CMC.

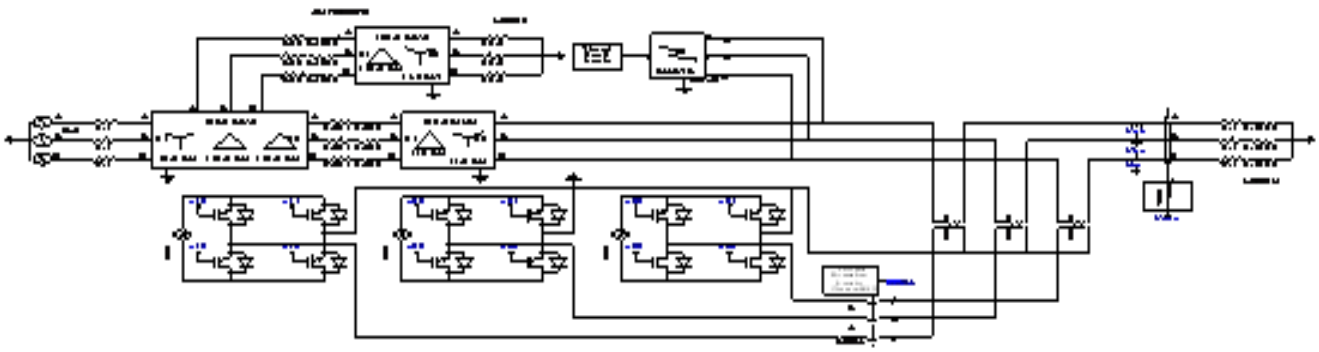


Fig. 10. Simulation model of DVR based three-level CMC test system in PSCAD/ETMDC

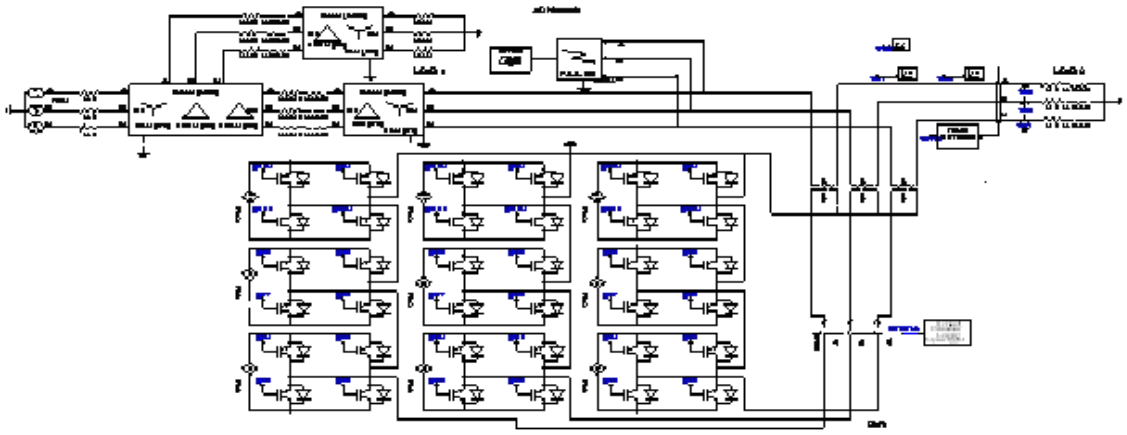
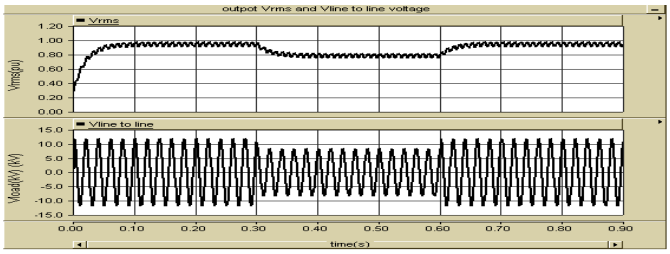
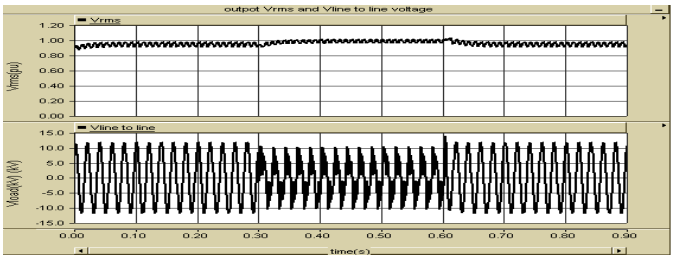


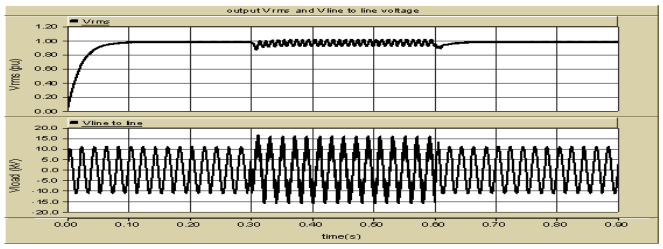
Fig. 11. Simulation model of DVR based seven-level CMC test system in PSCAD/ETMDC



(a)

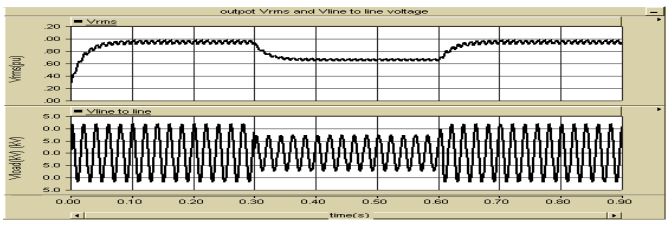


(b)

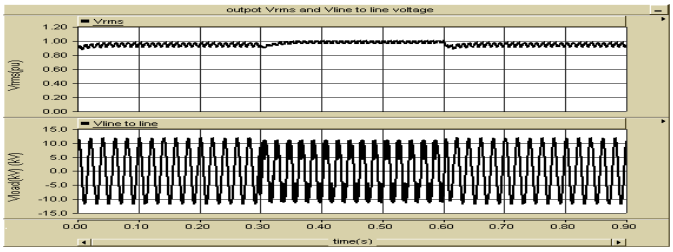


(c)

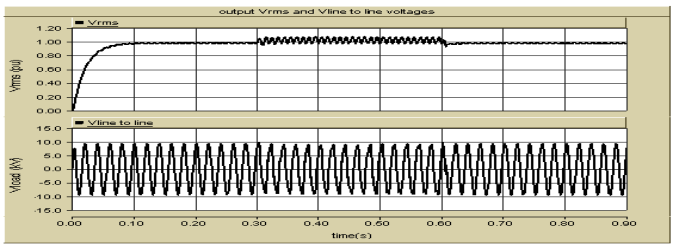
Fig. 12. Load voltage during line-to-ground fault: (a) without DVR, (b) with three-level CMC based DVR, (c) with seven-level CMC based DVR



(a)

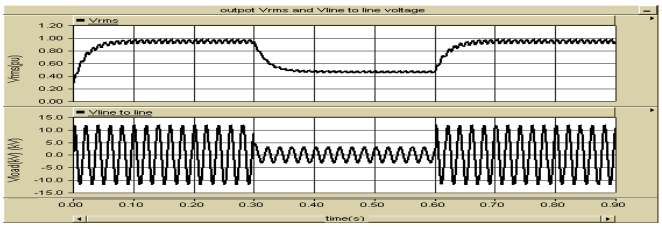


(b)

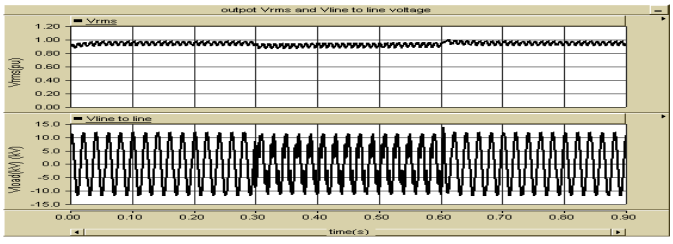


(c)

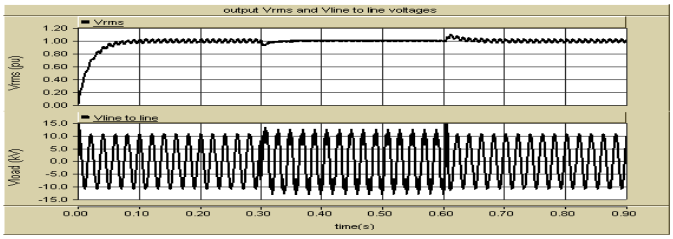
Fig. 13. Load voltage during line-to-line-to-ground fault: (a) without DVR, (b) with three-level CMC based DVR, (c) with seven-level CMC based DVR



(a)

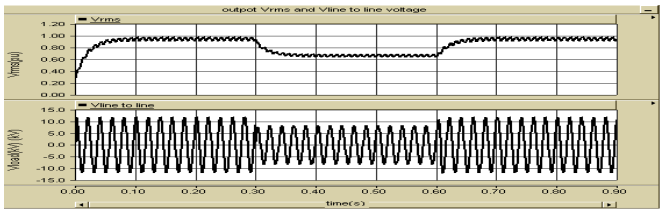


(b)

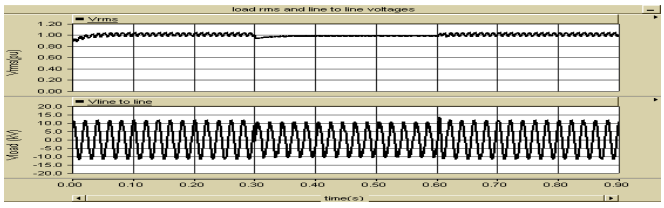


(c)

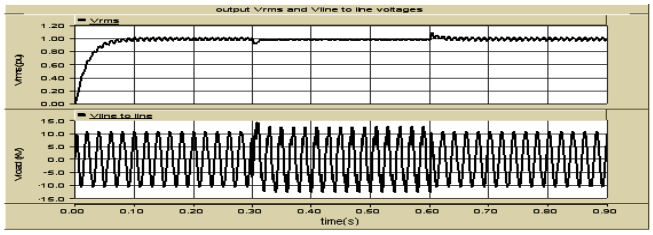
Fig. 14. Load voltage during line-to-line fault: (a) without DVR, (b) with three-level CMC based DVR, (c) with seven-level CMC based DVR



(a)

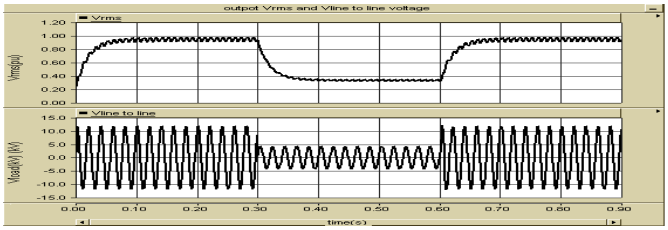


(b)

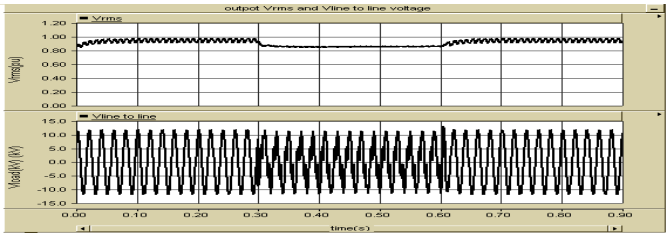


(c)

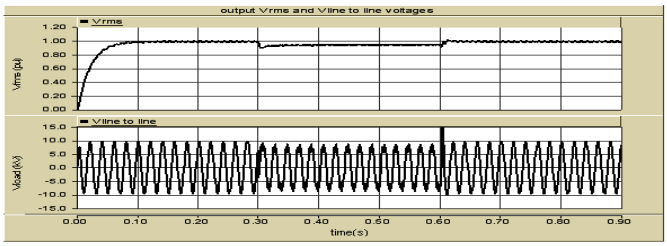
Fig. 15. Load voltage during three-phase-to-ground fault: (a) without DVR, (b) with three-level CMC based DVR, (c) with seven-level CMC based DVR



(a)



(b)



(c)

Fig. 16. Load voltage during three-phase fault: (a) without DVR, (b) with three-level CMC based DVR, (c) with seven-level CMC based DVR

Table .1
VOLTAGE SAG VALUES OF TEST SYSTEM WITHOUT DVR AND WITH OF DVR FOR VARIOUS FAULTS

Fault type	Load Vrms sag without DVR	Vrms with 3level CMC based DVR	Load Vrms with 7level CMC based DVR
Single L-G	80%	100%	100%
Double L-G	64%	100%	100%
Double L-L	48%	96%	100%
3phaseL-L-L-G	66%	99%	100%
3phase L-L-L	36%	88%	94%

The uni-polar and SPWM control schemes employed with CMC are shown to control the magnitude and phase of injected voltages, restoring V_{rms} to its initial value of 1.0 pu. It can be seen that the voltage sag mitigation is performed and a smooth, stable, and rapid DVR response is observed with acceptable overshoots when the DVR comes in and out of operation. It should be noted that passive filters are not used in simulation models. Table.1 shows the worst cases of faults, three-phase and double-line faults, where V_{rms} decreases to 36 % and 48 %, respectively from the reference value. The impact of DVR based three and seven-level CMC for voltage sag mitigation during the faults is clearly demonstrated.

C. Simulation of CMC based D-STATCOM

Based on the schematic model of D-STATCOM and power system as shown in Fig. 3, a PSCAD/EMTDC model is developed as similar to DVR shown in Figs. 10 and 11. Simulations are performed on the test system employing three loads, R-L, R and C, respectively, together with the D-STATCOM. The simulation results are shown for a period of 1.4 s. as shown in Figs. 17, 18(a) and 19(a). The simulation results are analyzed in three intervals when different loads are used and the D-STATCOM is not in operation as follows:

(i). In the simulation period 0.3 s to 0.6 s, the load1 (R-L) is connected by closing the circuit breaker B1. It is observed that the voltage drop is about 30 % as shown in Fig. 17.

(ii). At t = 0.6 s, the Load1 is disconnected by opening the circuit breaker B1. A rise in load voltage is observed very close to the reference value of 1.0 pu.

(iii). In the period 0.9 s to 1.2 s, the circuit breaker B2 is closed, connecting load3 (C) which is a capacitor bank on the high voltage side of the network. It can be seen that the load voltage has increased by 22 % from the reference value as shown in Fig. 17.

Similarly, a new set of simulations were carried out but now when the three and seven-level CMC based D-STATCOM is connected to the test system. The simulation results for the same time intervals as explained above are shown in Figs. 18 and 19, where the very effective voltage regulation provided by the seven-level CMC based D-STATCOM can be clearly appreciated. Figs. 18(b) and 19(b) show the voltage THD of the load2 when three and seven-level CMC based D-STATCOM are in operation. It can be seen that the THD of the load is significantly reduced to 24.023 % when seven-level CMC based D-STATCOM is used from 44.056 % as in case of three-level CMC based D-STATCOM. The THD introduced in the test power system with three and seven-level CMC based D-STATCOM is higher than the IEEE standard because the simulation is carried out without the use of passive filter to damp the IGBT switching harmonics.

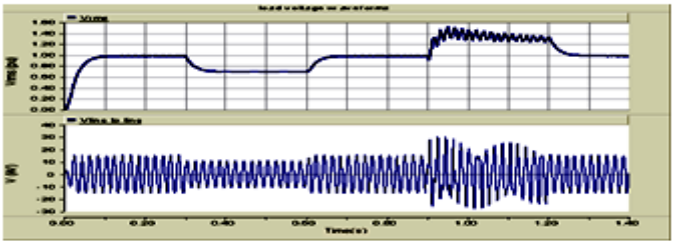
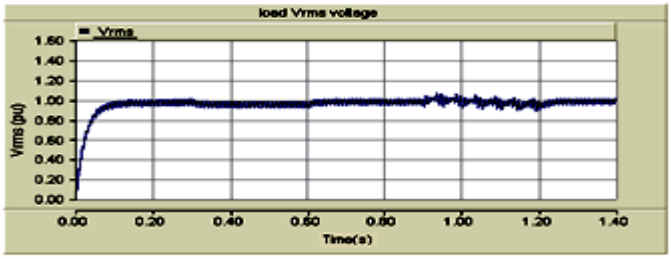
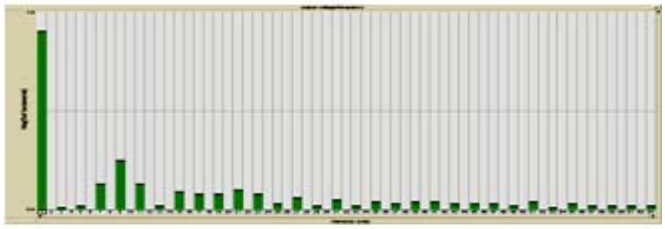


Fig. 17. Load voltage without D-STATCOM

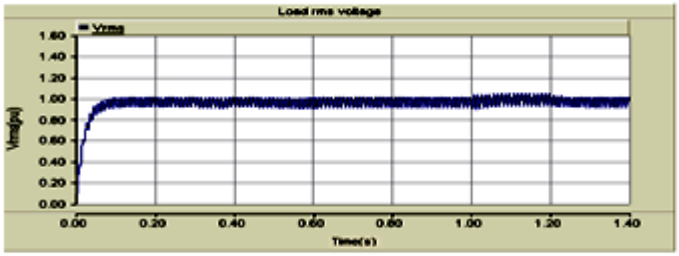


(a)

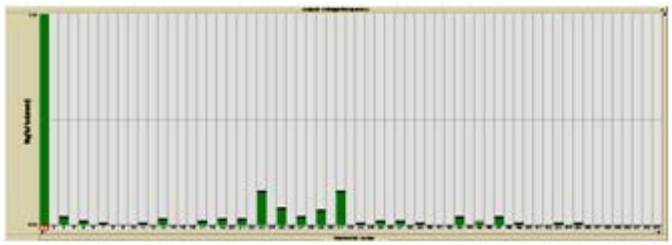


(b)

Fig .18. (a) Load voltage, (b) Load voltage harmonics, THD = 44.056 % with three-level CMC based D-STATCOM



(a)



(b)

Fig. 19. (a) Load voltage, (b) Load voltage harmonics, THD = 24.023 % with seven-level CMC based D-STATCOM

CONCLUSIONS

This paper presents simulation models of two of the custom power equipment namely, three and seven-level CMC based DVR and D-STATCOM in a distribution system. Uni-polar and PSHM based SPWM techniques are used to control the DVR and D-STATCOM. The simulation results have demonstrated the effectiveness of the DVR and D-STATCOM under different fault conditions and provided excellent voltage regulation capability by increasing the number of levels of CMC.

REFERENCES

[1]. A. Ghosh, G. Ledwich, Power Quality Enhancement Using Custom Power Devices, Kluwer's Power Electronics and Power System Series Editor, M. A. Pai, Kluwer, Academic Publishers,PP.241-376,2002.

[2]. A. K. Schoo, T. Thyagarajan, "Modeling of facts and custom power devices in distribution network to improve power quality," Third International Conference on Power Systems, Kharagpur, India, pp.1-7, December 27-29, 2009.

[3]. O. A. Lara, E. Acha, "Modeling and analysis of custom power systems by PSCAD/ETMDC," *IEEE Transaction on Power Delivery*, pp.266-272, January 2002.

[4]. H. Hatami, F. Shahnia, A. Pashaei, S. H. Hosseini, "Investigation on D-STATCOM and DVR operation for voltages control in distribution networks with a new control strategy," *IEEE Power Tech*, pp.2207-212, June 2008.

[5]. P. Vasudevanaidu, M. Tech, Y. N. Kumar, "A new simple modeling and analysis of custom power controllers," Third International Conference on Power Systems, Kharagpur, India, pp.1-6, December 27-29, 2009.

[6]. S. E. Jafarabadi, G. B. Gharehpetian, "A new ISPWM switching technique for THD reduction in custom power devices," Department of Electrical Engineering, Amirkabir University of Technology, 15914 Tehran, Iran.

[7]. Z. A. Zakaria, B. Chen, M. O. Hassan, "Transient studies of custom power equipments and static var compensator using PSCAD," International Journal of Electrical Power and Energy Systems Engineering, 2008.

[8]. A. Cetin, M. Ermis, "VSC- based D-STATCOM with selective harmonic elimination," *EEE Transactions on industry applications*, May 2009.

[9]. C. Sharmeela, G. Uma, M. R. Mohan, "Multi-level distribution STATCOM for voltage sag and swell reduction," *IEEE Power Energy Society General Meeting*, August 2005.

[10]. G. V. R. Satyanarayana, S. N. V. Ganesh, "Cascaded 5-level inverter type DSTATCOM for power quality improvement," *IEEE Student Technology Symposium,* India, April, 2009.

[11]. F. Z. Pheng, J. S. Lai, "Dynamic performance and control of a static var generator using cascade multilevel inverter," *IEEE Transactions on Industry Applications*, May/June, 1997.

G-Flash: An Authoring Tool for Guided Digital Storytelling

Jumail, Dayang Rohaya Awang Rambli, Suziah Sulaiman
Department of Computer and Information Science
Universiti Teknologi PETRONAS
Malaysia
jumail.wastam@gmail.com

***Abstract*— This paper describes the conceptual design of G-Flash, an authoring tool for supporting guided digital storytelling among young children. The basic idea of G-Flash revolves around guidance concept with the aim of assisting young children quickly generate a story according to the intended learning objectives. Tutored condition, a mid-level form of guidance giving was selected as the guided learning approach to allow the student getting only the right amount of assistance without compromising on the learner's creativity and motivation as well as to learn on their own within the assistance withholding condition. An important feature of G-Flash is the use of flashcards, a familiar and widely used tool to teach children, as the main media element to create the digital story was highlighted. A review of existing tools was provided and benefits of guidance concept, not present in existing digital storytelling tool, were discussed.**

***Keywords*—Digital Storytelling; Guided Learning; Tutored Approach; Illustrated Flaschcards; Assistance Giving**

I. INTRODUCTION

Despite the diverse ways digital storytelling (DST) can be used, the recent years has seen its growing use among educators to support learning and teaching activities, motivate and encourage student engagement through interactive approach [1-3], constructive learning, edutainment approach, game, and collaboration [4] [5] [6] [7]. Basically digital storytelling refers to the use of digital forms of media to tell the stories. Actors, music, sound effect, film images are several digital elements that have been used in storytelling [8]. However, with the advantage of technology era, storytelling can be told in a more interesting and engaging manner. Recent development in digital technology has made the resultant digital stories to reach the audience further through interactive digital media such as video games, interactive TV, DVDs, web technologies, and personal computer.

Crafting digital stories especially interesting and engaging ones may involve lots of creativity and motivation and time consuming. Thus, the presence of authoring tools eases the digital storytelling process. Numerous multimedia tools are available in the market to serve this purpose; however, most of them are general tools and not specifically designed for digital storytelling process. Hence, some of the research focuses in digital storytelling is the design of a model of such tool. The G-Flash authoring tool, proposed in this paper is one such effort with children as the target user. Most existing tools allow children to produce their own ideas freely in self-learning condition within the digital storytelling process. Conversely, the aim of G-Flash, is to provide guided learning or assistance giving within the digital storytelling application so young children can be encouraged to receive help, motivation, hints and assistance when they need it. Assistance should not lower the motivation of the student to learn on they own, or keep the balance of giving and withholding assistance [9]. As such, assistance should only be provided to the student when they require it. However, indirect guidance should also be presented to assist students to achieve the learning goal. This later concept is build into our system architecture and framework through both elements of tutored approach and flashcards.

Illustrated flashcards are provided in G-Flash authoring tool as a media to help student understand the story that student plan to create. The illustrated flashcards is used to represent the topic of the story and provide the story materials for creating a story related to the selected topic. The illustrated images on the flashcards provides a theme of idea to the learner to recall previous knowledge or experience or even generate new ideas f or the content of the story.

G-Flash prototype system design and architecture, and design implementation issues presented in Section III and IV respectively. Prior to that Section II provides a review of related works. Finally Section V concludes this paper with direction of future work.

II. RELATED WORKS

The focus of most research works in digital storytelling has been on examining the effectiveness of digital storytelling as a communication media in teaching and learning [10] [11] [12] [13]. As a learning method, digital storytelling has become a powerful tool that helps children to have a logical sense of complex stories, by creatively presenting their experiences through crafting a storyline [14] [15]. Thus,, the storytelling concept has been applied in many discipline such as entertainment, education, engineering, and sciences.

The digital storytelling process has been made easy and interesting due to the presence of numerous multimedia tools. However, most of these tools are either general tools such as Flash, Director, 3DS, Maya, Toonz, Virtools, Quest3D, Blender, or GameStudio, which are commonly used to create interactive stories respectively multimedia application and digital games [16] or may offer certain functionality only. Often, creating an interesting and engaging media rich digital story requires combination use of several tools. Thus, the need for tools

specifically designed for digital storytelling motivates an alternative line of research among digital storytelling researchers. As a result, several models of such tools has been proposed and developed. The following paragraphs provides a review of those tools related to our work, in particular describing how the tool work has been built, the media elements used to tell story, the target audience, objectives of the works is, and how the tool works,

KidPad [4] developed by Hourcade et al., is a collaborative story authoring tool that helps children to collaborate and create a story freely by drawing, writing and zooming through the 2D information space. KidPad provides a tool on the offline platform, work in one computer only; the children interact freely with the tools which are provided in icon form menus. KidPad support self-expression and provides an advanced interaction technique in a collaborative environment. KidPad has been tested by adult and young children 6-11 years old. KidPad support a collaborative storytelling, and self-expression, however it provide no assistance giving within the design.

Wayang authoring [5] developed by dimeb Research Group of Bremen University has been built as an authoring tool with a 2D graphical character "Wayang Puppet" as a medium to help children to share their cultural diversities through enhancing digital storytelling and self-expression. "Wayang authoring" is developed on an online platform and allows children to build their own stories from their own ideas, save their stories and share them with each other. Children interact by speech, text, and 2D characters. Targeted for 6-11 years old children, Wayang authoring provides the tutorial as the guide purposes, how to use the tool.

oTTomer [7] developed by valinho et al. provides story for young children (6 to 12 years), presented in episodes at a far away planet. The concept of oTTomer is to present the story scene in a different world, a distant galaxy where there exists a little planet called oTTomer. oTTomer is a quiet and peaceful place to live until the day horrific mutants called Odoracs invaded the oTTomer. This work provides several settings, which are important in their concept: the Story, the Character, and the rooms. Children can collect story elements and interact with specific situations in each room, and change the story progress. The main goal that children should achieve is to avoid a horrific escape from the black cave and to lock any Odorac that arrives, unless he refuses to leave. oTTomer uses audio, video, animation graphic, and text as the media within tool. Tutorial and rules of the game are provided to helps user to understand how to use the tool.

The FaTe2 [17] developed by HOC-hypermedia open center offers a combination of storytelling, edutainment, and collaborative interaction paradigms. Besides, it provides a web-based, multi-user, 2D and 3D virtual space where children can meet, chat, explore, play and perform storytelling activities collaboratively. Through the FaTe2, children can interact in 2D space, watch, read and listen to multimedia fairy tales, personalize characters, write dialogues, and modify or create a scene. Children at 7-11 years old are the potential target audience of the tool. FaTe2 provides avatar, it will appear to propose which activities to undertake, to assign penalties for improper behavior, and scores for ability game.

The review of the tools described in the preceding paragraphs and as summarized in Table 1, highlighted a few important points. First, the concept or the means of telling the story differentiate one tool from another. Secondly, the environment, the characters, and the action can be produced, alone or cooperative [18] in [5]. Finally, provision for self-expression and creativity are most commonly highlighted in existing approaches that is most tools allow users to freely create their story.

Digital storytelling can be produced by any types of media, as long as this can support student to express, describe, and share their experiences within the storyline. As figure 1 shows the interaction design of the storytelling approach that commonly highlighted in numerous of works. In our previous work [19] [20], we proposed an alternative media, the illustrated flashcards as a means to not tell but also create the story. Whilst illustrated flashcards have been used widely as the learning tool, however it has never been employed a media element in digital storytelling. Researchers asserted that it is helpful to improve memory and recall [21] [22]. Thus, illustrated flashcard is incorporated in our tool to motivate children as well helps them recall their experience be creative in describing their digital stories.

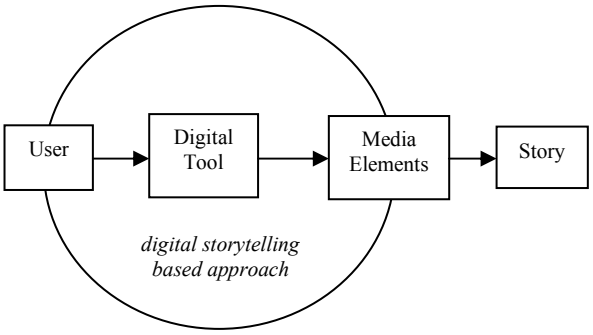


Figure 1 Interaction design of digital story based approach

Most existing tools allow users to freely design their stories. For children, our proposed target audience, this may have an adverse effect on the learning process especially when there is a specific objective need to be achieved. While self-expression led students to be creative, however, this may also led to the leaning objective not being attained. According to [23] guidance is essential to support the student thinking. Others asserted that guidance encourage children's thinking in developing concept and skill through understanding of the subject [24]. Thus, guidance was also integrates into the tool design framework [16] [9]. In particular, tutored approach, a form of guided learning was incorporated. Tutored approach provides balance of assistance giving to assist young children as the learners when they feel they need helps, in other condition it did not rob the motivation of the learners to learn on their own within withholding condition. In the tutored condition they may ask for help only when they really felt they needed it [9]. The conceptual design and the proposed system prototype are described in the next sections.

TABLE I. LIST OF DIGITAL STORYTELLING TOOL FOR CHILDREN

No	Tool Name	Concepts	Media Used	Audiences (Ages)	Assistances
1	KidPad	Collaborative Storytelling: Drawing, Writing, Printing	2D zoomable space, Iconic menus	6-11	-
2	Wayang Authoring	Interactive Storytelling: Imagining, Seeing, Composing: Writing, Talking	2D Wayang Puppet characters, Text, Audio	6-11	Tutorial
3	OTTomer	Game based Storytelling: Interacting based on game scenario by fighting the horrific mutants.	Scenario, Audio, Video, Animation, Graphic, Text	6-12	Tutorial
4	Fate2	Edutainment based Storytelling: Writing, Character Dialogue, and Collaborating.	2D environment: Scenario, Characters, Objects. 3D interaction space.	7-11	Tutored Condition with avatar designed as the assistance during the process of story creation

III. G-FLASH PROTOTYPE SYSTEM DESIGN AND ARCHITECTURE

Generally, for existing designs of digital storytelling which are meant for teaching and learning, the designs metaphors are built as interaction with the system – not interaction with the information that learners are looking for. In this case, the interaction is system-centered; that is, the focus is not on the needs of the learner. According to [25], learner-centered designs focus on developing a learner's understanding, rather than on improving usability issues. Rabin et al [26] further argue that the design framework developed through this process should support the learner's needs by giving the instructor option to help them through adaptable tasks. The design of our tool is based on the later. The following subsection described our system further.

A. System Conceptual Design

The overall aim of the design of the tool is provide guidance to user in creating the digital story through the use of illustrated flashcards. Thus the design of the tool is based on the two key elements described in the preceding sections: Guided learning (tutored approach) [9] and Illustrated Flashcards [27]. Both are interrelated and complement each other in terms of functionalities. Basically, the flashcards provides guidance throughout the story creation process, from topic selection to the composing of the story itself. To further assistance in the story creation, students are free call upon the virtual tutor at any time when needed. Figure 2 illustrates the system conceptual design and the relations between the key elements.

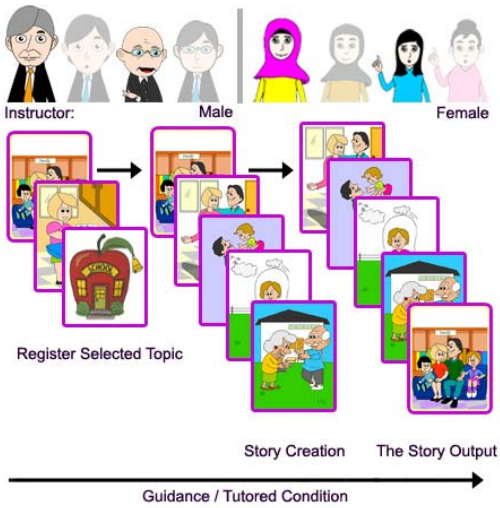


Figure 2. A G-Flash authoring prototype conceptual design and relation between the key elements

B. System Architecture

The G-Flash prototype is a Flash-based application developed using Adobe Flash CS3, and Action Script 2.0 as the core design platform. It is designed as a web-based application supported by PHP 5 (for the server) and MySQL (for the database). Initially the system was proposed as a standalone application; however, due to accessibility issue in which more audience could be reached, an internet based option was selected.

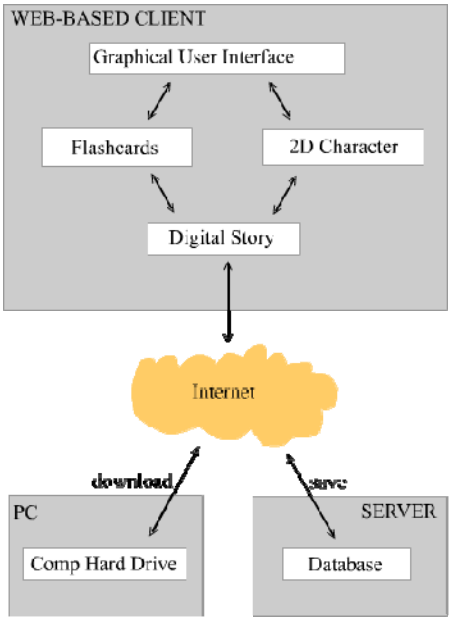


Figure 3. System Architecture for G-Flash.

The G-Flash system architecture is shown in Figure 3. From the figure, the user interacts with the system through a web-based client. A graphical user interface was provided by the application for user interaction with the system. The flashcards are employed as media elements to select the topic of the story and within the digital story composition. An instructor based on 2D character design was created to assist children along the digital story composing process. A database, which serves as a storage space for personal information and story information, resides at the server. However, an executable file is generated as the output of the story creation process and the children can download it and save it into their own personal computer hard drive.

Overall, the G-Flash authoring tool treats the application as a collection of cards and objects. Children register a card as the main theme of the story based on the selected topic, and then register a 2D character as assistance representative object, that designed as the "assistance or instructor" during the process of story creation.

C. *System Flow*

Figure 4 illustrates the system flow for the G-Flash authoring tool application.

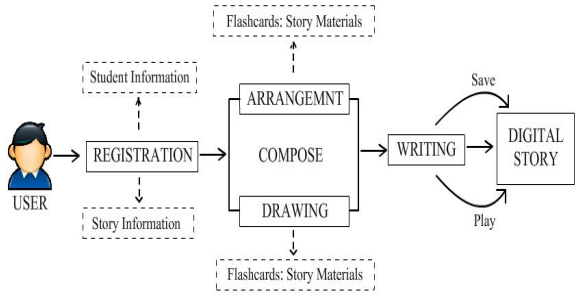


Figure 4. The system flow of G-Flash authoring tool.

From the figure 4, the learner begins the interaction process in the *Registration* stage. *Arrangement* and *Drawing* are the storytelling methods, to compose a digital story by using illustrated flashcards as the story media and materials. *Writing* is the next stage, in which the learner needs to describe each flashcard that was successfully arranged. Finally a digital story will be saved, and an executable file will be generated to allow young learners to play their own stories in personal computer. Figure 5 and 6 shows the webpage of the Registration, Arrangement and Drawing respectively. The final output, that is the completed digital story, presented in the form of free-flow or user-controlled flashcards animation including the card description is shown in Figure 7.



Figure 5. The story registration page

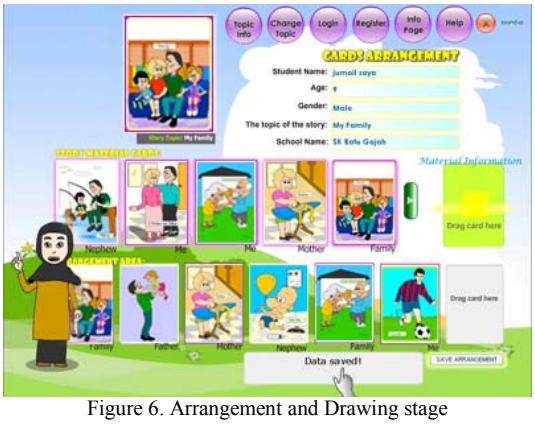


Figure 6. Arrangement and Drawing stage



Figure 7. Example of a final output, the complete digital story

IV. Design And Implementation Issues

Several design & issues arises during the development and initial testing of the prototype system. One major drawback of the system is on the number of flashcards presently at only seven for each story limits the choice of user to create the story. Thus, more flashcards for each story are needed for user to create more interesting sto-

ries. Moreover, creative written scripts for the virtual instructor are needed to motivate students.

In terms of the list of topics, currently the user is limited to what is available in the system. However, the challenge is to provide a suitable list of topics commonly used by teachers and children to relate their experience through digital storytelling. Generating this list may require conducting survey on the target user.

V. CONCLUSION

In this paper, we describe the design framework of an authoring tool to facilitate the digital storytelling process for children. While free expression in story design allows users to be creative, some form of guidance is still seen as necessary for users to achieve the stated objective in learning. Thus guided learning or tutored approach concept, which is lacking in existing tool, was incorporated in the design to provide guidance on the story creation. In our tool design, we introduce the use of illustrated flashcards to act as a guide in the terms of a `tool for memory recall of user experiences as well as idea generation. As a media element, the series of flashcards is used to guide story creation. The presence of virtual tutor or guide which can be called at any time further provide users with assistance in composing the story as well as on how to use the tool itself. As an online tool, user interacts with the system using a web-based client using internet as the running platform. A database is built in a server to save user personal information, story information, and documenting completed stories.

Future works includes conducting usability studies on the system as well as examining its acceptance and usefulness among potential users through comprehensive evaluation.

ACKNOWLEDGMENT

We wish to express sincere thanks and gratitude to the Department of Computer and Information Science of Universiti Teknologi PETRONAS for providing the environment, lab, and supporting tools in which this work has been made possible. This work is sponsored in part by the Fundamental Research Grant provided by the Ministry of Higher Education of Malaysia. Without that support we would not have been able to achieve the result presented herein.

REFERENCES

[1] T. U. o. Houston. "The educational uses of digital storytelling," 2009. [Online]. Available: http://digitalstorytelling.coe.uh.edu/. [Accessed: Dec. 16, 2009].

[2] J. Lambert. "Digital storytelling cookbook and travelling companion," Version 4.0. *Digital Dinner Press*. May. 2003.

[3] M. Jenkins, J. Lonsdale. "Evaluating the efectiveness of digital storytelling for children reflection," Center For Active Learning. Uiversity of Gloucestershire. *Proc. Ascilite Singapore 2007*.

[4] J. P. Hourcade, B. B. Baderson, A. Druin, G. Taxen. " KidPad: Colaborative Storytelling for Children, " *Proc. Human Factor in Computing System (CHI 2002)*, ACM press, April.2002, pp. 500-501.

[5] W. A. Widjajanto, M. Lund, H. Schelhowe. "Wayang Authoring: A Web-based Authoring Tool for Visual Storytelling for Children," *Proc. MoMM 2008, Nov. 2008*, pp. 464-467

[6] Vaucelle, C., Jehan, T. "Dolltalk: A computational toy to enhance children creativity," Short Talk: Portporri: Children and Virtual Reality. *CHI 2002, April 20-25, 2002*. Minneapolis, Minnesota, USA. ACM 1-58113-454-1/02/0004.

[7] P. Valinho, N. Correia. "oTTomer: An interactive adventure system for children," *SRMC'04, October 15, 2004*, New Tork, New York, USA, p. 71-74.

[8] C. H. Miller. "Digital Storytelling: A Creator's Guide to Interactive Entertainment," (Focal Press, 2004). ISBN 0-240-80510-0. p. 3-10.

[9] Borek, A. McLaren, M, B. et al. (2009). How Much Assistance is Helpful to Student in Discovery Learning. U. Cress, V. Dimitrova, and M. Speecht (Eds): EC-TEL 2009, LNCS 5794, pp. 391-404, 2009.

[10] Brian, M.L.: 'Storytelling with digital photographs: supporting the practice, understanding the benefit'. *Proc. CHI '08* extended abstracts on Human factors in computing systems, Florence, Italy2008 pp. 2657-2660.

[11] McLellan, H.: 'Digital storytelling in higher education', *Journal of Computing in Higher Education, 2007*, 19, (1), pp. 65-79

[12] Sanchez, T. Zam, G. Lambert, J.: 'Story Telling as an Effective Strategy in Teaching Character Education in Middle Grade Social Studies', *Journal for The Liberal Arts and Science, 2009*, (2), pp. 14-23

[13] Kimiko, R., Michael Jongseon, L., and Jonathan Micah, B.: 'Children's storytelling and programming with robotic characters'. Proc. Proceeding of the seventh ACM conference on Creativity and cognition, Berkeley, California, USA2009 pp. 19-28

[14] F. V. Gils. "Potential applications of digital storytelling in education," 3rd Tweenty Student Conference in IT, Enschede June 2005. University of Twente, Faculty of Electrical Engineering, Mathematics and Computer Science.

[15] A. Sadik. "Digital Storytelling: a meaningful technology-integrated approach for engage student learning," *Education Tech Research Dev, 2008*, pp. 487-506, doi: 10.1007/s11423-008-9091-8.

[16] Gobel, S., Salvatore, L. (2008). Storytec: a digital storytelling platform for the authoring and experiencing of interactive and non-linier stories. U. Spierling and N. Szilas (Eds). *ICIDS 2008*, LNCS 5334, pp. 325-328, 2008.

[17] F. Garzotto, M. Forfori. "FaTe2: Storytelling Edutainment Experiences in 2D and 3D Collaborative Speces," *IDC'06*, Jun 7-9, 2006, pp. 113-116.

[18] When, K. 2004. Machinima – Was Ego–Shooter und puppentheater gemeinsham haben. Telepolis. (15 August 2008). http://www.heise.de/tp/r4/artikel/17/17818/1.html

[19] Jumail; Rohaya, D.; Rambli, A.; Sulaiman, S.; , "A design framework for flashcards based guided digital storytelling," *Computer and Automation Engineering (ICCAE), 2010 The 2nd International Conference on* , vol.3, no., pp.4-8, 26-28 Feb. 2010

[20] Jumail; Rambli, D.R.A.; Sulaiman, S.; , "A guided digital storytelling prototype system using illustrated flashcards," *Information Technology (ITSim), 2010 International Symposium in* , vol.1, no., pp.1-6, 15-17 June 2010

[21] Palombella, A.L., and Johnson, D.P. (2004) "The Design Use and Evaluation of Hypermedia Flashcards as A teaching Tool," *TechTrends,* Vol 49, No.2. pp.46-54.

[22] Hayter, S., Scott, E., et al. (2007). The Use Modified Direct Instruction Flashcards System With Two High School Students with Developmental Disability. Publish online: 28 June 2007.

[23] B. K. Bayer. "Improving student thinking. A comprehensive approach," Forward by A. L. Costa. 2004. ISBN 0-205-15062-4. p. 168.

[24] Department for Education and Skill "Pedagogy and Practice: Teaching and Learning in Secondary School," 2004. [Online]. Available: http://www.sjl.herts.sch.uk/teachingtoolkit/PDF/Guided Learning.pdf. [Accessed: April. 18, 2010].

[25] Soloway, E., Guzdial, M., and Hay, K.E. (1994). Learner-centered design: The challenge for HCI in the 21st century. *Interactions*. 1(2): p. 36-48.

[26] M. D. Rabin, M. J. Burns. Multimedia Authoring Tool. In Conference Companion on Human Factors in Computing Systems: Common Ground," Vancouver, British Colombia,

Canada, April 13-18, 1996. M. J. *Tauber, ed. CHI'96*, ACM, New York, 1996, pp. 380-381.

[27] ESL Flashcards.com. “Free ESL Flashcards,” [Online]. Available: http://www.eslflashcards.com/. [Accessed: Feb. 24, 2011].

GIS Integrated DNA Computing for Solving Travelling Salesman Problem

R.Sridhar,
Sri Ramakrishna Mission Vidyalaya
College of Arts and Science
Bharathiyar University,
Coimbatore, India

Dr S Balasubramaniam,
DRDO-BU CLS,
Bharathiyar University,
Coimbatore, India

Abstract

DNA computing is a new method of simulating biomolecular structure of DNA and computing by means of molecular biology technological computation. It introduces a fire-new data structure and calculating method, providing a new way of solving NP-complete problem of traveling salesman. It is a new computational method by harnessing the enormous parallel computing ability and high memory density of bio-molecules, which brings potential challenges and opportunities to cryptography, steganography, Signature and Authentication. In this paper, DNA computing is integrated with GIS to find shortest path of traveling salesman problem with geocomputational method and DNA Computing method without using laboratory. Both methods show the same result proving that problems of GIS could be solved using DNA computing.

Keywords : DNA Computing, GIS, Shortest path, Geocomputational

I. Introduction

DNA computing is a form of computing which uses DNA, biochemistry and molecular biology, instead of the traditional silicon-based computer technologies. DNA computing, or, more generally, molecular computing, is a fast developing interdisciplinary area. It was started when Leonard Adleman, father of DNA Computing spawned the field with his paper "Molecular Computation of Solutions of Combinatorial Problems"[1], solved Travelling Salesman Problem and obtained solution using DNA experiment. Since then, Adleman has demonstrated how the massive parallelism of a trillion DNA strands can simultaneously attack different aspects of a computation to crack even the toughest combinatorial problems, such as the government's supposedly uncrackable Data Encryption Standard [2]. Quyang presented a molecular biology-based experimental solution to the maximal clique problem[3]. Liu designed a DNA Computing model system to solve the satisfiability problem [4]. Benenson designed a programmable and autonomous computing machine made of biomolecules, on which a finite automation can run [5]. Independently of the future technological success of DNA computing, this area has led already to interesting new computing paradigms which are certainly enriched our understanding of the nature of computation[6].

II. DNA and DNA computing

A. DNA

DNA(Deoxyribonucleic Acid) is the germ plasm of all life styles. It is a kind of biological macromolecule made up of nucleotides. In a DNA molecule, deoxyribonucleotides are joined into a polymer by phosphodiester bond between the 5' hydroxyl of one ribsose and the 3' hydroxyl of the next, thus left a free 5' end and a free 3' end. DNA molecules are directed polymers written from the 5' to the 3' end. Each nucleotide contains a single base. There are four kinds of bases, which are Adenine(A) and Thymine(T) or Cytosine(C) and Guanine(G). DNA most commonly occurs in nature as the well-known "double-helix" but both single and double DNA string fragments can be synthesized outside the cell. In a double helix DNA string, two strands are complementary in terms of sequence that is A to T and C to G according to Watson-Crick rules.

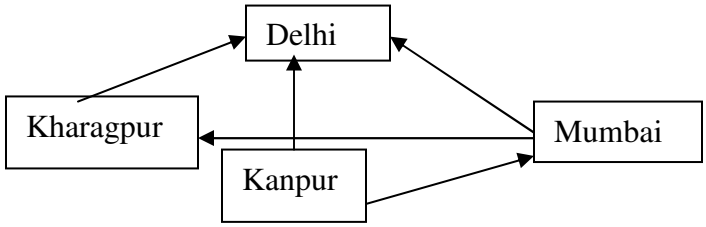
B. DNA Computing

Adleman used fragments of DNA to compute the solution to a complex graph theory problem. Adleman's method utilizes sequences of DNA's molecular subunits to represent vertices of a network or graph. Thus, combinations of these sequences formed randomly by the massively parallel action of biochemical reactions in test tubes described random paths through the graph. Using the tools of biochemistry, Adleman was able to extract the correct answer to the graph theory problem out of the many random paths represented by the product DNA strands. The algorithm that Adleman [8][9] implemented in the first DNA Computation.

III Methodology

A. DNA Computing Algorithm

Step 1: Generate a large number of paths through the graph He took a pinch (about 10^{14} molecules) of each of the different sequences and put them into a common test tube[10]. To begin the computation he simply added water - plus ligase, salt and few other ingredients to approximate the conditions inside the cell. Altogether only about one fiftieth of a teaspoon of solution was used. Within about the one second, he held the answer to the Hamiltonian path problem in his hand.To see what remains in the test tube: for example, the Kanpur to Mumbai flight number (TCGAGTAC) and the complimentary name of Mumbai (CATGTGAT) might meet by chance. By design, the first sequence ends with GTAC and the second sequence starts with CATG. As these sequences are complimentary to each other, they will stick/anneal together. If the resulting sequence now encounters the Mumbai-to-Kharagpur flight number (ACTACGAT), it too, will join with the resulting sequence because the first sequence (TGAT) is complimentary to the beginning of the second (ACTA). In this way the resulting sequence will grow in length, with DNA flight numbers together by complimentary DNA city names. The addition of ligase in the mixture will then permanently concatenate the chains of DNA flight numbers. Hence the test tube contains molecules that encode random paths through the different cities. Because he began with such a large number of DNA molecules and the problem contains just a handful of cities, there was a virtual certainty that at least one of the molecules formed would encode the Hamiltonian path. It was amazing to think that the solution to a mathematical problem could be stored in a single strand. For the above graph, the following are some of the paths that are generated after step1.



City	DNA Name	DNA Name Complement
Kanpur	ATCGTCGA	TAGCAGCT
Mumbai	GTACACTA	CATGTGAT
Delhi	TCAGACGA	AGTCTGCT
Kharagpur	CGATCGAT	GCTAGCTA

Flight Number	DNA Flight
Kanpur-Mumbai	TCGAGTAC
Kanpur-Delhi	TCGATCAG
Mumbai-Delhi	ACTATCAG
Kharagpur-Delhi	CGATTCAG
Mumbai-Kanpur	ACTAATCG

Kanpura →Delhi
5"TAGC AGCT AGTC TGCT3"
3"TCGA TCAG 5"

Kanpura→Mumbaia →Delhi
5" TAGCAGCT CATGTGAT AGTCTGCT 3"
3" TCGA GTACACTA TCAG 5"
Kanpura →Mumbaia →Kanpura →Mumbaia →Delhi
5"TAGCAGCTCATGTGATTAGCAGCTCATGTGATAG TCTGCT3"
3'TCGAGTACACTAATCGTCGAGTACACTATCAG5"

Kanpura→Mumbaia→Kharagpura→Delhi
5"TAGCAGCTCATGTGATGCTAGCTAAGTCTGCT3"
3"TCGAGTACACTACGATCGATTCAG5"

Step2: Amplification of paths by PCR:

Unfortunately, although he held the solution in his hand, he also held about 100 trillion molecules that encoded paths were not Hamiltonian. After performing PCR(polymerase chain reaction), the following are the paths that begin at Kanpur end at Delhi.

Kanpura -→Delhi
5"TAGCAGCT CATGTGAT AGTCTGCT3"
3"TCGA GTACACTA TCAGA5"

Kanpura→Mumbaia →Delhi
5"TAGC AGCT CATGTGAT GCTAGCTA AGTC TGCT3"
3"TCGAGTACACTACGATCGATTCAG5"

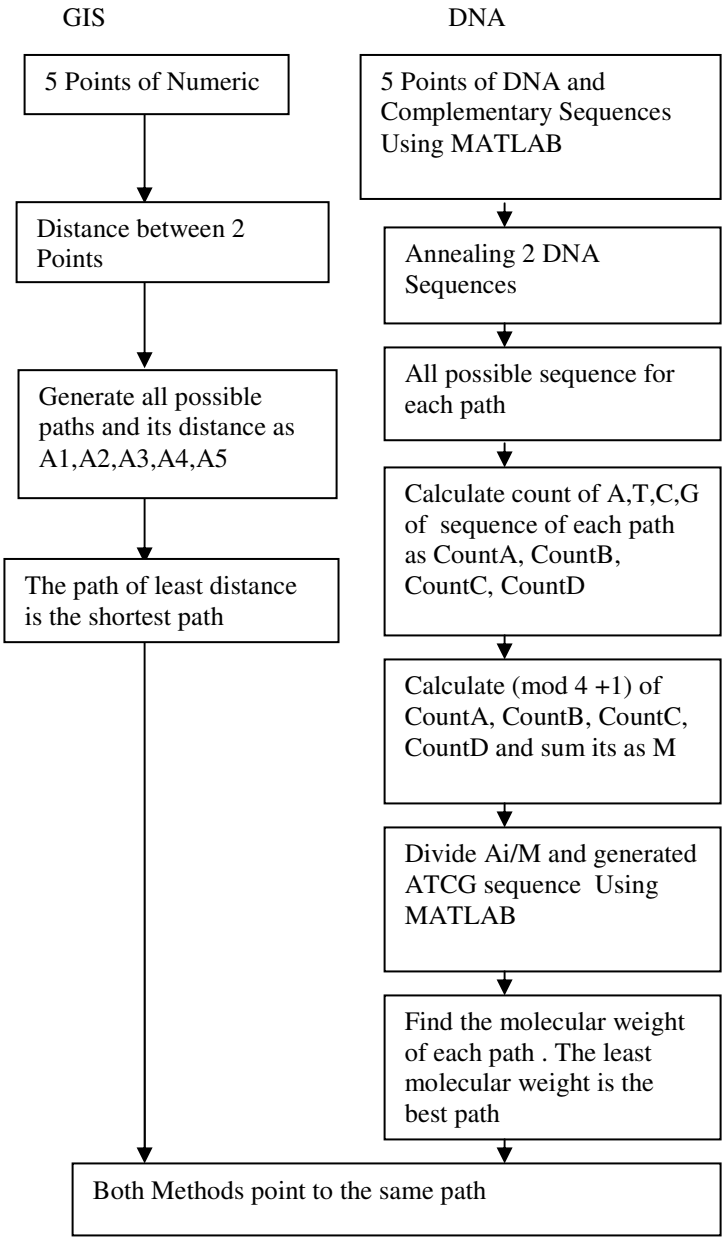
Kanpura →Mumbaia →Kanpura→Mumbaia →Delhi
5"TAGCAGCT CATGTGAT TAGCAGCT CATGTGAT AGTCTGCT3"
3"TCGAGTACACTAATCGTCGAGTACACTATCAG5"

Kanpura→Mumbaia→Kharagpura→Delhi
5"TAGCAGCT CATGTGAT GCTAGCTA AGTCTGCT3"
3"TCGA GTACACTA CGATCGAT TCAG5"

Step3: Gel-Electrophoresis
Next, he used gel electrophoresis to identify those molecules that had the right length (in our example a length of 24). All other molecules were discarded. For the above graph, after the completion of gelelectrophoresis the following path would be identified as length 24.

Kanpura→Mumbaia→Kharagpura→Delhi
TCGAGTACACTACGATCGATTCAG

IV. Flowchart of Integeration of GIS and DNA to compute the shortest path



V. Explanation and Result

A.. Explanation of GIS integrated DNA Computing for solving Travelling Salesman Problem

Step 1: Latitude and Longitude is known for a given map. A set of map points are plotted on the map whose values are displayed in the Grid which is marked sequentially shown in the Table 1. For each point a random sequence of ATCG of length 10 is generated using function Ranseq() of Matlab . Its complimentary is also generated which is shown in the Table 2.

Step 2: Once source and destination are given, the different paths from source to destination for a given set of points are generated shown in the Table 5

Step 3: Distance between two points of latitude and longtitude is calculated using an algorithm . pathdistance() array stores all possible paths and its distance. Shortest path by geocomputional method is shown in the Figure 1 and its algorithm shown below.

```
For i=1 to number of paths
For j=1 to number of ways for a given path
Const Radius = 6378007
'radius of Earth in meters
Const Pi = 3.141592
Const Circumference = Radius * 2 * Pi
Const metersPerLatDD = 111113.519
deltaXdd = Abs(ddX1 - ddX2)
deltaYdd = Abs(ddY1 - ddY2)
centerY = (ddY1 + ddY2) / 2
metersPerLongDD = (Cos(CenterY * (Pi / 180)) *
 Circumference) / 360
deltaXmeters = metersPerLongDD * deltaXdd
deltaYmeters = metersPerLatDD * deltaYdd
ddDistanceMeters = Sqrt(deltaXmeters^2 + deltaYmeters^2)
  distance= distance +dddistancemeters
  next
  pathdistance(i)=distance
  distance = 0
  next
```

Step 4 : DNA sequence generated in step 2 for which different Permutations are calculated. Let us consider first point as ATCGAAGTAG and second point as CAACTGAAGA. The 1->2 will be AGTAGCAACT and 2->1 will be GAAGAATCGA. This is being repeated for all set of Points are shown in the table 4.

Step 5: A set of sequence is calculated using step 4 for each path.

Step 6: Find the smallest value in the array of pathdistance. Shortest DNA sequence of each path are calculated as follows:

Step a: Find the count of A,C,T,G and represent it as countA, countC, countT, countG.

Step b: Find the remainder of CountA, countC, countT, countG by 4. Add 1 to it. Sum up their results. Divide Geographic distance by their sum. Generate a sequence accordingly, which is not shown in the table , but its length is shown in the Table 6.

Step c: Find the shortest length of the sequence shown in the Table 6

B. Results

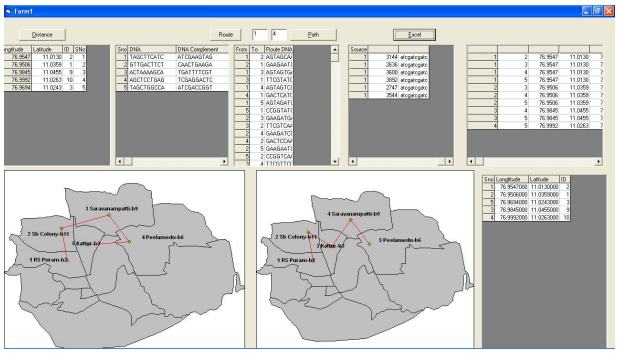


Figure 1. First Map shows 5 points selected by the user, Second Map shows the shortest path from source to destination

Table 1:
Longtitude and Latitude for a given point

Longtitude	Latitude	ID	SNo
76.9547	11.013	2	1
76.9506	11.0359	1	2
76.9845	11.0455	9	3
76.9992	11.0263	10	4
76.9694	11.0243	3	5

Table 2:
DNA elements for a given point

Sno	DNA	DNA Complement
1	TAGCTTCATC	ATCGAAGTAG
2	GTTGACTTCT	CAACTGAAGA
3	ACTAAAAGCA	TGATTTTCGT
4	AGCTCCTGAG	TCGAGGACTC
5	TAGCTGGCCA	ATCGACCGGT

Table 3:
Since 5 points are plotted on the map, their Different Permutations of Distance between set of points

Point 1	Point 2	Latitude of point1	Longtitude of point1	Latitude of point2	Longtitude of point2	Distance(m)
1	2	76.9547	11.013	76.9506	11.0359	2583.634
1	3	76.9547	11.013	76.9845	11.0455	4862.315
1	4	76.9547	11.013	76.9992	11.0263	5081.897
1	5	76.9547	11.013	76.9694	11.0243	2038.714
2	3	76.9506	11.0359	76.9845	11.0455	3854.351
2	4	76.9506	11.0359	76.9992	11.0263	5416.137
2	5	76.9506	11.0359	76.9694	11.0243	2425.005
3	4	76.9845	11.0455	76.9992	11.0263	2670.369
3	5	76.9845	11.0455	76.9694	11.0243	2875.893
4	5	76.9992	11.0263	76.9694	11.0243	3263.6

Table 4:
Different Permutations of DNA elements between set of points shown in the above Table 1.

From	To	Route DNA
1	2	AGTAGCAACT
2	1	GAAGAATCGA
1	3	AGTAGTGATT
3	1	TTCGTATCGA
1	4	AGTAGTCGAG
4	1	GACTCATCGA
1	5	AGTAGATCGA
5	1	CCGGTATCGA
2	3	GAAGATGATT
3	2	TTCGTCAACT
2	4	GAAGATCGAG
4	2	GACTCCAACT
2	5	GAAGAATCGA
5	2	CCGGTCAACT
3	4	TTCGTTCGAG
4	3	GACTCTGATT
3	5	TTCGTATCGA
5	3	CCGGTTGATT
4	5	GACTCATCGA
5	4	CCGGTTCGAG

Table 5:
All possible paths from Source to Destination and its Distance

Source	Via 1	Via 2	Via 3	Destination	Total Distance (m)
1	2	3	5	4	12577.4777
1	2	5	3	4	10554.9005
1	3	2	5	4	14405.2706
1	3	5	2	4	15579.3492
1	5	2	3	4	10988.439
1	5	3	2	4	14185.0948

Table 6:
DNA distance is computed without using PCR and Gel- Electrophoresis

DNA Route from source to Destination	Length of the sequence	Molecular weight
AGTAGCAACT,GAAGATGATT, TTCGTATCGA,CCGGTTCGAG,	3144	261260.00
AGTAGCAACT,GAAGAATCGA, CCGGTTGATT,TTCGTTCGAG,	2636	219050.00
AGTAGTGATT,TTCGTCAACT, GAAGAATCGA,CCGGTTCGAG,	3600	299150.00
AGTAGTGATT,TTCGTATCGA, CCGGTCAACT,GAAGATCGAG,	3892	323410.00
AGTAGATCGA,CCGGTCAACT, GAAGATGATT,TTCGTTCGAG,	2747	228300.00
AGTAGATCGA,CCGGTTGATT, TTCGTCAACT,GAAGATCGAG,	3544	294500.00

V Conclusion

On comparison of Geographical distance and DNA distance, it is being found that 1-2-5-3-4 is the shortest path distance for a given source as 1 and destination as 4. DNA sequence of each path will be tested as per procedure given by Adelman experiment in the Laboratory using PCR and Gel-electrophroesis. We hope that the result obtained through the above procedure will remain the same as of geographical distance.

Research on DNA computing is in child state but it has massive parallelism which can overcome the difficulties that may not be trackable by silicon computers.The concept of DNA Computing has wide opening in the fields of cryptography and steganography for developing a better algorithms than the existing one.

References

[1] L.M Adleman, "Molecular computation of solutions to combinatorial problems", Science, 266, 1994, 1021-1024

[2] Gehani A, LaBean T H, Reif JH, DNA-based cryptography. Dismacs Series in Discrete Mathematics and Theoretical Computer Science,2000 54:233-349.

[3] Ouyang, Q.et al. DNA solution of the maximal clique problem, Science,1997,278:542

[4] Liu,Q et al. DNA computing on surfaces Nature 2000 403:175

[5] Beneenson,Y et al. Programmable and autonomous computing machine made of biomolecules. Nature, 2001, 414:430.

[6] Kamei, T et. al. NA-containing inks and personal identification system using them without forgery, Jpn, Kokai Tokkyo Koho, 2002, 8 pp Kawai J, Hayashizakhi Y, DNA book, Genome Res, 2003, 13, 1488-1495.

[7] R.J.Lipton, "DNA solution of HARD Computational Problems", Science,268,1995,542-545.

[8] Masahita Yamamoto, Nobuo Masuura, "Solution of Shortest Path Problem by Concentration Control", DNA based computers 5, DIMACS series in Discrete Mathematics and Theoretical Computer Volume 54,2000, 101-110.

[9] V Shekhar, Ch.V.Ramana Murthy, .V.Gopalacaharyulu and G.P Rajasekhar, "DNA Solutions to the shortest path problem", ICADS-2002, Dec22-24, Dept of Mathematics, IIT Kharagpur.

[10] Martyn Amos, Gheorghe Paun, Grzezorg, rozenberg and Arto Salomaa, "Topics in the theory of DNA computing," Theoretical computer science, 287,2000,3-38

Illuminance Distributions, Visual Response and Limits for Conservation of Exhibits in Admiral Cheng Ho Gallery, Malaysia

N. Ahmad[1], S. Sh Ahmad[1, 2] and A. Talib[1]
[1] Faculty of Architecture, Planning & Surveying,
[2] Research Management Institute,
Universiti Teknologi MARA, 40450 Shah Alam, Malaysia
e-mail: sabar643@salam.uitm.edu.my

***Abstract*—This paper presents i) literature review of illuminance limits for conservation of exhibits; ii) pilot study on illuminance levels and distributions, air temperatures and relative humidity, RH and iii) survey results on visitors' visual feedbacks on the exhibits' conditions conducted at the Admiral Cheng Ho Gallery (Museum of History and Ethnography), Stadthuys, Melaka, Malaysia. Indicators for visual discomfort are observed from objectives ii and iii. The fieldwork was a pilot survey in the west facing gallery during high period of daylight distributions (14.00 -16.00hr) for a full week in March 2010. Results showed illuminance levels exceeded allowable exposure limits for some showcases. Measured air temperatures were much higher than accepted comfort range especially with opened windows in the afternoon and the RH levels were within the prescribed range. The survey identified the combination of natural daylight and artificial lighting deteriorated the exhibits' conditions through fading, distortion, dirt and dust. The showcases were placed against and opposite the fully opened windows. Thus, the presence of sunlight, daylight and provision for external views in the gallery produced glare and veiling reflections problems on the glass showcases. These situations may demonstrate the need for proper maintenance and appropriate controlled shading system. The evaluation of daylight distributions may serve as future conservation measure for the exhibits.**

***Keywords* – Historic Building; Daylit museum gallery; Light Damage; Conservation Limits; Daylight Control; Tropical Climate.**

I. INTRODUCTION

Light degrade and damage museum exhibits over time [1]. Factors that contribute to its damaging effects are the material of artefact, the type and intensity of light they are exposed to and the duration of the exposure. The visible and ultraviolet components of light can cause materials to fade. Excessive heat from light may cause certain materials to become dehydrated and show damages of shrinkage [2]. Although fading and deterioration of museum artefacts caused by light is unavoidable over time, protection of indoor environment can considerably lessen decline of artefacts and protect the collection [3]. Thus, monitoring and controlling museum lighting is key factors in ensuring the long-term preservation of museum artefacts.

The objectives of this study are to assess levels and distribution of measured daylight and artificial light and analyse visitors' visual response and feedback on the exhibits' conditions in the showcases.

II. LITERATURE REVIEW

A. *Lighting Limits for Conservation of Artefacts*

Macleod, 1978 in this review paper on lighting limits for artefact conservation [4] recommended safe lighting levels; a maximum of 50lux for light-sensitive objects (water colours, tapestries, etc.), a minimum of 150 lux for other items, and up to 300 lux for more robust materials (stone, metals, etc.). Pearson 1979 recommended lighting levels for several museum objects as shown in Table 1 [4].

TABLE 1
LIGHTING LEVELS [4]

Material	Illumination (Lux)	UV (W/lm)	UV (W/m^2)
Oil and tempera paintings, undyed leather, lacquers, wood, horn, bone and ivory.	150	80	12000
Textiles, watercolours, furniture, prints, and drawings, manuscripts, stamps, miniatures, wallpapers, dyed leather, and natural history exhibits.	50	30	1500

Thomson [5] recommended a simple two-level sensitivity approach for the illuminance of art objects: (i) daylight and artificial light level for moderately sensitive materials is 200±50 lux and (ii) artificial light for sensitive material is 50 lux. In either case the ultraviolet radiation was recommended not to exceed 75w/lm. These limiting values in Table 2 have been accepted by CIBSE, more acknowledged within the museums community [6].

TABLE 2
PHOTOCHEMICAL RESPONSIVITY CATEGORY OF MUSEUM OBJECTS [6]

Responsivity Category	***Objects***
I- Highly responsive	*Textiles, costumes, tapestries, paper, parchment, dyed leather, painted or dyed wood, natural history exhibits i.e., botanical specimens, fur and feathers.*
II-Moderately responsive	*Oil and tempera painting, fresco, undyed leather, horn, bone, unpainted wood and lacquer, some plastics*
III-Non-responsive	*Metal, stone, glass, ceramics, enamel, most minerals*

The Illuminating Engineering Society of North America (IESNA) has drastically changed its recommendations for art galleries & museums, and has specified maximum annual exposure in lux hours (lx hr y^{-1}) as discussed by Cuttle [7]. Meanwhile, Michalski [8] determined the sum of exposure or quantity of light on a surface is the result of light intensity

(lux) and time (hours) = Lux hours. This is an alternative approach that restricts annual exposure of artefacts to illuminance and hours of exposure. This method has been accepted as option recommendation by CIBSE, and the limiting values of both CIBSE and IESNA are shown in Table 3 [8].

TABLE 3
LIMITING CUMULATIVE EXPOSURE LIMITS (lx hr y^{-1})
ACCORDING TO RESPONSIVITY CATEGORY [8]

Responsivity category	CIBSE	IESNA
Highly responsive	150 000	54 000
Moderately responsive	600 000	500 000
Non-responsive	-	-

Westerhuis [8] discussed that Padfield, 1996 also emphasized that the illumination of an object (in Lux), does not calculate the destructive photochemical property of light. Problem lies when the lighting standard is commonly based on illumination of the object or based on intensity without understanding the underlying photochemistry [8]. Material fading is cumulative and depends on the light dose, regardless of rate [8]. The restriction on cumulative annual dosages must be based on amount calculated from the maximum illuminance levels x visiting hours, as opposed to division of commonly accepted dosages related to material and artefact deterioration [9].

Wilson [10] highlighted that some well monitored daylighting systems (rooflights/skylights) maintain 200 lux on the sensitive objects, but the lux hour proved to be more passive method to restrict dosages and maintain artefact preservation requirements. Wilson proposed figures in Table 4 which should be considered based on the premise that full positive reception of colour is not attained when illumination falls below 250lux. The recommended light levels for artefacts exclude the use of daylight.

TABLE 4
EXPOSURE LIMITS [10]

	Maximum Illuminance (Lux)		Maximum accumulated yearly exposure (Lux-hours)	
	UK	US	UK	US
Sensitive objects (eg. watercolours)	50	50	150,000	50,000
Medium sensitive objects (eg. oil painting)	200	200	600,000	480,000

Similar to the above, Balocco et al. [11] stated that Italian Standards prescribed that illuminance levels recorded on the surface of the tapestries, that is the "annual dose of light" or "maximum annual light energy exposure" should not surpass 200 klx*hours/year and the maximum illuminance value is 50 lx.

B. Visual Discomfort

Museums have the most difficult lighting criteria of all building types. Its application is necessary to enhance and view museum objects, but at same time the exhibition and conservation needs must be balanced. Previous studies indicated that several lighting problems in museum galleries were mainly due to direct sun penetration over the display areas. Many visual comfort problems were found associated to high illuminance levels, glare, high contrast areas, and lack of visual adaptation and overheating.

Menzies et al [12] highlighted that daylight can give rise to visual discomfort such as glare, reflections, light veiling or shadows. They reported that Boubekri and Boyer found that facades with window to wall ratio of between 40 and 55%, perceived above average visual discomfort due to glare. Osterhaus [13] explained that glare from windows are the result of direct sunlight or sunlight reflection off exterior surfaces that "enter a room and shine into the eyes of occupants or reflected off visual tasks and surrounding surfaces."

IESNA [14] defined glare as ''the sensation produced by luminance within the visual field that is sufficiently greater than the luminance to which the eyes are adapted to cause annoyance, discomfort or loss in visual performance and visibility". Glare consists of disability glare and discomfort glare. Disability glare is the "effect of stray light in the eye whereby visibility and visual performance are reduced" [14]. It causes discomfort and does not inevitably interfere with visual performance or capability.

Wilson [10] highlighted that objects displayed against windows are displayed against a high luminance (very bright) background. The surface colour and reflectance can also have a key impact on the level of illuminance in an interior [10]. Highly bright light sources may produce reflections in the glass of display cabinets, thus affecting the visibility of objects within the cabinet [10] and cause veiling. Our sensitivity to veiling reflection depends on the balance between the brightness of the reflection and the object. A low reflectance surface on the background of the glass cabinet can also reduce the adaptation level of the eye, and improves the visibility of the exhibited object [10].

The above literatures discussed on lighting limits for artefact conservation using cumulative annual exposure and visual discomfort issues.

III. METHODOLOGY

Two methods of research were employed for this pilot study which was based on a selected museum gallery, namely field measurement and survey on visitors' visual perception of exhibit conditions.

A. Case Study

The Admiral Cheng Ho Gallery, Melaka was chosen for this pilot study to understand issues and refine research methods before a more comprehensive study is embarked. This case was selected because it presented indoor daylighting with showcases of highly to non-sensitive materials, allowing for comparison between showcases placed on adjacent window wall and showcases placed on opposite window wall. All of them have the same light level demand, with similar museum exhibits (printed materials) but with different showcase placements.

The west facing gallery is located on the right porch of the Stadthuys (Museum of History and Ethnography), also known as the Dutch Square. This 1650 building, the oldest remaining Dutch building in the Orient, has been preserved in its original architectural form. It is situated in the historic precinct of Melaka city (latitude 2^{O} 11' 40.02" N, longitude102^{O} 14' 58.00" E, elevation 13m). This gallery

displays the stories of Cheng Ho's journey to the southern seas and his success in building the relationship between China and the African and Asian countries, as well as one who opened the doors to fair trade.

Originally designed as the office of the Dutch Governor and Deputy Governor, the gallery has a floor area of 43.4 m^2 and is side-lighted by pivoted wooden windows fitted with traditional louver (as shading device) located on the west wall (Fig.1). This may not be appropriate for its current function as gallery due to solar and UV radiation coming in contact with the exhibits.

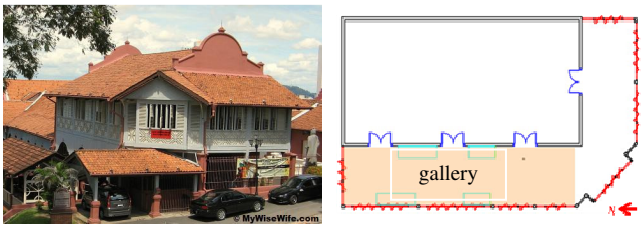


Fig. 1. External view and plan of the Admiral Cheng Ho Gallery, Melaka.

In the gallery area, where the measurements and surveys were done, daylight came from opened windows, periodically shaded with manually controlled traditional window louvers, which allow for visual link to the outside. Artificial lights were mainly diffused, located on the ceiling and walls. The direct artificial light came from spotlights directed pointed to the exhibits inside the showcases. The showcases' display walls are covered with velvety red fabric, which enhanced the exhibits displayed. Fig. 2 shows the gallery's exhibition hall on the first floor showing side windows on the west wing.



Fig. 2. Typical showcases' placement and combination of daylight and artificial lights at the west facing Admiral Cheng Ho Gallery

B. *Field Measurements*

The objective of the field research was to do pilot measurements on daylighting performance at the Admiral Cheng Ho Gallery. Illuminance measurements using luxmeters were conducted for quantitative analysis of lighting conditions for one week in March 2010. Air temperatures and relative humidity (RH) were also measured concurrently with the illuminance measurements between 14.00 and 16.00h, due to west facing orientation that experience higher occurrences of sunlight in the afternoon and late afternoon.

This pilot study is an essential step before doing more comprehensive field measurements in order to establish suitable design strategies for lighting museums, specific for this region, while focusing on placement and condition of collections. It is hoped that data from field measurements will shed more light on visual discomfort caused by direct sunlight into the west facing gallery space. Hence, measurements were taken between 14.00 and 16.00h when the gallery was in use. These hours were selected to gauge the luminous response of the gallery space to low solar positions as direct sunlight penetrates into the gallery in the afternoon hours (Fig.3). Furthermore, visual discomfort due to glare for west orientation showed maximum daylight glare index of 15.45 hours in correspondence to the maximum detected in exterior luminance [15].



15.00h 16.00h

Fig. 3. Daylight distributions

C. *Questionnaire Survey*

A questionnaire survey on the visual responses and opinion on the exhibits' condition in the gallery was conducted and then monitored closely to a random visitors' sample. For each questionnaire, the author was on hand to explain the positions of the artefacts and the conditions of the parameters related to the questionnaires. These visitors' feedbacks were gathered and compared concurrent with light measurements.

IV. RESULTS AND DISCUSSION

A. *Measured illuminance results*

The gallery space has a floor area of 43.4 m^2 and it is mainly illuminated by side windows and supplemented by artificial lights. After gathering the data, the illuminance values were recorded on interior layout plan for quick comparisons between different space illuminance levels, according to different times of day.

The plan in Fig. 4, at 14.00h, shows the combination of daylighting and artificial lighting presented considerably higher illuminance levels (Table 5). The level of light in the gallery decreased slightly at 15.00 and 16.00h, probably due to higher incidents of clouds in the sky. However, as the light level dropped slightly, the air temperatures rose slightly between 14.00 and 16.00h (Fig.6).

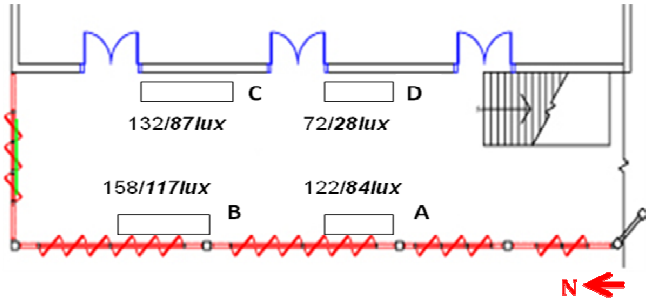


Fig. 4. Maximum illuminance level for daylight & artificial light exposure (opened window/***closed***) in March 2010 at 14.00h.

TABLE 5.
MAXIMUM ILLUMINANCE LEVEL OF DAYLIGHT & ARTIFICIAL LIGHT EXPOSURE (lx)

Time (h)	**Closed window with traditional louvers (lx)**	**Opened window with traditional louvers (lx)**
14.00	117	158
15.00	116	130
16.00	114	135

Under intermediate sky conditions in March, the combined illuminance of daylight and artificial light registered by luxmeter varied between 28 and 158 lx, while increased illuminance was observed on the wall of C and D showcases, which consisted of a gradual increase in illuminance recorded between 14:00 and 16:00h (Table 6). This west facing display areas located on the first floor showed higher indoor illuminance values on horizontal surfaces (Fig. 3).

Table 6 illustrates average 1 week illuminance level of daylight and artificial light measured in March 2010. The illuminance data of daylight and artificial light for both opened and closed louvered windows showed similar natural daylight patterns which fluctuated between 28 and 117lx; 72 and 158lx for closed and opened window with traditional louvers shading respectively.

TABLE 6
AVERAGE 1 WEEK ILLUMINANCE LEVEL OF DAYLIGHT & ARTIFICIAL LIGHT EXPOSURES.

Closed window with traditional shading louvers				
Time	Showcase A	Showcase B	Showcase C	Showcase D
14.00	84	117	87	28
15.00	83	116	94	30
16.00	83	114	108	30
Opened window with traditional shading louvers				
14.00	122	158	132	72
15.00	110	128	130	79
16.00	100	124	135	85

The illuminance levels remained low with shading as shown in Fig. 5 as excess daylight was periodically controlled by means of traditional louvers, which somewhat protected the collections. Nevertheless, showcases B and C experienced higher illuminance exposures and periodic opening for exterior historical context views showed needs of proper maintenance.

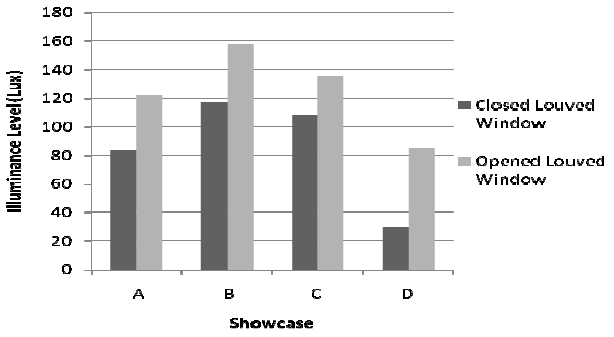


Fig. 5. Average 1 week illuminance level of daylight & artificial light exposures.

Table 6 illustrates the illuminance level of natural daylighting and artificial lighting. This simple analysis helps to illustrate how daylight and artificial lighting contributed to the total exposure. In this illustration and in comparison to Fig. 8, combination of daylight and artificial lighting clearly had a dominating effect on the exhibits according to the visitors' visual response.

The measured illuminance levels belonged to groups I, II and III (Table 2) in which objects that are non-sensitive to high light sensitivity are exhibited. The exhibits displayed in this gallery ranged from paper documents to miniature brocade. The exhibits maximum illuminance level of both daylight and artificial light exposures ranged from 135 to 158 lx and 114 to 117 lx for both opened and closed louvered windows respectively (Table 5). These 1 week exposures for some showcases were slightly above the maximum recommended values. This pilot study indicated that daylight and artificial light levels were not appropriately quantified and explored in the gallery.

B. Air Temperatures and Relative Humidity

Fig. 6 and 7 illustrate the illuminance, indoor temperature and relative humidity (RH) measured in the gallery. There were significant difference with indoor temperature between closed and opened windows. Both conditions recorded temperatures above the upper limit of comfort of 28.6°C [16]. Opened windows registered much higher temperature of up to 3.5°C than closed windows (Fig. 6). The reverse was observed for RH where the indoor RH is lower by up to 25% with opened windows (Fig. 7). These situations of high temperatures and high RH also created thermal discomfort.

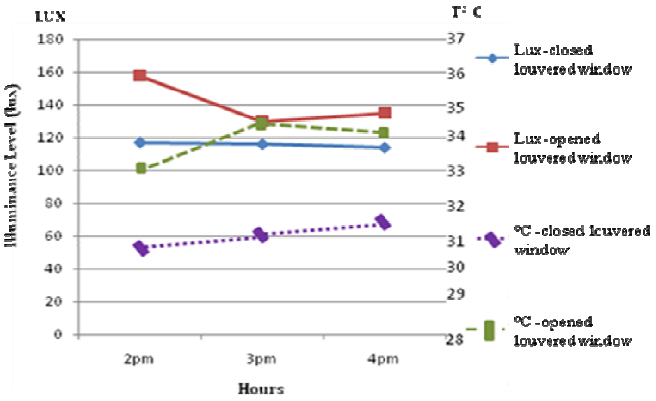


Fig. 6. One week average Maximum Daylight and Artificial Light Exposure and Temperature Level in the gallery.

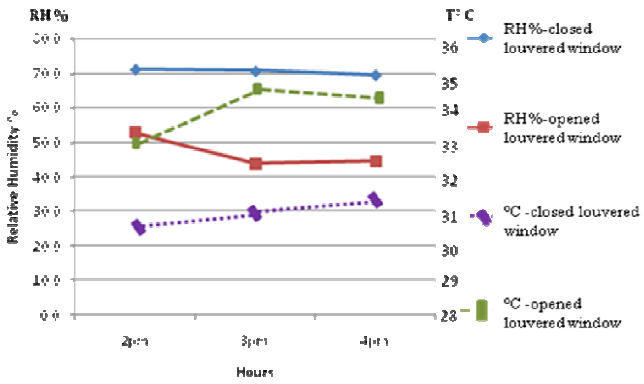


Fig. 7. One week average Maximum Relative Humidity and Temperature Level in the gallery.

C. Questionnaire Survey Results

From observation, an estimate of forty two visitors visited this gallery during this pilot survey. However, due to the specific nature of the survey, only twenty visitors managed to participate in the survey. According to the findings on the survey questionnaires, the preference factors in the afternoon were the temperature, followed by daylight. Figure 8 shows the survey results on visitors' opinions towards the exhibits' condition. The results showed that out of 20 questionnaires distributed and returned, 30% of respondents noticed problems in showcases C and D which were located opposite the windows, namely distortion, dirt and dust. Meanwhile, only 5% of respondents noticed fading in showcase A, and 15% and 10% of respondents noticed dirt and dust in showcases A and B respectively. Both showcases were located adjacent to window wall.

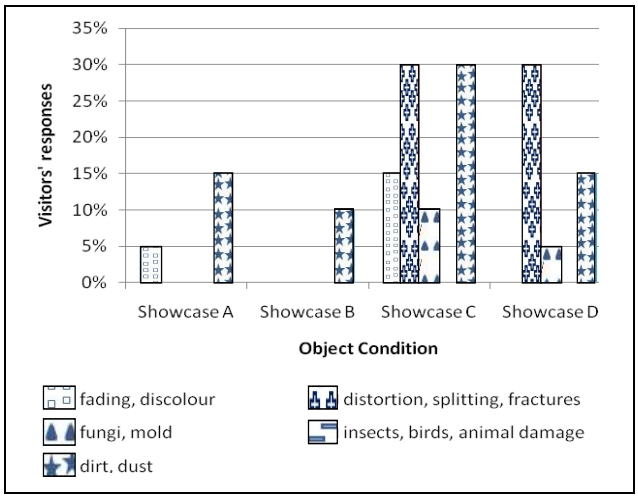


Fig. 8. Visitors' responses on exhibits condition.

The gallery used the potential of the building's historical context and the availability of daylight and views. Fig. 9 shows exhibit showcases placed directly on the reddish wall, directly opposite the opened windows. Windows across the showcase were opened during most of the daytime, but were closed when the lower angles of the late afternoon sun caused glare and reflections in the gallery. Daylighting through side windows created some reflections that need to be controlled by appropriate shading devices. It was observed that while the fully opened windows opposite the showcase offer external views, they increased incidents of veiling reflections on the glass showcase. Higher occurrences of glare discomfort were observed from windows facing west due to lower late afternoon sun angles. This provided conflict between providing effective shading devices and offering external view.



Fig. 9. Showcase showing reflections of louvered windows, placed on the reddish wall, directly opposite the opened windows

Meanwhile, Fig. 10 shows daylit exhibition space with showcases placed directly on the west-facing white wall which is adjacent to the opened windows. These windows offer views of historical sites of Malacca. While glare from direct sunlight were mostly absent in the morning, it was observed to occur during the late afternoon.



Fig. 10. Showcases placed directly on the west-facing white wall which is adjacent to the opened windows.

Survey results (Fig. 11) showed that out of 20 questionnaires distributed and returned, 45% of respondents observed worst glare condition at orientation E, at which visitors faced the showcases and back wall and windows are at their back. Meanwhile, 30% of respondents observed most preferred light level at orientation A, at which they faced the showcases and window directly. The 20 participants gave indicative results for future research when around 100 participants will be surveyed for more thorough findings.

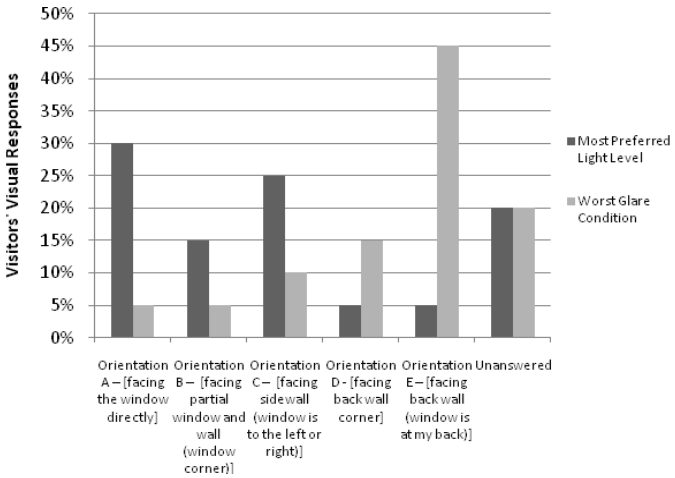


Fig. 11. Visitors' visual responses on most preferred light level and worst glare condition.

V. CONCLUSIONS

The results of the pilot measurement and survey gave indicative result for further study. There is a need for future research that include larger investigation and bigger survey population for more detailed findings. Generally, issues related with light level or illuminance control and cumulative exposure limits, in terms of object preservation, were observed in this gallery. From the overall analysis, some points can be concluded and noted as follows:

- Results showed measured illuminance levels exceeded allowable exposure limits for some showcases and higher temperature conditions were recorded during both opened and closed louvered windows in the afternoon.

Measured air temperatures were much higher than accepted comfort range especially with opened windows in the afternoon and the RH levels were within the prescribed range. The problems observed were related to lack of proper maintenance or financial problems to improve the lighting and ventilation systems.

- The limiting values of light exposure are based on traditional recommended exposure limits of various standard materials. Nevertheless, the problem observed when combination of total natural daylight and artificial light levels were not correctly explored and quantified. The traditional point measurements for showcases do not offer detailed information about continuous changes in natural lighting exposure, which take place throughout the day or year. This suggests future need of systematic light monitoring programme in the exhibition gallery.
- The survey identified the combination of natural daylight and artificial lightings affected the exhibits' conditions such as fading, distortion, dirt and dust. The showcases were placed against and opposite the fully opened windows. Thus, the presence of daylight and especially sunlight in the gallery created problems of glare and veiling reflections on the glass surface of showcases. These situations may demonstrate the need for appropriate controlled shading system that allows enough light for the exhibits without sacrificing external view.

The measurement of daylight with artificial light in this gallery was conducted as a preliminary study in view of further studies to find the optimal criteria and placement of each showcase as well as studies on better lighting design strategies for similar museum galleries.

ACKNOWLEDGMENT

This work was funded by Excellence Fund and monitored by the Research Management Institute, University Teknologi MARA (UiTM).

REFERENCES

[1] T. Padfield, "The role of standards and guidelines: Are they a substitute for understanding the problem or a protection against the consequences of ignorance? ," http://conservationphysics.org/ppubs/dahlem.pdf, 1994.

[2] A. Huber, "Problem-zone window in museum microclimates," in *Journal of American Institute of Conservation*, T Padfield & K Borchersen ed: National Museum of Denmark, 2007.

[3] S. Westerhuis, "Preventive Conserving," http://www.westerhuis-restauratie nl.pdf, 2004.

[4] J.M. Ayres et al., "Museum Environmental Requirements: A Literature Survey," *ASHRAE Transaction*, vol. n pt 2, pp. 112-121, 1990.

[5] G. Thomson, *The Museum Environment*, 2nd ed. London: Butterworths, 1986.

[6] C. Cuttle, "Damage to museum objects due to light exposure," *Lighting Research Technology*, vol. 28(1), pp. 1-9, 1996.

[7] C. Cuttle, "Lighting works of art for exhibition and conservation," *Lighting Research Technology*, vol. 20(2), pp. 43-53, 1988.

[8] S. Michalski, "Light, Ultraviolet and Infrared," Canadian Conservation Institute, http://www.cci-icc.gc.ca/crc/articles/mcpm/chap08-eng.aspx, 2010.

[9] S. C. Brook, "Daylighting museum galleries: a review of performance criteria.," *Lighting Research Technology*, vol. 32(3), pp. 161-168, 2000.

[10] M. Wilson, "Lighting in museums: Lighting interventions during the European demonstration project 'Energy efficiency and sustainability in retrofitted and new museum buildings' (NNES-1999-20)," *International Journal of Sustainable Energy*, vol. Vol. 25, No. 3–4, pp. 153-169, 2006.

[11] C. Balocco et al., "Natural lighting in the Hall of Two Hundred. A proposal for exhibition of its ancient tapestries (Case Study)," *Journal of Cultural Heritage* vol. 11, pp. 113–118, 2010.

[12] G.F. Menzies et al., "Windows in the workplace: examining issues of environmental sustainability and occupant comfort in the selection of multi-glazed windows," *Energy and Buildings* vol. 37, pp. 623–630, 2005.

[13] W. K. E. Osterhaus, "Discomfort glare assessment and prevention for daylight applications in office environments," *Solar Energy* vol. 79, pp. 140–158, 2005.

[14] *The IESNA Lighting Handbook; Reference & Application*. New York: IESNA Publication, 2000.

[15] A. Piccolo, Simone,F., "Effect of switchable glazing on discomfort glare from windows," *Building and Environment* vol. 44, pp. 1171-1180, 2009.

[16] S. S. Ahmad, "The performance of a partially airconditioned apartment building in Kuala Lumpur " *in the Proceeding of 24th International Conference of Low Energy and Architecture: PLEA 2007*, pp. 608-614, 2007.

Finite Difference Error Analysis of Geometry Properties of Implicit Surfaces

Pan Zheng[1], Bahari Belaton[1], Iman Yi Liao[1], Zainul Ahmed Rajion[2]
School of Computer Sciences[1], School of Dental Sciences[2]
Universiti Sains Malaysia, Penang, Malaysia
panzheng@gmail.com, bahari@cs.usm.my, iman@cs.usm.my, zainul@kck.usm.my

Abstract- In this paper we investigate the impact of different finite difference method (FDM) on estimation of the curvatures and other geometry properties of an implicit surface extracted from volumetric data. The FDM estimation case studies of the geometrical features are conducted on the surface in different resolutions which are refined surface, medium surface and coarse surface. A ground truth is established on each resolution to be compared with the experiment results. Then we apply relative error analysis on the results to find the influences of FDM that can be utilized in the estimation.

I. INTRODUCTION

It is easier to obtain the geometry property of a surface when an analytical function is given, however in real life science and engineering field, surfaces extracted from various data may not have explicit mathematical functions. Therefore certain estimation and approximation methods are needed. Finite different methods (FDM) are always used to estimate derivatives of differential equations. In domain of computer graphics and geometry, directly or indirectly FDM can be used to estimate various geometry properties of a surface. The general geometry properties of a surface are normal vectors, mean curvature, Gaussian curvature, principal direction vectors and principal curvatures. These properties are very important to further explore the nature of a surface.

In this study we focus on the geometry property of a surface extracted from a volumetric data with implicit polygonizer [1, 2]. Implicit polygonizer is considered because it is a cube traversal surface construction method and it has major advantages over conventional exhausted surface extraction methods. It has a complexity approximated to $O(n^2)$. By defining different cube sizes, surfaces in different resolution can be obtained, which is desired in our experiment to see how FDM works in different environment. We first experiment on syntheses surfaces of mathematical functions. Based on syntheses function, we establish some ground truth of the geometry properties, and then compare two sets of results to analyze the errors and stability of FDM in generating of those properties. Geometry property estimation can also be achieved by using surface fitting and interpolation methods, yet the complexity is enormous and not the concern of this study. Different from conventional pure mathematical analysis, our study focuses on the practical results of geometrical implementation. Qualitatively we look into the actual error effects mapped visually on a surface. Quantitatively we conduct relative error analysis by forming histograms for comparisons.

II. LITERATURES AND MATHEMATICAL BACKGROUND

Implicit surface is construed as a set of points $\{p \in \Re^3 : f(p) = I\}$, where I is the isovalue and f(p) is the implicit surface function. For any given point P, if $f(p) = I$ is satisfied, then the point is on the surface; else it is not. Implicit surface function can easily decide the location of the given points and construct surface in arbitrary form, which shows great flexibility on isosurface extraction of volumetric data. The implicit surface geometry properties that we are interested in are normal vectors, principal curvatures and principal directions. For normal vectors, William E. Lorensen and Harvey E. Cline [3] provided a solution to generate the normal vectors of the surface. The gradient of the data density around the isosurface can be computed as the normal vectors of the isosurface (figure 1), because the two areas where the target surface is in between have different isovalue (density).

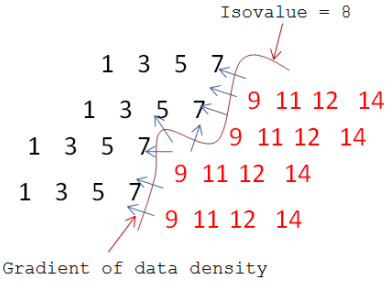


Fig. 1. Illustration of data density gradient as isosurface normal vectors

Based on this idea, the normal vectors of isosurface can be calculated with FDM's central difference.

$$n_x = \frac{f(x+\Delta,y,z)-f(x-\Delta,y,z)}{2\Delta}$$
$$n_y = \frac{f(x,y+\Delta,z)-f(x,y-\Delta,z)}{2\Delta}$$
$$n_z = \frac{f(x,y,z+\Delta)-f(x,y,z-\Delta)}{2\Delta}$$
$$n_f = \sqrt[2]{n_x^2+n_y^2+n_z^2}$$

Therefore the normalized normal vector is

$$n = \left(\frac{n_x}{n_f}, \frac{n_y}{n_f}, \frac{n_z}{n_f}\right)$$

To calculate principal directions and principal curvatures, we employed the formula derived by Jean-Philippe Thrion and Alexis Gourdon[4]

$$k_{1,2} = S \pm \sqrt{\Delta}$$
$$\Delta = S^2 + K$$

$k_{1,2}$ is the maximal and minimal curvatures. S is the mean curvature and K is the Gaussian curvature.

$$S = \frac{1}{h^2}\left[f_x^2\left(f_{yy}f_{zz} - f_{yz}^2\right) + 2f_yf_z\left(f_{xz}f_{xy} - f_{xx}f_{yz}\right) + f_y^2\left(f_{xx}f_{zz} - f_{xz}^2\right) + 2f_xf_z\left(f_{yz}f_{xy} - f_{yy}f_{xz}\right) + f_z^2\left(f_{xx}f_{yy} - f_{xy}^2\right) + 2f_xf_y\left(f_{xz}f_{zy} - f_{zz}f_{yx}\right)\right]$$

$$K = \frac{1}{2h^{\frac{3}{2}}}\left[f_x^2\left(f_{yy}+f_{zz}\right) - 2f_yf_zf_{yz} + f_y^2(f_{xx}+f_{zz}) - 2f_xf_zf_{xz} + f_z^2\left(f_{xx}+f_{yy}\right) - 2f_xf_yf_{xy}\right]$$

$$h = f_x^2 + f_y^2 + f_z^2$$

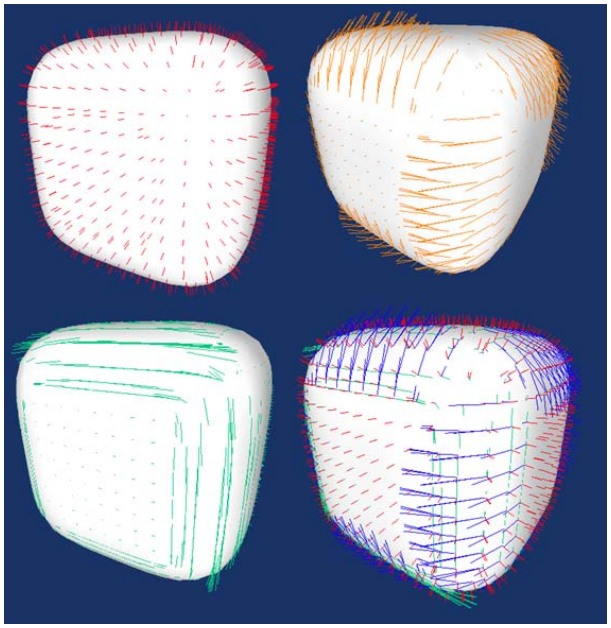


Fig. 2. Illustration of normal vectors, maximal principal direction, minimal principal direction and all-in-one

Principal directions can be computed with formula below

$$\overrightarrow{t_{1,2}} = \left(\alpha_x \pm \sqrt{\Delta}(f_z - f_y), \alpha_y \pm \sqrt{\Delta}(f_x - f_z), \alpha_z \pm \sqrt{\Delta}(f_y - f_x)\right)$$

$$\begin{aligned}\alpha_x = -\frac{1}{2h^{3/2}}(&-2f_z^3f_{xy} + f_y^3f_{zz} + 2f_y^2f_zf_{xy} \\ &+2f_z^2f_xf_{yz} + 2f_z^2f_yf_{xz} - 2f_y^2f_xf_{yz} - 2f_zf_xf_{zz} \\ &+2f_xf_yf_{yy} + f_y^2f_zf_{xx} - 2f_z^2f_xf_{xz} + f_x^2f_zf_{zz} \\ &-f_x^3f_{yy} + 2f_z^2f_yf_{yz} - f_y^2f_zf_{zz} + f_z^3f_{xx} \\ &-f_z^3f_{yy} - 2f_y^2f_xf_{xz} + 2f_x^2f_yf_{yz} - f_y^3f_{xx} \\ &+2f_z^2f_xf_{xy} - f_z^2f_yf_{xx} - 2f_y^2f_zf_{yz} + f_z^2f_yf_{yy} \\ &-2f_x^2f_zf_{yz} + 2f_y^2f_xf_{xy} + f_x^2f_yf_{zz} - f_x^2f_yf_{yy})\end{aligned}$$

α_y and α_y can be obtained by circular permutations of subscript x,y and z of above formula. f_x, f_y, f_z are as first order derivatives. f_{xx}, f_{yy} and f_{zz} are 2nd order derivatives and f_{xy}, f_{xz} , f_{yz} are 2nd order partial derivatives. They are in the direction denoted by the subscripts. With the knowledge of a given implicit functionf(x), finite difference methods can be applied to obtain different ordered derivatives in different direction.

Error of finite difference approximation is usually obtained by Taylor series [5]. Khan and Ohba [6] provided a new type of Taylor series based finite difference approximation for higher-degree derivatives calculation of a function. Nehrbass, Jevtic and Lee [7] presented an optimized method to reduce the numerical phase error without defining finer resolution or implementing higher order of FDM, which is time and memory efficient. Curvature estimation has been intensively studied by many researchers. The studies can be classified into two categories based on the nature of the data. Worring and Smeulders [8] did thorough investigation on 2D image curvature estimation along with error analysis. The curvature estimation and error analysis are also put forward for 3D image data [9, 10]. In our study, we address the FMD error impact on estimation of geometry properties of an implicit surface in 3D practically, rather than analyzing the error in a pure mathematical way.

III. Experiments and Results

It is straightforward to obtain derivatives for an explicit function, since the function has a well-defined mathematical representation. For a surface extract from practical data by an implicit function, it has no congruous representation. The extracted surface depends on characteristic of the data. Apparently the approximation of geometry properties of an implicit surface is keenly contingent on the derivatives of the implicit function. Ergo, the approximation of derivatives comes into picture. The purpose of this study and experiment is to compare the approximation results of the different finite difference method on computing the geometry properties of an implicit surface function. The experiment is designed in a two-fold manner. In the first step, we established a ground truth result (figure 2) by conducting the calculation of geometry properties of a specific equation. In this case, we took $f(x,y,z) = x^4 + y^4 + z^4 - 0.64$ which is a smooth cube surface for experiment. In the second step, we input this smooth cube function to implicit surface polygonizer with an isovalue of 0.64 and approximate geometry properties with different FDM. We also adjusted the resolution of the surface to investigate the performance of FDM. Three resolutions are defined, which are refined surface, medium surface and coarse surface. We achieve these by altering the traversal cube size of the implicit polygonizer.

Central difference approximation (CDA) is one of FDM. It has a form of

$$f_x = \frac{f(x+d) - f(x-d)}{2d}$$

for first order derivatives and

$$f_{xx} = \frac{f(x+d) - 2f + f(x-d)}{d^2}$$

for second order derivatives. In a mixed situation we can have

$$f_{xy} = \frac{1}{4d^2}(f(x+d, y+d, z) - f(x-d, y+d, z) - f(x+d, y-d, z) + f(x-d, y-d, z))$$

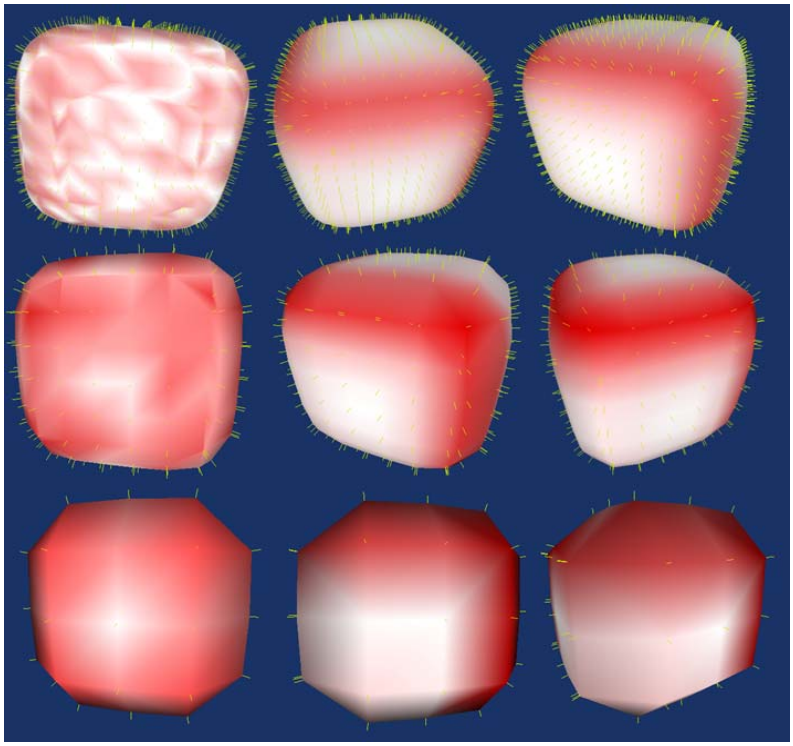


Fig. 3. The relative error of normal vector approximation overlay display on the surface (left column: CDA; middle column: FDA; right column: BDA with different surface resolution in each row)

Forward difference approximation (FDA) has the form of

$$f_x = \frac{f(x+d) - f(x)}{d}$$

$$f_{xx} = \frac{f(x+2d) - 2f(x+d) + f(x)}{d^2}$$

$$f_{xy} = \frac{1}{d^2}(f(x+d, y+d, z) - f(x, y+d, z) - f(x+d, y, z) + f(x, y, z))$$

Backward difference approximation (BDA) has the form of

$$f_x = \frac{f(x) - f(x-d)}{d}$$

$$f_{xx} = \frac{f(x) - 2f(x-d) + f(x-2d)}{d^2}$$

$$f_{xy} = \frac{1}{d^2}(f(x, y, z) - f(x-d, y, z) - f(x, y-d, z) + f(x-d, y-d, z))$$

The subscript can be substituted as the need of calculation in other directions.

Surface normal and principal curvatures are vector quantities. In order to measure the error in vectors, we need to measure the size or norm of a vector. In this study, the relative error is analyzed based on two-norm of the vectors. Hence, the relative error of each surface normal vector is computed by following formula

$$RE = \frac{|\overrightarrow{n_t} - \overrightarrow{n_a}|_2}{|\overrightarrow{n_t}|_2}$$

$\overrightarrow{n_t}$ is the true value of the normal vector, and $\overrightarrow{n_a}$ is approximated normal vector. Two-norm is taken for the calculation. The normal vectors we obtained are normalized. Therefore the denominator will be 1. So the equation can be simplified as

$$RE = |\overrightarrow{n_t} - \overrightarrow{n_a}|_2$$

Figure 3 shows the qualitative display of relative error overlaying the implicit surface. The regions highlighted in red are the concentration of the error. We can see the error of normal vectors estimated by CDA is fairly sparse and spreads over the surfaces. Since the central region of the smooth cube surface has minimal curvature, the error tends to be minimal as well. The error estimated by FDA and BDA has similar behaviour. The agglomerate of the error appears in certain high curvature portion of the surface. We create three histograms (figure 4, 5, 6) to show the error distribution against the curvature for different FDM. The maximum value of the curvature is 1.643438 in this case. From 0 to 1.643438, we divided the curvature into 10 even intervals. In each interval the average relative error (ARE) is calculated with formula below

$$\mathrm{ARE} = \frac{\sum_{i=1}^{n} \mathrm{RE(v)_i}}{n}$$

where n is the number of vectors that fall into the interval and v is the corresponding vector. For the refined surface, the relative error of CDA for normal vector estimation is accurate to 5 decimal. The relative error of FDA and BDA is approximated to 2 decimal.

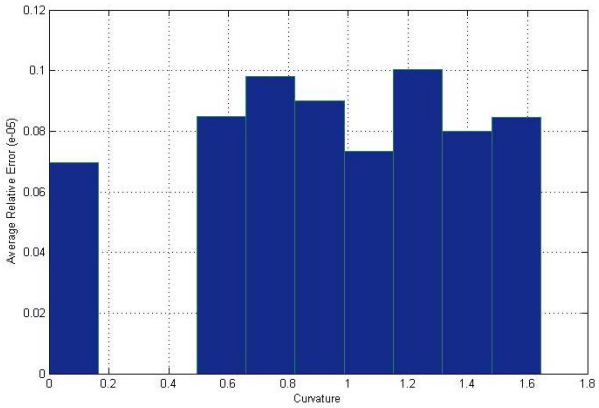


Fig. 4. The histogram of ARE of CDA against curvature for the refined surface (normal vectors)

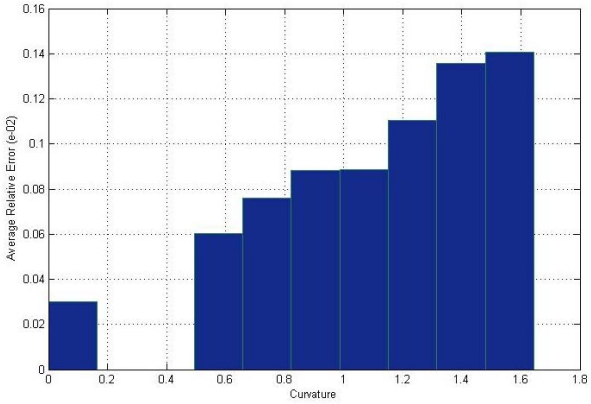


Fig. 5. The histogram of ARE of FDA against curvature for the refined surface (normal vectors)

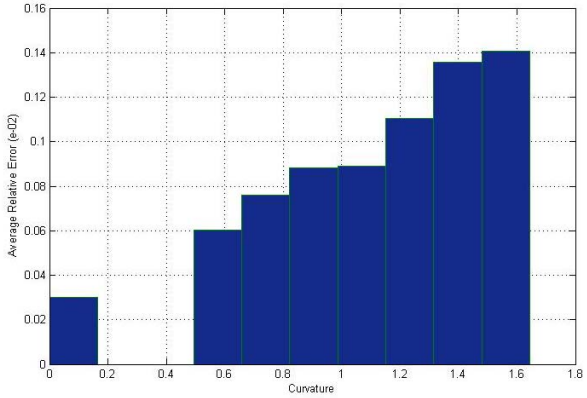


Fig. 6. The histogram of ARE of BDA against curvature for the refined surface (normal vectors)

The histograms of medium surface and coarse surface show the similar observation**.**

In case of maximal and minimal principal direction, the errors are carried out in similar fashion (figure 9, 10). As shown, the error accumulated in low curvature regions which contrast the error region of normal vectors. In ground truth case, these regions generally have curvature value of zero. This is caused by accumulated numerical errors brought by FDM in the formulas.

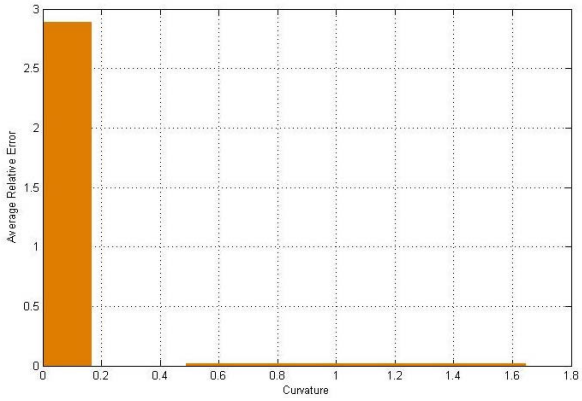


Fig. 7. The histogram of ARE of CDA against curvature for the refined surface (maximal principal direction)

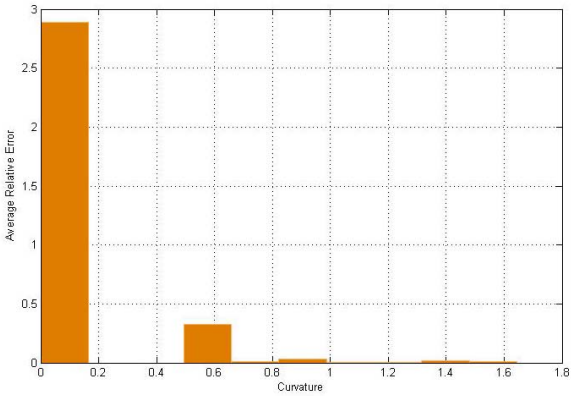


Fig. 8. The histogram of ARE of FDA against curvature for the refined surface (maximal principal direction)

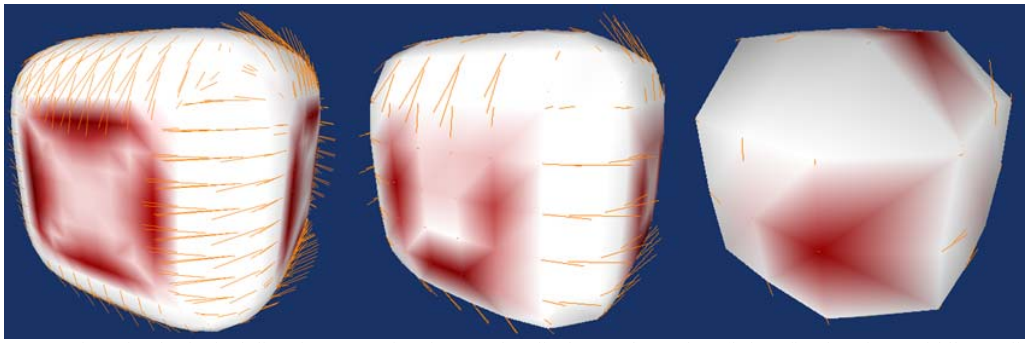


Fig. 9. The relative error of maximal principal direction approximation overlay display on the surface (left: refined surface; middle: medium surface; right: coarse surface)

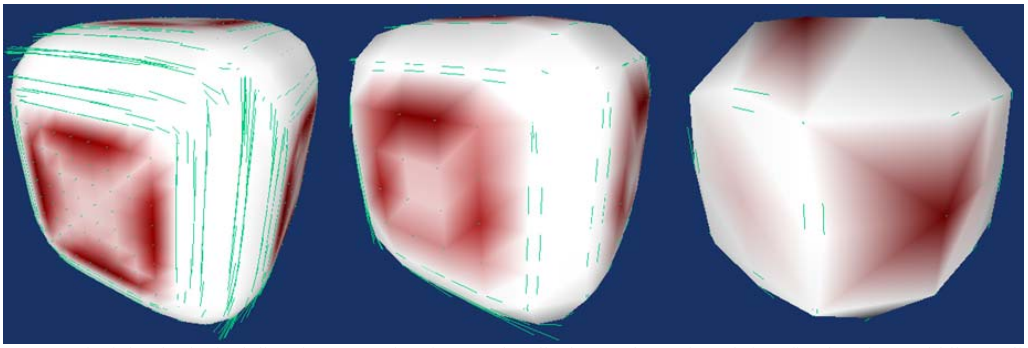


Fig. 10. The relative error of minimal principal direction approximation overlay display on the surface (left: refined surface; middle: medium surface; right: coarse surface)

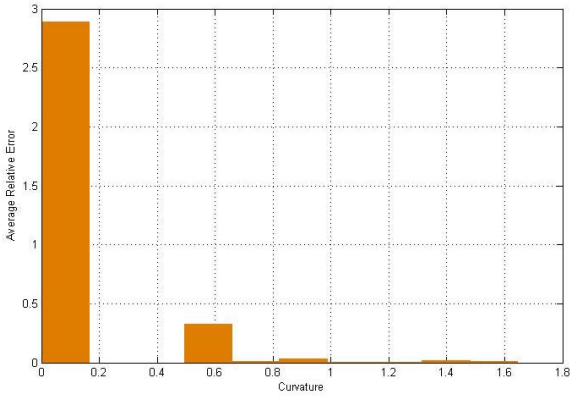


Fig. 11. The histogram of ARE of BDA against curvature for the refined surface (maximal principal direction)

Figure 7, 8 and 11 manifest the histograms of ARE of three different FDM on estimation the principal directions.

Principal curvatures are scalar values. Relative error can be obtained by dividing absolute error with the true value.

$$RE = \frac{|k_a - k_t|}{k_t}$$

The histograms of FDM approximation on principal curvatures accord with the histograms of principal directions. The two sets of histograms have similar trends (figure 12, 13, 14).

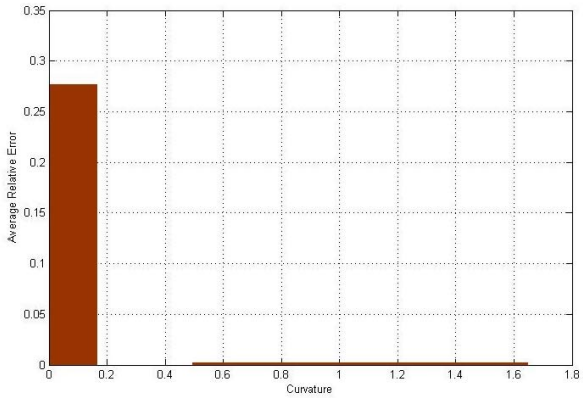


Fig. 12. The histogram of ARE of CDA against curvature for the refined surface (minimal principal curvature)

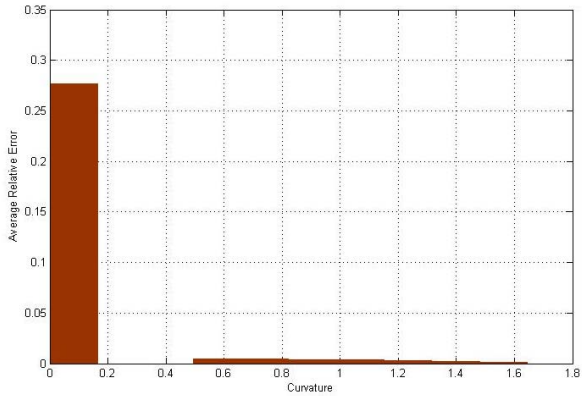


Fig. 13. The histogram of ARE of FDA against curvature for the refined surface (minimal principal curvature)

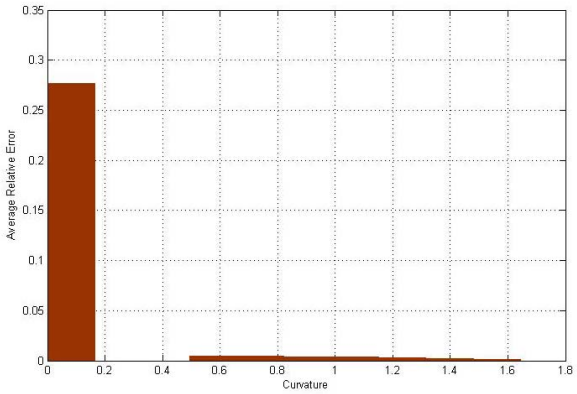


Fig. 14. The histogram of ARE of BDA against curvature for the refined surface (minimal principal direction)

Figure 15 shows the relative error of principal curvature approximation overlay display. The error overlay displays of maximal and minimal curvatures are similar, so only illustration of maximal curvature error is shown. The results are generated using CDA, whilst the results calculated by FDA and BDA are constantly alike.

Through this study, we can see several impact of FDM on approximation of geometry properties of implicit surface. Error is apt to increase on a low resolution surface, due to lack of sampling values. For curvature estimations, the low curvature regions are more sensitive to numerical error, whereas normal vector approximation is responsive to high curvature.

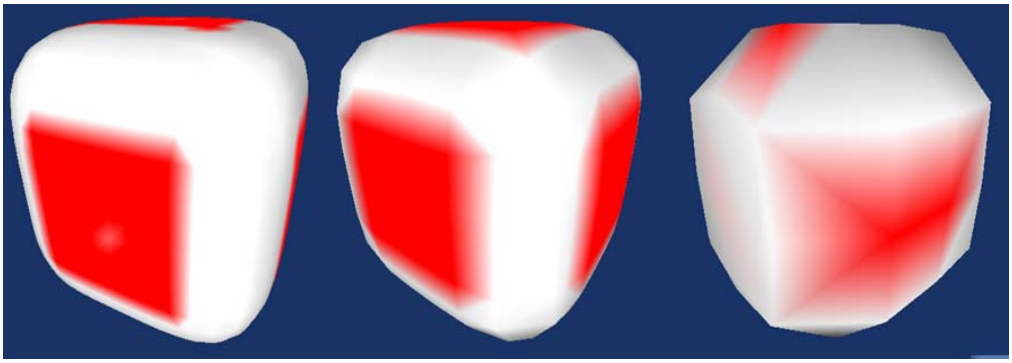


Fig. 15. The relative error of maximal curvature approximation overlay display on the surface (left: refined surface; middle: medium surface; right: coarse surface)

IV. CONCLUSION

This investigation of finite difference error analysis on geometry properties of implicit surface serves as a thorough case study. We try to provide some insight on how the different finite difference methods influence the approximation of geometry properties such as normal vectors, principal directions and principal curvatures of an implicit surface. It shows that central difference approximation method performs better on a convex manifold surface. This study is limited to one particular implicit surface function. In future the experiment may be conduct on more surfaces with distinct shapes and resolutions.

ACKNOWLEDGEMENT

This study is supported by Universiti Sains Malaysia Research University Fund (1001/PKOMP/814109).

REFERENCES

[1] Jules Bloomenthal, "Polygonization of Implicit Surfaces", Computer Aided Geometric Design, vol. 5 1988, pp. 341-355.

[2] Pan Zheng, Bahari Belaton, Iman Y.Liao, "Isosurface Extraction of Volumetric Data Using Implicit Surface Polygonization", Proceeding of Third Asia International Conference on Modeling & Simulation, 2009 pp. 555-559.

[3] E. Lorensen and Harvey E. Cline, "Marching cubes: A high resolution 3D surface construction algorithm", Computer Graphics, vol.21, No.4, 1987, pp. 163—169

[4] Thirion, J. P., Gourdon, A. (1996). "The 3D Marching Lines Algorithm", Graphical Models and Image Processing, 58 (6), pp.503-509

[5] William F. Ames, Numerical Methods for Partial Differential Equations, Section 1.6. Academic Press, New York, 1977

[6] Ishtiaq Rasool Khan, Ryoji Ohba, "Taylor series based finite difference approximations of higher-degree derivatives", Journal of Computational and Applied Mathematics, Volume 154 Issue 1, 1 May 2003, pp.115-124

[7] J.W. Nehrbass, J.O.Jevtic, R. Lee, "Reducing the phase error for finite-difference methods without increasing the order", IEEE Transactions on Antennas and Propagation, Volume 46 Issue 8, Aug 1998, pp.1194-1201

[8] M. Worring, A. W. M. Smeulders, "Digital Curvature Estimation", CVGIP: Image Understanding, Volume 58, Issue 3, November 1993, pp.366-382

[9] Nabih N. Abdelmalek, "Algebraic error analysis for surface curvatures and segmentation of 3-D range images", Pattern Recognition, Volume 23, Issue 8, 1990, pp.807-817

[10] Iman Y.Liao, Pan Zheng, Bahari Belaton, "Error analysis on curvature-based crest lines extraction on iso-surface of medical CT data", Proceeding of ECCOMAS Thematic Conferences on Computational Vision and Medical Image Processing, Porto, Portugal,2009, pp.133-138

Image Mosaics with Wavelet Domain Seam-lines

Paul Bao
Department of Information Technology
University of South Florida
pbao@poly.usf.edu

Abstract -Scene mosaics are a technique for building a panoramic view of a scene from a set of small views. When overlapped scene images are pasted, the mixed radiometry of the overlap areas may cause artifacts and blurred areas. The seam-line scene mosaics can avoid such artifacts and blurred areas. We propose a seamless scene mosaic scheme in the wavelet domain of the edge images, where the correspondence search and the seam-line search are performed. The homographic transformation obtained through wavelet domain correspondence research is applied for the original scene images for the geometric correction and the seam-line in the wavelet domain is reverse wavelet transformed to form a seam-line in the original spatial domain for the image pasting. This scheme can significantly improve the performance of the scene mosaics while achieving seamless scene mosaics of the scene.

Index terms: *Rendering, Wavelet, Seam-lines, Image Synthesis*

1. Introduction

Scene mosaics [3,5,9,10], a mechanism to align different views of a scene (overlapped) onto a larger image and seamlessly paste the images together, is considered to be a fundamental technique in image-based rendering systems [4,5] to generate wide angled and high resolution views of the scene, such as panoramas.

The kernel of scene mosaics is the *scene registration* [3], which derives the alignment transformations from the known image sequence. Though image registration algorithms have been studied for several decades, most existing approaches focus on either finding the local correspondences between images or extracting important image features for matching. These approaches suffer from the presence of occlusion or image noise near the features and result in merely local optimal solutions. More recently the phase-based correlation method provides a global solution by using *Fourier transform* technique for registering images. However, Fourier transform is known to be very poor in spatial localization. Instead, wavelet transform is a new promising approach in image processing with inherently strong spatial and frequency locality. The complex version of wavelet transform also promises the property of scale invariance and translation invariance and the interpolation convenience. There is very little work being reported on using the complex wavelet transform for the coarse-to-fine image registration.

2. Wavelet-based Scene Mosaics with the Seam-Lines

The wavelet-based scene mosaics scheme with seam-lines can be briefly described as the following phases (Fig. 1).

1. *The edge information is first extracted from the mosaicking images.*
2. *The edge images are then wavelet transformed into the baseband and the detailed multilevel subbands.*
3. *The correspondence is searched in the baseband and hierarchically in the detailed subbands if necessary to form the homographic transformation.*
4. *A simple radiometric correction is applied to overlap area of the mosaicking images.*
5. *The homographic transformation is then applied to the radiometric-adjusted images to inlay the images onto the mosaic coordinate system.*
6. *The least visible seam-line is searched from basebands using the least cost path algorithm.*
7. *The images are registered along the seam-line.*

3. Complex Wavelet Decomposition Representation

We start at searching a *uniform*, *global* and *hierarchical* representation model of the scene images. In this regard, the multiresolution wavelet decomposition is a desirable choice. For image registration, some additional requirements must be considered, namely scaling-, translation- and rotation-invariance, which imply that the matching algorithm can work independent of the motion of scene, objects and camera under the given representation model as well as the matching strategies. Scaling invariance is known to be an inherent characteristic of wavelet transform itself.

With the focus on image-based virtual reality in which we

usually register images taken with fixed viewpoint or along a principle axis or with little rotation angle, we may assume that there is no or little rotation between the images. Thus the rotation invariance for the wavelet transform is not required which allow us to focus on the image registration given the scaling and the translation invariance of the complex wavelet transform. Wavelet transform is a well-known method developed as a signal decomposition approach to overcome the shortcomings of the *Window Fourier Transform* [4]. In general, given a discrete image $f(x,y)$, the real-value wavelet pyramid is constructed by computing the filtered coefficients of four matrices A_j , $D_{j,p}$ $p=1,2,3$, on each level j respectively. The procedure is illustrated in figure 4 (a).

Translation-invariance of a wavelet implies that the decomposed signals are represented everywhere as the scaled and translated copy of the mother wavelet, they all look the same on the real domain, as illuminated in figure 5(b). Generally, image is defined on a bounded region of the real domain, so real-value image wavelet decomposition is known to be neither translation invariant nor rotation invariance (figure 5(c)). This gives rise to its inapplicability for image registration because the matching search may fail to locate the correlated coefficients in another image wavelet pyramid.

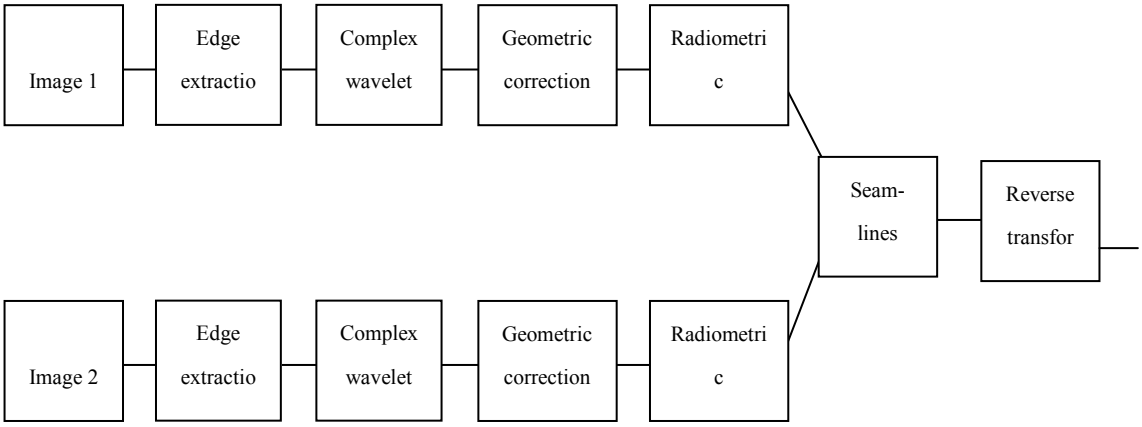


Figure 1: Schematic description of the system



Figure 2. *Lenna* Original image; Visual noise sensitive edges extracted by *Canny* operator; Two-level wavelet decomposition of the edge image.





Figure 3. The edge extraction of the left and right mosaicking images; the baseband of the edge images; the mosaic image

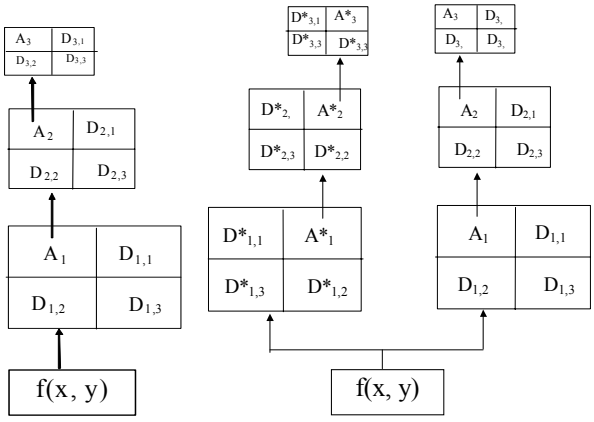


Figure 4 (a) Real-value wavelet (b) Complex wavelet

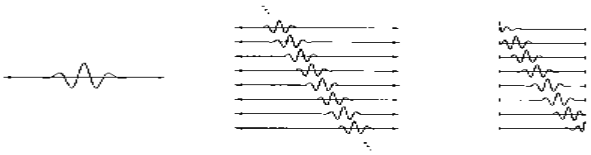


Figure 5. Translation-invariance and –variance wavelet. A mother wavelet; translation-invariance wavelet; translation-variance wavelet.

A separable complex value discrete wavelet transform is a proper representation in this regard because it can decompose an image into a hierarchically sub-sampled, directionally tuned spatial frequency subband domain. The bandpass filters can be defined so that translation in the spatial domain is represented as a phase rotation of the corresponding subband coefficients. This relation gives rise to not only the ability of matching the coefficients, but also the interpolability of the coefficients at the fractional accuracy, and hence leads to the accurate matching through the multilevel of complex wavelet pyramids. Figure 4 (b) is an illustration of complex wavelet pyramid, where $\{A_j^*, D_{j,p}^*, p=1,2,3\}$ is a conjugate mirror set of coefficient matrices $\{A_j, D_{j,p}, p=1,2,3\}$. The 2D complex wavelet filters so formed will contain both the first and the second quadrants, where the most significant information of real discrete images in the frequency domain is located. The particular complex wavelet employed in the scheme is the *Magarey-Kingsbury* Complex wavelet [7]. The wavelet and scaling filters g and h are a complex pair of even-length modulated windows, i.e. *Gabor* filter:

$$\begin{aligned} g_k &= w(k+0.5)e^{iw(k+0.5)} \\ h_k &= \tilde{w}(k+0.5)e^{i\tilde{w}(k+0.5)} \end{aligned}, \quad k = -N, -N-1, \ldots, N-1 \quad (1)$$

where w, $\tilde{w}$ are a pair of real-value low-pass window modeled as *Gaussian* windows:

$$w_1(k) = \exp\left(-\frac{k^2}{2\sigma_1^2}\right), \quad \tilde{w}_1(k) = \exp\left(-\frac{k^2}{2\tilde{\sigma}_1^2}\right) \quad (2)$$

The most compact supported window length is *4*, and *N=2*. The modulation frequencies w_1 and $\tilde{w}_1$ are assumed as complementary: $w_1 + \tilde{w}_1 = \pi$, and $\tilde{w}_1 < w_1$ [8,11]. An approximate version of g and h is given by *MKC-4*:

$$h = \frac{1}{10}[1-i, 4-i, 4+i, 1+i],$$

$$g = \frac{1}{14}[-1-2i, 5+2i, -5+2i, 1-2i] \quad (3)$$

To obtain fractional accuracy, the estimation of non-integer-index coefficients is needed. One nice feature of complex wavelet family is its interpolability. The down-sampled complex-valued coefficients of subbands can be interpolated by modulating a low-pass filter Ω, and convolving with the modulated kernel. The simplest complex interpolation formula is given below for the small fractional offset:

$$D_{j,p}(k+u, l+v) \approx D_{j,p}(k,l)\, e^{i \bullet \Omega_{j,p} \bullet (u,v)} \quad (4)$$

4. Geometric Correction

The general image registration problem can be formulated as a homographic transformation

$$I_2(k', l') = I_1(G(M; (k,l)) \quad (5)$$

where G is a homographic transformation from the pixels of image I_1 to that of image I_2, M is the transform parameters vector: $M = (m_0, m_1, \ldots, m_7, m_8)$. In terms of homogeneous coordinates, G can be re-written as

$$\begin{pmatrix} u \\ v \\ \mu \end{pmatrix} = \begin{bmatrix} m_0 & m_1 & m_2 \\ m_3 & m_4 & m_5 \\ m_6 & m_7 & m_8 \end{bmatrix} \bullet \begin{pmatrix} k \\ l \\ 1 \end{pmatrix}, \begin{pmatrix} k' \\ l' \\ 1 \end{pmatrix} = \begin{pmatrix} u/\mu \\ v/\mu \\ 1 \end{pmatrix} \quad (6)$$

where (u, v, μ) denotes a homogeneous coordinate point, its corresponding Cartesian coordinates are: $k' = u/\mu$, $l' = v/\mu$. This choice is satisfied robustly under the most situations of scene mosaics in IBR applications. When two images share the same viewpoint, we need only to recover other eight parameters with $m_8=1$, and then equation (5) can be rewritten as

$$\begin{cases} k' = \dfrac{m_0 k + m_1 l + m_2}{m_6 k + m_7 l + 1} \\ l' = \dfrac{m_3 k + m_4 l + m_5}{m_6 k + m_7 l + 1} \end{cases} \quad (7)$$

4.1 Similarity Measurement

The first task of the geometric correction is to find the partial correspondence between the two images. Our algorithm is similar to that in [11] except for two important differences. First, we re-define the pattern vector according to the physical characteristics of each of the subbands. Second, experiments show that the finer the level, the more zero coefficients in the subbands. Therefore, we may consider the base band coefficients only when calculating the similarity distance. These simplifications contribute to the reduction of the complexity of the similarity distance calculation, which is the densest computation in the matching procedure.

Let $PA_{j,q}(k,l)$, q=1,2 and $PD_{j,p}(k,l)$, p =1,2,…,6 denote the pattern vectors in the base band and the detailed subbands on a center position of pixel respectively.

$$PA_{j,q}(k,l) = [\, A_j(k+r,l+c) \,;\, (r,c)\in N] \quad q=1,2 \quad (8)$$

$$PD_{j,p}(k,l) = [\, B_{j,p}(k+r,l+c);\, (r,c)\in N_p \,] \quad p= 1,2,\ldots,6 \quad (9)$$

$$B_{j,p}(k,l) = \frac{D_{j,p}(k,l)}{\left|A_j(k,l)\right|}, \qquad p = 1,2,\ldots,6$$

is called the normalized detail subbands of wavelet transform. And $|\cdot|$ denotes the L_2 metric. $N = \{(0, 0),(-0.5, -0.5), (-0.5, 0.5), (0.5, -0.5), (0.5, 0.5)\}$, $N_1, N_4 = \{(0, 0), (-0.5, 0), (0.5, 0)\}$, $N_2, N_5 = \{(0, 0), (0 ,0.5), (0, -0.5)\}$, and $N_3, N_6 = N$ are a small neighborhood including the center point of the pixel as well as several grid points around it. The advantage of using pattern vector is that the coherence of the local parallax is being taken into account. The neighborhoods are defined with respect to the features of different frequency band-pass filters. For example, in the horizontal low and vertical high frequency subbands, we define the neighborhood as N_1, N_4, while in the vertical low and horizontal high frequency subbands, the neighborhood is defined as N_2, N_5. The complex values of the four grids points can be calculated using the interpolating formula (4), where $\Omega_{j,p}$ and $\Omega_{j,q}$ denote the pair of the modulation frequencies in x- and y-directions for q-th and p-th subband respectively on the level j,

$$(\tilde{w}_j, w_j),(w_j, \tilde{w}_j),(w_j, w_j),(-\tilde{w}_j, w_j),(-w_j, \tilde{w}_j),(-w_j, w_j),$$
$$(\tilde{w}_j, \tilde{w}_j),(-\tilde{w}_j, \tilde{w}_j),$$

where w_j *and* $\tilde{w}_j$ satisfy:

$$w_1 = \frac{5\pi}{6}, \qquad \tilde{w}_1 = \frac{\pi}{6}, \qquad w_j = 3\tilde{w}_j, \qquad w_j = \frac{w_{j-1}}{2} \quad (10)$$

The similarity distance between two corresponding pixels (k, l) in image I_1 and (k', l') in image I_2 is defined by:

$$S_j((k,l),(k',l')) = \sum_{q=1}^{2} SA_{j,q}((k,l),(k',l')) \sum_{p=1}^{6} SD_{j,p}((k,l),(k',l')) \quad (11)$$

where $SA_{j,q}$, $q=1,2$ and $SD_{j,p}$, $p= 1,2,\ldots,6$ are similarity distances of each subband, defined by

$$SA_{j,q}((k,l),(k',l')) = 1 - \frac{\left|PA_{j,q}(k,l) \bullet \overline{PA'_{j,q}(k',l'))}\right|}{\left|PA_{j,q}(k,l)\right| \left|PA'_{j,q}(k',l')\right|}, \quad q =1,2$$

$$SD_{j,p}((k,l),(k',l')) = \left|PD_{j,p}(k,l) - PD'_{j,p}(k',l')\right|$$

, $p=1,2, \ldots,6$

In our experiments, it shows that on higher resolution levels, most of the coefficients of $B_{j,p}$ approach to zero. Therefore, the second summation in equation (11) can be neglected in these levels. This strategy speeds up the matching calculation on higher resolution levels twice as much.

4.2. Correspondence Search

According to the similarity distance defined in the previous section, the matching algorithm can be performed

automatically in most cases. If large parallax exists, some interactions are needed. The algorithm starts at the coarsest level of the two reference images. First, the similarity measurement defined in (11) is employed to find the best matched central area of one image to another. Second, the parallax vector is propagated from central to border ring by ring until the boundary of correspondence region is reached and fine-tuned via (11). Third, the correspondence map resulted from the two previous steps is applied for the registration algorithm to fit an alignment transformation. The result is then used for initializing the correspondence map on the next finer level.

Note that the problem of the image matching mentioned here is different from the one in the stereo matching [11], where there is very little parallax between left and right views, and thus the matching is nearly complete and relatively easy. Here in the image mosaics, we face a partial correspondence problem, and thus it is necessary to mark the boundary of correspondence region. We identify the boundary pixel simply by:

$$\left| S_j((k,l),(k',l')) - S_j((k,l),N(k',l')) \right| > T_s \quad (12)$$

where $N(K', l')$ is neighbor pixel of (K', l'). T_s is a threshold value of boundary. When (12) is satisfied, the current neighbor pixel can be determined as a boundary pixel.

5. The least Visible Seam-lines

After the geometric correction, images are ready to project onto the mosaic coordinate system. In this scheme, the mosaic is done by directly placing images onto the mosaic coordinate system; the frontier between two images can be artificial. This artificial frontier is a *least visible seam-line*, which passes through the radiometrically similar areas, or along common edges. We search for the least visible seam-line in the baseband of the wavelet domain and then transform the baseband seam-line to the spatial domain using the reverse wavelet transform. The seam-line in the spatial domain may be scattered since it is transformed from only the baseband. A simple linear interpolation will be applied to smooth the seam-line. Due to the strong spatial localization of wavelet transform, the transformed least visible seam-line remains *least visible* in the original spatial domain.

The least visible seam-line in the baseband can be found by searching for the *least-cost path* through a criterion image using the dynamic programming algorithm. There are two criteria for the seam-line to be least visible [1]: either cutting through the radiometrically-equal areas, or along common edges between two images. The criterion image is defined as

$$c(l,k) = c_{dif}(l,k) - \lambda c_{edge}(l,k)$$

$$c_{diff}(l,k) = \frac{1}{N_v} \sum_{i,j \in V} \left| I_1(l+i,k+j) - I_2(l+i,k+j) \right|$$

$$c_{edge}(l,k) = Min(G_1(l,k), G_2(l,k))$$

where I_1 and I_2 are the coefficients in the baseband images and G_1 and G_2 are the gradient norms on them.

The radiometry differences c_{diff} between the two baseband images are averaged in a rectangular V and the common edges are computed by applying a gradient operator. The coefficient λ is a weighting variable determined by the following criterion. If the overlap area is lying on a homogenous area, the intensity part of the equation will be more important; if the overlap area is lying on a complex area with many edges, the edge part of the equation will be more important. In general, λ is set to 1 to reflect the equal importance of the intensity and edges of the ordinary images.

6. Experiment

Table 1 shows the time complexity based on different levels of the wavelet transform. The overhead of the wavelet transform is neglected. Each row represents the CPU processing time on the baseband of a certain resolution level. The larger the level number, the coarser the resolution. The experiment is conducted with *Matlab* 5.0 on *Pentium* 133 PC, which gives a very slow time in general. However, this table illustrates that wavelet-based seam-line scene mosaics outperform that of the spatial domain seam-line mosaics scheme 2, 2.83, and 3.24 times at levels 2, 3.and 4 respectively. Note that performance at wavelet level 5 possesses a little improvement over that at level 4.

References

[1] Duplaquet, M., Building Large Image Mosaics with Invisible Seam-lines, *The proceedings of SPIE Aerosense Conference,* **3387**, April 1998, Orlando.

[2] Bao, P., & Xu, D., "Complex Wavelet-based Image Mosaics using Edge-Preserving Visual Perception Modeling", *Computers and Graphics,* **23**(3), June, 1999

[3] Bao, P. & Xu, D., Visual Perception Based Complex Wavelet Thresholding For Panoramic Image Mosaics, *The Proceedings of IEEE Conference on Systems, Man and Cybernetics,* 4614-4619, October, 1998

[4] Brown, L. G. A., Survey of Image Registration Techniques, *ACM Computing Surveys,* **24**(4), December 1992, 325-376.

[5] Chen, S. E. and William. L., View Interpolation for Image Synthesis, *Computer Graphics (SIGGERAPH'93),* 1993, 279-288.

[6] Chen, S. E., QuickTime VR — An Image-Based Approach To Virtual Environment Navigation. *Computer Graphics (SIGGERAPH'95),* 1995, 29-38.

[7] Debevec, P. E., Taylor, C. J. and Malik, J., Modeling and Rendering Architecture from Photographs: A Hybrid Geometry–And Image-Based Approach. In *Computer Graphics (SIGGRAPH' 96*), 1996, pp. 11-20.

[8] Magarey, J. and Kingsbury, N. G., Motion Estimation Using Complex Wavelets. *Technical report,* Cambridge University, Department of Engineering, 1995.

[9] Pan, H. P., Uniform Full-Information Image Matching Using Complex Conjugate Wavelet Pyramids, *XVIII ISPRS Congress, Vienna,* 1996. *Intern. Arch. of Photogeometry and Remote Sensing*.

[10] Szeliski, R. and Coughlan, J., Hierarchical Spline-Based Image Registration, Proc. *IEEE Computer Soc. Conf. Computer Vision and Pattern Recognition (CVPR 94),* IEEE CS Press, Los Alamitos, Calif., 1994, 194-201.

[11] Canny, J., A Computational Approach to Edge Detection, *IEEE Trans. On Pattern Analysis and Machine Intelligence,* **8**(6), 24-32, November 1986.







Figure 7. Hong Kong Airport. The first three) are the source images. The middle two are the edge images extracted by *Canny* operator. The last is the mosaic image using 3 level wavelet transform.

Phases	Spatial domain seam-line scheme	Wavelet domain seam-line scheme			
Level		2	3	4	5
Correspondence	0.37	0.11	0.027	0.006	0.0017
Radiometric correction	0.03	0.03	0.03	0.03	0.03
Homographic transformation	0.18	0.18	0.18	0.18	0.18
Seam-line searching in baseband	0.10	0.026	0.0067	0.0018	0.0006
Total	0.68	0.34	0.24	0.216	0.21

Table 1: Performance comparison of spatial-based and wavelet-based seam-line mosaic.

Contour layer Extraction from Colour Topographic map by Feature Selection approach

Sandhya Banda, Arun Agarwal, C.Raghavedra Rao, Rajeev Wankar
sandhyab16@gmail.com, aruncs@uohyd.ernet.in, crrcs@uohyd.ernet.in, wankarcs@uohyd.ernet.in
University Of Hyderabad
India

***Abstract*—Contour layer of topographic maps can provide useful information for many vector based GIS applications. A topographic map consists of various semantic layers of overlapping information, differentiated primarily based on colour. Hence, to extract the contour layer from a topomap, colour segmentation algorithms are employed. However due to scanning and inherent features of topomap, colour space selection which provides efficient segmentation results becomes essential. The method proposed uses PCA as feature selection approach to select the colour features of topomap. The clusters are further processed to map to the layers of topomap using spatial properties.**

***Keywords*-Topographic map, Contour layer, Colour clustering, Principal Component Analysis**

I. Introduction

A topographic map gives a detailed and accurate graphic representation of cultural and natural features of the terrain based on topological surveys [1]. Topomaps describe spatial data using entities, attributes and relationships in an unstructured representation. Entities on maps are described by point, line, and area objects. Symbols, Text, Color are commonly used on maps to represent attributes associated with the entities. Relationships among entities are depicted visually. A scanned topographic map, which is in raster form, is one of the primary sources of spatial data in geographic databases and is used in a wide variety of GIS applications. A topomap consists of multiple layers of data, where each layer depicts a specific characteristic of earth's surface such as vegetation cover, hydrology, topography etc. Colour is primarily used to differentiate between these layers. A sample map is shown in figure 1. In this map, water bodies are shown in blue, grid lines in red, toponyms in black, contour lines in brown. For applications in GIS, each of these raster layers should be separated so that in each cell of a particular layer, there is one and only one thematic attribute or value. Automatic separation of different layers of information in topomaps poses an immense challenge due to the heavy interconnectedness of these layers. Our focus is on the generation of layer pertaining to contours, which has a tremendous application to geo scientific modelling due to the potential 3D representation of the terrain (which is a demanding tool from Geoscientists to take the advantage of visualization tools). Contour lines are represented by curves with 2-4 pixels width when scanned at a resolution of 300dpi, brown in colour. The lines are labelled indicating the elevation values. In [2] is presented various challenges of automatic extraction and vectorization of contour lines from colour topomaps. A layer corresponding to contours will invariably have noise, discontinuities and gaps. The extraction of a contour layer thus introduces a challenging problem of filtering unwanted text, identification of gaps and filling them, for realistic automatic vectorization. This chapter focusses on separating the contour layer from topomap using colour clustering algorithm and then filtering text and noise from the extracted contour layer.

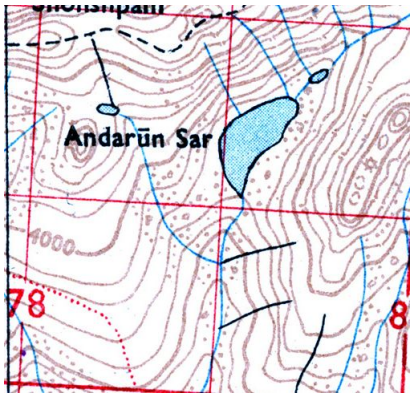


Figure 1. Contour layer Extraction

II. Related Work

The first step in the conversion of topomaps is color based separation of features. However existence of color in topomaps introduces other dimensions to the problem : false colours, aliasing which are induced by the scanning process [2].

Literature survey indicates that extensive work has been done in improving the segmentation of topomaps using various segmentation algorithms such as threshold based, histogram based, region based (region growing and merging),

and hybrid approaches. Each of the segmentation algorithms use any one of the colour spaces like RGB, HIS, Lab etc. Early segmentation methods on topomaps concentrated on color space selection. Ansoult et al. [3] use the mean and variance of the hue channel for discriminating soil types on a digitized soil map. Ebi et al. [4] transform the input RGB color space into another color space considering the chromaticity. Khotanzad et al. [2] addressed the problem by proposing a method to build a color key set for linear and area features of standard USGS topomaps and a non parametric clustering algorithm based on multidimensional histogram of the topomap. Yang Chen et al. [5] extended this work beyond the standard USGS maps to common conditioned maps by using the features extracted from the gray version of the same color map along with the color coded map. Carol Rids et al. [6] used color edge detection - vector angle edge detector, with a saturation-based combination of hue and intensity planes, and color clustering (minimum variance quantization) to extract the contour lines from color coded maps.

Khotanzad et al. developed a colour key set technique to compensate for aliased and false colours for USGS topographic maps and to address the problems associated with thin, closely spaced linear features and intersecting features. However, besides USGS topographic maps, other topographic maps in use, especially published in old age, are often non-USGS with poor conditions. Hence the focus of work has been to select the colour feature set, which can efficiently segment any kind of topographic map, than to improve the segmentation algorithm. This has been attempted as a feature selection problem by considering the colour features of various colour spaces.

III. Proposed Method

Major steps of the algorithm is as follows

1) Select the colour features of the topomap using Principal Component Analysis.
2) Quantize the feature set using Uniform Quantization
3) Cluster the quantized feature set by a Histogram based Non Parametric Clustering Algorithm. [7]
4) Merge the clusters to map to the layers of topomap by Spatial analysis.

Each of the steps are explained in detail in the following sections.

A. Feature Selection

Colour is perceived by humans as a combination of tristimuli R (red), G (green), and B (blue) which are usually called three primary colors. From R,G, B representation, we can derive other kinds of colour representations (spaces) by using either linear or non-linear transformations. Several colour spaces, such as RGB, HSI, CIE L*u*v* are utilized in color image segmentation, but none of them can dominate the others for all kinds of color images. Selecting the best colour space still is one of the difficulties in color image segmentation [8]. Hence the approach followed is to select a Hybrid colour space [9], consisting of the best features which can describe a particular topomap. It is addressed as a feature selection, selecting best features from all the color spaces for a given image. Principal Component Analysis (PCA) which is one of the most widely used technique for feature selection, has been employed.

The topomap is scanned and stored as a colour image using RGB colour space. The colour features of various colour spaces like HSV,YCbCr,YIQ etc are computed for each pixel of the image by transforming the RGB values.

Data is generated from the feature set of the image. Principal component vectors and values are computed as explained in the algorithm 1. The image is then transformed along the first three principal components and the transformed image is used for further processing as explained in the subsequent sections.

B. Quantization

The colour of pixel is represented by three dimensional vector, RGB where each channel can have a value between 0 and 255. A 24-bit color image contains at most 2^{24} = 16777216 different colours. Though a limited set of colours are used in topomap for representing the various features, scanning process introduces false colours. For example, in a simple scanned USGS map consisting only of blue, brown, black and purple, over 42000 distinct colours can be detected[[10]]. Thus , by employing color quantization full color RGB images, where each pixel is typically described by three 8-bit color samples, is represented in an approximate fashion by a relatively small number of colours. Thus the full color space, consisting of about 16 million pixels (2^{24}), is divided into a small number of regions, and for each region, a single representative color is used for each pixel that falls into the region. Main objective of any quantization algorithm is to minimize the overall distortion. Various colour quantization algorithms have been described in the survey. The colour topomap which is represented using Hybrid color space is quantized as follows:

1) PCA transformed colour image is represented as a cube with three components $P1, P2, P3$ along X,Y,Z axis respectively.
2) The minimum and maximum values along each axis of the cube are chosen from the input data i.e for example $X_{min} = P1_{min}, X_{max} = P1_{max}$
3) The cube is partitioned into sets of non overlapping cells. If the quantization levels are $(Q_C, C = P1, P2, P3)$,the whole cube is divided into $Q_{P1} * Q_{P2} * Q_{P3}$ cells. It is to be noted that the range of values to be divided differ along each axis based on minimum and maximum values of the corresponding axis.

Feature Selection Algorithm

{ *Input Arguments*
I_m *: Topomap image*
$N_r \times N_c$ *: Size of input image*
Output Arguments
I_f *:Image represented using selected features*
Functions called
eigval : Computes the eigen vectors.
Colour space conversions:
rgb2hsv : Transforms RGB to HSV.
rgb2yiq : Transforms RGB to YIQ.
rgb2ycbcr : Transforms RGB to YC_bC_r.
rgb2lab : Transforms RGB to L*a*b*.
rgb2xyz : Transforms RGB to CIE XYZ.
}
$n_p = N_r \times N_c$
{Feature extraction}
$F(1:N_r, 1:N_c, 1:3) = I_m$
$F(1:N_r, 1:N_c, 4:6) = rgb2hsv(I_m)$
$F(1:N_r, 1:N_c, 7:9) = rgb2yiq(I_m)$
$F(1:N_r, 1:N_c, 10:12) = rgb2ycbcr(I_m)$
$F(1:N_r, 1:N_c, 13:15) = rgb2lab(I_m)$
$F(1:N_r, 1:N_c, 16:18) = rgb2xyz(I_m)$
{Data matrix formation}
for $i = 1$ *to* N_r **do**
  for $j = 1$ *to* N_c **do**
    $X((i-1) * N_c + it2, 1:18) = F(i, j, 1:18)$
  end for
end for
{ Centre X by subtracting off column means, μ is the vector of column means}
$Y = X - \mu$
{Computing Covariance matrix, Σ of Y}
$\Sigma = Y^T Y \times 1/(n_p - 1)$
{The principal component coefficients are the eigenvectors of Σ}
$coeff = eigval(\Sigma)$
{Project Y onto the first 3 principal component axes to get the output.}
$I_f = Y \times coeff(:, 1:3)$

4) The tristimuli values of each pixel of the input image are mapped to a quantization level between 1 & Q_C.

$limit_{low} = X_{min}$
$limit_{up} = limit_{low} + Q_{P1}$
$V_{P1} = 0$
while $limit_{up} \leq X_{max}$ **do**
  $V_{P1} = V_{P1} + 1$
  if $P1 \geq limit_{low}$ AND $P1 < limit_{up}$ **then**
    return
  end if
  $limit_{low} = limit_{up}$
  $limit_{up} = limit_{up} + Q_{P1}$
end while
if $P1 > X_{max} - Q_{P1}$ AND $P1 \leq X_{max}$ **then**
  return
end if

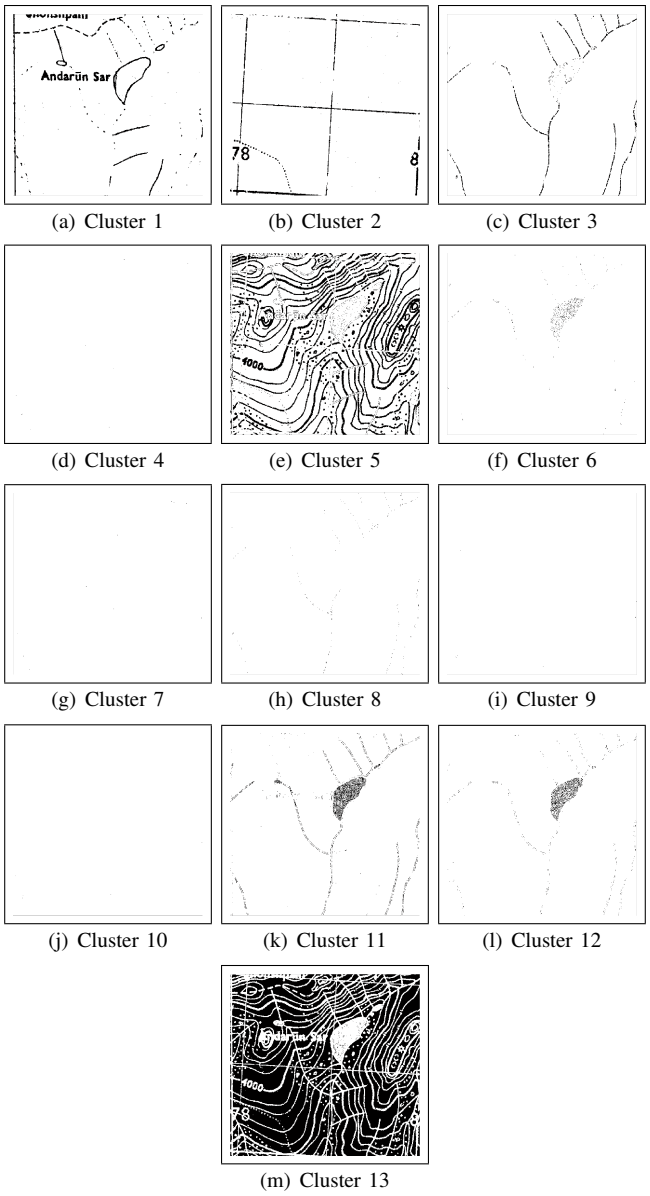
C. Clustering algorithm

The topomap segmentation has been performed using a non parametric histogram based clustering algorithm proposed by Khotanzad et.al. [7]. The quantized image is clustered by computing the histogram and finding the peaks of histogram using peak climbing approach. This algorithm is non parametric i.e. requires no parameters from the user as input. A three dimensional histogram of the quantized image is computed by counting the number of pixels in each cell of the cube, i.e a $Q_{P1}XQ_{P2}XQ_{P3}X1$ matrix is formed which stores the count of each cell of the cube. Clustering is performed by locating the peaks of the multidimensional histogram using peak climbing algorithm developed by [11]

1) The clustering operation requires the examination of all the neighbouring cells of all non-empty cells. The number of neighbours for each discrete cell is a function of the dimension of the space. The number of possible neighbours in the two and three dimensional representation are 8 and 26 respectively.
2) By examining the counts of neighbours of a particular cell, a link is established between that cell and the closest cell having the largest count in the neighbourhood. If two or more neighbouring cells have the same count for a particular cell, one of them is arbitrarily chosen as a parent.
3) At the end of the link assignment each cell is linked to one parent cell, but can be parent of more than one cell.
4) A peak is defined as being a cell with the largest density in the neighbourhood, i.e. a cell with no parent.
5) A peak and all the cells which are linked to it are taken as a distinct cluster representing a mode of the histogram.

Thus, the clustering process starts from each peak and identifies all the other cells linked to its peak by following the connectivity of the cells through the links. It can be noted that the method is completely automatic and can be applied on any colour image. It is amenable to parallel processing as the image can be divided and method applied on different parts of the image.

The results of applying the method are shown in the figure 2. It can be noted that number of clusters obtained is greater than the number of distinct colours present in a topographic map, due to presence of false colours and aliasing. Hence a post processing stage is necessary which can map the clusters to the layers of topomap. However, as the PCA transforms the color image, once the clusters are obtained



(a) Cluster 1 (b) Cluster 2 (c) Cluster 3

(d) Cluster 4 (e) Cluster 5 (f) Cluster 6

(g) Cluster 7 (h) Cluster 8 (i) Cluster 9

(j) Cluster 10 (k) Cluster 11 (l) Cluster 12

(m) Cluster 13

Figure 2. Clusters obtained from topomap in figure 1

from initial clustering, the same space cannot be used for further processing of clusters. For example, distance metrics cannot be used to merge the clusters. Hence, clusters are merged using spatial properties of pixels, described in the next section.

D. Merging the clusters

The clusters obtained on a PCA transformed colour topomap, are mapped to the layers. Neighbourhood analysis is used for this purpose. Number of pixels belonging to each cluster i.e. cluster size is computed. Based on the cluster size, the clusters which have relatively very less pixels compared to the image size, can be considered as noise. The cluster of maximum size, belongs to background and so not considered. In the remaining clusters, which belong to objects, the following procedure is applied on the clusters with size less than maximum size of object cluster.

Let $C_t, t = 1toN_{tc}$,be the clusters where N_{tc} are the total number of clusters. Let N_{rc} be the clusters after removing noise and background. For each pixel p in the cluster, C_i

1) Consider a $w \times w$ neighbourhood of p. Count the number of pixels in the neighbourhood which belong to each cluster in the list N_{rc}
2) If the number of pixels which belong to a particular cluster $C_j, j \neq i$ is more than $(w^2-1)/2$, assign pixel p to cluster C_j from cluster C_i
3) Iterate the above procedure on each cluster, until its size does not change between the two iterations.

Spatial analysis of clusters

{ *Input Arguments*
C_t : Clusters of topomap image
w : Size of window
Output Arguments
cnt :matrix of size $N_{rc}XN_{rc}$.
(Gives number of pixels of each cluster, assigned to each other cluster.)
Functions called
clussize : Gives the number of pixels in the image which belong to cluster
}
for $i = 1$ *to* N_{rc} **do**
  while true **do**
    for each pixel p in C_i **do**
      Find wXw neighbours of p.
      Let these be set S_p
      for $j = 1toN_{rc}$ **do**
        Find number of pixels in C_j from S_p, pN_{ij}
        if $pN_{ij} > (w^2-1)/2$ **then**
          p belongs to C_j
          $cnt(i,j) = cnt(i,j) + 1$
          break
        end if
      end for
      if clustsize(i) remains same **then**
        break
      end if
    end for
  end while
end for

4) Based on the number of pixels of cluster C_i belonging to other clusters,an adjacency matrix of size $N_{rc} \times N_{rc}$ is formed. The value at a position (i, j) is 1 if in the cluster C_i, number of pixels whose neighbourhood

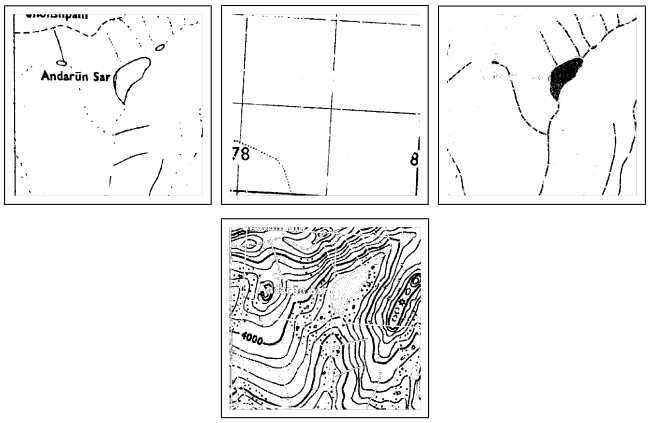


Figure 3. Layers of topomap in figure 1

Table I
CONFUSION MATRIX

		Predicted class	
		Contour	Other
Test outcome	Contour	True Positive(tp)	False Positive(fp)
	Other	True Negative(tn)	False Negative(fn)

belong to cluster C_j is maximum and is greater than a threshold i.e. if $cnt(i,j) = max(cnt(i,:))$.

5) Clusters are merged from the components obtained by backtracking the adjacency matrix. The figure 3 shows the merged clusters, which form the layers of topomap shown in figure 1

E. Results

The significance of using a feature selection on all the colour features for clustering the topomap can be observed by comparing the same clustering algorithm applied against a RGB colour space.

The results are illustrated using the test images shown in Figure 4. The test images are parts of topomaps prepared by Survey Of India, of scale 1:50000. They are scanned with a resolution of 300dpi. The first step is systematic sampling over the set of processed map documents, i.e training data is prepared for each sample image, by manually assigning pixels to the layer of topomap it belongs to. For each image a limited random number of pixels have been selected under each layer. care has been taken to select the pixels all across the topomap. For example, figure shows the pixels selected for contour layer in . After employing clustering, the layer index of each of the sampled pixel is stored. A confusion matrix is created using the clustered and labelled pixels, as shown in I. Measures derived from the confusion matrix are recall and precision for the contour layer. Precision is a measure of the accuracy provided that contour pixels have been predicted. It is defined by:

$$Precision = tp/(tp + fp)$$

where tp and fp are the numbers of true positive and false positive predictions for the considered class. Recall is a measure of the ability of a prediction model to select instances of contour pixels from a data set. It is commonly also called sensitivity, and corresponds to the true positive rate. It is defined by the formula:

$$Recall = Sensitivity = tp/(tp + fn)$$

where tp and fn are the numbers of true positive and false negative predictions for the considered class. tp + fn is the total number of test examples of the considered class.

Table II shows the results on 5132 pixels sampled from twelve maps, shown in figure 4. It can be seen that the same clustering algorithm performs better in the case of PCA space than the RGB space. For few images, using RGB space contour layer could not be separated from background. For images Topomap 8 and Topomap 10, using quantization level 16, along each axis, the contour layer could notbe separated from background. However using quantization level 32, the contour layer could be obtained. Hence the algorithm is sensitive to the quantization level.

IV. CONCLUSION

A colour topographic map is clustered into layers like contour, vegetation, water bodies etc. based on colour features. The results of applying the method using PCA transformed space are compared against RGB space for a set of topomaps. The clustering algorithm performs better when used with the transformed space. Also the algorithm can be implemented using a parallel architecture. It can be noted that the proposed method can be used on any colour document and is fully automatic with no manual intervention.

REFERENCES

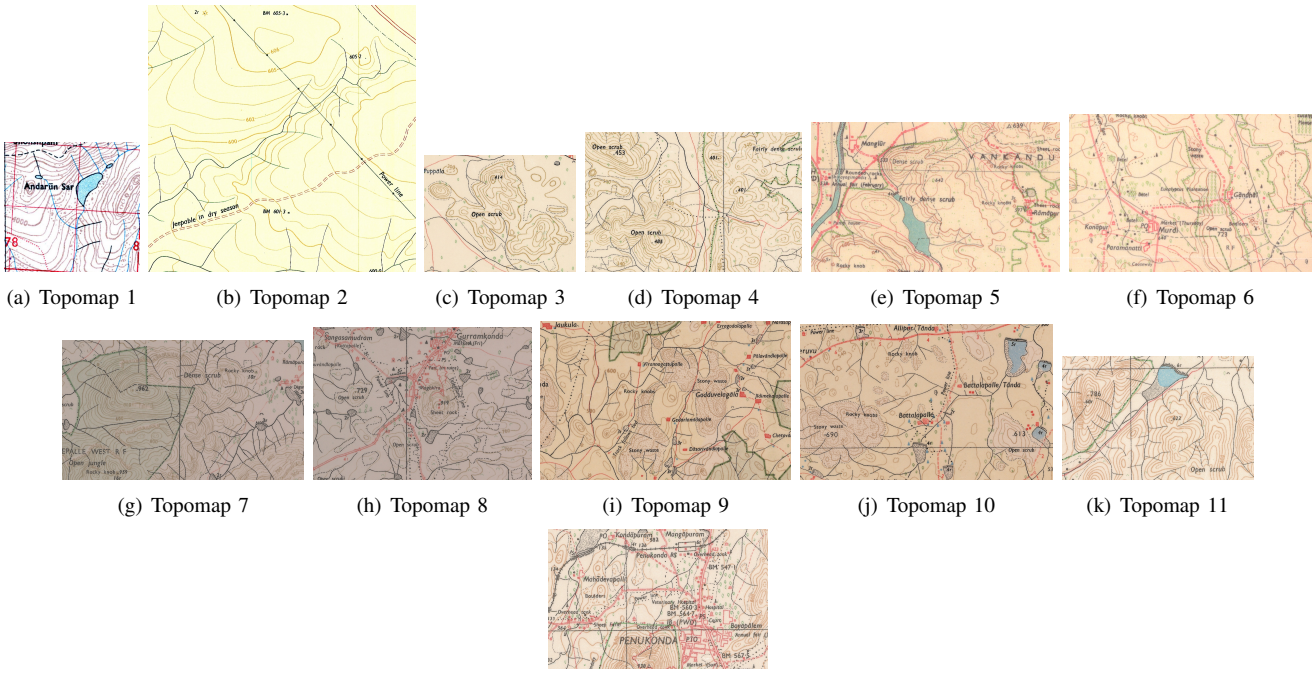
[1] C. Albert and K.W.Yeung, *Concepts and techniques of Geographic Information Systems*. India: PH Series in Geographic Information Science, Prentice-Hall.

[2] A. Khotanzad and E. Zink, "Contour line and geographic feature extraction from usgs color topographical paper maps," *IEEE Transactions on Pattern Analysis and Machine Intelligence*, vol. 25, no. 1, 2003.

[3] M. Ansoult, P. Soille, and J. Loodts, "Mathematical morphology: A toolfor automated gis data acquisition from scanned thematic maps," *Photogramm.Eng. Remote Sens*, vol. 56, no. 9, p. 1263 1271, 1990.

[4] N. Ebi, B. Lauterbach, and W. Anheier, "An image analysis system for automatic data acquisition from colored scanned maps," *Machine Vision Applications*, vol. 7, no. 3, p. 148 164, 1994.

[5] Y. Chen, R. Wang, and J. Qian, "Extracting contour lines from common-conditioned topographic maps," *IEEE Transactions on Geoscience and Remote Sensing*, vol. 44, no. 4, April 2006.



(a) Topomap 1 (b) Topomap 2 (c) Topomap 3 (d) Topomap 4 (e) Topomap 5 (f) Topomap 6

(g) Topomap 7 (h) Topomap 8 (i) Topomap 9 (j) Topomap 10 (k) Topomap 11

(l) Topomap 12

Figure 4. Test Images

Table II
RESULTS OF ACCURACY ASSESSMENT

Image	Size	Quantization	No of pixels		RGB		PCA	
Map		level	Total	Contour	Precision	Recall	Precision	Recall
1	484 X 506	16	336	77	89.16	96.10	96.15	97.40
2	1001 X 1001	16	242	98	100	59.18	100	71.43
3	583 X 755	16	296	85	51.27	95.29	100	87.06
4	695 X 1083	16	400	131	NaN	0	98.77	61.07
5	746 X 1243	16	402	141	98.21	78.01	99.09	77.3
6	787 X 1212	16	414	124	97.98	86.29	99.07	86.29
7	695 X 1205	16	401	105	NaN	0	79.46	84.76
8	760 X 1092	32	560	169	NaN	0	100	47.83
9	790 X 1249	16	332	104	NaN	0	49.15	83.65
10	774 X 1264	32	487	100	NaN	0	97.37	74
11	617 X 954	16	672	197	62.89	92.89	99.44	89.85
12	693 X 1095	16	590	112	72.06	87.5	98.18	96.43

[6] C. Rids, C. Rusu, and J. Astolu, "Contours extraction from a colour coded relief scanned map," *International Conference on Image Processing (ICIP)*, 2004.

[7] A. Khotanzad and A. Bouarfa, "Image segmentation by a parallel, nonparametric histogram based clustering algorithm," *Pattern Recognition*, vol. 23, no. 9, pp. 961 – 973, 1990.

[8] H. Cheng, X. Jiang, Y. Sun, and J. Wang, "Color image segmentation: advances and prospects," *Pattern Recognition*, vol. 34, pp. 2259 – 2281, 2001.

[9] R. Raveaux, J.-C. Burie, and J.-M. Ogier, "A colour document interpretation: Application to ancient cadastral maps," *International Conference on Document Analysis and Recognition(ICDAR)*, pp. 1128 – 1132, September 2007.

[10] A. Pezeshk and R. L. Tutwiler, "Contour line recognition and extraction from scanned colour maps using dual quantization of the intensity image," *IEEE Southwest Symposium on Image Analysis and Interpretation (SSIAI)*, pp. 173 – 176, March 2008.

[11] W. Koontz, P. M. Narendra, and K. Fukunaga, "A graph theoretic approach to non-parametric cluster analysis," *IEEE Transactions on Computers*, vol. C-25, pp. 936 – 944, 1976.

An Efficient Multimodal Face Recognition Method Robust to Pose Variation

Ali Cheraghian, Karim Faez, Hamidreza Dastmalchi, Farhad Bagher Oskuie
Dept. Electrical Engineering
Amirkabir University of Technology (Tehran Polytechnic)
Tehran, Iran
Ali_cheraghian@aut.ac.ir

***Abstract*- In the recent years, face recognition has obtained much attention. Using combined 2D and 3D face recognition is an alternative method to deal with face recognition. A novel multimodal face recognition algorithm based on Gabor wavelet information is presented in this paper. The Principal Component Analysis (PCA) and the Linear Discriminant analysis (LDA) have been used for size reduction. The system has combined 2D and 3D systems in the decision level which presents higher performance in contrast with methods which use only 2D and 3D systems, separately. The proposed algorithm is examined with FRAV3D database that has faces with pose variation and 95% performance that is achieved in rank-one for fusion experiment.**

***Keywords*— Principal Component Analysis; Gabor filter; Depth image; Multimodal face recognition**

I. INTRODUCTION

Face Recognition (FR) is one of the attractive methods in biometric systems, because face recognition provides a good trade-off between reliability and social acceptance. There are five major problems in face recognition which affect performance of the system: 1) Illumination variations 2) Pose changes 3) expression variations 4) time delay 5) occlusions [1]. As it has been mentioned, one of the challenges is pose variation. Algorithms presented for pose variation are divided in two main categories in related to their type of gallery images [1]. First, Multi-view face recognition system (FRS) which requires several poses for every subject in gallery. Another category identifies probe faces which have different poses with gallery face. In real situations, a frontal face in gallery is available but probe faces have unpredicted pose variations so, the system must be robust to these situations.

In [2], after a pose estimation step, a template-based on correlation-matching scheme has been used to align the probe image with the candidate pose in the gallery images.

In [3], a framework for recognizing faces with large 3D pose variations has been presented which applied a parametric linear subspace model for representing each known person in the gallery. In [4], a 3D face recognition method has been proposed. This method segments the convex regions in the range images based on the sign of the mean and the Gaussian curvatures. In the 3D face recognition method proposed by [5], an iterative closest point (ICP) approach was used to match face surfaces. In [6], 3D faces in the gallery are represented by third order tensors which are indexed by a 4D hash table. During online recognition, tensors are computed for a probe image and are used to calculate votes for the tensors in the gallery using the hash table. In this paper, experiments were performed on a database of 277 subjects. The algorithm achieved a rank one recognition rate of 86.4%.

Most face recognition researches have focused on the 2D intensity images. As shown in Face Recognition Vendor Test 2002 [7], one of the problems of these algorithms is the pose variation. According to the discriminating power of recognizing people, depth images are more powerful than intensity images [8].

Face recognition algorithms which combine 2D and 3D data have been recently proposed. In [9], it is shown that combining 2D and 3D results by using a simple weighting scheme, outperforms either 2D or 3D. In [10], a HMM approach was proposed to combine depth and intensity images, and finally a recognition rate of 90.7% for intensity images and 80% for depth images has been reported. When both intensity and depth images were combined, the system reached a rate of 91.67%,

In [11], Gabor wavelet was used for feature extraction, and a novel system was proposed to combine depth and intensity information. A recognition rate of 91% in images which have pose variation was achieved.

In this paper, we present a multimodal face recognition system as shown in Fig. 1.

In this research, Gabor wavelets have been used for feature extraction. Since the dimensions of data was large, it was reduced by using PCA (principal component analysis).To improve the discrimination between classes LDA (Linear Discriminant analysis) was used. In the next step, 2D and 3D system outputs have been combined in the decision level.

This paper is outlined as following: section II introduces the preprocessing which includes 3D face normalization and extraction depth and intensity images. In section III, Gabor wavelet was implemented for feature extraction and PCA+LDA for dimension reduction. This step for 2D system is as same as 3D system. In section IV, fusion strategy is introduced for combining 2D and 3D systems. Section V discusses about experimental results. At the last section, a conclusion summarizes made points in the paper and experiments.

II. PREPROCESSIN

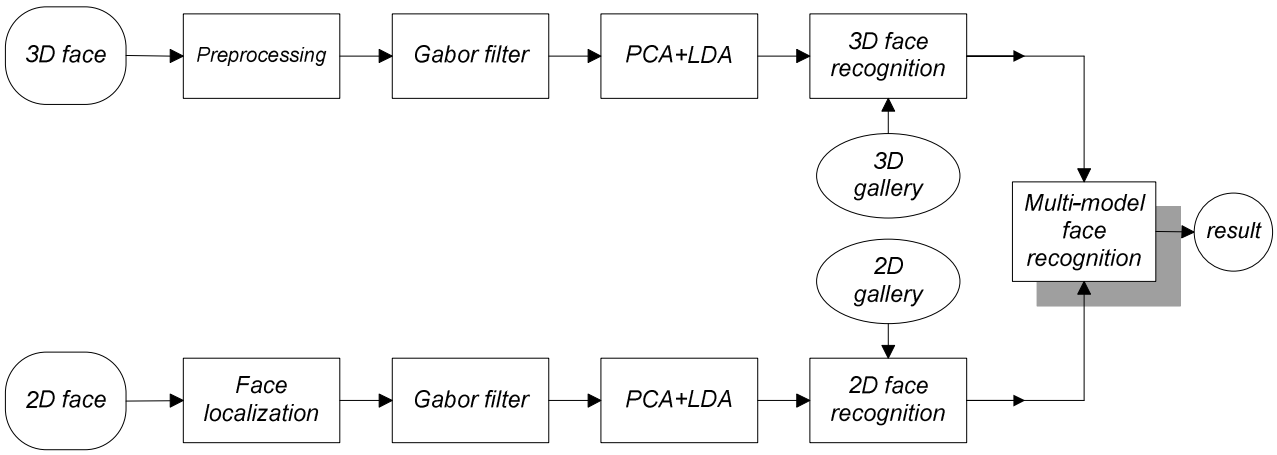


Fig. 1. General block diagram of our system for multimodal face recognition.

A. 3D face normalization and depth extraction

Since acquired 3D faces are noisy, they are not in correct coordinates and choosing the region of interest (ROI) in the face is essential, a preprocessing is needed before the feature extraction is done. The preprocessing includes three steps. First, in order to remove spike noises, a median filter has been used. A 3×3 window was utilized to remove spike noises. Using larger windows may cause to lose important information. In second step, in each face, a ROI has been selected. Hairs, shoulders and neck are not useful for face recognition, therefore, for selecting a suitable ROI, a rectangular region with size of 160×160, we landmarked center of eyes manually. In the third step, faces have been aligned to same coordinates. This step has an important role in robust identification. In order to align faces to the same coordinates the ICP algorithm has been applied [12]. In this algorithm, a frontal face with natural expression is selected as fixed model, and all 3D faces are rotated and translated to have minimum distance with the fixed model. These three steps provide clean data for the extracting the depth face. The size of the depth image is 120×120 pixels.

The flow diagram of these steps has been presented in Fig. 2.

B. intensity images

Intensity images are independent from 3D face. Center of eyes has been landmarked manually, and a rectangle with size of 160×160 pixels has been selected to extract ROI from faces. After this process, all images have been resized to 120×120 pixels. Finally, faces are ready for feature extraction.



Fig. 2. A flow diagram of the preprocessing Procedure.

III. FEATURE EXTRACTION

A. Gabor wavelet

In this paper, we used 2D Gabor wavelet for feature extraction from depth and intensity images. Gabor wavelets were first defined by D. Gabor [13], then generalized to two dimensions by J. Daugman [14]. A Gabor wavelet is complex sinusoids which are modulated by a 2D Gaussian function and represents the properties of spatial localization, orientation selectivity, spatial frequency selectivity, and quadrature phase relationships [15].

Image I(t) has been convolved with a wavelet transformation function:

$$Z_i = \int I(t)\,\psi(x-t)dt \qquad (1)$$

Where $\psi(x)$ is a Gabor kernel as follow:

$$\psi(x) = \frac{K_{\alpha,\beta}^2}{\sigma^2}\exp\left(-\frac{k_{\alpha,\beta}^2 x^2}{2\sigma^2}\right)\left[\exp\left(jk_{\alpha,\beta}x\right) - \exp\left(-\frac{\sigma^2}{2}\right)\right] \qquad (2)$$

In which, x=(x,y), α and β are orientation and scale of Gabor wavelet and $\sigma = 2\pi$.

Five different scales $\beta \in [0,1,2,3,4]$ and eight orientations have been used. Each image has two Gabor parts: amplitude and phase. Here, we only use the amplitude for face recognition.

B. Principal component analysis

The Gabor wavelet generates 40 images from each image. The dimension of available data is too high. Hence, a reduction in the data dimension seems to be necessary. PCA is popular in feature extraction and is used to find a low dimension representation of data. The face images are considered as random vectors. By solving the scatter matrix eigenvalues, a new orthogonal base is extracted and all of the face images are projected to a new subspace. Then, the feature

vector is extracted for every image. In PCA, every image must be transformed to a 1D vector. The set which has been used to train is $X = [X_1, X_2, \cdots, X_n]$ and the obtained set after subtracting the mean vector from all images is $R = [R_1, R_2, \cdots, R_n]$. In the next step, the covariance matrix R has been calculated as follow:

$$C = \frac{1}{M}\sum_{i=1}^{M} RR^T = AA^T \quad (3)$$

M is number of classes which were used to train. Then, the largest eigenvalues of covariance matrix and their corresponding eigenvectors were chosen. The transformation matrix will be obtained as:

$$W_{pca} = A.V \quad (4)$$

Where, V is the set of eigenvectors. Utilizing this matrix, Equation (5) has been resulted and will be used in feature extraction of each image.

$$\omega = W_{pca}^T(image_i - avg) \quad (5)$$

C. *Linear Discriminant Analysis*

LDA is utilized to reduce the high dimensional data into a low-dimensional space to combine data from the same class, while data of different classes are separated easily from each other by using the class information. In this case, LDA is better than PCA because it is a supervised algorithm [16].

To find W, we should maximize the following ratio,

$$J(W) = \frac{W^T S_b W}{W^T S_W W} \quad (6)$$

Where,

$$S_W = \sum_{j=1}^{C}\sum_{i=1}^{N_i} N_i\left(x_i^j - \mu_j\right)\left(x_i^j - \mu_j\right)^T \quad (7)$$

is the within-class scatter matrix, and

$$S_b = \sum_{i=1}^{C} N_i(\mu_i - \mu)(\mu_i - \mu)^T \quad (8)$$

is a between-class scatter matrix. x_i^j is also the projective vector extracted from PCA and μ is the mean vector, and the number of classes is C.

Since, S_w is usually singular, first the PCA has been opted for reduction of the dimensionality of the data, then LDA has been used for reduction of the dimensionality to C-1.

IV. CLASIFIER

In this paper, k-NN [17] has been used for classification. In this method, we classify x by assigning it to the class label ĉ (most frequently represented among the k nearest neighbor) which has the minimum distance among all the classes,

$$d(x, x_{ci}) = \min_{1\le c\le C, 1\le i\le n_c} d(x, x_{ci}) \quad (9)$$

Where, $d(x, x_{ci}) = \|x - x_{ci}\|$ is the Euclidean Norm.

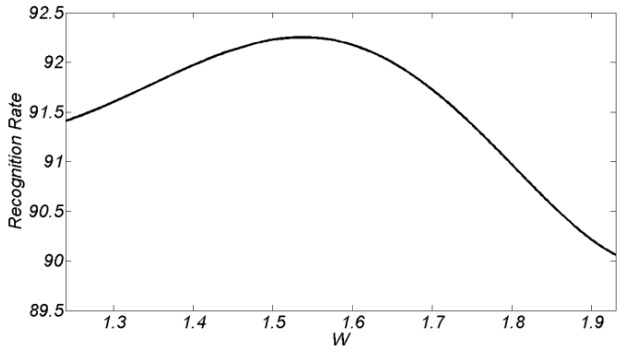


Fig. 3. Recognition rate versus w, weight for fusion of classifiers

A. *Fusion of classifiers*

2D system and 3D system has been combined with in the decision level. If a face considered for recognition to the 2D system, it results in 106 distances at the output of the classifier and the same procedure applied for the case of 3D system. Combination of the 2D and 3D systems has been performed by the weight factor ω.

$$D = \sqrt[2]{d_{2D}^2 + \omega \times d_{3D}^2} \quad (10)$$

This factor will be derived in a training process. In this process, a recognition rate of the system in rank one has been obtained with images that have 25^o pose variation for various values of weight factor and considering the ω corresponding to the maximum recognition rate.

V. EXPERIMENTAL RESULTS AND DISCUSSION

A. *3D face database*

In this paper the FRAV3D [18] database has been considered. This database has 106 subjects, and a ratio of one woman to three men approximately.

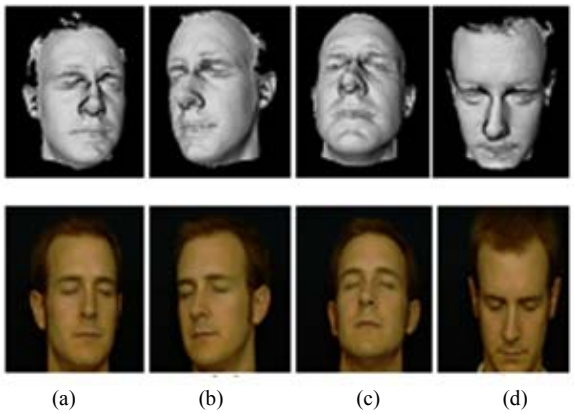


Fig. 4. Some samples of FRAV3D database: (a) Left turn 5º (respect to Y axis). (b) Right turn 25º (respect to Y axis). (c) Looking upwards. (d) Looking downwards.

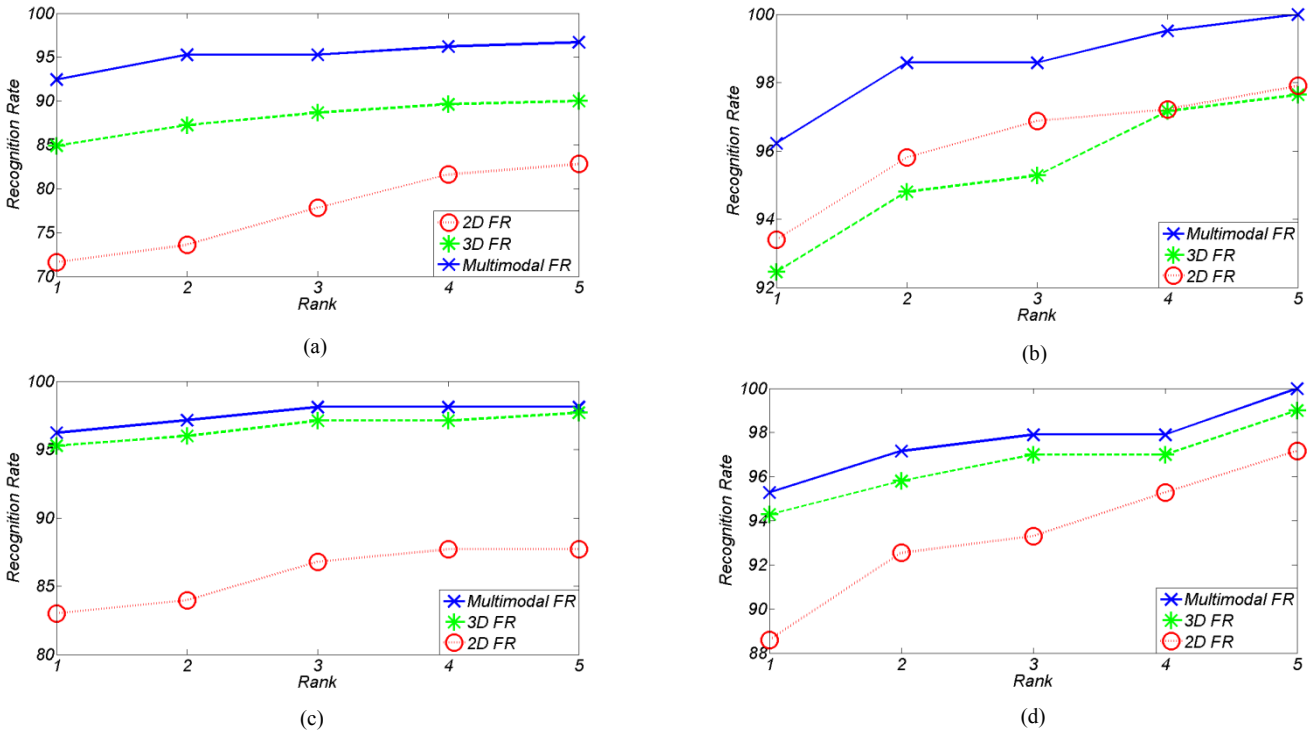


Fig. 5. Cumulative identification plots for (a) the right-rotated, (b) left-rotated, (c) up-rotated, and (d) down-rotated

The data were acquired with a Minolta VIVID 700 scanner. In this database, there are texture information (2D image) and a VRML files are existed (3D image). For each person there are 16 captures with pose, expression and light variation.

We only used faces with pose variation in this study.

B. Experimental results

In the present investigation the sizes of depth and texture images after preprocessing are 120×120 and after Gabor wavelet, 40 images were obtained for every face; consequently, a variety of dimensions for each image were observed, and it is necessary to reduce the sizes of each image by means of feature reduction method. Since LDA usually has some problems associated with singular values, PCA is considered in the first stage, and then LDA is utilized. After LDA algorithm, a vector with size of 105 for each image is obtained. Therefore, the size of images has been reduced considerably. Note that, K-NN classifier is utilized for texture and depth image and finally outputs of the two systems combined with a weight factor.

C. Identification results

In this experiment four frontal faces of each person were utilized for the training stage and other faces were used to test the system. In this step, system was examined by faces which have pose variation in right, left, up and down directions. Comparison of the recognition rate for the multimodal system with 2D and 3D systems is depicted in Fig. 5. As shown in figure, it is obvious that multimodal system has better performance. The proposed Method is also compared with multimodal PCA which is a fundamental method. In the multimodal PCA system, the PCA just used for feature extraction and combination of 2D and 3D systems that this combination occurred in the decision level. It is clear that the presented method exhibited better performance.

TABLE1
Comparing the proposed method with multimodal PCA

Rank-one rate	Multimodal PCA	Our method
25° right	66%	92.4%
5° left	84.4%	96.2%
Up	83%	96.2%
Down	80%	95.3%
mean	78.35%	95%

V. CONCLUSIONS

A multimodal face recognition based on Gabor feature has been proposed in this paper. Serial projection-based method is way of reducing the amount of data. There are two steps for data reduction in our algorithm. First, the principal component analysis (PCA); and second, Linear Discriminant analysis (LDA).The accurate recognition results show quite clearly that we are not discarding significant features during these steps an only the redundant information is discarded. This system has been combined 2D FRS and 3D FRS in the decision level which has shown a higher performance than systems with

separate FRS. In the present study, a sufficient investigation has been considered on the pose variation problem in face recognition. The results of all of the experiments demonstrate significant accuracy improvements over the baseline scenarios in pose variation. According to the obtained experimental results, the proposed method achieved the rank-one recognition rate of 95% on faces which have pose variation comparing to 78% success rate in PCA base method.

REFERENCES

[1] A. F. Abate, M. Nappi, D. Riccio, G. Sabatino, "2D and 3D face recognition: A survey," Pattern Recognition Letters, pp. 1885–1906, 2007.

[2] D.J. Beymer, "Face recognition under varying pose," A. I. Memo No. 1461, December 1993.

[3] K. Okada, C. vonder Malsburg, "Pose-invariant face recognition with parametric linear subspaces,". In: Fifth IEEE Internat. 2002.

[4] J.C. Lee, E. Milios,"Matching range images of human faces", Int. Conf. Comp. Vis., pp. 722–726, 1990.

[5] G. Medioni, R. Waupotitsch, "Face recognition and modeling in 3D", in: Proceedings of IEEE International Workshop on Analysis and Modeling of Faces and Gestures, pp. 232–236, 2003.

[6] A. S. Mian, M. Bennamoun and R. A. Owens, "Matching Tensors for Pose Invariant Automatic 3D Face Recognition" Int. Conf. CVPR, 2005.

[7] P. Phillips, P. Grother,, R. Micheals, D. Blackburn, E. Tabassi, M. Bone, "Face Recognition Vendor Test 2002" : Evaluation Report.

[8] C. Xu, Y. Wang, T. Tan, L. Quan,."Depth vs. intensity:Which is more important for face recognition?," In: Proc. 17th Internat. Conf. 2004

[9] K. Chang, K. Bowyer, P. Flynn."An evaluation of multi-modal 2D + 3D faces biometrics," IEEE Trans. Pattern Anal. Machine Intell., 2004.

[10] F. Tsalakanidou, D. Tzovaras, M. G. Strintzis,. "Use of depth and colour Eigenfaces for face recognition," Pattern Recognition Lett. Vol. 24, pp. 1427–1435, 2003.

[11] C Xua, StanLia, TieniuTana, , LongQuanb., "Automatic 3D face recognition from depth and intensity Gabor features," Pattern Recognition, vol. 42, pp. 1895—1905, 2009.

[12] P.J.Besl,N.D.Mckay,"A method for registration of 3D shapes," IEEE Trans. Pattern Anal. Machine Intell. vol. 14, pp. 39–256, 1992.

[13] D. Gabor, "Theory of communication", IEE, vol. 93, pp. 429–457, 1946.

[14] J. Daugman." Uncertainty relation for resolution in space, spatial Frequency and orientation optimized by two-dimensional visual Cortical filters". Journal of the Optical Society of America, pp. 1160-1169, 1985.

[15] J. Jones,L.Palmer. "An evaluation of the two-dimensional Gabor wavelet model of Simple receptive fields in catstriatecortex," Journal of Neurophysiology, pp. 1233–1258, 1987.

[16] A R. Webb,."Statistical Pattern Recognition," Second Edition. John Wiley & Sons, Ltd. 2002.

[17] T. M. Cover, P. E. Hart,"Nearest neighbor pattern classification,".IEEE Trans. Inform. Theory, IT-13, vol. 1, pp. 21–27, 1967.

[18] http://www.frav.es/databases/FRAV3D/

Towards MPEG4 Compatible Face Representation Via Hierarchical Clustering-Based Facial Feature Extraction

Alireza Ghahari
Department of Electrical and Computer Eng.
University of Connecticut,
Storrs, CT, 06269-2157 USA
alireza.ghahari@uconn.edu

Mohsen Mosleh
Department of Electrical Eng.
Sharif University of Technology,
Tehran, Iran
mosleh@alum.sharif.edu

Abstract- **Multi-view imaging and display systems has taken a divide and conquer approach to 3D sensing and visualization. We aim to make more reliable and robust automatic feature extraction and natural 3D feature construction from 2D features detected on a pair of frontal and profile view face images. We propose several heuristic algorithms to minimize possible errors introduced by prevalent imperfect orthogonal condition and non-coherent luminance trying to address the problems incurred with illumination discrepancies on common surface points in accommodation of multi-views. In our approach, we first extract the 2D features that are visible to both cameras in both views. Then, we estimate the coordinates of the features in the hidden profile view based on the visible features extracted in the two orthogonal views. After that, based on the coordinates of the extracted features, we deform a 3D generic model to perform the desired deformation based modeling. Finally, the face model is texture-mapped by projecting the input 2D images onto the vertices of the face model. As the reconstructed 3D face model is MPEG4 compliant, it can be readily animated by standard MPEG4 facial animation parameters (FAPs). Present study proves the scope of modeling procedure for real-time applications such as face recognition and performance driven facial animation.**

Keywords- Multi-view imaging; 3D sensing; 2D features; deformation; MPEG4 compliant

I. INTRODUCTION

A multi-view vision-based system is the assembly of units such as modeling, quantification, segmentation, fusion, interpretation and visualization. Geometric modeling is primarily concerned with method for the representation and manipulation of curves and surfaces. The more impressive unit, visualization, is concerned with the techniques for the transformation of data into pertinent, computer-generated images.

There are many approaches to enable creation of facial models in a virtual world, but two stand out. Firstly, laser scanning is used to register the 3D shape of human head. This approach focuses on reconstructing a remarkable shape, but ignores the face structure information and the characteristics of the target face [1]. Secondly, a more convenient way of 3D objects creation is reconstruction from 2D-photo information. Some researchers are using a stereo pair of images or video sequences to create a facial model by finding pixel correspondence between cached frames or stereo-pair. Tang and Haung [2] proposed an MPEG4 real-time performance-driven avatar via robust automatic tracking of facial movements in live video. Head motion parameters as well as local deformation parameters were estimated through a two-step algorithm solving an overconstrained system of linear equations. The estimated parameters were then converted into thirty one Facial Animation Parameters (FAPs) for each video frame to drive an MPEG4-compliant face model. Others use frontal and profile view to reconstruct a 3D facial model [3-5]. Specifically, feature positions at facial landmarks give a lot of information of the human characteristic and features provide the key to build the 3D structure of the person's face. Therefore, the feature extraction on views and how to make correspondence between them have been profound objectives when making a robust facial model. To detect 2D features, some methods have drawbacks such as too few points to guarantee individualized shape from a very different generic head, while others make much use of filtering operators such as Gabor wavelet based filter banks [6].

In this paper we present an efficient method for automatic feature extraction and 3D face modeling in the case of imperfect orthogonal condition and non-coherent luminance of frontal and profile view images.

The rest of this paper is organized as follows. In Section 2, we propose a global matching scheme to find locations of features. In Section 3, we describe a facial feature extraction method for detailed matching. In Section 4, the features in the profile views are estimated by utilizing the features obtained from the frontal view. Section 5 presents results of 3D model deformation and texture mapping process. Section 6 presents some discussions about the efficacy of proposed method in 3D face modeling. Finally, in Section 7, we offer concluding remarks with future scopes.

II. FEATURE GLOBAL MATCHING

A. Preprocessing

The input images are high resolution pictures, including frontal, half-profile and profile view with neutral facial

expression. The MIT-CBCL database [7] is well recognized for target applications of face modeling to recognize frontal and profile faces including a test set consisting of 200 images per subject and variation of the illumination, pose (up to about 30 degrees of rotation in depth) and the background. The preprocessing step consists of face scale normalization and histogram equalization operations to reduce the probable effects of non-perfect orthogonal and non-coherent luminance conditions. In addition, we assign a rectangular region of interest that holds the head in the frontal view in all frames.

B. *Feature clusters extraction*

In this step we estimate the global position of facial features. We assume the face consists of several structures such as the eyes, lips, nose, etc. Each feature such as an eye can be regarded as a structural assembly of micro features, which are small units of the feature that are being searched. There is also another implicit assumption pointing out that the features cannot appear in arbitrary arrangements. For instance, given the positions of two eyes, it is obvious that the other feature assemblies can only settle within specific area of facial landmarks. We use such a knowledge-based approach to develop a method for micro features assembly localization.

The eyes' texture is different from the skin and has a higher reflection rate than other features. In the discriminative C_b channel of the YC_bC_r color space, the reflection in the pupil may interrupt the processing trend and may strengthen the edges around an eye. Wrinkles on the eyelid may also hinder the localization process. Besides resolving these issues, using the C_r channel makes the method more robust to low-quality images.

Wide variety of works accomplished by the template-based matching methods, moderate filtering techniques, statistical Bayesian approaches, and error back-propagation neural networks for feature localization results from the extremely case-dependent image segmentation problem. They are not reliable since their parameters are too sensitive depending on each individual's facial image.

In this work, we use an extended form of the BMCA[1] [9], the sequential cluster detection algorithm (SCDA), adapted for cases in which feature clusters are not properly represented by a single representative.

C. *Sequential Cluster Detection Algorithm (SCDA)*

Having utilized basic morphological operators (opening and closing) on the thresholded C_r channel of the frontal view, the feature assembly clusters are determined using one sequential clustering scheme according to the following steps:

1) The $V(\mathbf{x})$ neighborhood of one non-processed micro feature, $\mathbf{x}$, is determined.

2) If $V(\mathbf{x})$ contains at least α, a threshold of the density of the $V(\mathbf{x})$, micro features then

a) One search loop creates a new cluster that includes:

- The point **x.**
- All points $\mathbf{y}$ for which there exist a sequence of c_y
- Points, $\mathbf{y}_k$, k = 1 , ... , c_y, such that $\mathbf{y} \in V(\mathbf{y}_1)$, $\mathbf{y}_k \in V(\mathbf{y}_{k+1})$, k= 1 , ... , $c_y - 1$, $\mathbf{y}_{cy} \in V(\mathbf{x})$.
- The executed points are considered as processed.

b) Else

- $\mathbf{x}$ is considered as processed.

Allocating sub-images to feature clusters is accomplished by some parameter definitions related to within scatter matrices of extracted clusters. These parameters are obtained through training on a set of facial patches. In this stage, Left eye window is established. Then, considering some underlying information of C_b channel, the right eye window is localized. Finally, prior knowledge about the face geometry in conjunction with feature clusters scattering details is used to build the nose and mouth windows as shown in Fig. 1.

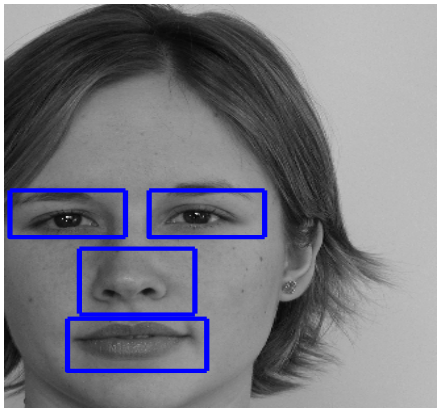


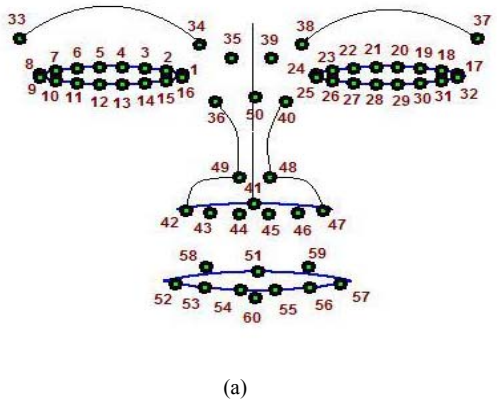
Figure 1. Features assembly sub-images of a sample from the MIT-CBCL database.

III. FEATURE EXTRACTION IN THE FRONTAL VIEW

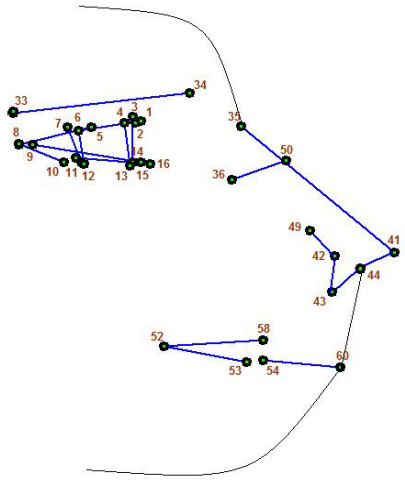
In the global matching, the facial feature landmarks are extracted automatically. In this section, we intend to extract allotted number of feature points, those which are the most characteristic points used to represent a face, from the both frontal and profile views. Fig. 2a shows 60 marked feature points in the frontal view and Fig. 2b shows 31 corresponding feature points in the visible profile view.

Using an edge detector operator, our purpose is to emphasize the representative weak edges and force it to remove other edge fragments. Although the Canny edge detector is customary for the pure edge extraction and is robust to extract weak edges, it does not perfectly extract the tokens. We provide edge linking for the Canny-processed i-

[1] Binary Morphology Clustering Algorithm



(a)



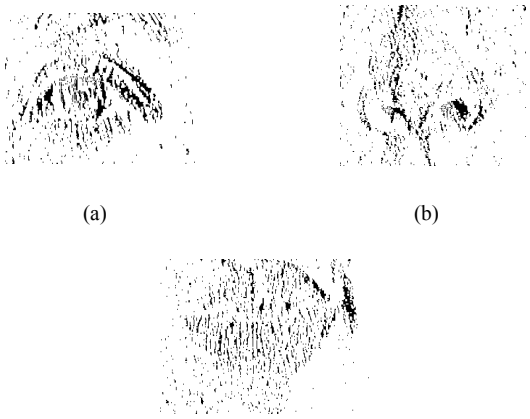
(b)

Figure 2. Marked facial feature points in the frontal and profile view images: (a) Frontal view. (b) Profile view.

mages as a by-product of one double thresholding scheme to reduce the effect of false positive errors. Fig. 3 shows the processed feature point landmarks for the image in Fig. 1. To extract the 2D feature points picked out from the frontal view, the hierarchical clustering approach in [8] has been adopted. Final results for the frontal view of the case of Fig. 1 are given in Fig. 5a. Then, the feature locations can be used to detect the shapes in detail by performing the convex hull operation.

IV. 3D COMPUTATIONS IN THE PROFILE VIEWS

In this section, we address the problem of features depth estimation in the profile and hidden profile views. The problem is how to make correspondences between 2D feature points, (X,Y), on frontal view and ones on the visible profile view, (Z,Y). We then make use of symmetry between facial features which scatter at each side of the face and the resulted coordinates from the frontal view and the visible profile view to estimate the Z coordinate of features in the hidden profile view.



(a) (b)

(c)

Figure 3. Facial landmarks processed with modified Canny edge detector: (a) Right eye. (b) Nose. (c) Mouth.

A. *Visible Profile View*

Assuming some functionality such that the Y coordinates on the frontal and profile views share the same value, the challenging issue is the non-perfect orthogonal feasible condition. In order to minimize the errors that may be introduced by the orthogonality constraint, we utilize an algorithm on detected 2D features aiming to decrease the dependency of orthogonality of face images.

In order to search for the feature points Z coordinate around their corresponding Y coordinate in the visible profile view, a heuristically obtained algorithm, self organizing intensity correlation (SOIC), has been exploited. According to the following flowchart (Fig. 4), in this algorithm, the Y coordinate of feature points visible to both cameras in both views construct the primitive search line. Then, an adaptive scheme considers a soft margin for each search line to minimize the induced square error. Using a 5*5 intensity correlation kernel, the algorithm self organizes the margin 'd' in order to force the solution Z coordinate to lie toward the middle of the d=0 solution region in hopes of improving generalization of resulting depth estimator. Considering the margin d_i, the correlation result with minimum value determines the Z coordinate of each feature point in the profile view. Fig. 5b shows the extracted feature points which correspond to the right (visible) side of the Fig. 5a.

B. *Hidden Profile View*

After fulfilling 3D computations in the visible profile view, we estimate the coordinates of the features hidden in the profile view based on the 2D facial features extracted in the frontal view and in the visible profile view. Making use of facial symmetry between the visible (r) and hidden (l) sides, with a 3D origin established at the middle distance between two eye centers (o), the 3D distance between the or-

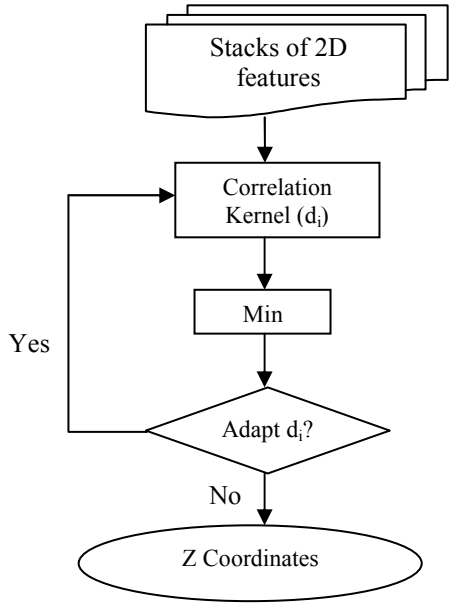


Figure 4. SOIC algorithm evolution.

igin to one of the symmetrical features at one side of the face (d_{or}), is the same or close to the distance from the origin to the corresponding feature at the other side of the face [3]. Consequently, the relative depth of each feature point in the hidden side of the profile view is calculated using

$$Z_l = \sqrt{d_{or}^2 - (X_l - X_o)^2 - (Y_l - Y_o)^2} + Z_o. \quad (1)$$

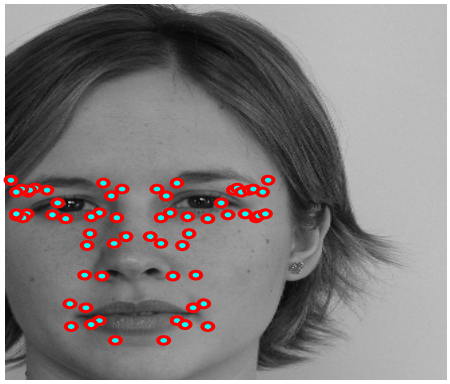
The result gives a predefined number of 3D features created from 2D features detected on two face images of a subject. Fig. 5c shows the computed feature points which correspond to the left (hidden) side of the Fig. 5a.

V. Generic Model Modification and Texture Mapping

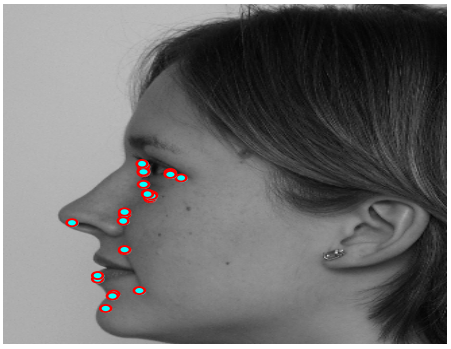
Using 3D feature points as control points for deformation, we deform a 3D generic model to create a 3D cloned model. A host of 3D generic face models are available at the literature. In order to design multifaceted patches, we should specify the coordinates of each unique vertex and a matrix that specifies how to connect these vertices to form the faces. Using NURBS[2] curve segments for vertices definition and Delaunay triangulation solution as the connection principle, a modified version of the well- known Candide model with 140 vertices and 264 surfaces has been designed. Then we modify the shape of the generic model to bring its vertices as close as possible to the corresponding 3D coordinates of the feature points calculated in the section 4.

We adopt the procrustes analysis, summarized in [3], and the Dirichlet Free-Form Deformation, which belongs

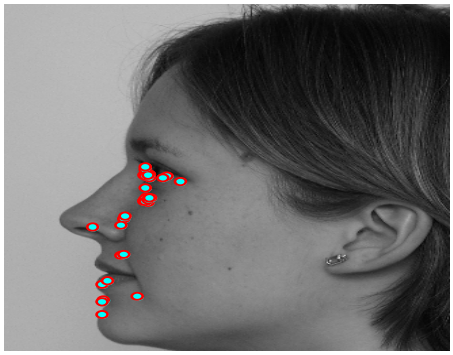
[2] Nonuniform, Rational B-Spline



(a)



(b)



(c)

Figure 5. Final representation of the facial features extracted from frontal and profile view images: (a) Frontal view. (b) Profile view (c) Hidden profile view.

to a wider class of geometric deformation tools, as modification functions to probe the results. Then to increase photo-realistic looking of cloned models, we utilize texture mapping. Texture mapping needs both a

texture image and texture coordinates. In order to reduce the effects of non-perfect orthogonality and non-coherent luminance condition, a two step process should be considered to provide properly smooth texture image:

1) Image deformation: Defining two feature lines (right and left lines) on the frontal image, the profile image is deformed to be connected to the frontal image. The profile image is deformed with translation to match to the right feature line, while flipping it across to the vertical axis matches the deformed profile image to be connected to the left feature line.

2) Image mosaic: Mosaicing of boundaries between the three combined images has been done to resist non-coherent luminance. The mosaicing is obtained using three-level wavelet packet decomposition.

In texture fitting, we first project a cloned 3D head onto three planes, the frontal (x,y), the right (y,z), and the left (y,z) planes. Then the projected points on one of three planes are transferred to the 2D-image space and finally to the combined image space. Fig. 6 presents the final modeling results for 1 out of the 10 cases that we tested. The first row shows frontal and profile views followed by wavelet packet tree and approximate coefficients in second level. The second row shows the textured head with corresponding deformed vertices of the face model on it and reconstructed face models rendered incorporating a high resolution 3D face model deploying generic model toolkits.

VI. Discussion

This section embraces a brief discussion about the applications of the current research and some experimental results considering the performance of the proposed automatic 3D face modeling system. To create a 3D cloned model, a dual process should be taken into account. The first is to extract discriminating features on the frontal and profile view images. The second is to create a 3D individualized facial model using extracted feature information. We stress the fact that a host of feature points are the best representatives since more information from images lead to better adaptation of an individual. Also, as the reconstructed 3D face inherits the same structure from the generic model with all parametric information, it can be animated immediately with parameters extracted from an automatic facial expression analysis system [8]. At the highest level, animation is controlled by a script containing speech and emotions with their duration. Another application of 3D facial cloning is 3D face recognition.

Training a moderate distance-related classifier, Ansari and A-Mottaleb [3] calculate the distances between each of the 29 feature vertices in the test model and the corresponding vertices in the database models. Testing their algorithm with 26 faces in the database, a recognition rate of about 96.2% achieved. In their recent multimodal approach [4], they extract a total of 68 facial features from the 2D intensity images. Then, by virtue of information from the facial features from the 2D modality and that of the 3D modality obtained from the stereo images, the induced modality integration leads to a 95% identification rate and 92% verification rate at 0.1% false positive rate for an application of face recognition in a112 training space.

Automatic facial feature extraction plays a vital role in robust 3D face modeling from a pair of frontal and profile face images. We are not only concern about the mean square error (MSE) of the transformation between the feature points from our database and the corresponding feature vertices of the 3D model, but also we expect that the deformation functions deserve acceptable processing time for modifying a 3D generic model to create a 3D cloned model. In our experiments, averaging the results over 10 images from the database [7], the normalized MSE of the transformation, with respect to the number of extracted feature points, has been calculated. The result is shown in Fig. 7 for the specified number of feature points. The extension of Ansari's method has been obtained by using 3D interpolation between the initial 29 feature points. Up to the specified number of feature points ($\cong 70$), Ansari's methods [3,4] outperforms our method, but ours surpasses his work as the number of feature vertices increases. Also, using the DFFD deformation tool produces slightly better results than procrustes program. Furthermore, we observed that with regard to time complexity, in the lower bounds of feature point's cardinality (i.e., < 90), the procrustes program is faster than DFFD tool, but the situation reverses in the upper bounds. Our system is implemented in Matlab on a Pentium IV with 2.20 GHz PC.

VII. Conclusions

We fully presented an automatic framework for facial feature extraction and robust 3D face modeling modifying the shape of an already well-prepared model using feature information extracted from 2D features of frontal and profile view images. Firstly, we introduced the sequential cluster detection algorithm (SCDA) thanks to the feature global matching and feature points localization. Putting the information from the detailed matching facial feature extraction together with SCDA-processed feature clusters, the automatic feature extraction pipeline set up for sample frontal images. After this process, employing the principle of one-to-one correspondence, the 3D coordinates of facial feature points visible in both face images were extracted using the proposed self organizing intensity correlation (SOIC) algorithm. Then, 3D computations of the features hidden in the profile view enabled us to deform the corresponding facial vertices of the generic 3D model. Finally, the face texture was extracted from the input images and RGB texture colors were mapped to the 3D face model. The result was remarkable enough to explore real-life applications of 3D face modeling in fields like face recognition and performance-driven facial animation. Our future study topic is to construct an MPEG4 parameter- based facial expression animation system using extracted facial animation parameters over a live performance and the compatible reconstructed models.

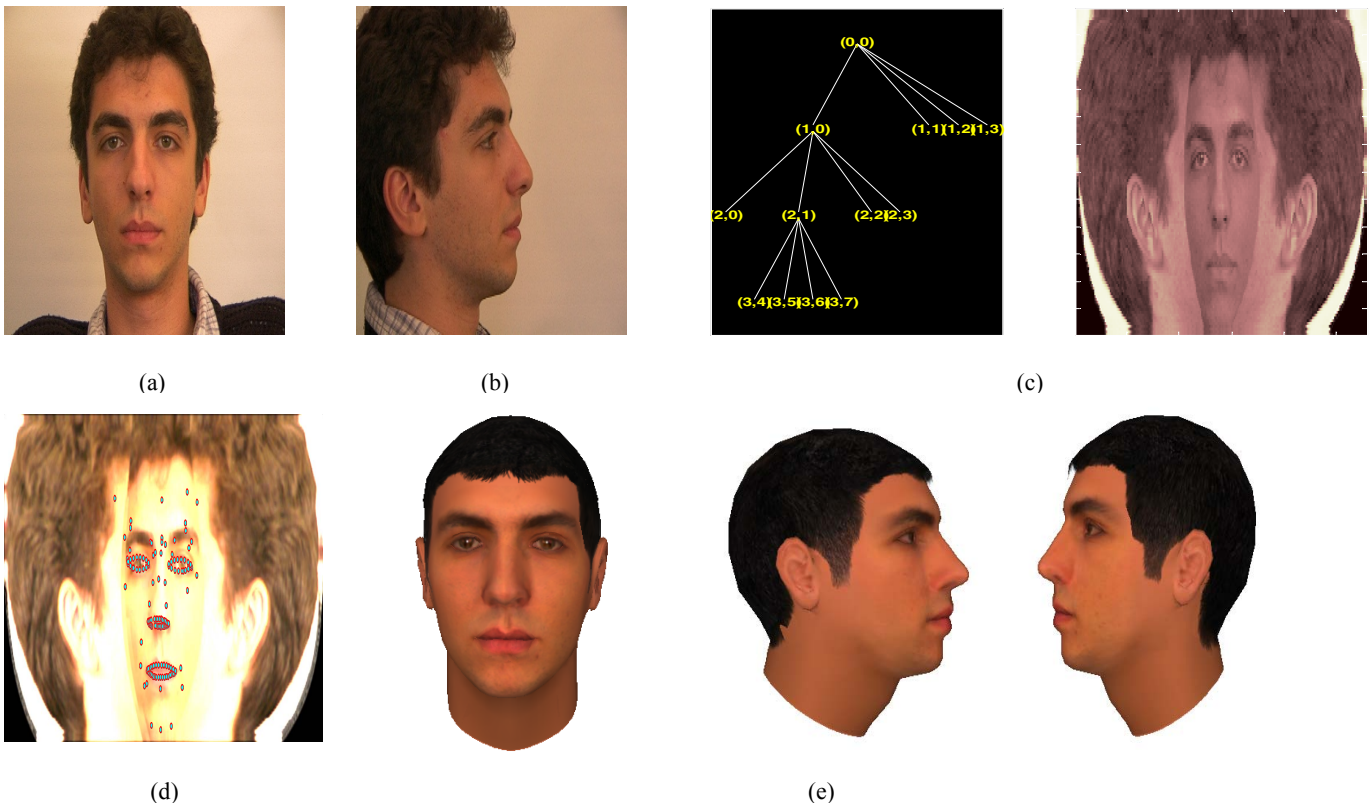


Figure 6. Snapshot of the proposed visualization pipeline: (a) Input frontal image. (b) Input profile image. (c) Three-level wavelet packet decomposition of deformed image. (d) Texture image and projected deformed feature vertices. (e) Subspace of the synthesized face model.

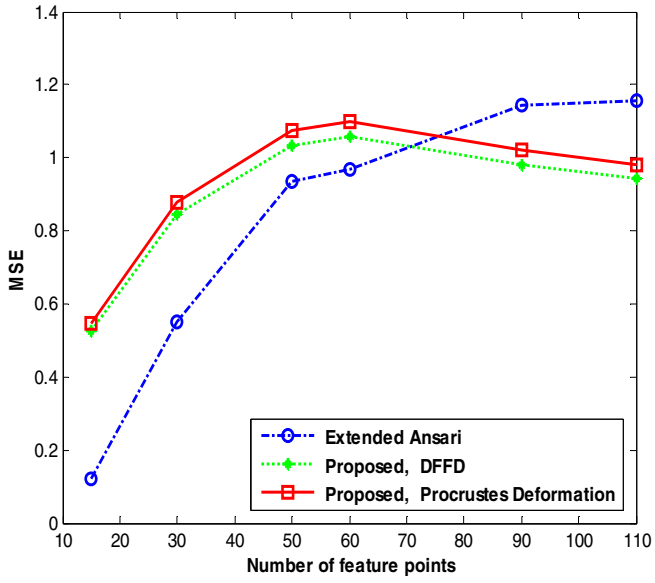


Figure 7. Comparison of the ensemble-averaged MSE performance.

REFERENCES

[1] W-S. Lee, and N. M-Thalmann, "Fast head modeling for animation," Image and Vision Computing **18** (2000) 355-364.

[2] H. Tang, and T.S. Huang, "MPEG4 performance-driven avatar via robust facial motion tracking," IEEE International Conference on Image Processing (ICIP'08), San Diego, CA, pp. 249-252, October 2008.

[3] A-N. Ansari, and M. A-Mottaleb, "Automatic facial feature extraction and 3D face modeling using two orthogonal views with application to 3D face recognition," Pattern Recognition **38** (2005) 2549-2563.

[4] A-N. Ansari, M. A-Mottaleb, and M. Mahoor, "A multimodal approach for 3D face modeling and recognition using 3D deformable facial masks," Machine Vision and Applications, vol. 20, 2009, pp. 189-203.

[5] T. Goto, W-S. Lee, and N. M-Thalmann, "Facial feature extraction for quick 3D face modeling," Signal Processing: Image Communication **17** (2002) 243-259.

[6] S. Bashyal, and G. K. Venayagamoorthy, "Recognition of facial expressions using Gabor wavelets and learning vector quantization," Engineering Applications of Artificial Intelligence **21** (2008) 1056-1064.

[7] B. Weyrauch, J. Huang, B. Heisele, and V. Blanz, "Component-based face recognition with 3D morphable models," Proc. of the 1st IEEE Workshop on Face Processing in Video, Washington, USA, pp. 1314-1317, December 2004.

[8] A. Ghahari, Y. Fatmehsari, and R. Zoroofi, "A novel clustering-based feature extraction method for an automatic facial expression analysis system," Proc. of the 5th IEEE Int. conf. on IIH-MSP, Kyoto, Japan, pp. 1314-1317, September 2009.

[9] S. Theodoridis and K. Koutroumbas, *Pattern Recognition*. San Diego: Academic Press, 2nd edition, 2003.

Performance of Real Time Cooperative MIMO using an SDR Platform

Hassaan Ajaz, Omer Ihsan, Usman Javed, Moaaz Ali Hafeez, Adnan A. Khan, Safwat Irteza

EE Department, Military College of Signals, National University of Science and Technology (NUST), Rawalpindi. 46000

R & D Department, National Radio Telecommunication Corporation (NRTC), Haripur. 22620

E-mail:{hassaan.ajm, omrihsan, usmanjavedchd, moaaz.ali.hafeez, adkhan100, safwatirteza}@gmail.com

***Abstract*—Fading remains the prime problem in wireless communications, and line of sight communication is not possible everywhere. Multiple Input Multiple Output (MIMO) is a technique used to mitigate multi path fading effects by physically placing multiple antennas to create independent channel realizations. Cooperative MIMO on the other hand generates the effect of MIMO through cooperation of distributed radio nodes within the network. The paper identifies performance gains achieved in terms of frame error rate versus average signal to noise ratio of cooperative communication networks over conventional SISO and multiple collocated antenna array systems. An experimental testbed is developed on a Software Defined Radio (SDR) platform comprising of three distributed network nodes operating in the 2.4GHz unlicensed ISM band. A Selective Decode and Forward (DF) cooperative protocol is developed and established between the nodes. The results have been evaluated in terms of diversity gains as measured from the experimental curves of FER versus average SNR. A comparative analysis reflects that at a fixed value of SNR the FER of CMIMO communication systems is less than SISO, SIMO and single antenna cooperation networks.**

I. INTRODUCTION

MIMO communication networks make use of spatial diversity by physically placing multiple antenna arrays at the transmitting and receiving stations. The antenna array mitigates multipath fading by creating independent channel realizations. A limitation to the implementation of MIMO systems is the physical size of the platform that hosts the antenna array apart from the requirement of added power used to energize the array. The antennas on a single platform must be separated by at least the correlation distance. Cooperative diversity [1]-[4] is used to combat multipath fading effects by producing transmit space diversity through relaying without physically placing multiple antennas at the usually small transmitting nodes of the network.

MIMO and cooperative MIMO networks make use of spatial diversity. Distributed antenna systems can achieve a higher spatial diversity gain due to the degree of spatially distributed location of antennas. The independent channel realizations thus achieved have no antenna correlation. The channel realizations thus formed, fade independently.

There are several types of cooperation possible between network nodes depending upon the network architecture, the channel conditions and the network node processing capabilities. Owing to such diverse parameters for the choice of the type of cooperation between nodes, the reconfigurable technology of software-defined radio (SDR) [5] is an ideal platform on which to experiment with cooperative protocols. Experimental implementations of cooperative communication schemes provide a valuable opportunity to study the interaction between theoretical concepts and architectural choices.

II. Related Work

There are relatively few experimental evaluations of cooperative communications when compared with the large amount of theoretical literature on the topic. A full cooperative communications system which operates in real-time over real wireless channels is developed in [6]-[7]. The performance evaluation shows a clear benefit to using amplify and forward relays, demonstrating a significant BER improvement under realistic wireless conditions. The custom OFDM-based physical layer uses a distributed version of the Alamouti block code, where the relay sends one of the branches of Alamouti-encoded symbols using WARP, an FPGA based SDR. [8] provides a concrete example of implemented virtual antenna arrays and sheds light onto the interactions needed among the physical, data, and routing layers in cooperative diversity schemes highlighting the implementation challenges in cooperative diversity systems.

The WINNER (Wireless World Initiative New Radio) project is a consortium of 41 partners co-ordinated by Nokia Siemens Networks working towards enhancing the performance of mobile communication systems. The project deliverables 3.5.1 and 3.5.2 [9] present relaying concepts and assessment of relay based deployment concepts. The presented performance assessment results in [9] show the potential of the investigated MIMO cooperative relaying technique to increase the average user throughput by 50% compared to single-path MIMO relaying.

The IEEE 802.16j WiMAX standard specifies OFDMA physical layer and medium access control layer enhancements to IEEE 802.16 to enable the operation of relay stations. Coverage area and throughput of the system is analyzed in [10] for WiMAX relaying networks.

Finally a platform which is also used as a reference

platform for a testbed implementation is in [11]. Performance gains of simple and selective Decode and Forward (DF) techniques are quantified in comparison to direct transmission. The network is implemented in a time division manner with a central control for the radio nodes which is somewhat artificial and limits system capacity due to loading of the SDR processors. The cooperative network is composed of three SISO links. Thus in general [11] evaluates BER vs SNR curves for relay diversity in SISO communication.

III. System Model

Figure 1 shows the network nodes identified by Source (S), Relay (R) and Destination (D) which represent distributed radio entities within the created experimental network. Each node is an SDR platform having individual baseband processing capabilities thus reducing to some extent, the capacity limitation imposed due to central control of radio nodes. The source and relay nodes create transmit space diversity and virtually generate the effect of a multi transmit antenna array through cooperation. The receiver node hosts multiple antennas. Thus the developed cooperative network is composed of a single SISO (S-R) and multiple SIMO (S-D and R-D) links. Signal combining techniques are applied at the receiver to output a single signal stream resulting into a Cooperative MIMO (CMIMO) network. Cooperative networks provide the advantage of independent channel realizations with minimum antenna correlation and maximum amount of spatial diversity gain due to spatially distributed network antennas. Multiple antennas at the receiver generate a receive diversity gain in addition to the cooperative transmit diversity gain to generate a MIMO effect.

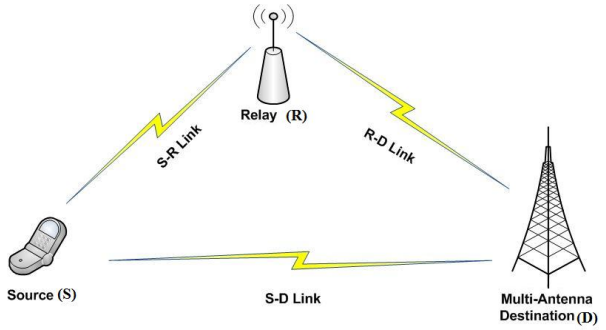


Fig. 1. Simplified System Model

Cooperation of radio nodes is broadly classified as Amplify and Forward (AF) and Decode and Forward (DF). A relay node in AF cooperation acts as a repeater and only amplifies the received signal before transmission. A relay node for DF cooperation is much more complex and has the capability to decode the received signal and take a forwarding decision. The advantage of using one of the techniques depends upon a number of conditions of which the relative distance between radio nodes, the channel conditions and transmit power of the nodes is important. The distance and channel effects of the S-R link is decisive in adopting a technique. Generally when the inter distance of Source and Relay is less AF is preferred for its ease of implementation and requirement of a less complex radio node. When the channel is noisy and the S-R distance is great then AF provides no diversity gain and thus DF is preferred.

IV. Experimental Setup and Considerations

A. Collision Control and Medium Access

Cooperative communication, assumes that the Destination node can separately receive the transmitted and relayed signal transmissions from the Source and Relay respectively. This is accomplished by transmitting the two signals orthogonally. The most straightforward method is separation in time, that is, the users data and relayed data are transmitted in non-overlapping time intervals.To ensure multiple access without collision of data from source and relay at the destination, a time division scheme is adopted as suggested in [12]. The source and relay take turns to transmit the same data to the destination.

Cooperative relaying systems have a minimum requirement of three network nodes, a Source, a Relay and a Destination. The systems can though, have more than one relaying nodes. The presence of multiple relays complicates the network layer protocol but at the same time provides a greater amount of spatial diversity gain. To account for the number of relays that a cooperative network can accommodate with time orthogonality, the delay time between frame transmissions is of paramount importance. The transmission time of a frame, T_f can be calculated as

$$T_f = \frac{N_b}{R} \tag{1}$$

where N_b is the number of bits per frame and R is the bit rate of the transmission link. Greater the frame size, greater the frame transmission time. A minimum separation in successive frame transmissions must be equal to at least the coherence time. The number of relays that the network can support without collision of frames from Source and Relays can be determined using the delay time between frame transmissions

$$N_{relays} = \frac{delay_{T_f}}{T_f} \tag{2}$$

where N_{relays} is the maximum number of relays the system can accommodate with the corresponding delay and frame transmission time. Greater the amount of delay between successive frames, greater the number of relays that can be accommodated. The throughput of the system degrades with increasing delay time between frame transmissions so there is a trade off between system throughput and the number of relays incorporated for

diversity.

For the cooperative platform developed a bit rate of 500kbps is used with the frame size of 256 bits including overheads. The frame transmission time then comes out to be $T_f = 256/500\text{k} = 512\mu\text{s}$. A frame delay time of 5ms which constitutes the guard time is used. This corresponds to $N_{relays} = (5\text{ms}/T_f)$ which comes out to be 9 relays.

B. Multi Antenna Reception

The destination hosts multiple antennas to capture the Source and Relay signals to create a MIMO effect at the receiver. The antennas are hosted on a single radio platform making it a collocated antenna receiver system. The signal streams received at the antennas are combined using the equal gain combining (EGC) for MIMO systems. The resultant signal is the weighted averaged signal of the two streams at the antennas.

The receiver accepts any one of the two similar packets reaching via any of the two independent channels after combining the signal streams. The signal streams are weighted with a constant ratio. The ratio should represent the average channel quality and therefore should not take account of temporary influences on the channel due to fading or other effects. The EGC can be expressed as

$$y_d[n] = \sum_{\mathbf{i=1,2..k}} w_i.y_i[n] \tag{3}$$

where w_i denotes weighting of the incoming signal y_i Using one relay station, the equation simplifies to

$$y_d[n] = w_{s,d}.y_{s,d}[n] + w_{s,r,d}.y_{r,d}[n] \tag{4}$$

where $w_{s,d}$ denotes the weight of the direct link and $w_{s,r,d}$ the weight of the multihop link.

C. SDR Platform and Signal Generation

An open source SDR platform called the Universal Software Radio Peripheral (USRP) is used, provided by Ettus Research [13]. The network is composed of three distributed nodes having independent baseband processing capabilities. The platform can host different RF ends to provide communication in different frequency bands. A base motherboard has analog to digital converters and digital to analog converters for the digitization and reconstruction of signals. There is an onboard FPGA for signal processing at IF and frequency translation to baseband. The USRP is interfaced with the computer running GNU Radio [14], which is the software toolkit for the software radio nodes, via a USB link. The platform functions in the unlicensed 2.4GHz ISM band. The platform is programmed to function with 2.45GHz as the center frequency and 3dB signal bandwidth of around 1MHz as depicted in Figure 2

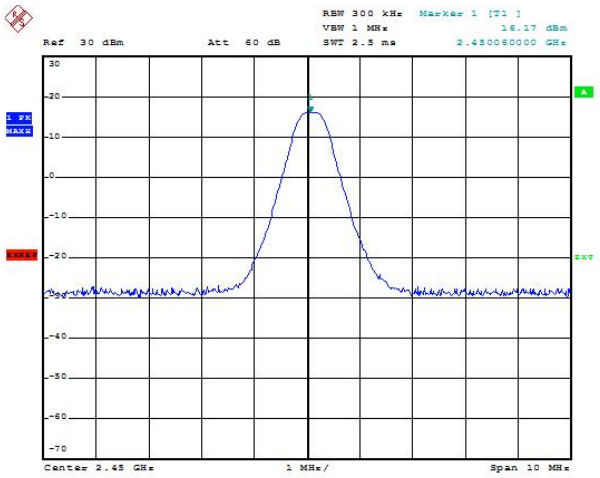


Fig. 2. Input Signal-Power and Frequency Characteristics

which is the signal input as depicted on a spectrum analyzer.

Figure 3 shows the constellation diagram of the transmitted signal for GMSK which is the selected modulation scheme for the developed cooperative network.

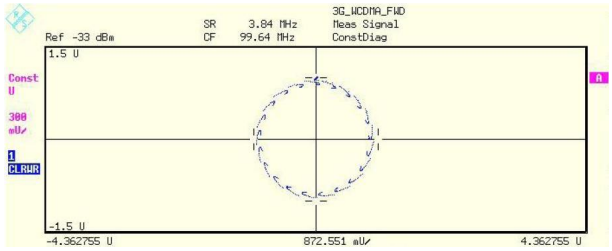


Fig. 3. Constellation of the Input GMSK Signal

D. Cooperative Relaying: Selective DF

The relay forwards data it receives from the transmitter using a Selective Decode and Forward (DF) cooperation technique. A data forwarding decision is made on the bases of an appended Cyclic Redundancy Check (CRC). A Fixed Decode and Forward (DF) technique forwards any data that it receives which cancels out any diversity gain in the network. The Fixed DF scheme due to this nature is not analyzed here and all simulation and practical results are compiled for the Selective DF scheme.
A datalink layer is established that determines if a packet is correctly received by checking the appended CRC of the received frame. A module is developed that calculates the number of packets in error out of the total packets received. A comparative study of various communication schemes is thus provided.

E. Experimental Setup Characterization

Coherence distance is the distance a radio node must be separated from another radio node to observe an inde-

pendent channel realization. A common approximation of coherence distance is one quarter of the carrier wavelength as

$$D_{coh} = \frac{\lambda}{4} \tag{5}$$

With the operational frequency of 2.45GHz, the coherence distance comes out to be approximately 3cm. Experimenting in the ISM 2400 MHz band provides greater number of multipaths as compared to the lower 400 MHz band [11] which makes it ideal for experimentation without having to make the experimental platform mobile.

With the frame transmission delay incorporated in the system, the channel acts as a slow fading channel. A physical testbed model as in [11] is created with multiple receive antennas and the network nodes are shielded using metal plates from one another as shown in Figure 4. Shielding the LOS helps in analyzing diversity gains.



Fig. 4. Experimental Platform with Three Equidistant Software Radio Nodes

V. Simulation

Simulation results of the developed cooperative Selective DF scheme are in Figure 5 to give an idea of the relative theoretical gains provided by cooperation as compared to the practical outcomes in Figure 8. In wireless communications, the presence of reflectors in the environment surrounding a transmitter and receiver creates multiple paths. As a consequence, the receiver will receive the reflected, diffracted and scattered signals from all directions. The receiver sees the superposition of multiple copies of the transmitted signal; a phenomenon called multipath fading. This can result in either constructive or destructive interference, amplifying or attenuating the signal power seen at the receiver.

A. Simulation Environnment

Rayleigh fading is most applicable to model heavily built-up environments where there is no line of sight (LOS) between the transmitter and receiver. The Rayleigh distribution is frequently used to model multipath fading with NLOS path. If 'r' is defined as a Rayleigh distribution random variable, the probability density function (pdf) is given by [15]

$$P_{(R)}(r) = \frac{r}{\sigma^2} \exp^{\frac{-r^2}{2\sigma^2}} \tag{6}$$

A channel is generally referred to as introducing slow fading if $T_0 > T_s$ where T_0 is the channel coherence time and T_s is the time duration in which the channel behaves in a correlated manner. In a slow fading channel T_0 is long compared with the time duration of a transmission symbol. The simulation results are based on a slow Rayleigh fading channel.

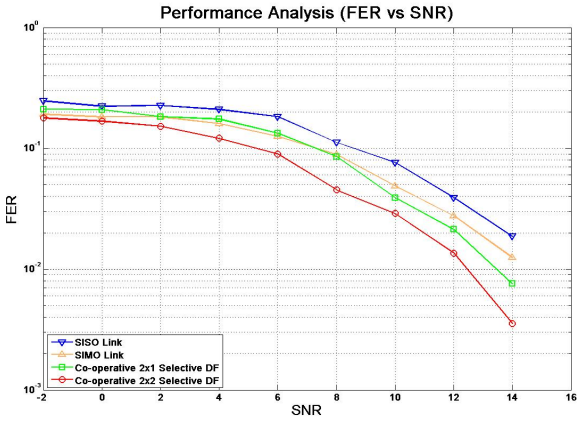


Fig. 5. Simulation results for FER vs SNR

VI. Experimental Results

A. Conventional Performance Parameters

A conventional performance parameter to analyze performance gains of cooperative systems is the outage capacity. When a source cannot reach its destination due to severe fading, it will not be of much help to keep trying by leveraging repeating transmission protocols such as ARQ. If a third party that receives the information from the source could help via a channel that is independent from the source-destination link, the chances for a successful transmission would be better, thus improving the overall performance. For cooperative networks there is path redundancy for signals via the relay hop.

Figure 6 shows a screen shot of a software radio receiver that is receiving signals from both the transmitter(T) and relay(E). In case of an outage event as in Figure 7 where the S-D link is under a deep fade the information still reaches the destination via the relay (E), multihop link. Thus by incorporating path redundancy, outage capacity of systems is enhanced.

```
------------E-RELAY---------------------- pktno =  40
------------T-TRANSMITTER------------------- pktno =  41
Packet Required 41 Packet Received 41
------------E-RELAY---------------------- pktno =  41
------------T-TRANSMITTER------------------- pktno =  42
Packet Required 42 Packet Received 42
------------E-RELAY---------------------- pktno =  42
------------T-TRANSMITTER------------------- pktno =  43
Packet Required 43 Packet Received 43
------------E-RELAY---------------------- pktno =  43
------------T-TRANSMITTER------------------- pktno =  44
Packet Required 44 Packet Received 44
------------E-RELAY---------------------- pktno =  44
------------T-TRANSMITTER------------------- pktno =  45
```

Fig. 6. Path Redundancy-Signal from Independent Channels

```
------------T-TRANSMITTER------------------- pktno =  125
Packet Required 125 Packet Received 125
------------E-RELAY---------------------- pktno =  125
------------T-TRANSMITTER------------------- pktno =  126
Packet Required 126 Packet Received 126
------------E-RELAY---------------------- pktno =  126
------------T-TRANSMITTER------------------- pktno =  127
Packet Required 127 Packet Received 127
------------E-RELAY---------------------- pktno =  127
------------E-RELAY---------------------- pktno =  128
Packet Required 128 Packet Received 128
------------E-RELAY---------------------- pktno =  129
Packet Required 129 Packet Received 129
------------E-RELAY---------------------- pktno =  130
Packet Required 130 Packet Received 130
------------E-RELAY---------------------- pktno =  131
```

Fig. 7. Information reaching Receiver via Relay(E) when Direct Link is Under a Fade enhancing Outage Capacity

B. FER vs SNR : Comparitive Analysis

Although precise SNR knowledge is not necessary for the plotting of BER curves, the relative increase in SNR between data points should be accurate in order to reproduce the desired graph geometry. Average SNR is a function of the transmit power and the distance between two given nodes. In the experimental setup the inter node distances are kept equal, the path loss for individual links is the same and gradual increase in the transmit power of the signal as measured in Figure 2 ensures relative increase in SNR between data points.

In [11] Simple and Selective Decode and Forward techniques with Single Antenna Cooperative nodes are analyzed in comparison with direct transmission. It is shown through experimental results that the simple DF did not provide discernible diversity gain. The Selective DF however provided a measurable diversity gain which is here tested against various communication systems with a Multi Antenna Cooperative receiver node.

Figure 8 shows the performance curves of various communication schemes including Direct transmission (SISO), Single input Multiple Output (SIMO), Single Antenna Cooperative (2x1) Network and Multi Antenna Cooperative (2x2) Network. Software Radio (SDR) helped in testing of all results on the same constructed platform using the same radio nodes for different types of communication schemes canceling effects of equipment efficiency differences in the final results.

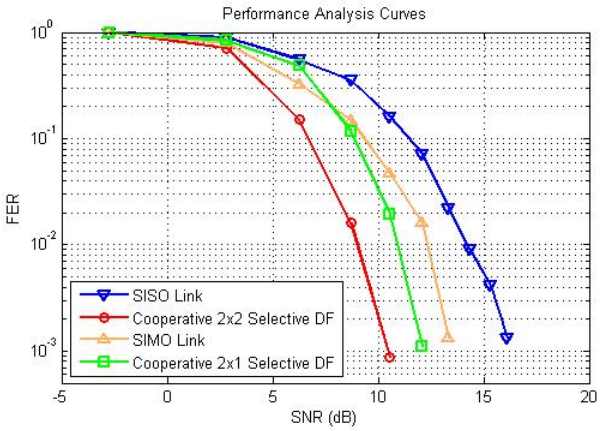


Fig. 8. Performance Gain of Cooperative MIMO over SIMO and SISO (Direct) communication

The diversity gain is quantified as the slope of the FER-SNR curve. Steeper the curve, the better the gain provided by the system. SISO systems have no diversity gain. Their performance is a function of SNR. SIMO systems host multiple collocated antennas at the receiver enabling receive diversity. The performance curves for SIMO are thus, more steep than SISO curves signifying diversity gain. A most interesting behavior is shown by the Single Antenna Cooperative (2x1) Network. At low SNR values, performance of SIMO systems is better than Single Antenna Cooperative networks. This is because the Single Antenna Cooperative Network is basically composed of multiple SISO links which show no diversity gain without cooperation. Once the relay starts to receive considerable frames without error, performance of the overall system is enhanced due to transmit diversity effects. Thus the S-R channel characteristics are most important. According to [16] a 2x1 system is equivalent to a 1x2 system. This is only true for collocated antenna systems. Since cooperative networks have a distributed nature, their performance curves differ from SIMO systems. At higher values of SNR the performance of the 2x1 cooperative network is better than SIMO due to the spatially distributed antenna platforms of the cooperating network nodes.

The performance of the devised and implemented Multi Antenna Cooperative (2x2) Network (also known as Cooperative MIMO or Virtual MIMO) has the steepest curve and thus the maximum diversity gain. It has advantages of both receive and transmit diversity with the additional gain provided by the spatial distribution of the transmitting antennas.

The amount of diversity gain depends upon the diversity order of the system. This can be verified by

mentioning that direct transmission is a 1x1 system, the SIMO system and the Single Antenna Cooperative system is a 2x1 system while CMIMO systems are 2x2 systems. In fact the transmit diversity gain provided by cooperative networks is higher than conventional collocated antenna array systems (MIMO) because of the spatial geographic distribution of the antennas.

VII. Conclusion

A framework to analyze spatial diversity gain for Cooperative Selective Decode and Forward (DF) technique is developed. Different communication schemes are tested on a uniform platform with uniform channel conditions. CMIMO provides enhanced reliability but at a cost of node complexity. The functional complexities of a cooperating node depend upon the technique used for cooperation. The experimental results achieved suggest that Cooperative Selective DF provides reliable communication with lesser FER at a reference SNR value thus improving system performance. As per the experimental curves in Figure 8 at a reference SNR value of 10dB cooperative 2x2 networks have approximately 10 times less FER than cooperative 2x1 networks and approximately 100 times less FER than SISO networks. Furthermore outage capacity is enhanced through path redundancy provided by relaying thus reducing the probability of an outage event.

References

[1] A. Sendonaris, E. Erkip and B. Aazhang, *"User cooperation diversity - Part I: System description", IEEE Transactions on Communications, vol. 51, pp. 1927-1938, November 2003*

[2] A. Sendonaris, E. Erkip and B. Aazhang, *User cooperation diversity - Part II: Implementation aspects and performance analysis", IEEE Transactions on Communications, vol. 51, pp. 1939-1948, November 2003*

[3] K.R. Liu, A. Sadek, W. Su and A. Kwasinski (2008), *Cooperative Communications and Networking*

[4] J.N. Laneman, D.N.C. Tse, and G.W. Wornell, *Cooperative diversity in wireless networks: Efficient protocols and outage behavior, IEEE Transactions on Information Theory, vol. 50, pp. 30623080, December 2004*

[5] J. Mitola, *The software radio architecture, IEEE Communications Magazine, pp. 2638, May 1995*

[6] M. Knox, E. Erkip, Kshitij K. Singh, *Cooperative Coding Implementation at the Physical Layer," in Proc. Wireless and Optical Communications Conference (WOCC), May 2009*

[7] WARP project: Wireless Open-Access Research Platform, Rice University, http://warp.rice.edu/

[8] A. Bletsas, A. Lippman, *Implementing Cooperative Diversity Antenna Arrays with Commodity Hardware",IEEE Communications Magazine, pp. 3340, December 2006*

[9] Wireless World Initiative New Radio, http://www.ist-winner.org/deliverables.html

[10] Robert Bestak, Pavel Mach, *"WiMAX Throughput Evaluation of Conventional Relaying", Personal Wireless Communications: International Federation for Information Processing (IFIP), Aug. 2007*

[11] G.J. Bradford, J. Laneman, *An Experimental Framework for the Evaluation of Cooperative Diversity", Conf. Inform. Sci. and Syst. (CISS), Baltimore, MD, Mar. 2009*

[12] J.N. Laneman, G.W. Wornell, *Distributed SpaceTime-Coded Protocols for Exploiting Cooperative Diversity in Wireless Networks", IEEE Transactions on Information Theory, 2003*

[13] Universal Software Radio Peripheral, http://www.ettus.com/

[14] GNU Radio, http://gnuradio.org/redmine/wiki/gnuradio

[15] M. Yu and J. Li, *Is amplify-and-forward practically better than decode-and-forward or vice versa?, IEEE ICASSP 05, vol. 3, pp. 365368, Mar. 2005"*

[16] S.M. Alamouti, *A Simple Diversity Technique for Wireless Communications,IEEE J. Sel. Ar. Comm., vol.16, no.8, pp. 1451-1458, Oct. 1998*

Video Transmission Over WiMedia-UWB Using Subpacket Hybrid ARQ

Gek Hong SIM
Faculty of Engineering
Multimedia University
Cyberjaya, Malaysia
sim.allyson@gmail.com

Yoong Choon CHANG
Faculty of Engineering
Multimedia University
Cyberjaya, Malaysia
ycchang@mmu.edu.my

Teong Chee CHUAH
Faculty of Engineering
Multimedia University
Cyberjaya, Malaysia
tcchuah@mmu.edu.my

Abstract— **Ultra-wideband (UWB) serves the high bandwidth demand for high definition video transmission over short-range wireless networks. Nevertheless, bursty errors due to harsh channel conditions during video transmission greatly deteriorate video quality. In order to improve the quality of video transmission over UWB, we propose the use of a subpacket based hybrid automatic repeat request (HARQ) scheme instead of the conventional packet based HARQ scheme. The proposed subpacket based HARQ scheme only retransmits erroneous subpackets and avoids retransmission of other correctly decoded subpackets. Simulation results show that in comparison with the conventional packet based HARQ scheme, the proposed subpacket based HARQ scheme achieves significant performance improvement in terms of delay, percentage of overhead, throughput and reconstructed video quality.**

Keywords- Ultra-Wideband, WiMedia-UWB, Subpacket, wireless video transmission.

I. INTRODUCTION

In recent years, ultra-wideband (UWB) technology has attracted considerable interest from the technical community due to its high data rate, low power and short range wireless communications properties, thus making it attractive for deployment in wireless personal area networks (WPANs). WiMedia, one of the UWB standardization bodies, promotes the interoperability between devices in WPANs and specifies the physical (PHY) layer and medium access control (MAC) layer in the ECMA-368 standard for UWB technology [1].

In wireless communication systems, transmission errors as a result of poor channel conditions may result in severe distortions to the reconstructed video at the receiver. In this case, the received erroneous video bit-streams have to be retransmitted in order to retrieve the information lost. Type-I and Type-II Hybrid Automatic Retransmission reQuest (HARQ) are two commonly used retransmission techniques in communication systems, including WiMedia-UWB [2-3].

Compared with packet based HARQ, subpacket based HARQ can significantly minimize transmission delays and improve throughput efficiency by retransmitting only the erroneous subpackets [4-6]. This technique is particularly important in bursty wireless channels as the conventional packet based HARQ scheme may result in excessive video transmission delay. Although subpacket based HARQ has been proposed for other communication systems [7], to the best of our knowledge, the performance of subpacket based HARQ in WiMedia-UWB for video transmission has never been investigated.

The focus of this paper is to fill the above mentioned gap by improving the quality of video transmission over WiMedia-UWB networks using subpacket HARQ. In particular, we conduct a mathematical analysis on the impact of subpacket based retransmission technique on system throughput as well as percentage of overhead. Performance analyses were carried out on two different HARQ techniques proposed for WiMedia-UWB, i.e., Type-I and Type-II HARQ. We also demonstrate that the proposed subpacket retransmission technique for Type-I and Type-II HARQ schemes in WiMedia-UWB outperforms the conventional packet based retransmission technique, in terms of providing a better video quality to the end users without affecting other system parameters such as delay, throughput and percentage of overhead.

The paper is organized as follows. In Section II, we provide an overview of the benchmarking techniques, namely packet based retransmission technique for Type-I and Type-II HARQ. Later in the section, we present the proposed subpacket based retransmission technique for the abovementioned HARQ schemes for video transmission over WiMedia-UWB. In Section III, a mathematical analysis on determining the allowable retransmission time as well as the percentage of overhead is made for packet and subpacket based retransmission techniques. Section IV presents the simulation results followed by a conclusion in Section V.

II. SYSTEM OVERVIEW

In this section, details of the system model for packet and subpacket based HARQ schemes are discussed. As mentioned, both of the retransmission techniques will be evaluated on Type-I and Type-II HARQ, which were proposed for WiMedia-UWB in [2-3]. The physical layer model built in the simulator is fully compliant to the physical layer specification by WiMedia-UWB (ECMA-368) [1].

Fig. 1 shows the WiMedia-UWB overall system model with packet and subpacket based HARQ. The encoder structures in the shaded blocks of Fig. 1 are shown in Fig. 2 and Fig. 3 for packet and subpacket based HARQ,

respectively. The error detection encoder (EDE) is used to encode a cyclic redundancy check (CRC) code. For error correction, we utilize a convolutional encoder and the Viterbi decoder as in the ECMA-368 WiMedia-UWB standard. The advantage of subpacket based retransmission technique is only apparent for retransmission systems because each block of the compressed video bit-stream is appended with the CRC code which will result in the increased of transmission overhead. Therefore, packet transmission is a more favorable technique for non-retransmission system as fewer parity bits are required for packet transmission. The detailed simulation flow for subpacket Type-I and Type-II HARQ retransmission schemes is illustrated in Fig. 4.

III. PERFORMANCE ANALYSIS

In contrast to the work in [5], which determines the optimum size of subpacket and its effect towards throughput and delay, in this section, we analyse the total allowable retransmission time and the percentage of the overhead bits for both packet and subpacket retransmission techniques in Type-I and Type-II HARQ systems.

A. *Total Allowable Retransmission Time for Packet and Subpacket Type-I HARQ*

The retransmission time is limited by the maximum allowable retransmission delay hence we show in the following, the mathematical analysis for determining the maximum allowable retransmission time for packet and subpacket based Type-I and Type-II HARQ retransmission schemes.

As shown in Fig. 2, the packet of length L_p is equivalent to the sum of message block of length L_{block} with CRC code of length L_{crc}, whereas L_{fec} is the length of redundancy bits that provide error correction whose length is determined by the code rate of the encoder. In each transmission, the time needed to transmit a packet is equivalent to (1), where i represents the number of retransmissions, r is the information transmission rate and T_i is the time needed for i^{th} retransmission.

$$T_i = \frac{L_p + L_{fec}}{r} \tag{1}$$

The total number of retransmission depends on the maximum delay time allowed by the system. Assume that T_{total} is the total tolerable delay time for a wireless video streaming system, the maximum allowable number of retransmission (n_{max}) is derived as follows:

$$T_{total} = \frac{L_p + L_{fec}}{r} + n_{\max} \times \frac{L_p + L_{fec}}{r} = (n_{\max} + 1) \times [\frac{L_p + L_{fec}}{r}] \tag{2}$$

$$n_{\max} = \left[\frac{T_{total} \times r}{L_p + L_{fec}} \right] - 1 \tag{3}$$

On the other hand, derivation of the maximum allowable retransmission time for subpacket based retransmission is shown next. In subpacket based transmission, a packet is segmented into sub-block before it is appended with error detection code. The subpacket is then coded for error correction purposes with an effective code rate as in (4) where, $R_{effective}$ and $L_{sub\text{-}fec}$ are the effective code rate and the length of the redundancy bits added for error correction in each subpacket, respectively.

The length of a subpacket, L_{sp} is obtained by adding the length of sub-block (L_{sb}) with CRC code ($L_{sub\text{-}crc}$). The total number of redundancy bits in a packet computed as in (5) and the total time required for the first subpacket transmission is shown in (6).

$$R_{effective} = \frac{L_{sb}}{L_{sb} + L_{sub-fec}} \tag{4}$$

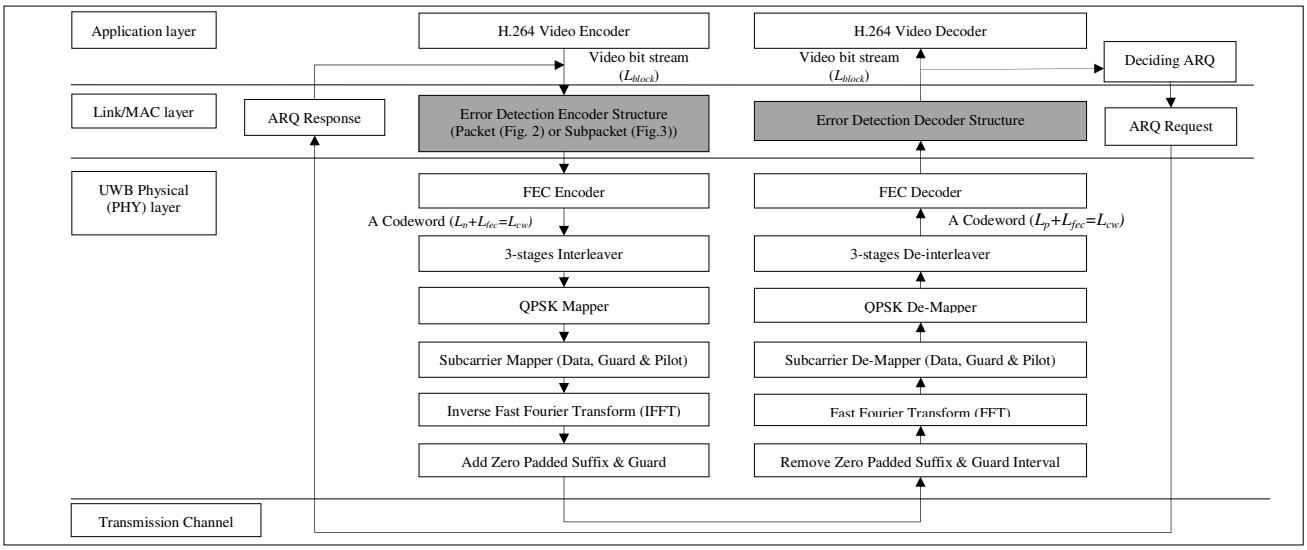


Figure 1. Overall WiMedia-UWB system block with packet or sub-packet based HARQ.

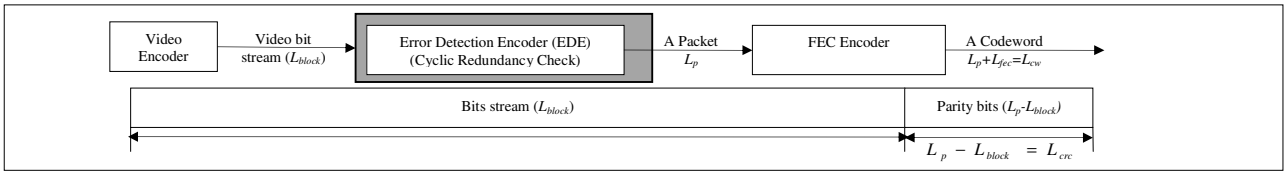


Figure 2. Encoder and packet structure for the conventional packet based retransmission technique.

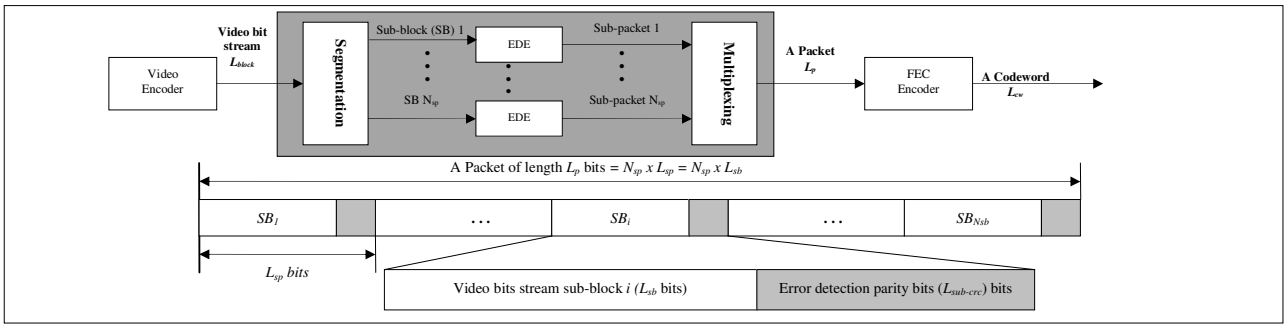


Figure 3. Encoder and packet structure for the proposed subpacket based retransmission technique.

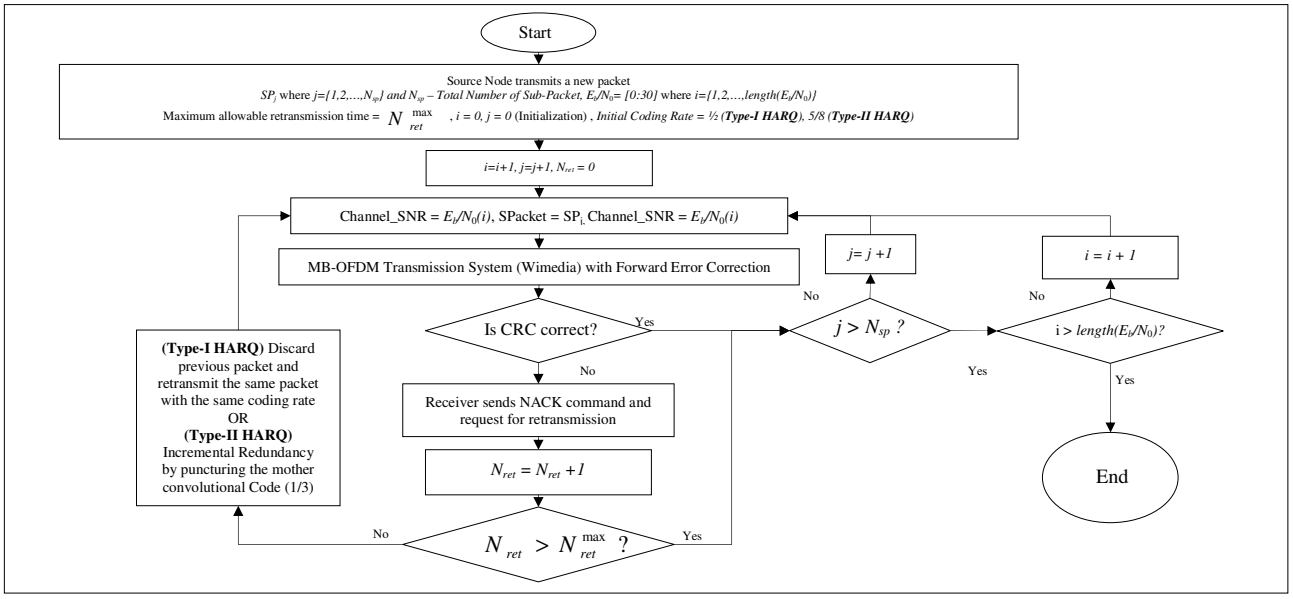


Figure 4. Flow chart of the proposed subpacket based retransmission in Type-I and Type-II HARQ systems.

$$L_{fec} = N_{sp} \times L_{sub-fec} \tag{5}$$

$$T_1 = \frac{N_{sp} \times L_{sp} + N_{sp} \times L_{sub-fec}}{r} = \frac{N_{sp}(L_{sp} + L_{sub-fec})}{r} \tag{6}$$

By subtracting (1) with (6), we can obtain the additional time taken (T_d) for first subpacket transmission as compared to packet transmission.

$$T_d = L_{sub-crc}(N_{sp} - 1) \tag{7}$$

On the other hand, the subpacket retransmission time depends on the number of subpackets requested to be retransmitted. Assuming that the number of subpackets in error for the i^{th} retransmission is $m(i)$, the time needed for the i^{th} retransmission is thus T_i as in (8). The total retransmission duration (T_{ret}) which depends on the number of maximum retransmission allowable is shown in (9) and the total transmission and retransmission duration (T_{total}) needed for a packet using the subpacket scheme is as in (10).

$$T_i = \frac{m(i) \times L_{sp} + m(i) \times L_{sub-fec}}{r} = \frac{m(i)(L_{sp} + L_{sub-fec})}{r} \tag{8}$$

$$T_{ret} = \frac{\sum_{i=1}^{n_{max}} m(i) \times [L_{sp} + L_{sub-fec}]}{r} \tag{9}$$

$$T_{total} = \frac{N_{sp} + (n_{max} \times N_{sp}) \times (L_{sp} + L_{sub-fec})}{r} \tag{10}$$

Finally, the maximum allowable retransmission time, which is dependent on $T_{total,}$ is as follows

$$n_{max} = \frac{1}{N_{sp}} \left[\frac{r \times T_{total}}{L_{sp} + L_{sub-fec}} \right] - 1 \tag{11}$$

B. Total Allowable Retransmission Time for Packet and Subpacket based Type-II HARQ

In Type-II HARQ, additional redundant bits for error correction are added during re-transmission, thus higher throughput is achievable for the same number of retransmission as compared to Type-I HARQ. The following is the analysis for packet and subpacket based Type-II HARQ scheme.

The retransmission time for the i^{th} retransmission (T_i) only includes the redundancy bits to be combined with previously received bits as shown in (12), where L_{fec_i} is the length of the added redundancy bits for the i^{th} packet retransmission time. The total number of retransmissions for a packet to be successfully delivered with a restricted delay of T_{total} is given by (13).

$$T_i = \frac{L_{fec_i}}{r} \tag{12}$$

$$\begin{aligned} T_{total} &= \frac{(L_p + L_{fec})}{r} + n_{\max} \times \frac{L_{fec}}{r} \\ n_{\max} &= \frac{r.T_{total} - L_p - L_{fec}}{L_{fec}} \end{aligned} \tag{13}$$

Using the similar approach as in Section A, we can obtain the total allowable delay duration for transmission and retransmission of subpacket based Type-II HARQ as in (14) and the maximum allowable retransmission time as in (15).

$$T_{total} = \frac{N_{sp}(L_{sp} + L_{sub-fec} + n_{\max}.L_{sub-fec})}{r} \tag{14}$$

$$n_{\max} = \frac{r.T_{total} - N_{sp}(L_{sp} + L_{sub-fec})}{N_{sp} \times L_{sub-fec}} \tag{15}$$

C. Percentage of Overhead Bits in Type-I HARQ

In our work, we take into account the overhead in the link and physical layers which are the error detection code and error correction code, respectively. At the first transmission, the length of overhead for packet (L_{oh}^{p}) and subpacket (L_{oh}^{sp}) transmission are given by (16) and (17), respectively, where $N_{tsp}^{i}, N_{sb}, L_{sb}$ and L_{block} are the number of subpackets to be retransmitted for the i^{th} retransmission, the number of sub-blocks, the length of sub-block and the length of the video bit stream, respectively.

$$L_{oh}^{p} = L_{block}.(1 - R_{code}) + L_{crc} \tag{16}$$

$$L_{oh}^{sp} = N_{sp}.L_{sb}(1 - R_{code}) + N_{sp}.L_{sub-crc} \tag{17}$$

D. Percentage of Overhead Bits in Type-II HARQ

For Type-II HARQ, the code rate and the method of overhead computation are given by (18) to (21). Assume that the maximum number of retransmissions is two, the total number of transmissions is thus equal to three.

During the first transmission, the overhead bits are equivalent to the length of error correction codes added with the error detection codes. The total length in bits for overhead count using packet and subpacket transmission is shown in (18) and (19), respectively where, R_{code} is the effective code rate. The code rates, R_{code1}, R_{code2} and R_{code3} are in descending order.

$$L_{oh}^{p} = L_{block}.(1 - R_{code\ 1}) + L_{crc} \tag{18}$$

$$L_{oh}^{sp} = N_{sp}.L_{sb}(1 - R_{code\ 1}) + N_{sp}.L_{sub-crc} \tag{19}$$

On the other hand, the total number of overhead for the first and second retransmission for packet and subpacket transmission is as in (20) and (21), respectively.

$$\begin{aligned} L_{oh}^{p} &= L_{block}.(1 - R_{code\ 2}) - L_p.(1 - R_{code\ 1}) \\ L_{oh}^{sp} &= N_{tsp}.L_{sb}(1 - R_{code\ 2}) - N_{tsp}.L_{sb}(1 - R_{code\ 1}) \end{aligned} \tag{20}$$

$$\begin{aligned} L_{oh}^{p} &= L_{block}.(1 - R_{code\ 3}) - L_p.(1 - R_{code\ 2}) \\ L_{oh}^{sp} &= N_{tsp}.L_{sb}(1 - R_{code\ 3}) - N_{tsp}.L_{sb}(1 - R_{code\ 2}) \end{aligned} \tag{21}$$

Finally, the percentage of overhead for packet (P_{oh}^{p}) and subpacket (P_{oh}^{sp}) retransmission techniques are obtained by dividing the total overhead bits, with the total transmitted bits during transmission and retransmission(s) cycles as in (22) and (23).

$$P_{oh}^{p} = L_{oh(total)}^{p} \Big/ (n_{\max} + 1) \times L_p + L_{fec} \tag{22}$$

$$P_{oh}^{sp} = L_{oh(total)}^{sp} \Big/ N_{sp} + (n_{\max} \times N_{sp}) \times (L_{sp} + L_{sub-fec}) \tag{23}$$

IV. Results and Discussion

In this section, we present the simulation results obtained from our proposed subpacket based retransmission technique, in comparison to the conventional packet based retransmission technique. The Carphone video sequence at quarter common intermediate format (QCIF) is used in the simulations.

The bit error rate (BER) performance is shown in Fig. 5. At poor channel conditions whereby the E_b/N_0 is lower than 10dB, the overall BER performance of subpacket based HARQ is almost identical to that of packet based HARQ because most of the erroneous packets and subpackets are no longer recoverable due to poor channel conditions. As the channel conditions improve (E_b/N_0 > 9dB), the overall error rate of subpacket based HARQ is lower compared with that of packet based HARQ. This is because subpacket transmission is less prone to bursty errors compared with packet transmission.

Fig. 6 shows the delay difference between packet and subpacket based HARQ schemes. At very low E_b/N_0 values (0-3dB), the delays of subpacket based HARQ are slightly higher than packet based HARQ because almost all the subpackets need to be retransmitted and the total number of parity bits is very high as each subpacket is appended with the CRC code. When channel conditions improve, only erroneous subpackets are retransmitted in subpacket based HARQ, hence resulting in lower delays. On the other hand, in packet based HARQ, the whole erroneous packet needs to be retransmitted and this

causes a higher delay in packet based HARQ. The delay performance of both schemes is similar for E_b/N_0 values higher than 27dB because very few retransmissions are required for packet and subpackets based HARQ in good channels.

The percentage of overhead at different E_b/N_0 values as shown in Fig. 7 is obtained according to the analysis presented in Section III. At very low E_b/N_0 values (0-3dB), the percentage of overhead is slightly higher for subpacket based HARQ because the retransmission of each subpacket is appended with one CRC code. On the other hand, the retransmission of a packet only requires one CRC code for the entire packet. As the E_b/N_0 is higher, a lower number of subpackets is required for retransmission hence less error correction bits need to be retransmitted. Therefore, the high number of error correction and information bits to be retransmitted for packet based HARQ causes it to suffer from a larger overhead.

Fig. 8 compares the throughput performance of the proposed subpacket retransmission technique with the conventional packet retransmission technique. At very low E_b/N_0 values, both packet and subpacket based Type-I and Type-II HARQ experience a low throughput as the number of successfully transmitted bits is low compared to the number of bits transmitted. The throughput of subpacket based HARQ achieve a significant improvement for E_b/N_0 values between 3dB and 29dB because the retransmission of each erroneous subpacket ensures a certain amount of successful decoded bits at the decoder. Nevertheless, as explained for the BER results in Fig. 5, the retransmitted packets still encounter some errors due to channel errors hence reducing the percentage of successfully transmitted bits as compared to packet based HARQ. Nonetheless, packet and subpacket based retransmission techniques achieve similar performance for Type-I and Type-II HARQ retransmission schemes at high E_b/N_0 values (> 29dB) as low BER results in high number of successful transmitted bits. In short, subpacket outperforms packet retransmission technique for both Type-I and Type-II retransmission schemes in terms of throughput at E_b/N_0 values between 3dB and 29dB.

Finally, the objective reconstructed video quality in terms of peak signal-to-noise ratio (PSNR) is shown in Fig. 9. It can be seen from Fig. 9 that the PSNR performance of the proposed subpacket based HARQ outperforms the packet schemes at all channel conditions for both of the retransmission schemes. On the other hand, the PSNR performance of each frame at E_b/N_0 values of 15dB is shown in Fig. 10. Figs. 9 and 10 show that the subpacket based retransmission scheme is able to provide better received video quality for all E_b/N_0 values in both HARQ schemes in WiMedia UWB systems. Observing Fig. 10, we can conclude that subpacket Type-I HARQ-based UWB system can provide a significant PSNR performance improvement. On the other hand, subpacket Type-II HARQ-based UWB system can provide a PSNR performance improvement of 3dB to 9dB at E_b/N_0 value of 15dB.

Summarizing the performance of subpacket retransmission scheme, the subjective quality of our proposed subpacket based retransmission technique for Type-I and Type-II HARQ schemes is shown in Fig. 11. It can be seen from Fig. 11 that our proposed subpacket retransmission technique results in better reconstructed video quality, in comparison with packet based retransmission.

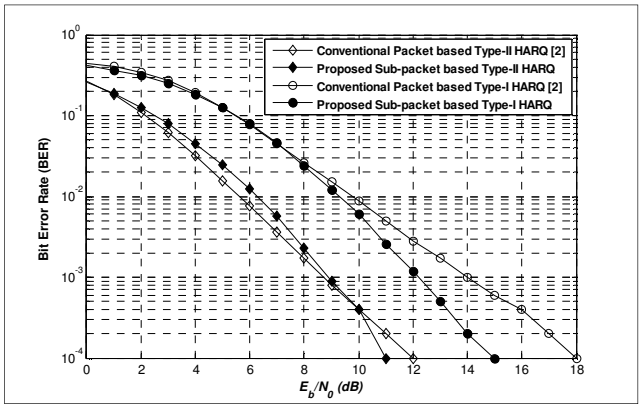


Figure 5. BER performance of the proposed subpacket retransmission technique, in comparison with the conventional packet retransmission technique.

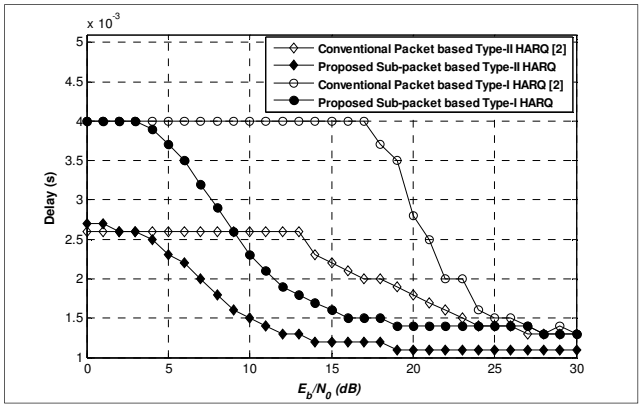


Figure 6. Transmission delay of the proposed subpacket retransmission technique, in comparison with the conventional packet retransmission technique.

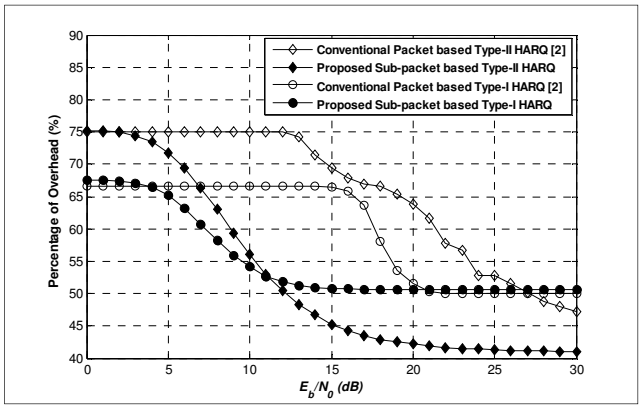


Figure 7. Percentage of overhead of the proposed subpacket retransmission technique, in comparison with the conventional packet retransmission technique.

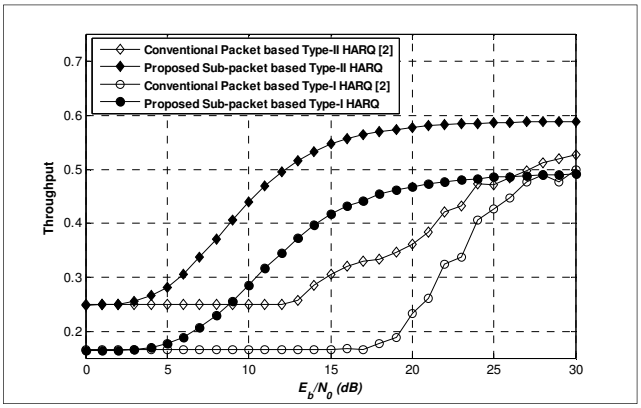


Figure 8. Throughput performance of the proposed subpacket retransmission technique, in comparison with the conventional packet retransmission technique.

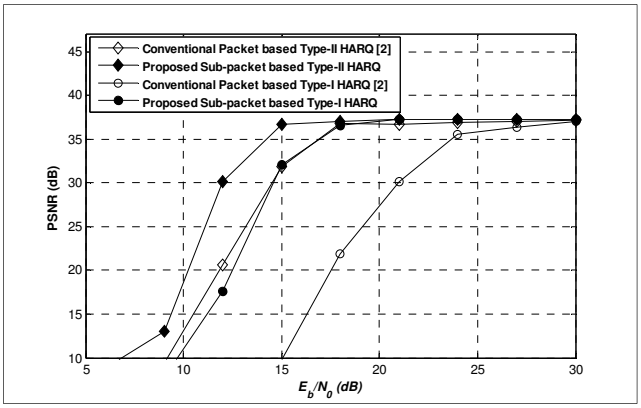


Figure 9. PSNR performance of the proposed subpacket retransmission technique, in comparison with the conventional packet retransmission technique.

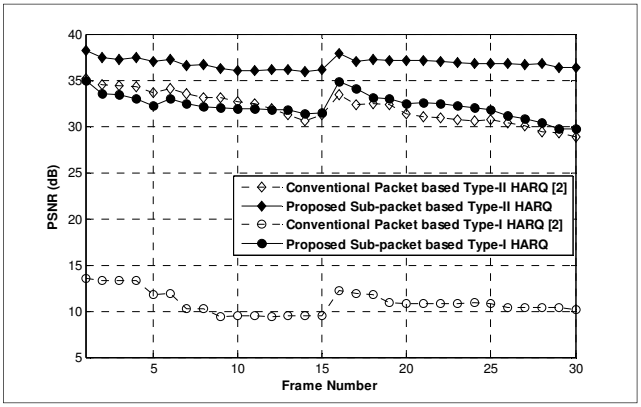


Figure 10. Frame-by-frame PSNR performance of the proposed subpacket retransmission technique, in comparison with the conventional packet retransmission technique.

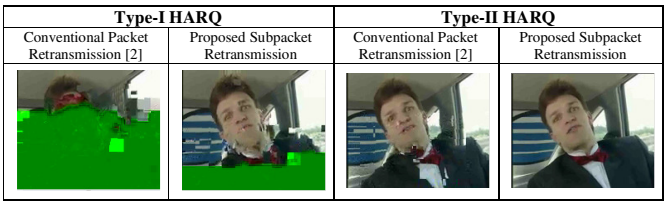


Figure 11. Subjective quality of the proposed subpacket retransmission technique, in comparison with the conventional packet retransmission technique.

V. CONCLUSION

This paper presents subpacket based retransmission technique in Type-I and Type-II HARQ transmission systems for video transmission over WiMedia-UWB network. The proposed subpacket based retransmission scheme give noticeable performance improvement in terms of the overall BER, delay, percentage of overhead, throughput, as well as the reconstructed video quality over the conventional packet retransmission techniques.

REFERENCES

[1] ECMA-368. (Dec 2008). High Rate Ultra Wideband PHY and MAC Standard. Available: http://www.ecma-international.org/publications/files/ECMA-ST/ECMA-368.pdf

[2] D. Lowe and H. Xiaojing, "Hybrid Automatic Repeat Requests for MB-OFDM Ultra-Wideband," in Proceedings of Third International Conference on Wireless and Mobile Communications, 2007, pp. 13-13.

[3] W. Cheng-Xiang, R. Heung-Gyoon, C. Hsiao-Hwa, and H. Yejun, "Hybrid ARQ with Rate Adaptation in Multiband OFDM UWB Systems," in IEEE International Conference on Communications, 2009, pp. 1-5

[4] Y. Q. Zhou and J. Wang, "Optimum sub-packet transmission for turbo-coded hybrid ARQ systems," in IEEE International Conference on Communications, 2003, pp. 3080-3084 vol.5

[5] Z. Yiqing and W. Jiangzhou, "Optimum subpacket transmission for hybrid ARQ systems," IEEE Transactions on Communications, vol. 54, pp. 934-942, 2006.

[6] M. L. B. Riediger and P. K. M. Ho, "A Probabilistic Subpacket Retransmission Scheme for ARQ Protocols," in IEEE International Conference on Communications, 2008, pp. 4809-4813

[7] N. Guo, F. Khaleghi, A. Gutierrez, J. Li, and M. H. Fong, "Transmission of high speed data in cdma2000," in IEEE Wireless Communications and Networking Conference, 1999, pp. 1442-1445 vol.3

Improving Connectivity and Coverage of Wireless Sensor Networks Using Mobile Robots

Chiraz Houaidia[#1], Hanen Idoudi[#2], Leila Azouz Saidane[#3]

[#]*Ecole Nationale des Sciences de l'Informatique (ENSI), Manouba University*
Campus Universitaire de la Manouba, Tunisia

[1]houaidia.chiraz@gmail.com

[2,3]{hanen.idoudi,Leila.saidane}@ensi.rnu.tn

Abstract — **Wireless sensor networks are often deployed in hardly accessible or hazardous fields. Their main goal is to monitor the target field and transmit surveillance data to a sink. Therefore, connectivity of the sensor network and the coverage ratio of the monitored area are the most relevant concerns to reach these goals. In this paper, we propose to use several mobile robots to assist sensor networks redeployment in order to enhance the network connectivity and the coverage ratio of the monitored area. We model the sensor network as an islets-based topology and we propose to use robots to detect and heal connectivity and coverage holes availing the sensors redundancy. Preliminary simulations showed that our new scheme can significantly enhance the connectivity ratio of the initial network and improve the coverage ratio by using few numbers of robots.**

Keywords — **wireless sensor networks, robots, connectivity, coverage, redeployment.**

I. INTRODUCTION

A wireless sensor network (WSN) is a complex structure consisting of a large number of sensor nodes distributed over a target region. Each sensor has limited computational and storage capacity, a restricted sensing and communication radius, and a finite power supply [3]. A large number of these devices could be deployed in a targeted field to create a sensor network for both monitoring and control purposes. Connectivity of the network is a main concern since sensors are in most cases required to deliver messages to a central device called sink. Furthermore, many WSN applications are required to perform certain tasks whose efficiency can be measured in terms of coverage. Thus, in order to properly sense the phenomena of interest, sensor nodes must be deployed appropriately to reach an adequate coverage level for the successful completion of the issued sensing tasks [2].

However, in many potential working environments, such as remote and large harsh fields or disaster areas, initial deployment of the sensor network cannot be performed manually and precisely. In these scenarios, the initial topology could be partially disconnected form the sink and/or doesn't insure a sufficient coverage ratio of the monitored field. Hence, it is necessary to redeploy the network so that redundant sensors are efficiently re-distributed to fill the coverage holes and maintain the network connectivity.

Many studies have been proposed within this scope. Most of them focused on mobile sensor networks where all or partial of the sensor nodes have motion capability [2,5,6,7,8]. These propositions relay on autonomous mobility of nodes based on distributed decisions. However, using mobile sensors could be too expensive or not possible particularly in large scale networks. On the other hand, owing to the difficulty of human intervention, wireless sensors assisted by robots have received a growing attention from the research community in the past years [4]. In such networks, once sensors are deployed over the area of interest, robots are then disseminated in the network to relocate redundant nodes so that they guarantee a sufficient level of sensing coverage and network connectivity.

In this context, we propose a new scheme to assist the redeployment of the sensor network using several mobile robots. Our main purpose is to enhance the connectivity and the coverage of a randomly deployed sensor network. According to our proposition, sensors form initially a clustered architecture to elect some nodes responsible of collecting redundancy information, and communicating with robots. This aims at reducing the energy consumption of some nodes. Then we use robots to probe all the target area in order to discover the sensor network topology and to redeploy it. We define a mobility model and a cooperation protocol for the robots functioning to ensure the global connectivity and a better coverage of the network at minimum time.

This paper is organized as follows. In the following section we present existent techniques for sensor networks redeployment. Afterwards, we introduce our new scheme based on the islets-based topology and the mobile robots assisted redeployment. In section 4, we display the results of simulations which enabled us to highlight the impact of our solution on enhancing sensing coverage and network connectivity. Section 5 concludes our paper.

II. RELATED WORK

Several researchers have investigated techniques to enhance the initial deployment of sensor networks using motion capabilities of sensors. In such schemes, sensors (or a subset of them) form a self-reconfigurable network and can move dynamically in order to adjust the topology according to the monitoring needs over the target area.

In [9] the sensors are modeled as particles of a compressible fluid, in [10] the theory of gas is used to model sensor movements in the presence of obstacles. A similar approach is

used in [11] to give a unified solution to the problem of deployment and dynamic relocation of mobile sensors in an open environment. The Voronoi approach is used in [12], where mobile sensors move from densely deployed areas to sparse areas on the basis of a local calculation of the Voronoi diagrams. In other solutions, [13] propose the use of Delaunay triangulation techniques to obtain a regular tessellation of the area of interest. Two principal approaches are used to define the movement of the selected sensor. In the first one, redundant nodes are the only nodes involved in the redeployment process and move directly to the area to cover. Nevertheless, this solution is costly in terms of energy consumed by implicated nodes and creates a long period delay to significantly improve the coverage. To balance the energy cost and the replacement time, a cascading movement was proposed in [5]. Once the coverage hole is detected, nodes move toward it along a carefully selected path. Algorithms related to potential field and virtual forces that relocate nodes are presented in [7]. Areas of redundancy or high density will be reduced thanks to the repulsive forces exerted between neighbouring nodes. Redundant nodes are moved to heal coverage holes.

However, in WSN and particularly in large-scale sensor networks, mobility can lead to rapid and important power consumption of sensors. Furthermore, mobility is an expensive feature. The relative analysis of increased message complexity of simulated mobility and the subsequent high energy consumption has given birth to Wireless Sensor and Actors Networks (WSAN). Indeed, actors, robots for instance, can be used to perform maintenance tasks on stationary sensor networks. Mobile robots could assist the redeployment of the network so that redundant sensors are relocated to sparse areas. Although using robots to assist deployment or maintenance of sensor networks is an attractive solution, few studies have focused on proposing new schemes in such context.

Y. Mei et al. proposed in [1] the use of some mobile robots to assist the replacement of exhausted sensors. All the robots are mobile and can take and drop sensors in pre-calculated positions. When a node becomes inoperative due to its energy's depletion, a robot moves to the target position, replaces the faulty sensor by a functional one or recharges the battery of the exhausted sensor. In a first centralized manager algorithm, a central manager receives failure reports from sensors and forwards them to individual robots. However in the distributed version, each robot functions as both a manager and a maintainer. Nevertheless, in this work, authors do not precise how to locate and collect redundant sensors. R.Soua et al. considered in [4] one mobile robot to assist the deployment of static sensor networks. The proposed deployment scheme uses permanent grid and cluster concepts to reduce the number of packets used in creating and maintaining a grid structure. The proposed solution is based on graph theory and combinatory optimization in order to reduce the robot's motion and efficiently guide the robot to redeploy sensors. However, a grid-based architecture is not feasible in a network in which nodes are relatively randomly deployed. The cost of organizing sensors into grids is high. Moreover, redeploying sensors in a large field with a single robot is challenging. Indeed, algorithms here described take potentially several iterations to terminate. They may not meet the requirements of a fast redeployment.

III. ROBOTS-ASSISTED SENSOR NETWORK REDEPLOYMENT

In this section, we present first the network model we used. We adopt a hexagonal cells pattern of the field and an islet-based topology for the initially deployed sensor network. We detail thereafter the clustering scheme proposed based on this model and we finally present our proposed technique for robots functioning during the sensors redeployment procedure.

A. Network Modelling

In our work, we consider initially a random deployment which consists on spreading a large amount of sensors on the field from, for instance, an airplane.
Such deployment could lead up to the formation of isolated clusters or sets of nodes (Fig.1) called here *islets* (or *islands*). An islet is a subset of connected sensors. We call *Mainland*, the islet that includes the sink node. Islets are disconnected from the Mainland; hence, connectivity of all sensors with the sink is not ensured nor the total coverage of the field.

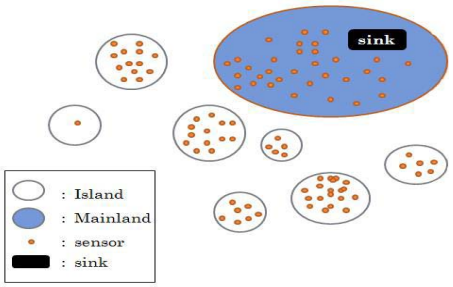


Fig. 1 Islets-based topology

We first organize sensors in a clustered architecture based on hexagonal cells pavement. This architecture aims at reducing the number of exchanged packets with robots and conserving sensors energy.

We assume that each sensor of the network is aware of its location, using GPS or any other localization technique. Furthermore, we make the assumption that for each sensor, the communication range is at least twice of the sensing range. Authors in [14] prove that this condition is sufficient to ensure that a full coverage of a convex area implies connectivity among active nodes inside it.

To facilitate the location of redundant sensors, we use a hexagonal partitioning of the field such that any two sensors in two adjacent cells can still communicate [16] (Fig 2).
Let C_1 and C_2 be two neighbouring cells and s_1 and s_2 two sensors then:

$$\forall (s_1, s_2) \in (C_1, C_2);\ distance(s_1, s_2) \leq Rc \qquad (1)$$

With Rc the maximum communication range of all nodes.

Thus, connectivity between nodes belonging to different cells is ensured by the construction of hexagons (Fig.4-(b)).

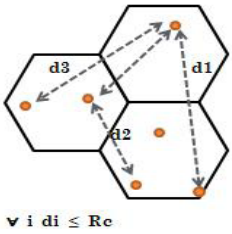


Fig. 2 Hexagonal cells

B. Clustering Mechanism

We adopt a clustering scheme to collect information about the positions of redundant nodes and the energy consumed on each islet. This information will be used during robots functioning. We propose therefore a clustering algorithm based on the hexagonal paving model. The principle of our algorithm is to consider each islet as a cluster. For each cell, a *Master* node should be elected and remains in the active state to provide coverage within the cell and gather location and energy information. Other nodes of the same cell will be considered as redundant and pass into the sleeping mode. Master nodes are elected based on their residual energy.

Among all the master nodes on an islet, one node should be chosen as the *Island-Head* to be the local coordinator within the islet. The *Island-Head* is chosen according to its residual energy and its position within the islet. *Island-Heads* collect information about the number, positions and the energy of redundant nodes on each islet and provide robots with this information when needed. This intends to reduce the number of packets exchanged with robots and to reduce energy consumption of sensors.

C. Robots Functioning

In islet-based sensor networks, the considered topology needs to be redeployed and reconfigured to obtain the sufficient coverage and network connectivity. To fulfil this goal, we propose to use several robots to enhance the topology.

Our proposed mobile robot based redeployment uses the clustered architecture of sensors to detect connectivity and coverage holes, locate redundant sensors and to redeploy them while exchanging minimum number of packets within Island-Heads.

We assume that robots are mobile and carry, initially, a fixed number of sensors (corresponding to their maximum load) to deploy them when needed. Each robot can deploy on field some of its carried sensors and can retrieve some redundant sensors from the field as long as its maximum load is not reached. We assume also that the total number of available sensors (those initially deployed in addition to sensors hold by robots) is quite sufficient to cover the target field.

In a multi robot approach, the challenge in the redeployment of the network is, on the one hand, to optimize the number of robots and on the other hand to coordinate their movement and communication.

1) Movement pattern of robots

We consider here N mobile robots with $N \geq 2$ in order to highlight the cooperation between neighbouring robots. The position of the sink node is not essential for our proposed method and it could be unknown beforehand. We assume that all robots have the same perception range R. This radius R is defined as follows:

$$R = (7/2) * Hexa_cote \quad (2)$$

With *Hexa_cote* the side's length of a hexagonal cell.

In the proposed mobility pattern, we assume that the robots have to cross over a bounded field. We divide the target field into R-width zones and we assign each zone to a robot. A robot can eventually treat iteratively several zones if the number of zones exceeds the robots number. Each robot acts on zones delegated to it and can collaborate with neighbouring robots.

As shown in Fig. 3, robots are initially lined up on the first horizontal edge of the field. Each robot have to travel through its zone to move toward the opposing field's edge while leading the coverage process (arrows in Fig.3 show the trajectory of robots). Once arrived at the opposite edge, a robot move a distance d, in horizontal way (on the X-axis) to access the edge of another untreated zone. Accessing the edge of a new zone and after communicating with neighboring robots, it has to travel across the new zone in the opposite direction. The same steps are repeated by all robots untill all zones are treated.

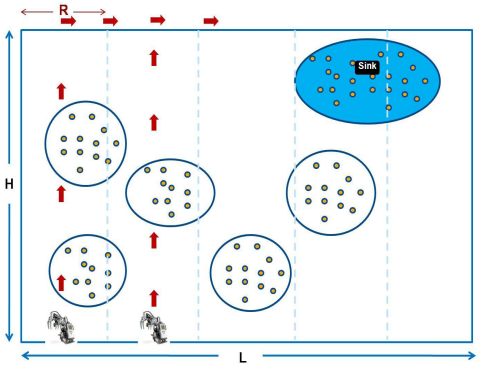


Fig. 3 Mobility of robots

The horizontal shift d to reach other zones depends on the width of the target field and the number of robots. Each time a robot reachs a horizontal edge of the field, it have to shift horizontally by a distance :

$$d = N*R \quad (3)$$

With N the total number of robots and R, a zone's width.

At a given step of their movement and considering L the width of the surface, if L is multiple of d then each robot does the shift itiratively until completing the field crossing. Otherwise, in the last itiration, only a subset of robots should make the shift to treat the remaining zones.

In some cases, a single pass all over the targed field is not sufficient to heal all the coverage holes and to connect all the islets. Hence, robots can re-iterate the same mobility pattern

as mush as necessary to fulfill these goals. Furthermore, continuous field crossing by the robots could be used for network maintenance. Thus, robots can, for instance, detect and replace faulty sensors.

2) Topology enhancement process

We distinguish three main tasks assigned to robots namely: topology discovery, collection of redundant sensors and their placement.

- *Topology discovery*

While moving, the robots broadcast *HELLO-ROBOT* messages to detect the presence of islets. If a sensor receives this message, it responds by transmitting the ID and position of its 'island-head'. The robot moves thus towards the 'island-head' and get back the number and positions of redundant nodes within the islet.

If after a certain delay, the robot does not receive a response to its message *HELLO-ROBOT*, it concluded that the cells visited are not covered and decided in this case to proceed to the placement of sensors, if available.

- *Collecting of redundant sensors*

At each islet discovered, the robot decides, based on information collected from the *island-head*, to collect redundant sensors therein without exceeding its capacity. Indeed, the robot having initially a number of sensors to deploy if needed, when it discovers a redundant sensor and if its capacity is not yet reached, it gathers the required number of sensors therein otherwise it memorise their positions and eventually come back in a second round to gather them.

- *Sensors placement*

While discovering the topology, the robots place sensors to cover the detected holes in the area. The new nodes should be deployed in an optimal way in order to minimize the number of sensors required to ensure a global coverage of the area of interest. For this purpose, we establish a relation between *Rs*(perception or sensing radius) and *Rc*(communication radius), which allows us to use the maximum capacity of perception and communication of nodes and ensures effective deployment in terms of number of sensors placed.

In fact, a cell, as constructed in the previous section, is covered just by having one active node (*Master node*) in the cell. Since the Master can be at any position, the hexagon diagonal should be equal to the sensing radius *Rs* of this node. It follows from this relationship a second optimization of the number of sensors placed considering a single sensor for every three neighbouring cells as shown in Fig.4-(a).

To benefit further more from communication capacity of sensors, we propose to define a cell so that the distance between two extreme points of two adjacent cells is less than or equal to *Rc* (Fig. 4-(b)).

If the robot lacks of sensors, it memorizes the position of the coverage hole to try to cover it in a second crossing of the field.

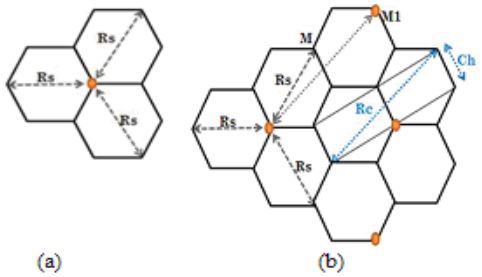


Fig. 4 Optimal placement of sensors

- *Behaviour of new sensors :*

A newly placed sensor acquires first a new identity and calculates its cells by executing the algorithm of the hexagonal paving of the area.

However, given the proposed approach for the network redeployment, the new node will, by definition, be 'master' of three cells at once (as it will be placed at the intersection of every three adjacent cells as detailed in the previous section). Thus, the sensors newly introduced in the surface are self-designated masters of cells to which they belong and avoid the election process.

On the other hand, as mentioned previously, new sensors are deployed in order to cover the holes between islets and thus have to join the existing islets by the following algorithm:

- Once introduced into the network, the new node sends a *HELLO-HEAD* message containing its ID and its cells coordinates in order to detect the nearest islet to join it.
- A sensor, belonging to the nearest islet and having received the *HELLO-HEAD* message, responds with a configuration message indicating the ID of the islet and its 'Head'.
- If the new node receives a response to his *HELLO-HEAD* request, he joins thus the designated islet.
- Otherwise it self-designates itself as *island-head* of the islet formed by cells to which it belongs.

3) Robots cooperation

Along the coverage procedure, robots can be, according to the redundancy, lacking of sensors to deploy in order to cover the empty cells. Therefore, to complete the coverage task, robots can communicate and lend sensors between each other according to a cooperative protocol for the exchange. For that, we define a limited number of sensors (*Threshold)* below which a robot is able to claim an exchange with at least one of its two immediate neighbours.

The exchange algorithm is as follows:

- Once reaching a horizontal edge of the surface and before moving to the edge of a new zone, a robot *Ri* have to stop for a given period of time T. During T, it sends periodically a *HELLO-NEIGHBOR* message, containing its ID and the number of sensors N_i on its disposal to announce its arrival to its neighbours robots (namely robots with ID *Ri-1* and *Ri+1* if the robot *Ri* is not placed initially at one vertical edge of the field).

- If (N_i < *Threshold*) then:
  - If it receives *HELLO-NEIGHBOR* messages from its neighbours mentioning that their respective load of sensors are less than the threshold number, then none of its neighbours is able to lend. In such case it abandons its request and continues its move to another zone.
  - If at least one of its neighbours presents a number of sensors superior to the required limit, it sends then a request asking the neighbour to lend him a given number of sensors.
  - If it receives a confirmation, it moves towards its neighbour to perform the exchange.
  - If after a given delay, it does not receive confirmation, then it sends its request to the second neighbour.
- Otherwise (*Ni*> *Threshold*)
  - If it receives requests from its neighbours, it confirms the exchange with the one having the fewest number of sensors. The number of sensors proposed to lend would be ((*Ni - Threshold) / 2*).
  - Otherwise, it continues its round to another zone.

IV. Simulation Results

We implemented our solution under the WSNet simulator [15]. For our preliminary simulations, we intended to study the performance of our proposed approach after one single crossing of the target field, i.e., after robots have made the first trip through the target field and treated all zones once. We measured the connectivity ratio and the coverage ratio of the resulting topology.

We carried our experiments while varying the number of robots and the initial topology. We varied the number of robots in order to study the optimal number of robots required to adjust the connectivity and the coverage ratios. On the other hand, we varied the initial network topology (the number of islets) in order to study the impact of redundancy on coverage and connectivity. The following table summarizes the different simulation parameters we used.

TABLE I. Simulation parameters

Parameter	Value
Network dimensions ($L \times H$)	600*600 m^2
Side's length of a cell (*Hexa_cote*)	7.5 m
Number of sensors (*N*)	200
Sensor communication radii (*Rc*)	30 m
Sensor sensing radii (*Rs*)	15 m
Initial load of a robot	20 sensors
Robot's communication range (*R*)	17,5 m
Robot's threshold of sensors (*Threshold*)	5

We used an initial topology of 200 sensors deployed randomly but organised into islets. We vary the number of islets for each scenario.

1) Connectivity ratio

The connectivity ratio (CR) is determined by the number of connected islets (among the initial islets) to the Mainland after the robots functioning. Thus, two connected islets are considered as a single one. This number corresponds to the difference between the initial number of islets and the final number of still isolated islets. Thus, we define the connectivity ratio as follows:

$$CR = (\text{initial number of islets} - \text{final number of islets}) / \text{initial number of islets} \quad (4)$$

As expected, simulations showed that increasing the number of robots improves the connectivity ratio reached at the end of the first round (Fig. 6). Moreover, using at least 2 robots allows a good connectivity ratio (up to 80%) in case of a 10 initial islets topology. Furthermore, as shown in Fig. 6, we notice that the connectivity ratio increases while using topologies with higher number of islets. This is explained by the fact that in initial topologies with a high number of islets, sensors are more scattered through the field than in few islets topologies. Hence, islets are separated by few cells and connectivity could be reached more quickly by placing some sensors to connect islets.

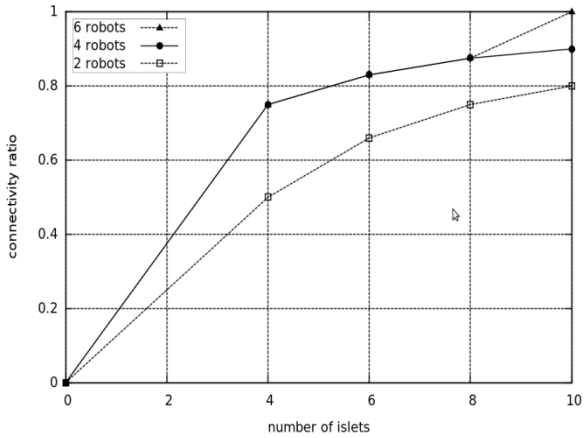


Fig. 6 First Round Connectivity Ratio

2) Coverage ratio

A cell is covered unless it contains at least one sensor. The coverage ratio (COR) is determined by the number of covered cells. We define it as follows:

$$COR = \text{number of covered cells} / \text{total number of cells} \quad (5)$$

Figure 7 shows the coverage ratio at the end of one field's pass when using 2, 4 or 6 robots. It follows that with more robots, we have automatically best coverage results. We point out also that the more the number of islets increases, the less the coverage ratio is. This is explained by the fact that redundancy decreases when sensors are scattered into multiple islets. Indeed, a redundant node, according to the optimal placement proposed in the previous section, is used to cover three cells at once; thus, minus a redundant node makes three extra uncovered cells. Furthermore, if we consider figure 8, we notice the very important enhancement of the coverage ratios of all subsequent topologies in comparison to the ratios of the initial topologies. Under such improvement, we can

easily predict that a total coverage could be reached in only few more passes of the field.

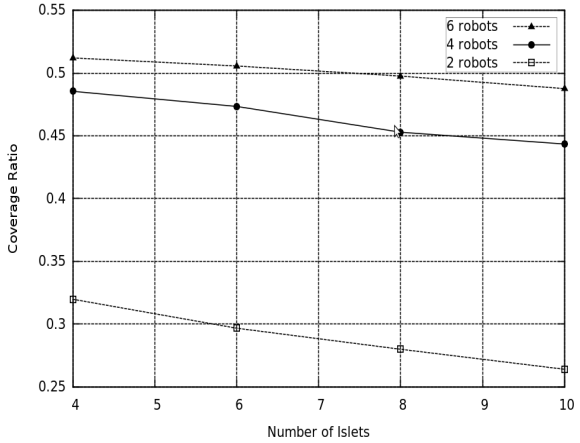


Fig. 7 First Round Coverage Ratio

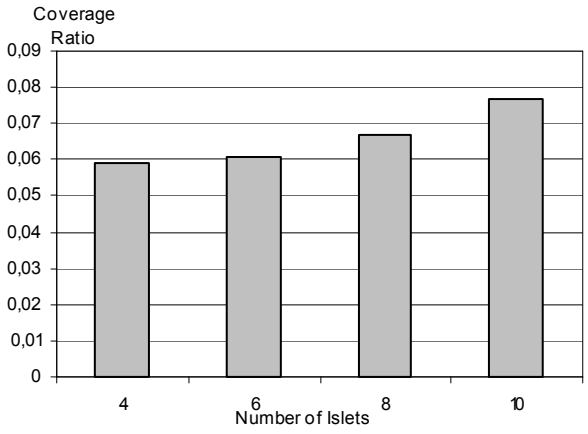


Fig. 8 Initial Coverage Ratio

V. Conclusion and Future Work

Robot-assisted WSNs is a promising paradigm in ubiquitous robotics since robots represent a vital means to avoid human intervention on sensor networks deployed in hazardous fields.

In this paper we proposed a new scheme for sensor networks redeployment assisted by mobile robots aiming essentially at improving the coverage and the connectivity of the monitored area. Our proposal was focused on how to exploit the redundancy generated by the initial random deployment to fill the connectivity and coverage holes. Our solution is based on a particular topology where sensors are first arranged on islets. We used a hexagonal area paving and a clustering algorithm appropriate to this hexagonal partition. Robots perform the network redeployment in a cooperative way while exploring the sensor network. Simulation results showed the efficiency of our solution in terms of both coverage and connectivity enhancement. Results have proven that using only few mobile robots has an important impact on reaching a total connectivity of the network while significantly enhancing the coverage ratio after a single robots crossing of the monitored area.

In our future work, we intend to study the trade off between the number of used robots and the time needed to reach total connectivity and coverage of the field (with multiple iterations). Also, the impact of our proposal on sensors energy will be studied in order to bring out the compromise between the cost introduced by the use of multiple robots and the effectiveness of the proposed approach towards the coverage and connectivity objectives. On the other hand, for a comparative purpose, other mobility strategies for robots would be implemented and evaluated. We also intend, in order to maintain the coverage within the area, to assist robots to systematic monitoring for detecting and replacing faulty sensors.

References

[1] Y. Mei, C. Xian, S. Das, Y. C. Hu, and Y. H. Lu, Sensor replacement using mobile robots, Computer Communications 30 (2007) 2615-2626.

[2] G. Wang, G. Cao, T.F. La Porta, and W. Zhang, Sensor Relocation in Mobile Sensor Networks, In Proceedings of the IEEE INFOCOM, Miami, FL, USA, March 2005; pp. 2302 - 2312.

[3] F.Pedraza, A.L.Medaglia, A.Garcia, Efficient Coverage Algorithms for Wireless Sensor Networks, Systems and Information Engineering Design Symposium, 2006 IEEE.

[4] R.Soua, L.Saidane, P.Minet, Sensors Deployment Enhancement by a Mobile Robot in Wireless Sensor Network, Networks (ICN), 2010 Ninth International Conference on, 10.1109/ICN.2010.29

[5] A. Howard, M. J. Mataric and G. S. Sukhatme, "An Incremental Self-Deployment Algorithm for Mobile Sensor Networks," *Autonomous Robots, Special Issue on Intelligent Embedded Systems*, September 2002

[6] A. Howard, M. J. Mataric and G. S. Sukhatme, "Mobile Sensor Networks Deployment Using Potential Fields: A Distributed, Scalable Solution to the Area Coverage Problem," *the 6th International Symposiumon Distributed Autonomous Robotics Systems*, June 2002.

[7] Y. Zou and K. Chakrabarty, "Sensor Deployment and Target Localization Based on Virtual Forces," *INFOCOM*, 2003.

[8] G. Wang, G. Cao, T.L. Porta, W. Zhang, Sensor relocation in mobile sensor networks, in: IEEE Infocom, 2005, pp. 2302–2312.

[9] N.Bartolini, T.Calamoneri, Emanuele G.Fusco, A.Massini, S.Silvestri, Autonomous Deployment of Self-Organizing Mobile Sensors for a Complete Coverage, Computer Science, 5343/2008.

[10] Kerr, W., Spears, D., Spears, W., Thayer, D.: Two formal fluid models for multiagent sweeping and obstacle avoidance. In: Kudenko, D., Kazakov, D., Alonso, E.(eds.) AAMAS 2004. LNCS, vol. 3394. Springer, Heidelberg (2005).

[11] Garetto, M., Gribaudo, M., Chiasserini, C.F., Leonardi, E.: A distributed sensor relocation scheme for environmental control. In: The Fourth ACM/IEEE Int. Conf. on Mobile Ad-hoc and Sensor Systems, MASS(2007).

[12] Wang, G., Cao, G., Porta, T.L.: Movement-assisted sensor deployment. IEEE Transaction on Mobile Computing 6 (2006).

[13] Ma, M., Yang, Y.: Adaptive triangular deployment algorithm for unattended mobile sensor networks. IEEE Transactions on Computers 56 (2007).

[14] X. Wang, G. Xing, Y. Zhang, C. Lu, R. Pless, and C.D. Gill, *Integrated coverage and* connectivity configuration in wireless sensor networks, ACM Transactions on Sensor Networks,Vol. 1, No. 1, August 2005.

[15] WSNET simulator. http://wsnet.gforge.inria.fr. Last Access 10/5/2010.

[16] V.Coskun, Relocating Sensor Nodes to Maximize Cumulative Connected Coverage in Wireless Sensor Networks, ISSN 1424-8220 2008.

Mobility Models for Vehicular Ad-hoc Network Simulation

Mrs. Vaishali D. Khairnar
Research Scholar, Nirma Institute of Technology, Ahmedabad. & Asst. Prof., Terna Engg. College, Nerul Navi-Mumbai.
email-id: vaishali_khairnar@rediffmail.com

Dr. S.N. Pradhan
Institute of Technology Under Nirma University, Ahmedabad.
email-id: snpradhan@nirmauni.ac.in

Abstract-**Vehicular mobility has some special characteristics of node mobility such as the high speed of cars, the strict constraints on nodes movement patterns, the periodicity of dense and sparse network areas, the clustering of users at intersections, or in traffic jams. These phenomena can only be captured with a limited level of realism in the simulated cars movement, and their impacts on the network performance cannot be ignored or assumed a priori, but need to be studied to guarantee the network simulation outcome to be reliable. We will study vehicular mobility models, which will describe an increasing level of detail in the vehicular movement. Also inter-vehicle communications metrics and the suitability of both existing and novel ad hoc protocols to car-to-car and car-to-road communication. One of the emerging applications that belongs to a ambient systems is to transparently and directly interconnect vehicles on roads, making an ad-hoc network that enables a variety of applications through distributed software's without the need of any fixed and dedicated infrastructure. The network as well as the embedded computers and sensors in the vehicle will be invisible to the driver, who will get the required services during his journey. Vehicular Ad-hoc Network (VANET), in which vehicles constitute the mobile nodes in the network. Most research work in VANET relies on simulations for evaluation purpose, so the key concept for VANET simulations is a real world vehicular mobility model which will ensures conclusions drawn from simulation experiments will carry through to real world deployments. In this paper we propose Random way-point model evaluate its effect in VANETs by ns-2 simulations.**

Keywords— **VANET, Mobility Model, Random way-point, Simulations, Real World, NS-2 etc.**

I. INTRODUCTION

VANET communication is becoming an important and popular research topic in the area of wireless networking as well as in the automobile industries. VANETs are distributed, self-organizing communication networks built by moving vehicles, and are thus characterized by very high node mobility patterns. Goal of this research paper is to develop a vehicular communication system which will enable quick and cost-efficient distribution of packet data for the benefit of passenger's safety and comfort. Simulations are commonly used as a first step in the protocol development for VANET research. Several communications network simulator already exist to provide a platform for testing and evaluating network protocols, such as NS-2 [1], OPNET [2] and Qualnet [3]. Tools are basically designed to provide generic simulation. Difficulties in the conducting large-scale and extensive field trials of logistic, economic and technological nature make simulation the mean of choice in the validation of networking protocols for vehicular networks. [13-14]It is a common practice in the preliminary stages of real-world technologies development. A vehicular environment is made especially challenging features like nodes mobility, such as the speed of cars, the constraints on nodes, movement patterns, the periodicity of dense and sparse network areas, the clustering of users at intersections or traffic jams[10-11]. This can be done by limited level of realism in the simulated cars movement. Simulation outcome has to be reliable to support mobility models. Variety of simulation tools are available such as PARAMICS [4], CORSIM [5] and VISIM [6], VanetMobiSim [7], MOVE [8], SUMO [9], etc which have been developed to analyze transportation scenarios at the micro- and macro-scale levels. We have implemented Random way-point mobility model using NS-2 (2.34) and MOVE.

II. VEHICULAR MOBILITY MODELING

Modeling Mobility is one of the important aspects in Vehicular Network. Various approaches can be adopted in modeling the movement of vehicles [15, 16] . Mobility models can be commonly classified into the following categories:

1) Macroscopic models: Vehicular traffic is regarded as a continuous flow, and gross quantities of interest, such as the density or the mean velocity of cars, are modeled, often using formulations borrowed from fluid dynamics theory.

2) Mesoscopic models: Individual mobile entities are modeled at an aggregate level, exploiting gas kinetic and queuing theory results or macroscopic-scale metrics, such as velocity/density relationships, to determine the motion of vehicles.

3) Microscopic models: Each vehicle's movement is represented in great detail, its dynamics being treated independently from those of other cars, except for those near enough to have a direct impact on the driver's behavior. Microscopic models are able to reproduce fine-grained real world situations, such as front -to-rear car inter-action, lane changing, flows merging at ramps, and inter-sections. Although macroscopic and mesoscopic descriptions are employed to capture the dynamics of large -scale vehicular systems, such as those occurring

over road topologies covering whole regions or countries, microscopic models, due to their high computational cost, are usually applied to reproduction of traffic in smaller areas, such as single highways or urban areas. However, the traditional branching of models into macroscopic, mesoscopic, and microscopic becomes less meaningful when considering vehicular mobility models employed in network simulation. Thus, a different, better fitting classification could be constructed by differentiating on the nature of the diverse analytical representation of car motion encountered in the vehicular networking literature. We propose the following categorization.

4) Stochastic models: Vehicle movement is regarded at a microscopic level which is constrained on a graph representing the road topology, mobile entities follow casual paths over the graph, traveling at randomly chosen speed. Stochastic models are the most trivial way to mimic car mobility, and were introduced by pioneering works in the field of vehicular networking.

5) Traffic stream models: Vehicular mobility is observed from a high level and treated as a continuous phenomenon. Traffic stream models determine cars' speeds, leveraging fundamental hydrodynamic physics relationships between the velocity, density, and outflow of a fluid, and thus fall into the macroscopic or mesoscopic categories defined before.

6) Car-following models: The behavior of each driver is computed on the basis of the state (position, speed, and acceleration) of the surrounding vehicles.

7) Flows-interaction models: Built upon an instance of one of the previous categories, flows interaction characterizes the mutual dynamics that merging vehicular flows induce reciprocally, e.g., at highway ramps or urban intersections.

III. EXISTING VANET MOBILITY MODELS

In this section we present the models that were proposed for simulating VANETs. Basically, these models simulate movements in rout es. As we will see, the considered parameters differ from one model to another. For instance, some models use route intersections, and others just assume continuous movement at these points. Some assume routes to be single lane, some others support multi-lanes routes.

1) Freeway Mobility Model (FMM): Freeway is a generated-map -based model, defined in [17].The simulation area, represented by a generated map, includes many freeways, each side of which is composed of many lanes as shown in the Fig.1. No urban routes, thus no intersections are considered in this model. At the beginning of the simulation, the nodes are rand omly placed in the lanes, and move using history-based speeds. A security distance should be maintained between two subsequent vehicles in a lane. If the distance between two vehicles is less than this required minimal distance, the second one decelerates and let the forward vehicle moves away. The change of lanes is not allowed in this model. The vehicle moves in the lane it is placed in until reaching the simulation area limit, then it is placed again randomly in another position and repeats the process. This scenario is definitely unrealistic.

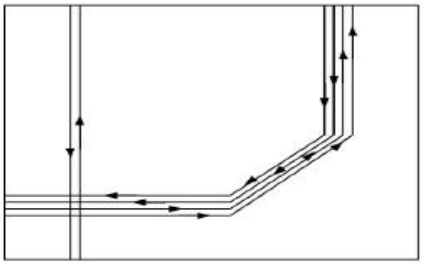


Fig. 1 Freeway Mobility Model

2) Manhattan Mobility Model (MMM): This is also a generated-map-based model, introduced in [17] to simulate an urban environment. Before starting a simulation, a map containing vertical and horizontal roads is generated as shown in the Fig 3. Each of these latter includes two lanes, allowing the motion in the two directions (north/south for the vertical roads and east/west for the horizontal ones). At the beginning of a simulation, vehicles are randomly put on the roads. They then move continuously according to history -based speeds (following the same formula like the freeway model). When reaching a crossroads, the vehicle randomly chooses a direction to follow. That is, continuing straightforward, turning left, or turning right. The probability of each decision is set by the authors respectively to 0:5, 0:25, 0:25.The security distance is also used in this model, and nodes follow the same strategy as in the freeway model to keep this distance. But contrary to the previous model, a vehicle can change a lane at a crossroads. Nonetheless, there is no control mechanism at these points (crossroads), where nodes continue their movements without stopping, which is unrealistic.

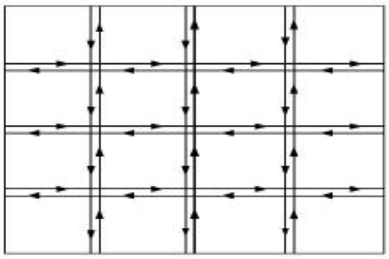


Fig. 2. Manhattan Mobility Model

3) Random-Way point Mobility Model: The node speed in the Random Waypoint model is uniformly distributed between 9 and 16 m/s covering the speed limits of the different road categories present in the simulation scenarios. The pause time between subsequent trips is uniformly distributed between 0 and 10 seconds to simulate a short stop at the destination. The initial values for a node's position and speed are set according to the steady-state initialization method [18].

IV. MOVE ARCHITECTURE

MOVE is implemented in Java and runs on top of an open source micro-traffic simulator SUMO. Following steps to implement MOVE First implement java sdk 1.6 and NS-2 Version 2.34 on Fedora 13 operating system. Next implement XML parser 3.11, FOX toolkit, PROJ

and GDAL on Fedora version 13 OS. Next configure SUMO with FOX, PROJ and GDAL. Execute MOVE by jar file.

MOVE consists of two main components:- Map Editor & Vehicle Movement Editor, as shown in Fig.3,4

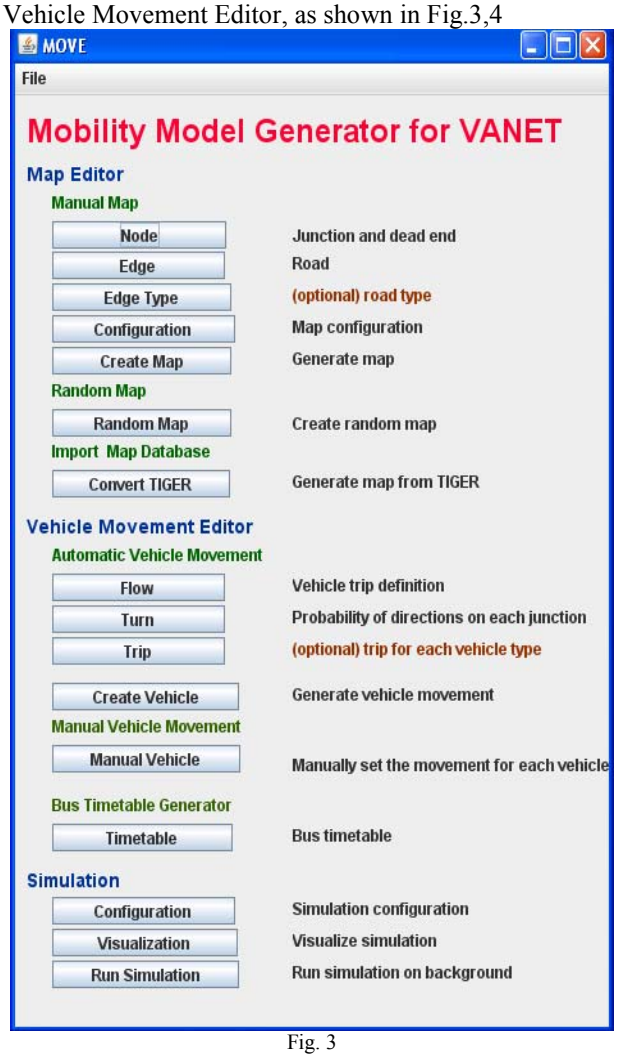


Fig. 3

The Map Editor is used to create the road topology. Basically implementation provides three different ways to create the road map.

_ The map can be manually created.

_ Generated automatically

_ Imported from existing real world maps such as Google maps.

Screen shots of Map Editor to create road topology as shown in Fig. 5. The Vehicle Movement Editor allows user to specify the trips of vehicles and the route that each vehicle will take for one particular trip Fig.6.

Three different methods to define the vehicle movements:-

_ The vehicle movement patterns can be manually created

_ Generated automatically Fig. 7.

_ Specified based on a bus time table to simulate the movements of public transportations. Fig.3.

Users inputs the information in the Map Editor and the Vehicle Movement Editor then this information is fed into SUMO to generate mobility trace which can be immediately used by NS- 2 version 2.34 to simulate real world vehicle movements. We can also visualize the generated mobility trace by clicking on the "Visualization" button on Main Menu, as shown Fig, 8.

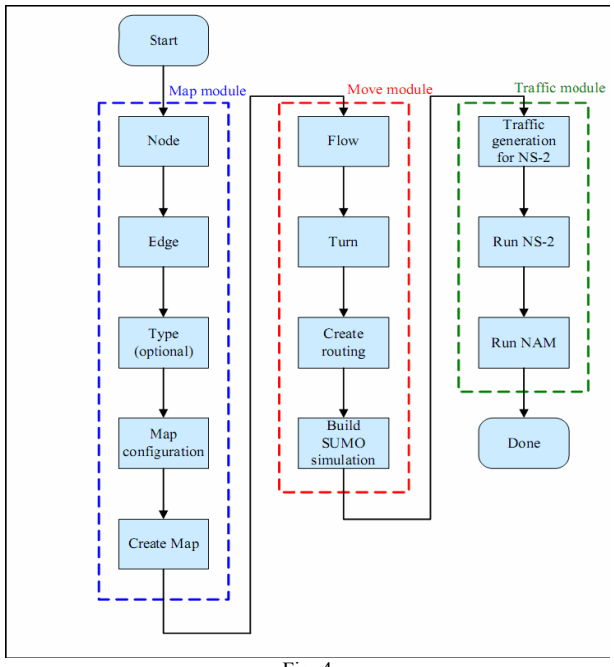


Fig. 4

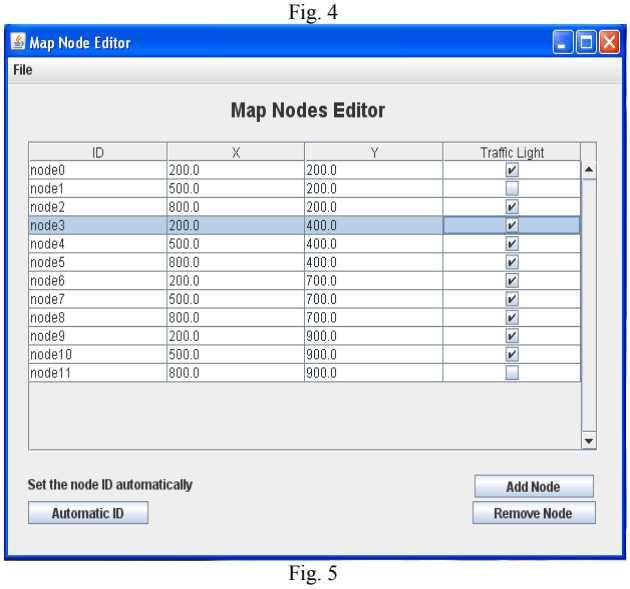


Fig. 5

A. MAP Editor: In MOVE, the road map can be generated manually, automatically or imported from a real world map. Manual generated of the map requires inputs of two types of information, nodes and edges as shown in Fig.5, 9. A "node' Fig. 4 is one particular point on the map which can be either a junction or the dead end of the roads. Furthermore, the junction nodes can be either normal road junctions or traffic lights. The edge Fig. 9 is the road that connects two points (nodes) on a map. The attributes associated with an edge include speed limit, number of lanes, the road priority and the road length. Fig.4 and Fig.8 shows snapshots of nodes editor and edge editor.

We can integrate Google Earth into MOVE. Google Earth is a tool that enables its user to view the satellite image map of any place on earth. The functionality that

Google Earth provides is called “Place mark” which allows the user to put a mark on any location of the Google earth map. Each place mark contains the longitude and latitude information of the selected locations and can be saved into a file in KML format [12]. One can define the node location on the Google map and then extract the node information by processing the saved KML file. This allows MOVE users to generate a map for any real-world road on earth for their simulations.

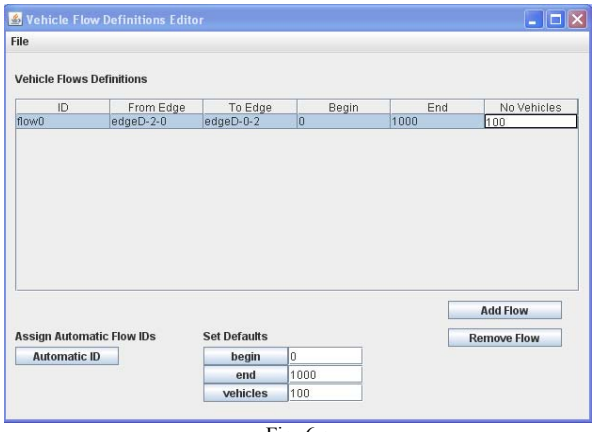


Fig. 6 a

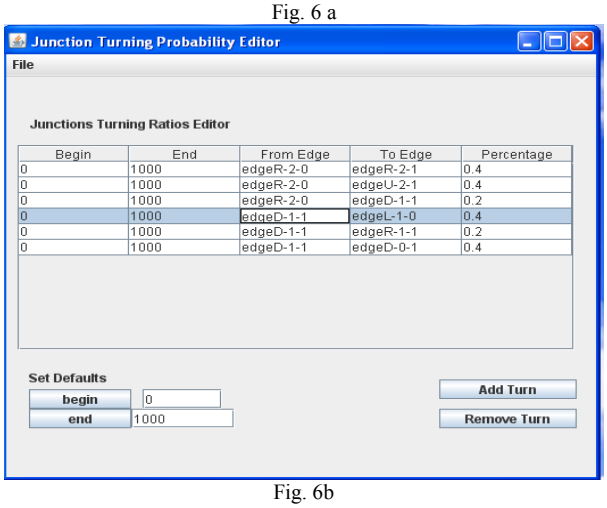


Fig. 6b

The road map can also be generated automatically without any user input. Three types of random maps are currently available (Fig. 7b):- grid, spider and random networks. There are some parameters associated with different types of random maps such as number of grids and the number of spider arms and circles. One can also generate a real world road map by importing real world maps from publicly available database.

B. Vehicle Movement Editor: The movements of vehicles can be generated automatically or manually using the Vehicle Movement Editor. The Vehicle Movement editor allows users to specify several properties of vehicle routes including the number of vehicles in a particular route, vehicle departure time, origin and destination of the vehicle, duration of the trip, vehicle speed etc. We can define the probability of turning to different directions at each junction in the editor Fig. 5, 9. MOVE allows users to enter the bus time table to simulate the movements of public transport. We model the bus as one type of vehicle which has similar parameters, such as speeds, routes, etc, associated with it as other vehicles. In addition, one needs to define the departure times of the first and the last bus and the bus inter-arrival time (which is assumed as constant) to simulate the bus time table Fig. 11.

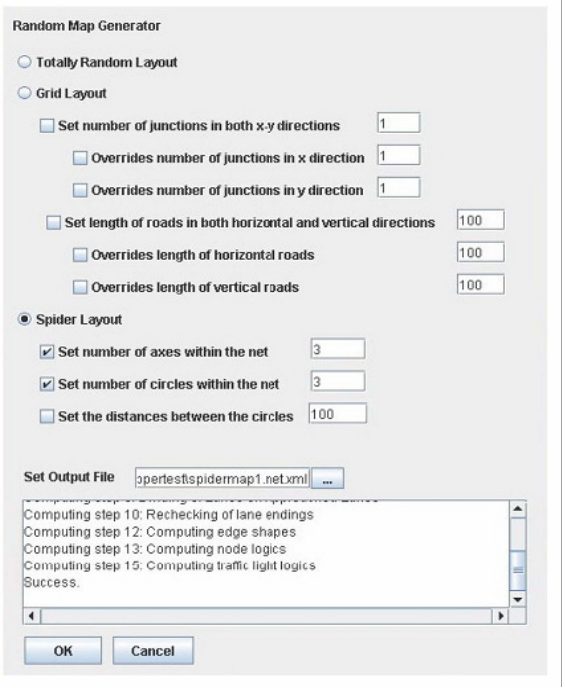


Fig. 7a

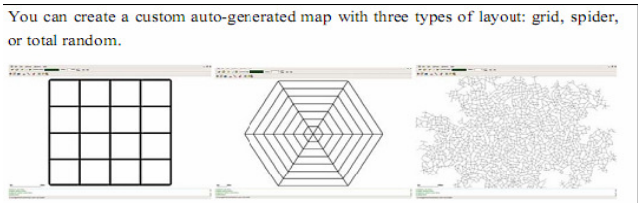


Fig. 7b

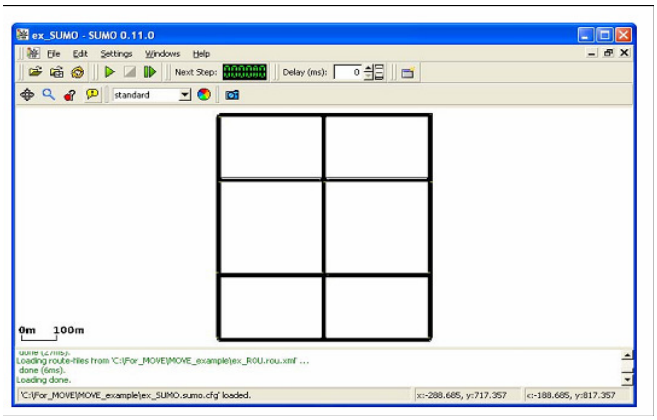


Fig. 8

V. EVALUATION

We evaluate the impact of mobility models generated by MOVE on the performance of ad-hoc routing protocol. We compare the performance of AODV when used with

the random waypoint model to that using the MOVE mobility model.

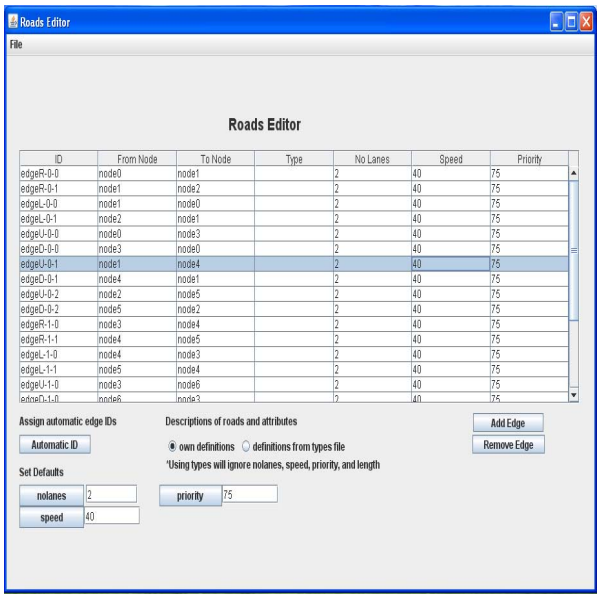


Fig. 9

The simulation experiments were carried out in NS-2 version 2.34 on fedora 13 operating system. Each simulation lasts for 900 seconds. We generated scenarios for 150 nodes moving in an area of 4 square kilometers. The number of source nodes from 10 to 50, each of which is a CBR traffic source transmitting UDP packets of a size 64 bytes at the rate of 4 packets per second. All nodes use 802.11 MAC operating at 2Mbps. The propagation model employed in the simulation is the log normal shadowing model. We used a path loss exponent 2.56 with standard deviation 4.0 based on real world measurement data from an inter-vehicle experiment. Fig. 12 shows the packet delivery ratio of AODV with different number of traffic sources. Each data point represents the average of six runs and the error bars represent the range of observed packet delivery ratios. Overall, the packet delivery ratios increase as the number of traffic sources increases, which suggest a higher density of nodes can increase the network performance as long as the increasing density does not create more radio interference.

The packet delivery ratios of AODV when using MOVE mobility models are lower than when using Random Waypoint model and have larger variations. The larger variance in MOVE data points is possibly due to unstable network connectivity imposed by constrained node movements by roads and traffic control mechanisms.

VI. CONCLUSION

In this paper, we describe the implementation and execution of Random Way-point Mobility Model using MOVE and Ns-2 Simulator which is based on an open source micro-traffic simulator SUMO. MOVE allows user to quickly and easily generate real world mobility

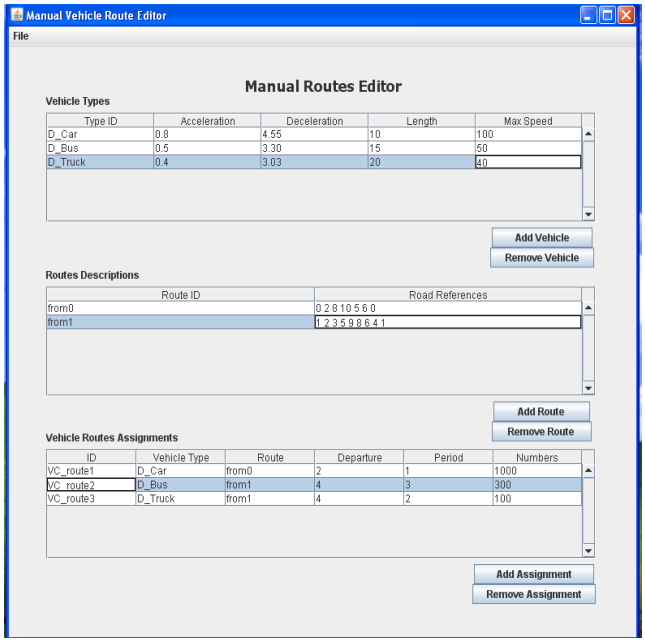


Fig. 10

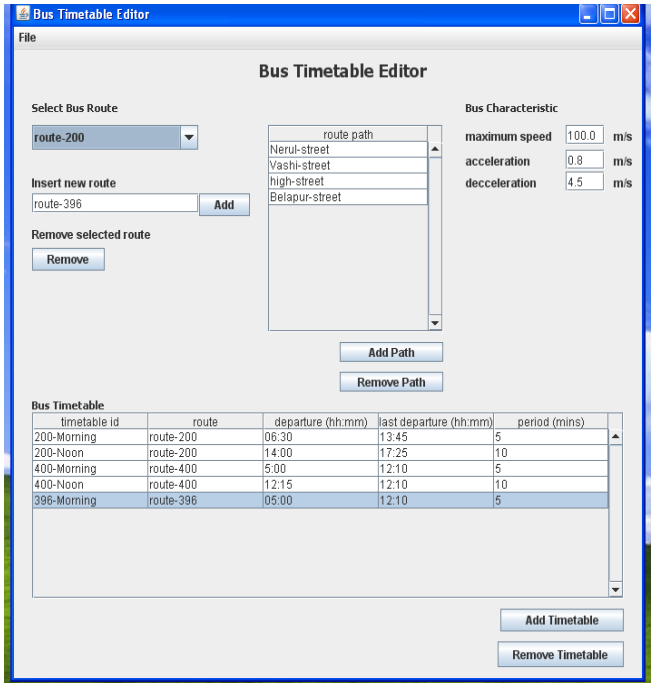


Fig. 11

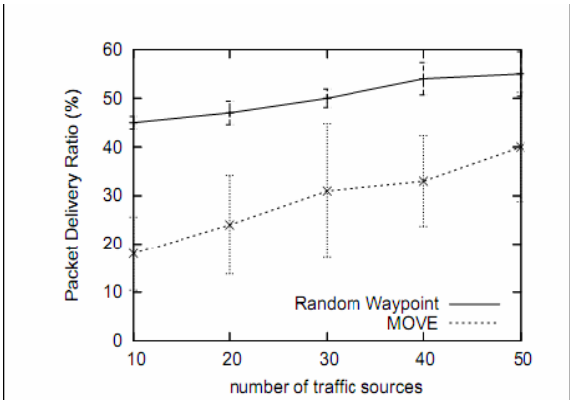


Fig. 12

models for vehicular network simulations. MOVE is publicly available and can be easily downloaded while SUMO is also publicly downloaded via following URL http://sumo.sourceforge.net/. Next step is to use this tool to understand the effect of level of details in context of VANET simulation. The movements of vehicles are based on static configurations defined in the Vehicle Movement Editor. The mobility model is first generated off-line and then used by network simulator NS-2 version 2.34.

REFERENCES

1) The Network Simulator NS-2 version 2.34.
2) http://www.isi.edu/nsnam/ns/index.html.
3) OPNET Simulator. http://www.opnet.com/.
4) QualNet Network Simulator. http://www.scalable-networks.com/.
5) Pamramics: Microscopic traffic Simulation. http://www.paramics-online.com/.
6) CORSIM. http://www.fhwa-tsis.com/.
7) PTV simulation VISSIM. http://www.english.ptv.de/.
8) VanetMobiSim. http://en.pudn.com/downloads160/sourcecode/app/detail720214_en.ht ml
9) MOVE http://www.cs.unsw.edu.au/klan/move/.
10) SUMO http://sumo.sourceforge.net/.
11) Amit Kumar Saha and David B. Johnson. Modeling mobility for vehicular ad hoc networks. In Proc. Of the 2nd ACM International Workshop on Vehicular Ad hoc Networks (VANET), October 2004.
12) John Heidemann, Nirupama Bulusu, Jeremy Elson, Chalermek Intanagonwiwat, Kun chan Lan, Ya Xu, Wei Ye, Deborah Estrin, and Ramesh Govindan. Effects of detail in wireless network simulation. In Proc. Of Communication Networks and Distributed Systems Modeling and Simulation Conference, January 2001.
13) KML tutorial. http://www.keyhole.com/kml/kml_tut.html
14) Realistic Mobility Models for Vehicular Ad hoc Network (VANET) Simulations , Kun-chan Lan and Chien-Ming Chou , National Cheng Kung University Department of Computer Science and Information Engineering Tainan, Taiwan.
15) Packet Transmission Analysis in Vehicular Ad Hoc Networks using Revival Mobility Model , K.Prasanth , Dr.K.Duraiswam,K.Jayasudha, Dr.C.Chandrasekar.
16) J. Luo and J.-P. Hubaux, "A survey of inter-vehicle communication," School of computer and Communication Sciences, EPEL, Tech. Rep. IC/2004/24, 2004.
17) A.Mahajan, N. Potnis, K. Gopalan, and A.I.A.Wang, "Urban mobility models for vanets" in Proceedings of the 2nd IEEE International Workshop on Next Generation Wireless Networks, December 2006.
18) F. Bai, N. Sadagopan, A. Helmy,"The IMPORTANT Framework for Analyzing the Impact of Mobility on Performance of Routing for Ad Hoc Networks", Ad Hoc Networks Journal - Elsevier Science, Vol. 1, Issue 4, pp. 383-403, November 2003.
19) William Navidi and Tracy Camp. Stationary distributions for the random waypoint mobility model. IEEE Transactions on Mobile Computing, 3(1):99–108, 2004.

BER Performance Evaluation for Multicarrier Code Division Multiple Access over Generalized κ-μ Fading Channels

James Osuru Mark, Brahim Belhaouari Samir and Mohammed Naufal
Department of Electrical & Electronic Engineering,
Universiti Teknologi PETRONAS,
Bandar Seri Iskandar 31750,
Tronoh, Perak, Malaysia.
E-mail: osurumark@gmail.com, brahim_belhaouari@petronas.com.my, naufal_saad@petronas.com.my

Abstract— Multicarrier code division multiple access (MC-CDMA) system has received a considerable attention from researchers owing to its great potential in achieving high data rates transmission in wireless communications. Due to the detrimental effects of multipath fading the performance of the system degrades. Similarly, the impact of non-orthogonality of spreading codes can exist and cause interference. This paper addresses the performance of multicarrier code division multiple access system under the influence of frequency selective generalized κ-μ fading channel and multiple access interference caused by other active users to the desired one. The average bit error rate is derived and expressed in Gauss hypergeometric functions. Maximal ratio combining diversity technique is utilized to alleviate the deleterious effect of multipath fading.

Index Terms —MC-CDMA, generalized κ-μ fading, average bit error rate, maximal ratio combining

1. INTRODUCTION

Multicarrier Code Division Multiple Access (MC-CDMA) is a digital modulation and multicarrier scheme which results from the combination of Orthogonal Frequency Division Multiplexing (OFDM) and Code Division Multiple Access (CDMA). Based on this combination, three multiple access techniques are formed, viz: Multicarrier (MC)–CDMA, Multicarrier Direct Sequence (DS)-CDMA and Multitone (MT)-CDMA. Hence, these multicarriers techniques are further classified into frequency domain and time domain spreading codes. In case of frequency domain , the original datastream is spread using spreading code and modulate different subcarriers with each chip while for time domain, original datastream is serial to parallel converted and spread using spreading code, then each subcarrier is modulated differently with each of the datastream. The main aim for these multicarrier access schemes is to provide sprectral efficiency, interference suppression capability and high data rate transmission over frequency selective fading channels. Similarly, the issue of how to spread the signal bandwidth without increasing the effect of delay spread is also addressed [1]. Hence, the other two multicarrier techniques will not be treated in this paper.

For the case of MC-CDMA system, it is assumed that the number of subcarriers and the processing gain have to be the same. Suppose the original symbol rate is high enough to become subject to frequency selective fading, then the signal should first be converted from serial to parallel before spreading over the frequency domain. This is to ensure that multicarrier transmission over each subcarrier should be frequency non selective fading. Therefore, MC-CDMA system transmits the same data bit over all subcarriers without changing the original baud rate [2].

The Bit Error Rate (BER) performance of the MC-CDMA system over frequency selective fading channels was addressed using equal gain combining and maximal ratio combining [3]. Effects of multipath delay on multicarrier received signals was investigated and a new closed form formula for BER was derived based on the orthogonal MC –CDMA system [4]. The authors [5] proposed a simple and efficient receiver design for frame based MC-CDMA in multipath Nakagami-*m* fading channels. The performance of the model were illustrated using different fading Nakagami-*m* parameters, modulation schemes (4, 16, and 64 QAM) and different number of users. In [6] the system performances were compared with that of the conventional DS-CDMA, it was observed that the multicarrier system outperforms when the system parameters are properly selected. The investigation of the performance of the MC-CDMA

system in uplink channel with frequency selective Rayleigh fading channels was conducted [7].

This paper tackles the effects of multiuser interference on performance of MC-CDMA wireless communication system over generalized κ-μ fading channels. The maximal ratio combining diversity method is applied to mitigate the severe impact of multipath fading. The average bit error probability (ABEP) for measuring the performance of the MC-CDMA wireless communication system is derived and expressed in Gauss hypergeometric functions. The paper is organized as follows: Section 2 outlines system and channel models. Analysis of the received signal is explained in section 3, while the application of Gaussian approximation method to analyse the received signal is described in section 4. In section 5, ABEP for the MC-CDMA system is derived, meanwhile the numerical results and discussion is explained in section 6. Finally, section 7 deals with conclusions.

2. System And Channel Model

2.1 *MC-CDMA Transmitter Model*

MC-CDMA system transmits datastream by first carrying out serial to parallel conversion and then spreads datastream in frequency domain (*F*-domain). The symbol duration of the transmitted signal is $T_s=qT_b$, where q is the number of substreams and T_b is the bit duration before conversion. Hence, after conversion each datastream is spread over N_p subcarriers using spreading code of $C_k[0]$, $C_k[1]$, .., $C_k[Np-1]$ assigned to user k in *F*-domain. The separation between two adjacent subcarriers is assumed to be $1/Ts$. The spreading codes are assumed to be random variables with values -1 or +1 having equal probability. In this case, each chip of data symbol is transmitted in parallel on different subcarrier. Then, the k th user transmitted signal is given by [8].

$$S_k(t)=\sqrt{\frac{2P}{N_p}}\sum_{i=1}^{q}\sum_{j=1}^{N_p} b_i^k(t)C_k[j-1]\cos\left(2\pi f_{ij}t+\phi_{ij}^k\right), \quad (1)$$

where P denotes transmitted power per bit, Np represents the number of subcarriers and q is the number of bits, f_{ij} is a subcarrier frequency, $b_i^k(t)$ is the i th binary data stream of user k $b_i^k(t)=\sum_{n=-\infty}^{\infty} b_i^k[n]P_{TS}(t-nT_s)$, where $b_i^k[n]$ is assumed to be a random variable which takes the value of +1 or -1 with equal probability, $P_{TS}(t)$ represents a rectangular waveform defined as $p_\tau(t)=1, 0\le t\le \tau$ and zero elsewhere, ϕ_i^k denotes a random phase introduced by carrier modulation assumed to be uniformly distributed in $[0,2\pi)$.

2.2 *Channel Model*

The link between the transmitter and the corresponding receiver is assumed to be slowly flat fading channel for each subcarrier. Therefore, the fading envelope of the received signal is modelled as generalized κ-μ fading distribution. Hence, the impulse response for the k th transmitted signal over the i th subcarrier is given by [9]

$$h_i^K(t)=\alpha_i^K\,\delta(t-\tau_k)\exp\left(-j\psi_i^k\right), \quad (2)$$

where $\alpha^k{}_i$, τ_k, $\psi^k{}_i$ and $\delta(.)$ denote the attenuation factor, delay, phase shift and Dirac delta function respectively. The delay is assumed to be uniformly distributed over $[0,T_s)$. Therefore, attenuation factor, delay and phase shift are assumed to be constant over a symbol period.

The κ-μ distribution is a generalized fading distribution that can be used to represent small scale variation of the fading signal in line of sight condition and fits well the experimental data. It includes the Nakagami-*n*, Nakagami-*m*, Rayleigh and One-Sided Gaussian fading distribution. This distribution considers a signal composed of clusters of multipaths waves propagating in a nonhomogenous environment [10]. Hence, in each cluster the phases of the scattered waves are random and have similar delay times, with delay time spreads of different clusters being relatively large [10]. The multipath waves within a cluster are assumed to have identical powers and each cluster has a dominant component with arbitrary power. Hence, if α follows a generalized κ-μ distribution, then the pdf of the instantaneous signal to noise ratio is given by [10], [11]

$$f(\gamma)=\frac{\mu(1+\kappa)^{\frac{\mu+1}{2}}}{\kappa^{\frac{\mu-1}{2}}\exp(\mu\kappa)\bar{\gamma}^{\frac{\mu+1}{2}}}\gamma^{\frac{\mu-1}{2}}\exp\left(-\frac{\mu(1+\kappa)}{\bar{\gamma}}\gamma\right)\times I_{\mu-1}\left(2\mu\sqrt{\frac{\kappa(1+\kappa)}{\bar{\gamma}}\gamma}\right), \quad (3)$$

where $\mu=\frac{E^2(\gamma)}{Var(\gamma)}.\frac{1+2\kappa}{(1+\kappa)^2}$, $\kappa\ge 0$ is the ratio of the total power of the dominant components to that of the scattered waves. E(.) is the expectation or average and var(.) is the variance, $I_x(.)$ is a modified Bessel function of the first kind and order x.

2.3 *MC-CDMA Receiver Model*

We assume that K asynchronous CDMA users simultaneously communicate with the base station employing MC-CDMA system. It is also presumed that the users exploit the same number of bits as well as subcarriers. Similarly, the state of perfect power control is assumed. Then the received signal at the base station is given by [8].

$$r(t) = \sqrt{\frac{2P}{N_p}} \sum_{k=1}^{K} \sum_{i=1}^{q} \sum_{j=1}^{N_p} \alpha_{ij}^{k} b_i^{k} (t - \tau_k) C_k[j-1] \times Cos\left(2\pi f_{ij} t + \varphi_{ij}^{k}\right) + n(t), \quad (4)$$

where *n(t)* is the Additive White Gaussian Noise (AWGN) with zero mean and double sided power spectral density (PSD) of $N_0/2$, $\varphi_{ij}^{k} = \phi_{ij}^{k} + \psi_{ij}^{k} - 2\pi f_{ij}\tau_k$, ψ_{ij}^{k} is a random phase introduced by the channel, φ_{ij}^{k} is assumed to be random variable uniformly distributed in $[0,2\pi)$, τ_k is the misalignment of user *k* with respect to the reference user, α_{ij}^{k} is a random variable which denotes the amplitude attenuation due to the channel.

3. Received Signal Analysis

In this case, the receiver makes use of all the received signal energy of an N_p – chip code scattered in the *F*-Domain. In frequency selective fading channels, different subcarriers can experience amplitude attenuation and phase shift differently. Therefore, this results in destroying orthogonality of the subcarrier which leads to interchannel interference. The statistic decision variable Z_u of the *0* th data bit in *u* th data subcarrier for the reference user is given by [8]

$$Z_u = \sum_{v=1}^{N_p} \int_0^{T_s} r(t) C[v-1] M_{uv} Cos\left(2\pi f_{uv} t + \varphi_{uv}\right) dt, \quad (5)$$

where M_{uv} is a parameter for identifying diversity combining techniques. Hence, the above equation can be expressed as

$$Z_u = D + I_1 + I_2 + \eta_0, \quad (6)$$

where *D* is the reference user or desired user, I_1 is a multiuser interference due to subcarriers having the same frequency, I_2 is multiple access interference due to other subcarriers with different frequencies. Assume that the received signal *k*=1 is the reference user, $\tau_k = \tau_1 = 0$ and the phase difference is also zero. Then, the desired user is given by

$$D = \sqrt{\frac{P}{2N_p}} T_s \sum_{u=1}^{N_p} \alpha_{uv} M_{uv} b_n[0], \quad (7)$$

where b_n *[0]* is the *0* th data bit transmitted by *uv* subcarriers of the reference user. Similarly, the MAI due to the same subcarrier frequency is expressed as

$$I_1 = \sqrt{\frac{P}{2N_p}} \sum_{k=2}^{K} \alpha_{uv}^{k} M_{uv} Cos\,\theta \int_0^{T_s} b_i^{k}(t-\tau_k) C_k[v-1] C[v-1] dt, \quad (8)$$

where $\theta = \varphi_{ij}^{k} - \varphi_{uv}$, also the MAI due to other active users with different subcarriers frequencies is

$$I_2 = \sqrt{\frac{P}{2N_p}} \sum_{k=2}^{K} \sum_{i=1}^{q} \sum_{j=1}^{N_p} \sum_{v=1}^{N_p} \alpha_{ij}^{k} M_{uv} \int_0^{T_s} b_i^{k}(t-\tau_k) C_k[j-1] C[v-1] \times Cos\left\{2\pi\left(f_{ij} - f_{uv}\right)t + \theta\right\} dt, \quad (9)$$

and finally, noise due to AWGN is expressed as

$$\eta_0 = \sum_{v=1}^{N_p} M_{uv} \int_0^{T_s} C[v-1] n(t) Cos\left(2\pi f_{uv} t + \varphi_{uv}\right) dt \quad (10)$$

4. Interference Analysis

The analysis of the interference caused by the other users to the desired one is carried out using Gaussian approximation technique. This method is used for determining the bit error rate of the multiple access communication system depending on decision statistic [12]. The interfering components to the desired one are assumed to be zero mean Gaussian random variables. Similarly, AWGN is a Gaussian random process and is a zero mean Gaussian random variable [13].

4.1 *Noise Analysis*

The noise engendered by AWGN is described by (10). Hence, this noise term is assumed to be Gaussian random variable with zero mean and variance[13]

$$Var[\eta_0] = \sum_{v=1}^{N_p} \frac{\alpha_{uv}^2 N_0}{2E_b}, \quad (11)$$

where E_b is the energy per bit.

4.2 *Multiple* Access *Interference (I_1)*

This multiple access interference (MAI) is caused by the subcarrier having the same frequency. Then, it is assumed to be Gaussian random variable with zero mean and variance[14]

$$Var[I_1'] = \frac{\alpha_{uv}^2}{3}, \quad (12)$$

where

$$I_1^{'} = \sqrt{\frac{P}{2N_p}}\alpha_{uv}^k M_{uv} Cos\,\theta \int_0^{T_s} b_i^k (t-\tau_k) C_k[v-1] C[v-1] dt$$

4.3 *Multiple* Access *Interference (I_2)*

Similarly, this MAI imposed by user k on desired one is contributed by the other subcarrier signal associated with $i=u$ and $j\neq v$ and is modelled by Gaussian random variables of zero mean and variance [14]

$$Var\left[I_2^{'}\right] = \frac{\alpha_{uv}^2}{2\pi[(i-u)+(j-v)q]^2}, \quad (13)$$

where

$$I_2^{'} = \sqrt{\frac{P}{2N_p}} \frac{\alpha_{ij}^k M_{uv}}{T_s} \int_0^{T_s} b_i^k (t-\tau_k) C_k[j-1] C[v-1] Cos\{2\pi(f_{ij}-f_{uv})t+\theta\} dt$$

Therefore, the decision variable is given by[8]

$$Z_u = \sqrt{\frac{P}{2N_p}} T_s \sum_{v=1}^{N_p} \left[D_{uv} + \sum_{k=2}^{K} I_1^{'} + \sum_{k=2}^{K}\sum_{i=1}^{q}\sum_{j=1}^{N_p} I_2^{'} + \eta_0 \right] \quad (14)$$

The mean of the decision variable is

$$E[Z_u] = b_u[0] \sum_{v=1}^{N_p} \alpha_{uv} M_{uv}, \quad (15)$$

and the variance is[14]

$$\sigma^2 = \left[\frac{N_p N_0}{2E_b} + \frac{K-1}{3} + (K-1)(N_p-1) q I_m \right] \sum_{v=1}^{N_p} \alpha_{uv}^2, \quad (16)$$

where $I_m = \frac{1}{qN_p} \sum_{u=1}^{q} \sum_{v=1}^{N_p} I(u,v)$ and

$$I(u,v) = \frac{1}{q(N_p-1)} \sum_{i=1}^{q} \sum_{j=1}^{N_p} \left\{ \frac{1}{2\pi^2[(i-u)+(j-v)q]^2} \right\}$$

Hence, if the maximal ratio combining is employed, i.e., $\alpha_{uv}=M_{uv}$, then the signal to interference noise ratio (SINR) is given by

$$SINR = \frac{\bar{\gamma}\left(\sum_{v=1}^{N_p} \alpha_{uv}^2 \right)^2}{\sum_{v=1}^{N_p} M_{uv}^2} = \bar{\gamma} \sum_{v=1}^{N_p} \alpha_v^2, \quad (17)$$

where

$$\bar{\gamma} = \left[\frac{N_p N_0}{2E_b} + \left(\frac{K-1}{3} \right) + (K-1)(N_p-1) q I_m \right]^{-1}$$

Therefore, the instantaneous signal to interference noise ratio is given by

$\gamma = \bar{\gamma} \sum_{v=1}^{N_p} \alpha_v^2$. Then, the fading envelope α can be modelled as generalized κ-μ distribution random variable and assuming multipath intensity profile (MIP) to be uniformly distributed for the MC-CDMA scheme. Therefore, $\sum_{v=1}^{N_p} \alpha_v^2$ obeys non-central Chi-square distribution with $2N_p$ degrees of freedom. The pdf of the instantaneous SINR is expressed as [11]

$$f(\gamma) = \frac{\mu N_p (1+\kappa)^{\frac{\mu N_p+1}{2}}}{\kappa^{\frac{\mu N_p-1}{2}} \exp(\mu N_p \kappa) \bar{\gamma}^{\frac{\mu N_p+1}{2}}} \gamma^{\frac{\mu N_p-1}{2}} \exp\left(-\frac{\mu(1+\kappa)}{\bar{\gamma}} \gamma \right) \times I_{\mu N_p-1}\left(2\mu \sqrt{\frac{N_p \kappa (1+\kappa)}{\bar{\gamma}} \gamma} \right) \quad (18)$$

5. Bit Error Rate Analysis

Since the transmitted signal is coherently modulated using binary phase shift keying (BPSK) , then, the conditional probability of error is given by [15] ,[16]

$$P_b = Q\left(\sqrt{2\gamma}\right) = \frac{\Gamma(0.5,\gamma)}{2\sqrt{\pi}}, \quad (19)$$

where Q(.) is Gaussian Q-function and Γ(.) is gamma function.

Hence, the unconditional probability of error is given by [15]

$$P_b(E) = \int_0^{\infty} Q\left(\sqrt{2\gamma}\right) f(\gamma) d\gamma \quad (20)$$

Equation (18) is expressed in series form of modified Bessel function [11] as

$$f(\gamma) = \frac{1}{\exp(\mu\kappa N_p)} \sum_{j=0}^{\infty} \frac{(\kappa N_p)^j (1+\kappa)^{\mu N_p+j} \mu^{\mu N_p+j}}{\bar{\gamma}^{\mu N_p+j} j! \Gamma(\mu N_p+j)} \times \gamma^{\mu N_p+j-1} \exp(-\beta\gamma) \quad (21)$$

This series converges for all values of γ except for $\gamma=0$. Therefore, the average error probability is given by [16]

$$P_b(E) = \frac{1}{\exp(\mu\kappa N_p)} \sum_{j=0}^{\infty} \frac{(\kappa N_p)^j (1+\kappa)^{\mu N_p+j} \mu^{\mu N_p+2j}}{\bar{\gamma}^{\mu N_p+j} j! \Gamma(\mu N_p+j)} \times \frac{\Gamma(\mu N_p+j+0.5)}{(\mu N_p+j)(1+\beta)^{\mu N_p+j+0.5}} {}_2F_1\left(1, \mu N_p+j+0.5; \mu N_p+j+1; \frac{\beta}{1+\beta}\right), \quad (22)$$

Where $\beta = \frac{\mu(1+\kappa)}{\bar{\gamma}}$ and ${}_2F_1(.)$ denotes Gauss hypergeometric function.

6. Numerical Results And Discussion

The graphs illustrated below show the BER performance analysis of MC-CDMA system over generalized κ-μ fading channels using (22). In this case, the number of iterations employed in the series evaluation which yields better results is 20 times.

Fig. 1 illustrates average BER versus SNR, then we observe that the average BER increases as the number of users increases. Hence, the performance of the system degrades. Similarly, in fig. 2, μ=2 is fixed while κ varies, the average BER decreases as κ increases, hence, the system performance improves. On the other hand, κ is set constant and μ is varied, the performance of the system improves as depicted in fig. 3.

As shown in fig. 4, we observe that, the average BER decreases as the SNR increases and increases as the number of users increase as well. Therefore, the performance of the systems improves as SNR increases and degrades as the number of users increase.

Fig. 5 depicts average BER versus the number of subcarriers. We observe that the BER decreases as the number of the subcarriers increase and increases as the number of users increase. Similarly, fig. 6 shows the BER versus the number of users, hence, the BER decreases when the number of users reduces and increases when the number of users increase as well.

7. CONCLUSION

The BER performance analysis for MC-CDMA system over frequency selective generalized κ-μ fading channels has been investigated. We analysed the multiuser interference using Gaussian approximation technique. The average bit error probability is derived and expressed in Gauss hypergeometric function. We observed that the performance of the system improves when SNR increases. Similarly, improvement in the system performance was obtained when the number of subcarriers is increased. We also deduced that the sytem performance enhancement is obtained when either of the parameters κ or μ is constant and the other varies. Generally, the application of the maximal ratio combining diversity technique has made the performance of the multicarrier system better. Finally, the degradation in system performance occurs when the number of users increase. This is due to the overlop of the transmitted signal spectra.

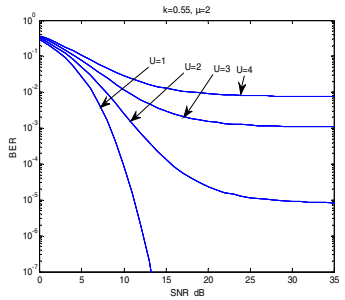


Fig. 1. MC-CDMA system performance over generalized κ-μ fading channels (μ=2, κ=0.55)

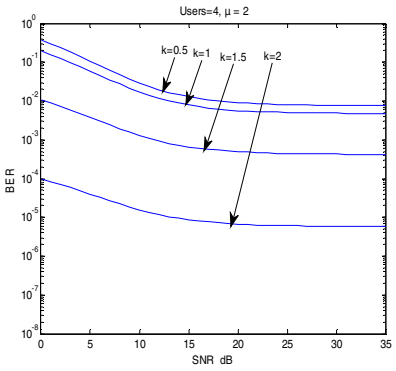


Fig. 2. BER performance for MC-CDMA system with constant μ and varying κ (Users=4, μ=2, κ=0.5,1,1.5,2)

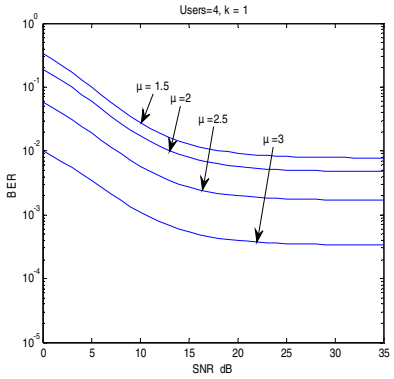


Fig. 3. BER performance for MC-CDMA system with constant κ and varying μ (Users=2, κ=1, μ=1.5,2,2.5,3)

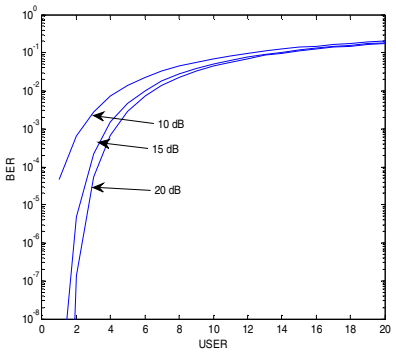


Fig. 4. Effect of signal power on MC-CDMA system performance over generalized κ-μ fading channels.

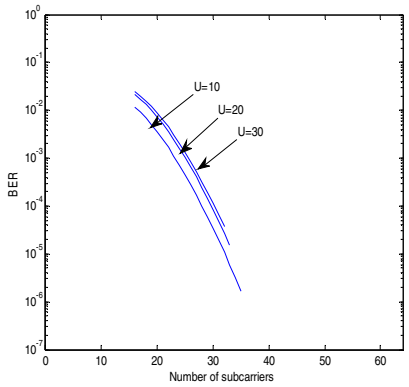


Fig. 5. Effect of active users on MC-CDMA system performance over generalized κ-μ fading channels.

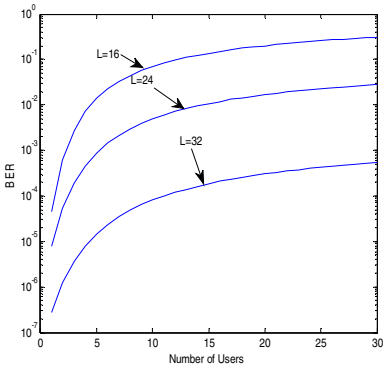


Fig. 6. Impact of subcarriers on performance of MC-CDMA system over generalized κ-μ fading channels.

ACKNOWLEDGMENTS

The authors would like to recognize and express thankfulness to PETRONAS for financial support.

REFERENCES

[1] Shinsuke Hara and Ramjee Prasad, "Overview of Multicarrier CDMA," in *Proc. IEEE 4 th Int. Symp. Spread Spectrum Techniques and Applications*, Mainz, Sept. 22-25, 1996, pp. 107-114.

[2] N. Yee, J. P. Linnartz and G. Fettweis, " Multicarrier CDMA in indoor Wireless Radio Networks," *Proc. Of IEEE PIMRC'93*, Yokohama, Japan, pp.109-113. Sept. 1993.

[3] Xiang Gui and Tung Sang Ng, "Performance of Asynchronous Orthogonal Multicarrier CDMA System in Frequency Selective Fading Channel,"*IEEE Trans. Commun*., vol. 47, NO. 7, pp. 1084-1091, July 1999.

[4] Mingqi Li, Qicong Peng and Yubai Li, " Performance Analysis of Multicarrier CDMA Systems in Multipath Fading Channels," *IEEE International Conf. on Commun*., vol 1, pp. 303-307, 2002.

[5] Hassan M. Elkamchouchi and Ahmed M. Medra, "Efficient Receiver Design for Frame Based MC-CDMA in Multipath Nakagami-*m* Fading Channels," *26 th National Radio Science Conference(NRSC2009)* March 17-19, 2009.

[6] Essam Sourour and Masao Nakagawa, "Performance of Orthogonal Multi-Carrier CDMA in a Multipath Fading Channel,"IEEE Trans. Commun., vol. 44(3) pp. 356-367, March 1996.

[7] Md. Rezaul Haque Khan, Md. Akbar Hossain, AHM Razibul Islam and Ju Bin Song, " SINR Performance of Multicarrier CDMA system in Frequency Selective Rayleigh Fading Channels,"International Conference on inf. And Commun. Tech., Dhaka, Bangladesh,7-9 th March 2007

[8] Lie-Liang Yang, *Multicarrier Communications*, John Wiley & Sons Ltd., 2009.

[9] Besma Smida, Lajos Hanzo and Sofiene Affes, " Exact BER Performance of Asnchronous MC-DS-CDMA over Fading Channels," *IEEE Trans. Wireless Commun*., vol. 9. NO. 4, pp.1249-1254, April 2010.

[10] Michel Daoud Yacoub, "The *K*-μ distribution and the η-μ distribution," *IEEE Antennas and Propagation Magazine,* Vol. 49, No. 1, pp.68-81, Feburary 2007.

[11] D. B. da Costa and M. D. Yacoub, " Moment Generating Functions of Generalized Fading Distribution and Applications," *IEEE Communnications Letters*, Vol. 12, No. 2, pp.112-114, Feburary 2008.

[12] Michael B. Pursley, " Performance Evaluation for Phase-Coded Spectrum Multiple-Access Communication-Part I: System Analysis," *IEEE Trans. Commun*., vol. Com-25, NO.8, pp.795-799, August 1977.

[13] Joseph C. Liberti and Theodore S. Rappaport, *Smart Antennas for Wireless Communications IS-95 and Third Generation CDMA applications*, Prentice Hall PTR, 1999..

[14] Lajos Hanzo, Lie-Liang Yang, E-L Kuan and K. Yen, *Single- and Multicarrier DS-CDMA Multiuser detection, Space-Time Spreading, Synchronization and Standard*., John Wiley & Sons Ltd. 2003.

[15] Marvin K. Simon and Mohamed-Slim Alouini, *Digital Communication over Fading Channels*, 2 nd Edition, John Wiley & Sons Ltd, Newjersey, 2005.

[16] I. S. Gradshteyn and I. M. Ryzhik, *Table of Integrals, Series and Products*, Fourth Edition, New York, Academic Press, 1965.

The Application of FSP Models in Software Performance Engineering: A Multi-Threaded Case-Study

Omid Bushehrian[1], Hassan Ghaedi[2]
Department of Computer and IT, Shiraz University of Technology, Shiraz, Iran
[1]bushehrian@sutech.ac.ir, [2]H_ghaedi@yahoo.com

***Abstract*— Detecting and fixing the performance obstacles of software during the early stages of software development process is the main objective of Software Performance Engineering(SPE) activities. SPE is mostly depended on the formal modeling languages due to the fact that these languages enable us to simulate the software and analyze the performance parameters. Various modeling languages such as queuing networks(QN), layered queues (LQ), Petri Nets and Stochastic Process Algebras are suggested for modeling distributed systems. There are several issues that are needed to be addressed when translating software architectural models to a target formal model, which are synchronous and asynchronous invocations, active and reactive objects, multi-threading, object deployment over computational nodes and process (thread) scheduling for resource utilization.**

In this paper, first we present a one-to-one translation rule set that is used to translate software Sequence and Deployment Diagrams into their corresponding FSP(Finite State Process) model considering the above mentioned issues. The resulting model then is analyzed through discrete event simulation tools such as LTSA from the performance perspective. Second, we have applied our translation rule set on a real world multi-threaded web application to obtain its FSP model. The simulation results are also presented.

I. INTRODUCTION

The performance of a distributed software system has always been of critical importance to the designers of such systems. Software Performance Engineering (SPE) aims at detecting and predicting performance problems at the early stages of development process by evaluating the software design or deployment using simulation, modeling or measurement [1]. There has been many works in automatic generation of performance models from software architectural models and then analyzing these generated performance models to locate the performance problems [2][3]. In order to solve these performance problems at design level, one approach is to manually optimize design decisions represented in performance models [4]. Automated techniques for optimizing the distributed software design or deployment with respect to performance have also been researched much so far [5][6]. One of the important factors affecting the performance of a distributed software is the way that software objects or components are assigned to the computing resources. For instance, deploying certain objects on the same computing node eliminates the network delay caused by message passing. Co-locating objects and resources they may need such as files, devices or special network links can also reduce the network delay. Furthermore, careful assignment of object replicas can lower the overall network delay caused by remote access to those replicas from other objects [6].

SPE activities are mostly relying on the formal modeling languages. Particular ability of a model is the prediction and estimation of non-functional characteristic of one system, before it has been made. Nowadays, the various types of analyzable formal models are used for modeling a distributed system, including queuing networks, layered queues, Petri Nets and Finite State Process (FSP) [8][9]. FSP's, are abstract machines used to model the behavior of concurrent and distributed systems [11]. Each process of distributed system can be modeled by a FSP that perform sequence of actions repeatedly. A distributed system is a collection of such processes that some of their actions are synchronized with each other [8][9].

The main problem is to find a method by which we can easily transform software models such as deployment and sequence diagrams into simulate able models in architectural level.

Current methods in performance modeling and evaluation haven't presented an exact and complete algorithm for the transformation of UML models into simulate-able models. These methods have only sufficed at examples of how transformation can be preformed. Specifically, in the previous methods, the communication model of objects(synchronous or asynchronous), object types(active or reactive), creation of threads, scheduling of threads on nodes and deployment of the objects haven't been considered when transforming a UML model into its corresponding formal model. To overcome these shortcomings in this article an algorithm for automatic transformation of software deployment and sequence diagrams into FSP [11] as a simulate-able model is presented, So that by simulating the resulting FSP model different performance factors such as response times, length of queues, objects

population can be measured. To achieve this, we use UML sequence diagrams that are annotated with SPT profile[10]. As shown in Figure 1 in this profile, performance tags can be augmented to sequence diagrams which explain the performance aspects of the modeled software.

II. RELATED WORKS

There are many researchers in the field of transforming architectural software models such as use-case models, sequence diagrams and deployment diagrams to analyzable formal models. Mainly queuing and Petri nets are used in this direction [12][13][14][15][16]. In [15] and [16] an algorithm is presented for automatic transformation of software architectural models into Petri net models for performance analysis. Queuing networks are another approach for modeling. In [12] automatic algorithms are presented for transforming architectural models into queuing models for various performing analysis. In [8] and [9] FSP models are used as destination model in transforming software architecture models.

In summary we can say that in presented algorithms in previous researches for transforming UML models to Petri and queuing models, following shortcomings are observed: (1) Deployment diagrams that are particularly important in distributed software are not considered. (2) In the previous methods, the issues such as communication models of objects (synchronous or asynchronous), object types (active or reactive), creation of threads, scheduling of threads on nodes and the deployment of the objects haven't been considered when transforming a UML model into its corresponding formal model. In this article by selecting FSP model as the destination model of the transformation, a 1-to-1 transformation algorithm is presented for transforming deployment and sequence diagrams to FSP's.

III. FINITE STATE PROCESS

FSP's, are abstract machines used to model the behavior of concurrent and distributed systems [11]. Each process of distributed system can be modeled by a FSP that perform sequence of actions repeatedly. A distributed system, is a collection of such processes that some of their actions are synchronized with each other[8][9]. For transforming sequence and deployment diagrams to FSP's, we must transform objects, threads, CPU's and communication links to FSP's. Each FSP is indeed an automata with several states that transits between states[11].

A simple sequence diagram that is annotated with SPT profile for performance, is illustrated in Figure 1. SPT profile introduces a large set of stereotypes for annotating UML models with performance information.

The annotation on the lifeline of the user object has a <<PAopenLoad>> stereotype indicating that it is a input workload with a specific intensity of the input requests made on the system by the users of the scenario. Here, the interval between requests is exponentially distributed with a mean of 40 ms. The <<PAstep>> stereotype is used to specify the amount of time (and its distribution) required for completing an operation on an object. For example the client object offers a *prepareResults()* operation whose completion time follows an exponentially distribution with 20 ms as the mean value.

The translation scheme generates an FSP process for each object specified in the sequence diagram. The order of operations shown on the timeline of each object is used to determine the events in each state of an FSP process. The sequence of messages specified in the sequence diagram for each object are translated to the actions in the FSP, e.g. *request*, *delegate* and *do*. The open arrowhead on the request message in Figure 1 implies that several users may be requesting the client object at the same time and hence that there is an implicit queue (of undefined capacity) at this object[8][9].

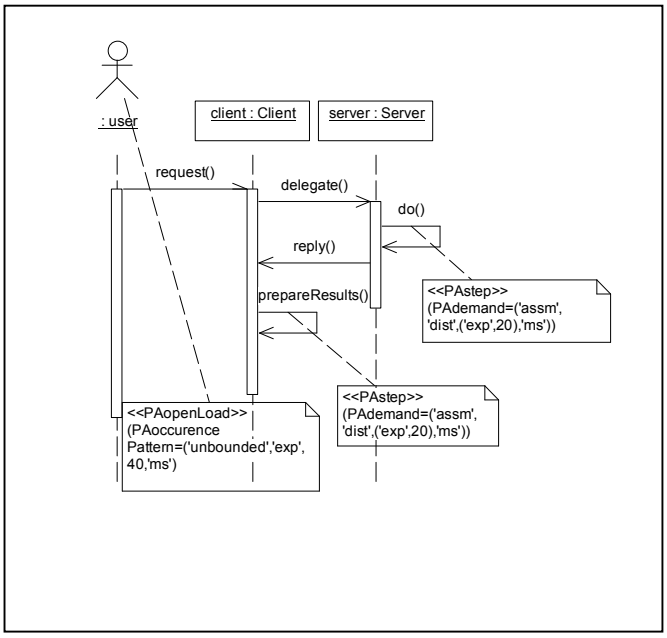


Fig. 1. Sample sequence diagram annotated with performance information according to SPT profile

The examples of transformation of an SPT annotated sequence diagram into FSP model is presented in [8][9]. The resulting FSP model then is used to simulate the corresponding use-case with an arbitrary input workload. The simulation is performed with a discrete event simulator tool such as LTSA [7][11].

IV. TRANSLATION RULES

In order to translate sequence and deployment diagrams corresponding to use-case scenarios, each object within the sequence diagrams should be translated to an FSP process. For multithreaded objects, a predefined number of instances of the FSP process should be created. Furthermore, According to the object type (active or reactive) the translation rule is different. Moreover, for each object, all incoming and out-going messages are analyzed to determine their types(Asynchronous or Synchronous) and translated accordingly.

Corresponding to each node within the deployment diagram an FSP process is created. The number of instances of this process is determined according to the number of CPU's installed on the node. The translation rules should synchronize

the threads and CPU's in the FSP model such that the maximum utilization is achieved during the simulation (no CPU is idle while threads are blocked due to the lack of CPU). The structure of the translation algorithm is shown in Figure 2.

```
Algorithm FSPmodel UMLtoFSP(model m)
  Begin
    FSPmodel f=create FSPmodel();
    For each SequenceDiagram sd in m
      For each object o in sd
        f.AddObject(o);
    For each DeploymentDiagram d in m
      For each Node n in d
        f.AddNode(n);
      For each Link l in d
        f.AddLink(l);
    f.Synchronize(m),
end
```

Fig. 2. Transformation Algorithm

A. Definitions

Sets O,L,M and C denote the set of objects, the set of links, the set of messages and the set of CPU's respectively. Each object *o* in O is specified by following multiplex that consists of name, type, node, first message, last message and the set of sent and received message by *o* respectively:

o:(Name, Type, Node, FirstMessage, LastMessage, MessageSet)

Each message *m* in M is specified by following multiplex that consists of name, sender object, receiver object, communication delay at the sender side, computational delay at the receiver side and message index respectively:

m:(Name,Sender,Receiver,Type,ComunicationDelay, ComputationalDelay,Index)

Each link l in L is specified by following multiplex that consist of two various nodes:

l(N,M)

Each node *n* in N is specified by a node name and the number of CPU's installed on it.

n(Name,Number)

In the subsequent subsections, the transformation algorithm body shown in Fig.3 will be explained. Note that each function within the algorithm body generates a set of FSP codes and augments them to the final FSP model. *Emit()* method is used for this purpose.

B. Translation Objects to FSP's

For each object, if it is a thread or reactive one then we need a Thread-Pool and if it is an active object, we need a queue. For generating the FSP'code corresponding to an object like o, the sent and received messages by o, represented in the corresponding sequence diagram, are examined consecutively. Each message *m* can be described by an ordered pair *<messageType, messageDirection>* in which *messageType* can be synchronous(denoted by S), asynchronous (denoted by A) or return message(denoted by R) and *messageDirection* can be out-going (denoted by G) or incoming (denoted by I) . If *m* is an out-going message network link is acquired and if *m* is an incoming message CPU is acquired. The body of each object o is formed as a sequence of actions each corresponding to an out-going or incoming message. The getStatus() function in the following code returns the ordered pair *<messageType, messageDirection>* for each message m and object o:

```
// Object Body Transformation
  For each m in o.MessageSet
  Emit( «o.Name»=(
    switch( getStatus(m.Type,o) )
    case (S,I):
     Emit( «m.Name»->«o.Name»acquirecpu-> )
     case (R,I):
     Emit( «m.Name»->«o.Name»acquirecpu-> )
    case (S,G):
     Emit( «o.Name»acquirelink ->«m.Name»-> )
    case (R,G):
     Emit( «o.Name»acquirelink ->«m.Name»-> )
    case (A,G):
     Emit( «o.Name»acquirelink->«m.Name»-> Other[index],
    Other[index]=(otherwork[index]->Other[index]| )
    case (A,I):
    Emit( «m.Name»->«o.Name»acquirecpu->Other[index],
    Other[index]=(otherwork[index]->Other[index]| )
    Else Emit( «m.Name»->«o.Name»acquirecpu )
    Emit( «o.Name»). )
```

C. System Composition

The following algorithm is used to compose all the previously generated processes. These processes include links, nodes, objects and queues. For objects with more than one replica or thread, a set of FSP processes is generated:

```
For all Links l in L
  Emit(Link«l.n»to«l.m»||)
For all nodes n in N
  Emit( [1.. «n.number»]:Cpu«n.Name»||)
For all Queues
  Emit(Queue«o.Name»||)
For all objects o in O
  Emit( [T]: «o.Name»||)
```

Variable T represents the number of object replicas corresponding to an active or re-active object. For synchronizing two FSP's P1 and P2 on action m1 and m2, where there are T replicas or threads available for P2 the action synchronization code is generated as follows:

```
Emit(/{[T].m2/m1,)
```

Corresponding to each message *m* sent by object S and received by object R, the receiver object R should acquire CPU to perform the computation of *m*. Therefore there should be synchronization between *getcpu* action of the corresponding CPU process and *acquirecpu* action of R which is placed before action *m*:

«o.Name»acquirecpu/[i]getcpu «n.Name»

In the above synchronization, *[i]getcpu«n.Name»* denotes the *getcpu* action corresponding to the i^{th} CPU process installed on node *n*. Node *n* is the node on which object *o* is deployed according to the deployment diagram. If a node n has more than one CPU installed on it, the allocation of CPUs to

objects deployed on *n* should be specified before generating the synchronization codes.

D. Thread Scheduling

For an object o deployed on Node *n* with T threads or replicas the code generation algorithm fairly divides the T threads among the number of CPU's *c* installed on *n*:

```
For each object o in O
    Emit(
     [0..T/c].«o.Name»acquirecpu/[1].getcpu«n.Name»,
    [(T/c)+1..2*T/c].«o.Name»acquirecpu/
    [2].getcpu«n.Name»,…
    [(c-1)/c*T+1..T].«o.Name»acquirecpu/
    [c]. getcpu«n.Name»
    )
```

The acquired CPU by an object *o* on receipt of message *m* should also be released after the completion of *m.* Therefore, the FSP corresponding to *o* should contain *a releasecpu* action which follows action m. Moreover, there should be synchronization between *releasecpu* action of the corresponding CPU process and *releasecpu* action of object o. The generated code is similar to the one for *getcpu* synchronization (see the above code).

The sender object of each remote message *m* should acquire the connecting link between the node on which the sender resides and the node on which the receiver resides before sending *m*. Therefore the *acquirelink* action of the sender process of *m* and the *getlink* action corresponding to link process should be synchronized

V. CASE STUDY: A MULTI-THREADED APPLICATION

This case-study is a real world web application used in ISP companies by which a customer can purchase an account for accessing Internet. This is a Multi-threaded application in which each customer transaction is handled by a separate thread. The main success scenario of the *Purchase-Account* use-case is as follows:

(1)The customer navigates to the purchase page. (2) The system shows available Internet packages. (3) The customer selects a package and confirms. (4) The system navigates to the bank payment page. (5) The customer pays the package price. (6) The system verifies the payment and creates an account in AAA software and submits the created account to the customer.

In this case study, not only the *purchase-account* requests to the web application is often high, but also the AAA software is very busy due to processing of many authentication requests from different Access Points inside the company network. The communication diagrams corresponding to the *purchase-account* and *Authenticate* use-cases are shown in Fig. 3. The computing nodes and their associated resources is also listed in Table I. For each computing node i, property C_i (in Table I) indicates the processing capacity of node i that is 100 unit for each processor installed on node i.

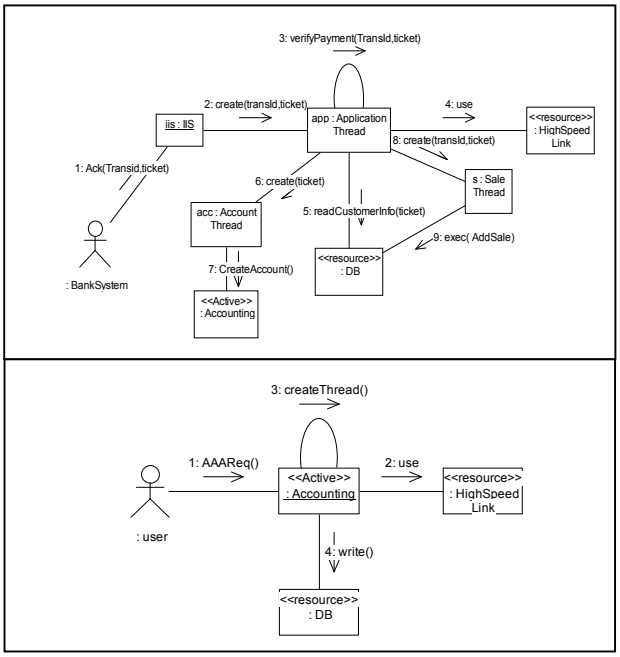


Fig. 3. *Purchase-Account* scenario (top), *Authenticate* scenario (bottom)

TABLE I
The computing nodes and their associated resources

	Properties	Associated Resources
Node1	C_1=200	High speed link to Internet
Node2	C_2=200	
Node3	C_3=200	
Node4	C_4=200	Sale and Accounting DB
Network Links	$B_{m,n}$=1000	

VI. DEPLOYMENT STRATEGY

Our observation showed that without correct deployment of this software over the available resources, many purchase requests to the application fails at step (6) (of the above scenario) due to the overloaded web application. Therefore it is essential to find the optimal deployment for this software over the available computing resources of the company in order to achieve the best performance. Note that objects with *<<resource>>* stereo-type represent system resources and have fixed location as listed in Table I. We have used the deployment algorithm proposed in [6] to find the optimal deployment of objects over the computational nodes. In [6], an ILP (Integer Linear Programming) algorithm for optimizing the deployment of software objects is proposed which evaluates each deployment in the search space, considering its *communicational* and *computational delays*. The former indicates the amount of delay resulted from remote communication of objects (assigned to different nodes) and the latter is defined as the delay resulted from sharing a node by several objects. The resulting deployment is shown in Fig. 4.

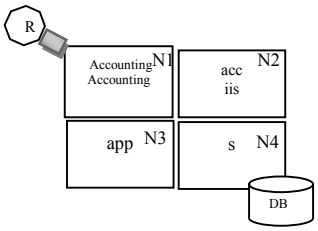


Fig. 4. *The optimal deployment of the case-study*

We translated the whole system to an FSP model using our translation algorithm. The performance attributes according to SPT convention for the case-study is presented in Table II and is used for translation. The number of threads in the system is assumed 50 in the translation process. We have simulated both scenarios as a single concurrent system using LTSA [7][11] to measure three metrics U_o, P_o and RT_i. U_o The utilization of object o, P_o is the average number of instances of active (or reactive) object o which are running simultaneously in the system. And RT_i is the mean response time of invocation I_i of an object. These values can be calculated easily by the LTSA tool after simulation. For calculating the response time of an object invocation like I_i, a variable of type *timer* should be defined in LTSA. For instance consider the simple sequence diagram in Fig. 5. The resulting FSP for this sequence diagram is as follows [8][9]:

a=(start→<?exp(1/20)?>do→end→a)

In order to measure the response time of invocation *start()* during the simulation in LTSA, variable *rt* of type *Timer* should be defined as follows:

Timer rt<start,end>

The above line of code tells LTSA to start a timer once the *start* action is fired and stop that once *end* action is fired. The resulting elapsed time between these two actions is kept in variable *rt* and the mean value of *rt* is reported by the LTSA at the end of simulation. Likewise, for measuring the metric U_a, a counter variable should be defined in LTSA as follows[8][9]:

Measure util <start,end>

The mean value of counter variable *util* during the simulation is reported by the LTSA as the utilization of object a.

After translating the *Purchase-Account* scenario to FSP model, it was simulated with an exponentially distributed input workload with four mean values: 500^{ms}, 1000^{ms}, 1500^{ms} and 2000^{ms} (which are the *interval between requests*). The input workload for the simulation of *Authenticate* scenario was also chosen exponentially with mean values: 200^{ms}.
The simulation results are presented in Table III for input workload 1000ms.

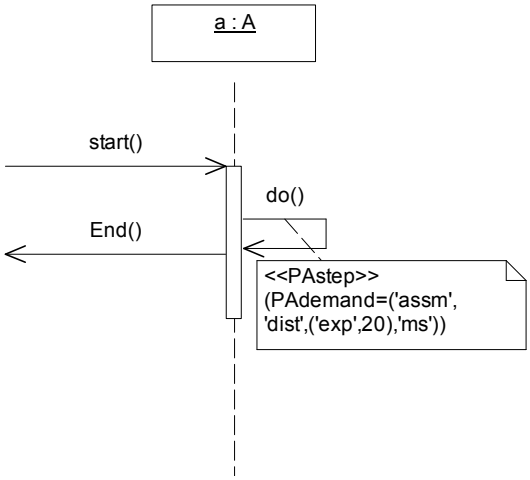


Fig. 5. *A simple sequence diagram*

TABLE II
The performance attributes according to SPT convention for the case-study

Message No.	Stereotype	Value
PurchaseAccount:1	OpenWorkLoad	occurencePattern=('unbounded','exp',$v,'ms')
PurchaseAccount:3	Pastep	PAdemand=('assm','dist',('exp',400),'ms')
PurchaseAccount:4	Pastep	PAdemand=('assm','dist',('exp',200),'ms')
PurchaseAccount:5	Pastep	PAdemand=('assm','dist',('exp',1000),'ms')
PurchaseAccount:7	Pastep	PAdemand=('assm','dist',('exp',1500),'ms')
PurchaseAccount:9	Pastep	PAdemand=('assm','dist',('exp',2000),'ms')
Authenticate:1	OpenWorkLoad	occurencePattern=('unbounded','exp',$v,'ms')
Authenticate:2	Pastep	PAdemand=('assm','dist',('exp',200),'ms')
Authenticate:3	Pastep	PAdemand=('assm','dist',('exp',40),'ms')
Authenticate:4	Pastep	PAdemand=('assm','dist',('exp',900),'ms')

TABLE III
The simulation data resulted from input workload=1000

Object	**Type**	**U_o**	**P_o**	**RT_i(ms)**
iis	Active	92%	-	3400
Accounting	Active	74%	-	1980
acc	Thread	0%	17	-
s	Thread	0%	16	-
App	Thread	24%	18	-
DB	Resource	100%	-	RT_5=1800RT_9=2900

VII. CONCLUSION AND FUTURE WORKS

In this paper a set of translation rules for converting the architectural models of a multithreaded application to simulate

able FSP models is presented. In previous researches for transforming UML models to analyzable formal models, Deployment diagrams that are particularly important in distributed software are not considered. In the previous methods, the issues such as communication models of objects (synchronous or asynchronous), object types (active or reactive), creation of threads, thread scheduling and deployment of objects haven't been considered when transforming a UML model into its corresponding formal model. We applied the translation rules on our case study (a multithreaded web-application) and measured factors that are important for performance. This case study has various characteristics such as synchronous and asynchronous calls, network communications (links), active and reactive objects. There are cases in distributed systems that their modeling is not possible by FSP's particularly when several replicas of a resource (like CPU) exist. Modeling resource scheduling algorithms is not possible by FSP's as well. For the future work, our objective is to extend FSP models to overcome these deficiencies.

REFRENCES

[1] M. Woodside, G. Franks, D. Petriu, "The Future of Software Performance Engineering", IEEE, 2007

[2] S. Balasmo, A. Dimarco, P. Inverardi, A. Simeoni, "Model-based performance prediction in software development", IEEE Trans. on Software Engineering, 30(1): 295-310, 2004

[3] S. Balsamo, M. Marzolla, "Performance evaluation of UML software architectures with multi-class queuing network models", Proc. 5th Int. workshop on Software and Performance (WOSP), ACM SIGSOFT ,2005

[4] A. Bennett, J. Field, "Performance engineering with the UML profile for schedulability, performance and time: a Case-Study", Proc. 12th annual Int. Symposium on Modeling, Analysis and Simulation of Computer and Telecommunication Systems, IEEE, 2004

[5] M. Bastarrica, R. Caballero, A. Demurjian, A. Shvartsman, "Two optimization techniques for component-based systems deployment", Proc. 13th Int. Conference on Software Eng. and Knowledge Eng., 2001

[6] B. Boone, F. Truck, B. Dhoedt, "Automated deployment of distributed software components with fault tolerance guarantees", Proc. 6th Int. Conference on Software Engineering Research, Management and Applications, IEEE, 2008

[7] T. Ayles, A.J. Field, J.N. Magee, "Adding performance evaluation to the LTSA tool", Proc. 13th Int. Conference on Computer Performance Evaluation: Modeling Techniques and Tools, LNCS 2794, 2003

[8] A. Bennett, A. J. Field, "Performance engineering with the UML profile for schedulability, performance and time: a Case-Study", Proc. 12th annual Int. Symposium on Modeling, Analysis and Simulation of Computer and Telecommunication Systems, IEEE, 2004

[9] A. Bennett, A.J. Field, M. Woodside, "Experimental Evaluation of the UML Profile for Schedulability, Performance and Time", LNCS 3273, 2004

[10] Object Management Group, UML profile for schedulability, performance and time specification, 2003

[11] J. Magee, J. Kramer, Concurrency:State Models and Java Programs, John Wiley and Sons, Chichester, England, 1999

[12] H. Youn, S. Jang, E. Lee, "Deriving Queuimg Network model for UML for software performance prediction", fifth Int. Conf. on Software Engineering Research, Management and Applications, IEEE, 2007

[13] V. Cortellessa, R. Mirandola, "Deriving a Queuing Network based performance model from UML diagrams" , ACM proc. Int. workshop on software and performance , 2000

[14] D. Petriu, M. Woodside, "Software performance models from system scenarios in Use-Case maps", Proceedings of the 12th International Conference on Computer Performance Evaluation, Modelling Techniques and Tools, Springer, London, 2002

[15] R. Pettit, H. Gomaa, "Modelling Behavioral design patterns of Concurrent Objects", Proceedings of the 28th international conference on Software engineering, 2006

[16] R. Pettit, H. Gomaa, "Analyzing behavior of concurrent software desgins for embeded systems", Proceedings of the 10th IEEE International Symposium on Object and Component-Oriented Real-Time Distributed Computing, 2007

Research and Implementation of ARINC653 Configuration Tool Based on AADL

Jianhua Xu
Southwest Jiaotong University
ChengDu, China
Email: xujh2011@163.com

Yun Li
University of Electronic Science and Technology of China
ChengDu, China
Email: dr_liyun@sina.com

Yang Meng
University of Electronic Science and Technology of China
ChengDu, China
Email: mengyang1005@126.com

***Abstract*—Applications must be integrated into a system configuration which satisfies all the requirements of applications in the ARINC653 system. The goal of this paper is to assist system integrator to generate correct configuration tables. Architecture Analysis and Design Language (AADL) is widely used in avionics systems modeling and analysis. In order to model and analyze avionics systems that meet the ARINC653 standard, we need to extend AADL existing standard to satisfy the requirements of ARINC653. This paper presents an approach to augment the modeling ability of AADL to describe ARINC653 configuration instance, details a modeling approach exploiting the new property sets of AADL for the design of ARINC653 architectures, and implement an automatic ARINC653 configuration tool based on AADL which generates the static configuration files that meet the qualification of ARINC653 schema for the instance model. The correct configurations generated by this tool verify the validity and feasibility of this method.**

***Keywords*—AADL; ARINC653; Property set; Configuration tables; Configuration instance; ARINC653 XML-Schema**

I. INTRODUCTION

ARINC653 [5] avionics standard is widely used in domain of avionics system. It defines an environment that allows full portability and reuse of application source code. Applications must however be integrated into a system configuration which satisfies the functional requirements of the applications and meets the availability and integrity requirements of the aircraft functions. The system inte-grator and the application developer are responsible to define the instance file for the configuration being integrated. XML is used to describe the configuration data. The XML instance should based on the ARINC653 XML-Schema format requirements. There are some universal business XML tools, however they are not intuitionistic and convenient for the users, and they did not provide functionalities such as data checking and data analysis.

The ARINC653 Configuration Tool based on AADL presented in this paper assist the system integrator and the application developer to generate system configurations and manage the configuration data, and furthermore it can analysis the non-functional attributes of the system such as reliability, availability, timing, security etc.

The Architecture Analysis and Design Language (AADL) [3] which based on MDE propose a component-based approach that fits with safety-critical systems needs. It is composed of several specialized hardware and software components that can be extended or refined to model safety-critical architectures with their requirements and properties. It is not only fit for modeling embedded real-time system, but also can describe the important performance-critical aspects such as timing requirements, fault and error behaviors, time and space partitioning, and safety and certification properties. Such description allows a system designer to perform analyses of the composed components and systems such as system schedulability, sizing analysis, and safety analysis.

In this paper, we present an approach for modeling a configuration instance of ARINC653 systems using AADL. We describe the modeling guidelines we elaborated in the extended property set of the AADL standard for the design and analysis of ARINC653 architectures. The goal of the ARINC653 configuration tool is to transform the AADL instance to XML instance file according to the ARINC653 XML-Schema and validate the integrality, validity of the configuration file. This paper details the implementation of ARINC653 configuration tool and the process of generating and verifying.

The paper is structured as follow. We first present the ARINC653 standard in Section 2 and the AADL in Section 3. Then, we detail the mapping relationship between ARINC653 configuration attributes and AADL component properties, and introduce the contents of the extended AADL property sets for the specific ARINC653 architectures in Section 4. Section 5 details the implement procedure of the configuration tool. Section 6 uses a case-study to illustrate the tool, validate the validity of this tool by generate correct static configuration file for an ARINC653 model. The section 7 presents the related work and the section 8 summarizes present works and makes a plan for latter works.

II. A RINC653

This section gives an overview of the ARINC653 standard. ARINC653 [4] is an industrial standard that defines a set of functions for the design of safety-critical avionics systems.

The standard is focused on safety-criticality, by partitioning applications. ARINC653 proposes the concept of partitioning and the Healthy Monitor mechanism.

Next subsections detail ARINC653 core functions.

A. Partitioning Management

Central to the ARINC653 philosophy is the concept of partitioning. One purpose of a core module in an IMA system is to support one or more avionics applications and allow independent execution of those applications. This can be correctly achieved if the system provides partitioning. The unit of partitioning is called a partition. A partition is therefore a program unit of the application designed to satisfy these partitioning constraints. Each partition is isolated in terms of time (temporal partitioning) and space (memory partitioning) and runs as if it was executed on a single processor. A robustly partitioned system allows partitions with different criticality levels to execute in the same core module, without affecting one another space or time.

The isolation is performed at two levels: time and space.

（1）Time partitioning

Time partitioning implies that each partition has a fixed timeframe for its execution.

In the ARINC653, Partitions are scheduled on a fixed, cyclic basis. To assist this cyclic activation, the core module system maintains a major time frame of fixed duration, which is periodically repeated throughout the module's runtime operation. Partitions are activated by allocating one or more partition windows within this major time frame, each partition window being defined by its offset from the start of the major time frame and expected duration. This provides a deterministic scheduling methodology whereby the partitions are furnished with a predetermined amount of time to access processor resources. Time partitioning therefore ensures each partition uninterrupted access to common resources during their assigned time periods.

The partition windows of ARINC653 are illustrated in Fig.1.

（2）Space partitioning

Space partitioning means that each partition has a dedicated address space to store its code and data and that communications between partitions are supervised by the module. Each partition has predetermined areas of memory allocated to it. These unique memory spaces are identified based upon the requirements of the individual partitions, and vary in size and access rights. At most, one partition only has write access to any particular area of memory. Memory partitioning is ensured by prohibiting memory accesses outside of a partition's defined memory areas.

B. Health Monitor

In ARINC653, the Health Monitor (HM) is the function of the O/S responsible for monitoring and reporting hardware, application and O/S software faults and failures. HM uses three health-monitor tables, namely System HM table, Module HM table and Partition HM table to handle occurring errors. The System HM table defines the level of an error (Module, Partition, and Process) according to the detected error and the state of the system (module init, system function execution, partition init, etc). The Module HM table defines the recovery action (e.g., shut down the module, reset the module) associated with the detected error for each module level error. The Partition HM table defines the recovery action (e.g., stop the partition, restart the partition in warm or cold mode) associated with the detected error for each partition level error. Each partition has a separate table.

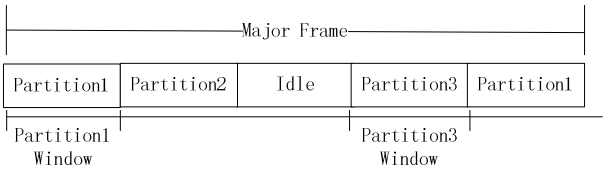


Figure.1 Time Partitioning
There are 3 partitions in the module.
Each partition has a static time slot in the major frame.

C. Configuration tables

The goal of modularize-system development is to integrate various application and system kernel code effectively. Each application should access to its required resources when executing on the module.

The system integrator is responsible for allocating partitions to core modules. The resulting configuration should allow each partition access to its required resources and should ensure that each application's availability and integrity requirements are satisfied. Hence the system integrator should therefore know the timing requirements, memory usage requirements and external interface requirements of each partition to be integrated. It is the responsibility of the application developer to configure the processes within a partition.

Configuration tables are required by the ARINC653 for ensuring that the system is complete during initialization and to enable communications between partitions. Configuration tables are static data areas accessed by the O/S. Verifying the information provided by the configuration tables before implementation make it is possible for system integrator to find out configuration errors as early as possible, and enhance the veracity and efficiency of system integration.

D. ARINC653 XML-Schema

ARINC653 standard defines the mechanism for specifying configuration data, in a standard format, that does not depend on the implementation of the ARINC 653 OS. This provides an intermediate form of the configuration definition that allows the systems integrator to create configuration specifications in a form that can be readily converted into an implementation specific configuration.

The ARINC 653 XML-Schema defines the structure of the data needed to specify any ARINC 653 configuration. The XML-Schema is the reference standard to which instance files are defined. The XML-Schema consists of tagged pairs that describe the attributes and their relationship to the whole. And the detailed content and structure of XML-Schema are shown in section 4.

III. AADL

This section details the AADL language.

AADL is a standard published by the Society of Automotive Engineers (SAE). It defines a component-centric language which allows the modeling of both software and hardware components. It focuses on the definition of block interfaces, and separates the imple-

mentations from these interfaces. The standard proposes both graphical and textual representation of the syntax.

An AADL description is made of components. The AADL standard defines software components (data, thread, thread group, subprogram, and process), execution platform components (memory, bus, processor, device, virtual processor, and virtual bus) and hybrid components (system).

AADL allows properties to be associated with AADL model elements. Properties are typed and represent name/value pairs that represent characteristics and constraints. The standard includes a pre-declared set of properties and users can introduce additional properties through property definition declarations.

The AADL version 1 is not amenable to represent some specific architectures of ARINC653, AADL provides two methods to extend its modeling ability: user-defined property sets and annex library. This paper presents an approach that defines extended property sets to augment AADL modeling ability. The details mapping rules between ARINC653 and AADL and new defined property set are presents in later section.

IV. MODELING ARINC653 ARCHITECTURES WITH THE AADL

This section details the direct mapping rule of AADL to ARINC653. And according to the ARINC653 XML-Schema, we extend a new AADL property set named ARINC653 that including all the required properties.

A. The concrete mapping rules

Refer to the AADL to ARINC653 [3] and the requirements of ARINC653 XML-Schema, we use the mapping rules.

(1) An ARINC653 Process is represented by means of a thread component in AADL.

(2) An ARINC653 Partition is represented by means of a process component in AADL.

(3) An ARINC653 Sampling port is represented by means of a data port in AADL.

(4) An ARINC653 Queuing port is represented by means of a data event port in AADL.

(5) An ARINC653 Channel is represented by means of a connection in AADL.

(6) ARINC653 Memory requirements is represented by means of a memory component in AADL.

B. ARINC653 XML-Schema Element Relationships

The XML-Schema is the reference standard to which instance files are defined. The XML-Schema defines the structure of the data. The XML-Schema consists of tagged pairs that describe the attributes and their relationship to the whole.

The ARINC 653 XML-Schema has been constructed based on Fig.2. The square boxes represent the schema elements and the attributes are represented by the text inside the box. This diagram represents the major elements and their attributes. The figure shows the major element relationships used to define the ARINC 653 XML-Schema.

The complete details of the schema and the details of the relationship between elements of schema are found in the detailed schema definition (Appendix G and H of

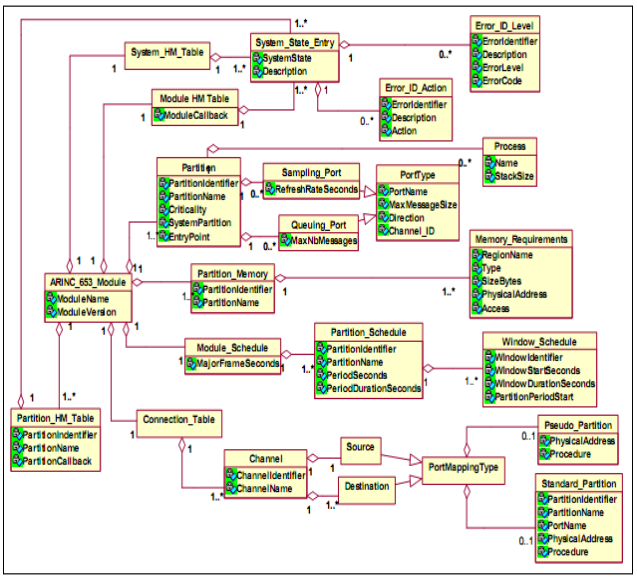


Figure.2 XML Schema Element Relationships

ARINC653 standard). Due to limited space, these are not detailed in this paper. In next subsection, we extended the property set based on the ARINC653 XML-Schema.

C. Extended AADL property set for ARINC653

According to the mapping rules between AADL components and ARINC653 architecture, and the specific definition of ARINC653 XML-Schema , the final property set include 5 major parts.

- **Partitions:**

  In this part, there are 6 attributes need to be defined:

  Partition_Identifier—the serial number of partition.

  Partition_Name—the name of partition.

  IsSystem_Patition—denotes whether this partition is a sys-tem partition.

  PartitionType—denotes whether this partition is a standard partition or a pseudo one.

  Criticality—denote the criticality of the partition.

  EntryPoint—the entry point.

- **HM tables**

  In this part, there are ten attributes need to be defined:

  System_State_Id—denotes the system state identifier.

  System_State_Entry—describes the system state.

  HM_Errors_Id—denotes the error identifier.

  HM_Errors_Description—describes the occurring errors.

  HM_Errors_Level—defines the risk level of current errors, include 3 levels: module level, partition level, process level.

  HM_Errors_code—the module is in the "process execution" system state, when a process level error occurs, the description will be get by the system.

  Module_HM_Action—defines the actions to be taken when a module level error occurs.

  Partition_HM_Action—defines the actions to be taken when a partition level error occurs.

  Module_HM_Callback—the entry address of Module call-back function.

Partition_HM_Callback—the entry address of Partition call-back function.

- **Schedule Table**

In this part, there are 9 attributes need to be defined:

Module_Major_Frame—define the major frame length,it is the ARINC653 specific schedule attribute.

Slots_Allocation—mapping to the Partition_Duration in order.

Partition_Duration—definite the time slot of each partition.

Partition_Period—definite the period of the partition.

Slots_Allocation_start—mapping to the Window_Identifier in order. Indicate the window corresponds to which partition.

Window_start_Seconds—denote the offset of each window from the start of major frame.

Window_Identifier—the time window identifier.

Window_duration_Seconds—the time slot of the time window.

Partition_Period_start—denote whether the new period of corresponding partition is start.

- **Memory**

In this part, there are 4 attributes need to be defined:

RegionName—never use.

Access_Type—definite the competence to access the mem-ory, include:read,write,read &write.

PhysicalAddress—the physical address of memory.

Memory_Kind—definite the content of the memory, include:code,data,input & output.

- **Port:**

In this part, there are 3 attributes need to be defined:

RefreshRateSeconds—denote the refresh rate of sampling port.

MaxMessageSize—denote the maximum size of the unsegmented message of sampling port and queuing port.

MaxNbMessages—denote the maximum size of a segment of queuing port.

V. IMPLEMENTATION OF CONFIGURATION TOOL

The implementation and the specific execution flow of the tool are presents in this section.

A. The kernel design point

To improve the efficiency and precision of this tool, we use the following major technology.

(1) Interaction class

We use the Drools to match every component of AADL model, the input of Drools engine should be a java object. Then we set an interaction class as the input of rule engine to keep the information of the AADL model.

(2) Drools rules engine

Drools rules engine is a component embedded in the Java program, its task is to test and compare the Java Data Object which submitted to the engine with the rules, activate the rules that consistent with the current data state, based on the implementation logic statement, and trigger the corresponding operation of the application.

Avionics model file contains a lot of components, each component also contains its own characteristics, sub-component, subprogram, channel, etc. The avionics model which to be analysis maybe a very complicated one, hence we need a common, accurate, and efficient rules engine to match all the branches of an unknown model. And thereby automatically complete the corresponding action under the matching condition.

By access to an existing interaction class object, use the conditions – determine statement(that is, if-else), call the java I / O operation functions can also implement the configuration generation, but it is a deeply nested structure and a confusing logical. There will be a large number of if-then statements, the code will be very messy, and more importantly is that it may make against code expansion. Rules engine is a good solution to the lack of this method.

Business logic of rules engine is clear, rules are independent of each other, we can increase the conversion rule directly without affect other rules, therefore, we choose Drools rules engine to generate and validate the configuration file.

(3) Dom4j

Dom4j is an easy to use, open source library for working with XML, XPath and XSLT on the Java platform using the Java Collections Framework and with full support for DOM, SAX and JAXP.

The ability of Dom4j to parse XML documents is very good, Various API provided by Dom4j can accurately find every node of XML documents, and get the node property values and store them into the interaction class object. This completes the analysis of Aaxl document, and ultimately converts the AADL model to a Drools engine operational interaction class object.

Dom4j also provide API to write XML document accurately. It is called by the rules after matching successfully, and writes the configuration document based on the ARINC653 XML-Schema.

B. The specific execution flow of the tool

In this section, we present the automatic generating procedure of ARINC653 configuration files. The detailed flow chart is depicted in Fig.3.

1. Based on the extended property set and the ARINC653 XML-Schema, modeling an ARINC653 XML-Schema instance file using AADL. It including: system HM table, module HM table, partition HM table for each partition, partition tables, partition memory, partition schedule table, channel table.

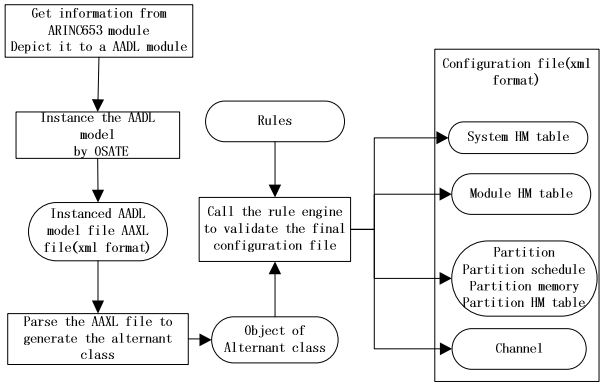


Figure.3 Tool Execution Flow

2. Instantiate the AADL model by OSATE tool and generate the AAXL file which is XML format.

3. Hence parse the features, properties, connections of AADL components. Put all the information into the corresponding interaction class object which is already set.

4. Call the rule engine to verify the integrity and legitimacy of all the configure information, after matching all the rules then call the API provided by the DOM4j to generate complete configuration files.

Pack the configuration tool to a plug-in file and it can be used in the OSATE development environment directly.

VI. CASE STUDY

Based on the extended property set, we set different models to test the response of the tool. The tool will prompts an error message related to the corresponding section of the model which is data missing or data formats error or data associated with issues. These messages prompt system integrator to correct the relevant errors, and configurations can be accurately generated only until all those errors been corrected and fully meet the relevant constraints.

The following case study sets an overall framework of the avionics system, illustrates the use of our tool for the verification and generation of ARINC653 configuration.

An example of an ARINC653 configuration instance represented with AADL graphical diagrams is shown in Fig.4. In this example, we define one ARINC653 module with four partitions (Partitions are described with processes.). The system management partition is a system partition, the other three partitions are not. Each partition holds its own memory segments. Partition1 and partition2 communicate via a channel, this connection is from an out data port of partition2 to an in data port of partition1. Partition3 contain two threads that they share a same data memory segment.

The specific time allocation of each partition in this example are depict in Fig.5. Partition 1 and partition 3 all have 2 time windows in the major frame of the module. Partition 2 is assigned 4 time windows and partition 4 is assigned 1 time window in the major frame. The duration and start time of every time window are depicted in Fig.5.

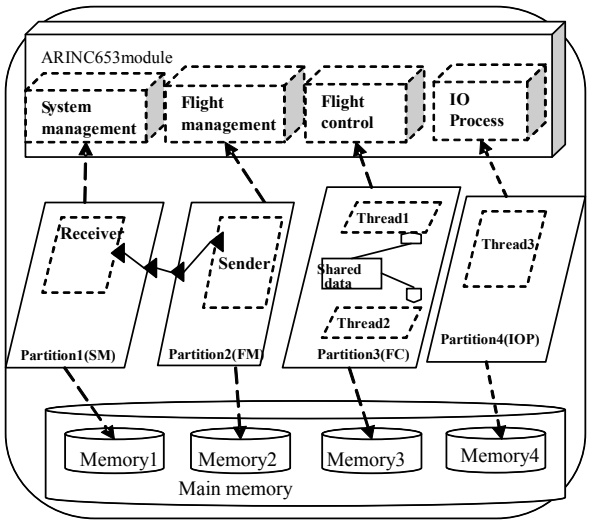


Figure.4 Case Study

Fig.6 presents the part of the static configuration file generated by our tool, due to a lack of space, we just put the partition schedule table into this paper. The configuration Information is consistent with the original time assignment presents in the Fig.5.

VII. RELATED WORKS

A number of related approaches have been proposed. Delange[3] presents an approach for the modeling, verification and implementation of ARINC653 systems using AADL. It details a modeling approach exploiting the new features of AADL version 2 for the design of ARINC653 architectures.

In this paper, we focus on the generation of system configuration. Our main contribution is we present a practical and efficient method to a5ugment the modeling ability of AADL to describe ARINC653 configuration instance and implement an automatic ARINC653 configuration tool.

Also, a number of tools are available that address the issues discussed in this paper. CHEDDAR [14] is a free real-time scheduling tool. It is designed for checking task temporal constraints of a real time application/system which is described with AADL or a CHEDDAR specific language. CHEDDAR provides a number of features to ease the development of specific schedulers and task models, and it relies on OCARINA [15] to provide schedulability analysis of AADL models. OCARINA allows model manipulation, generation of formal models, to perform scheduling analysis and generate distributed applications. OCARINA allows code generation from AADL descriptions to Ada.

VIII. CONCLUSION

Verification and generation of ARINC653 configuration tables are complex tasks due to their criticality and their dedicated services (time and space isolation).

The goal of this paper is to assist system integrator to generate and validate configuration tables for ARINC653

```
:Module_Schedule MajorFrameSeconds="10.0">
 <Partition_Schedule PartitionIdentifier="1" PartitionName="system_manage
  PeriodDurationSeconds="1.0" PeriodSeconds="5.0">
   <Window_Schedule WindowDurationSeconds="1.0" WindowIdentifier="101"
    WindowStartSeconds="0.0" />
   <Window_Schedule WindowDurationSeconds="1.0" WindowIdentifier="102"
    WindowStartSeconds="7.0" />
 </Partition_Schedule>
 <Partition_Schedule PartitionIdentifier="2" PartitionName="flight_controls"
  PeriodDurationSeconds="2.0" PeriodSeconds="5.0">
   <Window_Schedule WindowDurationSeconds="1.0" WindowIdentifier="201"
    WindowStartSeconds="1.0" />
   <Window_Schedule WindowDurationSeconds="1.0" WindowIdentifier="202"
    WindowStartSeconds="3.0" />
   <Window_Schedule WindowDurationSeconds="1.0" WindowIdentifier="203"
    WindowStartSeconds="6.0" />
   <Window_Schedule WindowDurationSeconds="1.0" WindowIdentifier="204"
    WindowStartSeconds="8.0" />
 </Partition_Schedule>
 <Partition_Schedule PartitionIdentifier="3" PartitionName="flight_managem
  PeriodDurationSeconds="1.0" PeriodSeconds="5.0">
   <Window_Schedule WindowDurationSeconds="1.0" WindowIdentifier="301"
    WindowStartSeconds="2.0" />
   <Window_Schedule WindowDurationSeconds="1.0" WindowIdentifier="302"
    WindowStartSeconds="5.0" />
 </Partition_Schedule>
 <Partition_Schedule PartitionIdentifier="4" PartitionName="io_process"
  PeriodDurationSeconds="1.0" PeriodSeconds="10.0">
   <Window_Schedule WindowDurationSeconds="1.0" WindowIdentifier="401"
    WindowStartSeconds="9.0" />
 </Partition_Schedule>
```

Figure.6 Partition Schedule Table of XML configuration

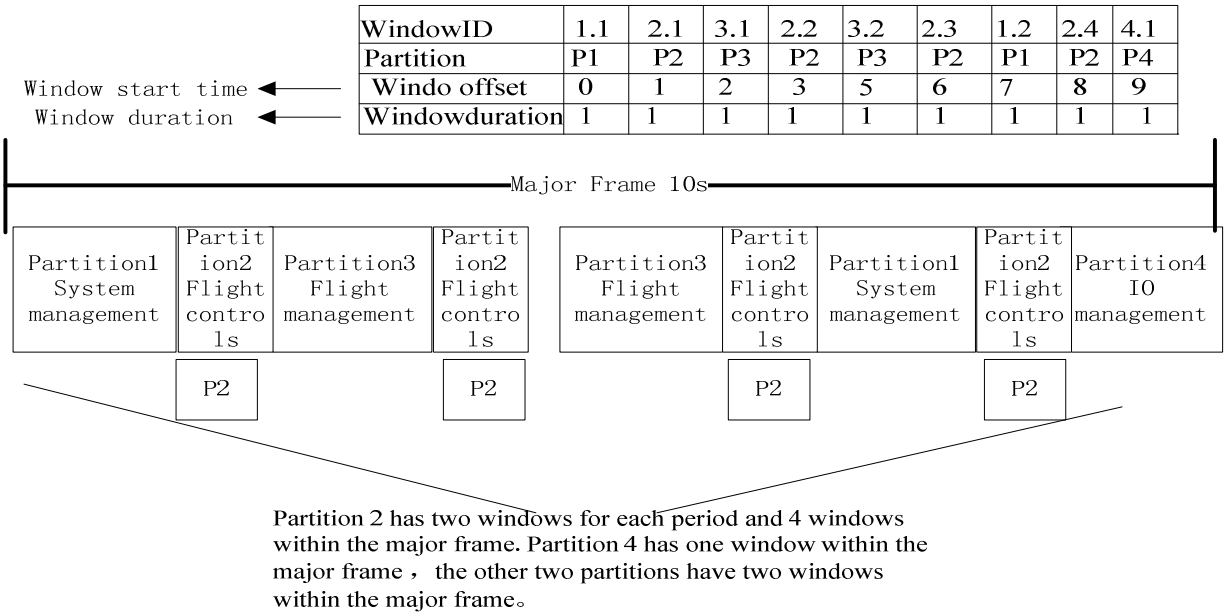


Figure.5 Partition Window Time Requirements

applications. The AADL was selected as a backbone language for our development process because its semantics is suitable for the modeling of safety-critical archi-tectures. This paper presents an approach to augment modeling and analysis capabilities of AADL by extending its property sets. By modeling an ARINC653 confi-guration instance case using AADL and generate static configuration by our tool. The final accuracy of the static configuration file shows that our configuration tool is effective. One of our future works is to improve the verification function of our automatic configure tool and generate configurations with different format applicable for different Operating Systems.

ACKNOWLEDGMENT

This work was supported by Natural Science Foundation of China under Grant 90718019.

REFERENCES

[1] J. Delange, L. Pautet. “ARINC653, AADL annex.” *TELECOM Paris Tech*.2008.

[2] Honeywell. “AADL to ARINC653.” Advanced Technology Platforms and Software, 2009

[3] SAE. Architecture Analysis & Design Language v2.0 (AS5506), September 2008.

[4] J. Delange, L. Pautet, A. Plantec and F. Kordon. “Validate, simulate and implement ARINC653 systems using the AADL.” *SIGAda '09 Proceedings of the ACM SIGAda annual international conference on Ada and related technologies,* vol.29 Issue 3, December 2009

[5] Airlines Electronic Engineering. “Avionics Application Software Standard Interface.” *Technical report, Aeronautical Radio, INC*, 1997

[6] J. Chilenski. “Aerospace Vehicle Systems Institute Systems and Software Integration Verification Overview.” *AADL Safety and Security Modeling Meeting*, Nov. 2007.

[7] P. H. Feiler, D. P. Gluch, and J. J. Hudak. “The Architecture Analysis and Design Language (AADL): An Introduction.” *Technical report*, 02 2006.

[8] SAE-AS5506: Architecture analysis & Design Language(AADL) , International Society of Automotive Engineers[S]. As-2 Embedded Computing Systems Committee,USA,2009.

[9] P. Dissaux and F. Singhoff. “Stood and Cheddar : AADL as a Pivot Language for Analysing Performances of Real Time Architectures”. Proceedings of the European Real Time System conference. Toulouse, France, Jan. 2008.

[10] POK Website. http://pok.gunnm.org/, 2009.

[11] J. Hugues, B. Zalila, L. Pautet, and F. Kordon. “From the Prototype to the Final Embedded System Using the Ocarina AADL Tool Suite”. *ACM Transactions in Embedded Computing Systems (TECS)*, 7(4):1–25, jul 2008.

[12] W. Barnes. “ARINC 653 and why is it important for a safety-critical RTOS”. April 2004.

[13] J. Delange, L. Pautet. “ARINC653 annex Overview.” *TELECOM Paris Tech*.2008

[14] F. Singhoff, J. Legrand, L. Nana, L. Marc´ e, “Cheddar: a Flexible Real Time Scheduling Framework,” *Proc of the ACM SIGAda International Conference*, Atlanta, US, 2004

[15] J. Hugues, B. Zalila, L. Pautet, “Rapid Prototyping of Distributed Real-Time Embedded Systems Using the AADL and Ocarina,” *Proc of the 18th IEEE/IFIP International Workshop on RSP ’ 07*, Brazil, 2007

An Insight into Real Software Industry Paradigms and Software Engineering Research

Rehan Akbar, Mohd Fadzil Hassan, *Azrai Abdullah, Sohail Safdar, Muhammad Aasim Qureshi
Department of Computer and Information Sciences
*Department of Management and Humanities
Universiti Teknologi PETRONAS, Malaysia.

rehankb@yahoo.com, mfadzil_hassan@petronas.com.my, azraia@petronas.com.my, sagi_636@yahoo.com, maasimq@hotmail.com

***Abstract*- Since years software development industry is trying hard to show a remarkable performance in its project development work. Issues related to the software processes improvement, risk management, people's factors and effective project management still exist. Though academic researchers have produced good quality work on software industry issues, but unluckily, software industry could not get benefit of it as was being expected. Software engineering research work also seems unable to identify and understand the real industry problems and providing hands on solutions. The gap between researchers and actual industry practitioners is the sole reason behind it. It is the foremost need to learn from the academic research work and experiences of real software development industry practitioners. The objective of this study is to bridge this gap by highlighting the root causes of differences between software engineering research works and actual industry practices. An analysis of real industry projects, academic projects, research publications, and industry people is made to complete this research work. The outcome of this research is twofold. First, the identification of factors behind the academic-industry gap; second, presenting a set of measures to bridge this gap to produce actual industry based research works.**

Keywords- Gap; Industry; Practitioners; Research Contribution

I. INTRODUCTION

From last two decades, many software engineering models, frameworks, practices and standards have produced by the researchers. Inspite of this large number of research works, software development processes are still the most investigated areas by the researchers. Software process improvement, process customizations, risk analysis and management, and project management issues are the most concerned areas related to the IT industry. Very sophisticated work is presented in such areas, for example [1], [2], [18 - 21]. In parallel to these research trends, there is a paradigm shift from traditional software engineering practices to the new revolutionary agile based practices [8], [22]. Where globalization has changed the overall socio-economic aspects, cultural trends and other areas of our society, IT industry has also been greatly affected with its consequences [6].

Project outsourcing has emerged as a common practice in effect to these global software development paradigms [6], [10]. Factors such as cheap labor, minimizing cost, fast development, market competition, use of advanced tools and technologies are driving force of project outsourcing [7], [8]. High expectations of client as a result of project outsourcing have made agile methodologies the preferred choice of developers [23]. Agile methodologies though do not suit to all kind of development environments but response to these practices by software teams is overwhelming [3], [4], [5].

Software industry rapidly changes its software development practices. Many factors such as project requirements, client's requirements, and better tools & technologies are behind such rapid changes. Software development practices vary from project to project and company to company. Centralized teams have been dislocated to distributed teams [6], [9]. Clients are offshore and teams are geographically distributed. Minimizing project cost and fast development have realized as the main factors of rapidly changing scenarios [7], [10].

In this globalization of software development, research work that has been produced is unable to address the industry problems in current circumstances. One question which arises in every IT person's mind is that why software engineering research is unable to solve the software industry problems? The answer can be found in other questions such as: Does the research works that is being produced meet the requirements of the software industry? Does the research work currently being produced is the same as required by the industry practitioners? Do industry practitioners consult software engineering research to find the solutions? Not really, the answer to all the questions. The basic reason behind this is the gap between academic research and actual software industry practices and requirements. Software engineering research methodology is also considered as one of the factors in such scenarios. Parallelism between software engineering research methodology and software methods has also discussed by [12]. The models and frameworks of software engineering research though provide strong basic grounds to build up strategies and develop customized practices, and process improvement techniques but they lack industry factor is also a fact. Software engineering research is unable to portray the real picture of the industry. Proper planning is required to conduct the software engineering research [13]. Ignoring or un-accepting this reality is at the cost of projects, resources and investments.

This paper highlights those factors that need to be considered by the researchers when devising strategies, and developing model or framework of software engineering. It also addresses the lack of interest of industry practitioners to become a part of software engineering research. Real software engineering is that which is being practiced during software development projects in software development companies. Our research work is based on analysis of real industry projects, research publications and projects, and industry

people. Personally, in our research group one researcher is also working in the software industry at a key management position. Contribution of that researcher made our analysis, findings and solutions more realistic. The outcome of this research is twofold. First, identification of those factors that are basic reasons behind this research deficiency and academic-industry gap; second, it presents a set of measures to bridge this gap and produce realistic industry based research work.

II. Analysis Overview

An extensive analysis and observations are made to complete this study. Exploratory type of case study is performed to complete the analysis of projects. Data is collected in the capacity of observing participant with actual software development teams. Archival data has also been used during analysis. Moreover, unstructured interviews of people from the industry, analysis of industry projects, reading and comparing software engineering research papers and study of academic projects, all are made to reach some conclusion.

Table 1 presents the summary of our sources of information analysis. Each observation is made on one basic principle that whether it provides solution to some industry problem or not? The models and frameworks presented in software engineering research works are compared with actual industry practices carefully to see their usability. A close case analysis is conducted in the study. Solution to industry problems and process improvement strategies were tried to find from the presented research models. Our findings are based on the ratio of industry problem to the solutions from research works.

Far rare contribution and combined efforts from both industry people and academic researchers are observed. Though in few cases academic researchers have contributed to the industry work but that is not significant.

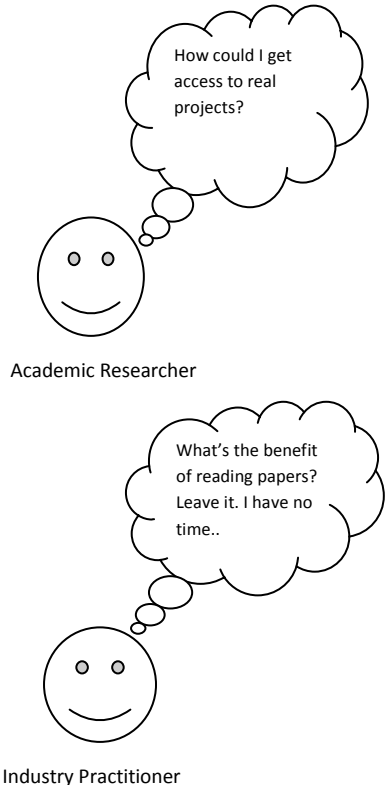


Fig 1. Academic – Industry Actors

TABLE 1
ACADEMIC-INDUSTRY GAP

Source	Type	Analy-sis Durat-ion	Contribu-tion to research from Industry	Contribu-tion to projects from Academics
Software Projects (Industry)	Offshore, onsite, multiple domains	1+ years	No	No
Industry practitioners	Project managers, Developers, Team leads, Senior management	1 – 2+ years	Only 1-2	Only 2-3
Research Publications	Research papers, Articles, Reports	2+ years	1-2 out of each 100	3-4 out of each 100
IT Projects (Academics)	Academic projects	7 years	No	Not directly related to industry issues and practices.

Neither contribution of software engineering research community to the industry projects or industry projects to the academic research work was observed. A very few (1-2) people from industry were contributing to the software engineering research works. This encouraging practice was limited to only those practitioners who had some sort of research background. The contribution in the form of research publications from industry practitioners and on the projects from academic researchers was not found that much encouraging (see table 1). Likewise, IT projects running in the academic institutions are not really of industry based. Except one or two cases, we couldn't find any industry person reading or consulting research publications to get guidance or seeking help from it. For Example, the industry oriented research work produced by the researchers such as process tailoring frameworks, process creation and improvement models and meta-models, requirement gathering and tracking processes, standardized practices and risk analysis frameworks were never consulted by the industry people. Same observations were made in the case of industry based work. Except one or two cases, no industry based practices such as interaction communication processes, requirement management processes, configuration management processes and internal

team based processes were ever published. Factors such as uncertain project durations, resources constraints, inaccessibility to real projects and data, company's privacy policies, busy schedule of industry people, lack of links or contacts between academicians and practitioners creates this misbalance and increase the gap. The way of thinking of both is entirely different and contradictory with each other as shown in figure 1.

Mainly work of academics researchers is based on the published work presented by other researchers in the form of models, frameworks, practices and standards. Finding similarities and differences is one of the part of research work. This approach of consulting and referring research work of other researchers is highly appreciated in the existing circumstances where researchers do not have proper access to the industry projects and data. That's why they rely more on previously presented works. This practice builds up the habit of thinking to inaccessible industry project as shown in figure 1.

On the other hand, industry people consider research work as a useless practice in the context of their own work. They prefer to consult quick online resources such as libraries, APIs and different forums to find the solutions. Reading a research paper is a non productive and time consuming activity for them as shown in figure 1.

In our analysis such incompatibilities were very prominent. Based on our case study analysis, factors responsible for such dilemma of software engineering research and industry, and a set of measures are presented in section III and IV respectively.

III. ACADEMIC – INDUSTRY GAP

On the part of academic researchers their contribution seems more positive and responsive as compare to the industry practitioners. The discipline of software engineering, its various studies and aspects are continuously being discussed and investigated to establish and improve the software processes. Requirement engineering, development and testing phases and project management in software engineering studies covers all such aspects of a software development projects. Software engineering research too revolves around software process development and improvement methodologies [11]. Inspite of such rich studies, the industry is unable to get benefit of it. Rarely any research based model is adopted by the companies. The situation becomes more adverse in case of small and medium scale organizations. Large organizations though have resources to adopt research models according to their requirements but improper knowledge about published work and its importance is a big hurdle.

The problem with the software engineering research work is that it seems more likely unable to meet the industry requirements. Same kind of thinking has been developed among the industry people. The research community also does not involve themselves to the actual development processes that make them unaware of real industry based issues and scenarios [14]. Indeed, the contribution from the academic researchers is outstanding; their work is of very good quality. Deep insights into software engineering processes, process improvement models, risk analysis and project management strategies from various angles are presented through exhaustive research work by the researchers.

On contrary, the contribution from industry practitioners is also observed quite discouraging. According to our study, rarely any project manager, team lead or a developer is found consulting the published work in order to improve and learn. Based on analysis as summarized in table 1, mainly following factors are found responsible for this dilemma:

a) Lack of collaboration and coordination between researchers and practitioners.
b) Research work is based on partial analysis of real projects, simulations [24] and incomplete case studies, therefore, does not address the real industry problems properly.
c) Non-cooperative behavior of industry people for the academic researchers and research work due to their busy and tight schedules.
d) Restrictions on accessibility of real data due to company's privacy policies and statements.
e) Un-interested and un-motivated project managers, team leads and developers to consult the researchers and published work to find the solutions.
f) Academic researchers don't have resources or links in the industry to conduct their research in real environments.
g) Uncertain project durations are obstacles to complete research work based on real projects.
h) Lack of motivation in the industry practitioners to consult published work.
i) The actual industry practices are never published by the actual practitioners in the form of research work.
j) Practitioners are not aware of how to write a paper and publish their work.
k) Communication gap and inaccessibility to published work.

Much good quality research works remains unable to be accessed and consulted by the industry people because of these factors. Similarly, many best practices and processes of the industry remain unpublished and academic researchers never come to know about them. Many models, framework and practices proposed by the academic people are not appreciated and encouraged by the industry people because of not meeting their requirements. A gap between software engineering research community and industry people has quite prominently been developed due to such factors.

IV. COVERING THE GAP

Recent trends of software development have increased the gap between the academics and industry. Factors discussed in section III prevails most frequently. Reasons behind such factors are very fundamental and can easily be overcome. Following realistic measures can effectively be adopted in this regard:

a) Software industry is entirely client based; project teams prefer client's requirements and try to satisfy him/her in each and every respect for successful

progress of project. Therefore, standardized processes are not really followed by the organizations. Research work, models and framework presented are based on standards and most of them do not really address client factors greatly. Best approaches in this regard need to be adopted appropriately.

b) Applied research projects in collaboration with the software industry need to be started effectively.
c) Need a framework for the involvement of academicians in the real industry projects.
d) Seeking help and expertise of industry people while devising a software engineering model or framework.
e) Motivating industry practitioners to publish their real processes and practices in the form of research papers and articles so that academicians could get benefit of it.
f) Well established and concrete software engineering methodology should be made to perform and complete the case studies of real projects while project's duration is quite uncertain.
g) More systematic communication and coordination strategies are required.
h) Identification of real industry problems by the researchers in consultation with the industry people and providing solutions through applied research methodologies.

As said earlier that real software engineering is one which is being practiced in the software industry. Client based software development and real industry practices are two main factors that create the difference of work at both ends. These factors need to be considered while proposing a model or framework. During analysis as summarized in table 1, lack of motivation of industry people towards research is obviously found. Many software companies are now motivated to improve the quality of work, increasing productivity of their teams and reducing development time to compete the market [16]. Thinking that motivation is a key success factor in education and training by [17] also applies to the industry practitioners learning research skills. Their way of thinking is found different from academic researchers (see figure 1). How software engineering researchers conduct their research and evaluate quality results is also not properly presented [13]. Even in majority of the cases they even are not aware of any model or framework presented by the researchers and whether it is useful for their project or not. A big gap between two software engineering key players is quite alarming. Minimizing and covering this gap is the ultimate need to produce the beneficial research work and to use it for the improvement in the industry.

V. CONCLUSION

Realistic thinking both by the researchers and industry practitioners is required to produce effective software engineering work that is actually the demand of IT industry. From last few years industry has realized the importance of people problems as an important factor for the project progress [15]. Researchers need to collaborate with industry in such requirements of the industry. Models and frameworks that are not used by the industry people are not considered as successful work. Identification of actual industry requirements, their processes and strategies need to be done. Research work produced then would be more effective and result oriented. Presence of gap between researchers and industry people may raise a big question on the applicability of current research work. Factors identified in this paper and guidelines that are provided to cover up this gap are the priority measures to be taken.

VI. FUTURE WORK

The issue that we have presented needs more discussions and investigation. Further aspects need to be given attention. A real option thinking coordination framework would be presented as an extension to our current work. Strategies for combined work of both key players of software engineering community would be made. The framework would suggest how the academic researchers and industry practitioners can collectively produce quality research work that really addresses the industry problems. The software engineering models produced then would be more productive.

REFERENCES

[1] N. Feng, M. Li and H. Gao, "A Software Project Risk Analysis Model Based on Evidential Reasoning Approach", World Congress on Software Engineering, IEEE Computer Society, IEEE. 2009, vol. 2, pages. 224-228.

[2] K. Bandyopadhyay, P. P. Mykytyn, and K. Mykytyn, "A Framework for Integrated Risk Management in Information Technology," Management Decision, MCB University Press, UK, 1999, vol. 37, pages. 437-444.

[3] J. Highsmith and A. Cockburn, "Agile Software Development: The Business of Innovation," IEEE Computer, 2001, vol.34, no.9. pages. 120-122.

[4] B. Boehm, "Get Ready for Agile Methods, with Care ," IEEE Computer, 2002, vol.35, no.1, pages.64-69.

[5] Manifesto for Agile Software Development, Agile Alliance, 2001, http://agilemanifesto.org/.

[6] J. Cho, "Globalization and Global Software Development," Issues in Information Systems, 2007, Volume VIII, No.2. pages. 287-290.

[7] R. Phalnikar, V. S. Deshpande, and S. D. Joshi, "Applying Agile Principles for Distributed Software Development," Proceedings of International Conference on Advanced computer Control, IEEE. 2008, pages. 535-539.

[8] A. Cockburn, J. Highsmith, "Agile Software Development: The People Factor," 2001, IEEE Computer. pages. 131-133.

[9] A. Rusu, A. Rusu, R. Docimo, C. Santiago, and M. Paglione, "Academia-Academia-Industry Collaborations on Software Engineering Projects Using Local-Remote Teams," Proceedings of SIGCSE'09, ACM, 2009, vol. 41, no. 1, pages. 301-305.

[10] A. Gopal, T. Mukhopadhyay, and M. S. Krishnan, "The Role of Software Processes and Communication in Offshore Software Development," Communications of the ACM, 2002, Vol. 45, No. 4ve, pages 193-200.

[11] A. Farooq, and R. R. Dumke, "Research Directions in Verification & Validation Process Improvement," ACM SIGSOFT Software Engineering Notes, 2007, Vol. 32, No. 4.

[12] E. Marcos, "Software Engineering Research versus Software Development," ACM SIGSOFT Software Engineering Notes, 2005, Vol. 30, No. 4.

[13] M. Shaw, "What Makes Good Research in Software Engineering," International Journal of Software Tools for Technology Transfer, 2002, Vol. 4, No. 1, pp. 1-7.

[14] P. Xu, and B. Ramesh, "Using Process Tailoring to Manage Software Development Challenges," Process Management, Published by IEEE Computer Society, 2008, pages. 39-45.

[15] C. B. Seaman, "Qualitative Methods in empirical Studies of Software Engineering," IEEE Transactions on Software Engineering, 1999, Vol. 25, No. 4. pp. 557-571.

[16] D. J. Paulish, and A. D. Carleton, "Case Studies of Software-Process-Improvement Measurement," IEEE Computer, 1994, pages. 50-57.

[17] A. Drappa, and J. Ludewig, "Simulation in Software Engineering Training," Proceedings of ICSE'00, ACM, Limerick, Ireland, 2000, pages. 199-208.

[18] X. Lu, Y. Ge, "Risk Analysis in Project of Software Development," IEEE, 2003, pages. 72-75.
[19] D. Kang, I. Song, S. Park, D. Bae, and H. Kim, "A Case Retrieval Method for Knowledge-Based Software Process Tailoring Using Structural Similarity," Proceedings of 15th Asia-Pacific Software Engineering Conference, IEEE Computer Society, IEEE, 2008, pages. 51-58.
[20] Y. Xiaoguang, W. Xiaogang, L. Linpin, and C. Zhuoning, "Research on Organizational-Level Software Process Improvement Model and Its Implementation," International Symposium on Computer Science and computational Technology, IEEE Computer Society, IEEE, 2008, pages. 285-289.
[21] C. Wu, W. Chang, I. K. Sethi, "A Metric-Based Multi-Agent System for Software Project Management," 8th IEEE/ACIS International Conference on Computer and Information Science, IEEE Computer Society, IEEE, 2009, pages. 3-8.
[22] C. Ferreira, and J. Cohen, "Agile Systems Development and Stakeholder Satisfaction: A South African Empirical Study," SAICSIT'08, ACM, 2008, pages. 48-55.
[23] G. B. Wills, N. Abbas, R. Chandrasekharan, R. M. Crowder, L. Gilbert, Y. Howard, D. E. Millard, S. C. Wong, and R. J. Walters, "An Agile Hypertext Design Methodology," Proceedings of HT'07, ACM, 2007, pages. 181-184.
[24] J. S. Carson, "Introduction to Modeling and Simulation," Proceedings of the 2005 Winter Simulation Conference, 2005, pages. 16-23.

A Collective Intelligence Based Business-Matching and Recommending System for Next Generation E-Marketplaces

Youssef IGUIDER* and Hiroyoshi MORITA**
* SRI International, Information Science and Engineering Department. Tokyo, Japan
** The University of Electro-Communications. Graduate School of Information Systems. Tokyo, Japan

***Abstract*- The present work proposes and describes a novel approach to business-matching and recommending systems, for the next-generation e-marketplaces, with a focus on the needs and realities of small business. The proposed matching system makes use of Collective Intelligence (IC) means to identify and recommend the best matching business opportunities for the user. At first, the content of business proposals and companies' profiles are parsed and indexed. The search engine starts by expanding the keyword of interest, to enable an intuitive-like search. The look-up results are then filtered based on a compatibility scoring mechanism. The customized business-matching results and recommendations are later served to the user via a novel visual interactive graphical interface. A prototype system applying the proposed and described approach is currently being developed and experimentally tested, to fully demonstrate the capabilities of the proposed system on real-world data. Although the prototype is at an early stage, the initial experiments show promising results.**

***Keywords**: Collective Intelligence, e-marketplace, business matching, recommending systems, small business.*

I. INTRODUCTION

A. Collective Intelligence (CI):

This work is inspired by the vision of Dr. Douglass Engelbart [1] regarding the use of technology to improve our c*ollective intelligence* for the betterment of humanity, by integrating social-cultural strategies with new technology to create a new way to portray information [1]. Dr. Engelbart (who is also a colleague and mentor to one of the authors) is often considered as the main founder of the field of *Collective Intelligence (CI)* [2][3]. CI is defined as the capacity of human collectives to engage in intellectual cooperation, in order to build new conclusions from independent contributors [4]. This study is an attempt to apply CI approach to the e-marketplaces for small businesses.

B. "Small Business – Big Impact!"

In most countries, the small business sector accounts for over half of all industrial activities. It is the major source of employment and a mainstay of regional economies, and has therefore a major role to play in the creation of new growth industries and the betterment of nations' economies. In the United States, for instance, small businesses provide 55% of all jobs, and contribute with 54% of all U.S. sales [5]. In Japan, the small business sector is also the economy's engine [6]. The small and mid-size enterprises (SME) representing 99.7% of the 4,973 thousands registered companies, employ 70.2% of Japan's workforce, and their contribution to the shipment in the manufacturing market is estimated at 51.1% [6].

It is however a fact that only about 50% of small businesses can still trade after their first 3 years [7]. Small businesses are exposed to bigger threats because they do not have the back-up of extra finance and resources that larger companies possess. "Difficulties to commercialize their products"; "mismatched trading", and the "lack of finding funding partners" are often listed among the top challenges commonly faced by small businesses, which lead to their failure [5][7][8]. Our aim is to design a business-matching and recommending system, which can enable e-marketplaces to address these issues.

C. Existing e-Marketplaces:

Business consulting and business matching for small and large businesses is mostly provided offline. A service that usually comes with more costly expenses than what small business can usually afford. Moreover, the recommended business matches are often geographically limited to local or regional partners. Few online e-marketplaces provide international business matching services. And most of these platforms simply list the same static information from their databases similarly to all users. Without truly taking into account the specific needs and background of the user.

In the present paper, we attempt to propose and introduce a new business-matching and recommending system, which would enable e-marketplaces to provide each user with personalized results customized to the specific needs of her/his business. The recommended business matches are served via a novel visual interactive graphical interface.

The following section discusses the evolution of information systems, and anticipate the coming trend of information systems, and therefore the motivation behind this research. The section III introduces and describes the proposed system. The section IV provides an overview about the initial experimental studies.

II. TARGETED INFORMATION SYSTEM

Information systems (IS) are combinations of information technology and people's activities using that technology to support operations, management, and decision-making.

A. Hardware management based IS:

Early IS solutions were operating based on primitive systems that used machine codes and data, to have the central processing unit of computing devises execute specific instructions. These primitive systems often executed one program at a time, and operated mainly as specific hardware-dependent systems. We represent this era of information systems as the "Hardware Management" stage, in Fig. 1.

B. Software management based IS:

Later, in the 60s through the 80s, after hardware capabilities evolved to allow similar software to run on more than one platform, advanced operating systems were born. Which enabled multi-tasking information systems to operate a large amount of software applications. Which help the users perform common tasks and activities in the real world. We represent this era of information systems as the "Software Management" stage, in Fig. 1.

C. Knowledge management based IS:

The expansion of the World Wide Web and the explosion of Internet interactions, led to the constantly increasing production of a huge amount of online data, which is doubling approximately every six months [9]. Therefore, we believe that there is an emerging need for new data management systems, able to take advantage of these large amounts of data, by uncovering new, implicit and potentially useful knowledge from them. And also creating new knowledge out of their interlinked characteristics. This knowledge operating information systems would play a vital role in the information industry. We represent this era of information systems as the "Knowledge Management" stage, in Fig. 1.

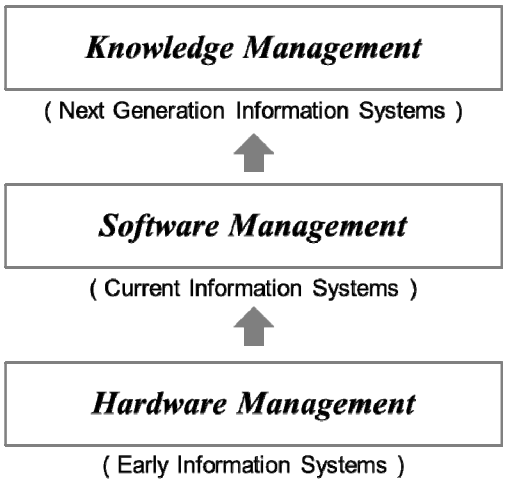


Fig. 1. Evolution of information systems

D. Collective Intelligence based knowledge managing IS:

This work attempts to propose a knowledge managing IS model, based on collective intelligence, which we later apply to develop a new business-matching system for next generation e-marketplaces.

"*Collective Intelligence (CI)* is a multidisciplinary philosophical framework, which integrates social-cultural strategies with new technology to create a way to portray information, with the goal to include, view, and aggregate as much information as possible in order to enable people to act strategically to solve complex problems" [1][10][11].

The basic idea behind our proposed knowledge-managing system is illustrated below in Fig. 2. Which is, by the way, very similar to the Intelligence producing cycle used by the Intelligence Community in the United States and many other countries [12]. The process is described below:

Collective-Intelligence Collection: Acquiring data and information from independent users, then provisioning that data in a way which ensures a later optimal processing.

Intelligence Processing: Converting the collected data into a form suitable for producing intelligence. By conducting various detailed analysis, comparisons and information correlation among the collected data.

Personalized Services: Reducing the information overload, by focusing on the consumer's specific need, to interpret the processed information into a finished intelligence product that may help the user draw analytical conclusions.

New Knowledge Creation: Aggregating and recombining the collected data and processed information, to systematically and dynamically create new knowledge that may convert questions (lacking information) into expanded intelligence.

Customized Expertise Servicing: Conveying expanded intelligence in a usable form, to support the user's decision-making with personalized and relevant insights and expertise.

"Smart & Intuitive" User Interface: Creating new ways of structuring facts, and using new ways of interacting with the system, is key to extending the people's capability to collect information, create, manipulate and share knowledge [1]

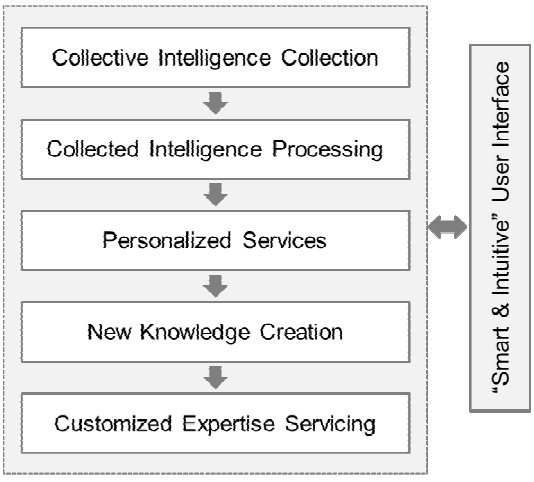


Fig. 2. CI based knowledge management

III. A CI Based System For E-Marketplaces

This section attempts to apply the approach introduced and discussed in the previous section, with the goal to propose a CI based new business-matching and recommending system model for e-marketplaces.

Unlike most existing e-marketplaces, where the system usually simply matches companies and lists to the user straightforward search results from available static databases, the proposed system model (Fig. 3) uses a CI approach toward the process of business-matching and business opportunity recommending.

As shown in Fig. 3, at first, various data are collected from the collectively submitted users' business (selling or buying) proposals, as well as from their company's profile and background. The collected data are then processed and carefully indexed. Then, based on the user's query, and also based on his/her recorded business background and company's profile, the system conducts various analysis and correlation operations, on the user's data vs. the data of the potential candidate partners, and their business proposals and needs. With the goal to reduce the search result overload, and instead convey to the user personalized business recommendations specific to his/her needs, interest and background. The goal is also to enable the user uncover new relevant business opportunities that might not be easily reachable though straightforward search of a static database.

TABLE I. illustrates an example, where a part of the user's information is scored and matched against the data of other identified business-partner candidates. With the goal to evaluate the user's compatibility with the identified business-partner candidates, and qualify the potential of their proposed business opportunities, the user's attributes are mapped against the attributes of the identified partner-candidates, via several correlation means, including the matching via Euclidean Distance Scoring (1).

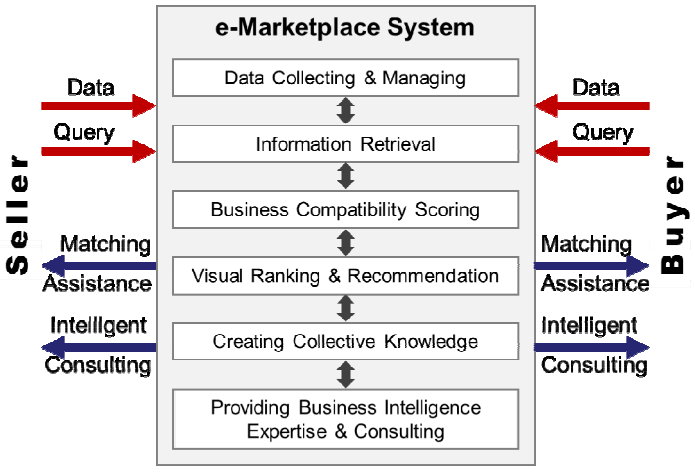


Fig. 3. CI based system for e-marketplaces

TABLE I
COMPATIBILITY SCORING

Attribute #	Attributes Description	User	Candidate Partners				
			P-1	P-2	P-3	...	P-n
A_1	Company Country	$S_0(A_1)$	$S_1(A_1)$	$S_2(A_1)$	$S_3(A_1)$	...	$S_n(A_1)$
A_2	Business Category	$S_0(A_2)$	$S_1(A_2)$	$S_2(A_2)$	$S_3(A_2)$	...	$S_n(A_2)$
A_3	Company Age	$S_0(A_3)$	$S_1(A_3)$	$S_2(A_3)$	$S_3(A_3)$	...	$S_n(A_3)$
A_4	Capital	$S_0(A_4)$	$S_1(A_4)$	$S_2(A_4)$	$S_3(A_4)$	...	$S_n(A_4)$
A_5	Business Volume	$S_0(A_5)$	$S_1(A_5)$	$S_2(A_5)$	$S_3(A_5)$	...	$S_n(A_5)$
A_6	Employees	$S_0(A_6)$	$S_1(A_6)$	$S_2(A_6)$	$S_3(A_6)$	...	$S_n(A_6)$
A_7	Offer type (Proposal)	$S_0(A_7)$	$S_1(A_7)$	$S_2(A_7)$	$S_3(A_7)$	...	$S_n(A_7)$
A_8	Product/Service category	$S_0(A_8)$	$S_1(A_8)$	$S_2(A_8)$	$S_3(A_8)$	...	$S_n(A_8)$
A_9	Minimum order ($)	$S_0(A_9)$	$S_1(A_9)$	$S_2(A_9)$	$S_3(A_9)$	...	$S_n(A_9)$
A_{10}	Targeted region/s	$S_0(A_{10})$	$S_1(A_{10})$	$S_2(A_{10})$	$S_3(A_{10})$	...	$S_n(A_{10})$
A_{11}	Non acceptable countries	$S_0(A_{11})$	$S_1(A_{11})$	$S_2(A_{11})$	$S_0(A_{11})$	...	$S_n(A_{11})$

$$C_{(i,j)} = \sqrt{\sum_{k=1}^{11} \left(S_i(A_k) - S_j(A_k)\right)^2} \qquad (1)$$

where,

$C_{(i,j)}$ - Compatibility between two partner-candidates i and j

$S_i(A_k)$ - Score of a partner-candidate i with regard to the attribute A_k

To comply with the recommendation of Dr. Engelbart (CI's founder) about the importance of creating new ways and symbols for structuring facts, in order to extend the users capability of manipulating the created knowledge [1], the business matching results and personalized recommendations are later conveyed to the user via a new visual graphic interface, which is illustrated by Fig.4 and TABLE II.

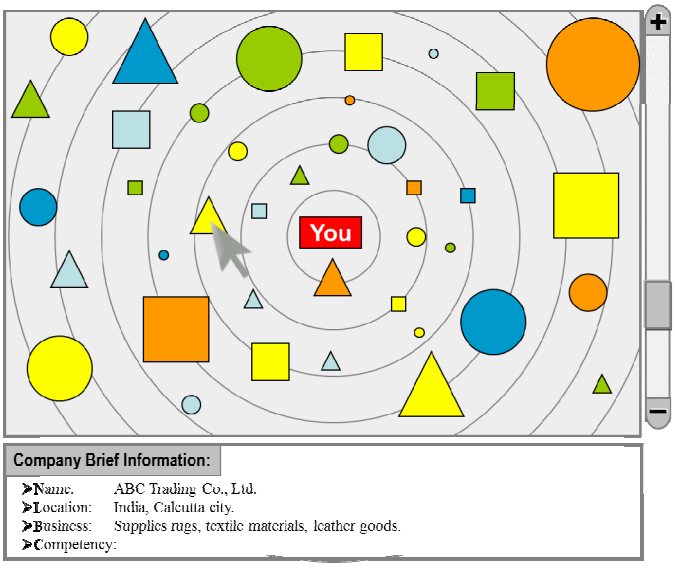


Fig. 4. Visual representations of the business-matching results

TABLE II
GRAPHIC SYMBOLS INTERPRETATION

Business Category	Color
Supplier	
Buyer	
Investor	
Consultant	
Logistic Service	

Company Location	Symbol
Same city	
Same country	
Same continent	
Other continent	

Company Size (number of employees)	Symbol Size
1-10	
11-100	
101-500	
501-1000	
1001 or more	

Colors, shapes and sizes are used to symbolize characteristics of the candidate partners, in order to help the user visually explore and interact with the recommended business opportunities via a graphical navigational interface.

Automated Business Consulting System

As a later stage, our research aims at creating a CI business-matching system, which enables the e-marketplace to perform as an automated business consulting platform. The system aggregates and recombines the collected data, to create new relevant knowledge. By systematically applying the best practices used in the market by business development experts. The created personalized expertize can be served to the user, to support his/her decision-making, and enhance his/her market strategy insights and business intelligence. Fig.5 illustrates an example, where the targeted automated consulting system would systematically uncover business partnering opportunities to the user. To provide him/her with expert level personalized consulting about how to strategically proceed with the uncovered business partnering opportunities.

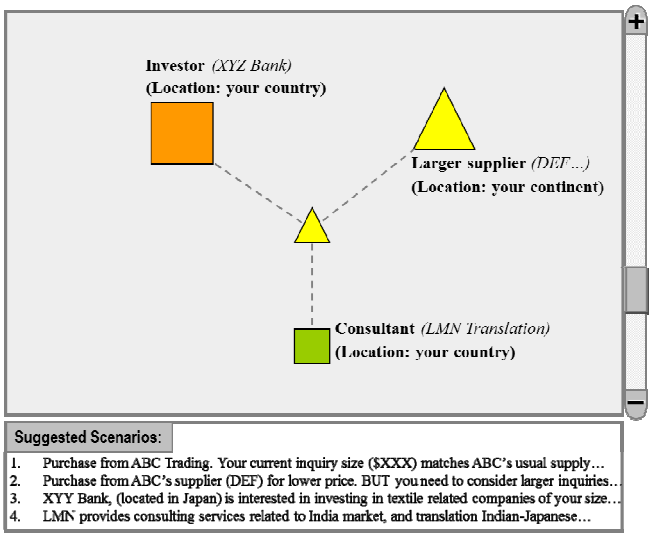


Fig. 5. CI Based Automated Consulting

IV. EXPERIMENTAL STUDIES

To experimentally study the proposed CI based business-matching and recommending system for e-marketplaces, we are currently developing a prototype that can process advanced business matching and generate recommendations, based on real-word business opportunities.

JETRO (Japan External Trade Organization (JETRO)'s online Business Matching Database

With goal to study our prototype based on real-word business matching data, the experimental studies and simulations conducted in this research are based on contents and data collected from JETRO's online business matching database. JETRO is a Japanese governmental organization, which promotes mutual trade and investment between Japan and the rest of the world. JETRO is running a free online business matching service "Trade Tie-up Promotion Program" (TTPP) [13]. Which allows business people (especially small and medium companies) to browse through over 20,000 business proposals in various industrial fields (TTPP: http://www.jetro.go.jp/ttppoas/)

The system's components of the experimental prototype are shown in Fig. 6. At first, an experimental simulation was developed, using Python programing language [14], for parsing JETRO's business proposals. The BeautifulSoup classes were used to screen-scrap and parse the web content of JETRO's entries (Fig.7 shows an example of an entry, business proposal). The result of this parsing led to compiling information from each entry (business proposal) in JETRO database. The following is an actual sample of the information that was automatically extracted from a current entry:

Proposal Title: Hawaiian Rugs
URL: www.jetro.go.jp/ttpp/EAN.CR06_EAN?id=1088642&corner_id=999
Proposal #: 1088642
Business Type: Export and Import of Products / Parts
Offer Type: Offer to sell products / parts
Proposal Category: None
Country Area: Tokyo, Japan

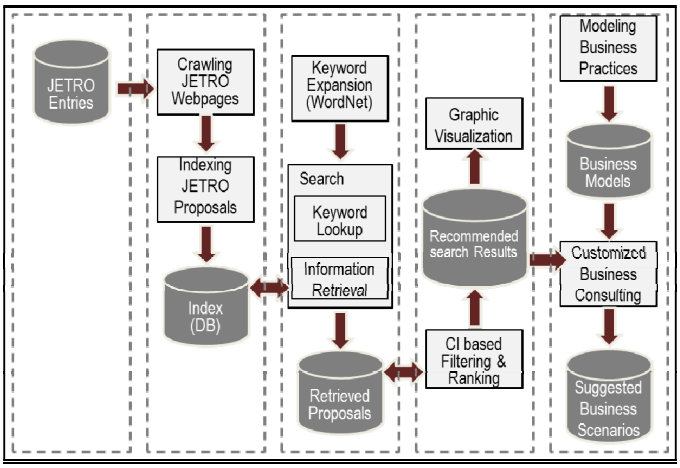


Fig. 6. Experimental business-matching and recommending prototype

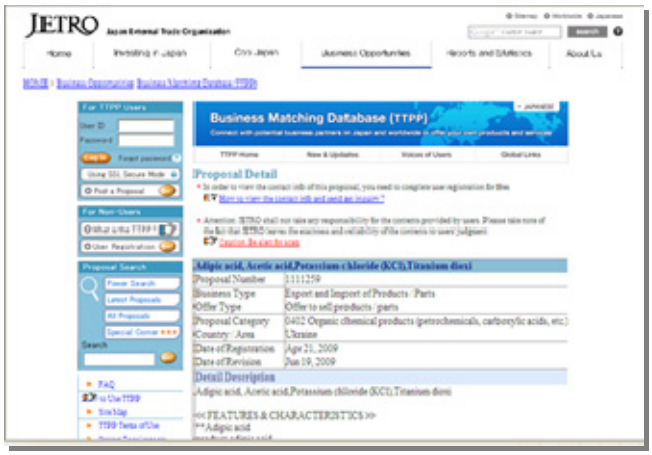


Fig.7. Sample-entry (business proposal) from JETRO's TTPP

Indexing TTPP business proposals:

In order to process the TTPP business proposals in depth, a set of business proposal entries were indexed into a SQLite database. To proceed, the contents were parsed, by randomly looping through the TTPP URLs, to crawl their entry contents. The experimental crawler was designed to ignore a set of words which carry no important meaning. The system was also designed to identify and ignore the URL of the business proposals that were either expired or deleted by the users. As results, the crawled and parsed TTPP business proposals were automatically indexed into a SQLite database, which was automatically created and saved for further use. The figures below show samples of the indexed data, where the database was populated with, (Fig.8) a list of the automatically generated and processed URLs, (Fig.9) parsed and processed words, and (Fig.10) information about how each word is associated to its corresponding proposal, along with the position of that word within the proposal page.

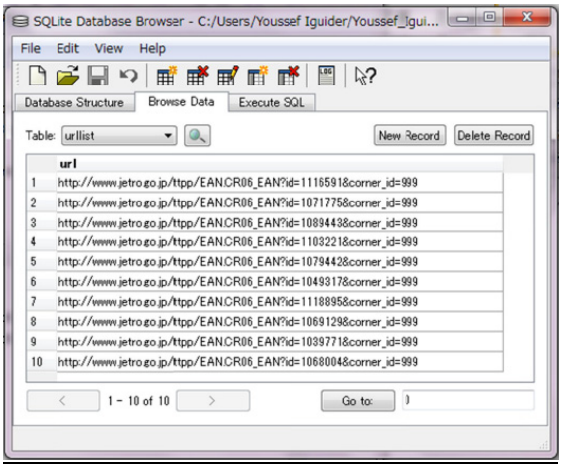


Fig. 8. List of the automatically processed and indexed URLs

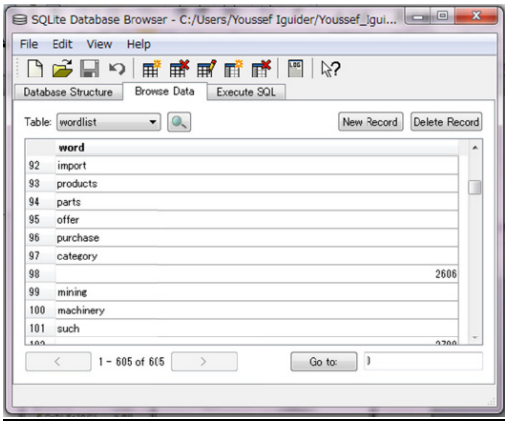


Fig. 9. List of the parsed and indexed words

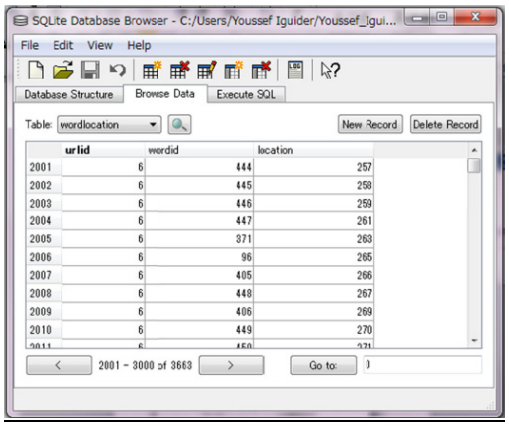


Fig. 10. Linking words to proposals, and their positions in the text.

Keyword expansion based on WorldNet:

To enable an intuitive-like search, the system uses WordNet allow identifying all words that may be relevant to the query submitted by a user when searching for a business opportunity. This may help uncovering hidden business opportunities that may be of interest to the user, but may not include the keyword that was submitted by the user. The following illustrate an example where the system is trying to expand a submitted keyword - "carpet".

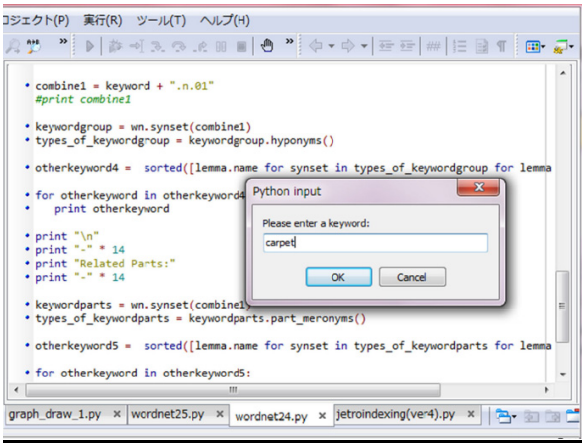


Fig. 11. Submitting a query keyword

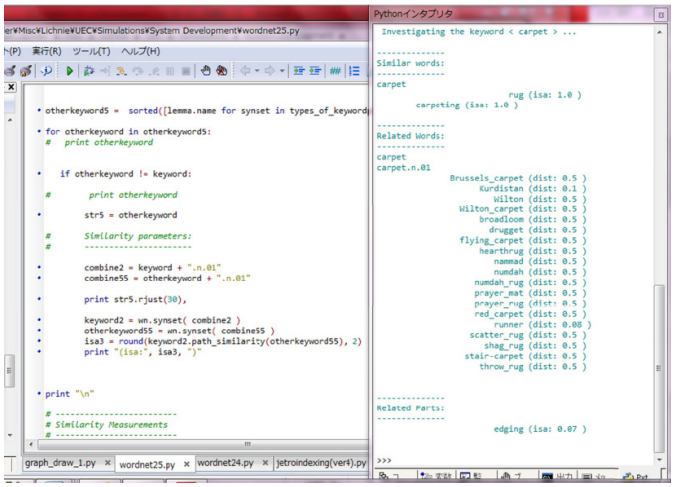


Fig. 12. Expanding the keyword “carpet”

As an example, the keyword expansion of the word “carpet” led to the following suggested results:

Similar words: carpet, rug, carpeting
Related Words: Brussels_carpet, Kurdistan, Wilton, Wilton_carpet, broadloom, drugget, flying_carpet, hearthrug, nammad, numdah, numdah_rug, prayer_mat, prayer_rug, red_carpet, runner, scatter_rug, shag_rug, stair-carpet, throw_rug
Related Parts: Edging

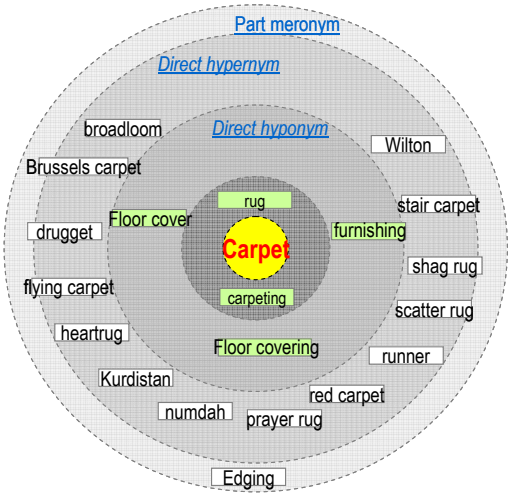


Fig. 13. Expansion of the keyword “carpet” by using WorldNet

Further, the prototype is simulated to look up the submitted keyword along with the expanded keywords in the indexed SQLite database. The data and content of the identified business proposals are then mapped to the attribute related to the user, by using the CI approach discussed above.

We currently are developing an experimental visualization system, to allow us convey the business-matching results and recommendations, via a visual graphic interactive interface, similar to what was described in Fig.4 and TABLE II.

V. Conclusion

The proposed and discussed business-matching and recommending system for e-marketplaces is expected to take the business matching process to a new level. The system makes use of a Collective Intelligence (IC) approach to identify and recommend the best matching business opportunities for the user. The results are later served to the user via a novel visual interactive graphical interface. A prototype system applying the proposed and described system is currently being developed and experimentally tested, to fully demonstrate the capabilities of the proposed system on real-world data. Although the prototype is at an early stage, the initial experiments show promising results.

References

[1] D. Engelbart , “Boosting Collective IQ,” *The Doug Engelbart Institute (www.dougengelbart.org/about/collective-iq.html)*

[2] P. Lévy, “From Social Computing to Reflexive Collective intelligence,” *IEML Research Program, CRC, FRSC, University of Ottawa. August 2009.*

[3] Stanford University’s archive “Doug Engelbart 1968 Demo” *(http://sloan.stanford.edu/mousesite/1968Demo.html)*

[4] T. Segaran, “Programming Collective Intelligence,” *O’REILLY ISBN:978-0-596-52932-1, 2007.*

[5] The United States Department of The Treasury. Various reports about the Economic Recovery *(www.treas.gov)*

[6] Japan’s Ministry of Economy, Trade and Industry, “Census of Manufactures,” *2008. (www.meti.go.jp/english/statistics/)*

[7] E.J. O’Donoghue, N. Key, and M.J. Roberts, “Does risk matter for farm businesses? The effect of crop insurance on production and diversification, “*Report of Economic Research Service, USDA.*

[8] B.S. Cromie, “Entrepreneurial Networks,” *International Small Business Journal 9, 57-74, 1991.*

[9] Federal Communications Commission (FCC 98-225), “MEMORANDUM OPINION AND ORDER,” *September 14, 1998.*

[10] MIT Center for Collective Intelligence *(http://cci.mit.edu/)*

[11] Wikipedia - The Free Encyclopedia, on “Collective Intelligence” *(http://en.wikipedia.org/wiki/Collective_Intelligence)*

[12] “INTELLIGENCE COLLECTION ACTIVITIES AND DISCIPLINES,” *Operations Security INTELLIGENCE THREAT HANDBOOK, OPSEC, April 1996*

[13] Trade Tie-up Promotion Program. The Japan External Trade Organization (JETRO) *(http://www.jetro.go.jp/ttppe/)*

[14] M. Lutz. "Programming Python," *3rd Edition. O'Reilly Media, August 2006.*

Three-phase Four-Leg Shunt Active Power Filter to Compensate Harmonics and Reactive Power

Izzeldin Idris Abdalla*, K. S. Rama Rao**, N. Perumal***
Universiti Teknologi PETRONAS, Dept. of Electrical and Electronic Engineering
31750 Tronoh, Malaysia
E-mail: * izzeldin_abdalla@yahoo.com, ** ksramarao@petronas.com.my, *** Perumal@ petronas.com.my

***Abstract*- This paper presents a compensating system for the harmonics and the reactive power using four-leg shunt active power filter (SAPF) in a three-phase four-wire distribution network and aims to minimize the harmonics and neutral current. Two control approaches p-q theory based hysteresis current control and load current detection based hysteresis current control are proposed. To validate the compensation performance of SAPF a distribution network with nonlinear loads is simulated using MATLAB/Simulink software. Simulation results are presented to assess the performance of SAPF to minimize the total harmonics distortion (THD) and neutral current, as well as to compensate the reactive power.**

***Keywords* - Harmonics mitigation, nonlinear loads, reactive power compensation, three-phase four-leg SAPF, total harmonic distortion.**

I. INTRODUCTION

Nowadays the power electronic equipments are widely used in distribution networks which act as nonlinear loads. Many power quality disturbances such as harmonics pollution, unbalanced load currents, and reactive power problems are caused by the nonlinear loads. As a result poor power factor, weakening efficiency, over heating of motors and transformers, malfunction of sensitive devices etc. [1]-[4] are encountered.

Three-phase three-wire active power filters (APFs) are previously not implemented in power net works, because of unavailability of high speed power switching devices. Recently the power electronic development spurred the interest in IGBTs, MOS-FETs etc [5], [6] and then APFs are developed incorporating power electronics technology to support the needs of industry. APFs conventionally used to mitigate harmonics, and to compensate reactive power in industrial networks, were already established in around 1970s [5], [7]-[9]. Shunt, series, and hybrid configuration are the three main types of three-phase, three-wire active power filters and their merits and de-merits are discussed in [10].

A voltage source inverter (VSI) is the heart of an active power filter. Various kinds of VSI classified according to their power converter types, operation modes, and phase numbers are presented in [9], [11]. Basically dc storage elements and power switches are the main components of VSI. An isolation transformer and an interface inductor are mandatory when APFs are implemented on power networks. The parameters of VSI play a very important role in the operation of APF as reported as in [4], [9], [11]. The APF unlike the passive filter is small in size, flexible, applicable for different voltage level networks, superior in filtering performance, and has minimum cost and operating losses [12].

Basically APF is applied to the medium voltage level networks and for use in high voltage level network, it should be connected via a three-phase transformer for the purpose of protection and design cost minimization [6], [13]. Also APF has high efficiency of approximately 94.4 % [14] and deal with lower-order harmonics such as 5th, 7th, 11th, 13th which are generated by the nonlinear loads [14], [15]. Actually, in several areas power is distributed through three-phase four-wire system and a traditional APF is inadequate for harmonics, reactive power compensation and power factor correction. To overcome this shortage, a three-phase four-wire SAPF has been introduced in the 1980s [16]-[20].

Basically there are two main kinds of three-phase, four-wire SAPF depending on their connection with the neutral wire. In the first type the neutral wire is connected to the midpoint of supply by means of a capacitor divider. In the second type the neutral wire is connected to the additional fourth leg [21]-[23]. The three-phase four-leg inverter topology is superior over the three-wire type, in mode of operation of power switches, number and compensation performance.

This paper concentrates on the three-phase four-leg SAPF which is adoptable to compensate harmonics and neutral current, generate or absorb reactive power, as well as improve the power factor. This paper also proposed two kinds of controllers, based on p-q theory, introduced earlier in [24], and load current detection using PLL. The two controllers are developed in MATLAB and fine tuned to control a three-phase four-leg SAPF. The mitigation of harmonic current components is accomplished by injecting compensation currents at the point of common coupling (PCC) with the same magnitude and opposite phase of distorted components.

II. MATHEMATICAL MODEL OF SAPF

Fig. 1 show a single line diagram configuration of the three-phase four-leg SAPF connected at the PCC of a three-phase four-wire AC system supplying mixed nonlinear loads.

By applying KCL at the PCC the source currents are as in (1).

$$i_s = i_L - i_{inv} \tag{1}$$

Applying KVL, the instantaneous source voltages are expressed as in (2).

$$v_s - v_B = R_s i_s + L_s \frac{di_s}{dt} \tag{2}$$

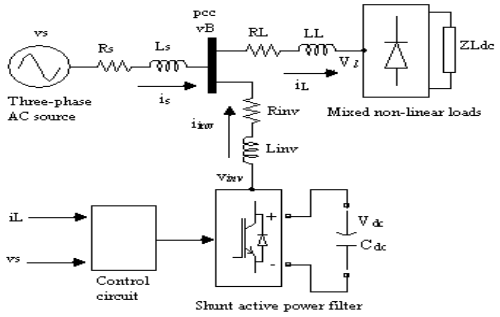


Fig. 1. Distribution network with shunt active power filter

Using Clark transformation, the source voltages and load currents can be transformed from a-b-c coordinates to $\alpha - \beta - 0$ coordinates as in (3) and (4).

$$\begin{bmatrix} v_0 \\ v_\alpha \\ v_\beta \end{bmatrix} = \sqrt{\tfrac{2}{3}} \begin{bmatrix} 1/\sqrt{2} & 1/\sqrt{2} & 1/\sqrt{2} \\ 1 & -1/2 & -1/2 \\ 0 & \sqrt{3}/2 & -\sqrt{3}/2 \end{bmatrix} \begin{bmatrix} v_{sa} \\ v_{sb} \\ v_{sc} \end{bmatrix} \tag{3}$$

$$\begin{bmatrix} i_0 \\ i_\alpha \\ i_\beta \end{bmatrix} = \sqrt{\tfrac{2}{3}} \begin{bmatrix} 1/\sqrt{2} & 1/\sqrt{2} & 1/\sqrt{2} \\ 1 & -1/2 & -1/2 \\ 0 & \sqrt{3}/2 & -\sqrt{3}/2 \end{bmatrix} \begin{bmatrix} i_{La} \\ i_{Lb} \\ i_{Lc} \end{bmatrix} \tag{4}$$

The real, imaginary and zero-sequence instantaneous powers in three-phase four-wire system are expressed as in matrix equation (5).

$$\begin{bmatrix} p_0 \\ p \\ q \end{bmatrix} = \begin{bmatrix} v_0 & 0 & 0 \\ 0 & v_\alpha & v_\beta \\ 0 & -v_\beta & v_\alpha \end{bmatrix} \begin{bmatrix} i_0 \\ i_\alpha \\ i_\beta \end{bmatrix} \tag{5}$$

The instantaneous real and imaginary powers include AC and DC components and are expressed as in (6)

$$p = \overline{p} + \tilde{p}\ , q = \overline{q} + \tilde{q}\ , p_0 = \overline{p}_0 + \tilde{p}_0 \tag{6}$$

The DC components, $\overline{p}$, $\overline{q}$ are the average real and imaginary powers originating from the fundamental component of the load current. The AC components, $\tilde{p}$, $\tilde{q}$, are the oscillating or ripple real and imaginary powers resulting from harmonics, p_h, q_h and negative sequence components of the load current. After successful compensation the AC component of real power, and the total imaginary power, will be eliminated or exist with small values. At that time the source current is sinusoidal, and in-phase with the source voltage and the power factor will be very close to unity [15], [25]-[27]. The zero-sequence instantaneous power is eliminated from (5), and then taking inverse transformation and separating real and imaginary parts, the matrix equation (7) was obtained.

$$\begin{bmatrix} i_\alpha \\ i_\beta \end{bmatrix} = \tfrac{1}{\Delta} \left\{ \begin{bmatrix} v_\alpha & -v_\beta \\ v_\beta & v_\alpha \end{bmatrix} \begin{bmatrix} p \\ 0 \end{bmatrix} + \begin{bmatrix} v_\alpha & -v_\beta \\ v_\beta & v_\alpha \end{bmatrix} \begin{bmatrix} 0 \\ q \end{bmatrix} \right\} \cong \begin{bmatrix} i_{\alpha p} \\ i_{\beta p} \end{bmatrix} + \begin{bmatrix} i_{\alpha q} \\ i_{\beta q} \end{bmatrix} \tag{7}$$

The active and reactive components of current in (7) can be expressed as in (8) and (9).

$$i_{\alpha p} = v_\alpha * p / \Delta\ , i_{\alpha q} = -v_\beta * q / \Delta \tag{8}$$

$$i_{\beta p} = v_\beta * p / \Delta , i_{\beta q} = v_\alpha * q / \Delta \tag{9}$$

The three-phase reference currents from the above reactive components of current can be obtained as in (10) and (11), respectively.

$$\begin{bmatrix} i_{fa}^* \\ i_{fb}^* \\ i_{fc}^* \end{bmatrix} = \sqrt{\tfrac{2}{3}} \begin{bmatrix} 1/\sqrt{2} & 1 & 0 \\ 1/\sqrt{2} & -1/2 & \sqrt{3}/2 \\ 1/\sqrt{2} & -1/2 & -\sqrt{3}/2 \end{bmatrix} \begin{bmatrix} i_{f\alpha}^* \\ i_{f\beta}^* \end{bmatrix} \tag{10}$$

$$i_{fn}^* = i_{fa}^* + i_{fb}^* + i_{fc}^* \tag{11}$$

III. THE PROPOSED CONTROL STRATEGIES

For the complicated control algorithm of three-phase four-leg SAPF, engineers seek the most simple and effective control method. This paper has developed and extended p-q theory introduced in [15] to control three-phase four-leg SAPF. Fig. 2 shows the proposed current control circuit consisting of the hysteresis current control block and the p-q theory based reference current calculation. The inverter receives the gating signals from hysteresis current control block.

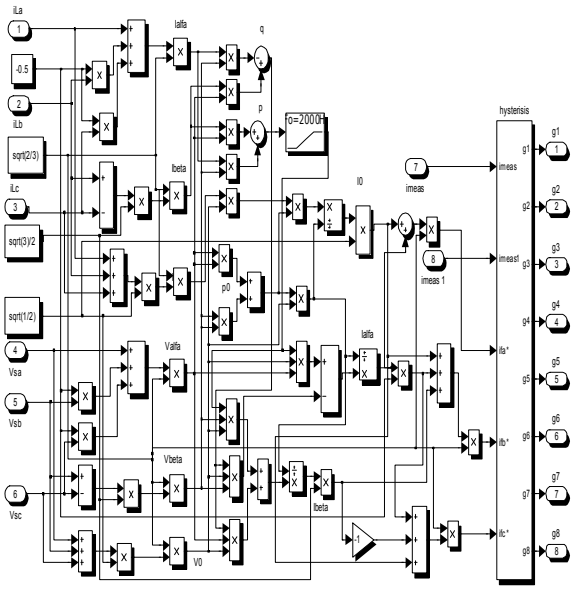


Fig. 2. Control circuit using p-q theory-based compensation strategy

The control circuit is implemented using equations (3) up to (11). AC component of active power can be obtained by extracting the dc component using a high-pass filter.

In the second proposed control strategy only the load current is detected by PLL to generate the reference currents.

The current control circuit, shown in Fig. 3 consists of the hysteresis current control block and the load current detection based reference current calculation.

The inverter receives the gating signals from the hysteresis current control block as shown in Fig. 3.

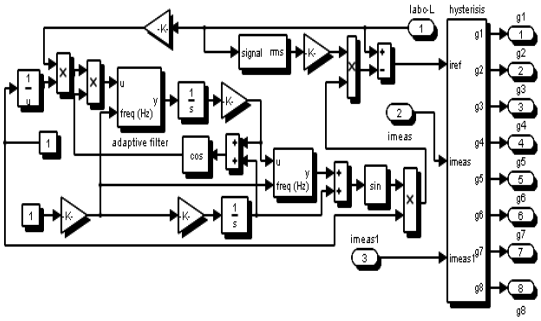


Fig. 3. Control circuit using load current detection strategy

IV. SIMULATION AND RESULTS

The parameters of the system for simulation are obtained from reference [14]. A three-phase and three single-phase diode rectifiers considered as nonlinear loads, are connected to the phases ‘a’, ‘b’ and ‘c’ of the distribution network which is depicted in Fig. 4.

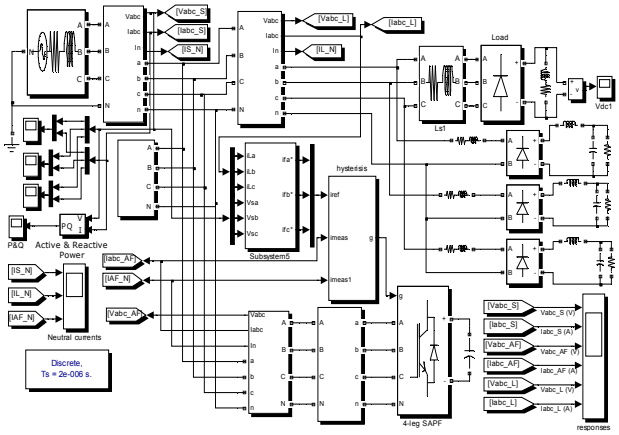


Fig. 4. Simulink model of the three-phase four-leg SAPF

The proposed control schemes and the power circuit of a four-leg SAPF is simulated using MATLAB/Simulink 7.9.0 software package. Simulation of the distribution network without compensation and with compensation under proposed control topologies are carried out. Figs. 5 to 11, represent simulation results of voltages, currents and powers without SAPF.

Fig. 5 show the waveform of source voltages, and the source voltages are observed to be sinusoidal.

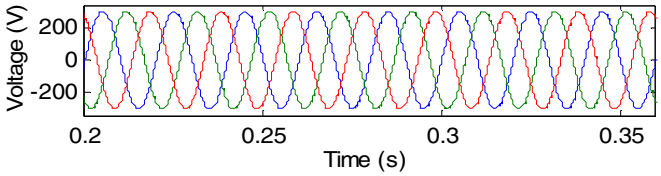


Fig. 5. Source voltages

Fig. 6 represents the behavior of the three-phase four-wire system source currents, which are highly distorted.

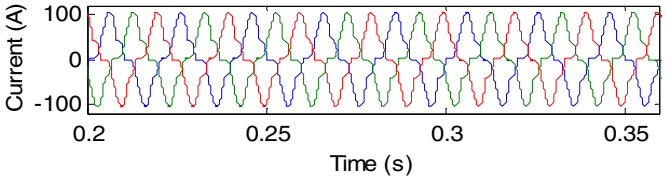


Fig. 6. Source currents

Fig. 7 shows the harmonic spectrum of source current for phase ‘a’ and the THD is observed to be equal to 31.17 %. Similar values of THD are obtained for phases ‘b’ and ‘c’.

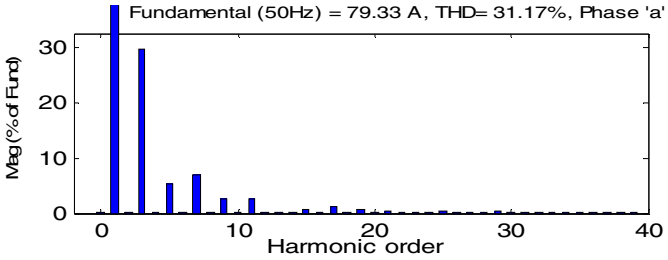


Fig. 7. Harmonic spectrum

Fig. 8 shows the three-phase four-wire system load currents. It is observed that the load current waveforms are similar with both the control techniques.

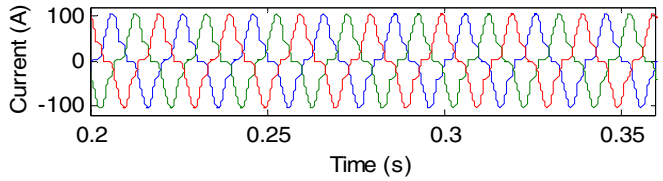


Fig. 8. Load currents

Fig. 9 shows the three-phase four-wire system source neutral current.

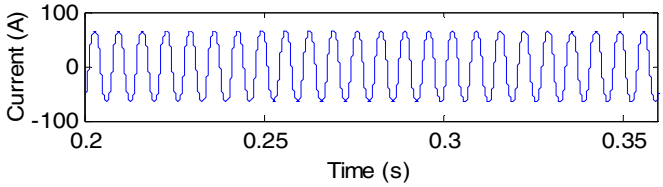


Fig. 9.source neutral current

Fig. 10 shows the three-phase four-wire system source voltage and current for phase ‘a’ which are both non-sinusoidal and the current is not in phase with the source voltage. Similar results are obtained for phases ‘b’ and ‘c’ also. It is clear from Fig. 10 that the supply side has poor power factor, excessive amount of reactive power and high THD.

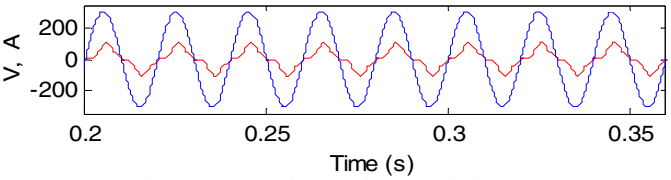


Fig. 10. Source voltage and current of phase ‘a’

Fig. 11 shows the real and imaginary powers and it is observed that the value of the imaginary power is very high.

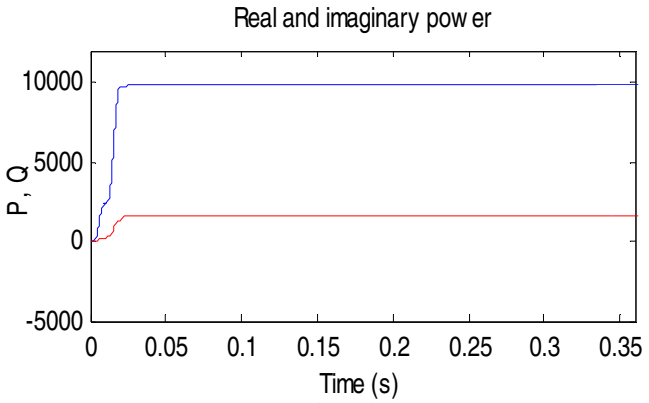


Fig. 11. Real and imaginary power

Figs. 12 to 17 show the simulation results of the distribution network using SAPF under p-q theory reference currents calculation and hysteresis current control. Fig. 12 represents the source currents, after compensation. It is observed that the currents are very close to sinusoidal as compared to the results obtained before filtering.

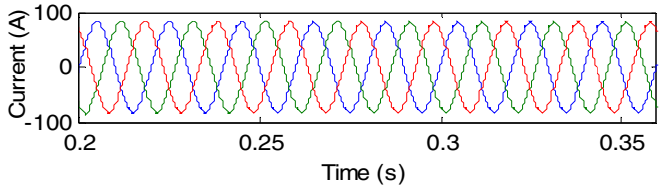
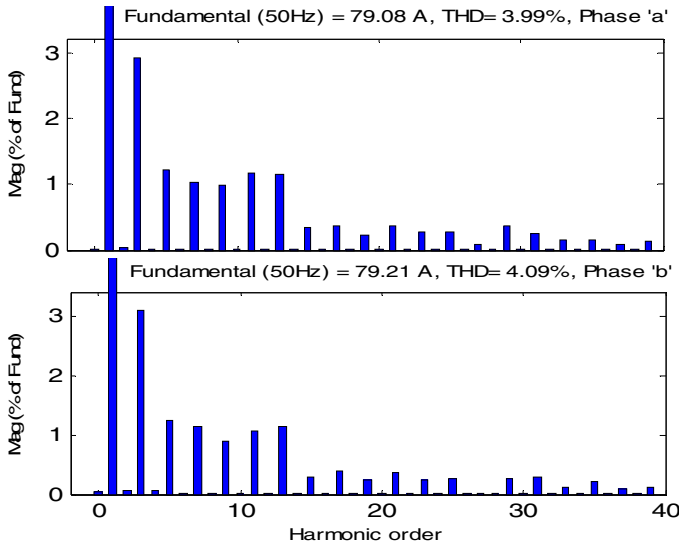


Fig. 12. Source currents

Fig. 13 represents the harmonic spectrum of source currents which proved the ability of SAFP for THD minimization as well as for reactive power compensation. For all the three phases the THD is proved to be less than the IEEE-519 standards.



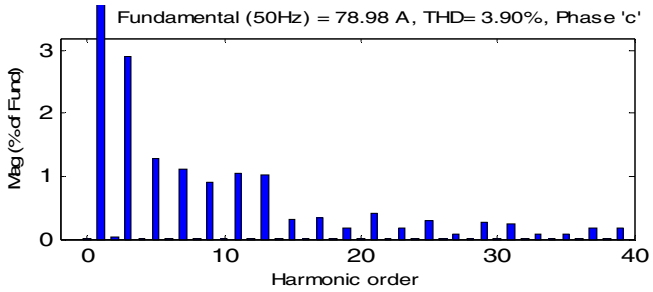


Fig. 13. Harmonic spectrum of sourse current phases ‘a’, ‘b’ and ‘c’

Fig. 14 show the current injected by the SAPF in phase ‘a’. Similar currents are injected in phases ‘b’ and ‘c’ also.

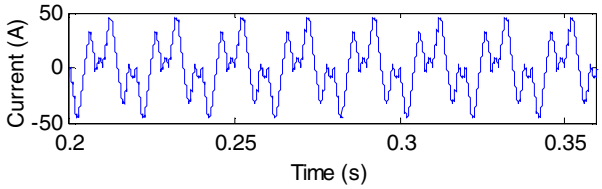


Fig. 14. SAPF compensation current

Fig. 15 shows the source neutral current after filtering, which is observed to be very close to zero.

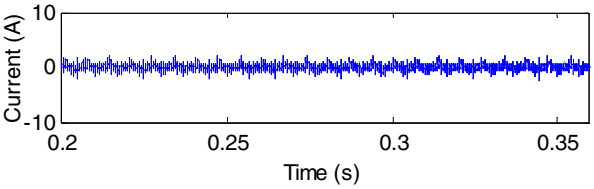


Fig. 15. Filtered source neutral current

Fig. 16 shows the source voltages and currents of phases ‘a’, ‘b’ and ‘c’ which are observed to be sinusoidal, and are also in phase. Thus, it can be concluded that the developed SAPF with proposed controller has successfully compensated the reactive power as well as improved the source side power factor close to unity.

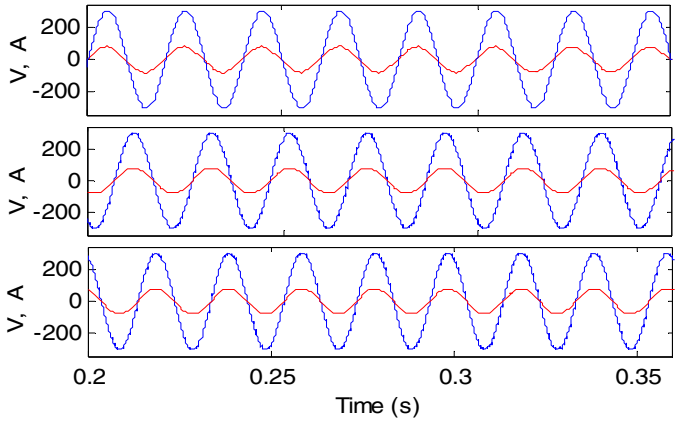


Fig. 16. Source voltage and current of phases ‘a’, ‘b’ and ‘c’

Fig. 17 shows the real and imaginary powers after compensation and the reactive power is observed to be successfully compensated as compared to Fig. 11.

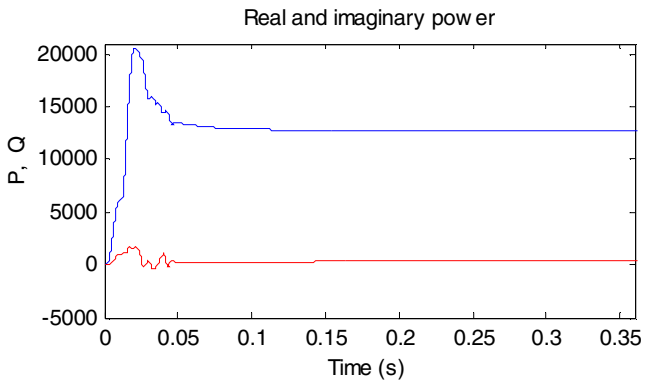


Fig. 17. Real and imaginary power after compensation

Figs. 18 to 23, represent the simulation results using SAPF with load current detection method for reference currents calculation and hysteresis current control. From Fig. 18 it is observed that the source currents are close to sinusoidal.

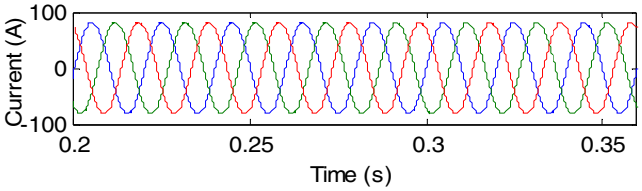


Fig. 18. Source currents

Fig. 19 shows the harmonic spectrum of source currents in phases ‘a’, ‘b’ and ‘c’. As observed the source current THD is successfully minimized to a very low value as compared with the result before compensation which also shows that the reactive power and harmonics are successfully compensated.

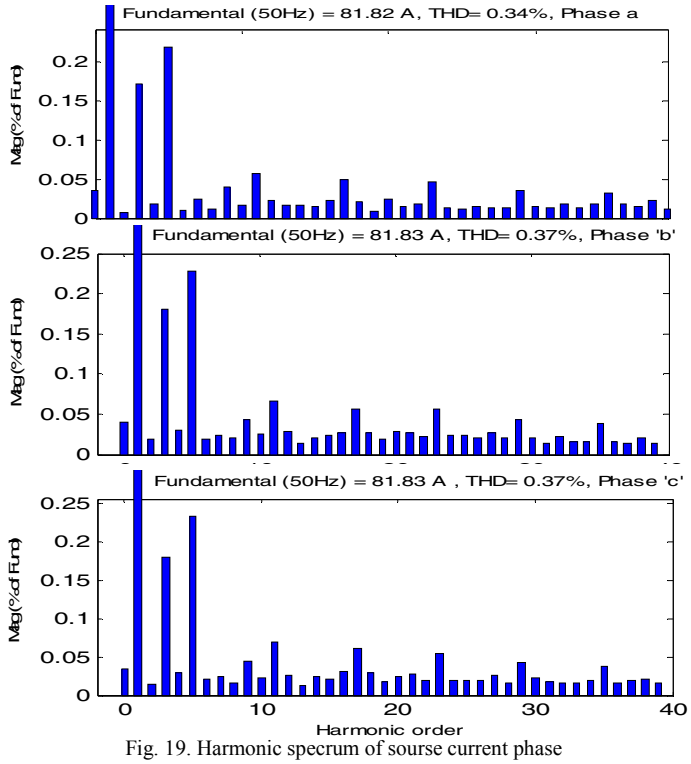


Fig. 19. Harmonic specrum of sourse current phase

Fig. 20 shows the current injected by the SAPF in phase ‘a’. and similar currents are injected in phases ‘b’ and ‘c’ also.

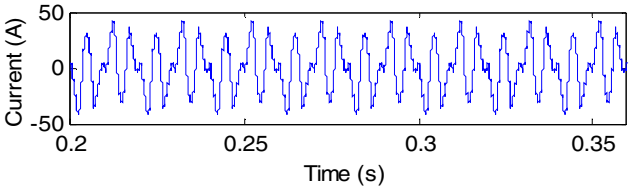


Fig. 20. SAPF compensation current

Fig. 21 shows the source neutral current after filtering, which is observed to be very close to zero.

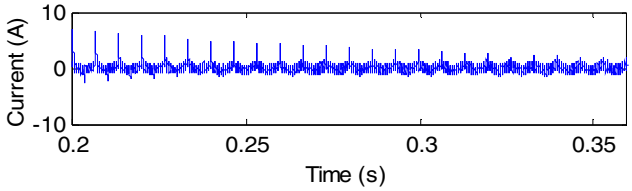


Fig. 21. Source neutral currents

Figs. 22 (a) to (c) represents the source currents and source voltages of the phases ‘a’, ‘b’ and ‘c’ after filtering which are observed to be sinusoidal, and are also in phase.

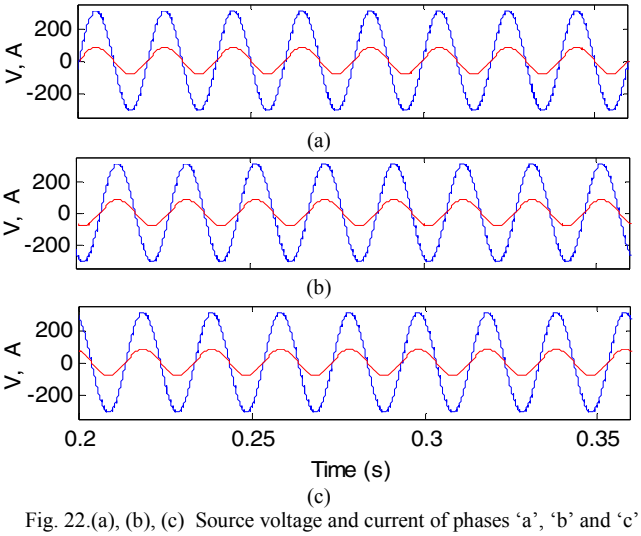


Fig. 22.(a), (b), (c) Source voltage and current of phases ‘a’, ‘b’ and ‘c’

Fig. 23 shows the real and imaginary powers after compensation and the reactive power is observed to be successfully compensated as compared to Fig. 11.

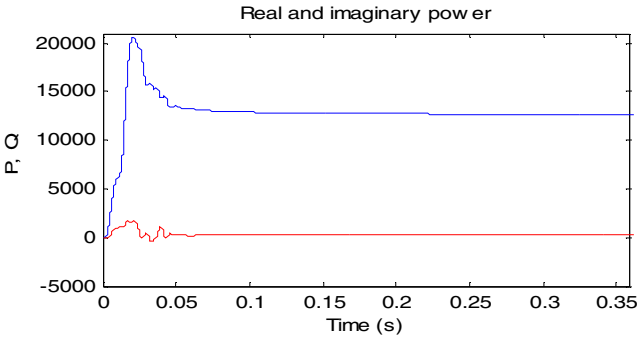


Fig. 23. Real and imaginary power after compensation

The THD of the source currents in phases 'a', 'b' and 'c' are observed to be 3.99 %, 4.09 % and 3.90 % respectively, when SAPF is used by p-q theory based hysteresis current controller, and 0.34 %, 0.37 % and 0.37 % respectively, when SAPF is controlled by the load current detection based hysteresis current controller. The % THD obtained by both the control techniques is observed to be within the prescribed limit of 5 % as recommended by IEEE-519 standards.

IV. CONCLUSIONS

Two control schemes, a p-q theory based hysteresis current control and a load current detection based hysteresis current control, for a three-phase four-leg SAPF in a three-phase four-wire distribution network supplying nonlinear loads are presented. It is shown that both the control techniques minimized the THD and neutral current. Simulation results have shown successful reactive power compensation, power factor correction and minimization of harmonics by the SAPF. The neutral current is minimized and THD is shown to be within the prescribed limits of IEEE-519 standards. Furthermore it is proved that the three-phase source currents are sinusoidal and are in phase with source voltages validating the good performance of SAPF in three-phase, four-wire distribution system supplying non-linear loads.

ACKNOWLEDGMENT

The authors gratefully acknowledge the support provided by Universiti Teknologi PETRONAS, Malaysia.

REFERENCES

[1] S. Hive, K. Chatterjee, and B.G. Fernandes, "VAr compensation and elimination of harmonics in three-phase four-wire system based on unified constant-frequency integration control," 11th International Conference on Harmonics and Quality of Power (IEEE Cat. No.04EX951), Ieee, 2004, pp. 647-651.

[2] M. George and K.P. Basu, "Modeling and control of three-phase shunt active power filter," American Journal of Applied Sciences, vol. 5, Aug. 2008, pp. 1064-1070.

[3] "A fuzzy logic controlled sliding mode control (SMC) of inverter in shunt active power filter for power quality improvement," International Journal of Electrical and Power Engineering, vol. 2, 2008, pp. 398-402.

[4] B. Singh, A. Chandra, and K. Al-Haddad, "Reactive power compensation and load balancing in electric power distribution systems," International Journal of Electrical Power & Energy Systems, vol. 20, Aug. 1998, pp. 375-381.

[5] I. Zamora, A.J.M.P. Eguia, I. Albizu, K.J. Sagastabeitia, and E. Fernhdez, "Simulation by MATLAB / simulink of active filters for reducing THD created by industria1 systems," Power Tech Conference Proceedings, IEEE Bologna, 2003.

[6] I.I. Abdalla, K.S.R. Rao, and N. Perumal, "Harmonics mitigation and power factor correction with a modern three-phase four-leg shunt active power filter," *IEEE International Conference on Power and Energy*, 2010, pp. 156-161.

[7] H. Akagi, "Active harmonic filters," Proceedings of the IEEE, vol. 93, Dec. 2005, pp. 2128-2141.

[8] F. Hamoudi, A. Chaghi, M. Adli, and A. Hocine, "A Comparative study between two strategies for four-wire shunt active filter control.

[9] P. Lohia, M.K. Mishra, K. Karthikeyan, and K. Vasudevan, "A minimally switched control algorithm for three-phase four-leg VSI topology to compensate unbalanced and nonlinear load," IEEE Transactions on Power Electronics, vol. 23, Jul. 2008, pp. 1935-1944.

[10] Z. Salam, T.P. Cheng, and A. Jusoh, "Harmonics mitigation using active power filter : a technological review," Elektrika, vol. 8, 2006, pp. 17-26.

[11] M.K. Mishra and K. Karthikeyan, "A study on design and dynamics of voltage source inverter in current control mode to compensate unbalanced and non-linear loads," International Conference on Power Electronic, Drives and Energy Systems, Ieee, 2006, pp. 1-8.

[12] H. Akagi, "Modern active filters and traditional passive filters," Bulletin Of The Polish Academy Of Sciences, Technical Sciences, vol. 54, 2006, pp. 255-269.

[13] J. Dixon, S. Member, Y. Valle, M. Orchard, M. Ortúzar, L. Morán, S. Member, and C. Maffrand, "A full compensating system for general loads , based on a combination of thyristor binary active power filter," IEEE TRANSACTIONS ON INDUSTRIAL ELECTRONICS, vol. 50, 2003, pp. 982-989.

[14] A. Unsal, A.R.V. Jouanne, and V.L. Stonick, "A DSP controlled resonant active filter for power conditioning in three-phase industrial power systems," Elsevier science, vol. 82, 2002, pp. 1743 - 1752.

[15] M. Ucar and E. Ozdemir, "Control of a 3-phase 4-leg active power filter under non-ideal mains voltage condition," Electric Power Systems Research, vol. 78, 2008, pp. 58-73.

[16] C. a Quinn, N. Mohan, and H. Mehta, "A four-wire, current-controlled converter provides harmonic neutralization in three-phase, four-wire systems," Eighth Annual Applied Power Electronics Conference and Exposition,, Ieee, 1993, pp. 841-846.

[17] D. Wu, Y. Che, and K.W.E. Cheng, "Design and performance of a shunt active power filter for three- phase four-wire system," 3rd International Conference on Power Electronics Systems and Applications, 2009, pp. 1-4.

[18] M. Aredes, J. Hafner, and K. Heumann, "Three-phase four-wire shunt active filter control strategies," IEEE Transactions on Power Electronics, vol. 12, Mar. 1997, pp. 311-318.

[19] M. Pakdel and H. Farzaneh-fard, "A Control strategy for load balancing and power factor correction in three-phase four-wire systems using a shunt active power filter," IEEE International Conference on Industrial Technology, ICIT, 2006, pp. 579-584.

[20] W. Xiaogang, X. Yunxiang, and S. Dingxin, "Three-phase four-leg active power filter based on nonlinear optimal predictive control," 27th Chinese Control Conference, Ieee, 2008, pp. 217-222.

[21] Z. Juan, W.U. Xiao-jie, G. Yi-wen, and D.A.I. Peng, "Simulation research on a SVPWM control algorithm for a four-leg active power filter," Journal of China University of Mining & Technology, vol. 17, 2007, pp. 590-594.

[22] A. Bellini and S. Bifaretti, "A Simple control technique for three-phase four-leg inverters," International Symposium on Power Electronics, Electrical Drives, Automation and Motion, IEEE, 2006, pp. 18-23.

[23] D.C. Patel, R.R. Sawant, and M.C. Chandorkar, "Control of four-leg sinewave output inverter using flux vector modulation," 34th Annual Conference of Industrial Electronics IECON , IEEE, 2008, pp. 629-634.

[24] G.W. Chang, S.K. Chen, and M. Chu, "An efficient a–b–c reference frame-based compensation strategy for three-phase active power filter control," Electric Power Systems Research, vol. 60, 2002, pp. 161- 166.

[25] H.H. Tumbelaka, "Power Flow in A Load-Current Sensorless Shunt Active Power Filter," Jurnal Teknik Elektro, vol. 7, 2007, pp. 1-7.

[26] H. Akagi, E.H. Watanabe, and M. Aredes, "chapter-3, the instantaneous power theory," Instantaneous power theory and applications to power conditioning, 2007, pp. 41-107.

[27] M.K. Syed and B.S. RAM, "Instantaneous power theory based active power filter: a MATLAB/simulink approach," Journal of Theoretical and Applied Information Technology, pp. 536-541.

3D Object Tracking Using Three Kalman Filters

Yasir Salih
Department of Electrical & Electronic Engineering
Universiti Teknologi PETRONAS
Perak, Malaysia
Email: yasir_g01297@utp.edu.my

Aamir S. Malik
Department of Electrical & Electronic Engineering
Universiti Teknologi PETRONAS
Perak, Malaysia
Email: aamir_saeed@petronas.com.my

***Abstract*—In the recent years, 3D tracking has gained attention due to the perforation of powerful computers and the increasing interest in tracking applications. One of the most common tracking algorithms used is the Kalman filter. Kalman filter is a linear estimator that is based on approximating system's dynamics using Gaussian probability distribution. In this paper, we provide a detailed evaluation of the most common Kalman filters, their use in the literature and their implementation for 3D visual tracking. The main types of Kalman filters discussed are linear Kalman filter, extended Kalman filer and unscented Kalman filter.**

***Keywords*—3D tracking, Kalman filter, LKF, EKF, UKF, vehicle tracking.**

I. INTRODUCTION

Tracking is one of the important applications of computer vision. In the recent year, 3D tracking has been widely researched due to the increasing interest in 3D tracking application for monitoring and security purposes. In addition, the availability of powerful and cheap computers has contributed to the increasing use of Kalman filter in 3D tracking applications. This paper summarizes some of the recently published work about 3D tracking using Kalman filters. These filters, which are known as stochastic filters, consider uncertainties when estimating state values. This makes it more robust to noise and interferences [1]. 3D tracking using Kalman filters has been used in many applications such as:

1) Security and monitoring

3D tracking is used for detection of loitering especially in sensitive areas such as airport and government building. It is also used in measuring crowd flux statistics and abnormal gatherings [2].

2) Vehicle tracking and traffic control

3D tracking is used for highways monitoring and surveillance of the transportation infrastructures. This helps in reducing accident rates by detecting vehicles that exceed speed limits. Tracking is also used in monitoring car parks and detecting vehicles going in a wrong direction [3].

3) Computer games

3D tracking is used in computer games and virtual reality applications. Head tracking and hand tracking are mostly used for virtual reality applications. The most famous games that use 3D tracking are the Nintendo Wii console which uses IR camera [4].

4) Robot navigation

3D tracking is used for navigating robots and unmanned vehicles. Tracking enables these machines to examine hostile environments such as mine field, space exploration and inspecting bags that might contain a bomb [5,6].

This paper addresses 3D tracking with emphasis on Kalman filters. The discussed filters are linear Kalman filter, extended Kalman filter and unscented Kalman filter. Kalman filter is a linear estimator that assumes variables have a normal probability distribution. This paper is organized as follows; Section 2 summarizes the published work in the last decade about Kalman filters. Section 3 addresses the technical details of these Kalman filters. Section 4 gives a thorough evaluation for these three filters by comparing their performance subjectively and objectively. Finally, section 5 concludes the study by summarizing the overall work and the future directions of the field.

II. RELATED WORK

Although Kalman is considered as a simple stochastic filter, yet it provides optimal estimation for linear systems that has Gaussian distribution. In this section, we summarize the published work about the three types of Kalman filters; linear Kalman filter, extended Kalman filter and unscented Kalman filter.

A. Linear Kalman filter

Linear Kalman filter has been used in [7] for implementing a generic tracking algorithm. At the beginning of the tracking process, the object of interest is selected interactively by user. After that, the region of interest is segmented using region growing method. For measurement, the dominant object color is computed using K-means clustering method. The method had a large computational time (around 1.5 second per frame) which is not convenient for real time tracking. In another work [8], the linear Kalman filter is being used for detecting the head of the vehicle occupant by using a 3D range camera mounted in the vehicle. The data of the range camera is represented using Reeb graphs. These graphs generate a list of locations for possible head candidates. Then these possible head locations are evaluated using multiple hypothesis trackers. Multiple hypothesis trackers are linear Kalman filters that evaluate all the possible values

for head candidates and retain the most likely one.

Robot navigation is most common application for using linear Kalman filter because it has low computation. In [5], Fernandez et al. used linear Kalman filter for navigating a mobile robot in a room. The vision system is not mounted on the robots but rather at a central processing unit which guides these robots using radio signals. Each one of these robots is equipped with IR sensors that form a T shape pattern in order to ease the detection of these robots. The algorithm has small errors. However, not having processing onboard is a major disadvantage for this work.

B. Extended Kalman filter

Ababsa [9] has used extended Kalman filter for estimating camera pose. The pose is estimated by finding the correspondence between 3D lines of a known room and 2D edges. Then the correspondence is obtained by estimating the rotation and translation matrices of the affine transform that matches the projected 3D lines with edges. This filtering process is repeated iteratively until error threshold is less than a predetermined value. One of the disadvantages of this work is that the 3D lines of the scene have to be known prior to estimation.

Geo et al. [10] used multiple extended Kalman filters to construct a generic object tracking algorithm. The idea of using multiple Kalman filters is to reduce the error by firstly estimating new object location. Then this location is evaluated with reference values using normalized cross-correlation. Then a second Kalman filter is used to give better estimation. In this work, three extended Kalman filters were used sequentially. Although multiple filters will incur additional computation; the estimation error has been reduced greatly.

In [11], an adaptive extended Kalman filter is used for navigating a robotic arm. The adaptive filter has the ability to update noise covariance in order to reduce errors. However, this reduction of errors comes at the cost of increase in computational time. In a similar work [3], extended Kalman filter is used for autonomous vehicle navigation. The robot estimates the target location as well as its own location. The measurements are color features of the tracked object and stereo disparity map. In order to have accurate measurements about the robot location, the robot is equipped with motion sensors that detect the displacement in robot location and provide ground truth data about the robot location.

C. Unscented Kalman filter

Unscented Kalman filter is used for nonlinear motions that cannot be approximated using extended Kalman filter. Gauso et al. [12] have used unscented Kalman filter for hand pose estimation using multiple cameras. The hand is represented by an articulated model of 12 degree of freedom and the motion is in form of translation distances and rotation angles. For measurements, the hand is represented in a voxel model which is generated from these images using background subtraction. The algorithm has high computational time due to complex degree of freedom model used. In another work [13], unscented Kalman filter was used for vehicle tracking using a camera mounted on a moving vehicle. Thus, the filter estimates the motion of the tracked vehicle and the host vehicle. The vehicle is detected by firstly projecting the previously detected location of current image. Then the location of this box is varied until it matches with the ROI of current image.

From the previously surveyed work, it is clear that linear and extended Kalman filters are the popular Kalman filters used due to their low computational requirements. Unscented Kalman filter has been used only in cases when the other two filters give poor results.

III. KALMAN FILTERING ALGORITHMS

Filtering is about attempting to estimate the next state of the system given the previous state and measured observations. This section discusses the algorithms and the concepts of Kalman filters.

A. Basic principles

Kalman filter is an iterative prediction-correction process to estimate the state of the system. Let's consider a system represented by a state space as shown in equation (1) and (2). F is the state transition matrix which transforms last estimation to the current one and $\boldsymbol{H}$ is the measurement matrix. Both $\boldsymbol{F}$ and $\boldsymbol{H}$ has size of [n x n] where n is the dimension of the state space, v_k is the process noise with covariance $\boldsymbol{Q}$ and e_k is the measurement noise with noise covariance $\boldsymbol{R}$.

$$x_k = Fx_{k-1} + v_k \tag{1}$$

$$z_k = Hx_k + e_k \tag{2}$$

B. Linear Kalman filter

The linear Kalman filter gives an optimal estimation for the next state using linear equations assuming that the variables have a Gaussian probability distribution. Equations (3) until (7) show the steps for linear Kalman filter:

a) Propagate the mean value for next state

$$\hat{x}_k^- = F\hat{x}_{k-1} \tag{3}$$

b) Propagate covariance of next estimation

$$P_k^- = FP_{k-1}F^T + Q \tag{4}$$

c) Calculate Kalman gain

$$K_k = P_k^- H^T (HP_k^- H^T + R)^{-1} \tag{5}$$

d) Correct the mean value

$$\hat{x}_k = \hat{x}_k^- + K_k(z_k - H\hat{x}_k^-) \tag{6}$$

e) Correct the covariance

$$P_k = (I - K_k H)P_k^- \quad (7)$$

$\hat{x}_k$ is the estimated state at time k and P_k is the error ($e_k = x_k - \hat{x}_k$) covariance. K_k is Kalman gain which is chosen to minimize the covariance error. z_k is the actual measurement and I is the identity matrix. Linear Kalman filter is designed to work with motions that have linear dynamics and the noise is Gaussian. These conditions are considered as the main limitations of Kalman filter [14].

C. Extended Kalman filter

When the system's dynamics is not linear, linear Kalman filter performs poorly because the basic assumptions of Kalman filter are not met. This problem can be solved by linearizing the estimation around the mean of previous state; which is known as Extended Kalman filter. In the same manner as linear Kalman filter, extended Kalman filter follow similar estimation steps as in equations (7) until (11).

Steps for extended Kalman filter:

a) Propagate the mean value for next state

$$\hat{x}_k^- = \hat{x}_{k-1} \quad (8)$$

b) Propagate covariance of next estimation

$$P_k^- = P_{k-1} + Q \quad (9)$$

c) Calculate Kalman gain

$$K_k = P_k^-(P_k^- + R)^{-1} \quad (10)$$

d) Correct the mean value

$$\hat{x}_k = \hat{x}_k^- + K_k(z_k - \hat{x}_k^-) \quad (11)$$

e) Correct the covariance

$$P_k = (I - K_k)P_k^- \quad (12)$$

D. Unscented Kalman filter

Unscented Kalman filter represents the state with a minimal set of carefully chosen sample (sigma) points. $2n + 1$ sigma points are selected around the previous estimation where n represent the dimensions of the state space[11]. Then a probability weight is assigned to these sigma points. After that, these sigma points are transformed using the unscented transformation. This transformation gives a new estimation for the state variables which are then corrected by transforming sigma point through the measurement model in order to compute the Kalman gain. Finally, the estimation is corrected using the Kalman gain in a similar manner to the linear and extended Kalman filters.

Sigma points are selected around the previous mean by adding to the mean the square root of covariance matrix. Then the weight of the first sigma point is set randomly, while other weights are proportional to it [15].

Compared to the extended Kalman filter, unscented Kalman filter approximates the mean of estimation by a third order Taylor series while the extended Kalman filter linearizes it using a first order Taylor series. The covariance in unscented Kalman filter has less error compared to the covariance of the extended Kalman filter. However, the computation time of unscented Kalman filter is larger than the ones for the extended Kalman filter [11].

IV. Results and Discussion

The three algorithms have been tested on different video sequences and evaluated quantitatively using root mean square error (RMSE). In this section, firstly we describe how measurements have been extracted from images. Then the results are displayed and analyzed.

A. The experiments

The data has been collected using CCD camera in indoor and outdoor scenes. Measurements have been extracted from these video sequences using motion and shape cues. Figure 1 shows measurement extraction process. The measured variables are the object location and size of the bounding box which are extracted using background subtraction and shape extraction techniques from the background subtracted image.

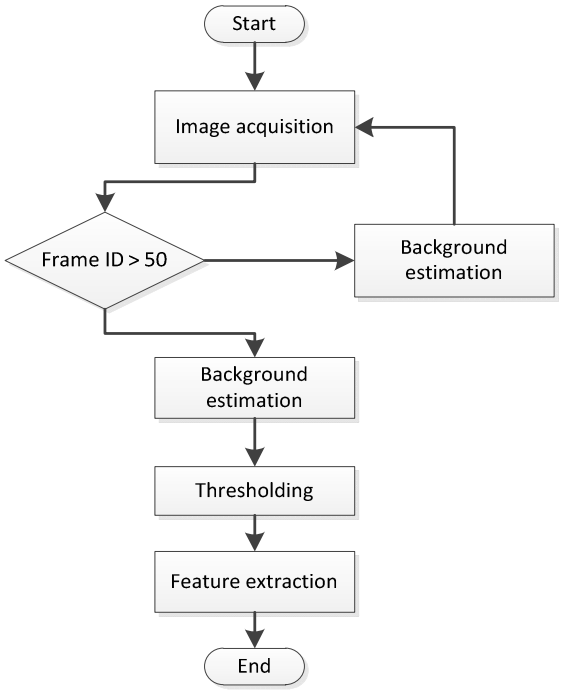


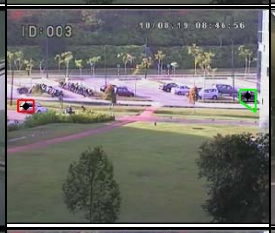
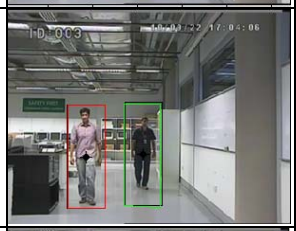
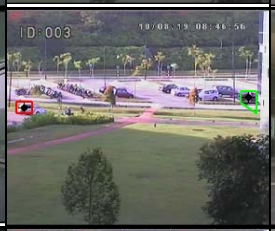
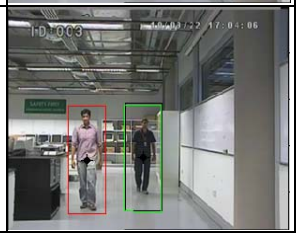
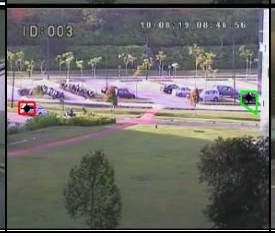
Figure 1. Measurements extraction process.

B. Results and discussion

The three Kalman filters have been evaluated subjectively a shown in table 1 which shows tracking results for various scenarios. The measured object location is represented by a black box while boxes of other colors represent the estimated object location. In table 2, the results of the three filters are identical for both the object location and the size of bounding box.

TABLE I.

TRACKING RESULTS OF THREE KALMAN FILTERS

Filter	Sequence #1	Sequence #2	Sequence #3	Sequence #4
Original image				
Linear Kalman filter				
Extended Kalman filter				
Unscented Kalman filter				

Similar results can be seen in table 2 where we implemented these tracking algorithms on one video sequence by considering random frames. The three filters have performed accurately where the measured object location and estimated one overlap completely which is indicated by the overlapping bounding boxes (the black box is been overlaid by the green bounding box).

The accuracy of the estimation is been measured quantitatively using RMSE measure. Looking at the RMSE analysis, unscented Kalman filter has smaller errors than linear Kalman filter and extended Kalman filter as it is shown in figure 2. Unscented Kalman filter has the ability to estimate nonlinear variables through the unscented transformation, this make the filter able to overcome linearity limitation associated with the other types of Kalman filter. Also we can see that the extended Kalman filter has slightly better accuracy than the linear Kalman filter, because the extended Kalman filter approximate nonlinear system using first order derivative which gives acceptable results with the system dynamics is slightly nonlinear.

The RMSE value for the object position is smaller than the one for the size of the bounding box. The size of the bounding box relies on the algorithms ability to extract the full size of the tracked object. In some cases and due to lighting variations the algorithm fails to extract the accurate size of the tracked object. These variations are highly nonlinear which and tend to have non-Gaussian dynamics. At the contrary, the object position follows a linear dynamics model and it has a Gaussian probability distribution, thus Kalman filters yields higher accurate estimation for object position rather than bounding box size.

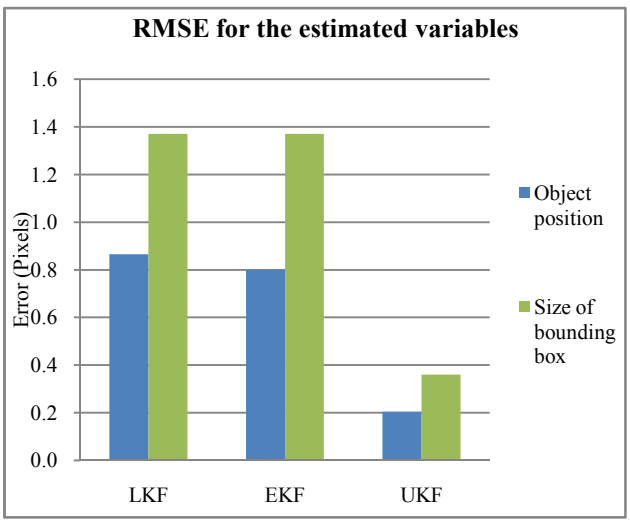


Figure 2. Estimation error (RMSE) for object location and bounding box.

TABLE II.
TRACKING RESULTS OF THREE KALMAN FILTERS

Frame No.	70	151	270	367	490
Linear Kalman filter					
Extended Kalman Filter					
Unscented Kalman filter					

If we consider the computational time of these filters we can notice that the extended Kalman filter takes the shortest computational time because of the linearization effect that eliminate the computations requirement associated with transition matrices. The unscented Kalman filter has the largest computational time because of the unscented transformation.

V. CONCLUSION

Kalman filter is a powerful estimation tool for linear systems with Gaussian distribution. For linear system dynamics, linear Kalman filter provides an optimal estimation using the prediction-correction steps discussed earlier. If the system has nonlinear dynamics; a suboptimal estimation can be achieved by using the extended Kalman filter and unscented Kalman filter. Most of the published work on 3D tracking using Kalman filters based on linear Kalman filter and extended Kalman filter. Kalman filter is mostly used for navigating autonomous vehicles and robot tracking.

ACKNOWLEDGMENT

This work is supported by the E-Science grant funded by the Ministry of Science, Technology and Innovation (MOSTI), Government of Malaysia (No: 01-02-02-SF0064).

REFERENCES

[1] A. Yilmaz, O. Javed, and M. Shah, "Object tracking," ACM Computing Surveys, vol. 38, 2006, pp. 13-58.

[2] W. Hu, T. Tan, L. Wang, and S. Maybank, "A Survey on visual surveillance of object motion and behaviors," IEEE Transactions on Systems Man and Cybernetics, Part C: Applications and Reviews, vol. 34, 2004, pp. 334-352.

[3] Z. Jia, A. Balauriya, and S. Challa, "Sensor fusion-based visual target tracking for autonomous vehicles," Artificial Life and Robotics, vol. 12, 2008, pp. 317-328.

[4] J.C. Lee, S.E. Hudson, J.W. Summet, and P.H. Dietz, "Moveable interactive projected displays using projector based tracking," 18th annual ACM symposium on User interface software and technology - UIST '05, New York, New York, USA: 2005, pp. 63-72.

[5] I. Fernández, M. Mazo, J.L. Lázaro, D. Pizarro, E. Santiso, and P. Martín, "Guidance of a mobile robot using an array of static cameras located in the environment," Autonomous Robots, vol. 23, 2007, pp. 305-324.

[6] C. Tsai, K. Song, X. Dutoit, H.V. Brussel, and M. Nuttin, "Robust mobile robot visual tracking control system using self-tuning Kalman filter," IEEE International Symposium on Computational Intelligence in Robotics and Automation, 2007, pp. 161-166.

[7] S. Weng, C. Kuo, and S. Tu, "Video object tracking using adaptive Kalman filter," Journal of Visual Communication and Image Representation, vol. 17, Dec. 2006, pp. 1190-1208.

[8] P.R. Devarakota, M. Castillo-Franco, R. Ginhoux, B. Mirbach, S. Kater, and B. Ottersten, "3-D-skeleton-based head detection and tracking using range images," IEEE Transactions on Vehicular Technology, vol. 58, Oct. 2009, pp. 4064-4077.

[9] F. Ababsa, "Robust extended Kalman filtering for camera pose tracking using 2D to 3D lines correspondences," IEEE/ASME International Conference on Advanced Intelligent Mechatronics, 2009, pp. 1834-1838.

[10] J. Gao, a Kosaka, and a Kak, "A multi-Kalman filtering approach for video tracking of human-delineated objects in cluttered environments," Computer Vision and Image Understanding, vol. 102, Jun. 2006, pp. 260-316.

[11] V. Lippiello, B. Siciliano, and L.V. Ã, "Adaptive extended Kalman filtering for visual motion estimation of 3D objects," Control Engineering Practice, 2007, pp. 123-134.

[12] A. Causo, E. Ueda, Y. Kurita, Y. Matsumoto, and T. Ogasawara, "Model-based hand pose estimation using multiple viewpoint silhouette images and unscented Kalman filter," 17th IEEE International Symposium on Robot and Human Interactive Communication, 2008, pp. 291-296.

[13] D. Ponsa, A. Lopez, J. Serrat, F. Lumbreras, and T. Graf, "Multiple vehicle 3D tracking using an unscented Kalman filter," IEEE Intelligent Transportation Systems, 2005, pp. 1108-1113.

[14] G. Welch and G. Bishop, An introduction to the Kalman filter, University of North Carolina at Chapel Hill, 1995.

[15] G.A. Terejanu, "Unscented Kalman filter tutorial," Workshop on Large-Scale quantification of Uncertainty, Sandia National Laboratories, 2009, pp. 1-6.

Unbiased Plain Gradient Adaptive IIR Notch Filter for Echo Cancellation

S. Dhanawan, A. Charoenphol, C. Benjangkaprasert

Faculty of Engineering
King Mongkut's Institute of Technology Ladkrabang,
Bangkok, 10520 THAILAND
E-mail : s9061054@kmitl.ac.th, kbchawal@kmitl.ac.th

***Abstract*- An adaptive echo canceller based on adaptive IIR notch filter with unbiased plain gradient algorithm is proposed, for the echo cancellation in telephone network. The unbiased plain gradient algorithm employs the bias removal techniques to remove the bias existing in the estimated parameter, resulting in obtaining good estimate of parameter for the echo canceller. Simulation results show that the proposed canceller outperforms the canceller with the classical LMS algorithm in terms of echo return loss enhancement (ERLE).**

I. INTRODUCTION

Adaptive IIR notch filters are extensively used in various signal processing applications such as communication systems, radar, sonar, biomedical engineering and so on [1]-[14]. The classical application of adaptive IIR notch filter is an echo canceller in the long distance telephony network. Network echoes are a major source of impairment to speech quality in telecommunication systems. Echo return loss and impulse response are important characteristics of an echo path for the design of echo cancellers. The performance of echo cancellers depends on the choice of the adaptive filtering algorithm. It is found in the literature survey that the least mean square (LMS) adaptive algorithm [1] is the most commonly used technique for real time applications adaptive filtering due to its simplicity and ease of implementation. However, it suffers from the slow convergence since the echo path is usually very long and the speech signals are non-stationary and highly correlated and a large number of filter coefficient is needed. It is well known that the convergence speed of adaptive filter can be improved when the lattice form structure filter is used [2]. The modular lattice structure is very useful to vary filter and easy to consider its stabilization. The adaptive lattice form structure filter allows high performance than other structure.

The unbiased plain gradient(UPG) algorithm for adaptive IIR notch filter was proposed in [5]. The contributions of the unbiased plain gradient adaptive IIR notch filter were good convergence property and low bias as compared with the conventional LMS adaptive IIR notch filter [1]. Therefore, we interest this algorithm in this paper.

In this paper, an adaptive echo canceller based on unbiased plain gradient adaptive IIR notch filter with lattice form structure for echo cancellation in telephone network is presented. The unbiased plain gradient algorithm employs the bias removal technique to remove the bias existing in the estimate parameter. As a result, it is obtained good estimate of parameter for the echo canceller. The proposed adaptive echo canceller based on the unbiased plain gradient algorithm's performance is compared with the LMS algorithm. We have observed that the proposed canceller performs better in both the low and the high signal to noise ratio (SNR) situations in noise disturbance.

The paper is organized as follows. Section II, the system model for the echo cancellation scheme in the telephone network and the interest adaptive algorithms for the echo canceller are described. The results are demonstrated in Section III and finally Section IV concludes of this paper.

II. ECHO CANCELLER STRUCTURE AND ALGORITHMS

A. Echo Canceller Structure

Figure 1 shows the basic block diagram of an adaptive echo canceller.

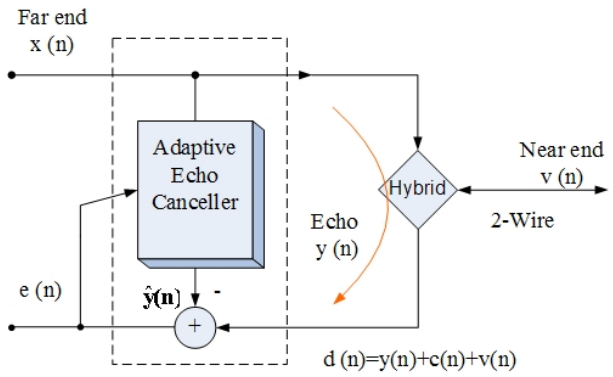


Fig. 1. Block diagram of an adaptive echo canceller for telephone network.

Consider the adaptive echo canceller described in Fig. 1, where $x(n)$ and $v(n)$ represent the far-end signal and near-end speech signal, respectively. Also $d(n)$, $c(n)$ and $\hat{y}(n)$ denote the received input signal to the echo canceller,

background noise, and the estimated echo signal, respectively. That can be described as follows[8]:

$$\hat{y}(n) = W^T(n)X(n) \tag{1}$$

$$e(n) = d(n) - \hat{y}(n) \tag{2}$$

$$d(n) = v(n) + y(n) + c(n) \tag{3}$$

where $W^T(n)$ is the filter coefficient vector of the echo canceller, $X(n)$ is the input vector and $e(n)$ is the error signal.

We assume the linearity of a finite duration (*n)* of the echo impulse response path with length of *n* samples containing the noise $c(n)$ are input $x(n)$ and the estimate echo are $\hat{y}(n)$ all can be expressed as follows [11]:

$$Echo\ \ path = \sum_{i=0}^{n} R_i \exp[-\frac{(i+1)}{880}]\delta(n-i) \tag{4}$$

where *n* is the numbers of samples and R_i is a random number within –2, +2 and $\delta(n)$ is the Dirac function, respectively.

The transfer function of adaptive echo canceller in the second-order adaptive IIR notch filter lattice form structure is given as follows [2]:

$$H(z) = \frac{1 + 2k_0(n)z^{-1} + z^{-2}}{1 + k_0(n)(1+\rho)z^{-1} + \rho z^{-2}} \tag{5}$$

The output signal of Eq. (5) can be expressed in time domain as follows :

$$\hat{y}(n) = u(n) + 2\hat{k}_0(n)u(n-1) + u(n-2) \tag{6}$$

$$u(n) = x(n) - \hat{k}_0(n)(1+\rho)u(n-1) - \rho u(n-2) \tag{7}$$

where $\hat{k}_0(n)$ is filter coefficient vector of adaptive lattice form structure filter at time *n,* and ρ is the pole constrain factor close to but less than unity to ensure the stability of the filter, respectively. The larger parameter ρ, the narrower notch bandwidth is obtained.

B. Adaptive Algorithms

In this paper we consider the LMS adaptive algorithm[1] and the unbiased plain gradient adaptive algorithm[5] applied to the echo canceller. There are briefly described the two algorithms in this subsection.

First, the adaptive algorithm to control the update filter coefficient by using the LMS algorithm for the canceller is described as follows:

$$\hat{k}_0(n+1) = \hat{k}_0(n) - 2\mu\hat{y}(n)\hat{e}(n) \tag{8}$$

where μ is step-size parameter controlling the speed of convergence, which is generally positive real number.

Next, the unbiased plain gradient adaptive algorithm is described. The adaptive algorithm based on the unbiased plain gradient algorithm for the canceller can be expressed as follows :

$$\hat{k}_0(n+1) = \hat{k}_0(n) - \mu\hat{y}(n)\{\hat{g}(n) - C\hat{k}_0(n)x(n)\} \tag{9}$$

where μ is step size parameter, $\hat{y}(n)$ is the output signal of the IIR notch filter and given by Eq. (6) and $\hat{g}(n)$ is the gradient of $\hat{y}(n)$ with respect to $\hat{k}_0(n)$, which is

$$\hat{g}(n) = 2u(n-1) \tag{10}$$

and the parameter *C* is defined by

$$C = \frac{\rho(1-\rho)}{(1+\rho)} \tag{11}$$

In the section III, the performances of the proposed echo canceller will be demonstrated.

III. Simulation Results

In this section, the performance of an echo canceller system using the proposed unbiased plain gradient(UPG) algorithm is compared to that using the classical LMS algorithm. The echo path is modelled as Eq.(4) and for fair comparison, convergence parameters are selected to equalize the same steady state performance. The assumed parameters of the proposed canceller and the LMS canceller are given as : $\hat{k}_0(0) = 0$, $\mu = 0.0001$, $\rho = 0.99$, and data range *N* = 1,000. The results are averaged over 100 runs and the measure of performance used for the adaptive echo canceller is echo return loss enhancement (ERLE) [1], which can be expressed as

$$ERLE\ \ (dB) = 10\log_{10}\frac{E[\hat{y}^2(n)]}{E[\hat{e}^2(n)]} \tag{12}$$

The objective of an echo canceller is to completely remove any emanating signal from impedance mismatching. Real systems are incapable of perfect cancellation for a variety of reasons. It is important, therefore to be able to quantify actual adaptive echo canceller performance and to understand system

and physical limitations that affect cancellation so that an adaptive echo canceller can be optimized for its environment.

Figure 2 compares the ERLE, using unbiased plain gradient algorithm and the LMS algorithm. The echo signal to background noise ratio is 60 dB. From Fig. 2, it is evident that the unbiased plain gradient algorithm for the echo canceller gives the same convergence speed as the LMS algorithm.

Tracking is another important aspect in echo cancellation, echo paths vary randomly and rapidly. Figure 3 compares the echo path tracking performance of the algorithms. From Fig. 3, it is demonstrated that the unbiased plain gradient algorithm also gives slightly same tracking performance as the LMS algorithm.

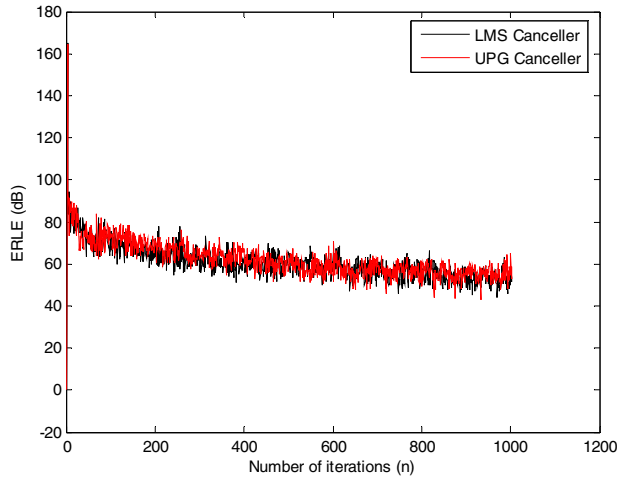


Fig. 2. ERLE of the cancellers by using unbiased plain gradient algorithm, the LMS algorithm and SNR is 60 dB.

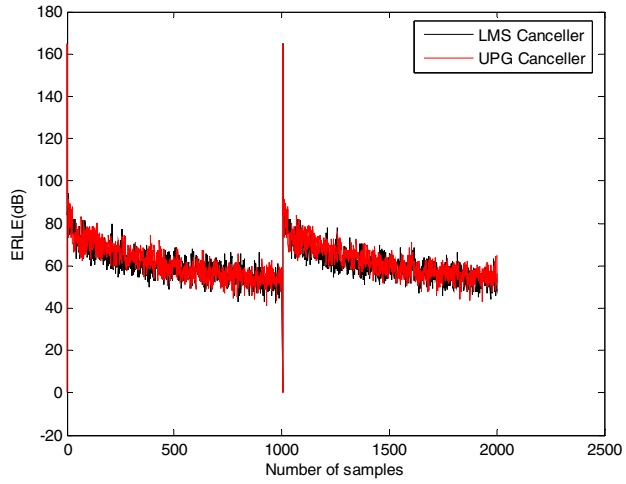


Fig. 3. Echo path tracking performance of the cancellers by using unbiased plain gradient algorithm and the LMS algorithm.

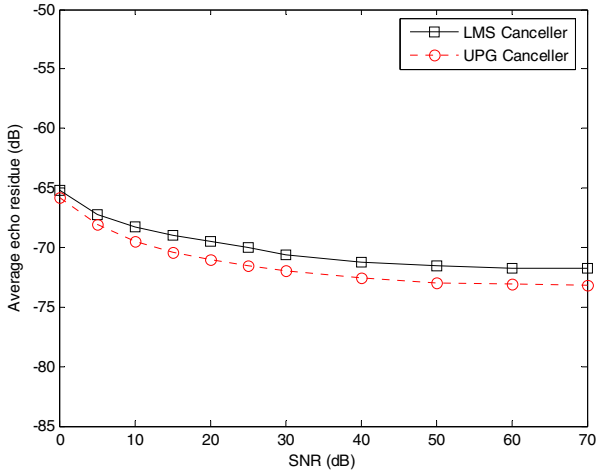


Fig. 4. Average echo residue of the cancellers by using unbiased plain gradient algorithm and the LMS algorithm.

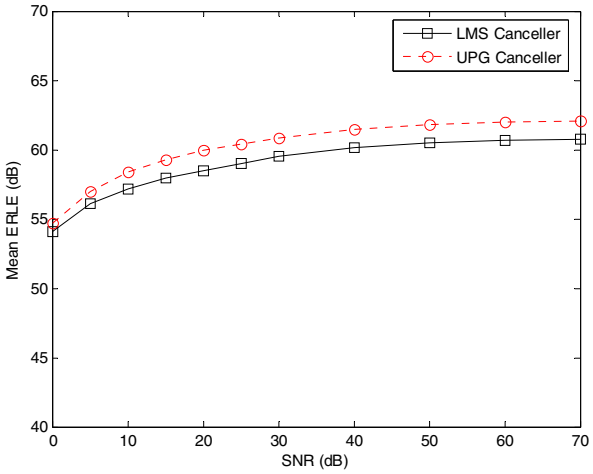


Fig. 5. Mean ERLE of the cancellers by using unbiased plain gradient algorithm and the LMS algorithm.

Figure 4 shows the average echo residue power comparison with the unbiased plain gradient algorithm and the LMS algorithm in various SNR within 0 dB to 70 dB. From Fig. 4, it is seen that the unbiased plain gradient algorithm for the echo canceller provides the lower average echo residue power than the LMS algorithm.

Finally, Figure 5 compares the mean value of ERLE of the cancellers. From this figure, it is evident that in both the low and the high SNR situations, the unbiased plain gradient algorithm for the echo canceller structure is excellent to improve high performance. We observe from the Fig. 5 that the unbiased plain gradient canceller achieves a performance improvement of approximately 1.5 dB compared to the LMS canceller.

IV. CONCLUSIONS

In this paper, an adaptive echo cancellation scheme using the unbiased plain gradient algorithm and the LMS algorithm is presented. The unbiased plain gradient algorithm employs the bias removal technique to remove the bias existing in the estimated parameter. Therefore, it is obtained good estimate of parameter for the echo canceller. From the simulation result, it is concluded that the unbiased plain gradient algorithm achieved better ERLE than the classical LMS algorithm.

REFERENCES

[1] B. Farhang-Boroujeny, *Adaptive filters : theory and applications*, Chic hester : John Wiley, 1998.

[2] N. I. Cho and S. U. Lee, "On the adaptive lattice notch filter for the detection of sinusoids," IEEE Trans. Circuits System., vol. 40, no. 7, pp. 405-416, July 1993.

[3] N. I. Cho and S. U. Lee, "Tracking analysis of an adaptive lattice notch filter," IEEE Trans. Circuits System., vol. 42, pp. 186-195, Mar. 1995.

[4] Y. Xiao, Y. Takeshita and K. Shida, "Steady-state analysis of a plain gradient algorithm for a second-order adaptive IIR notch filter with constrained poles and zeros," IEEE Trans. Circuit System II, Analog Digital Signal Processing, vol. 48, no. 7, pp.733-740, July 2001.

[5] R. Punchalard, W. Loetwassana, J. Koseeyaporn, and P. Wardkein, "Statistical analysis of an unbiased plain gradient algorithm for a constrained adaptive IIR notch filter," in Proc. 14th Asia Pacific Conference on Communications, pp. 1-5, Oct. 2008.

[6] W. Kenneth Jenkins, "An investigation of an adaptive IIR echo canceller: Advantages and Problems," IEEE Trans. Acoustics, pp.1819-1820, Dec. 1988.

[7] K. C. Ho, Q. G. Liu, R. Rabipour, and P. Yatrou. "A new sampling of echo paths in north America networks," in Proc. ICASSP '00, pp. 809-812, June 2000.

[8] C. Benjangkaprasert, S. Sukhumalwong, S. Teerasakworakun, and K. Janchitrapongvej, "The new variable step-size algorithm adaptive lattice structure for echo cancellation," in Proc. ICCAS2003, pp.2090-2092, Oct. 2003.

[9] J. H. Yoo, S. H. Cho, and D. H. Youn, "A Lattice/Transversal Joint (LTJ) structure for an acoustic echo canceller," in Proc. IEEE International Symposium on Circuits and Systems, vol. 2, pp. 1090–1093, Apr.-May 1995.

[10] J. F. Chicharo and T. S. Ng, "Gradient-based adaptive IIR notch filtering for frequency estimation," IEEE Trans. Acoustic, Speech, Signal Processing, vol. ASSP-38, pp. 769-777, May 1990.

[11] ITU-T Recommendation G.168 : Digital Network Echo canceller, 2003.

[12] K. C. Ho, Q. G. Liu, R. Rabipour, and P. Yatrou. "A new sampling of echo paths in north America networks," in Proc. ICASSP '00, pp. 809-812, vol. 2, June 2000.

[13] S. C. Pei and C. C. Tseng, "Adaptive IIR notch filter based on least mean *p*-power error criterion," IEEE Trans. Circuit System-II, vol. 40, pp. 525-529, Aug. 1993.

[14] T. Aboulnasr and K. Mayyas, "A robust variable step-size LMS-type algorithm analysis and simulation," IEEE Trans. Signal Processing, vol. 45, no.3, pp.631-639, March 1997.

Efficient Design of Local Binary Pattern for Image Retrieval

Rafi Md. Najmus Sadat[1], Abdur Rakib[2], Md. Musfequs Salehin[3], Naurin Afrin[3]
[1] *Gippsland School of Information Technology, Monash University*
[2] *Information and Communication Engineering, Rajshahi University*
[3] *Computer Science and Engineering, Rajshahi University of Engineering and Technology*
Email: najmus.sadat@monash.edu, {rakib.rajshahi, sohel16.bd, naurin.afrin}@gmail.com

***Abstract*—A novel image description method named Half-LBP has been proposed in this paper for image retrieval applications. Half-LBP transforms the relationship among the intensity levels of image local pixel blocks into a binary pattern in such a way that reduces the dimension of the descriptor significantly while keeping the retrieval accuracy comparable with the state of art methods. The basic operation is quite similar to the texture operator named Local Binary Pattern (LBP). However, the dimension of the LBP method and its variants are too high and take substantial amount of time to retrieve the images. To address this issue, Half-LBP image descriptor has been proposed which takes comparatively less time to find out the matched images from the database.**

***Keywords*-Local Binary Pattern; Image retrieval; Classification;**

I. Introduction

Image retrieval plays an important role in computer vision and image processing applications. Numerous algorithms for describing the image representation have been proposed for this purpose during the past decades. Among the image description methods, local binary pattern (LBP) [8] has received considerable attentions in many computer vision applications, such as face recognition [1], image retrieval [4] and motion analysis [2] , for its efficiency and simple computational complexity to build the image descriptor. However, the dimension of the descriptor of this method is much higher, that is why the post processes become slower. We propose an image description method which has almost similar performance as LBP yet having eight times less dimension to represent the image. Eventually, the proposed method takes substantially less amount of time to retrieve the desired images.

Most of the image description methods concentrate on effectiveness rather than efficiency. However, not only the accuracy, but also the processing speed is an important issue in the methods we are studying. Our research focuses to speed up the process by reducing the dimension of image descriptor. To get real time processing speeds, less dimension of the image descriptor is an important properties of the methods which take less time to build the feature and less time to retrieve the matched images. However, lower dimension usually has less distinctiveness than higher dimension. Therefore, we must need to take care of this trade-off while building the descriptor to represent the image.

Basically, LBP method had been proposed for texture analysis. This operator is defined as a monotonic illumination invariant texture measure, derived from local neighborhood. For each pixel in an image, a binary code is produced by thresholding center intensity value with the intensity value of the neighbor pixel. Then, A histogram, created to collect the occurrences of different binary patterns, is used to represent the image. The basic LBP operator considers only the eight neighbors of a center pixel [9], however the definition has been extended to include any number of circular neighborhoods by using the interpolation technique [8].

Our image description method splits up the neighborhoods into two separate categories based on the position of the pixels of the local pixel blocks and generates separate histograms from each of the categories. Finally, the descriptor is built by joining both of the histograms. So, the proposed histogram is lower in dimension and also keeps the relationship among the entire neighborhood.

Rest of the paper has been organized as follows. Section II describes related works on the image classification methods and the variants of Local Binary pattern. Section III and section IV present the construction of Local Binary Pattern and Half-LBP respectively. Experimental results are shown in section V. Finally, Section VI concludes the paper.

II. Related Works

Couple of variants of LBP, which are used in image retrieval, has been appeared in the literature and we will review the most noticeable ones in this section. The detail calculation of LBP is described in Section III. Hongliang Jin [6] noticed that LBP misses the local structure under certain circumstances and introduced improved LBP (ILBP) by including the center pixel into the pattern. However the dimension of ILBP is 512 (2^9) for nine neighbors and the dimension is higher than LBP (256). Huang et al. [5] pointed out that LBP can only reflect the first derivative information of images, but could not present the velocity of local variation. To solve this problem, they propose an extended version of Local Binary Patterns (ELBP) whose dimension is 295. Shu Liao et al. [7] proposed elliptical binary pattern (EBP) where elliptical neighborhood is defined to capture anisotropic structural information. The dimension of EBP

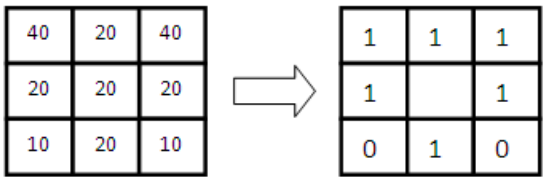


Figure 1: Calculation of Local Binary pattern

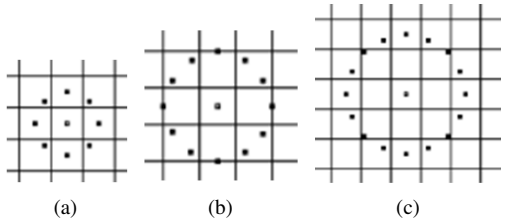


Figure 2: (a) 8 neighbors of radius 1, (b) 12 neighbors of radius 1.5 (c) 16 neighbors of radius 2.

is also based on the number of neighborhood which is higher than the circular neighborhood. Xiaoyang et al. [10] proposed local ternary patterns (LTP) to resolve the problem of the sensitivity to noise in near-uniform image regions. LTP uses 3-valued coding that includes a threshold around zero for the more precise coding of the local gray-scale difference. However, the dimension is 512 (2×2^8) which is higher than LBP as well.

Similarly, Hafiane et al. [3] proposed noise resistant texture descriptor called median binary patterns (MBP) where the localized binary pattern is obtained by thresholding the pixels against their median value of a neighborhood pixels instead of using the center gray value. However, the dimension of MBP is 512 (2^9). For the higher dimensionality of these methods, the image retrieval time is higher which is not suitable for real time applications.

III. Local Binary Pattern

Two most important characteristics of the LBP operator are (1) computational simplicity with its powerful discrimination and (2) the tolerance against illumination changes. In a basic LBP operator, the intensity value of a pixel is compared with the intensity value of its neighborhood pixels in a 3×3 pixel block. The comparison returns a sequence of binary code using equation 1.

$$s(Z) = \begin{cases} 1, & \text{if } Z \geq 0 \\ 0, & otherwise \end{cases} \tag{1}$$

where z is the comparison results between center pixel and neighborhood pixels. The sequence of the binary code is

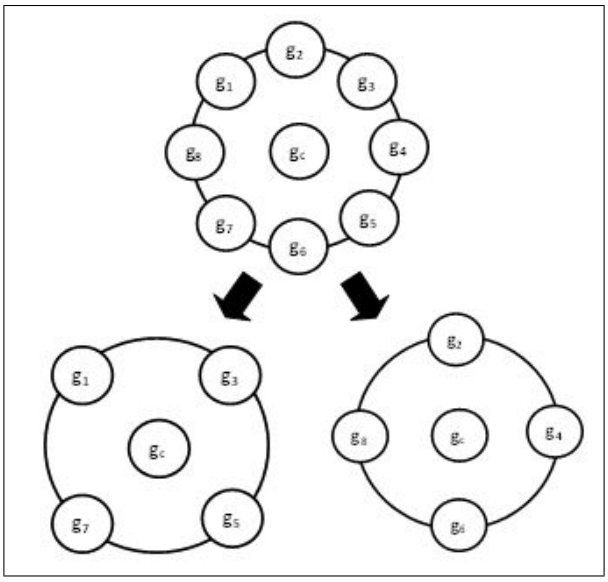


Figure 3: Process of splitting up the 3×3 pixel block

then converted to LBP value using equation 2.

$$LBP_{(P,R)}(x,y) = \sum_{p=0}^{P-1} s(g_c - g_p) * 2^p \tag{2}$$

where P and R are the number of neighbors and radius from the center pixel respectively. g_c and g_p are the center pixel and the neighbor pixels respectively. An example of calculating the LBP code from 3x3 pixel block has been illustrated in Figure 1. The number of neighbors can also be varied by using circular neighborhoods of different radius (R) and bi-linear interpolation as shown in Figure 2. LBP operator produces 2^P number of different patterns where P is the number of neighborhoods around a pixel.

IV. Half-LBP

Our main aim is to reduce the dimension of the LBP image descriptor. LBP is a very powerful operator which discriminates the pattern in a very well manner so that all kinds of local patterns in an image can be preserved. The key strength of LBP is that LBP keeps the intensity relationship among all the neighbors with the center pixel. Likewise, our proposed descriptor also considers all the neighbors to produce the binary code. However, it splits up the eight neighbors into two separate groups. That is why, we named the Binary pattern as Half-LBP. One of the groups has only the diagonal neighbors of a 3×3 local pattern and other has the rest. The process of splitting up the 3×3 pixel block is presented in Figure 3.

Now, if we build the histogram from four neighbors, then there will be $16(2^4)$ possible patterns to represent. Since, we have two groups of four neighbors pixel blocks, the

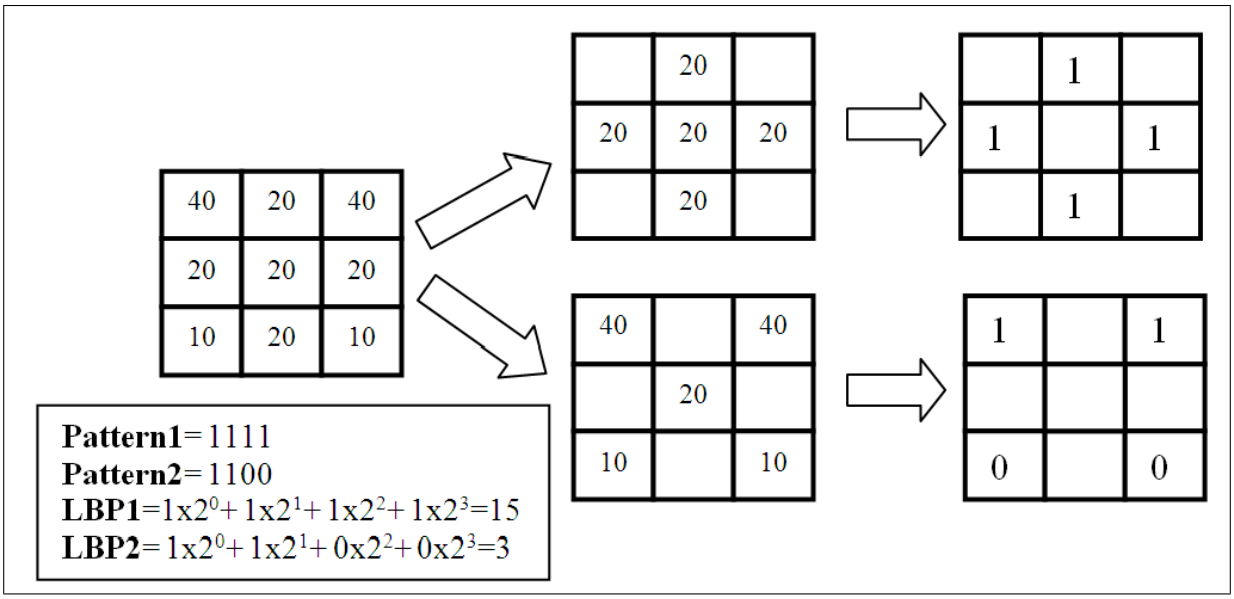


Figure 4: Process of calculating Half-LBP

dimension of this image descriptor will be 32 (2×16) which is eight times less than the original LBP method. Therefore, for retrieving images the proposed Half-LBP is much faster than the LBP and its variants, which have higher dimensional descriptor to represent the image. A simple example of calculating the Half-LBP is illustrated in Figure 4. The efficiency and the effectiveness of our proposed method is shown in Section V.

V. Experimental Result

To validate the effect of the proposed method, a textural image database for research purposes has been employed and the proposed results are compared with the results of Local binary Pattern (LBP) [8], Local Ternary Pattern (LTP) [10] and Median Binary pattern (MBP) [3]. Euclidean distance (L_1) is used as a similarity measurement criterion between two image descriptors in the experimental results.

K-Nearest Neighborhood (KNN) algorithm is one of the most popular and simplest methods for classifying patterns based on the closest training example in the feature-space. The KNN rule is to assign a given unlabeled example to the class that occurs most frequently among the k-nearest training samples. Usually the value of K is chosen based on the characteristics of the image database and the purpose of the applications. We have chosen the value of K as 3 in our experiment. So, if the majority of the neighbors from training image descriptors are from the same class as the test image descriptor, then the descriptor method is successful to classify the test image.

The experiments have been conducted over a large number of textured images from Outex [1] database. We have used 10 datasets (Outex_TC_00000 − Outex_TC_00009) from that database. Here, each dataset contains 24 different types of textures. There are total 44736 number of images in these 10 datasets. However, the number of images per dataset varies. Half of the images from each dataset have been used as training samples and half for the testing. The training and testing categorization have also been provided along with the benchmark dataset. Figure 5 shows few examples from each class of the database.

The goal is to speed up the classification process rather than outperform the existing texture descriptors in terms of accuracy. In Table I, the classification results of aforementioned datasets are presented. All the image descriptors are calculated considering eight neighbors of 3×3 pixel block. Unfortunately, any single image description method does not consistently perform well for all the Outex datasets. Half-LBP does not have higher accuracy in most of the cases which is quite expected as the dimension has been reduced. However, the performance of the proposed description method (Half-LBP) is comparable with others.

Table II shows the time taken by the methods for classifying the textures. We have used matlab implementation of all the methods in a desktop computer with 2.0 GHz Core 2 Duo processor and 2GB memory. Our proposed Half-LBP has taken the least amount of time among all the image descriptor methods. We have already mentioned that, the dimension of Half-LBP is eight times less than the original LBP. However, the time consumption ratio

[1]Textured image database: http://www.outex.oulu.fi/index.php?page=classification

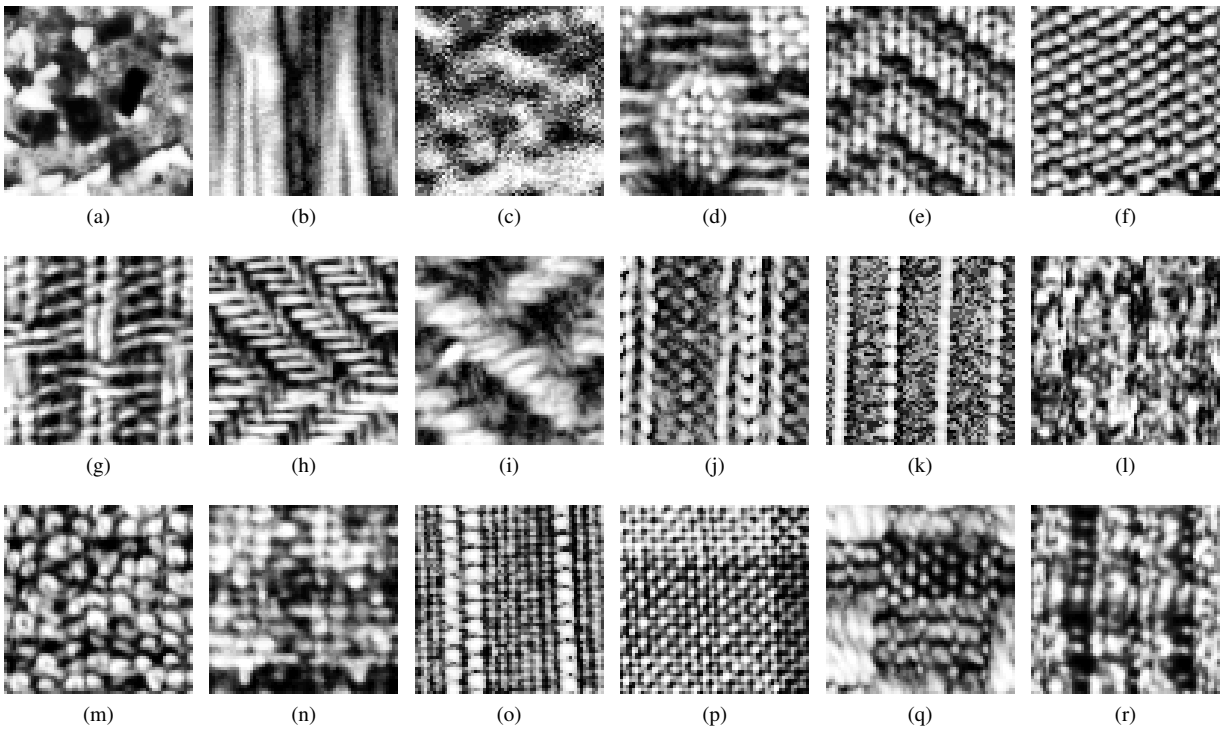


Figure 5: Sample textures of different classes from Outex database.

between Half-LBP and LBP is not always eight. Because, the priority of computing a job to the processor will not be the same for all the time. There is one more thing to mention about calculating the ratio of time complexity. We can mathematically derive that, the complexity of our proposed method is even much less than 8 times of LBP descriptor. For instance, the dimension of LBP and Half-LBP descriptor are d_1 and d_2 respectively. Now, if we have n number of training images for these methods to classify, then the number of iterations for the methods will be $n \times d_1^2$ and $n \times d_2^2$ respectively. As we know that, the dimension of Half-LBP is eight times less than the LBP descriptor i.e. $d_1 = 8 * d_2$. So, the ratio of the time complexity could be 64 (8^2). However, none of the experimental results have the expected ratio. Still, the computational time is very less compare to the other methods which we have claimed in this work.

VI. Conclusion

In this paper, we propose a new texture descriptor named Half-LBP for image retrieval applications. The motivation comes from the original LBP but the aim is to reduce the dimension of the image descriptor so that the retrieval process becomes faster. As shown in our experimental results, the proposed Half-LBP shows almost similar performance for classifying the benchmark texture database. However, it takes substantial amount of less time than other methods for the task of image classification. In this paper, we have

Dataset	**LBP**	**LTP**	**MBP**	**Half-LBP**
Outex_TC_000	**100.00**	**100.00**	99.58	**100.00**
Outex_TC_001	99.43	99.72	**99.81**	98.67
Outex_TC_002	94.81	**96.31**	95.95	90.10
Outex_TC_003	**100.00**	**100.00**	**100.00**	99.17
Outex_TC_004	99.62	99.53	**99.81**	98.58
Outex_TC_005	95.34	**96.44**	96.33	91.92
Outex_TC_006	99.19	99.35	**99.68**	98.05
Outex_TC_007	94.04	95.07	**95.23**	91.32
Outex_TC_008	99.03	**99.35**	**99.35**	98.21
Outex_TC_009	95.59	**96.16**	95.38	92.17

Table I: Classification accuracy (%) for Outex database [LBP=Local Binary Pattern, LTP=Local Ternary Pattern, MBP=Median Binary Pattern]

Dataset	**LBP (sec)**	**LTP (sec)**	**MBP (sec)**	**Half-LBP (sec)**
Outex_TC_000	0.32	1.03	0.98	**0.07**
Outex_TC_001	8.63	16.96	16.88	**0.55**
Outex_TC_002	129.90	318.98	316.94	**17.97**
Outex_TC_003	0.36	1.05	1.05	**0.07**
Outex_TC_004	8.76	17.09	17.12	**0.55**
Outex_TC_005	130.80	317.37	314.10	**17.74**
Outex_TC_006	2.69	6.23	6.18	**0.24**
Outex_TC_007	27.28	57.61	57.34	**1.62**
Outex_TC_008	2.70	6.44	6.36	**0.25**
Outex_TC_009	27.30	57.56	57.55	**1.64**

Table II: Computational time in seconds taken by the methods to classify the textures [LBP=Local Binary Pattern, LTP=Local Ternary Pattern, MBP=Median Binary Pattern]

only considered 8 neighbors and 3×3 image pixel block. However, the technique of Half-LBP can be applied on the other method with different radius values and different number of neighbors. This may bring more discrimination power with faster image retrieval applications. Our future work will consider these parameters and make the texture descriptor more distinctive.

REFERENCES

[1] T. Ahonen, S. Member, A. Hadid, M. Pietikinen, and S. Member. Face description with local binary patterns: Application to face recognition. *IEEE Transactions on Pattern Analysis and Machine Intelligence*, 28:2037–2041, 2006.

[2] P. Guo and Z. Miao. Motion description with local binary pattern and motion history image: Application to human motion recognition. pages 171 –174, 2008.

[3] A. Hafiane, G. Seetharaman, and B. Zavidovique. Median binary pattern for textures classification. *Image Analysis and Recognition*, pages 387–398, 2007.

[4] D. He and N. Cercone. Local Triplet Pattern for content-based image retrieval. *Image Analysis and Recognition*, pages 229–238, 2009.

[5] X. Huang, S. Z. Li, and Y. Wang. Shape localization based on statistical method using extended local binary pattern. *Proc. of Third Intl. Conf. on Image and Graphics*, pages 184–187, 2004.

[6] H. Jin, Q. Liu, H. Lu, and X. Tong. Face detection using improved lbp under bayesian framework. In *Proc. of Third Intl. Conf. on Image and Graphics*, pages 306 – 309, 2004.

[7] S. Liao and A. C. S. Chung. Face recognition by using elongated local binary patterns with average maximum distance gradient magnitude. In *ACCV: Proc. of the 8th Asian conference on Computer vision*, pages 672–679, 2007.

[8] T. Ojala, M. Pietikainen, and T. Maenpaa. Multiresolution gray-scale and rotation invariant texture classification with local binary patterns. *IEEE Trans. on Pattern Analysis and Machine Intelligence*, 24(7):971, 2002.

[9] T. Ojala, M. Pietikinen, and D. Harwood. A comparative study of texture measures with classification based on featured distributions. *Pattern Recognition*, 29(1):51 – 59, 1996.

[10] X. Tan and B. Triggs. Enhanced local texture feature sets for face recognition under difficult lighting conditions. *Trans. Img. Proc.*, 19(6):1635–1650, 2010.

Mobility Tolerant TDMA Based MAC Protocol for WSN

SandhyaSree Thaskani
MS by Research(ECE)
IIIT-Hyderabad
Hyderabad, India
thaskanisandhya@gmail.com

K.Vinod Kumar
BE (EEE)
NIT-Warangal
Warangal, India
vinodreddy.nitw@gmail.com

G.Rama Murthy
Associate Professor
IIIT-Hyderabad
Hyderabad, India
rammurthy@iiit.ac.in

Abstract*— Recent advancements in wireless communications and electronics have enabled the development of low cost sensor networks. Among the protocols of wireless Sensor Networks (WSN), Medium Access Control (MAC) protocols are given more priority as traditional MAC protocols are not suitable for Wireless communication. As many of the MAC protocols consider the sensor nodes to be stationary, and when these protocols are used in mobile environment the network performance decreases. In this paper, we introduce a new TDMA based MAC protocol which can be used in mobile wireless sensor network. This protocol uses TDMA based MAC scheme where the time will be divided into frames and then time slots. These slots are further divided into sections as channel request (CR), channel allocation (CA) and data section. We will also design an algorithm considering the energy efficiency of a wireless sensor network. Therefore the life time of the sensor nodes deployed in a wireless sensor network will be increased.

Keywords-Wireless Sensor Networks (WSN); MAC; TDMA; Communication Request; Channel Allocation; Data Section.

I. INTRODUCTION

The research area of Wireless sensor networks is an advancing technology which has opened new research issues. A sensor network is composed of a large number of sensor nodes that are densely deployed either inside the phenomenon or close to it. Some of the application areas are health, military and home. In military, for example, the rapid deployment, self organisation and fault tolerance characteristics of sensor networks make them a promising technology. In health, sensor nodes can also be deployed to monitor patients and assist disabled patients. Some other commercial applications include managing inventory, monitor product quality and monitor disaster areas.

Wireless Sensor Networks usually employ performance metrics that are different from those of more conventional data networks, emphasizing low power consumption and low cost rather than data throughput or channel efficiency. Since power is consumed every time a network device accesses the channel, the method by which the device can have a large effect on its power consumption and therefore the choice of a MAC protocol is crucial for a WSN.

The MAC protocol in a wireless multi hop self organising sensor network must achieve two goals. The first is the criterion of the network infrastructure. Since thousands of sensor nodes are densely deployed in a sensor field, the MAC scheme must establish communication links for data transfer. The second objective is to fairly and effectively share the resources between all the sensor nodes.

II. RELATED WORK

The Medium Access Control protocols can be broadly classified as following categories. They are: (1) Scheduling based and (2) Contention based. In this section some of the medium access protocols.

A. SMAC:

SMAC [3] is a contention based MAC protocol. SMAC uses three novel techniques to reduce energy consumption and support self-configuration. SMAC introduced a periodic sleep and wake up scheduling, which reduces energy consumption in listening to an idle channel. Neighboring nodes form virtual clusters to auto-synchronize on sleep schedules. SMAC also sets the radio to sleep during transmissions of other nodes. And it uses in-band signalling. Finally, SMAC applies message passing to reduce contention latency for sensor-network applications that require store-and-forward processing as data move through the network.

B. EMAC:

EMACS [2] In EMACS, time is divided into so called frames just like in TDMA but each frame is divided into timeslots and each slot contains three sections: communication request (CR), traffic control (TC), and data section. Each timeslot can be owned by only one network node. This network node decides what communication should take place in its timeslot. Other nodes can ask for data or notify the availability of data for the owner of the timeslot in the CR section. The owner of the slot transmits its schedule for its data section and broadcasts a table in the TC section, which tells to which other TC sections the node is listening. After the TC section, the transmission of the actual data packet follows. The Node goes into a standby sleep mode when at a certain time no transmissions are expected. It releases its slot and starts periodically listening to a TC section of a frame. When the node has to transmit some data (event driven sensor node), it can just fill up a CR section of another network node and agree on the data transmission, complete it and go back to sleep.

C. TRAM

In this MAC protocol time is divided into number of slots as we do in TDMA [8]. The network nodes switch in to idle mode or low power mode when they are not transmitting or receiving. A distribution election scheme is employed to determine which node to use a particular time slot. Time slots are not allotted to those nodes that do not have any data to transmit. This improves energy efficiency of the network significantly over TDMA.

D. Mobile TDMA

In [1] authors proposed TDMA-based MAC protocol for mobile sensor networks. This protocol works by first splitting a given frame into control part and a data parts. The control part is used to manage mobility, where as nodes transmit messages in data part. In data part, some slots are reserved for mobile node.

E. Mobility Models

The most widely used mobility model is random walk mobility model [4] (Brownian Movement). A slight enhancement to this model is Random Waypoint model [5]. In this model pauses are introduced between changes of direction and speed. A recent work in mobility models [6], argued that these models do not faithfully reflect reality, and developed a model based on social theory. The authors argue that, this model is well suited for MANETs. Mobility models of MANETs may not suitable for sensor networks as applications for sensor networks are tracking, monitoring, which is not the case of MANETs. However in [1] authors have introduced a novel mobility models which suit for sensor networks, viz Intra-cluster mobility and Inter-cluster mobility. In our protocol we are considering these models.

a. *Intra-cluster mobility:* When nodes are mobile, if they remain within their assigned cluster, the set of nodes within that cluster remains unchanged, though the topology may change. This is stated as intra-cluster mobility [1].
b. *Inter-cluster mobility:* When a node leaves its cluster, it will join in a new cluster due to mobility, causing the set of nodes in its original cluster to change and in new cluster also. This is stated as inter-cluster mobility [1].

In [1] authors have proven collision-freedom in intra- and inter-cluster mobility, if each node is assigned a distinct slot.

III. Problem Formulation

In this section we discuss the problems with the present medium access protocols.

- The major problem with TDMA is the excessive delay. Each node is given a particular time slot in which it has to send its data. If the node senses some data after its slot time is over, then it has to wait till it gets a chance to transmit in its own slot in the next time frame. This results in poor channel utilization and delay. Some times because of this delay, in some energy constrained networks like WSN there is probability that the node may die before it gets its slot in the next time frame and the data is lost with the node itself. Also lots of energy is being wasted by idle listening, which brings down the network lifetime significantly.
- TRAMA solves the problem of energy efficiency by switching in to low power mode when the node is not transmitting or receiving. But the problem of delay and poor channel utilization are not resolved.
- EMACS employs the idea of dividing the time slot into sections thereby decreasing the delay and improving the channel utilization to a certain extent. But this algorithm doesn't consider the case of two nodes compete for a particular time slot whose owner doesn't have any data to transmit. There is no discussion on what priority basis the nodes compete and get the time slot.
- Also none of the above said protocols consider mobility of the network nodes. They assume that the nodes are stationary or considerably low mobility. In [1] authors proposed an algorithm for mobile nodes based on TDMA. But this has problems of delay and poor channel utilization.

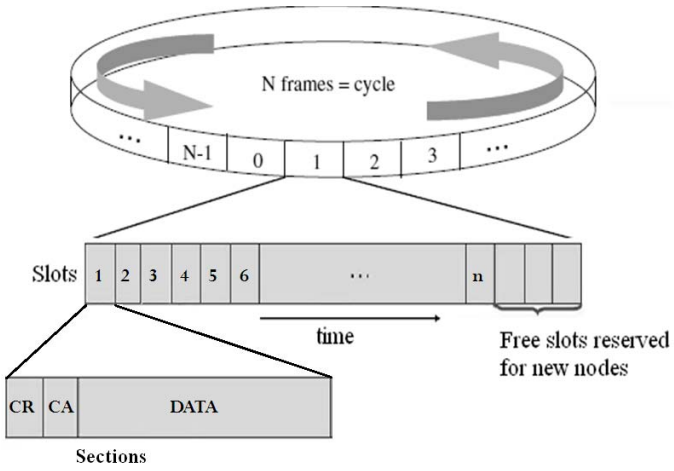


Fig. 1 Schematic of the proposed algorithm

IV. Assumptions

- Total network is static in the setup phase.
- Cluster head have relatively more battery power and less mobility when compared to other nodes in the cluster.
- Time synchronization for all nodes is done automatically.
- Except Cluster Head all other nodes have same capabilities.

V. Proposed Algorithm

We consider the whole network to be divided in to clusters using FLOC algorithm [7]. Each cluster has its own Cluster

Head. Now as in fig.1 time is divided in to frames (*N*) and in turn divided in to time slots. Before every time frame, the Cluster Head allocates a time slot to every node (*n*) in the cluster and *x* slots are left free for the nodes that join the cluster in later part of the time frame. This *x* is considered as 10% of number of nodes in a cluster. The node which holds the current slots is known as owner node.

Whenever a new node comes and joins the cluster, the Cluster Head allocates half of the free time slots (*x/2* slots) to this node. If another comes and joins the cluster, this time it gets half of the current free slots (*x/4*). Therefore a cluster will have some empty slot at anytime in the time frame to allocate to a new node that joins the cluster. Slot allotment to new nodes joined in a cluster is explained in section *V.A*. This deals with the problem of mobility of the network nodes efficiently. But if some of the mobile nodes leave the cluster or the particular owner node doesn't have any data to send and so the channel resources are wasted. To improve the channel utilization capability we split each timeslot in to three sections. They are:

1. Communication Request (CR)
2. Channel Allocation (CA)
3. Data Section (DS).

In communication request (CR) section, owner node collects the information about the surrounding nodes. All those nodes that have data to transmit will put requests to the owner node for the grant of slot for data transmission. If the owner node doesn't have any data to transmit then it will calculate the Priority Index (PI) of each node that has put a request for grant of a time slot. Among the slot requested nodes, the node with less PI is given more priority. PI calculation is explained in section *V.B*.

In Channel Allocation (CA) section, the node decides whether to send the data and keep the channel to it or allots the channel to a cluster node which has requested for a slot and has the highest priority.

Packets are transmitted or received in this Data Section. After the communication process is over the node goes into sleep as often as possible in order to save the battery power.

A. Slot allotment:

Inter-cluster mobility causes the nodes to move from one cluster and join in new cluster. New joined node needs a slot for its further communication. Cluster Head keeps track of nodes with the cluster, nodes leaving the cluster. When a new node enters into a cluster it requests Cluster Head for a slot.

Let *r* be the number of nodes left the cluster. These r slots are left unused as their owners left the cluster. *x* be the number of slots reserved for the nodes which joins cluster because of mobility. Total number of slots available for this instant is *r+x*. For the first r nodes which joins the cluster, Cluster Head allocates r free slots which are left unused as the owner nodes left the cluster. For next the nodes which joins the cluster, Cluster Head provides half of the free time slots i.e., x/2 and so for the next incoming nodes.

B. Calculation of PI:

Priority Index is the measure that decides whether a node gets the time slot of the owner node. Higher the PI, lower the priority. It is calculated based on the following factors.

- Priority Index is inversely proportional to mobility of node. If node has higher velocity the probability that it completely transmits the packet is less, so priority of packet should be more and so the priority index should be less.

$$PI \propto \frac{1}{V} \qquad (1)$$

- If battery power (BP_c) of the request node is less than threshold (BP_{th}) level, then the node cannot complete transmission of its packet, so the node should not transmit this packet. The priority of the packet should be more and hence the priority Index leads to inverse relationship.

  The PI of the packet should be inversely proportional to battery power if the battery power is less than threshold. If battery power is above the threshold level, then priority index of the packet should be more giving lower priority index values to the packets in nodes whose battery power is close to threshold value.

$$PI \propto BPc \quad \text{if} \quad BP_c \geq BP_{th}$$

$$PI \propto \frac{1}{BPc} \quad \text{if} \quad BP_c < BP_{th} \qquad (2)$$

$$B = Sgn(BP_C - BP_{TH}) \qquad (3)$$

- Depending on the difference of slot numbers between the owner nodes (s_o) and requested (s_r) node priority will be assigned.

  When the difference is positive, more difference causes more delay for transmission a packet. To reduce transmission delay, requested node (s_r) with more difference should be given more priority.

  When the difference is negative, lesser difference causes more delay for transmission a packet. To reduce delay, requested node with lesser difference should be given priority.

$$PI \propto \frac{1}{|S_o - S_r|} \quad \text{if} \; |S_o - S_r| \geq 0$$

$$PI \propto |S_o - S_r| \quad \text{if} \; |S_o - S_r| < 0 \qquad (4)$$

$$D = \text{sgn}(|S_o - S_r|) \qquad (5)$$

Where sgn stands for signum function which is defined as

$$Sgn(y) = 1 \quad if \quad y > 0$$
$$= 0 \quad y = 0$$
$$= -1 \quad y < 0$$

Considering all above equations PI is given as following

$$PI = B+D-v \qquad (6)$$

VI. Simulation Results

For the comparative evaluation, we simulate the protocols extensively in MATLAB. We consider a (100x100) m^2 sensor field and the nodes (both mobile and static) are randomly deployed all over the field. Each time frame is assumed to be 1ms long and is divided into 10 equal time slots.

The parameters of the nodes used in our simulation are as shown in the TABLE I.

TABLE I
NODE PARAMETERS

Parameters	**Values**
Simulation area	100 X 100 m^2
Number of nodes	100
Communication radius	30m
Sensing radius	3m
Total Initial Energy	1000J
Idle cost	0.0165 J/s
Transmission Power	10 J
Reception power	2 J

For static network:

Events are generated randomly at different times in a time frame. The average delay for a message generated in a particular time frame is calculated. This average delay is plotted against the number of events occurred in a time frame. It is evident from the fig. 2 that our proposed algorithm gives lesser delay when compared to traditional TDMA.

We assume Network Lifetime to be the time taken for 10% of the total nodes in the network to fail. We then plot the network lifetime obtained by simulating the traditional TDMA and the proposed protocol. The fig. 3 clearly shows that our algorithm outperforms the TDMA by 30% approximately.

For mobile network:

In this case, 10 mobile nodes are considered to be present initially in the simulation environment. These mobile nodes (x) have some amount of mobility (M_L). A random number of mobile nodes may join the cluster, which have mobility (M_C). Channel Utilization is assumed to be the percentage of channel that is utilized in a time frame.

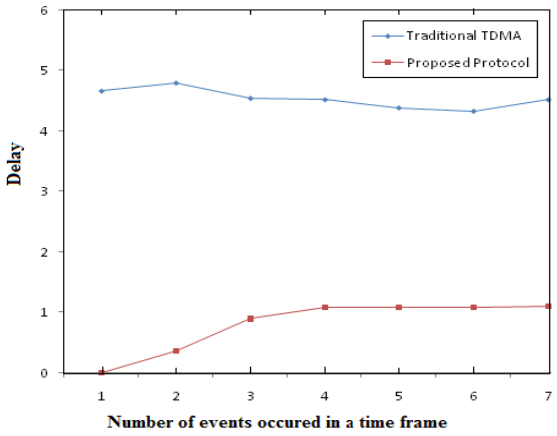


Fig. 2: Graph for Delay

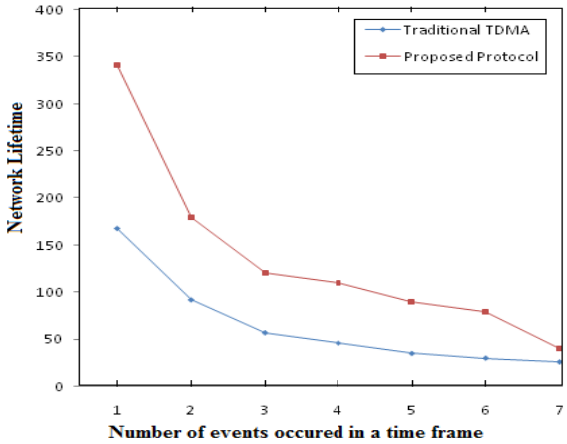


Fig. 3: Graph for Network Lifetime

When we maintain the mobility (M_L) of the nodes previously existing in the cluster to be constant and calculate the spectrum utility by varying the mobility of the incoming nodes and vice versa.

From fig. 4 and fig. 5 it is evident that our proposed protocol has good channel utilization capabilities when compared to mobile.

Conclusions

In this paper we have proposed energy efficient TDMA based MAC protocol. It has very good energy conserving properties comparing with traditional TDMA. Another interesting property of the protocol is that it has relatively very less delay when compared to traditional TDMA

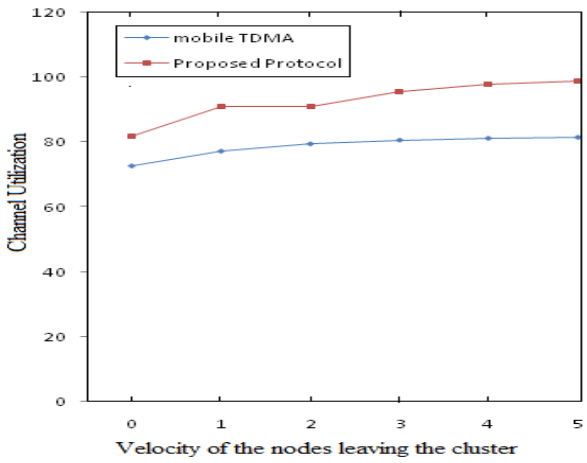


Fig. 4: Graph for Channel Utilization (I)

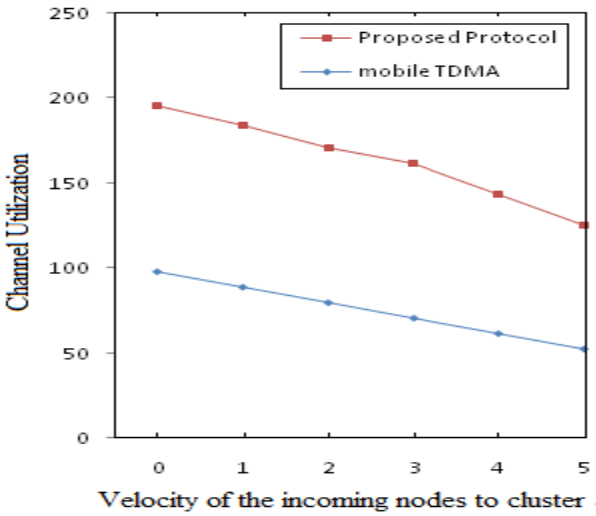


Fig. 5: Graph for Channel Utilization (II)

REFERENCES

[1] Arshad Jhumka, Sandeep Kulkarini "On the design of mobility-tolerant TDMA-based media access control (MAC) protocol for mobile sensor networks", 4th international conference on Distributed computing and internet technology, Bangalore, India, December 2007.

[2] S. Dulman, L. Hoesel, T. Nieberg, P. Havinga, "Collaborative Communication Protocols for Wireless Sensor Networks", *European Research on Middleware and Architectures for Complex and Embedded Systems Workshop*, Pisa, Italy, April 2003.

[3] W. Ye, J. Heidemann, and D. Estrin, "An energy-efficient MAC protocol for wireless sensor networks," in In Proceedings of the 21st International Annual Joint Conference of the IEEE Computer and Communications Societies (INFOCOM '02), New York, June 2002.

[4] Einstein, A.: "Investigations on the Theory of the Brownian Movement". Dover Publications,Mineola, NY (1956).

[5] Johnson, D.B., Maltz, D.A.: "Dynamic Source Routing in ad hoc Wireless Network",ch. 5, pp. 153–181. Kluwer Academic Publishers, Dordrecht (1996).

[6] Musolesi, M., Mascolo, C.: Designing mobility models based on social networks theory. Mobile Computing and Communications Review 1(2) (2007) .

[7] Demirbas, M., Arora, A., Mittal, V., Kulathumani, V.: A fault-local self-stabilizing clustering service for wireless ad hoc networks. IEEE Trans. Parallel Distrib. Systems 17(9), 912–922 (2006).

[8] V. Rajendran, K. Obraczka, and J.J. Garcia-Luna-Aceves, "Energy-Efficient, Collision-Free Medium Access Control for Wireless Sensor Networks", *The First ACM Conference on Embedde Networked Sensor Systems (SenSys 2003),* Los Angeles CA, Nov. 2003.

A New Hierarchal and Scalable Architecture for Performance Enhancement of Large Scale Underwater Sensor Networks

Majid Hamidzadeh [#1], Nosratallah Forghani [#2], Ali Movaghar [#3]

[#1] Sharif University of Technology, International Campus - Kish Island,
[#2] Department of Biomedical Engineering Toosi University of Technology Tehran, Iran
[#3] Department of Computer Engineering, Sharif University of Technology, Tehran, Iran

[#1] Hamidzadeh.majid@gmail.com
[#2] N_forghani@ee.kntu.ac.ir
[#3] Movaghar@sharif.ac.ir

Abstract— The different characteristics of UWSN and trade off between UWSN and WSN, have been discussed in many researches. Here, we aim to propose a new architecture for very large scale underwater sensor network. In deployment part of sensors, topology plays a crucial role in issues like communication performance, power consumption, network reliability and fault tolerance capabilities. Hence, it is so critical and should be analyzed how we deploy sensors in targets environment. For instance, to improve reliability of our networks in harsh conditions, it is so important to avoid deploying underwater sensors with single point of failure and bottleneck. For this purpose, we present enhanced clustering algorithm to build a topological architecture and we try to set some topological features for our proposed model. Scalability is regarded as the main advantage of clustering algorithms. In this paper, we comprise the pyramidal architecture with our proposed architecture, for building scalable UWSN with capability of fault tolerance and end to end delay estimation. We tried to calculate optimized number of nodes for using maximum number of deployed sensors into the water. Tree of Wheels (ToWs) improved our work of finding enhanced results. To the best of our knowledge, there is no study addressing the organized architecture due to enhance communication in underwater sensor networks. For simulation, we developed some MATLAB codes. Performance results are obtained taking into consideration different number of levels and sensors in along with the future works are mentioned. We believe that such a scalable architecture presents information that helps network designers to choose proper protocol and clustering algorithms depending on network situation and deployment environments.

Keywords: Underwater Sensor Network, Tree of Wheels, Scalability, Network Topology

I. INTRODUCTION

The largely unexplored vastness of the ocean, covering about two-thirds of the surface of Earth, has fascinated humans for as long as we have records. Recently, there has been a growing interest in monitoring aqueous environments. Although sensor networks have been deployed in a broad range of terrestrial applications [1-6], underwater use of sensors and sensor networks has been quite limited due to the harsh environment and high costs. Recently, there has been a rapidly growing interest in Underwater Wireless Sensor Network (UWSN) due to its advantages in a wide spectrum of applications in aquatic environments, such as lakes, ponds, rivers, and oceans. Potential applications of UWSNs include environmental underwater observation for scientific exploration, monitoring and data collection, disaster early warning, and underwater construction, commercial exploitation, coastline protection and target detection in military or terrorist events [2].

The way of deploying the nodes on the domain is very important for wireless sensor networks. In UWSN, usually we drop a large number of sensors into the water. Therefore, we don't have any anticipation for sensors` location due to define a topology or relation with them. They should announce their location to each other to figure out a random topology. Although, sink can plays the role of detecting the distribution of sensors for finding a desultory topology. In comparison with randomly deployed UWSNs, pre-configured UWSNs are superior in network performance in many aspects, including fault tolerance, delay time, data delivery ratio and energy consumption.

The hierarchal architecture needs new configuration because of three-dimensional characteristic. Therefore, we focus on building a Clustering method in way of hierarchal architecture and the way of set up this architecture in the form one topology, which has some related benefits.

The design of clusters and connection between them along with choosing the cluster head (CH) for this kind of network is a challenging issue in this decade. In several years, many researchers devoted themselves to these kinds of problems. In order to achieve the network scalability and better management, grouping sensor nodes into clusters has been widely pursued by the research community. Every cluster would have a leader, often referred to as the cluster-head (CH). Although many clustering algorithms have been proposed in basics of ad-hoc networks, the objective was mainly to generate stable clusters in environments with static and mobile nodes.

Many of such techniques care mostly about node availability and route stability, without much concern about critical design goals of WSNs such as network longevity and coverage. Recently, a number of clustering algorithms have been designed specifically for WSNs [7]. These proposed clustering techniques widely vary depending on the node deployment, bootstrapping schemes, the pursued network architecture, the characteristics of the CH nodes and the network operation model. It can localize the route set up within the cluster and thus reduce size of the routing table stored at the individual node. Clustering can also conserve communication bandwidth since it limits the scope of inter-cluster interactions to CHs and avoids redundant exchange of messages among sensor nodes.

A CH maybe elected by the sensors in a cluster or pre-assigned by the network designer. A CH may also be just one of the sensors or a node that is richer in resources. In addition to supporting network scalability, clustering has numerous advantages. The CH can also implement optimized management strategies for further enhancement of the network operation and prolong battery life of the individual sensors and the network lifetime. So that the sensors reties are avoided, redundancy in coverage can be limited and medium access collision is prevented [2]. Furthermore, a CH can aggregate the data collected by the sensors in its cluster and thus decrease the number of relayed packets [8].

In some applications, several thousands of sensor nodes might be deployed over the monitored region. For example, in biological oceanography scenarios, in environmental monitoring or in water coastline surveillance applications, such large-scale sensor networks would be necessary. Moreover, the diameter of the region might easily be several kilometers. In this case, scalability of the network is a very important design issue. In order to obtain a scalable network, the sensor nodes should be divided into clusters. The nodes within a cluster will then be connected to the sink nodes dedicated for that cluster [9].

The rest of the paper is organized as follows: section 2 reviews some related works. In section 3, we proposed our research work with clarification of our architecture. After that, in section 4, we listed our simulation results and at last, we conclude our paper on section 5.

II. RELATED WORK

This section reviews some scalability matter researches and categorizes clustering algorithms proposed in some literatures for WSNs. Different architectures and design goals/constraints have been considered for various presented algorithms of WSNs. At last, we summarize a collection of clustering algorithms and topological architectures for WSNs and present classification of various approaches about this topic.

Topology issues and clustering algorithms have been extensively studied in WSNs and recently in UWSNs. In [10] they proposed In-Network data processing, since sensor nodes might generate significant redundant data, similar packets from transmissions would be reduced. Data aggregation combines data from different source by using different factors such as min, max and average. Some of these functions can be performed either partially or fully in each sensor node with In-network data processing model. It is worth nothing that sometimes it may be necessary to assign backup CHs for cluster or rotate the role of being CH among sensors in cluster.

As in [11] researchers discussed, the deployment is either deterministic or self-organizing. In deterministic situations, sensors are manually placed and data is routed through pre-determined paths. In some cases CHs are excluded from sensing duties, in order to avoid depleting their energy rather quickly. As in [7] they review Baker and Ephremides proposed algorithm, Linked cluster algorithm (LCA) is among the early ones on clustering of wireless networks. In LCA focus is mainly on forming an efficient network topology that can handle mobility of nodes. By clustering, CHs are hoped to form a backbone network to which cluster members can connect while on the move. The objective of the proposed distributed algorithm is to form clusters so that a CH is directly connected to all nodes in its cluster. In [12], Nagpal and Coore proposed CLUBS, an algorithm that forms clusters through local broadcast and converge in a time proportional to the local density of nodes. Basically, cluster formation in CLUBS is based on the following three characteristics:

• Every node in the network must be connected to a cluster.

• Maximum diameter of all clusters in the network should be the same.

• Clusters should support the intra-cluster communication, which means nodes in a cluster must be able to communicate with each other.

The algorithm forms clusters with a maximum of two hops. The algorithm does not terminate unless all nodes in the network join some cluster as a CH or as a follower. Unlike most of the published schemes, the goal of Banerjee and Khuller is to form a multi-tier hierarchical clustering [13]. Figure 1 illustrates the concept of clusters' hierarchy. While grouping the nodes, a number of cluster's properties such as cluster size and the degree of overlap, which are useful for hierarchy's management and scalability, are also considered.

Low Energy Adaptive Clustering Hierarchy (LEACH) is one of the most popular clustering algorithms for WSNs [14]. It forms clusters based on the received signal strength and uses the CH nodes as routers to the base-station. All the data processing such as data fusion and aggregation are local to the cluster. LEACH forms clusters by using a distributed algorithm, where nodes make autonomous decisions without any centralized control. Initially, a node decides to be a CH with a probability p and broadcasts its decision. Each non-CH node determines its cluster by choosing the CH that can be reached using the least communication energy. DWEHC and HEED are other models which are similar in many ways; every node in the network participates in the clustering process, they do not make any assumption about the network size and consider energy reserve in CH selection [7].

III. CHALLENGES AND OUR CONTRIBUTION

Management and Scalability are two issues which are considered together. The sensors are expected to be deployed randomly in the area of interest by a relatively uncontrolled means, e.g. dropped by a helicopter in order to collectively

form a network in an ad-hoc manner. Given the vast area to be covered, the short lifespan of the battery-operated sensors and the possibility of having damaged nodes during deployment, large population of sensors are expected in most WSNs applications. It is envisioned that hundreds or even thousands of sensor nodes will be involved. Designing and operating of such large size network would require scalable architectural and management strategies. To support scalability problems, nodes are often grouped into disjoint and mostly non-overlapping clusters.

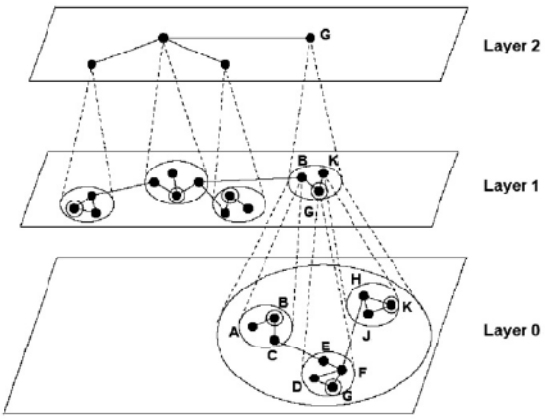


Figure 1. An Example of a multi-tier hierarchical clustering from [13]

In ground base WSN, several topologies concerning with pre-configured sensors, such as Mesh, Hexagonal, Pyranet or de Bruijn, were proposed by some researchers. (Pyranet) The common flaws among them are that the number of neighbors a node could has, has a significant effect on fault-tolerance capabilities and network throughput. Furthermore, a longer network diameter often introduces a considerable transmission delay, but because of limitations we do not have any pre-configured topology for UWSNs so far. There is a gap between topological architecture and sensor deployment for UWSNs.

Thus, for pre-configured WSNs which can adapt itself to randomly deployment of sensors, we propose efficient and scalable network architecture, named as ToWs. In ToWs, sensor nodes are first deployed as a Tree model, then, the children connect to each other like a wheel with virtual links but multi hop channel. In each wheel, they select their CH by using ranking algorithm. This algorithm can be one of previous discussed algorithms or one simple algorithm.

During the design phase of a large-scale sensor network, the designer should decide on the number of clusters, and considerably on the optimum locations and numbers of the sink nodes. Then, the number of sensors which obey one leader as cluster head should be estimated. In [9] they called this problem as the "multiple sink sensor network design problem". When they want to calculate relation between sink and other sensors, they try to provide some solutions.

Description of ToWs: A ToWs With amplitude M and level L denoted by a ToWs (K, L, M), can be constructed hierarchal. A ToWs (K, 1, 2) is a tree that its children are connected to each other like a Ring and beside, they have a center node (CN) that they are connected to it. Each CN with its brothers is one cluster. M is the number of nodes in the circumference. Thus, number of nodes within each cluster equals M+1. (For instance, ToWs (4, 1, 4) has 21 nodes like a normal tree with 4 children).

Network degree (ND) of this topology is 9, because each CN has M extra edges to its inter cluster`s nodes. More than that, each CN with 1 channel is connected to its father from outer cluster`s node and is similarly connected to its children (in contrast with normal Tree that each node is just connected to its father and children). Each node in ToWs (K, L, M) is labeled these three variable parameters (K, L and M). Similarly, each ToWs (K, L, M) has k sub networks ToWs (K, L-1, M), which are labeled with C index, where $2 < C < L$.

Therefore, with these three parameters such as (x, y, z), each node has unique address. They can be constructed by grouping basic building blocks. Figure 2 have illustrated one cluster of ToWs (K, L, 5) with its cluster head which is placed at the center of cluster. For larger networks, and in order to have more density, you can increase the number of K. For instance, you can have a ToWs with 10 nodes in each cluster. Therefore, it is an adaptive topology with consideration to our constraints in underwater sensor networks. Also, in figure 2, we see a cluster with 6 nodes and probable multi hop connection between follower nodes. In this figure, white node with black circumference is the cluster head. The blue sensor cannot communicate with CH directly; therefore, it is connected to CH with multi-hop channel which we named this links of communication as Virtual Link (VL). These kinds of VLs are made of some multi-hop channel, with number of hops limitation as we have assumed before.

Furthermore, for having more connected and reliable network, in each cluster, each node can be connected to its neighbors with direct links or multi-hop links but we assume all of the connection between brother nodes is virtual; because these virtual link increase connectivity and directly has more cost and complexity. The black node in figure 2 is the peak of one cluster. In each level, the peak node is a cluster head in previous level. This way of hierarchy makes it easy to deploy large number of sensors in a topological figure with high degree of flexibility.

For larger networks and in order to have more distributed networks, you can increase the number of K. For instance, you can have a ToWs with 10 nodes in each cluster. Therefore, it is an adaptive topology with consideration to our constraints in sensor networks. In figure 2, we see a cluster with 8 nodes and probable multi hop connection between follower nodes. In this figure white node with black circumference is the cluster head. The blue sensor cannot communicate with CH directly. Therefore, it is connected to CH with multi-hop channel which we named these links of communication as Virtual Link (VL). These kinds of VLs are made of some multi-hop channel, with number of hops limitation. In each cluster, each node is connected to its neighbors with direct links or multi-hop links but all the connections between brother nodes are virtual links. The black node in figure 2 is the peak of one cluster. In each level, the peak node is a simple follower or it is the cluster head

in previous level. This way of hierarchy makes it easy to deploy large number of sensors in a topological figure with high degree of connectivity.

CH selection in our proposed architecture is randomly or pre-assign. It has high cluster overlapping which is not interesting in this point of view, but because of its balanced clustering and its hierarchal characteristic, we can neglect it. Specific diameter and balanced clustering make it noticeable in other presented approaches.

Now we are going to clarify interconnections between sensors in bigger levels with all possible connections. For example, if we need a network with normal depth and little congestion (sparse) we can fix the number of levels and decrease K and M parameters.

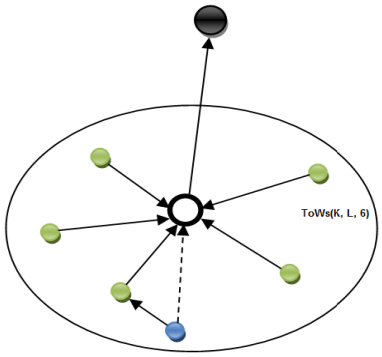


Figure 2. Inter cluster connection with one outlying follower (Virtual Link)

Figure 3 shows us ToWs (2, 3, 2). With order 2 tree, we just can cover our area of interest in 2 dimensions. Afterwards, if we need to increase the coverage in shallow water, this is possible to decrease K parameter and define M in a sufficient number and subsequently, decrease or stable number of L. Figure 4 illustrates ToWs (3, 3, 3). As you see in this figure, there is still a black hole at the middle of the three branches of this architecture. For covering this free space, in figure 6, we increased K and increased M for more connectivity. As a result, we have full coverage in our interested area.

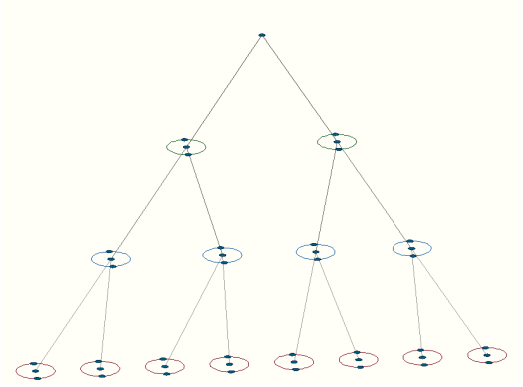


Figure 3. ToWs (2, 3, 2) for sparse covering and low degree of connections

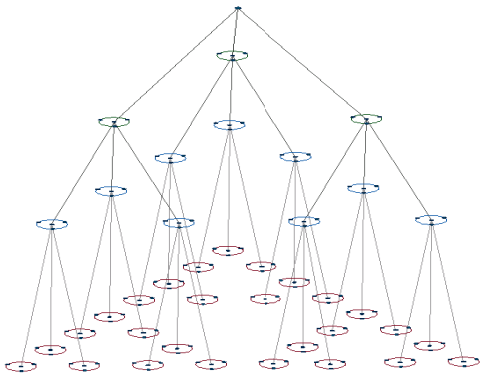


Figure 4. ToWs (3, 3, 3) for sparse covering with black hole in middle of the network

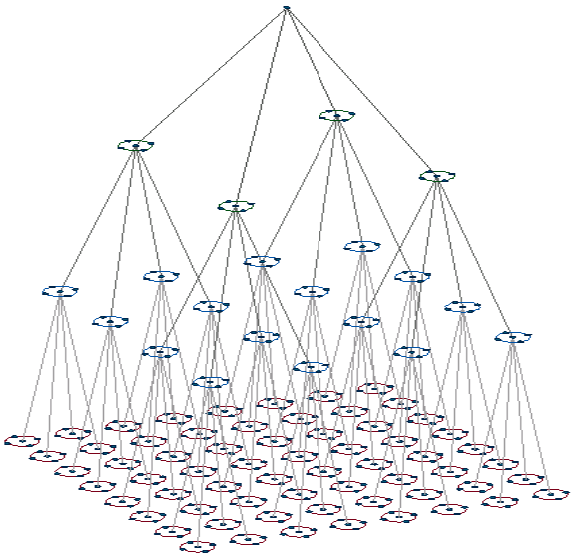


Figure 5. ToWs (4, 3, 4) with full coverage deployment

IV. Simulation Results

The Effect of Variation in K, L and M on Number of Nodes: As figure 6 shows, at the first experiment, we pursue increment of K as horizontal axis with different number of M and L. This figure shows us that the increment of K, with constant number of M and L in each curve, does not have considerable progression. These simulations have been conducted under the assumption that the deployed sensors are tethered and anchored to the ground and thus, there is no horizontal movement for the sensors. After that, figure 7, illustrates varying number of L along with constant numbers of M and K. last step, figure 8 shows different numbers of M along with constant numbers of K and L.

If we compares figure 6, 7 and 8, it is clear that in case of increment of Level, considerable progression of number of sensor exists. Because of increment of L is almost near to exponential curve but increment of M is like adding constant coefficient to function of number of nodes.

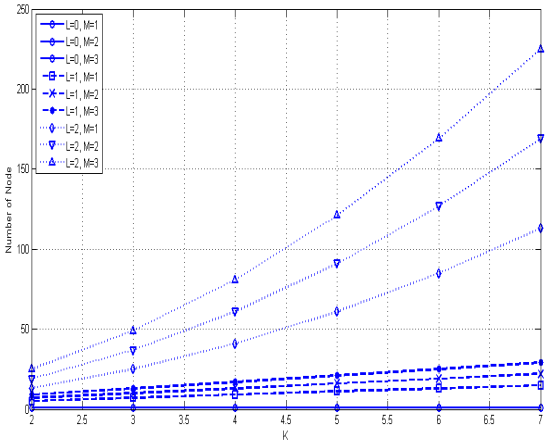


Figure 6. Number of nodes of ToWs with varying number of K

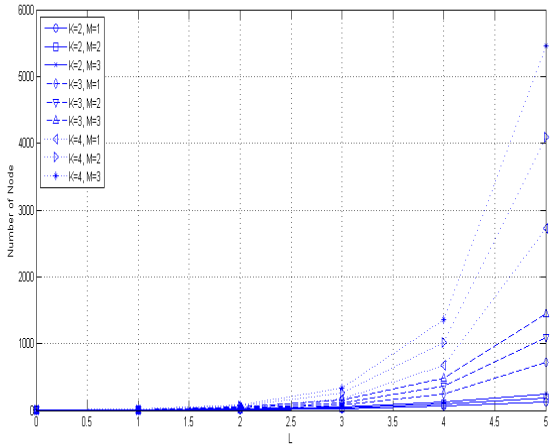


Figure 7. Number of nodes of ToWs with varying number of L

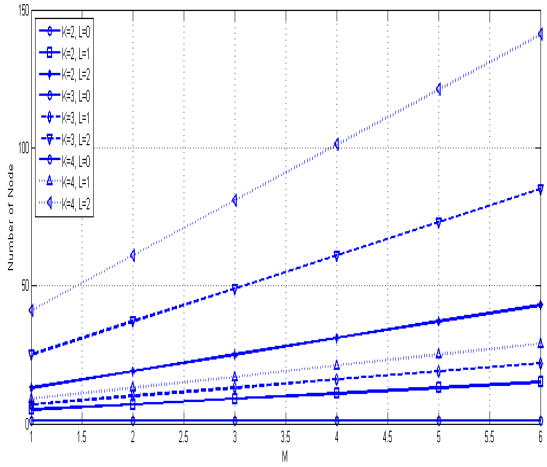


Figure 8. Number of sensors of ToWs with varying number of M

The Effect of Variation in K, L and M on Power Consumption: Now, it investigates the effect of variation of these parameters on the power consumption. For the first experiment, our assumptions were as we mentioned in previous chapter. We study power consumption in 2 kinds of messages and with considering constant parameters. First, for sampling message form sink to the entire network and second one for coming back data from underwater sensors to the surface.

In a comparison among figures 9 and 10 with figure 11, it can be understood that the effect of first parameters increment, on different values of L and M. This increment is useful for covering large scale of interested area. The results show us the increment of K and M does not have such a considerable effect on power consumption as L does. As it was predicted, power consumption line with increment of L behaves similar to exponential curve.

V. CONCLUSION

In this paper, we briefly examined the architectural and system clustering design issues for UWSNs. We believe that combination of scalable architecture with clustering algorithm improve the performance of large scale underwater sensor networks. Estimation of number of nodes and hops would be a main advantage of proposed scalable architecture in order to find new approaches for fault tolerance, power-saving mechanisms, scalability and efficient resource management which are the major challenges for UWSN designs. The unique features of our scalable architecture raise new challenges, but they also create opportunities to explore. In order to extend the lifetime of UWSNs, power efficiency should be pursued at both the node and network levels. Moreover, an accurate lifetime estimation model is necessary for UWSN designs and can help determine important design parameters to prolong lifetime. We aim to remove the gap between topological architecture and randomly deployment with proposing an adaptive topology for UWSNs which is estimable and computable. The ToWs can be help for protocol designer to imagine a regular network with hierarchal structure. High degree of scalability and flexibility are shown in this paper.

For improving analysis of our proposed research, we used Matlab simulation to show enhancement of our flexibility and we combined power consumption parameters as importance coefficient as function to our genetic algorithm. For this reason, we divided power consumption into two parts; First part was for sending broadcast messages from sink to sensors as sampling command, and second part (up to down) ,was data sensation from entire network to the sink (down to up). The results are shown in simulation part.

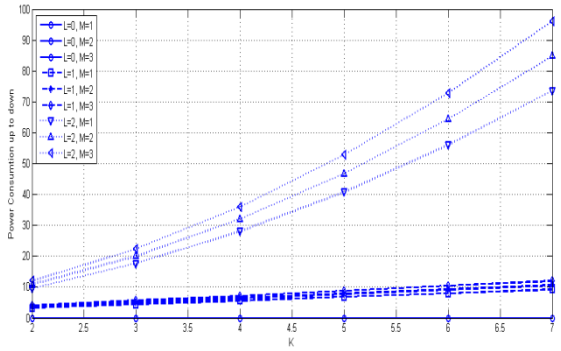


Figure 9. Power consumption from up to down with variation of K

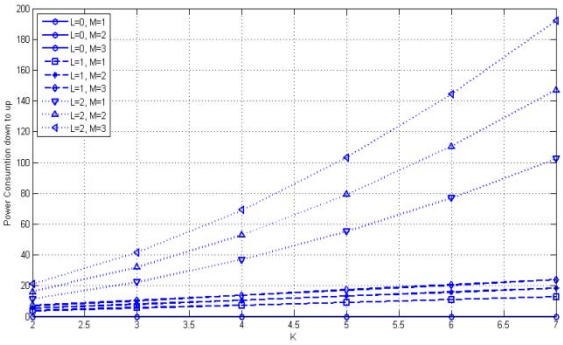


Figure 10. Power consumption from down to up with varying number of K

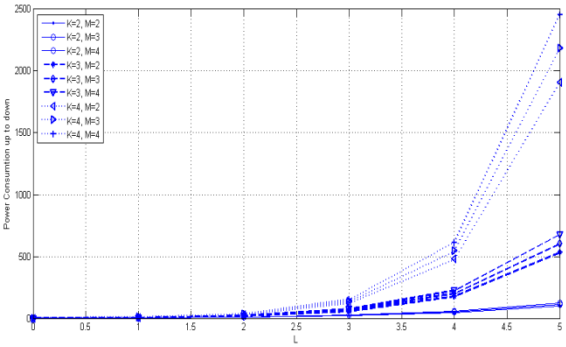


Figure 11. Power consumption from up to down with varying number of L

REFERENCES

[1] D. Pompili, T. Melodia, and I. F. Akyildiz, "Three-dimensional and Two-dimensional Deployment Analysis for Underwater Acoustic Sensor Networks," Ad Hoc Networks (Elsevier), vol. 7, no. 4, pp. 778-790, June 2009

[2] Z. Shi and Y. Fei, "Exploring architectural challenges in scalable underwater wireless sensor networks," in Annual Boston Area Computer Architecture Workshop (BARC), Feb., 2006.

[3] J. Kong, J. Cui, et al, "Building underwater ad-hoc networks and sensor networks for large scale real-time aquatic applications," IEEE MILCOM, 2005.

[4] J.-H. Cui, J. Kong, M. Gerla, S. Zhou, Challenges: building scalable mobile underwater wireless sensor networks for aquatic applications, in: Special Issue of IEEE Network on Wireless Sensor Networking, May 2006.

[5] A. Nimbalkar and D. Pompili, "Reliability in Underwater Inter-Vehicle Communications," Proc. of ACM International Workshop on UnderWater Networks (WUWNet), San Francisco, CA, September 2008.

[6] D. Pompili and T. Melodia, "Three-Dimensional Routing in Underwater Acoustic Sensor Networks," in Proc of ACM Intl. Workshop on Performance Evaluation of Wireless Ad Hoc, Sensor, and Ubiquitous Networks (PE-WASUN), Montreal, Canada, October 2005.A

[7] A. Abbasi and M. Younis, "A Survey on Clustering Algorithms for Wireless Sensor Networks," Journal of Computer Communications, Special Issue on Network Coverage and Routing Schemes for Wireless Sensor Networks, Vol. 30, pp. 2826–2841, 2007.

[8] M. Younis, M. Youssef, K. Arisha, Energy-aware management in cluster-based sensor networks, Computer Networks 43 May, 2003.

[9] E. I. Oyman and C. Ersoy. Multiple sink network design problem in large scale wireless sensor networks. In Proc. of ICC 2004, Paris, France, 2004.

[10] B. Krishnamachari, D. Estrin, S. Wicker, Modeling data centric routing in wireless sensor networks, in: Proceedings of IEEE INFOCOM, New York, NY, June 2002.

[11] K. Sohrabi et al., Protocols for self-organization of a wireless sensor network, IEEE Personal Communications 7 May. 2000.

[12] R. Nagpal, D. Coore, An algorithm for group formation in an amorphous computer, in: Proceedings of the 10th International Conference on Parallel and Distributed Systems (PDCS'98), Las Vegas, NV, October 1998.

[13] S. Banerjee, S. Khuller, A clustering scheme for hierarchical control in multi-hop wireless networks, in: Proceedings of 20th Joint Conference of the IEEE Computer and Communications Societies (INFOCOM' 01), Anchorage, AK, April 2001.

[14] W.B. Heinzelman, A.P. Chandrakasan, H. Balakrishnan, Application specific protocol architecture for wireless microsensor networks, IEEE Transactions on Wireless Networking (2002).

[15] Zhong Zhou, Jun-Hong Cui, Amvrossios Bagtzoglou, Scalable localization with mobility prediction for underwater sensor networks, in: Proceedings of IEEE INFOCOM'08, Mini-Conference, Phoenix, AZ, April 2008.

[16] Liang-Min Wang, Jian-Feng Ma, and Yan-Bo Guo, Node-failure Tolerance of Topology in Wireless Sensor Networks Vol. 7, No. 2, 2008

[17] Lucani, D. E., Stojanovic, M., Médard, M., "On the Relationship between Transmission Power and Capacity of an Underwater Acoustic Communication Channel", In Proceedings of IEEE Oceans Conference '08, 2008D.

[18] Pompili, T. Melodia, I. F. Akyildiz, "Routing Algorithms for Delay-insensitive and Delay-sensitive Applications in Underwater Sensor Networks," in Proc. of ACM Intl. Conf. on Mobile Computing and Networking (MobiCom), Los Angeles, CA, USA, Sept. 2006.

[19] M. Hoseiny Farahabady , H. Sarbazi-Azad, The WK-Recursive Pyramid: An Efficient Network Topology, Proceedings of the 8th International Symposium on Parallel Architectures,Algorithms and Networks, p.312-317, December 07-09, 2005.

[20] S. Suboh, M. Bakhouya, J. Gaber, and T. El-Ghazawi, An Interconnection Architecture for Network-on-Chip Systems, Kluwer Journal of Telecommunication Systems, Vol. 37, N 1-3, pp. 137-144, 2008.

[21] J. Huang, P. Hsu, K. H. Chen, "PyraNet: An Efficient and Reliable Pyramidal Wireless Sensor Network," 5th ACM Workshop on Performance Evaluation of Wireless Ad Hoc, Sensor, and Ubiquitous Network Vancouver, Canada, 50-53 , 2008.

Cache Balancing with Proportionate Cutting Strategy

Mohd Rohaizat Abdul Wahab,
Institute for Mathematical Research (INSPEM), UPM,
Serdang, Selangor, Malaysia
mrohaizat@gmail.com

Mohd Yunus Sharum,
Muhamad Taufik Abdullah,
Fac. of Comp. Science and Info. Technology, UPM,
Serdang, Selangor, Malaysia
{ myunus, taufik }@fsktm.upm.edu.my

Mat Rofa Ismail,
Institute for Mathematical Research (INSPEM), UPM,
Serdang, Selangor, Malaysia
rofa@math.upm.edu.my

Abstract—**Caching mechanism had been widely used in many applications particularly in CPU optimization, internet application, data structure etc. Our research in text processing reveals that caching mechanism is also applicable to solve performance problem of text analyzers. In this paper we describe the strategy called 'proportionate cutting' for balancing (maintaining) limited size cache. Our experiment shows that by proportionate cutting at 0.5 threshold's value gives good performance to the cache. This actually allows of using limited cache in text processing with high frequency words.**

Keywords- Cache; Caching Strategy; Text Processing

I. INTRODUCTION

Cache mechanism had been widely used in many applications. Such applications ranged from CPU processing, internet application i.e. web browsing, data structure and database, and so forth. In the processing by CPU, the cache was used to reduce the latency caused by memory access, which is slower compared to the processing of the existing CPU. Thus the cache mechanism is used as 'buffer' to ensure the CPU did not ends-up idle, waiting processing data to be transferred to/from the main memory. Another application of cache is in web browsing. As today's technology had becomes better, the same happened to the website's technology. Thus web pages are getting more advanced and heavily loaded with applets, client-side scripting etc. This subsequently makes the pages bigger and complex. But with the slower advancement of network technology compared to its content, this unbalanced progress had actually produced a bottleneck for web browsers in interaction with web servers. As a solution, caching was introduced for buffering the web pages so that the pages can be quickly reloaded and viewed without waiting for the slow transferring through network. In both examples, the cache acts as buffer to store and reuse previously accessed information. This allows the main process to skip repeating or time consuming sub processes, and thus subsequently speeds up the whole process.

A caching mechanism should be well-maintained with a good strategy. Otherwise two situations could happened – (i) the cache is not fully utilized, thus make the cache useless and latency may remains without any improvement, or – (ii) the caching mechanism produce more latency rather than reducing it. In such situations it is better for not to have the cache at all.

An example of using cache in text processing can be found in study conducted by Chen and Lee [1]. The caching approach was used with paragraph-scope analysis in identifying noun in Chinese text. In such analysis, the cache plays the role of keeping the information of the nearest neighbor for back referencing. The information of the cache will be reset when the analysis leave the scope of a paragraph. However, not much information is provided regarding the cache mechanism. The study discussed in this paper was actually a continuation from another related study conducted by Sharum et al. [2]. The study is about designing a caching strategy to solve performance's problems in morphological analyzers called MALIM [3], [4]. The study in [2] proposed a model of using unlimited cache as a caching strategy to improve the performance. But it shows that the limited size cache had caused some serious problems to the performance of morphological analyzer, thus by the proposed model we are only able to use the unlimited cache. However, unlimited size cache was not very practical, although applicable.

In this paper, we describe the technique for using limited size cache in processing text with high frequency words. But first we would like to elaborate briefly some important terms used in this paper. As the cache is limited, using it for processing text with very large amount of high frequency words would be problematic, especially if the number of words is much larger than the cache's size. In such situation, the cache mechanism used must be able to manage the cache very well to cope with its limited size. This process is referred as *cache balancing*. In order to maintain the size, some items must be removed to allow new items to enter. This process is defined as *proportion cutting*. Additionally, the cutting must maintain the balance between the affected, remaining items and the need for large space allocation. Thus the cutting must be of a *proportionate or balanced cutting*.

In the next section, we describe in more detail about the technique. Section III describes the experiment to evaluate the performance of our approach, while Section IV discusses the findings and results from the experiment. Final section draws the conclusion.

II. BALANCING LIMITED CACHE

A. Basic Approach

The easiest approach in balancing the items in limited size cache is based on the time when they were last accessed. If the

items are regularly referred, refreshed or visited, they will be kept in the cache and the record time will be updated. But if they not, the items will be removed to give some spaces for other regularly used items. However time is not the only mechanism for detecting infrequently used cache's items. Reference counting like the approach used in automatic garbage collector is also can be used for balancing cache.

Whatever the strategy is, at least the most required procedure in performing the cache balancing is to determine which cache item should be removed. This is because the cache size is limited and we had to ensure the items do not exceed outside the limit's boundary. In our approach, we use the simple method by keeping the timestamp of each item, and then each will be updated each time the items are visited. Once a new item needs to be inserted into the cache, we determined the candidate to be removed by traversing the cache and selecting the oldest or rarely visited items.

However this simple method produced latency due to the complexity of the approach. This is because we must traverse the entire cache to determine the suitable candidate to be removed. So, this process actually produces a complexity of n. Meanwhile, the removal will be performed each time an insertion is required on a full cache. If the application produced m insertions these subsequently produce m removals (assuming the cache is full). Thus the entire process of m insertions will produce mn complexity, since every insertion (which triggered the removal) will require n traversals.

In detailed examinations, we found that most of the worse performance of our limited size cache contains high numbers of removals. What seems to be the problem is that the excessive removals performed actually increased the complexity. This complexity then consumes more processing time for balancing the cache. If we are able to reduce the number of removals, the complexity would likely be reduced as well.

B. The Proportion-based Cutting Strategy

Generally, the removal is supposed to remove the cache's items to provide some space in the limited cache, and so new item can be stored. Each removal is triggered by a full cache state. Thus in order to avoid the removal we must ensure that the cache will always have some spaces for new items. Avoiding the full state will achieve the same effect of avoiding the removal. If we consider this in term of interval, we can reduce the frequency of removals by lengthening the interval between each removal, or lengthening the interval between the last removal and the next state where the cache becomes full.

This actually becomes the basis of the technique of the proportion-based cutting. The term proportion cutting means we remove some candidates from the cache based on certain proportion in ratio of the cache size. The term 'cutting' actually refers to the removal process. The larger proportion of the cache we removed means the longer interval for the cache to become full, since there are plenty of spaces to be filled by new items. This approach can be viewed as removing item one block at a time rather than by multiple pieces of the same block. The removing process will be much quicker since we perform single process instead of multiple processes. At the same time the large area consumed by the removed block will left a large space within an instance, but takes some times to be filled. So with this method, the removal becomes quicker and the frequency of the process would become lower (less removals).

The proportion-based cutting generally will affects large area of the cache. This might also affect some items which are referred frequently and supposed to stay in the cache. Thus, to avoid this from happening or at least reduce the effects, we have to ensure that the items of the same type are allocated contagiously. This is done by sorting them based on the last time they are referred. Once they are organized in groups, they can be treated by blocks. We then removed the block that contains the least referred items. However, in performing the cutting, we are still required to determine the proportion value or the size of the block. In the next section, we describe the experiment which is done to determine the best proportion value of the cutting.

An important aspect in proportion-based cutting is that we must balance between the proportion of the frequently referred items and the proportion of the space that becomes available. This is because if we remove too large block, we might have also removed the frequently referred items. Thus the cache would be devalued, since that is the main purpose of the cache – to contain the most referred items to enhance processing. However, if the removed block is too small, the proportion cutting may not be optimum in reducing frequent removals. Thus, a balanced approach must be developed to cater both aspects, and this brings us to the concept of proportionate cutting or a well balanced cutting.

In the proportionate cutting, the important aspect is to balance between the empty space produced with singe removal and the number of frequently referred items to stay in the cache. A proportionate value is the boundary value where we limit the cutting. We defined the *proportionate cutting value* or *pc-value* with a constant value as follows:

$$pc\text{-}value = 0.5$$

Besides simply as middle point between 0 and 1, this value actually was chosen since theoretically this minimized the chance of consuming too much frequently referred items but at the same time allows us to provide the most optimum space for inserting new items without performing removal too frequently. We use the following formula to calculate the proportion for cutting:

$$proportion = cache\text{-}limit \times pc\text{-}value \quad -(1)$$

Obviously this is similar as calculating a ratio. In order to perform the cutting, we also need to sort the cache. This is to ensure that items with similar removal criteria will be in contiguous positions thus can be removed as single block. We sort the items in descending order (most frequent to the least frequently accessed) and remove the cache's items from index [*proportion* - 1] until index [*cache-limit* - 1], assuming index

starts from 0. As a result, we can ensure no removal is required at least within the next *proportion* times of insertion.

III. EVALUATION'S METHOD AND EXPERIMENT

The pc-value actually was selected after conducting some experiments with several threshold values i.e. 0.25, 0.5, 0.75 and 1.0. Each evaluation of experimenting with these values was done using a morphological analyzer called MALIM described in [3], [4]. However, the analyzer was modified and fitted with new caching mechanism [2]. In the evaluation in this paper, the cache performance was evaluated by analyzing several sets of sample data. These sample data are described in Table I. Each sample data actually represents different text properties i.e. unique text without recurrence (Set W and TU) and text with high recurrence (Set T).

The evaluation was performed on a personal computer runs by 1.6GHz Intel Core-Duo's processor, along with 504Mb of memory. The Perl interpreter used for implementing the cache is the version 5.8.8 for Windows from the binary package distributed by ActiveState[1]. For each experiment, the cache size was limited to 10000 items. This limit was actually smaller than all the size of the sample data. For Set T we knew the size is still larger based on the size of Set TU. For the evaluation we want to ensure all the sample data have a full state cache at least once.

IV. RESULTS AND DISCUSSION

Table II displays the results of the first time execution of the analyzer with the cache, where the graphical results are displayed in Fig. 1. While in Table III displays the results of second execution and the graphical results are displayed in Fig II. However, to make the graph clearer, the results for threshold 0 in both Table II and III are not included in both figures.

The actual difference between first execution and second execution is on the utilization of persistent cache. The persistent cache is a simple technique where the cache contents are saved into a non-volatile storage which can be restored back later. Between the first and second time execution, the analyzer was unloaded and reloaded back to ensure the cache had been emptied before being restored with the persistent data. So in the first time execution, the analyzer starts with empty cache. However on the second time execution, the analyzer starts with a cache filled with the restored values from the previous cache.

TABLE I. SAMPLE DATA SET USED FOR EVALUATION

Words' set	Description
Set W	A set of 14319 unique words.
Set T	A collection of 172080 words, parsed from a collection of 263 Malay articles which was extracted from [5].
Set TU	A collection of 12685 unique words, produced by flattening (removing duplicate's words in) Set T.

[1] http://www.activestate.com

TABLE II. RESULTS OF FIRST TIME EXECUTION

Cutting threshold	Sample	Exec. time (s)	Frequencies of operation on cache		
			insert	retrieve	remove
0	Set W	95	14319	0	4319
	Set T	99	13129	158951	3129
	Set TU	91	12685	0	2685
0.25	Set W	39.847917	14319	0	2
	Set T	46.641868	18742	153338	4
	Set TU	30.688584	12685	0	2
0.5	Set W	39.785637	14319	0	1
	Set T	46.060241	18465	153615	2
	Set TU	30.50019	12685	0	1
0.75	Set W	39.741903	14319	0	1
	Set T	43.046282	17203	154877	1
	Set TU	30.455718	12685	0	1
1.0	Set W	39.795501	14319	0	1
	Set T	44.77234	17981	154099	1
	Set TU	30.247185	12685	0	1

TABLE III. RESULTS OF SECOND TIME EXECUTION

Cutting threshold	Sample	Exec. time (s)	Frequencies of operation on cache		
			insert	retrieve	remove
0	Set W	447	14319	0	14319
	Set T	226	8095	163985	8095
	Set TU	365	12685	0	12685
0.25	Set W	14.180069	5000	9319	2
	Set T	33.897803	13260	158820	5
	Set TU	12.315884	5000	7685	2
0.5	Set W	14.095241	5000	9319	1
	Set T	29.797199	11277	160803	2
	Set TU	17.628958	5000	7685	1
0.75	Set W	25.964807	9319	5000	1
	Set T	37.419095	14404	157676	2
	Set TU	22.467229	7685	5000	1
1.0	Set W	39.751367	14319	0	1
	Set T	42.178191	16850	155230	2
	Set TU	30.299053	12685	0	1

As we can see from Table II and III, the tested threshold values ranged from 0 to 1 (with interval 0.25 between each tested value). For the threshold 0, the cutting was not performed at all. The removal method is performed by removing only one item for each removal, while the rest of the threshold values used the cutting strategy. The most important aspect to be discussed is on the relation of execution time and the number of removals. From the tables II and III, we can see that there are huge differences between the threshold value 0 and the rest. First, the number of removals with threshold 0 was so high compared to other threshold values, which at most produced from 1 to 5 removals. We will not found 0 removals as we ensured that at least the removal is performed once. Subsequently, this difference affect the performance time as the complexity of removals consumes some processing time in each execution. Thus the higher the number of removals means the longer time in execution.

Yet the most important point in this experiment is to select the most optimum cutting value for balancing our cache. Based on Fig. 1 and 2 which compared among all the thresholds, we found that the most optimum value would be at threshold 0.5.

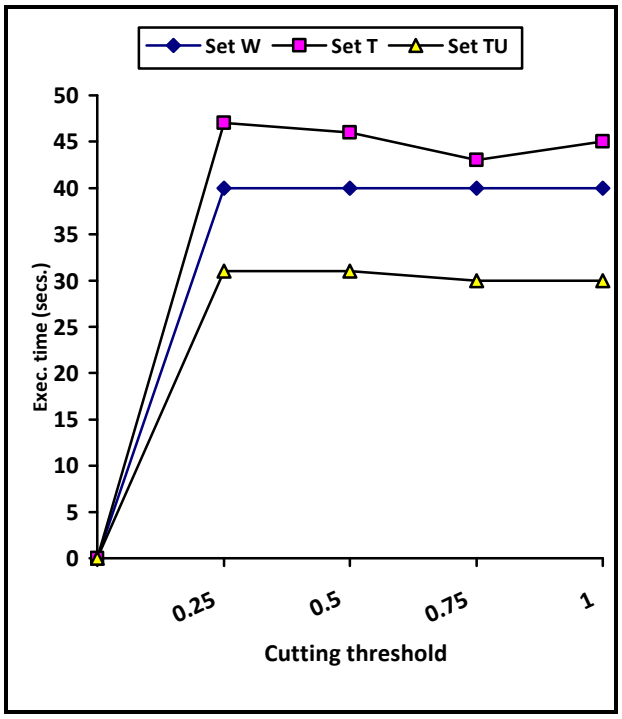


Figure 1. Text analysis without previously saved cache

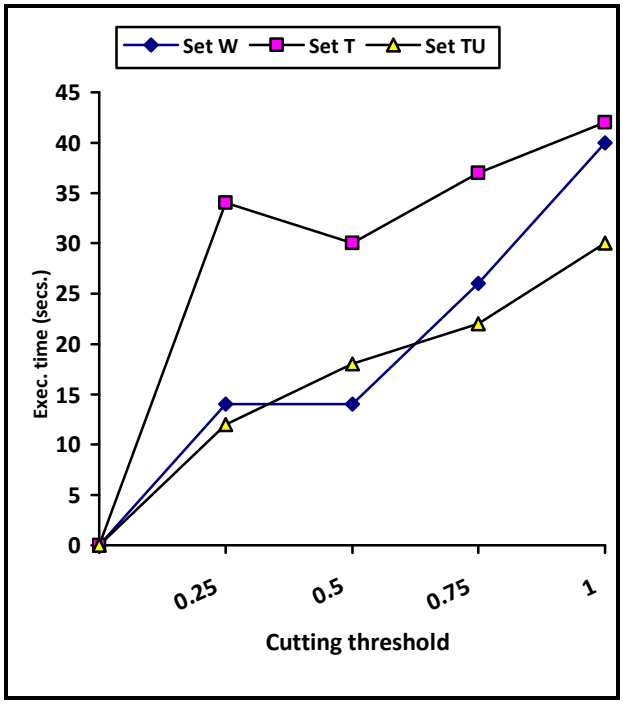


Figure 2. Text analysis with previously saved cache

If based on Fig. 1, most of the threshold values produced comparable execution time, with 0.75 produced a bit lower (execution time) than the others. However, Fig. 2 shows some significant differences. We can see thresholds 0.25 and 0.5 had actually produced low execution time, while 0.75 and 1.0 are much higher. Clearly thresholds 0.25 and 0.5 should be among the best candidates.

By considering between the thresholds, we referred back to Table II and III to determine the differences between the 0.25 and 0.5 thresholds. As we can see in Table II and III, the number of removal process for Set T (high frequency text) for 0.25 is a bit higher than 0.5. This actually a significant property as our target is to process any text, including with the high frequencies such as the Set T. We also consider that in the second time execution, the execution time for Set T in 0.5 is much lower than the 0.25. Based on these considerations, it is clear that 0.5 is the most balanced or optimum value for our cache compared with other tested values. However this does not represent other values within the range 0.25 to 0.5, which are not done in this experiment. However, based on the fact that 0.5 is the maximum value which produced lower execution time and better performance than 0.25, it would be safe to assume that 0.5 is the best for all values within the untested range.

V. Conclusion and Future Work

Based on the discussion, we proposed the threshold 0.5 as the proportionate cutting value for balancing limited cache. At the same time, the performance of unlimited cache will not degrades since removal is not required at all with the cache. As the conclusion, this paper had discussed the approach of using proportionate cutting for balancing limited size cache, where the most optimum cutting value is 0.5. However, we are not able to comment on using variable or fuzzy since it requires detailed study, which are not done. We expect that this strategy can be applied to any text processor which requires cache to improve the processing time. Based on the advantage gained in performance, it also indicates that this strategy could be used by text processors involved in processing text with high frequency words.

Acknowledgment

We would like to thank the anonymous reviewers who had generously provided us a lot of useful comments and feedbacks regarding the preliminary version of this paper.

References

[1] H. Chen and J. Lee "Identification and classification of proper nouns in Chinese texts," In Proceedings of the 16th Conference on Computational Linguistics: Copenhagen, Denmark, Volume 1, August 1996.

[2] M.Y. Sharum, M.R. Abdul Wahab and M.T. Abdullah, "Caching Strategy for Morphological Analyzer (A Preliminary Study)," URL: http://fsktm.upm.edu.my/~myunus/media/publication/yunus-report-2011-1.pdf, accessed on 10th Feb 2011.

[3] M.Y. Sharum, M.T. Abdullah, M.N. Sulaiman, M.A. Azmi Murad, and Z.A. Zainon Hamzah, "MALIM - A New Computational Approach of Malay Morphology," In Proceedings of 4th International Symposium on Information Technology – ITSim: KL, vol 2, pp. 837-843, June 2010. DOI: 10.1109/ITSIM.2010.5561561

[4] M.Y. Sharum, M.T. Abdullah, M.N. Sulaiman, M.A. Azmi Murad, and Z.A. Zainon Hamzah, "SAPI - New Algorithm for Malay Morphological Analyzer and Stemmer," In Proceedings of Artificial Intelligence Workshops 2010 (AIW2010) - Extraction of Structured Information from Texts in the Biomedical Domain (ESIT-BioMed 2010): Kuching, Sarawak, Malaysia, pp. 67-82, July 2010.

[5] "Utusan Online's archive" (http://www.utusan.com.my/utusan/search.asp)

Verification of Embedded System by a Method for Detecting Defects in Source Codes Using Model Checking

Yoshitaka Aoki
Graduate School of Engineering, Shibaura Institute Technology
Course of Electronic Engineering and Computer science
Saitama,Japan
m109002@shibaura-it.ac.jp

Saeko Matsuura
Graduate School of Engineering, Shibaura Institute Technology
Course of Electronic Engineering and Computer science
Saitama,Japan
matsuura@se.shibaura-it.ac.jp

Abstract—**We have proposed a method based on model checking for detecting hard-to-discover defects in enterprise systems. We apply our method to embedded system development to easily discover some defects caused by input/output data of the hardware which are influenced by the external environment before the software is integrated into the hardware. This paper discuss the effectiveness of our method using a case study to develop a line tracing robot.**

Keywords-component;Model checking,Software debugging,Software tools, Process Modeling, system verification

I. INTRODUCTION

Generally, enterprise systems consist of functions based on typical business logic. Business rules include many types of functions, and there are numerous combinations of execution orders and the conditions under which these orders must be executed. Programmers often have inadequate knowledge of business rules and hence may misunderstand the system designer's intentions. Moreover, programmers occasionally define the incorrect order in which business rules must be applied and the specific conditions under which these rules must be executed.

Because some programmers' decisions are incongruous with the designer's intentions, it becomes difficult to detect defects arising from the inappropriate definition of business rules by reviewing and testing of the code alone. Detection of such defects becomes a laborious task even if the inspector has the same knowledge as the system designer. Recently, a model-checking technique that facilitates thorough verification of every possible combination of states and thus ensures that the system reaches the desired state has been proposed as a promising approach for preliminary system development.

We have proposed a method for detecting defects in source codes using model-checking technique to reduce such a laborious task of developers[1]. To easily and definitely detect defects arising from such incongruous understanding of the specification, we have developed a tool which translates the target source code into a model that can be checked by the model-checking tool UPPAAL[4].

On the other hand, in embedded system development, it is hard that software properly controls input/output data of the hardware which are influenced by the external environment before being integrated into the hardware. This is because that incongruous understanding of the hardware specification takes place because it is hard to estimate entire behaviors of a target hardware being influenced by the external environments.

We apply our method to embedded system development by adding a step of modeling the external environments to capture the cause of the unstable behavior. The remainder of the paper is organized as follows. Section II discusses the UPPAAL model on the basis of a comparison with other model-checking tools. Section III discusses how defect source codes are translated into the UPPAAL model. Section IV describes the inspection process and Section V describes a case study. Section VI discusses related work.

II. MODEL−CHECKING TOOL

Model checking has been favored as a technique that helps improve reliability in the upper process of software. The model-checking tool uses temporal logic. It is inspected whether to fill a property in which a model is demanded from a system. When the specified state is not filled, the tool presents a counterexample. The process can be confirmed by the simulation facility. There are several model-checking tools, including SPIN[2] and PathFinder[3]. Table I presents a comparison of these tools with UPPAAL.

Enterprise system developers generally have little knowledge of model-checking techniques. As Table I shows, UPPAAL only provides a graphical visualization and recording of the dynamic behavior of a system description, so that we can confirm sequences of symbolic states of the system. It is easy to intuitively understand the phenomenon because UPPAAL can visually confirm laboratory results. As UPPAAL can accommodate time restrictions, it has the advantage of the modeling and verification abilities of real-time embedded systems. Furthermore, UPPAAL is easier to translate from not only Java but also other programming languages.

We adopted the model-checking tool UPPAAL because of the graphical view and fine simulation function in which counterexamples can be easily confirmed.

TABLE I. MODEL CHECKING TOOLS

Item	Model Checking tool		
	UPPAAL	PathFinder	SPIN
Model	UPPAAL Model	Byte Code	PROMELA
Limitation	None	Only Java	None
Graphical Model create	○	×	×
Graphical result	○	○	○
Partial inspection	○	●	○
Time pressure	○	×	×
Property add	New Model	Property class	New Model

The UPPAAL model consists of several locations and the transition arrows between them, as shown in Figure 1. A location expresses a state of the system, and the transition arrow indicates several conditions named Guard and a sequential processing during it named Update.

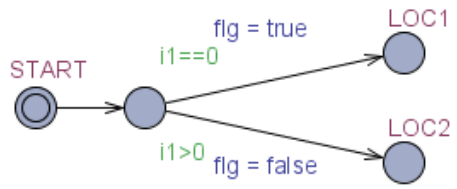


Figure 1. Basic Components of the UPPAAL Model

III. MODELING OF SOURCE CODE

A. Modeling Difficulties

To detect problems associated with the manner in which the execution orders and the necessary conditions are combined, the source code, including the defects, must be correctly translated into an UPPAAL model. If every point of finishing executing an expression in the source code translates into a location, there is a possibility of the number of states in the system increasing dramatically. As a result, testing may or may not be completed in time. However, the phenomena causing the defects must be correctly reproduced and the cause specified. Defining the cause of these defects enables specification of a sequence of transition arrows and the required conditions.

We must also devise a method for translating the source codes into UPPAAL models so as to identify the root cause of the defects.

B. Modeling Policy

To avoid state space explosion, source codes should be translated into the UPPAAL model to detect the anticipated defects. Generally, we intend to detect phenomena such as infinite loops, data overflow, time-out, and dead-lock problems. These phenomena are caused when the designers' intentions are not followed or when an incorrect combination of execution orders and the required conditions is employed.

In this study, we focus on the control flow model for an infinite loop. An infinite loop is caused by incorrect definition of the conditions for an iteration statement or selection statement. We limit the range of model checking to the target function, meaning the function call is abstracted by the appropriate variable in the target level.

C. Model of if Statement and for Statement

Figure 2 shows a model of the "if" statement. The top location expresses the start state of the "if" statement. This conditional expression is also translated into two transitions representing the true state [a] and the false state [b]. The body of the "if" statement is translated into the transition [c], which expresses the end point of the "if" statement. The transition [d] is replaced by the "else" statement.

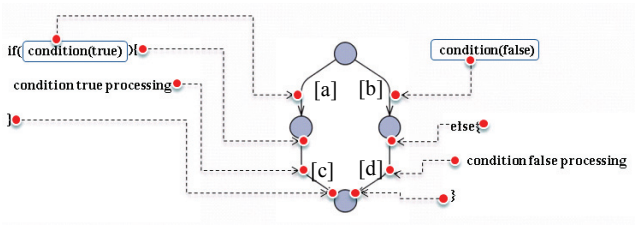


Figure 2. Model of if Statement

Figure 3 shows a model of the "for" statement. The top location expresses the beginning state of the "for" statement. The initialize and update expressions of the "for" statement are translated into transitions [a] and [b], respectively. The conditional expression is also translated into two transitions from these locations, which represent the true state [c] and the false state [d]. The body of the "for" statement is translated into transition [e] from this location, which expresses the end point of the statement.

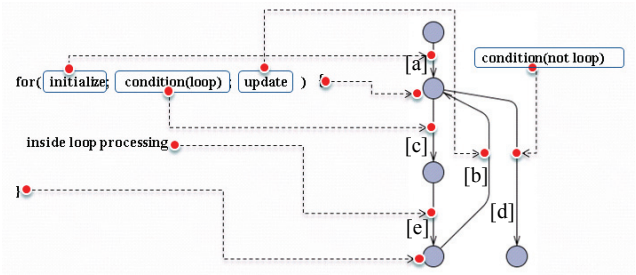


Figure 3. Model of for Statement

D. Abstraction of Other Statements

The other statements are translated into the UPPAAL model according to the following rules.

Firstly, statements that do not include any variables in the conditional expressions of the "if" or "for" statements are excluded from the UPPAAL model. This is because these statements have no influence on the execution of the control flow model.

Secondly, statements that include variables in the conditional expressions of the "if" or "for" statements are translated into statements in the UPPAAL model. Function call expressions are temporally defined by variations in the returned values. Various kinds of collection data types that are not included in UPPAAL are temporally defined by an array in this model.

IV. DEFECT DETECTION

A. Inspection Process

Inspection processes are divided into two parts, as shown in Figure 4. Firstly, for each method in the target source code, our supporting tool automatically generates a set of several graphs. We call it a structured diagram denoted by the red rectangle in Figure 4. Each graph is a representation of a method that has several loop structures and conditions by abstracting the target source code from the "if" statement and the "for" statement. Because the inspector can understand the basic specifications of the target source code, he/she can also understand the phenomenon caused by the defects. The defects being considered for inspection can then be selected from the structured diagram using the above methods. The UPPAAL model of the selected component is generated automatically. The Guard expression and the Update expression on each transition arrow are generated from the expression of the "if" statement and all expressions in the body.

When the generated expression is not suitable to the UPPAAL syntax rule, the inspector needs to modify it. Finally, the inspector defines a model for generating input data according to the expressions over a transition arrow. The inspector then starts to check the model using an expression that defines the occurrence of the infinite loop.

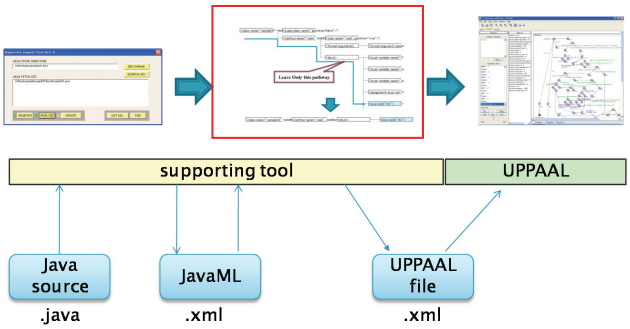


Figure 4. Inspection Process

B. Implementation

To facilitate the initial inspection process, we have developed a supporting tool using Microsoft Excel as an input-output interface. Various functions are described along with VBA. JJMLT [5] is used for the XML conversion of the Java source. The automatically generated model is inspected by UPPAAL. Microsoft Access is used to store the model definition used in the automatic generation of the model.

V. CASE STUDY

A. Outline

We have developed a program of a line tracing robot in Embedded Technology Software Design Robot Contest. The aim of this contest is to devise a program under the condition that all participants use the same hardware. The contest rule is that a robot drives along the specified course by using the light sensor and it stops after the specified number of laps by distinguishing two kinds of marks from the ordinary course. During the development, we were troubled by a phenomenon in which the behavior of this program is not stable so that the running sometimes succeeds and sometimes fails. Because the input and output values from sensors and actuators are sometimes different from the values assumed by the software, it is hard to reproduce the defect conditions.

As the contest is held every year and the course is changed a little bit, the program has continued to change by different novice programmers every year. Every year, they only do testing a robot actually and changing the program ad hoc. As they could not understand the essential cause, the phenomenon in the program remains unchanged.

B. Modeling Policy

The robot runs along a course colored with a black on a white background by using the value of the light sensor, which means brightness of a certain point in the external environment. Two kinds of marks are specified by a grey color and the length. The line tracing robot has such three main functions tracing a line, stopping at the goal, and recovering the course. Among these functions, the phenomenon that we have to investigate is to stop at the goal by correctly identifying the two kinds of marks. Although actual course has some curves, we assume that the shape of a course is a straight line and that a robot moves forward at a constant speed straightforward. This is because that such controls of a robot as steering, driving, and recoverying do not influence the above-mentioned phenomena. The randomness of value obtained by the light sensor can be determined by the nondeterministic property of UPPAAL.

C. Automatic Generation of the UPPAAL Model

The program is composed of three individual class files, that is, this program is enough small-scale for the inspector to understand the responsibility of these three classes. Then two classes unrelated with driving control function can be excluded from inspection by the judgement of the inspector. The navigation class related to the driving control is translated into UPPAAL model to be inspected.

Support tool automatically generate a test model by replacing items in the structured diagram with the predefined model as shown in Figure 2 and 3. Figure 5 represents a portion of the automatically generated model. The designated method is converted into a UPPAAL model being inspected. This model is named Model 1.

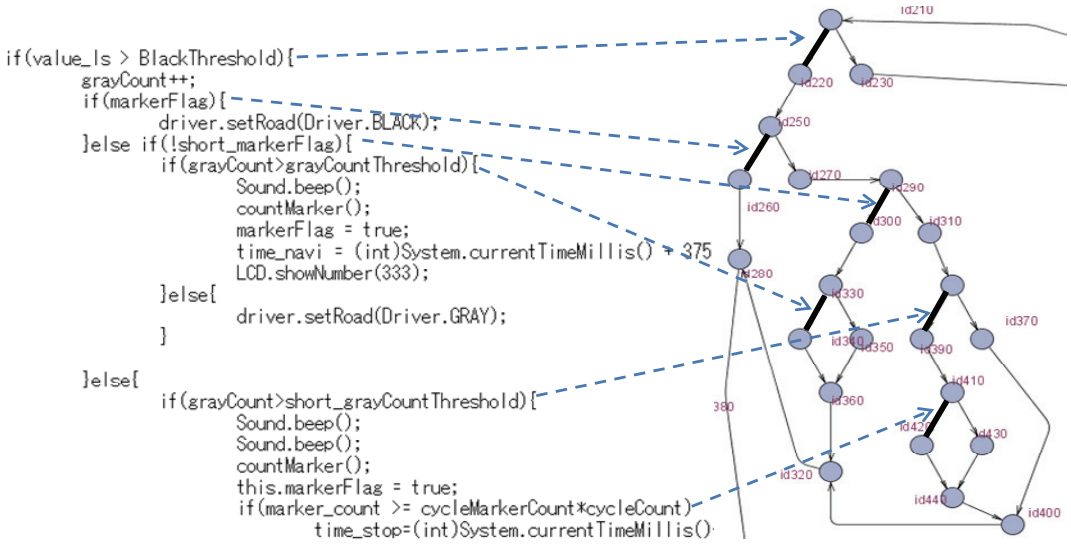


Figure 5. Example of model convert (Model 1)

D. *Modeling of External Environment*

1) *Modeling of output state*

We define the two kinds of output states in which we already recognized as the troublesome phenomenon. We define automatic stop state (AUTO_END) and manual stop state (MANUAL_END) by the model of UPPAAL. Automatic stop state is the state in which robot automatically stops after the specified number of laps. Manual stop state is the state in which robot automatically can't stop after the specified number of laps. These models are named Model 2(Figure 6).

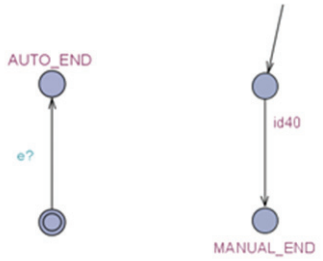


Figure 6. Model of automatic stop and manual stop (Model 2)

2) *Modeling of inputs state*

A course is colored with a black on a white background and two kind of markers are colored by a gray and have the different length. We call them a short marker and a long marker respectively

As a robot moves forward by using the value of the light sensor, which means brightness of a certain point in the external environment, the distance of the robot movement can be expressed numerically by the number of points being obtained by the light sensor, Figure 7 shows a model of the course.



Figure 7. Abstracted course

The course as shown in Figure 7 is translated into a UPPAAL model as shown in Figure 8. According to the movement distance on the course, we define five transitions on the model. Expression [A} on the model is a receiver of synchronizing with another process expressed by Model 1. Both expressions [B] and [C] are defined in the transitions from (1) to (5), which correspond to the five steps of movement distance. Expression [B] is the sending part of the synchronization process. This expression returns a handle to the caller. Expression [C] defines a range of values being obtained by a light sensor. Expression [D] is a combination of some conditions for transition based on five steps of movement distance. This expression limits the transition according to the distance. Expression [E] includes a variable which keeps a value of light sensor and a variable which keeps the robot position being increased one by one according to the movement.

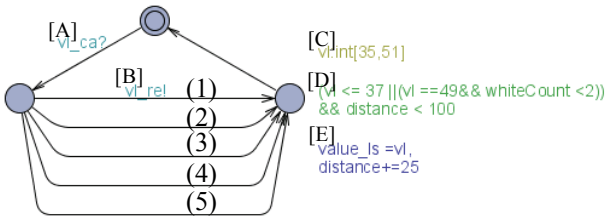


Figure 8. Model of light sensor (Model 3)

3) *Definition of time control*

A method System.currentTimeMillis () is used in this program. This method is a method of getting the current time. Instead of this method, the clock variable is available in UPPAAL. The source code is changed from an absolute timetable expression to a relative timetable expression by resetting the clock variable at the time of beginning to measure time as shown in Figure 9.

```
int currentTime = (int)System.currentTimeMillis();
time_stop=(int)System.currentTimeMillis()+1200;
```

↓

```
clock currentTime;
time_stop=1200;
currentTime=0;
```

Figure 9. Conversion of timer processing

4) Inspectiont model

Figure 10 shows the model formed by joining Models 1, 2, and 3. Each model is joined by the synchronization function of UPPAAL.

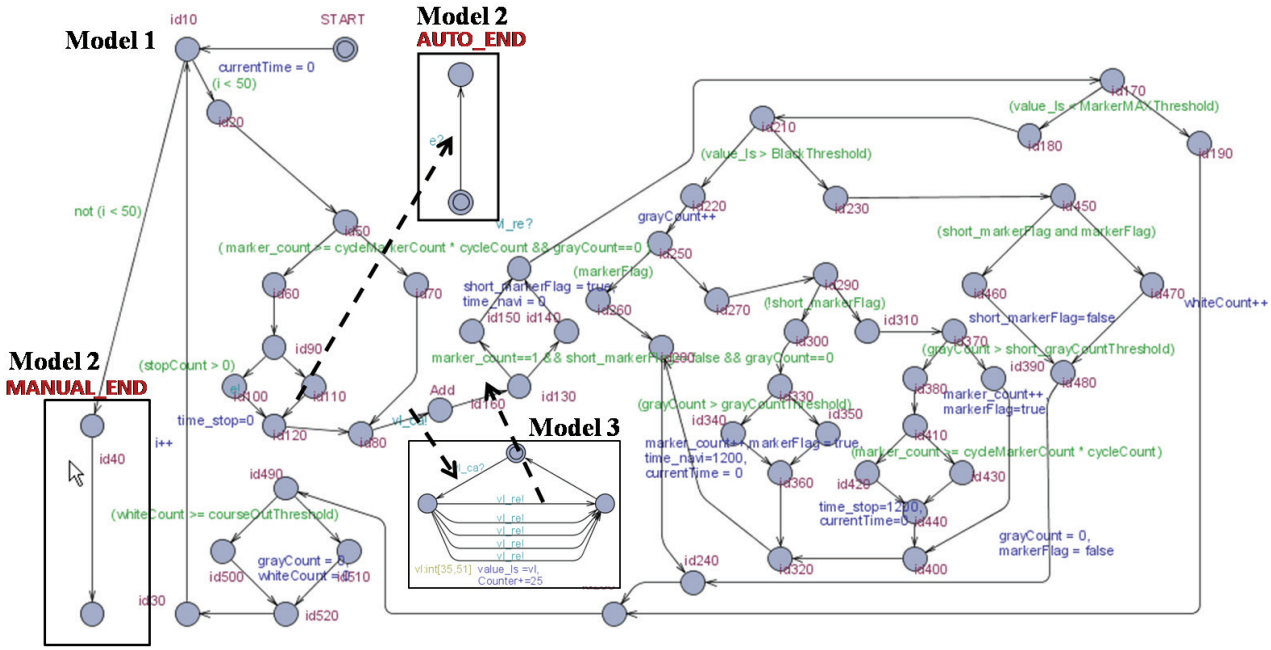


Figure 10. Inspection model

E. Model Checking

To do model-checking by the UPPAAL tool, we define the path formula for checking the model in UPPAAL as follows. Firstly we test that the location AUTO_END is not true in all reachable states. Inspection result is "Property is not satisfied", that is, the AUTO_END location is reachable through some path. Secondly, we test that the location MANUAL_END is not true in all reachable states. Inspection result is "Property is not satisfied", that is, the MANUAL_END location is also reachable through some path. We can confirm that both automatic stop and manual stop occur. Then we investigate the cause by using the simulation function of UPPAAL. As there is a high possibility that the robot misunderstands recognition of two kinds of markers, we extract all variables on the expression for branch conditions except variable which express threshold. Within these variables, markerFlag and short_markerFlag represent the state of passing each marker by boolean data. Table II shows the correspondence between the state of robot and these marker flags.

TABLE II. MEANING OF COMBINATION OF MARKER FLAG

markerFlag	Short_markerFlag	State of robot
FALSE	FALSE	On black color line
TRUE	FALSE	On line of gray, long marker
FALSE	TRUE	On black color line, next short marker
TRUE	TRUE	On line of gray, short marker

As Table III shows, we confirm the result of simulating of each on UPPAAL (distance on the course, the value of the timer, the value of the flag). The case where automatic stop can be done is inspection 1, and the case where automatic stop cannot be done is inspection 2. These marker flag are compared in Inspection 1 and Inspection 2. Figure 11 shows the correspondence between Table III and the course.

TABLE III. COMPARISON OF SIMULATION RESULTS

		1	2	3	4	5
Inspection1	markerFlag	FALSE	TRUE	FALSE	FALSE	TRUE
	Short_markerFlag	FALSE	FALSE	FALSE	TRUE	TRUE
	currentTime	>=0	>=0	>=0	>1200	0>=
	distance	0	275	425	475	800
Inspection2	markerFlag	FALSE	TRUE	TRUE	FALSE	FALSE
	Short_markerFlag	FALSE	FALSE	TRUE	TRUE	FALSE
	currentTime	>=0	>=0	>1200	>1200	>1200
	distance	0	275	300	425	425

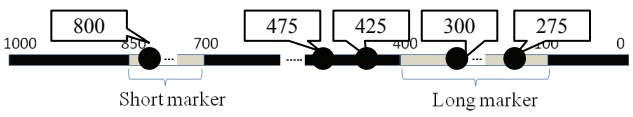


Figure 11. Comparison between marker flag transition and course

On the change of marker flags, there are difference in the third column of the Table III between Inspection 1 and Inspection 2. According to Inspection 2, at distance 300(in

long marker) on the course, the robot has the state of "Forecast of the short marker." During processing of recognition of the long marker, this state is set with the timer. When the time of timer passed before the robot slips out a long marker, the possibility that the processing outside assumption is executed turned out.

F. Re-model checking

Because there is problem with the control by timer, we changed old logic to new logic in which the count of marker and the count of gray color control. We execute the same inspection as the previous section for the modified model. We confirmed that the robot can stop automatically always. (It is not reachable to location MANUAL_END).

G. Check the actual application

We confirm the effect of the modified program by the real robot. Both the original program and the modified one has been tested 10 times by the robot. Table IV shows the result of testing, that is, the modified program can correctly stop the robot automatically in all tests.

TABLE IV. CONFIRM MODIFICATION RESULTS IN THE ROBOT

	Number of successful automatic stop	Number of failed automatic stop
Before modification	6	4
After modification	10	0

VI. RELATED WORK

Achenbach [6] compared the abstraction techniques in various model-checking tools and applied these tools to real-world problems. For example, the open/close behavior of the File IO stream was modeled using the transition between states such as open, close, and error. This approach is very similar to ours. However, this paper only discusses an engineering method for the use of model-checking tools in the upper process of software development, omitting any method for detecting defects from the source code. Bao [7] and Achenbach [6] suggested a procedure for abstracting the program to pay attention to the state that needs to be confirmed. Thomas [8] has provided an UPPAAL model that has been correctly translated from the Java source code for real-time embedded systems. We have proposed several types of abstraction models for enterprise systems, but they have not proposed any guidelines for abstraction, for the sake of avoiding explosion of the number of states in the system. Jianguo [9] and Bradbury [10] aimed to improve the precision of the verification process through model checking and model testing. However, they could not design an accurate model translated from the source code including the defects.

VII. CONCLUSIONS

We have developed a technique based on model checking and selection of the necessary elements for identifying hard-to-detect defects in enterprise systems and for detecting the root cause of these defects. We have applied our method to such embedded system development as a line tracing robot. In this case, time restriction in UPPAAL was useful to modeling it. In embedded system development, it is often difficult to decide whether a cause of a failure depends on the hardware or software control. Because the input and output values via such hardware as sensors and actuators are sometimes different from the values that are assumed by software, it is hard to reproduce the phenomena of the defect. However, our method could detect the cause by modeling all the system that consists of the robot and the running course. In the future, we plan to develop a tool support and make improvements to the proposed method so that it can be used to treat more complicated models.

REFERENCES

[1] Y.Aoki and S. Matsuura, A Method for Detecting Defects in Source Codes Using Model Checking Techniques, Proc of COMPSAC2010,pp.543-544, 2010.

[2] SPIN, http://spinroot.com/spin/whatispin.html/,2010

[3] Pathfinder,http:// javapathfinder.sourceforge.net/,2010

[4] UPPAAL, http://www.uppaal.com/, 2010.

[5] JJMLT, http://www.hpc.cs.ehimeu.ac.jp/aman/project/JJmlt/, 2010.

[6] Achenbach, M., Ostermann, K,"Engineering Abstractions in Model Checking and Testing", Source Code Analysis and Manipulation, Proc. of .SCAM '09.,pp.137-146

[7] Bao, T., Jones, M.D. 2009. Test Case Generation Using Model Checking for Software Components Deployed into New Environments. Proc.of ICSTW '09 ,pp. 57-66,2009.

[8] Thomas Bogholm, Henrik Kragh-Hansen. 2008.Model-Based Schedulability Analysis of Safety Critical Hard Real-Time Java Programs, Proc. of JTRES 2008 , pp. 106-114.

[9] Jianguo, Chen.,Hangxia, Z.,Bruda, S.D. 2008. Combining Model Checking and Testing for Software Analysis ,Computer Science and Software Engineering,,pp.206-209

[10] Bradbury, J.S., Cordy, J.R., Dingel, J. 2007 Comparative Assessment of Testing and Model Checking Using Program Mutation. Testing: Proc. of TAICPARTMUTATION 2007. pp. 210-222

Model-Based Methodology for Implementing MARTE in Embedded Real-Time Software

Mohd Zulkifli Mohd Zaki
Department of Software Engineering
Faculty of Computer Science and Information Systems
Universiti Teknologi Malaysia 81310 Johor Malaysia
zulkiflizaki@utm.my

Dayang Norhayati Abg Jawawi
Department of Software Engineering
Faculty of Computer Science and Information Systems
Universiti Teknologi Malaysia 81310 Johor Malaysia
dayang@utm.my

Abstract—**This paper presents an integration of a model-based methodology for embedded real-time software with MARTE. However, although has being introduced as a new profile to overcome problem in previous profile, a sound and systematic methodology is necessary to tackle complexity problem that arise. The objective of this paper is to propose an integration of profile and method for satisfying embedded real-time software requirements and helping engineers to model their system, enhancing the structure and behavior modeling. For that, this paper describes a proposed methodology for the integration process, involving two elements: a profile and a method. The integration result will support to solve complexity whereby the profile is used to solve the lack of specific modeling language notation for embedded real-time system and the method can provide a systematical software process. The proposed integration component model is applied on a case study to show its enhancements.**

Keywords-Model-based Methodology; UML; MARTE; Component-Based Software Engineering; Embedded Real-Time Software; Mapping

I. INTRODUCTION

Software engineering discipline has covered almost most of application domain, including Embedded Real-Time (ERT) system. ERT software is unavoidably become more and more complicated and sophisticated. This has causes the need of more acceptable approaches rather than simply rely on a simplex traditional concept of procedural programming that no longer sufficient to overcome very large systems, which can carry a million or more lines of code, the programming level.

ERT software design has become an important research area due to the high complexity of the new generations of such systems [12]. ERT software differs from the traditional data processing systems are that they are constrained by non-functional requirements such as dependability and timing constraint [2]. These special features actually will correspond to the increased of complexity as it derives from the amount of functionality that is associated with those systems [12]. Specification, modeling, synthesis, simulation, and verification are required to cope with this increasing complexity, as the need of efforts in all areas of system level design.

In additions, designing and modeling ERT systems are becoming more difficult as the requirements to the systems are increasing due to the user's needs and demands, which direct to complexity problems [16]. Therefore, ERT software development must be able to cope with complexity, to adapt quickly to changes and capable to support extra-functionality.

This is where Unified Modeling Language (UML) has become a strong candidate for specifying and designing ERT systems, which is mainly because of the abstraction provided by this language. UML is a graphical language for visualizing, specifying, constructing, documenting and executing software systems [14]. UML was adopted by Object Management Group (OMG) as a fusion among several of the best OO methods such as Booch [18], Harel [19], Jacobson [20] and Rumbaugh et.al [21]. UML has gained popularity as a tool for specification and design of embedded systems, mainly due to the abstraction provided by this language [15]. The advantage of UML is that the providence of extension mechanisms, which allow customization of the language, enabling the definition profiles for specific domains [12]. But, UML stills developed and challenged by some important problems, such as the ability to cope with ERT unique requirements like real-time constraints, resource restrictions and modeling independent components [16][17].

Therefore, the use of Unified Modeling Language (UML) profiles for ERT modeling to develop ERT system can aids the development process especially for modeling complex ERT systems [3][4]. From this perspective, a UML for Modeling and Analysis Real-Time and Embedded (MARTE) appears to be the suitable approach for modeling ERT systems [7]. Intends to replaces the previous profile [5][6], MARTE has provides some new key features such as support for non-functional property modeling and adds rich time and resource models to UML. Therefore, a model-based methodology has been study to suite the need of MARTE, making the purpose of MARTE profile become more extensive and useful.

The layout of this paper is as follows: Section II briefly describes the motivation of this paper; Section III describes the integration methodology for the integration purpose; Section IV presents the integration result, based on the

proposed integration methodology, which involved the study, discuss results and applied on an ERT case study. Finally, Section V presents a brief summary and conclusion drawn from this paper.

II. MOTIVATION

However, there is no specific methodology or process with MARTE and this is the motivation of this paper [12]. This is because, beyond UML and its profiles, another focus is on its methodology and software process, whereby UML specification only specifies syntax and semantics of its notation, but does not determine how to apply its elements within a development process [17]. This is where Method for Component-Based Real-Time Object Oriented Development and Testing (MARMOT) is acceptable to fulfill the needs. Acts as a systematical and sound development method for component-based development (CBD) and model-driven, MARMOT has been derived from KobrA [22] to yield elements of developing ERT software.

The main objective of this paper is to integrate the MARTE Design package, which consists of its component model and other features with MARMOT method. The processes of the integration are including mapping between component models and combining several features to enhance current approach. This integration has been performed because the need of both profile and method in fulfill each other requirements. However, because not in the same family, the integration process of MARTE profile and MARMOT method has some difficulties in finding suitable features for the integration. Therefore, this paper has described a proposed methodology in order to facilitate the integration process.

As results, towards this integration, MARTE profile will act as the enhancement of the current implementation of modeling language, which has been adapted in MARMOT methods. As the purposes of MARTE itself will be used to enhance the elements, especially that are related to the development of ERT software. On other hands, with the integration, MARMOT indirectly has provided MARTE a proper and systematic software process and methodology, which one of the current disadvantages of MARTE profile [12].

III. INTEGRATION METHODOLOGY

Integration between MARTE profile and MARMOT is possible to be done. It is because both of them, although not in the same paradigm, still depend on UML as the core modeling language of both profile and method. This modeling language is the parent of MARTE profile, while has been used as the main modeling language in MARMOT.

To aid in the integration process, a methodology has been introduced. There are six steps in the methodology. The methodology is meant to show process flow how the integration process between MARTE and MARMOT is being done. During the integration, most of the process mostly focused on the relation of MARTE profile and MARMOT method elements and artifacts. This is because their relation obviously depends on the elements and artifacts in both profile and method. The integration methodology is illustrated in Fig. 1.

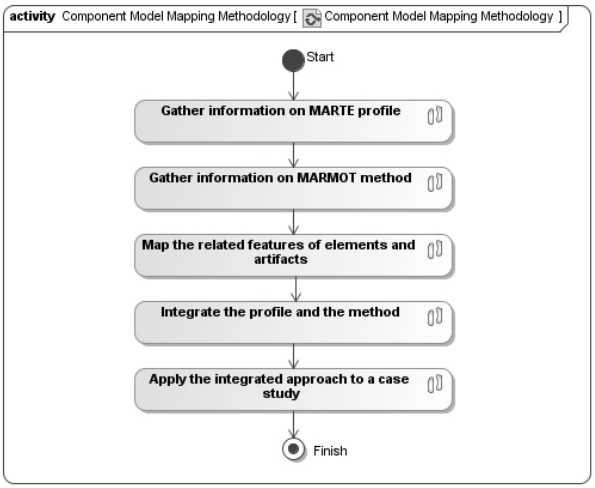


Figure 1. The Component Model Mapping Methodology

The first step is to understand MARTE profile. This is important to investigate how elements in MARTE profile can integrate with elements in MARMOT method approach with the newly proposed methodology. During this step, investigation and identification on MARTE elements, mostly related on model-based and CBD approach, will be conducted. Then, the second step understands MARMOT method and the elements and artifacts involved along the process. During this step, the identification on MARMOT elements, especially on structures and behavior modeling will be conducted and investigated.

The third step is mapping of MARTE profile elements and MARMOT method elements. The mapping is done by considering the relationship between both profile and method. This process is being done by mapping the related features of both elements and features of MARTE and MARMOT. The integration process continues with the fourth step, which is integrating both MARTE and MARMOT. The integration process will be done based on the elements, which has been identified during first and second steps, and the result contributed from mapping process in third steps.

Finally, the fifth step is applying the integrated approach into a case study. In this step, the applicability of the integrated approached will be verified using the case study by modeling the structure and behavior diagram. This can verified the newly enhancement which has been adopted during the integration.

IV. INTEGRATION RESULTS

A. Gather information on MARTE profile

OMG called for a new UML profile for MARTE [7]. MARTE is the first standard UML based for modeling ERT systems after more than three years of work, since October 2003. This UML profile for MARTE addresses modeling and analysis of real-time and embedded systems, including their software and hardware aspects. The MARTE specification consists of three main packages, which defines foundation concepts used in real-time and embedded domain, model-based design and model-based analysis.

MARTE is based on UML 2.0, Meta-model OCL2, and MOF 2.0 QVT and created as intentions to replace the

existing UML-SPT. Furthermore, MARTE also has establish an extension of the UML component model, called as Generic Component Model (GCM), which presents additional concepts from the usual component paradigm concepts that have been identified as necessary in order to address the modeling of artifacts in the context of ERT systems component based approaches.

MARTE consists in defining foundations for model-based description of real time and embedded systems. These core concepts are then refined for both modeling and analyzing concerns. Modeling parts provides support required from specification to detailed design of real-time and embedded characteristics of systems. MARTE concerns also model-based analysis. In this sense, the intent is not to define new techniques for analyzing real-time and embedded systems, but to support them. Intends to replaces the UML-SPT profile, MARTE also complies with UML 2.1 and other existing OMG standard.

Additionally, the MARTE GCM defines shortcut notations that help in simplifying the modeling and are useful in the application of component based strategies in the ERT domains.

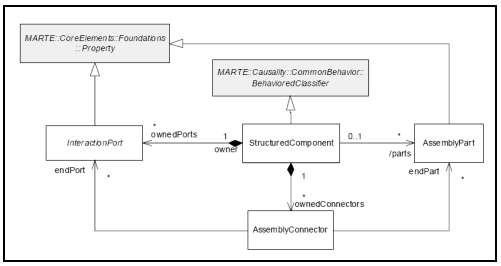


Figure 2. MARTE Generic Component Model package [7]

As shown in Fig. 2, the MARTE GCM introduced in this specification proposes mainly refinements to the UML structured classes. This model provides a common denominator among various component models, which in principle do not target exclusively the ERT domains. The purpose is to provide in MARTE a model as general as possible, that not tied to specific execution semantics, on which ERT characteristics can be applied later on. The MARTE GCM relies mainly on UML structured classes.

One of the main reasons to have refined the UML component model within this specification is to support both message-oriented and flow-oriented communication schemas.

B. Gather information on MARMOT methodology

MARMOT [22] is a system development method for embedded real time system. MARMOT aims to provide the ingredients to master the multi-disciplinary effort of developing embedded systems. It provides templates, models and guidelines for the products describing a system, and how these artifacts are built.

In MARMOT, component will identify at design and implementation phase. MARMOT method considers software and hardware in the development activities. MARMOT method will support by UML 2.0 for modeling. Advantages of MARMOT method are can give positive impact on reuse, effort and quality. MARMOT includes four activities, which consists of composition, decomposition, validation and embodiment.

MARMOT builds on the principles CBD by assuming its component model as shown in Fig. 3. MARMOT extends it towards the development of ERT systems. The specification is a suite of descriptive artifacts that collectively define the external interface of a component, so that it can be assembled into, or used by, a system. The realization abreacts collectively define a component's internal realization. By following this principle, each component is described through a suite of models as if it was an independent system in its own right.

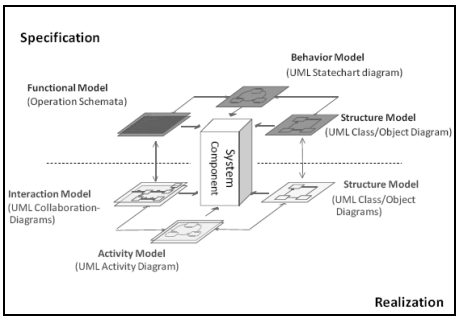


Figure 3. MARMOT Component Model [22]

MARMOT components follow the principles of encapsulation, modularity and unique identity that most component definitions put forward. In additions, encapsulation requires separating the descriptions of what a software a software unit does from the description of how it does it. These specifications are called specification and realization.

The concept of the MARMOT Component Model (CM) meta-model has been derived from [22]. Fig. 4 shows the MARMOT component, which consists of one or more structures, and one or more behaviors. Each structure and behavior has an internal part hidden from outside the component and an external part visible from outside. This external visible part also defines as an interface of the component.

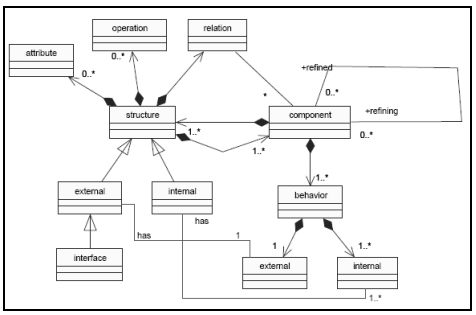


Figure 4. MARMOT Component Model meta-model [22]

The structure may contain specifications of attributes and operations of the component as well as the specifications regarding relationship with other components. Each external structure has an external behavior visible from outside. Each internal structure can have one or more internal behaviors specifying how externally visible operations of the component that has been specified in the external structure, are internally realized.

C. Mapping the related features and artifacts

According to finding and information from Step A and Step B, the suitable related features in both profile and method are the component model. Therefore, during the

integration process, most of the process mostly relied on the relation of MARTE GCM and MARMOT CM. By doing that, this integration process can focus on the relationships of CBD methodology that can support by the new UML profile for ERT.

In conjunction, investigation on MARTE component model also can help in determine the relation of formal CBD component model with MARTE component model. The result of relationships mapping from MARTE GCM to MARMOT CM elements are shown in Table 1.

TABLE I. MAPPING MARTE GCM TO MARMOT CM

Component element	MARMOT CM elements	MARTE GCM elements
Component	Uniformly represented as abstract component which consists of one or more structures and one or more behavior	A *StructuredComponent* and defines as a self-contained entity of a system, which may encapsulate data and behavior
Structure	May contain specification regarding the attributes and operations, and relationships with external component.	Specializes the *BehavoiredClassifier* classifier which own properties that can be used within internal component description and attributes.
Behavior	Attached to structure for specifying how externally visible operations are internally realized.	Enhancement of structure with Properties elements which make the compatibility regarding flow specifications and directions.
Interface	Represents by external structure and has external behavior visible from outside	Introduce *InteractionPort* and other mechanisms to support both message and flow oriented communication schemas.

Based on Table 1, the mapping of component model elements from both MARTE GCM and MARMOT CM is done. Mapping the similarities between both component models elements is doing the mapping process.

From the investigation, the similarities of both component models elements have been identified: Components, Behaviors and Interfaces. These elements actually are the basic elements of component model structures, which already being applied in MARMOT. Therefore, the mapping later on continues to find similarity between these elements with MARTE GCM elements. Using the similarities, the meta-model integration of both component models can be done.

Furthermore, the investigation on MARMOT CM can help in improving the current component model that has been implemented by MARMOT to a new enhancement. MARTE GCM will provide the enhancement elements.

D. Integrate the profile and the method

The integration of two component model meta-models is represented in Fig. 5. Using MARMOT component structure as the integration point does integration on both of the component model. This is because as to provide methodology to MARTE, the integration will mostly based on MARMOT method, and then will be enhanced using new elements from MARTE that has been introduced to support ERT systems development, mainly in designing and modeling phase.

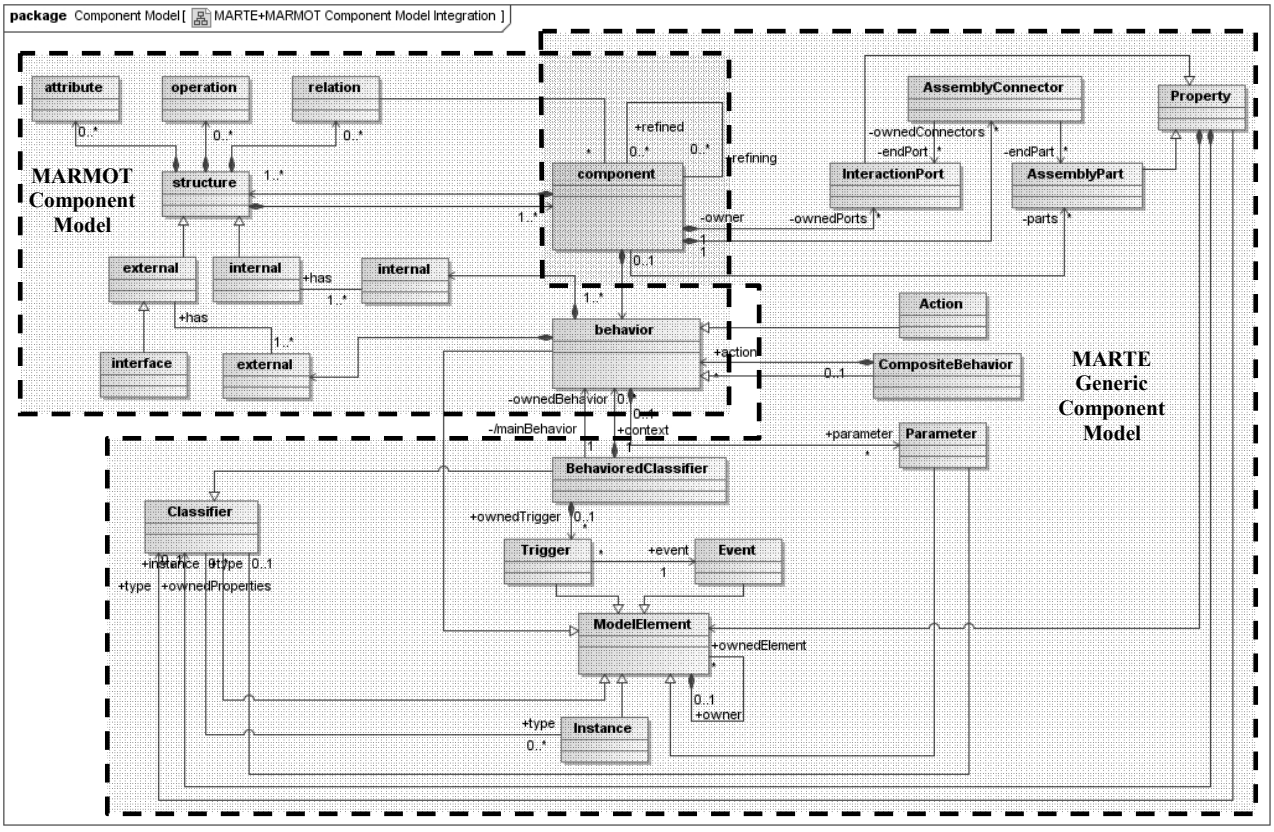


Figure 5. The Integration of MARTE GCM and MARMOT CM

During the integration process, there are no elements of meta-models; either from MARTE GCM or MARMOT CM has been removed from the original meta-models structures. Instead, the integration of the meta-models has considered more towards the similarity of the elements, which has been recognizing based on the mapping process. Therefore, the elements in both MARTE GCM and MARMOT CM will remain the same relationships.

Based on the integration, most of the enhancements are involving the capabilities of expressing the constraint requirements of ERT software directly into the modeling. This includes the introduction of new port mechanisms in structure and temporal properties mechanisms in behavior.

The application of the integrated component model meta-model will be used at development phases. Based on the integration meta-model, the current component model that has been adapted in MARMOT method will be enhanced. The enhancement will be supported by new elements that have been proposed in MARTE in supporting design and modeling for ERT systems.

E. Applying the integration

To demonstrate the application of the integration, this paper implement a case study of an AMR named Intelligent Mobile Robot 71848 series (IMR71848) case study. This application has been defined in context of an academic challenge, the goal of which was to provide a case study framework for benchmarking different kinds of design approaches to ERT systems.

This case study has been chosen because it is fairly representative of the problems encounter by ERT systems and software engineers when designing such systems, mainly in concentrating of multi-constraint properties and component-based development.

1) The IMR71848 Requirements. The case study introduces an intelligent mobile robot, IMR71848 as shown Fig. 6 for controlling the movement of the intelligent mobile robot in finding a passage and existing through the passage. It consists of a mobile robot, equipped with sensors and actuators, which communicates with a microcontroller.

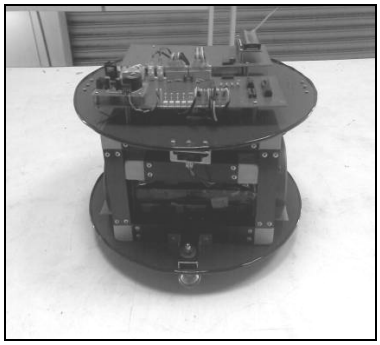


Figure 6. The IMR71848

The main function of the microcontroller, embed within the hardware is to move the servomotor which attached with wheels until the robot achieve or arrive its goal. Therefore, the software needs the ability to control the servomotor and at the same time, monitor the environment and navigate the robot. The software then will move the robot and achieve its goal by controlling the motor at each robot's drive wheels. Fig. 7 illustrate use case diagram for IMR71848 software.

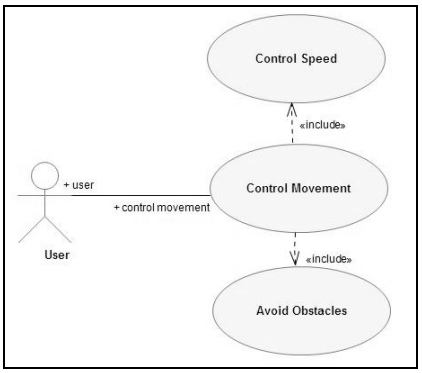


Figure 7. IMR71848 Use Case Diagram

The actor User will initiate and conducts all the task of the IMR71848.Later, the embedded controller will monitor its environment autonomously using the sensors and acts accordingly by giving responds to the actuator.

During a mission, the robot has to follow several rules in order to achieve the goals. The experiment of the mobile robot is carried out in an indoor environment. The environment is made up of stationary objects that shall be avoided by the robot. The stationary objects will be used as walls surrounded around the experimental environment except has a doorway passage. The IMR71848 will cruises around the environment to find a specific way that led to the doorway passage, at the same time, the robot need to avoid obstacles that exists within its environment.

2) Component Modeling

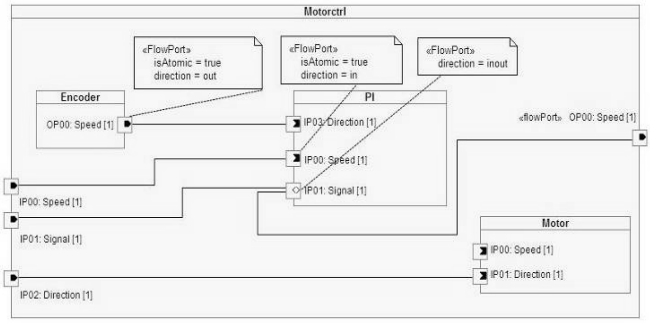


Figure 8. Example of Structure Modeling of Composite Class

Fig. 8 shows an example of structure modeling of *Motorctrl* components and indicates its context. The component reacts to signals and does not provide any operations to its environment. The *Motorctrl* component has inherited features such as enhancement of message port and flow port which is suitable to represent component for ERT software in design phase.

By using MARTE flow ports, it can enable data-flow oriented communications. The type of this value may either be given directly as the port type. Alternatively, if the data need to be send and received through the same port, MARTE has introduced flow specifications, which contain only properties. Instead, with the new enhancement using the integration meta-models, modeling component in MARMOT has become more detailed and specific with new notation introduced by MARTE, especially to support CBD development and design in ERT software. This detailing can helps developers in term of increasing understandability of ERT software design.

V. CONCLUSIONS

The main objective of using integrated approach in this research is to support MARTE profile with a sound and systematical CBD software process method. In order to integrate these profile and method, two component models are used: MARTE GCM and MARMOT CM.. MARMOT has been used as its extensions to support ERT system development using component technology.

This paper showed the flow of integration process of ERT profile and CBD method for ERT by using the proposed methodology. The proposed methodology consists of five main steps: First, the gathering information process of MARTE profile; second, the gathering information process of MARMOT method; third, relationship mapping process; fourth, focusing on the integration, and lastly; fifth, applying the integrated approach to a case study.

The result of paper is an integrated component model meta-model which map MARTE GCM to MARMOT CM. Besides, the mapping also in directly have detailed up MARMOT CM by adding multi-constraint requirement elements through property bundles from MARTE GCM. The new integration meta-model can support ERT systems with CBSE by considering issues of complexity of ERT software, multi-constraints extra-functionality and systematically software methodology and process for MARTE profile.

In addition, the integration also give the new enhancement during modeling a component, which give more specific modeling artifacts and more details design models, compared if model using UML 2.0. This enhancement can give advantages to the ERT software developers in designing and modeling ERT systems with more specific artifacts and notations.

ACKNOWLEDGMENT

Special thanks to Shahliza Abd Halim, Mohd Adham Isa and all EReTSEL members for their support, Ministry of Science, Technology and Innovation (MOSTI) Science Fund for the financing and funding and Universiti Teknologi Malaysia (UTM) for the facilities and infrastructures.

REFERENCES

[1] Sommerville, I. (2004). Software Engineering: Seventh Edition. Boston: Pearson Education Inc.

[2] Stankovic, J. A. (1996). Real-time and embedded systems. ACM Computing Surveys, Volume 28, Issue 1, 205-208.

[3] Douglas, B. P. (2004). Real Time UML Third Edition: Advances in the UML for Real Time Systems. Boston: Pearson Education Inc.

[4] Crnkovic, I. and Larsson, M. (2002). UML for Real: Building reliable component-based software systems. Boston: Artech House.

[5] OMG. (2002). UML Profile for Schedulability, Performance and Time (OMG document no.ptc/02-03-02). Retrieved from http://www.omg.org

[6] Woodside, C. M. and Petriu, D. C., (2004). Capabilities of the UML Profile for Schedulability Performance and Time (SPT). Workshop SIVOES-SPT on the usage of the SPT Profile, held in conjunction with the 10th IEEE Real-Time and Embedded Technology and Applications Symposium RTAS'2004, Toronto, Canada, May 2004.

[7] OMG. (2007a). MARTE specification beta 1. (OMG document.ptc/07-08-04). Retrieved from http://www.omg.org

[8] Urting, D., Berbers, Y., Van Baelen, S., Holvoet, T., Vandewoude, Y., and Rigole, P. (2002). A tool for component based design of embedded software. In Proceedings of the Fortieth international Conference on Tools Pacific: Objects for Internet, Mobile and Embedded Applications (Sydney, Australia). ACM International Conference Proceeding Series, vol. 21. Australian Computer Society, Darlinghurst, Australia, 159-168.

[9] Kuster, J.; Stroop, J., (2001). Consistent design of embedded real-time systems with UML-RT, Object-Oriented Real-Time Distributed Computing, 2001. ISORC-2001. Proceedings. Fourth IEEE International Symposium on, vol., no., pp.31-40, 2001

[10] Tesanovic, A. and Hansson, J. (2004). Structuring Criteria for the Design of Component-Based Real-Time Systems", in Proceedings of the IADIS International Conference on Applied Computing 2004, Mar. 2004.

[11] Bichler, L., Radermacher, A. and Schurr, A., (2002). Evaluating UML extensions for modeling real-time systems," Object-Oriented Real-Time Dependable Systems, 2002. (WORDS 2002). Proceedings of the Seventh International Workshop on , vol., no., pp.271-278, 2002

[12] Lisane B., B., Marcio E., K., and Luigi, C. (2009) UML as front end language for embedded system design, Behavioral Modeling for Embedded Systems and Technologies: Applications for Design and Implementation, July 2009

[13] Fateh, B., Mohammed, B., and Sebastien, B. (2009). UML2.0 Profile for Embedded Systems and Systems On a Chip (SOCs). Journal of Object Technology, Volume 8 (Issue No.1), pp. 135 – 157

[14] OMG. Object Management Group. (1997). Unified Modeling Language Specification, v1.0. Retrieved from http://www.omg.org

[15] Lavagno, L., Martin, G., and Selic, B. (Eds.) (2003). UML for real: Design of embedded real-time systems. Dordrecht, Netherlands: Kluwer Academic.

[16] Jochen, M.K. and Joachim, S. (2001). Consistent Design of Embedded Real-Time Systems with UML-RT. Object-Oriented Real-Time Distributed Computing, Fourth IEEE International Symposium on Object-Oriented Real-Time Distributed Computing, pp. 0031.

[17] Lutz, B., Ansgar, R., and Andreas, S. (2002). Evaluating UML Extensions for Modeling Real-Time Systems. Object-Oriented Real-Time Dependable Systems, Seventh IEEE International Workshop on Object-Oriented Real-Time Dependable Systems (WORDS'02), pp. 0271

[18] Booch, G. (1994). Object-Oriented Design with Applications, 2nd ed. Reading, Addison-Wesley.

[19] Harel, D. (1998). Modeling Reactive Systems with Statecharts. New York: Dorset House.

[20] Jacobson, I. (1992). Object-Oriented Software Engineering. Reading, Addison-Wesley.

[21] Rumbaugh,J., Blaha, J. M., Premerlani, W., Eddy, F., and Lorenson, W. (1991). Object-Oriented Modeling and Design. Englewood Cliffs, N.J. Prentice Hall.

[22] Choi, Y., Bunse, C. (2008) Towards component-based design and verification of a µ-controller. In: 11th International Symposium on Component-Based Software Engineering, pp. 196–211

[23] Mraidha, C., Tanguy, Y., Jouvray, C., Terrier, F. and Gerard, S. (2008). An Execution Framework for MARTE-based Models. 13th IEEE International Conference on Engineering of Complex Computer Systems. pp. 222-227.

Software Engineering Education: The Gap Between Industry's Requirements and Graduates' Readiness

Nurul Ezza Asyikin Mohamed Almi, Najwa Abdul Rahman, Durkadavi Purusothaman,
Shahida Sulaiman
School of Computer Sciences, Universiti Sains Malaysia
11800, USM, Penang, Malaysia
{neama100178, nar100166, dp104012}@student.usm.my, shahida@cs.usm.my

Abstract— **Software engineering is one of the most demanding jobs in software industry nowadays and its demand keeps on increasing. However, there are several issues arise with regard to readiness of Information Technology (IT) or Computer Science (CS) graduates from the point of views of software industry. This perspective causes the supply of graduates mainly in software engineering field seems to be insufficient. The industry claims that the software engineering graduates are not able to meet their requirements in software industry. This is really surprising to the academia that offers software engineering specialisation or related programmes in IT or CS field. This phenomenon creates the gap between industry's requirements and graduates' readiness which indirectly reflects the gap between software engineering education and industry. A number of studies and frameworks are available to ponder the issues on software engineering education and industry. This paper reports the gap between industry's requirements and graduates' readiness in software engineering perspectives to face the real world. From the findings, we conclude that there is a gap due to high demands from the industry in highly skilled fresh graduates. In contrast, future graduates are still lack of confidence and readiness though they specialise in software engineering field that has more job opportunities in IT or CS field.**

Keywords—**Software Engineering Education; Software Engineering Industry; Industry's Requirement; Graduates' Readiness**

I. INTRODUCTION

Unemployment among Information Technology (IT) and Computer Science (CS) graduates has been a concern either locally or globally. The unemployment rate keeps on increasing as if IT or software industry gets tougher for the graduates to enter and survive. Is the IT or software industry getting more competitive or is it the graduates are not marketable and not ready to meet the industry's requirements? This phenomenon also exists in software engineering industry though it is one of the most demanding jobs that require human capital resources. Besides, software is present everywhere in today's world and one of the most prominent, the most challenging and the toughest technology in the new area [1]. This reflects the reason why software industry requires high skilled fresh graduates mainly among software engineering specialisation.

In general, IEEE Std 610.12-1990 defines *software engineering* as "the application of systematic, disciplined, quantifiable approach to the development, operation, and maintenance of software" [2]. As the software engineering industry strives for skilful employers due to the gap between industry's requirements and graduates' readiness, there are several factors that cause this gap. One of the reasons why the gap keeps on increasing is the lack of preparation among graduates especially in software engineering field [3]. Karunasekera and Bedse [3] report that the least preparation for the professional career is one the common complaints utter by the industry. In addition, a rapid advancement of software engineering and an increase of software business demands are among the factors that create the gap [4]. Another factor is because software engineering curriculum does not align with what software engineering industry's needs [4] [5][6]. This shows that what the Software Engineering Education (SEE) provides does not fully satisfy the requirements of Software Engineering Industry (SEI).

In order to succeed in SEI, graduates' potential is based on some factors such as skills, attitude and knowledge [7]. Ledgard and Tauer [8] remind the graduates about the attitude and the team work issues that are described as egotistical individuals which may arise during working in team projects during their tertiary education. This is because the individual with such characteristic will ignore other team members and only focus on personal goals causing graduates to fail in the middle of their career [8][9].

Our study focuses on the gap between industry's requirements and graduates' readiness when facing the real world. The main objective is to propose a possible balance between SEE and SEI requirements in order to reduce the gap. This study is indeed an important effort and timely as it can provide the guidelines to graduates to prepare for the industry and provide them an exposure or knowledge about the industry's requirements before entering the industry especially in software engineering perspectives.

The following section will digest some related work, before we discuss the survey, its analysis and findings and finally conclude the work.

II. Related Work

A. Software Engineering

According to Roy and Veraat [10], software engineering discipline has been discussed over the last decade in term of SEE that has influences with regard to the problem in the gap between industry's requirements and graduates' readiness. The curriculum in SEE requires continuous enhancement and maintenance to produce software engineering graduates that fulfil the industry's requirements. In order to overcome this issue, current works propose some frameworks for SEE that could be guidelines to SEE [1] [3] [4] [5] [11] [12] [13].

Hamau-Lhadj et al. [11] propose a model-driven approach in SEE. This approach can help the graduates in SEI as it is the most current technique in software engineering. However, the work does not state whether graduates who study using this approach is highly demanded in the industry or not because it only discusses on how to prepare the graduates to meet the SEI's requirements. Another work proposes the use of learner-centred web-based approach model [12]. This approach is based on three ideas that are: (i) SEE must become more realistic; (ii) SEE has to move closer to the learner and (iii) it must take advantage of the Web. In this approach, the students learn better if they construct knowledge by themselves and make use the Web in their studies because the Web is a unique tool to change the education. The third example of a new framework is Group Projects approach [13]. This approach suggests that students should work independently as suggested by Hadjerrouit [12] and also work in team to achieve effective SEE programs. Mahmood [13] also describes on how undergraduates should perform and understand the real software engineering requirements, implements and references. In short, there are a number of frameworks that are available in order to enhance the curriculum in SEE and to ensure the graduates are equipped with what SEI requires. Most of the frameworks suggest some changes in SEE in order to reduce the gap between industry's requirements and graduates' readiness.

Besides, another way to reduce the gap is through collaboration between SEE and SEI [1] [4] [5] [14]. According to O'Leary et al. [5], the collaboration can help students to achieve what the industry requires or expects and ease them during the transition from education to industry. This will help them to get ready before facing the real world. According to Mahanti and Mahanti [1], collaboration between SEE and SEI can help students to keep abreast with the latest development and an example of collaboration programme is faculty from industry can visit and give lectures on emerging technologies in software industries and software engineering to the students. Furthermore, using collaboration to reduce the gap can also bring benefit to both parties [14]. Table I summarises the benefits to SEE and SEI by having collaboration according to Beckman et al. [14]. Therefore, by doing the collaboration between the SEE and SEI, all the parties can gain some benefits including the fresh graduates, who will be more ready to face the real working environment.

TABLE I
BENEFITS OF COLLLABORATION TO SEE AND SEI [14]

SEE benefits	SEI benefits
• Have easy placement of students. • Get special funding from corporate partners. • Have insight on corporate issues at the applied, practical level.	• Have influence on academic programs. • Have access to university researches. • Get new revenue sources. • Have cost-effective, customized education and training.

B. Industry's Requirements and Graduates' Readiness

There are huge demands on software development with large requirements of highly professional skilled individuals [1]. As the technology today are rapidly progressive in various fields including software engineering field, the employment demand also increases waiting for job seekers. However, there are several complaints from the industry sector about software engineering graduates who do not prepare well for their professional careers [3] [15] [16]. This issue arises because SEE environment differs from SEI environment. This is due to the nature in SEE that focuses more in theoretical concepts where more abstract and less practical in learning [1] [3] [6]. As a result, the SE graduates hardly understand the practical scale in the industry due to insufficient exposure in practical experience [3]. For this problem, Rayford et al. [17] suggest a few requirements that are needed by the industry from the graduates. Among the requirements are the ability to work under stress, good communication skills, and ability to follow processes, a solid work ethic and project management skills. These requirements are what most of the graduates lack of. They do not possess the skills needed by the industry which cause them to be not ready to enter the real work environment.

The main reason why the graduates could not gain the skills is because they choose the skills that they are already strong in and refuse to learn the area that they are weak or need to improve more while doing the project [3]. This choosy attitude causes them to focus in their interested area and discard other areas. However in reality, the industry requires graduates that are capable in various skills. To overcome the problem, that is lack of skills by the graduates, some of the companies need to provide training centres (both local in-house and external) to the graduates [18]. In a survey done by Taran and Rosso-Llopart [18], one of the respondents stated that, it was difficult to find engineers with all skills required by the industry, therefore in-house training need to be done for the newcomers and training is about the technical, people, management and company induction training. This shows that SEI confronts with some problems in recruiting new employees as fresh graduates are still not ready to face the real work environment. Hence, SEE must take action to equip the graduates with the requirements needed by the SEI and this can be done by enhancing the curriculum in SEE and create collaboration between SEE and SEI. Hence, our study will further justify the gap between software industry's requirements and graduates' readiness.

III. THE SURVEY STUDY

This section reports the survey we conducted to study the industry's requirements via interviews and graduates' readiness using questionnaire.

A. Objective

The main goal of the study has twofold: to examine the expectation of industry and employers and to survey the readiness of the final year students specialising in software engineering for the industry. The respondents were in their final year of School of Computer Sciences, specialised in software engineering and had just completed a five-month industrial training between May to September 2010. The objective was to survey on the aspects of: (1) what they had learned during studies especially in software engineering subjects, (2) what courses they learned that they had applied during the industrial training and (3) to know their opinions whether what they had learned under software engineering specialisation could make them feel ready to face the industry and also whether they are applicable during the industrial training. As for the industry, the purpose of study was to know the expectation of the software industry from the employer's perspectives with regard to the graduates marketable and the readiness.

B. Methods

We used cluster sampling method which involved twenty final year students specialising in software engineering and two companies involved in software development in Malaysia where the two main authors had their industrial trainings. The survey for the students was conducted by giving a set of questionnaire that requires the respondents' demographic background, their opinion about readiness to face the real world after undergoing the industrial training and mapping the software engineering subject they learned with the experience they had while undergoing industrial training. It consists of eleven questions of two parts (see Table II): Part A: Demographic background (A1-A4) and Part B: Information about the graduates' readiness (B1-B7). Some answers require reasons in order to justify respondents' opinion.

TABLE II
INFORMATION SOUGHT FROM THE QUESTIONNAIRE

Description	Question Number
Characteristic	
Specialisation in study	A1
The age of the respondents	A2
The generalization of the biological studies	A3, A4
The company type that respondents join	B1
Opinion	
Are SE subjects enough to apply in SE related jobs later?	B2
Are you ready to face the real working environment upon graduation?	B3
Did you apply SE subjects and how they were related during industrial training?	B4
Did you learn new things during industrial training?	B5
Does SE specialisation give an advantage in job market?	B6
Expectation	
What do you want to be upon graduation?	B7

As for the industry, we interviewed top level personnel. The interview aimed to investigate the expectations of employers towards the graduates specialised in software engineering, their opinion whether most graduates fulfil the industry's requirements, their evaluation on what graduates do not possess and their recommendation for the universities with regard to fresh graduates. The information sought is summarised in Table III.

TABLE III
INFORMATION SOUGHT FROM THE INTERVIEW

Question Number: Description
Opinion
I1: What are the expectations of the employer towards software engineering graduates?
I2: Do most graduates fulfil the expectations of the employer?
I3: What are the aspects that graduates do not have?
Expectation
I4: What are the recommendations to the universities to produce quality software engineering graduates?

IV. THE ANALYSIS

The analysis is based on 3 categories of data that are characteristic, opinion and expectation as in **Table II** and **Table III.** The questions that do not have any response were considered missing.

A. Characteristic

In characteristic element, the survey identified the properties of the final year students which include graduates' specialisation background, ages, personals (gender and race) and types of company they joined for the industrial training. As mentioned, all the respondents were major in software engineering specialisation. Their age was between 21 to 22 years old, all Chinese, consisted of 7 males and 13 females.

The types of company the respondents joined during their industrial training are shown in Fig. 1: 10% of the respondents joined Government Agencies (GA), 5% joined Public Higher Learning Education (PHLE), 30% joined Small/Medium Companies (SMC) and the highest rate that is 40% of the respondents joined Multi-national Companies (MNC) and finally 3 respondents (30%) did research training at USM instead of industrial training (OTH).

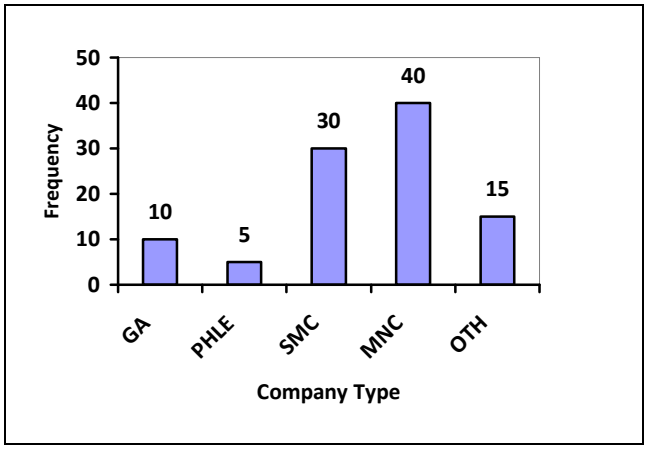


Fig.1. Type of companies chosen for industrial training

For the interview with practitioners, the two companies involved were a private software house and a government department. We interviewed five persons from the private company and one person from the government department. The four persons from the private software industry were the Chief Executive Officer (CEO), two Senior Software Engineers and one System Engineer, while from the government department the person interviewed was the higher officer in charge of IT department.

B. Opinion

Opinion element studied "What the final year students of software engineering thinks about the field" in term of subjects they had learned and their readiness to face the industry. Referring to Table IV, most of the respondents stated "Yes" and said what they had learned during their study were enough for them to apply to software engineering related jobs later (60%). On the hand, eight respondents said "No" that the subjects they already learned were not enough for them to apply in their jobs later.

TABLE IV
OPINION OF GRADUATES

Question Number: Description	Response Item	F	%
B2: Are SE subjects enough to apply in SE related jobs later?	Yes	12	60
	No	8	40
B3: Are you ready to face the real working environment upon graduation?	Yes	12	60
	No	8	40
B5: Did you learn new things during industrial trainings?	Yes	16	80
	No	4	20
B6: Does SE specialisation give an advantage in the job market?	Yes	17	85
	No	3	15

Note: F: Frequency, %: Percentage.

For element B3, twelve respondents (60%) said they were ready to face the real working environment once they graduated. For those said "Yes", they gave a reason that they understood better on what the working environment need and they experienced the real task during their industrial training. They also stated that they wanted to earn money upon graduation and could adapt to working environment. On the other hand, eight respondents stated "No" (40%) with the reasons that they were not ready to face the real working environment and they needed to improve themselves in term of required skills required by the industry. Some of the reasons included that they were too stressed and not ready.

The next element B5 shows that sixteen respondents said they had learned new things during industrial training (80%) while 20% of the respondents did not learn anything new during the industrial training. The new things the respondents had learned include Visual Basic, PHP, MySQL, PERL, Testing Life Cycle, Automated Testing Life Cycle, ColdFusion, ASP.NET, Oracle, Joomla, Wordpress and KAIZEN.

The last element that we surveyed was B6. There were seventeen respondents stated "Yes" that software engineering specialisation would give them an advantage in the job market. The respondents said that the market industry demand in IT were software engineering. They also stated that the job market was huge for SE specialisation. However, three respondents said "No". They gave the reasons that things in the job market rarely reflects what they have learned and they gave the reason that the actual skill they had was more important when getting jobs.

Regarding the related course they had learned (B4), there were eighteen respondents (90%) said "Yes" and chose the related course that they applied during their industrial training (See Table V). The subjects that the students applied during industrial training are depicted in Fig. 2. It shows that most of the students applied Programming Language Concepts & Paradigm (PLCP); and Software Project Management, Process and Evolution (SPMPE). On average, the students applied Software Requirements Analysis & Modelling (SRAM); Software Design & Architecture (SDA); and System Analysis & Design (SAD). While Design & Analysis of Algorithm (DAA) is the least related course that students applied during their industrial training.

TABLE V
OPINION OF GRADUATES ON SOFTWARE ENGINEERING COURSES

Question Number: Description	Response Item	F	%
B4: Did you apply SE subjects and how they were related during industrial trainings?	Yes	18	90
	No	2	10

Note: F: Frequency, %: Percentage

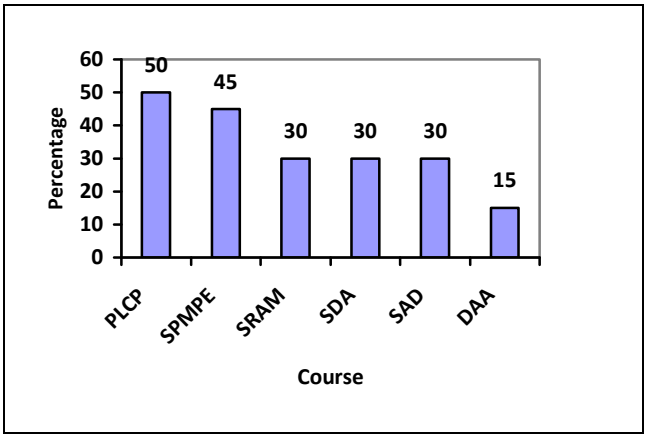


Fig. 2. Subjects in software engineering specialisation that students found being applied during industrial training

The opinion element for the interview (see Table VI) identifies "What are the expectations from the industry towards graduates". In I1 element, employers expect the fresh graduates to be confident in giving opinions and broaden their knowledge especially in computer skills. As for I2 element, employers stated that the graduates partially fulfil their requirements and were not creative in generating new ideas. Element I3 studied the aspects that employers could not find in graduates. They stated that among the aspects that they did not obtain from the graduates include communication skills, lack of team work, not good at sharing ideas and not independent in self improvements.

TABLE VI
OPINIONS DERIVED FROM THE INTERVIEW

Question Number: Description	Response Item
I1: What are the expectations of the employer towards software engineering graduates?	Confident in giving opinions, need to broaden the knowledge of the area (computer skills), think out of the box, creative, good analytical thinking, able to identify problems in existing systems and suggest the best solution.
I2: Do most graduates fulfil the expectations of the employer?	Fulfilled if graduates are able to finish the tasks on time. The tasks given to fresh graduates are partially easy like doing homework of what they have studied. However, this is not fulfilled if graduates are not creative in generating new ideas.
I3: What are the aspects that graduates do not have?	Communication skill, lack of team work, not good in expressing and sharing ideas among other team members, no creativity, not independent in knowing industries skills and future ideas.

C. *Expectation*

For the expectation among the respondents, we surveyed on the future career that they choose upon graduation and the suggestion for the university from industry's pratitioners.

Regarding element B7 (see Fig. 3), seven respondents wanted to be a Software Engineer (SE) upon graduation. While four respondents wanted to be a Software Analyst (SA) and two wanted to be a programmer (PG). On the hand, one respondent chose to be a Software Tester (ST) as their career and six respondents chose to do non-IT related jobs (OTH) such as a teacher, a professor, a businessman, a salesman and a computer gamer.

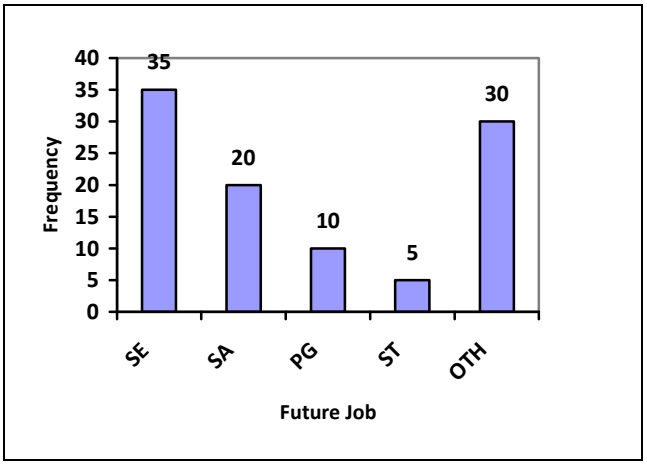


Fig. 3. Future careers chosen by SE graduates

As for I4 (see Table VII), the employers recommended some suggestions for universities to produce better performance graduates in future. The employers stated that the universities should expose the students with more technical skills. Moreover, employers also recommended that the universities should hire lecturers that have several years of working experience.

TABLE VII
EXPECTATIONS: EMPLOYEES

Question: Description	Response Item
I4: What are the recommendations to the universities to produce quality software engineering graduates?	- Keep up the industrial training exposure; it can develop students' confidence. Expose more to the real live working environment. - Expose the students with more technical skills. - Guide the students for preparation on how to become the employee and tell the employers' expectations. - Expose the students with the new technologies, languages and software.

V. THE FINDINGS

We anticipate that IT or CS graduates specialise in software engineering are not ready to face the real working environment as what always perceived by the stakeholders in software industries. However from our survey, 60% of final year students who were the respondents stated that they were ready to face the real working environment and claimed that what they had learned were enough for them to apply the job later. As the respondents had just completed their industrial training, this perspective could be due to least tasks they had during the industrial training and the time period of each given task was not so pressured. For example, one of the respondents who were not ready to face the real working environment said that the task during their industrial training was lighter than the real task working environment.

Even though, most of them claimed that they were ready to face the real work environment, 80% of them stated that they learned new technology or skills during their industrial training despite the fact that they learned the basic technologies in programming languages and databases before going out for industrial trainings. This reflects the fact that what the industry needs from the students are not enough as they still have to learn diverse technologies once they join a company upon graduation. This fact was also supported by the industry's claim through the interview we conducted that expect universities to expose more technical skills, new technologies, languages, and software.

The skills that industries expect from the graduates could not be educated during the studies [1].This shows that the employers' expectations from the interview could not be completely fulfilled such as 'think out of the box'. Another example, if students have the skill on C++ language but they need to develop a system using another language such as Java, they should be able to adapt to both languages as the methodologies of the languages and the skill required to solve the problems using the logical thinking are the same across all programming languages. This shows that industries should provide training to fresh graduates in the technology that their company adopts. This is due to the fact that software industry grows rapidly and its technologies are extremely diverse which are not possible for academia to expose all to their students mainly commercial technologies which are very costly for universities to purchase them.

The employers claimed that graduates are lack in creativity and the potential in creating new ideas, therefore students are advised to be more adventurous in trying new things and broaden their knowledge of new technologies in the industry instead of focusing their academic requirements only. Besides, the employers also highlighted that the low performance of graduates in terms of communication skill, lack of team work, not independent in knowing industry skill and other contributing factors might interrupt the growth of software industries.

VI. CONCLUSION

We conducted a survey among twenty final year students specialising in software engineering and interviewed five software related personnel in two companies. The study aims to investigate the gap between industry's requirements and graduates' readiness. We believe by addressing this issue to both SEE and SEI, they could get some insights on this issue to reduce the gap. The findings of the study also provide the guidelines to future CS or IT graduates and mainly software engineering graduates to prepare themselves before facing the real working environment later.

In short, industry has its own demands on hiring well trained and highly skilled graduates who comply with their requirements. However, students are still lack of required skills such as soft skills, managerial skills and technical skills. Our study deduces that both SEE and SEI should play their part and collaborate to ensure the SEE produces high skilled graduates that give benefit to the SEI. In addition, most graduates are still not ready to face the real working environment unless they attend some extra courses to enhance their soft skills, managerial and technical skills before they seek their first job once they graduate.

ACKNOWLEDGMENT

The authors would like to acknowledge the short term grant 304/PKOMP/6310044 for funding the related expenses with regard to this paper. The first three authors also thank to the School of Computer Sciences for the opportunity given to conduct this research under a related course.

REFERENCES

[1] R. Mahanti and P. K. Mahanti, "Software Engineering Education From Indian Perspective", *Proceeding of the 8th Conference on Software Engineering Education & Training (CSEET'05)*, IEEE Computer Society, April 2005, pp.111-117.

[2] IEEE Standard Glossary of Software Engineering Terminology, *IEEE Std 610.12-1990*, IEEE Computer Society, 1990, p.1.

[3] S. Karunasekera and K. Bedse, "Preparing Software Engineering Graduates for an Industry Career", *Proceedings of 20th Conference on Software Engineering Education & Training (CSEET'07)*, IEEE Computer Society, July 2007, pp.97-106.

[4] G. V. B. Subrahmanyam, "A Dynamic Framework for Software Engineering Education Curriculum to Reduce the Gap between the Software Organizations and Software Educational Institutions", *Proceeding of 22nd Conference on Software Engineering Education and Training (CSEET)*, Feb. 2009, pp.248-254.

[5] C. O'Leary et al., "Developing a Software Engineering Curriculum for the Emerging Software Industry in China", *Proceeding of the 19th Conference on Software Engineering Education and Training*, April 2006, pp. 115-122.

[6] H. Jaakkola, J. Henno, and I. J. Rudas, "IT Curriculum as a Complex Emerging Process", *IEEE International Conference on Computational Cybernetics (ICCC)*, Aug. 2006, pp. 1-5.

[7] A. Pilat et al., "Industry Feedback on Skills and Knowledge in Real-Time Software Engineering", *Proceeding of 19th EAEEIE Annual Conference (2008)*, IEEE Computer Society, June -July 2008, pp.129-133.

[8] H. Ledgard , J.Tauer, *Professional Software (Volume 1): Software Engineering Concepts*, vol. 1, Addison-Wesley Longman Publishing Co., Boston,MA, USA,1987, p.218.

[9] M. DiBernardo, "Don't Touch a Thing: How Adopting a Service Provider Attitude Can Boost Your Career", *ACM Software*, Crossroads, New York, vol.16, issue 1, pp. 3-5, 2009.

[10] G. G. Roy and V. E. Veraart, "Software Engineering Education: from an Engineering Perspectives", *Proceeding International Conference on Software Engineering: Education and Practice,* 1996, IEE Computer Society, Jan. 1996, pp.256-262.

[11] A. Hamau –Lhadj, A. Gherbi and J. Nandingam, "The Impact of the Model-Driven Approach to Software Engineering on Software Engineering Education", *Sixth International Conference on Information Technology: New Generations (ITNG'09)*, IEEE Computer Society, April 2009, pp.719-724.

[12] S. Hadjerrouit, "Learner-Centered Web-Based Instruction in Software Engineering", *IEEE Transaction on Education*, IEEE Education Society, vol. 48, issue 1, Feb. 2005, pp. 99-104.

[13] Z. Mahmood, "A Framework for Software Engineering Education : A Group Projects Approach", *International Journal of Education and Information Technologies – Powered GoogleDoc Journals*, vol. 1, issue 3, pp. 153 – 156, March 2007

[14] K. Beckman, N. Coulter, S. Khajenoori and N.R. Mead, "Collaboration: Closing the Industry-Academia Gap", *IEEE Software*, IEEE Computer Society, vol. 14, issue 6, Nov/Dec. 1997, pp. 40-57.

[15] A. Rusu, A. Rusu and R. Elloitt, "Work in Progress: Smoothing the Border between Academic and Professional Software Engineering Environment through Entrepreneurship", *Proceeding of 36th ASEE/IEEE Frontiers in Education Conference (2006)*, IEEE Computer Society, Oct. 2006, pp.17-18.

[16] K. Garg and V. Varma, "Software Engineering Education in India: Issues and Challenges", *IEEE 21st Conference on Software Engineering Education and Training 2008 (CSEET'08)*, IEEE Computer Society, April 2008, pp. 110-117.

[17] R. B. Vaughn and J. Carver, "Position Paper: The Importance of Experience with Industry in Software Engineering Education", *Proceeding of the 19th Conference on Software Engineering Education and Training Workshops 06 (CSEETW)*, IEEE Computer Society, April 2006, p. 19.

[18] G. Taran and M. Rosso-Llopart, "Software Engineering Education in Russia: A Comparative Study of People, Process and Technology a Four Year Perspective", *20th Conference on Software Engineering Education & Training (CSEET)*, IEEE Computer Siciety, July 2007, pp. 19-28.

The Process of Quality Assurance under Open Source Software Development

Atieh Khanjani[1], Riza Sulaiman[2]

[1,2]Schools of Industrial Computing & Computer Science
Faculty of Information Science and Technology
Universiti Kebangsaan Malaysia,
43600 UKM Bangi, Selangor Darul Ehsan,
Malaysia

[1]akhanjani *at* ftsm.ukm.my, [2]rs *at* ftsm.ukm.my

***Abstract*- Open Source Software (OSS) is software products available to the public, with its source code to study, change, and improves its design. Open Source Software Development (OSSD) is the process by which open source software is developed within the confines of software engineering life-cycle methods. However when open source used for commercial purpose, then an open source license is required. Open source software is very often developed in a public and collaborative manner. The quality assurance principle under open source software development is an approach to improve software product quality against traditional methods and techniques. Despite the fact that the open source developments have seen remarkable successful in recent years, there are a number of product quality issues and challenges facing the open source development model. Many industries and business sectors are following or using OSSD, since they realize the benefits, but they do have some reservations concerning quality assurance in the form of program code quality, maintenance of the code and its quality, over the life-cycle of the product and third party usage. This paper reviews the literature of the process of the latest quality assurance, under open source software development methods and techniques. The result from this review is to show the process of quality assurance of open source software and that how it can affect the overall quality assurance principal.**

Keywords: **Open source, licenses, quality assurance, OSSD model, process, procedures, and standards.**

I. INTRODUCTION

As today the stages of guarding and protecting a software after the development, is concerned more than just writing the code, every companies are looking for a methodology to support and maintain their software and improve the quality of their products. In this case software assurance plays a vital role to support companies with the standards and rules which they introduce; and open source software can overcome some drawback of traditional quality assurance because it is a kind of distributed software that use peer review technique in addition to make available source code for every volunteers who want to share their capabilities.
Moreover due to putting so many people to develop, test and evaluate the code, OSSD gets more benefits rather than traditional closed source software.
In terms of quality issues there are some important aspects:

- Improved services levels,
- Productivity, and
- End user satisfaction.

Due to the fact that open source code is available to the public, OSSD can improve quality in these three aspects, because it can enhance services levels which can increase efficiency for users and developers as well. Also because of having variety of ideas, that can participate to the project and modify the software code, the open source software can be more flexible. In terms of productivity, it is more suitable, because it can increase the motivation and performance of producing compared to close source software. Furthermore, the speed of bug defecting and resolving errors will be increased. However being a lot of volunteers, may make it dangerous because it needs a centralized organization to manage and maintenance. Moreover since the volunteers often develop software in their own path and even they may not consider the proper requirements, quality standards, and required tools to measure the quality, therefore it seems hard to document .
This paper focuses on reviewing the major concepts and process of quality assurance under OSSD model to improve the software quality. In Section 2, we have briefly outlined concepts of OSSD and quality assurance. In Section 3, quality assurance under open source software has been explained. In Section 4, we have presented the processes and procedures of quality assurance under OSSD, and finally we have concluded our work.

II. THE CONCEPTS OF OPEN SOURCE DEVELOPMENT

There are a lot of definitions for the concept of open source software development, according to OSD[1] a software which has ability to distribute freely with available source code through the Internet and using unpaid people that can modify the code freely, is open source software [1].
Some major concepts to identify open source software are as follow [2]:

- Distributed software.
- Free software.
- Available source code.
- Communicate through internet.

[1]*www.opensource.org/does/definition.html*

- Developers are users.
- Unpaid and large amount volunteers.

In the other words, open source software development is a kind of distributed software development that has a large amount of contributors and because of using Internet and make sharing freely it is so successful and useful that developers can communicate over the distance.

Due to having variety of contributors in OSS projects and the story of knowledge sharing among them the project can be more powerful and this might lead to improve even the position of contributors. For example they can move to the developers group from users or even in developers group move to the core developers [1]. Core developers are a small amount of expert developers, integrated to control and manage the system [3]. Co developers that are the people who have directly impact on software development in the project, also they effect on the code base and they can find issues on licensing [1, 4]. Figure 1 shows the structure of developers in open source methodology.

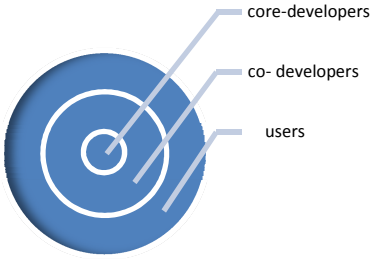


Fig. 1.The structure of developers and users in OSSD model

The pros and cons of open source software development versus traditional method have been presented (see table 1).

TABLE1
THE ADVANTAGES AND DISADVANTAGES OF USING OPEN SOURCE DEVELOPMENT MODEL

Features / Pros& Cons	For Users	For Developers	For System
Pros	1. Flexibility 2. Strong value 3.Participant in interested part 4.Code availability [4] 5.Ability to modify the code 6.Knowledge sharing 7.Increasing motivation 8. Greater choice and control	1. Allow to make own solution. 2. Reuse many existing functionalities. 3. Allow to survey problems freely. 4. Reduce damages in the beginning time of the system [5] 5. More motivation [5]	1. Bug detecting 2. OS tools 3. Reliability 4. Customizability 5. Sophisticated 6. Cost effective[6] 7. Rapid evolution 8. Portability 9. Extensibility 10. Reusability[7],[8] 11. Little cost 12. Multitude licensing [9, 10].
Cons	1. Useless documentation 2. Unstructured development 3. Irresponsible individuals	1. Lack of tools 2. Collaboration with new developers 3. Review of large projects	1. Lack of formal process; centralized management release and documentation. 2. Poor design 3. Hard estimation of man power [9] 7.No single responsibility for problem, lack of liability 8. Version proliferation 9.Complex licenses 10. High short term cost [10, 11]

III. THE CONCEPT OF QUALITY ASSURANCE UNDER OPEN SOURCE SOFTWARE

Quality Assurance (QA) is a systematic methodology that verifies whether products reach or exceed customer expectations or not. QA works by going through some process such as design, development or evaluation of the system by testing the result to reach the goals [10]. While the steps of the quality assurance process can modify according to the requirements and objectives of the companies, but the main goal in quality assurance issues, is delivering a high quality products and services for increasing customer satisfaction [11].

Quality assurance in open source development model, significantly, depends on two factors: code review and data testing. Availability of the code, allows anyone to analyze it and survey it as own viewpoint and detect more bugs.

Because of being unsuitable, some quality assurance techniques in some companies have to provide some guarantee to end-users of open source software, they have to be ensure the set of versions they select for distribution does not contain implicit violations of restrictions on inter component interactions. Then they perform code recheck for every change of source code in their enterprise level distributions before releasing security updates and service packs to enterprise customers.

In open source software, like the Apache HTTP Server[2], the Internet browser Mozilla Firefox[3], GNU/Linux[4] operating system, etc, due to sharing everybody's idea we have more chance to release bug, although the all bugs still cannot be eliminated. For developing these systems there are a specific methods and techniques of quality assurance that manage the quality of these products [15]. Due to having specific properties, such as having large community, sharing knowledgeable and interested users from whole the world, expert full time developers to manage and handle bugs, existing unpaid and even paid contributors, OSSD model in many ways can increase the quality [16, 17]. Furthermore using OS tools such as compilers, mailing list,

[2] *http://httpd.apache.org/*
[3] *www.mozilla.com/firefox/*
[4] *www.gnu.org/*

CVS [18], Gnu/Linux tools that naturally influence the quality of code can be another reason to improve quality of open source software development model. Applying suitable tools has a significant impact on the quality, therefore the adjustment of tools such as mailing lists should consider through management teams [19].

In open source software development, programmers freely provide improvements for recognition if their improvement is accepted and users do not pay a price; hence particularly attractive to users. Programmers are motivated to improve open source quality for an opportunity for recognition and future potential benefits [20]. The users for participating should register in some web sites, like *source forge.net* that it does offer facilities for users to record the skills they have [21].

In another perspective, Nakagawa [22] surveys the relationship between OSS quality and software architecture; and shows that the quality of OSS can be increased through attention to software architecture, with refactoring activity which results in software that matches with primarily established software architectures [23].

IV. The Processes and Procedures in Quality Assurance under Open Source

The process of OSSD model is iterative and parallel, with special properties and features that has been illustrated in Figure 2.

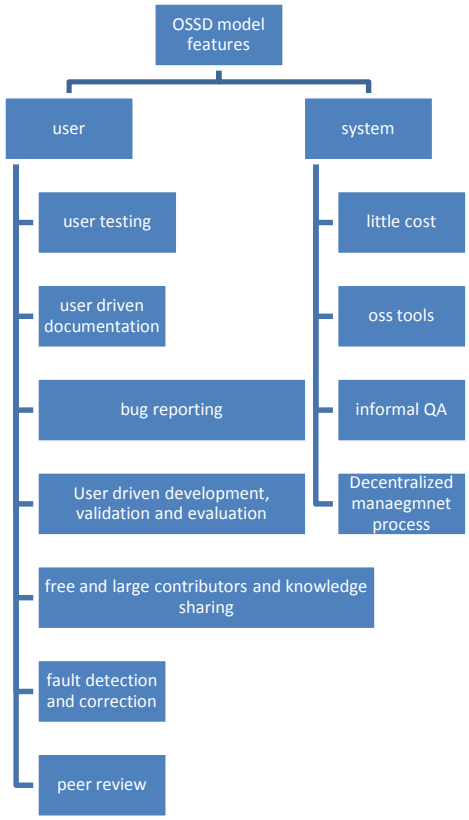


Fig. 2.The features of open source development model for quality assurance

The processes of quality assurance under open source software development model have been explained below.

A. *Requirement Definition and Design*

OSSD model is a parallel and repeatedly development technique with free participant user without central management, huge development communities and effective user testing. In this way, development methodology is not documented and the QA methodology is informally applied [20]. In open source, the problem of understanding user requirement has been almost resolved, because developers are typically as the same as users [24]. In terms of design, bug reports are one of the aspects to improve quality in OSSD model that allows to the software design process, and usability analyzes to inform interaction design in, all types of software development. Another advantage of OSSD is openness of this model that permits access to the design process that can only be derived in proprietary development by detailed, time consuming ethnographic observation [25]. Poor design leads to poor coding and therefore poor testing and quality issues. According to Porter [18], there is no formal design for OSS. It will be started by programming, or just applying documents design for documentation without modify. Moreover in distributed development environment, communication processes and a proper infrastructure with integrated instrument are very important to enable it. The projects to collect and gain a lot of people to cooperate need attraction to use the benefits of large teams. In addition the development process should attend to initial design activities to prevent quality assurance issues when the requirements evolve [19].

B. *Large Development Community*

Whatever project be more organized the efficiency of the project could be higher; if a system has a systematic and centralized hierarchy, it can be managed better. For example in Apache there are more than 2 levels for developers [1].Moreover the number of programmers and reviewers cannot guarantee the maintenance of code quality [17]. In addition the peer review in open source that is a beneficial and necessary technique to enhance the quality is performed universally [24].

C. *Testing*

In terms of testing in OSS issues, it is hard to estimate how much manpower should be delivered, how the developers should communicate, and which developers should team up closely [26].Testing issues in OSS, can be performed by all developers; also anyone can modify any part of codebase, but only committers can make changes official [8].When we use software testing, we can be sure whether the system satisfies its requirements or not. Open source according to Eric Raymond [1] that is an open source spokesman usually use “many eyeball” technique, to identify the bugs instead of formal testing methods. One of the problems in open source software testing is the lack of knowledge of participants to fix and test the entire architecture of open source software system.

D. *Maintenance*

Kozlov [27], in his paper focuses on relation between adaptive maintenance process and quality in open source software. He states maintainability is effected by analysis maintenance process, testability is effected by maintenance sub process, reliability is effected by design and delivery

maintenance sub process; while complexity, is effected by problem identification, design, implementation and test sub process; and finally the flexibility of software is effected by only delivery sub process [26]. The need for having professional developers especially in open source software is so clear because they provide accurate feedback. Furthermore too short release cycles could affect the software quality and frustrate end users due to less stability [28].

There are important activities in software maintenance such as post-delivery fault reporting and correction, which are performed before the software release. However in open source with having user feedback and several releases, the improvement of software quality will be easier; and it has significant effect on correctness, completeness and security as well. These activities are also applied to estimate the maintenance effort, guide decision making, support resource allocation, reduce risks and to measure and control software quality [29]. Also for having successful high quality products we have to implement the process that is produced in the past high quality properly [19].

E. Documentation

Documentation focuses on the style and coding guidelines. It is very important for developers especially in OSS projects; since useful documentation has a direct effect on quality degree and it allows to the new participant to know better about the system and understand the modification and evaluate the code. Due to in OSS projects, it performs by the individuals, good documentation according to the project structures is necessary. Useless user documentation, lack of date stamping and tools to check the documentation can make quality lower. Developers through documentation can describe the style that should use for source code and also when and who can make modification in a project's version control system [17].

F. Security Issues

In terms of security issues in open source, the security experts also improve open source program in addition to ordinary people due to pleasure gained from verification and review and trouble shooting of programs. One of the problems containing OSS is that some of the open source licenses emphasize that the software must remain open source, but this condition is not suitable for some companies that some of their customers want to use these products in their own application but not to make their product open source; and one of the solutions of this problem is to use Dual Licenses. In this case, a license is for free to use software but it makes users to present their new product to the market in form of an open source software program if they use the original open source software in the new product. However there is another license which the customer can buy and therefore the new product using the open source software has not to be presented to the market as an open source program [30].

V. CONCLUSION

OSSD model is a methodology to improve software quality assurance, it is faster and safer rather than traditional methodology, especially in case of large scale systems. However, open source has some restrictions if one were to use someone else's code for commercial gain. In this case the user of the code has to have a license agreement and pay some money to the owner or maintainer of the code. The license of open source is a copyright license but available to end users to modify the source codes for their own purposes such as troubleshooting or for non commercial redistribution. However all such silences have additional limitations such as preserve the name of author and a copyright statement inside the code. This paper reviewed the process of quality assurance under open source software development and how open source can improve quality assurance through its special features and properties**.** Also we have found out what is the motivation of participate too many people to this kind of software development and how it can be improved. This shows the reason that today organizations and customer attack to use open source**.**

One of the most arguable problems in OSSD model is the lack of good design that lead to reduce developer's motivation. Future work can be consist of some beneficial work regarding to solve problematic concepts in QA under OSSD model such as poor design and documentation and find a way to make them centralizes and strong.

REFERENCES

[1] C. Gacek and B. Arief, "The many meanings of open source," *Software, IEEE,* vol. 21, pp. 34-40, 2004.

[2] D. Cubranic and K. S. Booth, "Coordinating open-source software development," in *Enabling Technologies: Infrastructure for Collaborative Enterprises, 1999. (WET ICE '99) Proceedings. IEEE 8th International Workshops on*, 1999, pp. 61-66.

[3] Audris Mockus, "Two case studies of open source software development: Apache and Mozilla " *ACM Transactions on Software Engineering and Methodology (TOSEM)* vol. 11, pp. 309 - 346 2002.

[4] J. J. Heiss. (2007, August 2007). The meanings and motivations of open-source communities. Available: http://java.sun.com/developer/technicalArticles/javase/opensource_phipps/

[5] A. Khoroshilov, "Open source certification and educational process," in *Third InternationalWorkshop on Foundations and Techniques for Open Source Software Certification (OpenCert 2009)*, 2009, pp. 1-8.

[6] H. I. Hedberg, N.; Rajanen, M.; Harjumaa, L.; , "Assuring Quality and Usability in Open Source Software Development, " in *Emerging Trends in FLOSS Research and Development, 2007. FLOSS '07. First International Workshop on*, 2007, pp. 2 - 2.

[7] C. J. Xiong*, et al.*, "A model of open source software maintenance activities," in *Industrial Engineering and Engineering Management, 2009. IEEM 2009. IEEE International Conference on*, 2009, pp. 267-271.

[8] P. Aho*, et al.*, "Model-Driven Open Source Software Development - The Open Models Approach," in *Software Engineering Advances, 2009. ICSEA '09. Fourth International Conference on*, 2009, pp. 185-190.

[9] R. Abdullah*, et al.*, "The Challenges of Open Source Software Development with Collaborative Environment," in *Computer Technology and Development, 2009. ICCTD '09. International Conference on*, 2009, pp. 251-255.

[10] T. Waring and P. Maddocks, "Open Source Software implementation in the UK public sector: Evidence from the field and implications for the future," *International Journal of Information Management,* vol. 25, pp. 411-428, 2005.

[11] P. Maki-Asiala and M. Matinlassi, "Quality Assurance of Open Source Components: Integrator Point of View," in *Computer Software and Applications Conference, 2006. COMPSAC '06. 30th Annual International*, 2006, pp. 189-194.

[12] T. B. Dinh-Trong, J.M.; , "Open source software development: a case study of FreeBSD," *Software Metrics, 2004. Proceedings. 10th International Symposium on,* pp. 96-105, 2004.

[13] S. Kietzman. (2010, *What is Quality Assurance?* Available: http://www.wisegeek.com/what-is-quality-assurance.htm
[14] K. A. Johnson. (2010, *Mature Quality Assurance Processes*. Available: http://www.epam.com/quality-assurance-process.htm
[15] W. Y. Office. *Benefits of Using Open Source Software*. Available:http://open-source.gbdirect.co.uk/migration/benefit.html
[16] T. M. Otte, R.; Knoell, H.D.; , "Applied Quality Assurance Methods under the Open Source Development Model," *Computer Software and Applications, 2008. COMPSAC '08. 32nd Annual IEEE International* pp. 1247 - 1252, 2008.
[17] M. Michlmayr, Hunt, F., Probert, D, "Quality Practices and Problems in Free Software Projects," in *Proceedings of the First International Conference on Open Source Systems*, 2005, pp. 24-28.
[18] A. Porter, *et al.*, "Techniques and processes for improving the quality and performance of open-source software," *Software Process: Improvement and Practice,* vol. 11, pp. 163-176, 2006.
[19] T. Otte, *et al.*, "Development of a Quality Assurance Framework for the Open Source Development Model," in *Software Engineering Advances, 2008. ICSEA '08. The Third International Conference on*, 2008, pp. 123-131.
[20] S. Raghunathan, *et al.*, "Open source versus closed source: software quality in monopoly and competitive markets," *Systems, Man and Cybernetics, Part A: Systems and Humans, IEEE Transactions on,* vol. 35, pp. 903-918, 2005.
[21] S. C. G. Madey;, "Analysis of Activity in the Open Source Software Development Community " in *System Sciences, 2007. HICSS 2007. 40th Annual Hawaii International Conference on*, 2007, pp. 166b - 166b.
[22] E. Y. Nakagawa, *et al.*, "Software Architecture Relevance in Open Source Software Evolution: A Case Study," in *Computer Software and Applications, 2008. COMPSAC '08. 32nd Annual IEEE International*, 2008, pp. 1234-1239.
[23] E. Y. d. S. Nakagawa, E.P.M.; de Brito Murata, K.; de Faria Andery, G.; Morelli, L.B.; Maldonado, J.C.; , "Software Architecture Relevance in Open Source Software Evolution: A Case Study " in *Computer Software and Applications, 2008. COMPSAC '08. 32nd Annual IEEE International*, 2008, pp. 1234 - 1239.
[24] L. Barnett. (2004, *Applying Open Source Processes In Corporate Development Organizations*. Available: http://www.create.ucsb.edu/~xavier/EngPL/Forrester-ApplyingOSinCorporations.pdf
[25] M. B. Twidale and D. M. Nichols, "Exploring Usability Discussions in Open Source Development," in *System Sciences, 2005. HICSS '05. Proceedings of the 38th Annual Hawaii International Conference on*, 2005, pp. 198c-198c.
[26] H. Jongdae, *et al.*, "Extracting Development Organization from Open Source Software," in *Software Engineering Conference, 2009. APSEC '09. Asia-Pacific*, 2009, pp. 441-448.
[27] D. Kozlov, *et al.*, "Evaluating the Impact of Adaptive Maintenance Process on Open Source Software Quality," in *Empirical Software Engineering and Measurement, 2007. ESEM 2007. First International Symposium on*, 2007, pp. 186-195.
[28] T. Otte, *et al.*, "Applied Quality Assurance Methods under the Open Source Development Model," in *Computer Software and Applications, 2008. COMPSAC '08. 32nd Annual IEEE International*, 2008, pp. 1247-1252.
[29] Y. Liguo and C. Kai, "Evaluating the Post-Delivery Fault Reporting and Correction Process in Closed-Source and Open-Source Software," in *Software Quality, 2007. WoSQ'07: ICSE Workshops 2007. Fifth International Workshop on*, 2007, pp. 8-8.
[30] S. S.-S. Shirali-Shahreza, Mohammad; , "Various aspects of Open Source Software development " *Information Technology, 2008. ITSim 2008. International Symposium on*
vol. 4, pp. 1 - 7 2008.

A Hybrid TCP Congestion Mechanism to Improve Mobile WiMAX Networks

Jhonny Tay
Faculty of Computer Science
Information Technology
University of Malaya
Kuala Lumpur, Malaysia
E-mail jhonnytay@hotmail.com

Rafidah Md Noor
Faculty of Computer Science
Information Technology
University of Malaya
Kuala Lumpur, Malaysia
E-mail: fidah@um.edu.my

Abstract—**the traditional TCP was designed for wired network; implementing TCP protocol in wireless network may lead inaccuracy prediction and will results suffer performance degradation in network. A proposed TCP-Hybrid congestion mechanism is presented in this article to address the issues by improving TCP performance in wireless environments such as a mobile WiMAX. The model adapted the existing TCP congestion control which is based on TCP-Vegas and adopting a modification Scalable TCP aggressive rule to increase a window size. The experiment results have shown that while all TCP variants produces similar throughput, window size and round trip time, even they do in different ways. But however our propose mechanism has proven 1.3% to 3% more better throughput compared to TCP-Vegas and TCP-Scalable and also high window size contributed mechanism.**

Index Terms- Mobile WiMAX, TCP Congestion, NS-2

I. INTRODUCTION

The great convenience is bringing to a person who utilizing the technology of wireless due to it is getting more mature in nowadays. One of the main objectives of the next generation wireless network is to provide high data rate and support multimedia services to end users. The technology such as worsldwide interoperability for microwave access (WiMAX) based on IEEE 802.16, it is able to provide high bandwidth throughput over long-range coverage transmission and support fixed, nomadic and mobility transmission and one base station to multi mobile node called as point to multipoint mode and mesh mode. Even though WiMAX technology is being considered as the vast bandwidth providing at this time, but it doesn't mean it could often fulfill all kind of network applications required, abundant of demands along with heavy load of usage, low packet drop rate and small time delay is required although without any congestion experience is almost not possible, in other hand the popularity of internet has to increases the demand of necessity of high bandwidth, largely number widely dispersed internet sites in global network in fact has stressing the network traffic and resources, hence rises the issue of congestion in network traffic. Since its first time occurs in the traffic furthermore congestion avoidance in internet has become an important topic. In the early research [14]"network congestion in the internet has shown that much of the cause lies in transport protocol implementations (not in the protocol themselves)". The most well-known transport layer protocol is the transmission control protocol (TCP) is a connection-oriented based protocol, whereas the user datagram protocol (UDP) as a connectionless based. In October 1986, first congestion collapse occurred due to rapid growth of internet usage. Thereafter in detail [18] at RFC 2581 has defined four TCP congestion control algorithms: slowstart, congestion avoidance, fast retransmit and fast recovery. These four algorithms have had became as the fundamental of TCP congestion control mechanism due to minimize the congested experienced. TCP has proposed a multi-faceted congestion control strategy such as TCP Tahoe [14], Reno [8], New Reno [11], Veno [12], Vegas [3], Hybla [4], Highspeed [10], BIC [22], CUBIC [20], TCP-Illinois [17], and TCP-fusion [15], and Westwood cite3.

The rest of this paper is organized as follow; section II is shown the reviews related work, and wireless network such as WiMAX are discussed in section III. The section IV is to present several TCP congestion mechanisms. The proposed Hybrid TCP congestion model and experimental results are discussed in section V. Finally, section VI concludes the article.

II. RELATED WORK

As mentioned at early, TCP was originally designed for a wired network. It assumes the packet loss in the network is caused by the congestion problem, and the random bit error rate (BER) is negligible in a wired network. Therefore if the TCP protocol is employed in wireless environment may lead inaccurate congestion prediction, due to the TCP unable distinguish between different multi-factors of loss rather than caused by congestion in the networks. Unlike the traditional network, the wireless link manipulates the transmission through the air interface are might subject to many of interferences where it could be noises, multipath, mount obstacles, mobility (handoff) and so on. Previous studied has shown that wireless link generates higher bit error rate (BER) as the main issue to be faced in all wireless networks, and the limitation of radio coverage causes a frequent handoff in the mobile node consequently connects and disconnects to network [23]. On the other hand, the different wireless network may require or provide different mechanisms to interoperate with the TCP such as WiMAX employs automatic repeat request (ARQ) mechanism in their MAC layer which successful decrease the TCP from transmission losses [13].

Nowadays TCP become one of the most widely used protocols in transport layer, therefore without proper supports with TCP such as WiMAX would suffer performance degradation. Numerous congestion control mechanism are tries to addressed these issues. However in the previous studies [15] the existing congestion controls mechanisms could be fit into three categories such as a loss-based, a delay-based and a mixed loss-delay-based (i.e. hybrid). A loss-based congestion control is slowly increase the congestion window (cwnd) by 1 maximum segment size (mss) for every ACKs message receives and drastic decrease the cwnd size known as reactive control mechanism as an example, TCP Reno [8], Highspeed [10], scalable TCP [7], BIC-TCP [13], H-TCP [16] and TCP Westwood [5]. A delay-based is functioned as the proactive congestion control which is often checking the congestion condition by utilizing the round trip time (RTT) to predict the congestion before packet loss occurs. Example of delay-based congestion control mechanisms are TCP Veno [12], FAST-TCP [1], and TCP-Vegas [3].

The simulation results from TCP-fusion [15] shows that it could obtain the highest throughput in residual unused bandwidth network among other TCP variants by exploits the three characteristic of Reno, Vegas and Westwood. The results of [6] proposes congestion control known as TCP-Adaptive Reno (ARENO) which is can achieves better throughput over Reno, even High Speed TCP in varying buffer capacities with or without random early detection (RED) queue management. The conventional congestion control Reno is modified to dynamically adjust the response ability like faster increase congestion window size and less slow in decrease the window size after congested experienced in network. The other Reno enhancing work [7] add a scalable delay-based component which aims to monitor the network condition and rapidly increases sending rate if network is underutilized but gracefully reduce once the bottleneck is occured and has achieved good bandwidth scalability over a tradition TCP, called as Compound TCP (CTCP). The proposed hybrid mechanism, TCP-Illinois in [17] has a capability to predict the congested network situation based on loss as the main signal and delay which is the second signal also known as delay information. By adapting the standard congestion control (Reno, NewReno or SACK) and readjusting the congestion window size are refered to a delay information. Achieving a good throughput compared to the standard TCP and through the stochastic matrix models Illinois is shown fairly to allocate the network resource as well.

III. WiMAX Network

Worldwide Interoperability for Microwave Access (WiMAX) is a high speed wireless technology based on the IEEE 802.16 standards [2]. IEEE 802.16 offers two types of WiMAX network, fixed and mobile. The fixed WiMAX provides a wireless broadband coverage over a large area and has built-in QoS and security features. WiMAX has two type of implementations which are a LOS and Non Line-of-Sight (NLOS) and they work over a licensed spectrum. LOS exists when the WiMAX base station connects to another WiMAX base station using a microwave link. As for NLOS, it exists between the WiMAX base station and the WiMAX subscriber. Figure 1 illustrates the WiMAX network, LOS and NLOS.

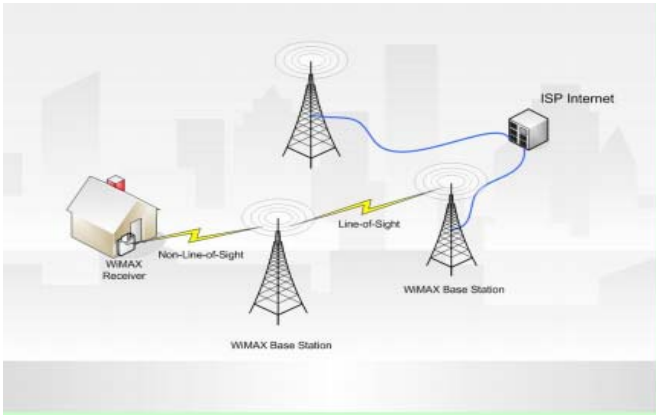


Figure 1. WiMAX: LOS and NLOS

The WiMAX standard provides a sophisticated Media Access Control (MAC) protocol that can share the channel across hundreds of users whilst providing QoS. It uses a request or grant access mechanism which eliminates collisions. The request or grant mechanism uses two modes of channel which are Time Division Duplex (TDD) and Frequency Division Duplex (FDD). In WiMAX networks, the base station controls the access of the inbound channel. Users who want to transmit packets, send a request on a contention-based access channel. The base station will grant the request by allocating the inbound channel access for the users. Therefore, the users who are allowed to use the inbound channel at one time will not experience any collisions. The advantage of requestor or grant mechanisms is the QoS support. The IEEE 802.16 standard offers four types of service flows which are an Unsolicited Grant Service (UGS), real-time Polling Service (rtPS), non real-time Polling Service (nrtPS) and Best Effort (BE) [19]. The service flows are defined to support multimedia applications. The UGS provides CBR flows for applications such as VoIP where it provides a bandwidth guarantee. The rtPS is designed for variable size data packets such as MPEG video. This service flow receives a minimum of bandwidth assurance. The nrtPS applications such as file transfer, support better than best effort services. The BE service flow is for background applications such as web browsing. The WiMAX architecture could be improved especially to support QoS mechanisms such as differentiated level of QoS, admission control, bandwidth management and policy.

IV. TCP Congestion Mechanism

This section discusses about the early TCP congestion mechanisms and the related TCP congestions.

A. *The Early TCP Congestion Mechanism*

Tahoe is the early TCP congestion control mechanism was implementing the first of three congestion control principles

[9] such as slow-start, congestion avoidance, fast retransmits known as TCP congestion principles. It very sensitive to packet loss 1% of loss could lead half portion decrease in throughput because of reset the window size to minimum value after packet loss experienced. Furthermore Reno are introduced which is implementing the all TCP congestion principles fast recovery after packet loss experienced but it lack in handle if two more segments are lost in the current window, fast recovery cannot retransmit all the lost packet until retransmit timeout, to overcome this issue NewReno has been introduced based on 3 acknowledgements and retransmit time out. In fact, the selective acknowledgment (SACK) mechanism are able to solve that lost in multi segment, unfortunately it has not been widely implemented. All these schemes are employs reactive flow control.

B. Related TCP Congestion Control

Vegas [3] select the minimal round trip time (RTT) as reference to estimate the optimal throughput and also records each sending rate in the sender during transmission to derive the actual throughput, RTT in Vegas is just become a parameter to calculate the timeout event and retransmits time, when dropped occurred in single or multi segment. In the retransmit mechanism, it is not based on n (3) duplicate ACKs, Vegas will do retransmits refers to; if Vegas obtain the duplicates ACK (acknowledgment) then it compare the current time to timestamp recorded when the result is greater. It rechecks to the first or second non duplicates-ACK after retransmits, when time interval since segment was sent is still greater the timeout value. The congestion window in Vegas should only decreased due to losses happened in this current sending rate but not for previous losses. The congestion avoidance by decreases the congestion window cwnd before the losses occur, therefore it is known as proactive control mechanism. The result has been reported Vegas delivered good achievement around 40% to 70% better than the traditional Reno. But at same research also found Vegas suffer severe performance degradation when inter-operated with other version of loss-based TCP control like Reno, and drop tail router.

Scalable TCP as aimed at speeding up the window update algorithm through replace the additive increase multiplicative decrease (AIMD) paradigm with more aggressive multiplicative increase multiplicative decrease (MIMD) algorithm in wide area network and constant recovery time from loss event regardless of window size. Scalable TCP is build on Highspeed TCP uses the same argument but it simplifies the implementation. The previous studies [21] Scalable TCP can achieve a good performance and dominate the bandwidth in high bandwidth-delay product over the other variants such standard TCP and HighSpeed TCP.

V. EXPERIMENT

Figure 2 below shows our simple network model and experiment in network simulator version 2 due to our research objective is to analyze the characteristic of WiMAX network, how TCP protocol sustain in wireless network and enhances the existing congestion mechanism, therefore the mobile WiMAX module has been integrated which developed by network institute of standard and technology (NIST) and Linux TCP congestion control. At early we present 1 mobile node (MN) which is connects to base station (BS) either one BS1 or BS2 with handover occur condition in point to multipoint mode, transmitting data through FTP application based on TCP Vegas, TCP Scalable and the proposes mechanism known as TCP-Hybrid each has attached with small packet size 500 Bytes, congestion window is 150 Bytes, link delay 100 ms with bandwidth is 1Mbps along 240 second traffic has set to stop for transmission data. Although as small packets size has been assigned, the experiment result shown in figure 3 that each of TCP mechanism produces with variety congestion window size during the transmission such as TCP- Vegas has donate the average around 42 Bytes, follow by TCP- Scalable 73 Bytes and the rest is our proposes mechanism has contributed 75 Bytes as the nearest congestion window size which is 150 Bytes, prove that TCP-Hybrid was exploit maximum size that is around 98 Bytes overcome the TCP- Vegas and TCP-Scalable.

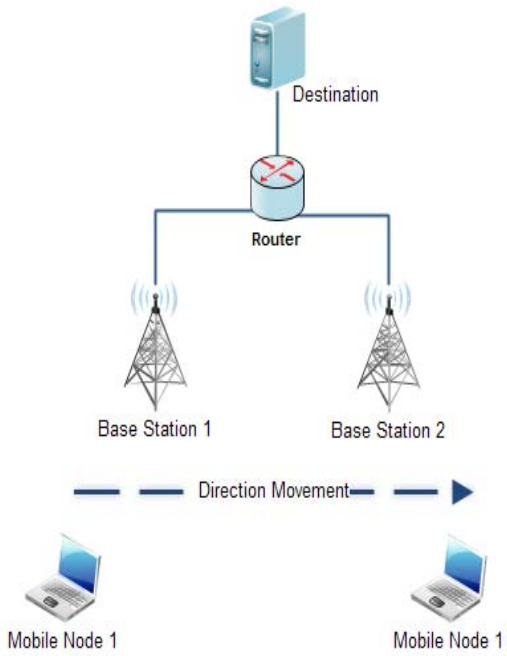


Figure 2. Network Topology.

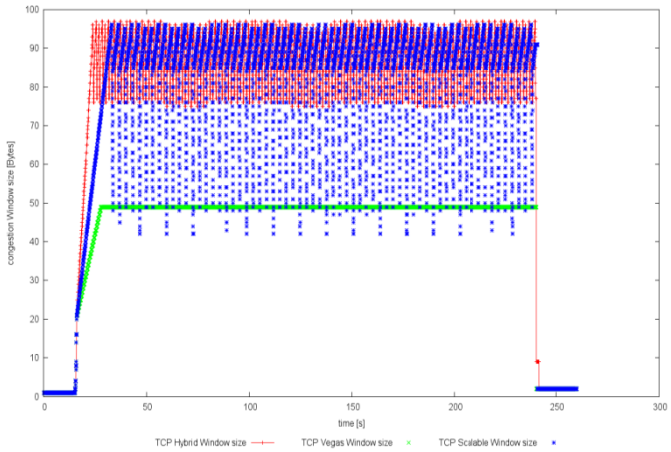


Figure 3. Congestion Window Size for 1 MN with 2 BS

Subsequently, through figure 4 shown that the round trip time (RTT) during transmitting data as the time it takes for reach the receiver and acknowledgment back to sender, in this case the proposes mechanism has generated highest averaging RTT around 0.45 ms due to the size of congestion window are greater than other TCP variants such as TCP-Scalable donated 0.37 ms and follow by TCP-Vegas is around 0.20 ms as the lowest throughput contributed.

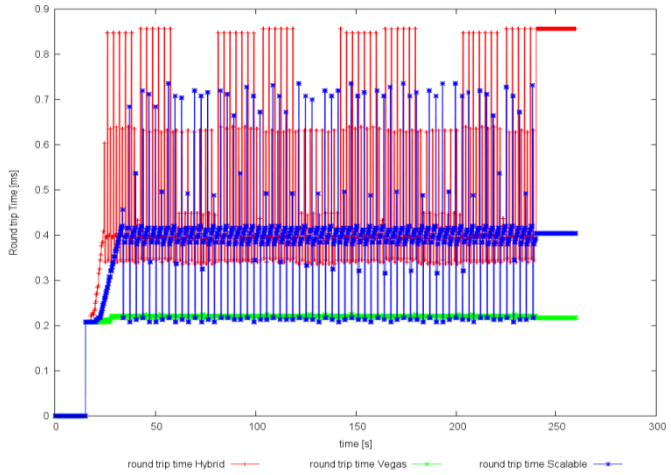


Figure 4. Round Trip Time for 1 MN with 2 BS

In figure 5 shown the average throughput rates for each of TCP variants such as TCP-Vegas around 754Kbps as the lowest throughput rate, follows by TCP-Scalable 767Kbps. fortunately our propose mechanism has contributed as highest average throughput which is at 777Kbps.

Furthermore we have set up a new experiment keep the same parameter as previous, hence by added link error from 1.5% to 5% to see how these three congestion mechanism sustain in that condition of network. Again proposes mechanism has donated the highest throughput even link error percentages increased every 0.5% follow by TCP-Scalable and TCP-Vegas in the lower line.

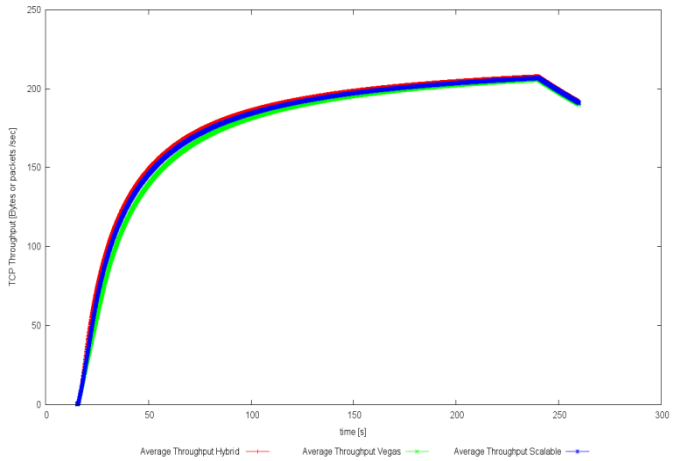


Figure 5. Throughput for 1 MN with 2 BS without Link Error Induced

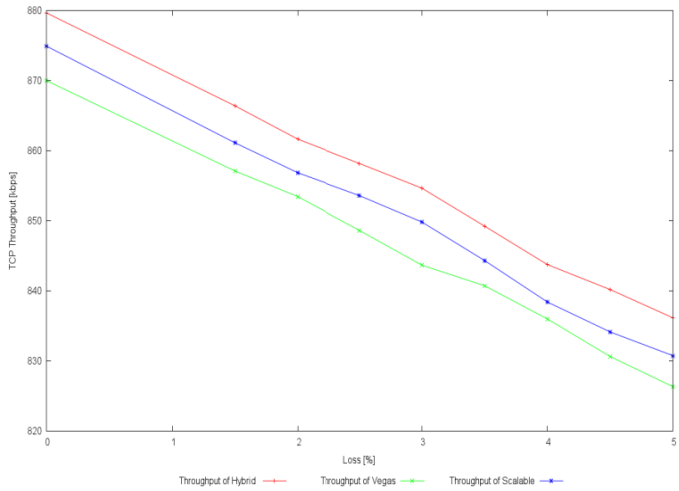


Figure 6. Throughput for 1 MN with 2 BS with Link Error Induced

A. Hybrid TCP Congestion Model

Our proposes congestion mechanism attempts to incorporate the congestion avoidance through exploit congestion window size and round trip time issues in most accurate way, it envisages two different modus losses-based and delay-based called as TCP-Hybrid control build on TCP Vegas [17] by adopting aggressive rule of Scalable TCP [16] three times more rapidly increase the sending window size until it reach the maximum size available and based on height RTT, which is exploit in loss-based mode, but if in delay-based it is acts as traditional Vegas uses proactive schemes to monitor the congestion condition in the network. Due to realize the idea a simple conceptual model for TCP-Hybrid is described in below work-flow is divided into two layers; a sender layer and receiver layer.

The sender layer consists of sender module, default setting and classification mechanism as the key conceptual mechanism; this proposes mechanism is just modifies the protocol on the sender-side. Both Sender layer and receiver layer are described below:

- Default setting also know as initializing value, there are several parameter have to be assigned before we can

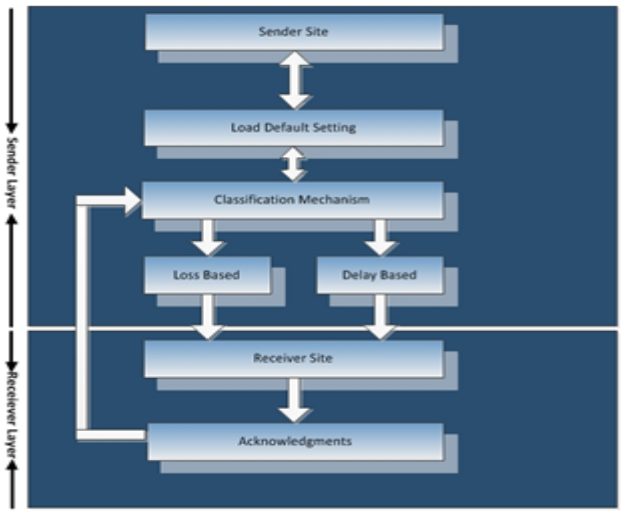


Figure 7. Hybrid TCP Congestion Proposes Model

use the congestion such as congestion window (cwnd), slow-start threshold (ssthresh), and round trip time (RTT).

- Classification is the most important part in this proposed control mechanism, it is automatically determined during sending packet occur, separated into two condition, while sending window size (cwnd) lower than the ssthresh default value, slow-start will operated as the mechanism to increase window sending size but obviously it took long time to climb over the rest of bandwidth (maximum size), therefore our propose mechanism will aggressively increase due to residual bandwidth in fact this is in loss-based mode. Afterward it will switch as delay-based mode once sending window size (cwnd) at maximum rate and acknowledgment (ack) time has been greater than the last RTT.
  - Loss-based which is based on scalable TCP mechanism with exploit multiplicative technique in order to increase their window size or on other hand, fully optimize residual bandwidth.
  - Delay-based is preserve the traditional TCP Vegas congestion avoidance mechanism is adjusting the congestion window to small size before the actual congestion is occurring.
- Receiver site and acknowledgement act as announcement to sender whether the packet arrives to receiver and with correct order or abnormal bit error, by sending back an acknowledgement includes the RTT, cwnd.

VI. CONCLUSION

This paper proposed a new TCP-Hybrid congestion control mechanism as the aims for improving TCP performance such as loss, optimize utilization congestion window size (cwnd) and produce high throughput over wireless network especially in mobile WiMAX environment. Our proposes mechanism is based on TCP Vegas by adopting modification Scalable TCP technique such as several time rapidly increase the window size (cwnd), from the simulation results we found that the TCP variants performed well in mobile WiMAX environment through ARQ (Automatic Repeat Request) successfully minimized the losses and our proposed mechanism has contributed as highest average throughput and sending window size.

REFERENCES

[1] FastTCPProject.2010, available at http://netlab.caltech.edu.

[2] IEEE Standard 802.16-2004. Technical Report IEEE Standard for Local and Metropolitan Area Networks, Air Interface for Fixed Broadband Wireless Access Systems. Last checked: 02/09/2010, available at http://www.ieee802.org/16/index.html.

3] Lawrence S. Brakmo, Sean W. O'Malley, and Larry L. Peterson. TCP Vegas: New Techniques for Congestion Detection and Avoidance. Proceedings of ACM SIG-COMM, 1994.

[4] C. Caini and R. Firrincieli. TCP Hybla: A TCP Enhancement for Heterogeneous Networks. INTERNATIONAL JOURNAL OF SATELLITE COMMUNICATIONS AND NETWORKING, 22:547–566, 2004.

[5] C. Casetti et al. TCP Westwood: Bandwidth Estimation for Enhanced Transport over Wireless Links. ACM Mobicom, 2001.

[6] H.Shimonishi et al. TCP-Adaptive Reno for Improving Efficiency-Friendliness Tradeoffs of TCP Congestion Control Algorithm. PFLDnet, 2006.

[7] K.Tan et al. Compound TCP: A Scalable and TCP- Friendly Congestion Control for High-Speed Networks. PFLDnetE, 2006.

[8] K. Fall and S. Floyd. Simulation-Based Comparisons of Tahoe, Reno and SACK TCP. Comp. Commun. Rev., 26, 1996.

[9] S. Floyd. Congestion Control Principles. Technical Report RFC2914, Network Working Group, 2000.

[10] S. Floyd. HighSpeed TCP for Large Congestion Windows. Technical Report RFC3649, Network Working Group, 2003.

[11] S. Floyd, T. Henderson, and et al. The NewReno Modification to TCP's Fast Recovery Algorithms. Technical Report RFC3782, Network Working Group. Last checked: 02/09/2010, available at http://www.ietf.org/rfc/rfc3782.txt.

[12] C. P. Fu and S. C. Liew. TCP Veno: TCP Enhancement for Transmission over Wireless Access Networks. IEEE JSAC, 21:216–228, 2004.

[13] E. Halepovic, Qian Wu, C. Williamson, and M Ghaderi. TCP over WiMAX: A Measurement Study. IEEE International Symposium on Modeling, Analysis and Simulation of Computers and Telecommunication Systems, pages 1–10, 2008.

[14] V. Jacobson. Congestion Avoidance and Control. Proc. SIG- COMM88, pages 314–329, 1988.

[15] K.Kaneko, T.Fujikawa, Z.Su, and J.Katto. TCP- Fusion: A Hybrid Congestion Control Algorithm for High-Speed Networks. PFLDnet, 2007.

[16] D. Leith and R.N. Shorten. H-TCP: TCP for High-Speed and Long-Distance Networks. In Proceedings of PFLDnet, 2004.

[17] S. Liu, T. Basar, and R. Srikant. TCP-Illinois: A Loss and Delay-Based Congestion Control Algorithm for High-Speed Networks. In Proc. First International Conference on Performance Evaluation Methodology Tools (VALUETOOLS), 2006.

[18] Allman M., Paxson V., and W Stevens. TCP Congestion Control. Technical Report RFC2581, Network Working Group, 1999.

[19] Loutfi Nuaymi. WiMAX Technology for Broadband Wireless Access John Wiley Sons, Ltd., 2007.

[20] I. Rhee and L. Xu. CUBIC: A New TCP-Friendly High-Speed TCP Variants. In Proceedings of PFLDNet, 2005.

[21] M. Tekala and R. Szabo. Evaluation of Scalable TCP,"Computer Systems and Applications. The 3rd ACS/IEEE International Conference, page 55, 2005.

[22] L. Xu, K. Harfoush, and I. Rhee. Binary Increase Congestion Control for Fast Long-Distance Networks. In INFOCOM, 2004.

[23] Y.Tian and et al. K.Xu. TCP in Wireless Environments: Problems and Solutions. IEEE Communications Magazine, 43:27–32, 2005.ss

Cooperative Architecture for QoS Management in Wireless 4G Networks

Nejd Ben Hamza[1], Slim Rekhis[2], and Noureddine Boudriga[3]
Communication Networks and Security Research Lab.
University of the 7^{th} of November at Carthage, Tunisia.
[1]nejdbenhamza@gmail.com, [2]slim.rekhis@gmail.com, [3]nab@supcom.rnu.tn

***Abstract*—The dynamics of the wireless links represent serious problems in guaranteeing quality of services (QoS). Combined with mobility, additional problems, arise like handoff delays and resource management, arise. In this work, we consider an interworking architecture composed of IEEE 802.11 and IEEE 802.16 access networks. We define a new set of Hybrid Units in charge of QoS management and handoff decisions, allowing to map quality of service classes, reduce the handoff blocking probability, and guarantee a fair distribution of users among the different access networks if they cover the same network area. The simulation results validate the efficiency of our approach.**

***Index Terms*—Hybrid Unit, QoS, vertical Handoff, IEEE 802.11, IEEE 802.16.**

I. Introduction

With the rapid development of wireless communication networks, integrating various radio access technologies, including, but are not limited to, cellular networks (e.g., GSM, GPRS, UMTS), and wireless IEEE 802.11 and 802.16 networks, into a universal access platform, known as fourth generation (4G) mobile communication system, has became an essential requirement. It is expected that the latter system will support seamless roaming across the multiple supported access networks to provide a continuous end-to-end data service.

Enforcing and managing Quality of Service (QoS) in 4G networks is a very challenging task [5], especially due to: a) the heterogeneity of the QoS models in the integrated access networks in terms of management mechanisms and resource reservation, and QoS definition and provision; b) the variety of supported services which include common known Internet services, traditional voice services, and real time applications; and the c) the non-uniform nature of service interfaces

In [2], a QoS Abstraction Layer (QoSAL) has been proposed, which is located between layers 2 (link) and 3 (network). The proposed QoSAL is characterized by the flexibility and modularity of QoS model that it defines. It provides an abstracted QoS service interface supporting the common aspects of some wireless technologies and puts up an efficient protocol allowing the reservation of QoS in remote APs on one hand and the handover preparation and execution on the other hand. The authors of [3] propose a Vertical Handoff Translation Center (VHTC) Architecture composed of WiFi wireless networks and WiMAX mobile communication systems to improve the transmission of QoS guarantees. The paper introduces new modules such as Packet Translation Module (PTM) which copes with packets format translation, QoS Mapping Module (QoSMM) which is responsible of classifying the data connections according to the new proposed mapping structures, and an Efficient Bandwidth Borrowing Management module (EBBM) which manages the bandwidth based on the classes of priority. Nevertheless, [3] is not totally suitable for wireless 4G networks and it does not address cooperation between the different access networks to perform an efficient QoS provision. In [1], an interworking architecture between WiMAX and WiFi technologies is proposed, which introduces a new entity, called WiMAX/WiFi Access Point (W²-AP). Within this architecture, the WiMAX Base Station (BS) manages many Subscriber Stations (SS) and multiple W²-APs located at its coverage area. A new MAC layer module is proposed that uses three components which are the W²-AP, the WiFi node and the WiMAX BS. While the proposed architecture does not require the implementation of separate QoS mapping mechanisms and guarantees continuity of QoS and consistency of bandwidth management throughout the network, the architecture is not easily extensible to address new types of access networks. Therefore, it cannot cope well with the properties of wireless 4G networks.

In this paper, we propose an interworking architecture composed of IEEE 802.11 and IEEE 802.16 networks that overlap with one another. Within this architecture a node, called Hybrid Unit (HU), is assigned to each access network. The latter can be a standalone equipment, or simply integrated to the base stations. The Hybrid Units are in charge of mapping QoS classes and parameters used by users when they hand over from an access network to another. Additionally, they are connected through the backbone network and cooperate, together by exchanging information regarding their load, pre-registered users, occupation of traffic management queues that are related to different QoS classes, and profiles of connected users. The aim is to reduce the rate of rejected handover requests, by allowing users to pre-register with the less overloaded network (with respect to the requested QoS class), and triggering handoffs when the network resources start to be overloaded so that users can be connected to another access network (which serves the same area from which the user is connected) without degrading the quality of service. In this paper, we define a set of functions to select the user to handoff in the case of QoS class overload, and estimate the percentage of resources to be reserved for handoff requests.

Three main contributions are depicted by this work. First, the proposed architecture and mechanisms can be easily ex-

tended to cope with other types of access networks, or support additional functionality such as security. Second, the proposed approach provides an optimal use of resources since users may get a higher QoS when a handover cannot be served using the QoS class they requested at the beginning. Third, the approach improves vertical handoff and reduces its delay. The simulation analysis shows that our approach reduces the handoff blocking rate by 20% with respect to a non-cooperative approach.

The remainder of this paper is organized as follows. The next section describes the different requirements for an efficient QoS management in an IEEE 802.11 and 802.16 based 4G network. Section III describes the proposed architecture. In Section IV the set of mechanisms to be executed by the hybrid units to manage the quality of service, are described. Section V describes the simulation scenarios and results. The last section concludes the work.

II. Requirements for an efficient management of QoS in 4G networks

In the following we describe a set of requirements that should be fulfilled by a 4G network in order to guarantee an efficient management of QoS.

a) Pre-registration: In 4G networks, since mobile devices may be equipped with a Network Interface Card (NIC) for each supported access network, the use of pre-registration scheme will be very advantageous. It allows the mobile device (MD) to manage many simultaneous connections at the same time (one active connection with the serving network and one or a set of inactive connections with other visible access networks), improves handoff latency, and helps providing an efficient handoff scheme with less energy consumption. Additionally, it helps selecting users to hand off in order to guarantee a fair distribution of users among the network. As some networks such as 802.16 support sleep mode procedure [4], such feature should be used, whenever possible, to let the mobile users perform pre-registration and move their network interface to the sleeping mode and reduce energy consumption.

b) Cooperation between hybrid units: Guaranteeing the quality of service in wireless 4G architecture is very challenging due to the heterogeneity of the QoS models and the parameters used by each access technology. A cooperative architecture with uses a set of nodes serving as bridges between the different access networks should be developed. These bridges need to cooperate together in order to enforce:

- A better management of the resources related to the supported QoS classes by asking retrieving from neighboring networks information regarding connected user profiles (e.g., requested QoS) and the occupation rate of their resources.
- A better resource provisioning by exploiting historical information regarding users in the network. These information include user mobility and the networks they pre-registered with.
- A reliable security service which addresses heterogeneity of the security schemes in terms of mechanisms of key distribution and supported protocols.

c) QoS mapping: Each access technology involved in the 4G network defines its own QoS model and parameters. For example, in IEEE 802.16 network five sorts of WiMAX QoS flow classes are defined while in IEEE 802.11 network eight types of QoS are supported. Therefore, a QoS mapping scheme should be defined allowing the translation of flow classes from one access network to another. Such a mapping should be performed transparently to users without affecting the handover delays.

d) QoS provision: In some situations where the network may be unable to offer to a user the QoS class it requested, the network may try map the connection of that user to a QoS class higher that the one it requested. This is done for the sake of guaranteeing the highest rate of user satisfaction. In this context, it would be interesting that the cooperating bridges, which belong to the different access networks, trigger handoffs to move some of their currently connected users to the access networks that cover the same (or part of the) area. The aim is to release resources and become able to accept handoff requests. A technique should be proposed to select the user (among the ones connected to current serving network) to handoff to another access network. Parameters such as the energy level of the user battery, and the expected staying period within the current network, would be interesting to use during decision.

e) User profile: With the aim to provide an efficient QoS in spite of nodes' mobility, the 4G networks must keep track of information regarding the status of connected mobile devices (e.g., remaining battery energy, user's service class, pre-registered networks). The collected parameters should be stored in a dedicated profile and transferred to the destination network whenever the user roams, enabling the 4G system to efficiently manage handover resources, and efficiently selecting the users to handoff from an access network without exhausting their battery energy.

f) Exploitation of the overlap: In wireless 4G networks different access networks can overlap with one another, sometimes allowing users to choose between different access technologies at the same location within the network. Typically, as user requests would be distributed over the different access networks that cover the same area, the wider is the overlapping area, the less will be the quantity of resources reserved for handover by these access networks. To efficiently manage the quality of service, network bridges should exploit the overlapping feature to optimize the quantity of resources reserved for handover and the number of users affected to each QoS class.

III. Architecture of the proposed network

In our proposed architecture, we consider an hybrid interworking approach composed of IEEE 802.11 and IEEE 802.16 networks that overlap with one another. Four main components are composing the latter architecture, namely radio access devices (WiMAX Base station, WIFI Access points), mobile nodes (MN) and hybrid units (HU) as illustrated in Figure1.

The hybrid unit is a node that may be a standalone equipment or integrated to a radio access element [6]. We assume that the latter entity will be responsible for managing the

quality of service of each access technology including the translation and mapping of QoS from WiFi or WiMAX QoS scheme to the proposed service classes and vice versa, the management of the latter QoS classes, and the provision and estimation of resources dedicated to handoffs. The Hybrid Unit is also in charge of performing a QoS based selection of user to handover and the determination of the less overloaded destination network.

We assume that all the access networks operate in infrastructure mode and each access technology is served by a unique dedicated HU. All of these HUs are interconnected together through an IP backbone. To be able to connect to any wireless technology (Wifi or MiMAX), each MN is equipped with a WiFi network interface and a WiMAX network interface. A user in the network can only manage one active connection which he uses to send and receive data. He can also pre-register with another access network of different technology using the second available network interface. The latter interface can then be switched to the sleep mode (in case of WiMAX network) or refreshed periodically in order to save energy while keeping an available connection with the pre-registered network. speak about maintaining connection in sleep mode(2)).

During the first admission of a given user in the architecture, a user profile will be created by the current serving hybrid unit. The data constituting the profile as well as rules used to update it will be detailed in the next section.

As users are mobile, handovers may occur. In our approach we mainly focus on vertical handover and highlight the cooperation between the hybrid units. The handoffs taken between two access points / base stations of the same network overlay will be transparent to the hybrid units.

The architecture brings out cooperative hybrid units allowing the support of new features such as:

- QoS mapping and management of new proposed service classes;
- QoS provision and estimation of resources dedicated to handoffs;
- Seamless handoff decisions based on historical connection and mobility of users

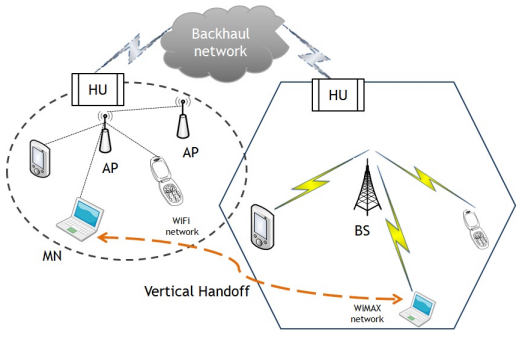


Figure 1. Proposed architecture

IV. QoS BASED FUNCTIONS EXECUTED BY HYBRID UNITS

Various features are added to each HU involved in the proposed architecture, providing an efficient QoS management.

A. QoS mapping

As in our approach, we are interested by a WiFi-WiMAX interworking architecture, a QoS mapping scheme between the two standards should be defined. To do so, we use the scheme defined in [3], where Eight QoS flow classes in Wifi based on the priority (four user priorities) are mapped to four WiMAX QoS flow classes as described in Table I.

WiFi (802.11e)	Proposed QoS classes	WiMAX (802.16)
VO (Voice; qo)	CBR	UGS (q0)
VI (Video; q1)	rtVBR	rtPS(q1)
BK (Background; q2)	nrtVBR	nrtPS(q2)
BE (Best Effort; q3)	MGBE	BE (q3)

Table I
PROPOSED QOS STRUCTURES

It should be noted that such a mapping does not consider the new class defined by the standard [7] called Extensible Real-Time Polling service (ErtPS). The latter service class is a scheduling service mechanism which is built on the efficiency of both UGS and rtPS. Consequently, the ErtPS scheduling service can be mapped to both CBR or rtVBR proposed structures, however, the first goal of designing ErtPS is the support of real-time service flows, that is why a possible alternative is to match the latter class of service with the rtVBR structure based on the fact that the main characteristic of the rtVBR structure is the dynamic allocation of resources.

Once defined, the HU will be able to translate the five sorts of WiMAX QoS flow classes and the eight priority classes of 802.11 QoS types according to the new proposed structures. Once the mapping to the new service class is performed, the HU subsequently handles the management of the latter classes. In fact, for each service class we provide a priority queue Q, which is used by a bandwidth management module. According to its requested or offered service class, each user traffic will be placed in a corresponding queue. Each queue can serve a defined number of users; we denote by $Capacity\,(Q)$ the function which returns the number of users whose traffic can be placed in the queue Q. We also denote by $OccRate\,(Q)$ the function returning the number of users whose traffic are currently placed in the queue Q. As we are proposing an architecture aimed to provide a seamless mobility, we allocate resources dedicated for handoffs in each access network per service class. $S_{Handoff}\,(Q)$ will denote the function which returns the maximal number of roaming users whose traffic can be served by the queue Q.

B. Collecting user profile

Each time a new user connects to an access network within its range, a user profile is created by the hybrid unit. This profile will contain two types of data:

The first type represents data to be directly retrieved from the user and updated periodically whenever it is attached to the current network. We distinguish three different parameters:

- The remaining energy in the battery of the mobile node: as the MN informs periodically its serving HU of its battery's level, the HU brings the user's profile up to date by inserting the available energy of the MN's battery.

- The Received Signal Strength (RSS) of the detected networks using the other inactive network interface. Whenever the MN detects new access networks within its range, it notifies its serving HU. In this context, the hybrid unit can decide which network the MN should pre-register with.
- The class of service (CS). Each user expresses his QoS preferences in terms of desired service class, in some cases, the network is unable to offer resources in the requested CS, so to satisfy the user request, the network may try map the connection of that user to a QoS class higher that the one it requested. As a consequence, the network must always know the desired CS and the provisioned CS for each user on the network in order to optimize the allocation of resources and offer users the best CS that meets their preferences.

The second type represents data generated by the network, and updated and forwarded to the next serving access network, once the user hands over. It essentially provides an idea on the user mobility in the network. In fact, the profile contains a value of the historical mobility of the user through the previous visited networks. Whenever the user hands over from one access technology to another, the old HU determines the visiting duration of the user in the last network. It updates the mean duration value (called historical mobility value), while assigning a high coefficient to the latter computed value. The aim is to make the mean value accurate and close the actual duration time

This profile has many advantages as its helps hybrid units to, later, deciding: when to execute handoffs, which user should be handed off, and to which network the user will be handed off or will pre-register with.

C. Pre-registering users

Before pre-registering with another access network of different technology, the mobile node informs its current serving HU about the access networks it detects on the second network interface, and the level of the computed RSS. After receiving the list of detected networks, the HU selects the network which has the least filled queue related to the class of service required by the mobile device.

Using its other network interface, the MD performs the network entry procedure and then enters to the sleep mode. When a handover procedure should be executed, the MS can easily switch to the new network (it as pre-registered with) by merely bringing back the second interface from sleep mode to awake mode. As users are mobile, a periodic refresh of the sleep process is executed to ensure seamless mobility and better use of the available resources in each visited network. Figure 2 illustrates such a scenario.

Unfortunately, the sleep mode operation is only defined in WiMAX, so when the MN is attached to a WLAN network, it can pre-register with a WiMAX network situated in the same coverage area and then enter the sleep mode. However, when the MN is connected to a WiMAX network, and after detecting a WLAN network within its range, the MD can perform the network entry procedure to the latter WLAN and cease to

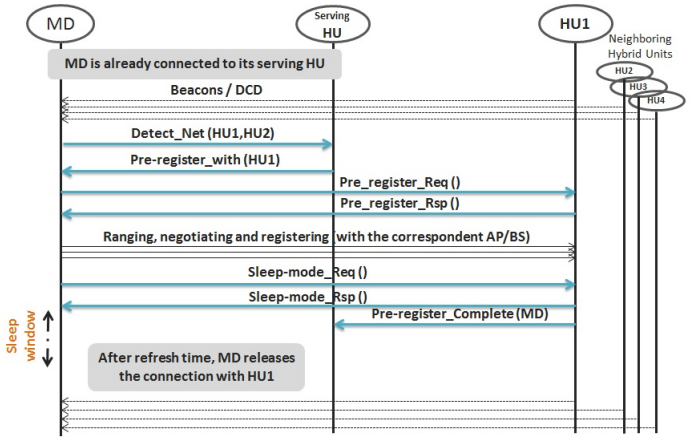


Figure 2. Pre-registration Scenario

communicate with it for some period. After the end of each period, a refresh is required to maintain communication with the access point and test whether the WLAN is still reachable.

The use of this procedure effectively improves and reduces the handoffs delays [4] and offers to the HU the opportunity to handover some pre-registered users in order to release resources and become ready to accept new handoff requests.

D. Management of proposed service structures

As described previously, the network may try map the connection of a given user to a QoS class higher than the one it requested when it is unable to offer him the QoS class it requested. Consequently, a mechanism for reallocation of users in the service classes is required to optimize QoS provision for each service class in the coming moments.

In this context, the HUs, belonging to overlapping 802.11 and 802.16 networks, may trigger handoffs to move some of their currently connected users from one access network to another in order to release resources and satisfy as more as possible handoff requests.

In order to decide which user (among the ones connected to current serving network) the HU should hand over to the network it is already pre-registered with, we identify the following parameters:

- Percentage of the battery level of $user_i$ returned by function $Bl(user_i)$;
- Received Signal Strength (RSS) of the network the user $user_i$ has preregistered with. Such value is returned by function $RSS_{Pre-register-Net}(user_i)$;
- Occupation rate of the priority queue related to the requested QoS class in the network that user $user_i$ has pre-registered with. This value is returned by function by $OccRate(Q(CS_{Pre-register-Net}(user_i)))$;
- Historical mobility (i.e., mean value of the user staying time within an access network) related to $user_i$, which is returned by function $Mob(user_i)$.

The determination of what user the HU should handoff to the pre-registered network is analyzed based on a computed static score S. The S can be defined as follows:

$S(user_i) = (w1 \times Bl(user_i) + (w2 \times 1/(OccRate(Q(CS_{Pre-register-Net}(user_i)))) + (w3 \times RSS_{Pre-register-Net}(user_i)) + (w4 \times 1/(Mob(user_i)))$

where $w1, w2, w3, w4$ are weights for each metric, which range from 0 to 1, such that their sum must be equal to 1. The values of these metrics are defined based on experimentation tests

We suppose that $OccRate(Q)$ will never return a null value and nodes are not stationary during their all their staying time in the network (i.e., $Mob(user)$ is different from zero). A candidate user, which has the highest score S, will be selected as the best user that the HU should hand over.

E. Estimating resources to be allocated to handoffs

In order to reduce the vertical handoff blocking rate between different access networks, our approach consists in using a dynamic scheme to let each HU reserve resources, per service class, for handing over users coming from neighboring networks. These resources can be traduced by entries in the priority queue related to the service class. We denote by $S_{Handoff}(Q(_{k_i}))$ the maximal number of roaming users whose traffic can be served by the queue Q_k (k is the QoS class) managed by the hybrid unit i. There are several factors that influence the estimation of the space dedicated to handoffs. We distinguish the following parameters:

- Percentage of highly mobile users (Highly mobile users are obtained by comparing their historical mobility value with a pre-defined threshold) in the current queue k which belong to the hybrid unit i. This value is obtained as follows: $P_{HighMobUsers}(Q_{k_i}) = (Number_{HighMobUsers}(Q_{k_i}))/(Number_{Users}(HU_i))$;
- Occupation rate of the corresponding queue k in the hybrid unit i. This value is denoted by $OccRate(Q_{k_i})$;
- Mean occupation rate in neighboring hybrid units denoted by $MeanOccRate_{NeighborNet}(Q_{k_i}) = \sum_{k \le p \le 4; 1 \le j \le N} OccRate(Q_{p_j})/((4-k+1) \times N)$ where k is the index of the QoS class and N is the number of the neighbor access networks;
- Overlapping factor representing the rate of the current access network area that is covered by other neighboring access networks. This value is given by $Overlap\,(i, N) = \sum_{1 \le j \le N; i \ne j} intersect(HU_i, HU_j)/Cov_{area}(HU_i)$ where $intersect(,)$ is a function that returns the common coverage areas of an access network and its neighboring N networks and $Cov_{area}()$ is a function that returns the coverage area of a given network.

Initially, we assume that each HU makes provision of resources dedicated to handoffs as follows:

$$S_{Handoff}(Q_{k_i}) = Capacity(Q_{k_i}) \times T_{IR} \quad (1)$$

whereT_{IR} is an Initial Reservation threshold.

After that, periodically, each HU exchanges the discussed parameters with its neighbors to update resources provision using the following equation

$S_{Handoff}(Q_{k_i}) = Capacity(Q_{k_i}) \times ((w1 \times P_{HighMobUsers}(Q_{k_i})) + (w2 \times MeanOccRate_{NeighborNet}(Q_{k_i})) + (w3 \times OccRate(Q_{k_i})) + (w4 \times 1/(Overlap(i, N))))$

where $w1, w2, w3, w4$ are weights for each metric, which range from 0 to 1, such that their sum must be equal to 1. The values of these metrics are defined based on experimentation tests.

V. Simulation

This section describes the simulation scenarios and results.

A. Simulation configuration

We conducted a software-based simulation to evaluate the effectiveness of our approach within an overlay area that integrates WiFi and WiMAX networks. Every access network is managed by an hybrid unit attached to the corresponding Access Point / Base Station. The mobile users are uniformly distributed over the covered network area. They move from a time slot to another by generating a random speed value that is uniformly distributed over the interval [0, 50] m/s, and random direction that is informally distributed over the interval [0, 360°]. To prevent nodes from leaving the simulation area, a border rule is defined. It consists in bouncing back the leaving node to the system area.

We choose to test the behavior of the HUs through 100 time slots (TS). The network attachment and the handover were chosen to take 1 TS and 3 TS, respectively. We assume that the maximum number of users that can be optimally served by all hybrid units is equal to 320.

We evaluate the performance of the networking model in terms of Satisfied Request Rate (SRR) and Handoff Blocking Rate (HBR). SRR and HBR are defined by the two following equations:

$$SRR = \frac{number\,of\,satisfied\,requests}{number\,of\,requests}$$

$$HBR = \frac{nb\,of\,dropped\,handoff\,requests}{total\,of\,handoff\,requests}$$

We considered two scenarios in this simulation. The scenario does not involve cooperation between HUs. In fact, each mobile node, which receives many signals from the different networks deployed within the network, will select the strongest RSS for each technology (RSS_{WiFi} and RSS_{WiMAX}). Therefore when a HU is unable to offer to a given user the QoS class he requested, the handoff request will be dropped. In the second scenario, the HUs cooperate together by exchanging the discussed parameters and triggering handoffs to move users to access networks that cover the same area (while maintaining the requested QoS or mapping the user traffic to a higher priority queue) in order to release resources and reduce the HBR value.

B. Simulation results

Figure 3 shows the variation of the satisfied requests rate in terms of the number of users. As the number of mobile nodes increases, the satisfaction rate increases proportionately. In the first scenario the rate of unsatisfied requests starts to

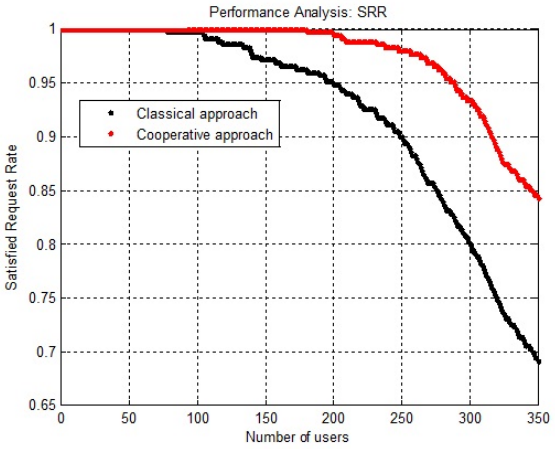


Figure 3. Satisfied requests rate

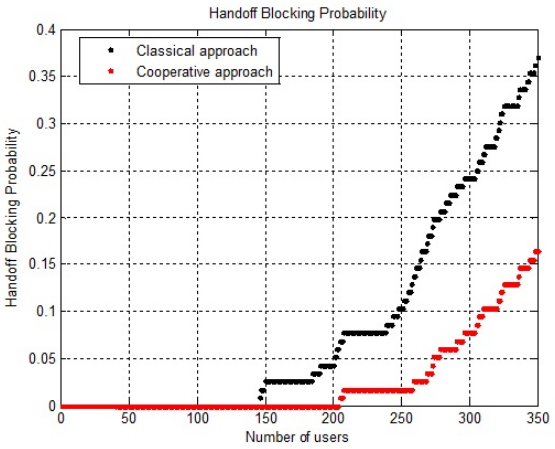


Figure 4. Handoff blocking probability

decrease (once the number of nodes reaches 75) quickly than the cooperative architecture (once the number of nodes approximately reaches 200 users). In addition, the SRR decreases more slowly when involving the cooperation between the HUs. It can be deduced from the Figure that cooperative approach allows an enhancement of 15% of the SRR value.

These enhancements can be explained by the fact that the cooperative approach supports new mechanisms for QoS management. In fact, even if the network cannot satisfy the user handoff requests for the QoS class newly requested (the case of a new connected user) or already granted (the case of a user that hands over), the hybrid unit will try to offer him a higher class of service. Moreover, the cooperative approach can hand over users to the networks they pre-register with if the latter are less overloaded and able to offer the same, or a better, quality of service. Consequently, resources are released and the quality service is slowly degraded.

Figure 4 shows the handoff blocking rate in terms of the number of nodes moving on the network. Whenever the number of users increases, new handoff requests are increasingly rejected. Contrary to the first scenario where a handoff blocking appears if the number of users reaches 150, in the second scenario, the handoff blocking is observed after the satisfaction of more than 200 requests. Moreover, we note that the handoff blocking rate increases more quickly in the second scenario (after rejecting 15% of users that can be served by all the HUs of the simulated architecture).

This handoff improvement is due to the fact that the hybrid units may trigger handoffs of specific users which are pre-registered with other networks. Therefore, each HU may become able to accept additional handoff requests. In addition, the hybrid units fairly re-distribute users among the available access technologies. Another feature that improves the handoff is the allocation of dedicated resources for handoffs. This allocation is estimated based on available resources on neighboring networks, mobility of users across the access wireless technologies, and the overlapping rate between these networks.

VI. Conclusion

In this paper, we have presented a cooperative architecture for QoS management in 4G networks that integrates 802.11 and 802.16 access technology. A set of hybrid units connected to every access network were proposed to be in charge of QoS mapping and management of QoS classes. As access networks may overlap, users are allowed to pre-register with another access network of different technology which is available within the same area. A cooperative technique was proposed to let hybrid units manage these QoS classes, and trigger vertical handoffs, so that users are fairly distributed among the access networks that cover the same area in the network. The aim is to release resources in the access networks, reduce the number of rejected handoff requests, and provide efficient QoS provision.

Simulation results showed that the new proposed QoS management scheme enhances the satisfied new connection and handoff requests rate by 15% and reduces the handoff blocking rate with 20% with respect to the classical approach (i.e., no cooperative hybrid units).

References

[1] Gustavo Carneiro, Carlos García, Pedro Neves, Zhikui Chen, Michelle Wetterwald, Manuel Ricardo, Pablo Serrano, Susana Sargento, and Albert Banchs. The daidalos architecture for qos over heterogeneous wireless networks. In *IST Mobile & Wireless Communications Summit*, June 2005.

[2] Gustavo J. A. M. Carneiro. *QoS Abstraction Layer in 4G Access Networks*. PhD thesis, FACULDADE DE ENGENHARIA DA UNIVERSIDADE DO PORTO, 2005.

[3] Yu-Chang Chen, Ja-Hsing Hsia, and Yi-Ju Liao. Advanced seamless vertical handoff architecture for wimax and wifi heterogeneous networks with qos guarantees. *Computer Communications*, 32(2):281–293, 2009.

[4] Kyeyoon Jang, Bongjhin Shin, and Daehyoung Hong. Fast vertical handover utilizing sleep mode in wlan and wimax heterogeneous networks. In *Proceedings of 14th Asia-Pacific Conference on Communications (APCC 2008)*, Tokyo, 14-16 October 2008.

[5] Xiaohuan Yan, Y. Ahmet Sekercioglu, and Sathya Narayanan. A survey of vertical handover decision algorithms in fourth generation heterogeneous wireless networks. *Computer Networks*, 54(11):1848–1863, August 2010.

[6] Faouzi Zarai. *Quality of Service and Security in Wireless Fourth Generation Networks*. PhD thesis, Communication School of Engineering. University of 7th of November at Carthage, Tunisia, February 2007.

[7] Yongqiang Zhang, Weihua Zhuang, and Aladdin Saleh. Vertical handoff between 802.11 and 802.16 wireless access networks. In *Proceedings of IEEE Global Telecommunications Conference*, 2008.

SL2R-HT and SL2R- LH: Securing Layer-2 Routing Protocol for WMN

Divya Bansal
Asst. Professor, CSE, PEC University of Technology
Chandigarh, India
divya@pec.ac.in

Sanjeev Sofat
Professor, CSE, PEC University of Technology
Chandigarh, India
sanjeevsofat@pec.ac.in

Prafulla Kumar
Director, Department of Information Technology
Ministry of Communication & Technology. New Delhi, India.

Abstract— **Earlier research efforts mainly focused on securing adhoc routing mechanisms. However, recently there has also been growing research interest in studying the security of the medium access control (MAC) and its impact on network performance. The impact will be even more severe in case of multi hop wireless networks. IEEE 802.11s being a multihop technology also derives similar security concerns. It also hence needs to ensure correct route establishment mechanisms, protection of routing information, and security of packet forwarding. In this paper two new schemes have been proposed to protect the IEEE 802.11s (draft) routing protocol: HWMP which is currently defined as the default protocol. The proposed schemes have been implemented in a simulation environment and the results have been compared with the existing protocol.**

Keywords-HWMP; Hashing; IEEE 802.11s; Routing;

I. INTRODUCTION

Unlike WLAN, mesh networks are self-configuring systems where each Mesh Point (MP) can relay messages on behalf of others, thus increasing the communication range and available bandwidth. In WLAN, the wireless AP has to be wired to the infrastructure, whereas in WMNs MPs can be connected to the rest of the network by wireless radio links only. WMNs are easy to install, require no cable cost, connections amongst nodes are automatic, offer network flexibility, discovery of newly added nodes, redundancy, and self healing reliability. WMNs are important for distributed applications that cannot rely on a fixed infrastructure, but require instant deployment, dynamism, self-configuration and self-organization. IEEE 802.11s (TG since May 2004) is a draft IEEE 802.11 amendment for mesh networking, defining how wireless devices can interconnect to create a mesh network. IETF did set a mesh networking TG to standardize IEEE 802.11s and the work is still in progress. Even though the standard is not final yet, the main traits of the standard have been already set which includes IEEE 802.11s architecture and routing using MAC addresses. The IEEE 802.11s TG did set HWMP (Hybrid Wireless Mesh Protocol) as a default routing protocol to be present in all 802.11s compliant devices. Besides, airtime has been set a default link quality metric to accompany HWMP. The standard is now planned to be released in January 2011. Although several standard drafts have been released by 802.11s, many issues still remain unsolved. The conventional WLAN security mechanisms such as WPA2/802.11i are still used as the standardized methods for authentication, access control and encryption between a wireless client and an access point. Since most wireless mesh solutions attempt to retain compatibility with commercial off-the-shelf WLAN client adapters, existing standardized WPA2 mechanisms are commonly retained making IEEE 802.11s inheriting its security framework from 802.11i with certain extensions. Due to the multihop mesh network architecture, security becomes even more challenging as the mesh points have to rely upon each other to make the traffic reach the ultimate destinations through several hops. Due to the architecture and the characteristics of WMN, attacks and consequences become even obvious. WMNs are extremely vulnerable to attacks due to their dynamically changing topology, absence of conventional security infrastructures and open medium of communication, which, unlike their wired counterparts, cannot be secured [9, 10]. In this paper, schemes to enhance security of mandatory routing protocol that facilitates prevention of authentication and integrity related external attacks have been proposed. Section II of the paper discusses the related work while section III describes the primitives of HWMP which is the default routing protocol of IEEE 802.11s (draft). Section IV analyzes the current security vulnerabilities of the protocol. In section V, the design of the two proposed schemes has been described. Section VI discusses the results so obtained after simulating the proposed schemes and also compares the two schemes with the existing protocol in terms of design parameters, security and performance. Finally Section VII concludes the paper.

II. RELATED WORK

Current research in the area of security and management in WMN is still in early stages. Several authors have investigated the performance related issues in upcoming IEEE 802.11s standard [8, 11, 12]. Most of the security solutions to the routing protocols have been derived from adhoc networks with little or no modifications [13]. In [14]

the author has introduced wormhole attack which can severely affect the performance of wireless multihop networks. The solution using Packet leashes which employ the use of hash chains and merkle tree has been proposed. In [15] author has identified security issues in WMN where DoS attacks due to vulnerabilities in routing protocols have been investigated. In the paper the authors have described various routing attacks affecting the performance of WMN which include Route Discovery, Route Maintenance and Data Forwarding. In [16] the authors have proposed the use of AODV protocol for routing in WMN with security extensions. The security has been enhanced using symmetric key cryptography with the use of Bloom's key pre distribution method. However the assumption that a central infrastructure is not available in WMN is invalid thus eliminating the need of proposed key distribution method. In [17] author has proposed a scheme which enhances the security of the HWMP routing protocol. However the approach described in [17] is still prone to replay attacks. Our approach also takes inspiration from the work described in [17] with some modifications to further improve the security of HWMP protocol. Our proposed approach is resistant to all type of attacks currently existing in the literature and does not cause extra overhead as it still uses the existing key hierarchy.

III. HYBRID WIRELESS MESH NETWORK PROTOCOL[1]

The Hybrid Wireless Mesh Protocol (HWMP) is a mesh routing protocol that combines the flexibility of on-demand routing with proactive topology tree extensions. The combination of reactive and proactive elements of HWMP enables optimal and efficient path selection in a wide variety of mesh networks (with or without infrastructure). HWMP uses a common set of protocol primitives, generation and processing rules taken from Ad Hoc On Demand (AODV) routing protocol adapted for Layer-2 address-based routing and link metric awareness. AODV forms the basis for finding on-demand routes within a mesh network while additional primitives are used to proactively set up a distance-vector tree rooted at a single root MP. The root role that enables building of topology tree is a configurable option of an MP. HWMP also supports two modes of operation depending on the configuration. These modes are:

- On demand mode: this mode allows MPs to communicate using peer-to-peer routes. The mode is used in situations where there is no root configured. It is also used in certain circumstances if there is a root configured.
- Proactive tree building mode: this can be performed by using either the RREQ or RANN mechanism.

These modes are not exclusive: on demand and proactive modes may be used concurrently. All HWMP modes of operation utilize common processing rules and primitives. HWMP control messages are the Route Request (RREQ), Route Reply (RREP), Route Error (RERR) and Root Announcement (RANN). The metric cost of the links determines which routes HWMP builds. In order to propagate the metric information between MPs, a *metric* field is used in the RREQ, RREP and RANN messages.

Routing in HWMP uses a sequence number mechanism to maintain loop-free connectivity at all times. Each MP maintains its own sequence number, which is propagated to other MPs in the HWMP control messages.

IV. SECURITY VULNERABILITIES IN HWMP

As per the current specification of HWMP protocol, the existing HWMP routing mechanism relies on the fact that all participating mesh entities cooperate with each other without disrupting the operation of the protocol. Without proper protection, the routing mechanism is susceptible to various kinds of attacks which are described as follows:

Flooding: Any malicious node which is not present in the network can broadcast the PREQ message to the destination. Hence all the nodes keep on forwarding the PREQ message resulting in poor network performance.

Route Disruption: This attack can be launched by a malicious node by modifying the mutable field values. In case a malicious node is present between two victim nodes, it may not allow creating path between them. As an example an attacker node can modify a metric field to zero while passing PREQ to other legitimate node forcing the destination node sending the PREP to pass it through attacker node. The attacker node can now drop the PREP message making the route discovery process to fail completely.

Route Diversion: A malicious node can launch a route diversion attack by modifying mutable fields in the routing information elements such as hop count, sequence number and metric field. A malicious node can divert traffic to itself by advertising a route to a destination with a Destination Sequence Number (DSN) greater than the one it received from the destination.

Routing Loop: A malicious node can create routing loops in a mesh network by spoofing MAC addresses and modifying the value of the metric field.

Current draft P802.11s/3.0, March 2009 does not provide any security measures for securing the HWMP control messages i.e. PREQ, PREP and RANN. The attacks described above are possible in HWMP because the malicious intermediate nodes might get the chance to alter the packet information and resend that packet into the network. It is the mutable fields that can be altered by the intermediate node. So as to provide security in HWMP, the mutable fields of the control packets need to be protected. In case the mutable fields of control messages- PREQ, PREP and RANN are secured using cryptographic techniques, the cost will be very high causing huge overhead to the network as in that case each packet will have to be encrypted and decrypted at each intermediate hop. The information elements in the HWMP contain fields that can be modified in the intermediate routers which we termed as mutable and those that cannot be modified termed as non-mutable fields. Some of the mutable fields are: Hop count field, TTL field, Metric field, Per destination flag.

V. SECURING HWMP

In order to secure the HWMP protocol, following is proposed:

- Protection of Non Mutable fields:

Non-mutable fields which need not be modified at the intermediate hops can be provided end-to-end security by applying any symmetric key encryption technique. Preferably we propose to use the existing key hierarchy i.e. GTK/PTK for protecting the non-mutable fields. The current draft proposes use of GTK/PTK for data frame protection. Hence without causing any additional burden, the same key hierarchy can be used to protect the non mutable fields from source to the destination.

- Protection of Mutable fields:

  Two different approaches have been proposed to protect the mutable fields in the current work. They are:

1. Tree based Hash Approach
2. Linear Hash Approach

In this proposed scheme, the mutable fields of the control messages are protected for authentication and integrity using tree based hash approach. The existing mutable and non-mutable fields are protected to design a secure layer-2 routing. In order to do so, the following has been done:

A. Use the existing key distribution of IEEE 802.11s
B. Symmetric key encryption is used to protect non-mutable fields using existing key hierarchy as they need to be decrypted at the final destination only.
C. Demonstrate that the mutable fields can be authenticated at every hop using the concept of hashed tree.

The two approaches are described below:

A. Secure Layer -2 Routing using Hash Tree (sl2r-ht)

Merkle Tree [2] approach has been used to formulate the hashed tree. It is a useful technique which can be used to build secure authentication and signature schemes from hash functions. [3]. The approach has also been successfully applied to secure routing in Wireless Sensor Networks (WSN). The µTESLA routing protocol is a popular protocol used for routing information in WSN. The Merkle tree hash is used to distribute and authenticate the parameters used in µTESLA. The method has been found to be efficient as it removes the authentication delay which is otherwise prevalent in many other known schemes. Deriving the similar concerns of introducing extra burden of keying and delays, the same approach has also been applied to protect the information elements of HWMP. A Merkle tree [4-6] is a complete binary-tree that has equipped with a function hash and an assignment function F such that for any interior node n parent and two child node n left and n right, the function F satisfies:

F(n parent) = hash(F(n left) & F(n right)).

Let the mutable fields of routing information elements that need to be authenticated are Y_1, Y_2,……Y_8. We hash each value Y_i into u_i with a one-way hash function HAMC using GTK and PTK for broadcast and unicast message respectively. Such as $K_i = h(Y_i)$. Then we assign the hash values to the leaves of the binary tree. To each internal vertex K of this tree, a value is assigned which is computed as the hash of the values assigned to the two children of K such as $K_{12} = h(K_1 \| K_2)$.

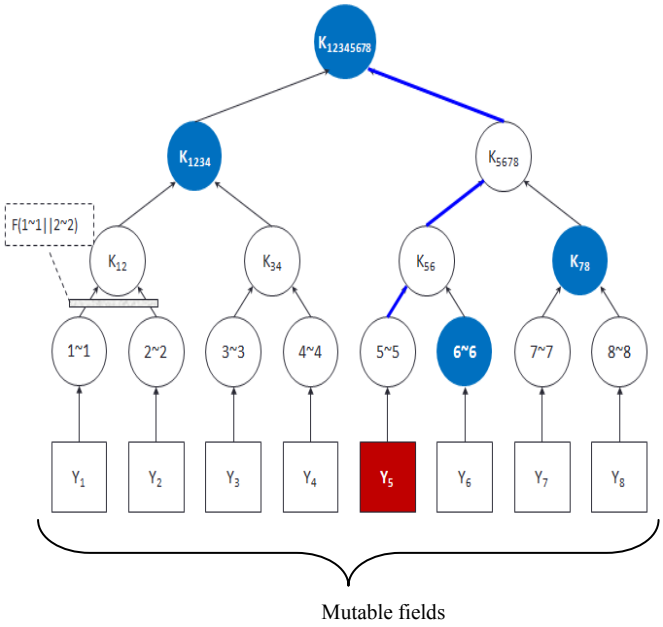


Figure 1: Formation of hash tree

Finally, the value of the root $K_{12345678}$ is computed which can be used for authentication purposes. The sender can reveal a value Y_i that needs to be authenticated along with the values assigned to the siblings of the vertices along the path from Y_i to root that is denoted as certification trail in the proposed scheme: cert-trail(Y_i). Sender sends these values to the receiver as an extra overhead. To authenticate the information received from the previous hop in the network, the receiver can hash the values of the certification trail in appropriate order to compute the root and create a MAC on the root using the derived key. It can then compare the values of the two MACs, if these two values are found to be the same, then the receiver can be assured that the value Y_i is authentic. Otherwise it is believed that the sender is not authenticated to network and mutable fields have been illegitimately modified by the malicious node. The receiver may now drop the entire forged frame received from the malicious sender. This makes the network secured from the external attacks launched by the malicious nodes. Fig.1 denotes a Merkle tree with 8 leaves and 8 leaf pre-images (Y_1, Y_2,……Y_8). Each leaf node is a hash of its corresponding pre-image and each internal node is the hash of the concatenation of two child values. Y_5 is the value of the pre-image needs to be verified and the root of the tree is known to be public. Value of Y_5 is verified if both the publicly known root ($K_{12345678}$) and computed roots are

same. The hash function used is a candidate one-way function such as SHA-1 [7].

The proposed scheme is explained with the following example. Consider a wireless mesh network where the route discovery process needs to take place from Source to Destination. Also consider M as the malicious node intending to disrupt the traffic. As per the SL2R-HT scheme, the Source which is a root in our case will initiate RANN broadcast. However, the RANN will be protected by the GTK of the root which is public and is known to all the neighbours. The non mutable fields will be protected using Root GTK and mutable fields using GTK of the Root/intermediate hop. The mutable fields will be authenticated using the certification trail as explained above. In case the values match, the intermediate receiving node will again create a MAC using its own GTK and forward it to its neighbours. The same will be received authenticated to the Destination. The Destination node will now reply with a unicast PREQ and send the same to its next hop after hashing it with its PTK. The process will be repeated at each intermediate hop where the mutable fields are verified and in case the root value matches, the node will again hash it with its PTK and forward it to the next hop. The Source will also receive the PREQ in the same manner. It will not be possible for the malicious node to participate in the route discovery process since the malicious node will neither have the GTK nor the PTK. The on demand mode routing information will also be protected in the same manner.

B. Secure Layer -2 Routing using LinearHash (sl2r-lh)

In the unicast control messages there are four mutable fields viz: Hop count, TTL, Metric, Destination Address

If these values are sent as it is in the network then there is an open opportunity for the malicious nodes to alter the fields and rebroadcast it into the network as already explained in earlier sections. In order to provide the security, a new scheme is proposed which also protects the mutable fields using hash technique, however over a linear function instead of tree formation.



Figure 2: Formation of Linear Hash

The hashed value will be broadcasted to the network for the integrity check of the packet. Since this value is intercepted by the intermediate nodes and the mutable fields can be easily modified, it is the responsibility of the receiving node to check the packet for integrity. If the packet doesn't pass through the integrity check then the receiving node will simply drop that packet. The details are explained

In SL2R-LH, mutable fields are first concatenated and then HMAC is applied. Since the unicast packets mostly contain four mutable fields, they all will be concatenated as shown in Fig. . Consider four mutable fields Y_1, Y_2,……Y4, then $K_{1234} = h(Y_1 \| Y_2 \| Y_3 \| Y_4)$ where function h uses GTK and PTK for broadcast and unicast control frames respectively. Sender appends this value (as an extra overhead) along with the actual frame and sends it to the receiver. In order to authenticate the mutable fields received, the receiver again applies the HMAC on received mutable fields it and compares it with the MAC value received from the sender. In case the two values match, the receiver is assured that the value is received from the authenticated node and in case the value does not match it is believed that the sender is not authenticated to the network and the mutable fields sent by this sender may actually have been the modified ones. The receiver can drop the entire frame received from this forged sender as in this case neither the sender node is said to be authenticated, nor is the integrity of the mutable fields assured. Hence our network remains secure.

VI. SIMULATION RESULTS AND DISCUSSIONS

The schemes have been analyzed for security and performance. The security analysis of both the schemes is done below:

Preventing Flooding: In the proposed SL2R-HT and SL2R-LH protocols, a node can participate in the route discovery process only if it has successfully establishes a GTK and PTK through key distribution mechanism of 802.11s. Thus it will not be possible for a malicious node to initiate a route discovery process with a destination address that is not in the network. Again, as the PREQ message is encrypted during transmission, a malicious node could not insert new destination address.

Preventing Route Disruption: This attack can be launched by any node by modifying the mutable field value. The attacker node if present between two victim nodes does not allow creating path between them. Attacker can modify the metrics field to zero while passing PREQ to other node hence destination node while sending PREP will have to pass it through attacker node. And now attacker node can drop the PREP message never allowing route discovery process. In the proposed SL2R-HT and SL2R- LH protocols, a node can participate in the route discovery process only if it has successfully establishes a GTK and PTK through key distribution mechanism of 802.11s. Thus it is not possible for attacker node to change the metrics value.

Preventing Route Diversion: A malicious node can launch a route diversion attack by modifying mutable fields in the routing information elements such as hop count, sequence number and metric field. A malicious node *M* can divert traffic to itself by advertising a route to a destination with a Destination Sequence Number (DSN) greater than the one it received from the destination. Here also the attacker could not change the mutable fields. So our network is secure.

Preventing Routing Loops: Formation of routing loops requires gaining information regarding network topology, spoofing and alteration of routing message. A malicious node can create routing loops in a mesh network by spoofing MAC addresses and modifying the value of the metric field. As malicious node will not have GTK and

PTK. They could not participate in path discovery process. So our network remains secure.
To evaluate the performance, the proposed schemes have been implemented in Qualnet 4.5[8] and analyzed for performance.

Table: 1 summarizes the status of the nodes configured in the simulation scenario and Table: 2 summarizes other parameters set for the conduct of simulation.

Node ID	***Configuration/Type***
11 and 12	Backbone
1 to 10	IEEE 802.11s Mesh Nodes
13 to 18	IEEE 802.11 STA
2	IEEE 802.11s Mesh Portal (Root)
1, 4, 7, 8, 10	IEEE 802.11s Mesh Access points (MAPs)
8→10, 15→16, 17→18.	Source Destination Pair sending and receiving CBR pkts
19 to 21	Attacker Nodes

Table 1: Node Configuration

Parameter	***Configuration***
Source of Application	CBR
No. of Data Packets	512 bytes
Rate	1 pkt/sec
Simulation Time	120 sec
Data Packets	100
Time delay between each data packet	1sec
Terrain Size	1500m×1500m

Table 2: Simulation Parameters

Each simulation is run ten times with different random seed numbers varying from 1 to 10. The averages are taken to collect statistics and the results are discussed and analyzed in next section.
In order to compare HWMP, SL2R-HT and SL2R- LH these approaches were run under identical traffic scenario. We consider the following security and performance metrics:
Packet Delivery Ratio: It determines the efficiency of the protocol to discover routes successfully since in the current scenario the attack is launched during the route discovery process. As shown in Figure 3(a), as the no. of malicious activities increase from 0% to 40%, packet delivery ratio reduces for HWMP whereas for SL2R-HT and SL2R- LH protocol it remains nearly constant. The reason for constant data packet received ratio for SL2R-HT and SL2R- LH approach is that both the approaches provide authentication to the mesh nodes during path discovery process and data packets are delivered when a secure path is established in mesh network. Since it is not possible for a malicious node to participate in the network, hence there is no loss of packets due to routing attacks.
Throughput: It determines the efficiency of the protocol. As shown in Figure 3(b), as the no. of malicious activity increase from 0% to 40%. Throughput reduces for HWMP whereas for SL2R-HT and SL2R- LH approaches, it remains to be nearly constant. The reason for constant throughput in case of SL2R-HT and SL2R- LH approach is that they both provide authentication to the mesh nodes during path discovery process and data packets are delivered when a secure path is established in mesh network. This leads to more no. of bits transferred over the network without getting lost due to malicious activity thus guarding the efficiency of the network from falling due to attacks.
Avg. End-to-End data packet delay: Average end-to-end delay refers to the average time elapsed from the source to the destination to deliver the packets. Figure 3(c)shows the average end-to-end delay comparison of all the three protocols. As the number of hops increase, the average end-to-end delay of the all three protocol also increases at the same rate. The results show that SL2R-HT and SL2R- LH protocol do not cause any extra overhead on avg. end to end delay between the data packets.
Path Discovery Delay: Path discovery delay refers to the delay in formulating path from source to destination. As shown in Figure 3(d) path discovery delay increases in HWMP, SL2R- LH and SL2R-HT in an increasing order. The difference between HWMP and SL2R-LH is almost negligible while the difference between HWMP and SL2R-HT is also quite small . Hence the security of the protocols can be given the preference over the little overhead caused. Also, it can be inferred that the SL2R- LH protocol can be preferred as it is secure as well as efficient when considering common application scenarios. However in case of critical applications demanding high level of security, SL2R-HT can be preferred.
Storage Overhead: In the proposed schemes, for a mesh node to be authenticated during routing process control packets need to store some extra storage information. In case of SL2R-HT, the root hash value and Certification trail need to be stored as an overhead while for SL2R- LH protocol, only one hash value needs to be stored in the form of an overhead. Figure 3(e) shows that the storage overhead of SL2R-HT is higher than SL2R- LH. But the difference is small and hence the security of the protocols can be given preference over the little overhead caused. Table:3 summarizes the ccomparison of HWMP,SL2R-HT and SL2R- LH approaches on the basis of protocol design characteristics and Table 4: summarizes the ccomparison of HWMP,SL2R-HT and SL2R- LH approaches for Security, Performance and Control Overhead.

Parameter	HWMP	SL2R- LH	SL2R- HT
Data Packet Received Ratio	Pkt. delivery ratio decreased with increase in malicious activity.	Remains constant but less secure than SL2R- HT method.	Remains constant and much secured than SL2R- LH method.
Path Discovery Delay	Less than SL2R-LH and SL2R- HT	Minimum	Little more than SL2R- LH
Throughput	Throughput decreases with increase in malicious activity.	Remains constant	Remains constant
Storage Overhead	Less than SL2R-LH and SL2R- HT	Minimum	Little more than SL2R- LH

Table 4: Comparison of HWMP,SL2R-HT and SL2R- LH for Security Performance/ Control Overhead

Parameter	HWMP	SL2R- LH	SL2R-HT
Key Hierarchy	-------	GTK, PTK	GTK, PTK
Concatenation	-------	At the base level	Tree to calculate root value
Security	-------	GTK, PTK	GTK, PTK
Algorithms used	-------	MD5	MD5, SHA1
Integrity Check	-------	Concatenate and then encrypt with HMAC using GTK, PTK as key	Tree formation, concatenated and then encrypt with HMAC using GTK, PTK as key
Formation	-------	Linear Hash	Hashed Tree

Table 3: Comparison of HWMP,SL2R-HT and SL2R- LH on the basis of protocol design characteristics

VI. CONCLUSION

One of the goals of the present research was to develop an authenticated, reliable and efficient Hybrid Wireless Mesh Protocol for IEEE 802.11s Wireless Mesh Network. To attain so the security vulnerabilities of candidate HWMP protocol were analyzed. The vulnerabilities mainly arise due to the fact that the fields of the routing information elements classified as mutable and non-mutable fields are unprotected in the current protocol and no security mechanism was specified in the current draft. The proposed approaches for securing HWMP protocol Hashed Tree approach (termed as SL2R-HT) and Linear Hash approach (termed as SL2R-LH). Both the approaches protect the non-mutable routing elements using encryption techniques and protect mutable routing elements using hashing techniques. From the results it can be clearly inferred that SL2R- LH method is slightly more efficient than SL2R- HT approach but is found to be broken in case high computation is available. Thus it can be can concluded that SL2R- HT approach is more secure, dependable and robust against the identified attacks, and causes only a small overhead over SL2R- LH.

ACKNOWLEDGMENT

This work is done in Cyber Security Research Center (CSRC), PEC University of Technology. The authors would like to thank Government of India, Ministry of Communications and Information Technology, Department of Information Technology, New Delhi, for funding the Project *"*Design and Development of Dependable, Secure and Efficient Protocol for Wireless Mesh Network(WMN)*"*, under which this research work has been done.

REFERENCES

[1] IEEE P802.11s™/D3.0, Draft STANDARD for Information Technology— Telecommunications and information exchange between systems— Local and metropolitan area networks— HWMP Specifications.

[2] Merkle, R.C.: "*A Certified Digital Signature (subtitle: That Antique Paper from 1979)"*. In: Brassard, G. (ed.) CRYPTO 1989. LNCS, vol. 435, pp. 218–238. Springer, Heidelberg (1990).

[3] Donggang Liu, Peng Ning, Security for wireless sensor networks, "Tree based Tesla", pp 43, 2007

[4] Edney, J. and Arbaugh, W. A – "Real 802.11 security: Wi-Fi Protected Access and 802.11i", Addison-Wesley 2004

[5] Stephen Asherson, Pieter Kritzinger and Paolo Pileggi - "Wireless Standards and Mesh Networks" Technical Report, Data Network Architectures Group 2007

[6] Lee, M.J. Jianliang Zheng Young-Bae Ko Shrestha, "Emerging standards for Wireless mesh technology", Wireless Communications, IEEE, April 2006, On page(s): 56- 63.

[7] FIPS 180-2: Secure Hash Standard (SHS) – Current version of the Secure Hash Standard (SHA-1, SHA-224, SHA-256, SHA-384, and SHA-512), 1 August 2002, amended 25 February 2004.

[8] www.scalable-networks.com

[8] Ling He; Jun Huang; Feng Yang, "A noval hybrid wireless routing protocol for WMNs", Electronics and Information Engineering (ICEIE), 2010 International Conference On Aug. 2010 , pp: Vol 1:281 - 285

[9] Bansal, D; Sofat, S; "Analysis of Denial of Service Attacks in IEEE 802.11s Wireless Mesh Networks" Springer, LNCS, Social Informatics and Telecommunications Engineering, Information Security and Digital Forensic, ISSN 1867-8211, Volume 41,2010

[10] Bansal, D; Sofat, S; "Security Challenges in Multihop Wireless Mesh Networks - A Survey" International LNCS, Social Informatics and Telecommunications Engineering, Information Security and Digital Forensic, ISSN 1867-8211, Volume 41, pp 92-101, 2010

[11] Garroppo, Rosario G.; Giordano, Stefano; Tavanti, Luca, "Experimental evaluation of two open source solutions for wireless mesh routing at layer two", 5th IEEE International Conference on Wireless Pervasive Computing (ISWPC), 2010, May 2010, pp : 232 - 237

[12] Kai Yang; Jian-feng Ma; Zi-hui Miao, "Hybrid Routing Protocol for Wireless Mesh Network", International Conference on Computational Intelligence and Security, 2009. CIS '09, Dec. 2009, pp: 547 - 551

[13] Ping Yi, Tianhao Tong, Ning Liu, Yue Wu, Jianqing Ma, " Security in Wireless Mesh Networking: Challenges & Solutions", Sixth International Conference on Information Technology: New Generations, 2009,pp: 423-428

[14] Hu, Y.-C.; Perrig, A.; Johnson, D.B, " Packet Leashes: A defense against Wormhole Attacks in Wireless Networks", INFOCOM 2003. Twenty-Second Annual Joint Conference of the IEEE Computer and Communications. April 2003,vol.3 pp: 1976 - 1986

[15] M.S.Siddiqui, Choong Seon Hong, " Security Issues in Wireless Mesh Networks", In Proc. of IEEE International Conference on Multimedia & Ubiquitous Engineering (MUE'07), 2007

[16] Celia Li, Zhuang Wang and Cungang Yang, "SEAODV: A Security Enhanced AODV Routing Protocol for Wireless Mesh Networks", TRANSACTIONS ON COMPUTATIONAL SCIENCE XI Lecture Notes in Computer Science, 2010, Volume 6480/2010, 1-16

[17] M.S. Islam, Y.J. Yoon, M.A. Hamid and C.S. Hong, " A Secure Hybrid Wireless Mesh Protocol for 802.11s mesh network, " In Proc. of ICCSA 2008, LNCS 5072, pp 972-985, 2008

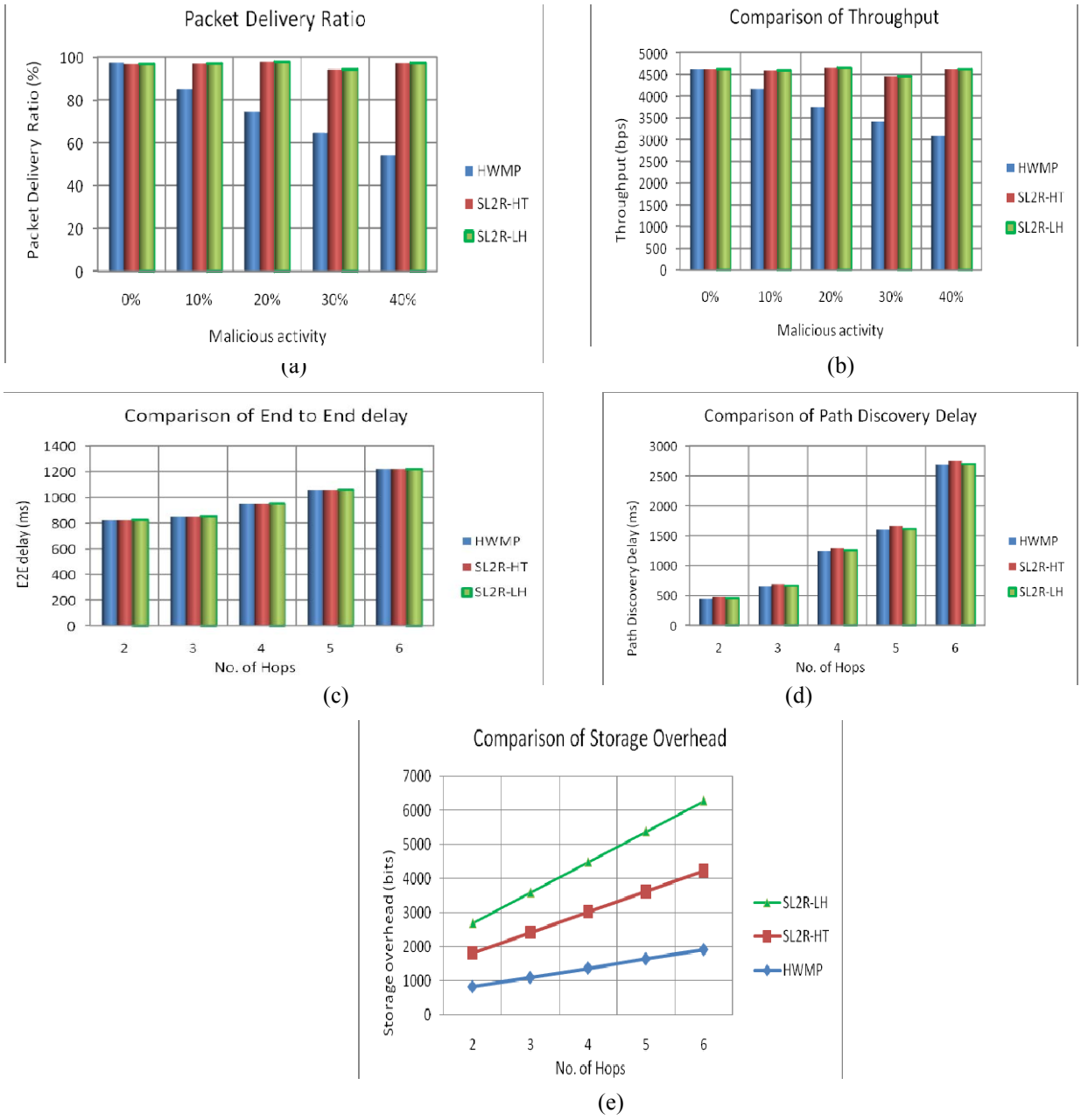


Figure 3:Performance Analysis of HWMP,SL2R-HT and SL2R- LH :
(a) Packet delivery ratio (b) Throughput (c) E2E Delay (d) Path doscovery delay (e) Storage Overhead.

Energy Efficient cross-layer design protocol by using token passing mechanism for WSN

SandhyaSree Thaskani
MS by Research(ECE)
IIIT-Hyderabad
Hyderabad, India
thaskanisandhya@gmail.com

K.Vinod Kumar
BE (EEE)
NIT-Warangal
Warangal, India
vinodreddy.nitw@gmail.com

G.Rama Murthy
Associate Professor
IIIT-Hyderabad
Hyderabad, India
rammurthy@iiit.ac.in

Abstract— **Recent advancements in processor, memory and radio technologies have enabled cheap and small sensors which are capable of sensing, communication and computation. Most of the Wireless Sensor Networks have limitation of battery power and in most of the applications it is not possible to replace the battery of a node. Considering this scarce energy and processing resources of WSN, we try to establish a joint optimization and design of networking layers i.e., cross layer design which could be a promising alternative to the inefficient traditional layered protocol design. In this paper we propose energy efficient cross layer design of the MAC and Routing protocol namely Energy Efficient cross-layer design protocol by using token passing mechanism for WSN. This proposed protocol proves to be better than some of the existing protocols and it is shown with the help of simulations.**

Keywords— **Wireless Sensor Network, Token Passing, Level, Sector, Sectroid,**

I. INTRODUCTION

Recent advancements in electronics and wireless communications enabled the manufacturing of cheap and small sensor nodes. A Wireless Sensor Network (WSN) consists of numerous sensor motes which sense the data, communicate with each other hop by hop and eventually report the data to the Base Station. Though WSN started for military applications, gradually it found to have very useful applications in wide range of areas like Health, Building Monitoring, Factory Automation etc. The main constraint in protocol design for WSN is Energy Efficiency as the motes have limitations due to battery operation. In many of the applications the sensor nodes are unattended and so battery replacement is not at all possible. Researchers have designed numerous protocols for each layer in the traditional layered protocol design. But by joint optimization of multiple layers by cross layer design gives more satisfactory results than our traditional layered design.

Medium Access Control (MAC) Protocols in Wireless Communications are broadly classified into three categories namely scheduled based, demand based and contention based MAC Protocols. TDMA, FDMA and CDMA are scheduled based MAC Protocols. Traditional methods like Trunking, Polling comes under demand based protocols. IEEE 802.11 standards define contention based protocols CSMA/CA. Token Ring is a combination of both contention based and scheduled based protocols.

Routing is a very important function carried out by network layer in the protocol stack. The routing layer protocols mainly emphasize on energy efficiency and throughput. Routing algorithms are broadly divided as data centric, hierarchical, fault tolerant, localization based [1]. In this proposed algorithm we make use of a innovative localization scheme proposed by [2] to reduce the redundancy. In [2] authors have localized by dividing the sensor field into levels and sectors. Using this localization technique combined with Token passing approach we propose a new approach Energy Efficient cross-layer design protocol by using token passing mechanism for WSN which proves to be better than many existing protocols for static WSN.

II. RELATED WORK

The previous scientific and experimental research reveals that the interactions between layers of the network stack play a very important role in improving the performance of the network. The inter dependency between the local contention and end to end congestion is an important factor to be considered in the protocol design. The interdependency between these network layers need cross layer mechanisms for efficient data delivery in WSNs. The design challenges and the importance of the cross layer design for meeting the application requirements in the energy constrained networks is discussed in [4].

Receiver based routing has been discussed in [5], the authors dealt with energy efficiency, time delay, multi hop and single hop performance. In [6] a TDMA based MAC scheduling routing algorithm is proposed where authors made use of sleep schedules which minimize the wastage of idle listening. Also the nodes will transmit in a particular time slot which is chosen based on the topology information. In this algorithm in addition to MAC scheduling, the route establishment is also dealt. The physical layer results in [7] are extended in [8] to compute the TDMA slot lengths to minimize the total energy consumption in a network with many transmitters and only one receiver.

Some protocols are designed based on the type of applications and other factors. For example, in [9] for periodic traffic in WSN, the nodes form distributed on-off schedules for each flow in network. This forms a route and max

efficiency could be achieved. The authors also showed a trade off between on-off schedules and the connectivity in the network.

III. ASSUMPTIONS & DEFINITIONS

1. Our first assumption is that all the sensors in the network are Topology – Aware.
2. The whole sensor network is densely deployed.
3. All nodes in network have equal capabilities.
4. Time synchronization for all nodes is done automatically.
5. **Token Frame (TC):** This is a control packet that circulates within group of nodes. It has number of fields which are as follows, Direction Flag (DF), Group Number (GN), Source Address (SA), Destination Address (DA), and Frame Control (FC). Fig. 1 shows the frame structure of token frame.

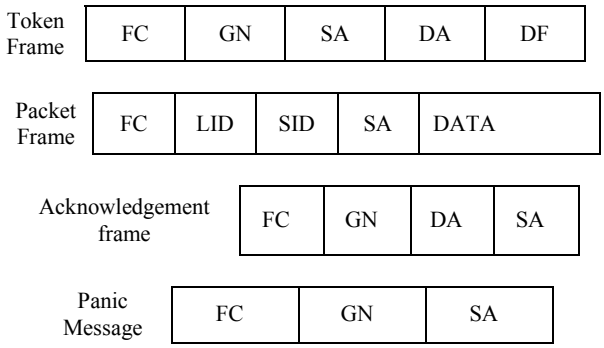


Fig. 1 Frame structure in our protocol

6. **Acknowledgement (ACK):** It is a control packet sent by a node to the adjacent node as a confirmation for the token packet reception. Fig. 1 shows the frame structure of acknowledgement.
7. **Panic Message:** It is a control message that is passed to the neighbours by a dying node. Fig. 1 shows the frame structure of panic message.
8. **Packet Frame:** This frame contains the data. This frame gives Level Id (LID), Sector Id (SID), source address (SA) and data (DATA). Fig. 1 shows the frame structure of packet frame.
9. **Network Lifetime:** The time taken for 10% of the total number of nodes in the network to fail is considered to be the Network Lifetime.
10. **Direction Flag:** This flag determines the direction of flow of the token. When the DF is set to be 0, the token is given to the left neighbour. If it is set to 1 then it is passed to the right neighbour, else if it is set to value 2 currently the node is not holding the token.

IV. PROPOSED ALGORITHM

The Proposed Algorithm is implemented in three main phases. They are as follows.

1. Sectroid (Group) Formation
2. Token Passing
3. Routing

1. Sectroid (Group) Formation:

Our basic assumption is that BS has capability of transmitting signals at various power levels. During the initial deployment the base station sends with minimum power level. All the sensor nodes which receive this broadcast message set their level id as 1. Then the Base Station steps up the power to the next higher value and broadcasts the signals. Now the nodes which receive the message for the first time will set their level id to 2. Like this the Base Station keeps on increasing the power of transmitting signal till all the nodes in the network are covered.

After levelling is completed the base station calculates the signal strength required for the broadcast to be heard by the farthest node in the network. Using this signal strength and a directional antenna which has a steerable beam, the sensor network is divided into equiangular sectors in clockwise or anti-clockwise direction. When the WSN is divided the base station sends some control packets using which all the nodes assign their sector ids.

2. Token Passing:

Every sectroid in the sensor network is assumed to be a group. In a group each node has two neighbours, left neighbour and right neighbour. Each group has two edge nodes, left edge node and right edge node. Left edge node's left neighbour is set to zero and right edge node's right neighbour is set to zero.A token is passed among all the nodes in a group and a node can transmit its data only when it holds the token. This actually avoids lots of collisions as at any point of time only a single node (from the whole group) is allowed to transmit the data.

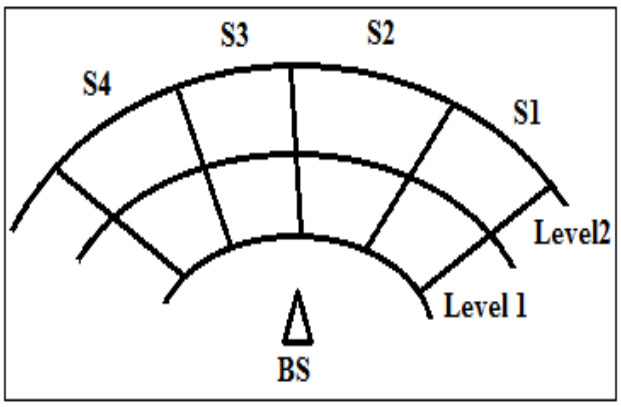


Fig. 2 Part of sensor field divided into sectroids (groups)

Initially a token is initialised by the left most nodes of all the groups in the whole network. If the Direction Flag (DF) is set to 0 then the token must be passed on to the left neighbour in the group else to the right neighbour in the group. Since the token is initialized in the right most node, the DF is set be 0. The first node holds the token for a fixed amount of time Hold Time (T_H) which is lesser than the transmission time (T_X). So that we can make sure that a node holding the token can complete the transmission completely. After this Hold Time the token is passed on to the next neighbouring node (left or right depending on the status of DF). When the token reaches the edge nodes i.e., the right most or the left most nodes, they invert the status of the DF and start passing the token again. Since there is always a chance that the token frame may be lost due to several reasons, we also give an acknowledgement packet for every token pass. If any node doesn't get back a token acknowledgement then it reinitializes the token with the same attributes which it stores temporarily in the cache memory.

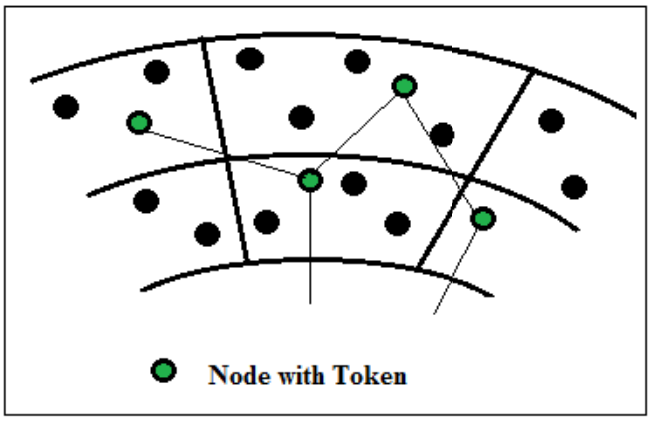


Fig. 3 Schematic of Token Passing Procedure

In case of node failure, that is when the energy of a node reaches certain threshold value then it sends out a panic message to both its neighbours. The neighbours will exclude the node from the chain of token passing and they make each other as their right and left neighbours. Typically when the edge node is about to die, there after the neighbouring node itself becomes an edge node.

3. Routing:

Whenever a sensor node gets a packet, it will see that it is forwarded only if it is from a higher level. This makes the flow of data only towards the base station not away from it. This is also considered as Directional Flooding. The packet is forwarded only when it is coming from the adjacent sectors. This make the flow of data converge as we move towards the base station. Effectively the levelling and clustering decreases redundancy to a great extent. The schematic flow of the algorithm can be seen as follows.

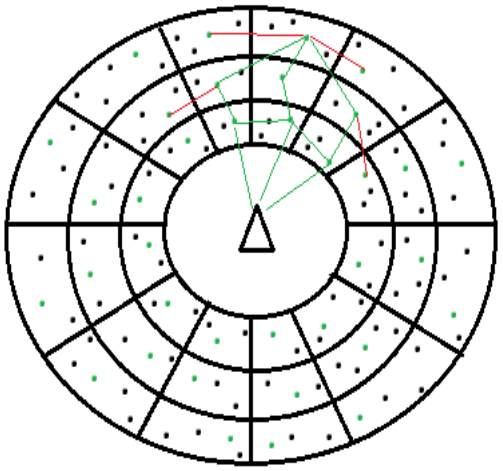


Fig. 4 Schematic of the Proposed Algorithm

1. When a node receives a data packet, it checks the level and sector id of the packet.
2. If the level id from the source is lesser than node's level then the packet is dropped.
3. If the level id from the source is larger than the node, then it checks whether the sector id is from the neighbouring sectors i.e., sectors with one hop distance. If not the packet is dropped.

V. Simulation Evaluation

In this section, we compare our proposed algorithm with traditional levelling [3] and PASCAL [2] algorithms. We calculate the network life time and number of average number of redundant messages received by base station using each algorithm. All implementation of protocols are done in MATLAB. Table I shows node parameters considered for this simulation study. All simulation results in this paper are average values after repeating 10 experimentations.

A. Experimental Methodology

In this paper we considered all nodes are distributed randomly in a flat ground. In case of MAC for Levelling and PASCAL, we considered simple MAC protocol CSMA/CA. For simplicity error free links are considered.

TABLE I
Node Parameters

Parameters	**Values**
Simulation Area	200 X 200 m^2
Number of Nodes	200 to 700
Initial Energy	500 J
Node Transmission Range	60m
Transmission Power	10 J
Reception Power	2 J

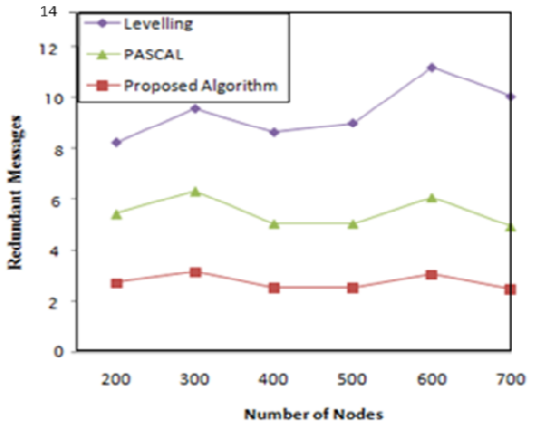


Fig. 5 Network Life Time

Fig. 5 shows the plot of Network Lifetime and Number of nodes comparing our proposed algorithm with traditional leveling and PASCAL. The graphs show that the proposed algorithm gives better network lifetime than leveling protocol and flooding. The network life time is defined as the number of events taken for the failure of 10% of nodes in the whole sensor network.

Fig. 6 shows the plot of average redundant messages and number of nodes comparing our algorithm with traditional levelling and PASCAL. The graph shows that the proposed algorithms have less number of redundant messages when compared to levelling and PASCAL protocols.

Experimental results shows that our proposed algorithm has better energy efficiency as the network life time is better when compared to levelling and PASCAL and average number of redundant message are lesser than levelling and PASCAL protocols.

VI. Conclusions

In this paper, we have proposed a token passing based cross-layer mechanism to serve the purposes of both MAC and routing layers. Total network is hierarchically formed into groups. Each group have a token. A node with token can only transmit data. After every T_H time token is passed to its next neighbour. All the nodes in a group are equally given change to transmit its data. By passing a light weight packet scheduling is done. By doing directional flooding routing is accomplished.

Experimental results have proven that our proposed cross-layer mechanism have better energy efficiency when compared to traditional levelling and PASCAL algorithms. Average number of redundant messages in our proposed algorithm is lesser than traditional levelling and PASCAL algorithms.

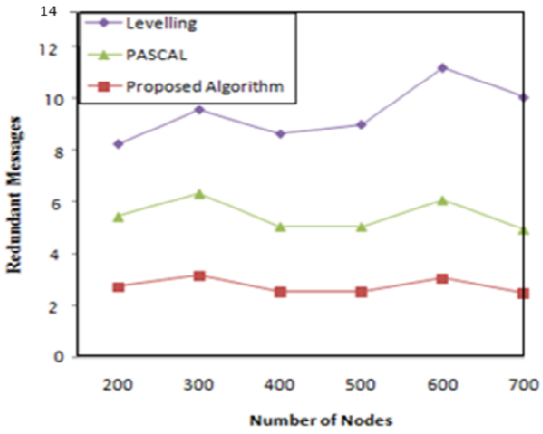


Fig.6 Average number of Redundant Messages

References

[1] Ian.F.Akyildiz, Weilian Su, Yogesh Sankarasubramaniam, and Erdal Gayirci, *"A Survey on Sensor Networks,"*IEEE Communications Magazine, August 2002.

[2]] Md.Aquil Mirza, Ramamurthy Garimella,*" PASCAL: Power Aware Sectoring Based Clustering Algorithm for Wireless Sensor Networks",* The International Conference on Information Networking (ICOIN), Chiang Mai, Thailand. January 20-24th,2009.

[3] R. L. Cruz and A. V. Santhanam, "Optimal routing, link scheduling and power control in multi-hop wireless networks," *IEEE INFOCOM*, 2003.

[4] A. J. Goldsmith and S. W. Wicker, "Design challenges for energy-constrained ad hoc wireless networks," *IEEE Wireless Communications Magazine*, 2002.

[5] P. Skraba, H. Aghajan, A. Bahai, "Cross-layer optimization for high density sensor networks: Distributed passive routing Decisions," in *Proc. Ad-Hoc Now'04*, Vancouver, July 2004.

[6] L. van Hoesel, T. Nieberg, J. Wu, and P. J. M. Havinga, "Prolonging the lifetime of wireless sensor networks by cross-layer interaction," *IEEE Wireless Communications*, vol. 11, no. 6, pp. 78 - 86, Dec. 2004.

[7] S. Cui, A. J. Goldsmith, and A. Bahai, "Energy-constrained modulation optimization," *IEEE Transactions on Wireless Communications*, vol. 4, no. 5, pp. 2349–2360.

[8] S. Cui, A. J. Goldsmith, and A. Bahai, "Joint modulation and multiple access optimization under energy constraints," *GLOBECOM*, 2004.

[9] M. L. Sichitiu, "Cross-layer scheduling for power efficiency in wireless sensor networks," 2004.

A Review on Modulation Techniques in Multiband-Orthogonal Frequency Division Multiplexing in Ultra-Wideband Channel

Chempaka Mohd Din, Wahidah Mansor, Roslina Mohamad
Faculty of Electrical Engineering
Universiti Teknologi MARA, 40450,
Shah Alam, Selangor.
pu3cempaka_0501@yahoo.com, wahidah231@salam.uitm.edu.my, roslina780@salam.uitm.edu.my

***Abstract* – This paper describes a review on mapping or modulation techniques used in multiband orthogonal frequency division multiplexing (MB-OFDM) in ultra-wideband (UWB) channel. QAM, BPSK and QPSK modulation techniques are commonly used in this system due to their smooth power spectrum, low bit error rate (BER) and low receiver complexity. The new constant envelop modulation technique is proposed since it has the capability to improve the power spectrum density and BER performance. Continuous phase modulation (CPM) scheme could be used to reduce the complexity at the receiver. The constant envelop characteristics of CPM has to be analyzed in order to adapt this scheme in (MB-OFDM) UWB system.**

***Keywords*--Multiband OFDM; Ultra-Wideband; Continuous Phase Modulation.**

I. INTRODUCTION

Ultra-Wideband (UWB) communication systems concepts was developed in late 1960's. Nowadays, UWB techniques have been improved and used in various applications such as radar, automobile collision avoidance, positioning system, liquid level sensing and others. The technique was developed for a wide range of applications. UWB refers to a transmission scheme that occupies a fractional bandwidth greater than 0.2 or a signal bandwidth of more than 500 MHz [1].

The three popular methods of modulating the ultra-wideband signal are Time Hop UWB (TH-UWB), Direct Sequence UWB (DS-UWB) and Multi-Band Orthogonal Frequency Division Multiplexing UWB (MB-OFDM) [2]. Among these three popular methods, (MB-OFDM) UWB is the best technique since it provides data rates as high as 480 Mbps. Since short-range communications are often accompanied with poor transmission channel condition such as indoor environments, MB-OFDM is a suitable modulation technique for UWB [3].

Some of well-studied modulation options in MB-(OFDM) UWB are binary-phase shift keying (BPSK), quadrature-phase shift keying (QPSK), pulse amplitude modulator (PAM), quadrature-amplitude modulation (QAM) and Frequency-shift keying (FSK). Currently, BPSK is one of the most popular modulation techniques in UWB application due to its smooth power spectrum and low bit error rate (BER). QPSK is widely used for applications that require low transmitting power and low complexity. Unfortunately, the synchronization and channel estimation for both modulations are not perfect under noisy condition, for example in the presence of additive white Gaussian noise (AWGN) which causes significant degradation in system performance. Higher order modulation ensures high data rate at the cost of poor BER in a noisy channel while lower order modulation for low data rate application is desired in poor channel condition. Noise level in wireless channels also influences the choice of modulation [4, 5].

This paper describes the modulation techniques used in (MB-OFDM) UWB including its function and performance. An overview of (MB-OFDM) UWB system and the modulation techniques used in this system are also discussed. The potential modulation technique that can overcome the limitations of the conventional techniques used in (MB-OFDM) UWB system is proposed at the end of this paper.

II. (MB-OFDM) UWB SYSTEM

(MB-OFDM) UWB signals provide large data-rates, low probability of interception, and the capability of estimating distances between the transceivers with a precision of a few centimeters, depending on their bandwidth [6]. It can support data transmission rates as high as 110 Mb/s over 10 meters, 220 Mb/s over 4 meters and 480Mb/s over 1 meter [7]. The transceiver architecture of (MB-OFDM) UWB system consists of scrambler, encoder, interleaver, modulator, inverse fast fourier transform (IFFT) module, de-scrambler, decoder, de-interleaver, demodulator and fast fourier transform (FFT) module as shown in Fig. 1

A. *Transceiver module*

Scrambler and de-scrambler are initialized with the same *seed value* which is chosen based on data sequence. They are called the *seed identifiers.* Scrambler will make

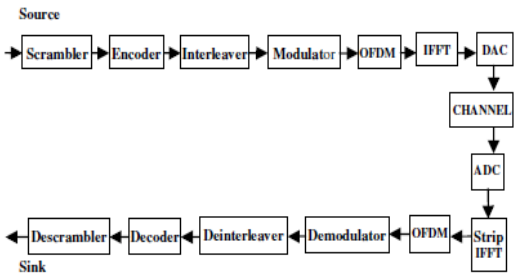


Figure 1. Transceiver architecture of (MB-OFDM) UWB system

binary data randomization process in order to improve anti-jamming ability. It converts a data bit sequence into a pseudorandom sequence that is free from long strings of simple patterns such as marks and spaces. Encoder and decoder function as channel codes which can improve the reliability of channel and overcome the effect of noise [7]. This block serves to add patterns of redundancy to the data in order to improve the signal to noise ratio (SNR) for more accurate decoding at the receiver [1].

Interleaver and de-interleaver provide robustness against burst errors. Bit interleaver operates through symbol interleaving and tone interleaving. In the *symbol interleaving*, the bits across data OFDM symbols are permuted to exploit frequency diversity across the sub-band. While in *tone interleaving*, the bits across data tone within an OFDM symbol are permuted to exploit frequency diversity across tones [1]. Data mapping or data modulation is essential to achieve mapping of binary bits onto UWB pulse waveform. There are multiple possible solutions to data mapping and the choice depends on design, application, data rate, BER and complexity requirements.

OFDM is a spectrally efficient way of implementing multicarrier modulation where multiple overlapping orthogonal carriers are used through fast fourier transform (FFT) and inverse fast fourier transform (IFFT) which is a core of the baseband of MB-OFDM transmitter [3, 4]. The bit streams will be modulated on various frequencies carrier by IFFT. For extremely high sampling frequency, analog-to-digital converter (ADC) is strictly needed to support a very large dynamic range to resolve the signal from the strong interferers [7].

B. *Frequency Spectrum*

The MB-OFDM system divides the UWB spectrum (3.1-10.6 GHz) into 528 MHz wide sub-bands and uses OFDM modulation to transmit the information in each sub-band [8, 9]. According to the standard, the MB-OFDM approach divides the UWB spectrum into 14 bands. The first 12 bands are grouped into 4 band groups consisting of 3 bands, and last two bands are grouped into a fifth band group. A total of 110 sub-carriers (100 data carriers and 10 guard carriers) are used per band. In addition, 12 pilot subcarriers allow for coherent detection (channel estimation purpose). The band is restricted to convolutional codes only for the channel coding. The concatenation of two or more codes leads to more robust channel codes than single code [10-12].

The analysis of the coexistence issue of UWB mainly focused on the coexistence between narrowband and (MB-OFDM) UWB systems as a narrowband jamming. [2, 13]. Typically, UWB receivers operating in band group 1 will suffer from potential interference. The interference could have significant impacts given the anticipated weak power levels of the UWB signal [14-16].

III. MODULATION TECHNIQUE IN (MB-OFDM) UWB

UWB faces several problems on the rise of noise level and interference by a number of UWB transmitters that puts a burden on existing communications services. This may be hard to bear for traditional systems designs and may affect the stability of such existing systems. The types of modulation technique used in (MB-OFDM) UWB can help to overcome some of the problems.

A. *Binary-phase shift keying (BPSK)*

BPSK or 2-PSK is the simplest form of PSK and uses two points on constellation diagram. It is the most robust modulation of all PSKs because the highest level of noise and distortion makes the demodulator reach an incorrect decision. BPSK is only being able to modulate 1 bit/symbol. Hence, it is not suitable for high data-rate application when the bandwidth is limited. This modulation was used by Mehbodniya *et al.,* [13] to investigate the effect of an MB-OFDM system as an interfering source to a UWB system. Magani *et al.,* [17] used various modulation schemes such as BPSK, QPSK, 8-PSK and 16-PSK modulators for the adaptive modulations to improve the BER performance in a frequency selective fading channel. Bhattacharya *et al.,* [9] worked on the production test of (MB-OFDM) UWB device by applying simple test stimulus for error vector magnitude (EVM) and complementary cumulative distribution function (CCDF) using BPSK modulation.

B. *Quadrature-Phase Shift Keying (QPSK)*

Quadrature-phase shift keying (QPSK) uses four constellation points for mapping and encodes 2 bit/symbol with gray coding to minimize BER. The advantage of QPSK over BPSK is it can transmit twice of the data rate at the same BER. QPSK is often used in a higher-order PSK implementation. Snow *et al.,* [18] compared spectrum estimation of coded MB-OFDM transmissions and WiMAX interference for various scenarios of interest. Matsumoto *et al.,* [15] and Mukarami *et al.,* [19] analyzed the interference of personal computer noises on (MB-OFDM) UWB system. Islam *et al.,* [10] proposed channel estimation technique for multipath time varying wireless channel. Fan *et al.,* [20] tried to improve the performance based on the characteristics of the practical indoor UWB multipath channel.

UWB standard channel by Lowe *et al.,* [21] was improved using the same modulation technique. The design of low-power UWB receiver by Li *et al.,* [14] was sufficiently robust against nearby interference. Nyirongo *et al.,* [3] worked on investigating the performance of concatenated Reed Solomon and convolutional codes for (MB-OFDM) UWB system. QPSK modulation was also used as a constellation mapping to avoid the speed bottleneck in add-compare-select operation by Maunu *et al.,* [22].

Tani *et al.,* [23] provided a performance analysis of a spectrum sensing algorithm based on statistical test that exploits the time periodically of the correlation induced by the cyclic prefix in WIMAX signal. A highly simplified phase tracking approach was proposed by Fan *et al.,* [24] to improve the system performance due to OFDM-based system which is sensitive to phase distortion. In other study, this modulation scheme was used to compare between the ranging accuracy of (MB-OFDM) and DS-UWB in an indoor environment by Cardinali *et al.,* [25]. The same modulation technique was used by Kim *et al.,* [11] in order to perform (MB-OFDM) UWB system with extra diversity.

C. Quadrature Amplitude Modulator (QAM)

QAM is both analog and digital modulation scheme which is a class of non-constant envelope scheme that can achieve higher bandwidth efficiency. QAM is widely used in the design of modems for telephone channels. The constellation point of QAM is usually the 2 power of n or (2^n). However, the points must be closed together to avoid noise and other corruption which produce high BER. A pre-distortion scheme was proposed by Yang *et al.,* [26] to overcome the impairments introduced by the multimode fiber using 16-QAM. Li *et al.,* [5] has reported that the performance of 4-QAM was found to be similar to the QPSK performance in (MB-OFDM) UWB system.

4-QAM was used by Liu *et al.,* [27] to overcome the low radio power and ultra wide bandwidth. Deergha *et al.,* [28] adapted 16-QAM to reduce the high peak to average power ratio (PAPR) by using clipping technique and turbo coding technique. 16-QAM was employed by Wylie-Green [29] to investigate the feasibility of detecting the downlink transmission from an indoor Fixed Service (FS) system.

D. Dual Carrier Modulation (DCM)

DCM is the principal of transmitting data by dividing the stream into several bit streams to modulate duo-carrier. The advantages of this modulation scheme are it is immune to multipath fading and less susceptible than single-carrier system to interference. However, it is difficult to synchronize the carrier and linear amplification is required. This scheme is used in some audio broadcast services and currently being adapted in OFDM. Viittala *et al.,* [30] compared the interference performance between MB-OFDM and DS-UWB, where the combination of DCM and QPSK were used. Lee *et al.,* [31] focused on reducing the loss in diversity of the system but using different mapping which was soft decision for both DCM and 16-QAM modulation. Tran *et al.,* [32] used DCM technique for high data rate and QPSK modulation for low data rate in order to quantify the pairways error probability (PEP).

E. Frequency Shift Keying (FSK)

Other modulation technique like FSK is seldom to be adapted. FSK is a frequency modulation where the digital information is transmitted through the frequency changes of a carrier wave. FSK modulation was employed in Gerrits *et al.,* [33] work to analyse the potential of low-power air interface for impulse radio (IR) UWB and frequency modulation (FM) UWB. The performance of data mapping scheme varies in practical scenario. Due to reflection, diffraction and scattering effect, the transmitted signal arrives at the receiver through multipath with different delays [4]. The performance of the modulation techniques used in (MB-OFDM) UWB system is shown in Table I.

Note that the potential constant envelop modulation which is continuous phase modulation (CPM) scheme has not been studied in UWB system. The CPM can be adapted in (MB-OFDM) UWB system due to its excellent performances such as power spectrum density, BER performance and spectral efficiency. It is believed that it will offer better performance than traditional methods.

IV. Continuous Phase Modulation

CPM is a desirable transmission format for narrowband tactical communication system and a special case for a large class of constant envelop modulation schemes for minimum shift keying (MSK) [34, 35]. With CPM, high spectral efficiency (bandwidth and power) can be achieved without the need of back-off full amplifier power [36, 37]. Some CPM schemes like MSK have been used in practical communication system, for example in NASA's Advanced Communication Technology Satellite (ACTS) system [38].

CPM is popular with the characteristics of low cost and high efficiency nonlinear amplifiers which are suitable for portable and mobile applications in CPM radio transmitter [35]. However, it has a limitation of high complexity at the receiver. Detectors for CPM typically consist of a number of matched filters and employ trellis

Performance Of (MB-OFDM) UWB System Obtained By Researcher Using Various Modulation Techniques

Purpose	Modulation Scheme	Classification Method	Performance
Design low-power UWB receiver against nearby interference [14]	QPSK	Platform-based design (PBD) methodology	Saving power = 3.1 mW Voltage gain = 27.5-29.2
Investigate the effect of NB OFDM system as an interfering source [13]	BPSK	Characteristics Function (CF) method	BER: M = 4, N_B = 3
Improving BER performance in a frequency selective fading [22]	BPSK, QPSK, 8-PSK, 16-PSK	Adaptive modulation (AM) Non-adaptive modulation (NAM)	AM: Gain = 8dB, BER = 1x 10^{-4} NAM: Gain = 4dB, BER = 1x 10^{-4}
Analyzing the potential of low-power air interface for impulse radio (IR) [33]	FSK	Constant envelop FM-UWB Direct digital synthesis (DDS)	Power = 4mW Gain = 34dB
Quantifying the pairways error probability (PEP) [32]	QPSK DCM	Space-Time-Frequency Code Implementation Maximum Likelihood decoding	QPSK: SNR = 5dB, BER = 10^{-4} DCM: SNR = 7.5, BER = 10^{-4}
Improving system performance due to OFDM-based system which sensitive to phase distortion [24]	QPSK	Phase tracking approach Classical approach	Power = 4.9 mW M1 & M2 = 1.2 x 10^{-4} M3 = 6 x 10^{-5}

based maximum likelihood estimation (MLE) [35, 36].

Numerous investigations have found that the Viterbi algorithm can be used for the purpose of decoding algorithm for CPM on an AWGN channel and performing MLE, however, the limitations are the complexity of the detector, a large match filter bank and many states in Viterbi decoder [38-41]. Viterbi algorithm is still compatible with some system depending on its purpose. Nowadays, new techniques and approaches have been developed by many researchers to overcome this problem while maintaining the system performance. The performance issue on CPM is achieving optimal bit error rate (BER) which related to the complexity reduction at the receiver.

CPM is a nonlinear modulation and more complex demodulator are needed. The information is encoded in phase, so CPM signals are sensitive to phase noise and frequency offset. However, the power and bandwidth efficiency of CPM are improved by the inherent trellis code caused by smoothed phase transition [36-38]. The performance issue on CPM is concerned on bit error rate (BER) which related to the complexity reduction at the receiver.

V. Complexity Reduction In CPM

The modulation and demodulation of CPM is complicated by the fact that the initial phase of each symbol is determined by the cumulative total phase of all previous transmitted symbols, which is known as the *phase memory*. Therefore, the optimal receiver cannot make decisions on any isolated symbol without taking the entire sequence of transmitted symbols into account. This requires a Maximum Likelihood Sequence Estimator (MLSE), which is efficiently implemented using the Viterbi algorithm as described in [36]. The complexity can be reduced using various techniques as discussed in the following subsections.

A. Match filter

In order to reduce the number of receiver match filters, the basis function expansion technique was used by Brown *et al.,* [35] which applicable for coherent or non-coherent CPM. This technique produces high spectral efficiency with the bandwidth of 25 kHz. Reducing 8 real filters to 2 result in an increase of power bandwidth to 99%. The layered-space-time technique by Zhao *et al.,* [42] was adapted to investigate the complexity and performance for single and multi antenna. For multi-antenna, the number of transmit and receive antennas were reduced by 6 and 4 respectively.

Perrins *et al.,* [43] used Optimal maximum likelihood sequence estimating (MLSE) to reduce the complexity of match filter. The match filter was reduced to 3 filters and the cumulative loss was only 2.6 dB at $1x10^{-5}$ of BER. Laurent representation was used in by Figuera *et al.,* [44] for the non-linear CPM modulation as a sum of time-offset pulse amplitude modulations which result in the reduction of match filter at the receiver while maintaining the optimum performance.

B. Trellis state

The analysis of the inherent trellis-encoder of CPM had been carried out by Huber *et al.,* [45] using maximum likelihood sequence estimation in order to reduce the receiver complexity. The state was reduced to 16 and the non-linear intersymbol interference was reduced by the use of decision feedback. Shen *et al.,* [46] used non-coherent detection algorithm which has the capability to reduce the complexity of trellis state. The energy per bit to noise density ratio (Eb/No) was less than 0.5 dB when the power spectral density, *N* was increased from 1 to 3. The performance degradation of the non-coherent detection algorithm with *N* equals to 2 compared to coherent detection maximum likelihood sequence estimation (MLSE) algorithm was about 0.5 dB. The non-coherent detection algorithm can provide the extremely good BER performance.

The CPM signal was decomposed by Cero *et al.,* [47] as a superposition of linearly modulated signals that had been proposed by Mengali [48] and using alternative reduced-complexity scheme such as decomposition and finite series expansion [45]. The decomposition proposed by [48] was suitable to be combined with the alternative technique to reduce trellis search. Özgül *et al.,* [49] proposed a channel pre-coding technique for multipath downlink channels and applied modulo-arithmetic operations to ensure stability in order to reduce complexity of trellis state in a mobile terminal. With channel pre-coding technique, there was no significant energy loss with roll-off-factor of 0.25. BER was 1×10^{-5} at 6.5 dB of performance gap Eb/No. The power efficiency of the system was improved by increasing the number of transmit antenna.

Besides the complexity reduction in trellis state by Hesse *et al.,* [50], the robustness to fading in systems that display good spectral and power efficiency need to be achieved. This can be made possible using an alternative separable implementation of L2-orthogonal space-time codes (STC) and reduced state sequence detection (RSSD) that had been revealed by Wang *et al.,* [51]. The results reported in [50] showed that even though the trellis was reduced to 20 states, the complexity of filter bank was remains unchanged. RSSD technique in [51] has managed to reduce the complexity of coded CPM detection efficiently with little performance loss.

C. Decoding and algorithm

Various methods have been investigated by previous researchers to reduce the complexity in the decoder. The new iterative search (ITS) detector based on maximum a posteriori (MAP) for non-coherent detection in the receiver proposed by Brown *et al.,* [52] has the potential to reduce the effect of jamming and signal interference of frequency hopped environment with BER performance of $1x10^{-3}$. In other study, matched filter bank which consist of analog filter and Walsh Space Approach was used by Svensson *et al.,* to reduce the complexity of Viterbi decoder [41]. In addition, using this approach, the performance degradation was higher for channel with significant adjacent channel. The trellis state was reduced to 32 states in AWGN channel.

Zhang *et al.,* [53] proposed the use of puncturing method at low-rate ring convolutional encoder outputs. They reported that the rate-2/3 punctured codes offered less performance degradation compared to the parent rate-1/2 codes, and the performance degradation increased when the rate was 3/4. Xian *et al.,* [54] also analyzed the same kind of complexity present in CPM, however, they used different technique which is orthogonal space-time block codes (OSTBC) for BCPM based on Laurent Decomposition for the purpose of achieving spatial

THE PERFORMANCE OF TECNIQUES USED TO REDUCE COMPLEXITY OF CPM

Types Of Complexity	Method / Approach	Performance
Reducing the number of match filter and signal terms in CPM [43]	MLSE based on PAM representation	Match filter = 3, Performance gain = 2dB, Cumulative loss = 2.6dB, BER = 1 x 10^{-5}
Reducing the number of match filter either coherent or non-coherent reception [35]	Basis Function Expansion	Efficiency = 2.56 Bandwidth = 25 kHz Power bandwidth = 99% Real filter = 2
Reducing the complexity of trellis state based on two transmit antennas OST-MCPM systems [46]	Non-coherent detection algorithm	Performance < 0.5 dB at 1<N<3
Reducing the complexity of trellis state in a mobile terminal and maintaining spectral efficiency by introducing only small envelop variation [49]	Channel precoding technique for multipath downlink channel Modulo-arithmetic operations for stability	no significant energy loss roll-off factor = 0.25 performance gap: 6.5dB at BER = 1 x 10^{-5} for $N_T = 6$ 15dB at BER = 1 x 10^{-3} for $N_T = 4$
Allowing a near optimum reception with very low complexity of MLSD [56]	Walsh space and M-algorithm	Power loss = 0.1 dB 0.5 time decrease for M-algorithm.

diversity at the cost of a high decoding complexity. Using this approach, the performance of quasi-static channel estimates was about 0.4 dB at a BER of 10^{-4} with much lower receiver complexity. Lampe *et al.,* [55] made the proper combination of non-coherent CPM with convolutional coding to improve power efficiency Maximum likelihood sequence detector (MLSD) which resulted in moderate transmitter and receiver complexity.

D. Maximum likelihood sequence detector (MLSD)

Francisco *et al.,* [56] reported that optimum reception could be achieved with very low complexity of MLSD using Walsh space and M-algorithm. By combining those techniques, the quasi-optimum experienced the low power loss which was only 0.1 dB. M-algorithm for 8-ary scheme was found to have 0.5 time degradation. In other study, Su *et al.,* [57] reduced the minimum Euclidean distance using single amplitude modulated pulse (AMP) based upon Laurent representation which in turn helps to reduce the complexity of MLSD.

E. Minimum mean square error (MMSE)

A Polyphase Matrix Model was introduced by Thillo *et al.,* [58] to reduce complexity of the existing Minimum Means Square Error (MMSE) channel equalizer and develop an existing high-performance frequency domain equalization approach for CPM signals. Lower BER can be obtained when the modulation index was increased. The CPM autocorrelation matrix can be approximated which reduced the complexity.

Özgül *et al.,* [59] worked on the same problem using a soft-information aided minimum mean-squared error (MMSE) equalizer and the frequency domain equalization (FDE) approach. They managed to obtain approximately 1 dB performance gain of the aforementioned scenarios when BER equals to 1×10^{-5}.

Other technique that was used to reduce the complexity of MMSE is Frequency Domain Equalization approach by Thillo et al., [60] which separated channel equalization on the one side and demodulation of the equalized CPM signal on the other. It can be concluded that MMSE complexity reduction technique can be applied for any modulation index without noticeable performance loss.

VI. DISCUSSION

As discussed previously, numerous investigations have been carried out in order to overcome the limitations of CPM and enhance the system performance at the same time. New approaches and models were proposed to ensure that the CPM becomes more efficient and is acceptable, and the complexity of CPM is successfully reduced. Table II summarizes the techniques used in the complexity reduction techniques of CPM.

Five classes of CPM complexity have been discussed; match filter, trellis state, decoding and algorithm, MLSD and MMSE. These classifications need to be observed very carefully in order to choose the best techniques of complexity reduction to ensure that CPM is suitable and compatible with (MB-OFDM) UWB system. Complexity reduction in the number of match filter in [35] using basis function expansion technique is applicable to coherent and non-coherent CPM. Non-coherent demodulation, such as envelop detection or square-law detection is commonly used to decrease the complexity and cost of the receiver of (MB-OFDM) UWB system.

The non-coherent demodulation is suitable for complexity reduction of CPM since it has the same properties as (MB-OFDM) UWB. In terms of complexity reduction in trellis state, [46] can be employed. This detection algorithm has the capability to analyze and examine the compatibility of the CPM scheme used in short range wireless transmission. Besides that, the non-coherent detection algorithm can provide extremely good BER performance.

Walsh space approach and M-algorithm can be used to reduce the complexity of maximum likelihood sequence detector (MLSD) [56]. This technique also compatibles to Viterbi decoder and suitable for CPM because (MB-OFDM) UWB is restricted to convolutional codes only for the channel coding and requires Viterbi decoder at the receiver. Hence, the performance of the system can be improved by reducing the number of Viterbi decoder.

VII. CONCLUSION

Modulation technique used in (MB-OFDM) UWB system has been discussed and the new possible mapping

or modulation technique, which is CPM for this system has been proposed. Since CPM has a limitation on its complexity at the receiver, appropriate techniques need to be applied to the system to overcome the problems. Techniques such as basis function expansion, non-coherent detection algorithm and Walsh space approach can be used to reduce the trellis state, the number of match filter, and the complexity of Viterbi decoder. The selection of the technique depends on the CPM characteristics and the wireless system of (MB-OFDM). Since the choice is considered a major challenge, it is crucial to choose the right modulation technique for the right purpose.

ACKNOWLEDGMENT

The authors would like to thank Minister of Higher Education, Malaysia (MOHE) for supporting this research through grant number 600-RMI/ST/FRGS5/3/ Fst(120/2010) and 600-RMI/ST/FRGS 5/3/Fst(164/2010)

REFERENCES

[1] W. P. Siriwongpairat and K. J. R. Liu, *Ultra-wideband communications systems: multiband OFDM approach*: Wiley-IEEE Press, 2007.

[2] M. Hamalainen, R. Tesi, and J. Iinatti, "On the UWB system performance studies in AWGN channel with interference in UMTS band," in *Ultra Wideband Systems and Technologies, 2002. Digest of Papers. 2002 IEEE Conference on*, 2002, pp. 321-325.

[3] N. Nyirongo, W. Q. Malik, and D. J. Edwards, "Concatenated RS-Convolutional Codes for Ultrawideband Multiband-OFDM," in *Ultra-Wideband, The 2006 IEEE 2006 International Conference on*, 2006, pp. 137-142.

[4] H. Arslan, Z. N. Chen, M. G. Di Benedetto, and I. Books24x, *Ultra wideband wireless communication*: Wiley Online Library, 2006.

[5] L. Changyi, Z. Guoxin, and W. Min, "Performance Analysis of Constellation Mapping and Channel Estimation in MB-OFDM UWB Systems," in *Wireless Communications, Networking and Mobile Computing, 2006. WiCOM 2006.International Conference on*, 2006, pp. 1-4.

[6] R. Blazquez, P. P. Newaskar, F. S. Lee, and A. P. Chandrakasan, "A baseband processor for impulse ultra-wideband communications," *Solid-State Circuits, IEEE Journal of,* vol. 40, pp. 1821-1828, 2005.

[7] J. Xu, X. Lu, H. Wu, Y. Bian, D. Zou, X. Zou, and C. Wang, "Implementation of MB-OFDM Transmitter Baseband Based on FPGA," in *Circuits and Systems for Communications, 2008. ICCSC 2008. 4th IEEE International Conference on*, 2008, pp. 50-54.

[8] A. M. Karim, M. S. Islam, and M. Othman, "Orthogonal Frequency Division Multiplexing Timing Synchronization in Multi-Band Orthogonal Frequency Division Multiplexing Ultra-Wideband Systems," *American Journal of Applied Sciences,* vol. 7.

[9] S. Bhattacharya, R. Senguttuvan, and A. Chatterjee, "Production test enhancement techniques for MB-OFDM ultra-wide band (UWB) devices: EVM and CCDF," in *Test Conference, 2005. Proceedings. ITC 2005. IEEE International*, 2005, pp. 10 pp.-245.

[10] S. M. R. Islam and K. Kyung Sup, "Winner-hopf interpolation aided kalman filter-based channel estimation for MB-OFDM UWB systems in time varying dispersive fading channel," in *Advanced Communication Technology (ICACT), 2010 The 12th International Conference on*, pp. 1184-1188.

[11] K. Jee-Hyun, S. Eu-Suk, Y. Hyun, S. Hyoung-Kyu, and Y. Young-Hwan, "Performance of MB-OFDM UWB Systems with Extra Diversity," in *Wireless Broadband and Ultra Wideband Communications, 2007. AusWireless 2007. The 2nd International Conference on*, 2007, pp. 25-25.

[12] C. Danfeng, F. Haipeng, C. Yunfeng, L. Wei, Y. Fan, L. Ning, and R. Junyan, "A sideband-suppressed low-power synthesizer for 14-band dual-carrier MB-OFDM UWB transceivers," in *Circuits and Systems (ISCAS), Proceedings of 2010 IEEE International Symposium on*, pp. 2139-2192.

[13] A. Mehbodniya and S. Aissa, "Effects of MB-OFDM System Interference on the Performance of DS-UWB," *Vehicular Technology, IEEE Transactions on,* vol. 58, pp. 4665-4669, 2009.

[14] L. Yanmei, W. Chang-Ching, A. Sangiovanni-Vincentelli, and J. M. Rabaey, "Design and Optimization of an MB-OFDM Ultra-Wideband Receiver Front-End," in *Circuits and Systems for Communications, 2008. ICCSC 2008. 4th IEEE International Conference on*, 2008, pp. 502-506.

[15] Y. Matsumoto, K. Fujii, A. Sugiura, and T. Murakami, "Impact of electromagnetic noises from PCs on the performance of MB-OFDM UWB systems," in *Consumer Electronics, 2009. ISCE '09. IEEE 13th International Symposium on*, 2009, pp. 430-433.

[16] A. Batra, S. Lingam, and J. Balakrishnan, "Multi-band OFDM: a cognitive radio for UWB," in *Circuits and Systems, 2006. ISCAS 2006. Proceedings. 2006 IEEE International Symposium on*, 2006, pp. 4 pp.-4097.

[17] M. Magani, G. Lu, and C. Xiaodong, "Improved BER performance on MB-OFDM UWB system using adaptive bit loading," in *Ultra-Wideband (ICUWB), 2010 IEEE International Conference on*, pp. 1-4.

[18] C. Snow, L. Lampe, and R. Schober, "Interference mitigation for coded MB-OFDM UWB," in *Radio and Wireless Symposium, 2008 IEEE*, 2008, pp. 17-20.

[19] M. Takahide, M. Yasushi, F. Katsumi, and S. Akira, "Interference potential of PC noises on MB-OFDM UWB systems," *Communications Letters, IEEE,* vol. 10, pp. 804-806, 2006.

[20] F. Xiangning, L. Bing, Z. Zaichen, and B. Guangguo, "Modified UWB channel estimation," in *Mobile Technology, Applications and Systems, 2005 2nd International Conference on*, 2005, pp. 6 pp.-6.

[21] D. Lowe and X. Huang, "Ultra-Wideband MB-OFDM Channel Estimation with Complementary Codes," in *Communications and Information Technologies, 2006. ISCIT '06. International Symposium on*, 2006, pp. 623-628.

[22] J. Maunu, M. Laiho, T. Koivisto, K. Virtanen, M. Pankaala, and A. Paasio, "Mixed-signal baseband processing chain for a MB-OFDM receiver," in *Electronics, Circuits and Systems, 2008. ICECS 2008. 15th IEEE International Conference on*, 2008, pp. 470-473.

[23] A. Tani and R. Fantacci, "A Low-Complexity Cyclostationary-Based Spectrum Sensing for UWB and WiMAX Coexistence With Noise Uncertainty," *Vehicular Technology, IEEE Transactions on,* vol. 59, pp. 2940-2950.

[24] F. Wen and C. Chiu-Sing, "Efficient and low complexity phase tracking method for MB-OFDM UWB receiver," in *Circuits and Systems (MWSCAS), 2010 53rd IEEE International Midwest Symposium on*, pp. 221-224.

[25] R. Cardinali, L. De Nardis, P. Lombardo, and M. G. Di Benedetto, "Lower bounds for ranging accuracy with multi band OFDM and direct sequence UWB signals," in *Ultra-Wideband, 2005. ICU 2005. 2005 IEEE International Conference on*, 2005, pp. 302-307.

[26] H. Yang, Y. Zheng, H. D. Jung, E. Tangdiongga, and A. M. J. Koonen, "Simulation of Multi-Band OFDM UWB Radio Over Multimode Fibre Using Pre-distortion Technique," 2008.

[27] L. Qi, Z. Luyong, Z. Zheng, and Y. Yabin, "A Novel Active Spectrum Sensing Scheme for Cognitive MB-OFDM UWB Radio," in *Cognitive Radio Oriented Wireless Networks and Communications, 2008. CrownCom 2008. 3rd International Conference on*, 2008, pp. 1-6.

[28] K. Deergha Rao and T. S. N. Murthy, "Effect of filtering and turbo coding on the performance of clipped MB-OFDM UWB signals," in *Information, Communications & Signal Processing, 2007 6th International Conference on*, 2007, pp. 1-5.

[29] M. P. Wylie-Green, "Dynamic spectrum sensing by multiband OFDM radio for interference mitigation," in *New Frontiers in Dynamic Spectrum Access Networks, 2005. DySPAN 2005. 2005 First IEEE International Symposium on*, 2005, pp. 619-625.

[30] H. Viittala, M. Hamalainen, and J. Iinatti, "Comparative Studies of MB-OFDM and DS-UWB with Co-Existing Systems in AWGN Channel," in *Personal, Indoor and Mobile Radio Communications, 2006 IEEE 17th International Symposium on*, 2006, pp. 1-5.

[31] L. Jee-Hye, B. Myung-Sun, and S. Hyoung-Kyu, "Improved Performance of Soft Decision Decoding for DCM in MB-OFDM System," in *Image and Signal Processing, 2008. CISP '08. Congress on*, 2008, pp. 165-169.

[32] T. Le Chung and A. Mertins, "Space-Time-Frequency Code implementation in MB-OFDM UWB communications: Design criteria and performance," *Wireless Communications, IEEE Transactions on,* vol. 8, pp. 701-713, 2009.

[33] J. F. Gerrits, J. R. Farserotu, and J. R. Long, "Low-Complexity Ultra-Wide-Band Communications," *Circuits and Systems II: Express Briefs, IEEE Transactions on,* vol. 55, pp. 329-333, 2008.

[34] F. Xiong and I. Books24x, *Digital modulation techniques*: Artech House Norwood, MA, USA, 2000.

[35] C. Brown and P. J. Vigneron, "Complexity reduction for continuous phase modulation using basis functions," in *Military Communications Conference, 2009. MILCOM 2009. IEEE*, 2009, pp. 1-7.

[36] R. Penrod, M. P. Fitz, Z. Weijun, and O. Takeshita, "A low complexity packet detection algorithm for a CPM modem," in *Signals, Systems and Computers, 2004. Conference Record of the Thirty-Eighth Asilomar Conference on*, 2004, pp. 1062-1067 Vol.1.

[37] A. Perotti, A. Tarable, S. Benedetto, and G. Montorsi, "Capacity-Achieving CPM Schemes," *Information Theory, IEEE Transactions on,* vol. 56, pp. 1521-1541.

[38] N. Zhang and P. Yang, "Reduced-State Detection for Continuous Phase Modulation (CPM) Signals," in *Intelligent Information Hiding and Multimedia Signal Processing, 2008. IIHMSP '08 International Conference on*, 2008, pp. 1205-1208.

[39] O. Dural and J. G. Proakis, "The performance of simplified maximum-likelihood sequence detector for continuous phase modulation scheme," in *Communications, 2000. ICC 2000. 2000 IEEE International Conference on*, 2000, pp. 641-645 vol.2.

[40] G. Colavolpe and R. Raheli, "Reduced-complexity detection and phase synchronization of CPM signals," *Communications, IEEE Transactions on,* vol. 45, pp. 1070-1079, 1997.

[41] T. Svensson and A. Svensson, "Reduced complexity detection of bandwidth efficient partial response CPM," in *Vehicular Technology Conference, 1999 IEEE 49th*, 1999, pp. 1296-1300 vol.2.

[42] Z. Wanlun and G. B. Giannakis, "Reduced complexity receivers for layered space-time CPM," *Wireless Communications, IEEE Transactions on,* vol. 4, pp. 574-582, 2005.

[43] E. Perrins and M. Rice, "Optimal and reduced complexity receivers for M-ary multi-h CPM," in *Wireless Communications and Networking Conference, 2004. WCNC. 2004 IEEE*, 2004, pp. 1165-1170 Vol.2.

[44] M. Figuera and J. V. Krogmeier, "Optimum and suboptimum receivers for M-ary CPM signals based upon the Laurent representation," in *Vehicular Technology Conference, 2002. Proceedings. VTC 2002-Fall. 2002 IEEE 56th*, 2002, pp. 2268-2272 vol.4.

[45] J. Huber and W. Liu, "An alternative approach to reduced-complexity CPM-receivers," *Selected Areas in Communications, IEEE Journal on,* vol. 7, pp. 1437-1449, 1989.

[46] S. Wenli and Y. Yanping, "Non-coherent detection for orthogonal space-time coded CPM systems," in *Anti-Counterfeiting Security and Identification in Communication (ASID), 2010 International Conference on*, pp. 334-338.

[47] A. Cero, D. Fertonani, G. Colavolpe, and M. P. Wylie-Green, "On Reduced-Complexity Soft-Output Detection of Continuous Phase Modulations," in *Vehicular Technology Conference, 2008. VTC Spring 2008. IEEE*, 2008, pp. 1092-1096.

[48] U. Mengali and M. Morelli, "Decomposition of M-ary CPM signals into PAM waveforms," *Information Theory, IEEE Transactions on,* vol. 41, pp. 1265-1275, 1995.

[49] B. Ozgul, M. Koca, H. Delic, and G. L. Stuber, "Pre-Equalization of Continuous Phase Modulation for Multipath Fading Channels," in *Wireless Communication Systems, 2007. ISWCS 2007. 4th International Symposium on*, 2007, pp. 166-170.

[50] M. Hesse, J. Lebrun, L. Lampe, and L. Deneire, "Separable Implementation of L2-Orthogonal STC CPM with Fast Decoding," in *Communications, 2009. ICC '09. IEEE International Conference on*, 2009, pp. 1-5.

[51] W. Haibo, L. Suoku, and J. Guodong, "Reduced State Sequence Detection for Ring Convolutional Coded Continuous Phase Modulation," in *Wireless Communications Networking and Mobile Computing (WiCOM), 2010 6th International Conference on*, pp. 1-4.

[52] C. Brown and P. J. Vigneron, "A reduced complexity iterative non-coherent CPM detector for frequency hopped wireless military communication systems," in *Military Communications Conference, 2005. MILCOM 2005. IEEE*, 2005, pp. 2345-2349 Vol. 4.

[53] Z. Lei, N. Jinnan, and Z. Honghui, "A Puncturing Method for Ring Convolutional Coded Continuous Phase Modulation," in *Networks Security Wireless Communications and Trusted Computing (NSWCTC), 2010 Second International Conference on*, pp. 412-414.

[54] X. Liang, R. Punnoose, and L. Huaping, "Simplified receiver design for STBC binary continuous phase modulation," *Wireless Communications, IEEE Transactions on,* vol. 7, pp. 452-457, 2008.

[55] L. H. J. Lampe, R. Schober, G. Enzner, and J. B. Huber, "Coded continuous phase modulation with low-complexity noncoherent reception," *Communications, IEEE Transactions on,* vol. 50, pp. 517-520, 2002.

[56] F. A. T. B. N. Monteiro and A. J. C. B. Rodrigues, "CPM reception combining complexity reduction techniques for schemes on minimum Euclidian distance upper bound and MSK," in *Information Theory, 2004. ISIT 2004. Proceedings. International Symposium on*, 2004, p. 218.

[57] S. Yi and Z. Shidong, "Performance estimation of P state coherent binary CPM receiver based on Laurent decomposition," in *Wireless Communications, Networking and Mobile Computing, 2005. Proceedings. 2005 International Conference on*, 2005, pp. 573-578.

[58] W. Van Thillo, J. Nsenga, R. Lauwereins, V. Ramon, A. Bourdoux, and F. Horlin, "Complexity Reduction of High-Performance Frequency Domain Equalization for CPM," in *Global Telecommunications Conference, 2008. IEEE GLOBECOM 2008. IEEE*, 2008, pp. 1-6.

[59] B. Ozgul, M. Koca, and H. Delic, "Double turbo equalization of continuous phase modulation with frequency domain processing," *Communications, IEEE Transactions on,* vol. 57, pp. 423-429, 2009.

[60] W. Van Thillo, F. Horlin, J. Nsenga, V. Ramon, A. Bourdoux, and R. Lauwereins, "Low-complexity linear frequency domain equalization for continuous phase modulation," *Wireless Communications, IEEE Transactions on,* vol. 8, pp. 1435-1445, 2009.

Defense Triangular of Routers (DTR) against traffic of packets in Internet Data Centers (IDC)

Hamid Mehdi
Islamic Azad University, Andimeshk Branch
Andimeshk, Iran
hamimehdi@gmail.com

Amir Masood Rahmani
Islamic Azad University, oloum Tahghighat Brach
Tehran,Iran
Rahmani74@yahoo.com

***Abstract*-These days many of the data centers are looking for new ways in order to increase the amount of responding to requests and also offering effectual and optimal services. Hence, in many of the data centers procedures like cache management of physical resources same as routers, load balancing, controlling over load, QOS mechanisms are utilized. One of the reasons that decrease the effectiveness of a router after a period of time is the reduction of the buffer level and the elimination of the packets by the router. It makes many unanswered requests or at least prolonged answering time. This article tries to offer an approach in order to increase the amount of the routers to improve the efficiency of an Internet Data Center (IDC). The article has shown an appropriate correspondence between the results and the hypothesis.**

Keywords-Internet Data Centers; Performance; Router; Defense Triangular of Routers

I. INTRODUCTION

There are involved elements in a growth in the amount of users' requests. The first one is high costs of stable communication and the second is lack of appropriate support in terms of new compulsory progresses.

Immediate accessibility to IDC (Internet Data Centers) is achievable through two procedures: first, direct access of the customers to the nearest servers [1-6] second, shifting Overcrowd links instead of near links [7, 8].

These two procedures will reduce the requesting time of the customers to the data, thus more requests will be responded.

In order to increase the efficiency of the data center hardware and software redundancy can be utilized; although it would make new costs. There are other procedures to increase the efficiency, such as alternation in terms of available protocol in away that TCP/IP packets store the maximum information that causes a reduction in the used bandwidth, reduction of packets in order to reduce overloads, a growth in bandwidth, overcrowd prevention.

Every router is able to respond to a number of packets in a time unit up to its structure, model and its company. And it uses memory, processor, and its buffer according to the amount of responses.

Figure 1 shows an effectiveness diagram of the router processor in the procedure of responding to users of a WebTV router. Many believe that when we talk about a processor or evaluation of router efficiency; an efficient router is one that is able to achieve 100% performance. Figure 1 Shows that the amount of a router performance in 300 seconds which is working 23.85% average. It is observed that the performance of the router is less than 30% and experimentally, it is believed that one should not allow the router performance make a rise above 40 or 45%. It will cause a decrease in buffer rate for the router. Consequently, the packets will be deleted because of buffer shortage.

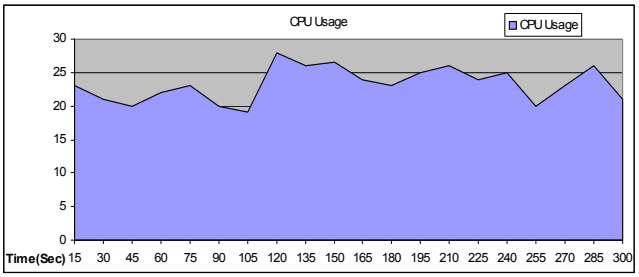


Figure 1.CPU Utilization of Router

If the performance of a router processor goes above 80%, it shows that the router is used as a Bottleneck. And it must look for sources of packet production on the net, which have caused an overcharge. Router designer companies such as Cisco offered some situation to resolve this problem such as interrupt and making new packets on the net. Many of the managers when this happen tries to change the procedures or upgrade the router or some will do an easier job, they buy routers with higher performances and use it on the net. There are three sources: 1. Width band which you can not send more than its capacity 2. Buffer zone, packet of the memory will be read, then they will stay in the buffer. If the buffer is not enough, the information will be dropped. 3. Router process or cycles which are the most signification elements of growth in the performance on the net.

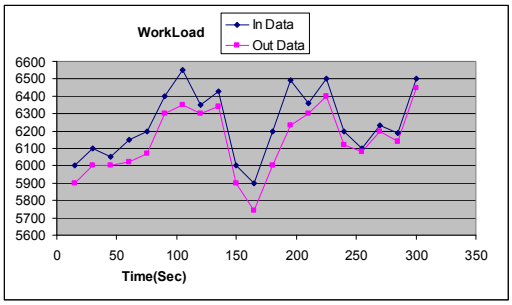


Figure 2. WORKLOAD

Figure 2 is load of a router in 300 seconds. In this figure the most incoming of packets in 63 %(

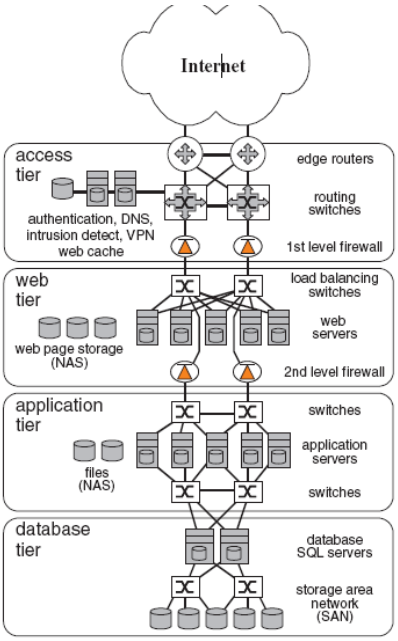


Figure. 3. IDC Four Tier Architecture

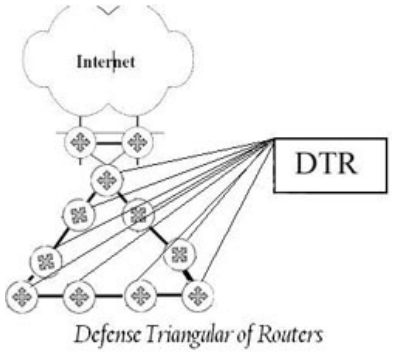


Figure 4. SYSTEM MODEL

6259.2kb.) And most outgoing of the packets is 5.5% (5488.7 kb/s). It shows a decrease of 0.8%, so packet deletion (dropping) happens.

According to figure 1 and figure 2 whenever workload goes up, the performance increases, too. And some of the packets will be deleted for some reasons. In the following parts: part2 will talk about current architecture of Data Centers. Part 3 offers an algorithm of a proposed way on traffic forecast. Part 4 show a simulation and part 5 discusses the conclusion.

II. ARCHITECTURE OF A DATA CENTER

Fig.4 shows four-tier architecture in accordance with current Internet Data Centers. Consider the necessities of an electronic trading session. First level of accessibility: here the requests will be checked then their rout will be distinguished. Then they will be sending to the server or the switcher based on the type of requests. At last, the information must pass the firewall to reach the next step.

In the next layer, load controllers will check the information. If they are requested information, they will be load-balanced and that layer will answer the user. Otherwise, information is send to the next layer. In the application layer, the applicable program extracts the information from Data Center layer and the extracted information will be displayed to the user.

Remember that in every session in Data Center that happens for a request, data Center will that information a unique sign. This will help information clusters not to interfere with each other.

A. A TYPICAL SYSTEM IN A SIMPLE WAY

In this section multilayer Internet Data Centers are considered crucial In order to talk about router management. As you can see in figure 4 the considered model is in access layer and available routers. In this way a router can be a transferable router (transfer is defined as a limited time from launching point of the router to the normal performance of it to get the information in order to response). That would be transferred to groups of answering routers based on the needs and rising of workload and after answering in consideration to the situation will be back on the last state.

III. PROPOSED ALGORITHM

Proposed algorithm, which is called Defense Triangular of Routers (DTR), has two router groups. Routers that are answering to incoming requests are called hot routers or working routers. Routers that are in the router set and time algorithm will decide their entrances are called cold or off routers.

This article tries to offer an algorithm according to hardware redundancy which is called DTR (Defense Triangular of Routers) to transfer the routers in a Data Center actively and automatically. The aim of the algorithm is to increase the number of answering when the incoming requests raise I Data Center. In order to get all the intended aims, algorithm must compute system behavior in all situations.

As a result, to study the situations of figure 4 a periodical manner of all working loads that go on the router (a periodical computing with a distinct T in a minute) is required. Furthermore, in the proposed algorithm of a router in transferring it from a hot group to a cold group, there is a delayed time which is called transferring time. Transferring time depends on some parameters in relation to its boot moment up to its accomplished moment. For example, transferring time can be of booting of a system and its working situation. Transferring time for routers can be a number between 1 to 10 minutes. Experimentally, transferring time is supposed to be 3 to 5 minutes. Besides, if a router is free, it must answer all the requests to be able to leave the router groups. The assumed time for a router to leave would be between 1 to 15 minutes.

In order to Proven methods provide an example,
Network managers of a Company calculate that their data center can answer up to 40 billion Requests; at the beginning of 1990 the rate of traffic was estimated 5.2 billion requests. If traffic growth rate of 2% and traffic

increase in constant therefore when network traffic reaches maximum?
Solution:
P= 5.2 billion = traffic primary
r=0.02 = growth rate
Traffic in year 1991 is:
(1.02) * (5.2) billion
Traffic in year 1992 is:
$(1.02)^2(5.2)$ billion
So traffic after n years is:
$(1.02)^n$ (5.2) billion.
Now Put in 40= $(1.02)^n$ (5.2) so n can be calculated by:

$$n\log(1.02) = \log\frac{40}{5.2}$$

Thus:

$$n = \frac{\log\frac{40}{5.2}}{\log(1.02)} = 102.02$$

Therefore in 103 +1990 = 2093 traffic reaches 40 billion packages.

In this example were calculated the traffic growth rate from Annual. Growing traffic at the end of each month is calculated, in the above example the growth rate per month equal to:

$$0.02/12 = \frac{2}{1200} = \frac{1}{600}$$

And Traffic after one month is:
$(1+\frac{1}{600})(5.2)$ Billion
And Traffic after two months is:
$(1+\frac{1}{600})^2(5.2)$ Billion
And Traffic in 1991 is
$(1+\frac{1}{600})^{12}(5.2)$ Billion
So Traffic after n years is:
$(1+\frac{1}{600})^{12n}(5.2)$ Billion

At last Traffic in 2092 year is:
$(1+\frac{1}{600})^{12*103}(5.2)$ Billion

$$\Rightarrow (1.001667)^{1236}(5.2) = 40.720818$$

If the traffic calculated daily, the growth rate in one day is: $(\frac{1}{600}/20) = (\frac{1}{18000})$
And Traffic after a year is:
$(1+\frac{1}{18000})^{12*3}(5.2)$ Billion
So Traffic after n years is:
$(1+\frac{1}{18000})^{36n}(5.2)$ Billion
At last traffic in 2093 Equal to:

$$(1+\frac{1}{18000})^{36*103}(5.2) = (1+\frac{1}{18000})^{3708}(5.2) = 40.796776$$

Billion.

If traffic calculated in each hour, now traffic growth rate equal to:

$$(1+\frac{1}{18000})/24 = \frac{1}{422000}$$

So Traffic in 2093 is:

$$(1+\frac{1}{422000})^{3708*24}(5.2) = (1.00000022)^{88992}(5.2) = 40.796776$$

If traffic calculated in the second, traffic in 2093 will be more and 40/799 billion packages.
This is better to look at the following article:

$$a_n = (1+\frac{1}{n})^n \qquad (1)$$

This sequence (formula) calculates for different values of n:

n	a_n
1	2
10	2.59374
100	2.70481
1000	2.71692
10000	2.71814
100000	2.71826

Theorem:

$$a_n = \lim_{n\to\infty}(1+\frac{1}{n})^n \qquad (2)$$

It is calling the number "***e***" and its value is 2.71. (e=2.71)
r is traffic growth rate And ***P*** for primary traffic so the traffic after t years show, ***P (t)***.
If the traffic calculated from Annual:

$$P(2) = (1+r)^2 P..., P(t) = (1+r)^t P$$

And

$$P(1) = (1+r)\ P$$

And if calculate the traffic in (1/n) year:
Therefore After t years if every (1\n) year calculate the traffic, traffic depends on the two variables t (time) and n (number of time-division). Therefore traffic equal to:

$$P_n(t) = (1+\frac{r}{n})^{nt} P \qquad (3)$$

If the n large and large, its mean traffic calculated in a short time and that will be close and closer to the real traffic model. Therefore if n desire to infinite, traffic calculated every moment. This model called continuous model and show it with ***P (t)***.
Therefore:

$$P_n(t) = \lim_{n\to\infty} P_n(t)$$

$$P_n(t) = \lim_{n\to\infty}(1+\frac{r}{n})^{nt} P$$

Assuming $x = \frac{n}{r}$ if $n \to \infty$ then

$x \to \infty$ So $P_n(t) = \lim_{x\to\infty}(1+\frac{1}{x})^{xrt} P$

But : $\lim_{x\to\infty}(1+\frac{1}{x})^{xrt} = \left[\lim_{x\to\infty}(1+\frac{1}{x})^{x}\right]^{rt}$

And it showed that:

$$\lim_{x\to\infty}(1+\frac{1}{x})^{x} = e \qquad (4)$$

So:

$$P(t) = \left[\lim_{x\to\infty}(1+\frac{1}{x})^{x}\right]^{n} P = Pe^{n}$$

Therefore a continuous traffic model is as follows:

$$P(t) = Pe^{n} = Pe^{rt} \qquad (5)$$

When **r** is positive it is calling ***development model*** and when r is negative it is calling ***deterioration model***.

Again traffic calculated in the example for 2093 year by formula 5:

$r = 0.02$

$t = 2092 - 1990 = 102$

Billion packets.

Therefore:

$P = 5.2$ Billion package.

Therefore, in 2093 as the year that the network is not able to answer traffic. This year, can be calculated as follows:

$$40 = P(t) = (5.2)e^{0.024}$$

Billion packages

$$\Rightarrow e^{0.024} = \frac{40}{5.2}$$

$$\Rightarrow 0{,}024 = \ln\frac{40}{5.2}$$

And where:

$$t = 50\ln\frac{40}{5.2} = 102.01104$$

And result is 2092:

2092 = 102 +1990

At last formula 5 computes the number of the traffic.

Therefore in every T_i some parameters would be evaluated for routers:

N_{Ro}: initial routers in the first layer

P(t): generate traffic every period

r: traffic factor

t: time factor.

P: traffic value in start time

N_{rn}: needed routers at the end of every time period…

N_{req}: number of request that any router can response. This value is defined for any router that designer company explain it [10].

$$N_{rn} = [P(t)/N_{req}] \qquad (6)$$

At last equation 6 computes the number of the routers, which must be in the line for the next period.

When a system is under a high workload the incoming requests maybe more than the answers prepared by the routers. Thus, N_{rn} is computed in the next period to answer more requests and algorithm will be allowed to compute the number of the routers in the period in high workload by using K, which is obtained in formula 1.

In equation 6 Number of the routers for the next period is computed by using a fixed factor. Algorithm DTR is studying the number of routers when $N_{ro} \neq N_{rn}$ which is the result of the computing. Here, redundancy, which is the result of the router transferred, may be able to change the number of the routers. Therefore, there are some to reduce the effect of the workload redundancy. First, increasing the time period of computing T. second, considering the fact that if the number of the routers is more than enough ($N_{rn} > N_{Ro}$) and there are routers from last period and in a LIFO are leaving the group, let them come back again in the group to answer. Or if ($N_{rn} < N_{Ro}$) the number of routers is less than enough do not let the last router to come in and connect the chain of the routers. Finally, computing the number of the routers in order to transfer from/to the group reduces redundancy effect.

First, it is supposed the routers have many requests. Then, the requests are going to be answered as FIFO. (In figure 4)

At last look at this example: N_{rc}: 2 and take P: 4000000 and t=30 , K= 0.02 , N_{req}=1500000 and traffic computed by A=4000000 * $e^{0.02 * 30}$ =7259024.293
Billion finally needed routers is obtained by and Nrn: [7259024.293/1500000] = 5. In this way when ($N_{rn} > N_{Ro}$) number of routers will be obtained to join N_{rn}-N_{Ro}=3 group.

IV. SIMULATION

Figure 4 is designed and utilized by YACSIM [9]. figure 5 shows all the information related to access layer for two routers in 300 seconds in different time period in FRM (fixed router management).

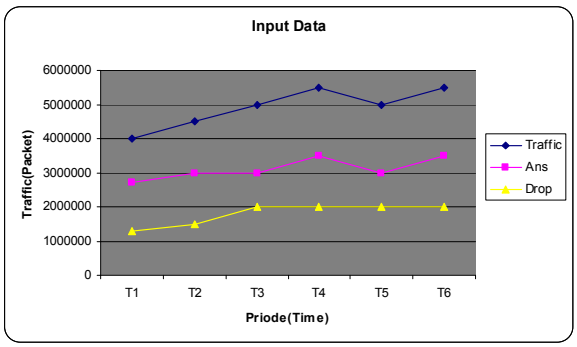


Figure 5. Input Data in FRM (Fixed Router Management

For example in T4 time period, there are 5500000 requests. 64% of all these requests are answered and 36% are deleted, because of reasons like: buffer space. Also there is 11 Ms. delayed time in responding. Workload average of the processor at the same time is 24%. 2000000 of requests are deleted and 3500000 the

packets are requested. In addition, all these numbers are an average of two routers in the first layer.

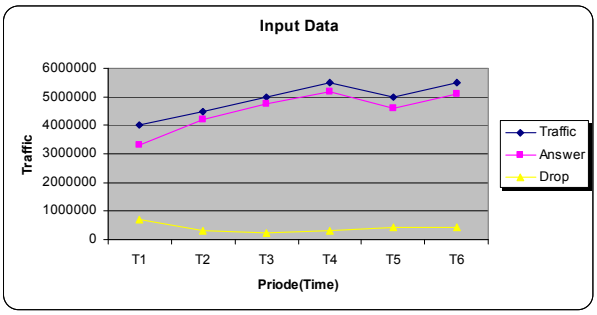


Figure 6. Input Data in DTR Method

Here, proposed DTR algorithm or a model of system in figure 4 with various routers is simulated and the results in figure 6 and 7 obtained. Remember that all the data in figure 5 are obtained by a normal approach in 300 seconds in six time periods. As an example T4 tome period and FRM (fixed router management) are studied here and the differences are displayed. There are 5500000 requests in this period in which 95 %(5200000) are responded and 5% (300000) are deleted. Also there is a 10ms-delay time. Processor's performance is 27.3. All these statistics are four routers. Now, all the columns in figure 5 and 6 are compared and algorithm performances to increase number of responses, is distinguished.

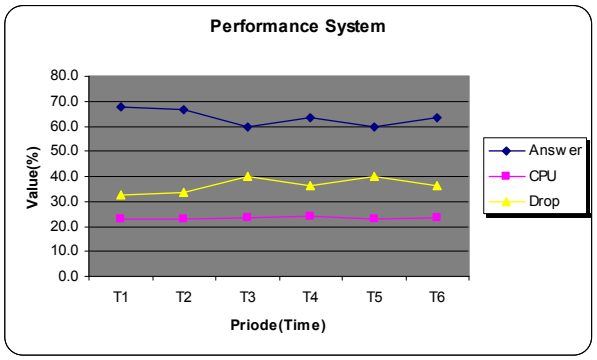


Figure 7. Performance System in FRM (Fixed Router Management)

Figure 7 shows the average percent of the responses for two ways. Number of responses these two ways. Number of responses in these two algorithms is equal (29500000) which are received in six time period in both. In figure 5, 18700000 of them are responded while in figure 6, 27120000 are answered. Comparing the parameters, it's clear that in DTR 91,9% of the responses are answered while in FRM 63.4% of the requests are responded (figure.7).

Figure 5, shows the average of packet dropping in both performances. There are different numbers of request deletion. In F figure 5, 10800000 requests are deleted but In figure 6, 2380000 requests are deleted.

Remember that high rate of responding is due to DTR operation which will cause redundancy costs.

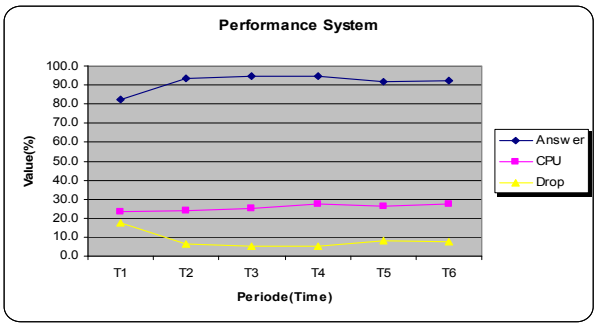


Figure 8. Performance System in DTR

In figure 7 and figure 8 processor operation rate is shown for both procedures. It shows that DTR is more efficient that FRM. And this will show that average working of the processor is high. Consequently, when there is a rise in responding there is a rise in the function of the processor that makes new costs.

V. Conclusion

In this article, it is tried to offer a way in order to increase the efficiency rate of the access layer. Comparing the current procedures (FRM) and the proposed procedure (DTR). It is obvious that DTR is more effective in a way that in number of responses and time period of responding it is more successful that FRM. DTR makes the responding level a rise up to 19.3% and the performance of the router processor increases. These costs are in accordance with high responses and low request deletion.

References

[1] J. Guyton and M. Schwartz, "Locating nearby copies of replicated internet servers," in *Proceedings of ACM SIGCOMM'95*, Cambridge,MA, Aug. 1995.

[2] A. Shaikh, R. Tewari, and M. Agrawal, "On the effectiveness of dns-based server selection," in *Proceedings of IEEE INFOCOM'01*, Anchorage, AK, Apr. 2001.

[3] Z. Fei, S. Bhattacharjee, E. Zegura, and M. Ammar, "A novel server selection technique for improving the response time of a replicated service," in *Proceedings of IEEE INFOCOM'98*, San Francisco, CA, Mar. 1998.

[4] D. Karger, E. Lehman, T. Leighton, M. Levine, D. Lewin, and R. Panigrahy, "Consistent hashing and random trees: Distributed caching protocols for relieving hot spots on the world wide web," in *ACM Symposium on Theory of Computing*, May 1997, pp. 654–663.

[5] L. Wang, V. Pai, and L. Peterson, "The effectiveness of request redirection on CDN robustness," in *Proceedings of OSDI'02*, Boston,MA, Dec. 2002.

[6] M. Karlsson and M. Mahalingam, "Do we need replica placement algorithms in content delivery networks," in *Proceedings of the 7th International Workshop on Web Content Caching and Distribution (WCW'02)*, Boulder, CO, Aug. 2002.

[7] Y. Chen, R. Katz, and J. Kubiatowicz, "Dynamic replica placement for scalable content delivery," in *Proceedings of IPTPS'02*, Cambridge, MA, Mar. 2002.

[8] L. Qiu, V. Padmanabhan, and G. Voelker, "On the placement of web server replicas," in *Proceedings of IEEE INFOCOM'01*, Anchorage, AK, Apr. 2001.

[9] R. Jump. Yacsim reference manual version 2.1. ECE epartment, Rice University.

[10] http://www.cisco.com.Troubleshooting High CPU Utilization on Cisco Routers

An Integrated Fusion Protocol for Congregating Sensor Data in Wireless Sensor Network

Buddha Singh
Sch. of Comp. & System Sciences
Jawaharlal Nehru University
New Delhi, India
e-mail: b.singh.jnu@gmail.com

Adwitiya Sinha
Sch. of Comp. & System Sciences
Jawaharlal Nehru University
New Delhi, India
e-mail: a.singh.jnu@gmail.com

Priti Narwal
Dept. of Computer Science
Manav Rachna International Univ.
Faridabad, India
e-mail: narwal.priti@gmail.com

***Abstract*- Effective fusion of data, accumulated from the sensors, can be regarded as a direct proportional factor to the successful deployment of a wireless sensor network. Two important fusion properties in support of the concerned area are: Correlation and Aggregation. This paper proposes an energy efficient data fusion protocol, which apart from employing power saving aggregation schemes, also implements network throughput enhancing routines via correlation of sensor signals. The protocol operates in dual mode to provide a perfect balance between the workload distributions among the sensor nodes during several parameter calculations. The notion of Connected Correlation Dominating Set is used to find out the clusters of active alive sensors, which actually involves in the transmission of data. On the basis of an Energy Model, the cluster heads are determined. To keep track of the error parameters, Least Squares (LS) estimation method along with the Linear Predictive Model is taken into consideration. Moreover, we simulate our algorithm using the Network Simulator (NS), ns-2.34.**

Keywords- Connected correlation dominating set; hyperedge correlation parameters; least squares; linear prediction; data aggregation & fusion.

General Terms- Integrated data fusion protocol, packet header formats, protocol modes, hypergraph & hyperedges, correlation graph, intersection graph.

I. INTRODUCTION

Rapid and profusive development in the field of sensor network has opened up many exiting portals of research. The large scale sensor networks can be found in varied applications, for instance, precision agriculture, geophysical and environment monitoring, remote health care, and security. The major challenge now is to effectively interpret the informations gathered from the sensors (nodes) and perform fusion over the accumulated data. However, energy that is a constrained property, still pose a threat to the fusion protocol design. In this paper, we concentrate on finding an initial connected correlation dominating set (which contains a considerable number of *active alive* nodes) and further apply intersection graph theory and energy model, to diminish the size of the set of sensor (actually transmitting), even less. We apply the idea of clustering to manage the energy utilization, thus lengthening the network lifetime.

II. RELATED WORK

Many researchers have been showing considerable interests in the field of data fusion in wireless sensor network. The work initiated in [1], have indeed boosted up the concerned area. However, the paper shows up much future prospects, which will be well addressed in this paper. The work in [1] does not support clustering technique and sensor mobility. Our paper responds both these drawbacks, and even finds a set of sensors (that relay data to the sink node), whose size is quite smaller than its existing counterpart. There are some effective mechanisms to find optimal size of the correlation dominating set [2], which also supports our exploration work. Moreover, some nodes can be made to sleep (dormant state) [3], while other active nodes are taken into account for the purpose of cluster formation and data transmission. Even there are various information fusion techniques [4] used to make inferences, estimate parameters, build feature maps (network scans), and compress sensor data.

III. NETWORK MODEL

A. Problem Statement

The aim is to devise a protocol for efficient data gathering from the sensor in wireless sensor network, in energy efficient manner and which calculates the connected correlation dominating set in a more optimized way, both in terms of: (a) size of the correlation dominating set, and (b) runtime cost of the algorithm.

B. Working Scenario

Let there be a given sensor field with substantial number of sensors, randomly deployed. Initially, all the sensors are in *alive* state. Then the neighborhood of each sensor is determined with the network simulation [5] commands. On gathering the knowledge about the neighboring sensors (Fig. 1), we execute the *basic protocol* to gather *d*-hop neighborhood information. In our simulation *d=2* (neighborhood span), i.e. spatial correlation [6] will be exploited to a degree of 2 in the proposed network model.

Next is the correlation structure computation phase, in which the hyperedge parameters are derived and error thresholds [7] are validated on basis of linear predictive

model of Least Squares (LS) estimation method. The outcome of the result is a set of sensors that form the *active* nodes from among the *alive* nodes, i.e. these sensors can be regarded as the *active alive* sensor nodes. The rest of the sensors are put to sleep state and are said to be the *dormant* sensor nodes. These *active alive* nodes form the connected correlation dominating set (connectivity informations are kept with the General Operations Director (GOD) [5] while simulating with ns), thus involving optimal communication cost [8].

The intersection graph reveals the clustering of the *active alive* nodes. Among the *active cluster members*, the node with maximum residual energy is appointed as the *Cluster Head* (CHs). The data transmission takes place between these CHs and the base station, thereby decreasing the actual nodes to transmit, radically. The concept of *epoch period* is further used to track the stability of the wireless sensor network, which when violated; the correlation structure is re-calculated with respect to the mobile network segment.

IV. Proposed Protocol

This section describes about the different modes in which the protocol functions. It also depicts the integrated sub protocols that constitute our data fusion protocol.

The working of the protocol is divided into the following modes:

- Online Mode (or In-Node Calculation)
- Offline Mode (or Off-Node Calculation)

A. Online Mode

- *Basic Protocol:* The purpose of the basic protocol is to accumulate *d*-hop neighborhood information (Fig. 2). In the primary phase, when the correlation structure of the network is not known, each node sends a beacon packet to its entire neighboring nodes. This packet is a control as well as data packet that is used for broadcasting a node's own sensor reading to all its neighboring nodes. After the *beacon* transaction is over, each node acquires 1-hop neighborhood information. On receiving the beacon packet, the receivers respond with a reply packet. This is a data packet that contains a sensors own data as well as its 1-hop neighborhood information also gets piggybacked, which was gathered in the *beacon* phase. Thus after the *reply* transaction all nodes will possess 2-hop neighborhood information. At the end, the correlation structure of the network (Fig. 3) is derived using the proposed estimator.
- *Correlation Based Clustering Protocol:* The purpose of this is to generate the network clusters, using least squares estimation technique and exploiting spatial correlation (Fig. 4). We have taken the euclidean distance metric for calculating the sensor distances. After 2-hop network information is gathered by each node, the hyperedge calculation is done, and once the *active alive* nodes are identified, correlation packet is used by the *active alive* nodes to discover its related active nodes, so as to form cluster. This is a control packet. On the receipt of this packet the sensors (*alive* nodes) answer with another control packet, correlation acknowledgement packet, so as to make sure that none of the *dormant* nodes are transmitting (cluster head). An intersection graph spanning over the *active alive* nodes will eventually result in adequate number of clusters.
- *Cluster Head Election Protocol:* The purpose of the cluster head election protocol is to select the node with maximum residual energy, from the set of active nodes, and is appointed as the cluster head. Once the clusters are formed (Fig. 5), the probe (control) packet searches for the *active alive* node that is having maximum residual energy, to elect such a node as the *cluster head*. On the receipt of this packet the sensors (*active alive* nodes) answer with another control packet, probe acknowledgement packet, so as to make sure that none of the non-cluster head nodes are transmitting (to the base station) (Fig. 6).

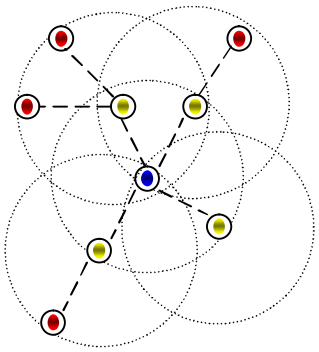


Fig. 1. Shows the 1-hop & 2-hop sensors of a particular node (blue colored) in the network. The yellow nodes are 1-hop neighbors & red ones are the 2-hop neighbors that escape the direct coverage of the concerned (blue node) sensor. The sensing ranges of the blue & yellow nodes are highlighted.

B. Offline Mode

The *offline mode* is engaged with the maintenance of sensor signal buffer of the respective sources during the execution of the basic protocol. Moreover, the mode also deals with the generation of reports on cluster formation and energy usage. The trace reports of the packet transmissions are also managed.

Thus, owing to the different working phases of the sub-protocols (which integrate the functioning of our fusion protocol), we entitle our proposed work as *Integrated Data Fusion Protocol* (IDFP).

V. Correlation Structure Computation

The existence of a hyperedge [1] in the network correlation graph is determined with the help of LS estimation method. A hyperedge *(S, s)* from a set of nodes *S* to a node *s* is drawn, if readings of the sensor *s* can be inferred from readings of sensors in *S*. Let *s[k]* and *s′[k]*

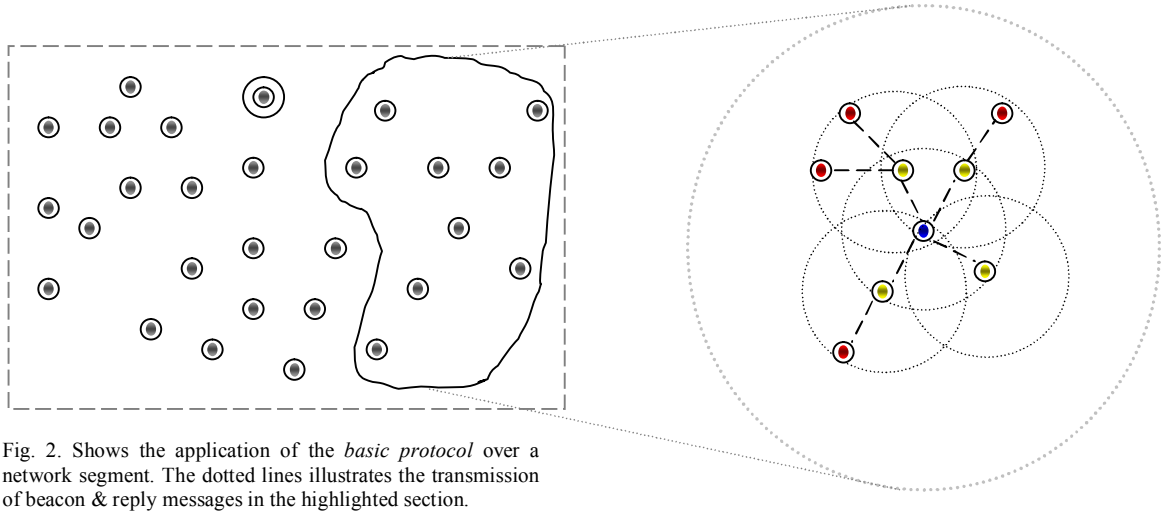


Fig. 2. Shows the application of the *basic protocol* over a network segment. The dotted lines illustrates the transmission of beacon & reply messages in the highlighted section.

denote the actual and predicted values of a sensor s at kth instant of time. Now, let $S = \{s_1, s_2 \ldots s_L\}$. We choose to use a linear predictive model to model the correlation, that is, we predict $s'[k]$ to be a fixed linear combination of $s_1[k], s_2[k], \ldots, s_L[k]$ for all k. More formally:

$$s'[k] = \sum_{l=1}^{L} \alpha_l s_l[k] \quad (1)$$

where α_l are weighting coefficients. The above equation can be easily generalized to handle temporal correlations as well. We have applied the Least Squares estimation method to minimize the error between the actual and computed readings. Further, a hyperedge (S, s) is constructed if the minimum error is within a certain application dependent bound. In particular, the weighted coefficients are chosen to minimize the least square error, $E(\alpha)$. Therefore, the least squares error, computed over K number of samples, is given by the formula:

$$E(\alpha) = \sum_{k=1}^{K} (s[k] - s'[k])^2 \quad (2)$$

Further, the weighted coefficients α_l are given [9,10] by:

$$[\alpha_1 , \alpha_2 , \ldots, \alpha_L]^T = (S^T S)^{-1} S^T s \quad (3)$$

In (3), $s = [s[1], s[2], \ldots, s[k]]^T$ signifies the actual readings sensed by the node s. Also, S symbolizes the $K \times L$ $(K>L)$ matrix of rank L representing the actual readings of the sensors in the set S, for the time period 1 to K.

$$E(\alpha) \leq \tau \quad (4)$$

Here, τ is the pre-defined error threshold determined by the programmer depending upon the network structure. If the error is within bounds, then the hyperedge will be added to the correlation graph, otherwise discarded. The interpretation of the 'adding of a hyperedge' is the 'correlation of a sensor node'.

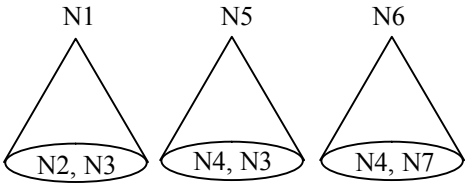


Fig. 3. Shows the correlation hypergraph of concerned network segment. This reflects that data of node *N1* is correlated with *N2* & *N3*, which means *N1* will enter dormant state. Overall (refer Fig. 5), in this part of the network, nodes 2,3,4,7 are actually transmitting, while others go to sleep state.

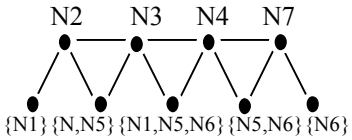


Fig. 4. Shows the application of the *correlation based clustering protocol* (over the network segment taken into consideration), by constructing the intersection graph. This clarifies that the nodes 2,3,4,7 are connected components & so form a cluster.

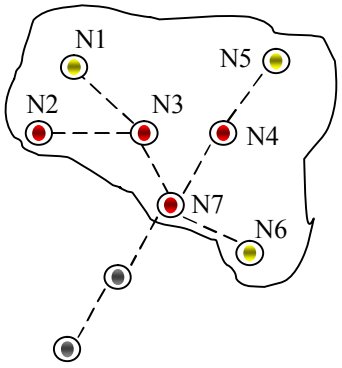


Fig. 5. Shows the cluster formation in the concerned network segment.

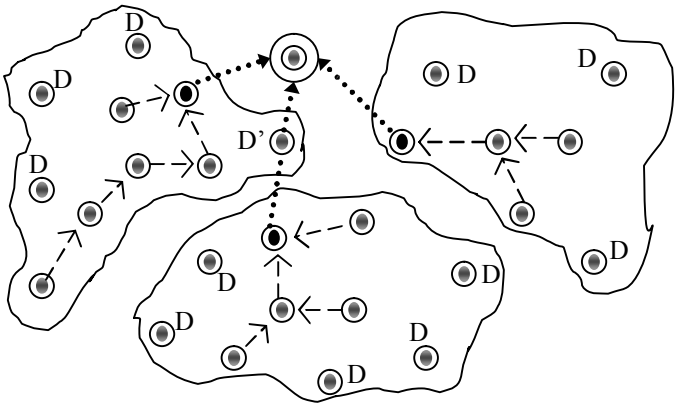


Fig. 6. Illustrates the actual data transfer after the usage of cluster head (CH) election protocol. From every cluster, only the CH (black nodes) is transmitting by taking the shortest route to the sink. Nodes with *D* marking refer to the dormant nodes which are in the sleep state. *D'* is the dormant node that acts as a bridge node to forward data.

VI. Simulation Results

The simulation is done in network simulator 2.34. We present model of our protocol, with comparison with *Naive Protocol* and the *Basic Protocol* (which refers to the *basic distributed* protocol in [1]).

The naive protocol represents the protocol, in which all the nodes transmit to the base station as per event schedules, without fusing data at different levels of cluster. Fig. 7 illustrates the graph of the number of dead sensors with regard to the ongoing day of data correlation & aggregation. The graph shows that though all the protocols perform almost similar up to 120-130 days, but after that, our protocol results in least number of dead sensors, owing to clustering of sensors and performing data aggregation. This interprets that the usage of our protocol eventually increases network lifetime. Fig. 8 demonstrates the stability of cluster structure. This is depicted by the average cluster head duration against the total number sensor nodes in the network. Cluster head duration refers to the period of time that a host becomes a cluster head.

With a neighborhood size (*d*) of 2, the figure shows that our proposed protocol has the longest cluster head duration. Fig. 9 shows the rate of successfully delivered packets with respect to the active alive nodes at the specific instant in the network. The chart shows that the performance of the proposed integrated protocol outperforms the basic & the naïve protocol. Fig. 10 depicts energy consumption per packet transmission against number of nodes in the network. It is clarified that our protocol expends comparatively least energy as the network spans over more number of nodes in the network.

VII. Conclusion & Future Scope

There are several promising avenues of research that this work can lead to. The proposed integrated protocol works in a sensor platform with very low degree of mobility. As a scope for future extension, the concerned protocol can be developed for adhoc environment, where the mobility degrees of the sensors are considerably high. Moreover, efficient estimators like: particle filter or Kalman filter [4], can be used to exploit the spatial correlation in the network.

The protocol is deployed in a two dimensional scenario and does not takes into account the uneven property of the terrains. Thus, to model it in a three dimensional simulation can yet be another challenging scope.

References

[1] H. Gupta, V. Navda, S. Das, V. Chowdhury, "Efficient gathering of correlated data in sensor networks," State University of New York, Stony Brook. *ACM Transactions on Sensor Networks*, vol. 4, no. 1, article. 4, January 2008.

[2] J. Li, C. H. Foh, L. H. L. Andrew, M. Zukerman, "Sizes of minimum connceted dominating sets of a class of wireless sensor networks," State University of New York, Stony Brook. *IEEE International Conference on Communications ICC'08*, May 2008, pp. 332-336.

[3] R. W. Haw, P. H. Haw, X. S. Shen, J. Zhang, "Sleep scheduling for wireless sensor networks via network flow model," University of Waterloo, Canada. *ScienceDirect on Computer Communications 29*, March 2006, pp. 2469-2481.

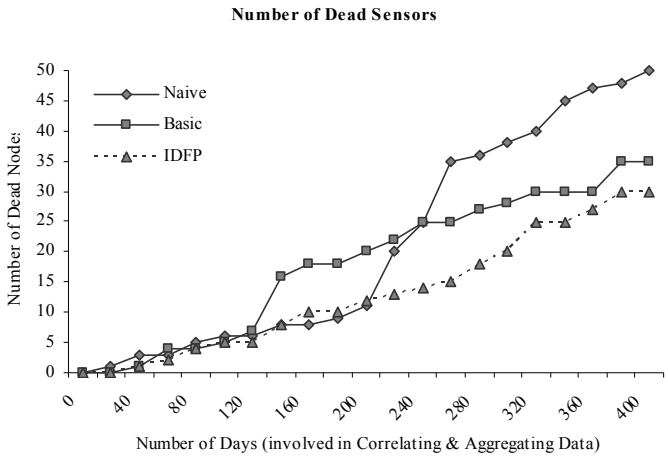


Fig. 7. Shows the no. of dead sensors over the no. of days.

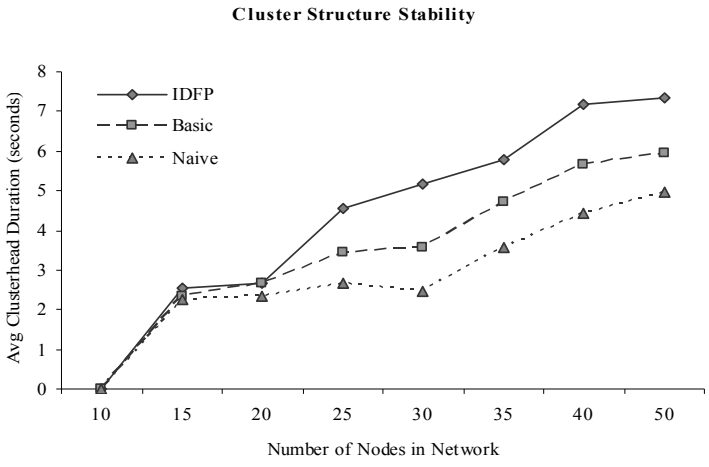


Fig. 8. Shows the stability of structure of the clusters in the network.

[4] E. F. Nakamura, Antonio. A. F. Loureiro, "Information fusion in wireless sensor networks," *ACM Transactions on Sensor Networks SIGMOD'08*, June 2008, pp. 1365-1372.

[5] K. Fall, K. Varadhan, "The ns Manual," The VINT Project, January 2009.

[6] S. Pattem, B. Krishnamachari, R. Govindan, "The impact of spatial correlation on routing with compression in wireless sensor networks," University of Southern California, *ACM Transactions on Sensor Networks*, vol. 4, no. 4, article 24, August 2008.

[7] S. Yoon, C. Shahabi, "The clustered aggregation (CAG) technique leveraging spatial and temporal correlations in wireless sensor networks," University of Southern California, *ACM Transactions on Sensor Networks*, vol. 3, no. 1, article 3, March 2007.

[8] J. Liu, M.Adler, Don Towsley, Chun Zhang, "On optimal communication cost for gathering correlated data through wireless sensor networks," University of Massachusetts, *The Twelfth Annual International Conference on Mobile Computing and Networking MobiCom'06*, 2006, pp. 310-321.

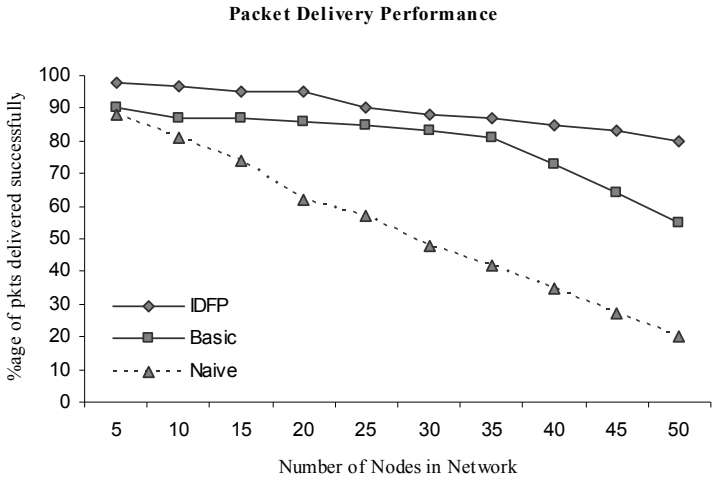


Fig. 9. Shows packet delivery performance of the network

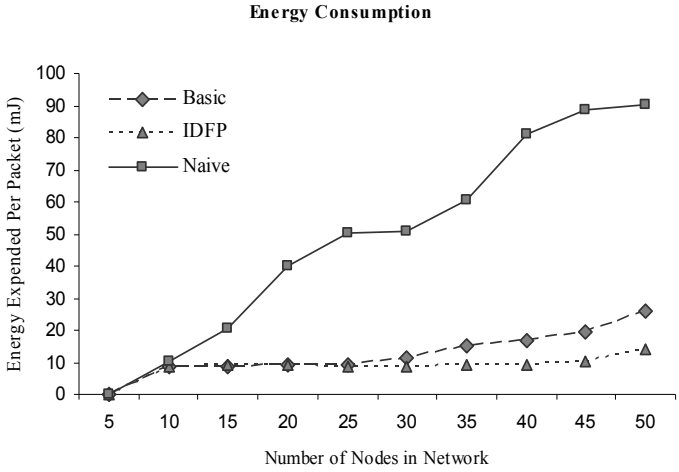


Fig. 10. Shows the energy consumption by nodes in the network.

Studies on the Planarity, Reliability and Energetic Efficiency in Wireless Sensor Networks

Kamil Staniec
Chair of Radiocommunications and Teleinformatics
Wroclaw University of Technology
Wroclaw, Poland
kamil.staniec@pwr.wroc.pl

Grzegorz Debita
Chair of Radiocommunications and Teleinformatics
Wroclaw University of Technology
Wroclaw, Poland
grzegorz.debita@pwr.wroc.pl

Abstract— **In the paper three most popular methods for spanning the wireless sensor networks (WSN) have been studied with respect to their offered reliability and intra-network radio interference. The authors proposed an algorithm for creating fully planar and reliable WSN structures that, unlike the other algorithms, considerably increase the Signal-To-Noise and Interference (SNIR) ratio in mesh networks, which advantage is particularly emphasized when directional antennas are used. Next, the influence of the number of sink nodes has been studied which ended with conclusion that a properly chosen sink nodes configuration may remarkably extend the network lifetime by bringing the number of necessary hops minimum.**

Keywords—**WSN, reliability, Signal-to-Noise, ZigBee**

I. INTRODUCTION

The environmental monitoring is quite a crucial issue particularly in densely populated habitats as well as in the proximity of large industrial facilities. Its main purposes are listed the following: - recording parameters defining the real environmental pollution and their comparison with intensities allowed in respective norms; - recording current meteorological conditions and forecasting thereof for the nearest future; - definition of the cause-and-effect relationships accounting for the source, the emitted amount, directions of flow determined by the topological and meteorological conditions etc.; - evaluating the threat of exceeding the allowed norms and taking respective precautions. Informing the public about hazards (if impossible to be coped with) and providing organizational instructions.

The environmental monitoring may encompass the air pollution with gases and dust, water and soil pollution, noise level, amount and composition of sewage as well as multiplicity of other elements of living nature, according to current circumstances. The recording of the measured parameters may, in turn, be performed either manually or automatically. It also facilitates the forecasting of the environmental condition at a given time. These forecasts may be grounds for administrative decision-taking process (both immediate or long-run) aiming at limiting further growth of the pollution intensities of various factors.

II. WSN NETWORK SPANNING ALGORITHMS

Every Wireless Sensor Network (WSN) begins with an unorganized deployment of sensors connected to radio modules (called hence forth nodes). It is assumed in this paper that the radio technology to carry information between nodes in the WSN is capable of operating in the mesh topology. Now, there are a few algorithms suitable for creating such connections in the initial unordered network. Two most popular solutions are the ZigBee native algorithms and Stojmenovič algorithms. Both will now be discussed together with an alternative solution proposed by the authors.

A. IEEE 802.15.4-ZigBee Local Minimum Spanning Tree Algorithm (LMST)

Both methods (i.e. ZigBee native algorithms and Stojmenovič) have one feature in common – it is the presence of the PAN (Personal Area Network) coordinator(s) to initiate the formation of the network. This is a device of extended functionality (as opposed to RFD's – Reduced Functionality Devices) with some pre-programmed intelligence for supporting the network formation. In LMST, however, the formation process starts in a few points of the unorganized network independently (nodes 8, 17, 18 and 19 in Fig. 1) – several FFD's start a network spanning routine to create connections in a star-topology around themselves (hence "local" in the algorithm name). Once all the local stars have been created, connections are made between these local individual stars to span the whole network.

B. Stojmenovič Minimum Spanning Tree Algorithm (MST)

The MST (or Stojmenovič, see [1], [2]) algorithm starts with the PAN coordinator broadcasting a beacon message heralding a new network formation, which is to announce that a new network is about to be created. Soon after this broadcast the PAN coordinator enters the listening mode to hear incoming response calls from nodes within the radio audible range. The successfully received calls are being collected for the duration of the, so called, listen window which – depending on the manufacturer – lasts for a few up to several seconds.

Now, after forming connections to the PAN coordinator each connected node performs the same searching routine to find nodes of its own neighbor set (further away from the PAN coordinator) and which have not connected to the PAN coordinator upon the primary broadcast.

Those nodes that respond within the listen window are recruited as neighbors. The procedure then continues throughout all the nodes in the entire area until eventually

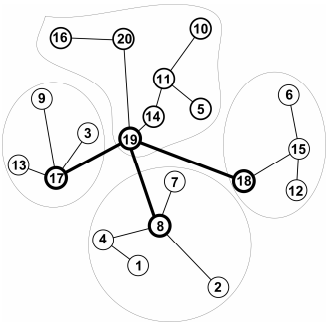


Figure 1. A result of LMST (ZigBee) network formation with four subnets

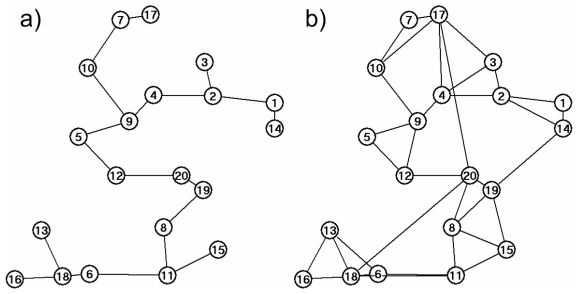


Figure 2. A result of MST (Stojmenovič) network formation with: a) the basic listen window; b) a doubled listen window

the minimum (global) spanning tree is formed (as shown in Fig. 2). It is assumed that the nodes which respond the fastest will be those that lie the closest to the broadcasting node, thus they may be considered as minimum-pathloss connections as compared to the calls that arrived after the listen window. This assumption, unfortunately, is not always true since some nearby nodes may simply not be able to respond as they can be, for instance, involved in transmission to the call from another node at a moment and thus be temporarily unavailable (see the comment in Section IV). Algorithms with a small (basic) window form a network initial structure. It is obvious that if the listen window is prolonged by a multiple of the basic listen window duration, more nodes will join in, thus forming redundant connections (referred to as a neighbor set). Based on this assumption, the topology-creating algorithms can be divided into two groups:

- those with a small listen window;
- those with a large listen window (i.e. a multiple of the small/basic listen window).

C. *The Proposal of a Reliable and Planar Algorithm (Authors'/planar)*

For the modeling of mesh systems the authors used theorems of the graph theory, one of which is the Gabriel's graph (GG). It is constructed by appropriately triangulating the network nodes: for every pair of interconnected nodes u and v separated by a distance d (along the edge l) no other nodes can exist within the circular area – with l being its diagonal – located between u and v (more on the subject can be found in [1]).

It is easy to notice that the structure presented in Fig. 1 and Fig. 2 do not satisfy the reliability theorem [3]. The theorem states that if in a given network S all connections are assigned equal unit weights and the maximum flow is calculated with the Fulkerson's method [4] for all nodes then if the flow value for each node is greater than two, the network guarantees that there will be an alternative connection in the case of failure of any intermediate node – if so, the network is regarded to be reliable.

The authors have created an algorithm (from now on called the authors'/planar algorithm) that assures connection of each node to at least two other nodes such that the connections do not intersect (whereby the whole network topology is said to be planar). Moreover, in order to account for the network physical nature (in reality the nodes are represented by transmit/receive modules such as ZigBee) – the proposed modified algorithm for GG creation checks the energy link budget of the new (redundant) connection and accepts it only if the pathloss L_{dB} (see Section IV) resulting from the distance between the connected nodes allows their mutual radio visibility. Such a procedure guarantees that connections will be of least attenuation (unlike structures made by ZigBee or Stojmenovič algorithms). The resultant topology spanned with the authors'/planar algorithm is depicted in Fig. 3

III. ZIGBEE (IEEE 802.15.4) SYSTEM

Out of the multiplicity of candidate solutions for effective creation of sensor networks is the ZigBee standard based on IEEE 802.15.4 specification [5]. It defines a low-cost, low-range, power-saving system allowing data rates – depending on the frequency band, of 20, 40 and up to 250 kbits/s and almost inexhaustible number of network nodes (typically 16 bit allocated for addressing with or 64 bits using extended addresses). Depending on the geographical region and local regulations, devices can found to operate in three distinct bands: 868 MHz (Europe, a single channel no. 0), 915 MHz (US, channels no. 1-10) and 2.4 GHz (global, channels no. 11-26). Since the latter frequencies offer both the greatest data rates (250 kb/s) and the greatest number of channels, it will be subject to studies in this paper.

IV. INTRA-NETWORK INTERFERENCE AND PATHLOSS CALCULATIONS FOR WSN

As will be treated in detail in later sections, the peer-to-peer topology, beside offering convenient network scaling and reliability/fault tolerance advantages, is quite prone to generating mutual radio interference between network nodes. As for the reliability provision, ZigBee does not offer any built-in capability assuring that each node will hold at least two other nodes as candidates for connections. As was shown in Section II.B this native method is also not optimal from the radio interference-mitigation viewpoint since each time a connection is to be established it is picked at random from the neighbor set.

Such a selection has an inherent weakness in that it

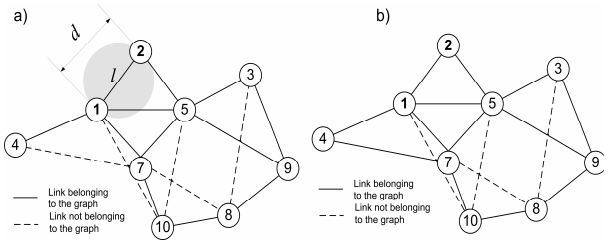


Figure 3. An example of the original Gabriel's graph (a) and modified GG (b)

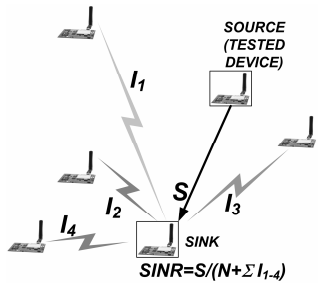


Figure 4. A conceptual scheme of SNIR calculation observed by a sink node from four interfering nodes

does not favor the least-pathloss candidates (hence much energy may be required to reach a distant neighbor).

For the k-th node it is given by (1), where S is the desired signal power in [W], k_B – Boltzman's constant in [J/K], T – ambient temperature in [K], BW – channel bandwidth in [Hz], NF – Noise Factor [–], N – the total number of network nodes, whereas the last term in the denominator denotes the sum of radiations from all other nodes (I_n) in the network (excluding, of course, the radiation from the k-th node for which SNIR is being calculated and the l-th node to which node k is transmitting, i.e. I_k and I_l, respectively). The desired signal power S as well as that of all interfering signals, can be found from one of the available pathloss models, e.g. the two-ray model which assumes up to some distance (a breakpoint) the power decays as $\sim 1/r^2$ and for further distances as $\sim 1/r^4$ (refer to [7], [8]). The model is quite fit for low-positioned antennas in the absence of other reflectors than the ground - the received power is assumed to be the phasor sum of the direct and the reflected wave.

$$SNIR_k\,|_{[dB]} = 10\log\left(\frac{S}{k_B \cdot T \cdot BW \cdot NF + \sum_{N/\{k,l\}} I_m}\right) \quad (1)$$

V. A Simplified Model of a Directional Antenna

Interference in WSN occurs mainly because even if direct line-of-sight directions between communicating nodes are not interfered, radio modules in the nodes can still hear transmissions from other nodes due to (most usually) omni-directional antennas installed in them.

The use of radiators with directional Antenna Radiation Patterns (ARP), as shown in Fig. 5a, could improve the situation by constraining emissions/receptions in only specified directions thus making the desirable transmissions immune to foreign transmissions arriving from angles outside the beamwidth θ_{3dB} in Fig. 5a. An example is provided in Fig. 5b: the communication session between nodes 1 and 2 is only affected by interference from node 3 to node 4 transmission direction but protected from transmission between node pairs 7-8 and 5-6 by attenuating those signals by 25 dB.

VI. Intra-Network Electromagnetic Compatibility in WSN Networks

In this section results will be presented of the research in the following domains:

- minimum beamwidth θ_{3dB} necessary to achieve the desired threshold SNIR (=5 dB, according to [5]);

- a number of nodes being effective interferes (i.e. such whose transmissions fall into the beamwidth of the node under test).

For this purpose an algorithm has been created for deploying nodes on a given area randomly with the assumption that each node is found within the radio range of at least two other nodes (refer to Section II.C). For each given number of nodes (10, 20, …, 90) ten scenarios have been generated. The final value of SNIR is an average calculated for all N nodes in all scenarios. Moreover, for each scenario results have been averaged over its tenfold realization. The reason for this was explained in Section where it was stated that in Stojmenovič and ZigBee algorithms neighbors for transmission are selected randomly. Therefore, by letting the neighbor be picked 10 times (each time computing the resultant SNIR presented to the tested node and eventually averaging the result) the resultant interference was made statistically robust and insensitive (to some degree) to variations following from the random neighbor selection before transmitting each individual packet, as is typical with ZigBee and Stojmenovič methods (see Section II.A-B).

A. Influence of the antenna beamwidth on SNIR

One of the obvious advantages stemming from the application of directional antennas (well-known and commonly utilized in e.g. cellular systems planning) is the reduction of the interfering signals arriving from the surrounding cells. However, as opposed to stationary systems, in WNS networks nodes are to be located not in sites guaranteeing the best area coverage with the minimum number of nodes, but rather in places where a given environmental factor is to be measured. It should also be noted that the cases to be analyzed in this section concern the worst-case scenario, i.e. such where all nodes attempt to transmit simultaneously. Admittedly, in real sensor networks such situations will occur extremely rarely e.g. on occasions of some natural disasters such as vast fire or flood. In ZigBee, such situations are avoided only in devices operating in the ISM 868 MHz band by imposing an upper limit on the duty cycle equal 1%, as specified in [6]. However, in majority of applications, the ISM 2.4 GHz band is used where no such restriction exists, giving way to such black scenarios of simultaneous transmission from multiple sources.

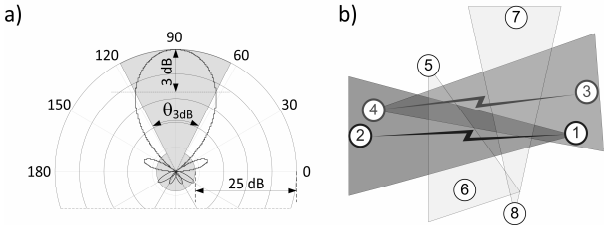


Figure 5. A simplified ARP model (a) and example of directional antennas used to reduce interference (b)

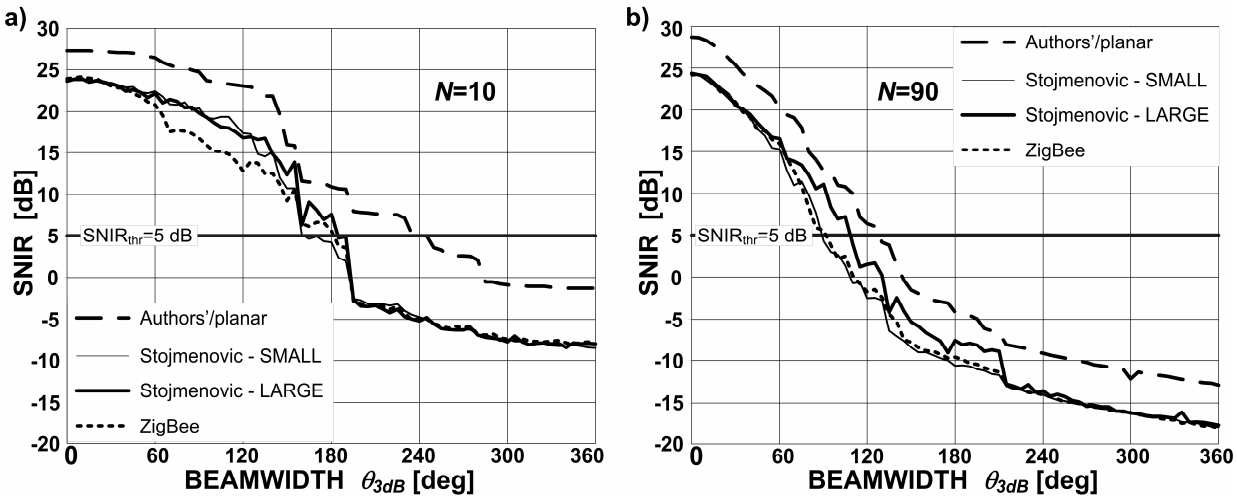


Figure 6. SNIR as a function of the beamwidth θ_{3dB} for: a) N=10; b) N=90

In Fig. 6 simulated results have been presented for two extreme cases regarding the number of nodes N on the same area i.e. 10 and 90. As was expected, the average level of interference introduced to each node is noticeably greater in the latter case which is expressed by the beamwidth θ_{3dB} needed for meeting the threshold $SNIR_{thr}$ of 5 dB. One can also see that ZigBee and Stojmenovič algorithms have similar trends except the 60°–150° range in Fig. 6a. Also, the kind of window in the Stojmenovič algorithm apparently does not have any significant effect on SNIR. It is evident, however, that the algorithm created by the authors has an advantage over the other algorithms in that it allows to obtain the same value of SNIR with a wider beamwidth, proving that the planarity is indeed an effective means of reducing the intra-network interference. In planar structures therefore, in WSN's of great nodes intensity (such as one presented in Fig. 6b) SNIR greater by c.a. 5 dB can be obtained as compared to non-planar networks for any beamwidth. Translating this conclusion to the minimum required beamwidth it can be stated that the desired $SNIR_{thr}$ is attained at θ_{3dB} wider by c.a. 20° than in ZigBee or Stojmenovič methods.

B. Influence of the network planarity on the number of interferers

It will now be demonstrated (Fig. 7) that modifications enforcing planarity and reliability (so called the authors'/planar model, see Section II.C), made to the existing spanning algorithms, will not be without effect on yet another factor, namely the number of interfering nodes.

Certainly, mere application of directional antennas can already reduce this number. However, it can be shown that by eliminating the possibility of intersecting nodes during the network spanning stage, this number will decrease even further. Interestingly, this effect is best emphasized with beamwidths around 180° (equivalent to installing a reflective screen on one side of the transmitting antenna) and looses its significance for both infinitely thin as well as omnidirectional beamwidths.

VII. ENERGETIC OPTIMIZATION FOR WSN

If a given environmental phenomenon is to be sensed across a given area, a mesh ZigBee-based WSN is a convenient solution. However, if the area itself is at a remote or hard-to-access location, there should exist a convenient way to send the readings collected from the sensor nodes (sources) of the WSN to a localized concentrator. It can be a WSN device with extended functionality (i.e. with a built-in dual ZigBee/GSM modem) for converting from ZigBee into GSM/GPRS frames and thereby acting as a gateway to the core network that will carry the information to the Customer Premises Equipment (CPE) for further storage, processing, modeling and/or forecasting as shown in Fig. 9.

There are at least two reasons for not equipping each WSN node with the GSM/GPRS modem (and thus becoming a sink for the data in the network). Firstly and technically, the sink node does not only concentrate traffic from numerous other nodes (which translates to its increased operational duty cycle) but is also responsible for communicating with the core network base station (BS).

Since it is thus expected to consume considerably more energy than the other network nodes, it should run on a reliable power supply, preferably different than the battery

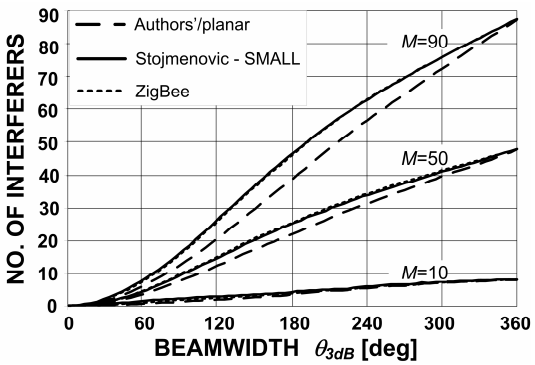


Figure 7. Average number of nodes interfering a statistical tested node

(though quite sufficient for all other nodes). Secondly and economically, beside the increased cost of reliable power supply, the price of devices with integrated dual ZigBee-GSM/GPRS modems is also remarkably higher than that of plain ZigBee radio modules.

In this section the authors will examine the energy consumption in the WSN part of the tele-transmission network depicted in Fig. 9. The energy is dispersed in the network mainly during the multi-hop transmissions of messages through the mesh WSN. Most ZigBee radio chips allow for controlling the output power within a broad range of dynamics, e.g. –17 dBm up to +3 dBm at 0.5 dB steps (based on Atmel AT86RF230 ZigBee radio module [9]) depending on the distance between the pair of communicating nodes. The planarity of the WSN topology in this respect has a noteworthy advantage over other network spanning algorithms by intrinsically assuring the least-attenuation links. However, even this situation can be improved by choosing an optimal number of sink nodes in a given WSN such that a trade-off is found between the energy consumption in the network and the economical/technical aspects discussed above. Since the energy is consumed mainly for conveying messages between nodes, the sum of all hops in the network (Σ_h) necessary to transfer a single message packet from each node to the sink (or sinks), has been chosen as a main determinant of the whole network energetic performance. As shown in Fig. 10 the use of multiple sinks is a tempting idea in terms of the total number of network hops. This example shows that Σ_h can change by almost half if the number of sinks is tripled. More general investigations will now be presented regarding the variation of Σ_h with increasing number of nodes N (ten different scenarios for each N as in Section VI).

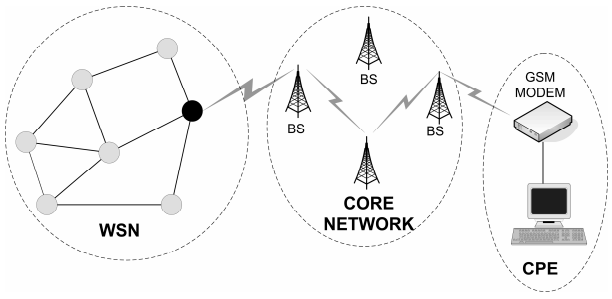


Figure 9. An example of the wide-area sensor network

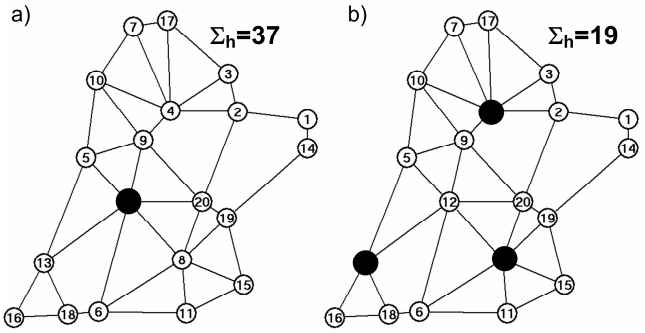


Figure 10. An example of a WSN consisting of N=20 nodes with a) M=1; b) M=3 sinks

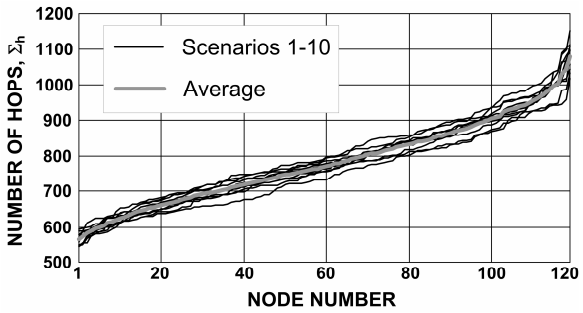


Figure 8. An example of a WSN consisting of N=20 nodes with a) M=1; b) M=3 sinks

At this point, however, one should pose a question as to the choice of the best candidate(s) for the sink node(s). As will now be presented, the choice of the proper node(s) should not be random; indeed it should be a result of careful analysis. In Fig. 8 the ordered values of Σ_h are presented for all ten scenarios with 120 nodes each. As can be seen a wrongly selected node for the global sink can significantly increase the total number of hops. The ratio of Σ_h between the worst sink node and the optimum one equals on average (over ten scenarios) 1.91, although in particular cases this ratio spanned from 1.73 even to 2.05. It must be remembered that the network expected longevity will vary at the same rate as it is linearly dependent of Σ_h in the network. Returning to the general studies of the total number of hops as a function of both, the number of network nodes N and that of sinks M, results are presented in a graphical form in Fig. 11. In Fig. 11a there are five bundles of ten curves each, representing, respectively, different values of N and the scenarios used in the simulations. Moreover, for each M in every scenario, an optimum combination of M nodes has been found, in terms assuring of the globally lowest sum of hops. The method used to find this optimum configuration was based on a brute-force technique of analyzing each possible configuration separately. Such an approach, though cumbersome with respect to the time of execution, assures that the M nodes selected as optimal are indeed the best choice in a global sense. As can be seen, Σ_h decreases exponentially with increasing M, which allows easy matching of best-fit approximations (see Fig. 11b and Table I) to the form given by (2). It appears that the inclusion of five sinks decreases the number of hops (and hence the energy consumption) over two times (from 205 down to 91 hops), especially for the dense network of 60 nodes in Fig. 11.

$$\Sigma_h(M) = d \cdot M^k \tag{2}$$

VIII. Conclusions and Further Research

The purpose of the paper was to provide a survey on some aspects that may improve a mesh sensor network operation. The first improvement consisted in assuring a fault-tolerant network (with at least two alternative links for every node) and, secondly, a planar network (whereby connections do not intersect). The former feature provides the reliability in the network while the latter reduces the intra-network radio interference.

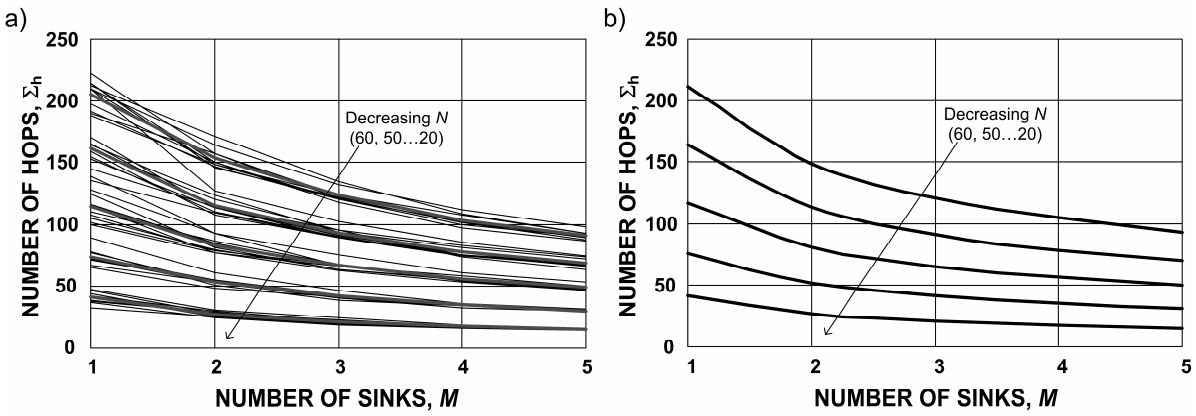


Figure 11. Number of total network hops as a function of the number of sinks a) bundles of curves plotted for N=20-60; b) best-fit exponential curves

The planarity is particularly useful when combined with directional antennas installed on the ZigBee radio modules. Thirdly (in Section VII), it was demonstrated that the energetic efficiency of the WSN greatly depends on the number of sinks which – when properly selected – may considerably optimize the energy consumption in the network. Results have been also presented of the number of hops in the network as a function of the number of sinks for various scenarios.

TABLE I.
ESTIMATED PARAMETERS OF THE NUMBER OF HOPS DEPENDENCY ON N

	Number of nodes, N				
	20	30	40	50	60
d	41.65	75.78	116.97	163.72	210.78
k	–0.62	–0.56	–0.53	–0.53	–0.51

This is quite time-consuming although it returns solutions optimal in the global sense. In future research, the authors intend to test other algorithms (such as tabu search, simulated annealing or genetic algorithms) for finding these optimal configurations.

ACKNOWLEDGMENT

This paper has been written as a result of realization of the project entitled: "Detectors and sensors for measuring factors hazardous to environment – modeling and monitoring of threats". The project financed by the European Union via the European Regional Development Fund and the Polish state budget, within the framework of the Operational Programme Innovative Economy 2007÷2013. The contract for refinancing No. POIG.01.03.01-02-002/08-00.

REFERENCES

[1] I. Stojmenovič, Handbook of Sensor Networks – Algorithms and Architectures. John Wiley & Sons, December, Ottawa 2004

[2] M. Pióro, D. Medhi, *Routing, Flow, and Capacity Design in Communication and Computer Networks*. Morgan Kaufmann Publishers, San Francisco 2004

[3] H. Frank, I.Frisch, "Analysis and design of survivable networks", *IEEE Transactions on Communication Technology*, vol. 18, issue 5, Oct. 1970, pp. 501-518

[4] L.R. Ford, D.R. Fulkerson, "Maximal flow through a network", *Canadian Journal of Mathematics*, Vol. 8, 1956, pp. 399–404

[5] IEEE, IEEE Std 802.15.4-2006, Part 15.4: Wireless Medium Access Control (MAC) and Physical Layer (PHY) Specifications for Low-Rate Wireless Personal Area networks (WPANs)

[6] CEPT, ERC Recommendation 70-03 Relating to the Use of Short Range Devices (SRD), Annex 1: Non-specific Short Range Devices. Version of 16 October 2009

[7] G. Debita, K. Staniec, "Reliable mesh network planning with minimization of intra-system interference", Proc. of *Broadband Communication, Information Technology & Biomedical Applications*, BROADBANDCOM'09, July 15-18, Wroclaw, Poland, pp. 243-244.

[8] K. Staniec, G. Debita, "Interference mitigation in WSN by means of directional antennas and duty cycle control", *Wireless Communications and Mobile Computing*, DOI: 10.1002/wcm.1089, Wiley, 2010

[9] AVR Low Power 2.4 GHz Transceiver for ZigBee IEEE 802.15.4 6LoWPAN, RF4CE and ISM Applications. Atmel. Available at: www.atmel.com

A QoS-Aware Routing Protocol for Mitigating End-to-End Delay in IEEE 802.11-based Mobile Ad hoc Networks

Khaled Abdullah Mohammed Al-Soufy
Department of Computer Engineering
Zakir Husain College of Engineering and Technology
Aligarh Muslim University
Aligarh - 202002, India.
Email: kalsoufi@gmail.com

Ash Mohammad Abbas
Department of Computer Engineering
Zakir Husain College of Engineering and Technology
Aligarh Muslim University
Aligarh - 202002, India.
Email: am.abbas.ce@amu.ac.in

***Abstract*—Providing quality of service (QoS) in a mobile ad hoc network is a challenging task due to its peculiar characteristics. This paper aims at presenting a routing protocol which identifies multiple node-disjoint paths between a given source and a destination. These multiple node-disjoint paths are examined for satisfying QoS in terms of end-to-end delay. In this paper, we analyze the end-to-end delay along the paths taking into account the IEEE 802.11 contention delays. To study the performance of our protocol, we have carried out simulation. The results show that the proposed protocol performs better in terms of QoS satisfaction ratio and the throughput as compared to an existing protocol proposed in the literature.**

***Index Terms*—Quality of service; delay; contention delay; contention area; re-sequencing delay; node-disjoint paths.**

I. Introduction

Devising a routing protocol for an ad hoc network with a provision of quality of service (QoS) is a challenging task due to their inherent characteristics. A lot of work is directed towards identification of multiple paths from the point of view of fault tolerance and load sharing [4]. Recently, the research is directed towards the use of multiple paths for the purpose of QoS provisioning in case of mobile ad hoc networks [5] [6]. In an ad hoc network, multiple paths between a given source and a destination may help in the provision of QoS in the following situations.

- In the situation where the resources of mobile nodes are limited, a single path may not be able to provide enough resources to satisfy the desired QoS. On the other hand, the resources along multiple paths that may exist between the given pair of nodes may suffice for the QoS requirements of the application.
- In the situation where enough resources are available along each path to satisfy the QoS requirements, the traffic can be shared across multiple paths. In other words, packets are sent along each path that is able to satisfy QoS requirements. This may help in achieving relatively larger throughput as compared to a single path.

Further, in case of single path routing, the failure of a path needs a new path to be rediscovered, which should also be capable of satisfying the QoS requirements. A new path may not be required to be rediscovered if there are multiple paths between the given source and the destination. Therefore, one would like to investigate the effect of multiple paths between a given source and a destination on the performance of the protocol that is aware of the QoS requirements of the application.

An issue that needs to be addressed while sending multiple packets along multiple paths is that packets may arrive at the destination out of order. Therefore, re-sequencing might be required at the destination which may further increase the overheads in terms of delays. The problem of re-sequencing in multipath routing is addressed using flow assignment in [8]. The issue of load balancing in multipath source routing for mobile ad hoc networks is addressed in [9], [10].

In this paper, we present a routing protocol that is aware of the QoS and may utilize multiple paths for traffic sharing. In our protocol, the source tries to identify multiple node-disjoint paths that are able to satisfy QoS requirements in terms of end-to-end delays for the real-time traffic and at the same time achieve high throughput while sending packets. The paths identified are selected for sending packets in such a manner so that contention delays along the paths and re-sequencing delays at the destination are alleviated.

The remaining paper is structured as follows. In section II, we describe some important concepts related to IEEE 802.11 based ad hoc network. In section III, we describe system model and some important assumptions related to the design of our protocol. Section IV contains end-to-end delay analysis. In section V, we analyze the throughput achievable for multi-hop wireless networks. Section VI contains the description of the proposed protocol. In section VII, we present results and discussion. The last section is for conclusion and future works.

978-1-61284-690-3/11/$26.00 ©2011 IEEE

II. IEEE 802.11 Overview

In a mobile ad hoc network, IEEE 802.11 is used as the *Medium Access Control* (MAC) protocol. IEEE 802.11 comes in different flavours, IEEE 802.11 with *Distributed Coordination Function* (DCF), is of particular interest in case of an ad hoc network because the mobile devices using DCF can be configured in ad hoc (or infrastructureless) mode. In the ad hoc mode, there is no need of a base station or an access point; and the devices themselves need to forward packets of one another towards their ultimate destinations. In IEEE 802.11, there is another coordination function called the *Point Coordination Function* (PCF), however, it works in infrastructure mode only, and therefore, it is not suitable for an ad hoc networks. Note that IEEE 802.11 DCF is based on *Carrier Sense Multiple Access* (CSMA) with *Collision Avoidance* (CA).

In a CSMA/CA based network, if a node i wishes to transmit, it senses whether the channel is busy or idle. If it finds the channel busy, it waits until the channel becomes idle. If the node finds the channel idle for a certain amount of time called the *Distributed Interframe Space (DIFS)*, it transmits the frame. The receiver node receives the frame and if it received the frame successfully, it waits for a time duration called *Short Interframe Space (SIFS)*, and sends an *Acknowledgment* (ACK) to the sender. If there is a collision, the node generates a random backoff number between 0 and $CW - 1$, where CW is called the contention window. The contention window, CW, may vary from CW_{min} to CW_{max}, where $CW_{max} = 2^m CW_{min}$. The node starts random backoff timer and counts down. During the count down phase, if the channel becomes busy, the node freezes the backoff counter. When the channel is idle again, the node resumes the count down of the backoff counter. When counter becomes zero, and the channel is idle for at least a DIFS time duration, it retransmits the frame. If again there is a collision, the node doubles its contention window and the backoff process is repeated until a specific number of retries. After the maximum number of retries either the frame is sent successfully or it is discarded. To reduce the probability of collision, there is an optional mechanism to reserve the channel using very small frames called *Request-To-Send* (RTS) and *Clear-To-Send* (CTS). If the medium remains idle, the node i tries to send a RTS control message and waits for a time duration called *Short Interframe Space (SIFS)*. Every node which receives RTS will defer its transmission including the receiver. When the receiver receives RTS, it waits for an SIFS and sends a CTS control message to the sender node, which is i, then starts to transmit the data packets using CSMA/CA.

III. System Model and Assumptions

Let there be an ad hoc network which can be represented by an undirected graph $G = (V, E)$, where V is a set of vertices or nodes and E is a set of edges or links that connect the nodes where $|V| = n$, and $|E| = m$. We assume that all the links are bidirectional and each node has transmission range R. Further assume that each node employs IEEE 802.11 based on CSMA/CA as a MAC protocol, where RTS/CTS mechanism can optionally be used to alleviate the hidden terminal problem. Note that a node can transmit to another node in its transmission range. However, a node contends for the channel with all nodes which are in its carrier sense range. Let (x_i, y_i, z_i) be the location of node i, and (x_j, y_j, z_j) be the location of node j, then node i and node j are neighbors of each other if $(x_i - x_j)^2 + (y_i - y_j)^2 - (z_i - z_j)^2 \leq R^2$, where R is the transmission radius of all nodes in the network. However, two nodes i and j may contend for the channel if $(x_i - x_j)^2 + (y_i - y_j)^2 - (z_i - z_j)^2 \leq R_{cs}^2$, where R_{cs} is called the carrier sense range. Generally, $R_{cs} = \alpha R$, where α is constant and is usually assumed to be 2 (see Figure 1).

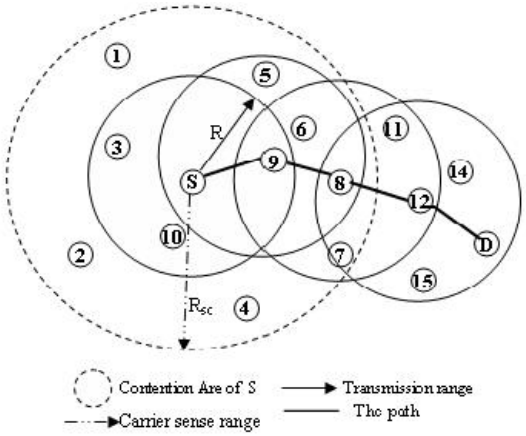


Fig. 1. The contention area of a given source node, S and the destination node D.

IV. End-to-End Delay Analysis

In our protocol, the source tries to estimate the average end-to-end delay based on per-hop delays. As mentioned earlier, IEEE 802.11 which is based on CSMA/CA is generally used as a MAC protocol in ad hoc networks. Hence, the contention delay at each node plays an important role and contributes to the major part of end-to-end delay. In this paper, we focus on contention delays along a path and try to minimize it. The actual procedure of how to minimize the contention delay shall be described later in this paper. The per-hop delays at each node, say node i, can be divided into three components which are as follows:

- T_s: Successful transmission time.
- T_c: Time consumed during collision.
- T_{bf}: Average backoff time at node i.

The total delay at node i is the summation of these delays and can be written as follows.

$$\Delta = T_c + T_{bf} + T_s. \tag{1}$$

Let us consider each of these delays separately.

The successful transmission time of the node i's packets, T_s, is as follows.

$$T_s = \frac{L}{C} + t_{ov} \tag{2}$$



Fig. 2. The channel is busy due to successful transmission.



Fig. 3. The channel is busy due to collision.

where, L is the length of the packet, C is the capacity of the link, and t_{ov} denotes the overhead incurred in transmitting the data frame. Using RTS/CTS mechanism, the time, t_{ov}, is given by,

$$t_{ov} = t_{ACK} + DIFS + 3SIFS + t_{RTS} + t_{CTS} \quad (3)$$

where t_{RTS}, t_{CTS}, and t_{ACK} are the times incurred in transmitting RTS, CTS and ACK control frames, respectively.

The backoff interval is selected randomly by using a backoff algorithm. During the backoff process, the actual time consumed between successive decrements of the backoff timer is not necessarily equal to τ (the slot duration). However, if the channel is sensed idle, the timer is decremented by τ. Otherwise, if the channel is sensed busy due to successful transmission of a neighboring node, the backoff timer is frozen and decrementing of the timer will be deferred during this time. Here, the probability of successful transmission is given by,

$$P_s = \frac{n(1-P)^{n-1}}{1-(1-P)^n}.$$

If the channel is detected busy due to collision, the backoff timer will be suspended time interval that equals T_c. In this case, at least one of the remaining nodes $(n-1)$ is in active mode. Hence, $P_c = 1 - P_I$ and $P_I = (1-P)^{n-1}$, whereas P is the probability that the remaining nodes can transmit a packet. See Figures 2,3. Thus,

$$P_c = 1 - (1-P)^{n-1}.$$

Hence, the average backoff time can be calculated as follows:

$$T_{bf} = \sum_{j=1}^{\overline{W_z}} \left[\sigma P_I + (1-P_I)\left(P_s T_s + P_c T_c\right)\right] \quad (4)$$

where the average number of backoff slots at attempt z,

$$\overline{W_z} = \frac{2^{z-1}}{2} CW_{min}.$$

The collision delay occurs when two nodes attempt to send packets simultaneously. As shown in Figure 3, the collision delay can be obtained as follows,

$$T_c = \sum_{j=0}^{r_{max}} (DIFS + t_{RTC}) \quad (5)$$

where r_{max} is maximum number of retries.

In the next section, we describe how one can achieve the optimal throughput.

V. Throughput Of a Multi-hop Network

In [17], an analysis throughput of IEEE 802.11 DCF is carried out under saturation conditions using Discrete-Time Markov Chain (DTMC). In [18], some new insights to the analysis of IEEE 802.11 DCF are presented using Fixed Point Theory. However, these analysis are for a single hop wireless networks. In [14], the analysis of a multihop networks is presented by extending the throughput analysis for a single hop network to a multihop network. An expression for the throughput of a single hope network is given in [13].
In this paper, we extend the analysis of the throughput of a single hop network to a multihop network. For that purpose, let us start with the analysis presented in [13].

It has mentioned in [13] that the mean time between successive renewals , $\overline{T}$, is as follows.

$$\overline{T} = \frac{1}{\nu\beta} + P_s T_s + P_c T_c \quad (6)$$

where, β is the exponential backoff parameter, and ν is the number of nodes in the single hop network. The The probability of collisions as a function of β is as follows [13].

$$P_c = 1 - e^{-(\nu-1)\beta\tau}. \quad (7)$$

The probability of transmitting the frame successfully as a function of β is given by [13].

$$P_s = 1 - P_c = e^{-(\nu-1)\beta\tau}. \quad (8)$$

Using (7) and (8), we can write (6) as follows.

$$\overline{T} = \frac{1}{\nu\beta} + e^{-(\nu-1)\beta\tau} T_s + T_c(1 - e^{-(\nu-1)\beta\tau}). \quad (9)$$

Let us denote the network throughput by Θ. According to the renewal and reward theorem [12], the network throughput is given by,

$$\Theta(\beta) = \frac{P_s L}{\overline{T}}. \quad (10)$$

Using (9) and (8), the expression for throughput of a single hop network can be written as follows.

$$\Theta(\beta) = \frac{e^{-(\nu-1)\beta\tau} L}{\frac{1}{\nu\beta} + e^{-(\nu-1)\beta\tau} T_s + T_c(1 - e^{-(\nu-1)\beta\tau})} \quad (11)$$

To extend the analysis of the throughput of a single hop network to a multihop network, we use the notion of transmission range and the carrier sense range. Note that a node can receive the transmission of another node if it lies in its

transmission range. However, while a node is transmitting a frame to its neighbor, there is a possibility of collision if any node in its carrier sense range starts transmitting a frame. As mentioned earlier, let $R_{cs} = \alpha R$ such that $\alpha >= 2$.

In a single-hop network, a node contends with $\nu - 1$ nodes, where ν is the number of neighbors of the node, and $\nu = \rho\pi R^2$. Here ρ is called the node density and $\rho = \frac{n}{A}$, where n is the total number of nodes in the network and A is the area deployment. In case of a network where there are multiple hops, h, between a given source and a destination, a node contends with, $\nu_{cs} - 1$, number of neighbors, where ν_{cs} is the number of nodes in the carries sense area, and $\nu_{cs} = \rho\pi R_{cs}^2$. The expression of throughput becomes as follows.

$$\Theta(\beta) = \frac{\frac{n}{\nu_{cs}h} L e^{-(\nu_{cs}-1)\beta\tau}}{\frac{1}{\nu_{cs}\beta} + (e^{-(\nu_{cs}-1)\beta\tau})T_s + (1 - e^{-(\nu_{cs}-1)\beta\tau})T_c} \tag{12}$$

To maximize the network throughput, we differentiate $\Theta(\beta)$ with respect to β and equate it to 0, we get

$$\begin{aligned} &- \frac{n}{\nu_{cs}h} L\tau(\nu_{cs}-1)e^{-(\nu_{cs}-1)\beta\tau} \\ &\{\frac{1}{\nu_{cs}\beta} + e^{-(\nu_{cs}-1)\beta\tau}T_s + T_c + T_c e^{-(\nu_{cs}-1)\beta\tau}\} \\ &- \frac{n}{\nu_{cs}h} L e^{-(\nu_{cs}-1)\beta\tau} \\ &\{-\frac{1}{\nu_{cs}\beta^2} - \tau(\nu_{cs}-1)e^{-(\nu_{cs}-1)\beta\tau}T_s + \\ &T_c\tau(\nu_{cs}-1)e^{-(\nu_{cs}-1)\beta\tau}\} = 0. \end{aligned} \tag{13}$$

The equation (13) can be written as follows,

$$\begin{aligned} &- \frac{-\frac{n}{h\nu_{cs}} L\tau\beta(\nu_{cs}-1)e^{-(\nu_{cs}-1)\beta\tau}}{\nu_{cs}\beta^2} \\ &- \frac{\frac{n}{h\nu_{cs}} L\tau T_c\beta^2(\nu_{cs}-1)e^{-(\nu_{cs}-1)\beta\tau}}{\nu_{cs}\beta^2} \\ &+ \frac{\frac{n}{\nu_{cs}h} L e^{-(\nu_{cs}-1)\beta\tau}}{\nu_{cs}\beta^2} = 0. \end{aligned}$$

Hence we get,

$$T_c\tau\nu_{cs}(\nu_{cs}-1)\beta^2 + \tau(\nu_{cs}-1)\beta - 1 = 0. \tag{14}$$

Solving for β in (14) by using the quadratic formula. Finally, we get

$$\beta = \frac{1}{2\nu_{cs}T_c}\left(\sqrt{1 + \frac{4T_c\nu_{cs}}{\tau(\nu_{cs}-1)}} - 1\right)$$

In what follows, we describe the proposed protocol.

VI. Proposed Protocol

In this paper, we propose A QoS-Aware Routing Protocol for Mitigating End-to-End Delay in Ad hoc Networks (QARMD). QARMD has two major phases: *route discovery* and *route maintenance*. Let us describe each of them as follows.

A. Route Discovery

When a source wishes to communicate to a destination and there is no valid path, then it generates a *Route Request (RREQ)* packet. An *RREQ* contains the following information.

<SourceAddress, DestinationAddress, SequenceNumber, TraversedHopList, DelayLimit, PathDelay, ContendingNeighbours, PathsDesired>.

The variable *SequenceNumber* denotes the broadcast-id of the *RREQ* generated by the source. Whenever a source node generates an *RREQ*, it increments the *SequenceNumber*.

Note that the tuple *<SourceAddress, DestinationAddress, SequenceNumber>* uniquely identifies an *RREQ*. Two or more *RREQs* having the same values in these fields are said to be the copies of one another. The field *DelayLimit* contains the end-to-end delay requirements to be satisfied for the packets. The field *PathDelay* contains the delay along the path up to the current node. It is initialized to 0 at the source. The variable *ContendingNeighbours* contains the number of neighboring nodes of a node and is also initialized to 0. The field *PathsDesired* contains the number of paths desired by the source, however, the source is open to any number of paths. When an intermediate node receives a copy of the *RREQ*, it examines whether its own address is already present in the *TraversedHopList* field of the *RREQ*. If yes, it discards the *RREQ*. Otherwise, it examines whether the *TraversedHopList* of the *RREQ* is disjoint with the *TraversedHopLists* of the *RREQs* already forwarded. If yes, it decides to forward the copy of the *RREQ*, otherwise, it discards the copy of the *RREQ*. Before forwarding the *RREQ* to its neighbors, let us consider what steps an intermediate node has to take when it receives an *RREQ*.

- It estimates the delay from its upstream neighbor to itself including the queueing delays. Let the delay estimated be *HopDelay*. It then adds the value of *HopDelay* to the value contained in *RREQ.PathDelay*. In other words,

  $$RREQ.PathDelay = RREQ.PathDelay + HopDelay.$$

- It compares *RREQ.PathDelay* with *RREQ.DelayLimit*. If

  $$RREQ.PathDelay > RREQ.DelayLimit$$

  it discards the *RREQ*.
- It determines the number of its neighbors, say *numNeighbors* using some beacon mechanism. It compares *numNeighbors* with *RREQ.ContendingNeighbors*. If

  $$numNeighbors > RREQ.ContendingNeighbors$$

  then

  $$RREQ.ContendingNeighbors = numNeighbors$$

- It appends its own address to the *TraversedHopList* of the *RREQ* before forwarding the *RREQ* to its neighboring nodes.

Note that when a copy of the *RREQ* arrives at the destination, *RREQ.PathDelay* contains the delay along the traversed path. On the same ground, the field *RREQ.ContendingNeighbors*

contains the maximum number of neighbors that may contend with any node along the path traversed by the copy of the *RREQ*.

Eventually, the copies of the *RREQ* arrive at the destination. The destination node collects the copies of the *RREQ* received until a timeout. It then computes the disjointness among the *TraversedHopLists* of the copies of *RREQ*. The destination examines whether the path satisfies the QoS requirements. For that it compares *RREQ.PathDelay* with the *RREQ.DelayLimit.* The destination discards the *RREQ* whose *RREQ.PathDelay* exceeds *RREQ.DelayLimit*. If there are more number of paths available than that of the *PathsDesired* (say k), the destination selects the first k shortest paths. If the number of hops along two or more paths are the same, then paths with smaller values contained in *RREQ.ContendingNeighbors* are selected. The destination generates *Route Replies (RREPs)* against the selected copies of the *RREQs* with disjoint *TraversedHopList.* The *RREPs* are sent towards the source along the reverse paths brought by the copies of the *RREQ* in their respective *TraversedHopLists.* The source collects *RREPs* received until a timeout. The source sorts the available paths to the destination in the ascending order of their end-to-end delays.

B. Route Maintenance

If a node senses a link failure, it informs upstream nodes along all those paths whose part the failed link was by unicasting a *Route Error (RERR)* message, one for each failed path. Every node that receives an *RERR* message, marks the path invalid and unicasts the *RERR* upstream. Eventually, the *RERR* arrives at the source. When the source receives an *RERR* message it marks the failed path invalid. The source then retransmits the data through alternate valid paths that are not yet failed and that satisfy QoS requirements of the application. If there is no such path, then the source initiates a new route discovery.

VII. Results and Discussion

To evaluate the performance of our protocol, we have developed our own simulator in C++. We generated topologies of the network where 100 nodes are distributed uniformly randomly in a region of area $1000m \times 1000m$. Each node is assumed to have a transmission range of 250m. The simulation time is 100 simulated seconds. The mobility model is *Random Way Point (RWP)*. In the *RWP* model, a node chooses a random speed uniformly distributed between a *min speed* and a *max speed*. It starts moving towards a randomly selected destination. When the node arrives at the destination, it takes a pause; and then again starts moving following the similar steps. The time for which the node takes a pause is known as the *pause time*. The medium access control (MAC) layer is assumed to be IEEE 802.11. The bandwidth of each link is assumed to be 2 Mbps. The traffic is *constant bit rate (CBR)*. The packet size is 512 bytes. While evaluating the performance of the protocol, we focused on the following parameters: (i) *Average end-to-end delay:* It denotes average latencies experienced by packets from the source to the destination.

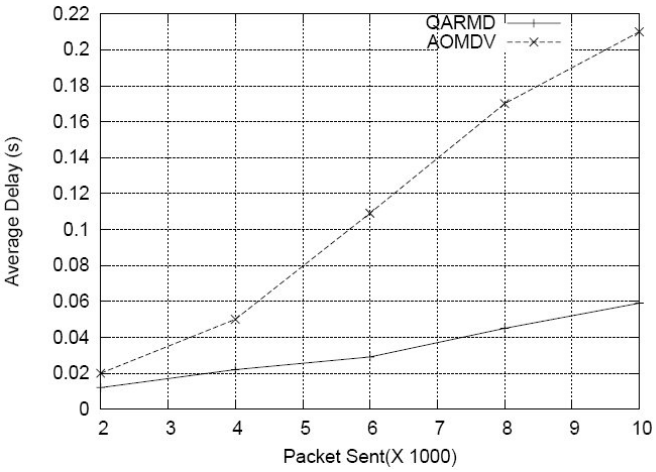


Fig. 4. Average end-to-end delay as a function of the number of packets sent by the source.

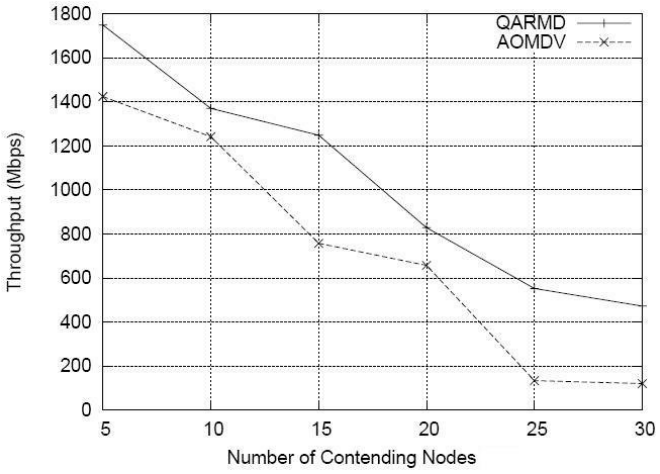


Fig. 5. Throughput as a function of the number of contending nodes.

(ii) *Throughput:* It denotes the average bandwidth occupied by packets that are sent to the destination. (iii) *QoS success ratio*: It represents how many packets arrive at the destination before the expiry of their respective deadlines divided by the total number of packets sent by the source. In other words, it represents the ratio of the number of packets whose QoS requirements (in terms of end-to-end delays) are satisfied to that of the total number of packets sent by the source. We compare the performance of the proposed protocol (QARMD) with AOMDV. The reason behind choosing AOMDV is that AOMDV is also a multipath routing protocol. In addition, we modified AOMDV in such a manner so that end-to-end delay can be used as a QoS parameter.

Figure 4 shows average end-to-end delays as a function of the number of packets sent by the source for a varying number of paths identified by the protocols. We observe that as the number of packets transmitted is increased, the average end-to-end delay increases. The reason is that with the increase in the

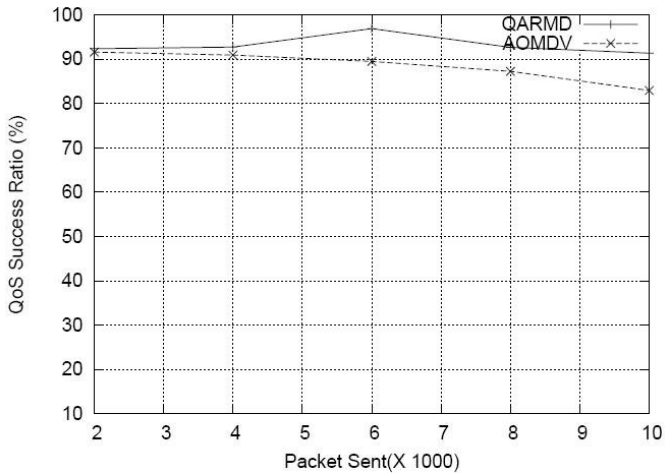


Fig. 6. QoS success ratio as a function of the number of packets sent by the source.

number of packets, the queueing delay is increased. However, QARMD incurs less delays as compared to AOMDV. The reason is that in case of QARMD, the path are selected in such a manner so that the contention delays and resequencing delays are mitigated.

Figure 5 shows that the throughput as a function of the number of contending nodes that are within carrier sense transmission range, R_{cs}, of the sender. We observed that when the number of contending nodes increases, the throughput of the network is decreased. The reason is that as the number of contending nodes increases, the possibilities of collisions and hidden terminal problems are significantly increased. As a result, the throughput of the network is decreased. As it is mentioned QARMD tries to identify node-disjoint paths with few contending nodes for mitigating the collisions and the hidden terminal problems, thus, the QARMD has significantly better throughput than AOMDV.

Figure 6 shows the QoS success ratio as a function of the total number of packets sent by the source. We observe that the QoS success ratio for QARMD is larger than that of AOMDV. The reason is that in case of QARMD packets follow paths with low contention delays. This reduces end-to-end delays experienced by packets and simultaneously enables more number of packets to reach before their respective deadlines, thereby, increasing the QoS success ratio.

VIII. Conclusion

In the proposed protocol, the source tries to identify multiple node-disjoint paths that satisfy QoS requirements in terms of end-to-end delays at the same time that achieve high throughput while sending packets. Since the contention delay at each node plays an important role and contributes to the major part of end-to-end delay, we focused on contention delays along a path and tried to minimize it. The source selects the paths that are expected to incur relatively low contention delays, hence, the data packets are shred among those paths according to the estimated delay of each path. We extended the analysis of the throughput of a single hop network to a multihop network then we tried to maximize it. In the simulation, the performance of the proposed protocol, QARMD is compared with AOMDV. We observed that QARMD provides an improvement over AOMDV in terms of end-to-end delay, QoS success ratio, and throughput.

References

[1] ANSI/IEEE Standard 802.11, "Information Technology, Telecommunications and Information Exchange Between Systems Local and Metropolitan Area Networks, Science Requirements, Part 11: Wireless LAN Medium Access Control (MAC) and Physical Layer (PHY) Specifications", 1999.

[2] G. Anastasi, E. Borgia, M. Conti, and E. Gregori. "IEEE 802.11b Ad Hoc Networks: Performance Measurements", *Cluster Computing*, Vol. 8, No. 2-3, pp. 135-145, 2005.

[3] M.M. Hira, F.A. Tobagi, and K. Medepalli., "Throughput Analysis of a Path in an IEEE 802.11 Multihop Wireless Network", *Proceedings Wireless Communications and Networking Conference WCNC*, pp. 441-446,2007.

[4] M.K. Marina and S.R. Das, "On-demand Multipath Distance Vector Routing for Ad Hoc Networks", *Proceedings of 9th IEEE International Conference on Network Protocols (ICNP)*, pp. 14-23, 2001.

[5] A.M. Abbas and Ø. Kure, "CQSR: A Correlation Aware Quality of Service Routing in Mobile Ad hoc Networks", *Proceedings of 3rd IEEE International Conference and Exhibition on Next Generation Mobile Applications, Services and Technologies (NGMAST)*, pp. 363-368, 2009.

[6] A.M. Abbas and Ø. Kure, "A Probabilistic Quality of Service Routing in Mobile Ad hoc Networks", *Proceedings of 1st IEEE International Conference on Networked Digital Technologies (NDT)*, pp. 269-273, 2009.

[7] N.T. Javan and M. Dehghan, "Reducing End-to-End Delay in Multi-path Routing Algorithms for Mobile Ad Hoc Networks", *Proceedings of 3rd International Conference on Mobile Ad hoc and Sensor Networks (MSN), Springer LNCS*, pp. 715-724, 2007.

[8] K.C. Leung, and V.O.K. Li, "Flow Assignment and Packet Scheduling for Multipath Networks". *Journal of Communication and Networks*, Vol. 5, No. 3, pp.230-239, 2003.

[9] S. Prasad, A. Schumacher, H. Haanpaa, and P. Orponen, "Balanced Multipath Source Routing", *Proceedings of International Conference on Information Networking (ICOIN)*, pp. 315-324, 2007.

[10] L. Zhang, Z. Zhao, Y. Shu, L. Wang, O.W., and W. Yang, "Load Balancing of Multipath Source Routing in Ad hoc Networks", *Proceedings of IEEE International Conference on Communications (ICC)*, Vo. 5, pp. 3197-3201, 2002.

[11] S. Mangold, S. Choi, P. May, O. Klein, G. Hiertz, and L. Stibor, "IEEE 802.11e Wireless LAN for Quality of Service", *Proceedings of European Wireless (EW)*, 2002.

[12] D.P. Heyman and M.J. Sobel. Stochastic Models in Operations Research :Volume I., *Lucent Technologies, Inc.*, 1983.

[13] A. Kumar, D. Manjunath, and J. Kuri, Communication Networking: An Analytical Approach, *Morgan Kaufmann Publishers*, 2004.

[14] R. Khalaf, I. Rubin, and J. Hsu, "Throughput and Delay Analysis of Multihop IEEE 802.11 Networks with Capture", *Proceedings of IEEE International Conference on Communications (ICC)*, pp. 3787-3792, 2007.

[15] M.M. Hira, F.A. Tobagi and K. Medepalli, "Throughput Analysis of a Path in an IEEE 802.11 Multihop Wireless Network", *Proceeding of Wireless Communications and Networking Conference (WCNC)*, pp. 441-446, 2007.

[16] T. Sugimoto, N. Komuro, H. Sekiya, S. Sakata and K. Yagyu, "Maximum Throughput Analysis for RTS/CTS-used IEEE 802.11 DCF in Wireless Multi-hop Networks",*Proceeding of International Conference on Computer and Communication Engineering (ICCCE)*, pp. 1-6, 2010.

[17] G. Bianchi, "Performance Analysis of the IEEE 802.11 Distributed Coordination Function", *IEEE Journal on Selected Areas in Communications*,Vol. 18, No. 3, pp. 535-547, 2000.

[18] A. Kumar, E. Altman, D. Miorandi, M. Goyal, "New insights from a fixed-point analysis of single cell IEEE 802.11 WLANs", *Journal IEEE/ACM Transactions on Networking (TON)*, Vol. 15, No. 3, pp. 588-601, 2007.

Fair and Reliable Multicast Routing for Wireless Mesh Networks

Nasrin Razavi[1], Mohammad Reaz Meybodi[2]

[1] Department of Computer Engineering, Islamic Azad University, qazvin Branch
qazvin, Iran
n.razavee@yahoo.com

[2] Department of Computer Engineering and IT, Amirkabir University of Technology
Tehran, Iran
m.meybodi@aut.ac.ir

Abstract

Multicast is a fundamental routing service in wireless mesh networks (WMNs) due to its many potential applications such as video conferencing, online games, and webcast. Recently, researchers proposed using link-quality-based routing metrics for finding high-throughput paths for multicast routing. However, the performance of such link-quality-based multicast routing is still limited by severe unfairness. Two major artifacts that exist in WMNs are fading which leads to low quality links, and interference which leads to unfair channel allocation in the 802.11 MAC protocol. These artifacts cause the multicast application to behave unfairly with respect to the performance achieved by the multicast receivers.

In some applications such as electronic test, competitions and etc. in addition to need for establishing the fairness among the members of the multicast group, it is need to reliable routing with 100% packet delivery ratio (PDR). one of proposed method for increasing PDR is Automatic Repeat Request(ARQ). Previously, numerous multicast protocols based on ARQ have been proposed to improve the packet delivery ratio. Therefore, these ARQ-based protocols can lead to excessive control overhead and drastically reduced throughput. Another technique for increasing PDR is Forward Error Correction (FEC) this method unlike the ARQ prevents of forward control packets and decreases overhead network partly.

In this paper, we present methods that in addition of the fairness improvement between the members of multicast group, increase PDR . two methods ARQ-based and FEC-based present in this paper, will be compared the gained fairness and PDR by 802.11.

Keywords: *wireless mesh network, multicast, routing*

1. Introduction

Wireless mesh networks (WMNs) have been proposed as an efficient solution for ubiquitous last-mile broadband access .The deployment and use of WMNs has increased significantly and several cities have planned and/or deployed WMNs [1-4]. WMNs are characterized by static mesh routers connected by wireless links to each other and to a few gateway nodes. These networks typically have low maintenance overhead, high data rates, and are not energy constrained. Compared to mobile Ad-hoc networks (MANETs), the static nature of mesh routers has shifted the major design challenges from maintaining connectivity among routers and conserving energy consumption to improving applications' performance, in particular, providing high-throughput and guaranteeing reliability in network access[5].

In a typical WMN environment, two major factors can severely affect both throughput and fairness of the whole network: fading and interference. Fading is the random attenuation of the signal due to reflections, scatterings and multipath propagation. Fading leads to inherently low quality links (even if the two end nodes are within transmission range) which can incur random packet losses.

Interference; when nodes defer their transmissions after sensing other transmissions, and packet drops, when the noise due to signals and multipaths from other transmitters decreases the SINR below the packet reception threshold. Hence, any practical solution that provides high throughput or reliability in a WMN has to deal with these two factors. Because of its random nature, more of papers don, t consider this about losing of data packets [6,7,8,9].

Multicast is another fundamental routing service in multihop mesh networks. It provides an efficient means of supporting collaborative applications such as video conferencing, online games, webcast and distance learning, among a group of users [10]. In spite of its significance, there has been little work on multicast routing in wireless networks. Moreover, there is no experimental work on providing fairness among multicast members in a multihop wireless network. Most recently, the authors of [11] studied link-quality-based routing metrics for finding high-throughput paths for multicast routing. Although these metrics have been shown to improve throughput compared to the widely used hop-count metric, one significant problem unfairness among different members of a multicast session remains unsolved.

In some application such as online game, video conferencing and etc. there is need to establishment of fairness among the multicast members until the group members obtain the equal throughput. In some of the applications such as electronic experiments, competitions and etc. in addition need to fairness establishment among the group members, there is the need to 100% PDR until questions, instruction packages and etc. attained to all members completely and simultaneously. In this paper, we present the methods that by MAC protocol namely IAFS [12] , automatic Repeat Request (ARQ) [13] and

Forward Error Correction (FEC) [13] methods, retained the fairness among the group and increased the packet delivery ratio(PDR).

The rest of this paper is as follows: in section 2, represent a method for fairness establishment among multicast group members. Sections 3 and 4, respective, are illustrated FEC and ARQ methods for increasing PDR. In sections 5 and 6, are illustrated the proposal method for fair multicast based on ARQ and FEC. In section 7, has been represented the simulation and evaluation results of given methods. In section 8 is represented a summary of the paper.

2. Fair establishment method among members of multicast groups

In this section, we present IAFS for multicast, a TDMA-like MAC solution to improve fairness and throughput of multicast in WMNs. We describe the four components of IAFS: the tree construction, the interference model, the scheduling algorithm, and the propagation of the schedule to the WMN nodes.

2.1. Tree construction

Constructing a good multicast tree is critical to the performance of any scheduling algorithm. In a realistic environment, if a tree consists mainly of lossy links due to fading, its performance will be poor, even with a perfect scheduling algorithm. In [13], the authors showed that SPP, which selects the path with the highest probability of packet delivery, gives the highest throughput among various link-quality-based metrics. Hence, in IAFS, we use SPP as the tree construction metric. SPP for a link is defined as the probability for a packet to be successfully transmitted from the sender to the receiver of that link, which can be easily calculated through offline measurements. The SPP for a whole path is equal to the product of the SPP values of the links constituting the path. A modified Dijkstra algorithm is used to find the paths with highest SPP value from the source to each receiver.

2.2. Interference model

In [14], Padhye et al. showed that it is difficult to accurately model interference among links and that simple heuristics (e.g., assuming that interference range is twice the transmission range) fail to provide accurate results. They also proposed an empirical methodology to predict pairwise interference in a network of n nodes using O(n2) measurements. For two links LAB and LCD, they define "broadcast interference ratio" (BIR) as follows:

$$BIR = (R_{AB}^{AC} + R_{CD}^{AC})/(R_{AB} + R_{CD})$$

where RAB, RCD are the packet delivery rates from A and C at B and D when only A or C broadcasts packets, respectively, and R_{AB}^{AC}, R_{CD}^{AC} are the packet delivery rates at B and D when both A and C broadcast packets simultaneously. The two links do not interfere when BIR is 1, and they interfere if BIR < 1.

In IAFS, since multicast forwarders use MAC layer broadcast to send data packets, the interference of interest is between nodes. This is in contrast to between links in [14], which is to be used for scheduling unicast. To measure the node interference, we perform all pairwise measurements similarly as in [28]. 2 However, since we consider nodes and not links in our scheduling, as we explain in the next section, we cannot use the BIR definition as above. We define two nodes A and C to be interfering if C's transmission affects the reception of any of A's children and vice versa. To measure the effect of C's transmission on A's child B, we measure the PDRs from A at B when only A broadcasts packets and when both A and C broadcast packets, respectively, and denote them as R_{AB}^{A}, R_{AB}^{AC}. We then define interference ratio (IR) as IRAC = min B ∈ children(A) R_{AB}^{AC} where $IR_{AB}^{AC} = R_{AB}^{AC}/R_{AB}^{A}$. Thus, node C is an interferer for link A → B (and it cannot transmit simultaneously with A), if IRAC < 1.

Similarly to the original BIR definition, the IR can take any value between 0 and 1. This gives us two different interference models. A schedule that assigns two forwarding nodes the same time slot only if they do not interfere as defined above guarantees fairness among all multicast receivers, assuming all tree links are of equal quality. We call this interference model the binary model. The binary model is conservative and may lead to long cycles and hence reduced sender rates (inversely proportional to the cycle lengths) and throughput. In this paper, we also consider the threshold-based model which considers node C as an interferer for node A only if IRAC < IT where IT is a selected interference threshold. The threshold-based model is more aggressive in finding nodes that can transmit simultaneously. This can lead to a reduced cycle length, which in turn leads to an increased sending rate and potentially increased throughput. However, it can also lead to unfairness as weakly interfering nodes are now competing to transmit in the same slot. Thus the threshold-based model effectively trades reduced fairness for increased throughput .We experimentally study this tradeoff in Section 5.

2.3. Scheduling algorithm

Our scheduling algorithm is based on spatial TDMA, first proposed in [15], and consists of three phases: compatibility matrix (CM) and compatibility graph construction, clique enumeration, and clique selection, similar to [16]. In the following, we explain the three phases of the scheduling algorithm using a single multicast tree in Fig. 1(a) as an example .We will explain how the algorithm can be easily extended for multiple concurrent trees at the end of this section. In this figure, the tree connects the gateway (node 1) to the receivers (nodes 5, 6, 7, 9, 10, 11). The solid lines denote the tree links, while the dashed lines denote links (with two end nodes within transmission range of each other) that are not part of the tree. In this example, S = {1}, R = {5, 6, 7, 9, 10, 11}, and FG = {1, 2, 3, 4, 8, 10}, and the scheduling algorithm has to schedule transmissions of nodes 1, 2, 3, 4, 8, 10.

CM construction: since forwarding nodes in IAFS use MAC layer broadcast to send data, the interference of interest is between nodes. This is in contrast to between links, as in the original spatial TDMA algorithm [15] and its later variations (e.g., [17,16]) which assign transmission rights to links.

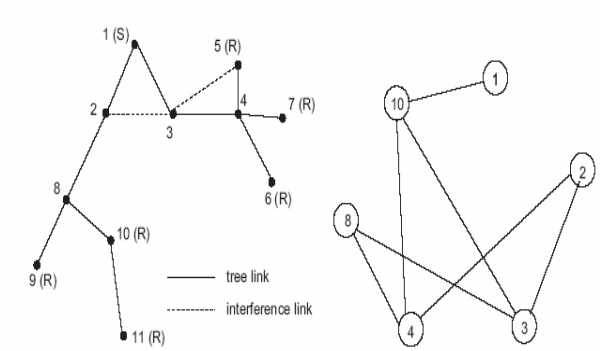


Fig1. Example physical tree formation and compatibility graph.

Consequently, in our scheduling algorithm, we define the CM to describe if pairs of nodes can transmit simultaneously. Specifically, we define CM as:

CM = [cmij], 1≤ i≤ j ||FG||

Where

$$cm_{ij} = \begin{cases} 0 & \text{if nodes } i, j \text{ cannot transmit,} \\ & \text{simultaneously,} \\ 1 & \text{otherwise.} \end{cases}$$

Two nodes cannot transmit simultaneously if any of the following two conditions hold: (i) any child node of node i is within transmission range of node j (collision), or (ii) one of the two nodes is an interferer for any of the children of the other node (interference). This second condition can be mathematically expressed as: $CM[ij] = 0$ if $IR^{ij}_{i\text{child}^k(i)} < IT$ for any k, where childk (i) is the kth child of node i. The reason condition (1) (collision) is not treated as a special case of condition (2) is that our interference measurement uses 802.11 CSMA and hence the child node of i may still get an IR above zero, which can cause nodes i and j to be scheduled in the same slot (e.g., if IR > IT).

The CM for the tree in Fig. 1(a), assuming IT = 1, is

$$CM = \begin{pmatrix} 0 & 0 & 0 & 0 & 0 & 1 \\ 0 & 0 & 1 & 1 & 0 & 0 \\ 0 & 1 & 0 & 0 & 1 & 1 \\ 0 & 1 & 0 & 0 & 1 & 1 \\ 0 & 0 & 1 & 1 & 0 & 0 \\ 1 & 0 & 1 & 1 & 0 & 0 \end{pmatrix},$$

where the rows correspond to nodes 1, 2, 3, 4, 8, and 10.

Using the CM, we can construct the compatibility graph shown in Fig. 1(b). In this graph, vertices correspond to nodes in FG, and an edge between two vertices denotes that these two nodes can transmit simultaneously.

Clique enumeration: After the CM construction, we enumerate all possible cliques in the compatibility graph. Although the problem of clique enumeration is NP-hard [16], the relatively small size of a WMN makes it easy to solve. For the graph in Fig. 1(b), the set of all cliques is

{{1}, {2}, {3}, {4}, {8}, {10}, {1, 10}, {2, 3}, {2, 4}, {3, 8}, {3, 10}, {4, 8}, {4, 10}}

Clique selection: We define a schedule as a set of cliques s that fulfills the following two conditions: (i) all nodes in FG are included in the schedule and (ii) each node in FG is included only once. Together, these two conditions ensure fairness among the receivers.

Given the list of cliques obtained in the previous step, we can enumerate the set S of all possible schedules. Each schedule s □ S corresponds to a cycle length Ts=||s|| , where ||s|| is the number of cliques in schedule s. To maximize spatial reuse, we need to select the schedule s□ that minimizes the cycle length:

$$T_{s^*} = \min_{s \in S} T_s.$$

Finding the optimal schedule requires an exhaustive search of all possible schedules. To reduce the computation cost, we propose a simple heuristic. The basic idea is to incrementally select and add to our schedule cliques that include many FG nodes, so that the total number of cliques is minimized. However, a straight forward implementation of the basic idea may not yield good schedules. For example, in Fig. 1(b), two possible schedules that may result from simply selecting cliques based on their sizes are

s1 = {{1, 10}, {4, 8}, {2, 3}}

s2 = {{4, 10}, {3, 8}, {2, }, {1}}

which have different cycles. This example shows that arbitrarily breaking ties may not lead to a good solution. To address this issue, we propose a heuristic called least overlapped first (LOF). In LOF, each clique is assigned a rank, equal to the number of common nodes this clique has with all other cliques of the same size. Then at each step of the scheduling algorithm, we select the clique that has the smallest rank, among the cliques of the same size. The intuition behind this heuristic is that if we can schedule a large clique that does not have many common nodes with other cliques of the same size, it will be easier to find other cliques with the same size, and form a schedule with a small cycle.

The steps of the LOF algorithm are as follows:

1. set s = {};
2. while not all nodes in FG are included in s

search for the clique CLi that includes the maximum number of nodes among the cliques that do not intersect with the members of s. If there are more than one cliques with the same number of nodes, select the one with the lowest rank.

add CLi to s.

The above LOF algorithm generates schedule s1 in the example of Fig. 1. In this example, clique {1, 10} has rank 2 as it overlaps with cliques {3, 10} and {4, 10}, cliques {2, 3}, {2, 4}, {3,8}, {4, 8} have rank 3, and cliques {3, 10}, {4, 10} have rank 4. Hence, LOF will first select the clique with the smallest rank, {1, 10}, and then two cliques with rank 3, resulting in schedule s1 with a cycle of three slots.

The main idea of the scheduling algorithm is common in many different scheduling algorithms, e.g., [18,19,20], although details may differ. In most of these works, the term flow contention graph or conflict graph is used, which is the complement term of compatibility graph in our paper, and the term independent set is then used instead of the term clique, which contains nodes that are not connected in the conflict graph. Then finding the minimum number of cliques to cover the compatibility graph is equivalent to finding the minimum number of independent sets to cover the conflict graph. We point out that the two approaches are essentially equivalent. We could have easily used the conflict graph-related terminology as well.

Scheduling multiple trees: The basic algorithm can be easily extended to schedule multiple multicast trees. In this case we simply enumerate each forwarder in each multicast tree separately in the CM construction. If the same node appears as forwarder in k multiple trees, it will appear as k separate nodes in the CM, and be assigned k time slots in a cycle, one for each of its tree appearance.

2.4. Schedule propagation

After computing the schedule, the network operator has to propagate it to the FG nodes. The schedule is propagated along the same tree the operator formed for the multicast session. However, since we need reliable delivery of the schedule to the forwarding nodes, each forwarding node unicasts it to its child nodes using hop-by-hop TCP sessions. The file of the schedule size is very small, containing only information of which nodes transmit at each slot of the cycle (and for which multicast session as there can be multiple concurrent ones).

3. Automatic Repeat Request

We selected ReMHoc [21] as a representative ARQ protocol for our comparison. ReMHoc follows the design principles of SRM [22], perhaps the most popular ARQ protocol for reliable multicast in the wired Internet. ReMHoc is receiver-initiated; each receiver is responsible for detecting losses, by detecting gaps in the packet sequence numbers. When a packet loss is detected, the receiver schedules a Request packet, asking for retransmission of the lost packet. To prevent the implosion of control packets, receivers wait for a random period of time before sending a request for a lost packet. If they receive a request for the same packet from another receiver before their timer expires, they postpone their own request by resetting the timer. This backoff is exponential in SRM, but linear in ReMHoc (proportional to the number of times this request has already been scheduled). This is because the loss rate is much higher in wireless networks than in the Internet, and hence faster response is required.

If the timer expires, a request is sent. But there is no guarantee that the request itself will not be lost, or that the repair packet will reach this receiver. Hence, the request timer is reset. In ReMHoc there is no upper bound on the number of times a request can be sent. However, we found that by allowing an infinite number of requests, the control overhead grows too fast and the PDR is reduced. Therefore, we decided to allow up to five retransmissions of t e same request. After requesting a packet for five times, a receiver considers this packet permanently lost and no further action is taken for that packet in the future. Request packets are multicast toward the whole group. Any multicast member that receives a request packet and has the requested packet, sends a Repair packet and does not propagate the request further.

Similarly as for the re- quest packets, a node postpones its transmission of a repair packet for a random period of time, and cancels it if in this time it hears another node retransmitting the same repair packet. Each repair packet is multicast to the whole group, so that all nodes that are missing the same data packet can recover by using the same repair packet.

4.Forward Error Correction

The key idea behind forward error correction (FEC) [23,24] is that k data packets are encoded at the sender to produce n encoded packets, where n > k, in such a way that any subset of k encoded packets suffices to reconstruct the original k data packets. Such a code is called an ń; kق FEC code and allows the receiver to recover from up to n _ k packet losses in a group of n encoded packets. A code is called systematic when the first k encoded packets are the original data packets. Systematic codes are much cheaper to decode and they allow partial reconstruction of data even when fewer than k encoded packets are received (with non-systematic codes receiving fewer than k packets is equivalent to receiving zero packets, since decoding is not possible). In a systematic code, the n _ k encoded packets that are different from the original k data packets are called parities.

In this paper we use a particular class of FEC codes, called Reed–Solomon (RS) codes, which use Vandermonde matrices to encode the data packets. In RS codes, k data packets are interpreted as the coefficients of a polynomial P of degree k _ 1. The encoding process involves multiplying the original data by an n _ k Vandermonde matrix G, and the decoding process requires the inversion of a k _ k submatrix G0 taken from G', and multiplication of the received data by G0_1. Rizzo [23] gives a description and a software implementation of RS codes which is used by many protocols, such as [25,26]. It works for packet sizes up to 1024 bytes, and the proposed values for k and n are 32 and 255, respectively.

5. Fair ARQ-based Multicast (FAM)

In this method, the data were forwarded to multicast members by given method in section 2, and if the receiver doesn't receive any packet because fading and etc. it forward the request packet with the aim of given ARQ method in section 3, and so enhanced PDR. The results of this method will present in section 7. the objection for ARQ method is the much overhead of it' s control packets, but by fair IAFS protocol, the rate of packet lost is less and the ARQ method doesn’t have much overhead.

6. Fair FEC-based Multicast (FFM)

In this method, the data was encoded before forward by source in presented FEC method in section 4. Then by means of given MAC protocol in section 2, were scheduled for data forwarding.

In this method the packet loss can be retrieval by forwarded parities in encoded packets. FFM unlike FAM has less overhead and also preservation fairness among the multicast members and increases the PDR. In section 7 , the results of this method is presented.

7. Simulation evaluation

7.1 simulation environment

We used the GloMoSim [29] simulator in our simulation study. We simulated a network of 50 static nodes placed randomly in a 1000m×1000m area, and we simulated 10 different topologies. The radio propagation range was 250m and the nominal bit rate was 2 Mbps (the data rate used for broadcast in 802.11 MAC protocol). environment. In our experiments, we used the two-ray propagation model, along with thermal noise and

Rayleigh fading. The noise factor was set to 7 dB. The Rayleigh fading model is appropriate for modeling environments with many reflectors, e.g., trees and buildings, where the sender and the receiver are not in line-of-sight of each other. Such environments are common in WMNs.Table.1. lists the general parameters that characterize the simulation environment. We compared results of our proposed methods with IAFS and 802.11 protocols.

Table.1.simulation environment

simulator	GlomoSim
Total Node	50
Simulation Time	400 seconds
Simulation Area	1000m ×1000m
Node Placement	Random
Radio Range	250m
Channel capacity	2 Mbps
Data Packet Size	1024 byte

7.2. Evaluation metrics

We use the following metrics in comparing our proposed methods with IAFS and 802.11.

PDR: the number of packets received by each receiver divided by the number of packets sent by the multicast source. PDR equals the throughput divided by the sending rate of the source.

1. Throughput (Kbps): the number of packets delivered to each receiver divided by the duration of the multicast session.

2. Fairness: fairness is characterized using the notion of Fairness Index γ defined in [10]. Although this metric is used in [10] to characterize spatial bias across comparable nodes in terms of hop-count and contention, the definition itself is not related to spatial bias and it simply gives an idea of the difference between throughputs received by different receivers.

Let the throughput of receiver i be denoted as Ti. To characterize the average fairness over all receivers, we define

$$\gamma_{ave} = average \quad \frac{\max(Tj, Tk)}{\min(Tj, Tk)} \mid \forall j,k \in [1..N]$$

and to characterize the worst case fairness over all receivers, we define

$$\gamma_{max} = \max \quad \frac{\max(Tj, Tk)}{\min(Tj, Tk)} \mid \forall j,k \in [1..N]$$

where N is the number of receivers. Ideally, γave=γmax=1 , but it is generally larger than 1 due to unfairness. The larger the γ value is, the more unfair the protocol is.

7.3. simulation results

In this section, we present the simulation results of proposed methods in PDR, fairness and throughput metrics, then compare the results with MAC 802.11 and IAFS protocols.

Fig.2. shows the packet delivery ratio by four approaches. So that, is clear in the figure the proposed approach in all scenarios is better than 802.11 and IAFS, but in comparing between FFM and FAM, can be seen that PDR in FFM almost in all cases is equal with 100%, and can obtained better results than FAM. In average case the PDR in FFM is equal with 100%. Therefore, FFM has been better results than FAM, IAFS and 802.11 respective, 2% , 7% and 23%.

Fig.3. a and b respective, shows the fairness average and worst case fairness by four approach in 10 different scenario. just as is clear of results, FAM gets better results than 802.11 protocols, but doesn't show good results than the two other approaches. IAFS and FFM get same results in most scenarios.

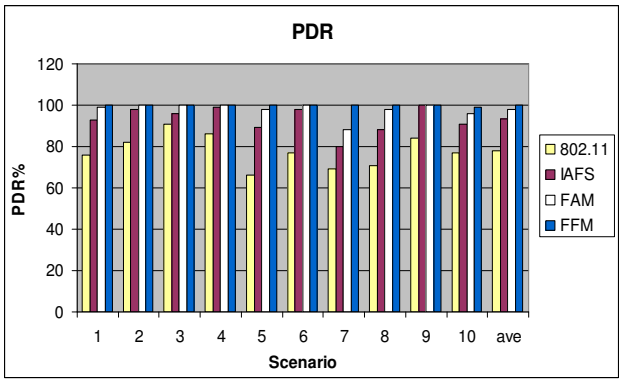


Fig.2. PDR comparison for 802.11, IAFS, FAM and FFM for 10 different scenarios

Just as is seen in fig.4.a , the gained fairness average by these two approaches in all scenario is equal with 1 and only in scenario 5 , fairness average isn't as good as another scenarios. Fig.3.b. shows the worst case fairness results in 10 scenarios. The results for IAFS and FFM are similar and better than two another approaches.

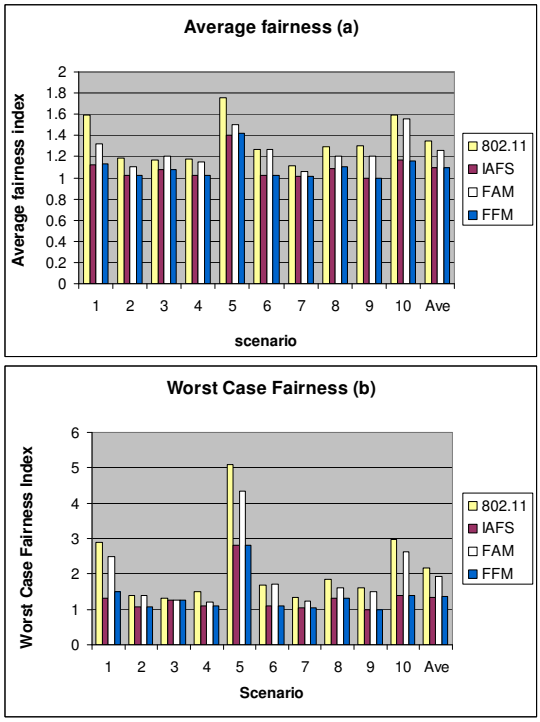


Fig.4. PDR comparison for 802.11, IAFS, FAM and FFM for 10 different scenarios.

Fig.4. shows throughput comparison for 802.11, IAFS, FAM and FFM for 10 different scenarios. Just as the results are clear, FAM doesn't get good results than the IAFS and FFM approaches. But FFM in all scenario gets better results than another approaches and the difference of the gained throughput by it with IAFS was 2 to 8 Kbps.
Just as is clear of results, FFM can with fairness established among multicast members, got to 100% PDR and higher throughput than another protocols.

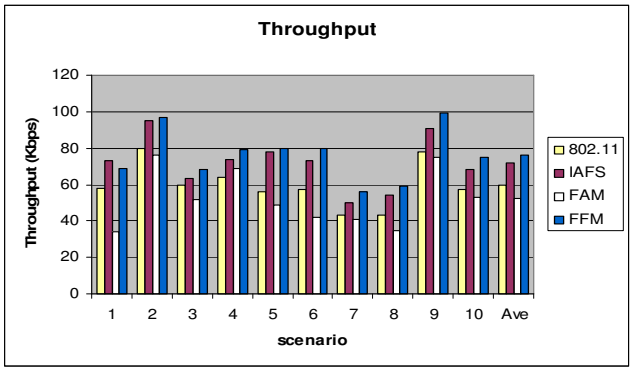


Fig. 3. throughput comparison for 802.11, IAFS, FAM and FFM for 10 different scenarios.

8. conclusion

In this paper, is presented two fair approaches for increasing packet delivery ratio in multicast for wireless mesh networks. In FAM, after data fair forward, each receiver requests the packet that it doesn't receive, further, so PDR has been increased. Just as the results show, this method have overhead partly for the forwarding control packets. But in FFM, first data encoded by RS method , then forwarded fairly. If the receiver doesn't take packet correctly, will retrieval the data by forwarding parities in encoded packets.
The results show that both proposed method increase PDR , but FFM has better throughput anf retain fairness among members correctly.

Reference

[1]ay area wireless users group, <http://www.bawug.org>.
[2] Champaign-Urbana community wireless network, <http://www.cuwireless.net>.
[3]MIT Roofnet, <http://www.pdos.lcs.mit.edu/roofnet>.
[4] Seattle wireless, <http://www.seattlewireless.net>
[5] D. Koutsonikolas and Y. Charlie Hu, Exploring the Design Space of Reliable Multicast Protocols for Wireless Mesh Networks, Journal of Ad Hoc Networks, 2009, Vol. 7, pp. 932–954
[6] D.S.J.D. Couto, D. Aguayo, J. C. Bicket, R. Morris, A high throughput path metric for multi-hop wireless routing, in: Proceedings of ACM MobiCom, 2003.
[7] R. Draves, J. Padhye, B. Zill, Routing in multi-radio, multi-hop wireless mesh networks, in: Proceedings of ACM MobiCom, 2004
[8] P. Gupta, P.R. Kumar, The capacity of wireless networks, IEEE Trans. Inform. Theory 46 (2) (2000) 388–404.
[9] M. Kodialam, T. Nandagopal, Characterizing achievable rates in multihop wireless networks: the joint routing and scheduling problem, in: Proceedings of ACM MobiCom, 2003.
[10] S.J. Lee, W. Su, M. Gerla, On-demand multicast routing protocol in multihop wireless mobile networks, ACM/Kluwer Mobile Networks and Applications 7 (6) (2002)
[11] S. Banerjee, A. Misra, Minimum energy paths for reliable communication in multi-hop wireless networks, in: ACM MobiHoc, 2002.
[12] D. Koutsonikolas, S. Das, Y. Charlie Hu, An interference-aware fair scheduling for multicast in wireless mesh networks, , journal of parallel and destributied computing , 2008, Vol. 68, pp. 372 – 386
[13] D. Koutsonikolas and Y. Charlie Hu, Exploring the Design Space of Reliable Multicast Protocols for Wireless Mesh Networks, Journal of Ad Hoc Networks, 2009, Vol. 7, pp. 932–954
[14] J. Padhye, S. Agarwal, V. Padmanabhan, L. Qiu, A. Rao, B. Zill, Estimation of link interference in static multi-hop wirele s networks, in: Proceedings of IMC, 2005.
[15] R. Nelson, L. Kleinrock, Spatial tdma: a colllision-free multihop channel access protocol, IEEE Trans. Comm. 33 (9) (1985).
[16] N.B. Salem, J.-P. Hubaux, A fair scheduling for wireless mesh networks, in: Proceedings of WiMesh, 2005.
[17] H. Luo, S. Lu, V. Bharghavan, A new model for packet scheduling in multihop wireless networks, in: Proceedings of ACM MobiCom, 2000.
[18] A. Ephremides, T.V. Truong, Scheduling broadcasts in multihop radio networks, IEEE Trans. Comm. 38 (4) (1990).
[19] H. Luo, P. Medvedev, J. Cheng, S. Lu, A self coordinating approach to distributed fair queueing in ad hoc wireless networks, in: Proceedings of IEEE Infocom, 2001.
[20] H. Luo, S. Lu, A topology-independent fair queueing model in ad hoc wireless networks, in: Proceedings of IEEE ICNP, 2000.
[21] A. Sobeih, H. Baraka, A. Fahmy, Remhoc: a reliable multicast protocol for wireless mobile multihop ad hoc networks, in:Proceedings of the IEEE Consumer Communications and Networkin Conference (CCNC), 2004.
[22] S. Floyd, V. Jacobson, C.-G. Liu, S. McCanne, L. Zhang, A reliable framework for light-weight sessions and application level framing, IEEE/ACM Transactions on Networking, 1997.
[23] L. Rizzo, Effective erasure codes for reliable computer communication protocols, ACM Computer Communications Review 27 (2) (1997).
[24] A.J. McAuley, Reliable broadband communication using a burst erasure correcting code, in: Proceedings of ACM SIGCOMM, 1990.
[25] J. Nonnenmacher, E. Biersack, D. Towsley, Parity based loss recovery for reliable multicast transmission, in:Proceedings of the ACM SIGCOMM, 1997.
[26] L. Rizzo, L. Visicano, Rmdp: an fec-based reliable multicast protocol for wireless environments, Mobile Computing and Communications Review 2 (2) (1998).

Author Biographies

Nasrin Razavi received the B.S. in Computer Engineering in Iran, in 2007. currently she is master in computer engineering in iran, in qazvin university. Her research interests include wireless networks, , learning systems, and distributed database.

Mohammad Reza Meybodi received the B.S. and M.S. degrees in Economics from Shahid Beheshti University in Iran, in 1973 and 1977, respectively. He also received the M.S. and Ph.D. degree from Oklahoma University, USA, in 1980 and 1983, respectively in Computer Science. Currently, he is a full professor in Computer Engineering Department, Amirkabir University of Technology, Tehran, Iran. Priorto current position, he worked from 1983 to 1985 as an assistant professor at Western Michigan University, and from 1985 to 1991 as an associate professor at Ohio University, USA. His research interests include wireless networks, fault tolerant systems, learning systems, parallel algorithms, soft computing and software development.

An Architecture for Real Time Television Audience Measurement

Debnath Mukherjee, Tanushyam Chattopadhyay, Siddharth Bhattacharya, Avik Ghose, Prateep Misra
{debnath.mukherjee, t.chattopadhyay, siddharth.bhattacharya, avik.ghose, prateep.misra}@tcs.com
TCS Innovation Labs, Tata Consultancy Services
Bengal Intelligent Park, Sector V, Salt Lake Electronics Complex, Kolkata – 700091, India

Abstract- **Currently, audience measurement reports of television programs are only available after a significant period of time, for example as a daily report. This paper proposes an architecture for real time measurement of television audience. Real time measurement can give channel owners and advertisers important information that can positively impact their business.**

We show that television viewership can be captured by set top box devices which detect the channel logo and transmit the viewership data to a server over internet. The server processes the viewership data and displays it in real time on a web-based dashboard. In addition, it has facility to display charts of hourly and location-wise viewership trends and online TRP (Television Rating Points) reports. The server infrastructure consists of in-memory database, reporting and charting libraries and J2EE based application server.

I. INTRODUCTION

Television Rating Points (TRP) is a measure of the popularity of a television channel or program. TRP is expressed as a number between 1 and 100 where one rating point equals 1% of a target television audience population. TRPs are measured using statistical sampling techniques from a target population.

TRP ratings are important for television broadcasters, media agencies, advertising agencies and advertisers. It has a huge impact on advertising expenditure and TV program scheduling. Hundreds of billions of dollars worth of air time buying and selling is done each year by media houses and companies based on TRP ratings.

Current methods of automated TRP measurements is based on placement of devices known as "People Meters" in the homes of the sample population. These devices are connected devices that measure viewing habits and periodically send reports to a back end system. Current methods used by "People Meters" are explained as follows.

1) **Audio Matching** – In this case the People Meter captures the audio content of a TV program , compresses the data and sends the data to a central backend server. In the server, the audio samples are compared with stored program audio data and thus viewership data is measured. This method is complex to implement and requires substantial investments in backend systems.
2) **Frequency Measurement** – This works with analog transmission systems, where the People Meter tracks the frequency of the tuned TV channel and sends this information to the backend. The backend maps the captured frequency with the channels and programs and is thus able to track viewer behavior. This method is the most popular method used in the country but is also most susceptible to errors / inaccuracies as there is no regulation or monitoring on local cable service providers with respect to the frequency of transmission.
3) **Watermarking** – In this technique watermarks are inserted in the program feed at the broadcasters end and is detected by the People Meter. The people Meters then transmits the detected watermark and timestamp to the backend. This method suffers from the fact that each program transmitted must be watermarked and that active cooperation from all broadcasters is required.
4) **Visual recognition** – In this case the People Meters looks for visual patterns and images from the displayed screen and thus tries to ascertain the program being watched. The proposed system uses this method of. TRP measurement.

The current TRP reports are sent on daily, weekly, monthly or quarterly basis, not in real time. Real time TRP reports can give an indication of current popularity of channels and thus help advertisers place their ads effectively.

The proposed system elegantly solves the problem of real time TV viewership tracking by using channel logo detection techniques. It uses sophisticated image processing techniques to detect the channels in real time based on stored signature of channel logos. The image processing is done by Digital Signal Processors present in the set top box known as HIP (Home Infotainment Platform). The detected channel and location is sent to a backend analytics server which shows the viewership data through dashboards and online reports. In some DTH systems, the channel being viewed can be found, however the set top box allows processing of analog RF cable as well. DTH has lower reach than cable, so this is significant.

The unique contribution of this paper is that it presents a novel application which helps advertisers and broadcasters view current trends of television viewership both in graphical and report format. It also reports current (real time) TRP of the various channels. The real time TRP will enable advertisers place advertisements based on current popularity of channels and also based on location factors.

978-1-61284-690-3/11/$26.00 ©2011 IEEE

III. Related Work

The related work is in the area of "digital signage" which Wikipedia describes as "a form of electronic display that shows information, advertising and other messages." These signs are displayed in out-of-home locations such as retail stores and corporate buildings. Some software such as Trumedia [6] helps advertisers give targeted advertisements by e.g. analyzing the current audience based on video analytics on the faces of the audience captured by a camera. The data about the audience is sent back to a backend server which helps display reports about the current audience. In TruMedia's integration with Cisco Digital Media Player, the real time information about the audience can be used to select the next message to play, thus enabling targeted advertising. Quividi [7] and CognoVision [8] are two other players in this market.

Our solution is for in-home TV displays and helps measure channel popularity in real time. This channel popularity can be used by advertisers to place ads at the right time.

III. Proposed System

The TV broadcast is routed to the device via composite A/V IN and output is given to the television via composite A/V OUT. Logo detection algorithms are run on the video using the digital signal processor in the HIP box. On recognition of the channel being viewed, the box constructs a tuple (channel identifier, location, timestamp) and sends it to the analytics server which displays various charts and reports.

The benefits of TRP tracking using HIP is as follows:

1) **Low cost TRP tracking** - The HIP platform is an extremely low cost device. It costs approximately an order of magnitude less than existing People Meters. Most importantly, TRP tracking is only one of the many applications that the device supports.
2) **Ease of deployment** - This is a software only solution that sits inside HIP. The primary purpose of HIP is not audience data measurement. This is an add-on software functionality.
3) **Real time audience measurement** – Data about viewership will be available in real time. This is as opposed to end of day or end of week data that current systems now provide.
4) **Increased accuracy** – Current systems are based on frequency monitoring are considerably less accurate since frequency of transmission in cable TV networks are changed arbitrarily from time to time by local cable TV operator.
5) **Larger sample size** – HIP being widely deployed will provide much larger sample sizes than the existing Peoplemeter devices.
6) **No possibility of data tampering by vested parties** – Since data is available to subscribers in real time, there is no scope for any manipulation of any stored data or doctoring of reports. Also secure channels from HIP platform will ensure complete integrity of measured data.

The deployment of the proposed solution is shown in Fig. 1.

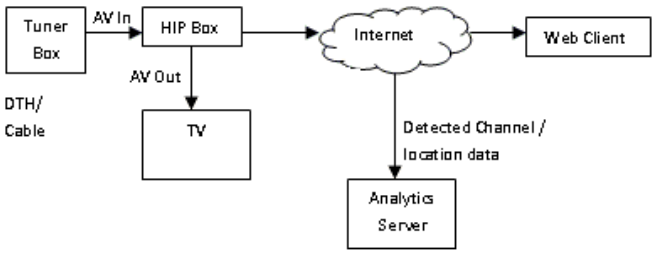


Fig 1. Deployment of the proposed solution

The basic working principle of this measurement system is as follows:

- HIP set top boxes detects logos of channels being viewed when channel is changed by the viewer
- HIP box transmits the detected channel id, current time stamp and IP address of the HIP box to an internet hosted analytics server using secure channels
- Geographic location is obtained using IP address. Each HIP box has a (static / dynamic) public IP address from which the geographic location of the box can be determined from Google API.
- Electronic Program Guide is obtained from internet sources
- Analytics server analyzes the data and creates dashboards, mashups, heat maps, real time trending and charts.
- Data from analytics server is available to authorized clients using a internet connection and browser

IV. Channel Logo Detection

A. Overview

The overview of channel logo recognition can be found from [1]-[3]. The steps are described in Fig. 2.

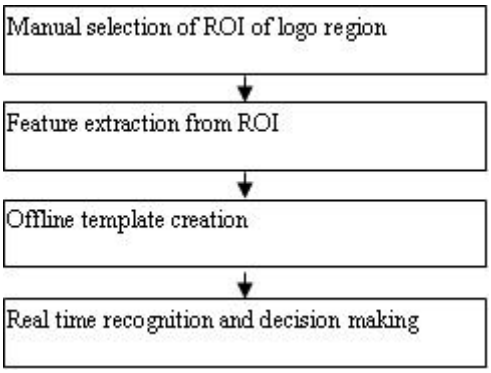


Fig. 2. Overview of Channel logo recognition

B. Manual selection of Region of Interest (ROI) of logo region

Initially the videos of all channels are recorded to create a single video file. Manual annotation is performed on the video file to generate an xml file containing channel code, start frame number and end frame number.

This video is played using a tool that enables the user to select the ROI (logo region) from the video using mouse. The tool takes the annotated xml file as input to generate a output xml file with ROI coordinates, height and width of ROI and features of the ROI.

The feature consists of quantized colors of the pixels in the ROI. We have used quantized colors to reduce the size of the template file.

C. Method of color quantization

The input candidate channel logo region image is UYVY format, which is converted to HSV color space to have separate information of color, intensity and impurities. These HSV values are quantized into 36 bins as described in [3].

D. Recognition of Channel logo

Once the candidate logo regions are found, each pixel is quantized to 36 values. Then the features of each candidate region are matched with the features of template logos stored in the database. In the proposed method a fuzzy multifactorial approach is used to recognize the channel logo. The factors and the reason behind selecting these factors are as below. (Details of the logo detection method can be found from [3]).

Bhattacharya distance: We have used a factor (f_bhat) based on that feature to find the histogram similarity between the candidate and the template. Details about this distance can be found from [5].

Crossing count and run length similarity: These are two shape invariant features used in OCR. We have constructed a Similarity matrix of size 36x36 and find the similarity between template and candidate using correlation coefficient. As the normalized correlation value also lies in the interval of (0,1), the factor value also in the same interval. The method of construction of the matrix is as below:

$$i \leftarrow quant[y][x],\ j \leftarrow quant[y][x+1],$$

$$cross_mat[i][j] = cross_mat[i][j] + 1,$$

$$\forall\ y \in (0, height)\ \forall x \in (0, width-1)$$

Where quant is the array of pixels with quantized color value, cross_mat is the matrix storing the crossing count feature

Flusser and Suk image moments: One simple Affine Moment Invariants (AMI) used for channel logo recognition. In [4] authors have used four such features. But other than the first one, rest is computationally expensive for implementation of a real time system in a DSP platform and it is found experimentally that the Affine Moment Invariant 1st Order Transformation (AMI 1) itself produces very good result.

Aspect Ratio: We have used another factor (f_asp) based on this feature can distinguish between different families of channel logos very efficiently. It is found that the aspect ratio of the logos of Star family varies with the same of Zee family. The method of assigning fuzzy weight to each of those factors is described in [3].

Construction of evaluation matrix

The evaluation matrix is formed using the factors values as described below

$$V = \begin{pmatrix} f_bhat_1 & f_bhat_2 & \dots & f_bhat_n \\ \dots & \dots & \dots & \dots \\ \dots & \dots & \dots & \dots \\ f_asp_1 & f_asp_2 & \dots & f_asp_n \end{pmatrix}$$

Construction of Additive Standard Multifactorial (ASM) function

Now, from the evaluation matrix V it is difficult to obtain any solution of the decision-making problem. So we define a mapping function M_m that maps the m-dimensional vector $f = (f_1, f_2, ..., f_m)$ into a one dimensional scalar i.e. $M_m(f) = M_m(f_1, f_2, ..., f_m)$

we apply ASM on V to obtain the multifactorial evaluation

$$V' = (v_1, v_2, ..., v_n)$$

$$\text{Where } v_i = M_m(v_{1i}, v_{2i}, ..., v_{ni})\ \forall i = [1, n].$$

Now we define a mapping function M_m as a simple arithmetic average over the m number of factors and thus it is defined as

$$M_n(d) = \frac{1}{m}\sum_{i=1}^{m} d_{in}$$

So we finally obtain the decision making matrix V' which is a row matrix and each element represents the confidence score of membership of the candidate region matching with the i^{th} logo.

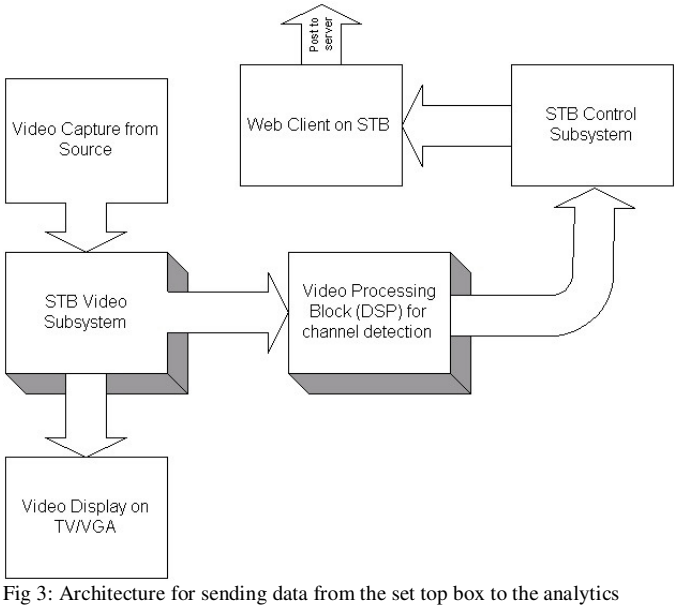


Fig 3: Architecture for sending data from the set top box to the analytics server

V. Reporting Of Data To The Analytics Server

The overall enhancements to the set top box is depicted in the architecture diagram (Figure 3). The sequence of events is as follows:

1. Video is captured using set-top-box (STB) video capture block
2. This video is then processed by logo detection algorithm running on DSP
3. The algorithm returns a channel id which is passed to the control sub-system of STB
4. The channel id and the time is recorded and fed to the box HTTP client
5. The HTTP client then posts this data at a 30 second (configurable) timer to the server

The web-poster utility runs in a timer loop and keeps posting channels watched, serial number (unique id), timestamp, location id and current time.

VI. Data Analytics On Streamed Data

A. *Overview of the Analytics Solution*

The architecture of analytics is shown in the following diagram.

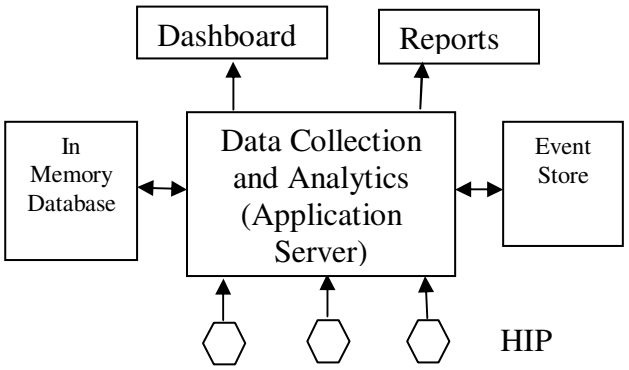


Fig. 4. Analytics Architecture

The steps in the data processing are explained in the following paragraphs.

Data is sent from the HIP boxes to a data collection application server implemented using J2EE technology. The data tuple consists of the location, timestamp and channel identifier.

The data is stored in an in-memory database. The database stores only a few minutes' worth of data. Data older than that is deleted. This database serves data to a real time display module which periodically takes snapshots of the data and displays on the web. Since real time current data is displayed, old data can be deleted; which helps to keep the size of the table small and improves the performance of the real time display module. The data in the in-memory database is also used to show the viewership statistics at various locations on a map of the country. This is done using Google Map Application Programming Interfaces.

The data is also stored in an event store, a relational database management system, for online reporting of:

- Television Rating Points (TRP) for a selected channel for a selected time period.
- Hourly trends of channel performance
- Location-wise trends of channel performance

Reports are published both as PDF and as HTML.

TRP for a channel during a time period is estimated as:
(total viewed time) / (total available time) * 100
Where "total viewed time" is the sum of the viewership of a channel during the selected time period and the "total available time" is the duration of the time period multiplied by the number of set top boxes deployed.

The system has been built using open standards such as Java/J2EE and SQL. This allows the system components to be replaceable with products from different vendors if needed.

The technology used in the implementation is as mentioned in Table I below.

TABLE I
TECHNOLOGY MATRIX

COMPONENT	TECHNOLOGY
Application Server	JBoss
Reporting library	Jasper Reports
Relational Database	MySQL InnoDB Engine
In-Memory Database	MySQL Memory Engine
Geographical Mashup	Google Maps API

B. *Features of the analytics solution*

The web frontend implements visualization of data in several "views". The available views are:

All Channels View – This view shows the performance of all the channels as bar charts – with viewership on the Y axis and the various channels on the X-axis.

Single Channel View – This view allows the user to select a location and a channel and display the viewership. The channel is shown on the X-axis and the viewership on the Y-axis.

City-wise Channel View- This view shows the performance of channels being watched at a particular city as bar charts - with viewership on Y axis and the various channels on the X axis.

Country-wide View - This view shows the performance of a particular channel across all geographic locations. Markers are placed at various locations on the map and on clicking on the marker a pop-up shows the viewership.

Reports View – This is divided into 3 kinds of reports

1. **Hourly Trend Report**- This view shows the viewership trend chart for a particular channel as it varies with time in the form of a line chart with number of viewers on the Y-axis and Hours on the X-axis. The data points are also shown in the report (hour, number of viewers).

2. **TRP Viewership Report**- This view shows the TRP value for a particular channel in a specified time window.

3. **Location based Trend Report**- This view shows the viewership trend chart for a particular channel and a specified location as it varies with time in the form of a line chart with number of viewers on the Y-axis and hours on the X-axis. The data points are also shown.

C. *Modules of the application*

The modules of the solution are explained below:

Data Collection Module – This module implements RESTful Web Service [9] to receive the data posted by the HIP boxes. A servlet processes the requests and writes to the in-memory database and the event store.

Image Generation Module – The real time display is implemented by taking snapshots of the data in the in-memory database periodically and generating PNG files. Different PNG files are generated for different views. Each image shows the viewership on the Y axis and the channels on the X-axis. The image generation is a background process.

Database Cleaner Module – As mentioned before, the old data in the in-memory database has to be deleted as old data is not required for showing real time charts. To achieve this, a background process is implemented.

Reports Module – Reports are generated using the JasperReports library. Each report shows a plot of the data at the top of the report and the actual data points below it in a tabular format.

Geographical Mashup module – The geographical plot is implemented using Google Maps API. Markers are placed at various locations where television audience measurement is done. On clicking on a marker, the viewership at that location is shown. This is a real time chart and Ajax technology is used from the web page to fetch the real time data from the in memory database.

VII. RESULTS

A. *Results for Channel logo detection*

The PC version of the code was tested over 280 different recorded videos from different channels. However, the current DSP based system can support upto 13 channels with recall and precision rate almost equal to 1. Recall (r) and Precision (p) can be defined as:

$$r = \frac{c}{c+m}, p = \frac{c}{c+fp}$$

where c is the number of correct recognition, m is the number of misses and fp is the number of false positives. For each channel we have tested the algorithm for 1 hour TV sequence taken at 20 different instant of time. The current software supports 13 channels. The average time to detect the logos is 1.87 milliseconds with a maximum of 1.95 ms and minimum of 1.8 ms. Code is developed using Texas Instruments(TI) Codec Engine framework.

B. *Results for Analytics*

This section shows screen shots of our TV Audience Measurement application. Figure 5 shows the geographical mashup. Figure 6 shows the hourly trend report. Figure 7 shows the TRP report and Figure 8 shows the All Channels view.

We simulated the set top boxes as threads running in a Java program. The various timing configurations are as follows:

1. The web poster on the STB posts once every 30 seconds
2. The image generator runs once every 5 seconds
3. The web screens are refreshed once every 10 seconds

Additionally, the network delay to send data from simulator to server was found to be 2 seconds.

Measurement on an Intel dual core 2.33 GHz processor with 2 GB RAM showed the average latency to reflect a channel change as 47.6 seconds.

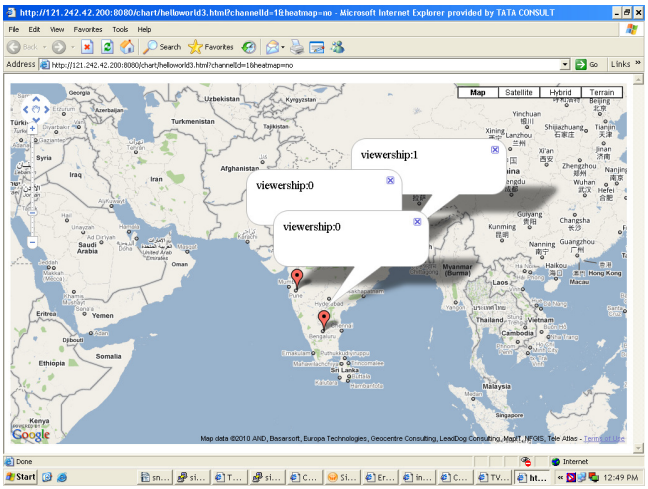


Fig. 5 Geographical mashup

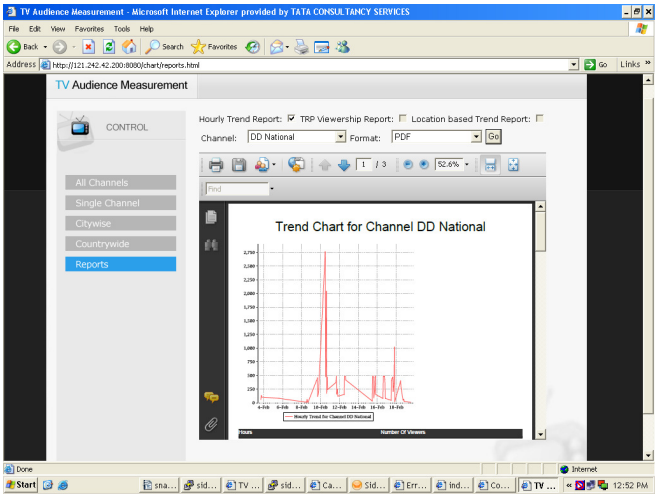


Fig. 6. Hourly trend report

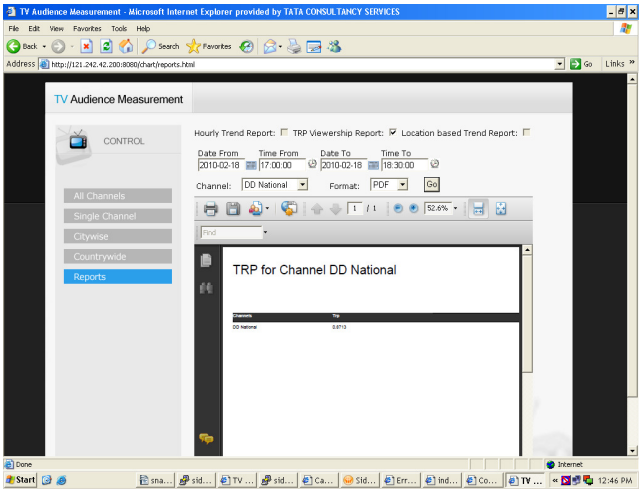


Fig. 7. TRP Report

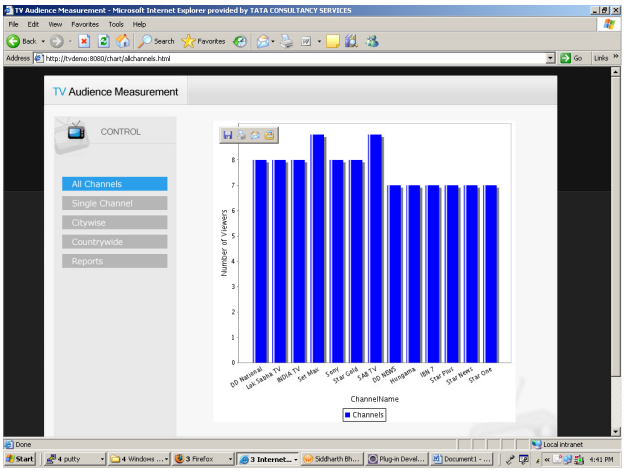


Fig. 8. All Channels View

VIII. Conclusion and Future Work

In this paper we have presented a novel application for real time measurement of TV audience. The application detects the logo of the currently playing channel and reports the channel and location to an analytics server. The analytics server helps the user to discover trends in viewership across channels and locations. This application would be useful for TV broadcasters and advertisers in their business efforts. In future work, we plan to investigate the possible application of Bayeux protocol [10].

IX. Acknowledgment

We acknowledge the involvement of Computational Research Laboratories (CRL) in this project.

References

[1] T. Chattopadhyay, Aniruddha Sinha, Arpan Pal, Debabrata Pradhan and Soumali Roy Chowdhury, "Recognition of Channel Logos from Streamed Videos for Value Added Services in Connected TV,"Proc. of the 29th International Conference on Consumer Electronics (ICCE'11), Jan, US, 2011

[2] T. Chattopadhyay, and ChandrasekharAgnuru, "Generation of Electronic Program Guide for RF fed TV Channels by Recognizing the Channel Logo using Fuzzy Multifactor Analysis", Proc. of the 14th International Symposium on Consumer Electronics (ISCE'10), 7-10 June, Germany, 2010.

[3] T. Chattopadhyay, Sounak Dey, Pritha Bhattacharya, Arpan Pal, "Electronic Program Guide for RF fed TV Channels," Proc. of the UKSim 4th European Modelling Symposium on Mathematical Modelling and Computer Simulation, (EMS 2010), Page(s), , Pisa, Itally, 2010

[4] J. Flusser, and T. Suk, "Affine Moment Invariants: A new tool for character recognition," Pattern Recognition Letters, Vol 15, page(s) 433-436, 1994

[5] T. Chattopadhyay, P Biswas, B. Saha and A. Pal, "Gesture Based English Character Recognition for Human Machine Interaction in Interactive Set top box Using Multi factor analysis", 6th Indian Conf. on Computer Vision, Graphics and Image Processing, ICVGIP, Page(s) 134-141, India, 2008

[6] Trumedia, http://http://trumedia.co.il/

[7] Quividi, http://www.quividi.com/

[8] Cognovision, http://www.cognovision.com/

[9] Representational State Transfer, http://en.wikipedia.org/wiki/Representational_State_Transfer

[10] The Bayeux Specification, http://svn.cometd.com/trunk/bayeux/bayeux.html

Recognizing User Activity Based on Accelerometer Data from a Mobile Phone

Media A. Ayu, Teddy Mantoro, Ahmad Faridi A. Matin, Saeed S. O. Basamh
Intelligent Environment Research Group (INTEG)
Kulliyyah of Information and Communication Technology (KICT)
International Islamic University Malaysia (IIUM), Gombak Campus, Kuala Lumpur, Malaysia
(media, teddy)@kict.iium.edu.my

Abstract— **Activity recognition refers to the ability of a machine/device to recognize the activity of users. This area of research has attracted many works especially related to the context aware and ubiquitous computing area. Wearable accelerometers have been explored for this activity recognition purpose; however the impracticality of attaching accelerometers to the user presents significant issues. Accelerometers today are embedded in many mobile devices. This paper explores the potential and possibility of using these accelerometer data to determine user activity recognition. The initial experiments show encouraging results with a very good accuracy rate of 92%. A simple prototype developed supports the implementation of the recognition process conducted.**

Keywords — **Activity recognition, Context awareness, Accelerometers, Ubiquitous Computing, Mobile devices**

I. INTRODUCTION

Supported by the increased competition by rivals and the increased demand by consumers, mobile device manufacturers have been, for the past few years, developing mobile devices that are smart and multi-functionally rich. Research and development on these devices are fast paced due to the nature of these devices (e.g. its mobility and size) that creates worlds of possibilities.

The introduction of embedded sensors in the design of these devices opened the door to many applications that would have been hard to implement in the past without the use of these sensors. Accelerometers, digital compasses, gyroscopes, GPS, microphones and cameras [1] are some of the examples of these sensors. These sensors provide raw data to be used in the implementation of many applications in these mobile devices. The GPS, for example, is used in location based applications; on the other hand light sensors are used in determining proximity between the user and the device [1]. Among the most interesting sensors is the accelerometer. An accelerometer is gravity sensitive, thus any changes in the orientation of the accelerometer will produce different readings [2]. These readings are the input for many applications in these devices, mainly for motion detection, posture sensing and human computer interaction [2][3]. Many games depend heavily on the data acquired from the accelerometer. The user interaction with the device, while engaging in these games, requires that the user constantly change the orientation of the device against the gravitational force. Another popular application of accelerometers in mobile devices is using the data acquired to change the screen view. When the user rotates the device from vertical to horizontal (or vice versa) the screen view will change accordingly. Many popular mobile manufacturers are currently implementing these functionalities as part of its design of its product line.

Activity recognition using accelerometers have been the interest of much research in this field. Wearable standalone accelerometers or systems with an accelerometer as its main component have been used in many research experiments [3][4][5]. Accelerometers were attached, in these experiments, to key areas of the human body. These experiments presented encouraging results however the problem is the impracticality of its implementation in the real world due to the wearable nature of these systems. With the increased popularity of accelerometer-embedded mobile devices, these accelerometers can be used for implementing context or/and activity recognition. Like wearable accelerometers, mobile devices are somewhat inseparable from its owner. Moreover, this kind of embedded accelerometer will enable a nonobtrusive activity monitoring for the user everyday usage. Also, it provides the flexibility and computational resources that is needed to process the data, which eliminates the need for external components to perform the computation. In this paper, we attempt to explore the potential and possibility of implementing activity recognition using data acquired from an accelerometer-embedded mobile phone.

Following this introduction part is Section II which presents a review on previous studies related to activity recognition research, especially the ones that utilized accelerometer. It is then followed by a brief description about the methodology used in our study work on the activity recognition using a mobile phone's accelerometer data. The discussion of some results yielded from our experiments is presented in Section IV. Lastly, this paper is closed by a conclusion and future work section.

II. RELATED WORK

Accelerometers, in its standalone form, have been favored for many years for activity recognition research. Wearable/attachable accelerometers or wearable systems

with accelerometers as the main components have been tested through various experiments [3][4][6].

Two-axis accelerometer was used in the works done by Bao and Intille [4]. For classification, decision tree algorithm classifiers were used which produced over 80% recognition accuracy for 20 everyday activities. The feature extraction method was based on the fast FFT. In another experiment, Yang et al. [7] used a triaxial accelerometer. Classification was based on a neuro-fuzzy classifier. This method achieved about 83%-93% recognition accuracy.

In general, raw data extracted from these accelerometers are in the values of the x,y and z axes at a particular instance of time. Attributes such as, the mean, standard deviation, frequency domain entropy and/or the correlation of acceleration data [3][4] are then calculated from the raw data and then classification are conducted based on some or all of these attributes.

High accuracy rates described in many papers provide encouraging indication of the feasibility of using accelerometers in activity recognition. However, these accuracy rates fail when activities being tested are part of a series of continuous events rather than controlled isolated events. This is because within continuous events, random actions may occur that produce readings that overlap with readings of *normal* events. Ravi et al. attempts to resolve this problem by combining microphones with accelerometers [3]. The microphone is used to capture sounds that will be used in the analysis to identify signal segmentation. The usage of the microphone was due to the assumption that the activities being tested on produced distinguishable sounds.

Accelerometers are widely used in various industries as it has various useful applications; the automotive industry is one of the earliest users of this technology which is evident in its usage of accelerometer in the airbag triggering technology. And lately, the hand-held gadget industry is increasingly using it in their devices to increase user interactivity.

Many electronic companies are slowly but steadily, introducing this technology. Some computers have built in accelerometers that provide a mechanism to detect sudden fall, also modern gaming consoles, such as the Wii™Nintendo ®'s WiiMote™ and the PlayStation® 3's dualshock ®3 joystick, use some sort of accelerometer to help in inputting purposes. However, perhaps the most known application for accelerometers in the electronic world is its application on modern handheld gadgets produced by companies such as Nokia, HTC, Sony Ericson and Apple. The accelerometer in mobile handheld devices is the one that is closest to general people use, as many people in the world are using mobile phones nowadays. Some developers have utilised accelerometer in mobile phones to create more interactive application in games and multimedia, such as skipping tracks in Windows Media Player mobile when the user shakes it [8].

The gaining popularity of accelerometer-embedded mobile devices in the past few years shifted research attention from wearable accelerometers to these devices. Several papers have discussed the possibility of using these mobile devices in activity/context recognition [1] [9][10]. Technically, the programmability and the computational capabilities [1] that these devices offer, creates the possibility in which accelerometer-based application development would be more convenient and accessible. Also, the nature of the phones and how it relates to people's lives are to some extent more favorable than wearable/attachable systems. Mobile devices/phones are more convenient to carry and also they tend to be inseparable from their owners, especially when the owners are commuting from one place to another..

III. METHODOLOGY

The works presented here is an initial works on user activity recognition as part of our context awareness research which aims for a creation of an intelligent environment. As mentioned in Gross and Specht [11], most definition of context considering four dimensions of context, i.e. location, identity, time and activity. Integrating those four dimensions will lead to the development of intelligent environment that will move users' distraction out of computer interaction [12].

This study focuses on the activity dimension of the context. The steps carried out in this research study are presented in Figure 1.

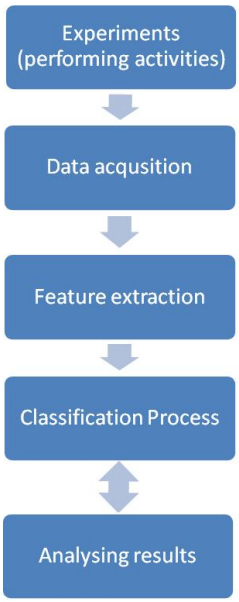


Figure 1. Our research study procedure

A. *Data Acquisition*

Various mobile device vendors provide accelerometers in their devices. In this paper, HTC mini was used. In order to acquire the x,y,z values of the accelerometer, a simple software application was developed to capture the data and store it in text form. Due to the unavailability (at the date of implementation) of official sensor API for the accelerometer in the HTC, a third party API [13] was used in the development of the data acquisition software application.

Our initial study only looked at five basic human activities, i.e. sitting, standing, walking, running and jumping. Each activity is performed by two individuals in certain period of time and the data related to these

activities were acquired. In the experiments, several repetitions are conducted for each activity. During these experiments the phone was always carried in right palm of the hand with the screen faced upwards. This way, we could minimize the accelerometer data noise. Later works will do data collection from accelerometer in different positions which are more 'natural' to the position of how usually people place their mobile phones.

B. Classification Process

Classification process for the activity recognition was carried out using Naïve Bayes algorithm classifier available in Weka machine learning tool [14][15][16]. Naïve Bayes is chosen based on previous works on accelerometer which reported the good accuracy of employing the algorithm in activity recognition [4][17] and its easiness compare to other algorithms, like kNN for instance. Data acquired from the experiments mentioned in Section A are used as the training data for this classification process. More experiments then also performed to gather some test data for the recognition process.

Our further works will look at the used of other classifier algorithms, and compare their performance in regard to the accelerometer data from mobile phones.

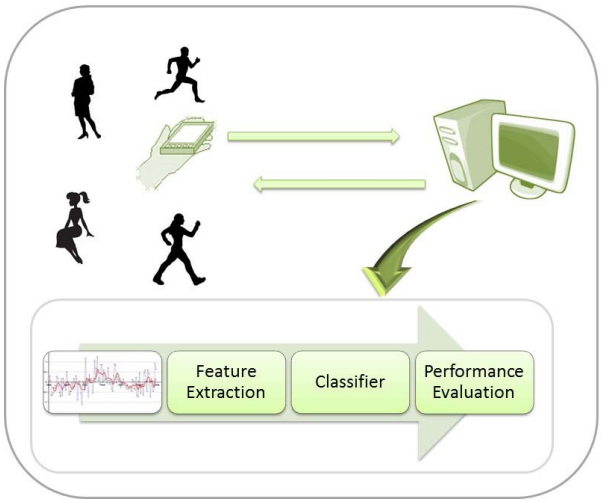


Figure 2. Our activity recognition framework

IV. DISCUSSION

Data acquired from the experiments conducted was plotted into graphs. Sample of data are depicted in Figure 3 (the y axis in the graphs represents time). The data shows the different behavior of the axes between the three activities. It shows how the z value varies extremely through time when the activity in concern is jumping (Figure 3). Another observation that can be deduced from these graphs is that the value of z in the case of sitting and standing shows no significance differences and they tend to be steady. On the contrary, the value of z fluctuates greatly in jumping activities. We believe that it is because of the significant changes of distance of the object from the ground. Based on the behavior of the data, we are confident that these x, y and z accelerometer data can be used for recognizing these three basic activities.

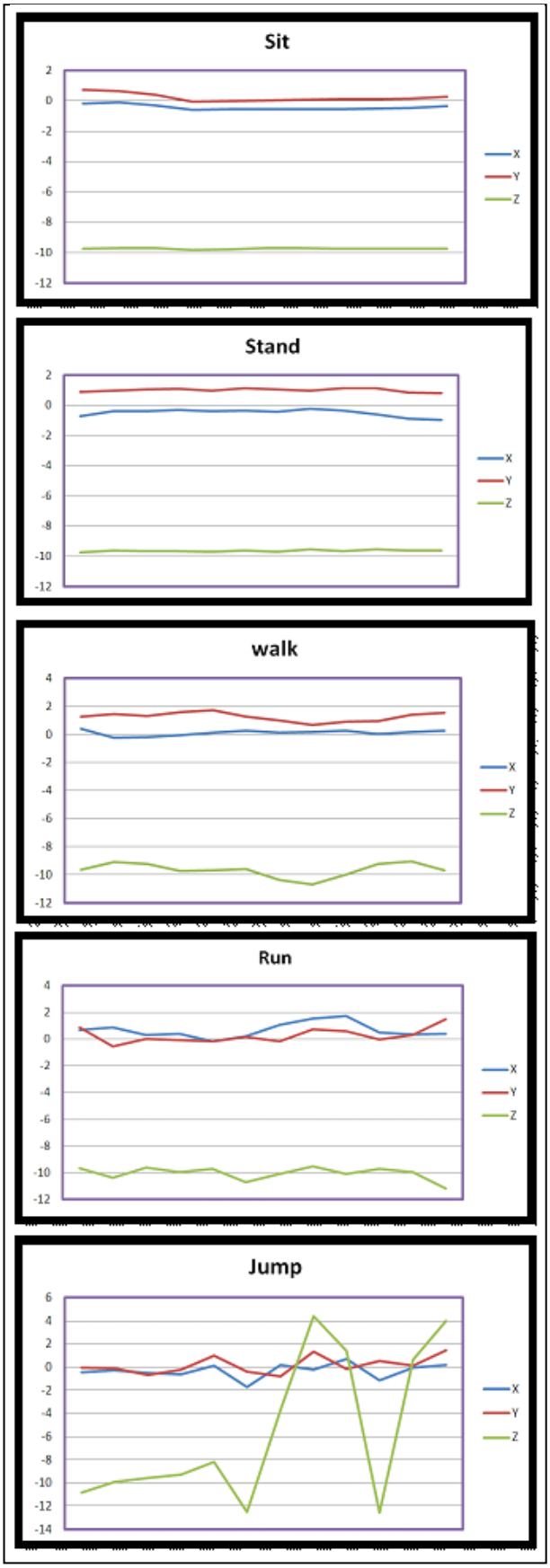


Figure 3. Accelerometer data behavior for the five basic activities

Two main features were calculated from the three axes accelerometer data i.e. the mean and standard deviation, in the pre-processing stage. Based on these data, we then have seven attributes to be fed to the Weka classifier tool for the classification process. The Naïve Bayes visualization tree created for the classification process can be seen in Figure 4.

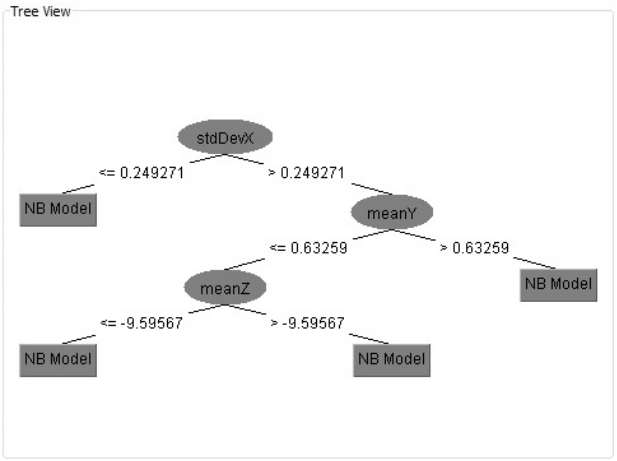


Figure 4. The Naïve Bayes tree used in the classification process

A good overall accuracy rate of about 92% was achieved in this activity recognition process. In terms of individual activities, accuracy rates varied. Overall relative error was around 13%. The standing activity showed the most accurate result with 100%, whereas sitting and walking have accuracy of more than 90% and running and jumping have less than 90% accuracy. The confusion matrix from the processing of the experimental data is presented in Table 1. The confusion matrix data explains the good accuracy mentioned above.

Table 1. Confusion matrix from the classification process

	sitting	standing	walking	running	jumping
sitting	22	2	0	0	0
standing	0	13	0	0	0
walking	0	0	22	1	0
running	0	0	0	20	3
jumping	0	0	0	3	24

The matrix in Table 1 shows that 101 out of 110 instances are classified correctly. Relating the confusion matrix to the accelerometer data, we can see that running and jumping show 'confusion' with each other. About 13% of running activity was incorrectly classified as jumping, and about 11% of jumping activity was incorrectly classified as running. We suspect that these are based on the nature of the accelerometer data of both running and jumping activities which having almost similar values of some attributes. Further exploration into this is needed to be performed. To understand more about the variation of accelerometer data more basic activities will need to be included in the near future works.

However, based on the encouraging results of this initial activity recognition process a simple prototype is developed in an HTC mobile phone to implement the activity recognition process in real time. The prototype has been developed based on the framework depicted in Figure 2. The prototype in action can be seen in Figure 5 below.

It is shown in Figure 5 that the user who was doing a walking activity will see the walking picture in his mobile which indicated that the mobile phone is able to recognize his activity in real time.



Figure 5. The prototype in action; the recognized activity is shown in the mobile phone

V. CONCLUSION AND FUTURE WORK

Using an HTC mini mobile device that has an accelerometer sensor, it is possible to distinguish basic activities by analyzing and classifying the data acquired from the accelerometer. The classification process based on Naïve Bayes algorithm using Weka machine learning tool has resulted a good accuracy rate of 92% in the activity recognition carried out in this study.

Future study in this area has been derived from the results shown on the initial works presented in this paper. The further exploration will include using activity recognition to estimate the location of individuals in closed environments where GPS signals are weak. The idea involves the usage of normal mobile devices to locate the whereabouts of users. The process of locating users is normally done by the use of GPS sensors. However, if the individual is inside a closed environment, GPS signals become weak and thus, it becomes unreliable. With the use of the accelerometer in these devices, it is then possible to estimate the location of these individuals inside these closed environments. For example, if a person goes through a tunnel, given the user's accelerometer data that shows that the person is walking and given the length of the tunnel, it is then possible to estimate the location of that individual.

Other works that can be derived from this study is the development of intelligent application that will integrate more than one context dimensions for user convenience and security, such as automatic switching mode based on

user location and activity, monitoring patients based on their identity, location and activity.

ACKNOWLEDGMENT

This project is sponsored by Research Management Center (RMC) of the International Islamic University Malaysia through EDW A 10-629 fund.

REFERENCES

[1] Nicholas D. Lane, Emiliano Miluzzo, Hong Lu, Kaniel Peebles, Tanzeem Choudhury and Andrew T. Campbell. "A Survey of Mobile Phone Sensing", IEEE Communication Magazine, September 2010.

[2] J. F. Knight, H. W. Bristow, S. Anastopoulou, C. Baber, A. Schwirtz, T.N. Arvanitis. "Uses of accelerometer data collected from a wearable system", Personal Ubiquitous Computing , 2007, pp 117-132

[3] N. Ravi, N. Dandekar, P. Mysore and M. L. Littman, "Activity Recognition from Accelerometer Data", Proceedings of the Seventeenth Conference on Innovative Applications of Artificial Intelligence. 2005.

[4] L. Bao and S. S. Intille. "Activity Recognition from User-Annotated Acceleration Data", PERSASIVE 2004, pp 1-17

[5] J. A. Ward, G. Tr□ster, P. Lukowicz and T. Starner "Activity Recognition of Assembly Tasks Using Body-Worn Microphones and Accelerometers", IEEE Transactions on Pattern Analysis and Machine Intelligence.

[6] J. S. Yi, Y. S. Choi, J. A. Jacko and A. Sears. "Context Awarensess via a single Device-Attached Accelerometer During Mobile Computing ", Proceedings of the 7th International Conference on Human Computer Interaction with Mobile Devices, 2005.

[7] J. Y. Yang, Y. P. Chen, G. Y. Lee, S. N. Liou and J. S. Wang. "Activity Recognition Using One Triaxial Accelerometer: A Neuro-fuzzy Classifier with Feature Reduction", International Federation for Information Processing. 2007.

[8] C. Mitchell, "Shake and skip to interact with your music", MSDN Magazine September 2009 Issue, accessed through http://msdn.microsoft.com/en-us/magazine/ee413721.aspx., retrieved May 2010.

[9] A. Ofstad, E. Nicholas, R. Szcodronski, R. Roy Choudhury. "AAMPL: Accelerometer Augmented Mobile Phone Localization.", Proceedings of the first ACM workshop on mobile entity localization and tracking in GPS-less environments.

[10] Z. He, L. Jin, L. Zhen, J. Huang. "Gesture recognitioin based on 3D accelerometer for cell phone interaction", IEEE Asia Pacific Conference on Circuits and Systems, 2008.

[11] T. Gross and M. Specht, "Awareness in Context-Aware Information Systems", in Mensh and Computer. 2001

[12] D. Sánchez, M. Tentori and J. Favela, "Hidden Markov Models for Activity Recognition in Ambient Intelligence Environments", Proceedings of the 8th Mexican International Conference on Current Trends in Computer Science, 2007.

[13] Sensor API, http://sensorapi.codeplex.com , retrieved April 2010.

[14] Andrew Roberts. A Guide to Weka. 2005. Accessed through http://www.andy-roberts.net/teaching/ai32/weka.pdf

[15] Weka Docs. http://wekadocs.com/ , retrieved July 2010.

[16]Weka Project Page, http://www.cs.waikato.ac.nz/ml/weka/, retrieved June 2010.

[17] T. Huynh and B. Schiele, "Toward Less Supervision in Activity Recognition from Wearable Sensors", Proceedings of the 10th International Symposium on Wearable Computers, 2006.

InteractiveDisplay: A Computer-Vision-Based Solution to Retrofit Existing Flat Displays into Interactive Surfaces

Lahiru L. Priyadarshana
Informatics Institute of Technology
Ramakrishna Rd, Colombo 06, Sri Lanka.
Email: llahiru@gmail.com

Kulari De Silva Lokuge
Informatics Institute of Technology
Ramakrishna Rd, Colombo 06, Sri Lanka.
Email: klokuge@gmail.com

***Abstract*- This paper outlines InteractiveDisplay, a novel and cost effective solution to create vision-based interactive surface systems by retrofitting existing regular displays. The proposed solution uses a regular off-the-shelf web camera as the main input device, and the raw image data captured by the web camera are processed using several image processing algorithms such as, background subtraction and skin color detection, to identify foreground objects. InteractiveDisplay's configuration addresses complexity and cost related issues with currently available computer-vision-based interactive surfaces. The proposed system provides an opening for more people to experience a new level of interactions with computing systems using the existing and commonly available technologies. The presented system is capable of responding in real-time for user interactions and provides a cost-effective configuration that requires minimum engineering efforts to set-up.**

I. INTRODUCTION

Keyboard and mouse are the most commonly used input devices for most of the conventional computing systems. These traditional input methods limit the ways of user interactions and increase the space between the users and the computing systems. Commonly used devices, such as mouse, only facilitate single pointer interactions. However, considering these limitations; recently, there has been a major effort in research in the field of Human Computer Interaction to innovate novel ways of interactions with computing systems. One of the major outcomes of the recent research is the ability to closely replicate the familiar hands-on experience of everyday object manipulation. These novel, comfortable and intuitive interactions are used in day-to-day life with interactive multi-touch based products such as, Microsoft Surface [1] and Apple iPhone [2]. They provide increased degrees of control over the traditional input methods and allow a new level of interactions between the computing system and the user that was unattainable previously with the traditional input devices.

This paper presents an alternative method to create an interactive surface with a regular flat display and an off-the-shelf web camera. The presented configuration is cost effective and requires a small number of commonly available hardware devices that address the installation issues that are typical of most interactive surface systems. The prototype that has been proposed is capable of detecting the 2-D positions and colors of circular tangible objects placed on the surface. Further, it identifies the user's hand regions and supports hands-on interactions.

II. MOTIVATION AND RELATED WORK

There are number of systems that use novel interaction methods to manipulate user interface components with natural hand gestures and two-handed manipulation. Most of the tabletop display systems and large wall displays have combined the displaying and sensing techniques together on one surface. Many systems such as PlayAnywhere [3] and WUW [4] have used video projection techniques for displaying and computer-vision-based techniques involving image processing and optical sensing or non-computer-vision-based special sensing techniques such as, capacitive coupling [5] for sensing. PlayAnywhere [3] uses projection for displaying and computer-vision techniques such as, shadow-based touch detection and visual bar code scheme for sensing.

By using systems based on optical sensing have confirmed to be mostly imposing in the richness of data capturing and the flexibility they can provide in processing and detecting arbitrary objects. For example it is possible to identify real world objects that are placed on the interactive surface using generic object recognition algorithms such as, bag-of-visual-words [6] based on SIFT [7]. However, a major drawback with most of vision-based interactive surface systems is the use of infrared based techniques with relatively expensive special hardware devices such as, infrared sensitive cameras and infrared illuminators. Another disadvantage of using infrared techniques is the absence of color information. Since the color information can be used to enhance the interactions with the user, it is considered as an important factor for interactive surfaces. However, one drawback using vision-based techniques is that they demand high computational power for processing, and the use of video projectors as the displaying technique may result in low-resolutions.

Tabletop interactive surface systems such as DiamondTouch [5] and SmartSkin [8] have special sensors embedded underneath the surface to recognize the user input. This method provides more accurate results and consumes low computational power. However, such systems have complex

architectural designs and the sensing devices they use are comparatively expensive.

Some researchers including Matsushita et al. [9] and Wilson [10] have identified the benefits of large wall displays that allow hands-on interactions for presentations and collaborative environments. However, with the use of infrared sensing techniques and video projection, these systems require high engineering efforts and expensive configurations.

There have been several efforts to retrofit existing regular flat displays (LCDs) into interactive surfaces in-order to have high-resolution and personal systems. In one approach Han [11] used Frustrated Total Internal Reflection (FTIR) method. His solution is relatively cost effective, but considering the infrared lighting system and other configurations; it requires a considerable engineering effort on installation. In another approach Hodges et al. [12] have described a method of using a special infrared based sensing system that is fully integrated into a thin form-factor display. This system provides more accurate sensing and an interface to interact with other devices using infrared signals. However, it requires tremendous engineering effort and is not a generic solution for all regular flat displays.

With the flexibility of computer-vision based sensing techniques it is also possible to retrofit an existing LCD using infrared lasers that addresses resolution issues with projection displays and increases the accuracy and responsiveness with minimum engineering effort. However, it has a huge safety concern for users and as well as developers, because of the strong infrared radiation emitting from the infrared lasers. This radiation is invisible to the human eye and the possibility of users tending to look directly into the lasers due to curiosity will be high.

Many of the systems that are based on the combination of projection for displaying and computer-vision based techniques for sensing address different issues within their defined scope. As discussed above, the issues with infrared techniques, engineering effort and expense are important facts with currently available interactive surfaces. Hence, InteractiveDisplay intends providing a solution for creating interactive surfaces that addresses the mentioned problems.

III. Implementation

InteractiveDisplay presents two main designs according to the role that its Sensing System takes at runtime.

First design combines the Sensing System with the Interactive Application creating one single component as shown in Fig. 1. This enables all the tasks including image capturing, processing and displaying to be carried out on a single computer.

Second design implements the Sensing System and the Interactive Application as two main components (see Fig. 2). In this design the Sensing System acts as a server that sends touch events to Interactive Client Applications using the standard protocol – TUIO [13].

As in most interactive surface systems, the hardware prototype of InteractiveDisplay consists of two separate sections; the sensing device and the displaying device.

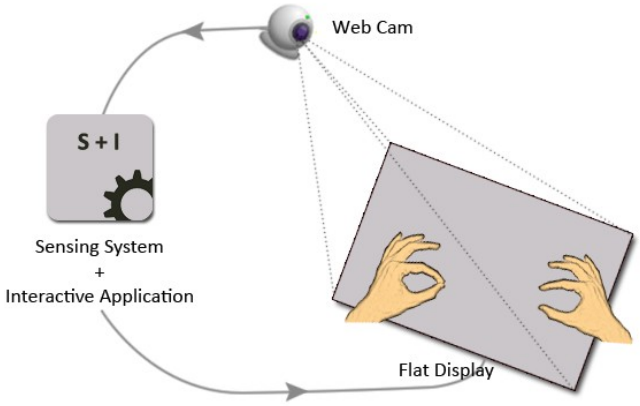


Fig. 1. Primary design of InteractiveDisplay. Sensing System and Interactive Application are combined

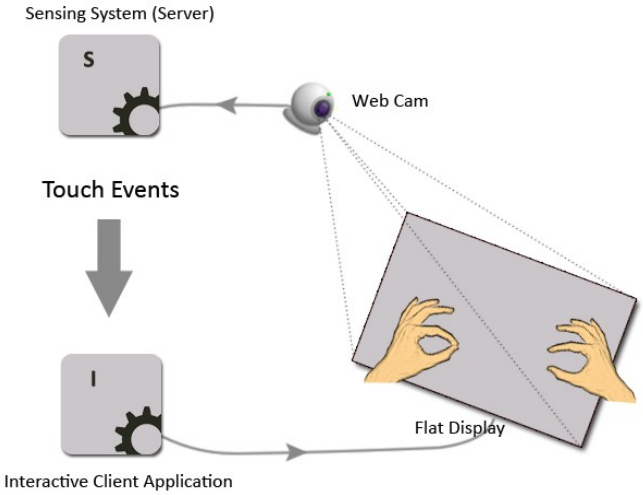


Fig. 2. Secondary design of InteractiveDisplay. Sensing System acts as a server and sends touch events to Interactive Client Application

The prototype uses a LCD monitor as the displaying device that is a 16:10 wide-screen with 1440x900 screen resolution. A low cost, off-the-shelf web-camera is used as the sensing device. The web-camera has two mega-pixel resolutions, and supports up to 30 frames per second. However, only 320x240 pixel resolutions is used in the prototype.

Fig. 3. shows the final setup of InteractiveDisplay hardware configuration. The web-camera is mounted above the LCD display as the only sensing device, capturing the surface area. User interactions are carried out directly on/over the LCD, and therefore it is considered as the surface or the interaction area. Additionally, a suitable apparatus (stand) is used to mount the LCD display and the web-camera to sustain the stability.

Regular web-cameras heavily depend on the ambient light of the working environment they operate. Therefore, a custom light source is used to gain controlled, evenly spread lighting on the surface area. This LED light source consists of 20 white



Fig. 3. InteractiveDisplay hardware configuration

LEDs (10 LEDs per row in two rows) and is considered as an optional hardware.

A. Color Recognition

Existing vision-based interactive surface systems that are based on infrared sensors are unable to capture color information. What they see is just a gray-scale world. In InteractiveDisplay we use a regular web-camera as the main sensing device. Therefore, InteractiveDisplay is capable not only of identifying 2-D positions but also the color information of the tangible objects placed on the surface. This is one of the major features that has been proposed in this paper, in related to interactive surfaces. Carom strikers covered with different colored fabrics are used as the tangible objects for demonstration purposes.

B. Trapezoid Transformation

As shown in Fig.4, the LCD panel is captured as a trapezoid in raw image data. Hence, a trapezoid transformation was employed to map the surface onto a rectangle view. Considering the distance from the web-camera to the displaying surface, the distortion caused by the camera lens was ignored.

C. Background Subtraction

InteractiveDisplay uses the HSV color space for background subtraction. Since luminance is represented as a separate channel in this color space, only hue (H) and saturation (S) are

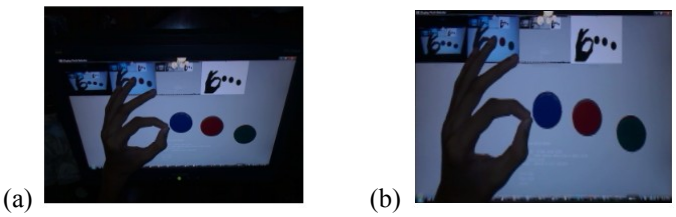


Fig. 4. Trapezoid transformation, (a) before applying trapezoid transformation, (b) resulted image

considered when performing the background subtraction. We use a screenshot of the currently displaying scene as the base model of the current background. In the color calibration stage, the surface area is captured with no foreground objects, and the average difference for each channel (hue and saturation) is calculated by computing the difference for each pixel on the 320 x 240 image. Consequently, two standard deviations of the difference for two channels are calculated. These average values and standard deviations are then used to separate the foreground from the background. If the calculated difference is between the range of average + half the standard deviation and average - half the standard deviation, the correspondent pixel is considered as a background pixel and otherwise a foreground pixel.

In this approach, the system has to capture the current background for each frame by taking a screenshot of the currently displaying scene. As the web-camera is highly sensitive for dramatic brightness changes, a controlled lighting and background is used. Also, the system renders less detailed graphics when making interactions as complex backgrounds would develop more noise in processed images.

D. Skin Color Detection

We use a histogram based skin color detection approach [14] to identify the hand regions. At the color calibration stage the system generates a histogram based on the user's skin color. This histogram is matched against the captured images using back projection and is used to identify the skin color pixels at the run-time. We use a two-dimensional histogram with hue and saturation values. Fig. 5. shows the resulted image of this approach. Further, additional noise is removed by applying morphological transformations [15].



Fig. 5. Skin color detection with histogram matching

InteractiveDisplay uses the pinching gesture as the main input method for hands-on interactions. We adopt the pinching gesture from Wilson's TAFFI [16] project. Consequently, our configuration brings the sensing area and displaying area onto a single surface.

After isolating foreground objects, a contour finder algorithm is used to detect the visible contours in the output image. 2-D positions of contours are then converted into gesture events and used in interactive applications.

As mentioned in Section 3, InteractiveDisplay's Sensing System can act as a server and pass the input events to Interactive Client Applications. The Sensing System sends input events to client applications through TUIO [13], which is an implementation of the standard communication protocol, Open Sound Control (OSC) [17]. The TUIO protocol facilitates the transmission of an abstract description of interactive surfaces, including touch events and tangible object states.

E. Polarized Filters

Regular LCD displays emit polarized light. Consequently, putting a polarizing filter perpendicular to the emitting light rays will block the visible light from the LCD. As an alternative approach, we introduce a piece of polarizing filter covering the web-camera lens, mounted perpendicular to the polarized light emitting from the LCD. Polarizing filters are relatively expensive, and they increase the complexity of the current configuration. As a cost effective method, polarizing filters that can be found in low-cost 3-D glasses or used/damaged LCD monitors, can be used for the above purpose. Nevertheless, this approach increases the accuracy of the system. Further, as the background (currently displaying scene of the LCD) is invisible to the web-camera, polarizing filters provide the ability to identify any foreground object regardless the complexity of the background.

IV. APPLICATIONS

We present few example applications to demonstrate the capabilities of InteractiveDisplay as an interactive surface.

A. Color Recognition

Color recognition is one of the main features has been proposed using this configuration. System can track different colored tangible objects and assign unique IDs based on their colors. This allows users to tag real-world objects and perform different tasks when the identified objects are placed on the surface.

An example application would assign IDs for circular colored objects and play different audio tracks once the correspondent object with correct color is placed on the surface. Also, a different colored object can be assigned as the volume controller and can be used to control the volume by sliding vertically.

B. Multi-Point Interactions

Placing more than one circular tangible object on the surface allows us to perform multi-point interactions. We demonstrate a simple map application using this feature. The user defines a secondary view by placing three circular objects in a triangular shape on a satellite map view, which is the



Fig. 6. Map application demonstrates the multipoint interactions of InteractiveDisplay

primary view of the application. As shown in Fig. 6. the system renders the correspondent street map view inside this specified triangular area.

C. Hands-on Interactions

InteractiveDisplay uses the pinching gesture to replicate day to day hands-on interactions. Zoom-in, zoom-out, rotate and move are the possible two-handed manipulations. Fig. 7. shows a user interacting with InteractiveDisplay using two-handed gestures.

V. RESULTS AND DISCUSSION

One of the primary advantages of using an off-the-shelf web-camera for creating interactive surfaces is the ability to capture more data such as color information. As a result, comparing to vision-based interactive systems such as, PlayAnywhere [3] and PlayTogether [18], InteractiveDisplay facilitates more attractive interactions that can be done by analyzing color information. However, this increases the level of noise in output images and demand higher computational cost for image processing techniques.

Pinching gesture facilitates more natural way of interaction, but it is difficult to interact with smaller UI components using this gesture. Also, occlusions take place when the hands are at the corners of the LCD screen. Consequently, this increases the number of false contours and decreases the accuracy of the sensing system. We use the center of the detected contour which is created when the thumb and forefinger are brought

together. As an improvement, the actual pinching point can be calculated using common image processing techniques.

As a future enhancement touch detection can be implemented on the current configuration using stereo-vision techniques. Stereo-vision can be used to track hands in 3-D space and detect when the fingers are touching the LCD panel.

Also, designing an advance prototype with improved portability, mobility and compact form factor would be another important enhancement.



Fig. 7. A user interacting with a photo manager application on InteractiveDisplay using two-handed manipulation

TABLE I
SUMMARIZATION OF FEATURES AVAILABLE IN INTERACTIVEDISPLAY

Feature	Availability	Comments
Color recognition	Yes	-
Object recognition	Yes	Capable of recognizing tangible objects that are placed on the surface
Hand gesture recognition	Yes	Currently only the pinching gesture is available
Multi-point interaction	Yes	Supports interactions involving multiple points
Touch detection	No	Considered as an improvement (using stereo vision)
Multi-touch detection	No	-
Real-time responsiveness	Yes	-
Cost effectiveness	Yes	Less than 180$ (including the LCD and off-the-shelf web-camera)

II. CONCLUSION

In this paper, we discussed a novel and cost-effective method to create interactive surfaces with commonly available hardware devices. Our solution allows more users to experience the novel ways of interactions and surface computing technologies in their day-to-day life with a minimum cost and engineering efforts.

We use background subtraction and histogram based skin color detection techniques to track tangible objects on the surface and to detect hands-on interactions, in real-time. In order to get more accurate results, we introduced another approach using polarized filters, which requires an additional engineering effort.

InteractiveDisplay augments the real-world objects with virtual media and supports hands-on interactions. It is capable of color detection and assign color-codes for object recognition.

ACKNOWLEDGMENT

We gratefully acknowledge Informatics Institute of Technology including, Alfred Perera and Naomi Krishnarajah, for providing us academic resources. We also thank all the academic and industrial professionals for spending their time on evaluating InteractiveDisplay. We are thankful to Johnny Lee and Pattie Maes for their thoughts on this project.

REFERENCES

[1] Microsoft Surface. [online] Microsoft Inc. Available from: <http://www.microsoft.com/surface> [Accessed 12 Oct 2008].

[2] Apple iPhone. [online] Apple Inc. Available from: <http://www.apple.com/iphone> [Accessed 15 Oct 2008].

[3] Wilson, A. D. 2005. PlayAnywhere: a compact interactive tabletop projection-vision system. In *Proceedings of the 18th Annual ACM Symposium on User interface software and technology* (Seattle, WA, USA, October 23 - 26, 2005). UIST '05. ACM, New York, NY, 83-92. DOI= http://doi.acm.org/10.1145/1095034.1095047.

[4] Mistry, P., Maes, P., and Chang, L. 2009. WUW - wear Ur world: a wearable gestural interface. In *Proceedings of the 27th international conference extended abstracts on Human factors in computing systems*, April 04-09, 2009, Boston, MA, USA. DOI= http://doi.acm.org/10.1145/1520340.1520626.

[5] Dietz, P. and Leigh, D. 2001. DiamondTouch: a multi-user touch technology. In *Proceedings of the 14th Annual ACM Symposium on User interface Software and Technology* (Orlando, Florida, November 11 - 14, 2001). UIST '01. ACM, New York, NY, 219-226. DOI= http://doi.acm.org/10.1145/502348.502389.

[6] Yang, J., Jiang, Y.-G., Hauptmann, A. G., and Ngo, C.-W. 2007. Evaluating bag-of-visual-words representations in scene classification. *In Proceedings of the international workshop on Multimedia Information Retrieval*, New York, NY, USA, 2007. ACM, 197–206.

[7] Lowe, D. 2004. Distinctive image features from scale-invariant keypoints. *International Journal of Computer Vision*, November 2004, 91-110. DOI= http://dx.doi.org/10.1023/B:VISI.0000029664.99615.94.

[8] Rekimoto, J. 2002. SmartSkin: an infrastructure for freehand manipulation on interactive surfaces. In *Proceedings of the SIGCHI conference on Human factors in computing systems: Changing our world, changing ourselves* (Minneapolis, Minnesota, USA, April 20 - 25, 2002). 113-120. DOI= http://doi.acm.org/10.1145/503376.503397.

[9] Matsushita, N., Rekimoto, J. 1997. HoloWall: Designing a Finger, Hand, Body and Object Sensitive Wall. In *ACM Symposium on User Interface Software and Technology (UIST)* (1997).

[10] Wilson, A. D. 2004. TouchLight: An Imaging Touch Screen and Display for Gesture-Based Interaction. In *Proceedings of the 6th international conference on Multimodal interfaces* (October 13-15, 2004, State College, PA, USA). DOI= http://doi.acm.org/10.1145/1027933.1027946.

[11] Han, J. 2005. Low-cost multi-touch sensing through frustrated total internal reflection. In *Proceedings of the 18th annual ACM symposium*

on User interface software and technology (Seattle, WA, USA, October 23 - 26, 2005). ACM, 115-118. DOI= http://doi.acm.org/10.1145/1095034.1095054.

[12] Hodges, S., Izadi, S., Butler, A., Rrustemi, A., & Buxton, B. 2007. ThinSight: versatile multi-touch sensing for thin form-factor displays. In *Proceedings of the 20th annual ACM symposium on User interface software and technology* (October 07-10, 2007, Newport, Rhode Island, USA). ACM, 259-268. DOI= http://doi.acm.org/10.1145/1294211.1294258.

[13] TUIO Protocol Specification 1.0, [online] TUIO.org. Available from: <http://www.tuio.org/?tuio10> [Accessed 25 Nov 2008].

[14] Bradski, G., Kaehler, A. 2008. *Learning OpenCV: Computer Vision with the OpenCV Library*, O'Reilly Media.

[15] Gonzalez, R., Woods, R. 2007. *Digital Image Processing: Third Edition*. Prentice-Hall.

[16] Wilson, A. D. 2006. Robust computer vision-based detection of pinching for one and two-handed gesture input. In *Proceedings of the 19th annual ACM symposium on User interface software and technology* (October 15-18, 2006, Montreux, Switzerland) ACM, 255-258. DOI= http://doi.acm.org/10.1145/1166253.1166292.

[17] Wright, M., Freed, A. 1997. Open Sound Control: A New Protocol for Communicating with Sound Synthesizers. In *proceedings of the International Computer Music Conference*. 1997.

[18] Wilson, A. D., Robbins, D. C. 2006 PlayTogether: Playing games across multiple interactive tabletops. In *IUI Workshop on Tangible Play: Research and Design for Tangible and Tabletop Games*, 2006.

An Electronic Policy Integrated Approach for Software Development (EPISoDe): A Case Study

Shahida Sulaiman, Umi Kalsom Yusof, Wan Mohd Nazmee Wan Zainon, Wan Muhammad Zulhafizsyam Wan Ahmad
School of Computer Sciences, Universiti Sains Malaysia,
11800 USM, Penang, Malaysia.
{shahida, umiyusof, nazmee}@cs.usm.my,
zulhafizsyam.com08@student.usm.my

Sarina Sulaiman
Faculty of Computer Science and Information System,
Universiti Teknologi Malaysia,
81310, Skudai, Johor, Malaysia.
sarina@utm.my

***Abstract*- Official websites of an organisation is a gateway to inform the public about its profiles, products or services, and other related information for the interested parties. Nevertheless such websites are sometimes not updated, do not provide required information or the worst case they are abandoned despite the fact that software developers have fulfilled the requirements of the users, and the systems have been deployed successfully. Hence, such websites require a dynamic web design that can delegate responsibility to each staff in ensuring the contents are always updated either to be shared among the staff or the public. This paper proposes an approach called EPISoDe that directly integrates organisations' policies as part of functional requirements in software development in this case we focus on website design and its implementation of higher learning institutions. We have deployed the proposed EPISoDe approach in a prototype called DyWeMS that provides an engine of a dynamic web design. We evaluated the approach on an official website of a school in a higher learning institution using DyWeMS dynamic engine. It implies that an organisational official website has the potential to be a one-stop information and knowledge centre that reflects organisations' history and legacy using the proposed EPISoDe approach that promotes delegation of responsibilities among the staff with the support of dynamic web design.**

***Keywords*—Official Websites; Dynamic Web Design; Software Development, Organisations' Policy**

I. INTRODUCTION

In tandem with the Internet advances, organisations promote their products and services via their official websites. Such websites act as the gateway for the public to know more about the concerned organisations' profiles. In addition they provide the information on products or services, announcements of their activities, organisations' news and press releases, and other information that may vary from one niche of an organisation to another. For example, a software company like Microsoft [1] highlights their products and trainings rather than their staff and research. On the other hand, a higher learning institution (HLI) such as Universiti Sains Malaysia (USM) [2] focuses more on their services that include academic programmes, academicians' expertise and research achievements.

In addition, organisations' websites could be the platform to collect information among the staff and process the information into useful knowledge that can assist top managerial levels to make decisions. For example, a HLI strategise its world rankings in order to position its status to the public. In this case, information must be properly captured to ensure the executives can derive the data that shows their key performance index (KPI) in order to decide what to be improved further. Our previous study on five faculties' websites of Malaysian HLIs shows that most websites have been developed according to users' basic requirements [3]. However they still encounter the risks of being abandoned by the users. Most home pages of the concerned websites were not updated. Besides, other linked web pages that should be updated by dedicated individuals mostly contain obsolete information.

One way to capture an organisation's information that can further be processed as knowledge to support decision making process is through knowledge management system (KMS). KMS provides the platform to capture information to be further processed based on users' demands mainly decision makers. Integrating KMS with organisations' official websites requires all staff to be involved in updating the related information. However there are many challenges to motivate users playing their roles in such systems. Hence, this motivates us to propose an approach that integrates an organisation's policy electronically using EPISoDe approach.

To the best of our knowledge, no existing work attempts to directly integrate organisations' policies in software development. Most of existing work studies the policies related to access controls, security and privacy such as the

work by He et al. [4]. Our work focuses on design and implementation for HLI official websites as the case study.

Section II discusses the proposed EPISoDe approach. The following Section III reports the case study. Section IV digests the related work. Finally, we conclude our work and its future work in Section V.

II. Electronic Policy Integrated Web-Based Software Design (EPISoDe)

From our previous study on existing faculties and schools of Malaysian HLIs [3], we found that the extensiveness of information provided still requires further improvement. More importantly, extensive information must be up-to-date too. This reveals the quality and reliability of the information provided for both visitors and users of the websites. We believe software engineers must integrate directly the policy aspects in their design and implementation of such websites to eliminate problems related to users' interventions in ensuring the contents of such websites are extensive, updated and reliable.

We propose an approach called EPISoDe that integrates organisations' policies in software development mainly in design and implementation of a website. Our study focuses on HLI website as the case study. The needs of HLI official websites are very different from product-based websites as their academic members are part of their products. Thus, information should come mainly from academic members who organise different activities, produce publication, involve in various projects, grants, and achievements. We anticipate the approach will improve the involvements of staff mainly the academic in updating the websites according to their roles.

For instance each academic should take the responsibility to update their own profiles, teaching, research, supervision and publication. The dean should update dean's speech in the website at least every new semester opens. The deputy dean of academic should update academic-related stuff under their job specifications. Each leader or coordinator of an activity must update the details of the activity. If the activity involves a competition then it becomes an achievement if the involved parties win. Once an activity ends, the coordinator must submit a report. Therefore, the administrator can focus on managing the system backups and housekeeping rather than updating data to the website. These roles are important to ensure everybody takes the responsibility to update the faculty's website. But how can we enforce the task to everybody involved? We hypothesise that a policy must be enforced and integrated to the design and implementation of the website. Thus, the proposed EPISoDe anticipates to contribute this aspect.

The proposed approach includes:

- Organisations' policies: What staff must follow to meet organisations' demands?
- Standard operating procedure (SOP): How staff should conduct an activity?
- Staff appraisals: What each staff has achieved yearly to achieve KPI?
- Yearly report: What organisations have achieved yearly to achieve overall KPI?
- Reminder: When to follow each SOP to meet organisation's policies?

Let P is a set of policy to be enforced in an organisation. Let S is a set of procedures for an activity A in the organisation. For each S there is a set of reminder R. Let X is staff yearly appraisal and Y is organisation's yearly report. Thus $[P = (S, A, R)] \rightarrow X, Y$ shows that a policy that consists of a set of procedures S, a set of activities A and a set of reminders R are sufficient conditions to generate yearly staff appraisal X and yearly organisation's report Y.

For example P = "Each activity must have a coordinator to manage it and a technical staff to take photos", S = {"Announce activity", "Report activity", "Upload photos"}, A = {"Conference", "Seminar", "Workshop",...}, R = {Date, Time} where Date = {day, month, year}, Time = {hours, minutes, seconds} that will be triggered to remind $S_i \subseteq S$ for $A_i \subseteq A$.

In term of requirement analysis, the policy P can be captured as a functional requirement. Thus a policy P should be a class by itself that captures all data about a policy to be enforced in an organisation when designing the website. A set of procedures S should be part of P. The relationship must be of type composition relationship in which when a policy is removed or terminated, the procedure must be removed too. Then a set of activities A should be part of S. This relationship should be of type aggregation. This is due to the fact that an activity can still exist even though the procedure is removed or disregarded. A set of reminder R should be tagged to each A as a temporal event. Fig. 1 shows the classes involved.

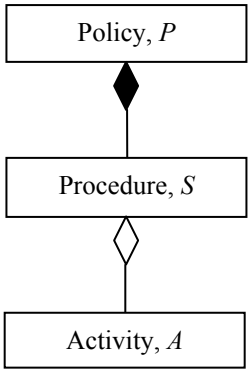


Fig. 1: Classes involved in the proposed EPISoDe

Fig. 2 illustrates the architecture that consists of the components in EPISoDe approach. The policies must be enforced by the top management. Each SOP must be

updated by authorised personnel. Each step or activity in SOP that requires a temporal event must be set with a reminder. Thus, the staff involved in documenting the SOP must update the relevant information to the website and automatically updated to KMS. Admin plays the role to backup data and perform housekeeping. Other staff must take part in the system to update related information or knowledge. At the end of the year, all the information will be further processed to support decision making related to an organisation's performance based on KPI. The information can be transformed as the faculty's yearly report. In addition, the yearly appraisal of each staff is generated via the system based on the information updated by them. Therefore, the proposed approach can assist top management to identify the staff who does not play the assigned roles in the system once they generate the yearly appraisal report. Hence, EPISoDe approach promotes software developers to consider organisations' policies and SOP in designing and implementing such websites mainly for HLI.

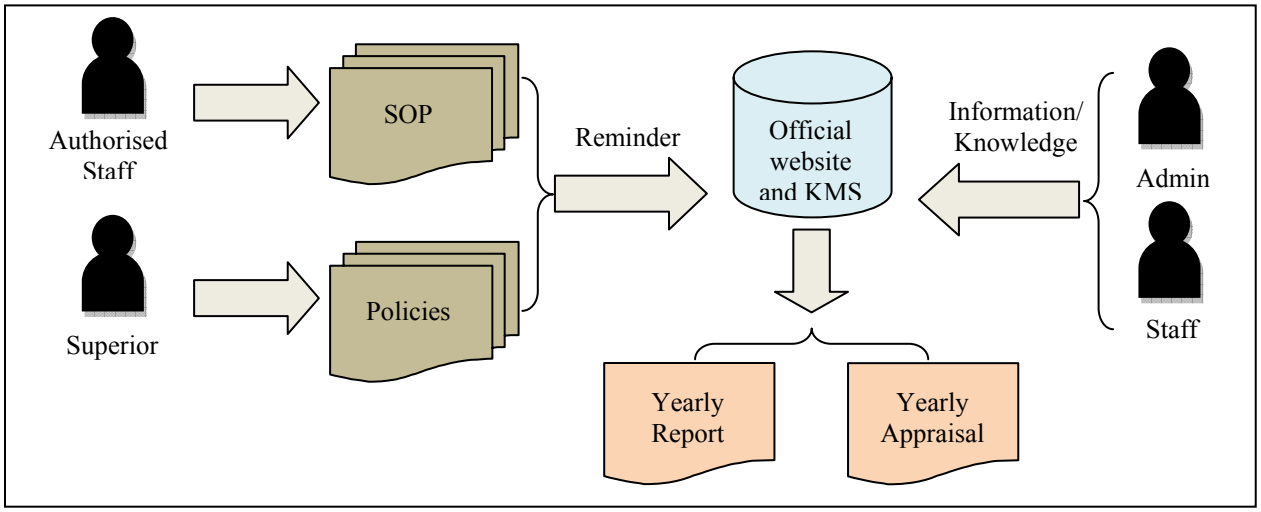


Fig. 2: The proposed architecture to integrate EPISoDe approach in web-based software design

III. Case Study

We have applied the proposed design approach to enhance the existing official website that is School of Computer Sciences, Universiti Sains Malaysia [5]. The current website (see Fig. 3) was improved to version 2 that has improved the interface as in Fig. 4. Then we enhanced the website to version 3 that integrates EPISoDe and DyWeMS engine in version 3 of the website [6].

Dynamic web design is very crucial in order to support the proposed EPISoDe. The dynamic features provided by DyWeMS dynamic engine include:

- Each staff plays the role to update their own profiles, relevant activities and achievements.
- Contents can be set dynamically to be displayed as announcements or news and events.
- Contents change status automatically based on the date of announcement, news or archive.
- Organisational chart is automatically generated based on staff's position in the organisation.
- Annual reports can be generated automatically based on contents posted by staff and admin.
- Images can easily be uploaded and displayed dynamically to highlight important events, news and other relevant information.

Comparison of the enhancement made from existing static web design with the new dynamic web design is listed in Table I. There are seven features to be compared with the current website [5] and the new one integrated with EPISoDe approach and DyWeMS dynamic engine [6].

The prototype was released to the staff for a beta testing since 15 April 2009. Initial response from the staff mainly academics showed positive feedbacks mainly towards delegation of roles in the school's website. Among the feedbacks include more authority and functionality to be given to the academic staff, ensure latest information is always updated to the website that shows the dynamic features provided really support and reduce administrator's tasks, and the layout must be more consistent in terms of font styles, sizes and colours.

The initial feedbacks reveals that the staff are willing to actively be part of content contributors to update their profiles and details, and relevant information such as teachings, publications, achievements and professional memberships. As we embed the dynamic engine and the proposed approach in the design; normal users cannot really see the differences between the old version 1 with the latest version 3 tested. However users with

administrator level can observe the burden has been lessened as the delegation of content contribution has been distributed to other staff.

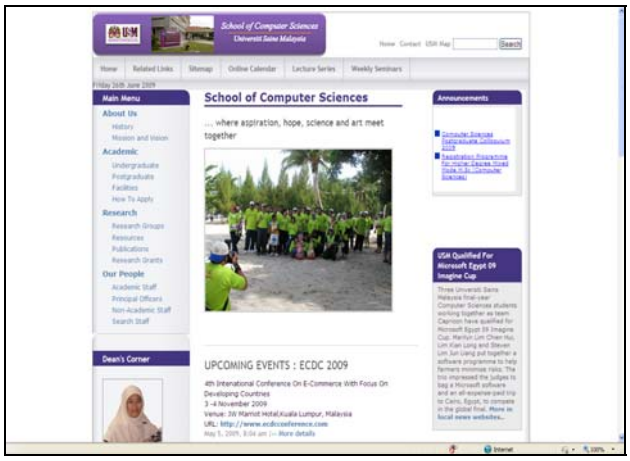


Fig. 3: Existing website chosen for the case study



Fig. 4: Enhanced design integrated with DyWeMS dynamic engine and EPISoDe approach in which users can login based on their roles

The case study shows that the proposed EPISoDe approach that integrates policy, SOP of activities as part of its software development mainly in HLI websites will ensure staff of an organisation plays the assigned role. This in turn will ensure data and information are always updated into KMS and further processed into related knowledge to support decision makers. With the support of dynamic web by DyWeMS' dynamic design method users are less burdened as compared to existing static web design and manual method. However there are challenges in the aspect of protecting the data, as KMS is now integrated with an organisation's official website thus Web security is vital.

TABLE I
COMPARISON BETWEEN STATIC WEB DESIGN VERSUS DYNAMIC WEB DESIGN

Features	Current [5]	New [6]
Role	Admin only.	Admin, authorised staff, superior, staff.
Nature	Static web design.	Integration of dynamic and KMS.
Input	Data only.	Data, information and knowledge.
Process	Data to information.	Data to information to knowledge.
Output	Display information only.	Display information, organisation's report, and staff's appraisal.
Status of contents	Manual housekeeping by admin.	Automatic housekeeping by temporal events.
Category of contents	Manual update by admin.	Can be set and displayed accordingly as announcement, or news and event.

IV. RELATED WORK

The related work covers three main topics: KMS, software design and web metrics, and content management system (CMS). EPISoDe proposes KMS to be integrated with official websites' design. We will see how issues in KMS inspire the proposed work. Besides, we stress the importance of having dynamic web design that supports dynamic features mainly in the scope of HLI. In addition we will discuss the quality of software design and why it is important to have up-to-date official websites for HLI in order to get better ranking in term of web metrics.

A. Knowledge Management System (KMS)

Data will be useful when we process it to be information. Selected information which is useful to organisations' will be knowledge to be shared among the staff. General knowledge known to all staff are classified as explicit knowledge. However tacit knowledge belongs to an individual is difficult to be shared. There are many studies in KMS that investigate the challenges faced by organisations in order to create knowledge sharing culture in their organisations.

A study by Ong et al. [7] used technology acceptance model (TAM) to evaluate the acceptance of KMS in semiconductor manufacturing companies in Taiwan. The study discovered five main points in terms of acceptance of KMS in the subject companies: (a) ensure employees that they will not lose power or influences when they share their knowledge, (b) the use of KMS can be the influences of friends, peers, superiors, or managers, (c) knowledge in KMS should be attractive and of high quality, (d) ease of use, (e) user friendliness. From the points only item (d) and item (e) can be considered as part of non-functional requirements in software analysis that can be captured while designing and implementing the system.

Hall [8] also highlights the importance of input-friendliness that can motivate knowledge sharing among intranets users. The work discusses some factors to motivate contributions that include provision of appropriate tools, the development of organisational culture to use KMS and reward systems. The factors are towards social aspects that are outside the boundary of KMS. In a more recent work of Hall [9], it describes the importance of perceiving the culture aspect in a broader angle that includes power issues, and organisational politics to explain both success and failure in motivating knowledge sharing. Gillies [10] also studied cultural obstacles to ensure successful use of KMS in large law firms. From the mentioned existing studies we find that most factors that influence the use of KMS relate to organisational and behavioural issues rather than technical issues. Only ease of use and user friendliness can be classified under technical aspects in software design.

On the other hand, software engineering community always measures the success of software systems based how much they fulfil users' requirements both functional and non-functional requirements. However there is little discussion on why good systems still fail in terms of their usage particularly in such KMS. Thus there is a gap between information science findings and the implementation of proposed solutions in the design of such KMS.

B. Quality Attributes for Software Design

A good software design will ensure the success of software systems developed for the users. Software metrics enable software designers or developers to measure the quality attributes of the system concerned. Some metrics can be used in the earlier stage of software development life cycle. This ensures the design is of high quality before software developers transform the design into corresponding codes.

Moore [11] suggests three main categories of quality attributes as the followings:

1) *Observable during execution:* can be measured when the system executes.
2) *Not observable during execution:* cannot be measured by executing the system only.
3) *Intrinsic to the architecture or design:* it is built-in to the software architecture and design.

The examples of attributes are also listed in Table II. The list of attributes is not exhaustive. The attributes are mostly based on non-functional requirements. For example performance attribute involves the measure of speed to process a functional requirement within the specified time. The issues of organisational and behavioural factors in KMS are outside the boundary of a computerised system. There are not classified directly under quality attributes except for usability which discovered in some KMS studies [7][10][11]. Thus we believe there is somehow a way to integrate organisations' policies that involve those human factors with software development. Those factors may be classified as functional or non-functional requirements depend on their nature.

TABLE II
QUALITY ATTRIBUTES OF SOFTWARE DESIGN [10]

Categories	Attributes
Observable during execution	Performance
	Reliability
	Usability
Not observable during execution	Portability
	Reusability
	Testability
Intrinsic to the architecture or design	Traceability
	Consistency
	Completeness

C. Web Publication Metrics

Cybermetrics Lab, a research group under Consego Superior de Investigaciones Cientificas (CSIC) introduced a metric for Web publication called 'webometrics'. The main goal of the metric is to promote Web publication in academic settings not to rank the universities. The metric generates the rankings based on unit for analysis of the independent institutional domain [12]. The main indicator is *Web impact factor (WIF)* based on link analysis that combines the external *inlinks* and the number of pages of the website using the ratio 1:1 between visibility and size. The indicators have respective weight. The indicators derived from the four main search engines (Google, Yahoo, Live Search and Exalead) are as the followings:

- Size (S): size components that is number of documents measured based on number of rich files in the web domain, and number of publications collected by Google Scholar database.
- Number of pages (n): Based on pages recovered from the four main search engines.
- Visibility (v): The total number of unique external links received (inlinks).
- Rich files (R): different format of files and their relevance to academic and publication activities, and scholar (Sc) counts the number of papers and citations for each academic domain.

From the metrics, we can observe the richness of information provided by the universities' websites in overall based on the indicators. See Fig. 5 for the list of rankings by webometrics [12]. Universiti Sains Malaysia is leading other Malaysian HLIs that is 585 for the world rank in the context of web metrics.

D. Content Management System (CMS)

For fast development of system to manage online contents we can use existing application called CMS. Web

CMS (WCMS) provides specific utilities for organisations to develop their official websites without the need to write extensive programming languages or markup languages. CMS provides a standard and professional look of websites. Examples of open source CMS include Mambo [13] and Joomla! [14]. Such CMS provides faster development of organisations' websites and more structured contents that are generic for such websites design. However using CMS may cause the organisation to feel losing of an identity as the layout of websites produced will be the same. Websites developed based on CMS will face the problem to be upgraded with new requirements or enhancements that are specific to certain organisations.

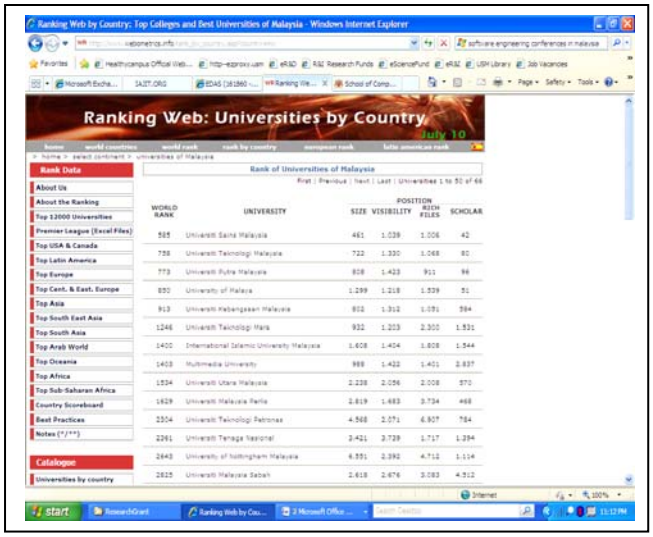


Fig. 5: Webometrics shows the ranking among Malaysian HLIs based on web metrics

V. Conclusion and Future Work

We propose EPISoDe approach that integrates organisations' policies in software development mainly for HLI. Based on our study on the challenges of knowledge sharing in KMS, we promote the idea that organisations' official websites should not only provide the necessary information to visitors of their websites. It should be a one-stop centre that archives all information and knowledge of an organisation. We deployed EPISoDe approach in an existing website as the case study. It is integrated with KMS and a dynamic web engine called DyWeMS. It ensures policies enforced can motivate the staff to work together to update the information and knowledge that are related to them. At the end of the year, all archives will be reported as faculty's yearly report and each staff can generate their yearly appraisal directly from the KMS. The case study shows that the staff involved were interested to be content contributors and to be given more autonomy to update their own profiles and related details to be further processed to meet organisation's KPI and specifically their own performance. Therefore, the website and KMS will both become the one-stop centre or archive of faculty's history and legacy over the years of its establishments.

Our future work includes the implementation of reporting module for staff's yearly appraisal report and the integration of data mining technique that can automatically capture data and information related to the staff from other portals such as IEEE [15] and SCOPUS [16]. This will reduce users' intervention and effort.

Acknowledgment

This work is supported by the USM short term grant: 304/PKOMP/6310044.

References

[1] Microsoft, www.microsoft.com, accessed on November 2010.
[2] Universiti Sains Malaysia, www.usm.my, accessed on November 2010.
[3] S. Sulaiman, U. K. Yusof, S. Sulaiman, "A Method to Integrate Organisations' Policies into Web Design," *The Fourth Malaysian Software Engineering Conference (MySEC'08)*, Malaysia, 16-17 December 2008, pp. 307-312.
[4] Q. He, P. Otto, A. I. Anton, L. Jones. "Ensuring Compliance between Policies, Requirements and Software Design: a Case Study, *Proceedings of the Fourth IEEE International Workshop on Information Assurance (IWIA'06)*, 2006.
[5] School of Computer Sciences, USM, www.cs.usm.my, accessed on June 2009.
[6] School of Computer Sciences, USM, www.cs.usm.my/v3, accessed on November 2010.
[7] C. -S. Ong, J. –Y., Lai, Y. –M. Wang and S. –W. Wang, "An understanding of power issues influencing employees' acceptance of KMS: an empirical study of Taiwan semiconductor manufacturing companies," *Proceedings of the 38th Annual Hawaii International Conference (HICSS'05),* January 2005, pp.1-10.
[8] H. Hall, "Input-friendliness: motivating knowledge sharing across intranets," *Journal of Information Science*, Jun 2001, vol. 27, pp. 139-146.
[9] H. Hall and M. Goody, "KM, culture and compromise: interventions to promote knowledge sharing supported by technology in corporate environments," *Journal of Information Science*, April 2007, vol. 33, no. 2, pp. 181-188.
[10] J. S. Gillies, "Cultural obstacles to a successful KM initiative in large law firms," *KMWorld & Intranets 2005 conferences & exposition,* San Jose, November 2005.
[11] J. W. Moore, "The road map to software engineering: a standards-based guide," *John Wiley & Sons.USA*.
[12] Webometrics, www.webometrics.info accessed on November 2010.
[13] Mambo, "Mambo CMS Latest Release", http://mambo-foundation.org/ accessed on November 2010.
[14] Joomla!, "Joomla CMS", http://www.joomla.org/ accessed on November 2010.
[15] IEEE, www.ieee.org accessed on November 2010.
[16] SciVerse Scopus, http://www.info.sciverse.com/scopus accessed on November 2010.

Review of Pricing Models for Grid & Cloud Computing

Parnia Samimi and Ahmed Patel[1]

School of Computer Science
Faculty of Information Science and Technology (FTSM)
Universiti Kebangsaan Malaysia (UKM)
43600 Bangi, Selangor Darul Ehsan, Malaysia

[1]Visiting Professor
Faculty of Computing Information Systems and Mathematics
Kingston University
Penrhyn Road, Kingston upon Thames KT1 2EE, United Kingdom.

parnia_samimi *at* yahoo.com, [1]apatel *at* ftsm.ukm.my

***Abstract*— Distributed system resources have become prevalent in ICT departments to lessen the burden of huge expenses incurred by very expensive storage computer systems. Add to this the continuous introduction and ever-growing evolution of simple to complex applications, the demand to access huge quantities of data, intensive computations, powerful simulations, maintaining and offering system resources and middleware infrastructure services the need to do all of this at an affordable and reasonable price is crucial. Distributed grid and cloud computing resources are currently considered to be one of the best technology options to provide this. They have many similar features and functions, and both of them are classed as distributed systems. They are capable of offering unaffordable resources and services at a reasonable price in a mass marketplace. The big question is: what is a reasonable price? How is pricing modeled and on what kind of economic principles is it based? Much of the issues surrounding these questions are very complex in themselves. This paper provides a comparative review of grid and cloud computing economic and pricing models from which appropriate tariffs and charging models can be chosen to meet particular business objectives. The actual choice depends on many other factors like enterprise regulations, tax laws, service level agreements and return on investments, are very important but outside the scope of this paper. In this paper we give the basic core principles and a comparative review of the latest and most appropriate economic and pricing models applicable to grid and cloud computing in order to propose better models for the future.**

Keywords*— *Grid computing, cloud computing, economic models, pricing models, charging models, service level agreement (SLA)

I. INTRODUCTION

Grid and cloud computing are emerging and evolving distributed technologies which offer considerable opportunities satisfying a variety of application and user needs. Technological advances, configurability of resources, applications operating and transferring of data at very high speeds at reasonable cost have come within the reach of the users over the last few years. Unfortunately, their uptake is hindered by the lack of proper and affordable economic and pricing models, tariff and charging structures within the framework of legal jurisdictions, tax and trading laws and business objectives.

For any viable business, economic models help in formulating the pricing and cost tariff structures to optimize return on investment, create critical mass of customers and manage resource deployment more efficiently. Very few existing economic models are used for real service business as an investment and income generator. They have been mainly studied and simulated for defining resource allocation algorithm rather than advocating and creating fully fledged proper economic model for grid and cloud computing business cases. There are many unresolved issues like how to determine and create tariff structures with a view to evolving a sustainable business over a long and last period term that need to be solved. Also, we have different pricing structures based on different economic models and conditions which are primarily based on pricing policy and business objectives that have conflicting goals [1]. Some of them have pricing schemes and tariff structures that include very stringent and overburdening rules for services which are prohibitive to users and makes the expected mass market user uptake very sluggish or unprofitable. [2]. Buyya et al. [3] noted that scheduling and resource management is a complex task because of the dynamically varying loads and availability in an ever-changing configuration of geographically distributed resources. Some of these resources are in-sourced (bought in) from various third party autonomous service providers having their own pricing policies and charging structures. All of this makes for complex accounting. The choice of particular pricing models and associated parameters depend on many factors which eventually have to be translated into fair and equitable service level agreement with ethical return on investment. These factors are complex and pose a constraining character of whatever pricing model or models are eventually produced for a real marketplace. They are important but they are outside the scope of this paper but will be addressed in a follow-up paper.

Presently, there is no single comprehensive model that can be applied for all instances of charging in the grid and cloud computing marketplace. Thus, in our research, we have studied and analyzed existing sets of pricing and charging models to eventually define a new model for cloud computing. To comprehend some of the complexities in specifying economic and pricing models, it is necessary to define what constitutes grid and cloud computing from different technology and business points of view, and show their relationship in order to propose more suitable models.

The goal of this paper is to present a comparative review of grid and cloud computing economic and pricing models to understand whether they are just studies or real-life candidates, and what are their advantages and shortcomings. The analyses from these models are important in order to define new realistic economic models for real grid and cloud computing marketplaces.

The paper is organized as follows. Section II presents the general view of grid and cloud computing architecture. Section III describes grid computing that includes the definition of grid computing, the general introduction of grid technologies, the classification and specification of grid economic and pricing models. Section IV provides the understanding of cloud computing that includes its definition, technologies and pricing models respectively. We then present a comprehensive comparison of these two approaches in Section V. Section VI concludes the paper by discussing the findings in this paper and highlighting our further research work for this specific research area.

II. GRID AND CLOUD COMPUTING ARCHITECTURE

Grid and cloud computing consist of services, protocols, resources and other management functions constituting six layers as shown in Fig. 1 with the following definition:

Grid and Cloud System Resources Fabric Layer 1: it is the heart of the grid and cloud system architecture. It is the lowest layer which is the foundation upon which all services are based. Various resources such as processors, storage and network are accessible in this layer.

Communication Connectivity Layer 2: it is responsible for security and communications. It identifies protocols for security functions such as authentication, access control, data integrity, confidentiality and data communication.

Unified Resources Layer 3: it is responsible for determining protocols for system configuration, accounting, monitoring, control, job initiation, negotiation, and payment of sharing operations on individual resources.

Collective and Composite Layer 4: coordinating different resources are the main roles of this layer, for example, directory services.

Middleware Layer 5: it is a software layer situated between the operating system and application which enables sharing information between multiple applications continuously. It is also considered as a standard for interconnecting components. Middleware employs brokers to act as its virtual service providers to resources in a transparent manner to shield the end-user from complex details.

Application Layer 6: this layer includes user applications which act in Virtual Organization environments. The applications used by users have the same ability to operate in both grid and cloud computing.

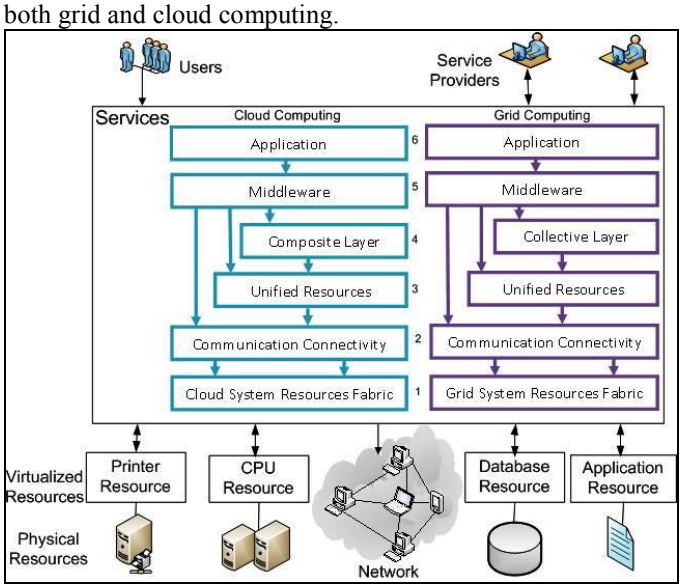


Fig. 1. Grid & Cloud Computing Resources, Services & Protocol Architecture

III. GRID COMPUTING

A. Grid Definition

Grid computing was first coined in 1990s by Ian Foster and Carl Kesselman and succinctly defined as: *Grid computing is coordinated resource sharing and problem solving in dynamic, multi-institutional virtual organizations"* [4].

In a basic grid computing networked environment, every computer can access the resources of every other computer. In this approach, multiple computers perform tasks via sharing in disparate geographical spaces. Computers may be connected by the Internet or any other network infrastructure. As a result, customers can have access to computing and storage resources on demand in real-time. It is frequently used for complicated intensive and extensive computation or massive data crunching that is done by several computers. Grid performs these computations in parallel in solving complex application or simulation, scientific, technical or business problems and in some instances, depending on the application, the results are harnessed and delivered to the target end-user.

There is no specific categorization for grids. Numerous IT/ICT suppliers, researchers, scientists have their own classification for grids on the basis of their insight, provision and usage. For example, Mike Ault and Madhu Tumma [5] jointly stated that IBM specified three types of grid:

1. Computational Grid: Nowadays even super computers are unable to provide computational power. Even if they did, it is not logical with a view to economical justification. Computational grid is defined as both a software and hardware infrastructure that provides high-end computational processing capabilities with consistent, inexpensive, dependable access.
2. Data Grid: It is a solution for managing, sharing, and controlling large amounts of scattered data. Remote or

local data is accessible through replica data grids offering the most cost effective solution.

3. Scavenging Grid: Jobs are transferred between machines in order to have smooth operating of the task by cycle-scavengers utilizing idling / free / available PCs.

B. Grid Technologies

The technologies that are used in grid computing include:

- Standardization: It helps IT departments of enterprises and organizations to decrease their systems costs and management, purchasing from multiple autonomous suppliers, and permitting cooperation between service providers as defined by Global Grid Forum (GGF) [6], which is a de facto standards body for grid Computing.
- Virtualization: a technique of dividing IT resources types such as simulation, time-sharing and Quality of service (QoS) is called virtualization that can add flexibility, scalability and better costing [7].
- Service orientation: Service-oriented architecture (SOA) enables enterprises to unite their dissimilar applications to reuse them instead of duplication.

C. Grid Economic and Pricing Model

The business model for grids emanates from non-commercial situations. They are mainly sponsored by research in academia or by huge government laboratory projects [8]. Thus, they are largely project-oriented in which the users or community of users participate in the project and are allocated a certain number of service units (i.e. CPU hours, storage space, load, etc.) that they can spend. These models are not very useful for creating real business models, but the set of service units' as parameters as "funny-money" are important factors that could be used in creating real economic models for tariff and pricing structures.

The pricing schemes investigated by Buyya et al. [3] are based on different parameters and methods including, flat price model, usage period and duration, voting, resource usage timings, demand and supply, customer loyalty, bulk purchase of services, cheaper prices, and SLA provisioning.

Grid economic service and pricing models are slowly evolving, with the most recent ones listed in Table1 [9]:

TABLE 1
ECONOMIC & PRICING MODELS OF GOODS & SERVICES

Economic Model	Description
Commodity Market Model	In this model, the price of service is defined based on amount of resource that users used. Different pricing models can be used in a Commodity Market Model like Usage Duration (Time), Flat fee, Subscription or Demand and Supply-based.
Posted Price Models	Both the posted price model and commodity market model are similar except that posted price model attracts customers through advertisement.
Bargaining Model	In this model, the resource brokers and grid service providers negotiate with each other to meet their objectives until they agree with the price.
Tendering/ Contract-Net Model	This model is mainly used for service haggling in a distributed problem solving system. In order to control services and goods exchange, this model is used on the contracting mechanism that is mainly used by businesses.
Auction Model	This model is based on negotiation between sellers and buyers. The auction rules which are acceptable by both the providers and customers are set by the auctioneer.
Bid-based Proportional Resource Sharing Model	In this model, the bid value defines the amount of resource share that is allocated to the customers. The users can access the resource through credits or tokens. The value of credits depends on demand.
Community/ Coalition/ Bartering Model	In this model, a unified computing environment is created by a group of individuals or institutions cooperating in a computing environment to share each other's resources.
Monopoly, Oligopoly	In this model, a Grid Service Provider (GSP) dominates the market. Since GSP is an individual provider of a specific service, users have to accept the price that is suggested by the individual GSP.

Table 2 provides an overall review of some of the important pricing schemes for resources in grid computing.

TABLE 2
PRICING SCHEMES FOR RESOURCES IN GRID

Pricing Model	Description	Economic Model	Where Implemented?
Autonomous Pricing Strategy[10]	Grid traders define the prices. This scheme is based on three strategies, decision making, bidding, and quoting-price.	Bidding	Theoretical study with simulation
Market-based Resource Allocation in Grids[11]	In this approach, producers and consumers make decision under their local knowledge and capabilities.	Continuous Double Auction model	Simulated in grid like environment
Game Theoretic Pricing Strategy [12]	This strategy is used for job allocation in mobile grids based on the Nash bargaining method. The mobile device and the Wireless Access Point (WAP) server are the two participants in bargaining game in order to define reasonable pricing strategy and effective job allocation for mobile device.	Bargaining	Simulated in heterogeneous grid system
Dynamic Resource Prices[13]	This approach consists of three types of agents; resource agents that are responsible for managing accessible resources, task agents that have the role of collecting requirements of resource combinations and mediating agents that accomplish the combinatorial auction for resource allocation.	English Auction	Theoretical framework simulated in an agent-based trading environment.
A Dynamic Price Model with Demand Prediction and Task Classification [14]	A Markov chain is used for prediction of resources. According to future demands a resource price-adjusting mechanism is defined. The process of price-adjusting consists of two steps; first is prediction of resource demand. Second step is to set the price. There are three types of pricing strategies; price decrease strategy, price	Commodity Market model	Theoretical study with simulation

	keeping strategy and price increase strategy.		
An Incentive Scheme[2]	This is a combination of two existing schemes double auction and a combinatorial auction. This approach has benefits of both technologies.	Auction	Studied in Europe-China Grid Internetworking (ECGIN) R&D Project.

IV. CLOUD COMPUTING

A. Cloud Definition

Cloud computing is a re-discovered technology topic which is gaining popularity, and expanding rapidly in service deployment environments. The idea was conceived by John McCarthy in 1961 [15]. Sharing resources, software and information via the Internet are the main functions of cloud computing in order to reduce cost, underutilization and to satisfy demand. The consumers of cloud computing can utilize applications without installation or configuration of special software and access their personal data from any computer over the Internet through centralized control but distributed management procedures.

It contains different elements, features, functions and dimensions covering many areas, including infrastructure as a service **(IaaS)**, platform as a service **(PaaS)** and software as a service **(SaaS):**

- IaaS: *Infrastructure as a Service* is a method in which enterprises lease equipments such as servers and network tools instead of purchasing from service providers through the internet.
- PaaS: *Platform as a Service* is a method whereby customers can lease resources such as computing equipment type of operating systems to develop and run applications through the Internet, etc.
- SaaS: *Software as a Service* method is where users or enterprises pay for software use and upgrades.

B. Cloud Computing Technologies

Some of the important technologies that contribute to cloud computing are specified [16] as:

- Virtualization: It is a method whereby resources are hosted on a virtual machine operating in a virtual environment between end users and the platform services.
- Web service and SOA: Service Oriented Architecture (SOA) is a set of services that is provided by distributed systems through middleware broker and web services accessible through networks. Both grid and cloud computing utilized them.
- Web 2.0 and Mashup: Web 2.0 refers to Web meta applications that permit sharing of information and collaboration through social network sites and other applications. For example, combining data from GoogleMap and Flicker as a remix meta application.
- Serviceflow and workflow orchestration: Is a collection of service structures by Cloud Computing on-demand in a one-stop shopping manner.
- Worldwide distributed storage system: A storage method that maps onto a single virtual storage system distributed over number of physical networked sites.

C. Cloud Pricing Model

According to traditional pricing model of software, customers should pay once-off for limitless usage. Since the recent evolution in software development from traditional method to SaaS, a new pricing method has become essential, considering many new factors for pricing.

Pricing model in cloud Computing is more flexible than traditional method. Every provider has its own pricing scheme. For example, Salesforce uses "pay per use" scheme [17]. Amazon uses "pay-per-use fixed pricing" for example First 50 TB / Month of Storage Used costs $0.150 per GB [18]. Some others use "pay for the resources" that are assessed based on speed of bandwidth or amount of storage (storage or bandwidth size). This method is more common in PaaS and IaaS.

According to Weinhardt et al. [17], the most prevalent method of pricing in cloud is pay per use, which is based on Units with constant price. Another common pricing model is subscription, whereby users sign a contract (subscribe) based on constant price of service unit and a longer period of time, for example six months or a year. Obviously, customers and providers would like to use static and simple pricing model in order to ease payment prediction. Nevertheless, for high-value services dynamic pricing can be more efficient.

Table 3 list several pricing schemes in cloud computing.

TABLE 3
PRICING MODELS IN CLOUD COMPUTING

Pricing Model	Description	Economic Model	Where Implemented ?
Dynamic Resource Pricing[19]	It is a type of dynamic pricing scheme used for federated cloud and supports various resource types. In this approach, Resource payments are determined based on demand and supply.	Auction	Theoretical study with simulation
Dynamic Auction Mechanism[20]	This mechanism used the approach of pricing, truthfulness and dynamic adjustment mechanisms. Dynamic adjustments tolerate fluctuation of users' distributions.	Marginal Bid and Sealed-bid Auction	Theoretical study with simulation
A Double Auction Bayesian Game-Based Pricing Model [21]	This framework enables people to buy resources from various providers and vacant resources can be exchanged with more flexibility.	Auction	This is a theoretical framework without any simulation experiments
Double-sided Combinational Auctions to Resource Allocation [22]	This is a market mechanism for service allocation that enables users and providers to deal through double-sided combinational auction. This mechanism is suitable for cases requiring various services and where many	Double-sided Auction	This is theoretical framework

	participants exist. Both users and service providers should be satisfied by the resource allocation mechanism. A double-sided auction model and K-pricing scheme were used in this mechanism.		with simulation

V. COMPARISON OF GRID AND CLOUD COMPUTING

Distinction of cloud and grid computing is an important issue. Although cloud and grid computing are technically and in generality different, they are similar in all other respect concerning offered services in the form of utility computing [23]. Both of these technologies are accessible through services over networks. They can be compared from technical viewpoints as:

- Usage: grid computing with a longer operational history was developed and operated publicly, but cloud computing originated and operated privately. Cloud is more popular in the nonacademic world while grid is applied in academia. Venders are far more successful in attracting nonacademic consumers to cloud because of its easy usage and accessibility. Again in cloud computing, an IP address is allocated to each virtual machine whereby consumers can access various applications directly via their machines.
- Standardization: grid customers can easily change their grid providers because of standardizing, but it is quite difficult in cloud. Rings et al. [24] expressed that there was a deficiency of standards and interoperation in cloud computing.
- Virtualization: Virtualization is one of the most vital elements of cloud computing especially for encapsulation and abstraction. Besides, it is also applied to achieve uniform interface to hide the defects, physical heterogeneity and geographical distribution. In grid computing, this application is used less as every organization which is fully responsible for controlling their resources. To achieve more reliability and better management of resources grid can use cloud technologies through virtualization layer [24]. Pricing models can easily reside at the virtualization level because it has a *global view* of all the underlying resources and service which is shielded from the user view.
- Pricing model and Service Level Agreement (SLA): In general, there are two schemes of pricing that used in economic models for shared resource allocation, fixed pricing and dynamic pricing in both cloud and grid computing. In dynamic pricing, the price is calculated based on pricing mechanism whenever there is a request. In some cases, the price of the resources is determined according to demand and supply. In fixed price, each seller defines price for resources that could be prohibitive and thus lead to a reduced customer base and decrease in revenue and profits. However, pricing models in cloud Computing are more flexible compared to the ones in grid Computing. In cloud environment, every provider has its own pricing model. It may be based on giga or tera bytes of storage space, CPU hour, network I/O transmission rates, data packet size or licensed cloud product [24]. But in order to achieve interoperability and collaboration within and outside grid computing requires standard services. Execution of the SLA in grid computing is largely not prevalent and still in its infancy but SLA for cloud computing has been proposed by several cloud service providers. There is a tendency to have SLAs for grid computing, which is will probably bring it into alignment with cloud computing trading.

The criteria and functions for grid and cloud computing is shown in Table 4 in a comparative manner, collated from Weinhardt et al. [17] and Luis et al. [25].

TABLE 4
GRID COMPUTING vs. CLOUD COMPUTING

Criteria	**Grid Computing**	**Cloud Computing**
Virtualization	Virtualization of data and computing recourses and in its beginning	Virtualization of hardware and software platforms and essential
Type of application	Batch	Interactive
Application development	Local	In the cloud
Access	Via grid middleware	Via standard web protocols
Organizations	Virtual	Physical
Business models	Sharing	Pricing
Service-Level agreements	Not yet enforceable	Essential
Control	Decentralized	Centralized (data center)
Openness	High	Low
Usability	Hard to manage.	User friendliness.
Switching cost	Low due to standardization	High due to incompatibilities
Architecture	Service orientated	User chosen architecture
Resource Heterogeneity	Aggregation of heterogeneity resources	Aggregation of heterogeneity resources
Resource Sharing	Collaboration (VOs, fair share).	Assigned resources are not shared.
Resource Allocation	On demand.	On demand.
Multitasking	Many users can perform different tasks.	Many users can perform different tasks.
Platform Awareness	The client software must be Grid-enabled.	The SP software works on a customized environment
Security	Security through credential delegations.	Security through isolation.
Software Dependencies	Application domain dependent software.	Application domain independent software.
High Level Services	Plenty of high level services.	No high level services defined yet.
Software Workflow	Applications require a predefined workflow of services.	Workflow is not essential for most applications.
Scalability	Nodes and sites scalability via load balancing.	Nodes, sites, and hardware scalability via load balancing.
Self-healing management	Re-configurability & partial self-healing	Re-configurability & self-healing
Payment model	Rigid	Flexible
User access	Access transparency for the end user.	Access transparency for the end user.
QoS Guarantees	Limited support, often best effort only.	Limited support, focused on availability and uptime.

VI. Discussion and Conclusion

We have presented and assessed the basic principles of cloud and grid from different viewpoints. In general, it can be surmised that these two technologies are similar in terms of ICT structures and service offerings. They have similar frameworks, architectures, use of technologies and pricing models. Moreover, both of them enable access to resources in order to reduce the cost of computing. However, the big difference is that cloud computing is more complex than grid computing because of its diversity and variety of services.

So far, different pricing mechanisms have been proposed or used by our contemporaries. From our analysis, they fall short in many different ways such as incomplete formulation of the pricing model and its association with SLA. We have presented the most recent available pricing models for grid and cloud computing in order to assess their relevance and applicability. However, most of them have a bias, by means of favoring the seller over the buyer in an unregulated trading environment. Overall, we have found from the 6 grid computing and 4 cloud computing pricing models that 90% of them are theoretical studies either with or without simulation, Only 1 pricing model, 10% of the total is deployed in grid computing, which is an Incentive Scheme, was implemented in real life. It appears that no single particular model fits all the possible criteria because of the varied nature of the enterprise policy and other business objectives.

Our initial analysis also shows that the features and functions of accounting and auditing procedures are not sufficiently included in these models for self-governance by service providers that meet the necessary legal requirements for accountability in a globally international trading space.

Defining a fair price for resources that benefit both providers and consumers is a fundamental step. It allows the creation and growth of critical mass customer uptake and use of the services to be modeled from the beginning. It has to be equitable in creating a just marketplace within the legal framework. It is envisaged that through process, the critical mass criteria can also be easily satisfied.

We are currently developing a new economic model to satisfy realistic requirements ranging from the variety of services to protecting the users as consumers within the regularity and legal frameworks. This model will serve as a framework for further developing tariff and pricing mechanisms within the scope of service level agreement practices to offer grid and cloud computing services. In addition, we will initially validate the model through simulation to test its effectiveness against various constraints as close to real-life and real-world grid and cloud computing service offerings. We believe that the proposed economic model will suffice for both grid and cloud computing regimes.

References

[1] Liang, Z., L. Zhang, S. Dong, and W. Wei, *Charging and Accounting for Grid Computing System*, in *Grid and Cooperative Computing*, M. Li, et al., Editors. 2004, Springer Berlin / Heidelberg. p. 644-651.

[2] Stiller, B. and D. Hausheer, *Design of Economic Grid Traffic Management and Security Mechanisms.* Rn, 2008. 1(R2): p. R1.

[3] Buyya, R., D. Abramson, and J. Giddy. *A case for economy grid architecture for service oriented grid computing*. in *Parallel and Distributed Processing Symposium., Proceedings 15th International*. 2001.

[4] Foster, I. and C. Kesselman, *The grid: blueprint for a new computing infrastructure*. 2004: Morgan Kaufmann.

[5] Ault, M. and M. Tumma, *Oracle 10g Grid & Real Application Clusters: Oracle 10g Grid Computing with RAC*. 2004: Rampant TechPress.

[6] *Open Grid Forum*. Available from: http://www.ogf.org/.

[7] Armstrong, S.R., *Survey of Computational Grid Systems and Virtualization in the Grid Space.* 2008.

[8] Foster, I., Y. Zhao, I. Raicu, and S. Lu, *Cloud computing and grid computing 360-degree compared.* ArXiv e-prints, 2008. 901: p. 131.

[9] Buyya, R., H. Stockinger, J. Giddy, and D. Abrams, *Economic models for management of resources in grid computing.* Arxiv preprint cs/0106020, 2001.

[10] Yang, J., S. Yang, M. Li, and Q. Fu. *An autonomous pricing strategy toward market economy in computational grids*. in *International Conference on Information Technology: Coding and Computing ITCC* 2005.

[11] Pourebrahimi, B., K. Bertels, G.M. Kandru, and S. Vassiliadis. *Market-Based Resource Allocation in Grids*. in *Second IEEE International Conference on e-Science and Grid Computing e-Science '06.* . 2006.

[12] Ghosh, P., N. Roy, S. Das, and K. Basu, *A pricing strategy for job allocation in mobile grids using a non-cooperative bargaining theory framework.* Journal of Parallel and Distributed Computing, 2005. 65(11): p. 1366-1383.

[13] Schwind, O. Gujo, and T. Stockheim. *Dynamic Resource Prices in a Combinatorial Grid System*. in *E-Commerce Technology, 2006. The 8th IEEE International Conference on and Enterprise Computing, E-Commerce, and E-Services, The 3rd IEEE International Conference on*. 2006.

[14] Xiangang, Z., X. Liutong, and W. Bai. *A Dynamic Price Model with Demand Prediction and Task Classification in Grid*. in *Sixth International Conference on Grid and Cooperative Computing GCC* 2007.

[15] McCarthy, J. *Life in the Cloud, Living with Cloud Computing*. 1961 12-1-2011]; Available from: http://computinginthecloud.wordpress.com/2008/09/25/utility-cloud-computingflashback-to-1961-prof-john-mccarthy/.

[16] Lizhe, W., T. Jie, M. Kunze, A.C. Castellanos, D. Kramer, and W. Karl. *Scientific Cloud Computing: Early Definition and Experience*. in *10th IEEE International Conference on High Performance Computing and Communications HPCC '08* 2008.

[17] Weinhardt, C., A. Anandasivam, B. Blau, and J. Stößer, *Business models in the service world.* IEEE IT Professional, Special Issue on Cloud Computing, 2009. 11(2): p. 28–33.

[18] *Amazon Simple Storage Service (Amazon S3)* Available from: http://aws.amazon.com/s3/.

[19] Mihailescu, M. and Y.M. Teo. *Dynamic Resource Pricing on Federated Clouds*. in *10th IEEE/ACM International Conference on Cluster, Cloud and Grid Computing (CCGrid)*. 2010.

[20] Lin, W.-Y., G.-Y. Lin, and H.-Y. Wei. *Dynamic Auction Mechanism for Cloud Resource Allocation*. in *Cluster, Cloud and Grid Computing (CCGrid), 2010 10th IEEE/ACM International Conference on*. 2010.

[21] Shang, S., J. Jiang, Y. Wu, Z. Huang, G. Yang, and W. Zheng, *DABGPM: A Double Auction Bayesian Game-Based Pricing Model in Cloud Market.* Network and Parallel Computing, 2010: p. 155-164.

[22] Fujiwara, I., K. Aida, and I. Ono, *Applying Double-sided Combinational Auctions to Resource Allocation in Cloud Computing*, in *10th Annual International Symposium on Applications and the Internet*. 2010.

[23] Brock, M. and A. Goscinski. *Grids vs. Clouds*. in *5th International Conference on Future Information Technology (FutureTech)*. 2010.

[24] Rings, T., G. Caryer, J. Gallop, J. Grabowski, T. Kovacikova, S. Schulz, and I. Stokes-Rees, *Grid and Cloud Computing: Opportunities for Integration with the Next Generation Network.* Journal of Grid Computing, 2009. 7(3): p. 375-393.

[25] Luis, M.V., R.-M. Luis, C. Juan, and L. Maik, *A break in the clouds: towards a cloud definition.* SIGCOMM Comput. Commun. Rev., 2009. 39(1): p. 50-55.

Requirement Engineering Techniques in Developing Expert Systems

Jac Ky Ang, Sook Bing Leong, Chin Fei Lee, Umi Kalsom Yusof
School of Computer Sciences
Universiti Sains Malaysia
11800 USM, Penang, Malaysia
ajk100075@student.usm.my, lsb100133@student.usm.my, lchinfei@gmail.com, umiyusof@cs.usm.my

Abstract— **Expert system has the least focus on requirement engineering. In facts, requirement engineering is important to get all the requirements needed for an expert system. If the requirements do not meet the clients' needs, the expert system is considered fail although it works perfectly. Currently, there are a lot of studies proposing and describing the development of expert systems. However, they are focusing in a specific and narrow domain of problems. Also, the major concern of most researchers is the design issues of the expert system. Therefore, we emphasize on the very first step of success expert system development - requirement engineering. Hence, we are focusing in the requirement engineering techniques in order to present the most practical way to facilitate requirement engineering processes. In this paper, we analyze expert system attributes, requirement engineering processes in expert system developments and the possible techniques that can be applied to expert system developments. Next, we propose the most appropriate techniques for the expert system developments based on the analysis. From this paper, a set of techniques for expert system development will be provided.**

Keywords- Requirement engineering technique, expert system

I. INTRODUCTION

Requirement engineering (RE) is the discipline of determining, analyzing, pruning, documenting, and validating the desires, needs, requirements of stakeholders for a system [1]. Jiang et al. [2] has stated that bad RE practice contributes to projects failure. Macaulay [3] has shown the benefits of RE by showing many empirical evidences while Nuseibeh et al. [4] have displayed the positive impact of using proper RE techniques to improve the software quality. In Expert System (ES), RE techniques are used to gather requirements to develop a system that can perform tasks that usually perform by human experts. ES contains a high density of problem solving knowledge that can act as a human expert from which the knowledge derive which distinguishes ES from other conventional programs. ES can be characterized by functional applications, project type, and role which are almost similar with the basis requirement of characteristics projects. They are application domain, requirements engineer types, information resources, user involvement and requirements properties. As ES is part of the artificial intelligence, a knowledge engineer is needed to study how human experts make options and translate the rules into condition that a computer can understand.

Our main goal of the research is to improve the quality of ES by proposing suitable RE techniques to be used during the development cycle of ES. Suitable techniques used can minimize the wasting of cost, time and scope and prevent rework during the development of ES. During the techniques selection process, we have to consider the technique attribute and project attribute in order to make a good justification of the techniques. In this paper, we will discuss the important factors in RE techniques selection based on these two main points.

The rest of this paper is organized as follows: Section II summarizes the problem background of the research. Section III discussed related work. Section IV presents the requirement of techniques and tasks to elaborate the analysis of ES development. For section V, we will propose a set of RE techniques that can be applied on ES development. Next, we discuss the implementation and needs of improvement in future. Before we end with conclusion in Section VII, we will also describe the future work.

II. PROBLEM BACKGROUND

One of the challenging tasks ES developments is selecting suitable RE techniques for a particular project as each project has different requirements. Hence, we need significant efforts in choosing different options and combinations of RE techniques. A careless mistake made in the process might lead to a great lost for the ES project. Many useful ES applications such as analysis, diagnosis, planning, predicting and computer aided instruction need RE techniques to gather all the important requirements for ES. Currently, there are some researches study on the RE techniques. Early work by Jiang et al., they described a *Methodology for Requirement Engineering Techniques Selection (MRETS)* to help requirement engineers to select suitable techniques for the projects on hands [5]. They applied MRETS to industrial software projects and provided preliminary information on the effectiveness of MRETS for the selection of RE techniques. In general, they presented the combination RE techniques by using a same methodology of MRETS. This is because Jiang et al. stated that there is no single technique could provide a solution for all RE problems [2]. On the other hand, a study related on requirement syntax [6] has stated that stakeholder requirements are written in unstructured natural languages (NL) which lead to some problems during the system development such as ambiguity, vagueness, complexity, omission, duplication, wordiness, inappropriate implementation and untestability. This indicates

there are common problems occurred during RE process. As a result, this affects the design and implementation process of ES directly.

Meanwhile, RE is always being ill-defined in the early stage of ES development. Lacking of concern in RE processes will cause under load or overload of information and hence knowledge engineers might waste times in researching a main problem domain in order to satisfy stakeholders. According to Mehdi Sagheb-Tehran [7], knowledge engineer is not general problem solver and do not know the limit of their own expertise. Hence, this research is important to provide guidelines for development teams during RE processes.

III. Related Work

In order to develop a high quality ES, we need active involvements of users, customers, and other stakeholders so that they can promote positive support for knowledge engineers to understand to their concerns. Stakeholders are people or organizations that have investments and commission in the content of a program, or in the extension and evaluation of a program (customers, users, project manager, analysts, developer, senior management, quality assurance staff etc.). They are a group or individual that can influence or is affected by the product throughout the product's life cycle directly and also indirectly. These stakeholders are from different backgrounds and have different technical skills. They are so important because the high quality of a product is depends on the customer's needs and intents. To have a successful of RE, we need to motivate and facilitate the active participation of stakeholders [8]. So, stakeholders have the potential to illuminate issues and involve during the progress of program or project implemented.

Adopting right RE techniques according to ES characteristics is very important in the system. Software engineers often face problem in selecting appropriate RE methods for a project. Engineers can make a good choice and have skills in applying the selected technique appropriately in order to effectively elicit, model, document, verify and validate requirements. If the engineering technique does not fit the project, the project is doomed to fail. Jiang et al. [5] has described the positive influence in project-oriented combination of RE techniques has on the success of software systems. They used interviews, workshops and evolutionary prototyping for requirement elicitation for a complete set of combination of RE techniques. Some of non-functional requirements are more easily elicited by specific techniques. About half of the ES applications were classified as being used for manufacturing or stakeholder service application. There was a need for dynamic requirement engineering that can work closely with an iterative release cycle because it was important to release it to stakeholder in market as early as possible so iterative and incremental development was used. In D.Mishra et al.'s [9] research, they described the process of applying RE techniques into the supply chain management system development. They only substantiate and extracted the suitable combination of RE techniques to be assumed in supply chain management system. So, all the requirement techniques can be based on the ES attributes.

In recent years, the application of ES technology to industrial and commercial problems has grown so wide. The applications ES are into most areas of knowledge work. They are more towards dealing with the significant amount of information that must be processed as a part of an environmental impact assessment. Moreover, they are depending on expert judgments whereas other collecting, processing, analyzing, and reporting information can be used in computer and information technologies. Experts are heavily affected in all aspects of the assessment. ES can help to identify the significant impacts, data collection, monitoring programs, provide judgments for specific impacts, and reducing or preventing impacts. Furthermore, ES are also having a roll play in another interesting field which derived from artificial intelligence. Looking at the nature of ES, it can solve the same problems without reprogramming within the same domain of the knowledge-base [10]. ES manage information demands and provide essential expertise. Developers of ES struggle to provide systems with the ability to imitate the capability of human experts, deal with incomplete knowledge, and provide logic for conclusions, provide wider distribution and provide systematic application of knowledge. The task need not to be repetitive as ES is algorithmic. However, it requires experts' generous thought and knowledge if bottleneck exists. ES has the rule-based approach with more powerful knowledge representations and more efficient mechanisms. So, this ES is capable of modeling and selecting suitable RE techniques for a software project.

IV. Expert System Requirement

In order to develop successful ES, it is important for us to understand the characteristic and attributes that will have influence to the project. Through understanding of the criteria to be considered in developing ES, we can define clearer requirements that are needed in developing ES. In addition, we will analyze on the RE process in ES development to identify the objectives and requirements. After that, we study on the specific techniques that can be applied in ES development by justifying the selected techniques.

A. Analysis of Expert System Development

In developing an ES, it is important for us to know that the criteria that are need to build a successful system. A system is considered successful when it can perform tasks as intelligence as human thinking and also it has the nature of intelligence [7]. In addition, cost of building an ES is always a concern for vendor to take in considerations, so it is important that error to made can be minimize to the lowest in order to save cost. As market demand, a user friendly expert system has slowly become a need because a user friendly system will save time and effort for end user when they first time expose to the system [7].

According to Tyran and George [11], there are many factors that can directly affect the success and failure of an ES. They have categorized the factors that associated to the successful of an ES into a few categories which is

organizational factors, implementations activities, technical factors, and also ease of use. Organizational factors are external factors that involve stakeholder such as commitment to the project, management support and also user's participation. Factors that are categorized in implementations activities are user needs assessment, demonstration of the system, training and also maintenance of the ES. They have also listed out the technical factors that can directly affect the ES success which is the technical expertise and ES software/development tools. There are also some factors that are not listed out, such as the unknown factors that changes unconsciously, realistic time and cost required in completing a project as well as resource requirements.

Meanwhile, attributes also are important factors in developing ES. It helps knowledge engineer in project characterization and also selection of RE techniques. The key attributes and characteristics that have direct effect on an ES are [1]:

i. Project size: the size of a project will affect on the requirement techniques that are going to be used in a project. Larger project need to use different RE techniques in completing it.
ii. Requirement volatility: project with high requirement volatility will need a more flexible technique in RE.
iii. Project category: different kind of project category will also affect the RE techniques to be used. For example, some of the project might require more user involvement and some might require more technical skills.
iv. Degree of safety criticality: higher the degree of safety critically, the more caution and serious techniques when handling it.
v. Project complexity
vi. Project cost constraint: cost constraint can affect the whole project, if the budget is not enough, then knowledge engineer will have difficulties in completing it.
vii. Project time constraint: with limited time to complete the project, the ES that develop might not meet its requirement.

B. *Analysis of Requirement Engineering Process in Expert System*

According to Cheng and Atlee [12], there are five main tasks in requirement engineering which are elicitation, modeling, requirements analysis, validation and verification and requirement management. The objectives and outputs are various in different stages. In the following section, we briefly describe the tasks on every stage.

Requirement elicitation – Requirement elicitation is a task of determining the problems and the needs of users to construct a system that resolve the problems and address customers' needs [4]. The objective of the task is to identify all the requirements to achieve the goal of ES. Meanwhile, success rate of ES project development will increase if we can collect as much of requirements during the early stage of elicitation. Hence, we need to identify all the stakeholders of ES. In addition to that, analogical techniques are needed to get more precise requirements [4]. The desired outputs of the process are increasing user commitment and fostering a sense of user ownership for a system [11].

Modeling – Modeling constructs abstract description that is amenable to interpretation [4]. It evokes the details that were missed in the initial elicitation. There are different categories of RE modeling approaches [4]. For ES development, we need to focus in data modeling, domain modeling and analyzing requirement analyzing model. Knowledge in ES is data and it is layered [13]. Therefore, we need to organize data and details gathered during initial elicitation so that it can be understood by all stakeholders. Regarding to this, we need to take times and effort to model the data in order to make the requirements clear.

Requirement analysis – According to Mylopoulos et al. [14], requirement analysis is a process of understanding functions, data and interface for new system. During the task of analysis, we can identify the ambiguity, inconsistency and incompleteness of the system [4]. It also analyzes non-functional requirements of ES developments such as quality, responses time and so on.

Validation and verification – It is important to ensure the requirements of ES are valid. In other words, we have to ensure the requirements are executable for the following development cycles. We require direct involvement of stakeholders to validate and evaluate the requirements by viewing the requirement artifacts [4]. Meanwhile, verification makes clear of ambiguous requirements. Therefore, we have to gather key stakeholders to review the processed requirements

Requirement management - Requirement management includes the tasks of managing the requirements for all the time. Development of an ES normally requires period of times. The refinement on knowledge may be done anytime and each changes results in requirement changes. Hence, we need to have series of techniques to manage the changes and requirement to ensure traceability of requirements for the coming system development cycles.

C. *Specific Requirement Engineering Techniques for Expert System*

There are a lot of RE techniques can be used for ES development in different tasks in RE process. In this paper, we have identified all the specific techniques out of the RE technique library proposed in the research done by Jiang et al. [2]. Meanwhile, the selecting factors will be based on the factor listed by Kheirkhah and Dareman [1]. The justification of the selected techniques is listed in Table 1.

V. PROPOSED WORK

In this section, we proposed suitable RE techniques for RE processes in ES development based on the previous analysis. In this project, we mainly focus on the existences and views of knowledge engineer as their knowledge in ES development is the major difference between ES and conventional software systems. The set of techniques suggested are shown in Fig. 1.

During elicitation, we propose interview, focus group and brainstorming. First, focus group is conducted to gather all the stakeholders to get the perceptions, opinions and comments about the ES. Furthermore, stakeholders are having different points of view and we need this chance to allow the team members to meet each other. Next, we interview the important stakeholders to gather initial background information. In the development of ES, knowledge engineer is a key stakeholder. For example, knowledge engineers view is the main concern to make the system user-friendly [7]. The system may be hostile if the knowledge engineer is not user-friendly concerned. Hence, we need to interview them to get more precise information and expert advices from them. We also suggest organizing a brainstorming sessions among the stakeholders to generate ideas.

In the process of modeling, we put the requirements into a model. We have chosen UML diagram to model the data and needs from stakeholder. In the modeling stage, we have chosen the ER diagram, UML and data flow diagram. ES is high complexity system where it deals with complex data. The models used normally do not show to the clients but they are kept throughout the development process [13]. The models can be used for references of the development team and each development team should have access of it.

During the process of analysis, we use the techniques of conflict management, card sorting and viewpoint based analysis. We use the card sorting to prioritize the requirements of ES. In addition to that, we have to solve the requirements conflicts that may arise during the analysis. Hence, the teams have to negotiate and solve the conflicts. The teams may gather the conflicted stakeholders and allow them to discuss for the conflicted requirements. During the analysis, it may need view point analysis to analyze the view of different stakeholders. To analysis the data of the requirements, we propose to use state machine and fault tree analysis as the project is high complexity.

In the stage of validation and verification, we use formal inspection, requirement checklist, requirement testing, and prototype. We first have a formal inspection to inspect the anomalies in the requirements analyzed. Then the team produces a list of requirements to ensure no requirements are left out.

We then further test the ES requirements for the feasibility by conducting requirements tests by building a test case and evaluate the tests. We also provide prototype to further prove the requirements are valid. The prototype focuses mainly on validating the raw data.

In task of requirement management, we document the requirements of the systems. We strongly suggest the organization provide a template for the development teams to standardize the document. The standardization can ensure the requirements can be easily understood by others in case there are following up tasks.

In summary, the suggested techniques are selected based on the ES attributes. The techniques are applied in each process of RE and they should be followed in sequences.

TABLE I.
SPECIFIC TECHNIQUES FOR EXPERT SYSTEM DEVELOPMENT

RE task	**RE techniques**	**Condition to apply this techniques**
Elicitation	JAD	1. The team consists of different stakeholders from various domains.
	Ethnograpghy	1. Functionality and usability are crucial 2. Elicitation of implicit knowledge is essential.
	Focus group	1. Able to facilitate communication. 2. Able to get domain knowledge.
	Interview	1. The opinion of some stakeholders are particular important.
	Brainstorming	1. Able to generate ideas.
Modeling	UML diagram	1. Project complexity is high.
	Data Flow diagram	1. Project complexity is high.
	ER diagram	1. Project complexity is high.
	Structured Natural Language Specification	1. Ability to help write unambiguous and precise requirements by using notation.
Analysis	State Machine	1. The project demands rigorous, precise, consistence and unambiguous descriptions and states.
	Fault tree analysis	1. The project complexity is very high.
	Goal-oriented analysis	1. The system has different goal for different users.
	Card sorting	1. Able to prioritize the requirements of system.
	Conflict management	1. Able to solve the conflict of requirements.
	Viewpoint based analysis	1. Able to identify different views of stakeholders.
Verification and validation	Formal inspection	1. Requirement preciseness and consistency are of major concern.
	Requirement checklist	1. Able to identify the incomplete requirement. 2. The system complexity is high.
	Prototype	1. Project complexity is high.
	Requirement testing	1. Able to test the involve stakeholders directly to review requirement artifacts.
Requirement management	Requirements management	1. The complexity is high. 2. The quality of the requirement specification and consistency is main concern.

VI. IMPLEMENTATION PLAN AND DISCUSSION

For most of the ES application in the world, there are a lot of problems faced when it comes to design and implementation phase. This is often caused by insufficient and ambiguous requirements from stakeholder in RE process. As a result of this, the ES developed does not meet stakeholder's needs. Company and organization might face a great lost in terms of money and time to fix the problem.

As we know, RE process is a very important process that can manipulate and it is the dominant of whole process in developing an ES. Currently, there is no existence of one complete RE techniques for all the stages in RE process that can be applied to all of the ES. Each stage has different requirements and also different techniques are required to complete the stage. RE techniques also vary in each project according to the project scales and others variables that affect the project. Besides considering the projects scales and attributes that affect the selection of RE techniques, there is also other factors that can affect the selection. The organization background and characteristics are such factors that can bring huge effect on selection process [1]. The size of the organization, the culture that are apply in the organization, the organization complexity and also the technical maturity in the organization are criteria that we should concern when selection of requirement engineering techniques.

Although there are a lot of decisive factors that we can analyze out before we make our decision, we have found out that a lot of non-functional principle that we cannot complete and satisfy in the project. Through series of techniques, the weaknesses from one technique can be covered by other technique. Hence, creating RE document can help knowledge engineer to model the prototype of the system.

We will carry out a series of experiments to make comparison of between ES that is developed using the technique we proposed and ES that is developed in usual way. For example, we will develop two similar systems, one with the set of RE techniques that we proposed and the other with the norms that are usually done by knowledge engineer. We will consider the criteria in testing the development process of both system and also how effectively our proposed set of techniques influences the overall process. These criteria that are in our consideration might be in software engineering area as well as in artificial intelligence area. In addition, we will carry out surveys and interviews with stakeholders to seek for comments on the current set of RE techniques. We will then review on the comments from stakeholders and make appropriate improvement and enhancement towards our proposed set of techniques.

VII. CONCLUSION AND FUTURE WORK

RE techniques is vital in determining how the ES will be implemented. Hence, selecting good and appropriate techniques during RE process is important. They contribute to the overall implementation of the whole ES project. A good document from RE process can definitely reduce the workload of the developer in the next step while a good reference of documentation will helps to prevent further maintenance problems. Therefore, we have chosen a list of RE techniques that is useful in developing ES project based on the criteria and project attributes of the particular ES. We have research on the pros and cons of each techniques involve in the RE process of ES. We have proposed a set of techniques for each stage of RE process based on our study on each of the suitable condition for that technique. We hope that with the suggested techniques for ES development, the result of design and implementation stage also will be-

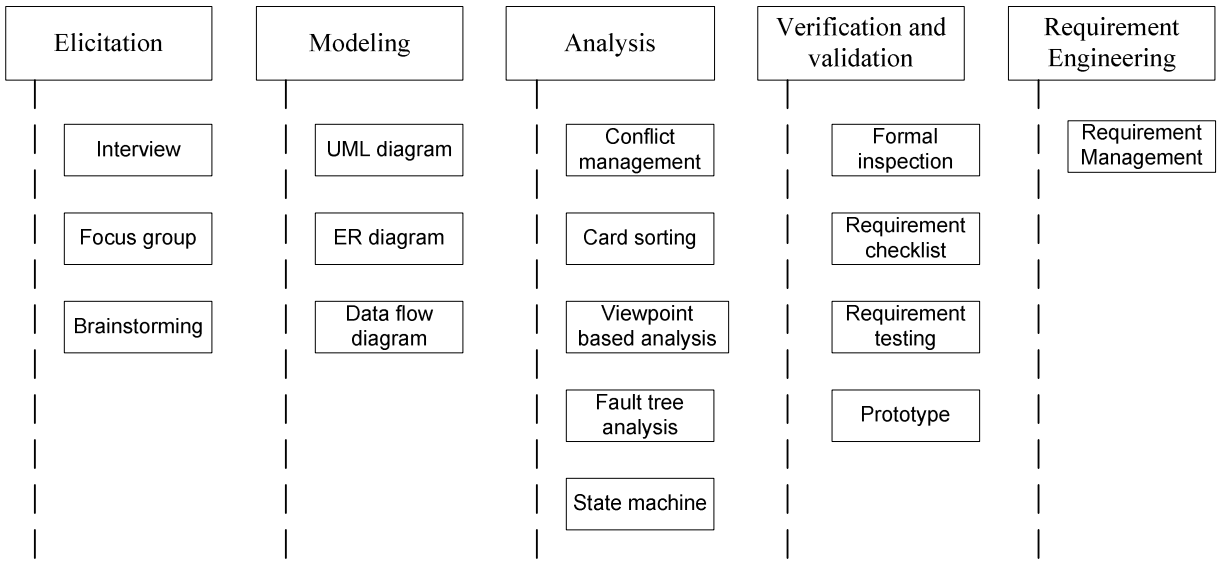


Figure 1. Series of requirement engineering techniques in expert system development

In future, we will also make good adjustments and corrections on the weaknesses of current proposed set of RE techniques so that it can fit in well in most of the projects and benefit to the development of ES. Meanwhile, we will include both functional and non-functional system requirement in choosing the technique so that the ES can meet the client's need. Developers might take this as the references when they are developing an ES. This will save the extra work for ES developers to analyse and justify for suitable RE techniques.

ACKNOWLEDGMENT

The main author wish to thank Universiti Sains Malaysia for the support of this research, under University Short Term Grant No: 304/PKOMP/639009 and APEX Incentive Grant.

REFERENCES

[1] E.Kheirkhah, and A.Deraman, "Important factors in selecting Requirements Engineering Techniques", *Proceedings of International Symposium on Information Technology (ITSIM 2008),* 2008, pp.1-5.

[2] L.Jiang, A.Eberlein, B.H.Far, and M.Mousavi, "A Methodology for the selection of Requirement Engineering Techniques", Software and Systems Modeling, vol.7, Iss.3, 2008, pp. 303-328.

[3] L.A.Macaulay, "Requirements Engineering. Applied Computing, Springer", 1996.

[4] B.Nuseibeh, and S.Easterbrook, "Requirements engineering: a roadmap", in Finkelstein, A. (ed.) the Future of Software Engineering, ACM Press, and New York, 2000.

[5] L.Jiang, A. Eberlien, and B.H.Far, "Combining Requirement Engineering Techniques-Theory and Case Study", *Proceeding of 12th IEEE International Conference and Workshops on the Enginering of Computer-Based Systems (ECBS'05),* 2005, pp. 105-112.

[6] A.Mavin, P.Wilkinson, A.Harwood, and M.Novak, "EARS (Easy Approach to Requirements Syntax)", *Requirements Engineering Conference, RE '09. 17th IEEE International,* 2009, pp. 317 - 322.

[7] M.Sagheb-Tehrani, "Expert Systems Development: Some Issues of Design Process", SIGSOFT Software Engineeering Notes, vol.30, Iss.2, Mar. 2005, pp. 1-5.

[8] I.Alexander, "A Taxonomy of Stakeholders, Human Roles in System Development", Issues and Trends in Technology and Human Interaction, Edited by Bernd Carsten Stahl, IRM Press, (Chapter 2) pp. 25-71, 2007.

[9] D.Mishra, A.Mishra, and A.Yazici, "Successful requirement elicitation by combining requirement engineering techniques", *Proceedings of 1st International Conference on the Applications of Digital Information and Web Technologies (ICADIWT 2008),* Oct. 2008, pp. 258-263.

[10] M.Lopez-Nores, J.Pazos-Arias, J.Garcia-Duque and B.Barragans-Martinez, "An agile approach to support Incremental Development of Requirements Specifications", *Proceeding of the 2006 Australian Software Engineering Conference (ASWEC'06*), 2006.

[11] C.K. Tyran, J.F.George, "The implementation of expert systems: A survey of Successful Implementation", 1993.

[12] Betty H.C.Cheng, Joanne M.Attle,"Research Directions in Requirement Engineering", *Proc. of IEEE Future of Soft. Eng.(FOSE'07)*,2007,doi:0-7695-2829-5/07.

[13] L.Longshu, X.Yi, L.Xuejun, L.Liang, F.Xianjin ,"Research on Software Architecture for Expert System in Practice",Pervasive Computing and Applications(ICPCA 2008),2008,pp.17 - 21.

[14] J.Mylopoulos, L.Chung, S.Liao, H.Wang, E.Yu, "Exploring alternative during Requirement Analysis", doi:10.1109/52.903174.

The Aspects of Choosing Open Source versus Closed Source

Atieh Khanjani[1], Riza Sulaiman[2]

[1,2]Schools of Computer Science & Industrial Computing
Faculty of Information Science and Technology
Universiti Kebangsaan Malaysia,
43600 UKM Bangi, SelangorDarul Ehsan,
Malaysia

[1]akhanjani *at* ftsm.ukm.my, [2]rs *at* ftsm.ukm.my

***Abstract*- Closed source software, is a type of software that is licensed under the exclusive legal right of its owner. It is also purchasable by users by paying amount of money. Open Source Software (OSS) is software available with its source code under an open source license to study and modify the code. Open Source Software Development (OSSD) is the process to develop OSS. Many industries try using OSSD as they see the advantages of open source compared to closed source software development. This research presents the reasons of recently using OSSD model rather than traditional closed source approach. The result is to show the differences between closed source and open source process and how open source can effect on quality through its particular features. It also identifies and addresses the challenges and benefits faced by the users against traditional closed source model.**

Keywords: licenses, closed source, OSSD model, process, procedures and open source.

I. Introduction

Today companies are looking for a methodology to support and maintain their software. This is because of increasing the attention of supporting and protecting software, after the development, rather than only building the code.

Therefore open source methodology due to having special characteristics plays a vital role to satisfy customers and companies as well. Unlike traditional methods which define teams and requirements, the processes in OSSD model is a parallel and repeatedly development techniques, with free user participant's, huge development communities and effective user testing.

Moreover due to putting so many people to develop, test and evaluate the code, OSSD gets more benefits rather than traditional closed source software. Although OSSD model has some problems to challenge, but still is a proper methodology especially for large scale software companies.

This paper presents a study between closed source software traditional development and open source software development model. In Section 2, we have mentioned closed source development methodology that is the previous form of software development. In section 3, we have briefly outlined concepts of OSSD model. In Section 4, we have provided a comparison between the aspects of using open source versus closed source. We also have the part of problems in OSSD model in section5 and finally we have concluded our work.

II. Closed Source Development Methodology

Closed source software or in fact proprietary software that belongs to a particular company or person, is software which is licensed under the exclusive legal right of its owner. It is also purchasable by users by paying amount of money to the one who has the right of publish under the certain condition. Therefore the economical aspect of this type of software compared to open source seems so important [1].

Proprietary software is naturally non-competitive. It also restricts interworking and interoperability between different manufacturer systems. Moreover in case of developing, selected expert developers with motivation of gaining money, will develop it [2]; and a dedicated group of programmers, will design and write the software code. In addition there is no individual work appearing in closed source, and it is all by team work[3]. In proprietary software the users purchase a binary version of the program not the source code; therefore the modification by users technically is impossible. In the other hand if there is a bug in the system users have to wait for a new release [4,5].

In terms of usability, proprietary software applies expert usability testing, guidelines, training course such as seminars and extensive support to help users. Moreover the cost of proprietary software varies from hundreds to thousands dollars depending on complexity, type of the system and requirements. Service and support is one of the major advantages of proprietary software because if the user has problem or the guide is not adequate they will resolve it instantly and that is why we can say that services are the one of the most important point to choose this software.

Furthermore, proprietary security software is typically developed in a managed and controlled environment by an integrated team with a common focus. The team reviews

and audits the codes alone, so the risks of back door Trojans will be reduced [6].

In comparison with traditional methodology, open source claims to be more useful and has more benefits, since commercial approach deals with visible features, but open source favors quality features [7]. The comparison will explain in section 4.

III. The Concepts of Open Source Development

A. A Brief History of Open Source

More than 50 years ago, when the first mainframes came to the market and were sold by firms hardware and software integrated together [8]. According to Hertel [9], in the 1960s, when the researchers start to use computers for their work, due to the lack of commercial software availability, they had to refer to software code open sharing at that time.

In 1960s, the possibility to send emails supported this free exchange code sources. Around 1969 IBM began to unbundle (separating hardware and software) and software became an independent product and was attended more and more. In 1981, the modification in the patent law in the United State and the emergence of the PC (Personal Computer) caused to the source code closing of the UNIX operating system [8]. In September 1983, Richard Stallman launched the GNU project (that initiated GNU operating system) to make a free UNIX-like operating system and he initiated the free software movement. He also pioneered copy left licenses like GNU General Public Licenses that is the most widely used free software license [10].

Open Source, then opened its place within the hackers–the people who love programming or do it for fun, or even for creating viruses [11].

B . The Definition of OSSD

Open source software development is a kind of distributed software development that has a large amount of contributors and because of using Internet and sharing idea freely it is so successful and useful for developers to communicate over the distance.

Usually the idea of starting an open source project comes from a draft idea or existing closed source software with personal motivations, needs or philosophy beliefs or to get portion of the market. Moreover for some individual participant it can be useful to measure their skills and capabilities. However it also can be a freedom of choices against huge previous business product such as Microsoft or IBM's which are controlling the software world or even comes from free thinkers or people who are not interested in making money but contributing to the well-being of the society [12].

There are some communities such as Open Source Observatory (SQO)[1] to help developers to improve their code quality in the open source software domain. The SQO-OSS system is a platform modeled around a simple, pluggable and extensible architecture that enables it to incorporate various types of data sources and is accessible through different user interfaces [13]. The OSS are training users or supporting usability to perform inspection effectively with a higher performance [14].

IV. Comparison of Open Source versus Closed Source

The biggest question, while choosing software is whether it is free or not. Unfortunately the decision is not clear cut and comes down to what you, the end user, needs. Below is a comparison of the strengths and weaknesses of both open and closed source software.

1. In traditional development model, the software is protected by copyrights and is sold to users to earn money, while in open source paradigm; the software is available to users freely to use and to change it.
2. In traditional way, development of a software is a systematic and formal work that is performed by skilled and expert developers to enhance the quality; and a centralized management team support it to improve software in new release, while in OSSD model there is frequent release that software improved by users and developers around the world. There are no special people or place to sit and discuss physically. In OSSD model, the improvement of quality of codes may depends on the personality of each individual who participates through registering in some host sites like *sourceforg.net;*[2]and it retains to the responsibility of each person against system to work better and enhance the quality.
3. The successful issue in quality of closed source is related to centralized management while in open source the quality is from its openness because many programmers examine it and can detect bugs. It also will be reevaluated more and more. Although it can be caused to have iterative correction and may some developers correct a same thing. Moreover the quality in OSSD model is improved rather than closed source because the process of developing software in open source such as reviewing and testing and maintainability performed parallel.
4. The property of openness in open source, helps to identify the user requirements, better than closed source software, because in this type of software, users themselves can contribute and have hand on it even as a developers [3].
5. The number of teams work on quality assurance is effective on quality assessment and this matter in closed source is kept by companies while in OSS it can be guessed by commit logs and source code itself [15].

[1] Reference to SQO [their website]

[2] http://sourceforge.net/

6. The target of closed source is software development to present to the public for gaining the market penetration and profit earning. While open source is a personal idea that can be spread with joining the other hands from all over the worlds to write and develop it, though coordinating of this large scale efforts, needs using standardization software to manage it [16].

7. Koru [17] states some reasons that traditional statistic modeling approaches are not well rather than OSSD. For example module size does not change significantly after a certain release, and because OSS often evolves the size measurement of OSS modules often changes over time, so traditional approach cannot be useful in OSSD setting until the second release.

8. In closed source software, developers start their work after releasing the software, while in OSS model developers are the same as users [12].

9. There is no ownership for open source and it is belong to the public while closed source belongs to one software firm and all the benefits will reverse to that company, but it is also possible to abuse from free codes or available ideas.

Comparing these two kinds of development presented in Table1.

TABLE1
PROPERTIES OF CLOSED SOURCE VERSUS OPEN SOURCE

Type / Property	Closed Source	Open Source
Copyright	Yes	No
Sold	Yes	No
Available Source Code	No	Yes
Free Software	No	Yes
Modify Code by Users	No	Yes
Systematic Development	Yes	No
Frequent Release	No	Yes
Openness	No	Yes
Parallel Process	No	Yes
Knowledge Sharing	No	Yes
Private License	Yes	No
Gaining Profit by Company	Yes	No

While comparing open source with closed source, open source methodology is more flexible and usable since it applies the idea of knowledge sharing and contributes too many people. Also the security terms is much more better than closed source, the bug reporting and defect handling is so faster; and testing issues is more reliable due to participating all developers and users. However in terms of documentation and central management, there is a problem with open source rather than closed source. Due to lack of responsible person for the projects, the users should wait until the problem has been resolved in anyway. Table2 shows how open source and closed source methodology behave with the similar features.

TABLE2
THE AFFECT OF OPEN SOURCE AND CLOSED SOURCE ON FEATURES

Features / Methodology	Security	Central Management	Design	Documentation	Testing	Bug Reporting
Open Source	Strong	No central management	Poor Design	Usually Useless and Unstructured User Documentation	Strong	Fast and Reliable
Closed Source	Depend on the Company Policy	Completely Central Management	Structured Design	Structured Documentation	Depend on Developers	Depend on Developers

V. PROBLEMS IN USING OPEN SOURCE

In case of collaboration problems, since communicating between developers should be very close in software development, and in open source it is only through the Internet, therefore the geographically distance and distributed collaboration leads to decrease communication among developers. Another problem is related to users that contribute the project until the end or not because there is no obligation to do and they are completely free. The release management policy demonstration is troublesome, because from the start of project, the release management guidelines are informal. Moreover when we do not have adequate contributors or interested users in OSS projects, it may have a negative effect on the motivation of volunteers, to keep maintaining the project. In addition any patch submitted to the project must pass the peer review process, in which code style, general quality and the interoperability with other parts of the application, are assessed [18]. Waring [19] notes the drawbacks of the open source software for business such as version proliferation that is the same problem with closed source, complex and numerous licenses, implementation issues that there is no single person is responsible for developing and resolving the problem of software, high short-term costs for OSS unlike the long-term costs that is lower than traditional model. Furthermore the economical challenge of open source to motivate volunteers to participate without money is also considerable [19]. Another disadvantage of using open source will clear, when we lose Internet or a fighting issue starts among programmers, which can hurt developing [20]. Moreover it may happen in

open source, which for a long time no updates for the system; and have to work with older version, since there is no certain responsibility to give the regular update for the software [21]. There is a similar issue for open source to support as well, because there is no support at all for open source unlike closed source, through a single company, especially, if we faced to an emergency problem that needs a quick answer [22]. In large OSS projects, large contributions can take longer to review, which can be problematic for volunteer developers [23].

VI. Conclusion

OSSD model is an approach to improve software quality, it is more usable and reliable rather than traditional methodology especially in case of large scale systems. This paper compares the two closed source software development model and OSSD model. The result shows that in terms of security, bug reporting and testing, is better to use open source methodology, rather than closed source, while there is a problem with documentation and design of using OSSD model, because of using novice volunteers and make a useless documentation. Also we have found out what the benefits and disadvantages of this methodology against traditional closed source software development are.

References

[1] t. f. e. Wikipedia. (2010, *Proprietary software*. Available: http://en.wikipedia.org/wiki/Proprietary_software

[2] P. Henkel. (2010, *Open source versus proprietary software: a discussion*. Available: http://www.matthewbarr.co.uk/opensource.htm

[3] S. Raghunathan, *et al.*, "Open source versus closed source: software quality in monopoly and competitive markets," *Systems, Man and Cybernetics, Part A: Systems and Humans, IEEE Transactions on,* vol. 35, pp. 903-918, 2005.

[4] t. f. e. Wikipedia. (2010, *Closed source - Definition*. Available: http://www.wordiq.com/definition/Closed_source

[5] T. W. J. C. s. wiki. (2007, *Advantages Disadvantages Of Open Source*. Available: http://timjimnetworktech.wikidot.com/advantages-disadvantages-of-open-source

[6] J. Daniel. (2009, *Open Source vs. Closed Source Software: The Great Debate*. Available: http://www.site-reference.com/articles/Website-Development/Open-Source-vs-Closed-Source-Software-The-Great-Debate.html

[7] W. Y. Office. *Benefits of Using Open Source Software*. Available: http://open-source.gbdirect.co.uk/migration/benefit.html

[8] S. Steiniger and G. J. Hay, "Free and open source geographic information tools for landscape ecology," *Ecological Informatics,* vol. 4, pp. 183-195, 2009.

[9] G. Hertel, *et al.*, "Motivation of software developers in Open Source projects: an Internet-based survey of contributors to the Linux kernel," *Research Policy,* vol. 32, pp. 1159-1177, 2003.

[10] t. f. e. From Wikipedia. (2010, *Richard Stallman*. Available: http://en.wikipedia.org/wiki/Richard_Stallman

[11] H. E. Pearson, "OPEN SOURCE LICENCES: OPEN SOURCE -- THE DEATH OF PROPRIETARY SYSTEMS?," *Computer Law & Security Review,* vol. 16, pp. 151-156, 2000.

[12] C. Gacek and B. Arief, "The many meanings of open source," *Software, IEEE,* vol. 21, pp. 34-40, 2004.

[13] V. K. Georgios Gousios, Konstantinos Stroggylos, Panagiotis Louridas, Vasileios Vlachos and Diomidis Spinellis, "Software Quality Assessment of Open Source Software," presented at the 11th Panhellenic Conference on Informatics, PCI 2007, Athens, 2007.

[14] F. P. D. Luyin Zhao, "Exploratory inspection: a learning model for improving open source software usability," in *Conference on Human Factors in Computing Systems,CHI '06 extended abstracts on Human factors in computing systems* Montréal, Québec, Canada 2006, pp. 1589 - 1594

[15] A. de Groot, *et al.*, "Call for Quality: Open Source Software Quality Observation," in *Open Source Systems*. vol. 203, E. Damiani, *et al.*, Eds., ed: Springer Boston, 2006, pp. 57-62.

[16] W. Ming-Wei and L. Ying-Dar, "Open source software development: an overview," *Computer,* vol. 34, pp. 33-38, 2001.

[17] A. G. Koru, *et al.*, "Modeling the Effect of Size on Defect Proneness for Open-Source Software," in *Software Engineering - Companion, 2007. ICSE 2007 Companion. 29th International Conference on*, 2007, pp. 115-124.

[18] K. V. Herwig Mannaert, "The use of open source software platforms by Independent Software Vendors: issues and opportunities presented at the International Conference on Software Engineering,Proceedings of the fifth workshop on Open source software engineering 2005.

[19] T. Waring and P. Maddocks, "Open Source Software implementation in the UK public sector: Evidence from the field and implications for the future," *International Journal of Information Management,* vol. 25, pp. 411-428, 2005.

[20] M. Bloch. (2010, *Open source software in your online business - advantages/disadvantages* Available: http://www.tamingthebeast.net/articles5/open-source-software.htm

[21] (2007, *Disadvantages of open source software*. Available: http://blog.ecomsolutions.net/index.php/2007/12/18/disadvantages-of-open-source-software .

[22] (2010, *advantages and disadvantages of open source software*. Available: http://www.softwarecompany.org/advantages-open-source-software.html.

[23] D. M. G. Peter C. Rigby, Margaret-Anne Storey and "Open source software peer review practices: a case study of the apache server," presented at the International Conference on Software Engineering, Proceedings of the 30th international conference on Software engineering 2008.

Reinforcement Learning in Power System Scheduling and Control: A Unified Perspective

Imthias Ahamed T. P., *Member, IEEE*, Jasmin E. A. and Essam A. Al-Ammar, *Member, IEEE*

***Abstract*—Reinforcement Learning (RL) has been applied to various scheduling and control problems in power systems in the last decade. However, the area is still in its infancy. In this paper, we present various research works in this area in a unified perspective. In most of the applications, power system problems – control of FACTS devices, reactive power control, Automatic Generation Control, Economic Dispatch, etc – are modeled as a Multistage Decision making Problem and RL is used to solve the MDP. One important point about RL is, it takes considerable amount of time to learn a control strategy. However, RL can learn off line using a simulation model. Once the control strategy is learned decision making can be done almost instantaneously. A major drawback of RL is most of the application does not scale up and much work need to be done. We hope this paper will generate more interest in the area and RL will be utilized to its full potential.**

***Index Terms*-- Reinforcement Learning, multistage decision making problem, Power system scheduling, Reactive power control, power system stability.**

I. Introduction

REINFORCEMENT Learning (RL) is a powerful computational tool used for scheduling, decision making and control. Since the publication of two books [1], [2] in the last decade, RL was used for various applications [3-7]. Researchers in the power systems also have started working in this area for more than a decade. However, practical applications of RL in power systems are still in its infancy. The objective of this paper is to present various research works in this area in a unified perspective and raise issues to be addressed so that this powerful tool could be utilized more efficiently for solving power system problems.

RL is a computational tool that learns – the best schedule, decision, action or parameters – by interacting with an actual system or a simulation model. At the outset we would like to emphasize on three points as far as RL applications are concerned. (i) RL can give only approximate solution; hence it should not be used when good analytical tools are available. (ii) RL is a model free method in the sense that they do not require precise mathematical model. However, it requires a simulation model. (iii) Even though it can give only an approximate solution RL is not a trial and error approach. RL has sound theoretical foundation. It can be viewed as approximate dynamic programming [1].

Applications of RL in power systems can be classified into two streams

1. Power system problem is scheduled as a multistage decision making problem (MDP) and RL is used to solve the MDP.
2. RL is used for parameter tuning of an existing controller.

In this paper we give a brief overview of these two streams and highlight the issues to be addressed.

The rest of the paper is organized as follows. In section II, we give a brief overview of MDP and RL. In section III and IV, we explain different streams of RL applications in power systems. In section V, we discuss the issues to be discussed in the future work and paper is concluded in section VI.

II. Reinforcement Learning

In this section, we explain how RL can be used to solve an MDP. There are various types of MDP. Here to introduce RL, an N stage decision making problem is explained. Let the system be in state x_0 in stage 0. If we take an action a_0, system will move to next state x_1. When the system moves from state x_0 to x_1, it will incur a cost $g(x_0, a_0, x_1)$. In general, in the k^{th} stage, if we take an action a_k, system will move from x_k to x_{k+1} and will incur a cost $g(x_k, a_k, x_{k+1})$. For an N stage MDP, system will reach an absorption state in the N^{th} stage. The total cost incurred when we start from x_0 and reach final state is $\sum_{k=0}^{N-1} \gamma^k g(x_k, a_k, x_{k+1})$, where γ is the discount factor. γ is chosen a value between 0 and 1 depending on the significance of future costs.

MDP is the problem of finding actions a_0, a_1, a_2, ..., a_{N-1}, such that the total expected cost $E\left[\sum_{k=0}^{N-1} \gamma^k g(x_k, a_k, x_{k+1}),\right]$ is minimized. In general, the cost $g(x_k, a_k, x_{k+1})$ could be a random variable.

Imthias Ahamed is with Saudi Aramco Chair in Electrical Power, E.E. Department, College of Engineering King Saud University, P O Box 800, Riyadh 11421, Saudi Arabia (email: iparambath@ksu.edu.sa)

Jasmin E. A. is with Department of Electrical and Electronics Engineering College of Engineering, Thrissur, Kerala, India (email: eajasmin@gmail.com)

Essam A. Al-Ammar is with Saudi Aramco Chair in Electrical Power, E.E. Department, College of Engineering King Saud University, P O Box 800, Riyadh 11421, Saudi Arabia (email: essam@ksu.edu.sa)

When the system is in state x, we will take an action a based on some "policy". Usually, policy is denoted by Π ( ). Thus, if we are following a policy Π ( ), the action taken in state *x* is Π(x). We can think of Π as a mapping

$$\Pi : X \rightarrow A$$

where X is the state space and A is the action space. There are several algorithms to find optimal policy [1], [2]. Here, we explain one algorithm, the Q learning algorithm.

Q learning algorithm involves learning the Q values. Q value for a state action pair (x, a) is defined as the total expected cost, if we start from state x, take an action a, thereafter follow the optimal policy, Π*.
That is,

$$Q(x,a) = E\left[\sum_{k=0}^{N-1} \gamma^k g(x_k, a_k, x_{k+1})\right], \quad \text{Where}$$

$$x_0 = x, a_0 = a; a_k = \pi^*(x_k) \; for k = 1,..... , N-1.$$

Let the Q values for all possible actions { a_i, i = 1....m } in state x', i.e., Q (x', a_1), Q(x', a_2),.....Q(x', a_m), be known. Then if Q (x', a*) < Q (x', a_i) for all $a_i \neq a^*$, we say a* is the optimal action in state x'. Mathematically, we write,

$$a^* = \arg\min_{a'} Q(x', a') \quad \ldots\ldots\ldots (1)$$

Similarly, if the Q values for all state action pairs are known, then we can find the optimal policy or best action in any state x, using the equation, $\Pi^*(x) = \arg\min_{a'} Q(x, a')$. Thus, by learning Q–values for different possible state – action pairs, we can find the optimal actions. Therefore, to learn the optimal actions, we have to first learn the Q-values. To learn the Q-values, we proceed as follows. We start with an initial guess for $Q(x_k,a_k)$ which we denote as $Q^0(x_k,a_k)$. At each time instant *k* the system is in state x_k, we take an action a_k based on the current estimate of $Q^*(x_k, a_k)$, $Q^n(x_k, a_k)$. .
Based on the action chosen and dynamics of the system, we reach a new state x_{k+1} and incur a cost of $g(x_k, a_k, x_{k+1})$. Using this data, we update the Q- value for the current state action pair using the following equation

$$Q^{n+1}(x_k, a_k) = Q^n(x_k, a_k) + \alpha[g(x_k, a_k, x_{k+1}) + \gamma \min_{a' \in A_{k+1}} Q(x_{k+1}, a') - Q^n(x_k, a_k)] \quad \ldots (2)$$

Where 'α', the learning index, indicates how much the Q-values are modified in each step.

Similarly, Q values of the state, action pair corresponding to all the states visited are updated. After N stages, system will reach the terminal state; then we say an episode is over. In general, N can be a random number. To learn the Q values corresponding to all the relevant state action pairs, we start the iteration from a new initial state and update the Q values of all states visited till the system reach the terminal state. In this manner a large number of episodes are repeated.

An important issue in RL is how to select the actions during the learning phase. It may be noted that if we know the optimal Q values, we can find optimal actions using (1). However, in the initial part of the algorithm, the optimal Q values are unknown; but, we have an estimate of Q values, $Q^n(x,a)$. The best action with respect to the estimate of the Q values is termed as the greedy action. Greedy action is given by the equation,

$$a_g = \arg\min_{a'} Q^n(x, a') \quad \ldots. (3)$$

One straight forward approach used in many RL applications is known as the ε-greedy algorithm. In ε greedy algorithm, on reaching any state, greedy action is selected with probability 1- ε and any other random action with probability ε. Now the issue is how to choose ε. In the initial part of the algorithm, ε is chosen close to 1 and as algorithm proceeds, ε is reduced to zero. There are various other sophisticated methods to judiciously balance the exploration and exploitation in RL literature [1], [2], [8].

III. Power System Problems Formulated AS A multi stage decision making problem

Automatic Generation Control (AGC), Economic Dispatch (ED) and Unit commitment Problem are important scheduling problems in power systems [9]. In AGC, a decision of by how much power generation should be changed should be made every 2 minutes or so. In ED, a decision of how much each unit should generate in the next 30 minutes should be made. That is, a decision has to be made every 30 minutes. UCP also is a multi stage decision making problem. In UCP, the problem is to decide which all units should be committed in each time slot. In [10], [11], [12], AGC, ED and UCP are formulated as MDP and RL algorithms are developed to solve the problem. Power Systems are forced to operate at reduced stability margins due to economical and environmental restrictions [13]. Various power electronic devices are utilized for power system stability control. In [14], how RL can be used to control dynamic brake and thyristor controlled series capacitor (TCSC) is presented. RL is also used for reactive power control by deciding the value of off line control settings so that the reactive power of the PV busses remain within the specified bounds [15].

Automatic Generation Control should make sure that each area generation (P_G) should be equal to the sum of the total load in the area and scheduled tie line exchange [13] (P_L + P_{tie}). The mismatch between P_G and P_L + P_{tie} is known as Area and Control Error (ACE). It can be shown that ACE= Δf + $B\Delta P_{tie}$ [13], where B is known as the Area Frequency Response Characteristics. The objective of the AGC is to make sure that ACE remains around zero.

In [10], RL algorithm has been applied to solve the AGC problem. ACE and derivative of the ACE are used as state variables and the required change in generation as the decision variable. ACE and derivative of ACE are quantized to 11 and 3 levels so that the state space is finite. Similarly the required change in generation is quantized to 11 levels. The reinforcement function g (x_k, a_k, x_{k+1}) is chosen as follows
g (x_k, a_k, x_{k+1}) = 0 if |ACE| is within a tolerance band
= 1 if | ACE| is outside the tolerance band.

If ACE is available, RL algorithm presented in section II can be used to learn an AGC strategy. Authors have shown that RL algorithm works well with a simple simulation model.

They have also presented various choices for state variables and reward functions [10]

Consider a Power System with N generators G_1, G_2, … supplying a total demand of P_D MW. Economic Dispatch is the problem of **deciding** the generations P_1, P_2, … such that total cost of generation $\sum_{i=1}^{i=N} C_i(P_i)$ is minimized and the constraints given below are satisfied.

$\Sigma P_i - P_T - P_L = 0$

$P_i^{min} \le P_i \le P_i^{max}$ *for* $i = 1$ *to* N

In [11], Economic Dispatch problem is formulated as an N stage Multistage Decision making Problem; where N is the number of generating units. In the first stage, the decision to be made is how much G_1 should generate given the total demand P_D. To use RL to solve ED, state space X, action space A, reward function g and transition function or a simulation model has to be defined. In this problem

$X = X_1 \cup \quad \cup \cdots$

Where X_1 is the set of all possible states in stage 1. Since total demand on the power system should be within the capacity

$$X_1 = \left\{ x : \sum_{i=1}^{N} P^i{}_{\min} < x < \sum_{i=1}^{N} P^i{}_{\max} \right\}$$

Similarly in stage k, the power to be dispatched by the remaining N-k units should be such that it is within the capacity of the N-k units. Therefore,

$$X_k = \left\{ x : \sum_{i=k}^{N} P^i{}_{\min} < x < \sum_{i=k}^{N} P^i{}_{\max} \right\}$$

In this problem the decision to be made or action to be taken in each stage is the amount of power to be dispatched by each generator. Therefore action space is

$A = A_1 \cup \quad \cup \cdots$

$$A_k = \left\{ a : \quad P^i{}_{\min} < a < P^i{}_{\max} \right\}$$

It may be noted that in [11], state space X and action space A are discretized. Next we require a simulation model which will give the next state x_{k+1}, given the current state x_k and action a_k. In the case of ED the model is very simple. In the first stage, state is the total power to be dispatched. That is, $X_1=P_D$. In the second stage, state is the total power to be dispatched among the remaining units.

Therefore, $x_2 = P_D - a_1 = x_1 - a_1$. Similarly

$$x_{k+1} = x_k - a_k$$

Finally to use RL, reward function has to be defined so that the objective of the decision making problem is captured. In [11] the reward function used when system go from stage k to stage k+1 is cost of generation of stage k. Therefore,

$$g(x_k, a_k, x_{k+1}) = C_k(a_k)$$

Where C_k is the cost function of the k^{th} generator. It may be noted that

$$\sum_{k=1}^{N} g(x_k, a_k, x_{k+1}) = \sum_{k=1}^{N} C_k(a_k)$$

Which is the total cost of the generation and the constraints are met by choosing the state space and action space judiciously. Now using the algorithm explained in section II, the optimal schedule can be learned for all loads.

Consider a power system having N generating units with load schedule for T hours given. UCP is the problem of deciding which all units have to be committed in the next T hours so that the total production cost is minimized [9]. In [12] UCP has been formulated as a MDP and RL was used to find the optimal solution. Mathematically UCP can be stated as given below.

Minimize the objective function,

$$\sum_{k=1}^{T}\sum_{i=1}^{N} [C^i(P^i{}_k)u^i{}_k + ST^i(u^i{}_k)(1-u^i{}_{k-1})]$$

where T is the time period (number of hours) considered, $C_i(P_{ik})$ is the cost of generating power $P^i{}_k$ units of power during k^{th} hour by i^{th} unit, ST^i is the start up cost of the i^{th} unit, $u^i{}_k$ is the status of the i^{th} unit during k^{th} hour and $u^i{}_{k-1}$ is the status of the i^{th} unit during the previous hour. Note that the superscript denotes the generating unit index and subscript denotes the time index.

The constraints are,

$$\sum_{i=1}^{N} P^i{}_k u^i{}_k = L_k \qquad 1 \le k \le T;$$

$$P^i{}_{\min} u^i{}_k \le P^i{}_k \le P^i{}_{\max} u^i{}_k \quad 0 \le i \le N-1; \quad 1 \le k \le T$$

$$T^i{}_{OFF} \ge D^i; \qquad T^i{}_{ON} \ge U^i \quad 0 \le i \le N-1;$$

Where

L_k - Load demand during hour k

$T^i{}_{OFF}$ – Number of hours the i^{th} unit has been OFF (down),

$T^i{}_{ON}$ – Number of hour's i^{th} unit has been ON (up)

U^i - Minimum up time of i^{th} unit.

D^i – Minimum down time of i^{th} unit.

The above problem can be viewed as a MDP. Each stage corresponds to a time slot. If we take one hour as a time slot, then the first hour is the first stage, and a T hour problem is a T stage problem. To apply RL, we have to define state space, X, action space A, simulation model and reinforcement function $g(x_k, a_k, x_{k+1})$.

First we give the definition of the action space A. The decision to be made in each stage is which all units have to be ON and which all units have to be OFF. Therefore, the action space is an N dimensional vector where N is the number of units. The decision in the k^{th} stage is denoted by a_k where $a_k = [a^1{}_k, a^2{}_k, ..., a^N{}_k]$ $a^i{}_k \in \{0,1\}$. Thus the action space

$$A = \{([a^1, a^2, ..., a^N]) : \quad a^i \in \{0,1\}$$

In each stage a decision is to be made based on the state of the system. State of the system should capture the necessary information to make the decisions in each stage. In the case of UCP state space, X, of the system is given by [12]

$X = X_1 \cup X_2 \cup \ldots X_T$

Where,

$$X_k = \quad \{(k, [p^1{}_k, p^2{}_k, ..., p^N{}_k]) : \quad -T \le p^i{}_k \le T\}$$

If $p^i{}_k > 0$, it denotes the number of hours unit has been ON up to the K^{th} hour. If $p^i{}_k \le 0$ it denotes the number of hours unit has been OFF up to the K^{th} hour.

To lean the optimal policy we also require a simulation model. That is, if

$x_k = [p^1{}_k, p^2{}_k, ..., p^N{}_k]$ and $a_k = [a^1{}_k, a^2{}_k, ..., a^N{}_k]$ are given we should be able to find x_{k+1} The transition function or an algorithm for finding x_{k+1} is given below.

$$\begin{aligned}
&if \quad p^i{}_k \le 0 \quad and \quad a^i{}_k = 1 \quad then \quad p^i{}_{k+1} = 1\\
&if \quad p^i{}_k \le 0 \quad and \quad a^i{}_k = 0 \quad then \quad p^i{}_{k+1} = p^i{}_k - 1\\
&if \quad p^i{}_k > 0 \quad and \quad a^i{}_k = 1 \quad then \quad p^i{}_{k+1} = p^i{}_k + 1\\
&if \quad p^i{}_k > 0 \quad and \quad a^i{}_k = 0 \quad then \quad p^i{}_{k+1} = -1\\
&if \quad p^i{}_{k+1} > T \quad then \quad p^i{}_{k+1} = T\\
&if \quad p^i{}_{k+1} < -T \quad then \quad p^i{}_{k+1} = -T
\end{aligned}$$

Finally to use the RL algorithm given in section 2, we have to define a reinforcement function. The reinforcement function used in [12] is given below.

$$g(x_k, a_k, x_{k+1}) = \sum_{i=1}^{N} [C^i(P^i{}_k)u^i{}_k + ST^i(u^i{}_k)(1 - u^i{}_{k-1})]$$

Once state space, action space, transition function and reward function are defined RL algorithm explained in section 2 can be used to find the optimal schedule. It may be noted that RL frame work allows flexibility in these choices. The ingenuity of the researchers is required in making these choices. In [16], effects of various choices of state variables are analyzed.

Another early work in application of RL in power systems is given in [14]. In this paper RL is used to decide when the resistive brake should be switched ON. The objective here is to damp large electro mechanical oscillations and loss of synchronism following a fault. An additional objective is to limit the time during which brake is switched ON. So in this case state space X, action space A, and reward function are designed keeping this objective in mind. The action space is given by A = {0, 1}. Zero denotes brake is OFF and '1' denotes brake is ON.

State should capture relevant information required to make the correct decision. In [14], a power system consisting of 4 generators and few loads are considered. Power system is grouped as two areas, with each area consisting of two generators. The relative angle and relative speed are considered as state variables. Therefore, state space $X = \{(\delta, \omega) : \delta \in [-\pi, \pi]; \quad \omega \in [-\omega_{\max}, \omega_{\max}]\}$. Now the reward function is chosen such that the objective is captured. The reward function used in [14] is given below.

$$\begin{aligned}
g(x_k, a_k, x_{k+1}) &= -|\omega_k| - ca_k \qquad if \ |\delta_k| \le \pi\\
&= -1000 \qquad if \ |\delta_k| > \pi
\end{aligned}$$

C determines by how much the algorithm penalizes for switching the brake ON. A very high negative reward is given for loosing synchronism. Depending on the action selected, simulation model of the 4 generator system gives the reward function and the next state x_{k+1}. In [14], to learn optimal policy Q – values are learned using model based learning method [1,2]. In model based learning instead of learning Q-values directly, transition probabilities $P(x_{k+1} / x_k, a_k)$ are first learned; hence Q-values are learned by solving the Bellmans equation.

$$Q(x_k, a_k) = g(x_k, a_k, x_{k+1}) + \gamma \sum_{x_{k+1} \in X} P(x_{k+1} / x_k, a_k) \max_{a' \in A} Q(x_{k+1}, a')$$

In [14], RL algorithm is also used to control TCSC devices [17]. The objective is to find appropriate value of series reactance so as to damp power system oscillations. In [14], action set is chosen as A= { -61.57, -46.18, -30.78, -15.39, 0}. The decision is to be made based on the present power flow and previous power flows and previous actions. The state is chosen as $x_k = (Pe_k, Pe_{k-1}, Pe_{k-2}, u_{k-1}, u_{k-2})$. Therefore, the state space is

$$X = \left\{ \begin{array}{r} (Pe_k, Pe_{k-1}, Pe_{k-2}, u_{k-1}, u_{k-2}) : P \in [-250, 250]; \\ u \in [-61.57, 0] \end{array} \right\}.$$

For the case study reported, power flow is less than 250 MW and *Pe* is discretized to 100 values and *u* is discretized to 5 values, which will result in a huge state space 25,000,000 (=100x100x100x5x5). The reward function chosen in [14] is given below

$$\begin{aligned}
g(x_k, a_k, x_{k+1}) &= -\left|Pe - \overline{Pe}\right| \qquad if \ |Pe| \le 250MW\\
&= -1000 \qquad if \ |Pe| > 250MW
\end{aligned}$$

Where $\overline{Pe}$ is the expected power flow through the transmission lines. From the reward function, we can see that penalty increases as power flow deviates from $\overline{Pe}$. States are obtained every 50ms and decisions are made based on ε-greedy algorithm. After 10hrs of learning, TCSC could limit the fluctuations in power flow.

In [15] RL algorithm is used to decide the values of off line control settings so that reactive power at PV busses and power flow along transmission lines are within specified bounds. These variables are called as constrained variables. To develop an RL algorithm, authors have modeled sequence of load flow solutions as an MDP. The state of the system can be determined from the solution of the load flow problem. Solution of the load flow consists of magnitude and angle of the node voltages. If solution of load flow and the constrained variables are chosen as the state of the MDP, the state space will become huge. In [15], authors have defined the state of the MDP as follows. Only constrained variables are chosen as state of the MDP and they are limited to take only binary values. The binary value corresponding to a constrained variable is taken as "0" if constrained is not violated else it takes a value "1". Thus state space is defined as

$$X = \{(b_1, b_2, ..., b_n) : b_i \in \{0, 1\}\}$$

Where n is the number of constrained variable and there will be 2^n elements in the state space.

Action set, A, is the off line control settings. For example, if there are 3 tap settings and one reactive compensation to be decided, action set is defined as follows [15]

$$A = \left\{ \begin{array}{r} (tap_1, tap_2, tap_3, b) : tap_i \in \{0.9, 0.91, 0.92, ..., 1.05\}; \\ b \in \{0, 0.03, ..., 0.27\} \end{array} \right\}$$

Reward function is chosen such that a negative reward is given whenever a constrain is violated. The magnitude of the negative reward increases as the number of constrains violation increases. The specific reward function chosen in [15] is given below.

$$g = -\frac{1}{n}\sum_{j=1}^{n}\left|\frac{2z_j - z_{j\max} - z_{j\min}}{z_{j\max} - z_{j\min}}\right|.$$

The new state of the MDP and reward function is obtained by solving the load flow equation. An optimal policy is learned using an algorithm similar to the given in section II.

IV. RL FOR PARAMETER ESTIMATION OF CONTROLLERS

RL algorithms have been used for finding the optimal values of controllers used in power systems. In [18], RL is used to find the optimal parameters of PID controller for Automatic Voltage Regulator (AVR) system. In [19], RL approach is used to find the gain of power system stabilizer (PSS).

AVR is used in power system to hold the terminal voltage of synchronous generator at a specified value. This regulator problem can be solved using PID controllers. However, for a power system, finding parameters of the PID controller-- K_P, K_I, K_D is challenging. In [18], Continuous Action Reinforcement Learning Algorithm (CARLA) is used to find K_P, K_I, K_D. In each learning step K_P, K_I, K_D are selected based on a cumulative probability distribution function (CPDF). Initially CPDF is chosen as a uniform distribution function and random values are selected for K_P, K_I, K_D; the step response of the system is obtained using simulation. From the step response the performance measures are obtained, using these measures CPDF are updated so that the CPDFs approach to Gaussian distribution with mean value near the optimal values.

Fast acting AVRs introduce negative damping. To improve the damping lead-lag compensators known as PSS are used. The transfer function of the PSS is of the form

$$G(s) = K\frac{1+sT_1}{1+sT_2}\frac{1+sT_1}{1+sT_2}.$$

In [19], RL algorithm is used to find optimal value of K. The choice of X, A, transition function and reward function is given below.

X={1,2,….,32}

A={+1,-1}

Transition function is $x_{k+1} = x_k + a_k$

$g(x_k, a_k, x_{k+1}) = 100$ if damping ratio > a specified value

= -1 if damping ratio < a specified value

V. ISSUES AND DIRECTIONS FOR FUTURE WORK

In the last two sections, we have seen several applications of RL in power systems scheduling and control. All applications involved choice of state space X, action space A and reward function g. For the same problem, there are various ways of choosing X, A and g. Here we discuss some issues in the choice of X, A and g, and give guide lines in choosing them.

"State" in the context of RL need not be the dynamic state of the system as defined in control system. It just need be the minimum information required to make appropriate decisions. For example, in the case of load frequency control of power system, state may be defined as the average value of frequency. To decide whether to increase or decrease generation can be made based on the current and past values of frequencies. It may be recalled that in [15], authors have not defined the entire solution of power flow as state variable but they have only used the status of the constrained variables as state. Another issue in defining the state variable is we should be able to obtain or compute the state from the actual system or the simulation model.

Another important issue while deciding the state variable is learning and storage of Q values. In almost all practical applications state variables and action variables are continuous and they are discretized so that number of (x,a) pair are finite. In all the applications, of RL presented in section III and IV state and action variable are discretized and Q values are stored in tables. If discretization step is small, table will become huge. For example, if $x = (P_1, P_2, P_3, P_4)$ say the power flows and $a = (tap_1, tap_2, tap_3)$ three tap settings and if power is discretized to 100 levels and tap setting to 10 levels, number of elements in the state space will be 10^8 and number of elements in the action space will be 10^3. Thus to store Q values, we require an array of size 10^{11} or a two dimensional matrix of size 10^8 x 10^3. The problem is not only with storage, time required for learning also will be exorbitant. It may be recalled that estimates of Q values in (2) will converge to optimal Q value only if all (x,a) pairs are visited infinitely often [1], [2]. Practically if we take 100 iterations as a large number, we require $100x10^{11}$ iterations to obtain a good approximation for Q values. In RL literature, various approaches like state aggregation and function approximation are present [1], [2], [20], [21]. In RL applications to power systems, neural networks [21] have been used for function approximation with some success [22], [23].

In most application choice of action space is straight forward. However, in many situations, action variables are continuous. Therefore, we have to discretize the action variable. If we go for very small discretization step, learning will be slow. Hence discretization step has to be judiciously chosen.

In most applications RL has been shown to perform well on simple systems. It is difficult to scale up the algorithms on systems of practical size as state space will become huge. Further work needs to be done to make the algorithms scale up.

VI. CONCLUSIONS

In this paper, we have reviewed various RL applications to power system scheduling and control. In particular, we have seen in a unified perspective how state space, action space and reward function are chosen for solving AGC problem, Economic Dispatch, UCP, controlling FACTS devices, reactive power control, tuning of AVR and PSS using RL algorithms. We hope this would provide guide lines for designing RL algorithms for other power system problems.

Even though there are various research work in this field, practical applications of RL in power system is still at its infancy. Further work need to be done to scale up the algorithms. One major issue in scaling up is the choice of state variable so that state space is not huge and Q values can be learned in reasonable time. By smart choice of state variables size of state space can be reduced. By using state aggregation and function approximation Q-values can be efficiently stored and learned. Further work need be done in this direction.

ACKNOWLEDGMENT

The authors are thankful to Saudi Aramco Chair in Electrical Power, King Saud University, Riyadh for supporting this work.

VII. REFERENCES

[1] D.P.Bertsekas, J.N.Tsitsikilis. Neurodynamic Programming, Athena Scientific, Belmount,MA., 1996.

[2] R.S.Sutton, A.G.Barto. Reinforcement Learning: An Introduction, Cambridge, MA:MIT Press, 1998

[3] G.J. Tesauro, TD Gammon. "Temporal difference Learning and TD gammon", Communications of ACM, 38 (3) (1995): 58 – 67.

[4] Robert H.Crites, Andrew G.Barto, "Elevator control using multiple Reinforcement Learning Agents" Kulwer Academeic Pulishers, Boston ,(1997).

[5] Hirashi Handa, Akira Ninimy, "Adaptive state construction forReinforcement Learning and its application to Robot Navigation problem", IEEE Transaction on Industrial Electronics, 7(2) 1436: 1441, 2001.

[6] Andrew Y.N., A.Coats, M.Diel, V.Ganpapthi, "Autonomous helicopterflight via Reinforcement Learning" Symposium on Experimental robotics, (2004).

[7] Farhad Sahba, Hamid R.Tizhoosh, "Application of Reinforcement Learning for segmentation of transrectal ultra sound images", BMC Medical Imaging, 2008

[8] M.A.L.Thathachar and P.S.Sastry, *Networks of Learning Automata: Techniques for on line stochastic optimization,* Boston: Kulwer Academic (2003).

[9] A.J.Wood, B.F.Wollenberg., "Power Generation and Control" John Wiley Sons 2002.

[10] T.P.Imthias Ahamed, P.S.nagendra Rao, P.S.sastry "A Reinforcement Learning approach to automatic generation control" Electric Power System research 63 (2002): 9-26

[11] E.A.Jasmin, T.P.Imthias Ahamed, V.P.Jagathiraj. *A Reinforcement Learning Algorithm for Economic Dispatch considering transmission losses,* Proceedings of IEEE International Conference (TENCON 2008), University of Hyderabad, November 2008.

[12] E. A. Jasmin, T. P. Imthias Ahamed, V. P. Jagathy Raj, Efficient Reinforcement Learning solution to Unit Commitment Problem through state aggregation*", Proceedings of International Conference on Control, Communications and Computing (ICCC 2010), College of Engineering, Trivandrum*, February 2010.

[13] P. Kundur, Power System Stability and Control. New York: McGraw-Hill, 1994.

[14] D. Ernst, M. Glavic and L. Wehenkel, " Power systems stability control : Reinforcement learning framework ", IEEE Transactions on Power Systems, February 2004, Volume 19, pages 427-435.

[15] John G. Vlachogiannis and Nikos D. Hatziargyriou, "Reinforcement Learning for Reactive Power Control", IEEE Transactions on Power Systems, August 2004, Volume 19.

[16] Jasmin.E.A. " Reinforcement Learning Approaches to Power System Scheduling", Ph.D Thesis, Cochin University of Science and Technology (2009).

[17] N. G. Hingorani and L. Gyugyi, *Understanding FACTS.* New York:IEEE Press, 2000.

[18] Mohammad Kashki, Youssef Lotfy Abdel-Magid, and Mohammad Ali Abido, "A Reinforcement Learning Automata Optimization Approach for Optimum Tuning of PID Controller in AVR System" Advanced Intelligent Computing Theories and Applications. With Aspects of Artificial Intelligence Lecture Notes in Computer Science 2008 Springer Berlin

[19] Hadidi, R. and Jeyasurya, B. "Reinforcement learning approach for controlling power system stabilizers", Canadian Journal of Electrical and Computer Engineering, 2009 pg 99-103

[20] Simon Haykin, Neural Networks: A Comprehensive Foundation, New York -1998

[21] Benjamin Van Roy, "Learning and Value Function Approximation in Complex Decision Processes", Department of Electrical Engineering and Computer Science, Massachusetts Institute of Technology 1998

[22] T. P. Imthias Ahamed ; P.S., Nagendra Rao; and P.S., Sastry (2006) "A Neural Network Based Automatic Generation Controller Design through Reinforcement Learning," *International Journal of Emerging Electric Power Systems*: Vol. 6 : Iss. 1, Article 6.

[23] E. A. Jasmin, T. P. Imthias Ahamed, V. P. Jagathy Raj, "Neural Network solution to Economic Dispatch through Reinforcement Learning", Proceedings of National Power System Conference , IIT Bombay, pp: 84 -89, December 2008.



Imthias Ahamed (M2009) was born in Tellicherry, India in 1966. He received his B.Tech degree in electrical engineering from Kerala university and M. Tech degree in Instrumentation and control from NIT-Calicut, India. He obtained his Ph.D from Indian Institute of Science, Bangalore, India in 2002. He is now an assistant professor in Electrical Engineering Department, King Saud University, Riyadh, Saudi Arabia. His current research include Reinforcement Learning, Neural Network and power system scheduling and control.



Jasmin.E.A was born in North Parur of Ernakulam district in 1974. She obtained her B.Tech from T.K.M.College of Engineering, Kollam, Kerala in the year 1995 and took M.Tech in Computer and Information sciences from School of Computer science, Cochin University of Science And Technology in 1997 and Ph.D from Cochin university of science and Technology in 2009. She is now serving as Senior lecturer at Govt. Engineering College, Thrissur, India. Her research interests include power system control and Reinforcement learning.



Essam Al-Ammar was born in Riyadh, Saudi Arabia. He received his BS degree (honor) in Electrical Engineering from King Saud University in 1997. From 1997-1999, he worked as a Power/software engineer at Lucent Technologies in Riyadh. He worked as an Instructor at King Saud University between 1999-2000. In 2003, he received his MS degree from University of Alabama, Tuscaloosa, AL, and the Ph.D. degree from Arizona State University in 2007. He is now an assistant professor in Electrical Engineering Department, King Saud University, Riyadh, Saudi Arabia. His current research and academic interests include dry-band arcing on fiber-optic cables, high voltage engineering, power system transmission, distribution and protection.

A Robust Mobile Business Card Reader Using MMCC Barcode

Siong Khai Ong, Douglas Chai and Alexander Rassau
School of Engineering
Edith Cowan University
270 Joondalup Drive
Joondalup WA 6027
Perth, Australia

***Abstract*—Business cards have existed since the 19th century and exchanging of business cards is common during introduction. The digital version, an electronic business card, helps to share information quickly and accurately. Also, it allows information to be stored and easily located. However, the current state of the art in business card readers using OCR technology usually fail in correctly reading all elements of the business card. Hence, in this paper, we proposed the use of an Mobile Multi-Colour Composite (MMCC) barcode printed on the business card. Containing the electronic version of the business card, the MMCC barcode allows cheap and accurate reading of the business card with a mobile phone camera. To highlight the effectiveness of the proposed method, we compared the results against commercially available business card readers, both in desktop and mobile versions.**

I. Introduction

Since the 19th century, the business card has been commonly used in promoting a person or business [1]. An example of such cards can be seen in Fig. 1. During introductions between two or more persons, the card is usually exchanged as an ice-breaker and it serves as a good memory aid to remember the person and their contact details.

Business cards contain information about their owners and the basic function of marketing the person has not changed over the years [2]. Obviously, more types of information such as telephone number, facsimile, mobile number, and email are included in today's business card as those types were not available then. Fig. 2 shows one of the business cards that is commonly used today.

Exchanging of information through digital means can ensure that information is shared quickly and accurately. An electronic business card allows information to be stored, organised and easily retrieved when required.

This led to the creation of vCard, one type of format for electronic business cards, which allows exchanges of information between different applications and systems as vCard is defined independent of the transportation method used to exchange information [3]. There are other formats that are available but in this paper, we will be using the vCard format as it is one of the most commonly used.

In order to convert a business card into digital form, often a business card reader is used. The current state of the art for business card readers using optical character recognition

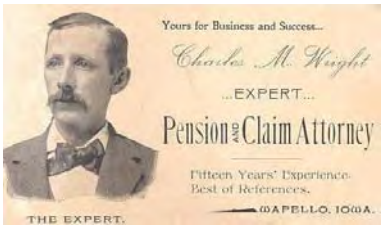


Fig. 1: An example of a business card used in 19th century [4]



Fig. 2: An example of a business card used today

(OCR) technology are still limited in their ability to provide 100% accuracy in recognition of the card. This is because business cards are designed differently from one another and it is challenging for the recognition algorithm to recognise all different design possibilities.

Also, an error can occur in types of information that has "zero error tolerance", such as email and phone numbers. When this happens, the whole process becomes useless.

Instead of solely depending on OCR technology to provide an accurate read out of the business card, a cheap and reliable method is to encode the digital version of the card (i.e. electronic business card) into a high data capacity barcode. Thereafter, the barcode is printed onto the business card. This allows the user to obtain the electronic business card easily by just capturing the image of the barcode, using a mobile phone camera.

A suitable high data capacity barcode for this application is the Mobile Multi-Colour Composite (MMCC) code. The MMCC barcode is a colour two dimensional (2D) barcode developed at Edith Cowan University for use with mobile

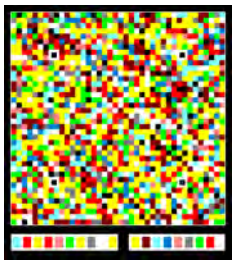


Fig. 3: An example of an MMCC barcode

phone camera [5]. An example of an MMCC barcode is presented in Fig. 3. There are other barcodes that might be suitable for this application. However, due to their limited data capacity, not all the important information that are shown on the business card can be encoded into these barcodes.

The aim of this paper is to propose the use of the MMCC barcode as part of a business card, so as to provide a cheap and accurate way to obtain the information shown on the business card electronically. Also, the electronic business card encoded into the MMCC barcode will be captured using a mobile phone camera to leverage on the mobility of the mobile phone and provide a convenient business card reader.

To highlight the effectiveness of this proposal, the accuracy will be tested against existing commercially available business card readers in both the desktop and mobile types.

This paper is organised as follows:

- A brief introduction to business cards and electronic business cards have been provided in this Section.
- In Section II, various types of business card reader and limitations in the current state of the art for business card readers are highlighted.
- Section III presents the proposed solution, using an MMCC barcode as an electronic business card.
- Experimental setup and results are presented in Section IV.
- Conclusions can be found in Section V.

II. Types of Business Card Reader

Generally, there are two different types of business card reader, both of which use OCR technology to extract the information found on business cards. One of them is the desktop business card reader while the other is the mobile business card reader.

A. Desktop Business Card Reader

A business card reader is a dedicated scanner that captures the images of the business card. The information shown on the card is extracted from the captured images using OCR technology. Usually, such business card readers are linked to a desktop computer or laptop. One such business card reader is illustrated in Fig. 4 and in this paper, this is referred to as a desktop business card reader.

After the information shown on the business card is extracted, these information is often imported into a contact organiser or saved as an electronic business card for easy organisation, storage and look-up.



Fig. 4: An example of a desktop business card reader



Fig. 5: An example of a business card reader operating on a mobile phone [7]

B. Mobile Business Card Reader

Over the last decade, there has been significant increase in the number of mobile phones [6] globally. Also, camera equipped mobile phones are becoming more common today. The mobile phone camera facilitates the business card reader to be "mobile" when a business card reader is installed onto the mobile phone. One example of such a business card reader is depicted in Fig. 5 and this is referred to as a mobile business card reader in this paper.

Using the mobile phone camera, the image of the business card is captured. Similar to the desktop business card reader, the mobile card reader also uses OCR technology to retrieve the information shown on the business card from the captured image.

Once the information is retrieved, the mobile card reader will import these information into a mobile contact organiser or simply saved it as an electronic business card.

C. Limitations in OCR Technology

Although the current state of the art in OCR technology can be considered quite accurate, any error in the recognition can cause the scanning process to be useless. This is especially true if the error occurs with a type of information which has "zero error tolerance", such as an email address or telephone number.

Since business cards are designed differently from each other, 100% correctly recognising all information becomes challenging and difficult for the OCR technology [8]. This is often true and can be seen from our experimental results in this paper, which will be presented later.

III. Use of MMCC as an Electronic Business Card

A cheap and reliable solution can be achieved through the use of a high data capacity barcode. The digital version of the



Fig. 6: An example of an MMCC barcode used on a businees card

business card is encoded into the barcode. In most cases, the information contained in the electronic business card can be similar to the physical business card. The "electronic business card" barcode is then printed onto the business card. An example of such a business card is highlighted in Fig. 6.

The user can retrieve information that is stored in the barcode by capturing the image of it using a mobile phone camera. With a barcode decoder, the mobile phone will extract the information of the electronic business card that is stored in the barcode. Similarly to both the desktop and mobile business card readers, the information can then be saved into a contact organiser or as an electronic business card, such as vCard.

Another advantage of using a high data capacity barcode to store information is that it allows the user to know whether the retrieved information is 100% accurate. If not, the user can just re-capture the barcode's image. However, in both the desktop and mobile business card readers, this is not possible as there is no error correction ability embedded in this approach. Hence, in order to ensure all the recognised information is correct, the user will have to manually compare the physical business card with the results produced.

In order to determine the suitability of the type of barcode used, we will need to first consider the types of information that the high data capacity barcode will need to encode. As much as possible, it shall encode all information that is found on the business card. However, it might not be possible as the amount of data capacity in the barcode has a limit.

A. Limitation in Barcode's Data Capacity

There are two ways to increase the data capacity of the barcode:

- having more cells, and/or
- having more colours.

However, both ways have their limitations.

When more cells are used, the physical size of those cells will be smaller. As our application is operating on a mobile phone, often images captured by the mobile phone camera can be blurred and together with the Joint Photographic Experts Group (JPEG) artifacts[1], correctly decoding the barcode can be challenging. Furthermore, the physical size of the whole barcode shall be small so that it can be printed on the existing business card.

[1]Currently, most mobile phone camera save images captured in JPEG.

TABLE I: Common types of information found in business card

S/No	Type of Information	Occurrence (%)
1	Name	100.0
2	Organisation	97.1
3	Job Title	76.5
4	Telephone number	82.4
5	Mobile number	82.4
6	Facsimile	79.4
7	Address	94.1
8	Universal Resource Locator (URL)	58.8
9	Email	88.2

If more colours are used, the Euclidean distance between each symbol will be closer to each other and this increases the risk of wrongly decoding the symbol. Also, the number of colour used should be limited so that the printing cost of the business card can still remain economical.

Hence, it is important to consider the types of information that are going to be encoded into the barcode so that the barcode can fulfilled its role as a robust electronic business card.

B. Information Commonly Found in Today's Business Cards

Although the business card's basic function of marketing its owner has not changed over the years, there are more types of information found in today's business cards. In this paper, 34 different business cards are used. Some types of information can be commonly found in those business cards while some are not.

In TABLE I, the nine different types of information that are most commonly found is presented.

Some of the business cards do contain other types of information such as the owner's qualification, business products and certification. However, such information is less than 10% of the 34 cards used in this paper. Hence, those types of information will not be considered in this paper.

C. Data Capacity Required for Barcode

In this paper, the vCard format is used as the electronic business card. It is one of the most commonly used formats for electronic business cards and the version used is 2.1 [3].

Based on the vCard format used and the types of information presented in TABLE I, the data capacity required to encode the barcode ranges from 135 to 352 bytes for those 34 business cards used in this paper.

D. Some Common Types of Barcode

Traditionally, one dimensional (1D) barcodes such as the one depicted in Fig. 7 have always been index to a database, and not the database entries themselves. This is because the data capacity of the 1D barcode is too low to fulfil the role as a database.



Fig. 7: An example of a traditional 1D barcode



Fig. 8: An example of a QR code

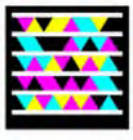


Fig. 9: An example of a Microsoft Tag [11]

TABLE II: Summarised findings of barcodes' suitability for business card application

Type of Barcode	Portable Database	Data Capacity more than 352 bytes
Traditional 1D barcode	No	No
Microsoft Tag	No	-
QR Code	Yes	No
MMCC barcode	Yes	Yes

However, newer barcode systems are becoming portable databases themselves and there is need for greater data capacity in order to fulfil the role as a database. Due to the need for greater data capacity, we are witnessing the evolution of barcodes from 1D to 2D [9].

One common 2D barcode that has been used widely is the Quick Response (QR) code developed by Nippondenso IS System [10]. An example of a QR code is shown in Fig. 8.

Microsoft's version of a colour 2D barcode called Microsoft Tag is highlighted in Fig. 9. As the Microsoft Tag reader requires an internet connection [11] to get the information associated with the barcode, it seems like the Tag is functioning more as an index, rather than as a portable database.

As mentioned earlier, another colour 2D barcode is the MMCC barcode which is illustrated in Fig. 3. MMCC is a high data capacity barcode which is designed for use with mobile phone cameras [5].

The use of QR code [8] and Microsoft Tag as electronic business cards are not something new. However, they are not suitable in this paper. The reasons are summarised in TABLE II.

Two important factors, whether are they portable database and their data capacity, must be considered. A suitable barcode for this paper will need to be a portable database. The traditional 1D barcode and Microsoft Tag are not considered in this paper as they function as an index to the database. If used, the mobile phone will require an internet connection in order to retrieve the information found in the electronic business card.

At times, especially when in overseas, an internet connection can be considered costly for such application. Furthermore, there is also possibility that there is no internet connection especially when the user is in remote area [12] or out to the sea. Holding on to the barcode and then captured it when there is data connection later on, defeat the purpose of leveraging the mobility provided by the mobile phone.

The barcode used in this paper must be capable of encoding at least 352 bytes of data. The 352 bytes exclude error correction. Hence, the total data capacity will have to be greater than 352 bytes. Also, the physical size of the barcode will be about 4 cm^2 and must still able to be decoded by the mobile phone. In this paper, the mobile phone used is a HTC Touch Diamond.

In our previous works [13], the QR code with data capacity of more than 250 bytes at about 9 cm^2 is not decodable by the HTC Touch Diamond. Therefore, QR code is not suitable for this paper due to its low decodable data capacity.

IV. Experimental setup and results

The First Read Rate (FRR) and Success Read Rate (SRR) are commonly used to validate the useability of barcode [14]. With a high FRR, it will mean that the barcode is easily read successfully at the first attempt. Having a high SRR, the barcode will be successfully decoded in most attempts.

The FRR and SRR can be computed based on the following:

$$\text{FRR} = \frac{\text{No of successful first read}}{\text{No of first read attempts}} \quad (1)$$

$$\text{SRR} = \frac{\text{No of successful read}}{\text{No of attempted read}} \quad (2)$$

To highlight the efficiency of the proposed method, the desktop and mobile business card readers are used to compare against the MMCC barcode in terms of FRR and SRR.

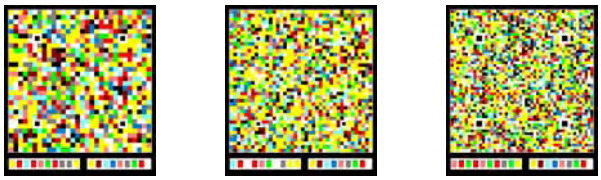
The desktop version used in this paper, CardScan executive, is a dedicated scanner linked to the desktop computer via a USB cable. After the business card is scanned, the desktop business card reader will extract the information of the card using the proprietary software[2] that is supplied together with the desktop card reader.

As for the mobile version, the WorldCard Mobile, installed on the HTC Touch Diamond is used for comparing the results against the proposed method. The business card image is captured using the mobile phone camera as shown in 10. After the image is captured, the business card reader installed on the mobile phone will extract the information of the business card using OCR technology.

[2]CardScan Executive, version 8.0.5.



Fig. 10: Capturing of image for mobile business card reader



(a) 30 by 30 cells (b) 40 by 40 cells (c) 50 by 50 cells

Fig. 11: Examples of different versions of MMCC barcode used

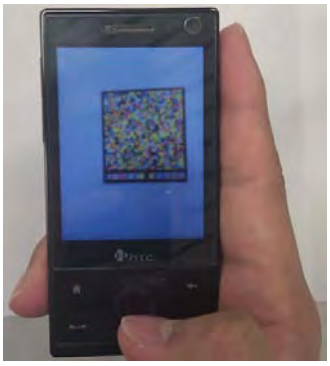


Fig. 12: An example of the way MMCC barcode is captured



Fig. 13: An captured image of the MMCC barcode

A. MMCC Encoder and Decoder

The encoder of the MMCC barcode has been developed using MATLAB and the colour barcode is printed with a physical size of 20 mm by 22.5 mm. Depending on the data capacity required to encode the electronic business card, three basic versions of the MMCC are used in this paper, namely 30 by 30 cells, 40 by 40 cells and 50 by 50 cells. The three different versions are presented in Fig. 11.

The decoder used for MMCC barcode is developed using Microsoft Visual Studio .NET Compact Framework environment with C#. This decoder is running on a HTC Touch Diamond mobile phone, a Windows Mobile 6.1 phone, with a 3.2 mega pixel camera.

All testing (including the mobile business card reader) are conducted in an office lighting environment. The barcode is captured using the mobile phone camera as presented in Fig. 12. Once the image is captured, the MMCC decoder will localise the barcode and decode the information stored in the barcode. An example of a captured MMCC barcode is illustrated in Fig. 13.

TABLE III: Resultant of the methods used

Method	Result of first read attempt
Desktop business card read	BEGIN:VCARD VERSION:2.1 N:Chai;Douglas;;Dr ORG:Australia TITLE:Senior Lecturer TEL;WORK;VOICE:(61 8) 6304 5874 TEL;WORK;FAX:(61 8) 6304 5811 ADR;WORK;PREF:;;100 Joondalup Drive; Joondalup;Western Australia;6027 URL;WORK:d.chai ecu.edu.auCRICOS IPC002796 END:VCARD
Mobile business card reader	BEGIN:VCARD VERSION:2.1 N:Dr Douglas Chai ORG:SCHOOL OF ENGINEERING TITLE:Senior Lecturer TEL;WORK;VOICE:(6i8)63045874 TEL;WORK;FAX:(618)63045811 ADR;WORK;PREF:;;100 Joondalup Drive, Joondalup Western Australia 6027 EMAIL:d.chai@ecu.edu.au END:VCARD
MMCC barcode	BEGIN:VCARD VERSION:2.1 N:Chai;Douglas;;Dr ORG:Edith Cowan University TITLE:Senior Lecturer TEL;WORK;VOICE:(61 8) 6304 5874 TEL;WORK;FAX:(61 8) 6304 5811 ADR;WORK;PREF:;;100 Joondalup Drive; Joondalup;Western Australia;6027 EMAIL:d.chai@ecu.edu.au END:VCARD

B. Results

Using the business card shown in Fig. 2 as an example, the outputs of the MMCC barcode, desktop and mobile business card readers are presented in TABLE III. The outputs are resulted from the first read attempts of the three methods.

TABLE IV: Data encoded in MMCC barcode for the business card shown in Fig. 2

Data encoded in MMCC barcode
BEGIN:VCARD
VERSION:2.1
N:Chai;Douglas;;Dr
ORG:Edith Cowan University
TITLE:Senior Lecturer
TEL;WORK;VOICE:(61 8) 6304 5874
TEL;WORK;FAX:(61 8) 6304 5811
ADR;WORK;PREF:;;100 Joondalup Drive;
Joondalup;Western Australia;6027
EMAIL:d.chai@ecu.edu.au
END:VCARD

TABLE V: Summarised results

	FRR (%)	SRR (%)
Desktop business card reader	14.7	8.2
Mobile business card reader	14.7	11.2
MMCC barcode	97.1	98.2

From the outputs shown in TABLE III, the desktop business card reader has wrongly decoded the email as an URL. As for the mobile card reader, it has wrongly decoded the "1" in the telephone number as an "i". In order to determine whether the MMCC barcode has decoded the information correctly, the output is compared to the data encoded in the MMCC barcode. These data are presented in TABLE IV. In this case, the MMCC barcode is correctly decoded.

The summarised results are tabled in TABLE V. With the MMCC barcode used, successful conversion of information from physical domain to the digital version has improved from less than 15% to more than 97% for both FRR and SRR. The downside of using an additional MMCC barcode as a business card reader is that the design of the business card has to be changed. However, this is not a major issue as the physical size of the MMCC barcode can be feasibly small and fit into existing business cards as presented in Figs 6 and 14.

V. Conclusions

The use of MMCC barcode has robustly improved the reading of business cards. The results of the successfully read cards significantly improved from less than 15% to more than 97%. Importantly, the physical size of the MMCC barcode is small enough to be fitted into existing business cards.

In future, more work will be done to look at porting this application into other popular mobile operating systems. Also, the research team will look at increasing the data capacity of the MMCC barcode so that more information, such as voice can be encoded into the mobile barcode.

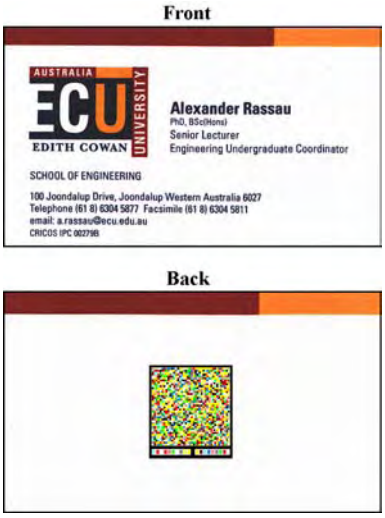


Fig. 14: An example MMCC barcode appearing at the back of a business card

References

[1] I. Stepanovska, "Business card history," Apr 2008. [Online]. Available: http://www.belightsoft.com/products/composer/history.php

[2] T. G. Holt, "Who invented business cards?" Jul 2010. [Online]. Available: http://www.articlesnatch.com/Article/Who-Invented-Business-Cards-/955889

[3] *vCard The Electronic Business Card Version 2.1*, versit Consortium Std., Sep 1996.

[4] "Brief history: Civil war pensions: The business card of one of the many attorneys specializing in pension claims, circa 1895. ssa history archives." Aug 2004. [Online]. Available: http://en.wikipedia.org/wiki/File:BusinessCardAttorney1895.jpg

[5] K. T. Tan, D. Chai, S. K. Ong, and H. Kato, "Data storage device and encoding/decoding method," Australia Patent 2 008 904 797, Sep 16, 2008.

[6] International Telecommunication Union, "The world 2009: ICT facts and figures," Oct 2009. [Online]. Available: http://www.itu.int/ITU-D/ict/material/Telecom09_flyer.pdf

[7] T. Onanuga, "Worldcard Mobile business card reader & scanner iPhone app," Jun 2010. [Online]. Available: http://www.latestgadgets.co.uk/www-apps/1136-worldcard-mobile-business-card-reader-scanner-iphone-app

[8] T. Dennis, "Business cards - ideal candidates for mobile barcodes," Feb 2010. [Online]. Available: http://mobile-barcode.tmcnet.com/topics/mobile-barcode-innovations/articles/75427-business-cards-ideal-candidates-mobile-barcodes.htm

[9] D. Barnes, J. Bradshaw, L. Day, T. Schott, and R. Wilson, "Two dimensional bar coding," *Purdue University, Tech*, vol. 621, 1999.

[10] R. Adams, "2-dimensional bar code page," Online, May 2008. [Online]. Available: http://www.adams1.com/pub/russadam/stack.html

[11] Microsoft, "Microsoft Tag," Jun 2010. [Online]. Available: http://tag.microsoft.com

[12] "Commnunications infrastructure and services availability in Australia 2008," Australian Communications and Media Authority and Australian Competition & Consumer Commission, Tech. Rep., 2008. [Online]. Available: http://www.acma.gov.au/webwr/_assets/main/lib310785/comms_infrastucture_and_svce_availability_in_aust_08.pdf

[13] S. K. Ong, D. Chai, and A. Rassau, "The use of alignment cells in MMCC barcode," *10th International Symposium on Communications and Information Technologies 2010 (ISCIT 2010)*, 2010.

[14] P. SYSTEMS, "Barcode design tips," May 2010. [Online]. Available: http://www.pointil.com/resources/barcodetips.htm

On Sequence Based Interaction Testing

Kamal Z. Zamli, Rozmie R. Othman, Mohd H.Mohamed Zabil
Software Engineering Group, School of Electrical and Electronic Engineering,
Universiti Sains Malaysia, Engineering Campus
14300 Nibong Tebal, Seberang Perai Selatan, Pulau Pinang, Malaysia

Abstract- T-way strategies aim to generate effective test data for detecting fault due to interaction. Different levels of interaction possibilities have been considered as part of existing t-way strategies including that of uniform strength interaction, variable strength interaction as well as input-output based relations. Many t-way strategies have been developed as a result (e.g. GTWay, TConfig, AETG, Jenny and GA for uniform strength interaction; PICT, IPOG and ACS for variable strength interaction; and TVG, Density and ParaOrder for input-output based relations). Although useful, all aforementioned t-way strategies have assumed "sequence-less" interactions amongst input parameters. In the case of reactive system, such an assumption is invalid as some parameter operations (or events) occur in sequence and hence, creating a possibility of bugs or faults triggered by the order (or sequence) of input parameters. If t-way strategies are to be adopted in such a system, there is also a need to support test data generation based on sequence of interactions. In line with such a need, this paper discusses the sequence based t-way testing (termed sequence covering array) as an extension of existing t-way strategies. Additionally, this paper also highlights the current progress and achievements.

I. INTRODUCTION

Software testing relates to the process of finding errors/defects and/of ensuring that a particular software of interest meets its specification. One of the key issues within software testing is on the generation of effective test data set for fault detection. Many useful test data generation strategies (e.g. boundary value analysis, cause and effect analysis, decision table, and equivalent partitioning) has been developed over the last 30 years [1]. Although helpful, these strategies have not been sufficiently adequate to generate test data for detecting faults due to interactions. For this reason, many new t-way interaction strategies (where t indicates the interaction strength), particularly based on covering arrays, have been developed in the literature.

In general, t-way strategies offer three levels of interaction possibilities for generating the test data (i.e. uniform strength, variable strength, and input output based relations). Uniform strength interaction forms the basis of interaction testing, where all input parameters are assumed to be uniformly interacting (i.e. with constant interaction strength (t) throughout). General T-Way (GTWay) [2, 3], In Parameter Order General (IPOG) [4], Multi-Core Modified IPOG (MC-MIPOG) [5], Automatic Efficient Test Generator (AETG) [6], TConfig [7], Jenny [8] and IBM's Test Case Handle (ITCH) [9] are amongst the strategies that deals with test data generation involving primarily with uniform strength interactions.

Unlike uniform strength interaction counterparts, variable strength interaction based strategies considers more than one interaction strength in the test data generation process. Practically, a particular subset of input parameters can have a higher interaction dependency than other parameters (indicating failures due to the interaction of that subset may have more significant impact to the overall system). As such, stronger interaction strength can be assigned accordingly. Simulated Annealing (SA) [10], Ant Colony System (ACS) [11] and Pairwise Independent Combinatorial Testing (PICT) [12] are examples of t-way strategies that adopt variable strength interaction.

While uniform strength and variable strength interaction based strategies assume that all input parameters interact with each other, input-output relations based strategies use the knowledge on the input-output relationships for test data generation. Strategies such as ParaOrder [13], Density[14], TVG [15], Union [16, 17] and Greedy [18] are amongst the strategies that support input-output based relations.

Despite being useful, all aforementioned t-way interaction strategies have assumed "sequence-less" interactions amongst input parameters. In many classes of (reactive) systems, some parameter operations (or events) occur in sequence [19] and hence, creating a possibility of bugs or faults triggered by the order (or sequence) of input parameters. If t-way strategies are to be adopted in such a system, there is also a need to support test data generation based on sequence of interactions. In line with such a need, this paper discusses the sequence based t-way testing (termed sequence covering array [19]) as an extension of existing t-way strategies. Additionally, this paper also highlights the current progress and achievements.

For the purpose of presentation, the rest of this paper is organized as follows. Section II discusses the background of interaction testing while Section III surveys the related work. Section V offers some insight into the current state-of-the-art on sequence based interaction testing. Finally Section VI gives our conclusions.

978-1-61284-690-3/11/$26.00 ©2011 IEEE

II. BACKGROUND

Consider a house alarm system (i.e. as reactive system) that consists of 4 input sensors shown in Table 1.

TABLE 1
HOUSE ALARM SYSTEM

Sensor	Function
A	Active when main door is opened
B	Active when any window is opened
C	Active when any window is broken
D	Detect any movement inside the house

When the alarm system is activated, the system will monitor these four sensors and produces an alarm messages when the system senses any unusual activities (e.g. in the presence of intruder). Here, the alarm system receives inputs from the sensors in random sequences. Main door may be opened first and then followed by any window opened or vice versa. Ideally, the house alarm system must be tested in all possible sequences so that no false alarm will be triggered due to sequencing faults. As seen in the sequence tree in Fig. 1, considering all possible sequences (with 24 tests) may not be practical and feasible in a mass factory production of the alarm system (i.e. due to time-to-market, resources, and cost constraints). For this reason, there is a need for a sampling mechanism that can help find the subsets of effective sequences for testing the overall system.

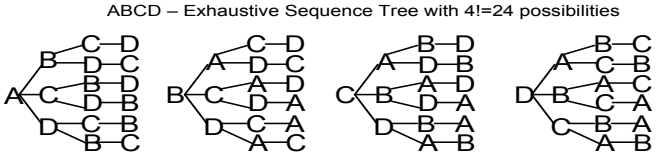


Fig. 1:Exhaustive Sequence Tree

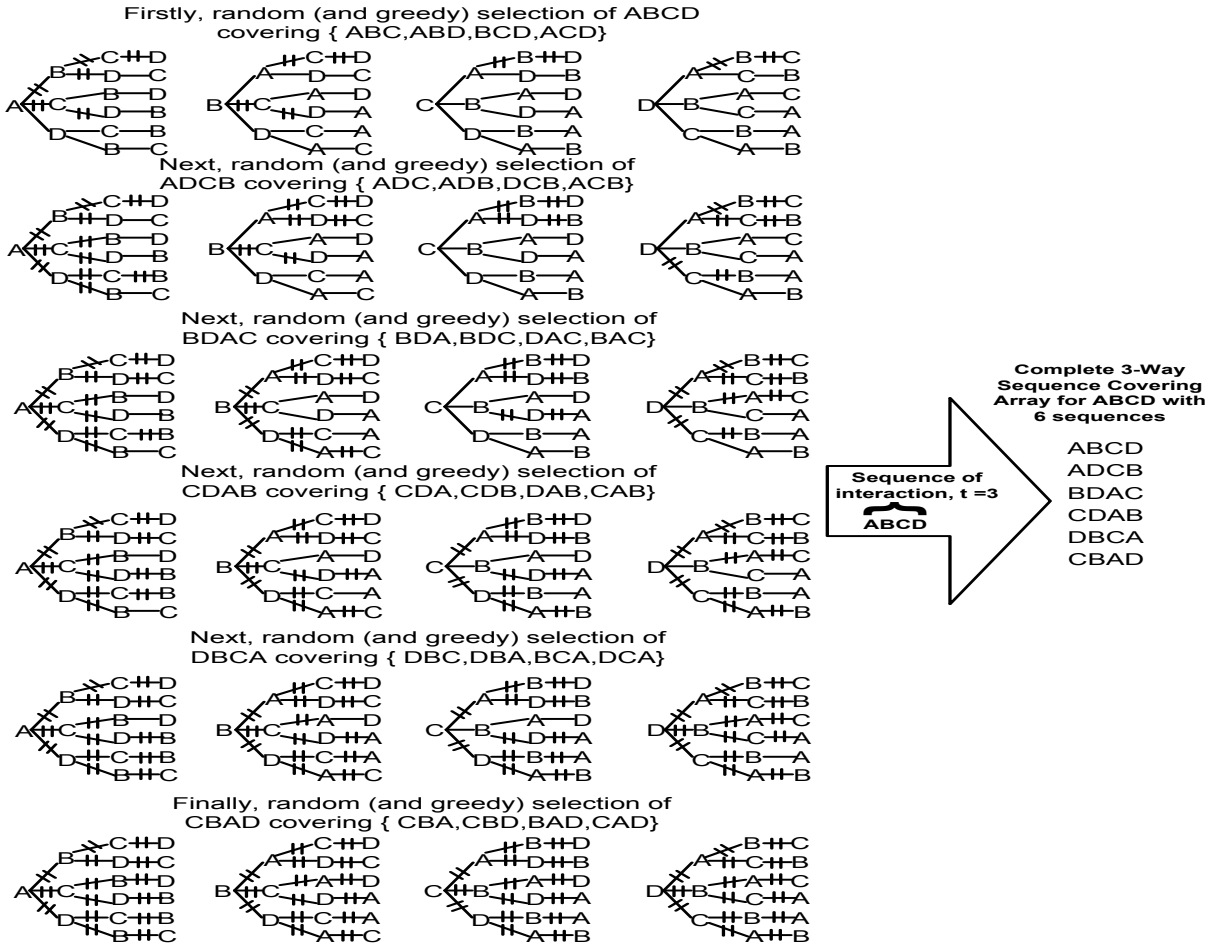


Fig. 2: Constructing 3-Way Sequence Combinations

Similar to conventional t-way testing, sequence based t-way testing also can support uniform sequence of interaction, variable strength sequence of interaction, and input output based relations. For uniform sequence of interaction, every t-way sequence must be covered at least once. Fig.2 from top to bottom illustrates possible construction of the 3-way sequence for ABCD. Assume that the sequence starts with A, and the sequence of ABCD is randomly selected. In this case, the 3-way sequences consisting of {ABC, ABD, BCD, ACD} are covered and are marked by | |. Again, from the first sequence tree starting with A, it can be seen that the next logical (and greedy) choice of sequence is ADCB or ADBC as either sequence has not contained | | marks as yet. Assuming that the sequence of ADCB is randomly chosen, the 3-way sequences of {ADC, ADB, DCB, ACB} is then covered and marked accordingly. Referring to the second sequence tree (from the top) in Fig. 2 for the sequence starting with B, the next greedy choice would be between BDCA and BDAC (i.e. as they do not contain any | | marks) Assuming that the random selection chooses BDAC, the 3-way sequences of {BDA,BDC, DAC, BAC} is then covered and marked. The whole process is continued until all the 3-way sequences are completely marked with | |. Here, the final test data set covering 3-way sequence for ABCD is then {ABCD, ADCB, BDAC, CDAB, DBCA, CBAD}. In terms of test reduction, there is a potential saving of 75%.

Concerning variable strength sequence of interaction, Fig. 3 illustrates the main sequence of interaction of t=2 for ABCD with the sub interaction sequence of t=3 for BCD. It should be noted that for t=2 (or pairwise), the sequences can simply be reversed in order to cover all the pairwise sequences. In the case of t=3, the 3-way sequence must cover BCD sequence exhaustively. Combining the main strength and the sub-strength, the final test data yields {ABCD, ABDC, ACDB, ACBD, ADBC, ADCB, DCBA}. In terms of test reduction, there is a potential saving of 70%.

As far as input output based relations is concerned, Fig. 4 highlights the case when two outputs are involved. Here, it is assumed that output 1, called f1, is significantly influenced by the sequence of AD and the output 2, called f2, is significantly influenced by the sequence of BC. To cover both for f1 and f2, there are only two possibilities {ABCD or DCBA}. If the goal is to cover the most sequence (i.e. greedy), the best selection is that of ABCD and DCBA. In term of test reduction, compared to exhaustive testing which required 24 tests, there is a potential saving of 83%.

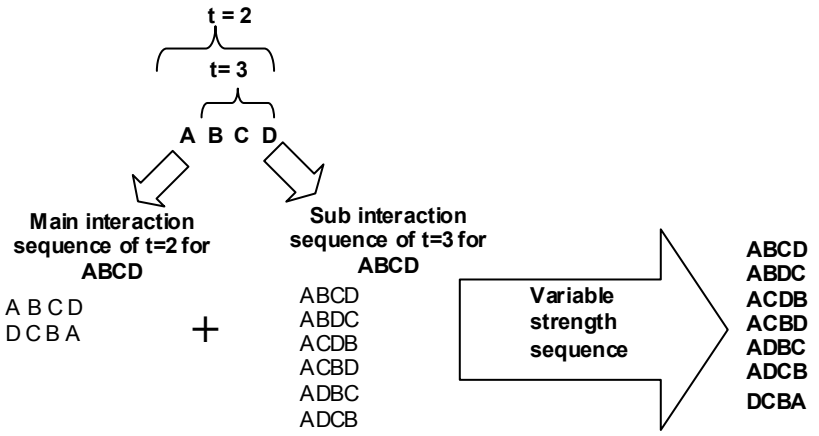


Fig. 3: Variable Strength Sequence of Interaction with t=2 and t=3

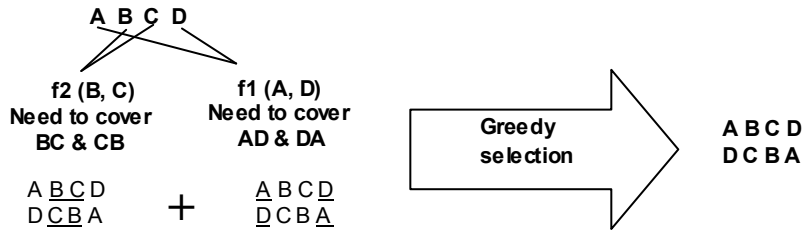


Fig. 4: Input Output Based Relations

Although useful as far as aiding understanding is concerned, it should be noted here that the strategy described in this section is not scalable due to the fact that it uses the exhaustive tree as the basis for selection. In the case of large parameters, using exhaustive tree can lead to combinatorial explosion problem.

III. RELATED WORK

Generally, existing interaction testing based strategy can be categorized in two different categories which are one-test-at-a-time (OTAT) strategy and one-parameter-at-a-time (OPAT) strategy. As the name suggests, an OTAT strategy generates one-test-case-at-a-time until all the interactions are covered. Based the main approach taken, the OTAT strategies can be further characterized into three categories, namely, iterative based, artificial life (AL) based, and heuristic based strategy.

Iterative based OTAT strategy executes a certain process iteratively to produce a test case. GTWay [2], ITCH [9], Jenny [8], TVG [15], PICT [12], UNION [16, 17] and Greedy [18] are the examples of iterative based OTAT strategy. GTWay iteratively used a backtracking algorithm in generating the test cases. As for ITCH, exhaustive searching algorithm is used during the generation of test cases.

Jenny, TVG and PICT are public domain tools which can be downloaded for freely from the developer's site. As for Jenny, the strategy generates the test data by constructing a test suite that covers 1-way interaction first before extending it to cover 2-way interaction. The process continues until the t-way interaction specified by the user is reached. Unlike Jenny, PICT generates the test data by selecting the first found uncovered pair and iteratively fills in the "don't care" value with the best fit value (i.e. value that covers the most uncovered pairs). TVG generates the test data based on 3 sets of algorithms: T-Reduced; Plus-One; and Random sets. Based on our experience with the tool, T-Reduced often produces the most optimal result as compared to Plus-One and Random sets. As for Union, the strategy iteratively generates a complete test data for every input-output relationship. Later, the strategy will remove any repetition (i.e. finding the union of test data) to find the final test suite. Unlike Union, Greedy uses the greedy algorithm in finding the best candidate for the final test suite.

The second category of OTAT strategy is the Artificial Life-based (AL) strategy. The strategies within this category utilize artificial life technique in generating the test data. Genetic Algorithm (GA) and Ant Colony Algorithm (ACA) are among artificial life techniques that are most commonly used for test data generation. GA based strategies starts by randomly creating a number of test data candidates, referred to as chromosomes. These chromosomes will undergo a series of mutation processes until certain criteria are met. After that, the best chromosome will be selected as final test data. For ACA, the test data is search using by colonies of ants on some possible paths. The selection of path is based on pheromone left by previous ant. The optimum paths correspond to the best test candidate to be included into the final test suite. Concerning related work, GA [20] and ACA [20] are Shiba's implementation of Genetic Algorithm and Ant Colony Algorithm respectively while GA-N [21] is Nie's implementation of Genetic Algorithm. In other work, Chen's implement Ant Colony Algorithm in his ACS [11] strategy.

The last category for OTAT strategy is the heuristic based strategy. Heuristic based OTAT strategy generates the test data based on some heuristic method. Density [14], Simulated Annealing (SA) [10] and Automatic Efficient Test Generator (AETG) [22] are amongst OTAT strategies that adopts heuristic method for generating test data. Density uses the global and local density calculation (improvising the "density" concept introduced by Bryce in [23, 24]) for constructing the test data. Unlike Density, SA starts with generating a feasible solution and applying a series of transformation to the solution until all interactions are covered. A binary search is adopted to find the most optimal solution. As for AETG, the strategy generates a list of test data candidates based on parameter-value configuration that cover the most uncovered tuples. A test data that covers the most uncovered tuples is selected from the test data candidates for the final test suite.

OPAT strategy refers to the strategy that adopts horizontal and vertical extension [4] for generating the test data. The strategy starts with generating an initial test suite (the exhaustive test suite for the selected number of parameters) and then extends the test suite by adding one parameter at a time (horizontal extension). To ensure maximum interaction coverage, a completely new test data may be added to the test suite during horizontal extension (and vertical extension). The OPAT based strategy is championed by Lei [25] based on his work on In-Parameter-Order (IPO) strategy. Later, Lei introduced IPOG [4] the extension of IPO to support higher order of interaction. Younis and Zamli propose a multi-core version of IPOG named MC-MIPOG [5, 26]. Moreover, Nie and William also come out with their own version of IPOG named IPO-N [21] and TConfig [7] respectively. Recently, Wang in [13] introduces two OPAT strategies, named ParaOrder and ReqOrder, which differs from its predecessor, IPOG in term of how the initial test suite is generated. IPOG generates the initial test suite in-defined-order-of-parameter found while ParaOrder generates the initial test suite for the first defined input-output relationship. As for ReqOrder, the selection of initial test case does not necessarily follow the first defined input-output relationship.

Last but not least, Kuhn is perhaps the first researcher to implement sequence based t-way strategy called the "quick and dirty" (QnD) strategy [19]. Since the implementation of the strategy has not been published in literature as yet, the details algorithm for QnD strategy is still unclear.

TABLE 2
SUMMARY OF EXISTING T-WAY STRATEGIES

Legend:		T-Way Strategies																				
Supported: √		OTAT Strategy															OPAT Strategy					
Not Supported: X		GTWay	ITCH	Jenny	PICT	TVG	Union	Greedy	QnD	GA	ACA	GA-N	ACS	Density	AETG	SA	IPOG	MC-MIPOG	IPO-N	TConfig	ParaOrder	ReqOrder
No Published Results: X*																						
Coventional T-Way Testing	Uniform Strength	√	√	√	√	√	X*	X*	X	√	√	√	√	√	√	√	√	√	√	√	√	X*
	Variable Strength	X	X	X	√	√	X*	X*	X	X	X	X	√	√	X	√	√	X	X	X	√	X*
	I/O Based Relation	X	X	X	X	√	√	√	X	X	X	X	X	√	X	X	X	X	X	X	√	√
Sequence Based T-Way Testing	Uniform Sequence	X	X	X	X	X	X	X	√	X	X	X	X	X	X	X	X	X	X	X	X	X
	Variable Sequence	X	X	X	X	X	X	X	X	X	X	X	X	X	X	X	X	X	X	X	X	X
	I/OBased Relation	X	X	X	X	X	X	X	X	X	X	X	X	X	X	X	X	X	X	X	X	X

IV. DISCUSSION

As discussed earlier, many t-way strategies for interaction testing do exist. Often, each strategy accommodates different types of interactions. Table 2 summarizes the type of interaction possibilities supported by existing t-way strategies. With the exception of QnD, all of the strategies support conventional t-way testing. ParaOrder [13], Density [14] and TVG [15] strategies support all three of the uniform strength, variable strength and input-output based relations. PICT [12], SA [10] and ACS [11] support uniform and variable strength interaction. Most other strategies support only uniform strength interaction.

It appears that only QnD [19] supports sequence based t-way testing. In particular, QnD supports uniform based sequence of interaction. As for variable strength and input output based relations for sequence based t-way testing, we have yet to discover any strategies which support these types of strength. In fact, as the generation of t-way interaction based test data is an NP-hard problem, it is expected that no single strategy can claim dominance as far as getting the most reduction in term of test data size.

As computer applications become larger in size and more complex and complicated in terms of process flow (e.g. embedded, web based, reactive and real time), existing t-way strategies are very useful to detect interaction fault between parameters especially when higher interaction strength is being used [27, 28]. But at the same time, not only interaction between parameters, the sequences of parameter occurrence also need to be tested. This is especially relevant when the system of interest involves event based reactive system in which sequence of parameter inputs plays pivotal role as far as the system operation is concerned. While many t-way strategies do exist to accommodate t-way interaction testing, we are still lacking of testing strategies that can support sequence based t-way testing.

Taking this into account, we are currently developing a new t-way strategy that supports not only conventional interaction strength, but also to support sequence based interaction of all strength possibilities. As far as implementation is concerned, the first version of our new tool is still under evaluation.

V. CONCLUSION

Although much progress has been achieved as far as t-way testing strategies are concerned, there are still rooms for improvements especially in terms of the support for sequence based t-way testing. It is hopeful that such a support would enhance the applicability of t-way strategies in the industry.

ACKNOWLEDGMENT

This research is partially funded by the generous fundamental grants – "Investigating T-Way Test Data Reduction Strategy Using Particle Swarm Optimization Technique" from Ministry of Higher Education (MOHE) and the USM research university grants – "Development of Variable Strength Interaction Testing Strategy for T-Way Test Data Generation".

REFERENCES

[1] K. Z. Zamli, M. I. Younis, S. A. C. Abdullah, and Z. H. C. Soh, *Software Testing*: First ed. KL Malaysia: Open University Malaysia, 2008.

[2] M. F. J. Klaib, "Development Of An Automated Test Data Generation And Execution Strategy Using Combinatorial Approach," PhD. Thesis, School of Electrical And Electronics, Universiti Sains Malaysia, 2009.

[3] K. Z. Zamli, M. F. J. Klaib, M. I. Younis, N. A. M. Isa, and R. Abdullah, "Design and Implementation of a T-Way Test Data Generation Strategy with Automated Execution Tool Support," *Information Sciences*, In Press

[4] Y. Lei, R. Kacker, D. R. Kuhn, V. Okun, and J. Lawrence, "IPOG: A General Strategy for T-Way Software Testing," in *Proceedings of the 14th Annual*

IEEE International Conference and Workshops on The Engineering of Computer-Based Systems, Tucson, AZ, 2007, pp. 549-556.

[5] M. I. Younis and K. Z. Zamli, "MC-MIPOG: A Parallel T-Way Test Generation Strategy for Multicore Systems," *ETRI Journal,* vol. 32, pp. 73-83, 2010.

[6] D. M. Cohen, S. R. Dalal, M. L. Fredman, and G. C. Patton, "The AETG System: An Approach To Testing Based on Combinatorial Design," *IEEE Transactions on Software Engineering,* vol. 23, pp. 437-444, 1997.

[7] A. W. Williams. *TConfig*. Available at: http://www.site.uottawa.ca/~awilliam/. Last Accessed on December 2010

[8] B. Jenkins. *Jenny Test Tool*. Available at: http://www.burtleburtle.net/bob/math/jenny.html. Last Accessed on December 2010

[9] A. Hartman, T. Klinger, and L. Raski. *IBM Intelligent Test Case Handler*. Available at: http://www.alphaworks.ibm.com/tech/whitch. Last Accessed on February 2010

[10] M. B. Cohen, P. B. Gibbons, W. B. Mugridge, C. J. Colbourn, and J. S. Collofello, "Variable Strength Interaction Testing of Components," in *Proceedings of 27th Annual International Computer Software and Applications Conference*, Dallas, USA, 2003, pp. 413-418.

[11] X. Chen, Q. Gu, A. Li, and D. Chen, "Variable Strength Interaction Testing with an Ant Colony System Approach," in *Proceedings of 16th Asia-Pacific Software Engineering Conference*, Penang, Malaysia, 2009, pp. 160-167.

[12] J. Czerwonka. *PICT Tool*. Available at: http://www.pairwise.org/tools.asp. Last Accessed on December 2010

[13] Z. Wang, C. Nie, and B. Xu, "Generating Combinatorial Test Suite for Interaction Relationship," in *Proceedings of 4th International Workshop on Software Quality Assurance (SOQUA2007)*, Dubrovnik, Croatia, 2007, pp. 55-61.

[14] Z. Wang, B. Xu, and C. Nie, "Greedy Heuristic Algorithms to Generate Variable Strength Combinatorial Test Suite," in *Proceedings of the 8th International Conference on Quality Software*, Oxford, UK, 2008, pp. 155-160.

[15] J. Arshem. *TVG*. Available at: http://sourceforge.net/projects/tvg. Last Accessed on December 2010

[16] P. J. Schroeder, "Black-Box Test Reduction Using Input-Output Analysis," PhD Thesis, Department of Computer Science, Illinois Institute of Technology, Chicago, IL,USA, 2001.

[17] P. J. Schroeder and B. Korel, "Black-Box Test Reduction Using Input-Output Analysis," *SIGSOFT Software Engineering Notes,* vol. 25, pp. 173-177, 2000.

[18] P. J. Schroeder, P. Faherty, and B. Korel, "Generating Expected Results for Automated Black-Box Testing," in *Proceedings of 17th IEEE International Conference on Automated Software Engineering (ASE'02)*, Edinburgh, Scotland, UK, 2002, pp. 139-148.

[19] D. R. Kuhn. *Combinatorial Testing for Event Sequences*. Available at: http://csrc.nist.gov/groups/SNS/acts/sequence_cov_arrays.html. Last Accessed on January, 2011

[20] T. Shiba, T. Tsuchiya, and T. Kikuno, "Using Artificial Life Techniques to Generate Test Cases for Combinatorial Testing," in *Proceedings of the 28th Annual Intl.Computer Software and Applications Conf. (COMPSAC'04)*, Hong Kong, 2004, pp. 72-77.

[21] C. Nie, B. Xu, L. Shi, and G. Dong, "Automatic Test Generation for N-Way Combinatorial Testing," in *Quality of Software Architectures and Software Quality*. vol. 3712, R. Reussner, *et al.*, Eds.: Springer Berlin / Heidelberg, 2005, pp. 203-211.

[22] D. M. Cohen, S. R. Dalal, A. Kajla, and G. C. Patton, "The Automatic Efficient Test Generator (AETG) System," in *Proceedings of the 5th International Symposium on Software Reliability Engineering*, Monterey, CA, USA, 1994, pp. 303-309.

[23] R. C. Bryce and C. J. Colbourn, "A Density-Based Greedy Algorithm for Higher Strength Covering Arrays," *Software Testing, Verification and Reliability,* vol. 19, pp. 37-53, March, 2009.

[24] R. C. Bryce and C. J. Colbourn, "The Density Algorithm for Pairwise Interaction Testing," *Software Testing, Verification and Reliability,* vol. 17, pp. 159-182, September, 2007.

[25] Y. Lei and K. C. Tai, "In-Parameter-Order: A Test Generation Strategy For Pairwise Testing," in *Proceedings of 3rd IEEE International Conference on High Assurance Systems Engineering Symposium*, Washington DC, USA, 1998, pp. 254-261.

[26] M. I. Younis, "MIPOG: A Parallel T-Way Minimization Strategy For Combinatorial Testing," PhD. Thesis, School of Electrical And Electronics, Universiti Sains Malaysia, October, 2010.

[27] M. I. Younis and K. Z. Zamli, "A Strategy for Automatic Quality Signing and Verification Processes for Hardware and Software Testing," *Advances in Software Engineering,* vol. 2010, pp. 1-7, 2010.

[28] K. Z. Zamli, N. A. M. Isa, M. F. J. Klaib, and S. N. Azizan, "A Tool for Automated Test Data Generation (and Execution) Based on Combinatorial Approach," *International Journal of Software Engineering and Its Applications,* vol. 1, pp. 19-35, 2007.

IPSec Authentication using Certificateless Signature in Heterogeneous IPv4/IPv6 Network

Nazrul M. Ahmad, Asrul H. Yaacob, Ridza Fauzi, and Alireza Khorram
Faculty of Information Science and Technology (FIST)
Multimedia University (MMU)
Jalan Ayer Keroh Lama,
75450 Melaka, Malaysia
Email: (nazrul.muhaimin, asrulhadi.yaacob)@mmu.edu.my

***Abstract*—This paper studies the incompatibilities issues on deploying IPSec Encapsulating Security Payload (ESP) in providing end to end security between heterogeneous IPv4 and IPv6 networks. The presence of IPv4/IPv6 translation gateway violates the TCP/UDP intrinsic functionalities due to the translation of the IP addresses in IP packets. We address these interoperability issues by modifying IKE negotiation with NAT-Traversal capability and some improvements on IPSec software. However, the implementation of the conventional IKE authentication mechanisms such as pre-shared key and Public Key Infrastructure (PKI) certificate-based requires both nodes either to be manually configured, or to exchange the certificates and the necessity to enrol to certain Certificate Authority (CA). This paper proposes a new Internet Key Exchange (IKE) authentication based on certificateless public key infrastructure in order to alleviate the limitation of the conventional IKE authentication. We also propose an efficient public and shared parameters distribution mechanism whereby the translation gateway acts as Key Generator Centre (KGC).**

I. Introduction

The emergence of IPv6 [1] enables new generation of applications and services such as peer-to-peer communication, security system, and sensor network that requires a huge address space. Since IPv6 is not designed to provide backward compatibility with IPv4, most IPv6 mission critical applications must be able to continuously interoperate with legacy IPv4 nodes. In the face of looming IPv4 address exhaustion and slow pace of IPv4 to IPv6 migration, a number of transition tools have been developed to ensure interoperability between heterogeneous address realms. Transition mechanisms can generally be categorized into three: Dual Stack [2], Tunneling [3], and Translation [4].

The most common transition mechanism nowadays is dual stack. A node with a dual stack allows co-existence and interoperability of IPv4 and IPv6 nodes using IPv4 or IPv6 packets. This permits gradual application-by-application upgrades into IPv6 environment without much disruption [2]. In IPv6 transition, tunneling is basically used to enable one network to send its data via another network's connections. Thus, 6to4 tunneling is done by encapsulating IPv6 packets within IPv4 packets and sends them as native IPv4 traffic. The tunnel provides virtual links over IPv4 physical network. When IPv4 and IPv6 nodes are not directly compatible and when IPv6 node wants to communicate with numerous IPv4 nodes, translation mechanism should be used. The translation mechanism such as Network Address Translation - Protocol Translation (NAT-PT) [4] was proposed without any modification to nodes on both ends whereby the router or translation gateway takes the responsibility of the translation. The gateway which is located at the boundary of IPv4 and IPv6 address realms translates IPv4 header into IPv6 header or vice versa.

To ensure end to end security between the end nodes, this paper considers the deployment of IPSec since IPSec has been widely applied in IP networks. IP Security (IPSec) [5] is a set of protocol designed to support secure exchange of IP packets which provides confidentiality, integrity, authentication, and non-repudiation. There are two main transformations that are applied to an IP packet: Authentication Header (AH) [6] and Encapsulating Security Payload (ESP) [7]. AH header is inserted into the IP packet immediately after the outer IP header. Then, AH authenticates the entire packet including the preceding IP header. The underlying of IPSec mechanism which preserves the end node addresses of IP packet will not work with the presence of translation gateway for most applications in practices [8]. When the translation gateway modifies the IP header from one address realm to another, IPSec evaluating this as violation of integrity and discards the packet. Therefore, AH and translation gateway simply cannot work. The IPSec ESP also employs a hash algorithm for packet authentication. But, unlike AH, it does not include outer IP header. This solves authentication problem.

IPSec requires a mechanism to authenticate the exchange of Security Association (SA) in the Internet Key Exchange (IKE) negotiation process. The conventional IKE authentication mechanisms outlined in [9] are pre-shared key and certificate-based asymmetric cryptosystems such as public-key encryption and digital signature. The use of pre-shared key is only feasible in the small scale network due to the difficulties in distributing the shared key to each pair of nodes. On the other hand, the use of certificate-based infrastructure requires a common Certificate Authority (CA) between two nodes. Because of the inherent incompatibility between IPv4/IPv6 translation gateway and IPSec and the inherent limitations of the existing implementation of IKE authentication, we propose a new IKE authentication scheme based on certificateless public key infrastructure. The proposed scheme offers significantly reduction in system complexity, eliminates the use of

978-1-61284-690-3/11/$26.00 ©2011 IEEE

certificate to guarantee the authenticity of public keys, and reduces the cost for establishing and managing the certificates.

The remainder of this paper is structured as follows: Section 2 describes the incompatibilities issues between translation gateway and IPSec. This section also gives background concepts on Public Key Infrastructure (PKI) and Identity-based Infrastructure. Section 3 presents the concepts of certificateless signature scheme. Then, Section 4 proposes a new IKE authentication by using Address Based Keys (ABK) with certificateless signature to alleviate the limitation of traditional pre-shared keys and PKI. Finally, Section 5 concludes this paper.

II. Technical Background

A. IPv4/IPv6 Translation Gateway Breaks IPSec

IPSec supports transport mode in providing end to end security between nodes. However, applying IPSec across translation gateway for this purpose violates TCP/UDP intrinsic functionalities. The co-existence of translation gateway and IPSec ESP is not feasible due to the IP header translation which causes the TCP/UDP checksum invalid. TCP/UDP checksum has a dependency on IP source and destination addresses through the inclusion of TCP/UDP pseudo-header in the calculation. Like normal Network Address Translation (NAT), while the translation gateway translates the IP addresses, it should also re-compute the checksum. Since IPSec ESP encrypts and authenticates ESP header and TCP/UDP header, any attempt to modify to checksum causes the integrity check to fail. Alternately, if translation gateway does not update the checksum, TCP/UDP verification will fail.

NAT-Traversal (NAT-T) [10] is designed to solve the problems inherent in using IPSec and translation gateway. The following section extensively describes the operation of NAT-T. With NAT-T, the UDP-ESP encapsulation [11] is deployed to support the IPSec packets from both end nodes to traverse the translation gateway and to avoid any problems with the IPSec-aware translation gateway. Let's imagine multiple connections are mapped to one allocated address. Since IPSec ESP does not use port information, the translation gateway can only utilize the protocol field in IP header to distinguish the packets. When the first IPSec connection is established, the translation gateway maintains the translation state information in the table so that all IPSec ESP packets will be routed to the first connection. However, when there is a new IPSec connection, the translation gateway replaces the entry in the table and thus breaking the first IPSec connection. UDP-ESP encapsulation gives the translation gateway an UDP header containing UDP port that can be used for multiplexing IPSec data streams.

1) IPSec across IPv4/IPv6 Translation Gateway.: To initiate secure end to end communication, IPSec uses IKE to negotiate and establish Security Association (SA) which contains parameters such as encryption and hash algorithm, keys, and encapsulation methods. IKE negotiation takes place in two phases. Phase 1 is the initial negotiation and an SA is established for IKE, so that the end nodes agree on common proposal for securely exchanging IKE messages. In phase 2, another SA is established for IPSec communication. This section discusses the necessary changes to the traditional IKE [9] negotiation in order to support IPSec across the translation gateway.

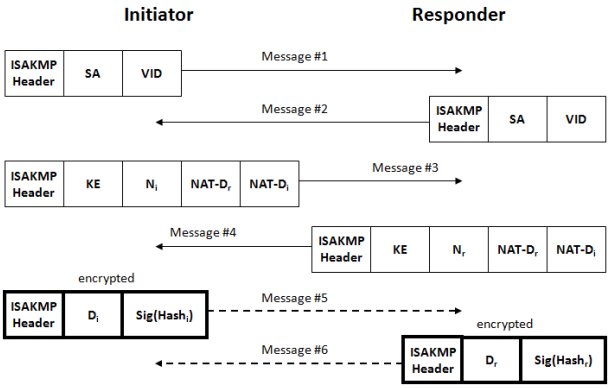


Figure 1. IKE Phase 1 with NAT Detection

NAT-T offers an effective and simple way to support IPSec across the translation gateway. Figure 1 shows NAT-T operation in the IKE Main Mode negotiation by using digital signature authentication. The first step of NAT-T operation is to detect the NAT-T capability of remote nodes. This is done by exchanging special Vendor ID (VID) in the first two messages IKE Phase 1 negotiation. Successful exchange of VID indicates that both ends support NAT-T. Upon agreeing both ends support NAT-T, the second step is to discover the presence of translation gateways along the communication path. The presence of translation gateway is determined by sending NAT-D (NAT-Discovery) payload. Both ends calculate and send the hashes of IP addresses and ports of both the source and destination. The NAT-D payloads are exchanged in the third and fourth messages of the Main Mode. Once received the NAT-D payload, both ends recalculate the hash value based on the IP and port addresses that they used in the IKE negotiation. If these hashes do not match, both ends discover that translation gateway exists somewhere in between.

The IPv4/IPv6 packet header translation by the translation gateway causes TCP/UDP checksum to fail. To validate the checksum, both end nodes need to exchange their original addresses used to construct the packets. The original addresses are embedded into a NAT-OA (Original Address) payload. This gives responder node accesses to required information so that the source and destination IP addresses can be checked and the checksum can be validated. The NAT-OA payloads are exchanged during the first and second messages of IKE Phase 2 as shown in Figure 2. On receiving NAT-OA payloads, the end nodes assemble the TCP/UDP pseudo-header based on the information contained in the NAT-OA payloads. This pseudo-header is appended to the original TCP/UDP segment for recalculating the checksum.

B. Public Key Infrastructure (PKI) and Identity-based Infrastructure

In the traditional Public Key Infrastructure (PKI), certificates are deployed to provide an assurance of the binding

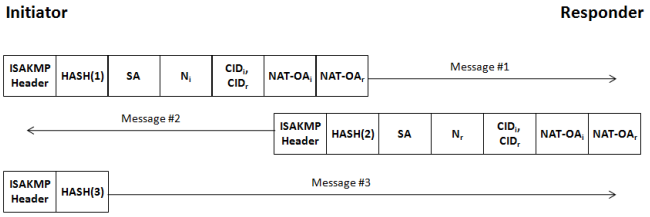


Figure 2. IKE Phase 2 with NAT-OA Payload

between public keys and users' identities that hold the corresponding private keys. The binding process is done by the trusted third party known as Certificate Authority (CA). The public/private key pairs in PKI can either be generated by the CA for the node or the node can generate the keys for itself and then verify with the CA for authenticity. The two main components of PKI are Registration Authority (RA) and Certificate Authority (CA). RA is responsible to accept requests for the certificates and to authenticate the identity. Once the validation process is complete, RA triggers the request to the CA. CA is responsible to generate and distribute the certificate that binds the public key to the identity of the node once the identity has been verified. However, PKI faces many obstacles in practises such as the scalability of the infrastructure and certificate management.

The idea of Identity-based cryptography was introduced by Shamir in 1984 [12]. In Identity-based cryptosystem, the public key of a node is created by applying a public hash function to the node's publicly known identifier such as E-mail address, username or the IP address. Then, the corresponding private key is generated from trusted third party known as Private Key Generator (PKG). The PKG uses a particular algorithm to generate the private key and returns it via a secure channel. In the key generation process, PKG generates a list of parameters. The parameters contain a master secret key, which is only known to the PKG, and a number of parameters that are distributed to all nodes relying on the particular PKG. Identity-based cryptosystem eliminates the need of certificates. However, we still need a convenient and reliable method of associating an identity string to a node. Moreover, there is an inherent key escrow in Identity-based cryptosystem since PKG is directly responsible in generating the node's private key.

Due to the complexity of certificate management in PKI and inherent key escrow in Identity-based, Al-Riyami and Paterson proposed the concept of certificateless public key cryptography in 2003[13]. Certificateless public key infrastructure combines the elements of trust model similar in traditional PKI and the absence of certificate in Identity-based. This infrastructure still makes use a trusted third party, but in contrast to Identity-based, the Key Generator Centre (KGC) does not generate node's secret key. Instead, the KGC generate an identity-dependent partial secret key that the node then combine with some secret known only to the node to produce secret key. In this paper, we propose a new IKE authentication by using certificateless signature scheme based on bilinear pairing.

III. Certificateless Public Key Cryptography

A formal Certificateless Signature (CLS) structure is a 7-tuple polynomial time algorithms: **Setup, Partial-Secret-Key-Extract, Set-Secret, Set-Secret-Key, Set-Public-Key, Sign** and **Verify**. The KGC will execute **Setup** and **Partial-Secret-Key-Extract** whereas the node will execute **Set-Secret, Set-Secret-Key, Set-Public-Key**. The algorithms is based on the proposed CLS scheme by [14] which provides a better performance compared to [15],[16]. We recall the details of the algorithm here. The discussion on the security and performance can be found in the original papers [14],[15],[16].

1) Setup: This algorithm calculates the parameters of CLS $params$ and master secret key msk. This algorithm runs as follows:

i. Run a generator to output two cyclic groups $\mathbb{G}_1$ and $\mathbb{G}_2$ of prime order r and a bilinear pairing

$$e : \mathbb{G}_1 \times \mathbb{G}_1 \longrightarrow \mathbb{G}_2 \tag{1}$$

ii. Choose an arbitrary generator $G \in \mathbb{G}_1$ and generate

$$g = e(G, G) \tag{2}$$

iii. Select a random $s \in \mathbb{Z}_r^*$ and set master public key

$$K_{KGC} = sG \tag{3}$$

iv. Choose hash function

$$\mathrm{H} : \{0,1\}^* \rightarrow \mathbb{Z}_r^* \tag{4}$$

The output of this algorithm are:

- the domain parameter which is public

$$params =< e, g, G, K_{KGC}, \mathrm{H} > \tag{5}$$

- master private key which is private to KGC

$$msk = s \in \mathbb{Z}_r^* \tag{6}$$

2) Partial-Secret-Key-Extract: This algorithm is executed by KGC when a node requests its partial secret key. The inputs of this algorithm are $params$,msk and the node identity ID. Prior to the release of the partial secret key, the node must be authenticated by the system. The algorithm returns

$$partial_key = (\mathrm{H}(ID) + msk)^{-1} G \in \mathbb{G}_1 \tag{7}$$

The key is transmitted over a secure channel to the node.

3) Set-Secret: This algorithm computes the secret value used in CLS. The node chooses a random $s_{ID} \in \mathbb{Z}_r^*$. This secret value will be used in the next algorithm to create the node's secret key.

4) Set-Secret-Key: This algorithm creates node's secret key. This key is kept safely by the node and it will be used in the signing process.

$$nsk = (partial_key, s_{ID}) \in \mathbb{G}_1 \times \mathbb{Z}_r^* \tag{8}$$

5) Set-Public-Key: This algorithm takes as inputs the $params$ and s_{ID} to compute the node's public key. This public key will be used to verify the signature. The public key corresponding to the node is

$$npk = g^{s_{ID}} \in \mathbb{G}_2 \tag{9}$$

6) Signing Process: Given a message $M \in \mathcal{M} = \{0,1\}^*$, this algorithm uses the $params$, and ID as well as its npk and s_{ID} to compute the signature, σ. The steps are as follows:

i. Choose randomly $x \in \mathbb{Z}_r^*$

ii. Compute

$$t = g^x \in \mathbb{G}_2 \tag{10}$$

iii. Calculate the hash

$$h = H\left(M||ID||npk||t\right) \in \mathbb{Z}_r^* \tag{11}$$

iv. Compute S

$$S = (x + h \cdot s_{ID}) \cdot partial_key \in \mathbb{G}_1 \tag{12}$$

v. The signature on M is

$$\sigma = (S, h) \in \mathbb{G}_1 \times \mathbb{Z}_r^* \tag{13}$$

7) Verification Process: To verify the authenticity of a message M with the signature $\sigma = (S, h)$, the other node computes

$$t' = e\left(S, H\left(ID\right)G + K_{KGC}\right)\left(npk\right)^{-h} \tag{14}$$

$$h' = H\left(M||ID||npk||t'\right) \tag{15}$$

The message is authentic if and only if $h' = h$.

IV. Address Based Keys (ABK) Authentication

The key exchange in Phase 1 of the IKE negotiation needs to be authenticated. Both end nodes require to prove their identity before proceed to Phase 2. A pre-shared key provides the simplest IKE authentication that is suitable for network with a limited and static number of IPSec nodes. Pre-shared key needs to be manually configured in each end node. Each end node finds the pre-shared key for its peer by using source IP address. With the presence of IPv4/IPv6 translation gateway, source IP addresses of both end nodes will be translated into new address realms. On top of that, IPv6-only node does not have a fixed translated IP address. This is due to dynamic mapping performed by the translation gateway by translating IPv6-only node address into one of the address allocated in IPv4 address pool. As the original IP addresses are only exchanged in Phase 2, it is impossible for the initiator and responder to select pre-shared key based on the peer's source IP address. Hence, the IKE negotiation with pre-shared key for authentication does not work with the presence of translation gateway.

On the other hand, IKE authentication by using digital signature and public key encryption are based on security certificates and are managed by using Public Key Infrastructure (PKI). In traditional PKI, a trusted third party known as Cetificate Authority (CA) is deployed to distribute and validate the certificate. The need for PKI to support certificate is commonly considered to be expensive to implement, use and maintain. In 1984, Shamir proposed Identity-based cryptosystem [12] whereby each node's public key can be an arbitrary string and hence, removes the need for certificates. Smetters and Durfee proposed to use Identity-based cryptosystem to secure IP-based network traffic [17]. In this system, a trusted third party called a Private Key Generator (PKG) is used to generate end node's private key. The major obstacle of this system is that the private key of all nodes is known by the PKG.

To eliminate key escrow problem which is inherent in Identity-based signature and the usage of certificate in traditional PKI, this paper proposes a new authentication scheme for IKE negotiation by using Address Based Keys (ABK) with certificateless signatures. ABK [18] is derived from Identity Based Cryptosystems (IBC). In IBC, any publicly known identifier such as email address or the IP address of a node can be used as a public key. For ABK, the IP address functions as the public key. In a certificateless signature scheme [13], a trusted third party known as Key Generation Centre (KGC) is deployed to communicate with end node for generation of public and secret keys. Unlike the trusted third party in PKI and Identity-based, the KGC does not have access to the node's secret key. Instead, the KGC generates a partial secret key and transmits it to the end node. Upon receipt of the partial secret key, the node combines partial secret key, KGC's public parameters, and node's secret value to produce node's secret key.

A. Implementation

As a preliminary proof of concept, we built this testbed under Linux platform. The IPv4/IPv6 internetworking environment for end to end IPSec support is illustrated in Figure 3. The initiator is an IPv6-only client and the responder is an IPv4-only legacy server. A translation gateway with NAT-PT capability is responsible for translating IPv6 packets to IPv4 packets, and vice versa. To facilitate IPv4 and IPv6 name to IP address mapping, Domain Name Service (DNS) server is used in IPv4 address realms. DNS is the protocol used to resolve the human-readable hostname, URL or email address into IP address. Since the nodes are distributed across the disparate address realms, DNS queries and responses need to cross the translation gateway. Therefore, DNS Application Level Gateway (ALG), an application specific agent that translates IPv6 addresses in DNS queries and responses into their IPv4 address bindings, is used in conjunction with NAT-PT to provide support for such application. To implement a new IKE authentication by using ABK with certificateless signature, we enhance the existing OpenSwan [19], an open source and a Linux-based IPSec implementation available under GNU general public license version 2.

A certificateless public key cryptosystem offers the simplicity compared to the PKI and eliminates the private key escrow problem in IBC. Hence, the system avoids the need of having a central trusted third party such as CA and PKG. Instead, a local KGC can be used [13],[20]. In this system, every domain deploys its own KGC and thus provides a truly distributed key management system. KGC is a standalone dual-stack node and is deployed at the edge of heterogeneous IPv4 and IPv6 networks. Based on this configuration, we propose to embed the KGC's functionality in IPv4/IPv6 translation gateway. The translation gateway has privileged to inspect IP packet in order to perform address translations and possible port multiplexing. Moreover, it also needs to snoop inside the IP

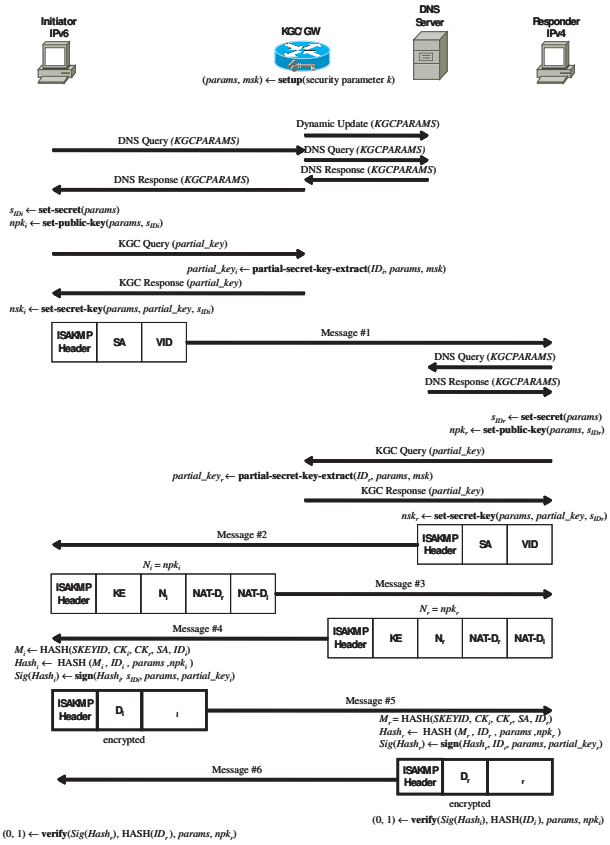


Figure 3. ABK Authentication with Certificateless Signature

payload that contains IP addresses for the protocol such as FTP and DNS. Since the translation gateway involves directly in examining the IP packets, we let the translation gateway acts as a KGC. Since the unconditional trust placed upon the translation gateway to perform the address translation, we invest roughly the same level of trust in translation gateway to act as a key generating and distributing centre.

B. Distribution of Shared, Public Paramaters

In certificateless public key infrastructure, all end nodes are required to know the domain public parameters *params* in order to generate their public/secret keys pair. The most feasible solution to distribute the KGC's *params* is to use the existing network infrastructure. Smetters and Durfee proposed to piggyback this information to DNS reply [17]. Due to the simplicity of the mechanism, we enhance this distribution technique for our implementation. Initially, KGC executes **setup** algorithm to generate *params*. Apart from the *params* generated in Section III, two additional parameters are listed. KGC_{ADDR} and KGC_{PORT} are IP address or hostname of the KGC and port on which the KGC is listening. KGC is then responsible to publish the *params* to DNS server. To provide secure and authenticating update to DNS server, KGC deploys Transaction Signature (TSIG) [21], a cryptographically means of identifying each endpoint of a connection that involves in making or responding to a DNS update. Under compromise attack, KGC is forced to regenerate and republish *params* to DNS server. Presumably, KGC is on a closely-monitored and

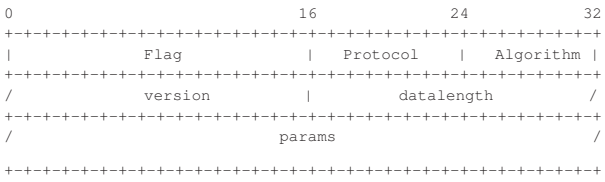


Figure 4. KGCPARAMS DNS Resource Record

well-protected node, frequent dynamic update can be avoided for a reasonably long period of time.

To realize the distribution of KGC's *params*, we introduce a new Resource Record (RR) type to DNS. In this section, we discuss the format of RR fields associated to the new RR type, i.e. KGCPARAMS, as shown in Figure 4. RDATA portion of KGCPARAMS RR utilizes the same format as that of KEY RR [22]. RDATA comprises of flags, protocol, algorithms and two additional fields, version and params. Version field is an integer that defines the version of the *params* generated in a single trust domain. Final field of RDATA represents a base64 encoding of the *params*.

To initiate the IPSec communication, the IPv6 client initially sends KGCPARAMS query to DNS server by setting the QNAME of the query to Fully Qualified Domain Name (FQDN) of the responder. If the DNS in IPv4 address realm, the DNS Application Level Gateway (ALG) on IPv4/IPv6 translation gateway will intercept and translate the query. Once obtained the DNS response, the IPv6 client extracts KGC_{ADDR} and KGC_{PORT} from *params* to contact KGC for requesting *partial_key*. Upon receiving the query from the IPv6 client, KGC runs **partial_secret_key_extract** algorithm by taking the client's identity, *params*, and *msk* as inputs to generate IPv6 client's *partial_key*. This *partial_key* is transmitted to the IPv6 client over a secure channel. Upon receipt of the *params* and *partial_key*, the IPv6 client generates public/secret keys pair (*nsk*, *npk*) based on equations (8) and (9). For the responder, the DNS query needs to be preformed once it received the first IKE message from the initiator. In this case, the responder is pre-configured with the FQDN of the KGC. As an example, the node could be configured with the name "kgc.testbed.com", where the testbed.com is the domain name. The responder generates a DNS query by setting the QNAME to the name of the KGC. The query has QTYPE set to KGCPARAMS so that the DNS server replies the *params* to the responder.

C. New IKE Authentication

We propose to implement ABK with certificateless signature in the Phase 1 of the IKE negotiation. This scheme is used to authenticate both end nodes and to provide the protection for the upcoming Phase 2 IPSec negotiation. To initiate IKE negotiation, the exchange of first two messages is identical to the existing scheme. The new scheme only has impact on the following subsequent exchanges. The nonce payloads N_i and N_r that are sent in third and fourth message usually include a large random number between 64 bit and 2048 bits. Instead of random number, this scheme transmits npk_x to remote end

node. This npk_x is used to validate and verify the signature that will be sent in the later stage of IKE negotiation.

The last two messages are strictly for exchanging the end node identity, proving the identity and retroactively authenticating all the previous messages. The ID payload contains information about the identity of the initiator or responder. The ID may be IP address, FQDN, email address, or something similar. The presence of IPv4/IPv6 translation gateway hides the end node identifiers. Prior to the exchanges of message 5 and 6, both end nodes are identified by using the translated IP addresses. Since the translated IP addresses are not fixed, this scheme proposes to populate initiator and responder original source IP addresses in ID payload. The recipient then can use the ID as a lookup key for IKE SA policy and the sender's public key npk, and as part of the security attributes that are related to the generation and verification of authenticators generated by the initiator and responder, $Hash_i$ and $Hash_r$, respectively.

Until the end of IKE message 4, all exchanges are not authenticated. To provide mutual authentication, both end nodes need to provide a digital signature in the exchange that the other node will verify. In this case, the initiator and responder authenticate their exchanges by sending signature σ_i and σ_r respectively. Equations (16)-(19) illustrate the authentication process for the initiator at the last two messages of the negotiation. As outlined in (10)-(13), the initiator executes the signing algorithm **sign** that takes $params$, $Hash_i$, initiator ID_i, and end node's secret key as input.

$$M_i \longleftarrow HASH\,(SKEYID, CK_i, CK_r, SA, ID_i) \quad (16)$$

where *SKEYID* is a session key between initiator and responder, and CK_i and CK_r are the initiator and responder cookies.

$$Hash_i \longleftarrow HASH\,(M_i, ID_i, params, npk_i) \quad (17)$$

$$Sig(Hash_i) \longleftarrow \textbf{sign}\,(Hash_i, s_{ID_i}, params, partial_key_i) \quad (18)$$

$$\sigma_i \longleftarrow (Sig(Hash_i), Hash_i) \quad (19)$$

Upon reception of IKE third exchange, the responder decrypts the messages to restore the ID payload and signature σ_i. Finally, the responder's verification algorithm **verify** inputs $Hash_i^{'}$ generated by the responder by using all the security attributes transmitted prior to this verification: ID_i, $params$, npk_i, and signature σ_i . The algorithm returns output 1 if the signature is valid ($Hash_i^{'}$=$Hash_i$) and 0 otherwise. To refer to the full execution of this process at the responder, we use (14) and (15) with the following notation. Figure 3 summarizes the new IKE authentication by using ABK with certificateless signature.

At the responder

$$(0,1) \longleftarrow \textbf{verify}\,(Sig(Hash_i), HASH(ID_i), params, npk_i) \quad (20)$$

V. Conclusion

This paper is intended to modify IKEv1 authentication to eliminate the need for certificate in IPSec and in turn, proposed a new IKE authentication based on certificateless signature. This is due to cryptosystem based on elliptic curve offers good security with smaller key size compared to RSA. We have also proposed to deploy translation gateway as KGC to reduce the exchanges of the messages in the network for securing end-to-end communication.

A performance analysis is accomplished to evaluate our CL-PKI scheme and it is compared with well-known RSA in terms of size of public key and signature block, and the speed of generating or verifying signature. Due to computationally expensive operation of pairing, the proposed scheme introduces extra processing overhead. Nevertheless, the proposed scheme offers significantly reduction in infrastructure complexity, eliminates the use of certificate to guarantee the authenticity of public keys and reduces the cost for managing the certificates.

Acknowledgment.: The research is funded by Ministry of Science, Technology, and Innovation (MOSTI), Government of Malaysia, under e-ScienceFund grant No. 01-02-01-SF0170.

References

[1] Deering, S., Hinden, R.: Internet Protocol, Version 6 (IPv6) Specification. RFC 2460, (1998)
[2] Nordmark, E., Gilligan, R.: Basic Transition Mechanisms for IPv6 Hosts and Routers. RFC 4213, (2005)
[3] Carpenter, B., Moore, K.: Connection of IPv6 Domains via IPv4 Clouds. RFC 3056, (2001)
[4] Tsirtsis, G., Srisuresh, P.: Network Address Translation - Protocol Translation (NAT-PT). RFC 2766, (2000)
[5] Kent, S., Atkinson, R.: Security Architecture for the Internet Protocol. RFC 2401, (1998)
[6] Kent, S., Atkinson, R.:IP Authentication Header. RFC 2402, (1998)
[7] Kent, S., Atkinson, R.:IP Encapsulating Security Payload (ESP). RFC 2406, (1998)
[8] Srisuresh, P., Holdrege, M.: IP Network Address Translator (NAT) Terminalogy and Consideration. RFC 2663, (1999)
[9] Harkins, D., Carrel, D.: The Internet Key Exchange (IKE). RFC 2409, (1998)
[10] Kevinen, T., Swander, B., Huttunen, A., Volpe, V. :Negotiation of NAT-Traversal in the IKE, RFC 3947, (2005)
[11] Huttunen, A., Swander, B., Volpe, V., DiBurro, L., Stenberg, M.: UDP Encapsulation of IPSec ESP Packets. RFC 3948, (2005)
[12] Shamir, A.: Identity-based Cryptosystems and Signature Schemes. Proc. of CRYPTO 1984, LNCS vol. 196, pp. 47-53, (1984)
[13] Al-Riyami, S., Paterson, K.: Certificateless Public Key Cryptography Advances in Cryptology. Proceedings of ASIACRYPT 2003, (2003)
[14] Routo T., Denise H. G.: A Certificateless Signature Scheme based on Bilinear Pairing Functions, Symposium on Cryptography and Information Security, (2007)
[15] Lifeng G.,Lei H., Yong L.: A Practical Certificateless Signature Scheme, Symposium on Data, Privacy and E-Commerce, (2007)
[16] Changji W., Hui H., Yong T.: An Efficient Certificateless Signature from Pairings, Symposium on Data, Privacy and E-Commerce, (2007)
[17] Smetters, D. K., Durfee, G.: Domain-Based Administration of Identity-Based Cryptosystems for Secure Email and IPSec. Proc. of the 12th Conference on USENIX Security Symposium, pp. 15-15, (2003)
[18] Arkko, J., Aura, T., Kempf, J.: Securing IPv6 Neighbor and Router Discovery. Proc. of 1st ACM Workshop on Wireless Security, pp. 77-86, (2002)
[19] OpenSwan, http://www.openswan.org
[20] Yum, D. H., Lee, P. J.: Generic Construction of Certificateless Signature. Lecture Notes in Computer Science, vol. 3108, pp. 200-211, (2004)
[21] Vixie, P., Gudmundsson, O., Eastlake, D., Wellington, B.: Secret Key Transaction Authentication for DNS (TSIG). RFC 2845, (2000)
[22] Eastlake, D.: Domain Name System Security Extension, RFC 2535, (1999)

Improved Extreme Programming Methodology with Inbuilt Security

Bala Musa S., Norita Md Norwawi
Faculty of Science and Technology
Universiti Sains Islam Malaysia
Nilai, Malaysia
Musa_bala@yahoo.com, norita@usim.edu.my

Mohd Hasan Selamat, Khaironi Yetim Sharif
Faculty of Computer Science and Information Tech.
Universiti Putra
Serdang, Malaysia
hasan@fsktm.edu.my, khaironi@fsktm.edu.my

***Abstract*—security in e-commerce is becoming an important issue to deal with as several cases of attacks to users' data are increasing exponentially. Therefore, there is absolute need for proper checks and balances to mitigate the lapses using the appropriate development framework. This paper provides as a candidate, Improve Extreme Programming Methodology by tightening security controls across the development stages without necessarily extending the process.**

***Keywords* — Development Framework; Extreme Programming; Security; Web engineering; E-commerce Security**

I. Introduction

This A report of Sysadmin Audit Network Security [1] on cyber security threads in 2009 have shown that Structured Query Language (SQL) Injection, Cross-site Scripting (XSS) and PHP File are the three most popular ways of compromising web applications. This points to the fact that web application layer is the initial focus of attackers where 75% of such attacks are XSS and SQL injection as contended by [2]. In another statistical survey according to [3], there are 80% potential threats to Web applications using cross-site scripting, while 62% as a result of SQL Injection, 60% Parameter Tempering and 37% Cookies Poisoning.

It therefore suffices to say that most of the threats in web application have little to do with Secure Socket Layer (SSL) or firewall which has been the understanding of security experts previously. It is much more to do with the application layer [4], [5] which according to [6] can be mitigated by inserting security checks and balances throughout the life cycle.

In addition, the cost of not doing an adequate work during the early stage of identifying design flaws may impact so much on any web system which may require re-architecture or shipping an unnecessary patches[7], [8].

Therefore, we present in this paper an improved Extreme Programming security framework for e-commerce as a candidate that tightens security across the lifecycle without extending it further.

II. Relevant Work

It has been argued by [9],[10], that there is no single methodology that is widely accepted as web methodology. However, researchers and practitioners tend to adopt or adapt from the existing software engineering methodology depending on the project type.

Some of these methods such as [11] proposes a web engineering framework that applied iterative requirement specification, analysis, design and implementation in obtaining feedbacks from users. They included an Agile Modeling Principle in their requirement and analysis phase.

Also, as a small web development such as those meant for students or non-commercial purpose, [12] and [13] proposes frameworks based on agile development which categorizes the stages into small web project, adopt modified XP process methodology, and apply XPMM. This is based on the fact that Agile methods are said to be the most preferred methods when it comes to developing web applications due to their rapid delivery nature and accommodation for change request [14].

It is interesting to note that, for the purpose of security in frameworks, none of the work mentioned earlier has actually considered inculcating security in the life cycle.

However, [15] describe an agile method that is integrated with software development for security purpose, while [16] provided a beginners sensitization framework that captures an early though for security such as use case and misuse cases in design and implementation.

Furthermore, [17] built in security checks around the feature driven development (FDD) by combining risk analysis within the FDD process with the aim of mitigating security lapses. It is argued that FDD approach is design and building phase centered instead of entire lifecycle [18].

But the most interesting work in relation to e-commerce security framework is proposed by [19] which is based on security engineering life cycle approach with security controls.

Therefore, to deal with the issue of e-commerce security in details, our approach inserts and tightens security in the entire development process using also the most efficient methodology in terms of all stallholders'

participation with pair reviewing code to double check areas of vulnerabilities.

III. Comparison Of Agile Methods Using Frameworks

Comparisons have shown the success of agile methods over traditional or heavyweight methods, researchers have also delved further into comparing the various agile methodologies using different frameworks and tools in order to give an insight on which agile method is appropriate for which home ground. Some of the most systematically guided comparisons are described by [20]. They selected XP and Scrum as the two well regarded agile methods for comparison. Used 4-Dimensional Analytic Tool mainly built for agile process, they carried out the comparison. It revealed from the comparison that XP has a significant high rating in terms of the most important agile values which is customer collaboration. Although it has more agile phases and less practices than Scrum methodology, the most significant advantage of XP over Scrum is the fact that it has quantitatively shown clean and simple code style with business culture.

Similarly, [21] compared nine agile methods using Lenses Analytical tool that measures the methods based on

A. Software development life cycle
B. Project management
C. Abstract principles/concrete guidelines
D. Universal pre-defined/situation appropriate and
E. Empirical evidence.

Their comparison has revealed the strength of different agile methods within the itemized perspective. It has further brought to light XP method of having solid empirical evidence in web application development and its complimentary support in providing project management for other methodologies such as scrum.

However, [21] has described some weaknesses in some of the agile methods such as Feature Driven Development which was described as putting more emphases on the design and implementation phase and hence requires the pairing of other approaches.

Scrum is said to have been more or less small approach that leaves out details of integration and acceptance testing.

Crystal Family of Methodology has a combination of methods such that choice of what method will suit what project happens to be a big task.

Dynamic System Development Method despite its prototyping approach, it has a secrecy policy that gives the consortium the custody of processes in the method.

Open Source Software Development is said to emphasis on code-free for members, but not an established methodology.

Rational Unified Process has additional tool support in its development without details of applicability in changing requirements.

Adaptive Software Development as the name implies, its adaptive culture imbibed by organization than full scale methodology.

Another comprehensive analysis using framework for agile methods that incorporated most of the criteria used by [21] and other additional criteria is described by [22] as shown in table 1.

Her findings show areas of commonality and difference in five selected agile methods.

Although the comparison has shown the different environment for the selected agile methods, it has also brought into light the customer collaboration that is associated with XP and its adaptation to changing request.

TABLE 1

COMPARISON OF AGILE METHODS USING ANALYTIC FRAMEWORK FOR AGILE METHODS

[22] Using Analytic Framework for Agile Methods	
Similarity	Difference
Agile methods are published between 1995 – 2002	DSDM and ASD adopt to technique from other methods
Authors based in US and UK	Scrum focus on project management XP adopt to change with efficient customer collaboration
Agile Methods shows objectivism technology solution to businesses	XP most commonly studied.
Agile Development in incremental and iterative	XP mostly combined with other agile methods
Agile User participation with team empowerment	XP activities are explicit with all encompass testing
Agile project team 3 to 5.	
Agile Communication is informal	
Agile Permit the use of UML model	
Agile allows for planning and control of iteration.	

IV. Improved Extreme Programming Methodology

This section presents the Improved Extreme Programming Framework that tightens security controls as it affects e-commerce environment. The model strength include the involvement of both the development team and business representatives at the very beginning which allows for identifying important security threats and dealing with such threats early enough in the lifecycle. Also, use/misuse cases are carried out from the requirement and design stage, while risk assessment is

done in iteration to uncover vulnerabilities that may scale through the initial phase.

Fig.1 is the architectural representation of the proposed framework.

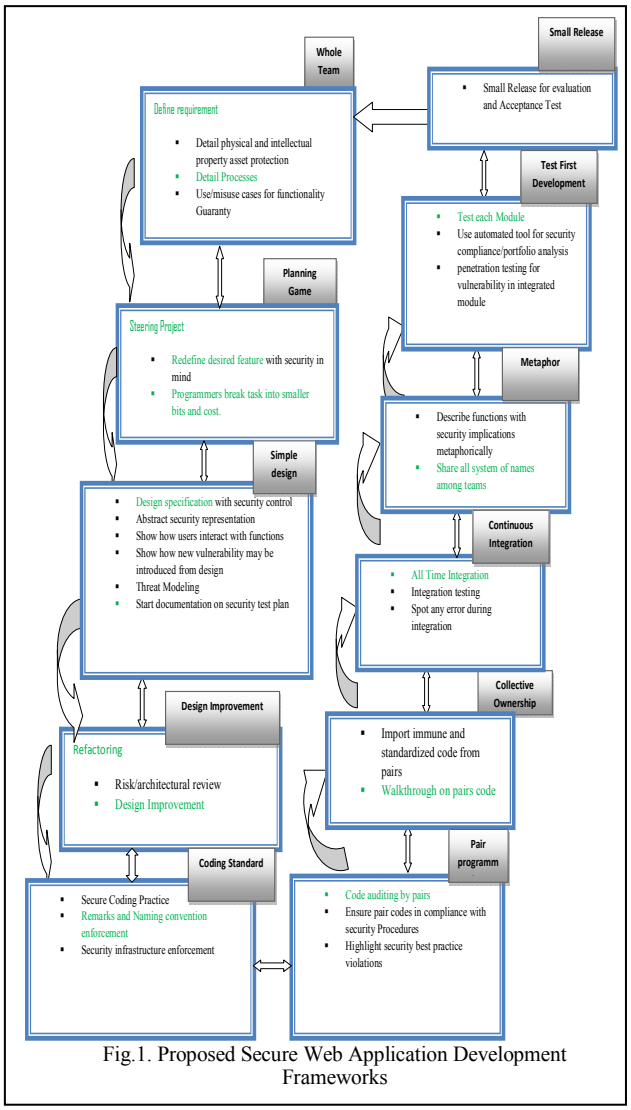


Fig.1. Proposed Secure Web Application Development Frameworks

We now further detail out each stage from the framework as thus:

A. Whole Team.

When stakeholders collaborate with web development teams such as System Analyst, Test team and developers, an opportunity is created for different teams to understand the perspective in which others view the system. Hence, business people may be enlightened on the risk involve when an attacker gains some openings in the system. Likewise the developers can have an insight on company policies and regulations. Therefore all stakeholders collaborate to define security requirement and acceptance testing requirement in the light of company rules and policies. Use/misuse cases are ways users/attackers view the system. Therefore, defining use/misuse case at requirement will guarantee how likely the system may be infiltrated and as such, a review of some security policies at earlier stage will be ensured, physical and intellectual property will also be considered.

B. Planning Game.

This involves defining expectation in stipulated period. Business representative at this stage uses the knowledge acquired in the previous phase to re-design their requirement with security consideration. The development team then split task into smaller units with time span and cost.

C. Simple Design.

Security control and how vulnerabilities are introduced are included at this stage. Risk analysis and threat model gears the development of security test plan which will be documented and used during Test-First Development. All designs are abstracted with details of security in each representation.

D. Design Improvement.

Refactoring is achieved at this level through revision until a standardized design is obtained while carrying out risk assessment for any vulnerability.

E. Coding Standard.

For collective ownership to be enforced, standardize codes are adapted by all developers working on different bits of modules. Furthermore, secure coding such as standard naming conventions, remarks and security infrastructure are enforced.

F. Pair Programming.

Pair review coding ensures that codes produced or written by an individual are reviewed by another pair which helps in double checking any error. Therefore programmers at this stage ensure that codes are in full compliance with security definitions and any non-compliance or violation is spotted and handle appropriately.

G. Collective Code Ownership.

For codes to be re-used by developers in separate development teams there has to be collective ownership of codes without necessitating any sort of privilege. Therefore, security alignment is the use of standardized and immune codes.

H. Metaphor.

This is identifying and separating with appropriate remark any function that has security implications to the development of the system.

I. Test – First Development.

For an effective test for vulnerabilities, feedbacks have to be gathered at all the stages in order to review each code released by the developing team. This gives some level of security assurance to the development. Source codes are also checked using automated tool for security compliance. The portfolio analysis checks the cross-enterprise risk that can have security impact.

J. Continuous Integration.

Keeping the system fully integrated enable errors become visible at early stage which might not be detected during testing.

K. Small Release.

Perfuming a small release enable customer evaluates the business requirement fulfillment and to accelerate the rapid development.

V. Case Study

The basic activities in development lie in the requirements, design, coding and testing. For the purpose of illustration, we examine the shopping cart activity in an online bookshop to explain two important stages in the model (Requirement, Design).

The requirement for an online bookshop is as follows:

a. Customer search for books on the home page using a keywords
b. The customer is expected to login and provide some basic information in order to add his choice of books to his cart and make a purchase
c. Customer makes an order

Therefore, the requirement definition will include:

A. Detail physical and intellectual property protection such as:
   i. Active content protection/secrecy
   ii. Client-to-server communication protection/confidentiality
   iii. Server protection from attacks like spoofing, defacement etc
   iv. Database server protection such as communication between client-to-database

B. Data processes
   i. Search books
   ii. Add to cart
   iii. Order books

C. Use Case
   i. Customer search books using keywords
   ii. Customer login to add to his cart the selected books
   iii. Customer make an order

D. Misuse case
   i. Attacker can craft a malicious code in the active content when placing a book in the cart
   ii. Attacker can try to reveal customer's personal information stored in cookies
   iii. Attacker can try to tamper with customers files through cookies
   iv. The web server used to display the link requested by the user can be circumvented if it is porous

The design follows the initial requirement set out. The fig 2 illustrates the use case diagram.

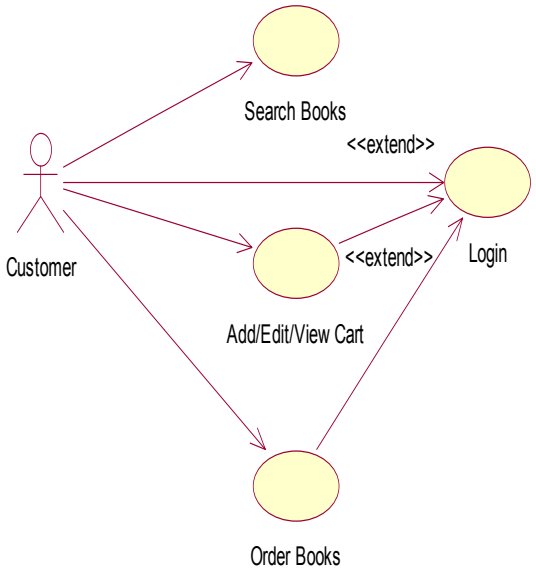


Fig 2: Use case diagram for Online Bookstore

The activity which requires special attention in the use case diagram is further detailed in fig 3 and 4 respectively

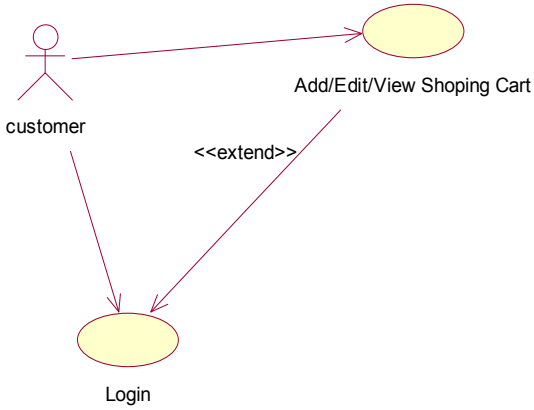


Fig 3: Use case diagram for Shopping Cart activity

a. The customer selects the sign-in button to display login form.
b. The customer submits his correct name and password to view the books available and cost.
c. On selecting his preferred books, the customer is displayed with details of his chosen books with add to cart option.
d. The customer add the book to his cart to obtain the status of his cart with quantity and cost updated

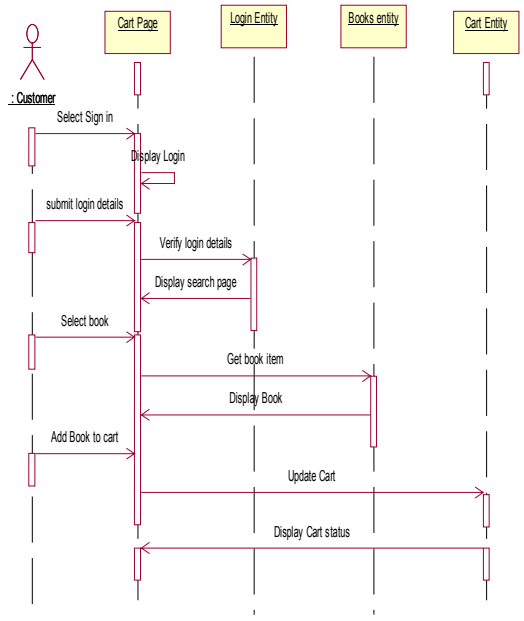


Fig 4: sequence diagram for shopping cart activity

The Misuse case in this context is illustrated in fig 5. The attacker can use different mechanism to circumvent the system during customer transmission of his details to the server.

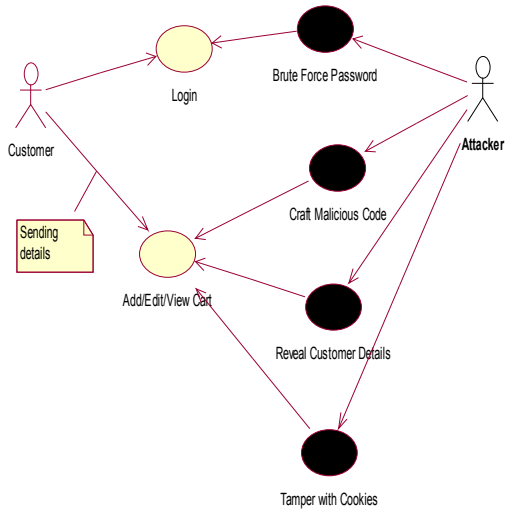


Fig 5: Misuse case diagram for Shopping Cart Activity

VI. Conclusion And Future Work

This approach presents a framework for e-commerce application development based on extreme programming methodology with inbuilt security checks and balances. The approach ensures the involvement of both the development team and business representatives at the very beginning which allows for identifying important security threats and dealing with such threats early enough in the lifecycle. Also, use/misuse cases are carried out from the requirement and design stage, while risk assessment is done in iteration to uncover vulnerabilities that may not have been detected from the initial phase.

This research will henceforth focus on improvement of the framework based on different environment and determining different frameworks in the context of e-commerce web application and their possible edge over one another in terms of security.

Acknowledgment

We wish to thank the Dean School of Post Graduate Studies (Prof. Dr. Bachok M. Tiab) for providing the logistics and guidance, and also the reviewers for their profound support and scrutiny which assisted tremendously towards this research

References

[1] Sysadmin Audit Network Security SANS/FBI, Top Cyber Security Risk. , in, SPI Dynamics Inc, 2009.
[2] O. Adrian, Web Application Vulnerability and IBM Rational AppScan, in, In IBM Rational Software Development Conference 2008, Orlando FL, 2008, pp. 6.
[3] A. Danny, Managing a growing threat: an executive's guide to Web application security., in, Web application security Executive brief, NY, USA, 2007, pp. 4.
[4] D. Stuttard, M. Pinto, The web application hacker's handbook : discovering and exploiting security flaws, Wiley Pub., Indianapolis, IN, 2008.
[5] V.K. Stijn, Threat Model for Web Application Using STRIDE Model, in, Information System, Royal Halloway University London, 2004, pp. 80.
[6] S. Caleb, Vincent, L. , InforSecWriters. Effective Controls for Attaining Continuous Application Security throughout the Web Application Development Life Cycle, in, 2007.
[7] S. Software Assurance Forum for Excellent in Code, Fundamental Practice for Secure Software Development, in, A Guide to the Most Effective Secure Development Practice in Use Today, 2008.
[8] M.S. Bala, M.N. Norita, S. Mohd Hasan, Secure E-commerce Web Development Framework. Information Technology Journal, DOI: 1812-5638, (2011).
[9] S. Hadjerrouit, Web-based application development: a software engineering approach. SIGCSE Bull. 33 (2001) 31-34.
[10] M. Jazayeri, Some Trends in Web Application Development, in, 2007 Future of Software Engineering, IEEE Computer Society, 2007, pp. 199-213.
[11] V.E.S. Souza, R.d.A. Falbo, An agile approach for web systems engineering, in, Proceedings of the 11th Brazilian Symposium on Multimedia and the web, ACM, Pocos de Caldas - Minas Gerais, Brazil, 2005, pp. 1-3.
[12] S. Hsieh, Software engineering for Web application development. J. Comput. Small Coll. 19 (2003) 10-19.
[13] H. Altarawneh, A.E. Shiekh, A Theoretical Agile Process Framework for Web Applications Development in Small Software Firms, in, Proceedings of the 2008 Sixth International Conference on Software Engineering Research, Management and Applications, IEEE Computer Society, 2008, pp. 125-132.
[14] R.S. Pressman, Software engineering: a practitioner's approach (2nd ed.), McGraw-Hill, Inc., 1986.
[15] H. Keramati, S.-H. Mirian-Hosseinabadi, Integrating software development security activities with agile methodologies, in, Proceedings of the 2008 IEEE/ACS International Conference on Computer Systems and Applications, IEEE Computer Society, 2008, pp. 749-754.
[16] D. Meledath, Secure Software Development Using Use Cases and Misuse Cases. Information Systems (2006).
[17] X. Ge, R.F. Paige, F.A.C. Polack, H. Chivers, P.J. Brooke, Agile development of secure web applications, in, Proceedings of the

6th international conference on Web engineering, ACM, Palo Alto, California, USA, 2006, pp. 305-312.
[18] S.R. Palmer, M. Felsing, A Practical Guide to Feature-Driven Development, Pearson Education, 2001.
[19] A. Sengupta, C. Mazumdar, M. Barik, e-Commerce security — A life cycle approach. Sadhana 30 (2005) 119-140.
[20] A. Qumer, B. Henderson-Sellers, An evaluation of the degree of agility in six agile methods and its applicability for method engineering. Inf. Softw. Technol. 50 (2008) 280-295.
[21] P. Abrahamsson, J. Warsta, M.T. Siponen, J. Ronkainen, New directions on agile methods: a comparative analysis, in, Proceedings of the 25th International Conference on Software Engineering, IEEE Computer Society, Portland, Oregon, 2003, pp. 244-254.
[22] D.E. Strode, The Agile Methods: An Analytical Comparison of Five Agile Methods and an Investigation of Their Target Environment, in, Massey University New Zealand, Palmerston North, pp. 224.

Data Hibernation Framework in Workflows Under Intrusion Threat

Sohail Safdar, Mohd Fadzil Hassan, Muhammad Aasim Qureshi, Rehan Akbar
Department of Computer & Information Sciences,
Universiti Teknologi PETRONAS,
Malaysia
sagi_636@yahoo.com, mfadzil_hassan@petronas.com.my, maasimq@hotmail.com, rehankb@yahoo.com

Abstract— **The main objective of the research is to define and propose a framework for data hibernation in the workflows under intrusion threat. When an intrusion is detected, the data services need to be discontinued immediately to retain the security and the integrity of the valuable data, till the system is recovered from the threat. By discontinuing data services, the end users may face inconveniences in using the system because of its temporary unavailability. Data hibernation addresses a mechanism of secure transferring of data and providing an access of the data alternatively keeping the data integrity intact. Data hibernation involves three steps i.e. designing an alternate schema for storing data, transferring data to that alternate storage and providing an access to that data. Hence the system can continue to provide data services securely to the end user even in the threat situations.**

Keywords— IDS (Intrusion Detection System), Data Hibernation, Dimensions, System Availability .

I. INTRODUCTION

World is experiencing the economic growth very rapidly. Every business organization is taking concrete measures to provide its customers with the quality of services and tries to gain maximum customer satisfaction. IT (Information technology) has provided all the business stakeholders an efficient mean of improving an in time delivery of quality services. But to provide quality services to the customers using IT infrastructure requires continuous research and development. Businesses are continuously optimizing their processes or workflows based on IT to meet the expectation of the world in the best possible way. With the remarkable development in the area of IT services, the number of security breaching attacks is also increased. Whenever there is a threat to the system, the executing workflows should be stopped and the services to the customers should be discontinued. This limitation promotes the area of ensuring secure availability of the quality services to the customer a very hot research area.

The current research is an effort in the same area and deals to overcome the problem of discontinuing the services when there is an intrusion attack to the system. Most of the existing solutions drive the system to shutdown the services temporarily by making the active transactions to be rollback in case of intrusion attack. Once the system is recovered from the attack and is considered as safe, the system becomes available again for the customers and end users. These solutions provide the security to the system along with maintaining the integrity of data. But doing so may cause inconvenience to the end users or customers. Customers are willing to use the quality services that are uninterrupted and available all the time. In this regard, an effort has been made by proposing a framework for alternate execution of workflows under threat. The framework is intended to deal with the situation when there is an intrusion threat to the system then it provides an alternate execution path for the system to continue its execution and provide the customers with the uninterrupted services all the time. The framework also ensures the security of system resources and maintains the integrity of the data. The whole workflow continues it execution robustly but in a secured fashion.

The current research is part of a framework for alternate execution of workflows under threat. This paper defines and describes the data hibernation framework in workflow under intrusion threat. The data hibernation framework is intended to work under the framework for alternate execution of workflows under threat. Therefore the current research is the detailed extension of the existing work and provides a firm basis to secure the data by maintaining its integrity during alternate execution of the system that is under threat. The overall execution of the system is continued robustly.

The problem that is addressed in this research is the discontinuation of the data services to the customers and users in case of intrusion threat for keeping the data integrity intact. The main objective of the research is to propose a data hibernation framework that can provide alternate data source and shifts the data from original to that alternate data source by giving the safe users an access to that data, so that the data services can be made securely available all the time even in the threat case.

The data hibernation framework defines the mechanism of the data to be hibernated in a similar way the animals are hibernated for a certain period of time. In this context, there is a need to model an alternate data source where the data is supposed to be shifted when the system goes under threat. The data hibernation cannot be considered as completed unless it provides an access of the hibernated data to the safe users. Data hibernation framework consists of the three steps based on the above mentioned concepts that is modeling alternate data source, transferring data to the alternate data source and providing access to the hibernated data. The proposed framework is intended to work for all the intrusions except that are corrupting the data.

The rest of the paper is organized as Section II discusses the background followed by section III that discusses the problem statement in specific as well as the objectives of the research. Section IV defines the concept of data hibernation. Section V discusses the complete data hibernation mechanism and the steps involved. Section VI describes the proposed framework in detail based on the steps discussed in section V followed by the conclusion.

II. BACKGROUND

Businesses are emphasizing a lot on improvement of their workflows in a way they are more robust and defensive to the threats. The major concern of the business is to provide uninterrupted quality services to acquire maximum customer satisfaction. Due to the high demand of business process optimizations the workflows management systems become very hot area of research. The current research directly addresses the secure system availability to the end users all the time even in the case of intrusion threat. In this manner the research is directly associated to the area of security and availability of workflows. Various efforts have been made for intrusion detection in the workflows and then system recovery. Multi-Version Objects [2][4] is an approach that involves multiple version of the same data objects and replaces the dirty objects with the clean version to recover the system. The system needs to be stopped when the threat is detected and the system is brought to the previous safe state using these clean data object versions. When the system is recovered then all the active transactions have to be repeated from the start [17][18]. Trace back recovery [2][5] mechanism that is based on Flow-Back Recovery Model monitors the traces of the flow of execution and then provide the recovery based on traces by cleaning the related data [19]. Workflow specifications can also be used to detect the intrusions. "Attack Tree Model" [3][6][7] proposes a method to describe the major goals and sub goals of the attack and then recover the system through dynamic regeneration of the workflow specification. Intrusion detected by the IDS (Intrusion Detection System) can be recovered by the dynamic regeneration of workflow specification using BPEL (Business Process Enterprise Language) Engine and Prolog Engine for intelligently [2][3][6][7]. All of the above mentioned methods follows undo and redo mechanism i.e. in case of intrusion threat all of the current activities need to be stop and undo and the system goes down. All the activities will be redone when the system is recovered and active again [20]. By undo and redo, the system can be brought to the consistent state again [14][15][16]. Some other approaches like Do-It-All-Up-Front, All or Nothing, Threat Modeling and Big Bang approach etc. ensures security on web environment based on undoing everything in case of intrusion threat is detected [2][3][8][9][10][11]. Making the system wait for the recovery purpose and redoing the tasks sometimes annoys the customer and user. Hence making the system available even in the unsafe state is desirable that is addressed for the first time in the framework for alternate execution of the workflows under threat [2][3]. The data can sometimes be encrypted for protection specially user information [12][13].

The framework for alternate execution of workflows under threat describes that whenever system goes under some intrusion threat, all of the users should forcefully be logout of the system. The data should be hibernated to the alternate location and meanwhile the users are login back to the system via special authentication [1][2][22] having strong password [21], the system is ready to execute the entire requests using alternate execution path. The whole phenomenon can be seen in the figure 1 [2].

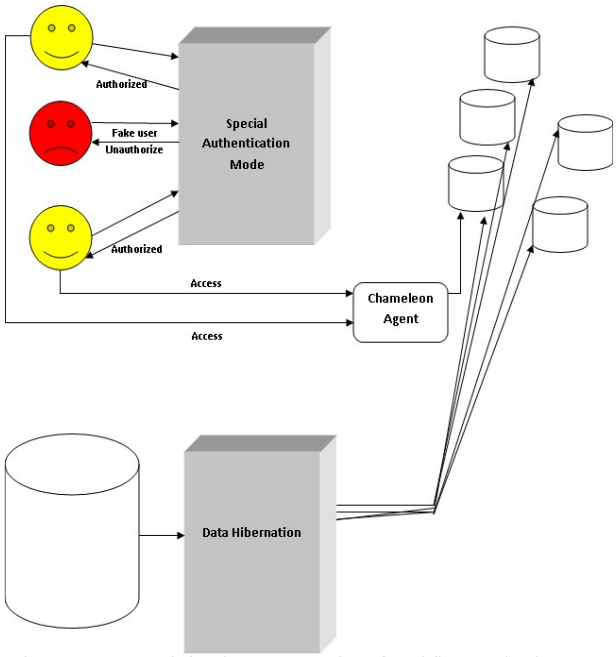


Figure 1: Framework for alternate execution of workflows under threat

The current research addresses the data hibernation part of this framework. Data Hibernation is formalize in to a framework to explain the details of the processes involve in it and hence in this paper the whole mechanism of data hibernation is addressed in detail.

III. OVERVIEW OF THE PROPOSED RESEARCH

A. *Problem Statement*

Whenever the workflow system goes under some intrusion threat, the system needs to remain available to avoid the services discontinuation to the customers. Hence it is required for the data to remain available securely to the customers that may not be possible using the same data source. Hence the following objectives need to be achieved.

B. *Objectives*

The main objective of the research is to propose a data hibernation framework that can work under intrusion threat situation as following.

- Model and provide the alternate data source.
- Conduct data transfer to the alternate data source securely.
- Provide successful connectivity to that data in alternative data source ensuring the data integrity remain intact.

Providing such services by the data hibernation framework, the system can continue to execute on an

alternate path along with other components having the data available for processing all the time in a secured fashion.

IV. DATA HIBERNATION

Data Hibernation is inspired by the concept of animal hibernation. Like animal hibernation data can also be hibernated, but the question arises where the data should be hibernated. Considering the animal's hibernation phenomenon that hibernate themselves in to the soil i.e. in the similar place where they use to live. Similarly, data can also be claimed to hibernate in the similar place where it used to be stored originally. If the data is originally stored in the file it may store in another file that is specially hidden from others. If the data is originally stored in a database then it may also be stored in another database of same or small sized database schema that can be logically mapped to the original database [2][3]. This paper describes the data hibernation in the context of databases.

Data hibernation is defined as the process of transferring data from the original data source to the designed alternate data source/s. It is required to make sure the alternate data source/s is designed in such a way that it is logically maps with the original data source.

V. PROPOSED DATA HIBERNATION MECHANISM FOR WORKFLOWS UNDER THREAT

It is proposed that data hibernation should only be conducted when there is a need of it. In the current case, it is proposed that data hibernation should be done if an intrusion threat is detected in the workflows and the system is desired to be continued without the discontinuation of the data services to the end user. Data hibernation majorly involves the transferring of data from the original data source to the alternative designed data source. Hence an important measure that is required to be taken for data hibernation is to design an alternate data source that is in compliance with the original data source. If the alternate data source/s is in compliance with the original one, only then it is possible to transfer the data from original to the alternate data source/s. Once the data is available in the alternate data source/s, it should be used by giving the access of the appropriate alternate location/s to the safe users. Safe users are considered to be those users who re-authenticate using some special secure mechanism during the unsafe state of the system due to intrusion threat [1][2][22].

Data hibernation is considered to be completed if the following three very important measures have been taken.

i) Designing alternate data source/s.
ii) Transferring of data from original to alternate data source.
iii) Providing the access to the end user on the data in the alternate data source.

A. Modeling Alternate Data Source/s

The first and very important measure to be taken is the designing of alternate data source/s that is incompliance with the original data source. Designing the alternate data source is one time step that should be done prior to run the system in an open environment. So the alternate data sources are always ready whenever they are required and data can be transferred to them successfully. Data sources for handling data that are considered in this research are databases. Hence the alternate database/s should be designed such that it can be mapped logically to the original database. It is proposed that there are two possible methods to design the alternate data sources. One is to design a complete single database similar to the original database but with different name and with a modified schema with respect to original database. The other method is to design multiple databases that are the subset of the original database. These subset databases are smaller than the original database and contain all aspects of the original database schema. Based on the above discussion, two following design approaches should be considered while designing alternate data source/s.

1) Single Original with Single Alternate Database

Single alternate database should be designed to handle the data completely with respect to the original database. One way is to design the same copy of the original database that can handle the data similar to the original one but on an alternate path or source address. But in this approach, if the source address of alternate database is hacked somehow then it becomes very easy to extract and steal data with the same commands as used for the original database [2]. To overcome this problem, the other way is that the alternate database may be designed with different name and the modified schema provided it should not negate the aspects of the original database. It may have different logical schema but it should be completely mapped with the original database schema. It is mandatory for both the databases to exist uniquely but support the achievement of common goals. The net effect on the data remains the same with respect to the original database before and after the processing once the alternate database is used. In this way it is not possible to extract the data using the same commands as from the original database and hence if the data source address is hacked, the data is likely to remain safe as compared to the previous approach.

2) Single Original with Multiple Alternate Databases

In this approach, multiple small size databases should be designed as an alternate data sources for the original single database. The designed small alternate databases should be the subset of the original databases as they contain partial logical schema in the normalized form that is existed in the original database. These small subset databases are called dimensions. Hence the dimensions are designed subset of the original database that works alternatively in the absence of the original database during the threat scenarios [2]. Designing and engineering the dimensions require additional rules to follow and should be designed in such a way that these are completely mapped to the original database using some logical translation. Making dimensions provide extra benefits in terms of security of data as compared to the previous approach of single alternate data source. In this case no intruder can hack the source addresses of all of the dimensions. Therefore it is not possible to steal the information completely by any mean and moreover the way to access information is also different from the one in the original database.

B. Data Transfer

This step is the heart of data hibernation and the definition of the data hibernation is majorly based on it. This step has to be done every time the system goes under threat

and becomes unsafe. In the case of system intrusion, alternate data source has to become active and data from the original database should be shifted to the alternate data source that may be single database or the dimensions. As the data is going to be shifted from one data source to the other therefore ETL (Extract, Transform and Load) [23] command set is required. Hence it is proposed that whenever the system goes in to unsafe state due to intrusion, the original data source becomes inactive or offline and ETL is performed on it to shift the data to the alternate data source. Consider dimensions as the better modeled alternate data source. ETL extract the data and then transform the data from one normalized schema in to another normalized schema and then load it unlike the ETL used in Data warehouse where it transforms the data from normalized schema to non-normalized schema and vice versa. Hence it may be noted that ETL command set in hibernating the data may not take that much time and cost as compared to the data warehousing. Moreover ETL used in data hibernation will be less complex as compared to the ETL used in Data warehousing based on the above facts.

C. Data Access from Alternate Source

Third Important step is to access the hibernated data in the alternate data source. Considering dimensions as the better modeled alternate data source, the connection strings for the dimensions can be derived from the metadata that maps the original database to the dimensions and dimension to the tables. The following are such metadata tables that are based on the rules that each database can have multiple dimensions and each dimension have multiple tables/entities provided tables cannot be the part of more than one dimension.

TABLE I
ENTITIES

Attributes	Description
Table_Name (PK)	Table/Entity name
Dim_Name (FK)	Dimension Name

TABLE II
DIMENSIONS

Attributes	Description
Dim_Name (PK)	Dimension Name
Orig_DB_Name (FK)	Name of database of which the dimension is the subset of.

The active table name can be extracted from the query and search the appropriate dimension name. After verifying the database of which it is a part, the appropriate connection string is used built the connection to that dimension.

VI. PROPOSED FRAMEWORK FOR DATA HIBERNATION IN WORKFLOWS UNDER THREAT

The proposed framework for data hibernation in workflows under threat follows the three steps discussed above. Without the completion of the above mentioned three steps, data hibernation can never be considered as completed. Data hibernation framework is based on the modeled dimensions i.e. the subset of original database to be used as the alternate data sources. Proposed framework categorizes the whole three steps involved in data hibernation in to the regions that is based on their frequency of occurrence. The first most important step of modeling dimensions as alternative data source has to be done once for the successfully running system. The modeled dimensions are then integrated with the system so that the system is ready to coordinate with the alternate data sources when it is required in the case of intrusion threat. Second important step is to transfer the data from the original data source to the dimensions and this step has to be taken whenever the intrusion threat is recognized by IDS (Intrusion Detection System) in the workflows. Then the third step is to provide the access to the data hibernated in the dimensions and the frequency of this step depends on the usage of the system. Therefore the three steps can be divided in to two regions based on the frequency of occurrence. One region can be termed as Modeling and the other one as Execution.

A. Explanation

As discussed the data hibernation framework is based on three steps that are distributed in two regions classified by the frequency of occurrences of the steps. The two regions are as following.

1) Modeling Region

Modeling region is the area in which the frequency of the all participating activities is one. Modeling region involves modeling of dimensions and their integration in the system. The activities in this region have to be completed before the system is made operational. This is a very important region because success of the overall alternate behavior of the system depends on the integration of successfully modeled dimensions.

2) Execution Region

Execution region involves the activities whose frequency of occurrence is more than one. This region involves two steps that are transferring the data to the alternate integrated dimensions and to provide safe users the access to the data that is hibernated in the dimensions.

Considering these two regions, the following are the steps of the framework using which the data hibernation can be completed.

- Start with the modeling region.
- Devise the rules for modeling the dimensions.
- Model the dimensions based on devised modeling rules from the original database.
- Integrate the dimensions in the system as the alternate data source.
- If the IDS (Intrusion Detection System) detect an intrusion threat in workflow system then the flag value is true.
- Enters in to the execution region.
- Start by transferring the data from the original database to the alternate dimension using ETL command set.
- Once the data transfer is completed, provide the access of that data to safe users.

The whole phenomenon of data hibernation can be seen as a complete framework in the following figure 2, figure 3 and figure 4. Figure 2 shows the activities involved in the modeling region where the rules for making dimensions are set and hence the dimensions are modeled on the basis of these rules and then the designed dimensions are implemented and integrated with the system. Figure 3 deals

with the activities involved in the execution region. Execution region becomes active only when the threat to the system is detected and flag is set to true. The data from the original source is then transferred to the alternate dimensions using ETL. Then the access is provided to the safe users. Figure 4 gives the complete picture of the whole framework of data hibernation and every step involved in this.

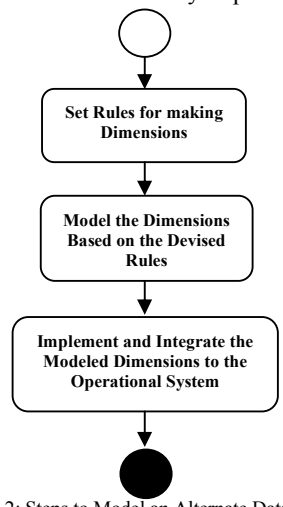


Figure 2: Steps to Model an Alternate Data Source in Modeling Region.

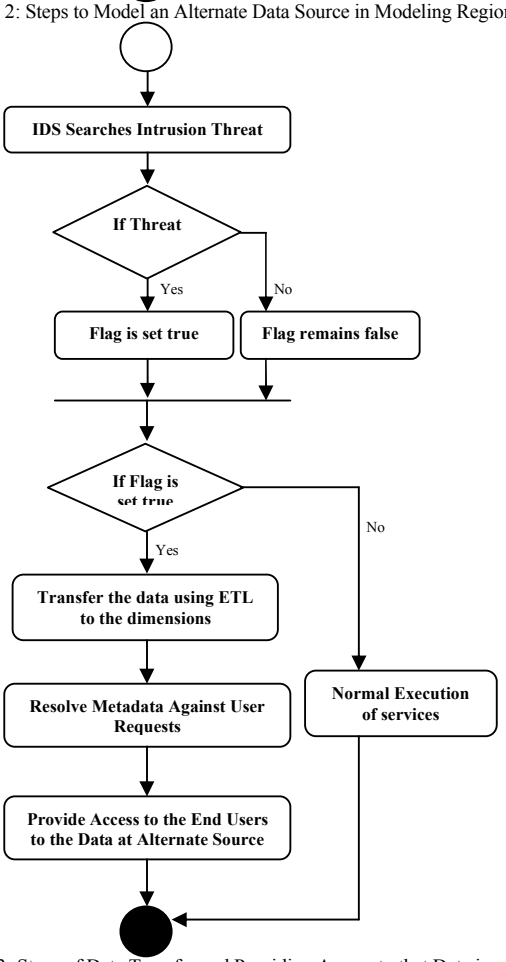


Figure 3: Steps of Data Transfer and Providing Access to that Data in Execution Region

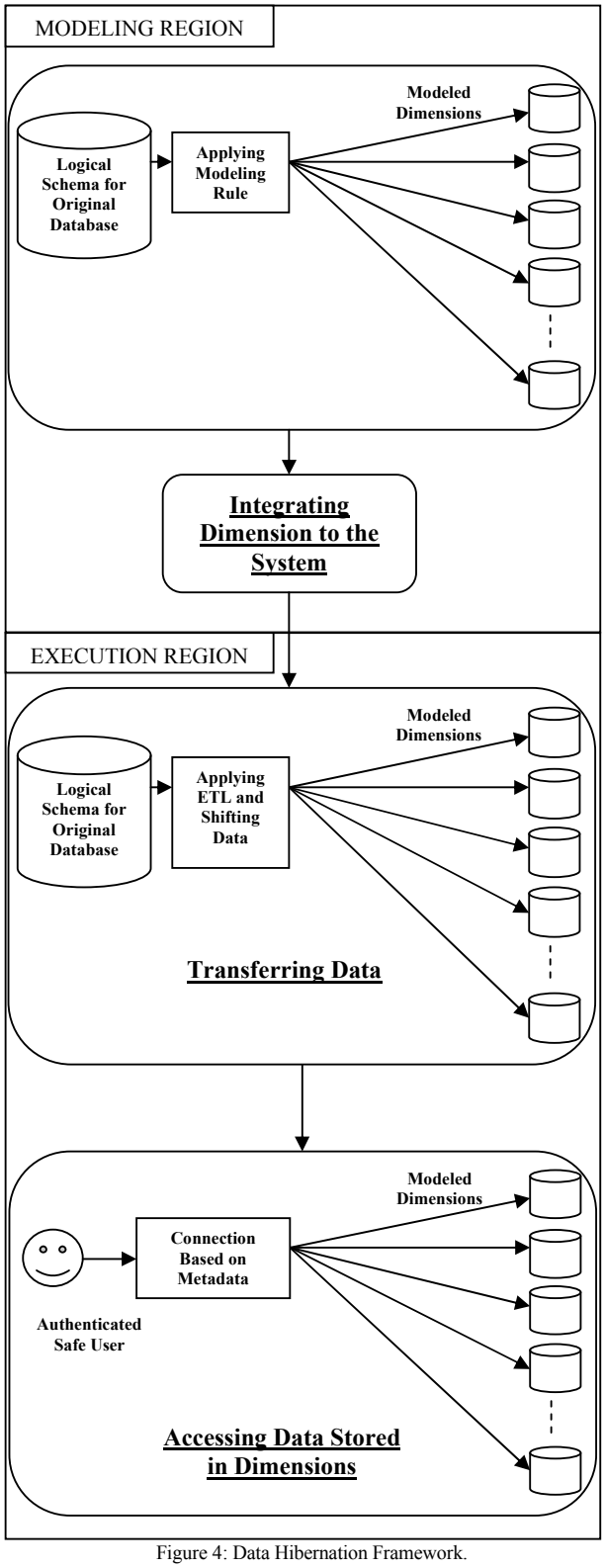


Figure 4: Data Hibernation Framework.

Figure 4 shows the complete mechanism of data hibernation in the form of a framework. The framework

contributes in providing the data availability keeping its integrity intact.

By far there is no approach that is addressing the data hibernation mechanism in case of intrusion threat. However, there are techniques of data transfer using ETL in data warehousing that are handling data transfer in a different context as compared to the current case.

VII. CONCLUSION

The data hibernation framework provides a detailed picture of how data hibernation can be carried out and hence contributes a remarkable mechanism in the framework for alternate execution of workflows under threat. Data hibernation framework not only provides the data transfer to the alternate source but also ensures the security of the data at the modeling level. While modeling the alternate data source, the method of modeling of dimensions gives more secure alternate data paths as compared to the normal one. Data hibernation can be used in various security related scenarios where it is desired to execute an alternate path no matter which particular framework is followed. Data hibernation framework can be integrated to the customized solutions. In future this research may lead to derive different techniques to design dimensions and handling them. The framework is workable for the intrusions that are meant for stealing data and have not affect data physically. In Future it can be extended to the data that becomes dirty due to intrusions.

REFERENCES

[1] Sohail Safdar, Mohd Fadzil Hassan, "Moving Towards Two Dimensional Passwords", International Symposium on Information Technology 2010, ITSIM 2010, Malaysia, June 2010.

[2] Sohail Safdar, Mohd Fadzil Hassan, Muhammad Aasim Qureshi, Rehan Akbar, "Framework for Alternate Execution of workflows under threat", 2nd International Conference on Communication Software and Networks, ICCSN 2010, Singapore , Feb 2010.

[3] Sohail Safdar, Mohd Fadzil Hassan, Muhammad Aasim Qureshi, Rehan Akbar, "Biologically Inspired Execution Framework for Vulnerable Workflow Systems", International Journal of Computer Science and Information Security, Vol.6 No.1, IJCSIS 2009.

[4] Meng Yu, Peng Liu, Wanyu Zang, "Multi-Version Attack Recovery for Workflow Systems", Proceedings of the 19th Annual Computer Security Applications Conference, ACSAC 2003 IEEE, 1063-9527/03, 2003.

[5] Meng Yu, Peng Liu, Wanyu Zang, "Self-Healing Workflow Systems under Attacks", Proceedings of the 24th International Conference on Distributed Computing Systems, ICDCS', IEEE, 1063-6927/04 2004.

[6] Casey K. Fung, Patrick C. K. Hung, "System Recovery through Dynamic Regeneration of Workflow Specification", Proceedings of the Eighth IEEE International Symposium on Object-Oriented Real-Time Distributed Computing, ISORC', IEEE, 0-7695-2356-0/05, 2005.

[7] Casey K. Fung, Patrick C. K. Hung, William M. Kearns, Stephen A. Uczekaj, "Dynamic Regeneration of Workflow Specification with Access Control Requirements in MANET", IEEE International Conference on Web Services, ICWS', 0-7695-2669-1/06, 2006.

[8] Kun Xiao, Nianen Chen, Shangping Ren, Kevin Kwiat, Michael Macalik, "A Workflow-based Non-intrusive Approach for Enhancing the Survivability of Critical Infrastructures in Cyber Environment", Third International Workshop on Software Engineering for Secure Systems, SESS', IEEE, 0-7695-2952-6/07, 2007.

[9] Gernot Goluch, Andreas Ekelhart, Stefan Fenz, Stefan Jakoubi, Simon Tjoa, Thomas M¨uck , "Integration of an Ontological Information Security Concept in Risk-Aware Business Process Management", Proceedings of the 41st Hawaii International Conference on System Sciences, IEEE, 2008.

[10] "Web Application Security Engineering", IEEE Security Magazine, Published By The IEEE Computer Society, 1540-7993/06, p-16 – 24, 2006.

[11] Margie Virdell, "Business processes and workflow in the Web services world", 2003, http://www.ibm.com/developerworks/webservices/library/ws-work.html, 03-03-09.

[12] Scott Mitchell, "Encrypting Sensitive Data in a Database", MSDN Spotlight, 2005.

[13] Sung Hsueh , "Database Encryption in SQL Server 2008" Enterprise Edition SQL Server Technical Article, 2008.

[14] Paul Ammann, Sushil Jajodia, and Peng Liu., "Recovery from malicious transactions". IEEE Trans on Knowledge and Data Engineering, 14:1167–1185, 2002.

[15] P. A. Bernstein, V. Hadzilacos, and N. Goodman., "Concurrency Control and Recovery in Database Systems". Addison-Wesley, Reading, MA., 1987.

[16] P. Chrysanthis. ACTA, "A framework for modeling and reasoning out extended transactions". PhD thesis, University of Massachusetts, Amherst, Amherst, Massachusetts, 1991.

[17] J. Eder, W. Liebhart., "Workflow Recovery". In Proceeding of Conference on Cooperative Information Systems, pages 124–134, 1996.

[18] M. M. Gore, R. K. Ghosh., "Recovery in Distributed Extended Long-lived Transaction Models." In Proceedings of the 6th International Conference DataBase Systems for Advanced Applicationns, pages 313–320, 1998.

[19] B. Kiepuszewski, R.Muhlberger, M. Orlowska., "Flowback: Providing backward recovery for workflow systems". In Proceeding of the ACM SIGMOD International Conference on Management of Data, pp. 555–557. 1998.

[20] C. Lala, B. Panda., "Evaluating damage from cyber attacks." IEEE Transactions on Systems, Man and Cybernetics, 31(4):300–3, 2001.

[21] "Random Password Strength", http://www.redkestrel.co.uk/Articles/RandomPasswordStrength.html, 14-09-09.

[22] Sohail Safdar, Mohd Fadzil Hassan, Muhammad Aasim Qureshi, Rehan Akbar, "Authentication Model Based on Reformation Mapping Method", International Conference on Information and Emerging Technologies ICIET IEEE, Pakistan, June 2010.

[23] M. Mrunalini , T.V. Suresh Kumar , K. Rajani Kanth , "Simulating Secure Data Extraction in Extraction Transformation Loading (ETL) Processes", Third UKSim European Symposium on Computer Modeling and Simulation, IEEE, 2009.

Intrusion Tolerant Serializability for Transaction-based SAN Environments

Yacine Djemaiel, Noureddine Boudriga
CN&S Research Lab., University of the 7th of November at Carthage, Tunisia.
{yacine.djemail, nab}@supcom.rnu.tn

***Abstract*—The serializability of transactions is among the properties that should be implemented in order to ensure the correct processing in transaction-based environments. When the system is compromised, the serializability in addition to the relevant properties of transaction-based environments may be affected. Ensuring the serializability of transactions in compromised systems is among the needs in order to enable the processing of interrelated transactions and avoiding blocking situations with the inability of committing transactions or some available sub-transactions. In this context, this paper proposes an approach to ensure an intrusion tolerant serializability in a compromised transaction-based environment. This approach is built on a new concept that is based on the definition and the use of virtual nodes instead of the detected malicious nodes. These virtual entities ensures the processing of transactions and sub transactions in a secure manner even if the running environment is compromised. They ensure the continuous running of transactions without experimenting the blocking of interleaved transactions and therefore to ensure the serializability even if the monitored system is compromised. A serial schedule graph is also generated and used by the Central Security Node in order to make decisions concerning the nodes and the set of data and transactions that are threatened by a malicious activity by attaching to each component a set of security parameters. The behavior of the proposed intrusion tolerant serializability scheme in addition to its efficiency is illustrated through a case study describing a SAN system that ensures the monitoring of cars activity and generates infractions and warning messages on road in order to prevent the occurrence of car accidents.**

***Index Terms*—: serializability, transaction, commit, intrusion tolerance, virtual node, SAN, serial schedule graph, storage area network.**

I. Introduction

Several issues should be considered when dealing with the processing of a set of interleaved transactions in a transaction-based environment. In most cases, these issues are due to the concurrent access to the same data by several transactions or the dependency relationship between running transactions. To ensure a correct and reliable processing of such transactions in transaction-based environments, an important property should be ensured that is the serializability. Ensuring serializability in a compromised transaction-based environment is among the main goals that should be achieved by the research community. Several constraints related to such environments in addition to the particularities of running components should be considered in order to protect running transactions and the handled data. Moreover, preventing the execution of some transactions that have been detected as malicious may be not authorized if the transaction system have to ensure some properties such serializability. This issue needs to be handled carefully by an intrusion tolerant transaction-based system by providing the way to prevent the damage to storage components and at the same time ensure the processing in a highly secure transaction processing and storage environments. Considering these issues and constraints, we propose in this paper an intrusion tolerant serializability scheme for transaction-based environments that ensures serializability even if the system is compromised based on a novel concept that is related to the use of the virtual node concept and the generation and the process of a serial schedule graph that holds a set of security parameters related to the nodes and operations performed on the data stored in SAN system storage devices.

The remaining of this paper is organized as follows. In Section II, we introduce the serializability concept and we make a survey of the existing approaches for intrusion detection and tolerance for transaction-based systems in addition to the works that have dealt with the serializability and the virtual machine concept. In Section III, we introduce the novel concept that is used to ensure the serializability in a compromised transaction-based environment. Section IV presents the proposed intrusion tolerant serializability scheme by defining the set of components and structures needed and the behavior of the introduced components in order to ensure an intrusion tolerant serializability. The next section presents a case study that illustrates the behavior and the efficiency of the proposed scheme against a compromised transaction-based SAN. Section VI concludes the paper.

II. Related work

Before introducing the major works related to the serializability in transaction-based environments, a definition of this concept should be given. The serializability is the definition of correctness for concurrency control in database systems. The execution of transactions one at a time or serially is among the possible restriction that could be imposed by a database management system in order to ensure that the execution of interleaved transactions is correct [5]. If each transaction that belongs to a schedule is correct, then a schedule comprising any serial execution of these transactions is considered as correct. Although the order of execution of operations in this serial execution is different from the interleaved execution, the effect of each operation is exactly the same as in the interleaved execution [2]. Compromising the serializability process has as impact on the violation of the data integrity.

When an attack is targetting the running transaction management system, this serializability mechanism should continue to process even if the system is compromised and the malicious transactions are running.

Several works have taken interest to the serializability concept especially when trying to check the correctness of the transactions to be executed. In [7], a technique is proposed to check the correctness of complex implementations of software transactional memory (STM) by verifying the execution runs using a checker that runs in parallel with the STM. Among the correctness criterion that is subject of verification is the serializability of transactions. A concurrency control protocol is generally used to ensure the serializable execution of transactions. Among the ways to recognize conflict serializable executions is to construct a directed graph called a serialization graph, as described in [2]. This graph has a node for each transaction and an edge $T_i \rightarrow T_j$ if T_i executes an operation which conflicts and precedes some operations executed by T_j. An execution is conflict serializable if and only if its serialization graph is acyclic [2]. Several efficient concurrency control protocols have been proposed including two-phase locking, timestamp ordering, optimistic and serialization graph testing. The protocols based on locking delay the execution of conflicting operations by using shared and exclusive locks for read and write operations. Shared locks allow several read operations to execute concurrently whereas exclusive locks ensure that a write operation is executed in isolation.

The conflict-serializability consistency model can reduce abort rates and improve performance in STMs. In [1], a discussion have been provided to show how this model can be supported on hardware-based TM systems. The conflict-equivalent serial schedule is constructed by determining a serializability order number (SON) for each transaction. The SON is an integer that indicates the relative order of a transaction among all transactions in the conflict-equivalent serial schedule that is being constructed.

Among the additional concepts that are used to handle the processing of transactions is the virtual concept. In [2], a virtual partition (VP) algorithm has been designed so that a transaction never has to access more than one copy to read a data item. Thus, the closest copy available to a transaction can always be used for reading. The basic idea of VP is for each site A to maintain a view, consisting of the sites with which A "believes" it can communicate. The view of a transaction, is the view of its home site. If the view changes before the transaction commits, then the transaction will be aborted. This virtual concept may be extended in order to protect handled data in storage devices. Moreover, the virtual machine concept is also used in order to ensure fault and intrusion tolerance such as the work proposed in [6] showing that virtualization promotes a hybrid fault model that allows tolerating malicious intrusions in application domains with little overhead.

In addition to the check of correctness, there are some additional researches that have interested to the protection of running systems against malicious activity such as the scheme proposed in [3]. This scheme is able to monitor heterogeneous traffic and to detect and tolerate attacks targeting transaction based applications interoperating in wireless environments. The scheme deals with the commit and the rollback operations in order to propose a solution to detect and tolerate attacks without considering the serializability concept and the way to tolerate it. Based on this survey, we can remark that the serializability has been studied in a legitimate environment without considering the possible threats and the effect of the malicious activity on the monitored serial schedule and therefore on the correctness of running transactions.

III. The virtual node concept

The serializability may be affected if a transaction that belongs to the processing schedule is processed by a compromised node. In this way, the proposed system should provide a solution in order to ensure the continuity of the processing of the transaction system even if some participant nodes are compromised. The solution to this issue, consists on the instantiation of a secure virtual entity that is able to process in a secure manner. In this section, we introduce first this concept then we detail the processing of such virtual entities in addition to the way to protect them from malicious activities.

A. Definition of a virtual node

A virtual node is a sotware entity that is instantiated by the Central Security Node (CSN) in order to process transactions that belong to the serial schedule. This entity is considered highly secured since it runs in a secured and highly protected environment. The virtual node may be seen as an object that has a set of attributes and methods. The methods represent the set of instructions needed to process incoming transactions. This virtual entity uses processing and storage resources relevant to the CSN in order to process the transaction or the sub-transaction instructions. The transactions processed by the virtual nodes are stored temporary in the Virtual Contaminated Area until the commit requests are validated or rejected by the CSN by issuing respectively a rollback. The commit may be performed locally or globally as described previously in [3].

B. Virtual node processing

The virtual node is instantiated by the Node Instantiator (NI) module that is described in the following section. This module takes as input the set of instructions that belong to the transaction to be processed. It generates a software instance that is composed of a set of methods that are responsible of the following tasks : 1) Executes the set of instructions associated to the transaction to be processed; and 2) Ensures the mutual authentication with the CSN. The authentication is embedded to the generated instances in order to reinforce the security and to prevent that an intruder loads and controls a malicious virtual node instead of a legitimate one. Each virtual node has a certificate that is generated when the node is instantiated and stored in a highly secured area called the Protected area that is accessed only by the administrator and that is defined previously in [4]. The NI manages the processing of the virtual node, it is able to start the running of a virtual node, to stop temporarily the running due to the detection of some problems related to performance or to make an end to the processing of a virtual node.

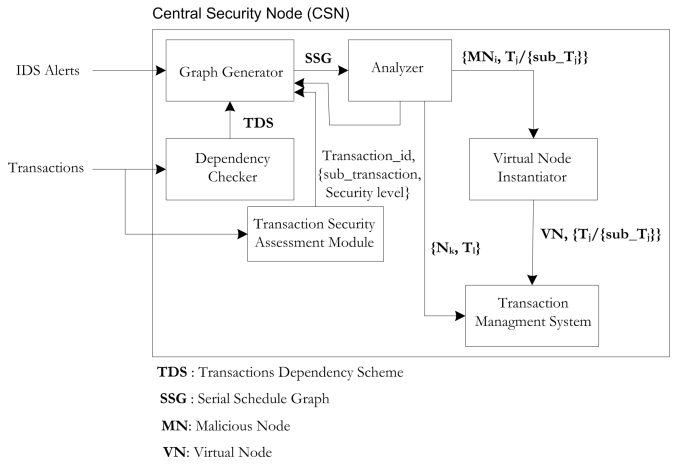


Figure 1. CSN architecture

IV. The intrusion tolerant serializability scheme

Before introducing the proposed scheme, we define first the intrusion tolerant serializability as a mechanism that ensures the serializability and guaranties the correct processing of the transactions that belong to the serial schedule even if the transaction processing environment is compromised.

A. Assumptions

The following set of assumptions should be considered in order to ensure the serializability even if the system is compromised:

- An intrusion detection and tolerance system that ensures the monitoring of the the transaction-based environment should be deployed.
- The detection of malicious activities are performed by a compromise independant component by implementing detection at the storage level.
- Additional structures are needed in order to monitor the status of running transactions and the issued local and global commits and aborts, as defined in [3].
- The CSN should be highly protected in order to ensure a secure environment for virtual nodes instantiation and transaction processing management.
- Each operation performed on the storage device is associated to a ratio that is defined based on its security impact on the handled data.

B. The CSN's Architecture

The CSN is composed of the following set of modules that are required to process transactions and to ensure an intrusion tolerant serializability process (Cf. Figure 1).

The Dependency Checker (DC): This module analyzes the set of transactions that belong to a selected serial schedule in order to determine the dependency relationships between them. These dependencies may be an input/output relationship between the transactions in addition to the shared access to data. These dependencies are written in a specific format that includes as fields: the identifier of transactions that are interrelated, the type of transactions dependency (input/output dependency, access to shared data, execution by the same participant node, etc.). This dependency is determined based on the analysis of the set of transactions that belong to the serial schedule in addition to the set of accessed data and the required participant nodes needed to process them. Moreover, this module analyzes the set of transactions in order to generate the serial schedule by returning as output the order of execution of transactions in addition to the order of elementary operations in each transaction.

The Graph Generator (GG): This module allows the generation of the serial schedule graph by considering the transaction dependency scheme generated by the DC in addition to the set of alerts generated by the intrusion detection and tolerance system. The output of this module is the generated graph that is composed of the set of transactions and handled data in addition to the set of parameters attached to the requested operations. Information on the participant node is also appended to this graph by mentioning if it is malicious or not. In addition, this module affects two orders for transactions that belong to the graph. The first order is associated to the transactions in the schedule. The second order is attached to each elementary operation that belongs to the whole schedule. This order is needed when there is a set of operations that should be executed in a new order to compensate the time needed to initiate a virtual node or if a malicious activity is detected after the processing of the transaction or the issue of the local commit.

The Transaction Security Assessment Module (TSAM): This module is responsible of the analysis of the set of transactions that belong to the defined serial schedule in order to affect to each area (a set of instructions that may be sequential or not) a security level that gives an information on the requested resources and the impact of the executed instruction on the security of the whole transaction-based system. This security level is computed based on different criteria related to the executed transaction. These criteria include the criticity of the handled data, the constraints associated to the application handling such data such as the case for the real-time applications compared to another application like a word processor, etc. This module takes as input a configuration file

holding the different level of criticity related to the handled data and applications that are available in the monitored SAN. Each elementary operation is assigned a security level that is denoted as OSL (Operation Security Level). The same operation that belongs to different transactions of the same schedule may be affected different levels of security since they handle data having different security levels (see Figure 2). A high security level is associated to the set of instructions and data that should not be tolerated to be executed in any malicious environment. A middle security level is attached to the set of instructions or data that may be tolerated when a malicious activity is detected. The last security level (low) is associated to the set of instructions that may be handled by an intruder and that are excluded from the intrusion tolerance process without affecting the security of the whole monitored system.

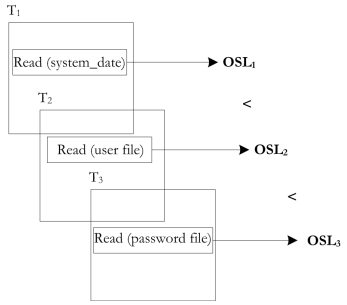


Figure 2. Sample of operation security levels

The Virtual Node Instantiator (VNI): This component ensures the instantiation of virtual nodes based on the information received from the Analyzer by using the set of transactions or sub-transactions that should be executed. This module creates a software entity that uses the resources of the CSN in terms of memory and free processing units. Upon the initialization of the new virtual node, a mutual authentication process is executed in order to check if this instance is authorized to process the requested transaction. This module sends a transaction execution status to the transaction management system in addition to the commit and rollback requests in order to manage these virtual entities.

The Analyzer: This component checks the generated graph in order to identify the list of malicious nodes that should be replaced by a set of virtual nodes in addition to the set of sub-transactions to be executed in this case. These information are forwarded to the VNI. The remaining transactions that are not identified as malicious are forwarded to the transaction management system in order to be executed. This component implements a set of decision algorithms in order to determine malicious nodes and transactions based on the security levels defined for each sub-transaction in addition to the ratios affected to each operation performed on the available data in the SAN. In order to determine which intrusion tolerance strategy should be applied, this module computes the total of ratios associated to the elementary operations that target the same data and compares it to the defined threshold to determine the appropriate intrusion tolerance strategy.

Three thresholds are defined: $thres_l$, $thres_m$, $thres_h$. If the computed ratio $ratio$ is between $thres_l$ and $thres_m$ then the intrusion tolerance process is not initiated and the operations are executed as if they are legitimate. If $ratio$ value is between $thres_m$ and $thres_h$ then the intrusion tolerance process is initiated. For a $ratio$ value that is greater than $thres_h$ a rollback should be generated and a request to instantiate a virtual node is forwarded to the VNI.

The Transaction Management System (TMS): It is a set of modules that are responsible of the processing and the management of running transactions in a transaction-based system. This components manages and controls the execution of transactions in addition to the set of commit and rollback operations that are local or global as described in a previous work ([3]). The functionalities and the particularities of this system is out of the scope of this paper and that are well detailed in [5]. The functionalities performed by the Scheduler and the transaction manager are implemented at the CSN.

C. The Serial Schedule Graph

In order to monitor the processing of transactions and to ensure the serializability, a serial schedule graph is needed. This graph is a directed acyclic that is formed by a collection of vertices and directed edges, each edge connecting one vertex to another, such that there is no way to start at some vertex v and follow a sequence of edges that eventually loops back to v again. This graph is used by our scheme with some introduced enhancements. The node in the proposed graph does not only represent the transaction identifier but also the processing node identifier in addition to a pair of flags that have two possible values: M or L. M_{T_i} means that the running transaction T_i is detected as malicious by the deployed intrusion detection and tolerance system. M_{N_i} signifies that the participant node N_i is malicious. The second flag may have in the same manner two possible values (L_{T_i} and L_{N_i}) meaning that the transaction T_i (respectively the node N_i) is considered legitimate during the running of the transactions schedule. This graph includes in addition to the transaction and the processing nodes, the set of requested data and the kind of operations performed on them (read/ write).

An example of a generated graph is described by the Figure 3.

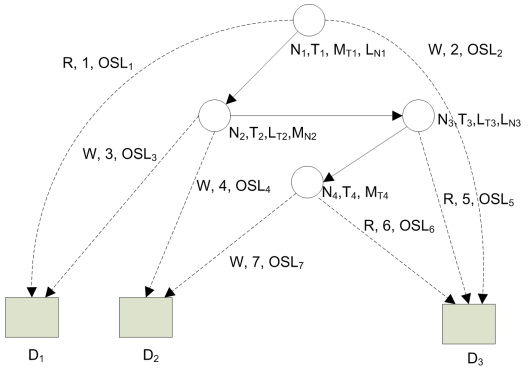


Figure 3. A sample serial schedule graph

Ratios are affected based on the impact of the operation on the data. If we consider the basic operations performed

on the data, the ratio affected to the write operation is much greater than the ratio affected to the read operation. The analyzer decides whether the operation will affect or not the security of the system based on the comparison of the total of ratios associated to the legitimate operations compared to the malicious one.

The generated graph is not static since it can be updated during the processing of the set of transactions that belong to it. In this context, the analyzer may detect some new malicious threats that appear as consequence of the execution of transactions such as the handling of malicious data as input to the processed transaction. In such case, the analyzer notifies the TMS and the VNI and updates the generated graph based on these new detected threats.

D. The intrusion tolerant serializability scheme

The CSN monitors the processing of the running transactions and ensures the serializability by generating a serial schedule graph. In addition to the monitoring task, this component ensures the management of running transactions by handling the rollback and commit operations.

The intrusion tolerance process is enabled once a malicious activity is detected in the generated serial schedule and based on the aforementioned possible attack sources (see Section IV-D). The first step of this process is to check if there are some malicious nodes that are selected to process transactions. Then, the transactions or elementary operations that are malicious are identified. The next step consists on computing the set of ratios associated to requested operations as mentioned in Section IV-B.

Before introducing the set of rules that are needed to ensure the intrusion tolerant serializability scheme, there are several situations that should be considered dealing with the detection of a malicious node or threat to data on the set of storage devices. An example of a serial schedule and the possible malicious activities detection points are illustrated by the figure 4 and that are considered in the set of defined rules.

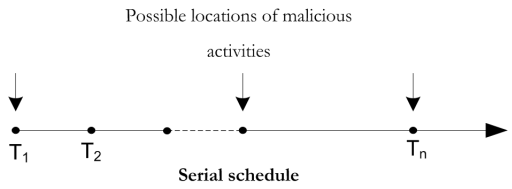


Figure 4. Possible detection points for a serial schedule

The malicious activity targetting the transaction-based system may be originated from different sources. The first attack source is the transaction that includes a set of malicious instructions that have as target the data on the storage devices. The second possible attack source is the SAN node that is responsible of the processing of the transaction and that has been compromised by an intruder by exploiting for example a vulnerability related to a running service on it.

According to this process, the intrusion tolerance process starts by checking if there are some malicious nodes in the graph in order to instantiate the needed virtual nodes to process transactions that belong to the serial schedule. After performing this task, if there are a set of malicious transactions then according the different security levels associated to the operations that will be executed there are basically three situations to handle 1) Operations that will be authorized for execution; 2) Operations that will handle data located at the virtual contaminated area and that are a copy of the legitimate data that are requested; and 3) Operations that will not be executed since it may affect the whole system status. For the last case, the processing of the serial schedule may continue if the output that is the result of processing of these operations is not required by the remaining transactions that belong to the serial schedule, otherwise a global rollback will be issued to make an end to the processing of the serial schedule since the serializability could not be ensured for such kind of threats. If a set of malicious transactions are detected as malicious after the starting of the serial schedule then they will be rexecuted by respecting the defined order in this serial schedule. After checking the participant nodes and the transactions, the last check is performed on the requested data. For each data, an addition of the OSL associated to the different operations performed on it is computed and the obtained value is compared to the defined thresholds in order to authorize the processing without applying an intrusion tolerance strategy or copying the data to the virtual contaminated area instead of the legitimate one or to block access to this data if it is critical. Since intrusion tolerance is applied partially on transactions according to the security level, the move of data will be partially performed as a consequence to this approach and that reduces the processing and storage overhead. The introduction of the security assessment module that enables the reduction of the set of data that will be handled in the virtual contaminated area and therefore the size of the structures used to manage the data in both area (the virtual contaminated and healthy area) is also optimized.

Since there are some transactions that may be re-executed, a delay may be introduced at this level and may be not accepted for some interactive applications presenting some strict temporal constraints. In order to reduce the introduced delay and if there some transactions that are not dependent then they may be executed before the malicious one that should be re-executed. In order to ensure the coherence of the whole serial schedule, the order of execution of each transaction and also the additional order for each elementary operations that are added to the generated graph, are used.

V. CASE STUDY

In order to illustrate the way to ensure intrusion tolerant serializability for running transactions, we consider a SAN system that is used to monitor the car traffic in roads and prevent the occurrence of accidents and determine infractions made by cars such as the excess of speed. In this context, the SAN system should include a set of components that integrate a set of sensors that log a set of information such as the access time, the speed and a set of information that are needed to identify the car (such as the registration number) and to extract the required information related to the car owner and the car

type. To fulfill these needs, the studied SAN system includes a set of components that are illustrated by the figure 5.

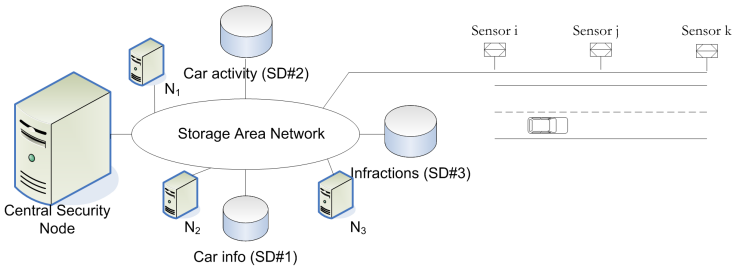


Figure 5. The car monitoring SAN system

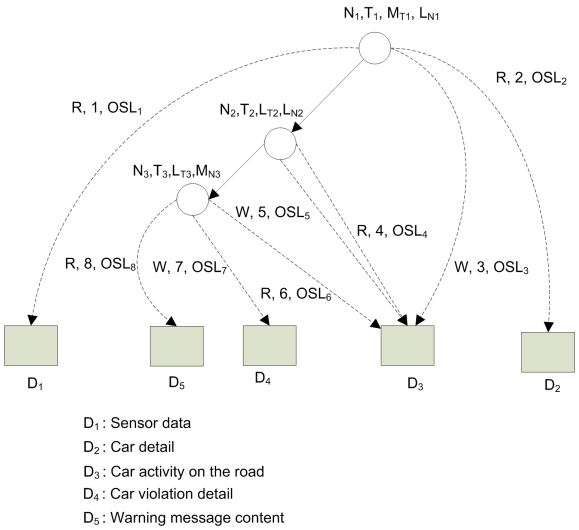


Figure 6. Serial schedule graph for car monitoring system

Based on the set of sensor deployed at different locations in the monitored road, information about the speed and the time of access is forwarded through the SAN system to the CSN in order to be processed and to determine if there is infactions concerning the speed or some warning messages that may be displayed on the road for the driver in order to prevent the occurrence of possible accidents. A set of transactions are to be executed by the studied SAN in order to ensure the aforementioned functions. To ensure the processing for such system, three transactions are required: T_1, T_2, T_3. The first transaction (T_1) ensures the processing of incoming data from sensors (identified by their $sensor_id$). It ensures the extraction of data identifying the car that is used to request the SD#1 to get the required data on the monitored car then adds the collected car activity to the SD#2. The second transaction T_2 reads data related to the car from the SD#2 in order to compute the car speed and compares it to the maximum authorized speed in the monitored area. If a violation is detected then it updates the infraction field (two possible values : yes or no). The transaction T_3 requests SD#2 in order to find entries that has an infraction field having the value "yes". For each entry, it reads information on the violated car from SD#1 then adds an entry to the SD#3. After that, it checks the current position of the car and it sends a warning message to be displayed in the near next board on the road. A serial schedule is defined using the aforementioned transactions. According to the serial schedule graph generated by the proposed scheme and illustrated by Figure 6, a virtual node N_3 is instantiated in order to process T_3. In addition to this malicious node, T_1 is detected as malicious and there is a dependency relationship between the two transactions: T_1 and T_2 since they access the same data D_3. As a consequence, the analyzer computes the $\sum OSL_i$ where $i = \{3, 4, 5\}$ and compares the obtained value to the defined thresholds. The obtained value is between the used $thres_m$ and $thres_h$ so the intrusion tolerance process should be applied for such transactions in addition to the instantiation of the virtual node. The serial schedule is executed even if the system is compromised without blocking the processing for N_1 and a part of D_3 is handled by N_1 that is located in the virtual contaminated area and the mapping between the healthy and the contaminated area is managed only for the fragments that are affected by the malicious operation performed by T_1.

VI. Conclusion

In this paper, we have proposed a novel scheme that ensures an intrusion tolerant serializability for running transactions based on a novel concept that is the generation of a highly secured virtual nodes in addition to the management of a generated serial schedule graph. This scheme is well suitable for transaction-based systems that manage a set of interleaved transactions that access the same data stored in the same storage device or that have a dependency relationship between each others. The efficiency of the proposed scheme is illustrated through a case study describing a transaction-based car monitoring SAN system that is exposed to a set of attacks trying to prevent the serializability of running transactions. In the near future, the proposed scheme will be tested for real scenarios and an enhancement of this scheme is studied in order to support wireless transaction-based environments and to present optimization capabilities for storage and memory requirements for the instantiated virtual nodes in order to handle efficiently a large number of virtual instances without affecting the normal processing of the CSN.

References

[1] Utku Aydonat and Tarek Abdelrahman. Hardware support for serializable transaction: a study of feasibility and performance. In *TRANSACT '09: 4th Workshop on Transactional Computing*, feb 2009.

[2] Philip A. Bernstein, Vassos Hadzilacos, and Nathan Goodman. *Concurrency Control and Recovery in Database Systems*. Addison-Wesley, 1987.

[3] Yacine Djemaiel and Noureddine Boudriga. Intrusion detection and tolerance for transaction based applications in wireless environments. In *IPDPS*, pages 1–8, 2009.

[4] Yacine Djemaiel, Slim Rekhis, and Noureddine Boudriga. Intrusion detection and tolerance: A global scheme. *International Journal of Communication Systems.*, 21(2):211–230, 2008.

[5] Ahmed K. Elmagarmid, editor. *Database Transaction Models for Advanced Applications*. Morgan Kaufmann, 1992.

[6] Hans P. Reiser and Rüdiger Kapitza. Fault and intrusion tolerance on the basis of virtual machines. In *Tagungsband des 1. Fachgesprch Virtualisierung (Feb 11-12, 2008, Paderborn, Germany)*, 2008.

[7] Arnab Sinha and Sharad Malik. Runtime checking of serializability in software transactional memory. In *IPDPS*, pages 1–12. IEEE, 2010.

Distributed Cross Layer Approach For Detecting Multilayer Attacks In Wireless Multi- hop Networks

Divya Bansal
Asst. Professor, CSE, PEC University of Technology
Chandigarh, India
divya@pec.ac.in

Sanjeev Sofat
Professor, CSE, PEC University of Technology
Chandigarh, India
sanjeevsofat@pec.ac.in

Prafulla Kumar
Director, Department of Information Technology
Ministry of Communication & Technology. New Delhi, India.

Abstract- **To deter internal attacks, Intrusion Detection Systems are the most favorable solutions for detecting intrusions and raising alerts for desired action since using encryption software for secure communication is not enough. A number of intrusion detection systems have been proposed for ad-hoc networks. Such intrusion detection systems cannot perform well for wireless mesh networks due to its multihop decentralized architecture. The selection of optimal and secure routing path and detection of multilayer security attacks cannot be achieved using traditional single layer IDS. Most of the MAC layer attacks occur due to non compliance of protocols by the nodes. Such a malicious behavior cannot be detected using conventional IDS. In this paper, a Cross Layer based Intrusion detection system has been proposed which takes advantage of the information available across different layers of protocol by activating multiple layer monitoring and detection. The proposed Cross layer based IDS is novel in its architecture and is able to detect multi layer attacks of compound nature. It can also detect low intensity attacks and attack switching behaviors which have been the major shortcoming of most of the existing IDS for Wireless Networks.**

Key words: Wireless Mesh Networks, multi layer attacks, Cross Layer Approach, Intrusion Detection Systems.

I. INTRODUCTION

Unlike WLAN, mesh networks are self-configuring systems where each Mesh Point (MP) can relay messages on behalf of others, thus increasing the communication range and available bandwidth. In WLAN, the wireless AP has to be wired to the infrastructure, whereas in WMNs MPs can be connected to the rest of the network by wireless radio links only [1, 2]. WMNs are easy to install, require no cable cost, connections amongst nodes are automatic, offer network flexibility, easy discovery of newly added nodes, redundancy, and self healing reliability. WMNs are important for distributed applications that cannot rely on a fixed infrastructure, but require instant deployment, dynamism, self-configuration and self-organization. Due to the architecture and the characteristics of WMN, attacks and consequences become obvious. WMNs are extremely vulnerable to attacks due to their dynamically changing topology, absence of conventional security infrastructures and open medium of communication, which, unlike their wired counterparts, cannot be secured [5,6].

The past research work has extensively focused on the data confidentiality, integrity and mutual authentication for wireless security. As another essential security requirement, availability has not been considered sufficiently. Nowadays, Denial of Service (DoS) attacks can reduce the availability of resource and result in massive service disruption. From the point of view of security and management, a robust WMN application should be resilient to DoS attacks and should be able to defend against such attacks launched either by the end devices or other adversaries. DoS attacks appear to be inevitable due to the physical characteristics of wireless links. WMNs suffer from yet another type of attacks which are termed as MAC misbehavior attacks. MAC layer misbehavior can be introduced by several techniques which include tweaking the MAC protocol or not complying with the protocols. These attacks can also affect the availability of resources for other legitimitate nodes leading to DoS attacks. Such a misbehaving technique does not depend upon security weaknesses of the standard. They are simpler and more efficient than known methods for misbehaving in the network [9]. Handling such MAC Layer misbehavior is also an important requirement to prevent DoS attacks and thus guaranteeing service availability. In this paper a cross layer based IDS has been proposed which can successfully detect the mis behaviour attacks for WMN. The attack strategies of smart selfish nodes have been implemented and analyzed. In the first part of this paper it has been demonstrated that most of the MAC misbehavior related attacks are practical to implement in WMN and the range of their practical effectiveness has been investigated on 802.11s standard. The effects of these attacks on network performance and other parameters have also been experimented and analyzed. A new cross layer based distributed and cooperative architecture of IDS for WMN has been proposed.

II. RELATED WORK

Current research in the area of security and management in WMN is still in early stages. The technology has been implemented mostly in the form of the experimental testbeds with little production use. Most of the IDS which act as an important line of defense have been proposed and implemented for 802.11 WLAN, MANETs or WSNs. Watchers[10] have been proposed for distributed environments. They can detect network traffic anomalies and misbehavior attacks but have huge memory requirements increasing cost. Watchdog & Pathraters [11, 12] detect

intrusions for mainly network layer and are based on DSR routing. CONFIDANT [13] is based on reputation based approaches and is efficient mostly for packet dropping attacks. It cannot detect protocol deviation based attacks. Several research efforts have been made in developing approaches based on Cross layer designs [14,15]. The results clearly show that Cross Layer based designs outperform single layer based IDS and are especially efficient for multihop wireless networks. In [14] a cross layer based IDS has been proposed for adhoc networks which can detect attacks at link layer and network layer. However the IDS is host based and does not exploit the advantages offered by WMN. In [16] Cross layer IDS has been proposed for multihop networks. It has been designed mainly for MANETs and WSNs which are highly constrained with energy. In [17] a novel cross layer based IDS has been proposed for WMN which detects attacks based on information collected from different layers. However the current design does not consider attacks based on protocol deviation and the implementation is for local systems and does not examine the performance overheads. In [18] the cross layer IDS called CRADS has been proposed based on non linear machine learning technique. However the design only considers routing attacks. Most of the IDS under research cannot detect attacks of compound form and cannot be directly extended to WMN. This paper introduces Cross Layer based Intrusion Detection System which takes advantage of the information available across different layers of protocol by activating multiple layer monitoring and detection. The proposed Cross layer based IDS is novel in its architecture and is able to detect multi layer attacks of compound nature and attack switching behaviors which have been the major limitation of most of the existing IDS for Wireless Networks.

III. THREAT MODEL AND ASSUMPTIONS

Standard protocols are implemented in the form of software and firmware improvising higher flexibility thus making wireless network devices easily programmable. An attacker can tamper with software and firmware to modify its default parameters ultimately forcing the protocol to deviate from its normal intended behavior. The objective, however, may vary from a selfish user trying to obtain better access to the valuable wireless resources such as bandwidth, channel access, etc to a malicious user attempting to disrupt network services to other legitimate users. As already discussed WMN are susceptible to many kind of threats. In our threat model it is assumed that an attacker can launch any attack or combination of attacks compounding the attack scenario. Our threat model considers attacks at both routing layer and MAC layer and is specified in Table I. In a mesh network, the MAC layer has to ensure that no station is starved of bandwidth. Ensuring fairness includes two distinct aspects: access to the radio channel and access for traffic forwarded through a given station. The former is the MAC layer's responsibility, and the latter falls to the routing or path-selection protocols [3]. The attacks considered in our threat model are described in next sub section.

TABLE I
THREAT MODEL

Layer	Associated Parameters	Attacks
Routing Layer	Optimal & Secure Path Selection	Packet dropping and route misdirection leading to blackhole, greyhole, wormhole
MAC Layer	Fairness, bandwidth, throughput, media access delay	Unfairness, Selfish MAC

A. Routing Layer Attacks

Packet Dropping: The adversary node can drop packets resulting in denial of service to the destination node. Any of the control or data packets can be dropped by the attacker node. This directly affects the availability of resources for the source node whose packets were dropped.

Route Misdirection: This attack occurs when an attacker node forwards the packet of the source node to a wrong destination node. This also affects the availability of resources for the source node whose packets were misdirected.

B. MAC Layer Attacks:

Misbehaving nodes in WMN typically misbehave to improve their own performance which includes nodes that refuse to forward packets on behalf of other nodes in order to conserve energy. Greedy nodes may exploit the vulnerabilities of IEEE 802.11 to increase their share of bandwidth at the expense of other users. The possible attacks due to MAC misbehavior have been explained below [4, 8]:

1. Shorter than DIFS Time Attack (ShDIFS):

In 802.11 networks, the stations before sending the packets and after sensing the channel to be idle wait for Distributed Coordination Function Inter Frame Spacing (DIFS) amount of time in order to avoid collision. DIFS is equal to *2*slot time + SIFS*. However as per the protocol, whenever the channel is sensed to be idle sender node should not send data before waiting for the required DIFS amount of time slots. While performing shorter than DIFS attack, the malicious node instead of waiting for DIFS amount of time either waits for SIFS amount of time or equal to slot time. It thus helps the attacker in getting faster access to the channel. Meanwhile all the other stations as per the protocol wait for DIFS amount of time before starting their backoff timers. The malicious node waits for only SIFS amount of time and starts its backoff timer. The misbehaving node thus gets the priority of accessing the media thereby delaying the media access of other competing nodes.

2. Oversized NAV Attack (ONAV):

In 802.11, to avoid collisions prior to sending packets, the stations send RTS(Request to Send) and CTS (Clear to Send). On listening to these RTS and CTS the nodes in the vicinity of communicating nodes stop their transmissions and set their net allocation vector fields (NAV) as per the duration id specified in RTS/CTS. The duration field in RTS/CTS specifies the period for which communication will takes place between the sender and the receiver (sending RTS and CTS) and for that specified duration the neighboring nodes suspend their transmission. In case of oversized NAV attack, the attacker

node sets the duration field value to a maximum possible value repeatedly. The receiving nodes update their NAV according to the received duration value. As a consequence, if the misbehaving node has more packets to transmit, it may get access to the channel for a longer duration as compared to other well-behaving nodes thereby increasing its throughput and reducing its latency compromising the fair access to channel by other legitimate stations. Another purpose of setting maximum NAV is to keep the channel occupied so that no other node is able to access the channel.

3. Reduced backoff Value Attack (Rboff):

Reduced backoff attack is another type of attack in which the attacker node deviates from the protocol. According to 802.11 MAC protocol, all the nodes desirous of transferring data select a random backoff time from a fixed contention window (for 802.11a CW_{min}=15 and CW_{max}=1023 while in case of 802.11b/g CW_{min}=31 and CW_{max}=1023) and then waits for the selected time before the packet transmission. In case of collisions and subsequent retransmissions, backoff interval is increased according to the predefined set of rules. In case of reduced backoff attack, the attacker does not follow the predefined contention window or the contention window used by the other nodes. Instead it follows a smaller contention window (say CW_{min}=1 and CW_{max}=4). By using the smaller backoff values, the attacker node will be able to access the channel more often than the legitimate and well behaved neighboring nodes. The advantage of selecting the smaller contention window is that even after collision when the node is required to double the size of backoff, the attacker node has a small impact. This is so because the initial size of contention window chosen by attacker node is quite small and hence the backoff value remains smaller than other nodes even if it doubles after the collision. Thus, the misbehaving node attains faster access to the channel in comparison to other competing well behaved nodes.

C. Implementation of Threat Model

To study the impact of the attacks on the draft IEEE 802.11s, various attacks were implemented in Qualnet 4.5 [7] which otherwise were not available as a part of the standard library.
In the scenario simulated for evaluating the attacks, two nodes have been configured as backbone network which are connected to a mesh portal. Two nodes are configured as both AP and MPs as they receive data from 802.11 STA and then forward them using the MPs. Thus configuring them as AP helps them in being able to receive data from the stations which follow 802.11 MAC protocol and MP configuration helps them in forwarding packets between MPs. Eight nodes 6have been configured as stations which are communicating with each other at application level. One node has been configured as the root MP while four nodes have been configured as are MPs. The initialization time for sending data is set to 13 sec since MPs take around 12sec to create the path amongst them and if the data is sent at the same time then there are chances of collisions between the mesh path formation data and data of the stations. The CBR links are established between the nodes: Node 8 ->11, Node 12->7, Node 10->13, Node 6->9. Node 6 is configured as the attacker node and the results are observed at 4 different seed values. Seed is a random number generator which is used to validate the results. There are certain cases when the seed favors a particular node and hence the effect of attack is visible but is very marginal. While performing the attacks different number of packets i.e. 25, 35, 45, 60, 75, 100 and 500 are used and then their average is considered.

To study the impact on different parameters of malicious node pair, duration field of NAV of the malicious sender was increased and the graph was plotted for difference in throughput obtained after and before the attack. In oversized NAV attack the default value of duration field is 3030 microseconds. To perform the attack the value of duration field is multiplied by 60. Thus the new value of duration field is 60*3030 microseconds. To study the impact of backoff attack on malicious node pair, backoff of the malicious sender was decreased and the graph was plotted for difference in average end to end delay after and before the launch of attack. In reduced backoff attack, the attack is performed by reducing the contention window size of attacker node. The default contention window is CW_{min} = 31 and CW_{max} = 1023. To perform the attack, the attacker node's contention window time was reduced to: CW_{min} = 1 and CW_{max} = 4. To study the impact of ShDIFFS attack of malicious node pair, the malicious node was made to wait for time shorter than DIFS (DCF Inter Frame Spacing) and the graph was plotted for difference in number of packets received

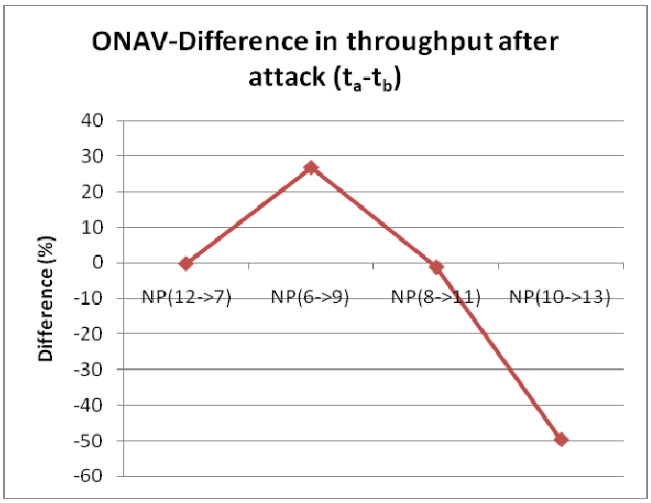


Figure 1: Difference in throughput after and before attack

after and before the launch of attack. In shorter than DIFS attack, the attack is performed by reducing both the DIFS waiting time and Tx DIFS time to SIFS time. The value of DIFS for legitimate node is SIFS + (2* Slot Time) and for Tx DIFS is also txSIFS + (2* Slot Time). When the attack is performed the value for malicious node is kept as DIFS = SIFS and txDIFS = txSIFS.

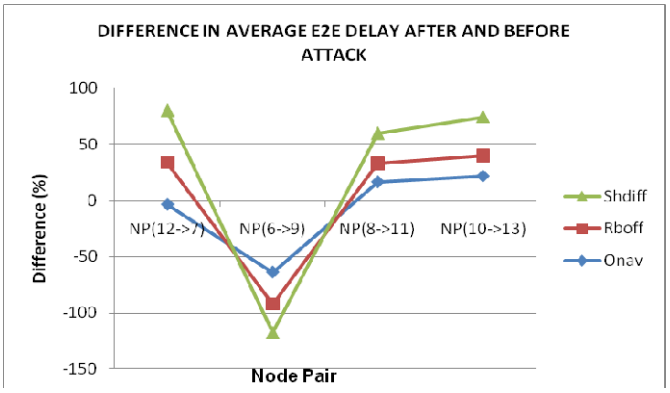


Figure 2: Difference in average E2E Delay after and before attack

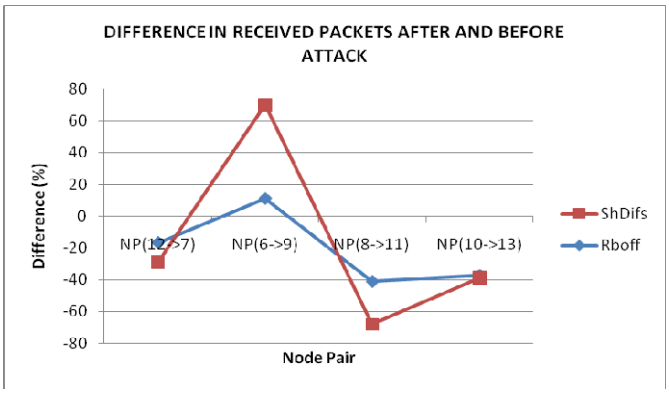


Figure 3: Difference in received packets after and before attack

Throughput:

From the Figure 1 it can be seen that there is an increase in the average throughput of the node 9, which receives packets from the attacker node while for all other nodes the throughput either decreases or remains constant. This is attributed to the fact that the attacker node sets a higher value of duration field completely occupying the channel resulting in a decreased throughput for other nodes and hence favorable network conditions. This results in a faster transfer of bits with lesser collisions and hence improved throughput.

End to End Delay(E2E):

End-to-end delay refers to the time taken for a packet to be transmitted across a network from source to destination. It includes transmission delay, propagation delay and processing delay. The processing delay also includes the queuing delay which is a key component of network delay. It is the time for which the packet remains in queue till it can be executed. The impact of oversized NAV attack, Rboff attack and ShDIFS attack on E2E delay is shown in Figure 2. In case of ONAV attack, higher value of duration field set by malicious node decreases the E2E delay of the malicious node. This is because the channel access time for malicious node decreases in this case and so does the time between two consecutive packets of the malicious node. As a result, the malicious node is able to send more number of packets after a single RTS. This in turns increases the E2E delay of the legitimate nodes because the malicious node occupies the channel for higher duration due to which the contention period for legitimate nodes increases, raising the channel access time. The packets remain queued for a longer duration for other legitimate nodes leading to higher E2E delay.

Similarly, for Rboff attack, end to end delay has decreased for the malicious node pair since the malicious node is able to acquire the channel on highest priority. This is so because it deviated from the protocol and waited for a very small backoff time and hence started its transmission of packets much earlier. The packets of malicious node did not have to wait in the queue for long and also the contention time for the node was also the lowest reducing the average end to end delay of the malicious node to be the minimal. Meanwhile for all other legitimate nodes the end to end delay has increased due to increased contention time and hence higher queuing delay. Similarly for ShDIFF attack, it can be seen that average E2E delay for the malicious node has decreased considerably in comparison to the legitimate nodes. This attributes to the fact that malicious node is able to acquire the channel faster and more frequently. While the packets of all other legitimate nodes had to wait in the queue till the channel gets idle. Further, since the other nodes contest at the same time so the number of retransmissions of other nodes also increase which results in overall increase in E2E delay of the legitimate node.

Total number of received packets:

As seen from the Figure 3 the total number of packets received by the malicious node pair is highest in case of both Rbof and ShDIFS attack. This is so because the attacker node waits for least amount of time to access the channel and also acquires the access to the channel more frequently and thus sends more number of packets as compared to other legitimate nodes in the network. Meanwhile, received total number of packets for all other nodes in the network have been decreased. This attributes to the fact that since the malicious node waited for the smallest amount of time (as all other nodes waited for DIFS or higher backoff), it could get an access to the channel faster and more frequently and hence was able to send its packets without collisions and retransmissions. All other nodes had been waiting for the channel to get idle since malicious node could always acquire the channel first by the virtue of protocol deviation, so the packets to be sent for all other legitimate nodes remain queued up. As soon as the contention period starts, all the nodes start contesting after long waiting leading to more number of collisions and hence more retransmissions, due to which the total number of packets of legitimate nodes decreases as compared to that of malicious node.

IV. CROSS LAYER BASED INTRUSION DETECTION FOR WMN

In the present work, cross layer intrusion detection system or CIDS is designed to determine the attacks which seek parameters from one layer but their effects are visible on the other layer. These attacks are difficult to detect when a single layer IDS is used because such attacks mainly take place

between two layers and hence cannot be determined by single layer IDS. CIDS can be employed to detect such attacks which take place between two layers. In IEEE 802.11s (draft), routing is embedded over MAC layer and below network layer. It uses some parameters from MAC layer but do not use entire functions of MAC layers to perform path selection and forwarding. Since mesh layer lies between MAC and network layer hence there are some attacks which cannot be detected by single layer IDS developed for either of these layers. This is so because protocol at mesh layer use parameters from MAC layer but their effect is seen in layer above i.e. mesh layer. The WLAN Mesh protocol layer supports set of services which include control, management, and other operation, including the transport of MSDUs between MPs within the WLAN Mesh.

This cross layer interactions can therefore enable IDS to make more informed decision about the intrusion in the network. The design goals of Cross layer Intrusion detection system are as follows:

- Increase true positives by correlating information from multiple layers
- Detect multi layer attacks targeting different layers in protocol stack
- Increase detection accuracy by selecting parameters from MAC layer and network layer

The proposed design architecture exercises two levels of intrusion detection. Level-I detection monitor intrusions at a single layer and informs other layers. Level-II detection detects multiple intrusions at the same layer using information received from other layers. To confirm the suspicious behaviour of the malicious nodes, the information obtained from various layers of protocol stack are combined and analyzed. Collecting information from different layers increases information about the malicious node thus aiding in identifying malicious nodes with more accuracy.

A. Components of CIDS

The proposed cross layer intrusion detection approach shall have following components:

- Monitoring Component: This is used for local events monitoring. The monitoring component will implement the detection algorithm. Algorithm is the core component and the efficiency and accuracy of detecting and responding intrusion is totally dependent on the underlying algorithm.
- Intrusion database: It consists of the records of recent misbehaviours and reputation value of the neighbouring nodes. The monitoring algorithm will generate a suspicious list based on the monitoring results of single layer. This will go as input to the analysis engine for further processing. This list is also sent to all neighbours who can use it as additional information and decide its own response.
- Analysis Engine: It collects inputs from multiple layers in the form of suspicious list. It will correlate information to confirm intrusions. The complexity of the analysis engine will depend upon the environment for which IDS has to be deployed. However for simplicity we have considered statistical approaches in our analysis engine. The analysis engine will update the intrusion list after confirming the status of the misbehaving node.
- Response component: It is used to respond in case intrusion is detected. The response in the form of global intrusion list is broadcasted to all the nodes. The list is also protected using PTK/GTK like other data packets to ensure integrity of the list. The working of the CIDS is shown in the form of a flowchart in Figure 4. The algorithms which will be used for monitoring and hence detection of attacks considered have been given in Table II.

TABLE II
MONITORING ALGORITHMS

Algorithm for detection of reduced backoff attack	
Determine the time of last ACK received, T_{ack} Determine the time of last ACK received, T_{ack} Determine the time of latest RTS sent, T_{rts} Determine if the node id of the receiver of ACK and the sender of RTS is same If the node id is same Then determine k = (T_{rts} – T_{ack}) -DIFS If (k<31) $f(k_s,k_w)$= $\begin{cases} \text{malicious list if } (ks > p \text{ and } kw < (k-p)) \\ \text{Well behaved if } (ks < p \text{ and } kw > (k-p)) \end{cases}$ Set SA = k_s Then node will be declared as malicious	*//where 31 is the CW $_{min}$ for 802.11a/g* *//SA is the selfish Aspect; WA is the Well behaved aspect*
Algorithm for detection of shorter then DIFS attack	
Determine the time of last ACK received, T_{ack} Determine the time of last ACK received, T_{ack} Determine the time of latest RTS sent, T_{rts} Determine if the node id of the receiver of ACK and the sender of RTS is same If the node id is same Then determine k = (T_{rts} – T_{ack}) –Backoff time If (k< Min. calculated DIFS time) $f(k_s,k_w)$= $\begin{cases} \text{malicious list if } (ks > p \text{ and } kw < (k-p)) \\ \text{Well behaved if } (ks < p \text{ and } kw > (k-p)) \end{cases}$ Set SA = k_s	*//DIFS=SIFS+2*slot time*
Algorithm for detection of Oversized NAV Attack	
Determine the duration field of received RTS, D_{rts} for k transmissions If (D_{rts} <=3031). $f(k_s,k_w)$= $\begin{cases} \text{malicious list if } (ks > p \text{ and } kw < (k-p)) \\ \text{Well behaved if } (ks < p \text{ and } kw > (k-p)) \end{cases}$ Set SA = k_s	*//duration field for data packet is constant, in case of normal node it is 3030* *// k_s: SA, k_w: WA* *//SA is the Selfish Aspect denoting reputation at the monitor node*
Algorithm for detection of Packet Dropping	
Packet drop is found, denote it as suspected node If (source add. of packet drop≠ suspicious list)	*//Packet drop can be monitored using watchdog/ pathrater* *//Packet dropping*

Initiate route discovery from itself to original destination	*could be due to source nodes' malicious behavior*
If suspected node □ newroute No Congestion	*//Existence of suspected node in new route implies no Congestion*
Attack detected and declared as the malicious node, insert the node details in suspicious list Else : Node is congested	*//Packet drop due to malicious node*

Algorithm for detection of Route Misdirection

If node forwards packets
if (source address of forwarded packet == source address sent by itself)
If (DA of pkt ≠ DA of original pkt)
Detect node as misdirecting packets to a different destination

B. ARCHITECTURE OF CIDS

A new type of architecture called asymmetric distributed and cooperative IDS is proposed for WMN environment which

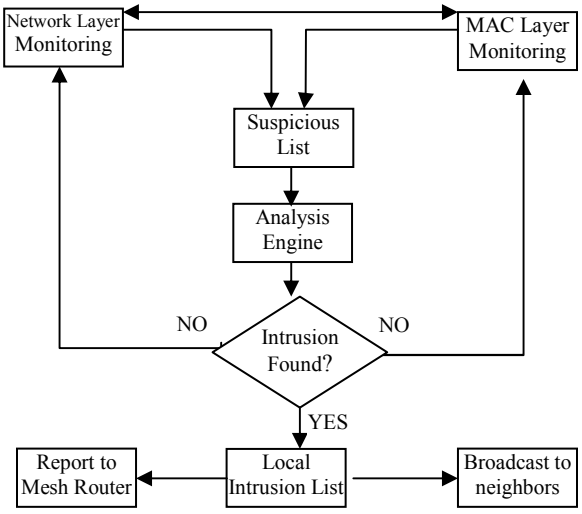


Figure 4: Working of IDS

complements the hierarchical structure of WMN. IDS deployed in each tier of WMN will use distributed collaborative approach to monitor and analyze traffic, however there shall be different responsibilities for different nodes (MPs/MAPs/MPPs).

Three-Tier Architecture has been designed for environments with relatively higher scale of mesh deployments where MAPs and MPs have different functionality and mesh spans across much larger areas. In this case MAPs will perform the monitoring and send the information to their MPs as per the hierarchy. The receiving MPs will perform monitoring as well as detect local level intrusions and hence trigger local intrusion lists to be used by their neighbours as well as MAPs in their domains. Each one is independently responsible for local intrusion, and the neighboring nodes cooperatively monitor a wider scope or realize rapid detection. But the response is local. The information so generated by MPs will also be sent to the mesh portal for further analysis. IDS central agent works on Mesh portal on the basis of information collected from mesh IDS agents (MPs) as well as its own collected information. Mesh portal collects all such local intrusion lists, performs analysis and generates a global intrusion list along with the reaction to be taken for each malicious node. This list is received by all the mesh points that will follow the reaction as specified in the global intrusion list. In case of multiple mesh portals, multiple global lists will evolve. The three tier architecture is shown in figure 5.

CONCLUSION

In this paper it has been demonstrated that most of the misbehavior related attacks are practical to implement in WMN. The results show that the selfish nodes can achieve significant resources by deviating from the standard media access protocols degrading the performance of well behaved nodes. Our proposed detection model for selfish MAC misbehavior stacks detects can detect these attacks by considering several parameters at different layers. The proposed cross layer Intrusion Detection System can detect

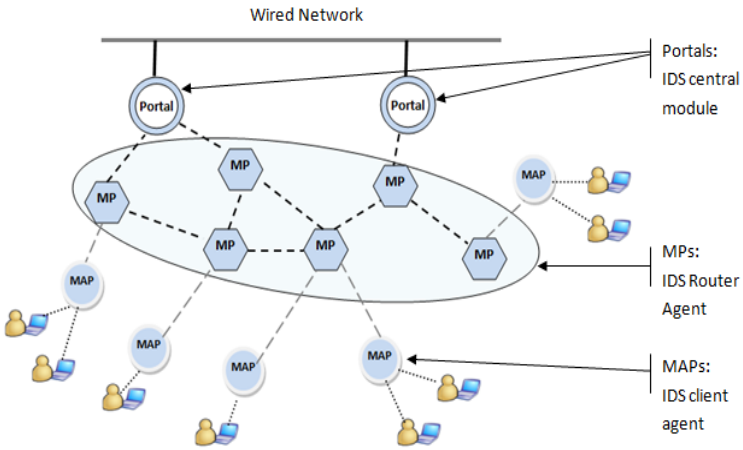


Figure 5: Two-Tier IDS Architecture

multilayer internal attacks of compound nature which are very difficult to circumvent using traditional single layer based IDS..

ACKNOWLEDGMENT

This work is done in Cyber Security Research Center (CSRC), PEC University of Technology. The authors would like to thank Government of India, Ministry of Communications and Information Technology, Department of Information Technology, New Delhi, for funding the Project *"Design and Development of Dependable, Secure and Efficient Protocol for Wireless Mesh Network(WMN)"*, under which this research work has been done.

REFERENCES

[1] G. R. Hiertz, S. Max, R. Zhao, D. Dee, L. Berlemann, *"Principles of IEEE 802.11s"*, in proceedings of 16th International Conference on Computer Communications and Networks (ICCCN), Honolulu, Hawaii, USA, Aug. 2007.

[2] G. R. Hiertz, S. Max, T. Junge, L. Berlemann, D. Denteneer, S. Mangold, and B. Walke, *"Wireless Mesh Networks in the IEEE LMSC"* in Proceedings of the Global Mobile Congress 2006, Beijing, China, Oct.2006, pp. 6.

[3] S.M. Faccin, C. Wijting, J. Kenckt, A. Damle, *"Mesh WLAN networks: concept and system design"*, IEEE Wireless Communications, Apr 2006.

[4] L. Guang and C. Assi. "*On the resiliency of ad hoc networks to MAC layer misbehavior*", in Workshop on PE-WASUN, ACM MsWiM, October 2005.

[5] Akyildiz, I.F.; Xudong Wang *"A survey on wireless mesh networks"* in Communications Magazine, IEEE Volume 43, Issue 9, Sept. 2005 Page(s): S23 - S30 .

[6] F. Akyildiz, X.Wang, W. Wang, "*Wireless mesh network: a survey*", Computer Networks, Volume 47, Issue 4, 15 March 2005, Pages 445-487.

[7] http://www.scalable-networks.com/products/QualNet/

[8] M. Raya, J. P. Hubaux, and I. Aad, "DOMINO: Detecting MAC Layer Greedy Behavior in IEEE 802.11 Hotspots," to appear in IEEE Trans. Mobile Computing, 2006.

[9] Lei Guang, Chadi Assi and Abderrahim Benslimane, "MAC Layer Misbehavior in Wireless Networks: Challenges and Solutions" IEEE Wireless Communications, Aug 2008.

[10] Chen M., Kuo S., Li P., and Zhu M., Intrusion Detection in Wireless Mesh Networks, CRC Press, 2007.

[11] Caballero J., "Vulnerabilities of Intrusion Detection Systems in Mobile Ad-hoc Networks: The Routing Problem," in Proceedings of TKK T-110.5290 Seminar on Network Security, Japan,pp. 1-2, 2006.

[12] Rafsanjani K., Movaghar A., and Koroupi F., "Investigating Intrusion Detection Systems in MANET and Comparing Idss for Detecting Misbehaving Nodes," in proceedings of World Academy of Science, Engineering and Technology, Canada, pp. 123-128, 2008.

[13] S. Buchegger, J-Y. Le Boudec, "Performance analysis of the CONFIDANT protocol (Cooperation of Nodes: Fairness in Dynamic Ad-hoc Networks)," 3rd ACM Int. Symp. on Mobile Ad Hoc Networks and Computing, Switzerland, 2002, pp. 226-236.

[14] Geethapriya Thamilarasu, Ramalingam Sridhar, "CIDS: cross-layer intrusion detection system for mobile ad hoc networks", International Journal of Mobile Network Design and Innovation 2009 - Vol. 3, No.1 pp. 10 - 20

[15] Jim Parker, Anand Patwardhan, Anupam Joshi Cross-layer Analysis for Detecting Wireless Misbehavior Consumer Communications and Networking Conference, 2006. CCNC 2006. 3rd IEEE, Vol. 1, Jan. 2006, pp. 6 – 9

[16] Shafiullah Khan, Kok Keong Loo, Zia Ud Din, "Cross layer design for routing and security in multi-hop wireless networks" in Journal of Information Assurance and Security 4 (2009) pp.170-173.

[17] Xia Wang, Johnny S. Wong, Fred Stanley, Samik Basu, "Cross-Layer Based Anomaly Detection in Wireless Mesh Networks," saint, pp.9-15, 2009 Ninth Annual International Symposium on Applications and the Internet, 2009

[18] C.J. John Felix*, A.Das, B.C.Seet*, B.S.Lee, 2008, CRADS: Integrated Cross Layer Approach for Detecting Routing Attacks in MANETs, IEEE Wireless Communications and Networking Conference (WCNC) 2008.

Automatic Arabic Digit Speech Recognition and Formant Analysis for Voicing Disordered People

Ghulam Muhammad [1], *Khalid AlMalki*[2], *Tamer Mesallam*[2], *Mohamed Farahat*[2], *and Mansour Alsulaiman*[1]

[1] Department of Computer Engineering, College of Computer and Information Sciences, King Saud University, Riyadh, Saudi Arabia

[2] Research Chair of Voice And Swallowing Disorders, King Abdul Aziz University Hospital, King Saud University, Riyadh, Saudi Arabia

{ghulam, kalmalki, tmesallam, mfarahat, msuliman}@ksu.edu.sa

Abstract

In this paper, analysis of speech from voice disordered people is performed from automatic speech recognition (ASR) point of view. Six different types of voicing disorder (pathological voice) are analyzed to show the difficulty of automatically recognizing their corresponding speech. As a case study, Arabic spoken digits are taken as input. The distribution of first four formants of vowel /a/ is extracted to show a significant deviation of formants from the normal speech to disordered speech. Experiment result reveals that current ASR technique is far from reliable performance in case of pathological speech, and thereby we need attention to this.

Index Terms: speech recognition, voice disorder, formants, Arabic digits

1. Introduction

There has been a growing interest of objective assessment of pathological speech (voice disordered speech) in recent years. Voice pathology detection and classification is one of the hot topics in voice analysis to which international community devotes great efforts [1]. Most of the works are concentrated on automatically diagnosis of pathology using digital signal processing methods [2 – 5]. For example, five pathologies are detected using Mel-frequency cepstral coefficients (MFCC) and fundamental frequencies in [2]. The highest and the lowest classifications were achieved with paralysis and hyper tension pathology, respectively. Discrimination of normal and pathological voices was analyzed using correlation between different types of acoustic descriptors in [3]. The descriptors were two types: temporal descriptors included energy, mean, standard deviation, and zero crossing, while spectral domain included delta, mean, several moments, decrease, roll-off, etc. Spectral decrease and the first spectral tristimulus in the Bark scale gave the best results in their experiments. The performance of linear predictive coding (LPC)-based cepstral analysis to discriminate pathological voices of speakers affected by vocal cord edema were evaluated in [4]. Estimation of glottal noise from voice signals using short-term cepstral was used to classify pathological voice in [5].

All of the above mentioned methods used only sustained vowel /a/ in their experiments. Comparative evaluation between sustained vowel and continuous speech for acoustically discriminate pathological voice was studied in [6]. It was found in their experiments that classification of pathology was easier for sustained vowel than for continuous speech. Automated intelligibility assessment was performed with context dependent phonological features using 50 CVC words from six different types of voice disordered speakers in [7]. Automatic recognition of Polish words was carried out where the input was speech from voice disordered Polish children in [8]. They used MFCC and human factor cepstral coefficients (HFCC) to recognize words with confusing phonemes. In a recent work, automatic recognition system was evaluated for speech disorder in head and neck cancer, where the speakers were German natives [19].

In this paper, conventional automatic speech recognition (ASR) system is evaluated for six different types of voice disorder patients speaking Arabic digits. MFCC and GMM (Gaussian mixture model) / HMM (hidden Markov model) are used as features and classifier, respectively. Recognition result is analyzed for types of diseases. Effects on performance before and after clinical operation are also investigated. Later first four formants (F1, F2, F3, and F4) of vowel /a/ present in the digits are extracted to make a comparison of distortion in terms of formants for different voice disorder. We believe that this is the first such work in Arabic speech, and that the comparison of performance between pre and post operation is interesting towards other language community as well.

The paper is organized as follows. Section 2 describes data used in the experiments, with a small description of diseases; Section 3 defines the ASR system, and gives experimental results with analysis; Section 4 compares formants with different types of diseases; finally, Section 5 concludes the paper and gives suggestions for future work.

2. Data

Two sets of data are used: one for training and other for testing. For training we use speech from speakers who have no voicing disorder (normal speaker). An in-house database is created from all Arabic digits (1 to 10) for training [9]. A total of fifty speakers utter all the ten Arabic digits with ten repetitions. First 40 speakers are used in training, while the rest 10 are reserved for testing. All speakers are Arabic native with age range from 18 to 50 years and without voicing disorder. The sampling rate is 16 kHz. Table 1 lists all Arabic digits with syllable structure.

For test data, total 62 speakers of six different types of voicing disorder give their Arabic digit speech. For each type of voicing disorder we have at least 10 speakers. The speakers' age range from fifteen to fifty years and all of them are native Arab. Test data set is recorded in different sessions at Research Chair of Voice and Swallowing Disorders, King Abdul Aziz University Hospital, King Saud University,

Riyadh by professional doctors at controlled environment. The sampling rate is 16 kHz.

Table 1. *List of Arabic digits.*

Symbol	Digit	Arabic Writing	Syllables	No. of Syllables
D1	Wahed	و احد	CV-CVC	2
D2	Athnayn	أثنين	CVC-CVCC	2
D3	Thalathah	ثلاثه	CV-CV-CVC	3
D4	Arbaah	أربعه	CVC-CV-CVC	3
D5	Khamsah	خمسه	CVC-CVC	2
D6	Setah	سته	CVC-CVC	2
D7	Sabaah	سبعه	CVC-CVC	2
D8	Thamanyah	ثمانيه	CV-CV-CV-CVC	4
D9	Tesaah	تسعه	CVC-CVC	2
D10	Ashra	شرةع	CVC-CVC	2

The six types of voicing disorder considered in this work are cyst, gastro-esophageal reflux disease (GERD), spasmodic dysphonia (SD), sulcus vocalis, nodules, and polyp. Here we give a brief description of these diseases and their effects on voice [10 – 14].

(a) Cysts are subepidermal epithelial-lined sacs located within the lamina propria, and may be mucus retention or epidermoid in origin. Mucus retention cysts form when a mucous gland duct becomes obstructed retaining glandular secretions. The voice often sounds diplophonic (particularly with epidermoid cysts), whereby there is great pitch instability and there is splitting of the fundamental frequency overtones.

(b) GERD is the retrograde movement of gastric contents (acid and enzymes, such as pepsin) into the laryngopharynx leading to symptoms referable to the larynx, hypopharynx, and nasopharynx. Symptoms include dysphonia, globus pharyngeus, mild dysphagia, chronic cough, excessive throat mucus, chronic throat clearing, etc.

(c) SD is a neuromuscular disorder. It is characterized by breathy voice quality with pitch and phonatory breaks and difficulty coordinating respiration with phonation.

(d) Sulcus vocalis is a linear depression on the mucosal cover of the vocal folds, parallel to the free border, of variable depth, usually bilateral and symmetrical. It inhibits closure of the vocal folds or causes stiffness in the vocal fold mucosa.

(e) Nodules are defined as bilateral symmetric epithelial swelling of the anterior/mid third of the true vocal folds. These are seen in children, adolescents, and predominantly female adults working in professions with high voice demands. Vocal fold nodules frequently interfere with vocal fold closure, so hoarseness and breathiness are common symptoms.

(f) Polyps are unilateral, occasionally pedunculated masses encountered on the true vocal fold. They occur more often in males, after intense intermittent voice abuse, history of aspirin or anticoagulant use, or other vocal trauma, such as endotracheal intubation. Polyps result in excess air egress during phonation (with a relatively breathy voice), and earlier vocal fatigue, frequent voice breaks in singers, and worsening hoarseness with high-pitched soft phonation.

3. Experiments with ASR system

The experiment in this work is conducted on a connected phoneme task constituting isolated Arabic digit. Each phoneme is modeled by a three state HMM. The state transition is left-to-right. Observation probability density functions are modeled using GMM. The number of mixtures of each state is varied to 1, 4, 8, and 16. All training and recognition experiments have been implemented with the HTK package [15]. Training is performed using normal speech, while testing is performed using normal and voice disordered speech.

The parameters of the system are: 16 kHz sampling rate with a 16 bit sample resolution, 25 milliseconds Hamming window with a step size of 10 milliseconds, and the pre-emphasis coefficient is 0.97. As features, 12 MFCC and 24 MFCC (12 MFCC plus their delta coefficients) are used.

Fig. 1 and 2 show recognition accuracy (%) of each type of voice using 12 MFCC and 24 MFCC, respectively. Table 2 shows best accuracy obtained in different parameters.

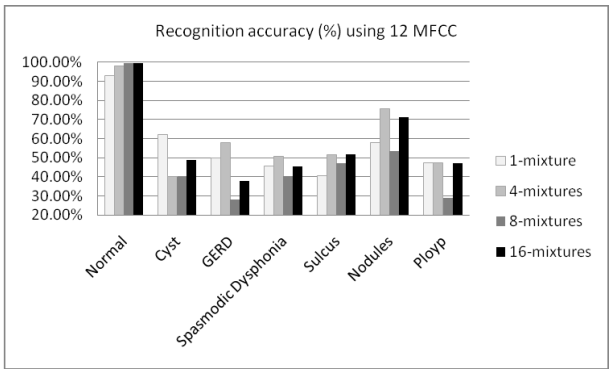


Fig. 1: *Recognition accuracy (%) of different voicing conditions using 12 MFCC features.*

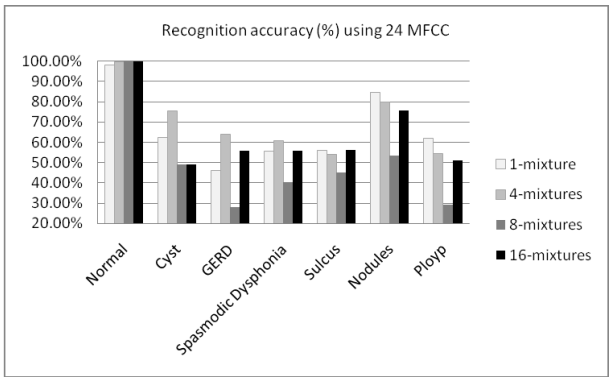


Fig. 2: *Recognition accuracy (%) of different voicing conditions using 24 MFCC features.*

From Fig. 2 and 3, and Table 2, we can see that though we obtain 100% recognition accuracy of Arabic digits spoken by normal speakers, there is a significant loss of accuracy while spoken by voice disordered people.

For example, Arabic digits spoken by people with polyp disorder have recognition accuracy of 47% using 12 MFCC and 4 mixtures, and 61% using 24 MFCC and 1

Table 2. *Best accuracy (%) obtained in different parameters.*

	Best mixture	Best feature	Best accuracy
Normal	8 / 16	24	100%
Cyst	4	24	75 %
GERD	4	24	64%
Spasmodic Dysphonia	4	24	60%
Sulcus	1 / 16	24	56%
Nodules	1	24	84.50%
Ployp	1	24	61 %

Table 3. *Best accuracy (%) obtained in pre and post operation of speakers.*

	Pre - operation	Post - operation
Cyst	72%	74%
GERD	62%	66%
Spasmodic Dysphonia	59%	62%
Sulcus	54%	60%

mixture. Among the six different types of voice disorder, the least accuracy is with sulcus disease (maximum accuracy of 56%) and the best with nodules disease (maximum accuracy of 84.50%).

In terms of performance of mixtures, it is found that there is no pattern of mixture for the best performance. In some of the disorders, the best performance is achieved with mixture 1, some with mixture 4, and some with mixture 8 and 16. In all of the disorders, 24 MFCC performs the best. It indicates that adding time derivatives to the feature can improve the performance with voice disorder, as it is the general case with normal speech.

An interesting experiment is also carried out with both pre and post operation voice disordered people to see whether there is any improvement of ASR after the operation. For post operation data, we could manage only five patients each with spasmodic dysphonia, sulcus, cyst and GERD, whose speech was recorded before the operation as well (test set). Speech of GERD, spasmodic dysphonia and sulcus were taken three months after the operation, while that for cyst was taken 12 days after the operation. The recognition performances of Arabic digits ASR with pre and post operation speakers are given in Table 3. The experiment is conducted with those speakers who have both pre and post operation data. In the table, only the best performances are shown. The table indicates that is no significant improvement in ASR performance achieved after the operation. For example, operation on GERD patients improves ASR performance from 62% to only 66%. This can be attributed to the fact that operation makes the patient speak easier than before from clinical point of view, however, it fails to improve ASR performance by large.

4. Formant analysis of /a/ for different types of voicing disorder

In Arabic, there are six vowels: /a/, /i/, /u/ and their longer counterparts /a:/, /i:/, /u:/. Some researchers consider Arabic vowels to number eight in total by counting the two diphthongs as vowels and, this is normally considered to be the case for modern standard Arabic (MSA) [16]. By changing the vocal tract shape, different forms of a perfect tube are produced, which in turn, can be used to change the desired frequencies of vibration. Each of the preferred resonating frequencies of the vocal tract (corresponding to the relevant bump in the frequency response curve) is known as a formant. These are usually referred to as F1 indicating the first formant, F2 indicating the second formant, F3 indicating the third formant, etc. [17].

In this current work, a formant based analysis of the Arabic vowel /a/ is carried out for different types of voicing disordered speech. First four formants of the vowel /a/ present in Arabic digits are analyzed. This vowel is present in all of the ten Arabic digits (see Table 1). Three frames in the middle of vowel /a/ in each utterance are considered to minimize the co-articulation effects. Middle frames are manually detected. Formant values of these frames are averaged to determine final four formants. Praat software, which is freely available in the internet, is used for analysis. This analysis is expected to be helpful in future Arabic speech processing tasks such as vowel and speech recognition and classification with voicing disorder.

Table 4 shows first four formants (F1, F2, F3, and F4) of vowel /a/ in different voicing conditions. The table also gives standard deviation of each formant and deviation of formant values from normal condition. All the formants listed are in Hz. The formant values of /a/ for normal speech are <710, 1492, 2467, 3647>. These obtained values (F1 and F2) differ slightly from the values reported in [17, 18]. In Ref. [17], F1 and F2 values for /a/ are <591, 1102>, while in Ref. [18] those are <695, 1590>.

All the six types of voicing disorder speech have significantly deviated formant values for /a/. For instance, cyst has F1 of 528 Hz which is 182 Hz less than normal /a/, and F2 of 1145 Hz which is 347 Hz less than that of normal; F3 value is comparable to normal, while F4 is 354 Hz higher than that of normal. F1 value deviates from the normal the most for cyst, followed by Spasmodic Dysphonia. The same is true for F2 value. F3 that corresponds to phoneme quality has the highest deviation from the normal in polyp, while F4 that corresponds to voice quality deviates most in cyst.

The formant values are not consistent even in same type of disorder. It varies between different samples and sometimes within the samples. This is studied in terms of pitch in [5]. From Table 4, we see that F1 in sulcus has standard deviation of 324 and polyp has 377. The high standard deviation indicates unstable nature of formants in each type of voicing disorder. For every formant value with each type of disorder, the standard deviation is more than 100 with the exception of F2 in nodules and polyp cases. This is one of the reasons of low recognition accuracy of Arabic digits uttered by disordered people. Formants of the vowels can be studied further to embed it in feature extraction module of Arabic ASR designed for pathological voice. The reason behind this is that every word and syllable in Arabic language must contain at least one vowel.

5. Conclusions

Arabic digits ASR performance in six different voicing disorder conditions was evaluated. Recognition accuracy varied between 56% and 82.50% in voice disordered

condition, while it was 100% in normal condition. Performance was also checked in post operation condition, where there was no high achievement. In addition, first four

Table 4. *First four formants (F1, F2, F3, and F4) of vowel /a/ present in Arabic digits in different voicing disorder conditions. SD represents standard deviation within the same condition.*

Disorder	F1			F2			F3			F4		
		SD	Mean deviation from normal		SD	Mean deviation from normal		SD	Mean deviation from normal		SD	Mean deviation from normal
Normal	710	4	0	1492	53	0	2467	16	0	3647	45	0
Cyst	528	107	-182	1145	107	-347	2452	115	-15	4001	115	354
GERD	747	107	37	1345	107	-147	2398	115	-68	3668	115	21
Spasmodic Dysphonia	582	101	-128	1178	101	-314	2687	132	220	3536	132	-111
Sulcus	658	324	-52	1202	108	-289	2512	439	45	3532	118	-115
Nodules	612	104	-98	1301	95	-191	2598	360	131	3899	166	252
Ployp	821	377	111	1431	28	-61	2880	250	413	3892	83	245

formants of /a/ in Arabic digits were analyzed in these conditions. The formant values varied significantly across and within conditions. Our future study will be to extract meaningful features to improve pathological ASR performance.

6. Acknowledgements

This work has been supported by the Research Chair of Voice And Swallowing Disorders (RCVASD), King Abdul Aziz University Hospital, King Saud University, Riyadh, Saudi Arabia.

7. References

[1] Manfredi, C. and Kob, M., "New trends in voice pathology detection and classification", *Biomedical Signal Processing and Control*, Editorial, (4):171-172, 2009.

[2] Dibazar, A.A., Berger, T.W., and Narayanan, S. S., "Pathological voice assessment", *Proc. IEEE Engineering in Medicine and Biology Society (EMBS) Annual International Conference,* NY, 2006.

[3] Dubuisson, T., Dutoit, T., Gosselin, B., and Remacle, M., "On the Use of the Correlation between Acoustic Descriptors the Normal/Pathological Voices Discrimination", *EURASIP Journal on Advances in Signal Processing*, Article ID 173967, 2009.

[4] Costa, S.C., Neto, B.G.A., Fechine, J.M., Correia, S., "Parametric cepstral analysis for pathological voice assessment", *Proc. the 2008 ACM symposium on Applied computing*, pp. 1410-1414, 2008.

[5] Murphy, P. J. and Akande, O. O., "Noise Estimation in Voice Signals Using Short-term Cepstral", *Journal of the Acoustical Society of America*, pp. 1679--1690, Vol. 121, No. 3, March, 2007.

[6] Parsa, Vijay and Jamieson, D. G., "Acoustic Discrimination of Pathological Voice: Sustained Vowels versus Continuous Speech", *Journal of Speech, Language, and Hearing Research*, Vol. 44, pp 327--339, April, 2001.

[7] Middag, C., Martens, J.P., Nuffelen, G.V., and Bodt, M., "Automated Intelligibility Assessment of Pathological Speech Using Phonological Features", *EURASIP Journal on Advances in Signal Processing*, Article ID 629030, 2009.

[8] Wielgat, R., Zieliński, T.P., Woźniak, T., Grabias, S., and Krol, D., "Automatic Recognition of Pathological Phoneme Production", *Folia Phoniatr Logop*, 60:323–331, 2008.

[9] Alotaibi, Y.A., Mamun, K.A., Muhammad, G., "Noise Effect on Arabic Alphadigits in Automatic Speech Recognition", *Proc. The 2009 International Conference on Image Processing, Computer Vision, and Pattern Recognition (IPCV'09),* Las Vegas, 2009.

[10] Jiang, J., Stern, J., Chen, H.J., et al., "Vocal efficiency measurements in subjects with vocal polyps and nodules: a preliminary report", *Ann Otol Rhinol Laryngol*, 113:277-82, 2004.

[11] Koufman, J.A., "The otolaryngologic manifestations of gastroesophageal reflux disease (GERD): a clinical investigation of 225 patients using ambulatory 24-hour pH monitoring and an experimental investigation of the role of acid and pepsin in the development of laryngeal injury", *Laryngoscope,* 101:1-78, 1991.

[12] Hirano, M., Yoshida, T., Tanaka, S., et al., "Sulcus vocalis: functional aspects", *Ann Otol Rhinol Laryngol*, 99:679-83, 1990.

[13] Ludlow, C.L., Naunton, R.F., Terada, S., et al., "Successful treatment of selected cases of abductor spasmodic dysphonia using botulinum toxin injection", *Otolaryngol Head Neck Surg,* 104:849-55, 1991.

[14] Bouchayer, M., Cornut, G., Witzig, E., et al., "Epidermoid cysts, sulci, and mucosal bridges of the true vocal cord: a report of 157 cases", *Laryngoscope*, 95:1087-94, 1985.

[15] Young, S., et. al., "The HTK Book (for HTK Version. 3.4)" Cambridge University Engineering Department, 2006.

[16] Elshafei, M., "Toward an Arabic Text-to -Speech System", *The Arabian Journal for Science and Engineering*, 16(4B):, 565–583, 1991.

[17] Alotaibi, Y. and Husain, A., "Formant Based Analysis of Spoken Arabic Vowels", *J. Fierrez et al. (Eds.): BioID_MultiComm2009, LNCS 5707*, pp. 170–177, 2009.

[18] Newman, D.L. and Verhoeven, J., "Frequency analysis of Arabic vowels in connected speech", *Antwerp papers in Linguistics 100*, pp. 77-86, 2002.

[19] Maier, A., Haderlein, T., et al., "Automatic Speech Recognition Systems for the Evaluation of Voice and Speech Disorders in Head and Neck Cancer", *EURASIP Journal on Audio, Speech, and Music Processing,* Article ID 926951, 2010.

Measuring Pairwise Distances Among Sequences of the miR-15/107 Group of miRNA Gene

Sim-Hui Tee
Multimedia University
Cyberjaya
63100 Selangor
Malaysia

***Abstract*- The miR-15/107 group of miRNA gene has been recognized as an important regulatory mechanism for main biochemical pathways in human. It has significant role to play in regulating gene expression that relevant to cardiovascular diseases, cancers and neurodegenerative diseases. Notwithstanding the fact that miRNA has strong implication on human health, an exhaustive taxonomic classification for the miR-15/107 group is impossible because the phylogeny of this group is incomplete. This paper aims at measuring pairwise distances among sequences of the miR-15/107 group of miRNA gene. The distance function allows bioinformaticians to compare the sequence of miR-15/107 group of miRNA gene and predict its target sites.**

I. INTRODUCTION

MicroRNAs (miRNAs) are short (~22 bases) RNA molecules that regulate gene expression by base pairing with complementary sequences in mRNAs (messenger RNAs) [1]. Its discovery in 1993 (*lin-4)* has enhanced scientific understanding of the mechanism of gene expression [2]. An eukaryotic genome usually contains hundreds of miRNA genes [3] that appear to be the regulators in maintaining genomic integrity [4]. Abundant of recent evidences suggested that miRNAs are important in cell division, metabolism, growth, mobility, stress response, angiogenesis, and apoptosis [5-7]. This implies that miRNAs have varying patterns of gene expression. Studies had also found that misregulation of miRNAs in gene expression is a disaster to human's health, which has implication in cancers [8-9], cardiovascular diseases, and neurodegenerative diseases [5].

The miR-15/107 group of miRNA gene has been recognized as one of the most important groups of miRNA that has significant role in biochemical pathways in human. The understanding of its regulatory role in gene expression is important for bioinformaticians and medical practitioners to unveil its impact on human diseases. Moreover, predicting the complementary binding of miRNAs with mRNAs is vital for functional studies and for the design of artificial RNAs [10].

Similar to other RNAs, miRNAs in one species of eukaryotes always have homologues in others. This fact suggests that there exists a common ancestral gene. Homologous miRNAs across different species provide a platform for gene comparison between human and other mammals.

miRNAs are the products of cleavage of a longer precursor transcript in the presence of enzymes [1]. They are first transcribed into long primary transcripts (pri-miRNAs) in the nucleus, then being cleaved into a ~70 bases hairpin precursor called pre-miRNA [4]. This pre-miRNA is then transported to cytoplasm and cleaved again to its mature form (~22 bases) [4]. The short length of miRNAs makes the gene alignment and comparison less complicated than longer RNA and DNA. However, alignment errors may still occur in phylogenetic reconstruction of miRNA using sequence-based methods. Furthermore, homoplastic sites where identical character appears in two distinct sequences by back and parallel mutation pose problem by introducing misleading signal and noise in data [11]. Notwithstanding the fact that miR-15/107 group of miRNA gene has strong implication in human health, an exhaustive taxanomic classification is impossible because the construction of phylogeny is incomplete [5].

Experimental detection of miRNA target sites on mRNA is time-consuming [12]. Although the studies reported that each miRNA may bind to 300-400 target mRNAs, the miRNA-mRNA interactions stored in the TarBase database is far less than the actual mi-RNA targeting [12]. It has been widely recognized that computational prediction of miRNA-mRNA interactions is valuable for the reconstruction of the complex miRNA target binding [12]. The successful computational reconstruction of miRNA target sites can potentially identify the biologically relevant condition of normal and cancer cells [9]. Such prospect encourages bioinformaticians to devise a robust distance function for the comparison of different miRNAs (especially miR-15/107 group) across species in order to understand the role of miR-15/107 group in preventing human disease.

This paper aims at measuring pairwise distances among sequences of the miR-15/107 group of miRNA gene. The secondary and tertiary structure of the target RNA sequences can be inferred from the correspondence of the aligned sequences [13].

II. BACKGROUND

Sequence alignment is a fundamental method to infer homology and function of miRNA. Most sequence comparisons use distance function to represent the insertion, deletion, and substitution of neucleotides. Some of the major computational methods of sequence alignment are Dot Matrix, Dynamic Programming, Hidden Markov Models, word-based

methods (i.e. BLAST and FASTA), subword composition [14], and Scoring Matrices. The methods using sequence conservation or structural similarity are relying on binary classifications by which a non-miRNA class is generated based on the absence of features used to define the positive class [15].

The solution to the genomic distance problem for linear genomes provided by Hannenhalli and Pevzner (so-called HP theory) is a complicated distance measure that models inversions and translocations only [16]. Many of the mutation types are not modeled by this theory. Yancopoulos et al, on the other hand, devised a new approach called Double Cut and Join (DCJ), which is much simplified as compared to Hannenhalli and Pevzner's HP theory. DCJ is used typically to model advanced neucleotide spatial feature such as transposition and block interchanges [17].

Bergeron et al has attempted to integrate HP theory into DCJ [18] by computing a new HP distance via the introduction of a variable of extra cost *t* [18]. The extra cost variable in Bergeron et al's model is computed in linear time by a tree data structure associated to a genome [18]. Bergeron et al's model assumes that DCJ distance equals to HP distance given $t=0$. However, according to Bergeron et al's proposition, a component of genome is oriented if either its permutation has positive and negative elements, or its adjacency graph has two even paths [18]. This proposition leads to a situation where the DCJ distance of two genomes is less than the corresponding HP distance given that unoriented components are present [18]. Bergeron et al proposed a solution to treat the components with paths separately from the components without paths [18]. However, they did not provide a validation for this solution.

Arribas-Gil et al [19] proposed a stochastic sequence evolution model to obtain alignments between two homologous sequences. This proposed algorithm is much efficient because a pair hidden Markov structure is used for alignments [19]. However, Arribas-Gil et al's statistical model is only catered for insertion and deletion of necleotides.

Chen and Chen [20] used joint entropy and mutual information in their study of the mutual regulation among miRNAs. The related miRNA pairs are more relevant as they took sequence and secondary structure into consideration in the similarity measure [20]. Their approach has strength in finding the relation between miRNA genes and the target prediction. However, the pairwise distance between miRNA genes is not measured in their approach.

Feng et al [21] proposed a new approach to measure pairwise distances among primary sequences. They defined a discrimination measure using the primitive discrimination substrings of two sequences for the similarity analysis [21]. The discrimination measure must satisfy the triangle inequality on top of all the distance conditions [21]. This model is not only applicable to DNA primary structure. It can be extended to measuring pairwise distance among sequences of miR-15/107 group of miRNA gene.

The sequence similarity of the members of miR-15/107 group is the common sequence of AGCAGC at the 5' end [22]. There are 12 annotated human genes in the microRNA Registry that exhibit this common sequence [22]. The members of miR-15/107 group and their sequences are given in Table 1 [5].

TABLE 1
SEQUENCES OF THE MEMBERS OF miR-15/107 GROUP

miRNA genes	Nucleotide sequences	Length (base)
hsa-miR-107	AGCAGCAUUGUACAGGGCUAUCA	23
hsa-miR-103	AGCAGCAUUGUACAGGGCUAUGA	23
hsa-miR-15a	UAGCAGCACAUAAUGGUUUGUG	22
hsa-miR-15b	UAGCAGCACAUCAUGGUUUACA	22
hsa-miR-16	UAGCAGCACGUAAAUAUUGGCG	22
hsa-miR-195	UAGCAGCACAGAAAUAUUGGCC	22
hsa-miR-497	CAGCAGCACACUGUGGUUUGU	21
hsa-miR-503	UAGCAGCGGGAACAGUUCUGCAG	23
hsa-miR-424	CAGCAGCAAUUCAUGUUUUGAA	22
hsa-miR-646	AAGCAGCUGCCUCUGAGGC	19

The similarity study between human miR-15/107 group and other species shows that all of them (as listed in Table 1) are conserved in *Pan troglodytes* [22]; all but hsa-miR-646 are conserved in *Macacca mulatta* [22]; all but hsa-miR-646, hsa-miR-424, and hsa-miR-503 (partial) are conserved in *Mus musculus* [22]. High conservation rate of miR-15/107 group of genes between human and these mammals suggests a homology of genes. This makes possible the reliable tracing of the evolution of gene function within a gene family [23]. However, the conservation rate of miR-15/107 gene group is low between human and non-mammals. For instance, there is no conserved pattern being observed between human and *Drosophila melanogaster* [22].

III. METHODS

A. Data Source

microRNA data were retrieved using Entrez. Complete sequence of miR-107 of *Capra hircus* and *Homo sapiens* were handled. In addition, miR-646 sequence of *Pan troglodytes* was handled as well.

B. Measuring Pairwise Distances

In this paper, pairwise distances among sequences of miR-15/107 group of genes were calculated based on Feng et al's Discrimination Measure (DM) algorithm [21]. Feng et al's three definitions [21] are adopted in measuring pairwise distances of miR-15/107 genes. Given that S and Q are sequences of a genome, $S(i)$ and $S(j)$ denote the ith and jth element of S, and $S(i,j)$ be the substring of S [21].

Definition 1. *S(i,j)* is a discrimination substring (DS) that distinguishes *S* from *Q* if $S(i,j) \notin Q$. Such substring *S(i,j)* is called a primitive discrimination substring (PDS).

Definition 1a. $\Delta(S,Q)$ is a set of PDSs that distinguishes *S* from *Q*.

The Definition 1a is derived from Definition 1, where $\Delta(S,Q)$ is not an empty set provided that $S(i,j) \notin Q$ and $Q(i,j) \notin S$ hold.

Definition 2. $DM(S_1 \rightarrow S_2)$ denotes the discrimination measure that S_1 distinguishes from S_2.

$$DM(S \rightarrow Q) = \sum_{u \in \Delta(S,Q)} t / [(l(S) - k + 1)\log_2(k+1)] \quad (1)$$

$$DM(Q \rightarrow S) = \sum_{v \in \Delta(Q,S)} t' / [(l(Q) - k' + 1)\log_2(k'+1)] \quad (2)$$

Where $l(u)=k$, $l(v)=k'$, number of appearances of *u* in *S* is *t*, and number of appearances of *v* in *Q* is *t'*. $DM(Q \rightarrow S)$ is different from $DM(S \rightarrow Q)$ as $\Delta(S,Q) \neq \Delta(Q,S)$

Definition 3. The discrimination measure of *S* and *Q* is

$$DM(S,Q) = \sqrt{(DM(S \rightarrow Q))^2 + (DM(Q \rightarrow S))^2} \quad (3)$$

Equation (3) is a distance function derived from (1) and (2).

However, Feng et al's model (Definition 1-3 above) does not take the repetition-free longest common subsequence (RFLCS) into consideration. RFLCS is a variant of longest common subsequence (LCS), which is a fundamental problem in stringology and biological applications [24-26]. In the scope of this paper, the repetition-free longest common subsequence is the longest common nonsuperstring which is solvable in linear time [27]. RFLCS is defined as below [25,28].

Definition 4. Given two sequences S_1 and S_2, a RFLCS is a subsequence of both S_1 and S_2 that contains at most one occurrence of each symbol. The longest common subsequence of S_1 and S_2 of length *k* is a sequence of indices $1 \le i_1 < \ldots < i_k \le n$ and $1 \le j_1 < \ldots < j_k \le m$.

In this paper, RFLCS was used to compute an examplar sequence which contains only one representative for each family of duplicated genes. RFLCS enables the repetitive longest common subsequence be filtered in sequence analysis.

IV. RESULTS AND DISCUSSION

In this research, miR-107 and miR-646 genes of three species were studied. The results for *Capra hircus* miRNA miR-107 were presented in Table 2.

TABLE 2
CAPRA HIRCUS MIR-107

Source	*Capra hircus*
Base pair	23
Locus	EF638077
Sequence	agcagcattg tacagggcta tca

Sequence alignments of miR-107 between *Capra hircus* with four organisms were presented in Table 3.

TABLE 3
SIGNIFICANT ALIGNMENTS OF MIR-107 BETWEEN CAPRA HIRCUS WITH FOUR OGRANISMS

Accession	Organism	Max score	E value
NR_034814.1	*Ornithorhynchus anatinus*	46.1	0.002
NR_031863.1	*Rattus norvegicus*	46.1	0.002
NR_032024.1	*Pan troglodytes*	46.1	0.002
NR_029524.1	*Homo sapiens*	46.1	0.002

In Table 4, the sequence results for *Homo sapiens* miR-107 were presented.

TABLE 4
HOMO SAPIENS MIR-107

Source	*Homo sapiens*
Base pair	81
Locus	NR_029524
Sequence	ctctctgctt tcagcttctt tacagtgttg ccttgtggca tggagttcaa gcagcattgt acagggctat caaagcacag a

The relevant sequence alignments of miR-107 between *Homo sapiens* with four organisms were presented in Table 5.

TABLE 5
SIGNIFICANT ALIGNMENTS OF MIR-107 BETWEEN HOMO SAPIENS WITH FOUR OGRANISMS

Accession	Organism	Max score	E value
NR_034814.1	*Ornithorhynchus anatinus*	135	2e-29
NR_031863.1	*Rattus norvegicus*	145	3e-32
NR_032024.1	*Pan troglodytes*	150	7e-34
NR_032162.1	*Monodelphis domestica*	122	2e-25

Table 6 demonstrates the sequence results for *Pan troglodytes* miR-646.

TABLE 6
PAN TROGLODYTES MIR-646

Source	*Pan troglodytes*
Base pair	92
Locus	NR_035966
Sequence	atcaggagtc tgccagtgga gtcagcacac ctgcttttca cctgtgatcc

	caggagagga agcagctgcc tctgaggcct caggctcagt gg

The relevant sequence alignments of miR-646 between *Pan troglodytes* with four organisms were presented in Table 7.

TABLE 7
SIGNIFICANT ALIGNMENTS OF MIR-646 BETWEEN PAN TROGLODYTES WITH HOMO SAPIENS

Accession	Organism	Max score	E value
NR_030376.1	*Homo sapiens*	171	7e-40

Table 2 and 4 enumerate the nucleotide sequences of miR-107 of *Capra hircus* and *Homo sapiens*. Although two genes were descended from a common ancestral gene, there are varieties in the exhibited patterns. The results of sequence alignment as shown in Table 3 and 5 reveal that the miR-107 of *Pan troglodytes* is more similar to that of *Homo sapiens*. The results in Table 7 further suggest that miR-646 between *Pan troglodytes* and *Homo sapiens* are largely conserved.

V. CONCLUSION AND FUTURE WORKS

This paper presented a way to measuring pairwise distances among sequences of the miR-15/107 group of miRNA gene. The method allows bioinformaticians to compare the sequence of miR-15/107 group and predict its target sites. In future, the pairwise distances among sequences of more individual miR-15/107 genes will be computed. Furthermore, more species will be involved in the sequence alignment in order to understand the phylogenic features better.

REFERENCES

[1] B. Lewin, *Genes VIII*, USA: Pearson Prentice Hall, 2004.

[2] R.C. Lee, R.L.Feinbaum, V.Ambros, "The C.elegans heterochronic gene lin-4 encodes small RNAs with antisense complementarity to lin-14", in *Cell*, Vol 75, No 5, 1993, pp 843-854.

[3] D.P. Bartel, "MicroRNAs: target recognition and regulatory functions", in *Cell*, Vol 136, No 2, 2009, pp215-233.

[4] R. Shalgi, Y. Pilpel, and M. Oren, "Repression of transposable-elements—a microRNA anti-cancer defense mechanism?", in *Trends in Genetics*, Vol 26, No 6, 2010, pp 253-259.

[5] J.R. Finnerty, W-X, Wang, S.S. Hébert, B.R. Wilfred, G. Mao and P.T. Nelson, "The miR-15/107 group of microRNA genes: evolutionary biology, cellular functions, and roles in human diseases.", in *Journal of Molecular Biology*, Vol 402, 2010, pp 491-509.

[6] V. Ambros, "The functions of animal micrornas", in *Nature*. Vol 431, 2004, pp 350-355

[7] T. Du, and P.D. Zamore, "Beginning to understand microrna function" in *Cell Research*, Vol 17, 2007, pp 661-663.

[8] K.P. Porkka, M.J. Pfeiffer, K.K. Waltering, R.L. Vessella, T.L. Tammela, and T. Visakorpi, "MicroRNA expression profiling in prostate cancer", in *Cancer Research*, Vol 67, No 13, 2007, 6130-6135.

[9] B. Liu, J. Li, and A. Tsykin, "Discovery of functional miRNA-mRNA regulatory modules with computational methods", in *Journal of Biomedical Informatics*, Vol 42, 2009, 685-691.

[10] S.E. Seemann, A.S. Richter, J. Gorodkin, and R. Backofen, "Hierarchical folding of multiple sequence alignments for the prediction of structures and RNA-RNA interactions", in *Algorithms for Molecular Biology*, 5:22, 2010, doi: 10.1186/1748-7188-5-22

[11] A.W.M. Dress, C. Flamm, G. Fritzsch, S. Grűnewald, M. Kruspe, S.J. Prohaska, and P.F. Stadler, "Noisy: identification of problematic columns in multiple sequence alignments", in *Algorithms for Molecular Biology*, 3:7, 2008, doi: 10.1186/1748-7188-3-7

[12] M. Sturm, M. Hackenberg, D. Langenberger, and D. Frishman, "TargetSpy: a supervised machine learning approach for microRNA target prediction", in *BMC Bioinformatics*, 11:292, 2010, doi: 10.1186/1471-2105-11-292

[13] A. Polanski and M. Kimmel, *Bioinformatics*, Berlin: Springer, 2007.

[14] A. Apostolico and O. Denas, "Fast algorithms for computing sequence distances by exhaustive substring composition", in *Algorithms for Molecular Biology*, 3:13, 2008, doi: 10.1186/1748-7188-3-13

[15] M. Yousef, S. Jung, L.C. Showe, and M.K. Showe, "Learning from positive examples when the negative class is undetermined- microRNA gene identification", in *Algorithms for Molecular Biology*, 3:2, 2008, doi: 10.1186/1748-7188-3-2

[16] S. Hannenhalli, P.A. Pevzner, "Transforming men into mice (polynomial algorithm for genomic distance problem)", in Proceedings of FOCS, 1995, pp 581-592.

[17] S. Yancopoulos, O. Attie, R. Friedberg, "Efficient sorting of genomic permutations by translocation, inversion and block interchange", in Bioinformatics, 21, 2005, pp 3340-3346

[18] A. Bergeron, J. Mixtacki, J. Stoye, "A new linear time algorithm to compute the genomic distance via the double cut and join distance", in *Theoretical Computer Science*, Vol 410, 2009, pp 5300-5316.

[19] A. Arribas-Gil, D. Metzler, and J-L Plouhinec, "Statistical alignment with a sequence evolution model allowing rate heterogeneity along the sequence", in *IEEE/ACM Transactions on Computational Biology and Bioinformatics*, Vol 6, No 2, 2009, pp 281-295.

[20] F. Chen and Y-P.P. Chen, "Exploring cross-species-related miRNAs based on sequence and secondary structure", in *IEEE Transactions on Biomedical Engineering*, Vol 57 No 7, 2010, pp 1547-1553.

[21] J. Feng, Y. Hu, P. Wan, A. Zhang, and W. Zhao, "New method for comparing DNA primary sequences based on a discrimination measure", in *Journal of Theoretical Biology*, Vol 266, 2010, pp 703-707.

[22] S. Griffiths-Jones, "The microRNA Registry", in Nucleic Acids Research, Vol 32, 2004, pp D109-D111.

[23] P.D. Thomas, "GIGA: a simple, efficient algorithm for gene tree inference in the genomic age", in *BMC Bioinformatics*, 11:312, 2010, doi: 10.1186/1471-2105-11-312

[24] T.H. Cormen, C.E. Leiserson, R.L. Rivest, C. Stein, *Introduction to Algorithms*, Cambridge: MIT Press, 2001.

[25] P.A. Pevzner, *Computational Molecular Biology: An Algorithmic Approach*, Cambridge: MIT Press, 2000.

[26] O. Keller, T. Kopelowitz, M. Lewenstein, "On the longest common parameterized subsequence", in *Theoretical Computer Science*, Vol 410, 2009, pp 5347-5353.

[27] J.C. Na, D.K. Kim, J.S. Sim, "Finding the longest common nonsuperstring in linear time", in *Information Processing Letters*, Vol 109, 2009, pp 1066-1070.

[28] P. Bonizzoni, G.D. Vedova, R. Dondi, and Y. Pirola, "Variants of constrained longest common subsequence", in *Information Processing Letters*, Vol 110, 2010, pp 877-881.

Using Emergency Re-admission Time Window to Design the Re-admission Prediction Feature in Electronic Medical Record (EMR) Systems

Sim-Hui Tee
Multimedia University
Cyberjaya
63100 Selangor
Malaysia

***Abstract*- Electronic Medical Record (EMR) systems are the most innovative information technology infrastructure in the recent decades that facilitate the improvement of healthcare quality, efficiency and safety. EMRs are used by medical practitioners in storing, handling, and consulting the patients' data. Decision support is one of the most useful and promising features of EMRs, which is yet to be fully adopted in healthcare sector. The reason of the uncommon use of the decision support feature is partly due to the complexity of medical processes and protocols, and partly due to the technological constraint. In this research, the re-admission prediction feature was investigated as a part of decision support in EMRs. The emergency re-admission time window was used to design the proposed re-admission prediction feature. This research also examined how the appropriateness of the width of a time window contributes to the design factor of the proposed re-admission prediction feature. This research demonstrated that the use of emergency re-admission time window is appropriate in the design of re-admission prediction feature. The research outcome allows the users of EMRs to manage the re-admission case in hospital.**

I. INTRODUCTION

Electronic Medical Record (EMR) systems are the most innovative information technology infrastructure in the recent decades that facilitate the improvement of healthcare quality [1-3], efficiency [4-5] and safety [6-7]. It is also expected that EMR will reduce the health care cost [8] which has a tendency of increase in recent decades. EMRs are used by medical practitioners in storing [9], handling [10], and consulting the patients' data [9]. According to a medical treatment task analysis, an EMR system should assist medical practitioners in medical treatment, nursing, data archiving, and documentation [11]. The EMR-assisted medical treatment can be sophisticated, such as surgical-related EMR system [11].

A useful EMR system should be achieving interoperability with other hospital information systems, such as Radiology Information System and Picture Archival and Communication Systems (PACS) [12]. Furthermore, the embedded decision support feature will enhance the functionality and role of EMR drastically. Today, decision support still remains as one of the most useful and promising features of EMRs, which is yet to be fully adopted in healthcare sector. The underdevelopment of decision support in EMRs is primarily due to the technical complexity that involved, as medical systems are far more complicated than the commercial IT systems. A robust clinical decision support EMR system should enable clear critical decisions [13], which is a target yet to be achieved.

Currently, there are EMRs that equipped with partial decision support features. However, the usage rate is not always positive. The reason of the uncommon use of the decision support feature is partly due to the complexity of medical processes and protocols, and partly due to the technological constraint.

In this research, the re-admission prediction feature was investigated as a part of decision support in EMRs. This feature is based upon the admission data that captured in the system [14] when the patients are admitted. The emergency re-admission time window was used to design the proposed re-admission prediction feature. This research also examined how the appropriateness of the width of a time window contributes to the design factor of the proposed re-admission prediction feature. This research demonstrated that the use of emergency re-admission time window is appropriate in the design of re-admission prediction feature. The research outcome allows the users of EMRs to manage the re-admission case in hospital more efficiently.

II. METHODS

The chosen time window in defining the days of re-admission can be varying, depending on the diseases that patients are suffering from [15]. Despite the fact that a frequently chosen time window is 28 days after discharge, shorter or longer periods have also been suggested depends on the risk group of patients [15]. In view of this, this research adopts a Bayesian approach to determine the optimal time window in defining re-admission. In determining an optimal time window, patients are categorized into group of "high re-admission risk" and "low re-admission risk" [15]. Using a mixture distribution with probability density function [15-16], we yield the function in equation (1).

$$f(x) = pf_1(x) + (1-p)f_2(x) \quad (1)$$

where x denotes time to re-admission.

In Demir et al's model of time to re-admission [15], Coxian phase-type model was used by which only three rates of re-admission were adopted, where q_{10} denotes re-admission rate for high-risk (Φ_1) patients; q_{12} denotes transfer rate from high-risk to low-risk category; and q_{20} denotes re-admission rate for low-risk (Φ_2) patients. The limitation of this model is that it does not consider the possibility of transfer rate from low-risk to high-risk, which might be due to the wrong diagnosis or other reasons. In this research, q_{21} denotes such case.

In equation (1), the probability of a patient being in the high-risk group, *p*, is re-defined as:

$$P = \frac{q_{10}}{q_{10} + q_{12} + q_{21}} \tag{2}$$

According to Demir et al's model [15], $f_1(x)$ in equation (1) is the probability density function for Φ_1. Since we have introduced q_{21} as a transfer rate from low to high risk group, we re-adjust the parameter λ_1 for the high-risk group, as shown in equation (3)

$$\lambda_1 = q_{10}+q_{12}+q_{21} \tag{3}$$

From equation (3), we get

$$f_1(x) = \lambda_1 e^{-\lambda_1 x} \tag{4}$$

According to Demir et al's model [15], $f_2(x)$ in equation (1) is the probability density function for Φ_2. Due to the introduction of q_{21}, we re-adjust the parameter λ_2 for the low-risk group as in equation (5)

$$\lambda_2 = q_{20}+q_{21} \tag{5}$$

From equation (5), we yield

$$f_2(x) = \frac{\lambda_1}{\lambda_1 - \lambda_2}\lambda_2 e^{-\lambda_2 x} + \frac{\lambda_2}{\lambda_2 - \lambda_1}\lambda_1 e^{-\lambda_1 x} \tag{6}$$

Using Bayesian approach, a patient is assigned to Φ_1 if $p(\Phi_1 | x) > p(\Phi_2 | x)$, and to Φ_2 if otherwise [15]. The optimal cutoff time to re-admission is [15]:

$$\Psi = \frac{\ln[\lambda_2(1-p)/(-2p\lambda_2 + p\lambda_1 + \lambda_2)]}{(\lambda_2 - \lambda_1)} \tag{7}$$

III. INTEGRATING RE-ADMISSION PREDICTION FEATURE IN EMR

The re-admission prediction feature that was designed using emergency re-admission time window in Section II was integrated in an EMR. This paper categorized the EMR system into three modules based on its capabilities. Patient administrative module of an EMR encompasses the administrative workflow such as patient registration record, medical notes generator, and discharge summary generator. This module is the interface between medical secretary and patient. However, physicians and nurses do handle some features of the patient administrative module. The data accuracy for admission date and duration of stay of a patient is important as it is linked to other modules of the EMR.

The second module of EMR is basic module. The basic module process, retrieve and store the data either originated from the patient administrative module or input from its sub-modules (which is normally specialized modules). The basic module of EMR operates as a platform that support the parallel functions of the specialized modules, such as nursing documentation sub-modules, picture archive and communication system (PACS), operation planning system, radiology information system (RIS), cardiac telemonitoring system [17], high-resolution MRI [18], and ambulatory system [19].

The third module of an EMR is functionally dependent on the second module (specialized module) to operate. This module is a decision support module that enhances the functionalities of the respective specialized modules. The inputs to the decision support module are largely carried out in the specialized module.

The schematic view of this 3-module EMR system is illustrated in Fig 1.

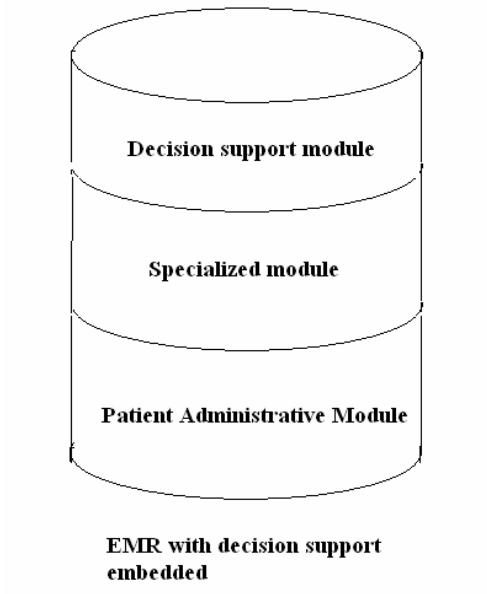


Fig. 1. Schematic view of an EMR with decision support embedded

The re-admission prediction feature, as one of the decision support tool, requires input of time to re-admission and date of admission. Such input normally is captured at the patient administrative module. Other variables from specialized module might be needed (although it is optional to the physicians), such as the prescribed drugs, medical images and lab test results. The data flow integration of the re-admission prediction tool is illustrated in Fig 2.

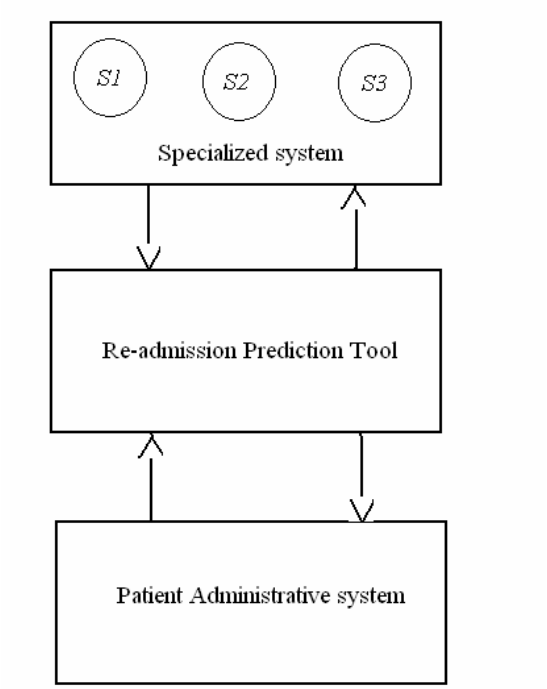


Fig. 2. Data flow integration of the re-admission prediction tool in an EMR system

Fig 2 exhibits that re-admission prediction tool, as a component of decision support module, requires mutual data flow with patient administrative system and the specialized system. The number of specialized system that interacts with re-admission prediction tool is dependent on each hospital's needs and budgets.

The re-admission prediction tool should not be maintained as a subset of individual specialized system. It is because such practice increases the complexity of EMR and costs. Furthermore, it contributes to the difficulty in system maintenance and evolution.

IV. CONCLUSION

In this research, re-admission prediction feature of an EMR system is designed using emergency re-admission time window. The re-admission is defined in term of optimal time. A schematic integration of re-admission prediction tool in EMR system shows that it is a subset of decision support module that requires data flow between patient administrative system and specialized system. Seamless integration of the re-admission prediction tool in an EMR system is important to the enhancement of hospital admission flow management.

REFERENCES

[1] J.G. Beun, "Electronic healthcare record; a way to empower the patient", in *International Journal of Medical Informatics*, Vol 69, 2003, pp 191-196.

[2] E.Ammenwerth and H.P. Spötl, "The time needed for clinical documentation versus direct patient care", in *Methods of Information in Medicine*, Issue 1, 2009, pp 84-91.

[3] M.G. Kahn and D. Ranade, "The impact of electronic medical records data sources on an adverse drug event quality measure", in *Journal of the American Medical Informatics Association*, Vol 17, 2010, pp 185-191.

[4] R.T.O'Connell, C. Cho, N. Shah, K. Brown, and R.N. Shiffman, "Take Notes (s): Differential EHR satisfaction with two implementations under one roof", in *Journal of the American Medical Informatics Association*, Vol 11, 2004, pp 43-49.

[5] V.L. Patel, J.F.Arocha, and A.W. Kushniruk, "Patients' and physicians' understanding of health and biomedical concepts: relationship to the design of EMR systems", in *Journal of Biomedical Informatics*, Vol 35, 2002, pp 8-16.

[6] H.Cao, P. Stetson, and G. Hripcsak, "Assessing explicit error reporting in the narrative electronic medical record using keyword searching", in *Journal of Biomedical Informatics*, Vol 36, 2003, pp 99-105.

[7] L. Poissant, J. Pereira, R. Tamblyn, and Y. Kawasumi, "The impact of electronic health records on time efficiency of physicians and nurses: a systematic review", in *Journal of the American Medical Informatics Association*, Vol 12, 2005, pp 505-516.

[8] K. Trimmer, J. Beachboard, C. Wiggins, and W. Woodhouse, "Electronic medical records use – an examination of resident physician intentions", in *Proceedings of the 41st Hawaii International Conference on System Sciences*, 2008, pp 1-10.

[9] A. Taddei, C.Carpeggiani, M. Emdin, R. Balocchi, S. Dalmiani, G. Cecchetti, A. Macerata, D. Pierotti, and C. Marchesi, "Development of an electronic medical record for patient care in cardiology", in *Computers in Cardiology*, Vol 24, 1997, pp 641-644.

[10] R.I.Kitney, S. Bickram, S. Claesen, "Clinical trials of an electronic medical record system", in *Computers in Cardiology*, Vol 25, 1998, pp 201-204.

[11] S. Wakui, N. Yoshikai, K. Minami, "An electronic medical record system for surgeons and its evaluation in the field", in *IEICE*, 2008, pp 35-40.

[12] A. Traina, N.A. Rosa, and C.Traina, "Integrating images to patient electronic medical records through content-based retrieval techniques", in *Proceedings of the 16th IEEE Sysmposium on Computer-Based Medical Systems*, 2003, 6 pages.

[13] L.A.E. Al-Safadi, "Semantic-based exchanger for electronic medical record", in *Proceedings of Third International Conference on Convergence and Hybrid Information Technology*, 2008, pp 962-967.

[14] P.S.C. de Mello, R.M.V.R. Almeida, W.C.A. Pereira, "A computerised information system for the analysis of hospital admission flow and characteristics", in *International Journal of Medical Informatics*, Vol 61, 2001, pp 11-20.

[15] E. Demir, T. J. Chaussalet, H. Xie, and P.H. Millard, "Emergency readmission criterion: a technique for determining the emergency readmission time window", in *IEEE Transactions on Information Technology in Biomedicine*, Vol 12, No 5, 2008, pp 644-649.

[16] M.J. Faddy and S.I. McClean, "Analysing data on lengths of stay of hospital patients using phase-type distributions", in *Applied Stochastic Models in Business and Industry*, Vol 15, 1999, pp 311-317.

[17] A. Alesanco and J. García, "Clinical assessment of wireless ECG transmission in real-time cardiac telemonitoring", in *IEEE Transactions*

on Information Technology in Biomedicine, Vol 14, No 5, 2010, pp 1144-1152.

[18] A. Rengle, M.Armenean, R. Bolbos, J-C. Goebel, A. Pinzano-Watrin, H.Saint-Jalmes, P. Gillet, and O. Beuf, "A dedicated two-channel phased-array receiver coil for high-resolution MRI of the rat knee cartilage at 7 T", in *IEEE Transactions on Biomedical Engineering*, Vol 56, No 12, 2009, pp 2891-2897.

[19] H.A. Shaban, M.A. El-Nasr, and R.M. Buehrer, "Toward a highly accurate ambulatory system for clinical gait analysis via UWB radios", in *IEEE Transactions on Information Technology in Biomedicine*, Vol 14, No 2, 2010, pp 284-291.

Medical Simulation Platform

J. S. S. Melo[1], L. M. Brasil[2], R. Balaniuk[3], E. Ferneda[3] and J. S. Santana[4]
[1] University of Brasília (UnB), Department of Post-Graduation in Electrical Engineering, Brasília, Brazil
[2] University of Brasília (UnB), Gama College (FGA), Gama, Brazil
[3] Catholic University of Brasília (UCB), Technology and Science Center (CCT), Brasília, Brazil
[4] University of Brasília (UnB), Medicine Department, Brasília, Brazil

***Abstract*- The Medical Simulation Platform (MSP), developed and validated by teachers and students of the medical area, tried to present the architecture of a virtual platform that integrates formal content in the form of texts, ontologies, 3D images and simulation. A case study was accomplished in the area of the skull bone anatomy for graduation courses in the area of Health.**

I. INTRODUCTION

Informatics applied to the area of Health has been gaining emphasis in the last years. It has been contributing, for instance, to the medical decision making process by helping and suggesting diagnoses, as well as to the improvement in the medical teaching. Concerning the information technology available for the area of Health today, it is possible to bring about a jump in quality by means of platforms that are able to quickly provide selected, lapidated and modeled data to support the medical decision process [1].

Informatics in Health has been making use of new computational tools and technologies, like Artificial Intelligence (AI), Virtual Reality (VR), Multimedia, Hypermedia and the Internet. Nowadays several initiatives try to make the association of these approaches to obtain greater precision from the medical information manipulated.

More specifically, the demand of the medical area for teaching innovation is evidenced by the increasing interest in Intelligent Tutoring Systems [2] applied to several areas in Health, such as Anatomy, Physiology, Pathology and simulation of surgery procedures. The human anatomy is one of the basic disciplines in the teaching of Health sciences, being frequent the need for consultation of text books, anatomy atlas and even the manipulation of cadavers. These facts motivated the development of the ITS Medical Simulation Platform (MSP), presented as follows.

This work is organized into five topics. In the first one it is presented a general view of the theoretical reference of this work, aiming at the comprehension of the concepts, methodologies and platforms used as basis, such as: (*i*) Intelligent Tutoring Systems, (*ii*) Ontologies, (*iii*) Virtual Reality, (*iv*) Inference machines. The requisites for validation, analysis and evaluation of MSP are expressed in the other topics, results, discussion and conclusion.

II. MEDICAL SIMULATION PLATFORM

A. Architecture

Today most of the ITS available try to emphasize the relation between text and image in a learning sequence determined by an expert with the support of pedagogical agents [2]. With the possibility of interaction with virtual platforms, the learner gets one more study tool. However, the learning semantics defined and modeled by an expert is not structured on a 3D platform. That is to say the virtual platform becomes a mere 3D object visualizing device. The objective of this work is to investigate the aggregation to the virtual platform of the same learning semantics defined for the ITS, so that it can be created a communication and interaction channel between ITS and VR [3], through the sharing of the same knowledge basis, for example. In this sense, the MSP System initially tries to make the relationship between ITS and VR closer, taking advantage of the concept of ontologies [4]. Such concept permits guaranteeing a form of access to the knowledge in an organized, formal manner and with a unique vocabulary. It also makes it possible to browse the knowledge in a hierarchical (knowledge within the domain of Anatomy) and lateral way (knowledge in Pathology and Physiology), through the relationships produced among the classes.

The knowledge is obtained from the ontology through comments added to the classes, the definition of the hierarchies and relationships, the vocabulary associated to the class, the axioms represented and the restrictions and domains added to each class.

The ontology elaborated within the ambit of this work had as its basis the *Foundational Model of Anatomy* (FMA) [5] - ontology developed by the University of Washington and destined to the formalization of the knowledge in Anatomy. The FMA project brings in its set of relationships a primary association as to the 3D visualization domain. However, the ontology proposed here improves the relationship between the two domains. The ontology related to the VR domain had as its basis the 3D and tactile processing framework architecture developed by the University of Stanford, CHAI3D [6], whose hierarchy is presented in Figure 1.

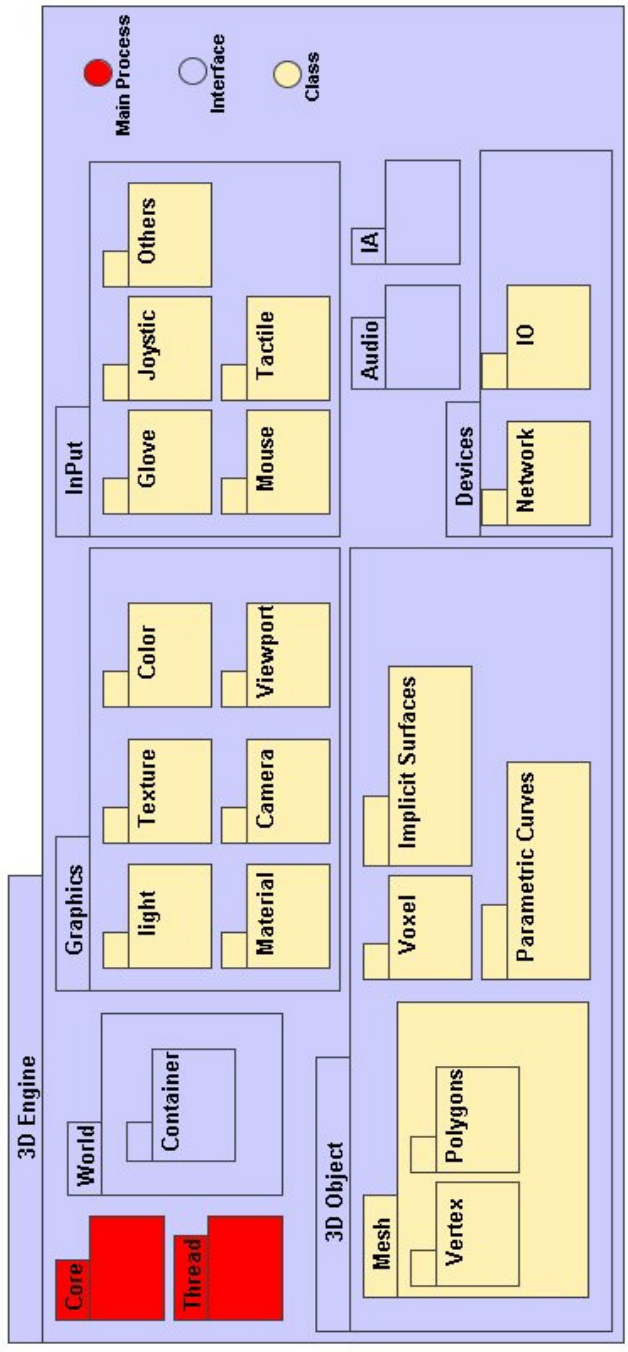


Fig. 1. CHAI3D Architecture

The ontology was developed on the Protégé platform [5], representing the hierarchy of classes, attributes, properties, restrictions, axioms and the internal relationships described in CHAI3D. This ontology, associated to FMA, made it possible the match of 3D objects with descriptive information about the human anatomy. It is possible, thus, to visualize the classes described in FMA under different focus, as it can be seen in Figure 2.

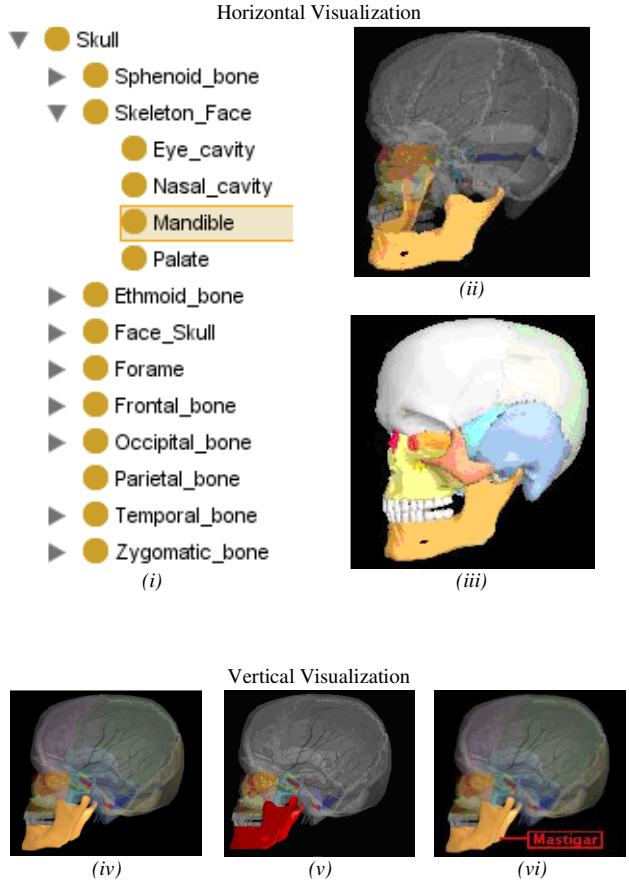


Fig. 2. *(i)* Hierarchical Visualization of the *(ii)* mandible compared to the (iii) skull. Lateral visualization concerning the domains of *(iv)* anatomy, *(v)* pathology and *(vi)* physiology

After the integration of the two ontologies, they were submitted to the inference machine RACER PRO [7], trying to evidence the generation of possible hypotheses about the relationships described and a better redistribution of the original classes shown in Figure 1. Among the alterations proposed by the inference machine, there are: (*i*) the incorporation of *class AI* by class *mathematics* due to the equality of the attributes and (*ii*) the incorporation of classes *3D Object, Graphics* and *Input* as subclass of class World due to the association of attributes. In this sense, MSP can be considered an ITS, because it generates knowledge out of a set of pre-processed pieces of information. As to the hypothesis derivation lines, MSP is classified as a forward one, in which the solution to a problem has data or ideas as its starting-point [8].

The integration of ontologies into VR platforms, like MSP, contributes to the current teaching techniques, since it incorporates the possibility of browsing and interchange among different knowledge domains. MSP provides a reactive teaching, that is to say it depends on the solicitation of the learner for the change in a context. The context and structure selected are visualized on a 3D platform according to the associations and attributes formalized in the ontology, as it can

be observed in the visualization of the maxilla bone disposed in Figure 3. The maxilla stands out from the other nearby bones so that it can evidence the class hierarchy and the attributes of dimension, position and weight defined in the domain *Anatomy*.

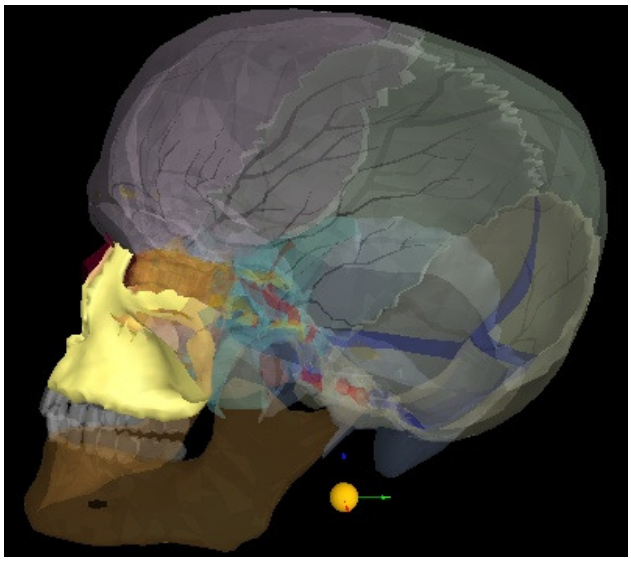
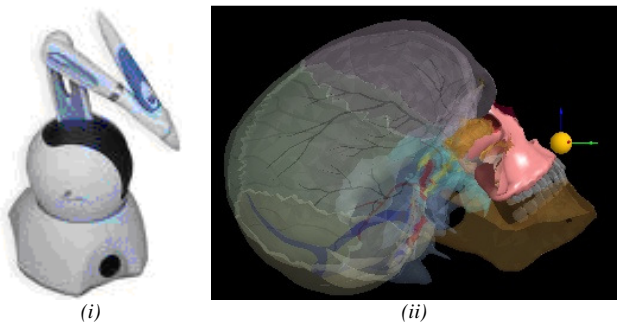


Fig. 3. Visualization of the maxilla bone under coordination of ontologies

The ontology, when centralizing the pieces of knowledge, permits MSP to make it available content bidirectional browsing functionalities. That is to say both ITS and VR have access to the different domains formalized, permitting the learner to choose the most convenient way of browsing.

Another resource also integrated to the system by means of ontology was a tactile interface, as shown in Figure 4. A Phantom Omni robotic arm permits tactile contact with 3D structures selected making it possible to the student tactile sensations like dimensions, textures and physical properties like weight, toughness, elasticity.



(i) *(ii)*

Fig. 4 *(i)* Phantom Omni integrated to MSP and *(ii)* its interaction with the VR platform

B. *Validation Process*

The validation process of the architecture proposed was accomplished in the area of the bony skull anatomy and counted on the support of teachers and a group of 120 students of the area of Health from two Brazilian universities (UCB and UnB), as shown in Table 1.

TABLE I
Distribution of validation

Group	Course	Quantity	
		UCB	UnB
A	Medicine	30	30
	Nursery	-	30
B			
	Biomedicine	-	30

Since they are courses with distinct characteristics, the validation was divided into two groups: Group A, made of students of Medicine from both education institutions, validated the architecture and the technology, and group B, made of students of Nursery and Biomedicine under the responsibility of the same teacher, validated the concepts and the content. The objective was to verify if the utilization of the tutoring system would bring about any learning performance gain.

MSP was made available on a Web Platform. The validation of the proposed architecture was accomplished based on the integration of an electronic questionnaire. Its objective was to verify its pedagogical advantage compared to the traditional means of teaching.

The evaluated points were [3]:

- Graphical design;
- Textual content;
- Facility, simplicity, system access availability through the *internet*;
- Visualization and 3D browsing;
- Inter-relationship among the different concepts of Anatomy (vertical browsing) and the concepts of Physiology and Pathology (horizontal browsing);
- Interaction with the 3D structure based on tactile interfaces;
- Facility for bidirectional browsing (ITS ⇔ VR).

C. *Result*

In function of the experimentation, some operational problems were detected and solved. These problems were related to (i) the stability of the system on a multi-user platform with different types of operational systems, (ii) capacity of management of the remote server, (iii) file storage and recovery and (iv) location and visualization of the 3D structures.

Despite the limitation related to the statistic meaning, the stimulating results indicate more than indexes and eventual tendencies. As to the technology and the architecture applied, it was observed that all the purposes were reached. Concerning Group A:

- 86% were for the use of Web technology for the dissemination of knowledge in the medical area;
- 78% considered that VR contributed to a better understanding of the human anatomic structures;
- 63% considered that the direct manipulation of 3D objects contributed to a better understanding of the anatomic structures;
- 63% approved the utilization of Web systems in the teaching of medical procedures;
- 67% evaluated as positive the utilization of tactile interfaces associated to VR in the teaching of anatomy.

Concerning the organization and quality of the content presented, 67% of Group B considered MSP a support tool that improved the presential teaching of Anatomy.

After the accomplishment of the research, MSP was divulged in many lists of experts of several Brazilian universities, and there were 514 requests for registration afterwards, for courses of Physiotherapy, Nutrition, Biology and Psychology, which kept a positive evaluation as to MSP.

III. Conclusion

The architecture of the MSP system proposed in this work turned out to be interesting for contributing to the areas of Biomedical Engineering, Informatics in Education and Education in Health, since it proposed an ITS that (i) formalizes its content in the form of ontologies, (ii) makes it possible the relationship among different knowledge domains in Health (Anatomy, Physiology and Pathology) through horizontal and vertical browsing of the content, (iii) associates VR and ontologies, (iv) makes it possible the visualization of 3D structures of the human anatomy on a Web platform, (v) makes it possible the manipulation of anatomic structures modeled on a 3D platform by means of tactile interfaces and (vi) makes it possible bidirectional browsing between ITS and VR

ACKNOWLEDGMENT

This work was partially financed by the Brazilian agency FINEP (Study and Project Financer).

REFERENCES

[1] B. Orgun, J. Vu. HLontology and mobile agents for interoperability in heterogeneous medical information systems. Computers in Biology and Medicine, v.36, n.7–8, p.817–836B, 2005.

[2] B. Ig. Plataforma para construção de ambientes interativos de aprendizagem baseados em agentes. 2006. 133f. Dissertação (Mestrado em Computação) – Faculdade de Tecnologia, Universidade Federal de Alagoas, Maceió, 2006.

[3] J. S. S. Melo. Integrando realidade virtual em sistema tutores inteligentes no domínio da saúde. 2007. 115f. Dissertação (Mestrado em Gestão do Conhecimento e Tecnologia) - Centro de Ciência e Tecnologia, Universidade Católica de Brasília, Brasília, 2007.

[4] J. Bezivin, R. Lemesle. Ontology-based Layered Semantics for Precise OA&D Modeling. In: WORKSHOP ON PRECISE SEMANTICS FOR OBJECT-ORIENTED MODELING TECHNIQUES, 1., 1997, Finaland. Proceedings… Local: FIN/Finland, 1997.

[5] O. R. Dameron, M. Musen. Challenges in converting frame-based ontology into owl: the foundational model of anatomy case-study. American Medical Informatics Association Fall, p.181-185, Washington DC, 2005.

[6] F. Coti. "Environment Chai3D". Departamento de Robótica de Stanford. http://www.chai3d.org <acessado em janeiro de 2008>.

[7] V. Haarslev, R. Möller, M. Wessel. Querying the Semantic Web with Racer + nRQL, Proceedings of the KI-04 Workshop on Applications of Description Logics, Ulm, Germany, September 20-21, 2004, available online as CEUR Workshop Proceedings 115, 2004.

[8] S. Russel, P. Norvig. Artificial intelligence: a modern approach. prentice hall, New Jersey – EUA, 1995.

Emerging Computational Strategy for Eradication of Malaria

[1]Monday Eze, [2]Jane Labadin and [3]Terrin Lim
Faculty of Computer Science and Information Technology,
Universiti Malaysia Sarawak, 94300 Kota Samarahan, Malaysia
[1]eze_monday@yahoo.com, [2]ljane@fit.unimas.my and [3]terrin@fit.unimas.my

Abstract: **Even with a lot of efforts by researchers, malaria eradication is yet to become a reality. The link between malaria infected and non-infected human beings, which led to transmission of the disease, is bridged by infected malaria vectors, through blood sucking bites. Such bites take place either in residential homes or public places. Suppose the residential homes are placed under reliable vector control, malaria transmission will still persist unless the public places are taken into consideration. The emerging computational strategy is about leveraging on the interactions between human beings and mosquitoes in public places to build realistic network models with the ultimate aim of applying relevant search techniques to such models, so as to determine the public places which act as reservoir of infected malaria vectors. The overall result will form a key resource for realistic vector control. Hence the idea is to be more proactive and offensive against malaria vectors, by locating the vectors in their hiding places, rather than human beings being located and bitten by the infected vectors. The emerging computational strategy discussed here is part of an ongoing research project in application of computational techniques towards eradication of malaria. This paper documents the result of an initial survey on malaria vector existence in public places.**

I. INTRODUCTION

A number of public places, such as bars and restaurants have been reported to close outdoor terraces or shut down completely as customers cannot sit outside because of what experts described as 100 billion mosquitoes invasion [1]. The importance of public places in disease transmission could be proved by referring to research by [2] and [3] which shows that contact rate between infectious and susceptible individuals could be reduced as much as 50% by closing some public places. While closing down public places is not the best solution, this finding however underlines the importance of public places in disease propagation. It has been shown that the number of individuals in a household drastically affects the size of disease outbreaks [2]. This implies that the more the number of people interacting in a place, the more the probability of disease transmission in that location. A recent literature survey carried out as part of this research revealed that the average household size for all the countries studied spans between 2.2 and 7.4. For instance Bangladesh [4] is 5.6, Norway [5] is 2.3, Switzerland [6] is 2.2, Japan [7] is 2.7, Afghanistan [8] is 7.4, Australia [9] is 2.6, China [10] is 3.7, Egypt [11] is 4.9, USA [12] is 2.57 and Canada [12] is 3.1. Since most public places (eg. schools, markets, airports etc) accommodate thousands of people, the probability of disease spread is very high in such places, and hence the need for studying malaria transmission in public places.

II. RESEARCH HYPOTHESES:

The hypotheses for this research experiment are:

Hypothesis1: Some public places where human beings visit for their daily socio-economic activities harbor malaria vectors.

Hypothesis2: These public places contribute to propagation of malaria due to blood sucking bites by mosquitoes in these locations.

Hypothesis3: The control of malaria resulting from human migration from location to location will remain very difficult to deal with, as long as malaria vectors thrive in public places.

Hypothesis4: Network Modeling can be used to study the dynamics of malaria transmission in public places.

Hypothesis5: Even if vectors are controlled effectively in the residential homes, malaria will still persist if the public places are not taken into consideration.

III. MATERIALS AND METHODS

A survey research was carried out in Sarawak State of Malaysia in June 2010 on vector existence in public places. A total of 525 valid responses were obtained from respondents drawn from ten countries, though the indigenes (Malaysian citizens) constituted a greater percentage. The foreigners involved were those who visited or were living in Malaysia at the time of this research. The aim of this survey is to determine previous experiences of mosquito bites in 16 carefully selected type of public places (see TABLE I). The respondents also had the option of indicating three most critical public places, and ranking them in the order of perceived degree of vector existence (or mosquito bites experiences), as well as suggesting other public places apart from the sixteen. The vector control strategies used in residential homes were also studied. Various modeling and data analysis techniques were applied to derive relevant outputs. The two popular correlation coefficients (Spearman and Pearson Correlation Coefficients) were applied for relevant validation of the research findings.

IV. DATA EXTRACTION

The VEXCount (vector existence count) table was built from the questionnaire data. This is the frequency distribution table which cumulates all the binary responses against each of the public places under consideration. This table is shown below as extracted from the experimental data. This implies that out of the 525 respondents, 398 experienced mosquito bites in a school, 156 in a football pitch, 317 in a bus stop, etc in that order.

TABLE I
VEXCOUNT TABLE

S/N	PublicPlace	Respondents Count
1	School	398
2	FootBallPitch	156
3	BusStop	317
4	Market	247
5	SwimPool	86
6	Restaurant	207
7	Airport	30
8	Road	226
9	BarbSaloon	26
10	River	442
11	Zoo	249
12	Mountain	283
13	Hotel	76
14	Office	60
15	CinemaHall	50
16	NightClubs	26

The distribution of respondents according to country of origin is shown in TABLE II.

TABLE II
RESPONDENT NATIONALITY TABLE

Country	Respondents Count
China	1
Germany	1
Indian	3
Indonesia	5
Korea	1
Libya	1
Nigeria	3
Pakistan	1
Palestine	2
Malaysia	507
TOTAL	525

Data analysis for respondents who have suffered from malaria revealed that vector controls were actually applied in their residential homes. The three tools indicated are *Bednets* (mosquito nets covering beds in the bed room), *Windownets* (nets that bar mosquitoes from entering through the windows), and *Insecticides*. The distribution of these tools is shown in TABLE III, with a total of five respondents indicating that they do not apply any measure in controlling mosquito vectors in their homes.

TABLE III
VECTOR CONTROL TOOLS TABLE

Tools	Respondents Count
BedNets	19
WindowNets	26
Insecticides	42
None	5

Also extracted is the multiple control strategy data which shows the distribution of how these respondents apply combination of vector control strategies in the residential homes. The result is TABLE IV with column codes *NoneSTRAT*, *SingleSTRAT*, *DoubleSTRAT*, *TripleSTRAT* representing 0,1,2, and 3 number of strategies in that order.

TABLE IV
MULTIPLE CONTROL STRATEGY TABLE

Combination of Strategies	Respondents Count
NoneSTRAT	5
SingleSTRAT	15
DoubleSTRAT	21
TripleSTRAT	10

The cumulative rank (*CUMRank*) table was built by extracting the three ranks (*Rank1, Rank2, Rank3*) assigned by the respondents to each of the public places under investigation, and then cumulating these ranks to get *CUMRank* score as shown in TABLE V.

TABLE V
THE CUMRANK TABLE

Public Places	Rank1	Rank2	Rank3	CUMRANK
AirPort	1	0	0	1
BuStop	30	50	54	134
Cinema	1	4	7	12
Football Pitch	13	28	19	60
Market	17	48	40	105
Mount	94	78	36	208
NightClub	2	0	1	3
Pool	11	0	7	18
Restaurant	10	15	29	54
River	200	110	44	354
Road	15	31	43	89
School	70	41	62	173
Zoo	31	47	72	150
Hotel	0	2	6	8
Office	0	0	3	3
Saloon	0	1	1	2

In order to study the variation between vector existence and top ranking, the *VEXCount* and *CUMRank* tables were merged giving rise to TABLE VI. This table was used for validation of the experiment through computation of correlation between the measure of vector existence and the cumulative ranking.

TABLE VI
MERGING CUMRANK & VEXCOUNT

S/N	PublicPlace	VEXCOUNT	CUMRANK
1	School	398	173
2	FootBallPitch	156	60
3	BusStop	317	134
4	Market	247	105
5	SwimPool	86	18
6	Restaurant	207	54
7	Airport	30	1
8	Road	226	89
9	BarbSaloon	26	2
10	River	442	354
11	Zoo	249	150
12	Mountain	283	208
13	Hotel	76	8
14	Office	60	3
15	CinemaHall	50	12
16	NightClubs	26	3

The experimental data was mined for information related to *vector bite without infection* (VBWO) and *vector bite with infection* (VBWI). The VBWO data displayed on the left side of TABLE VII shows respondents who visited public places and were bitten by mosquitoes, but did not suffer from malaria. The VBWI data on the right side of the same table shows the respondents who visited public places and were bitten by mosquitoes, and then got infected by malaria within the last two years. The common column "*PPCount*" stands for public place count and it represents the total number of public places where the respondents had mosquito bites. The total numbers of people involved are 474 and 51 for VBWO and VBWI categories respectively.

TABLE VII
VECTOR BITE WITH & WITHOUT INFECTION (VBWO & VBWI)

VBWO		VBWI	
Respondents	PPCount)	Respondents	PPCount
8	1	0	1
16	2	2	2
109	3	9	3
69	4	11	4
69	5	7	5
69	6	6	6
48	7	4	7
27	8	2	8
22	9	2	9
11	10	5	10
10	11	2	11
6	12	0	12
4	13	0	13
4	14	0	14
1	15	0	15
1	16	1	16
474		51	

TABLE VIII
RE-RANKED TABLE

S/N	PublicPlace	Re-rank of VEXCount (RV)	Re-rank of CUMRANK (RC)	RC-RC (d)	d^2
1	School	2	3	-1	1
2	FootBallPitch	9	8	1	1
3	BusStop	3	5	-2	4
4	Market	6	6	0	0
5	SwimPool	10	10	0	0
6	Restaurant	8	9	-1	1
7	Airport	14	15	-1	1
8	Road	7	7	0	0
9	BarbSaloon	15	14	1	1
10	River	1	1	0	0
11	Zoo	5	4	-1	1
12	Mountain	4	2	2	4
13	Hotel	11	12	-1	1
14	Office	12	13	-1	1
15	CinemaHall	13	11	2	4
16	NightClubs	16	13	3	9

V. DATA ANALYSIS AND VALIDATION

The extracted data was analyzed for correctness, and various outputs like histograms, pie charts and graphs were generated. The Pearson Product Moment method was used to calculate the correlation coefficient of the survey data, with particular attention on the relationship between vector existence and top ranking. This validation is necessary since *vector existence* does not automatically qualify a public place as *top ranked*, but the reverse is always true, as every *top ranked* public place automatically qualifies as having *vector existence*. A high correlation coefficient between vector existence and top ranking could therefore be used as a basis for validation of the survey. The Pearson Product Moment Correlation coefficient is given by:

$$r(x,y) = \frac{\mathrm{N}\sum \mathrm{xy} - (\sum \mathrm{x})(\sum \mathrm{y})}{\sqrt{\mathrm{N}\sum x^2 - (\sum \mathrm{x})^2}\sqrt{\mathrm{N}\sum y^2 - (\sum \mathrm{y})^2}} \qquad (1)$$

where $\boldsymbol{x}$ is the CUMRANK and $\boldsymbol{y}$ is the VEXCount (from TABLE VI). The terms in equation (1) can be calculated as:

$$\sum \mathrm{x} = 2879, \quad \sum \mathrm{y} = 1374, \quad \sum \mathrm{xy} = 433697,$$

$$\sum x^2 = 797141, \quad \sum y^2 = 264982, \quad \mathrm{N} = 16 \quad .$$

Therefore, ***r(x,y)*** is evaluated to be:

$$\frac{16(433697) - (2879)(1374)}{\sqrt{16(79741) - (2879)^2}\sqrt{16(264982) - (1374)^2}}$$

Hence r(x,y) = 0.92059.

To calculate the Spearman's Rank Correlation Coefficient on the experimental data, the *VEXCount* and *CUMRANK* were both re-ranked in order of magnitude as 1^{st}, 2^{nd}, 3^{rd},.. $16^{th.}$, giving rise to TABLE VIII which was then used for correlation analysis. The Spearman's Rank Correlation Coefficient is given by:

$$R = 1 - \frac{6\sum d^2}{\mathrm{N}(N^2 - 1)} \qquad (2)$$

where d = RV-RC (see TABLE VIII)

$$R = 1 - \frac{6 \text{ x } 29}{16(16^2 - 1)} \qquad Hence\ R = 0.95735$$

The calculated values of both correlation coefficients are very high, therefore validating the experiment.

VI. RESULTS

Various scenarios were analyzed using the extracted tables. The key visual outputs are shown in the following diagrams, and their significances discussed in relevant sections of this paper.

The vector existence histogram was plotted as shown in Fig 1 visualizing the relationship between the public places and number of respondents who experienced mosquito bites in

such places. Furthermore, the pie chart in Fig 2 was also plotted to visualize the experimental data. The result indicated that "Rivers", "Schools", "Bus Stops", "Mountains" in that order are the topmost reservoirs of malaria vectors.

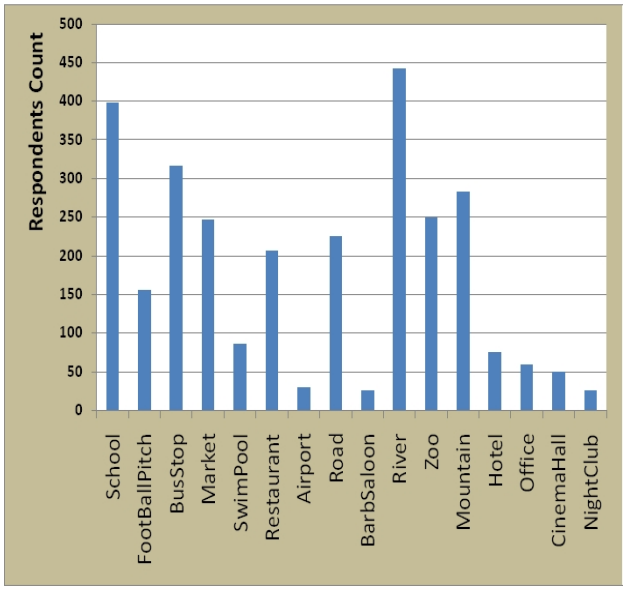


FIG 1: HISTOGRAM OF VECTOR EXISTENCE IN PUBLIC PLACES

One important deduction from Fig 1 and Fig 2 is that there are malaria vectors in public places.

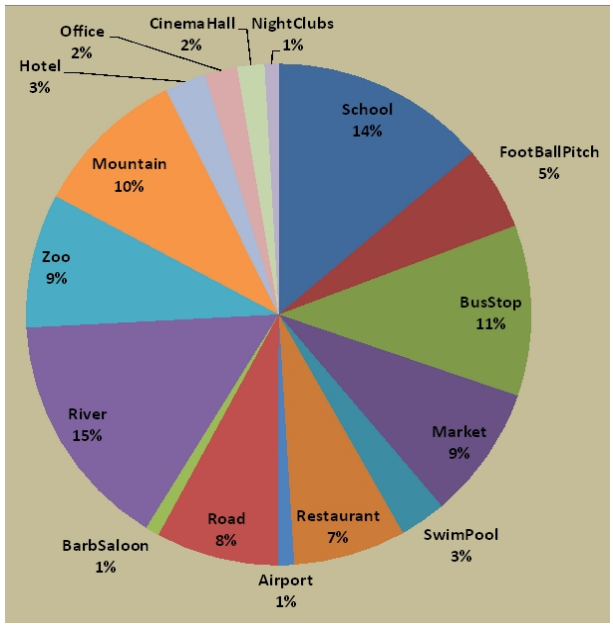


FIG 2: PIE CHART OF VECTOR EXISTENCE IN PUBLIC PLACES

In the research survey, each of the respondents were required to indicate the three public places perceived as most infested with malaria vectors, based on their past experiences of mosquito bites. The result of this is the graph in Fig 3 with the corresponding indicators "Rank3','Rank2' and "Rank1" clearly shown. The same data was used to generate the histogram in Fig 4.

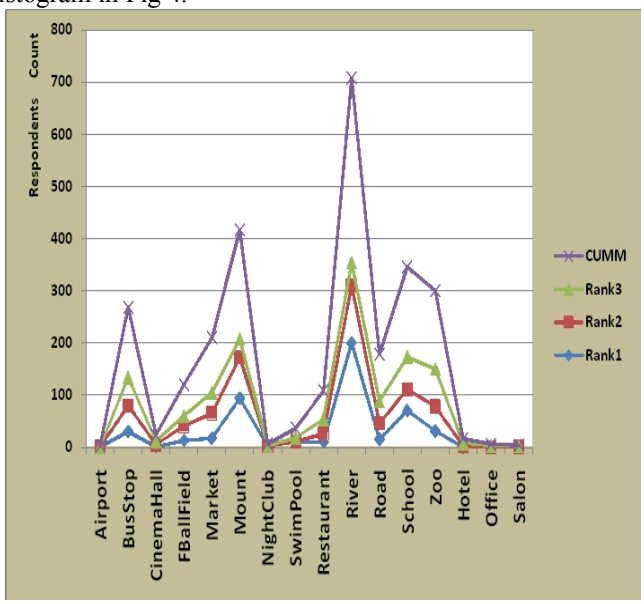


FIG 3: GRAPH OF RANKING OF VECTOR EXISTENCE

The fourth plot in Fig 3 with indicator "CUMM" is the cummulative rank, derived by summing up the three top ranks for each of the respondents. This derivative plot is of key significance.

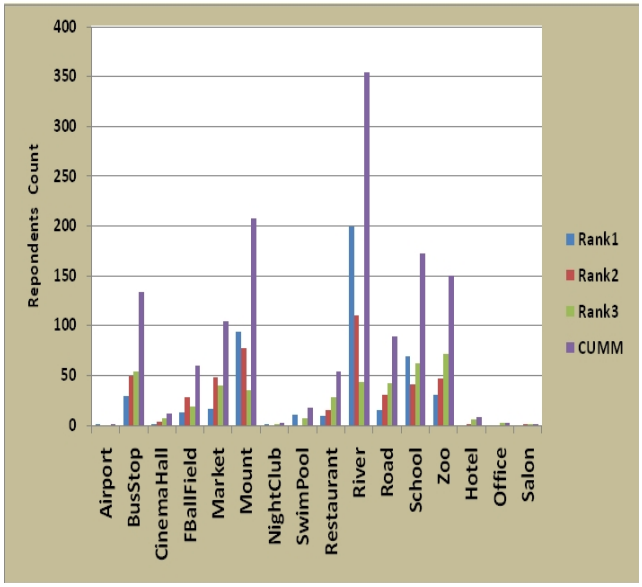


FIG 4: HISTOGRAM OF VECTOR EXISTENCE RANKING

First is that it could be used to derive the mean rank by simply dividing the cummulative rank by 3. Secondly, it acts as a visual validator, since it is expected to superimpose on top of the other three top rank plots. This is in line with the result of the numerical validation done using correlation coefficients as earlier stated.

The result of analysis on vector control tools used by respondents in their residential homes is Fig 5.

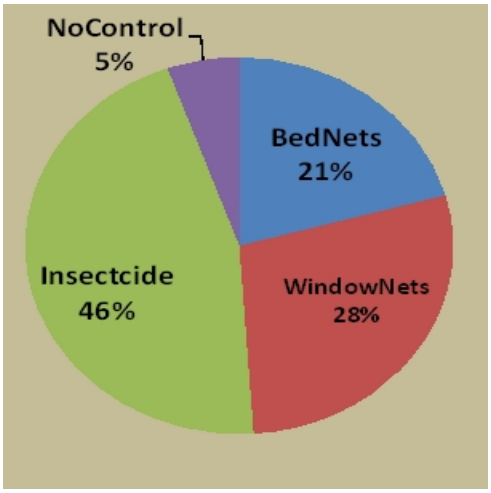


FIG 5: VECTOR CONTROL TOOLS CHART

As already mentioned in the data exctraction section and shown in TABLE III, the target group represented by this figure are the respondents who have suffered from malaria.

As much as 95% of the respondents use vector control tools in their residential homes, while only 5% live without vector controls. It is therefore very interesting to note that even at this, these respondents still suffered from malaria. The pertinent question is, "Why then do they still suffer from malaria?". The quest to answer this led to further analysis on combination of vector control strategies. Fig 6 clearly shows that as much as 62% of these respondents use a combination (of either double or tripple) vector control strategies but still suffered from malaria. Since it is assumed that the respondents are not naïve in the use of vector control tools, there is one way to account for why they still suffer from malaria even after applying vector controls in their residential homes. That is the fact that they must have contacted the malaria from the public places rather than in their residential homes.

The result of this experiment also supported the fact that not all mosquito bites led to malaria. For instance, of all the 525 respondents who have had mosquito bites at one time or the other, only 51 of them had malaria (within the last 2 years). Since malaria transmission is through bites by infected mosquitoes, this scenario can only be explained by deducing that the rest of the people who did not suffer from malaria must have been bitten by non-infected mosquitoes. The graph of bites with infection and bites without infection are shown in Fig 7 and Fig 8 respectively. In each of these graphs, the number of respondents was plotted against the number of public places where these respondents visited and experienced mosquito bites.

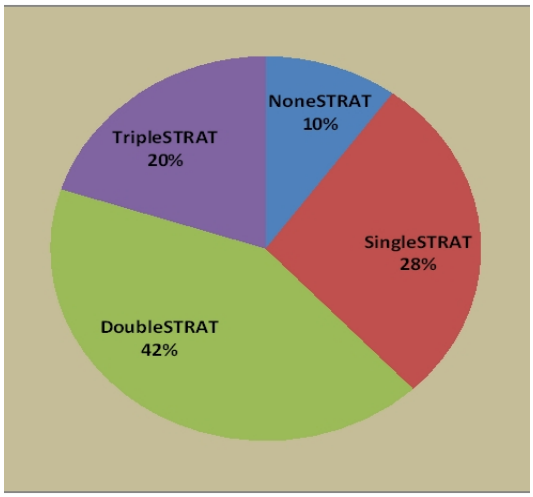


FIG 6: COMBINATION OF VECTOR CONTROLS CHART

A closer look at the shapes of Fig 7 and Fig 8 reveals a fairly common trend. For instance, both graphs rise up steadily, reach a peak, and then descend. Many facts can be deduced from these graphs. First is that there must be a public place or a combination of public places that account for the highest vector density, otherwise there would not have been any peak point on these graphs as observed. Secondly, there is a limit to number of places people can effectively visit and be bitten by mosquitoes. For instance a larger percentage of respondents visited and were bitten by mosquitoes in 1 to 6 public places, while very negligible number were able to visit between 11 to 16 places.

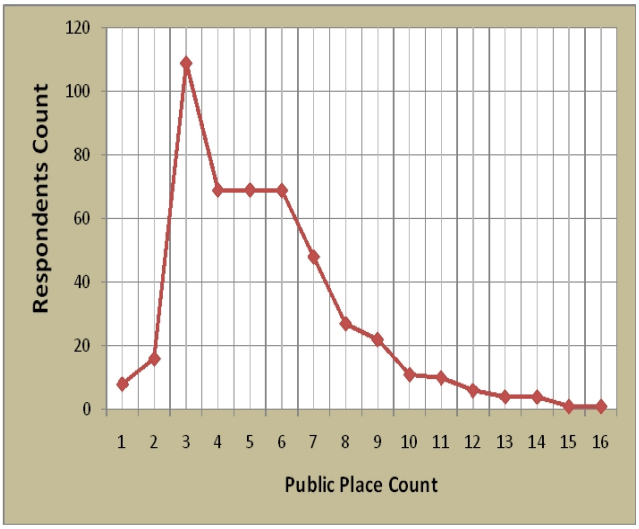


FIG 7: GRAPH OF BITES WITHOUT INFECTION

The fact that each of the respondents could accurately recollect the public places where they experienced mosquito bites is a clear indication that networks of human hosts and public places can be constructed for modeling malaria transmission.

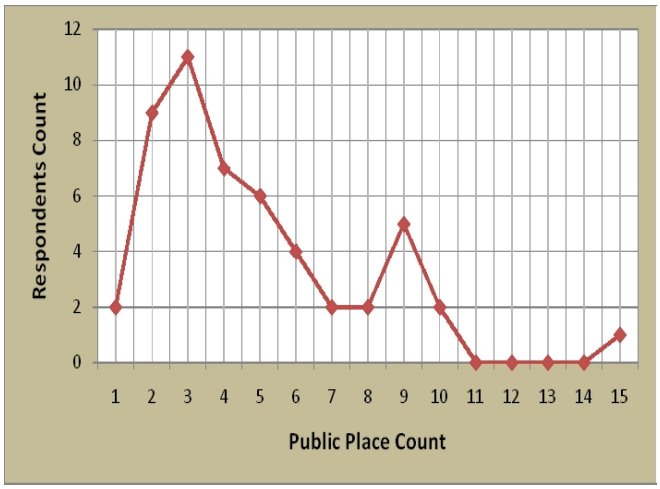


FIG 8: BITES WITH INFECTION GRAPH

VII. DISCUSSIONS ON RESEARCH OUTCOMES AND HYPOTHESIS

The result of this research has shown that there is indeed vector existence in public places. For instance, every of the 525 respondents mentioned at least one public place where they have had mosquito bites, with up to 2 respondents experiencing bites in all the 16 public places under investigation. It can also be deduced that the concept of vector existence in public places is not limited to Malaysia alone, since respondents were drawn from 10 countries. Result of this experiment also clearly proves that even if vectors are effectively controlled in residential home, malaria will still persist as long as the public places still harbor by malaria vectors.

The research also shows that it is possible to rank the degree of existence of vectors, though the present scope only gives an idea of type of public places of serious concern, rather than the exact location of those places. Prediction of the exact public places is the work in progress task of this ongoing research.

The concept of malaria vector bites without infection underlines the need to focus computational efforts on discovering the hotspots for infected vectors. Without achieving this, policy makers could waste limited vector control resources on areas of less immediate concern. In line with the hypothesis, it is clear that malaria resulting from human migration to other countries cannot be stemmed without effective vector control in public places. For instance, when a traveler enters a foreign country, the first point of interaction is the public places like airports, hotels, etc. If mosquitoes thrive in such public places, they bite the infected foreigner and subsequently bite the citizens of the host country to infect them. Malaria is therefore propagated. In the same way, while leaving the host country, the foreigner could also contact malaria and take back home to spread in his/her home country.

VIII. CONCLUSION

The entire hypothesis put forward can be seen to hold based on the results of this experiment. Though this experiment does not pinpoint the particular public places (or exact locations), it gives clues to types of public places of serious concern. It can therefore be concluded that research on malaria transmission through public places is a necessity for complete eradication of malaria. This research has revealed that malaria vector reservoirs could be further classified into natural (eg. river) and man-made habitats (eg. school, hotel). Such an understanding will definitely be useful in vector control, since the man-made reservoirs could be much easier to deal with than the natural reservoirs.

IX. FUTURE RESEARCH:

Work is currently in progress on building realistic network models and applying relevant computational techniques to determine the specific public places of serious concern.

ACKNOWLEDGMENT

The authors acknowledge with gratitude to the Ministry of Higher Education for financial support through the Fundamental research grant scheme FRGS/2/10/SG/UNIMAS/02/04

REFERENCES:

[1] D. Rogers, “Experts warn of 100Billion mosquito hell”, Austrian Times, July 17, 2009.
[2] D. Aleman and B. Schwartz, “Accounting for Individual Behaviours in a Pandemic Disease Spread Model”, Proceedings of the 2009 Winter Simulation Conference, University of Toronto http://www.informs-sim.org/wsc09papers/190.pdf
[3] M. Haber, D. Shay , X. Davis , R. Patel, X. Jin, E. Weintraub, E. Orenstein, and W. Thompson, “Effectiveness of interventions to reduce contact rates during a simulated influenza pandemic”, Emerging Infectious Disease 13 (4): 2007, 581–589.
[4] http://www.discoverybangladesh.com/meetbangladesh/people.html
[5] Norway Government Census, "Population and Housing Census 2001:Steady increase of small households", Statistic Norway, Nov 3, 2001
[6] Swiss Federal Statistics Publication. http://www.bfs.admin.ch/bfs/portal/en/index/themen/01/04/blank/key/haushaltsgroesse.html
[7] S.R. Quah, "Major Trends Affecting Families in East and Southeast Asia,: Major Trends Affecting Families: A Background Document”, Report for United Nations, Department of Economic and Social Affairs, Division for Social Policy and Development, Program on the Family , March 2003, pp 17.
[8] I. De Silva, "Demographic and Social Trends Affecting Families in the South and Central Asian Region : Major Trends Affecting Families: A Background Document”, Report for UN, Dept . of Economic and Social Affairs, Division for Social Policy and Development, Program on the Family, May 2003, pp4
[9] Australian Bureau of Statistics, http://www.abs.gov.au/ausstats/abs@.nsf/mf/3236.0
[10] China National Statistics Bureau, http://www.chinatoday.com/general/population.htm
[11] H. Badran, “Major Trend Affecting Families”, United Nations Program on Family, Division for Social Policy and Development (UNDESA) http://www.un.org/esa/socdev/family/Publications/mtbadran.pdf
[12] U.S. Census Bureau Reports & Statistical Abstract of the United States, 2008 http://www.infoplease.com/ipa/A0922165.html

Relationships Between Emotional Evaluation of Music and Acoustic Fluctuation Properties

Ryosuke Yamanishi, Yuya Ito, and Shohei Kato
Dept. of Computer Science and Engineering
Nagoya Institute of Technology
Gokiso-cho, Showa-ku, Nagoya 466–8555, Japan
Email: {ryama, yyitoh, shohey}@juno.ics.nitech.ac.jp

***Abstract*—We studied the relationships between the acoustic fluctuation properties of music and the emotional evaluations of music as a component technology for an automated song selecting system based on instinct and human emotion. When people listen to music, they select songs reflect their own feelings at the time, and then they emotionally evaluate the song. We believe that our emotional evaluation of songs are influenced by the fluctuation properties of both the volume and pitch of songs. Thus, we focused on the fluctuation properties containing dynamic ideas concerning music, and extracted thirty six fluctuation properties concerning both the volume and pitch from each song using the Fast Fourier Transform. We also prepared a subjective evaluation experiment for plural songs using the Semantic Differential method, and obtained an emotional evaluation of the songs. Then, we studied the relationships between the extracted properties and the emotional evaluations of the songs by conducting a multiple discriminant analysis. As a result, a high percentage of the questions were answered correctly and low discriminant errors were shown, and therefore, we suggested that the fluctuation properties of the songs influenced the emotional evaluations of them. Furthermore, we confirmed the especial properties related with the emotional evaluation of the music by taking into consideration the coefficients of the liner discriminants of the canonical variates that describe the discriminant spaces.**

***Keywords*—Music; Acoustic prperties; Fluctuation; Emotion; Multiple Discriminant Analysis**

I. Introduction

Music has recently attracted attention as the one of the media that enriches human cultural lives. It has recently become reasonable to suppose that music is regarded as the important factor in human lives considering the widespread use of portable music players. The innovation of media information processing enables portable music players with a large-capacity memory. People also have started collecting and taking along a lot of music data. People who are searching for songs that they want to listen to by using text data, e.g., the name of a song, the name of an artist, the name of an album, or the name of a genre. However, it is difficult to search for the song that the people want to listen to using only the text data as the capacity of music data increase. Therefore, a song selection method based on the given instincts, in other words the emotional evaluation of the song, is needed.

Furthermore, people can relax when they listen to a song whose mood is the same as their feelings at the given time [1], [2]. So, the song selection method based on the given instincts enables us to not only select the song from a large-capacity database based on our feelings at the time , but also enjoy the psychological and biological effectiveness.

To compose the song selection system based on the instincts, we need to know what emotional evaluation each song has in the database as the first step. We studied the relationships between the emotional evaluation of music and the acoustic fluctuation properties.

We extract the acoustic fluctuation properties that can explain the features of music described in section II by conducting an acoustic analysis. In addition, we obtained the results from an emotional evaluation of music using adjectives described in section III by conducting subjective evaluation experiment. We then found the acoustic properties that influence the emotional evaluation by considering the relationships between the extracted acoustic properties and the emotional evaluation of music results through a multiple classification analysis described in sections IV and V.

II. Acoustic fluctuation properties

There are plural music features that people can perceive. Pitch and volume are regarded as the more important factors for expressing music above all other factors [3], and it is reasonable to say that any temporal variation in pitch and volume influences the emotional evaluation of a song. The time concept has also been regarded as the one of the more important factors for music in the field of cognitive psychology [4]. We extracted the acoustic fluctuation properties concerning both the pitch and volume that show temporal variation for this paper. Existing studies [3], [5] detected the emotion or mood of music with the audio signals. However, fluctuation properties that can explain the time concept of music were not covered in these studies. We believe that it is necessary to cover the fluctuation properties for revealing the relationships the emotional evaluation of music and the acoustic properties.

A. Fluctuation properties of music

Rhythm, melody, and harmony are the three major factors for composing music [6]. They are signed and sealed as the time structures of both the pitch and volume, and are different for each song. The emotional evaluations of songs can be influenced by their differences. We believe that this idea about music and emotion is plausible to the people widely.

Rhythm is signed and sealed by the temporal regularity of both the pitch and volume. The melody is composed of

the temporal alteration of both the pitch and volume, and the harmony is composed of the relative relations of sounds that are pronounced at the same time and have a definite action during the passage of time.

The fluctuation properties of music can be used to interpret songs from a time standpoint, and capture the factors composing the music. Therefore, we focused on the fluctuation properties of both the pitch and volume, and extracted the properties of the fluctuation spectrum by conducting an acoustic analysis.

B. Extracting properties

Since we would like to extract the acoustic properties that people can precisely perceive, we did not use songs stored as MIDI formatted data but songs stored as WAV format data. An acoustic analysis of WAV formatted song data enables us to visualize the structures about both the time and fluctuation of music. All the song data used in an analysis are taken from Compact Discs and stored as stereo data, the sampling frequency is 44100 Hz, and they were linear quantized to 16 bits in order to standardize the acoustic quality.

We believe that not only the acoustic properties of music for an entire frequency band, but also the ones on several frequency bands influence the emotional evaluations. So, we prepared five kinds of frequency bands. They were Low, Middle, High, Ultrahigh, and All. The acoustic properties of music were extracted from these five frequency bands. In this paper, the Low frequency band, Middle frequency band, High frequency band, Ultrahigh frequency band, and All frequency band are each defined as a band lower than 200 Hz, 200 - 800 Hz, 800 - 2000 Hz, more than 2000 Hz, and a band that is as long as we can calculate, respectively.

1) Fluctuation property about volume: The power spectrums for each frequency band at each time are calculated from the WAV formatted song data using a short-time Fourier transform (Hanning window, length of window 2048 points, resolution time is 25 ms). For each time, the values of the integral of each power spectrum are calculated with respect to each frequency band. The values of the integral are regarded as the volume on each frequency band. The fluctuation properties of the volume are generated by regarding the volume at given each time as the time-series data with respect to each frequency band. Then, the fluctuation spectrum concerning the volume on each frequency band is generated from the fluctuation property for the volume on each frequency band using the Fast Fourier Transform.

2) Fluctuation property concerning pitch: The pitch at each given time is detected by using zero-cross detection. The $Pitch_t$ at each time t is calculated by using the following equation.

$$Pitch_t = \frac{smp \cdot count_0}{2}, \tag{1}$$

where, smp and $count_0$ are the sampling frequency and number of zero-cross in the window at time t. The fluctuation property of the pitch is generated by regarding the pitch at each given time as the time-series data. Then, the fluctuation spectrum concerning the pitch can be generated from the fluctuation property of the pitch by using the Fast Fourier Transform.

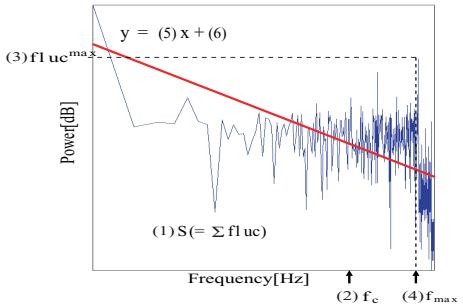


Fig. 1. Example of fluctuation spectrum

TABLE I
SONG PROPERTIES

Index	Features
1 - 6	Properties of fluctuation spectrum about volume on All frequency band (1) ∼ (6)
7 - 12	Properties of fluctuation spectrum about volume on Low frequency band (1) ∼ (6)
13 - 18	Properties of fluctuation spectrum about volume on Middle frequency band (1) ∼ (6)
19 - 24	Properties of fluctuation spectrum about volume on High frequency band (1) ∼ (6)
25 - 30	Properties of fluctuation spectrum about volume on Ultrahigh frequency band (1) ∼ (6)
31 - 36	Properties of fluctuation spectrum about pitch (1) ∼ (6)

C. Properties of fluctuation spectrum for a song

Figure 1 shows an example of a fluctuation spectrum. The properties of the fluctuation spectrum on a song are calculated from each fluctuation spectrum that is generated in II-B1 and II-B2. When $fluc(\omega)$ represents the fluctuation spectrum on frequency band ω, and n is the number of the spectrums, the properties of a song are shown by using the following equations with respect to each frequency band. TABLE I lists the properties and their index.

(1) Value of integral S:

$$S = \int fluc(\omega) d\omega.$$

(2) Centroid frequency f_c:

$$f_c = \frac{\int \omega \cdot fluc(\omega) d\omega}{S}.$$

(3) Max value of the fluctuation spectrum $fluc^{max}$:

$$fluc^{max} = \max_{\omega > 0.1} \left(fluc\left(\omega\right) \right).$$

(4) Max frequency of the spectrum $fluc^{max}$:

$$f_{max} = \arg \left(\max_{\omega > 0.1} \left(fluc\left(\omega\right) \right) \right).$$

(5) The slop of the regression line α:
The slop of the regression line for $fluc(\omega)$ is calculated by using the least-squares method.

$$\alpha = \frac{n\sum^{n}\omega \cdot fluc(\omega) - \sum^{n}\omega\sum^{n} fluc(\omega)}{n\sum^{n}\omega^2 - \left(\sum^{n}\omega\right)^2}.$$

(6) The intercept of the regression line β:
The intercept of the regression line for $fluc(\omega)$ is calculated by using the least-squares method.

$$\beta = \frac{\sum^{n}\omega^2\sum^{n} fluc(\omega) - \sum^{n}\omega \cdot fluc(\omega)\sum^{n}\omega}{n\sum^{n}\omega^2 - \left(\sum^{n}\omega\right)^2}.$$

The thirty six above-mentioned features are considered the properties of a song. The properties of songs are each normalized, and then the average property value and standard deviation of all songs reach each zero, and one, respectively.

III. Emotional Evaluation

This study is different from the existing studies in [7], [8] in that this study is not for the classification of the music genre but for revealing the relationships between the emotional evaluation of music and the features of music. It has been proposed that the emotional evaluation is important when considering the significance and effectiveness of music, and has been studied in some related works [4], [9]. We obtained the emotional evaluation of music by conducting a subjective evaluation experiment based on the Semantic Differential method whose criteria were varied [10].

A. Presentation songs and objects to be evaluated

We prepared one hundred and fifty songs that were arbitrarily selected from several genres, e.g., Pop, Classical, Jazz, Rock, House and so on. Almost all of the songs provide people with different emotional impressions throughout a song. Then, we used an arbitrarily-prescribed phrase that was extracted from a song and it was about ten seconds long and used as the object to be subjectively evaluated. Hereafter, we use our evaluation of this one phrase as the emotional evaluation of a song.

B. Subjective evaluation experiment

We prepared eight pairs of adjectives for evaluating the songs. TABLE II lists the eight pairs of adjectives. All the prepared songs were evaluated on a scale of one to seven for the eight adjectives based on the Semantic Differential Method. Eighteen healthy men and women (fifteen men, and three women) in their twenties participated in our evaluation. The subjects listened to and evaluated all the songs in random order through a prepared interface on the given web browser. With this interface, the songs are played by using the Windows Media Player on each subject's own personal computer. So the subjects could rewind and play back the songs over and over again.

TABLE II
Adjectives

Index	Evaluation on a one-to-seven scale						
	-3	-2	-1	0	+1	+2	+3
1	Bright - Dark						
2	Mellifluence - Harsh						
3	Rich - Poor						
4	Clear - Murky						
5	Agitato - Peaceful						
6	Heavy - Light						
7	Soft - Hard						
8	Thick - Thin						

TABLE III
Number of appropriate songs of each adjective for analyzing

Index of adjectives	1	2	3	4	5	6	7	8
The number of songs	131	122	82	125	133	91	108	91

C. Emotional evaluation of songs

Twelve thousand emotional evaluations of the songs (eight adjectives for one hundred fifty songs) were obtained from the subjective evaluation. Then, we used the mode for all the subjects' evaluations of a song as the emotional evaluation of a song. The evaluations that had a dispersion from all the subjects' evaluations of more than a two were considered inappropriate, and removed from the group of analytical objects. The numbers of appropriate songs for analysis are listed in TABLE III.

IV. Discriminant analysis

The numbers of analytical songs for each adjective are listed in TABLE IV. We can see that there is no song in +3, index eight (Thick - Thin). In general, the class that has less than three data do not satisfy the homoscedasticity and is unsuitable for discriminant analysis [11]. Therefore, we removed the classes that had less than three data from the analytical objects, and the adjectives whose indices are three and eight were analyzed as they each have five and six classes respectively.

A. Feature selection

The contributory features for discriminating x_i (i means index of property) were selected from the thirty six different properties of the songs listed in TABLE I with respect to each adjective, and are listed in TABLE V. The appropriate features are selected by using a stepwise method, and the Fisher's linear discriminant function was used as the evaluation function [12].

B. Canonical discriminant analysis results

Canonical discriminant analysis was conducted using songs listed in TABLE III, where the explanatory and dependent variables are the properties of the songs selected in IV-A and the classes of each adjective, respectively.

1) Considering percentage of questions correctly answered and errors: The percentage of questions correctly answered and the errors are listed in TABLE VI. We can obtain more than double the percentage of questions correctly answered

TABLE IV
NUMBERS OF EVALUATIONS OF SONGS FOR EACH CLASS, ADJECTIVES

Index	Evaluation on one-to-seven scale						
	-3	-2	-1	0	+1	+2	+3
1	7	39	29	3	32	17	4
2	5	26	39	4	21	22	5
3	2	22	29	11	13	4	1
4	9	26	43	3	27	12	5
5	9	25	40	3	22	21	13
6	5	6	20	5	28	22	5
7	9	18	29	5	29	14	4
8	4	14	41	14	15	3	0

TABLE V
SELECTED FEATURES

Index of adjectives	Song properties
1	x_7, x_{10}, x_{21}
2	x_{17}, x_{27}, x_{31}
3	x_2, x_5, x_9, x_{20}
4	x_6, x_7, x_{16}
5	x_2, x_3, x_6, x_7, x_{14}, x_{15}
6	x_{31}, x_{32}
7	x_2, x_{15}, x_{20}, x_{33}
8	x_8, x_{10}, x_{11}, x_{17}, x_{32}

TABLE VI
PERCENTAGE OF QUESTIONS CORRECTLY ANSWERED AND ERRORS

Index of adjectives	Percentage of questions correctly answered	Error
1	0.493	0.95
2	0.475	0.95
3	0.569	0.68
4	0.44	1.10
5	0.556	0.74
6	0.473	1.02
7	0.472	1.01
8	0.593	0.68

TABLE VII
CONTRIBUTING RATES OF CANONICAL VARIATES

Index of adjectives	CV1	CV2	CV3	CV4	CV5	CV6
1	0.61	0.22	0.17	-	-	-
2	0.61	0.3	0.09	-	-	-
3	0.48	0.32	0.19	0.01	-	-
4	0.56	0.31	0.13	-	-	-
5	0.52	0.24	0.1	0.09	0.03	0.01
6	0.67	0.33	-	-	-	-
7	0.56	0.21	0.16	0.07	-	-
8	0.37	0.29	0.21	0.10	0.03	-

from the theoretical values when it is randomly discriminated. Above all, the percentage of questions correctly answered about adjectives with three, five, and eight indices are relatively-good, and we can suggest that a reasonable level of discrimination was confirmed. Moreover, there was less than one error for adjectives whose indices were one, two, three, five, and eight. This shows that almost all the songs are discriminated in the classes next to the true classes even if a misclassification happened.

2) Considering discriminant spaces: The contributing rates of each canonical variate (CV) are listed in TABLE VII. Point diagrams of songs for each adjective are generated from CV1 and CV2, and are shown in Figure 2. We can confirm that the positives and negatives from the evaluation are discriminated along with CV1 for adjectives whose indices are one, two, and five. In particular, songs for each class are continuously-distributed with CV1 for adjectives whose index is five. Moreover, for adjectives whose indices are three and eight, the songs of each class are mixed even though the percentage of questions for discrimination that were correctly answered and the errors are well associated (TABLE VI). We believe it is caused by the relatively-low contribution rates of CV1 and CV2 (TABLE VII), and in fact, it is difficult to discriminate them using only CV1 and CV2 as the adjectives whose indices are three and eight.

V. RELATIONSHIPS BETWEEN EVALUATION AND ACOUSTIC PROPERTIES

We would like to focus our attention in this paper on the adjectives whose indices are one, two, and five. The emotional evaluations of songs for these adjectives are discriminated well by CV1 and CV2, which are composed of prepared acoustic properties (Figure 2). TABLE VIII lists the acoustic properties and coefficients of the liner discriminants (LD) of CV1 and CV2 with respect to the adjectives whose indices are one, two, and five. Therefore, it seems reasonable to suppose that the coefficients of LD for each acoustic property can be regarded as the influence rate of each acoustic property for each CV.

- Adjective 1, Bright - Dark
  Figure 2 shows that Bright songs and Dark songs are each in the minus area and the plus area of CV1, respectively. As for the adjective whose index is one (Bright - Dark), TABLE VIII shows that the coefficient of the liner discriminant for CV 1 of x_{21} that represents the max frequency of the fluctuation spectrums concerning the volume on the High frequency band is relatively big number in negative. In addition, the coefficient of the liner discriminant for CV1 of x_7 that represents the value of the integral of the fluctuation spectrums concerning the volume on the Low frequency band, and that x_{10} that represents the max frequency of of the fluctuation spectrums concerning the volume on the Low frequency band are both negative. It seems from these that the songs with a volume on the High frequency band that passionately sway, and of deep bass (for example, drums, or bass) that passionately change are discriminated as Bright songs.
- Adjective 2, Mellifluence - Harsh
  Figure 2 shows that Mellifluence and Harsh songs are each in the minus and plus areas of CV1, respectively. As for the adjective whose index is two (Mellifluence - Harsh), TABLE VIII indicates that the coefficients of the liner discriminants for a CV1 of x_{17}, which represents the slop of the regression line concerning the fluctuation spectrums of the volume on the Middle frequency band, and x_{31}, which represents the value of the integral of the fluctuation spectrums concerning the pitch, are both relatively big numbers in positive. When the slop of the

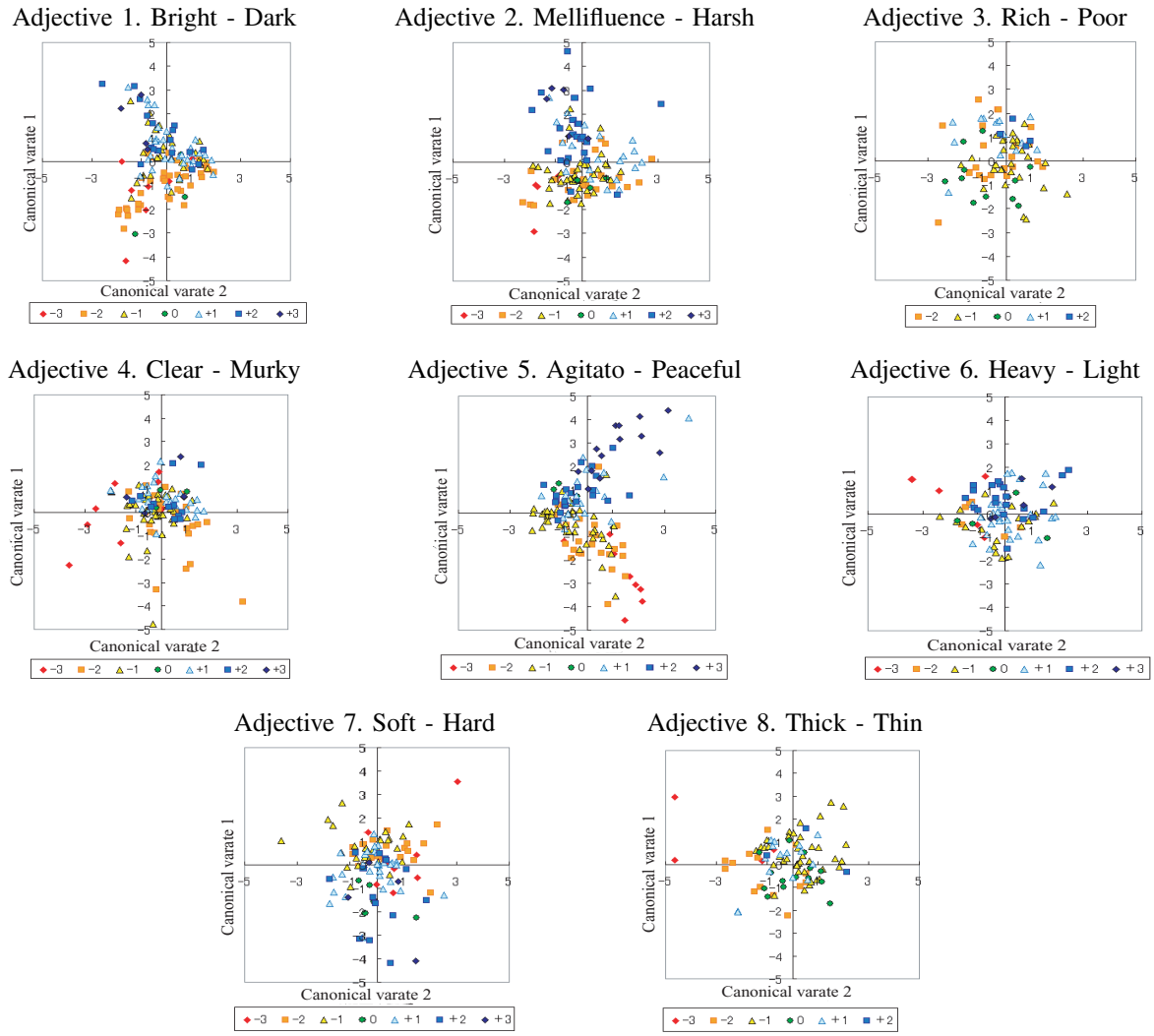


Fig. 2. Point diagrams of songs for each adjective

TABLE VIII
COEFFICIENTS OF LINER DISCRIMINANTS OF CANONICAL VARIATE ONE AND TWO FOR EACH ADJECTIVE

Adjectives	Properties	Coefficients of LD1	Coefficients of LD2
1	x_7	**-0.412**	0.28
	x_{10}	**-0.46**	0.69
	x_{21}	**-1.05**	-0.48
2	x_{17}	**1.12**	-0.41
	x_{27}	-0.01	0.86
	x_{31}	**0.52**	0.61
5	x_2	**0.77**	-0.63
	x_3	**-1.89**	1.04
	x_6	-0.06	-0.69
	x_7	**-0.80**	-0.42
	x_{14}	-0.5	0.16
	x_{15}	**1.33**	-0.59

regression line for the fluctuation spectrums increases, the value of the short-period power spectrums increases. The high-frequency waves of the fluctuation spectrums for the volume are related to the instrument assuming the rhythm with a short cycle, for example, the drums. It seems that the songs are harsh from these when their pitch passionately changes, and the volume of the instrument assuming the rhythm increases and decreases frequently.

- Adjective 5, Agitato - Peaceful
Figure 2 shows that Agitato and Peaceful songs are each in the minus and the plus area of CV1, respectively. In addition, each evaluation is distributed in a continuous way along CV1. As for the adjective whose index is five (Agitato - Peaceful), TABLE VIII indicates that the coefficients of the liner discriminants for CV1 of x_3, which represents the max frequency of the fluctuation spectrums concerning the volume on the All frequency band, and x_7, which represents the value of the integral of the fluctuation spectrums concerning the volume on the Low frequency band, are both relatively big number in negative. The coefficient of the liner discriminant of CV1 of x_{15}, which represents the max frequency of the fluctuation spectrums concerning the volume on the Middle frequency band, and x_2, which represents the

TABLE IX
PERCENTAGES OF QUESTIONS CORRECTLY ANSWERED AND ERRORS BY LEAVE-ONE-OUT CROSS VALIDATION

Index of adjectives	Percentage of questions correctly answered	Error
1	0.47	0.98
2	0.46	0.98
3	0.49	0.79
4	0.42	1.13
5	0.53	0.79
6	0.44	1.02
7	0.43	1.08
8	0.56	0.75

centroid frequency on the All frequency band, are both relatively big number in positive. For these, it seems that the songs are agitato when their max volume on the All frequency band is high and the volume on the Low frequency band is also high. However, it seems that the songs are peaceful when the max volume on the Middle frequency band is high. Accordingly, we can suggest that this adjective (Agitato - Peaceful) is influenced by the dynamic idea of the fluctuation concerning the volume on each frequency band.

Regarding the adjectives whose indices are three, four, six, seven, and eight, the classes of evaluation are mixed in each discriminant space even though the percentages of the questions correctly answered are sufficient. It can be assumed that they can not be discriminated by using the discriminant spaces that are composed by only CV 1 and CV2. In addition, TABLE V indicates that there are few acoustic properties for discriminating classes of adjectives whose index is six (Heavy - Light), basically there are only two properties. For this reason, we believe that the properties for discriminating classes of this adjective are not with in the thirty six properties that were prepared.

VI. CROSS VALIDATION

We confirmed the availability of the prepared properties by using a leave-one-out cross validation. TABLE IX lists the percentage of questions correctly answered and the errors by conducting the leave-one-out cross validation. From this, the percentage of questions correctly answered and the errors are both sufficient for use as test data, and we can suggest that the prepared acoustic properties are available.

VII. CONCLUSION

We extracted the acoustic fluctuation properties and analyzed the relationships between the results from an emotional evaluation of music and the acoustic fluctuation properties by conducting a multiple discriminant analysis. As a result, we could obtain a high percentage of questions correctly answered and low number of errors for all the prepared adjectives, and suggested that the acoustic fluctuation properties influenced the results from an emotional evaluation of music. Moreover, we confirmed the acoustic properties that influence the discrimination for the classes of adjectives, such as for Bright - Dark, Mellifluence - Harsh, and Agitato - Peaceful.

The future direction of this study is as follows.

- Increasing the number of song:
  There were not enough appropriate songs to fairly evaluate the use of adjectives (Tables III and IV). We will prepare more and a variety of songs for analysis.
- Detailed recognition for high-dimensional discriminant spaces:
  In this paper, we focused our attention on and took into consideration the adjectives that are easily discriminated by using only CV1 and CV2. However, the discriminant of some of the adjectives might depend on not only CV1 and CV2, but also more CVs (TABLE VII). So, we will take more CVs into consideration by using some more techniques that can be used to describe multiple dimensions, such as the Varimax rotation [13].
- Application for automated song selecting system based on instinct:
  We will create a song selection system that is based on common instinct while reflecting the results of this study. We will then evaluate its usability by conducting a subjective evaluation experiment using the system.

ACKNOWLEDGMENT

This work was supported in part by the Ministry of Education, Science, Sports and Culture, Grant–in–Aid for Scientific Research under grant #20700199, and Research Foundation for the Electrotechnology of Chubu.

REFERENCES

[1] M. E. Donald. and P. Joseph, *Music Therapy In Principle And Practice*. Charles C Thomas Pub Ltd, 2005.
[2] K. Momose, Y. Fujisawa, and A. Uchiyama, "Effects of music on physiological measurements and mood states, and their correlation with impression of the music," *Journal of International Society of Life Information Science*, vol. 22, no. 2, pp. 545–551, 2004.
[3] L. Lu, D. Liu, and H.-J. Zhang, "Automatic mood detection and tracking of music audio signals," *IEEE Trance on Audio, SPEECH, And Lang Processing*, vol. 14, 2006.
[4] L. B. Meyer, *Emotion and Meaning in music*. University of chicago Press, 1956.
[5] P. Synak and A. Wieczorkowska, "Some issues on detecting emotions in music," *Lecture Notes in Computer Science*, vol. 5097/2008, pp. 164–174, 2008.
[6] S. Feldstein, *Practical Theory Complete: A Self-Instruction Music Theory Course*. Alfred Publishing Company, 1982.
[7] T. Kitahara, Y. Tsuchihashi, and H. Katayose, "Music genre classification and similarity calculation using bass-line features," *Proceesings of the 10th IEEE International Symposium on Multimedia, Workshop on Multimedia Audio and Speech Processing*, pp. 574–579, 2008.
[8] D.-N. Jiang, L. Lu, H.-J. Zhang, J.-H. Tao, and L.-H. Cai, "Music type classification by spectral contrast feature," *Proceedings of IEEE International Conference on Multimedia and Expo, 2002.*, vol. 1, pp. 113–116, 2002.
[9] P. N. Juslin and J. A. Sloboda, *Music and Emotion: Theory and Research*. Oxford University Press, 2001.
[10] C. E. Osgood, W. S. May, and M. S. Miron, *Cross-Cultural Universals of Affective Meaning*. University of Illinois Press, 1975.
[11] C. M. Bishop, *Pattern Recognition and Machine Learning*. Springer, 2006.
[12] H. Liu and H. Motoda, *FEATURE EXTRACTION CONSTRUCTION and SELECTION: A data Mining Perspective*. KLUWER ACADEMIC PUBLISHERS, 1998.
[13] H. F. Kaiser, "The varimax criterion for analytic rotation in factor analysis," *PSYCHOMETRIKA*, vol. 23, no. 3, pp. 187–200, 1958.

A-Class: A Classroom Software with the Support for Diversity in Aptitudes of Autistic Children

Md. R. Rahman, Shujon Naha, Proteek C. Roy, Ishrat Ahmed, Samiha Samrose, Md. M. Rahman, S. I. Ahmed
Department of CSE, Bangladesh University of Engineering and Technology (BUET),
Dhaka, Bangladesh.
Email: {helloratul, shujon76, proteek_buet,ishratahmedmren, samiha_mumu, mazy_buet}@yahoo.com,
ishtiaque@csebuet.org

***Abstract*—The burgeoning growth of the e-Learning technologies implies the fact that the future education system will largely depend upon the electronic devices and computer aided technologies. It has already been proved that the computer aided teaching techniques are much more effective for the children than the traditional teaching system in most of the cases. A large number of software has been designed to assist the teachers in the classroom to teach and evaluate the students. Although those software systems are good enough for a class with normal (neurotypical) children, those very often fail to address the special needs of the autistic children. Hence, the autistic children face various challenges in participating with neurotypicals in the same classroom. We have addressed this problem by designing and implementing an intelligent classroom software, named "A-Class", which takes care of the diversity of tastes among the autistic children of a classroom and helps the teacher to teach in a class participated by both autistic and neurotypical children. In this paper we discuss the idea, design and implementation of A-Class based upon our five months of intervention with the autistic children at Autism Welfare Foundation (AWF) in Dhaka.**

***Keywords*—Autism, Classroom, E-Learning**

I. INTRODUCTION

The autism spectral disorders are defined by the qualitative impairments in social communication. Although the true reason for autism is still unknown to the medical sciences; it has been proved to be the result of abnormal and irregular growth of cerebral neurons of human brains[1]. People suffering from autism very often demonstrate a poor performance in social interactions; and hence find it difficult to communicate to other people. On the other hand, it is equally difficult for others to communicate to them in the usual ways. As the number of autistic people has been reported to increase at a high rate throughout the world in recent decades, it has become necessary to discover effective ways for communicating to them. One of the bigger challenges is to ensure proper education to the autistic children in a proper way so that they can develop their skills and contribute to the society being within their limitations.

The autistic children have a different way of thinking than the expected pattern of the neurotypicals. Due to the abnormal cerebral structure, their thinking style is very much different. They very often have a strong attraction to some particular persons, objects, tasks, places or environments. During our intervention for more than three months with the autistic children of Autism Welfare Foundation (AWF) located at Dhaka, Bangladesh, we observed this important feature among most of the autistic children. This type of abnormal attraction makes them unique from their other peers. Some autistic children were found be attracted by the underwater objects, while some were found to be fond of vehicles. Some liked foods, some liked trees, some liked sports etc. Their attraction level is very intense and most of them do not feel comfortable if they are not dealing with something related to the things they liked. For example, an autistic boy who was fond of vehicles did not get interest in playing a fishing game; rather got the racing game more interesting and engaging. On the other hand, the autistic boy who was attracted to the underwater objects got little interest in playing a racing game but he enjoyed playing the fishing game very much. Any effort on teaching an autistic child with something they are not interested in was proved to be unfruitful. Hence the diversity in aptitude should be considered with utmost care while designing a learning method for autistic children.

The parents of the autistic children very often face the problems while choosing schools for their kids. For their special needs, most of the general schools which are designed for the neurotypicals fail to provide an autistic child with the proper care. In the special schools made for the autistic children, there are a good numbers of autistic children with different aptitudes and hence, the teachers get it difficult to customize the teaching method for each of them. The electronic teaching software available in CD/DVDs cannot be customized for a special child, to our best knowledge. Hence, the proper teaching with customized method for every child has become very difficult to get.

In this paper, we focus on this particular problem and design a software which can provide with a customized platform for every child attending a large classroom. This software takes care of the diversity of aptitude of each of the children and releases the teacher from the responsibility of customizing the teaching for each of the students. Further, this software can be used in a classroom where there can be autistic children. So, it offers a platform for making the general schools able to accept the autistic children and assure them proper learning environment.

II. Related Previous Works

Not very much remarkable works have been done on the idea we are proposing in this paper. But there have been a number of efforts for teaching the autistic children. Some of the raditional efforts involve using "Clue Cards". "Clue Cards" are cards with pictures drawn on them. The teacher shows the
children the cards so that they can memorize the concept of the picture more easily. As autistic children are diverse in their aptitudes, one card cannot be applicable for all of them. Hence, the traditional "Clue Cards" do not address the issue of diversity in autism. The effect of interacting video and attractive pictures or interface on children learning has been analyzed and proved [2]. So eventually number of softwares are available on CD/DVDs which offer an animated environment for the students to learn a new topic. There have been two problems associated with these softwares:
i) Most of these are not inter-active ii) These are not customizable according to the diversity of the autistic children.

Hence, if the autistic child does not like the environment offered by the software, teaching becomes difficult. On the top of that, none of these softwares were made for a whole classroom dealing with autistic children along with neurotypicals. Another attempt is Story Listening Systems (SLS), a model of technology and literacy development, are shown to promote language skills development in children through storytelling with a virtual peer [3]. However, SLS make several assumptions about children [4]. Very recently, Hoque [5], [6] used the open source game developing platform "*Scratch*" to make customizable games for the development of speech for the autistic children. In their paper, they emphasized the necessity of customization according to the aptitude of the autistic children. The easy customization option of Scratch offers a suitable platform to make computer games according to the aptitude of an autistic kid. Their games were targeted to develop the loudness and intelligibility in the speech of the autistic children. A number of classroom softwares are available for the modern classrooms equipped with facilities of computers, multimedia, local area networks, internet (etc.). Very recently, use of 3G mobile phones has been studied in the classroom for teaching and checking the responses of the students. All of these systems have been made for the neuro-typical students who behave like "expected patterns". To our best knowledge, no classroom software has been made for the autistic children, which takes care of the diversity of aptitudes among the autistic children.

III. Our Works

We have addressed the issue of diversity in aptitudes among autistic children while designing the learning environment with the help of our classroom software. As we know communication skills for autistic children differ from the norm, including their thinking process. Children with autism find words too busy, so it's easier to retain information through pictures. Through remembrance of pictures, autistic children are able to understand others and express themselves [8]. If we use a sing-song voice or robot-like tone will help them to communicate more frequently [9]. In our design we have tried to address these issues with help of implementing the applied behavior analysis (ABA), one of the most effective education methodologies of autistic children [10].

For the time being we have designed our class room as an alphabet learning classroom which is software based. In our proposed classroom, there will be computer before every student and the teacher. All computers will be interconnected by the Local Area Network (LAN). The students' computers will show the item chosen by the teacher. While teaching, the teacher will choose the item in his/her computer and a corresponding message will be broadcasted over the network. Each of the computers before the students will receive that message. The item that becomes visible in a student's computer for a particular message depends on the profile of the student who is using that computer. Each of the autistic children will get his favorite environment in his monitor according to his profile. The general students, on the other hand, will see the general environment that is applicable in typical cases. We use Java socket based networking technology for the networking purpose. The front end has been designed by the swing components of Java. In the back-end an Oracle database server works. The profile of each of the students, which will include his/her aptitude, is assumed to be set before the student attends the class. For the time being, we have selected a number of themes targeted for a number of autistic children and the topic for the classroom has been set as the English alphabet (A-Z). There are provisions for extending the software with more themes and topics.

IV. The Design Of Proposed Classroom

The classrooms should be equipped with the following components: i) Computers ii) Local Area Network iii) Java Development Kit (JDK).

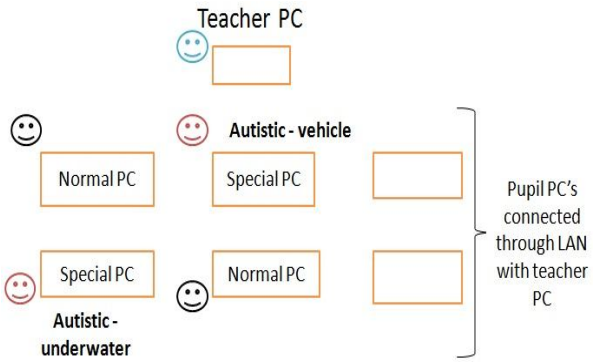


Figure. 1: Diagram of the proposed classroom

The diagram of proposed classroom is given in Figure 1. There is a computer in front of every pupil of classroom. The computer denoted special means it has autistic pupil in front of it. All the computers are connected through lan. Based on the login (username and password) our intelligent system will identify the computers in front of autistic pupils and it will also extract the information of their field of interest which will be previously stored in database. So all normal pupils will see same interface but every autistic pupil will see different interfaces based on his own interest. Now when teacher wants to show them 'A' she presses button 'A' and the students will see like this :

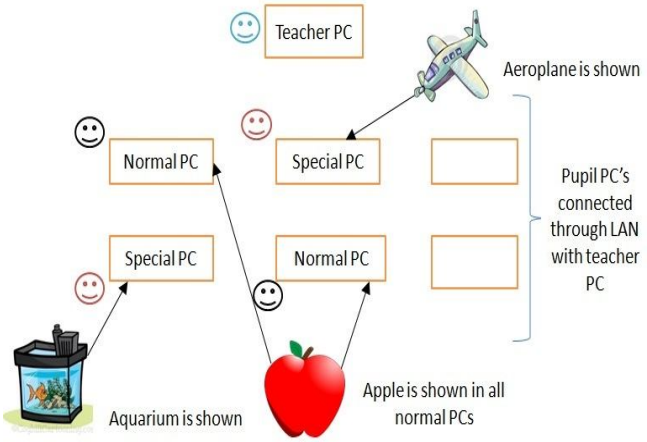


Figure. 2: Diagram of the proposed classroom

So in all normal pupil pc a typical image is shown, here 'A' for apple is shown in all normal computer but the autistic pupil who likes vehicles, in his interface 'A' for aeroplane will be shown and the autistic pupil who likes underwater, in his interface 'A' for aquarium will be shown. Thus all the letters will be shown with different pictures to different computers.

Some sample interfaces :

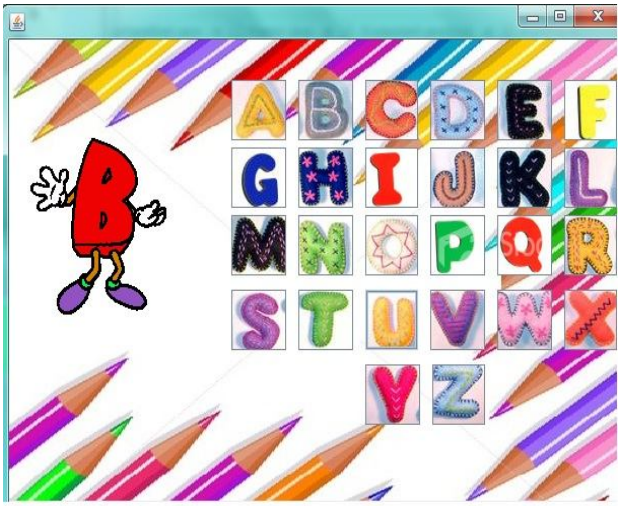


Figure. 3: Teacher interface



Figure. 3: Normal pupil interface



Figure. 4: Autistic pupil interface

V. THE E-R DIAGRAM

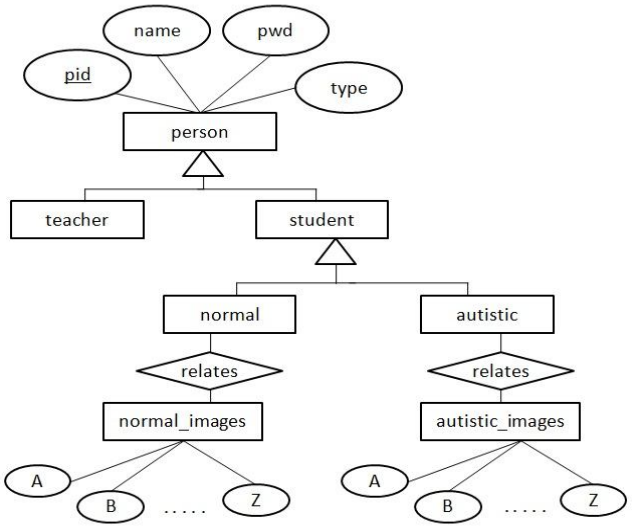


Figure. 5. E-R diagram

VI. THE REQUIREMENTS AND INSTALLATION

A. Hardware specification

We have tested our software in the following PC configuration.

1) Intel Pentium 4 processor 2.66GHz.
2) 1 GB of Memory
3) 80 GB of Hard Disk.

B. Software specification

1) First we need to install j2se 6.0 [11] for both server and client.
2) Then in server computer we need to install tomcat server 6.0.20 [12] and mysql Version 14.14 Distribution 5.1.41 [13].
3) Then first create a database named 'autism' and then import the SQL files in MySQL server.
4) Finally unzip the autismServer.zip file in the Root directory of your tomcat server, which contains the war file and the image directory.

VI. USING THE SOFTWARE

The software can be used to teach alphabet to a class of student containing both neurotypical and autistic children. It has three types of users: i) Administrator ii) Teacher iii) Student

A. For the Administrator

i. Admin should entry the teachers and students name and corresponding password in database.

B. For the teacher

i. Teacher must login first to start the program using her username and password.
ii. Then teacher will press the start button shown to view the alphabet panel.
iii. To teach an alphabet the teacher will then press the corresponding button showing the alphabet and it will be broadcasted to all students.

C. For the Students

i. Student must login first to start the application in her pc.
ii. Then she has to wait until the teacher press the "Start" button.
iii. Finally when the teacher press an alphabet button, according to the login information the student will see the corresponding images of the alphabet.

Evaluation: The final part of this software is the "Evaluation". In this stage, the success of teaching the students is measured by testing the students with a set of questions. The method of this examination is very simple. The students are given a letter and a set of pictures before them. The pictures will show different items (according to their personal choice) and only one of those objects has the name starting with the letter shown in that context. The task for the children is to find out the correct picture. For this, the students just need to click upon the right picture. The answer will be locally judged and the evaluation is sent to the teacher. The teacher, in this way, will get the result of evaluation of each of the students in his/her screen after taking the class.

This Evaluation part ensures the scope for improving the teaching materials for the right method of pedagogy. It also will provide the teacher with an option for visualizing the individual performances of each of the students in context of the whole class.

The pictures shown in the evaluation part might be chosen from the same set of pictures used for teaching them. Alternatively, we might choose different picture of the same object to test the student's skills to identify the objects. This particular portion leaves a number of research option open for the future improvement. The learning method can be developed in a scalable way so that the teacher can get the option to set the right level of difficulty while setting the questions for the evaluation.

VII. FUTURE WORKS

Although for the time being we know the field of interest of every autistic pupil by consulting their parents, we have a plan to develop an artificial intelligence system to understand about the autistic pupils likings and to determine his field of interest by integrating machine

learning, pattern matching and emotion analyzing. Soon we will add different kind of singing tunes or robotic tones in our software. We have the plan to develop and add different relevant gaming environment for their learning. Also we have vision to develop real time interaction between intelligent programs with autistic pupils using software and hardware interface. We have the plan to innovate motivating environment which will influence autistic pupil to develop his communication skill and socialization. Another improvement can be the transformation of the current system to a mobile platform. In many cases, mobile devices were proved to be the better way of communication in a classroom. In particular, the evaluation system can be shifted to the mobile devices to eliminate the possible confusion of clicking on wrong icon. The system can then be tried to upgrade to a "multi-mouse single screen" system. We might add some gaming concepts to it and make the learning more interesting to the students.

VIII. CONCLUSION

The world of autism is still a mystery to the science. While the medical therapies are being devised with medicine and physical exercises, the necessity for ensuring equal opportunity for the autistic children in every sphere of life should be approached by technology. *A-Class* is a big step toward developing an equal educational environment for both the autistic and the neuro-typical children. This software can lead toward devising more technological support for the autistic population for helping them in achieving equal facilities in every sphere of their life.

IX. REFERENCES

[1] Autistic Spectrum Disorder (ASD) and Attention Deficit/ Hyperactivity Disorder (AD/HD): A Comparison - Sally Bloch-Rosen, Ph.D.,Licensed Clinical Psychologist .

[2] Baskett, C.B. The effect of live interactive video on the communicative behavior in children with autism, University of North Carolina at Chapel Hill, Chapel Hill, 1996.

[3] Cassell, J. (2004). Towards a model of technology and literacy development: Story listening systems. Applied Developmental Psychology, 25, 75-105.

[4] Tartaro, A. Storytelling with a virtual peer as an intervention for children with autism. SIGACCESS Access. Comput.

[5] M. E. Hoque, Analysis of Speech Properties of Neurotypicals and Individuals Diagnosed with Autism and Down Syndrome, 10th ACM conference on Computers and Accessibility (ASSETS), Halifax, Nova Scotia, October, 2008.

[6] M. E. Hoque, J. K. Lane, R. elKaliouby, M. Goodwin, R. W. Picard, Exploring Speech Therapy Games with Children on the Autism Spectrum, In Proceedings of InterSpeech, Brighton, UK, September, 2009.

[7] http://www.prometheanworld.com/upload/pdf/USA TODAY_Classroom Tech_2.pdf

[8] http://ezinearticles.com/?Learn-Why-Autistic-Children-Think-in-Pictures-Instead-of-Words&id=2690229

[9] Autism (Symptoms and Treatment) - Bonita Darula, http://www.autismintoawareness.com/

[10] O.I. Lovaas, "Behavioral treatment and normal educational and intellectual functioning in young autistic children", Jl of Cons. & Clinical Psychology, vol. 55, 1989, pp. 3–9.

[11] http://java.sun.com/javase/downloads/index.jsp

[12] http://tomcat.apache.org/download-60.cgi

[13] http://dev.mysql.com/downloads/

Architectural digital images. Quality and emotional evaluation based on the visualization environment

D. Fonseca
GTM - Grup de Recerca en Tecnologies Media, La Salle – Universitat Ramon Llull
Quatre Camins 2, 08022 Barcelona, SPAIN

J. Duran
DEVP - Comunicació Audiovisual – Universitat de Barcelona
Pg. Vall d'Hebron 171, 08035 Barcelona, SPAIN

Abstract- **The visualization of architectural images has always been associated with physical models, panels and displays on large format computer screens. However, technological developments in the past decades have produced new interesting devices such as Smartphones or immersive displays. This evolution has created a new workflow that enables on-site management, virtual visualization and decision making through the viewing of information on those devices. In this paper, we will conduct a statistical study to evaluate the emotional differences on visualization architectural images in different environments and the relationship with the quality perceived by the users related with their previously experience in the architectural framework. The results show that factors related to the user such as gender or previous experience with the typology of images, and the type of device, influence the user's emotional reaction.**

I. INTRODUCTION

In recent years, the new immersive techniques of visualization and the modern Smartphones have led to the control of big volumes of increasingly complex multimedia information, therefore facilitating its analysis, interpretation, and manipulation as in [1, 2].

On the one hand, immersive systems have gained popularity because they permit major interaction capabilities through an increasing number of natural and ergonomic interfaces, thereby extending their range of utility from the analysis of information to application in art, entertainment, and education as in [3]. At the same time, immersive systems isolate a user from its environment in order to ensure that the stimulus reaches more directly, thereby increasing the communicative capacity of the message.

On the other hand, the modern Smartphones can make calls, play music, take and store photographs, browse Internet, and of course, they are able to manage and view anywhere the information related to the architectural framework [4].

Undoubtedly, one of the most researched themes on the use of these new technologies is information visualization (IV). IV is a well-established discipline that proposes graphical approaches to help users better understand and make sense of large volumes of information as in [5].

This paper includes a multidisciplinary approach that intends to examine a user's emotional response according to the technique features of an image and its display where it is visualized, in order to make headway in generating images with accurate parameters that will optimize the manner in which the user visualizes an architecture project.

To carry out our work, and based on the methodology and results of previous studies of this work that we can see in "Reference [6]", we focus on the evaluation of emotion reflected by the user as a result of the visualization exercise of certain type of images (based on the perceived quality and the relationship between the color model and level of compression). This approach is intended to complement traditional studies where user perception and the characteristics of the human visual system have received little attention as in [7].

II. RELATED WORK

A. Image Perception

In a psychological area, we used works that would allow us to evaluate the differences of perception by the user [8], as well as measure the type and amount of emotions that the image provokes in the viewer [9]. We can find cultural differences as to how the user assigns different descriptors [10]. The interpretation of the colors, for instance, can have a direct influence on the emotions that the visual message generates in the viewer [11], and for this reason we believe that it is very important to find the best way to store them (the emotions).

Paul Ekman, a professor in psychology at San Francisco University and one of the major recognised experts in this subject, has demonstrated that, by studying the facial expressions, these emotions are universal [12]. Simply put, they can be studied [13]:

- By the use of a scale "pleasant-unpleasant"
- By the use of a scale "active-passive"
- By studying cultural and social differences, as emotional reactions are learned in a specific environment

Centered in the field of psychology and neuropsychology, the main study of how the user reacts in front of a digital image is the IAPS (International Affective Picture System

[14]), revised and replied in several studies to check out its validity within diverse cultural frameworks [15]. In the case of the original IAPS system, the emotions are grouped into three variables: *valence* (i.e. pleasantness) which differentiates positive (pleasant) from negative (unpleasant) emotional states; *arousal* (i.e. activation) differentiates exciting, arousing states from calm, relaxed states; and *dominance* or level of control sensation. This system is defined as an effective method to check out abnormal behavior and emotional dysfunction in several types of users [16, 17].

B. Quality Perception

Currently, the study of quality perception of images has generated a considerable interest due to business requirements. However, it is extremely difficult to define and measure the concept of quality in an image [18]. Initially, quality depends on physiological aspects of each user [19]. In order to work with users for defining a few quality perception scales it is necessary to define different stages in the following manner:

- Psychophysical study in order to quantify perception scales. In other words, empirically examine human visual response models, in which different concepts such as color, special and temporal sight, and different iterations that lead to the conclusion, are interrelated.
- Modeling of visualization to include all stimuli.
- Iteration for verification.

The study and understanding of the relationship among different elements, by which the quality of a perceived image can be determined, enables us to define all the features that an image possesses in order that the user's visualization exercise is satisfactory and can be adapted to every requirement, an assertion on which this study is based.

C. Browsing Pictures

The image adaptation problem (to display large information in several types of displays) has also been studied by researchers for some time [20].

Browsing large photos, drawings, or diagrams, is more problematic on mobile devices, in front of computer screens or virtual environments, because of the reduce screen (between 2,2" and 4"), the low resolution (normally 320x240 with a maximum resolution of 800x400) and the power of the hardware (specially CPU and RAM). To reduce the number of scroll and zoom operations, researchers are adapting text visualization techniques such as RSVP (rapid serial visual presentation) to enable users to view information through selected portions of a picture. For example, some studies propose an RSVP browser for photographs that use an image-processing algorithm to identify possible centers of interest.

Compared to smaller screens, larger screens magnify images of objects, therefore, they appear closer, which implies that the attractive or aversive stimuli from the depicted images seems closer, thus, increasing the urgency and intensity of responses to those stimuli [21]. Larger images increase the automatic allocation of resources to attention because the peripheral vision is influenced, increased visual processing is required, and larger images generate larger mental visions [22].

If we employ immersive technology, the size and details of the image and peripheral vision of a user increases, thereby increasing the communicative capacity of the environment and message, since the user is mentally absorbed by the environment [23].

III. Methodology and Procedure

In this paper we focused on studying data transcoding technology [24, 25] (the process of converting the data format according to client device capability), and in particular the evaluation of user emotion during the visualization of images with variations of color system, compression format, or both operations.

Emotional responses are stronger when negative or positive stimuli appear closer, like those evoked by images on large screens. References [26, 27, 28] were studies that have determined the effects of screen size on valence, which was comparable to its effect on arousal:

- Positive and negative images on larger screens evoked stronger positive and negative responses, respectively.
- Large format displays are associated to more positive reactions regardless of stimulus.

We have employed two models of images in the test design: the first is a representative selection from the IAPS system [14], which were used as control images and placed at the beginning (7 images) and at the end (7 images) of the test. The second group of images related to the architectural project have been split into the following diverse sub-groups: infographic images generated by computer (18 images), explanatory photographic images of a concrete project (Bridge AZUD, Ebro River in Zaragoza, Spain, Isidro Navarro, 2008, 19 images), composition panels (used in the course "Informatics Tools, Level 2.," Architectural Degree, La Salle, Ramon Llull University, 7 images), and HDR photographic images (6 images).

Our two models combine original images of the IAPS system (color images with a resolution of 1024x768) and architectural color images (with resolutions between 800x600 and 4900x3500). There are also images that have been modified in terms of color (converted to black and white), and level of compression (JPG changes into JPG2000 with compression rates of between 80% and 95%). We used JPEG 2000 (an international standard ISO-15444 developed in open source code) because of its most obvious benefit [29]: its increased compression capability which is especially useful in high resolution images [30, 31]. Another interesting aspect of the JPG2000 format is the ROI (region-of-interest) coding scheme and spatial/SNR scalability that provide a useful functionality of progressive encoding and display for fast database access as well as for delivering various resolutions to terminals with different capabilities in terms of display and bandwidth [20].

In our study we have related positive and negative images as follows:

- Positive neutral and negative control images based on the categories from IAPS system [10].
- Positive architectural images have high definition (high resolution and without visual errors related to rate of compression).
- Negative architectural images have low definition (low resolution and/or with visual errors of compression).

We used two test models: the system used in previous phases [12] where the images are mounted inside a PowerPoint® presentation (for mobile environment visualization because of the preliminary test that showed low usability of our web system [32] on small screens (we need a lot of "panning actions")), and on-line model (used on computer screen and HMD), that lets us upload images insider a on-line manager for their visualization and evaluation. The test method involved the following steps:

1. Compilation of general information about the test environment: local time, date, place, and information about the screen, type, size, resolution.
2. The facilitator (or web system) displays the two previous images to test the evaluation methodology. Without providing a definite time limit, the facilitator explains the manner in which the user must evaluate the images.
3. Finally, the user evaluates the images on three levels: valence, arousal (emotion evaluation proposed from IAPS system), and quality perceived (personal research). Users had to mark a punctuation in a questionnaire ranging from "1", minimum level or disagree option, to "9", maximum level of agreement or satisfaction. The three levels of the test are based on the original SAM (Self Assessment Manikin, that we can see in the Fig. 1), developed by the IAPS [14].

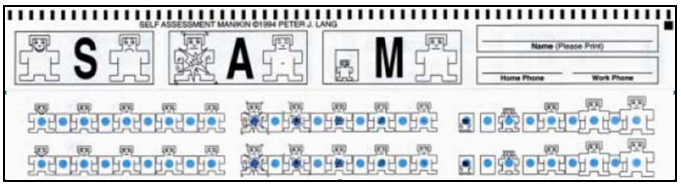


Fig 1. SAM test

The test was conducted using a qualitative approach with a representative selection of different type of users in three different devices:

- **Generic computer screen**: 17" diagonal distance with a resolution of 1280x1024 and 0.4–0.5m between user and the screen. A sampled of 34 users was involved in the evaluation: 12 women (Average Age (Av): 27.7; Standard Deviation (SD): 7.2) and 22 men (Av: 28.86; SD: 7.01).
- **Head Mounted Display** (5DT HMD 800-40): 0.49" equivalent to 44" at 2m visualization (real visualization distance: 0.03–0.04m), resolution of 800x600 per display. We tested 14 users: 6 women (Av: 25.83; SD: 6.36) and 8 men (Av: 27.25; SD: 6.45). We can find more about the results of this experiment in "Ref [33]".
- **Smartphone** (Nokia n97 mini): 3.2", resolution of 640x360 and 0.3–0.4m of distance visualization. We tested 20 users: 10 women (Av: 28.7; SD: 4.74) and 10 men (Av: 26.5; SD: 6.47).

To analyze our research proposal, two working hypotheses will be enunciated and expanded:

- H1: The emotion is related to quality: if the perceived quality increases, the emotional level will also increases. Based on the above statement, the quality and therefore emotion levels measured will be higher when the user views smalls screens in front of larger or high definition screens (in similar conditions of visualization: relation between distance of visualization and diagonal screen). On a small screen size is more difficult to perceive the errors of compression or bad resolution and therefore the level of perceived quality is higher.
- H2: Architectural images in black and white do not convey the entire message (they lose information about materials and lighting), and their quality and emotional affect is reduced in all environments and especially on smaller screens (on a mobile screen) compared to larger ones (computer and HMD) because of the very difficult to see detailed information. On the other hand, HDR images improve the assessment against their original, especially in environments of low quality or small-format screens.

IV. Results

A. *First Study*

Fig. 2, shows the first analysis we performed was to compare the overall quality perceived by users in the evaluation of architectural images in the three devices tested (computer screen, HMD and mobile screen):

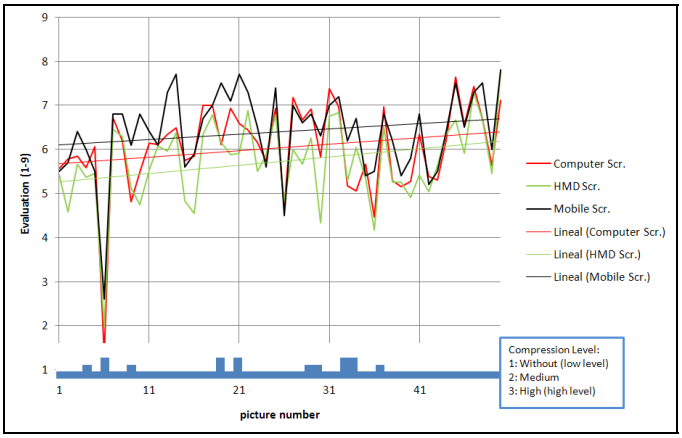


Fig 2. Overall quality evaluation (Y axis: evaluation from 1 to 9, minimum and maximum values of SAM test, X axis: image number of the test)

Fig. 3, compares the results of quality and emotion (focusing on the level of the *valence*) we break down the results by type of image compression (axis-X, 1: Color without compression, 2: Color JPG2000 with 80% rate compression, 3: Color JPG2000 with 95% rate compression, 4: Black and white image without compression, 5: Black and white JPG2000 with 80% rate compression, 6: Black and white JPG2000 with 95% rate compression):

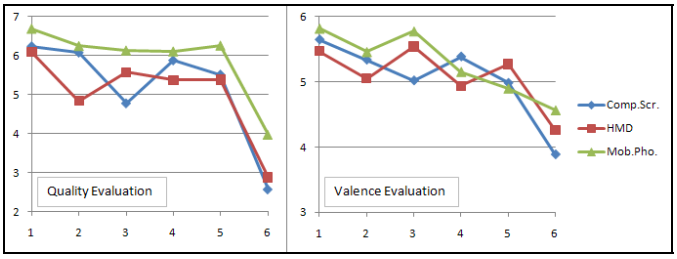


Fig.3 Quality and *valence* evaluation (Y axis: evaluation from 1 to 9 of SAM test)

It became clear that the best quality assessment was yielded by viewing on a mobile screen (even though this screen has the lower resolution, Figures 2 & 3). Including the control images, the average is 6.27 (SD: 1.87) for viewing on a mobile screen, 5.71 (SD: 1.85) for viewing on a computer screen and 5.54 (SD: 1.63) for the use of HMD. It is emphasized that the only image with a significantly lower resolution value (Figure 2, picture nº 6, 200x142), was the worst rated (Av: 2.6; SD: 1.6), about 40% lower than in high compression cases (average 8 pictures with 95% compression rate: 4.7; SD: 2.09).

If we analyze the statement of Hypothesis 1, we find that is true for color images, but not for all types of processed images in black and white. As we can see, color images regardless of the degree of compression, they score higher in quality and *valence* on mobile phone screen, but for black and white images only our Hypothesis is valid for images with a higher compression ratio (X axis number 6: JPG2000 with 95% rate of compression). If we simplify the analysis by averaging all the images in color and black and white together, the Fig. 4, confirms our H1:

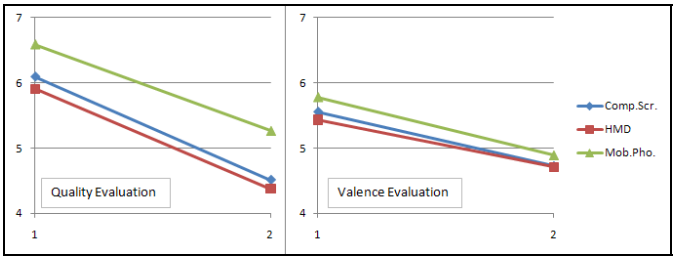


Fig.4. Quality and *valence* evaluation (Y axis: evaluation from 1-9 of SAM test, X axis: 1-Color images, 2-Black and white images)

Based on multiple previous studies [6], we can find defined an interesting index for our research: IOV, Index of Optimum Visualization. This index is the result of dividing the screen diagonal distance among the distance visualization. Checking the recommendations, the value of 0.31 is the optimum rate. In Table I, we can find the following average IOVs of our study:

TABLE I
IVO AVERAGE

Computer Screen	HMD	Mobile Phone
0,43	0,16	0,24

Extreme values of IOV (very close or far away the screen), generate a decrease of quality perceived (Figure 4, computer screen and HMD plots) and the closest value to IOV optimum rate (Mobile Screen) generates better perceived quality and value of valence.

B. *Second Study*

Linking with the second Hypothesis, we can see (Fig. 3 & 4) that architectural images in black and white have lower values that the same ones visualized with color model. Analyzing the results by the type of compression (Fig. 3), it is interesting to note as black and white architectural visualization penalizes both the quality and the valence. Comparing the images without any type of compression (values 1 & 4 from the X-axis), the black and white always yield a value less than their original color as we can see in the Table II:

TABLE II
QUALITY

	Comp. Screen		HMD		Mobile Phone	
	Average	SD	Average	SD	Average	SD
JPG Color	6,23	1,94	6,08	1,69	6,68	1,84
JPG2000 Color (95%)	4,78	1,89	5,56	1,39	6,13	1,74
JPG B&W	5,87	1,94	5,37	1,61	6,10	1,94
JPG2000 B&W (95%)	2,58	1,20	2,88	1,31	3,97	1,78

The apparent loss of quality (not real) that the user perceives when viewing the image in black and white, is diminished if it is observed on a small screen or with low resolution, generating affective values similar to other environments for images without high compression rates (values 4 & 5) and significantly improving the response when a high compression rate (value 6) as we can observe in the Table III:

TABLE III
VALENCE

	Comp. Screen		HMD		Mobile Phone	
	Average	SD	Average	SD	Average	SD
JPG Color	5,64	1,68	5,47	1,50	5,82	1,63
JPG2000 Color (95%)	5,02	1,87	5,54	1,58	5,78	1,71
JPG B&W	5,38	1,57	4,93	1,76	5,16	1,93
JPG2000 B&W (95%)	3,88	1,76	4,26	1,89	4,57	1,65

In Fig.5, we get another interesting result when we analyze the behavior of the *arousal* dimension:

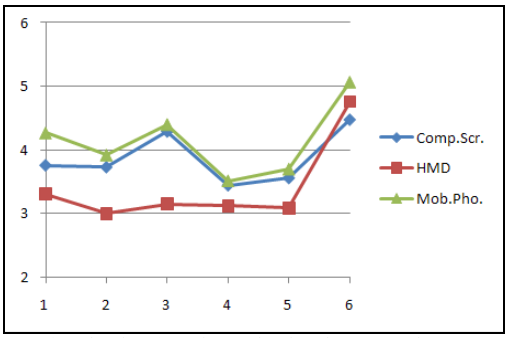


Fig.5. *Arousal* evaluation (Y axis: evaluation from 1-9 of SAM test, X axis: type of image compression and color model, see description in Figure 3)

Negative stimuli (pictures with high compression, values 3 & 6 from the X-axis) generated a higher degree of excitement, especially when the image was displayed in black and white model (value 6).

In line with previous phases of our investigation [19], in the case of conversion to black and white a sharp reduction is seen, regardless of the resolution and level of compression of the infographic image: about 13% on mobile and computer screen, and 25% on HMD. This information tells us that the use of black and white in architectural framework is not valid.

In Table IV, we test our affirmation about the usefulness of HDRi in small format screens. First, we review the perceived quality of images in HDR format and their original in color and black and white model:

TABLE IV
HDR AVERAGES OF IMAGE QUALITY PERCEIVED

Image Nº	Resolution	Color / Compr.	Comp.Sc.	HMD	Mobile
52	2816x1880	Original	7,64	6,67	7,50
	2816x1880	B&w	6,56	5,92	6,50
	2816x1880	HDR	7,43	7,29	7,30
55	2816x1880	Original	6,69	6,67	7,50
	2816x1880	B&w	5,63	5,46	6,00
	2816x1880	HDR	7,12	7,75	7,80

As we can see, the perceived quality of the images processed using HDR technique lies in the most high ratings in all environments (Av: 7.45, SD: 0.21; compares with original in color Av:7.11, SD:0.04; and black and white modification Av:6.01, SD: 0.05), especially in the visualization in HMD (valuing the difference between the modes of color image).

If we analyze our emotional variables, we have the following average values showed in the Tables V and VI:

TABLE V
HDRI VALENCE

	Comp. Screen		HMD		Mobile Phone	
	Average	SD	Average	SD	Average	SD
Original Color	6,56	1,58	6,15	1,41	6,45	2,16
Black and white model	5,84	1,57	5,46	2,29	5,25	2,01
HDR transformation	6,14	1,76	6,31	1,84	6,25	2,18

TABLE VI
HDRI AROUSAL

	Comp. Screen		HMD		Mobile Phone	
	Average	SD	Average	SD	Average	SD
Original Color	3,64	1,54	2,50	1,34	2,90	1,83
Black and white model	3,02	1,56	3,08	1,40	2,70	1,32
HDR transformation	4,24	1,85	2,83	1,86	3,95	2,12

The combined results of emotional framework show that viewing such images has a *valence* higher in environments where it is better perceived the quality of an image (HMD). However, in other environments studied, HDR images are getting very high values of *valence* and prominently, we can observed as *arousal* rates are much higher (HDR:3.68, SD:1.95; Color: 3.01, SD:1.57; B&W: 2.93, SD:1.42), than for the original and processed images in black and white.

V. CONCLUSIONS

With the results of the first study we have demonstrated our first Hypothesis, and we can conclude it is necessary to increase image quality or limit the degree of compression when the visualization exercise combines low-resolution screen and short distances.

Refer to second study, we can certainly conclude that images in black and white are not a good model to show the information of architectural project (as we discussed in the statement of H2), but against our hypothesis, the quality and emotional evaluation of small interfaces increase in front of the other environments compared. We assume that this adverse result of our initial Hypothesis it could be because of the same idea proposed in H1: low quality image (compression or model color), visualized on small screens has higher evaluation than on larger screen.

HDR images improve the assessment against their original, especially in environments of low quality (high quality perceived, with high *valence* and low *arousal*) but not in small-format screens (where the assessment by users is closer to medium format screens such as computers displays).

In conclusion, both working hypotheses have been proven (the second one with some exceptions), which means that the display of images on small format screens generate greater empathy from the user (to be linked to the perceived quality of emotion [13]), including for images with high compression or that are in black-and-white, which are the least suited for use in architectural environments.

REFERENCES

[1] André, E. The Generation of Multimedia Presentations. A Handbokk of Natural Language Processing: techniques and applications for the processing of language as text. *Marcel Dekker Inc.*, 2000, págs. 305-327.

[2] Robbe-Reiter, et al. Expression constraints in multimodal human-computer interaction. *Intelligent User Interfaces.* New Orleans , 2000, págs. 225-228.

[3] Otero, A. (2003). Sistemas Inmersivos y Aplicaciones de Realidad Virtual. Santiago Compostela. *Universidad de Santiago Compostela.*

[4] Sousa, R., Nisi, V., & Oakley, I. (2009). Glaze: A visualtization Framework for Mobile Devices. *Springer* Berlin. DOI= 10.1007/978-3-642-03655-2_95

[5] Carmo, M. B., Afonso, A. P., & and Matos, P. P. (2007). Visualization of geographic query results for small screen devices. *Proceedings of the 4th ACM workshop on Geographical information retrieval* (pp. 63-64). Lisboa

[6] Fonseca, D., Garcia, O., Duran, J., Pifarre, M., & Villegas, E. (2008). An Image-Centred "Search and Indexation System" based in User's

Data and Perceived Emotion. In ACM (Ed.), *Proceeding of the 3rd ACM international Workshop on Human-Centered Computing* (pp. 27-34). Vancouver, Canada: HCC '08, ACM,

[7] Fan, X., Xie, X., Ma, W., & Zhang, H. Z. (2003). Visual Attention Based Image Browsing on Mobile Devices. *Proceedings of the 2003 International Conference on Multimedia and Expo (ICME)* (pp. 53-56). Baltimore: IEEE Computer Society.

[8] Pask, A. M. (2005). Art Historians' Use of Digital Images: a Usability Test of ARTstor. *A Master's Paper for the M.S. in L.S. degree*.

[9] Hong, S., Ahn, C., Nah, Y., Choi, L. Searching Color Images by Emotional Concepts*. 3rd International Conference on Human.Society@Internet*, Tokyo, Japan, July 27-29, 2005. Springer Vol. 3597/2005. DOI: 10.1007/11527725,

[10] Mikels, Fredrickson, Larkin, Lindberg, Maglio, Reuter-Lorenz. (2005). Emotional category data on images from the IAPS. *Behaviour Research Methods*, 37 (4), 626-630.

[11] J. H. Xin 1, K. M. Cheng, G. Taylor, T. Sato, A. Hansuebsai Cross-Regional Comparison of Colour Emotions Part I. Quantitative Analysis*. Color Research & Application, Vol. 29, pp. 451-457.* Wiley Periodical Inc., 2004,

[12] Ekman Paul. Facial Expressions of emotion, 1979

[13] Ekman Paul. A methodological discussion of nonverbal behavior, *Journal of Psychology*, 1957, 43, 141-149.

[14] Lang, P., Bradley, M., & Cuthbert, B. (1997). International Affective Picture System (IAPS): Technical Manual and Affective Ratings*. NIME*, Gainesville, Florida, USA.

[15] Bruno Verschuere, Geert Crombez, Ernst Koster. (2007). Cross Cultural Validation of the IAPS. Ghent, Belgium: *Ghent University*.

[16] L. Hollink, A.Th, Schreiber, B.J. Wielinga, M. Worring. Classification of user image descriptions**.** *International Journal of Human-Computer Studies, Vol. 61,* Elsevier Ltd. - Academic Press, Inc, 2004, págs. 601-626. DOI: 10.1016/j.ijhcs.2004.03.002.

[17] Houtveen JH, Rietveld S, Schoutrop M, Spiering M, Brosschot JF. (2001). A repressive coping style and affective, facial and physiological responses to looking at emotional pictures. *International Journal of Psychophysiology*, 42, 265-277.

[18] Mark D, F. (2002). Image quality measurement and modeling for digital photography. *ICIS*, (pp. 318-319). Tokyo.

[19] Coursaris, C., Swierenga, S., & Watrall, E. (2008). An Empirical Investigation of Color Temperature and Gender Effects on Web Aesthetic. *Journal of Usability Studies , 3* (3), pp. 103-117.

[20] Chen, L., Xie, S., Fan, X., et al. (2003). A visual attention model for adapting images on small devices. *Multimedia Systems , 9* (4), 353-364. DOI=10.1007/s00530-003-0105-4

[21] Bellman, S., Schweda, A., & Varan, D. (2009). Viewing Angle Matters-Screen Type Does Not. *Journal of Communication* , pp. 609-634.

[22] Reeves, B., Lang, A., Kim, E., & Tatar, D. (1999). The effects of screen size and message content or attention and arousal. *Media Psychology* , pp. 49-67.

[23] Henden, C., et al, (2008). A sorround display warp-mesh utility to enhance player engagement. *ICEC Proceedings.* Pittsburgh: Carnegie Mellon University Entertainment Technology Center.

[24] Han, R., Bhagwat, P., LaMIare, R., Mummert, T., Perret, V., & Rubas, J. (1998). Dynamic Adaptation in an image transcoding proxy for mobile web browsing. *IEEE Pers Commun , 5* (6), 8-17.

[25] Ma, W., Bedner, I., Chang, G., Kuchinsky, A., & Zhang, H. (2000). Framework for adaptive content delivery in heterogeneous network environments. *Proc SPIE* (pp. 86-100). Palo Alto: Multimedia Computing and Networking. The Smithsoniana/NASA Astrophysics Data System.

[26] Codispoti, M., & De Cesarei, A. (2007). Arousal and attention: Picture size and emotional reactions. *Psychophysiology* , pp. 680-686.

[27] Mühlberger, A., Neumann, R., Wieser, M., & Pauli, P. (2008). The impact of changes in spatial distance on emotional responses. *Emotion* , pp. 192-198.

[28] Reeves, B., & Nass, C. (1996). The media equation: How people treat computers, television, and new media like real people and places. New York: *Cambridge University Press*.

[29] Bernier, R. (2006). An introduction to JPEG 2000. *Library Hi Tech News , 23* (7), 26-27.

[30] Hughitt, V., Ireland, J., et al (2009). Helioviewer.org: Browsing Very Large Image Archives OnLine Using JPEG2000*. The Smithsonian/NASA Astrophysics Data*.

[31] Rosenbaum, R., & Schumann, H. (2005). JPEG2000-based image communication for modern browsing techniques. *Proceedings of the SPIE (Image and Video Communications and Processing)* (pp. 1019-1030). Rostock: The International Society for Optical Engineering.

[32] Fonseca, D., Garcia, O., Navarro, I., et al, (2009). Iconographic WEB image classification based on Open Source Technology. In IIIS (Ed.), *Proceedings of the 13th World Multi-Conference on Systemics, Cybernetics and Informatics 2009 (WMSCI09). 3*, pp. 184-189. Orlando: IIIS.

[33] Fonseca, D.; Moreno, P.; García, O.; Paniagua, F.; , "Categorization of user behaviour: Digital imaging architectural visualization in immersive media," *Information Systems and Technologies (CISTI), 2010 5th Iberian Conference on* , pp.1-4, 16-19 June 2010

Measuring User Reaction to Reduce Internet Anxiety

Santosh Kalwar
Lappeenranta University of Technology
Department of Information Technology
Lappeenranta, Finland
santosh.kalwar@lut.fi

Kari Heikkinen
Lappeenranta University of Technology
Department of Information Technology
Lappeenranta, Finland
kari.heikkinen@lut.fi

Jari Porras
Lappeenranta University of Technology
Department of Information Technology
Lappeenranta, Finland
jari.porras@lut.fi

***Abstract*- The Internet has recently emerged with new kind of services, applications and countless contents. User reaction plays essential role in interacting with the Internet. The theoretical concepts on feelings are extracted from psychology, phenomenology and computer science. It is understood that feelings are subjective experience of users aroused from different emotions. As feelings changes based on time, circumstance, people and environment, it is extremely difficult to assess feelings objectively. User's interaction on the Internet is based on contents (text, audio and video materials) and context (past experience, surroundings, circumstances, environment, background, or settings). Thus, the potential of understanding feelings and its measure is very important. In this paper, a systematic measure of *feelcalc* module is introduced to measure user's reaction in order to reduce human anxiety on the Internet.**

Keywords: feelings; user; anxiety; Internet; human; reduce; measure

I. INTRODUCTION

"*You cannot make yourself feel something you do not feel, but you can make yourself do right in spite of your feelings*."
–Pearl S. Buck

When Pearl S. Buck said above wise lines, he must have understood that feelings are not something that can be easily controlled. In addition, why not, feelings are range of emotions one inhibits during a life span. A user may feel tense and annoyed when a web browser suddenly crashes. Another user may feel anxious of not understanding terminologies on the Internet. Yet another use may feel fearful of losing money while doing online banking transactions. These are some examples of feelings associated with people who use wide range of activities, services, and applications on the Internet.

The state of feeling anxiousness could happen when one is using the Internet. Consuming lots of information online could cause anxiousness or stress. The anxiety might cause serious problems of mental illness among different age groups. One cannot deny that the anxiety on the Internet is an unreal phenomenon. Moreover, there is a practical need to address some of the present challenges (e.g. Addiction, Pornography, Online pathological usage, online behavior). In the developed world, the Internet has become part of our daily habits. As a part of the daily habit, user may never forget to 'log in' into their Facebook account or update their 'tweets' using popular micro-blogging application. On positive note, the reason behind such behavior is understandable simply because we have popular tools such as social networking services (SNS) and tools (e.g. Facebook, MySpace, Twitter, and YouTube) currently available. In order to enhance effective interaction of users on the Internet, one needs to address how one behaves on these popular tools. By an informal observation, it is obvious while interacting with the Internet that we utilize our time by updating and reading recent information using popular social networking services (SNS) and tools. Thus, the proliferation of interactive, eye-catching, crispy web application tools, mainly collaborative and interactive, can have negative impacts on user's behavior.

User reaction might be associated with user's feelings and thoughts. There is variety of such feelings associated with browsing experiences. In general, any type of feeling is part of an emotion. It seems that the emotion inhibited is due to tools used on daily basis. This also affects on user's satisfaction [1]. An emotion of a user on the Internet could be divided into two major parts: thoughts and feelings. Thoughts and feelings maybe related to one another. A simple categorization of emotion is cogitated and plotted in Figure 1. Nevertheless, what you think is not necessarily, what you feel and what you feel is not necessarily, what you think. Therefore, the feelings and thoughts may be inter-related but not completely related. There are several keywords associated with feelings such as anxious, depressed, angry, sad, nervous, jealous, happy, joyful, cheerful, excited, disgusted, frightened, mad, irritated, panicky, discouraged, uneasy, frustrated, and tense. On the contrary, it is hard to find keywords associated with thoughts. Corresponding to Descartes famous statement, "*cognito ergo sum*" or, "*I think, therefore I am*.", people often use, "*I think…, in my opinion, and in my viewpoint*" which in simpler terms that might relate to positive, negative and neutral for some events, activities and things. In this paper, a feelcalc module is introduced, an algorithm is illustrated briefly, and a simple visualization is created to measure Internet anxiety. We first describe about users study, feelcalc module and finally, we conclude briefly with future direction of the work.

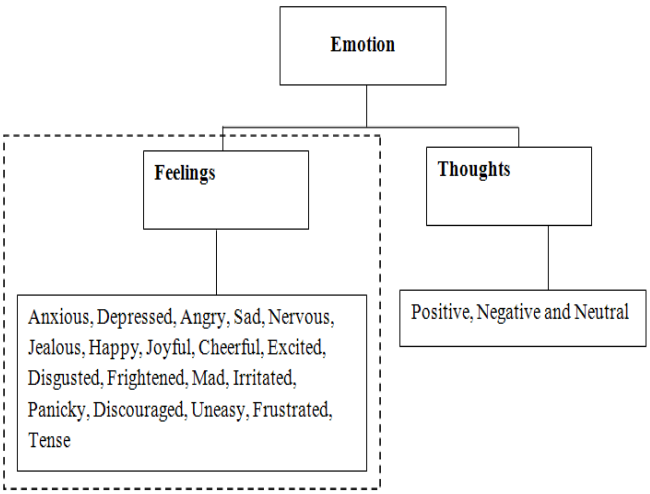


Figure 1: A sketch showing types of emotion.

II. Internet Anxiety

In our past study, we have identified seven types of Internet anxiety [2]. Our seven types of Internet anxiety are based on user's experiences and feelings. It is understood that users/human feelings are hard to extract. Suppose an anxiety could be broadly categorized and the categorization is based on positive, negative and neutral feelings.

A. Positive feelings

First, it is important to categorize the Internet anxiety based on positive feelings. The keywords associated with positive feelings could be cheerful, excited, joyful, and happy and so on.

B. Negative feelings

Second, it is also important to categorize the Internet anxiety based on negative feelings. Some of the keywords associated with negative feelings could be anxious, depressed, angry and sad.

C. Neutral feelings

Third, it is important to categorize the Internet anxiety based on neutral feelings. Some of the keywords associated with neutral feelings could be "I feel nothing, I do not know, and I cannot say what is my feeling right now".

III. Related Work

Feelings are subjective experience of the users and it is hard to find subjective experience measured objectively. It is understood that Internet can cause anxiety [3]. There are numerous reports of problem encountered on daily basis from the contents on the Internet. People experience numerous sorts of feelings on the Internet. On the other hand, the user interface and user experiences might be the cause of Internet anxiety, and not just the contents. Other researchers have used the terms; "problematic Internet use" [4], "the pathological Internet use" [5], "Internetomania", "Internet addiction disorder" [6, 7]. The terms about problematic Internet use has been used interchangeably. The users with "pathological Internet use" have been drawn towards interpersonal use of the Internet [4, 8, 9, and 10]. There is very little evidence from literature about measuring feelings of users to reduce Internet anxiety. Recently, some studies has focused on investigating user's emotion in the area of computer based learning and games. In one study [11], student's emotions were measured using "An agent, which acted out their emotions and talked with the student expressing full sentences of cognitive, meta-cognitive and emotional feedback". Similarly, In order to investigate user's emotions, pedagogical agents for providing emotional feedback is used in another recent study [12] where the study reports that intelligent tutors used for automatic recognition of and response to human emotions. In yet another intelligent tutoring system creation, one study reports usage of "sensor features to predict so-called 'yes!' events" [13].The Figure 2 shows emotional pedagogical agents with range of emotions.

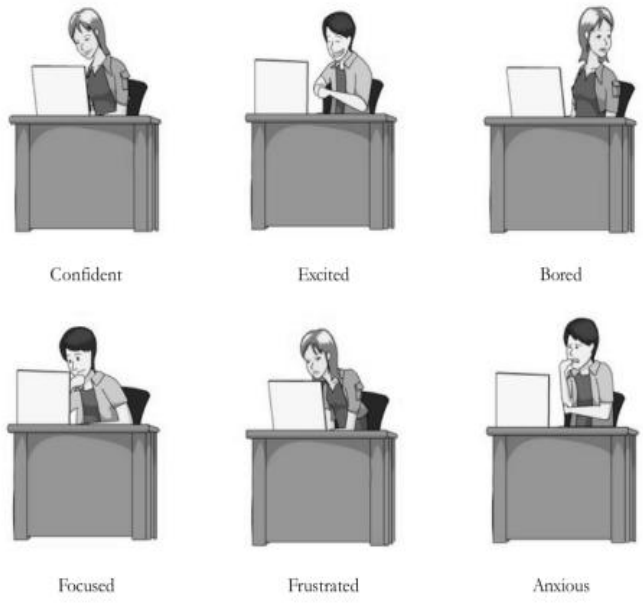


Figure 2: Emotional pedagogical agents showing a range of emotion [11].

IV. User's Study

Before we began our study, it was very important to study the user who is constantly on the Internet. First, an observation of users was made for two consecutive weeks in the university library. Each working day, about twenty-five minutes of time were dedicated to these individual users for mere observations. This observation was performed with formally informing these users. Finally, for two weeks time period note were taken and an observation of fifty users were made.

Observations

- Users felt quite excited when accessing social networking services (Facebook, MySpace).

- Many users accessed the SNS services intensely. Due to overwhelmingly popularity of using such services, library staffs had to put warning signs for users.
- Users carried out the interepretation of warning sign as, "*The use of social networking sites like Facebook is strictly prohibited.*"

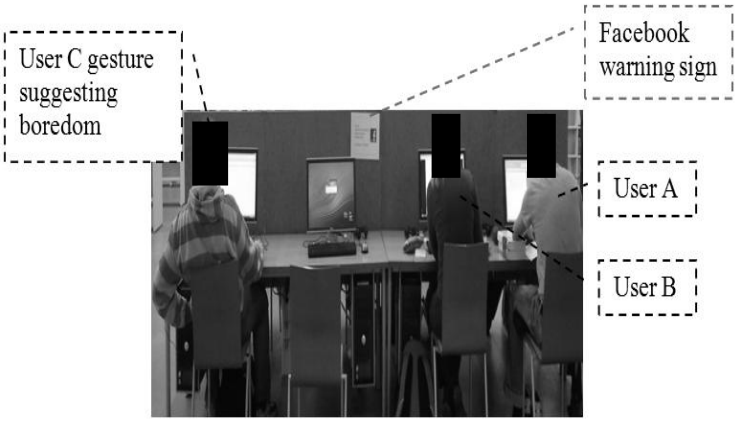


Figure 3: Users accessing the Internet in a library.

- From the Figure 3, three users (User A, User B and User C) are working in a library. It can be seen that User A and User B are working and they are close to screen. On the contrary, the
- user C gesture suggests of boredom. The User C is leaned back and remotely trying to access the system. The warning sign is shown in the dotted red.
- If we assume that, all these users are experiencing Internet anxiety. Furthermore, a User A is feeling positively and User C is feeling negatively and User B is neutral about her feeling then we have three cases to explore in three different categories of feelings.
- A user 'A' is positive about his feelings. He might feel cheerful, excited, joyful, and happy. While interacting with the Internet contents, he possesses no anxiety. He has not encountered any problems such as broken web links, hard web accessibility, and nervousness of performing online monetary transactions.
- A user 'B' is neutral about her feelings. She does not know what kind of feelings she has experienced. She cannot say much after interacting with the contents on the Internet. She is unaware of any anxiety. She has not encountered any problems of using the contents.
- A user 'C' is negative about his feelings. He is anxious and depressed with the contents on the Internet. He does not know what else to do without social networking sites. He cannot access Facebook. His body gesture suggests anxiousness. His feelings are anxious, depressed and sad.
- Based on the near-distant observation, the interpretations of User's feeling were presumed to be positive, negative and neutral. The Table 1 summarizes behavior patterns and feelings of users. The user's study adhered by creating simple prototype visualization for the sake of measuring user's reactions.
- An unbiased observer was involved in the study for taking notes & monitoring their actions/reaction.

Table 1: Few keywords that summarize the behavior patterns and feelings of users

Users	Behavioural affects	Initial Feelings	Later Feelings	Third Party Observer
A	higher excitement, positive arousal, high enthusiasm	curious, gratified, motivated, cheerful	joyful, no major changes in feelings noticed	focus, eagerness, no sweating of palms
B	medium excitement, neutral arousal, medium enthusiasm	neutral, unknown, untraceable	minor changes in feelings	difficult to extract any conclusion, no intervention
C	low excitement, negative arousal, low enthusiasm	boredom, depressed, confused most of the times	anxious, major changes in feelings noticed	leaning back, lack of focus, helplessness

V. FEELCALC MODULE

In this chapter, short and brief explanation of feelcalc module is introduced. Moreover, the high-level view of feelcalc module has been devised. It consists of four major elements i) Identifying user's input or the patterns of the inputs via multi-modal, speech, touch, haptic technology ii) processing the input using feelcalc engine, using an algorithm iii) measuring user's reaction which could be either physical or cognitive and finally, iv) advancement of user's productivity in human cognition. The Figure 4 illustrates the high-level conceptual view of the feelcalc module.

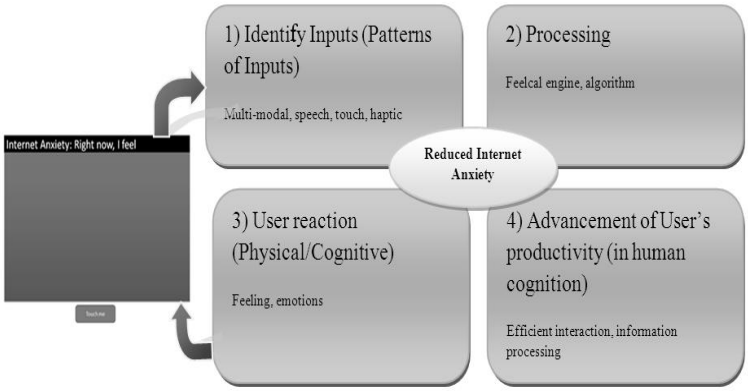


Figure 4: High level Conceptual View of Feelcalc module

A. *Feelcalc algorithm*

The preliminary feeling calculation algorithm has been created to measure feelings of users in order to reduce Internet anxiety. The algorithm 1 is very simple in nature, a self-explanatory in process.

Algorithm 1

```
1: procedure FEEL
2:     initialize-sate()
3:     loop
4:         options ⟵ option-generator (queue)
5:         selected_options ⟵ intended (options)
6:         update(selected_options)
7:         execute()
8:         add-successful-feelings()
9:         drop-unsuccessful-feelings()
10:    end loop
11: end procedure
```

1. *Procedure Feel:* The procedure feel calculates the feelings associated with users. It has initial state where in this stage; all the feelings keywords are initialized.
2. *Initialize:* The state method initializes the three different states of feelings. These state could be positive, negative or neutral states.
3. *loop* runs for each number of states.
4. *option* variable is used and the option generator generates the various options from the queue of options. The option generator generates feeling constructs for example color to identify if the users feelings.
5. *selected option* are selected based on intended feelings options.
6. *Selection:* The update method updates the selected option of feelings.
7. *execute:* The execute method is responsible for executing the updated selected feelings.
8. *add sucessful feelings* method takes care of adding feelings in the database and the unsucessful feelings are removed. The types of feelings can be seen from Figure 1.
9. Those unindentified feelings are dropped through *drop-unsuccessful feelings* method.
10. The loop contintinues from step 3-10 until filtered feelings are generated
11. The procedure ends.

B. *Feelcalc engine*

The feelcalc engine consists of feature extraction engine. The role of feature extraction engine is self-explanatory. In addition, body gesture techniques such as leaning back, movement, sweating of palms/fingers, shrugging, simple facial expressions, and non-verbal clues has been used to extract feelings and emotional arousal from a user. Apart from that, a skin conductance, for example, galvanic skin response and sensors could have been used. In latter case, it might be significantly easy to measure a response from a user. Once the response is achieved, we could then categorize the user's response based on its type. The Figure 5 illustrates how feelcalc engine might work.

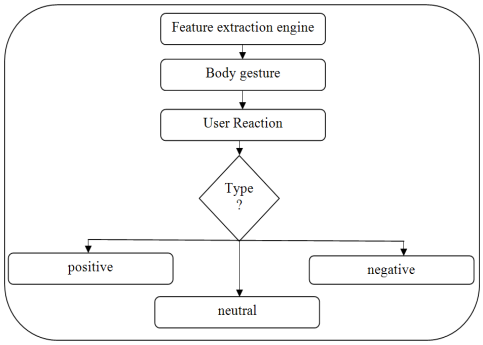


Figure 5: Schematic diagram of feelcalc engine.

C. *Prototype Visualization*

A simple prototype has been implemented which is shown in the Figure 6.There are three sets of color identifying three different types of feelings. The red color indicates "extremely anxious", the blue color indicates "moderately anxious" and the "green color" indicates "not at all anxious". The preliminary idea behind this prototype implementation is to enquire with users different sets of feeling they inhibited. A user clicks on the respective color and the system shows the number of sites visited and the time spend in each website (in seconds). In short, the system shows the graphical representation of site, time spent and severity of anxiousness.

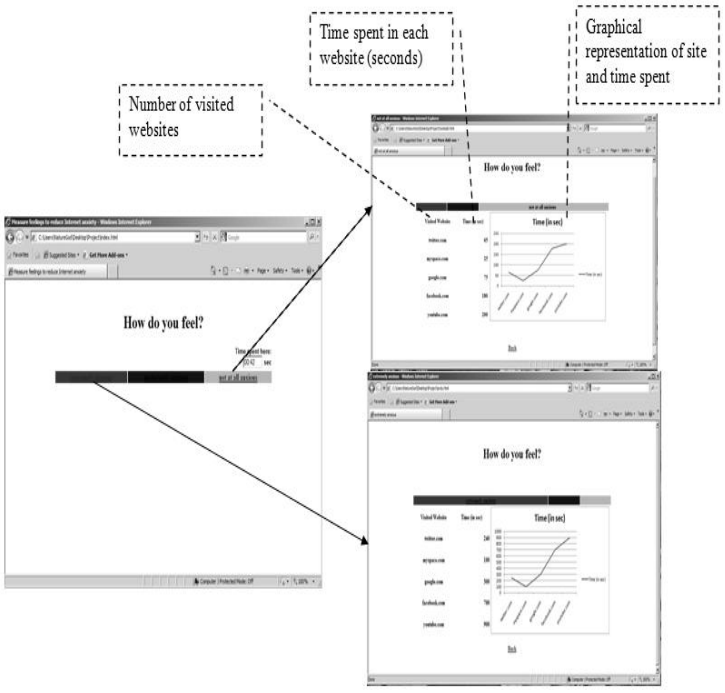


Figure 6: A simple prototype visualization illustrating types of feelings associated with users.

Three users (A, B and C) tested the prototype and they got three different results based on the colors selected. A "user A" was feeling positively and a user was found having no anxiety at all. The "green" colored tab was clicked, which showed number of website visited and the graphical representations of the sites. Similarly, a "user B" was feeling neutral and similar results prevailed. Likewise, a "user C" clicked on the red button and the similar results were shown. During the final process of research, users were advised to answer checklist questionnaires. Very simple questionnaires, for an instance, "How do you feel about your Internet usage?" was imposed on users. The question was used in order to determine if their action/reaction has been reduced, increased or has remained constant throughout. The summary Table 2 for measuring user reaction in contemplation of reducing human anxiety is shown.

Table 2: Users measurement through a working prototype visualizations

Users	Selected Colours/buttons	Type of feelings	Thoughts	Checklist Questionnaires
A	green	not at all anxious	neutral	constant
B	blue	moderately anxious	neutral	constant
C	red	extremely anxious	negative	reduced

VI. Conclusion And Future Work

To the best of our knowledge, we believe that this is the first study that measures the user's reaction to reduce Internet anxiety. The observation, note taking, algorithm, and prototyping visualization were successfully carried out. The algorithm is very simple in nature, which demonstrates types of categories of feelings such as positive, negative and neutral to be selected and successful selection of feelings for execution. Moreover, the simple prototype visualization, which was built, assisted users to notify the types of website they visited, graphical representation showed the time spent on each website and colors helped to measure their reaction. We think this is valid tool for user's notification of feelings. The negative feeling was subdivided into "extremely anxious", "moderately anxious" and "not at all anxious" which were measured with the users. However, in this preliminarily stage, it is hard to generalize if the user's feelings were reduced. Therefore, there is few limitation of this work. First, the prototype was not tested with large number of participants. Second, the efficiency of algorithm was not measured. When we began our study on Feelcalc module, we thought that there were just few technical questions such as building methods, techniques, and algorithmic intelligence. Nevertheless, we found very little evidence insofar and are working towards building more sophisticated and simplistic model of feeling algorithms. More importantly, in our pursuit for improving user's experiences by measuring user's reaction for reducing Internet anxiety, we still have long way to go. In that thrust, the research on a development of feelcalc engine has just begun. In our future work, we should measure all the categories of the feelings and built more enhanced version of preliminary prototype for feelcalc module.

Acknowledgement

The author thanks anonymous reviewers for their helpful suggestions in this paper. Author would also like to thank all the participants for their voluntary participation for this research work.

References

[1] D. A. Norman, "Emotional design: Why We Love (or Hate) Everyday Things, " Basic Books, New York, U.S.A., 2004.

[2] Santosh Kumar Kalwar. Cyberpsychology, Behavior, and Social Networking. August 2010, 13(4): 443-446.

[3] M. Macaulay, The effects of web-assisted learning on students' anxiety, Journal of Educational Computing Research 28 (3), 2003, pp. 221–230.

[4] Caplan, S. E. (2002). Problematic Internet use and psychosocial well-being: development of a theory-based cognitive-behavioral measurement instrument. Computers in Human Behavior, 18, 553–575.

[5] Davis, R. A. (2001). A cognitive-behavioral model of pathological Internet use. Computers in Human Behavior, 17, 187–195.

[6] Shapira, N. A., Lessig, M. C., Goldsmith, T. D., Szabo, S. T., Lazoritz, M., Gold, M. S., & Stein, D. J. (2003). Problematic Internet use: proposed classification and diagnostic criteria. Depression and Anxiety, 17, 207–216

[7] Shih-Ming Li, Teng-Ming Chung, Internet function and Internet addictive behavior, Computers in Human Behavior, Volume 22, Issue 6, November 2006, Pages 1067-1071, ISSN 0747-5632, DOI: 10.1016/j.chb.2004.03.030.

[8] Caplan, S. E. (2003). Preference for online social interaction: A theory of problematic Internet use and psychosocial well-being. *Communication Research, 30*, 625–648.

[9] McKenna, K. Y. A., & Bargh, J. A. (2000). Plan 9 from cyberspace: The implications of the Internet for personality and social psychology. *Journal of Personality & Social Psychology*, *75*, 681–694

[10] Morahan-Martin, J., & Schumacher, P. (2000). Incidence and correlates of pathological Internet use among college students. *Computers in Human Behavior, 16*, 13–29

[11] Beverly Woolf, Winslow Burleson, Ivon Arroyo, Toby Dragon, David Cooper, Rosalind Picard, Affect-Aware Tutors: Recognizing and Responding to Student Affect (2008), Available at: http://centerforknowledgecommunication.com/publications/recentPubsandAwards/2008/Tech%20Education_Final.pdf

[12] Woolf, B., Arroyo, I., Cooper, D., Burleson, W., Muldner, K. (2010). Affective Tutors: Automatic Detection of and Response to Student Emotion. In R. Nkambou, J. Bourdeau & R. Mizoguchi (Eds.), Advances in Intelligent Tutoring Systems (Vol., 308, pp. 207-227): Springer Berline/Heidelberg.

[13] Muldner, K., Burleson, W., & VanLehn, K. (2010). "Yes!": Using Tutor and Sensor Data to Predict Moments of Delight during Instructional Activities. In P. De Bra, A. Kobsa, D. Chin, K. Muldner, W. Burleson & K. VanLehn (Eds.), User Modeling, Adaptation, and Personalization (Vol. 6075, pp. 159-170): Springer Berlin / Heidelberg

Study on Service Diffusion in Mobile Social Network

Feng Chen, Rui Ni, Leixin Mai, Xiaowei Qin and Guo Wei

University of Science and Technology of China, Hefei, 230027
E-mail: {chfeng, ruini, sammai}@mail.ustc.edu.cn, {qinxw, wei}@ustc.edu.cn

***Abstract* – How to popularize the own Mobile Value-added Services (*MVS*s) in current mobile networks is interesting and important to many SP/CPs (Service Providers/Content Providers). In this paper, we focus on the study of service diffusion of *MVSs* and provide a novel methodology, which investigate that from a new perspective of epidemic spread. Firstly, we argue about the characteristics of Mobile Social Network (*MSN*), which is composed of mobile users, and analyze various factors that impact the subscribers to customize the *MVS*s. Then epidemic dynamics is used to depict the service diffusion and some conclusions including marketing strategy have been carried out thereinafter. Finally, through a series of experiments, we find that: 1) by using Acquaintance-First marketing strategy, the MVSs will quickly pop up at a low cost; 2) SP/CPs should do efforts to the effective spreading rate, which can result in a higher popularity of the service.**

Keywords: *Mobile Social Network (MSN), Mobile Value-added Services (MVSs), epidemic dynamics, service diffusion, effective spreading rate*

I. INTRODUCTION

In the latest decades, with the great technical advances in the mobile telecommunication and the diversification of customers' requirements, pure voice phone and simple data services cannot satisfy the need of the subscribers, causing a decrease of the Average Revenue Per User (APRU) and then increasing the probability of departure rate simultaneously. Thus, various MVSs continuously emerge. These services, which are designed to be personalized and with varied contents apart from the traditional information, are launched by Service Providers/Content Providers (SP/CPs) to absorb the customers and improve the ARPU. In order to exploit the services which satisfies the users' needs, operating and popularizing them to be killer applications becomes one of the major topics of interest and a key priority for many SP/CPs, which can be stated as service diffusion process.

Service diffusion dynamics, discussed based on empirical evidence, that impact on the service adoption have been widely presented in the academic literature and the business and technology press [8]. Note that, the determinants are always political, cultural, economical and geographical. Sarker had paid his attention on the mobile devices, and discussed the motivations and circumstances surrounding mobile device use and the adoption with characteristics of individuals, technologies, and context though use process analysis in [4]. Bobby Swar *et al.* analyzed the impact of national culture on the adoption and diffusion of mobile phone services by using Hofstede's cultural dimension values and Bass diffusion model, which has been described as one of the most famous empirical generalizations in marketing [5]. Yamakami enumerated a wide range of the value-added mobile Internet services that had been used in Japan in order to identify the evolution driving force, and then presented a 2-dimentional-factor model to identify the market positions of the value-added mobile Internet services [3]. Timo Ali-Vehmas *et al.* talked about the strategic actions related to the standardization, system architecture, vendors' product strategies, substitutes, regulation and service provision to advance the service diffusion of push on talk over cellular [6]. An analysis of the telecommunication services diffusion process in Commonwealth of Independent States was proposed by Nurilla Mahamatov *et al.* and they found tele-services (telecommunication services) in Commonwealth of Independent States (CIS) are mostly complementary to each other [7].

In this paper, we aim at providing a novel methodology to view over the service diffusion from a new perspective of epidemic spread. Physicists and sociologists have found that when people participate in the mobile telecommunication, MSN comes into being [1], which possesses small-world scale-free property [2] and forms the basis of service diffusion. We introduce some valuable researches on the mobile value produced by MVSs and two critical probabilities are mapped onto. And then, we analyze the service diffusion from the viewpoint of epidemic dynamics in complex networks; obtain the effective service spreading threshold in MSN. Moreover, we propose some strategies about earlier marketing to get a large diffusion rate and a high service popularity. Finally, through simulated experiments, we evaluate those and get some conclusions which may be favor to improve the popularity of MVSs.

This work was supported by the National Basic Research Program of China (973 Program) (2007CB310602), the National High Technology Research and Development Program of China (863 Program) (2009AA011506) and the China-Finland International S\&T Cooperation Program (2010DFB10570).

978-1-61284-690-3/11/$26.00 ©2011 IEEE

The remainder of this paper is organized as follows. In Section II, we argue about MSN and the emerging MVSs about their properties and values to the customers. Section III introduces the service diffusion in MSN using SIS/SIR threshold model. To quickly pop up and chase a high popularity, we propose some strategies for service promotion in Section IV. Section V presents our experimental results and relative discussions. Concluding remarks are placed in Section VI.

II. MSN AND MVSs

Sociologists have proposed the definition that "a mobile social network can be defined as the user's patterns of interconnection with others emerging through the social use of mobile devices" [1]. So, by using MVSs to communicate or experience, people who join in the mobile telecommunication society then form a MSN, where the users are described as network nodes and the connection between two of them represents the possibility that they contact each other for a period of time. Empirically, MSN here attributes to be a human social network, which has been found to exhibit small-world and scale-free properties. Assuming that user i has n_i connections to his acquaintances individually then n_i follows a power-law distribution

$$p(n_i) \sim n_i^{-\gamma} \tag{1}$$

where $p(n_i)$ denotes the probability that user i has n_i connections and $\gamma > 0$ is the characteristic exponent. Fig. 1 depicts a power-law distribution in a small-world and scale-free network. As shown there, only a few people have numerous acquaintances, which is suited to the realities today. Abello and Aiello et al. studied the call graph of long-distance telephone calls made during a single day, finding that the degree distributions of the outgoing and incoming edges followed a power law with exponent $\gamma_{in} = \gamma_{out} = 2.1$ [2].

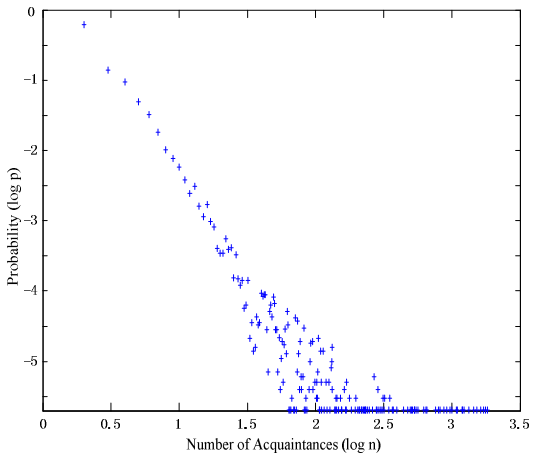


Fig. 1 Probability of user i having n_i connections versus n_i

Great achievements in the mobile communication technologies have facilitated many kinds of MVSs, such as mobile TV, online-game, multimedia streaming and et cetera. They are always channel integrating, network mediating and mobile commerce end-user services, designed to meet various needs of the consumers and described as the specialized and personalized applications. To obtain widespread adoption of these services, a set of requirements should be met, which are technological, business strategic and behavioral.

Bill Anckar et al. proposed an analytical framework to evaluate the suitability of specific services/application for m-commerce in [8], where mobile value offered by the MVSs was analyzed and classified to time-critical arrangements, spontaneous decisions and needs, entertainment needs, efficiency ambitions and mobile situations, etc (see Fig. 2). These five different settings can create mobile value, thus being driving force to the adoption of the MVSs.

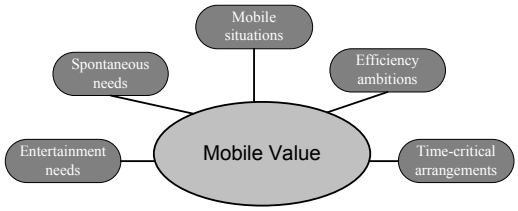


Fig. 2 Mobile value brought by the MVSs

A more systematic work was proposed by Pedersen in [9] to explore the behavioral adoption requirements of end-users of mobile commerce services, which are always technological, business strategic and often vary across end-users, contexts and roles. By integrating domestication research findings into the traditional model of Information Communication Technology (ICT) adoption, they developed a theoretical model of the adopters' decision to use mobile commerce services (see Fig. 3), where the users' expectations are considered. This literature reviewed on both adoption and, in particular, on domestication research indicates that social issues such as interpersonal and external influence are more important to the adoption of mobile services than to the adoption of traditional ICT-services adopted for purely functional reasons.

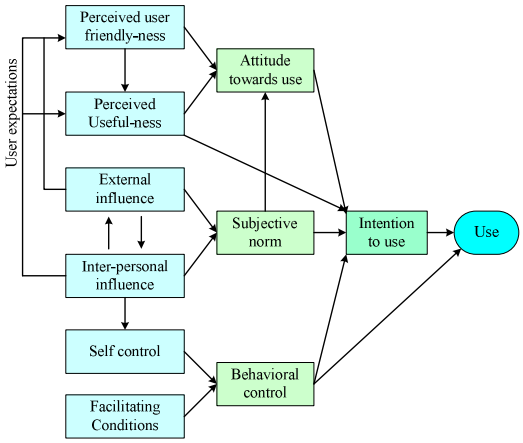


Fig. 3 Service behavioral adoption model [5]

III. SERVICE DIFFUSION

In the canonical model of epidemic contagion, the individual of the population always belongs to three basic states, which can be described as susceptible (*S*), infected (*I*) and removed (*R*). The diffusion model is always named according to the transformation among them, e.g. if the susceptible population are infected and then removed to be immune, it can be modeled as SIR model; similarly, if they are removed to be susceptible again, it would be called SIS model. Here, we follow the same terms of the states of the users next and adopt SIS model [8] to analyze the service diffusion process.

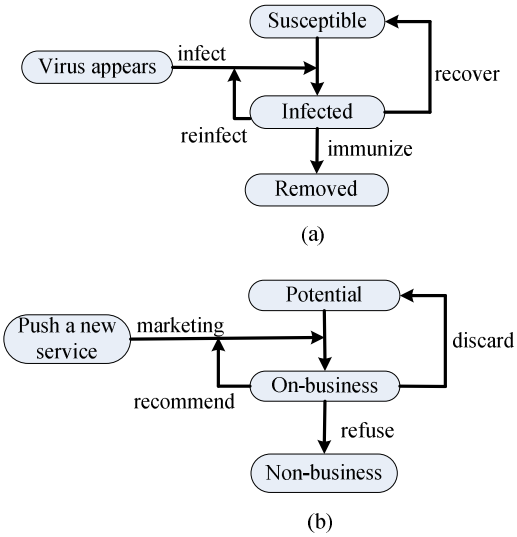


Fig. 4 Epidemic spread versus service diffusion

Considering there are N users in MSN, who is in one of those three states S (susceptible), I (infected), or R (removed). For a mobile value-added service (e.g. VoD), we assume that, at each time step t, the probability of a 'susceptible' user who turns to be 'infected' is η_e, and the probability that the 'infected' user drops the service is η_d. For simplicity, we call them as the probability of service-employment and service-dropping respectively. Then, we define an effective spreading rate $\lambda = \eta_e / \eta_d$.

Assuming the relative density $\rho_k(t)$ of 'infected' users with given acquaintances k, represents the probability that a user with k connections is 'infected'. The dynamical reaction rate equations can thus be written as:

$$\frac{\partial \rho_k(t)}{\partial t} = -\eta_d \rho_k(t) + \eta_e k[1-\rho_k(t)]\Theta(\rho_k(t)) \quad (2)$$

where $\Theta(\rho_k(t))$ is the probability that any given link points to an 'infected' user. When in steady state, $\rho_k(t)$ turns to ρ_k, then we can get an expression:

$$\rho_k = \frac{k\lambda\Theta(\lambda)}{1+k\lambda\Theta(\lambda)} \quad (3)$$

For MSN, the probability that a connection points to a user with s acquaintances is proportional to $sP(s)/ < k >$, thus,

$$\begin{aligned}\Theta(\lambda) &= \frac{1}{< k >}\sum_k kP(k)\rho_k \\ &= \frac{1}{< k >}\sum_k kP(k)\frac{\lambda k\Theta}{1+\lambda k\Theta}\end{aligned} \quad (4)$$

Here, we define λ_c as the spreading threshold. And if $\lambda > \lambda_c$, the service will be popular finally, which means $\Theta > 0$. For a nonzero λ_c,

$$\frac{d}{d\Theta}\left(\frac{1}{< k >}\sum_k kP(k)\rho_k\right)|_{\Theta=0} \geq 1 \quad (5)$$

Which yields the solution

$$\lambda_c = \frac{< k >}{< k^2 >} \quad (6)$$

For scale-free networks (e.g. MSN), which has a power-law distribution $p(k) = (1+\gamma)m^{1+\gamma}k^{-2-\gamma}$ with the exponent $\gamma > 0$, where m is the minimum connectivity of any user [8]. Let $N \to \infty$, so

$$< k >= \int_m^\infty kp(k)dk = \frac{1+\gamma}{\gamma}m \quad (7)$$

and

$$< k^2 >= \int_m^\infty k^2 p(k)dk \to \infty \quad (8)$$

then $\lambda_c \to 0$, which means if the effective spreading rate is kept to nonzero, the service will be popular finally.

Combing Eq. (3) (4) and the distribution mentioned above to compute self-consistently the probability ρ:

$$\rho \sim \lambda^{1/(1-\gamma)} \quad (9)$$

For a fixed γ, we obtain $\rho \propto \lambda$ (See details in Ref.[10]), which means if the high popularity of the MVSs wanted by SP/CPs, they should do efforts to improve λ, i.e. increase the probability of service-employment and decrease the probability of service-dropping.

IV. STRATEGIES FOR SERVICE PROMOTION

Nowadays, many diverse and highly differentiated services, which run for communication, entertainment, information or business, have already been or will be promoted through a variety of service platforms. These services are always targeted and personalized to meet different needs, thus keeping novel to the customers. Therefore, the procedure for the subscribers to learn, try, compare, familiarize and habituate themselves to those above is strongly required, which can be called as "experience time". But, how to choose the right people to experience them and thus spread them, due to the limited costs, remains a problem.

Scale-free network is a robustless net, which is vulnerable to virus attacks and then leads to the epidemic. So it strongly needs some immunization strategies to prevent that. Similarly, in scale-free-like MSN, we

should adopt appropriate marketing methods to make the novel service quickly pop up, which can be listed as follows:

i) Push-On-Random (POR): This randomly choose the people in MSN to experience the under promoted service. It ignores the differences between the big-degree users and the small-degree ones.

ii) Targeted-Push (TP): Considering the inhomogeneity of the scale-free networks, pushing the novel service selectively to the consumers should be efficient way, e.g., selecting the few people who contact others most frequently (Big-Degree First, BDF) to experience it. These people have a long buddy-list and are prone to spread the new service to their acquaintances, then causing a high service popularity. But, to our empirical knowledge, it needs to know the global information about the MSN, which remains difficult.

iii) Acquaintance-First (AF): Here, we firstly select a candidate population, whose ratio is p, from all the users randomly. Then we choose the people, who are the acquaintances of the candidate ones, as the marketing targets to experience the services. Obviously, using this approach, it is no need to get the global information, but acquaintances only. It should be noted that the big-degree user always has a lot of connections with other people, for which he would easily been chosen, which then turns to the second method in fact, but without knowing any global information.

V. Simulation Results

In this section, we investigate the service diffusion using SIS model based on simulation experiments. This simulation adopts time-driven simulation approach that has been widely used in the mobile telecommunication network studies. Considering a mobile network that has $N = 10000$ users. As mentioned in Seciton II, this net is a MSN, who has a pow-law distribution. We set $\gamma = 2.1$ in this experiment, and other parameters are configured according to varied situations. Our experiment focuses on the MVS' diffusion in MSN, especially the popularity in final steady state, under different service marketing strategies, varied probabilities of service-employment and service-dropping.

Fig. 5 depicts a general MVS diffusion in MSN by using some different marketing strategy. Here, we set $\eta_e = 0.2$ and $\eta_d = 0.1$. In Fig. 5, we clearly find that by using BDF strategy, the proportion of service adoption grows most quickly. AF follows next, and POR stands in the last. As mentioned in Section IV, if using BDF, global information about the MSN, especially the detailed distribution of users' acquaintances should be understood, which remains difficult and expensive. And POR, which randomly choose the customers to experience, needs only few costs, but leads a slowest increase of the proportion of service adoption. With appropriate service promotion rate, AF marketing strategy employs the mediate costs between BDF and POR, which just means that AF can strike the right balance between the costs and the rate of service diffusion.

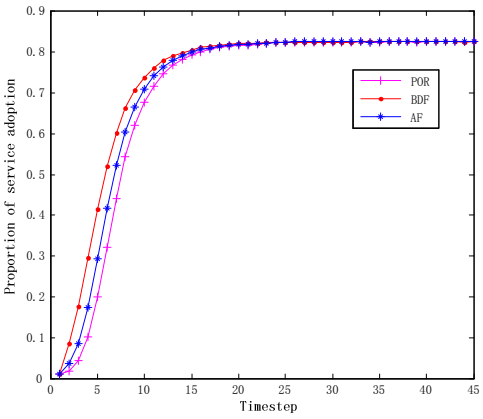


Fig. 5 The popularity of general service versus timestep

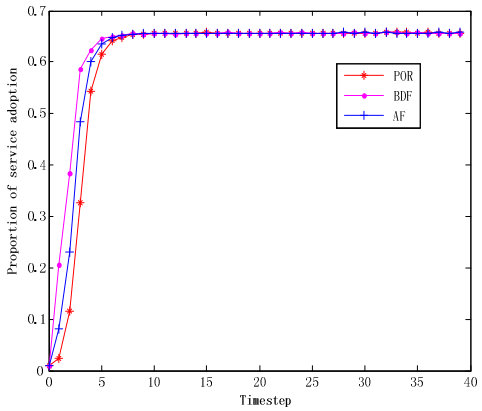


Fig. 6 Proportion of big-degree-oriented service adoption versus timestep

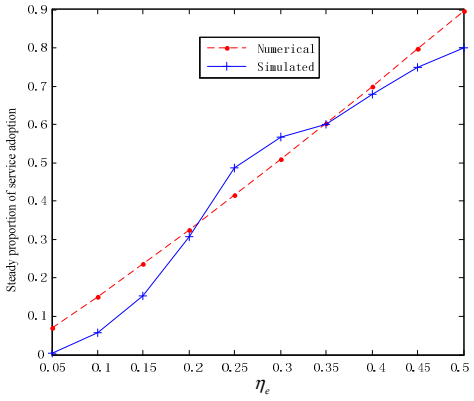


Fig. 7 Steady proportion of service adoption versus η_e with $\eta_d = 0.1$

MVSs, which are always designed to meet various needs of the consumers, exhibit personalized and specialized. Here, we argue about a specialized service, which may be designed to the customers having a big-degree property, e.g. mobile yellow pages for business men, and observe its diffusion procedure under BDF, POR and AF respectively. We know that, for this service, the more acquaintances results in the higher η_e and the lower η_d.

Fig. 6 figures out the related diffusion procedure. It can be seen that the service diffusion process is similar to Fig. 5. As shown therein and comparisons above, we found that AF marketing strategy also emerges relative superiority than the other ones.

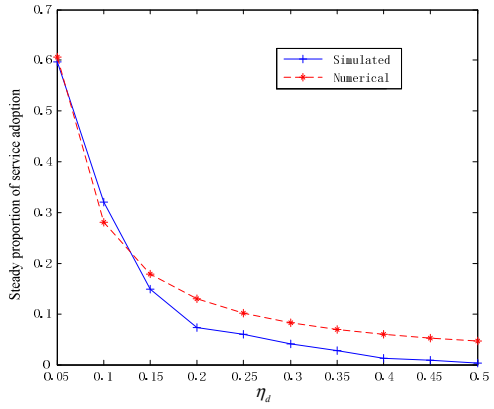


Fig. 8 Steady proportion of service adoption versus η_d with $\eta_e = 0.2$

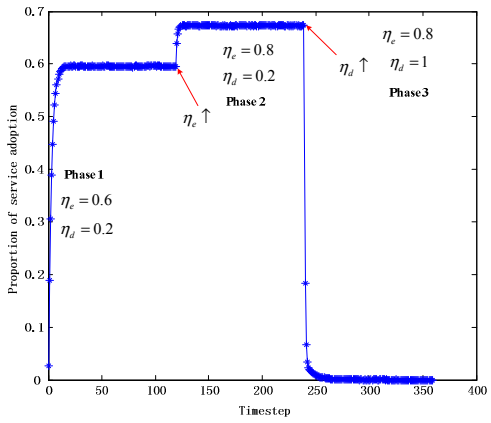


Fig. 9 Proportion of service adoption versus timestep

In Fig. 7, the blue curve represents the steady proportion of service adoption ρ when the probability of service-employment η_e varies from 0.05 to 0.5 with the probability of service-dropping $\eta_d = 0.1$, and the red one denotes the fitting curve according to Eq.(9): $\rho = a\lambda^{1/(1-0.1)}$. The similar curves are shown in Fig. 8, where η_e equals to 0.2 and η_d changes from 0.05 to 0.5. From these two figures, we find that, although a little deviation to the numerical ones, it still shows that ρ increases when γ remains const and the effective spreading rate λ grows up, which has proved that $\rho \propto \lambda^{1/0.9}$ obtained in Section III. So, for a high popularity, SP/CPs should do their efforts to improve the service experience to make λ larger, i.e. increase the probability of service-employment and relatively decrease the probability of service-dropping.

Fig. 9 describes the service diffusion procedure and the steady proportion of service adoption when facing different activities of SP/CPs or users, which can be used to prove the conclusions mentioned above. As shown, in the first phase, which a new service is proposed, SP/CPs always do their best ($\eta_e = 0.6$) to promote and lead a nice initialization. For more revenues, SP/CPs increase input in improving Quality of Service (QoS) ($\eta_e = 0.8$) and then a higher proportion of service adoption is received in Phase 2. After a period of time(last phase), the users lose their interests in the adoption of this service ($\eta_d = 1$), causing the sharp decline in the proportion of service adoption (at most 0% finally).

VI. CONCLUSIONS

How to facilitate the MVSs and then turn them to be killer applications in the mobile telecommunication, becomes a challenge but interesting to SP/CPs. In this paper, we investigate the service diffusion from a new perspective of epidemic spread. We argue about MSN firstly, which is composed of mobile consumers, and its small-world scale-free properties, then analyze various factors that impact on the adoption of MVSs of the customers and map them to two critical parameters. After that, epidemic dynamics and SIS model is used to analyze the service diffusion in MSN. And we get some threshold properties. From experimental results, we can clearly know: 1) by using Acquaintance-First marketing strategy, the MVSs will quickly pop up at a low cost; 2) SP/CPs should do efforts to improve the effective spreading rate to chase a higher popularity.

It should be noted that, dynamic probability of service employment and service dropping which may vary with different timestep and different number of acquaintances, has not been argued in this paper. And we will do more detailed researches in the future.

REFERENCES

[1] Giuseppe Lugano, "Mobile social networking in theory and practice", *First Monday*, vol. 13, no. 11., 2008.

[2] R. Albert and A. L. Barabasi, "Statistical mechanics of complex networks," *Reviews of Modern Physics,* vol. 74, pp. 47–97, 2002.

[3] Toshihiko Yamakami, "A 2-dimensional evolution model of value-added mobile Internet services", *AINA'05*, vol. 2, pp. 758-761, 2005.

[4] S. Sarker and J. D. Wells, "Understanding mobile handheld device use and adoption", CACM, vol. 46, no. 12, pp. 35-40, 2003.

[5] Swar. B., Jedong Kim, Duk Hee Lee and Junghoon Moon, "Impact of Culture on Mobile Phone Service Adoption and Diffusion: A Cross-Country Analysis", *ICCIT'09*, pp. 1442-1444, 2009.

[6] Ali-Vehmas, T., Luukkainen, S., "Service diffusion strategies for push to talk over cellular", *ICMB. 2005*, pp. 427-433, 2005.

[7] Mahamatov, N., Jongsu Lee and Minkyu Lee, "Telecommunication services diffusion in CIS: dynamics of competition and complementarity among telecommunication services", *ICI 2007*, pp.1-5, 2007.

[8] Bill Anckar and Davide D'Incau , "Value-Added Services in Mobile Commerce: An Analytical Framework and Empirical Findings from a National Consumer Survey", *HICSS'02*, pp. 1444-1453, 2002.

[9] Per E. Pedersen, "Adoption of mobile commerce: An exploratory analysis", SNF-REPORT NO.51/01, 2001.

[10] Pastor-Satorras R, Vespignani A, "Epidemic dynamics and endemic states in complex networks", *Phys. Rev. E*, vol. 63, 2001.

[11] Dodds P S, Watts D J, "Universal behavior in a generalized model of contagion," *Phys. Rev. Lett.*, vol. 92, 2004.

Capacity and Resource Reservation in Broadband Internet

Raenu Kolandaisamy
Faculty of Computer Science
Information Technology
University of Malaya
Kuala Lumpur, Malaysia
Email: kraenu@yahoo.com

Rafidah Md Noor
Faculty of Computer Science
Information Technology
University of Malaya
Kuala Lumpur, Malaysia
Email: fidah@um.edu.my

***Abstract*—The aim of this paper is to introduce a model to providing Internet service charging according to a capacity and usage based charging. A charging model is introduced according to the user interests and preferences. The model provides resource optimization to the mobile network through a capacity and resource parameters where it generates a cost-effective method to optimize the resources. Experiments are conducted using a network simulator to evaluate the model and analyze the results. The results will be useful for Telecommunication Networks and accounting policy planning for the Broadband Internet Charging Quality of Service.**

***Index Terms*—Broadband Internet, Capacity, Resource Reservation, Optimization, QoS**

I. INTRODUCTION

In the next generation of network, more interactive applications are expected to be carried by mobile users such as video chatting, real time video gaming, and voice over IP, at any time and any where. In a mobile network, the frequent mobility of the users implies more difficult challenges to provide a Quality of Service (QoS) guarantee in Internet service. Two QoS architectures widely known, Integrated Services [2] and Differentiated Services [1] proposed by the Internet Engineering Task Force(IETF). integrated services(IntServ) reserves resources according to the individual flows. A path must be set up to reserve resources before data is transmitted. The Resource ReSerVation Protocol (RSVP) is a protocol to set up the packet path [12]. The protocol carries information such as traffic characteristics and resource requirements. There are two main types of messages in RSVP, a PATH and a RESV. The PATH message is sent by a sender node to its destination receiver. It carries information about source traffic and characteristics of the path between the sender and receiver. DiffServ reserves resources according to a group of traffic classes or services. In DiffServ, traffic is divided into a small group, which is called a forwarding class. In each forwarding class, there is a predefined forwarding treatment in terms of traffic priority and bandwidth allocation. In a DiffServ network, each router (e.g., edge router or core router) has its own functionality. When traffic arrives at the edge router, it will perform two basic operations which are packet classification and traffic conditioning. At the core router, traffic is forwarded according to the forwarding class in a packet header.

In voice service, billing is based on the duration of the call; GPRS allows charging based on transmitted information volume (for data services). However, sometimes it is not convenient to charge per megabyte downloaded. The user will rarely download a song if it is cheaper to purchase a CD in a store. On the other hand, tracking real-time events while on move (e.g., downloading a video clip immediately after a scored goal in a football game) or previewing a clip from cinema movie is a different situation, where the user will pay for recent news, interesting information, or entertainment. However, many operators are moving from a traditional time-based billing approach to a model of billing that sets a fee for a certain service over a longer period (e.g., a week or a month), while giving users freedom to use that service as much as they want or within certain limits (in number of events, in time usage, or in data volume). Of course, different tariff models and different associated QoS classes should be used to optimize the utilization of the network resources.

The rest of this paper is organized as follow; section II discusses the related work, and the broadband Internet is discussed in section III. The section IV presents the charging model which contains the capacity based charging and resource based charging. Section V presents the experimental and evaluation results. Finally, section VI concludes the article.

II. RELATED WORK

Savage.S. and M.Waldman.D [10] examine the consumer preferences for internet bandwidth by focusing on the ability and urban or rural locations as the source of the preference heterogeneity. They came up with an economic model to show the ability that decreases the effective price of bandwidth. According to their prediction, a decrease in price may give total effect of an increase in ability and also increase in the demand for bandwidth. The proposed model will be used to explain the reasons exist of various high-ability consumers value bandwidth and suggests that demographic proxies for ability also should be included in experimental specifications of internet demand. Boutaba, Li and Iraqi [8] examine the interrelation between pricing and admission control for multi

domain DiffServ networks by studying the pricing and user behaviours. A system had been modelled as a market to show the price of a service class to be a sign of the available resource inside the network. Evaluation on pricing strategy and admission control scheme also has been done throughout the study. A Tariff based architecture has been proposed to separates the pricing for core networks from end-to-end pricing through domain abstraction and maintains domain and global price tables at the access networks.

Cicconetti et al. [4] recommended a mechanism to be employed by the Subscriber Stations named as Bandwidth Request Reiteration(BR2) which put a stop to deadlock from occurring. The researchers used detailed packet-level stimulation, they compare Bandwidth request reiteration to an alternative approach based on timeout and showed that Bandwidth Request Reiteration accomplish good performance in terms of the average transfer delay. QoS-aware bandwidth provisioning is a significant issue concerning the commercial operation of service providers. Tran and Ziegler [11] worked together and proposed an adaptive bandwidth provisioning schemes enabling the quality of service quality of service guarantees. They developed novel adaptive provisioning schemes named as PS 1 and PS2 where its features based on traffic measurements, the Gaussian traffic model and appropriate traffic predictions.

Bandwidth estimation is becoming a main problem of fundamental internet engineering. There is difficult in determining the bandwidth required to carry traffic with a specific bit rate offered to an internet link and satisfy the quality-of-service requirements. Jin, William & Don [3] provide bandwidth estimation and also find a solution to the problem of best-effort traffic. The researchers built a simple statistical model and the model is validated by using a queuing theory and an extensive empirical study. It has been proved that the model is valid for traffic with 64 host-pair connections or more.

Hoffler [5] found that there was an issue on infrastructure competition opposing welfare effects and finally decided to estimate the welfare effects from broadband access competition. The gain from reduced deadweight loss may compensated by the inefficient duplication of an existing infrastructure. This paper investigates about the development of broadband internet access in Western Europe for the period of 2000-2004 and investigates which effects prevails empirically.

III. Broadband Internet QoS Requirements

Quality of Service depends on the statistical nature of traffic through three main phenomena [9]:

- Transparency is referring to time and semantic integrity of transferred data. A certain degree of data loss in an acceptable for streaming traffic but not for elastic traffic, however it is acceptable for delays that occasioned by network queuing or congestion but should preserve the semantic integrity.
- Throughput is quality of service measure for elastic traffic defined as the document size divided by the transfer time. Throughput for web documents can be reached up to ten or hundreds of kilobits/seconds but for transferring larger documents such as video or databases may require higher rates.
- Accessibility is the probability of admission refusal and the delay for set up in case of blocking. This is relevant to a network that employed an admission control. The probability of blocking rate is depending on a transaction and network provider where it has a certain maximum rate to achieve.

This is relevant to a network that employed an admission control. The probability of blocking rate is depending on a transaction and network provider where it has a certain maximum rate to achieve.

Three types of charging options are:

- Flat rate pricing. A fixed charge is applied to a traffic volume that produced by the network such as weekly or monthly. On one hand, the advantage of using flat rate pricing is the simplicity where it does not increase a network operating cost. On the other hand, its disadvantage is unfairness where a lower usage user has to pay as much as a higher usage user.
- Congestion pricing. A congestion pricing allows users to pay for the level of quality of service they estimated. The pricing is covered for the network congestion only rather than cost of the network. An advantage of congestion pricing is allowing the users to pay for their traffic value and gaining the priority in accessing the network resources. However, a network provider may give a poor network service to the users as a result the users pay because of inefficient provider.
- Transaction pricing. A transaction pricing is depending on predicting resource demand, giving announced charges and to size the network to avoid network congestion when the demand is prevailed. There is a price value for users to pay that allowing the network operator to cover the network cost. The advantage of using transaction pricing is able to predict resource demand in the future if using one type of network service such as telephone network but if applied to multiservice network, the pricing charging will be come more complex due to many parameters such as traffic characteristics, performance requirements of transaction, bandwidth and buffer capacity of network types.

IV. Charging Model

A cyclic dependency breaks [7] the calculation steps into three: the capacity planning, pricing and demand estimation. However, by referring to this model, we extend each of the modules so that it fit into our framework and case studies.

A. Capacity Charging

Referring to Karsten et al. [6], first they determined the optimum prices then they provided the capacity according to the demand. But in our case a capacity planning is the most important part in calculation process, where we can estimate the number of users based on the contract subscription (fixed contract) and non subscription contract (flexible contract).

Therefore, we divided the capacity planning into two that are class based planning and user based planning.

QoS services			Period of time	Minimum Bandwidth	Minimum Bandwidth (for period of time)	Data rates (Mbps)
Flexible Contract	Per-class	Premium	60 minutes	4 Mbit/s	14,400	100
			120 minutes		28,800	
			180 minutes		43,200	
			up to 4 hours		57,600	
		Intermediate	60 minutes	2 Mbit/s	7,200	100
			120 minutes		14,400	
			180 minutes		21,600	
			up to 4 hours		28,800	
		Default	60 minutes	1 Mbit/s	3,600	100
			120 minutes		7,200	
			180 minutes		10,800	
			up to 4 hours		14,400	
	Per-user	High Level User	60 minutes	4 Mbit/s	14,400	100
			120 minutes		28,800	
			180 minutes		43,200	
			up to 4 hours		57,600	
		Secondary Level User	60 minutes	2 Mbit/s	7,200	100
			120 minutes		14,400	
			180 minutes		43,200	
			up to 4 hours		57,600	
		Lower Level User	60 minutes	1 Mbit/s	3,600	100
			120 minutes		7,200	
			180 minutes		10,800	
			up to 4 hours		14,400	

Fig. 1. Flexible Contract with Minimum Bandwidth Guaranteed.

- Class based planning In class based planning, there are three types of classes (Premium, Intermediate and Default) where amount of resources allocated for each class can be expected. Let consider a simple example for a premium class capacity planning. A minimum requirement for Voice over IP (VoIP) is 4 Mbit/seconds. The maximum period of time the flexible contract user can access is 60 minutes hence the expected capacity to provision is 14,400 Mbit (see Figure 1).
- User based planning In user based planning, the amount of resources allocated for different level of users is equivalent to different types of classes. However, the users are given a preference of how to use the resources where they can access any type of applications.

B. Resource Charging

The users are charged according to the contracts that they subscribed. In fixed contract, a user paid the Internet charging in advance according to his/her monthly subscription while in flexible contract, user paid the resources according to number of minutes that they want to access the Internet such as 60 minutes, 120 minutes or more than 180 minutes. The minimum bandwidth allocated for flexible contract is shown in Figure 1. There are two types of charging in fixed and flexible contracts which are a capacity based charging and usage based charging. On the first hand, the capacity based charging is charged based on resource allocated to different types of application (per-class QoS service) where amount of resources are provisioned by referring to the classes subscribed (premium, intermediate or default). The resources are charged according to the maximum amount of resources allocated to the subscriber for a certain period. On the other hand, the usage based charging is charged based on the resources used by different level of users (per-user QoS service).

For example, a user who subscribed (fixed contract) to a premium class paid a monthly charged, Y. The maximum amount of resources allocated for premium class subscriber is N. The premium charge rate is Pr. A fixed contract discount rate is Fxr. The capacity based charging is as follow:

$$Y = [Pr \times N \times 30] - Fxr \tag{1}$$

Let take another example of usage based charged. A user who paid a monthly charged, Z for higher level user subscription (fixed contract). The maximum amount of resources allocated for higher level user is M. The higher level user rate is Hr. A fixed contract discount rate is Fxr. The usage based charging is as follow:

$$Z = [Hr \times M \times 30] - Fxr \tag{2}$$

The maximum amount of resources given to the premium class and higher level user is similar. In flexible contract, the user is charged according to the application basis and user basis which is similar to fixed contract. As explained before, the user paid the resources according to the minutes allocated. For example, a user who wants to access the Internet according to different types of application (Premium, Intermediate or Default) for 60 minutes paid K.

C. Accounting Policy

To control and sharing of network resources, charging is required. Charging can be done in multi-service networks either by reservation or actual used of resources. Charging is an important concept in reservation because it preludes other users from using the reserved resources. However, if charging is limited to reservation parameters only, the applied charge depends on the ability of the user to give a good prediction of the expected traffic characteristics.

The chosen charging schemes may influence the accounting requirements for the provider. Some charging scheme may be very highly demanding or lead to zero accounting requirements. Volume-based charging schemes require the measurement of the transmitted volume and this increases the complexity for accounting. Whilst, the providers may offer different accounting services (e.g. accounting indication, itemized invoice, etc.) Accounting describes the collection of data about resource consumption. This includes the control of data gathering, transport and storage of accounting data. For accounting process, a user or provider must authenticated and authorized. This functions are performed by the Authenticate Authorize Accounting (AAA) Server. Listed below is an excerpt of accounting policy algorithm.

```
Accounting-Policy:
      if subscription_type==Premium {
      set meter_location = access-point(network1)
      set record_type =detailed
      set report_interval = 100s
      set report_target = ip_address
}
QoS-Meter-Policy:
      if metric==one-way-delay {
      set method = passive
      set timestampsize = 24 bits
      set ingress_meter_location
              = access-point(network1)
      set egress_meter_location
              = access-point(network2)
```

}

The network is divided into two sub domains. The mobile network domain and service provider domain contain all the policy message which broadcasted through a wireless channel. The mobile network domain consists of three level of QoS, i.e. premium, intermediate and default. Each QoS class carries customer policy, service policy and flow policy. Whilst the message exchange between the mobile network and the service provider is charging and accounting policy. Whilst, the service provider domain contains the metering policy. Figure 2 shows the use case diagram for capacity and resource reservation in Broadband Internet.

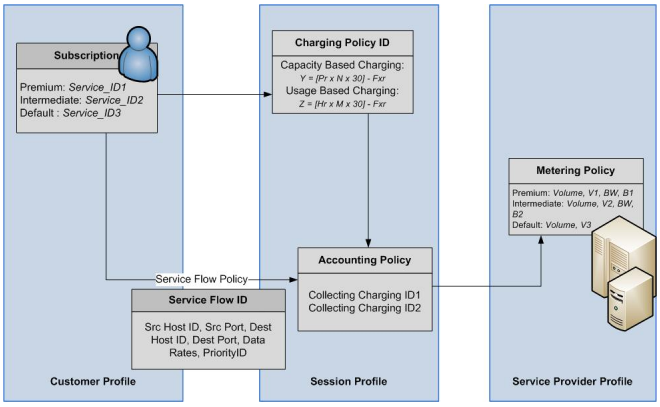


Fig. 2. Use Case Flow Diagram.

V. Experiment and Evaluation

In this experiment, the subscription user parameters were defined. Then the service flow identifier (ID) were declared in each of the traffic class. The charging policy attributes were defined in the service provider domain. The attributes were discussed in previous section. The accounting policy module was implemented in the service provider domain too. Therefore it calculates the related pricing and charging according to the user subscription modules, i.e. Premium, Intermediate and Default. Later the metering module is calculated to provision resources according to the traffic classes. Figure 3, 4 and 5 below shows the subscription contract between three different users, i.e. Premium, Intermediate and Default.

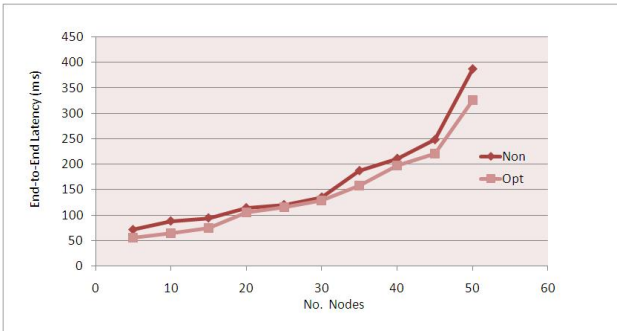


Fig. 3. End-to-End Latency for Premium Subscriber.

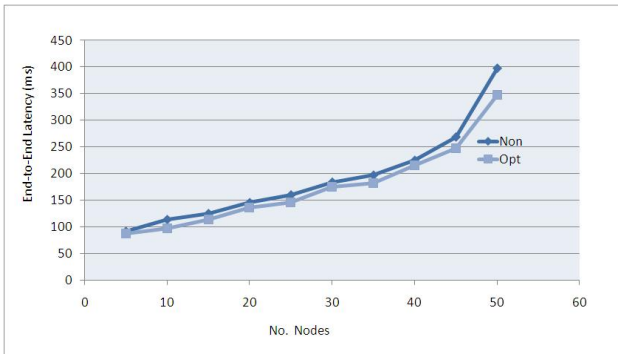


Fig. 4. End-to-End Latency for Intermediate Subscriber.

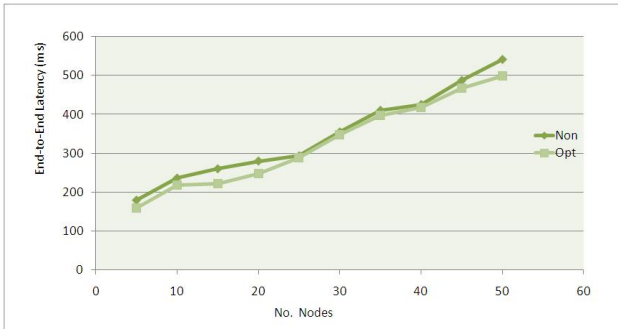


Fig. 5. End-to-End Latency for Default Subscriber.

VI. Conclusion

The relations between the different roles of the user and service provider may affect the accounting process. However, this article presented the Quality of Service model when the charging, accounting policy and metering are integrated into the mobile network. The results have shown that the user who subscribed to a comprehensive subscription, i.e. Premium may not encountered bandwidth problem and less latency.

In the future, the complete model needs to be simulated using a simulator tool, NS-2 to show that it works well in the network mobility context. We also plan to extend the model and look at whether it fits if the mobile network gets more complex (i.e. a nested mobile network).

References

[1] Steven Blake, David L. Black, Mark A. Carlson, Elwyn Davies, Zheng Wang, and Walter Weiss. An Architecture for Differentiated Services. Technical Report RFC2475, Network Working Group, 1998.

[2] Bob Braden, David Clark, and Scott Shenker. Integrated Services in the Internet Architecture: an Overview. Technical Report RFC1633, Network Working Group, 1994.

[3] Cleveland W. S. Sun D. X. Cao, J. Bandwidth Estimation for Best-Effort Internet Traffic. *Statistical Science*, 3(19), September 2004.

[4] C. Cicconetti, L. Lenzini, and E. Mingozzi. A Bandwidth Request Reiteration Mechanism for IEEE 802.16 Wireless Networks. *Wireless Networks*, (16), 2010.

[5] F Hoffler. Cost and Benefits from Infrastructure Competition. Estimating welfare Effects from Broadband Access Competition. *Telecommunications Policy*, (31), September 2007.

[6] M. Karsten, J. Schmitt, L. Wolf, and R. Steinmetz. Cost and Price Calculation for Internet Integrated Services. In *Proceedings of KiVS 99*, 1999.

[7] Brett A. Leida. Cost Model of Internet Service Providers: Implications for Internet Telephony and Yield Management. In *Masters Thesis, Massachusettes Institute of Technology, Cambridge, MA, USA*, 1998.
[8] T. Li, Y. Iraqi, and R. Boutaba. Pricing and Admission Control for QoS-Enabled Internet. *Computer Networks*, (46), 2004.
[9] James W. Roberts. Quality of Service Guarantees and Charging in Multiservice Networks. In *Special Issue on Traffic Control, IEICE Transactions Communications*, 1998.
[10] S. J. Savage and D. M. . Waldman. Ability, Location and Household Demand for Internet Bandwidth. In *International Journal of Industrial Organization*, 2009.
[11] H. T. Tran and T. Ziegler. Adaptive Bandwidth Provisioning with Explicit Respect to QoS Requirements. *Computer Communications*, (28), 2005.
[12] John Wroclawski. The Use of RSVP with IETF Integrated Services. Technical Report RFC2210, Network Working Group, 1997.

Resource Allocation Algorithm for WiMAX Systems

Mr. Wankhede Vishal A.
Electronics Department
SVNIT / SNJBs COE
Surat / Chandwad, India
wankhedeva@gmail.com

Mr. Jha Rakesh
Electronics Department
SVNIT
Surat, India
Jharakesh.45@gmail.com

Prof. Dr. Upena Dalal
Electronics Department
SVNIT
Surat, India
upena_dalal@yahoo.com

Abstract

WiMAX presents a very challenging multiuser communication problem: Different users in same geographic area requiring high on-demand data rates in a finite bandwidth with low latency. To make resource allocation more practical, in mobile WiMAX instead of individual subcarriers a group of them is allocated to different users in both frequency and time. There are several ways to allocate subchannels in mobile WiMAX, three for downlink:FUSC (Fully Utilised Subchannelisation), PUSC (Partially Utilised Subchannelisation) and AMC (Adaptive Modulation and Coding). This paper aims to study the performance of low complexity adaptive resource allocation in downlink of OFDMA for WiMAX systems with variable rate requirements. Objective of the proposed algorithm is to maximize total throughput while maintining rate proportionality among the users. The proposed algorithm prioritizes the user with the high sensitivity to the subcarrier allocation. Simulation results shows that proposed method performs better than previous method in terms of significantly decreasing the computational complexity and achieve higher capacities, while being applicable to a more general class of systems.

Index terms— Downlink OFDMA, Subcarrier allocation , power allocation.

I. INTRODUCTION

Multiple-access techniques typically endeavor to provide orthogonal , noninterfering , communication channels for each established link. The most common way to divide the available dimensions for different user is through the use of time , frequency and also using code division multiplexing. WiMAX has very challenging multiuser communication problem means users in one geographic area needs high on-demand data reates in a finite bandwidth with very less latency. Multiple-access techniques allow different users to share the available bandwidth by allocating individual user small part of the total system resources. In WiMAX multiple-access problem is quite complicated as WiMAX traffic- VoIP, data transfer and video streaming- and for system deployment- mobility , neighboring cells , requirement of bandwidth efficiency. It is difficult to implement efficient and flexible multiple-access strategy to improve WiMAX system performance. OFDM is a modulation technique that creates independent streams of data which can be used by different users , but OFDM is not a multiple-access tactic. For this reason Mobile WiMAX use different approach which is known as orthogonal frequency division multiple access (OFDMA), where subcarriers and time slots are allotted to different users. To increase multi user diversity designer have to increase freedom in scheduling the users. OFDMA come with a few outlay like overhead in downlink and uplink as base station(BS) needs channel information for its users , and Mobile station(MS) needs to know which subcarrier it has been assigned. Multiple access techniques like Frequency division multiple access (FDMA) , Time Division Multiple Access (TDMA) and Code Division Multiple Access (CDMA) entails its own pros and cons so recompense of OFDMA is that best features of each technique can be achieved. OFDMA is hybrid of FDMA and TDMA where users are vigorously assigned subcarriers (FDMA) in different time slots (TDMA). So OFDMA comes with advantages like robust multipath suppression and frequency diversity. In addition , OFDMA is a flexible technique that can put up many users with varying data rates and Quality of Service (QoS) requirements.

To lay a hand on variety of traffic from different applications in WiMAX network , it is essential to find a resource management elucidation. Assigning subcarriers and power to users in Mobile WiMAX system has recently been an area of active research. In [1] novel downlink resource management framework for multiservice WiMAX networks was proposed where the demands of both WiMAX service providers and subscribers are taken into account. For optimization problems algorithms like fairness-constrained greedy revenue for downlink adaptive power allocation and a utility-constrained greedy approximation for downlink call admission control was developed in [1]. In [2] adaptive bandwidth allocation and admission control scheme for polling service in WiMAX is proposed using game formulation. Solution for non cooperative game is formulated by Nash equilibrium for the amount of bandwidth offered to a new connection. Resource allocation algorithms are core part of Physical layer of WiMAX , their aim is to pursue efficiency in resource usage in terms of power consumption, reducing interference and capacity provisioning. Resource allocation issues is been covered in [3]. OFDMA and Adaptive Modulation and Coding (AMC) mode is provided to manage physical layer resources and leaving scope for the development of algorithms in [3]. For "last mile" Internet access OFDMA-Time Division Duplexing (TDD) system was proposed in[4] to provide high spectrum efficiency on both uplink and downlink channels .

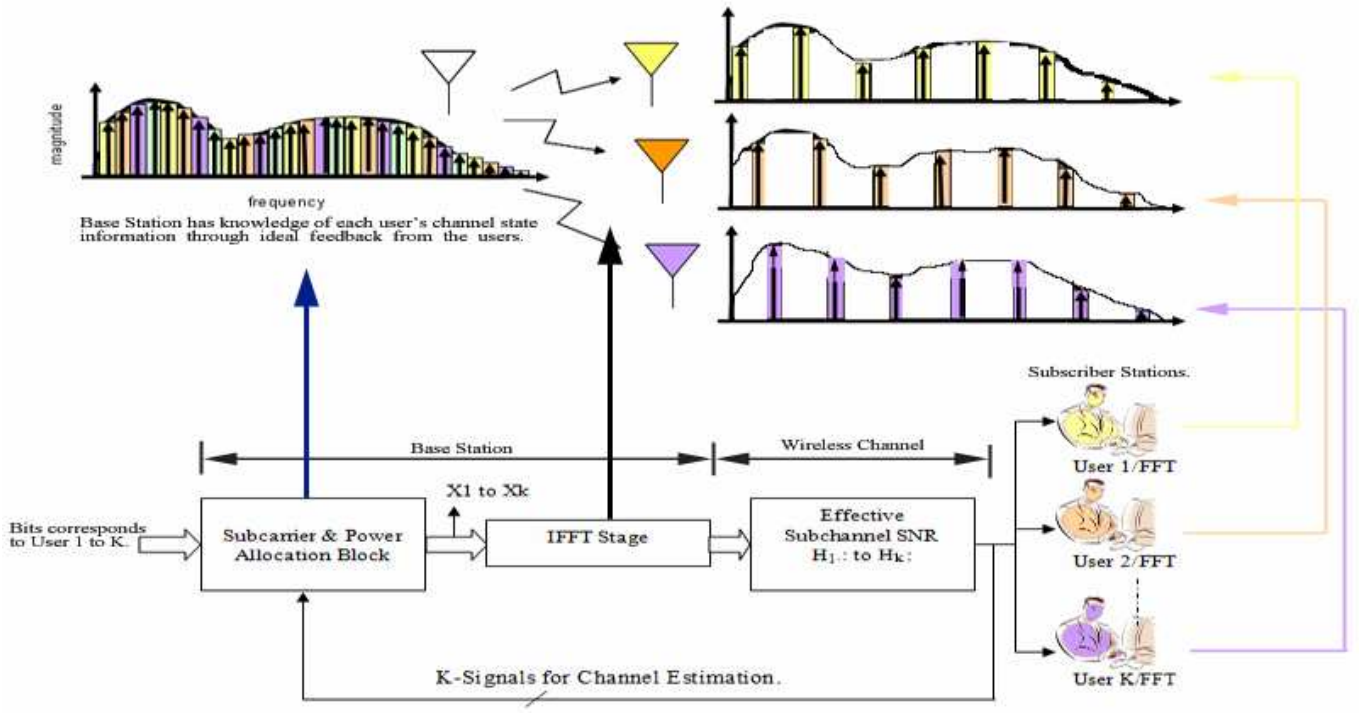


Fig. 1. Block diagram of Downlink OFDMA for K Users.

In [5] problem of dynamic subcarrier allocation, adaptive power allocation, admission control and capacity planning is tackled using Hungarian method transforms for wireless metropolitan area networks. A low complexity adaptive resource allocation in downlink of OFDMA systems with fixed and variable rate was proposed in [6]. In [6] total throughput of the system increases while maintaining rate proportionality among the users, also priority is assigned to users to allocate more resources.

II. SYSTEM MODEL

Block diagram for resource allocation in OFDMA is shown in Fig. 1. Proposed system is only applicable for downlink traffic. In the downlink Base Station (BS) of WiMAX system applies the combined subcarrier and power allocation algorithms. BS assign subcarriers to live users and the number of bits per OFDM symbol from each user to be transmitted on each subcarrier. The Power calculation for each subcarrier is depends on number of assigned bits and type of modulation scheme used at that instant. Table I shows the list of notations used to design mathematical model of the system with values used in our simulation.

TABLE I. NOTATIONS USED TO DESIGN MATHEMATICAL MODEL

Notation	Description	Value
K	Number of Users	16
N	Number of Subcarriers	64
n	Each or Individual Subcarrier (n) , following 1≤n≤N	1 to 64
k	Individual user following 1≤k≤K	1 to 16
$p_{k,n}$	Power assigned to particular user	
B	Bandwidth	1MHz
$g_{k,n}$	Channel gain of kth user in nth subcarrier with Additive White Gaussian Noise (AWGN) σ2 =N0 B / N where N0 is noise spectral density.	--
N_0	Noise Power spectral density	
$h_{k,n}$	Subchannels signal-to-noise ratio (SNR)	$gk,n^2/\sigma^2$
P_{tot}	Total Power	1W
R_k	Total data rate for user	
Φ	Proportionality constant	

For proposed system k^{th} user's received SNR on subcarrier n is defined as $\gamma_{k,n}=p_{k,n}\ h_{k,n}$. For proposed system wireless channel is modeled as time varying frequency selective Rayleigh channel .

In downlink transmitter of typical OFDMA system K users information bits are allocated to N subcarriers and each subcarrier n of user k following constraint $1\leq k\leq K$ is assigned a power $p_{k,n}$. While subcarriers are allotted to different users allotted subcarrier shouldn't be allot to another users till that user finish his work. For this purpose control channel is used which is responsible for keeping track of allotted subcarriers to different users. E.g. User 1 decodes allotted subcarriers only. We follow two assumption for proposed system first is that each user experiences independent fading and second is that each user is able to estimate the channel perfectly also these estimates are made known to transmitter through feedback network. Channel gain of user k in subcarrier n is denoted as $g_{k,n}$ with

AWGN. At the end resource allocation algorithms receive channel estimates as a input.

It is assumed that systems can give service to K number of users with N subcarriers. Frequency selective Rayleigh fading channel is modeled. Additive white Gaussian noise(AWGN) with power spectral density of Noise $\sigma^2=N_0B/N$. Bit error rate can be approximated to $BER \leq 10^{-3}$. Resource allocation allow each user to choose better subcarrier for him. Number of bits transmitted in downlink can be formulated as,

$$r_{k,n} = \log_2(1+\frac{\gamma_{k,n}}{\Gamma}) = \log_2(1+p_{k,n}H_{k,n}) \qquad (1)$$

Where $\Gamma = -1*ln(5BER)/1.6$ is a constant signal to noise ratio gap and $H_{k,n}=h_{k,n}/\Gamma$ is the effective subchannel or group of subcarrier's signal to noise ratio. The resource allocation algorithms objective formulated as follows where $c_{k,n}$ acts as an indicator for subcarrier allocation so that when $c_{k,n}=1$ then only subcarrier n is assigned to user k.

$$\max_{c_{k,n},p_{k,n}} \max \frac{B}{N}\sum_{k=1}^{K}\sum_{n=1}^{N} c_{k,n}\log_2(1+p_{k,n}H_{k,n}) \qquad (2)$$

To follow aim in (2) system have to strictly pursue following constraints

Constraint 1 : $c_{k,n} \in \{0, 1\}$ for all values of k and n.

First constraint tells to algorithm that if subcarrier is allocated to particular user then set value of $c_{k,n}$ to 1 so that another user cant get that subcarrier. If value of $c_{k,n}$ is 0 means subcarrier can be taken by any user.

Constraint 2: $p_{k,n} \geq 0$ for all values of n.

Second constraint tells to algorithm that value of k^{th} users n^{th} subcarrier's power should always be greater than or equal to 0.

Constraint 3:

$$\sum_{k=1}^{K} c_{k,n} = 1 \qquad \text{for all values of } n.$$

Third constraint tells to algorithm that allocate k^{th} users n^{th} subcarrier to user ranges in between $k=1$ to K only once.

Constraint 4:

$$\sum_{k=1}^{K}\sum_{n=1}^{N} c_{k,n}p_{k,n} \leq P_{total}$$

Fourth constraint tells to algorithm that sum of the product of subcarriers allotted to user ranges in between 1 to K and power allotted to each user's allotted subcarriers should be less than or equal to total available power. This constraint also called as power constraint.

Constraint 5:

$$\frac{R_i}{R_j} = \frac{\Phi_i}{\Phi_j}, \text{ for all values of } i.$$

and $j \in \{1,2,3,....,K\}$

$i \neq j$ for $k=1,2,3,...,K$.

where R is the data rate for the user and Φ is proportionality constants only one thing should keep in mind that sum of proportionality constant for users in the range 1 to K should be equal to one. It is simply like a probability for different codes which we want to transmit, sum of probability of all available codes is equal to 1.

Total data rate (R_k) for k^{th} user given as

$$R_k = \frac{B}{N}\sum_{n=1}^{N} c_{k,n}r_{k,n} \qquad (3)$$

III. PROPOSED ALGORITHM

We utilize a combination of the approaches in [7,8,9] to develop the nature of the problem also we are trying to reduce complexity while preserving performance of the system. Following are the steps of proposed algorithm.

a. Calculate number of subcarriers N_k assigned to each user.
b. Assign subcarriers to each user to achieve proportionality.
c. Assign total power P_k to each user maintaining proportionality.
d. Assign $p_{k,n}$ for each users subcarriers subjected to P_k constraints.

In proposed algorithm proportionality constraints are used to differentiate different services so that service provider can give priority to specific users based on different billing methods.

In proposed algorithm proportionality constraints are used to differentiate different services so that service provider can give priority to specific users based on different billing methods. Assuming a flat transmit power over the entire bandwidth, each subcarrier adds fraction of total power equal to P_{tot}/N. Proposed algorithm aims to maximize throughput per user with lesser complexity. Instead of prioritizing the user with lesser throughput the user with highest data rate to achieve is giving priority to choose available subcarrier. Above a to g steps can be represented mathematically as follows.

Step 1:

To satisfy proportionality constraints subcarriers assigned to each user should approximately same as data rates after power allocation.

$N_1:N_2:\text{-----}:N_K=\Phi_1:\Phi_2:\text{-----}\Phi_K$.

$N_k=[\Phi_k N]$

This may lead to $N_{\text{var}} = N - \sum_{k=1}^{K} N_k$, where N_{var} means unallocated subcarriers. Second step takes care of how N_k subcarriers for k^{th} user and N_{var} subcarriers.

Step 2: Initialization

$c_{k,n}=0$, for all the values of $k \in \{1,...,K\}$ and for all values of $n \in \{1,...,N\}$.

$R_k=0$, for all values of $k \epsilon \{1,...,K\}$
$P=P_{tot}/N^2$.
Set of Number of Subcarriers $(N_{set})=\{1,2,...,N\}$

Step 3: Running Iterations from $k=1$ to K.
Sort $H_{k,n}$ in ascending order
$n=arg\ max_{\ n \epsilon Nvar1} | H_{k,n} |$
$c_{k,n}=1$
$N_k=N_k-1$, $N_{set}=N_{set}/\{n\}$

$$R_k = R_k + \frac{B}{N}\log_2(1+pH_{k,n}) \qquad (4)$$

Step 4: Define Data Rate and calculation of unallocated subcarriers.
In for loop's condition check for $||\ Nset\ || > Nvar$.
$K_{set}=\{1,2,...K\}$
$k=arg\ min\ k \epsilon K_{set} R_k/ \Phi_K$.
$n=arg\ max\ n \epsilon N_{set} |Hk,n|$
if $N_k > 0$
$c_{k,n}=1$
$N_k=N_k-1$, $N_{set}=N_{set}/\{n\}$

$$R_k = R_k + \frac{B}{N}\log_2(1+pH_{k,n})$$

else
$K_{set}=K_{set}/\{k\}$

Step 5: Allocate remaining subcarriers.
$K_{set}=\{1,2,...K\}$
for $n=1$ to N_{var}
$k=arg\ max_{\ k \epsilon Kset} |H_{k,n}|$
$c_{k,n}=1$

$$R_k = R_k + \frac{B}{N}\log_2(1+pH_{k,n})$$

$K_{set}=K_{set}/\{k\}$
For power allocation among users we use same as in [10,11]. Waterfilling across the subcarriers is been performed. The flowchart of the proposed algorithm is shown in Fig. 2. Above steps number 1 to 5 explained in easy way using flowchart.

IV. Simulation Results

The frequency selective multipath channel is modeled of six Rayleigh multipaths. Doppler frequency of 50Hz is assumed with delay spread of channel 5µs. The total power was assumed to be 1W and total bandwidth as 1MHz. Rest of the parameters are already been mentioned in section II.

As shown in the Fig. 3., the channel gains of User 1, have a less amount of channel gain from 0.55 to 0.66 i.e. 0.11 while for User 2 channel gains varies from 0.15 to 0.33 i.e. 0.18 for first two subchannels. This information is shown in following TABLE II. This is due to multiuser diversity as each user experiences different channel fading. However, how different users undergo fading could be measured by their channel gain variance as shown in TABLE II.

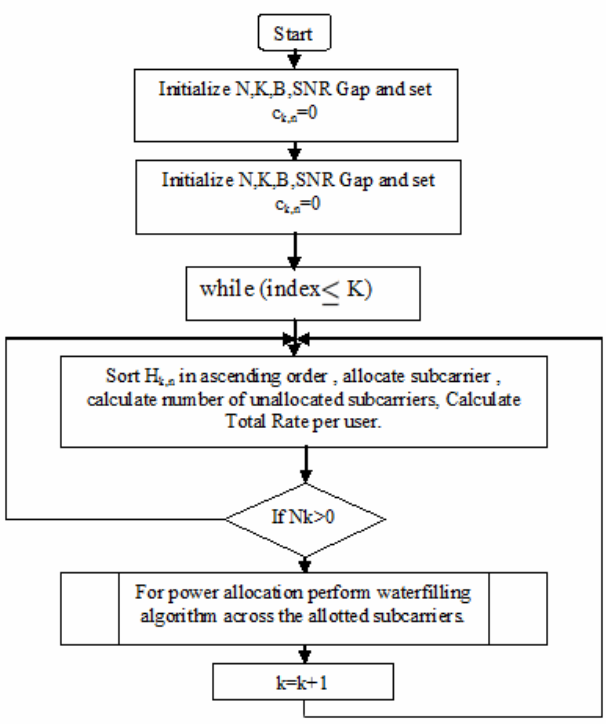


Fig. 2. Flow chart for the simulated model

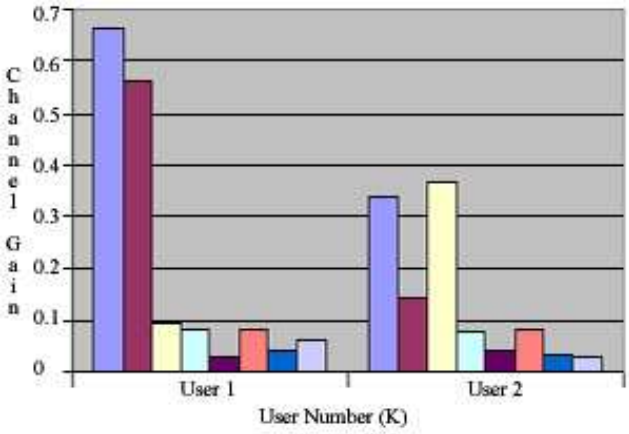


Fig. 3 Channel with only two users with eight subchannels.

TABLE II. The channel characteristics of a two user system shown in Fig. 3.

User Index	1	2
Minimum channel gain	0.55	0.15
Maximum channel gain	0.66	0.33
Variance	0.11	0.18

Fig. 4 shows the normalized proportions of the normalized rate for each user averaged over 100 channel samples. The normalized capacities are given by $R/\sum_{k=1}^{16} R_k$ and observed for both proposed algorithm and

ROOT-FINDING algorithm. This result is compared to the normalized proportional constraints $\{\phi_k\}_{k=1}^{16}$. It is been observed that proportionality among the users for the proposed method is no longer being strictly enforced as compared to ROOT-FINDING.

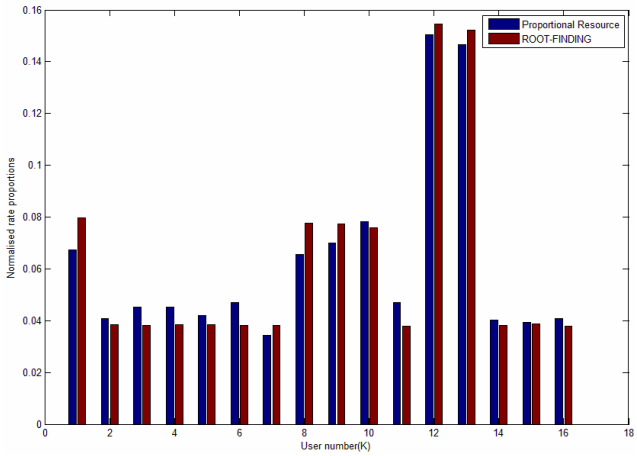


Fig.4 Normalized capacity ratios per user for SNR=30dB, K=16 and BER=10-3.

Fig. 5. show the comparison of total capacities between the proposed method and ROOT-FINDING. As the number of users increases capacities increases. This is the effect of multiuser diversity gain, which is outstanding in systems with bigger number of users. The proposed algorithm has a consistently higher total capacity than the ROOT-FINDING method for all the numbers of users for this set of simulation parameters. Normalized capacity ratios per user for 16 users averaged over 100 channels, proportions Φ_k taken as input for both algorithms for each user. The proposed algorithm has minimal deviation from the required proportions, but ROOT-FINDING stick on to it much better. Proposed algorithm achieves the best performance for the most underserved user, with a slight gain for optimal power allocation over its allocated subcarriers relative to an equal-power allocation. Also proposed algorithm results in a starved worst-case user; in fact , it is typical for several users to receive no resources at all for substantial periods.

TABLE III. SUMMARY OF PERFORMANCE COMPARISON

Performance Criterion	Proposed Algorithm	ROOT-FINDING
Subcarrier Allocation Complexity	*O(KNlog2N)*	*O(KNlog2N)*
Power Allocation Complexity	*O(K)*	*O(nK),n≈9*
Achieved Capacity	High	Low
Adherence probability	Slack	Stretched
Assumption on subchannel SNR	None	Required

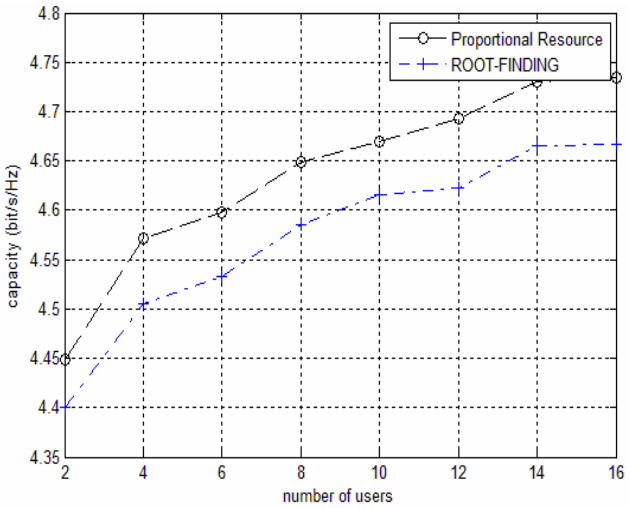


Fig. 5 Users average capacity versus number of users. There are 64 subcarriers and BER=10^{-3}.

V. CONCLUSION AND FUTURE SCOPE

The problem of multiuser downlink resource allocation in Mobile WiMAX system was studied. Simulation results show that information fed back and association among subcarriers play vital role to improve system performance. A reduced complexity resource allocation was proposed and seems especially attractive as the number of users increases. It is observed through simulation that the proposed method performs better than previous method in terms of significantly decreasing the computational complexity and achieve higher capacities, while being applicable to a more general class of systems. As a possible future work, our algorithm , could be tested using Fuzzy logic and Genetic algorithms. The fairness issue for the different user in the same service class is another topic in our research schema. The effects of imperfect channel state information due to estimation error and feedback latency are also comes under future study.

REFERENCES

[1] Bo Rong, Yi Qian and Kejie Lu, "Integrated Downlink Resource Management for Multiservice WiMAX Networks", IEEE Transactions On Mobile Computing, VOL.6 , NO.6, JUNE 2007.

[2] Dusit Niyato and Ekram Hossain, "Radio Resource Management Games In Wireless Networks: An Approach to Bandwidth Allocation and Admission Control for Polling Service in IEEE 802.16", IEEE Wireless Communications, February 2007.

[3] Leonardo Badia, Andrea Baiocchi ,Simone Merlin, Silvano Pupolin, Andra Zanella and Michele Zorzi, "On The Impact of Physical Layer Awareness on Scheduling and Resource Allocation in Broadband Multicellular IEEE 802.16 Systems", IEEE Wireless Communication, February 2007.

[4] Bo Rong and Yi Qian, "Adaptive Power Allocation and Call Admission Control in Multiservice WiMAX Access Networks", IEEE Wireless Communications, February 2007.

[5] Syed Hussain Ali, Ki-Dong Lee and Victor C.M. Leung, "Dynamic Resource Allocation in OFDMA Wireless Metropolitan Area Networks", IEEE Wireless Communications, February 2007.

[6] Sanam Sadr, Alagan Anpalagan and Kaamran Raahemifar, "Suboptimal Rate Adaptive Resource Allocation for Downlink OFDMA Systems", Hindawi Publishing Corporation, International Journal of Vehicular Technology, Volume 2009.

[7] Mo-Han Fond, Robert Novak, Sean McBeath and Roshni Srinivasan, "Improved VoIP Capacity in Mobile WiMAX Systems Using Persistent Resource Allocation", IEEE Communications Magazine, October 2008.

[8] Spyros Xergias, Nikos Passas and Apostolis K. Salkintzis, "Centralized Resource Allocation for Multimedia Traffic in IEEE 802.16 Mesh Networks", Proceedings of the IEEE, Vol. 96, No.1 , January 2008.

[9] Fen Hou, James She, Pin-Han Ho and Xuemin Shen, "A Flexible Resource Allocation and Scheduling Framework for Non-real-time Polling Service in IEEE 802.16 Networks" , IEEE Transactions On Wireless Communications, VOL. 8, NO. 2, FEBRUARY 2009.

[10] Jianwei Huang, Vijay G. Subramanian, Rajeev Agrawal and Randall A. Berry, "Downlink Scheduling and Resource Allocation for OFDM Systems.", IEEE Transactions On Wireless Communications, VOL. 8, NO. 1, JANUARY 2009.

[11] Nassar Ksairi and Walid Hachem, "Resource Allocation for Downlink Cellular OFDMA Systems-Part I: Optimal Allocation", IEEE Transactions on Signal Processing, Vol. 58, No. 2, February 2010.

Study of Mobility Effect on Energy Efficiency in Medium Access Control Protocols

Mahdi Zareei[1*], Rahmat Budiarto[2], Tat-Chee Wan[3]
[1*]mza09_sa0008@student.usm.my, ([2]rahmat, [3]tcwan)@cs.usm.my
School of Computer Sciences
Universiti Sains Malaysia

Abstract- **Wireless sensor networks (WSN) became popular in recent years, with big variety of applications from environmental monitoring to disaster recovery. Energy efficiency is a key characteristic of todays wireless sensors. In energy constraint sensor network, mobility handling can cause some additional challenges in sensor protocol design. Recently there are many MAC protocols have been proposed and adopted specially for sensor networks. Most of the proposed MAC protocols in wireless sensor network assumed nodes to be static. However some application like medical care and disaster response make use of mobile sensors essential. In this paper, we take closer look at S-MAC, T-MAC (which are well-known energy efficient MAC protocols) and IEEE 802.15.4 (which is the ZigBee standard) MAC protocols and studies their performance in terms of energy efficiency in different situation of mobility.**

I. INTRODUCTION

Wireless sensors are compact-size, low power, inexpensive devices which are capable to measure local environmental conditions or other parameters such as temperature, acceleration, lighting level, humidity, pressure, movement, etc. and forward such information to a sink for proper processing. Wireless sensor networks (WSNs) are already being used in academic pilot projects and commercial projects alike. WSNs have a wide range of applications such as environmental monitoring [1], biomedical research [2], human imaging and tracking [3], and habit monitoring [4].

Implementations of the applications introduced above impose some requirements to the network. Such as Implementation price, Limited range of wireless sensor nodes, Network lifetime. All these requirements depend on energy efficiency directly. For example by decreasing power consumption of communication between nodes, we can increase network lifetime. Due to this implementation cost is reduced and we can deploy our network densely to cover all our areas. So energy efficiency is a key characteristic of WSNs.

The need for energy efficient operation and energy constraints of sensor nodes has driven lots of research on sensor networks. Assumed that the transceiver is the most power consuming component of a typical sensor node, then large advantageous could achieve at the link layer where the medium access control (MAC) protocol is controlling the usage of the radio unit.

In this paper, we take closer look at S-MAC, T-MAC (which are well-known energy efficient MAC protocols) and IEEE 802.15.4 (which is the ZigBee standard) MAC protocols and studies their performance in terms of energy efficiency in different situation of mobility.

The rest of paper organized as follows. In Section 2, we describe the MAC layer and reviewing the S-MAC, T-MAC and IEEE 802.15.4 MAC protocols as well. Simulation scenario and results are discussed and analyzed in Section 3. Finally we summarize the conclusion in section 4.

II. MAC PROTOCOLS

By their nature wireless sensor network have to communicate. Therefore node communication device has to be carefully managed to allow efficient and effective communication. For wireless communication each node needs to have radio device and transfers data between adjacent network nodes, which is part of data link-layer work.

An important part of the data link layer is the medium access control (MAC) protocol. This protocol defines when nodes are allowed to transmit packets and when they are allowed to receive. One of the major tasks of the MAC protocol is to avoid collision from interfering nodes. So MAC protocol has tight control over energy efficiency, delay, mobility, and other metrics of the network [5].

Sensor network is different from traditional wireless network in many points. First of all, nodes in sensor networks are battery powered, and mostly it is difficult to change batteries for all nodes. Second, nodes in wireless sensor network often deployed in ad-hoc manner and they organize themselves into communication powered network rather than with careful pre-planning similarly used in traditional wireless network. Third, in some cases nodes are not stationary. And finally, most traffic in the network is triggered by sensing events. All of these characteristics make that traditional MAC protocols are not suitable for wireless sensor networks.

There are many MAC protocols have been developed for traditional wireless network such as Time division multiple access (TDMA), frequency division multiple access (FDMA), and code division multiple access (CDMA), which are widely used in modern cellular communication system. Although researchers have done some steps in implementing the MAC protocols for sensor networks but most of them assumed sensor nodes are static. In the rest of this part we discussed some well-known MAC protocols.

A. S-MAC

S-MAC [6] is one of the well-known energy efficient MAC protocols which specially designed for sensor network. S-MAC is a contention-based protocol based on IEEE 802.11. The main idea behind S-MAC is adopt a periodic listen-sleep cycle to reduce idle listening time, thus extending battery life

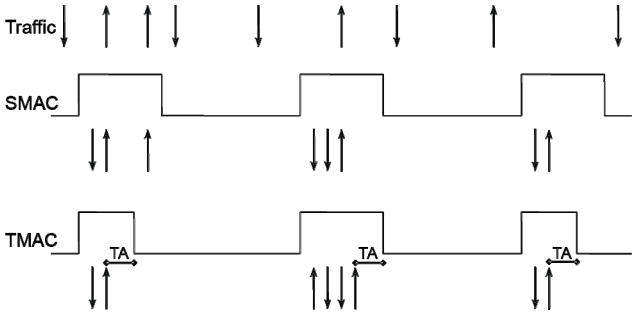


Fig 1. Comparing S-MAC and T-MAC protocols

time for sensor nodes. In S-MAC approach, each node sleep for some time, during sleep time, the node turn off its radio and set the timer to awake itself later. When the timer fired node wake up and listen to see if any other node wants to talk to it.

All nodes are free to choose their own listen/sleep schedule. However to reduce control overhead S-MAC divided nodes in different virtual cluster. Neighboring nodes from each virtual cluster set up a common sleep schedule. Bordering nodes can follow both schedules of overlapping virtual cluster, so it can bridge communication between different virtual clusters. The drawback of this method is that these bordering nodes consume more energy since they have less time to sleep. Also it is possible when two nodes follow completely different schedules they miss each other for ever. To solve this problem S-MAC introduce periodic neighbor discovery, so each node periodically listen to the whole synchronization period.

The channel access time in S-MAC divided into periods of fixed duration T consisting sleep mode (radio-off) and active mode (radio-on). In active mode (listen periods) nodes exchange SYNC packets to informs neighbors of its schedule (the time to the next activation periods) to avoid collision. These periods called synchronization periods. For collision avoidance SYNC message are preceded by carrier sense contention.

The SYNC packet is very short and includes the address of the sender and the time of its next sleep. In order for a node to receive both data and SYNC packets in listen interval, S-MAC divided listen period into two parts, first is for SYNC and the second is for data packet. Also RTS/CTS and ACK packets exchanges are used for data transfer to avoid collision.

B. T-MAC

Fixed duty cycle in S-MAC drives some problem for adaptation to the variation of network environment and it cause high latency and lower throughput in some cases. To this end, T. Van Dam and K. Langendoen at year 2003 [7] propose an enhanced version of S-MAC called Timeout MAC (T-MAC). T-MAC enhances S-MAC by introducing adaptive duty cycle feature. Figure 1 shows the difference between S-MAC and T-MAC.

T-MAC propose dynamically determine the length of active time under variable load, to reduce idle listening by transmitting all messages in burst and put the node in sleep

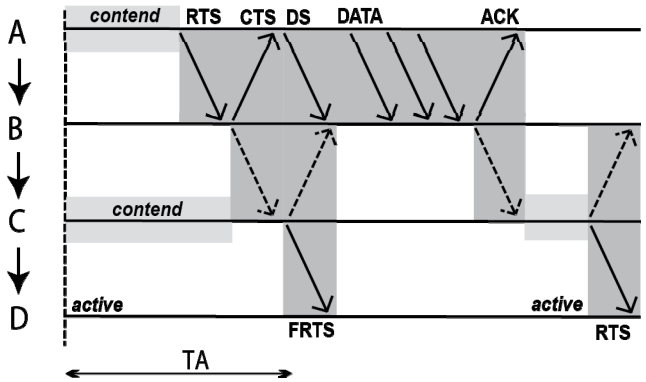


Fig. 2. The future-request-to-sent packet scheme (source [7])

mode when no activation event has occurred for a time threshold *TA*. This time-out value, *TA*, is set to span a small contention period and an RTS/CTS exchange. If a node does not detect any activity (an incoming message or a collision) within interval *TA* it can assume that no neighbor wants to communicate with it and goes to sleep. On the other hand, if the node engages or overhears a communication, it simply starts a new time-out after that communication finishes.

The adaptive duty-cycle allows T-MAC to adjust to fluctuations in network traffic. S-MAC, on the other hand, operates with a single active-time for all nodes, which must be chosen conservatively to handle worst-case traffic. The most important drawback of T-MAC is aggressive power-down policy, because of that that nodes often go to sleep too early, namely called *early sleeping problem* as a node goes to sleep when a neighbor still carry on the messages for it.

The T-MAC propose future-request-to-send (FRTS) packet to solve this problem. The idea is to let another node know that there are still messages to read. T-MAC works as follow: if a node overhears a CTS packet destined for another node, it may immediately send a FRTS, like node C in Figure 2. The FRTS packet contains the length of the blocking data communication (this information was in the CTS packet). A node must not send an FRTS packet if it senses communication right after the CTS, or if it is prohibited from sending due to a prior RTS or CTS.

C. IEEE 802.15.4 Slotted CSMA/CA MAC

IEEE 802.15.4 standard [8] for low rate wireless personal area networks (WPAN) is considered as one of the standards for wireless sensor networks, since it supports small, cheap, energy-efficient devices operating on battery power sensors. This protocol shows great potential to adopt different requirement of WSN applications. Figure 3 shows the Structure of IEEE 802.15.4 protocol stack.

In IEEE 802.15.4 standard MAC layer defines two types of nodes: Reduced Function Devices (RFDs) and Full Function Devices (FFDs). FFDs are equipped with a full functionality of MAC layer, so they can operate as a network coordinator, a link coordinator or as just another communications device.

An FFD can talk to other FFDs and RFDs. FFDs discover other FFDs and RFDs to establish communications. Nevertheless RFDs can only act as end-devices and are

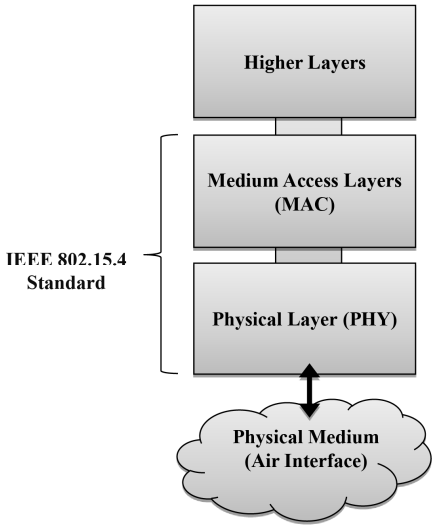


Fig 3. Structure of IEEE 802.15.4 protocol stack

equipped with such as a light switch or a passive infrared sensor.

An IEEE 802.15.4 network requires at least one FFD to act as a network coordinator and provide synchronization services to other devices or other coordinators. After an FFD (which may have greater computational resources) is activated for the first time, it may establish its own network and become the PAN coordinator.

IEEE 802.15.4 operates in two beacon-enabled networks and non-beacon networks modes. In a non-beacon-enable network, device simply transmits its data using unslotted CSMA/CA, while in beacon-enable network devices use the slotted CSMA/CA as a MAC to synchronize to the superframe structure and contend for the usage of channels. In a beacon-enable network, the coordinator indicates in the beacon that the data is pending. The device periodically listens to the beacon and transmits a MAC command request using slotted CSMA/CA if necessary.

III. SIMULATION ENVIRONMENT

We performed simulation to compare performance of S-MAC, T-MAC and IEEE 802.15.4 CSMA/CA MAC. Castalia [9] has been used in this experiment. Castalia simulator mainly developed on OMNET++ [10] to support sensor network simulations. 300×300 m^2 field consisting of 60 nodes which uniformly placed over the field has been set up. Each cycle of simulation runs for 300 seconds and results are averaged over 10 simulation runs with different random seeds. CC2420 [11] employed as a RF transceiver with power consumption 62 mW in receive, 62 mW in transmit and 1.4 mW in sleep mode. Data rate set to 250 kbps.

We study protocols performance with a different ratio of mobility in the network and with varies speed. The performance of protocols in terms of energy efficiency has been evaluated in different situation. The effect of node mobility on the performance of the discussed protocols shown

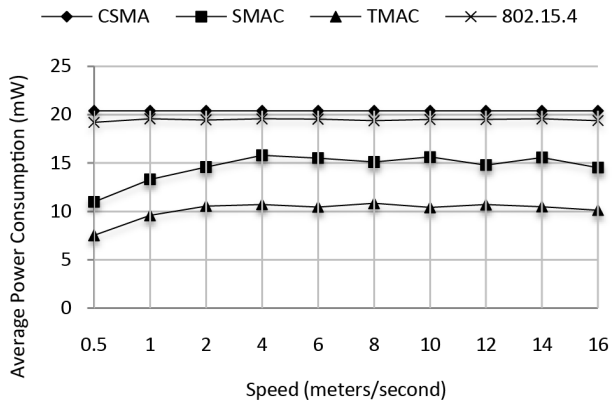


Fig. 4. Average power consumption (all nodes are mobile, the sink is stationary)

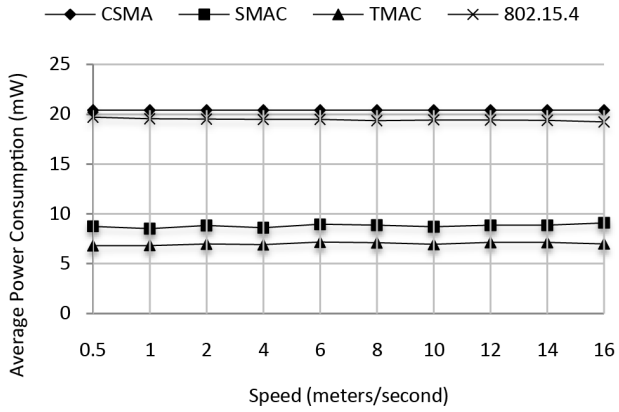


Fig. 5. Average power consumption (all nodes are stationary, the sink is mobile)

in Figures 4, 5 and 6. In the first scenario, we assume the sink in the middle of our simulation field and set it as a static node, and the rest of the nodes distributed uniformly in the field with mobility option. Figure 4 plotted the average power consumption versus mobility speed while we increase the speed of nodes from 0.5 to 16.

The CSMA MAC sets as a comparison point, in order to compare the performance of other protocols. As we expect CSMA has highest power consumption among studied protocols. Meanwhile it does not use any energy conservation scheme and the radio of node is always on, thus mobility does not have any impact on power consumption of CSMA protocol. IEEE 802.15.4 to some extent has similar performance with CSMA, even though IEEE 802.15.4 uses Carrier Sense Multiple Access with Collision Avoidance (CSMA/CA) it could conserve more energy than CSMA, although power consumption still higher than S-MAC and T-MAC. T-MAC shows the lowest power consumption among protocols. Meanwhile it uses dynamic duty cycle it can adopt better with mobility in the network. Besides, T-MAC uses some extra power conservation than S-MAC. S-MAC and

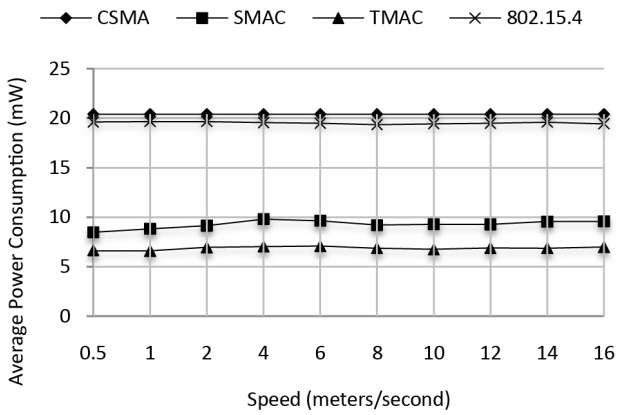


Fig. 6. Average power consumption (20% of nodes are mobile, the sink is stationary)

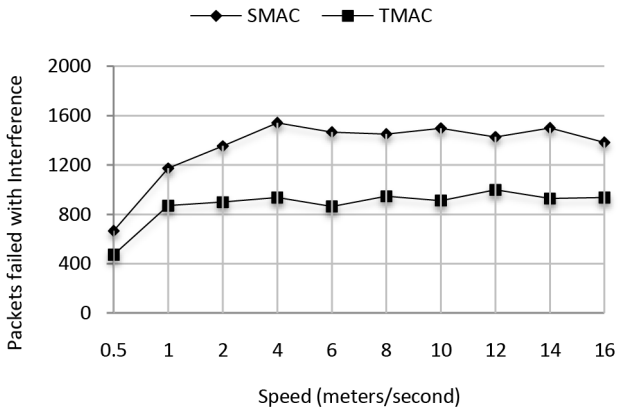


Fig. 7. Average packets failed with interference versus speed.

T-MAC were shown highest power consumption when node speed is 4 m/s. Since in this scenario all nodes are moving, we believe increasing speed after 4 m/s do not have more impact on protocols while protocols cannot handle this highly dynamic network.

Figure 5 shows the result of our second scenario while we have Stationary nodes with a mobile sink. In this case we assume nodes are stationary, deployed uniformly in the field, and single sink is moving among them. In this scenario again T-MAC performs better than S-MAC although the difference is not too much like in the first scenario. However all nodes are stationary and just sink is moving so increasing the speed do not have visible impact on the power consumption. IEEE 802.15.4 and CSMA revealed the same result as the first experiment. We already mentioned that IEEE 802.15.4 and CSMA do not have any energy conservation mechanism, the energy consumption do not change noticeably in mobility.

Figure 6 illustrates the result of the third scenario, when 20% of nodes are mobile with randomly distribution, and the sink is set in the center of the virtual field. It is shown that with increasing the speed of nodes, power consumption of S-MAC increase slightly while for T-MAC we have almost flat line and it is because with using dynamic duty-cycle T-MAC has better adoption with network conditions. In this scenario for both S-MAC and T-MAC fluctuation of power consumption is negligible since just 20% of nodes are mobile. Mobility increases the contention between interfering nodes, thus it causes more packet drop. Nodes try to retransmit the packet and it is the reason for more energy consumption.

Figure 7 shows the average packets failed with interference in the network when all nodes are mobile and sink set to be stationary in the center of the field (scenario 1). It shows the sharp increase in terms of packet failed during the rises in speed value from 0.5 to 4 meters per second. Here also T-MAC shows quite better performance than S-MAC. As we already mentioned in T-MAC section adaptive duty-cycle allows T-MAC to adjust better to fluctuations in network traffic as compare to S-MAC.

In this paper we just consider power consumption to compare the protocols. The simulation results show that protocols face performance degradation while network topology change. We believe that more research need to justify the impact of mobility on the performance of MAC protocols by considering more parameters such as packet delivery ratio, delay as well as power consumption.

IV. CONCLUSIONS

This paper has presented an overview of the three popular MAC protocols, S-MAC, T-MAC and IEEE 802.15.4 Slotted CSMA/CA MAC along with comparing their performance in terms of power consumption in different mobility situations. From the simulation result we can conclude T-MAC shows better performance among other studied protocols. Using adaptive duty-cycle allows T-MAC to adjust the fluctuations in the network much better than IEEE 802.15.4 Slotted CSMA/CA and S-MAC. The results indicate that, energy consumption increases with the mobility in the network and also number of mobile nodes. As mobility increases the chance of contention rises, nodes need more retransmission and energy consumption increases accordingly.

ACKNOWLEDGMENT

This research has been partially supported by the computer science school under Grant number: 1001/PKOMP/817047.

REFERENCES

[1] F. Stann and J. Heidemann, "RMST: Reliable data transport in sensor networks," in Proceedings of the First International Workshop on Sensor Net Protocols and Applications, 2003, pp. 102-112.

[2] L. Schwiebert, et al., "Research challenges in wireless networks of biomedical sensors," in Proceedings of the 7th annual international conference on Mobile computing and networking, 2001, pp. 151-165.

[3] S. D. Feller, et al., "Tracking and imaging humans on heterogeneous infrared sensor arrays for law enforcement applications," Fitzpatrick Center for Photonics and Communication Systems and Department of Electrical and Computer Engineering, Duke University, Durham, NC, vol. 27708, 2002.

[4] A. Mainwaring, et al., "Wireless sensor networks for habitat monitoring," in Proceedings of the 1st ACM international workshop on Wireless sensor networks and applications, 2002, pp. 88-97.
[5] I. Demirkol, et al., "MAC protocols for wireless sensor networks: a survey," Communications Magazine, IEEE, vol. 44, pp. 115-121, 2006.
[6] W. Ye, et al., "Medium access control with coordinated adaptive sleeping for wireless sensor networks," IEEE/ACM Transactions on Networking (ToN), vol. 12, p. 506, 2004.
[7] T. Van Dam and K. Langendoen, "An adaptive energy-efficient MAC protocol for wireless sensor networks," 2003, pp. 171-180.
[8] IEEE. (2003). IEEE 802.15.4 standard. Available: http://standards.ieee.org/getieee802/download/802.15.4-2003.pdf
[9] OpenNICTA. Castalia Simulator. Available: http://castalia.npc.nicta.com.au/
[10] Omnet++ web page. Available: http://www.omnetpp.org/
[11] A. Chipcon, "CC2420 2.4 GHz IEEE 802.15. 4/ZigBee-ready RF Transceiver," Chipcon AS, Oslo, Norway, vol. 4, 2004.

Performance of Alamouti Coded MIMO Systems with Switch and Examine Combining

Gourab Maiti and Aniruddha Chandra
Department of Electronics and Communication Engineering
National Institute of Technology, Durgapur, India
{gourab_maiti@sify.com, aniruddha.chandra@ieee.org}

Abstract—**In this paper, we have considered a 2 x *L* multiple input multiple output (MIMO) system employing Alamouti coding at transmitter and switch and examine combining (SEC) at receiver. At first, analytical expressions for capacity and outage probability, in Rayleigh fading channel, are found. Next, the symbol error rate (SER) for *M*-ary phase shift keying (MPSK) modulation is calculated. The derived expressions are in closed-form and conform to the simulation results. For more than two (*L* > 2) receiver antennas, SEC performs significantly better than the traditional switch and stay combining (SSC).**

Keywords—**Alamouti code; switched combining; capacity; outage probability; Rayleigh fading; MPSK; SER**

I. INTRODUCTION

Major 4G wireless standards, like WiMax and LTE, have already adopted the MIMO capability as an integral part of their air interface specifications [1]. Use of multiple antennas at transmitter (Tx) and receiver (Rx) results in additional diversity/ multiplexing/ array gain, enhanced channel capacity, and fewer errors during transmission. A simple MIMO configuration, with 2 Tx antennas, may be realized through Alamouti coding [2]. On the other hand, at the receiver side, traditional combining schemes may be used to realize diversity.

Recently there has been an upsurge of literature concerning performance analysis of Alamouti coded MIMO systems with some sort of receiver diversity [3-8]. Although many variants of receiver diversity combining algorithms exist, the authors in these papers focused largely on maximal ratio combining (MRC) or selection combining (SC). In an earlier paper [9], we have evaluated the error performance of a 2 x *L* MIMO system equipped with SEC, instead of MRC or SC. However, error rates for only binary phase shift keying (BPSK) modulation were provided. The current text is a direct extension of our previous work in that the framework for error probability analysis now covers MPSK as well. In addition, expressions for capacity and outage probability are also derived.

The remainder of this paper is organized as follows. The system model under study is presented in Section II followed by expressions for probability density function (PDF) and cumulative distribution function (CDF) of the instantaneous signal-to-noise ratio (SNR) at each branch of the receiver. Next, using the model in Section II, analysis of capacity, outage probability, and SER for MPSK are described in Section III, IV, and V respectively. The paper finally ends with some concluding remarks in Section VI.

II. SYSTEM MODEL AND NOTATIONS

The system model with 2 Tx and L Rx antennas is shown in Fig. 1. Let s_1 and s_2 denote the equivalent baseband signals corresponding to two successive information bits which are sent using a 2×1 Alamouti code [2]. For a slow fading channel it may be assumed that the channel transfer function remains constant over two consecutive bit intervals, and accordingly the received signals on nth branch in these two intervals can be expressed as

$$r_{1n} = h_{1n}s_1 + h_{2n}s_2 + n_{1n} \tag{1a}$$

$$r_{2n} = -h_{1n}s_2^* + h_{2n}s_1^* + n_{2n} \tag{1b}$$

where $\{s_1^*, s_2^*\}$ are the complex conjugates of $\{s_1, s_2\}$, $h_{mn} = \alpha_{mn}\exp(j\theta_{mn})$; $m \in \{1,2\}, n \in \{1,2,\cdots,L\}$ is the complex channel gain between the mth Tx antenna and the nth Rx antenna with α and θ being the random amplitude and phase variations respectively, and the additive noise n_{mn} is a zero-mean circularly symmetric complex Gaussian random variable (RV) having a variance N_0.

At the receiver, the space time (ST) combiners attached to each branch process the signal to produce an output pair $\{y_{1n}, y_{2n}\}$ given by

$$y_{1n} = \hat{h}_{1n}^* r_{1n} + \hat{h}_{2n} r_{2n}^* \tag{2a}$$

$$y_{2n} = -\hat{h}_{1n} r_{2n}^* + \hat{h}_{2n}^* r_{1n} \tag{2b}$$

where $\hat{h}_{mn}$ is an estimate of h_{mn}. If the channel estimator produces perfect channel state information (CSI), it can be shown that

$$y_{mn} = \left(\alpha_{1n}^2 + \alpha_{2n}^2\right)s_m + w_{mn} \quad ; \quad m \in \{1,2\} \tag{3}$$

by substituting (1) in (2) and using the definition of h_{mn}. As the RV w_{mn} has a variance of $2N_0$, the instantaneous SNR available at the ST combiner output would be

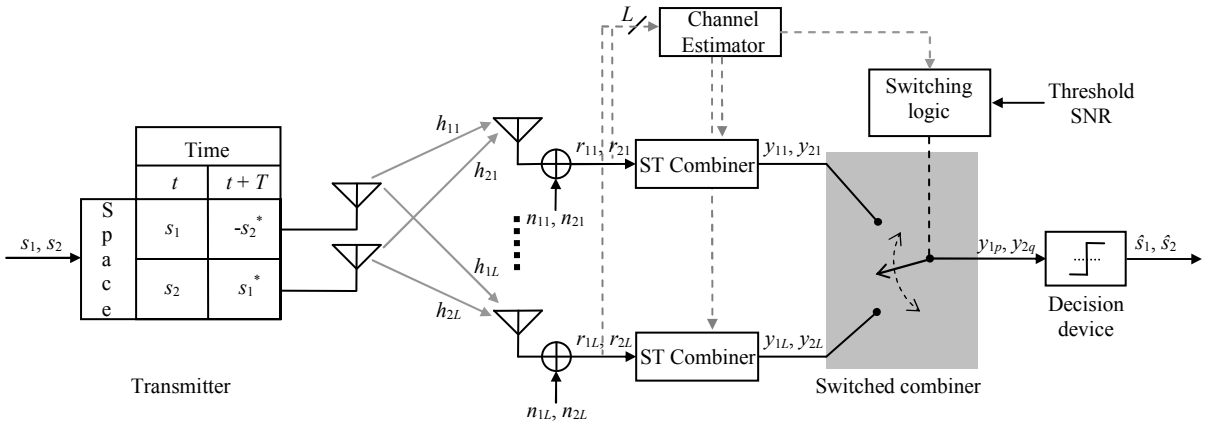


Figure 1. Transmission model of a 2×*L* MIMO system employing Alamouti code at transmitter and pre-detection switch and examine combining at receiver.

$$\gamma_n = \frac{\eta}{2}\left(\alpha_{1n}^2 + \alpha_{2n}^2\right) \;\; ; \;\; n \in \{1,2,\cdots,L\} \tag{4}$$

where, $\eta = (E/N_0)$ is the SNR in additive white Gaussian noise (AWGN) channel and E is the symbol energy. For a Rayleigh fading channel, the distribution of $\{\alpha\}_{m=1,n=1}^{2,L}$ is [10]

$$f_\alpha(\alpha) = \frac{2\alpha}{\Omega}\exp\left(-\frac{\alpha^2}{\Omega}\right) \;\; ; \;\; E\{\alpha^2\} = \Omega, \;\; \alpha \geq 0 \tag{5}$$

Accordingly, the PDF of γ_n will follow a central chi-square distribution with four degrees of freedom

$$f_\gamma(\gamma_n) = \frac{4\gamma_n}{\bar{\gamma}_n^2}\exp\left(-\frac{2\gamma_n}{\bar{\gamma}_n}\right) \;\; ; \;\; E\{\gamma_n\} = \bar{\gamma}_n, \;\; \gamma_n \geq 0 \tag{6}$$

and the corresponding CDF would be

$$F_\gamma(\gamma_n) = 1 - \left(1 + \frac{2\gamma_n}{\bar{\gamma}_n}\right)\exp\left(-\frac{2\gamma_n}{\bar{\gamma}_n}\right) \;\; ; \;\; \gamma_n \geq 0 \tag{7}$$

which can be derived by expressing the CDF, $F_\gamma(x) = \int_0^x f_\gamma(\gamma_n)d\gamma_n$, with an incomplete gamma function [11, (8.350.1)], and further reducing the same with [11, (8.352.1)].

For SEC, the diversity combiner operates in discrete time fashion, i.e. the branch switching occurs at time $t = uT$, where u is any integer. As the ST combiners give out the pair $\{y_{1n}, y_{2n}\}$ after every $2T$ amount of time, a parallel to serial conversion (not shown in Fig. 1) is necessary before the output can be fed to the combiner. The channel estimator estimates the current SNR in different branches at every $t = uT$. Using the information, the switching logic block triggers the selector to switch from the current branch to the next branch if SNR in current branch falls below some threshold value (generally found from a table that stores the optimum thresholds for different SNR).

Let us assume that the pth and qth branches are selected during the two signalling intervals of interest. The output of the combiner $\{y_{1p}, y_{2q}\}$ is then hard-decoded

$$\{\hat{s}_1, \hat{s}_2\} = \sqrt{E}\,\mathrm{sgn}\left(\Re\{y_{1p}, y_{2q}\}\right) \tag{8}$$

to produce an estimate of the original signal pair $\{s_1, s_2\}$.

III. Analysis of Capacity

It is well known that the capacity for an AWGN channel is given by Shannon's formula, $C(\eta) = B\log_2(1+\eta)$, where B is the signal bandwidth. In fading channel, however, the capacity, $C(\gamma) = B\log_2(1+\gamma)$, becomes a function of the instantaneous SNR. In order to find the average capacity for Alamouti coded MIMO system with SEC, we need to average $C(\gamma)$ over the PDF of the combiner output SNR, i.e.

$$C = \int_0^\infty C(\gamma) f_{\gamma,SEC}(\gamma)d\gamma \tag{9}$$

where, $f_{\gamma,SEC}(\gamma)$ is the PDF of γ at SEC output. Assuming independent and identically distributed (IID) fading, $f_{\gamma,SEC}(\gamma)$ can be expressed as [10, (9.341)]

$$f_{\gamma,SEC}(\gamma) = \begin{cases} f_\gamma(\gamma)\left[F_\gamma(\gamma_{th})\right]^{L-1} & ;\gamma < \gamma_{th} \\ f_\gamma(\gamma)\sum_{j=0}^{L-1}\left[F_\gamma(\gamma_{th})\right]^j & ;\gamma \geq \gamma_{th} \end{cases} \tag{10}$$

where, $f_\gamma(\gamma)$ and $F_\gamma(\gamma)$ are given by (6) and (7) respectively. Substituting the value of $C(\gamma)$ and $f_{\gamma,SEC}(\gamma)$ in (9) we get

$$\begin{aligned} C = {} & B\log_2 e\left\{\left[F_\gamma(\gamma_{th})\right]^{L-1} - \sum_{j=0}^{L-1}\left[F_\gamma(\gamma_{th})\right]^j\right\}\int_0^{\gamma_{th}}\omega(\gamma)d\gamma \\ & + B\log_2 e\sum_{j=0}^{L-1}\left[F_\gamma(\gamma_{th})\right]^j\int_0^\infty\omega(\gamma)d\gamma \end{aligned} \tag{11}$$

where, $\omega(\gamma) = \ln(1+\gamma)f(\gamma)$. The first integration may be readily solved through integration by parts

$$
\begin{aligned}
I_1 &= \frac{4}{\bar{\gamma}^2}\int_0^{\gamma_{th}} \ln(1+\gamma)\gamma\exp\left(\frac{-2\gamma}{\bar{\gamma}}\right) \\
&= 1-\left(\frac{2\gamma_{th}}{\bar{\gamma}}+1\right)\exp\left(-\frac{2\gamma_{th}}{\bar{\gamma}}\right)\ln(1+\gamma_{th}) \\
&\quad -\exp\left(-\frac{2\gamma_{th}}{\bar{\gamma}}\right)+\left(1-\frac{2}{\bar{\gamma}}\right)\exp\left(\frac{2}{\bar{\gamma}}\right)\times \\
&\quad \left[E_1\left(\frac{2}{\bar{\gamma}}\right)-E_1\left(\frac{2(1+\gamma_{th})}{\bar{\gamma}}\right)\right]
\end{aligned} \tag{12}
$$

where, $E_1(x)=\int_x^{\infty} t^{-1}\exp(-t)dt \;\; ; \; x>0$ is the exponential integral of first order [12, (5.1.1)].

To solve the second integral we make use of the following result [13]

$$
\begin{aligned}
&\frac{\mu}{(\lambda-1)!}\int_0^{\infty}\ln(1+x)(\mu x)^{\lambda-1}\exp(-\mu x)dx \\
&\qquad = P_{\lambda}(-\mu)E_1(\mu)+\sum_{q=1}^{\lambda-1}\frac{1}{q}P_q(\mu)P_{\lambda-q}(-\mu)
\end{aligned} \tag{13}
$$

where $P_q(x)=\sum_{v=0}^{q-1}\left(x^v/v!\right)\exp(-x)$ is the poission CDF. Thus, the second integral

$$
\begin{aligned}
I_2 &= \frac{4}{\bar{\gamma}^2}\int_0^{\infty}\ln(1+\gamma)\gamma\exp\left(-\frac{2\gamma}{\bar{\gamma}}\right)d\gamma \\
&= \left[P_2\left(-\frac{2}{\bar{\gamma}}\right)E_1\left(\frac{2}{\bar{\gamma}}\right)+P_1\left(\frac{2}{\bar{\gamma}}\right)P_1\left(-\frac{2}{\bar{\gamma}}\right)\right] \\
&= \left[\left(1-\frac{2}{\bar{\gamma}}\right)\exp\left(\frac{2}{\bar{\gamma}}\right)E_1\left(\frac{2}{\bar{\gamma}}\right)+1\right]
\end{aligned} \tag{14}
$$

Substituting (12) and (14) in (11) we get

$$
\begin{aligned}
C = B\log_2 e\left\{\left[F_{\gamma}(\gamma_{th})\right]^{L-1}-\sum_{j=0}^{L-1}\left[F_{\gamma}(\gamma_{th})\right]^j\right\}I_1 \\
+ B\log_2 e\sum_{j=0}^{L-1}\left[F_{\gamma}(\gamma_{th})\right]^j I_2
\end{aligned} \tag{15}
$$

Fig. 2 shows a plot of (15) for $\gamma_{th}=3$ dB, i.e. the capacity of an Alamouti based SEC MIMO system in Rayleigh fading channel for a fixed threshold. For, L = 2, SEC operation becomes identical with SSC system. Further, for larger values of L, the capacity increases only when average SNR $(\bar{\gamma})$ is close to the γ_{th} value.

In order to exploit the capacity advantage throughout the SNR axis, the combiner needs to operate with optimum switching threshold (γ_{th}^*) which may be found by differentiating (15) with respect to γ_{th}, and setting the result to zero, i.e. $\partial C/\partial\gamma_{th}\big|_{\gamma_{th}=\gamma_{th}^*}=0$. A closed-form expression for γ_{th}^* is, however, unattainable and numerical minimization technique was used to tabulate γ_{th}^* (shown in table I) for each value of average SNR $\bar{\gamma}$.

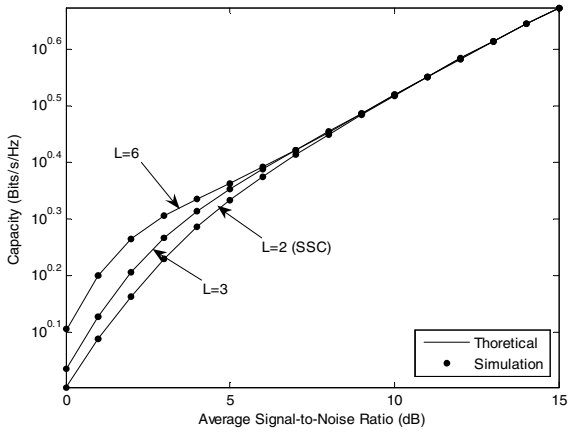


Figure 2. Capacity curves for Alamouti based SEC system with fixed threshold (γ_{th} = 3 dB) for different numbers of Rx antennas.

The corresponding plot of optimum capacity, for both theoretical and simulated values is given in Fig. 3. The results show that capacity values increase with additional Rx antennas throughout the whole SNR range.

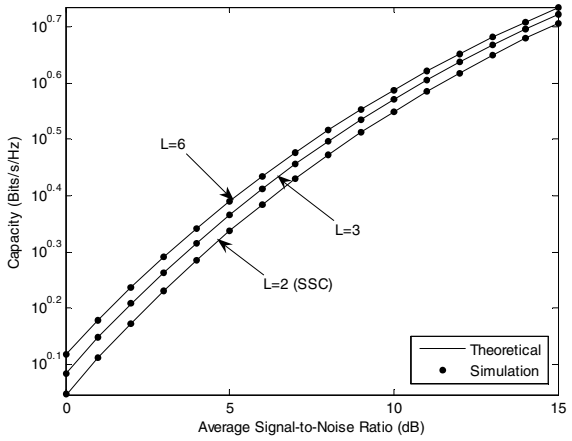


Figure 3. Capacity curves for Alamouti based SEC system with optimum threshold (as found from Table I) for different numbers of Rx antennas.

IV. Analysis of Outage Probability

The outage probability P_{out} of the combiner is defined as the probability that its output SNR γ falls below a given target threshold γ_0 i.e. $\Pr(\gamma<\gamma_0)$. Quite naturally P_{out} is a function of both target threshold γ_0 and switching threshold γ_{th}. The outage probability can be calculated by integrating the PDF $f_{\gamma,SEC}(\gamma)$, given by (10) in the range $[0,\gamma_0]$ over the random variable γ as

TABLE I
Optimum switching threshold for capacity as a function of increasing average SNR per branch for different Rx antennas

$\bar{\gamma}$ (dB)	Optimum common switching threshold		
	L=2 (SSC)	*L*=3	*L*=6
0	-0.51	0.22	1.27
1	0.45	1.16	2.23
2	1.43	2.12	3.22
3	2.38	3.07	4.17
4	3.29	4.02	5.13
5	4.23	4.98	6.12
6	5.18	5.96	7.08
7	6.14	6.93	8.06
8	7.10	7.88	9.03
9	8.06	8.86	10.01
10	9.02	8.83	10.98
11	9.99	10.8	11.98
12	10.97	11.78	12.97
13	11.94	12.76	13.96
14	12.92	13.75	14.97
15	13.90	14.75	15.98

$$P_{out} = p(\gamma < \gamma_0) = \int_0^{\gamma_0} f_{\gamma,SEC}(\gamma) d\gamma \tag{16}$$

Inserting (10) in (16) we obtain

$$P_{out} = \left\{ \left[F_\gamma(\gamma_{th})\right]^{L-1} - \sum_{j=0}^{L-1} \left[F_\gamma(\gamma_{th})\right]^j \right\} \int_0^{\gamma_{th}} f(\gamma) d\gamma + \sum_{j=0}^{L-1} \left[F_\gamma(\gamma_{th})\right]^j \int_{\gamma_{th}}^{\gamma_0} f(\gamma) d\gamma \tag{17}$$

Solving the integrals through integration by parts

$$I_3 = \int_0^{\gamma_{th}} f(\gamma) d\gamma = 1 - \frac{2}{\bar{\gamma}} \left(\gamma_{th} + \frac{\bar{\gamma}}{2} \right) \exp\left(-\frac{2\gamma_{th}}{\bar{\gamma}} \right) \tag{18}$$

and

$$I_4 = \int_{\gamma_{th}}^{\gamma_0} f(\gamma) d\gamma = 1 - \left(\frac{2\gamma_0}{\bar{\gamma}} + 1 \right) \exp\left(-\frac{2\gamma_0}{\bar{\gamma}} \right) \tag{19}$$

Substituting (18) and (19) in (17), the final outage probability expression becomes

$$P_{out} = \left[F_\gamma(\gamma_{th})\right]^L - \sum_{j=0}^{L-1} \left[F_\gamma(\gamma_{th})\right]^{j+1} + \sum_{j=0}^{L-1} \left[F_\gamma(\gamma_{th})\right]^j I_4 \tag{20}$$

Fig. 4 shows the outage probability performance of Alamouti coded SEC in Rayleigh fading channel for a fixed switching threshold of $\gamma_{th} = 2$ dB and a target threshold of γ_0 =3 dB. The horizontal axis (x-axis) is normalized with respect to target threshold.

Like the capacity case, the outage probability also attains its minimum value when the combiner operates with optimum switching threshold γ_{th}^*, which may be obtained by setting $\partial P_{out} / \partial \gamma_{th} \big|_{\gamma_{th} = \gamma_{th}^*} = 0$. It can be easily shown that [10], for $\gamma_{th} = \gamma_0$, $P_{out} = \min\{P_{out}(\gamma_{th}, \gamma_0)\}_{\gamma_{th} = \gamma_0} = P_{out}^*$, and we get the optimum performance. The corresponding plot for $\gamma_{th} = \gamma_0 = 3$ dB is shown in Fig. 5.

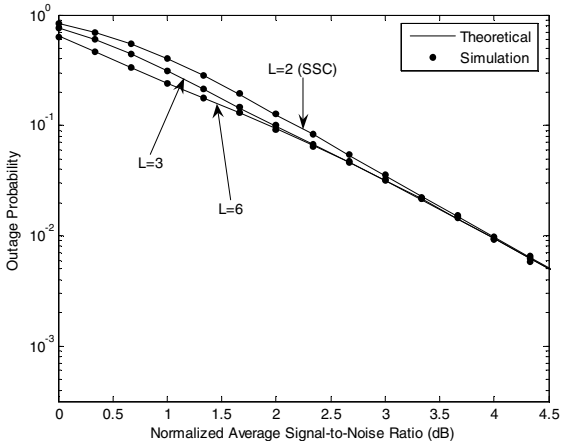


Figure 4. Outage probability curves for Alamouti based SEC system with fixed threshold (γ_{th} = 2 dB) for different numbers of Rx antennas.

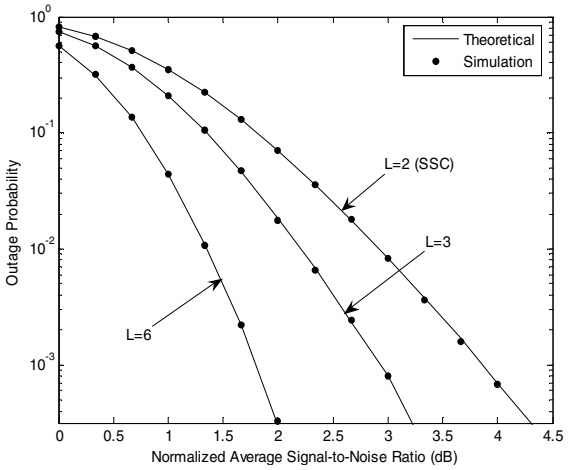


Figure 5. Outage probability curves for Alamouti based SEC system with optimum threshold for different numbers of Rx antennas.

V. ANALYSIS OF SER

After discussing capacity and outage probability, in this section, we would derive the expression of SER for MPSK in conjunction with our 2 x *L* MIMO system. For MPSK modulation, the symbols are equally spaced on a circle of radius $\sqrt{E}$, and the angle between two consecutive symbols is $\phi_i = 2(i-1)\pi/M$, where i =1, 2, … , *M*. Further, for optimum coherent detection, the SER of MPSK in an AWGN channel is given by

$$P_s = \frac{1}{\pi} \int_0^{\frac{\pi(M-1)}{M}} \exp\left[-\eta \sin^2\left(\frac{\pi}{M} \right) \Big/ \sin^2\theta \right] d\theta \tag{21}$$

For fading channel, the SER, $P_s(\gamma)$, becomes conditional on the fading SNR γ, which may be obtained from (21) by replacing η with γ.

A Multil-branch Switch and Examine Combining

With the assumption of statistical independence between fading and noise, the average SER (P_s) can be calculated by averaging the conditional error probability $P_s(\gamma)$ over the underlying fading random variable (γ) as

$$P_s = \int_0^{\infty} P_s(\gamma) f_{\gamma,SEC}(\gamma) d\gamma \tag{22}$$

where $f_{\gamma,SEC}(\gamma_s)$ is as mentioned in (10). Interchanging the integration limit, we get

$$P_s = \frac{1}{\pi} \int_{\theta=0}^{\frac{\pi(M-1)}{M}} \int_{\gamma=0}^{\infty} f_{\gamma,SEC}(\gamma) \exp\left(-\frac{\sin^2\left(\frac{\pi}{M}\right)}{\sin^2\theta} \gamma \right) d\gamma d\theta \tag{23}$$

and after some more algebraic manipulations

$$P_s = \frac{1}{\pi}\frac{4}{\bar{\gamma}^2}\left[\sum_{j=0}^{L-1} \left[F_\gamma(\gamma_{th})\right]^j \int_0^{\frac{\pi(M-1)}{M}} \Xi(\theta) d\theta + \left\{ \left[F_\gamma(\gamma_{th})\right]^{L-1} - \sum_{j=0}^{L-1} \left[F_\gamma(\gamma_{th})\right]^j \right\} \times \int_0^{\frac{\pi(M-1)}{M}} \left(\Xi(\theta) - \Lambda(\theta) - \gamma_{th} \frac{\Lambda(\theta)}{\sqrt{\Xi(\theta)}} \right) d\theta \right] \tag{24}$$

where $\Xi(\theta) = 1/\left(D + 2/\bar{\gamma}\right)^2$, $\Lambda(\theta) = \exp\left[-\left(D + 2/\bar{\gamma}\right)\gamma_{th}\right]\Xi(\theta)$, and $D = \sin^2(\pi/M)/\sin^2\theta$.

Fig. 6 shows the SER performance of MPSK for Alamouti coded multi-branch SEC system over Rayleigh fading channel for a fixed threshold of $\gamma_{th} = 3$ dB and different M values.

For BPSK (M = 2) the expression given in (24) reduces to [3]

$$P_e = \frac{1}{2}\left[F_\gamma(\gamma_{th})\right]^{L-1}\left[1 - \Theta(\bar{\gamma})\right] + \sum_{j=0}^{L-2}\left[F_\gamma(\gamma_{th})\right]^j \times \left[\left\{1 - F_\gamma(\gamma_{th})\right\} Q\left(\sqrt{2\gamma_{th}}\right) - \Theta(\bar{\gamma}) Q\left(\sqrt{2\xi(\gamma_{th})}\right) - \frac{1}{\bar{\gamma}+2}\sqrt{\frac{\gamma_{th}}{\pi}} \exp\{-\xi(\gamma_{th})\} \right] \tag{25}$$

where $\Theta(\bar{\gamma}) = \sqrt{\bar{\gamma}/(\bar{\gamma}+2)}\{(\bar{\gamma}+3)/(\bar{\gamma}+2)\}$ and $\xi(\gamma_{th}) = \gamma_{th}\{(\bar{\gamma}+2)/\bar{\gamma}\}$.

B Dual-branch Switch and Stay Combining

Substituting L = 2 in (25), one can obtain the error probability for Alamouti coded SSC scheme

$$P_e = \frac{1}{2}\left[F_\gamma(\gamma_{th})\right]\left[1 - \Theta(\bar{\gamma})\right] + \left[\left\{1 - F_\gamma(\gamma_{th})\right\} Q\left(\sqrt{2\gamma_{th}}\right) - \Theta(\bar{\gamma}) Q\left(\sqrt{2\xi(\gamma_{th})}\right) - \frac{1}{\bar{\gamma}+2}\sqrt{\frac{\gamma_{th}}{\pi}} \exp\{-\xi(\gamma_{th})\} \right]. \tag{26}$$

It may be noted that the error rate may also be minimized (like capacity or outage probability) by finding optimum switching threshold through the equality $\partial P_e / \partial \gamma_{th}\big|_{\gamma_{th}=\gamma_{th}^*} = 0$. Unfortunately, no closed-form expression exists for γ_{th}^*. Numerical minimization technique was used to tabulate γ_{th}^* as given in Table II for M = 2.

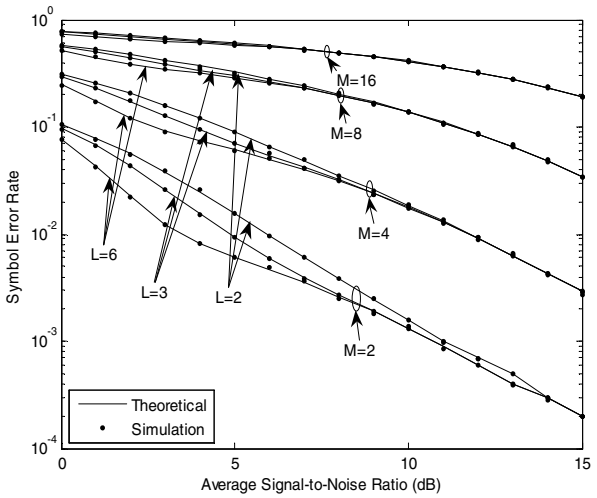


Figure 6. SER curves for Alamouti based SEC system with fixed threshold (γ_{th} = 3 dB) for different M and for different numbers of Rx antennas.

TABLE II
Optimum switching threshold for SER as a function of increasing average SNR per branch for different Rx antennas

$\bar{\gamma}$ (dB)	Optimum common switching threshold		
	L=2 (SSC)	L=3	L=6
0	-1.43	-0.62	0.57
1	-0.62	0.20	1.43
2	0.16	1.00	2.24
3	0.90	1.77	3.05
4	1.60	2.50	3.80
5	2.30	3.20	4.54
6	2.92	3.86	5.25
7	3.52	4.50	5.93
8	4.08	5.09	6.60
9	4.60	5.65	7.20
10	5.09	6.19	7.79
11	5.55	6.69	8.35
12	5.98	7.16	8.89
13	6.38	7.60	9.40
14	6.75	8.04	9.90
15	7.10	8.44	10.4

VI. CONCLUSIONS

Closed-form analytical expressions for capacity, outage probability, and SER have been obtained for a 2 x L MIMO

system employing Alamouti code and SEC diversity. For verification of the derived expressions, extensive Monte Carlo simulations were carried out. It was found that the theoretical values (represented by solid lines) show excellent match with the simulation results (represented by black dots). Graphical plots indicate that if the SEC system is run with optimum threshold, it can outperform the SSC system by taking advantage of the extra diversity branches.

REFERENCES

[1] A. Q. Li, G. Li, W. Lee, M. Lee, D. Mazzarese, B. Clerckx, and Z. Li, "MIMO techniques in WiMAX and LTE: A feature overview," *IEEE Commun. Magz.*, vol. 48, no. 5, pp. 86-92, May 2010.

[2] S. M. Alamouti, "A simple transmit diversity technique for wireless communications," *IEEE J. Select. Areas Commun.*, vol. 16, no. 8, pp. 1451-1458, Oct. 1998.

[3] W. Li and N. C. Beaulieu, "Effects of channel errors on receiver selection-combining schemes for Alamouti MIMO systems with BPSK," *IEEE Trans. Commun.*,vol. 54, no. 1, pp. 169-178, Jan. 2006.

[4] A. Jemmali and J. Conan, "BER analysis of the Alamouti coding scheme using receive antenna selection," *Proc. IEEE ICWMC,* Nov. 2010, pp. 155-159.

[5] W. Li, N. C. Beaulieu and Y. Chen, "Generalized receiver selection combining schemes for Alamouti MIMO systems with MPSK," *IEEE Trans. Commun.*, vol. 57, no. 6, pp. 1599-1602, Jun. 2009.

[6] F. J. L. Martinez, E. M. Naya, K. –K. Wong, and J. T. Entrambasaguas, "Closed-form BER analysis of Alamouti-MRC systems with ICSI in Ricean fading channels," *IEEE Commun. Lett.*, vol. 15, no. 1, pp. 46-48, Jan. 2011.

[7] S. Thoen, L. Van der Perre, B. Gyselinckx, and M. Engels, "Performance analysis of combined transmit-SC/receive-MRC," *IEEE Trans. Commun.*, vol. 49, no. 1, pp. 5-8, Jan. 2001.

[8] Z. Chen, J. Yuan, and B. Vucetic, "Analysis of transmit antenna selection/maximal-ratio combining in Rayleigh fading channels," *IEEE Trans. Veh. Tech.*, vol. 54, no. 4, pp. 1312-1321, Jul. 2005.

[9] G. Maiti and A. Chandra, "Error probability of Alamouti coded MIMO system with multibranch switch-and-examine combining," *Proc. IEEE CASCOM PGSPC 2010*, vol. 1, no. 2, Nov. 2010, pp. 5-8.

[10] M. K. Simon and M. S. Alouini, *Digital Communication over Fading Channels*, NJ, NY: Willey-Interscience, 2nd ed., 2005.

[11] I. S. Gradshteyn and I. M. Ryzhik, *Table of Integrals, Series, and Products*, New York: Academic, 7th ed., 2007.

[12] M. Abramowitz and I. A. Stegun, *Handbook of Mathematical Functions with Formulas, Graphs, and Mathematical Tables*, NY: Dover, 9th ed., 1970.

[13] D. Haccoun, M. Torabi, and W. Ajib, "Performance analysis of multiuser diversity with antenna selection in MIMO MRC system," *Physical Commun.*, vol. 3, no. 4, pp. 276-286, Dec. 2010.

Energy Balanced Clustering Method with Use of Learning Automata

Batool.Abadi khasragi
Electronic, Computer & IT Department
Islamic Azad University Osku Branch
Osku, Iran
Batool.abadi@gmail.com

Abstract— Increasing miniaturization and sensor communication abilities make them invisible and expand the availability everywhere in any time. Sensor network applications, increase the challenging issues related to design network protocols have emerged. One of them is increasing energy efficiency and lifetime in the network. Sensor nodes with limited energy reserves are deployed, so the network must operate with minimal energy overhead. This article focuses on improving the network lifetime by using energy efficient arrangement of nodes in a state primary goal to reduce energy waste with using energy balance. Therefore, learning automata capabilities - to solve issues in sensor networks is appropriate is used. For the purpose mentioned above, energy balanced clustering technique based on learning automata is proposed that learning automata residing in the cluster head, for balance the best node is selected according to the amount of energy remaining as the new cluster head. Proposed technique with the NS2 simulator to simulate the behavior is evaluated. Results show that the calculated energy balance improves the life time of sensor network substantially.

Keywords- *Sensor networks, energy balance, learning Automata, clustering, nodes classification.*

I. INTRODUCTION

Sensor networks should be able to dynamically, network backbone and data path in response to changing network conditions put the reorganization. [10]This especially is important for energy efficiency .Because of the nodes have limited energy storage. Nodes are generally unattended and automated so that store their energy is irreplaceable. [6] According to the organizing techniques of objective reasons, nodes should be increasing nodes lifetime. Better mechanism for improving the network lifetime should calculate energy consumption over a unique node address. Since the energy remaining after the death of the network, wasting energy is a network without a network residual energy than the amount of energy is wasted. If the battery is an empty node, on which neighbors to communicate with other parts of the network have relied on that node will affect. Organizing techniques node energy consumption should consider the total network nodes to receive and delay exhaustion. It is thought that nodes in a similar time trend to analysis, although this position due to the different nodes in the network traffic is impossible rough. Which leads to main station is forced to further operations in the boundary nodes which have to do. Because thay have to relay data of other nodes to the main station. Methods of organizing the nodes along the network service quality by providing full coverage and connectivity are important. To reduce the information exchanged, a small group of nodes is called the cluster can take shape. [8,13,14]

However, periodic exchange of information related to the network even in a small group may also be non efficient in terms of energy. Instead continuously reviewed in sensor networks where nodes are activated only when the network quality decreased, can take the form of agreement. [3] These methods cannot predict the lack of stored energy, but increase network lifetime.

If you wear a sensor network nodes will be effectively less important, will reduced network quality. To protect nodes from being early exhaustion, energy consumption across the network should be smooth. Smooth consumption of energy - while its neighboring nodes still have enough energy - the nodes due to exhaustion and constant excessive consumption of energy will be protected.

Energy consumption of a node directly proportional to the tasks that the node runs. To balance energy consumption duties should be shared between nodes to balance the energy consumption for the mechanism is efficient division of tasks and also to consider sensing regional conditions and network. Dynamic network control protocol, enables the distribution functions requires, in accordance with the current node has ability.

In order to answer the question "What technique can increases lifetime of sensor nodes and organized effective network with many nodes are deployed?" techniques to organize the sensor nodes in the network literature [7, 3, 11] have been studied and concluded that these techniques due to low efficiency in management of network energy restrictions are in increasing lifetime. Therefore, developing a organization of balanced energy technique that can control nodes with a low overhead organization and operational nodes and network lifetime increase is the purpose of this article. This technique called learning automata based energy balanced clustering (LAEBC), in this, nodes themselves into clusters based on their

ability in terms of residual energy levels are organized. Network so that when the environment can vary dynamically be reconstructed. The best performance provides the limited energy storage and maintain nodes from sudden exhaustion. Thus the network for a long time reducing wasted energy storage, will remain active. The results show that compared with existing techniques to organize nodes, LAEBC lifetime balance rate increases because standard deviation of energy levels at least 20% less than the remaining techniques are available.

II. EXISTING ORGANIZATION NODES TECHNIQUES

Basic method for information sharing network initially organized sensor network topology is proposed. High energy overhead due to information sharing network, a different layout techniques such as clustering its [7,12,13] hierarchical [4,9] or adaptive topology [2,3] has been proposed. These methods can also reduce the network control overhead and energy consumption over the life of uneven energy consumption of nodes considered unique because they produce. Uneven node energy consumption, by the uneven distribution of lifetime for the nodes are created. Being depleted at an early result of a major node, quality of service and network coverage as well as the connection decreases.

III. SUGGESTED SOLUTION

Existing protocols to organize and deploy are concentrated only on local energy efficiency, while the overall energy consumption to reduce energy dissipation is important. Method proposed in this paper, the nodes in the network if the energy is balanced, which organizes the operational lifetime of the network nodes using preserved early analysis increases and classification technique based on residual energy storage is provided. Category nodes to detect high-energy nodes - which may do a greater tasks beside of sensing. Then nodes based on their capabilities for sharing the duties of low-energy nodes to neighbors with high energy are organized. Classification based on residual energy reserves that have been proposed nodes to nodes with high-energy and low-energy are classified as energy consumption is divided among them. Energy consumption of a node directly with the tasks that will run is proportional. Therefore, if the duties are shared, energy consumption will be balanced. Tasks involved in lifetime sensor nodes are identified as sharing the duties between the neighboring nodes provide.

A. Classified nodes

Nodes based on current energy levels are classified as capable for performing duties neighboring nodes with lower energy are identified. Initially assume that all nodes have the same energy residuals. As soon as nodes start their activity, their levels of energy decreases gradually. Since, the tasks in different phases at different energy levels are used, the remaining energy at any given time all nodes will be different. For example, in comparison sensing gateway node may be more energy than the others used to relay data. Such additional duties should be balanced between the nodes to make energy is re-distributed. Equitable distribution of duties must ensure that a node if only the minimum energy required for sensing and data transmission has to run its additional duties to be considered.

Node energy residual is the only variable parameter that every node has the same memory and processing power is reduced. This leads to the sensor nodes based on their residual energy levels we identified. Two types of sensors nodes with excess energy (Excess Energy Node (EEN)) and node energy needs (Necessary Energy Node (NEN)) have been assigned. Energy nodes which are sufficient for performing extra duties and EEN are called nodes which just enough energy to run their own duties to sensing NEN are called nodes.

B. Determine the type of node (EEN / NEN)

Node types using the energy levels of residual energy intake or a node is calculated. If the energy required to send and receive a packet is already marked, the remaining energy of nodes can be closed and generation packet rate and arrival packet rate be calculated depending on which type of diagnostic work EEN / NEN for the node will provide. Compared with the residual energy level and a predefined threshold (E_{th}), the energy level of a node with maximum residual battery capacity and normalization to 100 are graded. [4] Normalized energy level leading to easy handling even for heterogeneous nodes with different battery capacity. Battery capacity based on the lowest level of energy level that is shown E_{th}, is defined. E_{th} value is dependent on the application form and the minimum energy requirements for performing specific tasks for a given time a node is introduced. Nodes which have energy levels higher than E_{th} called EEN otherwise called NEN. When a node is savings all his energy analysis is considered.

C. Learning automata based energy balanced clustering method (LAEBC)

A learning automata based energy balanced clustering method (LAEBC) to organize sensor nodes based on the type has been proposed. This method actually a generalization of standard clustering methods [1, 5, 13, 14, 15] for balanced energy distribution network. Small groups of nodes organized into clusters to share the energy levels. Learning Automata resident in each cluster head based on calculated residual energy levels increases energy exhaustion the chance of cluster head of the cluster members and decrease it when energy exhaustion. Automata gradually, learns which nodes of the cluster members can act as a gateway.

At the start as $p_i = 1/(n-1)$ probability that n is the number of nodes in each cluster and the maximum is seven to eight nodes. Since, in beginning work in the energy level of nodes is equal, therefore first randomly selected member of the cluster is selected as a gateway. After a period, send and / or receiving operations, environment response to favorable or unfavorable choice of gateway node will prompt the desired cluster. Desirable or undesirable environmental response on the base of the hypothetical gateway selection algorithms result this algorithm has a low complexity as a function of energy works. With performance of this algorithm one of the member of cluster is assumed gateway. Now if the node marked by the node selection algorithm and the environment should be the

same answer automata favorable environment and B_i (n) = 0 otherwise undesirable response and B_i (n) = 1 will be. If the response of the environment is undesirable nodes selected by Automata enough power to not being a gateway. In general, if the desired response and B_i (n) = 0 node that is selected as the gateway will be rewarded and the rest nodes are not be rewarded. If B_i (n) = 1, that nodes are not be rewarded and rest of other cluster members are rewarded. Influence coefficients penalties and rewards to the node where the gateway goes to the replacement node that has enough energy to push for passage. Set action of Learning Automata is equal {A1, A2, ..., An}, which are as an input environment. Considering the environmental response to any favorable response to surgery i, B_i (n) = 0 or undesirable B_i (n) = 1 and P-model environment is binary. Considering the possibility of analyzing the energy of early cluster head, the next repetitions automata learns member of the cluster that the chances of more and enough energy to relay data members of the cluster has the information cluster head past as a new cluster head selected. In fact, with selected action A_i by Automata all of cluster head data transferred in to node i. Thus the lifetime of such a cluster head has been increased and avoid early exhaustion and help to maintain connectivity and coverage network. Selecting energy cluster head or gateway from EEN nodes type energy is balanced and if a gateway to become a state NEN becomes as a none gateway node, to save remaining energy. Gateway node selection algorithm as the energy function is executed. If all nodes are converted to NEN themselves as network organizations, all of them always active [3] and they operate as gateway. When a gateway node and a cluster is forming, neighbors the gateway should automatically be a member of the cluster.

Thus providing the required connections, crossings are selected beyond the end of a passage in communication range of each gateway and thus, clusters are overlapping and overlapping clusters of organs may have multiple gateway to send their data.

D. Gateway Selection Algorithm (energy function)

While the clusters are formed around the gateway, the gateway selects input nodes of the network EEN. When a node EEN gateway mode is entered, it informs your neighbors with using confirmation message of gateway. After receiving the confirmation message, nodes table for gateway -related data are updated to send data. Each node the ability to send data at least need one gateway. Each node, to start gateway selection procedure distributed on the gateway requests messages between neighbors when it failures.

Algoritm1: Gateway Selection Algorithm

Assume:
Each node has a gateway information table to store at most G_{th} number of Gateway info .

Let :
NType : type of node G_{No}:no of gateways
G_{th}:gateway threshold State:state of the node
Msg:control message Table:gateway info
t_p:predefined wait time t_s: random wait time

1.1 When *gateway request message received;*
1.2 if NType $\neq$ NEN AND $G_{no} \neq 0$ AND $G_{no} \leq G_{th}$ then
1.3 $State_{prev} \longleftarrow State_{current}$;
1.4 $State_{current} \longleftarrow State_{transition}$;
1.5 Broadcast($Msg_{willingness}$);
1.6 Waite(t_p);
1.7 if $Msg_{received} == Msg_{willingness}$ then
1.8 Waite(t_s);
1.9 if $Msg_{received} == Msg_{willingness}$ then
1.10 Update(Table);
1.11 $State_{current} \longleftarrow State_{prev}$;
1.12 end
1.13 else
1.14 Broadcast($Msg_{confirmation}$);
1.15 $State_{current} \longleftarrow State_{gateway}$;
1.16 end
1.17 end
1.18 else
1.19 Broadcast($Msg_{confirmation}$);
1.20 $State_{current} \longleftarrow State_{gateway}$;
1.21 end
1.22 end

IV. EFFICIENCY ANALYSIS

Experimental evaluation of different schemes to compare with LAEBC have been implemented. Nodes organized two major projects, namely LEACH [7] and ASCENT [3] also compare against LAEBC have been implemented. Since the method of All-active [2] is the basic method for organizing nodes as a baseline for comparison will be discussed.

Simulation environment includes sensor nodes that are randomly distributed and assume nodes are similar in terms of architecture. Each node have a same energy, memory and operation ability also nodes have a same sensing and communication region. Communication between the nodes is two-way. Nodes spread from 100 to 500 for varies the varied network density. To test the results discussed, when the average node transmission range is less than 5 to a network, sparse called, otherwise it's called dense network. Number of created packet, have been distributed among nodes uniformly. For collecting data from sensors spread there are 50 sink nodes or base station. Will assume that the sink or base station connected to the main power residual and data packets to sink node along multiple paths of data communication are conducted. Environmental profile is shown in Table 1. Performance measurement techniques to organize and pattern standard deviation of node energy levels and the residual network lifetime have been used as a parameter. Standard deviation of node energy shows how much the network is balanced, while the lifetime of the network shows how much each method can be used to keep network.

Three different defined of network lifetime to compare different techniques from different view points were expressed that their definitions are below:

- Required time for exhaustion of first node in the network .
- Required time to rupture first occurs in the network. (The first network segmentation occur).
- Required time for exhaustion half of the spread nodes.

TABLE 1 - PROFILE SIMULATION ENVIRONMENT FOR IMPLEMENTING PLANS TO ORGANIZE

Parameter	Value
Number of nodes (S)	Varied from 100 to 500
Number of nodes per transmission range (t_r)	2 to 10
Initial node energy (E)	100 unit power
Data transmission cost (E_t)	0.04 unit power
Data receiving cost (E_r)	0.02 unit power
Data transmission range (t_r)	4 unit distance
Energy threshold (E_{th})	30%
Gateway threshold (G_{th})	≤ 3
Gateway selection rate for LEACH (Δ)	20 unit time
Node active to inactive time ratio for ASCENT (ε)	0.4
Sensing rate	Uniformly random
Data generation rate	Uniformly random

For each of the cases, residual energy levels of sensor nodes are registered to the standard deviation of residual energy and network lifetime are calculated.

A. Definition of a lifetime1: Time needed for becoming the first node exhaustion.

Comparison of techniques for organizing the layout and the various nodes, residual energy levels and standard deviation of network lifetime - when the first node analysis goes - have been measured. When the data nodes to the main station through the Multi-Hop Communications data are sent, closer nodes to the main station are distributed further data in comparing with further nodes. Many important nodes for keeping connected between the main station and other network nodes exist. Such nodes due to the implementation of tasks will be depleted sooner. When nodes are depleted, in terms of operational networks thay are non-efficient. Therefore, the time needed for analysis as the first node network lifetime is discussed.

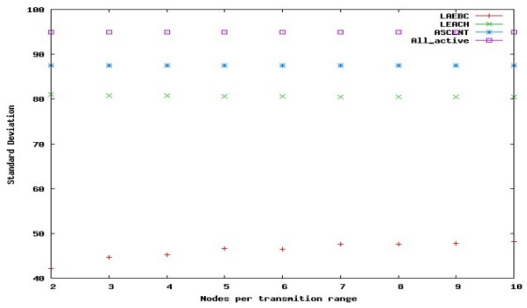


Chart 1 - Standard deviation of residual energy when the first node is exhausted

In real mode nodes are randomly distributed and the nodes in different situations, for various tasks are performed. None of the All-active and ASCENT methods doesn't have any criteria duties or energy balance in the organization and layout plans but LAEBC to this task when the energy level is lower than a certain threshold level fall, will distribute. LEACH also to periodic rotation of duties gives the nodes to be balanced energy consumption. Due to predicted energy balance LEACH and LAEBC in compared with All-active and ASCENT have less energy waste.

LEACH has no explicit criteria for same nodes as LAEBC wont maintain therefore, can not become cluster head node that has less energy and its neighboring nodes still have enough energy to prevent.

Chart 2 shows when the first node analysis goes as a function of transmission range of nodes. Form to clearly indicate that LAEBC better than other available techniques can be implemented. LAEBC energy levels based on the remaining will category nodes to EEN and NEN. Nodes with high energy EEN and raised nodes and only one EEN can be as a gateway. While the energy level of a gateway node to fall below E_{th}, the mode of crossing lifetime to enhance their lives. There was not available such technique in existing organize techniques.

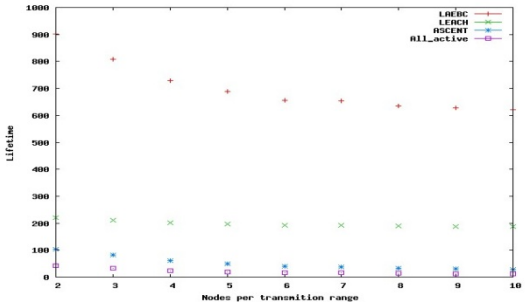


Chart 2 - Network lifetime when the first node is exhausted.

High-density network in the network lifetime of a longevity for all relevant methods in low node density decreases. Lifetime due to increased number of neighbors is reduced. High number of neighbors it implies that a node has gateway, close to relay more data.

Increase - has been fixed.≥Significantly the network lifetime for LAEBC - When the number of nodes to move within 5 LAEBC network connection using the threshold crossing (G_{th}) controls the maximum number of crossings of the cluster G_{th} allows. G_{th} the simulation is set to 3 and the network, when the number of nodes to move to within five reaches is saturated. Same threshold used for LEACH well controls connection plug. Therefore, a similar behavior shows LAEBC. Nodes in high density, chart 2 also shows that a node in the network lifetime LAEBC have a 600sim times is at the least 400sim times over other techniques.

B. Definition of lifetime 2: When the first rapture occurs.

When a node being depleted due to all its neighbors are isolated or discrete network is called discrete. Amount of time it takes to rupture first occurs in the network, which is

measured efficiency is an important parameter because it can lead to segmentation of the network is being ineffectively. Standard deviation of residual energy levels and the network lifetime when the rapture occurs first investigated and results are described below. Standard deviation residual energy when the first rapture occur in Figure 3 is shown.

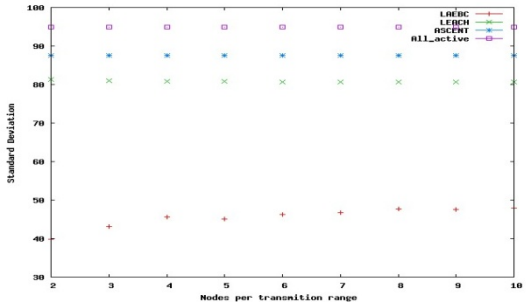


Chart 3 - Standard deviation of residual energy when the network first segmentation occurs.

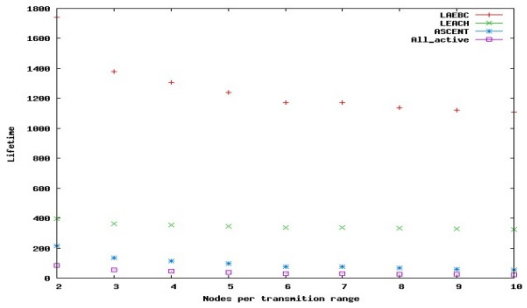


Chart 4 – Lifetime of network when the first network segmentation at the network occurs.

Chart 4, time taken for different node density before at least one node is isolated from the network shows.

C. Definition of lifetime3: when 50 percent of the total nodes are empty.

In this, time needed for analysis as 50 percent of the nodes lifetime are discussed. Because some of existing works such as [2,3] of the same parameters as the network lifetime of use. Network may not be effective to the extent, however, for work completed testing is done. Standard deviation of residual energy among nodes - when half the nodes have died - in Figure 5 is shown. Due to the energy balance criterion standard deviation LAEBC cluster head movement and politics in LEACH energy curve for the two methods are uniformed. Chart shows when the empty half of the nodes are spread LAEBC minimum waste of energy is compared with other methods. Chart 6 lifetime for 50% of nodes die shows. While the density of nodes varies, the time difference between the first node to become empty nodes, and 50% for one important feature being depleted for the different techniques shows. Ideally, all nodes must be depleted at the same time, but due to different tasks and work that nodes are running; this is impossible. For example, a node closer to the main station, is forced to relay more data pack.

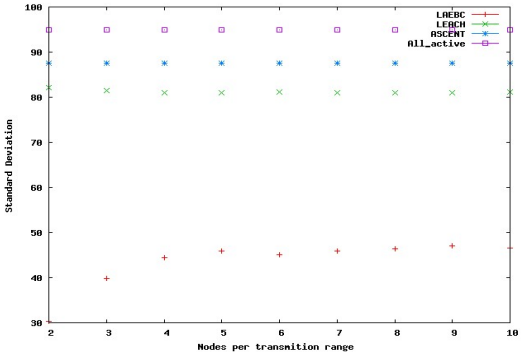


Chart 5 - Standard deviation of residual energy when 50% of the nodes are empty.

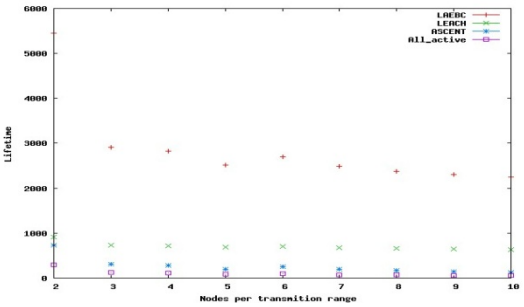


Chart 6 - Lifetime when 50% of network nodes are empty.

LAEBC lifetime of time needed to analyze the first node to the time needed to analyze 50% of nodes was increases. LAEBC minimum difference between the first node to analyze the nodes is 50%. This indicates that this is LAEBC able to near ideal conditions of operation compared to existing methods. Chart 6 also shows that LAEBC has the ability to network lifetime than LEACH in all network density increases. Also LAEBC - when the network is spars - better execute from ASCENT and All-active methods is in High node density lifetime differences between the compared methods decreases, but still LAEBC is run better than other methods.

V. DESCRIBING CONTENTS

In this paper, the existing organizing methods, namely All-active [2], LEACH [7] and ASCENT [3] are compared against with each other and the results of the test methods defined for three different network lifetime show. Standard deviation of residual energy levels and network lifetime as criteria efficiency are discussed and the results of the methods mentioned nodes are organized.

LAEBC enables sharing tasks can be better than other energy techniques in all cases provide balanced. This implies that when a LAEBC network is not active, less energy is wasted. LEACH in periodically spin gateway based on

parameters including residual energy levels and also is balances energy among neighbors. LEACH has a more energy wasted than LAEBC. LEACH because of the preserved nodes being depleted early fails. ASCENT as adaptive network with using of activate nodes in cases where death occurs will deploy. Since ASCENT allows nodes to be empty - while the neighbors are good energy - on average 85% standard deviation for all three lifetime energy has been compared. All-active method of any parameter does not preserve energy thus wasted energy, the highest rate at about 95% for every definition of lifetime was compared. Energy balance can extend the network lifetime. For example LAEBC has a lowest energy waste and the network lifetime longer than the other techniques.

VI. CONCLUSIONS AND FUTURE WORK

High difference in energy consumption could lead to a early segmentation of the network. Contrary to organize a balanced technique called Learning Automata Based Energy Balanced Clustering Method(LAEBC) is proposed in this paper. Load balancing in distributed systems is very common that the nodes of the added burden will stop. Similar methods using self-assembly capacity utilization for a node sharing tasks among neighbors has been taken.

Making responsibilities for balancing between neighbors that have high and low energy levels, sensor nodes based on energy levels are classified and inside of cluster nodes are classified according to type of nodes. LAEBC can be prevent a node of tasks that the residual energy is lower than the threshold, so, with using of energy depleted to protect of nodes from early exhaustion. Experimental performance evaluation of the time the first node being depleted as measured by lifetime expectancy are resulted that LAEBC increases network lifetime compared with existing techniques. The experimental results have shown that LAEBC can increase efficiency of network in compared with other methods. We mean; when the time required for efficient segmentation of the first network to be created or when half of nodes spread is defined to be empty, it can be increases efficiency of network .

In this article all of the extended nodes for arrange of network are required. Some of these nodes may be common with neighbors in the region of cover. These nodes can be the cause of energy consumption are redundant activities that can shorten the network lifetime. Nodes can contain repetitive tasks known to be inactive to improve overall energy efficiency. Some nodes may replace dead nodes to increase the operational lifetime of the network be used. Investigated of how nodes can be repetitive tasks to face in the deaths of nodes could be used in future work.

REFERENCES

[1] S. Bandyopadhyay and E. J. Coyle. *"An energy efficient hierarchical clustering algorithm for wireless sensor networks"*. In The 22nd International Annual Joint Conference of the IEEE Computer and Communications Societies (INFOCOM'03), pages 1713–1723, San Francisco, CA, USA, 2003.

[2] A. Cerpa and D. Estrin. *"ASCENT: Adaptive Self-Configuring sensor Networks Topologies"* .In The 21st International Annual Joint Conference of the IEEE Computer and Communications Societies (INFOCOM'02), pages 1278–1287, New York, NY, USA, June 2002.

[3] A. Cerpa and D. Estrin. *"ASCENT: Adaptive Self-Configuring sensor Networks Topologies"* .IEEE Transactions on Mobile Computing, 3(3):272–285, July 2004.

[4] X. Cheng, B. Narahari, R. Simha, M. Cheng, and D. Liu. *"Strong minimum energy topology in wireless sensor networks: NP-completeness and heuristics"*. IEEE Transactions on Mobile Computing, 2(3):248–256, July 2003

[5] J. Deng, Y. S. Han, W. B. Heinzelman, and P. K. Varshney. *"Scheduling sleeping nodes in high density cluster-based sensor networks"*. ACM/Kluwer MONET: Special Issue on Energy Constraints and Lifetime Performance in Wireless Sensor Networks, 10(6):813–823, Apr. 2005. URL http://web.ntpu.edu.tw/ yshan/monet04.pdf.

[6] D. Ganesan, A. Cerpa, W. Ye, Y. Yu, J. Zhao, and D. Estrin. *"Networking issues in wireless sensor networks"*. Journal of Parallel and Distributed Computing (JPDC), Special issue on Frontiers in Distributed Sensor Networks, 64(7):799–814, July 2004.

[7] W. Heinzelman, A. P. Chandrakasan, and H. Balakrishnan. *"An application specific protocol architecture for wireless micro-sensor networks"*. IEEE Transactions on Wireless Communications, 1(10):660–670, Oct. 2002.

[8] X. Hong, M. Gerla, R. Bagrodia, T. Kwon, P. Estabrook, and G. Pei. *"The mars sensor network: efficient, energy aware communications"*. In IEEE Military Communications Conference (MilCom'01), pages 418–422, McLean ,Virginia USA, Oct. 2001.

[9] Y. Ma and J. H. Aylor. *"System lifetime optimization for heterogeneous sensor networks with a hub-spoke topology"*. IEEE Transactions on Mobile Computing, 3(3):286–294, July 2004.

[10] P. Santi. *"Topology control in wireless ad hoc and sensor networks"*. ACM Computing Surveys,37:164–194, June 2005.

[11] B. Sinopoli, C. Sharp, L. Schenato, S. Scha ert, and S. Sastry. *"Distributed control applications within sensor networks"*. Proceedings of the IEEE, 91(8):1235–1246, Aug. 2003.

[12] K. Sohrabi, W. Merrill, J. Elson, L. Girod, F. Newberg, and W. Kaiser. *"Methods for scalable self-assembly of ad hoc wireless sensor networks"*. IEEE Transactions on Mobile Computing,3(4):317–331, Oct. 2004.

[13] L. Subramanian and R. H. Katz. *"An architecture for building self-configurable systems"* .In IEEE/ACM symposium on Mobile and Ad hoc networkig and computing, pages 63–73,Boston, MA, USA, Aug. 2000.

[14] K. J. Taek, M. Gerla, V. Varma, M. Barton, and T. Hsing. *"Efficient ooding with passive clustering an overhead-free selective forward mechanism for ad hoc/sensor networks"*.Proceedings of the IEEE, 91(8):1210–1220, Aug. 2003.

[15] W. Ye, J. Heidemann, and D. Estrin. *"An energy-efficient MAC protocol for wireless sensor networks"*. In The 21st International Annual Joint Conference of the IEEE Computer and Communications Societies (INFOCOM'02), pages 1567–1576, New York, NY, USA, June 2002.

Telemedicine in a cloud – A Review

Shaftab Ahmed
Department of Computer Science and Engineering
Bahria University, Islamabad, Pakistan
Shaftab_2010@yahoo.com,

Azween Abdullah
Department of Computer and Information Sciences
Universiti Teknologi Petronas, Bandar Seri Iskandar
31750 Tronoh, Perak, Malaysia
azweenabdullah@petronas.com.my

Abstract –

The Information communication Technologies (ICT) has assumed an important role in all domains of life today. The computation requirements are often larger than resources available at hand in an enterprise and it would like to outsource it for high speed computation or data management requirements. In other cases a small enterprise would like to lease computation or data archiving resources as per demand. Cloud computing is a new paradigm which may be used to handle such situations. It offers a virtual environment at a small initial investment by entrepreneurs planning to develop large applications scalable as the scope and workload increases. The computer hardware and software are available in virtualized environments of cloud computing offering Software as a Service (SaaS), Infrastructure as a Service (IaaS), and Platform as a Service (PaaS) through Datacenters and Cloud Service Providers (CSP). The paradigm shift provides elastic infrastructure, efficiency of resource utilization, reduction in upfront capital investment and focus on core activities. A model for cloud computing for telemedic services is being developed to cater for large data archive of Clinical Data Records (CDR), Decision Support Systems (DSS) and event based notification and monitoring system in a typical hospital. In this paper we have reviewed the rapid growth in cloud computing activities, available opportunities and services with the early birds in this technology. Beside this the hospital information and medical data services architecture using cloud services has been discussed in the context of the model being developed. Data storage service, Security service, scalability and performance issues have been discussed.

Keywords: CSP, SaaS, PaaS, IaaS, CDR, WSDL, WAFL, ZFS

I. INTRODUCTION

The new millennium started with an asset of wonderful scientific and engineering developments among which the impact of computer technology and the infiltration of the Information Communication Technologies (ICT) in everyday life, commerce and industry has been phenomenal. Grid computing remained the hype of the last one decade where the computer professionals were excited to deliver commodity computing power over the internet for high performance systems along with availability of large data archives on demand anywhere any time.

Although the grid computing was initially meant for scientific and engineering purposes the natural desire of computer professionals was to take it to the social commercial domains. Data grids, medical grids etc were developed to meet the challenges of computer industry capitalizing on high capacity networks and communication systems for electronic data processing and presentation. In spite of many success stories of grid computing paradigms it lacked support of e-commerce activities especially for computing applications which require guaranteed security of data during archiving, distribution, processing and disposal afterwards on the host computing system like the medical information systems.

The cloud computing technology was born out of the growing scope of computing technologies for both high performance and large data storage management systems. The data centers are used to store and manage large volumes of data dynamically generated over the time. They have become essential to provide efficient work load distribution and query servicing applications. They are capital intensive requiring high upfront costs. Hence the developers start with a prototype and then go for full scale solution. Cloud computing offers a virtual environment at a small initial investment by entrepreneurs planning to develop large applications scalable as the scope and workload increases.

II. BACKGROUND AND RELATED WORK

Cloud computing was in the vision of the computer scientists as early as the year 1961 when John McCarthy of Stanford university predicted that "computation may one day be organized as a public utility". The idea is gaining ground now and acceptability in the ICT community for this paradigm shift from prevailing computation services is growing. Cloud computing paradigms are being developed to provide computer hardware and software services as utilities in virtualized environments. The Datacenter hardware and Software are provided by a Cloud Service Provider (CSP) to the prospective users. The qualities of new compute and business models have promoted virtualized, scalable, solutions with low up front investment leading to, "pay as you go" philosophy. Many research groups in universities like Berkeley [1] and Stanford are making research contributions in development of cloud computing standards

The paradigm shift offered by cloud computing will provide elastic infrastructure, efficiency of resource utilization, reduction in upfront capital investment and focus on core activities. The application software is expected to migrate to the service providers. Ian Foster [2] defined cloud as, "a computing paradigm which is a pool of abstracted, virtualized, dynamically scalable, managed, computing, power storage platforms and services for on demand delivery over the internet". This has given a framework based on Software as a Service (SaaS), Infrastructure as a Service (IaaS), and Platform as a Service (PaaS) [3]. The clouds can be implemented at Private, Enterprise and External levels. The clouds may also be federated into virtual private clouds [4]. The community clouds may also be formed by joining trustful

978-1-61284-690-3/11/$26.00 ©2011 IEEE

domains of similar activities together to share computing and data storage resources. The community clouds may remove dependence on cloud service providers like Amazon, Google and Microsoft. This will lead to a struggle between the proprietary and open software developers. The advantages of computing cloud [3] include openness, competitiveness, and graceful failure, convenience in control and environment sustainability.

The Web 2.0 has a number of new features suitable for cloud computing architecture to cater for processing pipelines, batch processing systems, web engineering, service provisioning under "pay as you go" contract which suits Data centers, P2P computing, utility computing and Grid computing. Applications are being developed to provide ubiquitous access to cloud service providers for dynamic discovery, composability of services meeting QOS, speed, reliability and scalability considerations for prospective users.

The core infrastructure is composed of Virtual Machines (VM), Peer to Peer Networking (P2P), Distributed Identity and trust management, Distributed Persistence, Distributed parallelism, Bandwidth management and tariff of services. Rajkumar [4] has added the concept of Service Level Allocator (SLA) to the definition of cloud and has proposed four layers for cloud service architecture i.e. Users/ Brokers, Service level Agreement (Resource Layer), Virtual Machine and Physical Hardware as shown in figure 1

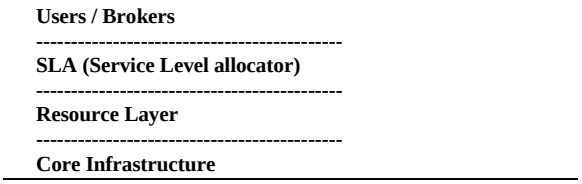


Figure 1 Cloud Services Layers

The service allocator uses resources offered by multiple participants through distributed service repository using the business model of execution. Virtualization of machines is done on the resource layer which deals with distributed computation, distributed persistence, bandwidth management and e-commerce. The core infrastructure is composed of physical machine, P2P networking and distributed trust management.

The physical machines are maintained by the data centers who present them as virtual machines providing flexibility in hardware and software selection for configuring a platform. The hypervisor technologies are used to compose virtual machines on demand, dynamically managed and provisioned over the web services resource framework. The customer is charged by cloud service provider for the virtual machines provided / leased and duration of usage. The SLA examines the user requests against admission control policy, pricing, accounting and metering the service over virtual machines.

The cloud computing supports machines virtually presented by the cloud service providers who charge the usage of the hardware and software services by a mutually agreed tariff. It provides an opportunity to new entrepreneurs and small business centers to start with small applications which may grow into larger applications over the time. It is also useful for larger enterprises handling huge data sets and high performance computing systems to use service providers shifting the capital investment to operational investment considerations relieving the developer from some of the managerial issues.

Cloud computing platforms and service providers at present are Amazon Compute Cloud EC2 and the Data Cloud S3, Google AppEngine, Microsoft Azure, Live mesh, Sun Microsystems Sun Grid and the Grid Lab Aneka of Manjrasoft. They offer computation and data storage services at very low upfront costs easily scalable to match the user requirements. We present a brief description of these as under:

Amazon Elastic Computing Cloud (EC2) [7] offers a library of available Amazon Machine Images (AMI). The user may configure an AMI of his choice as well and exercise control over software starting from Kernel upwards. There is no limit on number of applications to be hosted. The Simple Storage Service (S3) of Amazon is used to upload the selected or composed AMIs before execution. Amazon charges the user by instance / hour for each machine instance and data storage in GB-month basis. Data transfer is charged in tera bytes. Application engine for Web Services (AWS) offers a number of higher level managed services for use in conjunction with EC2.

Google Application Engine offers web application services through web based Admission Console (AC) to manage and run web applications. It supports an API for data storage, email services etc. The AppEngine has impressive automatic scaling and high availability features [1] [8]. The Mega store based on Bigtable data storage is available to the AppEngine applications. However AppEngine is not suitable for general purpose computing

Microsoft Azure [6] applications are developed using .NET libraries and compiled using Common Language Routine (CLR). The Azure is intermediate between compute application framework of AppEngine and the hardware virtual machine of EC2. The system supports general purpose computing. The libraries provide a degree of automatic network configuration and failover / scalability.

Microsoft Live Mesh [9] aims to provide centralized location for user to store applications and data. The user can access or upload applications and data through web based Live Desktop. A user may offer his devices through live mesh software which is password protected through windows live login.

Ubuntu Enterprise Cloud Architecture [10] offers Linux distribution for cloud services. The mission of Ubuntu is to select best components from open source, refine and provide them to users. Its strategy includes multi vendor support and procedures to avoid "data lock in" to counter the fear that monopolies in cloud industry might emerge. The three components developed are as under:

- Ubunto Server edition on Amazon EC2 (IaaS)
- Ubuntu Enterprise Cloud powered by Eucalyptus (IaaS)
- Ubuntu One (SaaS)

Ubuntu 9.04 Server edition offers Eucalyptus using KVM hypervisor which allows deployment of a cloud with API matching that of AWS [6]. The Eucalyptus being the main component of Ubuntu Enterprise Cloud (UEC) supports following elements [10]:

- Cloud Layout Controller (CLC)
- Walrus Storage Controller (WS3)
- Elastic Block Storage (EBS)
- Cluster Controller (CC)
- Node Controller (NC)

Aneka is a .NET based service oriented platform for grid/cloud applications. It is built on a de-centralized architecture consisting of executers accessible over the internet through a configurable container.

Cloud computing is being projected as the fastest growing technology with the inclusion of heavy weights ready to field data centers providing solutions to customers in almost all fields. However a lot of road blocks have yet to be cleared. A de facto standard for application development and deployment over the cloud is required to avoid monopolization of services. Interoperability and portability between clouds has to be ensured by international acceptable practices to build confidence of the end users and entrepreneurs to field their applications without any hesitation. They may flexibly migrate to desired cloud service provider without compromising security and functionality of intellectual assets.

Cloud Computing has a wide range of applications ranging from social networking, web hosting, data archiving presentation and high performance computing. The composition of services for a cloud computing application is a challenging task involving configuration and deployment over the virtual environment offered by a service provider. Hence cloud simulation can play an important role in the design phase by conceiving and operating computer architecture and applications on a simulator. The Cloudsim [5] is a simulator which supports a virtualization engine and services model to field an application. It provides an opportunity to test an application in a repeatable and controllable environment to tune for performance, speed, availability and other measuring parameters before setting up an application on a real Cloud computing environment.

III. CLOUD COMPUTING FOR TELEMEDIC SERVICES

A. Cloud User – Doctor, Researcher, Nurse

The users of cloud services include patients, doctors, nurses, researchers and the administrative staff. Hence role based model of security and accessibility has to be used, supplemented by Authentication, Authorization and Access Control procedures supported by a transaction logging mechanism for consistency. The data modified or appended should be visible at various levels governed by suitable policies. Report generation on selectable parameters and access to decision support tools have to be provided. The access to other cloud domains should be through single sign on for seamless access. Evolving standards for managing clinical research information [20] are focused on replication, secure and universal access, presentation tools, and data exchange and metadata management.

B. Data Archiving

To handle the Data archiving and availability on demand in-house image archiving and storage involves expenditure on infrastructure, IT staff and operational procedures. In the wake of new technologies, up gradation of hardware and software remains a problem for a dynamic enterprise. Cloud based service model relieves the enterprise from periodic disposal of obsolete hardware, procurement and installation of new hardware, program / data transport to new platforms and re installation of software framework to ensure continuity of services. The data cloud S3 of Amazon [7] is an example of large storage system.

The electronic healthcare and telemedic services have become a convenient way for the patients and medical doctors. The data generated in modern electronic diagnostic procedures like MRI, PET, CT [12] etc. is quite large for which adequate archiving and presentation methods have to be developed. The data is expected to be maintained for a long time although some of it may be required actively while the rest may be accessed occasionally. Hence a hierarchy of storage has to be maintained to provide quick services for active data while keeping the rest of data in background with higher access time.

In many cases the implementation of security procedures by the Cloud Service Providers may be more reliable as compared to self managed archives in the hospitals. The data confidentiality and auditability requirements of Human Services Health Insurance Portability and Accountability (HIPPA) [13] have to be ensured for archiving and presentation of medical data. A case study was performed by TC3 a healthcare company [14] in their HIPPA compliant application development using AWS [11] [1]. Iron Mountain's Digital Record Center for medical images [15] is another example of cloud service.

Migration of data to cloud service providers poses a host of new challenges. The users are at the mercy of service provider for availability and integrity [10] of data. More over the "data lock in" may allow the vendor to monopolize the resource activity as proprietary software tools will hamper migration of data. Hence if a user wants to migrate to a different cloud he has to get the data extraction in required format. Continuity of business activities with flexible switch over to new service providers can be ensured by using open data formats and standards implemented on non proprietary

basis [6]. Such models will allow switching between CSPs through same APIs for example Amazon provides API and AMI tools like Euca2tools without license, facilitating developers to use compatible applications. Ubuntu 9.04 has adopted Amazon Web Services (AWS) [7] Elastic Compute Cloud (EC2) for storage and presentation of images. It uses Eucalyptus for software development and AWS APIs. This is applicable to both private and public clouds hence the time for development and transition is significantly reduced.

C. Distributed Event based notification servicess

The electronic data received through an event monitoring system is analyzed on line to raise alerts to request for a service. In many cases the data received may be used with archived data to proactively generate warnings and alarms. A medical monitoring system attached to the patient's body generates on line data for monitoring and archiving which can be analyzed by intelligent agents to raise alerts and messages on the monitoring console. Knairig [16] has proposed a medical event monitoring system using Session Initiation Protocol (SIP) which helps establishment, modification and termination of sessions between participants. For this purpose Invite and Subscribe procedures are used. An event subscribed to signal the monitoring system may execute a procedure to generate an alert.

D. Engagement with cloud service provider,

The Cloud Service Provider (CSP) hosts datacenters services PaaS and IaaS are provided to the users under a contract to provide on demand service, broad band access, rapid elasticity and measured service [19]. The guaranteed uptime and availability in failures through replicated domain servers is essential for healthcare applications. The CSP should agree to auditability of data and services provided to avoid malicious use. Adequate measures have to be conceived before deployment over the cloud to avoid data lock in situation. Such situation may lead to monopoly and blackmail by a CSP who owns the tools required to extract the data for the customer. Hence Vendor Neutral (VN) medical data archiving and presentation should be preferred.

The datacenters being presented by the Cloud Service Providers are dedicated and have specific hardware software configuration which might lead to problems in cross cloud service provider interoperability and data communication. Hence before adoption of cloud services by a medical hospital the following points must be considered [2].

- The sensitive data processed is accessible and propagated to privileged users only
- Regulatory compliance through external audits, Security Certification, investigation and support tools is ensured
- Data location by specifying where the CSP will store data for processing, the computed data output etc. so that the client can exercise validation checks etc.
- Data recovery procedure in disaster and data retrieval agreement to avoid data lock in has to be decided.

The data storage, integrity and fault tolerance can be provided by management information system like that provided by SUN ZFS (Zeta File System) or WAFL (Write Anywhere File Layout), which can be used for quick recovery from faulty condition.

E. Decision support tools

The data available to a user may be of various kinds organized in groups of tables and reports. Structured queries are used to extract data of interest. For intelligent and on demand information usage and to derive inferences often specialized Decision Support tools are required. In medical diagnosis the Clinical Decision Support System (CDSS) [17] is used to access on line data to match and select similarities in cases available in computerized knowledge base for assessment and seeking clinical guidelines.

Typical CDSS consists of Liveware, Hardware and Software. The Liveware deals with human activity i.e. patients, doctors, medical staff, data administrators etc. governed by policies for data entry, management, processing and presentation. The hardware deals with storage capacity speed of access and use of On Line Transaction Processing (OLTP) or On Line Analytical Processing (OLAP) for making required data available. The software categories include Application software, data modeling and presentation components. Application software performs data Extraction, Transformation and Loading functions (ETL). Modeling software creates relationships in data or meta data for analysis purposes. The presentation tools offer output options which allow export of data to other applications in selected formats.

F. Security service

Data security is an important issue in any IT infrastructure. It is even more important in medical services because of personal information of a patient. HIPPA has laid out the guidelines for this purpose. When moving to cloud infrastructure new dimensions are of concern. The availability of service on demand, assurance of computation integrity through auditability of cloud service provider operations and transparent regulation are important challenges to be met by cloud computing before its acceptance and usage by medical community.

The encryption methods used to archive data are applicable to cloud data services; however the data storage of clinical data and the medical repository should be seamlessly integrated in the cloud infrastructure through trusted computing methods [18]. Inclusion of Third Party Auditor [7] who has expertise and capabilities to assess the risk of cloud storage services may add confidence of a user. The encrypted storage in trusted domains is considered to be safer than un-

encrypted data maintained within the clinics. For adoption of cloud services by a medical hospital combination of high assurance, remote server integrity and sound cryptographic methods are required.

The additional security concerns and risks involved in data management in cloud environments are loss of governance, data lock in, compliance risks, data protection and insecure or incomplete procedure for data deletion from storage systems. European Network and Information Security Agency (ENISA) [21] in its report has emphasized that these issues must be carefully covered and cautiously monitored before outsourcing data management to Cloud Service Providers.

IV. VIRTUAL HOSPITAL OVER THE CLOUD

A. Clinical Data Records & Electronic Patient Journal

The archives consist of structured Clinical Data Repository (CDR), case histories and medical procedures along with unstructured data like reports of radiology, surgical procedures, pathology, EEG etc. These reports are often text oriented. A data access and control framework is required to handle variety of activities originating from the doctor and staff, these activities is interactive and often requires data collection and aggregation. The researchers are interested in cross patient history queries based on their choices of data

The medical data archive has to be multi tiered and accessible through client server applications. The top most is the virtualization layer which can be used by a barely computer aware person through any suitable browser. The middle tier receives data service requests e.g. query, transaction or data entry. It responds with a suitable way i.e. the queries are referred to database server for data extraction from archives; the transactions like medical report entry or clinical measurements are handled by a data collection and archiving service. The lowest tier supports many simultaneous connections of clients to the repository. The hardware used to store information may be in-house, outsourced to service provider (CSP) or both.

The archiving of data may be classified in layered hierarchy, figure 2 shows a typical stack of hardware and software layers to virtualized client and server interaction where the hardware may be in house or outsourced to cloud service provider (CSP). The cloud service providers for archiving and storage of data may be required to store consolidated data archives in the backend, whereas the recent data and CDRs be maintained by high speed Storage Area Networks (SAN).

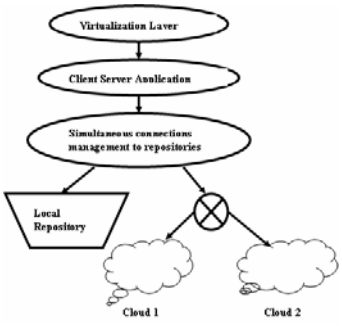


Figure 2 Layered hierarchy of storage

Figure 3 shows an architectural view of the virtualized storage management system which extend the enterprize to virtual storage domains which may support multiple client interaction available to a datacenter. This may be extended to join datacenters in a bigger context

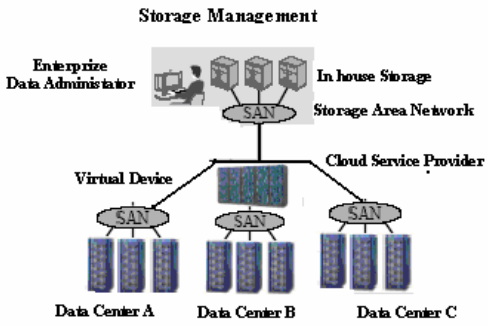


Figure 3 Architecture of virtualized storage system

The repository of clinical data records (CDR) should be reliably and consistently available to authorized users anywhere anytime through presentation tools whenever required. Wherever possible the integration of patient history and transactions regarding clinical measurements / diagnostics should be seamlessly integrated

B. Decision Support System

The electronic data generated for a variety of medical diagnostics have been presented through special decision support tools. The query processing for various levels of users and selecting suitable tool is a complex and challenging task. The data storage should support accessibility from different operating environments and should adopt prevailing standards of software in the industry, like object oriented, modular designs, relational database technology etc. The decision support tools required for a medical hospital can be divided into following main categories [20]

- **a)** Patient Specific Tools
- **b)** Clinical Data Record Access Tools
- **c)** Clinical Research Tools
- **d)** Personal Productivity Tools

We are in a process of developing decision support tools in line with the guidelines discussed. These tools will integrate in a bigger model using cloud based services for out sourcing activities to CSPs and cross enterprise data sharing. New communication models will be developed to have an integrated medical community.

C. *Medical event monitoring system*

An event monitoring system is useful in ehealthcare system where the ICT services increase the interactivity between patients and medical community. The events may be normal scheduling of diagnostic tests, medicine schedule along with alerts which require attention of patient or the medical staff. The medical history is proactively analysed by intelligent agents embedded in the system which raise alerts of various nature. Some of the alerts may require only a normal response and others may have to be acknowledged by the staff within specified time failing which the alert may be passed on to a higher level in the system. This is particularly important in aged patients, post operation rehabilitation and special citizens where the medical service provider assumes a higher level of reponsibility and vigilance.

A prototype system is being developed to cater for the requirements of a medium sized hospital. Wireless and land based connectivity are both being used for this purpose.

V. Conclusion and Future Work

Cloud Computing is an important new platform which is a challenge for both the software developers and the service providers. The success depends on acceptance by all the players with a trust like we usually have in banking system, where we can safely assume that no serious mishandling will go unnoticed. Beside this the confidence to get the services as per demand anywhere anytime has to be built. The migration of a client / enterprise from one CSP to another should be seamless. It is feared that data lock in or fear of compromise of the resources held in one system will not allow the users to migrate easily. On the contrary the CSP may monopolize and create problems for the end user.

The ICT developers, service providers and stake holders in the industry are looking forward to major changes and developments with the advent of Web 2.0. Cloud computing is going to assume a very important paradigm shift in the way the enterprises like hospitals, data processing and archiving systems think. The end users will also find a major change where he does not have to carry a laptop everywhere, instead he can use a small PDA to ride on the web and interact with datacenters and resource providers effortlessly. This will also help release the pressure in office accommodation, the communities of users will be able to share and communicate their data and development work without any hassle.

VI. References

[1] Michael Armburst, Armando Fox and group, “Above the Clouds: Berkely View of Cloud Computing”, UC Berkeley, adaptive Distributed Systems Laboratory, February 10, 2009

[2] Ian Foster, Yong Zhao, Ioan Raicu, Shyong Lu, “Cloud Computing and Grid Computing 360-Degree Compared”, Department of Computer Science University of Chicago

[3] Gerald Briscoe, Alexandros Marinos, “Digital Ecosystems in Clouds: Towards Community Cloud Computing”, Department of Media and Communications London School of Economics and Political Sciene.

[4] Rajkumar Buyya, Chee Shin Yeo, Srikumar Venugopal, “Market-Oriented Clou Computing: Vision, Hype and Reality for Delivering IT services as Computing Utilities” Manjrasoft Pvt Ltd, Melbourne, Australia

[5] Rajkumar Buyya, Rajiv Ranjan and Rodrigo N. Calheiros, “Modeling and Simulation of Scalable Cloud Computing environments and the CloudSim Toolkit: Challenges and Opportunities”, 2009

[6] Jinesh Varia, “Cloud Architecture” Amazon Web Services

[7] Amazon Elastic Compute Cloud (EC2), http://www.amazon.com/ec2

[8] Google App Engine, http://appengine.google.com

[9] Microsoft Live Mesh, http://www.mesh.com

[10] Windows Azure Platform http://windowsazure.com

[11] Simon Wardley, Etiene Goyer, Nick Barcet, “Ubuntu Enterprize Cloud Architecture” Technical white paper August 2009

[12] Habib Zaidi, “ Medical Imaging: Current status and future perspectives”, Genava University Hospital Switzerland

[13] “Protecting Personal Health Information in Research: Understanding the HIPPA Privacy Rule”, Department of Health and Human Services, USA,NIH Publication Number 03-5388 http://www.hhs.gov/ocr/hippa

[14] TC3 Healthcare Case Study: Amazon Web Services available at http://aws.amazon.com/solutions/case studies/tc3-health

[15] Brian Babinean, “Iron MountainReduces Medical Image storage costs” Enterprise Strategy Group, publication June 2009

[16] Knarig Arabshian and Henning Schulzrinne, “ a SIP-based Medical Event Monitoring system” Department of Computer science, Columbia University

[17] Steven A. Ponedal and Michael Tucker, “ Understanding Decision support sytems” Journel of Managed Care Pharmacy March 2002

[18] Junwei Cao, “Implementation of Grid Enabled Medical Simulation Applications using Workflow techniques” Procedings of 2nd international workshop on Grids and Cooperative Computing”, Shanghai 2003

[19] Nigel Shadbolt, Paul Lewid, “ MAIKT: Combining Grid and Web Services for Collaborative Medical Decision Making”, University of Southampton

[20] Cong Wang, Qian Wang, “Ensuring Data Security in cloud computing”, Department of ECE, Illinois Institute of Technology.

[21] “Cloud Computing, risks and recommendations for information security”, enisa – European Network and Information Security Agency report -2009

[22] Yasutomo, Yasungri, Masahide, “Recent trends of storge system technologies”, Hitachi

[23] Dawai Sun, Xiaoyu Zhang, “Grid Based Secure Web Services Framework for Bioinformatics”, California State University San Marcos.

[24] L.Seitz, “Encrypted storage of medical data on a grid”, LIRIS,INSA Villeurbanne cedex, France

[25] http://medical.nema.org DICOM (Digital Imaging and Communication in Medicine)

[26] Feancesco Fedele, “Healthcare and Distributed Systems Technology”, ANSAworks 95, Cambridge, UK 1005

[27] Chris North, Ben Shneiderman and Catherine Plaisant, “Visual Information Seeking in Digital Libraries: The Human Explorer

[28] Seigfried Benkner, “GEMSS: Grid Infrastructure for Medical Service Provision”, University of Vienna, Vienna, Austria

A Parametric Study to Investigate Skin Prestretch

Jamaluddin Mahmud
Faculty of Mechanical Engineering
Universiti Teknologi MARA
40450 Shah Alam, Selangor, MALAYSIA
jm@salam.uitm.edu.my

Cathy A Holt & Sam L Evans
School of Engineering
Cardiff University, The Parade,
Cardiff, CF24 3AA, UNITED KINGDOM
Holt@cf.ac.uk; EvansSL6@cf.ac.uk

***Abstract*—This paper for the first time assesses the significance of skin pre-stretch using numerical analysis. The derivations of mathematical models based on Ogden's constitutive equation which both ignore and include the pre-stretch term are presented. A programme was written to conduct the parametric study. This is novel as no similar approach has been reported before. The results show that pre-stretch is a significant parameter in describing skin behaviour. It is found that a 0.1 unit difference in prestretch, λ_p ($\Delta\lambda_p = 0.1$) produced a larger effect than a 10 unit difference in Ogden's coefficient, μ ($\Delta\mu = 10$ Pa) and 4 unit difference in Ogdens's exponent, α ($\Delta\alpha = 4$).The current stress-stretch graph is also compared and seems in good agreement with results found by the other researchers. The result of this study could contribute to the development of the constitutive models for skin in the future. Therefore, further analysis should be carried out to investigate this. Nevertheless, this study has contributed to the knowledge about skin behaviour.**

Keywords: Skin prestretch, Ogden model, hyperelasticity.

I. INTRODUCTION

From an engineering standpoint, the mechanical behaviour of skin is of wide interest [1] and many studies have been undertaken to assess its functions and properties for cosmetic and clinical applications [2]. Nonetheless, skin behaviour is still not well understood [3] and determining the mechanical properties of this largest organ of the human body has always been a great challenge. Although experiments have been the most common and widely used approach to describe skin behaviour, attempts have also been made to develop the numerical model for skin. To date, no constitutive equations specifically developed for human skin has been reported. The mechanical properties of skin were determined by adapting the constitutive model for other materials (e.g. rubber, theory of elasticity). The numerical analysis is complicated due to the complex structure of skin. Skin is multilayered, anisotropic and viscoelastic; it is also known that skin is an inhomogeneous material whose mechanical behaviour is nonlinear load-deformation relationship and pre-stressed [4]. It is ideal to incorporate all these properties into the model. However, to analyse them simultaneously would be extremely difficult. Although there were attempts to model skin viscoelasticity [5], the more common approach is to assume skin to be hyperelastic, where notably proposed by Danielson [6], Tong and Fung [7] and Lanir [8]. The linear elastic models do not accurately described skin model. Therefore, the idealisation of hyperelasticity provides a means of modelling the stress-strain behaviour of materials, whose stress-strain relationship can be defined as non-linearly elastic, isotropic, incompressible and generally independent of strain rate; though according to Ogden [9] a hyperelastic material refers to an elastic material for which a strain-energy function exists. Hyperelastic materials are characterised by the strain energy function, W and the deformation gradient F. Ogden [10] proposed the strain energy function, W (isotropy and incompressible):

$$W = \sum_{i=1}^{N} \frac{\mu_i}{\alpha_i}\left(\lambda_1^{\alpha_i} + \lambda_2^{\alpha_i} + \lambda_3^{\alpha_i} - 3\right) \qquad (1)$$

λ_i are the principal stretches; μ_i and α_i are the material parameters with the function's order of N.

This paper for the first time assesses the significance of skin pre-stretch using numerical analysis. The derivations of mathematical models which both ignore and include the pre-stretch term are presented and a programme was written to conduct the parametric study. This is novel as no similar approach has been reported earlier. The result of this study could contribute to the development of the constitutive models for skin in the future.

II. METHODOLOGY

A. Stage 1: parametric study

Considering the Ogden model (1), where the material is assumed to be isotropic, hyperelastic and incompressible,

the relation of engineering stress, σ_E and principal stretches, λ, is described by

$$\sigma_E = \frac{\mu}{\lambda}\left(\lambda^{\alpha} - \lambda^{-\alpha/2}\right) \quad (2)$$

This equation has been used by Evans and Holt [11] to compare their results with others. A brief derivation of it is represented in Appendix A. Before applying this approach to the current results, a parametric study designed to investigate the sensitivity of Equation 2 to the variation in μ and α is investigated.

B. Stage 2: Evaluating the prestretch term in the stress-stretch relation

The current analysis attempts to add the prestretch, λ_p to investigate its contribution to the stress-stretch relation. For this purpose, based on Equation 1, the relation of engineering stress, σ_E and principal stretch, λ, (2) was re-derived to include the prestretch term:

$$\sigma_E = \frac{\mu}{\left(\lambda + \lambda_p\right)}\left(\left(\lambda + \lambda_p\right)^{\alpha} - \left(\lambda + \lambda_p\right)^{-\alpha/2}\right) \quad (3)$$

Using (3), a parametric study was designed and conducted to:

(i) analyse the sensitivity of the parameters, μ, α and λ_p to the solution.

(ii) prove the non-uniqueness of the current solutions; and determine several sets of parameters that producing similar solution.

III. RESULTS AND DISCUSSION

A. Stage 1: parametric study

The result showing the sensitivity of (2) to the variations in μ and α is presented in Fig. 1. For this purpose, two sets of curves are plotted to observe the boundaries. The first set aimed to observe the effect of variations in μ. Therefore, while keeping α constant (α = 26; as proposed by Evans and Holt [11], μ was varied from 5 to 15 Pa ($\Delta\mu$ = 10 Pa). The second set aimed to observe the effect of variations in α. Therefore, while keeping μ constant (μ = 10 Pa; as proposed by Evans and Holt, [11], α was varied from 20 to 30 ($\Delta\alpha$ = 10). Evans and Holt [11] parameter (μ = 10 Pa, α = 26) is included as a reference. It is observed that the boundary for a 10 unit difference in α ($\Delta\alpha$ = 10) is twice significant than μ ($\Delta\mu$ = 10 Pa). This shows that (2) is very sensitive to a change in α and the effect of this must be considered when determining skin properties or comparing skin properties for different subjects.

B. Stage 2: The effect of pre-stretch

The result showing the sensitivity of (3) to the variations in μ, α and λ_p is presented in Fig. 2. The current study included the prestretch term, which has been omitted in the previous stage (*A*). Therefore, three sets of curves are plotted to observe the three boundaries. The first set aimed to observe the effect of variations in μ. Therefore, while keeping α and λ_p constant (α = 26, λ_p = 0.2), μ was varied from 5 to 15 Pa ($\Delta\mu$ = 10 Pa). The second set aimed to observe the effect of variations in α. Therefore, while keeping μ and λ_p constant (μ = 10 Pa, λ_p = 0.2), α was varied from 20 to 30 ($\Delta\alpha$ = 10). The third set aimed to observe the effect of variations in λ_p. Therefore, while keeping μ and α constant (μ = 10 Pa, α = 26), λ_p was varied from 0.15 to 0.25 ($\Delta\lambda_p$ = 0.1). Evans and Holt [11] parameter (μ = 10 Pa, α = 26, λ_p = 0.2) is included as a reference.

It is observed that a 0.1 unit difference in λ_p ($\Delta\lambda_p$ = 0.1) produced a larger boundaries than a 10 unit difference in μ ($\Delta\mu$ = 10 Pa). A 10 unit difference in α ($\Delta\alpha$ = 10) produced a twice significant effect (twice larger boundary) than a 10 Pa difference in μ ($\Delta\mu$ = 10 Pa). This shows that (3) is very sensitive to a change in λ_p and α and its effect is significant when comparing skin properties for among subjects or loading directions.

When applying the curve fitting technique, it is known that several equations could fit into a curve. A similar effect could be seen when performing the inverse finite element procedure. The possible solution (optimised material parameters) is not single. During conducting a FEA, a set of material parameters will produce one set of skin deformation. In contrary, several sets of material parameters could produce a similar skin deformation. To demonstrate this, several material parameters were investigated and the result is shown in Table 1 and Fig. 3. It is observed that the curves for several material parameters (Table 1) could match one another (Fig. 3).

The findings deduced from the current parametric study provided a better understanding in interpreting the results from the stress-stretch diagrams with an inclusion of the prestretch effect. The knowledge could be used to interpret and compare skin properties among subjects.

Compared to stage 1, the current study introduces a stress-stretch relation (3) that includes a prestretch term. By adding the prestretch term, the curves shifted to the left compared to the previous analysis (Fig. 1). This reveals that prestretch increases skin stiffness. Therefore, it is found that prestretch is a significant parameter in defining skin properties and should not be ignored when plotting the stress-stretch diagram. Moreover, as shown in Fig. 2, the stress-stretch diagram is very sensitive to the change of prestretch value. As described earlier, a 0.1 unit difference in λ_p ($\Delta\lambda_p$ = 0.1) produced a larger effect than a 10 unit difference in μ ($\Delta\mu$ = 10 Pa) and 4 unit difference in α ($\Delta\alpha$ = 4).

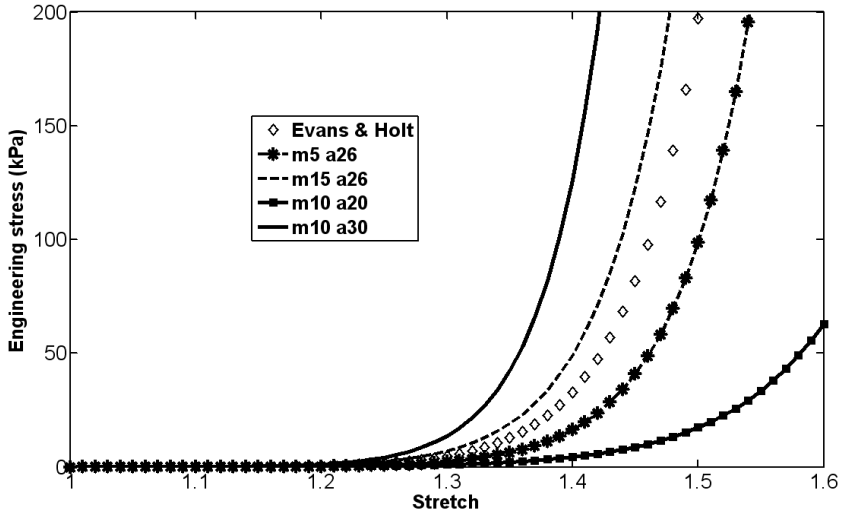


Figure 1: The bounds for variations in μ (Δμ = 10 Pa, dotted lines) and α (Δα = 10, continuous lines).

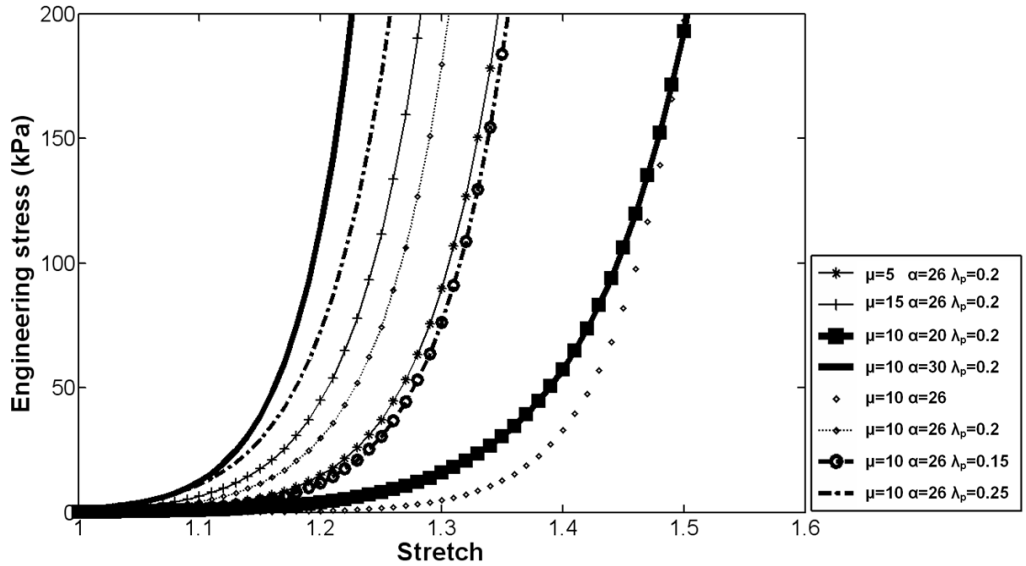


Figure 2: The bounds for variations in μ (Δμ = 10 Pa, thin solid lines), α (Δα = 10, thick solid lines) and λ_p ($\Delta\lambda_p$ = 0.1, dotted lines)

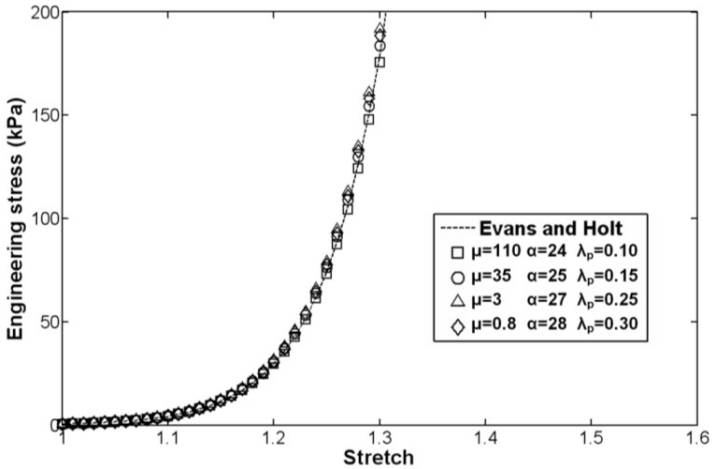


Figure 3: The curves for a few sets of material parameters which fit into one another.
Evans and Holt (2009) data (μ = 10 Pa, α = 26, λ_p = 0.20, dotted line) is used as a reference

However, including the prestretch effect increases the complexity in the analysis. By adding the prestretch term, the non-uniqueness of the current optimisation solution becomes more significant as now it needs to consider three parameters for optimal solution. Fig. 3 reveals that the solution that can fit into one stress-strain curve is not unique. The current study; which included an additional parameter (prestretch), produced a more variety of parameter sets that could match the experimental data. Moreover, skin prestretch is a measured quantity and its actual value is always not easy to measure using *in vivo* experiments. Therefore, it proves that the current study is useful and significant in determining skin properties as it includes the prestretch effect.

IV. CONCLUSION

The objective to investigate the significance of skin prestretch numerically has been achieved successfully. The current study found out that skin stretch is an important parameter in describing skin properties although it will increase the complexity of the analysis. The findings deduced from the current parametric study has provided a better understanding in interpreting skin behaviour using the stress-stretch diagrams, especially when considering the prestretch effect. The result of this study could contribute to the development of the constitutive models for skin in the future.

REFERENCES

[1] Mahmud J, Holt CA, Evans SL. "An innovative application of a small scale motion analysis technique to quantify human skin deformation *in vivo*". Journal of Biomechanics. 2010, vol. 43, pp 1002-1006.

[2] Payne PA. 1991. "Measurement of properties and function of skin". Clinical Physics & Physiological Measurement. 1991. vol. 12(2). pp 105-129.

[3] Evans SL. 2009. "On the implementation of a wrinkling hyperelastic membrane model for skin and other materials". Computer Methods on Biomechanics and Biomedical Engineering. vol. 12(3). pp 319-332.

[4] Tran HV, Charleux F, Rachik M, Ehrlacher A, Ho Ba Tho MC. "In vivo characterization of the mechanical properties of human skin derived from MRI and indentation techniques". Computer Methods in Biomechanics and Biomedical Engineering. 2007, vol. 10(6), pp 401-407.

[5] Shoemaker PA, Schneider D, Lee MC, Fung YC. A constitutive model for two-dimensional soft tissues and its application to experimental data. Journal of Biomechanics. 1986, vol. 19(9), pp 695-702.

[6] Danielson DA. "Human skin as an elastic membrane". Journal of Biomechanics. 1973, vol. 6, pp 539-546.

[7] Tong P, Fung YC. "The stress-strain relationship for the skin". Journal of Biomechanics. 1976, vol. 9(10), pp 649-657.

[8] Lanir Y. "Constitutive Equations for Fibrous Connective Tissues". Journal of Biomechanics. 1983, vol. 16, pp 1-12.

[9] Ogden RW. Non-linear Elastic Deformation, 1984. Ellis Horwood.

[10] Ogden RW. "Large deformation isotropic elasticity: on the correlation of theory and experiment for incompressible rubberlike solids". Proceedings of Royal Soc London. 1972, vol. 326, pp 565-584

[11] Evans SL, Holt CA. 2009. "Measuring the mechanical properties of human skin *in vivo* using digital image correlation and finite element modelling". Journal of Strain Analysis for Engineering Design. 2009, vol. 44(5), pp 337-345.

[12] Holzapfel GA. Nonlinear Solid Mechanics: A Continuum Approach For Engineering. 2000. John Wiley and Sons Ltd.

V. APPENDIX A

Deriving engineering stress

Ogden's strain energy function [10], W, in its general form :

$$W = \sum_{i=1}^{N} \frac{\mu_i}{\alpha_i}\left(\lambda_1^{\alpha_i} + \lambda_2^{\alpha_i} + \lambda_3^{\alpha_i} - 3\right) - p(J-1) \qquad \text{(A.1)}$$

As described in Section 4.4.1.4, λ_i are the principal stretches; and μ_i and α_i are the material parameters with the function's order of N. The incompressibility constraint is introduced via the term $p(J–1)$, where p is the hydrostatic pressure and J is the volume ratio $\lambda_1\lambda_2\lambda_3$.

For incompressible isotropic hyperelastic material, the second Piola-Kirchoff stress, S_a, in terms of the Cauchy stress, σ_a, is [12]:

$$S_a = \lambda_a^{-2}\sigma_a \qquad , a = 1, 2, 3 \qquad \text{(A.2)}$$

Re-arranging (A.2);

$$\sigma_a = \lambda_a^2 S_a \qquad \text{(A.3)}$$

Considering an incompressible material under uniaxial tension (with single pair of Ogden parameter, N=1), the second Piola-Kirchoff stress [3]:

$$S_1 = \mu\left(-\lambda_1^{-2-\frac{\alpha}{2}} + \lambda_1^{\alpha-2}\right) \qquad \text{(A.4)}$$

Substituting (A.4) into (A.3) and generalising the equation, the Cauchy stress, σ:

$$\sigma = \lambda^2\mu\left(-\lambda^{-2-\frac{\alpha}{2}} + \lambda^{\alpha-2}\right) \text{ or } \sigma = \mu\left(\lambda^{\alpha} - \lambda^{-\frac{\alpha}{2}}\right) \qquad \text{(A.5)}$$

Cauchy (or true) stress is represented by force, F, measured per unit surface area, A_i, defined in the current configuration [12]:

$$\sigma = \frac{F}{A_i} \qquad \text{(A.6)}$$

The engineering (or nominal) stress, σ_E, is represented by force measured per unit surface area, A_o, defined in the reference configuration:

$$\sigma_E = \frac{F}{A_o} \qquad \text{(A.7)}$$

The relation between the current and reference configurations relate the areas to be:

$$A_i = \frac{1}{\lambda} A_o \tag{A.8}$$

Substituting (A.8) into (A.7) yields:

$$\sigma_E = \frac{F}{\lambda A_i} \tag{A.9}$$

Therefore, the relation of Cauchy and engineering stresses becomes:

$$\sigma_E = \frac{1}{\lambda}\sigma \tag{A.10}$$

Substituting (A.5) into (A.10) yields:

$$\sigma_E = \frac{\mu}{\lambda}\left(\lambda^{\alpha} - \lambda^{-\frac{\alpha}{2}}\right) \tag{A.11}$$

Name Extraction for Unstructured Malay Text

Mohd Yunus Sharum, Muhamad Taufik Abdullah,
Md Nasir Sulaiman, Masrah Azrifah Azmi Murad
Fac. of Comp. Science and Info. Technology, UPM,
Serdang, Selangor, Malaysia
{ myunus, taufik, nasir, masrah }@fsktm.upm.edu.my

Zaitul Azma Zainon Hamzah,
Fac. of Modern Language and Communication, UPM,
Serdang, Selangor, Malaysia
zaitul@fbmk.upm.edu.my

Abstract—**Names are categorized as proper nouns. Identifying nouns in unstructured text is very challenging since the number is almost unlimited. Name recognition can be used for part-of-speech (POS) tagging or automatic term acquisition in natural language processing (NLP). In this paper we proposed a general approach to recognize names in Malay text. Using the proposed approach, we implement an application of free indexing for indexing names from a collection of Malay texts. Our evaluation shows that the application reach 92% precision score, 54% recall score, and F-score 68% in indexing names from news' articles.**

Keywords-Malay text processing; Pattern recognition; Name recognition; Name extraction

I. INTRODUCTION

Natural language processing (NLP) involved processing of unstructured as well as structured text. Structured text is easier to be analyzed as they are arranged in some fixed or known pattern, like tagged text in HTML or XML format. However, analyzing unstructured text is difficult because of their dynamic and free form characteristic. Analysis on these documents is quite challenging as we had to determine the general pattern of the information before we can analyze them.

Syntax analysis is one of the processes in NLP, which is to analyze and retrieve semantical information or to check the validity of a sentence in text document. Part-of-speech (POS) or word class is one of the information that is required for the syntax analysis. Partially, this information can be produced from morphological analyzers such as MALIM [1], [2]. Word classes group words according to their grammatical role in sentence, such as the noun, verb, adjective, adverb and function words. Words of certain classes are easier to be analyzed as their numbers are limited. Some required information can be stored in dictionary or lexicon, while some can be synthesized based on the information given in the lexicon. However, certain class of words may not be easily analyzed especially the nouns.

Analyzing unstructured text to recognize noun becomes challenging since the number is almost unlimited. We cannot store information regarding all nouns. To define and record all existing nouns is difficult as new words like the proper nouns may be easily created while the existing may already began to disappear or be obsolete. Thus, even if it is possible to collect and store all of the existing nouns, such approach would not be economical while at the same time is not promised to be effective. However, by determining the characteristics and common properties of nouns would allow us to recognize nouns even if they are not yet stored in lexicon or dictionary. Name is a type of noun, and to recognize names would help us to develop approach in recognizing nouns.

Our research work focused on developing minimal technique to recognize names, and the main purpose of this paper is to describe the general approach that we have developed to recognize names in unstructured Malay text document. There are several applications for this technique, and one application is also described in this paper. Section II describes the related work that had been done previously. In section III, we describe the approach for recognizing names. Section IV describes the application of the proposed approach in implementing a names' indexer and the evaluation of its effectiveness using Precision and Recall. In the final section we draw the conclusion.

II. RELATED WORK

There has been enormous work on identifying nouns in other languages, especially for English. However, only few researches had been found on recognizing noun for Malay text. Bali [3] developed a framework to analyze and classify Malay words from Malay text. The framework consists of several filtering steps, in which each filter analyzed and filtered out specific type of words. Some of the filters recognized a set of nouns and special names, which also consists the abbreviation. Specifically, the procedures indentify the following word types:

- acronyms and abbreviations based on sequence of capital letters (two or more alphabets e.g. AO, CGR; sequence of consonants e.g. PBPKNM; or sequence of vowels e.g. UIA), and parenthesis containing such words,
- person's name based on title e.g. *Datuk Seri Khaled Nordin, Professor Syed Naquib Al-Attas*,
- proper nouns (e.g. organization's name) based on collocation of abbreviations, capitalized initial letters and words preceding known abbreviation.

Besides that, the framework also contains a procedure to recognize loan words and use the morphological analyzer to filter affixed words.

The approach of using title for word recognition was used by Baldwin and Awab [4]. However, the title was only meant to separate words rather than for classifying names. The title's abbreviations were found among the abbreviations used by a tokenizer to extract word as token[1]. The abbreviations include ***Abd., Ab., Mohd., Md., Muhd***., Bhd., ***Drs., Dr., Dt***., Inc., Sdn., St., Jln., ***Kapt***., kg., kump, LL.B., LL.M, ***Lt.***, per., ***Pn.***, Pt., Rp., Tmn., ***Tn.***, Tkt., Tj., ***Y.bhg, ABD., AB., MOHD., MD., MUHD***., BHD., ***DRS., DR., DT***., INC., SDN., ST., JLN., ***KAPT.***, KG., KUMP, LL.B., LL.M, LT., PER., ***PN.***, PT., RP., TMN., TN., TKT., TJ., ***Y.BHG***. Beside title and names (in bold text), some of these abbreviations refer to other proper nouns which are usually found as part of the name of places, company, organization etc.

It is common that some words are widely used as names. Most of Muslim males will include words like *Muhammad* and its variants (e.g. *Muhd, Muhamad* etc.), and also *Abdul* or *Abd*. While the females also use common words like *Siti* or *Nor*. Certain community may also apply common characteristics for names like '*Singh*' for the Sikh, and three words for Chinese which some include common family names (like *Lee*, *Chong* etc.). There are also common syllables used for names such as for the Indians *('Vijay…', '...samy…', '...mala'*) and Sikh (*'...jit'*). Of all these common words found in names, we identify the most common so we may use them as guide to identify names. It is impractical to specify all of the existing names. But the problem for this approach is that there had been no statistical data i.e. the frequencies; that we can use to identify the most used words in names that exist in Malay text. However we still can select popular or common names based on some general observation.

A. Some issues with names identification

Generally each initial characters of a multi words name are written with capital letters. However, a lot of other proper nouns for non-person entities are also written with initial in capital letters, like '*Seminar Kesenian dan Kebudayaan*' (event), '*Bangunan Parlimen*' (building) etc. This approach might be used to recognize proper nouns but is not reliable just to recognize person's names. Sometimes non-related words that are not part of a name might also have capitalized initial due to punctuation mark i.e. full-stop. Thus, a person's name may be preceded by word with capitalized initial although is not part of the name, such as in '*... sebagainya. Maka Sultan Ismail pun …*'. Capturing '*Maka Sultan Ismail*' as person's name is wrong since *maka*/so is only a function word. In such case we may require a proper lexicon on function words to exclude the extra part. Fortunately it is possible to create such lexicon since there is only small number of function words exist. However, it could still be a problem if the extra word is also a noun like '…. *Perlantikan Salleh Abbas sebagai* …' (*perlantikan* / appointment).

Words with capitalized initials which look like a person's name may not refer to a person but instead to other entities like building, places, organization, events etc. This is due to the tradition of giving person's names in naming non-human entities. Example is like '*Jambatan Sultan Ismail'* (Sultan Ismail's Bridge) or '*Jalan Tun Sambanthan*' (Tun Sambanthan's Road). By the title we may recognize some part of the entity as person's name and carelessly referring it as person's names instead of a bridge or a road. To handle this problem we could scan and capture the text from the word *Jambatan* or *Jalan*. However, this problem is not an issue if the names will be filtered or we just want to capture proper names.

Using title as name identifier does not fully guarantee a person's name as they are sometimes misleading. Ambiguities can occur on titles based on job post or profession like *Presiden*, *Jeneral*, *Hakim*, *Majistret*, *Pengetua*, *Peguam*; which are commonly used in front of names to indicates the person's profession or status i.e. *Hakim Tun Salleh Abbas*. As the title could also become part of proper nouns e.g. '... *Hakim Mahkamah Tinggi, Tun Salleh Abbas ...*', it require extra analysis to differentiate between the two forms. This is different with the terms 'doctor' or 'engineer' where they are commonly used in names by abbreviations i.e. 'Dr.' and 'Ir.', thus easier to be recognized. In ambiguous situation we may capture word like *Komisioner Jeneral Penjara* (which actually refers to a job post) as person's name, since by the title *Jeneral* we expect *Penjara*/prison as a person's name. In similar case, we may extract both *Presiden Suharto* and *Presiden Indonesia* as person's names, as we are not able to differentiate between person and country's name. Unless, we have the information for disambiguation like *Suharto*=person, *Indonesia*=country. Some of these titles are rarely found with person's name while others are common. The common title may be ambiguous, while others may not. Thus to reduce the possibilities of errors, we may only select the titles commonly found with person's name which is not ambiguous (e.g. *Hakim*), while leaving ambiguous title like *Presiden*.

Using titles for names identification may also becomes problematic due to different customs. Indonesian used *Bapak* or *Ibu* for titles, as *Tuan* and *Puan* for Malaysian. But due to different customs these titles may be used redundantly in certain languages, while others may not. For example, title *Ibu* is used to formally address female's name for Indonesian. But in Malaysian text it is also used for non-person entities such as *Ibu Pejabat ...*/headquarters, *Ibu Pertiwi*/motherland etc. which to indicate 'main of something'. Thus to recognize person's name using title *Ibu* is a bit ambiguous for Malaysian Malay, even though such ambiguity may seldom occurs for Indonesian Malay.

III. RECOGNIZING PERSON'S NAME

A. Basic approach

Our objective is to develop a technique to recognize person's names. Generally the easiest approach is to scan for words with capitalized initials. However, this characteristic is very general and common for all proper nouns. Instead, for the basic approach we develop our recognition technique by scanning for known titles. The approach based on titles is effective as other nouns would not use titles at the beginning of name. Even though we still have to handle some issues regarding the use of titles - such as the ambiguity and the possibilities to be part of non-person's names.

[1] The tokenizer also said credited to John Carroll, in turn adapted from code by Guido Minnen, Erik Hektoen, and Greg Grefenstette.

We also implement an approach of scanning for common first name. Most Malay male generally use variants of *Muhammad* like *Mohd*, *Muhd* or simply as *M.* (initials of *Muhammad*) for first names. Some may use other common name such as *Ahmad* or *Abdul*. Common first names also exist with Malay female's name and other communities as well like Chinese and Indian. Traditionally the Chinese will maintain their family name as the first word of their name. Some people may share common names as the family name is shared along the same descendant. As the results, we may found common names like *Chang, Tan, Chong* etc. among the Chinese. The Indian Hindus also tend to have names in common due to the tradition of using their god or goddess' names in naming their children. For the Sikh, names like *Singh* or *Kaur* are commonly found as final names. In general certain names are actually popular with certain community, thus we may found that they are commonly used as person's names. So these names (first name, final name, etc.) can be used as identifiers for recognizing person names. However, we may only select the most popular or commonly used since we do not want to specify all of them. Table I shows some of the titles and part of names that are normally found with person's names in Malay text.

There is another characteristic regarding person's names in Malay text. It is also common for Malaysian's to include the kinship terms to their names or other Malaysian. Such characteristic could be manipulated to detect names. Table II lists some of the kinship terms that normally exist with Malaysian's name. For people with other unique customs, they might use distinct convention for their names. For instances, the men from Middle East would use *Ibnu* or *Ibn*, while for some Englishman they might use 'Sr.', 'Jr.' or roman's number (i.e. II, III, IV etc.) at the ends of name. These sometimes are retained in Malaysian text e.g. '*Raja Henry III*'/King Henry III. However, not all common characteristics with foreign text necessarily exist or appear in Malay text. For example, the name title *San* might be used within the Japanese text. However in Malay text, the word are rarely found or used even for Japanese names. Generally to implement pattern related with customs we have to learn more on the customs to identify the common pattern.

TABLE I. SOME COMMON TITLES AND PART OF NAMES FOUND WITH NAMES IN MALAY TEXT

Type	List
Abbreviated title	Sdr, Sdri, En, Tn, Pn, Hj, Hjh, YBhg, Sen, Prof, PM, Dr, Drs, Ir, YB, YAB, Kol, Brig, Jen, Kapt, Sjn, DYMM, DYTM *etc.*
Title	Tunku, Tengku, Tun, Toh, Tan Sri, Datok, Dato', Datu, Datuk, Datin, Seri Paduka, Senator, Profesor, Kolonel, Brigidier, Jeneral, Komisioner, Mejar, Kapten, Sarjan, Leftenan, Lans, Koperal, Inspektor, Laksamana, Cif *etc.*
First name	Ahmad, Muhd, Mohd, Muhamad, Muhammad, Mohamed, Mohammed, Md, Mat, M., Syed, Abd., Abdul, A., Siti, Noor, Nor, Nur, Nurul, Ku, Wan, Nik, Che, Chong, Lee, Tan *etc.*
Final name	Singh, Kaur

TABLE II. LIST OF KINSHIP TERM EXIST WITH MALAYSIAN'S NAME

Word / Abbreviation	Meaning
Bin, B.	Son of (Malay)
Binti, Bt.	Daughter of (Malay)
Anak, Ak., A/K	Child of (Bumi's /Native)
Al., A/L	Son of (non-Malay)
Ap., A/P	Daughter of (non-Malay)

Another unique characteristic with person's names is on the use of initials like *M. Jegathesan* and *James T. Brown*. This also can be used to detect person's names.

Based on the characteristics discussed so far, we summarize in general that person's names may be found in several forms as follows:

- Name with known titles - e.g. *Prof Dr Ramlah Adam*
- Name with known first name - e.g. *Mohd Shafie*
- Name with kinship - e.g. *Nor Ishak bin Yaakub*
- Name with known final name - e.g. *Raja Henry III*
- Name with initials - e.g. *J.P. Morgan*

B. Some heuristics to improve recall

In improving recall, we also scan some words which contain person's names like *Jambatan Sultan Ismail* or *Yayasan Halim Saad*. But we only capture the part that is identified as the person's names based on the characteristics summarized above. In certain occasions, we may have to scan words from the back especially if using the final names. But this procedure is prone to error as we do not know exactly where the actual name starts (i.e. in '*Menurut Peguam Jagjit Kaur …*' we need to exclude '*Menurut*'*)*. So, to reduce the possibility of error we limit the scanning only for the first word to the left. This avoids overscanning person's names that may includes non-related words. Generally this approach is for the purpose of improving recall.

Based on the summarized characteristics on person's name above, we can confirm certain words as person's name. Thus for any words that we have selected by the characteristics, we can put some confidence on the words as person's names. Subsequently, we may apply some heuristics to search for other possible names. For names with title, we may try to locate the same name which may be written in the text with shorter version or without the full title, as they could not be found by direct comparison and searching. The use of multiple variations of name in a same text is very common especially in newspapers' article. For example, in the first paragraph, a name generally specified in full name like '*Prof. Datuk Dr. X*' but in further paragraphs the name is cited simply as '*X*' or '*Dr. X*'. Thus, using the truncation technique might help us improve the recall by scanning the location of the shorter names.

We might also detect some other names which might coincidently similar with the name without the title, but refers to a different person. Using a recursive truncation and searching, we may improve the coverage to cover these names. For example, in a newspaper's article the reporter may cite

somewhere the name of '*Datuk Abdul Khalid*'. Using the truncation approach, we could use the shorter words (i.e. '*Abdul*', '*Khalid*') as 'seed' to extract names like '*Khalid Salleh*' or '*Abdul Rahman*' if they are coincidently occurred within the same text. This will improve the recall as well.

IV. EVALUATION'S METHOD AND EXPERIMENT

A. Design and methodology

Using the recognition approach described above, we developed an application called 'name indexer', which is used for free indexing (see Fig.1). An indexing generally would create inverted file, which can be used to improve searching performance. Free indexing (or automatic indexing) is a type of term indexing where the process is not authorized or lack of intervention by human [5]. With the implementation of automatic acquisition, we collect all existing person's names as many as possible and build a comprehensive index for the names. This index will list all existing names complete with links to the documents containing the indexed name. It is generated into a form of hypertext markup language (HTML) document that contains hyperlinks to all of the indexed items.

We implemented the application using Perl scripting language, where all the recognitions are performed using regular expression (RE). Generally the recognition approach is easier to be implemented with RE, and based on our implementation most of the recognition' steps can be described using the RE which is currently supported by Perl version 5.8.8. Besides Perl, many other scripting and programming languages also can support RE thus they might be used either.

For the evaluation's experiment, we had collected a series of 117 Malay newspapers' articles that were published on 1st July 2010 from Utusan Online's website [6]. The collection contains different types of text, comprising several articles from different topics. Through some brief analysis, we found that some of these articles contain a lot of names while others contain less or do not have any names at all. Thus, by combining all these different topics allow us to test our technique on different kind of name's density and text's types. Generally this is sufficient for the purpose of evaluating the 'name indexer'. Our evaluation is also limited to Malaysian Malay as the sample collection was extracted from Malaysian newspapers. In the experiment, the articles will be used as input data to be analyzed by the 'name indexer'.

The application's performance was evaluated using Precision and Recall method. In the context of our measurement, a 'relevant' item is defined as *a person's name*. This means that a relevant name in the text must refer to a person. If the person's name exists as part of the name of non-human entities, it is not considered as relevant. E.g. the name *Indira Gandhi* is relevant, but *Lapangan Terbang Antarabangsa Indira Gandhi* (Indira Gandhi's International Airport) is not; even though the latter contains a person's name. Another consideration for relevancy is that the name searched must be part of the topic discussed in the text.

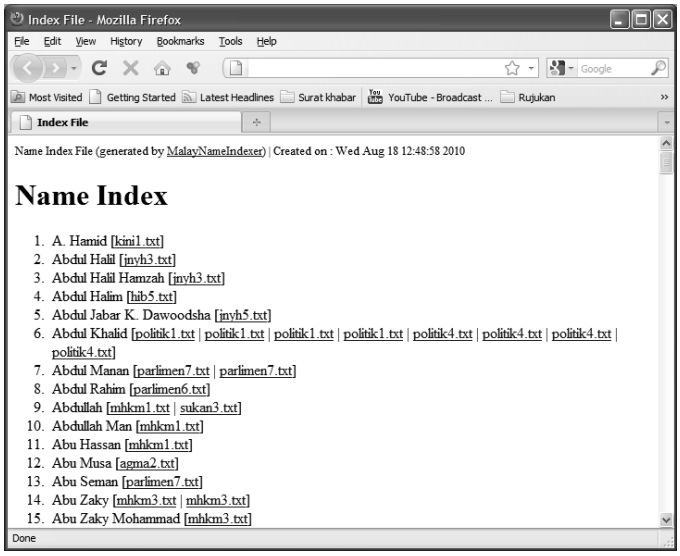


Figure 1. The screenshot of the index file produced by the 'Name Indexer'

If it is auxiliary (i.e. author's name) or not related with the topics discussed or reported, they are considered not relevant. For evaluation's process, first the texts are manually analyzed and the exact set of the existing names is identified (i.e. represents the expected result). Then the text is processed by the name indexer for indexing (which produced the analyses results). Once the indexing is done, the results are manually compared and categorized.

B. Experiment results

Table III shows the overall result of indexing names from the newspapers' articles using the 'name indexer'. Overall, the F-score for the performance of the indexing is only at 68%. From the results, apparently the 'name indexer' achieved high precision with average precision score is over 92% with the number of fall-out only at 11%. However, the average recall score is quite low with the value just slightly above 54%. Based on the results, it shows that our approach performed precise analysis but yet does not able to cover a lot of person's names existing in the newspapers' articles. Technically, we found that most of the non-recognized names are actually unknown names like the foreign names. Besides that, the 'poor' recall is also due to unknown pattern i.e. names which do not belong to any of the defined forms. Thus they are not recognizable. However the analyzer did not produce too many errors or wrong analysis. We only found some minor errors like *P. Pinang*, *Tuanku Presiden* or *Sultan Kelantan*; which actually are not person's names. As consequences, these errors eventually misguided the heuristics to search for irrelevant 'name' like *Pinang*, *Presiden* or *Kelantan*.

TABLE III. OVERALL RESULTS OF INDEXING NAMES IN MALAY TEXT DOCUMENTS

Average Precision	Average Recall	F-score	Fall-out
0.9213	0.5368	0.6784	0.1122

If categorized according to the topics, the low recall score is highly occurs with business news articles, world news or with less formal reports like entertainment and sports. However, on more formal topics like politics and local news that involved authorities, VIPs or honorable persons, the indexing produced better performance in its precision and recall scores. Apparently most of these topics contain a lot of person's names with known titles, thus recognizable by the analyzer. The heuristics also works well since there are some names with titles where the heuristics can be based on. Generally the common names also improve the recognition for people without titles.

V. CONCLUSION AND FUTURE WORK

As conclusion, we found that the approach of recognizing person's names can be performed and returns precise result. However, it requires more comprehensive rules or patterns so that it can cover most of existing names that can exist in Malay text. We also found that the high recall can be accomplished using some heuristics to recognize more names automatically. So, some improvement will be made especially to improve the recall.

REFERENCES

[1] M.Y. Sharum, M.T. Abdullah, M.N. Sulaiman, M.A. Azmi Murad, and Z.A. Zainon Hamzah, "MALIM - A New Computational Approach of Malay Morphology," In Proceedings of 4th International Symposium on Information Technology – ITSim: KL, vol 2, pp. 837-843, June 2010. DOI: 10.1109/ITSIM.2010.5561561.

[2] M.Y. Sharum, M.T. Abdullah, M.N. Sulaiman, M.A. Azmi Murad, and Z.A. Zainon Hamzah, "SAPI - New Algorithm for Malay Morphological Analyzer and Stemmer," In Proceedings of Artificial Intelligence Workshops 2010 (AIW2010) - Extraction of Structured Information from Texts in the Biomedical Domain (ESIT-BioMed 2010): Kuching, Sarawak, Malaysia, pp. 67-82, July 2010.

[3] Ranaivo-Malançon Bali. Identifying and classifying unknown words in Malay texts. Proceedings of the Seventh International Symposium on Natural Language Processing (SNLP2007), Pattaya, Thailand, pp. 299-304, December, 2007.

[4] T. Baldwin and S. Awab, "Open Source Corpus Analysis Tools for Malay", In Proceedings of the 5th International Conference on Language Resources and Evaluation (LREC2006), Genoa, Italy, pp. 2212-5, 2006.

[5] C. Jacquemin and D. Bourigault, "Term Extraction and Automatic Indexing" in The Oxford Handbook of Computational Linguistics (eds R. Mitkov), Oxford University Press. pp 599-615. 2003.

[6] "Utusan Online's archive" (http://www.utusan.com.my/utusan/search.asp)

Electromagnetic (EM) Cavity Resonance Residual Life Indicator

A. Mason[1], A. Thomas[2], H. Keele[2] and A.I.Al-Shamma'a[1]
[1]School of Built Environment, Liverpool John Moores University (LJMU), Liverpool, L3 2ET, UK.
[2]Dstl, Porton Down, Salisbury, SP4 0JQ, UK.
Email: A.Mason1@ljmu.ac.uk

***Abstract*- This paper presents part of a joint venture between Dstl and LJMU. The purpose of this work is to investigate the interaction of electromagnetic (EM) waves within a resonant microwave cavity to sense and characterise filter materials for residual life indication. This paper looks at a single filter material, ASZM-TEDA activated carbon, which is commonly used for military applications where personnel are likely to come under attack from chemical agents. The paper briefly introduces activated carbon, discusses theory relevant to the work, the methodology used for investigation, and finally a selection of pertinent measurements taken using a bespoke microwave cavity resonator.**

I. INTRODUCTION

Activated carbon (sometimes also referred to as activated charcoal [1]) includes a wide range of processed carbon based materials, and has a microcrystalline structure. Its use in filtration is brought about by the fact that it has a high level of porosity and hence a large surface area where adsorption or chemical reactions may take place.

The preparation of activated carbons involves two main steps [2]: the carbonisation of raw material at temperatures less than 800°C in an inert atmosphere, and the activation of the carbonised product. During the carbonisation process, most of the non-carbon elements (e.g. oxygen, hydrogen and nitrogen) are eliminated as volatile gaseous species by the decomposition of the starting material. The residual elementary carbon atoms group themselves into stacks of flat sheets cross-linked in a random manner; the irregular arrangement of these sheets gives rise to pores. These pores are further enhanced through the activation process, which is usually carried out in an atmosphere of air, CO_2, or steam at 800-900°C. This results in an oxidation of some of the regions within the char in preference to others so that as combustion proceeds, a preferential etching takes place. This results in the development of a large internal surface area which can be as high as $2500m^2/g$ [3], although areas in the region of $500m^2/g$ to $800m^2/g$ are more typical [4].

Activated carbon is available in a number of different forms, including powder and granules. The ASZM-TEDA product under test in this work is in a granule form, and contains a number of inorganic impregnant. These are Copper, Silver, Zinc, Molybdenum and Triethlyenediamine, and are present in order to improve the effectiveness of product against warfare gases [2, 5]. Fig. 1 and 2 show a sample of the ASZM-TEDA product as viewed by a scanning electron microscope (SEM) at varying levels of magnification. Fig. 2 shows the macroscopic pores on the surface of an activated carbon granule.

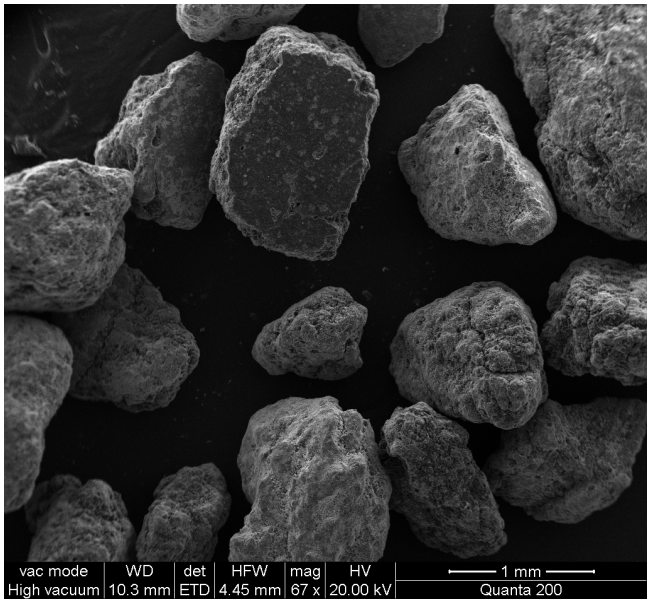


Fig. 1. Activated carbon granules as viewed with a SEM.

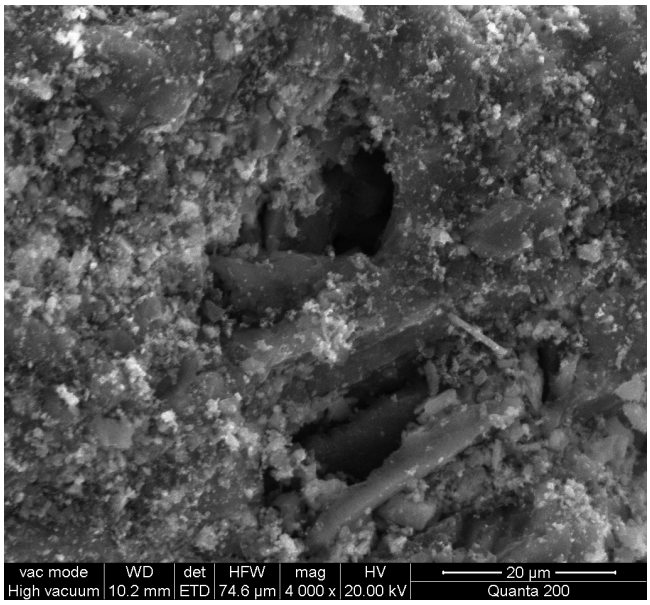


Fig. 2. A highly magnified view of an activated carbon granule as viewed with a SEM, showing macroscopic surface pores.

Activated carbons have a number of applications, including gas and water purification, sewage treatment as well as being used in air filtration for clean-rooms and gas masks. The later application is of particular interest in this work since an issue has been raised in military circles in relation to gas masks which utilise activated carbon filters. At present there is no convenient method for determining the residual life of a filter leading to a conservative filter change policy. This policy results in significant wastage as usable filters are discarded. The aim of this research is to tackle this problem and find a sensing method which can be used to easily define the residual life of an activated carbon filter.

II. Microwave Theory

Using microwave cavity resonator techniques with activated carbon began under the assumption that as the product is aged (i.e. through adsorption of material from the air) its relative permittivity (ε_r) must change.

One method which can be used to find the ε_r of a substance is to monitor the effect it has on the resonant frequencies of an electromagnetic (EM) cavity. An EM cavity, consisting of a hollow structure with conducting walls, will resonate when it is excited at an appropriate frequency by a small antenna placed inside the structure. The resonant modes occur when the electric and magnetic fields form standing waves, and so depend upon the internal dimensions of the cavity and the permittivity of any material placed inside. For a cylindrical cavity resonator (see section III) the fundamental modes are TE_{111} and TM_{010}. TE (Transverse Electric) Modes have a magnetic component in the propagation direction and TM (Transverse Magnetic) Modes have an electric component in the propagation direction. Each mode will generate a resonant peak with a quality factor (Q), which is inversely proportional to the power dissipated in the cavity for each applied EM oscillation. A high Q indicates a sharp resonant peak that will be more readily analysed and improve the accuracy of the sensor.

The resonant frequency for TE_{nml} and TM_{nml} modes in a cylindrical cavity [6] can be calculated using equation (1).

$$f_{nml} = \frac{c}{2\pi\sqrt{\mu_r \varepsilon_r}} \left[\left(\frac{p_{nm}}{a} \right)^2 + \left(\frac{l\pi}{d} \right)^2 \right]^{1/2} \quad (1)$$

Where:

c is the speed of light
μ_r is of the relative permeability
ε_r is the relative permittivity
p_{nm} is the m^{th} root of the of Bessel function of the n^{th} order for TM modes or the m^{th} root of the first derivative of Bessel function of the n^{th} order for TE modes
a is the radius of the cavity
d is the depth of the cavity

All EM modes therefore have the same dependence upon $\sqrt{\varepsilon_r}$, so when the cavity is excited by an appropriate range of frequencies and the resulting spectrum is captured, the resonant peaks corresponding to these modes will shift to lower frequencies as the permittivity is increased.

III. Experimental Setup

A. Sample preparation

In order to determine a microwave response to activated carbon relating to residual life, ASZM-TEDA activated carbon granules were artificially aged. Briefly this procedure included placing the carbon granules in shallow trays at a maximum depth of 2cm and exposing them to an atmosphere of 40°C and 80% relative humidity. The carbon remained in this controlled environment for 7 months, being riffled on a weekly basis to ensure even exposure to the ambient air. The carbon was sampled every month and two 150g samples were taken and placed in sealed containers; one sample was sent to LJMU and the other tested for toxic gas break through times. The later results are shown in Fig. 3 in terms of residual life [7].

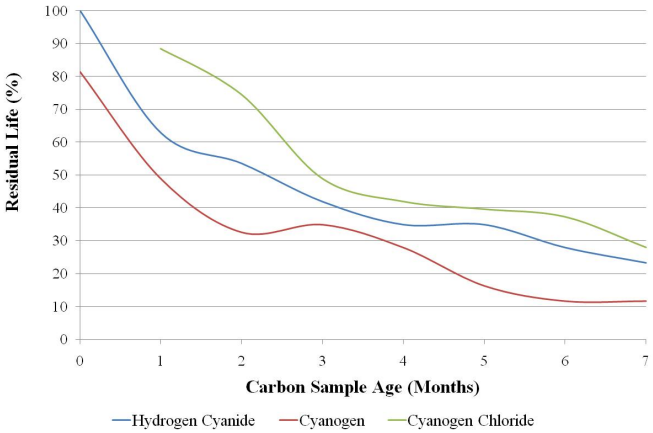


Fig. 3. Measured residual life for toxic gases as carbon ages. **Note:** No measurement was possible for cyanogen chloride at month 0.

TABLE I
Sample information, including sample age, sample number and the colour coding used for results in section IV.

Sample number	Weight (g)	Age (months)	Comment	Results Colour
1	--	--	Distilled water	
2	10.19	0	ASZM-TEDA	
3	12.44	1	ASZM-TEDA	
4	12.61	2	ASZM-TEDA	
5	12.65	3	ASZM-TEDA	
6	12.79	4	ASZM-TEDA	
7	12.96	5	ASZM-TEDA	
8	12.65	6	ASZM-TEDA	
9	12.76	7	ASZM-TEDA	

Upon arrival at LJMU, the carbon material was placed into 15ml polypropylene centrifuge tubes, weighed and then tested in a bespoke cylindrical microwave cavity. Table I gives a brief description of the samples under test for the purposes of this paper. Note that water is included also as a basis for comparison.

B. Data acquisition

The apparatus used for testing of the carbon samples is shown in Fig. 4. It comprises a Marconi 6200A microwave test set, capable of power magnitude measurements between 20MHz and 20GHz, and a cylindrical microwave cavity. The cavity allows for measurement of reflected (S_{11}) and transmitted (S_{21}) power. Both measurements are taken over the full frequency range of the test set using a bespoke software application (see Fig. 5) which acquires data in defined frequency intervals in order to maximise data resolution. For the purposes of these experiments data was captured at 500MHz intervals, with 1601 data points per interval. Each carbon sample was tested 6 times consecutively and then the average of these measurements taken.

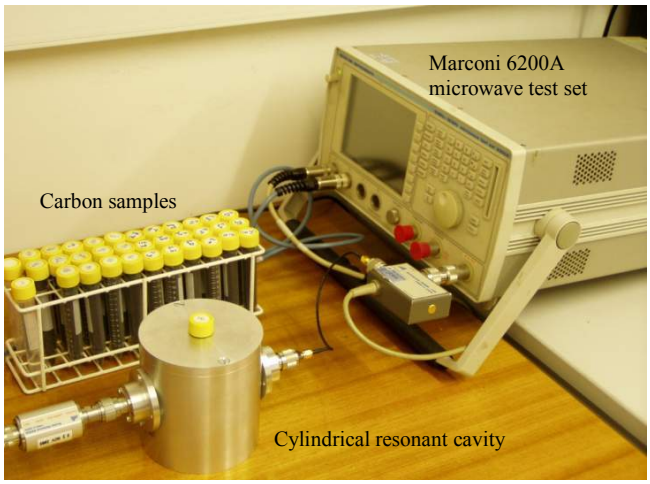


Fig. 4. Marconi 6200A microwave test set, resonant cavity and activated carbon samples under test.

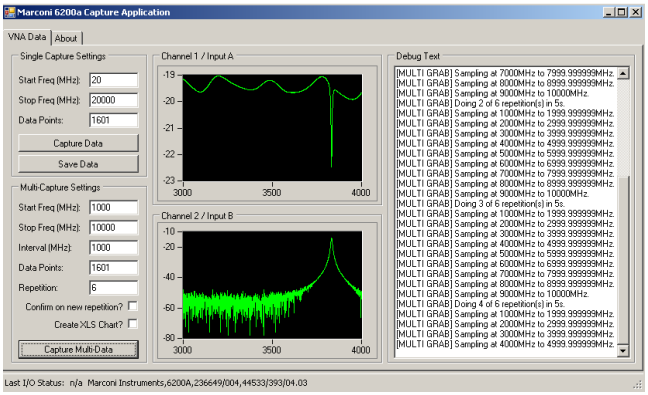


Fig. 5. A screen grab of the bespoke data acquisition software which interfaces with the Marconi 6200A microwave test set.

IV. RESULTS

Responses shown by materials exposed to microwave radiation in a resonant cavity are often specific to that material. This means that one has to look through the entire measured spectrum (20MHz – 20GHz in this case) looking for frequencies where interesting features are present. Fig. 6 to 9 show selected results of measurements using the apparatus previously described. Fig. 6 to 8 are concerned with S_{11} measurements and Fig. 9 S_{21} measurements. All of the measurements show a distinctive pattern (highlighted in Fig. 6 and 9) which suggests that it is possible to distinguish between activated carbon samples of different ages using a resonant microwave cavity.

Initially it was wondered if the response was simply due to increased water content in the carbon samples. During the aging of the samples they are exposed to high humidity, therefore taking on moisture from the atmosphere. However, the samples do this relatively quickly; the samples increase in weight significantly between months 0 and 1, but in subsequent months the weight remains relatively stable. Therefore the measured response must be as a result of some other feature of the carbon, which appears to be linked to its aging. It is known that the carbon is aging due to the reduced gas breakthrough times shown in Fig. 3.

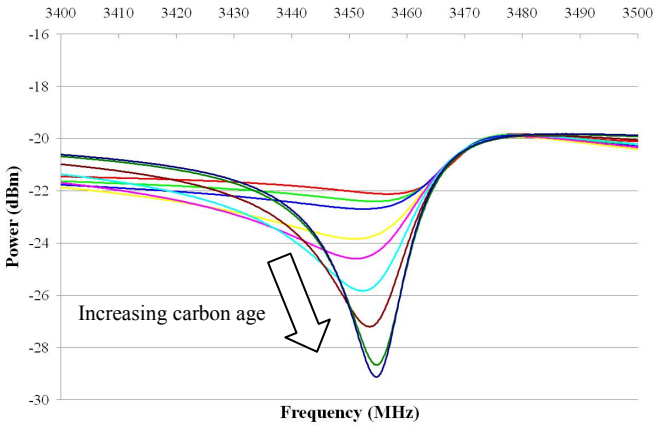


Fig. 6. S_{11} measurements between 3400MHz and 3500MHz.

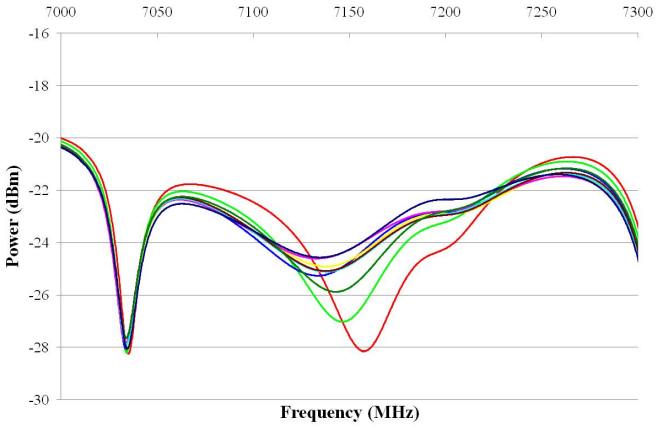


Fig. 7. S_{11} measurements between 7000MHz and 7300MHz.

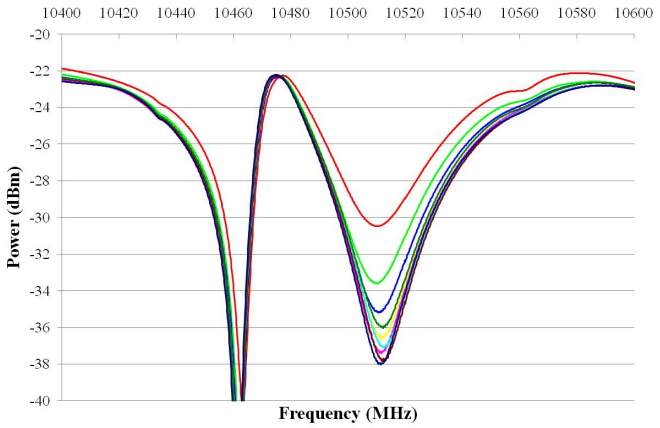


Fig. 8. S_{11} measurements between 10400MHz and 10600MHz.

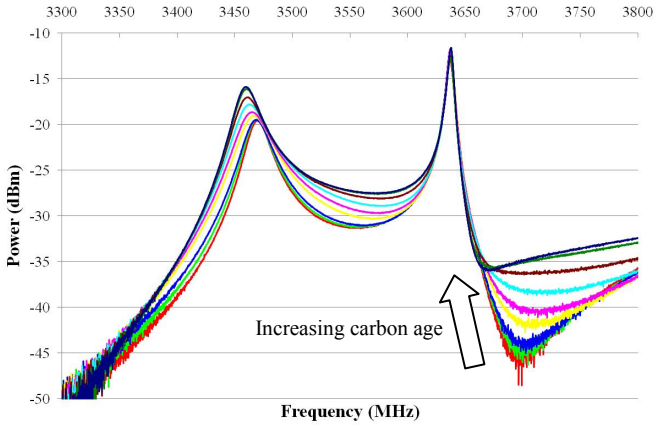


Fig. 9. S_{21} measurements between 3300MHz and 3800MHz.

V. Conclusions and Future Work

This paper presents a novel application of a resonant microwave cavity in order to determine the residual life of activated carbon samples. The work thus far suggests that the method is able to distinguish between samples of different ages; the sample residual life has been verified via gas breakthrough testing.

The most obvious application of this work would be for testing gas mask filters before they are taken onto the battle field in order to ascertain the remaining useful life. This will help to reduce the current levels of waste. In addition, the technology could be applied to the manufacture of activated carbon as a quality control tool.

Future work will look at quantifying the change in the microwave spectrum as a result of aged samples. In order to do this, samples aged using a different temperature condition will be tested (i.e. 22°C in addition to 40°C). The lower temperature samples should age more slowly and therefore will experience a different rate of gas breakthrough time degradation. By doing this we can more reliably determine the correlation between changes in the microwave spectrum and breakthrough time.

Additional work will also include co-aging two further batches of activated carbon to determine the robustness of the measurement technique. The research has scope for testing of other filter materials – work has already been published for measurements involving high efficiency particulate air (HEPA) filters [8].

References

[1] Carbon Resources. (07/11/2010). *Activated Charcoal Information*. Available: http://www.carbonresources.com/activated-charcoal.html

[2] R. C. Bansal and M. Goyal, "Activated carbon and its surface structure," in *Activated Carbon Adsorption*, 1st ed Boca Raton: CRC Press, 2005, pp. 1-9.

[3] H. Marsh and F. Rodríguez-Reinoso, "Porosity in Carbons: Modelling," in *Activated Carbon*, 1st ed: Elsevier, 2006, p. 96.

[4] S. Jhadhav, "Value Added Products from Gasification - Activated Carbon," Indian Institute of Science 2005.

[5] H. Marsh and F. Rodríguez-Reinoso, "Activated Carbon," in *Activated Carbon*, 1st ed: Elsevier, 2006, p. 10.

[6] D. M. Pozar, *Microwave Engineering*, 3rd ed. New York: John Wiley and Sons, 2005.

[7] A. Thomas, "Annual Report 2009-2010," Dstl, Salisbury, UK Unclassified, Annual Report 2010.

[8] A. Mason, S. Wylie, A. Thomas, H. Keele, A. Shaw, and A. I. Al-Shamma'a, "HEPA Filter Material Load Detection Using a Microwave Cavity Sensor," *International Journal on Smart Sensing and Intelligent Systems,* vol. 3, pp. 322-337, 2010.

Development of a Non-Deterministic Input-Output Based Relationship Test Data Set Minimization Strategy

Ong Hui Yeh and Kamal Zuhairi Zamli
School of Electrical and Electronic Engineering
Universiti Sains Malaysia, Engineering Campus
14300 Nibong Tebal, Penang, Malaysia
e-mail: yeh_1985@hotmail.com, eekamal@eng.usm.my

***Abstract*- Numerous efficient interaction testing strategies have been proposed in the past literatures to generate optimized test cases for software system under test (SUT). Meanwhile, most of the reported tools enumerate their test cases by covering all *t*-interactions of parameters involved, which are also known as uniform strength interaction testing. Later on, variable strength interaction testing has been proposed to allow certain subsets to cover higher *t*-interactions. Nevertheless, this consideration is still insufficient to generate test cases based on actual interactions. In fact, recent researches claimed that neither uniform nor variable strength interaction testing is capable to exactly cover actual factors interaction. Recently, interaction testing based on input-output relationship is reported to accommodate the actual interactions for SUT. This approach claimed that the interaction testing should focus on those input combinations that affect a program output, rather than considering all possible input combinations. The problem of generating minimal test cases is considered NP-complete as no single strategy in input-output interaction testing can generate the most efficient test cases. Therefore, a non-deterministic input-output based relationship test data sets minimization strategy, TIOR, has been proposed in this paper. The benchmarking inputs that reported in the literatures have been executed on TIOR in order to demonstrate its effectiveness and TIOR generally gives competitive results against other strategies.**

I. INTRODUCTION

Design of Experiment (DOE) technique has been commonly applied to address quality control issues in various domains such as agriculture, chemistry, medicine, and industrial design for several decades. DOE aims to maximize the amount of information gained in an experiment by optimizing the combinations of independent variables [1, 2]. In software engineering context, software testing that applied DOE methods is referred as interaction testing or *t*-way testing (where *t* indicates the interaction strength). Interaction testing is an effective and efficient sampling technique been used to detect faults that caused by interaction between parameters in component-based software systems [3]. Specifically, interaction testing generates optimized test cases (experiments) that fulfill the coverage of all *t*-way parameters interactions for a typical system. The rationale for *t*-way testing stemmed from the fact that from empirical observation, the number of parameters involved in software failures is relatively small (i.e. in the order of 2 to 6), in some classes of software [4, 5].

Numerous efficient interaction testing strategies have been proposed in the past literatures [6-9], to generate optimized test cases for software system under test (SUT). Meanwhile, most of the reported tools enumerate their test cases by covering all *t*-interactions of parameters involved, which are also known as uniform strength interaction testing. However, in most actual scenarios, not all faults from a typical SUT are solely constituted by these *t*-interactions. Practically, a particular subset of parameters can have a higher degree of interaction than others, which indicating failures due to the interaction of that subset may have more significant impact to the overall system [4]. For example, consider a subset of components that control a safety-critical hardware interface. A stronger coverage is desired in that area (i.e. t=3) but the rest of the components may be sufficiently tested with pairwise testing (t=2). In this case, variable strength interaction testing strategy is then been proposed in order to support this practical need [4, 11]. With this consideration, variable strength of coverage can be assigned to any subset of components as well as to the whole system.

Variable strength interaction testing facilitates its flexibility by allowing certain subsets to cover higher *t*-interactions. Nevertheless, this consideration is still insufficient to generate test cases based on actual interactions. In fact, recent researches claimed that neither uniform nor variable strength interaction testing is capable to exactly cover actual factors interaction. To address this issue, Schroeder P. J. et al. [11] proposed that input-output based relationship interaction testing can accommodate the actual interactions for SUT. They claimed that the interaction testing should focus on those input combinations that affect a program output, rather than considering all possible input combinations. This is indeed a favorable concern in real software systems since the input-output interaction testing gives actual parameters interactions and thus enhances the systems robustness and improves the fault detect ability [12]. On the other hand, the problem of generating minimal test cases is considered NP-complete [13] as no single strategy in input-output interaction testing can

generate the most efficient test cases. Therefore, a non-deterministic input-output based relationship test data sets minimization strategy, TIOR, has been proposed in this paper. The benchmarking inputs that reported in the literatures [12] have been executed on TIOR in order to demonstrate its effectiveness and TIOR generally gives competitive results against other strategies.

The rest of the paper is structured as follows: Section 2 gives the mathematical background on interaction testing. Section 3 discusses the recent related work on input-output based relationship interaction testing whereas in Section 4, the implementation of TIOR is further illustrated and clarified. In Section 5, we compare and discuss our results with other existing tools. Lastly, we conclude our work in Section 6.

II. MATHEMATICAL BACKGROUND

Mathematically, interaction testing can be abstracted to a covering array (CA). CA is a combinatorial object that been extensively used to generate interaction test cases in software systems when all factors (parameters) have equal number of levels (options). A covering array, CA (N; t, k, v), is an array with N rows and k columns that satisfies the criteria that each t-tuple occurs at least once within these rows [14, 15]. When N is unknown or unspecified, the notation CA (t, k, v) can be used. Note that t is known as interaction strength, k is the number of factors and v is the number of options associated with each factor. For covering array, the value of v is the same for all k.

Mixed-level covering array is a generalization of covering array that allows for different alphabet sizes for different rows [16]. The mixed-level covering array is denoted as MCA (N; t, k, (v_1, v_2, ..., v_k)), an N x k array on v symbols [17], where $v = \sum_{i=1}^{k} v_i$ [27], with the following properties:

1. Each column i ($1 \le i \le k$) contains only elements from a set S_i with $| S_i | = v_i$.
2. The rows of each N x t sub-array cover all t-tuples of values from the t columns at least once.

A shorthand notation can be used to describe MCA (also for CA, VCA and IOR) by combining the same v_i's and representing this number as a superscript [18]. For instance, three v_i's each with two options is written as 2^3. In this manner, an MCA (N; t, k, (v_1, v_2, ..., v_k)) can also be written as an MCA(N; t, (s_1^{p1}, s_2^{p2}, ..., s_r^{pr})) where $k = \sum_{i=1}^{r} p_i$.

Variable strength covering array, denoted as VCA (N; t, (v_1, v_2, ..., v_k), C), is an N x k mixed level covering array, of strength t containing C, a vector of covering arrays each of strength greater than t and defined on a subset of the k columns. Ordering of the columns in the representation of a VCA is important since the columns of the covering arrays in C are listed consecutively from left to right [19, 20].

Differ from CA, MCA and VCA, input-output based relationship covering array needs not generate test cases to cover all t-way interactions but only required to cover all actual interactions. This covering array can be denoted as IOR (N; (v_1, v_2, ..., v_k), R), an N x k mixed level covering array which covers interaction relationship, R, of a typical software SUT. R consists of w number of interaction coverage requirement, r, which specified the actual interactions for that SUT and is defined as $R = \{r_1, r_2, ..., r_w\}$ [11, 12]. Each r indicates a set of inputs (factors) that are interacting and is constitute to a specified interaction coverage requirement.

III. RELATED WORK

Considering the support of input-output interaction testing, much useful effort is also emerging. First of all, Schroeder P. J. et al. proposed the model of input-output based relationship testing method and give three different test generation algorithms [11, 21, 22] to solve the problem of test generation for software with complex input-output relationship. Their first approach implemented a brute force algorithm to explore all possible combinations of test to discover the correct minimal test set [11]. However, this is an inefficient algorithm as it consumed a lot of computational resources in order to generate test set. Then, they proposed the Union algorithm by generating a serial of test suite (a set of test cases) for each output variable to cover the interaction among the associative inputs variables respectively, and then taking the union of them in order to obtain a final test suite [21]. This algorithm is simple but not producing small test suite. Lastly, Schroeder P. J. proposed the Greedy algorithm [22]. This algorithm works by selecting an unused test case that covers the greatest number of uncovered combinations of input values each times until all interactions have been covered by the selected test suite. It indeed generate a much smaller test suite than the Union algorithm, but with a bad time and space performance since this method must check all test cases in a huge search space. In their later work [23], they implemented a problem reduction method, which is based on the color graph, to enhance the efficiency of the Greedy algorithm. Nonetheless, it should be noted that this method is applicable when the number of edges in associated color graph is much smaller than that of complete graph with the same number of edges. And the algorithm with reduced technique may generate some redundancy test cases.

Later on, Wang Z. Y. et al. [12] analyzed and improved the Union algorithm. They suggested that all the positions corresponding to each "don't care" factor shall not be assigned until a coverage requirement which include this factor is dealt. The improved Union algorithm generates better results in term of test set size reduction if compared with the previous Union algorithm. Despite of Union algorithm, they also implemented input-output interaction testing by adopting the in-parameter-order strategy [13]. For this strategy, an initial test suite will be constructed for a sub-system with small number of factors. The system is then extended by adding a new factor to get a test suite for the new sub-system. The extending process is repeated

until all factors have been added into the sub-system. This approach gives comparable results against the Greedy algorithm [12].

IV. Overview of TIOR Strategy

TIOR is implemented based on one-test-at-a time basis (which is first used by AETG [24]) to construct test cases. Basically, TIOR strategy is composed from two algorithms: Interaction Pair Generation algorithm and Test Suite Construction algorithm. In order to illustrate how TIOR strategy exploits Interaction Pair Generation algorithm, consider a typical factor set that consisting of 4 factors (parameters) of 2 levels (options) for each, F = $\{2^4\}$. Table I summarized this factor set in terms of symbolic value to facilitate our discussions. We also assumed that the interaction coverage requirements in this case are: P1P2, P1P3, P1P4 and P2P3P4.

TABLE I
SYMBOLIC NOTATIONS FOR F = $\{2^4\}$

Parameter	P1	P2	P3	P4
Base Values	0	0	0	0
	1	1	1	1

Based on this example, there are 4 groups of parameter interaction (corresponding to interaction coverage requirements of P1P2, P1P3, P1P4 and P2P3P4). Denoted that the parameter involves in parameter interaction is termed as interaction element throughout this paper.

Upon generation of aforementioned parameter interaction groups, Interaction Pair Generation algorithm proceeds to generate all possible interaction pairs. For each parameter interaction group, exhaustive combinations will be formed within its interaction elements whereas the don't care ('X') values are assigned on the corresponding non-interacting elements. Table II depicts the resultant interaction pairs for the example and Fig. 1 shows the pseudo code for Interaction Pair Generation algorithm.

TIOR adopts dynamic partitioned base data structure in Interaction Pair Generation algorithm to hold the generated interaction pairs since it offers systematic and well organized space search rather than the unpartitioned base data structure, in which every search always begin from the first data of the bulky irregular data structure. The number of partition for data structure relies on the number of groups of parameter interaction. In this example, TIOR used 4 partitioned data structure to store the resultant interaction pairs accordingly.

TABLE II
THE RESULTANT INTERACTION PAIRS

Parameter Interaction	**P1P2**					**P1P3**					**P1P4**					**P2P3P4**			
Parameter	**P1**	**P2**	**P3**	**P4**		**P1**	**P2**	**P3**	**P4**		**P1**	**P2**	**P3**	**P4**		**P1**	**P2**	**P3**	**P4**
Interaction Pairs	0	0	X	X		0	X	0	X		0	X	X	0		X	0	0	0
	0	1	X	X		0	X	1	X		0	X	X	1		X	0	0	1
	1	0	X	X		1	X	0	X		1	X	X	0		X	0	1	0
	1	1	X	X		1	X	1	X		1	X	X	1		X	0	1	1
																X	1	0	0
																X	1	1	1
																X	1	1	0
																X	1	1	1

```
Algorithm of Interaction Pair Generation(factor set, F and interaction coverage requirements, R)
1: begin
2: let F = {f0……fm-1} where F represents number of values defined for each factor, f and m =
   number of factor
3: let R = {r0……rz} where R represent the set of interaction coverage requirements
4: initialize IE = { }, where IE represents interaction pairs partitioned base data structure
5: for each interaction coverage requirement, ri
6: {
7:   for each combination of parameter interaction in ri
8:   {
9:   if (factors are interaction elements)
10:     generate interaction pair for interaction elements;
11:  else
12:     append don't care ("X") values for non-interacting elements;
13:  store the interaction pair (with "X") into IE[i];
14: }
15:}
16: return IE;
17: end
```

Fig. 1. Pseudo Code for Interaction Pair Generation Algorithm

Once the interaction pairs are generated, TIOR summons Test Suite Construction algorithm to generate test suite. First of all, a test case is proposed by forming the first combination of exhaustive combinations (for interaction elements) and assigning a random value (within the range) to each non-interacting element from the first group of parameter interaction. Base on partitioned base data structure as well, TIOR subsequently verifies the number of interaction pairs could be covered by that test case. This test case is promptly sent to final test suite if only if it covered all of its corresponding interaction pairs (indicating an optimized test case been found). Otherwise, TIOR will reassign another set of random values and check for its covering pairs. As long as the optimized test case has not been discovered, TIOR will repeat the assigning and checking process for n (number of iterations) times, and choose the test case with best number of covered pairs among the n test cases proposed. The corresponding covered pairs in partitioned data structure are then eliminated before the system proceeds to propose next test case. The final test suite is considered completely formed as all pairs in partitioned data structure are covered. Fig. 2 illustrates the pseudo code for Test Suite Construction algorithm.

Note that in TIOR, the users can decide on the value of n. Given a typical input specifications, TIOR generates test suite accordingly as described before. With this customizable looping system, if the TIOR user chooses a larger value of n for typical input, there is higher chance for TIOR to give more optimized test suite. This is due to the fact that, by having more iterations (corresponding to higher value of n) on assigning additional set of random values and checking corresponding covered pairs routine, TIOR gets higher possibility to obtain the test case which has more covered pairs. Though, TIOR consumes extra computational time for these. In other side of coin, TIOR generates less optimized test suites with smaller n value but less execution time. This notable customization provides the flexibility for TIOR users to decide their preference (either the optimality of test suite or generation time concern) on generating the test suite.

```
Algorithm Constructing Test Suite (number of iterations, n and interaction pairs, IE)
1: begin
2: initialize τ = { }, where τ represents final test suite
3: initialize α = { }, where α represents a test case that will be comprised of a set of
   factors
4: initialize β = { }, where β represents covered pairs
5: for each interaction coverage requirement, ri
6: {
7:   for each combination of parameter interaction in ri
8:   {
9:     generate interaction pair for interaction elements;
10:    for n times of iterations
11:    {
12:      assign a random value for each non-interacting element;
13:      form α;
14:      check β on IE;
15:      if (maximum # of β)
16:        break;
17:      else
18:        update weight;
19:    }
20:    add α into τ;
21:    remove β in IE;
22:    if (IE is null)
23:      break;
24:}
25: if (IE is null)
26:   break;
27:}
28: return τ
28:end
```

Fig. 2. Pseudo Code for Test Suite Construction Algorithm

V. RESUTLS AND DISCUSSION

In this section, we attempt to evaluate TIOR with the current benchmarking tools in input-output based relationship interaction testing. Notes that all the results are obtained using Windows XP with a 2.80 GHz Core 2 Duo CPU and 2 GB RAM with Java (JDK 1.6) installed. As TIOR is non-deterministic in nature, 20 independent runs have been performed and the best results of these runs are reported for each input. Besides that, the number of iterations is set to 200 throughout the experiments as well. It is noted that the data of other works (i.e. Density, ParaOrder, UNION, and TVG) are collected from Wang Z. Y. et al. [20]. Lastly, no fair comparison for test cases generation time is able to be performed due to the differences or unspecified of computing environments in the published literatures; thus, this aspect is excluded in our discussion.

In order to evaluate the effectiveness of TIOR against other tools, similar input specifications as specified by Wang et al. are applied to our strategy. For instance, 2 set of factors are chosen to represent the systems with fixed-level factors and mixed-level factors respectively. The fixed-level factors are consisted of 10 factors (parameters) where each factor have 3 levels (options) and defined as $F_1 = \{3^{10}\}$ whereas mixed-level factors are 3 factors of 2 options, 3 factors of 3 options, 3 factors of 4 options and a factor with 5 options and denoted as $F_2 = \{2^3 \times 3^3 \times 4^3 \times 5\}$. TIOR are then required to generate test cases for these factor sets based on predefined input-output interactions. The input-output interactions are built by selecting coverage requirements from a pool of coverage requirements in [12]; they are also attached in appendix along this paper. In brief, there will be 6 iterations in the experiment for each factor set. The first 10 coverage requirements will be included for the first iteration and defined as $|R| = 10$. With these, the input-output interactions are then added with another 10 following coverage requirements for consecutive iteration. Table III and Table IV show the generated test suites size from TIOR as well as other published tools.

Based on Table III and Table IV, Density can produce smallest test suites for almost all inputs. However, TIOR also producing the considerable results in this case. For instance, TIOR gives the optimized test suite at $|R| = 10$ for $F_2 = \{2^3 \times 3^3 \times 4^3 \times 5\}$ and produces better results than ParaOrder as well as TVG in some other cases. Particularly, TIOR always gives the smaller size than UNION for each input-output interaction.

TABLE III
COMPARISON OF DIFFERENT STRATEGIES FOR $F_1=\{3^{10}\}$ AND DIFFERENT SIZE OF R

|R|	Density	ParaOrder	UNION	TVG	TIOR
10	86	105	503	86	89
20	95	103	858	105	99
30	116	117	1599	125	132
40	126	120	2057	135	139
50	135	148	2635	139	147
60	144	142	3257	150	158

TABLE IV
COMPARISON OF DIFFERENT STRATEGIES FOR $F_2=\{2^3x3^3x4^3x5\}$ AND DIFFERENT SIZE OF R

|R|	Density	ParaOrder	UNION	TVG	TIOR
10	144	144	505	144	144
20	160	161	929	161	182
30	165	179	1861	179	200
40	165	183	2244	181	207
50	182	200	2820	194	222
60	197	204	3587	209	230

VI. CONCLUSIONS

This paper has discussed the development of an interaction testing strategy, TIOR, that supporting the input-output based relationship interaction testing. The experimental data shown TIOR always produces competitive test suites for both fixed-level and mixed-level inputs. As part of future work, additional practical feature such as implementation of automated actual data output mapping system can be considered to integrate within TIOR to further enhance its reliability and usability.

ACKNOWLEDGMENT

This research is partially funded by the generous fundamental grants – "Investigating T-Way Test Data Reduction Strategy Using Particle Swarm Optimization Technique" from Ministry of Higher Education (MOHE) and the USM research university grants – "Development of Variable Strength Interaction Testing Strategy for T-Way Test Data Generation" and PRGS – "Implementing Distributed T-Way Test Data Generator by Using Tuple Space Technology". The first author is the recipient of the USM postgraduate fellowship.

REFERENCES

[1] D.R. Kuhn and V. Okum, "Pseudo-Exhaustive Testing for Software," *30th Annual IEEE/NAS Software Engineering Workshop. SEW '06*, vol., no., pp.153-158, April 2006.

[2] D. Hoskins, R.C. Turban, and C.J. Colbourn, "Experimental Designs in Software Engineering: D-Optimal Designs and Covering Arrays," *WISER 2004 - ACM Workshop on Interdisciplinary Software Engineering Research*, pp. 55-66, 2004.

[3] D.R. Kuhn and M.J. Reilly, "An Investigation of the Applicability of Design of Experiments to Software Testing," *27th Annual NASA Goddard/IEEE Software Engineering Workshop, Proceedings*, pp. 91-95, December 2002.

[4] K.Z. Zamli and M.I. Younis, "Interaction Testing: From Pairwise to Variable Strength Interaction," *2010 Fourth Asia International Conference Mathematical/Analytical Modelling and Computer Simulation (AMS)*, pp.6-11, May 2010.

[5] D.R. Kuhn, D.R. Wallace, and A.M., Jr. Gallo, "Software fault interactions and implications for software testing," *IEEE Transactions on Software Engineering,* vol.30, no.6, pp. 418- 421, June 2004.

[6] J. Kim, K. Choi, D.M. Hoffman, and G. Jung, "White Box Pairwise Test Case Generation," *Seventh International Conference Quality Software, QSIC '07.*, pp.286-291, Oct. 2007.

[7] Y. Cui, L. Li, and S. Yao, "A New Strategy for Pairwise Test Case Generation," *Third International Symposium Intelligent Information Technology Application, IITA*, vol.3, pp.303-306, November 2009.

[8] Y. Lei, R. Kacker, D.R. Kuhn, V. Okun, and J. Lawrence, "IPOG: A General Strategy for T-Way Software Testing," *14th Annual IEEE International Conference and Workshops*, *Engineering of Computer-Based Systems, ECBS '07.* pp.549-556, 26-29 March 2007.

[9] M.F.J. Klaib, K.Z. Zamli, N.A.M. Isa, M.I.Younis, and R. Abdullah, "G2Way A Backtracking Strategy for Pairwise Test Data Generation," *15th Asia-Pacific Software Engineering Conference, APSEC '08*, pp.463-470, 3-5 December 2008.

[10] M.B. Cohen, P.B. Gibbons, W.B. Mugridge, and C.J. Colbourn, "Constructing Test Suites for Interaction Testing," *Software Engineering, Proceedings. 25th International Conference,* pp. 38- 48, 3-10 May 2003.

[11] P. J. Schroeder and B. Korel. "Black-Box Test Reduction Using Input-Output Analysis," *Proceedings of the International Symposium on Software Testing and Analysis (ISSTA2000)*, *ACM SIGSOFT Software Engineering Notes*, vol. 25, no.5, pp. 173-177, 2000.

[12] Z. Wang, C. Nie and B. Xun, "Generating Combinatorial Test Suite for Interaction Relationship." *Proceeding of 4th International Workshop on Software Quality Assurance (SOQUA2007)*, pp. 55-61 September, 2007.

[13] Y. Lei and k. C. Tai, "In-Parameter-Order: A Test Generation Strategy for Pairwise Testing," *Proceedings. Third IEEE International High-Assurance Systems Engineering Symposium,* pp.254-261, 13-14 Nov 1998.

[14] M. B. Cohen, c. J. Colbourn and A. C. H. Ling, "Augmenting Simulated Annealing to Build Interaction Test Suites," *14th International Symposium on Software Reliability Engineering, ISSRE 2003*, pp. 394-405, 17-20 Nov. 2003.

[15] C. Yilmaz, M. B. Cohen and A. A. Porter,"Covering Arrays for Efficient Fault Characterization in Complex Configuration Spaces," *IEEE Transactions on Software Engineering,* , vol.32, no.1, pp. 20- 34, Jan. 2006

[16] L. Zekaoui, "Mixed Covering Arrays on Graphs And Tabu Search Algorithms", *Ottawa-Carleton Institute for Computer Science*, University of Ottawa, Canada, Master Thesis (2006).

[17] R. C. Bryce and C. J. Colbourn, "The Density Algorithm for Pairwise Interaction Testing," *Software Testing, Verification and Reliability*, 17(3), pp. 159–182, 2007.

[18] Y. Jun and Z. Jian, "Backtracking Algorithms and Search Heuristics to Generate Test Suites for Combinatorial Testing," *30th Annual International Computer Software and Applications Conference (COMPSAC'06),* vol. 1, pp.385-394, 2006.

[19] M. B. Cohen, P. B. Gibbons, W.B. Mugridge, C. J. Colbourn and J. S. Collofello, "Variable Strength Interaction Testing of Components," *27th Annual International Computer Software and Applications Conference,* pp.413, 2003.

[20] Z. Wang, B. Xu and C. Nie , "Greedy Heuristic Algorithms to Generate Variable Strength Combinatorial Test Suite," *The Eighth International Conference on Quality Software, QSIC '0,* pp.155-160, 12-13 Aug. 2008.

[21] P. J. Schoeder, "Black-Box Test Reduction Using Input-Output Analysis." *Ph.D. Thesis*, Department of Computer Science, Illinois Institute of Technology, Chicago, IL,USA, 2001.

[22] P. J. Schroeder, P. Faherty and B. Korel, "Generating Expected Results for Automated Black-Box Testing." *Proceedings of 17th IEEE International Conference on Automated Software Engineering (ASE'02)*, 2002.

[23] C. Cheng, A. Dumitrescu and P. J. Schroeder. “Generating Small Combinatorial Test Suites to Cover Input-Output Relationships,” *Proceedings of Third International Conference on Quality Software*, pp. 76-82, Nov 2003.

[24] D. M. Cohen, S. R. Dalal, M. L. Fredman and G. C. Patton, "The AETG System: An Approach to Testing Based on Combinatorial Design," *IEEE Transactions on Software Engineering*, vol.23, no.7, pp.437-444, Jul 1997.

APPENDIX

The collection of coverage requirements in experiment is as shown below. There are 10 factors in both F_1 and F_2, which is $F = \{f_1, f_2, f_3, f_4, f_5, f_6, f_7, f_8, f_9, f_{10}\}$. These 10 factors could be denoted by their corresponding sequence numbers, and then the factor set is described as F = {0, 1, 2, 3, 4, 5, 6, 7, 8, 9} for short [12].

COLLECTION={{1, 2, 7, 8}, {0, 1, 2, 9}, {4, 5, 7, 8}, {0, 1, 3, 9}, {0, 3, 8}, {6, 7, 8}, {4, 9}, {1, 3, 4}, {0, 2, 6, 7}, {4, 6}, {2, 3, 4, 8}, {2, 3, 5}, {5, 6}, {0, 6, 8}, {8, 9}, {0, 5}, {1, 3, 5, 9}, {1, 6, 7, 9}, {0, 4}, {0, 2, 3}, {1, 3, 6, 9}, {2, 4, 7, 8}, {0, 2, 6, 9}, {0, 1, 7, 8}, {0, 3, 7, 9}, {3, 4, 7, 8}, {1, 5, 7, 9}, {1, 3, 6, 8}, {1, 2, 5}, {3, 4, 5, 7}, {0, 2, 7, 9}, {1, 2, 3}, {1, 2, 6}, {2, 5, 9}, {3, 6, 7}, {1, 2, 4, 7}, {2, 5, 8}, {0, 1, 6, 7}, {3, 5, 8}, {0, 1, 2, 8}, {2, 3, 9}, {1, 5, 8}, {1, 3, 5, 7}, {0, 1, 2, 7}, {2, 4, 5, 7}, {1, 4, 5}, {0, 1, 7, 9}, {0, 1, 3, 6}, {1, 4, 8}, {3, 5, 7, 9}, {0, 6, 7, 9}, {2, 6, 7, 9}, {2, 6, 8}, {2, 3, 6}, {1, 3, 7, 9}, {2, 3, 7}, {0, 2, 7, 8}, {0, 1, 6, 9}, {1, 3, 7, 8}, {0, 1, 3, 7}}.

Multi-Sensor Spot Welding Monitor using Wireless Sensor Network Technology

J.D. Cullen, A. Mason, M. Al-Jader, N. Wylie, A. Shaw, A.I. Al-Shamma'a
Built Environment and Sustainable Technologies (BEST) Research Centre,
Liverpool John Moores University, Byrom Street, Liverpool, L3 3AF, UK.
email : J.D.Cullen@ljmu.ac.uk

***Abstract*- Resistance welding is used extensively in manufacturing industries, the most popular being spot welding in the automotive industry. Despite spot welding being in use for over a century, there has been relatively little development of sensors for monitoring the process in real-time. Most existing systems use current, voltage and electrode force to give an indication of welding quality, however these systems do not provide warning of changes in the welding environment. These changes could include material variability or electrode condition, which could result in weak weld nuggets.**

Presented in this paper is an investigation of a system that utilises an array of sensors, including current, voltage, infrared and ultrasonic that is capable of monitoring the spot welding process as it is performed. This system utilises wireless sensor technology to transmit data from the welding arms to a sensor connected to a base computer where the data can be analysed. The wireless link is particularly useful when retrofitting the sensor cluster to existing installations.

I. INTRODUCTION

Spot welding is an important welding technique that has been long established and extensively used in industry, especially the automotive industry [1]. The main quality control tests are the destructive chisel test and peel test, which are carried out on welds obtained from the production line of the product [2]. The failure rates are then detected, examined, and evaluated. If there is substantial failure rate increase, then the whole batch of products is rejected as faulty. The labour costs incurred while performing this type of testing also make this approach unattractive. Industry typically demands increased productivity and reduced production costs. This indicates that the traditional method of testing is not desirable; they are therefore receptive to newer testing methods, especially non-destructive methods that allow the sample under test to be used in production. Ideally, for the manufacturer, there would be no destructive testing methods because of product wastage. Conventional resistance welding process control has been based upon monitoring the voltage and current, or their derivatives, power and resistance [3,4]. While these sensors work well under ideal conditions, surface contaminants or metal impurities can result in weak or under sized welds to be formed while retaining the same voltage and current values as for welds conforming to the ideal standards [5-7].

Fig. 1 shows an image taken from a high speed camera running at 5000 frames per second of a specially adapted welding tip, being used to create a weld on the edge of two pieces of galvanised steel of thickness 1mm. Visible in the picture is the expelled zinc from the coating, and the molten pool of metal which, when cool, forms the spot weld nugget. However, as experts in industry would testify, simply having the right conditions for weld formation does not mean that a weld has been formed. Therefore, other parameters must be examined as well in order to give a complete picture of the quality of weld formation [8].

To counter the need to destructively test so many spot welds the use of a sensor cluster comprising a series of sensors was investigated to meet industrial requirements. The multiple outputs of the sensor cluster would give a prediction of the nugget size, upon which a decision of weld quality was made. An additional sensor input to the cluster is the condition of the electrode, since a poor electrode changes the current density through the metal, resulting in either excessive or insufficient heating.

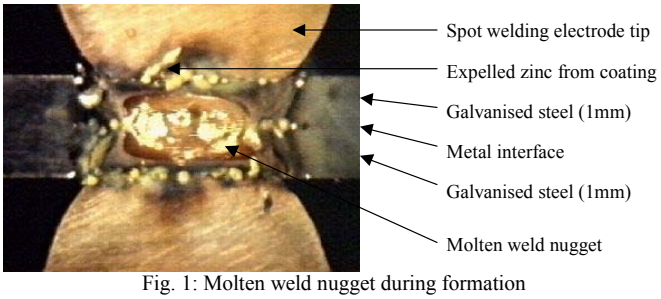


Fig. 1: Molten weld nugget during formation

II. EXPERIMENTAL SETUP

There are many types of spot welders available [9]. For these investigations the pedestal type spot welder is used. The pedestal type, as shown in fig. 2(a), has a fixed vertical pedestal frame and integral transformer and control cabinet. The bottom arm is fixed to the frame and is stationary during welding, taking the weight of the work piece. The top arm is hinged to move down in an arc. The pivoting arms are adjustable so as to have an adjustable gap between the electrodes. The arms are easily adjusted in the hubs and various length arms are able to be fitted giving access to difficult joints. The unit used had fully adjustable current levels suitable for light and medium industrial use.

The sensors under investigation, shown in fig. 2(b), are placed in relevant positions for most effective detection, see fig. 2(c). The current sensor (not visible) is a Rogowski (air cored) coil. This sensor gives a voltage output proportional to the current induced through the arms of the spot welder, while the voltage sensor is, simply, two leads connected to each spot welder electrode. This signal is then passed through a buffer/amplifier circuit and into a data logger within a PC. The infrared sensor is a photoelectric infrared-diode, mounted in the cluster, at 45° and at a distance of 70mm from the electrode tips, also passed through the buffer/amplifier circuit.

All the data from these sensors have their readings captured using a data acquisition board on a PC. The data-acquisition program is specifically written for this research work in the Pascal based Delphi environment. The signals are sampled at 1 kHz each for current, voltage, infrared and ultrasonic envelope. All the data is continuously streamed into the PC, and analysed to provide a prediction of each weld [10]. Typical industrial welding times for 0.8mm galvanised steel are 0.2s for the weld duration, the pre time of data capture is 0.3s and the post time is 0.4s. This allows the data to be captured from before the electrodes are in contact with the metal, to after the electrodes are removed from the metal, which provides a full data set for the ultrasonic profile. After the system was tried in the laboratories at Liverpool, it was installed in a 'test cell' at Jaguar Cars (Halewood), which allowed the system to be tried on industrial robots and welding machines, without the pressure of operating within the confines and needs of a production line. Fig. 3 shows the robot welding system in the test cell.

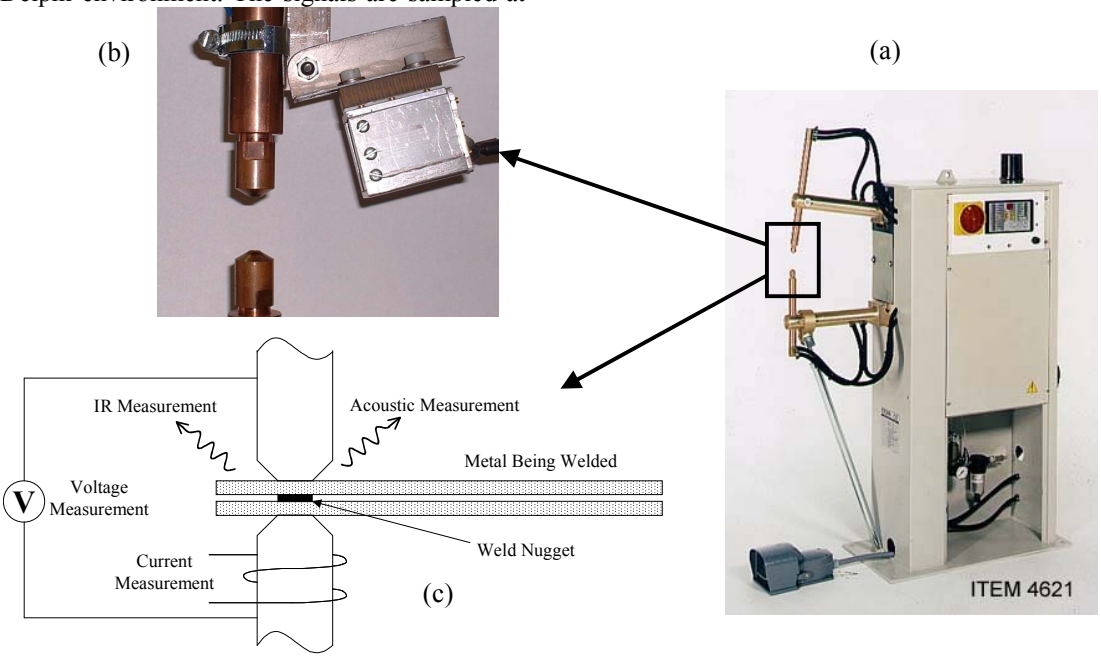


Fig. 2: (a) Pedestal spot welding machine, (b) Experimental setup of the sensors cluster, (c) diagram of sensors used.

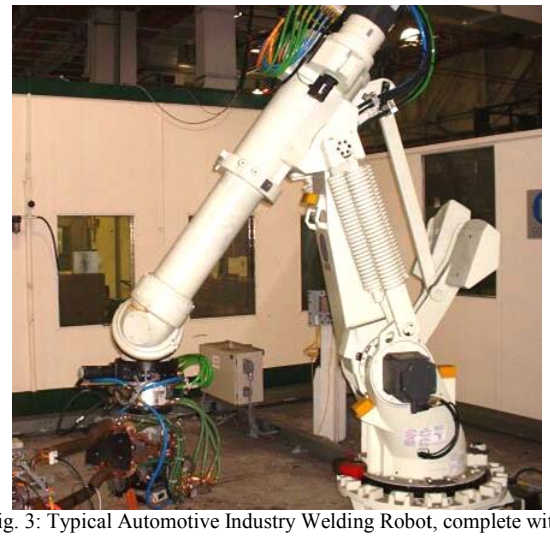


Fig. 3: Typical Automotive Industry Welding Robot, complete with interchangeable head

There is a problem with using such a monitoring system with pre-existing installations. A large proportion of the robots involved in under body manufacture (technically called 'body in white') have multiple heads which are exchanged for different tasks, or for different vehicle types being assembled. This results in having to rework the robot to include additional cabling for the sensors. This is highly expensive, and therefore is a barrier to the implementation of the new sensor technology. The answer to this is to use Wireless Sensor Networks (WSNs) to provide the link between the spot welding sensors.

III. Implementation of a WSN Spot Welding Sensor

To demonstrate the principle of WSN operating in an automotive scenario, it was decided to utilise a single sensor rather than implement the entire sensor cluster previous mentioned, as each sensor would require some amount of

conditioning logic for its output to be compatible with the MicaZ [11] mote ADC interface. This is a result of many of the sensors having an output range greater than that of the mote ADC (minimum = 0V, maximum = current battery voltage).

The single sensor chosen to be adapted for connectivity to the MicaZ motes was for current sensing. Many industrial spot welders have inbuilt current sensors [12] but this is not the case with the pedestal spot welder used in this research, hence the use of a Rogowski coil as previously mentioned. This sensor is placed around one of the welder arms. When current flows during welding a current is induced in the coil which results in a voltage output. It is driven from a 9V battery and its output varies between ±4.5V, which meant that a conditioning circuit was required.

A conditioning circuit was designed to take the output of the current sensor and reduce the signal amplitude as well as shifting it such that it varied over the range of approximately 0.1-2.1V. Fig. 4 shows the measured results from the circuit once it was built. Measurements were taken with a GDS-810S oscilloscope.

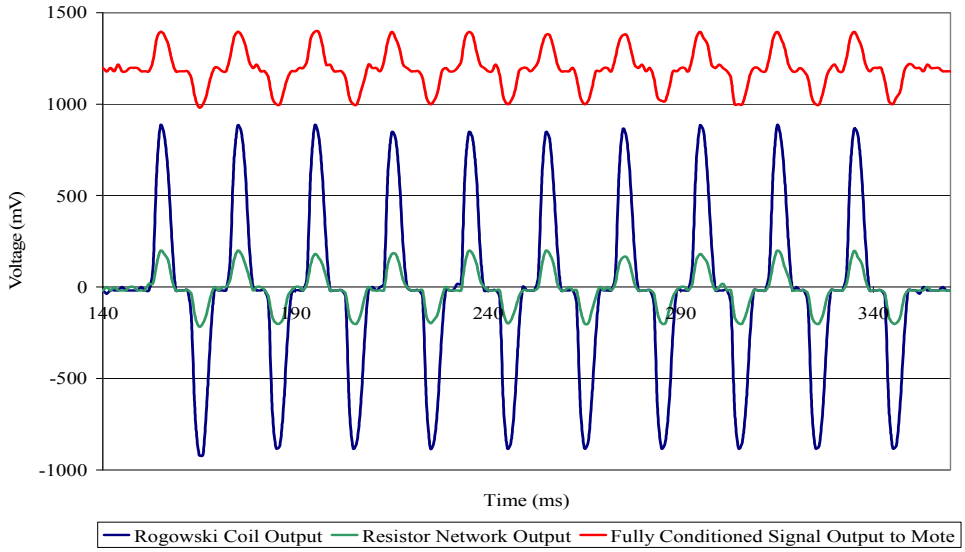


Fig. 4: Measured signal levels from sensor conditioning circuit

Fig. 4 shows that the conditioning circuit converts the output to a range useable by the MicaZ motes. The circuit, along with a copy of the mote interface board, was boxed in order to prevent it from becoming damaged, Fig. 5.

As previously mentioned, sampling was performed at 1kHz to obtain a good resolution (20 data points per cycle) of the 50Hz AC signal. It is possible for the MicaZ motes to sample at much higher frequencies but this is the sampling frequency used for the previously mentioned sensor cluster. The mote transfers data via broadcast messaging to a base node, which in turn passes the data to a Delphi [13] written GUI, as shown in Fig. 6. Broadcast routing was utilised for this demonstration simply because there was only a single welding machine to test the system.

The GUI displays data such as the number of samples taken, the minimum and maximum voltage readings as well as the mean voltage during a weld. The software then uses this to determine whether a weld was good or bad and shows an alert based upon this decision.

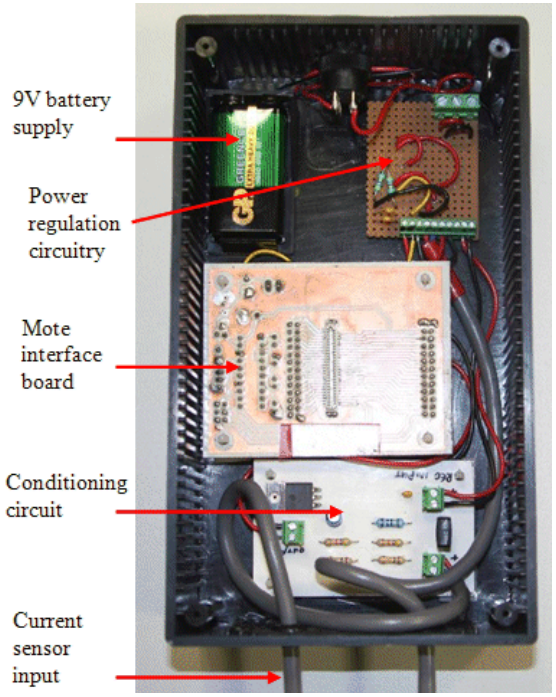


Fig. 5: Conditioning circuit and mote boxed to prevent damage

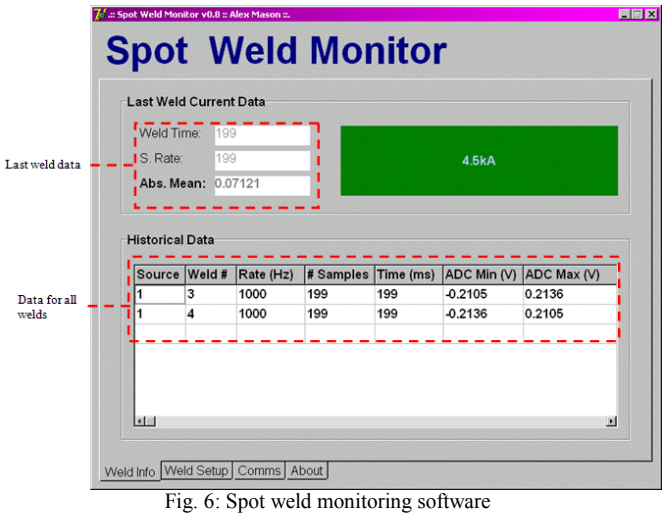


Fig. 6: Spot weld monitoring software

IV. Calibration And Testing

To calibrate the software to correctly correlate the mean voltage detected with the welding current used, weld data from around 250 welds was used. Current data used for calibration was taken from the control unit mounted on the spot welder, which allows one to set the current used for a weld. The weld current was increased from 2kA to 8kA in 0.5kA steps. It is noteworthy that the selected current was often different to the current displayed on the control unit after a weld. It is thought that this is caused by the control unit seeking the selected current during a weld, and so the value displayed after a weld is actually an average of the current used; evidence for this is shown in Fig. 4 where the voltage peaks are of slightly differing heights. Therefore, it is the post weld current value which is reflected in the calibration results shown in Fig. 7.

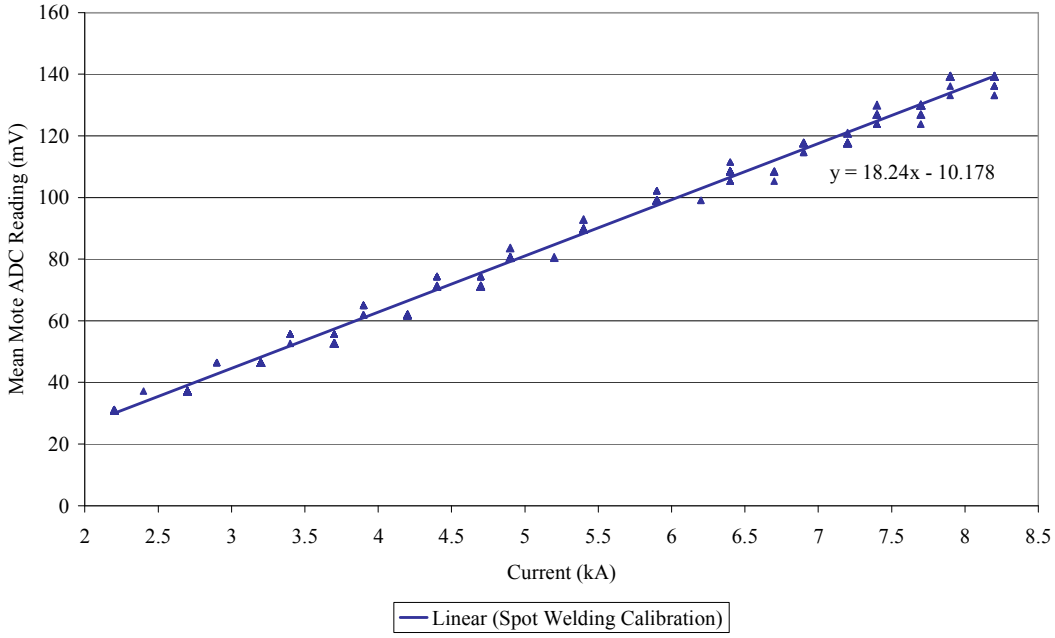


Fig. 7: Calibration of the spot welding sensor system

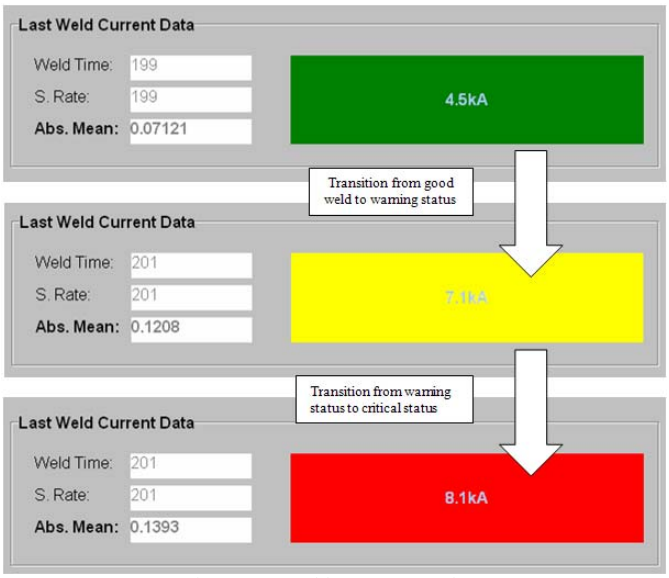


Fig. 8: Spot weld system user alert

Using the calibration results with the system software, it was possible to demonstrate the system – Fig. 8 shows the user alerts being triggered based upon different current levels.

There is the possibility for this system to be taken much further, but for the purposes of this project the aim was to show that it was possible to integrate a mote into industrial spot weld monitoring. It has been shown in this chapter that the motes can operate in highly metallic environments and so such a system provides the perfect tool for retrofitting sensors to expensive robotic welders, making it a cost effective solution for quality control and energy saving in automotive spot welding processes.

V. Conclusions And Further Work

This paper has shown that it is possible to measure various process parameters during the spot welding operation. This is not only limited to the traditional parameters such as voltage and current; it would also be possible to add in new, indirect sensing methods such as thermal emission and ultrasonic during the welding process [10]. From these sensors, additional information can be derived, such as dynamic resistance and spot welding power.

By the use of wireless sensor technology, it has been shown that the spot welding data can be transmitted from the spot welding machine, without having to run additional cables through the robot wiring looms.

Further work on the system needs to be done to expand the scope of the system. This system is only a demonstrator of a single robot head communicating with a base station, it can be expanded further to have multiple robot heads communicating with a single base station. The spot welding analysis can also be assisted by analysing the quality of the electrode tip, so having the capability for image capture and transmission on the head could be beneficial, which would require the use of image compression libraries to transmit the data in real-time.

Acknowledgements

The authors would like to thank the industrial partners including, but not limited to Corus, and Jaguar Cars for their kind support.

References

[1] C.F.Larson, “Bibliography on Resistance Welding”, Welding Journal, 51, 1972, pp. 1950-1971.
[2] R.J.Krieger, S.A.Wenk, R.C.McMaster, “Non destructive test methods for inspection of welded joints”, Welding Journal 33,1954, pp. 1118-1129.
[3] A.G.Livshits, “Universal Quality assurance method for resistance spot welding based on dynamic resistance”, Welding Research Supplement, 1997.
[4] W.F.Savage, E.F.Nippes, F.A.Wassel, “Dynamic contact resistance of series spot welds”, Welding Journal 57 (2), 1978, pp. 43s-50s.
[5] AWS 1966 Recommended Practices for Resistance Welding.
[6] AWS 1988 Recommended Practices for Automotive Weld Quality - Resistance Spot Welding.
[7] British Standards 1993 Specification for Resistance spot welding of uncoated and coated low carbon steel, BS 1140.
[8] K.Matsuyama, “Spot welding system and method for sensing welding conditions in real time”, US Patent No. 6,506,997 B2, 2003.
[9] Tecna 2003, Tecna S.P.A website, http://www.tecna.net/
[10] J. D. Cullen, et al., "Multisensor fusion for on line monitoring of the quality of spot welding in automotive industry," Measurement, vol. 41 , 2008, pp. 412-423.
[11] Crossbow: “MPR/MIB Users Manual”, Crossbow Technology Inc, 4145N First Street, San Jose, California, http://www.xbow.com/.
[12] J. D. Cullen, A. M. A. El-Rasheed, A. I. Al-Shamma’a, W. Lucas: “Multi Sensor Fusion for On Line Monitoring of the Quality of Spot Welding in Automotive Industry”, GARS-2005 Conference, Liverpool John Moores University, 22 June 2005.
[13] Borland Corporation: “Borland Delphi 7”, http://www.borland.com/, 2001